Geological Survey of Canada
Commission géologique du Canada

GEOLOGICAL INFORMATION DIVISION
JAN 21 1985
DIVISION DE L'INFORMATION GÉOLOGIQUE

This document was produced by scanning the original publication.

Ce document est le produit d'une numérisation par balayage de la publication originale.

PAPER 85-1A
ÉTUDE

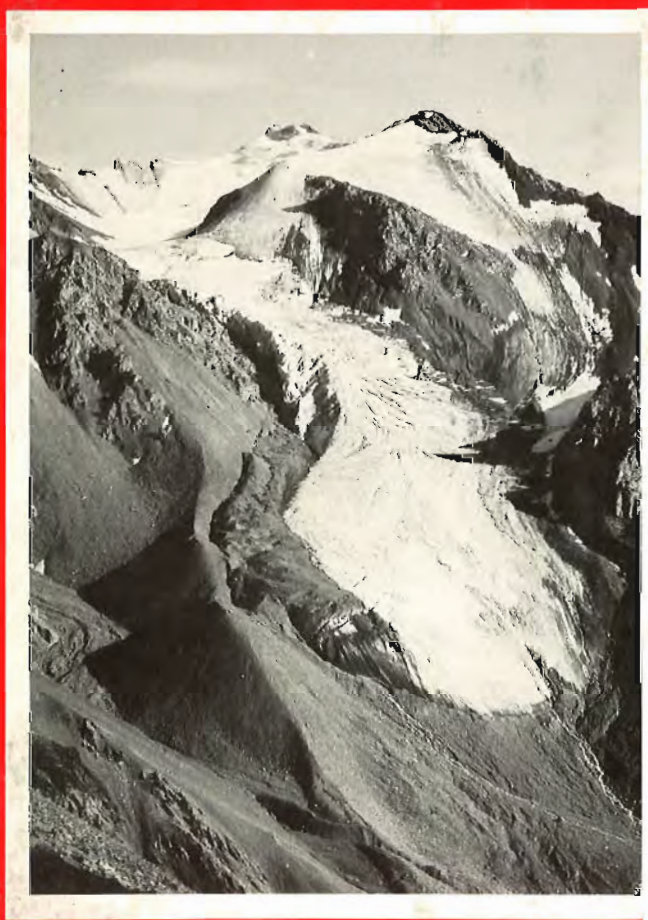

CURRENT RESEARCH

RECHERCHES EN COURS

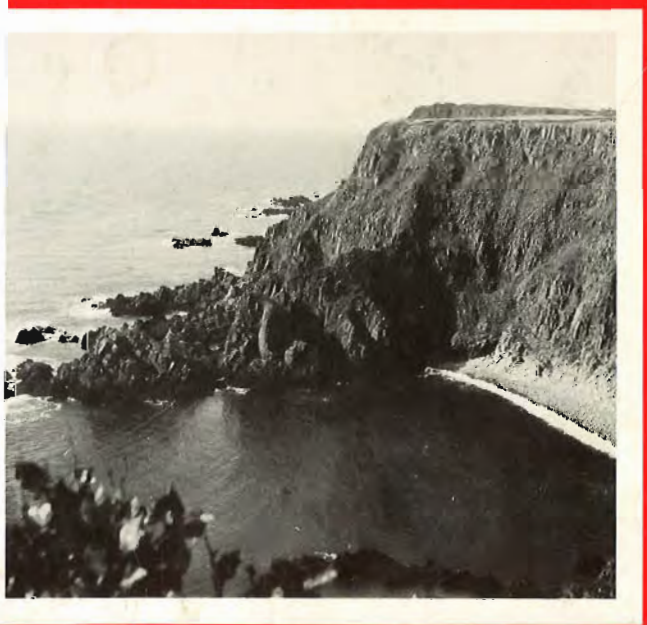

PART A
PARTIE

1985

Canada

Notice to Librarians and Indexers

The Geological Survey's twice-yearly *Current Research* series contains many reports comparable in scope and subject matter to those appearing in scientific journals and other serials. All contributions include an abstract and bibliographic citation. It is hoped that these will assist you in cataloguing and indexing these reports and that this will result in a still wider dissemination of the results of the Geological Survey's research activities.

Avis aux bibliothécaires et préparateurs d'index

La série Recherches en cours *de la Commission géologique paraît deux fois par année; elle contient plusieurs rapports dont la portée et la nature sont comparables à ceux qui paraissent dans les revues scientifiques et autres périodiques. Tous les articles sont accompagnés d'un résumé et d'une bibliographie, ce qui vous permettra, nous l'espérons, de cataloguer et d'indexer ces rapports, d'où une meilleure diffusion des résultats de recherche de la Commission géologique.*

Technical editing and compilation
Rédaction et compilation techniques

R.G. Blackadar
W.C. Morgan
H. Dumych
P.J. Griffin
N.C. Ollerenshaw
M.-F. Dufour
L.E. Vincent

Production editing and layout
Préparation et mise en page

M.J. Kiel
Debby Busby

Typed and checked
Dactylographie et vérification

Jacinthe Caron-Blais
Janet Gilliland
Shirley Kostiew
Janet Legere
Sharon Parnham

GEOLOGICAL SURVEY OF CANADA
PAPER 85-1A
COMMISSION GÉOLOGIQUE DU CANADA
ETUDE 85-1A

CURRENT RESEARCH
PART A

RECHERCHES EN COURS
PARTIE A

1985

© Minister of Supply and Services Canada 1985

Available in Canada through

authorized bookstore agents and other bookstores

or by mail from

Canadian Government Publishing Centre
Supply and Services Canada
Ottawa, Canada K1A 0S9

and from

Geological Survey of Canada offices:

601 Booth Street
Ottawa, Canada K1A 0E8

3303-33rd Street N.W.,
Calgary, Alberta T2L 2A7

100 West Pender Street
Vancouver, British Columbia V6B 1R8
(mainly B.C. and Yukon)

A deposit copy of this publication is also available
for reference in public libraries across Canada

Cat. No. M44-85/1AE Canada: $15.00
ISBN 0-660-11756-8 Other countries: $18.00

Price subject to change without notice

Cover

(left) *Alpine glacier, Kaskawulsh map-area; Yukon Territory. (GSC 123515)*

(right) *Cliffs in Triassic basalt showing columnar jointing; Grand Manan Island, New Brunswick. (GSC 98550)*

NOTE TO CONTRIBUTORS

Submissions to the *Discussion* section of *Current Research* are welcome from both the staff of the Geological Survey and from the public. Discussions are limited to 6 double-spaced typewritten pages (about 1500 words) and are subject to review by the Chief Scientific Editor. Discussions are restricted to the scientific content of Geological Survey reports. General discussions concerning branch or government policy will not be accepted. Illustrations will be accepted only if, in the opinion of the editor, they are considered essential. In any case no redrafting will be undertaken and reproducible copy must accompany the original submissions. Discussion is limited to recent reports (not more than 2 years old) and may be in either English or French. Every effort is made to include both *Discussion* and *Reply* in the same issue. *Current Research* is published in January and July. Submissions for these issues should be received not later than 1 November and 1 May respectively. Submissions should be sent to the Chief Scientific Editor, Geological Survey of Canada, 601 Booth Street, Ottawa, Canada, K1A 0E8.

AVIS AUX AUTEURS D'ARTICLES

Nous encourageons tant le personnel de la Commission géologique que le grand public à nous faire parvenir des articles destinés à la section discussion *de la publication* Recherches en cours. *Le texte doit comprendre au plus six pages dactylographiées à double interligne (environ 1500 mots), texte qui peut faire l'objet d'un réexamen par le rédacteur en chef scientifique. Les discussions doivent se limiter au contenu scientifique des rapports de la Commission géologique. Les discussions générales sur la Direction ou les politiques gouvernementales ne seront pas acceptées. Les illustrations ne seront acceptées que dans la mesure où, selon l'opinion du rédacteur, elles seront considérées comme essentielles. Aucune retouche ne sera faite aux textes et dans tous les cas, une copie qui puisse être reproduite doit accompagner les textes originaux. Les discussions en français ou en anglais doivent se limiter aux rapports récents (au plus de 2 ans). On s'efforcera de faire coincider les articles destinés aux rubriques* discussions *et* reponses *dans le même numéro. La publication* Recherches en cours *paraît en janvier et en juillet. Les articles pour ces numéros doivent être reçus au plus tard le 1er novembre et le 1er mai respectivement. Les articles doivent être renvoyés au rédacteur en chef scientifique: Commission géologique du Canada, 601, rue Booth, Ottawa, Canada, K1A 0E8.*

GEOLOGICAL SURVEY OF CANADA
COMMISSION GÉOLOGIQUE DU CANADA

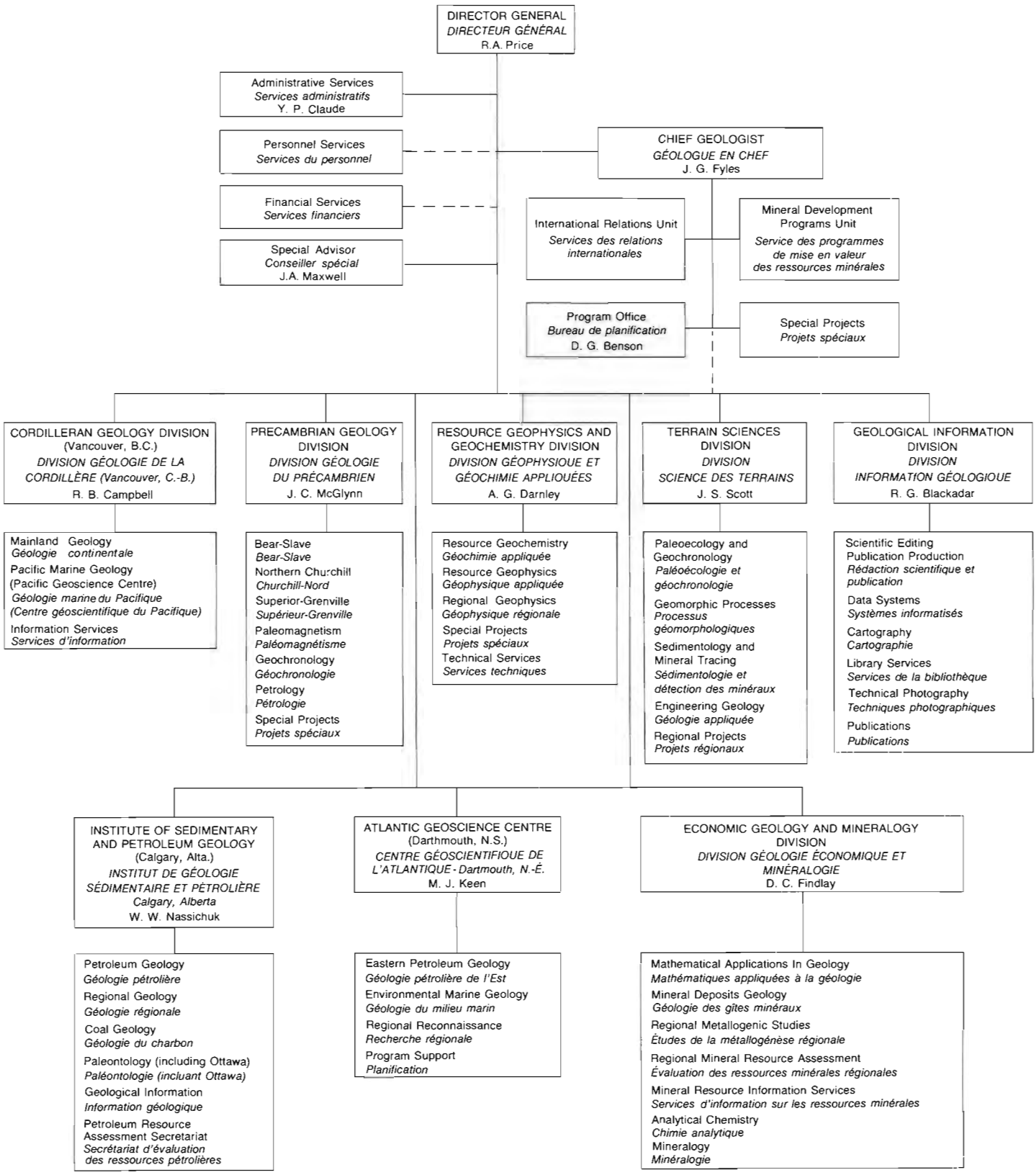

April 1984

Avril 1984

Separates

A limited number of separates of the papers that appear in this volume are available by direct request to the individual authors. The addresses of the Geological Survey of Canada offices follow:

601 Booth Street,
OTTAWA, Ontario
K1A 0E8

Institute of Sedimentary and Petroleum Geology,
3303-33rd Street N.W.,
CALGARY, Alberta
T2L 2A7

Cordilleran Geology Division
100 West Pender Street,
VANCOUVER, B.C.
V6B 1R8

Atlantic Geoscience Centre,
Bedford Institute of Oceanography,
P.O. Box 1006,
DARTMOUTH, N.S.
B2Y 4A2

When no location accompanies an author's name in the title of a paper, the Ottawa address should be used.

Tirés à part

On peut obtenir un nombre limité de "tirés à part" des articles qui paraissent dans cette publication en s'adressant directement à chaque auteur. Les adresses des différents bureaux de la Commission géologique du Canada sont les suivantes:

601, rue Booth
OTTAWA, Ontario
K1A 0E8

Institut de géologie sédimentaire et pétrolière
3303-33rd, St. N.W.,
CALGARY, Alberta
T2L 2A7

Division de la géologie de la Cordillère
100 West Pender Street
VANCOUVER, Colombie-Britannique
V6B 1R8

Centre géoscientifique de l'Atlantique
Institut océanographique de Bedford
B.P. 1006
DARTMOUTH, Nouvelle-Ecosse
B2Y 4A2

Lorsque l'adresse de l'auteur ne figure pas sous le titre d'un document, on doit alors utiliser l'adresse d'Ottawa.

PUBLICATIONS
FEB 5 1985
FEV
SENT / EXPÉDIÉES

SCIENTIFIC AND TECHNICAL REPORTS
RAPPORTS SCIENTIFIQUES ET TECHNIQUES

ECONOMIC GEOLOGY/GÉOLOGIE ÉCONOMIQUE

V. RUZICKA and G.M. LECHEMINANT: Summary on uranium in Canada, 1984 15

R.K. STEVENSON: An occurrence of amazonite, gahnite, and sphalerite near Portman Lake, Northwest Territories 23

J. RIMSAITE: Petrography, petrochemistry and mineral associations of selected rocks and radioactive occurrences north of Mont-Laurier, Quebec: a progress report 47

G.E. LOWEY and D.G.F. LONG: Preliminary investigation of the sedimentology of auriferous strata in the Early Aphebian (Huronian) Lorrain Formation, between Sault Ste. Marie and Elliot Lake, Ontario 97

R.T. BELL and V. RUZICKA: Uranium in the Circum-Ungava Belt, northern Quebec and Labrador: new information from the central Labrador Trough 145

C.D. ANGLIN and J.M. FRANKLIN: Gold mineralization in the Beardmore-Geraldton area of northwestern Ontario 193

C.W. JEFFERSON, W.E. NELSON, R.V. KIRKHAM, J.H. REEDMAN, and R.F.J. SCOATES: Geology and copper occurrences of the Natkusiak basalts, Victoria Island, District of Franklin 203

D.C. GRÉGOIRE: Extraction of organically-bound gold in surficial materials 223

S.S. GANDHI: Geology of the Artillery Lake Pb-Zn-Cu district, District of Mackenzie 359

R.V. KIRKHAM: Base metals in upper Windsor (Codroy) Group oolitic and stromatolitic limestones in the Atlantic Provinces 573

J.W. LYDON, W.D. GOODFELLOW, and I.R. JONASSON: A general genetic model for stratiform baritic deposits of the Selwyn Basin, Yukon Territory and District of Mackenzie 651

J.W. LYDON, I.R. JONASSON, and K.A. HUDSON: The distribution of gold in the TEA barite deposit, Yukon Territory 661

C.J. MWENIFUMBO: Mise-à-la-masse mapping of gold-bearing alteration zones at the Hoyle Pond gold deposit, Timmins, Ontario 669

GEOCHRONOLOGY/GÉOCHRONOLOGIE

F.C. TAYLOR and W.D. LOVERIDGE: A Rb-Sr study of granitoid intrusive rocks of the Cape Smith Belt, northern Quebec 65

K.M. CONNARE and R.H. McNUTT: Rb-Sr geochronology of the Nobel gneiss and McKellar gneiss, Parry Sound region, Ontario 175

GEOPHYSICS/GÉOPHYSIQUE

B.S. DAUDIER and E.J. SCHWARZ: An interpretation method for gravity and magnetic data for areas peripheral to the Canadian Shield 421

L.E. STEPHENS and B.W. GRAHAM: An electromagnetic survey over the Gloucester Landfill Site for the detection of contaminated groundwater 431

P.H. MCGRATH and J.B. HENDERSON: Reconnaissance ground magnetic and VLF profile data in the vicinity of the Thelon Front, Artillery Lake map area, District of Mackenzie ····· 455

D.F. POLEY and D.C. LAWTON: Acquisition and processing of high resolution reflection seismic data from permafrost affected areas of the Canadian part of the Beaufort Sea ····· 491

S.P. CHEADLE, M.B. BERTRAM, and D.C. LAWTON: Development of a physical seismic modeling system, University of Calgary ····· 499

P.J. HOOD, M.E. BOWER, C.D. HARDWICK, and D.J. TESKEY: Direct geophysical evidence for displacement along Nares Strait (Canada-Greenland) from low-level aeromagnetic data: a progress report ····· 517

A.R. BAYS, D.F. POLEY, and S.M. BLASCO: DMAPS: a new experimental digital marine reflection seismic acquisition and processing system ····· 523

D.V. WOODS: Large-scale electromagnetic induction investigation of the Kapuskasing Structural Zone, northern Ontario ····· 533

C.J. YORATH, R.M. CLOWES, A.G. GREEN, A. SUTHERLAND-BROWN, M.T. BRANDON, N.W.D. MASSEY, C. SPENCER, E.R. KANASEWICH, and R.D. HYNDMAN: LITHOPROBE – Phase 1: southern Vancouver Island: preliminary analyses of reflection seismic profiles and surface geological studies ····· 543

PALEONTOLOGY/PALÉONTOLOGIE

T.E. BOLTON and J.R.P. ROSS: The cryptostomate bryozoan **Sceptropora** (Rhabdomesina, Arthrostylidae) from Upper Ordovician rocks of southern Mackenzie Mountains, District of Mackenzie ····· 29

M.J. ORCHARD: Carboniferous, Permian and Triassic conodonts from the central Kootenay Arc, British Columbia: constraints on the age of the Milford, Kaslo and Slocan groups ····· 287

A.E.H. PEDDER: Lower Devonian rugose corals of Lochkovian age from Yukon Territory ····· 587

PETROLOGY/PÉTROLOGIE

K.L. CURRIE: An unusual peralkaline granite near Lac Brisson, Quebec-Labrador ····· 73

K.L. BUCHAN and K.D. CARD: Preliminary comparison of petrographic and paleomagnetic characteristics of Nipissing Diabase intrusions in northeastern Ontario ····· 131

S.M. ROSCOE: The Booth River Intrusive Suite, District of Mackenzie ····· 141

QUATERNARY GEOLOGY/GÉOLOGIE DU QUATERNAIRE

Inventory mapping and stratigraphic studies/Inventaire cartographique et stratigraphique

D.A. ST-ONGE and L.A. DREDGE: Northeast extension of glacial Lake McConnell in the Dease River Basin, District of Mackenzie ····· 181

R.W. KLASSEN and W.J. VREEKEN: Quaternary geology of southwestern Saskatchewan ····· 187

C. TARNOCAI, S. SMITH, and O.L. HUGHES: Soil development of Quaternary deposits of various ages in the central Yukon Territory ····· 229

L.A. DREDGE and E. NIELSEN: Glacial and interglacial deposits in the Hudson Bay Lowlands: a summary of sites in Manitoba ····· 247

D.R. SHARPE: The stratified nature of deposits in streamlined glacial landforms on southern Victoria Island, District of Franklin ····· 365

R. GILBERT, J.P.M. SYVITSKI, and R.B. TAYLOR: Reconnaissance study of proglacial Stewart Lakes, Baffin Island, District of Franklin ····· 505

Paleoecology and geochronology/Paléoécologie et géochronologie

T.W. ANDERSON, R.J. MOTT, and L.D. DELORME: Evidence for a pre-Champlain Sea glacial lake phase in Ottawa valley, Ontario, and its implications ····· 239

Sedimentology and geomorphology/Sédimentologie et géomorphologie

D.G. HARRY, H.M. FRENCH, and W.H. POLLARD: Ice wedges and permafrost conditions near King Point, Beaufort Sea coast, Yukon Territory ····· 111

R.N.W. DILABIO: Gold abundances vs. grain size in weathered and unweathered till ····· 117

D.M. DUGGAN and J.L. LUTERNAUER: Development-induced tidal flat erosion, Fraser River delta, British Columbia ····· 317

REGIONAL GEOLOGY/GÉOLOGIE RÉGIONALE

Appalachian Region/Région des Appalaches

D. NANCE: Alleghenian deformation in the Mispec Group, Saint John Harbour, New Brunswick ····· 7

H. PINTSON, P.S. KUMARAPELI, and M. MORENCY: Tectonic significance of the Tibbit Hill Volcanics: geochemical evidence from Richmond area, Quebec ····· 123

D.J. FUREY: Geology of the Belleoram pluton, southeast Newfoundland ····· 151

M. COYLE, D.F. STRONG, D. GIBBONS, and E. LAMBERT: Geology of the Springdale Group, central Newfoundland ····· 157

L.M. CUMMING: A Halifax slate graptolite locality, Nova Scotia ····· 215

H. WILLIAMS, N.P. JAMES, and R.K. STEVENS: Humber Arm Allochthon and nearby groups between Bonne Bay and Portland Creek, western Newfoundland ····· 399

Cordilleran Region/Région de la Cordillère

P. DOUCET, E.D. GHENT, and P.S. SIMONY: Metamorphism in the Monashee Mountains east of Blue River, British Columbia ····· 69

R. PARRISH, S.D. CARR, and R.L. BROWN: Valhalla gneiss complex, southeast British Columbia: 1984 field work ····· 81

S.D. CARR: Ductile shearing and brittle faulting in Valhalla gneiss complex, southeastern British Columbia ····· 89

L.C. STRUIK: Pre-Cretaceous terranes and their thrust and strike-slip contacts, Prince George (east half) and McBride (west half), British Columbia ····· 267

D.W. KLEPACKI, P.B. READ, and J.O. WHEELER: Geology of the headwaters of Wilson Creek, Lardeau map area, southeastern British Columbia ····· 273

D.W. KLEPACKI and J.O. WHEELER: Stratigraphic and structural relations of the Milford, Kaslo and Slocan groups, Goat Range, Lardeau and Nelson map areas, British Columbia ····· 277

T. HARMS: Pre-emplacement thrust faulting in the Sylvester allochthon, northeast Cry Lake map area, British Columbia ····· 301

L.C. STRUIK: Dextral strike-slip through Wells Gray Provincial Park, British Columbia ····· 305

R.J. SCAMMELL: Stratigraphy and structure of the northwestern flank of Frenchman Cap Dome, Monashee Complex, British Columbia: preliminary results ····· 311

M.D. GERASIMOFF: Postmetamorphic thrust faulting on the northeastern margin of the Shuswap metamorphic complex, Wells Gray Provincial Park, British Columbia ····· 327

M. BARDOUX: The Kelowna detachment zone, Okanagan valley, south-central British Columbia ····· 333

J.W.H. MONGER: Structural evolution of the southwestern Intermontane Belt, Ashcroft and Hope map areas, British Columbia ····· 349

Canadian Shield/Bouclier canadien

J.A. PERCIVAL: The Kapuskasing structure in the Kapuskasing-Fraserdale area, Ontario ····· 1

C.W. JEFFERSON: Uppermost Shaler Group and its contact with the Natkusiak basalts, Victoria Island, District of Franklin ····· 103

L. CORRIVEAU: Precambrian syenitic plutons, Central Metasedimentary Belt, Grenville Province of Quebec ····· 165

T. FRISCH, I.R. ANNESLEY, and C.A. GITTINS: Geology of the Chantrey belt and its environs, Lower Hayes River and Darby Lake map areas, northern District of Keewatin ····· 259

R.S. HILDEBRAND and C.F. ROOTS: Geology of the Rivière Grandin map area (Hottah Terrane and western Great Bear Magmatic Zone), District of Mackenzie ····· 373

J.A. PERCIVAL, R.A. STERN, and M.R. DIGEL: Regional geological synthesis of western Superior Province, Ontario ····· 385

R. TIRRUL: Nappes in the Kilohigok Basin, and their relation to the Thelon Tectonic Zone, District of Mackenzie ····· 407

J.B. HENDERSON and R.I. MACFIE: The northern Artillery Lake map area: a transect across the Thelon Front, District of Mackenzie ····· 441

D.T. JAMES: Geology of the Moraine Lake area and the Thelon Front, District of Mackenzie ····· 449

A. DAVIDSON, L. NADEAU, S.M. GRANT, and L.L. PRYER: Studies in the Grenville Province of Ontario ····· 463

T.M. GORDON, S.L. JACKSON, and E. ZALESKI: Metamorphic processes in the Kisseynew metasedimentary gneiss belt, Manitoba ····· 511

M. SCHAU and K.E. ASHTON: High grade metamorphic rocks of northwestern Melville Peninsula, District of Franklin ····· 527

P.H. THOMPSON, N. CULSHAW, D.L. THOMPSON, and J.R. BUCHANAN: Geology across the western boundary of the Thelon Tectonic Zone in the Tinney Hills- Overby Lake (west half) map area, District of Mackenzie ····· 555

G.M. NARBONNE, H.J. HOFMANN, and J.D. AITKEN: Precambrian-Cambrian boundary sequence, Wernecke Mountains, Yukon Territory ····· 603

G.D. JACKSON, T.R. IANNELLI, R.D. KNIGHT, and D. LEBEL: Neohelikian Bylot Supergroup of Borden Rift Basin, northwestern Baffin Island, District of Franklin ····· 639

G.M. ROSS and T.L. SMITH: Physical volcanology and stratigraphy of the Seton Formation: foredeep volcanism in Athapuscow Aulacogen, District of Mackenzie ····· 681

STRATIGRAPHY/STRATIGRAPHIE

M. TEITZ and E.W. MOUNTJOY: The Yellowhead and Astoria carbonate platforms in the Late Proterozoic Upper Miette Group, Jasper, Alberta ····· 341

E.W. MOUNTJOY, R. FOREST, and R. LEONARD: Structure and stratigraphy of the Miette Group, Selwyn Range, between Ptarmigan and Hugh Allan creeks, British Columbia ····· 485

B.D. RICKETTS: Volcanic breccias in the Isachsen Formation near Strand Fiord, Axel Heiberg Island, District of Franklin ····· 609

J.R. DIETRICH, J. DIXON, and D.H. MCNEIL: Sequence analysis and nomenclature of Upper Cretaceous to Holocene strata in the Beaufort-Mackenzie Basin ····· 613

J.C. HARRISON, Q.H. GOODBODY, and R.L. CHRISTIE: Stratigraphic and structural studies on Melville Island, District of Franklin ····· 629

SCIENTIFIC AND TECHNICAL NOTES
NOTES SCIENTIFIQUES ET TECHNIQUES

NOTES

F.H.A. CAMPBELL: Stratigraphy of the upper part of the Rae Group, Johansen Bay area, northern Coronation Gulf area, District of Franklin ····· 693

K. MORAN and H. CHRISTIAN: Triaxial shear strength testing facility for the Western Arctic ····· 697

S.K. TANOLI, R.K. PICKERILL, and K.L. CURRIE: Distinction of Eocambrian and Lower Cambrian redbeds, Saint John area, southern New Brunswick ····· 699

K.W. CONWAY and J.L. LUTERNAUER: Evidence of ice rafting and tractive transfer in cores from Queen Charlotte Sound, British Columbia ····· 703

S.A. EDLUND: Lichen-free zones as neoglacial indicators on western Melville Island, District of Franklin ····· 709

D.C. HARRIS and R.I. THORPE: Occurrence of copper arsenides in the East Arm area, Great Slave Lake, District of Mackenzie ····· 713

M.C. ROBERTS, H.F.L. WILLIAMS, J.L. LUTERNAUER, and B.E.B. CAMERON: Sedimentary framework of the Fraser River delta, British Columbia: preliminary field and laboratory results ····· 717

J.M. DUKE: An overview of the Sudbury Timmins Algoma Mineral Program (STAMP), Ontario ····· 723

K.G. ROOT: Reinterpretation of the age of a succession of Paleozoic strata, Delphine Creek, southeastern British Columbia ····· 727

P.A. EGGINTON: Moles as agents of erosion in the Ottawa area, Ontario ····· 731

FEDERAL-PROVINCIAL MINERAL DEVELOPMENT PROGRAMS 1984–89 AND OTHER FEDERAL PROGRAMS

PROGRAMMES FÉDÉRAUX-PROVINCIAUX DE MISE EN VALEUR DES RESSOURCES MINÉRALES, 1984 à 1989, ET AUTRES PROGRAMMES FÉDÉRAUX

B. MERCER, D.F. STRONG, D.H.C. WILTON, and D. GIBBONS
The King's Point Complex, western Newfoundland 737

P.D. VAILLANCOURT
Sandstone lithology in the Silver Mine Formation and its relation to galena occurrence in the Yava deposit, Cape Breton Island, Nova Scotia 743

S.L. JACKSON and T.M. GORDON
Metamorphism and structure of the Laurie Lake region, Manitoba 753

A. GALLEY, D. AMES, and J.M. FRANKLIN
Preliminary investigation of gold occurrences in the Flin Flon-Snow Lake Belt, Manitoba and Saskatchewan 761

H.D. ROGERS
Geology of the igneous-metamorphic complex of Shelburne and eastern Yarmouth counties, Nova Scotia 773

A.J. SEXTON and A.A. COTIE
Petrogenesis and economic geology of the Sporting Mountain pluton, Cape Breton Island, Nova Scotia 779

Y.D. GAGNON and R.A. JAMIESON
Geology of the Mont Albert region, Gaspé Peninsula, Quebec 783

B.H. O'BRIEN
Preliminary report on the geology of the LaHave River area, Nova Scotia 789

J.B. WHALEN
The McGerrigle plutonic complex, Gaspé, Quebec: evidence of magma mixing and hybridization 795

Author Index/Index des auteurs 801

-1-

THE KAPUSKASING STRUCTURE IN THE KAPUSKASING-FRASERDALE AREA, ONTARIO

Project 820006

John A. Percival
Precambrian Geology Division

Percival, J.A., The Kapuskasing structure in the Kapuskasing-Fraserdale area, Ontario; in Current Research, Part A, Geological Survey of Canada, Paper 85-1A, p. 1-5, 1985.

Abstract

The northeast-striking Kapuskasing structural zone of high-grade metamorphic rocks is not present in the 60 km wide area between Kapuskasing and Fraserdale. Amphibolite-facies orthogneiss occurs between the southern Groundhog River and the northern Fraserdale-Moosonee high-grade metamorphic blocks. The southern block consists of tonalite, mafic gneiss and paragneiss metamorphosed to the granulite and upper amphibolite facies. It is in fault contact with granite to the east and gneiss in the amphibolite facies to the west. To the north, the Fraserdale-Moosonee Block is made up of anhydrous granulite of psammitic metasedimentary and intermediate igneous composition. A major pseudotachylite zone separates the granulites from granitoid rocks and gneiss in the amphibolite facies to the east; smaller fault zones occur within the block as well as between it and orthopyroxene-bearing metasedimentary gneiss of the Quetico belt to the west. Within the 120 km long zone of granulites in the Quetico belt, the proportion and grain size of orthopyroxenes and garnet increases toward the east at the expense of biotite, suggesting that metamorphic grade increases toward the anhydrous granulites of the Fraserdale-Moosonee Block. Although this apparent metamorphic pattern requires further study by geothermobarometry, it appears to support the model of a tilted crustal section west of the Kapuskasing structure.

Résumé

La zone tectonique de Kapuskasing, orientée vers le nord-est et composée de roches à métamorphisme intense ne se manifeste pas dans la bande de 60 kilomètres de large qui se trouve entre Kapuskasing et Fraserdale. De l'orthogneiss à faciès amphibolite se présente entre la rivière Groundhog au sud et les blocs de roches fortement métamorphisées de Fraserdale-Moosonee au nord. Le bloc sud se compose de tonalite, de gneiss mafique et de paragneiss métamorphisés jusqu'au faciès granulite et au faciès supérieur amphibolite. Une faille le met en contact avec du granite à l'est et du gneiss dans le faciès amphibolite à l'ouest. Au nord, le bloc Fraserdale-Moosonee se compose de granulite anhydre de composition psammitique métasédimentaire et ignée intermédiaire. Une grande zone de pseudotachylite sépare les granulites des roches granitiques et des gneiss du faciès amphibolite vers l'est; de plus petites zones de failles se présentent à l'intérieur du bloc et entre celui-ci et le gneiss métasédimentaire à orthopyroxène de la zone de plissement de Quetico à l'ouest. Dans la zone à granulites, de 120 kilomètres de long, à l'intérieur de la zone de Quetico, la proportion et la granulométrie des orthopyroxènes et des grenats augmentent vers l'est aux dépens de la biotite, ce qui laisse croire que le degré de métamorphisme augmente plus on s'approche des granulites anhydres du bloc Fraserdale-Moosonee. Bien qu'il faudra entreprendre d'autres études géothermobarométriques de ce modèle métamorphique apparent, celui-ci semble appuyer le modèle d'une section lithosphérique inclinée à l'ouest de la structure de Kapuskasing.

Introduction

The Kapuskasing structure is a narrow, 500 km long, northerly-trending zone of high-grade metamorphic rocks and positive gravity and aeromagnetic anomalies that interrupts the easterly-striking belts of the Superior Province. A recent study by Percival and Card (1983, in press) suggested that the high-grade rocks of the southern Kapuskasing zone are the basal part of a west-dipping slab of upthrust continental crust characteristic of the deep regions beneath the Abitibi-Wawa greenstone belt. In that area, the Kapuskasing zone is bounded by a fault on the east whereas the western contact is complex and gradational (Percival, 1985). Although exposure is poor farther north, strong lineaments visible on aeromagnetic maps (Geological Survey of Canada, 1984) suggest that the Kapuskasing zone is fault-bounded on both the east and west sides (MacLaren et al., 1968; Bennett et al., 1967; Thurston et al., 1977). A limited field program was initiated in 1984 to examine available outcrops in critical areas with a view toward better understanding of the history of the Kapuskasing structure over its entire (500 km) exposed length. M.R. Digel provided cheerful field assistance under trying conditions.

Under consideration are a more southerly area where the Kapuskasing structure cuts the east-trending greenstone-granite terrane of the Wawa and Abitibi belts (Fig. 1.1) and a northern area where it transects metasedimentary gneiss of the Quetico and Opatica belts. The Kapuskasing zone forms the boundary between the Wawa and Abitibi belts, which have similar lithological, stratigraphic and geochronological characteristics and are thus considered to be parts of a once-continuous belt, now divided by the Kapuskasing zone. Similarly, the Kapuskasing zone is the boundary between the Quetico belt of metasedimentary schist and gneiss and granite that extends 1200 km to the west, and the poorly-exposed Opatica belt, also dominantly of metasedimentary origin (Card, 1982).

Groundhog River area

In the Groundhog River area (Fig. 1.1, 1.2), high-grade metamorphic rocks of the Kapuskasing zone, sharply defined aeromagnetically (MacLaren et al., 1968), are bounded on the west by tonalitic gneiss of the Wawa belt and on the east by granodiorite of the Abitibi belt. A positive gravity anomaly, which coincides with high-grade rocks of the Kapuskasing structure over most of its length, diverges up to 30 km to the west of the Groundhog River Block.

Tonalitic gneiss comprises much of the Wawa belt west of the Kapuskasing structure. West of the Groundhog River Block are sparsely xenolithic hornblende-biotite tonalite and tonalitic gneiss. Xenoliths are mainly hornblende-plagioclase amphibolite with local clinopyroxene. Dykes and sills of pink leucocratic granite, aplite and pegmatite cut the gneiss. Foliation and gneissosity form chaotic to gently rolling patterns.

Exposure in the Groundhog River Block is minimal. Rock types include felsic orthogneiss, with some mafic gneiss and paragneiss (Thurston et al., 1977; Bennett et al., 1967). Tonalitic orthogneiss contains orthopyroxene in addition to hornblende, biotite, magnetite and some clinopyroxene. Mafic gneiss is made up of clinopyroxene, plagioclase, hornblende and magnetite, with variable proportions of garnet, orthopyroxene and quartz. A unit of garnet-orthopyroxene-biotite paragneiss was reported by Thurston et al. (1977). Northerly-trending dykes, perhaps part of the Matachewan swarm, cut the high-grade rocks and are offset by brittle faults and cut by pseudotachylite zones.

East and northeast of the Groundhog River Block are homogeneous granodiorite and hornblende-biotite tonalitic gneiss, part of the Abitibi belt.

Areas near the eastern and western boundaries of the Groundhog River Block are exposed locally. In the Wakusimi River area (Fig. 1.2), part of the western boundary is exposed over a distance of some 200 m. Mafic gneiss consisting of garnet, clinopyroxene, magnetite and plagioclase with minor hornblende, and cut by mafic dykes, is in contact with tonalitic rocks to the west. In the mafic gneiss, pseudotachylite zones become more abundant to the west. Tonalite is fractured and friable and is recognizable only on the weathered surface; the fresh surface is black, fine grained to aphanitic, and individual minerals cannot be identified. The rock has no planar fabric but is thoroughly altered and is thus termed cataclasite. Although the contact between mafic gneiss and tonalite cataclasite could represent the boundary fault between the Groundhog River Block and Wawa belt, poor exposure does not allow elimination of the possibility that the contact is within the Groundhog River Block but near the boundary fault. Zones of pseudotachylite are common in high-grade rocks of the Groundhog River Block at several locations near the western boundary.

An area near the eastern boundary of the Groundhog River Block is exposed 0.2 km west of the Groundhog River on Highway 11. Migmatitic biotite-plagioclase-quartz gneiss and pegmatite are cut by several sets of small brittle faults and associated phyllonite and cataclasite. Small-scale offsets of migmatitic layering and pegmatite dykes permit determination of movement sense on individual fault surfaces. Northeast-striking faults with dips 35°N to 50°S are most common. Movement on these appears mainly dextral transcurrent with a component of southeast-side-up along shallow (15-30°) northeast-plunging lineations. Part of the outcrop shows northwest-side-up movement on northeast faults along moderate (30-50°) northwest-plunging lineations. Northeast faults are locally offset by small-scale northwest-striking, northeast-dipping faults showing sinistral transcurrent movement. These two main fault directions are possibly part of a conjugate set; the principal strain axis (σ_1) would be oriented east-west.

At its northern end, the Groundhog River aeromagnetic anomaly trends northerly toward the Clay-Howells alkalic rock complex (Sage, 1983). Linear anomalies that correspond to faults farther south are weak in this area and the central positive anomaly fades near Moonbeam, close to the most northerly exposure of high-grade rock. On strike to the north in the Remi Lake area are hornblende-biotite tonalite gneiss

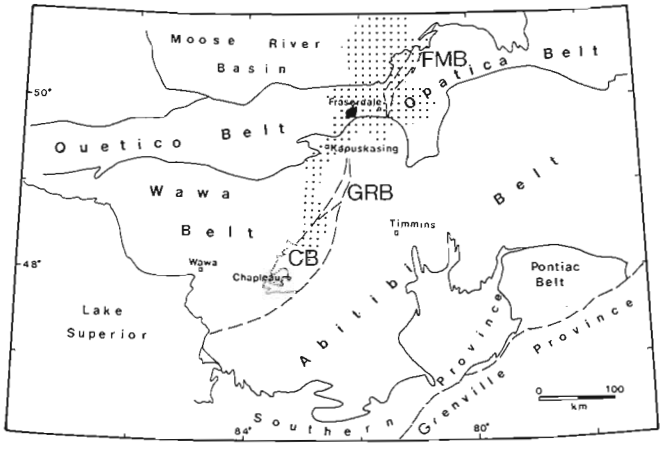

Figure 1.1. *Sketch map showing major lithological subdivisions of the Superior Province. Kapuskasing structural zone is divided into Chapleau Block (CB), Groundhog River Block (GRB) and Fraserdale-Moosonee Block (FMB). Dotted pattern indicates positive gravity anomaly, defined by -25 mGal Bouguer anomaly contour.*

and granite, similar to rocks to both the east and west. High-grade rocks and the aeromagnetic anomaly do not appear to extend north of Highway 11 and there is apparent lithological continuity across the trend of the Kapuskasing structure in this area. Some 60 km northeast of the north end of the Groundhog River Block is the southern tip of the Fraserdale-Moosonee Block of high-grade metamorphic rocks and associated positive aeromagnetic anomaly.

Fraserdale-Moosonee Block

The Fraserdale-Moosonee Block is defined over its 200 km length by a distinct aeromagnetic anomaly with a maximum width of 25 km. High-grade rocks in the block are in fault contact with biotite-bearing paragneiss and granite to the east (MacLaren et al., 1968; Bennett et al., 1967). Cataclastic zones, indicating faults, are also present near the geophysically-defined western boundary, a contact zone with metasedimentary granulites of the Quetico belt which Skinner (in MacLaren et al., 1968) indicated to be gradational in character.

A reconnaissance trip was made on the North French River and spot checks conducted on the Little Abitibi River. The north-flowing North French River traverses the northeast-trending Fraserdale-Moosonee Block obliquely (Fig. 1.2). At the southern end of the North French traverse, paragneiss and diorite-monzonite are the common rock types. Farther north, minor paragneiss is interlayered with pyroxene-bearing tonalite containing inclusions of mafic granulite.

Common rock types in the Fraserdale-Moosonee Block are paragneiss, mafic gneiss and a suite of diorite-monzonite composition; also abundant are tonalitic rocks. Enclaves of gabbroic anorthosite occur in diorite and tonalite at one locality. Paragneiss consists of melanosome with garnet - orthopyroxene - plagioclase - quartz - magnetite ± biotite and leucosome with plagioclase - K-feldspar - quartz ± orthopyroxene on the 1-5 cm scale. Medium- to coarse-grained homogeneous foliated rocks with garnet - orthopyroxene - biotite - plagioclase - quartz assemblages are considered to be homogeneous diatexite, derived from paragneiss. Mafic gneiss commonly occurs as large enclaves or layers in tonalite and diorite and comprises assemblages of orthopyroxene - clinopyroxene - magnetite - hornblende - plagioclase or garnet - clinopyroxene - magnetite - hornblende - plagioclase ± scapolite. Tonalitic gneiss consists of interlayered dark and light laminae on the 1-10 cm scale of orthopyroxene - clinopyroxene - plagioclase - quartz and plagioclase - K-feldspar - quartz respectively. Rocks of the diorite-monzonite suite are medium grained, foliated to augen-textured, and consist mainly of clinopyroxene, hornblende and plagioclase with variable quantities of orthopyroxene, biotite, K-feldspar and minor quartz.

Planar structures are defined by compositional layering in gneiss, alignment of biotite and in some areas by planar alignment of ribbon quartz. Rare lineations, defined by rodded quartz grains, plunge gently to the northeast. Planar structural elements strike northeasterly or north with moderate dips to the west or northwest. Zones of pseudotachylite are thicker and more common in the eastern 5 km of the block than farther west. They trend northeasterly and dip moderately northwest to steeply southeast. A 2-m wide, northeast-striking, southeast-dipping pseudotachylite zone exposed on the North French River consists of layers of aphanitic flinty rock and cataclasite with porphyroclasts of granitoid and mafic rock. The outcrop appears to be part of the main eastern fault zone separating the Fraserdale-Moosonee Block from lower-grade rocks to the east. Narrow northeast-trending, northwest-dipping shear zones are recognized in the Fraserdale-Moosonee Block by mylonitic textures such as ribbon quartz in pegmatite, fine granular feldspars and pyroxene augen. Pseudotachylite cuts mylonitic rock locally. Zones rich in pseudotachylite separate areas of differing composition and structural trend within the Fraserdale-Moosonee Block, suggesting that northeasterly brittle faults have juxtaposed and re-oriented deep crustal fragments. A small body of websterite on the North French River may be one such fragment. It consists of altered pyroxenes, amphibole and chlorite, and is bounded to the southeast by a major pseudotachylite zone and to the northwest by a chloritic shear zone.

Mafic dykes are common in the Fraserdale-Moosonee Block. Small (5-30 cm) fine grained dykes of mafic to ultramafic composition have orientations between northeast, with steep southeasterly dips, to north, with moderate to steep easterly dips. Dyke margins are locally offset sinistrally by brittle northeast faults. The inconsistency of dyke orientations suggests possible post-intrusion re-orientation of the host rock on the ubiquitous fault zones. Larger (10-30 m) fresh northeast-striking dykes with coarse ophitic texture and probable olivine could be members of the Abitibi swarm.

East of the Fraserdale-Moosonee Block are parts of the poorly exposed Opatica and Partridge River belts. East-trending units of biotite-bearing gneiss of metasedimentary origin and derived granitic plutons characterize the Opatica belt. To the north, the Partridge River belt consists dominantly of granitic and gneissic rocks and small east-trending greenstone belts (MacLaren et al., 1968; Bennett et al., 1967). Outcrops adjacent to the Fraserdale-Moosonee Block are characterized by a northeast-trending rodding or mineral lineation plunging 30-40°.

An aeromagnetic lineament defines the boundary between the Fraserdale-Moosonee Block and the Quetico belt to the west in some areas. However, the boundary is not readily defined on the basis of lithology or metamorphic grade. In the Fraserdale area, some 5 km west of the magnetic anomaly, homogeneous diatexite with metasedimentary xenoliths contains the assemblage orthopyroxene-biotite-plagioclase-quartz ± garnet. Associated meta-igneous rocks include layered gabbro-diorite-anorthosite with orthopyroxene and garnet-clinopyroxene-hornblende-plagioclase mafic gneiss. Lithological layering and foliation strike east to southeast and dip moderately northwards.

Rocks up to 6 km east of the Fraserdale-Moosonee Block are cut by zones of pseudotachylite and mylonite striking north and northwest, dipping steeply east or west.

To the west and northwest, east-striking, steeply-dipping units of migmatitic paragneiss consist of melanosome of garnet-biotite-plagioclase-quartz ± orthopyroxene ± biotite. Rare occurrences of garnet-cordierite-sillimanite migmatites associated with garnet-orthopyroxene assemblages represent pelitic compositions (Fig. 1.2). Orthopyroxene occurs as coarse (5-10 mm) crystals comprising up to 20 per cent of the rock as far west as Guilfoyle Lake (Fig. 1.2) but is finer (2-3 mm) and less abundant to the west. Spot checks indicated the presence of orthopyroxene in garnetiferous paragneiss as far west as Missinaibi River (Fig. 1.2), some 120 km west of the Fraserdale-Moosonee Block. Areas underlain by rocks with abundant orthopyroxene coincide approximately with the broad positive gravity anomaly which includes the Fraserdale-Moosonee Block but extends some 100 km to the west.

At least three types of mafic dykes occur in the eastern Quetico belt. North and northeast of Fraserdale, a group of dykes has north to northwest trends and steep easterly dips. The dykes are 2-10 m thick and some contain plagioclase megacrysts, characteristic of the Matachewan swarm.

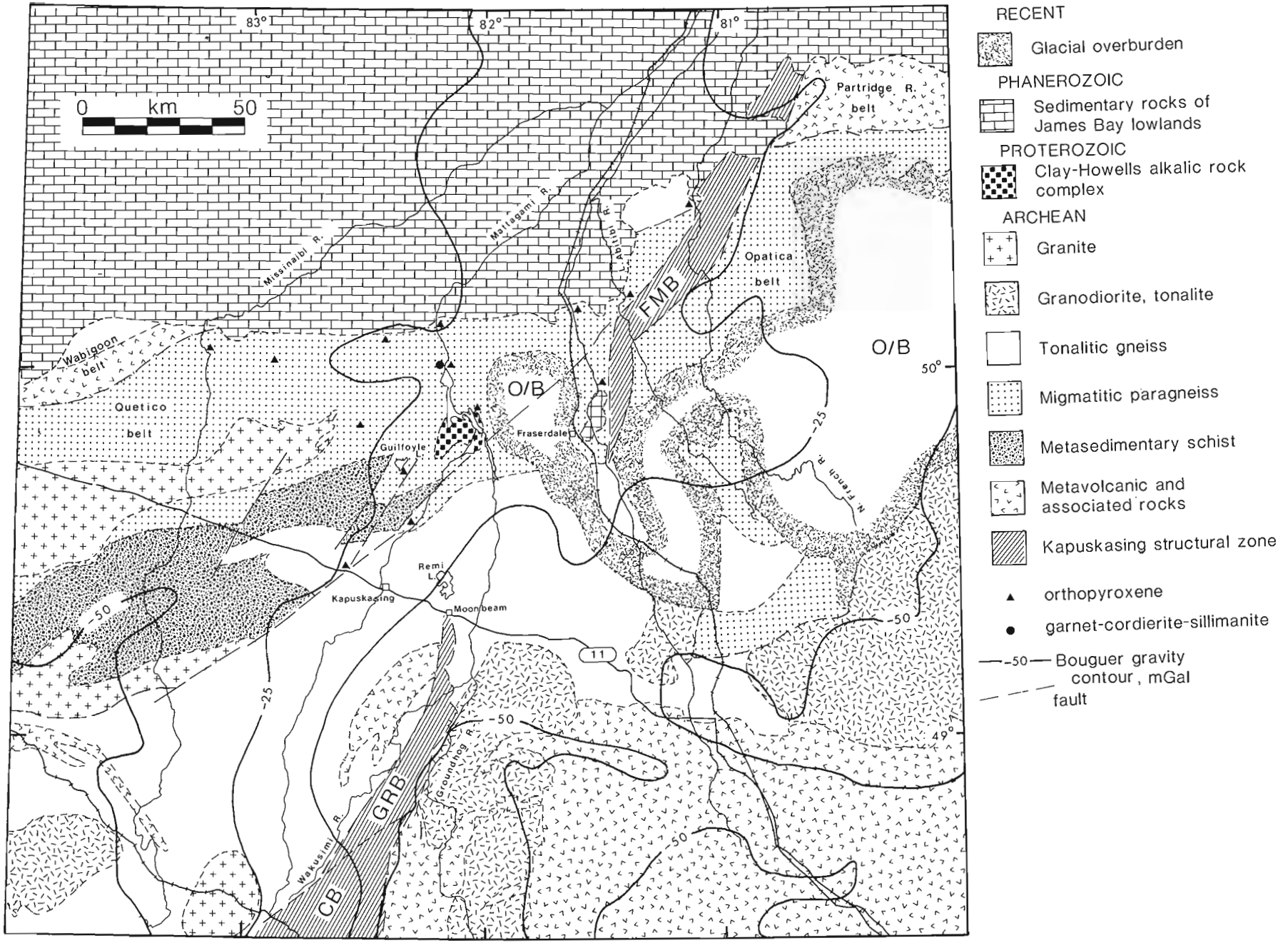

Figure 1.2. *Generalized geological map of the Kapuskasing structural zone in the Kapuskasing-Fraserdale area (modified after Card and Sanford, 1983). CR: Chapleau Block; GRP: Groundhog River Block; FMR: Fraserdale-Moosonee Block. Orthopyroxene is widespread in the Kapuskasing structural zone; individual occurrences are not shown.*

Two members of a group of 15 dykes exposed on the Little Abitibi River contain central zones rich in xenocrysts(?) of euhedral pyroxene and carbonate. Dykes in this group have sharply irregular margins and numerous apophyses and are altered to chlorite schist or local shear zones. Development of pseudotachylite in country rock appears to predate dyke emplacement; for the most part the dykes are fresh whereas the homogeneous diatexite country rock is riddled with shear zones, pseudotachylite and late planar schistose zones. Apparently, only these latest schistose zones affect the dykes. The irregular margins suggest that the dykes intruded fractured rock.

Two types of dykes with northeast trends are also present in the Fraserdale area. Green-grey weathering, medium grained ophitic diabase dykes up to 15 m wide contain sparse plagioclase megacrysts to 2 cm. They are fresh for the most part but are cut locally by thin shear zones and are similar to Kapuskasing dykes in the Chapleau area (Card et al., 1981). Brown-weathering, medium- to coarse-grained diabase dykes with ophitic texture also have northeasterly trends and thicknesses of 10-20 m. They appear fresh and are probably members of the Abitibi swarm.

On the basis of the widespread occurrence of orthopyroxene, granulite-facies metamorphism characterizes the eastern 120 km of the interior of the Quetico belt. Although the metamorphic assemblage, garnet-orthopyroxene-biotite-plagioclase-K-feldspar-quartz, does not change over the distance, orthopyroxene and garnet are coarser and more abundant in the east. Similar rock compositions in the Fraserdale-Moosonee Block have mainly anhydrous garnet-orthopyroxene-plagioclase-K-feldspar-quartz ± biotite assemblages, the main difference between paragneiss in the two terranes being in the proportion of biotite. Plans are underway to assess metamorphic conditions (P-T-a_{H_2O}) in granulites of the eastern Quetico belt and Fraserdale-Moosonee Block using garnet-orthopyroxene-biotite-plagioclase-quartz geothermobarometry. This will further test the hypothesis, developed in the Wawa-Timmins area to the south (Percival and Card, 1983), that the crust west of the Kapuskasing structure was tilted by rotation on a west-dipping thrust fault to reveal an oblique crustal cross-section.

References

Bennett, G., Brown, D.D., George, P.T., and Leahy, E.J.
1967: Operation Kapuskasing; Ontario Department of Mines, Miscellaneous Paper 10.

Card, K.D.
1982: Progress report on regional geological synthesis, central Superior Province; in Current Research, Part A, Geological Survey of Canada, Paper 82-1A, p. 23-28.

Card, K.D. and Sanford, B.V.
1983: Geology of the Timmins (NM-17) map sheet, Ontario and Quebec; Geological Survey of Canada, Open File Map 956.

Card, K.D., Percival, J.A., Lafleur, J., and Hogarth, D.D.
1981: Progress report on regional geological synthesis, central Superior Province; in Current Research, Part A, Geological Survey of Canada, Paper 81-1A, p. 77-93.

Geological Survey of Canada
1984: Magnetic anomaly map Timmins (NM-17) Map NM-17-M, Scale 1:1 000 000.

MacLaren, A.S., Anderson, D.T., Fortescue, J.A.C., Gaucher, E.G., Hornbrook, E.H.W., and Skinner, R.
1968: A preliminary study of the Moose River Belt, northern Ontario; Geological Survey of Canada, Paper 67-38.

Percival, J.A.
1985: A possible exposed Conrad discontinuity in the Kapuskasing uplift, Ontario. Submitted to "Deep Structure of the Continental Crust: Results from Reflection Seismology"; American Geophysical Union Geodynamics Series (edited by M. Barazangi and L.D. Brown).

Percival, J.A. and Card, K.D.
1983: Archean crust as revealed in the Kapuskasing uplift, Superior Province, Canada; Geology, v. 11, p. 323-326.

– Structure and evolution of Archean crust in central Superior Province, Canada; in Archean Supracrustal Sequences, ed. L.D. Ayres and P.C. Thurston; Geological Association of Canada, Special Paper. (in press)

Sage, R.P.
1983: Geology of the Clay-Howells Alkalic rock complex; Ontario Geological Survey, Open File Report 5402, 187 p.

Thurston, P.C., Siragusa, G.M., and Sage, R.P.
1977: Geology of the Chapleau area, districts of Algoma, Sudbury and Cochrane; Ontario Division of Mines, Geoscience Report 157.

ALLEGHENIAN DEFORMATION IN THE MISPEC GROUP, SAINT JOHN HARBOUR, NEW BRUNSWICK

Project 730044

Damian Nance[1]
Precambrian Geology Division

Nance, D., Alleghenian deformation in the Mispec Group, Saint John Harbour, New Brunswick; in Current Research, Part A, Geological Survey of Canada, Paper 85-1A, p. 7-13, 1985.

Abstract

East of Saint John Harbour, three phases of Alleghenian deformation affect the grey lithic arenites (Lancaster Formation) and underlying, pink polymict conglomerates and siltstones (Balls Lake Formation) of the Carboniferous Mispec Group. The first (D_1) produced a widespread cleavage (S_1) that dips gently southeast and is axial planar to rare mesoscopic folds (F_1) of northwest vergence. The second (D_2) was not a fabric-forming event but a period of gentle warping which produced the broad domes and basins (F_2) that define the regional structure. The third (D_3) produced a second cleavage (S_3) that is less widespread but locally overprints that of D_1. S_3 dips moderately northwest and is axial planar to frequent mesoscopic folds (F_3) that verge southeast. On a regional scale, the Mispec Group is flat-lying, large-scale overturned structures are absent, and the intensity of Alleghenian deformation increases southward. Relationships support a parautochthonous Mispec terrane in which the Balls Lake and Lancaster formations reflect both proximal fan and more distal fluvial facies deposited in advance of, and subsequently overridden by, an allochthonous Alleghenian terrane to the south. This contrasts with relations west of Saint John where the Mispec Group is itself allochthonous and lies south of the Alleghenian (Variscan) front.

Résumé

A l'est de Saint John Harbour, trois phases de la déformation alléghanienne ont affecté les arénites lithiques grises (formation de Lancaster) et, au-dessous, les conglomérats polygéniques roses et les siltstones (formation de Balls Lake) du groupe carbonifère de Mispek. La première phase (D_1) a produit un clivage étendu (S_1) qui plonge doucement vers le sud-est et qui se trouve dans le plan axial de rares plis mésoscopiques (F_1) de vergence nord-ouest. La deuxième phase (D_2), qui n'a pas agi sur la structure des roches, a été une période de gondolements de faible amplitude qui a donné naissance aux larges dômes et bassins (F_2) qui définissent la structure régionale. La troisième (D_3) a créé un deuxième clivage (S_3) qui est moins étendu que le premier mais qui se superpose par endroits à D_1. S_3 présente un pendage modéré vers le nord-ouest et se trouve dans le plan axial de plis mésoscopiques nombreux (F_3) de vergence sud-est. A l'échelle régionale, le groupe de Mispek est plat; on n'y rencontre pas de structures déversées sur une grande échelle et l'intensité de la déformation alléghanienne s'accroît vers le sud. Les relations observées appuient l'hypothèse d'un terrain (Mispek) parautochtone dans lequel les formations de Balls Lake et de Lancaster correspondent à un faciès proximal en éventail et à un faciès distal d'origine fluviatile qui se sont déposés avant l'arrivée, au sud, d'un terrain alléghanien allochtone qui les a subséquemment recouverts. Ces constatations contrastent avec les relations observées à l'ouest de Saint John, où le groupe de Mispek est lui-même allochtone et s'étend au sud du front de la déformation alléghanienne (Variscan).

[1] Department of Geological Sciences, Ohio University, Athens, Ohio 45701

Introduction

In the northern Appalachians, deformation associated with the Alleghenian (Variscan/Hercynian) event is largely localized within late Paleozoic basins of the Avalon terrane, whose development is dominated by right-lateral, strike-slip displacements (Bradley, 1982). This, however, is not the case in southernmost New Brunswick where Alleghenian deformation has produced a belt of stacked thrust sheets. The belt, which trends east-northeast, terminates across a prominent thrust zone that is considered to separate the strongly deformed Carboniferous sediments of the Mispec Group from those of the essentially undeformed Kennebecasis Formation to the north (Ruitenberg and McCutcheon, 1982). The coarse redbeds of the Kennebecasis Formation are locally derived (Currie, 1984; Currie et al., 1981) and probably reflect alluvial and fluvial sedimentation within fault-bounded, strike-slip basins. The siltstones and conglomerates of the Mispec Group, in contrast, are of uncertain depositional environment and largely unknown provenance. As the two successions are likely to be, at least in part, penecontemporaneous (Currie, 1984), the thrust zone that separates them is widely held to be a major tectonostratigraphic boundary that marks the Alleghenian (Variscan) front in Maritime Canada (Rast and Grant, 1973). Accordingly, the Mispec Group is viewed as an allochthonous terrane that has been transported northwestward from its site of deposition, along a thrust that defines its northern limit of outcrop. This interpretation is well documented to the west of Saint John (Rast et al., 1978, 1975) where

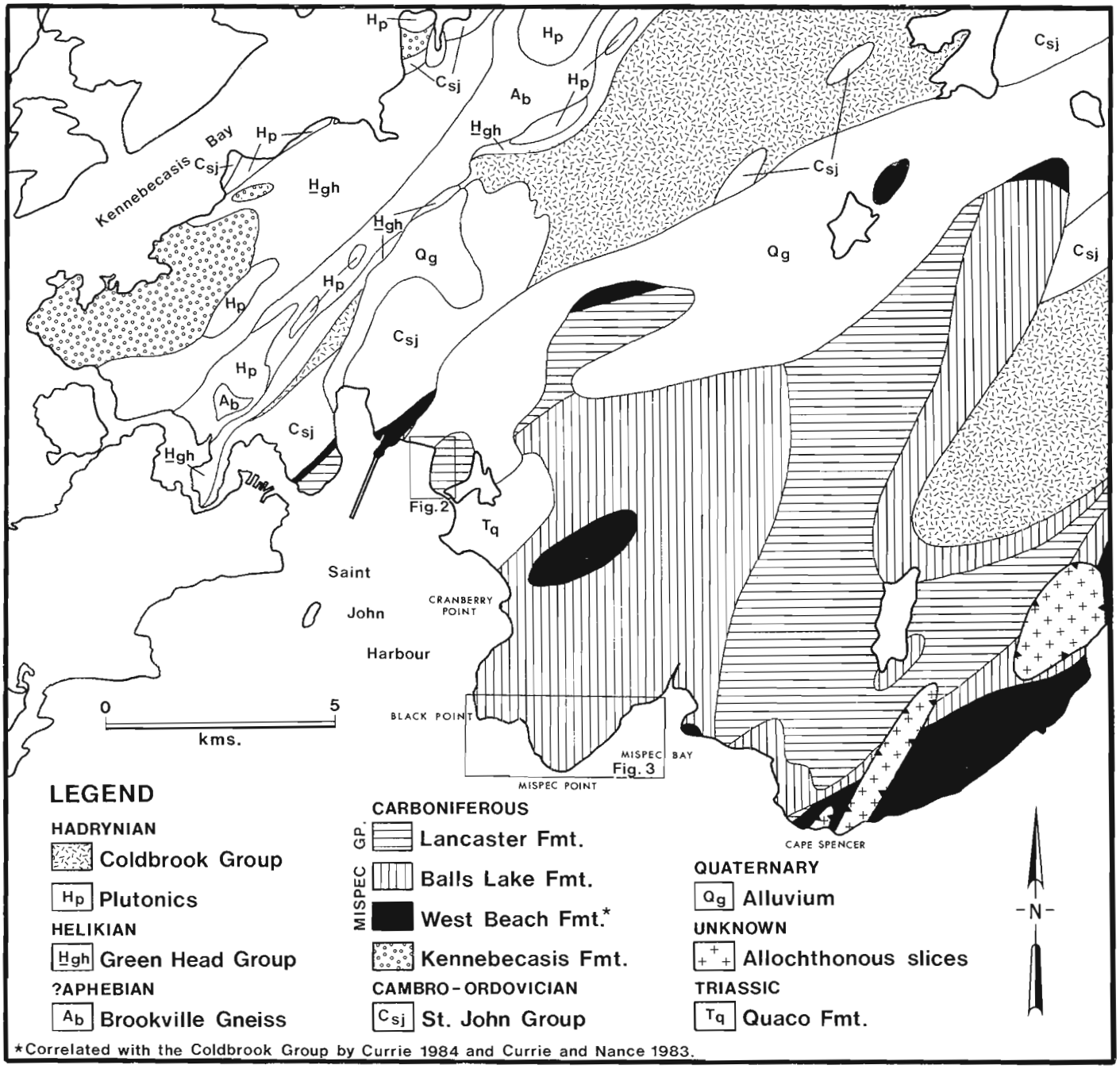

Figure 2.1. Simplified geological map of east Saint John (modified after Currie, 1984; Currie and Nance, 1983; and Currie et al., 1981).

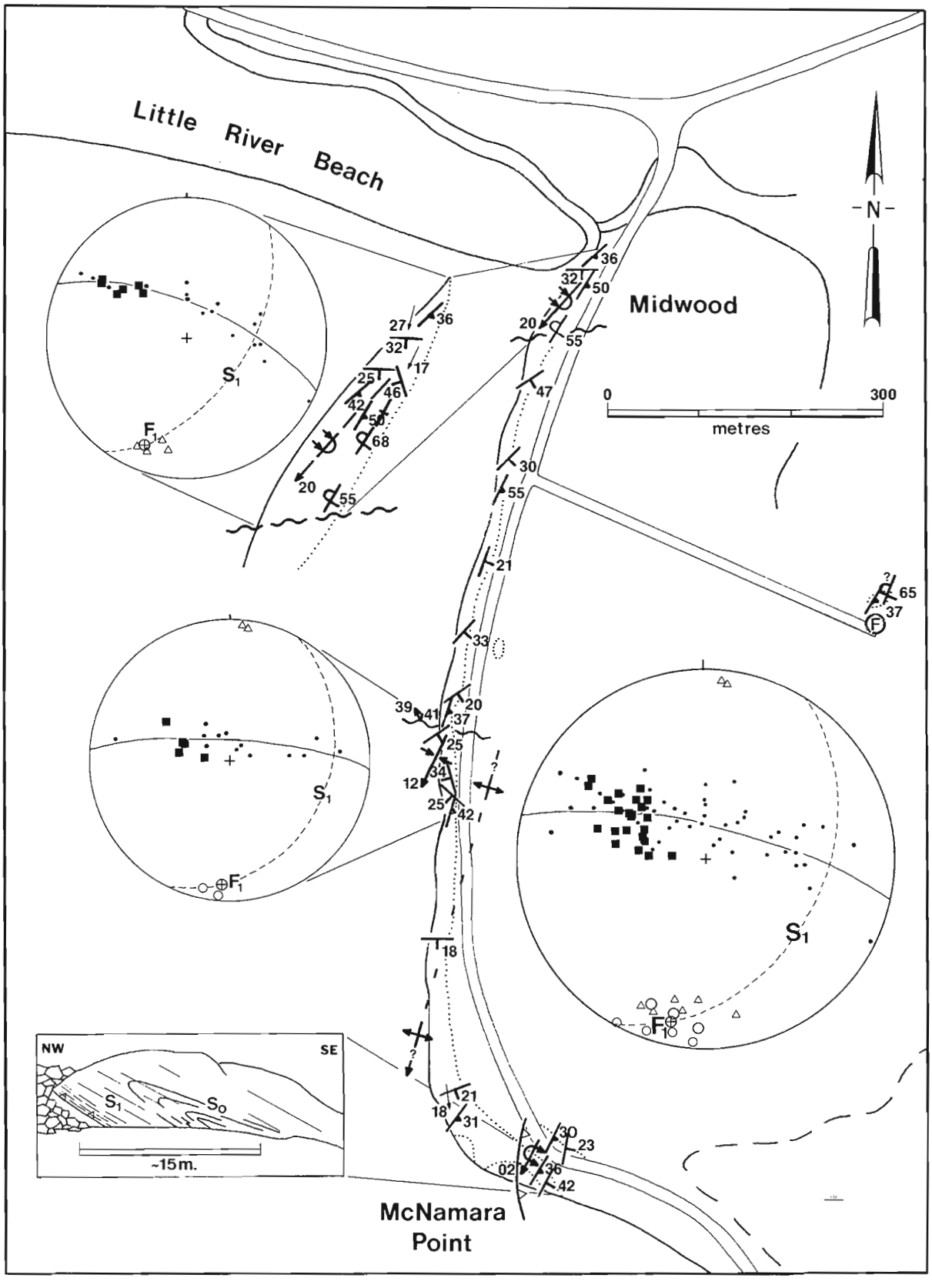

Figure 2.2. D_1 *structural relations in the Lancaster Formation between Little River Beach and McNamara Point (see Fig. 2.1 for location, and Fig. 2.3 for legend).*

sediments of the Mispec Group are involved in major overturned structures and nappe-like complexes of regional extent.

To the east of the city, however, the Mispec Group is broadly flat-lying, large-scale overturned structures are absent, and the intensity of its deformation increases to the south rather than the north (Currie and Nance, 1983). As a result, the position of the Alleghenian front in this region is uncertain and, in the absence of evidence for major thrusting, the relationship of the Mispec Group to penecontemporaneous units farther north remains unclear.

This report, which documents the structural geometry of the Mispec Group along the eastern shore of Saint John Harbour, represents a preliminary step in a larger project aimed at resolving the nature of the Alleghenian front east of Saint John, and the relationship of this thrust belt to the regional strike-slip faulting that is the main deformational response to the Alleghenian event in the northern Appalachians.

Stratigraphy

The diverse Carboniferous sediments of the Mispec Group have traditionally been subdivided into three formations (Hayes and Howell, 1937; Alcock, 1938). The Lancaster Formation largely comprises grey lithic arenites with occasional thin siltstone beds that contain poorly preserved plant fragments of Pennsylvanian age (Westphalian B; Stopes, 1914). The Balls Lake Formation consists of red to pink polymict conglomerates, siltstones, shales and minor sandstones. The West Beach Formation is predominantly a bimodal volcanic unit comprising acid and basic tuffs, agglomerates, and both rhyolitic and locally pillowed basaltic flows, interbedded with maroon siltstones and sandstones.

Despite this simple subdivision, the stratigraphy (and hence structure) remains uncertain, as complete disagreement exists with respect to the sequence of these formations. Hayes and Howell (1937) believed that the Lancaster Formation (their Little River Series) was sequentially overlain by the Balls Lake and West Beach formations. Alcock (1938), in contrast, placed the Lancaster Formation above the West Beach and Balls Lake formations, an order supported by Ruitenberg et al. (1979). Wardle (1978), however, concluded that the West Beach Formation was overlain by the Balls Lake and Lancaster formations in the exact reverse order to that of Hayes and Howell (1937). The latter stratigraphy has been substantiated by Currie and Nance (1983), and provides the basis for the ongoing re-examination of the structural and depositional history of the Mispec Group.

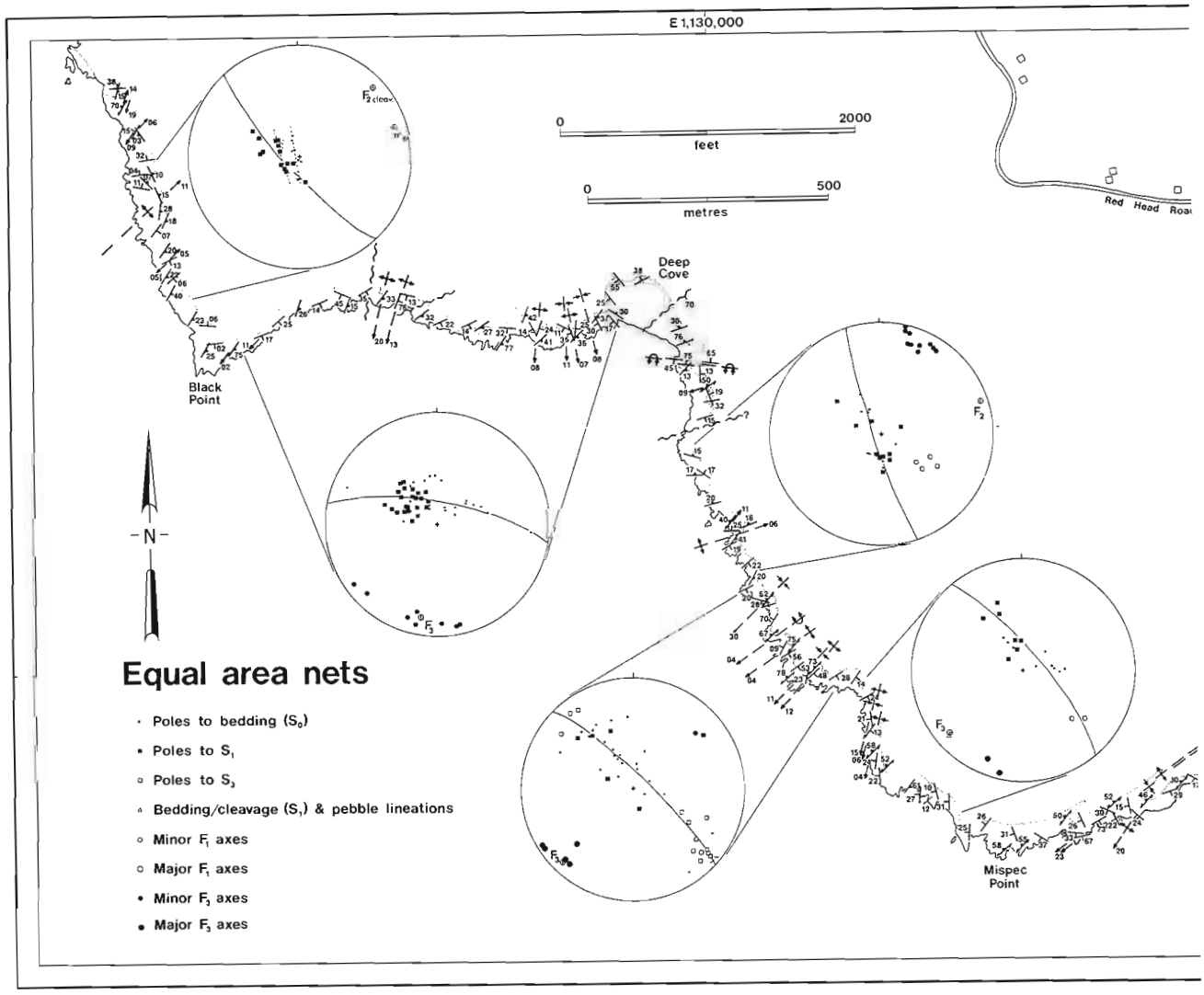

Figure 2.3. *Structural map of the Balls Lake Formation between Black Point and Mispec Bay (see Fig. 2.1 for location. Co-ordinates after 1:4800 New Brunswick Topographic Series).*

Currie and Nance (1983) also established evidence for a correlation between much of the West Beach Formation and the bimodal, late Precambrian and recently identified Eocambrian (Currie, 1984) volcanics and volcaniclastics of the nearby Coldbrook Group (Fig. 2.1). As this would entirely remove the West Beach Formation from the Carboniferous Mispec Group and dramatically affect interpretations of the regional structure, further substantiation of this correlation is a high priority of the ongoing reinvestigation. The West Beach Formation, however, was not encountered in the areas described in this report.

Structural geometry

Three phases of Alleghenian deformation affect the Balls Lake and Lancaster formations along the eastern shore of Saint John Harbour. Two of these are locally major fabric-forming events such that the three phases may be placed in sequential order on the basis of overprinting. All three are not everywhere developed, however, and while the first two affect all lithologies of the Mispec Group from Saint John to Cape Spencer (Fig. 2.1), the third is absent north of Cranberry Point and progressively intensifies southward.

D_1 structures

The earliest deformational structures take the form of a variable but widespread cleavage (S_1) that is broadly axial planar to rare, mesoscopic folds (F_1) of consistent northwest vergence. In the sandstones of the Lancaster Formation between Little River Beach and McNamara Point (Fig. 2.2), D_1 constitutes the only phase of mesoscopic structuring and its style is spectacularly displayed at the mouth of Little River (insert; Fig. 2.2) where well-defined beds (S_0) of the Lancaster Formation are deformed about an F_1 syncline that plunges gently south-southwest. Diagnostic sedimentary criteria for younging are absent, but the overturned nature of the southeastern limb of the fold is clearly demonstrated by the relationship of bedding to the strongly developed axial planar cleavage (S_1). This dips moderately southeast and locally gives rise to a prominent bedding/cleavage intersection lineation (L_1). A similar, asymmetric rather than overturned, syncline occurs midway between Midwood and McNamara Point (Fig. 2.2), where it plunges due south. At McNamara Point itself, D_1 structuring is associated with displacement along a minor thrust fault (insert; Fig. 2.2). Marked by a few decimetres of cataclasite, the thrust parallels an S_1 cleavage that progressively intensifies toward the thrust surface and defines the axial plane of a strongly asymmetric F_1 anticline developed in the hangingwall. As at

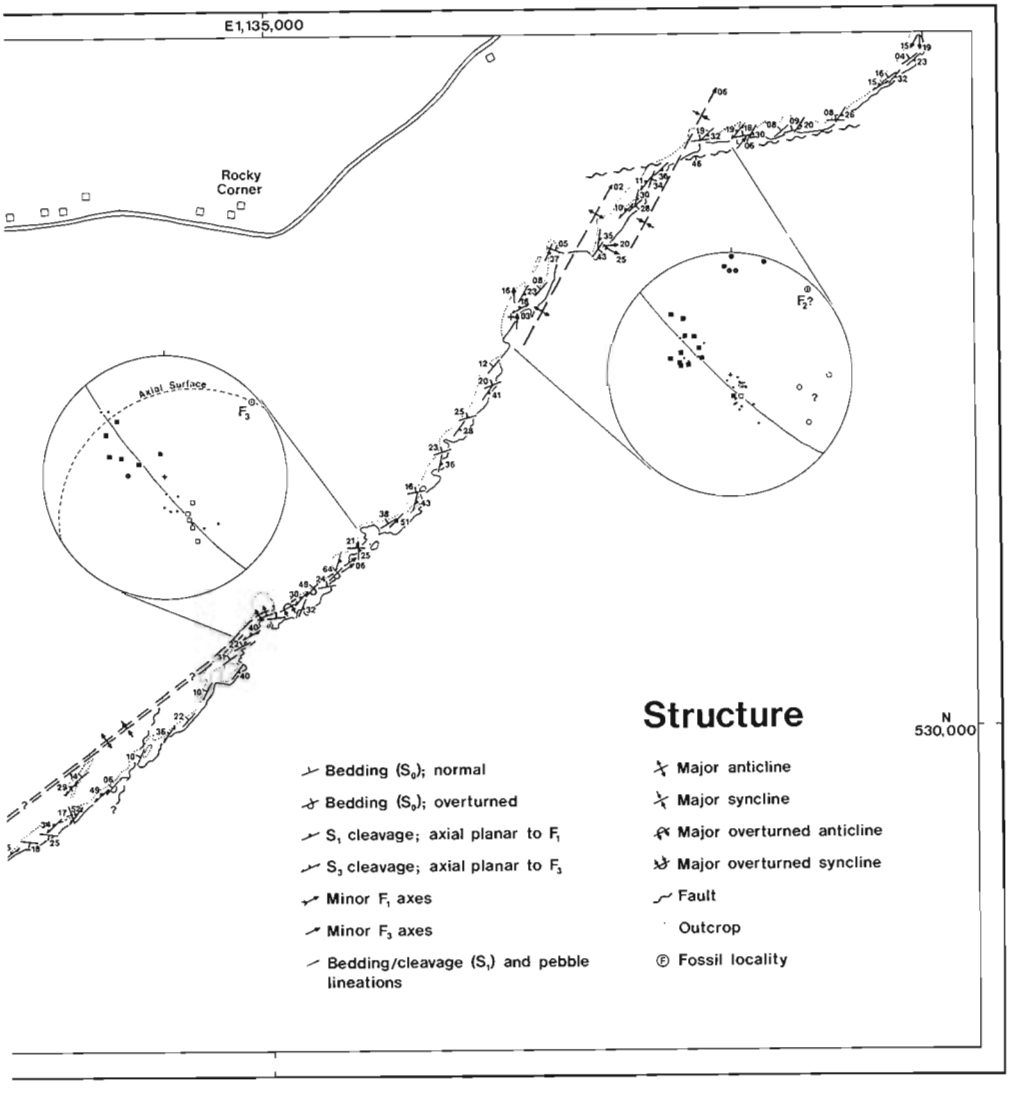

Little River Beach, the fold displays a tight Class 1C profile, and is overturned toward the northwest. Displacement on the thrust surface, however, is likely to be small. Conglomerate pebbles at McNamara Point are flattened within the S_1 cleavage and locally extended parallel to the F_1 axes and the L_1 intersection lineation.

Farther south, in the redbeds of the Balls Lake Formation between Black Point and Mispec Bay (Fig. 2.1), mesoscopic F_1 folds have not been observed, and S_1 takes the form of a bedding-subparallel cleavage. Dips to the southeast still predominate but they are gentle and locally range through northeast to northwest under the influence of subsequent folding (Fig. 2.3). As with the Lancaster Formation, conglomerates, such as those at Deep Cove, may locally show strong L-S tectonite fabrics.

D_2 structures

The second deformation reflects a period of gentle warping rather than a fabric-forming event, but produced the broad domes and basins that characterize the pattern of regional structuring (Fig. 2.1). Fold axes (F_2) are subhorizontal and plunge northeast and southwest, broadly parallel to those of F_1. However, the event produced no minor structures and is recognizable only as a regional sinuosity in the orientation of bedding and the S_1 cleavage. That it post-dates D_1 is clearly demonstrated in the Balls Lake Formation north of Black Point (Fig. 2.3) where S_0 and S_1 define a gentle, northeast-plunging flexure within which individual outcrops (tie-lines on insert; Fig. 2.3) maintain a constant angular relationship (11°) between cleavage and bedding as these are traced around the fold closure. South of Deep Cove (Fig. 2.3), a more open F_2 fold is well exposed and locally causes the S_1 cleavage to dip northwest. Megascopic flexures of S_0 and S_1 in the Balls Lake Formation east of Rocky Corner (Fig. 2.3), and the Lancaster Formation north of McNamara Point (Fig. 2.2), are also considered F_2 folds.

D_3 structures

The final deformation represents the second fabric-forming event which is less widespread but locally overprints that of D_1. D_3 is largely absent north of Black Point, and has not been observed in the Lancaster Formation of the Midwood section (Fig. 2.2). In the Balls Lake section of Mispec Point (Fig. 2.3), it takes the form of a locally prominent cleavage (S_3) that is similar in appearance to S_1 and is likewise axial planar to mesoscopic folds (F_3). The cleavage, however, dips consistently northwest at moderate angles such that F_3 folds are asymmetric or overturned to the southeast. S_3 is unaffected by, and hence post-dates, the F_2 flexuring. The style of D_3 structuring is well displayed at Mispec Point (Fig. 2.4) where conglomerates of the Balls Lake Formation are deformed about a tight F_3 fold-pair that plunges gently southwest. Fold profiles are of Class 1B to 1C style with a strong axial planar (S_3) cleavage that has almost entirely overprinted the scarcely recognizable S_1 fabric. The fold-pair may reappear on the coastline farther to the northeast as an overturned structure that plunges gently northeast (Fig. 2.3). D_3 structuring is also developed to the east and south of Deep Cove (Fig. 2.3) where F_3 fold-trains with wavelengths on the order of 100 m are associated with intensification of the S_3 cleavage. Away from F_3 closures, however, an often gently dipping S_3 cleavage is more weakly developed such that the S_1 cleavage is preserved. On the coast east of Rocky Corner (Fig. 2.3), for example, excellent flat-lying, polyphase cleavage occurs that is commonly modified by strong refraction of both cleavages across alternating conglomerate and siltstone beds. The cleavages intersect to produce a rhombic pattern except in areas of F_3 minor folding where S_3 is axial planar to folds in S_1. Sedimentary structures, however, are often well preserved and demonstrate that the succession is consistently upward-younging.

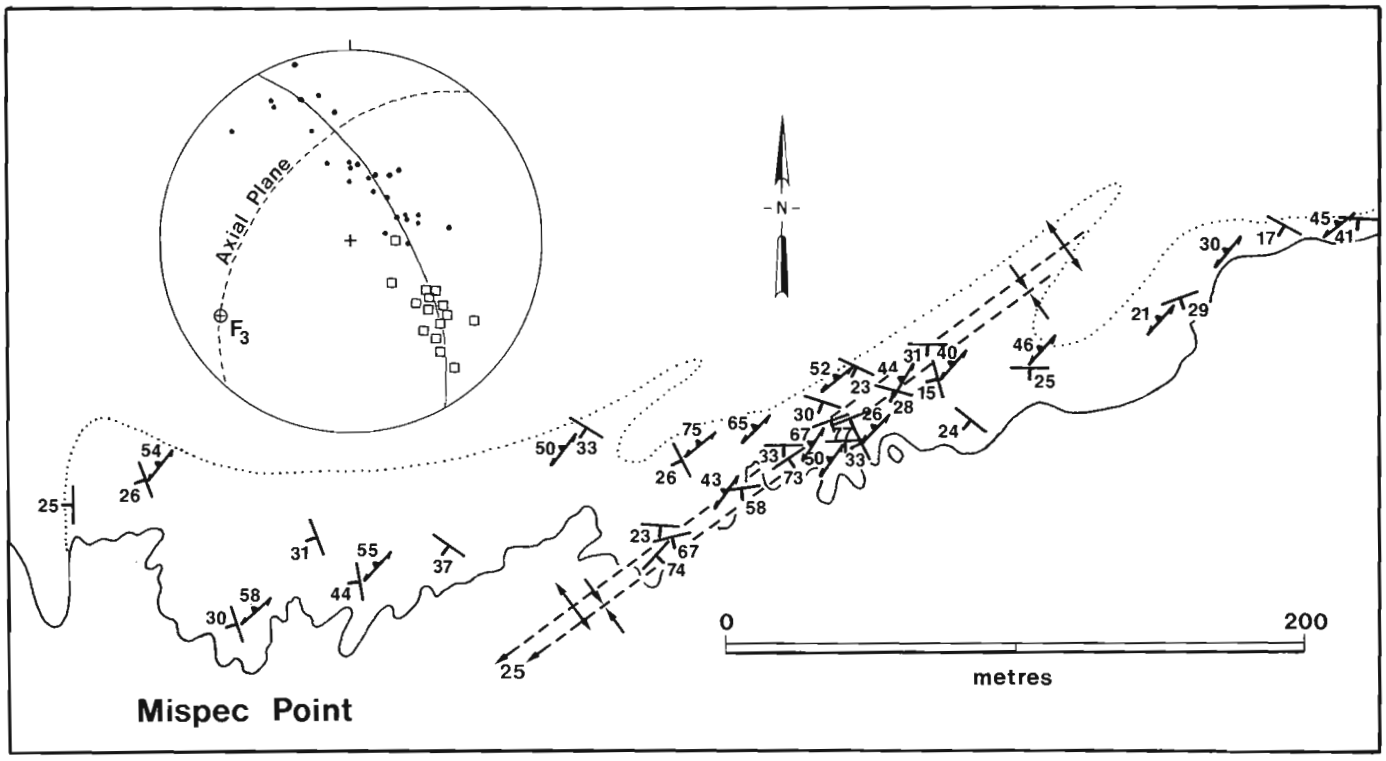

Figure 2.4. D_2 structural relations in the Balls Lake Formation at Mispec Point (see Fig. 2.3 for location).

Summary and discussion

Deformation in the Mispec Group east of Saint John Harbour records two phases of cleavage formation separated by a period of regional warping. Both cleavage phases have also been recognized in the Mispec Group farther east (Ruitenberg et al., 1979), although their regional significance will remain uncertain until a firm Carboniferous stratigraphy is established. Nevertheless, both local and regional (Currie and Nance, 1983) studies suggest that the two phases of deformation produced only mesoscopic structures in a region dominated by essentially flat-lying sequences that consistently young upwards. This contrasts with the Alleghenian structure west of Saint John (Rast et al., 1978, 1975) where the first and principal cleavage is axial planar to regional overturned structures that are displaced along cleavage-subparallel thrust surfaces. The cleavage dips gently southeast but steepens and intensifies toward the northwestern limit of the Mispec Group, as the Alleghenian front is approached. Minor refolding during a second deformational phase produced an axial planar cleavage that dips gently northwest.

East of the city, deformation associated with the northwestern margin of the Mispec Group is not appreciable, but rather intensifies southward from Mispec Bay to Cape Spencer (Fig. 2.1), where largely transposed and stratigraphically uncertain lithologies of the Mispec Group are tectonically overlain by a granitic unit of unknown affinity (Currie and Nance, 1983). Such relationships seem incompatible with an allochthonous Mispec terrane bound by an Alleghenian front along its northwestern edge. Instead, the observations suggest an autochthonous or parautochthonous Mispec terrane bound by an Alleghenian front to the south. This interpretation is compatible with the revised Mispec stratigraphy and supports the tentative proposal of Currie and Nance (1983), that the Balls Lake and Lancaster formations respectively comprise proximal fan and more distal fluvial facies deposited in advance of, and subsequently overridden by, an allochthonous Alleghenian terrane to the south.

Acknowledgments

The author greatly benefitted from field discussions with Ken Currie, Saifullah Tanoli, Ishmail Patel and Ron Pickerill. Financial support was provided by the Ohio University Research Council (OURC 9637) and is gratefully acknowledged.

References

Alcock, F.J.
1938: Geology of the St. John region, New Brunswick; Geological Survey of Canada, Bulletin 210, 65 p.

Bradley, D.C.
1982: Subsidence in late Paleozoic basins in the northern Appalachians; Tectonics, v. 1, p. 107-123.

Currie, K.L.
1984: A reconsideration of some geological relations near Saint John, New Brunswick; in Current Research, Part A, Geological Survey of Canada, Paper 84-1A, p. 193-201.

Currie, K.L. and Nance, R.D.
1983: A reconsideration of the Carboniferous rocks of Saint John, New Brunswick; in Current Research, Part A, Geological Survey of Canada, Paper 83-1A, p. 29-36.

Currie, K.L., Nance, R.D., Pajari, G.E., Jr., and Pickerill, R.K.
1981: Some aspects of the pre-Carboniferous geology of Saint John, New Brunswick; in Current Research, Part A, Geological Survey of Canada, Paper 81-1A, p. 23-30.

Hayes, A.O. and Howell, B.G.
1937: Geology of Saint John, New Brunswick; Geological Society of America, Special Paper 5, 146 p.

Rast, N. and Grant, R.H.
1973: Transatlantic correlations of the Variscan-Appalachian orogeny; American Journal of Science, v. 273, p. 572-579.

Rast, N., Grant, R.H., Parker, J.S.D., and Teng, T.C.
1978: The Carboniferous deformed rocks west of Saint John, New Brunswick; in Guidebook for field trips in southeastern Maine and southwestern New Brunswick, ed. A. Ludman; New England Intercollegiate Geological Conference 70th Annual Meeting, Queens College Press, Flushing, New York, p. 162-173.

Rast, N., Pajari, G., Grant, R., Wardle, R., O'Brien, B., and Patel, I.
1975: Geology of southwestern New Brunswick – Field Guide; Geological Society of America, Penrose Conference Field Guide.

Ruitenberg, A.A., Giles, R.S., Venugopal, D.V., Buttimer, S.M., McCutcheon, S.R., and Chandra, J.
1979: Geology and mineral deposits, Caledonia area; Mineral Resources Branch, New Brunswick Department of Natural Resources, Memoir 1, 213 p.

Ruitenberg, A.A. and McCutcheon, S.R.
1982: Acadian and Hercynian structural evolution of southern New Brunswick; in Major structural zones and faults of the northern Appalachians, ed. P. St.-Julien and J. Beland; Geological Association of Canada, Special Paper 24, p. 131-148.

Stopes, M.C.
1914: The "Fern Ledges" Carboniferous flora of Saint John, New Brunswick; Geological Survey of Canada, Memoir 14.

Wardle, R.J.
1978: The stratigraphy and tectonics of the Greenhead Group: Its relationship to Hadrynian and Paleozoic rocks, southern New Brunswick; unpublished Ph.D. thesis, University of New Brunswick, Fredericton, New Brunswick.

-3-

SUMMARY ON URANIUM IN CANADA, 1984

Project 750010

V. Ruzicka and G.M. LeCheminant
Economic Geology and Mineralogy Division

Ruzicka, V. and LeCheminant, G.M., Summary on uranium in Canada, 1984; in Current Research, Part A, Geological Survey of Canada, Paper 85-1A, p. 15-22, 1985.

Abstract

Field and laboratory investigations of recently discovered uranium occurrences and deposits have revealed that (a) the mineralization processes that formed the Cigar Lake deposit, Saskatchewan were similar to those reported for the McClean Lake deposit; (b) the recently discovered Boomerang Lake occurrence related to the sub-Thelon unconformity occurs in a geological environment similar to that hosting deposits related to the sub-Athabasca unconformity; (c) additional occurrences of mineralization similar to the Black Sturgeon Lake showing, Ontario, will be restricted to areas containing uraniferous igneous rocks adjacent to ferruginous metavolcanic rocks in areas affected by Keweenawan hydrothermal activity; (d) uranium occurrences in the Otish Basin, Labrador Trough, Central Mineral Belt of Labrador and the Nonacho Basin were formed by epigenetic processes.

Résumé

Des études en laboratoire et sur le terrain d'accumulations et de gisements d'uranium récemment découverts ont révélé que (a) les processus de minéralisation à l'origine du gisement de Cigar Lake (Saskatchewan) sont analogues à ceux qui ont supposément concouru à la formation du gisement de McClean Lake; (b) le gisement récemment découvert de Boomerang Lake, que l'on rattache à la discordance sous-jacente à la formation de Thelon, se présente dans un environnement géologique semblable à celui qui renferme les gisements associés à la discordance sous-jacente à la formation d'Athabasca; (c) d'autres minéralisations comparables à l'accumulation superficielle de Black Sturgeon Lake (Ontario) se limitent à des régions qui contiennent des roches ignées uranifères adjacentes à des roches métavolcaniques ferrugineuses, elles-mêmes situées dans des régions qui ont été soumises à l'activité hydrothermale de Keweenawan; (d) les minéralisations d'uranium découvertes dans le bassin d'Otish, dans la dépression du Labrador, dans la zone minérale centrale du Labrador et dans le bassin de Nonacho ont été formées par des processus épigénétiques.

Introduction

Geological studies of Canadian uranium deposits and uranium-bearing areas continued in 1984 commensurate with uranium exploration activity in Canada, which remained almost on the same level as in 1983. Locations of the main exploration targets in 1984 are shown in Figure 3.1. Selected key deposits and areas in Saskatchewan, Northwest Territories, Quebec and Ontario were studied in detail by the authors in the course of a biennial assessment of Canadian uranium resources conducted on behalf of the EMR Uranium Resource Appraisal Group. Some results are presented in this paper.

Athabasca Basin region, Saskatchewan

The Athabasca Basin region was the main subject of geological studies and also the main target of uranium exploration in 1984 because the world's largest high grade uranium deposits occur in this region. Results of some of these studies have recently been published by, among other authors, Wallis et al. (1984), Ruzicka (1984), Artru et al. (1984), Ey (1984), Grauch et al. (1984), and Darnley et al. (1984). Extensive exploration for uranium was conducted in the region by Cogema Canada Limited, Eldor Resources Limited, AGIP Canada Limited, Saskatchewan Mining Development Corporation, Minatco Limited, Uranerz Exploration and Mining Limited, Amok Limited and by other companies associated with these operations.

The main exploration targets (Fig. 3.2) were: (1) the Waterbury Lake area including the Cigar Lake deposit, Tibia Lake, Longyear Bay and Close Lake prospects; the Dawn Lake and McArthur River blocks including the Dawn Lake zones and the BJ prospect; (2) the Collins Bay area including the B zone; the Studer-Umpherville block including the Sand Lake prospect; the Hatchet Lake and the Fife Island areas; (3) the Key Lake area including Boundary Lake segment; (4) the Carswell Structure; and (5) the Stoney Rapids area. All of these target areas contained either ore bodies or mineralization associated with the sub-Athabasca unconformity.

Waterbury Lake area

A brief description of the mineralization was reported by Ruzicka and LeCheminant (1984, p. 44). It occurs in an altered zone mainly within the lowermost part of the clastic

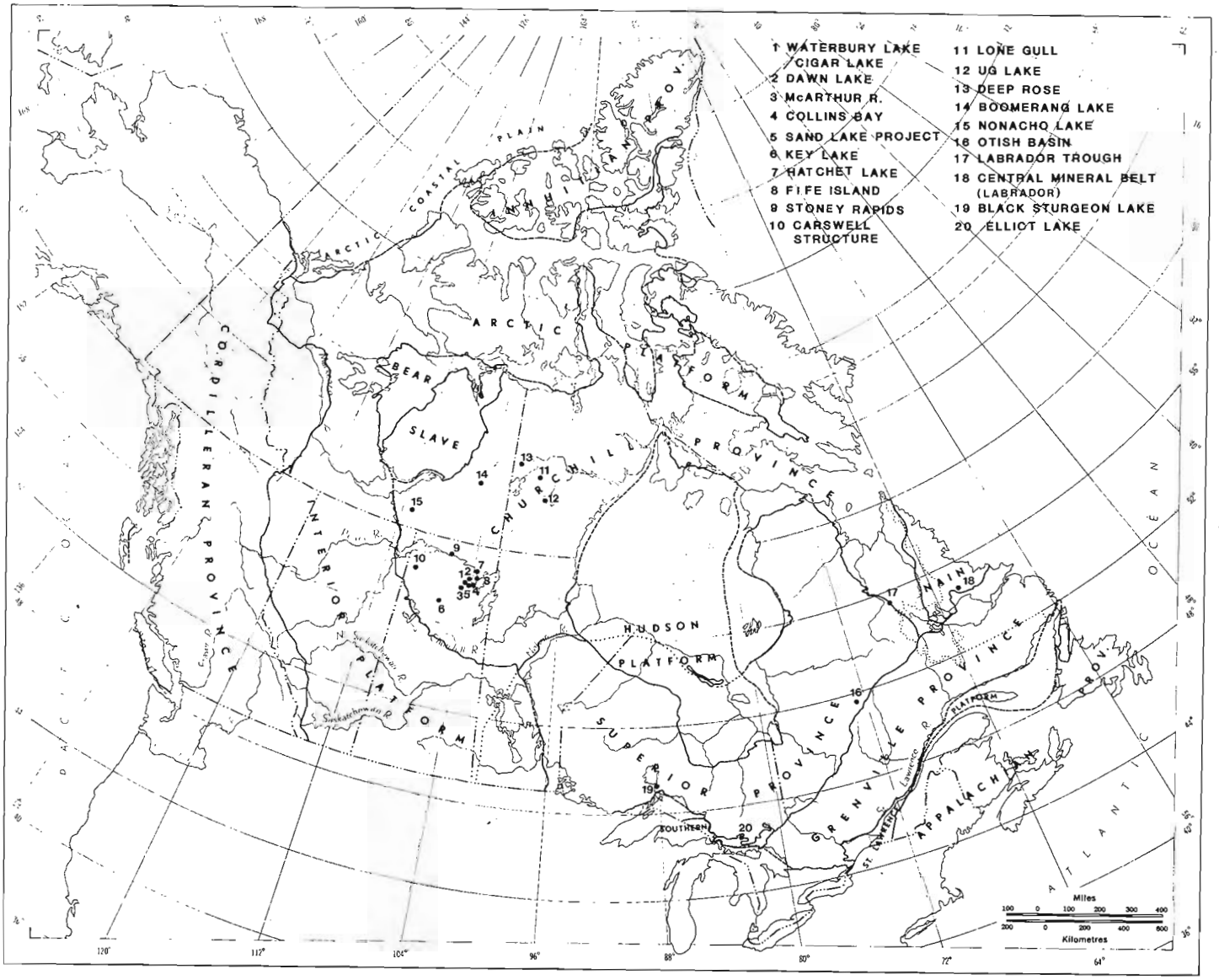

Figure 3.1. *Main uranium exploration targets in Canada, 1984.*

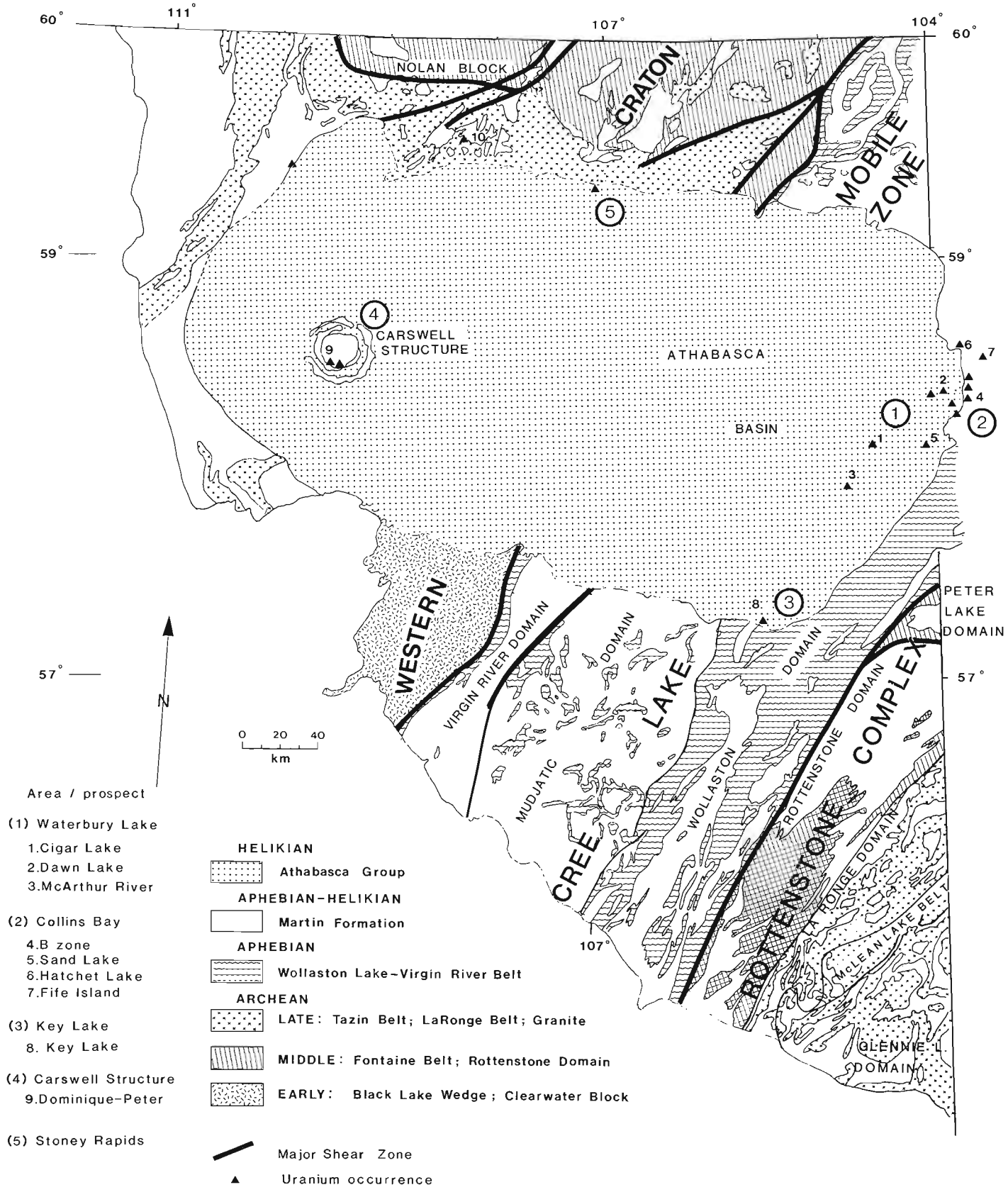

Figure 3.2. *Main uranium exploration targets in the Athabasca Basin region, Saskatchewan, 1984.*

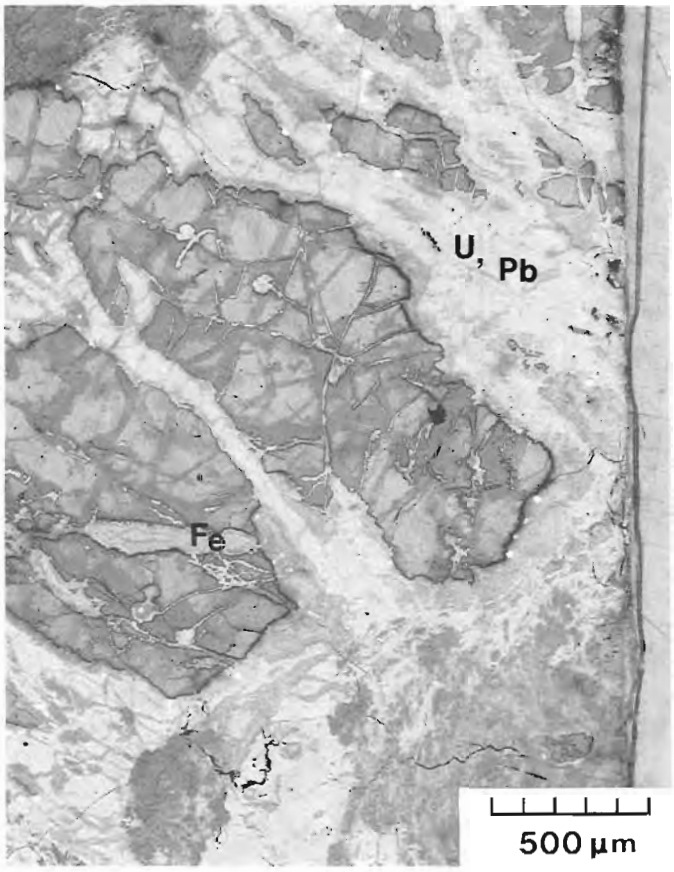

Figure 3.3. *Relict quartz clasts (light grey) replaced by iron oxide (Fe) and surrounded by later pitchblende (U, Pb). Cigar Lake deposit, Saskatchewan. (Reflected light)*

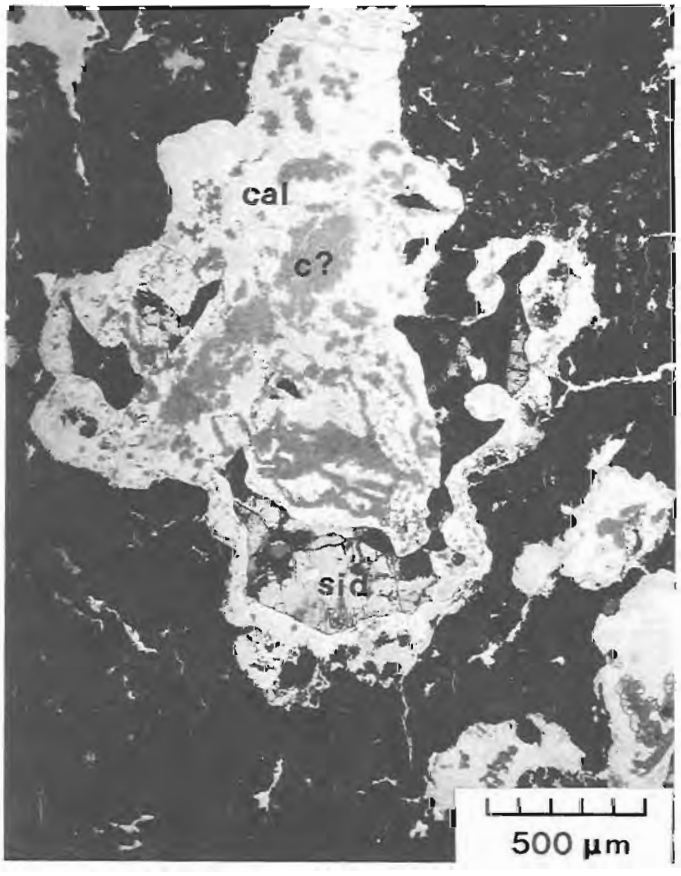

Figure 3.4. *A vug in matrix of sandstone filled with calcite (cal) containing subhedral siderite (sid) and patches of, apparently, chamosite (C?). Cigar Lake deposit, Saskatchewan. (Transmitted light)*

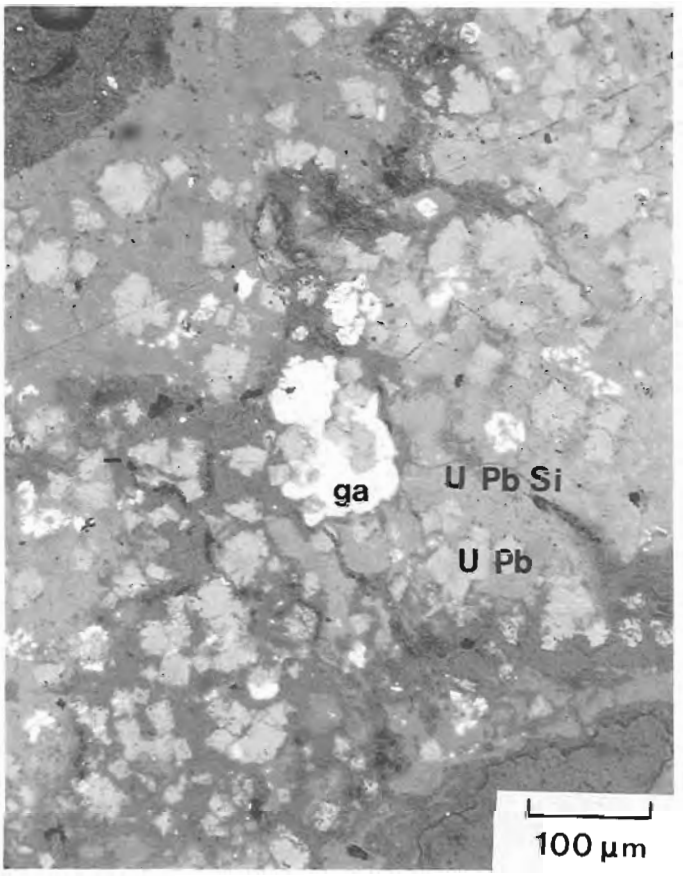

Figure 3.5. *Clusters of cubic (U, Pb) and massive (U, Pb, Si) pitchblende associated with galena (ga) in matrix of sandstone. Cigar Lake deposit, Saskatchewan. (Reflected light)*

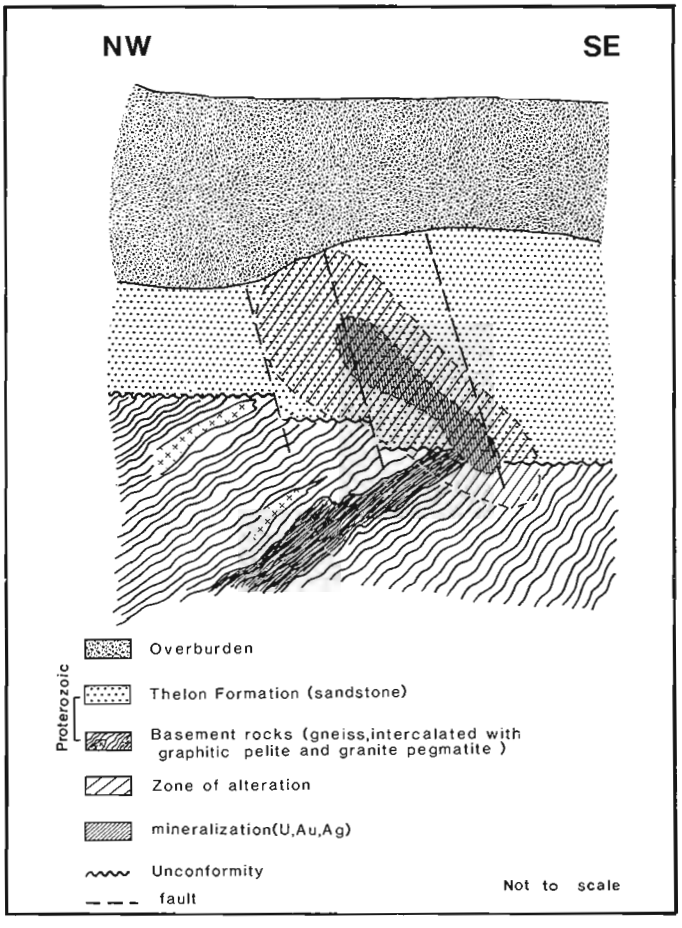

Figure 3.6. *Schematic section through the Boomerang Lake occurrence, Northwest Territories.*

sedimentary rocks of the Athabasca Group at a depth of 410 to 440 m (Saskatchewan Mining Development Corporation, 1984).

The basement rocks consist of: augen gneiss, and graphitic metapelite with pyrite; calc-silicate rocks and granite-pegmatite. The basement rocks are locally mylonitized, fractured, faulted and, in the vicinity of the mineralization altered to chlorite and clay.

The sandstone at the base of the Athabasca sequence consists of subangular quartz clasts in a matrix of illitic clay-mica (glauconite-celadonite) and kaolinite. Some of the quartz has been replaced by iron oxides and pitchblende. The youngest gangue minerals are siderite, chamosite and calcite (Fig. 3.3). In the vicinity of the mineralization the sandstone contains vugs filled with druses of euhedral quartz or calcite with subhedral siderite and patches of chamosite (Fig. 3.4).

The mineralization occurs in two associations: (a) polymetallic containing pitchblende and Ni-, Cu-, Pb- and Ti- minerals, commonly accompanied by chlorite, illite and carbonates; this assemblage occupies, as a rule, the lowermost portions of the mineralized bodies; (b) as pitchblende/coffinite concentrations associated with iron oxides, iron sulphides and clay minerals; this assemblage generally occupies upper portions of the mineralized bodies.

The pitchblende occurs in several forms and at least in two generations: in addition to massive, disseminated, vein, breccia and botryoidal forms (Ruzicka and LeCheminant, 1984), it occurs in clusters of cubic grains (Fig. 3.5) which resemble the alpha-uranium-heptaoxide described by Dahlkamp (1978) from the Key Lake deposit.

Microscopic and megascopic observations indicate: (a) ore formation took place in several stages, the polymetallic phase being the earliest; (b) distribution of the mineralization was structurally controlled by the sub-Athabasca unconformity, which is intersected by a zone of fracturing; (c) mineralization apparently took place at the interface of ascending and reducing hydrothermal fluids with oxidizing descending or laterally moving solutions; (d) alteration processes included: authigenic formation of illitic clay-mica (glauconite-celadonite), chamosite,(?) chlorite and kaolinite; partial dissolution of clastic quartz, its recrystallization in vugs or redeposition in silicification haloes; deposition of late stage carbonates.

These observations are compatible with a model for development of the McClean deposits proposed by Wallis et al. (1984) and with genetic considerations summarized by Darnley et al. (1984).

Baker Lake – Thelon region, Northwest Territories

In addition to the Lone Gull and UG Lake (Lac Cinquante) deposits, known for some years, several other uranium occurrences have been discovered in the Baker Lake – Thelon region and exploration has continued during recent years. Most of the exploration was oriented towards discovery of deposits associated with the sub-Thelon unconformity using a conceptual genetic model derived from deposits in the Athabasca Basin region. Although most of the deposits and occurrences in the Baker Lake – Thelon region exhibit features fitting at least in part the model for Athabasca-type deposits (Tremblay, 1982; Wallis et al., 1984) the best example of this type is apparently the occurrence discovered by Urangesellschaft Canada Limited at Boomerang Lake in the southwestern part of the Thelon Basin (Fig. 3.1).

Boomerang Lake occurrence

The occurrence was discovered by drill-testing geochemical and geophysical anomalies on claims optioned by Urangesellschaft Canada Limited from Dome Mines Limited (Indian and Northern Affairs, Canada, 1983).

The uranium/polymetallic mineralization occurs in an illite-chlorite-kaolinite altered zone at the sub-Thelon unconformity. This unconformity separates Proterozoic basement rocks – biotite-garnet gneiss with intercalations of graphitic and pyritic pelite and granite pegmatite – from locally limonitized and bleached sandstone of the Thelon Formation. The bedrock is covered by thick overburden (Fig. 3.6). In addition to uranium, which occurs in massive pitchblende, the mineralization contains Pb, Ni, Co, V, Cr, Zr, Zn, Au and Ag. The upper part of the basement rocks is regolithic and contains hematite pseudomorphs after garnet.

Sibley Basin, Ontario

Lithostratigraphic similarities between the Athabasca and Sibley basins led about eight years ago to a search for uranium deposits spatially related to the sub-Sibley unconformity in an area between Nipigon, Pass Lake and Black Sturgeon Lake. This search was spurred by discoveries of uranium mineralization associated with the unconformity at the Enterprise mine (Ruzicka, 1977) and by studies of occurrences in the Nipigon area (Franklin, 1978).

Discovery of a uranium occurrence near Black Sturgeon Lake triggered field and laboratory studies by the Geological Survey (Ruzicka and LeCheminant, 1984) and Carleton University (Thompson, 1984). Additional results of subsequent studies follow.

Black Sturgeon Lake occurrence

Uranium mineralization of the Black Sturgeon Lake occurrence is confined to: (a) albitic granite pegmatite and (b) fractures in adjacent ferruginous rocks.

Uranium- and thorium-bearing minerals in the pegmatite are irregularly distributed (Fig. 3.7) in a coarse grained rock composed of large multigranular quartz grains with sutured internal grain boundaries, anhedral dusty orthoclase and minor plagioclase with albite twinning. The rock locally contains myrmekite. The main radioactive minerals are thorite (Fig. 3.8) and brannerite embedded in orthoclase (Thompson, 1984).

The ferruginous rocks are apparently volcanics, rich in magnetite and ilmenite, with biotite-muscovite or an amphibole-rich matrix, with abundant titanite as a separate phase or closely intergrown with ilmenite. Prehnite occurs in narrow veins associated with calcite, or as large laths in the matrix with amphibole and chlorite, suggesting hydrothermal alteration. The mineralization filling fractures in the ferruginous rocks is epigenetic and consists of thorium-free pitchblende. It is associated with hematite; magnetite, commonly altered to hematite along the contact with the pitchblende; a chlorite-actinolite-hornblende assemblage (Fig. 3.9); titanium-bearing minerals (Fig. 3.10); a magnetite-biotite-amphibole assemblage (Fig. 3.11); or with prehnite and/or calcite. Accessory minerals in the fracture fillings locally are pyrite, galena and sphene (Fig. 3.12); apatite, chalcopyrite and covellite.

On the basis of these and previous observations (Ruzicka and LeCheminant, 1984; Thompson, 1984) the genesis of the Black Sturgeon Lake occurrence can be

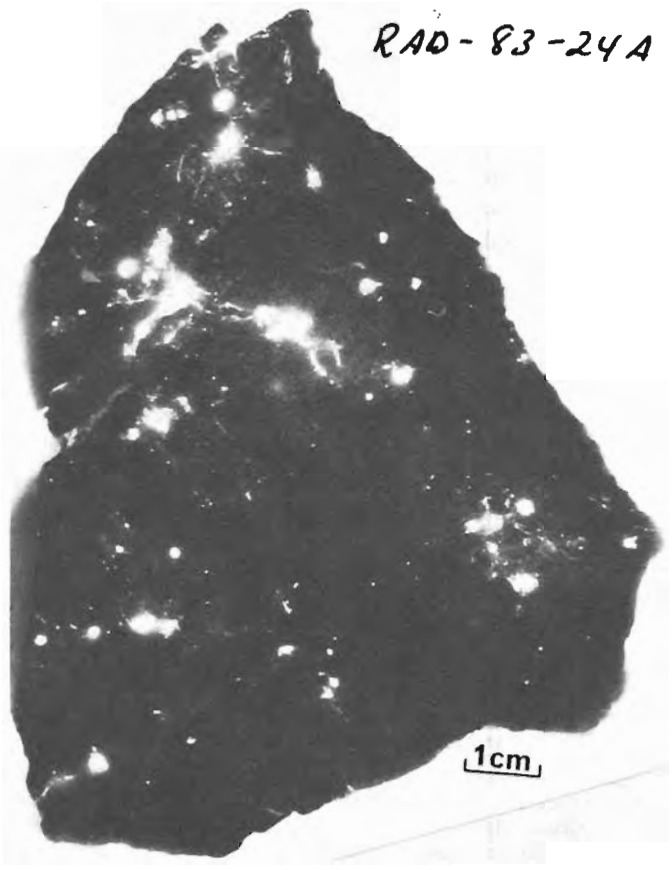

Figure 3.7. Autoradiograph of albitic granite pegmatite containing grains of thorite and minor amounts of brannerite. Black Sturgeon Lake occurrence, Nipigon area, Ontario. Positive image.

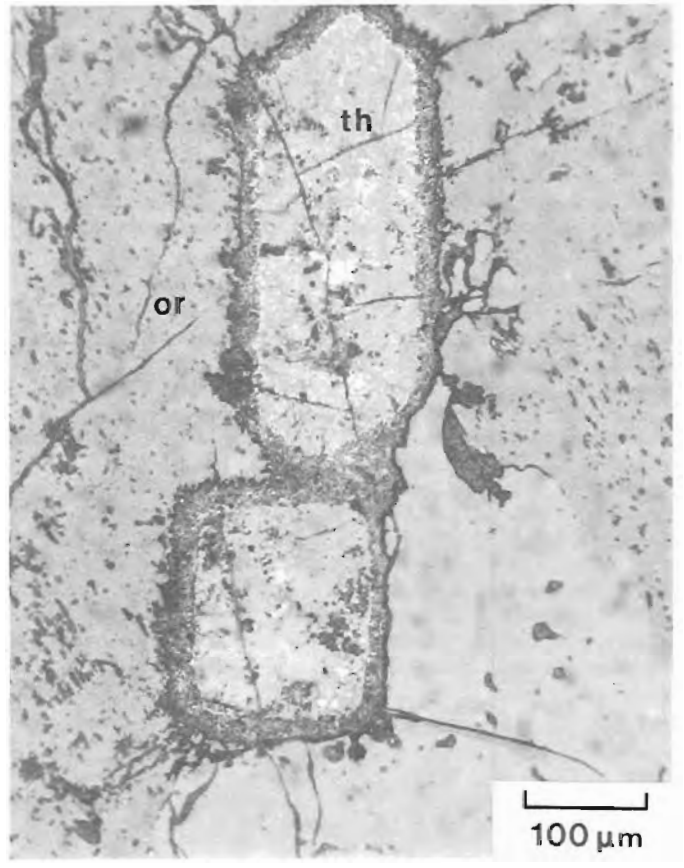

Figure 3.8. Thorite (th) embedded in orthoclase in granite pegmatite. Black Sturgeon Lake occurrence, Nipigon area, Ontario. (Reflected light)

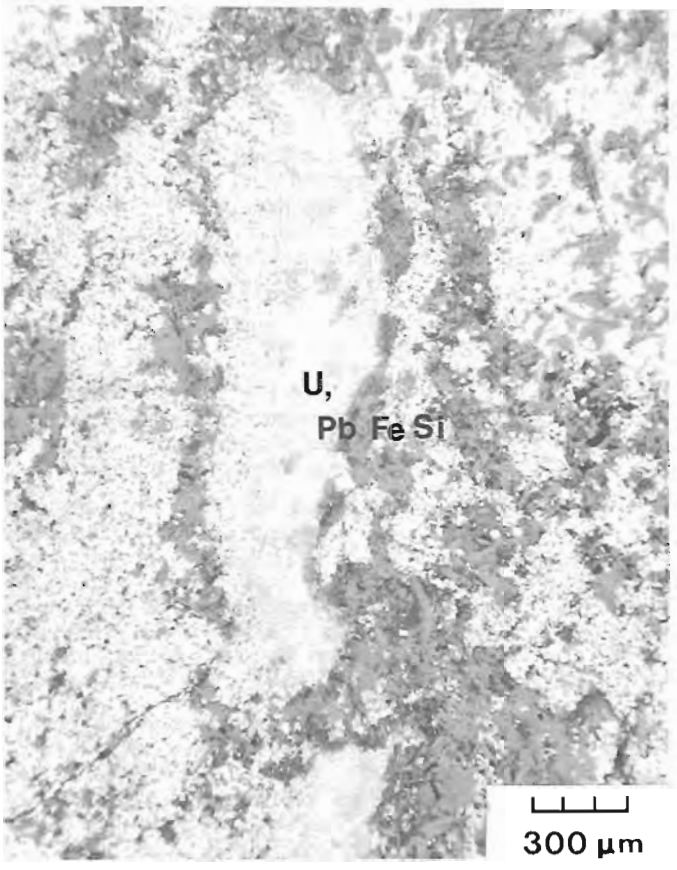

Figure 3.9. Pitchblende (U, Pb, Fe, Si) occurring in elongate patches in a matrix of chlorite, actinolite and hornblende. Black Sturgeon Lake occurrence, Nipigon area, Ontario. (Reflected light)

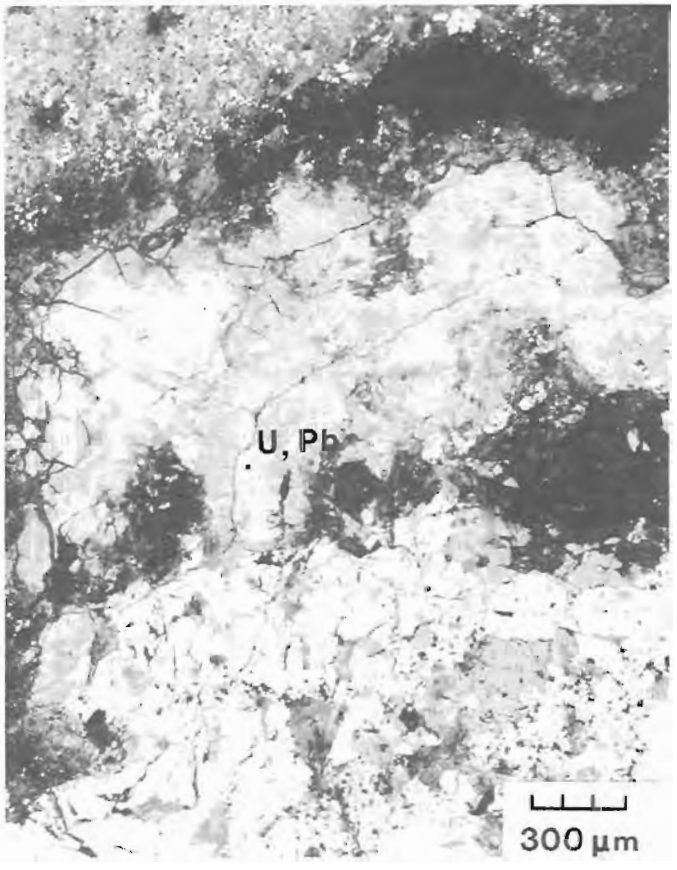

Figure 3.10. Pitchblende (U, Pb) intimately associated with titanium minerals in a sandstone matrix. Black Sturgeon Lake occurrence, Ontario. (Reflected light)

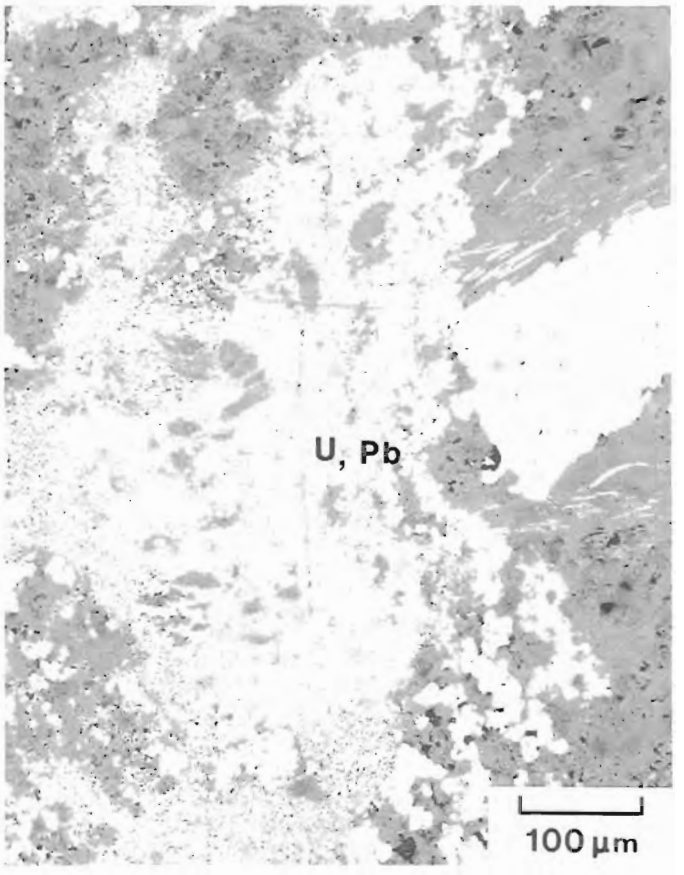

Figure 3. 11. Pitchblende (U, Pb) associated with a magnetite-biotite-amphibole assemblage. Black Sturgeon Lake occurrence, Nipigon area, Ontario. (Reflected light)

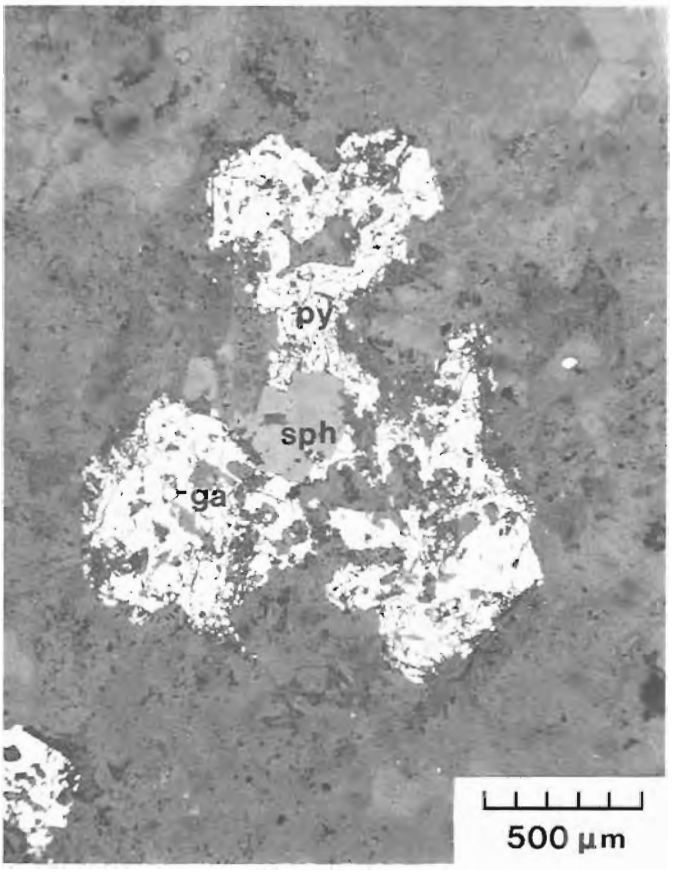

Figure 3.12. Fracture filling containing local lenses of granular calcite and, in addition to pitchblende, (not shown), galena (ga), sphene (sph) and pyrite (py). Black Sturgeon Lake occurrence, Nipigon area, Ontario. (Reflected light)

interpreted as follows: (a) the source of uranium was apparently the albitic granite pegmatites; (b) uranium was carried from the source to the site of deposition in hydrothermal solution; (c) propulsion of the solutions was caused by Keweenawan igneous activity; (d) deposition of uranium-bearing minerals, caused by interaction between the solutions and the ferruginous rocks, was associated with development of hematite and chlorite. Therefore, the potential for discovery of this type of mineralization is restricted to areas containing uranium-bearing igneous rocks adjacent to ferruginous metavolcanic rocks and in the vicinity of Keweenawan diabase bodies.

Other areas

The remaining areas explored for uranium in 1984 were: Otish Basin, Quebec; Labrador Trough, Quebec and Labrador; Central Mineral Belt of Labrador; and Nonacho Basin, Northwest Territories. A limited amount of exploration was conducted in the Elliot Lake area, Ontario.

Metallogenic features of the Otish Basin relating to uranium mineralization were reported by Ruzicka and LeCheminant (1984) and are being analyzed in more detail. Some of the uranium occurrences contain epigenetic mineralization and are located at the contact between gabbro sills and dykes and the units of the Otish Group. The host rocks are usually epidotized, chloritized, albitized and carbonatized.

Uranium occurrences in the Schefferville – Lac Romanet area of the Labrador Trough are described by Bell and Ruzicka (1985). These reports are complementary to previous reports, such as by Kish and Tremblay-Clark (1978) and Kish and Cuney (1981).

Exploration activity for uranium in the Central Mineral Belt of Labrador has been recently revived in the Heggart Lake segment of the belt (Smyth et al., 1978). In addition to the occurrence reported by Smyth et al. (ibid.), uranium mineralization was identified in this area in the following environments: (a) as veins or scattered grains of opaque minerals (brannerite?) in very fine grained volcanic rocks consisting of subhedral plagioclase in a greenish aphanitic matrix of chlorite and opaques. The uranium minerals are accompanied by small amygdules of chlorite or chlorite-chalcopyrite-galena-carbonate; locally the plagioclase is sericitized; (b) as cuspate zones of a radioactive metamict mineral (brannerite?) associated with chalcopyrite, in the plagioclase-rich reddish matrix of a dolomite breccia; (c) in a mudstone – marl (?) consisting of a chlorite-carbonate-quartz assemblage as a partly metamict uraninite-like phase (according to XRD analysis); and (d) in a chlorite-quartz aphanitic rock as an unidentified uranium-bearing phase (XRD analysis yielded only a chlorite group pattern) associated with disseminated pyrite.

Uranium occurrences additional to those reported by Gandhi (1978) and Gandhi and Prasad (1980) were discovered in the Nonacho Basin area, Northwest Territories, by

exploration companies. Several of the occurrences are related to the sub-Nanacho unconformity and occur as fracture fillings in both the Nonacho cover and in the Archean basement rocks. Some of the occurrences in the Nanacho Basin and adjacent areas are related to sodic metasomatic processes (albitization).

Acknowledgments

The authors acknowledge the co-operation of geologists and management personnel from the following exploration and mining companies: Cogema Canada Limited, Urangesellschaft Canada Limited, Uranerz Exploration and Mining Limited, Saarberg-Interplan Canada Limited and PNC Exploration (Canada) Co. Limited.

References

Artru, P., Berville, M., Moreau, M., and Tona, F.
1984: Geological environment of vein-type deposits in the Aphebian basement of the Carswell Structure on the Athabasca Plateau (Northern Saskatchewan). Comparison with other deposits of the same type; in 'Abstracts', Volume IX, Part 1, 27th International Geological Congress, Moscow, 4 – 14 August, 1984, p. 328-329.

Bell, R.T. and Ruzicka, V.
1985: Uranium in Circum Ungava Belt: Northern Quebec and Labrador, New Information from the Central Labrador Trough; in Current Research, Part A, Geological Survey of Canada, Paper 85-1A, Report 19.

Dahlkamp, F.J.
1978: Geological Appraisal of the Key Lake U-Ni Deposits, Northern Saskatchewan; Economic Geology, v. 73, p. 1430-1449.

Darnley, A.G., Wallis, R.H., and Ruzicka, V.
1984: A review concerning the origin of the Athabasca, Saskatchewan, Canada, uranium deposits; in 'Abstracts', Volume IX, Part 1, 27th International Geological Congress, Moscow, 4 – 14 August, 1984, p. 342.

Ey, F.
1984: Alterations and structural setting of a uranium Proterozoic unconformity deposit: Cluff Lake D orebody (Saskatchewan, Canada); in 'Abstracts', Volume IX, Part 1, 27th International Geological Congress, Moscow, 4 – 14 August, 1984, p. 346.

Franklin, J.M.
1978: Uranium mineralization in the Nipigon area, Thunder Bay district, Ontario; in Current Research, Part A, Geological Survey of Canada, Paper 78-1A, p. 275-282.

Gandhi, S.S.
1978: Geological observations and exploration guides to uranium in the Bear and Slave Structural provinces and the Nonacho Basin, District of Mackenzie; in Current Research, Part B, Geological Survey of Canada, Paper 78-1B, p. 141-149.

Gandhi, S.S. and Prasad, N.
1980: Geology and uranium occurrences of the MacInnis Lake area, District of Mackenzie; in Current Research, Part B, Geological Survey of Canada, Paper 80-1B, p. 107-127.

Grauch, R.I., Leventhal, J.S., and Harper, C.T.
1984: Organic material from the Cluff Lake (Canada) uranium district, its nature and paragenetic implications of the included mineral assemblages; in 'Abstracts', Volume IX, Part 1, 27th International Geological Congress, Moscow, 4 – 14 August, 1984, p. 351-352.

Indian and Northern Affairs, Canada
1983: Exploration Overview; Mining, Exploration and Geological Investigations, Northwest Territories 1983; Geology Division, Northern Affairs Program, Yellowknife, N.W.T.

Kish, L. and Cuney, M.
1981: Uraninite-albite veins from the Mistamisk Valley of the Labrador Trough, Quebec; Mineralogical Magazine, December, v. 44, p. 471-483.

Kish, L. and Tremblay-Clark, P.
1978: Geochemistry and radioactivity in the Labrador Trough, 56 degrees 00'-58 degrees 30'; Gouvernement du Québec, Ministère des Richesses Naturelles, Service des Gîtes Mineraux; DPV-567, 69 p.

Ruzicka, V.
1977: Conceptual models for uranium deposits and areas favourable for uranium mineralization; in Report of Activities, Part A, Geological Survey of Canada, Paper 77-1A, p. 17-25.

1984: Unconformity-related uranium deposits in the Athabasca Basin region, Saskatchewan; in 'The IAEA Handbook on Proterozoic Unconformity and Stratabound Uranium Deposits', ed. J. Ferguson; International Atomic Energy Agency, Vienna, p. 228-283.

Ruzicka, V. and LeCheminant, G.M.
1984: Uranium deposit research, 1983; in Current Research, Part A, Geological Survey of Canada, Paper 84-1A, p. 39-51.

Saskatchewan Mining Development Corporation
1984: Cigar Lake; Press Release, May 29, 1984, Saskatoon, Saskatchewan.

Smyth, W.R., Marten, B.E., and Ryan, A.B.
1978: A major Aphebian-helikian unconformity within the Central Mineral Belt of Labrador: definition of new groups and metallogenic implications; Canadian Journal of Earth Sciences, v. 15, no. 12, p. 1954-1966.

Thompson, S.V.
1984: Uranium mineralization of the Black Sturgeon Lake uranium occurrence, District of Thunder Bay Ontario; unpublished B.Sc Thesis, Carleton University, Ottawa, 80 p.

Tremblay, L.P.
1982: Geology of the uranium deposits related to the sub-Athabasca unconformity, Saskatchewan; Geological Survey of Canada, Paper 81-20, 56 p.

Wallis, R.H., Saracoglu, N., Brummer, J.J., and Golightly, J.P.
1984: The geology of the McClean uranium deposits, northern Saskatchewan; The Canadian Mining and Metallurgical (CIM) Bulletin, v. 77, no. 864, p. 69-96.

AN OCCURRENCE OF AMAZONITE, GAHNITE, AND SPHALERITE NEAR PORTMAN LAKE, NORTHWEST TERRITORIES

Project 820011

Ross K. Stevenson[1]
Precambrian Geology Division

Stevenson, R.K., An occurrence of amazonite, gahnite and sphalerite near Portman Lake, Northwest Territories; in Current Research, Part A, Geological Survey of Canada, Paper 85-1A, p. 23-28, 1985.

Abstract

Emerald green amazonite occurs as 2-20 mm crystals in a coarse, peraluminous biotite granodiorite in the Portman Lake area, Northwest Territories. Increasing concentration of lead in the potassium feldspar results in a gradual change in colour from white (Pb-poor) to green (Pb-rich). Increasing concentration of zinc results in the formation of a zincian spinel (gahnite) and, eventually, sphalerite (and pyrrhotite, pyrite and galena) as sulphur becomes available. Gahnite, sphalerite, pyrrhotite, pyrite and galena are found in a much finer grained portion of the same granodiorite. The fine grained granodiorite is a product of rapid crystallization caused by volatile loss through rapid decompression. The most plausible mechanism to explain the enrichment in lead and zinc appears to be contamination of the granodiorite by suitable host rocks, but the rocks sampled nearby are not considered appropriate.

Résumé

L'amazonite vert émeraude se présente sous forme de cristaux de 2 à 20 mm dans une granodiorite à biotite peralumineuse, à grains grossiers, dans la région de Portman Lake (Territoires du Nord-Ouest). L'augmentation de la concentration du plomb dans le feldspath potassique se traduit par un passage graduel de la couleur du blanc (feldspath pauvre en plomb) au vert (feldspath riche en plomb). De même, à mesure que s'accroît la concentration du zinc, apparaissent successivement du spinelle zincifère (gahnite), puis, en présence du soufre, de la sphalérite (ainsi que de la pyrrhotite, de la pyrite et de la galène). La gahnite, la sphalérite, la pyrrhotite, la pyrite et la galène se trouvent dans une partie de la granodiorite à grains beaucoup plus fins. La granodiorite à grains fins résulte d'une cristallisation rapide causée par une perte de matières volatiles sous l'effet d'une décompression brusque. L'explication la plus plausible de l'enrichissement en plomb et en zinc semble être une contamination de la granodiorite par des roches mères ayant les propriétés voulues, mais les échantillons prélevés dans le voisinage ne sont pas jugés appropriés.

[1] Department of Geological Sciences, McGill University, 3450 University Street, Montreal, Quebec H3A 2A7

Introduction

A small but striking occurrence of emerald to apple green amazonite (lead-bearing potash feldspar) granodiorite and mineralized granodiorite forming part of a regional granodiorite complex is poorly exposed in the Portman Lake area of the Hill Island Lake sheet (76 C), Northwest Territories. The occurrence is part of the northern extension of the Northeast Granodiorite-Diorite Complex mapped by Koster (1962) in adjacent northern Saskatchewan where it contains hornblende dated by the K/Ar method at 2370 ± 40 Ma (Koster et al., 1970). According to Koster et al. the massive synkinematic to late kinematic composite pluton consists of various granitic, granodioritic and dioritic rocks that display nebulitic structures considered consistent with an anatectic origin. The amazonite occurrence was discovered by K. Ashton while engaged in preliminary reconnaissance of the Hill Island Lake sheet for the Geological Survey of Canada in 1979.

The occurrence is 340 m south-southeast of a datum point on the southeastern shore of a small lake in the southern part of the map area (long. 109°08'W, lat. 60°04'N, Fig. 4.1). The anhedral to subhedral crystals of amazonite, up to 2 cm across, make up the K-feldspar component of a biotite granodiorite that outcrops in the area shown in Figure 4.1. Blocks of amazonite-bearing granodiorite are found in talus below the outcrop. The amazonite-bearing granodiorite is surrounded by similar biotite granodiorite in which the K-feldspar is white. Two sulphide-bearing lenses in the same outcrop contain sphalerite, pyrrhotite, pyrite, galena, chalcopyrite and spinel (principal end-members $FeAl_2O_4$ and $Zn_3Al_2O_4$). The lenses of mineralized fine-grained granodiorite apparently are younger than the coarse-grained granodiorite.

The granodiorite-diorite complex contains small bodies of fine- to medium-grained pink granite composed of pink microcline, quartz and albite, one of which lies across the northern extremity of the amazonite occurrence. The contacts of this body with the granodiorite are ambiguous; pink granite veins cut the granodiorite, suggesting that the pink granite is younger than the granodiorite; but because the main contacts are gradational the bordering granite could have been remobilized during intrusion of granodiorite magma. Neither pink granite nor the granite veins contain sulphides. North of Saskatchewan – Northwest Territories boundary, the eastern and western limits of the enclosing granodiorite pluton have yet to be mapped.

Acknowledgments

The field work for this project was completed by the author while employed by the Geological Survey of Canada. I thank Dr. Hewitt H. Bostock for providing the opportunity to study the occurrence. The invaluable assistance of Donald Watanabe in the field is also greatly appreciated. My thanks go to Robert F. Martin for his constructive comments on the manuscript. Support for this project was provided by the Geological Survey of Canada and an operating grant (# A7721) from NSERC to Robert F. Martin.

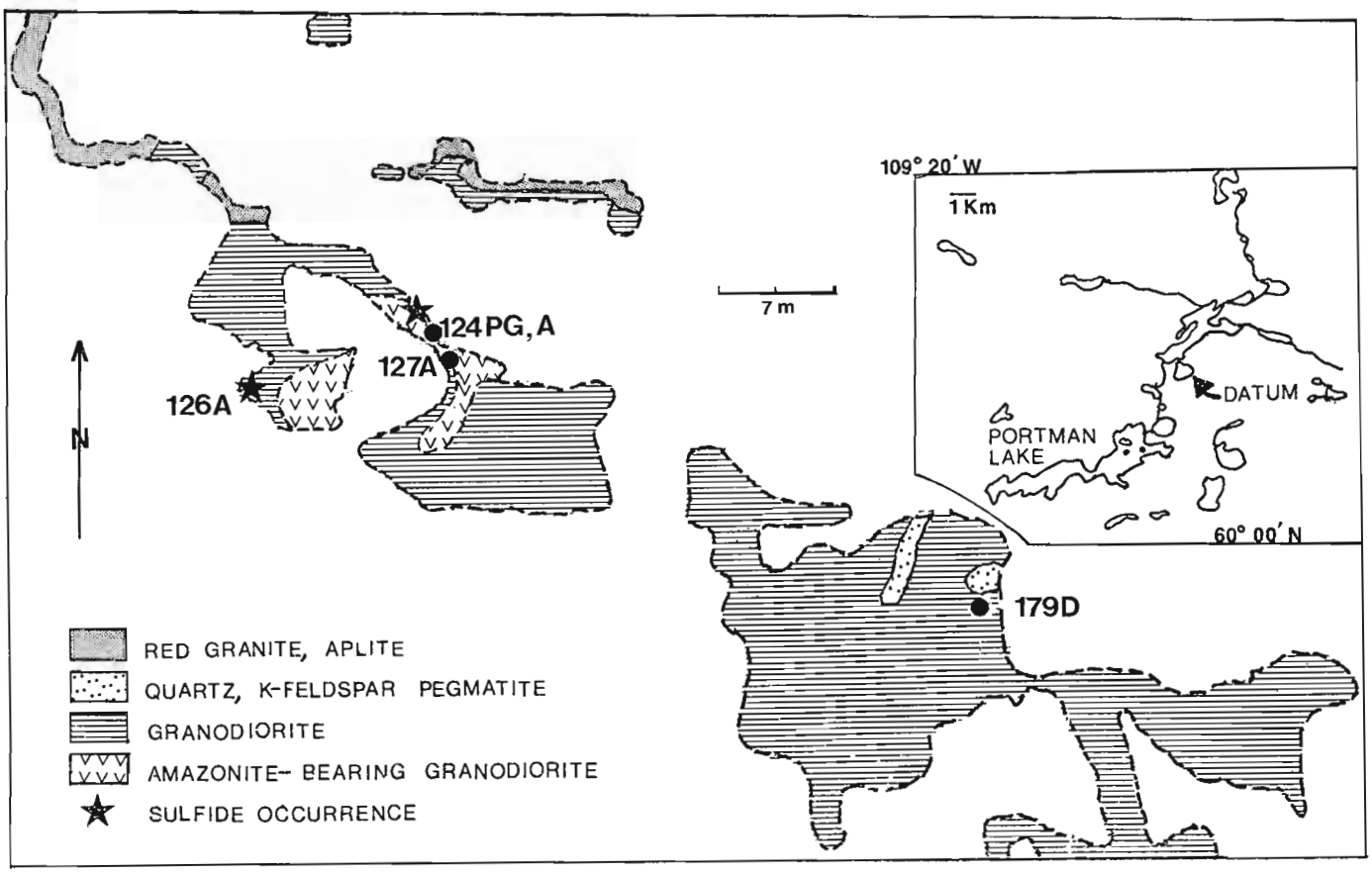

Figure 4.1. Geology of the amazonite occurrence. Dashed lines indicate limit of outcrop. Inset map shows the location of the datum (reference point) with respect to Portman Lake. The occurrence is 340 m at 155° from the datum. Dots denote sample locations. Note that 126A is from a sulphide occurrence.

Petrography

The coarse grained granodiorite and granite are composed of plagioclase (andesine), microcline, quartz, biotite, garnet ± hornblende, epidote and pyrrhotite; accessory apatite, zircon and ilmenite are found largely as inclusions in flakes of biotite up to 15 mm across. Hornblende is associated with biotite. Plagioclase and microcline are generally both white except in a 15 m^2 area, where the colour of the microcline gradually progresses from white through pale green to emerald green. The amazonite-bearing granodiorite is also in contact along one side with a lens of sulphide-bearing, fine grained granodiorite. The amazonite (Fig. 4.2) is texturally similar to white microcline that is present in other parts of the pluton. The colour of each grain is homogeneous (i.e., there is no colour zoning). Inclusions of quartz, biotite, plagioclase and apatite are common. The microcline (either green or white) appears microperthitic to mesoperthitic. Almandine garnet forms subhedral 1-3 mm grains that are largely nonpoikilitic. Trace amounts of pyrrhotite are interstitial to silicate minerals in the amazonite granodiorite.

Chemical compositions of both normal and amazonite-bearing granodiorite are given in Table 4.1. Normative corundum indicates that the series has a peraluminous character. Note the striking difference in Pb content between the normal granodiorite (179D: 53 ppm Pb) and the amazonite-bearing granodiorite (124PG: 1817 ppm Pb). The unmineralized granodiorite is surprisingly rich in iron (up to 9.6% Fe_2O_3, total iron expressed as Fe_2O_3) and depleted in magnesium. The iron is probably largely Fe^{2+}, as ilmenite is the only opaque oxide present. Pb and Zn contents are generally low (92 and 43 ppm, respectively) in the pink granite.

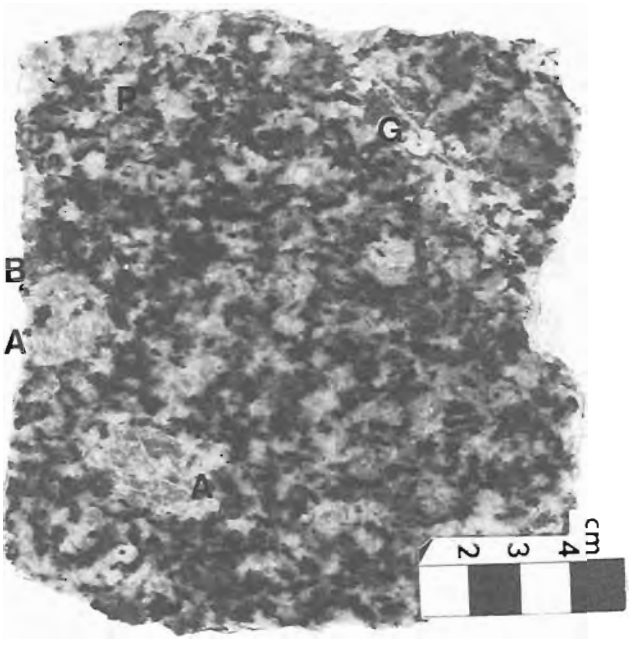

Figure 4.2. *An amazonite-bearing granodiorite; amazonite (A), biotite (B) and plagioclase (P). The linear feature (G) in the top right corner is a granitic vein containing pink microcline and some epidote.*

Table 4.1. Chemical composition of Granodiorite and Sulphide-bearing rock, Portman Lake, Northwest Territories

	179D 1	127A 2	124PG 3	124A 4	126A 5
SiO_2	63.07	64.03	70.68	61.56	68.66
TiO_2	0.76	1.08	0.83	0.20	0.44
Al_2O_3	15.65	14.31	13.85	11.26	13.42
Fe_2O_3*	8.58	9.60	5.87	11.05	8.89
MnO	0.13	0.15	0.46	0.10	0.07
MgO	1.11	0.82	0.31	0.26	0.29
CaO	3.34	3.22	2.86	0.16	0.25
Na_2O	2.65	2.69	2.99	1.62	1.65
K_2O	3.49	3.33	1.29	2.66	2.97
P_2O_5	0.26	0.30	0.06	0.04	0.03
BaO	0.15	0.20	0.04	0.04	0.06
SrO	0.05	0.04	0.02	0.01	0.01
LOI	1.56	0.83	0.15	4.82	3.14
Total	100.78	100.58	99.41	93.77	99.85
Trace elements (ppm)					
Nb	20.0	18.6	4.2	0.0	13.5
Zr	320.4	289.5	214.8	97.2	191.4
Y	29.9	16.9	96.7	0.0	0.0
Rb	95.4	140.3	52.0	61.0	68.1
Th	5.4	0.0	31.9	35.3	11.8
Pb	53.0	268.6	1817.0	3662.0	751.0
Zn	462	326	182	7.5%	5100
Cu				177	243

1. Coarse grained granodiorite with white microcline
2. Coarse grained granodiorite with pale green amazonite
3. Biotite-poor, coarse grained granodiorite with emerald green amazonite
4. Sulphide-bearing sample from talus: best assay
5. Fine grained granodiorite, sulphide-bearing sample from outcrop

* Total iron expressed as Fe_2O_3. The samples were analyzed by X-ray fluorescence at McGill University. LOI: loss on ignition.

Within the same 15 m^2 area, two lenses of fine grained granodiorite contain sphalerite, pyrrhotite, pyrite, galena and chalcopyrite, in decreasing order of abundance. These lenses also contain a greater amount of quartz and lesser amounts of biotite, plagioclase and K-feldspar than the coarser granodiorite. The fine grained granodiorite lenses contain occasional glomerophyric clusters of xenocrysts of coarse biotite and plagioclase derived from the coarse granodiorite. Also present are muscovite and gahnite, which together may comprise up to 40 per cent of mineralized specimens. The feldspars have been partly altered to sericite, and spinel grains are commonly rimmed by muscovite.

The sulphides are interstitial to the silicate minerals and are usually enclosed in a mesh of intergrown muscovite and fine grained white mica. Pyrite forms subhedral cubes that may be partly enclosed by pyrrhotite or sphalerite (Fig. 4.3). Both pyrrhotite and chalcopyrite also occur as minor exsolution-blebs in sphalerite. Inclusions of spinel are common in the sulphides. Galena is found as minute disseminated grains in the fine grained granodiorite as well as in a 3-mm-wide vein with pyrrhotite and epidote. The vein cuts the coarse grained granodiorite. Between the two compositions of sulphide-bearing granodiorite reported (Table 4.1), sample 124A represents the best assay, but is taken from talus. Sample 126A is derived from an outcrop and is more representative of the sulphide-bearing granodiorite.

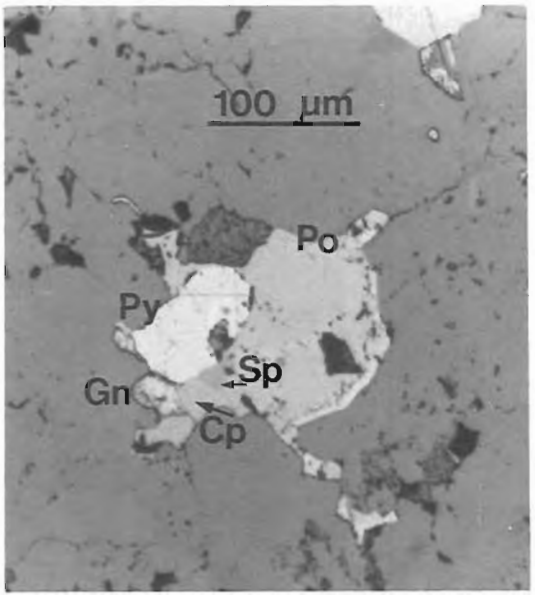

Figure 4.3. Sulphides from a mineralized fine grained granodiorite lens adjacent to the amazonite occurrence: Py – pyrite; Sp – sphalerite; Po – pyrrhotite; Gn – galena; and Cp – chalcopyrite. Weathering has produced a pyrite rim on some grains of pyrrhotite.

Mineral composition

The chemical composition of selected minerals of the Portman Lake occurrence was determined using a Cameca Microbeam model MB-1 electron microprobe (Table 4.2). Conditions of analysis and the standards used are reported in Table 4.2.

Microcline compositions vary between Or_{88} and Or_{94}. The three sets of data in Table 4.2 illustrate, at constant Or composition, the effect of the progressive change in colour from white to green: the microcline increases in Pb content from 160 through 2790 to 14800 ppm. The only element to show any covariation with intensity of colour is lead. Polished-sections show that amazonite grains are completely free of galena. Microcline contains virtually no Fe or Mg, but may contain Ba (up to 1.2% BaO). No compositional zoning is apparent within grains.

Mn and Cu generally amount to less than 1 wt.% in sphalerite from the sulphide zone (Table 4.2). The assemblage sphalerite-pyrite-pyrrhotite may allow a geobarometric study if the degree of alteration proves to be insignificant and if the sphalerite equilibrated with hexagonal pyrrhotite. The Fe content of the sphalerite varies from 7% to 7.5% within single grains and from 6% to 7.5% between samples.

Gahnite is quite variable within a single hand-specimen (Table 4.2), with Zn and Fe varying by as much as 10 per cent on the scale of a thin section. The gahnite is in fact a Fe-Zn-Mg solid solution ranging in this case from hercynite ($Hc_{64.1}Gh_{30.3}Mg\text{-}Sp_{5.6}$) to gahnite ($Hc_{40.4}Gh_{52.3}Mg\text{-}Sp_{7.3}$). The Ti content of the spinel is negligible. There is no apparent compositional zoning in any of the sulphides or within gahnite.

Discussion

Amazonite, typically a blue-green perthitic microcline, is found in pegmatites or metasomatized rocks (Smith, 1974). However, there are rare exceptions. Cech et al. (1971) proposed that the definition be broadened to include a green orthoclase from a pegmatite at Broken Hill, Australia. Furthermore, the occurrence of amazonite in granodiorite at Portman Lake also appears to be an exception to the generalization made above.

The Pb content of amazonite from Portman Lake reaches as much as 18850 ppm (2.03% PbO); more commonly, however, the deepest emerald green amazonite contains, on average, 14 000 ppm Pb. These specimens have few equals in the world, in terms of lead content. Alker (1959; in Cech et al., 1971), reported on amazonite with 1.35% Pb from a pegmatite at Pack, Austria, and Hofmeister (1984) and Cech et al. (1971) reported values of lead up to 2% in amazonite from Broken Hill, Australia. Foord and Martin (1979) showed that the change from white K-feldspar to amazonite is accompanied by an increae in lead content, as at Portman Lake (Table 4.2). The increase in lead content with increasing intensity of the green colour of the microcline is also evident from the whole-rock compositions.

Table 4.2. Compositions of selected minerals from the Portman Lake suite

	179A 1	127G 2	124E 3		125C 4	125C 5
SiO_2	63.52	64.85	62.80		0.0	0.03
Al_2O_3	19.20	19.02	19.26		58.19	56.65
FeO	0.0	0.02	0.0		26.00	16.88
MnO					0.90	0.16
MgO	0.0	0.0	0.0		1.26	1.70
CaO	0.02	0.02	0.0		0.0	0.0
Na_2O	0.82	0.82	0.87		0.41	
K_2O	15.37	15.09	14.32			
BaO	0.99	0.84	0.80			
PbO	0.02	0.30	1.59			
ZnO					13.94	24.58
Total	99.93	100.95	99.64		100.70	99.91
Ab	7.5	7.6	8.4	Hc	64.1	40.4
Or	92.4	92.3	91.6	Gh	30.3	52.3
An	0.1	0.1	0.0	SP	5.6	7.3

	124A 6	124A 7
Fe	7.06	61.88
Cu	0.07	0.13
Zn	59.30	0.06
Mn	0.03	0.0
S	33.88	38.06
Total	100.33	100.13

1. white microcline
2. pale green amazonite
3. emerald green amazonite
4-5. hercynite-gahnite solid solution
6. sphalerite
7. pyrrhotite

Note: The analyses were done on a Cameca Microbeam model MB-1 electron microprobe. Accelerating voltage: 15 kV, beam current 10 nA; most elements were counted for 10 seconds except Ba (50 s) and Pb (150 s). The following standards were used: orthoclase (Si, Al, K), andradite (Fe, Ca), Mgo (Mg), albite (Na), $BaSO_4$ (Ba), vanadinite (Pb), and willemite (Zn) for the silicate minerals. Sulphide standards included sphalerite (Zn), chalcopyrite (Cu, Fe, S) and MnTiO (Mn). Olivine (Mg), spessartine (Mn, Si, Al), andradite (Fe, Ca), willemite (Zn), MnTiO (Ti) and albite (Na) were used for the spinel.

The zinc content of the Portman spinel is relatively low compared to that of gahnite found in some metapelitic rocks (Frost, 1973; Dietvorst, 1980; Sunblad, 1982). However, a similar concentration of zinc is found in the spinel in metapelites at the Geco base-metal deposit, Manitouwadge, Ontario, but in this locality, the spinel is much richer in Mg and poorer in Fe.

The occurrence of gahnite-hercynite solid solution is generally regarded as a result of the metamorphism of a zinc-iron-bearing assemblage (Spry, 1982; Ririe, 1982; Dietvorst, 1980). However, evidence of regional metamorphism, such as foliation or an assemblage of clearly metamorphic minerals, is lacking in the granodiorite. Cerny and Hawthorne (1982) and Cerny et al. (1981) noted that gahnite is not an uncommon constituent of peraluminous granitic pegmatites and that it occurs almost exclusively in sulphide-poor assemblages. The presence of gahnite at Portman may indicate that the initial oxygen and sulphur fugacities favoured the formation of gahnite, which appears to have crystallized early, relative to sphalerite, which is interstitial.

In the general case of an evolving sulphur-poor granitic melt, one may envisage the treatment of Pb and Zn as incompatible elements, concentrated in progressively more differentiated melts until they become saturated at the pegmatitic stage. At this point, Pb may be forced to substitute for K in K-feldspar, to form amazonite, and Zn may appear as gahnite (Foord and Martin, 1979; Cerny and Hawthorne, 1982). This process may be viable so far as lead is concerned, because it does show increased concentration in the amazonite-bearing granodiorite before the appearance of galena. Zinc, on the other hand, shows no conspicuous concentration except in the mineralized granodiorite. However, neither the mineralized granodiorite nor the amazonite-bearing granodiorite resembles a late-stage pegmatitic fraction.

Dietvorst (1980) suggested that the zinc content of metamorphic biotite decreases with temperature and that during the waning stages of metamorphism, zinc is released from the biotite to form spinel. Thus, a rather rapid decrease in the temperature of the Portman granodiorite would have facilitated the liberation of Zn and Pb. But the late (subsolidus) crystallization of amazonite and gahnite is difficult to visualize and is not supported by textural evidence. The presence of interstitial sulphides indicate that sulphur became available only at a late stage; the formation of amazonite and gahnite would have to predate the influx of sulphur.

A third alternative is to propose local contamination of the granodioritic melt. If the melt digested wall rock enriched in Pb and Zn, the granodiorite may have become locally enriched in these metals. This could lead to early saturation of lead and zinc in the granodioritic melt and subsequent primary crystallization of amazonite and gahnite. Contamination may also result in the dilution of other components, such as sulphur, thus forcing Pb and Zn to first partition into amazonite and gahnite until sufficient sulphur had accumulated to form sphalerite and galena at a later stage. Alternatively, the melt may have been sulphur-poor, in which case dilution would not be necessary.

The most likely contaminant might be though to be the pink granite, because of its close proximity to the amazonite – sulphide occurrence, but as already noted, the pink granite sampled contains no sulphides and has low lead and zinc contents. Furthermore, there is some question as to whether the pink granite predates or postdates the granodiorite. An ideal contaminant would be a sulphide-bearing rock of sedimentary affinity, to account for the enrichment in Pb and Zn and the peraluminous character of the granodiorite. The possibility of more than one contaminant increases the complexity of the problem. Current research is aimed at determining the process(es) and conditions that result in the concentration of lead and zinc and the crystallization of amazonite and gahnite.

Although the actual mechanism that concentrates the Pb and Zn is in question, the formation of the sulphide-bearing, fine grained granodiorite could be described as follows: The coarse texture of the granodiorite suggests a slow cooling of the pluton. The fine grained lenses, however, denote a more rapid nucleation and growth of crystals. This could be facilitated by the fracturing of the granodiorite, resulting in sudden decompression and flow of volatiles outward from the pluton (Jahns and Burnham, 1969). This flow of volatiles may aid in the concentration of Pb, Zn and Fe in the rapidly crystallizing fine grained granodiorite. The oxygen and sulphur fugacities were such that Pb crystallized in amaxonite and Zn in gahnite until sufficient sulphur accumulated to result in late-stage formation of interstitial sulphides, and even later, vein galena.

References

Cech, F., Mosar, Z., and Povondra, P.
1971: A green lead containing orthoclase; Tschermaks Mineralogische und Petrographische Mitteilungen, v. 15, p. 213-231.

Cerny, P. and Hawthorne, F.C.
1982: Selected peraluminous minerals; in Granitic Pegmatites in Science and Industry, ed. P. Cerny; Mineralogical Association of Canada Short Course Handbook, v. 8, p. 163-186.

Cerny, P., Trueman, D.L., Ziehlke, D.V., Goad, B.E., and Paul, B.J.
1981: The Cat Lake – Winnipeg River and the Wekusko Lake pegmatite fields, Manitoba; Manitoba Department of Energy and Mines, Economic Geology Report ER80-1, 215 p.

Dietvorst, E.
1980: Biotite breakdown and the formation of gahnite in metapelitic rocks from Kemio, southwest Finland; Contributions to Mineralogy and Petrology, v. 75, p. 327-337.

Foord, E.E. and Martin, R.F.
1979: Amazonite from the Pikes Peak Batholith; The Mineralogical Record, v. 10, p. 373-382.

Frost, B.R.
1973: Ferroan gahnite from quartz-biotite-almandine schist, Wind River, Wyoming; American Mineralogist, v. 58, p. 831-834.

Hofmeister, A.M.
1984: A spectroscopic and chemical study of the coloration of feldspars by irradiation and impurities, including water; PhD thesis, California Institute of Technology, 405 p.

Jahns, R.H. and Burnham, C.W.
1969: Experimental studies of pegmatite genesis. I. A model for the derivation and crystallization of granite and pegmatite; Economic Geology, v. 64, p. 843-864.

Koster, F.
1962: The geology of the Thainka Lake area (east half), Saskatchewan; Saskatchewan Department of Mineral Resources, Report No. 71, 27 p.

Koster, F. and Baadsgaard, H.
1970: On the geology and geochronology of northwestern Saskatchewan. I. Tazin Lake region; Canadian Journal of Earth Sciences, v. 7, p. 919-930.

Ririe, G.T.
1982: A model for gahnite and magnetite formation during metamorphism of sulfide-rich rocks; Geological Society of America, Abstracts with Programs, v. 14, p. 227-228.

Smith, J.V.
1974: Feldspar minerals, v. 1. Crystal Structure and Physical Properties; Springer-Verlag, New York, 627 p.

Spry, P.G.
1982: An unusual gahnite-forming reaction, Geco base-metal deposit, Manitouwadge, Ontario; Canadian Mineralogist, v. 20, p. 549-553.

Sunblad, K.
1982: Distribution of gahnite-bearing sulphidic deposits in the Scandinavian Caledonides; Transactions of the Institution of Mining and Metallurgy, v. 91B, p. 214-218.

-5-

THE CRYPTOSTOMATE BRYOZOAN **SCEPTROPORA** (RHABDOMESINA, ARTHROSTYLIDAE) FROM UPPER ORDOVICIAN ROCKS OF SOUTHERN MACKENZIE MOUNTAINS, DISTRICT OF MACKENZIE

Project 740084

Thomas E. Bolton and June R.P. Ross[1]
Director General's Office

*Bolton, T.E. and Ross, J.R.P., The cryptostomate bryozoan **Sceptropora** (Rhabdomesina, Arthrostylidae) from Upper Ordovician rocks of southern Mackenzie Mountains, District of Mackenzie; in Current Research, Part A, Geological Survey of Canada, Paper 85-1A, p. 29-45, 1985.*

Abstract

*The arthrostylid bryozoan **Sceptropora facula** Ulrich occurs from 17 to 64.5 ± m below the base of the Silurian in the Avalanche Lake region of the Mackenzie Mountains. Disarticulated segmental forms of widely diverse shape are included in the species. A Late Ordovician Richmondian age is established for this interval within the Whittaker Formation by the associated conodont and ostracode faunas.*

Résumé

*Le **Sceptropora facula** Ulrich (arthrostylidé, bryozoaire) se rencontre dans l'intervalle 17-64, 5 m, sous la base du Silurien, dans la région d'Avalanche Lake (monts Mackenzie). Cette espèce renferme des individus segmentés de formes diverses. D'après les conodontes et ostracodes qui lui sont associés, cet intervalle de la formation de Whittaker appartiendrait au Richmondien (fin de l'Ordovicien).*

[1] Department of Biology, Western Washington University, Bellingham, Washington, U.S.A. 98225

Introduction

Slender, minute dendroid bryozoans of the cryptostomate suborder Rhabdomesina are found in many of the Paleozoic marine sediments of the world. Representatives of the rhabdomesine family Arthrostylidae are most abundant in Ordovician and Silurian rocks particularly throughout the Canadian-Siberian faunal realm. Their small size, however, renders them difficult to recognize both in the field and laboratory and hence they are generally overlooked.

The present paper describes several well preserved silicified specimens found in acid residues from the Whittaker Formation limestones analyzed for trilobite and conodont material by B.D.E. Chatterton, University of Alberta, and G.S. Nowlan, Geological Survey of Canada. We thank Dr. Chatterton for permission to describe the bryozoan fauna, and Drs. Copeland and Nowlan for information on the associated ostracode and conodont faunas. M.J. Copeland provided the SEM photographs (Cambridge Stereoscan 180) and J.W. Kempt the thin section photographs.

The samples were collected by B.D.E. Chatterton and D.G. Perry in 1979 and by B.D.E. Chatterton and D.J. Over in 1983 from the stratigraphic sections 79 AV1 (62°24'N, 127°04'W; 20, 46, 53.5, 54 and 60 m above base of section), and 83 AV4B (62°23'N, 127°03'W; 80.25 and 94.5 m above base of section), located in the southern Mackenzie Mountains about 10 km east of Avalanche Lake (see Chatterton and Perry, 1983, text-figs. 1-3). The thin bedded, limestones and shales forming these intervals are regarded as moderate to deep water sediments deposited close to the continental shelf/continental slope boundary (Chatterton and Ludvigsen, 1983, p. 146).

In section 79 AV1, the samples are stratigraphically located from 35.5 to 75.5 m below the first occurrence of the Silurian conodont **Distomodus kentuckyensis** Branson and Branson by Chatterton and Perry (1983), or between 24.5 and 64.5 m below the first sample containing the Silurian conodont **Ozarkodina hassi** (Pollock, Rexroad and Nicoll) as recognized by G.S. Nowlan (1984, personal communication), or between 39 and 79 m below the highest occurrence of recognizable Ordovician ostracodes (M.J. Copeland, 1984, personal communication). In section 83 AV4B, the samples are located from 17 to 31.25 m below the Ordovician-Silurian boundary as based on conodonts (G.S. Nowlan, 1984, personal communication) and at least 42 to 55.75 m below the last recognized Ordovician ostracodes (M.J. Copeland, 1984, personal communication).

Sceptropora facula Ulrich in these intervals was most abundant at the 53.5 and 54 m levels of section 79 AV1 and the 94.5 m level of section 83 AV4B, where it is associated with a ptilodictyoid **Stictopora**? sp. and the rhabdomesines **Ulrichostylus** sp. (Pl. 5.1, fig. 5) and **Nematopora** cf. **lineata** (Billings) (Pl. 5.2, figs. 1, 7). Two specimens (GSC 80123, 80124) of **Enallopora**, an Ordovician-Silurian genus occurring in both North America and Europe (Kiepura, 1962, p. 393), were the only bryozoans identified in the conodont-defined boundary beds (111.5 m) of section 83 AV4B. The solitary coral **Grewingkia** (R.J. Elias, personal communication, 1984), another Late Ordovician-Early Silurian genus, is present in the same boundary beds.

Ross (1982, Pl. 2, fig. 6), in the only previous description of bryozoan faunas from this general region, recognized one specimen of **S. facula** from Ludvigsen's section R 625 of the Whittaker Formation farther to the northwest in the Dusky Range (lat. 63°17'N, long. 125°21'W; Ludvigsen, 1978, text-fig. 1), associated with **osburnostylus** sp., **Ulrichostylus**, a phylloporinid, and trepostome bryozoans. This fauna is located 140 m below the Ordovician-Silurian boundary as defined by Ludvigsen (1979, p. 54), and was considered by him within the Edenian **Whittakerites planatus** trilobite zone. Ross (1980) noted that **S. facula** had so far been found only in the Richmondian.

The genus **Sceptropora** ranges throughout the Upper Ordovician (Edenian to Richmondian), and possibly into Lower Silurian (Llandovery). The possible Lower Silurian occurrence is based on one North American species, **S. fustiformis** Ulrich, 1889, whose syntypes (U.S.N.M. 43474) were believed by Ulrich to have been derived from the Middle Silurian "Clinton" at Hamilton, Ontario. Subsequently, Bassler (1913) assigned those specimens to the Upper Median (Cataract). These dumbell-shaped forms are in a thin bedded, medium grey, argillaceous limestone, associated with a coquina of minute bryozoans (Boardman, R.S., 1984, personal communication; **Helopora fragilis** Hall by Ulrich, 1889, p. 46). Until additional examples of **S. fustiformis** have been actually collected from the Silurian sequence at Hamilton, the Early Silurian age for the genus should be questioned. The only other Silurian-assigned species, **S.**? **obscura** Astrova, 1965, is not a **Sceptropora**; hence the published Wenlock? age based on this European occurrence of the genus should be disregarded.

S. facula itself occurs in the Stony Mountain Formation of Manitoba (Ulrich, 1889, p. 46), the Vaureal Formation of Anticosti Island, Quebec (Twenhofel, 1928, p. 160), both Richmondian units, and in several Upper Ordovician sections of the north-central United States. It has also been reported from the Marathon Basin of Texas (King, 1937, p. 41).

Conodonts associated with **S. facula** in the Avalanche Lake region include **Oulodus rohneri** Ethington and Furnish and **Pseudobelodina vulgaris vulgaris** Sweet, forms characteristic of Richmondian Conodont Fauna 12 (G.S. Nowlan, 1984, personal communication; McCracken and Nowlan, 1984). Ostracodes from this same interval include forms characteristic of the Late Ordovician **Platybolbina (Reticulobolbina) lenzi** Copeland assemblage (Copeland, 1977, text-fig. 2).

SYSTEMATIC PALEONTOLOGY

Genus **Sceptropora** Ulrich, 1888

Type species. **Sceptropora facula** Ulrich, 1888.

Diagnosis. "Zoarium articulated; segments numerous, short, sceptre or club-shaped, the lower half striated, non-celluliferous, its extremity bulbous; upper half more or less expanded, celluliferous, and with a large socket at the centre of the top; occasionally with two sockets when the segment had articulated with two succeeding joints. Zooecia subtubular, radially arranged about a central axis, their apertures subovate, and arranged between vertical lines." (Ulrich, 1888, p. 228; 1889, p. 46).

Sceptropora facula Ulrich, 1888

Plate 5.1; Plate 5.2, figures 2-6, 8-10;
Plates 5.3 to 5.6; Plate 5.7, figures 1-4, 6-8

Sceptropora facula Ulrich, 1888, p. 229, figs. 1a-d.
Sceptropora facula Ulrich. Ulrich, 1889, p. 46, figs. 2a-d.
Sceptropora facula Ulrich. Bassler, 1911, p. 153, figs. 74a-d.
Sceptropora facula Ulrich. Twenhofel, 1928, p. 160.
Sceptropora facula Ulrich. Ross, 1982, pl. 2, fig. 6.
Sceptropora facula Ulrich. Blake, 1983, p. 565, figs. 279a-g.

Description. Zoarium dendroid (Pl. 5.7, figs. 2, 4, 6); segments usually straight to slightly curved (Pl. 5.6, fig. 9), varying from indian club to bell (Pl. 5.7, figs. 1-3, 7, 8) to mushroom shape (GSC 80117), 0.92 to 2.0 mm in length

(Table 5.1); proximal end slender, striated (Pl. 5.1, fig. 3, 4, Pl. 5.2, figs. 3, 4, 6, 8), zooecia absent, normally terminating in a short smooth bulb (Pl. 5.2, figs. 3, 6; Pl. 5.4, figs. 7, 8; Pl. 5.6, fig. 2), a distinct brim developing in more stubby forms (Pl. 5.4, figs. 2, 7, 8); segments expand distally to a sharp brim from 0.56 to 1.96 mm in diameter, below which are two to rarely three rows of subcircular zooecia apertural openings distally aligned in ten or more rows; distally from the brim each segment contracts rapidly to a point (Pl. 5.2, figs. 4, 8) or in more stubby forms end in centrally located single, shallow to deep (Pl. 5.1, figs. 3, 4, 6; Pl. 5.2, figs. 3, 6, 9; Pl. 5.3, fig. 8; Pl. 5.4, figs. 1-9; Pl. 5.6, figs. 7, 9; Pl. 5.7, figs. 3, 4, 7, 8), or double, deep attachment sockets (Pl. 5.5, figs. 1, 3, 4; Pl. 5.6, figs. 1-5, 8, 10); distal end surrounded normally by two to three rows of 10 to 18, rarely up to 25, apertures separated by prominent longitudinal ridges (Pl. 5.5, figs. 1, 3, 4).

In transverse section, axial region composed of a well-developed longitudinal axial wall (Pl. 5.3, figs. 2, 3, 5, 7; Pl. 5.5, figs. 2, 6; Pl. 5.6, fig. 6), that in the distal end of regular shaped zoaria and in the wider, stubby forms may be thickened (Pl. 5.5, fig. 5); zooecial walls thick with dark, distinct boundaries; wide extrazooecial skeletal zone. Above the brim, zooecial openings externally are oval and internally, triangulate in shape (Pl. 5.5, figs. 2, 6); the dividing structure can be more of a strut or bar (Pl. 5.1, figs. 6, 7; Pl. 5.2, figs. 6, 9) rather than a continuous wall (Pl. 5.4, fig. 5), present only at or near the surface.

In longitudinal section (Pl. 5.1, fig. 5; Pl. 5.3, figs. 1, 4, 6; Pl. 5.4, figs. 4, 6; Pl. 5.7, figs. 1, 8), zooecia recumbent, varying in length, opening at a low angle to surface, from .06 to .14 mm in diameter, lacking diaphragms and acanthopores; attachment sockets floored by extrazooecial skeletal material.

Discussion. A wide variety of shapes are included in this species, ranging from narrow, nearly brimless through indian club to wide stubby to bell to short mushroom (GSC hypotype 80116). All forms occur together at the 94.5 m level of section 83 AV4B and at the 53.5 m level of section 79 AV1. The typical indian club form also occurs at the 80.25 m level in section 83 AV4B and ranges from 53.5 to 60 m in section 79 AV1; the bell-shaped form in section 79 AV1 ranges from 46 to 54 m.

The inclusion of double socketed forms, with highly grooved upper surfaces (Pl. 5.5, fig. 3), conforms with Ulrich's original generic diagnosis. Similar variation in shape and size, and the development of dichotomous branching, is evident in the material from the erratic boulders of Poland described by Kiepura (1962) as **S. facula** (compare Kiepura, Pl. 10, fig. 3 with Pl. 5.6, figs. 1, 4, 5, 10 herein).

S. estoniensis Brood, 1980 (formerly **S. facula** Ulrich by Bassler, 1911 and Kiepura, 1962) from the Hirnantian Porkuni Stage of northern Estonia, glacial erratic boulders of Poland, and stage 5b at Ullerntangen in Ringerike (Oslo region), Norway, is more robust, with acanthopores and smaller zooecial apertures than typical **S. facula.** The stubby forms herein included in **S. facula**, however, are even more robust at their proximal ends than **S. estoniensis** and are closer in apertural size than the club-shaped segments, but in longitudinal section there is a close resemblance to some specimens of **S. estoniensis** (i.e., compare Brood, 1980, fig. 3A with Pl. 5.4, figs. 4, 6). The bell-shaped **S. facula** slightly relates to the holotype of **S. florida** Kiepura; **S. spinosa** Kiepura is quite distinct.

Types. Syntypes, USNM 43478, 240848-240851, GSC 774, Stony Mountain Formation, Stony Mountain, Manitoba. Hypotypes, USNM 240847, Vaureal Formation, High Cliff, Anticosti Island, Quebec; USNM 240852, Elkhorn Formation, Ohio, U.S.A.; GSC 8309, Stony Mountain Formation, Stony Mountain, Manitoba; GSC 80068-80071, 80117, 80127, section 79 AV1 – 54 m; 80072-80079, 80118, section 79 AV1 – 53.5 m; 80080, section 79 AV1 – 46 m; 80081, 80119, section 79 AV1 – 60 m; 80082-80116, 80120, 80128, 80129, section 83 AV4B – 94.5 m; 80125, 80126, section 83 AV4B – 80.25 m, Whittaker Formation, east of Avalanche Lake, Mackenzie Mountains, District of Mackenzie.

Table 5.1. Sceptropora facula Ulrich dimensions (in mm), club, bell and stubby segments

	Syntypes			Hypotypes, GSC												
	USNM 240848	USNM 240849	GSC 774	8309	80115	80127	80069	80125	80119	80081	80126	80068	80076	80070	80086	80082
Total length of segment	1.48	1.50	1.60	1.80	.92	1.06	1.08	1.16	1.20	1.24	1.24	1.24	1.28	1.32	1.32	1.32
Diameter proximal end	.20	.34	.16	.20	.20	.16	.16	.16	.20	.20	.20	.20	.28	.16	.20	.16
Diameter distal brim	.92	.94	1.12	.76	.72	.68	.76	.68	.72	.68	.64	.68	.80	.68	.84	.56
Diameter socket	-	.22	-	-	.20	-	-	-	.12	-	-	.24	.28	-	-	-

	Hypotypes, GSC															
	80128	80084	80089	80085	80118	80079	80117	80078	80077	80093	80090	80129	80091	80096	80097	80101
Total length of segment	1.40	1.40	1.40	1.52	1.16	1.20	1.28	1.36	1.48	1.42	1.44	1.60	1.64	1.68	1.76	2.0
Diameter proximal end	.20	.24	.28	.20	.20	.16	.20	.36	.20	.16	.16	.20	.20	.80	.76	.84
Diameter distal brim	.64	.76	.80	.60	1.72	1.48	1.80	1.04	1.40	.84	.92	1.04	1.00	1.36	1.40	1.96
Diameter socket	-	-	.16	-	-	.20	.28	.40	.16	.60	.60	.92	.88	.84	.84	.80 .68

References

Astrova, G.G.
1965: Morphology, evolutionary history, and systematics of Ordovician and Silurian bryozoans; Akademya Nauk SSSR Paleontologii Instituta, 106.

Bassler, R.S.
1911: The Early Paleozoic Bryozoa of the Baltic Provinces; Smithsonian Institution, United States National Museum, Bulletin 77.

1915: Bibliographic index of American Ordovician and Silurian fossils, volume 2; Smithsonian Institution, United States National Museum, Bulletin 92.

Blake, D.B.
1983: Systematic descriptions for the Suborder Rhabdomesina; Geological Society of America University of Kansas, Treatise on Invertebrate Paleontology, Part G, Bryozoa Revised, v. 1, p. 550-592.

Brood, K.
1980: Late Ordovician Bryozoa from Ringerike, Norway; Norsk Geologisk Tidsskrift, v. 60, p. 161-173.

Chatterton, B.D.E. and Ludvigsen, R.
1983: Trilobites from the Ordovician-Silurian boundary of the Mackenzie Mountains, northwestern Canada; Paper for the Symposium on the Cambrian-Ordovician and Ordovician-Silurian boundaries, Nanjing, China, October, 1983, Nanking Institute of Geology and Palaeontology, Academia Sincia.

Chatterton, B.D.E. and Perry, D.G.
1983: Silicified Silurian odontopleurid trilobites from the Mackenzie Mountains; Palaeontographica Canadiana, no. 1.

Copeland, M.J.
1977: Early Paleozoic Ostracoda from southwestern District of Mackenzie and Yukon Territory; Geological Survey of Canada, Bulletin 275.

Kiepura, M.
1962: Bryozoa from the Ordovician erratic boulders of Poland; Acta Palaeontologica Polonica, v. 7, no. 3-4, p. 347-428.

King, P.B.
1937: Geology of the Marathon Region, Texas; United States Geological Survey, Professional Paper 187.

Ludvigsen, R.
1978: Middle Ordovician trilobite facies, southern Mackenzie Mountains; Geological Association of Canada, Special Paper 18, p. 1-33.

1979: A trilobite zonation of Middle Ordovician rocks, southwestern District of Mackenzie; Geological Survey of Canada, Bulletin 312.

McCracken, A.D. and Nowlan, G.S.
1984: Conodonts from Ordovician-Silurian boundary strata, Whittaker Formation, Avalanche Lake, Mackenzie Mountains, Northwest Territories, Canada; Geological Society of America, Abstracts with Programs 1984, v. 16, no. 3, p. 179.

Ross, J.R.P.
1982: Middle and Upper Ordovician ectoproct bryozoan faunas from the southwestern District of Mackenzie, Canada; Third North American Paleontological Convention, Proceedings, v. 2, p. 447-452.

Twenhofel, W.H.
1928: Geology of Anticosti Island; Geological Survey of Canada, Memoir 154 (1927).

Ulrich, E.O.
1888: On Sceptropora, a new genus of Bryozoa, with remarks on Helopora Hall, and other genera of that type; The American Geologist, v. 1, no. 4, p. 228-334.

1889: On some Polyzoa (Bryozoa) and Ostracoda from the Cambro-Silurian rocks of Manitoba; Geological Survey of Canada, Contributions to the Micro-Palaeontology of the Cambro-Silurian Rocks of Canada, Part II, p. 27-57.

Plate 5.1

Figures 1-7. **Sceptropora facula** Ulrich. Whittaker Formation, District of Mackenzie.

1. Oblique proximal view showing longitudinal ridges, struts and open zooecia below brim, x 70, section 79 AV1 – 54 m; hypotype, GSC 80068.
2. Side view of proximal end showing 2 rows of zooecia below and above brim, and pointed distal end, x 80, section 79 AV1 – 54 m; hypotype, GSC 80069.
3, 6, 7. Side view showing struts and open zooecia above brim, single socket, x 40, x 80, x 160, section 83 AV4B – 94.5 m; hypotype, GSC 80082.
4. Side view showing club-shaped segment, 2 rows of zooecia below and above brim, single socket, x 70, section 79 AV1 – 54 m; hypotype, GSC 80070.
5. Longitudinal thin section of stubby form, single socket, section 79 AV1 – 53.5 m; hypotype, GSC 80072.

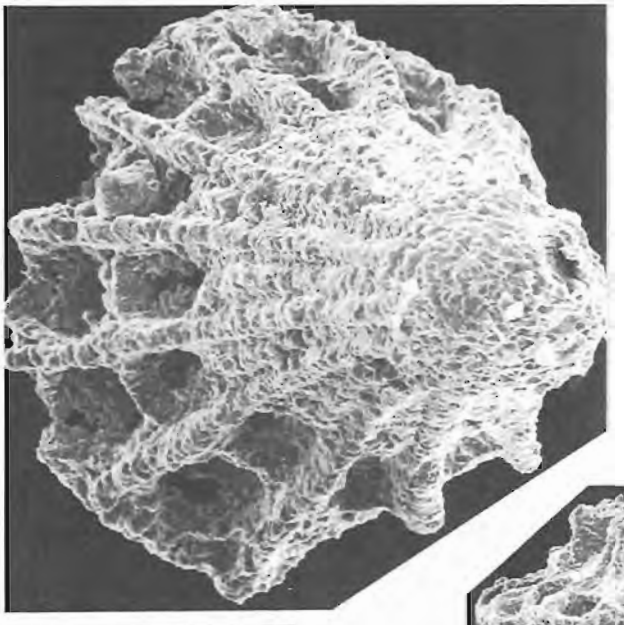

1

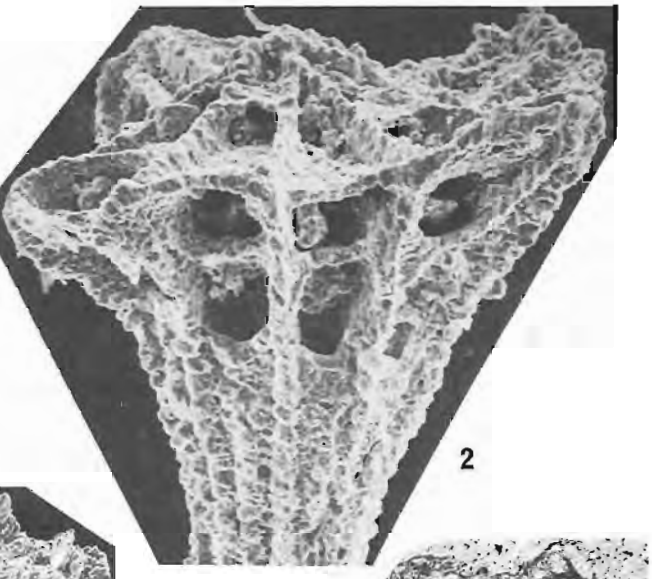

2

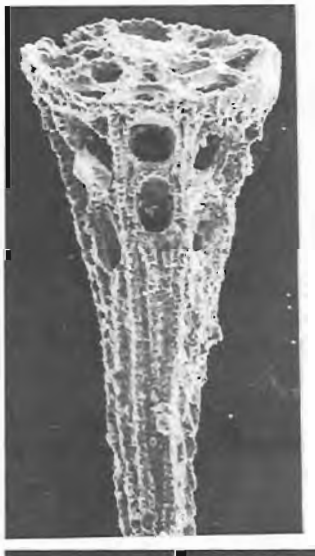

3

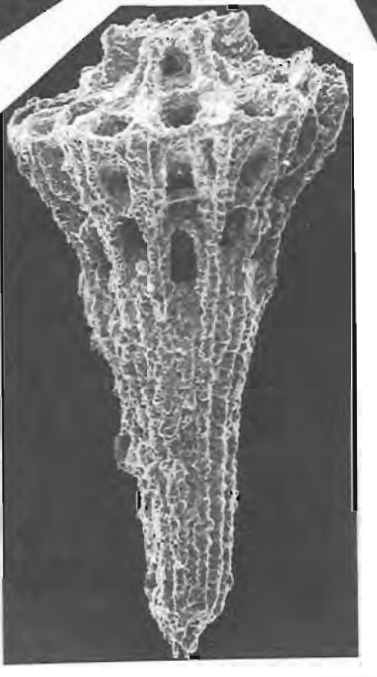

4



5

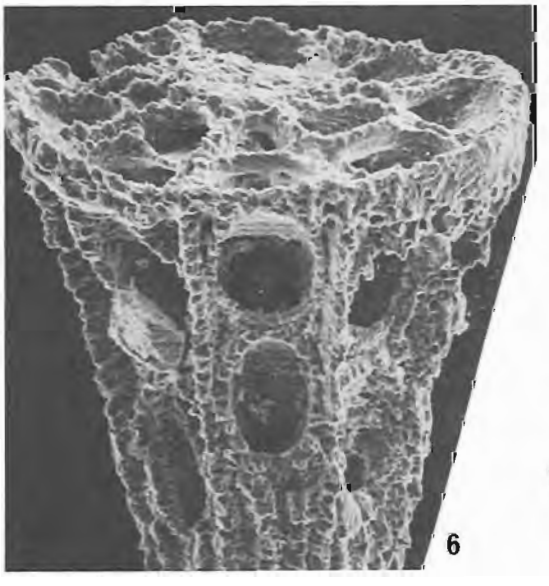

6

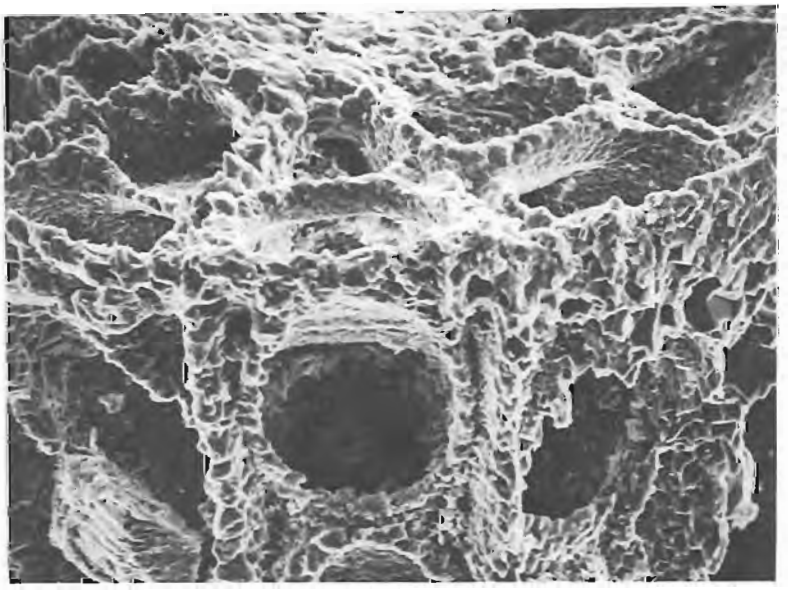

7

Plate 5.2

Figures 1, 7. **Nematopora** cf. **lineata** (Billings). Side view showing apertural arrangement, x 40 and x 80, section 83 AV4B – 94.5 m; Whittaker Formation, District of Mackenzie; hypotype, GSC 80121.

Figures 2-6, 8, 9. **Sceptropora facula** Ulrich. Section 83 AV4B – 94.5 m, Whittaker Formation, District of Mackenzie.

2,8 Side view of narrow segment with large zooecia below brim and smaller zooecia above, pointed distal end, x 80 and x 40; hypotype, GSC 80083.

3,5. Side view showing club-shaped segment with expanded proximal end and narrow brim, x 40 and x 80; hypotype, GSC 80084.

4. Side view of segment showing narrow brim and pointed distal end, x 40; hypotype, GSC 80085.

6,9. Side view of segment with struts and open zooecia, x 40 and x 160; hypotype, GSC 80086.

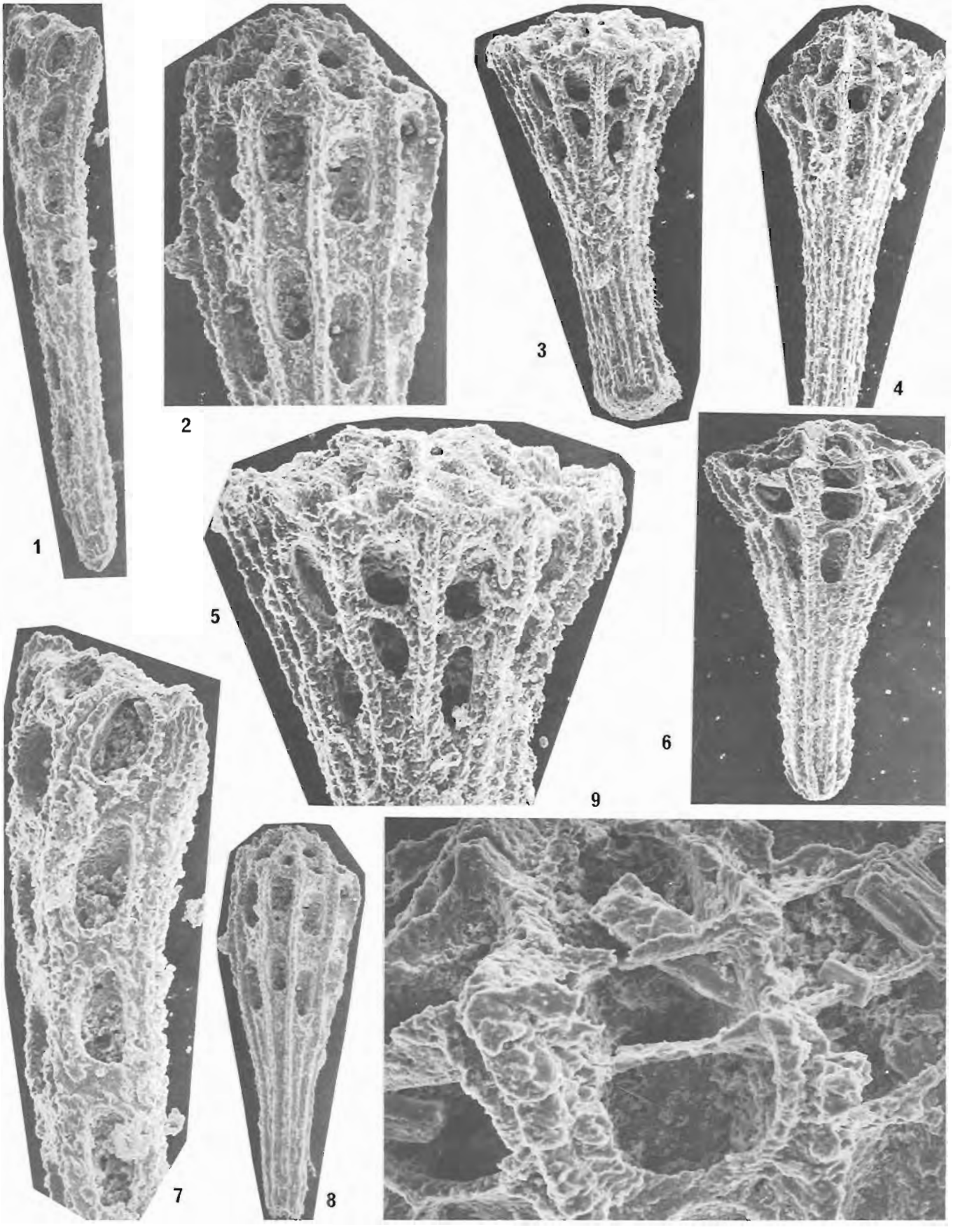
1
2
3
4
5
6
7
8
9

Plate 5.3

Figures 1-8. **Sceptropora facula** Ulrich. Whittaker Formation, District of Mackenzie.

1. Longitudinal section, slightly off-centre, through wide attachment socket, showing recumbent zooecia of club-shaped segment, and wide extrazooecial skeleton, x 100, section 83 AV4B – 94.5 m; hypotype, GSC 80087.

2,3. Natural transverse section showing wall structure of club-shaped segment, x 300 and x 100, section 83 AV4B – 94.5 m; hypotype, GSC 80088.

4. Longitudinal section through centre of club-shaped segment, x 50, section 79 AV1 – 53.5 m; hypotype, GSC 80073.

5,7. Transverse sections just below brim and near proximal end of club-shaped segments, x 130, section 79 AV1 – 53.5 m; hypotypes, GSC 80074, 80075.

6. Natural longitudinal section of club-shaped segment showing recumbent zooecia, x 110, section 79 AV1 – 60 m; hypotype, GSC 80081.

8. Side view of club-shaped segment with large central attachment socket, x 60, tilt 12°, section 83 AV4B – 94.5 m; hypotype, GSC 80089.



1

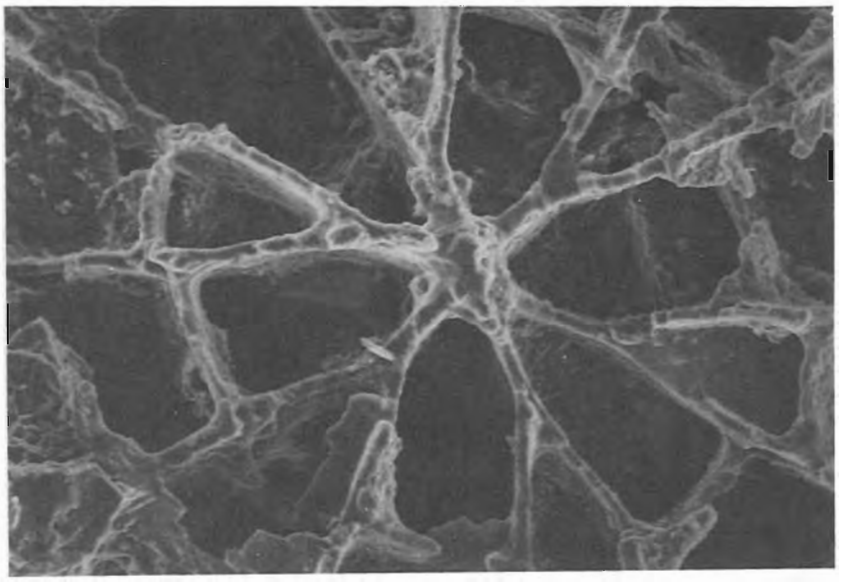

2

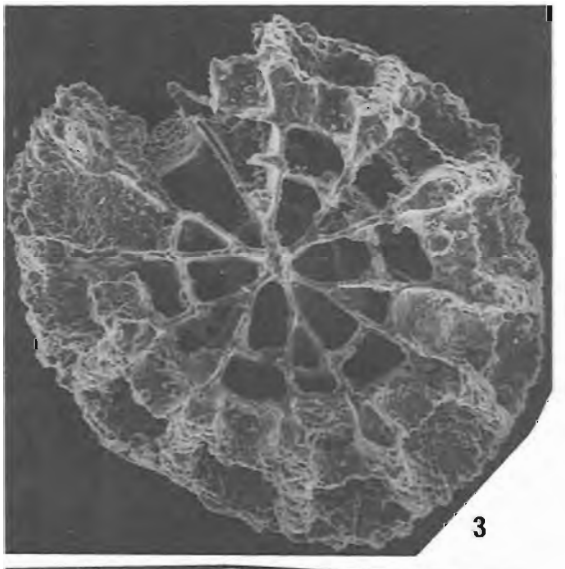

3

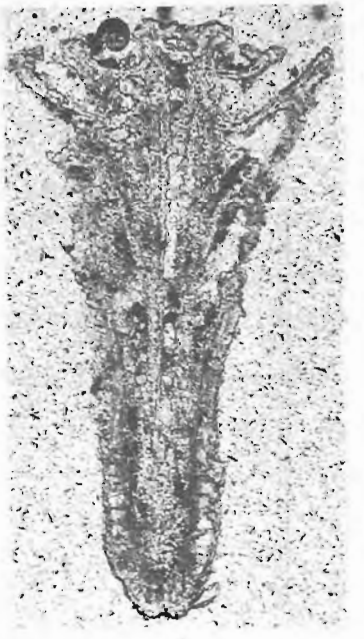

4

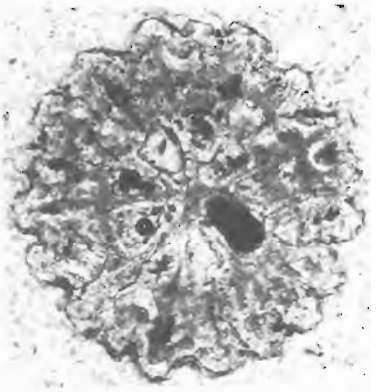

5

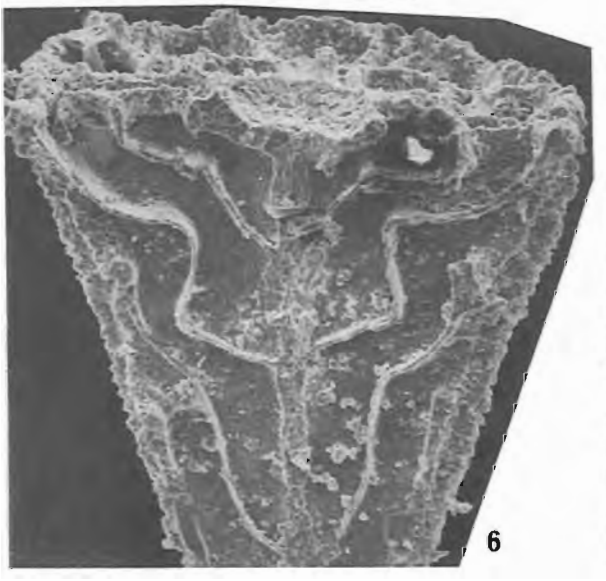

6

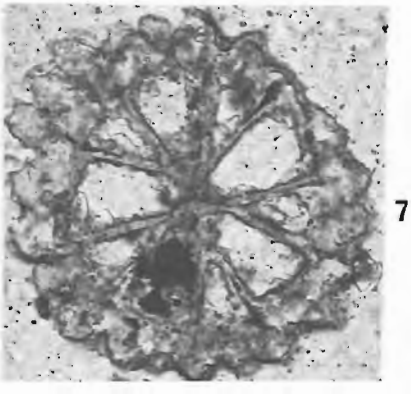

7

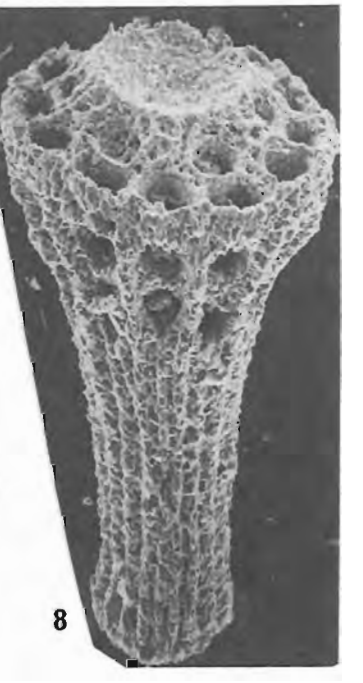

8

Plate 5.4

Figures 1-9. **Sceptropora facula** Ulrich. Section 88 AV4B – 94.5 m except Fig. 5, Whittaker Formation, District of Mackenzie.

1,2. Distal and side views of stubby segment showing 2 rows of zooecia below and above brim and large central attachment socket, x 35; hypotype, GSC 80096.

3. Distal view of stubby segment with many small zooecia around large central attachment socket, x 35; hypotype, GSC 80097.

4,6. Longitudinal sections of stubby segments with wide extrazooecial skeleton, x 50; hypotypes, GSC 80094, 80095.

5. Distal view of bell-shaped segment with three rows of zooecial apertures and large central attachment, x 130, section 79 AV1 – 54 m; hypotype, GSC 80071.

7. Side view of stubby segment showing large central attachment socket and smaller side socket, x 60, tilt 12°; hypotype, GSC 80090.

8. Side view of stubby segment with large single central attachment socket, x 50; hypotype, GSC 80091.

9. Distal view of club-shaped segment with small central attachment socket, x 110, tilt 32.2°; hypotype, GSC 80092.

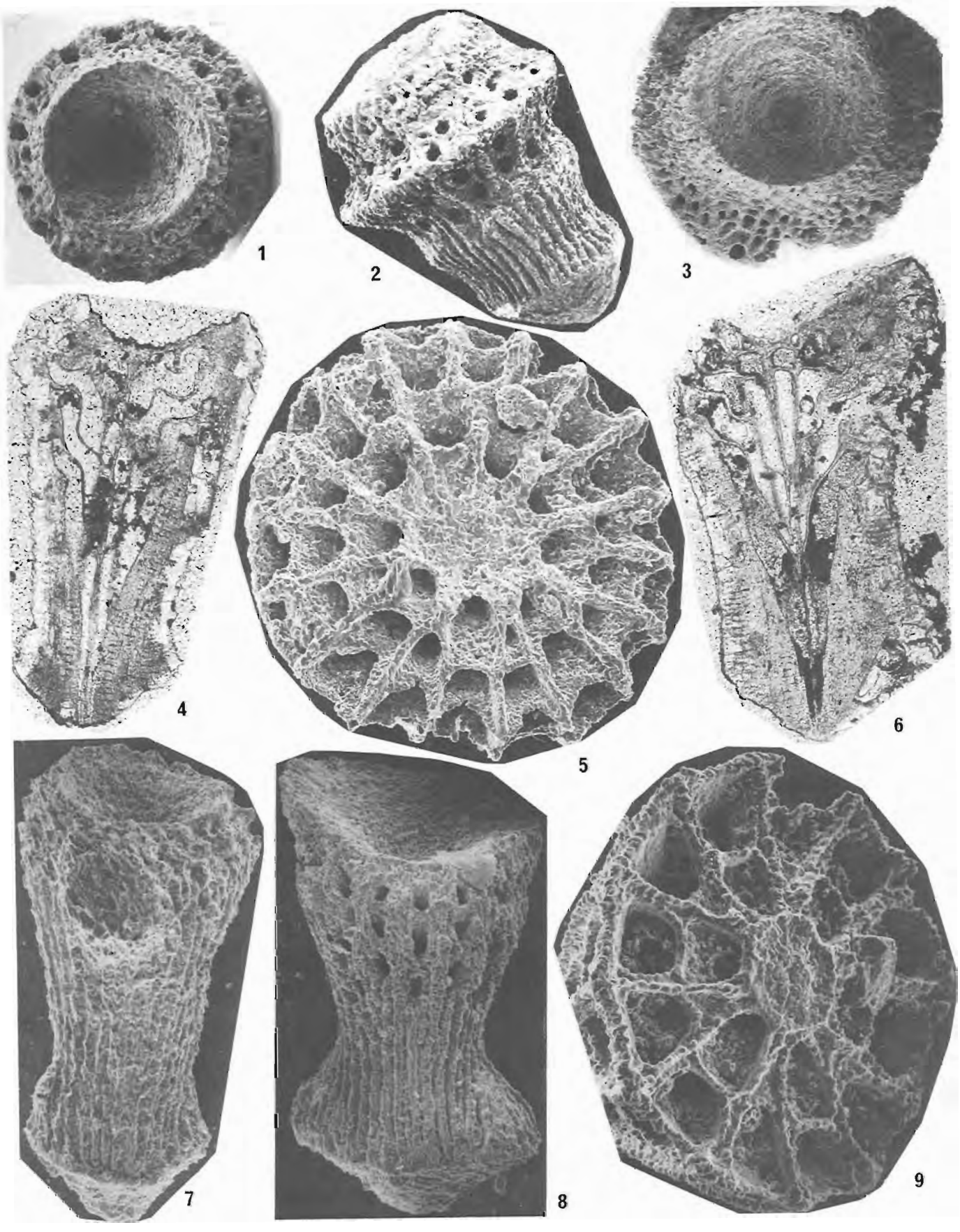
1
2
3
4
5
6
7
8
9

Plate 5.5

Figures 1-6. **Sceptropora facula** Ulrich. Section 83 AV4B – 94.5 m; Whittaker Formation, District of Mackenzie.

1,3,4. Side and distal views of stubby segment displaying widely separated double, deep attachment sockets and longitudinal ridges, x 35, x 70 and x 35; hypotype, GSC 80101.

2,5. Transverse sections, near distal end and below brim of stubby segments with wide extrazooecial skeleton, x 90 and x 100; hypotypes, GSC 80102, 80103.

6. Transverse section near distal end of club-shaped segment displaying 2 rows of unequal size zooecia, x 130; hypotype, GSC 80104.

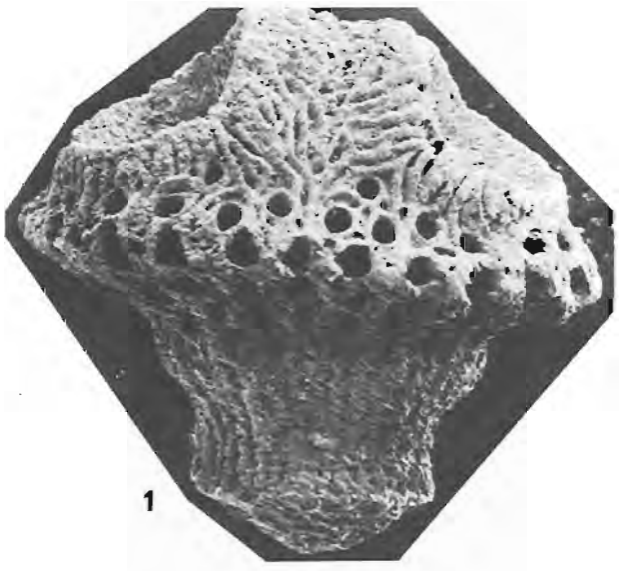

1

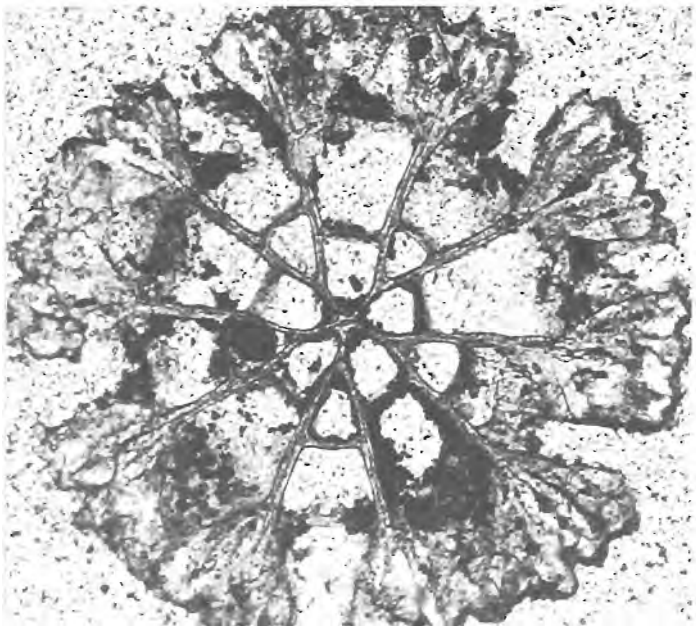

2

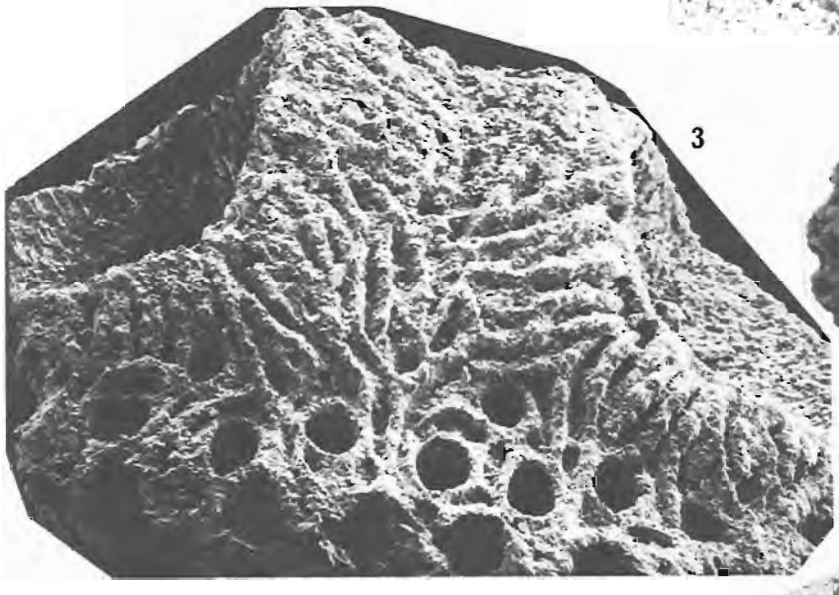

3

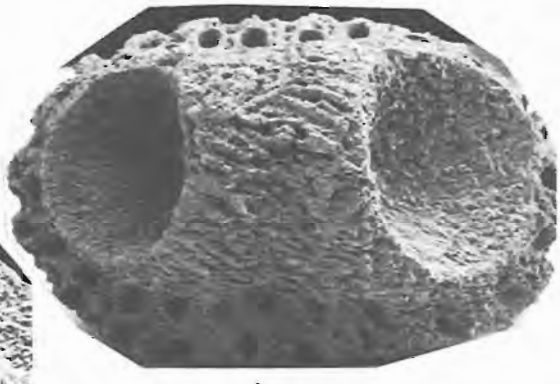

4

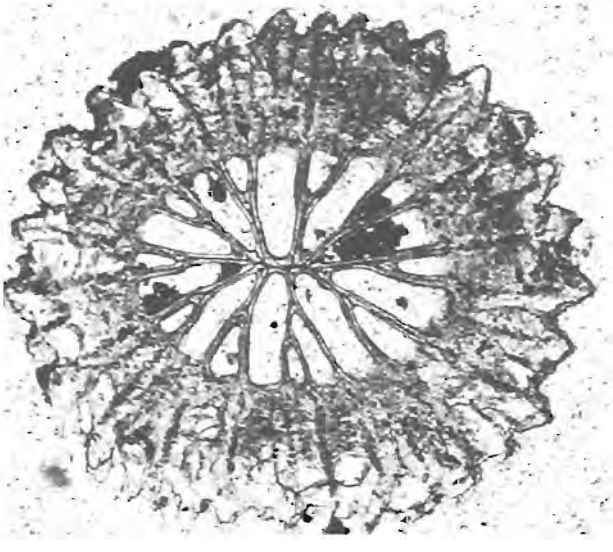

5

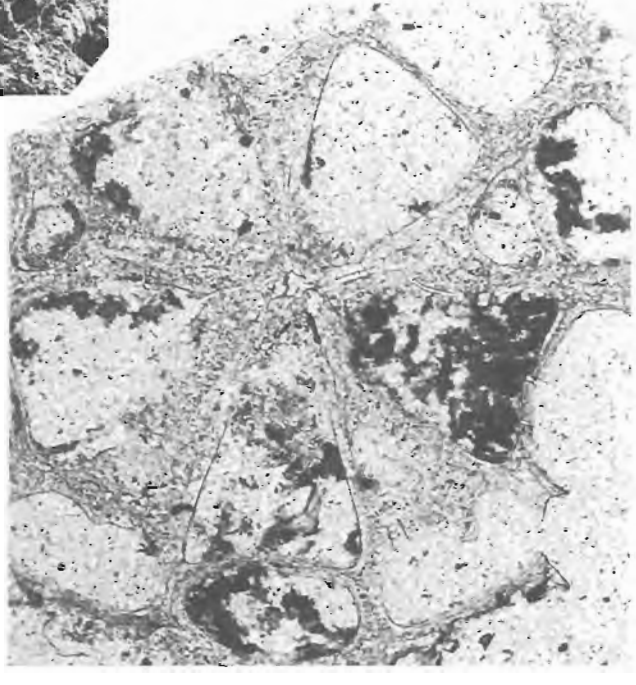

6

Plate 5.6

Figures 1-10. **Sceptropora facula** Ulrich. Section 83 AV4B – 94.5 m, Whittaker Formation, District of Mackenzie.

1,2. Side views of a stubby and club-shaped segments with pointed distal end between large double attachment sockets, x 35 and x 35, tilt 30°; hypotypes, GSC 80105, 80106.

3,10. Distal and side views of thick club-shaped segment showing large double attachment sockets separated by narrow ridge, x 70 and x 70, tilt 30°; hypotype, GSC 80107.

4,5. Side views of thick club-shaped segments showing single rim of zooecial apertures above brim, large double attachment sockets separated by medium width ridge, x 70 and x 70, tilt 35°; hypotypes, GSC 80108, 80109.

6. Transverse section near distal end of stubby segment showing 2 rows of unequal size zooecia around central axis and wide extrazooecial skeleton, x 130; hypotype, GSC 80110.

7. Oblique distal view of stubby segment with central attachment socket surrounded by 2 rows of zooecial apertures, x 35, tilt 59°; hypotype, GSC 80111.

8. Side view of thick club-shaped segment with small double attachment sockets separated by very wide porous ridge with incomplete second row of zooecial apertures, x 70, tilt 30°; hypotype, GSC 80112.

9. Side view of curved, thick club-shaped segment with large central attachment socket surrounded by one row of zooecial apertures, x 70, tilt 30°; hypotype, GSC 80113.



1



2

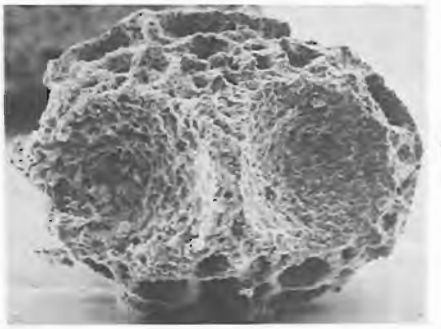

3

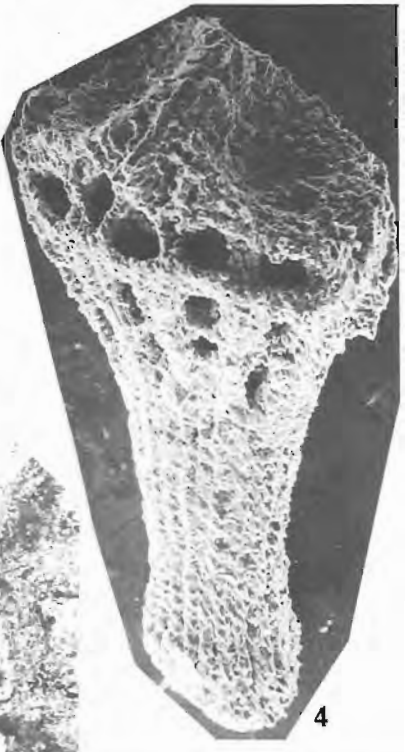

4

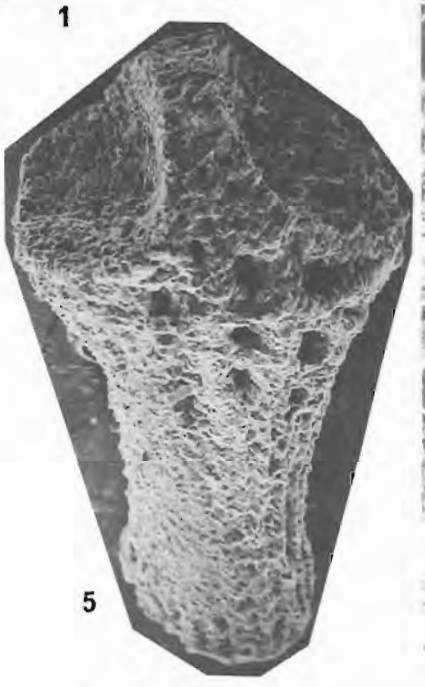

5

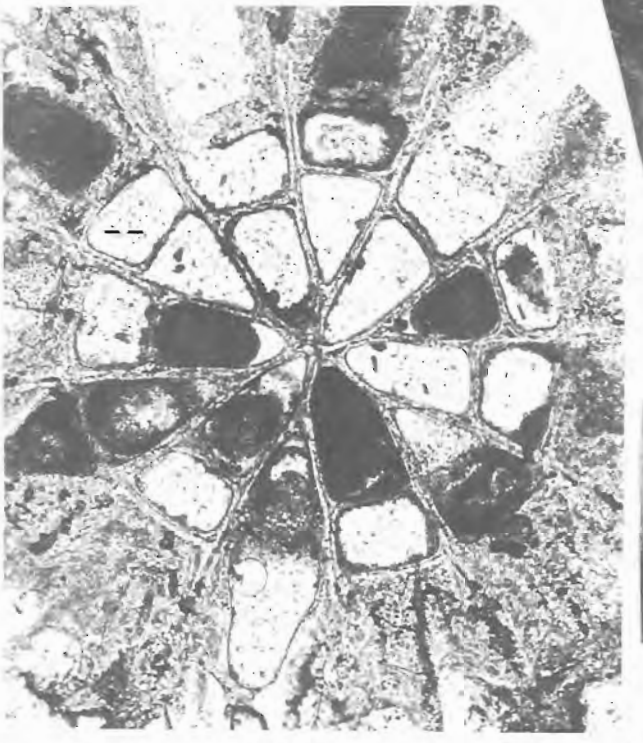

6

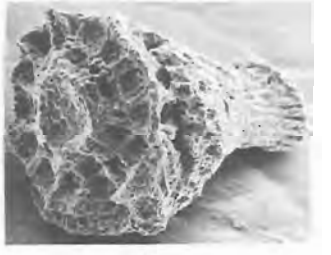

7

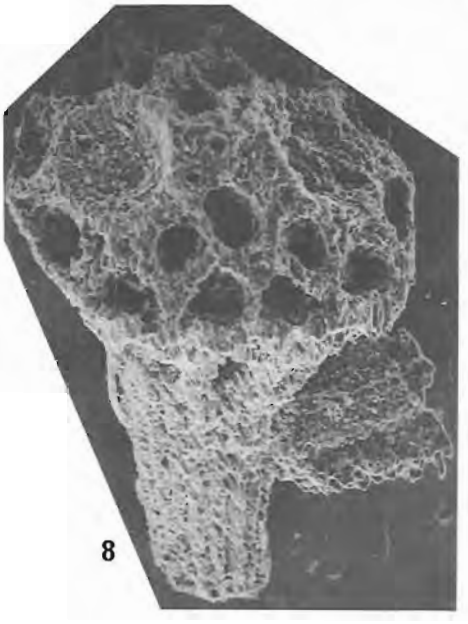

8

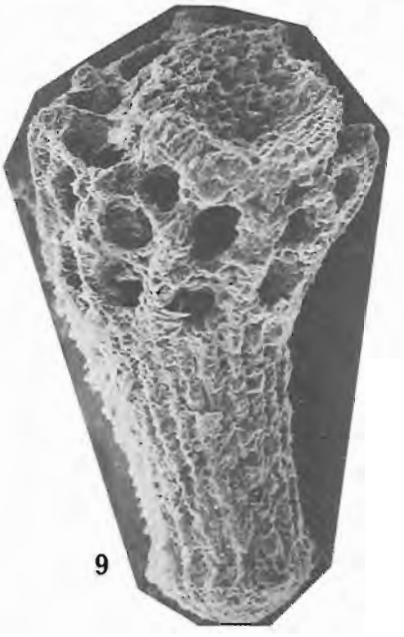

9

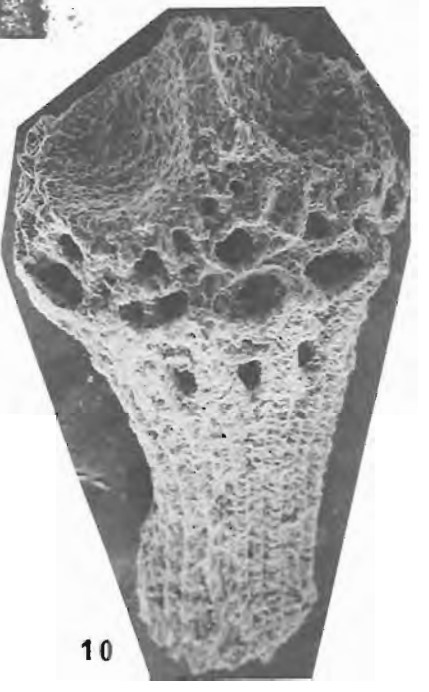

10

Plate 5.7

Figures 1-4, 6-8. **Sceptropora facula** Ulrich. Whittaker Formation, District of Mackenzie.

1. Natural longitudinal section of a bell-shaped segment, x 80, section 83 AV4B – 94.5 m; hypotype, GSC 80114.
2. Articulated zoaria of bell-shaped segments, x 44, section 79 AV1 – 46 m; hypotype, GSC 80080.
3,7. Side and distal views of bell-shaped segments with shallow central attachment sockets, x 55 and x 70, tilt 68°, section 79 AV1 – 53.5 m; hypotypes, GSC 80077, 80079.
4. Articulated zoaria of club-shaped segments, x 53, section 83 AV4B – 94.5 m; hypotype, GSC 80115.
6. Articulated zoaria of thick club-shaped segments displaying a pair of horizontal attachments, x 35, section 79 AV1 – 53.5 m; hypotype, GSC 80078.
8. Natural longitudinal section of a bell-shaped segment with large raised central attachment socket, x 65, section 83 AV4B – 94.5 m; hypotype, GSC 80116.

Figure 5. **Ulrichostylus** sp. Side view of zoarium showing apertural arrangement and longitudinal ridges, x 65, tilt 18°, section 79 AV1 – 53.5 m; hypotype, GSC 80122.

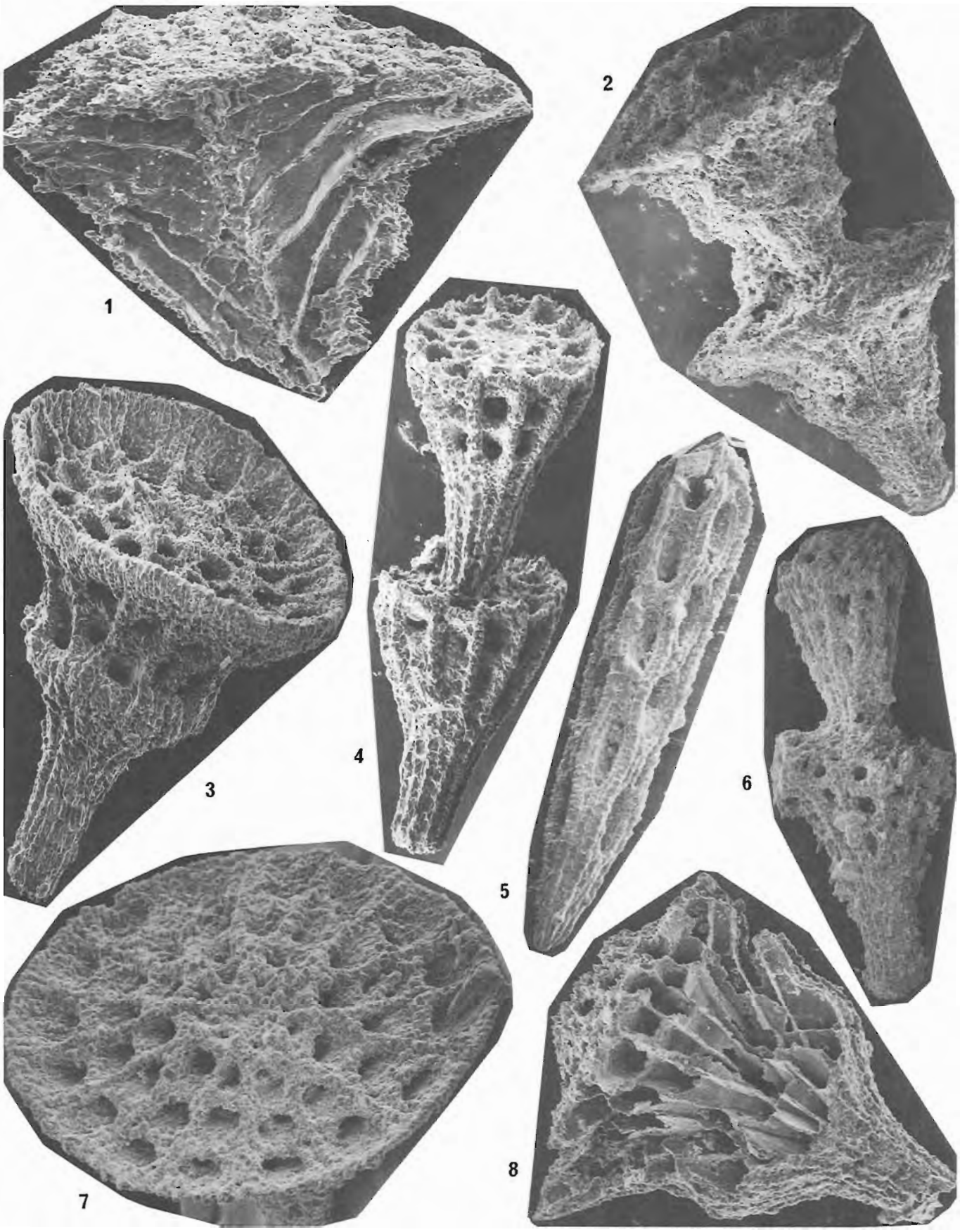
1
2
3
4
5
6
7
8

PETROGRAPHY, PETROCHEMISTRY AND MINERAL ASSOCIATIONS OF SELECTED ROCKS AND RADIOACTIVE OCCURRENCES NORTH OF MONT-LAURIER, QUEBEC: A PROGRESS REPORT

Project 770061

J. Rimsaite
Economic Geology and Mineralogy Division

Rimsaite, J., Petrography, petrochemistry and mineral associations of selected rocks and radioactive occurrences north of Mont-Laurier, Quebec: a progress report; in Current Research, Part A, Geological Survey of Canada, Paper 85-1A, p. 47-64, 1985.

Abstract

This paper documents additional results of laboratory studies, including SEM-EDS and isotope analyses, and discusses mineral associations in the following:

1. *selected mafic, felsic, hybrid and ore grade rocks;*
2. *mineralized gneissic and white heterogeneous pegmatites;*
3. *mineralized pegmatites associated with quartzite and with pyrite-bearing biotite gneisses;*
4. *mineralized migmatites associated with microcline pegmatites;*
5. *pegmatites associated with mafic skarn and biotite gneisses.*

Mineralization occurs in primary and secondary minerals.

Uranium mineralization occurs in contact zones between microcline pegmatite and paragneisses, as well as between paleosome and neosome phases. Radioactive REE-bearing occurrences are common at contacts between the pegmatite and mafic skarn.

Résumé

Cette étude rend compte des résultats de certaines études en laboratoire, notamment des analyses au microscope électronique à balayage (EDS) et isotopiques, et traite des associations minérales observées dans:

1. *des roches mafiques, felsiques, hybrides et minéralisées choisies;*
2. *des pegmatites minéralisées gneissiques et hétérogènes de couleur blanche;*
3. *des pegmatites minéralisées associées à de la quartzite et à des gneiss à biotite pyritifère;*
4. *des migmatites minéralisées associées à des pegmatites à microclines;*
5. *pegmatites associées à du skarn mafique et à des gneiss biotitiques.*

Les minéralisations apparaissent dans les minéraux primaires et secondaires.

La minéralisation de l'uranium a lieu dans les zones de contact entre la pegmatite à microclines et les paragneiss, de même qu'entre des composantes d'âge différent. Les accumulations radioactives sont communes aux surfaces de contact entre la pegmatite et le skarn mafique.

Introduction

Mineral associations from selected minerals and rocks collected in 1977 and 1979 north of Mont-Laurier, Quebec are discussed and analyses presented in this paper.

Geological features have been discussed by Kish (1977) and Tremblay (1974). For sampling localities see Figure 9.1 in Rimsaite, 1978.

The analyzed samples represent basement gneisses and migmatites of Patibre Formation, calc-silicate rocks (skarn), biotite-hornblende and pyrite-bearing biotite gneisses and metamorphic pegmatites of La Force Formation of the Grenville Group which contains scattered radioactive occurrences, and metamorphosed intrusive mafic and felsic rocks.

Table 6.1 presents results of rapid chemical and spectrographic analyses for major and minor constituents, neutron activation analyses for uranium, and X-ray fluorescence analyses for thorium of the whole rocks. Table 6.2 summarizes semiquantitative SEM-EDS* analyses of selected minerals and of their alteration products.

Other laboratory studies included separation of heavy minerals for isotope studies, microscope studies of minerals in oil immersion mounts and petrograpic examination of thin sections and of polished thin sections in reflected light; X-ray identification of minerals, and Pb, U, Th isotope studies of zircon concentrates and of minerals coated with secondary radioactive mineral aggregates (Table 6.3).

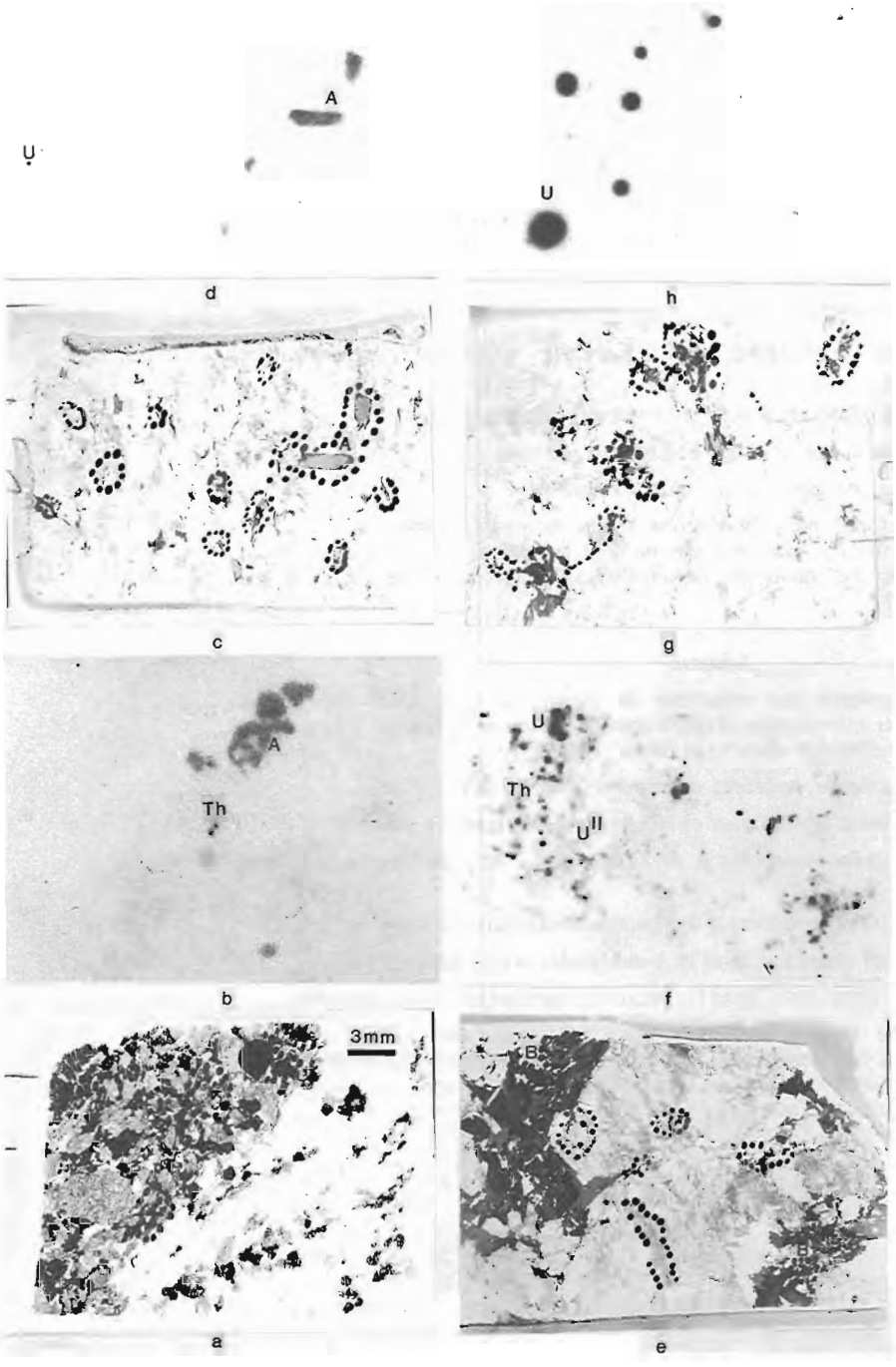

a. *Polished thin section of a radioactive contact between mafic hornblende-titanite rock (dark, left) and granite pegmatite (Table 6.1, analysis 18).*

b. *Autoradiograph of 6.1a showing distribution of radioactive allanite (A) and a few small grains of uranothorite (Th).*

c. *Allanite-bearing pegmatite adjacent to skarn. This rock contains 153 ppm U and 140 ppm Th. See Figure 6.2 for details.*

d. *Distribution of coarse grained allanite (A) and fine grained uraninite (U).*

e. *Radioactive pegmatite with prominent patches of biotite (B) adjacent to altered, pyrite-bearing biotite schist. This rock contains 230 ppm U and 472 ppm Th. See Figures 6.4, 6.5 for details.*

f. *Distribution of fine grained uranothorite (Th) and diffuse lines of secondary uranium minerals (U^{II}) in, and adjacent to, patches of biotite.*

g. *Radioactive pegmatite adjacent to the allanite-bearing pegmatite (c) and to skarn. This pegmatite contains 1120 ppm U and 278 ppm Th. For details see Figure 6.7*

h. *Autoradiograph of polished thin section (g) showing distribution of coarse grained uraninite (U) which is associated with remnant biotite.*

Figure 6.1. *Polished thin sections and autoradiographs showing distribution of radioactive minerals in selected radioactive occurrences north of Mont-Laurier, Quebec. Black circles mark areas selected for scanning electron microscope (SEM) and energy dispersive spectrometer (EDS) analyses. All photographs were taken in transmitted light at the same magnification as in (a).*

* SEM = scanning electron microscope; EDS = energy dispersive spectrometer

Table 6.1. Partial chemical analyses of the principal rock types and selected, biotites from radioactive occurrences north of Mont-Laurier, Quebec*

	Sample location symbols**																		
	RPL	TDN-2	JMV-4		JMV-1	RPL		PP-2			JMV-1	JMV-3		TDN-2			S of M-50	
Sample**	Mafic 1	Mafic sk 2	Mig 3	Mig 4	Peg 5	Gr 6	Gr 7	Apl 8	Peg 9	Bio 10	Bio 11	Bio 12	Mig 13	Mig 14	Sk 15	Sk 16	Sk 17	Mafic 18	Bio 19
SiO_2%	47.9	52.3	72.3	72.9	73.0	63.0	61.2	74.0	85.6	36.8	37.5	34.6	65.1	67.4	71.9	74.3	77.3	35.0	34.3
TiO_2	1.9	0.3	0.4	0.2	0.2	0.5	0.4	0.2	0.0	3.3	3.3	3.4	1.5	0.3	0.4	0.1	0.1	7.1	3.3
Al_2O_3	11.8	3.2	14.0	14.7	14.3	18.2	18.8	13.5	8.9	15.3	15.6	16.3	6.4	16.5	14.7	13.4	14.0	6.4	15.0
Fe_2O_3	1.8	0.9	1.5	0.3	0.1	1.3	0.4	0.2	0.0	5.5	5.0	10.1	0.3	0.6	0.9	0.3	0.9	24.7	6.4
FeO	9.0	7.5	1.2	1.0	1.0	2.4	2.4	1.8	0.2	16.3	16.7	14.6	4.1	1.4	1.8	0.3	0.0	10.2	14.1
MnO	0.2	0.3	0.3	0.3	0.1	0.1	0.1	0.1	0.1	0.7	0.7	0.4	0.2	0.1	0.1	0.1	0.1	0.3	0.3
MgO	9.4	12.2	0.7	0.4	0.2	1.3	1.1	0.5	0.0	9.0	8.9	6.6	2.8	0.4	0.5	0.5	0.3	0.1	9.0
CaO	11.1	20.7	1.6	1.3	0.7	1.6	1.6	1.3	1.5	0.0	0.0	0.2	6.5	2.2	1.6	0.7	1.1	0.0	1.7
Na_2O	2.0	0.1	3.7	3.0	2.9	2.7	2.7	3.1	3.0	0.0	0.0	0.0	0.0	3.7	3.9	2.3	3.8	0.6	0.0
K_2O	1.8	0.2	4.3	5.6	6.3	8.5	8.6	4.2	0.2	9.0	8.7	8.9	3.2	6.0	3.6	6.7	3.3	2.7	7.9
H_2O	1.6	0.7	0.5	0.6	0.6	0.7	0.5	0.4	0.0	3.2	3.4	3.6	1.1	0.5	0.8	0.4	0.4	0.4	5.0
Cl	.11	.07	.05	.06	.07	.03	.04	.02	.00	.15	.18	.20	.02	.02	.05	.02	.01	0.0	0.1
F	.21	.06	.05	.04	.35	.07	.07	.05	.00	.85	1.30	.40	.35	.05	.07	.03	.04	0.1	0.3
P_2O_5	1.50	.09	.15	.09	.04	.63	.54	.07	.00	.00	.00	.02	.64	.57	.14	.03	.00	2.4	1.1
CO_2	.00	1.10	.10	.20	.10	.00	.00	.10	.10	.20	.20	.02	.21	.00	.10	.30	.20	0.1	0.0
S	.07	.01	.03	.00	.00	.02	.01	.13	.00	.02	.00	.07	.08	.02	.06	.00	.02	.06	.07
Ba	.10	.01	.09	.12	.10	.15	.15	.05	.01	.03	.02	.03	.01	.15	.04	.07	.03	.07	.03
Rb	.01	.00	.02	.02	.03	.03	.03	.02	.00	.10	.10	.07	.01	.02	.02	.03	.01	.01	.06
Sr	.10	ND***	ND	ND	.03	.05	.05	.02	.01	.00	.00	.00	.00	.03	ND	.03	.02	ND	.00
Zn	.01	.01	.01	.00	.00	.01	.00	.00	.00	.05	.05	.05	.06	.00	.01	.00	.00	.03	.04
Zr	.03	ND	ND	ND	.03	.03	.01	.20	.01	.04	.04	.00	.02	.03	ND	.02	.00	.5	.00
U ppm	4.6	4.5	5.3	2.3	5.1	4.0	3.4	1380	20	190	180	929	>5000	54	98	397	243	89	1120
Th ppm	ND	16	22	18	ND	ND	ND	219	ND	ND	ND	104	845	ND	171	211	ND	331	756

* Analysts and laboratories are listed in "Acknowledgments".
** Sample location symbols are the same as those on sketch map (Rimsaite, 1978, Fig. 9.1).
Samples: Mafic mafic rock; sk skarn; Mig migmatite; Peg pegmatite; Gr granite; Apl aplite; Bio biotite. (See Appendix 1 for description of samples).
*** Not determined

Table 6.2. Semiquantitative SEM-EDS analyses of selected radioactive and accessory minerals and of their alteration products from radioactive occurrences north of Mont-Laurier*

	Sample locations** and host rocks																			
	PP-1, gneissic pegmatite (1-8)							JMV-1, contact gneiss/pegmatite (9-12)					TDN-2, white heterogeneous pegmatite (13-21)							
Sample**	Bio a 1	U 2	Th 3	Rim U 4	Zr-agr 5	Ep-Al 6	Rim Al 7	REE g 8	U 9	U a Fe 10	U a Ti 11	Uph 12	Bio 13	Th 14	U in Th 15	Si in Th 16	U 17	Rim U 18	Cof 19	Zr 20	Zr in Th 21
MgO	1.3	-	-	-	-	3.3	0.7	-	-	-	-	-	10.3	-	-	-	-	5.6	-	-	-
Al_2O_3	8.3	-	-	-	0.4	18.9	4.5	-	-	-	-	-	14.7	0.3	-	1.1	-	12.5	0.8	0.4	-
SiO_2	21.3	1.3	4.2	8.9	7.7	39.8	13.3	-	1.3	3.9	6.0	13.7	37.3	9.4	18.0	47.9	-	24.0	17.5	30.8	8.9
P_2O_5	0.5	-	0.9	-	-	-	-	-	-	-	-	-	-	-	0.4	-	-	0.5	-	-	-
Cl	-	-	-	-	-	-	-	-	-	-	-	-	0.4	-	-	-	-	-	-	-	-
K_2O	1.7	-	-	-	-	2.6	0.5	-	-	-	-	-	9.6	-	-	-	-	-	-	-	-
CaO	1.1	0.6	-	-	1.7	1.4	2.2	7.3	0.3	0.3	0.6	6.2	-	1.4	0.5	0.8	0.5	0.8	1.1	3.6	1.7
SrO	-	-	-	-	-	-	-	2.4	-	-	-	-	-	-	-	-	-	-	-	-	-
TiO_2	0.3	-	-	-	30.1	-	0.3	-	-	-	15.4	-	3.0	-	-	0.3	-	-	-	-	3.0
MnO	-	-	-	-	-	0.6	-	-	-	-	-	-	0.3	-	0.3	-	-	1.3	-	0.6	-
FeO***	8.5	0.3	5.7	50.6	3.1	17.0	3.9	-	6.2	13.4	9.5	0.5	19.4	1.0	1.3	2.0	0.3	28.9	0.8	1.8	22.4
ZrO_2	-	-	-	-	2.4	-	-	-	-	-	-	-	-	-	-	-	-	-	-	57.0	6.2
HfO_2	-	-	-	-	-	-	-	-	-	-	-	-	-	-	-	-	-	-	-	2.2	-
Cr_2O_3	-	-	-	-	-	-	-	-	-	-	-	-	0.3	-	0.3	0.3	0.3	0.3	-	0.6	-
Y_2O_3	0.3	5.3	3.0	0.5	-	-	1.3	-	-	-	-	-	-	-	0.5	-	1.0	-	3.0	-	4.3
Yb_2O_3	-	-	1.4	-	-	-	-	-	-	-	-	-	-	-	-	-	-	-	-	-	-
Er_2O_3	-	-	1.1	-	-	-	-	-	-	-	-	-	-	-	-	-	-	-	-	-	-
La_2O_3	2.1	-	-	-	-	0.7	4.0	16.1	-	-	-	-	-	-	-	-	-	-	-	-	-
Ce_2O_3	4.9	-	0.5	-	3.4	2.0	10.6	28.0	-	-	-	-	-	-	-	-	-	-	-	-	-
Pr_2O_3	-	-	-	-	-	0.2	1.4	2.3	-	-	-	-	-	-	-	-	-	-	-	-	-
Nd_2O_3	2.6	-	0.5	-	1.4	1.2	6.2	9.6	-	-	-	-	-	-	-	-	-	-	-	-	0.9
Sm_2O_3	0.5	-	-	-	-	0.5	1.2	-	-	-	-	-	-	-	-	-	-	-	-	-	-
PbO	1.9	8.6	5.0	16.2	5.0	2.4	2.2	-	10.8	7.6	8.9	-	-	4.5	1.1	4.5	11.0	1.5	3.5	-	3.2
ThO_2	4.1	4.1	6.8	0.6	0.6	1.3	6.2	-	9.3	10.5	1.4	-	-	55.7	40.8	8.9	9.3	-	1.1	-	18.5
UO_2	3.6	69.4	43.6	1.8	26.4	2.5	4.1	-	66.4	52.2	44.1	59.3	-	10.4	28.7	30.3	70.1	-	63.5	0.2	6.6
U/Th	0.9	16.9	6.4	3.0	44.0	1.9	0.66	-	7.0	5.0	31.5	-	-	0.18	0.7	3.4	7.5	-	57.7	-	0.36
Pb/U	0.5	0.12	0.11	9.0	0.19	1.0	0.5	-	0.16	0.14	0.2	-	-	0.43	0.04	0.15	0.15	-	0.05	-	0.48
Pb/Th	0.49	2.1	0.73	27.0	8.3	1.8	0.35	-	1.16	0.72	6.3	-	-	0.08	0.02	0.5	1.18	-	3.18	-	0.17

* Analysts and laboratories are listed in "Acknowledgments".

** For sample location see text and Fig. 9.1 in Rimsaite, 1978. Samples: Bio a biotite altered; U uraninite; Th thorite, uranothorite; Rim U (Al) rim on uraninite (allanite); Zr agr Zr-bearing aggregates; Ep-Al epidote-allanite; REE g REE-bearing grain; U-Fe (Ti) uraninite altered to Fe(Ti)-bearing phase; Uph uranophane; U (Si,Zr) in Th U (Si,Zr)-bearing phases in uranothorite.

*** Total iron reported as FeO.

Table 6.3. Preliminary isotopic data* for zircons and radioactive crusts

Mineral concentrate**	Location	Sample weight mg	U%	Th%	Pb%	Common Pb (% of total)	$^{207}Pb/^{235}U$	$^{206}Pb/^{238}U$	$^{208}Pb/^{232}Th$	$^{207}Pb/^{206}Pb$	Apparent Isotopic age (Ma) $^{208}Pb/^{232}Th$
Zircon 1	JMV-3	37.6	0.31	0.007	0.0025	3.5	0.776	0.083	0.085	852.0	1655.8
Zircon 2	JMV-3	39.0	0.05	0.026	0.0128	33.9	1.560	0.155	0.045	1013.0	857.9
Zircon 3	JMV-3	56.0	6.34	0.307	0.03	34.1	0.027	0.003	0.044	983.0	878.0
Zircon 4	JMV-1	18.2	0.83	0.107	0.12	24.5	1.176	0.115	0.029	1052.7	570.9
Titanite	JMV-1	0.2	0.29	0.55	0.12	84.	34.17	3.73	-	821.	
Biotite	H-50	70.0	0.61	0.24	0.6	3.7	1.550	0.114	0.132	1031.0	2507.8

* Preliminary isotopic data from GEOSPEC Consultants Ltd., research contracts OGY80-01086 and OSQ81-00033.

** Notes on mineral concentrates (Hand-picked from a few hundred to 40 000 grains).

1. Zircon fragmented, rounded, stained red with Fe-oxide.
2. Zircon, many types: zoned, rounded overgrown by clear rims and composite.
3. Zircon, mainly clear prisms, some are coated with galena, coatings less than 1 μm thick.
4. Barrel-shaped zircon (Fig. 6.7a).
5. Titanite coated with uraniferous crusts.
6. Biotite flakes with uraniferous crusts in fractures.

Because of alterations, overgrowths and of metamict nature of most of the REE** and Th minerals, some difficulties have been encountered with separation of clean minerals for isotope studies and with X-ray identification of poorly crystallized and metamict minerals. Approximately 20 per cent of minerals studied were metamict or amorphous to X-rays.

Petrography, petrochemistry and mineral associations are correlated in the following specimens:

1. selected mafic, felsic, hybrid and ore grade rocks;
2. mineralized gneissic and white heterogeneous pegmatites in Pond Lake prospect;
3. mineralized pegmatites associated with quartzite and with pyrite-bearing biotite gneisses south of Beaudette Creek;
4. mineralized migmatites associated with microcline pegmatites along base lines 1 and 3 in prospects formerly owned by Canadian Johns Manville Co.;
5. pegmatites associated with mafic skarn and biotite gneisses between Patibre Lake and Tom Dick Creek.

Acknowledgments

The following assistance is greatly appreciated: rapid chemical and spectrographic analyses of rocks by the staff of the Analytical Chemistry Section, X-ray identification of minerals by A.C. Roberts, scanning electron microscope studies by D.A. Walker and semiquantitative SEM-EDS analyses by D.A. Walker and G.J. Pringle, all of the Mineralogy Subdivision, Geological Survey of Canada. This study was also supported by neutron activation analyses for uranium by the Atomic Energy Canada Limited; X-ray fluorescence determinations of thorium by Bonder-Clegg and Company Ltd., and isotope studies by the GEOSPEC Consultants Ltd., research contracts OGY80-01086 and OSQ81-00033. I wish to thank N. Prasad of the Geological Survey of Canada for his assistance in the field and to J.R. Beauchamp who guided us to the Pond Lake prospect and to R.F. Kaltwasser who showed us properties owned by the Canadian Johns Manville Company Limited in 1977.

Selected mafic, felsic, hybrid and ore grade rocks

A comparison of petrochemical data in Table 6.1 and in additional published and unpublished analyses (Table 3.1 in Rimsaite, 1982a) indicates that uranium mineralization occurs in felsic rocks and at the contact between a mafic rock or a xenolith and microcline pegmatite (Table 6.1, analysis 18). Biotite-bearing felsic rocks having an intermediate to high silica content appear to be favourable hosts for uranium and thorium mineralization, However, some felsic rocks can be very similar in chemical composition but quite different in degree of their radioactivity. The following discussion attempts to compare stratigraphic position and chemical, textural and mineralogical differences and similarities between barren and mineralized rocks, the latter containing 50 ppm U or more.

Mafic rocks

Three types of mafic rocks are compared: metagabbro, mafic skarn and a contact zone between Ti-rich mafic rock and pegmatite (respectively analyses 1, 2 and 18 in Table 6.1*). The metagabbro and mafic skarn have similar quantities of U (ca 5 ppm), of Fe and Mg (ca 20 per cent) but different concentrations of Ti, Al, Ca, alkalis, P and CO_2. Skarn contains more Ca and CO_2 as a result of abundant calcic amphibole and scapolite, whereas metasomatic biotite, alkali feldspars and abundant titanite and apatite account for higher Al, K, Na, Ti and P content in the metaggabro.

** REE = rare-earths elements

* hereafter analyses from Table 1 are referred to simply by bracketed number, i.e. (1)

The third mafic rock contains only 35 per cent SiO_2 and represents a contact zone between mafic, Fe-Ti-oxide-rich rock and microcline pegmatite (Fig. 6.1a, b, analysis 18 in Table 6.1). Ilmenite, magnetite, titanite and microcline account for relatively high concentration of Ti, Fe, Al and K in this hybrid rock. Allanite, apatite and uranothorite which crystallize along a few centimetres wide contact zone, account for elevated values of P, U and Th.

Migmatite in Patibre Formation

Fine grained gneissic portion of the migmatite (3) is similar in chemical composition to coarser grained pegmatitic phase (4), but the latter contains slightly more K due to the presence of porphyroblastic K-feldspar. These basement rocks contain 5.3 ppm and 2.3 ppm U and 22 ppm and 18 ppm Th.

Barren granite pegmatite

The granite pegmatite (5) is very similar in chemical composition to the pegmatitic phase of the migmatite from Patibre Formation (3, 4), but contains 5.1 ppm U and more potassic feldspar and more fluorine.

Porphyritic granites

Red (6) and grey (7) porphyritic granites are almost identical in chemical composition. They contain high concentrations of alumina (18 per cent) which suggests their sedimentary origin from clay-rich pelites. Ferric iron which apparently has been introduced and crystallized in microcline fractures has produced the red coloration of the red porphyritic granite.

White heterogeneous radioactive pegmatite

Within a distance of a few centimetres, the heterogeneous pegmatite (8 to 11) varies in grain size, mineralogy, abundance of biotite-rich xenoliths and degree of their recrystallization and assimilation. Radioactivity of the heterogeneous pegmatite is related to the grain size, mineralogy and yellow stains produced by films and coatings of secondary radioactive mineral aggregates. Quartz-rich, coarse grained portions of the pegmatite are less radioactive than adjacent finer grained biotite-bearing phases (8, 9 and 10). With the exception of higher concentrations of U, Th and Zr, the finer grained radioactive portion of the heterogeneous pegmatite is similar in chemical composition to the barren pegmatite (8 and 5). Recrystallized flakes of biotite in pegmatite and those in biotite-rich xenoliths are similar in chemical composition and contain 190 ppm and 180 ppm U which can be accounted for by the presence of secondary uraniferous mineral aggregates in biotite fractures. Biotite concentrate from xenoliths contains more fluorine than recrystallized biotite in the same pegmatite. However, biotite concentrates from other pegmatites, such as from the oxidized pegmatite in locality JMV-1 and H-50, differ in chemical composition (10, 11, 12, 19). Biotite associated with muscovite (12) and chloritized biotite (19) contain higher proportions of ferric iron and more uranium than biotites from white pegmatite. In biotites from oxidized pegmatites, ferric oxide and uranyl-bearing aggregates have crystallized along (001) cleavage planes of the biotite, commonly as goethite, uranophane and kasolite.

Moderately radioactive migmatite

This migmatite (14) is enclosed in pegmatite adjacent to quartzite and metabasite. Migmatite is made up of porphyroblastic microcline perthite veined by albite, coarse grained quartz and biotite which has crystallized between feldspar and quartz. Biotite contains abundant radioactive accessory minerals, probably coated with radioactive crusts, including apatite, allanite, molybdenite and zircon. Several morphological types of ziron were concentrated for isotope analyses (Table 6.3).

Radioactive pegmatite associated with mafic skarn

Radioactive pegmatites (15 to 17) adjacent to mafic skarn contain abundant allanite-epidote which is overgrown by Th-rich rim. This Th-rich allanite accounts for most of the radioactivity and for relatively high Th/U ratio of about 2 in the host rock (Fig. 6.1c, d; analysis 15 in Table 6.1). The other two rock specimens are from white heterogeneous pegmatite, a few hundred metres away from outcropping skarn. The finer grained phase of the pegmatite contains more U and K than the coarse grained quartz-rich phase (16, 17).

Barren and mineralized pegmatites are very similar in their chemical compositions (5, 8, 16) indicating that petrochemical properties alone without supporting textural and mineralogical studies cannot be considered reliable criteria to determine favourable environment for uranium mineralization. Heterogeneous granitoid rocks (Rimsaite, 1982a) and stratigraphic position, namely La Force Formation, provide more favourable environment for mineralization than basement rocks of the Patibre Formation (Kish, 1977).

Mineralized gneissic and heterogeneous pegmatites in Pond Lake Prospect (Fig. 6.2, 3, analyses 1-8 in Table 6.2)

Pond Lake prospects are located in Leman Township (see Fig. 9.1 in Rimsaite, 1978). The radioactive pegmatites were discovered, cleared of glacial cover and investigated by J.R. Beauchamp*. Prospects PP-1 and PP-2, located a few hundred metres apart, are separated by a creek and by glacial and alluvial debris. In locality PP-1, the gneissic pegmatite is underlain by mafic skarn and consists of medium grained radioactive gneissic phases which grade into coarse grained barren phases.

The heterogeneous pegmatite in PP-2 occurrence is made up of xenoliths, fine grained feldspathic phases, coarse grained patches of recrystallized biotite, porphyroblastic microcline perthite, antiperthite overgrown by clear rims of albite, and barren phases composed mainly of quartz and rare prisms of tourmaline.

The radioactive phase of gneissic pegmatite is prospect PP-1 is made up of biotite streaks and bands which contain abundant inclusions of allanite, apatite, titanite and zircon, and scattered grains of uraninite and uranothorite and rare grains of pyrite in a quartzo-feldspathic groundmass (Fig. 6.2, 6.3). Zircon and allanite are commonly concentrated in alternating biotite bands, one containing abundant allanite, the other dominantly zircon. Allanite grains apparently replace host biotite. Allanite is metamict, heterogeneous, and surrounded by zoned Th- and REE-rich rims; it contains disseminated grains of yttrian unranothorite, and is partly replaced by poorly crystallized hydroxyl-bastnaesite, chlorite and serpentine group mineral aggregates (analyses 3-6 in Table 6.2, Fig. 6.2f, h, i; Rimsaite, 1982c, Fig. 31.6 a-e). Locally zircon grains are intergrown with uraninite and with uranothorite (Fig. 6.2g).

Uraninite crystallizes in biotite and is surrounded by prominent iron-rich rims and an alteration halo in the host biotite (Fig. 6.3; analyses 1 and 2 in Table 6.2). Fresh portions of uraninite contain relatively high concentration of yttrium (5.3%), moderate concentrations of lead (8.6%) and thorium (4.1%). Along fractures, uraninite is replaced by a Si-Fe-Th-bearing phase which contains variable proportions of U, Th, REE and other elements (analysis 3 in Table 6.2).

* Mr. J.R. Beuachamp (private communication, 1977)

Rim surrounding uraninite extends into fractures. It is heterogeneous and contains Fe-rich, Pb-rich and U-rich phases (Fig. 6.3a-i). Uranium liberated from altered uraninite reacts with other leached ions and precipitates in biotite fractures as chemically complex compounds, the most common being U-Ti-Th-, Si-U-Fe-Pb-, and U-Si-Th-Zr-bearing crusts (Fig. 3.7f, g, h in Rimsaite, 1983a).

The white heterogeneous pegmatite in prospect PP-2 contains scattered grains of uraninite, uranothorite, allanite, zircon and abundant secondary uranium minerals, mainly uranophane and rare thorobastnaesite associated with chloritized biotite (analyses 8-11 in Table 6.1). Pegmatite is fractured and some of the fractures are filled with pyrite associated with molybdenite and rare chalcopyrite. The pyrite bands are overgrown by green phengitic muscovite.

Gneissic pegmatite adjacent to mafic skarn contains REE-bearing minerals; heavy REE crystallize in uraninite and in secondary mineral aggregates associated with U and Th, and light REE precipitate in metamict allanite and as poorly-crystallized or amorphous hydroxyl-bastnaesite group

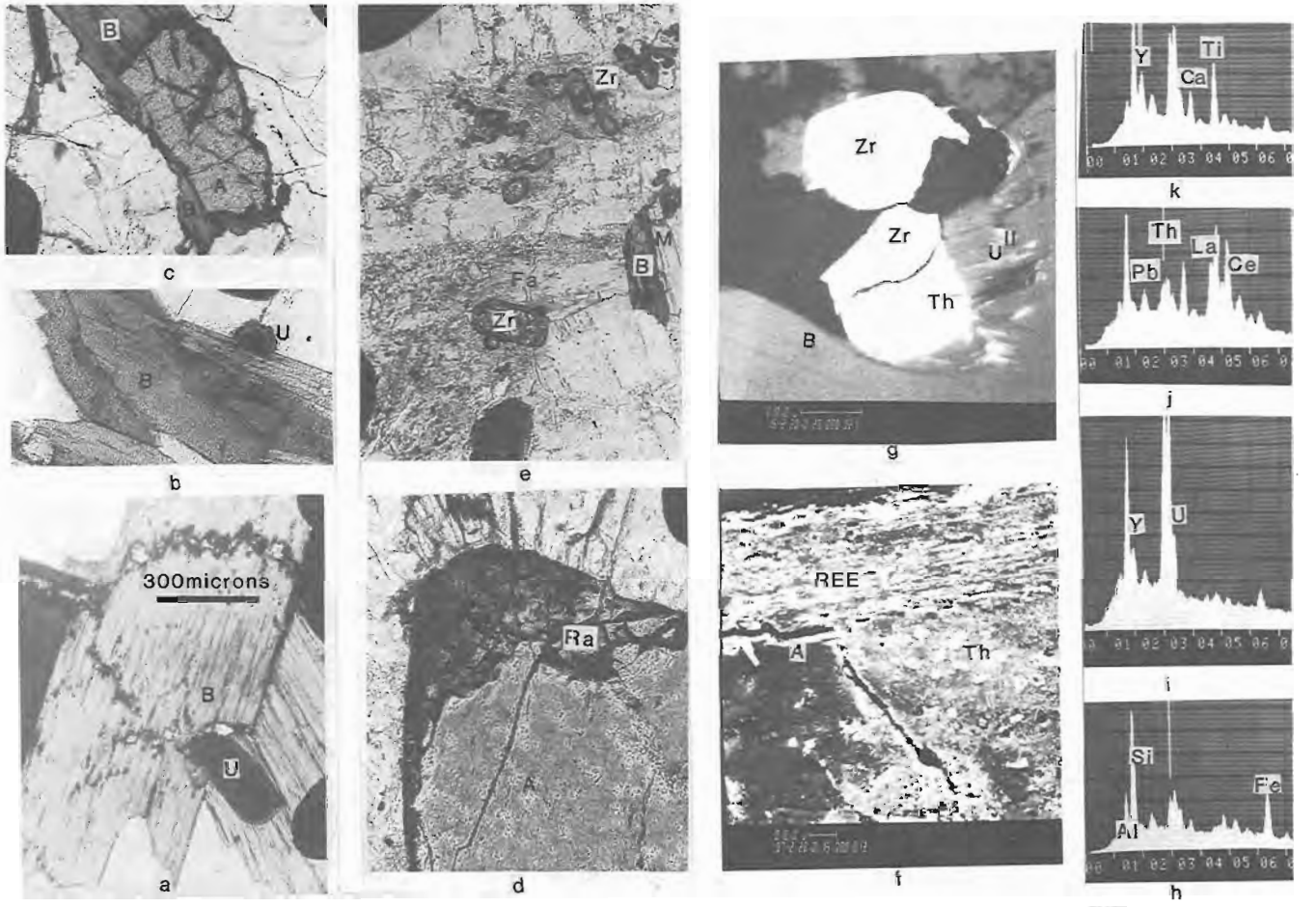

a. Biotite flakes (B) with inclusions of coarse grained uraninite (U).

b. Small grain of uraninite (U) adjacent to biotite flakes (B).

c. Allanite (A) surrounded by dark pleochroic halo replaces host biotite (B).

d. Coarse grained epidote-allanite (A) with bright-orange radioactive rim (Ra). Prominent fractures radiate from the allanite. For an autoradiograph of the allanite and uraninite in Figure 6.2b see Figure 6.1d.

e. Zircon grains (Zr) and biotite flake (B) partly replaced by muscovite (M) in altered feldspar (Fa).

f. Backscattered electron image (BEI) of heterogeneous rim on altered allanite (A). White specks of thorite (Th) crystallize under the REE-rich rim (REE). Figures f-k on GSC-203414-H).

g. Zircon grains intergrown with uranothorite (Zr, Th) in biotite (B). Fractures in biotite are filled with secondary uranium-bearing mineral aggregates (U^{II}).

h. Energy dispersive spectrum (EDS) of altered epidote-allanite in Figure 6.2f. Element lines listed in order of decreasing intensities are: Si > Fe > Al = Th, U > Pb > Ca > Ce > La.

i. EDS of Th-rich specks in (f): Th > Si > U > Y > Fe > Pb > Ce, Al.

j. EDS of REE-rich bands in zoned rim of allanite in (f): Si > Ce > La = Ca > U, Th > Pb, Fe > Al, Y.

k. EDS of white specks adjacent to the rim of altered allanite in (f): Si > Th, U > Ti > Y > Ca > Pb > Fe > Al > Ce.

Figure 6.2. *Illustrations of radioactive and accessory minerals from pegmatites in locality TDN-2 (a-e) and PP-1 (f-k). See Figure 9.1, in Rimsaite, 1978. Photomicrographs (a-e) were taken in transmitted light at the same magnification as (a).*

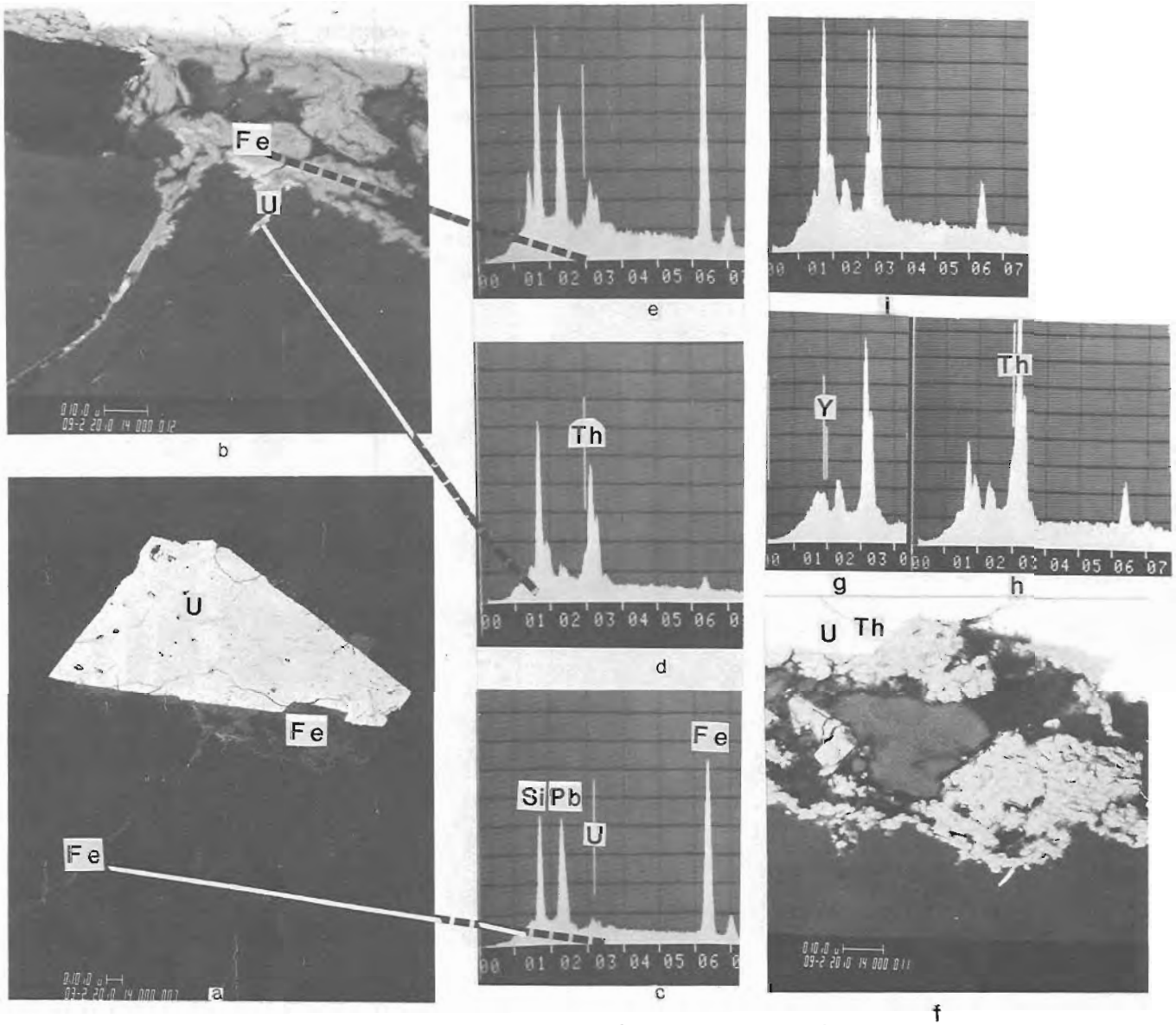

a. *BEI of uraniite (U) and of Fe-rich rim (Fe) which extends into fractures (Fe).*

b. *BEI of the rim on uraninite in (a), enlarged from (a). The rim consists of Fe-Si-Pb-rich flaky groundmass (Fe) and U-rich specks and bands (U, white).*

c. *EDS of radioactive Fe-rich mineral aggregates filling fractures away from uraninite in (a): Fe > Si = Pb > U.*

d. *EDS of white, strongly radioactive bands and specks in Fe-rich rim in (b): Si > U > Y > Th > Pb = Fe.*

e. *EDS of the principal component of the rim in (b): Fe > Si > Pb > Al > U > Th, analysis 4 in Table 6.2.*

f. *BEI of the edge of uraninite (U) in (a), adjacent to rim in (b), showing part of the Fe-rich rim (Fe) and Th-bearing crusts (Th) filling fractures in uraninite.*

g. *EDS of unaltered portion of uraninite in (f): U > Pb > Y, analysis 2 in Table 6.2.*

h. *EDS of thorian mineral aggregates filling fractures in uraninite in (f).*

i. *EDS of uraniferous spots in the outer portion of the rim on uraninite in (f). The spectrum is similar to that in (d) but shows stronger intensities of U and Fe: Si = U > Th = Y = Fe > Pb.*

Figure 6.3. *Illustrations of rimmed uraninite and of radioactive Fe-rich mineral aggregates filling fractures in gneissic biotite-allanite-zircon-bearing pegmatite. (GSC 203755-C)*

mineral aggregates. In the Pond Lake prospect, mineral associations represent primary, secondary and supergene parageneses which resulted from the following geological processes:

I. Pegmatitic crystallization phase. Paragenesis of primary minerals related to crystallization of pegmatites include rock-forming minerals, namely biotite and feldspars followed by quartz, and radioactive and accessory minerals: uraninite, uranothorite, apatite, tourmaline and zircon which in turn were followed by recurring zonal growth of zircon and by crystallization of accessory minerals which replace biotite. These include titanite and allanite. The latter overgrows and engulfs zircon grains.

II. Hydrothermal phases. Introduced hydrothermal mineralizing solutions followed fracturing and caused interactions between already formed minerals, further growth and alteration of primary minerals along fractures, and crystallization of chlorite, muscovite, serpentine, pyrite, molybdenite, chalcopyrite, galena, hydroxyl-bastnaesite, thorobastnaesite, Fe-rich silicate crusts and complex U-, Th-, REE, Zr-bearing compounds in rims on radioactive minerals and in fractures. Redistribution of alkalis and myrmekitic and albitic overgrowths are also related to this phase.

III. Supergene or weathering phases. These involved further hydration and alteration of minerals leading to leaching, transportation and reprecipitation of mobilized radionuclides, REE and other ions as coatings on minerals and rocks exposed to surface weathering.

Mineralized pegmatities associated with quartzite and with oxidized pyrite-bearing gneisses south of Beaudette Creek (Fig. 6.1e, f; 6.4; 6.5a, f; and 6.7a)

Mineralized pegmatites south of Beaudette Creek and north of JMV-1 prospect are poorly exposed on the northern slope of the hill as bands in quartzite (Fig. 6.1e, f) and adjacent to pyrite-bearing biotite gneisses (Fig. 3.2a, b in Rimsaite, 1982a). The pegmatite bands vary in width from a few centimetres to a few metres, and because of their hardness and better resistance to weathering and erosion than the surrounding paragneisses, the pegmatites stand out as ridges or form step-like slopes on hillsides.

Grey impure quartzite which hosts radioactive pegmatite contains 89% SiO_2, 4% Al_2O_3, 0.1% Na_2O, 1.6 K_2O, 0.6% TiO_2, 3.2 ppm U and 13 ppm Th. The adjacent silica-rich pegmatite contains 230 ppm U and 472 ppm Th (see Table 3.1, analysis 28 in Rimsaite, 1982a). The granite pegmatite is made up of abundant quartz, antiperthite which is veined by barite, and biotite which is partly replaced by muscovite. The high concentration of silica in this pegmatite (80 per cent) apparently reflects its affinity to the host quartzite.

Radioactivity increases at the contact between the pegmatite and its host rock and in mica bands (Fig. 6.1e, f). Biotite contains inclusions of uranothorite, uraninite which in turn contains inclusions of molybdenite rimmed by galena, titanite and elongated crystals of zircon which has crystallized along the boundary between biotite and muscovite (Fig. 6.4a, b, c, d). Poikilitic textures, resulting from porphyroblastic and recurring growth of minerals, fracturing and alterations along fractures are common features in this area. Some examples include (1) zoned zircon grains which have engulfed three crystals of apatite; (2) uraninite which is partly replaced by thorian and iron-rich phases; and (3) feldspars stained red by iron oxides filling fractures. Radionuclides mobilized during alteration of radioactive minerals also reprecipitated in fractures. EDS analysis (not shown here) has indicated that crusts filling fractures in biotite contain U and Th; rims on uranothorite are heterogeneous and consist of Th, Si, Fe, Zr, Pb phase in the inner portion of the rim and of Fe, Si, Y, Th, Pb phase in the outer portion of the rim. Titanite contains some Nb.

This granite pegmatite contains a complex association of primary and secondary minerals, namely: quartz, antiperthite, biotite, muscovite, titanite, apatite, uraninite, uranothorite, zircon, molybdenite, galena, barite, iron oxides and chemically complex uraniferous crusts filling fractures and interstices.

Two radioactive pegmatites associated with pyrite-bearing biotite gneisses have been cleared from debris by bulldozing. One pegmatite is migmatitic, adjacent to oxidized gneiss and contains 62 ppm U and 31 ppm Th. The other pegmatite is about 50 m north down the slope from the migmatitic pegmatite. It is strongly radioactive and contains 2580 ppm U and 608 ppm Th. The size and extent of the radioactive occurrences on the slope of the hill cannot be estimated because only small areas have been cleared from surficial materials.

Chemical analyses of the rusty pyrite-bearing gneiss and of the strongly radioactive mica pegmatite are given in Table 3.1, analyses 25 and 27 in Rimsaite, 1982a. The pegmatite contains primary and secondary radioactive minerals in biotite bands and in epidote which fills fractures in plagioclase (see Fig. 3.2a, b and also 3.3 a-e in Rimsaite, 1982a). Mineralogy of the pegmatites in this area is similar, but proportions of quartz, of potassic and sodic feldspars, of radioactive minerals and of oxidation products are different. Oxidized pyrite and chalcopyrite liberated sulphur, iron and copper which precipitated in fractures and on the surface as yellow coatings of native sulphur, as hematite and goethite in fractures of pyrite, as jarosite in altered biotite, and as blue and green coatings of azurite and malachite on chalcopyrite (Fig. 6.5f-h; see also Fig. 38.6b and Fig. 38.8c in Rimsaite, 1982b). Iron-rich rims on uraninite, coatings of galena on zircon, and chemically complex crusts filling fractures in biotite and feldspar (Fig. 6.5a-f and Fig. 6.7a; see also Fig. 3.4 in Rimsaite, 1983a) probably formed during the hydrothermal stage. The complex association of primary and secondary minerals suggests the following sequence of crystallization: plagioclase and biotite, followed by fracturing, then epidote in plagioclase fractures, followed by uraninite-ilmenite intergrowths in epidote; then Fe-rich rims and radioactive fracture fillings in biotite and in other minerals, then crystallization of sulphides and alteration of primary minerals during hydrothermal stages and finally supergene reactions resulting in oxidation of sulphides and crystallization of hematite, goethite, jarosite, native sulphur, malachite and azurite. Biotite flakes overgrown by secondary uranyl-bearing mineral aggregates, titanite and barrel-shaped zircon grains were concentrated for isotope analyses (Fig. 6.5a; 6.7a).

Mineralized migmatites along base lines 1 and 3 in properties formerly owned by Canadian Johns Manville Company (Fig. 6.6; analyses 13, 14 in Table 6.1; analyses 9-12 in Table 6.2)

A contact rock between pyrite-bearing hornblende – biotite gneiss and microcline pegmatite (analysis 13, Table 6.1) was collected on a southern slope of the hill between Beaudette Creek and Patibre Lake. The harder pegmatite layers form steps in softer gneissic phases which are susceptible to alteration and erosion. The radioactive contact zone consists of medium grained altered plagioclase, biotite, brown hornblende and quartz which grade to coarse grained, porphyroblastic microcline. This zone is enriched in radioactive and accessory minerals, notably uraninite, Fe-poor titanite, apatite and a few grains of galena,

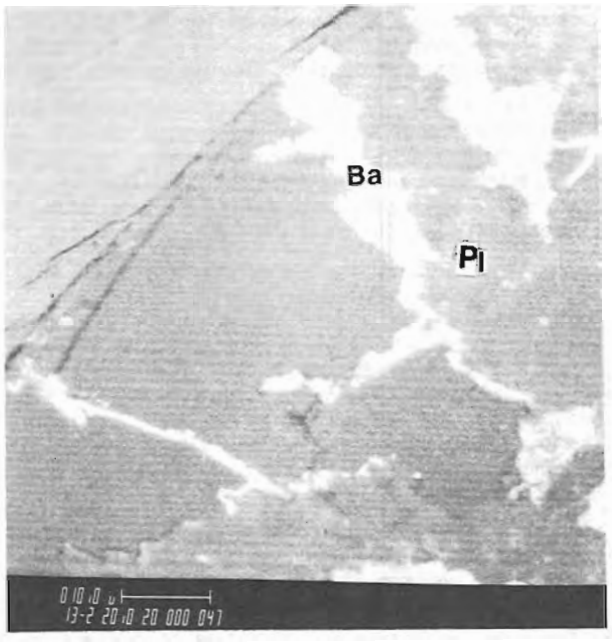

c

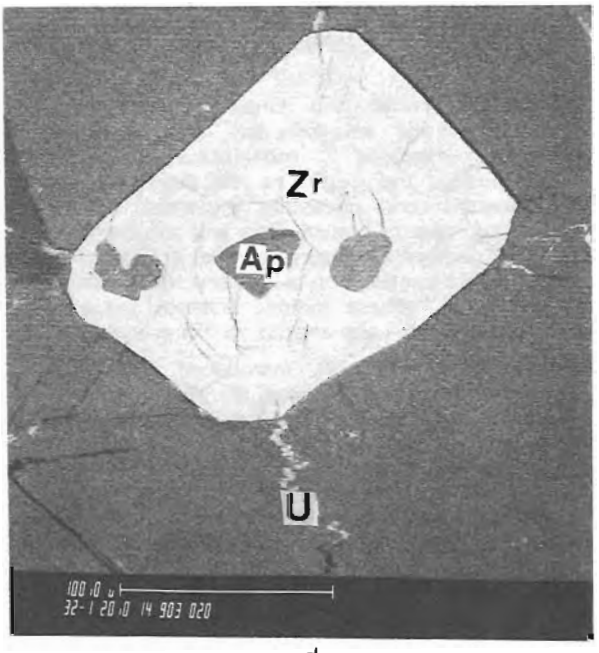

d

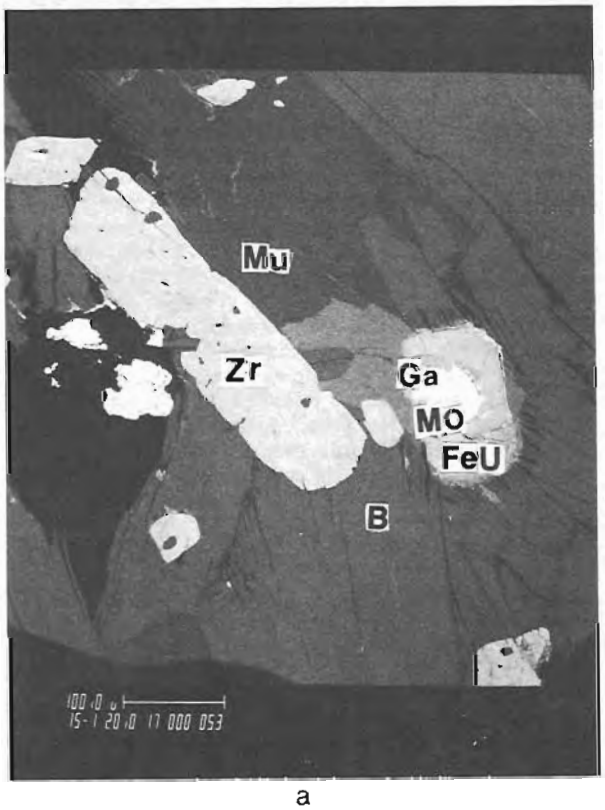

a

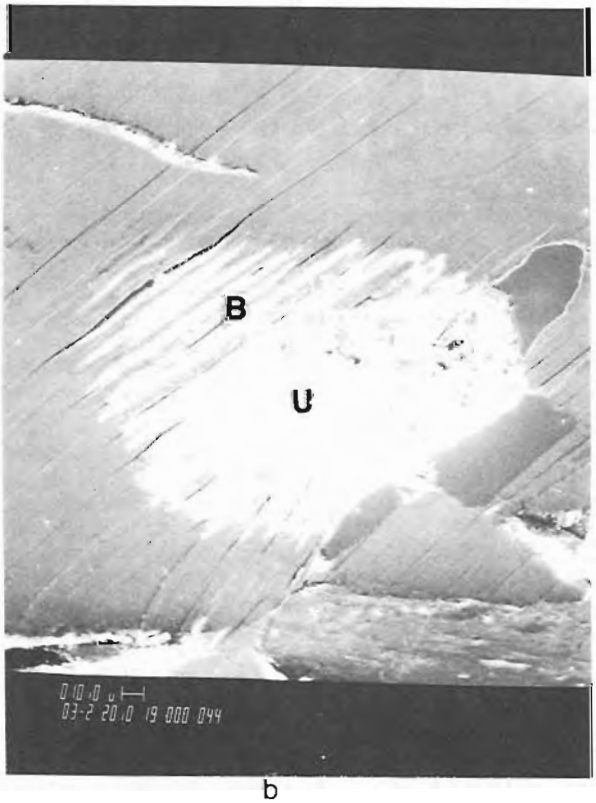

b

a. *BEI of a complex mineral association at the boundary between biotite (B) and muscovite (Mu): Zircon (Zr), uraninite, partly replaced by Fe-rich phase (Fe, U) with inclusion of molybdenite (Mo) overgrown by galena (Ga).*

b. *SEI (secondary electron image) of uraninite (U) in biotite (B). Biotite has exfoliated adjacent to uraninite. Fractures in micas are filled with Fe-rich and U-rich mineral aggregates.*

c. *BEI of barite (Ba) in fractures of plagioclase (P).*

d. *BEI of zoned zircon (Zr, white) which as overgrown three apatite grains (Ap, grey). Fractures filled with secondary uraniferous and Fe-rich mineral aggregates (U) radiate from the zircon grain.*

Figure 6.4. *Associations of radioactive and accessory minerals and of mobilized radionuclides and other ions which precipitated in fractures of radioactive pegmatite in Figure 6.1e. (GSC 203724)*

pyrite and zircon. Fractures filled with uranophane which is associated with iron oxides, uranophane overgrowths on uraninite, titanite and biotite, and various types of altered uraninite are the characteristic features of these migmatites and provide mineralogical and petrographic evidence of a complex history of mineralization (Fig. 6.6 and see also Fig. 3A-F in Rimsaite, 1982d). Scanning electron micrographs illustrate resorption and further healing and overgrowths of altered uraninite and replacement of galena by Ca-sulphate (Fig. 6a, h). The apparently older, rounded and fractured patches of uraninite have been partly healed and overgrown by a more compact uraninite phase, thus resembling several phases and overgrowths in heterogeneous zircon (Rimsaite, 1981). Some grains of uraninite have been corroded, leached and partly replaced by silicates and Fe-rich uraniferous phases (Fig. 6.6b, g) which produced "transparent uraninites" described by Tremblay (1974). Fractured remnants of uraninite (Fig. 6.6a) may represent detrital grains; healed and euhedral grains are pegmatitic; uranophane overgrowths on uraninite probably formed during hydrothermal stage, whereas thin radioactive coatings on fractured titanite and on biotite flakes (Fig. 6.6h, i) probably formed during hydrothermal phase and continued growing in a weathering environment. Two types of uranophane, one (Fig. 6.6c, d) relatively coarse grained, compact and having higher Pb content is apparently older; the other, Pb-poor

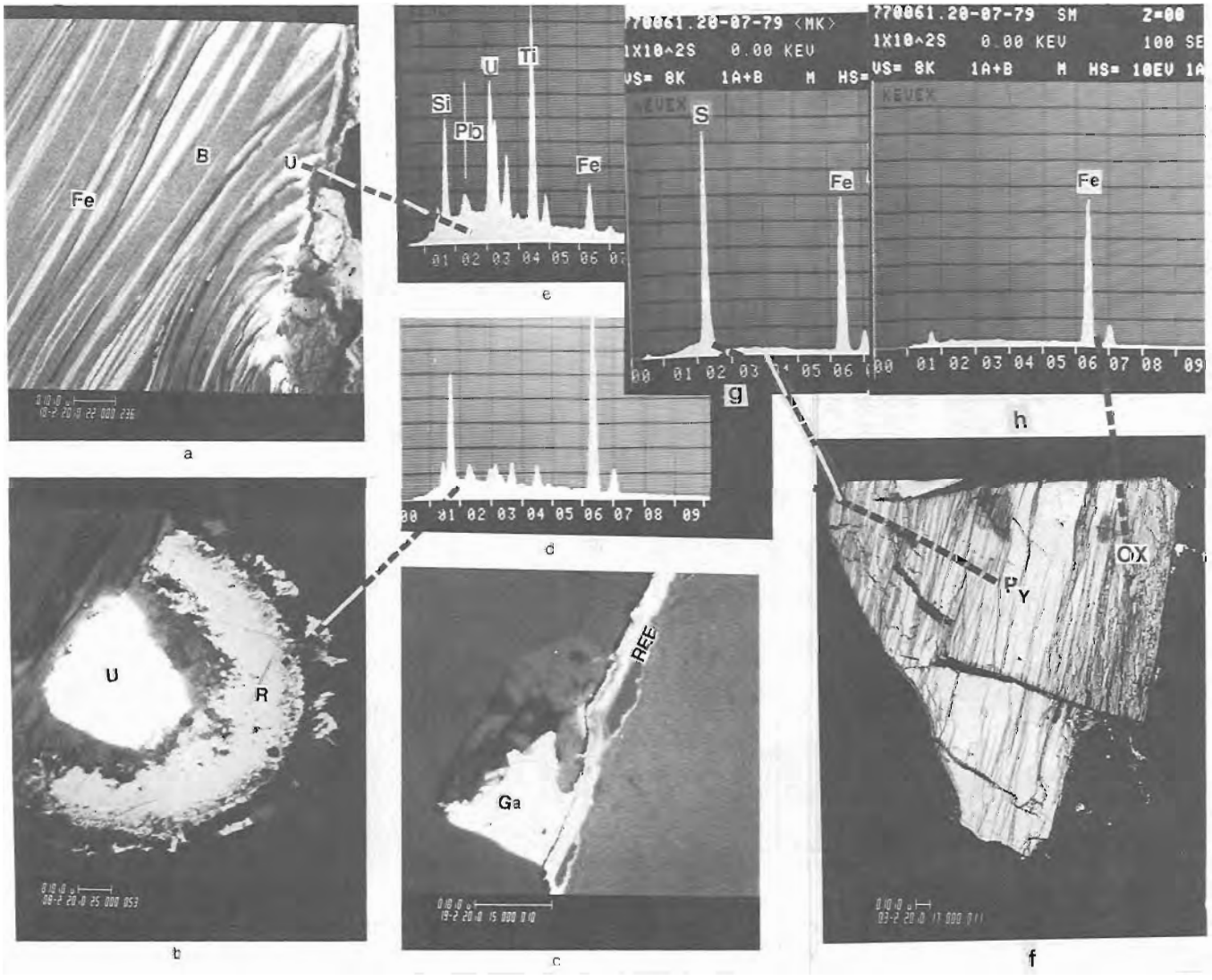

a. BEI of fractured biotite (R) with Fe-rich and U-bearing mineral aggregates (U) in its (001) fractures.

b. BEI of uraninite (U) which is surrounded by Fe-rich rim (R). The uraninite is the same as that in Figure 6.2.

c. BEI of galena (Ga, white) and REE-bearing mineral aggregates which migrated and precipitated along intergranular fractures.

d. EDS of chemically complex Fe-rich rim in (b): Fe > S > Al = Th, U, Ca, Ti.

e. EDS of Ti-U-rich crusts in biotite fractures in (a): Ti > U > Si > Ca > Fe > Pb.

f. BEI of oxidized pyrite (Py, white) with dark oxidized bands (OX) along fractures.

g. EDS of pyrite in (f): S > Fe.

h. EDS of iron oxide in (f): Fe.

Figure 6.5. *Examples of oxidation and migration of liberated radionuclides and associated REE and Fe along fractures. (GSC 203532, 203724)*

fluffy and soft is probably younger and supergene thus suggesting different environments of crystallization and age for these uranophane aggregates.

Fresh portions of uraninite contain relatively high concentration of Th (9.3%) and are slightly contaminated with Fe and Si. Iron, Ti, Si and Ca commonly replace altered grains of uraninite under supergene conditions of weathering and alteration; however, assuming possible detrital origin of some uraninite remnants, part of Fe, Si and Ca could have been present in these uraninites before recent supergene alteration (analyses 9 to 12 in Table 6.2).

Hornblende at the contact is brown (dehydrated?) but is green away from the contact. This apparently dehydrated hornblende and relatively high Th content in uraninite suggest an elevated temperature at the contact. On the other hand, presence of Th as a thorite phase which replaced uraninite along fractures in association with Fe-rich silicate rims (Fig. 6.3f) suggests their crystallization after fracturing at a lower temperature, probably during the hydrothermal stage. The presence of abundant uranophane accounts for a U/Th ratio of >5 in this contact zone between pegmatite and migmatite.

The other migmatite (analysis 14, Table 6.1) which is enclosed in, and thus older than the pegmatite, has only 54 ppm U. The migmatite contains abundant accessory minerals which have been described in section 1. Barren quartz-tourmaline and muscovite-sillimanite-bearing leucocratic pegmatites outcrop west and north of the radioactive migmatite.

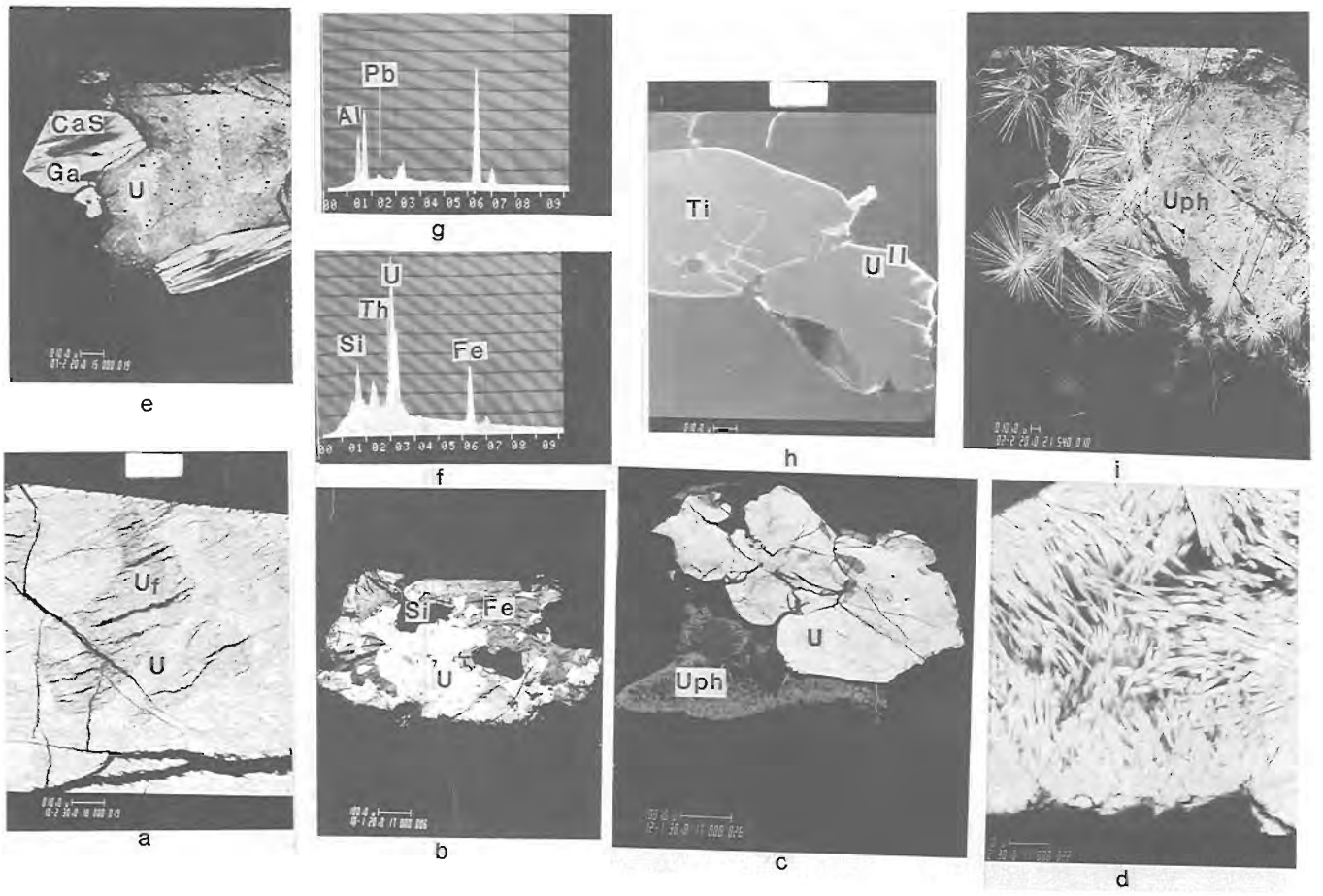

a. BEI of fractured and mottled uraninite (U) with irregular patches of apparently older grey uraninite which is traversed by parallel fractures (Uf).

b. BEI of uraninite remnants (U, white) in a grain which is partly replaced by silicates (Si) and Fe-rich phase (Fe).

c. BEI of fractured uraninite (U) which has been overgrown by uranophane (Uph).

d. BEI of uranophane, enlarged from (c).

e. BEI of mottled uraninite (U) with adhering grains of galena (Ga) which has been replaced by Ca sulphate in the centre (CaS, black).

f. EDS of Fe-rich phases which have partly replaced uraninite in (b).

g. EDS of Fe-rich silicate which has invaded uraninite in (b).

h. BEI of fractured titanite (Ti) with bright rims and crusts in fractures which have formed by precipitating secondary uranium minerals (U^{II}).

i. BEI of radiating needles of uranophane (white) which crystallized as thin films and mat-like coatings on biotite flakes.

Figure 6.6. *Examples of uraninite and of its alteration products in mineralized migmatite, locality JMV-1. See Table 6.1 analyses 13 and 14 and Table 6.2, analyses 9-12 for chemical composition of minerals and of the host rock. (GSC 203577-R, 203414-G).*

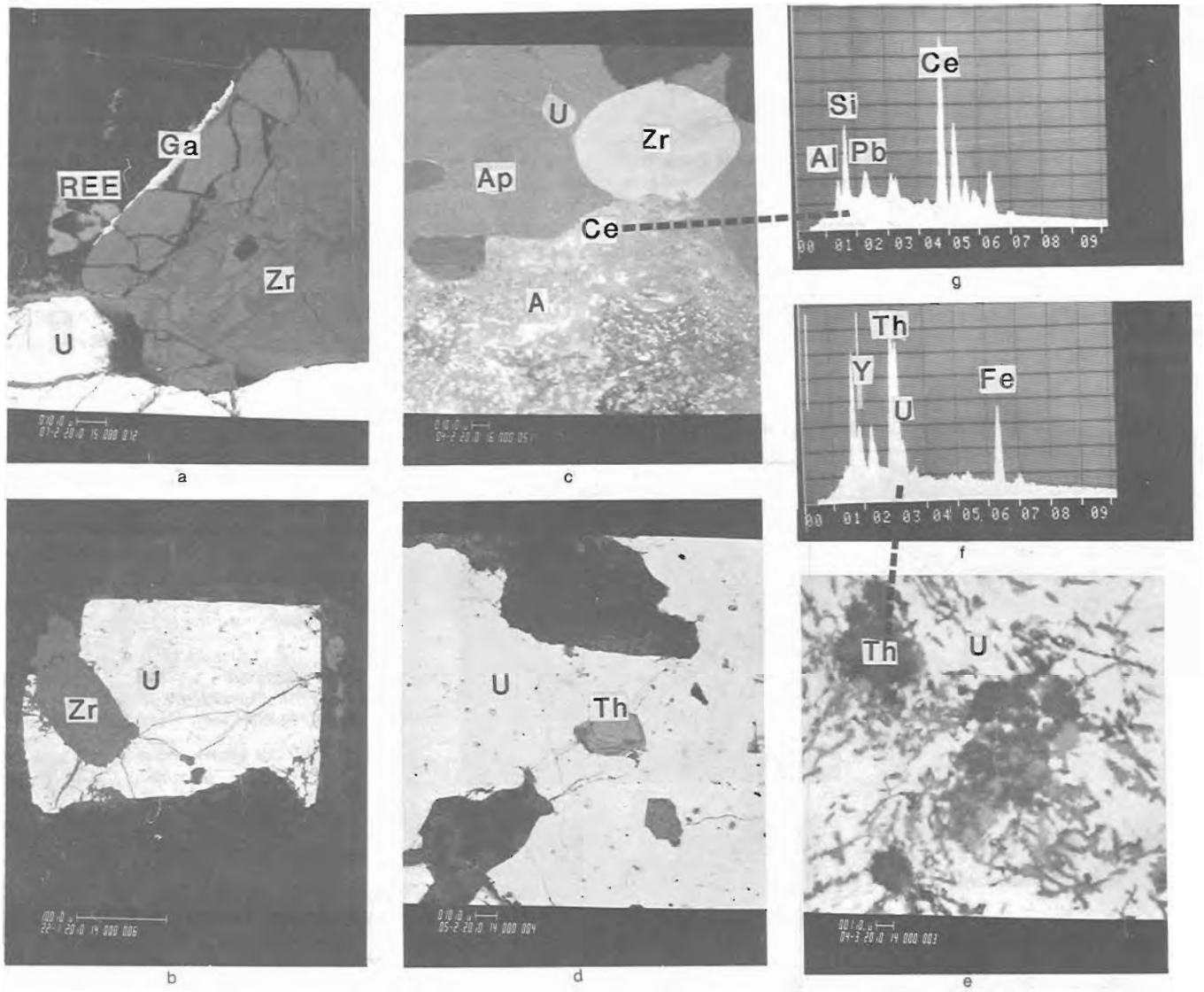

a. *BEI of uraninite (U) which has overgrown zircon (Zr). The fractured zircon consists of darker (altered, softer) and lighter grey (fresh, hard) phases and contains white rim of galena (Ga) and adhering REE-bearing specks (REE).*

b. *BEI of uraninite (U) with enclosed zircon (Zr).*

c. *BEI of mineral association: allanite (A), apatite (Ap), uraninite (U) and zircon (Zr). The allanite is altered and coated with small Ce-rich specks (Ce).*

d. *BEI of uraninite with inclusions of uranothorite (Th).*

e. *BEI of heterogeneous uraninite at high magnification. It has a pitted appearance and consists of fresh Pb-bearing uraninite (U, white) and of Th-bearing chemically complex phase (Th, dark grey).*

f. *EDS of Th-bearing phase in uraninite in (e): Th > Si > Fe > Pb = Y > U.*

g. *EDS of Ce-rich specks on allanite in (c): Ce > Si > Fe > Pb > U = Al.*

Figure 6.7. *Showing mineral associations in locality TDN-2. See Figure 6.1d, h for distribution of radioactive minerals in these rocks. (GSC 203755-N).*

Pegmatites associated with mafic skarn and with biotite gneisses between Patibre Lake and Tom Dick Creek
(Fig. 6.1c, d, g, h; 6.2a-e; 6.5b, c, d; 6.7b-g; 6.8; analyses 15-17 in Table 6.1; analyses 13-21 in Table 6.2)

Prospects with numerous scattered radioactive occurrences in white pegmatites between Patibre Lake and Tom Dick Creek belong to Mont-Laurier Uranium Mines Ltd. Two examples illustrate the mineralogy of this area: (1) radioactive pegmatites adjacent to mafic skarn and (2) a white heterogeneous pegmatite adjacent to biotite gneiss, approximately 500 m from the exposed mafic skarn.

In the occurrence adjacent to skarn a band of biotite gneiss is also present, and within a distance of about 20 m the rocks display the following changes from the mafic skarn towards the radioactive pegmatite. Mafic skarn contains only 0.3 ppm U and 3 ppm Th. It consists mainly of calcic amphibole and calcite. Towards the pegmatite, mafic skarns grade into a green, granular, diopside-rich rock which contains interstitial scapolite and metasomatic phlogopite, and slightly more U (4.5 ppm) and Th (16 ppm). Adjacent gneissic bands containing from 12 ppm to 22 ppm U and from 60 to 80 ppm Th grade into porphyroblastic microcline pegmatites which contain from 76 ppm to 153 ppm U and from 69 ppm to 171 ppm Th. These pegmatites contain remnants of older (paleosome) plagioclase-biotite-bearing phases, locally with scattered zircon grains (Fig. 6.2c). Plagioclase grains are overgrown by albite and clouded by fine grained sericite and other speckled alteration products which locally recrystallize to coarse muscovite patches. Biotite flakes are recrystallized and contain inclusions of allanite, apatite, titanite, uraninite, uranothorite and zircon. Microcline porphyroblasts and veinlets of quartz (neosome) replace and engulf older minerals. Proportions of paleosome and neosome phases vary within less than 1 metre. The pegmatites locally contain remnants of pyroxene-bearing xenoliths surrounded by titanite and apatite which are overgrown by allanite. Allanite overgrows REE-poor, epidote-like cores, titanite, apatite and zircon, and locally replaces biotite and remnant pyroxene, reaching 1 cm in size (Fig. 6.1c, d). Allanite is metamict, overgrown by radioactive and REE-rich rims and it is commonly altered to poorly crystallized aggregates of hydroxyl-bastnaesite group minerals (Fig. 6.2b-e; 6.5b, c, d; 6.7c, g). Allanites from all radioactive occurrences north of

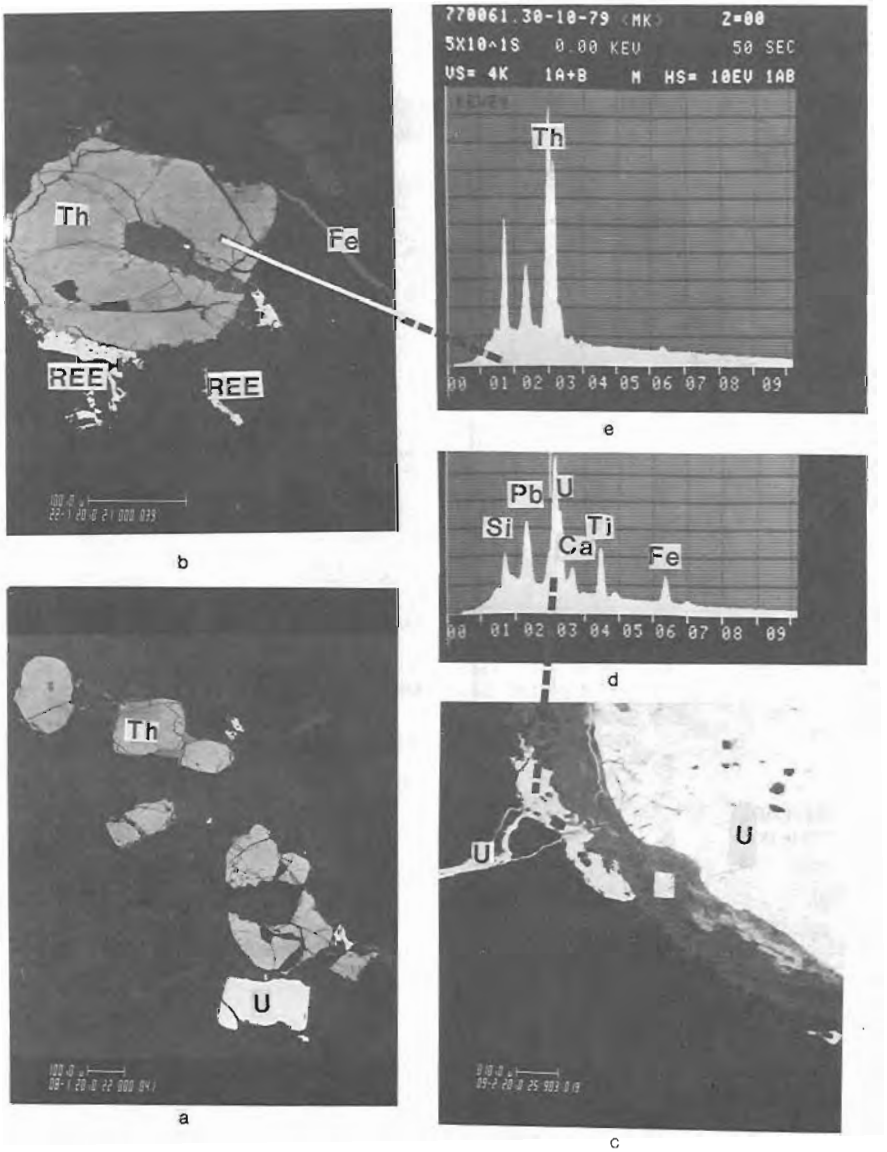

a. BEI of disseminated grains of uranothorite (Th, grey) and of one crystal of uraninite (U, white).

b. BEI of uranothorite (Th) with a REE-rich rim (REE). Unidentified Fe and REE minerals have also precipitated in fractures (REE, white; Fe, grey).

c. BEI of uraninite (U) with a heterogeneous rim (R, grey). Outermost uraniferous portion of the rim extended into fractures (U, white).

d. EDS of the uraniferous portions of the rim on uraninite in (c): U > Pb > Ti > Si = Ca, Fe.

e. EDS of uranothorite in (b): Th > Si > Pb, U.

Figure 6.8. *Illustrations of radioactive minerals from white pegmatite in locality TDN-2. See Table 6.1, analyses 16, 17, for chemical composition of pegmatite and Table 6.2, analyses 13-21 for chemical composition of minerals (GSC 203755-I).*

Mont-Laurier are altered and metamict. Zdorik et al. (1964) who studied allanites from carbonatites and albitites, postulated that metasomatic allanites which have crystallized at low temperature in fractures retained their crystal structure whereas allanites which have crystallized at elevated temperatures became metamict.

Unlike coarse grained hexagonal bastnaesite (1 to 6 mm plates) from hydrothermal REE-occurrences described in the literature (Gerasimovskyi, 1964), fine grained aggregates of hydroxyl-bastnaesite group minerals which replace allanite in the area north of Mont-Laurier are poorly crystallized and amorphous, similar to poorly crystallized bastnaesites described by Sverdrup et al. (1959).

The allanite-rich pegmatite is fractured and veined by galena and REE-bearing mineral aggregates (Fig. 6.5c). Chemical composition, and rock-forming minerals of allanite-rich pegmatite are almost identical to those of adjacent uraninite-rich pegmatite which contains 1120 ppm U and 278 ppm Th (analysis 15 in Table 6.1; analysis 26 in Table 3.1 in Rimsaite, 1982a). The strongly radioactive portion of the pegmatite contains porphyroblastic uraninite grains which have engulfed zircon and uranothorite, and which in turn have been locally replaced by Fe-Th-bearing phases (Fig. 6.1g, h; 6.7b, d, e, f). Uraninite grains have crystallized at the contact between paleosome and neosome phases in biotite which has been partly replaced by muscovite.

Some white heterogeneous pegmatites have been cleared from glacial and alluvial cover by bulldozing. The cleared pegmatites vary in size from a few metres to 150 m in length and 70 m in width. Within a distance of a few centimetres, radioactive pegmatites vary in texture, grain size, proportion of older plagioclase-bearing phase clouded by alteration, in size and abundance of xenoliths, in clear neosome phases which consist of porphyroblastic microcline, quartz and recrystallized biotite, and in radioactivity. Uranium mineralization commonly occurs at the contact between paleosome and neosome phases, in biotite and in adjacent quartz. Roughly parallel bands of recrystallized biotite, veined by fractured quartz, contain crystals of uraninite and uranothorite surrounded by prominent heterogeneous rims (Fig. 6.2a). Depending on proportions of older plagioclase and newly formed albite rims on plagioclase, of microcline and quartz, concentrations of major constituents vary particularly the proportions of Na and K. Specimens from mineralized spots contain from 70 ppm to 400 ppm U and 200 ppm Th (analyses 16 and 17, Table 6.1).

Accessory minerals have also crystallized preferentially at the contact between paleosome and neosome phases, commonly in biotite. In biotite, apatite has crystallized adjacent to quartz, and zircon adjacent to microcline. Several morphological types of zircon are present: small composite and fragmented rounded grains stained red by iron oxide crusts. These were probably derived from a sediment. Clear slender prisms and coarse grained, barrel-shaped cyrtolite grains which are zoned and have enclosed older zircons and other minerals are typically pegmatitic. Because of the presence of coarse grained zircons, pegmatites commonly contain ten times more zirconium than the enclosing country rocks. Other accessory minerals include titanite, pyrite, allanite and molybdenite.

Uraninite and uranothorite are heterogeneous. They contain inclusions, chemically complex rims and differ in extent and degree of alteration (analyses 14-18, Table 6.2).

Uraninite from fine to medium grained partly reworked xenolith contains less Th (6.6%) than uraninite from coarse pegmatitic phases (9.3% Th; analysis 17, Table 6.2; and see analysis 9, Table 3.1 in Rimsaite, 1983a).

Uranothorite grains contain U-rich patches and are overgrown by heterogeneous rims which locally contain 63% of light REE and 1.5% yttrium (see analysis 19, Table 3.2 in Rimsaite, 1983a). Iron- and REE-rich rims on uraninite and on uranothorite extend into fractures (Fig. 6.8). Other minerals filling fractures include hematite, goethite, molybdenite, galena, U-Pb-rich crusts, U-Th-Ti-bearing compounds and prehnite filling fractures in biotite. Alteration and replacement of minerals (such as of plagioclase by muscovite, sericite and calcite; of biotite by chlorite, muscovite and prehnite), crystallization of complex mineral aggregates in fractures and rims on radioactive minerals; and reactions between adjacent minerals, such as thorite and zircon (analyses 20 and 21, Table 6.2) took place during hydrothermal stage in areas which have been permeable to hydrothermal solutions.

Note on isotopic data in Table 6.3

Zircon concentrates from a block of migmatite enclosed in pegmatite, represent the following types: red, fragmented grains stained by Fe-oxides (zircon 1); average concentrate (zircon 2) and clear slender prisms (zircon 3) which are similar to those illustrated previously in Figure 11.1b in Rimsaite (1983b). Concentrate (zircon 4) represents barrel-shaped crystals from pegmatite, some probably coated with thin films of sulphides as in Figure 6.7a. Specimens 5 and 6 represent titanite and biotite concentrates which are coated with secondary uranium minerals. Most of these specimens were contaminated with minute inclusions and impurities stuck to their surfaces and fractures which is apparent from high proportions of common lead. Consequently only apparent ages calculated from their $^{207}Pb/^{206}Pb$ ratios are considered as meaningful and merit a short discussion. Barrel-shaped zircon grains yielded the oldest apparent age of 1053 Ma, followed by radioactive mineral aggregates filling fractures in biotite from pegmatite H-50 (1032 Ma); average zircon concentrate from migmatite yielded 1013 Ma and clear prismatic zircon 983 Ma. Fragmented and stained zircon, believed to be of detrital sedimentary origin, apparently lost much of its radiogenic lead and yielded a relatively low apparent age of 852 Ma. The youngest apparent age of 821 Ma was obtained on titanite coated with secondary uranium minerals and contaminated with 84% common lead. This attempt to date (1) zircons from migmatite some of which could represent detrital zircons in the original sediment, (2) zoned metamorphic and hybrid zircons which consist of anisotropic core and isotropic rims, and (3) clear pegmatitic prismatic and barrel-shaped zircons, as well as (4) secondary uranium minerals representing mobilization and redeposition of leached uranium, should be continued. Isotope studies using acid-washed concentrates to remove surface impurities, and/or ion probe studies on selected parts of a single grain would aid in providing time limitations to the ages of sedimentation, metamorphism, pegmatitic and hydrothermal activity and subsequent migration and reprecipitation of liberated radionuclides in fractures.

Summary and conclusions

Twenty mineral occurrences were examined in a 26 km by 15 km radioactive belt north of Mont-Laurier, Quebec. The belt extends in northerly direction east of Lievre River; north of Patibre Lake it continues in an easterly direction. Uranium mineralization occurs in a few centimetres wide contact zone between microcline pegmatite and the following gneisses of La Force Formation: (1) impure metaquartzite (U = 230 ppm; Th = 472 ppm), (2) pyrite-bearing biotite and

biotite-hornblende paragneisses (U = 5000 ppm; Th = 845 ppm), (3) mafic skarn (contact zone contains abundant allanite, U = 98 ppm; Th = 171 ppm), (4) mafic skarn and biotite paragneiss (1120 ppm U; 278 ppm Th); and (5) white heterogeneous pegmatites containing scattered radioactive spots or bands, commonly at the contact between paleosome and neosome phases, along xenoliths and in biotite (U ranges between 70 ppm and 2580 ppm; Th between 200 and 610 ppm).

Some occurrences contain abundant secondary uranyl-bearing mineral aggregates which in part account for a U/Th ratio of 5 or greater. In contrast, some oxidized and altered pegmatites contain low U/Th ratio resulting from destruction of uraninite and other U minerals and removal of the leached uranium.

Mineralized and barren granitoid rocks are similar in their chemical composition, but their textures, petrography and mineral associations provide more useful criteria for predicting zones for mineralization, notably along contacts between neosome and paleosome phases and between mafic rocks and microcline pegmatites.

The occurrences studied are made up of detrital-sedimentary, metamorphic, pegmatitic, hydrothermal and supergene minerals. Examples of selected associations of primary and secondary minerals in mineralized gneissic pegmatite, in a contact zone between hornblende-biotite paragneiss and microcline pegmatite, in high grade portions of a heterogeneous pegmatite and in an oxidized pegmatite are as follows:

1. uraninite, uranothorite, secondary radioactive and REE-bearing mineral aggregates, zircon, apatite, allanite, hydroxyl-bastnaesite, biotite, chlorite, feldspar, quartz;
2. uraninite, uranothorite, uranophane, hematite, goethite, titanite, apatite, zircon, biotite, hornblende, microcline, altered plagioclase, albite, quartz;
3. uraninite, uranothorite, ilmenite, titanite, cyrtolite, apatite, allanite, secondary uranothorite, thorobastnaesite, hydroxyl-bastnaesite, molybdenite, galena, pyrite, chalcopyrite, biotite, muscovite, prehnite, chlorite, gypsum, calcite, barite, epidote, malachite, azurite, feldspars, quartz;
4. U-free thorite, thorogummite, chemically complex U-Th-Ti-Zr-bearing crusts in biotite fractures, hematite, goethite, jarosite, biotite, chlorite, microcline, quartz, altered plagioclase, sericite.

Preliminary isotope studies of zircons and of secondary uranium-bearing mineral aggregates filling fractures in biotite and titanite indicated a spread of apparent $^{207}Pb/^{206}Pb$ ages between 1053 Ma (barrel-shaped pegmatitic zircon) and 821 Ma (secondary U-bearing mineral aggregates on titanite). Further isotope studies are warranted to determine limits to the ages of sedimentation, metamorphism, pegmatitic and hydrothermal activities and supergene alterations.

References

Gerasimovskyi, V.V.
1964: Bastnaesite and parisite from northern Pribaikal; Academy of Sciences of U.S.S.R., Mineralogical Museum, Transactions no. 15, p. 194-202.

Kish, L.
1977: Patibre (Axe) Lake area; Preliminary Report; Ministère des Richesses Naturelles, Service des Gites Mineraux, DPV-487, 13 p. and geological map 1:20 000 of DPV-487.

Rimsaite, J.
1978: Mineralogy of radioactive occurrences in the Grenville structural province, Ontario and Quebec; a preliminary report; in Current Research, Part B, Geological Survey of Canada, Paper 78-1B, p. 49-58.

1981: Isotope, scanning electron microscope and energy dispersive spectrometer studies of heterogeneous zircons from radioactive granite in the Grenville structural province, Quebec and Ontario; in Current Research, Part B, Geological Survey of Canada, Paper 81-1B, p. 25-35.

1982a: Mineralogical and petrochemical properties of heterogeneous granitoid rocks from radioactive occurrences in the Grenville structural province, Ontario and Quebec; in Uranium in Granite, ed. Y.T. Maurice; Geological Survey of Canada, Paper 81-23, p. 19-30.

1982b: Mode of occurrence of secondary radionuclide-bearing minerals in natural argillized rocks: a preliminary report related to a barrier clay in nuclear waste disposal; in Current Research, Part A, Geological Survey of Canada, Paper 82-1A, p. 247-259.

1982c: The leaching of radionuclides and other ions during alteration and replacement of accessory minerals in radioactive rocks; in Current Research, Part B, Geological Survey of Canada, Paper 82-1B, p. 253-266.

1982d: Alteration of radioactive minerals in granite and related secondary uranium mineralizations; in Ore Genesis – The State of the Art, ed. G.C. Amstutz, et al.; Springer Verlag, Berlin, Heidelberg, New York, p. 269-280.

1983a: Selected mineral associations in radioactive occurrences in the Grenville structural province: a progress report; in Current Research, Part B, Geological Survey of Canada, Paper 83-1B, p. 23-37.

1983b: Mineralogical, petrochemical and petrographic-textural studies of ore grade and lower grade radioactive rocks from the Bancroft area, Ontario; in Current Research, Part B, Geological Survey of Canada, Paper 83-1B, p. 93-108.

Sverdrup, T.L., Bryn, K.O., and Saebo, P.C.
1959: Contributions to the mineralogy of Norway: No. 2 bastnaesite, a new mineral for Norway ; Norsk Geologisk Tidsskrift, v. 39, p. 237-247.

Tremblay, P.
1974: Mineralogy and geochemistry of the radioactive pegmatites of the Mont-Laurier area, Quebec; unpublihsed M.Sc. thesis, Queen's University, Kingston, Ontario, 133 p.

Zdorik, T.B., Kupriyanova, I.I., and Kumskova, N.M.
1964: Crystalline allanite from several metasomatic occurrences in Siberia; Academy of Sciences of U.S.S.R., Mineralogical Museum, Transactions, v. 15, p. 208-214.

Appendix 1

Notes on samples in Table 6.1

1. Metagabbro, away from mineralization: mainly hornblende grains ranging in size from 20 µm to 500 µm and biotite in a groundmass of plagioclase. Abundant apatite, magnetite and titanite.
2. Mafic skarn adjacent to mineralized pegmatite "15": mainly diopside and amphibole and a few grains of phlogopite and titanite in a groundmass of microcline, quartz and scapolite.
3. Migmatite from Patibre Formation containing biotite and hornblende grains disseminated in, and interbanded with, a granular mosaic of plagioclase, microcline and quartz.
4. Migmatite "3" grading to porphyroblastic plagioclase-microcline pegmatite.
5. Barren pegmatitic granite: paleosome made up of altered plagioclase grains overgrown by clear rims of albite and myrmekite and a few laths of chloritized biotite engulfed in porphyroblastic microcline perthite and strained quartz.
6. Pink porphyritic granite: biotite bands, pushed aside by microcline and quartz porphyroblasts which form clear patches 1-2 cm in size giving this rock a porphyritic appearance. Pink colour is due to red iron oxides filling fractures.
7. Grey porphyritic granite, similar to "6" but has erratic distribution of biotite. Groups of clustered clear microcline and quartz grains give a porphyritic appearance to this granite. Both porphyritic granites contain the following accessory minerals (listed in decreasing order of abundance): apatite, titanite, allanite and zircon.
8. Leucocratic radioactive aplite-like portion of a white pegmatite composed of medium grained plagioclase, microcline and quartz. A few laths of biotite and enclosed radioactive minerals are altered to chlorite, thorobastnaesite (? XRD = 65522) and to secondary uranium compounds which coat fractures in micas. Pyrite veinlet, enclosed in muscovite, transects the rock.
9. Coarse grained quartz-rich portion of the pegmatite adjacent to "8".
10. Biotite flakes coated with secondary uranium minerals from biotite segregations in pegmatite associated with "8" and "9". This sample contains also 510 ppm Li and 110 ppm Cs.
11. Biotite concentrate prepared from a biotite-rich xenolith in "9".
12. Biotite concentrate from radioactive two-mica rock made up of plagioclase, quartz, microcline and micas. Biotite flakes contain inclusions of uraninite and uranothorite and are partly replaced by muscovite. For illustrations see Fig. 3.2a, b and 3.3a, b, c, d in Rimsaite, 1982a.
13. Mineralized migmatite at the contact between biotite-hornblende gneiss and microcline pegmatite. The contact zone contains abundant accessory minerals: apatite, titanite, allanite, uraninite, uranothorite, secondary uranium minerals and zircon. For analyses of radioactive minerals see Table 6.2, analyses 9-12.
14. Migmatite at the contact between biotite schist and microcline, plagioclase, quartz pegmatite. Accessory minerals at the contact include allanite, titanite, apatite, zircon and uraninite.
15. Radioactive pegmatite made up mainly of microcline perthite, quartz, remnant plagioclase and biotite, and very large zoned crystals of allanite. Allanite grows on titanite and epidote. Allanite has been partly replaced by poorly crystallized aggregates of bastnaesite – hydroxyl-bastnaesite series (XRD = 65534). Small grains of uraninite and of uranothorite enclosed in prominent rims, crystallize in biotite, along the edges of allanite and/or in fractures and interstices between paleosome plagioclase and neosome quartz.
16. Microcline-rich portion of pegmatite "17" made up of altered plagioclase, two generations of microcline (one perthitic with plagioclase inclusions, the other fine-grained interstitial), strained quartz and biotite. Biotite contains inclusions of allanite and disseminated grains of uraninite. Plagioclase alters to speckled aggregates (clay) and to sericite-muscovite.
17. Coarse grained portion of pegmatite associated with "16". Altered plagioclase grains have clear rims of albite and myrmekite. Porphyroblastic microcline and quartz push aside biotite flakes into elongated bands. The biotite is partly replaced along (001) fractures by prehnite (XRD = 65533).
18. Radioactive rocks northeast of Mont-Laurier, south of H-50. Titanite-rich contact between metagabbro and granite. Other accessory minerals include allanite, apatite and magnetite. In addition, this rock contains 0.2% Ce and 0.1% La.
19. Biotite concentrate from microcline pegmatite H-50. Biotite flakes are slightly altered to chlorite. Crusts of secondary uranium minerals crystallize in biotite fractures and account for 1120 ppm U. Thorite inclusions in biotite are U-free. For chemical composition of radioactive minerals see Table 3.1, analyses 13-16 in Rimsaite, 1983a.

Appendix 2

Notes on analyzed spots in Table 6.2

Minerals from sampling locality PP-2 (1-8, Fig. 6.3).

1. Altered biotite adjacent to enclosed uraninite grain in (2).
2. Fresh portions of uraninite.
3. Thorite (Th, Si) in fractures of uraninite.
4. Iron-Si-Pb-rich rim on uraninite.
5. Uranium-Zr-bearing mineral aggregates in fractures of biotite; see Fig. 3.7 f in Rimsaite, 1983a.
6. Altered REE-poor epidote-allanite; note high iron content.
7. REE-bearing portions of the rim on allanite.
8. REE-rich grain adjacent to allanite. Unidentified; X-ray lines: 2.92, 2.05, 3.93 A.

Minerals from sampling locality JMV-1 (9-12, Fig. 6.6)

9. Mottled uraninite, relatively fresh.
10. Uraninite partly replaced by Fe-Th-U-bearing phase.
11. Uraninite partly replaced by Ti-Fe-Si-bearing phase.
12. Uranophane aggregates which crystallize in fractures and as coatings on other minerals.

Minerals from sampling locality TDN-2 (13-21, Fig. 6.7, 8)

13. Biotite which hosts uraninite and uranothorite.
14. Uranothorite in biotite in (13); see analysis 19, Table 3.2 in Rimsaite, 1983a for chemical composition of REE-rich portions of the rim on this uranothorite.
15. Uranium-rich spots in uranothorite.
16. Silica-rich phases in fractures of uranothorite.
17. Uraninite.
18. Iron-rich portion of the rim on uraninite.
19. Coffinite-like mineral aggregates filling fractures in feldspar adjacent to uraninite.
20. Slightly altered zircon.
21. Iron-rich Zr-bearing patches in uranothorite.

-7-

A Rb-Sr STUDY OF GRANITOID INTRUSIVE ROCKS OF THE CAPE SMITH BELT, NORTHERN QUEBEC

Project 830029

F.C. Taylor and W.D. Loveridge
Precambrian Geology Division

Taylor, F.C. and Loveridge, W.D., A Rb-Sr study of granitoid intrusive rocks of the Cape Smith Belt, northern Quebec; in Current Research, Part A, Geological Survey of Canada, Paper 85-1A, p. 65-67, 1985.

Abstract

Rb-Sr age measurements on samples from two granitoid intrusive plutons located near the western end of the Cape Smith Belt yield the following results: Pecten Harbour pluton: isochron, age 1786 ± 14 Ma, initial ratio 0.70216 ± 0.00005, MSWD 0.06. Lanyan Lake pluton: errorchron, age 2050 ± 167 Ma, initial ratio 0.7019 ± 0.0004, MSWD 9.8. The isochron age of the Pecten Harbour pluton is considered to date the intrusive event whereas the errorchron age may reflect some incorporation of the older host rocks within the measured samples of the Lanyan Lake pluton.

Résumé

Les datations au Rb-Sr exécutées sur des échantillons prélevés dans deux plutons intrusifs granitoïdes à proximité de l'extrémité ouest de la zone de Cape Smith donnent les résultats suivants: pluton de Pecten Harbour, âge isochrone (c'est-à-dire établi d'après le diagramme isochrone) 1786 ± 14 Ma, rapport initial 0,70216 ± 0,00005, écart moyen quadratique pondéré 0,06; pluton de Lanyan Lake, âge non isochrone 2500 ± 167 Ma, rapport initial 0,7019 ± 0,0004, écart moyen quadratique pondéré 9,8. L'âge isochrone du pluton de Pecten Harbour indique théoriquement la date de l'événement intrusif, tandis que l'âge non isochrone tient compte du fait que les échantillons mesurés du pluton de Lanyan Lake contiennent peut-être des roches mères plus anciennes.

Geological setting

Although granitoid intrusive rocks are rare in the Cape Smith Belt and the Labrador Trough, small plutons of granodiorite and tonalite that intrude rocks of the former belt near its west end (Taylor, 1982; Fig. 7.1) are suitable for geochronological studies. Whereas most of the plutons, such as the one at Lanyan Lake, intrude amphibolite facies rocks, the pluton at Pecten Harbour cuts rocks in the greenschist facies. The contact between the granodiorite and the country rock at Lanyan Lake is typical of most of the intrusions in that it is gradational, but the tonalite and granodiorite pluton at Pecten Harbour clearly crosscuts the country rocks and contains inclusions of them.

Analytical procedures and results

Analytical procedures for the extraction of Rb and Sr from whole rock samples were based on those described by Wanless and Loveridge (1972). Analyses were performed on a MAT-261 solid source mass spectrometer in the multicollector mode. In this mode, the three major isotopes of strontium, ^{88}Sr, ^{87}Sr and ^{86}Sr are collected simultaneously in three separate, precisely positioned Faraday cups. ^{85}Rb is monitored and ^{84}Sr is measured for isotope dilution studies by peak switching. Isotope dilution measurements of rubidium contents are also performed in the multicollector mode with the ^{85}Rb and ^{87}Rb ion beams entering the ^{86}Sr and ^{88}Sr cups. The relative gains of the amplifiers associated with the individual cups are determined by use of a constant current source.

Analytical results are listed in Table 7.1 and displayed on an isochron diagram (Fig. 7.2). The average of 18 measurements of the $^{87}Sr/^{86}Sr$ ratio for the strontium isotopic standard NBS-987 during this period of time was 0.71025 with a standard deviation (S.D.) of 0.00004. Eleven measurements of the E and A standard (Eimer and Amend, lot 492327) yielded an average $^{87}Sr/^{86}Sr$ of 0.70804, S.D. = 0.00003.

Table 7.1. Analytical data, whole rock samples, granitic rocks north of Cape Smith Belt

Sample No.	Rb ppm	Sr ppm	$^{87}Rb/^{86}Sr$	$^{87}Sr/^{86}Sr$
1. Pecten Harbour pluton				
GV 169B	8.937	600.0	0.0431	0.70325
GV 60	9.510	610.7	0.0450	0.70330
GV 54	14.14	537.2	0.0761	0.70413
GV 168J	23.00	549.4	0.1210	0.70528
GV 168	21.55	495.2	0.1258	0.70540
GV 168C	28.39	493.4	0.1664	0.70645
GV 168E	49.87	490.4	0.2940	0.70971
GV 168F	47.34	290.8	0.4707	0.71421
GV 168I	29.37	107.4	0.7908	0.72248
Repeat	29.61	106.8	0.8014	0.72277
2. Lanyan Lake pluton				
GV 171B	12.09	584.4	0.0598	0.70374
GV 171A	19.46	706.6	0.0796	0.70415
GV 172C	33.69	760.3	0.1281	0.70567
GV 172A	33.74	707.2	0.1379	0.70611 ±0.00025
GV 172F	43.89	697.1	0.1820	0.70703
Repeat	44.39	694.1	0.1849	0.70706 ±0.00015
GV 172G	44.31	555.8	0.2305	0.70894
			±1%	±0.00010 except as noted

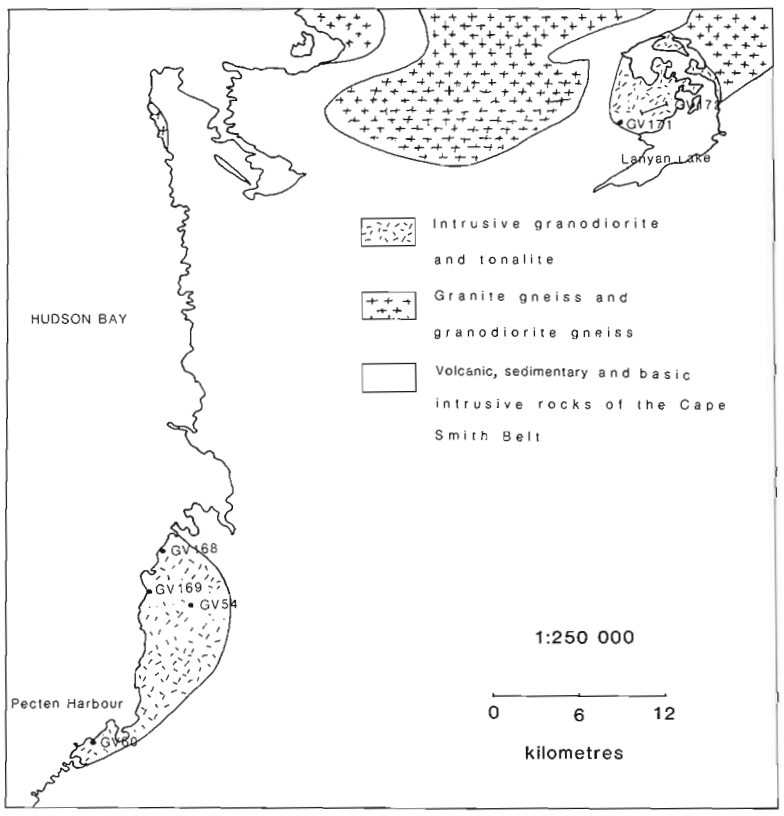

Figure 7.1. *Sample localities, western Cape Smith Belt.*

Discussion

Samples were collected at Pecten Harbour at the sites indicated in Figure 7.1 and along a traverse line at the Lanyan Lake pluton (GV 172) as well as at site GV 171. Fifteen samples were analyzed. The results of analysis of the nine samples from the Pecten Harbour pluton show an excellent spread (inset, Fig. 7.2) and form a well defined isochron at 1786 ± 14 Ma, initial ratio 0.70216 ± 0.00005 and a very low MSWD of 0.06. This initial Sr^{87}/Sr^{86} ratio, when plotted on a strontium isotope development diagram, lies within the zone indicative of relatively uncontaminated mantle magma. The seven data points from the Lanyan Lake pluton show a good spread but do not all either lie on the same line as those from Pecten Harbour or clearly describe another. Two of these points (GV 171A, and 171B) lie close to the 1786 Ma line of the Pecten Harbour samples but the rest scatter above that line. All seven together suggest an errorchron age of 2052 ± 167 Ma, with an initial ratio of 0.7019 ± 0.0004 and MSWD 9.8.

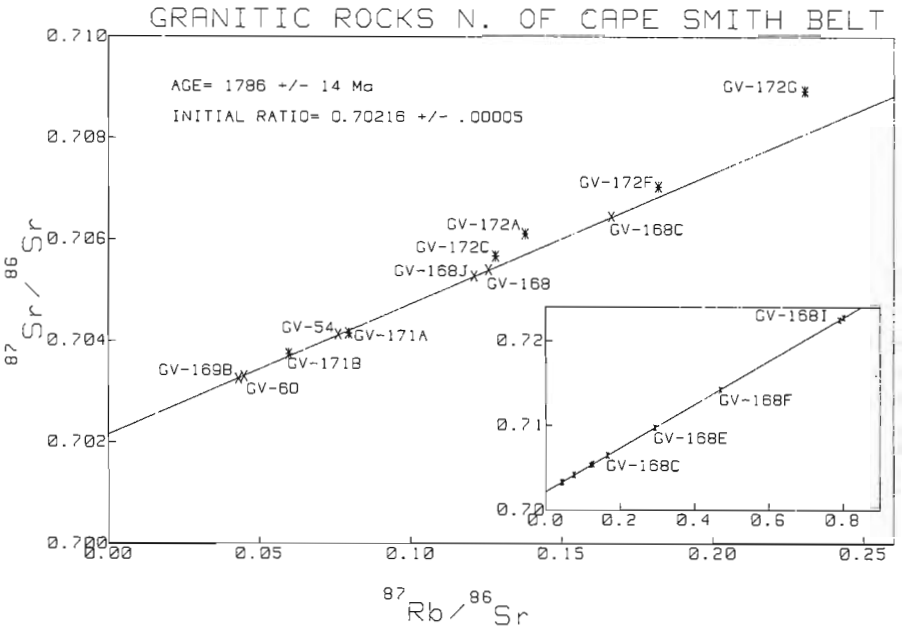

Figure 7.2. *Rb-Sr isochron plot. Crosses, Pecten Harbour pluton; asterisks, Lanyan Lake pluton. The isochron parameters are derived from the Pecten Harbour pluton results.*

The Lanyan Lake pluton data points fall into two groups. Those from site GV 171 have relatively low Rb/Sr ratios and provide a reasonable fit to the Pecten Harbour isochron. Those from the GV 172 traverse are higher in rubidium and scatter above the isochron. In the Pecten Harbour and GV 171 rocks there is a generally consistent inverse relationship between Rb and Sr content; the Sr content falls as the Rb content rises (Table 7.1). In the GV 172 samples, both the Rb and the Sr contents are comparable with the highest Rb and Sr contents in the Pecten Harbour samples. Three characteristics of the GV 172 samples, relatively high Rb contents, high Sr contents, and high $^{87}Sr/^{86}Sr$ ratios (with regard to the associated Rb/Sr ratios) are compatible with variable contamination from an older source relatively rich in Rb and Sr.

From the geological viewpoint, the Pecten Harbour rocks are more suitable for age determination than those from Lanyan Lake. Although inclusions of the country rock occur in the tonalite and granodiorite of the Pecten Harbour pluton, these are, in general, unassimilated and show clean unabsorbed contacts with their host. The contact itself is sharp and uncontaminated in comparison with that at Lanyan Lake, which is gradational over 60 m on its west side. Therefore, we consider the Pecten Harbour samples to be representative of the intrusion and not contaminated with older host rock. Hence, 1786 ± 14 Ma indicates the age of the intrusion of these granitoid rocks and the 2052 Ma result from the Lanyan Lake pluton probably reflects some contamination with older material.

References

Taylor, F.C.
1982: Reconnaissance geology of a part of the Canadian Shield, northern Quebec and Northwest Territories; Geological Survey of Canada, Memoir 399.

Wanless, R.K. and Loveridge, W.D.
1972: Rubidium-strontium isochron age studies, Report 1; Geological Survey of Canada, Paper 72-23.

-8-

METAMORPHISM IN THE MONASHEE MOUNTAINS EAST OF BLUE RIVER, BRITISH COLUMBIA

EMR Research Agreement 200-04-84

P. Doucet, E.D. Ghent, and P.S. Simony
Cordilleran Geology Division

Doucet, P., Ghent, E.D., and Simony P.S., Metamorphism in the Monashee Mountains east of Blue River, British Columbia; in Current Research, Part A, Geological Survey of Canada, Paper 85-1A, p. 69-71, 1985.

Abstract

Upper amphibolite facies metasedimentary rocks of the Hadrynian Horsethief Creek Group underlie the Monashee Mountains of southeastern British Columbia. Metamorphic grade increases gradually southward from the south margin of the Malton Gneiss, with coexisting kyanite and sillimanite (fibrolite) present in a zone about 16 km wide and at least 1.5 km thick north of Mud Lake. Fibrolite alone is found south of Mud Lake. The broad kyanite-sillimanite zone contrasts markedly with the zones of coexisting aluminosilicates observed to the west across the west-side-down North Thompson normal fault and to the east at Mica Creek where isograds are sharply defined and isogradic surfaces are steep. Metastable fibrolite produced from thermal metamorphism associated with extensive plutonism in the southern part of the study area may account for the abundant sillimanite, but a more plausible explanation resides in the rotation of the isogradic surface to a subhorizontal orientation in the region studied.

Résumé

Les roches métasédimentaires du faciès supérieur à amphibolites du groupe hadrynien, de Horsethief Creek, reposent sous la chaîne de Monashee dans le sud-est de la Colombie-Britannique. Le degré de métamorphisme s'accroît graduellement vers le sud à partir de l'extrémité sud du gneiss de Malton; de la cyanite et de la sillimanite (fibrolite) sont présentes dans une zone d'environ 16 km de largeur et d'au moins 1,5 km d'épaisseur, au nord du lac Mud. On trouve de la fibrolite seule au sud du lac Mud. La vaste zone de cyanite-sillimanite tranche de façon marquée sur les zones d'aluminosilicates coexistants qui se trouvent vers l'ouest, de part et d'autre de la lèvre affaissée de la faille normale de la rivière Thompson-Nord, et, à l'est, au ruisseau Mica, où les isogrades sont très bien définies et les surfaces isogrades abruptes. L'abondance de la sillimanite pourrait être due à la production de fibrolite métastable par métamorphisme thermique associé au plutonisme étendu dans la partie sud de la région étudiée; par contre, une autre explication plus plausible, suppose une rotation de la surface isograde qui a donné une orientation subhorizontale.

Department of Geology and Geophysics, University of Calgary,
Calgary, Alberta T2N 1N4

Introduction

The northern margin of the Shuswap Metamorphic Complex east of the North Thompson River, part of the Canoe River map sheet (NTS-83D) (Fig. 8.1), was mapped on a reconnaissance scale by Campbell (1968). The metamorphic zones he delineated in the area included a garnet zone between Bone Creek and the mountain range north of Mud Lake, staurolite-kyanite zones north of Bone Creek and north of Mud Lake, and a sillimanite zone south of Mud Lake. Reconnaissance mapping along the northern slope of the Mud Lake valley by Pell and Simony (1981) resulted in the tentative relocation of the kyanite-sillimanite isograd approximately 1 km north of Mud Lake.

Detailed mapping, at a scale of 1:24 000, and extensive sampling initiated during the summer of 1984 to accurately delineate the kyanite-sillimanite isograd and preliminary petrographic studies, indicate that sillimanite is much more widespread than was previously imagined. Coexisting kyanite and sillimanite were observed from Mud Lake northward to the northern slope of the Bone Creek valley.

Lithology

The major rock units in the study area each include a variety of metamorphosed clastic, carbonate and mafic igneous rocks belonging to the Hadrynian Horsethief Creek Group. The stratigraphic succession can be described using the nomenclature of Poulton and Simony (1980) established in the Purcell and Selkirk mountains and that of Pell and Simony (1981) established in the southern Cariboo Mountains.

The Lower Pelite unit is composed of a sequence of thick interbedded pelite and semipelite, lesser psammite, and rare amphibolite layers. Aluminosilicate minerals are abundant throughout the unit.

The Lower Marble unit which normally tops the Lower Pelite has not been observed.

The Semipelite-Amphibolite unit outcrops widely. It consists of thickly interbedded semipelites, pelites and psammites, numerous thin amphibolite layers, and a few calc-silicate bands. Aluminosilicate minerals are not as abundant in these pelites and semipelites as in the Lower Pelite unit.

The Middle Marble unit is characterized by two thick pure marble beds, with variable amounts of impure dolomitic marbles and calc-silicates, separated by pelite, psammite and semipelite beds.

Above the Middle Marble is the Upper Clastic unit which is characterized by abundant psammite and semipelite and lesser pelite.

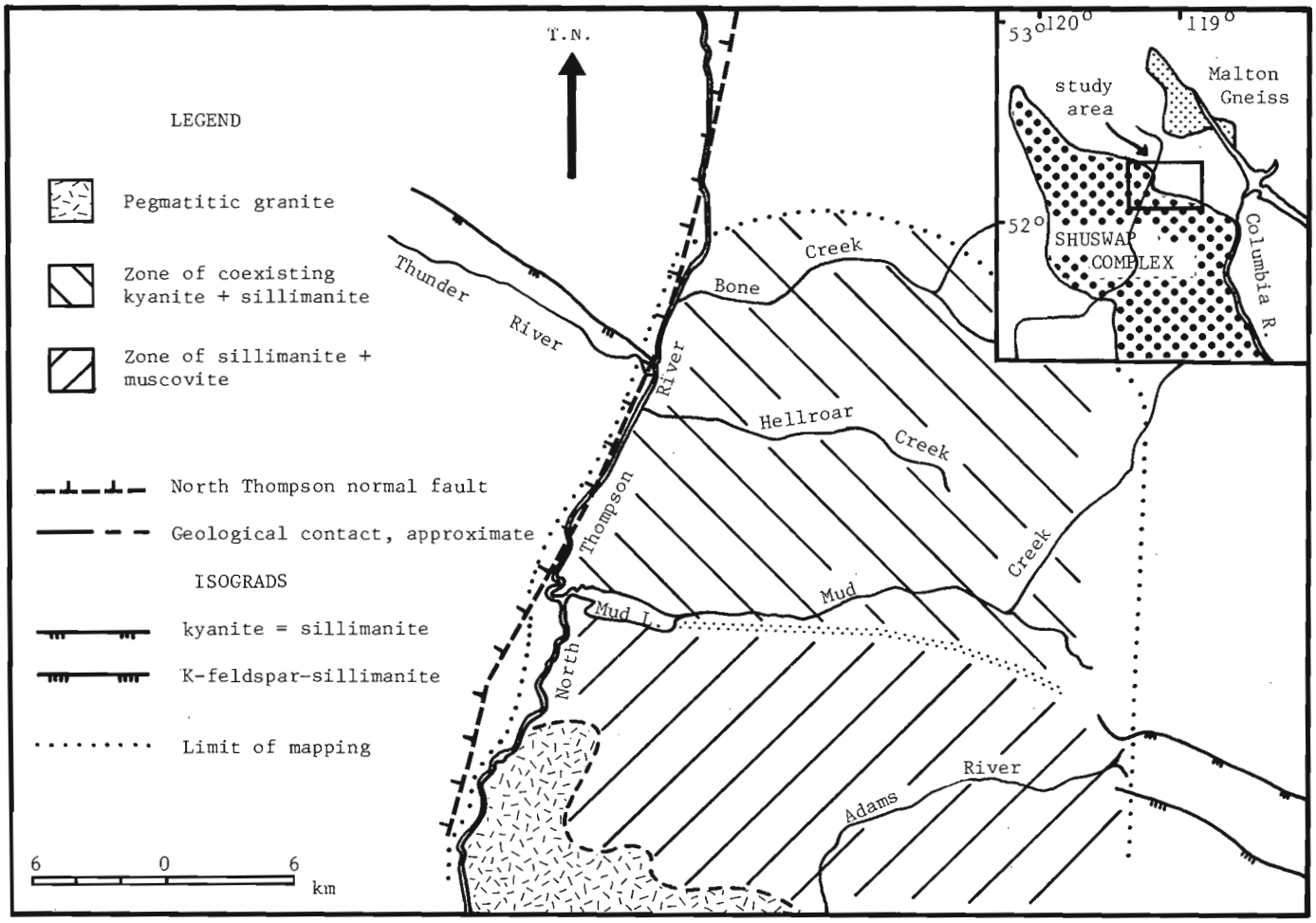

Figure 8.1. Metamorphic map of the Monashee Mountains. Isograds after Pell and Simony (1981) and Raeside (1982).

Structure

Three sets of folds, F_1, F_2 and F_3 are found in superposition within the area. The foliations S_1 and S_2 associated with the first two fold sets generally cannot be distinguished except in the hinge zones of major F_2 folds. The regional foliation present in the various rock types therefore have to be mapped as S_{1+2}, an approach that has been taken by other workers in nearby areas (see Simony et al., 1980; Raeside, 1982; Dechesne et al., 1984). The regional foliation defines a large scale subhorizontal open S-surface oriented northeast.

The dominant mappable structures within the study area are second generation (F_2) antiforms and synforms, generally with a shallow southeast axial plunge. These folds vary from open to very tight and are characterized by well developed axial planar cleavage. A first phase of folding (F_1), coaxial to F_2, has been identified in adjacent areas (Ghent et al., 1977; Simony et al., 1980; Raeside, 1982; Dechesne et al., 1984). These juxtapose identical but opposite facing stratigraphic packages. Similar large F_1 nappes have not yet been identified in the study area. Late folding, tentatively assigned to a third phase of deformation, followed peak regional metamorphic conditions. It is responsible for small scale crenulations in the S_{1+2} foliation, best demonstrated by bent and broken mica flakes.

The west-side-down North Thompson normal fault separates a terrane of comparatively low pressure metamorphism on its west side from the region under present investigation, to which higher pressures of metamorphism have been tentatively assigned (Pell and Simony, 1981).

Metamorphism

Regional metamorphism within the study area reached the upper amphibolite facies. The metamorphic grade increases gradually from a staurolite-free kyanite zone in the north to a broad muscovite-sillimanite zone in the south. A very broad zone, nearly 16 km wide, situated between Mud Lake and the northern boundary of the region studied, is characterized by coexisting kyanite and sillimanite (fibrolite), whereas sillimanite alone occurs in pelites and semipelites south of Mud Lake (Fig. 8.1). This broad kyanite-sillimanite isograd is in marked contrast to that observed in either the Mica Creek-Scrip Range region to the east (Ghent et al., 1977; Raeside, 1982) or the southern Cariboo Mountains to the west (Pell and Simony, 1981), where the isogradic surfaces are subparallel to the main structures and quite steep.

The isogradic surface may also be broadly subparallel to the layering in the study area but there it has been rotated to a nearly horizontal orientation. Kyanite and sillimanite are found together from the valley bottoms to the mountain tops, indicating that the zone of coexistence is at least 1.5 km thick. An overabundance of metastable sillimanite, resulting from thermal metamorphism associated with widespread granitic plutonism in the southern part of the region, might also account for the broad kyanite-sillimanite zone, but does not account for the wide distribution of kyanite.

Raeside (1982) noted that high grade pelites in the Scrip Range contained both fibrolite and granoblastic sillimanite. Preliminary petrographic examination of pelites from the study area revealed only fibrolite to be present.

Conclusion

Rocks of the Hadrynian Horsethief Creek Group in the Monashee Mountains were affected by three phases of deformation. Upper amphibolite facies regional metamorphic conditions were attained late in the second deformation phase, third phase folding being largely postmetamorphic. The North Thompson normal fault subsequently dropped the assemblage on its west side, resulting in a significant difference in metamorphic pressure observed across the fault. The attitude of the kyanite-sillimanite isograd across the fault is markedly different. The zone of coexisting kyanite and sillimanite west of the fault, and at Mica Creek, is narrow and the isograd is steep; conversely, the zone is more than 16 km wide and at least 1.5 km thick in the study area while the isogradic surface appears to be subhorizontal.

References

Campbell, R.B.
1968: Canoe River, British Columbia; Geological Survey of Canada, Map 15-1967.

Dechesne, R.G., Simony, P.S., and Ghent, E.D.
1984: Structural evolution and metamorphism of the southern Cariboo Mountains near Blue River, British Columbia; in Current Research, Part A, Geological Survey of Canada, Paper 84-1A, p. 91-94.

Ghent, E.D., Simony, P.S., Mitchell, W., Perry, J., Robbins, D., and Wagner, J.
1977: Structure and metamorphism in the southeast Canoe River area, British Columbia; in Report of Activities, Part C, Geological Survey of Canada, Paper 77-1C, p. 13-17.

Pell, J. and Simony, P.S.
1981: Stratigraphy, structure, and metamorphism in the southern Cariboo Mountains, British Columbia; in Current Research, Part A, Geological Survey of Canada, Paper 81-1A, p. 227-230.

Poulton, T.P. and Simony, P.S.
1980: Stratigraphy, sedimentology, and regional correlation of the Horsethief Creek Group (Hadrynian, Late Precambrian) in the northern Purcell and Selkirk Mountains, British Columbia; Canadian Journal of Earth Sciences, v. 17, p. 1708-1724.

Raeside, R.P.
1982: Structure, metamorphism and migmatization of the Scrip Range, Mica Creek, British Columbia; unpublished Ph.D. thesis, University of Calgary, Calgary, Alberta, 204 p.

Simony, P.S., Ghent, E.D., Craw, D., Mitchell, W., and Robbins, D.B.
1980: Structural and metamorphic evolution of northeast flank of Shuswap Complex, southern Canoe River area, British Columbia; Geological Society of America, Memoir 153, p. 445-461.

-9-

AN UNUSUAL PERALKALINE GRANITE NEAR LAC BRISSON, QUEBEC-LABRADOR

Project 680071

K.L. Currie
Precambrian Geology Division

Currie, K.L., An unusual peralkaline granite near Lac Brisson, Quebec-Labrador; in Current Research, Part A, Geological Survey of Canada, Paper 85-1A, p. 73-80, 1985.

Abstract

The Lac Brisson (Strange Lake) pluton forms an almost circular body 7 km across which consists of crudely layered, porphyritic alkali feldspar-quartz-arfvedsonite-acmite (± astrophyllite ± enigmatite) granite. A late phase or layer of the intrusion contains high concentrations of unusual sodium and calcium-bearing Be, Zr and rare earth minerals. Geochemically the pluton exhibits an unusual differentiation trend with Ca increasing with differentiation, and agpaitic index decreasing in the most Zr and rare earth-enriched phases. These trends may be due to concentration of F in residual melts. The pluton yields a K-Ar age on amphibole of 1270 ± 30 Ma, identical to a zircon age of 1270 ± 10 Ma from the Flowers River peralkaline granite. The pre-drift configuration of the Late Proterozoic Greenland-Labrador alkaline province probably was equant, rather than elongate. The peralkaline granite shows chemical affinities to a contiguous rapakivi granite suite suggesting an indirect genetic link among anorthosites, rapakivi granites, peralkaline granites and peralkaline syenites.

Résumé

Le pluton Lac Brisson (Strange Lake) forme une masse presque circulaire d'un diamètre de 7 kilomètres qui se compose de granite porphyrique à feldspath alcalin, à quartz, à arfvedsonite et à acmite (± astrophyllite ± énigmatite) grossièrement stratifié. Une phase ou couche tardive de l'intrusion contient de fortes concentrations insolites de béryllium et de zirconium sodiques et calciques et de lanthanides. Le pluton présente une différenciation géochimique anormale, la teneur en Ca augmentant avec la différenciation et l'indice agpaitique diminuant dans les phases les plus enrichies en zirconium et en lanthanides. Ces tendances pourraient être dues à une concentration de F dans le magma résiduel. La datation au K-Ar de l'amphibole donne un âge de 1270 ± 30 Ma pour le pluton, ce qui est identique à l'âge de 1270 ± 10 Ma obtenu par Hill (1982) pour du zircon extrait du granite peralcalin de Flowers River. Avant la dérive continentale, la configuration de la province alcaline Groeland-Labrador du Protérozoique récent était vraisemblablement équidimensionnelle plutôt qu'allongée. Le granite peralcalin présente des affinités chimiques avec un cortège granitique rapakivique contigu, ce qui laisse croire qu'il existe un lien génétique indirect entre les anorthosites, les granites rapakiviques, les granites peralcalins et les syénites peralcalines.

Introduction

Zajac et al. (1984) reported an unusual niobium-zirconium-rare earth deposit (Strange Lake deposit) occurring within a peralkaline granite pluton on the Quebec-Labrador border, and discusses its discovery by tracing of float from a fluorine anomaly detected by the Uranium Resources Program of the Geological Survey of Canada. The peralkaline pluton hosting this deposit was examined by the author during four days of field work in 1980, undertaken at the request of the Iron Ore Company of Canada. This note records the result of these observations and some subsequent analyses.

Geological setting

The peralkaline pluton lies southeast of Lac Brisson (Fig. 9.1) in a region of rolling upland barrens and shallow bouldery lakes. Valleys tend to be filled with moraine, eskers and other glacial deposits, but outcrop is moderately abundant on the higher ground. The bedrock belongs to the Nain province of the Canadian Shield according to the reconnaissance geological mapping compiled by Taylor (1975). This mapping did not distinguish the peralkaline pluton from other Proterozoic granitoid rocks, but comparison with more recent work shows the peralkaline pluton to lie on the contact of a mass of rapakivi granite to the south and a diverse suite of gneisses and migmatites to the north.

The gneiss complex (unit 1) consists mainly of mesocratic, fairly homogeneous biotite oligoclase-quartz gneiss containing 5-10 per cent of salic schlieren and lenticles of oligoclase+perthite+quartz. To the east of the complex these lenticles become more numerous and larger and the gneiss passes into migmatite or agmatite (unit 1a) in which the biotite gneiss appears as boudins or spindle-like masses. The gneiss complex contains relatively sparse 30 to 100 cm bands of gneissic mafic granulite consisting of granoblastic andesine, pyroxene (variously uralitized and chloritized) and minor quartz. Orthopyroxene and clinopyroxene coexist in some specimens, but others contain only one pyroxene. These bands may represent transposed mafic dykes. In general the gneiss complex trends a few degrees west of north and dips steeply to the east, but intricate, locally ptygmatic small folding occurs in some areas. K/Ar dating of similar rocks north and west of Lac Brisson returned cooling ages of 1750-1800 Ma (Taylor, 1975) implying an Archean or Aphebian age for the protolith.

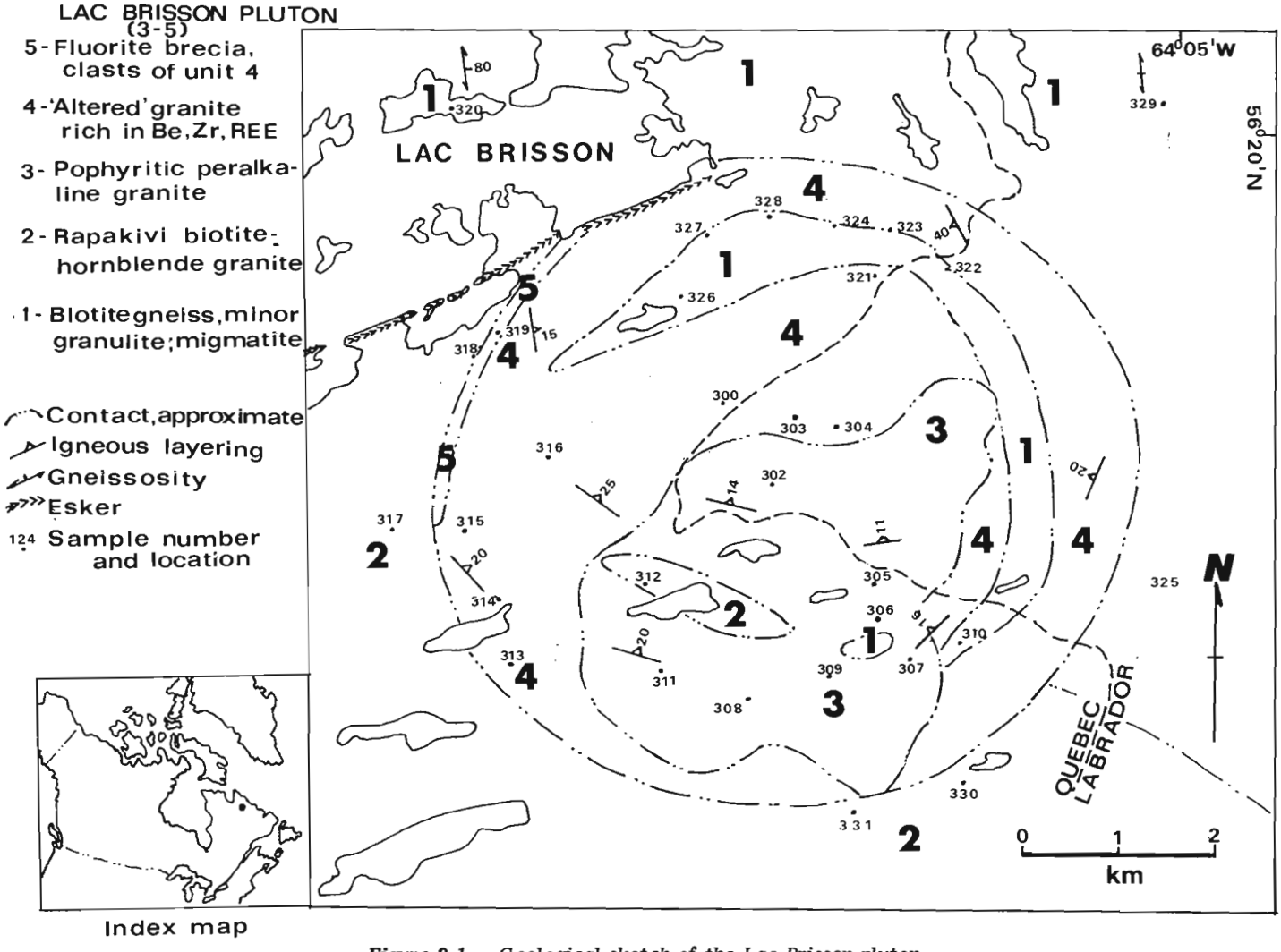

Figure 9.1. Geological sketch of the Lac Brisson pluton.

On its southern and western side the peralkaline pluton contacts a batholithic mass of essentially massive rapakivi granite (unit 2) which contains up to 60 per cent ovoid alkali feldspars with white-weathering plagioclase rims. The ovoids typically lie in the range 2 to 4 cm across with scattered individuals up to 10 cm. The cores of the ovoids contain abundant small oikocrysts of mafic minerals which define or emphasize internal zones. Quartz forms euhedral to subhedral grains. Hornblende, commonly mantled by biotite, is the principal mafic mineral, but some large grains contain cores of hedenbergite. Purple fluorite was observed as a sparse accessory. Microscopically, the feldspar is mainly perthitic microcline. The distinctive appearance and mineralogy of this mass identify it as one of a suite of Elsonian rapakivi granites, probably related to the nearby Mistastin batholith (Emslie et al., 1980). The age of this suite probably lies in the range 1350-1500 Ma. On its northeastern side the rapakivi granite contains inclusions of the gneiss.

Geology of the peralkaline pluton

The peralkaline granite appears to form an almost circular body about 7 km in diameter. The pluton consists of crudely layered, porphyritic feldspar-quartz-arfvedsonite-acmite (± astrophyllite ± enigmatite) granite. An upper layer, or late saucer-shaped phase, contains high concentrations of zirconium, niobium beryllium and rare earth minerals. Their presence in surface samples can be detected by brightly coloured patches in the rock. The pluton contains screens and pendants of variously altered country rocks as well as a multitude of smaller inclusions of doubtful origin. Due to the numerous screens, definition of the contact of the pluton would be difficult in any case, but the contacts are not exposed. To the south and west a broad arcuate valley separates peralkaline granite from rapakivi granite. To the northwest, sparse outcrop and boulders suggest that the boundary of the pluton is strongly brecciated and mineralized by fluorite. The curvilinear features bounding the southern, western and northern sides of the pluton appear to be of

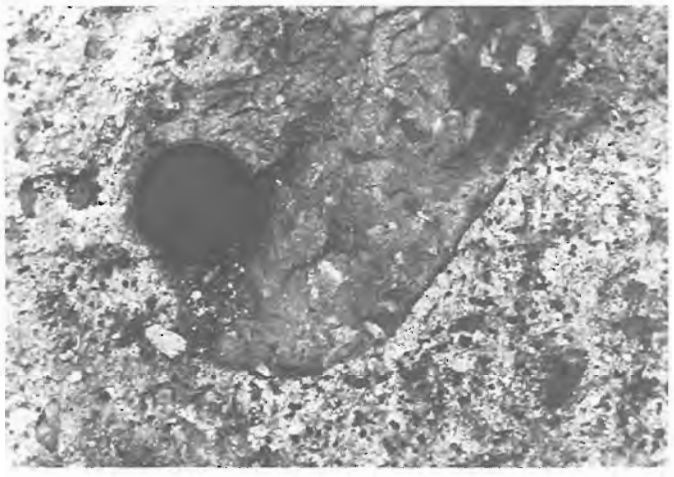

Figure 9.2. *Inclusion of amphibolite in peralkaline granite. Note the prominent alkali feldspar porphyroblasts in the inclusion. Lens cap is 3.5 cm in diameter. (GSC 204153-I)*



Figure 9.4. *Small mafic inclusions not showing feldspar porphyroblastesis. Compare to Figure 9.2. These inclusions may be restite. (GSC 204153-J)*



Figure 9.3. *Strongly metasomatized salic gneiss. The gneissic appearance of this inclusion is identical to that of the host rocks, but its chemistry is peralkaline (specimen 322). (GSC 204153-K)*

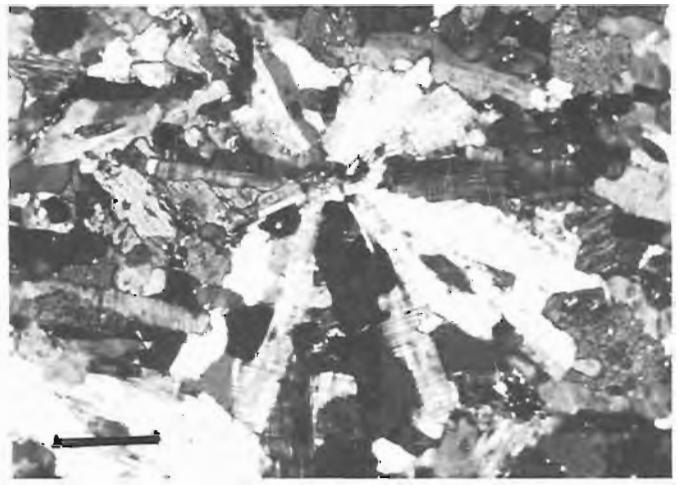

Figure 9.5. *Rosette of feldspar laths in peralkaline granite. The scale bar is 0.2 mm in length. (GSC 204153-G)*

regional extent, but deflected around the pluton, suggesting that emplacement may have used and deformed older faults. On the east side of the pluton a vertical contact is exposed for 10 m between granite and a large screen of gneiss. The granite is rather fine grained but exhibits the characteristic porphyritic texture. A rim of acicular amphibole 1 cm thick radiates into the granite from the actual contact. The gneiss appears unaffected more than 30 cm from the contact. Within this distance the structure and texture of the gneiss appear unaffected, but the salic schliers noted above carry fine arfvedsonite needles, giving them a distinctive bluish tinge.

A semi-continuous screen of country rocks lying several hundred metres within the pluton displays all of the varieties recognized in the surroundings of the pluton. Within the screen, up to 400 m wide, the country rocks have been variably metasomatized. Porphyroblastic feldspar occurs ubiquitously in mafic rocks (Fig. 9.2) and some salic gneisses have been so transformed that their original character is preserved only in strong foliation (Fig. 9.3) and association with mafic gneiss. However, many small inclusions in the granite appear dense, and lack any evidence of significant metasomatism (Fig. 9.4). These inclusions may be relicts of the protolith of the granite ("restite"), or possibly fragments of older intrusive phases of the pluton.

The pluton, where fresh exhibits a pale grey colour, locally with a faint steely blue tinge (unit 3). The rocks are commonly distinctly porphyritic with euhedral feldspar and poikilitic amphibole phenocrysts up to 5 mm long in a fine grained matrix of quartz and feldspar. The rocks virtually all display foliation ranging from moderate alignment of feldspar to compositional banding on a scale of 10 to 100 cm, with slightly darker finer grained layers and paler, coarser layers. The layering in the southern part of the pluton dips northerly at angles of 5 to 25 degrees, parallel to a pervasive jointing. The layering appears to define an asymmetric saucer-like structure, but the number of observations in the northwest quadrant is insufficient to be certain.

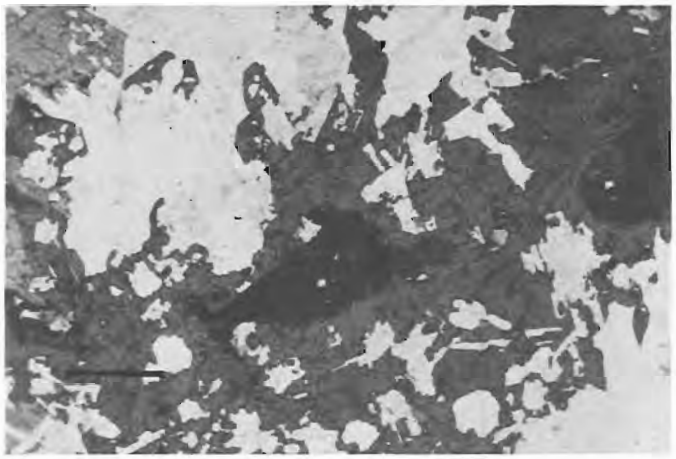

Figure 9.6. *Large amphibole crystal with enigmatite core (dark colour). Note the euhedral shape of many of the salic inclusions, suggesting that much of the amphibole is late adcumulus overgrowth. Scale bar is 0.2 mm. (GSC 204153-F)*

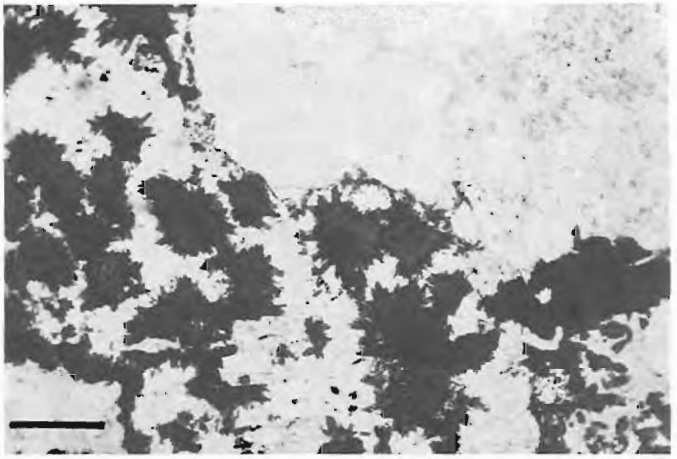

Figure 9.8. *Rosettes of gittinsite (black). Gittinsite is colourless, but is here marked by gel-like iron oxides. The gittinsite is probably pseudomorphous after elpidite. (GSC 204153-E)*

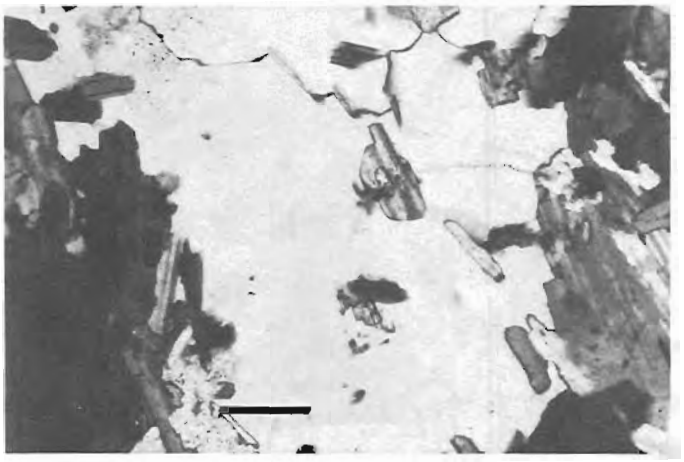

Figure 9.7. *Large quartz grain with acmite (pale grey) and elpidite (colourless) inclusions. Note that the colour of the pyroxene is identical to that of contiguous grain, suggesting the quartz may be partly replacive. Length of scale bar is 0.2 mm. (GSC 204153-D)*



Figure 9.9. *Fluorite breccia. The matrix consists of rose to purple flourite, the fragments of 'altered' peralkaline granite. (GSC 204153-L)*

Table 9.1. Chemical analyses of the Lac Brisson pluton and country rocks

	Gneiss complex				Rapakivi granite				Dykes		unaltered peralkaline granite						
Specimen	329	320	310	326	317	325	330	331	327	328	306	308	309	311	302	305	307
SiO_2	75.2	72.6	49.9	50.9	71.1	73.2	75.1	70.7	62.8	62.0	71.4	71.3	71.7	71.0	70.8	71.4	71.3
TiO_2	0.04	0.47	1.27	0.61	0.30	0.07	0.25	0.53	0.33	0.34	0.37	0.19	0.20	0.28	0.27	0.39	0.24
Al_2O_3	13.8	13.6	15.8	15.9	13.1	13.2	11.9	12.8	15.3	15.5	11.2	11.4	11.9	11.8	11.6	10.5	10.4
Fe_2O_3	0.3	0.5	1.8	0.9	1.4	0.2	0.7	0.9	4.5	4.8	2.4	2.8	1.8	3.2	1.9	3.3	3.1
FeO	0.0	2.8	11.0	6.8	0.5	1.1	1.2	3.4	2.3	1.9	2.3	2.1	2.7	2.2	2.4	1.7	1.8
MnO	0.01	0.05	0.23	0.15	0.03	0.02	0.02	0.07	0.10	0.09	0.12	0.11	0.09	0.10	0.11	0.13	0.10
MgO	0.16	1.18	5.39	8.64	0.52	0.33	0.15	0.39	0.21	0.35	0.11	0.06	0.14	0.13	0.11	0.03	0.11
CaO	2.32	2.78	8.92	10.5	2.24	1.22	0.68	1.56	1.68	2.77	0.89	0.38	0.49	0.43	0.64	0.51	0.57
Na_2O	3.5	3.7	2.8	1.9	3.7	2.4	2.6	3.0	7.7	9.2	4.9	4.9	5.3	4.8	4.9	5.1	5.1
K_2O	2.94	1.64	1.73	0.96	5.00	5.99	5.82	5.32	3.27	1.85	4.87	4.95	4.92	4.89	4.83	5.09	4.41
H_2O	0.45	0.97	1.64	1.52	0.84	0.91	0.82	0.81	0.72	0.83	0.41	0.35	0.32	0.32	0.53	0.44	0.55
CO_2	0.2	0.1	0.2	0.5	0.3	0.0	0.3	0.3	0.2	0.1	0.2	0.3	0.3	0.1	0.2	0.1	0.6
P_2O_5	0.04	0.09	0.14	0.30	0.09	0.06	0.02	0.12	0.07	0.07	0.01	0.05	0.02	0.04	0.02	0.03	0.04
Ba(ppm)	410	440	400	960	650	2400	500	1300	140	130	65	75	83	77	79	87	61
Be	–	–	38	–	16	–	–	–	13	18	43	20	24	21	32	24	75
Ce	90	290	40	50	110	120	280	130	520	510	1300	700	450	530	600	950	1200
Co	–	11	38	29	–	–	–	–	–	–	–	–	–	–	–	–	–
Cr	–	22	51	110	5	9	–	–	9	10	9	6	6	6	6	8	10
Cu	9	17	42	47	14	11	15	13	24	15	15	10	11	12	16	18	15
La	40	160	30	60	110	120	180	100	330	300	630	410	240	310	300	450	600
Rb	80	50	140	40	340	140	210	170	230	180	830	610	450	520	540	800	730
Sr	390	420	410	2100	190	420	160	210	130	150	110	56	50	33	58	45	95
V	23	73	240	130	39	30	26	9	30	27	29	18	20	16	14	17	26
Y	–	–	–	–	27	21	20	46	210	250	910	340	320	230	480	770	600
Yb	–	8	–	–	10	6	8	8	26	33	81	54	28	38	53	85	58
Zn	40	50	150	80	130	70	60	80	310	260	660	550	360	430	410	500	480
Zr	130	460	110	260	320	110	380	510	2400	2400	3700	2670	2240	1300	4650	6010	5960
Agpaitic index	0.65	0.58	0.41	0.26	0.88	0.79	0.89	0.84	1.06	1.11	1.19	1.18	1.18	1.12	1.15	1.32	1.27

	altered peralkaline granite							metasomatized rocks				Average dyke	Average fresh granite	Average altered granite
Specimen	300	303	304	313	314	315	321	318	323	322	324			
SiO_2	72.1	72.3	74.0	71.8	72.0	72.6	72.1	58.5	62.8	69.9	56.0	62.40	71.27	72.41
TiO_2	0.67	0.15	0.26	0.23	0.24	0.26	0.27	0.33	1.19	0.42	0.87	0.33	0.29	0.30
Al_2O_3	9.1	8.8	9.5	9.3	9.0	10.2	8.6	13.8	13.7	8.8	14.5	15.40	11.26	9.21
Fe_2O_3	2.4	3.6	3.6	4.9	3.9	3.2	4.3	4.1	2.0	5.1	3.3	4.65	2.64	3.70
FeO	2.9	2.3	1.3	1.0	2.1	0.1	0.6	0.1	4.1	1.3	5.0	2.10	2.31	1.47
MnO	0.14	0.13	0.13	0.16	0.14	0.12	0.17	0.02	0.10	0.22	0.19	0.10	0.11	0.14
MgO	0.34	0.00	0.25	0.53	0.68	0.31	0.48	0.45	1.64	0.25	1.98	0.28	0.10	0.37
CaO	1.03	0.62	0.56	0.68	0.88	1.25	1.72	10.4	2.91	1.80	4.34	2.23	0.56	0.97
Na_2O	3.3	3.0	3.6	4.4	3.4	3.6	3.1	5.1	2.9	2.3	6.3	8.95	5.00	3.49
K_2O	4.18	4.53	4.22	3.72	4.11	3.72	3.18	4.58	4.54	5.74	3.33	2.56	4.85	3.95
H_2O	0.83	0.63	0.63	0.68	0.86	0.54	1.05	1.80	1.88	0.74	2.40	0.77	0.42	0.74
CO_2	0.5	0.2	0.3	0.3	0.2	0.3	0.3	0.1	0.1	0.3	0.1	0.15	0.26	0.30
P_2O_5	0.02	0.10	0.07	0.03	0.02	0.02	0.03	0.08	0.42	0.03	0.28	0.07	0.03	0.04
Ba(ppm)	60	54	70	44	31	35	38	31	4000	140	750	135	75	47
Be	35	27	92	120	130	50	95	–	–	68	12	15	34	75
Ce	880	1200	1300	1900	2300	14000	11000	110	240	2000	420	515	820	3600
Co	14	17	9	17	12	15	11	–	11	17	11	–	–	12
Cu	18	22	23	25	58	47	53	14	22	22	20	19	14	27
La	390	520	560	730	1000	6700	6100	80	180	1100	330	325	420	2310
Rb	910	960	880	790	790	780	770	320	160	770	560	205	640	840
Sr	74	86	79	120	100	220	210	160	1000	190	370	140	65	130
V	33	27	23	26	25	30	28	45	89	30	75	28	20	38
Y	960	1200	1100	1600	1300	1900	2100	19	42	1700	240	230	520	1450
Yb	130	180	160	170	100	68	78	49	8	190	24	29	55	125
Zn	770	1100	1100	1030	1370	540	830	80	120	830	1170	285	485	960
Zr	12800	17000	10870	13040	7830	22400	23500	130	930	23500	1250	2400	3790	15350
Agpaitic index	1.09	1.12	1,10	1.21	1.12	0.98	0.99	0.97	0.71	0.99	0.96	1.08	1.20	1.09

Analyses by Rapid Methods Group, Geological Survey of Canada, J.L.Bouvier, supervisor
– not detected

The central and marginal parts of the pluton contain a granite phase (unit 4) notably rich in unusual Zr, Be and rare earth minerals. This phase can readily be recognized in hand specimen by brightly coloured, roughly circular or ellipsoidal patches 1 to 5 mm in diameter. These spots however seem to be the result of a very superficial late alteration, suggesting that at depth this "altered" granite would not show alteration.

Table 9.2. Chemical balance calculations for peralkaline granite

	1	2	3	4	5	6	7
SiO_2	62.40	60.96	71.27	71.27	69.71	72.41	69.71
TiO_2	0.33	0.34	0.29	0.29	0.28	0.30	
Al_2O_3	15.40	16.07	11.26	11.26	14.06	9.21	14.06
FeO(t)	6.29	6.55	4.69	4.69	4.03	5.17	4.03
MnO	0.10	0.10	0.11	0.11	0.07	0.14	
MgO	0.28	0.30	0.10	0.10	*	0.37	
CaO	2.23	2.50	0.56	0.56	0.00	0.97	
Na_2O	8.95	9.59	5.00	5.00	7.18	3.49	7.18
K_2O	2.56	2.19	4.85	4.85	6.07	3.95	6.07
H_2O	0.77	0.83	0.42	0.42	0.00	0.74	
CO_2	0.15	0.13	0.26	0.26	0.21	0.30	
P_2O_5	0.07	0.08	0.03	0.03	0.02	0.04	
Ba(ppm)	135	145	75	75	105	47	
Be	15	12	34	34	*	75	
Ce	515	465	820	820	*	3600	
Cr	10	10	7	7	*	16	
Cu	19	20	14	14	*	27	
La	325	310	420	420	*	2310	
Rb	205	135	640	640	440	840	
Sr	140	152	65	65	*	130	
Y	230	183	520	520	*	1450	
Yb	29	25	55	55	*	125	
Zn	285	252	485	485	10	910	
Zr	2400	2175	3790	3790	*	15350	

1. Average dyke (Table 9.1), assumed parental to columns 2, 3.
2. Material extracted from 1 by fractionation (assumed 86 weight per cent of parent).
3. Residual after extraction of 2 from 1. Compare average fresh granite of Table 9.1.
   (Note that the high proportion of extract (86 weight per cent) is required in order that the extract be silica-saturated. See text.)
4. Average fresh peralkaline granite (Table 9.1), assumed parental to 5, 6.
5. Material assumed extracted from 4 by fractionation (42 weight per cent of column 4). Percentage extracted fixed by assumption that CaO cannot be less than 0 in the extract. Asterisks mark values which compute as negative numbers, and hence cannot be explained by fractionation.
6. Residual after extraction of 5 from 4. Compare average altered granite from Table 9.1.
7. Composition of a mixture of stoichiometric albite (43.6%), orthoclase (30.5%), riebeckite (10.3%) and quartz (14.6%), with 1.3% free Na+ and 0.9% free K+. Compare to column 5.

Microscopically, the typical peralkaline granite (unit 3) displays large rounded quartz phenocrysts, some zoned, large poikolitic amphibole euhedra, and assemblages of feldspar phenocrysts ranging from grid twinned microcline perthite through albite+microcline (not perthitic) assemblages, to mainly albite, all set in a matrix dominated by fine alkali feldspar laths (Fig. 9.5). The amphibole phenocrysts contain a dense core, but much of the large crystals appears to be adcumulus overgrowth (Fig. 9.6) enclosing feldspar and relicts of enigmatite. The amphibole exhibits pale olive to opaque blue pleochrism. Preliminary electron probe data suggest that it lies between riebeckite and arfvedsonite with high K_2O content (more than 1.3 weight per cent). Many of the large amphiboles exhibit a partial or complete rim of acmitic pyroxene, faintly pleochroic from pale buff to pale green, sometimes with deeper green cores. Some specimens contain swarms of minute, aligned astrophyllite needles in felsic portions. Colourless to pale purple fluorite and pale yellow pyrochlore, commonly associated with amphibole occur commonly as accessories, while more exotic minerals occur rarely.

The "altered" granite noted above has a rather different structure. Large quartz grains contain numerous aligned inclusions of amphibole and elpidite (Fig. 9.7). Albite occurs as rosettes of fine laths, and much of the amphibole is converted to a red-brown mass of alteration products. Accessory minerals in this phase include many unusual minerals now being investigated by other workers. Minerals identified in the present work by optic properties and X-ray diffraction include narsarsukite, elpidite, gittinsite, and gagarinite-like mineral. Narsarsukite can be readily identified by X-ray diffraction, but the optic properties (colourless prismatic, $-2V=48°$, $n_X=1.53$, $n_Z-n_X=0.012$) are anomalous, possibly due to high Ca content. Elpidite is a ubiquitous accessory. Much of the material appears to diverge from the theoretical composition ($Na_2ZrSi_6O_{18}\cdot 3H_2O$) toward a Ca-rich analogue (J. Jambor, personal communication, 1984). In some specimens the elpidite has been completely isomorphously replaced by gittinsite ($CaZrSi_2O_7$), locally accompanied by acmite needles and gel-like iron oxides (Fig. 9.8). A mineral giving an X-ray pattern like gagarinite ($NaCaYF_6$) occurs in several specimens. The Russian literature specifies this mineral to be water soluble. Possibly the Lac Brisson material is an insoluble Ca-rich analogue. Zircon and sphene occur in spectacular, very late spherulites of fine fibers, apparently replacing earlier minerals.

The northwestern contact of the pluton exposes a crescentic zone of fluorite-rich breccia (unit 5) which seems to form the latest phase of the pluton. The fragments in the breccia are mainly of altered country rocks, most commonly of unit 4, and this unit consistently fringes the fluorite-rich zone, suggesting that there may be some genetic connection between them. The breccia (Fig. 9.9) contains well rounded fragments, many of which are partially broken up, forming streams of small chips, in some cases giving a distinct, steeply-dipping foliation to the rock. The breccia resembles diatreme or tuffisitic breccia, but the fluorite matrix is more abundant.

Geochemistry of the pluton

Twenty-eight chemical analyses of the pluton, made from powders obtained from 1 kg specimens collected to obtain fresh rock without obvious inclusions, are presented in Table 9.1. Major element analyses were made by X-ray fluorescence, with H_2O and CO_2 determined by infra-red methods. Trace elements were determined by a combination of X-ray fluoresence and spectroscopy. Sample locations are

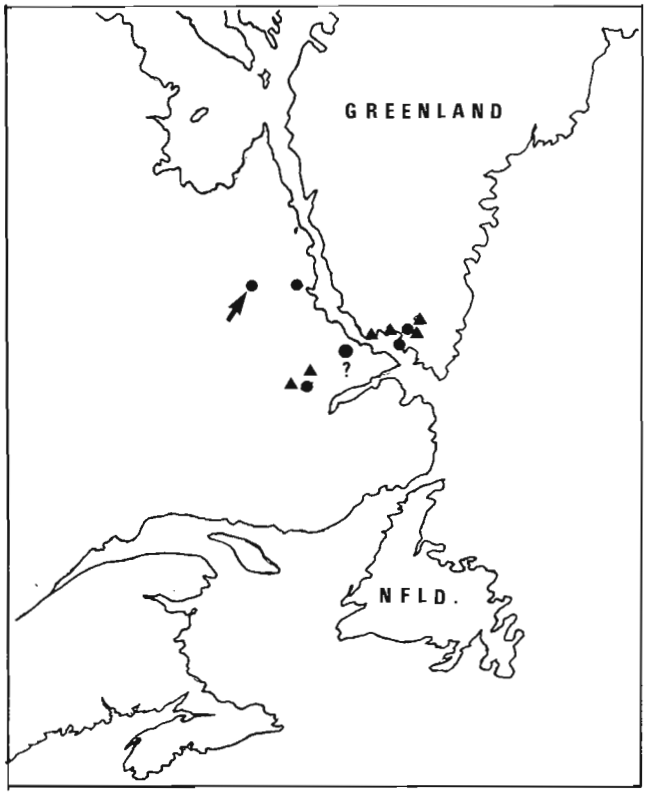

Figure 9.10. Occurrences of peralkaline rocks in Greenland and Labrador, restored to their probable position prior to Mesozoic drift. Triangles – peralkaline undersaturated rocks, nepheline syenite, naujaite, lujavrite, kakortokite. Circles – peralkaline granite, rhyolite, quartz syenite. Arrow marks the position of the Lac Brisson pluton. Question mark shows the position of riebeckite granite of possible metasomatic origin.

shown in Figure 9.1. The sampling was not systematic, but an attempt was made to sample widespread varieties and avoid small pockets of unusual composition.

The results of the sampling may be summarized as follows. The gneiss complex has generally granitoid compositions in the leucocratic parts and gabbroid compositions in the mafic granulites. All gneisses show Na greater than K, moderate Ca contents appropriate to the silica values and low agpaitic index (molecular Na+K/Al). Rb contents are relatively low, and Sr/Rb is greater than 3. By contrast, the rapakivi granite has a distinctive high K chemistry, low Ca content, and moderate to high agpaitic index. The Rb content is relatively high and the Sr content low so that Sr/Rb averages close to 1.0. The peralkaline pluton exhibits high Fe^3/Fe^2, very low MgO and CaO contents, and agpaitic index greater than 1.0. Ba and Sr are strongly depleted and Rb enriched, so that Sr/Rb is less than 0.25, and K/Rb less than 100. Be, Zn, Zr and rare earths are strongly enriched.

The peralkaline pluton poses difficult geochemical problems, notably the original source of the peralkaline magma and the processes leading to the concentration of Be, Nb, Zn, Zr and rare earths. Some light can be cast on the first problem by considering analyses of aphyric dykes (analyses 327,328). Compared with the average peralkaline granite these dykes are more mafic and less agpaitic. They could serve as a parental composition from which the granite could be derived by crystal fractionation. To assess this possibility, a chemical balance calculation is shown in Table 9.2, assuming the dykes to represent parental liquid, the average granite to represent residual liquid, and calculating the composition of extracted material. To avoid weighing small, possibly fictitious, differences in composition, the calculation considered only SiO_2, Al_2O_3, FeO(t), CaO, Na_2O and K_2O for which the differences are large and unmistakable. The results are constrained by SiO_2 content. The parent, daughter and all known phenocryst phases are silica-saturated. Hence the extract must also be silica-saturated. This requires about 86 per cent of the parental liquid to crystallize, leaving 14 weight per cent of the liquid to form the observed granite. The extracted material is roughly equivalent to a mixture of arfvedsonitic amphibole and albitic feldspar. Note that all major and trace elements can be balanced by this procedure so that the dyke composition could represent a parent to the granite, but this initial composition is itself highly evolved as shown by the high Na, Zr, rare earth, Fe/Mg and agpaitic index of the dykes. The simplest method of returning such a composition toward more common values would be to add diopsidic pyroxene with a small Al content, leading to a pyroxene syenite composition with agpaitic index near 1. Such rocks are well known in the nearby Mistastin batholith (Emslie et al., 1980).

According to standard petrologic theory, peralkaline intrusions tend to become more peralkaline with differentiation, leading to spectacular concentration of Na-rich minerals in late pegmatites (Upton, 1974; Linthout, 1984). The pluton in question displays an opposite trend. The agpaitic index falls in Zr and REE enriched specimens, and in the most enriched (315 and 321) is less than 1.0. The Ca content (which normally falls with differentiation) noticeably increases in these rocks. Comparing the composition of fresh and "altered" granite (Table 9.2) suggests that extraction of a mix of quartz, alkali feldspar riebeckite, and a small amount of alkali-rich fluid (assumed responsible for metasomatism around the pluton) from the fresh granite could account for the major element composition of the "altered" granite, but this process cannot account for any of the trace element contents which are enriched in the "altered" granite. Such enrichment appears to require some form of metasomatism.

Age of emplacement

Although Taylor (1975) did not distinguish the peralkaline pluton from surrounding Proterozoic granites, he showed a K/Ar age determination on amphibole of 1138 ± 44 Ma from a site underlain by peralkaline granite. This specimen is no longer available for examination. A large specimen of fresh, porphyritic granite collected by I.S. Zajac was submitted for age determination. Clean, unaltered pleochroic dark blue to violet amphibole with no visible contamination analyzed 2.36 per cent K_2O, returned 96.7 per cent radiogenic argon, and yielded an age of 1271 ± 30 Ma. This age is significantly greater than that obtained by Taylor (1975), leaving the age of emplacement of the pluton somewhat uncertain. However, the age is identical to the 1270 ± 10 Ma obtained by Pb-U concordia on zircon from peralkaline granite of the Flowers River suite 100 km to the east (Hill, 1982). Hill (1982) compiled a number of ages and found that the peralkaline suite seemed to be slightly younger than Elsonian suite of anorthosites and rapakivi granites (1300-1500 Ma), but the age gap was slight.

Discussion

The Lac Brisson (Strange Lake) pluton forms another occurrence of peralkaline oversaturated felsic rocks in Labrador. When combined with previously known occurrences

(Hill, 1982; Curtis and Currie, 1981) in Labrador and the occurrences in west Greenland (Upton, 1974) which were contiguous prior to Mesozoic continental breakup (Srivastava, 1978), this peralkaline province forms a roughly equant region some hundreds of kilometres across. The southern part of the province was subsequently transected by the "Grenville front" leading to spectacular deformation and metamorphism of southern occurrences (Curtis and Currie, 1981) but leaving northern occurrences such as Lac Brisson virtually pristine.

Like the other occurrences, Lac Brisson pluton appears to be a high level intrusion derived by crystal fractionation from an already highly evolved parent. The ultimate source of the parent remains uncertain. An association with anorthosite has been persistently suggested (Bridgwater and Harry, 1968; Upton, 1974), but derivation from pyroxene syenites of the rapakivi granite suite spatially associated with the anorthosites seems more plausible on chemical balance grounds. Emslie (1978) pointed out that the link between anorthosite and rapakivi granite suites may be indirect, depending on heat transfer in the crust rather than direct descent.

Evolution of the Lac Brisson (Strange Lake) pluton appears unusual because concentration of Be, Zr and rare earths was marked by decrease in alkali content, decrease in agpaitic index, and increase in Ca. Part of this may be due to loss of Na in metasomatizing solutions, but Ca increased and Na/Ca decreased during the presumably igneous phase of differentiation (Table 9.2). A possible explanation may lie in concentration of F in residual melt (Manning et al., 1980). If water escapes in a hydrothermal phase, then residual melt will become extremely rich in F and elements complexed with it, notably Ca, Zr and rare earths. This might account for progression from "altered" granite to fluorite-rich breccia. In place of late hydrothermal alteration, late alteration would be due to an essentially anhydrous F- (and Ca-) rich fluid, suggested by replacement of elpidite by gittinsite, narsarsukite by sphene, and development of gagarinite. The effects of this metasomatizing fluid may also be reflected in the anomalously high trace element contents of the "altered" granite. If this reasoning is correct, the most favourable sites to prospect for deposits similar to Strange Lake should be fluorite-rich peralkaline granites, particularly those with late fluorite concentrations such as the fluorite breccia at Lac Brisson.

Acknowledgments

I am much indebted to the Iron Ore Company of Canada, and particularly to I.S. Zajac, for the opportunity to study the Lac Brisson pluton. A.C. Roberts made the X-ray diffraction identifications. J.C. Jambor gave much needed guidance on the mineralogy. Discussion with Tyson Birkett has substantially improved the manuscript. I am particularly indebted to I.S. Zajac for a copy of his oral presentation to the CIMM 1984 meeting.

References

Bridgwater, D. and Harry, J.T.
1968: Anorthosite xenoliths and plagioclase megacrysts in Precambrian intrusions of south Greenland; Meddelser om Gronland, bd. 185, no. 2, p. 1-243.

Curtis, L.W. and Currie, K.L.
1981: Geology and petrology of the Red Wine alkaline complex, central Labrador; Geological Survey of Canada, Bulletin 294, 61 p.

Emslie, R.F.
1978: Anorthosite massifs, rapakivi granite and Late Proterozoic rifting of North America; Precambrian Research, v. 7, p. 61-98.

Emslie, R.F., Cousens, B., Hamblin, C., and Bielecki, J.
1980: The Mistastin batholith, Labrador-Quebec, and Elsonian Composite Rapakivi suite; in Current Research, Part A, Geological Survey of Canada, Paper 80-1A, p. 95-100.

Hill, J.P.
1982: Geology of the Flowers River-Notakwanon River area, Labrador; Newfoundland Department of Mines and Energy, Report 82-6, 140 p.

Linthout, K.
1984: Alkali zirconosilicates in peralkaline rocks; Contributions to Mineralogy and Petrology, v. 86, p. 155-158.

Manning, D.A.C., Hamilton, D.L., Henderson, C.M.B., and Dempsey, M.J.
1980: The probable occurrence of interstitial Al in hydrous F-bearing and F-free aluminosilicate melts; Contributions to Mineralogy and Petrology, v. 75, p. 257-262.

Srivastava, S.P.
1978: Evolution of the Labrador Sea and its bearing on the early evolution of North America; Journal Royal Astronomical Society, v. 52, p. 313-357.

Taylor, F.C.
1975: Lac Brisson, Quebec-Newfoundland; Geological Survey of Canada, Map 1439A.

Upton, B.G.J.
1974: The alkaline province of southwest Greenland; in The Alkaline Rocks, ed. H. Sorenson; Interscience, 221-238.

Zajac, I.S., Miller, R., Birkett, T., and Nantel, S.
1984: The Strange Lake deposit, Quebec-Labrador, Canadian Institute of Mining and Metallurgy, Bulletin, v. 77, p. 60.

-10-

VALHALLA GNEISS COMPLEX, SOUTHEAST BRITISH COLUMBIA: 1984 FIELD WORK

Project 830006

Randy Parrish, Sharon D. Carr[1], and Richard L. Brown[1]
Precambrian Geology Division

Parrish, R., Carr, S.D., and Brown, R.L., Valhalla gneiss complex, southeast British Columbia: 1984 field work; in Current Research, Part A, Geological Survey of Canada, Paper 85-1A, p. 81-87, 1985.

Abstract

Field studies in 1984 focused on mapping rock units of the Valhalla gneiss complex south to the Columbia River with an emphasis on kinematics indicators and shear zones. East-directed sense of shear is characteristic of most granitic sheets throughout the complex; brittle faulting on the east side of the complex postdates east-directed ductile shear within granitic rocks of Paleocene-Eocene age. West-directed shear on the west side of the complex along west-dipping zones postdates earlier east-directed shear and may be related to uplift. It is not clear whether compressional or extensional tectonic models, or both, best explain the field and geochronological data.

Quartzite pebble conglomerate identified and mapped in upper Gwillim Creek has helped outline an early north-northwest-trending antiform of >500 m amplitude which repeats stratigraphy. The age of most metasedimentary rocks and of several igneous rock units is uncertain, although many of the metasedimentary rocks of the Nemo Lakes area on the north side of the complex are now regarded as metamorphosed Slocan Group.

Résumé

Les études entreprises sur le terrain en 1984 se sont concentrées sur la cartographie des unités lithostratigraphiques du complexe granitique de Valhalla vers le sud jusqu'au fleuve Colombia, notamment sur l'identification des indicateurs cinématiques et des zones de cisaillement. Un cisaillement dirigé vers l'est caractérise la plupart des couches granitiques du complexe; la formation de failles cassantes sur la marge est du complexe a été postérieure au cisaillement ductile vers l'est qui s'est produit à l'intérieur de roches granitiques paléocènes-éocènes. Le cisaillement vers l'ouest qui s'est produit sur la marge occidentale du complexe le long des zones inclinées vers l'ouest a été postérieur au cisaillement vers l'est plus ancien et pourrait être lié au soulèvement. On ne sait pas encore si un modèle tectonique en compression ou en extension ou les deux expliquent le mieux les données géochronologiques et les données prélevées sur le terrain.

Un conglomérat à galets de quartzite identifié et cartographié sur le cours supérieur du ruisseau Gwillim a permis de délimiter une ancienne structure anticlinale à orientation nord-nord-ouest dont l'amplitude est supérieure à 500 m et qui répète la stratigraphie. L'âge de la plupart des roches métasédimentaires et plusieurs unités ignées est encore incertain bien qu'un grand nombre de roches métasédimentaires de la région des lacs Nemo sur la marge nord du complexe soient maintenant considérées comme faisant partie du groupe métamorphisé de Slocan.

[1] Ottawa-Carleton Centre for Geoscience Studies, Department of Geology, Carleton University, Ottawa, Ontario K1S 5B6

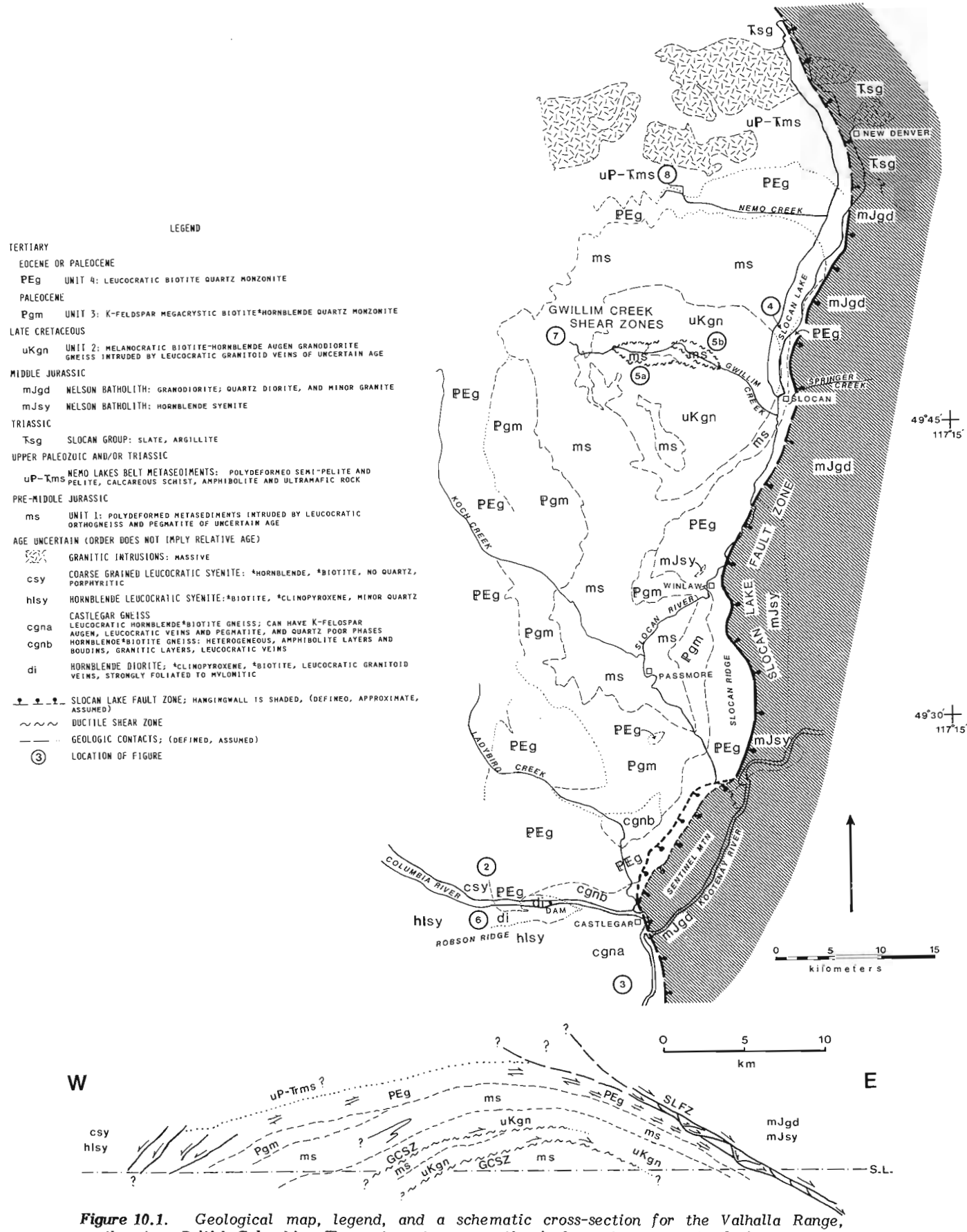

Figure 10.1. *Geological map, legend, and a schematic cross-section for the Valhalla Range, southeastern British Columbia. The east-west cross-section is drawn to represent relations between rock units in the vicinity of Gwillim Creek and Slocan. On the section the west-directed shears on the left (west) side are projected northwards from the Columbia River area.*

Introduction

Field data from the previous summer (Parrish, 1984), recorded the presence of an important east-dipping ductile shear zone of considerable thickness associated spatially with a brittle east-dipping fault zone on the east flank of the Valhalla gneiss complex. Together, this zone was termed the Slocan Lake fault zone and was shown to extend from the north end of Slocan Lake (Parrish, 1981) southwards for over 100 km, joining the Champion Lake fault of Simony (1979) and Corbett and Simony (1984). The age of the feature was thought to be early Tertiary since it affected a granitic rock unit known to be Paleocene in age.

The 1984 season involved the mapping of rock units from the fault zone westwards across the north-south culmination of the complex, and southwards from the Passmore Dome (Reesor, 1965) to Robson Ridge, south of the Columbia River at Castlegar (Fig. 10.1). Additional work within metasedimentary units of the complex exposed in Gwillim Creek drainage, revealed that early fold structure and stratigraphy can be recognized. These structures shed light on the early history of the area, prior to development of east-directed shear zones and extensive granitic plutonism. In addition to summarizing rock units and structure, preliminary age determinations are summarized, and possible tectonic models are briefly discussed.

Results of mapping, southern Valhalla Complex

Mapping was conducted over a two month period; the details are shown in Figure 10.1 and discussed more extensively in Carr (1985) and only a brief summary is given here. The Valhalla complex south of Koch Creek is similar to that described farther north by Reesor (1965) in that several sheets of granitoid rock, each up to 2 km thick, are arched over a north-south culmination whose axis is approximately 10 km west of the Slocan Lake fault zone. In addition the main units close to the south, wrapping around the southern end of the complex. All of these granitoid units are variably deformed. Relationships on the western flank are not well understood, but some syenitic rocks, generally having minor or no ductile deformation, are prevalent. Some are intrusive whereas others have probable faulted contacts with deformed granitoid rocks to the east. The Castlegar gneiss of Simony (1979), in part, has intrusive relationships to rocks of the complex near Castlegar.



Figure 10.2. *Deformed syenite of unit* ***csy*** *near Syringa Creek. View looks north; C-S fabric (Berthe et al., 1979) in this west-dipping shear zone indicates movement is left side down. Black layers in lower right may be either black mylonite or possibly basaltic dykes which are deformed as well, as described in text. (GSC 204049-J)*

Lithologies of igneous rocks

Map units 2, 3, and 4, labelled in Figure 10.1 as **uKgn, Pgm,** and **PEg,** have been described by Parrish (1984) and Carr (1985). Their ages, however, are now known to be Late Cretaceous, Paleocene, and Paleocene-Eocene, respectively, based on zircon U-Pb dating at well-exposed localities within the ductile shear zone along or near the Slocan Valley. Map unit **PEg,** the biotite leuco-quartz monzonite which is extensively truncated by the brittle fault on the east side of the complex, can be traced almost continuously around the entire gneiss dome over an area of 80 km by 30 km, and is in places over 2 km thick. A total lack of hornblende, the presence of smoky quartz and only a few per cent mafic minerals are characteristic of this very homogeneous granitoid unit. Comparison to Little (1960), and in particular, his discussion of the 'Valhalla plutonic series' reveals that the southern Valhalla Range, underlain in part by this extensive sheet-like unit, is the type locality of this plutonic series, previously considered to be early Cretaceous or Jurassic in age. Clearly, revision or abandonment of the term 'Valhalla plutonic series' is in order in light of this information and its implications. An additional point is that unit **PEg** thins to the south and last outcrops on the north slope of Robson Ridge where it has been observed to intrude syenitic and dioritic rocks described below.

The upper contact of unit **PEg** is only exposed on the north and west sides of the complex. Generally, the contact is characterized by a zone of leucogranitic sills concordant with metasedimentary rocks on the south side of the Nemo Lakes belt (Parrish, 1981). The Nemo Lakes stock, a term used to describe a leucogranite sheet-like body on the south side of the metasedimentary belt, is now considered to be part of this larger granitic unit. A previous four-point Eocene "errorchron" age for the stock (Parrish, 1981) is consistent with this reassignment in the regional geological context. The revised relationship is incorporated into Figure 10.1.



Figure 10.3. *Castlegar gneiss (unit* ***cgna****) as inclusions within cross-cutting granite, both of uncertain age. (GSC 204049-Q)*

A variety of syenitic rocks is exposed on the southwest flank of the complex, in the vicinity of the Columbia River west of Castlegar, and on Robson Ridge (Figure 10.1). At least five different syenitic rocks have been observed; we believe they can be separated into two groups – those with pink to tan K-feldspar, which probably belong to the distinctive Eocene Coryell plutonic suite (see Little, 1960, p. 90-94) and which have no ductile deformation, and those which have white K-feldspars, are ductilely deformed to varying degrees, and have an uncertain, but older age than the true Coryell syenites. The Coryell syenites have only been observed as small plugs and bodies from Syringa Creek westwards and are not shown on Figure 10.1. Of all the syenitic rocks, most common is a hornblende leuco-syenite (map unit **hlsy**, <5% quartz) which closely resembles the syenite previously termed unit 6 near Winlaw in the upper plate of the Slocan Lake fault zone (Parrish, 1984). The syenite near Winlaw has also been dated using its zircons and is mid-Jurassic in age, clearly related to the Nelson batholith in time. A coarser grained syenite (unit **csy**) containing hornblende ± biotite occurs near Syringa Creek and is shown in Figure 10.2. Another syenitic rock is melanocratic with >50% mafic minerals, including clinopyroxene. We believe these white feldspar-bearing syenitic rocks west of Castlegar to be related since contacts appear transitional and nondistinct, although they are shown as separate units in Figure 10.1.

The Castlegar gneiss, occurring in the vicinity of Castlegar, is a heterogeneous unit containing at least two mappable lithologies, some also disposed in sheets. North of Columbia River, the Castlegar gneiss clearly underlies Unit **PEg** and is invaded by abundant leucogranitic dykes, lenses, and sills. Detailed descriptions of the Castlegar gneiss are provided in Carr (1985). A main K-feldspar megacrystic hornblende-bearing monzonite or quartz monzonite (unit **cgna**) is apparently transitional in lithology with the hornblende leucosyenite previously described and may be related in origin. Southwest of Castlegar, the Castlegar gneiss is clearly cut by a small body of undeformed fine grained granite (Fig. 10.3, not shown in Fig. 10.1) whose age is uncertain. A heterogeneous layered gneiss can also be distinguished (unit **cgnb**, Fig. 10.1). A grey hornblende ± biotite diorite (unit **di**) is exposed at the deepest structural level along the Columbia River near Keenleyside Dam and generally underlies leucocratic syenitic units and megacrystic Castlegar gneiss (Fig. 10.1).

Four types of dyke rocks have been recognized, but are not shown on Figure 10.1 as they are at most 5 m in width. Foliated basic dykes of uncertain age are involved in discrete, west-directed, west-dipping shear zones present between Keenleyside Dam and Deer Park along Lower Arrow Lake. They clearly crosscut units **PEg** and **csy** near Syringa Creek, but are strongly sheared and recrystallized. Crosscutting, north-trending, ~70° east-dipping planar basaltic dykes with chilled margins are common west of Keenleyside Dam. Often, fractures are present in identical orientation but without dykes. This dyke set is likely middle or late Eocene in age. One unusual dyke of similar orientation was found on the south shore of Lower Arrow Lake near the dam. It is also basaltic but contains abundant xenocrysts of mantle origin (Cr-diopside, orthopyroxene, olivine, augite, some with reaction rims) along with less common xenoliths of granite. Although it occurs only a few metres from other inclusion-free basaltic dykes, it may be considerably younger as most rocks of this type are Miocene or younger in southern British Columbia (Ross, 1983). Aplite dykes have been observed both near Syringa Creek within granitoid and other units and in the central part of the complex near central Gwillim Creek. In general they are northerly-trending, steeply-dipping, and at locale 5a of Figure 10.1 are entirely undeformed. This is not true of similar appearing dykes in lower Gwillim Creek (locale 5b of Fig. 10.1) where they are deformed (see Fig. 10.5, discussed later).

Structural fabric and shear zones

Features within unit PEg

Early in the 1984 field season, it became apparent that an east-directed sense of shear was well-developed within unit **PEg** in the south-central and southwestern parts of its exposure, particularly near Columbia River and Ladybird Creek (Fig. 10.1, Carr, 1985). By east-directed we imply the relative sense of displacement of the upper member of the shear couple as determined from kinematic indicators in outcrop or oriented specimens. This observation is at variance with preliminary generalizations of Parrish (1984), which were based on limited field data. An implication of this is that ductile fabric, and the shear zone which it represents, are in part arched over the complex, diverging from the north-south brittle fault zone on the east side of the complex, discussed in more detail by Carr (1985). On the west side of the complex, the ductile east-directed fabric of unit **PEg** is not as uniformly developed as on its east side and it increases in intensity upwards; the fabric is more annealed, and the ductile strain probably occurred at higher temperature than farther east where chlorite-muscovite-quartz assemblages are widespread. The development of porphyroblastic muscovite near Slocan Ridge, near Springer Creek, and elsewhere (Fig. 10.1 and Parrish, 1984, p. 327) is thought to be metamorphic in origin, forming at the expense of biotite in response to low greenschist conditions late in the history of the shear zone. Thin section examination has revealed that these porphyroblasts are kinked and deformed, although they postdate much of the strain in the rock. The syenite directly in the hangwall is now known to be Jurassic, and therefore could not have caused contact metamorphic growth of mica.

In addition to these observations, on the east side of the complex thin, restricted, pseudotachylite veins are developed in the upper kilometre of the lower plate. One of these is shown in Figure 10.4 cutting the foliation within unit **PEg**. The vein is in part parallel to the foliation and in part crosscutting; the vein itself is not deformed and must have formed very late in the ductile strain history of the rock.

Gwillim Creek area

East-directed stretching lineation is developed within metasedimentary and pegmatitic lithologies of unit **ms** near the head of Gwillim Creek. This stretching lineation is the prominent east-west lineation recorded by Reesor (1965), and it is clearly superimposed on older fabrics, summarized below. Within unit **uKgn**, foliation and moderately- to highly-strained augen of K-feldspar are present everywhere; determination of internal shear sense has not yet been possible despite careful examination at many places. In addition, lineation in unit **uKgn** is very weakly developed.

The external relationships of unit **uKgn**, as first observed by Reesor (1965, p. 12) are in part intrusive and in part tectonic in origin. The upper contact with metasedimentary rocks of unit **ms** is transitional and indicative of an intrusive origin, as outlined by Reesor (1965). The lower contact of unit **uKgn**, exposed in two zones or slices (Fig. 10.1, cross-section), is everywhere very sharp. Unit **uKgn** near the contact with unit **ms** is an augen-free hornblende-biotite schist without leucocratic veins (Reesor, 1965) and is extensively recrystallized and annealed. We believe this contact to be a shear zone of considerable displacement. We term these two zones, which constitute an

apparent duplication of the same rock units along a distance of more than 10 km, the Gwillim Creek shear zones (Fig. 10.1). Features of the lower of the two are shown in Figure 10.5; the geometry of this zone is outlined in the schematic cross-section shown in Figure 10.1. Undeformed planar north-south trending aplite dykes intrude the upper Gwillim Creek shear zone (locale 5a, Fig. 10.1) and postdate all displacement. Although not yet examined in detail, the dykes of the lower shear zone (locale 5b) which crosscut foliation in Figure 10.5 are variably deformed, generally indicating east-directed shear. Although not yet proven, this sense of shear is believed to be the sense for the bulk of the strain within the Gwillim Creek shear zones. These aplitic dykes are very late in the total strain history, because some of them are continuous across the **ms-uKgn** contact and are merely folded and flattened. An important implication is that if the aplitic dykes of these two shear zones are the same age, the lower of the two was active later than the upper one. We tentatively interpret the Gwillim Creek shear zones as resulting from structural duplication of a single sheet of unit **uKgn**, thus implying large displacement.

West-directed shears near Columbia River

Discrete west-directed, west-dipping shear zones are extensively developed within diorite, syenites, and granitic rocks near Columbia River west of Keenleyside Dam (Fig. 10.2; Carr, 1985). These cut older east-directed fabric, where present, within unit **PEg**. The west-directed fabric is penetrative only within the diorite (unit **di**) near Keeleyside Dam. Within this diorite, feldspar layers have pulled-apart veins with infilling hornblende, actinolite, epidote and calcite (Fig. 10.6). Steeper more discrete zones of shear cut earlier more penetrative and shallower zones, and both have similar west-directed shear sense. These shears have no evidence of retrogression and probably formed at amphibolite facies conditions. Details of these structures are discussed in Carr (1985). The shears are developed on scales up to ~20 m displacement and ~5 m width but may have much larger analogs; the contact between units **PEg** and **csy** may be one such zone (Fig. 10.1). Both rocks are strongly foliated in the vicinity of the contact, which is unfortunately covered for 3 km north of the Columbia River.

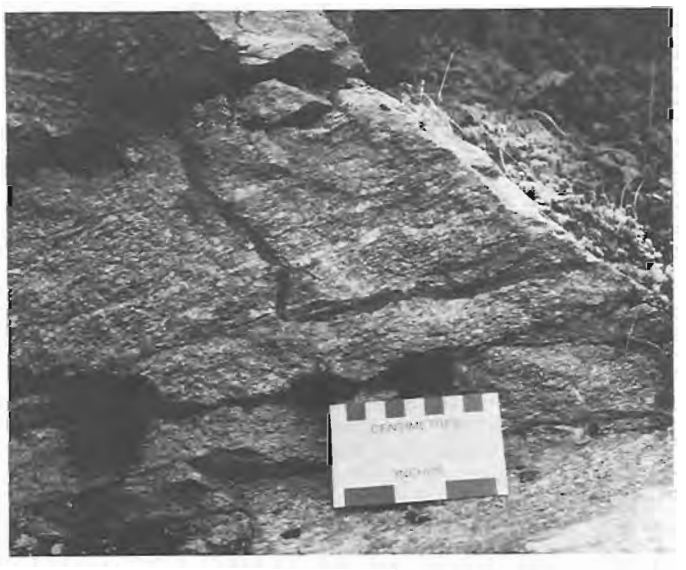

Figure 10.4. *Pseudotachylite vein possibly generated during frictional heating; vein is both parallel and discordant to mylonitic foliation of unit* ***PEg*** *near Cape Horn north of Slocan. View to south. (GSC 204049-H)*



Figure 10.5. *Northeast view of lower Gwillim Creek shear zone (locale 5b); rusty metasediments of unit* ***ms*** *below, grey granitoid gneiss of unit* ***uKgn*** *above. White dotted line indicates the contact, veins are orthogonal to layering and relatively undeformed. Some veins off the right side of the photo (not shown) actually cut across the contact without disruption, although they are folded. Amphibolitic layers are broken and extended as relatively rigid bodies. Cliff is about 30 m high. (GSC 204049-B)*

Structure and stratigraphy of metasedimentary units ms and uP-TRms

A careful examination of rocks in upper Gwillim Creek was made to ascertain the potential of recognizing any stratigraphic succession which might be useful in delineating fold structures.

Despite the large (>50%) amount of migmatite and intrusive leucogranitic rock in this high grade zone (K-feldspar-sillimanite zone), several distinctive rock units were recognized. The most useful was a deformed quartz-pebble conglomerate of variable thickness in a succession of pelite, semipelite and calcareous gneiss. The conglomerate (Fig. 10.7) is composed almost entirely of quartzite clasts in a semipelitic to calc-silicate matrix. Most commonly the clasts are matrix-supported, but this is not always true. The thickness of the conglomerate varies from about two metres to several tens of metres, and there may be more than one conglomerate horizon. Minor northwest-trending folds were observed to be consistent with the presence of a much larger northwest-trending isoclinal antiform which repeats marker units and has an amplitude in excess of 500 m. It is shown schematically in the section of Figure 10.1. This fold has been traced about 5 km along strike but may extend considerably farther. The age of this metasedimentary sequence is uncertain. Quartzite-pebble conglomerates exist in the Windermere, Hamill, and Milford groups of the Kootenay arc, as well as near the base of mantling gneisses of uncertain age in the Monashee complex. Most of the quartz-pebble conglomerates within the Kootenay arc are associated with quartzite, and in the Valhalla Range, the absence of associated quartzite is inconsistent with direct lithologic correlation with Cambrian or older formations; recently, Klepacki (1985, and personal communication, 1984) has described quartzite pebble conglomerates without prominant quartzite in the McHardy Assemblage of the Milford Group, making this a possible candidate for lithologic correlation.



Figure 10.6. *Pull-apart veins infilled with hornblende, calcite, actinolite and epidote within a felsic layer within the diorite of unit* ***di****; south side of Columbia River near Keenleyside Dam. (GSC 204049-M)*

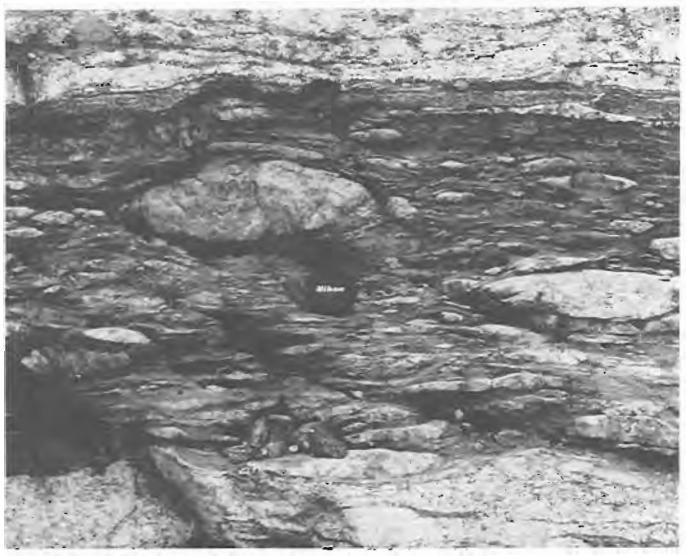

Figure 10.7. *Quartz pebble matrix-supported conglomerate of unit* ***ms*** *near the head of Gwillim Creek. (GSC 204049-C)*

The Nemo Lakes belt was reexamined by one of us (Parrish) with D. Klepacki. Rocks above the ultramafite in the succession described by Parrish (1981) were confidently concluded to be Slocan Group, with marbles low in the sequence being possible equivalents to the Whitewater and related limestones near Sandon. Above the ultramafite for over 500 m, minor folds are absent, the rocks are little deformed and crossbeds were discovered for the first time indicating that the sequence is northwest-facing and right side up (Fig. 10.8). Rocks below the ultramafite are well exposed but only about 300 m of section is present. They lack distinctive lithologies and could be correlated with any of several pre-Triassic lithologic units in the Kootenay Arc, including the Milford Group.

More specific structural and stratigraphic correlation between metasedimentary rocks of the Gwillim and Nemo Creek areas must await mapping in intervening areas.

Age constraints of granitoid units

U-Pb age determinations summarized previously (Parrish, 1984) indicated that units **uKgn** and **Pgm** are about 90 Ma and 63 Ma old, respectively. Additional U-Pb zircon determinations from unit **Pgm** from Slocan Ridge, structurally within 1 km of the Slocan Lake fault, support this Paleocene age assignment. Two determinations from unit **PEg** at Slocan demonstrate that it is late Paleocene or early Eocene, but it contains more inherited zircon, and further work must be done to more precisely determine its numerical age. Two age determinations of zircon from the syenite near Winlaw (unit **mJsy**) show that it is Jurassic in age, clearly part of the hanging wall of the Slocan Lake fault. As the fabrics of units **Pgm** and **PEg** are similar, it can be confidently concluded that much of the ductile deformation in plutonic rocks is of Eocene age. Earlier deformation is clearly evident as dykes of unit **PEg** cut highly deformed metasedimentary rocks near the bottom of the granite, but as yet, the age of earlier folds and fabrics is uncertain.

Preliminary tectonic model and discussion

A plausible tectonic model of the Valhalla Range must take into account the following observations, listed in broadly chronological order:

1. large-scale northwest-trending folding of stratigraphic rocks of uncertain age;
2. emplacement of plutonic rocks at least as old as late Cretaceous and as young as early Eocene;
3. development of extensive easterly-directed shear zones in part contemporaneous with emplacement of plutonic rock;
4. progressive development and probable younging of such shear zones structurally downward with apparent duplication of a plutonic sheet;
5. north-south arching of the area, warping both shear zones and sheets of plutonic and metamorphic rock;
6. development of west-directed, west-dipping ductile shears on the west flank near the Columbia River and east-directed, east-dipping brittle and possibly ductile faults or shears along the east flank of the complex.

The large-scale northwest-trending folds are the earliest structures recognized and may correlate with regional Jurassic deformation evident elsewhere in Omineca Crystalline Belt. Subsequent development of east-directed shear zones, with apparent duplication of rocks over a distance in excess of 10 km (see section, Fig. 10.1) is consistent with a model of a structural duplex developing during regional crustal shortening, similar in geometry to that of Brown et al. (in press) for the Monashee complex. We caution, however, that ductile strain in the rocks of the complex may not all be of similar age or even of similar tectonic setting. For instance, east-directed shear strain within unit **PEg** may have been produced by either progressive crustal shortening as above or by a regime of regional extension as proposed in the model of Wernicke (1981), as long as uplift and arching occurred later. The last phases of movement, items 5 and particularly 6 above, are interpreted as having resulted from regional extension, perhaps at different levels of the crust.

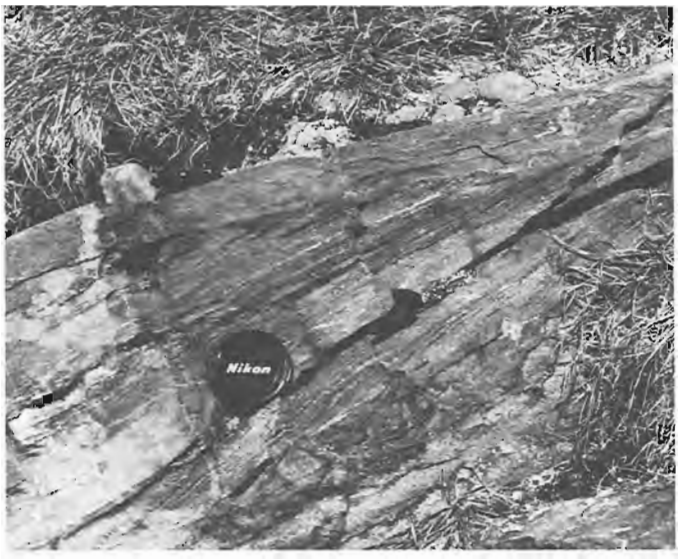

Figure 10.8. *Psammitic bed truncating inclined forset beds within sillimanite schist of the Nemo Lakes belt (unit* ***uP-TRms****). View is to the northwest with tops to the northwest. This locale is thought to be metamorphosed basal Slocan Group. (GSC 204049)*

A final choice between compressional or extensional tectonic models for the bulk of the ductile strain may be possible when more information is available regarding the ultimate location of the root(s) of the shear zones, flattening strain and metamorphic juxtaposition along the shear zones, and more precise timing constraints and cooling history. This work is presently being pursued by the Geological Survey of Canada and Carleton University.

Acknowledgments

David Bethune and Camille Parrish are thanked for very pleasant field assistance and insightful questions; David Klepacki is thanked for generously spending two days with one of us (Parrish) studying the stratigraphy of the Nemo Lakes belt. Phil Simony and Cynthia Corbett kindly shared their experience south of Castlegar which helped orient us with respect to the Castlegar and Trial gneiss and the Champion Lake fault. This manuscript was reviewed by C. Roddick.

References

Berthe, D., Choukroune, P., and Jegouzo, P.
1979: Orthogneiss, mylonite, and non-coaxial deformation of granites: the example of the South Armorican shear zone; Journal of Structural Geology, v. 1, p. 31-42.

Brown, R.L., Journeay, J.M., Lane, L.S., Murphy, D.C., and Rees, C.J.
– Obduction, back-folding and piggyback thrusting in the metamorphic hinterland of the Canadian Cordillera; Journal of Structural Geology. (in press)

Carr, S.D.
1985: Ductile shearing and brittle faulting in Valhalla gneiss complex, southeastern British Columbia; in Current Research, Part A, Geological Survey of Canada, Paper 85-1A, Report 11.

Corbett, C.R. and Simony, P.S.
1984: The Champion Lake Fault in the Trail-Castlegar area of southeastern British Columbia; in Current Research, Part A, Geological Survey of Canada, Paper 84-1A, p. 103-104, 1984.

Klepacki, D.
1985: Stratigraphic and structural relations of the Milford, Kuslo and Slocan Groups, Goat Range, Lardeau and Nelson map areas, British Columbia; in Current Research, Part A, Geological Survey of Canada, Paper 85-1A, Report 36.

Little, H.W.
1960: Nelson map-area, west half, British Columbia (82F W 1/2); Geological Survey of Canada, Memoir 308, 205 p.

Parrish, R.R.
1981: Geology of the Nemo Lakes belt, northern Valhalla Range, southeast British Columbia; Canadian Journal of Earth Sciences, v. 18, no. 5, p. 944-958.

Parrish, R.
1984: Slocan Lake fault: a low angle fault zone bounding the Valhalla gneiss complex, Nelson map area, southern British Columbia; in Current Research, Part A, Geological Survey of Canada, Paper 84-1A, p. 323-330.

Reesor, J.E.
1965: Structural evolution and plutonism in Valhalla gneiss complex, British Columbia; Geological Survey of Canada, Bulletin 129, 128 p.

Ross, J.V.
1983: The nature and rheology of the Cordilleran upper mantle of British Columbia: inferences from perioditite xenoliths; Tectonophysics, v. 100, p. 321-357.

Simony, P.S.
1979: Pre-Carboniferous basement near Trail, British Columbia; Canadian Journal of Earth Sciences, v. 16, p. 1-11.

Wernicke, B.
1981: Low-angle normal faults in the Basin and Range province: nappe tectonics in an extending orogen; Nature, v. 291, p. 645-648.

DUCTILE SHEARING AND BRITTLE FAULTING IN VALHALLA GNEISS COMPLEX, SOUTHEASTERN BRITISH COLUMBIA

Project 830006

Sharon D. Carr[1]
Precambrian Geology Division

Carr, S.D., Ductile shearing and brittle faulting in Valhalla gneiss complex, southeastern British Columbia; in Current Research, Part A, Geological Survey of Canada, Paper 85-1A, p. 89-96, 1985.

Abstract

Valhalla gneiss complex comprises arched layers of paragneiss and granitoid sheets. The structurally highest sheet, a homogeneous biotite quartz monzonite, is Paleocene-Eocene in age. It wraps around the dome and has been ductilely deformed under middle greenschist or higher facies metamorphic conditions, prior to doming of the complex. Asymmetry of mylonitic fabric elements gives an upper member easterly-directed sense of shear on both the east and west flanks of the culmination.

Discrete west-dipping, westerly-directed ductile shears on the southwest flank are late stage features.

The Slocan Lake fault zone, an east-dipping, easterly-directed detachment fault on the eastern margin of the complex is a fairly linear feature which postdates easterly-directed ductile deformation. The fault zone may either be related to doming of the complex or it may postdate this deformation.

Résumé

Le complexe du gneiss de Valhalla se compose de couches arquées de paragneiss et de roches granitiques. La couche la plus élevée, une monzonite quartzifère à biotite, date du Paléocène-Eocène. Elle entoure le dôme et a subi, avant le bombement du complexe, une déformation ductile dans des conditions métamorphiques menant au faciès moyen des schistes verts ou à un faciès plus évolué. L'asymétrie des éléments structuraux mylonitiques donne au terme supérieur une direction de cisaillement vers l'est sur les versants est et ouest de la crête.

Les cisaillements ductiles discrets inclinés et orientés vers l'ouest sur le versant sud-ouest sont les produits du dernier stade de déformation.

La zone de failles du lac Slocan, qui est un décollement orienté et incliné vers l'est sur la marge est du complexe, est quasi linéaire, postérieur à la déformation ductile orientée vers l'est. La formation de cette zone de failles peut être liée au bombement du complexe ou être postérieure à cette déformation.

[1] The Ottawa-Carleton Centre for Geoscience Studies, Department of Geology, Carleton University, Ottawa, Ontario K1S 5B6

Introduction

This report focuses on structural features at high levels in Valhalla gneiss complex. Ductile deformation fabrics and kinematics of the uppermost granitoid sheet in the complex are examined, and a further discussion of the Slocan Lake fault zone, a brittle detachment fault described by Parrish (1984) is presented. A general overview of Valhalla gneiss complex geology, the structural geology at lower levels in the dome and possible tectonic models are discussed by Parrish et al. (1985).

General geology

Valhalla gneiss complex

Valhalla gneiss complex is a domal structure comprised of high grade paragneiss structurally overlain and interlayered with thick granitoid sheets. Four map units (Fig. 11.1) have been defined in the complex (after Reesor, 1965). Unit ms, consists of polydeformed sillimanite grade metasedimentary rocks, and generally discordant leucogneiss and pegmatite of uncertain age, disposed in three sheets or slices. In Gwillim Creek, the lower two sheets have ductiley sheared contacts with overlying unit uKgn (Parrish et al., 1985). Unit uKgn is a melanocratic granodiorite gneiss which has been dated by Parrish (1984) as late Cretaceous. This package of repeated ms and uKgn is overlain by a third sheet of unit ms up to 3 km thick which outcrops around the core of the entire complex. These units are overlain by unit Pgm, a megacrystic quartz monzonite of Paleocene age (Parrish, 1984), and unit PEg, a homogeneous layer of biotite quartz monzonite of Eocene – Paleocene age (Parrish et al., 1985). To the north, unit PEg appears to intrude up-TRms of the Nemo Lakes metasedimentary belt.

General structure. The rock units which form Valhalla gneiss complex have undergone one or more ductile deformation events. Unit ms is multiply deformed; in the Gwillim Creek area large scale northwest-trending folds have been overprinted by a penetrative east-west stretching lineation (see Parrish et al., 1985). The granitoid units vary from massive to foliated to mylonitic in fabric; where deformed, they also commonly exhibit an east-west stretching lineation.

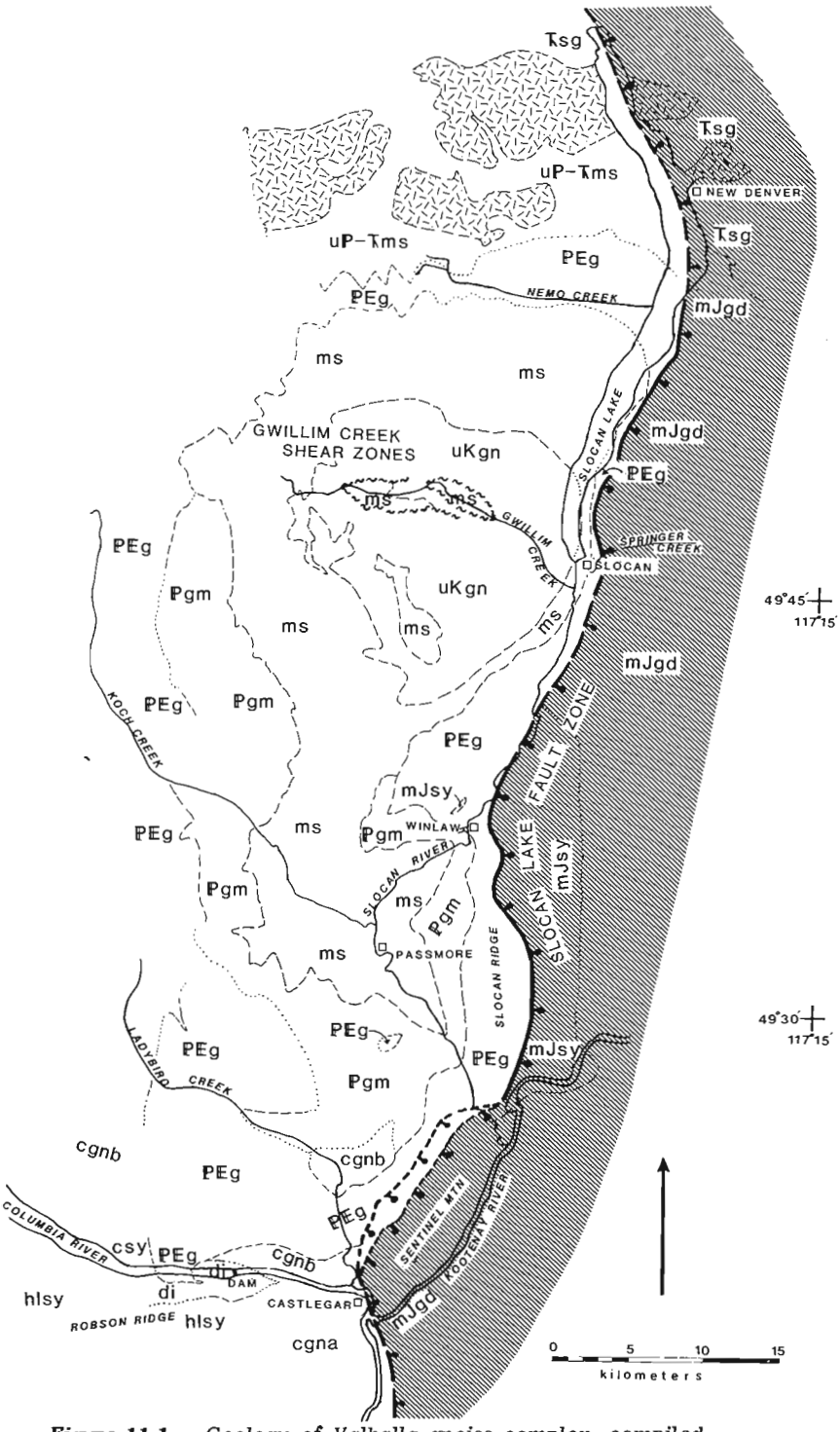

LEGEND

TERTIARY

EOCENE OR PALEOCENE

PEg UNIT 4: LEUCOCRATIC BIOTITE QUARTZ MONZONITE

PALEOCENE

Pgm UNIT 3: K-FELDSPAR MEGACRYSTIC BIOTITE*HORNBLENDE QUARTZ MONZONITE

LATE CRETACEOUS

uKgn UNIT 2: MELANOCRATIC BIOTITE-HORNBLENDE AUGEN GRANODIORITE GNEISS INTRUDED BY LEUCOCRATIC GRANITOID VEINS OF UNCERTAIN AGE

MIDDLE JURASSIC

mJgd NELSON BATHOLITH: GRANODIORITE; QUARTZ DIORITE, AND MINOR GRANITE

mJsy NELSON BATHOLITH: HORNBLENDE SYENITE

TRIASSIC

Tsg SLOCAN GROUP: SLATE, ARGILLITE

UPPER PALEOZOIC AND/OR TRIASSIC

uP-Tms NEMO LAKES BELT METASEDIMENTS: POLYDEFORMED SEMI-PELITE AND PELITE, CALCAREOUS SCHIST, AMPHIBOLITE AND ULTRAMAFIC ROCK

PRE-MIDDLE JURASSIC

ms UNIT 1: POLYDEFORMED METASEDIMENTS INTRUDED BY LEUCOCRATIC ORTHOGNEISS AND PEGMATITE OF UNCERTAIN AGE

AGE UNCERTAIN (ORDER DOES NOT IMPLY RELATIVE AGE)

GRANITIC INTRUSIONS: MASSIVE

csy COARSE GRAINED LEUCOCRATIC SYENITE: *HORNBLENDE, *BIOTITE, NO QUARTZ, PORPHYRITIC

hlsy HORNBLENDE LEUCOCRATIC SYENITE: *BIOTITE, *CLINOPYROXENE, MINOR QUARTZ

CASTLEGAR GNEISS

cgna LEUCOCRATIC HORNBLENDE*BIOTITE GNEISS; CAN HAVE K-FELDSPAR AUGEN, LEUCOCRATIC VEINS AND PEGMATITE, AND QUARTZ POOR PHASES

cgnb HORNBLENDE*BIOTITE GNEISS: HETEROGENEOUS, AMPHIBOLITE LAYERS AND BOUDINS, GRANITIC LAYERS, LEUCOCRATIC VEINS

di HORNBLENDE DIORITE; *CLINOPYROXENE, *BIOTITE, LEUCOCRATIC GRANITOID VEINS, STRONGLY FOLIATED TO MYLONITIC

SLOCAN LAKE FAULT ZONE; HANGINGWALL IS SHADED, (DEFINED, APPROXIMATE, ASSUMED)

DUCTILE SHEAR ZONE

GEOLOGIC CONTACTS; (DEFINED, ASSUMED)

STRIKE AND DIP OF MYLONITIC FOLIATION, TREND AND PLUNGE OF STRETCHING LINEATION, ARROW INDICATES DIRECTION OF MOVEMENT OF UPPER MEMBER OF SHEAR COUPLE (FIGURE 2)

Figure 11.1. *Geology of Valhalla gneiss complex, compiled from Reesor (1965) and Parrish (1984).*

The granitoid bodies have a sheetlike configuration, although their original intrusive geometry is unknown. The sheets comprising Valhalla gneiss complex have been arched into two domal culminations in which compositional layering, metamorphic layering and mylonitic foliation dip gently outward from the centres of the culminations, west of Slocan and near Passmore (Fig. 11.2).

Ductile fabrics and kinematics. On the eastern margin of Valhalla gneiss complex, units PEg and Pgm have a pervasive, moderate to strong mylonitic fabric which consistently indicates an easterly-directed[1] sense of shear. Kinematic indicators used to deduce sense of shear (after Brown and Murphy, 1982; Berthe et al., 1979) include asymmetry of shear plane (C surface) defined by compositional layering, and the mylonitic foliation or flattening plane (S surface). The flattening plane is identified by the orientation of elongate feldspar crystals, pulled-apart feldspars, quartz ribbons, biotite "fish" and elongate strain shadows (Fig. 11.3, 11.4). Shear bands are often well developed and their inclination to the shear plane was also used as a kinomatic indicator (Fig. 11.4). Biotite occurs in pressure shadows of feldspars indicating that biotite was stable during ductile deformation. In unit PEg, in the Slocan lake fault zone, muscovite, chlorite, epidote, calcite, quartz and pyrite occur in fractures in pulled-apart feldspar porphyroclasts. This indicates that at least part of the ductile deformation occurred under greenschist facies metamorphic conditions.

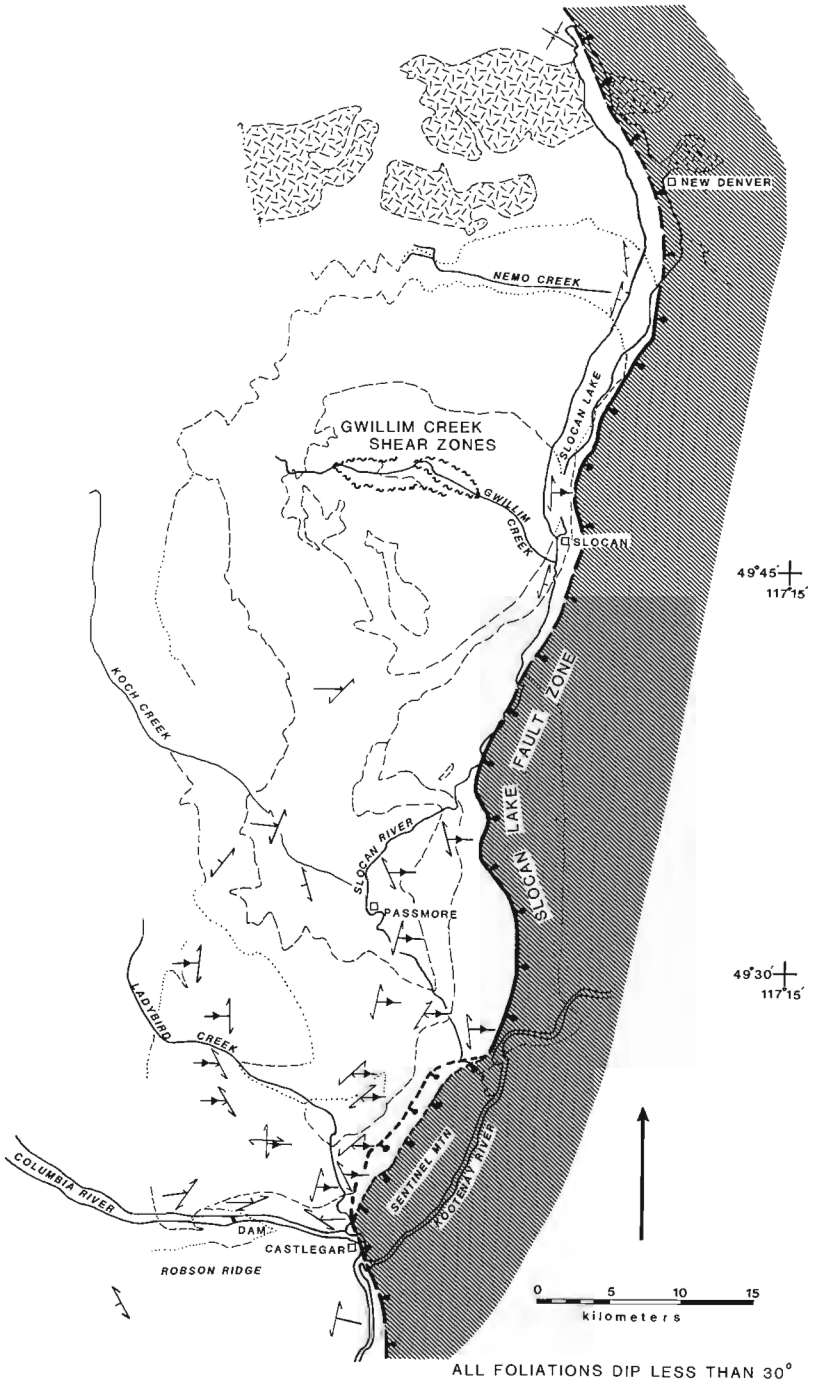

Figure 11.2. *Structure map of Valhalla gneiss complex shows location and sense of shear of kinematic indicators. Data distribution reflects areas studies; for supplementary structural information refer to Reesor (1965).*

Easterly-directed shear sense in unit PEg has been documented across the domal culmination in the Ladybird Creek area. West-dipping mylonitic foliation on the west side of the dome has the same easterly-verging sense of shear as east-dipping mylonites on the east side of the dome. Mylonitic fabric on the west side of the complex, however, tends to be weaker and more discontinuous to the east. Feldspars tend to behave in more brittle fashion and the fabric appears partially annealed. This is the subject of continuing study.

The fabric in unit Pgm on the west side of the complex in Koch Creek is predominantly igneous in nature; the intensity of fabric increases eastward. Where mylonitic fabric is present in units PEg and Pgm, the stretching lineation is consistently oriented due east-west ±10°. More work must be done to determine the bounding geometry of the easterly-directed shear zone which produced mylonitic fabrics in units PEg and Pgm.

Near Passmore, schist and concordant orthogneiss of unit ms underlie mylonitic units Pgm and PEg. Sillimanite-garnet-K-feldspar-graphite schist has a strong east-plunging lineation developed within metamorphic and compositional foliation, which parallels the mylonitic foliation of the overlying units. In this area, sillimanite is stable and the foliation and lineation are strongly developed although partially annealed. Retrogression is almost nonexistent. Easterly-directed kinematic indicators are present, although it is not known whether this high temperature fabric is synchronous with ductile shearing in unit PEg and Pgm (see Parrish, 1985 for discussion of structure, fabric and contact relationships of this rock unit in the core of the dome).

Ladybird Creek area

Eight kilometres north of Castlegar in Pass Creek valley, units Pgm and PEg overlie a window of heterogeneous hornblende-biotite gneiss (unit cgnb). It is a layered

[1] easterly-directed: indicates movement of upper member of shear couple

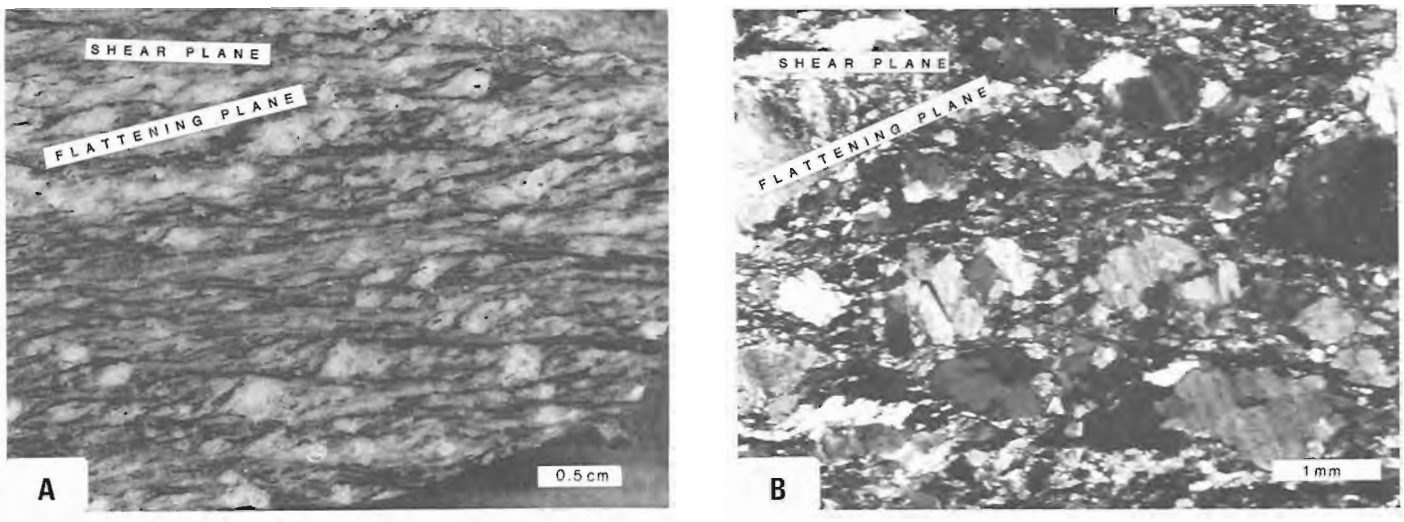

Figure 11.3. *Mylonitic unit PEg exhibits easterly-directed sense of shear. Dextral shear couple indicated by acute angle between mylonitic compositional layering interpreted as plane of shear and elongate and pulled-apart feldspar porphyroclasts which lie in flattening plane. A: rock slab; B: photomicrograph.*

quartzo-feldspathic paragneiss at least 200 m thick, which contains layers and lenses of amphibolite. Abundant leucocratic and pegmatitic veins are irregular and often folded. Lithologiclaly this gneiss can be correlated with unit cgnb of Castlegar gneiss. Although the gneiss contains layers of K-feldspar-augen-hornblende-biotite orthogneiss which may be sills of unit Pgm, the gneiss is not thought to be equivalent to this unit.

The geometry of units cgnb, PEg and Pgm in the Ladybird Creek area is not well understood. The gneiss window of unit cgnb does not occur in the core of a structural culmination as would be expected from the map pattern (Fig. 11.2); the units dip gently southeastward. Biotite quartz monzonite of unit PEg which typically overlies unit Pgm, outcrops on the south side of Ladybird Creek on a steep ridge. On the north side of the creek valley, unit Pgm outcrops at an equivalent elevation. The critical contacts have not yet been observed. The map pattern could be explained if intrusive contacts of units PEg and Pgm with each other and with unit cgnb do not parallel the paragneiss foliation. It could also be accounted for structurally by a west-northwest-trending normal fault in Ladybird Creek.

Columbia River/Castlegar area

Unit PEg intrudes and overlies a complicated package of gneissic and plutonic rocks at the southern end of the complex in the Castlegar area. These rocks include the Castlegar gneiss described by Simony (1979) and a suite of mildly alkaline plutonic rocks which lie to the west of Castlegar in the Columbia River area (Fig. 11.1). The relative ages of these units are unknown at present.

Castlegar gneiss (unit cgna) is a light grey weathering leucocratic, K-feldspar-augen-hornblende paragneiss which is well exposed 1 km west of Castlegar at river level and outcrops on the east end of Robson Ridge west of Castlegar (Fig. 11.1). Minor biotite is present. The amount of quartz varies from negligible to approximately 20 per cent. Accessory minerals include zircon, apatite and sphene. Leucocratic pegmatite and fine grained mafic-rich layers are present. Unit cgna has a strong foliation, minor small scale folds, small scale ductile shears with minor displacement and a moderately well developed east-west lineation. Hornblende-feldspar aggregates and some K-feldspar augen lie in the lineation; however, large hornblende porphyroblasts and K-feldspar augen are often variably oriented. Some asymmetry of fabric elements was observed indicating that it may be possible to determine the sense of shear in this rock unit.

Unit cgnb of Castlegar gneiss is a rusty weathering, layered hornblende-biotite-quartzofeldspathic paragneiss. It outcrops east of Keenleyside Dam on the north side of the river, and in Pass Creek valley 10 km north of Castlegar. It is generally medium grained with up to 35 per cent quartz. Large K-feldspar augen are sometimes present. Granitic intrusions, leucocratic veins and amphibolite layers are variably folded, boudinaged and transposed. Unit cgnb has a well developed foliation and an east-west hornblende lineation. This gneiss is more heterogeneous and mafic than unit cgna which it interdigitates and possibly underlies.

Unit di, a melanocratic hornblende diotite, outcrops on both sides of the Columbia River and in north-facing cliffs on Robson Ridge near Keenleyside Dam. It underlies cgnb on the north side and unit hlsy on the south side. The diorite is homogeneous, but is crosscut by leucocratic veins, pink syenite veins and granite dykes, all of which are variably folded and strained. The fabric in unit di varies from massive to very highly strained where discrete shears have developed. Hornblende, actinolite, epidote, calcite and quartz are observed in extension fractures, necks of boudins and across joint surfaces.

Unit hlsy coutcrops in the western part on Robson Ridge. It is a generally massive leucocratic hornblende syenite which varies to quartz syenite and quartz monzonite. Megacrystic phases have been observed on Robson Ridge. This unit is believed to be gradational with unit cgna of Castlegar gneiss.

Unit csy is a coarse grained, quartz-free porphyritic syenite. It outcrops west of unit PEg on the north shore of the Columbia River. Constituent mafic minerals include hornblende, biotite and clinopyroxene. Unit csy is crosscut by north-trending, steeply-dipping basaltic dykes and pink syenite veins and intrusions which are thought to be of Coryell affinity (for discussion of possible correlations of alkalic rocks see Parrish et al., 1985). Unit csy is deformed

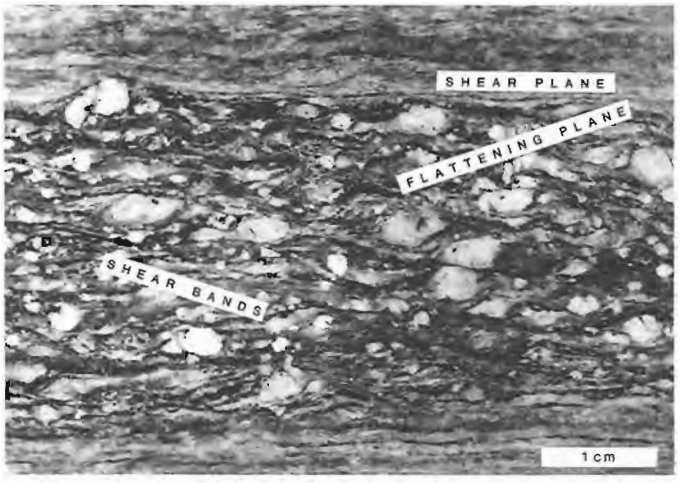

Figure 11.4. *Easterly-directed dextral shear sense in unit PEg indicated by relationship between shear plane, flattening plane and shear bands.*



Figure 11.5. *Discrete shear in coarse grained syenite (unit csy) 12 km west of Castlegar. Photo looking north; sense of displacement is top side down to the west. White aplite vein at right.*

by discrete minor ductile shears (Fig. 11.5). Units csy and hlsy appear to be in gradational contact with melanocratic clinopyroxene-biotite phases (not shown on map), which outcrop on the shoreline west of Syringa Creek.

Unit PEg has a gradational igneous contact with underlying unit cgnb where PEg intrudes and contains inclusions of Castlegar gneiss. The quartz monzonite (unit PEg) thins suddenly and terminates on the south side of the river where it intrudes the hornblende diorite (di). To the west, massive layering in PEg appears to be truncated by unit csy, although the contact has not been observed.

These rock units in the Castlegar/Columbia River area form a gentle culmination centred west of Keenleyside Dam (Fig. 11.2). This could be the continuation of a broad north-south trending anticline mapped by Simony (1979) in Castlegar and Trail gneiss farther south.

Discrete shear zones. Discrete ductile shear zones with displacements of centimetres to metres have been observed in all rock units in the Columbia/Castlegar area except the leucocratic hornblende syenite (unit hlsy). These shears are best developed and most common on the west side of the culmination in units di, PEg, and csy west of Keelyside Dam (Fig. 11.5, 11.6). Most of the shears dip moderately to the west with a westerly-directed sense of displacement. Approximately 20 per cent of the shears dip eastward with the opposite sense of displacement.

North-trending basaltic dykes in the general area crosscut ductile easterly-verging fabric in PEg. These dykes are involved in discrete west-side-down shears indicating that these shears are relatively late features (Fig. 11.6). Hornblende is stable in the shear zones. This requires that high temperatures prevailed in this area until late in the deformation history.

The Slocan Lake fault zone

The Slocan Lake fault zone is an approximately 100 km long north-south trending feature. It is a gently east-dipping (<35°), detachment fault in which the upper plate moved down to the east. This feature is a cataclastic zone characterized by brecciated rock and by discrete fault planes which occur in both fault breccia and coherent rock.



Figure 11.6. *West-dipping westerly-directed discrete ductile shear in unit PEg 10 km west of Castlegar. Basaltic dykes are involved in the deformation.*

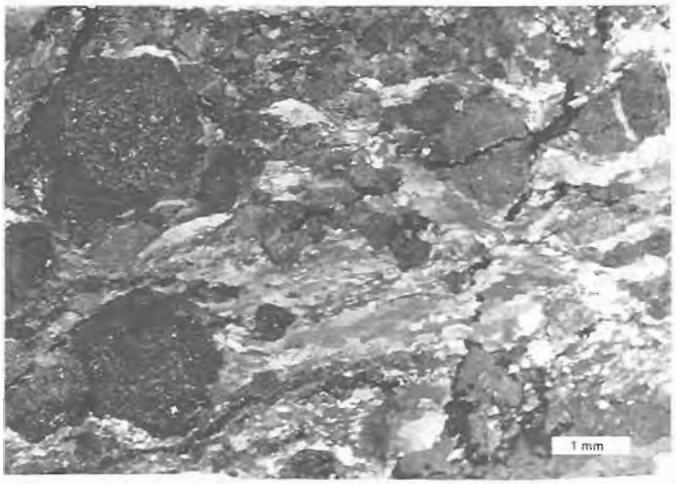

Figure 11.7. *Photomicrograph of cataclastic biotite quartz monzonite (Unit PEg) in the footwall of the Slocan Lake fault zone. Elongate quartz grains, quartz subgrains and recrystallized matrix are relict mylonitic features which are clearly crosscut by quartz filled fractures. Feldspar crystals are altered to sericite.*

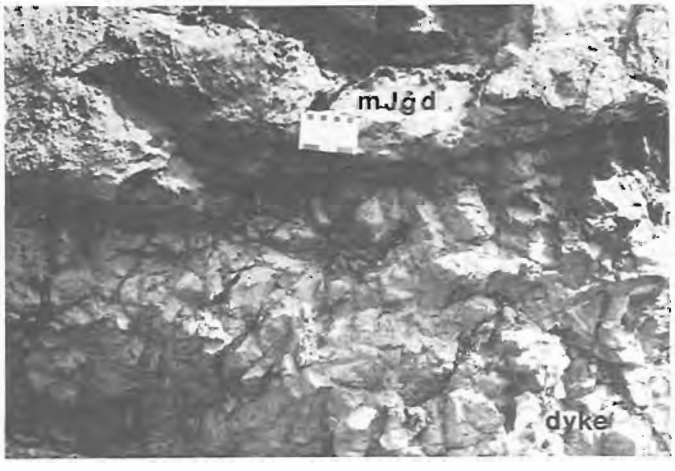

Figure 11.8. *Brecciated granodiorite (unit mJgd) and basaltic dyke in hanging wall of Slocan Lake fault zone.*

Local (<0.5 m thick) mylonite zones associated with discrete, apparently small scale, faults are present on Slocan Ridge and at Cape Horn north of Slocan, but the most significant deformation in the Slocan Lake fault zone is brittle. In the Slocan area, the fault zone is 40-250 m thick, but it appears to be thicker to the south on Slocan Ridge. The Slocan Lake fault zone is characterized by retrograde alteration, although retrograde mineral assemblages are not confined to the fault zone. The fault zone, mapped in creek valleys in the Slocan area, was found to dip 25-35° to the east, roughly paralleling the mylonitic foliation in unit PEg. In this area, the cataclastic fault zone is up to 250 m thick in unit PEg and approximately 50 m thick in Nelson batholith (unit mJgd). Stepped mineral fiber growth on polished and grooved surfaces are the main indicators of movement direction. For most of its length, the Slocan lake fault zone juxtaposes middle Jurassic Nelson batholith in the hanging wall against mylonitic unit PEg in the footwall.



Figure 11.9. *Flat lying fault crosscuts brecciated unit PEg. Relict mylonitic fabric in the hanging wall dips westward. Mylonitic fabric has been completely overprinted by cataclastic fabrics in the footwall.*

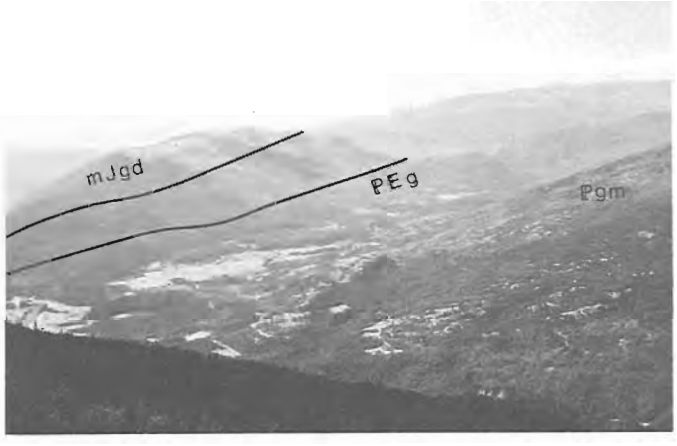

Figure 11.10. *View looking north towards Sentinel Mountain with proposed fault traces of the Slocan Lake fault zone.*

The footwall is characterized by brittley deformed unit PEg. Cataclastic textures include fault breccia, protocataclasite and cataclasite (see Sibson, 1977). Relict mylonitic fabric is clearly crosscut by brittle fracturing and brecciation (Fig. 11.7) and in places by pseudotachylite. The fault zone cuts across section in the footwall; north of Slocan unit ms is in fault contact with Nelson batholith and unit PEg is not present.

In the fault zone, unit PEg has been retrograded to chlorite grade. Chlorite is ubiquitous and feldspars are altered to sericite and clays, giving the rocks a mottled pink and green weathering colour. Epidote, calcite and pyrite occur on joint and fracture planes. Rare quartz veins are present. Biotite, which is usually stable in unit PEg, is not present in the fault zone but muscovite porphyroblasts are. They are generally oriented in the stretching lineation, are slightly deformed and are sometimes pulled-apart. Muscovite growth may have taken place during late stages of the ductile easterly-directed shearing event in unit PEg, or it may have occurred at early and/or lower level stages of movement on the Slocan Lake fault zone.

In the immediate hanging wall of the fault, the Nelson batholith rocks are cataclastic with chlorite alteration. Veins and quartz-infilled fractures are observed in fault breccia in the Slocan Lake area. The Nelson batholith is considerably less deformed than the underlying mylonitic quartz monzonite, and relict igneous fabric can still be recognized. Figure 11.8 shows a fractured basaltic dyke in granodiorite fault breccia.

West-dipping mylonitic foliation is often observed in the fault zone, as are east-dipping faults which crosscut both ductile and cataclastic fabric (Fig. 11.9). It is suggested that these faults are listric normal faults which cause the originally east-dipping fabric to be rotated into a west-dipping orientation. This geometry would account for the elongate lens of retrograded and brecciated middle Jurassic hornblende syenite (unit mJsy), which overlies a package of west-dipping mylonitic biotite quartz monzonite in the footwall of the major fault zone near Winlaw.

Sentinel Mountain

Further work must be done to delimit the geometry and fault trace of the Slocan Lake fault zone in the Sentinel Mountain area north of Castlegar. A massive to weakly deformed biotite quartz monzonite similar in lithology to unit PEg, but more heterogeneous in grain size and fabric, outcrops on the western flank of Sentinel Mountain. Its lower contact is generally recessive, but brecciated zones are observed at the top of the underlying mylonitic unit PEg. Its upper contact with Nelson batholith, observed in one locale, is a discrete mylonite zone. The age of this quartz monzonite is unknown. If this unit is in fault contact with Nelson batholith (as shown in Fig. 11.1, 11.10), then the Slocan Lake fault zone splays, creating a fault bounded footwall horse. If the upper contact is not faulted, then a hanging wall/footwall cutoff exists within unit PEg, implying that there is relatively little displacement on the Slocan Lake fault zone. If the quartz monzonite is part of the Nelson batholith, then the originally proposed fault trace suggested by Parrish (1984) is correct.

Continuation of the fault zone

To the north of Valhalla gneiss complex, the Nemo Lakes belt metasedimentary rocks (unit uP-TRms) and slate of the Slocan Group (unit TRsg) have been intruded by unfoliated granitic stocks (Parrish, 1981). Continuation of the Slocan Lake fault zone along the northern half of Slocan Lake is implied by structural and metamorphic discontinuities in these rocks across the lake. A large-scale, northwest-trending syncline on the northwest shore of Slocan Lake does not continue across the lake. High grade uP-TRms metasedimentary rocks on the western lakeshore oppose low grade slates of TRsg on the eastern shore (Parrish, 1981). The presence of retrograded cataclastic zones in the granitic stocks north of New Denver on the east shore support this argument. They are interpreted to be part of the hanging wall assemblage. The Slocan Lake fault zone is assumed to die out to the north; perhaps its displacement is taken up by incompetent rocks of the Slocan Group (unit TRsg).

At its southern end, the Slocan Lake fault zone is thought to feed into the Champion Lake fault (described by Corbett and Simony, 1984), which continues southward in the Columbia River valley towards Trail. Unfortunately, outcrop along the fault trace in the Castlegar area is poor due to glaciation. Retrograde cataclastic zones occur in Nelson batholith on the southwest end of Sentinel Mountain and on the south shore of the Kootenay River near the confluence of the Columbia and Kootenay rivers. The proposed hanging wall and footwall rock units in the Castlegar area have general characteristics which are similar to those seen at corresponding structural levels farther north in the Slocan River valley. The Bonnington pluton in the hanging wall of the Champion Lake fault in the Castlegar area is equivalent in age and lithology to Nelson batholith in the hanging wall of the Slocan Lake fault zone (Little, 1960). The Castlegar gneiss, forming the footwall of the Champion Lake fault, has undergone a complex high temperature ductile deformation history, as have rocks in the footwall of the Slocan Lake fault zone. As suggested by Corbett and Simony (1984), it is probable that the Castlegar gneiss and Bonnington pluton are separated by a brittle feature, the northward continuation of the Champion Lake fault, which is continuous with the Slocan Lake fault zone.

Conclusion

The Slocan Lake fault zone is a dominantly brittle fault which clearly postdates ductile shearing in unit PEg. Mylonitic fabric in the footwall is brecciated and retrograded to chlorite grade. Nelson batholith appears to be faulted as a fairly coherent sheet. Most of the deformation has been accommodated in the footwall. However, the faulted, "back-rotated" syenite near Winlaw and deeply incised linear topographic features in Nelson batholith indicate that there are internal structural complexities in the hanging wall rocks. As yet no certain hanging wall/footwall cutoffs exist, so there is no means of determining the order of magnitude of the displacement on the fault. North of Slocan where unit ms is in fault contact with Nelson batholith, the fault zone has cut down-section removing unit PEg. In this area the minimum displacement is 400 m, which is the minimum thickness of unit PEg.

Discussion

Paleocene – Eocene biotite quartz monzonite of the uppermost sheet (unit PEg) of Valhalla gneiss complex wraps around the dome and was ductilely deformed under middle greenschist or higher grade metamorphic conditions. Sense of shear determined from well-developed mylonitic C and S surfaces and shear bands is consistently easterly-directed on both east and west flanks of the culmination. Development of this consistent fabric must have predated arching implying that the doming and at least some of the ductile deformation of Valhalla gneiss complex are early Tertiary events. Further work will be undertaken to determine the relationship between shearing in unit PEg and deformation at lower structural levels in the dome.

The Slocan Lake fault zone, an east-dipping, easterly-directed detachment fault on the east flank of Valhalla gneiss complex is a relatively late, dominantly brittle feature. Discrete west-dipping, westerly-directed ductile shears on the west flank are late stage features. Further study of the orientation of these structures and strain analysis may resolve interrelationships between these features and easterly-directed shearing in unit PEg.

The implications of this study are discussed further by Parrish et al. (1985).

Acknowledgments

This project was in part funded by National Research Council of Canada Operating Grant A6293 to R.L. Brown. I am grateful to Randy Parrish and Dick Brown for their help and advice and to Dave Bethune for assistance in the field.

References

Berthe, D., Choukroune, P., and Jeguzo, P.
1979: Orthogneiss, mylonite and non-coaxial deformation of granites: the example of the South Armerican Shear Zone; Journal of Structural Geology, v. 1, p. 31-42.

Brown, R.L. and Murphy, D.C.
1982: Kinematic interpretation of mylonitic rocks in part of the Columbia River fault zone, Shuswap terrane, British Columbia; Canadian Journal of Earth Sciences, v. 19, p. 456-465.

Corbett, C.R. and Simony, P.S.
1984: The Champion Lake Fault in the Trail-Castlegar area of southern British Columbia; in Current Research, Part A, Geological Survey of Canada, Paper 84-1A, p. 103-104.

Little, H.W.
1960: Nelson map area, west half, British Columbia (82F W½); Geological Survey of Canada, Memoir 308, 205 p.

Parrish, R.R.
1981: Geology of the Nemo Lakes belt, northern Valhalla Range, southeast British Columbia; Canadian Journal of Earth Sciences, v. 18, no. 5, p. 944-958.

Parrish, R.R. (cont.)
1984: Slocan Lake fault: a low angle fault zone bounding the Valhalla gneiss complex, Nelson map area, southern British Columbia: in Current Research, Part A, Geological Survey of Canada, Paper 84-1A, p. 323-330.

Parrish, R.R., Carr, S.D., and Brown, R.L.
1985: Valhalla gneiss complex, southeast British Columbia: 1984 field work; in Current Research, Part A, Geological Survey of Canada, Paper 85-1A, Report 10.

Ressor, J.E.
1965: Structural evolution and plutonism in Valhalla gneiss complex, British Columbia; Geological Survey of Canada, Bulletin 129, 128 p.

Sibson, R.H.
1977: Fault rocks and fault mechanisms; Journal of the Geological Society of London, v. 133, p. 191-213.

Simony, P.S.
1979: Pre-Carboniferous basement near Trail, British Columbia; Canadian Journal of Earth Sciences, v. 16, p. 1-11.

PRELIMINARY INVESTIGATION OF THE SEDIMENTOLOGY OF AURIFEROUS STRATA IN THE EARLY APHEBIAN (HURONIAN) LORRAIN FORMATION, BETWEEN SAULT STE. MARIE AND ELLIOT LAKE, ONTARIO

DSS Contract 15SQ. 23233-4-0198

G.W. Lowey[1] and D.G.F. Long[1]
Precambrian Geology Division

Lowey, G.W. and Long, D.G.F., Preliminary investigation of the sedimentology of auriferous strata in the early Aphebian (Huronian) Lorrain Formation, between Sault Ste. Marie and Elliot Lake, Ontario; in Current Research, Part A, Geological Survey of Canada, Paper 85-1A, p. 97-101, 1985.

Abstract

Stratiform gold concentrations are associated with hematite laminae and hematitic pebble bands in the middle Lorrain Formation between Sault Ste. Marie and Elliot Lake. The middle Lorrain Formation consists of three members, a lower red quartzite member, a jasper conglomerate member and an upper red quartzite member. The upper and lower red quartzite members can be interpreted in terms of deposition from sandy braided fluvial systems with characteristics in part similar to the South Saskatchewan and Platte river systems. The jasper conglomerate member was deposited from rivers with characteristics similar to proximal parts of the Platte River and the Donjek River. Gold concentrations, while low, appear to be associated with heavy mineral concentrations. They may represent primary placer concentrations or diagenetically altered magnetite-ilmenite placers affected by acid oxidized groundwaters.

Résumé

Dans le milieu de la formation médiane de Lorrain, entre Sault Ste Marie et Elliot Lake, des concentrations d'or stratiformes se présentent en association avec des lamines d'hématite et des sables caillouteux de nature hématitique. La formation médiane de Lorrain est constituée de trois membres, un conglomérat de jaspe intercalé entre des couches de quartzite rouge. On peut attribuer la mise en place des membres inférieur et supérieur de quartzite rouge à l'action des systèmes fluviaux anastomosés à lits sablonneux, dont les caractéristiques rappellent en partie les systèmes des rivières South Saskatchewan et Platte. Quant au conglomérat de jaspe, son dépôt est attribué à des rivières dont les caractéristiques s'apparentent à celles des parties proximales des rivières Platte et Donjek. Les concentrations d'or, bien que faibles, semblent être associées à des concentrations de minéraux lourds. Il peut s'agir de concentrations de placers primaires ou de placers de magnétite-ilménite qui ont subi une altération diagénétique et les effets d'eaux souterraines oxydées et acides.

[1] Department of Geology, Laurentian University, Sudbury, Ontario, P3E 2C6

Introduction

The Lorrain Formation is a thick (0-2.5 km) arenaceous sequence of early Aphebian age. It forms part of the Huronian Supergroup (Cobalt Group), which outcrops in a broad belt between Sault Ste. Marie (41 J), Ontario, and Noranda, Quebec (Fig. 12.1). The discovery of stratiform gold concentrations in the Lorrain Formation in the Cobalt Plain (Colvine, 1982; Long et al., 1982) in concentrations of up to 1200 ppm led to a renewed interest in the potential for placer related gold deposits (Mossman and Harron, 1984) both in the Cobalt Plain (Colvine, 1983; Long, 1984) and in outcrops of Lorrain Formation between Sudbury and Sault Ste. Marie (Tortosa, 1984). The latter study, which formed part of the Sudbury, Timmins, Algoma, Minerals Program (STAMP) funded by the federal government, was designed around a regional geochemical sampling program intended to identify anomalous metal concentrations (including gold) in Lorrain Formation. The present study was initiated to determine the stratigraphic and sedimentological controls on gold distribution in the formation, so as to provide a basis for future exploration. In addition numerous samples were collected from areas not accessible during tenure of the STAMP program in order to provide more comprehensive geochemical coverage. This report provides a brief outline of research undertaken during the first year of this study, and concentrates on the area between Sault Ste. Marie and Elliot Lake.

Previous work

Stratigraphy

The area between Sault Ste. Marie and Elliot Lake has long been a focus of geological activities. According to Frarey (1977) the earliest geological observations were those of Bigsby (1821, 1863) who described strata now included in the Gowganda and Lorrain formations. Bigsby was followed by many notable geologists, including Murray, Logan, and Collins, with the area between Sault Ste. Marie and Thessalon becoming known as the "original Huronian area" (Frarey, 1977). Details of the prior history of investigation, and the sedimentary and tectonic framework of the area are to be found in papers by Collins (1925), Roscoe (1969), Robertson et al. (1969), Card et al. (1972), Robertson (1973), Wood (1973), Frarey (1977) and Young (1973, 1983). The greater part of the area has been mapped by Frarey (1977), with additional detailed mapping by Robertson (1970), Chandler (1973), Wood (1975), Siemiakowska (1977, 1978) and Bennett (1982).

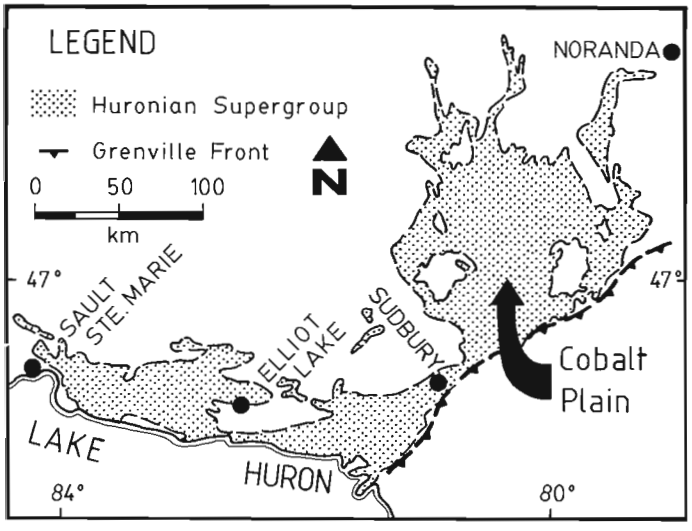

Figure 12.1. *Distribution of Huronian rocks.*

On a regional scale, Collins (1925) and Young (1973) recognized three major subdivisions in the Lorrain Formation. The basal unit consists of varicoloured planar and trough cross-stratified feldspathic and sericitic sandstone with minor mudstone and pebble conglomerate. This is overlain by a middle unit of massive and planar cross-stratified coarse quartz sandstone associated with lenticular beds of quartz and jasper pebble conglomerate. The upper unit consists of white, coarse to medium grained quartz sandstones with only minor amounts of quartz pebble conglomerate. On a local scale the Lorrain can be subdivided into five (Hadley, 1968) to seven (Bennett, 1982) members. Frarey (1977) distinguished six members (Fig. 12.2) and noted that all contacts between members are conformable and gradational.

Sedimentology

Parts of Lorrain Formation have been interpreted in terms of deposition in shallow water marine or lacustrine environments (Collins, 1925; Robertson, 1963; Hadley, 1968), delta fringe and beach environments (Hadley, 1968) and fluvial environments (Bain, 1924; Pettijohn, 1957; Wood, 1973; Young, 1973; Frarey, 1977). The only comprehensive regional sedimentological investigation of the formation to date is that of Hadley (1968) who calculated the mean paleoflow direction in the Bruce Mines – Sault Ste. Marie area to be towards 153 degrees. He determined that at most locations paleoflow was consistently to the south and southeast, with only minor variations between members (Hadley, 1968, p. 164). Hadley (1968) noted that most paleocurrent distributions in Lorrain Formation were unimodal, a feature typical of fluvial deposits, yet he interpreted Lorrain Formation in terms of shallow marine and (pro) delta fringe environments (lower Lorrain), succeeded by "overwhelmed beach" (minor fluvial influence) and "efficient beach" environments in the middle and upper parts of the formation. Hadley's main objection to a fluvial model for the bulk of the Lorrain Formation was the absence of distinct fining upwards cycles, a feature typical of many high-sinuosity (meandering) stream deposits. As Hadley's work predates the proliferation of works on braided river systems (Smith, 1970; Miall, 1977, 1978; Rust, 1978; Long, 1978) his confusion is understandable. Young (1973), utilizing Smith's (1970) observations, suggested that with the exception of the transitional beds at the base of the formation, all of the lower and middle Lorrain Formation are of fluvial origin. Young (1973, p. 113) interpreted the

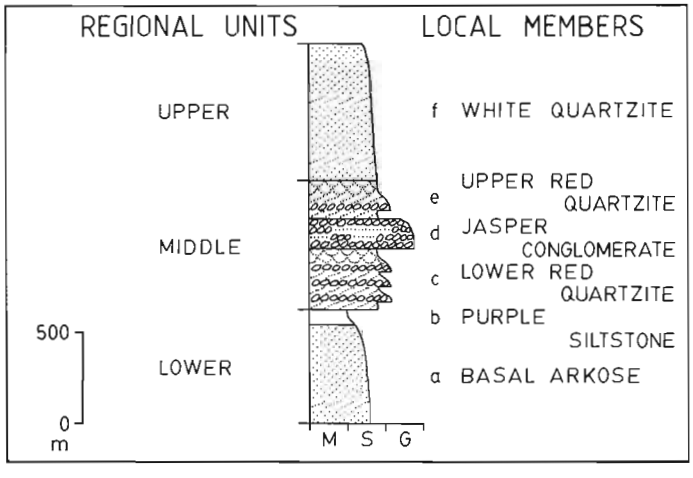

Figure 12.2. *Generalized stratigraphy of the Lorrain Formation in the Sault Ste. Marie – Elliot Lake area (after Young, 1973 and Frarey, 1977).*

uppermost part of the Lorrain (white quartzite member) as coastal plain deposits, which include desert lag and perhaps eolian deposits, in part reworked during marine transgression.

Site of anomalous gold values

Observations by Colvine (1981, 1982, 1983) indicate that, in the Cobalt Plain, hematitic intervals in the middle Lorrain have the greatest gold potential. Colvine (1983) found that where mature hematitic quartz-pebble conglomerates are present in this unit, gold concentrations were considerably above the background value of 2 ppb, with highs from 55 to 1200 ppb. Regional geochemical analysis of Lorrain Formation in the area between Sudbury and Sault Ste. Marie (Tortosa, 1984), indicated that the upper red quartzite member (middle Lorrain) has the highest average gold content (Table 12.1) and that on a smaller scale gold is concentrated in hematite laminae and hematitic pebble bands. Whereas the absolute values obtained by Tortosa (1984) were low (maximum 0.007 oz/ton) they are consistent with the interpretation that gold concentrations are related to primary or diagenetically altered placer concentrations (Colvine, 1981, 1982, 1983; Long and Lloyd, 1983; Long, 1981).

Present study

Sedimentology of the auriferous middle part of Lorrain Formation

Most of the Lorrain Formation appears to have been deposited in a braided fluvial environment. A comprehensive discussion on the sedimentology of the Lorrain Formation is beyond the scope of this preliminary report as some areas of the formation have still to be examined and much of the field data remains to be analyzed. Hence comments are restricted to units in the middle of the formation which are considered to have the greatest gold potential.

The middle Lorrain consists of the lower red quartzite member, the jasper conglomerate member and the upper red quartzite member. Preliminary investigation of these units is consistent with a braided fluvial depositional environment. Both the upper and lower red quartzite members contain less than ten per cent conglomerate (based on the cumulative thickness of conglomerates in all measured sections) in beds from 1 to 20 cm thick. The conglomerates commonly lack visible internal structures and are clast supported. Grain size ranges from granule to pebble grade, with a maximum grain size (apparent intermediate diameter) of 5 cm. Associated sandstones are typically trough and planar cross-stratified, coarse or medium grained quartz arenite, with local pebble concentrations. Trough cross-stratification occurs as cosets in units 10 to 100 cm thick. Planar cross-stratification, in some cases exhibiting graded foresets, normally occurs in solitary sets in beds 10 to 50 cm thick. Specular hematite is concentrated along foreset laminae in planar cross-stratified beds, and near and at the base of trough crossbeds. Hematite is also found in the matrix of some of the conglomerates in the upper and lower red sandstone members.

Conglomerates in the upper and lower red sandstone members probably represent channel lags. Trough crossbedded units are interpreted as the product of deposition from migrating sinuous crested sand dunes, while planar cross-stratification can be related to migration of straight crested bedforms. The greater composite thickness of trough cross-stratified sets may indicate that they accumulated in slightly deeper water than the planar cross-stratified sets. The association of conglomerates and planar and trough cross-stratified sandstones seen in the upper and lower red sandstone members is similar to that proposed for the South Saskatchewan braided river model by Miall (1978). Composite sets of small scale planar cross-stratification, trough cross-stratification and ripple cross-lamination, which Cant and Walker (1978) suggested are typical of sand-flat growth in the South Saskatchewan River, are not obvious in any of the sections observed in the Lorrain Formation. Another departure from the South Saskatchewan River model is the general absence of overbank fines, and greater abundance of conglomerates in the upper and lower red sandstone members of Lorrain Formation. While a sand flat model may not be directly applicable, a mechanism involving simple channel aggradation may be. Cant and Walker (1978) indicated that in the South Saskatchewan River, this type of sequence would be dominated by trough crossbedding, decreasing in scale upwards, with only minor, isolated planar cross-stratified sets related to cross-channel bar formation (sequences like this have been observed in the upper red quartzite member). An alternative to the South Saskatchewan analogue is a proximal Platte type river model (cf. Miall, 1978). While this type of river system is characterized by dominance of planar cross-stratification in sandy reaches, more proximal parts, such as the reach of the South Platte near Denver, contain longitudinal gravel bars with only minor transverse sand bars, hence producing sequences with a lower abundance of planar cross-stratification (Smith, 1970).

The jasper pebble conglomerate member contains between 10 and 90% conglomerate, in units 10 to 700 cm thick. The conglomerates are typically clast supported, massive, crudely planar stratified, or in some cases planar cross-stratified. Median grain size is from granule to cobble grade, with a maximum observed clast size of 15 cm. Interbedded with the conglomerates are massive, plane bedded and planar cross-stratified, very coarse to medium grained quartz arenites, in units 10 to 400 cm thick.

Conglomerates in the jasper pebble conglomerate member represent deposits produced by the migration of longitudinal and transverse gravel bars, as well as channel lag deposits. These probably accumulated in the deeper parts of the alluvial channels, while the massive and planar cross-stratified sands were formed by transverse bars at lower flow stages and in shallower parts of the channels. Some may have accumulated in overbank areas during floods although as the stream banks were essentially unconsolidated due to the absence of organic binding (plant roots) the normal response to increased runoff would be rapid broadening of the channel (cf. Wolman and Brush, 1961), rather than deepening and extensive overbank flooding. Strata in the jasper pebble conglomerate member include sequences which resemble the Donjeck type river model of Miall (1978) or a proximal variant of the Platte model (cf. Smith, 1970).

Table 12.1. Gold content (ppb) of samples from the Lorrain Formation (after Tortosa, 1984)

Member/Lithology	Number of samples	Range	Mean	Standard deviation
White Quartzite	331	0-197	1.5	11.8
Upper Red Quartzite	103	0-197	10.6	26.4
Jasper Conglomerate	74	0-20	1.4	3.3
Lower Red Quartzite	248	0-60	2.4	8.0
Basal Arkose	102	0-160	6.9	22.4
Hematite laminae	94	0-192	7.4	25.0
Pebble beds	191	0-87	2.2	8.2
Hematitic pebble beds	94	0-62	4.4	12.0
Other	500	0-197	3.3	4.7

Regional trends observed in the middle Lorrain include a progressive decrease in both maximum grain size and composite bed thickness from north to south. These trends are consistent with existing (Hadley, 1968) and newly observed paleocurrent observations, and support the interpretation that the Lorrain changes from proximal to distal in this direction. The middle Lorrain does not represent the deposits of a single river system, more likely it was deposited on a composite alluvial braid plain, involving a series of coalescing humid region (wet) alluvial fans.

Discussion and preliminary conclusions

The highest average gold values observed during the STAMP program (Tortosa, 1984) were obtained from the upper red quartzite member. This member is approximately 190 m thick, is widely distributed and as such represents an extensive exploration target.

Based on the assumption that in a simple placer model coarser grained gold (and thus higher values) will accumulate in areas closest to the source areas, Tortosa (1984) proposed that proximal facies of the upper red quartzite member represent the best exploration targets. Placer concentrations are known to occur in both proximal (Witwatersrand: Minter, 1978) and distal facies (Van Horn Sandstone: McGowan and Groat, 1971) of humid region braided alluvial fan deposits. Moreover, Singerland (1984) has shown that regionally heavy mineral concentrations occur in zones parallel to depositional strike, and that their location depends on a complex interaction of original grain size distribution combined with downstream changes in frictional velocity and bed roughness in the depositional system.

A further complication is that the occurrence of gold in the Lorrain may not reflect a primary gold placer concentration but diagenetic concentration during alteration of magnetite/ilmenite placers by acid oxidized groundwater (Clemmey, 1981; Clemmey and Badham, 1982; Long and Lloyd, 1983; Long, 1984, in press). While no additional comments can be made on the distribution of gold in the Lorrain of the Sault Ste. Marie – Elliot Lake area prior to completion of further chemical analysis, the concept that gold concentrations are placer related (primary or diagenetic) does allow some speculation. Singerland (1984) has shown that it is theoretically possible to predict the location of placers in a depositional system if the initial size distribution of the heavy minerals is known, and frictional velocity and bed roughness can be calculated. Application of this approach to middle Lorrain strata may allow for better prediction of target areas, irrespective of primary or secondary character of the gold concentrations.

References

Bain, G.W.
1924: Alluvial fan deposits in the upper Huronian; American Journal of Science, Series 5, v. 8, p. 54-60.

Bennett, G.
1982: Geology of the Two Horse Lake area, district of Algoma; Ontario Geological Survey, Report 210, 63 p.

Bigsby, J.J.
1821: Geological and mineralogical observations on the northwestern portion of Lake Huron; American Journal of Science, 1st series, v. 3, p. 254-272.

1863: On the Cambrian and Huronian Formations; Quarterly Journal, Geological Society of London, v. 19, p. 36-52.

Cant, D.J. and Walker, R.G.
1978: Fluvial processes and facies sequences in the sandy braided South Saskatchewan River, Canada; Sedimentology, v. 25, p. 625-648.

Card, K.D., Church, W.R., Franklin, J.M., Frarey, M.J., Robertson, J.A., West, G.F., and Young, G.M.
1972: The Southern Province; in Variations in Tectonic Styles in Canada, ed. R.A. Price and J.W. Douglas; Geological Association of Canada, Special Paper 11, p. 335-380.

Chandler, F.W.
1973: Geology of McMahon and Morin townships, District of Algoma; Ontario Division of Mines, Geological Report 112, 77 p.

Clemmey, H.
1981: Some aspects of the genesis of heavy mineral assemblages in lower Proterozoic uranium-gold conglomerates; Mineralogical Magazine, v. 44, p. 339-408.

Clemmey, H. and Badham, N.
1982: Oxygen in the Precambrian atmosphere: an evaluation of the geological evidence; Geology, v. 10, p. 141-146.

Collins, W.H.
1925: North shore of Lake Huron; Geological Survey of Canada, Memoir 143, 160 p.

Colvine, A.C.
1981: Reconnaissance of the Lorrain Formation, northern Cobalt Embayment; in Summary of Field Work, 1981, by the Ontario Geological Survey, ed. J. Wood et al.; Ontario Geological Survey, Miscellaneous Paper 100, p. 87-189.

1982: Summary of activities, Mineral Deposits Section, 1982; in Summary of Field Work, 1982, by the Ontario Geological Survey, ed. J. Wood et al.; Ontario Geological Survey, Miscellaneous Paper 106, p. 172-175.

1983: Mineral deposit studies in the Huronian Supergroup; in Summary of Field Work, 1983, by the Ontario Geological Survey, ed. J. Wood et al.; Ontario Geological Survey, Miscellaneous Paper 116, p. 253-255.

Frarey, M.J.
1977: Geology of the Huronian belt between Sault Ste. Marie and Blind River, Ontario; Geological Survey of Canada, Memoir 383, 87 p.

Hadley, D.G.
1968: The sedimentology of the Huronian Lorrain Formation, Ontario and Quebec, Canada; Ph.D. thesis, Johns Hopkins University, Baltimore, Maryland, U.S.A., 301 p.

Long, D.G.F.
1978: Proterozoic stream deposits: some problems of recognition and interpretation of ancient sandy fluvial systems; in Fluvial Sedimentology, ed. A.D. Miall; Canadian Society of Petroleum Geologists, Memoir 5, p. 313-341.

1981: The sedimentary framework of placer gold concentrations in basal Huronian Strata of the Cobalt Embayment; in Summary of Field Work, 1981, by the Ontario Geological Survey, Miscellaneous Paper 100, p. 218-223.

Long, D.G.F. (cont.)
1984: Geology and placer related gold potential of the Huronian Supergroup along the western margin of the Cobalt Plain: Preliminary investigation of parts of NTS 41P/3 and 41P/6; in Summary of Field Work, 1984, by the Ontario Geological Survey, Ontario Geological Survey, Miscellaneous Paper (December 1984).

– Stratigraphic and depositional setting of placer gold concentrations in basal Huronian Strata of the Cobalt Plain; Ontario Geological Survey, 123 p. (in press)

Long, D.G.F. and Lloyd, T.R.
1983: Placer gold potential of basal Huronian strata of the Elliot Lake Group in the Sudbury area, Ontario; in Summary of Field Work, 1983, by the Ontario Geological Survey, ed. J. Wood et al.; Ontario Geological Survey, Miscellaneous Paper 116, p. 256-258.

Long, D.G.F., Leslie, C.A., and Colvine, A.C.
1982: Placer gold in the Huronian of the Cobalt Plain (Abstract); in Geoscience Research Seminar, December 8-9, 1982, Abstracts, Ontario Geological Survey, p. 16.

McGowan, J.H. and Groat, C.G.
1971: Van Horn Sandstone, West Texas: an alluvial fan model for mineral exploration; Bureau of Economic Geology, The University of Texas at Austin, Report of Investigations, No. 72, 57 p.

Miall, A.D.
1977: A review of the braided river depositional environment; Earth Science Reviews, v. 13, p. 1-62.

1978: Lithofacies and vertical profile models in braided river deposits: a summary; in Fluvial Sedimentology, ed. A.D. Miall; Canadian Society of Petroleum Geologists, Memoir 5, p. 597-604.

Minter, W.E.L.
1978: A sedimentological synthesis of placer gold, uranium and pyrite concentrations in Proterozoic Witwatersrand sediments; in Fluvial Sedimentology, ed. A.D. Miall; Canadian Society of Petroleum Geologists, Memoir 5, p. 801-829.

Mossman, G.A. and Harron, G.A.
1984: Witwatersrand-type paleoplacer gold in the Huronian Supergroup of Ontario, Canada; Geoscience Canada, v. 11, p. 33-40.

Pettijohn, F.J.
1957: Paleocurrents of Lake Superior Precambrian quartzites; Geological Society of America Bulletin, v. 68, p. 469-480.

Robertson, J.A.
1970: Township 1A, district of Algoma; Ontario Department of Mines and Northern Affairs, Preliminary Geological Map P.610, scale 1 inch to 1/4 mile.

1973: A review of recently acquired geological data, Blind River – Elliot Lake area; in Huronian Stratigraphy and Sedimentation, ed. G.M. Young; Geological Association of Canada, Special Paper 12, p. 169-198.

Robertson, J.A., Card, K.D., and Frarey, M.J.
1969: The Federal-Provincial Committee on Huronian stratigraphy progress report; Ontario Department of Mines, Miscellaneous Paper 31, 26 p.

Roscoe, S.M.
1969: Huronian rocks and uraniferous conglomerates in the Canadian Shield; Geological Survey of Canada, Paper 68-40, 205 p.

Rust, B.R.
1978: Depositional models for braided alluvium; in Fluvial Sedimentology, ed. A.D. Miall; Canadian Society of Petroleum Geologists, Memoir 5, p. 605-625.

Siemiakowska, K.M.
1977: Geology of the Wakomata Lake area, District of Algoma; Ontario Division of Mines, Geological Report 151, 57 p.

1978: Geology of the Endikai Lake area, District of Algoma; Ontario Geological Survey, Geological Report 178, 79 p.

Singerland, R.
1984: Role of hydraulic sorting in the origin of fluvial placers; Journal of Sedimentary Petrology, v. 54, p. 137-150.

Smith, N.D.
1970: The braided stream depositional environment: a comparison of the Platte River with some Silurian clastic rocks, north-central Appalachians; Geological Society of America Bulletin, v. 81, p. 2993-3014.

Tortosa, D.
1984: Results of the Sudbury, Timmins, Algoma, Minerals Program (STAMP), Project 3: Huronian Supergroup lithogeochemistry; Geological Survey of Canada, Open File 1089.

Wolman, M.G. and Brush, L.M., Jr.
1961: Factors controlling the size and shape of stream channels in coarse non-cohesive sands; in Physiographic and Hydraulic studies on Rivers, 1956-1961, United States Geological Survey, Professional Paper 282-G, p. 183-210.

Wood, J.D.
1973: Stratigraphy and depositional environments of upper Huronian rocks of the Rawhide Lake – Flack Lake area, Ontario; in Huronian Stratigraphy and Sedimentation, ed. G.M. Young; Geological Association of Canada, Special Paper 12, p. 73-95.

1975: Geology of the Rawhide Lake area, NTS 41J/NE, Algoma District, Ontario; Ontario Division of Mines, Geoscience Report 129.

Young, G.M.
1973: Tillites and aluminous quartzites as possible time markers for middle Precambrian (Aphebian) rocks of North America; in Huronian Stratigraphy and Sedimentation, ed. G.M. Young; Geological Association of Canada, Special Paper 12, p. 97-127.

1983: Tectono-sedimentary history of early Proterozoic rocks of the northern Great Lakes region; in Early Proterozoic geology of the Great Lakes Region, ed. L.G. Medaris, Jr.; Geological Society of America, Memoir 160, p. 15-32.

UPPERMOST SHALER GROUP AND ITS CONTACT WITH THE NATKUSIAK BASALTS, VICTORIA ISLAND, DISTRICT OF FRANKLIN

Project 840003

C.W. Jefferson
Economic Geology and Mineralogy Division

Jefferson, C.W., Uppermost Shaler Group and its contact with the Natkusiak basalts, Victoria Island, District of Franklin; in Current Research, Part A, Geological Survey of Canada, Paper 85-1A, p. 103-110, 1985.

Abstract

The Natkusiak Formation overlies the Shaler Group with low-angular unconformity. The uppermost unit of the Shaler Group is a distinctive quartzarenite that is restricted to the southwest sector of the Holman Island Syncline area. The quartzarenite unconformably overlies the Kilian Formation and is here proposed as the Kuujjua Formation. It is cliff-forming, conglomeratic to fine-sand-sized and contains abundant tabular and trough crossbeds. Paleocurrent data suggest local fluvial transport from the south and reworking of the sands in a shallow marine tidal environment.

The uppermost Kilian Formation is informally divided into four members which are bevelled beneath the Kuujjua Formation in the southwest sector and beneath the basalts in the northeast sector. Stratigraphic and paleocurrent data suggest that the Holman Island Syncline was the site of a gently subsiding trough which was uplifted and eroded before eruption of the Natkusiak basalts. The evaporites, sabkha limestones and dolostones of the Kilian Formation are lithologically similar to the Thundercloud Formation in Mackenzie Mountains. Evaporites and red alluvial mudstones of the Redstone River Formation, which overlies the Thundercloud, appear to have no counterparts on Victoria Island.

Résumé

La formation de Natkusiak repose en discordance subhorizontale sur le groupe de Shaler dans l'île Victoria (Territoires du Nord-Ouest). L'unité supérieure du groupe de Shaler est une quartzite sédimentaire caractéristique trouvée uniquement dans le secteur sud-ouest de la région du synclinal de l'île Holman. L'auteur propose de lui donner le nom de formation de Kuujjua. Cette quartzite forme des escarpements et sa granulométrie varie du conglomérat au sable fin. Elle contient d'abondants faisceaux de feuillets obliques séparés par des surfaces tabulaires et en gouttière. Les données sur les paléocourants laissent croire qu'il y a eu transport fluviatile local à partir du sud et remaniement des sables dans un milieu intertidal marin peu profond.

La partie supérieure de la formation de Kilian est divisée officieusement en quatre membres qui sont tronqués sous la formation de Kuujjua dans le secteur sud-ouest et sous les basaltes du secteur nord-est. Les données sur la stratigraphie et les paléocourants laissent croire que le synclinal de l'île Holman a été l'emplacement d'une gouttière qui s'affaissait doucement et qui a été soulevée et érodée avant l'éruption des basaltes de Natkusiak. La lithologie des évaporites, des calcaires de sebkha et des dolomies de la formation de Kilian ressemble à celle de la formation de Thundercloud des monts Mackenzie dans les Territoires du Nord-Ouest. Les évaporites et les pélites allluviales rouges de la formation de Redstone River, sus-jacentes à la formation de Thundercloud, ne semblent pas avoir d'équivalent dans l'île Victoria.

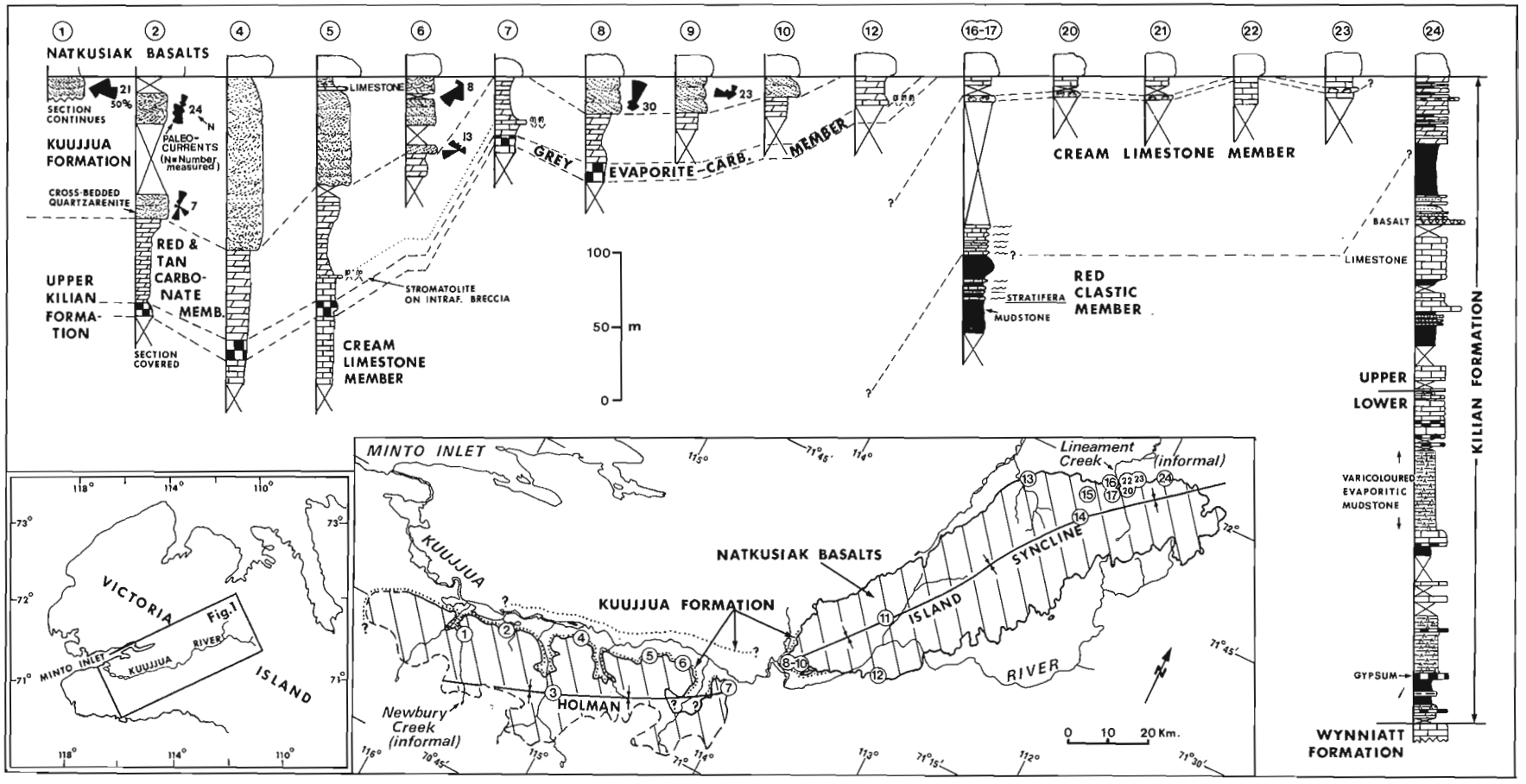

Figure 13.1. *Measured sections of the uppermost Shaler Group, located around margin of Natkusiak basalts (diagonal lines) in northwestern Victoria Island. Sections are numbered in sequence with those of Jefferson et al. (1985).*

Introduction

This paper is a result of reconnaissance evaluation of the copper potential of the Natkusiak basalts (Jefferson et al., 1985). Study of the contact between the Shaler Group and Natkusiak basalts (Thorsteinsson and Tozer, 1962) was prompted by two considerations. First, was the possibility that strong lineaments transecting the Holman Island Syncline were growth faults with concommitant facies and thickness changes (Seeber, 1970; Nelson, 1983). Using this concept, upper Shaler Group strata were considered to have potential for copper deposits formed by downward percolating meteoric waters that leached the cupriferous basalts. A second consideration was the suggestion by Jefferson (1978) and Young et al. (1979), contested by Eisbacher (1978), that the stratigraphy and corresponding mineral potential of the uppermost Shaler Group on Victoria Island resembles that of the Redstone River Formation (Ruelle, 1982; Jefferson and Ruelle, in press) in the Mackenzie Mountains. This study shows that the uppermost Shaler Group more closely resembles the Thundercloud Formation which underlies the Redstone River Formation.

Stratigraphy

Stratigraphic units discussed in this report are summarized in Table 13.1 and measured sections are illustrated in Figure 13.1. The uppermost part of the Kilian Formation (Thorsteinsson and Tozer, 1962) was studied in order to elucidate the nature of the contact between the Shaler Group and Natkusiak basalts. Areas around pronounced lineaments were investigated in detail for possible facies changes and copper occurrences. These investigations led to subdivision of the upper Kilian into three informal members and separation of the uppermost unit as a new formation. The lower Kilian was not examined.

Thicknesses were measured by graduated staff and by altimeter. The units studied outcrop immediately below the Natkusiak basalts near the centre of the Holman Island Syncline. The syncline is divided for descriptive purposes into northeast and southwest sectors, the axes of which trend 040° and 070° respectively. The stratigraphy of the uppermost Shaler Group is continuous between the two sectors.

Upper Kilian Formation

Red clastic member (informal)

The lowest studied stratigraphic section of the Kilian Formation was measured in the "Lineament" Creek (informal name) area (Fig. 13.1) of the northeast sector. At least 40 m of red, quartzose, fine grained sandstone to mudstone contain desiccation cracks, lenticular bedding and ripple marks. In the absence of paleocurrent data this could be a fluvial, lacustrine or intertidal sequence. Correlation of this section is uncertain; it possibly corresponds to the upper part of section N illustrated by Young (1981, Fig. 12.15), here reproduced in Figure 13.1.

The red clastic rocks grade upward through 30 m of section containing at least eight transgressive shoreline (?tidal) cycles of red to green fine grained clastic units, overlain by tan limestones with planar to wavy fine laminae, Stratifera stromatolites, ripple marks, desiccation cracks and hopper-shaped halite casts.

Table 13.1. Stratigraphy of the uppermost Shaler Group, Victoria Island

Formation	Member (Thickness)	Lithology
NATKUSIAK		Basalt flows.
SHALER GROUP		LOW-ANGLE UNCONFORMITY
KUUJJUA (≤90 m)		Mainly coarse grained quartz sandstone but includes lower quartz-pebble conglomerate, upper fine sand and minor limestone. Unidirectional to locally bipolar paleocurrents from trough and tabular cross beds. Fluvial to shallow marine. Not present in northeast sector.
		LOW-ANGLE UNCONFORMITY
	RED & TAN CARBONATE (0-70 m)	Alternating red and tan coloured recessive shaly limestone grading upward to bluff-forming dolomitic mudstone, with one stromatolite biostrome. Sabkha environment. Not present in northeast sector.
UPPER KILIAN (>200 m)	GREY EVAPORITE-CARBONATE (~ 100 m)	Similar sabkha carbonates to above, but grey, with several white to rose-cream coloured gypsum beds.
	CREAM LIMESTONE (~ 100 m)	Aphanitic limestone: finely laminated, flat chip conglomerate, small-scale tepees, ripple cross laminae, one stromatolite biostrome, recessive middle not exposed, bottom 20 m algal limestone with chert nodules.
	RED CLASTIC (>70 m)	Lower part: red, quartose siltstone to sandstone with desiccation cracks, lenticular bedding and ripple marks. Upper part cyclic: red to green sandstones and siltstones with halite casts, overlain by pale tan algal limestone. Transgressive marginal marine.
LOWER KILIAN (>200 m)		Varicoloured evaporitic mudstone and bedded gypsum/anhydrite (Yong, 1981).

Cream limestone member (informal)

The red clastic member is overlain by 20 m of shallow marine limestones containing Stratifera stromatolite biostromes, nodular chert units and laminated shaly limestone interbeds. These limestones are well exposed beneath a thick, columnar jointed sill. Cherty limestone near the basal contact of the sill has been altered to serpentine. In the Lineament Creek area (Fig. 13.1) about 100 m of strata are inferred above the sill, but only a maximum of 40 m are exposed immediately beneath the Natkusiak Formation. Thin basalt flows (Young, 1981, Section P) and evaporites may be present in the covered interval, but the exposed strata consist almost entirely of finely laminated, aphanitic, pale tan limestones which contain desiccation cracks, dewatering structures, concretions, flat pebble conglomerates (both vertically and horizontally stacked), small-scale tepee structures, beach rock, ripple marks and ripple cross laminae. This sequence is interpreted to be of shallow marine to coastal sabkha in origin.

One well-identified nodular chert bed overlain by a columnar stromatolite biostrome outcrops a maximum of 20 m below the basalts in the Lineament Creek area. The stromatolite biostrome was traced 5 km laterally from southwest to northeast where it is bevelled at the sub-Natkusiak unconformity and where its characteristic lithology occurs as hematite-coated boulders in a thin basal conglomerate immediately beneath the basalts.

The lowest Kilian rocks that were examined in the southwest sector (Section 5) are lithologically very similar to the uppermost Kilian rocks in the northeast sector. They are the same colour, composition and contain the same sedimentary structures. A maximum of 40 m of these limestones were measured south of Kuujua River but stromatolites were not noted. These limestones are inferred to be stratigraphically equivalent to, or higher than those exposed at the top of the Lineament Creek succession. A coastal sabkha environment of deposition is inferred.

Grey evaporite-carbonate member (informal)

In the southwest sector the cream-coloured limestones are overlain by 10 to 15 m of recessive, greenish grey to grey dolomitic mudstones. These contain sedimentary structures similar to those in the cream limestone but also include several 10- to 30-cm interbeds of white, pink or pale green gypsum that are thought to represent shallow coastal lagoonal evaporite deposits.

Red and tan carbonate member (informal)

The thin evaporitic member is overlain by alternating tan and red coloured limestone to dolomitic mudstone, containing the same sedimentary structures but with very well developed flat pebble conglomerates which are oriented vertically in polygonal arrays (Fig. 13.2) and characterize a strandline environment. One bed of flat pebble conglomerate 1 to 2 m thick that is overlain locally by columnar stromatolites is correlated between sections more than 40 km apart. This bed is overlain by recessive, maroon and tan dolomitic mudstone which contains the same sedimentary structures indicative of a coastal sabkha environment. The dolomitic mudstone becomes more prominent near the top.

The total thickness of Kilian above the grey evaporitic member decreases from about 70 m in the central part of the southwest sector, to 30 m or less toward the northeast (Fig. 13.1). This decrease in thickness at the top of the succession is due to successive thinning of the maroon and tan mudstones, and their ultimate removal north of latitude 71°25' N and east of longitude 113°50 W. This stratigraphic thinning is interpreted to be caused by erosion prior to deposition of the overlying quartzarenites. Although the section described by Thorsteinsson and Tozer (1962, p. 35) was not examined in detail, sections on either side of their section were measured. Their unit 2, described as red siltstone and fine grained sandstone, is correlated with the red and tan carbonate member.



Figure 13.2. *Stacked, oriented flat pebble conglomerate in red and tan carbonate member, upper Kilian Formation, Section 7. Divisions on rod are 20 cm. (GSC 204187-C)*

Kuujjua Formation (proposed) and two unconformities

The unconformity bounded nature and distinct lithology of this easily traceable, lenticular (0 to 120 m thick) cliff-forming quartzarenite suggest that it should be considered a distinct formation, although its narrow outcrop expression precludes it being mapped separately from the Kilian Formation in which it was formerly included (Thorsteinsson and Tozer, 1962). It is restricted mainly to the southwestern sector, where it is nearly continuously exposed north and south of Kuujjua River. Section 4 at 71°13'N, 115°7'W is here proposed as the type section. It appears to be the thickest, best exposed section and was measured and described by Thorsteinsson and Tozer (1962, p. 35-37), who also recognized the potential individuality of this unit.

The precise basal contact of the Kuujjua Formation is generally obscured by talus. At Sections 8 to 10, the quartzarenite sharply overlies red dolomitic mudstones which are green and chloritic in the 5 cm immediately below it. The contact is scoured but quartzarenite locally infills polygonal cracks of the underlying mudstones. The basal contact may be conformable as well as gradational in the centre of the southwest sector at Section 5 where red, desiccation-cracked mudstone is interlaminated with silty quartzarenite across about 20 cm of the contact zone. An unconformity is suggested to the northeast, however, by thinning of the red and tan carbonate member between the grey evaporite-carbonate member and the Kuujjua Formation (Fig. 13.1).

The quartzarenite is thickest on the south side of Kuujjua River in the centre of the southwest sector. It thins to the northeast and southeast and also appears to thin toward the north and west. The lower part of the formation is composed dominantly of quartz, from pebble to fine sand size but is generally coarse grained sand. Locally overturned planar (Fig. 13.3), and trough crossbeds are abundant. The top 50 m of Section 5 consists mainly of medium- to fine-grained quartzarenite, grading up to poorly exposed green and maroon sandstones and shales with desiccation cracks. Thin limestone interbeds contain possible stromatolites.



Figure 13.3. *Unidirectional tabular and overturned crossbeds in quartzarenite of the Kuujjua Formation (proposed), at Section 8. Hammer for scale in lower left. (GSC 204187-A)*

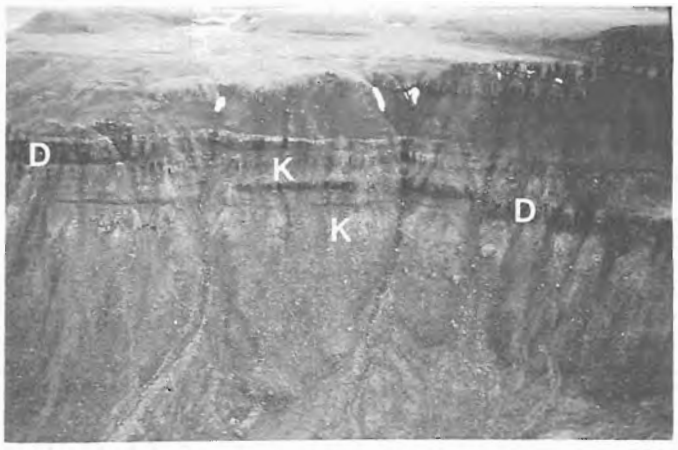

Figure 13.4. *Diabase sills (D) intruding and enclosing rafts of Kuujjua quartzarenite (K) in cliff exposure between sections 4 and 5 (Fig. 13.2). Height of view is about 100 m. (GSC 204187)*

Unidirectional paleocurrents (Fig. 13.1) and weakly fining- and thinning-upward tabular crossbedded packages 5-15 m thick (Fig. 13.3) suggest a fluvial origin for parts of the quartzarenite. At the top of the quartzarenite, however, a marine influence is suggested by local bimodal-bipolar paleocurrent patterns and limestone interbeds. Unimodal paleocurrents trend northerly at the northeast limit of the quartzite, southwesterly near the centre, and easterly in the southwest. Most crossbeds in the lower part of the formation are straight, tabular sets 2 to 20 cm thick, suggesting migrating bars as the predominant bedform. The vertical and areal variability of the limited paleocurrent data presented here indicate that many more paleocurrent data are required to document the detailed paleogeography of this formation.

The precise upper contact of the Kuujjua Formation is also obscured by talus. The quartzarenite is intruded by numerous diabase sills (Fig. 13.4). There are, however, no intercalated Natkusiak basalt flows. Where excavated by the author, the top 10 cm of the quartzarenite are intensely hematitic, overlain by a few centimetres of mudstone and then abruptly overlain by a basalt flow. At Sections 7 and 12 (Fig. 13.1) the quartzarenite thins to zero toward the southeast and northeast. These directions were also the provenance of the quartzarenite as shown by well-defined northerly to northwesterly paleocurrents at Sections 8 and 9. Thin siltstone and carbonate beds which occur at the top of Section 5 are absent to the east. The quartzarenite in eastern sections (8 to 10) resembles the lower part of the type section (5) which is coarse grained and has thick tabular crossbeds. These data suggest that upper siltstone and carbonate beds may originally have been present at Sections 8 to 10 but were removed by erosion prior to eruption of the Natkusiak basalts. The unconformity between Kilian limestones and Natkusiak basalts in the northeast sector may be a composit of both unconformities which bound the quartzarenite. The unconformity in the northeast sector differs from both unconformities in the southeast: it is clearly angular (Fig. 13.5) and is marked locally by hematitic, imbricated basal conglomerate.

Discussion

Sedimentary history and development of the Holman Island Syncline

The upper Kilian strata, as redefined, are laterally extensive with no marked facies changes. The strata record a minor transgression and clastic starvation from a lacustrine

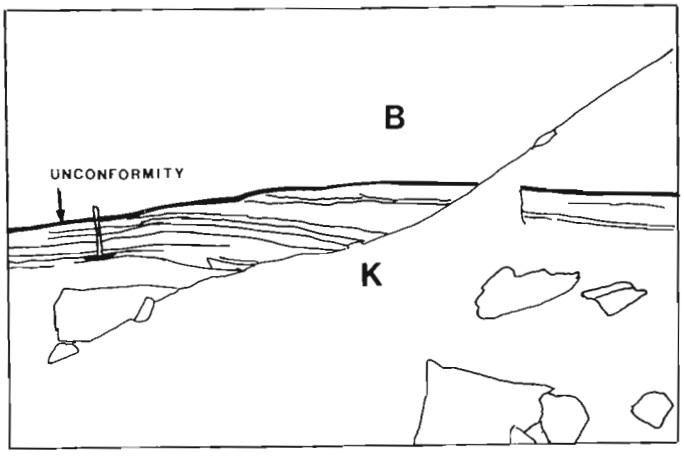



Figure 13.5. *Angular unconformity between Natkusiak basalt (P) and underlying cream limestone member of the Kilian Formation (K), Section 15. Sketch (a) on left, hammer for scale. (GSC 20421-X)*

or upper intertidal environment in which fine grained clastic sediments were deposited, to a very shallow subtidal marine and coastal sabkha environment punctuated by at least one period of basin restriction, during which evaporites (sulphate) were deposited. These dominantly carbonate strata were gently uplifted, tilted and bevelled, although the deepest part of the basin in the southeast area may not have undergone erosion.

An extensive alluvial system transported clean extra-basinal quartz pebbles and coarse- to medium-grained sand of the Kuujjua Formation into the southwest sector of the Holman Island Syncline area, where it was locally reworked under shallow marine tidal conditions. The northeast sector contains little record of this event. In the southwestern sector a second episode of gentle tilting and erosion is inferred from bevelling of the Kuujjua Formation toward the southeast and northeast, and possibly also to the northwest and southwest. The northeastern sector records this bevelling and perhaps also the previous bevelling as a thin, discontinuous, locally imbricated hematitic basal conglomerate. Here the northwestern side is documented to have been gently tilted toward the south.

Combined, the above data suggest that a gentle trough developed along the present axis of the Holman Island Syncline, possibly during and probably after deposition of the Kilian and Kuujjua formations, but was bevelled before eruption of the Natkusiak basalts. This inference can be tested by careful investigation of more exposures on the north side of Kuujjua River in both sectors.

Age and correlations

The unconformably overlying basalts and intrusive sills have been dated by K-Ar at approximately 700 Ma (see discussions in Baragar and Loveridge, 1982; Palmer et al., 1983). Attention has been drawn to the similarity of succession between late Proterozoic rocks of the Amundson Embayment and Late Proterozoic rocks of the

Table 13.2. Tentative correlation between upper Late Proterozoic rocks of Victoria Island and Mackenzie Mountains, N.W.T.

Mackenzie Mountains[1]			Victoria Island[2]	
GROUP	FORMATION	MEMBER	MEMBER	FORMATION
PALEOZOIC FORMATIONS			PALEOZOIC FORMATIONS	
UNCONFORMITY			UNCONFORMITY	
SHEEPBED				
RAPITAN	KEELE TWITYA SHEZAL SAYUNEI MOUNT BERG			
UNCONFORMITY				NATKUSIAK
COATES LAKE	COPPERCAP	Allodapic limestone		
		Transition Zone		
	REDSTONE RIVER	Red bed		
		Evaporite		
	THUNDERCLOUD	Dolostone	UNCONFORMITY	
		Sandstone		KUUJJUA
		Maroon and Tan Carbonate	Upper (incl. basalt?)	KILIAN
		Evaporite	Lower	
		Volcaniclastic		
UNCONFORMITY			no correlative?	
LITTLE DAL	UPPER CARBONATE	Basalt		
		UC 7-12	Lower Kilian?	
		UC 1-6	main	WYNNIATT
	RUSTY SHALE		lower	
	GYPSUM			MINTO INLET
	GRAINSTONE		middle & upper	REYNOLDS PT.
	BASINAL		middle	
	MUDCRACKED		lower-middle	

[1] After Aitken (1981), Jefferson (1983) and Jefferson and Ruelle (in press).
[2] After Thorsteinsson and Tozer (1962) and Young (1981).

Mackenzie Mountains (Young, 1981; Jefferson, 1978; Aitken, et al., 1978a, b). The Shaler Group has been correlated on a formation-for-formation basis with Hl, Tsezotene Formation, Katherine Group and Little Dal Group. In particular the evaporites of the Kilian Formation were postulated to be correlative with evaporites of the Redstone River Formation (Jefferson, 1978; Young et al., 1979, contested by Eisbacher, 1978) which is in the middle of the newly defined Coates Lake Group (Jefferson and Ruelle, in press), above the Little Dal Group. This study has described sedimentary rocks of the Kilian Formation that are very similar lithologically to sequences at the top of the Little Dal Group and within the Thundercloud Formation which is the basal unit of the overlying Coates Lake Group (Aitken, 1981; Jefferson, 1983; Jefferson and Ruelle, in press). The Thundercloud and Kilian formations both contain evaporite-dominated members overlain by tan and maroon carbonates with features that are typical of coastal sabkha environments. If these similarities imply stratigraphic correlation, then the Kilian Formation is laterally equivalent to the Thundercloud Formation. In consequence, evaporites and redbeds of the Redstone River Formation have no counterparts on Victoria Island (Table 13.2). The unconformity-bounded Kuujju Formation is of uncertain correlation.

Other differences have long been apparent between the two areas. For example, a very thick basalt (Natkusiak) is the uppermost Proterozoic unit on Victoria Island but in Mackenzie Mountains the relatively thin Little Dal lavas underlie most of the Proterozoic sabkha carbonates and quartzarenites. The difference in stratigraphic position can be used to suggest that the Little Dal basalts are older than the Natkusiak basalts. The thin basalt flow reported by Young (1981, Fig. 12.15) to be within the Kilian Formation (Fig. 13.1) is possibly closer in age to the Little Dal basalts. The Mackenzie Mountains also contain extensive younger sequences of stratiform, sabkha-hosted copper occurrences (Redstone Copper Belt); grey allodapic limestones (Coppercap Formation); glaciomarine deposits and iron formation (Rapitan Group) and younger Proterozoic strata that are not present on Victoria Island. The absence of these strata gives some indication of the time gaps that must be accounted for in unconformities below and above the Natkusiak basalts.

Acknowledgments

C.W. Jefferson was ably assisted in the field by K. MacDonald. N.E. Nelson, J.H. Reedman and W. Gibbins are thanked for discussions in the field. Drafts of this manuscript were read by M.P. Jackson, M. Henderson, W.R.A. Baragar, G.M. Young, R.V. Kirkham, W.E. Nelson, R.F.J. Scoates, R.T. Bell and J.D. Aitken, all of whom contributed valuable comments.

The contribution is ancillary to resource assessment of Banks Island and northwestern Victoria Island (GSC Project No. 840003) which received rotary and fixed wing support from Polar Continental Shelf Project, coordinated by F. Hunt and B. Hough. Logistic support and generous hospitality from Panarctic Oils Limited is also gratefully acknowledged.

References

Aitken, J.D.
1981: Stratigraphy and sedimentology of the Upper Proterozoic Little Dal Group, Mackenzie Mountains, Northwest Territories; in Proterozoic basins of Canada, ed. F.H.A. Campbell; Geological Survey of Canada, Paper 81-10, p. 47-71.

Aitken, J.D., Long, D.G.F., and Semikhatov, M.A.
1978a: Progress in Helikian stratigraphy, Mackenzie Mountains; in Current Research, Part A, Geological Survey of Canada, Paper 78-1A, p. 481-484.

1978b: Correlation of Helikian strata, Mackenzie Mountains-Brock Inlier-Victoria Island; in Current Research, Part A, Geological Survey of Canada, Paper 78-1A, p. 485-486.

Baragar, W.R.A. and Loveridge, W.D.
1982: A Rb-Sr study of the Natkusiak basalts, Victoria Island, District of Franklin; in Current Research, Part C, Geological Survey of Canada, Paper 82-1C, p. 167-168.

Eisbacher, G.H.
1978: Two major Proterozoic unconformities, Northern Cordillera; in Current Research, Part A, Geological Survey of Canada, Paper 78-1A, p. 53-58.

Jefferson, C.W.
1978: Stratigraphy and sedimentology, Upper Proterozoic Redstone Copper Belt, Mackenzie Mountains, N.W.T. – a preliminary report; in Mineral Industry Report for 1975, Northwest Territories, Canada Department of Indian and Northern Affairs, E.G.S. 1978-5, p. 157-169.

1983: The Upper Proterozoic Redstone Copper Belt, Mackenzie Mountains, N.W.T.; unpublished Ph.D. thesis, The University of Western Ontario, London, Ontario, 445 p.

Jefferson, C.W. and Ruelle, J.H.
– The Late Proterozoic Redstone Copper Belt, Mackenzie Mountains, N.W.T.; in Mineral Deposits of Northern Cordillera, ed. J.A. Morin; C.I.M. Special Volume. (in press)

Jefferson, C.W., Nelson, W.H., Kirkham, R.V., Reedman, J.H., and Scoates, R.F.J.
1985: Geology and copper occurrences of the Natkusiak basalts, Victoria Island, N.W.T.; in Current Research, Part A, Geological Survey of Canada, Paper 85-1A, Report 27.

Nelson, W.H.
1983: Report on the field program, summer 1982. Unpublished assessment report, Panarctic Oils Ltd., Filed with Department of Indian Affairs and Northern Development, Yellowknife, 87 p.

Palmer, H.C., Baragar, W.R.A., Fortier, M., and Foster, J.H.
1983: Paleomagnetism of Late Proterozoic rocks, Victoria Island, Northwest Territories, Canada; Canadian Journal of Earth Sciences, v. 20, p. 1456-1469.

Ruelle, J.C.L.
1982: Depositional environments and genesis of stratiform copper deposits of the Redstone Copper Belt, Mackenzie Mountains, N.W.T.; in Precambrian Sulphide Deposits, H.S. Robinson Memorial Volume, ed. R.W. Hutchinson, C.D. Spence and J.M. Franklin; Geological Association of Canada, Special Paper 25, p. 701-737.

Seeber, O.A.
1970: Geological Report on the Cam Group, 87-H-10; Assessment report for Grandroy Mines Ltd., Project 0829, Toronto, Canada; Assessment files, Department of Indian and Northern Affairs, Yellowknife, 25 p.

Thorsteinsson, R. and Tozer, E.T.
1962: Banks, Victoria and Stefansson Islands, Arctic Archipelago; Geological Survey of Canada, Memoir 330, 85 p.

Young, G.M.
1981: The Amundsen Embayment, Northwest Territories; relevance to the upper Proterozoic evolution of North America; in Proterozoic Basins of Canada, ed. F.H.A. Campbell; Geological Survey of Canada, Paper 81-10, p. 203-218.

Young, G.M., Jefferson, C.W., Delaney, G.D., and Yeo, G.M.
1979: Middle and Late Proterozoic evolution of the northern Canadian Cordillera and Shield; Geology, v. 7, p. 125-128.

ICE WEDGES AND PERMAFROST CONDITIONS NEAR KING POINT, BEAUFORT SEA COAST, YUKON TERRITORY

Project 840014

David G. Harry, Hugh M. French[1], and Wayne H. Pollard[2]
Terrain Sciences Division

Harry, D.G., French, H.M., and Pollard, W.H., Ice wedges and permafrost conditions near King Point, Beaufort Sea coast, Yukon Territory; in Current Research, Part A, Geological Survey of Canada, Paper 85-1A, p. 111-116, 1985.

Abstract

Observations of ice wedges near King Point, Yukon Territory, permit inferences to be made regarding their growth, contribution to ground ice volume, and use as indicators of recent climatic change. At this site, ice wedges underlie 18-20% of terrain and account for up to 21% of the total ground ice volume of the upper 5 m of permafrost. Both modern and buried, fossil ice wedges are recognized. Identification of fresh veinlets within the frozen active layer suggests that 38% of modern wedges cracked during the winter of 1983-84. More than half of the wedges examined possess one or more growth stages superimposed upon the primary wedge. The permafrost aggradation responsible for this rejuvenation provides further evidence of recent climatic cooling in the western Arctic.

Résumé

L'examen des coins de glace près de la Pointe King, au Yukon, permet de formuler certaines hypothèses sur leur croissance, leur contribution au volume de glace dans le sol et leur utilité en tant qu'indicateurs des changements climatiques récents. À cet endroit, les coins de glace se présentent sous 18 à 20 % du terrain et représentent jusqu'à 21% du volume de glace dans les cinq premiers mètres du pergélisol. On y reconnaît des coints de glace récents et des dépôts enfouis de remplacement de coins de glace. L'identification de petits filons récents dans le mollisol gelé porte à croire que 38% des coins récents se sont fendus au cours de l'hiver de 1983-84. Plus de la moitié des coins examinés présentent au moins une étape de croissance superposée sur le coin primaire. L'aggradation du pergélisol responsable de cette réjuvénation est une autre indication du refroidissement récent du climat dans l'ouest de l'Arctique.

[1] Departments of Geology and Geography, University of Ottawa, Ottawa, Ontario K1N 6N5
[2] Department of Geography, University of Ottawa, Ottawa, Ontario K1N 6N5

Introduction

Ice wedges represent one of the most common types of ground ice occurring within surficial deposits on the Yukon coastal plain (Rampton, 1982). Ice-wedge polygons are ubiquitous on the horizontal and pediment-like surfaces which characterize the terrain of this region. It is likely, therefore, that wedge ice forms a major component of the total ground ice volume in near-surface permafrost, as reported from other areas of the western Canadian Arctic (e.g., Pollard and French, 1980; French and Harry, 1983) and Alaska (e.g., Brown, 1967). Stratigraphic analysis of ice-wedge characteristics provides a useful tool in paleoenvironmental reconstruction (e.g., Mackay, 1975a, 1976a; French et al., 1982; Mackay and Matthews, 1983). Since ice-wedge growth is controlled by surface geomorphic and climatic conditions, it follows that events such as their burial, thaw-truncation, or rejuvenation reflect sequential changes in the surface environment.

Along much of the Beaufort Sea coast of Yukon Territory, rapid shoreline recession has occurred in association with the erosion of ice-rich permafrost sediments (Mackay, 1963; Lewis and Forbes, 1974). This provides an opportunity to examine extensive cliff sections, containing excellent exposures of ice wedges along continuous transects up to 500 m in length. This report describes the distribution and morphology of ice wedges near King Point, Yukon Territory (Fig. 14.1). These observations permit inferences to be made regarding the growth of ice wedges, their contribution to ground ice volume, and their significance as an indicator of recent environmental change. The possible development of offshore oil and gas resources, with associated land-based facilities to be located along the Yukon coast, provides further incentive for documenting local permafrost and ground ice conditions.

Regional climate and permafrost conditions

The Yukon coastal plain experiences an arctic maritime climate, characterized by long cold winters and short cool summers (Burns, 1973). Data recorded at Shingle Point DEW-line site during the period 1957-1980 indicate a mean annual air temperature of -10.4°C. The region is underlain by continuous permafrost, probably extending to depths in excess of 300 m (Judge, 1973). Active layer thickness ranges from less than 0.3 m in fine grained sediments overlain by organic deposits, to 1-2 m in areas of partly vegetated sands and gravels (Rampton, 1982). Ground ice distribution is highly variable, reflecting the wide range of geological and geomorphic environments, and the complex permafrost history of the region. Borehole data show that almost all fine grained sediments in this area possess high ice contents (Rampton, 1971). In addition to ice wedges, ground ice occurs in the form of pore ice, reticulate ice-vein systems, segregated ice lenses, and thick tabular sheets of massive ice.

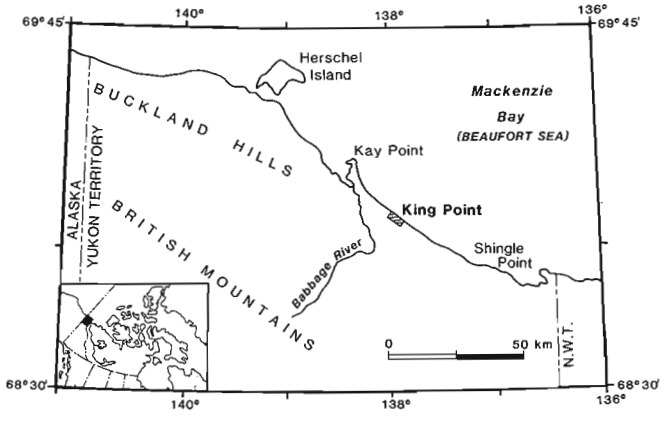

Figure 14.1. Location map of King Point, Yukon Territory.

Site description

The study site is located approximately 3 km southeast of King Point, within a terrain unit mapped by Rampton (1982) as postglacial lacustrine plain. This section of coast is characterized by the development of a major retrogressive thaw flow slide (cf. Rampton, 1982, Fig. 25). The headwall of this feature is between 5 and 20 m in height and extends laterally for approximately 1.2 km (Fig. 14.2). Rapid scarp retreat has truncated an area of high-centre polygon terrain, exposing the underlying ice-wedge network in vertical section. The erosion process is polycyclic and thus the extent and location of actively eroding faces varies from year to year.

A reconnaissance visit was made to this site on May 30, 1984, followed by more detailed fieldwork on June 4-5, 1984. At this time, a permafrost exposure approximately 370 m in length and 1-6 m in height was available for examination, the remainder of the scarp being either inactive or obscured by snowbanks (Fig. 14.3). Fieldwork was undertaken in early spring for three reasons: first, in order to gain access to the site before summer thaw rendered the face dangerously unstable and the scarp foot impassable; second, to utilize snowbanks to reach the upper

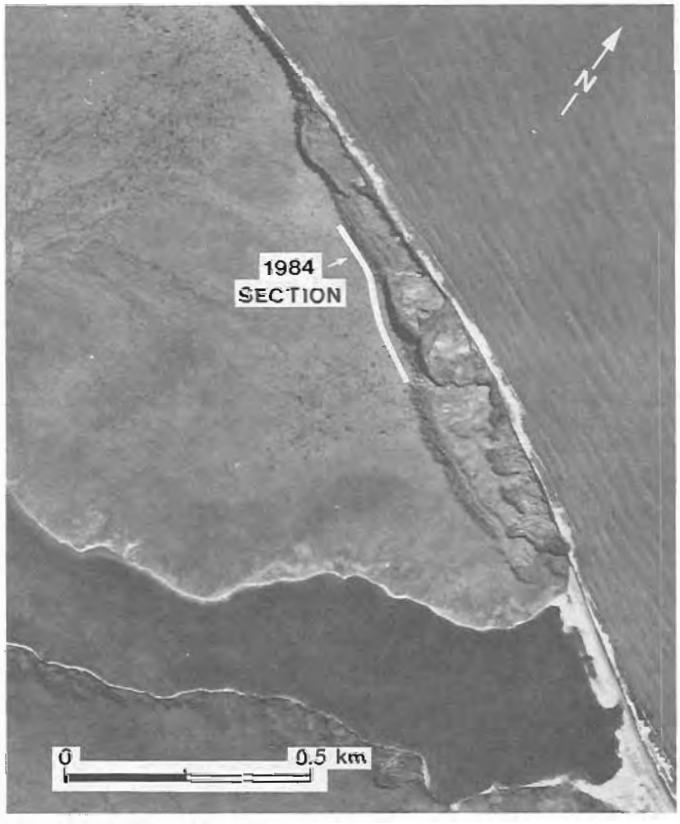

Figure 14.2. Air photograph of the area southeast of King Point, indicating the approximate location of the permafrost exposure examined in May and June 1984. (NAPL A21831-101, 18 August 1970)

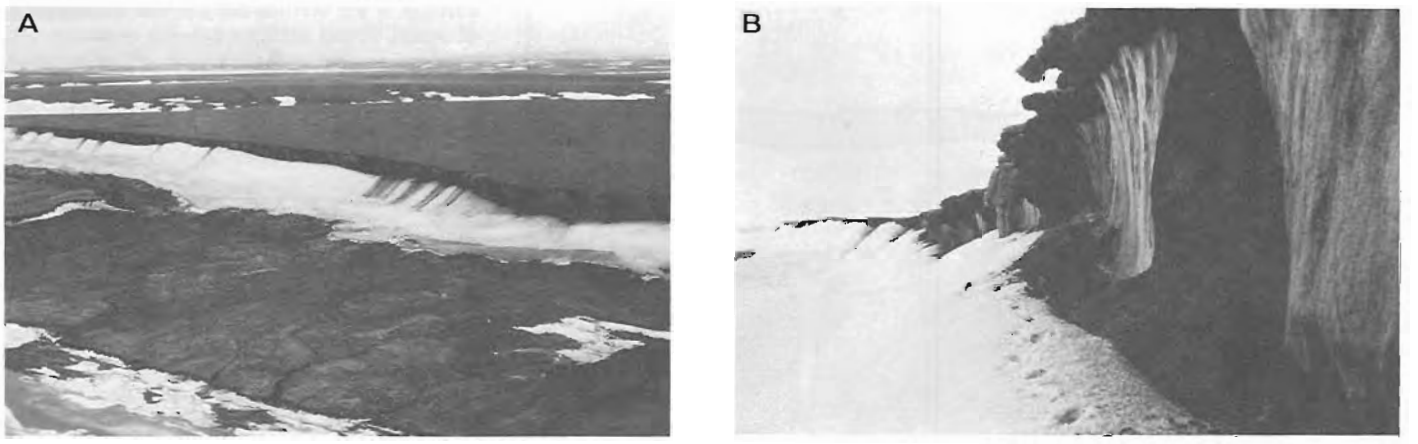

Figure 14.3

A – Oblique aerial view of permafrost exposure near King Point, 30 May 1984. (GSC 204081-J)
B – Detail of exposure showing modern ice wedges enclosed by clay diamicton. (GSC 204081-E)

part of the exposure within which the ice wedges are developed; third, to examine the upward extensions of ice wedges through the frozen active layer prior to the onset of thaw.

Five stratigraphic units may be recognized at this locality (Fig. 14.4). The basal unit consists of a tabular sheet of massive ice at least 5 m in thickness which has controlled the development of the thaw flow slide. This unit was almost completely obscured by snowbanks at the time of visit and therefore was not studied in detail. The massive ice is overlain by up to 1.5 m of diamicton, consisting of grey silty clay containing sporadic angular clasts up to 30 cm in diameter. The clay contains 5-10% excess ice, in the form of small lenses. This material has a gradational upper contact with approximately 2.5 m of horizontally stratified sandy silt, locally containing pods of organic material particularly near the upper boundary of the unit. Small ice lenses and veins contribute to excess ice contents of 10-40% within the sandy silt. This unit is overlain by a peat layer varying in thickness from 1.0-2.5 m and showing a well developed decompositional profile. Surface sediments consist of 0.4 m of eolian sand.

Within the Quaternary stratigraphic framework established by Rampton (1982), the diamicton is interpreted as Buckland Till of possible early Wisconsin age, whereas the overlying sandy silt unit represents the deposition of postglacial lacustrine sediments. Ice wedges appear to have grown epigenetically within this sediment sequence, following postlacustrine permafrost aggradation.

Ice-wedge characteristics

A total of 50 ice wedges, forming part of a contiguous net, were examined in detail to determine their distribution, size, and morphological characteristics. They may be classified according to their degree of activity and structure (Fig. 14.5). Both modern and fossil, buried wedges are recognized. Modern wedges extend upward to within 1 m of the ground surface and appear to be related to the tundra polygon network. They may be further categorized as single- or multi-stage wedges according to their structure. Modern wedges may be either active (i.e, periodically cracking) or inactive under present environmental conditions. At this locality, 80% of the wedges examined were classified as modern. The remainder appear to be fossilized or buried, in that they bear no apparent relation to the present surface and presumably have ceased growing. The tops of these fossil wedges are located 1.0-3.8 m below the surface and are well below the present permafrost table. These features are also much smaller than modern wedges, ranging from 0.05-1.0 m in apparent width.

Two properties of ice wedges are readily measured in linear exposures: their apparent spacing and apparent width (Fig. 14.6). At this locality, the apparent spacing of modern wedges ranges from a maximum of 15 m to an effective minimum of zero, in cases where the scarp face truncates two intersecting ice wedges. The frequency distribution is approximately normal, with a mean value of 8.7 m and a standard deviation of 2.9 m. The apparent maximum width of modern wedges ranges from 0.1-10.0 m, with a mean of 3.6 m and a standard deviation of 2.3 m. The positively skewed distribution is biased by a small number of high values which represent measurement of ice wedges in very low-angle oblique section. In two cases, the scarp face parallels ice-wedge axes, providing continuous exposure of wedge ice along a polygon boundary.

Mackay (1977) has shown that, in randomly oriented vertical exposures, the apparent spacing of ice wedges is much less than the maximum plan diameter of ice-wedge polygons and thus the true spacing of ice wedges. Conversely, the mean true width (w) of a number of equal-sized ice wedges is less than the mean apparent width (a) and is given by:

$$w = 0.64\ a \qquad (1)$$

These relationships suggest that the mean true width of the King Point ice wedges is approximately 2.3 m, and their true spacing is greater than 9 m. Measurements made from 1:13 000 scale aerial photographs indicate a mean polygon diameter in this area of 12-13 m. These latter values suggest that modern wedge ice underlies approximately 18-20% of the land surface in the vicinity of King Point.

Data on ice-wedge height (i.e. maximum vertical extent) are incomplete, since the base of almost all wedges was obscured either by snowbanks or by contact with massive ice in the lower part of the exposure. Most wedges, however, have minimum heights of between 4.5 and 6.0 m. Assuming, therefore, a mean height of 6 m and a mean true width of 2.3 m, these observations suggest that ice wedges in this area have height- to- width ratios of approximately 2.6:1.

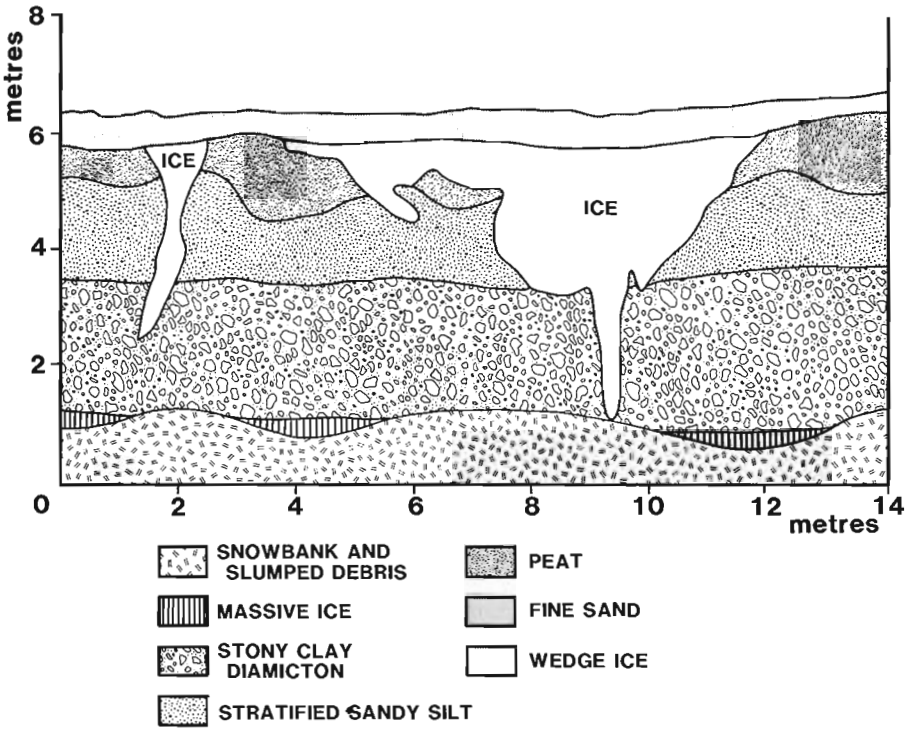

Figure 14.4. *Measured section illustrating permafrost stratigraphy near King Point.*

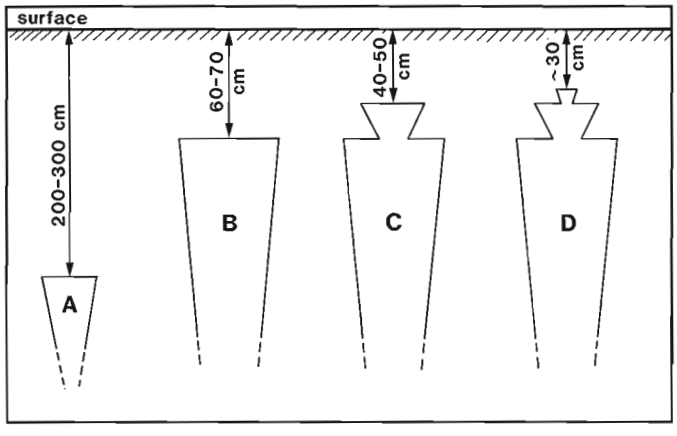

Figure 14.5. *Schematic diagram illustrating classification of ice wedges observed near King Point: A – Fossil, buried; B – Modern, single-stage; C – Modern, two-stage; D – Modern, multi-stage. Only wedges of types C, D, and rarely B, show evidence of active cracking.*

Ice-wedge contribution to ground ice volume

Two components contribute to the total volume of ice contained within near-surface permafrost exposed southeast of King Point: the ice wedges and the pore and segregated ice contained within their enclosing sediments. Measurement of ice-wedge morphology and sediment ice content permits an evaluation of the relative importance of the two components.

Assuming modern ice wedges to be, on average, 2.3 m wide, 6.0 m high, and spaced 12.0 m apart, these features account for approximately 11.2% by volume of the upper 5 m of permafrost. An additional 0.2% by volume is accounted for by the occurrence of small, fossil wedges 1.5-4.0 m below the surface. The contribution of pore and segregated ice to the total ice volume may be calculated from measurements of gravimetric ice content of sediments, using the method of Pollard and French (1980). Representative values of volumetric ice content for this section are presented in Table 14.1. Analysis suggests that ground ice accounts for approximately 55% by volume of the upper 5 m of permafrost at this site. Of the total ice volume, approximately 21% represents the contribution of ice wedges.

These results are consistent with calculations of ground ice volume in other areas of the western Canadian Arctic (Table 14.2). In comparison to data from Richards Island (Pollard and French, 1980), ice wedges at King Point comprise a rather higher percentage of the total volume of earth materials but contribute equally to total ground ice volume. Their contribution to both volume of earth materials and ground ice volume is, however, less than values calculated for southwest Banks Island (French and Harry, 1983). This reflects the absence at King Point of large buried ice wedges, as observed on southwest Banks Island (French et al., 1982).

Ice-wedge growth and recent permafrost history

The morphology of ice wedges at King Point may be used to make a number of inferences regarding their growth history. By identifying ice veinlets extending upwards from wedge tops through the still frozen active layer, it was possible to determine that 15 out of 40, or approximately 38%, of modern ice wedges had cracked during the previous winter. This observation is in excellent accord with long term studies on Garry Island, where Mackay (1974) has concluded that on average nearly 40% of ice wedges crack in any given year. More than half of the modern ice wedges at King Point exhibit a complex structure, with one or more growth stages superimposed upon the primary wedge (Fig. 14.5); 55% of wedges possess a secondary stage and a further 7.5% possess a smaller tertiary stage. In general, the primary wedge tops occur at 60-70 cm below the surface, and the narrow superimposed segments extend upwards for a further 20 cm.

Multiple ice-wedge structures of this type are common in the western Arctic (e.g., Mackay, 1974, Fig. 17, 18) and have probably developed in response to a recent climatic cooling trend (Mackay, 1976b). The tops of primary ice wedges mark a former permafrost table. During a period of warm climate, this represented the lower boundary of an active layer which was significantly thicker than at present. Subsequent climatic deterioration and concomitant upwards aggradation of permafrost led to ice-wedge rejuvenation, marked by new growth stages extending upwards to the present frost table. The existence of multiple growth stages demonstrates that the cooling trend has not been continuous, and may have been interrupted by at least one warmer period. This was not, however, of sufficient magnitude or duration to allow active layer deepening to the tops of primary wedges.

The decrease in active layer thickness implied by ice-wedge rejuvenation may be illustrated by plotting depth to the top of each primary wedge against depth to the top

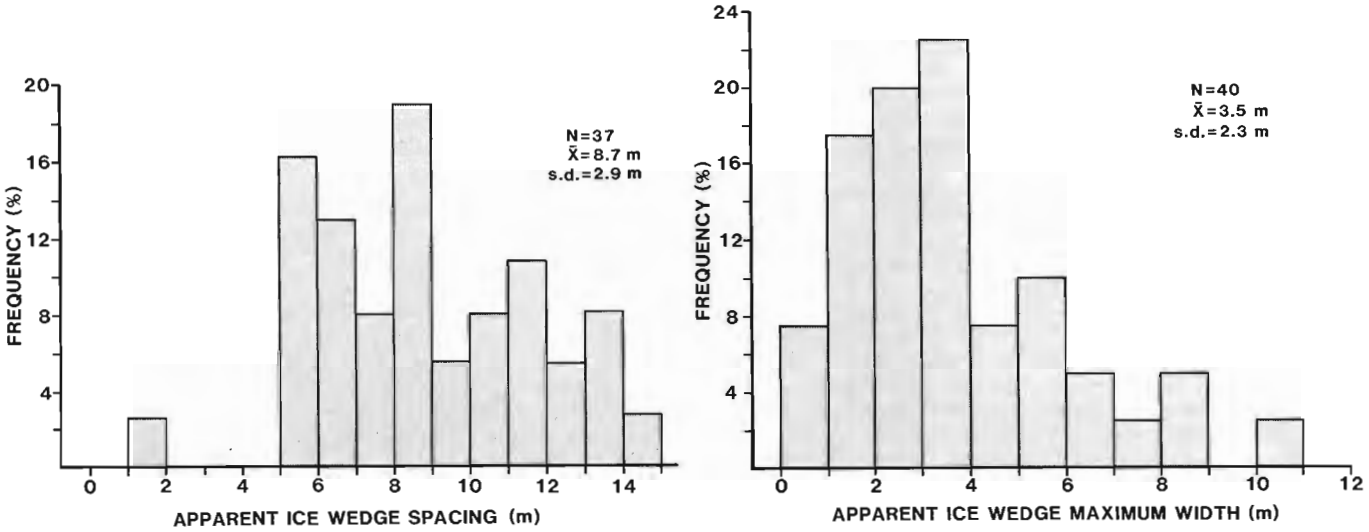

Figure 14.6. Histograms illustrating distribution and size of ice wedges near King Point.

Table 14.1. Representative values of ground ice volume in permafrost near King Point

Depth (m)	Material	Pore/Segregated ice A %	Pore/Segregated ice B %	Wedge ice %	Total ice %
0.5-1.0	Peat	50.0	40.8	18.4	59.2
1.0-2.0	Peat	50.0	41.7	16.7	58.4
2.0-3.0	Sandy silt	43.2	37.5	13.2	50.7
3.0-4.0	Sandy silt	56.7	51.3	9.6	60.9
4.0-5.0	Silty clay	47.0	44.0	6.4	50.4
5.0-6.0	Silty clay	47.0	45.1	4.0	49.1

Notes: 1. Column A indicates ice content of sediments enclosing ice wedges. Column B indicates contribution of pore and segregated ice to total volume of earth materials.

2. Ice contents of peat represent visual estimates only.

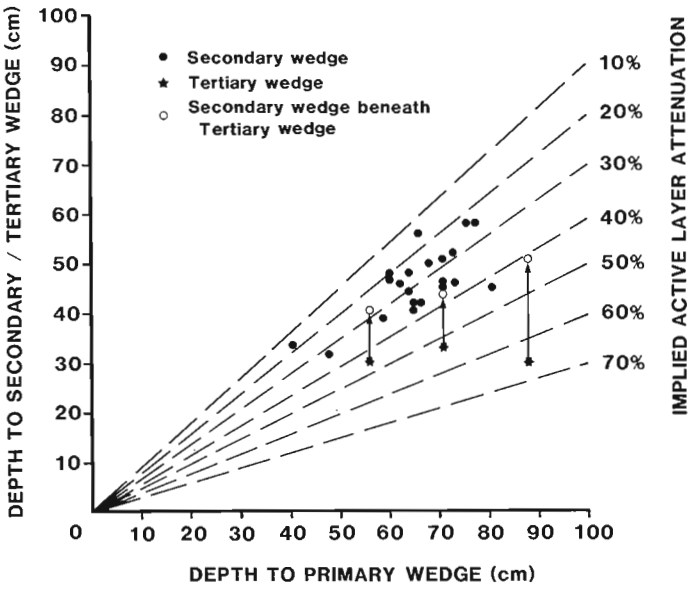

Figure 14.7. Graph showing depth below surface of ice wedge tops and implied active layer attenuation in the vicinity of King Point.

Table 14.2. Ground ice volume in the upper 5 m of permafrost in selected areas of the western Canadian Arctic

Area	Pore/Segregated ice	%	Wedge ice %	Total ice %
King Point, YT	43.5	(79.2)	11.4 (20.8)	54.9 (100.0)
Richards Island, NWT	28.3	(79.3)	7.5 (21.0)	35.7 (100.0)
Southwest Banks Island NWT	38.7	(66.2)	19.8 (33.8)	58.5 (100.0)

Notes: 1. Values in parentheses indicate percentage contribution of ground ice types to total ice volume.

2. Richards Island data after Pollard and French, 1980.

3. Banks Island data after French and Harry, 1983.

of the corresponding secondary or tertiary wedge (cf. Mackay, 1976b, Fig. 47.1). Measurements of ice wedges observed near King Point indicate an active layer attenuation of 20-40%, with a mean estimate of 30.7% (Fig. 14.7). Although the range in both present and former active layer thickness is relatively small, reflecting data collection from a geographically limited area, the results are consistent with observations made elsewhere in the western Arctic (Mackay, 1976b). Of the 15 single-stage wedges observed near King Point, only two possessed 1984 veinlets. This is also consistent with Mackay's (1976b) suggestion that, in most cases, only multi-stage ice wedges are actively growing.

The small size of rejuvenated wedge segments (0.1-0.3 m) suggests that active layer attenuation represents a relatively recent phenomenon in this area, probably limited to the last hundred years at most. Systematic climatic records have been maintained for less than thirty years on the Yukon coast. However, on the basis of long-term climatic data collected at four subarctic stations (Burns, 1973), Mackay (1975b, 1976b) has suggested that the cooling trend may have begun in the late 1940s and resulted in a 2°C decline in mean annual air temperature. The widespread nature of this trend is supported by data from high arctic stations, which also indicate a persistent downward temperature trend from the 1940s onward (Thomas, 1975).

Conclusions

Observations of ice wedges exposed near King Point, Yukon Territory, indicate that wedge ice forms a major component of near-surface permafrost in this area of the Yukon coastal plain. Wedge ice underlies nearly 20% of the terrain and accounts for up to 21% of total ground ice volume in the upper 5 m of permafrost. Ice-wedge characteristics at this locality may be used in support of several current theories regarding ice-wedge growth and recent permafrost history. Field evidence suggests that 38% of ice wedges examined cracked during the winter of 1983-84, as indicated by the presence of a veinlet penetrating the frozen active layer. More than 50% of wedges show signs of rejuvenation, in response to upward permafrost aggradation. This provides further evidence of recent climatic cooling in the western Arctic. Most ice wedges which have not been rejuvenated during this period appear to be inactive.

Acknowledgments

Fieldwork expenses for H.M. French and W.H. Pollard were provided by EMR Research Agreement No. 136 and by NSERC operating grant A8367 (HMF). We wish to thank J.A. Heginbottom for his comments on this manuscript.

References

Brown, J.
1967: An estimation of volume of ground ice, Coastal Plain, northern Alaska; United States Army Corps of Engineers, Cold Regions Research and Engineering Laboratory, Hanover, N.H., Memorandum, 22 p.

Burns, B.M.
1973: The climate of the Mackenzie Valley – Beaufort Sea; Department of the Environment, Climatological Studies, no. 24, v. 1,2, 227 p, 239 p.

French, H.M. and Harry, D.G.
1983: Ground ice conditions and thaw lakes, Sachs River Lowlands, Banks Island, Canada; in Mesoformen des Reliefs im heutigen periglazialraum, ed. H. Poser and E. Schunke; Abhandlungen der Akademie der Wissenschaften in Gottingen, Math.-Physik. Klasse, Nr. 35, p. 70-81.

French, H.M., Harry, D.G., and Clark, M.J.
1982: Ground ice stratigraphy and late-Quaternary events, southwest Banks Island, Canadian Arctic; in The R.J.E. Brown Memorial Volume; Proceedings, Fourth Canadian Permafrost Conference; National Research Council of Canada, Ottawa, p. 81-90.

Judge, A.S.
1973: Deep temperature observations in the Canadian North; in Permafrost, North American Contribution to the Second International Conference (Yakutsk, USSR), National Academy of Sciences, Publication 2115, p. 35-40.

Lewis, C.P. and Forbes, D.L.
1974: Sediments and sedimentary processes, Yukon Beaufort Sea coast; Environmental-Social Program, Northern Pipelines, Task Force on Northern Oil Development, Report 74-29.

Mackay, J.R.
1963: Notes on the shoreline recession along the coast of the Yukon Territory; Arctic, v. 16, p. 195-197.

1974: Ice wedge cracks, Garry Island, Northwest Territories; Canadian Journal of Earth Sciences, v. 11, p. 1366-1383.

1975a: Relict ice wedges, Pelly Island, N.W.T.; in Report of Activities, Part A, Geological Survey of Canada, Paper 75-1A, p. 469-470.

1975b: The stability of permafrost and recent climatic change in the Mackenzie Valley, N.W.T.; in Report of Activities, Part B, Geological Survey of Canada, Paper 75-1B, p. 173-176.

1976a: Pleistocene permafrost, Hooper Island, Northwest Territories; in Report of Activities, Part A, Geological Survey of Canada, Paper 76-1A, p. 17-18.

1976b: Ice wedges as indicators of recent climatic change, western arctic coast; in Report of Activities, Part A, Geological Survey of Canada, Paper 76-1A, p. 233-234.

1977: The widths of ice wedges; in Report of Activities, Part A, Geological Survey of Canada, Paper 77-1A, p. 43-44.

Mackay, J.R. and Matthews, J.V.
1983: Pleistocene ice and sand wedges, Hooper Island, Northwest Territories; Canadian Journal of Earth Sciences, v. 20, p. 1087-1097.

Pollard, W.H. and French, H.M.
1980: A first approximation of the volume of ground ice, Richards Island, Pleistocene Mackenzie delta, Northwest Territories, Canada; Canadian Geotechnical Journal, v. 17, p. 509-516.

Rampton, V.N.
1971: Ground ice conditions, Yukon coastal plain and adjacent areas; in Report of Activities, Part B, Geological Survey of Canada, Paper 71-1B, p. 128-130.

1982: Quaternary geology of the Yukon coastal plain; Geological Survey of Canada, Bulletin 317, 49 p.

Thomas, M.K.
1975: Recent climatic fluctuations in Canada; Department of the Environment, Climatological Studies, no. 28, 92 p.

-15-

GOLD ABUNDANCES VS. GRAIN SIZE IN WEATHERED AND UNWEATHERED TILL

Project 780016

R.N.W. DiLabio
Terrain Sciences Division

DiLabio, R.N.W., Gold abundance vs. grain size in weathered and unweathered till; in Current Research, Part A, Geological Survey of Canada, Paper 85-1A, p. 117-122, 1985.

Abstract

The abundance of gold was determined in up to ten grain size fractions separated from the matrix (< 4.0 mm) of till collected at five gold deposits in the Canadian Shield and Appalachian Orogen. In the unoxidized till samples, gold is most abundant in grain size fractions at and finer than the grain size of the primary gold-bearing minerals in the ore deposit. In the oxidized till samples, gold is most abundant in silt and finer sizes. The optimum grain size range for geochemical analysis of till varies among the deposits but is readily determined by this type of fractionation as part of an orientation survey.

Résumé

La teneur en or a été déterminée dans un maximum de six classes granulométriques séparées de la matrice (< 4 mm) du till provenant de cinq gisements aurifères dans le Bouclier canadien et l'orogène des Appalaches. Dans les échantillons de till inaltéré, l'or est plus abondant dans les classes égales et inférieures à la granulométrie des minéraux aurifères primaires du gisement. Dans les échantillons de till oxydé, l'or est plus abondant dans les classes dont la taille est égale ou inférieure à celle du limon. La granulométrie optimale pour l'analyse géochimique du till varie en fonction des gisements, mais elle est facilement déterminée par cette méthode dans le cadre d'une étude d'orientation.

Introduction

A common problem in the geochemical analysis of till in mineral exploration is the choice of a representative and geologically meaningful grain size fraction for analysis. For each specific set of source rocks and ore minerals, enough data should be available so that one can choose an optimum size fraction for analysis so that subtle anomalies are not missed and so that the metal content of the analyzed fraction is not controlled by variations in the till's content of "inert" rock-forming minerals. The size range will include the specific size fraction to which the ore minerals are glacially comminuted. Dreimanis and Vagners (1971), Lindén (1975), and Haldorsen (1977) investigated these so-called "terminal grades" for common rock-forming minerals in till. Recently, more emphasis has been placed on the comminution behaviour of ore minerals and the effects of weathering on trace metal levels vs. grain size (Kauranne, 1967; Shilts, 1973, 1984; Smith and Gallagher, 1975; Ayras, 1977; Klassen and Shilts, 1977; Eriksson, 1973; DiLabio, 1979, 1981, 1982), although the amount of published information on the partitioning of metals and minerals in till is still quite small.

When extending this type of experiment to gold exploration, consideration must also be given to the original form of the gold (native, oxide-, or sulphide-bound) and the possibility of remobilization and reprecipitation of gold during postglacial weathering. This report presents results of tests of gold abundance with respect to grain size in till from several sites and demonstrates the value of such simple tests as part of an orientation survey.

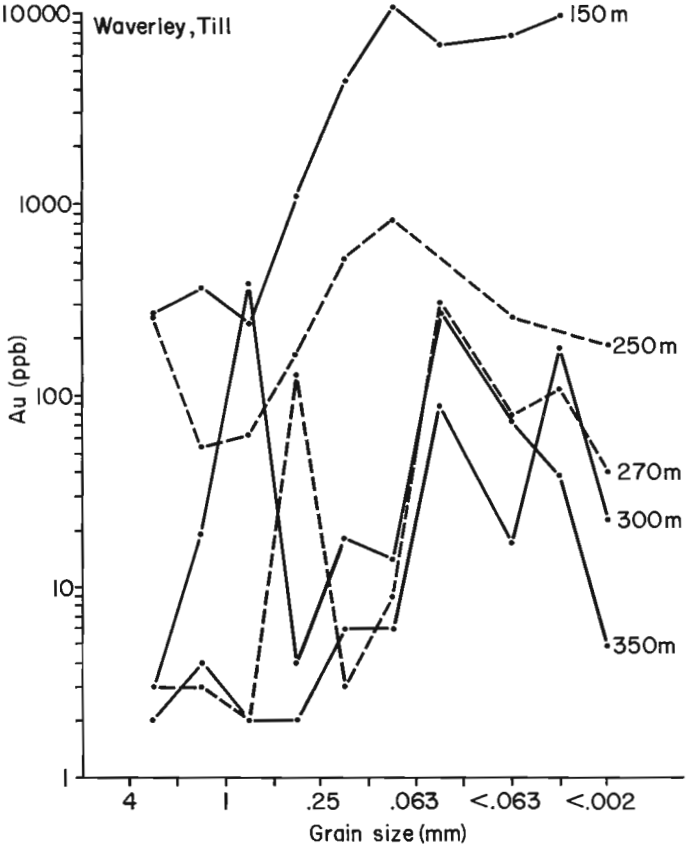

Figure 15.1. Abundance of gold vs. grain size of analyzed fraction of oxidized till at varying distances down-ice from the gold deposit at Waverley, Nova Scotia. Curve for 250 m is the average of data for eight samples; other curves represent one sample each.

Methods

Each sample of the <4 mm matrix of till was dry sieved to recover samples of fines in fractions such as <0.037 or <0.063 mm. The oversized sediment was wet sieved to wash out adhering fines, dried, and dry sieved at 1ϕ intervals using stainless steel sieves of 2.0, 1.0, 0.5, 0.25, 0.125, and 0.063 mm sizes. Fractions coarser than 0.063 mm were ground to powder (<0.063 mm) prior to analysis. When samples were large enough, a fraction <0.002 mm was recovered by centrifugation and decantation of a separate portion of each raw sample.

Gold analysis was performed by the fire assay – atomic absorption technique after digestion in $HCl-HNO_3$. Ten grams of sample was analyzed, except for the <0.002 mm fraction, of which only 1.0 to 2.5 g was available for analysis. Tungsten analysis was performed by colorimetry after sintering. Base metals were determined in the <0.002 mm fraction of selected samples by atomic absorption techniques after a hot $HCl-HNO_3$ digestion. Analyses were performed by Bondar-Clegg and Co. Ltd., Ottawa.

Heavy minerals were recovered from the 0.25 to 0.063 mm fraction of selected samples using methylene iodide (s.g. = 3.3) as the heavy liquid. These separates were examined with a scanning electron microscope using displays of both secondary and backscatter electron images to guide the examination. Qualitative analyses of grains seen in the displays were obtained using energy dispersive X-ray methods.

Results

At Waverley, Nova Scotia, quartz-carbonate veins in Meguma Group greywackes contain coarse grained native gold, scheelite, and arsenopyrite. Oxidized till was collected from shallow test pits at several distances down-ice from the deposit (Fig. 15.1). Close to the deposit, most grain size fractions are gold-rich. Moving down-ice, the overall gold content of the till drops sharply and the most auriferous grain sizes are isolated in the fine fractions. Only in the most gold-rich sample was particulate gold seen, in an SEM search of sand-sized heavy minerals; grains of gold were not seen in searches of finer fractions. Most of the gold in these weathered samples must be present in an adsorbed form on

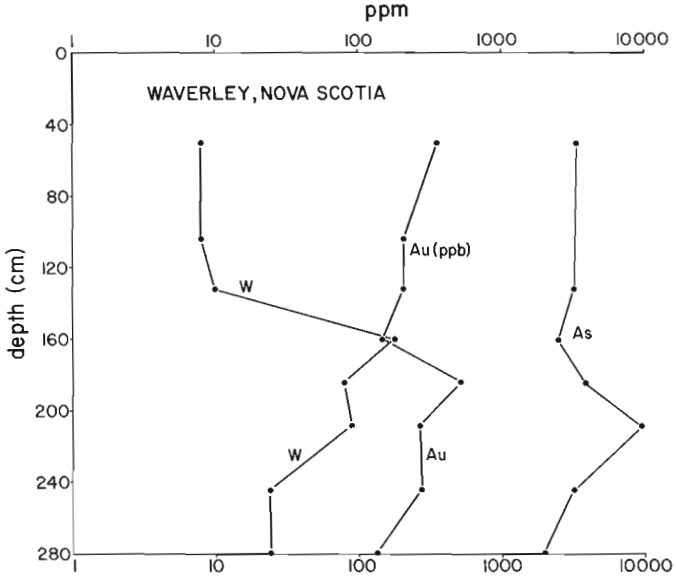

Figure 15.2. Variations in W, Au, and As abundances in the <63 μm fraction of till in a soil profile at Waverley.

iron and manganese oxides and hydroxides, and on clay minerals. It appears that a fine fraction such as <0.063 mm (<250 mesh) would be the best choice for analysis of samples collected at this scale.

Detailed sampling of a soil profile (Fig. 15.2) allows study of the behaviour of gold during pedogenesis. Assuming the resistate scheelite has the same bedrock source as the gold, the curves of tungsten and gold levels vs. depth in the profile should be similar in shape. Because they diverge in the upper part of the profile, one could suggest that gold has been hydromorphically enriched in the upper part of the profile. Note should also be made of the shifts in gold levels at this scale of sampling; this is "normal" for gold in soil profiles.

At the Pandora deposit, near Cadillac, Quebec, gold is present in bedrock, mostly in pyrite and rarely in native form. Till was collected at depths of 2 to 6 m at four sites along the down-ice edge of the deposit. Fractionation of two oxidized till samples shows that gold is most abundant in finer fractions (Fig. 15.3). Results for the two unoxidized samples tested (Fig. 15.4) suggest that gold is most abundant in sand-sized fractions. Gold levels are erratic in these samples because the sample sizes were small. A percussion drill was used to collect rather small original samples and the fractionation was done on remnants after other tests. In general, the gold seems to be present in sand-sized pyrite in fresh till, and in iron oxides and on silt and clay grains in weathered till.

At Onaman River, near Beardmore, Ontario, Cu-Ag-Au mineralization carries gold in chalcopyrite and pyrite. A map of Cu levels in till (Fig. 15.5) and the positions of Cu-rich boulders best define the size and shape of the dispersal train

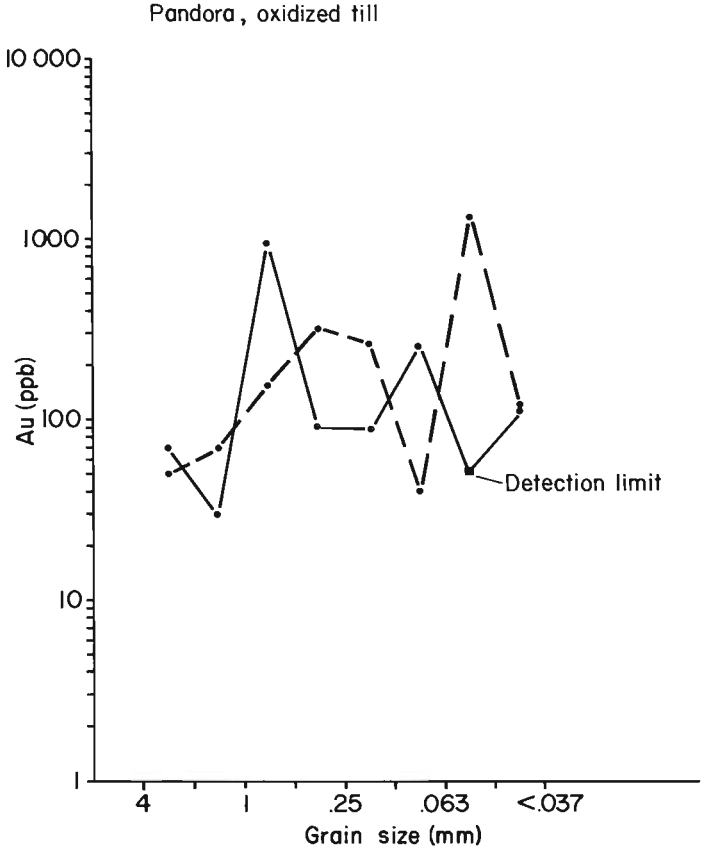

Figure 15.3. Abundance of gold vs. grain size of analyzed fraction of two samples of oxidized till at the Pandora deposit, Cadillac, Quebec.

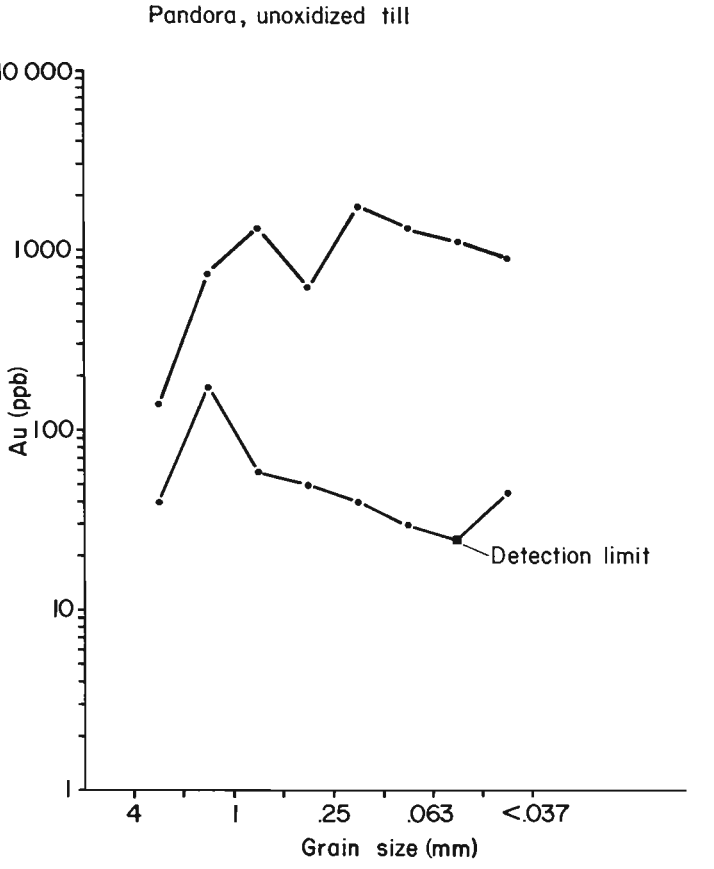

Figure 15.4. Abundance of gold vs. grain size of analyzed fraction of two samples of unoxidized till at the Pandora deposit, Cadillac, Quebec.

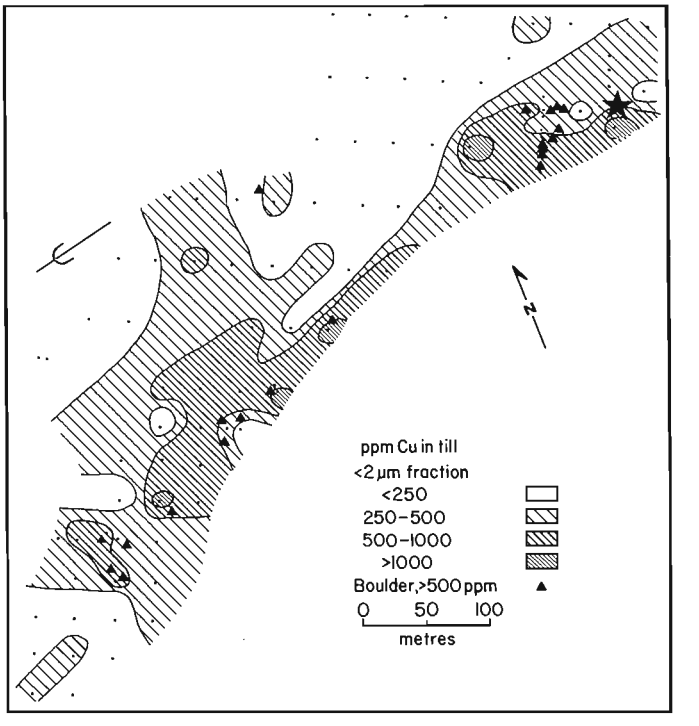

Figure 15.5. Map of copper abundances in the <2 µm fraction of till at Onaman River, Ontario. Mineralized bedrock is shown by the star.

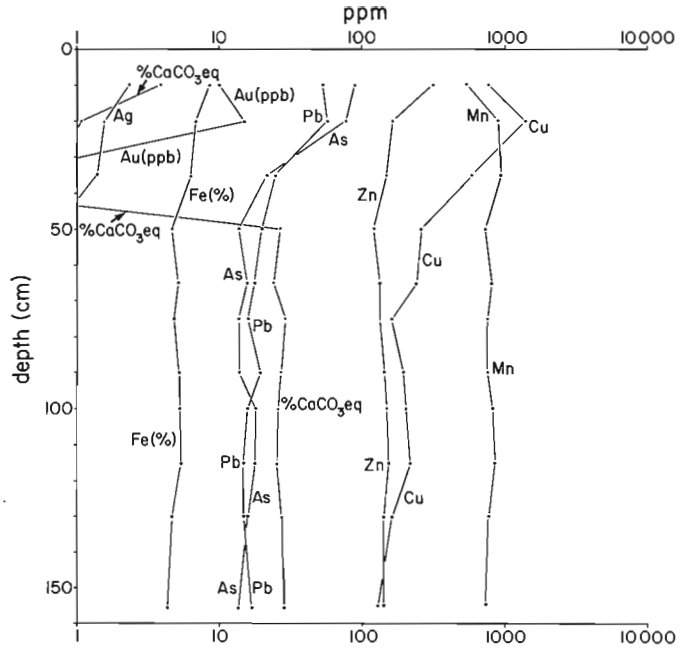

Figure 15.6. Variations in trace elements in the <2 μm fraction and gold and $CaCO_3$ equivalent in the <63 μm fraction of till in a soil profile at Onaman River, Ontario.

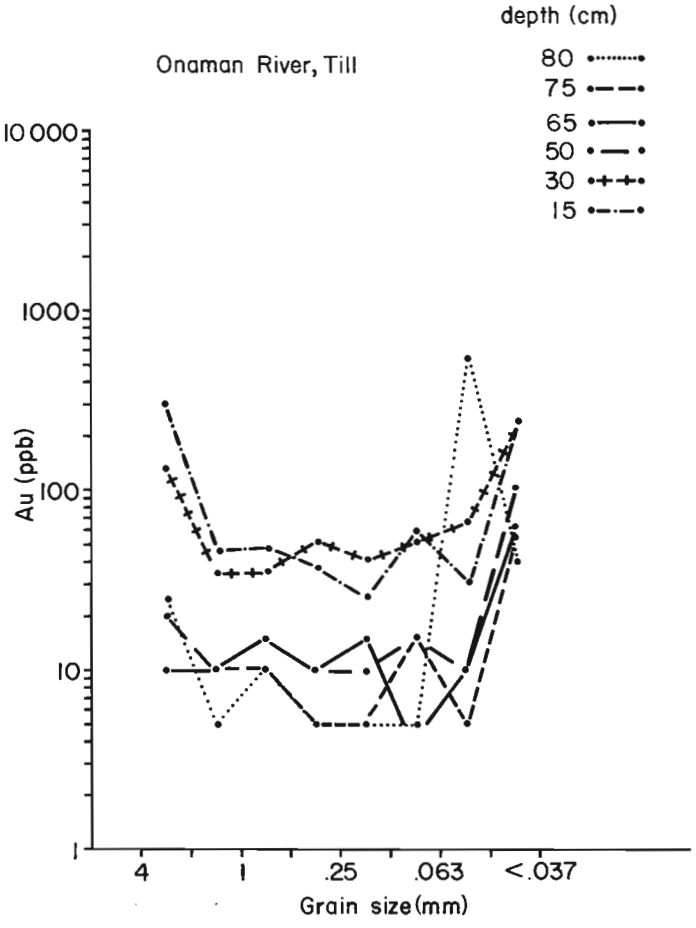

Figure 15.7. Abundance of gold vs. grain size of analyzed fraction of till at varying depths below surface in a dispersal train at Onaman River, Ontario.

derived from the mineralization. In exploration trenches, soil profiles developed on till were sampled in detail. Gold content was found to vary with copper and silver contents (Fig. 15.6) in each of six sampled trenches. Figure 15.6 shows data on 11 samples from a section through a thin edge of the dispersal train where the metalliferous till is the upper 40 cm of the sequence. In another section of this type, Au levels in six samples increase up the section, and the most Au-rich fractions are the finest ones (Fig. 15.7). The most gold-rich samples also show gold enrichment in coarse fractions, grain size fractions that consist predominantly of rock fragments. Regardless of the depth or gold content of the samples in the profile, the partitioning curves have roughly the same shape and they all display gold enrichment in fine fractions, presumably because the gold released during weathering of the sulphides is very fine grained or is adsorbed on fine grained minerals. Superimposing the set of partitioning curves for Cu in the same samples (Fig. 15.8) shows similar patterns to Au and the enrichment in fine sizes that is characteristic of the behaviour of chalcophile elements in oxidized till, lending support to the idea that Au is remobilized in the soil profile and may behave like some base metals during weathering (DiLabio, 1979; Shilts, 1984).

At the Agassiz deposit at Lynn Lake, Manitoba, Au is contained in fine grained pyrite. Fractionation of a sample of oxidized till shows variable gold levels, but again suggests that the fine fractions are the most gold-rich (Fig. 15.9).

At the base of the thick Quaternary sequence at the Owl Creek gold deposit near Timmins, Ontario, a green muddy till and its oxidized equivalent are preserved. The unoxidized green till contains abundant fresh pyrite and Paleozoic carbonate rock fragments; most of these are

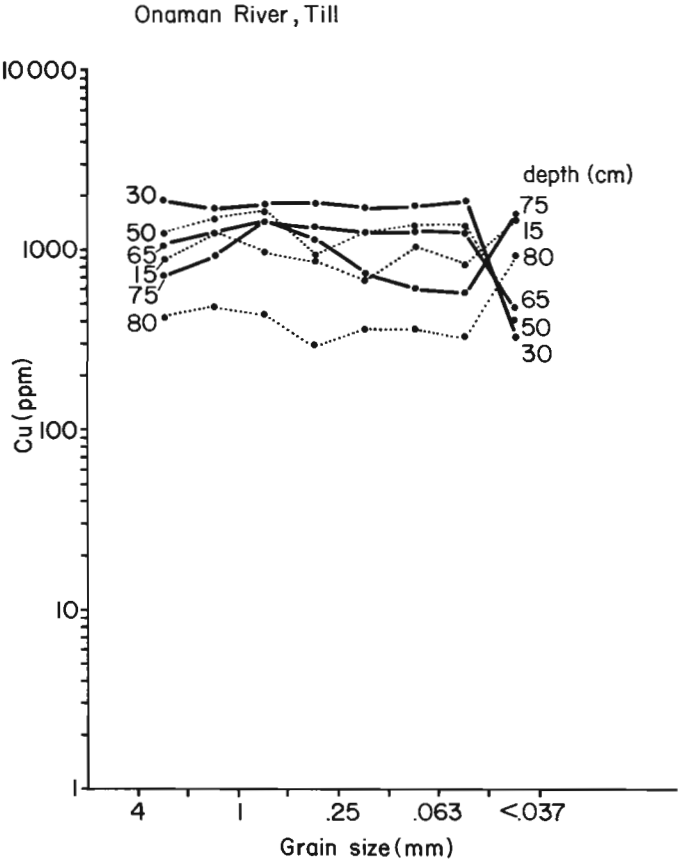

Figure 15.8. Abundance of copper vs. grain size of analyzed fraction of the same samples of till as in Figure 15.7.

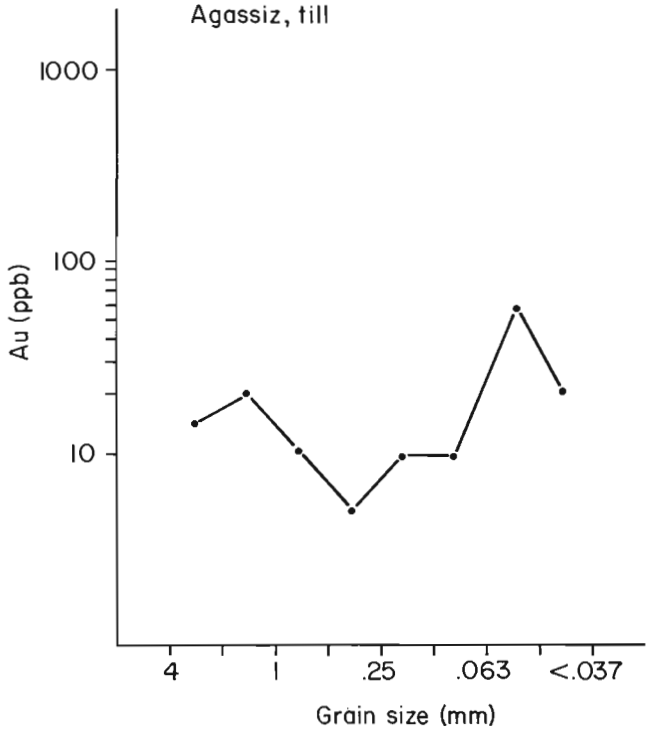

Figure 15.9. Abundance of gold vs. grain size of analyzed fraction of a sample of oxidized till from the Agassiz deposit, Lynn Lake, Manitoba.

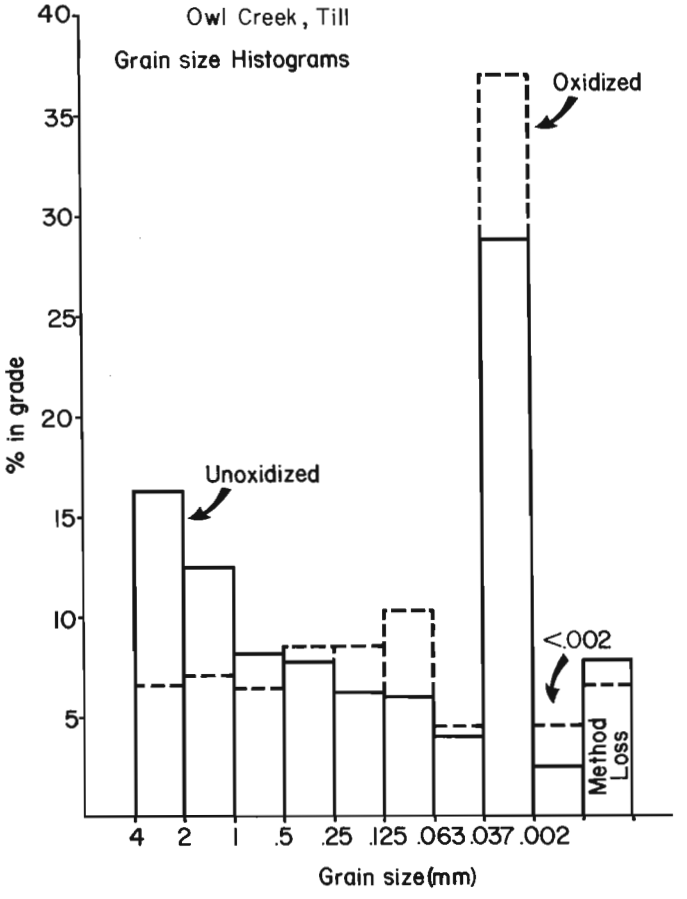

Figure 15.10. Grain size histograms of a gold-bearing unoxidized till sample and its oxidized equivalent at the Owl Creek deposit, Timmins, Ontario.

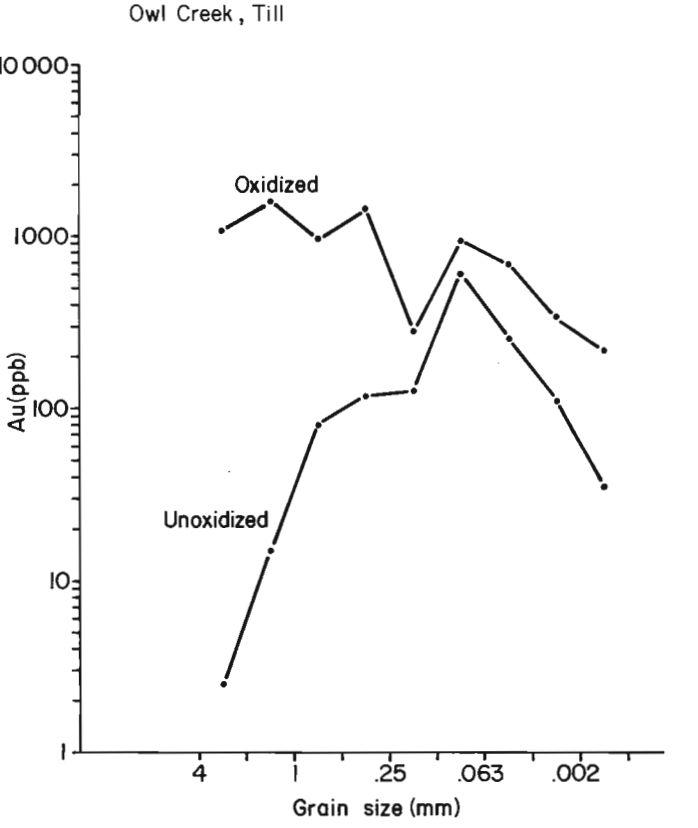

Figure 15.11. Abundance of gold vs. grain size of analyzed fraction of a sample of unoxidized till and its oxidized equivalent at Owl Creek, Timmins, Ontario.

decomposed in the oxidized layer. Weathering also shows up in the differing grain size distributions of the two units; the weathered till has more mud and less coarse sediment than the unweathered till (Fig. 15.10). Partitioning curves for the two units (Fig. 15.11) show strong gold enrichment in sand sizes in the unoxidized till and in coarse sizes in the oxidized till. The oxidized till is also much more auriferous in all size fractions than the unoxidized till. It appears that gold has been added to the oxidized till, perhaps from groundwater flowing down the bedrock-controlled gradient. The extra gold cannot be accounted for by volume loss caused by the decomposition of pyrite and carbonates.

Scanning electron microscopy shows that the sand-sized heavy minerals in the unoxidized till are dominated by euhedral pyrite, which may explain the sand-sized peak in gold content. Gold grains were not seen, although they should be present because the ore contains a small amount of free gold. Heavy minerals in the oxidized till are dominated by earthy limonite-goethite grains and corroded pyrite remnants. Again, no gold grains were seen. It appears that the gold in the oxidized till is tied up in the secondary iron oxides.

Conclusions

Gold in unweathered till is most abundant in grain size fractions that reflect the grain size of the glacially liberated and comminuted native gold and oxide or sulphide host minerals. It is more difficult to understand why gold is most abundant in finer sizes of weathered till; this could reflect one or more of the following: the original grain size of native gold; the grain size of gold released from weathering sulphides; and the grain size of gold-adsorbing phases; the last reason is favoured by the author.

It appears that a significant part of the gold in weathered till has been transported in groundwater and some is present as reprecipitated grains.

Fractionation experiments of this type are relatively easily done and can provide valuable information to guide geochemical exploration programs. In particular, the choice of an optimum grain size fraction for geochemical analysis of till at a given site can be made on the basis of the results of fractionation of samples collected during an orientation survey. From the examples cited in this study, the traditionally used minus 80 mesh (<0.177 mm) fraction often would be diluted by gold-poor, fine and very fine sand, and the optimum grain size fraction should be chosen instead to selectively isolate the gold-rich grain sizes of the till.

Acknowledgments

I thank the following people for allowing access to properties and for providing samples: D. Thorsteinson; M.E. Holt and A.C. Durocher, Camflo Mines Ltd.; W.B. Coker, R. Snow, and D.J. Bird, Kidd Creek Mines Ltd.; and E. Nielsen, Manitoba Department of Energy and Mines. R.W. Boyle made several helpful comments on the manuscript. Able field assistance was given by R. Jordan, J.R. Laidlaw, B. Prieur, M. Rupners, and P.H. Wyatt.

References

Ayras, M.
1977: Statistical observations on the element distribution in the fine material of till, Sodankyla, northern Finland; Geological Survey of Finland, Report of Investigation No. 14, 41 p.

DiLabio, R.N.W.
1979: Drift prospecting in uranium and base-metal mineralization sites, District of Keewatin, Northwest Territories, Canada; in Prospecting in areas of Glaciated Terrain 1979; Institution of Mining and Metallurgy, London, p. 91-100.

1981: Glacial dispersal of rocks and minerals at the south end of Lac Mistassini, Quebec, with special reference to the Icon dispersal train; Geological Survey of Canada, Bulletin 323, 46 p.

DiLabio, R.N.W. (cont.)
1982: Gold and tungsten abundance vs. grain size in till at Waverley, Nova Scotia; in Current Research, Part B, Geological Survey of Canada, Paper 82-1B, p. 57-62.

Dreimanis, A. and Vagners, U.J.
1971: Bimodal distribution of rock and mineral fragments in basal tills; in Till – A Symposium, ed. R.P. Goldthwait; Ohio State University Press, Columbus, p. 237-250.

Eriksson, K.
1973: The distribution of some metals in different till fractions; Bulletin of the Geological Institutions of the University of Uppsala, v. 5, p. 157-164.

Haldorsen, S.
1977: The petrography of tills – a study from Ringsaker, south-eastern Norway; Norges Geologiske Undersøkelse, no. 336, 36 p.

Kauranne, L.K.
1967: Facts to be noticed in pedogeochemical prospecting by sampling and analysing glacial till; in Geochemical Prospecting in Fennoscandia, ed. A. Kvalheim; Interscience, New York, p. 273-277.

Klassen, R.A. and Shilts, W.W.
1977: Glacial dispersal of uranium in the District of Keewatin, Canada; in Prospecting in Areas of Glaciated Terrain 1977; Institution of Mining and Metallurgy, London, p. 80-88.

Lindén, A.
1975: Till petrographical studies in an Archaean bedrock area in southern central Sweden; Striae, v. 1, p. 1-57.

Shilts, W.W.
1973: Drift prospecting; geochemistry of eskers and till in permanently frozen terrain, District of Keewatin, Northwest Territories; Geological Survey of Canada, Paper 72-45, 34 p.

1984: Till geochemistry of Finland and Canada; Journal of Geochemical Exploration, v. 21, p. 95-117.

Smith, R.T. and Gallagher, M.J.
1975: Geochemical dispersion through till and peat from metalliferous mineralization in Sutherland, Scotland; in Prospecting in Areas of Glaciated Terrain 1975, ed. M.J. Jones; Institution of Mining and Metallurgy, London, p. 134-148.

-16-

TECTONIC SIGNIFICANCE OF THE TIBBIT HILL VOLCANICS: GEOCHEMICAL EVIDENCE FROM RICHMOND AREA, QUEBEC

EMR Research Agreement 244/04/83

H. Pintson[1], P.S. Kumarapeli[2], and M. Morency[1]
Precambrian Geology Division

Pintson, H., Kumarapeli, P.S., and Morency, M., Tectonic significance of the Tibbit Hill Volcanics: geochemical evidence from Richmond area, Quebec; in Current Research, Part A, Geological Survey of Canada, Paper 85-1A, p. 123-130, 1985.

Abstract

The Tibbit Hill Volcanics of the Sutton Mountains region have been interpreted as being rift-facies volcanic rocks associated with the opening of the Iapetus Ocean. This interpretation is based on their tectonic-stratigraphic setting and bimodal character.

The volcanics are extensively altered to epidosites and have been metamorphosed to the blueschist-greenschist transition facies. Despite the combined effects of epidotisation/metamorphism, which have resulted in the redistribution of most of the major elements, the majority of the incompatible element patterns (Nb, P, Hf, Zr, Ti, Y and REE) have remained intact. Variations in the abundances of these immobile elements are attributable to fractional crystallization. The total abundances of these elements and their normalized patterns are similar to those of transitional or alkalic basalts. Plots of various immobile elements on discrimination diagrams attest to their "Within Plate" tectonic setting. Since the Tibbet Hill Volcanics are part of a continental rise/slope assemblage the setting would be continental as opposed to oceanic.

Résumé

Les roches volcaniques de Tibbit Hill dans la région des monts Sutton sont interprétées comme étant des roches de fosse tectonique associées à la formation de l'océan Japet. Cette conclusion est fondée sur le milieu tectono-stratigraphique et la nature bimodale de ces roches.

Les roches volcaniques ont été altérées en épidotites sur de vastes étendues et métamorphisées jusqu'au faciès de transition entre les schistes bleus et les schistes verts. Malgré les effets combinés de l'épidotisation et du métamorphisme, qui ont provoqué la redistribution de la plupart des éléments principaux, la plus grande partie des motifs produits par les éléments incompatibles (Nb, P, Hf, Zr, Ti, Y et lanthanides), sont demeurés intacts. La cristallisation fractionnée entraîne des variations du nombre considérable de ces éléments immobiles. La somme totale de ces éléments et leurs motifs normalisés sont similaires à ceux des basaltes transitionnels ou alcalins. Les diagrammes de discrimination de ces divers éléments immobiles révèlent qu'ils se sont accumulés dans un milieu tectonique à l'intérieur de la plaque. Étant donné que les roches volcaniques de Tibbit Hill font partie d'un assemblage talus-glacis continental, ce milieu serait continental plutôt qu'océanique.

[1] Département des Sciences de la Terre, Université du Québec à Montréal, Montréal, Québec H3B 3H5
[2] Department of Geology, Concordia University, Montreal, Quebec H3G 1M8

Introduction

Late Precambrian/early Cambrian volcanic sequences such as the Catoctin lavas of central Virginia and southern Pennsylvania and the Lighthouse Cove lavas of western Newfoundland are regarded as volcanic rocks related to continental rifting which occurred as a prelude to the opening of the Iapetus Ocean. This interpretation is based on their setting in the overall Appalachian tectonic-stratigraphic framework and on their petrochemistry (Strong and Williams, 1972; Rankin, 1976). Another volcanic unit which has similar tectonic and stratigraphic relations is the Tibbit Hill Volcanics of the Sutton Mountains region of Quebec and Vermont.

The Tibbit Hill Volcanics are exposed in four principal outcrop areas (Fig. 16.1) including the area in the Notre Dame Mountains, Quebec (Charbonneau and St. Julien, 1981; Kumarapeli et al., 1981). These areas coincide with axial culminations of the westernmost anticline of the Sutton Mountains Anticlinorium. The rocks are predominantly basaltic except in Waterloo area, Quebec where rhyolitic rocks are locally present (Osberg, 1965; Rankin, 1976).

The age of the volcanics is not precisely known. They are probably the oldest Appalachian rocks exposed in the Sutton Mountains region and are presumed to lie directly on a circa 1000 Ma Grenvillian basement (Doll et al., 1961; Baer et al., 1971). They form the lowermost exposed part of a continuous stratigraphic succession, the Oak Hill Group (Clark, 1934, 1936), the middle part of which is early Cambrian in age. Thus, a late Hadrynian/early Cambrian age indicated by the stratigraphic relations, is similar to the age assigned to the Catoctin Formation and the Lighthouse Cove lavas.

The Tibbit Hill Volcanics are pervasively polydeformed and thrust towards the northwest (St. Julien and Hubert, 1975; Ando et al., 1983; St. Julien et al., 1983) probably during the Taconic orogeny. The rocks are commonly characterized by greenschist metamorphism, except in Richmond area, where abundant development of crossitic amphibole suggests blueschist-greenschist transition facies metamorphism (Trzcienski, 1976). The full significance of the above and other occurrences of high P-low T mineral assemblages in the Appalachians is not yet understood. However, Zen (1983) concluded that such rocks should be found on the North American cratonic side of a possible subduction zone, and consequently, the ancient margin of North America cannot be farther northwest that these occurrences.

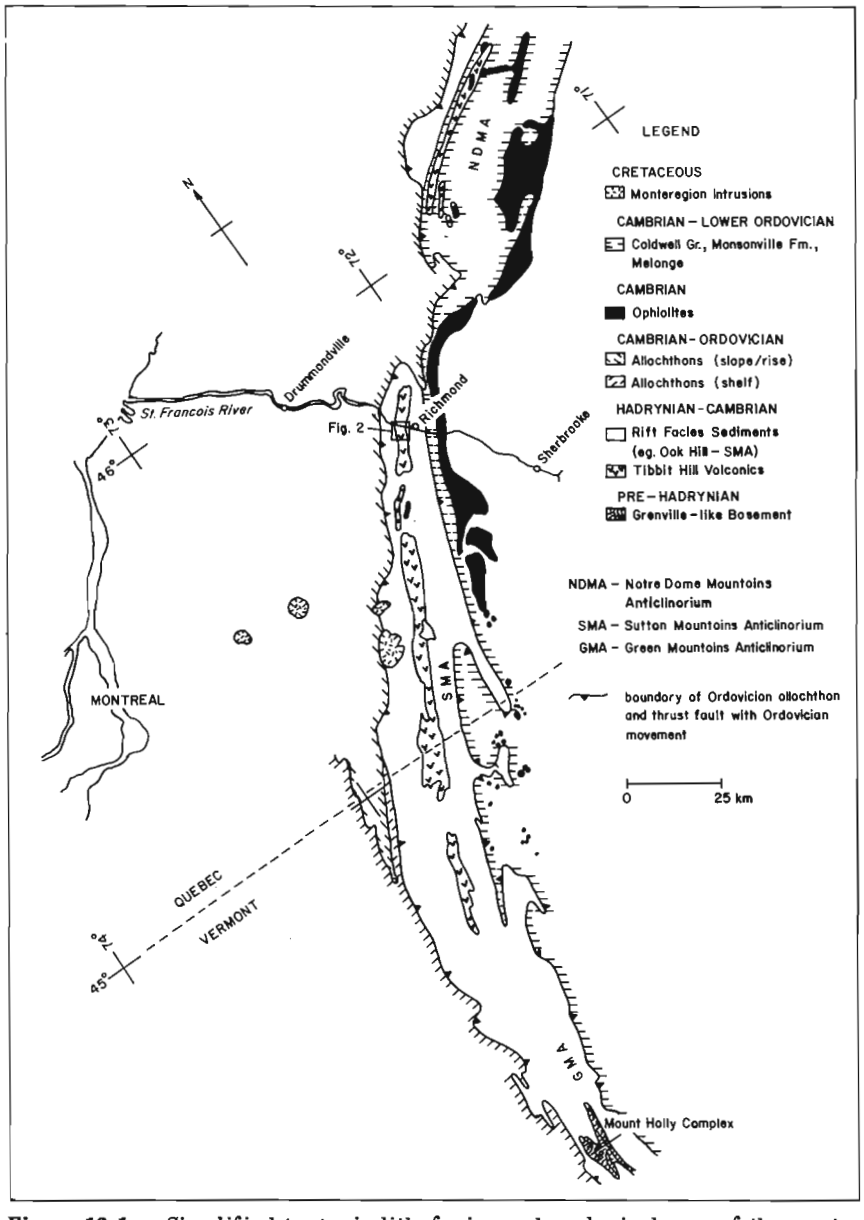

Figure 16.1. *Simplified tectonic lithofacies and geological map of the western margin of the Notre Dame-Sutton-Green Mountains' anticlinoria showing the occurrence of the Tibbit Hill Volcanics (after Baer et al., 1971; Williams, 1978; St. Julien et al., 1983), and the location of the study area.*

From a study of the gravity and magnetic anomalies associated with Tibbit Hill Volcanics, Kumarapeli et al. (1981) have shown that the seemingly minor belt defined by the outcrop areas is actually the surface expression of a much larger volcanic unit which is only slightly exposed at the present level of erosion. The gravity-magnetic model of Kumarapeli et al. (1981) indicates a continuous belt of mafic volcanic rocks, about 250 km long, being widest (~45 km) and thickest (~8 km) in its mid-section. In plan, the model has the shape of a boomerang, the apex of which points approximately in the directions of the trends of the Ottawa Graben and the Grenville dyke swarm. However, it should be noted that the original configuration of these elements may have been somewhat modified by northwest thrusting. Kumarapeli et al. (1981) and Kumarapeli (in press) have marshalled the above space relations and other lines of arguments to suggest that the Volcanics formed at an rrr triple junction – the Sutton Mountains triple junction – of a rift system (eo-Appalachian or Iapetan rift system), in an environment analogous to that of the Afar triangle. The failed arm of the three-pronged rift is considered to be the Ottawa Graben.

Important as these rocks seem to be to an understanding of the tectonic evolution of the Iapetus and hence of the Appalachian foldbelt, detailed studies of their petrology and geochemistry are sparse although a knowledge of these aspects could provide

additional constraints to models of their tectonic significance. With this in mind, we undertook a detailed study of the petrology and geochemistry of a 10-km segment (Fig. 16.1) of the volcanic belt in Richmond area, Quebec. The area was selected on the basis of its excellent rock exposure along several recent roadcuts. Also, the volcanic rocks probably attain their maximum thickness in this general area. The area was mapped at 1:10 000 to gain insight into the local structure and volcanic stratigraphy of the Tibbit Hill Volcanics and to provide a framework for sampling for petrological and geochemical studies (Pintson, 1982). A problem that was not addressed in this study is the significance of crossitic amphibole which as mentioned earlier is abundantly developed in the THV of Richmond area. The only other part of the THV whose petrology and geochemistry has been studied in some detail is in Vermont (Coish, personal communication, 1983; Pieratti, 1976).

Tibbit Hill Volcanics

Field relations and petrography

Detailed geology of these Volcanics in Richmond area, Quebec is given in Pintson (1982 and M.Sc. thesis). The following is a brief summary of the local geology and petrography of the rocks. Detailed mapping at a scale of 1:10 000 has shown that a volcanic stratigraphy is not discernible within the volcanics. The rocks are mappable as two main units – greenstones and epidosite-bearing greenstones (Fig. 16.2). Other rock types, such as intercalated phyllites and laminated schists of mixed volcanic and sedimentary origin, are also present but these are volumetrically insignificant and probably have little bearing on the overall geochemistry of the Tibbit Hill Volcanics.

Greenstones constitute just over half of the exposed metavolcanic rocks. They are fine grained, massive to schistose, locally amygdaloidal, and rarely porphyritic. They consist essentially of albite, chlorite, epidote, crossitic and/or actinolitic amphibole, phengite, sphene and FeTi-oxides (with some associated rutile). Approximate modes for the samples studied for this report are given in Table 16.1. Occasionally rare cores of kaersutite occur within crossite and along with the FeTi-oxides represent the only primary minerals remaining in these rocks (Trizcienski, 1976). Coupled with the almost complete transformation of primary mineralogy has been the total destruction of original textures with rocks exhibiting well developed penetrative deformational textures. Even in amygdaloidal or porphyritic varieties the groundmass has been totally altered.

The presence of amygdules indicates that the greenstones have been derived from lava flows. Clear examples of other primary structures such as pillows, columnar jointing and even flow contacts were not observed. The amygdules are of various shapes and sizes, may or may not be aligned in the plane of schistosity, and consist essentially of albite, quartz, calcite, epidite and chlorite. They may be filled wholly by one of the above minerals or with several of them occurring as irregular intergrowths or in concentric layers.

Porphyritic greenstones, where found, commonly contain 1-5 mm long prismatic shapes, now preserved as albite, which probably were labradorite phenocrysts originally. Some rocks also contain 1-2 mm patches of chlorite which may represent olivine or pyroxene phenocrysts.

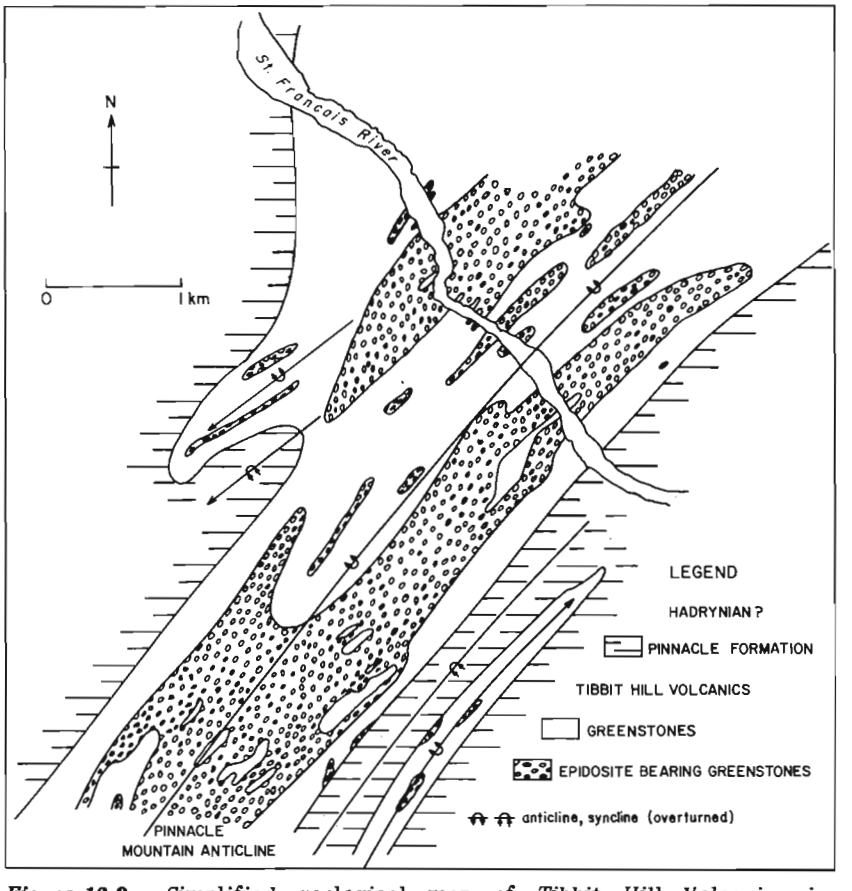

Figure 16.2. *Simplified geological map of Tibbit Hill Volcanics in Richmond area, Quebec. Note the abundance of epidosite-bearing greenstones.*

The epidosite-bearing greenstones make up the majority of the remaining exposed rocks within the Tibbit Hill Volcanics and occur in isolated bodies or in large continuous zones (Fig. 16.2). These rocks consist of nodules or "knots" of epidosite (epidote-quartz rock) set in a groundmass which is commonly identical to the greenstones described above. The contacts between the greenstones and epidosite-bearing greenstones are gradational over several metres. The epidosites occur as ellipsoids, spheroids and lenses, ranging in size (longest dimensions) from 0.5-100 cm, have their two main axes aligned parallel to the regional schistosity and make up from 1-40% of an outcrop. Contacts between the epidosites and the host greenstones are usually sharp, though in some cases they may also be gradational over 1-5 cm. The epidosites consist essentially by blocky epidote (50-70 modal %), quartz, sphene and crossite/actinolite, with minor calcite, FeTi-oxides and rare albite. Although most epidosites stand out as distinct masses, with the epidote concentrated in localized zones, some of the surrounding greenstones may exhibit pervasive epidotisation, containing up to 30% epidote. One epidosite (RTH-2) has been studied for this report and its mode is given in Table 16.1.

Epidosites have been described from the Vermont segment of the Tibbit Hill Volcanics as well (Booth, 1950) and they seem to be a common feature of many basaltic to andesitic rocks that have undergone low-grade metamorphism (eg. the Cliefden outcrop, Australia, Smith, 1968; the Catoctin lavas, Virginia, Reed and Morgan, 1971; the Keweenawin lavas, Michigan, Jolly and Smith, 1972; Archean lavas, Abitibi area, Jolly, 1980; and others). The conclusions

Table 16.1. Major and trace element analyses* and approximate modal compositions** of the Tibbit Hill Volcanics from the study area. RHT-2 is an epidosite, all the rest are greenstones.

	RTH-1	RTH-2	RHT-3	RTH-4	TRH-5	RTH-6	RTH-7	RTH-8
SiO_2(wt.%)	46.08	48.26	46.06	46.85	44.87	47.91	46.33	45.86
TiO_2	2.93	2.55	2.58	3.06	3.43	3.27	3.64	3.89
Al_2O_3	15.05	15.10	15.84	15.32	16.03	14.30	14.32	15.04
Fe_2O_3	14.10	11.28	13.09	13.50	14.71	13.80	14.44	15.98
MgO	6.84	1.30	7.85	6.75	8.22	7.02	5.14	5.69
MnO	0.16	0.18	0.25	0.28	0.28	0.21	0.21	0.22
CaO	6.13	18.22	6.45	7.35	3.52	4.53	6.46	4.27
Na_2O	3.21	0.43	4.08	2.99	4.70	3.43	2.51	4.00
K_2O	2.29	0.05	0.51	0.01	0.68	2.17	4.02	2.28
P_2O_5	0.41	0.35	0.32	0.43	0.48	0.46	0.59	0.65
LOI	3.08	1.82	3.36	4.13	4.02	3.17	2.34	2.65
Total	100.28	99.54	100.39	100.67	100.94	100.27	100.00	100.53
Rb (ppm)	36.7	-	-	-	-	34.9	65.2	30.9
Nb	18.4	15.1	14.6	26.3	21.4	22.2	28.9	32.2
Sr	529	3154	831	676	155	192	312	267
Hf	6.06	5.50	4.55	5.59	7.46	7.32	8.38	8.78
Zr	214	219	157	201	248	248	289	319
Y	36.7	33.9	27.7	33.6	41.7	40.1	43.3	47.1
La	23.7	22.2	19.3	25.4	28.2	31.3	35.0	41.1
Ce	59.1	52.6	44.3	57.8	67.3	73.6	89.9	104
Nd	40.5	33.7	26.7	31.5	38.6	40.2	45.0	50.2
Sm	8.43	7.78	5.90	7.21	9.54	9.33	10.9	12.1
Eu	2.56	2.45	2.04	2.39	2.90	2.77	3.27	3.39
Tb	0.95	0.88	0.81	0.96	1.08	1.22	1.24	1.23
Yb	3.46	3.07	2.60	2.93	3.84	4.29	4.05	4.20
Lu	0.52	0.46	0.41	0.45	0.59	0.65	0.59	0.63
Albite	35	tr.	32	45	38	30	12	48
Chlorite	9	-	25	35	38	16	5	10
Epidote	14	68	28	9	1	1	9	1
Crossite/ Actimolite	8	8	5	-	1	14	22	-
Phengite	22	-	-	-	3	20	25	14
Sphene	5	12	4	4	4	10	14	12
Calcite	-	1	-	3	-	-	2	-
Quartz	-	11	-	1	1	-	-	-
FeTi-oxides	7	tr	6	3	14	9	11	15

*Analytical notes in Pintson (M.Sc. in preparation); precision of the trace element data is generally better than 10%; - indicates below detection limit (10 ppm).

**Based on visual estimates of single thin sections: tr trace, - absent

reached by all workers cited above is that the epidosites were formed essentially by the isochemical redistribution of the major elements (except for some leaching of K_2O and the addition of water) within the volcanic pile.

Throughout the study area the Tibbit Hill Volcanics are always overlain by the Pinnacle Formation (Fig. 16.2), consistent with the basal stratigraphy of the Oak Hill succession (Clark, 1934, 1936).

Geochemistry

Major and trace element analyses of the Tibbit Hill Volcanics for the study area are presented in Table 16.1. Within the greenstones, and particularly between the greenstones and the epidosite, compositional variations are largest for K_2O, Na_2O and CaO. Lesser variations are observed for Fe_2O_3 and MgO, whereas Al_2O_3, SiO_2, TiO_2 and P_2O_5 are fairly constant. It should be noted that there is a systematic increase in TiO_2 and P_2O_5 from samples RTH-3 through to RTH-8, a feature that will be discussed below. Variations in the major elements are also related to modal mineralogy. For example, the high CaO content of the epidosite correlates with abundant epidote, and similarly, the high K_2O content of sample RTH-7 correlates with abundant phengite.

In previous studies of epidotisation (eg. Reed and Morgan, 1971) the behaviour of CaO and Na_2O were found to best characterize the process. Since CaO is enriched in the

epidosites, it is depleted in the greenstone – the opposite would occur for Na_2O. Such relationships are present in the greenstones of this study for their average CaO content (5.72 wt.%) is well below that of the average basalt (9.66 wt.%) or tholeiite (10.35 wt.%) while their average Na_2O content (3.68 wt.%) is higher than that of the average basalt (2.97 wt.%) or tholeiite (2.44 wt.%) (basalt-tholeiite averages from Le Maitre, 1976), indicating that epidotisation was probably a redistribution process. A fuller discussion of the behaviour of the major elements will be given in Pintson (M.Sc. thesis in preparation) where variations in most of these elements are shown to be indeed due to redistribution. These variations preclude the use of the major elements in defining the petrological affinities of these rocks, although their SiO_2 contents, which are still fairly representative of the protolith, indicate that they are truly basaltic.

Unlike the major elements, the trace elements, particularly the immobile ones (including TiO_2 and P_2O_5), fall within a consistent range and vary systematically from one sample to the next. These relationships are probably inherited from an original magmatic differentiation process, unaffected by epidotisation/metamorphism. Normalized incompatible element patterns for an epidosite (RTH-2) and its host greenstone (RTH-1) are compared in Figure 16.3. The patterns show the following features: (1) they are relatively smooth patterns enriched in the more incompatible elements; (2) Rb, K and Sr show large variations in their normalized abundances; (3) the abundances of the immobile trace elements (excepting Zr) are higher in the greenstone than in the epidosite; and (4) Nb and P normalized abundances are low relative to the smooth curves produced by the other elements (excluding Rb, K, Sr).

The first feature indicates that despite alteration/metamorphism, the immobile element pattern of these rocks has remained largely intact since such relatively smooth curves are commonly characteristic of fresh basalts (excluding Volcanic Arc Basalts) where normalized abundances of Nb, Sr, P, Hf, Zr, Ti and Y correlate with the Rare Earth Elements (REE) (Sun et al., 1979; Sun, 1980). The wide variations in Rb, K and Sr, the second feature shown by the patterns, attest to their highly mobile nature. Depletion of Rb and K within the epidosite has resulted in these two elements becoming enriched within the greenstone. Similarly, the enrichment of Sr within the epidosite has resulted in this element's depletion within the greenstone. Such behaviour for Sr would be expected since its distribution parallels that of Ca. The third feature, the overall lower abundances of the immobile trace elements (excluding Zr) in the epidosite (by about 10%) may be due to dilution. The dilutants are probably quartz (11%) and calcite (1%) which occur as open space fillings in the epidosite. In contrast to the immobile trace elements, Zr poses an enigma, by being apparently enriched in the epidosite. However, considering that the indicated enrichment is only about 2%, its significance is questionable. Finally, the lower Nb and P normalized abundances relative to the overall smooth curves of the immobile elements seem to be primary features and not due to epidotisation since they occur in both samples. Such depletions have been ascribed to crustal contamination (eg. Thompson et al., 1983) and is discussed below. Thus, excepting the postulated complications brought about by crustal contamination during magma ascent and dilution during or after epidotisation, the most salient point arising from the comparative study of the epidosite and its host greenstone is that the immobile trace element pattern of the rock survives, virtually intact, the process of epidotisation. Similar conclusions have been reached by Condie et al. (1977) and Muecke et al. (1979) who studied the trace element distributions in epidosites and their host rocks from other localities.

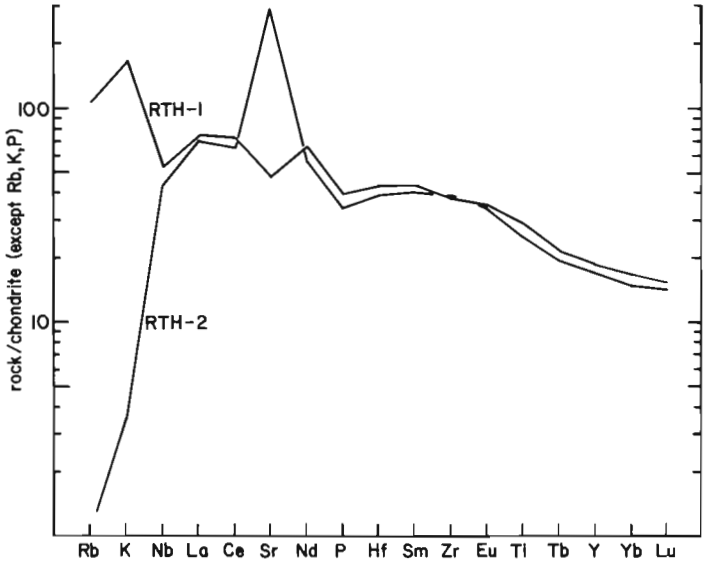

Figure 16.3. *Normalized incompatible element patterns for samples RTH-1 (greenstone) and RTH-2 (epidosite). All elements have been normalized to chondritic abundances except Rb, K and P which have been normalized to terrestrial abundances. Normalizing values are from Sun (1980), except for Hf which is from Ehmann and Rebagay (1970). The order of the elements is based approximately on their increasing incompatibility from right to left.*

Normalized patterns for four greenstones, showing the range of values observed in the rocks of this study, are shown in Figure 16.4. Again, the salient features as discussed above are present. REE, Nb, P, Hf, Zr, Ti and Y have remained immobile whereas Rb, K and Sr have been highly mobilized during epidotisation. In addition, low Nb and P normalized abundances persist. The normalized pattern for the epidosite is also included in Figure 16.4 to illustrate the similarities of the curves for the immobile elements and thus, to further demonstrate that even such a highly altered rock can be useful in geochemical studies.

Significance of the immobile elements

Since it has been shown that the REE, Nb, P, Hf, Zr, Ti and Y have not been demonstrably modified during the epidotisation and metamorphism of the Tibbit Hill Volcanics these element abundances can be used for two purposes: (1) to define the tectonic setting in which the volcanics formed, and (2) to gain insight into the origin and evolution of the parent magma. A number of discrimination diagrams

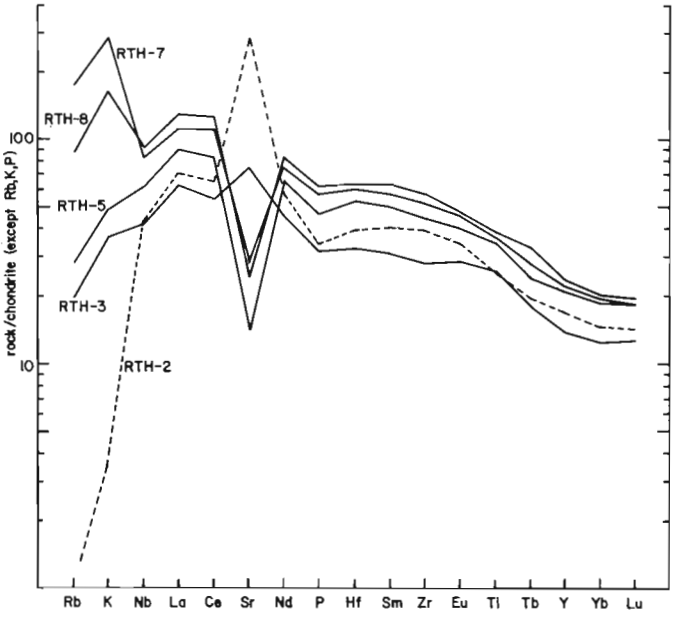

Figure 16.4. *Normalized incompatible element patterns for four greenstones of this study. Sample RTH-2 (epidosite) is also included for comparison.*

relating trace element abundances and/or ratios with tectonic setting are shown in Figure 16.5. In all diagrams the data for the greenstones and the epidosite plot consistently in the "Within Plate Basalt" fields and define rather smooth linear trends. Since "Within Plate Basalts" comprise either Ocean Island Basalts or Continental Rift Basalts additional criteria are needed to further discriminate between these two environments. These criteria are provided by field relations. Considering that Tibbit Hill Volcanics are the lowermost exposed rocks of the Oak Hill Group in the Sutton Mountains region, that the Oak Hill Group unconformably overlies a continental basement (Grenville) in the Green Mountains region (Doll et al., 1961) and that the relationships are probably similar in the Sutton Mountains region as well, a continental environment is assigned to the Volcanics.

The linear trends of the data (Fig. 16.5) are taken as further evidence that these elements have remained immobile during epidotisation/metamorphism and that their variation is a result of a primary magmatic process. This process is identified as fractional crystallization because of the parallel nature of the normalized patterns with increasing total abundance of the immobile incompatible elements (Fig. 16.4) and because, in a diagram such as La/Sm vs. La (Fig. 16.6) the points plot along a straight nearly horizontal line, a feature restricted solely to fractional crystallization (Allègre and Minster, 1978).

Based on the Nb/Y ratio (Fig. 16.5d) Tibbit Hill Volcanics would be classified as tholeiitic basalts. This is at variance with their higher total incompatible element abundances with the presence of relict kaersutite. The abundances of the incompatible elements within the Tibbit Hill are comparable to those of transitional or alkalic basalts. In addition, the occurrence of kaersutite is restricted to rocks of alkaline composition (Aggarwal et al., 1984). Thus, Tibbit Hill Volcanics are interpreted to be transitional or alkalic basalts with anomalously low Nb/Y ratios.

Normalized patterns (immobile elements only) for one of the rocks of this study (RTH-7) and a transitional mildly alkalic basalt from the Boina Centre, Afar Rift, Ethiopia (S51, Barberi et al., 1975) are shown in Figure 16.7. These two patterns are compared for two reasons. Firstly, to show that the shapes and abundances of these two patterns are similar (although RTH-7 is more enriched in all elements because it is more evolved). Secondly, to show the expected distributions of Nb and P within a typical basalt (S51) as generalized by Sun (1980, excluding Volcanic Arc Basalts). For S51, Nb plots along an extension of the light REE while P correlates with Nd. This is in contrast to the rocks of this study, where these two elements show a characteristic depletion (Fig. 16.3, 16.4, 16.7). As mentioned above, such Nb and P depletions are believed to be the result of crustal contamination (eg. Thompson et al., 1983). Also included in Figure 16.7 is the normalized pattern for the

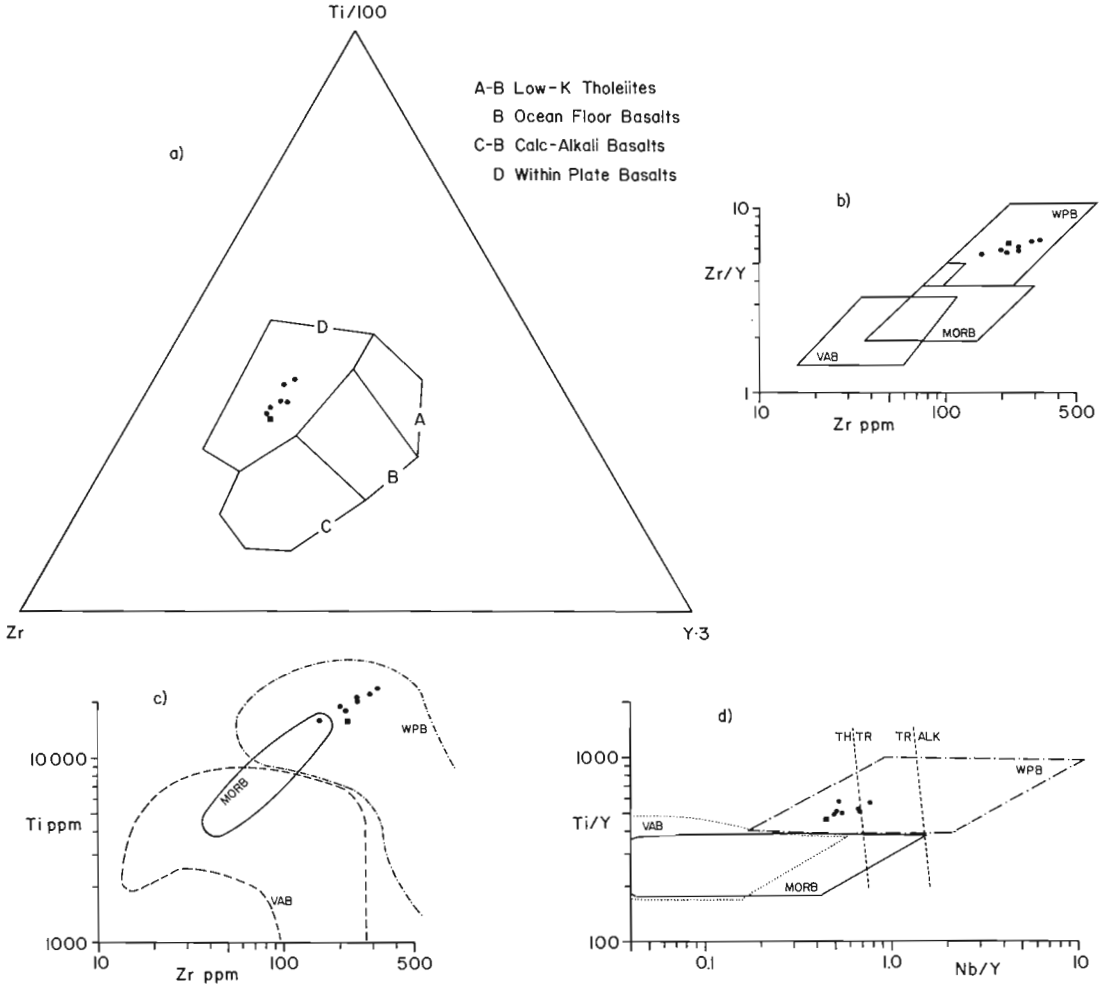

Figure 16.5. *Various discrimination diagrams relating geochemistry with tectonic setting. WPB = within plate basalts, MORB = mid-oceanic ridge basalts, VAB = volcanic arc basalts; a) from Pearce and Cann (1973), b) from Pearce and Norry (1979), c) and d) from Pearce, 1982; in d) TH = tholeiitic, TR = transitional, ALK = alkalic;* ● *= greenstones,* ■ *= epidosite.*

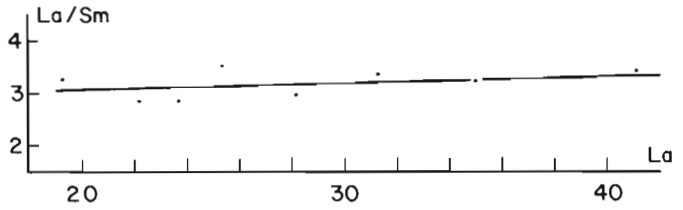

Figure 16.6. La/Sm vs. La diagram for the rocks of this study (the line is a "least squares" best fit).

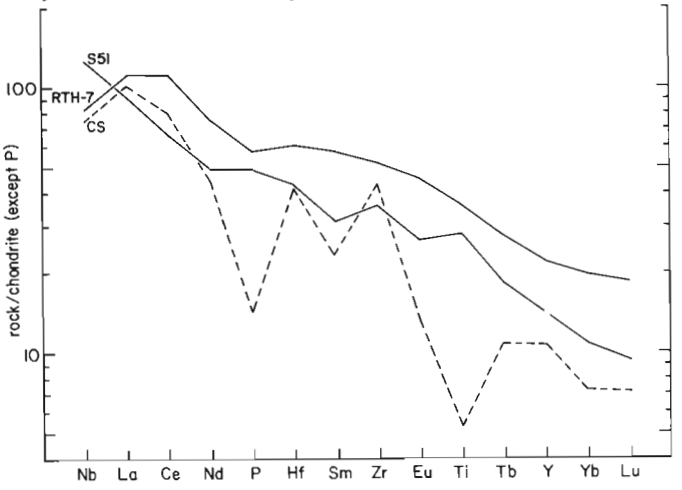

Figure 16.7. Normalized immobile incompatible element patterns for greenstone RTH-7 (this study); a transitional basalt from the Boina Centre, Afar Rift, Ethiopia (S51, Barberi et al., 1975); and the average for these elements within the Precambrian Canadian Shield (CS, Shaw et al., 1967, 1976). For S51, Nb has been derived by multiplying Ta by 17.5 the chondritic Nb/Ta ratio (eg. Thompson et al., 1983).

average of the elements of interest within the Precambrian Canadian Shield (CS, Shaw et al., 1967, 1976). This pattern is shown as an example of the distribution of these elements within the continental crust. Although there is a wide scatter of points, the low Nb and P abundances are apparent and are a characteristic feature of the majority of proposed crustal contaminants (eg. Thompson et al., 1983). Thus, Tibbit Hill Volcanics may have been contaminated by a crustal (continental) component characteristically low in Nb and P, but with a more regular distribution of elements from Hf to Lu than in the example shown (CS). If crustal contamination was indeed a factor in the petrogenesis of the Tibbit Hill then it further suggests that these rocks were erupted in a continental within plate setting.

Conclusions

Five main features of the Tibbit Hill Volcanics have been established in this study:

1. despite alteration (epidotisation) and metamorphism (blueschist-greenschist transition facies) the REE, Nb, P, Hf, Zr, Ti and Y have remained immobile;
2. when plotted on discrimination diagrams all data fall consistently in the "Within Plate Basalt" field. This coupled with the field relations of the Tibbit Hill indicates a continental within plate setting and not an oceanic island within plate setting;
3. variations between the samples studied are attributable to fractional crystallization;
4. total abundances of these elements and their normalized more incompatible element enriched patterns are similar to transitional or alkalic basalts, consistent with the presence of relict kaersutite in these rocks, despite tholeiitic Nb/Y ratios;
5. anomalously lower Nb and P normalized abundances may indicate contamination by continental crust, consistent with the idea that the Volcanics formed in a continental rift environment.

Thus the geochemical studies agree with the previous reasonings that the Tibbit Hill Volcanics erupted through continental crust. That they are transitional to alkaline in composition as well, lends support to the idea that they are rift related volcanic rocks that formed at an rrr triple junction, possibly over a mantle plume (Dewey and Burke, 1974).

Acknowledgment

This work was supported by an EMR Research Agreement to PSK and MM.

References

Aggarwal, P.L., Fujii, T., and Nesbitt, B.E.
1984: Magmatic composition and tectonic setting of altered, volcanic rocks of the Fennell Formation, British Columbia; Canadian Journal of Earth Sciences, v. 21, p. 745-752.

Allègre, C.J. and Minster, J.F.
1978: Quantitative models of trace element behaviour in magmatic processes; Earth and Planetary Science Letters, v. 38, p. 1-25.

Ando, D.J., Cook, F.A., Oliver, J.E., Brown, L.D., and Kaufmann, S.
1983: Crustal geometry of the Appalachian orogen from seismic reflection studies; in Contributions to the Tectonics and Geophysics of Mountain Chains, ed. R.D. Hatcher, Jr., H. Williams and I. Zietz; Geological Society of America, Memoir 158, p. 83-101.

Baer, A.J., Poole, W.H., and Sanford, B.V.
1971: Rivière Gatineau, Quebec-Ontario; Geological Survey of Canada, Map 1334A, Sheet 31.

Barberi, F., Ferrara, G., Santacroce, R., Treuil, M., and Varet, J.
1975: A transitional basalt-pantellerite sequence of fractional crystallization, the Boina Centre (Afar Rift, Ethiopia); Journal of Petrology, v. 16, p. 22-56.

Booth, V.H.
1950: Stratigraphy and structure of the Oak Hill succession in Vermont; Geological Society of America Bulletin, v. 61, p. 1131-1168.

Charbonneau, J.M. and St. Julien, P.
1981: Analyse structurale et relations déformation-métamorphisme, Groupe d'Oak Hill, région du mont Sainte-Marguerite, Appalaches du Québec; Canadian Journal of Earth Sciences, v. 18, p. 1051-1064.

Clark, T.H.
1934: Structure and stratigraphy of southern Quebec; Geological Society of America Bulletin, v. 45, p. 1-20.

1936: A Lower Cambrian series from southern Quebec; Royal Canadian Institute Transactions, v. 21, pt. 1, p. 135-151.

Condie, K.C., Viljoen, M.J., and Kable, E.J.D.
1977: Effects of alteration on element distributions in Archean tholeiites from the Barberton Greenstone Belt, South Africa; Contributions to Mineralogy and Petrology, v. 64, p. 75-89.

Dewey, J.F. and Burke, K.
1974: Hot spots and continental break-up: Implications for collisional orogeny; Geology, v. 2, p. 57-60.

Doll, C.G., Cady, W.M., Thompson, J.B., Jr., and Billings, M.P.
1961: Centennial geological map of Vermont; Vermont Geological Survey.

Ehmann, W.D. and Rebagay, T.V.
1970: Zirconium and hafnium in meteorites by activation analysis; Geochimica et Cosmochimica Acta, v. 34, p. 649-658.

Jolly, W.T.
1980: Development and degradation of Archean lavas, Abitibi Area, Canada, in light of major element geochemistry; Journal of Petrology, v. 21, p. 323-363.

Jolly, W.T. and Smith, R.E.
1972: Degradation and metamorphic differentiation of the Keweenawan tholeiitic lavas of northern Michigan, U.S.A.; Journal of Petrology, v. 13, p. 273-309.

Kumarapeli, P.S.
– Iapetan aulacogens and fracture zones in the Canadian Shield; Proceedings Fifth International Conference on Basement Tectonics, Cairo, Egypt. (in press)

Kumarapeli, P.S., Goodacre, A.K., and Thomas, M.D.
1981: Gravity and magnetic anomalies of the Sutton Mountains region, Quebec and Vermont: Expressions of rift volcanics related to the opening of Iapetus; Canadian Journal of Earth Sciences, v. 18, p. 680-692.

Le Maitre, R.W.
1976: The chemical variability of some common igneous rocks; Journal of Petrology, v. 17, p. 589-637.

Muecke, G.K., Pride, C., and Sarkar, P.
1979: Rare-earth element geochemistry of regional metamorphic rocks; in Origin and Distribution of the Elements, ed. L.H. Ahrens; Proceedings of the Second Symposium, UNESCO, Pergamon Press, Physics and Chemistry of the Earth, v. 11, p. 449-464.

Osberg, P.H.
1965: Structural geology of the Knowlton-Richmond area, Quebec; Geological Society of America Bulletin, v. 76, p. 223-250.

Pearce, J.A.
1982: Trace element characteristics of lavas from destructive plate boundaries; in Andesites, ed. R.S. Thorpe; J. Wiley & Sons, p. 525-548.

Pearce, J.A. and Cann, J.R.
1973: Tectonic setting of basic volcanic rocks determined using trace element analyses; Earth and Planetary Science Letters, v. 19, p. 290-300.

Pearce, J.A. and Norry, M.J.
1979: Petrogenetic implications of Ti, Zr, Y, and Nb variations in volcanic rocks; Contributions to Mineralogy and Petrology, v. 69, p. 33-47.

Pieratti, D.D.
1976: The origin and tectonic significance of the Tibbit Hill metavolcanics, northwestern Vermont; Unpublished M.Sc. thesis, University of Vermont, 136 p.

Pintson, H.
1982: Geology of a part of the Tibbit Hill Volcanics near Richmond, Quebec; Unpublished B.Sc. thesis, Concordia University, Montreal, Quebec, 75 p.

Rankin, D.W.
1976: Appalachian salients and recesses: late Precambrian continental break up and the opening of the Iapetus ocean; Journal of Geophysical Research, v. 81, p. 5605-5619.

Reed, J.C., Jr. and Morgan, B.
1971: Chemical alteration and spilitization of the Catoctin greenstones, Shenandoah National Park, Virginia; Journal of Geology, v. 79, p. 526-548.

St. Julien, P. and Hubert, C.
1975: Evolution of the Taconian orogen in Quebec Appalachians; American Journal of Science, v. 275-A, p. 337-362.

St. Julien, P., Slivitsky, A., and Feininger, T.
1983: A deep structural profile across the Appalachians of southern Quebec; in Contributions to the Tectonics and Geophysics of Mountain Chains; ed. R.D. Hatcher, Jr., H. Williams and I. Zietz; Geological Society of America, Memoir 158, p. 103-111.

Shaw, D.M., Dostal, J., and Keays, R.R.
1976: Additional estimates of continental surface Precambrian Shield composition in Canada; Geochimica et Cosmochimica Acta, v. 40, p. 73-83.

Shaw, D.M., Reilly, G.A., Muysson, J.R., Pattenden, G.E., and Campbell, F.E.
1967: An estimate of the chemical composition of the Canadian Precambrian Shield: Canadian Journal of Earth Sciences, v. 4, p. 829-853.

Smith, R.E.
1968: Redistribution of major elements in the alteration of some basic lavas during burial metamorphism; Journal of Petrology, v. 9, p. 191-219.

Strong, D.F. and Williams, H.
1972: Early Paleozoic flood basalts of northwestern Newfoundland: their petrology and tectonic significance: Geological Association of Canada Proceedings, v. 24, no. 2, p. 43-54.

Sun, S.-S.
1980: Lead isotopic study of young volcanic rocks from mid-ocean ridges, ocean islands and island arcs; Philosophical Transactions of the Royal Society of London, v. A297, p. 409-445.

Sun, S.-S., Nesbitt, R.W., and Sharaskin, A.Y.
1979: Geochemical characteristics of mid-ocean ridge basalts; Earth and Planetary Science Letters, v. 44, p. 119-138.

Thompson, R.N., Morrison, M.A., Dickin, A.P., and Hendry, G.L.
1983: Continental Flood Basalts...Arachnids Rule OK?; in Continental Basalts and Mantle Xenoliths; ed. C.J. Hawkesworth and M.J. Norry; Shiva Publishing Limited, p. 158-185.

Trzcienski, W.D., Jr.
1976: Crossitic amphibole and its possible tectonic significance in the Richmond area, southeastern Quebec; Canadian Journal of Earth Sciences, v. 13, p. 711-714.

Williams, H.
1978: Tectonic lithofacies map of the Appalachian Orogen; Memorial University of Newfoundland, St. John's, Newfoundland, Map No. 1.

Zen, E-an
1983: Exotic terranes in the New England Appalachians – limits, candidates, and ages: A speculative essay; in Contributions to the Tectonics and Geophysics of Mountain Chains; ed. R.D. Hatcher, Jr., H. Williams and I. Zietz; Geological Society of America Memoir 158, p. 55-81.

PRELIMINARY COMPARISON OF PETROGRAPHIC AND PALEOMAGNETIC CHARACTERISTICS OF NIPISSING DIABASE INTRUSIONS IN NORTHEASTERN ONTARIO

Project 820005

K.L. Buchan and K.D. Card
Precambrian Geology Division

Buchan, K.L. and Card, K.D., Preliminary comparison of petrographic and paleomagnetic characteristics of Nipissing Diabase intrusions in northeastern Ontario; in Current Research, Part A, Geological Survey of Canada, Paper 85-1A, p. 131-140, 1985.

Abstract

Nipissing Diabase sills of northeastern Ontario commonly carry one of two distinct directions of remanent magnetization. The primary or secondary nature of each remanence and their relative age is controversial.

In a regional comparison of the paleomagnetic and petrographic characteristics of the Nipissing Diabase it is shown that both magnetizations are carried by petrographically fresh samples. This implies that either two ages of Nipissing intrusions are present or that there has been thermal overprinting with no accompanying chemical alteration. Altered gabbro, on the other hand, may be unstable (as in the deformed Sudbury-Blind River zone) or stably magnetized (as in the less deformed Cobalt-Sault Ste. Marie zone).

Résumé

Habituellement, les filons-couches de la diabase de Nipissing dans le nord-est de l'Ontario présentent une des deux orientations magnétiques rémanentes. On n'a pas encore déterminé avec certitude l'âge relative de chaque rémanence ni s'il s'agit de rémanences primaires ou secondaires.

Une comparaison régionale des caractéristiques paléomagnétiques et pétrographiques de la diabase de Nipissing révèle que les deux orientations magnétiques sont présentes dans les échantillons récents du point de vue pétrographique, ce qui laisse entendre qu'il existe deux intrusions de Nipissing d'âges différents ou qu'il y a eu surimpression thermique sans altération chimique. Par contre, le gabbro altéré peut être instable (comme dans la zone déformée de Sudbury-Blind River) ou magnétisé de façon stable (comme dans la zone moins déformée de Cobalt-Sault Sainte-Marie).

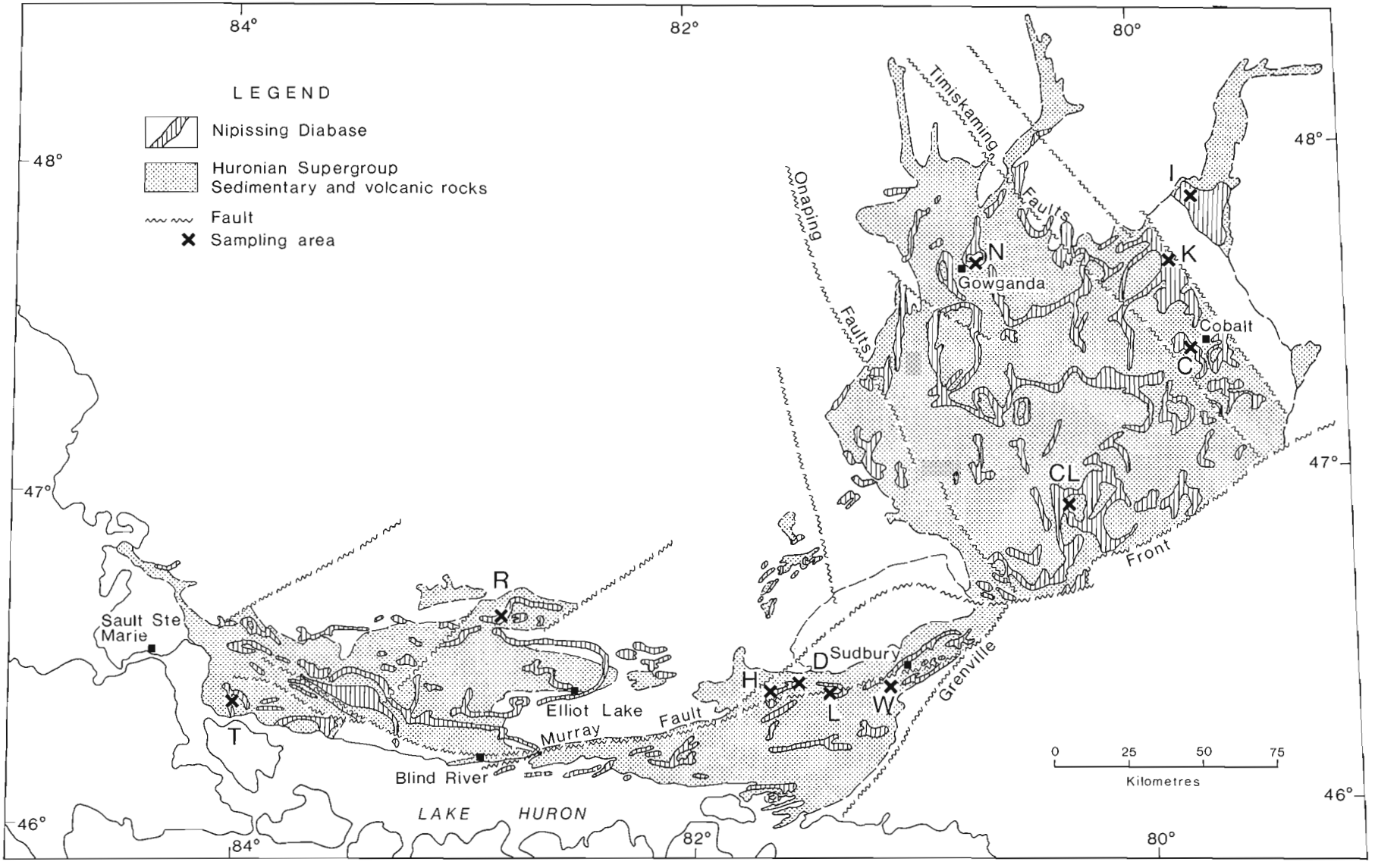

Figure 17.1. *Geological setting of the Nipissing Diabase. The Murray Fault is approximately the boundary between the relatively highly metamorphosed Sudbury-Blind River zone and the little metamorphosed Cobalt-Sault Ste. Marie zone. Sampling areas are labelled as follows: C = Coleman; CL = Clement; D = Drury; H = Hyman; I = Ingram; K = Kerns; L = Louise; N = Nicol; R = Raimbault; T = Tarbutt; W = Waters.*

Introduction

Tholeiitic gabbro intrusions of Early Proterozoic age, collectively referred to as "Nipissing Diabase", occur throughout the southern part of the Canadian Shield between Sault Ste. Marie and Cobalt, Ontario (Fig. 17.1). They are closely associated with and intrude Early Proterozoic supracrustal rocks of the Huronian Supergroup and their Archean granite-greenstone basement. The Nipissing intrusions were emplaced after early deformation of the Huronian strata but before secondary deformation events and regional metamorphism that were concentrated in the south-central part of the region between Sudbury and Blind River, Ontario (Card, 1978). Rubidium-strontium whole rock isochron ages of about 2100 Ma have been obtained from Nipissing intrusions in the Blind River area by Van Schmus (1965) and in the Gowganda area by Fairbairn et al. (1969).

In the north, in the region extending from Cobalt in the east to Sault Ste. Marie in the west, Nipissing Diabase intrusions are generally unmetamorphosed and little deformed (Card and Pattison, 1973). In contrast, in the Sudbury-Blind River area, Nipissing intrusions are generally deformed and, along with the Huronian rocks, regionally metamorphosed under conditions ranging from low greenschist to low amphibolite facies of the low-pressure facies series as defined by Miyashiro (1961). The available geological and geochronological data indicate that this metamorphic event occurred about 1850 to 1900 Ma ago and is probably correlative with the Early Proterozoic Penokean Orogeny that affected the Southern Province of the Canadian Shield (Fairbairn et al., 1969; Card, 1978).

Paleomagnetic characteristics of the Nipissing Diabase and their interpretation are complicated. Numerous local studies have reported one or other of two stable magnetizations. One magnetization, commonly referred to as N1, is directed either north and up at approximately 40° or south and down at 40°. The second, N2, is steeply down to the west. In a few localities, both magnetization directions have been observed.

There have been various interpretations of the N1 and N2 magnetizations. Some authors (Symons and Londry, 1975) believe N1 to be primary and N2 a viscous overprint. Others (Roy and Lapointe, 1976) consider N2 primary and N1 a metamorphic overprint. Identification of the primary nature of N1 and N2 has usually been based on a positive baked contact test with surrounding Huronian sediments. Since positive baked contact tests have been reported for both N1 (Symons, 1967; Morris, 1979) and N2 (Roy and Lapointe, 1976) magnetizations, it has been suggested that intrusions of two ages are included in the Nipissing suite (Morris, 1979; Stupavsky and Symons, 1982). Regardless of whether one or several ages are present, the relative age of N1 and N2 is still unclear.

Since the Early Proterozoic apparent polar wander path for North America is based in part on the assumed relative age of N1 and N2 (see, for example, Irving, 1979; Stupavsky and Symons, 1982), it is important to ascertain whether one of the Nipissing components can be associated with metamorphic overprinting. Hence, samples of fresh and altered Nipissing Diabase were collected at localities throughout the region (Fig. 17.1) to test the effect of metamorphism on their paleomagnetic properties.

Geology of the Nipissing Diabase

Nipissing Diabase intrusions form sills, dykes, cone-sheets, and irregular bodies ranging in thickness from a few metres to several thousand metres (Fig. 17.1). Contacts with the country rocks are sharp and narrow marginal chill zones and thermal metamorphic aureoles are commonly present. The diabase is massive, although in the Sudbury-Blind River area many bodies have foliated border zones and erratic interior zones of foliation. The general spatial relationship between Nipissing Diabase intrusions and Huronian supracrustal sequences suggests that they have a genetic relationship. Major faults that initially formed the Huronian depositional basins at a later stage may have provided passageways for mantle-derived mafic magmas. These magmas, rising in the form of dykes through the underlying Archean granitoid crust, would tend to spread laterally, forming sills and cone-sheets within the overlying stratified Huronian rocks.

Nipissing Diabase intrusions consist mainly of pyroxene gabbro and hornblende gabbro. Differentiation locally results in more mafic varieties, including metagabbro and feldspathic pyroxenite, and more leucocratic and felsic varieties, including gabbroic anorthosite and granophyre. These differentiates form distinct layers in some bodies.

The foregoing rock types are composed essentially of varying proportions of calcic plagioclase (labradorite-bytownite), clinopyroxenes (augite, pigeonite), orthopyroxene (enstatite-bronzite), hornblende, quartz, granophyre, and iron-titanium oxides with minor sulphides and apatite. Forsteritic olivine is present in several intrusions.

The Nipissing intrusions are medium- to coarse-grained rocks; grain size is typically variable over short distances. In gabbroic rocks the pyroxene/plagioclase ratio is typically about 1:1 and the dominant pyroxene, augite, is anhedral and fills interstices between euhedral plagioclase laths. In mafic gabbro and pyroxenite, orthopyroxene and clinopyroxene are present in approximately equal proportions, forming euhedral grains with interstitial plagioclase. The primary oxides are lamellar intergrowths of ilmenite-magnetite and ilmenite-hematite.

Metamorphism of the Nipissing Diabase

Nipissing Diabase intrusions have been metamorphosed under conditions ranging from deuteric alteration through subgreenschist to lower amphibolite facies of regional metamorphism. Metamorphism involves uralitization of the pyroxenes, saussuritization of plagioclase, and alteration of the primary oxide minerals. Regional variations in metamorphic grade displayed by mineral assemblages in Huronian rocks are matched by changes in Nipissing metagabbro assemblages, although in the metagabbro, remnants of the original magmatic rock are commonly preserved. Preservation of unaltered gabbro and pyroxene in the interiors of large Nipissing Diabase bodies in the Sudbury-Blind River area, where regional metamorphic grade is up to amphibolite facies, is due to the impermeable nature of these rocks. Metamorphism of the gabbro, which is controlled by availability of water, begins around the margins and along joints and fractures within the intrusions. Pyroxenes are replaced by actinolite, or mixtures of actinolite, talc, and chlorite. Fine grained oxides, probably both magnetite and ilmenite, are formed by uralitization of the pyroxenes. Calcic plagioclase is altered to albite and epidote; these react with actinolite, and probably also with iron-titanium oxides, to form blue-green aluminous hornblende. The primary ilmenite-magnetite and ilmenite-hematite intergrowths are replaced by magnetite-sphene-leucoxene aggregates.

In summary, the change from gabbro to metagabbro involves the addition of water and proceeds by reactions such as:

pyroxene + water = actinolite + magnetite
calcic plagioclase + water = albite + epidote

Table 17.1. Petrographic and paleomagnetic characteristics of Nipissing Diabase samples

Area	Sample	Alteration Percent	Alteration Type	Oxide Mineralogy	Magnetic Direction	$J_N(A/m)$	Blocking Temp.(°C)	Remanence Carrier
				Sudbury-Blind River zone: fresh gabbro				
Drury	820101	2	A	Large lamellar magnetite-ilmenite intergrowths. Fine magnetite along alteration veins. Sulphides.	other	$.5x10^{-2}$		
Drury	820103	0		Similar to 820101, except no fine grained oxides.	other	$.1x10^{-1}$	550-580	magnetite
Drury	820106	1	A	Similar to 820101.	other	$.8x10^{-2}$		
Drury	820202	1	A	Lamellar magnetite-ilmenite intergrowths.	other	$.6x10^{-2}$	450-580	magnetite
Louise	820401	0		Lamellar magnetite-ilmenite intergrowths. Sulphides.	N2	$.7x10^{-1}$	500-560	magnetite
Louise	820403	15	A	Large lamellar magnetite-ilmenite grains. Fine grained oxides (magnetite and ilmenite?) along alteration veins.	N2			
Louise	820410	10	A	Lamellar magnetite-ilmenite intergrowths. Fine grained oxides in alteration veins.	N2	$.4x10^{-1}$	500-570	magnetite
Waters	820504	2	A	Lamellar magnetite-ilmenite intergrowths.	other	$.4x10^{-1}$		
Waters	820506	25	A	Similar to 820504 plus fine grained oxides (magnetite?) in alteration veins.	N2	.2	500-570	magnetite
Waters	835703	0		Magnetite with small hematite exsolution lamellae.	N2	.3	500-570	magnetite
Waters	835704	10	A	Similar to 835703.	N2			
Drury	835802	1	B	A few single-phase (magnetite) grains and sulphides.	unstable	$.5x10^{-2}$	20-530	
Drury	835803	2	A	Similar to 835802.	other	$.1x10^{1}$	200-570	magnetite?
				Sudbury-Blind River zone: partly altered gabbro				
Drury	820201	50	Di	Large grains with irregular intergrowths of magnetite and ilmenite. Small grains of magnetite and ilmenite(?) disseminated through uralitic amphiboles.	unstable	$.2x10^{-3}$		
Drury	820301	50	Di	Lamellar magnetite-ilmenite intergrowths. Oxide-silicate intergrowths (magnetite and ilmenite intergrown with sphene).	weak	$.4x10^{-4}$		
Drury	820303	50	Di	Similar to 820301.	weak	$.7x10^{-4}$		
Louise	820411	30	C	Lamellar magnetite-ilmenite intergrowths. Fine grained oxides in altered phase.	N2	$.2x10^{-1}$		
Waters	835701	70	A	Magnetite with small hematite exsolution lamellae.				
				Sudbury-Blind River zone: highly altered gabbro				
Drury	820107	100	C	Single grains of magnetite and ilmenite. Abundant sulphides.	unstable	$.1x10^{-2}$	250-300	pyrrhotite?
Drury	820109	100	C	Large lamellar magnetite-ilmenite intergrowths. Fine magnetite and ilmenite. Sulphides.	unstable	$.1x10^{-3}$	?	
Louise	820406	100	C	Lamellar magnetite-ilmenite grains surrounded and replaced by sphene-leucoxene aggregates. Sulphides.	other	$.4x10^{-1}$	100-550	
Waters	820501	100	C	Minor oxides (secondary?).	unstable	$.3x10^{-2}$	20-550	
Louise	835601	100	C	Fine grained oxides intergrown with silicates.	unstable	$.7x10^{-4}$		
Hyman	835902	100	C	Single-phase (magnetite) grains.	other	.6	200-350	pyrrhotite?
Hyman	836001	100	C	Single-phase (magnetite) grains intergrown with sphene.	other	.6		

Table 17.1 (cont.)

Area	Sample	Alteration Percent	Alteration Type	Oxide Mineralogy	Magnetic Direction	$J_N(A/m)$	Blocking Temp.(°C)	Remanence Carrier
Hyman	836002	100	C	Similar to 836001 with abundant sulphides.	unstable?	$.2x10^{-2}$	200-300	pyrrhotite?
Hyman	836005	100	C	Similar to 836001.	unstable	$.6x10^{-1}$	20-500	
				Cobalt-Sault Ste. Marie zone: fresh gabbro				
Clement	820607	20	C	Lamellar magnetite-ilmenite grains. Sulphides.	N1	$.1x10^{1}$	530-570	magnetite
Kerns	822601	1	B	Lamellar magnetite-ilmenite intergrowths. Sulphides.	N1	$.8x10^{-1}$	450-570	magnetite
Ingram	833901	2	B	Single-phase (magnetite?) grains and irregular multi-phase oxide intergrowths.	other	.2	20-575	
Ingram	834005	10	C	Similar to 833901.	other	.1	20-575	
Nicol	836204	5	B	Single-phase (magnetite?) grains.	N1	.1	500-560	magnetite
				Cobalt-Sault Ste. Marie zone: partly altered gabbro				
Clement	820604	50	Di	Lamellar magnetite-ilmenite grains.				
Kerns	822604	50	C	Large magnetite grains. Silicate-oxide intergrowths.	N1	$.8x10^{-1}$		
Raimbault	831605	50	C	Lamellar magnetite-ilmenite intergrowths.	N1	$.5x10^{-1}$		
Raimbault	831802	50	C	Primary magnetite-ilmenite intergrowths altered, leaving oxide laths in sphene-leucoxene aggregate.	N1	$.2x10^{-1}$	520-570	magnetite
Coleman	833602	50	C	Some single-phase (magnetite?) grains. Much fine grained oxide intergrown with silicates.	semistable	$.5x10^{1}$	?	
Nicol	836302	50	C	Lamellar magnetite-ilmenite intergrowths. Sulphides.	N1+N2	.5	20-560	
Nicol	836501	50	Dii	Irregular two-phase intergrowths (magnetite and ilmenite?)	N1+N2	$.4x10^{1}$	20-560	
Nicol	836504	30	C	Irregular two-phase intergrowths (magnetite and ilmenite?)	N1+N2	$.2x10^{1}$	20-550	
				Cobalt-Sault Ste. Marie: highly altered gabbro				
Clement	820609	99	C	Fine grained oxides and oxide-silicate intergrowths. Sulphides.	N1	.1	500-570	magnetite
Tarbutt	832701	100	C	Lamellar magnetite-ilmenite grains. Irregular intergrowths of magnetite, ilmenite and hematite?	N1+N2?	$.2x10^{1}$	100-580	
Tarbutt	832901	100	C	Original lamellar magnetite-ilmenite grains altered to oxide-silicate intergrowths.	?	$.8x10^{-3}$	?	
Coleman	833701	100	C	Irregular intergrowths of several oxides.	N2	$.3x10^{1}$	20-570	

Sampling areas are located in Figure 17.1.

Percent alteration is based on silicate mineralogy. Fresh samples are less than 20% altered, partly altered samples are 20 to 80% altered and highly altered samples are more than 80% altered.

The dominant type of alteration is listed as: (A) vein alteration along discrete veins or fractures; (B) deuteric alteration or marginal alteration of pyroxene (or pyroxene and plagioclase); (C) pervasive alteration of pyroxene (to uralitic amphibole or blue-green hornblende) and plagioclase (saussuritization); (D) selective alteration in which (i) pyroxene is completely altered while plagioclase remains fresh (magmatic) or (ii) plagioclase is saussuritized while pyroxene is fresh or only partly uralitized.

Stable directions of magnetization (N1, N2 and other) are discussed in the text.

J_N is intensity of natural remanent magnetization.

Blocking temp. gives the range of observed blocking temperatures.

Remanence carriers are postulated on the basis of observed blocking temperatures.

With increasing metamorphic grade, the retrograde assemblages are transformed to greenschist and amphibolite facies assemblages through reactions such as:

actinolite + albite + epidote + magnetite =
blue-green hornblende + quartz

Iron oxide minerals are involved in several of these reactions and, hence, metamorphism may have an effect on the paleomagnetic characteristics of the rocks.

Paleomagnetism

Sampling and laboratory procedure

About 5 drill cores or block samples were oriented with sun and magnetic compass at each of 70 Nipissing sill sites throughout the region. Sites were selected to obtain a representative sampling of fresh pyroxene gabbro, fresh gabbro with alteration veins, and altered gabbro. In the present report we outline results of 30 sites (from 11 sampling areas in Fig. 17.1) from which 44 polished thin sections have been prepared.

Usually, one specimen per core was demagnetized in stepwise fashion to peak alternating fields (AF's) of 0, 2.5, 5.0, 10, 15, 20, 25, 30, 35, 40, 50, 60, 70, 80, 90, and 100 mT to test the stability and direction of magnetization. Selected specimens were then thermally cleaned to peak temperatures of 20, 100, 175, 250, 300, 350, 400, 450, 500, 530, 550, 560, 570, 580, and 600°C in order to examine their blocking temperature spectra and establish the carriers of stable remanence.

Alteration veins were cut from several fresh gabbro cores (procedure described in Buchan, 1979) to determine if differences in paleomagnetic stability or direction could be detected between fresh and altered material at this scale. Orientation markings were transferred to both fresh and altered segments. Fresh and altered material were then AF demagnetized separately.

Results

Petrographic and paleomagnetic stability characteristics are summarized in Table 17.1 for each of the cores for which a polished thin section was examined. Samples from the Sudbury-Blind River zone and the Cobalt-Sault Ste. Marie zone are listed separately.

For convenience each core is categorized as fresh, partly altered or highly altered on the basis of the estimated percent alteration observed in the silicate minerals. Fresh samples are <20% altered, partly altered samples are 20 to 80% altered, highly altered samples are >80% altered.

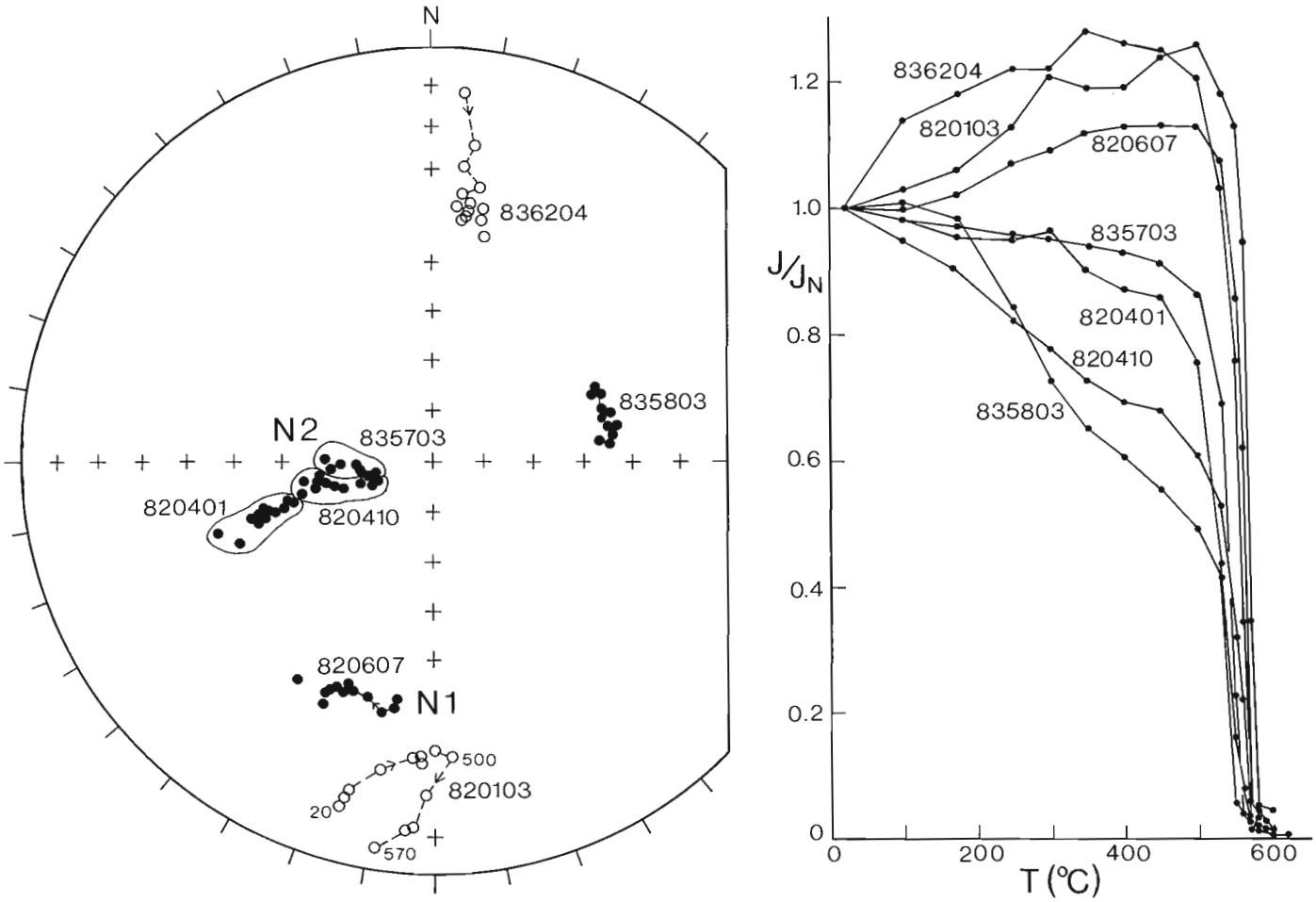

Figure 17.2. Thermal demagnetization characteristics of typical fresh pyroxene gabbro samples. Directions are plotted with respect to horizontal on an equal-area projection with closed (open) symbols indicating positive (negative) inclinations. Scattered directions above 570 or 580°C are not shown to avoid congestion. N1 and N2 represent the downward projection of the two standard Nipissing magnetizations which are reported in the literature (see text). Samples 820103, 835803 – Drury Township; 820401, 820410 – Louise Township; 820607 – Clement Township; 835703 – Waters Township; 836204 – Nicol Township.

The dominant type of alteration is also specified: (A) vein alteration along discrete veins or fractures; (B) deuteric alteration or marginal alteration of pyroxene (or pyroxene and plagioclase); (C) pervasive alteration of pyroxene (to uralitic amphibole or blue-green hornblende) and plagioclase (saussuritization); (D) selective alteration in which (i) pyroxene is completely altered while plagioclase remains fresh (magmatic), or (ii) plagioclase is saussuritized while pyroxene is fresh or only partly uralitized.

Natural remanent magnetization (NRM) intensity is listed, along with the direction of magnetization (referred to the present horizontal) after stepwise AF and/or thermal demagnetization. The dominant magnetic blocking temperature range and most likely carrier of stable magnetization are also reported.

Fresh gabbro from both the Sudbury-Blind River and Cobalt-Sault Ste. Marie zones (Table 17.1 and Fig. 17.2) almost always carries a single component magnetization at a given sampling site. From sampling area to sampling area, however, the direction of magnetization varies. The N1 and N2 magnetizations reported in earlier studies of the Nipissing Diabase are most common. For example, sample 836204 (Fig. 17.2) from the Nicol area attains a stable N1 direction on AF demagnetization, while Louise sample 820410 gives the N2 direction. Other stable directions (e.g. sample 835803 from the Drury area) occur sporadically. The degree to which folding of Nipissing sills may explain some of these anomalies, especially in the more deformed Sudbury-Blind River zone, is unclear.

Magnetic blocking temperatures (see the intensity decay curves of Fig. 17.2) are concentrated near 580°C, indicating that magnetite is the dominant remanence carrier in fresh gabbro. Polished thin section studies (Table 17.1) confirm the presence of abundant magnetite, usually in the form of lamellar magnetite-ilmenite intergrowths in these samples. These results agree with a study of Nipissing Diabase west of Elliot Lake (Patel and Palmer, 1974) in which stable N1 magnetization was correlated with magnetite-ilmenite exsolution intergrowths.

The paleomagnetic behaviour of altered gabbro is much more complex than that of fresh gabbro. Samples from the Sudbury-Blind River zone behave quite differently from those of the Cobalt-Sault Ste. Marie. Hence, it is best to examine the results from each zone separately.

In the Sudbury-Blind River zone there is a clear loss of magnetic stability with increasing degree of alteration (Table 17.1). Partly altered and highly altered cores are often unstable and of lower intensity than fresh samples. Altered samples which do maintain a stable direction rarely, if ever, exhibit the N1 or N2 direction. Instead, their directions are widely scattered. Examples of thermal demagnetization of highly altered samples from the Sudbury-Blind River zone are illustrated in Figure 17.3a-17.3e.

Blocking temperatures are no longer concentrated near 580°C but may form a broad range between room temperature and 580°C (Fig. 17.3b, 17.3e) or a discrete range well below 580°C. The broad range of blocking temperatures may be associated with oxide-silicate intergrowths which have replaced the lamellar magnetite-ilmenite intergrowths of fresh samples, or with single-phase magnetite grains observed in some samples. In several samples (Fig. 17.3a, 17.3c) a narrow blocking temperature range near 300°C suggests that pyrrhotite may carry much of the remanence. This correlates with an abundance of sulphides observed in the polished thin sections of these samples (Table 17.1).

Alteration veins are common in fresh gabbro throughout the Sudbury-Blind River zone. To see whether the loss of magnetic stability with alteration, which is observed between sampling sites, occurs on the scale of individual samples, alteration veins were cut from two cores in the Waters sampling area and one from the Louise area. Oriented segments of fresh and altered material were then AF demagnetized and measured separately.

The most dramatic difference is observed in Waters sample 820506 (Fig. 17.4a, 17.4b). Fresh material (segment 820506A of Fig. 17.4a) gives a very stable magnetization with a smooth intensity decay, while the vein (segment 820506B) shows an erratic intensity decay and direction. The NRM intensity per unit volume is also different, being 50 times higher in the fresh segment.

Results from the other two vein separations are, however, much less convincing. In Waters sample 835704 (not shown) the altered segment contains two narrow veins plus intervening fresh material which proved too difficult to remove. In Louise sample 820403 (not shown) the separation appears to be more complete. In both cases, fresh and altered segments have the same stable magnetization direction on AF demagnetization. The only observable difference is in NRM intensity per unit volume which is two or three times higher in the fresh portion. It is not clear whether the stable magnetization of the altered segments is carried by contaminating fresh material (as seems likely in the case of Waters 835704) or whether the alteration veins in these samples contain a stable magnetization similar in direction to that of the fresh material, but of lower intensity.

In the Cobalt-Sault Ste. Marie zone there is no dramatic loss of stability with increasing degree of alteration (Table 17.1), as is observed in the Sudbury-Blind River zone. Indeed, highly altered or partly altered samples (Fig. 17.3f-17.3h) are often as stable as fresh samples. For example, highly altered sample 820609 (Fig. 17.3f) from the Clement area has a similar stability and direction as the largely fresh sample 820607 (Fig. 17.2) from a nearby sampling site.

Altered gabbro in the Cobalt-Sault Ste. Marie zone is not associated exclusively with the N1 or the N2 magnetization. In a few cases systematic swings are observed in partly or highly altered gabbro (e.g. Tarbutt sample 832701 of Fig. 17.3g). Although such swings indicate the presence of two components of magnetization (usually N1 and N2), it has not been possible, as yet, to associate one or the other component with the alteration.

Blocking temperatures of single component samples are usually near 580°C, while those of two-component samples occupy a broad range up to 580°C. See, for example, the intensity decay curves of Figure 17.3f-17.3h. As is the case in the Sudbury-Blind River zone, oxide-silicate intergrowths have replaced the lamellar magnetite-ilmenite intergrowths of fresh samples.

Fresh and altered segments were separated in only a single core from the Cobalt-Sault Ste. Marie zone. Both segments of Clement area sample 820607 showed similar stable directions on AF demagnetization (Fig. 17.4c and 17.4d), while the NRM intensity per unit volume of fresh material was twice that of the altered material.

Discussion

It is clear from Table 17.1 and the description above that neither the N1 nor the N2 magnetization is associated exclusively with petrographically fresh or with altered gabbro. In fresh gabbro from the Sudbury-Blind River zone, N2 is observed most frequently, while N1 dominates in the Cobalt-Sault Ste. Marie zone.

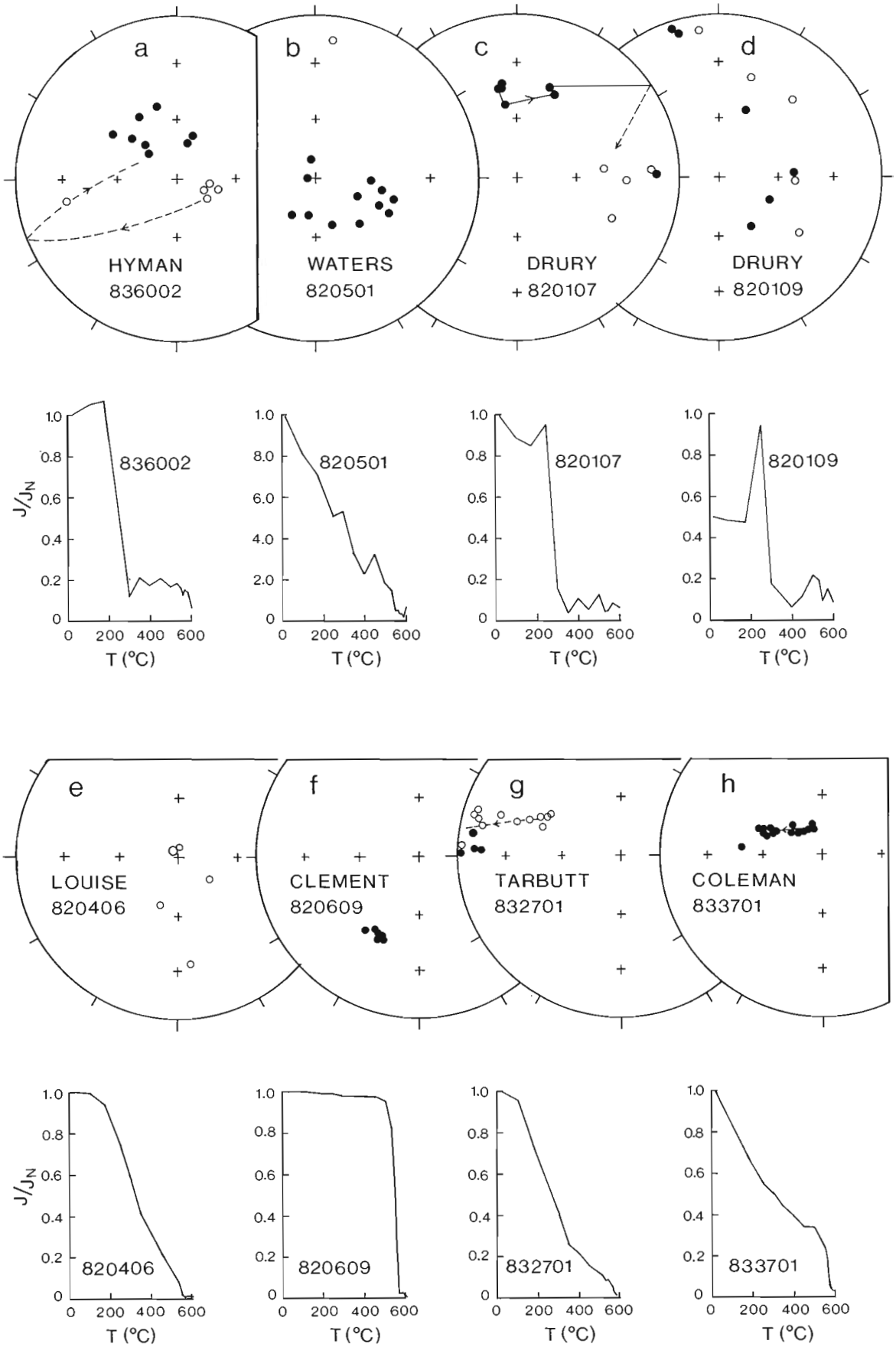

Figure 17.3. *Thermal demagnetization characteristics of representative highly-altered gabbro samples. Symbols are the same as in Figure 17.2. Directions above 580°C are not shown. Directions are plotted with respect to the horizontal.*

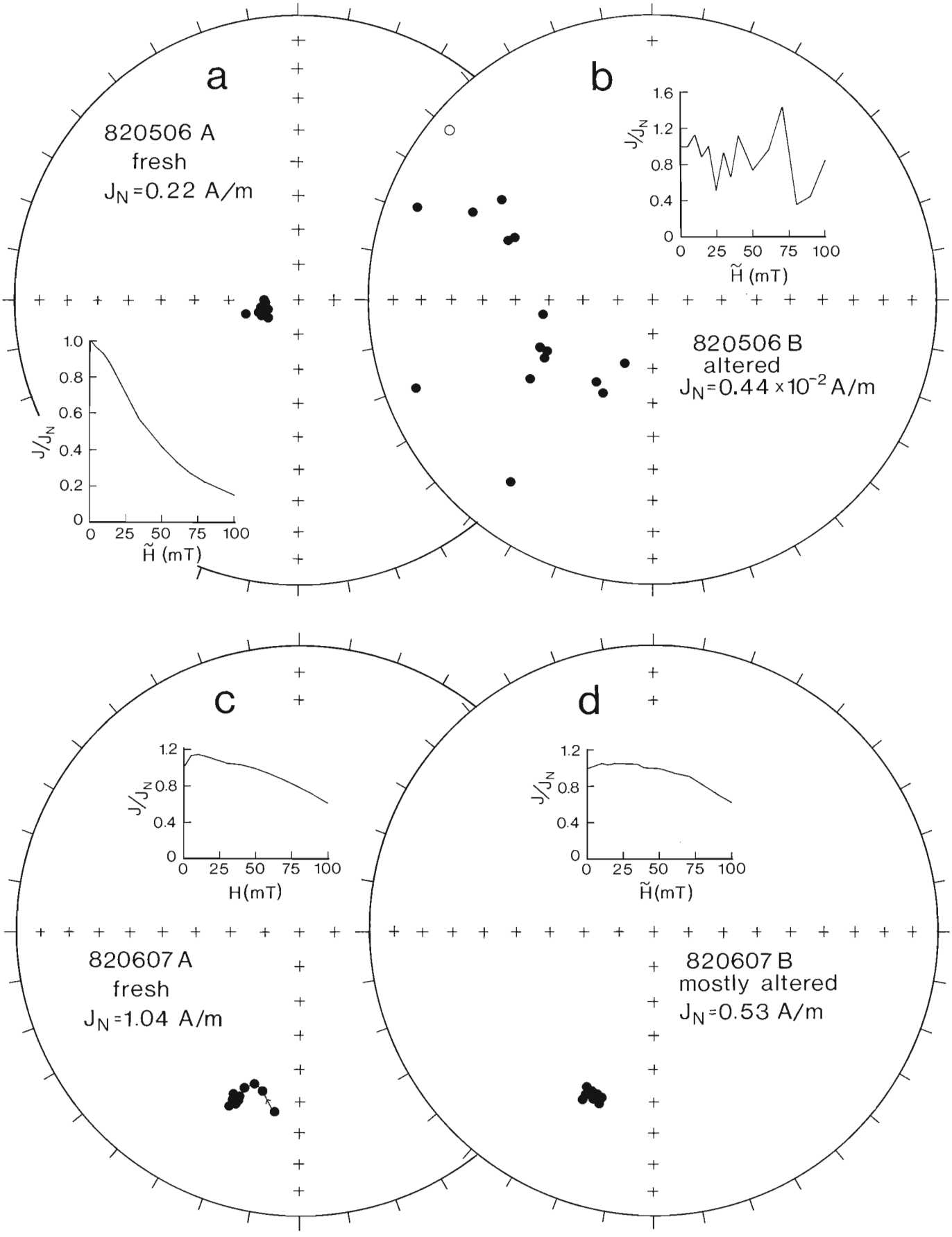

Figure 17.4. *AF demagnetization characteristics of fresh and altered separates. Symbols are the same as in Figure 17.2. Directions are plotted with respect to the horizontal.*

Such results can be interpreted in two ways. If petrographically fresh gabbro always carries a primary remanence, at least two ages of Nipissing intrusions are required, with fresh N1 units of a distinctly different age from fresh N2 units. However, if some petrographically fresh gabbro units have acquired a magnetization by thermal overprinting with no accompanying chemical alteration, then one or both magnetizations could be secondary. Thermal overprinting is more likely to have occurred in the Sudbury-Blind River zone where temperatures during regional metamorphism probably reached 350-550°C (Card, 1978), temperatures which may be sufficient to thermally reset magnetite (Pullaiah et al., 1975; Dunlop, 1983). In the Cobalt-Sault Ste. Marie zone, however, temperatures during metamorphism are unlikely to have exceeded 350°C, probably insufficient to thermally reset magnetite.

Results from altered gabbro are difficult to interpret on a regional basis since different paleomagnetic behaviour is observed from one sampling area to another. In the Sudbury-Blind River zone samples from altered sites are unstably magnetized or have stable but scattered directions. The loss of the stable (usually N2) magnetization observed in fresh samples may be explained by the replacement of lamellar magnetite-ilmenite intergrowths by oxide-silicate intergrowths. These intergrowths and other alteration products (single-phase magnetite and sulphides) are often unstable.

In the Cobalt-Sault Ste. Marie zone, on the other hand, stable N1 (occasionally N2) directions are observed at some altered sites, while N1 and N2 are superimposed at others. The reason for the stability of the magnetization of these samples, which also contain oxide-silicate intergrowths and single-phase magnetite of the N1 and N2 magnetizations, is not clear and requires further study, especially of sites where the two remanences are superimposed.

Acknowledgments

We are grateful to T. West and L. Madore for assistance in the field and laboratory. Vein segments were cut by G. Freda. The manuscript was critically reviewed by J.A. Percival and W.F. Fahrig.

References

Buchan, K.L.
1979: Paleomagnetic studies of bulk mineral separates from the Bark Lake diorite, Ontario; Canadian Journal of Earth Sciences, v. 16, p. 1558-1565.

Card, K.D.
1978: Metamorphism of the Middle Precambrian (Aphebian) rocks of the eastern Southern Province; in Metamorphism in the Canadian Shield, Geological Survey of Canada, Paper 78-10, p. 269-282.

Card, K.D. and Pattison, E.F.
1973: Nipissing diabase of the Southern Province, Ontario; in Huronian Stratigraphy and Sedimentation, ed. G.M. Young; Geological Association of Canada, Special Paper 12, p. 7-30.

Dunlop D.J.
1983: Viscous magnetization of 0.04-100 m magnetites. Geophysical Journal of the Royal Astronomical Society, v. 74, p. 667-687.

Fairbairn, H.W., Hurley, P.M., Card, K.D., and Knight, C.J.
1969: Correlation of radiometric ages of Nipissing Diabase and Huronian metasediments with Proterozoic orogenic events in Ontario; Canadian Journal of Earth Sciences, v. 6, p. 489-497.

Irving, E.
1979: Paleopoles and paleolatitudes of North America and speculations about displaced terrains; Canadian Journal of Earth Sciences, v. 16, p. 669-694.

Miyashiro, A.
1961: Evolution of metamorphic belts; Journal of Petrology, v. 2, p. 277-311.

Morris, W.A.
1979: A positive contact test between Nipissing diabase and Gowganda argillites; Canadian Journal of Earth Sciences, v. 16, p. 607-611.

Patel, J.P. and Palmer, H.C.
1974: Magnetic and paleomagnetic studies of the Nipissing diabase, Lake Matinenda area, Ontario; Canadian Journal of Earth Sciences, v. 11, p. 353-361.

Pullaiah, G., Irving, E., Buchan, K.L., and Dunlop, D.J.
1975: Magnetization changes caused by burial and uplift; Earth and Planetary Science Letters, v. 28, p. 133-143.

Roy, J.L. and Lapointe, P.L.
1976: The paleomagnetism of Huronian red beds and Nipissing diabase; Post-Huronian Igneous Events and apparent polar path for the interval -2300 to -1500 Ma for Laurentia; Canadian Journal of Earth Sciences, v. 13, p. 749-773.

Stupavsky, M. and Symons, D.T.A.
1982: Extent of Grenvillian remanence components in rocks of the Southern Province; Canadian Journal of Earth Sciences, v. 19, p. 698-708.

Symons, D.T.A.
1967: Paleomagnetism of Precambrian rocks near Cobalt, Ontario; Canadian Journal of Earth Sciences, v. 4, p. 1161-1169.

Symons, D.T.A. and Londry, J.W.
1975: Tectonic results from paleomagnetism of the Aphebian Nipissing Diabase at Gowganda, Ontario; Canadian Journal of Earth Sciences, v. 12, p. 940-948.

Van Schmus, W.R.
1965: The geochronology of the Blind River-Bruce Mines area, Ontario, Canada; Journal of Geology, v. 73, p. 774-780.

-18-

THE BOOTH RIVER INTRUSIVE SUITE, DISTRICT OF MACKENZIE

Project 770055

S.M. Roscoe
Economic Geology and Mineralogy Division

Roscoe, S.M., The Booth River Intrusive Suite, District of Mackenzie; in Current Research, Part A, Geological Survey of Canada, Paper 85-1A, p. 141-144, 1985.

Abstract

A large layered mafic-ultramafic intrusion with associated granitic rocks has been recognized in the northern part of Slave Structural Province. The intrusive rocks, mostly cumulate textured, are termed the Booth River Intrusive Suite. They intrude Archean metagreywacke, metavolcanic rocks, and granitic rocks and are unconformably overlain by Aphebian strata of the Goulburn Group. Geophysical data indicate that the latter strata cover the main body or component lobes of Booth River intrusive rocks beneath a 40 km-wide section of the Burnside River Synclinorium. Rims of the intrusion(s) are exposed on the northwest flank of this structure at Booth River and along the southeast flank. An erosional remnant of similar rocks, surrounded by Archean rocks, is present 60 km to the west.

The presence of these distinctive early Aphebian or very late Archean intrusive rocks along a younger structural trough trending northeasterly across the Slave Province suggests a sequence of geological events there that parallel those in the much better developed northeasterly-trending East Arm trough. The Booth River Intrusive Suite could contain significant concentrations of various commodities associated with comparable layered complex intrusions, notably PGM, Cr, Ni, Cu, Ti, V, and Sn.

Résumé

Une grande intrusion mafique-ultramafique stratifiée et des roches granitiques associées ont été identifiées dans la partie nord de la province structurale des Esclaves. Les roches intrusives, surtout à cumulats, forment le cortège intrusif de la rivière Booth. Elles ont pénétré des métagrauwackes, des roches métavolcaniques et des roches granitiques de l'Archéen et reposent en discordance sous les couches aphébiennes du groupe de Goulburn. Les données géophysiques indiquent que ces couches aphébiennes recouvrent la masse principale ou les lobes composants des roches intrusives de la rivière Booth sous une section de 40 km de large du synclinorium de la rivière Burnside. Les bords de l'intrusion sont exposés sur le versant nord-ouest de la structure à la rivière Booth et le long du versant sud-est. Un reste érodé de roches similaires, entouré de roches archéennes, se présente à 60 km à l'ouest.

La présence de ces roches intrusives caractéristiques de l'Aphébien ancien ou de l'Archéen très récent le long d'une dépression tectonique plus récente qui est orientée vers le nord-est en travers de la province des Esclaves laisse croire qu'il s'est produit une série d'événements géologiques similaires à ceux qui ont eu lieu dans la fosse d'East Arm beaucoup mieux développée, à orientation nord-est. Le cortège intrusif de la rivière pourrait contenir d'importantes concentrations de divers produits associés à des intrusions complexes stratifiées comparables, notamment les métaux du groupe platine, le chrome, le nickel, le cuivre, le titane, le vanadium et l'étain.

Introduction

Layered noritic intrusive rocks outcrop along the northwest and southeast flanks of the Burnside River Synclinorium in NTS 76 K/14 and in 76 K/3 and 6 (Fig. 18.1). They are not distinguished on regional geological maps (Fraser, 1964; Campbell, 1976) from younger, more extensive, thin gabbro sheets intruded along or near the unconformity between Archean rocks and strata of the Aphebian Goulburn Group. Pyroxenite noted by Fraser (1964) along the south limb of the synclinorium, however, has been found to be a component of the older layered intrusion.

The layered intrusive rocks include coarse grained leuconorite, melanorite, websterite, troctolite, dunite, gabbro, monzonite, and quartz monzonite. They have distinctive aeromagnetic signatures shared in part by a coarse perthite granite body in 76 K/12. Similar granite was noted in 76 K/4. The Gumbo Lake Intrusion in 76 L/6, an isolated plate-like remnant of layered ilmenite-rich leuconorite, is considered to belong to the same suite. Rocks of this suite were initially recognized in 76 K/14 along Booth River, a tributary of Hood River, and the suite is herein called the Booth River Intrusive Suite. It represents a magmatic event comparable to the intrusion of the Blachford Lake Intrusive Suite (Davidson, 1978) in the southern part of the Slave Province.

History of investigations and acknowledgments

The intrusive complex at Booth River is marked by a conspicuous, extensive gossan developed on ilmenite-rich rock containing minor amounts of sulphides (locality 1 in Fig. 18.1). Canadian Nickel Company drilled a short hole in this zone around 1958, and subsequently prospectors for Roberts Mining Company noted chalcopyrite nearby (DIAND assessment files). I made a brief helicopter stop at the gossan in 1981 and the following year spent one day examining and sampling the complex (point 2) assisted by M. Fysson. Conimag readings were taken along the sampled section. J.M. Duke and R.F. Emslie provided advice on petrographic studies of samples.

In 1983, R.F. Emslie, D.C. Findlay, and S.B. Green joined me in field studies in the area through a two week period during which outcrop areas of the Booth River Intrusive Suite were outlined as shown in Figure 18.1. I collected samples across intrusions at localities 4 and 6 assisted by H.E. Roscoe who took conimag readings. Emslie, Findlay, and Green sampled southern exposures of layered mafic rocks at locality 7 using a rock drill. They also obtained a series of core samples across a younger gabbro sill at locality 3. I visited the Gumbo Lake ilmenite-rich noritic intrusion (8) which had been reported by Borealis Syndicate (DIAND files). Jon Scoates and I made several traverses in the southern area in 1984 between points 6 and 11. We also examined early mafic phases of the Blachford Lake Intrusive Suite noting similarities with the Booth River Intrusive Suite. Petrological studies of collected samples are continuing. This paper is intended to provide the geological setting for such studies. It has been reviewed by Jon Scoates.

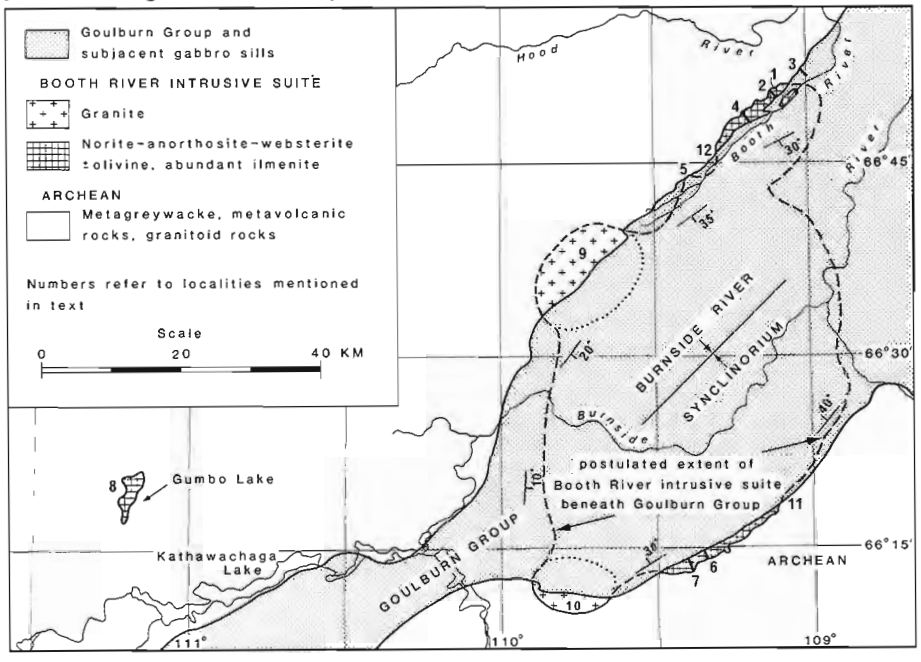

Figure 18.1. *General geology of Booth River Intrusive Suite.*

Northern rim of noritic intrusion at Booth River (76 K/14)

The northern outcrop area of Booth River intrusive rocks is 14 km long and up to 2 km wide. The noritic intrusion is bordered on the northwest by its floor of steeply-dipping, southerly-striking Archean metagreywacke, and on the southeast by a younger gabbro sheet which separates it from basal strata of the Goulburn Group. Its irregular north border reflects gentle southerly dips of the basal intrusive contact. Compositional and textural variations are apparent across horizontal distances of as little as one metre across strike and smaller scale layering dipping 10 to 30 degrees southeast is suggested by vague banding on some steep rock faces. No exposures of the basal contact or of metagreywacke immediately beneath it were observed.

The lowermost intrusive rocks observed at locality 4 (Fig. 18.1) are fine- to medium-grained dunite and websterite containing disrupted thin layers rich in oxides including magnetite. One sample consists of cumulus olivine with intercumulus pyrrhotite containing small amounts of chalcopyrite. Cumulus ilmenite is present in one specimen. Another contains millimetre scale layers of dunite, troctolite, websterite and oxides. Similar rocks were noted in several places at the base of the intrusion southwest of locality 4. Near 12, basal fine grained gabbro-norite appears to be overlain by websterite. At locality 2, the lowermost exposed rock of the intrusion is xenomorphic-textured gabbro that coarsens southeastward through a 10 or 20 m horizontal distance to gabbro-norite that contains cumulus plagioclase up to 1 cm or more long.

Coarse grained leucocratic gabbro norite that locally approaches anorthosite, websterite, peridotite and troctolite, in composition forms the bulk of the northern exposure of intrusive rocks of the Booth River Suite. A websterite layer with abundant magnetite was noted about 300 m south of the northern margin of the intrusion at locality 4. This is overlain by melanonorite that in turn is overlain by poorly exposed ilmenite-rich rock. Intercumulus ilmenite is ubiquitous in all of the noritic rocks and is very abundant in zones or lenses at more than one stratigraphic level. One such zone is near the southeast edge of the intrusion south of 4, and an extensive ilmenite-rich zone at locality 1 extends to the margin of the younger gabbro sill. Minor amounts of pyrrhotite are present in the latter zone.

The southwest and northeast extremities of the rim of the intrusion are overlapped by a thin gabbro sheet

intruded at the base of the Goulburn Group. The intrusion re-emerges from beneath the gabbro sill as a small patch of intrusive breccia and sulphide-bearing pyroxenite at point 5 about 6 km southwest of the main overlap. The breccia consists mainly of granitoid clasts in a gabbro matrix.

A separate small area of Booth River rocks flanked by gabbro is exposed in the Booth River valley south of locality 1. This is interpreted as a window through the younger fine grained gabbro sill. Here, Booth River rocks comprise rusty-weathered, altered, amphibole-rich rock with 1-3 mm seams of hercynite and pyrrhotite (with chalcopyrite and pentlandite) that dip gently southeast. Steeply-dipping sulphide seams are also present.

Southern rim of noritic rocks (76 K/3 and 6)

The southern rim of mafic intrusive rocks similar to those at Booth River is 20 km long and up to 2 km wide. Its southern margin, a gently north-dipping basal intrusive contact marked by extensive brecciation and alteration of underlying metagreywacke, is highly irregular in plan. The intrusion is overlapped to the north by quartzite and siltstone of the Western River Formation which is intruded by a 40 m thick sill of gabbro about 30 m above its base. Aeromagnetic maps (GSC Maps 3622G, 3628G) indicate that a narrow magnetic zone extends along strike within the exposed area of rocks of the Booth River Intrusive Suite and also continues beneath cover rocks beyond the extremities of this exposure. This zone is interrupted and apparently shifted about 1 km dextrally at a locality near the base of the Goulburn Group 5 km northeast of sampling line 6. The Goulburn strata are not disrupted here so the Booth River Intrusive Suite may have been faulted prior to deposition of the Goulburn Group.

The basal contact of the intrusion is very close to the magnetic zone in some places but elsewhere it diverges considerable distances south of the zone. At locality 7 (Fig. 18.1), it is 1 km south of this more regular marker zone. The basal breccia zone contains blocks of metagreywacke in a gabbroic matrix. Many outcrops are gossaned, reflecting irregularly distributed concentrations of sulphides. In some places injections of gabbro and sulphides extend tens of metres southerly along fractures in the underlying metagreywacke. Upper parts of the zone contain rotated blocks of metagreywacke and, commonly, agmatitic gabbro. Scoates made the important field observation that some inconspicuous, fine grained, pale-weathering rocks in the basal contact zone between points 6 and 7 (Fig. 18.1) contain millimetre- and centimetre-scale layers composed of varying proportions of cumulus plagioclase, olivine, orthopyroxene, and oxide minerals. The laminae are disrupted and segmented. This layered zone, locally up to 15 m wide, was traced several hundred metres along strike.

Compositional and textural variations in the coarse grained noritic rocks are not as apparent in the field in the southern area as in the north. The general position of the magnetic zone, referred to above, was determined along sampling line 6 by conimag measurements but no outcrops of rock containing especially abundant magnetite were found. Several thin zones containing ilmenite and/or abundant sulphides are present between reference points 6 and 7 (Fig. 18.1). Emslie noted that K-spar is present in rocks along sampling line 7 and that quartz is also present in rocks in the upper part of this section. Accordingly, some of these rocks could be termed pyroxene monzonite and quartz monzonite. Thin dykes of aplite or granophyre, granite, and pegmatitic muscovite granite intrude noritic rocks in the western part of the southern rim. These dyke rocks are considered to be members of the Booth River Intrusive Suite.

Biotite perthite granite

Coarse grained leucocratic granite outcrops sparsely within a semi-circular area in 76 K/12 designated locality 9 in Figure 18.1. This area corresponds with an aeromagnetic high similar to and contiguous with magnetic highs associated with the noritic Booth River rocks to the northeast. A gravity high shown on the gravity map of Canada is centred over Goulburn rocks a short distance south of locality 9 so it seems likely that an appreciable thickness of mafic Booth River rocks underlies not only the sedimentary cover rocks but also at least part of the granitic body. Our field work has not eliminated the possibility that a mafic rim may extend around parts of the west and north margins of the granite. Similar granite is present at the southern margin of the Goulburn Group at locality 10 in 76 K/4.

The granite has a distinctive texture not unlike the cumulate texture of most of the noritic rocks. Plagioclase, K-spar, quartz, biotite, muscovite, amphibole and zircon occur in interstices between dominant, closely spaced, large amoeboid shaped grains of perthite. Most quartz occurs in large, irregular compound grains. Reddish brown biotite which is the principal and commonly the only mafic mineral, is chloritized in some specimens.

Gumbo Lake ilmenite-rich noritic intrusion

The Gumbo Lake intrusion (locality 8) in 76 L/6 overlies a gently-dipping floor of Archean metavolcanic and metasedimentary rocks. The lowermost layers observed are gabbro norite but the intrusion consists mainly of leuconorite with layers containing abundant to nearly massive ilmenite through appreciable but undetermined thicknesses. Numerous muscovite granite and granite pegmatite dykes intrude the complex. These are similar to dykes in Booth River rocks at the south side of the Burnside River Syncline.

Late gabbro sheets

The thin gabbro sheets along the northwest and southeast flanks of the Burnside River Synclinorium (not shown in Fig. 18.1) are segments of a group of such intrusions present nearly everywhere at the base of the Goulburn and Epworth groups throughout the region. It is unlikely that they have any relationship to the older Booth River Intrusive Suite. They are noteworthy, however, inasmuch as they obscure relationships between the Booth River intrusive rocks and the basal strata of the Western River Formation.

The northern sill contains granophyric phases. Medium grained gabbro at the south side of the Booth River near locality 1 contains plates of granitoid rock up to 1.5 m thick. It is not clear whether these are dykes or rafts, or whether the host gabbro is part of the Booth River Intrusion or part of the younger gabbro sheet which is chilled against hornfelsized Western River siltstone about 50 m to the south. Evident hornfels does not extend more than a metre or so away from the sill. A thin partition of similar hornfels separates the base of the sill from underlying Booth River norite at the south end of sampled section 4. At point 3, a partition of basal Western River quartz pebble conglomerate and quartzite appears to be recrystallized beneath the sill.

The gabbro sill along the south flank of the syncline intrudes Western River quartzite about 25 m stratigraphically above Booth River monzonorite at locality 7. Epidote and tremolite have been formed in carbonate nodules as far as 10 to 15 m below the sill. Farther east at point 6, dark grey siltstone stratigraphically below the quartzite, and probably little more than 10 m above Booth River intrusive rocks, is not perceptively metamorphosed.

Age and regional geological significance of Booth River Intrusive Suite

Exposures of rocks herein considered to belong to the Booth River Intrusive Suite, excepting the Gumbo Lake outlier, are parts of an intrusive complex, or of a cluster of consanguineous intrusions, 80 km long and 50 km wide. Very large volumes of magma were injected into a huge chamber or several chambers whose roof rocks could hardly fail to have been disrupted and intensely metamorphosed. There is no sign of any such effects in superincumbent Goulburn strata although the Booth River rocks appear to have been faulted in places. Hornfels in overlying sedimentary rocks is adjacent to gabbro sills and is entirely attributable to intrusion of the sills. Accordingly, on the basis of presently available evidence the Booth River Intrusive Suite must be considered pre-Goulburn. The original roof rocks, perhaps a sequence of gently-dipping earlier Aphebian rocks or very late Archean rocks, were apparently eroded in their entirety and the unroofed intrusions themselves also eroded prior to deposition of the Goulburn Group. Thus the Booth River Intrusive Suite may indicate that an important chapter in the geological history of this part of the Slave Province has been lost from the record.

It is interesting to speculate that there may be some connection between the intrusion of rocks of the Booth River Suite and the later development of the Burnside River Synclinorium. This structure, together with Rockinghorse structural basin, defines a trough extending northeasterly across the central part of the Slave Province parallel to the Athapuscow Alocogen (Hoffman et al., 1977) in the East Arm of Great Slave Lake. The trans-Slave structure coincides with a zone of moderately positive gravity, analogous perhaps to the East Arm gravity high. The history of development of the trans-Slave structure may parallel that of the East Arm more closely than has been realized. Intrusion of the Booth River Suite may have accompanied early Aphebian rifting, and later downwarping within the fractured zone may have produced a sedimentary and structural trough across the Slave Province. The Booth River Intrusive Suite is comparable in many ways to the early gabbroic and some of the granitic rocks of the early Aphebian Blachford Intrusive Suite in the East Arm area (Davidson, 1978).

Economic geology

No economically interesting mineral concentrations have been found in Booth River rocks. The noritic rocks, however, contain disseminations and some concentrations of sulphides. Minor amounts of pentlandite as well as chalcopyrite have been noted in pyrrhotite in some sulphide-rich layers, so the mafic-ultramafic intrusive rocks and particularly their basal breccias could contain significant nickel-copper concentrations. Oxide layers in highly differentiated rocks at the base of the intrusive suite have not yet been studied. If any of these are found to contain chromite, this would justify prospecting for platinum group metals as well as chromite. Vanadiferous magnetite is another conceivable target, and ilmenite might be of interest. Ilmenite at Booth River contains titanium and iron in stoichiometric proportion and about 0.5% vanadium. Borealis Syndicate sampled the titanium content of extensive bodies of ilmenite-rich rock in the Gumbo Lake Intrusion. There is no information, however, on the thicknesses of the ilmenite zones. A possibility that tin deposits might be associated with the biotite perthite leucogranites is worth consideration. Hyperalkalic rocks in the Blachford Lake Intrusive Suite at Thor Lake contain important beryllium, niobium-tantalum, and rare earth element concentrations. Such rocks have not been recognized in the Booth River Intrusive Suite but they could be present. Most importantly, it should be realized that more intrusions of rocks of the Booth River Intrusive Suite are likely to be present along the trans-Slave structure and that possibilities of finding these are not confined to the borders of gabbro sills at the base of the Goulburn Group. There are many magnetic anomalies that should be investigated.

Conclusions

Rocks considered part of the Booth River Intrusive Suite have been found through an area 115 km long and up to 50 km wide on the flanks of the Burnside River Synclinorium in NTS 76 K and L in the central northern part of the Slave Structural Province. Cumulate textured noritic rocks with intercumulus ilmenite are most characteristic of the suite. Intrusive breccias and gently dipping layers of ultramafic rocks and oxides are present in some places at bases of intrusive bodies exposed at the margins of Aphebian cover rocks of the Goulburn Group on both sides of the synclinorium. Elsewhere, the basal rocks are gabbro-norite. Bodies of perthite granite occur in separate outcrop areas.

The Booth River Intrusive Suite was emplaced in Archean rocks and unknown roof rocks subsequent to Archean orogenic activity. The intrusive rocks were unroofed and significantly eroded prior to deposition of the Goulburn Group. They may also have been faulted in pre-Goulburn time.

A northeasterly trending zone in the Slave Province marked by synclines and basins of Aphebian strata, by the occurrence of the Booth River Intrusive Suite, and by a moderately elevated gravity signature requires study.

The Booth River mafic-ultramafic-granitic intrusive rocks bear many similarities to layered intrusions elsewhere in the world that have been subjects of particularly intensive investigations. Some of these, most spectacularly the Bushveld Complex, have been important sources of metals and other commodities. The Booth River Intrusive Suite warrants special geological studies and prospecting programs.

References

Campbell, F.H.A. and Cecile, M.P.
1976: Geology of the Kilohigok Basin, Goulburn Group, Bathurst Inlet, Northwest Territories; Geological Survey of Canada, Open File 332, 1:500 000 scale.

Davidson, A.
1978: The Blachford Lake Intrusive Suite: an Aphebian Alkaline Plutonic Complex in the Slave Province, Northwest Territories; in Current Research, Part A, Geological Survey of Canada, Paper 78-1A, p. 119-134.

Fraser, J.A.
1964: Geological notes on Northeastern District of Mackenzie, Northwest Territories; Geological Survey of Canada, Paper 63-40.

Hoffman, P.F., Bell, I.R., Hildebrand, R.S., and Thorstad, L.
1977: Geology of the Athapuscow Aulocogen, East Arm of Great Slave Lake, District of Mackenzie; in Report of Activities, Part A, Geological Survey of Canada, Paper 77-1A, p. 117-129.

URANIUM IN THE CIRCUM-UNGAVA BELT, NORTHERN QUEBEC AND LABRADOR: NEW INFORMATION FROM THE CENTRAL LABRADOR TROUGH

Projects 750010, 750069

R.T. Bell and V. Ruzicka
Economic Geology and Mineralogy Division

Bell, R.T. and Ruzicka, V., Uranium in the Circum-Ungava Belt, northern Quebec and Labrador: new information from the central Labrador Trough; in Current Research, Part A, Geological Survey of Canada, Paper 85-1A, p. 145-149, 1985.

Abstract

Uranium occurs in several environments in the Circum-Ungava Belt. Newly recognized styles of mineralization in the Labrador Trough include occurrences hosted by black, cherty, and phosphatic shale and by dolostone.

An additional occurrence in albitized rocks is documented. In general there are potential sources for uranium within clastic rocks, particularly in black shales, potential sources for scavenging agents in sequences containing evaporites, and appropriate thermal agencies and structural traps provided by widespread volcanism and attendant intrusions. Together these provide excellent conditions to form high-grade vein deposits in albitites within the Circum-Ungava Belt.

Résumé

Il y a de l'uranium dans plusieurs milieux de la zone circum-Ungava. De nouveaux modes de minéralisation ont été identifiés dans la fosse du Labrador, dont des venues d'uranium trouvées dans les schistes noirs, siliceux et phosphatiques et dans des dolomies.

Une autre venue est identifiée dans des roches albitisées. En général, il peut y avoir des sources d'uranium dans les roches clastiques, notamment les schistes argileux noirs et des sources possibles d'agents d'épuration dans des séquences à évaporites; le volcanisme étendu et les intrusions connexes produisent des agents thermiques et des pièges structuraux appropriés. Ensemble, ces éléments fournissent les conditions idéales pour la formation de gisements filoniens à forte teneur dans les albitites de la zone circum-Ungava.

Introduction

This report summarizes data on uranium/thorium occurrences, including new occurrences, and speculates on uranium metallogeny in the Circum-Ungava Belt. For this region we follow the stratigraphy of Dimroth et al. (1970), Dimroth (1978), and Wardle and Bailey (1981). For details the reader is referred to these excellent studies.

In this report we summarize data on occurrences described by other workers (Kish and Tremblay-Clark, 1978; Kish and Cuney, 1981) and contribute some descriptive data on new occurrences investigated by us during the 1984 field season. The main groups of occurrences are briefly summarized below.

Occurrences

1. Uraninite-albite veins

a. Mistamisk area (after Kish and Cuney, 1981; Kish and Tremblay-Clark, 1978). The showings occur in north-northwest-trending, vertical albite veins about 20 cm thick by 15 m long near Mistamisk Lake (for location, see: Kish and Cuney, 1981). The veins are in argillites of the Dunphy Formation.

Kish and Cuney (1981) identified albite, lesser amounts of dolomite and chlorite, and minor calcite, quartz and hematite accompanied by uraninite, tellurides (melonite, altaite), sulphides (chalcopyrite, covellite, pyrite, bravoite, galena, molybdenite), clausthalite, minor organic material and traces of native gold. Pitchblende and secondary uranium minerals as well as goethite are also present. The uraninite occurs in the axial parts of the veins and contains significant yttrium but only traces of thorium and rare-earth elements.

Concerning the genesis of these veins Kish and Cuney (1981) suggest metasomatic alteration with fluids (at 300 degrees C and 2.5 kb) derived during an Hudsonian event from sodic schists with an evaporitic origin. Their U/Pb isotope data suggest thermal events at 500 and 100 Ma.

b. GM occurrence, Romanet River area (new occurrence). The GM showing (56°23'N, 67°50'W) is described in company assessment reports by Smith (1979). It occurs in brecciated argillites and slates either in the Dunphy Formation (as mapped) or possibly in a stratigraphically higher unit, perhaps the Uvé. At this locality the pelites are brecciated and sygmoidal, coarse albite ± quartz ± dolomite veins trending roughly west-northwest are developed. Radioactivity is spotty. Preliminary studies by mineralogists at the Geological Survey indicate this is mainly due to disseminated, coarse uraninite and veinlets of uraninite and coffinite in both wall rock and in albite veins. Clausthalite, marcasite, pyrite and molybdenite are common. Chalcopyrite and copper stain are present but uncommon. Locally some opaque uranium-bearing minerals are associated with chlorite in dolomite, which is in turn accompanied by lenses of quartz, apatite and bands of muscovite.

The GM appears comparable with the Mistamisk showings. Mineralization at the GM however occurs not only in albitite veins but in the wall rock; the sygmoidal nature of the albite veins may be due to the change in trend of the Mistamisk Romanet uplift zone along Romanet River.

At GM, the brecciation of the country rock may be due to faulting or intrusion events preceding metasomatism, or partly to volume change accompanying the metasomatism. Some brecciation may be synsedimentary. Similar monomictic breccias with border phase heterolithic breccias occur a few kilometres west associated with mafic intrusions, probably feeders to the Bacchus Formation. If these breccias are all related, perhaps the metasomatism is older than Hudsonian, and associated with thermal events related to one or more of the volcanic episodes during the development of the Trough.

We speculate that the main metasomatic and mineralizing event is earlier than Hudsonian and that fluids were mobilized by the volcanic and intrusive events from shale and evaporitic regimes within the Trough rocks.

Granites and pegmatites to the east of Romanet Lake should be prospected for similar mineralization. Sequences adjacent to and beneath areas of extensive volcanism such as that of the Bacchus Formation, especially around the margins of horst or graben blocks that were formed in the Aphebian, are accorded high favourability.

2. Uraninite-copper sulphide pods. Romanet Lake area (new showing)

A short (8 m) concordant pod, up to 30 cm wide, of coarse disseminated digenite-chalcopyrite-covellite ± quartz and ferroan dolomite occurs in well bedded siliceous dolomites of Dunphy Formation just west of Romanet Lake (56°16'N, 67°48'W). Disseminated uraninite occurs in the pod; secondary uranium and copper minerals are also present. The copper sulphides are selenium-bearing.

The podiform, concordant nature of the showing suggests that this occurrence results from weak mobilization of uranium and copper from carbonate rocks. This type of Cu and Cu-U occurrence in carbonate and clastic rocks is an aspect of the Copperbelt of Africa and of the Adelaidian in Australia. While these may not in themselves be important mineral deposits, their presence enhances the overall potential of an area and should encourage further investigation.

3. Uraniferous phosphatic black shales; Iron Arm (new occurrences).

The Labrador Mining and Exploration Company is currently conducting detailed studies on its leases around Schefferville and identified radioactive anomalies that occur stratigraphically just above the Sokoman Formation, and are summarized below.

a. radioactive carbonaceous and phosphatic shale and fine sandstone horizons and resedimented fragments of these rocks in conglomeratic turbidite layers within 10 m of the lower contact of the Menihek Formation (in drill core from 54°44'N, 67°03'W and 54°45'N, 67°03'W; Figure 19.1);

b. radioactive carbonaceous, phosphatic, calcareous breccias within 3 m of the contact (54°43'N, 66°16'W; Figure 19.2); and

c. radioactive seeps and calcareous tuffa around cold springs (54°53'N, 65°55'W, and 54°36'N, 65°58'W).

The first type of showing contains uranium in the 10 to 100 ppm range and represents stagnant, starved, "black shale" type accumulations (see Bell, 1978). The second contains uranium in the 1000 ppm range and represents remobilization from the first type into dilatant structures during regional folding. The phosphates have enhanced the entrapment of uranium here. The third type presumably represents leakage from the other two under present groundwater movements; here most of the radioactivity appears to be due to daughter elements.

We also briefly investigated areas south of Schefferville to determine whether there was evidence for uranium mobilization during the deep weathering of that area during the Mesozoic. No radioactive anomalies were found within

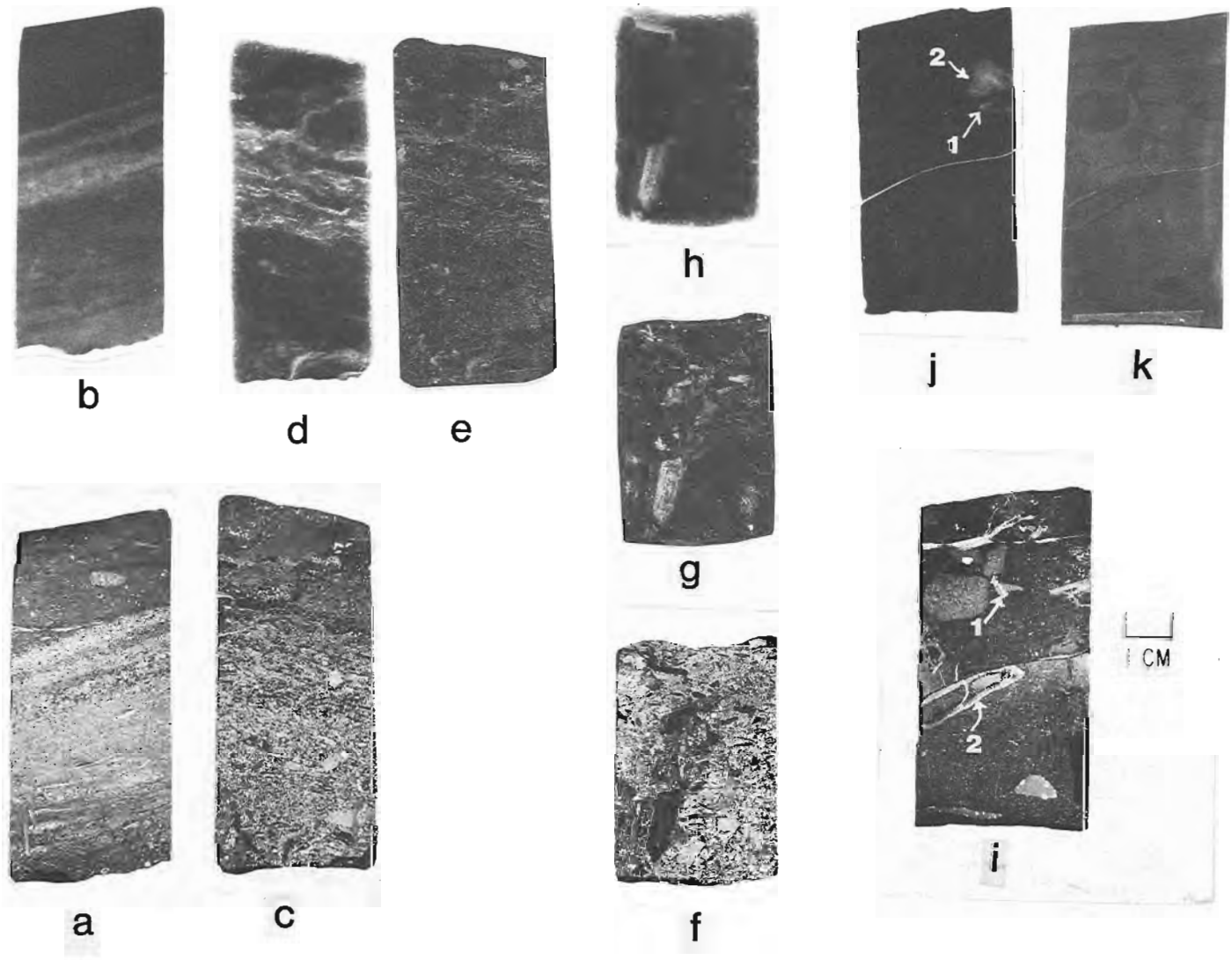

Figure 19.1. *Uraniferous black clastics in Menihek Formation (54° 44'N, 67° 03'W and 54° 45'W, 67° 03'W).*

All taken from polished slabs of drill core in lower 5 m of drillholes east of Schefferville. All are black clastics.

(a) RL photograph of sandstone-siltstone, slightly calcareous pyritic and carbonaceous

(b) AR of specimen in (a)

(c) RL photograph of conglomerate sandstone, highest reflectant material of pyrite and dots of fine pyrite, lesser reflectant material highly siliceous or phosphatic chert

(d) AR of specimen in C; most radioactivity in matrix

(e) PR of specimen in C

(f) RL of conglomerate in turbidite sequence

(g) PR of specimen in f; the highly carbonaceous material shows as white

(h) AR of specimen in f; most radioactivity in black shale fragments

(i) RL of conglomerate in turbidite; highest reflectant material pyrite, lesser reflectant mainly chert or phosphatic chert; note pyrite fragment at arrow (1) and rimming chert clast at (2); speckled nature of matrix due to small clots (100 μ m size) of finely crystalline pyrite (5 μ m size).

(j) AR of specimen in (i); note two radioactive clasts in upper left, (1) phosphatic chert and (2) carbonaceous shale

(k) PR of specimen (i); most strongly siliceous fragments appear as dark grey

RL – reflected light photograph of polished surface
AR – autoradiograph of polished surface; white most radioactive
PR – acetate-peel replica of slightly (HF) etched polished surface, contact print.

Approximate scale shown in (i).

the Sokoman Formation although fractures in the black shales of the Menihek nearby were anomalous. Two radioactive shear zones were discovered by the authors in a pit in Menihek shale west of the main access road to the Redmond 1 mine. One of the zones is exposed on the northwest wall of the pit. The radioactivity is associated with limonitic gangue and yielded radiometric response about 7 times background. Strike of the shear zone is 300°, dip 75° to northwest and width 5 to 8 cm. The second shear zone is parallel in strike to the first but dips 75° to southwest with a width of about 20 cm and with similar radiometric response.

4. Other occurrences in the Labrador Trough. (after Kish and Tremblay-Clark, 1978)

Kish and Tremblay-Clark (1978) documented the Snowball Prospect (69°2'W, 56°32'N) where 3 to 50 times background radioactivity occurs in a basal sandstone sequence of red quartz-pebble conglomerates and coarse grained arkose. The radioactivity is mainly due to thorium (up to 1300 ppm) which is in minerals of probable detrital origin. These rocks are equivalent to lower Seward Subgroup.

Kish and Tremblay-Clark (1978) also documented the Chioak Prospect, 80 km west of Fort Chimo in the northern Labrador Trough. It is in green and red arkose and conglomerates of the Chioak Formation which lie on Allison, Fenimore and Dragon formations (equivalent to the Ferriman Subgroup) and probably also on Archean basement rocks.

The uranium in the Chioak Prospect is hosted by poorly sorted conglomeratic, coarse grained arkose. The radioactive material occurs in the matrix as unevenly distributed clusters of grains; some lithic fragments are also radioactive. Some of the Chioak occurrences were tested by drilling (more than 100 drillholes) by Imperial Oil Limited in 1974-1978 (Boyd, 1978) about 2.5 km west of the northwest point of Lac Jourdau. The best intersection contained 0.1%U_3O_8 and 0.15% Cu over 4.8 m. Pyrite and chalcopyrite are common. Thorium content is low.

The significance of the Chioak Prospect is that epigenetic sandstone type mineralization is demonstrated within the Trough rocks. Therefore the lower Seward Subgroup of the Knob Lake Group, the Chioak (here) and perhaps its equivalents in the Tamarack Group at the south

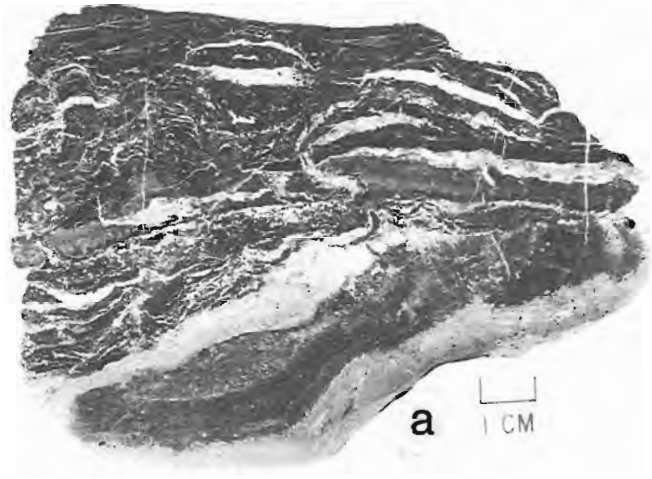

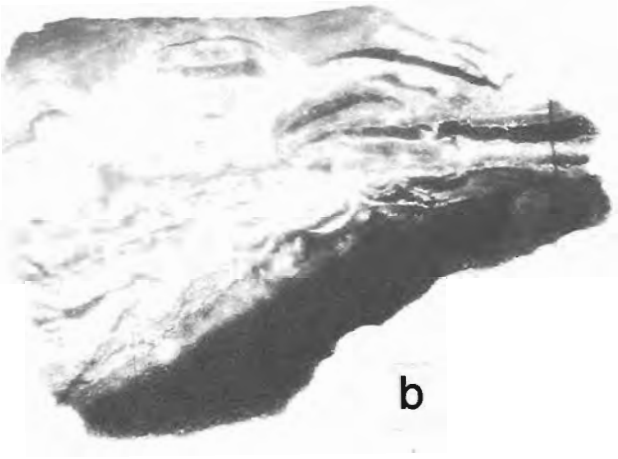

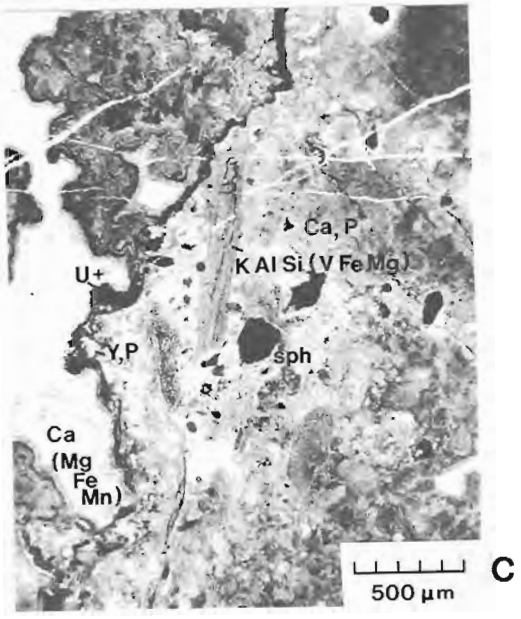

(a) RL photograph of polished slab, weathered zone adjacent to scale

(b) AR of (a); note weathered zone is weakly to non-radioactive

(c) Photomicrograph (transmitted light) of zone of high radioactivity in this specimen. Brecciated phosphatic chert with carbonate cement (Ca, (Mg, Fe, Mn)) and matrix mainly of microcrystalline apatite (Ca,P). The shale-like inclusions are a mixture of phosphate (Ca,P) and a vanadium-bearing mica (K, Al, Si, (V, Fe, Mg)). Sphalerite (Sph) and galena are present in the chert. The opaque zone adjacent to the carbonate filled vug is U-bearing with pyrite and phosphate with irregular compositional response (mainly Si, Fe, S, Ca, P, U, (Pb) ± Ti). One clear grain at the edge of this zone is probably xenotime. (Results of microprobe investigations by G. LeCheminant)

Figure 19.2. *Uraniferous cherty phosphorite breccia at Iron Arm (54° 43'N, 66° 16'W).*

end of the Trough and certainly the post-Trough Sims Formation are favourable for successor basin, sandstone type uranium or for the unconformity – related (Athabasca – type) mineralization.

Discussion

In their study, Kish and Tremblay-Clark (1978) identified detrital (thorium high) and epigenetic (uranium high) mineralization in clastic rocks of the Trough. Generally uranium contents of the various units in the Trough were fairly low; although fragments of pelitic rocks in the Chioak arkoses suggest that Ferriman equivalent rocks may be locally anomalous.

In this study we identified synsedimentary concentrations in phosphatic black shales of the Menihek Formation. Syngenetic protore concentration in other pelite units such as the Otelnuk Formation could have been reconcentrated by metamorphism and metasomatism accompanying the many intrusive events in the Trough as well as during subsequent orogenies.

The uranium-bearing veins such as those at Mistamisk and Romanet River are important first in that they demonstrate (re)mobilizations of a high-grade nature and second in opening up a broader terrain for exploration. The role of evaporites as suggested by Kish and Cuney (1981) may be an important and unifying aspect in providing a strong scavenging agent and perhaps a primary source (see Dunsmore, 1977).

Finally we suggest that the intrusions accompanying Aphebian volcanism could provide the structural and thermal components for the development of high grade vein type deposits throughout the Circum-Ungava Belt.

Acknowledgments

We acknowledge in particular the cooperation in both field visits and extensive discussions during 1984 of T. Avison, J.L. Caty, Serge Chevé, J. Kearvell, and L. Kish. Mineral identifications were made by D. Roberts, G. LeCheminant and D. Harris of the Geological Survey.

References

Bell, R.T.
1978: Uranium in black shales – a review; in Short course in uranium deposits, their mineralogy and origin, ed. M.M. Kimberly; Mineralogical Association of Canada, October 1978, p. 307-329.

Boyd, W.F.
1978: Summary report on 1978 exploration activity on the Chioak project by Esso Canada; Ministère de l'Énergie et des Ressources du Québec; Service de la documentation téchnique, fiche GM 33890.

Dimroth, E.
1978: Région de la fosse du Labrador entre les latitudes 54°30' et 56°30'; Ministère des Richesses Naturelles, du Quebec, Direction générale de la Recherche Géologique et Minérale, Rapport geologique 193, 396 pages avec 14 cartes.

Dimroth, E., Baragar, W.R.A., Bergeron, R., and Jackson, G.D.
1970: The filling of the Circum-Ungava geosyncline; in Symposium on basins and geosynclines of the Canadian Shield, ed. A.J. Baer; Geological Survey of Canada, Paper 70-40, p. 45-142.

Dunsmore, H.E.
1977: A new genetic model for uranium-copper mineralization; Permo-Carboniferous basin, northern Nova Scotia; in Report of Activities, Part B; Geological Survey of Canada, Paper 77-1B, p. 247-253.

Kish, L. and Cuney, M.
1981: Uraninite-albite veins from the Mistamisk valley of the Labrador Trough, Quebec; Mineralogical Magazine, v. 44, p. 471-483.

Kish, L. and Tremblay-Clark, P.
1978: Géochimie et radioactivité dans la fosse du Labrador; Ministère des Richesses Naturelles, Direction générale des Mines, Service des gîtes mineraux, DPV-567, 69 pages.

Smith, M.
1979: Report of 1978 field program, exploration permit 636, Townships 4852, 4951, and 4952, New Quebec for Quebec Ungava Mining Company Limited; Ministère de l'Énergie et des Ressources du Québec; Service de la documentation téchnique, fiche GM 34788.

Wardle, R.J. and Bailey, D.G.
1981: Early Proterozoic sequences in Labrador, in Proterozoic basins of Canada, ed. F.H.A. Campbell; Geological Survey of Canada, Paper 81-10 supplement, p. 331-359.

GEOLOGY OF THE BELLEORAM PLUTON, SOUTHEAST NEWFOUNDLAND

Project 840025

D.J. Furey[1]
Precambrian Geology Division

Furey, D.J., Geology of the Belleoram pluton, southeast Newfoundland; in Current Research, Part A, Geological Survey of Canada, Paper 85-1A, p. 151-156, 1985.

Abstract

The Belleoram pluton is an example of bimodal plutonism. The first phase is an equigranular hornblende-biotite granite intruded into Precambrian and Cambrian sediments and volcanics. At the contact, pipes and veins of granite intrude country rock and xenoliths of the country rock have been included in the pluton. Numerous finer grained and darker granitoid enclaves are homogeneously distributed throughout the pluton. The enclaves have been generated by amoeboid-shaped dykes of fine grained, darker granitoids which intrude the main body of the pluton. The second intrusive phase consists of hornblende microgranites and synplutonic composite dykes. The dykes are composite, with either quartz-feldspar rhyolite or microgranite cores, which gradually change composition and grain-size towards the dacitic margins. This phase was followed by the intrusion of alaskitic granite of the Harbour Breton pluton.

Résumé

Le pluton de Belleoram est un exemple de plutonisme bimodal. Dans sa phase initiale, le pluton est constitué d'un granite équigranulaire à hornblende et à biotite qui a fait intrusion dans des roches sédimentaires et volcaniques précambriennes et cambriennes. Au point de contact, des cheminées et des filons de granite ont fait intrusion dans la roche encaissante et des xénolites de la roche encaissante se sont ajoutés au pluton. Un grand nombre d'enclaves granitoïdes plus sombres et à grain plus fin sont réparties également partout dans le pluton. Ces enclaves ont été produites par des dykes amiboïdes de granitoïdes plus sombres à grain fin qui ont fait intrusion dans la masse principale du pluton. La seconde phase intrusive comprend des microgranites à hornblende et des dykes intrusifs composites synplutoniques. Les dykes intrusifs sont composites, leur noyau étant composé soit de rhyolite à quartz et à feldspath, soit de microgranite; la composition et la granulométrie changent progressivement à mesure qu'on s'approche des marges dacitiques. Cette seconde phase a été suivie par l'intrusion du granite à alaskite du pluton de Harbour Breton.

[1] Department of Geology, Memorial University of Newfoundland, St. John's, Nfld., A1B 3X5

Introduction

The Belleoram pluton occupies an ellipsoidal area of approximately 30 km^2 between Belleoram and Harbour Breton, southeast Newfoundland (Fig. 20.1). It is a granite-microgranite-rhyolite porphyry complex intrusive into late Precambrian to Devonian sediments and volcanics. The pluton was comprehensively described by Widmer (1950) as part of a regional survey of the Hermitage Bay – Fortune Bay area. Ermanovics et al. (1967) proposed that assimilation of country rock xenoliths had modified the composition of the intruding magma. Strong et al. (1974) included the pluton in a geochemical survey of granitoid rocks of eastern Newfoundland. Hughes and Smith (1978) studied the contact aureole of the pluton in the Great Bay de L'eau Formation.

During the summer of 1984, the author completed detailed mapping of the Belleoram pluton and traverses through the east lobe of the Harbour Breton pluton, the Pass Island pluton and the Farmer's Cove plug. Laboratory studies are now in progress. This report concentrates on field aspects: the relationships between the country rocks and the pluton, the internal lithological, textural and structural variability of the pluton, and its association with local dyke swarms.

Country rocks

The Belleoram pluton is located in the Avalon Terrane (Williams, 1983), southeast of the Dover-Hermitage Fault, in Precambrian to Upper Cambrian volcanic and sedimentary rocks and Devonian conglomerates.

The oldest country rocks are fine- to medium-grained, grey-black hornfelsed basalts of the late Precambrian Belle Bay Formation (map unit 1; Fig. 20.1) which outcrop in the English Harbour Hills north of Cluett's Pond. The contact with the pluton is sharp. The unit is conformably overlain by the Mooring Cove Formation (map unit 2) outside the field area (Williams, 1971).

The Mooring Cove Formation (map unit 2), is best exposed along the coast and in the hills north of the community of Belleoram. It consists of deep red to pink flow-banded, locally autobrecciated rhyolite and crystal-lithic tuffs, with minor agglomerate. The unit is conformably overlain by purple sandstone and conglomerate (map unit 2a). Minor pyrite is developed in the volcanics on Iron Skull and the south coast of Long Island. The pluton-country rock contact has been traced along the base of these hills, enclosing the Mooring Cove Formation as inliers in the pluton. Xenoliths of rhyolite occur in the granite and 2 mm to 50 cm veins of granite intrude up to 5 m into the country rock.

The Rencontre Formation (map unit 3) is exposed inland and along the coastline north of Belleoram, on Chapel and Long islands, and southeast of Salmonier Cove Pond. On Chapel and Long islands the unit consists of red, coarse grained, crossbedded arkosic sandstone and conglomerate, which grades upward into the Chapel Island Formation (map unit 4). Near the pluton it has been hornfelsed (map unit 3a) and on the west shore of Chapel Island partially assimilated by the Farmer's Cove plug (map unit 9e). Southeast of Salmonier Cove Pond, the Rencontre Formation is a fine- to medium-grained, white-yellow arkosic sandstone.

The Cambrian (Williams, 1971) Chapel Island Formation (map unit 4) outcrops along the coast between English Harbour West and St. Jacques, on Chapel Island, northeast of Cluett's Pond, atop the English Harbour Hills and southeast of Wreck Cove. The formation consists of grey to green, micaceous, ripple-marked siltstone and thinly bedded, fine grained grey sandstone. Near the contact with the Belleoram pluton, the formation has been converted to either a hard, fine grained grey hornfels or a kinked and folded light to dark grey, micaceous metapelite (map unit 4a). The contact is exposed on Chapel Island as an impressive display of veins, pipes and dykes of granite intruding up to 30 m into the country rock. Xenoliths of the Chapel Island Formation are common in the pluton near the contact. Northeast of English Harbour West and north of Wreck Cove, the hornfelsed sediments host magnetite and hematite mineralization (map unit 4b).

The Blue Pinion Cove Formation (map unit 5) conformably overlies the Chapel Island Formation and is overlain by the Chamberlains Brook Formation (map unit 6) at Blue Pinion Cove. The formation consists of blue-white, crossbedded orthoquartzite, with minor red and grey sandstone and shale horizons. The country rock-pluton contact is well exposed along the coast west of St. Jacques. Within 30 to 50 m of the contact, numerous angular xenoliths of the Blue Pinion Cove Formation comprise up to 30 per cent of the inclusion population. Two west-trending faults cut sediments northeast of English Harbour and a swarm of quartz-feldspar rhyolite porphyry dykes intrude the unit west of St. Jacques.

The Chamberlains Brook Formation (map unit 6) consists of red and green shale, with sandstone and conglomerate beds near its base, and shale and limestone horizons in the upper part. It conformably overlies Cambrian sediments (map unit 5) at Blue Pinion Cove where it is separated by a sharp angular disconformity from the overlying Great Bay de L'eau Formation (map unit 8). The Formation does not come in contact with the Belleoram granite.

The Late Silurian or Devonian (Williams, 1971; Calcutt, 1974) Cinq Isles Formation (map unit 7), a grey and red crossbedded sandstone, red and grey quartz-pebble conglomerate with minor limestones, is exposed along the coast from Wreck Cove to the outlet of Salmonier Cove Pond. The contacts with older and younger sediments are not exposed. Rare 30 to 50 cm wide veins of granite intrude the sediments.

The Upper Devonian (Widmer, 1950; Green, 1974) Great Bay de L'eau Formation (map unit 8) is the youngest sedimentary formation in the map area. It outcrops inland and along the coast between Coombs Cove and Blue Pinion Cove, where it overlies Cambrian sediments with a sharp angular unconformity. The formation consists of reddish to green-grey to buff pebble to boulder conglomerate with lenses of slate and sandstone and minor red and black shales. Subrounded to well rounded clasts of granite, quartzite, shale, siltstone and minor amounts of white quartz and rhyolite pebbles are loosely cemented in a clayey to sandy matrix. Bedding is locally poorly to well developed and consistently dips from 10 to 25 degrees to the southeast; graded bedding and crossbedding are common.

A 10 to 100 m wide thermal aureole (map unit 8a) has hornfelsed the conglomerate near the contact with the Belleoram pluton. The hornfels forms a series of hills between Mose Ambrose and Coombs Cove. The contact is steeply dipping at angles of 50 to 70 degrees (Smith, 1976). Pebbles have not been deformed or distorted, and sedimentary textures are not absent in the aureole. The contact was exposed at three localities where, over a 60- to 90-cm-wide zone, a fine grained sediment grades into a rock of equigranular granitic texture. This restricted granitization at the contact could nowhere be traced into the sediments for more than one metre, suggesting a localized contact effect. Biotite and garnet have been locally developed. A garnet isograd can be traced along the contact north of Coombs Cove for approximately one kilometre.

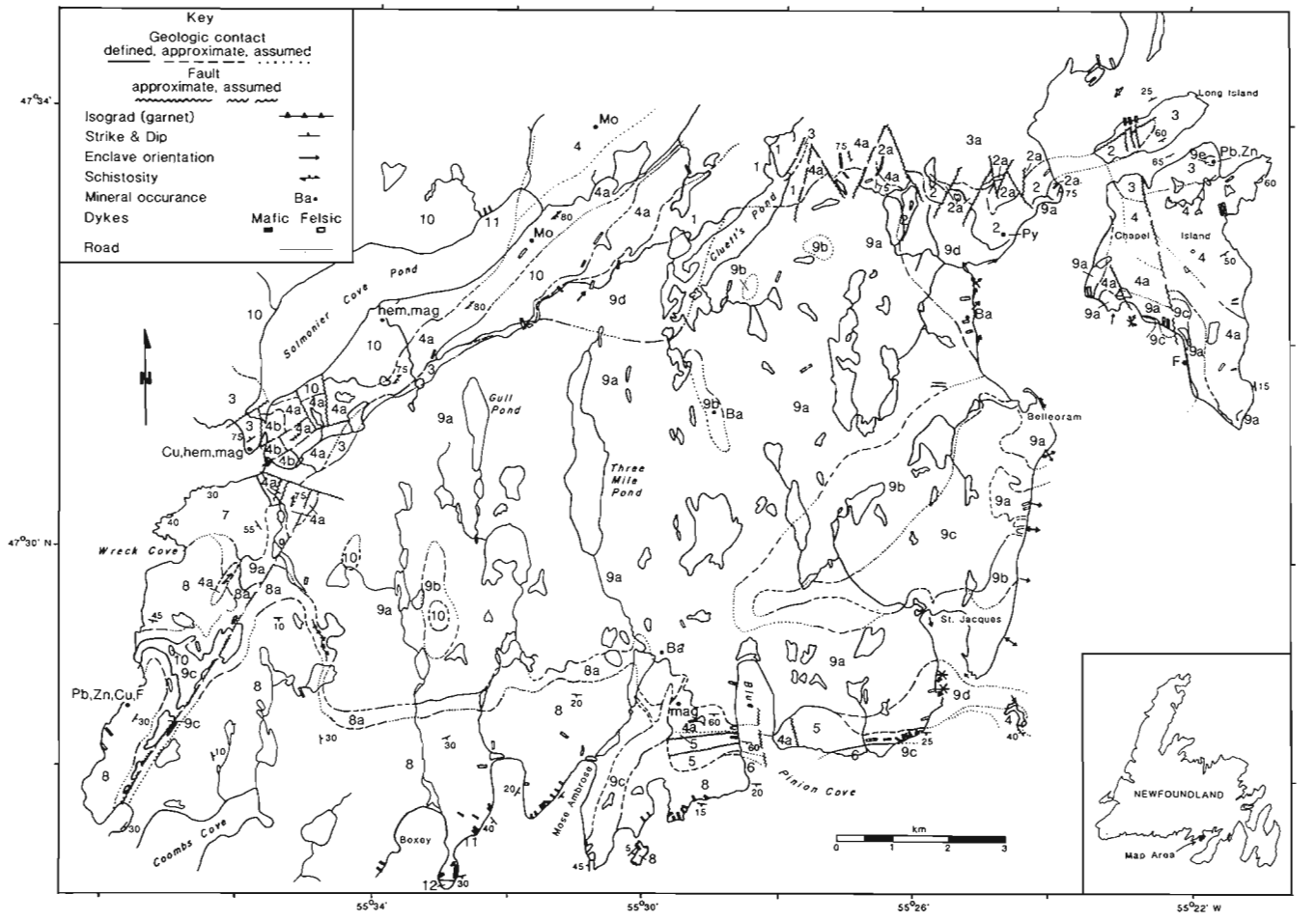

Figure 20.1. *Geological map of Belleoram Pluton.*

LEGEND

BELLEORAM MAP AREA

Devonian:

12 Boxey Head Basalt – fine- to medium-grained dark grey to purple amygdaloidal basalt.

11 Mafic Dykes – fine- to medium-grained, commonly amygdaloidal, dark green diorite and diabase dykes.

10 East Harbour Breton Pluton – medium- to coarse-grained pink to red, alaskitic biotite granite.

9 Belleoram Pluton – (9a) fine- to medium-grained, grey to pink enclave-rich quartz monzonite; (9b) medium-grained green-brown granodiorite; (9c) orange-red quartz-feldspar rhyolite porphyry and miarolitic microgranite; (9d) xenolith-bearing quartz diorite border phase; (9e) Farmer's Cove plug – buff to pinkish inclusion-rich rhyolite with quartz and feldspar phenocrysts.

8 Great Bay de L'eau Formation – buff-pink, locally crossbedded, pebble to boulder conglomerate, with lenses of slate and sandstone; (8a) hornfelsed conglomerate.

Devonian or earlier:

7 Cinq Isles Formation – red to grey quartz-pebble conglomerate and crossbedded sandstone.

Cambrian or Eocambrian:

6 Chamberlain's Brook Formation – red and green shale, with quartzose sandstone and pink limestone beds.

5 Blue Pinion Cove Formation – crossbedded orthoquartzite, with minor red-grey sandstone and shale.

4 Chapel Island Formation – grey, micaceous, ripple-marked siltstone, shale and sandstones; (4a) hornfelsed sediments, locally host (4b) to hematite and/or magnetite mineralization.

Hadrynian:

Long Harbour Group:

3 Rencontre Formation – crossbedded purple sandstone, pebble conglomerate and red argillite; (3a) hornfelsed sediments.

2 Mooring Cove Formation – pink-orange, flow-banded rhyolite, rhyolite tuff and agglomerate; (2a) purple-red crossbedded sandstone and grey shale.

1 Belle Bay Formation – fine- to medium-grained, dark grey to black hornfelsed mafic volcanics.

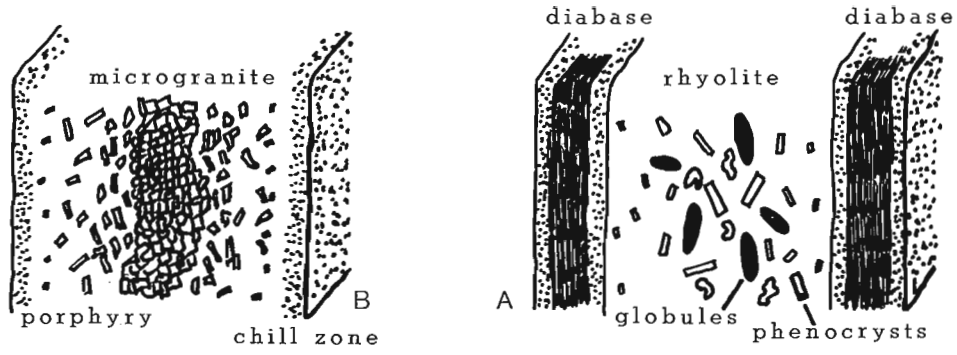

Figure 20.2. Schematic cross-sections of composite dykes. (A) Quartz-feldspar rhyolite porphyry dykes, containing quenched globules of diabase magma, normally bounded by two diabase dykes chilled against the rhyolite dyke and the country rock. (B) Dyke with red microgranite core, orange-brown feldspar rhyolite porphyry transitional zone, and dark green diabase margin which chills against the country rock. Type A dykes are more abundant in the northeast region of the map area while Type B dykes are most common in the southeast.

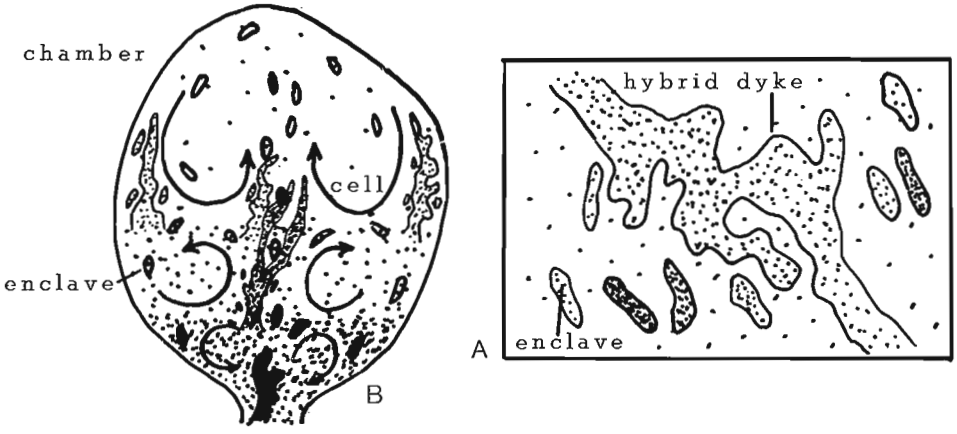

Figure 20.3. (A) Schematic diagram of typical hybrid granitoid dyke showing the lobate and cuspate nature of its contact with the host granite. Local ellipsoidal granitoid enclaves are generally of the same composition and texture as the dyke rock. (B) Possible model for enclave genesis. A convecting and zoned magma chamber, more mafic towards the base, with hybrid granitoid dykes intruding from depth and generating enclaves. (Figure 20.3B modified from Vernon, 1983.)

The formation (map unit 8) has also been cut by numerous northwest-trending dark green diabase and pink quartz-feldspar porphyry dykes along the coast from Mose Ambrose to Boxey, where it is overlain by the Boxey Head Basalt in slight angular unconformity. Thin calcite veins, with minor amounts of galena, fluorite, sphalerite and chalcopyrite mineralization, cut the formation along the coast south of Wreck Cove.

Intrusives

The Belleoram Pluton (map unit 9a) was the main focus of the present investigation. It generally outcrops, over an area of approximately 130 km^2 along a northeast axis, as a series of parallel ridges north-trending with cliff faces and scree slopes facing west. In the English Harbour Hills the ridge trend follows the east-northeast boundary, and between Blue Pinion Cove and Belleoram they trend northeast. This latter physiographic trend distinguishes the major subdivision of the pluton into grey granite (map unit 9a) and pink-orange microgranite (map unit 9c) units. Throughout the pluton joint patterns generally trend east and north, and subhorizontal joints give the appearance of subhorizontal sheeting.

The relatively undisturbed nature of the Great Bay de L'eau Formation led Widmer (1950) to propose a late Devonian to Carboniferous age for the pluton. Potassium-argon isotopic dating of biotites by Wanless et al. (1965, 1967) gave ages of 400 ± 20 and 342 ± 20 Ma. The first date was considered to be anomalous due to the loss of potassium or excess argon resulting from the alteration of 30 per cent of the biotite to chlorite.

The pluton has been subdivided into two major units (1) an equigranular, fine- to medium-grained grey to pink quartz monzonite (map unit 9a) intruded by (2) a fine grained, feldspar-porphyritic, orange to red microgranite (map unit 9c). The first unit is characterized by granitoid enclaves, amoeboid-shaped hybrid dykes and xenoliths of hornfelsed country rocks near the contacts. The second unit outcrops between Blue Pinion Cove and Belleoram and as a large dyke south of Wreck Cove. At the first location, an equigranular medium grained grey to green quartz monzonite (map unit 9b) surrounds the microgranite.

The granite consists of approximately equal amounts of alkali feldspar and plagioclase, and 15 to 25 per cent milky quartz. The plagioclase crystals display normal and

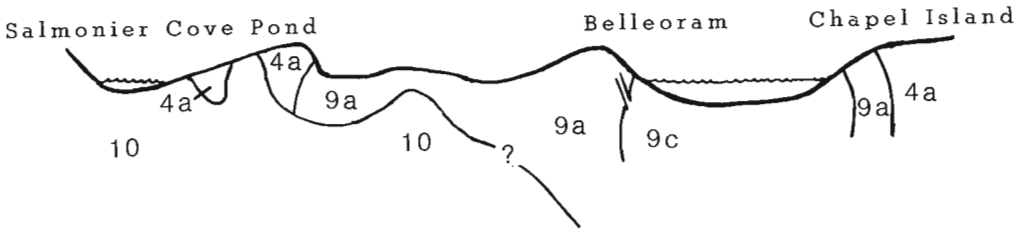

Figure 20.4. *Idealized cross-section between Salmonier Cove Pond and Chapel Island (see Fig. 20.1). The Harbour Breton pluton (map unit 10) is intrusive into the Chapel Island Formation (map unit 4a) in the west and into the Belleoram granite (map unit 9a) to the east. The microgranite (map unit 9c) intruded into the enclave-rich granite. The contact between the granite and the Chapel Island Formation (map unit 4a) is exposed on Chapel Island.*

oscillatory zoning, are inclusion-rich, and have been extensively altered. Accessory minerals are biotite, hornblende, rare clinopyroxene, zircon and irregularly-shaped grains of magnetite. The hornblende may be altered to biotite or chlorite. Epidote is also developed as a secondary mineral. The microgranite phase contains the same minerals as the granite, but is finer grained, miarolitic and pink-orange. Miarolitic cavities are commonly filled with limonite.

A fine grained, red to pink quartz-diorite border phase, ranging from absent to approximately 10 m wide, occurs at pluton-country rock contacts from Iron Skull to the area north of Three Mile Pond. Ermanovics et al. (1967) suggested that the margin of the pluton may have been basified near the contact with the shale, and that xenoliths of shale have been altered to compositions of the host pluton.

Both the country rocks and the granite phase of the Belleoram pluton have been intruded by felsic dykes (map unit 9c). These range in lithology from fine grained microgranite with 1 to 2 mm long phenocrysts of feldspar, to quartz-feldspar rhyolite and quartz latite porphyry. They generally discolour the pluton for a metre from their contacts. Their composition varies from red rhyolite porphyry cores which grade into a brown intermediate transitional zone to a dark green dacitic margin (Fig. 20.2A). Other dykes have red microgranite cores, transitional zones of feldspar rhyolite porphyry, and dacite margins chilled against both the core and the country rock (Fig. 20.2B). The dacite margins sometimes contain amygdules filled with quartz. The relative widths of the core, transition, and dacitic zones may vary from absent to 4 m, to the extent that dykes of either rhyolite or dacite may occur. These composite dykes are generally 2 to 7 m wide with the symmetrical green outer zones rarely more than one metre in width. The core porphyry has euhedral phenocrysts of pink to orange alkali feldspar, embayed quartz, zoned plagioclase, and accessory biotite and magnetite, with secondary chlorite and sericite. The porphyry has enclaves of the dacitic marginal phase from 2 to 30 cm in diameter.

Many dykes to the south of the map area are either dacitic or rhyolitic and lack the other phase. Medium grained, grey to pink porphyritic dykes of intermediate composition are also common. These are found along the entire margin of the pluton and five have been noted within the pluton. Orange and brown porphyritic xenoliths of the dyke rock are seen in areas (map unit 9d) adjacent to centres of dyke intrusion, suggesting that the dykes range in age from pre- to post-Belleoram plutonics. One dyke (map unit 9c), trending northeast and located immediately east of the community of English Harbour West, is approximately 500 m by 4000 m. It appears to pinch out before making contact with the Belleoram pluton.

The Farmers Cove plug (map unit 9e), exposed on the northeast side of Chapel Island in a 15 to 30 m high cliff, intrudes the red sandstone conglomerates of the Rencontre Formation (map unit 3), including xenoliths near its border. Widmer (1950) suggested that xenoliths in the core of the plug represent different degrees of digestion of fragments of the Rencontre Formation. The xenolith-rich nature and proximity of the plug to the Belleoram pluton suggested to Widmer (1950) that it was an extension of the Belleoram pluton. In fact, little evidence exists to support or contradict this assertion.

It is a buff to greyish pink rhyolite with phenocrysts of quartz and feldspar in a fine grained matrix. The rocks have been altered to epidote and muscovite, with minor amounts of galena and sphalerite mineralization.

The Harbour Breton pluton (map unit 10) outcrops on the shores of Salmonier Cove Pond and as a 5 km long northeast-trending body intruded into Chapel Island Formation (map unit 4) sediments 500 m east of Salmonier Cove Pond. Outcrops of this unit are also found within the main body of the Belleoram pluton; as a 3 m by 10 m intrusion into the rhyolite dyke (map unit 9c) south of Wreck Cove; and, as a 1 to 4 m wide dyke in the main phase of the Belleoram pluton on the west side of Chapel Island.

The pluton consists of medium- to coarse-grained, homogeneous, pink, alaskitic granite or porphyritic biotite granite, locally hosting xenoliths of country rock. Molybdenum and fluorite occurrences in quartz veins and as fillings along joint surfaces are common along the southern margin of the pluton.

A swarm of fine grained, dark green to black diabase dykes (map unit 11) outcrop along the coast between Blue Pinion Cove and Boxey, and intrude the Harbour Breton pluton along the shore of Salmonier Cove Pond. Along the east shore of Mose Ambrose, one of these dykes intrudes a rhyolite porphyry dyke (map unit 9c), and may intrude along the contacts of earlier intruded quartz-feldspar rhyolite porphyry dykes. Some of these dykes have been auto-brecciated. These dykes are similar in appearance to the dacite margins bordering many of the felsic dykes, and may be a later stage of a progressive intrusive event.

The Boxey Head Basalt (map unit 12) is exposed on the east side of Boxey Point and on Boxey Head. It overlies the Great Bay de L'eau Formation (map unit 8) with a slight angular unconformity and has been assigned a Carboniferous or Triassic age by Smith (1976). It consists of flows of fine- to medium-grained, dark grey to purplish grey basalt separated by thin intervals of red sandstone and shale. Upper and lower portions are amygdaloidal, with amygdules which Green (1976) states are filled with calcite and zeolites.

Quaternary glacial outwash is best exposed along the coast between St. Jacques and Blue Pinion Cove, and in a gravel pit in Mose Ambrose. Sands and gravels are found in marine terraces.

Inclusions

The variety of inclusions in the Belleoram pluton has posed problems to previous workers. Ermanovics et al. (1967) suggested that the inclusions originated from both shales

altered to compositions approaching those of the Belleoram granite, and through the alteration of the Great Bay de L'eau conglomerate (map unit 8a) into a granite, with outlines of cobbles preserved. Williams (1971) suggested that the inclusions resulted from explosive brecciation prior to granite emplacement, but failed to observe the ellipsoidal nature of most of the inclusions. In fact, there are two different types of inclusions in the first phase of the Belleoram pluton: xenoliths and enclaves (terminology of Vernon, 1983).

Xenoliths are generally restricted to within less than 5 m of the contacts. An exception is the contact with the Blue Pinion Cove Formation, in the vicinity of which angular or broken pieces of the blue orthoquartzite constitute from 2 to 30 per cent of the total inclusion population. They are seen approximately 30 to 50 m from the contact, and gradually increase in abundance as the contact is approached. Angular to subangular, lenticular, black hornfelsed pelite xenoliths are distributed throughout the entire granite, but are more abundant near the contact of the Chapel Island Formation.

Xenoliths of felsic and mafic dyke material (map units 9c, 11) occur along the north-central, northeast and southeast perimeters of the pluton in areas (9d) adjacent to dykes. In the north, xenoliths are restricted to within 2 to 4 km of the contact with the country rock, and are either orange-brown porphyry or black aphanitic diabase, surrounded by reaction halos. They may have originated with the destruction of synplutonic dykes and reinclusion of the resulting fragments into the Belleoram groundmass.

A few xenoliths display sharp contacts between a very fine grained, dark grey granite and a medium grained lighter-coloured granite. These inclusions are preserved fragments of brecciated hybrid dykes associated with ellipsoidal enclaves of granite.

The enclaves range from ellipsoids almost indistinguishable from the host granite, through increasing degrees of darkening and decreasing grain-size, to dark gabbroic-textured ellipsoids (Fig. 20.3A). Most are rounded to ellipsoidal with cuspate margins. The rounded shape is primary, and may represent globules of more mafic magma that have mingled and quenched in a granitoid host magma. The abundance of the enclaves is not related to pluton contacts and is homogeneous throughout the pluton. Dark enclaves, which may contain 1- to 2-cm feldspar crystals, are similar in composition and texture to local hybrid granitoid dykes.

Summary

The intrusion of the Belleoram granite locally altered the country rocks to hornfels, shooting veins and dykes of granitic material into the hornfels. Xenoliths from the country rocks were mixed with an enclave-rich granitic magma, the enclaves having been derived from granitic dykes of granitic composition intrusive from deeper within the magma chamber. A simple model (Fig. 20.3B) proposes that the observed variations in grain-size and texture of the enclaves result from layered convection cells within the magma chamber, and the ability of hybrid granitoid dykes to intrude into overlying magma.

Synplutonic dykes of rhyolite and dacite composition might be explained by rapid unmixing after separating from the magma chamber. These dykes are associated with the microgranite phase of intrusion and barite veining in the granite phase. Fluorite and quartz veining found in the microgranite preceded the intrusion of the Harbour Breton pluton (Fig. 20.4), which is associated with molybdenum and fluorite occurrences.

Acknowledgments

The author would like to thank D.F. Strong for suggesting this project, reviewing this paper, and guidance throughout the project; R.H. Vernon for discussion concerning the enclaves and xenoliths in the Belleoram granite; B.A. Green and C.F. O'Driscoll who supplied reference materials in preparation for field work; and Brian Sears, who provided invaluable field assistance and photographic expertise.

References

Calcutt, M.J.
1974: The stratigraphy and sedimentology of the Cinq Isles Formation, Fortune Bay, Newfoundland; unpublished M.Sc. thesis, Memorial University of Newfoundland.

Ermanovics, I.F., Edgar, A.D., and Currie, K.L.
1967: Evidence bearing on the origin of the Belleoram Stock, southeastern Newfoundland; Canadian Journal of Earth Sciences, v. 4, p. 413-431.

Green, B.A.
1974: Harbour Breton Map Area; in Newfoundland Department of Mines and Energy 1974 Report of Activities, p. 3-9.

1976: Harbour Breton Miscellanea; in Newfoundland Department of Mines and Energy 1976 Report of Activities, p. 2-5.

Green, B.A. and O'Driscoll, C.F.
1975: Gaultois map area; in Newfoundland Department of Mines and Energy 1975 Report of Activities, p. 56-63.

Hughes, C.J. and Smith, M.M.
1978: A Claim of High Level Granitization Refuted; Maritime Sediments, v. 14, p. 11-14.

O'Driscoll, C.F.
1977: Geology of the Hermitage Peninsula, Southern Newfoundland; unpublished M.Sc. thesis, Memorial University of Newfoundland, 144 p.

Smith, M.
1976: Geology of an area around Mose Ambrose, English Harbour West, South Coast, Newfoundland; unpublished B.Sc. thesis, Memorial University of Newfoundland, 38 p.

Strong, D.F., Dickson, W.L., O'Driscoll, C.F., and Kean, B.F.
1974: Geochemistry of Eastern Newfoundland Granitoid Rocks, Newfoundland Department of Mines and Energy, Report 74-3, 140 p.

Vernon, R.H.
1983: Restite, Xenoliths and Microgranitoid Enclaves in Granites; Journal and Proceedings, Royal Society of New South Wales, v. 116, p. 77-103.

Wanless, R.K., Stevens, R.D., Lachance, G.R., and Rimsaite, R.Y.H.
1965: Age Determinations and Geological Studies. Part 1 – Isotopic Ages, Report 5; Geological Survey of Canada, Paper 64-17 (Part 1), 126 p.

1967: Age Determinations and Geological Studies. Part 1 – Isotopic Ages, Report 7, Geological Survey of Canada, Paper 66-17, 120 p.

Widmer, K.
1950: The Geology of the Hermitage Bay area, Newfoundland; unpublished Ph.D. thesis, Princeton University, New Jersey, 439 p.

Williams, H.
1971: Geology of the Belleoram map area, Newfoundland (1 M/11); Geological Survey of Canada, Paper 70-65, 39 p.

1983: Appalachian Suspect Terranes; Geological Society of America, Memoir 158, p. 33-58.

-21-

GEOLOGY OF THE SPRINGDALE GROUP, CENTRAL NEWFOUNDLAND

Project 840024

Marylou Coyle[1], D.F. Strong[1], D. Gibbons[2], and E. Lambert[3]
Precambrian Geology Division

Coyle, M., Strong, D.F., Gibbons, D., and Lambert, E., Geology of the Springdale Group, central Newfoundland; in Current Research, Part A, Geological Survey of Canada, Paper 85-1A, p. 157-163, 1985.

Abstract

The Silurian Springdale Group comprises interbedded basaltic flows, silicic and intermediate ash-flow tuffs, and fluviatile red sandstones and conglomerates derived mainly from the volcanic rocks. They occur along the western margin of the Lower Paleozoic central volcanic belt of Newfoundland in a synformal basin, intruded on its margins by younger or cogenetic granitoid rocks; on its eastern margin it is faulted against older volcanic and intrusive rocks of the central volcanic belt. Ten volcanic-sedimentary and four intrusive lithotypes have been recognized within the group, some of which are repeated both stratigraphically and structurally. They are symmetrically disposed about the synformal axis, and are readily interpreted as a caldera-fill sequence.

Résumé

Le groupe silurien de Springdale se compose d'une série de coulées basaltiques, de tufs volcaniques à cendres siliceux et intermédiaires et de grès et conglomérats rouges fluviatiles dérivés surtout des roches volcaniques. Ces matériaux interstratifiés se présentent le long de la marge ouest de la zone volcanique centrale du Paléozoïque inférieur de Terre-Neuve, dans un bassin synforme dont les marges ont été coupées par des roches granitoïdes plus récentes ou cogénétiques, ou dont la marge est a été faillée contre les roches volcaniques et intrusives plus anciennes de la zone volcanique centrale. Dix lithotypes volcano-sédimentaires et quatre lithotypes intrusifs sont reconnus dans le groupe; certains d'entre eux se répètent stratigraphiquement et structuralement. Ils sont disposés symétriquement autour de l'axe synforme et sont aisément identifiés comme étant une séquence de matériaux de remplissage de caldéra.

[1] Department of Geology, Memorial University of Newfoundland, St. John's, Nfld. A1B 3X5
[2] Department of Geology, Dalhousie University, Halifax, N.S. B3H 3J5
[3] La Scie, Newfoundland A0K 3M0

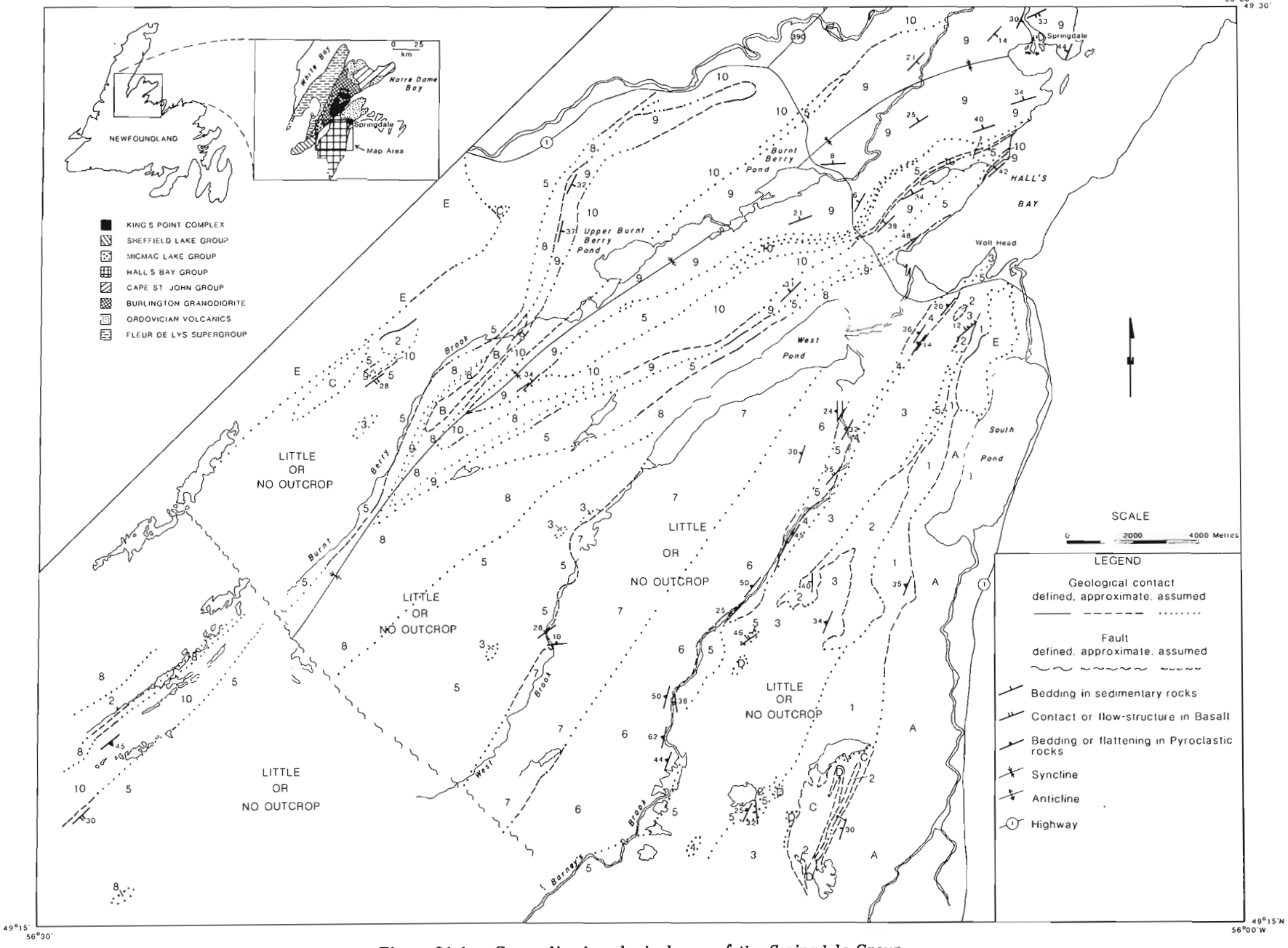

Figure 21.1. *Generalized geological map of the Springdale Group.*

Introduction

Williams (1967) recognized nine different "belts" of Siluro-Devonian rocks on the island of Newfoundland, the largest of which are the Springdale and Botwood belts of the central Newfoundland "mobile belt" or "Dunnage terrane". This report deals with the Springdale Belt as exposed in Springdale map area (12H/8), which was mapped during the summer of 1984 at a scale of 1:25 000. This belt extends continuously for 60 km from Springdale southward to Millertown Junction, or more than 100 km southwestward if volcanic inliers within the Topsails Complex are included (see Whalen and Currie, 1983, Fig. 2.2), and reaches a maximum width of 30 km across the centre of the belt (Fig. 21.1).

Wessel (1975) reviewed the confusion arising from the terms "Springdale Formation" and "Springdale Group", and suggested that the first be used only for the uppermost sedimentary unit, and changed the group name to the Halls Bay Group. The term Springdale Group is entrenched in the literature, but we recognize that formational status will be assigned to the other volcanic and sedimentary units as this study advances and that a revision along the lines suggested by Wessel (1975) may be required at a later time.

LEGEND

Map units of the Springdale Group
(not necessarily in stratigraphic order)

Unit

1. Red, fractured, moderately welded, lithic-crystal (plagioclase, alkali feldspar, biotite) ash-flow tuff.
2. Laharic and explosion breccia; poorly sorted; composed of blocks of varied composition in an ashy-muddy volcanogenic matrix.
3. Intermediate composition flows and intrusions.
4. Intermediate to silicic pyroclastic breccias, crystal-lithic and lapilli ash-flow tuffs.
5. Basaltic flows, breccias and scoria.
6. Silicic lithic ash-flow tuffs, with a basal lithophysae horizon, overlain by welded lithic lapilli tuffs and breccias.
7. Brown, densely welded, massive flinty silicic ash-flow tuffs.
8. Red and pink rhyolitic vitric tuffs, locally vitroclastic, strongly divitrified, spherulitic or welded.
9. Red and maroon, polymictic cobble conglomerate with medium grained matrix, coarse to fine sandstones and sandy siltstones. All units are dominated by volcanic debris, with local concentrations of granitoid clasts.
10. Quartz-feldspar crystal-lithic tuffs; densely welded, with widely dispersed ultramafic-mafic clasts.

Intrusive Rocks

A. Foliated amphibolitic granodiorite.
B. Massive to flow-banded rhyolite.
C. Massive microdiorite.
D. Felsic microporphyry sills and dykes.
E. Younger granitoid rocks.

The Springdale Group is not fossiliferous, and its age has only been indirectly inferred to be Silurian by correlation with lithologically similar fossiliferous rocks of the Botwood belt. More recently a U/Pb date on zircon from a felsic volcanic unit (unit 10) has yielded a Lower Silurian date supporting this correlation (F. Chandler, personal communication).

Although Wessel (1975) considered the northern part of the Springdale Group to be "bounded by a transcurrent strike-slip fault with apparent dextral displacement" (the Lobster Cove fault), it has long been known that this fault is in fact the site of overthrusting of Lower Ordovician (Lushs Bight Group) pillow lavas onto the Springdale Group. Furthermore, outcrops of the Springdale Group are known to the north of this fault, where they lie unconformably on the Lushs Bight Group. To the northeast at Pilleys Island the Springdale Group lies unconformably on the Roberts Arm Group, a thick sequence dominated by basaltic pillow lavas of disputed age between Lower Ordovician and Lower Silurian (see review by Nowland and Thurlow, 1984).

Along its southeastern boundary the Springdale Group lies unconformably on a basement of foliated granodiorite and diorite which we correlate with the Mansfield Head Complex (Bostock et al., 1979) and the Hungry Mountain Complex (Thurlow, 1981). Whalen and Currie (1983, Fig. 2.2) also show rocks of the Hungry Mountain Complex as occurring on the southwestern margin of the group. Although contacts are rarely seen, and may be fault-modified. Strong contact metamorphic effects indicate that both the basement rocks and the Springdale Group are intruded by granitoid rocks. We correlate these with various phases of the Topsails Complex, which also intrudes the group on its southern and western margins (Fig. 21.1).

As shown on Figure 21.1, exposure in the area is extremely sparse, except along the main brooks, the coastline of Halls Bay, several highway intersections, some linear ridges, and rare isolated outcrops.

A single north-plunging synclinal axis extends through the Springdale Group from Springdale southwestwards through Burnt Berry Pond and just east of Upper Burnt Berry Pond. The syncline (Fig. 21.1) closes sharply about 10 km to the southwest of Upper Burnt Berry Pond. Sedimentary rocks of the Springdale Group are inclined up to 50 degrees on either side of the axis, which is also sporadically marked by a steeply-dipping, spaced fracture cleavage. Wessel (1975) considered the syncline to reflect the earlier geometry of the basin in which the Springdale Group was deposited.

Faults in the area are indicated by local shearing, jointing and inferred offsets of units, but only one is shown on Figure 21.1 and even this is based mainly on interpretation of topographic and aeromagnetic patterns, as were the numerous faults shown by Kalliokoski (1953). The linear eastern and western boundaries of the group, although intruded by granitoid rocks, are taken as reflecting early faults along which the group was down-dropped, and which possibly controlled volcanism and sedimentation, and even the subsequent intrusion of the granitoids. Basal units 1 to 4 are eliminated from the west central part of the map area by intrusion and subsequent uplift of granitoid rocks.

Description of map units

Volcanic and sedimentary units

Unit 1 is located along the eastern margin of the map area, and extends as an elongate lens toward the south at least 15 km southwest of South Pond. It forms the stratigraphic base to the other volcanic units to the west, (units 2-10), is intruded by younger granitoid rocks (unit E), and is thought to have a fault-modified unconformable relationship with the older granodiorite (Unit A) to the east.

Unit 1 is a moderately welded, lithic-crystal tuff, commonly highly fractured or sheared along its eastern margin. It differs from the other overlying ash-flows in that fractured and broken crystals of both plagioclase and K-feldspar are present, along with accessory biotite, quartz, and rare opaques. The lithic component includes clasts of plagiophyric basalt, andesite, ultramafics, and red jasper. The matrix includes shards, rock and crystal fragments, and partially welded pumice lapilli with a eutaxitic texture. Perhaps the most important aspect of this early tuff is the occurrence of two feldspars and biotite in its crystal component, suggesting that it was extracted from a relatively deep, water-saturated, magma chamber.

Unit 2 is a distinctive laharic and explosion breccia composite unit, best developed along the eastern border of the volcanic terrane, but also mapped along the western margin of the Springdale Group. The eastern exposures of this unit form an 8 km long band only metres wide in the north, which expands southwards to cover an irregularly shaped lobate area about 1 km wide. Separate elongate ridges of this unit are also found to the south of the main lobate area, extending the unit by 8 km. The western equivalent is found in two separate smaller exposures, a northern one about 1 km^2, and a southern one about 1 by 2.5 km. Unit 2 has a variety of relationships with the other units, eg. stratigraphically overlain by unit 3, interbedded with units 5 and 8, and intruded by units C and D.

Unit 2 comprises a number of lithologies, dominantly laharic flows, along with tuffites, volcanic conglomerates, and volcanic explosion breccias. In general these volcaniclastic lithologies are characterized by poor sorting and massive to very coarse bedding. The lahars have dominantly subangular blocks, weighing up to one ton, in a locally vesicular muddy or ashy matrix. Both the coarse and fine fractions of these deposits vary from basalt to rhyolite. Bedding is commonly absent in the lahars, but where present it is reversely graded, with the finer basal horizon much thinner than the overlying coarse beds. The fabric of the laharic flows is isotropic, with local imbrication of elongate clasts.

The tuffites are composed of predominantly pyroclastic debris and reworked volcanic clasts, and could be further subdivided into tuffaceous conglomerates and tuffaceous breccias. Boulders in these units are not as large as those of the lahars, but are also commonly subangular to subrounded. The composition of the larger clasts ranges from basaltic scoria and bombs to rhyolitic tuffs of varied texture. The matrix is dominated by vitric shards and broken crystals with minor lithic fragments, and is locally vesicular.

Volcanic conglomerates differ from the above lithotypes in that they have been more extensively reworked and redeposited as a clastic sedimentary rock. They contain large, subrounded to rounded boulders and cobbles in a sand-sized matrix; there is no clay-sized fraction. Most of the clasts are silicic volcanics, with fewer of andesitic and basaltic composition, and pumiceous material is absent. Sorting ranges from poor to good. Bedding is common, and may be thick and structureless, thin and finely laminated, or crossbedded. These deposits commonly show normal grading, especially obvious in scour fills or channel deposit horizons.

Explosion breccias are very similar to monomictic lahars with a microbrecciated matrix component. They are commonly composed of intermediate or basaltic volcanic material, as both clasts and matrix. Bedding is commonly absent and the fabric is isotropic or shows "streaming" from a gas brecciation process.

Unit 2 was produced by a wide variety of physical mechanisms. The predominant feature in all of its subunits is the large size of the clasts, carried in a finer matrix, ie. with a strongly bimodal size distribution. These units represent facies variation developed during volcanic activity, ranging from near-source explosion deposits, to more distal, fluvially reworked deposits. Some debris flows may have been activated on unstable slopes and rapidly deposited, whereas others could have had long periods of reworking.

Unit 3 includes intermediate flows, flow breccias, and intrusives, distributed along the eastern and southern border of the volcanics in a belt about 14 km long and 3 km wide. A number of isolated exposures are also found in the central and western portions of the map area. Unit 3 is interbedded with units 1, 2, 4, and 5, and in part intrudes units 5 and 3. It consists of intermediate composition nonvesicular flows (dacite, andesite), commonly aphanitic, locally with phenocrysts of flow-aligned plagioclase. The massive flows are typically brecciated. Intrusions of massive andesite are also found. A minor phase of this unit consists of interbanded silicic and mafic compositions on the scale of centimetres and smaller. The flows and intrusions of unit 3 represent a period of volcanism dominated by intermediate chemistry, unlike the other major lava flows, which are of basaltic composition.

Unit 4 forms a narrow band, about 500 m wide, of intermediate ash-flow tuff, extending from southern Hall's Bay over 10 km toward the south-southwest. It overlies unit 3 and is succeeded by flow unit 5, and may be locally gradational into unit 6. It ranges in composition from rhyolite to andesite, although it is predominantly dacite. Lithologies include pyroclastic breccia and crystal-lithic and lapilli ash-flow tuffs.

In the lithic-dominated portions, the cognate clasts are andesite and aphanitic rhyolite in an ashy matrix. These lithic tuffs are generally bedded, tend to have reverse grading, and vary in degree of welding. The tuff breccias contain angular and flattened pumice fragments (>65 mm long) in an ashy matrix, with minor lithic fragments, and also show variable degrees of welding. The lapilli tuff, or lapilli stone, has pumice fragments from 2 to 65 mm long, in a welded ashy matrix. These lithologies tend to be discontinuous along strike and often pinch out. Unit 4 was deposited as ash-flows from an andesitic to dacitic source.

Unit 5 consists of at least four lenses of basaltic flow rocks, in a band up to 35 km long and 3 km wide. They are distributed throughout the entire area, with prominent and representative exposures along the southwest coast of Hall's Bay, and Barney's, Burnt Berry, and central West brooks. Barneys Brook closely follows the contact between unit 5 and the overlying unit 6 (Fig. 21.1). Smaller outcrops are found at the southwestern extremity of the Springdale map area (Fig. 21.1) and along the northwestern margin of the Springdale Group, within the King's Point map area to the north of Figure 21.1. These basaltic flows are typically aphanitic, with local spectacular concentrations of plagioclase phenocrysts, and tend to be highly vesicular, with amygdules of quartz, calcite and chlorite.

Unit 6 consists of silicic ash-flow tuffs, exposed continuously along Barney's Brook, in conformable contact with basaltic flows of unit 5, over a strike length of 14 km with a maximum width of 3 km. These "Barney's Brook ash-flows" are red to grey and display varying proportions of crystals, lithic fragments, and vitroclasts. The basal part of the unit is a thick, lithophysae-rich horizon resting on irregular flow tops of the basaltic unit 5. The individual lithophysae may be as large as 10 cm in diameter, with central cavities partially or completely filled with quartz crystals, radiating microlites, and chalcedony. This horizon grades upwards into a partially welded, ashy, crystal-lithic lapilli tuff. The phenocrysts are plagioclase and quartz,

commonly broken and concentrated in the matrix in preference to the pumice vitroclasts. A crude "bedding" is defined by flattening of the lapilli during welding.

The partially welded zone is succeeded upwards by a vitroclastic breccia tuff. Pumice bombs are flattened and some are as much as a metre in length. Concentrations of the large vitroclasts define a bedding which can be either normal or reversely graded. Throughout the partially welded zones. There are local concentrations of lithic fragments. They are dominantly silicic volcanics, andesite and rarely basalt, and commonly define a bedding which is normally graded. Unlike unit 4, these horizons are constant along strike, in terms of both their thickness and continuity.

A densely welded equivalent of the more northerly tuffs is found along the southern section of Barney's Brook, where the welding extends to its basal contact with underlying unit 5. The densely welded portions of unit 6 are maroon, vitric crystal ash-flow tuffs. A welding lamination is seen on weathered surfaces, but on fresh surfaces they look massive and structureless. Phenocrysts are plagioclase and quartz, which vary in relative proportions in a streaky manner. This unit is locally extremely massive and has the superficial appearance of an intrusive quartz-feldspar porphyry.

Unit 6 represents a number of pyroclastic flow units, each characterized by different proportions of lithics, vitroclasts, etc. They cooled as a simple cooling unit suggesting that the flows followed one another in rapid succession, with no substantial development of internal thermal gradients. In such sequences the degree of welding is greatest near the base, with partial welding in the middle of the unit and little or no welding near the top.

Unit 7 comprises massive silicic tuffs found along West Brook and the hills east of West Pond, as intermittent outcrops in a northeast-trending band for approximately 15 km with an average width of about 3 km. Although exposure is very poor and no contacts are seen, it appears that unit 7 overlies and grades into unit 6.

This unit is dacitic to rhyolitic, contains massive, vitric, strongly welded ash-flow tuffs, vitroclastic breccia, and in one location along West Brook, is overlain by a crystal-lithic sandstone. Welding can be observed on weathered surfaces, but it is commonly too dense to distinguish on fresh surfaces. Curvilinear joint surfaces are very common in the massive portions of the vitric tuff, and internal plastic shear zones or local brecciation can be seen as well as flow folds. The massive tuffs are locally porphyrytic, with small euhedral quartz and plagioclase phenocrysts in a brown to maroon ashy vitric matrix.

Another zone within unit 7 is a welded vitroclastic breccia, with very angular pumice fragments which may be flow-folded and have very chaotic orientations. No bedding is apparent in these rocks, but a flattening orientation can be measured from welding in the finer units.

Unit 8 forms a rhyolitic ash-flow tuff sequence extending throughout the central portion of the volcanic area, as two major bands folded about a synformal axis. On the northwestern limb, a band of unit 8 is less than 1 km wide and extends for 14 km to the fold closure. Exposures on the southeastern limb form two horizons, (1) an outer one 15 km long, several hundreds of metres wide in northern extremity of the limb and broadening toward the southwest to 2 km and (2) an inner band that is only several hundred metres or less wide and 7 km long. Another extensive tract of this lithotype is found in the southwestern corner of the map area, as two northeast-trending belts, one 1 km by 3 km, the second 500 m by 6 km. Unit 8 is interbedded with units 2, 5, 9, 10, may locally grade into unit 9, and is intruded by unit B.

Unit 8 includes an assemblage of dominantly devitrified, welded, pink and red rhyolitic ash-flow tuffs and breccias, displaying a variety of features which represent processes of flow, autobrecciation, and devitrification in viscous rhyolitic flow tuffs. Since this ash-flow tuff grades into a sandstone at a few localities, it may be part of a complex cooling unit rather than a simple cooling unit. Certain parts of the unit are very massive due to intense welding, and others consist of unwelded vitroclastic tuffs with large individually devitrified shards, each showing independent development of spherules. Other phases of the ash-flow breccias are not strongly divitrified, all with internal auto- or gas-brecciation textures. These breccias have clasts of plastically deformed rhyolitic lava and pumice. The vesicles are commonly infilled with pink to milky quartz.

The finer tuffs comprise a simple cooling unit with a sequence of massive welded ash-flows, a partially welded horizon with lithophysae and spherulitic zones, and an upper breccia horizon. In the upper unit, mixed magmas are found within the breccias, with alternating thin basaltic and silicic bands. The silicic tuffs are intruded by a rhyolitic plug (unit B), the crosscutting intrusions also cutting one another in a number of places.

Unit 9 comprises a sequence of redbed sediments distributed in the central portion of the synform, forming belts 18 km long, 3 km wide in the northeast and narrowing to 500 m at the inner fold closure. An outer band of sediments is disposed about the central axis over a length of 15 km and a width of between 2 and 0.5 km. Unit 9 is interbedded with units 5, 10 and 8, and grades into unit 8 in a few locations. The sedimentary rocks are also intruded by unit B along the northwestern limb.

These sedimentary rocks have been described in detail by Wessel (1975), who termed them the "Springdale Formation". We point out that this unit includes several separate sedimentary units which might in future justify separate formational names. In general the sequence consists of two types of conglomerate, sequences of sandstones, and sandy siltstones with localized development of caliche. These sedimentary facies are repeated in varying proportions in the total thickness of the fluvially deposited succession. Features such as crossbedding, ripples, laminations, rip-up horizons, and scour channels, are present, and have been evaluated in some detail by Wessel (1975).

A distinctive polymictic cobble conglomerate is found at local interfaces with the volcanic rocks of the Springdale Group. These conglomerates are commonly massive to poorly bedded, with bedding marked by sandy scour channels which pinch and swell and are thus not informative for true bedding orientations. The larger clasts can be imbricated and large-scale coarsening upward sequences can be recognized.

The cobble-sized clast population is subrounded to subangular. It essentially consists of detritus of silicic volcanic debris, predominantly aphanitic and porphrytic rhyolites, intermediate volcanics, and rarer basaltic and granitoid clasts. The cobbles are supported in a medium grained sandy matrix which varies in colour from pale beige to maroon. The grains of the fine fraction tend to be more angular and fractured than the coarser fragments, but are composed of the same lithic material plus abundant alkali feldspar and quartz.

A pebble conglomerate is found throughout the sedimentary package, but it mainly delineates basal portions of sandy cycles, and thus occurs many times through the sequence. The pebble conglomerates are usually massive and indurated, with little recognizable grading or other internal structures. Pebbles in this conglomerate are subrounded, and composed of silicic volcanic rocks, red and green cherts, and

rare ultramafic, basaltic, and granitoid clasts. These pebbles are supported in a fine- to medium-grained matrix of subangular sand which is composed of the same lithic components as the pebbles and a high proportion of quartz and feldspar.

Fine- and medium-grained red and maroon sandstones dominate the sedimentary sequence. They are commonly well bedded, and graded. Excellent examples of prograding sequences can be found, as well as asymmetrical ripples, trough and normal crossbeds and finely laminated horizons. In the finer sandstones there are concentrations of muddy rip-up clasts.

The sandy beds commonly grade up into very fine sandy siltstone. These upper horizons are finely laminated, and well graded or massive. Most have caliche prominently developed in their uppermost portions. Discrete accumulations of caliche can coalesce to form horizons or beds, and carbonate cement is typical of the sandstones which host the caliche.

Unit 10 occurs as a densely welded crystal-lithic tuff in the interior of the central syncline of the Springdale Group. Another area of exposure is found in the southwestern extremity of the Springdale map area. The larger synclinal exposure trends northeast for 18 km with the northwestern limb formed by a broader band as wide as 2.5 km in the centre and narrowing both northwards and southwards. The southeastern limb is up to 1 km wide, becoming less than 150 m at its northern limit on the coast of Halls Bay. The southwestern exposures form a belt about 6 km long by 1.25 km wide.

This crystal tuff is very massive and, like unit 8, so strongly welded as to look like an intrusive porphyry. It differs however, in that it has large obvious phenocrysts of quartz and feldspar with fragments of green ultramafic and red jasper. The feldspars are often zoned and fractured, and together with the quartz can make up to 60 per cent of the rock. The crystals are in a red, brown or orange vitric aphanitic matrix. The lithics are commonly angular, and may have reaction halos, especially the ultramafic clasts.

Intrusive units

Unit A is a highly deformed amphibolite-grade foliated granodiorite marking the southeastern boundary of the Springdale Group. It extends from west of central South Pond southwards for at least 18 km along a faulted unconformable contact. In the north it is intruded by the younger granitoid rocks of Topsails affinity.

The unit represents basement to the volcanics. It is green and black, medium- to fine-grained diorite, with hornblende and biotite, intruded or net veined by a pale, fine grained granite, with a typical tectonic fabric emphasized by amphibole alignment.

Unit B is an intrusive rhyolite occurring as a lens 4 km by 500 m, along the northwestern limb of the syncline, that cuts both units 8 and 9. It is massive, aphanitic, and pink or maroon. At the contacts between it and the pyroclastic sequences, an autobrecciation and gas brecciation is commonly observed. Curvilinear jointing and ductile flow-shear features are found within the body of rhyolite.

Unit C is a fine grained microdiorite exposed along both margins of the Springdale Group. In the southeast it covers an area 2.5 by 5 km and on the western margin it is at least 1 km by 3 km. It is black, very fine grained and tends to be massive. It is seen to intrude units A and 2, and is contemporaneous with or intruded by unit D. Unit E may also intrude it in the west, although this contact is altered by faulting.

Unit D, a felsic microporphyry, is found in only a few isolated exposures, commonly in conjunction with the microdiorite (unit C), exposed in narrow elongate patterns in the southeastern corner of the map area. It may represent dykes and sills related to the younger granitoid suites. Unit D is either contemporaneous with or intrudes unit C, it intrudes unit 2 along bedding as a sill, and is also found as an isolated exposure, cut by intermediate dykes near Barney's Brook.

Unit E, the younger granitoid rocks, appears to have been intruded along faults bounding the Springdale Group. An elongate exposure is found along the western side of South Pond, at the northeastern corner of the volcanic terrane. It is 1 km by 4 km, and a contact aureole is observed although not distinguishable at the scale of Figure 21.1. The western and southern margins of the Springdale Group are also marked by these younger granitoid rocks, and they extend through hundreds of square kilometres southwards throughout the Topsails Complex (Whalen and Currie, 1983).

The younger granitoid rocks include red and pink equigranular biotite granite, which ranges from coarse- to fine-grained to porphyritic. Quartz monzonite and less commonly granodiorite are also present. Along the northwestern boundary with the volcanics, the granites tend to be highly sheared and altered, possibly resulting from the faulting responsible for uplift and elimination of units 1 to 7 in this area.

Discussion

It is premature to speculate on precise correlations between volcanic rocks of the Springdale Group and other Siluro-Devonian sequences of western Newfoundland, but several features are worth noting. For example, no peralkaline rocks were recognized anywhere within the Springdale Group. It does contain biotite-bearing ash-flows, intermediate andesitic or dacitic flows, pyroclastics and abundant basaltic flows.

In these features it is similar to the Cape St. John Group, but it differs from the King's Point Complex, the MicMac Lake Group, and the commenditic rocks of the Sheffield Lake area. Given that the peralkalinity is a result of metasomatic processes near intrusive contacts (see Mercer et al., 1985), its absence in the Springdale and Cape St. John groups may simply reflect the fact that their subvolcanic plutons are not exposed, ie. that we are simply seeing a shallower depth of exposure where metasomatic fluids did not reach. On the other hand, the Topsails Complex, to the south of the study area, has both peralkaline and metaluminous suites (Taylor et al., 1980, 1981), and Whalen and Currie (1983) consider the former to be the younger. If direct correlations can be made, this may indicate that the metaluminous Springdale Group is somewhat earlier than the other peralkaline-bearing groups. This in turn would imply that magmatism migrated from one site to another, possibly with changes in the local tectonic regime.

Although it is fairly clear from the above descriptions that an abundance of volcanic facies typical of cauldron subsidence and related pyroclastic volcanism are represented in the Springdale Group, the precise tectonic controls of caldera collapse may well have been of more regional significance. It is well-known that calderas tend to be controlled by basement structures and regional tectonics, and it is not likely that those of western Newfoundland in Siluro-Devonian times were any exception. The evaluation of such questions awaits comprehensive mapping of these different suites, as well the results of detailed geochemical and other laboratory studies which are now in progress.

Compositional variation within the pyroclastic sequence points to a number of explosive events, and deeper levels of the magmatic system may have been tapped to produce the two-feldspar biotite-bearing crystal tuffs. Subsequent flows and pyroclastics of mafic to intermediate compositions may have resulted from processes of magma-mixing, for which there is also evidence from interbanded mafic and silicic welded ash-flow tuffs. The large areas of laharic breccia and pyroclastic breccia along the margins of the volcanic terrane are disposed as lobate forms reminiscent of debris flows off steep scarps around caldera margins. Younger granites along the margins appear to have been controlled by faulting, with uplift and erosion of the volcanic stratigraphy occurring along the western central margin. The precise volcanic stratigraphy has not yet been determined, both because of the poor exposure and the fact that some units appear to have overlapped in time, eg. the laharic and breccia flows and some andesitic and basaltic flows. Evaluation of these and other questions awaits further detailed field mapping, as well as petrographic and chemical study of a full range of representative samples.

Acknowledgments

We are grateful for assistance from M. Basha, K.L. Currie, W. Epp, B.F. Kean, D. Machin, J. Maloney, H. Sandeman, C. Saunders, G. Stapleton, and H.S. Swinden. We especially thank A.A. Burgoyne and R. Hewton of Brinco Mining Ltd. for use of their Springdale facilities, and the Springdale office of the Newfoundland Department of Forestry for access to their aerial photographs.

References

Bostock, H.H., Currie, K.L., and Wanless, R.K.
1979: The age of the Roberts Arm Group, north central Newfoundland; Canadian Journal of Earth Sciences, v. 16, p. 599-606.

Kalliokoski, J.
1953: Springdale, Newfoundland: Geological Survey of Canada Paper 53-5, 4 p.

Kean, B.F., Dean, P.L., and Strong, D.F.
1981: Regional geology of the central volcanic belt of Newfoundland; in Geological Association of Canada Special Paper 22, p. 65-78.

Mercer, B., Strong, D.F., Wilton, D.H.C., and Gibbons, D.
1985: The King's Point Volcano-Plutonic Complex, western Newfoundland; in Current Research, Part A, Geological Survey of Canada Paper 85-1A, Report 8.

Nowlan, G. and Thurlow, J.G.
1984: Middle Ordovician conodonts from the Buchans Group, central Newfoundland, and their significance for regional stratigraphy of the central volcanic belt; Canadian Journal of Earth Sciences, v. 21, p. 284-296.

Taylor, R.P., Strong, D.F., and Fryer, B.J.
1981: Volatile control of contrasting trace element distributions in peralkaline granitic and volcanic rocks; Contributions to Mineralogy and Petrology, v. 77, p. 267-271.

Taylor, R.P., Strong, D.F., and Kean, B.F.
1980: The Topsails igneous complex: Silurian-Devonian peralkaline magmatism in western Newfoundland; Canadian Journal of Earth Sciences, v. 17, p. 425-439.

Thurlow, J.G.
1981: The Buchans Group: its stratigraphic and structural setting; Geological Association of Canada Special Paper 22, p. 79-90.

Wessel,, J.M.
1975: Sedimentary Petrology of the Springdale and Botwood Formations, Central Mobile Belt, Newfoundland, Canada; unpublished Ph.D. thesis, University of Massachussetts, 216 p.

Whalen, J.B. and Currie, K.L.
1983: The Topsails igneous terrane of western Newfoundland; in Current Research, Part A, Geological Survey of Canada, Paper 83-1A, p. 15-23.

Williams, H.
1967: Silurian rocks of Newfoundland; Geological Association of Canada, Special Paper no. 4, p. 93-137.

PRECAMBRIAN SYENITIC PLUTONS, CENTRAL METASEDIMENTARY BELT, GRENVILLE PROVINCE OF QUEBEC

Project 760061

L. Corriveau[1]
Precambrian Geology Division

Corriveau, L., Precambrian syenitic plutons, Central Metasedimentary Belt, Grenville Province of Quebec; in Current Research, Part A, Geological Survey of Canada, Paper 85-1A, p. 165-174, 1985.

Abstract

The Mont Laurier area in the Central Metasedimentary Belt, embraces an igneous province of Precambrian potassic intrusions of alkaline affinity. Their rock associations include syenite, monzonite, diorite and biotite pyroxenite. Nepheline syenite or quartz syenite are usually minor components. The contact zones of the Kensington, Cameron, Gracefield and Lac Rouge plutons, located in the western part of the Metasedimentary Belt are characterized by heterogeneous syenite mixed with clinopyroxene-rich inclusions or patches. Country rocks adjacent to these zones are typically rich in calc-silicates. Emplacement of these plutons postdates the regional metamorphism and deformation, the latter being deflected around them. Dykes of syenite or pyroxenite and mafic veins associated with these plutons crosscut the country rock structure.

Résumé

La région de Mont-Laurier, située dans la zone métasédimentaire Centrale, abrite toute une série précambrienne de plutons potassiques de nature alcaline. Aux syénites qui constituent la majeure partie de ces plutons, sont associées des monzonites, des diorites ainsi que des pyroxénites à biotite. Les syénites à néphéline ou à quartz sont des éléments secondaires. Une unité syénitique très hétérogène qu renferme des domaines mafiques riches en clinopyroxène caractérise les contacts des plutons de Kensington, Cameron, Gracefield et Lac-Rouge, situés dans la partie ouest de la zone. Les roches encaissantes contiguës à ces zones se composent habituellement de calcsilicates. La mise en place de ces plutons est postérieure au métamorphisme et à la déformation régionale et les structures dues à ces phénoménes sont deviées autour des plutons. Des dykes de syénite ou de pyroxénite et des veines mafiques recoupent, par endroits, les structures des roches encaissantes.

[1] Department of Geological Sciences, McGill University, Montreal, Quebec H3A 2A7

Introduction

Study of a cluster of plutons of syenite and related alkaline mafic rocks in the Mont Laurier area, Quebec (Fig. 22.1), began in 1983, and initial findings were reported by Corriveau (1984). This paper presents the results of field work done in 1984 and petrographic studies on samples collected in 1983. Detailed geological maps have been made of four of these plutons: Kensington, Cameron, Gracefield and Lac Rouge. Particular attention was paid to the Kensington pluton, a petrochemical study of which will form the core of a Ph.D. thesis by the author at McGill University under the supervision of R.F. Martin, R. Doig and D. Francis. Field assistance was provided by Philippe Garneau. This study follows an initial assessment of the distribution of different types of plutonic rocks in the Central Metasedimentary Belt (Britton, 1979), and is part of an on-going study of this topic.

Kensington pluton

Field relationships

The Kensington pluton east of Maniwaki (Fig. 22.2) offers the largest variety of rock types among the potassic intrusions of the Mont Laurier area. It is an east-trending, ovoid body composed of five distinct plutonic phases intruded in the following order: (1) a crescent-shaped body (15 km^2) of pink, homogeneous, leucocratic syenite, in part recrystallized, occupies the western part of the pluton; an heterogenous phase occurs at the margin of much of this body; (2) an oval shaped intrusion of grey monzonite, diorite and pyroxenite forms most of the remainder of the pluton. The mineralogy of these three types is related and is quite different to that of the leucocratic syenite and its partial heterogenous envelope. Each type forms a mappable body, as follows: a) a marginal, crescent shaped body (6.5 km^2) of monzonite with a somewhat variable biotite and clinopyroxene content, that wraps around the west end of b) a biotite-bearing diorite body (11.6 km^2) with variable colour index; and c) a small, irregular body (0.6 km^2) of massive biotite pyroxenite that occupies the northeast extremity of the pluton; (3) an irregular mass (1.2 km^2) of heterogeneous monzonite intrudes the monzonite and diorite near the centre of the pluton.

Dykes and cognate inclusions are sporadically distributed throughout the pluton except in the central and eastern part of the diorite mass where they are numerous. The syenite crescent has many country rock xenoliths and a few inclusions and dykes of porphyritic syenite. No dykes associated with the pluton were found within the marginal country rocks. An heterogeneous syenitic to monzonitic phase containing diffuse, clinopyroxene-rich inclusions is found close to the outer contact of parts of the pluton, and also in the western syenite crescent adjacent to the monzonite unit. A similar rock forms a small crosscutting intrusion within the monzonite and diorite units. Along the western contact of the syenite the outer margin of this zone locally contains country rock xenoliths whose metamorphic foliation and layering is roughly parallel with the contact. The predominant xenolithic rock is marble, but xenoliths of quartzite, calc-silicate, metapelitic and quartzofeldspathic gneiss are also present. Zoned veins of clinopyroxene with or without amphibole, feldspar, titanite, calcite and scapolite cut across the contact zone and in places replace syenite.

The country rocks consist of impure quartzite with feldspar and biotite, intercalated with rusty quartzofeldspathic gneiss, biotite gneiss, massive diopsidite and pelitic gneiss. Granitic rocks occur near the western part of the pluton. They are massive or foliated, with variable grain size, and contain augite, titanite, biotite and magnetite. They locally include some massive calc-silicate. Marble predominates one-half kilometre from the pluton.

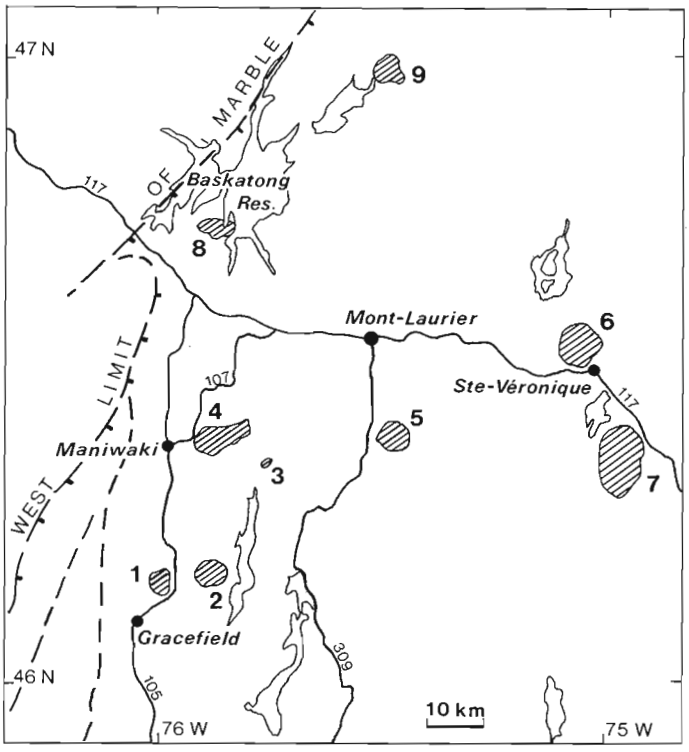

1. *Gracefield*
2. *Cameron*
3. *Satellite*
4. *Kensington*
5. *Lac-Rouge*
6. *Ste-Véronique*
7. *Loranger*
8. *Baskatong*
9. *Piscatosin*

Figure 22.1 *Location of syenitic plutons in the Mont Laurier area.*

Foliation and layering in the country rocks tend to be concordant with the contact of the pluton. Macroscopic isoclinal folds are common and have steeply plunging fold axes. Small, steep shear zones, some containing mylonite, occur near the pluton, and may be related to its emplacement. They are a few millimetres in width and can be traced for a few metres within marble; one shear zone a metre wide deforms a pegmatite dyke. Planar and linear structures in sheared marble east of the pluton are steeply inclined to the east, and C-and-S fabrics give a normal sense of displacement.

Internal structure

The Kensington pluton presents a coherent distribution of steeply dipping foliation formed by feldspar laths, that defines a crescentic pattern generally concordant with the internal contact between the different units. Disorder in this pattern occurs in the northwest part of the diorite body where it pinches out within the monzonite, and in the central and eastern parts where a generally northeast trend prevails. The pyroxenite body is massive. Megascopic discordances between units are present locally. For example, foliation in the syenite unit and its heterogeneous border phase appears to be crosscut by the southwestern apophysis of monzonite. The foliation that is common to both the monzonite and diorite units appears to cut across the southwest part of the contact between them. The pyroxenite body and its related dykes crosscut foliation within the adjacent diorite. At megascopic scale, foliation within the diorite is crosscut by

the heterogeneous monzonite body, which itself carries a foliation parallel to its contacts in the narrow, south-extending arm of this body.

The foliations within the plutonic rocks are considered to be of primary igneous origin, related to emplacement. They are modified by post-consolidation recrystallization, particularly in the monzonite apophysis and in parts of the syenite crescent. In addition, rocks of most units contain rare shear zones that can be traced for a few metres.

Petrography

The pink syenite of the western crescent is homogeneous, relatively leucocratic (CI 8 ± 5), and commonly massive. It is composed chiefly of 6-10 mm subhedral mesoperthite grains, in places rimmed by granular plagioclase and in places recrystallized to fine, granular aggregates of microcline and oligoclase. It contains a few per cent anhedral clinopyroxene and/or hornblende; the clinopyroxene is partly or wholly replaced by hornblende, which may be intergrown with a little quartz. Magnetite, ilmenite, titanite, pyrite, euhedral zircon and REE-bearing minerals are accessory, and a little secondary epidote and chlorite are present locally. Green biotite is associated with hornblende in the outer part of the syenite body.

The grey monzonite (CI 17 ± 9) is composed of subhedral perthite in up to 1 cm laths and varying proportions of smaller grains of plagioclase, biotite and clinopyroxene with accessory apatite, magnetite and ilmenite. Plagioclase shows diffuse zoning, includes clinopyroxene and apatite grains, and may be overgrown by alkali feldspar. Clinopyroxene is colourless to pale green in thin section, rarely displays diffuse colour zoning, and includes euhedral apatite and opaque oxide grains. It has coronae of amphibole, or is replaced by amphibole-quartz symplectite. Brown biotite occurs in flakes that include small apatite euhedra, contrasting with larger, subhedral apatites elsewhere in the rock. This relationship between biotite and apatite, also found in the diorite and pyroxenite phases, rules out a post-magmatic origin for the biotite, such as its formation through metasomatic or metamorphic processes. This igneous biotite is commonly surrounded by incomplete, narrow rims of titanite or opaque oxide, suggesting that it is a primary igneous phase that began to react with intergranular fluid during crystallization. A second generation of biotite cuts across these rims in some rocks, and also partly replaces the feldspars, clinopyroxene and its amphibole rims. Other secondary features include weak recrystallization of the feldspars, and the formation of titanite or biotite coronae around opaque oxides. Plagioclase grains show undulose extinction and bent twin lamellae, and are weakly sericitized or saussuritized. In the southwestern apophysis of monzonite, the intensity of recrystallization appears to increase toward the syenite crescent. Laths of alkali feldspar disappear through recrystallization, and clinopyroxene is completely replaced by biotite. These features are not present in the monzonite crescent along its contact with syenite north of the apophysis. Within the main monzonite crescent, minor heterogeneities consist of variation in colour index and mineral proportion, and are usually gradual and diffuse. Layering was observed at two localities, but has no more than a few metres lateral extent. Lack of layering, in fact, is the rule for all the plutonic phases.

The diorite is dark grey, relatively homogeneous, medium grained and mesocratic (CI 40 ± 10). It is composed of subhedral zoned andesine, clinopyroxene (zoned salite) and brown biotite, with accessory apatite, magnetite and ilmenite. Scattered laths of alkali feldspar occur in a few places, marking a link with the monzonite. Melanocratic and leucocratic phases are dispersed throughout the body and do not have a coherent distribution. Weakly preferred orientation of biotite and plagioclase laths commonly gives a weak foliation, although in a few places this is strongly developed. The microscopic texture and mineralogical relationships are similar to those of the monzonite.

The pyroxenite is massive, medium grained, fairly homogeneous and contains the same mineralogy as the diorite. The dominant clinopyroxene is usually weakly zoned, but shows strong colour zoning locally, with zones parallel to annular trains of opaque inclusions. It is subhedral and set in a subordinate groundmass of biotite and poikilitic plagioclase. Large poikilitic biotite flakes occur in places.

The heterogeneous monzonite is generally massive and has a colour index varying around 20. Subhedral to euhedral alkali feldspar in up to 1 cm laths are set at random in an hypidiomorphic matrix of clinopyroxene and plagioclase. Titanite, apatite, biotite, pyrrhotite, scapolite, epidote and calcite are accessory or secondary phases. This unit varies a great deal, from fine to coarse, and from syenitic to clinopyroxene-rich, over tens of centimetres. Variable zones are widely dispersed throughout the body, but are more concentrated near its western margin. This unit is similar to the heterogeneous marginal zone of the syenite crescent, and to other mixed rocks at or near the outer contact of the pluton, to which it may be related.

The main rock of the heterogeneous marginal zone of the syenite body ranges between syenite and monzonite, and is replete with diffuse, segregation-like masses and sharply bounded xenoliths rich in clinopyroxene. All these varieties have basically the same mineralogy, varying only in proportions. In addition, zoned veins containing varying proportions of clinopyroxene, amphibole, green spinel, feldspars, titanite, scapolite, biotite, calcite and pyrrhotite cut this rock as well as the adjacent country rocks. The masses included in the syenite are commonly elongate and contorted, their size varies from a few centimetres to more than a metre, and their abundance from 10 to 50 per cent. Other types of inclusions are rare, but include marble and interlayered calc-silicate and quartzite, the latter being injected by white syenite with minor clinopyroxene and titanite within a few tens of metres of the contact. In a few places are found cauliflower-like masses with clinopyroxene-rich margins grading inward to syenitic or monzonitic cores surrounded by clinopyroxene-plagioclase rims that may contain epidote and scapolite. Calcite may fill embayments in the syenitic cores, rimmed by garnet, amphibole or epidote.

Dykes

Numerous dykes occur within the Kensington pluton. Four categories are recognized: (1) dykes of pyroxenite, diorite and heterogeneous monzonite that are directly equivalent to plutonic phases; (2) dykes of texturally different but likely petrogenetically related rocks; (3) composite dykes of fine grained diorite injected with syenite, quartz syenite and aplite veins; (4) pegmatite and aplite dykes. The first two categories are dykes directly related to and occurring only within the Kensington pluton, whereas the other two are widespread throughout the Mont Laurier area. One small, east-trending diabase dyke was found within the country rock.

In the northeast part of the pluton, pyroxenite dykes constitute as much as one half of the exposures within a kilometre of the pyroxenite body, but become less numerous to the west. They are found as far west and southwest as the monzonite body, but were not observed within the syenite, nor in the country rocks. The pyroxenite dykes are straight, vertical, a few centimetres to several metres wide, and trend northeast. Dykes of medium grained diorite with stubby

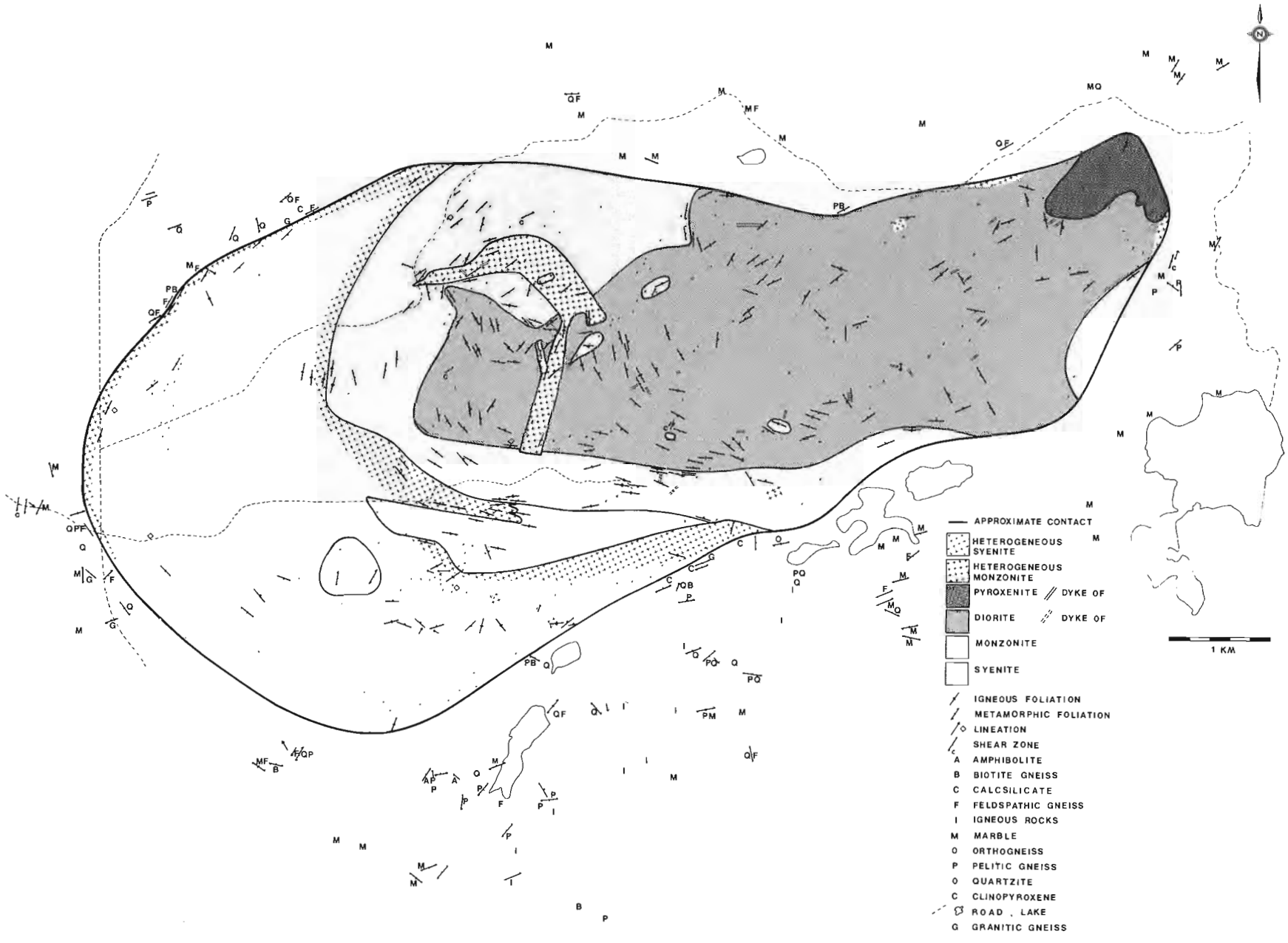

Figure 22.2. *Geology of the Kensington pluton.*

plagioclase crystals, like the diorite of the main mass, occur within the adjacent monzonite and are oriented at high angles to the contact between these two units. Dykes of heterogenous monzonite are found in all adjacent units, although relationships within the syenite crescent are not clear. None of these dykes have chilled margins, suggesting that they are all syn-plutonic. That they do not occur within the surrounding country rocks suggests that the mechanical properties of these rocks, particularly the marble, may have inhibited dyke formation at the time the pluton was emplaced.

Dykes of the second category, also consisting of pyroxenite, diorite and monzonite, as well as syenite, are not evenly distributed within the pluton. Few dykes were observed within the syenite crescent, and those that do occur consist essentially of pink syenite. A few dykes of syenite and meladiorite with poikilitic plagioclase crystals were observed within the pyroxenite body. Dykes of fine grained diorite, coarse grey syenite, and pyroxenite devoid of biotite are present within the heterogeneous monzonite body. The central part of the diorite mass is characterized by numerous dykes of diorite of different textures and grain size, and by a few coarse, grey, porphyritic syenite dykes. The most common phase is diorite with characteristic equant clinopyroxene grains, 2 mm in size, scattered in a fine grained granular matrix. Another phase of diorite has large poikilitic plagioclase crystals that appear partly deformed and recrystallized. There is one small mass of massive mafic rock near the southern edge of the diorite mass that contains large, non-oriented, poikilitic biotite flakes that enclose olivine and clinopyroxene grains. Other than this example, preliminary thin section examination of the first two categories of dykes shows that they contain the same suite of minerals and the same order of crystallization as the plutonic rocks they intrude.

The fine grained diorite of the composite dykes consists of 2-5 mm plagioclase phenocrysts with irregular borders, diffuse zoning and sericitized cores, dispersed in a very fine grained matrix of granular plagioclase, hornblende, magnetite and apatite. Some fine grained dykes are lamprophyric, with phenocrysts of clinopyroxene and/or biotite. The late pegmatites are essentially composed of quartz and microcline; traces of fluorite and molybdenite were observed locally. These pegmatites are not obviously related to the pluton.

Sequence of intrusion

The sequence of intrusion in the Kensington pluton is deduced from contact relationships between the various phases and dykes, bearing in mind that distinction between dykes of the first and second categories described above is critical. It is clear from field relationships (Fig. 22.2) that the heterogeneous monzonite body is younger than the monzonite and diorite masses, and from crosscutting relationships of dykes of the first category that the pyroxenite is younger than the diorite which in turn is younger than the monzonite. Age relations between the pyroxenite and heterogeneous monzonite are not known; despite the fact the the latter is cut by pyroxenite dykes, this pyroxenite is different in texture to that which forms dykes within the monzonite and diorite farther east.

The relative age of the syenite mass is hard to ascertain. This body appears to be devoid of either dykes or inclusions of monzonite, diorite and pyroxenite, but although syenite dykes are present within the more mafic units to the east, they do not have the same appearance as the syenite of the crescent. Critical in this relationship is the interpretation that an apophysis of monzonite intrudes the syenite crescent. This interpretation is based on the facts that the monzonite transects the syenite's heterogeneous border zone, and that its southern contact is locally discordant to foliation in the adjacent syenite. This crosscutting relationship is in accord with the textural interpretation that the syenitic crescent, being the most recrystallized body, is the earliest phase emplaced at the present level. Monzonite in the apophysis, however, also appears recrystallized. The relationship between the monzonite of the apophysis and of the main monzonite crescent to the north is uncertain; petrographic work may show whether the two are different, or whether the one is a more recrystallized equivalent of the other. Another uncertainty concerns the possibility that the heterogeneous monzonite body and the heterogeneous border zone of the syenite crescent may be related; they are certainly similar in appearance and mineralogy.

Cameron pluton

Field relationships

A variety of pink and grey syenites characterizes the Cameron pluton, an equant body 6 km in diameter centred 15 km northeast of Gracefield (Fig. 22.3). Except for one unit, the various syenites seem to grade into one another; in contrast to the Kensington pluton, no crosscutting relationships were observed. Five types of texturally and/or mineralogically different syenitic rocks are recognized: (1) pink, leucocratic syenite is characteristic of the outer margin, but occurs sporadically elsewhere in the northern part of the pluton; (2) a similar pink syenite, but carrying large biotite flakes, is also found in the marginal zone, but is more common in the central parts; (3) coarse, grey syenite is particularly well exposed in the southwest part of the pluton, where it apparently occludes the marginal pink phase, but is also common in the central and eastern parts; (4) medium grained, hypidiomorphic-granular syenite occurs in various places; (5) medium grained, pink, amphibole-bearing quartz syenite occurs as a large dyke cutting the coarse grey syenite in the south-central part of the pluton, but its relationship to the other pink syenites is not known. In addition, heterogeneous syenite with inclusions of country rock and clinopyroxene-rich rock are found along the outer contact of the pluton. The coarse, grey syenite contains rare inclusions of pyroxenite; in places decametric zones of melasyenite occur within this unit, appearing to either grade into or crosscut the normal phase. Figure 22.3 shows the observed distribution of the above rock types.

The outer contact of the pluton is sharp, and closely defined at several places. Massive diopsidite or pale green amphibolite layers of variable thickness intercalated with pyroxene-bearing quartzite and gneiss occur in a consistent way at the contact of the intrusion. These calc-silicate rocks have similar mineralogy to the heterogeneous syenite found close to the contact. This spatial association, also found at the contacts of other plutons in the Mont Laurier area, does not appear to be fortuitous, although similar rocks do occur locally within the metasedimentary gneisses at some localities removed from any exposed intrusions. Quartzite and quartz-rich gneiss with minor biotite, quartzofeldspathic and pelitic gneiss are the most abundant country rock types, but marble is present along the northeast and east sides. Planar structures in the country rocks wrap the pluton. They dip steeply toward it on the west side, away from it on the east side, and are essentially vertical along the north and south contacts. There is no evident formation of a new foliation or increase in the intensity of deformation as the contact is approached. Pegmatites in the country rocks vary from strongly foliated and lineated to essentially non-deformed. Although the pluton is wrapped by the country rock structure, the restriction of marble to the northeast suggests that the pluton lies astride the regional structure as defined by major metasedimentary units.

Internal structure

Foliation and lineation, whether due to igneous or recrystallization processes, are poorly or not at all developed in most of the Cameron pluton. Those observed close to the contact are parallel or subparallel to it and dip steeply outward. In the south-central part of the pluton there seems to be no relationship in orientation to the contact, or to the distribution of the various rock types. The somewhat irregular distribution of the pink and grey syenites and the absence of obvious crosscutting relationships between them, except for the large quartz syenite dyke, prompted a search for a more coherent pattern within the intrusion. At megascopic scale there appears to be a gradational variation in the distribution of the grey syenitic rocks, giving a pattern consisting of an eccentric core of more mafic, grey, clinopyroxene-bearing syenite that grades outward to a more leucocratic, pink, amphibole-bearing phase. This pattern is complicated by the presence of a crescent shaped area of pink syenite within the grey syenite. The limits shown in Figure 22.3 serve only to visualize gradations from a

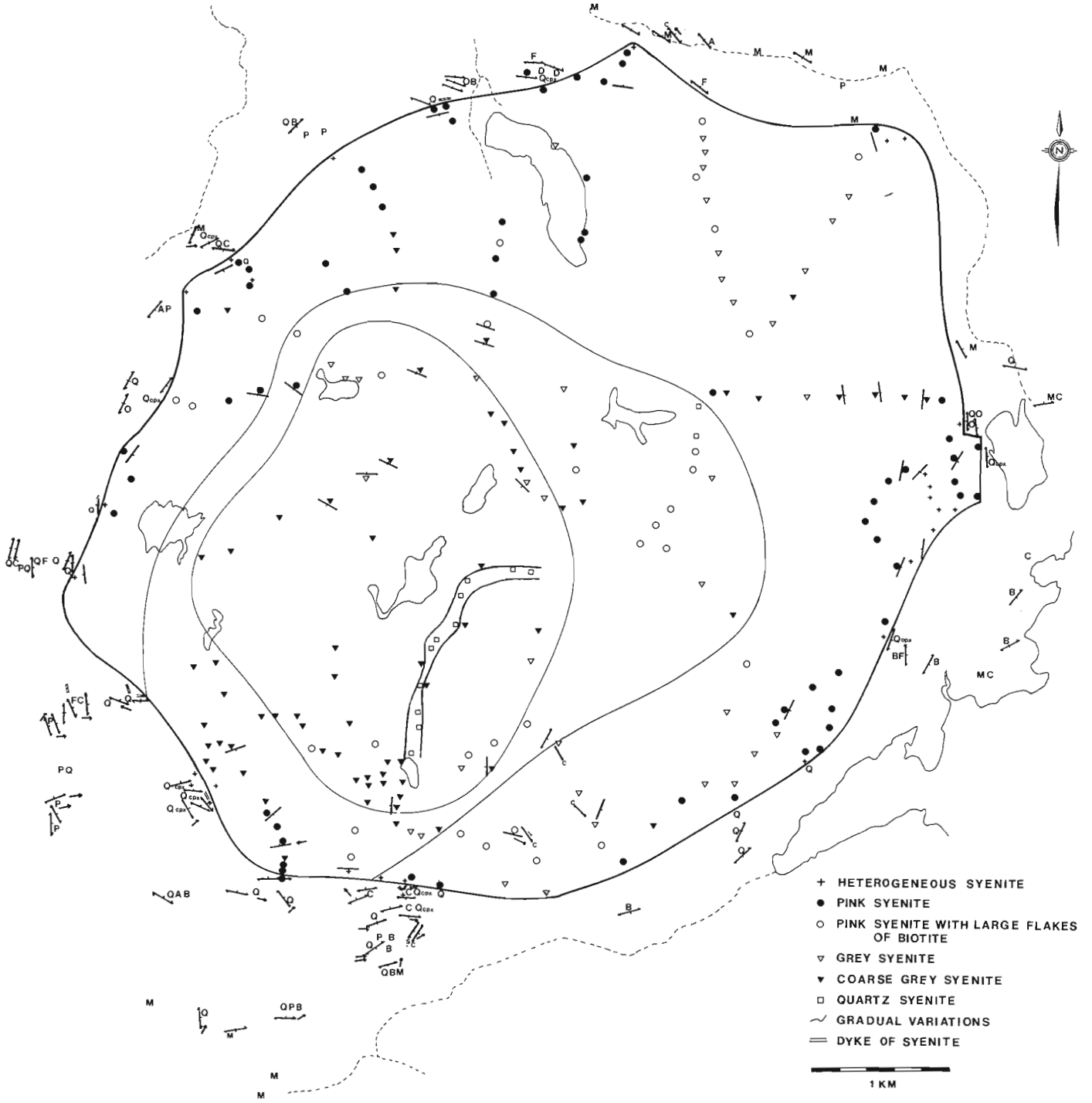

Figure 22.3. *Geology of the Cameron pluton. Symbols described in Figure 22.2.*

hornblende-bearing outer zone to a clinopyroxene-bearing core separated by a zone in which both mafic minerals occur; they should not be interpreted as contacts. Variations in texture and colour are probably due in large part to recrystallization processes, although the variation in colour index and composition is probable magmatic.

Small shear zones with mylonite occur in the southern part of the pluton. They trend either northeast or northwest and are between 1 and 10 cm wide. One of these shear zones deforms a late pegmatite dyke.

Petrography

Syenites of the Cameron pluton exhibit a spectrum of textures and mineralogical proportions. The two varieties of grey syenite differ mainly in grain size, and consist of stubby crystals of finely exsolved perthite dispersed in an hypidiomorphic groundmass of pale green clinopyroxene, reddish brown biotite and opaque oxide. Apatite grains are included in all these minerals. Plagioclase is minor and usually included in the perthite grains. Secondary minerals include minor biotite and titanite as rims around opaque grains, and local amphibole coronae around clinopyroxene. Limited recrystallization is shown by perthite, in the form of sutured grain boundaries and some sub-grain development.

The pink syenites are, in contrast, amphibole bearing. They show much more evidence for recrystallization. Chessboard-textured alkali feldspar has a variable grain size. Hornblende is anhedral, includes rare remnants of clinopyroxene, and is partly replaced by brown biotite. Individual biotite grains are subhedral and have ragged edges. Iron oxide grains have titanite rims and may be surrounded by biotite. Other accessory minerals are apatite and rare zircon; traces of secondary epidote occur locally.

Buff-weathering quartz syenite forms a dyke up to 50 m wide in the south-central part of the pluton. Although contacts were not observed, this unit appears to be the only distinctly later intrusive phase within the pluton. The main mafic component is green-brown amphibole that contains a few, small cores of clinopyroxene; biotite is subordinate. Quartz is variable in content, molded euhedral feldspar grains in quartz-poor rocks, but forming individual, rounded grains that are somewhat strained in rocks whose composition approaches that of granite. Opaque oxides and apatite are accessory.

Although the grey pyroxene syenite and the pink, leucocratic hornblende syenite are superficially different, there is an obvious correlation between colour, degree of replacement of clinopyroxene by hornblende and biotite, and degree of feldspar recrystallization. That there are no sharp or intrusive contacts between these rocks, except for the quartz syenite dyke, suggests that the Cameron pluton developed in situ from a single pulse of intrusive magma.

Clinopyroxene-rich inclusions, locally amounting to pyroxenite, have similar mineralogy and texture to the grey pyroxene syenite, except that the feldspar component is intersertal, plagioclase has the form of small, hypidiomorphic grains, and clinopyroxene has a marked, though diffuse, zoning. A very few samples of syenite collected from the centre of the pluton contain either orthopyroxene or brown amphibole; the relationship of these rocks to the predominant clinopyroxene-bearing syenite is not known. Heterogeneous syenitic rocks of the outer contact zone are similar in texture and mineralogy to those described for the Kensington pluton.

Dykes, veins and inclusions

Dykes of porphyritic syenite and quartz syenite crosscut the country rocks as well as the plutonic rocks. They have straight contacts, are up to a metre wide, and do not exhibit chilled margins. Where present, igneous foliation is parallel to the dyke walls. Irregular veins of syenite containing clinopyroxene and titanite invade calc-silicate rocks and clinopyroxene- or orthopyroxene-bearing quartzite immediately adjacent to the contact. Veins rich in clinopyroxene, amphibole and/or titanite replace the syenite as well as the country rocks, in places in spectacular fashion.

Brief comments on other syenite plutons

Gracefield

This pluton contains nepheline-bearing rocks and has been mapped as consisting of two syenite intrusions, one within the other (Durocher, 1977; Corriveau, 1984). New mapping reveals that nepheline syenite is not a phase of the outer syenite (syenite I), but occurs as two dyke-like masses that appear to crosscut this syenite and the country rocks (Fig. 22.4). The outer contact zone and to some extent the contact between syenites I and II are marked by heterogeneous rocks with well defined to diffuse inclusions rich in clinopyroxene. These inclusions have a centimetre-thick clinopyroxene selvage in sharp contact with the enclosing syenite, but grade inward to a feldspar-bearing core. Veins and cauliflower-like masses rich in clinopyroxene also occur at the contact.

Like the Kensington and Cameron plutons, foliation in the country rocks wraps around this pluton, dipping steeply toward it on the west and south and away from it on the north and east sides. Igneous foliation within the pluton, defined by oriented feldspar laths, is steeply dipping but does not form an obvious pattern. Later shear zones, some with mylonite, are common along the western margin of the pluton. These trend northeast, are steep, and carry a moderately plunging northeast lineation. Sense of displacement appears to be northeast side down.

Lac Rouge

The outline of this almost circular pluton, 5 km in diameter, is for the most part defined by its positive aeromagnetic anomaly and low topographic expression. Only twenty outcrops were found, most of them near the southwest contact (Fig. 22.5). Outcrops consist of coarse grained syenite, in places well foliated, except close to the contact where the rocks are heterogeneous, though not as rich in clinopyroxene as in the contact zones previously described. The country rocks close to the contact are granitic gneiss, amphibolite and clinopyroxene-bearing quartzite. Foliation in these rocks is steep and, as around the other plutons, parallel to the contact.

Baskatong

This pluton was not described in the previous report by Corriveau (1984). It is even more poorly exposed than the Lac Rouge pluton, and like that pluton can only be outlined on the basis of its aeromagnetic anomaly. Three types of plutonic rocks were encountered, among which monzonite predominates. The monzonite is either massive with idiomorphic feldspars and similar to the monzonitic phases of the Loranger pluton, or it deformed and recrystallized. In the latter case, biotite and amphibole define a variably developed metamorphic foliation that trends northeast. Two outcrops of well preserved, medium grained, pink to grey syenite occur at the centre of the aeromagnetic anomaly.

This rock is composed of alkali feldspar megacrysts up to 1 cm in size with interstitial amphibole, biotite, apatite, magnetite, titanite and clinopyroxene. On an island in Baskatong Reservoir at the northeast side of the anomaly, well preserved, medium grained, lilac-grey diorite is exposed, comprising plagioclase, clinopyroxene partly replaced by amphibole, biotite, magnetite and apatite; plagioclase euhedra reach a size of 1 cm. The mafic minerals locally define an igneous foliation. A wide range of dyke rocks is associated with this body. Dykes of both melano- and highly leucocratic diorite, monzonite, composite diorite-syenite, and fine grained grey diorite were observed. Contrary to the interpretation of Jacoby (1975, p. 20), these rocks are not metamorphosed; they resemble rocks of the Kensington pluton. Contacts of the pluton and the adjacent country rocks are not exposed.

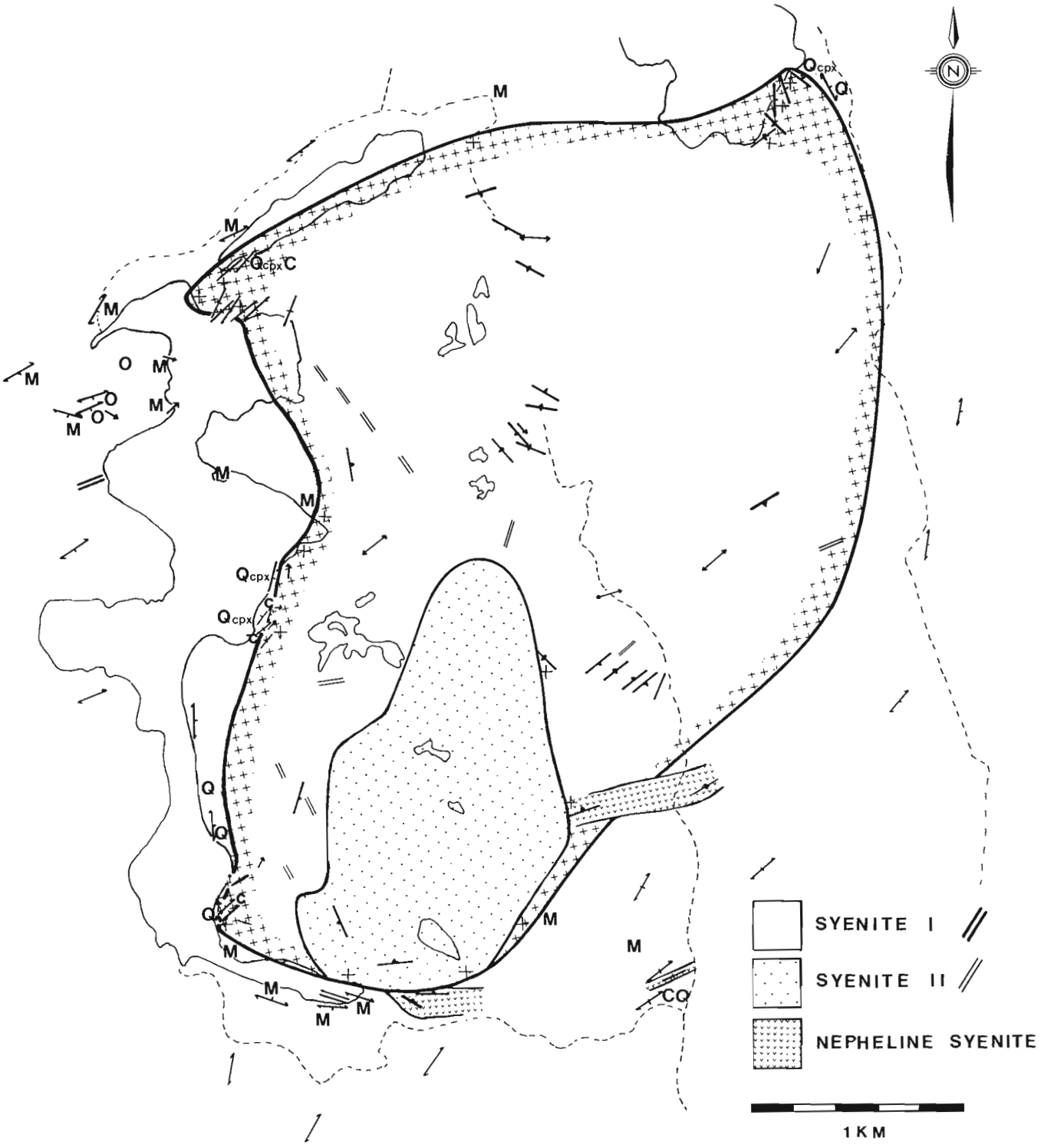

Figure 22.4. *Geology of the Gracefield pluton, modified after Durocher (1977). Symbols described in Figure 22.2.*

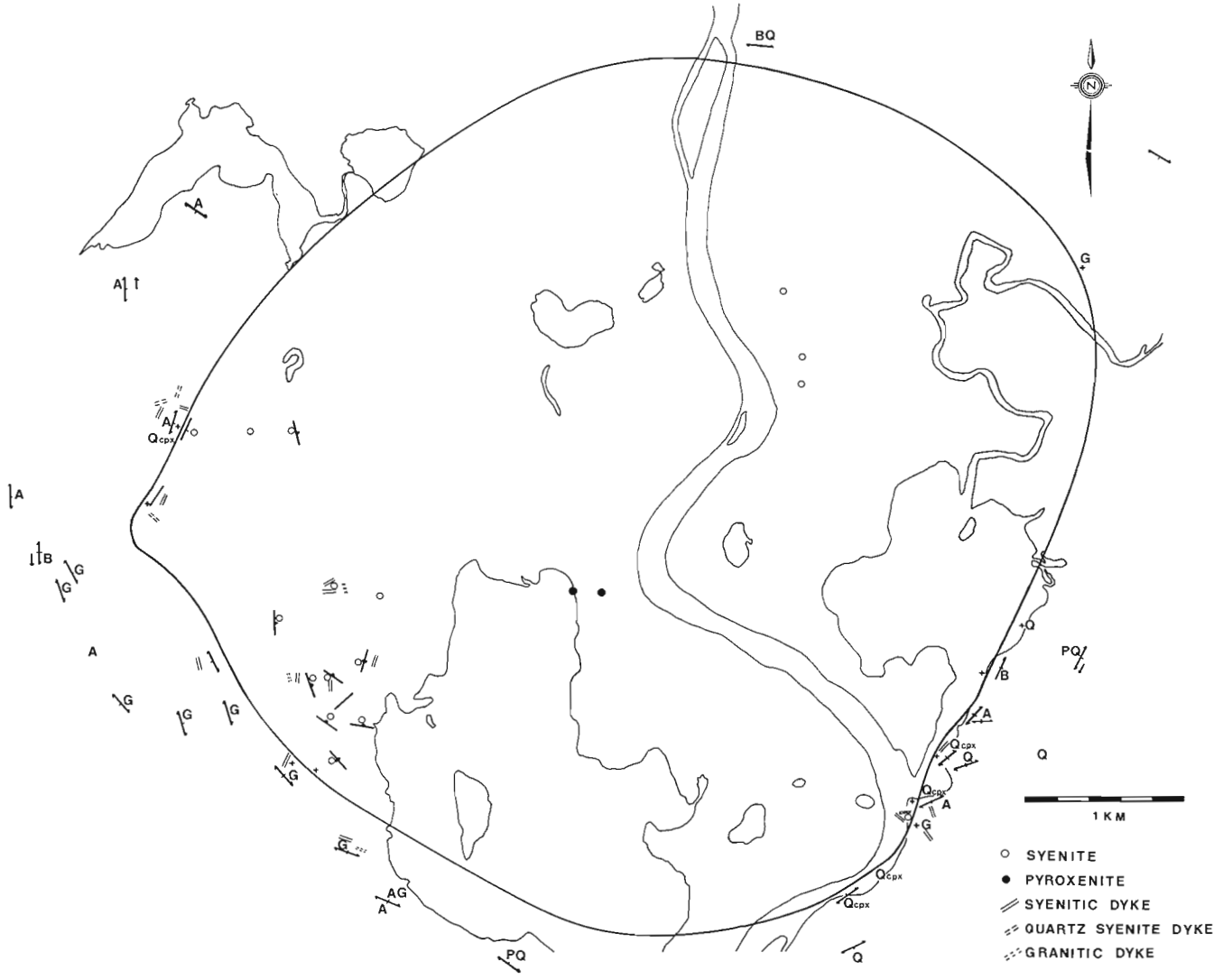

Figure 22.5. *Geology of the Lac-Rouge pluton. Symbols described in Figure 22.2.*

Like the Baskatong pluton, the Piscatosin pluton (9, Fig. 22.1) is poorly exposed and was not examined during this study.

Summary

This work contributes further documentation and understanding of the potassic plutons of alkaline affinity, first recognized by Wynne-Edwards et al. (1966) as a distinctive cluster of nine plutons in the Mont Laurier area. Their combined rock association includes biotite pyroxenite, diorite, monzonite, mela- to leucosyenite, and minor quartz or nepheline syenite. Their igneous crystallization sequence is clinopyroxene (mainly salite), apatite, titano-magnetite, plagioclase (andesine to oligoclase), alkali feldspar and biotite, but biotite may have started to crystallize before plagioclase in the more mafic rocks. Titanite, zircon and REE-bearing minerals are accessory in the more felsic rock types. Amphibole, some titanite and biotite are secondary reaction products around clinopyroxene and titano-magnetite, related to cooling from igneous temperatures rather than to later prograde metamorphism. In these alkaline rocks, potassium prevails over sodium, judging by the absence of minerals such as aegirine-augite and sodic amphibole (and even hornblende from the primary crystallization sequence), and the abundance of late biotite (though not muscovite). Most units show good preservation of primary igneous features such as flow foliation and zoning in plagioclase and clinopyroxene. The presence of gabbro and quartz monzonite, the dominance of monzonite, and the absence of biotite pyroxenite in the Loranger and Baskatong plutons raises some doubt regarding their relationship to the other, more clearly potassic alkaline plutons. The Loranger and Baskatong plutons may have been emplaced earlier than the other plutons, as their monzonitic phases are commonly more highly deformed. This interpretation would have to be verified by radiometric age determinations.

Another feature characteristic of most of the plutons is the presence of heterogeneous syenite zones close to the outer contacts and also internally between some units; this feature is particularly well developed in the southwestern plutons where marble and calc-silicate rock are common among the country rocks. Pyroxene-rich segregations and/or

inclusions in the heterogeneous syenite, and veins of similar material both within the plutonic and adjacent country rocks seem to be related to the proximity of calcareous rocks. Clinopyroxene-bearing quartzite and massive diopsidite associated with other calc-silicate rocks within the country rocks characterize narrow aureoles around the plutons. Although found elsewhere, such rocks are rare beyond the aureoles.

The potassic plutons intruded marble, quartzite, other forms of paragneiss and granitoid gneiss that were already highly deformed and metamorphosed to amphibolite or granulite facies. Lack of distinct metamorphic aureoles in rocks other than the calc-silicates just mentioned is probably due in part to the already relatively anhydrous state of the country rocks. The plutons and associated dykes of syenite and, at Ste.-Véronique, pyroxenite have clearly intruded the gneisses. The plutons have likely swelled in situ, pushing aside the gneisses to give a 'wrap-around' structure without superimposing a new foliation. Structures characteristic of diapiric emplacement were not observed. If in-place swelling occurred when some of the plutonic rocks were already essentially solid, it would account for the recrystallization encountered in many parts of the plutons and for the apparently insensible distribution and attitudes of primary igneous structures. Internal dykes related to specific plutonic phases suggest that intrusion continued after earlier phases had solidified; this would contribute to a swelling mechanism. Lack of chilled margins of both the main plutonic units and dykes within and beyond the plutons suggests that intrusion occurred at depth in a warm environment; this is supported by the occurrence of unrelated aplite and pegmatite dykes within the plutonic rocks. The fact that the plutonic rocks, particularly those near the sheared western margin of the Central Metasedimentary Belt (Fig. 22.1), contain post-consolidation shear zones with amphibolite facies minerals indicates that they are not entirely post-tectonic. Given that they are younger than the main imprint of deformation and metamorphism on the country rocks, late-tectonic would be the best label to apply to them.

References

Britton, J.M.
1979: Late-tectonic syenite and granite plutons of the Grenville Province of southwest Quebec and southeast Ontario; in Current Research, Part B, Geological Survey of Canada, Paper 79-1B, p. 163-166.

Corriveau, L.
1984: Account of field observations on rock units and structural features of the syenitic complexes of the Mont-Laurier area, Central Metasedimentary Belt of the Grenville Province; in Current Research, Part A, Geological Survey of Canada, Paper 84-1A, p. 303-306.

Durocher, M.E.
1977: Petrology of the Gracefield pluton; unpublished M.Sc. thesis, École Polytechnique de Montréal, 210 p.

Jacoby, R.
1975: Région du réservoir Baskatong; Ministère des Richesses naturelles du Québec, Rapport Géologique 167, 51 p.

Wynne-Edwards, H.R., Gregory, A.F., Hay, P.W., Giovanella, C.A., and Reinhardt, E.W.
1966: Mont Laurier and Kempt Lake map-areas, Quebec; Geological Survey of Canada, Paper 66-32, 32 p.

Rb-Sr GEOCHRONOLOGY OF THE NOBEL GNEISS AND MCKELLAR GNEISS, PARRY SOUND REGION, ONTARIO

K.M. Connare[1] and R.H. McNutt[1]
Precambrian Geology Division

Connare, K.M. and McNutt, R.H., Rb-Sr geochronology of the Nobel gneiss and McKellar gneiss, Parry Sound region, Ontario; in Current Research, Part A, Geological Survey of Canada, Paper 85-1A, p. 175-180, 1985.

Abstract

The Nobel granitic gneiss, located in the Britt domain gives a Rb-Sr whole rock age of 1330 ± 44 Ma with an initial $^{87}Sr/^{86}Sr$ value of 0.7033. This agrees with a previously published zircon U/Pb age and is interpreted as the time of intrusion of the unit. The McKeller gneiss, located in the Parry Sound granulite domain gives a Rb-Sr whole rock age of 1241 ± 12 Ma, interpreted as the time of Rb-Sr closure for the granulite grade metamorphic event.

Résumé

La datation de l'ensemble du gneiss granitique Nobel, situé dans le domaine Britt, donne un âge de 1330 ± 44 Ma; la valeur initiale du rapport $^{87}Sr/^{86}Sr$ est de 0,7033. Ce résultat concorde avec l'âge par la datation U/Pb du zircon déjà publié et correspond vraisemblablement au moment de l'intrusion de l'unité. La datation au Rb-Sr de l'ensemble du gneiss de McKeller, qui est situé dans le domaine des granulites de Parry Sound, donne un âge de 1241 ± 12 Ma, ce qui correspond vraisemblablement au moment de la fermeture Rb-Sr du métamorphisme ayant produit le faciès des granulites.

[1] Department of Geology, McMaster University, Hamilton, Ontario, L8S 4M1

Introduction

It is commonly found, when comparing the results of zircon U-Pb and Rb-Sr ages on high grade rocks, that the U-Pb method gives results significantly older than the Rb-Sr method (see for example Krogh and Davis, 1973). We present here the results of Rb-Sr age dating on the amphibolite grade Nobel gneiss and the granulite grade McKellar Gneiss from the Parry Sound region, Ontario. These results can be compared with the zircon U-Pb results of van Breeman et al. (1984). This report is part of a larger study on comparitive Rb-Sr and U-Pb geochronology of high grade metamorphic rocks.

Geological setting

The Parry Sound region has recently been the subject of reconnaissance mapping by Davidson and Morgan (1981) and Davidson et al. (1982) (Figure 23.1). They divided the region into several domains and subdomains based on differences in rock assemblages, metamorphic grade and structural style, separated by tectonic zones containing features of ductile deformation such as mylonite, boudinage and sheath folds. Davidson et al. (1982) interpreted the area to be stacked crust slices as a result of deep crustal thrusting with movement towards the northwest.

The Nobel gneiss is found at the eastern margin of the Britt Domain which consists of rocks of plutonic and supracrustal origin that have been deformed, metamorphosed and, in part, migmatized. These rocks were intruded by younger plutons that have also been deformed, metamorphosed and migmatized. One of these late-stage plutons is the Nobel gneiss.

The Nobel gneiss is an amphibolite grade, hornblende granite to hornblende quartz monzonite containing a tonalitic phase (Figure 23.2). It is composed of quartz, plagioclase, microcline and hornblende with minor biotite, sphene, allanite and zircon. Both hornblende and biotite show some alteration with biotite often showing iron oxide exsolution. Allanite is frequently opaque suggesting extensive destruction of the crystal structure by radioactivity.

The McKellar gneiss (Figure 23.3) is in the Parry Sound Domain, an area dominated by granulite grade mafic gneisses with subordinate marble and paragneiss. The McKellar gneiss is one of these mafic gneisses and is found in the central portion of the Parry Sound Domain occurring as one of several domal structures (Lacy, 1960). The immediately adjacent country rock is marked by the occurrence of marble (Figure 23.3). The other mafic gneiss units in the area appear

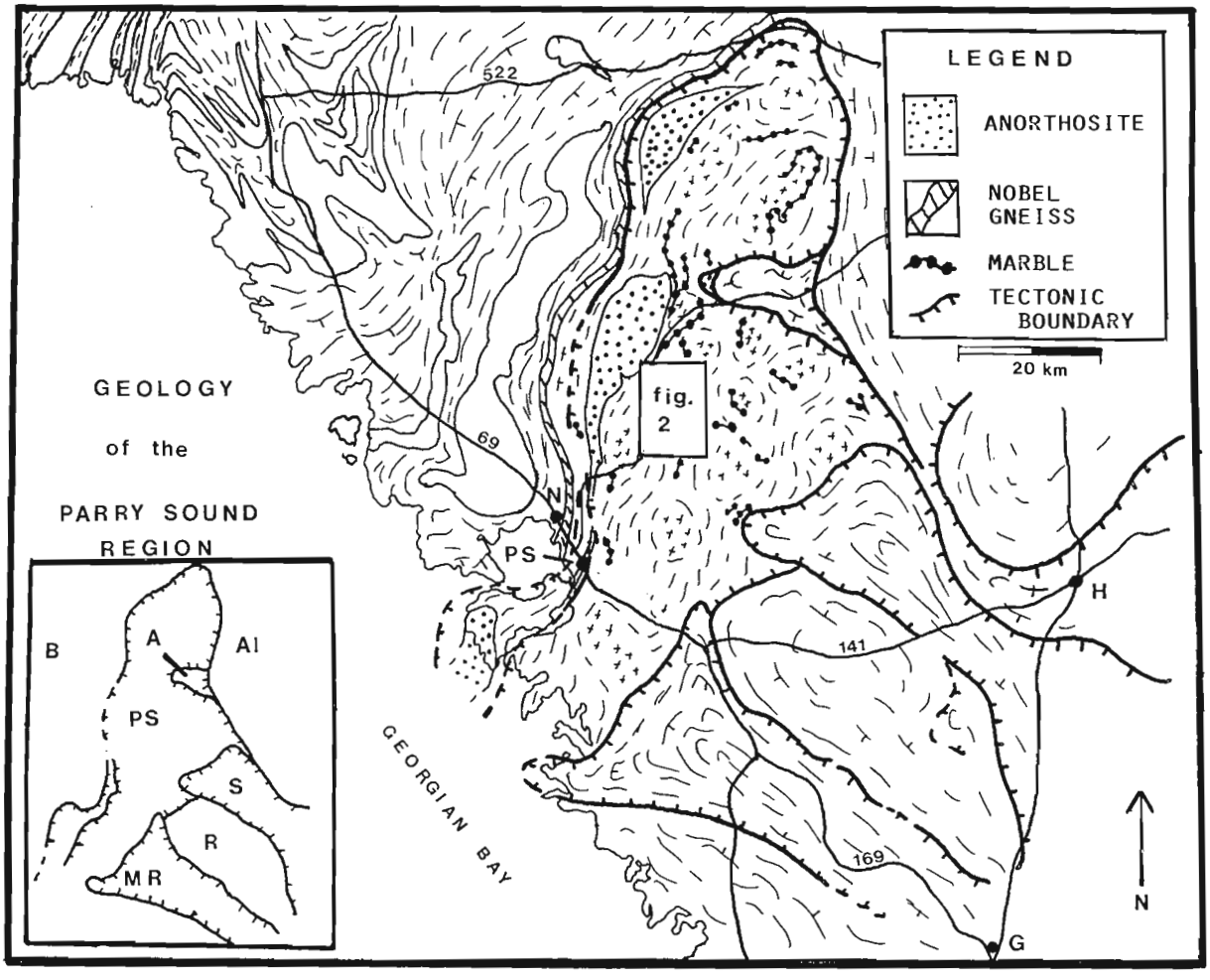

Figure 23.1. *Map of the Parry Sound Region. Abbreviations for the domains are as follows (see insert): A – Ahmic, Al – Algonquin, B – Britt, MR – Moon River, PS – Parry Sound, R – Rosseau, S – Sequin. On the Map: G – Gravenhurst, H – Huntsville, N – Nobel and PS – Parry Sound. Map modified after Davidson et al. (1982).*

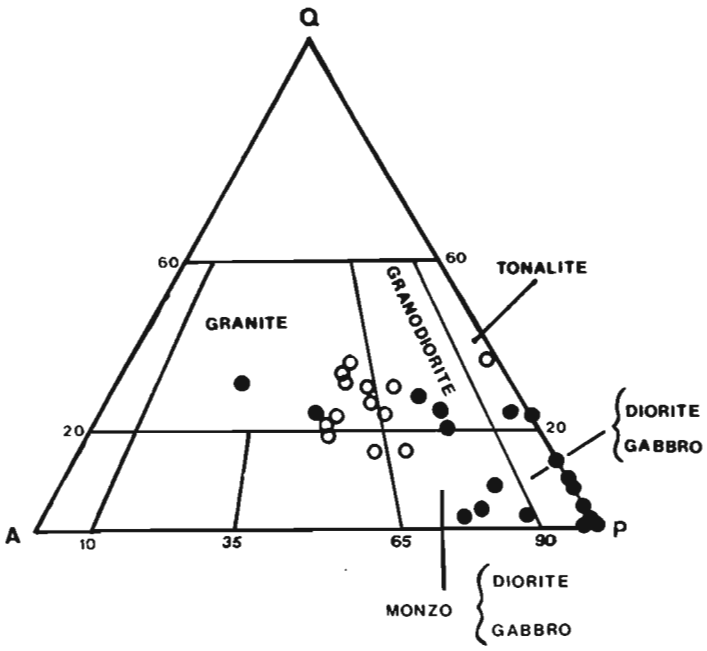

Figure 23.2. *Modal Analyses of the Nobel and McKellar Gneisses. Solid circles are McKellar, open circles are Nobel Gneiss.*

very similar to the McKellar gneiss and may prove to be essentially the same. We call such units McKellar-type gneiss.

The McKellar gneiss has a greasy-green colour typical of mafic granulites. Though it appears homogeneous in outcrop it has a variable composition and ranges from granite to diorite (Figure 23.2). Black mafic dykes are common and are of variable thickness. They have been metamorphosed along with the gneiss.

The samples collected for this study from the Parry Sound Domain have been divided into three groups:

1. The McKellar outcrop samples, consisting of fifteen samples from one outcrop located on Highway 124 near the village of McKellar. These form the basis of the geochronological study and have also been used for geochemical and petrographic analyses.
2. Ten samples collected regionally throughout the McKellar gneiss unit proper for geochemical and petrographic analyses.
3. Nine samples collected at, and away from, a shear zone located outside of and to the east of, the McKellar gneiss, but in McKellar-type gneiss. They were collected to determine what effect retrograde metamorphism had on the mineralogical and geochemical character of the McKellar-type gneiss.

The McKellar gneiss proper is composed of plagioclase, clinopyroxene, hypersthene, quartz, opaques and apatite. Potassium feldspar, hornblende, garnet and biotite may also be present. Plagioclase and potassium feldspar are frequently antiperthitic and perthitic, respectively. One sample from the McKellar Outcrop (MCGR-5) contains more than 40 per cent perthite. Hypersthene is rarely altered to a light brown mica.

The shear zone contains a pegmatite dyke, approximately two metres thick, emplaced before movement had taken place and now severely deformed. The core of the dyke is coarse grained with grain size decreasing towards the margin. This finer grained outer portion often contains rotated feldspar augens. Within a few metres of the shear zone, the McKellar-type gneiss has the typical granulite grade, greasy-green colour. Towards the shear zone, the rock undergoes a marked change in colour to black and white, reflecting the formation of hornblende from pyroxenes and the recrystallization of plagioclase. Foliation away from the shear zone is at a high angle but is deflected parallel within one metre of the contact.

The rocks collected furthest from the shear zone are composed of plagioclase, hypersthene, clinopyroxene and opaques with minor hornblende, apatite and biotite. Closer to the shear, the contents of plagioclase hypersthene, clinopyroxene and opaques decrease while quartz, hornblende and biotite increase. As the shear zone is approached the hornblende changes colour from olive green to blue-green. Hypersthene and clinopyroxene disappear about four metres from the contact. The mineralogical changes can be summarized in one of the following two equations:

1. hypersthene + clinopyroxene + plagioclase$_1$ + $H_2O \rightarrow$ hornblende + quartz + plagioclase$_2$
2. hypersthene + potassium feldspar + plagioclase$_1$ + $H_2O \rightarrow$ hornblende + biotite + quartz + plagioclase$_2$

(modified after Winkler, 1979)

Geochemistry

The Nobel gneiss is rather homogeneous in chemical composotion with the average composition similar to the calc-alkaline granite of Nockolds (1954) (Table 23.1). In comparison with trace element data from unmetamorphosed calc-alkaline granites, it is enriched in Ba, Y, Zr and the LREE.

Samples from the shear zone, both granulite and amphibolite grade, are the most homogeneous of the three McKellar gneiss groups. Comparison of granulite and amphibolite grade samples from this shear zone show virtually no differences in chemical composition. This homogeneity indicates to a first approximation, isochemical metamorphism with the exception of the introductions of volatiles.

Both major and trace element show that the McKellar gneiss is not depleted compared to other granulite terranes (e.g. Rollinson and Windley, 1980). These analyses also show that the McKellar outcrop is more heterogeneous than the other samples collected regionally from the McKellar gneiss. This heterogeneity is reflected in a workable spread in Rb-Sr ratios, allowing a geochronological study.

Geochronology

Eight samples from the Nobel gneiss have been analyzed by the Rb-Sr whole rock age method, giving an age of 1330 ± 44 Ma (MSWD = 1.67) with an initial $^{87}Sr/^{86}Sr$ ratio of .7033 ± 17 (Figure 23.4). The error in the initial ratio is due in part to the long extrapolation from the closely grouped data points to the origin. This age is in agreement with the U-Pb zircon results from van Breeman et al. (1984) who obtained an age of 1345 Ma for the Nobel gneiss (marginal Orthogneiss and their terminology). These ages are interpreted as the time of intrusion of the Nobel gneiss.

For the McKellar gneiss, of the twelve samples analyzed, eleven samples yield a well defined isochron giving an age of 1241 ± 12 Ma (MSWD = 2.23) with an initial $^{87}Sr/^{86}Sr$ ratio of .7036 ± 6 (Figure 23.5). One sample,

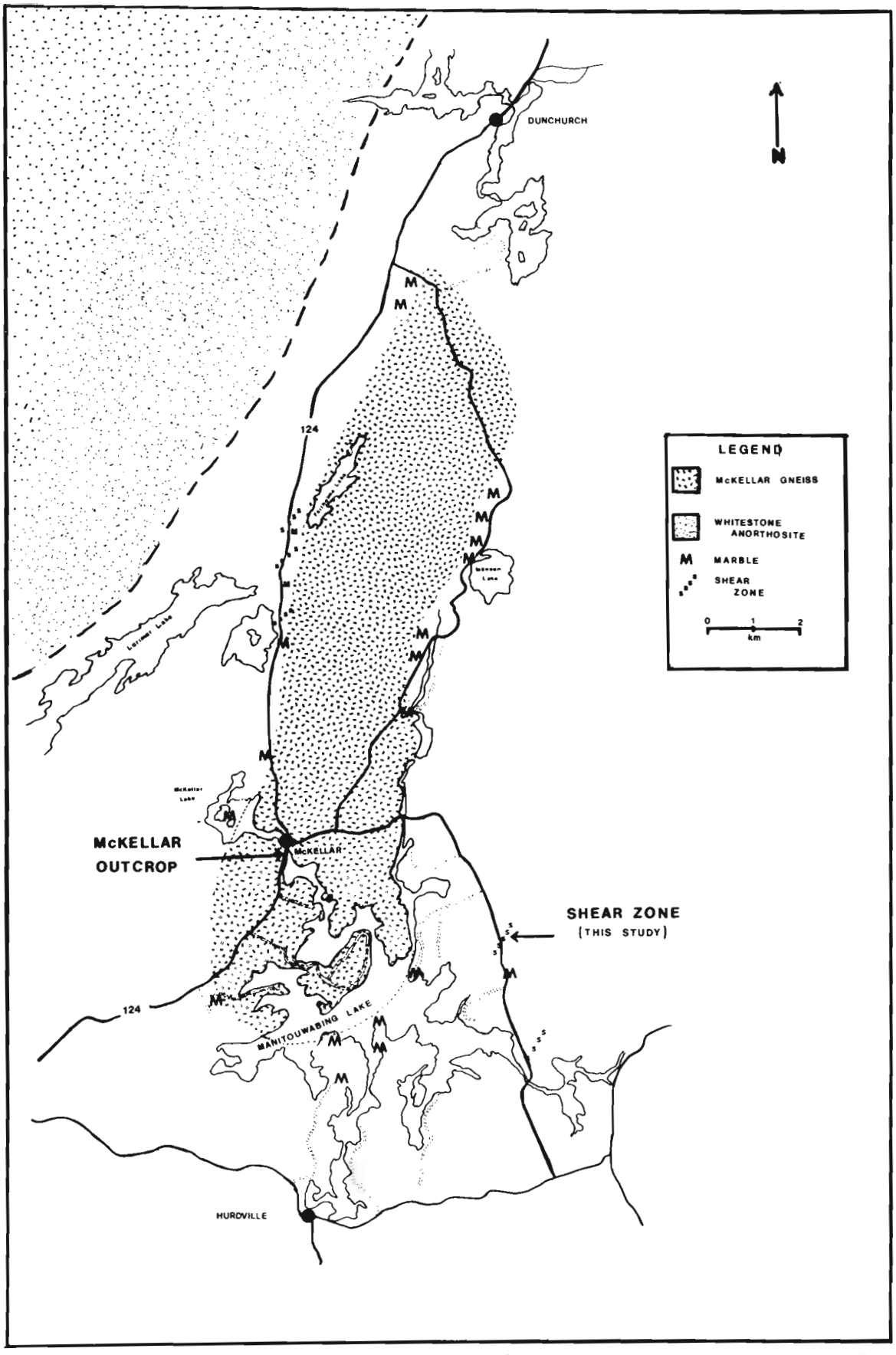

Figure 23.3. *McKellar Area Map, showing locations of the geochronological study on the McKellar outcrop and the location of the shear zone discussed in the text.*

Table 23.1

	1	2	3	4	5
SiO_2	69.89	58.39	54.23	53.59	52.64
TiO_2	.40	1.11	1.12	.96	.92
Al_2O_3	14.55	15.25	17.22	17.59	18.03
Fe_2O_3	3.81	7.41	9.51	9.31	8.95
FeO	*	*	*	*	*
MnO	.05	.13	.14	.14	.12
MgO	.87	3.35	4.60	5.23	6.44
CaO	1.60	5.24	8.10	7.40	7.56
Na_2O	3.06	4.03	3.58	3.80	3.52
K_2O	5.05	2.75	.97	1.18	1.18
P_2O_5	.09	.57	.27	.32	.38
H_2O				.42	.25
Ba	887.5	1096	392	614	468
Rb	99.4	39	13	12	12
Sr	132.6	470	800	894	952
Y	39.6	38	26	28	28
Zr	274.5	309	98	142	163
Nb	14.6	16	13	10	9
Ce	95.3	48	29	40	34
La	49.1	28	15	21	21
Nd	45.4	38	20	27	25
Pb	16.8	17	9	20	10

1 – Nobel Gneiss. Average of fifteen analyses.
2 – McKellar Gneiss-McKellar outcrop. Average of fifteen analyses.
3 – McKellar Gneiss-regional samples. Average of twelve analyses.
4 – Shear zone-amphibolite grade. Average of four analyses.
5 – Shear zone-granulite grade. Average five analyses.
* Total iron as Fe_2O_3

MCGR 5, plots to the left of the isochron. It was noted previously as containing 40 per cent perthite, thus it is probable that this sample lost Rb due to the exsolution processes during granulite facies metamorphism. The above age disagrees with results for U-Pb zircons determined by van Breeman et al. (1984), who obtained a lower intercept age of 1100-1200 Ma on concordia and an upper intercept age of 1350-1450 Ma, that they interpret as the time of granulite facies metamorphism and intrusion respectively.

Our age is from a single large outcrop with all samples collected within metres of each other. This was done to ensure, as far as possible, that the condition of a common initial $^{87}Sr/^{86}Sr$ is achieved. This resulted in a good linear array of points and a reasonable interpretation is, that it represents a "blocking temperature" for the Rb-Sr system during the granulite metamorphic event. Obviously more work is needed to resolve the differences in age, including some Sm/Nd studies.

Low initial ratios for the Nobel gneiss are within the mantle strontium ratios believed to be present for the Grenville during this time (Heaman, 1980). This value indicates little or no contamination by upper crustal material. If the 1241 Ma age is the time of granulite grade metamorphism, the value of .7036 is the maximum possible for the McKellar igneous protolith.

Acknowledgment

This work was funded by EMR grant 206 to RHM.

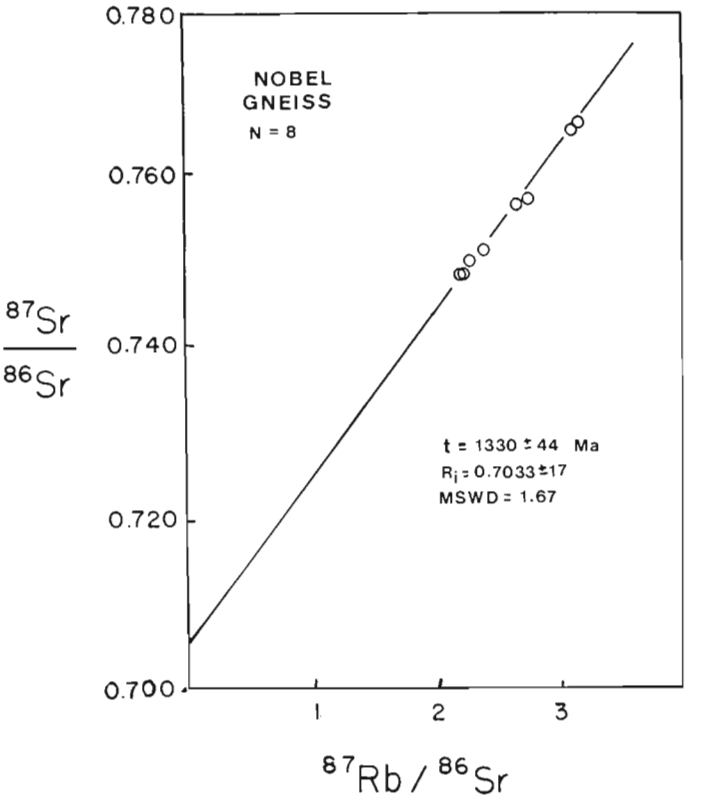

Figure 23.4. Rb-Sr whole rock isochron for the Nobel gneiss.

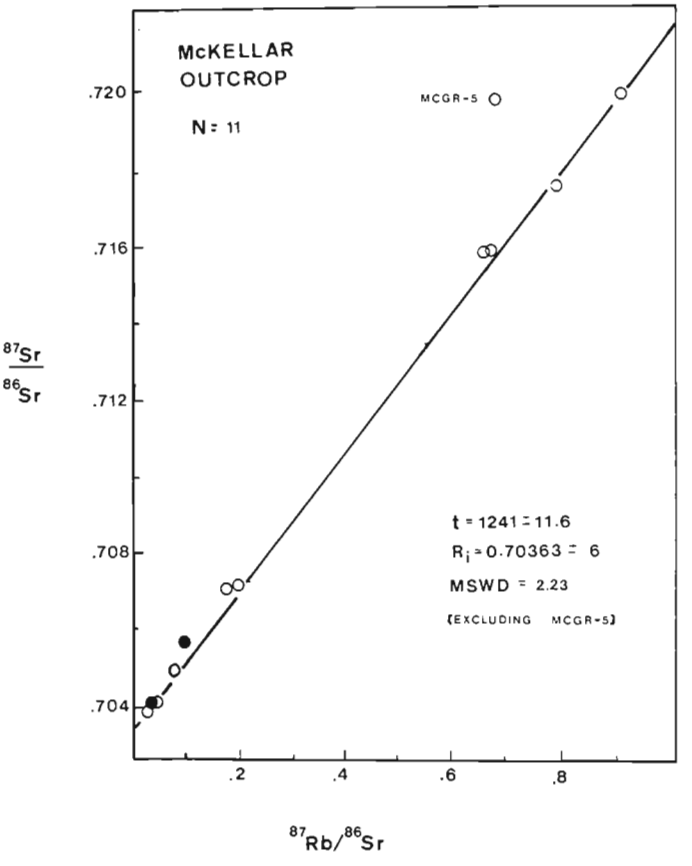

Figure 23.5. Rb-Sr whole rock isochron for the McKellar gneiss outcrop. The solid circles are mafic dyke samples.

References

Davidson, A. and Morgan, W.C.
1981: Preliminary notes on the geology east of Georgian Bay, Grenville Structural Province, Ontario; in Current Research, Part A, Geological Survey of Canada, Paper 81-1A, p. 291-298.

Davidson, A., Culshaw, N.G., and Nadeau, L.
1982: A tectonometamorphic framework for part of the Grenville Province, Parry Sound Region, Ontario; in Current Research, Part A, Geological Survey of Canada, Paper 82-1A, p. 175-190.

Heaman, L.M.
1980: Rb-Sr geochronology and isotope systematics of some major lithologies in Chandos Township, Ontario; unpublished M.Sc. thesis, p. 141.

Krogh, T. and Davis, G.L.
1973: The effect of regional metamorphism on U-Pb system in zircon and a comparison with Rb-Sr systems in the same whole rock and its constituent minerals; Carnegie Institute of Washington Yearbook, v. 72, p. 601-610.

Lacy, W.C.
1960: Geology of the Dunchurch Area, Ontario; Geological Society of America Bulletin, v. 71, p. 1713-1718.

Nockolds, S.R.
1954: Average chemical composition of some igneous rocks; Geological Survey of America Bulletin, v. 65, p. 1007-1032.

Rollinson, H.R. and Windley, B.F.
1980: An Archean granulite grade tonalite-trondjemite-granite suite from Scourie, N.W. Scotland: Geochemistry and origin; Contributions to Mineralogy and Petrology, v. 72, p. 265-281.

van Breeman, O., Davidson, A., Loveridge, W.D., and Sullivan, R.W.
1984: U-Pb zircon geochronology of Grenville tectonites, granulites and igneous precursors, near Parry Sound, Ontario, Abstract, 1984 GAC-MAC Meeting, London.

Winkler, H.G.F.
1979: Petrogenesis of Metamorphic Rocks; New York, Springer-Verlag, p. 348.

NORTHEAST EXTENSION OF GLACIAL LAKE MCCONNELL IN THE DEASE RIVER BASIN, DISTRICT OF MACKENZIE

Project 830017

D.A. St-Onge and L.A. Dredge
Terrain Sciences Division

St-Onge, D.A. and Dredge, L.A., Northeast extension of glacial Lake McConnell in the Dease River basin, District of Mackenzie; in Current Research, Part A, Geological Survey of Canada, Paper 85-1A, p. 181-186, 1985.

Abstract

Systematic mapping northeast of Great Bear Lake shows that a glacial lake once covered the Dease River basin as far as Lac Le Roux, Dismal Lakes, and possibly Lac Rouvière. Ice contact deltas, beaches, terraces, De Geer moraines, silty rhythmites, washed till, and pockets of sand lie at or below 290 m a.s.l. The northeastern limit of glacial Lake McConnell, which occupied the isostatically depressed basins of Great Bear Lake, Great Slave Lake, and parts of Lake Athabasca, has been extended to include the Dease River basin. The results of this study indicate that glacial Lake McConnell extended to Dismal Lakes and reached an elevation of 290 m.

Résumé

La cartographie systématique d'une région au nord-est du Grand lac de l'Ours démontre qu'un lac glaciaire occupait le bassin de la rivière Dease jusqu'aux lacs Le Roux, Dismal et, possiblement, Rouvière. Des deltas fluvioglaciaires, des plages, des terrasses, des moraines de De Geer, des rythmites silteuses, du till délavé et des placcages de sable prélittoraux jusqu'à 290 m marquent le niveau de ce lac. La limite nord-est du lac glaciaire McConnell qui occupait les bassins, déprimés par isostasie, du Grand lac de l'Ours, du Grand lac des Esclaves et d'une partie du lac Athabasca a été étendue pour inclure le bassin de la rivière Dease. Les résultats indiquent que la lac McConnell s'étendait jusqu'aux lacs Dismal et, qu'à son maximum, le plan d'eau était de 290 m.

Introduction

Glacial Lake McConnell is the high level proglacial lake that once occupied the combined basins of Great Slave Lake, Great Bear Lake, the western end of Lake Athabasca, and parts of the Peace and Athabasca river valleys (Fig. 24.1; Craig, 1965). This glacial lake formed along the glacially isostatically depressed margin of the receding continental Laurentide Ice Sheet. The McConnell phase ended when isostatic recovery reinstated the interfluves which separate the modern lake basins.

The former existence of a major high level lake was first recognized by McConnell (1890), who observed abandoned strandlines at the western end of Great Bear Lake that were lower than those reported earlier by Back (McConnell, 1890) at the eastern end. Bell (1900), Cameron (1922), and Raup (1946) further related raised strandlines to the pattern of ice retreat and subsequent isostatic readjustment. Taylor (1960) separated an early lake phase in the western end of the Athabasca basin – Lake Tyrrell – from other lake events. Craig (1960, 1965) summarized previous work, made further observations on raised lake shorelines, and reconstructed limits for a major glacial lake, which he named glacial Lake McConnell. His limits, shown in Figure 24.1, are based on the elevations of several deltas, on a number of spot elevations on the highest beaches, and contour extrapolations between. His use of the elevations of high beaches is somewhat problematical for two reasons: (1) He mentioned that the highest beaches fall below the highest lake levels as determined by deltas, and (2) He recognzed the possible existence of multiple lake levels but commonly assumed that widely spaced strandlines form a single water plane. Nevertheless, his reconstructions show a major glacial lake whose westerly limits in the Great Slave basin stand at elevations of between 228 m (west end) and 281 m (east and north ends); and in the Great Bear basin at between 182 m (Smith Arm) and 298 m (McTavish Arm). He postulated a rate of rise of 0.8–1.0 m/km towards the east. His limit in the vicinity of Dease Arm (Great Bear Lake), based on strandline determination, is 240 m. Fieldwork during the summer of 1984 indicates that the northern arm of glacial Lake McConnell was more extensive and higher than Craig had indicated.

Physiographic setting

Dease River and its tributaries drain a broad depression extending northeastward from Dease Arm of Great Bear Lake (Fig. 24.1). The basin forms a shallow amphitheatre-like depression rimmed on three sides by low bedrock hills.

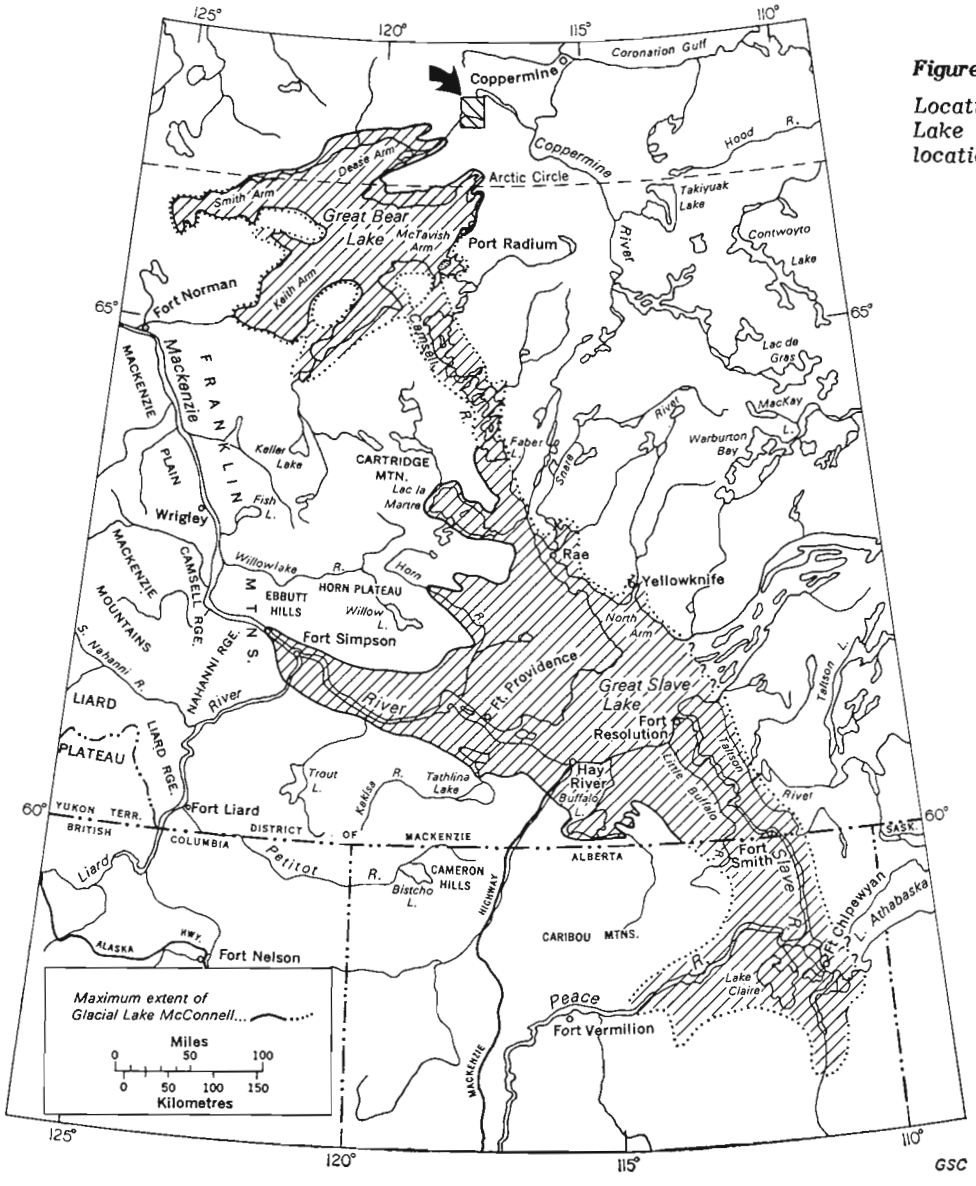

Figure 24.1

Location map showing extent of glacial Lake McConnell (after Craig, 1965) and location of present study.

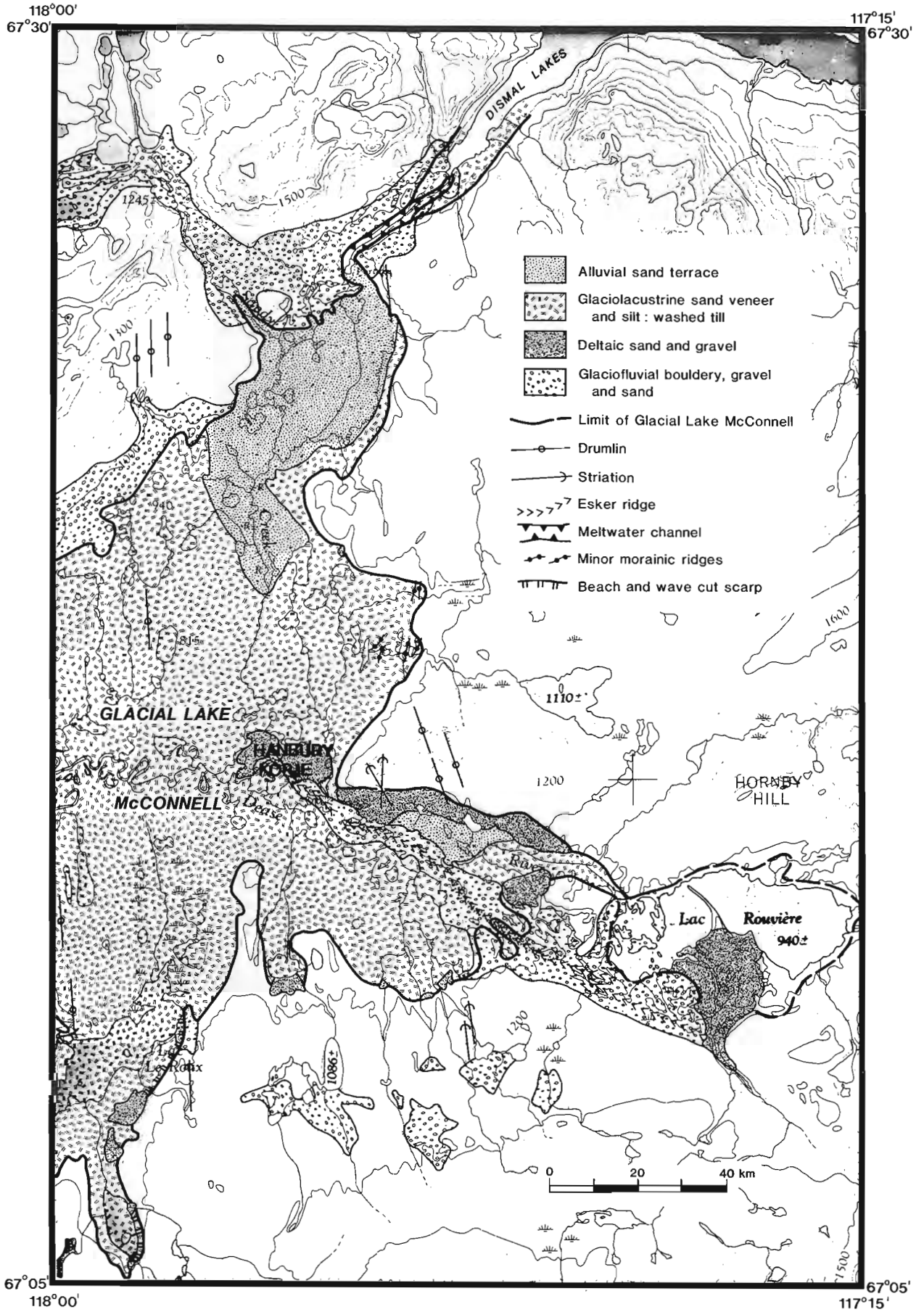

Figure 24.2. *Location of selected geologic features in Dease River basin.*

The area drained by Dease River and by its northern tributary Sandy Creek is extensively mantled by unconsolidated glacial deposits, predominantly sand and gravel, but the area around Lac Rouvière is bounded to the south and east by broad hills of granite and to the north by ridges of granite and sandstone (Baragar and Donaldson, 1973).

Mapping in this area during the summer of 1984 indicates that a glacial lake with a water level at approximately 290 m a.s.l. formerly occupied the basin (Fig. 24.2). The evidence includes: (1) numerous deltas between 280-290 m a.s.l.; (2) wave cut notches and beach ridges in the area of Lac Le Roux at similar elevations; (3) De Geer moraines, northeast of Hanbury Kopje (Fig. 24.2) below 290 m; (4) washed till below 290 m a.s.l.; and (5) the presence of silty rhythmites at the western end of Dismal Lakes at about 285 m.

The above evidence along with previous work strongly suggests that, at its maximum, glacial Lake McConnell extended into the basin of Lac Rouvière and coalesced with smaller ice marginal lakes in the Dismal Lakes basin.

Perched deltas and terraces

There are four types of deltas in the Lac Rouvière-Lac Le Roux basin: (1) triangular-shaped sand and gravel deposits which extend from south and east of Lac Le Roux to Lac Rouvière; (2) the esker delta forming a prominent hill known as Hanbury Kopje; (3) the delta terrace on the north side of Dease River between Hanbury Kopje and Lac Rouvière; and (4) the terraced sand deposit in the Sandy Creek basin.

A string of flat-topped triangular pads of fine to medium sand with granules on the surface are located at 290 m a.s.l. along the eastern margin of Lac Le Roux. The eastern edges of the pads grade into till or form minor gravelly ridges; the western edges form gentle but distinct slopes which are slightly terraced in places. These sand deposits are interpreted as a series of minor deltas deposited by small streams flowing into a lake 290 m a.s.l. The minor ridges at the apex of some of these deltas suggest that they were formed in contact with glacier ice. The minor terraces on the delta fronts are probably beaches, formed subsequent to the deltas, when lake level dropped.

A flat-topped outwash deposit at the northeast end of Lac Le Roux is easily distinguished from the delta sand by its higher elevation (305 m), its pitted surface, and the ubiquitous presence of collapsed structures. It predates the glacial lake. Minor beaches and notches have been formed on the west side of this deposit at 290 m a.s.l.

Between Lac Le Roux and Lac Rouvière there are several other sandy deltas, similar to those described above, which are all at 290 m a.s.l. The large delta between the esker ridge and Dease River (Fig. 24.2) differs from these by its larger size, higher and steeper foreslope, coarser grain size, and its gradation into an outwash complex. These features indicate high energy deposition and construction, in proximity to glacier ice, into the glacial lake at 290 m a.s.l.

The large delta on the south shore of Lac Rouvière is bounded by pitted outwash sand and gravel on either side; the main channel that cuts across its surface is terraced and pitted; its eastern edge is scarred by collapsed ridges. All these features clearly indicate that the delta, at the time of construction, was partly confined by masses of inactive glacier ice. Its surface elevation, at 300-310 m a.s.l., is only slightly above those of others which formed in glacial Lake McConnell. The delta may be a feature of Lake McConnell, but more likely it formed in a higher lake which was contemporary with, but was not necessarily a part of, the McConnell water plane.

Just east of where Sandy Creek flows into Dease River is a large deposit of ice contact sand which rises 40 m above the flat plain (Fig. 24.3). This hilly area known as Hanbury Kopje culminates in a flat-topped delta at 280-290 m a.s.l. The western part of the complex consists of subdued, rounded hills; a 20 m-high section in the western part shows that it consists of sandy silt and fine sand in planar beds, with internal ripple-drift crossbeds (Fig. 24.4). The eastern part of this delta complex is a broad, flat, plateau-like surface with steep sides to the north and east (hence the name kopje given the feature by early explorers). The surface, marked by a few channel scars, rises very gently to the south to merge with the esker (Fig. 24.2). This major delta complex was nourished by outwash waters flowing into a lake with a water plane at approximately 290 m a.s.l. The implications



Figure 24.3. *Hanbury Kopje showing ice contact features in the foreground and the flat-topped delta standing 40 m above sandy plain in background.*

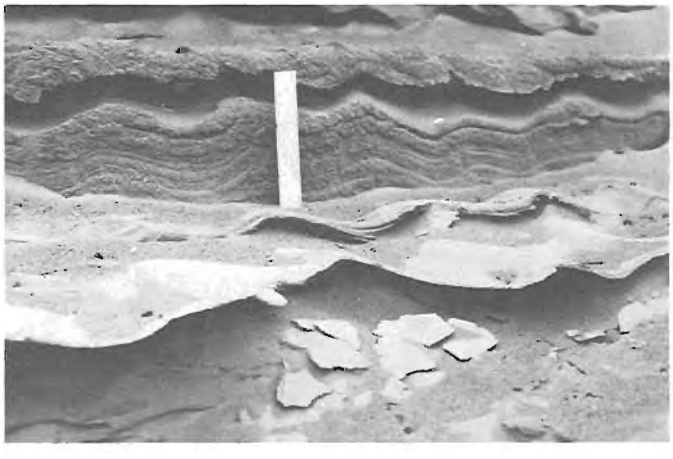

Figure 24.4. *Surface and cross-section of ripples within planar beds at Hanbury Kopje.*



Figure 24.5. Sand and fine gravel terraces east of Hanbury Kopje, north of Dease River. View west showing ice contact slope which formed against an ice lobe which occupied Dease valley (central background). Esker ridge is in the background.



Figure 24.6. Broad, steep-sided channel at the northwest end of Dismal Lakes. In this channel water flowed from Dismal Lakes basin to glacial Lake McConnell.

of this are (1) that stagnant ice occupied the broad depression east of Hanbury Kopje and (2) that for an unknown length of time glacial Lake McConnell was in contact with stagnant glacier ice.

East-southeast of Hanbury Kopje and north of Dease River, a broad, sandy terrace mantles the base of a ridge of granitic rocks (Fig. 24.5). The flat, terraced surface generally slopes gently (2-3°) towards the bedrock ridge to the north. The southern slope is steep and scarred by collapsed ridges, a clear indication that glacier ice was the southern confining element at the time of sand deposition. The elevation of this dissected terrace ranges from 290 m a.s.l. at its eastern end, declining to 280 m a.s.l. at its western extremity. This ice marginal sand deposit marks a phase in the disintegration of the ice mass which postdates the building of Hanbury Kopje.

Finally, 6 km southwest of the western extremity of Dismal Lake is an expanse of sand about 13 km long and 4 km wide. Its surface is scarred by a complex network of abandoned channels, meander scrolls, and oxbow lakes of Sandy Creek. The surface level of this shallow sand deposit is slightly above 280 m a.s.l. This "perplexing labyrinth of featureless gravelly barren" (Whalley, 1977, p. 59) is a delta built into the northernmost bay of glacial Lake McConnell by meltwaters flowing through a 6 km-long channel (Fig. 24.6) from the basin of Dismal Lakes. Ice filled the central part of the Dismal Lakes basin at the time, and a marginal lake occupied the area between the remnant ice mass and the valley sides. These conclusions, based on fieldwork during the summer of 1984, substantially modify an earlier interpretation which postulated that the channel at the western end of Dismal Lakes marked an outlet of glacial Lake Coppermine (St-Onge et al., 1981).

Beaches

South and east of Lac Le Roux the minor deltas are linked by a washing limit and notch at 290 m a.s.l. They mark the contact between a bouldery till and littoral sand deposits. One kilometre west of the strandline (i.e. into the basin) the material becomes a sandy diamicton, suggesting limited sedimentation of fines in the water body. On the west side of Lac Le Roux beach spits have been formed at 290 m a.s.l on a spur of a bedrock hill. These ridges were not investigated on the ground, but they appear to be composed of gravel and/or cobbles.

De Geer moraines

De Geer-type morainic ridges lie to the north of Hanbury Kopje where the 290 m contour makes a re-entrant to the east. The bottom of this broad valley is covered by smaller, irregular morainic ridges. A few sharp-crested elongated ridges trending north-south are asymmetrical, with a steep slope to the west. The location, orientation, and shape of these ridges strongly suggest that they are De Geer or cross-valley moraines (Andrews, 1963).

Washed till

Most of the area below 290 m forms a gently undulating marshy plain, consisting of low hummocks of bouldery till and sand-filled swales. The sand matrix has been washed out of the exposed till hummocks and redeposited in adjoining depressions.

In the lower part of the basin, erosion by Dease River and Sandy Creek has exposed up to 9 m of recent alluvium resting on till at river level. Silty deposits are absent below these fluvial sediments but the cause of this lack of fine sedimentation is uncertain. Possibly this part of the glacial lake could have existed for too short a period to allow any significant amount of silt to be deposited.

Dismal Lakes rhythmites

On the south shore of the narrow bay forming the extreme west end of Dismal Lakes, a coarsening upwards sequence of silt to gravel forms a prominent terrace at 290 m a.s.l. Lateral erosion by a small creek has exposed a 17 m-thick section.

At the base of the section 9 m of rhythmites are exposed. Each individual bed, up to 20 cm thick, is composed of a thinning upwards sequence ranging from fine sand to silty clay; a clay layer 3-5 cm thick separates each rhythmite (Fig. 24.7). The thickness of the sand-silty clay units and the relative coarseness of the material suggest that they are proximal rhythmites that were deposited in a lake marginal to a residual mass of glacier ice still occupying Dismal Lakes basin. Abundant sediments from the ice surface and from high hills immediately to the south rapidly filled this part of the narrow glacial lake, hence the coarsening upward sequence. The ice marginal waters flowed westward through the channel cut into the outwash deposits at the western end of the lake into glacial Lake McConnell (Fig. 24.2).



Figure 24.7. Rhythmites on the south side at the northwestern end of Dismal Lakes. Bands of sand/silt form units 20-30 cm thick separated by silty clay beds 3-5 cm thick.

Conclusion

A glacial lake occupied the basins of Dease River and Sandy Creek as far east as Lac Rouvière and as far north as the west end of Dismal Lakes. Lake level, defined by numerous deltas and strandlines was about 290 m a.s.l. Collapsed structures near the apex of deltas and at the margin of terraces indicate that the lake, at least in the basin of Lac Rouvière, was in contact with glacier ice. Because of the topographic continuity of the Dease River basin with Dease Arm, the lake that is recorded here must be an extension of glacial Lake McConnell. Craig (1960) determined the level of Lake McConnell to be only about 240 m (790') at Dease Arm, but about 298 m (980') in McTavish Arm, the next embayment south (Fig. 24.1). The 298 m level in McTavish Arm may be contemporaneous with the 290 m level in Dease basin, but the 240 m level is probably a lower lake stage. This means that the elevations of the water planes proposed by Craig (1960, 1965) do not relate to a single lake phase. The name glacial Lake McConnell should be used in a broad sense to refer to the series of ice marginal lakes that occupied the isostatically depressed basins now occupied by Great Bear Lake, Great Slave Lake, and Lake Athabasca. Its maxium limit does not reflect the elevation of a single isostatically deformed water plane.

Acknowledgments

We are grateful to the Department of Indian and Northern Affairs for providing logistical assistance to graduate students and for expert radio expediting service. Our colleague, V.K. Prest, provided stimulating discussion, both in the field and in the office. The following students provided not only assistance in the field but were also responsible for numerous independent observations for which we are very grateful: D. Kerr, A.M. Mercier, S. McGillivray, and Marie Tremblay. D.A. Hodgson critically read and substantially improved the original manuscript.

References

Andrews, J.T.
1963: The cross valley moraines of north-central Baffin Island, N.W.T.: A descriptive analysis; Geographical Bulletin, v. 19, p. 47-77.

Baragar, W.R.A. and Donaldson, J.A.
1973: Coppermine and Dismal Lakes map area, District of Mackenzie; Geological Survey of Canada, Paper 71-39, 20 p.

Bell, R.
1900: An exploration of Great Slave Lake, Northwest Territories; Geological Survey of Canada, Summary Report 1889, p. 103-110.

Cameron, A.E.
1922: Hay and Buffalo Rivers, Great Slave Lake and adjacent country, Northwest Territories; Geological Survey of Canada, Summary Report 1921, Part B, p. 1-44.

Craig, B.G.
1960: Surficial geology of north-central District of Mackenzie, Northwest Territories; Geological Survey of Canada, Paper 60-18, 8 p.

1965: Glacial Lake McConnell and the surficial geology of parts of Slave River and Redstone River map areas, District of Mackenzie; Geological Survey of Canada, Bulletin 122, 33 p., map.

McConnell, R.G.
1890: Report on an exploration in the Yukon and Mackenzie basins, N.W.T.; Geological Survey of Canada, Annual Report, v. 4, 1888-1889, pt. D.

Raup, H.M.
1946: Phytogeographic studies in the Athabasca-Great Slave Lake region, II; J. Arnold Arboretum, v. 27, no. 1, p. 1-85.

St-Onge, D.A., Geurts, M.A., Guay, F., Dewez, V., Landriault, F., and Léveillé, P.
1981: Aspects of the deglaciation of the Coppermine River region, District of Mackenzie; in Current Research, Part A, Geological Survey of Canada, Paper 81-1A, p. 327-331.

Taylor, R.S.
1960: Some Pleistocene lakes of northern Alberta and adjacent areas; Journal of the Alberta Society of Petroleum Geology, v. 8, p. 167-178, 185.

Whalley, G.
1977: The legend of John Hornby; Laurentian Library, Edition 51, MacMillan of Canada, Toronto, 367 p.

-25-

QUATERNARY GEOLOGY OF SOUTHWESTERN SASKATCHEWAN

Project 830024

R.W. Klassen and W.J. Vreeken[1]
Terrain Sciences Division, Calgary

Klassen, R.W. and Vreeken, W.J., Quaternary geology of southwestern Saskatchewan; in Current Research, Part A, Geological Survey of Canada, Paper 85-1A, p. 187-192, 1985.

Abstract

The unglaciated Cypress and Wood Mountain plateaus and surrounding glaciated terrain in southwestern Saskatchewan reflect significant age differences between not only Tertiary and Quaternary age terrain but within Quaternary age terrain as well. The oldest Quaternary surfaces in the Cypress area are nearly featureless, till-veneered, Tertiary gravel flats similar to the adjacent margin of the unglaciated plateau, whereas the youngest glaciated terrain several hundred metres lower, consists of sharply irregular hummocky terrain. Gently irregular to nearly flat till plains, interspersed with belts of mostly subdued hummocky terrain, occur over the remainder of the area and appear to be of intermediate age.

Absolute age dates have not been obtained from surfaces of Quaternary age in this region. The occurrence of paleosols, volcanic ashes, and fossiliferous sediments within the terrain of intermediate age, however, may provide the age dating control critical to deciphering the Quaternary history of this region.

Résumé

Les plateaux non glaciaires de Cypress et de Wood Mountain et le terrain glaciaire avoisinant dans le sud-ouest de la Saskatchewan présentent des différences chronologiques marquées entre les terrains tertiaires et quaternaires et aussi à l'intérieur des terrains quaternaires. Les surfaces quaternaires les plus anciennes de la région de Cypress sont des terrains plats graveleux tertiaires, presque sans particularité et recouverts d'un placage de till; ils sont similaires à la marge contiguë du plateau non-glaciaire. Par contre, le terrain glaciaire le plus récent, qui est situé à plusieurs centaines de mètres plus bas, est un terrain mamelonné très irrégulier. Des plaines de till légèrement ondulées ou presque planes, qui sont parsemées de zones mamelonnées surtout atténuées et qui semblent être d'âge intermédiaire couvrent le reste de la région.

On n'a pas encore déterminé l'âge absolu des surfaces quaternaires de cette région. La présence de paléosols, de cendres volcaniques et de sédiments fossilifères dans le terrain d'âge intermédiaire pourrait toutefois fournir le contrôle chronologique essentiel à la reconstitution de l'histoire du Quaternaire dans cette région.

[1] Department of Geography, Queen's University, Kingston, Ontario K7L 3N6

PART I (R.W. Klassen)

Introduction

The Cypress (72F) and Wood Mountain (72G) map areas include unglaciated uplands at about 1350 and 900 m elevation, respectively. These uplands stand some 400 to 200 m above the surrounding glaciated plains and the considerable contrast in the age and origin of these landscapes is unique to this part of the Canadian Prairies. This setting is ideal for comparative study of not only preglacial and glacial landscapes but also of glacial landscapes of different ages.

Surficial geology mapping, begun in 1983 (Klassen, 1984), was continued in the Cypress (72F) map area. Particular efforts were made to collect data relevant to the absolute and/or relative ages of the glaciated terrain. To date, absolute dates have not been obtained from postglacial deposits.

Previous studies in southern Alberta and Saskatchewan have led to a consensus among one group of workers who suggest that the Late Wisconsinan Laurentide Ice Sheet terminated along the Lethbridge moraine in southern Alberta and approximately along the northern slopes of the Cypress and Wood Mountain uplands in southwestern Saskatchewan (Reeves, 1973; Stalker, 1977; Jackson, 1979; Rutter, 1980; Mott and Jackson, 1982). This interpretation has been rejected in a number of regional syntheses that position the Late Wisconsinan ice margin well into Montana with the unglaciated uplands depicted as nunataks or within a major re-entrant into the continental glacier (Christiansen, 1979; Clayton and Moran, 1982; Mickelson et al., 1983; Shetsen, 1984).

The glacial landscape of this region consists mainly of gently irregular to flat till plains to the south and east of the Cypress Hills (Fig. 25.1). Hummocky moraine occurs in belts or patches around the upland, in the south-central part, and in the northwest corner of the map area. Outwash and

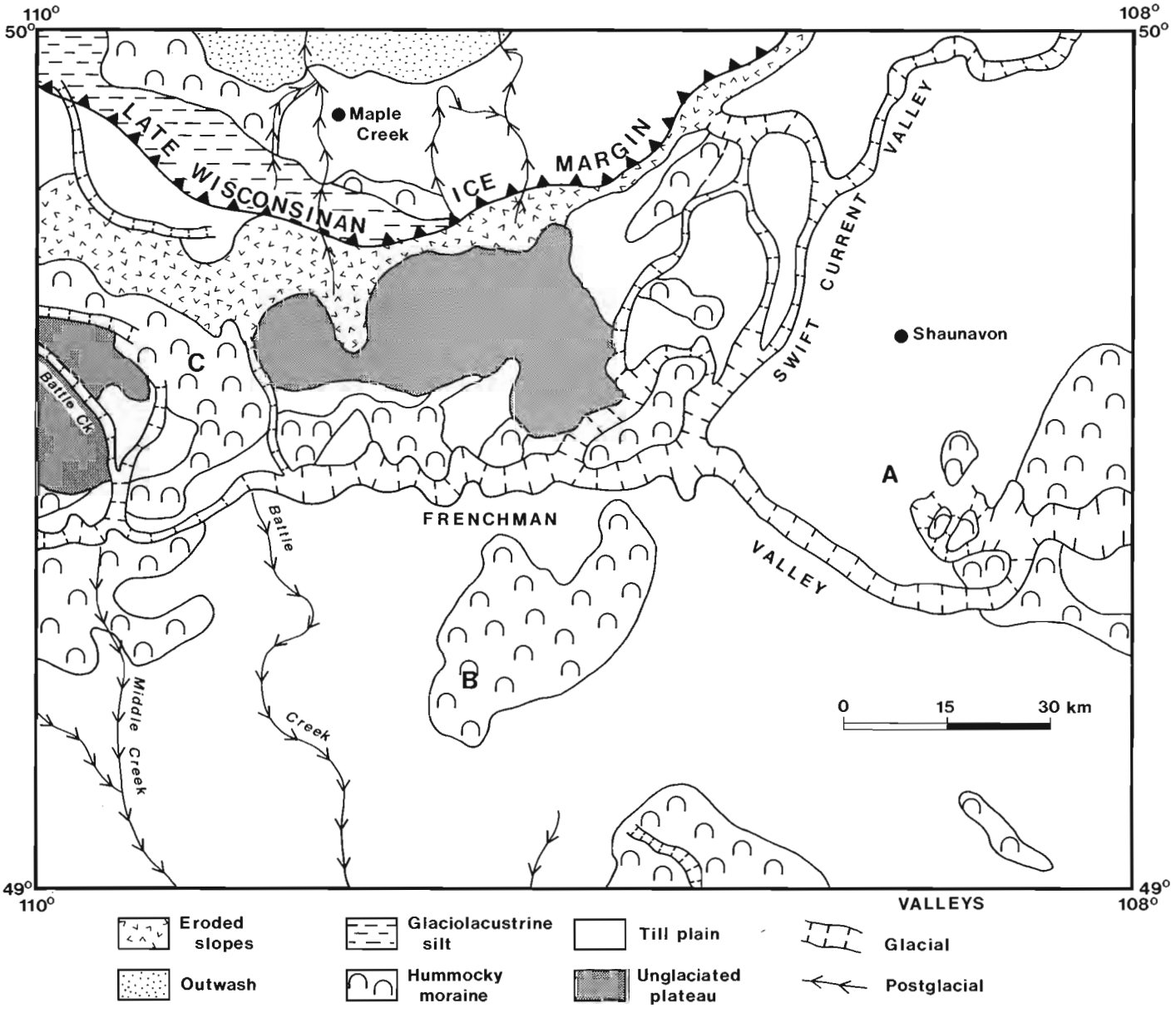

Figure 25.1. Generalized surficial geology map of the Cypress map area (72F), Saskatchewan. A, B, and C are sites described in the text.

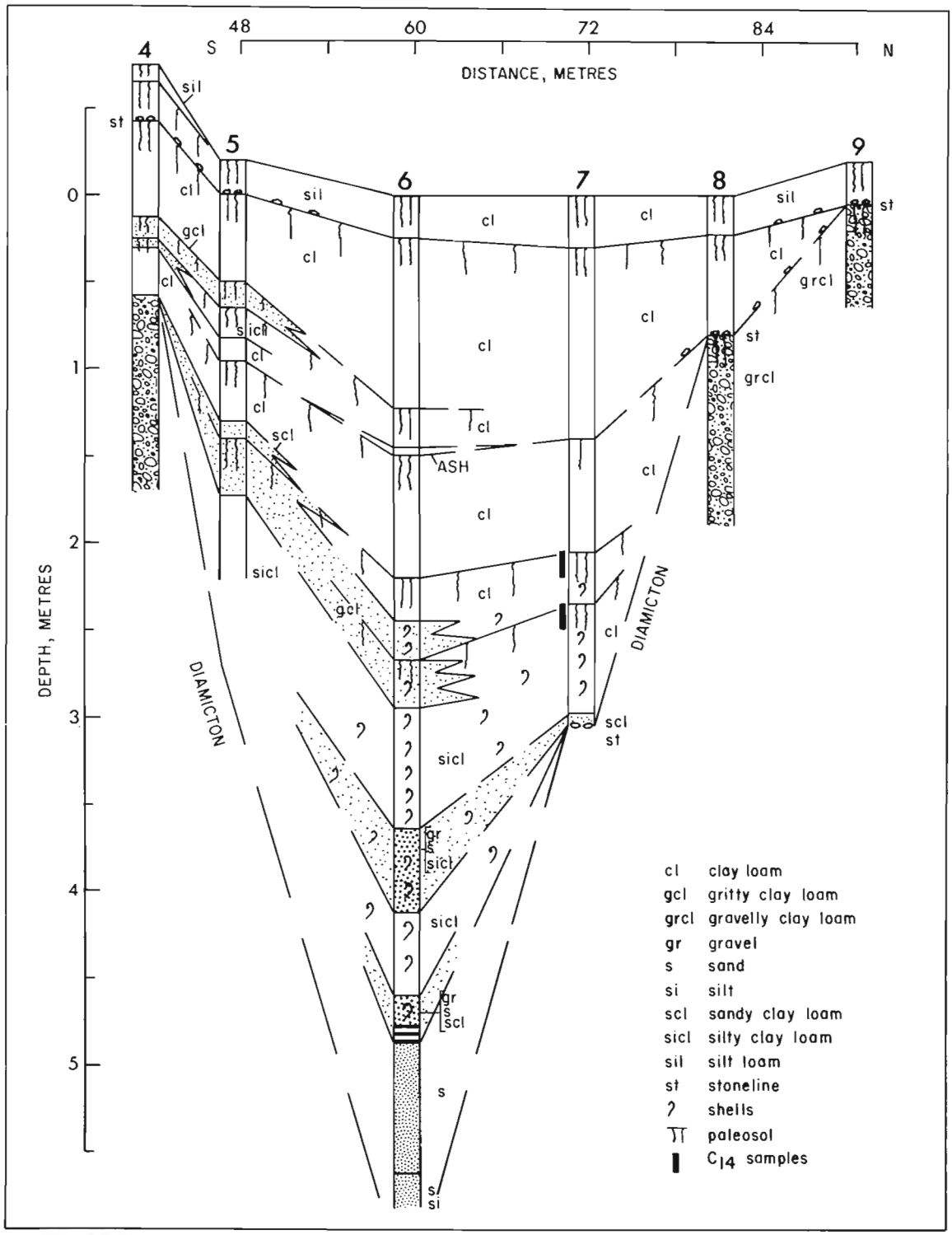

Figure 25.2. *Borehole stratigraphy of a depression in hummocky moraine between the west block and centre block of the Cypress Hills (49° 37'N, 109° 43'W). See Figure 25.1, Locality C.*

glaciolacustrine deposits are restricted mostly to the northwest part of the map area where the diversity of glacial deposits and landforms contrasts with the nearly featureless till plains elsewhere.

Studies to date have focused on establishing the age relationships of glacial landforms and deposits within the Cypress area. These investigations are based on assumptions discussed as follows:

1. The nature and thickness of postglacial sedimentation and erosion in similar types of terrain within units of different age should differ. If, for example, the hummocky moraine in the northwest part of the area (Fig. 25.1) is considerably younger (Late Wisconsinan) than the hummocky moraine elsewhere in the area (Early Wisconsinan or older), it should be possible to quantify differences in the above mentioned characteristics. Also, only the eastern part of Frenchman valley, a major east-west trending valley in regional sidehill position (Fig. 25.1), would have been occupied by Late Wisconsinan meltwater if the glacier margin did not extend beyond the northwest part of the map area. Differences in valley fill thickness and valley wall erosion may be evident along the segments if their ages differ significantly.
2. The effects of soil forming processes, surface weathering, and periglacial processes may be different on surfaces of significantly different ages.
3. The deposits of ice lobes of different domains and/or ages may be recognized by the distribution and surface weathering of glacial erratics associated with the surface till.

Progress and results

Hummocky moraine in the northwest part and elsewhere was compared through airphoto study and in the field. Specific features such as moraine plateaus and hummocks occurring south of the Cypress Hills commonly have a subdued appearance and gullying is evident, although isolated patches of moraine plateau and 'beaded' ridges appear as fresh as in the hummocky moraine in the northwest part of the map area.

Clayey sediments some 4 m thick overlying a paleosol in till were exposed in a fresh dug-out within a depression in hummocky moraine in the south-central part of the map area (B of Fig. 25.1, 49°13'N, 109°13'W). This paleosol may correlate with a paleosol in till and loess on the till plain to the northwest (A of Fig. 25.1; Klassen, 1984). Detailed analyses of samples collected for the purpose of obtaining datable material, soil information, and paleontological records remain to be completed. Shallow drilling was completed at several sites in hummocky moraine between the 'west-block' and 'centre block' of the Cypress Hills (C of Fig. 25.1) and is reported on in Part 2.

The western (pre-Late Wisconsinan?) segment and eastern (Late Wisconsinan) segment of Frenchman valley (Fig. 25.1) may reflect age differences. The westernmost part occupied by Battle Creek (Fig. 25.1) has gently sloping walls and present drainage (Middle Creek and Battle Creek) follows consequent courses southward out of the main valley. The easternmost segment, which carried Late Wisconsinan meltwater from the ice margin north of the Cypress Hills (Fig. 25.1), is much larger, has steeper walls, and is cut almost entirely in bedrock. The geomorphological differences between these segments are not necessarily the result of age differences and further study of landforms and sediments within the valley is required to determine the causes.

Comparative studies of surface and buried soils as an age dating method have been initiated. Paleosols in particular may provide useful information regarding absolute or relative ages of surfaces.

Shield rock types (mainly metamorphic and granitic) associated with the surface till in the southern part of the map area commonly are weathered to a visibly greater degree than are similar rock types in the northern part of the area. Marked contrasts can be seen in the surface texture of the above and below ground parts of Shield rocks in the southern part of the map area. The above ground parts are commonly spalled or have a jagged or sculptured aspect resulting from differential weathering of the mineral constituents. Age differences of the surface tills appear to be the most likely reason for the differences in the degree of weathering as it seems unlikely that local conditions such as moisture and soil chemistry are significant factors in causing the noted differences in weathering from north to south.

Relict periglacial structures in the form of polygonal ground patterns are preserved on parts of the unglaciated plateau as well as on glaciated surfaces bordered by hummocky end moraine in the southeast part of the Cypress plateau. Fresh roadcuts expose stony wedges or fine sediments that form subtle polygonal patterns on the flat glaciated surfaces bordering the hummocky moraine. Convoluted structures of probable periglacial origin were noted at one locality on the till plain (A of Fig. 25.1) east of the Cypress Hills (Klassen, 1984).

Conclusions

Studies to date suggest that glaciated surfaces of substantially different ages occur in the Cypress map area. The oldest surfaces are nearly featureless till-veneered Tertiary gravel flats between hummocky moraine and the unglaciated southern margins of the Cypress plateau (Fig. 25.1). The youngest glaciated terrain occurs as complexes of hummocky moraine, hummocky glaciolacustrine silt, and outwash north of the Cypress Hills upland. This part appears to correlate with the Late Wisconsinan maximum in Alberta as proposed by Stalker (1977). The largest part of the map area consists of glaciated terrain of intermediate age which may be Early Wisconsinan or older. Considerably more field data are required to establish the age inferences made.

PART 2 (W.J. Vreeken)

Introduction

Following field reconnaissance begun in the summer of 1983 (Klassen, 1984), a coring program was begun during the summer of 1984 in belts of hummocky terrain in the northwest part of the Cypress map area (Fig. 25.1).

The first two terrain units selected for analysis are crossed by the Cypress Hills Road (C of Fig. 25.1). This road connects the westernmost unglaciated plateau element (west block) of the Cypress Hills with the unglaciated centre element (centre block), which lies within Cypress Hills Provincial Park. The higher of these terrain units extends across the topographical saddle between the plateaus and onto the regional south-facing slope of the Cypress Hills complex. The other terrain unit is set within, and below, the higher unit. It does not extend across the saddle, but meltwater channels associated with it did drain across the saddle, through the present day Hungerford Lakes, into the Frenchman River meltwater channel system (Fig. 25.1). Depressions selected from within these terrain units were cored in transects along their principal axes. Corings were made with a trailer-mounted Giddings hydraulic coring device. The following is a report on data from a transect along the short axis of the depression in the higher terrain unit.

Borehole observations

Figure 25.2 depicts the borehole stratigraphy of the bottomland portion of a 156 m transect that connects surrounding hill crests. These crests and adjoining slopes are underlain by a gravelly clay loam diamicton, overlain by a stone concentrate which is capped by a thin and discontinuous silt loam veneer. The veneer is most likely of Eolian origin.

The bottomland sequence was cored, at Station 6 (Fig. 25.2) to a depth of 6.1 m, without penetrating diamicton. The basal increment of this sequence consists of interbedded fine sands and coarse silts, followed by 75 cm of well sorted medium sands. The middle increment measures about 265 cm; it includes materials ranging from gravel to clay loam in texture, whereas the coarser materials are confined to the lower 125 cm. At the base of this increment, several thin (<0.5 cm), black, clay-like intercalations occur within a sandy unit. These intercalations may well consist of colloidal organic matter. Gastropod shells occur throughout the middle increment. A distinct zone of organic enrichment extends to 50 cm below the top, and another one surmounts the top of the increment. Both zones can be correlated with equivalent zones at Station 7, where they were sampled for the purpose of radiocarbon dating.

The upper increment at Station 6 consists of 220 cm of dark-coloured clay loams. These are separated by several buried soils and by one layer of light-coloured volcanic ash.

Discussion of borehole data

The first increment at Station 6 (Fig. 25.2) is thought to have been deposited by running water. The abundance of well sorted sands precludes a provenance within the confines of the present day depression. An external provenance would be commensurate with fluvioglacial and therefore deglacial deposition.

The middle increment appears to represent a sequence of postglacial pond deposits of local provenance. During follow-up work, material for radiocarbon dating will have to be collected from its base. The samples already collected will date termination of the pond environment. The gastropod shells may reveal more about the paleoenvironmental conditions.

The third increment appears to represent the slough environment that prevails at present. This is characterized by steady infilling with humus-rich, very fine textured material. The buried soils may mark periods of drought of durations much longer than the annual dry season. The volcanic ash will have to be identified; it is probably Mazama ash and, if so, would have been deposited 6600 years ago (Westgate and Briggs, 1980). Volcanic ash was encountered at other sites during the past two years, both in the Maple Creek area of southern Saskatchewan and in adjacent Alberta. Some of these may represent Glacier Peak ash and, if so, would be about 11 200 years old (Westgate and Briggs, 1980).

Conclusion

This initial data base, though promising, requires considerable expansion. Borehole data can offer important information but do not offer any significant insight into sedimentary and paleosolic structures. Future studies therefore will endeavor to interface the coring program with a program of deep-trench studies.

References

Christiansen, E.A.
1979: The Wisconsinan glaciation of southern Saskatchewan and adjacent areas; Canadian Journal of Earth Sciences, v. 16, p. 913-938.

Clayton, L. and Moran, S.R.
1982: Chronology of Late Wisconsinan glaciation in middle North America; Quaternary Science Reviews, v. 1, p. 55-82.

Jackson, L.E.
1979: Glacial history and stratigraphy of the Alberta portion of the Kananaskis Lakes map area; Canadian Journal of Earth Sciences, v. 17, p. 459-477.

Klassen, R.W.
1984: Quaternary geology of southwestern Saskatchewan; in Current Research, Part A, Geological Survey of Canada, Paper 84-1A, p. 641-642.

Mickelson, D.M., Clayton, L., Fullerton, D.S., and Barnes, H.W.
1983: The Late Wisconsin glacial record of the Laurentide ice sheet in the United States; in Late-Quaternary Environments of the United States, ed. H.E. Wright, Jr.; volume 1, The Late Pleistocene, ed. J.C. Porter; University of Minnesota Press, Minneapolis, p. 3-37.

Mott, R.J. and Jackson, L.E., Jr.
1982: 18 000 years palynological record from the southern Alberta segment of the classical Wisconsinan "Ice-free Corridor"; Canadian Journal of Earth Sciences, v. 19, no. 3, p. 504-513.

Reeves, B.D.K.
1973: The nature and age of the contact between the Laurentide and Cordilleran ice sheets in the western interior of North America; Arctic and Alpine Research, v. 5, no. 1, p. 1-16.

Rutter, N.W.
1980: Late Pleistocene history of the western Canadian ice-free corridor; in The ice-free corridor and peopling of the New World, ed. N.W. Rutter and C.E. Schwager; Canadian Journal of Anthropology, v. 1, p. 1-8.

Shetsen, I.
1984: Application of till pebble lithology to the differentiation of glacial lobes in southern Alberta; Canadian Journal of Earth Sciences, v. 21, no. 8, p. 920-933.

Stalker, A.MacS.
1977: The probable extent of classical Wisconsin ice in southern and central Alberta; Canadian Journal of Earth Sciences, v. 14, p. 2614-2619.

Westgate, J.A. and Briggs, N.D.
1980: Dating methods of Pleistocene deposits and their problems, V. Tephrochronology and fission-track dating; Geoscience Canada, v. 7, p. 3-10.

GOLD MINERALIZATION IN THE BEARDMORE-GERALDTON AREA OF NORTHWESTERN ONTARIO: STRUCTURAL CONSIDERATIONS AND THE ROLE OF IRON FORMATION

Project 750098

C.D. Anglin and J.M. Franklin
Economic Geology and Mineralogy Division

Anglin, C.D. and Franklin, J.M., Gold mineralization in the Beardmore-Geraldton area of northwestern Ontario: structural considerations and the role of iron formation; in Current Research, Part A, Geological Survey of Canada, Paper 85-1A, p. 193-201, 1985.

Abstract

Gold deposits occur in deformed Archean sedimentary rocks that consist of a northerly assemblage (Group A), containing greywacke, iron formation, and conglomerate, feldspar porphyry and mafic intrusions, and a southerly greywacke sequence (Group B). Gold deposits are restricted to the northerly assemblage. The southern domain has a northeastward structural facing, but the northern faces west-southwest. The two domains are juxtaposed along a major dextral strike-slip fault which parallels the Bankfield-Tombill fault. Fault movement(s) produced a complex foliation pattern that deformed an earlier regional cleavage, and generated prominent Z-folds.

The gold mineralization occurs primarily in veins that parallel the major faults, and occupy cleavage that transects earlier structures. The pyrite and arsenopyrite that accompany gold replace oxide-rich iron formation. The gold in iron formation away from these sulphide zones is less than 10 ppb. Thus gold and attendant sulphides were introduced into the Geraldton area late in its tectonic history.

Résumé

Les gisements aurifères se présentent dans des roches sédimentaires déformées d'âge archéen qui comprennent, au nord, un assemblage (groupe A) de grauwacke, de formation ferrifère et de conglomérat, de feldspath porphyrique et d'intrusions mafiques, et, au sud, une séquence de grauwacke (groupe B). Les gisements aurifères se trouvent uniquement dans l'assemblage plus au nord. Le domaine sud a une orientation structurale nord-est et le domaine nord, une orientation ouest-sud-ouest. Ces deux domaines sont juxtaposés le long d'un important décrochement dextre qui est parallèle à la faille de Bankfield-Tombill. Le mouvement de la faille a produit une foliation complexe, cause de la déformation d'un clivage régional antérieur et de la production de plis proéminents en Z.

Les minéralisations aurifères se présentent surtout en filons parallèles aux principales failles et ont rempli des fractures recoupant les structures plus anciennes. La pyrite et l'arsénopyrite qui accompagnent l'or remplacent la formation ferrifère riche en oxyde. La teneur en or de la formation ferrifère éloignée de ces zones sulfurées est inférieure à 10 ppb. L'or et les sulfures connexes ont donc été introduits dans la région de Geraldton vers la fin de son histoire tectonique.

Introduction

The Beardmore-Geraldton gold district is situated in an 80 km long belt of metasedimentary and metavolcanic rocks which form part of the southern margin of the Archean Wabigoon greenstone belt of northwestern Ontario (Fig. 26.1). Metasedimentary rocks in the Geraldton area hosted eleven gold mines which produced, over a period of 34 years, approximately 2 900 000 ounces of gold with an average grade of 0.1 ounces per ton. In the Beardmore area, gold production, largely from metasedimentary rocks (one mine was hosted in metavolcanic rocks), totalled over 1 135 000 ounces with an average grade of 0.66 ounces per ton (Mason and McConnell, 1982).

The Geraldton area provides a particularly useful study area as its gold deposits exhibit close spatial relationship to specific stratigraphic, structural and intrusive elements that are common to many of the important gold districts of Superior Province (Franklin and Thorpe, 1983; Hodgson and MacGeehan, 1982). The present study was initiated to examine:

a. the degree to which gold mineralization is controlled by stratigraphy;

b. the significance of the localization of many of the producers along one of the important regional structures in the area, the Bankfield-Tombill fault;

c. the degree to which gold distribution is controlled by structure;

d. the relationship between gold mineralization and iron formation; and,

e. the role of the feldspar porphyry intrusions in the mineralization.

This report constitutes a summary of field observations carried out in the Geraldton area in the summers of 1982 and 1983, and emphasizes the structural interpretations and the role of iron formation. Geochemical data and a discussion of the intrusive rocks will be presented in a subsequent paper. Some preliminary geochemical data on the iron formation are also presented. Follow-up to this work is being done in the form of an M.Sc. thesis at Memorial University by C.D. Anglin.

Regional geology

Archean sedimentary and volcanic rocks are exposed from east of Geraldton westward to Beardmore, where they are covered by Lake Nipigon and Logan diabase sills, and then continue to the west of the lake (Fig. 26.2). The gold mineralization is hosted in a linear zone of sedimentary and volcanic rocks at the boundary between two Archean subprovinces, the Wabigoon to the north, and the Quetico to the south (Stockwell, 1964; Pirie and Mackasey, 1978). Wabigoon Subprovince is a typical granite-greenstone terrain consisting of thick accumulations of metasedimentary and metavolcanic rocks which are intruded by plutons ranging in composition from granite and syenite to gabbro (Card, 1983). Quetico Subprovince consists largely of metasedimentary rocks and their high grade gneissic and migmatitic equivalents, with tonalitic orthogneiss and massive granitic plutons (Card, 1983).

The position of the boundary between these two subprovinces is based mainly on changes in lithology, but also corresponds to changes in structural trend, and to some degree, style, and metamorphic grade. Card (1983) stated that the "Wabiggon-Quetico boundary is a lithological transition from metavolcanics to metasediments in the western part of the area (the Beardmore-Geraldton area) and a major fault, the Gravel River fault, in the east (east of Geraldton)." Mackasey et al. (1974) have presented a general stratigraphic column for the boundary zone consisting of: (1) a southern, narrow, mafic volcanic unit adjoining the Quetico metasedimentary rocks; (2) a central greywacke unit, which includes shale, heterolithic pebble conglomerate and oxide facies iron formation; and (3) a northern metavolcanic sequence (Fig. 26.2). They interpret the boundary as a facies change from a sediment-dominated terrain in the south to a mafic volcanic-dominated terrain in the north.

The central sedimentary unit defined by Mackasey et al. (1974) was subdivided by Bruce (1936) and Horwood and Pye (1951) into two distinct groups, mainly on the basis of lithological differences. The northern group, designated Group A, (Fig. 26.2) is a heterogeneous assemblage of greywacke, chlorite schist, conglomerate and oxide iron formation, intruded by hornblende gabbro and diorite, as well as feldspar and quartz-feldspar porphyries. The southern group, Group B, consists of a monotonous series of slaty greywacke with minor iron formation and no intrusions. Beds in both groups strike, on average, south of east, parallel and subparallel to a pervasive regional cleavage. Both bedding and cleavage dip steeply.

The regional cleavage appears to be related to broad-scale isoclinal folding, the style of which is similar in both groups of sediments. Later deformation of this cleavage occurs in a few locations and is related ot minor asymmetric folds with an attendant cleavage.

Current study

Structural facing of folds in the metasedimentary rocks

It is interesting to note, as did Horwood and Pye (1951), that of the two sedimentary packages only the northern group (Group A) is mineralized. No gold-bearing veins have been reported in the Group B sediments. Numerous occurrences

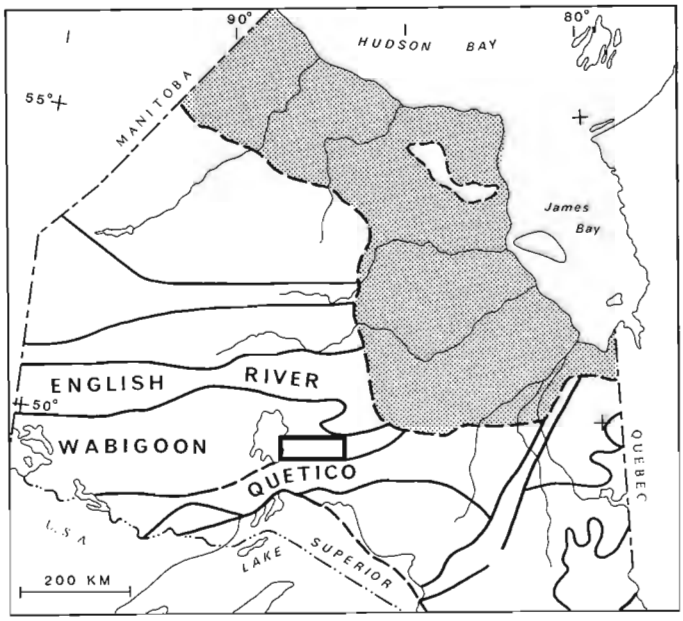

Figure 26.1. Map of Ontario showing the English River, Wabigoon and Quetico belts in relation to other structural zones and belts in central Superior Province. Stipple indicates Phanerozoic rocks. Beardmore-Geraldton area is shown in black rectangle.

are located in the metavolcanic rocks (to the north of the Group A sedimentary rocks in the eastern part of the belt, and to the north and south of the sedimentary rocks in the western part of the belt), but only one of these produced any gold (the Northern Empire Mine in Beardmore). All the major producers were hosted by Group A sedimentary rocks.

Structural studies were undertaken to document the contrast between the two sedimentary groups and, particularly, the nature of the contact between them. Bedding, cleavage and younging directions were noted at several locations in the belt (Fig. 26.3 and 26.4). It was observed that minor folds within the two groups consistently face in opposite directions. The structural facing (Cummins and Shackleton, 1955; Borradaile, 1976) of Group B is north-eastward, while that of Group A is west to southwestward (Fig. 26.2). Figure 26.4 is a schematic representation of the structural facing data observed in outcrop.

There are several ways of interpreting the common boundary between Group A and Group B rocks:

1. The discontinuity between the two groups may represent the axis of an earlier "first" isoclinal fold that has brought the two sedimentary packages together on opposite limbs and has subsequently been deformed (Fig. 26.5a). One problem with this interpretation is that the two groups are lithologically dissimilar. This could be the result of the fold hinge being located at a facies change within the sequence. This hinge may then be the locus for lateral movement, causing widely separated elements of the same stratigraphic package to be brought together.
2. A difference in structural facing between two juxtaposed rock units may also be due to an original difference in the orientation of the bedding, that is, an angular unconformity (Fig. 26.5b). This is not an acceptable explanation for the Beardmore-Geraldton area as the two groups have structural facings oriented parallel to or facing the discontinuity. If the boundary was an unconformity at least one of the domains would face away from it.
3. The discontinuity may simply represent a major fault that has juxtaposed two, possibly completely unrelated, "slices" of rock (Fig. 26.5c).

The contact between the Group A and Group B sedimentary sequences was observed in outcrop on the Bankfield Mine property, approximately 300 m south of the old shaft (Fig. 26.6). This outcrop consists of a northern section of strongly foliated greywacke and conglomerate in which sedimentary textures and structures are obscured due to the foliation; a middle, 4 m wide, section of "phyllite" (chlorite schist); and, a southern section of slightly foliated greywacke, in which bedding and grading are easily discernible. The contact between the conglomerate and the "phyllite" (probably phyllonite) was described by Pye (1951) as "... a sharply defined disconformity (which) shows as a clear but irregular line separating the band of conglomerate (Group A) from the underlying sediments of Group B." South of the phyllite there is little or no change in the character of these greywackes for several hundred metres across strike (Pye, 1951). Beds face north and are slightly overturned and bedding-cleavage relationships indicate an eastward structural facing. These sedimentary rocks do not appear to be highly deformed, nor do they host any significant quartz veins. In contrast, the sediments to the north of the phyllite are strongly foliated, highly quartz-veined, and host hornblende gabbro and quartz-feldspar porphyry intrusions. It is postulated that the "phyllite" unit may represent a fault or shear zone at the contact between Group A and Group B, and that the discontinuity between the two groups is a major fault which may or may not correspond to an early, large scale, fold hinge.

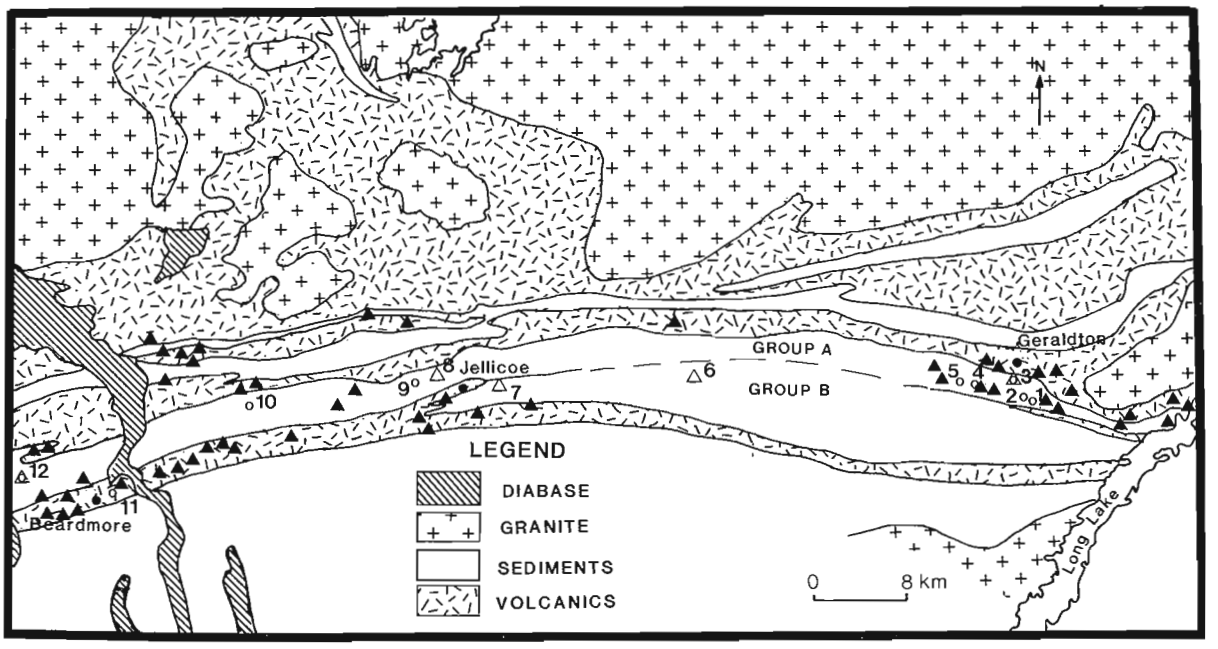

Figure 26.2. Geology of the Beardmore-Geraldton area (after Pye, 1951). Open circles are past producing gold mines, solid triangles are gold occurrences, open triangles are areas where structural facing data were obtained. Numbers indicate areas referred to in text: 1. Hardrock Mine; 2. MacLeod-Cockshutt Mine; 3. Little Long Lac Mine; 4. Magnet Mine; 5. Bankfield Mine; 6. Grant's Camp; 7. Jellicoe; 8. Oxaline Lake; 9. Solomon's Pillars Mine; 10. Watson Lake; 11. Northern Empire Mine; 12. Leitch Mine.

The Bankfield-Tombill fault

The main fault identified in this area, the Bankfield-Tombill fault (BTF), crosses the Bankfield property approximately 350 m north of, and is oriented approximately parallel to, the phyllite unit described above. The BTF is the most obvious and well-defined fault in the Geraldton area. It has been traced along strike, westward from south of Geraldton, for a total distance of about 10 km. Along its length the fault strikes 110 to 120° and dips steeply south at 60 to 70° (Pye, 1951). The minor features observed in the fault zone depend primarily on the rock type which the fault cuts. In metasedimentary rocks the fault has a brittle character and consists of a zone of highly silicified and carbonatized brecciated material, commonly showing evidence of multiple brecciation events, and often impregnated with small amounts of pyrite and chalcopyrite. Drilling on the Roxmark Mines Limited property (1 km east of the old Magnet Mine; see Fig. 26.2) in 1981 intersected the fault. In drill core the fault is seen to consist of 0.5 to 2.0 m of clay (fault gouge) with a zone of silicification and brecciation up to 20 m wide on either side. Here the fault is localized at the contact between metasediments (slaty greywackes and minor oxide iron formation) and very highly altered mafic rock. Immediately adjacent to the fault the metasediments have developed a penetrative cleavage which has given them a very fissile character. Fifty metres north of the fault the cleavage is less pronounced but the sediments show extreme development of asymmetric folds of several centimetres to several metres in amplitude.

Where the fault cuts through hornblende gabbro it has a much more ductile character and develops zones of highly carbonatized and intensely foliated chlorite schist which commonly contain a prominent stockwork of quartz and quartz-carbonate veins. Many parallel chlorite schist zones, ranging from several tens of centimetres to several metres in width, are intercalated with the relatively undeformed portions of the intrusion. This relationship is particularly well exposed in a series of outcrops adjacent to the Bankfield-Tombill fault on Highway 11, 2 km west of Geraldton. This fault is well-defined on strike to the east and west of these outcrops (Pye, 1951), and is characterized by the following features. Moderately foliated gabbro (Fig. 26.7a) can be traced into more foliated material (Fig. 26.7b) in which narow, anastomosing chloritic "shear" zones have developed, and into intensely foliated, rubbly-weathering, carbonatized chlorite schist (Fig. 26.7c) and very finely laminated chlorite-rich seams (Fig. 26.7d) all within a few metres. Figure 26.7d illustrates particularly well three steeply-dipping planar fabric elements within this fault zone. Throughgoing chloritic seams (a) bound domains which contain an oblique internal foliation (b), which in turn is cut by a secondary cleavage (c). The intersection line of these three cleavages plunges subvertically. The latter cleavage (c) consistently offsets the foliation (b) in a dextral sense. The conventional interpretation of this kind of fabric in shear zones is formation by dextral transcurrent shear motion (Berthe et al., 1979).

The amount of carbonate in these schists suggests that there has been a significant amount of fluid movement through these zones, resulting in intense alteration. The chemical mass-balance relationships between the various zones illustrated in Figure 26.7 are currently being examined.

The earliest record of movement along the BTF postdates the intrusion of the albite porphyry at the Bankfield Mine which was brecciated by the fault (Pye, 1951). A 650 m dextral offset is recorded by Proterozoic diabase dykes that are cut by the fault. This may or may not be the same movement that brecciated the porphyries and there may have been movement along the zone prior to the intrusion of the porphyries, but no clear evidence was found to support or refute this. It is interesting to note that the distribution of the porphyries, and to some extent the mafic intrusions, is roughly parallel and spatially closely related to the fault, implying that the BTF and related structural features may have acted to localize the intrusion of these rocks.

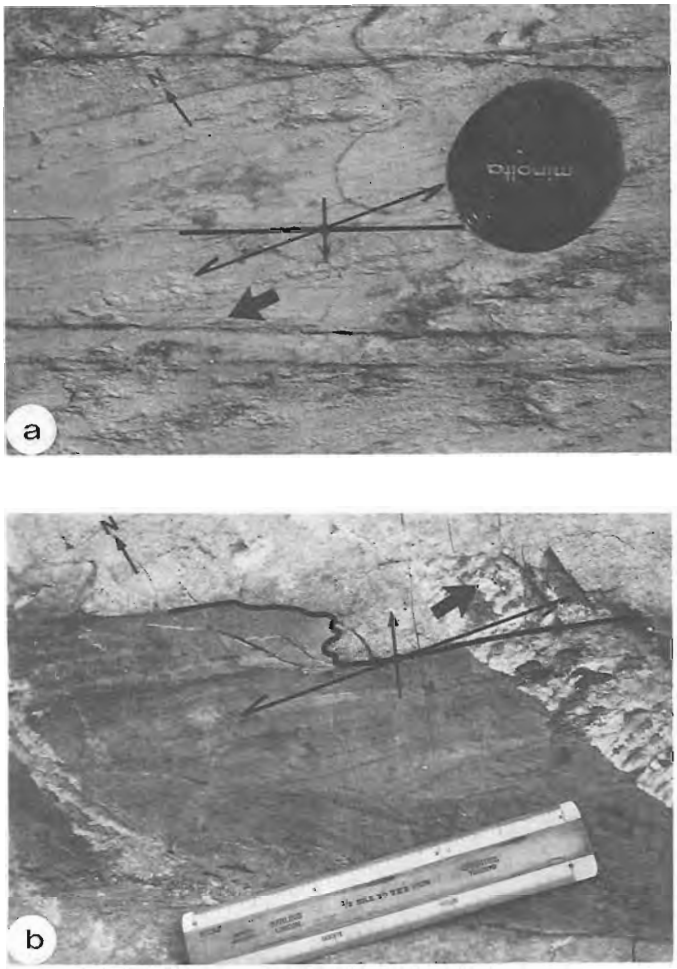

Figure 26.3. *Sedimentary rocks illustrating bedding, cleavage and younging relationships; (**a**) Oxaline Lake, Group A, structural facing is west-southwest (GSC 203327-S); (**b**) Grant's Camp on Highway 11, structural facing is to the east. (GSC 204078-B)*

All dislocative features (fracturing and displacement of pebbles in conglomerate, slip along cleavage planes, Z-shaped asymmetry of minor folds) in the vicinity of the fault indicate a dextral sense of movement consistent with the offset of the diabase dykes. Large-scale dislocative features, unfortunately, are rarely seen due to a lack of outcrop and the paraconformable nature of the rock units and the fault. The asymmetric folds are strongly developed in the vicinity of the fault and it is likely that they are directly related to the same regional stress regime that resulted in faulting.

Most of the producing mines in the east part of the belt were located very close to (within several 100 metres) this fault, implying that it may represent a major "break" similar to those identified in many other Superior Province gold camps. The Larder Lake Break and the Destor-Porcupine fault system are two such examples.

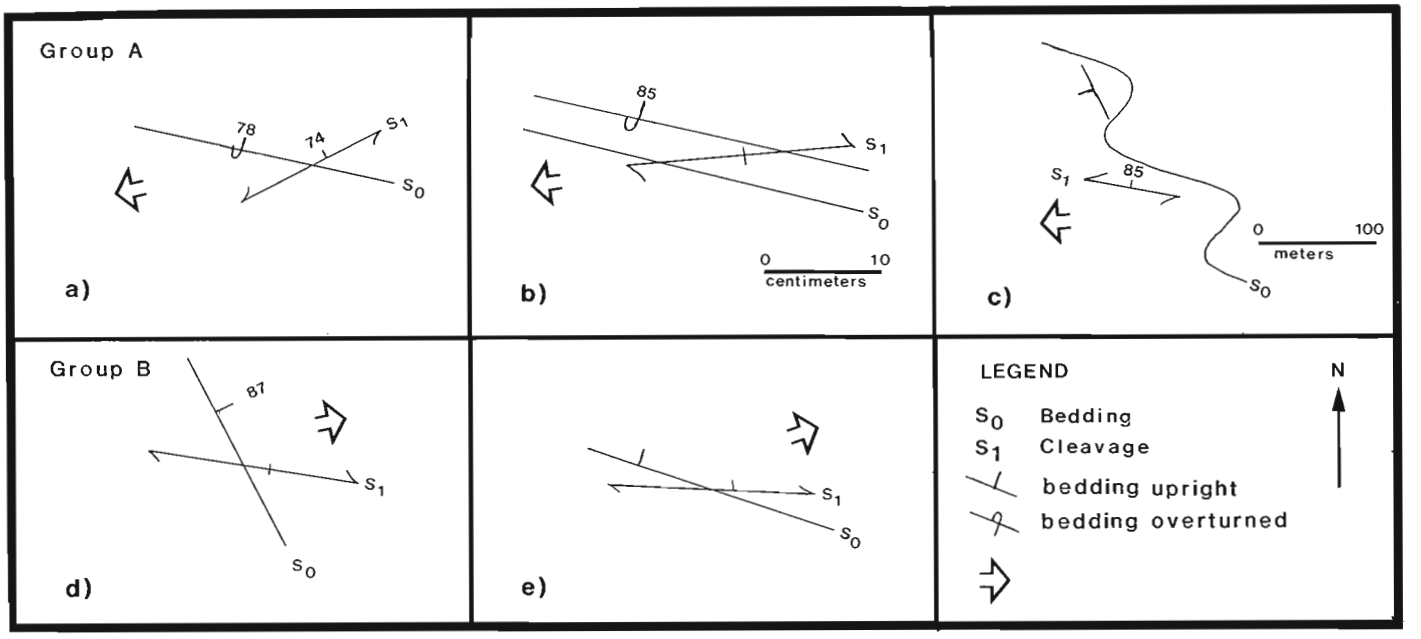

Figure 26.4. Schematic diagram illustrating bedding-cleavage relationships and structural facing at various locations in the Beardmore-Geraldton area (see Fig. 26.2 for location numbers). Group A sedimentary rocks; a) Leitch Mine-location 12; b) Oxaline Lake-location 8; c) Little Long Lac Mine-location 3. Group B sedimentary rocks; d) Jellicoe-location 7; e) Grant's Camp-location 6.

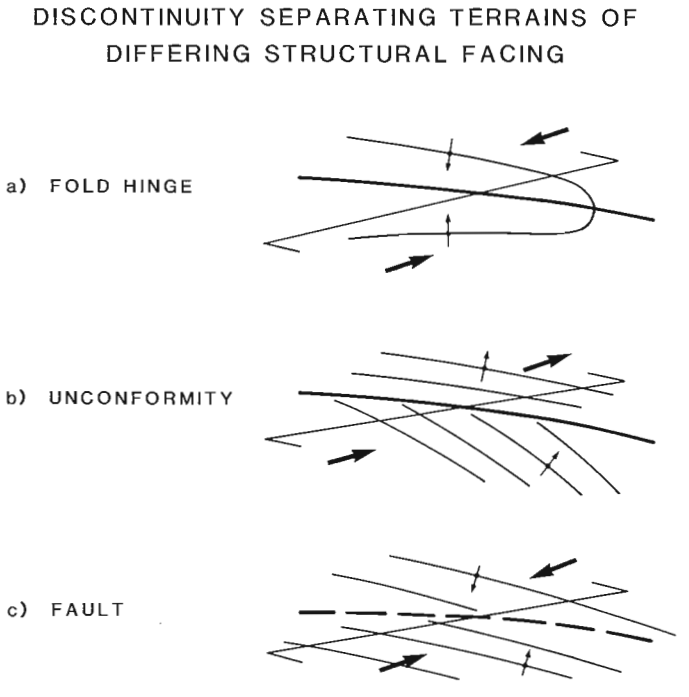

Figure 26.5. Schematic diagram representing three possible interpretations for differing structural facings.

Structural control of mineralization

The majority of ore bodies in the Geraldton area are vein-type. The veins are localized in the hinges of, or along the limbs of, minor flexures or asymmetric folds that have a shallow plunge to the west, and in zones of fracturing and intense foliation along the contacts between rocks of differing ductility (Horwood and Pye, 1951; Pye, 1951). One of the largest single orebodies in the area, the F zone in the Consolidated Mosher Mine (immediately west of the MacLeod-Cockshutt Mine), was of the latter type. It was located along a porphyry-greywacke contact and is estimated to have contained (on both the Mosher and MacLeod properties) in excess of 10 000 000 tons of ore grading approximately 0.15 ounces per ton gold.

The veins are, as a group, parallel to the major break (BTF) but individually "... are of limited lateral and vertical extent.." and "... tend to be arranged en echelon along the direction of the alignment." (Pye, 1951). Gold has been reported in small quantities in the fault zone itself, but no orebodies have been found within it (Pye, 1951). A major portion of the gold mineralization at Geraldton is thus in veins that cut the axial cleavage of the Z-folds.

The ore-bearing veins are related temporarily to the dilation of the cleavage which occurred during the development of the shear zones. The asymmetric folds and related axial cleavage, that are overprinted by the mineralization, may postdate the development of the discontinuity between the Group A and Group B sediments. Both the cleavage and the mineralization overprint the intrusive rocks. This places the mineralization fairly late in the development of the belt.

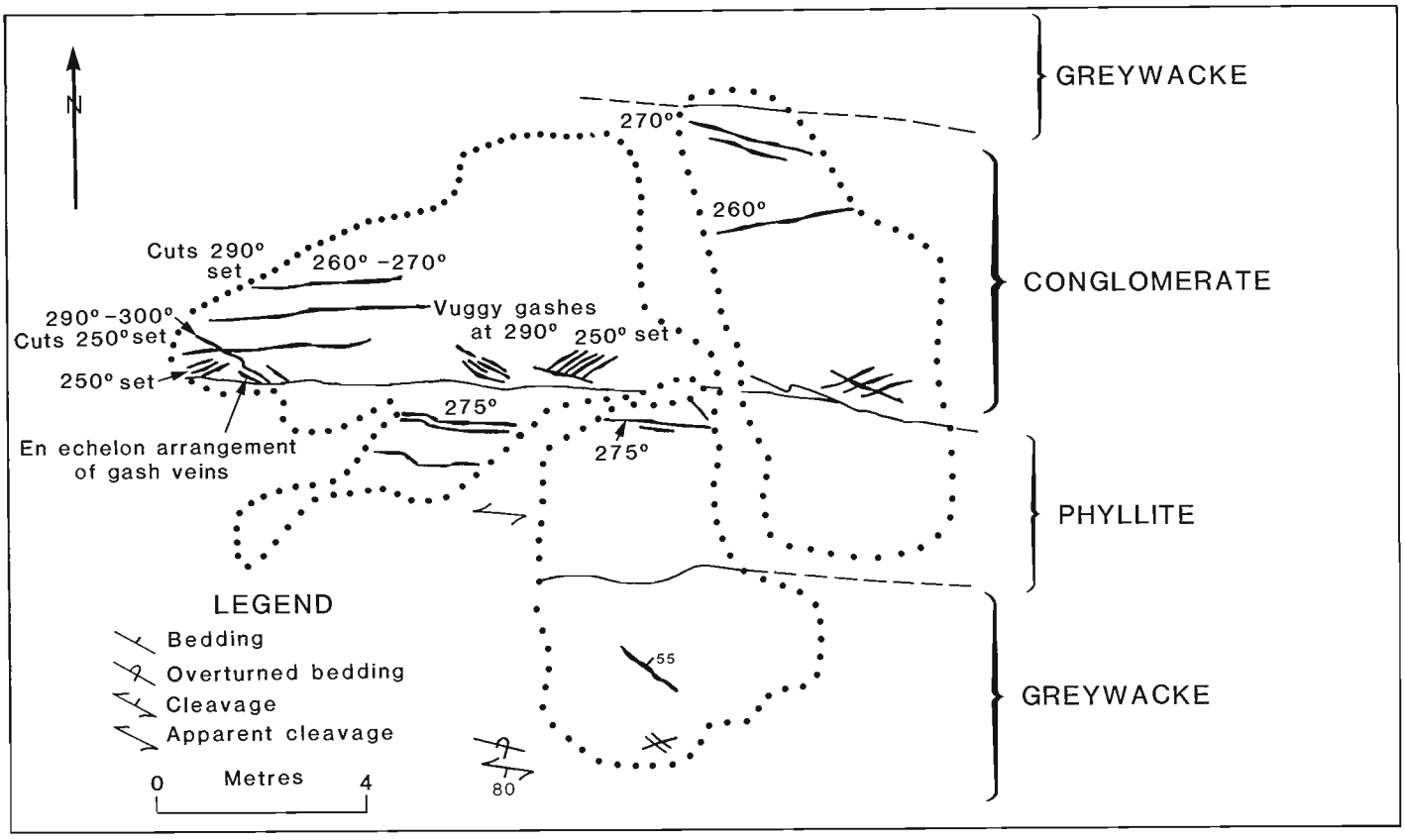

Figure 26.6. *Detailed map of contact between the Group A (conglomerate and greywacke) to the north, and the Group B (greywacke) sedimentary rocks to the south.*

Iron formation hosted gold

At the Hardrock and MacLeod-Cockshutt Mines, an important ore zone, the north ore zone, was hosted in intensely folded and fractured oxide iron formation and interbanded foliated greywacke. The gold is contained within irregular lenses of sulphide which are distributed along the north limb, and in the nose of, a westward-plunging asymmetric fold (Horwood and Pye, 1951). These lenses consist of quartz veins with quartz, pyrite and arsenopyrite replacing wallrock on one or both sides of the vein, and are associated with intense carbonate alteration (Fig. 26.8). The lenses are localized in zones of intense deformation along the contacts of greywacke and iron formation, and in the noses of small asymmetric folds in an orientation consistent with the axial planar cleavage of these folds. Thus, gold mineralization in iron formation is related to relatively late, structurally controlled, features (Thorpe, 1975; MacDonald, 1982; Kerswill and Anglin, 1984; Horwood and Pye, 1951).

Although there are abundant carbonate and sulphide minerals present in the depths, none of these are considered to reflect the presence of a primary carbonate or sulphide facies of iron formation. Indeed, only oxide facies iron formation, containing both magnetite and hematite, has been observed throughout the belt. In every instance where sulphide and carbonate minerals have been observed they can be seen to be superimposed on the oxide iron formation, and all other rock types in the vicinity, and to be localized by structural features.

By far the major part of the iron formation in the belt is unmineralized. Mineralization is associated with anomalous structural conditions and the presence of sulphide alteration. Also, it is worth noting that less than 30% of the gold production from Geraldton came from iron formation-hosted ore (MacDonald, 1982). Most of the production has been from the sedimentary rocks, particularly at or near the contact with feldspar porphyry intrusions. Oxide iron formation in the Geraldton area is therefore not a negative indicator of gold mineralization, but in itself, it is not a positive indicator. A more consistent spatial relationship with mineralization is seen with anomalous structural conditions, and felsic intrusive rocks.

Figure 26.7 *(facing)*

Photographs showing progressive development of shear zones within hornblende gabbro in outcrop on Highway 11 approximately 2 km west of Geraldton, Ontario.

a) *Moderately foliated gabbro; spotted texture is formed by 3-8 mm hornblende megacrysts;*

b) *increasingly foliated gabbro in which narrow anastomosing chloritic shear zones up to 2 cm wide have developed;*

c) *intensely foliated, rubbly weathering, carbonatized chlorite schist; the pitted texture results from the weathering of carbonate minerals;*

d) *very finely laminated chloritic schist indicative of intense deformation; three steeply dipping planar fabric elements are evident; 1) throughgoing chloritic seams (a) 2) oblique internal foliation (b) 3) secondary cleavage (c).*

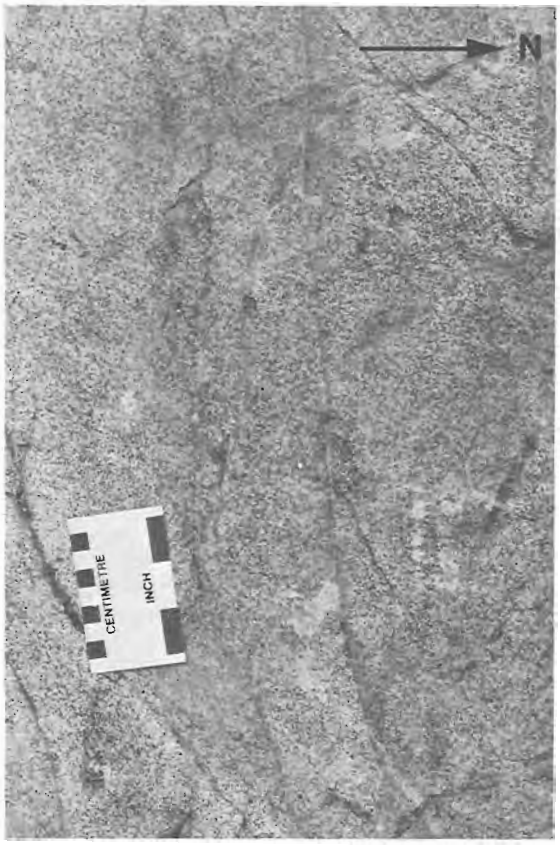

Figure 26.7a



Figure 26.7b



Figure 26.7c

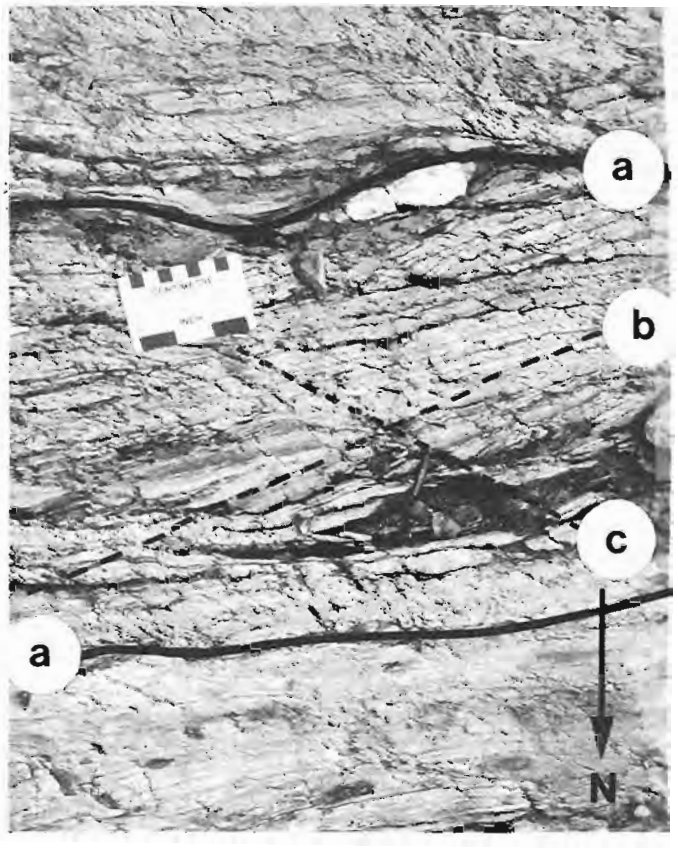

Figure 26.7d



Figure 26.8. Polished slab from Solomon's Pillars occurrence north of Jellicoe, Ontario. Note the irregular, replacement character of sulphides away from the vein. The host rock is cherty magnetite-hematite iron formation.

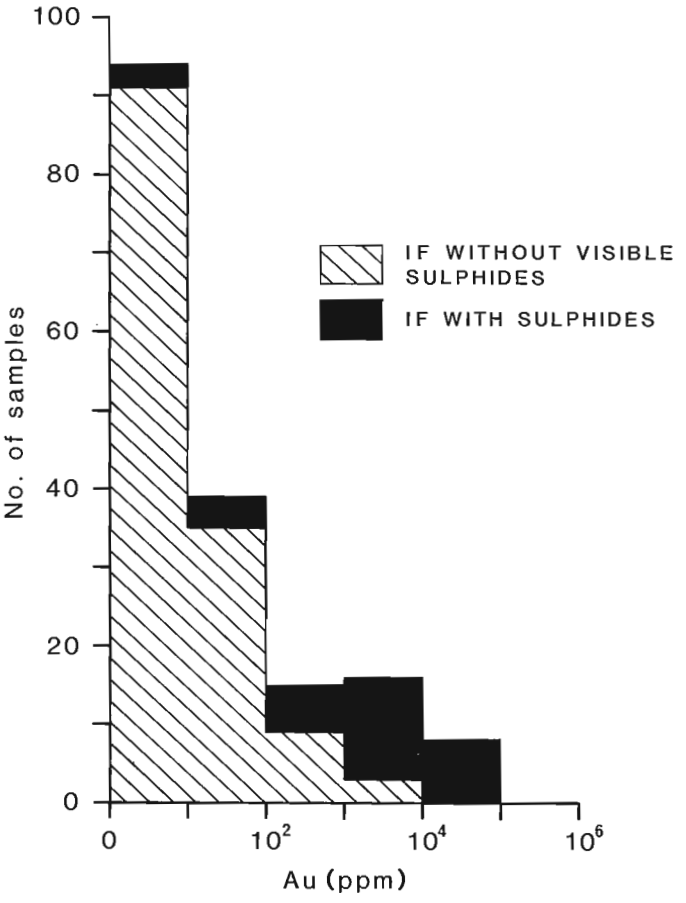

Figure 26.9. Frequency distribution of gold in iron formation in the Beardmore-Geraldton area.

Distribution of gold and base metals in iron formation

A total of 137 oxide samples (those with no visible sulphides) and 33 sulphide-bearing samples of iron formation from throughout the belt were analyzed for gold by delayed neutron activation analysis at X-Ray Assay Laboratories Ltd. (Toronto) and Chemex Laboratories Ltd. (Vancouver). Duplicate analyses from each laboratory indicate that results above 10 ppb are reproducible to ±25%. Those above 20 ppb may be somewhat better. Analyses below 10 ppb are probably reproducible at ±50% of the stated value. Analyses for Cu, Pb and Zn were done by atomic absorption spectrophotometry in the laboratory of the GSC in Ottawa, generally with a precision of ±15%.

The gold data have been plotted on a histogram (Fig. 26.9, note the logarithmic scale of gold content). Examination of the frequency distribution of gold content indicates that the data are bimodally distributed, with the content of gold in the sulphide-bearing samples clearly higher than the sulphide-free samples. Furthermore, the median gold value for the non-sulphide bearing samples is extremely low at less than 10 ppb (most of the samples were actually less than 2 ppb).

Arsenopyrite is ubiquitous in the sulphide replacement zones within the mineralized iron formations, however, there does not seem to be a direct correlation between the amount of arsenic and gold. Copper, zinc and lead contents of the iron formation are generally low and little change in their distribution is evident in the more gold-rich areas. Copper (average of 15 ppm in all iron formation) in the gold-rich samples is locally slightly enriched (up to a few 100 ppm) compared with gold-poor iron formation (typically 3 to 50 ppm) but a distinct correlation of copper and gold is lacking. Zinc (average content 36 ppm in all iron formation samples) and lead (average content approximately 2 ppm) are both low; even in sulphide-rich samples these elements are not notably enriched. This suggests that the sulphides are probably not the result of a volcanogenic massive sulphide-type hydrothermal system, but are the result of some other type of mineralizing system. This is consistent with the observation of Kerrich and Fryer (1979).

These data, and the distribution of sulphides in iron formation in cleavage and other structurally controlled zones, lead to the conclusion that the sulphides and the gold do not have a primary genetic relationship to the iron formation (Kerswill and Anglin, 1984; MacDonald, 1982). This is consistent with the findings of Phillips et al. (1984).

Discussion

The contact between the two major sedimentary groups in the Beardmore-Geraldton area is a fault or shear zone that is parallel to the boundary between the Wabigoon and Quetico subprovinces, and is also parallel to the Bankfield-Tombill fault, which is most closely related to the gold deposits. Other subparallel faults, including the Watson Lake fault east of Beardmore, the Paint Lake fault north of Jellicoe, and the Gravel River fault west of Geraldton, form the boundaries between the sedimentary and volcanic rocks, both north and south of the principal sedimentary area. Each fault-bounded "panel" bears little stratigraphic or lithological similarity to adjacent "panels", possibly indicating that each is a tectonically transposed "slice", juxtaposed well after the principal volcanic and sedimentary depositional events. Dextral strike-slip motion similar to that interpreted to have occurred along the Bankfield-Tombill fault may also have occurred along the margins of the other "panels", causing them to be tectonically stacked.

In the area of most of the past-producing mines near Geraldton, empalcement of the vein and disseminated gold mineralization was controlled by structures and overprint a) the pervasive regional cleavage; b) the intrusions which also are affected by the regional cleavage, and c) later asymmetric folds and associated structures. Thus gold was emplaced late in the structurla history of the region, during one of the late stages of fault movement.

Gold, with associated sulphides and attendant carbonate alteration, is clearly a structurally controlled chemical overprint. Primary sulphide-facies iron formation, and primary anomalous gold content in the iron formation, are absent in the Beardmore-Geraldton area.

Acknowledgments

The authors thank Howard Poulsen for many fruitful discussions and suggestions both in the field and in Ottawa. John Mason, Carig McConnell and Jerry White of the Thunder Bay office of the Ontario Ministry of Natural Resources provided considerable support in the field. James MacDonald and Moe Lavigne of the Ontario Geological Survey are conducting research in the area, and provided many new ideas and information. Fred Kehlenbeck of Lakehead University is thanked for his on the spot instructions on structural facing measurements. Lac Minerals Corp., Dome Mines Ltd., and Roxmark Mines Ltd. are gratefully acknowledged for allowing access to information and properties. Jim Donnelly is thanked for her invaluable assistance in the field.

References

Berthe, D., Choukroume, P., and Jegouzo, P.
1979: Orthogenesis, mylonite and non-axial deformation of granites; the example of the South American Shield; Journal of Structural Geology, v. 1, p. 31-42.

Borradaile, G.J.
1976: "Structural facing" (Shackleton's Rule) and the Paleozoic rocks of the Malaguide Complex near Velez Rubio, S.E. Spain; Proceedings Konnklijke Nederlandse Akademie Van Wentenschappen, Amsterdam, Series B, p. 330-336.

Bruce, E.L.
1936: The eastern part of the Sturgeon River area; Ontario Department of Mines, v. 45, part 2, p. 1-59.

Card. K.D.
1983: Regional geological synthesis, central Superior Province: reconnaissance investigations in the Nakina area, Ontario; in Current Research, Part A, Geological Survey of Canada, Paper 81-1A, p. 25-27.

Cummins, W.A. and Shackleton, R.M.
1955: The Ben Lui recumbent syncline (S.W. Highlands); Geological Magazine, v. 92, p. 325-363.

Franklin, J.M. and Thorpe, R.I.
1983: Comparative metallogeny of the Superior, Slave and Churchill provinces; H.S. Robinson Memorial Volume, Precambrian Sulphide Deposits, ed. R.W. Hutchinson, C.D. Spence, and J.M. Franklin; Geological Association of Canada, Special Paper 25, p. 3-90.

Hodgson, C.J. and MacGeehan, P.J.
1982: Geological characteristics of gold deposits in the Superior Province of the Canadian Shield; in Geology of Canadian Gold Deposits, ed. R.W. Hodder and W. Petruk; Canadian Intsitute of Mining and Metallurgy, Special Volume 24.

Horwood, H.C. and Pye, E.G.
1951: Geology of Ashmore Township; Ontario Department of Mines Annual Report, v. LX, part V, 105 p.

Kerrich, R. and Fryer, B.J.
1979: Archean precious-metal hydrothermal systems, Dome Mine, Abitibi Greenstone Belt. II. REE and oxygen isotope relations; Canadian Journal of Earth Sciences, v. 16, p. 440-458.

Kerswill, J.A. and Anglin, C.D.
1984: Some thoughts on gold deposits hosted by iron formation with particular reference to the Lupin Mine, Contwoyto Lake area, NWT, and to gold mineralization in the Geraldton Camp, Ontario; in Current Activities Forum 1984, Program with Abstracts, Geological Survey of Canada, Paper 84-8, p. 6.

MacDonald, A.J.
1982: The iron formation-gold association evidence from Geraldton area; in The Geology of Gold in Ontario, ed. A.C. Colvine; Ontario Geological Survey, Miscellaneous Paper 110, p. 75-83.

Mackasey, W.O., Blackburn, C.E., and Trowell, N.F.
1974: A regional approach to the Wabigoon-Quetico belts and its bearing on exploration in northwestern Ontario; Ontario Department of Mines, Miscellaneous Paper 58, 29 p.

Mason, J.K. and McConnell, C.D.
1982: Gold mineralization in the Beardmore-Geraldtona rea; in The Geology of Gold in Ontario, ed. A.C. Colvine; Ontario Geological Survey, Miscellaneous Paper 100, p. 84-97.

Pirie, J. and Mackasey, W.O.
1978: Preliminary examination of regional metamorphism in aprts of the Quetico metasedimentary blet, Superior Province, Ontario; in Metamorphism in the Canadian Shield, ed. J.A. Fraser and W.W. Heywood; Geological Survey of Canada, Paper 78-10, p. 37-48.

Phillips, G.N., Groves, D.I., and Martyn, J.E.
1984: An epigenetic origin for Archean banded iron-formation-hosted gold deposits; Economic Geology, v. 79, p. 162-171.

Pye, E.G.
1951: Geology of Errington Township, Little Long Lac area; Ontario Department of Mines, Annual Report v. LX, part VI, 140 p.

Stockwell, C.H.
1964: Age determinations and geological studies part II; Fourth report on structural provinces, orogenies and time classification of rocks of the Canadian Precambrian Shield; Geological Survey of Canada, Paper 64-17, pt. 2, p. 1-29.

Thorpe, R.I.
1975: Geology of gold deposits in Canada; in Report of Activities, Part A, Geological Survey of Canada, Paper 75-1A, p. 256.

GEOLOGY AND COPPER OCCURRENCES OF THE NATKUSIAK BASALTS, VICTORIA ISLAND, DISTRICT OF FRANKLIN

Projects 840003, 700059, 840012

C.W. Jefferson, W.E. Nelson[1], R.V. Kirkham, J.H. Reedman[2], and R.F.J. Scoates
Economic Geology and Mineralogy Division

Jefferson, C.W., Nelson, W.E., Kirkham, R.V., Reedman, J.H., and Scoates, R.F.J., Geology and copper occurrences of the Natkusiak basalts, Victoria Island, District of Franklin; in Current Research, Part A, Geological Survey of Canada, Paper 85-1A, p. 203-214, 1985.

Abstract

Copper showings occur throughout Late Proterozoic Natkusiak basalts that are here informally divided into seven regionally mappable members. The basalts unconformably overlie the Shaler Group and occupy the southwest-trending asymmetric Holman Island Syncline. Prominent northwest-trending lineaments transect the syncline but are not directly associated with facies changes, copper occurrences and most faults.

Native copper with prehnite is disseminated in vesicular flows, concentrated in veins occupying joints and fractures in massive basalt, or disseminated in quartz-prehnite veins. Several native copper occurrences are close to northeast-trending faults and lineaments. Native copper is associated with prehnite, pumpellyite, chlorite, quartz and calcite, products of sub-greenschist facies metamorphism. Chalcocite and minor bornite, tetrahedrite, chalcopyrite and pyrite occur with quartz, calcite and hematite in veins and sheeted vein systems. Economic copper concentrations have not yet been identified. Copper was probably redistributed during early burial metamorphism into porous stratigraphic and structural zones within the volcanic pile.

Résumé

Des indices de cuivre se présentent partout dans les basaltes tardiprotérozoïques de Natkusiak qui, dans le présent rapport, sont divisés officieusement en sept niveaux susceptibles d'être cartographiés à l'échelle régionale. Ils reposent en discordance sur le groupe de Shaler et occupent le synclinal asymétrique de Holman Island, orienté vers le sud-ouest. Des linéaments proéminents à orientation nord-ouest traversent le synclinal mais ne sont pas associés aux changements de faciès, aux indices de cuivre et à la plupart des failles.

Du cuivre natif et de la prehnite sont disséminés dans des coulées vésiculaires, concentrés dans des filons dans les diaclases du basalte massif ou disséminés dans des filons de quartz et de prehnite. Il y a plusieurs indices de cuivre natif près de failles et de linéaments à orientation nord-est. Le cuivre natif est associé à la prehnite, à la pumpellyite, à la chlorite, au quartz et à la calcite, qui sont les produits d'un degré de métamorphisme moins élevé que celui du faciès des schistes verts. La chalcocite, ainsi que de petites quantités de bornite, de tétraédrite, de chalcopyrite et de pyrite se manifestent avec du quartz, de la calcite et de l'hématite en filons et en réseaux de filons feuilletés. On n'a pas encore identifié de concentrations exploitables de cuivre. Le cuivre a vraisemblablement été réparti de nouveau dans des zones stratigraphiques et structurales poreuses au sein de la masse volcanique au cours d'une ancienne période de métamorphisme par enfouissement.

[1] Panarctic Oils Ltd., 815-8th Avenue S.W., Calgary, Alberta T2P 2H6
[2] J.H. Reedman and Associates Ltd., Box 1583, Winnipeg, Manitoba R3C 2Z6

Introduction

This report describes copper occurrences and their geological setting in Late Proterozoic rocks of the Holman Island Syncline, Victoria Island, Northwest Territories (Fig. 27.1). Work was concentrated on the Natkusiak basalts and their contact with the underlying Kilian Formation.

The Inuit have long known that the Natkusiak basalts contain native copper (see reports by V. Stefansson, 1913, p. 294 and Thorsteinsson and Tozer, 1962, p. 77). Minor native copper was found in the Natkusiak basalts by Thorsteinsson and Tozer (1962), Christie (1964) and Baragar (1976). Widespread exploration of the Natkusiak basalts in the late 1960s by Grandroy Mines Ltd. (Newbury, 1969; Seeber, 1970) and by Muskox Syndicate (Ekstrom and Pelette, 1968) verified the large exhumed plates of copper veins (up to 300 kg) which had been earlier reported by the Inuit as well as a variety of additional disseminated to vein-type native copper and copper sulphide occurrences.

The data presented here are based on a reconnaissance evaluation of the Holman Island Syncline (WEN, 1982-1984; CWJ, 1984), combined with detailed studies in two areas of pronounced physiographic lineaments (JHR and CWJ, 1984).

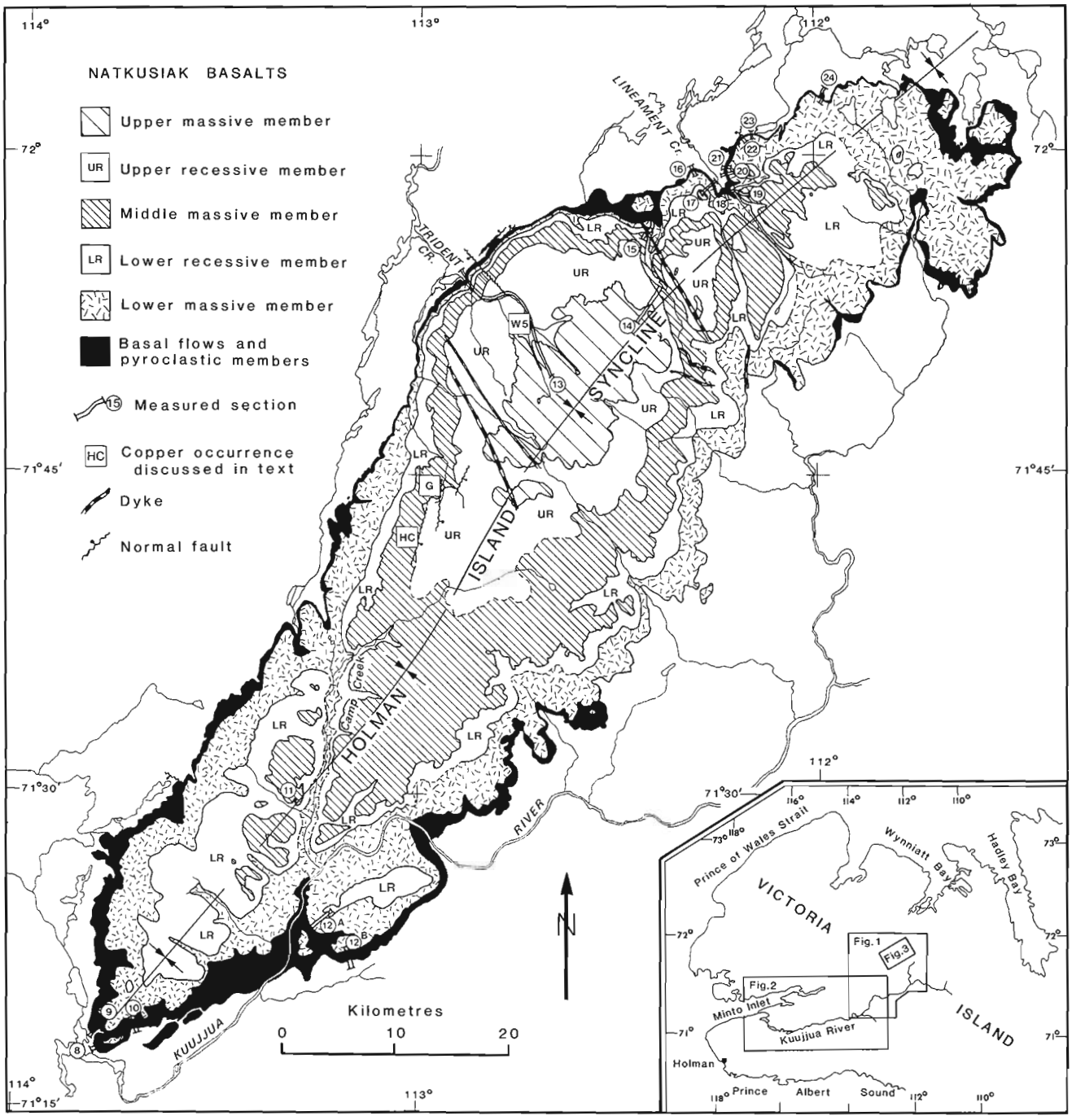

Figure 27.1. Geological map of Natkusiak basalts in the northeast sector of Holman Island Syncline. Copper occurrences discussed in text are shown by letter (W5, G, HC) or referred to measured sections (8 to 24).

RFJS and RVK (1984) provided detailed information for several measured sections and copper occurrences. All of us contributed to the discussion on genesis.

Stratigraphy

The main stratigraphic units of this report are summarized in Table 27.1. Two aggregate sections in the area of thickest basalts (Fig. 27.2, 27.3) comprise a series of vertically measured mini-sections which were compiled either by tracing out or lithologically correlating distinctive flows. Thicknesses were measured by graduated staff, by Abney level or by altimeter with corrections for dip where necessary. Aggregate thicknesses were checked by geologic cross-sections using the 1:250 000 topographic base. They roughly corroborate thicknesses reported by Baragar (1976). The Natkusiak basalts are separated by erosion into a well exposed northeast sector and a partially exposed southwest sector, both centred on the Holman Island Syncline (Fig. 27.1). Correlations suggest that the two sectors were originally contiguous, although local variations exist within and between them (see Jefferson, 1985).

The Natkusiak basalts and related sills have been dated by K-Ar at approximately 700 Ma (see discussions in Baragar and Loveridge, 1982; Palmer et al., 1983). Stratigraphic correlations relevant to the age of the basalts are discussed by Jefferson (1985).

Natkusiak Formation

The Natkusiak basalts are greater than 650 m thick at section 14 (Fig. 27.3) and 1100 m thick at "Trident Creek" (informal name; section 13) which is at the centre of the northeast sector. The basalt pile is here informally divided into seven regionally mappable members (Table 27.1, Fig. 27.1, 27.3). This informal subdivision was prompted by the need to consider copper occurrences in a stratigraphic context and was made possible by extensive exposure with distinct weathering characteristics of the members. The validity of this proposed stratigraphy is constrained by the lack of closely spaced stratigraphic sections, the reconnaissance nature of the field work and the consequent lack of systematic laboratory studies. Future field and laboratory studies of the Natkusiak basalts may result in modification of this proposed stratigraphy.

Table 27.1. Stratigraphy of the Natkusiak Formation, Victoria Island

Formation	Member (Thickness)	Lithology
DYKES (cm to dm wide)		Massive jointed diabase. Intrude entire Shaler Group and Natkusiak basalts. Two orientations, NE and NW.
SILLS (0 to >60 m thick)		Massive, columnar-jointed diabase: locally well developed internal layering, cumulate textures and granophyre. Intrude mainly Shaler Group, thin sills in basalts.
NATKUSIAK BASALTS	UPPER MASSIVE ($\geq$150 m)	4-8 flows: blue-green, orange-brown weathering, massive blocky to columnar jointed. Forms top plateau in Trident Creek area.
(>1100 m, 40-50 flows)	UPPER RECESSIVE ($\leq$500 m)	20-29 flows: dark green, mainly green-brown weathering, rubbly flaggy breaking.
	MIDDLE MASSIVE (80-90 m)	4-6 flows: blue-green, orange-brown weathering, massive blocky to columnar jointed, forms top plateau throughout much of region.
	LOWER RECESSIVE (20-200 m)	4-9 flows: dark brown-green to green, drab green-brown weathering. Locally includes pyroclastic rocks and pillowed lavas.
	LOWER MASSIVE (~75 m)	2-5 flows: blue-green to green-grey, orange-brown to brown weathering, massive, cliff-forming, blocky to columnar jointed, forms second lowest plateau.
	PYROCLASTIC (0- >100 m)	Lower ~10 m: locally sedimentary, green to maroon, upper $\leq$90 m: lithic lapilli tuff, local tuff-breccia, green (bottom) to maroon (top).
	BASAL (0- >70 m)	0-4 flows, blue-green to green-brown, orange-brown to green-brown weathering, massive, cliff-forming to rubbly. Locally spheroidally weathered or includes hyaloclastic breccia with lithic and volcanic inclusions; isolated to layered pillowed flows in amygdaloidal hyaloclastic matrix. Forms plateau in central and southwestern areas.
	LOW-ANGLE UNCONFORMITY	
SHALER GROUP		

Individual flows within these members are traceable for up to 30 km along strike. As noted by Baragar (1976) and Palmer et al. (1983) sampling is made difficult by extensive physical weathering. The flow bases are frost-shattered to felsenmeer and form blocky, rubbly bluffs. The amygdaloidal flow tops form gently sloping benches. Lenticular units of red mudstone and rare red to grey stromatolitic limestone were observed between flows in six places. These interflow sedimentary beds locally exceed one metre in thickness and several kilometres in lateral extent. Brief petrographic descriptions are given of typical samples from each member.

Basal member (informal)

The basal member, up to 70 m thick, and consisting of as many as four flows, each ranging from 0 to 30 m in thickness, is present throughout much of the region. The basal member pinches out locally as shown in Sections 16 and 24 (Fig. 27.3). Flows of the basal member range from amygdaloidal hyaloclastite to spheroidally weathered dark brown-green flows, to massive, columnar-jointed cliff-formers that weather brown-green to orange-brown. The hyaloclastic flow in the "Lineament Creek" (informal name) area contains abundant amygdules. It also includes small fragments to metre-long blocks of dark green, altered limestone, and very large interlayers and/or blocks of massive, columnar-jointed basalt.

The massive basalt consists of randomly oriented, partly sericitized plagioclase microlites ($An_{\sim 40}$?) with interstitial pigeonite and magnetite. Secondary minerals include chlorite (after glass?), calcite, minor quartz and hematite. Neither olivine nor olivine pseudomorphs were observed in the few samples examined here. However Baragar (personal communication, 1984) has noted that minor olivine occurs characteristically throughout the Natkusiak basalts.

In "Newbury Creek" (informal name) the basal member consists of 20 m of interlayered pillow lava and highly amygdaloidal hyaloclastic-pyroclastic debris with primary dips of 33° towards 160° (Fig. 27.4). The pillowed unit is tabular in shape and areally restricted, the top being bevelled against a subhorizontally overlying massive flow. As suggested by Baragar (1976) the basal flows were probably extruded into moderately shallow to very shallow water.

Lithic pyroclastic member (informal)

The lithic pyroclastic member extends over most of the region and ranges in thickness from less than 10 to more than 100 m. It was described as agglomerate by Thorsteinsson and Tozer (1962), bouldery conglomerate or volcanic breccia by Young (1981) and red volcanic sediments or red bed member by Baragar (1976).

In the Lineament Creek area it comprises a lower, recessive, sedimentary subunit up to 20 m thick and an upper lithic lapilli tuff from 10 to 30 m thick. The sedimentary subunit is very recessive but well exposed locally in the Lineament Creek area. It contains several complete but apparently shallow water turbidite cycles (Fig. 27.5) interbedded with trough-crossbedded, rippled, scoured and planar laminated mudstones to sandstones. The subaqueous turbidites may have originated as subaerial pyroclastic surges. The maroon to green sedimentary units are dominantly reworked volcanic material. The top third of the well bedded sedimentary subunit contains several massive to graded beds of accretionary lapilli, most of which range in diameter from 3 mm to 2 cm and have scoraceous cores (Fig. 27.6).

The main body of the pyroclastic member is a lithic lapilli tuff (Fig. 27.7). The coarser lithic "agglomerates" and breccias described by Thorsteinsson and Tozer (1962) and

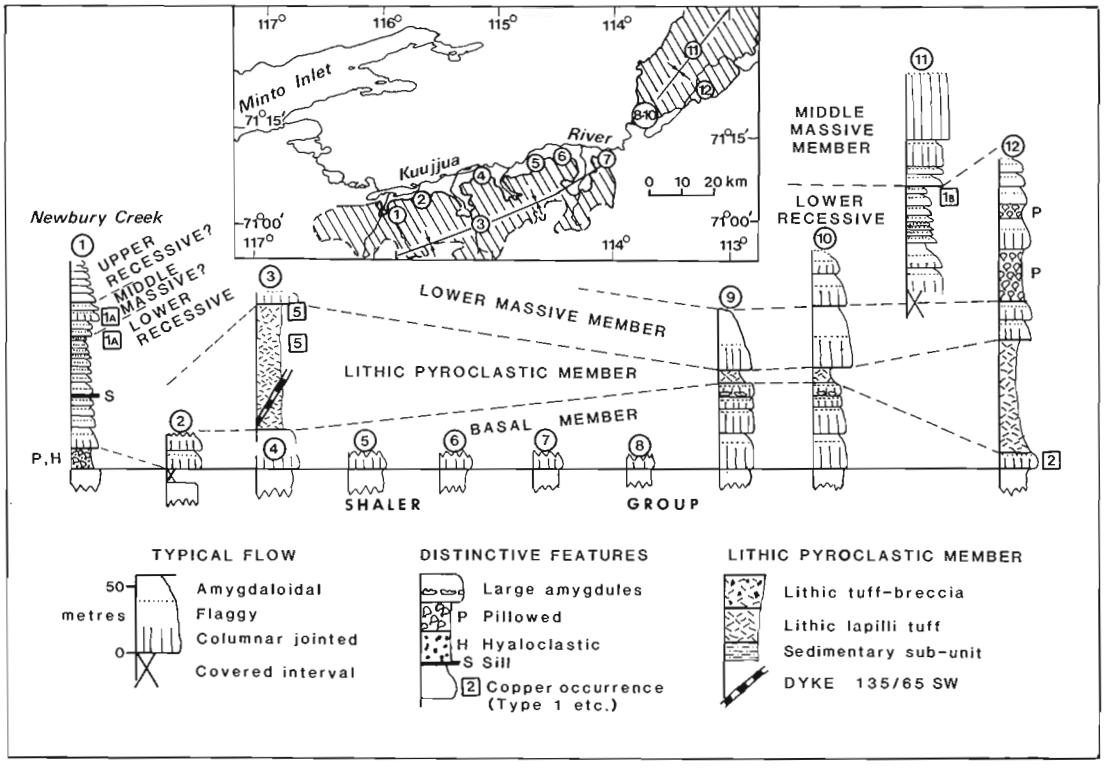

Figure 27.2. *Measured sections in the southwest sector of Holman Island Syncline, through the Natkusiak basalts at same vertical scale as Figure 27.3. Inset shows outline of Natkusiak basalts (diagonal lines) and location of sections along the Kuujjua River. Some legend items only for Figure 27.3.*

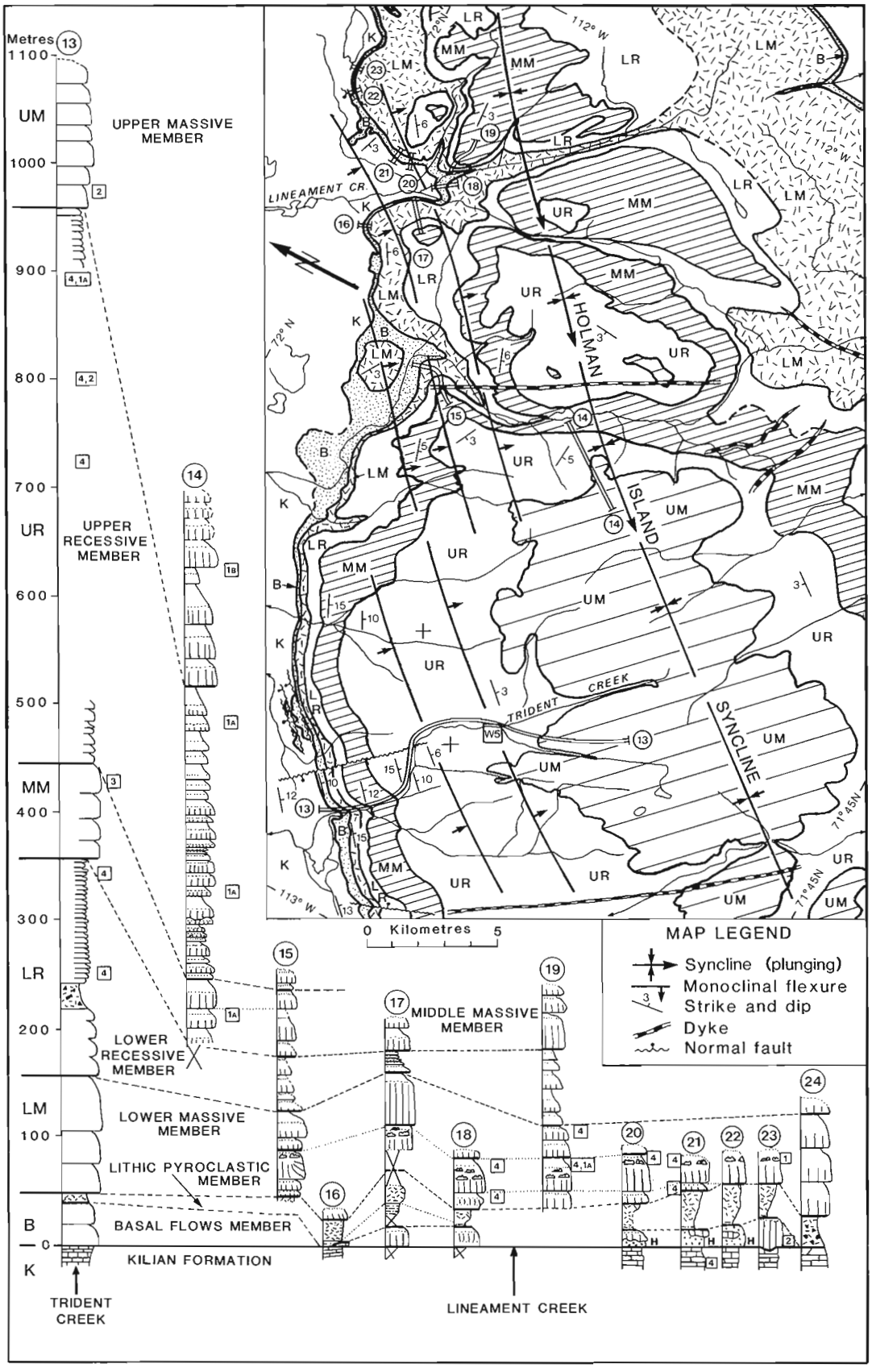

Figure 27.3. *Geological map of the Lineament Creek-Trident Creek area with stratigraphic sections through Natkusiak basalts at same vertical scale as Figure 27.2. Section 24 (location shown on Fig. 27.1) is after Thorsteinsson and Tozer (1962, p. 38). Sections 14, 19 and 20 are in approximately the same respective positions as sections 1A, 2B and 1B of Baragar (1976). Map legend is shown in inset; map units are keyed to Section 13. The legend for measured sections, shown as double lines on map, is given in Figure 27.2.*

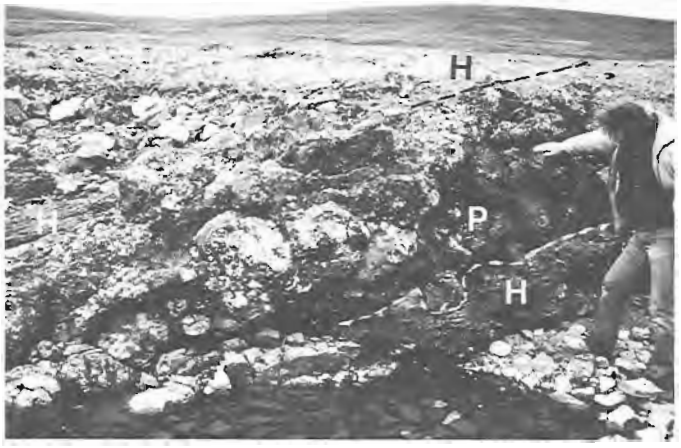

Figure 27.4. Southwest-dipping interlayered pillowed flows (P) and amygdaloidal hyaloclastite (H) at the base of Section 1, Newbury Creek area. Height of exposure is about 1.8 m. (GSC 204188-E)



Figure 27.5. Complete Bouma cycle (A B C D E) in lower sedimentary part of the lithic pyroclastic member, Section 17. Note shallow water symmetrical ripples (R) in overlying siltstones. Hammer for scale. (GSC 204121-G)

Young (1981) occur in the extreme northeast, locally at Trident Creek and south of Section 3 (Fig. 27.2). The lithic lapilli tuff consists of subrounded clasts, generally less than 3 cm in diameter, supported by a calcareous, felted lithic tuff matrix. The tuff tends to be drab green at the base grading to deep red at the top, although some sections are entirely maroon, and others are entirely green or drab earthy brown in colour. Large clasts are mostly cream to dark green, chloritic, aphanitic limestone. Finely crystalline massive and scoriaceous basalt fragments are also present. The fragment size coarsens upward in the lower part of the unit. The best exposures reveal several indistinct beds, 1 to several metres thick, of slightly differing fragment size within the unit. A strong horizontal fabric is defined by oriented fragments, the felted lithic matrix and compaction features. A sample examined in thin section showed the same features as observed macroscopically. The overall texture is thus seriate and unsorted. Welded textures were not observed. The top contact is baked against the overlying flow in several places, and vertical to inclined pipe amygdules are common at the base of the overlying flow.

The pyroclastic member probably originated from a number of explosive centres throughout the region, as suggested by its highly variable thickness (Fig. 27.2, 27.3). These were possibly from phreatic eruptions caused by hot solutions circulating in the underlying sedimentary rocks. Initial deposits were reworked by turbidites and traction currents (tidal?) to form cross beds and ripple marks in a shallow subaqueous environment. The accretion lapilli indicate at least local airfall origin, but the bulk of the overlying lithic pyroclastic beds appear to be mass flow deposits. The pillowed and hyaloclastic unit in Newbury Creek (Section 1, Fig. 27.2) may be an equivalent of the pyroclastic member. The top of the pyroclastic member is locally quite irregular on a metre scale, suggesting erosion prior to extrusion of the lower massive flows. This erosion may also be indicated by the red, oxidized top of the unit which could be due to weathering (and/or deposition?) in a subaerial environment.

Lower massive member (informal)

The lower massive member ranges from 20 to 80 m thick and includes two flow types, each 10 to 50 m thick. Green-brown discontinuous flows in the lower part of this unit are locally separated by sedimentary and pyroclastic rocks similar to those of the underlying pyroclastic member.

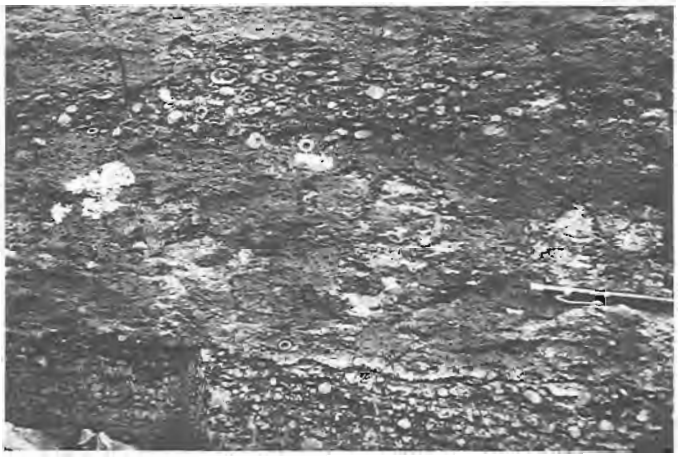

Figure 27.6. Indistinctly bedded accretionary lapilli tuff, typical of lithic pyroclastic member, Section 15. Pencil for scale is 15 cm long. (GSC 204121-Y)



Figure 27.7. Lithic lapilli tuff, upper part of pyroclastic member, Section 17. Height of view is 90 cm. (GSC 204121-D)

The main part of the lower massive member comprises two to three massive, columnar-jointed, cliff-forming flows (Fig. 27.8) that are blue-green-grey and weather orange-brown to brown. The most distinctive of these in the Lineament Creek area was termed the Rosetta flow by Baragar (1976). It is 25 to 30 m thick and contains large flat bottomed amygdules, with puffy tops, that range up to 20 cm wide and 10 cm high (Fig. 27.9). This distinctive flow was traced over 25 km from northeast to southwest. The lower massive member forms the lowest plateaus in the northwest sector. It forms the top of the succession in the central area and much of the southeast sector, west of 113°30'W.

The Rosetta flow is subophitic to microlitic and consists of altered plagioclase laths (An_{30}?) with interstitial clinopyroxene and dispersed magnetite. Alteration minerals include interstitial chlorite, hematite and minor carbonate in fractures. The amygdules are filled with chlorite, quartz, carbonate and locally prehnite, pumpellyite and native copper.

Lower recessive member (informal)

The lower recessive member comprises four to nine indistinct, dark green, drab green-brown-weathering flows. The unit ranges from 20 to 80 m thick with individual flows being 3 to 20 m thick. The flows form a series of low, rubbly, bluffs separated by gently sloping amygdaloidal flow-top terraces. Weathering renders these flows platy, crumbly and difficult to sample. Most flow tops and bases are difficult to distinguish and individual flows are difficult to trace laterally. Several flows are pillowed at Section 12. The unit as a whole, however, is readily mappable in the northeastern sector.



Figure 27.8. *Columnar joints in thick flow of lower massive member, Section 17. Height of view is 12 m. (GSC 204121-V)*

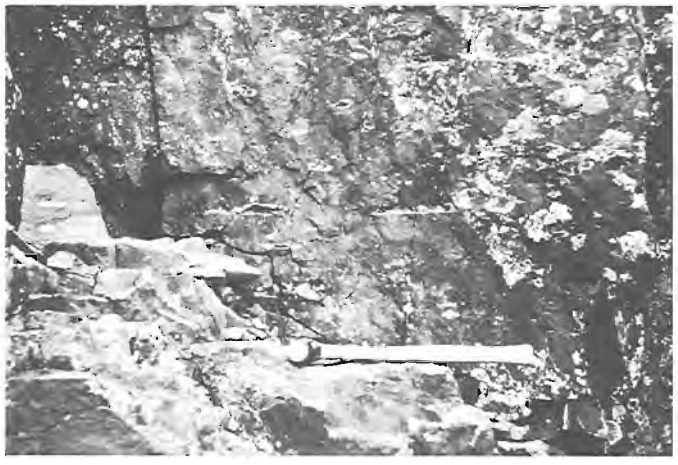

Figure 27.9. *Large flat-bottomed amygdules in Rosetta flow, lower massive member, Section 19. Hammer for scale. (GSC 204121-E)*

Some of the dark green, crumbly, lower recessive flows appear to be more mafic than normal basalt in composition. However they have not as yet been analysed petrographically or chemically to test this speculation.

Middle massive member (informal)

The middle massive member is approximately 70 to 90 m thick. It comprises four to six flows that are similar to flows of the lower massive member but that weather to brighter shades of orange-brown. The flows, which are each 10 to 50 m thick, generally do not form cliffs but constitute prominent bluffs of angular blocky felsenmeer revealing local, crudely developed columnar jointing. The middle massive member forms extensive plateaus throughout much of the northeast sector except in the Trident Creek area. It also forms the uppermost plateau in the southwest sector around Newbury Creek. Baragar's (1976) sections 2B and 3B are topped by this member.

These blue-green basalts contain abundant, prismatic, reddish brown crystals of hematitized ?clinopyroxene that are 1-2 mm long. The basalts weather locally to a knobby exterior, due to the presence of 2-5 mm amygdules of quartz, prehnite and pumpellyite which contain flecks of native copper. These may be the "quartz dacite" units referred to by Ekstrom and Pelette (1968).

A typical example of this member exhibits a fine grained ophitic texture with plagioclase laths enclosed by larger interstitial clinopyroxene crystals. The plagioclase and groundmass are altered to chlorite, carbonate, quartz and sericite. Distinct patches of chlorite and quartz are possibly devitrified glass. Magnetite is finely disseminated through the rock.

Upper recessive member (informal)

The upper recessive member is more than 270 m thick. It contains 20 to 29 flows which, like those of the lower recessive member, are thin, weathered and indistinct. Most are drab dark green and weather green-brown. They generally form low, rubbly bluffs with amygdaloidal, bench-forming flow-tops. Several of the darker flows weather spheroidally. Several orange-brown- to brown-weathering, massive blocky flows are similar to those of the middle and upper massive members. As in the lower recessive member, many of the darker green, crumbly and spheroidal-weathering flows may be more mafic than basalt in composition.

Two examples of this member have a subophitic texture; one of the two contains large plagioclase phenocrysts over 1 cm in length. The plagioclase-clinopyroxene primary mineralogy and alteration assemblages are not notably different from those of other members.

Upper massive member (informal)

The upper massive member forms the highest plateau at about 600 m elevation in the Trident Creek area. This unit is at least 150 m thick and comprises at least six flows which are massive, blue-green and weather orange-brown. The flows, which form high bluffs of angular coarse blocks topped by extensive flow-top benches, are laterally extensive; the number preserved being determined by the erosion level. Glaciers have removed amygdaloidal flow tops from most of

the broader terraces and plateaus, exposing well developed polygonal joints and polyhedral weathering patterns. The same feldspar microlites and prismatic brown hematite crystals noted in the middle massive member are present locally. This member possesses the same textures, primary and secondary minerals as the other massive members.

Dykes and sills

Two sets of dykes and related sills intrude the Natkusiak basalts. Numerous sills intrude the sedimentary rocks below (Baragar, 1976). Dykes of the northeasterly trending set are thin, fine grained and dip 45 to 70° to the southeast or northwest. One dyke of this array feeds a thin aphanitic sill which separates two flows. The northwesterly trending set comprises thin to thick, near-vertical to steeply dipping diabase dykes that extend to the top of the preserved volcanic pile. These dykes were documented by Baragar (1976) as feeders to sills beneath the Natkusiak basalts but have not been observed to feed any flows or sills within the basalt pile. No thick sills were observed by the writers within the Natkusiak basalts. Two discordant diabase sheets were, however, portrayed by Baragar (1976) and Palmer et al. (1983) at the tops of their sections 2A and 3A.

The northwesterly trending dykes have orientations that are similar to those of prominent northwesterly lineaments but cut across some lineaments at low angles (see below). The dykes weather prominently and none seem to be the cause of any of the major lineament valleys in the region. Stratigraphic relationships suggest that many if not all of the major dykes and thick sills are younger than the remaining Natkusiak basalts, although their paleomagnetic signatures are not radically different (Palmer et al., 1983). The thin dykes, axial to the Holman Island Syncline, may be related to extension of the basalts and possibly to some copper occurrences.

Structure

The Holman Island Syncline is the major structural feature of the region. It is canoe shaped with maximum plunges of 3° and a trend of 040° in the northeast sector, but trends subhorizontally at about 070° in the southwest sector. The change in orientation of the axis occurs near a prominent meander in the Kuujjua River at approximately 113°50'W longitude. Interference folds are not apparent at this position. In the northeast sector the northwest limb of the syncline comprises a series of flexures or steps with dips ranging from subhorizontal to 15° toward the southeast. A sketch map of the area between Lineament Creek and Trident Creek illustrates the structural style (Fig. 27.3).

Distinct steep-sided linear canyons transect the Holman Island Syncline and were thought to have fault offsets (Nelson, 1983) or to have large dolerite dykes (Baragar, 1976) associated with them. They trend 135° to 160°, as do major dykes intruding the basalts. Numerous other lineaments criss-cross the basalt plateaus in other directions e.g. 110°, 070°, 030° and 010°. However, offset on the Lineament Creek lineament (Fig. 27.3) was not detectable. A maximum of 40 m of late normal displacement was determined on one arm of Trident Creek that trends 160°. No evidence exists of the presence of dolerite dykes in these canyons and two large dykes cross canyons in the area of Trident Creek at oblique angles.

Several other minor faults in the region have been noted. These also have vertical offsets of only 20 to 40 m and trend about 000°, 195° and 215°-220°. Recognizable lineaments are not associated with these faults except for the 215°-220° set which are subparallel to the axis of the Holman Island Syncline in the northeast area. These faults,

Table 27.2. Copper Occurrences and Alteration, Natkusiak Basalts and Upper Kilian Formation

Type	Mineral	Host Rock	Associated Minerals[1]	Shape of Occurrence
1A	Native Copper (disseminated)	densely amygdaloidal parts of flows, any member	prehnite, quartz, chlorite, pumpellyite, calcite.	disseminated within amygdules and gas cavities, at junctions between prehnite crystals and fine wires and blebs within botryoidal masses of prehnite.
1B	Native Copper (disseminated)	middle and upper massive members: as 1A but with associated red interflow mudstones	prehnite, pumpellyite, chlorite, quartz, calcite; similar alteration in red mudstones.	thin veinlets in joints, disseminated in amygdules and in massive basalt, minor copper in veinlets and reduction spheres in red mudstones.
2	Native Copper (veins)	massive jointed flows with knobby, sparsely amygdaloidal texture	microscopic prehnite-pumpellyite-quartz	crystalline dendritic copper in the shape of blebs, and thin to thick veins along joints.
3	Native Copper (disseminated)	massive flows, any member	none (other than typical whole rock alteration)	disseminated fine to microscopic flecks in massive basalt.
4	Chalcocite (bornite, tetrahedrite, pyrite) (veins)	recessive members (mainly)	quartz, calcite, hematite, chlorite, pumpellyite	veins and vein-sets, commonly trending 120-130°, expanding laterally in amygdaloidal flow tops.
5	Pyrite, chalcopyrite (±arsenopyrite)	pyroclastic member	not known	very fine grained, disseminated in matrix and outlining clasts; locally forms massive clasts.
6	Chalcocite (veinlets)	upper Kilian, cream limestone member	none documented	steeply dipping veinlets near overlying Natkusiak basalts.

[1] Associated minerals listed approximately in order of decreasing proximity to copper, minor minerals in brackets.

clearly offsetting the Kilian-Natkusiask contact (Fig. 27.3) and following subtle lineaments which are visible on satellite images, appear to be deformed by younger structures. Other lineaments, which can be traced for several hundred kilometres, appear to be younger fractures which have been accentuated by physical weathering of vertically jointed basalts and glacial scour. The 215°-220° set may be older, but facies changes or other evidence of early faulting have not been noted.

Copper occurrences

Copper concentrations occur sporadically throughout the Natkusiak basalts and parts of the upper Shaler Group. To date however no deposits of economic grade and tonnage have been identified. Previous exploration by Muskox Syndicate and Grandroy Mines Limited was concentrated in the thickest parts of the volcanic pile (Ekstrom and Pelette, 1968; Newbury, 1969; Seeber, 1970). A variety of native copper and copper sulphide occurrences have been documented and are summarized in Table 27.2. Some typical copper and silver contents from grab samples are listed in Table 27.3.

Many of the occurrences are associated with distinct pale green patches where the basalts have been altered to prehnite, chlorite, pumpellyite, quartz and carbonate. Botryoidal prehnite with disseminated native copper occurs in amygdules and larger gas cavities in flow tops sporadically throughout the pile. Native copper also occurs in veins and as coatings along joints without macroscopic prehnite. In addition every basalt sample analyzed petrographically is altered to differing amounts of chlorite, calcite, quartz, prehnite and pumpellyite.

Native copper occurs in at least four forms (see Table 27.2). These are separated here, for descriptive purposes, but may be related in space and genetically. Type 1A is disseminated native copper in flow tops. The key association is with prehnite in permeable zones comprising large and small amygdules, flow-top rubble and large

Table 27.3. Copper and silver contents[1] in typical grab samples of Natkusiak basalts

Type	Sample No.[2]	Locality		Cu (%)	Ag (ppm)
1A	84-WEN-23	Newbury Creek (middle massive?)		0.39	9
	84-WEN-25	Newbury Creek (middle massive?)		1.17	4
	84-WEN-26	Newbury Creek (middle massive?)		1.22	2
	KQ-84-18B	Trident Creek, upper recessive		2.7	2
	KQ-84-18E	Trident Creek, upper recessive		0.2	0
	KQ-84-19B	Trident Creek, upper recessive		2.2	0
	KQ-84-19D	Trident Creek, upper recessive		0.9	0
1B	JP 84-387	Section 13, upper massive		260 ppm	n.d.
	JP 84-417BA	Genesis (G) middle massive		760 ppm	n.d.
	JP 84-417BB	Genesis (G) middle massive		1.0	n.d.
2	Holy Cow A	massive vein, middle massive		98.4	79
	Holy Cow B	massive vein, middle massive		95.2	114
	Genesis A	massive vein, middle massive		91.5	171
	Genesis B	massive vein, middle massive		80.2	167
	JP 84-412AB	Genesis, 2 cm adjacent to vein		8.9	9
3	84 JR501 to 509	9 chip samples of 24 m flow, lower massive member, Trident Creek		23 to 398 ppm mean ~210 ppm	n.a.
4	84 MKS-005	W5 chalcocite vein, upper recessive		10.08	14
	JR-0103	W5 chalcocite vein, upper recessive		61.8	62
	JR-0104	W5 wall rock beside vein - recessive		1.39	7
5	84-WEN-006	SE Lineament Creek		0.03	tr
	84-WEN-014	SE Lineament Creek	Lithic	3.73	14
	84 JSJ-4	South of Section 3	Pyroclastic	0.08	n.d.
	84 JSJ-329	South of Section 3	Member	0.03	12
	84 JSJ-5 to 12	South of Section 3		tr to 1.67	tr to 8
	84 JSJ-18	N of Section 3, top of lower rec.		4.88	n.a.
	84 JSJ-19	N of Section 3, top of lower rec.		0.03	n.a.
	84 JSJ-20	N of Section 3, top of lower rec.		4.22	n.a.

[1] JP and KQ samples analyzed by Atomic Absorption Spectrometry by Analytical Chemistry Section, Economic Geology Division, Geological Survey of Canada, Ottawa. All other samples analyzed for Panarctic Oils Ltd., by Loring Laboratories Ltd., Calgary.

[2] Samples collected by the following: WEN-WEN; KQ-RVK; JP-CWJ; HOLY COW-WEN; JR-JHR; MKS-M.K. Swartout; JSJ-J.S. Johaneson.

n.d. = not detected, tr = trace, n.a. = not analyzed.

gas cavities. Some of these occurrences appear to be laterally continuous and extensive, as noted by Newbury (1969), but the few occurrences that were continuously sampled have erratic copper contents. Detailed sampling is required to test most of these occurrences, particularly those in Newbury Creek.

Type 1B is a variant of 1A with the close association of red interflow sedimentary rocks being the main distinguishing feature. The sedimentary rocks are generally very fine grained, massive to laminated maroon dolomitic mudstones but locally include grey nodular limestones, silicified stratiform stromatolites and intraformational flat chip conglomerates. At Section 14, within the upper massive member, the flow top below a mudstone unit is deep red and highly amygdaloidal. Both flow top and mudstone are transected by a network of minute quartz and calcite veinlets. Native copper occurs in large amygdules and variably abundant veinlets in the overlying orange-weathering, massive, blocky flow. The apparent abundance of copper veinlets in outcrop is proportional to the thickness of the red mudstones along strike. Native copper is rare or absent along strike where the mudstone pinches out, but is present where the mudstone lenses in. Associated minerals (chlorite, quartz, prehnite, pumpellyite and late calcite) are concentrated within the veinlets and amygdules, and are not generally obvious in the massive basalt except in thin section.

Type 2 is native copper in veins. At the Genesis (G) showing (Fig. 27.1) Types 1B and 2 native copper occur within the top flow of the middle massive member which is overlain by an extensive bed of red mudstone. The mudstone bed is at least 1 m thick and is overlain by the upper recessive member. The underlying flow top is altered extensively to chlorite-pumpellyite and transected by numerous quartz-prehnite veinlets containing late calcite. Some of these veins also extend up into the recessive flow. Native copper is disseminated throughout the underlying flow top and concentrated near the veined zones. One of the veins, up to 40 cm wide and trending 130°, cuts deeper into the underlying flow and consists of native copper disseminated in prehnite, quartz, chlorite and pumpellyite. Late sparry calcite fills large voids. Still deeper in the same flow, native copper occurs in Type 2 vertical veins (Fig. 27.10) which have dendritic growth patterns. The veins preferentially fill the 035°-050°-oriented portions of polygonal columnar joints in the massive basalt. Similar veins at the Holy Cow (HC) showing strike approximately 125° and also fill triple junctions between polygonal joints. Exhumed plates of the veins range from less than 1 kg to more than 300 kg in weight. Abundant native copper has permeated the basalt beside the veins (Fig. 27.11). The massive basalt has a knobby weathered surface, apparently related to quartz and/or prehnite amygdules which also contain flecks of native copper.



Figure 27.10. *Exhumed native copper veins, HC showing (Fig. 27.1). Hammer for scale. (GSC 204188-D)*

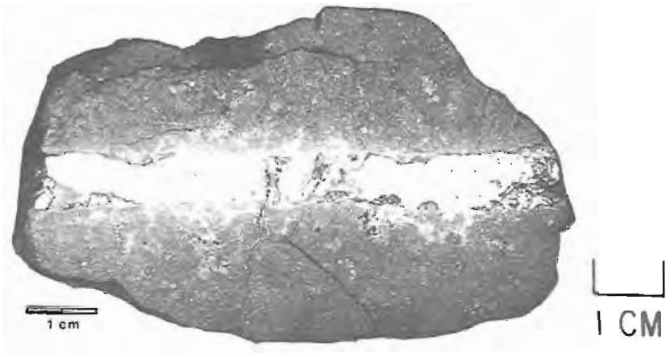

Figure 27.11. *Polished hand sample JP 84-412A illustrating invasion of disseminated native copper from vein (white) into host basalt. From G showing (Fig. 27.1). (GSC 204191)*

One occurrence of Type 3, a flow in the middle massive member at Trident Creek, was sampled in detail (Table 27.3). Minute grains of native copper, generally less than 1 mm in size are disseminated between the various silicate minerals of the basalt. Visible copper of Type 3 was found at two localities over two- to three-metre intervals within much thicker flows. Copper contents range from 24 to 398 ppm, the latter over a 2.3 m interval.

Chalcocite veins, Type 4, were studied by JHR extensively in the Trident Creek area (Fig. 27.3). The W5 vein system trends 140°, dips about 70-90° northeast and occurs mainly in the upper recessive member. It is a sulphide system, dominated by chalcocite with lesser bornite and minor pyrite, tetrahedrite and chalcopyrite. Gangue in the vein consists of quartz, calcite and hematite.

Numerous other similar vein systems also occupy mainly northwest to north-northwest trending fractures in the Trident Creek area. Most of these fractures are completely filled by chalcocite and the sulphides have permeated the basalt near the central veinlets. Copper may have been added to pre-existing pyrite, with progressive removal of iron and sulphur. In addition to those containing chalcocite, many fractures contain thin films of quartz. The copper sulphide veins occur throughout the section as do other veins containing native copper and flow tops with disseminated native copper, but the sulphide-bearing veins seem to cut several flows and to be discrete from the native copper which occurs in other veins (Type 2) and disseminated in flow tops (Type 1A).

The north-northwest fracture direction compares with that of the lineaments and some of the faults mapped along the contact with the Kilian Formation which have offsets up to 40 m. On the other hand the W5 fracture system and most other sulphide-filled fractures contain little evidence of displacement and appear to be relatively "tight". In contrast several northeast-trending faults repeat the Kilian-Natkusiak contact. Other northeast-trending lineaments offset northwest-trending lineaments. One northeast-trending fracture was also observed by CWJ near the W-5 zone. This fracture contains breccia with drusy, weathered quartz, carbonate, hematite and native copper in the matrix.

Extensive, but variable grade disseminated native copper (Type 1A) was also outlined by RVK and WEN in flow tops near the top of the upper recessive member in the W5 area (Table 27.3). Associated minerals include prehnite, quartz, calcite and pumpellyite. This variety of Type 1A shows a preference for large gas cavities several centimetres to greater than 1 m in diameter in flow tops.

In summary, copper sulphides in the Trident Creek area occur within northwest-trending fractures whereas the native copper occurs mainly within flow tops and subordinate amounts within northeast- and northwest-trending fractures. The sulphide and native copper systems appear to have different origins.

Type 5 consists of patchy to extensive areas where the pyroclastic member has been altered to mottled grey colours and contains variable amounts of disseminated pyrite and chalcopyrite. Copper abundances range from trace to more than 3.7% in grab samples. The sulphides occur in the matrix, concentrated around clasts, and locally constitute some of the clasts. Extensive rusty gossan zones at the southeast end of Lineament Creek and in the vicinity of Section 3 are the best examples of this type. Minor chalcocite veins also occur in the pyroclastic member at the colour transition from green to red and at the top of the member.

Genesis of copper occurrences

Copper occurrences on Victoria Island have been documented mainly in the Natkusiak basalts and a few in the top of the Kilian Formation. Disseminated copper in massive flows (Type 4), may have formed at the time of eruption during degassing and desulphurization of the lava. Most other occurrences, however, appear to be genetically related to redistribution of copper within the basalt pile. The redistribution processes also involved the aqueous transport of silica, calcium, aluminum, iron, silver, carbonate and sulphur to form the observed minerals. Alteration of the basalts and deposition of copper were concentrated in flow tops and fractures because of their inherent porosity and permeability. The prehnite-pumpellyite assemblage indicates that these processes occurred during low-grade, probably burial metamorphism, between greenschist and zeolite facies (Coombs, 1960; Liou, 1971). The extensive sills beneath the pile may have elevated the geothermal gradient, promoting this metamorphism. Occurrence of much prehnite and native copper in primary gas cavities suggests that this burial metamorphism occurred during or soon after eruption of the basalts. Present exposures of the Natkusiak basalts probably represent only a remnant of a much thicker and more extensive volcanic pile.

Red, fine grained clastic rocks and red, highly vesicular flow tops are spatially associated, although not exclusively, with some stratabound native copper occurrences (e.g. Sections 11, 14; the G showing). The red hematitic rocks may have served as oxidized source rocks or units within which oxidized copper-bearing solutions were able to migrate. Mineralizing solutions apparently moved laterally and upwards in some localities but downward in others.

Prehnite is closely associated with native copper at many localities in the Natkusiak basalts. A similar close association of native copper with prehnite, as well as with thin red subaerial flows, has been documented in the Triassic Karmutsen Group on Vancouver Island in British Columbia (Surdam, 1968; Lincoln, 1971). Essentially identical native copper with prehnite occurs in similar young Precambrian basalts of the Osler Group on Simpson Island, Ontario, on the north side of Lake Superior (RVK). Native copper is also known to occur with prehnite (among many other minerals) in deposits of the Keweenaw Peninsula in Michigan (Stoiber and Davidson, 1959; Jolly, 1974). As Lincoln (1971) suggested the copper was probably extracted from flows with a relatively high fO_2 and precipitated by reactions that produce prehnite and pumpellyite. These processes have led to the widespread deposition of prehnite and native copper in certain flow tops of the Natkusiak basalts. Although several of these occurrences appear to be laterally extensive, the copper grades and thicknesses documented to date have not indicated any economic deposits.

Airphoto interpretation and detailed mapping have failed to show any marked facies changes or other clearly defined relationships among normal faults, the prominent northwesterly trending lineaments and copper occurrences. The 120-130° preferred direction of copper sulphide veins is cut at low angles by these major lineaments without apparent effect. The possibility remains, however, that some vein systems are secondary structures that originated with the lineaments. On the other hand, northeast-trending lineaments are spatially associated and may also be genetically associated with both normal faults and some copper occurrences, for example the Holy Cow (HC) and Genesis (G) showings and "Camp Creek" (informal name) area.

The sulphide-bearing veins occupy fractures that, although containing minor breccia and slickensides, have no discernible offsets. The veins show evidence of copper-bearing solutions reacting with the basalts and with earlier-precipitated pyrite. The veins evidently cut several flows but are much better developed in flow-top zones. No demonstrable relationship exists between native copper in flow tops and copper sulphides in veins. The copper in the veins probably was derived from the basalts but possibly the sulphur was derived from the underlying Kilian Formation, as little evidence exists for significant sulphur sources in the lavas.

Acknowledgments

C.W. Jefferson was ably assisted in the field by K. MacDonald. W.E. Nelson and J.H. Reedman were assisted by M.P. Jackson, J.S. Johaneson, A. Bleakney, A. Duguid, M. Swartout and C. Hopper. M. Henderson and A. Roberts are thanked for mineral identification. G. Young assisted with drafting.

The contributions of W.E. Nelson and J.H. Reedman were made possible by Panarctic Oils Limited. We are grateful to Panarctic Oils Limited for transportation and hospitality to CWJ, RFJS, RVK and K. MacDonald, and for permission to publish this report.

The contribution by CWJ and RFJS is ancillary to resource assessment of Banks Island and northwestern Victoria Island which received rotary and fixed wing support from Polar Continental Shelf Project, Department of Energy Mines and Resources, coordinated by F. Hunt and B. Hough. W. Gibbins accompanied the group in the field from July 4 to 11 inclusive, shared logistic support from PCSP and contributed geological observations and discussions.

Drafts of this paper were read by M.P. Jackson, D.C. Waylett, G. Varney, M. Henderson, W.R.A. Baragar, D.C. Findlay and R.T. Bell. We appreciate their helpful comments.

References

Baragar, W.R.A.
1976: The Natkusiak basalts, Victoria Island, District of Franklin; in Report of Activities, Geological Survey of Canada, Paper 76-1A, p. 347-352.

1977: Volcanism of the stable crust; in Volcanic Regimes in Canada, eds. W.R.A. Baragar, L.C. Coleman and J.M. Hall; The Geological Association of Canada, Special Paper Number 16, p. 377-405.

Baragar, W.R.A. and Loveridge, W.D.
1982: A Rb-Sr study of the Natkusiak basalts, Victoria Island, District of Franklin; in Current Research, Part C, Geological Survey of Canada, Paper 82-1C, p. 167-168.

Christie, R.L.
1964: Diabase-gabbro sills and related rocks of Banks and Victoria Islands, Arctic Archipelago; Geological Survey of Canada, Bulletin 105, 13 p.

Coombs, D.S.
1960: Lower grade mineral facies in New Zealand; 21st International Geological Congress, v. 13, p. 339-351.

Ekstrom, R.L.V. and Pelette, W.B.
1968: Report of Work, 1968, Muskox Syndicate, Victoria Island properties, N.W.T.; Assessment Files, Department of Indian and Northern Affairs, Yellowknife, 27 p.

Jefferson, C.W.
1985: Uppermost Shaler Group and its contact with the Natkusiak basalts, Victoria Island, District of Franklin; in Current Research, Part A, Geological Survey of Canada, Paper 85-1A, Report 13.

Jolly, W.T.
1974: Behavior of Cu, Zn, and Ni during prehnite-pumpellyite rank metamorphism of the Keweenawan basalts, northern Michigan; Economic Geology, v. 69, p. 1118-1125.

Lincoln, T.N.
1981: The redistribution of copper during low-grade metamorphism of the Karmutsen volcanics, Vancouver Island, British Columbia; Economic Geology, v. 76, p. 2147-2161.

Liou, J.G.
1971: Synthesis and stability relations of prehnite, $Ca_2Al_2Si_3O_{10}(OH)_2$; The American Mineralogist, v. 56, p. 507-531.

Nelson, W.H.
1983: Report on the field program, summer 1982. Unpublished assessment report, Panarctic Oils Ltd., Filed with Department of Indian Affairs and Northern Development, Yellowknife, 87 p.

Newbury, M.C.
1969: Studies on the copper mineralization of the Natkusiak Formation, Victoria Island, Canada; unpublished B.Sc. thesis, Queen's University, Kingston, Ontario, 37 p.

Palmer, H.C., Baragar, W.R.A., Fortier, M., and Foster, J.H.
1983: Paleomagnetism of Late Proterozoic rocks, Victoria Island, Northwest Territories, Canada; Canadian Journal of Earth Sciences, v. 20, p. 1456-1469.

Seeber, O.A.
1970: Geological Report on the Cam Group, 87-H-10; Assessment report for Grandroy Mines Ltd., Project 0829, Toronto, Canada; Assessment files, Department of Indian and Northern Affairs, Yellowknife, 25 p.

Stefansson, V.
1913: My Life with the Eskimo; New York, Macmillan Company, 538 p.

Stoiber, R.E. and Davidson, E.S.
1959: Amygdule mineral zoning in the Portage Lake Lava series, Michigan copper district; Economic Geology, v. 54, p. 1250-1277 and 1444-1460.

Surdam, R.C.
1968: Origin of native copper and hematite in the Karmutsen Group, Vancouver Island, B.C.; Economic Geology, v. 63, p. 961-966.

Thorsteinsson, R. and Tozer, E.T.
1962: Banks, Victoria and Stefansson Islands, Arctic Archipelago; Geological Survey of Canada, Memoir 330, 85 p.

Wanless, R.K. and Loveridge, W.D.
1972: Rubidium-strontium isochron age studies: Report 1; Geological Survey of Canada, Paper 72-23, 77 p.

Young, G.M.
1981: The Amundsen Embayment, Northwest Territories; relevance to the upper Proterozoic evolution of North America; in Proterozoic Basins of Canada, ed. F.H.A. Campbell; Geological Survey of Canada, Paper 81-10, p. 203-218.

-28-

A HALIFAX SLATE GRAPTOLITE LOCALITY, NOVA SCOTIA

Project 760022

L.M. Cumming
Economic Geology and Mineralogy Division

Cumming, L.M., A Halifax slate graptolite locality, Nova Scotia; in Current Research, Part A, Geological Survey of Canada, Paper 85-1A, p. 215-221, 1985.

Abstract

During a study of the bedrock geology of Kejimkujik National Park an occurrence of ***Dictyonema*** *sp. and* ***Anisograptus*** *sp. was discovered near the village of Maitland Bridge. These dendroid and true graptolites occur at a stratigraphic horizon near the top of the Halifax Formation and confirm an Early Ordovician (Tremadoc) age for the upper part of the Meguma Group.*

Résumé

Des roches à ***Dictyonema*** *sp. et à* ***Anisograptus*** *sp. ont été découvertes près du village de Maitland Bridge au cours d'une étude de la géologie du socle rocheux du Parc national de Kejimkujik. Ces graptolites dendroïdes et véritables se présentent dans un horizon stratigraphique situé près du sommet de la formation d'Halifax et confirment que la partie supérieure du groupe de Meguma date de l'Ordovicien ancien (Trémadocien).*

Introduction

Kejimkujik National Park (21 A/6) is situated in Meguma terrane near the centre of the western peninsula of Nova Scotia (Leefe et al., 1982). Much of the eastern part of the Park is underlain by slates of the Halifax Formation (see Fig. 28.1). The bedrock of this slate area is mantled by glacial debris which has been moulded into a swarm of some 200 drumlins (Wilson, 1938). Outcrops in this slate area occur where glacial till is thin, as for example between drumlins; or where the till has been washed away, as along lake shores or along stream valleys. At a few Halifax slate outcrops, aboriginal Micmac petroglyphs are preserved on smooth and glacially polished surfaces (Bailey, 1898, p. 40 M; Molyneaux, 1983).

Fossils have not been previously found in the extensive area of Halifax slate that lies south of South Mountain Batholith. These slates extend from Annapolis County and through Queens and Lunenburg counties for a distance of 85 km across strike (Keppie, 1979).

However, **Dictyonema flabelliforme** (Eichwald) has long been known from Halifax slate exposed along the north side of South Mountain Batholith at a locality near New Canaan (Dawson, 1891; Crosby, 1962). The New Canaan locality is 90 km northeast of the Park. Also, a single graptolite specimen has been recorded from Meguma terrane near Goldenville, 520 km east of the Park (Poole, 1971).

The purpose of the paper is to describe a rare occurrence of graptolites in rocks of the Meguma Group or "Gold-bearing series" of Nova Scotia. Discovery of these fossils in cleaved Halifax slate was facilitated by bulldozing of outcrops during construction of a highway bridge at the village of Maitland Bridge. The fossil locality was noted during a general resource study of geology of Kejimkujik National Park (Cumming, 1979).

Acknowledgments

The writer thanks Chief Park Interpreter Peter R. Hope for his interest and co-operation. Several other officers of Parks Canada assisted in providing access to the park, including C. Drysdale, G. Cullen, J. Logan and Superintendents G.C. Myers and W.L. Wombolt. Two summer employees of Kejimkujik National Park, Larry Caldwell and Goldie Gibson, assisted in collecting fossils and the first **Dictyomen**a was found by L. Caldwell.

J.C. Smith, then of the Department of Mines and Energy of the Province of Nova Scotia, gave useful geological information and advice. P. Gimbarzevsky, Pacific Forest Research Centre, Victoria, B.C. provided valuable background information about park resources.

Halifax Formation of the Meguma Group

The Meguma Group is confined to Nova Scotia and adjacent offshore areas. The group has traditionally been subdivided, for the purpose of geological mapping, into an upper shaly unit (Halifax Formation) and a conformable, lower, sandy unit (Goldenville Formation; see Woodman, 1904, p. 368; Keppie, 1979).

The term "Meguma Group" has now generally replaced an older term "Gold-bearing series" which was preferred by earlier economic geologists such as Faribault, because it was a descriptive term (Faribault, 1913, p. 161). The most recently published geological maps of the Kejimkujik Lake area (GSC maps 437A and 438A by Faribault, Armstrong and Wilson, 1938) use Meguma Group and Gold-bearing series synonymously on the map legend.

The Kejimkujik Lake region displays important stratigraphic sections that are useful in determining the minimum thickness of the Halifax Formation and in describing its sequence of strata. A stratigraphic subdivision of a sequence of beds of the Halifax Formation at and near Kejimkujik Lake was recognized by several early workers.

An orderly succession of strata within the Halifax Formation of this area was first recognized by Prest (1895, p. 422). He listed a succession of 13 units of the "Meguma Group" which made up a total thickness of 26 000 feet (7900 m). These early findings were restated by Prest (1915, p. 21) in the following succession of 9 units comprising 10 050 feet (3060 m) of slates of the "Halifax Formation", which lay above his units 1 to 4 (Goldenville Formation).

Succession of "Meguma Group" by W.H. Prest (1915).
(in descending order)

	Thickness (feet)
13. Blue and bluish-grey slate	2000
12. Black slates with white sandy seams	1500
11. Bluish-black slate	2000
10. Bluish-grey and ribboned slate	500
9. Upper greenish-grey slate	1000
8. Upper purple slate	400
7. Middle greenish-grey slate	1500
6. Lower purple slate	150
5. Lower greenish-grey slate	1000
4. Bluish to greenish-grey whin and slate of same colour	5000
3. Upper bluish-grey quartzite and bluish-grey slate	3000
2. Bluish-grey quartzite with graphitic slate	2000
1. Lower bluish-grey quartzite with grey slate at bottom	6000
Total thickness about	26 000

In the Kejimkujik Lake region the lower and the upper purple slates of the Halifax Formation (units 6 and 8 of Prest, 1915) are well exposed along the shore of Mill Bay (Faribault et al., 1938). Bluish slates (units 10 and 11) outcrop along the east shore of the lake. Black slates (unit 12) outcrop along Mersey River and are exposed at Mill Falls near the Visitors Reception Centre of the Park. It is this same unit 12, of black slates, which trends northeast towards the village of Maitland Bridge and which contains graptolites in the bed of the Mersey River (see Fig. 28.1 to 28.3).

The above succession of strata of the Halifax Formation (units 5 to 13 of Prest, 1915) appears to be a local subdivision and has not been used in regional geological mapping in other areas of Meguma terrane. For example, Wright (1915, p. 5 and 1931, p. 313) described a more general succession of three lithological subdivisions of the Halifax Formation in nearby Lunenburg County. This succession, in descending order consisted of:-

black slates,
banded argillites
green slates

The black slates (upper subdivision of Wright) show a more pronounced slaty cleavage than the two underlying units because the black slates are softer and consist chiefly of thin-bedded carbonaceous layers with occasional interbeds of

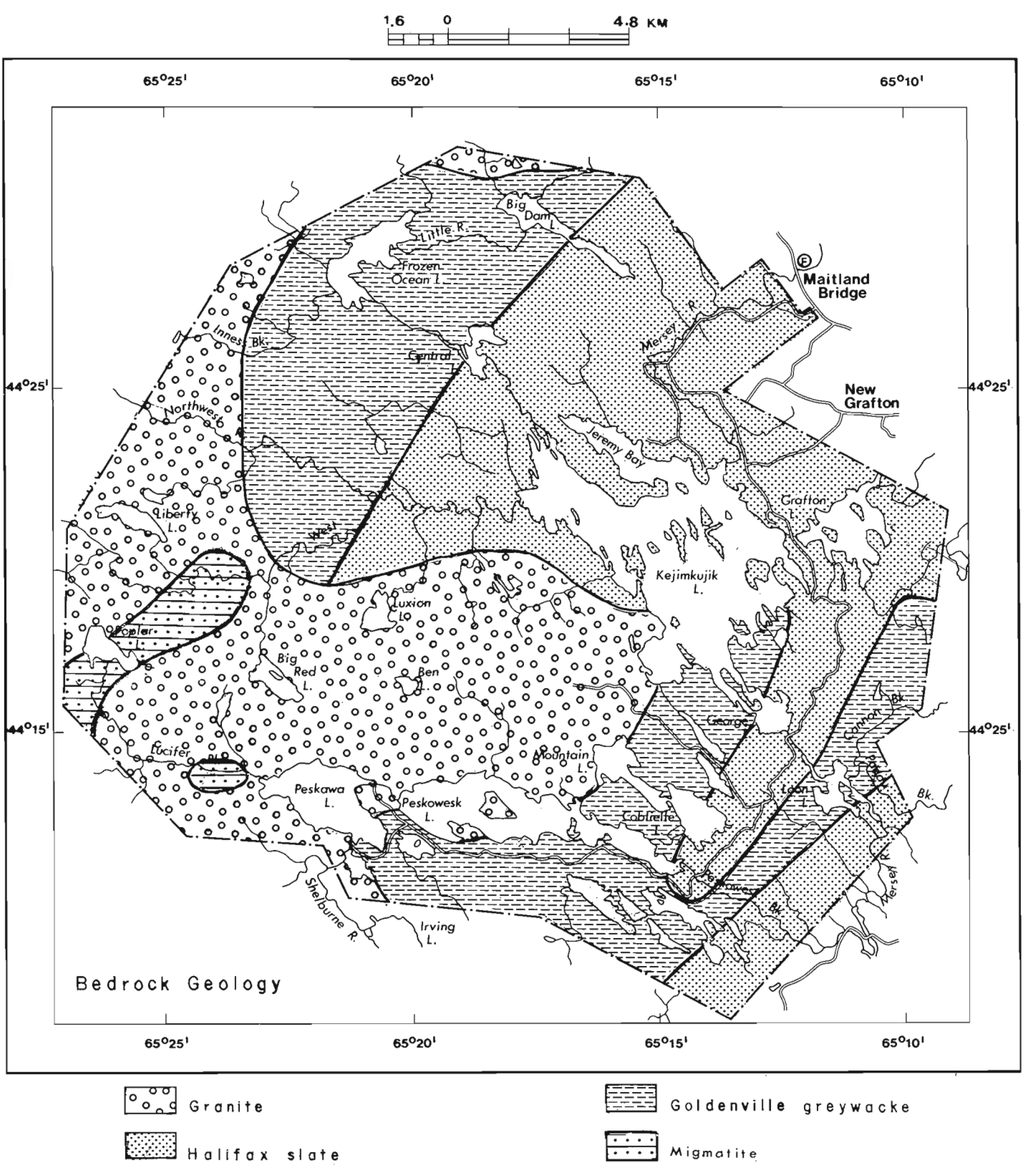

Figure 28.1. Distribution of major rock units in Kejimkujik National Park, showing an important fossil locality at Maitland Bridge. Note that the eastern part of the park lies mainly within a broad belt of slate of the Halifax Formation.

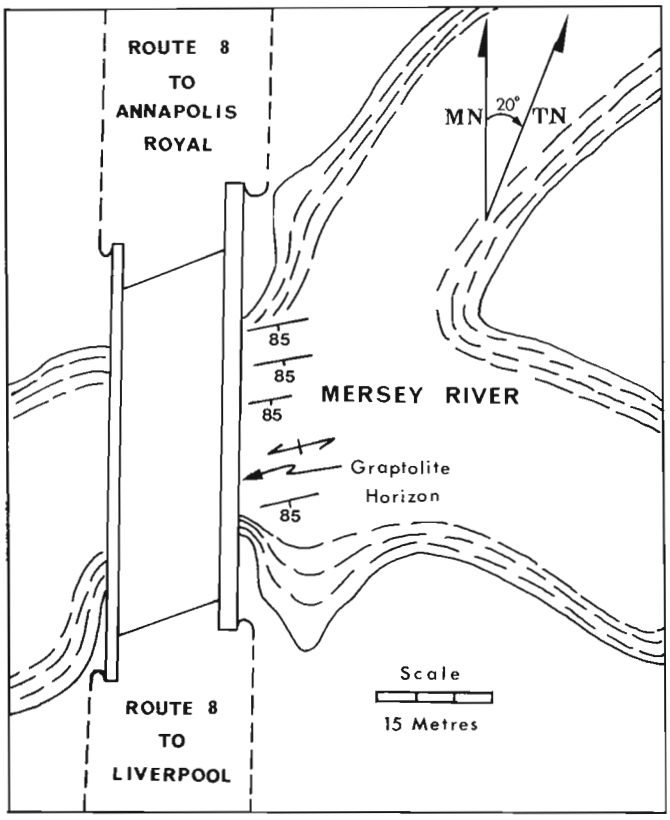

Figure 28.2. Sketch map showing general location of a graptolite locality beneath the highway bridge at Maitland Bridge, Annapolis County, Nova Scotia. At this locality, slaty cleavage is parallel, or nearly parallel, to bedding in strata of the Halifax Formation.

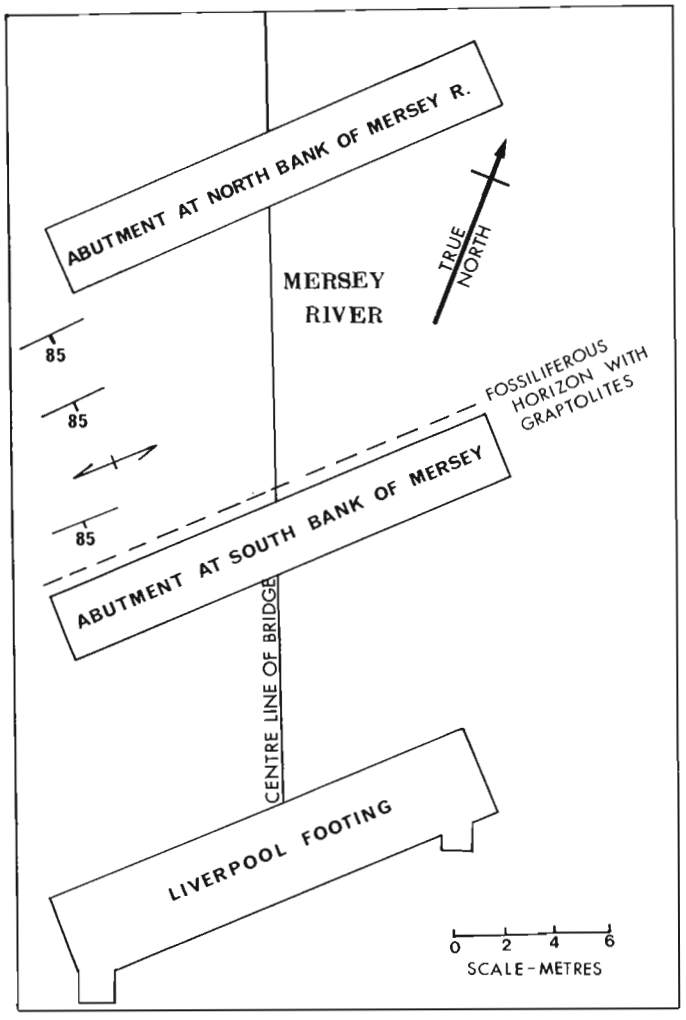

Figure 28.3. Sketch map showing the location and trend of a graptolite-bearing horizon in slates of the Halifax Formation in the stream bed of the Mersey River at Maitland Bridge.

dark grey argillites. These interbedded argillites and the underlying banded argillites are characterized by considerable pyrite in the form of well defined cubes, similar to those developed at Peter Point on Kejimkujik Lake.

The top of the Halifax Formation has been eroded away so that we have no way of estimating the original total thickness of the formation. A thickness of 11 700 feet (3560 m) was measured along Black River, Kings County, by Faribault, north of South Mountain Batholith. Sediments of the Halifax Formation were deposited under anoxic conditions. Similar thick, black shale sequences of Tremadoc age are widespread throughout the world and are typically developed at margins of large continental masses (Erdtmann, 1982).

Graptolite locality and collections

The general location of the graptolite locality at Maitland Bridge is shown on Figure 28.1. The bedrock geology shown on this map is the work of a number of geologists, including – L.W. Bailey, 1898; W.H. Prest, 1909; E.R. Faribault, P. Armstrong and J. Tuzo Wilson, 1938; B.E. Jones and F.S. Shea, 1964; F.C. Taylor, 1969; and L.M. Cumming, 1979.

Figure 28.2 shows in greater detail the location of the graptolite horizon in the streambed of the Mersey River beneath a highway bridge constructed in 1978. Figure 28.3 shows the trend of the graptolite horizon near the bridge abutment at the south bank of Mersey River. The graptolite fauna at this locality is imperfectly preserved, because of the pervasive slaty cleavage. The fauna consists of numerous specimens of **Dictyonema** sp. (Fig. 28.4) and a single specimen of **Anisograptus** sp. (Fig. 28.5) as well as traces of annelids (Fig. 28.6). GSC hypotypes 67802 to 67805 from this locality are in the type collections of the Paleontology Section, Geological Survey of Canada, Ottawa.

Additional samples are part of a representative collection of rocks stored at the Park Interpretative Centre at Jakes Landing, Kejimkujik National Park. A partial list of these specimens follows:-

Sample Number	Description
CE-42-3-78	Halifax slate with pyrite formed along a joint and capillary cracks.
CE-42-6-78	Annelid tracks on a slate fragment in which cleavage and bedding are nearly parallel.
CE-42-7-78	A thin slate layer with annelid tracks.



Figure 28.4. ***Dictyomema*** *sp. on slab of dark grey to black Halifax slate from the bed of Mersey River at Maitland Bridge (see GSC hypotypes 67804 and 67805). Slaty cleavage and bedding are parallel, or nearly parallel, at this locality and bedding dips 85° south. GSC 20282-F.*

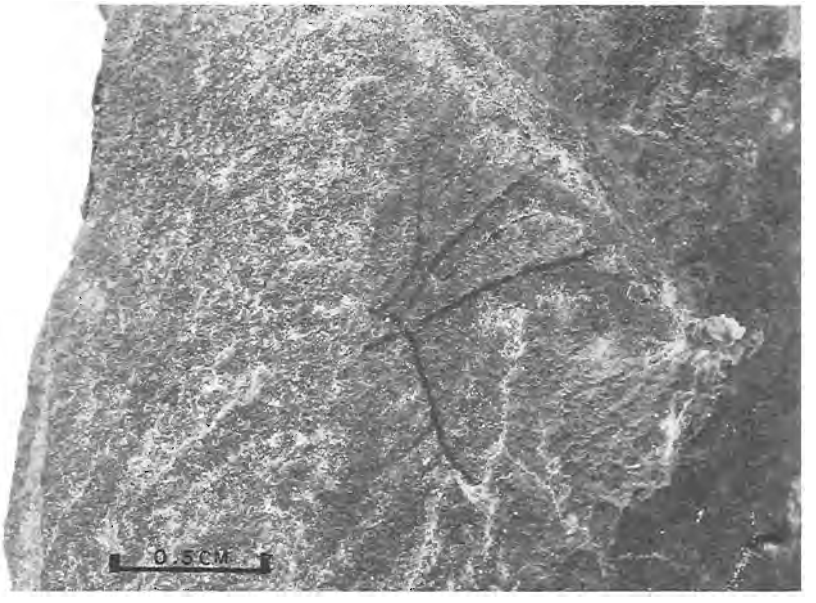

Figure 28.5

Broken fragment of ***Anisograptus*** *sp. from unit 12 (Prest, 1915) of the Halifax Formation at Maitland Bridge. GSC hypotype 67802. (X4 GSC 203522-H)*

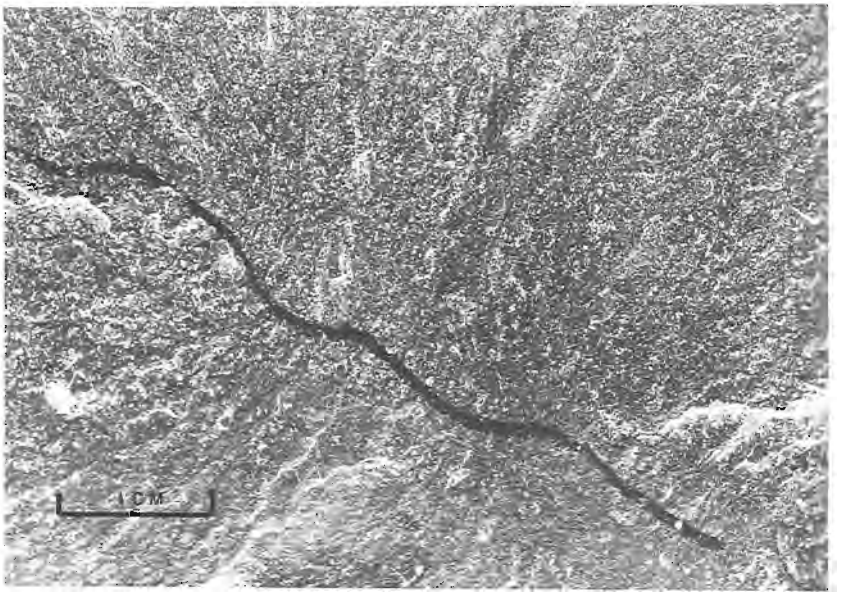

Figure 28.6

An annelid marking in slate of the Halifax Formation from the graptolite locality at Maitland Bridge, GSC hypotype 67803. (X2 GSC 203522)

CE-42-8-78	2 specimens; one is over 60 cm long, showing parallel cleavage and bedding of black Halifax slate.
CE-43-1-78	A thick slate layer showing numerous 7 mm pyrite cubes.
CE-43-4-78A,B and C	Annelid tracks on black slate.
CE-44-3-78	Crossbedding in a 3 cm white sandy band in Halifax slate with top indicated. This crossbedded layer shows that the sequence of beds beneath the bridge is not overturned, but simply tilted 85° to the east.
CE-44-4-78	Halifax slate cut by a 2 mm milky quartz vein.
CE-45-1-78	Black slate of the Halifax Formation with **Dictyonema** and an annelid track.

Age of the Meguma Group

The most recent studies of the Meguma Group assign the group to a Cambro-Ordovician age (e.g. Zentelli et al., 1984; Henderson, 1984) and the Goldenville Formation to a Cambrian age (Keppie, 1984). The stratigraphic position of a Tremadoc fauna at Maitland Bridge supports these age assignments.

The **Dictyonema** specimens from the Maitland Bridge locality are similar in form to those specimens described from New Canaan, Kings County. These were illustrated by Dawson (1891, p. 563) as **Dictyonema Websteri.** These specimens were re-identified by D.E. Thomas and O.M.B. Bulman as **Dictyonema flabelliforme** (Eichwald) sensu lato (in Crosby, 1962, p. 20-21; in Smitheringale 1973, p. 20-21). The current age assignment of the Meguma Group has been largely based on these rare fossil occurrences from the northwestern margin of the area of outcrop of the Meguma Group.

The dendroid graptolites at Maitland Bridge are similar to holotype No. 1077 at the Redpath Museum, McGill University (Alison and Carroll, 1972, p. 15). However, Bulman (1954, p. 7) in studying the general variability of **Dictyonema flabelliforme** found that no two individual specimens were exactly comparable and that there was a vast range of variation and diverse combinations of characters.

The general **Anisograpid** fauna as described by Bulman (1950) is of Tremadoc (Early Ordovician) age and is essentially a dendroid fauna comprising such epiplanktonic forms as **Dictyonema** and **Anisograptus.** The preservation of the Maitland Bridge graptolite fauna is such that the graptolites are only identified to a generic level. However the fauna is sufficiently distinctive to permit an Early Ordovician age assignment for a horizon near the top of the Halifax Formation.

It was the general scarcity of fossils in the Meguma Group which caused several earlier workers to regard these strata as Cambrian or Precambrian (e.g. Walcott, 1891; Woodman, 1908, p. 111). Faribault (1899, p. 6) summed up this problem as follows- "Although no well defined fossils have so far been found in the sedimentary rocks constituting the gold-measures, most geologists agree to classify them, provisionally, as Lower Cambrian." Faribault later had reservations about the age of these strata and frequently referred to them as Precambrian. For example, Faribault (1915), in discussing the age of the Meguma Group near the Park, in Queens County, stated

> "The age of the series cannot be determined by paleontology as it is practically barren of fossils. From lithological analogy, they have been regarded until recently as Lower Cambrian, but they are now believed to be late Pre-Cambrian in age."

Malcolm (1929, p. 13; reprinted in 1976 as GSC Memoir 385) also stated that the Gold-bearing series (Meguma Group) was "probably of Precambrian age."

Harris and Schenk (1975) recognized that megafossils occur sparingly in the Meguma Group and that **Dictyonema** occurrences near New Canaan indicated a Tremadoc age, while poorly preserved samples near the head of Tangier Harbour indicated an Arenig age. This suggested that the Meguma Group is "... Lower Ordovician in age. However, Cambrian and Middle to Late Ordovician strata, although as yet unrecognized, may be represented as well." (Harris and Schenk, 1975).

The (?) graptolites near the head of Tangier Harbour occur along Highway 7, 1.0 to 1.2 miles east of Tangier River. Samples of presumed graptolites from this area (GSC localities 82925 and 89773) examined by B-D. Erdtmann, Indiana University, were found to be almost completely obliterated by metamorphism. Also, B. Richards, Cambridge University, identified the same material as "possibly graptolites". Thus the Arenig age of rocks at these localities is in doubt and the outcrops may represent infolded, barren, slate along the crest of the Tangier anticline.

The placement of the Goldenville Formation entirely in the Cambrian was suggested by Pickerill and Keppie (1981, p. 36) after review of trace fossils found in the Meguma Group. The lower and upper age limits of the Goldenville Formation remain unsolved as indicated by recent correlation charts (Cook and Bally, 1976; Barnes et al., 1981).

References

Alison, D. and Carroll, R.
1972: Catalogue of type and figured fossils in the Redpath Museum; McGill University, Montreal, 173 p.

Bailey, L.W.
1898: Report on the geology of south-west Nova Scotia; Geological Survey of Canada, Annual Report, v. IX, part M, p. 1-154 and map.

Barnes, C.R., Norford, B.S., and Skevington, D.
1981: The Ordovician System in Canada, correlation chart and explanatory notes; International Union of Geological Sciences, Publication no. 8, 27 p. and 2 charts.

Bulman, O.M.B.
1950: Graptolites from the Dictyonema shale of Quebec; Geological Society of London, Quarterly Journal, v. XC1, part 1, p. 63-99.

1954: The graptolite fauna of the Dictyonema shales of the Solo region; Norske Geologisk Tidsskrift, v. 33, p. 1-40.

Cook, T.D. and Bally, A.W. (editors)
1976: Stratigraphic Atlas of North and Central America; Princeton University Press, 272 p.

Crosby, D.G.
1962: Wolfville map-area, Nova Scotia; Geological Survey of Canada, Memoir 325, 67 p.

Cumming, L.M.
1979: Bedrock Geology of Kejimkujik National Park; 252 pages, manuscript prepared for Parks Canada by Regional and Economic Geology Division, Geological Survey of Canada, Ottawa.

Dawson, J.W.
1891: The Geology of Nova Scotia, New Brunswick and Prince Edward Island or Acadian Geology; MacMillan and Co., London, 4th edition, 694 p.

Erdtmann, B.-D.
1982: Palaeobiogeography and environments of planktic dictyonemid graptolites during the earliest Ordovician; p. 9-27 in The Cambrian-Ordovician Boundary: Sections, Fossil Distributions, and Correlations, ed. M.G. Bassett and W.T. Dean; National Museum of Wales, Geological Series no. 3.

Faribault, E.R.
1899: The gold measures of Nova Scotia and deep mining; The Mining Society of Nova Scotia, p. 5-16.

1913: The goldbearing series of Nova Scotia; International Geological Congress, Guide Book no. 1, p. 158-192.

1915: Caledonia map-area, Queens County, Nova Scotia; Geological Survey of Canada, Summary Report for 1914, Sessional Paper no. 26, p. 103-106.

Faribault, E.R., Armstrong, P., and Wilson, J.T.
1938: Kejimkujik Lake sheets (East and West Half), Digby, Annapolis and Queens counties, Nova Scotia; Geological Survey of Canada, Map 437A and 438A.

Harris, I.M. and Schenk, P.E.
1975: The Meguma Group; Maritime Sediments, v. 11, no. 1, p. 25-47.

Henderson, J.R.
1984: Structural history of the Meguma Terrane in Nova Scotia from Sheet Harbour to Sherbrooke; abstract, Geological Society of America, Northeastern Section, Program, p. 23.

Jones, B.E. and Shea, F.
1964: Geological map of Kejimkujik National Park; Nova Scotia Department of Mines; scale 1 inch to 0.5 miles.

Keppie, D.J.
1979: Geological map of the Province of Nova Scotia; Nova Scotia Department of Mines and Energy; scale 1:500,000.

1984: Tectonics of the Meguma Terrane, Nova Scotia; abstract, Geological Society of America, Northeastern Section, Program, p. 28.

Leefe, J., Morrison, J., Evans, M., and Mullen, E.
1982: Kejimkujik National Park-a guide; Four East Publications Ltd., Tantallon, N.S., 115 p.

Malcolm, W.
1929: Gold fields of Nova Scotia; Geological Survey of Canada, Memoir 156, 253 p.

Molyneaux, B.
1983: The petroglyphs of Kejimkujik Lake, Nova Scotia; Rotunda, v. 16, no. 1, p. 36-43.

Pickerill, R.K. and Keppie, J.D.
1981: Observations on the ichnology of the Meguma Group (?Cambro-Ordovician) of Nova Scotia; Maritime Sediments and Atlantic Geology, v. 17, p. 130-138.

Poole, W.H.
1971: Graptolites, copper and potassium-argon in the Goldenville Formation, Nova Scotia; in Report of Activities, Part A, Geological Survey of Canada, Paper 71-1, p. 9-11.

Prest, W.H.
1895: Deep Mining in Nova Scotia; Nova Scotia Institute of Science, Proceedings and Transactions, v. VIII, p. 420-434.

1909: Map of west Caledonia, Queens County, Nova Scotia; manuscript map approximate scale 500 feet to an inch; Geological Survey of Canada files, 601 Booth Street, Ottawa.

1915: The Gold Fields of Nova Scotia (a Prospectors Handbook); Industrial Publishing Company, Ltd., Halifax, Nova Scotia, 158 p.

Smitheringale, W.G.
1973: Geology of parts of Digby, Bridgewater, and Gaspereau Lake map-areas, Nova Scotia; Geological Survey of Canada, Memoir 375.

Taylor, F.C.
1969: Geology of the Annapolis-St. Marys Bay map-area, Nova Scotia (21A, 21B East Half); Geological Survey of Canada, Memoir 358, 65 p. and map.

Walcott, C.D.
1891: Correlation Papers-Cambrian; U.S. Geological Survey, Bulletin 81, 447 p.

Wilson, J.T.
1938: Drumlins of south-west Nova Scotia; Royal Society of Canada, Transactions, section IV, p. 41-47.

Woodman, J.E.
1904: Nomenclature of the gold-bearing metamorphic series of Nova Scotia; The American Geologists, v. 33, p. 364-370.

1908: Probable age of the Meguma (gold-bearing) series of Nova Scotia; Geological Society of America, Bulletin, v. 19, p. 99-112.

Wright, W.J.
1915: Geology of the New Ross map-area with an introductory chapter on the Gold-bearing series and the granites of southern Nova Scotia; unpublished Ph.D. thesis, Yale University, 356 p.

1931: Data on the method of granitic intrusion in Nova Scotia; Royal Society of Canada, Transactions, section IV, p. 309-326.

Zentilli, M., Wolfson, I., Shaw, W., and Graves, M.
1984: The Goldenville-Halifax transition of the Meguma Group as a control for metallic mineralization; abstract, Geological Society of America, Northeastern Section, Program, p. 73.

-29-

EXTRACTION OF ORGANICALLY-BOUND GOLD IN SURFICIAL MATERIALS

Project 830041

D. Conrad Grégoire
Resource Geophysics and Geochemistry Division

Grégoire D.C., Extraction of organically-bound gold in surficial materials; in Current Research, Part A, Geological Survey of Canada, Paper 85-1A, p. 223-228, 1985.

Abstract

A method has been developed for the determination of organically-bound gold in soils, lake and stream sediments. A 10 g sample of soil or sediment is digested with a 5% solution of sodium hypochlorite. The recovery of organically-bound gold is nearly quantitative for lake and stream sediments high in organics. For stream sediments and soils low in organic content, the recovery of gold is complicated by the sorption of released gold by inorganic sample components. For these materials recoveries as low as 70% of the organically-bound gold is possible.

Résumé

Une méthode a été mise au point pour déterminer la présence de l'or lié aux matériaux organiques dans les sols et les sédiments lacustres et fluviatiles. Il suffit de faire digérer un échantillon de dix grammes de sol ou de sédiment dans une solution de 5 % d'hypochlorite de sodium. L'or lié aux matériaux organiques peut être récupéré presque entièrement dans le cas des sédiments lacustres et fluviatiles riches en matériaux organiques. Dans le cas de sédiments fluviatiles et de sols pauvres en matériaux organiques, la récupération est compliquée par l'adsorption de l'or libéré par les composantes inorganiques. Pour ces matériaux, il est possible de récupérer jusqu'à 70 % de l'or lié aux matériaux organiques.

Introduction

A knowledge of the gold species present in weathering products is essential to understanding the mechanism(s) of transportation of gold from mineralized areas and its subsequent deposition in soils, and stream and lake sediments. Information of this nature could also be used as a tool for exploration purposes.

The chemical separation of metals bound up or associated with various phases of a soil or sediment has been studied. A recent review of partial dissolution techniques by Chao (1984) emphasizes the importance of data thus obtained in geochemical exploration.

It is clear from the chemical literature that the role of organic materials in the surficial environment is great with respect to the transportation and concentration of metals (Stevenson, 1983; Kerndorff and Schnitzer, 1980). The chemistry of gold in soils and sediments has been investigated by Ong and Swanson (1969) and reviewed by Boyle (1979). These authors acknowledge the importance of humic substances in the stabilization of gold in soils and sediments.

Although many studies have been completed on the extraction of organically bound metals in soils and sediments, no work has been published to date on a method for the extraction of organically bound gold from these materials.

The development of methodology for the determination of gold from the organic phase of soils and sediments is made difficult by the very high organic content possible (up to 90%), the large sample size needed (typically 10 g) and the very low detection limit (less than 1 ppb) required for quantitative analysis. In addition to the analytical problems resulting from these factors, the choice of reagent for the extraction of gold from organic material is also problematic.

Two common reagents have been used to oxidize organic matter in surficial materials; hydrogen peroxide and sodium hypochlorite. The use of hydrogen peroxide as an oxidizing agent is not as effective or specific as sodium hypochlorite. In a comparative study of the two reagents, Lavkulich and Wiens (1970) have found that hydrogen peroxide does not destroy completely the organic material in the sample and also is more reactive toward the sesquioxides present, thus releasing metals associated with iron and manganese oxide and hydroxide phases. Chao and Sanzalone (1977) and Hoffman and Fletcher (1979) have determined that hydrogen peroxide can dissolve several sulphide minerals found in sediments and soils, whereas iron and manganese oxides (Rose, 1975) are not dissolved appreciably by sodium hypochlorite.

Ideally, the gold present in the organic phase of a soil or sediment could be extracted by the application of the appropriate reagent and no gold would be extracted from or lost (once released) by chemical reaction or adsorption to other phases. In practice, however, it is seldom possible to perform the quantitative dissolution of one phase without in some way affecting other phases. As a result, one may only be able to determine semi-quantitatively how much gold is associated with the organic phase.

The objective of this work was to develop methodology for the quantitation of gold bound in the organic phase of soils and sediments using sodium hypochlorite as the extracting reagent and to establish the accuracy and precision of the method.

Table 29.1. Solubility of gold in 5% sodium hypochlorite solution

Sample	Mass	Au/ppb	% Au leached
Precipitated gold	50 mg	-	< .01
MacInnis Lake rock	1 g	550[a]	1.2
PTC-1	1 g	650[b]	3.4

[a] Maurice, 1984
[b] McAdam et al., 1973

Experimental

Reagents and apparatus

All reagents used were of reagent grade. The 5% sodium hypochlorite (J.T. Baker) was used without prior adjustment of pH. Gold standard solutions were prepared by dilution of stock 1000 ppm auric chloride solution (Aldrich Chem. Co.) with distilled water.

All gold determinations were done on a Perkin-Elmer Model 5000 atomic absorption spectrophotometer equipped with a Model 500 graphite furnace.

Analytical procedure for the determination of total gold and gold in sodium hypochlorite extracts

For the determination of total gold, ten grams of prepared sample (minus 80-mesh, ball milled) were placed in a porcelain crucible and heated in a muffle furnace at a temperature of 650°C for one hour. The ash was transferred to a 250 ml beaker and 25 ml of aqua regia were added. The mixture was allowed to stand for one hour at room temperature. The contents of the beaker were heated gently on a hot plate and allowed to reflux for one hour before increasing the temperature and evaporating the sample to incipient dryness. To the residue were added 25 ml of concentrated hydrochloric acid. The contents were stirred and heated to boiling for five minutes. The resulting mixture was centrifuged for five minutes (2000 rpm) and the residue was rinsed twice with 5 ml aliquots of 3 M hydrochloric acid.

Table 29.2. Composition of barren sediments and soil

Sample	Au/ppb	Loss on ignition/%	Fe/%[a]	Mn/%[a]	Al/%[a]
CR-M	2.7	35.1	2.8	.025	4.0
CR-R	7.3	6.3	5.7	.044	8.3
S-5	4.0	5.3	6.0	.085	7.7

[a] Determined by X-Ray fluorescence

Table 29.3. Recovery of added gold from lake sediments and a soil treated with sodium hypochlorite

	% Recovery		
Extraction	CR-M	CR-R	S-5
NaOCl	57	72	66
pH = 2 HCl	20	8	4
pH = 1 HCl	17	2	1
pH = .5 HCl	5	1	2
	99	83	73

Table 29.4. Extraction of iron, manganese and aluminum from sediment and soil samples using 5% sodium hypochlorite and various concentrations of hydrochloric acid

	Percent Fe Extracted[a]			Percent Mn Extracted[a]			Percent Al Extracted[a]		
Extraction	CR-M	CR-R	S-5	CR-M	CR-R	S-5	CR-M	CR-R	S-5
NaOCl	.65	.02	< .01	0.8	0.5	< .05	.14	< .01	< .01
pH = 2	.87	.09	.08	2.0	.30	< .05	.22	< .01	.02
pH = 1	.93	.10	.06	2.0	.38	< .05	.30	.05	.01
pH = .5	.80	.11	.09	6.0	8.64	1.0	.35	.52	1.1

[a] percent of total metal present in sample

The combined supernates were then evaporated to dryness and made up to a final volume of 100 ml with 3 M hydrochloric acid.

Solutions resulting from the sodium hypochlorite digestion of soils and sediments contained a substantial quantity of dissolved organic material and unreacted hypochlorite and gold (III) could not be extracted directly into methyl isobutyl ketone (MIBK). To these solutions, 25 ml of 30% hydrogen peroxide were added and allowed to stand for three hours. During this time, the colour of the solution changed from a dark brown to a light amber. This step was necessary to prevent the formation of an emulsion upon extraction into MIBK. To the resulting solution was added 10 ml of concentrated hydrochloric acid to destroy any remaining hypochlorite in solution. The solution was then evaporated to incipient dryness and made up to 100 ml with 3 M hydrochloric acid.

Extraction procedure

Fifty millilitres of the prepared solution were extracted in a 125 ml separatory funnel into 5 ml of MIBK for ten minutes using a mechanical shaker (Eberbach Corp.). The aqueous layer was discarded. Ten millilitres of 0.1 M hydrochloric acid (saturated with MIBK) was used as backwash solution to remove excess iron from the MIBK extract (2 minutes extraction time). Standards using the appropriate quantity of auric chloride solution were prepared using the same procedure.

Gold in the MIBK extracts was determined by atomic absorption spectrometry using a graphite furnace atomization system. Ten microlitres of sample solution were delivered to the graphite furnace by means of an Eppendorf pipet fitted with disposable plastic tips. The following critical instrumental operating parameters were used; wavelength – 242.8 nm; drying cycle – 100°C for 20 seconds; charring cycle – 550°C for 20 seconds; atomization cycle – 2400°C for 5 seconds, maximum power.

All determinations were done in triplicate unless otherwise noted.

Table 29.5. Change in loss on ignition (%) with successive sodium hypochlorite treatments

	Sample		
NaOCl treatment	CR-M	CR-R	S-5
1	32.1	4.9	3.5
2	18.2	3.4	2.6
3	11.0	3.3	2.4
4	5.3	3.6	2.8
5	3.4	3.4	2.6

Preliminary studies

Solubility of gold and some gold bearing minerals in 5% sodium hypochlorite

The object of any metal speciation study is to determine the quantity of metal associated with each chemical phase of the sample. For gold, it is expected that much of the element in sediments and soils will be present in the form of metallic gold, associated with iron and manganese oxides and sulphide minerals or bound up in humic materials. Although gold is the noblest of metals and is quite resistant to chemical attack, the metal is soluble in strong oxidizing medium in the presence of complexing agents. When sodium hypochlorite is heated or acidified, chlorine is liberated and gold present in several phases may be released or dissolved. An important consideration is then the solubility of free and combined gold in minerals when these are treated with hypochlorite solution.

To determine the applicability of sodium hypochlorite as an extracting agent for organically bound gold, a study was made on the solubility of metallic gold and gold bound to sulphides in sodium hypochlorite solution.

Samples of precipitated gold metal, a gold bearing rock (MacInnis Lake basement rock) and PTC-1 sulphide concentrate (McAdam et al., 1973) were used as test materials. The gold in the MacInnis Lake sample was determined to be primarily metallic gold by microprobe analysis (Maurice, 1984).

Samples of each of these materials were equilibrated with 25 ml of 5% sodium hypochlorite for a period of 24 hours. The resulting mixture was warmed on a hot plate for three hours and centrifuged at 2000 rpm for ten minutes to separate the leach solution from the residue. The residue was washed twice with distilled water and the rinsings were combined with the original leach solution. To this solution, 10 ml of 12 M hydrochloric acid were added to destroy any remaining hypochlorite. The solution was evaporated to dryness, the salts dissolved in 3 M hydrochloric acid, and the gold (III) extracted into MIBK.

The results presented in Table 29.1 indicate that metallic gold is not appreciably dissolved during the hypochlorite treatment. It is reasonable to expect differences in the solubility of gold depending on the particle size of the gold and the reactivity of the matrix material

Table 29.6. Organically-bound gold in sediments and soils

Sample	Loss on ignition/%	Total gold ppb	NaOCl extractable gold (% of total)
Moose Lake sediment	47.0	6.4	65.7
Red Lake sediment	14.9	281.5	90.9
Moose Creek stream sediment - A	19.9	53.1	60.4
Moose Creek stream sediment - B	24.3	53.4	56.1
Soil 1 B-Horizon	8.0	14.9	63.0
Soil 2 B-Horizon	6.8	92.2	92.4

Table 29.7. Determination of organically-bound gold in Moose Creek stream sediment

Sample	Organically-bound gold % of total
1	58.1
2	51.9
3	54.7
4	57.1
5	50.9
6	61.0
7	55.6
Mean	55.6
Coefficient of variation	6.3%

toward sodium hypochlorite. This may explain the much higher solubility of elemental gold in the MacInnis Lake rock sample relative to finely divided precipitated gold. There is a possibility that some of the gold present in this sample is associated with sulphides (Maurice, private communication) which could also account for the higher solubility of gold in the sample. Although sulphides are clearly attacked by the hypochlorite treatment (Rose, 1975; Hoffman and Fletcher, 1979) the effect is not serious enough to preclude the use of sodium hypochlorite solution as an oxidizing agent for organic matter in sediments and soils.

Recovery of added gold from barren sediments

Gold lies at the very bottom of the electrochemical series and thus is capable of being reduced by many ions in solution to form colloidal particulate gold. When gold associated with organic material is released by the action of sodium hypochlorite solution, there is a possibility that the released metal could be precipitated to metallic gold by metallic ions in solution, adsorbed onto solid inorganic components or bound to residual organic material including carbon.

Composite samples of two lake sediments and one soil were selected to determine if gold released as a result of hypochlorite oxidation remained in solution. A known quantity of gold (III) was added to a slurry containing sample and sodium hypochlorite solution and the recovery of gold was determined. The natural gold content of these samples (determined by aqua regia digestion) was found to be below 7 ppb. Blanks were run simultaneously with test samples (triplicate determinations). Following this treatment, the residues were rinsed with hydrochloric acid of increasing strength to determine if gold lost to sorption could be mobilized. The amount of iron, manganese and aluminum leached from the sample by each experimental step was determined.

To 10 g of sediment or soil were added 0.25 micrograms of gold as auric chloride. Fifty millilitres of 5% sodium hypochlorite solution were added to the mixture and allowed to stand for 15 hours at room temperature. The solution was then heated to near boiling for three hours. After cooling, the leach solution was separated from the residue by centrifugation (2000 rpm for 10 minutes). The residue was rinsed twice with distilled water and then was equilibrated for a period of one hour with 50 ml of hydrochloric acid ranging in pH from 2 to 0.5. After each equilibration step, the residue was rinsed twice with 10 ml of hydrochloric acid of the same concentration.

The composition of the sample material used for this study is given in Table 29.2. The recovery of added gold from each step of this procedure is given in Table 29.3. The initial recovery of gold from the hypochlorite digestion was nearly the same for all three samples. With increasing acid strength of rinse solutions, the recovery of the gold remaining was high for the lake sediment samples but remained relatively low for the soil sample (S-5). It is evident that gold chloride is rather tightly bound to the inorganic components comprising the soil sample and that recovery of this metal is unlikely to be easy. It appears from these data that although some of the dissolved gold was bound to organic components, the association was fairly weak and could be broken with 0.1 M hydrochloric acid. One hypochlorite digestion was not sufficient to destroy completely the organic material in the CR-M sample.

The dissolution of iron, manganese and aluminum (Table 29.4) from the sample matrix was not appreciable for the hypochlorite extraction or for the rinsings with hydrochloric acid of pH down to 1.0. However, when the rinse solution was increased in acidity to pH 0.5, substantial quantities of manganese and aluminum were dissolved. Gold associated with manganese and aluminum minerals would be released and included with gold derived from the organic phase.

The procedure for the extraction of organic gold from soils and sediments could include several rinses with 0.1 M hydrochloric acid in order to desorb gold taken out of solution by inorganic components in the sample. It is clear, however, that if the integrity of the manganese oxide/hydroxide phase is to be preserved, that some of the gold will remain bound to other sample components. This will be particularly true for soils low in organic content where the recovery can be as low as 70%. The recovery of gold from the two sediment samples was quite high and was quantitative for the sample of very high organic content.

Destruction of organic matter in sediments and soils using 5% sodium hypochlorite solution

The range of molecular weights of organic matter found in sediments and soils is great, as is the range in the organic content of these materials. It is therefore unlikely that a single sodium hypochlorite digestion will suffice to destroy completely the organic matter found in all samples. Lavkulich and Weins (1970) reported that three hypochlorite digestions were necessary to oxidize completely the organic matter present in soils. Fulvic acids, which make up a large part of the organics have a lower range of molecular weights and a higher reactivity toward minerals and metals in solution than do humic acids or humins (Schnitzer and Kodoma, 1977). Fulvic acids are probably more susceptible to hypochloride oxidation than other organic components of higher molecular weight and thus most of the gold bound to organics would probably be released into solution during the first or second hypochlorite treatment.

Although the loss on ignition is not a quantitative measure of the organic content of a sample, the change in loss on ignition with successive hypochlorite treatments can be used as a measure of the extent of oxidation of humic material. Ten gram samples of prepared material (minus 80-mesh, ball milled) were digested with 50 ml of hypochlorite solution as previously described. The residues were washed twice with distilled water and oven dried at 80°C overnight. The loss on ignition was determined by heating the sample in a programmable muffle furnace at a temperature of 800°C for one hour (at the maximum temperature).

In Table 29.5 is given the loss on ignition with successive hypochlorite digestions for the two sediment and one soil sample discussed previously. For the highly organic (Table 29.2) CR-M sample, at least three digestions were required before there was no change in the loss on ignition. For the remaining lake sediment sample CR-R and soil S-5, little change was observed after the first hypochlorite digestion. From the data given here, it was concluded that three hypochlorite digestions would suffice for most samples. Only for more highly organic materials such as peat and humus would additional digestions be required. After completing three digestions, the residues ranged in color from a dull grey (CR-M) to a reddish-brown (S-5).

Results and discussion

Extraction of organically bound gold from surficial materials

The method developed for the extraction of organically bound gold from surficial materials was applied to a series of six composite samples obtained from mineralized areas. All samples with the exception of the Red Lake sediment were obtained from the Hemlo area of northwestern Ontario, Canada. The Red Lake sample is a composite of lake sediments obtained in the vicinity of Red Lake which is located in Ontario near the Manitoba border (Timperley and Allan, 1974). The two Moose Creek stream sediments were obtained from the same stream but from different locations. The two soils originated from two different sampling sites.

The procedure for the extraction of organically bound gold entailed three sodium hypochlorite extractions followed by two rinsings of pH = 1 hydrochloric acid. Before subjecting the samples to the hypochlorite procedure, all samples were extracted (2 hours) with a solution of 1 M ammonium acetate adjusted to pH 7 with ammonium hydroxide. This procedure was used to estimate the content of easily exchangeable gold in the sample material. No detectable quantities of gold were obtained from any of the samples with the exception of the Red Lake sediment. This sample contained 1.1% of its total gold in an easily exchangeable form. The results obtained using the hypochlorite procedure outlined above are presented in Table 29.6. Each value is the average of three separate determinations.

Lake sediments (particularly center-lake sediments) are expected to contain mostly organically-bound gold because it is unlikely that dense metallic gold would be transported to these areas. This has been verified for the Red Lake sediment sample but not for the Moose Lake sediment. The detection limit for the determination of gold in these materials is approximately 1 ppb. Materials which contain a very low level of gold such as the Moose Lake sediment (6.4 ppb) are subject to analytical error during the course of the extraction procedure. For this reason, the results obtained for this sample should be interpreted with caution.

The organic gold content of the two stream sediment samples (common source) agree well with one another indicating a high level of reliability for the method on repeated analyses. The two soil samples differ greatly in their abundance of organically-bound gold probably owing to natural differences related to the sampling site.

Accuracy and precision

Unfortunately, no reference materials exist with which to test the actual accuracy of the results obtained from the application of sodium hypochlorite as extractant for organically-bound gold. However, some semi-quantitative evaluation can be made based on the various data collected during this study.

It has been shown in this work that the sodium hypochlorite reagent does attack to some extent native gold and gold bound in sulphide minerals. However, the actual contribution of these is expected to be small. Of greater concern is the loss of released gold to other components present in the sample matrix.

For lake sediments and for highly organic stream sediments, the loss of released gold is not significant providing most of the organic material is destroyed and providing there is sufficient gold present in the sample to avoid serious analytical errors. In most cases, quantitative recovery of organically-bound gold can be expected for lake sediment samples.

For stream sediments of low organic content and for soils, the losses due to the interaction of matrix components with released gold can be substantial (Table 29.3). The results obtained for these samples could be low by as much as 30 per cent in the worst case. However, when applied to geochemical studies, natural anomalous values of organically-bound gold would be detected in these materials when data is compared from materials of similar composition.

The precision of the method was determined by the analysis of seven 10 g samples of Moose Creek stream sediment (B). The results presented in Table 29.7 demonstrate that the repeatability of the method is satisfactory. The coefficient of variation is 6.3%.

Acknowledgments

The author is grateful to P.W.B. Friske, J.J. Lynch and Y.T. Maurice for collecting and providing the sample material used in this study. W. Alexander is thanked for his able technical assistance with much of the experimental work.

References

Boyle, R.W.
1979: The geochemistry of gold and its deposits; Geological Survey of Canada, Bulletin 280, p. 51-57.

Chao, T.T.
1984: Use of partial dissolution techniques in geochemical exploration; Journal of Geochemical Exploration, v. 20, p. 101-135.

Chao, T.T. and Sanzalone, R.J.
1977: Chemical dissolution of sulfide minerals; in Journal of Research, U.S. Geological Survey; v. 5, p. 409-412.

Hoffman, S.J. and Fletcher, W.K.
1979: Selective sequential extraction of Cu, Zn, Fe, Mn and Mo from soils and sediments; in Geochemical Exploration 1978, ed. J.R. Watterson and P.K. Theobald; Association of Exploration Geochemists, Special Publication, v. 7, p. 289-299.

Kerndorff, H. and Schnitzer, M.
1980: Sorption of metals on humic acids; Geochimica et Cosmochimica Acta, v. 44, p. 1701-1708.

Lavkulich, L.M. and Wiens, J.H.
1970: Comparison of organic matter destruction by hydrogen peroxide and sodium hypochlorite and its effects on selected mineral constituents; Soil Science Society of America, Proceedings, v. 34, p. 755-758.

Maurice, Y.T.
1984: Gold, tin, uranium and other elements in the Proterozoic nonacho sediments and adjacent basement rocks near MacInnis Lake, District of Mackenzie; in Current Research, Part A, Geological Survey of Canada, Paper 84-1A, p. 229-238.

McAdam, R.C., Sutarno, and Moloughney, P.E.
1973: Noble-metal-bearing sulphide concentrate PTC: its characterization and preparation for use as a standard reference material. Department of Energy, Mines and Resources of Canada, Mines Branch Bulletin TB 176.

Ong, H.L. and Swanson, V.E.
1969: Natural organic acids in the transportation, deposition and concentration of gold; Quarterly Journal of the Colorado School of Mines, v. 64, p. 395-425.

Rose, A.W.
1975: The mode of occurrence of trace elements in soils and stream sediments applied to geochemical exploration; in Geochemical Exploration 1974, ed. I.L. Elliott and W.K. Fletcher; Elsevier, Amsterdam, p. 691-705.

Schnitzer, M. and Kodoma, H.
1977: Reactions of minerals with soil humic substances; in Minerals in Soil Environments, ed. J.B. Dixon, S.B. Weed, J.A. Kittrick, M.H. Milford, and J.L. White; Soil Science Society of America, Madison, Wis., p. 741-770.

Stevenson, F.J.
1983: Trace metal-organic interactions in geological environments; in The Significance of Trace Elements in Solving Petrogenic Problems and Controversies, ed. S.S. Augustithis; Theophrastus Publications, S.A., Athens, p. 671-691.

Timperley, M.H. and Allan, R.J.
1974: The formation and detection of metal dispersion halos in organic lake sediments; Journal of Geochemical Exploration, v. 3, p. 167-190.

-30-

SOIL DEVELOPMENT ON QUATERNARY DEPOSITS OF VARIOUS AGES IN THE CENTRAL YUKON TERRITORY

Project 790005

C. Tarnocai[1], S. Smith[2], and O.L. Hughes
Terrain Sciences Division, Calgary

Tarnocai, C., Smith, S., and Hughes, O.L., Soil development on Quaternary deposits of various ages in central Yukon Territory; in Current Research, Part A, Geological Survey of Canada, Paper 85-1A, p. 229-238, 1985.

Abstract

Soil development on Quaternary materials resulting from pre-Reid (0.12-1.2 Ma), Reid (80-120 ka), and McConnell (14-30 ka) glaciations was studied in order to aid in the differentiation of these deposits. The most useful morphological soil properties, which provide the basis for field separation of these materials, were: solum depth; colour of the B horizons; frequency, colour and thickness of clay skins; degree of weathering and soil matrix alteration; and periglacial and cryogenic features. The pre-Reid deposits are associated with well developed Luvisols (paleo). The Reid deposits are associated with relatively weakly developed Luvisols (paleo) and Brunisols (paleo). The McConnell deposits are associated with the least developed soils (Brunisols).

Résumé

Les auteurs ont étudié l'évolution du sol sur les matériaux quaternaires provenant des avancées glaciaires de Reid (de 80 à 120 milliers d'années) et McConnell (de 14 à 30 milliers d'années) et de glaciations antérieures à celle de Reid (de 0,12 à 1,2 million d'années) afin d'aider à distinguer ces dépôts. Les propriétés morphologiques les plus utiles à l'identification des matériaux sur le terrain sont les suivantes: la profondeur du solum, la couleur des horizons B, la fréquence, la couleur et l'épaisseur des pellicules argileuses, le degré d'altération et la transformation de la matrice du sol et, les caractéristiques périglaciaires et cryogènes. Les dépôts accumulés antérieurement à la glaciation de Reid sont associés à des paléoluvisols tandis que les dépôts correspondant à la glaciation de Reid sont associés à des paléoluvisols et paléobrunisols relativement peu développés. Les dépôts de McConnell, eux, sont associés aux sols les moins développés (brunisols).

[1] Agriculture Canada, Land Resource Research Institute, Ottawa, Ontario K1A 0C6
[2] Agriculture Canada, Land Resource Research Institute, Whitehorse, Yukon Territory

Introduction

During the 1983 field season, Quaternary deposits and the soils developed on them were investigated under a joint Terrain Sciences – Land Resource Research Institute project in the McQuesten map area (115 P) and parts of the Stewart River (115 O and N, E1/2) and Dawson (116 B and C, E1/2) map areas of central Yukon Territory. The principal objectives of the project were:

1. mapping of the distribution of the Quaternary deposits of the McQuesten map area;
2. characterization and comparison of soils developed on successive ages of glacial deposits within the region glaciated by the Cordilleran ice sheet;
3. comparison of those soils with soils developed on presumed correlative glacial deposits produced by successive advances of montane glaciers in the southern Ogilvie Mountains; and
4. evaluation of differences in the morphological, physical, and chemical properties of soils developed on successive ages of glacial deposits, and possible effects of those differences on geochemical exploration.

Major pedogenic differences, especially in clay mineralogy, have been demonstrated in soils developed in the area on drift of pre-Reid, Reid, and McConnell age by Rutter et al. (1978), Foscolos et al. (1977), and Hughes et al. (1972). Kodama et al. (1976) provided a detailed mineralogical study of two soils from the area.

In this report field observations of the morphological characteristics of various soils and their correlation with the three ages of Quaternary materials are presented.

Geological setting

Main Cordilleran ice sheet

In that part of central Yukon Territory glaciated by the main Cordilleran ice sheet, Bostock (1966) inferred four separate advances: Nansen (oldest), Klaza, Reid, and McConnell, with each successive advance less extensive than the preceding one. Landforms associated with the Nansen advance are so subdued that the Nansen limit cannot be interpreted with confidence from airphotos. The limit mapped by Bostock (1966) and shown in this report (Fig. 30.1) is to a considerable degree based on field observations of glacial erratics. In places there are landform features suggestive of a glacial limit intermediate between the Nansen limit and the more readily identifiable limit of Reid Glaciation. Bostock (1966) was able to link such features together locally to define a limit of Klaza Glaciation. Extensive areas exist, however, in which no distinction between Nansen and Klaza deposits can be made on the basis of landforms. In this report, all glacial deposits beyond the limit of Reid Glaciation are grouped as "pre-Reid". It is hoped, however, that laboratory analyses of pre-Reid soils will reveal criteria for distinguishing deposits of Nansen and Klaza age.

Moraines and other ice-marginal features marking the limit of the Reid advance are subdued by comparison with features related to the McConnell advance. Nevertheless, the highly digitate Reid limit can be traced, with interruptions, from the type locality (the term "type locality" refers to the location where a specific age of glacial landform was identified) near Reid Lakes (site 41, Fig. 30.1) southward then northwestward into the Snag map area in southwestern Yukon Territory where it joins with the limit of Mirror Creek Glaciation as defined by Rampton (1969, 1971).

Well preserved ice-marginal features related to the McConnell advance can be traced from the type locality 14 km southwest of Mayo, around the digitate margin of the northwestern part of the Cordilleran ice sheet during the McConnell maximum. The limit is traceable, with interruptions, into the Snag map area, where it joins with the limit of McCauley Glaciation as defined by Rampton (1969, 1971).

Montane glaciation of the southern Ogilvie Ranges

Thick drift of pre-Reid age deposited by the Cordilleran ice sheet occurs along upper Lake Creek (site 40, Fig. 30.1) west of the Willow Hills, along Stewart River downstream from where the river turns southwestward out of Tintina Trench and northwestward along Tintina Trench. The gently undulant drift surface in Tintina Trench is continuous with the upper surface of the Flat Creek beds (McConnell, 1905), which are composed of glaciofluvial gravel, glacial till, and silt. Lithology of the gravel and till indicates that they were deposited by montane glaciers originating in the southern Ogilvie Mountains. To the west of Tintina Trench, glaciofluvial gravel, termed Klondike River gravels or Klondike gravels by McConnell (1907), lies on a high bedrock terrace on the south side of Klondike River. At the mouths of Hunker and Bonanza creeks (near sites 52 and 53, Fig. 30.1), the Klondike gravels overlie White Channel gravel of presumed Late Pliocene – Early Pleistocene age. The bedrock terrace and overlying Klondike gravels merge at Yukon River with a terrace that continues northwestward beyond the mouth of Fortymile River. Flat Creek beds and Klondike gravels are the product of one or more "old" glaciations during which large montane glaciers flowed both northward and southward from the axis of the southern Ogilvie Mountains (Vernon and Hughes, 1966). High terraces along Fortymile River east of the Yukon – Alaska boundary appear to be the downstream continuation of terraces thought by Weber (1983) to relate to the Early (?) Pleistocene Charley River glacial episode and probably also the Middle (?) Pleistocene Mount Harper glacial episode.

Modified, but readily recognizable, moraines and other ice-marginal features of the southern Ogilvie Mountains were assigned by Vernon and Hughes (1966) to an "intermediate" glaciation. Glaciers in southward-draining valleys, such as the North Klondike (site 59, Fig. 30.1) and Chandindu (site 58, Fig. 30.1), reached to the northeast side of Tintina Trench. Terminal deposits are inset within inner valleys that are incised some 200 m below the upper surface of the Flat Creek beds, indicating a major erosional interval between old and intermediate glaciations of the area. The southward-flowing glaciers had northward-flowing counterparts that extended beyond the southern Ogilvie Mountains into adjacent Taiga Valley.

Moraines assigned to the "last" glaciation of the southern Ogilvie Mountains (Vernon and Hughes, 1966) are mostly confined to tributary valleys within the mountains, indicating a restricted advance.

Loess deposits

A thin veneer of loess occurs on morainal and outwash deposits of all ages within the area studied. Loess thickness typically ranges from 10 to 50 cm. In areas of pre-Reid and Reid deposits, the loess rests on paleosols, typically truncated, which have developed on the older deposits. Ventifacts that are either polished and fluted or pitted, depending upon rock type, are common at the interface between the paleosol and the overlying loess.

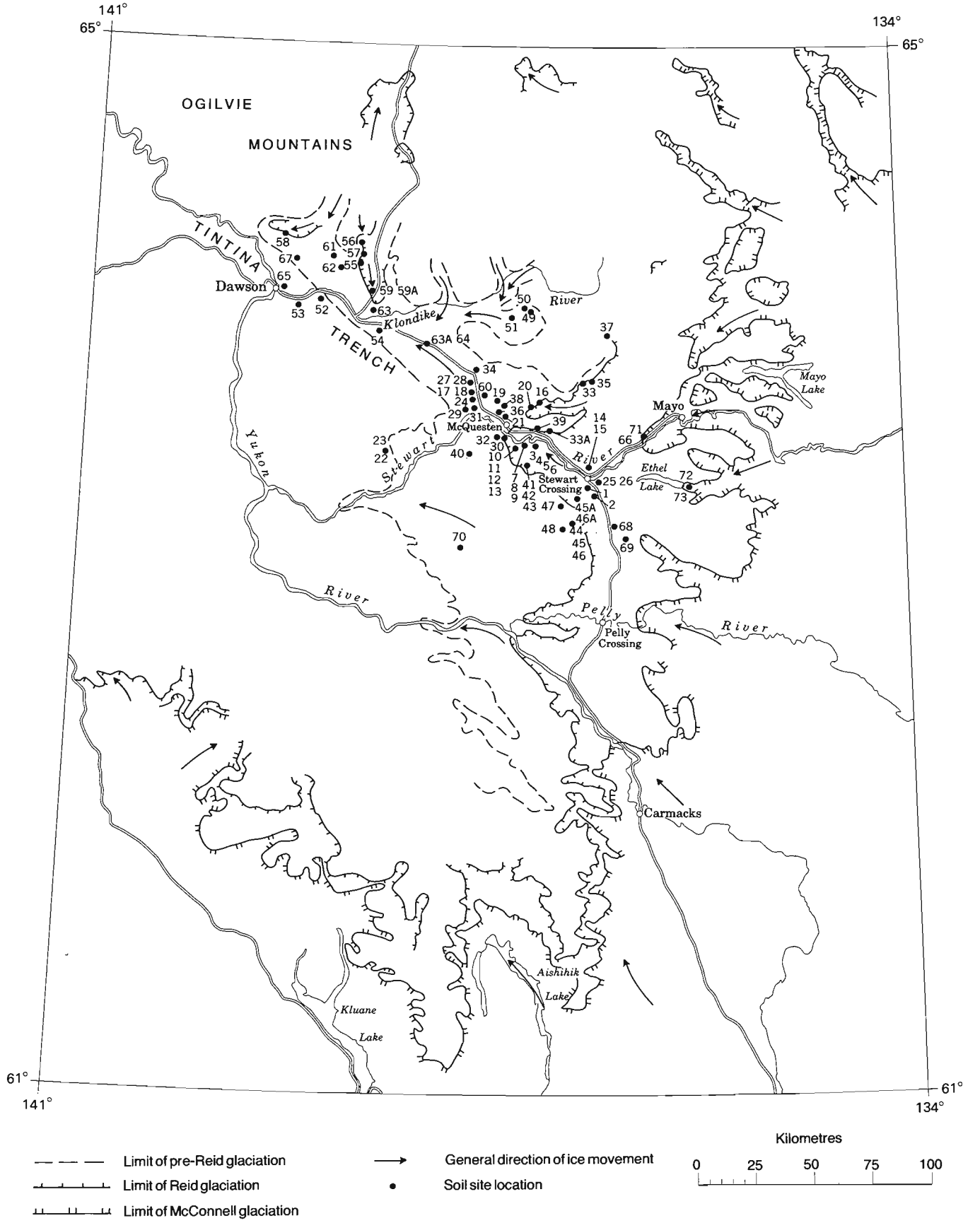

Figure 30.1. *Glacial limits in central and southern Yukon and location of soil sample sites.*

In 1983 ventifacts were best displayed in an elliptical turn-around area at the end of a side road leading to Jackfish Lake (near site 68, Fig. 30.1) in an upland between Pelly and Stewart rivers. There, the ventifact horizon lies at the truncated top of a Brunisol developed on pitted coarse outwash gravel of Reid age. Orientation of flutings on boulders ranged from 330° to 010°, generally parallel to the trend of U-shaped dunes in the upland area.

The loess is judged to be of late McConnell age with the exception of one site where it may be of Reid age. The truncated paleosols and the ventifact horizons together indicate that, during the McConnell Glaciation, areas of Reid and pre-Reid deposits were essentially devoid of plant cover and exposed to severe deflation. Loess began accumulating only in late McConnell time, when warmer and probably moister conditions permitted growth of sufficient vegetation to trap and stabilize loess.

Much of the loess likely originated from outwash plains that extended from the retreating McConnell ice margin. Loess derived from the outwash plains is characteristically calcareous. At sites where loess overlies soils developed on pre-Reid deposits, however, the loess is commonly noncalcareous. Such sites are, in general, far from the outwash plain sources. This suggests the possibility that such loess was derived by wind erosion from local sources such as the noncalcareous sola of Luvisols developed on the Reid and pre-Reid deposits.

Correlation and chronology

Drifts of the old, intermediate, and last glaciations in the southern Ogilvie Mountains correspond closely in morphology to pre-Reid, Reid, and McConnell drifts, respectively, deposited by the Cordilleran ice sheet. The suggested correlation is supported by the meagre radiometric data available.

Near Fort Selkirk, at the confluence of Pelly and Yukon rivers, a cemented till is overlain by gravel and sand, silt (loess?) containing 20 cm of Fort Selkirk tephra, basaltic lapilli containing charred remains of tree trunks and, at the top, more than 90 m of basalt of the Selkirk Group (Templeman-Kluit, 1974, p. 55). The tephra has yielded glass-fission-track ages of 0.84 ± 0.13 and 0.86 ± 0.18 Ma and a zircon-fission-track age of 0.94 ± 0.40 Ma (Naeser et al., 1982). A sample of basalt from immediately above the lapilli yielded a K-Ar age of 1.08 ± 0.05 Ma (M.L. Silberman, personal communication to J.V. Matthews, 1981). Bostock (1966) considered the till to be related to the Nansen or a still older advance, and glacial striae on the upper surface of the basalt to be related to the Klaza advance. It is suggested that an age of about 1 Ma is a minimum for the Nansen advance and a maximum for the Klaza advance.

Mosquito Gulch tephra, from a terrace of Bonanza Creek near Dawson, has a glass-fission-track age of 1.22 Ma (Naeser et al., 1982). The terrace was formed after Klondike River and tributaries such as Bonanza Creek began in incise through the Klondike gravels; hence the date is a minimum for the old glaciation(s) of the southern Ogilvie Mountains. The dates from Fort Selkirk and that of the Mosquito Gulch tephra indicate at least comparable antiquity for the Nansen advance of the Cordilleran ice sheet and the old glaciation(s) of the southern Ogilvie Mountains.

There are no dates directly relevant to the end of the Klaza advance or to the beginning of the Reid advance. Organic silt on the valley floor of Hunker Creek, a tributary of Klondike River upstream from Bonanza Creek, has been radiocarbon dated as greater than 53.9 ka (GSC-527, Lowdon and Blake, 1968, p. 229). This age is minimum for the incision of the Klondike drainage system, which preceded the intermediate glaciation of the southern Ogilvie Mountains. Incision may have been much earlier.

At Ash Bend (site 7, Fig. 30.1) on Stewart River, organic silt containing Sheep Creek tephra (J.A. Westgate, personal communication, 1984) overlies glaciofluvial gravel and till of Reid age. Wood from within the tephra was dated at greater than 42.9 ka (GSC-524, Lowdon and Blake, 1968). Bone associated with this tephra (originally reported to be Dome tephra) at Canyon Creek, Alaska, has yielded uranium-thorium and uranium-protactinium dates of 78 and 73 ka, respectively (Hopkins, 1982, p. 6). The dates indicate that Reid Glaciation had culminated and the Cordilleran ice sheet was in retreat before 42.9 ka and perhaps by about 80 ka.

There are no finite limiting dates from our study area for the beginning of McConnell Glaciation. At Tom Creek in the Liard Plain, organic material from Tom Creek silt beneath a surface till has been dated at 23.9 ± 1.14 ka (GSC-2811). At Silver Creek, near the southern end of Kluane Lake, organic beds overlain by Kluane till, the surface till of the area, have yielded dates as young as 29.6 ± 0.46 ka (GSC-769, Lowdon and Blake, 1970; Denton and Stuiver, 1967). Although these localities are distant from our study area, they suggest that McConnell Glaciation began perhaps by 30 ka and that the Cordilleran ice sheet continued to expand after 23.9 ka. There are no dates from our area relative to retreat of the Cordilleran ice sheet following the McConnell maximum. A basal sample of organic deposits within the limit of the last glaciation in the headwaters of Blackstone River in the Ogilvie Mountains has been dated at 13.74 ± 0.19 ka (GSC-515, Lowdon and Blake, 1968). A comparable date of 13.66 ± 0.18 ka (GSC-495, Lowdon et al., 1967) has been obtained from the base of an organic deposit above McCauley till in the southwestern Yukon. We adopt 14 ka as the approximate time of culmination of McCauley Glaciation of the southwestern Yukon, of the last glaciation of the southern Ogilvie Mountains, and of McConnell Glaciation in the central Yukon.

Soil investigations

Field methods

Site selection. The objectives of our soil investigations differed markedly from those of routine soil surveys. Virtually all soils in Canada are developed on parent material of Late Wisconsinan or Holocene age. In routine surveys all soils are examined and classified without need to distinguish between parent materials of distinctly different geological age. In our study area we were aware in advance that parent materials of three age categories, ranging from McConnell deposits (10 to 14 ka) to pre-Reid deposits, some of which may be more than 1.25 Ma, were present. Given our major objective of characterizing and comparing soils developed on the respective age classes of geological materials, a high degree of selectivity was needed to obtain adequate representation of each age class. To limit variability in soil development due to the nature of the parent material, sampling was concentrated in morainal and glaciofluvial deposits, within each age class. In addition, sites were carefully chosen to display both optimum soil development and good subsequent preservation of the soil.

Degree of preservation is an important consideration in dealing with soils developed on parent material of Reid and older age. Reid deposits were subjected to a period of severe periglacial conditions as adjacent areas were glaciated during McConnell Glaciation. Consequently, the soils were affected by varying degrees of cryoturbation, solifluction, and wind deflation in addition to conventional erosion. Soils developed on older materials may have been subjected to one million

years or more of alternations between glacial and interglacial climates. Hence it was necessary to select sites carefully which appeared to display both optimal soil development and good preservation.

Sample sites were located on morainal deposits at the type localities of the Reid and McConnell glaciations and at sites judged to be of Reid and McConnell ages based on airphoto tracing of glacial limits. Others were located on glaciofluvial (outwash) terraces that, from their geomorphic settings, were clearly related to either Reid or McConnell glacial deposits. Sample sites on deposits of pre-Reid age were selected in the zone between the limits of Reid and Nansen glaciations, as mapped by Bostock (1966, Fig. 1).

Description and sampling of soils. Once a pedon (a three-dimensional body of soil) had been selected, detailed descriptions were undertaken (McKeague, 1978, Canada Soil Survey Committee, 1978). The descriptive terminology used and the procedures for sampling followed were those outlined by the Expert Committee on Soil Survey (1983). Soil pits measuring 1 x 2 m in area and 2 m in depth were dug with the aid of portable, gasoline-powered jackhammers. In some locations, where a continuous vertical exposure over some distance was desired, trenches 1 m wide, several metres deep, and up to 20 m in length were dug. These were necessary to display location, shape, and periodicity of sand involutions. In conjunction with the trenches and some pits, horizontal cuts at specific depths (25, 50, and 75 cm) were examined using a procedure similar to that described by van Vliet and Langohr (1981). These were important for the description of the three-dimensional character of polygonal ground features. Sketches and photographs were made of the distribution of sand wedges, secondary carbonates, and cryoturbation features.

Morphological features such as structure, clay skin development, consistence, and texture were recorded for each soil horizon. Colour was described according to Munsell soil colour chart notation. The depth and thickness of each horizon were also measured. Samples 1 or 2 kg in size were collected from each horizon for laboratory analyses. Samples of forest floor materials were also collected at each site. Undisturbed samples were collected for preparation of soil thin sections for micromorphological studies.

Of the 77 sites described in detail and sampled for routine analysis, 56 were considered to be representative (i.e., not subjected to local disturbance or extreme truncation) of soils formed on pre-Reid, Reid, or McConnell drift surfaces. Field observations concerning these representative soils are summarized in this report. The nature of materials sampled and the number of pedons from which soils have been submitted for detailed analysis are presented in Table 30.1.

Soil development

A summary of the morphological characteristics of soils sampled on the three ages of surficial materials is found in Table 30.2. The periglacial and weathering features are summarized in Table 30.3. The term "solum" used in the following sections refers to the depth of weathering from the top of the respective drift material to the bottom of the lowermost B horizon. This solum depth does not include the overlying loess material. It should be noted that in some cases values reported are based on only a few soil profile descriptions and as such are likely to change as more field work is carried out in subsequent years.

Soils on pre-Reid outwash. The large variation in solum thickness (58-205 cm) on pre-Reid outwash is probably due to erosion removing part of the solum. Field observations lead to the conclusion that maximum solum development is at least 2 m and that the weathering effects (BC horizon) extend to a maximum of 5 m (roadcuts at site 28).

The colour of the upper Bt horizon was 5YR (reddish brown) and this colour gradually changed to 7.5YR in the lower Bt horizon. Locally a colour of 2.5YR, normally associated with strongly weathered soils found in southern temperate environments, was measured on these pre-Reid soils. These strong colours are especially significant for the interpretation of the past soil environment when they occur in combination with translocated clay.

These soils have Bt horizons with an angular or subangular blocky structure and many moderately thick clay skins, resulting from re-organization and/or translocation of clayey matrix material. Clay skins occur as coatings on ped and pebble surfaces and form bridges between sand grains.

Table 30.1. Structure and summary of survey data base

Soil parent material	Total pedons sampled	Representative pedons			Pedons for detailed analyses
		Total	Outwash	Moraine	
Pre-Reid	24	15*	11	4	10
Reid	26	16	5	11+	8
McConnell	6	4	1	3	3
Residual	2	1			1
Miscellaneous (unknown age, origin, or incomplete profile)	19				

* Representative pedons are those utilized to prepare soil morphological summaries presented in Table 30.2.

\+ Of these 11 Reid moraine pedons, 6 were located in material of Cordilleran glacial origin, 5 of montane (Ogilvie Mountains) origin.

Another characteristic of these pre-Reid outwash soils is the persistence of clay skins with depth. They are as common in the lower B horizons as in the upper B horizons although their thickness decreases with depth. They also occur more commonly as bridges between mineral grains in the lower part of the soil rather than as coatings on ped and channel surfaces. All of these soils show strong chemical weathering and most of the granitic and other rock types, with the exception of quartzite, are strongly altered due to weathering.

Most soils associated with pre-Reid outwash materials display strong cryoturbation in the form of disrupted and displaced soil horizons and oriented stones. Various sizes of sand wedges and sand involutions are also common. Ventifacts are commonly found at the pre-Reid soil surface.

Soils on pre-Reid morainal deposits. The average solum thickness in pre-Reid morainal materials (91 cm) is slightly less than the thickness found for pre-Reid outwash soils. This shallower depth is probably due to the finer texture of the till and greater truncation because these soils usually occur on sloping terrain.

Table 30.2. A summary of soil morphologies developed on various parent material underlying loess

Soil parent material	No. of pedons	Solum thickness** (cm)	Uppermost II B Horizons*			Lower II B Horizons	
			Thickness** (cm)	Dominant colour hue+	Consistence++ (moist)	Dominant colour hue+	Consistence (moist)
Pre-Reid outwash	12	x=109 (58-205)	x=25 (10-40)	5YR (reddish brown)	firm	7.5YR (dark brown)	friable
Pre-Reid moraine	4	x=91 (50-123)	x=30 (22-40)	7.5YR	firm	7.5YR	friable
Reid outwash	5	x=45 (9-90)	x=37 (9-70)	7.5YR	friable	10YR (yellowish brown)	very friable
Reid (Cordilleran) moraine	6	x=56 (14-106)	x=20 (16-26)	10YR	friable	10YR	very friable
Reid (Ogilvie Mtns) moraine	5	x=53 (40-69)	x=34 (22-43)	10YR	friable	10YR	very friable
McConnell drift	4	x=21 (0-40)	x=15 (14-17)	10YR	variable	not applicable	not applicable

Soil parent material	Dominant Primary Structure		% of profiles with II Bt horizons*	% of II B horizons with clay skins	Dominant Clay Skins		
	Type	Grade			Frequency	Thickness	Location
Pre-Reid outwash	blocky	weak-moderate	100	100	many++	moderately thick	bridges between sand grains and ped faces
Pre-Reid moraine	blocky=granular	moderate-strong	100	100	many=common	moderately thick	on all voids/channels, ped faces occasionally bridges between sand grains
Reid outwash	blocky=platy	weak-moderate	20	80	few	very thin	bridges between sand grains on some ped faces
Reid (Cordilleran) moraine	blocky=granular	weak-moderate	33	83	few>common	thin	bridges between sand grains
Reid (Ogilvie Mtns) moraine	granular>blocky	weak-moderate	80	80	few=common	thin	bridges between sand grains on many pebble surfaces
McConnell drift	variable	weak	25	50	none, few	thin	on some ped faces

* for definitions of soil horizons see Canada Soil Survey Committee (1978)
++ for definitions of soil morphological terms see Expert Committee Soil Survey (1983)
** mean thickness, range of values in brackets
\+ Munsell soil colour notation
= equal proportions
> first member dominant

Table 30.3. Periglacial and weathering features

Soil parent material	% of profiles with sand wedges/ involutions	% of profiles with strong cryoturbation	Coarse Fragments			
			Degree of weathering	Frost orientation	Silt or matrix cappings	Ventifacts
Pre-Reid outwash	34	50	strong chemical alteration	common	occasional	common
Pre-Reid moraine	75	100	strong chemical alteration	common	common	common
Reid outwash	20	0	moderate chemical, frost shattering	occasional	common	abundant
Reid (Cordilleran) moraine	0	20	moderate chemical, frost shattering	common	common	common
Reid (Ogilvie Mtns) moraine	0	20	moderate chemical, frost shattering	common	common	common
McConnell drift	0	0	slight to none	none	occasional	none

The colour of the uppermost B horizon is 7.5YR, one hue yellower than the pre-Reid outwash soils. The structure of pre-Reid morainal soils is moderately to strongly developed, subangular blocky and granular, and is the strongest structure of all soils in this study. Approximately 75% of the primary soil structure in the uppermost B horizons is moderate to strong and the structure of the remainder of the soil is moderate in development.

All pre-Reid morainal soils described had Bt horizons associated with reorganized or translocated clay. This clay occurs in the form of clay skins and clay bridges with frequency, thickness, and location of translocated clay similar to that of soils developed on pre-Reid outwash materials. Cryoturbated soil horizons were observed in all pedons examined. The degree of cryoturbation and the frequency of sand wedges and involutions are greater than in soils developed in pre-Reid outwash materials.

Soils on Reid outwash deposits. The solum thickness varied widely in these soils, with an average of 45 cm being less than half of the value for the pre-Reid outwash soils. Similarly, the maximum value of 90 cm is less than half of the maximum value for the pre-Reid outwash soils.

The dominant colour of the uppermost B horizon is 7.5YR but at one site (13) with strong morphological development, the uppermost B horizon was 5YR. Only a few of the Reid outwash soils were described as having Bt horizons, and the thin clay skins present were found on ped faces and pebbles and in places formed bridges between sand grains. Most of the horizons had angular or subangular blocky structure which was weakly to moderately, and locally very weakly, developed.

Sand wedges are less common in these soils than in pre-Reid soils and only one of the five pedons sampled was associated with sand wedges. These soils did not seem to have undergone strong cryoturbation. The chemical weathering was moderate in the Reid outwash soils. Ventifacts are common along the Reid outwash surfaces.

Soils on Reid morainal deposits. The mean solum thickness of the Reid morainal soils is slightly greater than that associated with the Reid outwash soils. The solum thicknesses in the Yukon Plateau and the Ogilvie Mountains areas were similar.

The uppermost B horizon in a quarter of the Reid morainal soils studied has a colour of 7.5YR; all of these soils had Bt horizons. The rest of the Reid morainal soils sampled have a colour of 10YR in the uppermost B horizon, which was either a Bt or a Bm horizon. In general, these dark brown upper B horizons were underlain by yellowish brown B horizons.

The dominant structure of the Bt horizons is moderately to strongly developed blocky to granular. The Bm horizons, on the other hand, generally have a weak to moderate blocky structure.

The Reid morainal soils whose uppermost B horizon was designated as Bt are all associated with clay skins which are generally thin and are found on ped and pebble faces and between sand grains. The soils with Bm horizons, however, had either no clay skins or very few, thin clay skins. No sand wedges or sand involutions occur in the soils examined. Cryoturbated soil features such as oriented stones and silt cappings are common. Ventifacts are regularly observed on the Reid soil surface. Weathering is moderate and frost-shattered coarse fragments are common. These coarse fragments, primarily those with non-quartzose lithologies, have undergone moderate chemical weathering.

Soils on McConnell deposits. Because of the limited number of pedons described in the McConnell deposits (two for outwash and two for morainal deposits), the characteristics of these soils are given together. As noted previously, the outwash and morainic materials and the overlying loess are essentially the same age and have been subjected to only one cycle of soil development. Thus the loess and subjacent material are treated as parts of a single soil profile.

The total solum thickness (including the loess) ranged from 37 to 49 cm with a mean value of 42 cm. This solum results basically from the removal of carbonates with little other evidence of pedological weathering.

The dominant colour of the B horizon in the McConnell soils is 10YR. Soil structures varied but all are weak. Illuviated clay in the form of clay skins is generally lacking. One solum did have a Bt horizon with common, thin clay skins. Whether these clay skins are the result of in-site reorganization of a clayey matrix or were produced by the processes of illuviation could not be determined solely by

field observations. The thin section samples and additional sampling of these soils in the future will, it is hoped, answer this question.

No periglacial or cryoturbated features were observed in soils developed on McConnell drift. Some silt or matrix cappings on coarse fragments are locally present in the lower solum.

Preservation of soil materials in reworked deposits

Soils were described and sampled on the most stable (level or near level) surfaces. Much of the study area, however, is steeply sloping and mountainous terrain. On sloping surfaces the old soils are eroded and their materials incorporated in the colluvial deposit. Soils on these surfaces show young (Brunisolic) development. Close and careful examination of some of the stones, especially the quartz and quartzite fragments, revealed that they contained remnants of former clay coatings, presumably formed when these fragments were incorporated within the solum (B horizon) of now eroded paleosols. These minute clay coatings, which are preserved in cracks and depressions of clasts, provide clues to the age of the material.

The colour of the clay coatings on fragments in colluvium derived from pre-Reid materials is generally reddish or reddish brown, and that of fragments derived from Reid materials is brown. In some cases (site 59) it appears that the coating on pebble surfaces and in the cracks has survived even glacial transport as coatings resembling those associated with pre-Reid soils were found in a soil developed on till of Reid age in the Benson Creek moraine.

Loess characteristics

A summary of loess morphology, based on field observations, is presented in Table 30.4. Loess thickness ranges from 5 to 50 cm with an average of about 22 cm. No significant differences were found in thickness of loess overlying surfaces of different ages except that the loess was thinnest on McConnell outwash.

Two basic types of loess occur in the study area, calcareous and noncalcareous. Calcareous loess is found at the sites northeast of Stewart River, between Stewart Crossing and McQuesten River. In these soils carbonate has moved downward from the loess to form irregular lenticular Cca horizons in the upper part of the underlying paleosol. This loess was presumably carried by prevailing southerly paleowinds of the region from broad outwash plains of McConnell age. Soils developed on calcareous loess lack an Ae horizon but do have a reddish Bm horizon (7.5YR and 5YR), indicating the process of Brunisolic soil formation through decalcification, hydrolysis, and oxidation. The remainder of the soils in the area are covered by noncalcareous loess. This noncalcareous loess may have been derived from wind erosion of the leached upper parts of paleosols on pre-Reid or Reid deposits. Ae horizons overlying a yellowish brown (10YR) Bm horizon are commonly observed on these noncalcareous loesses, suggesting incipient Luvisol formation within this surficial veneer.

Identification of surficial materials based on the associated soils

When soils are used to determine the relative age of a deposit, a stable surface should be chosen to ensure that the least eroded soil is selected. This soil should then be examined and described, with special attention being paid to those properties which aid in the differentiation. The most significant morphological properties, which provide the basis for field separation of soils developed on the three ages of deposits discussed in this report, are: solum depth; colour of the upper and lower B horizons; frequency, colour, and thickness of clay skins; degree of weathering; and periglacial and cryogenic features. A tentative field identification of these materials is presented in Tables 30.5 and 30.6, and soil descriptions, based on these properties, are given below. In selecting a site for soil description, care should be taken to choose a locality with a stable surface to ensure minimal truncation. In addition to describing morphological properties the soil should also be sampled for chemical, physical, and micromorphological analyses to further refine the classification of the soil.

Pre-Reid materials. These deposits are associated with well developed Luvisolic (paleo) soils with a deep solum. The depth of the solum may be as great as 200 cm for outwash materials and 125 cm for moraine materials. The colour of the upper B horizon is reddish brown, generally 5YR for outwash materials and 7.5YR for moraine materials. The colour of the lower B horizon in both deposits is 7.5YR.

Many reddish or reddish brown, moderately thick clay skins are present in soils developed on pre-Reid materials. These soils were strongly and very strongly weathered and most rock materials, except quartz, chert, and quartzite, show strong chemical alteration and disintegration. Sand wedges and involutions and strongly cryoturbated soil horizons are also common characteristics.

Reid materials. These deposits are associated with moderately developed Luvisolic (paleo) and Brunisolic (paleo) soils. They have a moderately deep solum with typical depths of 40-50 cm for outwash materials and 50-60 cm for moraine materials. The maximum depth could be as great as 1 m for

Table 30.4. Summary of loess morphology

No. of pedons	Underlying parent material	Thickness of loess	% Occurrence of Ae	Dominant colour of		Structure of uppermost B	Structure of lower B	% of Pedons showing distinct mixing with underlying material
				uppermost B	lower B			
2	McConnell drift	x=21 (5-49)	0	7.5YR	10YR	granular (weak)	granular	25
15	Reid drift	x=21 (8-50)	13	7.5YR	10YR	granular blocky (moderate to weak)	platy= blocky	40
11	Pre-Reid drift	x=23 (10-41)	45	10YR	10YR	granular > massive (weak)	platy > massive	36

both outwash and moraine materials. The soils associated with both types of deposits have a colour of 10YR in the B horizon. There is little difference in colour between the upper and lower B horizons, except for some Reid outwash soils in which the upper B horizon sometimes has darker colours. Where present, thin clay skins are brown, in contrast to the reddish brown clay skins associated with the pre-Reid soils. The Reid soils are moderately weathered. Soft rock materials, such as porphyry, in the solum show moderate weathering and disintegration. These soils can be moderately cryoturbated and are associated with fewer sand wedges and involutions than are the pre-Reid soils.

McConnell materials. These are the least developed soils found on the three ages of materials. The soils are predominantly Brunisols, similar to those found on Late Wisconsinan materials elsewhere in Canada under similar climatic conditions. The mean solum of these soils is about 20 cm deep with a maximum depth of only 40 cm. The B horizon is light brown and generally only one B horizon is present. These soils lack clay skins, cryogenic features, and sand wedges and involutions.

Conclusions

The nature of the pre-Reid soils (i.e., those formed during the period prior to the onset of Reid Glaciation) suggests that pedogenesis occurred over a long period of time under a relatively mild and humid climate. For at least some interval of time, a truly temperate climate must have existed in order to produce the strong alteration and deep weathering observed in this study. Conversely, the periglacial features, particularly sand wedges, illustrate the effects of an intensely cold and dry environment on the soil (Carter, 1983). In this study no differentiation of pre-Reid drift into Nansen and Klaza age was possible based on field-observable properties.

Table 30.5. Field identification of various surficial materials based on pedon features

Surficial material	Thickness of solum[x] (cm)	Dominant colour (hue) of uppermost II B	Dominant colour (hue) of lower II B	Dominant clay skins	Presence of Cca horizon	Soil classification°
Pre-Reid outwash	109* 205+	5YR	7.5YR	many, moderately thick	not present	Luvisol (paleo)
Pre-Reid moraine	91* 123+	7.5YR	7.5YR	many, moderately thick	not present	Luvisol (paleo)
Reid outwash	45* 90+	7.5YR	10YR	few, very thin	not present**	Luvisol (paleo) or Brunisol (paleo)
Reid moraine	56* 106+	10YR	10YR	few, thin	not present**	Luvisol (paleo)
McConnell drift	21* 40+	10YR	N/A++	none	present	Brunisol

* mean thickness
** secondary carbonate build-up may occur in the top of the uppermost B horizon due to the leaching of calcareous McConnell loess
\+ maximum thickness
++ there is usually one B horizon
x does not include the overlying loess
° soil classification according to Canada Soil Survey Committee 1978; the term "paleo" indicate soils whose development began during pre-Wisconsinan times

Table 30.6. Field identification of various surficial materials based on the rate of weathering and cryogenic features of the soil

Surficial materials	Rate of weathering in soil	Presence of ventifacts*	Rate of cryoturbation in soil	Sand wedges and involutions
pre-Reid outwash and moraine	strong and very strong chemical weathering and disintegration of most rock materials, except quartz and quartzite	common	very strong, especially in till; vertically oriented stones; cryoturbated Bt materials	common to very common
Reid outwash and moraine	moderate chemical weathering and disintegration of soft rock materials such as porphyry	common	moderate; vertically oriented stones; cryoturbated Bt materials, especially in till	few to very few
McConnell drift	very weak or no chemical weathering and disintegration in rock materials	not present	very little or none	not present

* on soil surface below the loess cover

Reid soils (i.e., those formed during the interval after Reid Glaciation) apparently formed under less temperate conditions than the pre-Reid soils and certainly over a shorter time period. Some Reid soils appear similar to some contemporary Luvisolic soils seen in more southern boreal regions of Canada but again exhibit periglacial features induced by the cold, dry periglacial climate. The general similarity of Reid soils found on Cordilleran drift to those found on moraines of montane glaciers in the southern Ogilvie Mountains supports the presumed correlation between these deposits although some difference in the occurrence of Bt horizons is apparent. In the period of time of formation of McConnell soils (during the last 14 000 years), the present cold boreal environment has produced only weakly developed soils markedly different from those preserved on older drift surfaces.

Because of these differences, soils may be used to help establish drift age relationships providing that suitable landscape positions are utilized when evaluating morphological development and collecting soil samples for analytical purposes.

Acknowledgments

Field assistance was provided by Dave Murray, Ted Fuller, Marg Nichol, and Alex Holland. Special thanks are extended to R.J. Fulton and J.A. McKeague for reviewing this manuscript.

References

Bostock, H.S.
1966: Notes on glaciation in central Yukon Territory; Geological Survey of Canada, Paper 65-36, 18 p.

Canada Soil Survey Committee
1978: The Canadian system of soil classification; Research Branch, Canada Department of Agriculture, Publication 1646, 164 p.

Carter, D.L.
1983: Fossil sand wedges on the Alaskan arctic coastal plain and their paleoenvironmental significance; Proceedings of the Fourth International Conference on Permafrost, Fairbanks, Alaska, National Academy Press, p. 109-114.

Denton, G.H. and Stuiver, M.
1967: Late Pleistocene glacial stratigraphy and chronology, northeastern St. Elias Mountains, Yukon Territory, Canada; Geological Society of America Bulletin, v. 78, no. 4, p. 485-510.

Expert Committee on Soil Survey
1983: The Canadian soil information system (CanSIS), Manual for describing soils in the field, ed. J.H. Day; Agriculture Canada, Ottawa, LRRI Contribution No. 82-52, p.

Foscolos, A.E., Rutter, N.W., and Hughes, O.L.
1977: The use of pedological studies in interpreting the Quaternary history of central Yukon Territory; Geological Survey of Canada, Bulletin 271, 48 p.

Hopkins, D.M.
1982: Aspects of the paleogeography of Beringia during the late Pleistocene; in Paleoecology of Beringia, ed. D.M. Hopkins, J.V. Matthews, Jr., C.E. Schweger, and S.B. Young; Academic Press, New York, p. 3-28.

Hughes, O.L., Rampton, V.N., and Rutter, N.W.
1972: Quaternary geology and geomorphology, southern and central Yukon (northern Canada); 24th International Geological Congress (Montreal), Guidebook, Excursion A11, 59 p.

Kodama, H., Miles, N., Shimoda, S., and Brydon, J.E.
1976: Mixed-layer kaolinite-montmorillonite from soils near Dawson, Yukon Territory; Canadian Mineralogist, v. 1, p. 159-163.

Lowdon, J.A., Fyles, J.G., and Blake, W., Jr.
1967: Geological Survey of Canada radiocarbon dates VI; Geological Survey of Canada, Paper 67-2, Part B, 42 p.

Lowdon, J.A. and Blake, W., Jr.
1968: Geological Survey of Canada radiocarbon dates VII; Geological Survey of Canada, Paper 68-2, Part B; reprinted from Radiocarbon, v. 10, 1968, p. 207-245.

1970: Geological Survey of Canada radiocarbon dates IX; Geological Survey of Canada, Paper 70-2, Part B; reprinted from Radiocarbon, v. 12, no. 1, 1970, p. 46-86.

McConnell, R.G.
1905: Report on the Klondike gold fields; Geological Survey of Canada, Annual Report, v. 14, Part B, p. 1-71.

1907: Report on gold values in the Klondike high-level gravels; Geological Survey of Canada, Publication 979.

McKeague, J.A.
1978: Manual on soil sampling and methods of analysis; Canadian Society of Soil Science, 2nd edition, 212 p.

Naeser, N.D., Westgate, J.A., Hughes, O.L., and Pewe, T.L.
1982: Fission track ages of late Cenozoic distal tephra beds in the Yukon Territory and Alaska; Canadian Journal of Earth Sciences, v. 19, no. 11, p. 2167-2178.

Rampton, V.N.
1969: Pleistocene geology of the Snag – Klutlan area, southwestern Yukon Territory, Canada; unpublished Ph.D. dissertation, University of Minnesota, Minneapolis, Minnesota.

1971: Late Pleistocene glaciations of the Snag – Klutlan area, Yukon Territory; Arctic, v. 24, no. 3, p. 277-300.

Rutter, N.W., Foscolos, A.E., and Hughes, O.L.
1978: Climatic trends during the Quaternary in central Yukon based upon pedological and geomorphological evidence; Proceedings of the Third York Quaternary Symposium, York University, Toronto, p. 309-359.

Templeman-Kluit, D.J.
1974: Reconnaissance geology of Aishihik Lake, Snag and part of Stewart River map areas, west-central Yukon; Geological Survey of Canada, Paper 73-41, 97 p.

van Vliet, B. and Langohr, R.
1981: Correlation between fragipans and permafrost with special reference to silty Werchselian deposits in Belgium and northern France; Catena, v. 8, p. 137-154.

Vernon, P. and Hughes, O.L.
1966: Surficial geology of Dawson, Larsen and Nash Creek map areas, Yukon Territory; Geological Survey of Canada, Bulletin 136, 25 p. (includes Maps 1170A, 1171A, 1172A).

Weber, F.R.
1983: Glacial geology of the Yukon – Tanana Upland – A progress report; University of Alaska Museum, Occasional Paper no. 2, p. 96-100.

-31-

EVIDENCE FOR A PRE-CHAMPLAIN SEA GLACIAL LAKE PHASE IN OTTAWA VALLEY, ONTARIO, AND ITS IMPLICATIONS

Project 780033

T.W. Anderson, R.J. Mott, and L.D. Delorme[1]
Terrain Sciences Division

Anderson, T.W., Mott, R.J., and Delorme, L.D., Evidence for a pre-Champlain Sea glacial lake phase in Ottawa valley, Ontario, and its implications; in Current Research, Part A, Geological Survey of Canada, Paper 85-1A, p. 239-245, 1985.

Abstract

Fossil ostracodes extracted from laminated sediments at six core sites between Lake Ontario and Ottawa valley show evidence for a freshwater glacial lake phase preceding the Champlain Sea incursion of Ottawa valley. Inferred ages for the correlative glacial lake phases of the Lake Ontario basin and succeeding low-water stage of Early Lake Ontario indicate that marine deposition in the Champlain Sea commenced in Ottawa valley between approximately 11 800 and 11 400 BP. This estimate conflicts with the Champlain Sea chronology based on marine mollusc shells and the calving bay concept developed to explain the early formation of Champlain Sea.

Résumé

Des ostracodes fossiles récupérés de carottes de sédiments laminés recueillies à six emplacements entre le lac Ontario et la vallée de l'Outaouais indiquent qu'un lac glaciaire d'eau douce a existé dans la région avant l'avancée de la mer Champlain dans la vallée de l'Outaouais. Les âges supputés des phases corrélatives de lac glaciaire du bassin du lac Ontario et du stade suivant d'étiage de l'ancien lac Ontario indiquent que le début de l'accumulation de sédiments marins dans la mer Champlain dans la vallée de l'Outaouais date d'environ 11 800 à 11 400 BP. Cette estimation va à l'encontre de la chronologie de la mer Champlain qui est fondée sur la présence de coquilles de mollusques marins et sur l'hypothèse d'une baie vêlante qui a été formulée pour expliquer la formation précoce de la mer Champlain.

[1] Aquatic Ecology Division, Canada Centre for Inland Waters, P.O. Box 5050, Burlington, Ontario L7R 4A6

Introduction

Rhythmically layered sediments underlying marine clay of the Champlain Sea occur at several localities in the Ottawa-St. Lawrence-Champlain Lowlands. Johnston (1917) was the first to recognize that the basal Champlain Sea clays of the Ottawa area are laminated and suggested that these sediments were derived from the meltwater of a nearby ice front. Antevs (1925) and subsequently Gadd (1962) found further evidence of rhythmic sedimentation beneath fossiliferous marine clay in Ottawa valley. Excavations for the St. Lawrence Seaway in the Long Sault area, Ontario, revealed a bottom to top sediment sequence of Fort Covington Till, coarse gravel, and cobbly stratified sand overlain by glaciolacustrine varved clay which in turn is overlain by marine clay (Terasmae, 1965). The glaciolacustrine clay was interpreted by Terasmae to have been deposited in an ice-dammed lake which existed between the glacier margin to the north and the high terrain to the south. Farther down river in the St. Lawrence Lowlands, rhythmites occur directly below marine clay of the Champlain Sea at several places along Nicolet River north of Ste-Monique-de-Nicolet, Quebec (Gadd, 1971) and sand containing a mixed fossil fauna of freshwater and marine molluscs underlies marine clay in the Verchères area (LaSalle, 1966). Piston cores collected from Lake Champlain by Freeman-Lynde et al. (1980) contain alternating layers of whitish grey and dark grey clay underlying fossiliferous dark grey clay. The alternating layers of the lower unit are interpreted as varved clays deposited in proglacial Lake Vermont, and the overlying fossiliferous clay as marine sediment of the Champlain Sea. The stratigraphic sequences at these localities imply: that an extensive freshwater lake occupied the Ottawa-St. Lawrence-Champlain Lowlands region, that this lake represented a northward extension of one or more of the glacial lake phases of the Lake Ontario basin, and that it was succeeded by the marine transgression of the Champlain Sea.

The concept of a freshwater glacial lake phase extending northward out of the Lake Ontario basin is not new. Leverett and Taylor (1915) suggested that Lake Frontenac, one of the post-Iroquois glacial lakes in the Lake Ontario basin, drained northward around the Adirondack Mountains into the Lake Champlain basin. Prest (1970), and more recently Clark and Karrow (1984), showed that lower lake phases of the Lake Ontario basin eventually became confluent with the Fort Ann phase of glacial Lake Vermont in the Lake Champlain basin. According to MacClintock and Terasmae (1960), the Fort Ann phase may even have extended westward as far as Ottawa. Dadswell (1974), in his study on the postglacial migration of freshwater crustaceans, showed evidence of pre-Champlain Sea glacial lake coverage into the upland areas southwest and north of Ottawa valley.

In this study stratigraphic and fossil invertebrate records are examined at six localities in a transect of lake cores extending from Lake Ontario to Ottawa valley. Implications concerning the temporal relationship between the Champlain Sea and events in the eastern Great Lakes region are presented.

Geological setting and site descriptions

Geological setting

The transect of lake cores straddles the Frontenac axis, an arch of Precambrian rocks connecting the Laurentian Highlands to the west and north with the Adirondack Mountains to the west, and extends into the Lake Ontario basin to the south and the Ottawa-St. Lawrence Lowlands to the north (Bostock, 1970; Chapman and Putnam, 1966).

Generally flat-lying Paleozoic limestones, shales, and sandstones underlie the lowland areas, whereas highly deformed and altered Proterozoic igneous and metamorphic rocks form the uplands (Sanford and Baer, 1981). Precambrian rocks of the Frontenac axis form the sill that controls drainage from Lake Ontario to St. Lawrence River.

The surficial geology of the area has been studied by several workers and deposits relating to Late Wisconsinan glaciation, glacial lakes, and Champlain Sea have been mapped. The approximate extent of maximum glacial lake coverage and approximate shoreline position of the Champlain Sea are shown in Figure 31.1. Recent papers by Gadd (1980) and Clark and Karrow (1984) contain reviews of the pertinent surficial geology and touch on some of the inconsistencies that have led to differing and often controversial interpretations of the deglacial history. These accounts and a review by Prest (1970) provide the basis for the sequence of events described in the following paragraphs.

Retreat of late Wisconsinan ice to the eastern end of the Lake Ontario basin resulted in the formation of glacial Lake Iroquois between the ice and the drainage divide, and the lake drained eastward into Mohawk valley near Rome, New York. Further retreat of the ice created a northern outlet around Covey Hill at the northern end of the Adirondack Mountains. The consequent lower glacial lake (Frontenac phase?) drained into the Champlain valley which was occupied by a glacial lake at a lower level (Fort Ann phase). Continued downslope migration of the outlet in the Covey Hill area resulted in consecutively lower lake phases in the Lake Ontario basin until a lake formed that was confluent with the lake in the Champlain valley (Belleville-Fort Ann phase). This lake remained in existence until the ice barrier preventing incursion of the sea was removed, and the Champlain Sea invaded the lowlands. Lake level in the Lake Ontario basin dropped and the lake (Trenton phase) drained into, or was coeval with, the Champlain Sea (Clark and Karrow, 1984).

Location of ice blocking the incursion of the Champlain Sea is critical to the deglacial history of the area. Gadd's (1980) hypothesis requires an ice barrier in upper St. Lawrence valley, separating glacial lakes in the Lake Ontario basin from a calving bay sea in lower St. Lawrence and Ottawa valleys. By contrast, Clark and Karrow (1984) and many other earlier workers suggest an ice barrier in lower St. Lawrence valley and extension of glacial lakes in the Ontario basin into upper St. Lawrence and Ottawa valleys.

Site descriptions

The locations of the core sites are shown in Figure 31.1. Table 31.1 summarizes the location, basal radiocarbon dates, ages inferred from pollen studies, stratigraphy, and sediment intervals analyzed. Sites 1 and 2 denote piston core stations from cruise numbers 70-0-37 and 67-0-18, respectively, in eastern Lake Ontario. Station 70-0-37-E30 is from the deepest sounding area of Lake Ontario; Station 67-0-18-28 is from the deepest part of the St. Lawrence trough (Sly and Prior, 1984). Sites 3, 4, and 5 are small lakes situated between Lake Ontario and the southwest shoreline of the Champlain Sea. Ross Lake (site 3) is situated well beyond, whereas Lambs Pond and Loon Lake (sites 4 and 5, respectively) are located close to the shoreline position of the Champlain Sea. In fact, the Lambs Pond basin is considered to have been an embayment of the Champlain Sea when the Sea was at its maximum. Dates of 9900 ± 100 BP (GSC-3127) and 10 500 ± 140 BP (GSC-3146) on wood and gyttja, respectively, were obtained for the spruce pollen maximum in nearby Waterton Bog (Fig. 31.1). The age

disparity between the gyttja and enclosed wood suggests that the gyttja date is too old by some 600 years. By inference, the 10 500 ± 110 BP date (GSC-3273) on the correlative spruce pollen maximum and 12 300 ± 230 BP date (GSC 3088) for the base of the spruce zone obtained in Lambs Pond are too old by about 600 years. Thus the basal gyttja in Lambs Pond is more accurately placed at 11 700 BP (Table 31.1). Site 6 represents a core of Champlain Sea sediments obtained at the LaRose Forest Research Station, located about 40 km east of Ottawa, 5 km south of Bourget, Ontario.

Methods

The cores from Lake Ontario were obtained during piston and gravity coring-echo sounding surveys of the bottom sediments of Lake Ontario from research vessels between 1966 and 1974. The full shipboard procedures are outlined in Thomas et al. (1972). The piston cores were recovered with a 450 kg Alpine piston corer fitted with a 12.2 m core barrel and a 5.7 cm I.D. plastic liner.

Cores from the small lakes (sites 3, 4, and 5) were recovered by means of the Brown and Livingstone samplers. Winter drilling from ice was carried out at site 3 by the Testing Laboratories Division, formerly in the Department of Public Works, using truck-mounted, heavy drilling equipment. Shelby tube cores were recovered from the deeper sediments which otherwise could not have been penetrated with the hand-operated Livingstone corer. The core from Champlain Sea deposits (site 6) was also obtained with the drilling equipment of the Testing Laboratories Division.

The cores were logged and described in the laboratory and samples were removed at selected levels or intervals in the cores for pollen and faunal analyses as well as radiocarbon dating. The methods for pollen analysis and extraction of macrofossil remains are described elsewhere (Mott et al., 1981). The laminated silty clay did not always disaggregate after routine soaking in water. Complete disaggregation, however, was achieved following periodic dehydration (heating the sample in an oven at 100°C) and wet sieving through a 149 μ sieve. Concentrates were examined under a dissecting microscope and all identfiable specimens were picked out and stored dry for later examination.

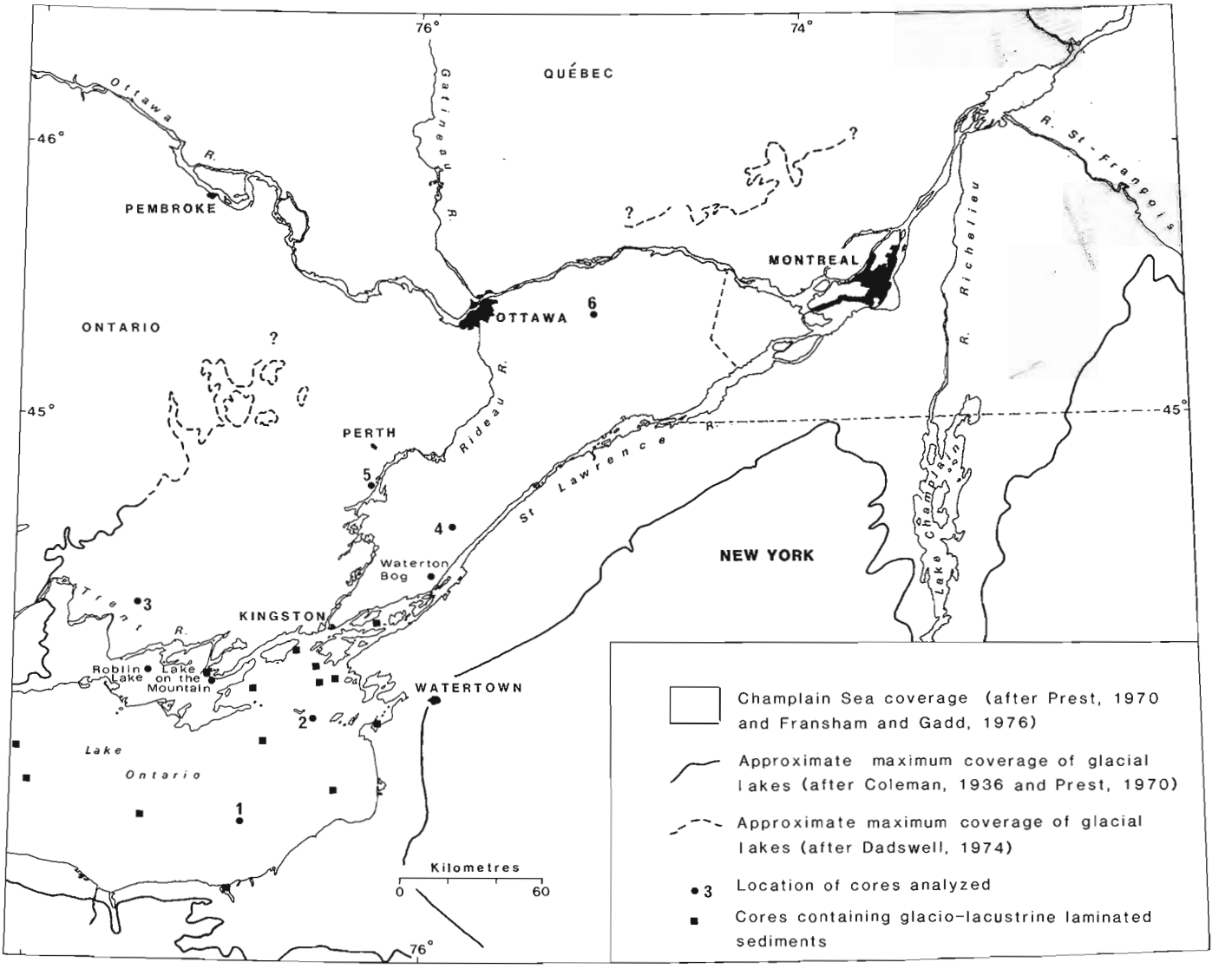

Figure 31.1. *Lake Ontario – upper St. Lawrence – Ottawa valley region showing approximate extent of glacial lake coverage, Champlain Sea shoreline, and locations of sites discussed in text.*

Table 31.1. Location, chronology, stratigraphy, and sediment intervals analyzed at core sites

Site number and name	Latitude	Longitude	Basal ^{14}C date BP (lab. no.)	Depth (m)	Inferred age from pollen stratigraphy BP	Sediment surface elevation (m a.s.l.)	Sediment interval analyzed (m)	Stratigraphy (m)	
1. Lake Ontario 70-0-37-E30	43°30.4'	76°54'		5.90	10 500	-148	6.10-12.00	0-7.0 7.0-10.9 10.9-16.5	Massive grey silty clay Laminated red and grey clay Massive grey clay
2. Lake Ontario 67-0-18-28	43°53.6'	76°32.6'		5.20	10 400	23	4.95-6.42	0-4.95 4.95-6.00 6.00-11.50	Massive grey silty clay Stratified fossilferous sand and silt Laminated red and grey silty clay
3. Ross Lake	44°19'	77°27.5'	11 350 ± 260[1] (GSC-625)	4.84-4.93		135	10.80-11.80	0-5.00 5.00-5.01 5.01-11.80	Gyttja, sandy at base Medium-coarse sand Laminated grey silty clay with occasional sand layers
4a. Lambs Pond	44°39.1'	75°48.1'	12 300 ± 230[2] (GSC-3088)	8.41-8.44	11 700	105	8.45-11.03	0-5.00 5.00-8.44 8.44-8.80 8.80-9.75 9.75-11.03	Banded marl Gyttja, sandy and clayey at base Massive grey silty clay Laminated grey silty clay Interbedded massive and laminated grey clay
4b. Lambs Pond	44°39.1	75°48.1'				105	7.40-9.60	0-3.86 3.86-7.18 7.18-9.66 9.66-9.91 9.91-10.58	Banded marl Gyttja, sandy and clayey at base Massive grey silty clay Laminated grey clay Interbedded massive and laminated grey clay
5. Loon Lake	44°46.7'	76°14'	10 700 ± 260[2] (GSC-3418)	10.25-10.30		112	10.48-10.84	0-10.30 10.30-10.46 10.46-10.66	Gyttja Massive grey clay Laminated grey silty clay
6. LaRose Forest Station	45°23.5'	75°08'				74	42.51-50.48	39.60-46.00 46.00-47.71 47.71-48.26 48.26-50.48	Massive to faintly banded grey silty clay Massive grey silty clay, marine fauna only No recovery Alternating units of laminated grey silt and clay; silt and clay laminae up to 2 cm thick below 49.0 m. Marine and freshwater fauna above 48.35 m; Freshwater fauna only below 48.35 m.

[1] From Lowdon and Blake (1968)
[2] This study

Faunal analysis

Fossil remains recovered from the core sites are listed in Table 31.2. Freshwater ostracodes dominate in the basal laminated clay units with **Candona subtriangulata** (C. cf. C. subtriangulata) common to all six sites. The majority of the specimens at sites 1 and 6 were immature forms and could only be identified as **C. cf. C. subtriangulata** or as **Candona** sp. Specimens denoted as **Candona** sp., however, do have similar shape and size to those identified as **C. subtriangulata** in Cronin (1977). **Limnocythere friabilis** is present at sites 2, 3, 4, and 5 and **Cytherissa lacustris** at sites 2, 3, and 4 only. The upper part of the laminated clay unit at site 3 is dominated by **Candona candida**, and minor occurrences of **Candona caudata, Candona paraohioensis, Cyclocypris ampla**, and **Limnocythere herricki**.

The **Candona** subtriangulata – **Cytherissa lacustris** – **Limnocythere friabilis** assemblage reflects deposition in a large oligotropic lake having few dissolved solids. It can be assumed that the depth of the lake was in excess of 180 m at the time of deposition based on the presence of **C. subtriangulata** and **C. lacustris** (Delorme, 1978). The assemblage is closely aligned to the modern analogues that characterize Lakes Superior, Huron, Erie, and Ontario. The **Candona candida** – dominated assemblage at site 3 implies shallower lake conditions upwards in the sequence.

Marine foraminifers, ostracodes, and molluscs are present in the sediment interval 42.51 to 48.35 m of the Champlain Sea core (site 6). Foraminifera occur in all intervals down to 48.35 m. Ostracodes are present in the upper intervals and mollusc shell fragments identified as **Portlandia arctica** and **Portlandia** sp. occur at two levels only (44.7 and 46.9 m). Where foraminifera are most abundant, the assemblages are dominated by two species, **Elphidium clavatum** and **Islandiella helenae. Maynesena orbicularis** is a common occurrence wheras **Pateoris hauerinoides** and **Elphidium incertum/asklundi** are rare. The marine ostracodes are represented by three species of **Cytheropteron** but number of specimens of each species is low.

The foraminifera assemblages imply a high salinity environment near the base of the marine sequences followed by decreasing salinity upwards in the core (C. Rodrigues, personal communication, 1984). The lowermost marine sediment interval (48.26-48.35 m) contains high salinity indicators such as **Islandiella helenae** in association with the freshwater ostracode **Candona** cf. **C. subtriangulata.** This mixed association represents a transitional interval between the initial freshwater phase at the base of the core and the full marine conditions inferred for the overlying sediments. The transitional interval presumably corresponds with the early Champlain Sea Transitional Phase of Cronin (1979a, b).

Discussion and conclusions

The laminated red and grey or grey clay units at all six sites are interpreted to be glaciolacustrine in origin on the basis of the laminated nature of the sediments and presence of freshwater ostracodes. Core sites 1 and 2 are particularly well situated to record possible evidence for the presence of Champlain Sea in the Lake Ontario basin. These sites occur in the deepest parts of two basins – the main basin of Lake Ontario and the shallower St. Lawrence Trough, respectively. If the Champlain Sea were present and had left a record in the Lake Ontario basin, surely it would have been preserved in the upper laminated clay at sites 1 and 2, especially at site 1. Marine evidence, however, is lacking in the

Table 31.2. Fossil occurrences at each site

TAXA	1	2	3	4a	4b	5	6
MARINE							
FORAMINIFERA							
Elphidium clavatum							+
Elphidium incertum/asklundi							+
Islandiella helenae							+
Maynesena orbicularis							+
Pateoris hauerinoides							+
Quinqueloculina seminulum							+
Polymorphinids							+
OSTRACODA							
Cytheropteron latissimum							+
Cytheropteron nodosum							+
Cytheropteron pseudomontroscense							+
MOLLUSCA							
Portlandia arctica							+
Portlandia sp.							+
FRESHWATER							
OSTRACODA							
Candona candida			+				
Candona caudata			+				
Candona paraohioensis			+				
Candona rawsoni		+					
Candona subtriangulata	+	+		+	+	+	
Candona cf. **C. subtriangulata**			+			+	+
Candona sp.	+		+	+	+		+
Cyclocypris ampla			+				
Cytherissa lacustris		+	+		+		
Limnocythere friabilis		+	+	+	+	+	
Limnocythere herricki			+				
Limnocythere sp.					+		

ostracode fauna at these sites. On the other hand, if Champlain Sea had entered the Lake Ontario basin, as suggested as early as 1890 by Gilbert and 1907 by Fairchild to as recently as 1984 by Clark and Karrow, it would have existed for such a short time and have been so diluted by the freshwater glacial lakes that marine-like conditions in all likelihood could not have become established.

Sediments identified as glaciolacustrine occur throughout the Lake Ontario basin (Thomas et al., 1972) and are confirmed by acoustic profiling and piston coring at several localities in the basin as shown in Figure 31.1 (Anderson and Lewis, 1975; Sly and Prior, 1984). Cores from Roblin Lake and Lake on the Mountain (Terasmae and Mirynech, 1964) similarly reveal units of glaciolacustrine varved clay overlying till and bedrock, respectively, and underlying gyttja. Henderson (1966, 1967, 1970, 1973) has mapped glaciolacustrine sands and clays in several areas northeast, north, and northwest of Kingston. Stratigraphic position and presence of freshwater fossil ostracodes indicate that these glaciolacustrine sediments are in part contemporaneous with the rhythmically layered sediments underlying the marine deposits in Ottawa valley.

The widespread distribution of glaciolacustrine sediments from Lake Ontario to the vicinity of Ottawa implies that a high-level proglacial lake extended northward out of the Lake Ontario basin to Ottawa valley. Dadswell (1974) provided independent evidence for the existence of such a lake. This proglacial lake encompassed the interval from glacial Lake Iroquois to the Trenton phase of the post-Iroquois "falling" lake phases (Clark and Karrow, 1984). The Candona **candida**-dominated assemblage that characterizes the upper 5 cm of the laminated sediments at site 3 may relate to, and provide evidence for, the "falling" lake phases. Stratified sand and silt containing freshwater ostracodes and pelecypods overlying glaciolacustrine laminated clay at four sites in Lake Ontario, including site 2, record a low-water stage of Early Lake Ontario which came into existence soon after the draining of glacial Lake Iroquois and the post-Iroquois lake phases (Anderson and Lewis, 1984).

The presence of freshwater glaciolacustrine sediments beneath marine sediments of the Champlain Sea in Ottawa valley sheds new light on the age of the Champlain Sea. Glacial Lake Iroquois came into existence shortly after 12 500 BP (Fullerton, 1980) and is generally thought to have drained soon after 12 000 BP (Karrow et al., 1975; Terasmae, 1980). The radiocarbon date of 11 760 ± 310 BP (GSC-626) on basal gyttja in Biddy Lake near Brighton, Ontario, provides a minimum age for isolation of this lake from glacial Lake Iroquois; furthermore, the date seems valid from pollen studies and correlation with the regional pollen record (Terasmae, 1980). This date is in agreement with an inferred age of 11 700 BP on basal sandy gyttja in Lambs Pond (site 4). The 11 700-year estimate similarly provides a minimum age for the draining of the proglacial lake and formation of an embayment of the Champlain Sea when the Sea reached its limit in the Lambs Pond area. Pollen evidence from low-level deposits in Lake Ontario documented in a paper entitled "Postglacial water-level history of the Lake Ontario basin", in preparation by T.W. Anderson and C.F.M. Lewis, shows that Early Lake Ontario may have reached its lowest level by 11 400 BP. The last of the glacial lake phases, the Trenton phase, therefore, drained between approximately 11 800 and 11 400 BP. Since the glacial lake phases of the Lake Ontario basin extended northward into Ottawa valley, and since the Trenton phase was apparently correlative with the Champlain Sea (Clark and Karrow, 1984), the Champlain Sea probably came into existence between about 11 800 and 11 400 BP. This estimate is in conflict with the Champlain Sea chronology based on marine mollusc shells (Richard, 1975, 1978) and with the calving bay concept of Gadd (1980); further discussion on this matter is beyond the scope of this report.

It is recommended that all known localities where rhythmically layered sediments are overlain by marine deposits of the Champlain Sea be examined for fossil ostracodes and for other fossil freshwater indicators such as the crustaceans, copepods, cladocerans, and diatoms. It might also prove useful to analyze these sediments especially the more southerly sites, for pollen content. Palynological studies on cores obtained from former embayment sites of the Champlain Sea in eastern Ontario and Ottawa valley are presently under way by Anderson.

Acknowledgments

The LaRose Forest Station core was obtained by M.J.J. Bik, formerly with the Geological Survey of Canada. The Ross Lake core was kindly provided by J. Terasmae of Brock University. C.F.M. Lewis collected most of the Lake Ontario cores including those analyzed in this study.

We are grateful to C. Rodrigues (University of Windsor) and M.F.J. Smith (National Museum of Natural Sciences) for identifying the foraminifera and mollusc shells, respectively, and to the Radiocarbon Dating Laboratory of the GSC for providing the radiocarbon dates.

Discussions with V.K. Prest and D.R. Sharpe were stimulating and helpful. We thank D.R. Sharpe and W. Blake, Jr. for critical reviews of the manuscript.

References

Anderson, T.W. and Lewis, C.F.M.
1975: Acoustic profiling and sediment coring in Lake Ontario, Lake Erie and Georgian Bay; in Report of Activities, Part A, Geological Survey of Canada, Paper 75-1A, p. 373-376.

1984: Postglacial water-level history of the Lake Ontario basin; Geological Association of Canada – Mineralogical Association of Canada Annual Meeting, London, Ontario, Program with Abstracts, v. 9, p. 41.

Antevs, E.
1925: Retreat of the last ice-sheet in Eastern Canada; Geological Survey of Canada, Memoir 146, 142 p.

Bostock, H.S.
1970: Physiographic subdivisions of Canada; in Geology and Economic Minerals of Canada, ed. R.J.W. Douglas; Geological Survey of Canada, Economic Geology Report No. 1, p. 10-30.

Chapman, L.J. and Putnam, D.F.
1966: The Physiography of Southern Ontario; University of Toronto Press, Toronto, Ontario, 386 p.

Clark, P. and Karrow, P.F.
1984: Late Pleistocene water bodies in the St. Lawrence Lowland, New York, and regional correlations; Geological Society of America Bulletin, v. 95, p. 805-813.

Coleman, A.P.
1936: Lake Iroquois; Ontario Department of Mines, Report 45, 36 p.

Cronin, T.M.
1977: Champlain Sea Foraminifera and Ostracoda: A systematic and paleoecological synthesis; Géographie physique et Quaternaire, v. xxxi, p. 107-122.

1979a: Foraminifer and ostracode species diversity in the Pleistocene Champlain Sea of the St. Lawrence lowlands; Journal of Paleontology, v. 53, p. 233-244.

Cronin, T.M. (cont.)
1979b: Late Pleistocene benthic foraminifer from the St. Lawrence lowlands; Journal of Paleontology, v. 53, p. 781-814.

Dadswell, M.J.
1974: Distribution, ecology, and postglacial dispersal of certain crustaceans and fishes in eastern North America; Publications in Zoology 11, National Museums of Canada, 110 p.

Delorme, L.D.
1978: Distribution of freshwater ostracodes in Lake Erie; Journal of Great Lakes Research, v. 4, p. 216-220.

Fairchild, H.L.
1907: Gilbert Gulf (marine waters in the Ontario Basin); Geological Society of America Bulletin, v. 17, p. 712-718.

Fransham, P.B. and Gadd, N.R.
1976: Geological and geomorphological controls of landslides in Ottawa valley, Ontario; in 29th Canadian Geotechnical Conference, Vancouver, British Columbia, p. v-1 – v-12.

Freeman-Lynde, R.P., Hutchinson, D.R., Folger, D.W., Wiley, B.H., and Hewett, M.J.
1980: The origin and distribution of subbottom sediments in southern Lake Champlain; Quaternary Research, v. 14, p. 224-239.

Fullerton, D.S.
1980: Preliminary correlation of post-Erie interstadial events (16 000-10 000 radiocarbon years before present) central and eastern Great Lakes region and Hudson, Champlain and St. Lawrence Lowlands, United States and Canada; United States Geological Survey, Professional Paper 1089, 52 p.

Gadd, N.R.
1962: Surficial geology of the Ottawa map-area, Ontario and Quebec; Geological Survey of Canada, Paper 62-16, 4 p.

1971: Pleistocene geology of the central St. Lawrence Lowland; Geological Survey of Canada, Memoir 359, 153 p.

1980: Late-glacial regional ice-flow patterns in eastern Ontario; Canadian Journal of Earth Sciences, v. 17, p. 1439-1453.

Gilbert, G.K.
1890: History of the Niagara River; New York Commission for State Reservation at Niagara, Annual Report, v. 6, p. 61-84 and Smithsonian Institute Annual Report for 1890, p. 231-257.

Henderson, E.P.
1966: Surficial geology, Gananoque-Wolfe Island, Ontario; Geological Survey of Canada, Map 13-1965.

1967: Surficial geology, Westport, Ontario; Geological Survey of Canada, Map 22-1966.

1970: Surficial geology of Brockville and Mallorytown map-areas, Ontario; Geological Survey of Canada, Paper 70-18 (Map 6-1970).

1973: Surficial geology of Kingston (north half) map-area, Ontario; Geological Survey of Canada, Paper 72-48, 6 p.

Johnston, W.A.
1917: Pleistocene and Recent deposits in the vicinity of Ottawa, with a description of the soils; Geological Survey of Canada, Memoir 101, 69 p.

Karrow, P.F., Anderson, T.W., Clarke, A.H., Delorme, L.D., and Sreenivasa, M.R.
1975: Stratigraphy, paleontology, and age of Lake Algonquin sediments in southwestern Ontario, Canada; Quaternary Research, v. 5, p. 49-87.

LaSalle, P.
1966: Late Quaternary vegatation and glacial history in the St. Lawrence Lowlands, Canada; Leidse Geologische Mededelingen, v. 38, p. 91-128.

Leverett, F. and Taylor, F.B.
1915: The Pleistocene of Indiana and Michigan and the history of the Great Lakes; United States Geological Survey, Monograph 53, 529 p.

Lowdon, J.A. and Blake, W., Jr.
1968: Geological Survey of Canada radiocarbon dates VII; Radiocarbon, v. 10, p. 207-245.

MacClintock, P. and Terasmae, J.
1960: Glacial history of Covey Hill; Journal of Geology, v. 68, p. 232-241.

Mott, R.J., Anderson, T.W., and Matthews, J.V., Jr.
1981: Late-glacial paleoenvironments of sites bordering the Champlain Sea based on pollen and macrofossil evidence; in Quaternary Paleoclimate, ed. W.C. Mahaney; GeoAbstracts, England, p. 129-172.

Prest, V.K.
1970: Quaternary geology of Canada; in Geology and Economic Minerals of Canada, ed. R.J.W. Douglas; Geological Survey of Canada, Economic Geology Report No. 1, p. 676-764.

Richard, S.H.
1975: Surficial geology mapping: Ottawa valley lowlands (parts of 31G, B, F); in Report of Activities, Part B, Geological Survey of Canada, Paper 75-1B, p. 113-117.

1978: Age of Champlain Sea and "Lampsilis Lake" episode in the Ottawa-St. Lawrence Lowlands; in Current Research, Part C, Geological Survey of Canada, Paper 78-1C, p. 23-28.

Sanford, B.V. and Baer, A.J.
1981: Geology, southern Ontario, Ontario-Quebec-U.S.A.; Geological Survey of Canada, Map 1335A.

Sly, P.G. and Prior, J.W.
1984: Late glacial and postglacial geology in the Lake Ontario basin; Canadian Journal of Earth Sciences, v. 21, p. 802-821.

Terasmae, J.
1965: Surficial geology of the Cornwall and St. Lawrence Seaway Project areas, Ontario; Geological Survey of Canada, Bulletin 121, 54 p.

1980: Some problems of late Wisconsin history and geochronology in southwestern Ontario; Canadian Journal of Earth Sciences, v. 17, p. 61-381.

Terasmae, J. and Mirynech, E.
1964: Postglacial chronology and the origin of deep lake basins in Prince Edward County, Ontario; Proceedings of the 7th Conference on Great Lakes Research, University of Michigan, Great Lakes Research Division, Publication 11, p. 161-169.

Thomas, R.L., Kemp, A.L.W., and Lewis, C.F.M.
1972: Distribution, composition and characteristics of the surficial sediments of Lake Ontario; Journal of Sedimentary Petrology, v. 42, p. 66-84.

GLACIAL AND INTERGLACIAL DEPOSITS IN THE HUDSON BAY LOWLANDS: A SUMMARY OF SITES IN MANITOBA

Project 750072

L.A. Dredge and E. Nielsen[1]
Terrain Sciences Division

Dredge, L.A. and Nielsen, E., Glacial and interglacial deposits in the Hudson Bay Lowlands: a summary of sites in Manitoba; in Current Research, Part A, Geological Survey of Canada, Paper 85-1A, p. 247-257, 1985.

Abstract

A complex sequence of glacial and nonglacial beds is exposed in many river sections in the Hudson Bay Lowlands of Manitoba. The stratigraphic column consists of two or more old tills; an interglacial formation comprising marine, lacustrine, fluvial, and terrestrial peat beds; several young tills separated by sand beds; and postglacial glaciolacustrine and marine deposits. The oldest till (Pre-Illinoian) was emplaced by ice from the north which crossed the entire region. A soil-forming period followed. It was succeeded by a major glaciation (Illinoian) when ice of eastern provenance covered the region. The Sangamon Interglaciation is recorded by beds of woody peat and inorganic sediments. Ice of both northern and eastern provenance covered the area during the entire Wisconsin Glaciation, but shifts in ice flow across the area left a series of till units separated in places by sand beds. The problematic sandy units are probably the overrun remains of radial and interlobate moraines.

Résumé

Une séquence complexe de couches glaciaires et non glaciaires paraît dans de nombreuses coupes le long de rivières dans les basses-terres de la baie d'Hudson, au Manitoba. La colonne stratigraphique comprend au moins deux tills anciens, une formation interglaciaire composée de couches de tourbe marine, lacustre, fluviatile et terrestre, plusieurs tills récents séparés par des couches de sable ainsi que des dépôts glaciolacustres et marins d'origine postglaciaire. Le till le plus ancien (pré-Illinoien) a été mis en place par la glace provenant du nord qui a traversée toute la région. Il y a eu ensuite une période de formation de sol qui a été suivie par une glaciation importante (Illinoien) au cours de laquelle les glaces en provenance de l'est ont envahi la région. L'interglaciaire du Sangamon est représenté par des couches de tourbe ligneuse et de sédiments inorganiques. La glace provenant à la fois du nord et de l'est a recouvert la région au cours de la glaciation du Wisconsin, mais les changements du sens de l'écoulement de la glace dans la région ont laissé une série d'unités de tills qui sont séparées par endroits par des couches de sable. Les unités sableuses dont l'origine est encore indéterminée sont vraisemblablement les vestiges de moraines radiales et interlobaires recouvertes par les glaces.

[1] Manitoba Energy and Mines, 555-330 Graham Avenue, Winnipeg, Manitoba R3C 4E3

Introduction

Recent investigations of river sections in northeastern Manitoba have revealed a complex sequence of glacial and nonglacial deposits, which span several glaciations and interglaciations. The oldest deposits preserved in sections may belong to a pre-Illinoian glaciation; the youngest were deposited in Holocene glacial lakes and in the postglacial sea which subsequently inundated substantial parts of the Lowlands. This report provides a general inventory of interglacial sites in northern Manitoba (Fig. 32.1). The descriptions and discussions are restricted to those deposits associated with or predating the last glaciation, and to sites along the Churchill, Nelson, Stupart, Gods, and Echoing rivers. The report is based on work conducted in 1984, but in some places data from previous studies have also been included. Much of the information about the Henday site is derived from a work in preparation by E. Nielsen, A. Morgan, R.J. Mott, and N.W. Rutter, entitled "Stratigraphy of glacial and nonglacial deposits in the Gillam area, Manitoba".

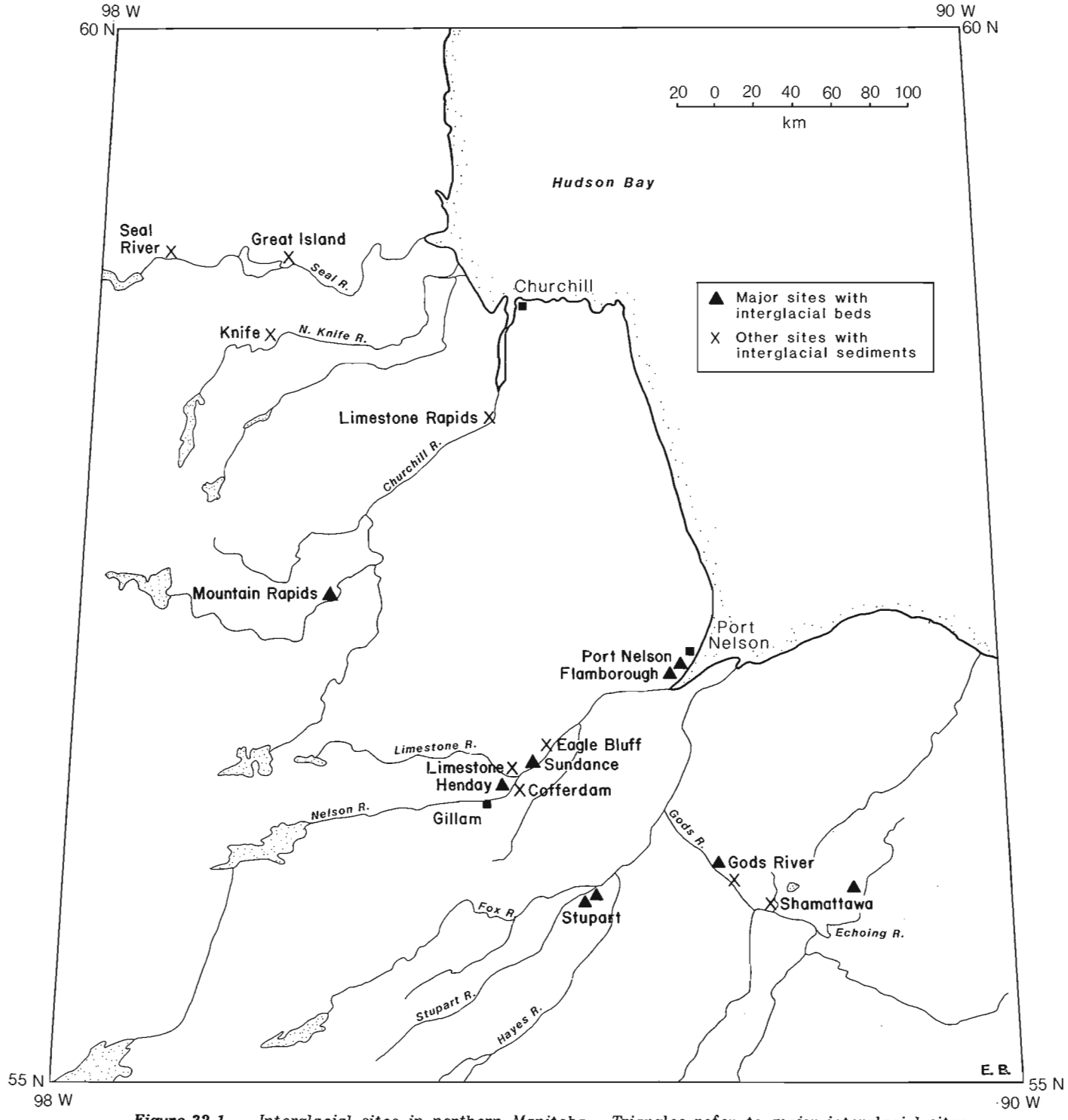

Figure 32.1. Interglacial sites in northern Manitoba. Triangles refer to major interglacial sites described in this report; Xs refer to sites with partial interglacial sequences.

General nature of the deposits

The stratigraphic record comprises both glacial and nonglacial deposits. The observed glacial deposits consist principally of lodgment and basal melt-out facies of till, which in some places have been glaciotectonically deformed. Aquatic flow diamictons were recognized in the till deposits of Holocene age but were not identified in older deposits. Several tills or depositional till facies were present at each site. These individual units were differentiated by colour, texture, compaction, carbonate content, stoniness, clast lithology, and sedimentary or tectonic structures, and the amount of oxidation inwards from joints. Most of the tills have a clayey silt matrix. The upper tills in the sequence are commonly brownish, whereas those below are commonly greyish, with heavy red-stained joint surfaces. The typical matrix carbonate contents for all the silty tills range from 20 to 40 per cent (by weight).

The nonglacial deposits are of two basic types. One, and sometimes two relatively thin sand beds, generally less than 1 m thick, commonly separate the brown tills. These beds consist of massive, medium grained sorted sand. Lower in the sections are multiple, stacked beds of gravel, sand and silt, clay, marl, and peat containing wood. Cobble gravels are possibly outwash deposits, whereas other sand and gravel sequences are of nonglacial fluvial origin. The fine sand and silt beds commonly display wavy planar laminae, or ripple-drift crossbeds and were probably deposited in relatively quiet water. The clay deposits are both varved and massive. Marl, richly fossiliferous, was found at only one site, but fibrous, slightly compressed peat and woody peat were found at several places, generally interbedded with sands. The stacked nonglacial sequences are 2 to 4 m thick.

The roots of a paleosol, developed in till, were identified at only one location (Sundance), although some of the coloration of the tills at other localities may also be related to soil-forming processes.

Major sites visited in 1984

Port Nelson

The Port Nelson section (Fig. 32.2) is clearly exposed along 2 km of bluffs between Harts Creek and Port Nelson. The uppermost marine and glaciolacustrine units overlie a crumbly, very stony unoxidized brown till. The unit contains a set of arcuate sand beds (Fig. 32.3) which may mark former shear planes within the glacier. Its loose nature and internal structures indicate that this till was deposited by basal melt-out of englacial debris. This upper unit is either separated from another brown till by a line of imbricated cobbles which dips towards Hudson Bay, or, in some places, grades into it.

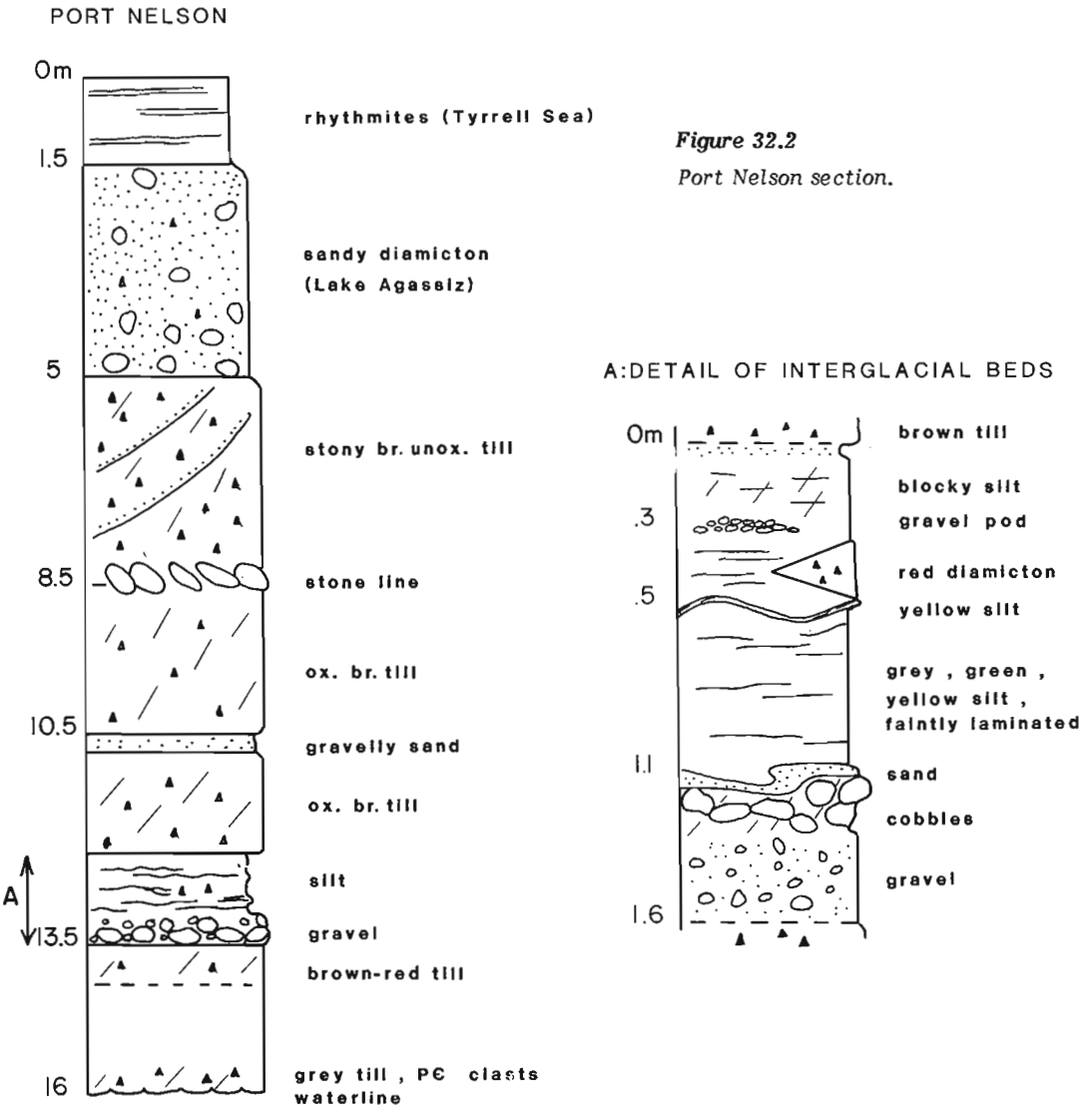

Figure 32.2

Port Nelson section.



Figure 32.3. *Arcuate sand beds marking shear planes in the original ice mass, in loosely compacted silty till at Port Nelson. (GSC 204037-I)*

The second till is also brown and calcareous but is noticeably less stony and contains brown oxidation along joints. Some zones within this till unit are substratified. It is underlain by another oxidized till unit but separated from it by a 60 cm bed of gravelly sand. The till contains "clasts" of grey silt derived from underlying lacustrine deposits.

The upper till sequence grades into about 1.5 m of stone-free silt, which includes both massive and laminated beds. The silts are thought to be lacustrine in origin. Poorly sorted, rounded, pebble gravel forms the base of the nonglacial unit and has a conformable contact with the silt and sand, which has filled some of the interstices in the upper part of the gravel unit.

The lowest unit in the section is a stony and very compact till. The upper 40 cm of this unit is brownish grey, but becomes distinctly redder at depth. A grey till with abundant Precambrian clasts is exposed along the tidal flats but was not exposed at the base of the section. This till is the basal till of the sequence and has significantly more granitic clasts than any of the overlying tills.

Flamborough

The Flamborough sections consist of a 4 km stretch of bluffs, with slumped portions, lying along the Nelson estuary northeast of Flamborough Head. The stratigraphic succession is similar to that described for the Port Nelson section, but in some areas organic units were found, particularly in slump zones; slope failure may be related to the organic-bearing beds. The main section (Fig. 32.4, Flamborough 3) contains

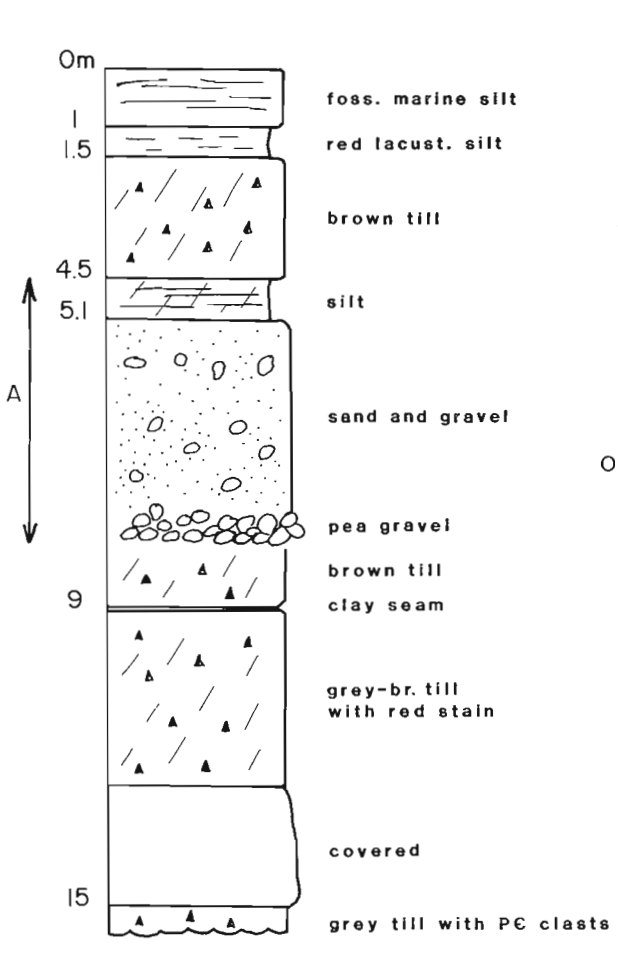

Figure 32.4

Sections at Flamborough Head, Nelson River.

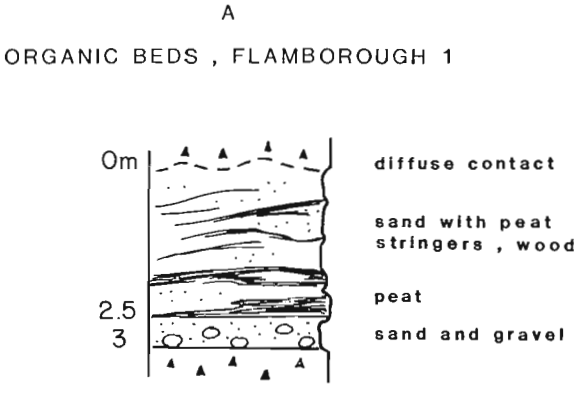

fossiliferous marine and nonfossilferous lacustrine deposits sharply underlain by loose, brown, calcareous unoxidized till with vestigal sand "shear" planes. A thick sequence of horizontally bedded grey silt containing thin sand beds conformably overlies poorly sorted sand and well sorted pea gravel. This nonglacial sequence is underlain by a grey-brown till with red oxidation staining. A grey till with granitic clasts forms the tidal flat.

A second section (Fig. 32.4, Flamborough 1) within a slump backwall, about 100 m west of Flamborough 3, exposes a less complete stratigraphic sequence but contains organic sand and peat layers (Fig. 32.5). In the upper part, consisting mainly of silty sand, the organic stringers and pods are fibrous, thin (1-2 cm), discontinuous, and undulating; towards the bottom of the unit they are up to 60 cm thick and consist of platy brown-black peat with some compressed twigs. The lower 50 cm of these beds consists of coarse sand and gravel, which is abruptly underlain by red-stained till.

Stupart River

Three sections with glacial/nonglacial sequences lie along Stupart River near its confluence with Fox River. The highest and most extensive exposures (Fig. 32.6A) show multiple brown tills with intervening horizontal, structureless sand beds of uncertain and controversial origin (see below). The upper till unit is looser and less oxidized than those below and contains sand shears. At Fox River the lowermost well exposed unit is a massive silty grey clay of marine or lacustrine origin.

The clay layer stratigraphically correlates with a subtill silt and clay bed at "Twisty Creek" (Fig. 32.6B). At this location the upper part of the section is tree covered, but the bottom 10 m exposes the nonglacial beds and their upper and lower contacts. The upper part of the exposure is a grey-brown, oxidized, relatively stony till. The till grades

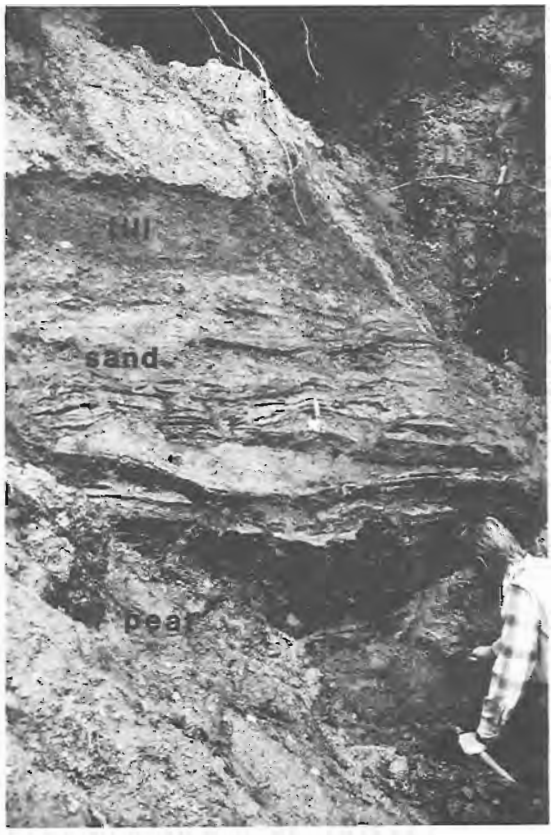

Figure 32.5. Interglacial sand and peat beds at Flamborough, section 1. (GSC 204037-E)

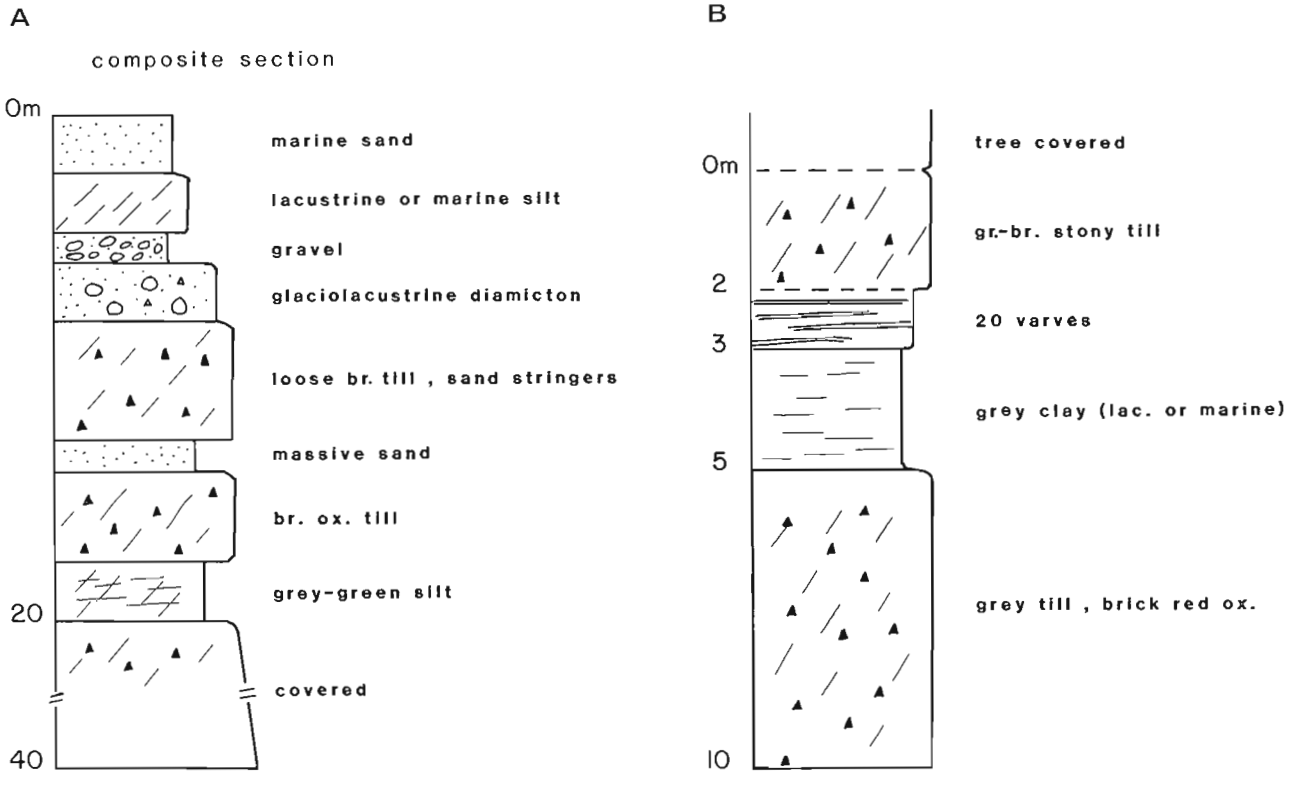

Figure 32.6. A. Composite section from Stupart River near its junction with Fox River. B. Lower part of the sequence at Stupart River at its junction with Twisty Creek.

downwards into a set of 20 couplets of buff silt and grey silty clay, which are interpreted as varves (Fig. 32.7). The couplets are of variable thickness, are draped over irregularities in the underlying bed, and have some internal erosional contacts (re-activation surfaces). The upper varves also display some deformation, produced by the glacier which overrode them. The varves are presumed to be lacustrine; below them is 2 m of steel grey, crumbly clay which may be either of lacustrine or marine origin. The clay contains dark mottles and has a sulphurous odour. The clay is separated by a sharp contact from at least 5 m of blocky grey moderately stony till which has brick red oxidation rinds on joint surfaces. The till breaks into large blocks, a contrast to the smaller fracture habit of the overlying brown tills.

Echoing River

This 18 m section lies along a meander cut in a tributary creek flowing into Echoing River. It was first noted by B.G. Craig in 1967 during Operation Winisk. The sedimentary record (Fig. 32.8) consists of glaciolacustrine silt and clay, an upper till, a major multi-bed nonglacial sequence, and possibly a lower till. The top part of the upper till unit consists of a yellow-brown silty till with unoxidized joints, which is separated from its underlying grey-brown counterpart by a stone line. The oxidized till becomes stone-free near its base; its lower contact is a contorted lamina of yellow silt. The subsequent 5 m (Fig. 32.8, 32.9) consists, from top to bottom, of grey massive clayey silt, brown irregularly laminated silt, compact platy peat with wood, white marl containing lacustrine macrofossils, varved brown silt and black clay with rip-up structures, contorted sand beds (at the contact of units 6 and 7 in Fig. 32.9), and blocky black stone-free clay. Below a depth of 40 cm the clay becomes blockier and stonier – generally more till-like than the clay above – but could equally be a glaciolacustrine or



Figure 32.7. Varved silt and clay, Stupart River section. (GSC 204037-F)

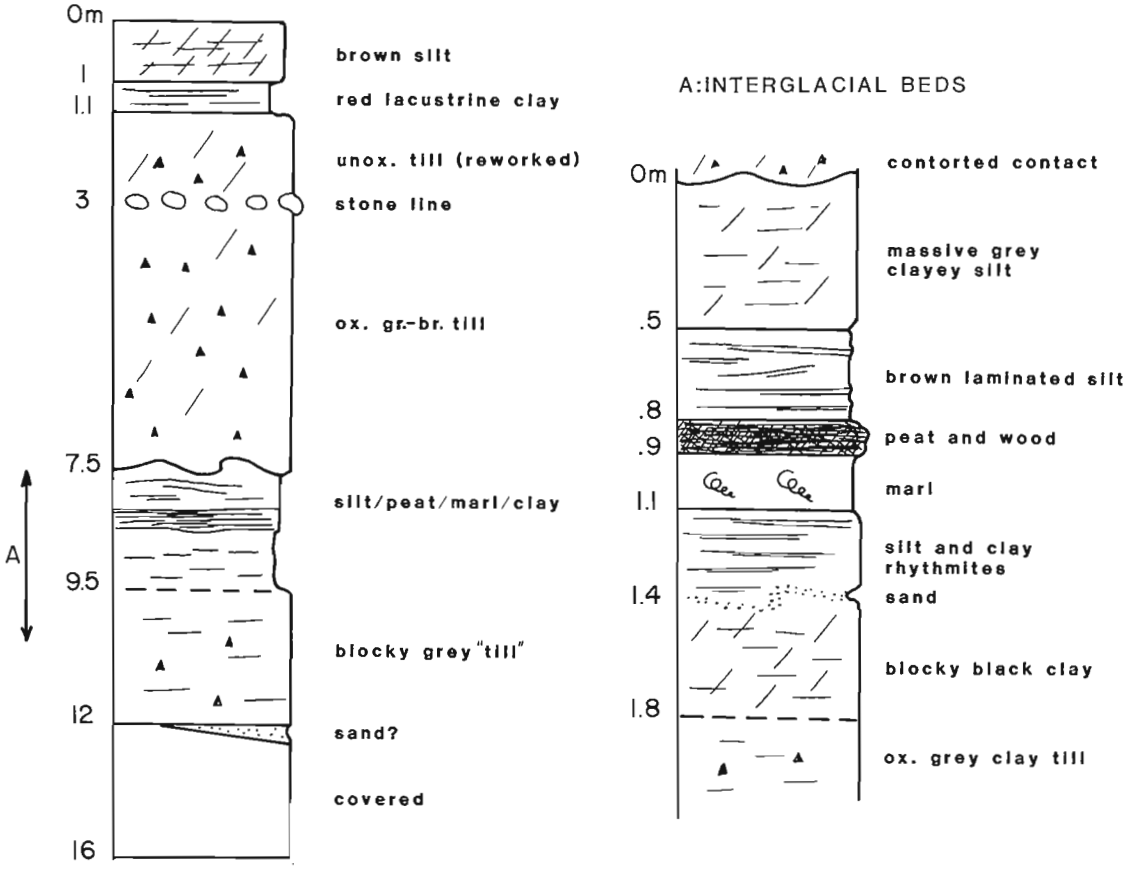

Figure 32.8. Echoing River section and detail of interglacial beds.



Figure 32.9. *Interglacial beds, Echoing River: (1) till, (2) clay-silt, (3) brown laminated silt, (4) peat and wood, (5) marl, (6) varved silt, (7) clay, and (8) stony clay diamicton. (GSC 204037-G)*

glaciomarine diamicton. The lowermost 4 m of the section is covered but there are some indications of a basal silty sand unit.

Gods River

The Gods River sections were the first major interglacial ones to be studied in detail in the western Hudson Bay Lowlands. Two sections were visited in 1984 to resample wood and peat beds for radiocarbon dating and paleoecological analysis. The sites were initially described and interpreted by Netterville (1974), who proposed the name Gods River Sediments, for the organic-rich nonglacial beds, and the name Twin Creeks Sediments for the sand beds higher up in the sections. The tills above the interglacial beds were called the Wigwam Creek Formation. The section shown schematically in Figure 32.10, together with others along the same stretch of river, shows a complex sequence of multiple tills separated by sand, silt, and peat. Beneath Tyrrell Sea sediments is a set of three brownish silty tills separated by horizontal sand layers which are traceable over long distances. The upper till is loose, crumbly, and grey-brown; the middle till is oxidized and irregularly jointed; and the lower till is olive grey, very compact, stony, and with wide-spaced columnar joints. The major nonglacial beds lie below these tills. The upper beds, which are more than 2 m in total thickness, are composed of silt, sand, and organic detritus, including wood. Peaty layers are black on fresh surfaces. The woody peat is underlain by sand and gravel containing less organics. The lowermost unit in the section is an olive grey till, with brick red oxidation adjacent to joints.

Henday

The 30 m-high Henday section (Fig. 32.11, 32.12A) extends about 250 m as bluffs along Nelson River and has been described previously by Nielsen and Dredge (1982, stop 4). The upper glacial unit is grey-brown oxidized till. It is underlain by a nonglacial unit of blocky, weakly stratified silt containing sand laminae (Fig. 32.11), having a maximum thickness of 3 m. One part of the bluff exposes a peat unit below the silt sequence. Pollen and beetle assemblages from this peat have been described elsewhere (Nielsen and Dredge, 1982).

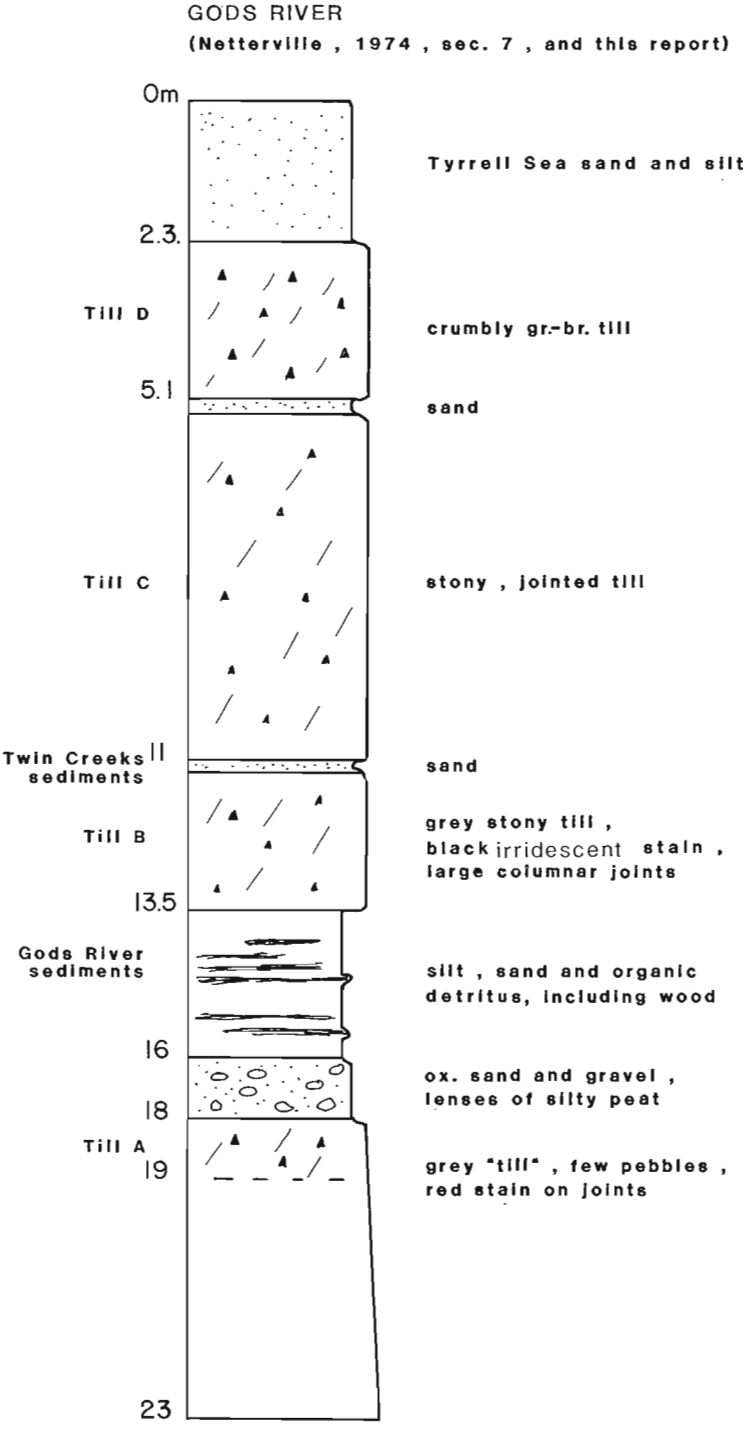

Figure 32.10. *Gods River section.*

The peat is underlain by a diamictic gravel which grades downwards into 12 m of compact grey till. At the base of one part of the bluff, striae trending 130°-140° are preserved on limestone outcrop. R.J. Mott concluded that the pollen assemblage represented climatic conditions similar to that presently experienced at Gillam, which lies within the boreal forest near the forest/tundra border. A.V. Morgan (University of Waterloo), however, suggested that the beetle population characterized cooler, tundra conditions. The two conclusions are not necessarily incompatible, since the deposits may span a range of climates. Aspartic acid ratios on wood from this site correspond to values on wood taken from the Missinaibi beds of the James Bay Lowlands.

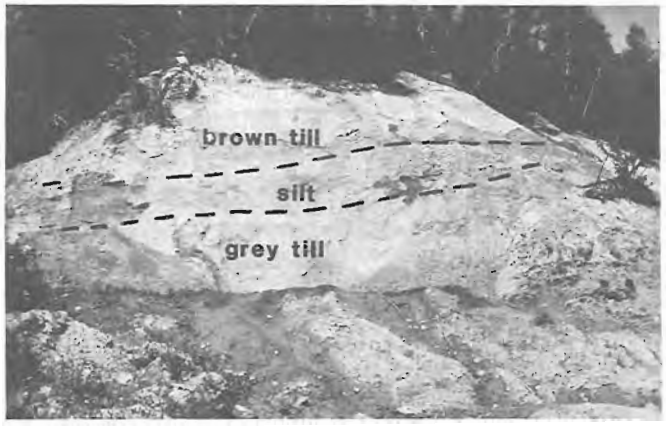

Figure 32.11. *Henday section, showing the interglacial silt beds (between dashed lines) between till sheets. (GSC 204037-H)*

Sundance

The 35 m-high Sundance section (Fig. 32.12B) has been logged previously by Nielsen (Nielsen and Dredge, 1982, stop 1). Its essential units within the till sequence consist of an upper, oxidized greyish silty till which correlates with the lowermost till exposed at Henday, underlain by highly fractured olive grey, silty sand till. An oxidized zone separates the two tills. Microscopic examination of the oxidized zone showed that it contains pollen and charcoal, suggesting that it is the root of a paleosol. The pollen assemblage is indicative of a subarctic or tundra environment.

Mountain Rapids

Mountain Rapids lies within the Canadian Shield about 50 km west of the Paleozoic/Precambrian contact along Churchill River. The 30 m-high bluff exposes multiple till units separated by sand and gravel beds. All the tills are silty and have a high carbonate matrix content (36-43%). The uppermost till is crumbly, loose, and contains few stones. It truncates beds of silt and sand containing tiny peat balls and partly flattened carbonized sticks, which have been dated at >32 000 BP (GSC-3074). The underlying three till units are

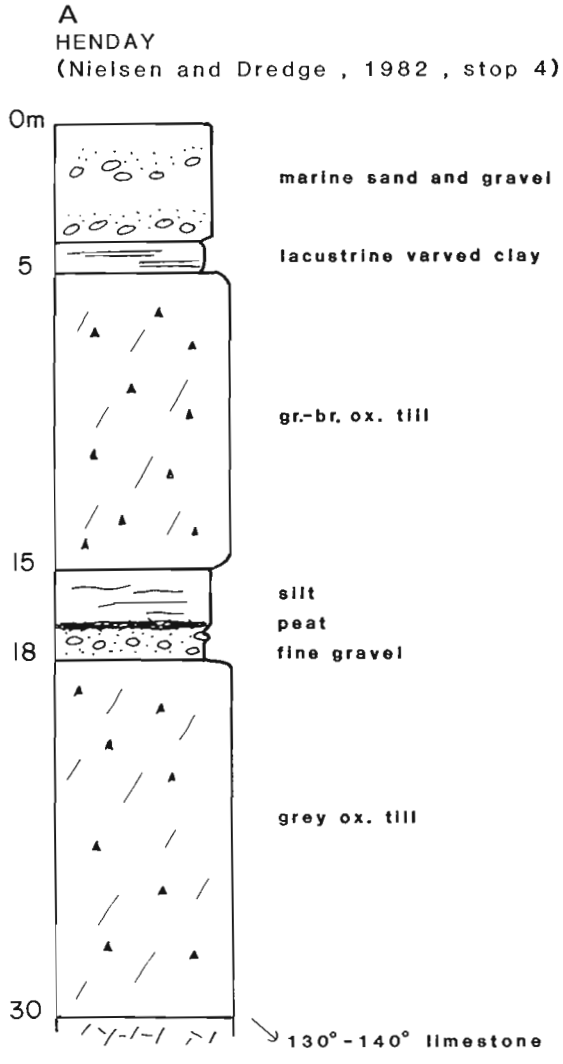

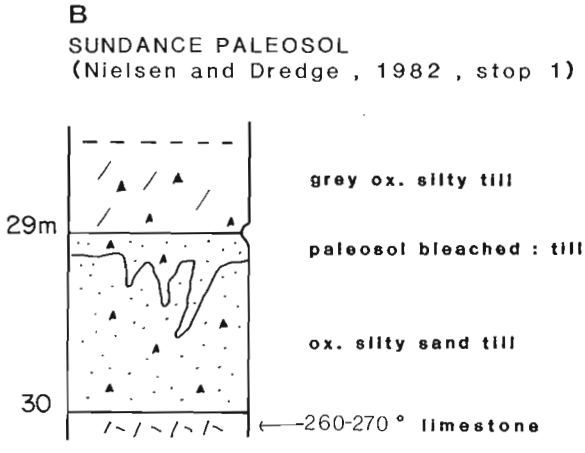

Figure 32.12

A. Section near Henday switching station, on Nelson River. B. Sundance paleosol. The lower part of the Sundance section completes the stratigraphic sequence at Henday.

olive brown, stony, blocky, and oxidized, although the lowest has a reddish hue. These tills are separated from each other by unfossiliferous beds of sand and gravel whose upper parts are intercalated with till and have till injections within them. Crossbedding in the lowest gravel bed indicates current directions towards the east.

The section (Fig. 32.13) is difficult to interpret: part of the section exposed and logged in 1980 was slumped in 1984, and vice versa; because the section lies near the zone of confluence of major Wisconsinan ice domains (Keewatin and Hudson), substantial provenance changes and multiple deposits could be present within a given glacial episode. On the basis of their silty nature and high carbonate content in the matrix, combined with the presence of eastern indicator lithologies (greywackes and pink sandstones), tills should all be of eastern provenance. However, because the upper two tills have much higher Precambrian clast contents than the lower two (50% vs. 19%), they may have been emplaced by ice from the north which reworked the lower silty tills, possibly during one main glacial event (see Discussion). The sand and gravel beds do not necessarily signify nonglacial events.

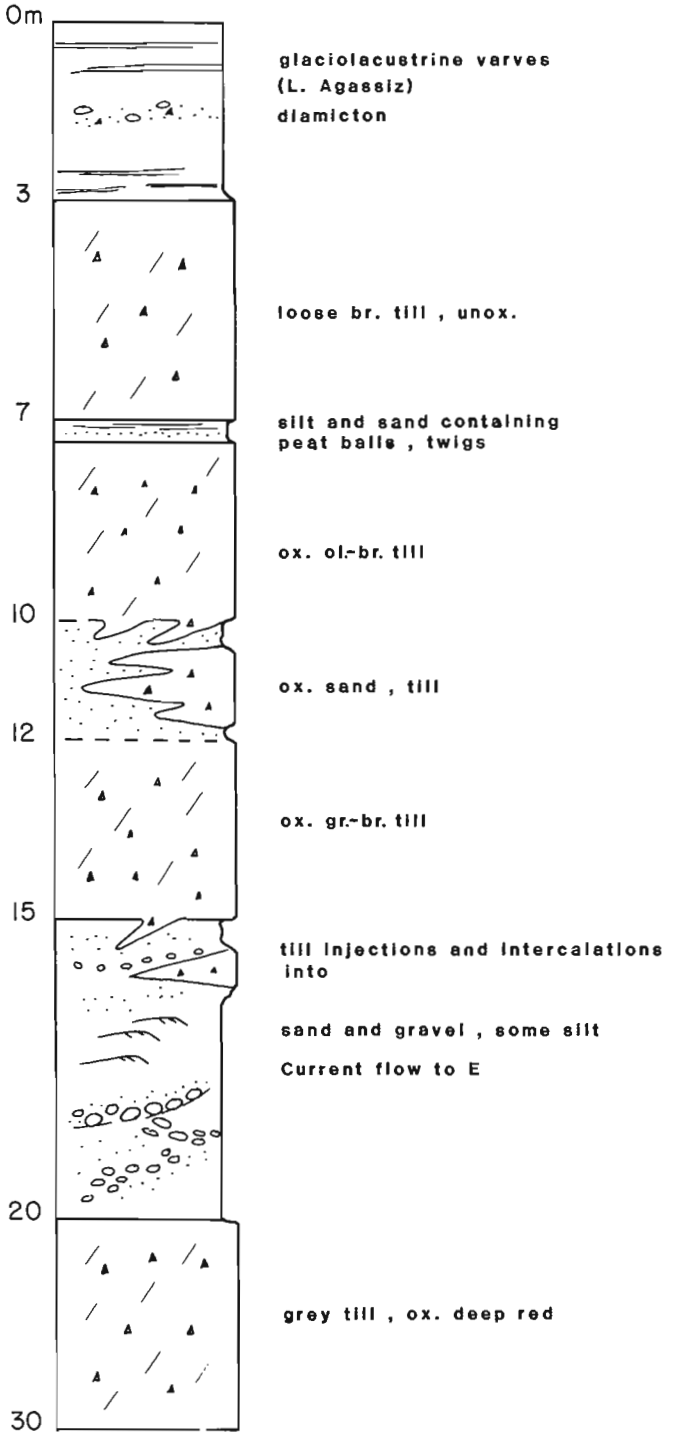

Figure 32.13. *Mountain Rapids, Churchill River. A composite section based on exposures logged in 1980 and 1984.*

Limestone Rapids

A three till sequence similar to that at Mountain Rapids was also encountered at Limestone Rapids, in Paleozoic terrain farther down Churchill River. Dredge et al. (in press; Fig. 32.14) logged a three-till sequence in which a thin organic-bearing sand bed separated the uppermost till from those below. Nielsen and Young (1981), at a nearby section, logged two stacked tills, overlying a cobble unit, with a lower till below. Although all the tills were of similar silty texture, the fabrics in the top and lowermost till indicated an ice movement from the north (155°-180°), whereas the middle till fabric indicated an easterly provenance (250°) for that unit. Pebble counts in the section logged by Dredge indicate a similar provenance for the succession of tills, but their stratigraphic position relative to the intertill gravel beds is different.

Other sites

Other sites containing both glacial and nonglacial deposits in the Hudson Bay Lowlands and adjacent parts of northeastern Manitoba are shown on Figure 32.1. The Limestone section was previously described (Nielsen and Dredge, 1982). The Great Island Site, which is at river level, consists only of cemented gravel and leaf casts (Taylor, 1961). The Seal River and Knife sections (Dredge et al., in press) also show partial sequences, as do the Cofferdam, Eagle Bluff, and lower Churchill River sections.

Discussion

Interglacial deposits

Two types of nonglacial deposits in the sections are exposed in the Hudson Bay Lowlands. The first type is a 1-4 m thick sequence of silt, sand, and organics; the second consists of structureless sand beds, generally less than 1 m thick, which are sandwiched between till units.

The organic beds and associated inorganic units in the Henday, Flamborough, Port Nelson, Stupart, Gods, and Echoing River sections were deposited in proglacial, lacustrine, terrestrial, and possibly marine environments, and are assumed to belong to the last interglaciation. This assignment is based on four aspects of their occurrence:

1. The pollen assemblage from peat at the Henday site reflects conditions at least as warm as present. The remaining sites are still under investigation.
2. Wood fragments from the Manitoba organic beds have the same aspartic acid ratios as wood from the Missinaibi interglacial unit.
3. These beds occupy a similar stratigraphic position as the Missinaibi beds in the James Bay Lowlands, which at present are assigned to the Sangamon Interglaciation (stage 5).

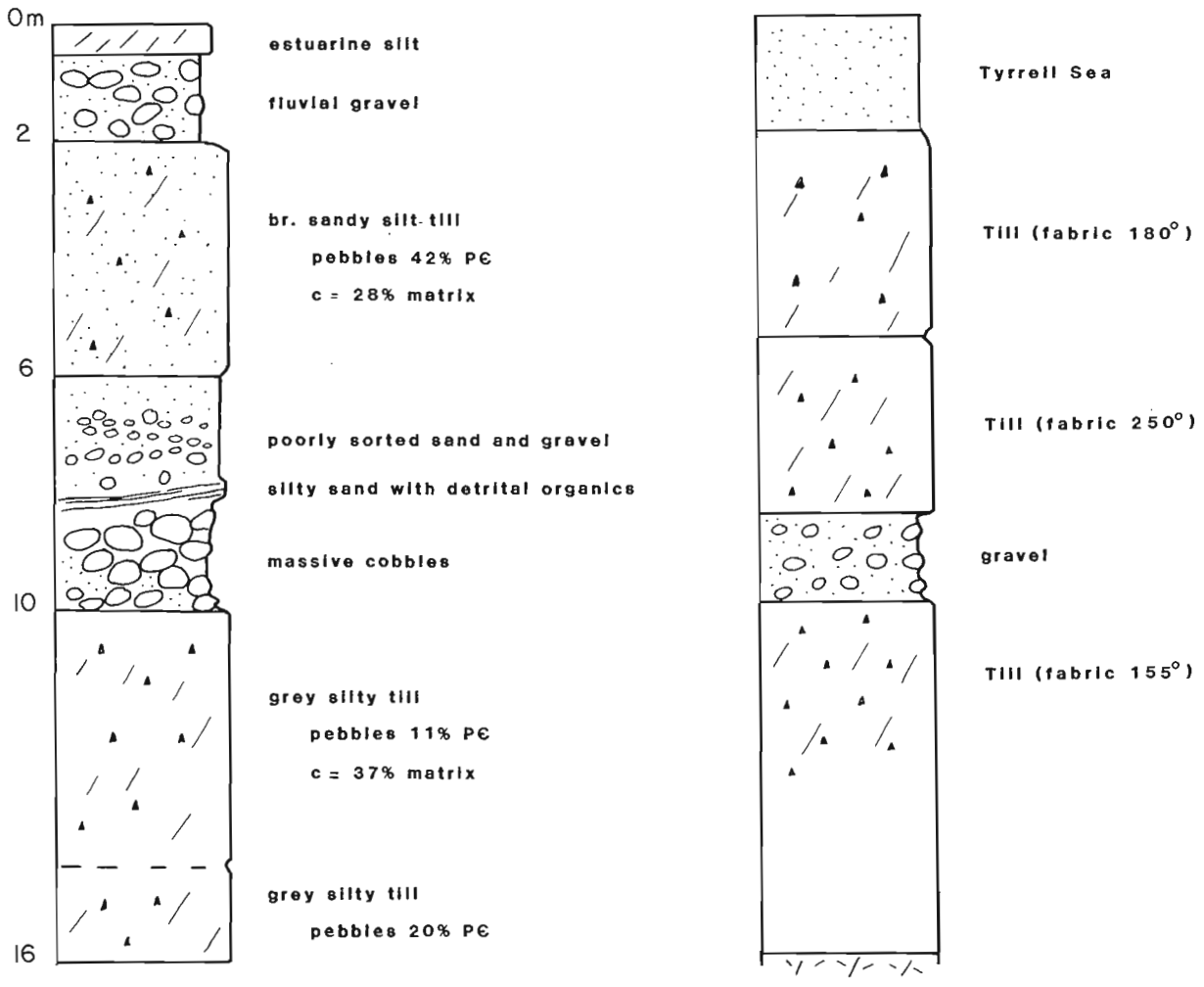

Figure 32.14. *Sections near Limestone Rapids, Churchill River.*

4. Position. They are the first (from the top) major subtill nonglacial deposits encountered in the sections and can be logically assigned to the first major interglaciation before present in the lowlands.

The paleosol at Sundance, however, has tentatively been assigned to a pre-Sangamonian nonglacial interval. The pollen assemblage from this paleosol differs from that of the other organic units studied, and the till which truncates it correlates with the pre-Sangamonian till at Henday. Lithic data and striae from a nearby site indicate that the till on which the paleosol has developed has a northerly provenance, whereas all others in the area were deposited by ice from the east.

Origin of structureless sand beds

At most sections studied several sand beds separate the tills which overlie the interglacial unit. The interpretation of these sand beds is important to deciphering the Wisconsinan glacial history of (and number of glacial units in) the Hudson Bay Lowlands, but the origin of these sand units is somewhat problematic. Previously, they have been inferred to be nonglacial beds associated with multiple deglaciations of Hudson Bay (Andrews et al., 1983). If the sand beds were nonglacial in origin, however, one might expect to see well defined fluvial crossbedding with current structures indicating flow towards Hudson Bay, incipient soils or oxidized zones on the fluvial units, erosional basal contact relations between the sand unit and underlying till, and correlatable till units above a given sand bed; these aspects were not observed in the sections examined in Manitoba. The number of beds differs from one site to the next, the "problematic" sand units lack well defined sedimentary structures, although they are texturally uniform across a given section, and the sand beds are commonly intercalated with or grade into till. On the basis of the observed field relationships we propose that these sand beds originated subglacially and englacially in association with an ice sheet whose centres of ice flow shifted during the course of the Wisconsin Glaciation.

Along Churchill and North Knife rivers the intertill sand beds separate tills that have major lithic (granitic vs. carbonate) and fabric (N-S vs. E-W) differences. These tills were emplaced by Keewatin and Hudsonian ice and reflect the repeated major shifts in ice flow across that region. The sand beds are interpreted as representing the remains of former interlobate moraines and subglacial drainage networks which lay along the passive zones of convergence between the two major ice domains. As the ice masses shifted, the sorted sandy deposits would have been entrained, smeared,

and homogenized (the sedimentary structures were destroyed) by the overriding ice. The sand beds in the Gods, Nelson, and Stupart sections separate tills with observable, but less dramatic differences than those crossing the Keewatin/Hudson convergence. Fabrics in tills above and below the intertill sands vary by 10°-45°, and the main lithological difference is in the ratio of red to buff carbonate pebbles. The sand beds in these areas are thought to have developed as radial moraines in zones of passive ice flow between ice streams within the Hudsonian Ice Domain.

The organics and twigs in the upper sand unit at Mountain Rapids suggest that this unit might be of nonglacial origin. Because the peat was in the form of tiny pellets, however, R.J. Mott (personal communication, 1982) has suggested that the organics are allochthonous, and were eroded and redeposited into the upper sand unit from material stratigraphically lower in the section. An alternative explanation for the organic sands is that they do actually represent the interglacial beds and that there is an exceptionally long glacial record at the Mountain Rapids site.

Not all sand beds are of the same origin, and some of the minor beds that are thin and discontinuous (e.g. at some Port Nelson sections) separate basal and englacial facies of the same till unit. Sand beds of this sort commonly display minor sedimentary structures and separate tills which are similar in colour and lithology, but different in compaction and joint habit.

Glacial events and ice flow directions

At least three major glaciations are represented in the sections examined. The earliest is recorded in the till beneath the paleosol exposed at Sundance and possibly by the till at river level (tidal surface) at Port Nelson. The lower till at Sundance is sandier than others and contains more Precambrian clasts than the overlying tills. Although striae directly under the Sundance till trend towards the west, those nearby at Henday indicate ice flow from the north-northwest and probably relate to the glacial event which emplaced the Sundance till. The tidal till also has abundant Precambrian clasts. These tills were emplaced by ice of northern provenance, whose centre may have lain in western District of Keewatin or eastern District of Mackenzie.

The bleached and oxidized upper part of the Sundance till has been interpreted as a paleosol which formed during a subsequent interglaciation when neither ice nor proglacial lakes were present.

The red-stained, grey till directly below the interglacial beds at all sites is silty, calcareous, contains abundant clasts from the Paleozoic rocks beneath Hudson Bay, and was emplaced by ice from the east and northeast during an Illinoian glaciation.

South of Churchill River, all tills above the interglacial beds are brownish, have similar clayey silty matrices, and contain mainly carbonate clasts. In the interpretation presented above for the intertill sand beds, all these tills belong to a continuous Wisconsinan glaciation; the variations in compaction, stoniness, fracture habits, and some of the variations in colour and structural features can be related to depositional environments and to slight provenance shifts during the Wisconsin Glaciation, which may or may not relate to climatic changes elsewhere. These provenance shifts are supported by fabric data from the tills (Nielsen and Dredge, 1982).

The upper part of the Wisconsinan till sheet at Mountain Rapids and Limestone Rapids was emplaced by ice from the north, although the lower part of the till sheet was emplaced by ice of eastern provenance, probably Hudsonian Ice. Fabrics from Limestone Rapids (Nielsen and Young, 1981) and clast counts from both Limestone Rapids and Mountain Rapids, which show a marked increase in Precambrian clasts (50% vs. 20%), indicate that Keewatin ice overran and in part re-incorporated the previous Hudsonian tills.

Summary

The oldest (pre-Illinoian?) till exposed at Sundance and Port Nelson was emplaced by ice from the north. A soil-forming period followed this glaciation, during which the Sundance paleosol developed. During the Illinoian Glaciation (immediately prior to the last interglaciation) ice originating in, or extending across Hudson Bay, reached as far west as Mountain Rapids, but possibly not as far north as Limestone Rapids, which appears to have been covered by ice flowing from the north. The succeeding Sangamon Interglaciation (isotope stage 5), left a series of alluvial, lacustrine, marine, and terrestrial organic deposits. Ice covered the area during the entire Wisconsin Glaciation. During the early part of the Wisconsin Glaciation, Hudsonian and/or Labradorean ice covered the area south of Knife River, while Keewatin ice lay to the north. During the middle and late Wisconsinan, ice flow from a Hudsonian centre was sustained or developed, and ice of eastern provenance continued to occupy the Gods and Nelson River areas, although there were some minor shifts in ice flow directions. During the late Wisconsinan there was a major directional ice-flow change in the northern part of the region, and the Churchill River area was overrun by ice from the District of Keewatin-Mackenzie.

Glaciofluvial sediments were deposited along zones of weakness and between ice lobes within the Wisconsinan Laurentide ice sheet. As flow centres shifted these deposits were overrun and homogenized; their vestiges are the intertill sand beds commonly observed within the Wisconsinan tills of the region.

References

Andrews, J.T., Shilts, W.W., and Miller, G.H.
1983: Multiple deglaciations of the Hudson Bay Lowlands, Canada, since deposition of the Missinaibi (Last-Interglacial?) Formation; Quaternary Research, v. 19, p. 18-37.

Dredge, L., Nixon, M.F., and Richardson, R.J.
– Quaternary geology and geomorphology, northwestern Manitoba; Geological Survey of Canada, Memoir 418. (in press)

Netterville, J.A.
1974: Quaternary stratigraphy of the lower Gods River region, Hudson Bay Lowlands, Manitoba; unpublished M.Sc. thesis, University of Calgary, Calgary, 79 p.

Nielsen, E. and Dredge, L.
1982: Quaternary stratigraphy and geomorphology of a part of the Lower Nelson River; Geological Association of Canada, Field Trip 5, Guidebook, 56 p.

Nielsen, E. and Young, R.V.
1981: Quaternary geology and aggregate resource inventory of the Thompson and Churchill areas; in Manitoba Mineral Resources Division, Report of Field Activities, 1981, p. 103-106.

Taylor, F.C.
1961: Interglacial conglomerate in northern Manitoba; Geological Society of America Bulletin, v. 72, p. 167-168.

GEOLOGY OF THE CHANTREY BELT AND ITS ENVIRONS, LOWER HAYES RIVER AND DARBY LAKE MAP AREAS, NORTHERN DISTRICT OF KEEWATIN

Project 820008

Thomas Frisch, Irvine R. Annesley[1] and Catherine A. Gittins[2]
Precambrian Geology Division

Frisch, T., Annesley, I.R. and Gittins, C.A., Geology of the Chantrey belt and its environs, Lower Hayes River and Darby Lake map areas, northern District of Keewatin; in Current Research, Part A, Geological Survey of Canada, Paper 85-1A, p. 259-266, 1985.

Abstract

The map area is underlain by Archean? gneissic rocks of plutonic origin and northeast-trending belts of supracrustal and granulite facies rocks.

Lower amphibolite grade metasediments of the Aphebian? Chantrey Group form a syncline 5 km wide and 175 km long. Marginal shallow-marine carbonate and quartzitic rocks are overlain by either fine grained metapelite/psammite, quartzite and dark, pyritic schist or, locally, metaconglomerate. Coarse andalusite is a common porphyroblast in pelitic rocks. Two periods of folding have severely deformed the Chantrey Group and its contact with basement is strongly sheared, with local overthrusting of basement.

Another supracrustal belt, of the same metamorphic grade but intruded by granite, comprises pelitic and metavolcanic rocks and subordinate Chantrey-type marble, quartzite and metaconglomerate.

A 10 km-wide belt of granulite facies rocks in southeastern Lower Hayes River area consists of garnetiferous gneisses and meta-intrusive garnet-orthopyroxene granite.

Résumé

La région cartographiée repose sur des roches gneissiques archéennes? d'origine plutonique et sur des zones à orientation nord-est de roches supracorticales et de roches à faciès de granulites.

Les métasédiments du faciès inférieur d'amphibolites du groupe aphébien? de Chantrey forme un synclinal de 5 km de large sur 175 km de long. Les roches carbonatées et quartzeuses qui se sont formées dans un milieu marginal peu profond sont recouvertes soit de métapélites-psammites à grain fin de quartzites et de schistes pyrileux sombres, soit par endroits de métaconglomérats. L'andalousite à grain grossier est un minéral porphyroblastique qui abonde dans les roches pélitiques. Deux périodes de plissement ont fortement déformé le groupe de Chantrey et, au contact du socle, on observe un cisaillement et, par endroit, un chevauchement.

Une autre zone supracorticale, qui a subi le même degré de métamorphisme mais dans lequel du granite a fait intrusion, se compose de roches pélitiques et métavolcaniques avec des quantités de moindre importance de marbre, de quartzite et de métaconglomérat similaires à ceux du groupe de Chantrey.

Dans le sud-est de la région du cours inférieur de la rivière Hayes, une zone de roches à faciés de granulites d'une largeur de 10 km se compose de gneiss grenatifères et de granites métaintrusif à grenat à orthopyroxène.

[1] Department of Geology, University of Ottawa, Ottawa, Ont. K1N 6N5
[2] Department of Geology, University of Toronto, Toronto, Ont. M5S 1A1

Introduction

The main focus of this project is the Aphebian(?) Chantrey Group of metasediments which form a northeast-trending belt across Chantrey Inlet, an arm of the sea into the mainland south of King William Island.

This area of the Churchill Structural Province of the Canadian Shield was mapped on a reconnaissance scale (1:506 880) in 1960 (Heywood, 1961), when the Chantrey Group was first recognized and its distribution and general aspect delineated. The bedrock geology of the region has received little attention since that time.

The major part of the Chantrey belt outcrops in Lower Hayes River area (NTS 56M) and continues eastward into Darby Lake area (56N); field work in 1984 was concentrated in the region shown in Figure 33.1. Chantrey Group rocks also occur in northeastern Montresor River area (66I), southwest of Lower Hayes River area; Montresor River area was mapped in 1982 (Frisch and Patterson, 1983). Thus the Chantrey belt runs almost continuously for 220 km.

The 1984 work completed the field component of this project.

Physiography

The "barren lands" of Lower Hayes River area are dominated by the physiographic features of Chantrey Inlet, the lower reaches of the Back and Hayes rivers and their coalescing deltas at the head of Chantrey Inlet. Most of the area is underlain by granitoid rocks, forming low hills separated by lakes and marshy areas. Relief is little more than 200 m. The Chantrey Group occupies a physiographically poorly defined, very shallow trough across central Lower Hayes River area.

The Hayes River is bordered by poorly consolidated Quaternary marine sand locally forming cliffs up to 75 m high. The deposits also extend northwards from the river near the eastern edge of Lower Hayes River area. This sand accumulated in a high stand of the sea during glacial retreat (Geological Survey of Canada, 1982).

Acknowledgments

We thank our field assistants, Ann Purdy and Terry Needham, for their help and enthusiasm; helicopter pilots M. Grubac and D.R. White and engineers D. Bryant and C. Arnott of Quasar Helicopters, Ltd. for their skill; and Janien Schwarz for her culinary efforts. The Polar Continental Shelf Project generously provided helicopter and Twin Otter flying time and accommodation at Resolute Bay. F.P. Hunt and B. Hough and staff at PCSP Resolute Bay extended numerous courtesies.

We are also grateful to Colin Dickie of the N.W.T. Government for much help and hospitality in Gjoa Haven and to Gideon Qitsualik of Gjoa Haven for his hard work caching supplies in the field.

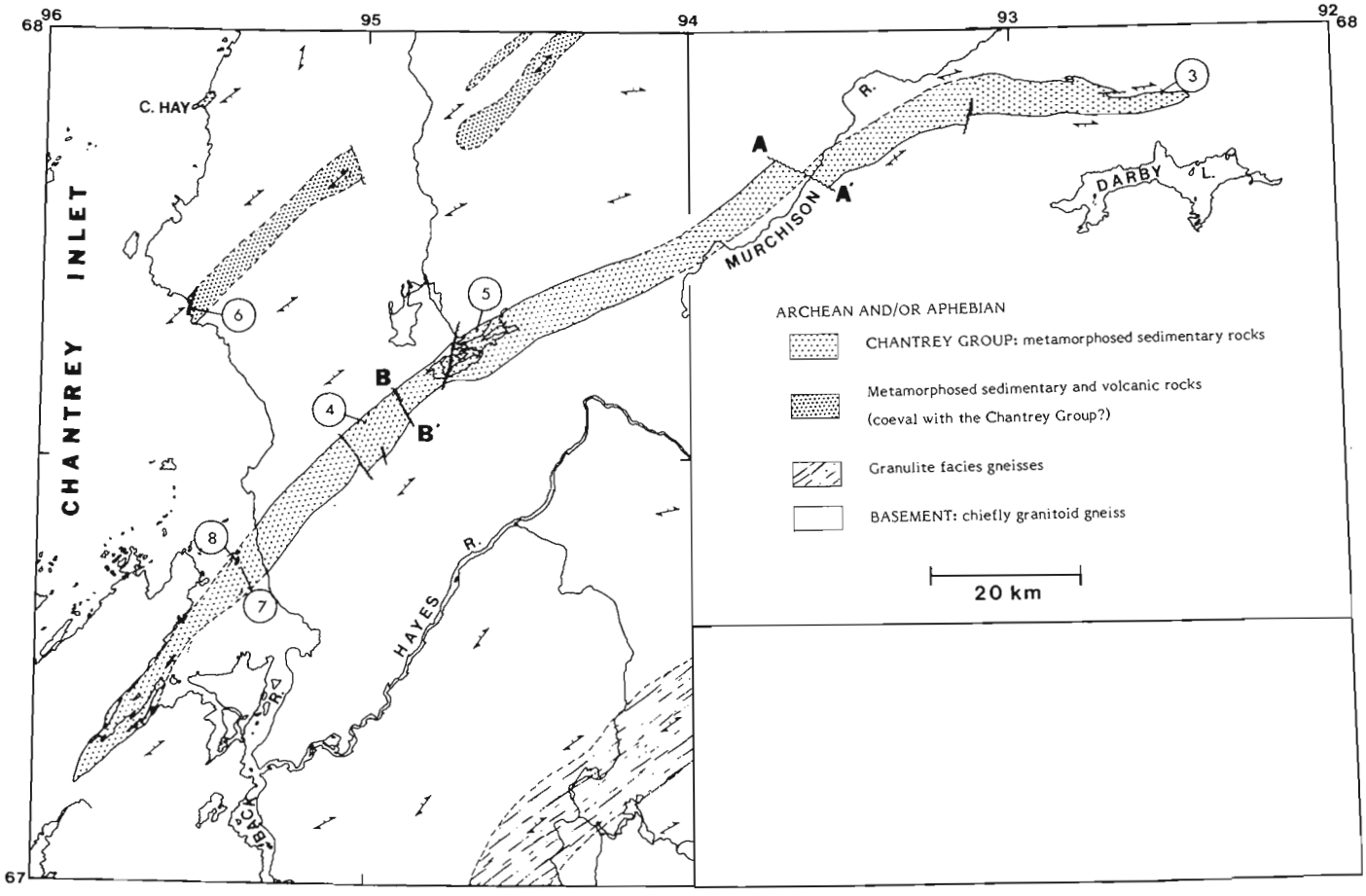

Figure 33.1. Geological sketch map of the environs of the Chantrey belt. A-A' and B-B' are faults that divide the belt into the three segments shown in Figure 33.2. Circled numbers refer to the localities depicted in Figures 33.3-33.8.

Basement complex

The (presumably Archean) basement complex of the region comprises a heterogeneous assemblage of plutonic granitoid rocks heavily and extensively covered by lichen. Little subdivision of the complex proved possible in the 1:250 000 mapping conducted.

Most of the basement consists of medium grained, gneissic, biotite-bearing granodiorite, commonly with porphyroblastic feldspar (generally K-feldspar). Grossly similar but more mafic rocks occur widely. These contain hornblende in addition to biotite and more plagioclase than K-feldspar.

Augen gneiss of granitoid composition predominates locally and tends to be mylonitized to varying degree. Some augen gneiss may be derived from a distinctive porphyroblastic granite seen in clean shoreline exposures along Chantrey Inlet. The K-feldspar porphyroblasts in this rock invariably show preferred orientation to some extent, at least. Indeed, except for pegmatite dykes, all the granitoid rocks have preceded or accompanied major deformation.

Migmatites are exposed at the head of Chantrey Inlet and present a complex mixture of plutonic granitoid rocks and supracrustals such as amphibolites, mafic schists and garnetiferous gneisses. Garnetiferous leucogranitic veins and layers are probably of anatectic origin.

Gneissic trends overwhelmingly bear northeast in Lower Hayes River area. Foliation generally dips steeply northwest but southward dips are common in the basement at the edge of the Chantrey belt.

Granulite facies rocks

A northeast-trending belt of granulite grade rocks cuts across the southeast corner of Lower Hayes River area (Fig. 33.1). The constituent rocks may be grouped into garnetiferous gneisses and K-feldspar porphyroblastic, garnet-orthopyroxene granite (garnetiferous charnockite). The gneisses are strongly layered, leucocratic, garnet-rich layers alternating with brownish weathering, more mafic layers. A sedimentary protolith is suggested by the high garnet content and heterogeneity of the gneisses.

The orthopyroxene granite is a distinctive rock. Euhedral, pale grey K-feldspar crystals up to 4 cm long are well aligned in a brown-weathering, greenish, medium grained matrix consisting of altered orthopyroxene, biotite, feldspar and quartz. Pink garnets, 0.5 to 1 cm across, are abundantly but unevenly distributed through the granite.

Schlieren-like lenses of fine grained, dark garnet gneiss and pyroxene gneiss are common in the granite and lie in the gneissosity plane. Relatively finer grain size of the orthopyroxene granite at contacts with gneiss also suggests an intrusive origin for the granite.

Although the borders of the granulite belt are gradational into, and concordant with, the surrounding gneiss, they can be fairly clearly delineated on a large-scale map. The granulite grade rocks are increasingly retrograded towards the margins of the belt, losing their greasy green lustre and becoming more biotite-rich. The end member of this process may resemble the augen gneiss so common in the basement complex. Age relations between granulites and basement are unknown.

The granulite belt appears to be traceable on aeromagnetic maps (Geological Survey of Canada, 1977a, b) southward into Mistake River area (NTS 56L), where it swings westwards and runs into eastern Montresor River area. There, Frisch and Patterson (1983) noted garnetiferous gneisses with anomalous structural trends. Subsequent work has shown that these gneisses of the "eastern sector" of Montresor River area include granulite facies rocks.

Supracrustal belts

Chantrey belt

Chantrey Group rocks in the area investigated in 1984 form a tightly folded synclinal structure extending northeastwards across Lower Hayes River area and in a more easterly direction for 50 km in the northern Darby Lake sheet (Fig. 33.1). The structure closes at both ends and plunges fairly consistently 10 to 20° northeast in Lower Hayes River area and the same amount west-southwest in Darby Lake area.

The Chantrey Group consists of sedimentary rocks metamorphosed to lower amphibolite grade. A simplified, preliminary geological map of the belt is presented in Figure 33.2. To facilitate designation of units on Figure 33.2, the units are identified by number. Although, in general, the higher units in the stratigraphic sequence have higher numbers, the numerical designation of any unit is based on its lithology rather than its relative age. Thus, for example, the two units labelled "3" at the western end of the Chantrey belt are lithologically similar but do not represent repetition of the same unit.

Lithology. The border of the eastern Chantrey belt is represented by a thin, resistant carbonate unit (Fig. 33.3). This unit (1 in Fig. 33.2) is highly siliceous and contains sprays of coarse, white diopside and rosettes of pale green tremolite.

Unit 1 is overlain by a quartzite (unit 2) of variable composition, which commonly forms the outermost unit of the western Chantrey belt. Near the contact with unit 1 or basement, the quartzite is impure and schistose and may even grade into quartz-mica schist. The schist locally carries quartz clasts and, at the northern edge of the belt on the east coast of Chantrey Inlet, abundant quartz lenses aligned in schist suggest the lenticular bedding characteristic of tidal deposits (Reineck and Singh, 1980). Thick sections of unit 2 contain a significant proportion of relatively pure white, grey or pink quartzite, rarely ripple marked and crossbedded; fuchsite is locally present.

At the eastern end of the Chantrey belt, ripple marked, fairly pure quartzite (5 in Fig. 33.2) overlies unit 2 and forms an extensively rubbly terrain (Fig. 33.3). Elsewhere in the belt, the overlying rock is a persistent carbonate unit (unit 3; Fig. 33.4), which can be followed practically the entire length of the Chantrey belt. Much of the unit is highly recrystallized, calcitic or dolomitic marble but siliceous interbeds and variegated calc-silicate layers are common. Well preserved stromatolites were found locally, as in segment 2 of the belt (Fig. 33.5), and provided useful way-up indications. Generally, however, stromatolites have been virtually destroyed by intense recrystallization and deformation.

Unit 3 thickens and thins rapidly and the western end of the Chantrey belt is marked by two carbonate units, the outer one of which includes calcareous metamudstone interbedded with marble.

Unit 3 is overlain by dark grey, finely laminated metasiltstone locally grading into fine grained metasandstone or -mudstone (unit 4). Over most of the Chantrey belt, unit 4 contains, particularly in more pelitic layers,

	Segment 1	Segment 2	Segment 3
⁘	Quaternary alluvium		
7		Metaconglomerate; polymict: clasts predominantly quartzose, also granitoid and mafic; schistose matrix	
6	Pelitic schist with porphyroblasts of biotite (and chloritoid?), andalusite and garnet; dark grey, pyritic; rare ripple marks		
5	Quartzite, relatively pure; locally hematitic, rarely grunerite?-bearing; rare crossbeds and ripple marks		Orthoquartzite, quartzite; locally hematitic; minor impure sandy and staurolite±garnet-bearing pelitic interbeds
4	Metasiltstone with porphyroblasts of garnet, andalusite and, rarely, biotite? or chloritoid?; finely laminated		Metasiltstone/mudstone; finely laminated; fine grained meta-sandstone/siltstone with cordierite at W end of belt
3, /	Marble with siliceous interbeds, subordinate calc-silicate; locally stromatolitic		Includes calcareous metamudstone and -siltstone at W end of belt
2	Impure quartzite, micaceous to schistose quartzite, locally fuchsitic; minor schist and schistose conglomerate; rare crossbeds and ripple marks		
1, /	Siliceous marble, calc-silicate; locally diopside- and tremolite-rich		
xxx	Basement: granitoid rocks		

N.B. Numerical designation of the units is mainly for convenience and does not necessarily indicate their relative ages or facies equivalents.

0 km 10

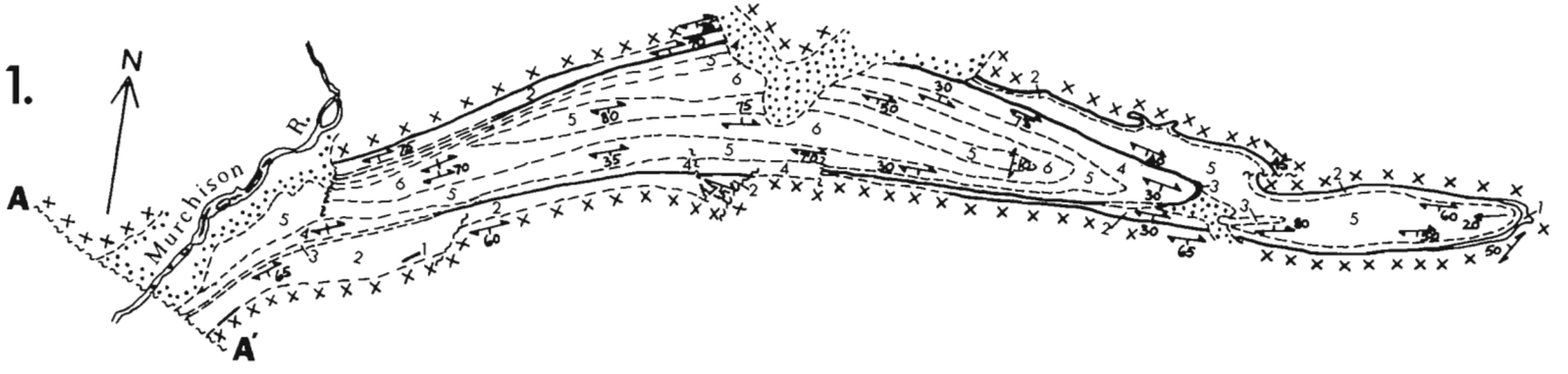

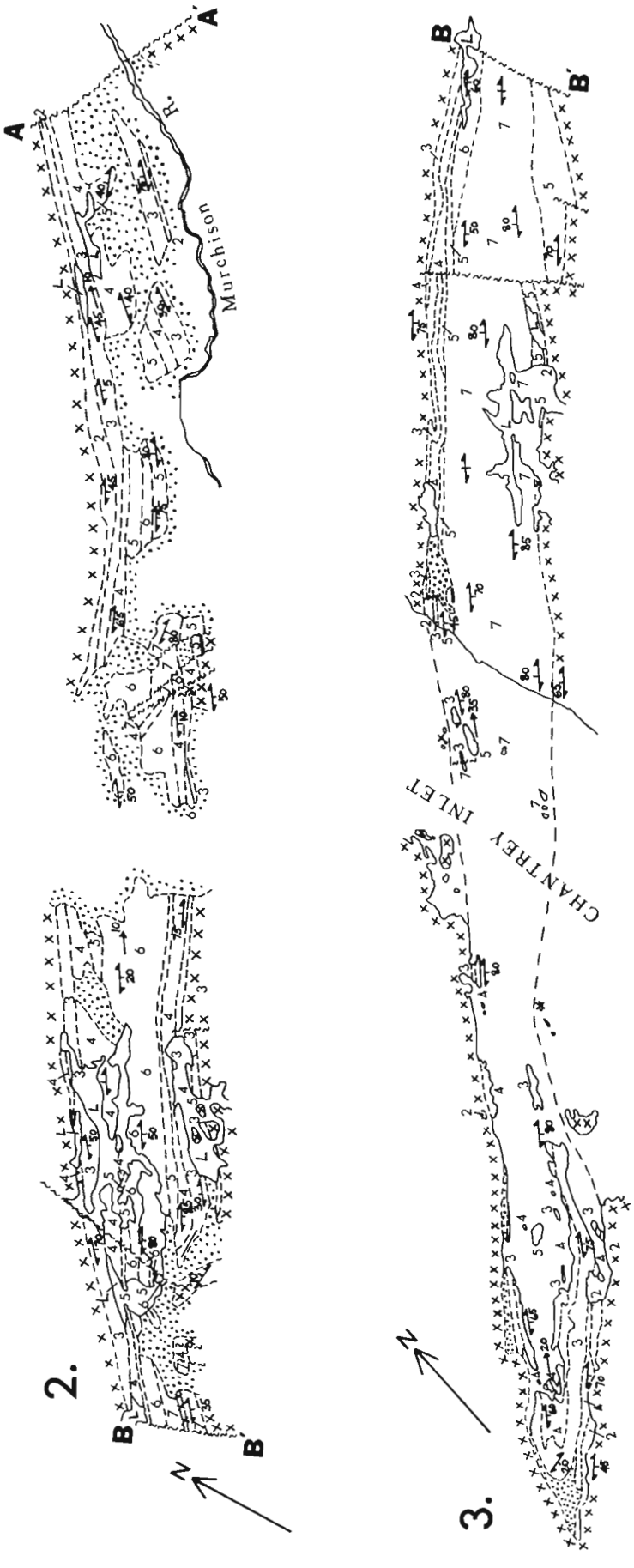

Figure 33.2. Geological sketch map of the Chantrey belt. The belt is divided into three segments separated by faults A-A' and R-R' (Fig. 33.1).

millimetre-size pink garnets and coarser blades of andalusite; rarely, tiny porphyroblasts of biotite (or chloritoid?) also occur. The andalusite blades lie randomly in the foliation plane and cross-sections show the cruciform arrangement of inclusions that characterizes chiastolite (Fig. 33.6). At the western end of the Chantrey belt, the upper marble unit is overlain by a fine grained, quartzose metasandstone/siltstone with poorly developed cordierite porphyroblasts.

The next younger unit (unit 5) is a generally massive quartzite, white, pink or grey. Although for the most part relatively pure, the quartzite is notably hematitic in places. Crossbedding in this unit is locally preserved well enough to be used for determination of tops. A highly impure variety of metasandstone with abundant amphibole, tentatively identified as grunerite, and pelitic laminae occurs stratigraphically above unit 4 in segment 2 of the Chantrey belt and has been included in unit 5. Crossbedded, pink to buff quartzite near the western end of the belt is interbedded with impure sandy and staurolite ± garnet-bearing layers, which are most common in the lower part of the unit.

The core of the syncline is occupied by either fine grained pelitic schist (unit 6) or metaconglomerate (unit 7). The pelitic schist is a remarkably dense, dark rock, almost black in places, rich in porphyroblasts of chiastolite (2-3 cm, exceptionally 25 cm long), garnet and biotite or chloritoid. Oval porphyroblasts, typically 5 mm long, of a glossy black, platy mineral were considered in the field to be chloritoid. However, an X-ray check and thin section of a single specimen of schist show the porphyroblasts to be brown biotite. It is the ubiquitous and abundant presence of biotite (or chloritoid) porphyroblasts that distinguishes unit 6 from much of unit 4. The schist tends to weather rusty due to disseminated pyrite. Ripple marks are present but not common.

Metaconglomerate (unit 7) is the major component of the Chantrey belt over a distance of some 20 km east of Chantrey Inlet. Although polymict, the metaconglomerate does not have a wide range of clast lithologies. Most clasts are of white, recrystallized quartz but granitoid (including gneissic) clasts are common and indeed predominate near the basement contact; subordinate mafic clasts are biotite schist and amphibolite, invariably lensoid. Clast size ranges from pebble to boulder (Fig. 33.7). Quartzofeldspathic clasts are rounded to angular and commonly stretched in the schistosity plane (length:width up to 10:1). The matrix is strongly schistose with variable quartz ± feldspar content; it becomes increasingly gneissic towards the basement contact. Locally, clast-rich metaconglomerate alternates with clast-poor schist (Fig. 33.7) but numerous traverses and observations in the metaconglomerate unit demonstrated the predominance of clast-rich lithologies.

East of Chantrey Inlet the metaconglomerate pinches out and gives way to pelitic schist (unit 6) – presumably due to facies change rather than structural control. Metaconglomerate appears again in the highly faulted block in the middle of segment 2 (Fig. 33.2) but is not found elsewhere in the Chantrey belt of Figure 33.1.

Structure. The Chantrey belt in the area of Figure 33.1 is essentially a canoe-shaped structure with a 10 to 20° plunge at each end. Axes of the NE-SW folds in the more central parts of the belt rarely plunge more than 10° but angles of up to 40° were recorded locally.

Two major episodes of folding have deformed the Chantrey Group. Early, tight, more or less upright folding with NE-trending axial planes probably pervades the entire belt but can only locally be directly observed. An unusually good exposure of these folds in garnetiferous pelites associated with quartzite (unit 5) is depicted in Figure 33.8; the plunge of 35° at this locality is exceptionally steep. We consider the severe shortening implied by these structures to have affected the entire Chantrey belt.

A second event produced more open and steeply plunging (50-60°) folds with SE- to S-trending axes, transverse to the strike of the Chantrey beds. These folds are most readily seen in the marble units (Fig. 33.4).

Numerous observations of southward dips and inverted stratigraphy along the southern contact indicate that the syncline is overturned to the northwest.



Figure 33.3. *View to the northeast of the northern margin of the Chantrey belt. Southward-dipping calc-silicate rock (unit 1) overlies basement. The rubbly terrain in the foreground is underlain by quartzite (unit 5).*



Figure 33.4. *Aerial view of second-generation, transverse, steeply plunging folds in marble unit (3) near the northern margin of the Chantrey belt (basement at top left).*

Basement-Chantrey Group contact. Intense deformation makes it difficult to determine the nature of the original basement-Chantrey Group contact. The presence of conglomeratic rocks, in particular rocks with gneiss clasts, at the border of the Chantrey belt suggests an unconformity. Moderate to profound angular discordance between Chantrey and granitoid rocks is evident locally.

In general, however, the apparently unconformable contact between Chantrey Group and basement has been drawn into concordance by tectonism. Severe shearing characterizes both basement and Chantrey rocks. Twenty kilometres from the western end of the belt a mass of quartzite several hundred metres long occurs as a tectonic inclusion in basement just north of the northern contact.

Deformation appears to have been particularly severe along the southern margin of the belt, where commonly several units are absent, presumably cut out by faulting. In places, basement has clearly been thrust northward over Chantrey Group. Overthrust basement also appears at the northern contact, 15 km from the eastern end of the belt.

Except for pegmatite and diabase dykes, no intrusive rocks are seen to cut the Chantrey belt. A narrow sliver of granite well inside the belt at the western end of segment 2 (Fig. 33.2) is thought to be a tectonically emplaced slice of basement.

The generally simple, linear, if highly sheared contact of the Chantrey belt contrasts with the complex interleaving of Chantrey Group and basement in Montresor River area (Frisch and Patterson, 1983).



Figure 33.5. *Exceptionally well preserved, laterally linked, domal stromatolites in marble unit (3) near the northern margin of the Chantrey belt.*



Figure 33.6. Chiastolite variety of andalusite in pelitic schist of the supracrustal belt north of the Chantrey belt. The nature and distribution of chiastolite is identical to that commonly found in pelitic schists of the Chantrey Group. Length of hammer shaft is 29.5 cm.



Figure 33.7. Metaconglomerate (unit 7) of the Chantrey Group in a glacially striated outcrop in Chantrey Inlet. The alternation of clast-poor and clast-rich rocks is probably somewhat atypical of unit 7.

Environment of deposition of the Chantrey Group. Shallow-water sedimentary structures (crossbedding, lenticular bedding, ripple marks, stromatolites), shallow-to deeper-water lithologies (reefoid carbonates, quartzites, dark, euxinic shales) and lack of igneous rocks indicate the Chantrey Group was deposited on continental crust in a progressively deepening near-shore marine environment (prograding delta?). The restricted occurrence of conglomerate points to sedimentation down a slope of limited extent, below which the euxinic shale protolith of the pelitic schist unit (unit 6) may well have been deposited.

Other supracrustal belts

Supracrustal rocks occur in northeast-trending belts north of the Chantrey belt (Fig. 33.1). The belt reaching the sea halfway between the Chantrey belt and Cape Hay is well exposed only on the coast. It consists mainly of pelitic and tuffaceous? rocks with garnet, staurolite, chiastolite

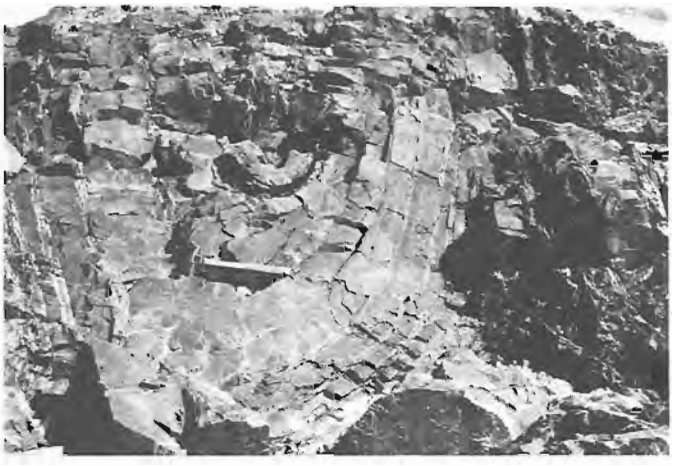

Figure 33.8. Early syncline-anticline pair plunging 35° away from the viewer in pelitic schist associated with quartzite (unit 5) of the Chantrey Group in Chantrey Inlet.

(Fig. 33.6) and cordierite. Minor components of the belt include quartz-eye schists (acid metavolcanics) and magnetite iron formation; amphibolite occurs towards the northeast. Also present locally are siliceous marble, white quartzite and metaconglomerate identical to rocks in the Chantrey belt. Although in part lithologically correlative with the Chantrey Group, the northern belt is generally more deformed and broken up by basement. In that respect it resembles the Chantrey belt in Montresor River area.

At Cape Hay, a few outcrops of coarse grained amphibolite, layered hornblende schists and minor acid metavolcanic interbeds are probably remnants of another NE-trending supracrustal belt, not exposed inland.

Dykes

Pegmatite dykes are common throughout the area and cut the supracrustal rocks in many places. Pegmatite intrusive into Chantrey rocks east of Chantrey Inlet yielded a muscovite K-Ar age of 1680 Ma (Heywood, 1961).

Diabase dykes are uncommon and poorly exposed. The aeromagnetic map of Lower Hayes River area indicates only one major dyke, running northwest from the southeast corner of the area. No outcrops of this dyke were found. A thin diabase dyke cuts the Chantrey belt along a NW-trending fault in the middle of segment 2.

In Darby Lake area, a large NW-trending diabase dyke is exposed cutting marble near the northern edge of the Chantrey belt. The diabase outcrops apparently owe their preservation to the resistant nature of the adjacent siliceous marble and calc-silicate rock.

Economic geology

No significant mineral showings of economic interest were found.

The rocks with the greatest potential for mineral exploration would appear to be those of the supracrustal belt north of the Chantrey belt and the dark pelitic schist (unit 6) of the Chantrey Group. The former include greenstone belt-type assemblages such as acid metavolcanics and iron formation. Pyritic shale, the inferred protolith of the Chantrey schist, is the major host of the Kupferschiefer and Zambian Copperbelt copper ores (Park and MacDiarmid, 1964).

References

Frisch, T. and Patterson, J.G.
1983: Preliminary account of the geology of the Montresor River area, District of Keewatin; in Current Research, Part A, Geological Survey of Canada, Paper 83-1A, p. 103-108.

Geological Survey of Canada
1977a: Lower Hayes River, District of Keewatin, Northwest Territories; Geophysical Series (Aeromagnetic), Sheet 56M; Geological Survey of Canada, Map 7675G.

1977b: Mistake River, District of Keewatin, Northwest Territories; Geophysical Series (Aeromagnetic), Sheet 56L; Geological Survey of Canada, Map 7653G.

Geological Survey of Canada (cont.)
1982: Surficial geology, Lower Hayes River, District of Keewatin; Geological Survey of Canada, Map 7-1981.

Heywood, W.W.
1961: Geological notes, northern District of Keewatin; Geological Survey of Canada, Paper 61-18, 9 p.

Park, C.F., Jr. and MacDiarmid, R.A.
1964: Ore Deposits; W.H. Freeman, San Francisco, 475 p.

Reineck, H.E. and Singh, I.B.
1980: Depositional Sedimentary Environments with Reference to Terrigenous Clastics, 2nd edition; Springer-Verlag, New York, 549 p.

PRE-CRETACEOUS TERRANES AND THEIR THRUST AND STRIKE-SLIP CONTACTS, PRINCE GEORGE (EAST HALF) AND MCBRIDE (WEST HALF), BRITISH COLUMBIA

Project 820014

L.C. Struik
Cordilleran Geology Division, Vancouver

Struik, L.C., Pre-Cretaceous terranes and their thrust and strike-slip contacts, Prince George (east half) and McBride (west half) map areas, British Columbia; in Current Research, Part A, Geological Survey of Canada, Paper 85-1A, p. 267-272, 1985.

Abstract

Prince George and McBride map areas are divided into five stratigraphically distinct terranes: Cache Creek, Quesnel, Slide Mountain, Barkerville, and Cariboo. Two structural successions of thrust-stacked terranes are separated by a southeast trending right-lateral strike-slip fault system along the Willow River. The western succession is capped by Quesnel, and the eastern by Slide Mountain Terrane. The floor thrust (Eureka Thrust) beneath Quesnel Terrane is cut by granite of the Naver pluton.

Résumé

Les régions cartographiées de Prince George et de McBride (moitié ouest) sont divisées en cinq terrains stratigraphiquement distincts: Cache Creek, Quesnel, Slide Mountain, Barkerville et Cariboo. Deux successions structurales de terrains chevauchés sont séparées par un réseau de failles à décrochements dextres latéraux à orientation sud-est le long de la rivière Willow. Le terrain de Quesnel recouvre la succession ouest et le terrain de Slide Mountain, la succession est. Le granite du pluton de Naver recoupe le chevauchement basal (chevauchement d'Eureka) sous le terrain de Quesnel.

Introduction

Mapping in Prince George (east half) and McBride (west half) map areas (Fig. 34.1) was undertaken to study the contacts between four terranes, Cariboo, Barkerville, Slide Mountain and Quesnel, which are thrust bounded in southwest McBride and northwest Quesnel Lake map areas (Struik, 1982, 1983a, b).

A system of right-lateral strike-slip faults along the Willow River separates two structural stacks of thrust imbricated terranes. The structural stacks have a common basement of metasedimentary and lesser amounts of metabasaltic rocks assigned to Barkerville Terrane. To the west the succession is capped by Quesnel Terrane phyllite and volcaniclastics floored by a thin serpentinite and amphibolite layer (Crooked Amphibolite) on the Eureka Thrust. To the east the top of the succession is Slide Mountain Terrane pillow basalt on the Pundata Thrust.

The similarity of structural stacking in the west (Crooked Amphibolite on Barkerville) and the east (Slide Mountain on Barkerville) led to an inferred correlation between the Crooked Amphibolite and Slide Mountain Terrane which had two implications. First, the Slide Mountain Terrane must have been in place prior to regional folding and metamorphism because the Crooked Amphibolite is folded and metamorphosed, locally to kyanite grade, along its entire length from Prince George to Crooked Lake in

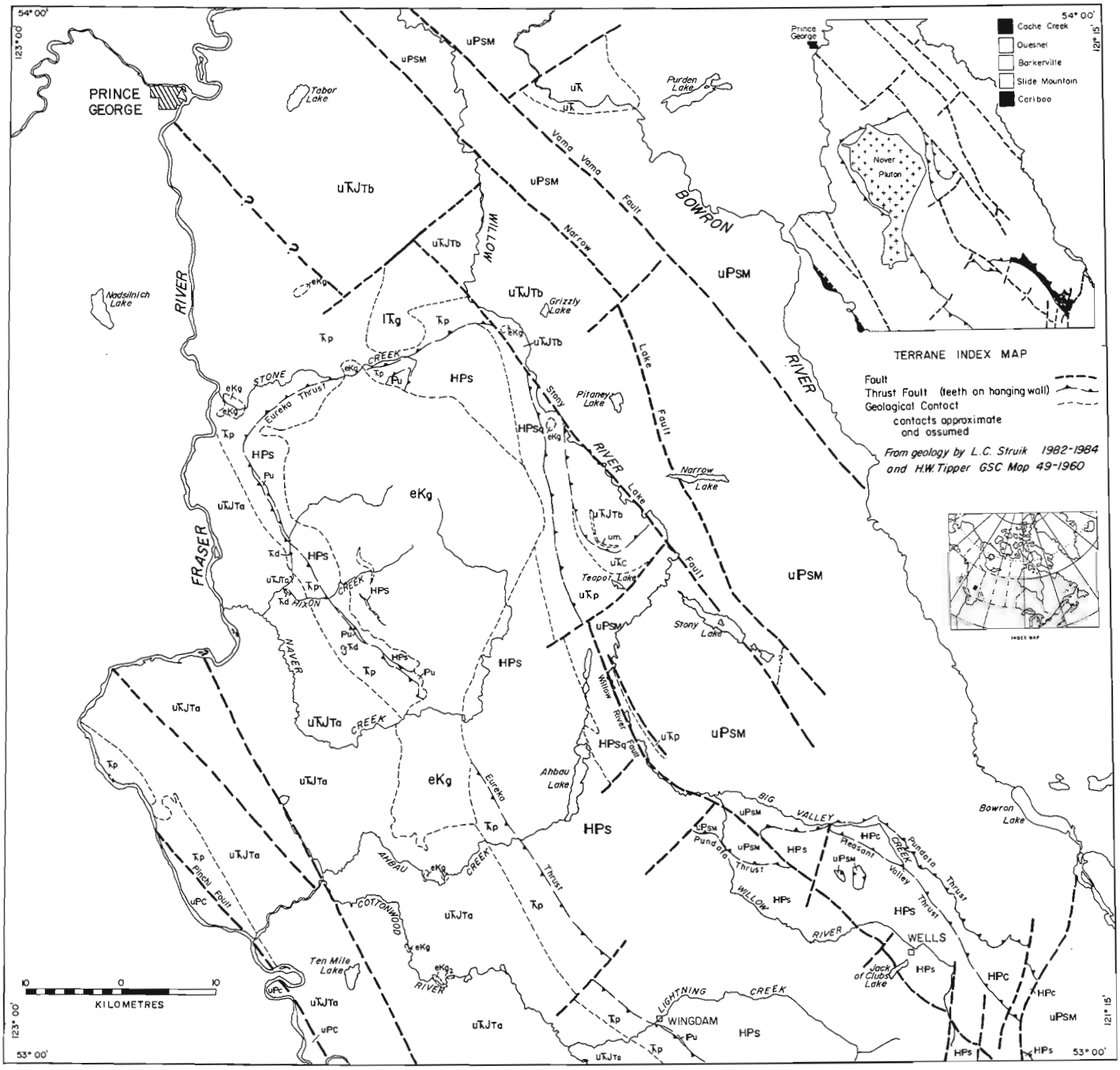

Figure 34.1. Pre-Cretaceous bedrock geology of Prince George east half and McBride west half map areas.

CACHE CREEK TERRANE

UPPER PALEOZOIC

uPc CACHE CREEK GROUP; basalt, chert

QUESNEL TERRANE

UPPER TRIASSIC AND/OR LOWER JURASSIC

Ʀd diorite

uƦJTb greywacke, siltstone, minor conglomerate

uƦJTa andesitic volcaniclastics, greywacke, slate

UPPER TRIASSIC

uƦc sandy limestone, limestone

uƦp siltite, pelite, limestone, minor bioclastic limestone

MIDDLE AND UPPER TRIASSIC

Ʀp phyllite, slate

UPPER PALEOZOIC?

Pu CROOKED AMPHIBOLITE; serpentinite, amphibolite

SLIDE MOUNTAIN TERRANE

UPPER TRIASSIC

uƦ shale, sandstone

UPPER PALEOZOIC

uPsM SLIDE MOUNTAIN GROUP; basalt, chert

BARKERVILLE TERRANE

HADRYNIAN AND PALEOZIC

SNOWSHOE GROUP

HPs undifferentiated grit, pelite, marble

HPsq grit, quartzite

CARIBOO TERRANE

HADRYNIAN AND PALEOZOIC

HPc CARIBOO GROUP; BLACK STRUART GROUP; WAVERLY, GUYET, GREENBERRY, AND ALEX ALLAN FORMATIONS

INTRUSIVE ROCKS

LOWER CRETACEOUS

eKg porphyritic granite

JURASSIC OR YOUNGER

um ultramfic intrusive

LOWER TRIASSIC

lƦg porphyritic granite

Quesnel Lake map area. Second, the Slide Mountain Terrane (represented by the Crooked Amphibolite) must thin to the west (it is locally missing) where it theoretically roots.

The differences in thickness, metamorphic grade, and structural fabric in these two suites preclude unqualified correlation, especially in view of the lack of a physical link between them within the map area.

The Naver Pluton, granite to granodiorite in composition, transects the Eureka Thrust along Naver Creek. The pluton twice dated by K-Ar on biotite yielded an average age of 105 Ma (Tipper et al., 1979), thereby providing a minimum age for the thrust.

Strike-slip displacement throughout the study area is part of the strike-slip system bounding the western flank of the northern Rocky Mountain Trench and as such indicates that the faults continue to the southeast from where they were described by Gabrielse (in press). The system is not trending into the Fraser Fault, but rather, parallels the regional southeasterly trend of the Shuswap Metamorphic Complex as suggested by Gabrielse (in press); implying that hundreds of kilometres of transcurrent displacement is accomodated throughout the Cariboo Mountains and Quesnel and Shuswap highlands.

Terranes

Prince George (east half) and McBride (west half) map areas are divided into five stratigraphically different terranes; from west to east they are Cache Creek, Quesnel, Slide Mountain, Barkerville and Cariboo (Fig. 34.1). A synopsis of the stratigraphy is given only where the interpretation varies from previous work or is useful background for the structural history. Rocks of Cariboo Terrane were described in Struik (1981, 1982).

Quesnel Terrane

For the purpose of this paper the Quesnel Terrane is divided into seven rock units (Fig. 34.1), from oldest to youngest: 1) Crooked amphibolite, 2) black pelite, 3) siltite, 4) limestone, 5) volcaniclastics, 6) greywacke, and 7) diorite. Whether the Crooked Amphibolite is actually stratigraphically linked to the overlying rocks of Quesnel Terrane is questionable.

Crooked amphibolite. Named after Crooked Lake in Quesnel Lake map area, this unit consists of serpentinite and amphibolite. The two rock types do not occur together but occupy the same structural position between Quesnel and Barkerville terranes. Talc is commonly found with the serpentinite. Tipper (1960) did not differentiate this unit from others in Prince George map area.

The serpentinite consists of irregular masses and prisms of serpentine which generally show no foliation or other regular structure. The amphibolite on the other hand consists mainly of foliated prismatic actinolite and hornblende crystals, less than 2 mm long. The unit is less than 200 m thick and commonly less than 60 m thick near Hixon Creek.

Black pelite. Black fine grained clastics and limestone that overlie the Crooked amphibolite are similar to those in the same structural position near Quesnel and Cariboo lakes where they have been tentatively dated as Middle and Late Triassic from extracted conodonts examined by M.J. Orchard (personal communication, 1984). They may be confused with younger black fine grained clastics of Quesnel Terrane or the upper part of the Snowshoe Group of Barkerville Terrane.

The unit underlies the area from Prince George to Wingdam in a thin belt. Tipper (1960) included these rocks in the Cariboo Group, however, in more recent maps (Tipper et al., 1979; Tipper et al., 1980) he placed them in an unnamed Upper Triassic unit. Within Prince George east half, the pelites are in chlorite to biotite grade of metamorphism. The thickness is unknown and the upper and lower contacts have not been seen.

Siltite. This unit consists of black siltite, pelite and limestone. It is distinguished from the black pelite unit by being more quartz rich and having abundant interbeds of graphitic black micritic limestone and locally grey bioclastic limestone.

It outcrops along the Willow River north of Teapot Lake and was included by Tipper et al. (1979) in an unnamed Upper Triassic black phyllite unit. The lower contact appears abruptly gradational (tectonic?) with grit of the Snowshoe Group southwest of Teapot Lake. The siltite is tentatively dated as Late Triassic from conodonts extracted from the bioclastic limestone (M.J. Orchard, personal communication, 1984).

Limestone. This unit consists of grey and light grey finely crystalline limestone and sandy limestone. It is distinguished from the darker limestone of the siltite unit by its colour, well defined thin bedding and ripple laminations.

The limestone is restricted to the hill north of Teapot Lake where it overlies the siltite unit. It was included by Tipper (1960) in unit 6a. Its lower and upper contacts were not seen.

Volcaniclastics. This unit consists of andesitic volcaniclastics, greywacke and slate. They are distinguished from rocks of the Slide Mountain Terrane by the lack of pillow basalt and ribbon chert and the well defined bedding of the volcaniclastics. Isolated exposures of the unit may be confused with the fragmental component of the Slide Mountain Terrane.

The sequence is found west of the black pelite unit. It was mapped as part of unit 6a in Tipper (1960) and part of the Takla Group in Tipper et al. (1979, 1980). Contact relationships with the black pelite and greywacke units are unknown.

Greywacke. This unit consists of grey and olive-grey, commonly fine grained greywacke, grey and dark grey siltstone and argillite, and minor conglomerate and tuff. Its thin, well bedded character, common ripples, grading and cross-stratification distinguish the unit from others within the terrane.

It is well exposed east of Prince George near Tabor Mountain. It was included by Tipper (1960) in unit 6a and Tipper et al. (1979) in a Jurassic sandstone and an Upper Triassic unit. It is assigned to the Upper Triassic because it is similar to Upper Triassic greywacke and siltstone of Dragon Lake near Quesnel (Struik, 1984).

Diorite. The unit consists of diorite, distinguished from that of the Slide Mountain Group by its lack of pyroxene, and outcrops on Government, Hixon and Terry creeks. It intrudes the black pelite and volcaniclastic units.

At Terry Creek it consists of hornblende and plagioclase with lesser amounts of quartz and sphene. Common alteration products are epidote, white mica, chlorite and albite. The hornblende is mainly prismatic.

Slide Mountain Terrane

Slide Mountain Terrane consists of mainly pillow basalt and chert of the Slide Mountain Group. In most places the predominance of pillow basalt and ribbon chert distinguish it from the mostly fragmental volcanics of Quesnel Terrane, but those criteria are useless along the western margin of Slide Mountain Terrane near Teapot Lake where agglomerates and fragmental rocks predominate. There, however, the presence of local pillow basalt and the absence of well bedded fragmental rocks distinguished the Slide Mountain Group from the Quesnel Terrane volcaniclastics.

Tipper et al. (1979) showed the Slide Mountain Group overlain by Upper Triassic sediments along the Bowron River. If the contact is stratigraphic the sediments would be part of Slide Mountain Terrane and are included therein for lack of opposing data.

Barkerville Terrane

The Barkerville Terrane consists of the Snowshoe Group (Struik, 1983a, b) of which one grit unit is herein described.

Grit. Grit, quartzite and pelite are differentiated from the Snowshoe Group because they are less micaceous, thereby being more resistant. The grit and quartzite are light grey and weather light grey to white. The pelite is olive-grey and grey and varies from garnet to biotite bearing.

Intrusive rocks of uncertain terrane affinity

Three units of intrusive rocks are described separately from the terranes because they either postdate the emplacement of the terranes or their affinities are uncertain.

Lower Triassic porphyritic hornblende granite west of Grizzly Lake has been isotopically dated as 176 Ma (see the Parsnip River map by Tipper et al., 1979). Except that the granite is hornblende-bearing rather than biotite-bearing, it is identical to the Naver pluton to the south. The Naver pluton, however, is dated as approximately 105 Ma.

A pyroxenite dyke(?), which seems to intrude Quesnel Terrane north of Teapot Lake, contains well formed pyroxene crystals up to 3 cm long. The crystals show no macroscopic tectonic fabric.

Lower Cretaceous granite of the Naver pluton is exposed between Stone and Ahbau creeks. It consists of biotite granodiorite to granite with potassium feldspar megacrysts. It is locally sheared and partly epidotized.

Structure

Layer-parallel faults separate four of the five terranes in the area: Quesnel, Slide Mountain, Barkerville, and Cariboo. The Cache Creek Terrane in contrast is separated from Quesnellia by a steeply dipping strike-slip fault. The moderately dipping faults showing components of strike-slip may be younger than the thrusts; however, timing is not well understood.

Terrane boundaries

Eureka Thrust. The Eureka Thrust (Struik, 1983b) separates Quesnel Terrane in the hanging wall from Barkerville Terrane in the footwall. The thrust is marked by discontinuous serpentinite and amphibolite of the Crooked amphibolite, which is never more than 200 m thick in the Prince George and McBride map areas. Metasediments of Barkerville Terrane are invariably sheared at the thrust contact, from mylonite to variably cataclastic.



Figure 34.2. *Stretched and compressed, partly spherulitic pillow basalt of Slide Mountain Terrane near the Willow River Fault. Note the planar fabric and the distended light coloured spherulites. The mineralogy of the rock is entirely secondary, consisting mainly of chlorite, epidote, albite, and white mica.*



Figure 34.3. *Cataclastic flow fabric in deformed basalt of Slide Mountain Terrane in the Willow River Fault near Pig Valley Creek. Note the extension features exemplified by the boudinage structure.*

The sediments of Quesnel Terrane are tightly folded, locally refolded, but generally are not sheared as intensely as the metasediments of Barkerville Terrane.

The Crooked amphibolite is exposed locally along the western margin of Barkerville Terrane, but has not been found along the eastern contact between Quesnel and Barkerville terranes. The structural sequence at Teapot Lake suggests that Quesnel is thrust onto Barkerville Terrane, but the bounding rocks show no obvious evidence of the event. The black calcareous phyllite unit at the base of Quesnel Terrane appears to be interlayered with Snowshoe Group dark grey grit.

Pundata Thrust. The Pundata Thrust, described in Struik (1981), separates the Antler Formation of Slide Mountain Terrane from the underlying Barkerville Terrane and is exposed in the southeast of the map area. In contrast to the Eureka Thrust the Pundata cuts relatively brittle rocks.

Pleasant Valley Thrust. The Pleasant Valley Thrust is a ductile fault separating Cariboo from underlying Barkerville Terrane in the southeast. It is moderately east-dipping and classified as a thrust fault becauuse it puts older over younger in the vicinity of Wells.

Strike-Slip Faults

Several moderately to steeply dipping faults are classified as strike-slip from their fabric geometry. Features such as extension parallel to the strike of the faults (Fig. 34.2) and the geometry of deformed inclusions indicate subhorizontal movement in a right-lateral displacement. The surface expression of the faults are tens of kilometres long and marked by prominent lineaments. For example, the Narrow Lake Fault is represented by the west-facing mountain front of Slide Mountain basalt against the low-lying drift-covered Willow River valley. As a system, the faults transect the map area on a northwest trend. They are not simple strike-slip faults, but are transpressional and ductile. Their mineral fabrics indicate intense cataclasis (Fig. 34.3) locally mylonitization. Though they are thought to crosscut the terrane boundary thrust faults there is some question as to whether the Willow River Fault, for instance, cuts the Pundata Thrust or passes into it, and thereby being one and the same.

The Narrow Lake-Stoney Lake-Willow River faults separate Quesnel from Slide Mountain Terrane. There is no typical Quesnel Terrane rock east of the fault system. The Slide Mountain Terrane on the Willow River near Big Valley Creek seems to be structurally the farthest west, but, that rests on the validity of the interpretation that the Pundata Thrust is not the continuation of the Willow River Fault.

The Willow River Fault system records transpressional displacements that offset and penetrate the Barkerville, Slide Mountain and Cariboo terranes to the southeast.

References

Gabrielse, H.
– Major dextral transcurrent displacements along the northern Rocky Mountain Trench and related lineaments in north-central British Columbia; Geological Society of America bulletin. (in press)

Struik, L.C.
1981: A re-examination of the type area of the Devono-Mississippian Cariboo Orogeny, central British Columbia; Canadian Journal of Earth Sciences, v. 18, p. 1767-1775.

1982: Bedrock geology of Cariboo Lake (93A/14), Spectacle Lake (93H/3), Swift River (93A/13) and Wells (93H/4) map areas, central British Columbia; Geological Survey of Canada, Open File 858.

Struik, L.C. (cont.)
1983a: Bedrock geology of Spanish Lake (93A/11) and parts of adjoining map areas, central British Columbia; Geological Survey of Canada, Open File 920.

1983b: Bedrock geology of Quesnel Lake (93A/10) and part of Mitchell Lake (93A/15) map areas, central British Columbia; Geological Survey of Canada, Open File 962.

1984: Stratigraphy of Quesnel Terrane near Dragon Lake, Quesnel map area, central British Columbia; in Current Research, Part A, Geological Survey of Canada, Paper 84-1A, p. 113-116.

Tipper, H.W.
1960: Prince George map area, Cariboo District, British Columbia; Geological Survey of Canada, Map 49-1960.

Tipper, H.W., Campbell, R.B., Taylor, G.C., and Stott, D.F.
1979: Parsnip River, British Columbia; Geological Survey of Canada, Map 1424A.

Tipper, H.W., Woodsworth, G.J., and Gabrielse, H.
1980: Tectonic assemblage map of the Canadian Cordillera and adjacent parts of the United States of America; Geological Survey of Canada, Map 1505A.

GEOLOGY OF THE HEADWATERS OF WILSON CREEK, LARDEAU MAP AREA, SOUTHEASTERN BRITISH COLUMBIA

Project 790041

D.W. Klepacki[1], P.B. Read[2], and J.O. Wheeler
Cordilleran Geology Division, Vancouver

Klepacki, D.W., Read, P.B., and Wheeler, J.O., Geology of the headwaters of Wilson Creek, Lardeau map area, southeastern British Columbia; in Current Research, Part A, Geological Survey of Canada, Paper 85-1A, p. 273-276, 1985.

Abstract

Structures and stratigraphy, particularly for the three assemblages of the Upper Mississippian and Lower Pennsylvanian Milford Group, have been traced from the Goat Range northwestward through upper Wilson Creek into Poplar Creek map area. Davis sedimentary assemblage lies east of Schroeder-Spyglass Fault. Keen Creek volcanic assemblage, west of this fault, unconformably overlies lower Paleozoic Lardeau Group within a window beneath Stubbs Fault. Much of the window and both faults are intruded by McKian Creek Stock. McHardy siliceous argillite assemblage, above Stubbs Fault, is cut by another thrust fault folded by Cascade Mountain Anticline in Poplar Creek area. Coarse conglomerate within the anticline was apparently derived in Late Mississippian time from a nearby source in the Lardeau Group. Near Kuskanax Batholith McHardy assemblage is separated by a zone of ultramafics (probably marking the location of Whitewater Fault) from the overlying amphibolite and minor pelitic schist which are correlated with the Lower Permian and (?)Carboniferous Kaslo and Upper Triassic Slocan groups, respectively.

Résumé

On a découvert les structures et la stratigraphie, notamment des trois assemblages du groupe de Milford du Mississipien supérieur et du Pennsylvanien inférieur, à partir du chaînon Goat vers le nord-ouest, en passant par la partie amont du ruisseau Wilson, jusque dans la région cartographiée du ruisseau Poplar. L'assemblage sédimentaire de Davis se trouve à l'est de la faille Schroeder-Spyglass. L'assemblage volcanique de Keen Creek est situé à l'ouest de cette faille et repose en discordance sur le groupe de Lardeau du Paléozoïque inférieur à l'intérieur d'une fenêtre tectonique sous la faille de Stubbs. Le massif de McKian Creek a pénétré les deux failles et une grande partie de cette fenêtre tectonique. L'assemblage d'argilite siliceuse de McHardy, qui est sus-jacente à la faille de Stubbs, est coupé par une autre faille de chevauchement qui a été plissée par l'anticlinal de la chaîne des Cascades dans la région de Poplar Creek. Un conglomérat à grain grossier à l'intérieur de l'anticlinal date du Mississipien récent et est vraisemblablement dérivé d'une source voisine dans le groupe de Lardeau. Près du batholite de Kuskanax, une zone de roches ultramafiques (qui marque vraisemblablement l'emplacement de la faille de Whitewater) sépare l'assemblage de McHardy des amphibolites et des schistes pélitiques secondaires sus-jacents qui ont été mis en corrélation avec les groupes de Kaslo du Permien inférieur et du (?)Carbonifère et le groupe de Slocan du Trias supérieur respectivement.

[1] Department of Earth, Atmospheric and Planetary Sciences, Massachusetts Institute of Technology, Cambridge, MA, U.S.A. 02139
[2] Geotex Consultants, Ltd., 100 West Pender St., Vancouver, British Columbia, V6B 1R8

Introduction

Two weeks of field work in 1984 in the headwaters of Wilson Creek were devoted to tracing rock units and structures mapped in the Goat Range study area (Klepacki and Wheeler, 1985) into Poplar Creek map area (Read, 1973; Fig. 35.1). Stratigraphy worked out in the less-deformed Goat Range study area, particularly in the western assemblages of the Milford Group, enabled a better resolution of the complicated map pattern worked out by Read (1973) in southwestern Poplar Creek map area and the recognition there of faults mapped earlier in the Goat Range.

Stratigraphy

The oldest rocks in the Wilson Creek (Fig. 35.2) area are grit, pelitic schist and minor calc-schist of the Broadview Formation. The exposures north of McKian Creek stock, unit 9a of Read (1973), were found to extend into the west wall of Wilson Creek.

The western assemblages of the Milford Group consist of the Keen Creek and McHardy assemblages. The Keen Creek assemblage, in the Goat Range south of McKian Creek stock, lies unconformably on the Broadview Formation (Klepacki and Wheeler, 1985). The assemblage consists essentially of two tholeiitic volcanic units (and related sediments) separated by a limestone unit yielding Late Mississippian and Early Pennsylvanian conodonts (Orchard, 1985). Sparse conglomerate occurs at the base of the assemblage. During the present study units of the Keen Creek assemblage were traced into the west wall of Wilson Creek valley west of McKian Creek stock. Volcanic and volcaniclastic units north of Keen Creek grade westward into rusty weathering quartz-plagioclase-biotite-muscovite-chlorite schists where they include some quartzite beds west of Wilson Creek. Amphibolite persists near the base of the assemblage. Limestone grades west of Wilson Creek into quartz-plagioclase-carbonate-biotite-actinolite granulite. The Keen Creek assemblage has also been identified north of McKian Creek stock in Poplar Creek map area. There, basal clastics composed of fine grained Broadview detritus also lie unconformably on the Broadview Formation. The succession above the basal beds, which is similar to the Keen Creek assemblage to the south, comprises two volcanic units and related sediments – units 13a, 13b and 19 of Read (1973) – separated by limestone (unit 14).

The McHardy assemblage in the Goat Range area is predominantly bedded, cherty or siliceous argillite underlain by a sequence, in descending order, of: dark grey limestone and white marble, boulder conglomerate and metagreywacke, and pink tuffaceous metasandstone. The limestone has yielded Upper Mississippian conodonts (Orchard, 1985). The conglomerate, 1500 m northwest of Mount Cooper, consists of diorite, mafic volcanic and rare granite boulders dated by U-Pb methods on zircons as Ordovician (Okulitch et al., in prep.). The McHardy assemblage commonly contains bodies of amphibolite and equigranular and porphyritic hornblende diorite of late Paleozoic age (Klepacki and Wheeler, 1985).

Siliceous argillite, diorite and amphibolite of the McHardy assemblage has been traced from the Goat Range area around the western and northern sides of McKian Creek stock into the Poplar Creek map area. There, west of the Spyglass Fault, the McHardy assemblage comprises unit 15 of Read (1973) as well as abundant limestone (unit. 14). The stratigraphic section beneath the limestone in the anticline south of Cascade Mountain is similar to that in the McHardy assemblage northwest of Mount Cooper. In particular it includes conglomerate similar to the conglomerate near Mount Cooper and contains boulders of quartz-pebble conglomerate, gneiss (with the foliation at an angle to the foliation in the matrix), greywacke, blue-quartz-granule grit identical to that in the Broadview Formation, and minor volcanics and diorite. The composition of the conglomerate suggests that a source in the Broadview and other units of the Lardeau Group was nearby.

A belt of amphibolite along the southeastern margin of the Kuskanax Batholith contains deformed pillows and is bounded on the southeast by one or two narrow zones of serpentinite, talc schist and equigranular diorite bodies (unit 13d of Read, 1973). These rocks are considered to be correlative with the upper plate units of the Lower Permian and (?)Carboniferous Kaslo Group in the Goat Range area. There they are floored by serpentinite along the Whitewater Fault which is intruded by the Early Permian Whitewater diorite (Klepacki and Wheeler, 1985).

Grey pelitic schist (unit 17 of Read, 1973) bordering the Kuskanax Batholith and overlying the amphibolite probably belongs to the Slocan Group on the basis of relationships in the Goat Range area where the Upper Triassic Slocan Group lies above and is deformed with the Kaslo Group. The intervening Lower Permian Marten conglomerate (Klepacki and Wheeler, 1985) was not observed in the Wilson Creek area.

Structure

Several of the major structures of the Goat Range area can be either traced into or identified within the Poplar Creek map area. These include the Stubbs and Whitewater thrust faults and the Schroeder west-dipping normal fault and its apparent continuation as the Spyglass Fault.

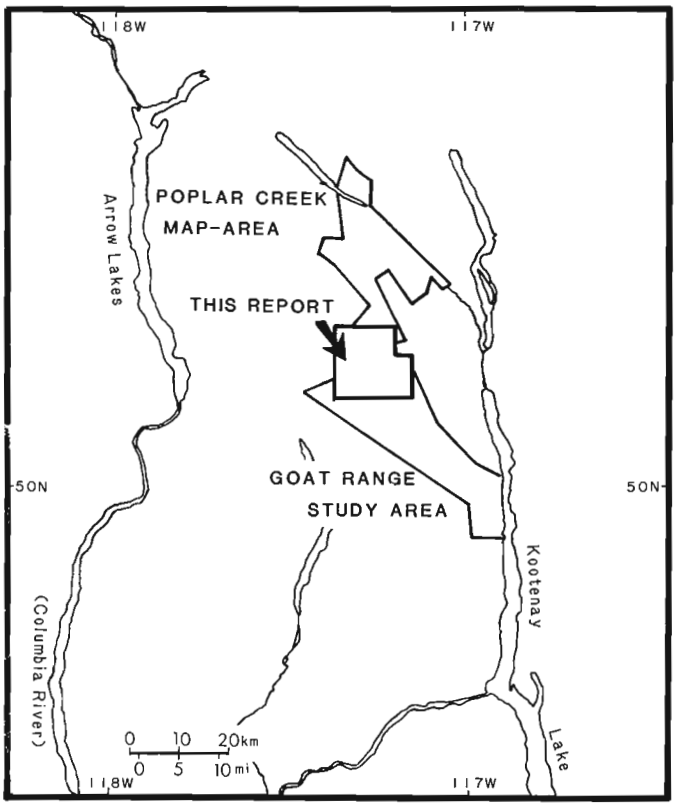

Figure 35.1. *Location of the area of detailed mapping around Wilson Creek headwaters, the Poplar Creek area mapped by Read (1973) and the Goat Range area mapped by Klepacki (Klepacki and Wheeler, 1985).*

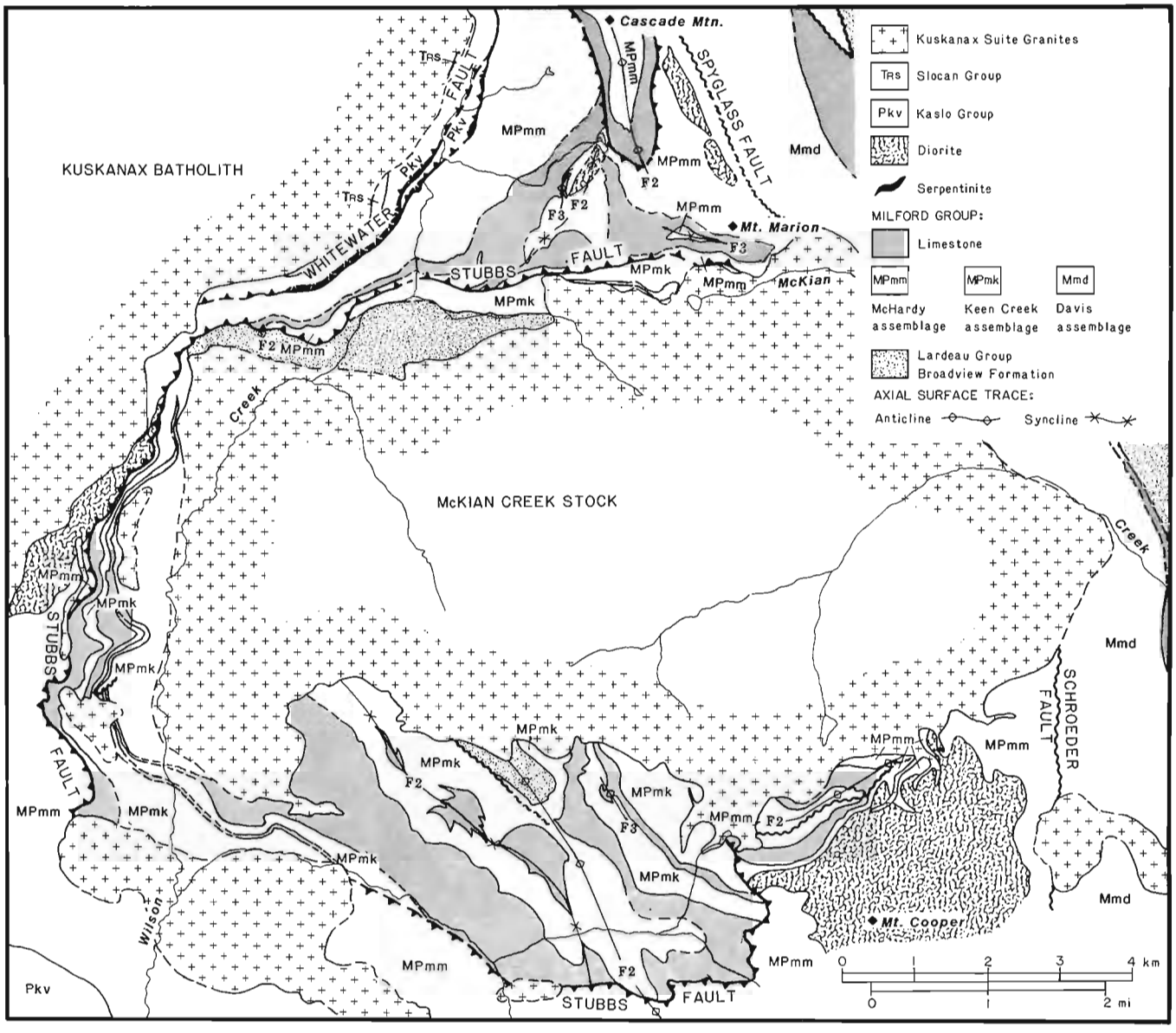

Figure 35.2. *Geological map of the headwaters of Wilson Creek.*

In the Goat Range area the McHardy assemblage and the overlying Kaslo and Slocan groups have been thrust over the Keen Creek assemblage along the Stubbs Fault. It was subsequently intruded by Middle Jurassic granitic plutons. The Stubbs Fault was traced from the Goat Range around the McKian Creek stock. The fault is recognized by the way it separates the Keen Creek and McHardy assemblages and truncates units within them both above and below the fault. It appears that the McKian Creek stock arched the thrust surface upon intrusion into all the assemblages of the Milford Group resulting in the exposure of the Keen Creek assemblage and the underlying Broadview Formation in a window flanking the McKian Creek stock.

The association of serpentinite, talc schist and diorite along the southeastern border of the "Kaslo" amphibolite southeast of Kuskanax Batholith suggests the location there of the Whitewater Fault and related splays. In the Goat Range the Whitewater Fault thrusts the upper plate of the Kaslo Group, floored by ultramafics, over the lower plate of the Kaslo Group underlain by the McHardy assemblage. It appears, therefore, that in Poplar Creek map area the lower plate of the Kaslo Group is missing and that its upper plate is thrust directly onto the McHardy assemblage.

The fold south of Cascade Mountain is interpreted as an anticline rather than a synform (Read, 1973) for the following reasons. The stratigraphic succession within the core of the fold, when compared with the similar succession northwest of Mount Cooper where the facing direction is known, suggests that the fold is an anticline. In addition, southeast-plunging minor folds on the limbs suggest that the fold is a southeast-plunging anticline not a synform. The fold also exposes a folded thrust in the saddle between Cascade Mountain and Mount Marion which repeats the section and truncates the McHardy limestone above the fault.

The limestone units of the Milford Group trace out a series of folds in the Wilson Creek area. Fabrics and fold interference patterns support the chronology of deformation worked out by Read (1973). F_1 folds are restricted to the Lardeau Group. F_2 folds are the earliest folds recognized in

Upper Mississippian and younger rocks. The foliation in these rocks is axial planar to these folds. F_2 folds generally have an "N"-shaped profile when viewed towards the north. F_3 folds are generally tight mesoscopic and macroscopic folds with a reversed "N" profile looking north. A fourth folding episode, locally well developed in the Goat Range area (Klepacki and Wheeler, 1985) but weakly developed in the Poplar Creek map area (Read, 1973, p. 59), has a similar profile to F_3 and may occur at Cascade Mountain. There the axial surface of the Cascade Mountain anticline changes from nearly vertical south of Cascade Mountain to easterly dipping near the summit.

Summary

The stratigraphy of the Goat Range study area, especially the revised upper Paleozoic Milford and Kaslo groups and their associated faults, were traced northward through Wilson Creek area into the Poplar Creek map area. This now provides a basis for re-interpreting the upper Paleozoic stratigraphy and for identifying the related faults farther northwest in the Poplar Creek area.

References

Klepacki, D.W. and Wheeler, J.O.
1985: Stratigraphic and structural relation of the Milford, Kaslo and Slocan groups, Goat Range, Lardeau and Nelson map areas, British Columbia; in Current Research, Part A, Geological Survey of Canada, Paper 85-1A, Report 36.

Okulitch, A.V., Read, P.B., Wanless, R.K., and Loveridge, W.D.
Paleozoic plutonism in southeastern British Columbia; (in prep.).

Orchard, M.J.
1985: Carboniferous, Permian and Triassic conodonts from the central Kootenay Arc: constraints on the age of the Milford, Kaslo, and Slocan groups; in Current Research, Part A, Geological Survey of Canada, Paper 85-1A, Report 37.

Read, P.B.
1973: Petrology and structure of Poplar Creek map area, British Columbia; Geological Survey of Canada, Bulletin 193, 144 p.

STRATIGRAPHIC AND STRUCTURAL RELATIONS OF THE MILFORD, KASLO AND SLOCAN GROUPS, GOAT RANGE, LARDEAU AND NELSON MAP AREAS, BRITISH COLUMBIA

Project 790041

D.W. Klepacki[1] and J.O. Wheeler
Cordilleran Geology Division, Vancouver

Klepacki, D.W. and Wheeler, J.O., Stratigraphic and structural relations of the Milford, Kaslo and Slocan groups, Goat Range, Lardeau and Nelson map areas, British Columbia; in Current Research, Part A, Geological Survey of Canada, Paper 85-1A, p. 277-286, 1985.

Abstract

Mapping of upper Paleozoic rocks was continued in order to understand the relationships between the Cordilleran accreted terranes and ancestral North America. The Upper Mississippian and Lower Pennsylvanian Milford Group comprises three assemblages linked by Early Namurian limestones. The eastern, sedimentary Davis assemblage and the central, tholeiitic Keen Creek assemblage both lie with angular unconformity on the lower Paleozoic Lardeau Group. Siliceous argillite of the western, McHardy assemblage is thrust eastward along Stubbs Fault over the Keen Creek assemblage. The overlying tholeiites and conodont-bearing cherty tuff of the Lower Permian and (?)Carboniferous Kaslo Group are repeated by the Early Permian Whitewater Thrust Fault. Diorite intruding the fault is overlain unconformably by the Lower Permian Marten conglomerate in turn succeeded by Upper Triassic sediments of the Slocan Group. All map units and related thrust faults were folded by Dryden Anticline which was later cut by Schroeder normal fault before intrusion of Middle Jurassic granites.

Résumé

On a continué de cartographier les roches du Paléozoïque supérieur afin de mieux comprendre les liens qui existent entre les terrains accumulés dans la Cordillère et l'Amérique du Nord primitive. Le groupe de Milford du Mississipien supérieur et du Pennsylvanien inférieur se compose de trois assemblages reliés par les calcaires du Namurien ancien. L'assemblage sédimentaire de Davis, à l'est, et l'assemblage tholéiitique de Keen Creek, au centre, reposent en discordance angulaire sur le groupe de Lardeau du Paléozoïque inférieur. L'argilite siliceuse de l'assemblage de McHardy, qui est situé à l'ouest, a été poussée vers l'est sur l'assemblage de Keen Creek, le long de la faille de Stubbs. Les tholéiites et les tufs siliceux à conodontes sus-jacents du groupe de Kaslo du Permien inférieur et du (?)Carbonifère sont reproduits par la faille chevauchante de Whitewater du Permien ancien. La diorite qui a fait intrusion dans la faille est recouverte en discordance par le conglomérat de Martin du Permien inférieur qui, à son tour, est recouvert par les sédiments du groupe de Slocan du Trias supérieur. Toutes les unités cartographiques et les failles chevauchantes connexes ont été plissées par l'anticlinal de Dryden que la faille normale de Schroeder a par la suite recoupé avant l'intrusion des granites du Jurassique moyen.

[1] Department of Earth, Atmospheric and Planetary Sciences, Massachusetts Institute of Technology, Cambridge, MA, U.S.A. 02139

Introduction

The Milford, Kaslo, and Slocan groups comprise sedimentary and volcanic assemblages deposited along and west of the North American continental margin from late Paleozoic to early Mesozoic time. The volcanic, ultramafic and related sedimentary rocks of Kaslo Group form part of the Eastern Assemblage of Monger et al. (1982) where they form the leading edge of the Cordilleran accreted terranes. Phyllite, limestone, calcareous flysch, and quartzite of Slocan Group are part of Quesnellia terrane lying directly west of the Eastern Assemblage. The purpose of this project is to examine in central Kootenay Arc the stratigraphic and structural relationships between the leading edge of the accreted terranes and the autochthonous rocks of ancestral North America.

Mapping from the 1982 field season (Klepacki, 1983) in the Goat Range study area (Fig. 36.1) was extended southeast in 1983 to connect with Ainsworth area (Fyles, 1967) and to the northwest, nearly to the Poplar Creek map area (Read, 1973). This report incorporates ages of rock units assigned from microfossils identified by M.J. Orchard (Orchard, 1985) from collections made by J.O. Wheeler in 1965, 1967, 1980 and 1981, by A.V. Okulitch in 1976, by P.B. Read in 1976 and 1978, by M.J. Orchard in 1981 and by D.W. Klepacki in 1982 and 1983.

The principal results of the 1983 field season include:

1. Milford Group can be divided into three structurally discrete, stratigraphic assemblages; an eastern (Davis) assemblage of limestone, clastic and volcanic rocks, a central (Keen Creek) assemblage of limestone, pillowed tholeiitic volcanics and volcaniclastic rocks, and a western (McHardy) assemblage of cherty sediments and minor volcanic rocks and limestone (Fig. 36.2).
2. A panel comprising the McHardy assemblage and the Kaslo and Slocan groups has been thrust along the Stubbs Fault over the Keen Creek assemblage which lies unconformably on the Lardeau Group.
3. A thrust fault within the Lardeau Group places Index and Jowett formations on top of the Broadview Formation and this thrust is truncated by the unconformity at the base of the Milford Group (Davis assemblage).
4. Thrusting within Kaslo Group and intrusion of diorite bodies occurred in Early Permian time.
5. Fault panels mapped in Ainsworth area (Fyles, 1967) contain stratigraphy similar to that identified in the study area, and faults bounding these panels splay off the Schroeder Fault.

Stratigraphy

Hamill Group

The oldest and structurally lowest rocks of the study area are pegmatitic mica schist and gneiss, grey quartzite, and micaceous quartzite mapped as Lower Cambrian Hamill Group by Fyles (1967). This unit occurs along the shore of Kootenay Lake, at the southeastern edge of the study area (Fig. 36.3).

Badshot Formation

Coarsely crystalline white marble mapped as Badshot Formation outcrops sporadically at low elevations east and north of Mount Buchanan. Fyles (1967) mapped this unit as Lower Cambrian Badshot Formation because it overlies quartzite of the Hamill Group and underlies calcareous schist of Lardeau Group.

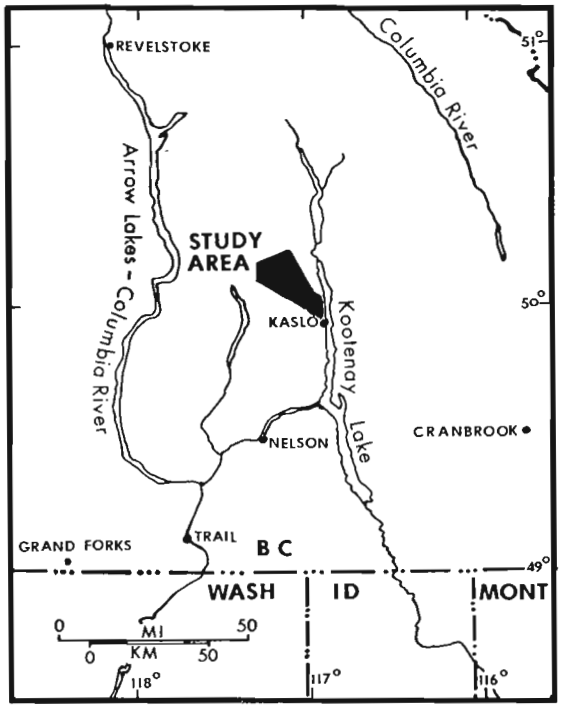

Figure 36.1. Location map of the Goat Range study area.

Lardeau Group, Index Formation

The stratigraphy of Lardeau Group is based on work farther north (Fyles, 1964; Read and Wheeler, 1976). Indicators of stratigraphic tops are scarce in the Lardeau Group in the study area but, where present, support the stratigraphic order outlined by earlier workers. Calc-silicate gneiss, quartzofeldspathic biotite-muscovite schist, and garnet-biotite schist and gneiss form the Index Formation. A white marble underlying the volcanic Jowett Formation is interpreted as Index Formation but may be Badshot marble. Index Formation is mapped along the southeastern margin of the study area.

Lardeau Group, Jowett Formation

Pyroxene-porphyry pillow lava, greenstone, and chlorite phyllite and schist are mapped as Jowett Formation. The unit forms two discontinuous belts: an upper belt which lies below the unconformity at the base of Milford Group and is locally truncated by it; and a lower belt which outcrops along the 5000-foot high ridge extending northeast from Milford Peak, 7.5 km north of Mount Buchanan. The Jowett Formation contains xenoliths of the underlying white marble thereby demonstrating that the strata face west.

Lardeau Group, Broadview Formation

Grey mica phyllite and schist, quartz-pebble conglomerate and blue-quartz-granule grit make up the Broadview Formation. The unit outcrops along the northeastern margin of the study area and northwest of Mount Cooper below the Keen Creek assemblage of Milford Group.

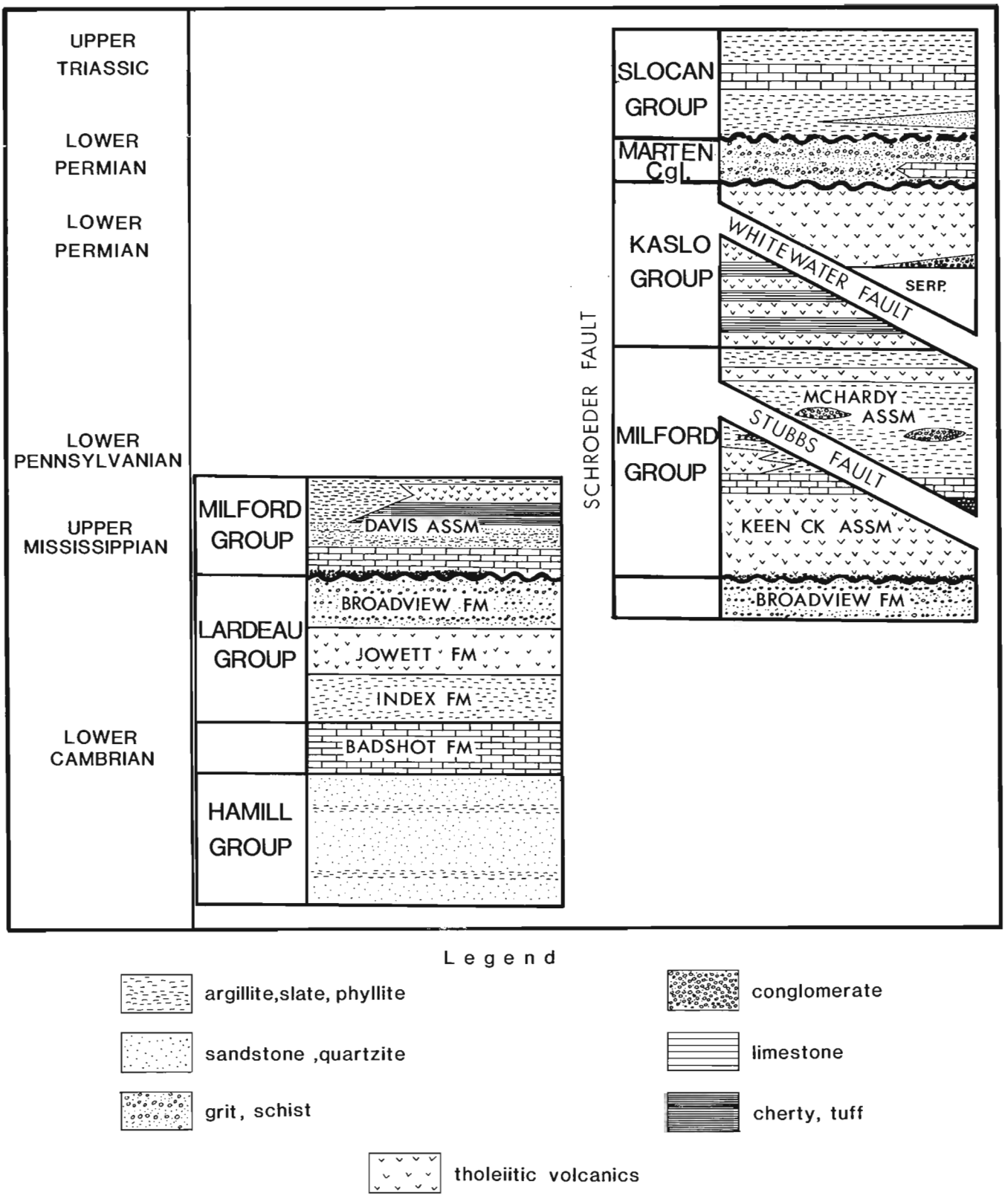

Figure 36.2. *Tectonic and stratigraphic relationships of stratified rocks in the Goat Range. Stratigraphic ages determined from fossil collections are shown on the left margin.*

Milford Group

Rocks previously mapped as Milford Group (Cairnes, 1934; Fyles, 1967; Read and Wheeler, 1976) can be divided into three stratigraphic assemblages. Consistent stratigraphic elements of all assemblages are:

1. An Upper Mississippian limestone near the base of the assemblage.
2. Siliciclastic rocks consisting of bedded cherty argillite, chert or quartz-pebble conglomerate, and slate or mica phyllite.
3. Volcanic rocks, including pyroxene-plagioclase pillow lava, pillow breccia, and tuffaceous greenstone.

While gross lithologies are similar and in part coeval, detailed stratigraphic correlation remains tentative, especially between McHardy assemblage and Milford Group farther east.

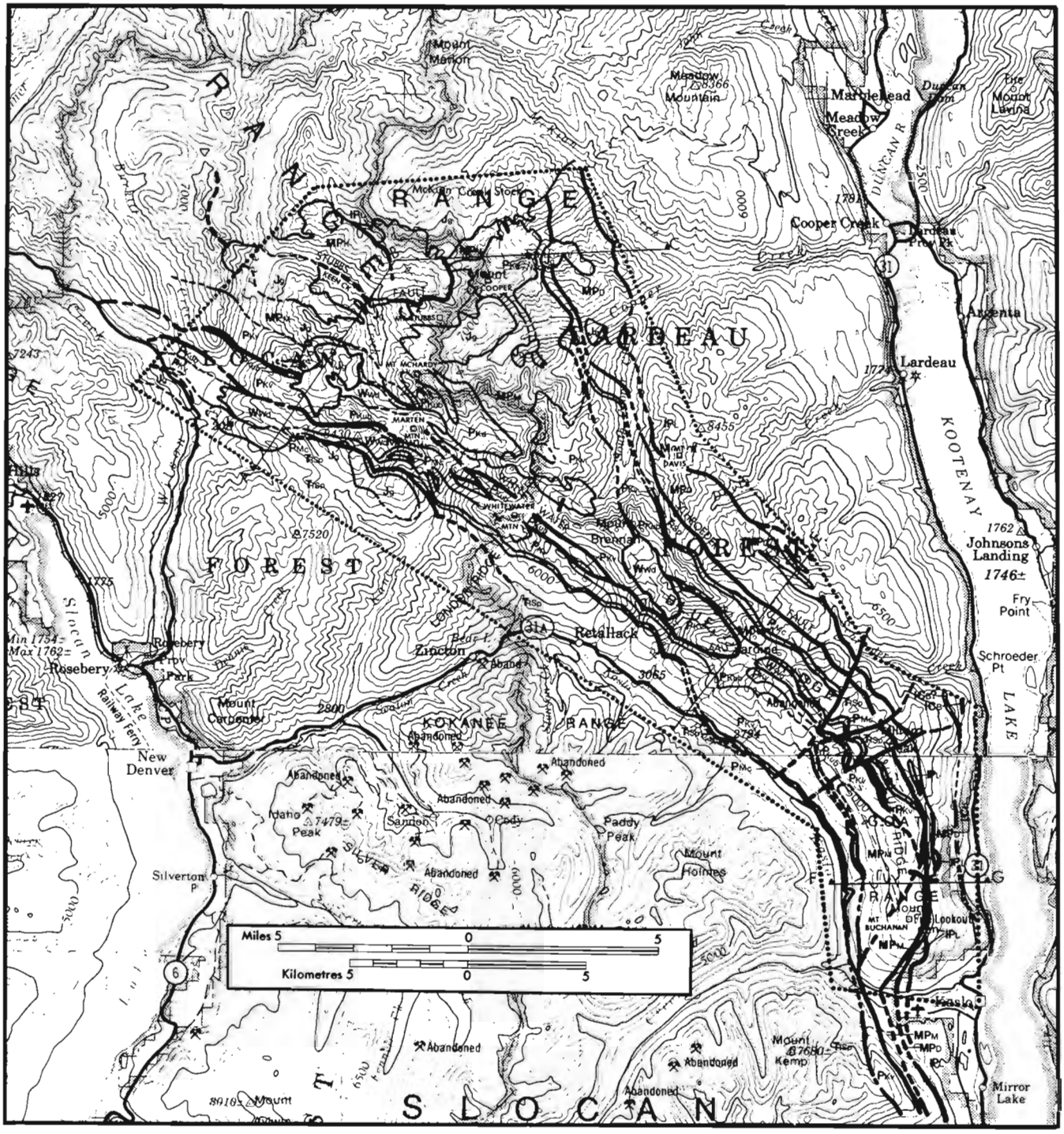

Figure 36.3. *Generalized geological map of the Goat Range study area from work of the 1982 and 1983 field seasons. Contour interval is 500 feet.*

Milford Group, Davis assemblage

The eastern belt of Milford Group lies unconformably upon grits and volcanics of Lardeau Group. This belt is informally named Davis assemblage because of good exposure of the sequence on Davis Ridge. This assemblage consists, in ascending stratigraphic order, of: rare basal quartz-pebble conglomerate, limestone, interbedded phyllite, limestone and metasandstone, cherty tuff and local phyllitic greenstone, overlain by grey siliceous argillite. The Davis assemblage forms a west-facing panel truncated to the west by the Schroeder Fault. Upper Mississippian (Early Namurian) conodonts have been obtained from the lower limestone and from a limestone lens in the cherty tuff unit (Orchard, 1985).

Milford Group, Keen Creek assemblage

The Keen Creek assemblage is exposed in the core of the Dryden Anticline, south of the McKian Creek Stock. Psammitic schist, quartzite, grit and quartz-pebble conglomerate, correlated with Broadview Formation of Lardeau Group, are unconformably overlain by a lower unit of sparse conglomerate and volcanics. The pyroxene-plagioclase pillow lavas, greenstone and green tuffaceous rocks are in turn overlain by a middle unit of light and dark grey banded limestone which has yielded Upper Mississippian (Early Namurian) and Lower Pennsylvanian (Late Namurian) conodonts (Orchard, op. cit.). The upper unit of the assemblage is composed in the east chiefly of pillow lavas

LEGEND for Figure 36.3

Geological Boundary: ——— Fault: ———

Axial Surface, Dryden Anticline: —+—

UPPER TRIASSIC

T_{RSD} SLOCAN GROUP:
Slate/phyllite, limestone, sandstone

Disconformity

LOWER PERMIAN

P_{MC} MARTEN Conglomerate:
Greenstone conglomerate

Unconformity

PERMIAN AND(?) CARBONIFEROUS

P_{KV} KASLO GROUP:
Tholeiitic volcanics

P_{KUB} KASLO GROUP:
Ultramafic Unit

UPPER MISSISSIPPIAN AND PENNSYLVANIAN

MP_M MILFORD GROUP
McHardy assemblage:
Siliceous argillite, diorite
tholeiitic volcanics, limestone

Stubbs Thrust Fault

MP_K Keen Creek assemblage:
Tholeiitic volcanics, limestone, clastics

MP_D Davis assemblage:
Siliciclastics, limestone, tholeiitic volcanics

Angular Unconformity

LOWER PALEOZOIC

IP_L LARDEAU GROUP:
Calcareous schist, mafic volcanics, grit

LOWER CAMBRIAN

$I\epsilon_B$ BADSHOT FORMATION
White marble, calc-silicate gneiss

$I\epsilon_H$ HAMILL GROUP
Mica Schist, quartzite, micaceous quartzite

INTRUSIVE ROCKS

MIDDLE JURASSIC

J_g KUSKANAX-NELSON Granitic rocks:
Hornblende-biotite granite, aegerine granite feldspar porphyry

LOWER PERMIAN

W_{Wd} Whitewater diorite:
Medium- to coarse-grained foliated diorite

PERMIAN AND(?) CARBONIFEROUS

P_{Kd} feeder diorite:
Medium-grained porphyritic hornblende diorite

and volcaniclastics which grade westward into tuffaceous rocks and then into meta-wacke, quartz-pebble (meta-chert?) conglomerate and grey siliceous phyllite. Conglomerate clasts are matrix supported. The matrix is a fine grained dark grey hornblende-biotite hornfels.

Milford Group, McHardy assemblage

The McHardy assemblage is separated from the underlying Keen Creek assemblage by the undulating Stubbs Fault. This assemblage was mapped earlier as Milford Group and, in part, as Kaslo and Slocan groups (Cairnes, 1934; Fyles, 1967; Read and Wheeler, 1976) and as Grey Siliceous Argillite Unit (Klepacki, 1983). The lowest unit is grey limestone and dark grey calcareous sandstone overlain by tuffaceous sandstone in turn overlain by a mostly matrix-supported boulder conglomerate. Clasts are boulder- to pebble-sized and consist of diorite, amygdaloidal and pyroxene-porphyry volcanics, and rare granite. The granite boulders have yielded an Ordovician isotopic date (U-Pb, zircons; Okulitch et al., in prep.). Exposure of this conglomerate unit is restricted to a tight, northeast-trending fold cut off by McKian Creek Stock northwest of Mount Cooper. This conglomerate is overlain by limestone succeeded by thick, complexly folded grey siliceous argillite with rare calcareous beds and conglomerate. Conglomerate beds contain clasts of chert, diorite and volcanic rocks. Near the top of the McHardy assemblage, but within siliceous argillite, are thin (3-5 m) beds of pyroxene-plagioclase porphyry pillow lava of tholeiitic composition. McHardy assemblage is also distinguished by numerous dykes and sills of hornblende diorite porphyry which feed overlying volcanic rocks.

Similar grey siliceous phyllite, cut by dykes and sills of hornblende porphyry, near Mount Buchanan also belongs to the McHardy assemblage. There the phyllite is apparently underlain by a limestone which has yielded Upper Mississippian (Early Namurian) conodonts (Orchard, op. cit.). This limestone may be correlated with that northwest of Mount Cooper.

Kaslo Group, ultramafic unit

Serpentinite breccia, talc schist, or talc-chlorite schist outline a discontinuous sheet traversing the length of the study area (Fig. 36.3). The Whitewater Fault, marked near Whitewater Mountain by a complicated sliver zone, occurs at the base of the ultramafic unit thereby dividing the Kaslo Group into two plates. Northwest of Whitewater Mountain, however, a splay off the Whitewater Fault creates a third plate within the Kaslo Group, intermediate in character between the upper and lower plates by virtue of containing important amounts of cherty tuff. Because the intermediate plate is floored by ultramafic rocks, it probably represents a repetition of the upper plate. North of Mount Buchanan, the ultramafic unit rests on McHardy assemblage. The ultramafic unit is interpreted as oceanic floor basement to the upper plate of the Kaslo Group (Klepacki, 1983).

Kaslo Group, lower plate units

The lower plate units at Whitewater Mountain comprise tholeiitic pyroxene-porphyry pillow lava, flows, and tuffaceous greenstone interbedded with green and white cherty tuff. This sequence lies with depositional contact on the McHardy assemblage. Within the intermediate plate of Kaslo Group northwest of Marten Mountain a cherty tuff sequence which lithologically resembles the lower plate sequence has yielded Lower Permian conodonts (Orchard, op. cit.). Zircons recovered from the top of the cherty tuff yielded a single discordant point with U-Pb ages of 245.58 ± 7.08 Ma (U^{238}-Pb^{206}) and 269.60 ± 12.70 Ma (U^{235}-Pb^{207}) (P. van der Heyden, R.L. Armstrong; personal communication, 1983). These dates provide a minimum age of the zircons present in this sequence and should not be interpreted as the age of the unit without additional data. Kaslo Group is assigned a Permian and(?) Carboniferous age in accordance with the structural position of fossil data.

Kaslo Group, upper plate units

The upper plate of the Kaslo Group is predominantly pillow lava. Sedimentary rocks are rare and consist of greywacke and volcanic conglomerate with clasts of volcanics, diorite, and serpentinite. The upper plate is floored by the ultramafic unit and overlain stratigraphically by the Marten conglomerate.

Marten conglomerate

Rusty-weathering greenstone conglomerate with clasts of pyroxene-porphyry pillow lava, diorite, limestone, and in two localities, serpentinite, overlies the Kaslo Group with angular unconformity. This mappable unit is well exposed in the headwaters of Marten Creek southwest of Inverness Mountain. The matrix of the conglomerate is commonly calcareous green or grey phyllite or limestone and is locally pyritic. The conglomerate also contains sparse lenses of limestone a few centimetres to 10 metres thick, one of which has yielded Lower Permian conodonts.

Slocan Group, phyllite-limestone-sandstone unit

The youngest sedimentary rocks in the study area comprise a thick unit of grey phyllite or slate, locally rhythmically bedded with grey quartzite and limestone layers. Limestone beds are up to 20 metres thick, although most are only a few centimetres thick. Limestone has yielded Upper Triassic (Carnian/Norian) conodonts (Orchard, op. cit.), shell and crinoid fragments, molluscs and cephalopods (Cairnes, 1934). Sandstone beds containing detrital mica occur southwest of Retallack and require granitoids or metamorphic rocks in the source terrane. Previous work (Cairnes, 1934; Klepacki, 1983) suggests a source area to the west.

Intrusive rocks

Three major types of intrusive rocks occur in the study area. These are: synvolcanic diorite, syntectonic diorite, and granitic rocks. Synvolcanic diorite is medium- to fine-grained foliated hornblende diorite porphyry commonly containing ductile shear zones, mineralized quartz-epidote ± carbonate veins, and breccia with mineralized fractures. Glomerophyric hornblende is common but not ubiquitous. Dykes of synvolcanic diorite can be traced into tholeiitic volcanics of the McHardy assemblage and the Kaslo Group. Accordingly, in the field, the synvolcanic diorite was referred to informally as the "feeder diorite". It is considered, therefore, to be of Permian and (?)Carboniferous age. Large bodies of "feeder diorite" occur at Mount Cooper and southeast of Mount McHardy.

Syntectonic diorite or "Whitewater diorite" is difficult to distinguish from "feeder diorite" where crosscutting relationships or glomerophyric textures characteristic of the "feeder diorite" are lacking. In general, Whitewater diorite is medium- to coarse-grained equigranular diorite with a lower colour index than "feeder diorite". Locally Whitewater diorite is intensely sheared with fine grained, mylonite-like ductile shear zones which suggest syntectonic emplacement. The unit is best exposed at Whitewater Mountain where it invades the Whitewater Fault and overlying Kaslo volcanics.

North of Marten Mountain, it includes large xenoliths of serpentinite and volcanics, including a body with the serpentinite-volcanic contact, interpreted as representing the Whitewater Fault. Because the Whitewater diorite intrudes the Kaslo Group of Lower Permian and (?)Carboniferous age and is unconformably overlain by the Marten conglomerate of Lower Permian age, the age of the diorite is Early Permian. The Whitewater diorite is restricted to the McHardy assemblage and the Kaslo Group.

Granitic rocks consist of hornblende and/or biotite granite and leucogranite, aegerine granite, and feldspar porphyry plugs and dykes. Isotopic dates farther north (Read and Wheeler, 1976; Parrish and Wheeler, 1983) and south (Nguyen, Sinclair and Libby, 1968) on Kuskanax and Nelson suite granitic rocks, and preliminary zircon analyses in the study area, suggest the granitoids are Middle Jurassic. Granitic bodies postdate folding events and plug all major faults, but are locally cut by faults with minor displacement (100 m).

Major structures and deformation

The distribution of Mississippian and younger rocks in the study area is controlled by four major structures: Whitewater Fault, Stubbs Fault, Dryden Anticline, and Schroeder Fault (Fig. 36.4). Pre-Mississippian rocks experienced additional deformation not associated with these structures. This earlier deformation is manifested as thrust faults and a pre-Mississippian foliation probably associated with folding. Northwest of Mount Cooper, two foliations are present in Broadview Formation of Lardeau Group, whereas only one occurs in the overlying Keen Creek assemblage of Milford Group(Fig. 36.5, 36.6, 36.7). Pebbles of quartzite in basal conglomerate of Keen Creek assemblage are stretched along the foliation associated with the Dryden Anticline. This foliation is present as crenulation cleavage in the underlying Broadview Formation. Southeast and east of Mount Buchanan, structurally upright marble and overlying Jowett Formation volcanics lie structurally on top of Broadview Formation in apparent thrust contact. The thrust

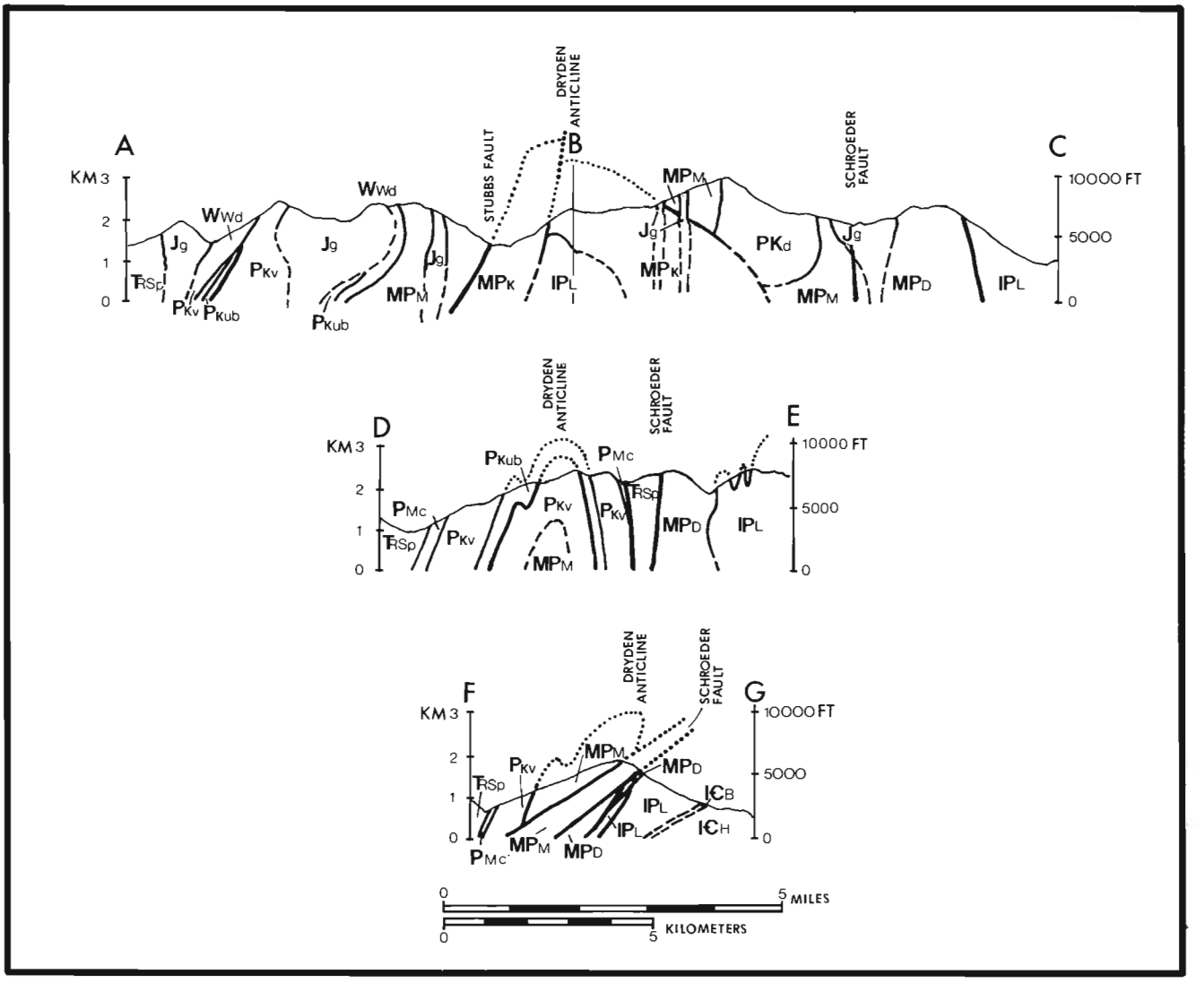

Figure 36.4. Vertical geological sections from the Goat Range study area. Location of the sections is keyed to Figure 36.3, with A-B-C the most northerly section and F-G the most southerly section. No vertical exaggeration.

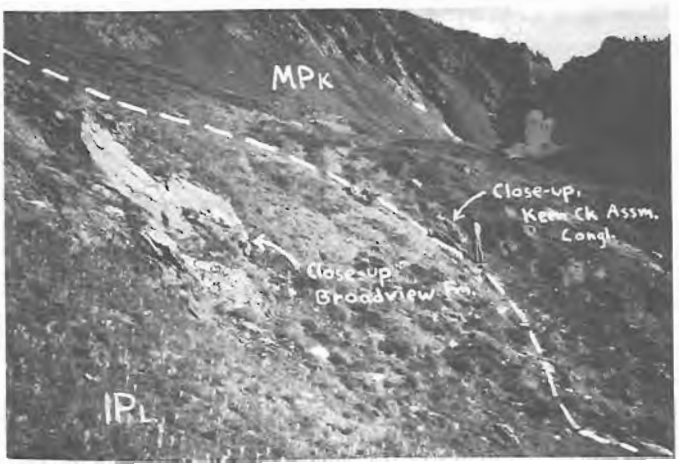

Figure 36.5. *Outcrops which define the angular unconformity between the lower Paleozoic Lardeau Group, Broadview Formation and the Mississippian and Pennsylvanian Keen Creek assemblage of the Milford Group. The locations of Figures 36.6 and 36.7 are outlined. This view is to the southeast (140°).*



Figure 36.6. *Outcrop of Proadview Formation micaceous quartzite directly below the unconformity. The dominant foliation ($S_1{}^L$) dips northeast and is defined by quartz-rich and mica-rich layers. A later foliation ($S_2{}^L$) dips southwest and the intersection of the two foliations is defined by microfold (crenulation) hinges. The photograph looks southeast.*

fault is interpreted to lie at the base of the marble and volcanics and is locally truncated by the overlying Milford Group indicating pre-Upper Mississippian thrusting (Fig. 36.3; Fig. 36.4, section F-G).

Whitewater Fault

The Whitewater Fault occurs at the base of Kaslo Group ultramafic unit and repeats the volcanic stratigraphy. Where exposed, the Whitewater Fault is a shear zone that is folded by folds associated with the Dryden Anticline. The Whitewater Fault cuts the Kaslo Group lower plate units, requiring the age of displacement to be younger than those Lower Permian and (?)Carboniferous strata. The Whitewater Fault is plugged by the Whitewater diorite, which not only truncates the fault but has a large xenolith containing part of the Whitewater Fault. Northwest of Marten Mountain, Whitewater diorite is overlain unconformably by the Lower Permian Marten conglomerate indicating an Early Permian age of movement along the fault.

Dryden Anticline

The first folding episode recognized in rocks younger than Mississippian generated the Dryden Anticline. Slaty and phyllitic foliation in the Keen Creek and McHardy assemblages, the Kaslo and Slocan groups, and, locally, the Whitewater and "feeder" diorites, is axial planar to this and related folds. Foliation in the Davis assemblage and crenulation in the Lardeau Group east of Schroeder Fault is axial planar to east-verging tight folds (Fig. 36.4, section D-E) which have similar orientation to the Dryden Anticline and may be of the same deformational event. The axial surface of Dryden Anticline is cut off by McKian Creek Stock in the northwestern section of the study area. From there it can be traced south to the Mount Buchanan area where it is apparently truncated by a thrust fault in the McHardy assemblage (Fig. 36.4, section F-G). These truncations and regional considerations (Read and Wheeler, 1976) suggest the Dryden Anticline was generated during the Middle Jurassic Columbian Orogeny.

The axial surface of Dryden Anticline is mostly steeply to moderately inclined to the southwest although it locally dips northeast due to interference of younger structures. In the northwest the fold plunges southeast at 15 degrees and in the southeast it plunges northwest at approximately 8 degrees. The Dryden Anticline thus forms a saddle-shaped structure with the depression occurring near the "elbow" bend of structural trends northwest of Mount Buchanan.

Stubbs Fault

The McHardy assemblage and Kaslo and Slocan groups have apparently been thrust onto the Keen Creek assemblage along the Stubbs Fault. The fault is well exposed on the northern flank of Mount Stubbs where the underlying upright, east-dipping limestone of Keen Creek assemblage becomes overturned to the east, suggesting east-directed movement along the fault (Fig. 36.8). The Stubbs Fault, as well as the Whitewater Fault, is folded by the Dryden Anticline (Fig. 36.4, section A-B-C). However, the Stubbs Fault also cuts folds associated with the Dryden Anticline, suggesting synchronism of folding and faulting. The Stubbs Fault is plugged by Middle Jurassic granites of Kuskanax Batholith affinity.

Schroeder Fault

The Schroeder Fault is traced the length of the study area and juxtaposes the east limb of the Dryden Anticline against the west-facing Lardeau Group and Davis assemblage. The Schroeder Fault has significant normal movement as it places Upper Triassic Slocan Group against Upper Mississippian Davis assemblage of Milford Group. Because the Schroeder Fault cuts Dryden Anticline structures, which apparently formed during the height of regional metamorphism, the faulting is postmetamorphic, similar to faults in the Ainsworth area (Fyles, 1967). South of Mount Buchanan, the Schroeder Fault splays into the Josephine and Lakeshore faults of the Ainsworth area. Northeast of Mount Cooper, the Schroeder Fault is plugged by a leucogranite stock of Kuskanax batholith affinity, thus reflecting pre-Middle Jurassic normal faulting northwest of Kootenay Lake.



Figure 36.7. Outcrop of conglomerate in rusty-weathering tuffaceous sediments at the base of Keen Creek assemblage. Clasts of quartzite are stretched out along foliation which dips southwest and is equivalent to $S_2{}^L$). This fabric is the primary foliation in Keen Creek assemblage.

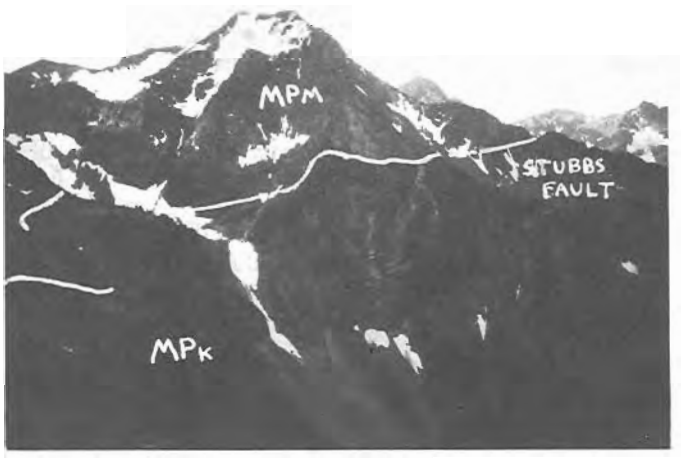

Figure 36.8. Mount Stubbs and the Stubbs Fault viewed from the northeast. The fault truncates the layered limestone unit. The footwall contains limestone and volcanics of Keen Creek assemblage. The hanging wall contains siliceous argillite and diorite of McHardy assemblage. Note how the east-dipping strata at the base of the mountain sweep up to steep westward dips directly below the fault trace, suggesting tectonic transport from the west (right).

Other fold phases

Two additional fold phases postdate the Dryden Anticline. Both phases are southerly plunging, westerly verging, and locally conjugate. The earlier phase has southeasterly striking axial surfaces and moderately plunging axes. The Whitewater drag fold, near Retallack (Hedley, 1945), is of this relative age. The absolute age of this event is uncertain.

The later phase is only locally well developed. Axial surfaces strike south to southwesterly and folds plunge moderately to steeply south and verge to the west. Slip-cleavage surfaces forming secondary foliation are locally developed, especially along Wilson Creek southwest of Marten Mountain and near the bend in regional structural trends north of Mount Buchanan where later folds are associated with southwesterly trending faults (Fig. 36.3). The age of this event is also uncertain except that the faults near the bend in structural trends postdate the Schroeder Fault and are possibly younger than Middle Jurassic. Interference relationships of these two later fold phases are exposed in outcrops of Slocan Group grey phyllite about 13 km along highway 31A, west of Kaslo village.

Late faulting

Moderately to steeply dipping faults with clay gouge zones are exposed along the eastern margin of the study area. Displacement along these faults is unknown but cannot be significant because the overall sequence of major rock units is not interrupted by these features. Granitic dykes are broken and warped in drag folds suggesting right-lateral movement along a fault in Davis assemblage 4.5 km east of Mount Cooper. These dykes are correlated with the Middle Jurassic granitic plutonism, so these faults are post-Middle Jurassic.

Mineral deposits

Gold and silver have been extracted from several mines and properties in the map area. Cairnes (1934) and Maconachie (1940) have described many of the mineral deposits in the area. In general, most properties are located on or near northeast-trending quartz-galena-sphalerite-pyrite-chlocopyrite veins with rusty-weathering carbonate alteration envelopes. Sulphide minerals are occasionally found in northwest-trending veins. Mineralized quartz veins are commonly found along the margins of the ultramafic unit and are spatially associated with feldspar porphyry or granitic dykes, although genetic relationships between dykes and veins are uncertain. Precious and base metal values have also been reported from alteration zones on the margins of granitic stocks along North Cooper Creek and from the Marten conglomerate near Kane Creek. Pyrite pods occur along bedding in Slocan grey phyllite and sandstone along Wilson Creek.

Acknowledgments

D.W. Klepacki is grateful for the assistance of Allan Vichert, Pikku Vichert, Cindi Klepacki, and Daniel Orange. Allan Vichert provided useful geological discussion in the course of field work. Discussions with and visits from James T. Fyles, Alain Leclair and John Reesor greatly contributed to an understanding of the regional setting of the study area and continuation of units to the south. B. Clark Burchfiel participated in mapping the Mount Buchanan and Mount Brennan areas. Peter Read, Geotex Consultants Ltd., kindly provided his unpublished and accurate field map of the Mount Buchanan-Milford Peak area for use during remapping of the area. Rodney Place provided willing and useful assistance to J.O. Wheeler in 1980.

References

Cairnes, C.E.
1934: Slocan mining camp, British Columbia; Geological Survey of Canada, Memoir 173, 137 p.

Fyles, J.T.
1964: Geology of the Duncan Lake area, Lardeau District, British Columbia; British Columbia Department of Mines and Petroleum Resources, Bulletin 49, 87 p.

Fyles, J.T. (cont.)
1967: Geology of the Ainsworth-Kaslo area, British Columbia, British Columbia Department of Mines and Petroleum Resources, Bulletin 53, 125 p.

Hedley, M.S.
1945: Geology of the Whitewater and Lucky Jim mine areas; British Columbia Department of Mines, Bulletin 22, 54 p.

Klepacki, D.W.
1983: Stratigraphic and structural relations of the Milford, Kaslo and Slocan groups, Roseberry Quadrangle, Lardeau map area, British Columbia; in Current Research, Part A, Geological Survey of Canada, Paper 83-1A, p. 229-233.

Maconachie, R.J.
1940: Lode gold deposits, Upper Lemon Creek area and Lyle Creek-Whitewater Creek area, Kootenay District; British Columbia Department of Mines, Bulletin 7, 50 p.

Monger, J.W.H., Price, R.A., and Templeman-Kluit, D.J.
1982: Tectonic accretion and the origin of the two major metamorphic and plutonic welts in the Canadian Cordillera; Geology, v. 10, p. 70-75.

Nguyen, K.K., Sinclair, A.J., and Libby, W.G.
1968: Age of the northern part of the Nelson batholith; Canadian Journal of Earth Sciences, v. 5, p. 955-957.

Okulitch, A.V., Read, P.B., Wanless, R.K., and Loveridge, W.D.
Paleozoic plutonism in southeastern British Columbia. (in prep.)

Orchard, M.J.
1985: Carboniferous, Permain and Triassic conodonts from the central Kootenay Arc: constraints on the age of the Milford, Kaslo and Slocan Groups; in Current Research, Part A, Geological Survey of Canada, Paper 85-1A.

Parrish, R.R. and Wheeler, J.O.
1983: A U-Pb zircon age from the Kuskanax batholith, Southeastern British Columbia; Canadian Journal of Earth Sciences, v. 20, p. 1751-1756.

Read, P.B.
1973: Petrology and structure of Poplar Creek map area, British Columbia; Geological Survey of Canada, Bulletin 193, 144 p.

Read, P.B. and Wheeler, J.O.
1976: Geology, Lardeau west-half, British Columbia; Geological Survey of Canada, Open File Map 432.

CARBONIFEROUS, PERMIAN AND TRIASSIC CONODONTS FROM THE CENTRAL KOOTENAY ARC, BRITISH COLUMBIA: CONSTRAINTS ON THE AGE OF THE MILFORD, KASLO AND SLOCAN GROUPS

Project 810028

M.J. Orchard
Cordilleran Geology Division, Vancouver

Orchard, M.J., Carboniferous, Permian and Triassic conodonts from the central Kootenay Arc, British Columbia: constraints on the age of the Milford, Kaslo and Slocan groups; in Current Research, Part A, Geological Survey of Canada, Paper 85-1A, p. 287-300, 1985.

Abstract

Carboniferous, Permian and Triassic conodont faunas are recorded and described from Lardeau and Nelson map areas. Those from the Milford Group gave a minimum age range within the Carboniferous of Tournaisian through Namurian, and are older in the west, younger in the east; they are characteristically of relatively shallow-water aspect. The Milford conodonts are compared with contemporaneous, relatively deep-water conodont faunas from the Eagle Bay Formation of the northern Kootenay Arc. The first fossils ever recorded from the Kaslo Group are conodonts of Early Permian age extracted from cherts. Conodonts from the Slocan Group are Carnian and Norian (Late Triassic). Four different ages and a possible hiatus were recognized by utilizing the recent Norian zonation of Orchard (1983).

Résumé

Des ensembles fauniques de conodontes du Carbonifère, du Permien et du Trias ont été enregistrés et décrits dans les régions cartographiées de Lardeau et de Nelson. Les conodontes du groupe de Milford datent au moins du Tournaisien jusqu'au Namurien du Carbonifère, et sont plus anciens vers l'ouest et plus récents vers l'est; ils sont caractéristiques d'un milieu relativement peu profond. Les conodontes de Milford sont comparés aux conodontes contemporains d'eau relativement profonde de la formation d'Eagle Bay dans le nord de l'arc de Kootenay. Les premiers fossiles a être reconnus dans le groupe de Kaslo sont des conodontes du Permien ancien qui proviennent de cherts. Les conodontes du groupe de Slocan datent du Carnien et du Norien (Trias récent). En utilisant la zonation norienne établie récemment par Orchard (1983), il a été possible d'identifier quatre âges distincts ainsi qu'une lacune possible.

Introduction

This paper presents all the conodont data currently available from the Milford, Kaslo and Slocan groups of southeastern British Columbia (Lardeau and Nelson map areas, NTS 1:250 000, 82 K, 82 F). The results represent both an accompaniment to the work of Klepacki and Wheeler (1985) and a supplement to the earlier work of Read and Wheeler (1976).

In ascending order, the Milford, Kaslo and Slocan groups constitute the upper Paleozoic and lower Mesozoic stratigraphy exposed in the central part of the Kootenay Arc, a major north-trending, arcuate structural zone near the ancient margin of cratonic North America. Because the rocks are complexly deformed and diagnostic macrofossils are uncommon, earlier correlations based on lithological similarities have resulted in erroneous stratigraphic interpretations. Hence, when Bancroft (1920, p. 40B) first presented a table of formations for the area, the "Milford Series" was regarded as "probably Jurassic" and the "Slocan Series" was thought to be Carboniferous. Later, Cairnes (1934) showed that the Milford lay beneath the Slocan but, as then conceived, both included Triassic sediments. More recently, Read and Wheeler (1976) reinterpreted the Triassic part of the Milford Group as infolded Slocan Group strata.

The Kaslo Group was correctly interpreted by Cairnes (1934) as occupying a stratigraphic position between the Milford and Slocan groups, an interpretation supported by the work of Klepacki (1983), and confirmed by the fossil data presented here. In contrast, Ross and Kellerhals (1968, p. 855) interpreted the Kaslo as lying beneath the Milford.

Rock unit nomenclature and fossil control: historical perspective

The Milford Group unconformably overlies the Lardeau Group of presumed early to middle Paleozoic age (Read and Wheeler, 1976). Originally described as the Milford Series by Bancroft (1920, p. 40B) the first use of the name is accredited to LeRoy (in Bancroft, 1920, p. 43B) who used it for rocks of the Blue Ridge or Milford Syncline, near Milford Peak. Based on that belt of rocks (shown on Map 1667, of the Slocan Mining Area, in Drysdale, 1917), which are now known to include both Milford and Slocan group rocks, the "Milford Series" was consequently regarded by Cairnes (1934) as embracing both Carboniferous and Triassic parts. The revision of Read and Wheeler (1976) essentially redefined the Milford Group as the older part of the former series.

The Milford Group includes limestones that often contain echinoderm remains. In addition, Early Carboniferous coral faunas are known (Bancroft, 1921, p. 100A) and some recent collections of these have been dated as early Late Viséan, as have accompanying foraminiferids (E.W. Bamber, personal communication). Brachiopod collections made in 1917 by Bancroft east of Mount Cooper were reported by Kindle (in Cairnes, 1934, p. 34) to be of probable Pennsylvanian age, although Late Mississippian conodonts are now known from the locality (Locs. 10-12).

The Kaslo Group, which overlies the Milford Group, includes a relatively minor amount of sediment and because fossils were previously unknown, its age has been problematic. Originally described as the Kaslo schists (McConnell, 1897, p. 24A) and later as the Kaslo Volcanics Group (Bancroft, 1919, p. 29B), its age was regarded as Triassic by Cairnes (1934, p. 49) because of its stratigraphic position between what was then thought to be Triassic Milford Group and Triassic Slocan Group. Later, on stratigraphic grounds, Read and Okulitch (1977) thought the group may be Permian but Ross and Kellerhals (1967, p. 855) interpreted it to be pre-Carboniferous.

The Slocan Group consists of a considerable thickness of largely pelitic rocks that unconformably overlie the Kaslo Group (Read and Wheeler, 1976; Klepacki, 1983). Although the first fossils collected from the Slocan Group were thought to be Carboniferous (Bancroft, 1919, p. 36B), poorly preserved belemnoids, ammonoids, corals and pentacrinoids have recently been regarded as of probable Triassic age (Cairnes, 1934, p. 60; Fyles, 1967, p. 34; Little, 1960, p. 53, 56-57). Late Triassic conodonts from the Slocan Group were first determined by B.E.B. Cameron in 1977 (GSC internal report).

Locality register

Locality numbers refer to sites shown in Figure 37.1. Following initials represent collector: D.W.K.=Klepacki; A.V.O.=Okulitch; M.J.O.=Orchard; P.B.R.=Read; J.O.W.=Wheeler. This is followed by the field number, and a description of the locality.

1. P.B.R. V78-2/3F: Road exposure of crinoidal limestone 0.65 km W of Catherine Lake. UTM Zone 11u, 0430300E, 5583700N. 50°24'11.3"N, 117°58'50.7"W.
2. M.J.O. WB81-49: Fissile, dark grey to black crinoidal argillaceous limestone at the topographic base of section at 6850 ft. elevation, 7.6 km at 245° from Comaplix Mountain. 50°48'10"N, 117°51'35"W.
3. M.J.O. WB81-50: Thick bedded to massive pale grey limestone with crinoids, brachiopods, indistinct ?corals. A few metres above Loc. 2.
4. J.O.W. WB81-52: Limestone 300 m NE of break in ridge and Loc. 3. 7000 ft. elevation, 7.1 km at 246° from Comaplix Mountain. 50°48'15"N, 117°51'10"W.
5. J.O.W. WB81-53: Crinoidal limestone 30 m NE of Loc. 4.
6. D.W.K. WBK83-48d: Limestone, 3.6 km NW of Mount Stubbs. 50°11'35"N, 117°15'20"W.
7. J.O.W. WB80-F9: Dark grey, brachiopod-bearing limestone; same horizon as Loc. 9. 8300 ft. elevation, 4.26 km at 294° from Mount Cooper. 50°11'30"N, 117°15'30"W.
8. J.O.W. WB80-F10: Dark grey, detrital limestone beneath Loc. 7. 8250 ft. elevation.
9. J.O.W. WB80-F14: Dark grey, brachiopod-bearing calc-arenitic limestone; same horizon as Loc. 7. 8100 ft. elevation, 4.31 km at 294° from Mount Cooper.
10. J.O.W. WB65-F5-2: Brachiopod-bearing carbonate, 7500 ft. elevation, 4.99 km N80°E of Mount Cooper. 50°11'10"N, 117°07'50"W.
11. M.J.O. WB81-42: Dark grey, brachiopod-bearing limestone, 7500 ft. elevation on ridge E of Mount Cooper, 8.2 km at 331° from Mount Davis. Approximates Loc. 10.
12. M.J.O. WB81-43: Dark grey, brachiopod-bearing limestone; E of and less than 3 m stratigraphically below Loc. 11.
13. D.W.K. WBK83-45a: Limestone on north face of Mount Stubbs. 50°10'35"N, 117°13'20"W.

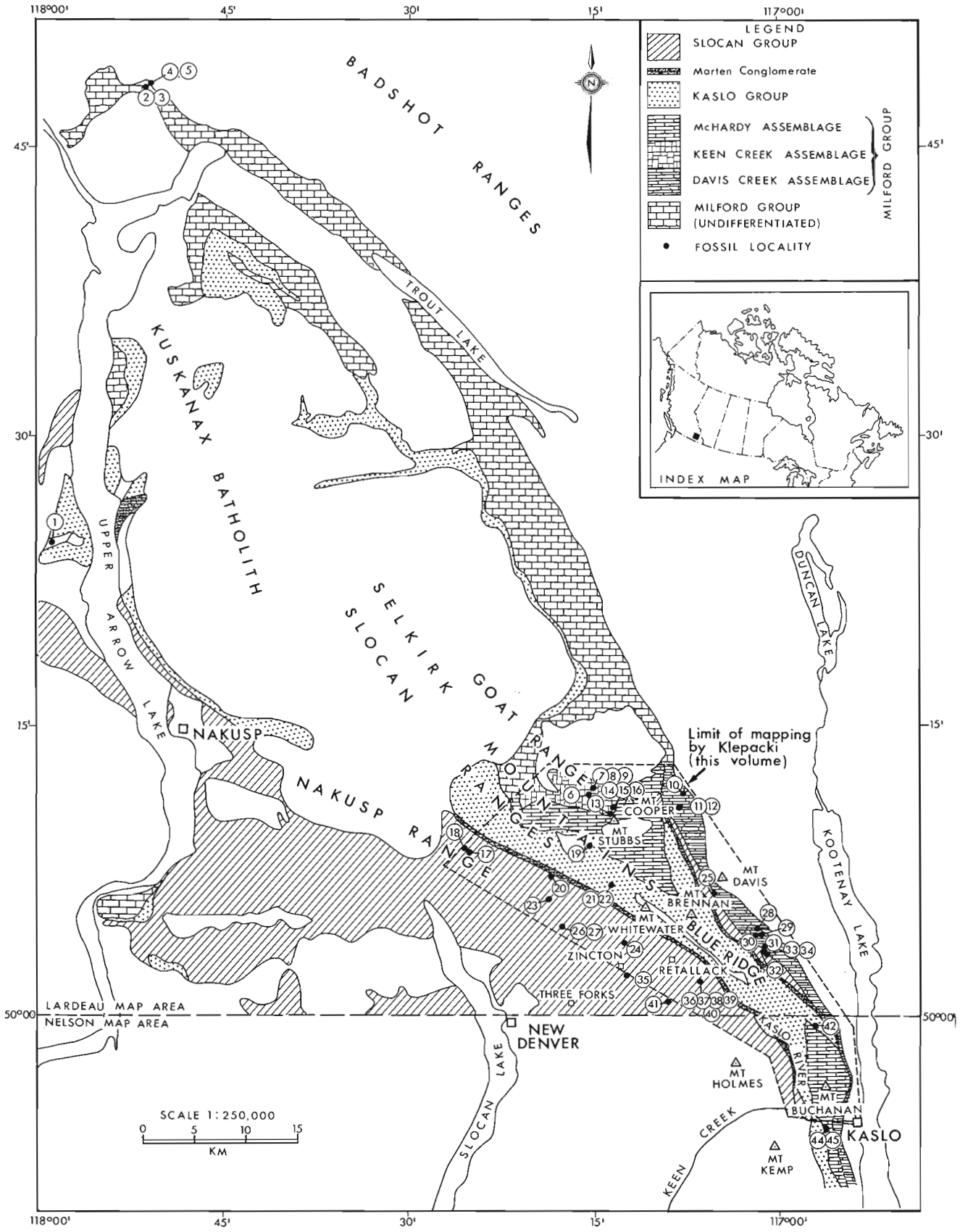

Figure 37.1. *Simplified geological map of the central Kootenay Arc showing localities of conodont collections 1–45. Geology based on (Read and Wheeler, 1976; Klepacki and Wheeler, 1985).*

14. M.J.O. WB81-46: Within 3 m of exposed base of light and dark grey detrital limestone. 7100 ft. elevation, 1.6 km at 250° from Mount Cooper; below Mount Stubbs. 50°10'00"N, 117°13'00"W.

15. J.O.W. WB80-F16: Float of dark grey limestone containing bioclastic beds. 7100 ft. elevation, 1.61 km at 250° from Mount Cooper. 50°10'00"N, 117°13'00"W.

16. J.O.W. WB80-F18: Medium grey calcarenite fossil hash bed, as Loc. 15.

17. J.O.W. WB65-F5-5: Limestone, 6300 ft. elevation, 3.86 km N. 62°W of junction of Fitzstubbs and Wilson creeks. 50°08'25"N, 117°25'15"W.

18. J.O.W. WB67-62-1A: Limestone, 7050 ft. elevation, on ridge separating Ranch Creek from Fitzstubbs Creek. 50°08'10"N, 117°25'40"W.

19. D.W.K. WBK83-53e1/2: Chert; composite sample collected through 320 m apparent thickness, near the headwaters of Keen Creek. 50°08'00"N, 117°16'45"W.

20. D.W.K. WBK83-39a: Limestone on logging road 1 km SW of Monitor-Dixie Creek junction. 50°06'45"N, 117°19'20"W.

21. D.W.K. WBK82-19i-ii: Limestone bed associated with the matrix of conglomerate. Inverness Mountain. 50°06'25"N, 117°15'22"W.

22. D.W.K. WBK82-19i-i: As 21. 50°05'25"N, 117°15'20"W.

23. J.O.W. WB67-26S-2A: Limestone on ridge separating Wilson Creek from the head of Marten Creek, at elevation 7025 ft. 50°05'40"N, 117°19'45"W.

24. D.W.K. WBK82-14d: Limestone on London Ridge. 50°05'20"N, 117°12'45"W.

25. D.W.K. WBK82-33a: Limestone on Davis Ridge-Mount Brennan Saddle. 50°05'21"N, 117°05'25"W.

26. J.O.W. WB65-F4-1G: Limestone, 7100 ft. elevation, 8.29 km at S 79°W of Whitewater Mountain. 50°04'30"N, 117°17'45"W.

27. J.O.W. WB65-4-1K: On ridge separating Dennis Creek from Marten Creek, W of Whitewater Mountain. 50°04'30"N, 117°17'45"W.

28. J.O.W. WB67-63-4A: Limestone on ridge separating Davis and Schroeder creeks, at 7500 ft. UTM Zone 11u, 0498000E, 5546700N. 50°4'28.3"N, 117°01'40.6"W.

29. J.O.W. WB80-F6: Grey, crinoidal limestone in float, identical with beds in place nearby. 7400 ft. elevation, 1.61 km at 0.05° from Mount Schroeder. 50°04'00"N, 117°01'30"W.

30. D.W.K. WBK83-30g: Limestone near headwaters of Schroeder Creek. 50°03'33"N, 117°00'15"W.

31. J.O.W. WB80-F5: Grey crinoidal limestone lens within cherty tuff. 7300 ft. elevation, 0.32 km at 110° from Mount Schroeder. 50°03'00"N, 117°01'30"W.

32. J.O.W. WB80-F4: Float of dark and light grey argillaceous limestone with layer of crinoidal debris; outcrop of similar rock nearby. 7250 ft. elevation, 0.48 km at 205° from Mount Schroeder. 50°03'00"N, 117°02'00"W.

33. J.O.W. WB80-F1: Dark grey, argillaceous limestone with sparse crinoidal fragments. 7300 ft. elevation, 1.13 km at 205° from Mount Schroeder. 50°02'30"N, 117°02'00"W.

34. J.O.W. WB80-F2: Dark grey, bioclastic limestone float near outcrop of same. As Loc. 33.

35. J.O.W. WB67-51-3D: Limestone breccia float on alluvial fan below waterfall at Lucky Jim Mine. 50°02'00"N, 117°12'55"W.

36. A.V.O. 14CAa76-1F: Limestone on Kaslo-New Denver Road, 1.13 km W of Rossiter Creek. 50°01'48"N, 117°07'00"W.

37. P.B.R. RL76-3F: Limestone. Same as Loc. 36.

38. P.B.R. RL76-4F: Limestone. Same as Loc. 36.

39. M.J.O. SL.80-1: Limestone. Same as Loc. 36.

40. A.V.O. Slocan I. Limestone. Same as Loc. 36. Locs. 36-40 were collected within a 90 m roadside outcrop.

41. J.O.W. WB67-25S-3B: Limestone in Stenson Creek at 5125 ft. elevation. 50°00'50"N, 117°09'20"W.

42. D.W.K. WBK83-25a: Limestone, unnamed mountain south of Milford Peak. 49°59'50"N, 116°57'45"W.

43. D.W.K. WBK83-4h: Limestone, Coffee Creek, 500 m W of Highway 31. 49°41'40"N, 116°55'30"W.

44. M.J.O. Landslide 1: Limestone exposed at side of old railway grade 4 km west of Kaslo. UTM Zone 11u, 0502500E, 5528600N. 49°54'42.2"N, 116°57'54.6"W.

45. M.J.O. Landslide 2: As 40. A few metres stratigraphically below (?) Loc. 43.

Plate 37.1

Upper views, unless stated otherwise. All specimens from the Milford Group.

Figure 1. **Pseudopolygnathus** sp. GSC 69063, x60, Loc. 1.

Figure 2. **Polygnathus** sp. GSC 69064, x80. Loc. 1.

Figure 3. **"Spathognathodus"** n. sp. A. GSC 69065, x60. Lateral view. Loc. 2.

Figure 4. **Hindeodus** cf. **H. penescitulus** (Rexroad and Collinson). GSC 69066, x60. Lateral view. Loc. 5.

Figures 5, 16. **Idioprioniodus** sp(p). Posterior views of:
5. metalonchodiniform element. GSC 69067, x60. Loc. 31.
16. ligonodiniform element. GSC 69078, x60. Loc. 3.

Figures 6, 10-14. **Gnathodus girtyi simplex**
6. GSC 69068, x75. Loc. 9.
10. GSC 69072, x75. Loc. 29.
11. GSC 69073, x50. Lateral view. Loc. 31.
12. GSC 69074, x75. Loc. 18.
13. GSC 69075, x50. Loc. 31.
14. GSC 69076, x80. Loc. 11.

Figure 7. Ichthyolith A. GSC 69069, x80. Loc. 5.

Figure 8. ?**Rhachistognathus muricatus** (Dunn). GSC 69070, x80. Loc. 44.

Figure 9. **Cavusgnathus altus** Harris & Hollingsworth. GSC 69071, x60. Oblique-upper view. Loc. 11.

Figure 15. **Neognathodus** sp. GSC 69077, x80. Loc. 16.

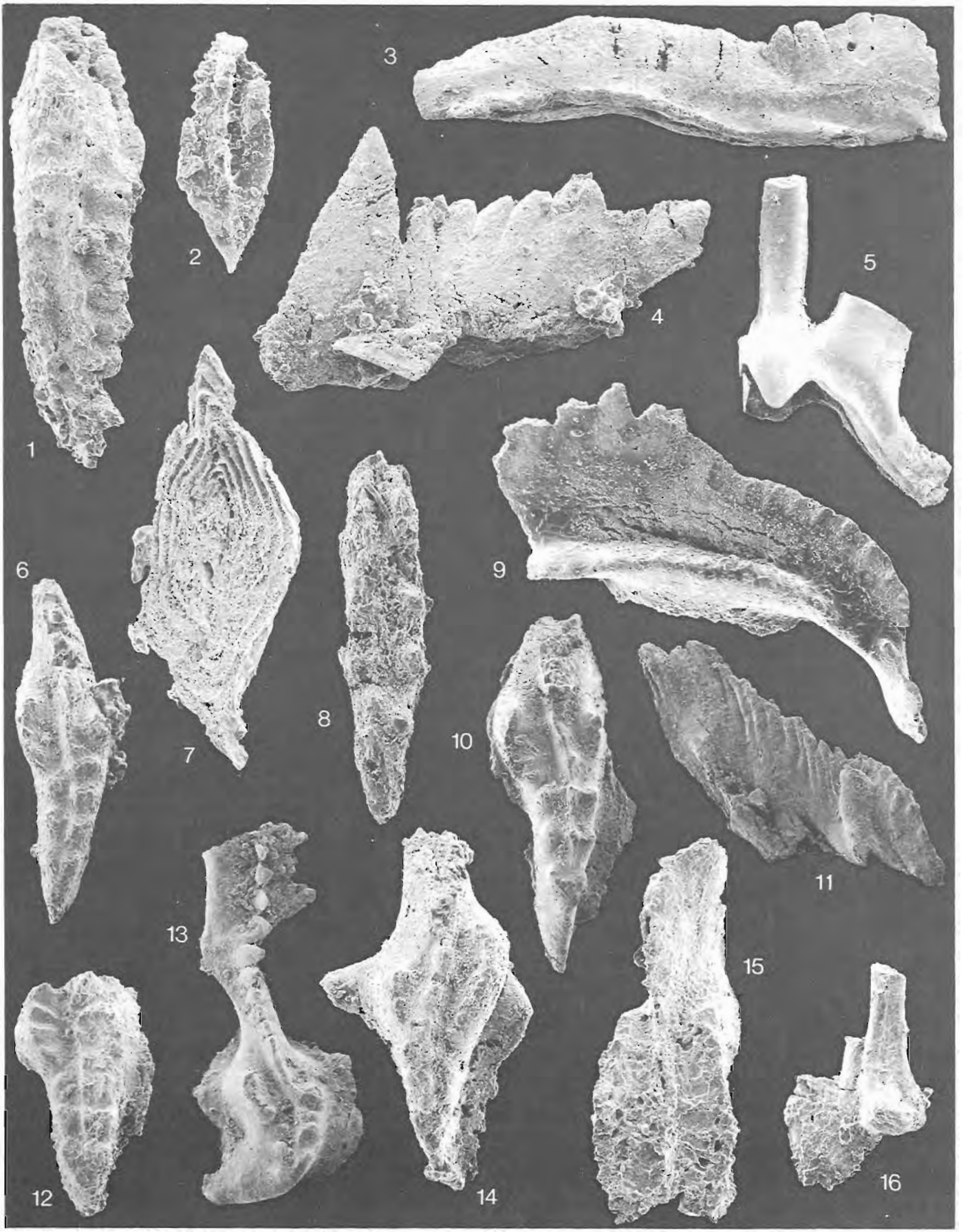
1
2
3
4
5
6
7
8
9
10
11
12
13
14
15
16

The conodonts

General features

Most conodonts recovered from the central Kootenay Arc are poorly preserved and fragmentary. Many show the effects of shearing (e.g. Pl. 37.1, figs. 11, 13), and all are thermally altered. The minimum CAI (Colour Alteration Index) values are 5 but commonly the conodonts are white and recrystallized (CAI=7-8), implying postdepositional temperatures in excess of 400°C. The metamorphism may have destroyed many conodonts, which may account for the generally low yields (of approximately 200 samples processed since 1980, 23 were productive, and most of these were small faunules). Low conodont diversity and abundance within the Milford Group suggests an inhospitable marine environment of deposition that often may not have supported conodont animals. This aspect of the Milford conodonts is discussed below. Another factor is the presumed rapid sedimentation of many of the units covered by this study, which would have diluted conodont yields.

Milford Group

Klepacki and Wheeler (1985) recognize three structurally discrete, stratigraphic assemblages within the Milford Group of the Goat Range, southern Lardeau map area, from east to west: the Davis, Keen Creek and McHardy assemblages. Carbonates from each of these yielded conodonts. Farther north in Lardeau map area near Comaplix Mountain, additional faunules have been recovered from undifferentiated Milford Group of Davis assemblage aspect. At the western edge of Lardeau map area, a single faunule was recovered from limestone included in the Slocan Group by Read and Wheeler (1976), but earlier regarded, correctly, as part of the Milford Group by Reesor and Moore (1971). Conodonts from throughout the region indicate a combined time span covering much of the Mississippian and part of the Pennsylvanian. Four conodont faunas (A-D) from the Milford Group are differentiated, and are discussed below in what is interpreted to be chronological order.

Fauna A – The oldest faunule (Locality 1, Fig. 37.1) was recovered from a crinoidal limestone lens near Catherine Lake in the extreme west-central part of the Lardeau map area. Although very poorly preserved, representatives of both **Polygnathus** and **Pseudopolygnathus** are distinguished. The age of the limestone is therefore no older than Late Famennian and no younger than Late Tournaisian.

The lower side morphology of the **Pseudopolygnathus** is characterized by a relatively broad pit, as is typical of the **P. dentilineatus** group of Lane et al. (1980, p. 123; = **P. primus** of Klapper, in Ziegler, 1981), which originated in the Late Devonian, but which was superseded by the **P. multistriatus** group in the Late Tournaisian. Therefore, this western development of the Milford Group may be no younger than Middle Tournaisian.

Fauna B – A series of faunules (Locs. 2-5) collected from limestones in the vicinity of Comaplix Mountain in the north-central part of the Lardeau map area are dominated by simple spathognathodids accompanied by **Hindeodus, Kladognathus**? and possibly **Idioprioniodus.** The ramiform elements that constitute the last two genera are all fragmentary and that fact, combined with the generally sparse nature of the faunules, precludes confident determination of multielement species. However, certain elements resemble **Ligonodina levis** (e.g. Pl. 37.2, fig. 4) and **Hibbardella abnormis** (e.g. Pl. 37.2, fig. 2), both of which were originally described from the upper part of the mid Mississippian Keokuk Formation at the Sylvan Beach locality of Branson and Mehl (1941, p. 181). The discrete element **L. levis** was regarded by Rexroad (1981, p. 11) as in an evolutionary line of descent leading to the discrete element **Kladognathus** of the Chesterian (Upper Mississippian) series, each of them representing the Sc element in multielement **Kladognathus** species. However, conservative elements such as **L. levis** also occur above the range of kladognathiform elements (Rexroad, 1981, p. 11) and in fact the species has been recorded through much of the Middle and Upper Mississippian strata of the North American Midcontinent (Rexroad and Collinson, 1963, 1965; Thompson and Goebel, 1968; Nicoll and Rexroad, 1975).

Hibbardella abnormis occurs in pre-Chesterian rocks in the Illinois Basin. In common with the younger discrete element species **Hibbardella milleri** and **H. fragilis** (Rexroad, 1981, p. 11), **H. abnormis** may have been the Sa element of a multielement **Kladognathus** species. A third element in the Milford fauna (Pl. 37.1, fig. 10) resembles the form-genus **Kladognathus** but the antero-lateral processes diverge from the anterior edge of the cusp rather than from an anterior denticle. That is the essential difference between all of these ramiform specimens from the Milford Group at Comaplix Mountain and **Kladognathus** sensu stricto. I regard the Milford association as a probable primitive multielement **Kladognathus** species, the age of which, in Mississippi Valley region terms, is possibly Late Valmeyeran.

The other elements of Fauna B do not currently provide a definitive means of dating it. The spathognathodiform elements are probably new, at least in part. Although some of the blade fragments are denticulate, most of the specimens are characterized by an adenticulate posterior part; only the anterior one-third, which constitutes a relatively high blade, bears discrete denticles. The basal cavity of these specimens, in so far as it is preserved, appears to extend below most of the posterior two-thirds of the unit. The basal configuration and the general profile of these spathognathodiform elements resemble that of other elements from British Columbia referred to **Bispathodus stabilis** sensu lato by Orchard and Struik (in press). One exceptionally large but incomplete specimen from the Greenberry Limestone (op. cit., GSC Loc. No. C-101911), of Late Tournaisian age, does in fact show complete fusion of the posterior blade, a feature that I regarded as gerontic within that population. However, in the Milford limestone faunule, the feature is not an aberration, but may reflect an evolutionary development within the **stabilis** lineage. The occurrence of **'Spathognathodus'** n. sp. A suggests that these faunules are pre-Late Mississippian, which is consistent with a Late Valmeyeran or, in European terms, a Viséan age.

One faunule (Loc. 5) grouped with Fauna B contains an element determined as ichthyolith A (Pl. 37.1, fig. 7). This element is also known to occur within unnamed carbonates, in west-central British Columbia, which are dated, by conodonts, as Early and/or early Middle Pennsylvanian. The Milford record of this ichthyolith implies that it ranges on both sides of the mid-Carboniferous boundary. A single associated hindeodid resembles **Hindeodus penescitulus** Rexroad and Collinson, A Viséan species.

Fauna C – The remainder of the conodont data from the Milford Group comes from the Goat Range of the southern Selkirk Mountains (Klepacki and Wheeler, 1985). Several faunules from this area are characterized by **Gnathodus girtyi simplex.** The Keen Creek Assemblage of Klepacki and Wheeler (1985) yielded only sparse Mississippian conodont faunules (Locs. 7, 8, 9, 14) in which probable representatives of this **Gnathodus** species are accompanied by a few, relatively conservative, long-ranging elements of **Idioprioniodus.** More abundant but otherwise identical

faunules were recovered from the Davis Assemblage in its southern outcrop near Mount Schroeder (Locs. 29, 31). A different conodont association, known only from the northern outcrops of the Davis Assemblage (Locs. 10-12), also include **G. girtyi** but is dominated by **Cavusgnathus** and **Kladognathus**, genera that are not recorded to the west.

Gnathodus girtyi simplex was originally described from the Bird Spring Formation in Southern Nevada (Dunn, 1965) in which it occurs second in abundance to **Adetognathus unicornis**, the characteristic species of the Grove Church Formation in Illinois, the topmost unit of the standard Chesterian. Subsequently, both Webster (1969) and Dunn (1970) recognized an uppermost Mississippian **G. girtyi simplex** Zone but as suggested by Lane and Straka (1974) and confirmed by Tynan (1980) the range of **G. girtyi simplex** is greater than originally thought and a zone based on its occurrence is a broad concept. Nevertheless, the species is a useful index for Upper Mississippian strata, ranging from within the **Kladognathus-Cavusgnathus naviculus** Zone of the mid-Chester (Collinson et al., 1971; Lane and Baesemann, 1982), that is Zone B of Tynan (1980), up to the top of the Mississippian, at which point it evolves into **Declinognathodus noduliferus**, the index for the base of the Upper Carboniferous (Lane and Baesemann, 1982). In Europe, **G. girtyi simplex** ranges within the Pendleian and Arnsbergian stages (E_{1-2}) of the Namurian (Higgins, 1975).

The specimens of **Cavusgnathus** from the Davis Assemblage resemble most closely **C. altus**, a species that is recorded in pre-Chesterian rocks in West Texas (Lane, 1974, p. 278), and ranges up to near the top of the Chester in the Illinois Basin (Collinson et al., 1971) and in Utah (Tynan, 1980). **Kladognathus** the faunal associate of **Cavusgnathus**, is a potentially useful index but, as in the

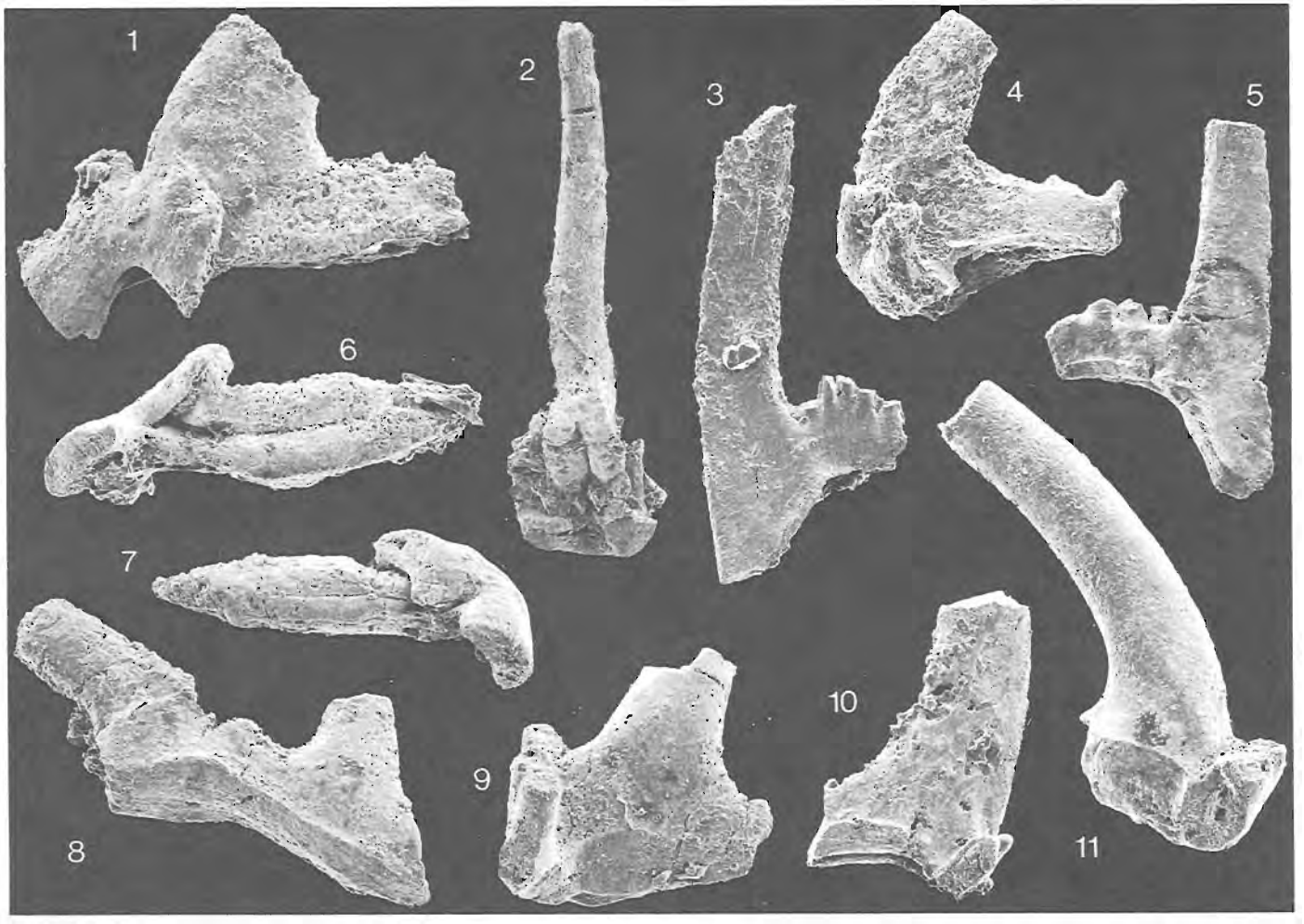

Plate 37.2

Inner-lateral views, unless stated otherwise. All specimens are from the Milford Group.

Figures 1-4, 6, 10. **Kladognathus**? sp. A. Specimens have relatively broad, shallowly excavated bases.
- 1,6. 'kladognathiform' (Sb?) element, GSC 69079, x80. Loc. 2. Lateral and lower views. Note concave anterior edge.
- 2. hibbardelliform (Sa) element, GSC 69080, x60. Loc. 3. Posterior, oblique-lower view.
- 3. neoprioniodiniform (M) element, GSC 69081, x60. Loc. 3.
- 4,10. ligonodiniform (Sc) elements, respectively GSC 69082, x80. Loc. 3. GSC 69087, x60. Loc. 4.

Figures 5, 7-11. **Kladognathus** sp. B. Specimens have relatively everted bases.
- 5. neoprioniodiniform (M) element, GSC 69083, x60. Loc. 12.
- 7. kladognathiform (Sb?) element, GSC 69084, x80. Loc. 11. Lower view. Note convex anterior edge.
- 8. 'ozarkodiniform' (P?) element, GSC 69085, x80. Loc. 12.
- 9,11. ligonodiniform (Sc) elements, respectively GSC 69086, x80. Loc. 12. GSC 69088, x60. Loc. 11.

Comaplix Mountain occurrences (Fauna B), poor preservation and sparse yields make specific determinations questionable. In the Davis Assemblage faunules, an element (Pl. 37.2, fig. 7) close to 'true' kladognathiform (**K. mehli**?) occurs. Additional elements (Pl. 37.2, figs. 9, 11) have a single antero-lateral process that emerges from a denticle anterior of the cusp (**'Kladognathus' tenuis**). These elements, combined as **Kladognathus** sp. B, are therefore regarded as more advanced than the species of Fauna B. In addition to the trend to develop antero-lateral processes farther forward of the cusp, there is a significant difference also in the lower surface morphology. All the elements of **Kladognathus** sp. B have narrower, more inverted basal regions compared with **Kladognathus**? sp. A, the elements of which have broader, somewhat flattened and more distinctly furrowed undersides (compare Pl. 37.2, figs. 6, 7).

The age of Fauna C from the Davis Assemblage is therefore correlated with the mid-Chesterian of the Mississippi Valley (Horowitz and Rexroad, 1982), and to Zone B of the Chainman Formation of Western Utah (Tynan, 1980). In Europe, **Cavusgnathus-Kladognathus** faunules are uncommon and most of the individual North American species are unrecorded. However, Higgins (1975) recognized a **Kladognathus-Gnathodus girtyi simplex** Zone in the basal Namurian (Pendleian, E_1) of Britain and a correlation with that zone appears probable.

The limestones from the southern part of the Davis Assemblage and those from the Keen Creek Assemblage are also Late Mississippian or Early Namurian based on **G. girtyi simplex** but theoretically they could be older, younger, or contemporaneous with the **Cavusgnathus-Kladognathus** bearing faunules. The presence of the latter taxa may reflect particular shallow-water conditions in the east, rather than any temporal difference (see below).

Two conodont collections made from an outcrop (Locs. 44, 45) near Kaslo in the northern part of the Nelson map area (NTS 82 F) were referred by Klepacki and Wheeler (1985) to the McHardy Assemblage. From one, a specimen of **Gnathodus girtyi** was recovered, and in the other a specimen referred to **Rhachistognathus**? sp. was found. The stratigraphic relationship of the two samples is uncertain, but they probably lay within 10 m of one another. The specimen of **Rhachistognathus** sp. is very poorly preserved, but the denticle distribution on the platform, although only just discernible, appears to correspond to that of **R. muricatus** (Dunn). This implies an age no older than the uppermost Mississippian, and possibly as young as Early Pennsylvanian (Lane and Straka, 1974; Lane and Baesemann, 1982). However, the nearby occurrence of **G. girtyi** suggests that the McHardy Assemblage at this outcrop, in common with those of the Davis and Keen Creek assemblages, is Late Mississippian.

Fauna D – The youngest fauna from the Milford Limestone occur within limestones of the Keen Creek Assemblage (Locs. 15, 16). Only four specimens were recovered, from two samples, and none of them are well enough preserved for specific determination. A species of **Idiognathodus** demonstrates that the limestone is no older than the mid-Morrowan, Early Pennsylvanian (Lane and Straka, 1974), or Marsdenian of the Late Namurian (Higgins, personal communication), although a minimum age for this genus is Early Permian. A probable **Neognathodus** species has strong, equally developed parapets that suggest a primitive condition such as is characteristic of **N. bassleri**. The occurrence of this specimen supports an Early Pennsylvanian rather than a younger age for the youngest Milford limestone. In European terms, the fauna is Late Namurian or Early Bashkirian.

Kaslo Group

Conodonts recovered from a channel sample across several hundred metres of chert outcrop are the only known fossils from the Kaslo Group. It is not known over what stratigraphic interval the conodonts originated, but since both black and white conodonts occur in the sample, they probably came from at least two stations, one of which was affected by higher temperatures related to associated igneous activity.

The conodonts are virtually all neogondolellid pectiniform elements, accompanied by a few ramiform fragments. The specimens of **Neogondolella** are of a relatively conservative morphology. They are characterized by elongate platforms, unornamented other than by microreticulation, by a generally terminal, relatively prominent posterior cusp, and a low carina that rises anteriorly into a low blade composed of laterally compressed denticles; the mid-platform margins are usually subparallel. They correspond to the popular concept of **Neogondolella idahoensis** (e.g. Kozur, 1978; Szaniawski and Malkowski, 1979; Wardlaw in Mytton et al., 1983) that characterizes Upper Lower Permian (Leonardian) strata elsewhere. They also resemble **N. slovenica**, a species from a comparable stratigraphic level in the Upper Lower Permian (Chihsian) of Slovenia, northwest Yugoslavia (Ramovs, 1982), and the slightly older **N. intermedia** Igo from Japan. In view of the limited

---

Plate 37.3

Upper views, unless stated otherwise.

Figure 1. ?**Ellisonia**? cf. **E. alienus** (Movschovitsch & Kozur). GSC 69089, x60. Lateral view. Loc. 22. Kaslo Group.

Figures 2, 4-10, 13. **Neogondolella** sp(p). Figs. 2, 5-7, 9, 10 from Kaslo Group, the remainder from the basal conglomerate of the Slocan Group.
2. GSC 69090, x80. Loc. 19.
4. GSC 69092, x80. Posterior fragment, early growth stage. Loc. 22.
5. GSC 69093, x80. Lower view. Loc. 19.
6, 7. GSC 69094, x80. Oblique-lateral and upper views. Loc. 19.
8. GSC 69095, x80. Loc. 22.
9. GSC 69096, x150. Early growth stage. Loc. 19.
10. GSC 69097, x150. Early growth stage. Loc. 19.
13. GSC 69100, x80. Posterior fragment, late growth stage. Loc. 21.

Figure 3. **Idiognathodus** sp. GSC 69091, x60. Loc. 15. Milford Group.

Figures 11, 12, 14. **Paragondolella polygnathiformis** (Budurov & Stefanov) sensu lato. Slocan Group.
11. GSC 69098, x80. Loc. 41. Elongate morph.
12. GSC 69099, x80. Loc. 18. Lower view, abbreviated morph.
14. GSC 69101, x80. Loc. 18. Abbreviated morph.

Figure 15. **Neogondolella navicula** (Huckriede) sensu lato. GSC 69102, x80. Loc. 34. Slocan Group.

Figures 16, 17. **Epigondolella primitia** Mosher. GSC 69103, x150, x80. Loc. 37. Slocan Group.

Figure 18. **Epigondolella** cf. **E. postera** (Kozur & Mostler). GSC 69104, x80. Loc. 38. Slocan Group. Specimen resembles also certain morphs of **E.** n. sp. C of Orchard, 1983.

Figures 19, 20. **Epigondolella bidentata** Mosher. GSC 69105, x80, x150. Loc. 23. Slocan Group.

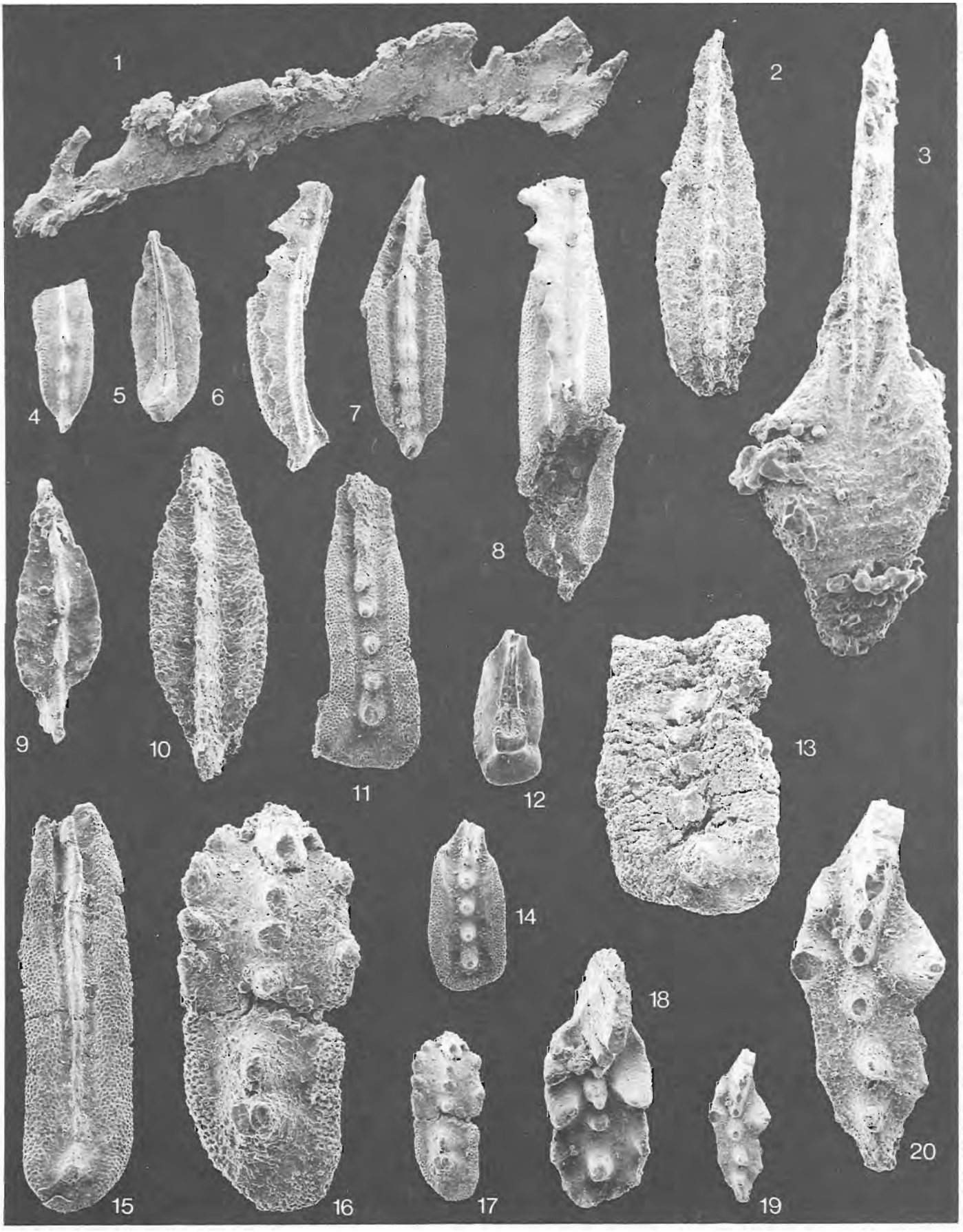
1
2
3
4
5
6
7
8
9
10
11
12
13
14
15
16
17
18
19
20

material and pending taxonomic revision of this group of Early Permian neogondolellids, the Kaslo specimens are kept in open nomenclature. Their morphology is, however, regarded as characteristic of the late Early Permian.

Marten conglomerate

Two samples from a limestone bed intercalated with conglomerate near the headwaters of Marten Creek at Inverness Mountain yielded poorly preserved specimens of **Neogondolella** and **Ellisonia**?. In most respects, the neogondolellids are the same as those from the Kaslo chert, although some are larger than any recovered from the latter. Hence, one large posterior fragment (Pl. 37.3, fig. 13) has a subquadrate platform termination and a cusp that is relatively 'submerged' by posterior platform growth. Such a morphology is to be expected in late growth stages of Early Permian **Neogondolella**; intermediate growth stages (Pl. 37.3, fig. 8) show the increased postero-lateral expansion that leads to this condition.

Another feature of at least one neogondolellid (Pl. 37.3, fig. 8) from the conglomerate is the anterior blade denticles that are partly fused and have, in profile, distinct arcuate inter-denticular spaces. This type of denticulation appears to be a feature of some illustrated Permian neogondolellids (e.g. Behnken, 1975, pl. 2, fig. 11), but I have not seen it in post-Early Triassic collections. On the basis of the available material, I regard **Neogondolella** from the Marten conglomerate as specifically indeterminate but, in common with those from the Kaslo Chert, morphologically indicative of Early Permian time.

Associated with the neogondolellids is a single specimen of a ramiform conodont characterized, at least in part, by an alternation of relatively large and small, discrete denticles.

Table 37.1. Locality number on Figure 37.1, GSC Loc. No., Rock unit, and age of conodont collections from the central Kootenay Arc.

Figure 1	GSC Loc. No.	Rock Unit	Age
1	C- 87703	Milford, lst.	Late Famennian-Tournaisian
2	C- 87715	Milford, lst.	Visean
3	C- 87716	Milford, lst.	Visean
4	C- 87717	Milford, lst.	Visean
5	C- 87718	Milford, lst.	Visean?
6	C-103466	Milford, Keen Ck. Ass., lst.	Carboniferous
7	C- 87160	Milford, Keen Ck. Ass., lst.	Early Namurian
8	C- 87161	Milford, Keen Ck. Ass., lst.	Early Namurian
9	C- 87165	Milford, Keen Ck. Ass., lst.	Early Namurian
10	O- 68715	Milford, Davis Ass., lst.	Late Visean-Early Namurian
11	C- 87712	Milford, Davis Ass., lst.	Early Namurian
12	C- 87713	Milford, Davis Ass., lst.	Early Namurian
13	C-103458	Milford, Keen Ck. Ass., lst.	indet.
14	C- 87714	Milford, Keen Ck. Ass., lst.	Early Namurian
15	C- 87167	Milford, Keen Ck. Ass., lst.	Late Namurian-Wolfcampian
16	C- 87169	Milford, Keen Ck. Ass., lst.	Late Namurian-Early Bashkirian
17	O- 68719	Slocan, lst.	Permo-Triassic
18	O- 93538	Slocan, lst.	Carnian
19	C-103451-2	Kaslo, chert.	Leonardian
20	C-103382	Slocan, lst.	Carnian
21	C-101310	Slocan? conglomerate, lst.	Leonardian?
22	C-101309	Slocan? conglomerate, lst.	Leonardian?
23	O- 93549	Slocan, lst.	Late Norian
24	C-101305	Slocan, lst.	Late Middle-Late Triassic
25	C-101314	Slocan (east), lst.	Middle-Late Triassic
26	O- 68707a	Slocan, lst.	Middle Norian
27	O- 68707b	Slocan, lst.	Carnian?
28	O- 93545	Milford, Davis A., lst.	Carboniferous?
29	C- 87156	Milford, Davis A., lst.	Early Namurian
30	C-103387	Milford, Davis A., lst.	Late Visean-Early Namurian
31	C- 87155	Milford, Davis A., lst.	Early Namurian
32	C- 87154	Slocan (east), lst.	Late Middle-Late Triassic
33	C- 87151	Slocan (east), lst.	Middle-Late Triassic
34	C- 87153	Slocan (east), lst.	Norian(?)
35	O- 93547	Slocan, lst.	Middle Norian
36	O- 93464	Slocan, Whitewater lst.	Late Carnian-Norian
37	O- 93467a	Slocan, Whitewater lst.	Carnian-Norian boundary
38	O- 93467b	Slocan, Whitewater lst.	Middle Norian
39	C-116333	Slocan, Whitewater lst.	Middle Norian
40	C-116336	Slocan, Whitewater lst.	Carnian-Norian boundary
41	O- 93548	Slocan lst.	Carnian
42	C-103373	Slocan (east), lst.	Middle-Late Triassic
43	C-103398	Milford, McHardy Ass.?, lst.	indet.
44	C-116334	Milford, McHardy Ass., lst.	Early-Mid-Namurian
45	C-116335	Milford, McHardy Ass., lst.	Early Namurian

This morphology is like that of **'Stepanovites' alienus,** which was based on three specimens from the Artinskian-Kungurian boundary beds of the Shurtan Formation exposed in the Kamai Ravine of the Perm District of the Urals (Movschovitsch et al., 1979, fig. 1, section 3; p. 102). A similar element was recorded by Szaniawski and Malkowski (1979, pl. 10, fig. 2) from the Ahlstrandodden section of the Kapp Starostin Formation in Spitsbergen. As in the Urals, the Spitsbergen element (described as "fragment 1") was associated with **Neostreptognathodus** in Upper Lower Permian (Leonardian) strata. Although the species is not well known, and the Kootenay element differs in overall morphology from the aforementioned specimens, its presence lends support to the Leonardian age suggested for the neogondolellids.

Hence, the present evidence suggests that the conodonts from Inverness Mountain (Locs. 21, 22) are quite close in age to those of the underlying Kaslo Chert.

Slocan Group

Limestones referred to the Slocan Group have yielded conodonts indicative of both Carnian and Norian (Late Triassic) age. Furthermore, recent refinement of Norian conodont zonation (Orchard, 1983) facilitates the recognition of a broad range of Norian time within the Slocan Group. The oldest Slocan faunules came from two localities (Locs. 18, 41) where morphs of **Paragondolella polygnathiformis** occur. This species ranges throughout the Carnian but was largely replaced in the latest Carnian by metapolygnathids, including **'Epigondolella' primitia,** a species that spans the Carnian-Norian boundary. The latter species occurs at Localities 37 and 40. Post-Early Norian species of **Epigondolella** occur in five faunules. At Localities 26, 35, 38 and 39, **E. postera** indicates the mid-Middle Norian and at Locality 23, **E. bidentata** morphs indicate Upper Norian strata. Significantly, faunules indicative of both the Carnian-Norian boundary and of the Middle Norian were recovered from within the same section of outcrop at Localities 35-40 and probably also at Localities 26-27. The former is the "Whitewater limestone" (see Hedley, 1945, p. 9), one of the principal mineralized beds within the Slocan Group. The reason for this close proximity of disparate ages may lie in intense structural interleaving but the complex structure may obscure a relatively condensed sequence, or some non-sequence. The latter possibility is supported by the absence of unequivocal Early Norian conodonts within the study area.

In the eastern belt of the Slocan (Locs. 25, 32, 33, 34, 42), **Epigondolella** has not been found. Whilst it remains a possibility that the faunules from this belt are wholly pre-Norian, this distribution of conodonts is more likely a reflection of differing environments (see below).

Conodont biofacies and comparisons within the Kootenay Arc

Conodont distribution within the Kootenay Arc partly reflects the environment of deposition of the sediments. Within the Carboniferous, the **Cavusgnathus-Kladognathus** biofacies (Horowitz and Rexroad, 1982) of the Milford Group (Davis Assemblage north) has generally been regarded as indicative of shallow-water, high energy and/or possibly euryhaline conditions. **Cavusgnathus** has been shown elsewhere to dominate the basal transgressive phase of a marine interval (e.g. Merrill, 1980) and its occurrence within the Milford Group is probably another example. It also seems probable that **Kladognathus,** and spathognathodids such as **'Spathognathodus'** n. sp. A, which accompanies **Kladognathus**? in the conglomerate basal facies of the Milford in its northeastern outcrop (also of Davis Assemblage aspect) are similar examples of environmentally restricted conodonts.

Table 37.2. Numerical data on conodont collections from the Milford Group.
Numbers at top shown on Figure 37.1. A, B, C, D refer to faunas described in text.

		1	2	3	4	5	6	7	8	9	10	11	12	13	14	15	16	28	29	30	31	43	44	45
A	*Polygnathus*	7	-	-	-	-	-	-	-	-	-	-	-	-	-	-	-	-	-	-	-	-	-	-
	Pseudopolygnathus	2	-	-	-	-	-	-	-	-	-	-	-	-	-	-	-	-	-	-	-	-	-	-
B	*Kladognathus?*	-	X	X	X	?	-	-	-	-	-	-	-	-	-	-	-	-	-	-	-	-	-	-
	'Spathognathodus'	-	8	2	3	-	-	-	-	-	-	-	-	-	-	-	-	-	-	-	-	-	-	-
	ichthyolith A	-	-	-	-	9	-	-	-	-	-	-	-	-	-	-	-	-	-	-	-	-	-	-
C&B	*Hindeodus*	-	-	-	-	1	-	-	-	-	-	1?	-	-	-	-	-	-	-	-	-	-	-	-
	Idioprioniodus	-	-	X	-	-	X	X	?	X	-	?	?	-	-	-	-	?	?	-	X	-	-	-
C	*Cavusgnathus*	-	-	-	-	-	-	-	-	-	3	6	2	-	-	-	-	-	-	2	-	-	-	-
	Gnathodus girtyi	-	-	-	-	-	-	1	3	11	-	1	1	-	2	-	-	-	21	-	31	-	-	1
	Kladognathus	-	-	-	-	-	-	-	-	-	-	X	X	-	-	-	-	-	-	-	-	-	-	-
	Rhachistognathus	-	-	-	-	-	-	-	-	-	-	-	-	-	-	-	-	-	-	-	-	-	1	-
D	*Idiognathodus*	-	-	-	-	-	-	-	-	-	-	-	-	-	-	1	1?	-	-	-	-	-	-	-
	Neognathodus	-	-	-	-	-	-	-	-	-	-	-	-	-	-	-	2	-	-	-	-	-	-	-
	indet. frags.	-	-	-	-	-	-	-	-	-	-	-	-	X	-	-	-	-	-	-	-	X	-	-
	C.A.I.	7	5	5	5	5	6	6-7	6	6	5-6	5-7	5-6	5-6	6	6-7	6-7	6	5-6	5-6	5	5	5	5

Table 37.3. Numerical data on conodont collections from the Kaslo and Slocan groups. Numbers at top shown on Figure 37.1.

		19	21	22	17	18	20	23	24	25	26	27	32	33	34	35	36	37	38	39	40	41	42
Perm.	*Ellisonia?*	-	-	1	-	-	-	-	-	-	-	-	-	-	-	-	-	-	-	-	-	-	-
	Neogondolella	36	11	8	-	-	-	-	-	-	-	-	-	-	-	-	-	-	-	-	-	-	-
Triassic	*Epigondolella*	-	-	-	-	-	1?	10	-	-	9	-	-	-	-	6	2	8	2	12	4	-	-
	E. primitia	-	-	-	-	-	?	-	-	-	-	-	-	-	-	-	?	X	-	-	X	-	-
	E. postera	-	-	-	-	-	-	-	-	-	X	-	-	-	-	X	?	-	X	X	-	-	-
	E. bidentata	-	-	-	-	-	-	X	-	-	-	-	-	-	-	-	-	-	-	-	-	-	-
	Neogondolella	-	-	-	-	-	-	1	2	1	-	-	9	1	7	-	-	-	-	-	-	-	4
	Paragondolella	-	-	-	-	6	2	-	1?	-	-	1?	-	-	-	-	1	-	-	-	-	1	-
	ramiforms indet.	X	X	-	X	-	X	X	X	-	X	-	-	-	X	?	-	-	-	-	-	-	-
	ichthyoliths	-	-	-	-	X	-	-	-	-	-	-	-	-	-	-	-	-	X	-	-	-	X
	C.A.I.	5,7	5	5	6	5-6	5	5	5	5	5	7	5	5	5	5	5-7	5-6	5,7	5-6	6-7	6	5

In the Late Famennian and Tournaisian, pseudopolygnathids and polygnathids, such as occur in the westernmost Milford (Fauna A) are also regarded as indicative of near- rather than off-shore marine environments. Neither palmatolepids (Devonian) nor siphonodellids (Tournaisian), which characterize more open marine environments, occur in Fauna A.

Within Upper Mississippian rocks, relatively offshore environments (biofacies 2 of Horowitz and Rexroad, 1982) are characterized by diverse faunas of **Gnathodus, Lochriea (Paragnathodus)** and **Idioprioniodus,** a biofacies that is only partly developed in the Keen Creek and Davis (south) assemblages. **Idioprioniodus** occurs throughout the region, but **Gnathodus** is represented by only one species (**G. girtyi**) and **Lochriea** is absent. In view of the fact that many gnathodid and paragnathodid species were extant during the time represented by Faunas B and C, their absence suggests an environmental control. Presumably **G. girtyi** was more tolerant of certain (shallow-water related?) conditions than those other taxa.

Within the Kootenay Arc, more or less contemporaneous Mississippian conodont faunas are known to the north in the Eagle Bay Formation (Okulitch and Cameron, 1976; Orchard, unpublished manuscript). Both Tournaisian and Late Viséan-Early Namurian faunas are known and interestingly both are characterized by diverse conodont populations that are dominated in the Tournaisian by **Siphonodella,** and include, in the younger Mississippian, abundant specimens of **Gnathodus bilineatus, G. texanus** and **Lochriea commutatus,** as well as **Idioprioniodus** and fewer representatives of **G. girtyi** and **Rhachistognathus.** These contemporary and far more diverse faunas are interpreted as an off-shore, deeper and more open marine equivalent of those that characterize the Milford Group.

Conodont distribution in the Slocan Group may also reflect some environmental control. All of the faunules from the western (main) belt of the Slocan are composed of either **Paragondolella** or its derivative **Epigondolella.** On the other hand, the eastern belt has yielded principally **Neogondolella.** Poorly preserved specimens of the latter are more difficult to identify but broad contemporaneity of the two belts is indicated. Evidence from elsewhere in Western Canada indicates that, within the Norian, **Neogondolella** and **Epigondolella** preferred different habitats, but the environmental controls are not presently understood.

Summary

Conodonts from the Milford Group of the central Kootenay Arc give a minimum age range of Tournaisian through Namurian, that is Early Mississippian through Early Pennsylvanian. There remains a possibility of this range extending downward into the Late Devonian (Late Famennian) and upward into the higher Bashkirian (Middle Pennsylvanian equivalent), but an extension into the basal Permian is considered unlikely. Dating in the extreme west (Locality 1), in the northeast (Locs. 2-5) and in the south-central (e.g. Loc. 7-12, 29-31) part of the Lardeau map area identifies successively younger levels within the Lower Carboniferous, respectively Tournaisian (or older), Viséan, and Namurian. There is thus an indication of an eastward transgressive onlap. The Milford conodont biofacies reflect relatively shallow-water, near-shore, restricted marine conditions (particularly in the northern Davis Assemblage) compared with correlatives in the Eagle Bay Formation of the northern Kootenay Arc.

Conodonts from the Kaslo Group are the first fossils from that unit and date it, in part, as Late Early Permian. The same age is attributed to conodonts from the overlying Marten conglomerate at Inverness Mountain.

Conodonts from the Slocan Group date it as Late Triassic. Based on **Epigondolella** and its antecedents, four distinct ages are recognized in the western belt: Carnian, Carnian-Norian boundary, mid-Middle Norian and Late Norian. The juxtaposition of the two intermediate Late Triassic faunules in two localities suggests a hiatus may exist within this part of the Slocan Group. In the eastern belt, **Epigondolella** is unknown and a **Neogondolella** biofacies is represented within probable correlative strata, implying some difference in environmental regime between the two belts.

Acknowledgments

I thank J.O. Wheeler for showing me the geology of the central Kootenay Arc in 1981 during which time I collected some of the samples reported on. Other samples that constitute the source of the data were collected by D.W. Klepacki, J.O. Wheeler, P.B. Read and A.V. Okulitch, all of whom have kindly contributed information on locality and stratigraphic context of samples. E.W. Bamber made available unpublished macrofossil data from the

Milford Group. B.E.B. Cameron was responsible for isolating the conodont collections made prior to 1979, and is acknowledged for first identifying Triassic conodonts from the Slocan Group. A.C. Higgins, D.W. Klepacki and J.O. Wheeler read the manuscript and made useful comment. P. Krauss did some of the conodont photography. B. Forman helped compile Figure 37.1, which was drafted by T. Oliveric. B. Vanlier typed the manuscript.

References

Bancroft, M.F.
1919: Southern Lardeau, Slocan District, B.C.; Geological Survey of Canada, Summary Reports 1917, pt. B, p. 35-41.

1920: Slocan map area, B.C.; Geological Survey of Canada, Summary Reports 1919, pt. B, p. 39-48.

1921: Lardeau map area, B.C.; Geological Survey of Canada, Summary Reports 1920, pt. A, p. 94-102.

Behnken, F.H.
1975: Leonardian and Guadalupian (Permian) conodont biostratigraphy in western and southwestern United States; Journal of Paleontology, v. 49, p. 284-315.

Branson, E.B. and Mehl, M.G.
1941: Caney conodonts of Upper Mississippian age; Journal of Denison University Science Laboratory, v. 35, p. 167-178.

Cairnes, C.E.
1934: Slocan Mining Camp, British Columbia; Geological Survey of Canada, Memoir 173.

Collinson, C., Rexroad, C.B., and Thompson, T.L.
1971: Conodont zonation of the North American Mississippian; Geological Society of America, Memoir 127, p. 353-394.

Drysdale, C.W.
1917: Slocan Area, Ainsworth and Slocan Mining Divisions; Geological Survey of Canada, Summary Reports 1916, p. 56-57, Map 1667.

Dunn, D.L.
1965: Late Mississippian conodonts from the Bird Spring Formation in Nevada; Journal of Paleontology, v. 39, p. 1145-1150.

1970: Conodont zonation near the Mississippian-Pennsylvanian boundary in western United States; Geological Society of America Bulletin, v. 81, p. 2959-2974.

Hedley, M.S.
1945: Geology of the Whitewater and Lucky Jim Mine Areas, Slocan District, British Columbia; B.C. Department of Mines, Bulletin 22.

Higgins, A.C.
1975: Conodont zonation of the late Viséan-early Westphalian strata of the south and central Pennines of northern England; Geological Survey of Great Britain, Bulletin 53.

1982: A mid-Carboniferous boundary in the western Europe conodont sequence; in Biostratigraphic data for a mid-Carboniferous boundary, ed. W.H.C. Ramsbottom, W.B. Saunders, and B. Owens; Subcommission on Carboniferous Stratigraphy, p. 13-14.

Horowitz, A.S. and Rexroad, C.B.
1982: An evaluation of statistical reconstructions of multi-element conodont taxa in middle Chesterian rocks (Carboniferous) in southern Indiana; Journal of Paleontology, v. 56, p. 959-969.

Klepacki, D.W.
1983: Stratigraphic and structural relations of the Milford, Kaslo and Slocan groups, Roseberry Quadrangle, Lardeau map area, British Columbia; in Current Research, Part A, Geological Survey of Canada, Paper 83-1A, p. 229-233.

Klepacki, D.W. and Wheeler, J.O.
1985: Stratigraphic and structural relations of the Milford, Kaslo and Slocan groups, Goat Range, Lardeau and Nelson map areas, British Columbia; in Current Research, Part A, Geological Survey of Canada, Paper 85-1A, Report 36.

Kozur, H.
1978: Beitrage zur Stratigraphie des Perms. Teil II: Die Conodontenchronologie des Perms; Freiberger Forschungsheft C 334, p. 85-161.

Lane, H.R.
1974: Mississippian of southeastern New Mexico and West Texas – a wedge – on wedge relationship; American Association of Petroleum Geologists Bulletin, v. 58, p. 269-282.

Lane, H.R. and Baesemann, J.F.
1982: A mid-Carboniferous boundary based on conodonts and revised intercontinental correlations; in Biostratigraphic data for a mid-Carboniferous boundary, ed. W.H.C. Ramsbottom, W.B. Saunders, and B. Owens; Subcommission on Carboniferous Stratigraphy, p. 6-11.

Lane, H.R., Sandberg, C.A., and Ziegler, W.
1980: Taxonomy and phylogeny of some Lower Carboniferous conodonts and preliminary standard post-**Siphonodella** zonation; Geologica et Palaeontologica, v. 14, p. 117-164.

Lane, H.R. and Straka, J.J.
1974: Late Mississippian and Early Pennsylvanian conodonts, Arkansas and Oklahoma; Geological Society of America, Special Paper 152.

Little, H.W.
1960: Nelson map area, west half, British Columbia; Geological Survey of Canada, Memoir 308.

McConnell, R.G.
1897: Report on Field Work in West Kootenay Area, British Columbia; Geological Survey of Canada, Annual Reports 1895, v. 8, p. 23A-37A.

Merrill, G.K.
1980: Preliminary Report on the Restudy of conodonts from the Barnett Formation; in Guidebook for the West Texas Geological Society Field Trip, ed. D. Winkle.

Movschovitsch, E.V., Kozur, H., Pavlov, A.M., Pnev, V.N., Polozova, A.N., Chuvashov, B.I., and Bogoslovkaya, M.F.
1979: Conodont assemblages of the Lower Permian in the sub-Ural region and problems of correlation of Lower Permian deposits; in Conodonts of the Urals and their stratigraphic significance, ed. G.N. Papulov and V.N. Puchkov; Symposium Sverdlovsk, 1979. USSR Academy of Sciences, Scientific Centre of the Urals, Proceedings of the Institute of Geology and Geochemistry, Issue 145, p. 94-131.

Mytton, J.W., Morgan, W.A., and Wardlaw, B.R.
1983: Stratigraphic relations of Permian units, Cassia Mountains, Idaho; Geological Society of America, Memoir 157, p. 281-303.

Nicoll, R.S. and Rexroad, C.B.
1975: Stratigraphy and conodont paleontology of the Sanders Group (Mississippian); in Indiana and adjacent Kentucky; Indiana Geological Survey, Bulletin 51.

Okulitch, A.V. and Cameron, B.E.B.
1976: Stratigraphic revisions of the Nicola, Cache Creek, and Mount Ida groups, based on conodont collections for the western margin of the Shuswap Metamorphic Complex, south-central British Columbia; Canadian Journal of Earth Sciences, v. 13, p. 44-53.

Orchard, M.J.
1983: **Epigondolella** populations and their phylogeny and zonation in the Upper Triassic; Fossils and Strata, No. 15, p. 177-192.

Orchard, M.J. and Struik, L.C.
– Conodonts and stratigraphy of Upper Paleozoic limestones in Cariboo Gold Belt, east central British Columbia; Canadian Journal of Earth Sciences. (in press)

Ramovs, A.
1982: Unterperm – Conodonten aus den Karawanken (Slowenien, NW Jugoslawien); Neues Jahrbruch Geologische Palaontologisch Abhandlungen, v. 164, p. 414-427.

Read, P.B. and Okulitch, A.V.
1977: The Triassic unconformity of south-central British Columbia; Canadian Journal of Earth Sciences, v. 14, p. 606-638.

Read, P.B. and Wheeler, J.O.
1976: Geology, Lardeau west-half, British Columbia; Geological Survey of Canada, Open File 432.

Reesor, J.E. and Moore, J.M., Jr.
1971: Petrology and structure of Thor-Odin Gneiss Dome, Shuswap Metamorphic Complex, British Columbia; Geological Survey of Canada, Bulletin 195.

Rexroad, C.B.
1981: Conodonts from the Vienna Limestone Member of the Branchville Formation (Chesterian) in southern Indiana; Indiana Geological Survey, Occasional Paper 34, p. 1-16.

Rexroad, C.B. and Collinson, C.
1963: Conodonts from the St. Louis Formation (Valmeyeran Series) of Illinois, Indiana, and Missouri; Illinois State Geological Survey, Circular 355, p. 1-28.

1965: Conodonts from the Keokuk, Warsaw, and Salem formations (Mississippian) of Illinois; Illinois State Geological Survey, Circular 388, p. 1-26.

Rexroad, C.B. and Thompson, T.L.
1979: A spathognathodont lineage of Mississippian conodonts; Lethaia, v. 12, p. 235-243.

Ross, J.V. and Kellerhals, P.
1968: Evolution of the Slocan Syncline in south-central British Columbia; Canadian Journal of Earth Sciences, v. 5, p. 851-872.

Szaniawski, H. and Malkowski, K.
1979: Conodonts from the Kapp Starostin Formation (Permian) of Spitsbergen; Acta Palaeontologica Polonica, v. 24, p. 231-264.

Tynan, M.C.
1980: Conodont biostratigraphy of the Mississippian Chainman Formation, Western Millard County, Utah; Journal of Paleontology, v. 54, p. 1281-1309.

Webster, G.D.
1969: Chester through Derry conodonts and stratigraphy of northern Clark and southern Lincoln counties, Nevada; California University Publications in Geological Sciences, 79, p. 1-121.

Ziegler, W. (ed.)
1977: Catalogue of Conodonts, v. 3, Stuttgart.

1981: Catalogue of Conodonts, v. 4, Stuttgart.

-38-

PRE-EMPLACEMENT THRUST FAULTING IN THE SYLVESTER ALLOCHTHON, NORTHEAST CRY LAKE MAP AREA, BRITISH COLUMBIA

Project 770016

Telka Harms[1]
Cordilleran Geology Division, Vancouver

Harms, T., Pre-emplacement thrust faulting in the Sylvester Allochthon, northeast Cry Lake map area, British Columbia; in Current Research, Part A, Geological Survey of Canada, Paper 85-1A, p. 301-304, 1985.

Abstract

The Sylvester Allochthon comprises a stack of fault-bounded slices of Upper Paleozoic oceanic lithologies emplaced onto the miogeocline sometime after the Triassic and prior to the mid-Cretaceous. A tonalitic intrusive, yielding a preliminary zircon age of Late Permian, has been shown to intrude across at least one of the characteristic slice-bounding faults within the Sylvester along the Rapid River. Although much of the internal structural style of the Sylvester Allochthon may be related to the emplacement process, at least some of the thrust faulting is earlier.

Résumé

L'allochtone de Sylvester se compose d'un amas de lambeaux aux lithologies océaniques du Paléozoïque supérieur qui sont limités par des failles et qui ont été mis en place sur le miogéosynclinal après le Trias et avant le Crétacé moyen. Une intrusion de tonalite qui, d'après la datation du zircon, date provisoirement du Permien récent, a pénétré au moins une des failles limitrophes caractéristiques dans l'allochtone le long de la rivière Rapid. Bien qu'une grande partie du style structural interne de l'allocthone puisse être liée au processus de mise en place, une partie au moins des failles chevauchantes est antérieure.

[1] Department of Geosciences, University of Arizona, Tucson, Arizona

Introduction

Since recognition of the upper Paleozoic Sylvester Group of north central British Columbia (Gabrielse, 1963) as an obducted oceanic assemblage (Monger, 1977; Gabrielse and Mansy, 1980) detailed study of the Sylvester has shown it to consist structurally of a stack of subhorizontal, fault-bounded, tectonolithologic sheets or slivers (commonly older-over-younger) resulting in a highly variable and shuffled tectonic "stratigraphy" (Harms, 1984; Gordey et al., 1982). The Sylvester Allochthon presently lies as an enormous klippe above North American migeoclinal carbonates (Fig. 38.1). The basal Sylvester fault is continuous and planar below the allochthon and shows no evidence of significant postemplacement imbrication or deformation. The age of emplacement of the allochthon is loosely constrained; it must be younger than Triassic, the age of the youngest rocks within the Sylvester assemblage (Gabrielse, 1963) and older than the mid-Cretaceous Cassiar batholith which intrudes both the Sylvester fault and the miogeocline. It has been assumed that the remarkable imbrication within the Sylvester Allochthon in some way resulted from or is related to the obduction process and is therefore also Triassic to mid-Cretaceous. However, relationships determined during the 1984 field season, and fossil ages together with zircon dating on samples collected during 1983, show that at least some of the internal Sylvester thrust faults significantly predate emplacement of the allochthonous body.

Tectonic and intrusive contact relationships

The complex tectonic stratigraphy which characteristically results from the structural style within the Sylvester Allochthon is shown in Figure 38.2 for the small portion of the allochthon that lies along Rapid River northeast of Cry Lake in Cry Lake and McDame map areas. Northwest of Rapid River a fairly widespread, green layered undated volcanic unit (Unit I) comprises interbedded layered basalt flows, green tuffaceous volcaniclastic rocks, and green banded chert. Immediately north of the river an Early to Middle Pennsylvanian limestone (conodont dating by M. Orchard) (Unit II) is in fault contact with, and structurally above the volcanic unit. The type section of the Sylvester Group (Mamet and Gabrielse, 1969), which occurs farther northwest along structural trend, includes a distinctive basal member consisting of a coarse calcarenite containing quartz and volcanic lithic grains, and unusually large crinoid columnals. In the type area, the Nizi Formation lies above the layered volcanics of Unit I. To the southeast the basal Nizi member is thrust northeastward over Pennsylvanian limestone (Unit II). Because of the presence of volcanic fragments in the basal Nizi member, the Nizi Formation was initially described as being depositional on Unit I in the type section (Mamet and Gabrielse, 1969). However, disharmonic folding between the two units, and the thrust fault contact relationships between the basal Nizi and Pennsylvanian limestone, and between Pennsylvanian limestone and Unit I volcanics, suggest the basal Nizi contact is structural rather than depositional. On the north side of Rapid River, the Pennsylvanian limestone unit is overlain by a strongly foliated and lineated siliceous tectonite (Unit III). Because of the abrupt change in grade of penetrative deformation, this contact, also, is believed to be a fault.

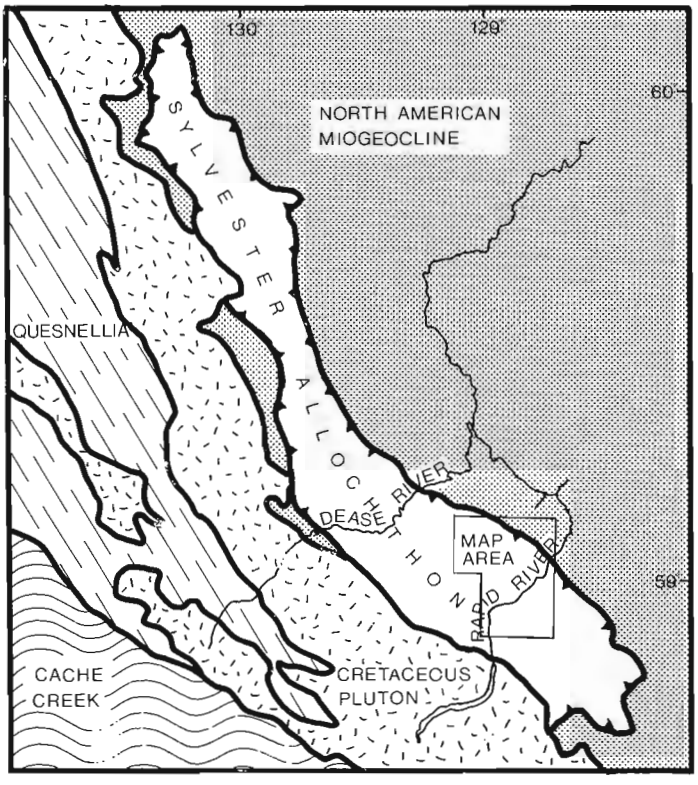

Figure 38.1. Regional setting of the Sylvester Allochthon and study area.

Northwest of the Rapid River the Pennsylvanian limestone is intruded by a distinctive tonalite body. The intrusive consists of euhedral plagioclase phenocrysts (40%), relatively abundant anhedral quartz phenocrysts (30%) and minor biotite (5%) in a chloritized, very fine grained, crystalline groundmass (25%). In some localities the tonalite may contain as much as 15% euhedral hornblende phenocrysts. Chemical analyses are not yet complete, but on the basis of hand specimen and thin section analysis, a tonalite composition is assigned. The tonalite also intrudes the basal Nizi where the Nizi is thrust over the Pennsylvanian limestone. Near Rapid River, however, none of the unit-bounding faults are intruded by the tonalite, nor are the siliceous tectonite (Unit III) or layered volcanic (Unit I) sheets.

A thick succession of the green layered volcanic unit (Unit I) is also found southeast of Rapid River. There, a sequence of basal Nizi calcarenite which is thinner than that in the type section occurs above the volcanics. Structurally above the basal Nizi member is an exceedingly thick sequence of banded chert (Unit IV). The base of this unit includes a section of interlayered carbonate, radiolarian chert, and quartz grit; the association suggests very fine imbrication at the base of, if not throughout, the thick chert sheet. The remaining 550+m of upper Nizi Formation is missing between the basal Nizi and Unit IV chert. A fault parallel with bedding responsible for removing the upper Nizi, must once have existed between these two units. Now, however, intervening between the two tectonic sheets is a generally tabular or sill-like body of the tonalite intrusive (Fig. 38.3). The tonalite is clearly intrusive into both the basal Nizi and layered volcanic units below, and the banded chert unit above. Septa, baked country rock, irregular intrusive contacts, and chilled tonalite are all visible along the tonalite contacts. The tonalite, therefore, crosscuts a typical Sylvester thrust fault.

Tonalite age and timing of deformation

Preliminary zircon dating from samples collected in 1983 from the tonalite north of Rapid River (Site B, Fig. 38.2) has been conducted by J.K. Mortensen at the University of British Columbia and suggests a Late

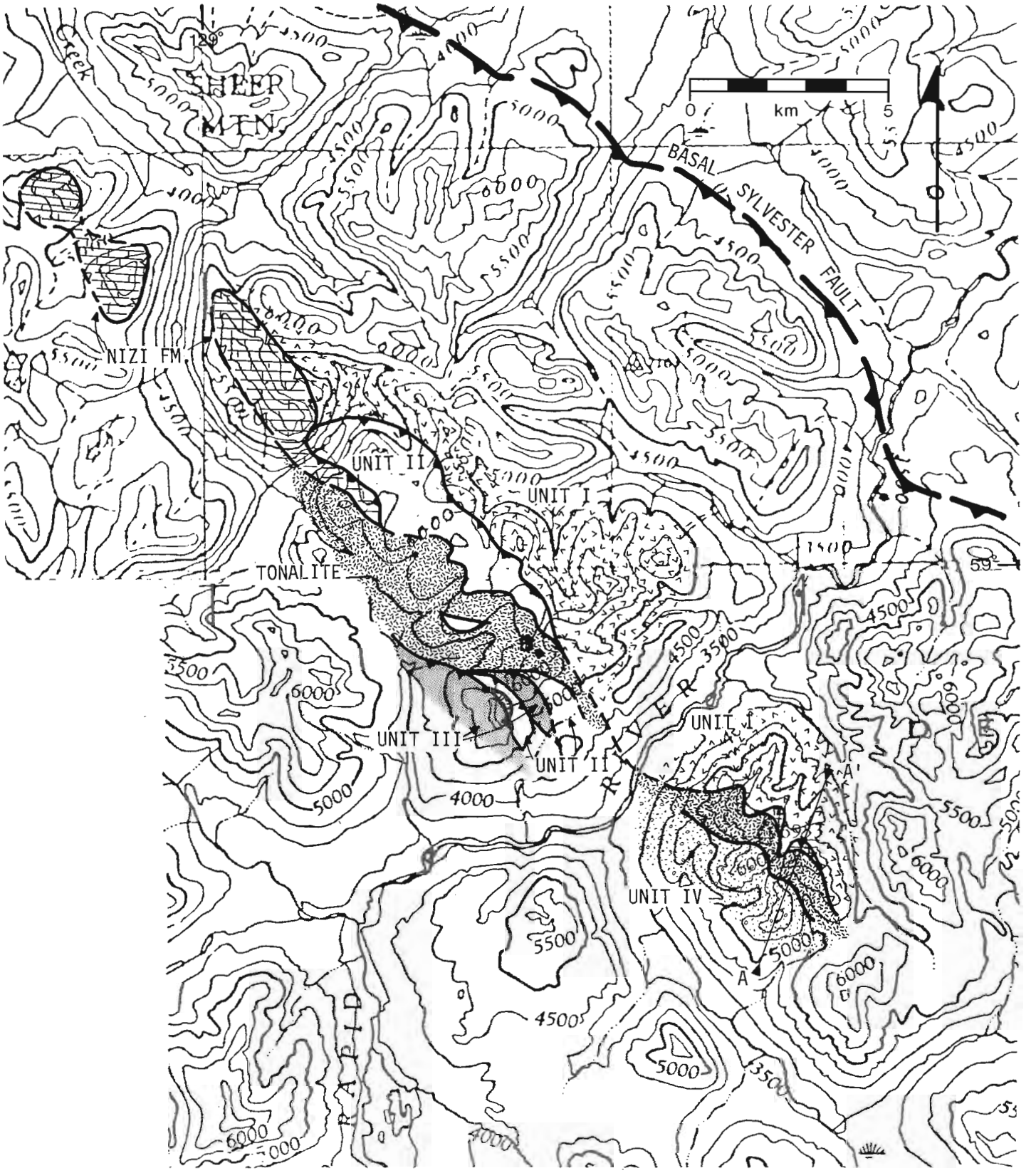

Figure 38.2. *Geological map of parts of the Sylvester Allochthon along Rapid River. Closed barbs; thrust faults, open barbs; presumed thrust faults. Nizi Formation contacts modified from Gabrielse, 1963.*

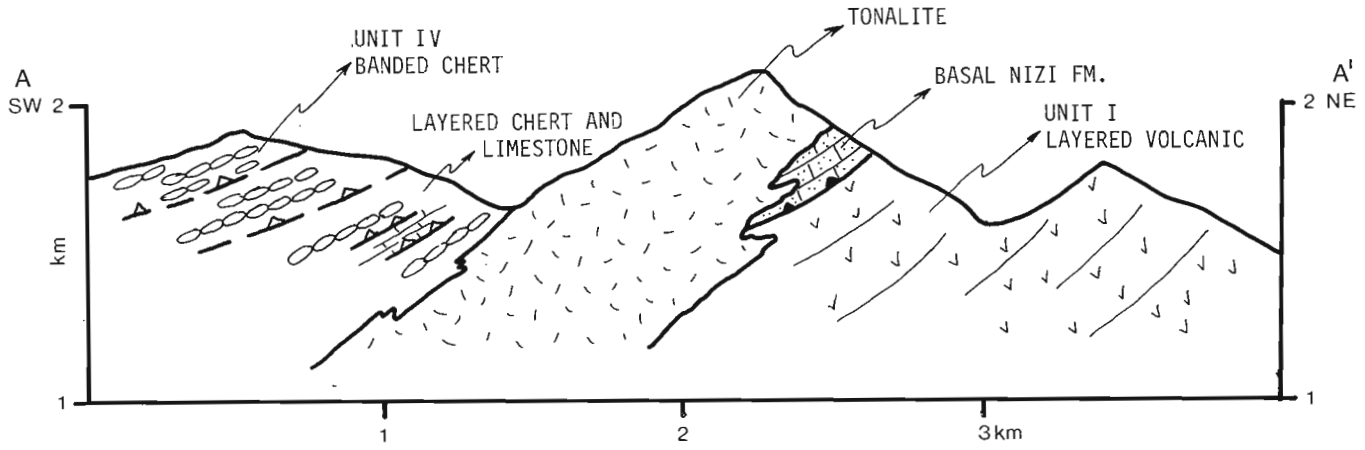

Figure 38.3. *Geological cross section. Line of section southeast of Rapid River, shown in Figure 38.2.*

Permian age. As the tonalite can be shown to straddle at least one of the tectonolithologic sheet-bounding faults along Rapid River, some of the imbrication characterizing the Sylvester Allochthon must have occurred prior to its emplacement and was carried to its present position. The pre-emplacement structures are physically indistinguishable in the field from others which may be emplacement related to the allochthon. Pre-emplacement deformation appears to be post-mid Pennsylvanian (Unit II) and is certainly pre-Late Permian; an interval during which other lithologies of the Sylvester Allochthon were still accumulating in an ocean floor environment (Gordey et al., 1982).

References

Gabrielse, H.
1963: McDame map area, British Columbia; Geological Survey of Canada, Memoir 319, 138 p.

Gabrielse, H. and Mansy, J.L.
1980: Structural style in northeastern Cry Lake map-area, north-central British Columbia; in Current Research, Part A, Geological Survey of Canada, Paper 80-1A, p. 33-35.

Gordey, S.P., Gabrielse, H., and Orchard, M.J.
1982: Stratigraphy and structure of Sylvester Allochthon, southwest McDame map area, northern British Columbia; in Current Research, Part B, Geological Survey of Canada, Paper 82-1B, p. 101-106.

Harms, T.
1984: Structural style of the Sylvester Allochthon, northeastern Cry Lake map area, British Columbia; in Current Research, Part A, Geological Survey of Canada, Paper 84-1A, p. 109-112.

Mamet, B.L. and Gabrielse, H.
1969: Foraminiferal zonation and stratigraphy of the type section of the Nizi Formation (Carboniferous System, Chesterian Stage) British Columbia; Geological Survey of Canada, Paper 69-16.

Monger, J.W.H.
1977: Upper Paleozoic rocks of the western Canadian Cordillera and their bearing on Cordilleran evolution; Canadian Journal of Earth Science, v. 14, p. 1832-1859.

DEXTRAL STRIKE-SLIP THROUGH WELLS GRAY PROVINCIAL PARK, BRITISH COLUMBIA

Project 820014

L.C. Struik
Cordilleran Geology Division, Vancouver

Struik, L.C., Dextral strike-slip through Wells Gray Provincial Park, British Columbia; in Current Research, Part A, Geological Survey of Canada, Paper 85-1A, p. 305-309, 1985.

Abstract

In northern Wells Gray Provincial Park, east-dipping dextral strike-slip faults offset 1) the thrust contact between Cariboo Terrane to the east and Barkerville Terrane to the west, 2) metamorphic isograds and 3) the Hobson Pluton of Cariboo Terrane. The strike-slip faults are the southeastern continuation of the Matthew Fault system and probably translate part of the dextral motion from the McLeod Fault of the Rocky Mountain Trench to the eastern boundary of the Shuswap Metamorphic Complex.

Résumé

Dans la partie nord du parc provincial de Wells Gray, des failles à décrochement dextre inclinées vers l'est produisent un décalage 1) du contact de chevauchement entre le terrain de Cariboo à l'est et le terrain de Barkerville à l'ouest, 2) des isogrades métamorphiques, et 3) du pluton de Hobson dans le terrain de Cariboo. Les failles de décrochement sont la prolongation sud-est du réseau de failles de Matthew et ont vraisemblablement transmis une partie du mouvement dextre de la faille de McLeod du sillon des Rocheuses jusqu'à la limite est du complexe métamorphique de Shuswap.

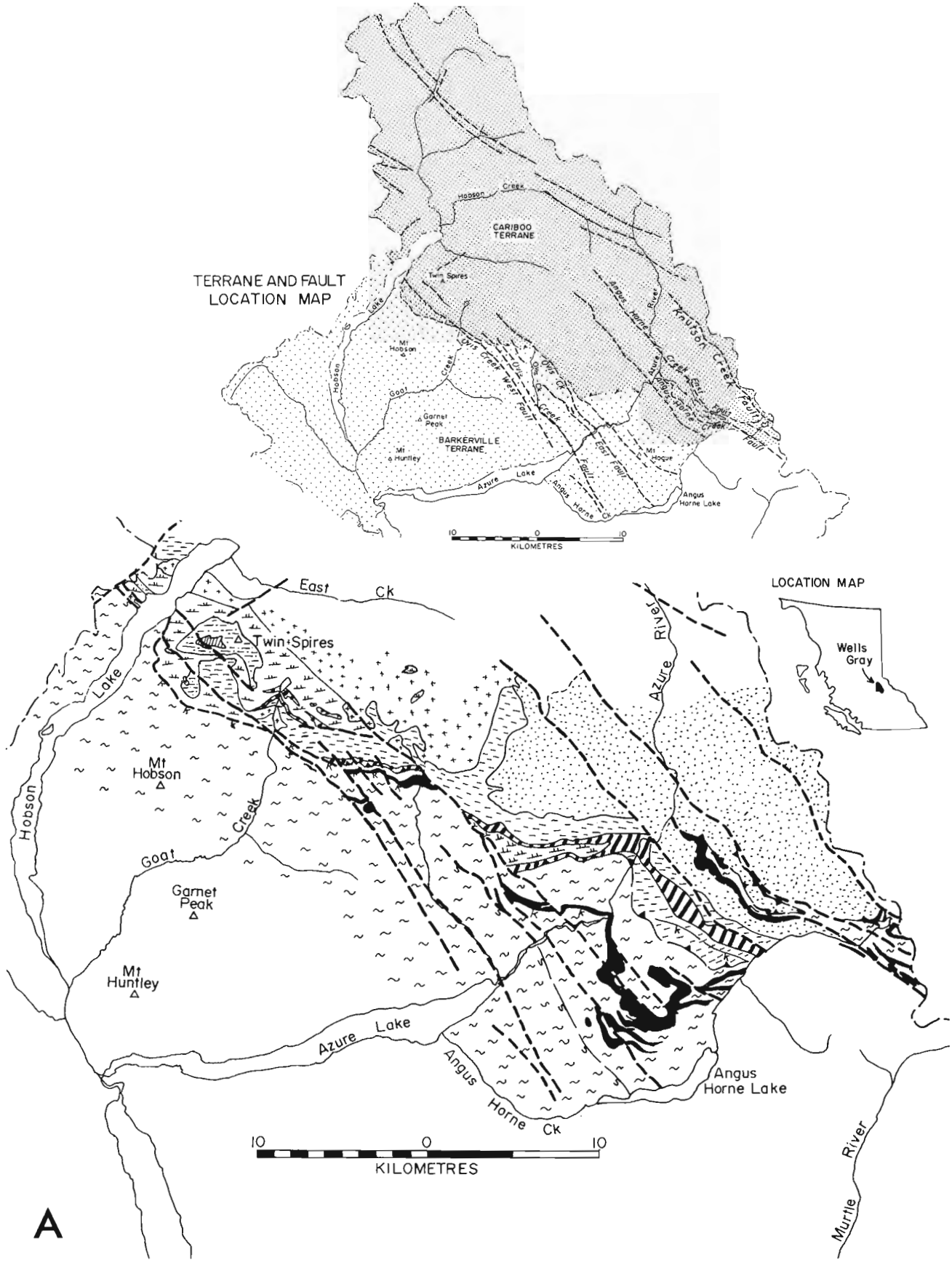

Figure 39.1. *Regional geology of part of the north of Wells Gray Provincial Park. The inset map displays the distribution of two distinct packages of rock, called Cariboo and Barkerville terranes, and some of the the faults forming the boundary between them.*

Introduction

Two regionally large and distinct rock packages are in fault contact from Barkerville southeast to Quesnel Lake, British Columbia. The eastern package, consisting entirely of sedimentary rocks, is referred to as Cariboo Terrane and is thrust (relatively) over the western package, which consists mainly of sedimentary rocks and some volcanics and is called Barkerville Terrane (Struik, 1983a, b). Both terranes are late Proterozoic (750 Ma) and Paleozoic (up to 260 Ma). The two terranes and the thrust fault that separates them can be traced into Wells Gray Park (Fig. 39.1) where they are offset by moderately northeasterly dipping strike-slip faults which may have a component of compression.

The Cariboo Terrane consists of the Cariboo and Kaza groups (Fig. 39.1, Campbell et al., 1973) within the map area and ranges in metamorphic grade from chlorite to garnet and locally to kyanite. The Barkerville Terrane consists of rocks mapped as Horsethief Creek to the south and Snowshoe Group to the north. The rocks are metamorphosed to kyanite grade or higher west of the Ovis Creek faults and to kyanite grade or lower to the east. In the stratigraphy of Pell and Simony (1982, 1984) the sequence is part of the semipelite and amphibolite, middle marble and upper clastic units of the Horsethief Creek Group. There is some question as to their correlation to the north. The middle marble unit, however, is much like the Bralco marble (Snowshoe Group) and the semipelite and amphibolite unit may be the Downey succession of the Snowshoe Group as mapped in Struik (1983b). Such correlations are contradictory, because Struik (1982, 1983a) describe those units of the Snowshoe Group as Paleozoic, whereas the Horsethief Creek Group is late Proterozoic.

The low-angle fault that carried Cariboo Terrane onto Barkerville Terrane is best exposed at the headwaters of Ovis Creek (Fig. 39.1) where Cunningham and Isaac formations of Cariboo Terrane are faulted onto grit, phyllite, marble and schist of Barkerville Terrane. The low-angle fault is the same in style and relative age as the Pleasant Valley Thrust at Mount Watt near the North Arm of Quesnel Lake (Struik, 1983b). It was mapped by Pigage (1978) as a premetamorphic slide.

The metamorphic grade is very similar directly across the thrust near the head of Ovis Creek, although it rises rapidly from garnet to kyanite grade to the southwest into Barkerville Terrane (see also Pigage, 1978). The thrust fault loses its definition to the southeast where Kaza Group of Cariboo Terrane directly overlies it.

The strike-slip faults are well exposed in deglaciated cirques and on some ridge tops. They transect the map area from Hobson Lake to the head of Angus Horne Creek and to the northwest are in line with the Matthew Fault at the head of the East Arm of Quesnel Lake. They offset the thrust fault at the base of Cariboo Terrane (Fig. 39.1) and penetrate much of the rock between Ovis Creek West Fault and Angus Horne Creek East Fault causing dislocations of metres to kilometres.

The faults have fabric geometry that indicates dextral strike-slip motion (with a possible component of compression), which is confirmed by the offset of map-scale geological structures such as the Cariboo-Barkerville Terrane contact (Fig. 39.1). The dextral motion trends into the Matthew Fault (Struik, 1983a, b) which in turn is in line with the McLeod Fault at the big bend of the Fraser River. Gabrielse (in prep.) suggests that dextral displacement on the system of faults west of the northern Rocky Mountain Trench is in part directed through the Cariboo Mountains by the McLeod Fault. The strike-slip faults of Wells Gray Park support that suggestion and prompt the proposal that the displacement continues even farther to the southeast along the western margin of the Shuswap Metamorphic Complex as marked by the sillimanite metamorphic isograd.

CARIBOO TERRANE

JURASSIC

Hobson Pluton

granodiorite, granite, diorite

LATE PROTEROZOIC

Cariboo Group

Yanks Peak and Midas Formations; quartzite, phyllite, siltite

Yankee Belle Formation; quartzite, phyllite

Cunningham Formation; limey marble

Isaac Formation

phyllite, calcareous phyllite, siltite, quartzite, marble

marble, phyllite

Kaza Group

grit, quartzite, phyllite

BARKERVILLE TERRANE

LATE PROTEROZOIC AND PALEOZOIC?

undifferentiated grit, gneiss, schist, marble, quartzite

marble

KEY

Geological contact (approx. and assumed)
Fault (approx. and assumed)
Thrust fault (approx. and assumed)
Metamorphic mineral-grades (symbols on high grade side of the contact line)
garnet-kyanite
kyanite-sillimanite
Wells Gray Provincial Park Boundary

B

Strike-slip faults

Southeast trending strike-slip faults consist of semiductilely sheared rocks of both Cariboo and Barkerville terranes. They can be distinguished from other faults by their offset of metamorphic isograds, folds and faults and by their extensional and dextral flow.



Figure 39.2. Dextral translation of an extension fault which offsets previously formed flow fabric in the Knutson Creek Fault. The feature is interpreted as one protracted period of rock flow. (photo is taken looking northeast)



Figure 39.3. Dextral shear of tension gashes in Kaza Group quartzite in the Knutson Creek Fault (northeast is to the top). The brittle extension in the quartzite is accommodated by ductile flow in bounding pelitic beds.

The faults transect the map area from the north end of Hobson Lake to the head of Angus Horne Creek. North of the map area they trend into the Matthew Fault as mapped by Fletcher (1972), Struik (1983a, b) and Kaplan (1984). They vary in length from hundreds of metres to tens of kilometres. The faults offset sillimanite, kyanite and garnet grade rocks, as well as the thrust at the base of Cariboo Terrane (at the head of Ovis Creek) and the Hobson Pluton.

The fault zones feature flaser grit, phyllonite, distended competent beds and quartz veins in ductile pelitic matrix, extension faults, mineral-filled tension gashes and lineations of elongate grains and other inclusions within metasediment and granitoids. The features formed at various times but are interpreted to mark the progression of a single protracted event.

Cataclastic rocks

Rocks involved in the faulting include grit, marble, quartzite, siltite, pelite, and granitoids of the Cariboo Terrane, and grit, marble and pelite of Barkerville Terrane.



Figure 39.4. Example of the common boudinage features through Cariboo and Barkerville terranes in northern Wells Gray Park. Distended calcite vein in Isaac Formation (Cariboo Terrane) calcareous pelite at the head of Goat Creek (white spot is a quarter for scale, looking northeast). Compare this feature to the similar one in highly strained gneiss shown by Hanmer (1984, Fig. 4F).

Most of the rocks are phyllonite or flaser quartzite although mylonite has been noted in marble and quartzite along the Angus Horne Creek East Fault. Locally, where the Hobson Pluton was sheared it is a feldspar augen granitoid. Some of the fault zones have more brittle structures such as losenge-shaped inclusions of quartzite coated with slickenside, composed locally of chlorite (Ovis Creek West Fault). The combination of brittle and semiductile structures in the same fault system may result because the system was active before and during uplift of the host rock.

Metamorphic minerals such as garnet and kyanite are distended and broken. Garnet is commonly partly chloritized, rotated and forms augen in the cores of mica sheaths. The metamorphic minerals are completely destroyed within the fault zones.

Minor structures in the strike-slip fault zones

Faults of small offset within the shear zones record a combination of extension and translation, well displayed by the Knutson Creek Fault (Fig. 39.2).

Quartz- and calcite-filled tension gashes, common in calcareous quartzite of Kaza Group, dip steeply to the northwest and are dextrally sheared along Knutson Creek Fault (Fig. 39.3).

Boudinage is common throughout the rocks of the area (Fig. 39.4), being particularly conspicuous in the ductile pelite and marble of the Isaac Formation. The orientation of the boudin axes is consistent with northwestward stretching, parallel to the strike-slip faults.

Mineral elongation, extension faults and boudinage provide an internally consistent sense of rock flow trending north-northwest to northwest. The flow, dextral shear fabric and regional and local dextral offsets are interpreted as components of a dextral strike-slip flow throughout the northern part of Wells Gray Provincial Park. It is extrapolated to the northwest as part of the Matthew and McLeod Lake faults and to the western margin of the Cariboo Mountains, in general including such faults as the Isaac Lake shear zone and Betty Wendle Creek Fault (Sutherland-Brown, 1963; Campbell et al., 1973).

Strike-slip faults of Prince George and McBride map areas (Struik, 1985) in combination with those of the western margin of the Cariboo Mountains would translate many kilometres of strike-slip displacement from northern British Columbia southeastward into the Shuswap Metamorphic Complex.

Acknowledgment

Pat Rogers, Park Superintendent of Wells Gray Provincial Park, has been helpful and encouraging with the project beyond his granting of permission to access the park for scientific purposes.

References

Campbell, R.B., Mountjoy, E.W., and Young, F.G.
1973: Geology of McBride map area, British Columbia; Geological Survey of Canada, Paper 72-35.

Fletcher, C.J.N.
1972: Structure and metamorphism of Penfold Creek area, near Quesnel Lake, central British Columbia; unpublished Ph.D. thesis, University of British Columbia.

Hanmer, S.K.
1984: The potential use of planar and elliptical structures as indicators of strain regime and kinematics of tectonic flow; in Current Research, Part B, Geological Survey of Canada, Paper 84-1B, p. 133-142.

Kaplan, J.
1984: Structure and metamorphism, north of Quesnel Lake and east of Niagara Creek, Cariboo Mountains, British Columbia; unpublished M.Sc thesis, University of British Columbia.

Pell, J. and Simony, P.S.
1982: Hadrynian Horsethief Creek Group/Kaza Group correlations in the southern Cariboo Mountains, British Columbia; in Current Research, Part A, Geological Survey of Canada, Paper 82-1A, p. 305-308.

Pell, J. and Simony, P.S. (cont.)
1984: Stratigraphy of the Hadrynian Kaza Group between the Azure and North Thompson rivers, Cariboo Mountains, British Columbia; in Current Research, Part A, Geological Survey of Canada, Paper 84-1A, p. 95-98.

Pigage, L.C.
1978: Metamorphism and deformation on the northeast margin of the Shuswap Metamorphic Complex, Azure Lake, British Columbia; unpublished Ph.D. thesis, University of British Columbia.

Struik, L.C.
1982: Bedrock geology of Cariboo Lake (93A/14), Spectacle Lake (93H/3), Swift River (93A/13) and Wells (93H/4) map areas, central British Columbia; Geological Survey of Canada, Open File 858.

1983a: Bedrock geology of Spanish Lake (93A/11) and parts of adjoining map areas, central British Columbia; Geological Survey of Canada, Open File 920.

1983b: Bedrock geology of Quesnel Lake (93A/10) and part of Mitchell Lake (93A/15) map areas, central British Columbia; Geological Survey of Canada, Open File 962.

1985: Pre-Cretaceous terranes and their thrust and strike-slip contacts, Prince George east half and McBride west half, British Columbia; in Current Research, Part A, Geological Survey of Canada, Paper 85-1A, Report 34.

Sutherland-Brown, A.
1963: Geology of the Cariboo River area, British Columbia; British Columbia Department of Mines and Petroleum Resources, Bulletin 47.

-40-

STRATIGRAPHY AND STRUCTURE OF THE NORTHWESTERN FLANK OF FRENCHMAN CAP DOME, MONASHEE COMPLEX, BRITISH COLUMBIA: PRELIMINARY RESULTS

EMR Research Agreement to R.L. Brown, 288-84

R.J. Scammell[1]
Cordilleran Geology Division, Vancouver

Scammell, R.J., Stratigraphy and structure of the northwestern flank of Frenchman Cap dome, Monashee Complex, British Columbia: preliminary results; in Current Research, Part A, Geological Survey of Canada, Paper 85-1A, p. 311-316, 1985.

Abstract

At the northwest end of Frenchman Cap dome high grade metamorphic autochthonous cover rocks of the Monashee Complex lie beneath the Monashee Décollement which separates them from overlying metamorphic rocks of the Selkirk Allochthon. Autochthonous cover rocks comprise an assemblage of clastics, carbonates and volcanics which suggests a tectonically active, shallow marine, platform environment. These form the overturned limb of the Sibley syncline and record two phases of synmetamorphic deformation. As the Monashee Décollement is approached from below, phase 2 folds become tighter, their fold hinges become subparallel to the regionally pervasive stretching lineation and their axial planes flatten to parallel the décollement. Allochthonous rocks above the décollement comprise a sequence of amphibolite with extensive pegmatite, pelite, quartzite and psammite. Only one phase of synmetamorphic tight to isoclinal folding has been recognized. A well developed east trending penetrative stretching lineation is present throughout.

North trending, possibly Tertiary, minor normal faults with down-side to the west crosscut the area. Kinematic indicators in local shear zones give both westward and eastward senses of shear. The Monashee Décollement, marked by a zone of pervasive concordant and discordant sheared pegmatite, truncates the stratigraphic succession in lower plate rocks.

Résumé

A l'extrémité nord-ouest du dôme de Frenchman Cap, les roches de couverture autochtones fortement métamorphisées du complexe de Monashee reposent sous le décollement de Monashee qui les sépare des roches métamorphiques sus-jacentes de l'allochtone de Selkirk. Les roches de couverture autochtones se composent d'un assemblage de roches clastiques, de roches carbonatées et de roches volcaniques qui se sont vraisemblablement accumulées sur une plate-forme marine peu profonde dans un milieu tectoniquement actif. Elles forment le versant inverse du synclinal de Sibley et révèlent qu'il y a eu deux phases de déformation synmétamorphique. Lorsqu'on s'approche du décollement de Monashee par en-dessous, les plis de deuxième phase deviennent plus fermés, leurs charnières sub-parallèles à la linéation d'étirement pénétrante que l'on trouve partout dans la région et leurs plans axiaux s'aplatissent pour devenir parallèles au décollement. Les roches allochtones au-dessus du décollement se composent d'une séquence d'amphibolites avec beaucoup de pegmatite, de pélite, de quartzite et de psammite. Une seule phase de plissement synmétamorphique qui a produit des plis fermés à isoclynaux a été identifiée. Une linéation bien développée à orientation est se présente dans toute la séquence.

La région est entrecroisée au nord de petites failles normales dont la lèvre est affaissée vers l'ouest et qui datent peut-être du Tertiaire. Les indicateurs cinématiques dans les zones de cisaillement locales révèlent que le cisaillement s'est produit vers l'ouest et vers l'est. Le décollement de Monashee, qui est marqué par une zone de pegmatites cisaillées concordantes et discordantes, coupe la succession stratigraphique dans la partie inférieure de la plaque.

---

[1] Ottawa-Carleton Centre for Geoscience Studies, Department of Geology, Carleton University, Ottawa, Canada, K1S 5B6

Introduction

Frenchman Cap dome is one of several structural culminations which outcrop in the Monashee Complex west of the Columbia River near Revelstoke (Fig. 40.1). Structural elements of the dome comprise: basement gneisses, and autochthonous cover of the Monashee Complex, and allochthonous cover (Selkirk Allochthon) separated by the Monashee Décollement (Fig. 40.1). The décollement, a zone of mylonitization and detachment faulting, is thought to be a product of Jurassic deformation during collision between North America and western allochthonous terranes (Brown et al., in press; Brown and Read, 1983; Read and Brown, 1981). Uplift from depths greater than 25 km is attributed to the development of a basement duplex (Brown et al., in press).

Although well defined in the eastern flank of Frenchman Cap dome, the Monashee Décollement is narrower and much more subtle in nature at the northwest end. The nature of the décollement and bounding rocks at this location forms the author's M.Sc. project. The results of a month-long preliminary study of the stratigraphy and structure at the northwest end of Frenchman Cap dome are presented in this report.

Stratigraphy

Autochthonous cover

Autochthonous cover rocks in the study area comprise an approximately 2 km-thick assemblage of amphibolite grade clastics, carbonates and volcanics. Brown (1980, 1981) has suggested a tectonically active shallow marine platform environment of deposition for these rocks. Within the map area, the cover has been subdivided into nine mappable units (Fig. 40.2). Most boundaries between these units are gradational over 2 to 50 m. The thicker these zones the more arbitrary the location of boundaries becomes. Since mapping has not yet been extended southward to the basement gneisses (Fig. 40.2), the stratigraphic position of cover relative to basement will not be considered (for earlier reconnaissance work see Brown, 1980 and Hoy and Brown, 1980).

The lowermost map unit (1) observed in the allochthonous cover is a light orange to light grey, fine- to medium-grained, 30- to 50-m-thick, quartzite. It is commonly white mica- or hornblende-bearing. Other than weak bedding no primary structures have been preserved.

Overlying the quartzite with sharp contact is a thinly layered hornblende-garnet-bearing gneiss 20- to 60-m-thick (unit 2). Similar in appearance to gneisses higher in the sequence it can be distinguished by its generally finer grain size and thinner compositional layers. Although more mapping is necessary, this unit appears to contain interbedded lenses of pelite which may be facies equivalents.

The above gneisses grade over 5 to 10 m into unit 3 composed of calc-silicate and impure marble. The calc-silicates are medium- to coarse-grained with red, green and grey beds up to several centimetres thick. Upwards within this unit sandy marble layers become dominant and bedding increases in thickness to layers of several metres. Diopside is found throughout this 5- to 30-m-thick unit.

The impure marble of unit 3 is abruptly overlain by a coarse grained biotite-kyanite-garnet-sillimanite-bearing pelite (unit 4). This rusty weathering 2- to 30-m-thick unit grades upwards into a 250- to 350-m-thick package of gneisses (unit 5) consisting dominantly of massive amphibolite-bearing hornblende gneisses, psammites, quartzites and minor pelite. Layering is generally in the decimetre range but may be thinner. The gneisses grade over 20 to 30 m into a biotite-kyanite-garnet-sillimanite-bearing pelite (unit 6), a distinctive unit up to 100 m thick which can be distinguished from pelitic rocks lower in the section by its generally finer grain and higher concentration of garnet porphyroblasts (up to 30 per cent). Layers of semipelite are also present in this unit. Since the unit thins to less than 5 m, it is probably a facies equivalent of the gneissic units which bound it. The pelitic unit grades upwards into gneissic unit 7 which is very similar to the underlying unit 5. The overlying gneiss of unit 7 differs from unit 5 in that quartzite and quartzofeldspathic gneisses are more common, and higher up in the unit a distinctive coarse grained amphibolite appears, which contains 5 to 12 cm radiating clusters of

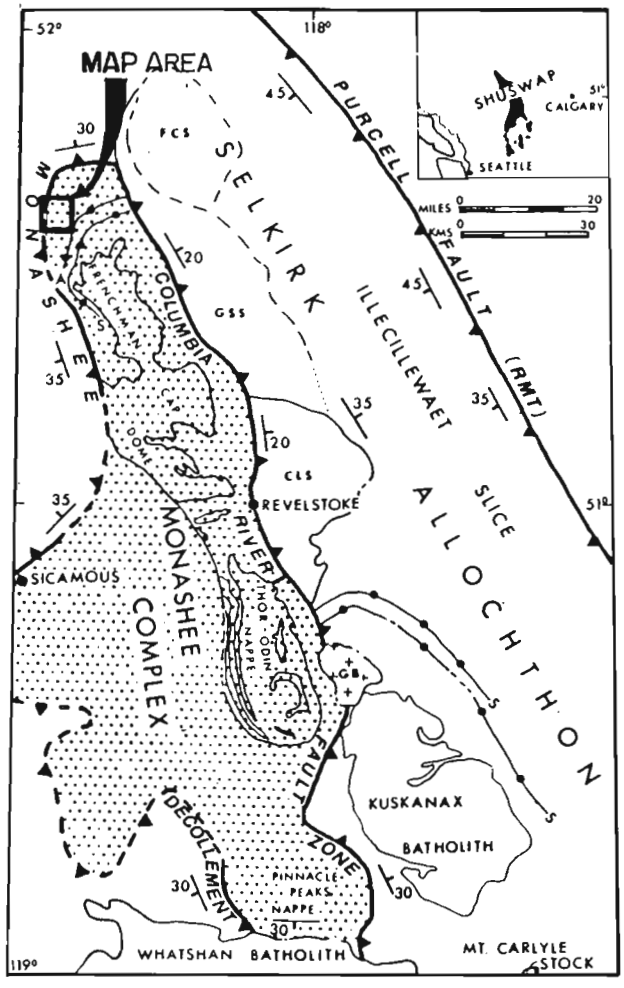

Figure 40.1. *Simplified regional map showing major tectonic elements of Shuswap terrane and location of map area. Stippled area outlines tectonic window of exposed Monashee Complex. Barbs on upper plate. FCS = French Creek slice, GSS = Goldstream slice, CLS = Clachnacudainn slice of Selkirk allochthon. S and A indicate selected axial surface traces of synforms and antiform, respectively, illustrating truncation of folds by Monashee Décollement and Columbia River fault. Strike and dip symbols indicate approximate attitudes of dominant foliation in upper and lower plates adjacent to décollement and in upper plate above Purcell fault. GB = Galena Bay stock (from Brown and Read, 1983).*

amphibole, 2 to 20 cm garnets and clusters of randomly oriented turquoise kyanite. The amphibolite ranges from 2- to 20-m-thick and displays both concordant and discordant relationships. The total thickness of gneissic unit 7 is 200 to 250 m.

Although hornblende- garnet- and mica-bearing quartzites increase in quantity upwards, the overlying unit (50 to 70 m thick) is dominantly amphibolite with interbedded quartzites (unit 8). Quartzite and amphibolite packages within the unit are 10 cm to 20 m thick with laminated to metre-scale bedding. Very coarse grained amphibolite with radiating amphibole clusters is most commonly found within this unit.

The uppermost unit (9) in the map area is dominantly quartzite locally interbedded with amphibolite and minor kyanite-bearing pelite. Compositional layering ranges from thin lamination to layers several metres thick. Quartzite and amphibolite packages range from 0.1 to 20 m in thickness. Pelitic rocks consist mainly of concordant 5 to 25 cm thick layers and rarely form 10- to 50-cm-thick discordant dyke-like bodies. Primary structures preserved within the quartzites include normal graded beds, decimetre-scale troughs and crossbedding. Amphibolite units are both concordant and discordant and most commonly display spectacular boudinage.

Pegmatite is common throughout the autochthonous cover rocks. Although most are composed of plagioclase and quartz, potassic feldspar-, muscovite-, diopside-, and kyanite-bearing varieties exist. They range from 5 cm to 3 m in thickness. Massive, sheared, discordant, concordant and folded varieties indicate that pegmatite was produced before, during and after deformation. Pegmatite increases in quantity as the Monashee Décollement is approached.

Allochthonous cover

Allochthonous cover rocks comprise two recognizable map units. The structurally lower unit (10), dominantly amphibolite with interbedded pelitic rocks, is extensively invaded by discordant and concordant pegmatite. Sillimanite and kyanite coexist within the pelitic rocks. This unit grades upwards into dominantly pelitic rocks of unit 11 with interbedded quartzite, psammite, semipelite, minor amphibolite and ubiquitous discordant and concordant pegmatite. Within the pelitic rocks sillimanite is the only aluminosilicate present.

Pegmatite is pervasive throughout the allochthonous cover. As in the autochthonous rocks massive, sheared, concordant, discordant and folded varieties exist. No stratigraphic top indicators have been found within either unit 10 or 11.

Structural geometry

Autochthonous rocks in the study area exhibit structural fabrics indicating polyphase deformation. They form the overturned limb of the Sibley syncline which has an axial surface dipping away from the dome at a moderate angle towards the northwest (Brown, 1980). Superimposed upon this limb are synmetamorphic reclined tight to isoclinal folds with axial surfaces dipping to the west and fold hinges generally parallel to a well developed penetrative westerly trending and plunging stretching lineation.

Within autochthonous rocks synmetamorphic first phase deformation is indicated by: 1) a weak foliation (S1) which is inclined to the compositional layering (S0), and is folded by later folds; 2) refolded folds; 3) garnets with internal foliations which define a foliation folded by later folds.

Second phase folds are the dominant structure in the autochthonous cover. They are tight to isoclinal reclined folds (as indicated by Fig. 40.3B, 40.3D), have westerly dipping axial planes (S2, Fig. 40.3) and fold hinges subparallel and parallel to the stretching lineation (LS, Fig. 40.3A, 40.3C).

As the décollement is approached several changes occur in the autochthonous footwall rocks. Second phase folds appear, they become tighter, their fold axes become parallel or subparallel to the stretching lineation, and compositional layering and axial surfaces flatten slightly to parallel the décollement (Fig. 40.4).

Compositional layers thin as the décollement is approached. Whether this is a primary structure and/or a product of high strain has yet to be determined. Thinning is also evidenced by numerous amphibolite boudins with long axes normal to the stretching lineation, and outcrop scale listric normal faults which have northerly strikes perpendicular to the stretching lineation and down-thrown blocks to the west. These attitudes are most consistent with thinning which may have occurred during easterly or westerly motion of upper plate allochthonous rocks over lower plate autochthonous rocks along the Monashee Décollement.

Within the highly strained allochthonous cover only one phase of deformation has been observed. Those are reclined tight to isoclinal folds and northwesterly dipping axial surfaces and northwesterly trending fold axes. Further investigation should reveal the relationship of these folds to folding in the autochthonous cover.

Throughout all rocks in the area there exists a well developed, penetrative, westerly trending and plunging stretching lineation (Fig. 40.3). This lineation is defined by quartz-rodding and commonly pulled apart aligned crystals of feldspar, hornblende, kyanite and sillimanite.

Shear zones have been observed in all rock units in the area. Most parallel the layering but some truncate compositional layering. These zones, 10 cm to 1 m thick, are usually pegmatitic. Most internal mesoscopic foliations within these zones are highly flattened and do not provide unambiguous kinematic indicators. Where internal fabrics are unambiguous their geometry at some locations indicate eastward, whereas at others westward transport of hanging wall with respect to footwall rocks. A microscopic kinematic study to determine the relationships and significance of the two opposing senses of shear will be undertaken.

The latest deformation to affect rocks in the map area induced vertical north trending normal faults with the downthrown blocks to the west. The most significant of these is marked on Figure 40.2. Although this fault is marked by a spectacular zone of intense fracturing, the displacement on the fault is no greater than 2 m at the north end of the study area. These faults may be a product of Tertiary extension.

Monashee Décollement

The Monashee Décollement, separating allochthonous upper plate rocks from autochthonous lower plate rocks, is well exposed in the map area. It is marked by a zone of extensive discordant and concordant pegmatite at the base of the structurally lower unit (10) in the allochthonous cover. The décollement is presently drawn at the base of this stratigraphic unit (Fig. 40.2) which truncates the lower plate stratigraphic succession at the northwest end and west flank of the area. Rocks which bound this detachment are highly strained.

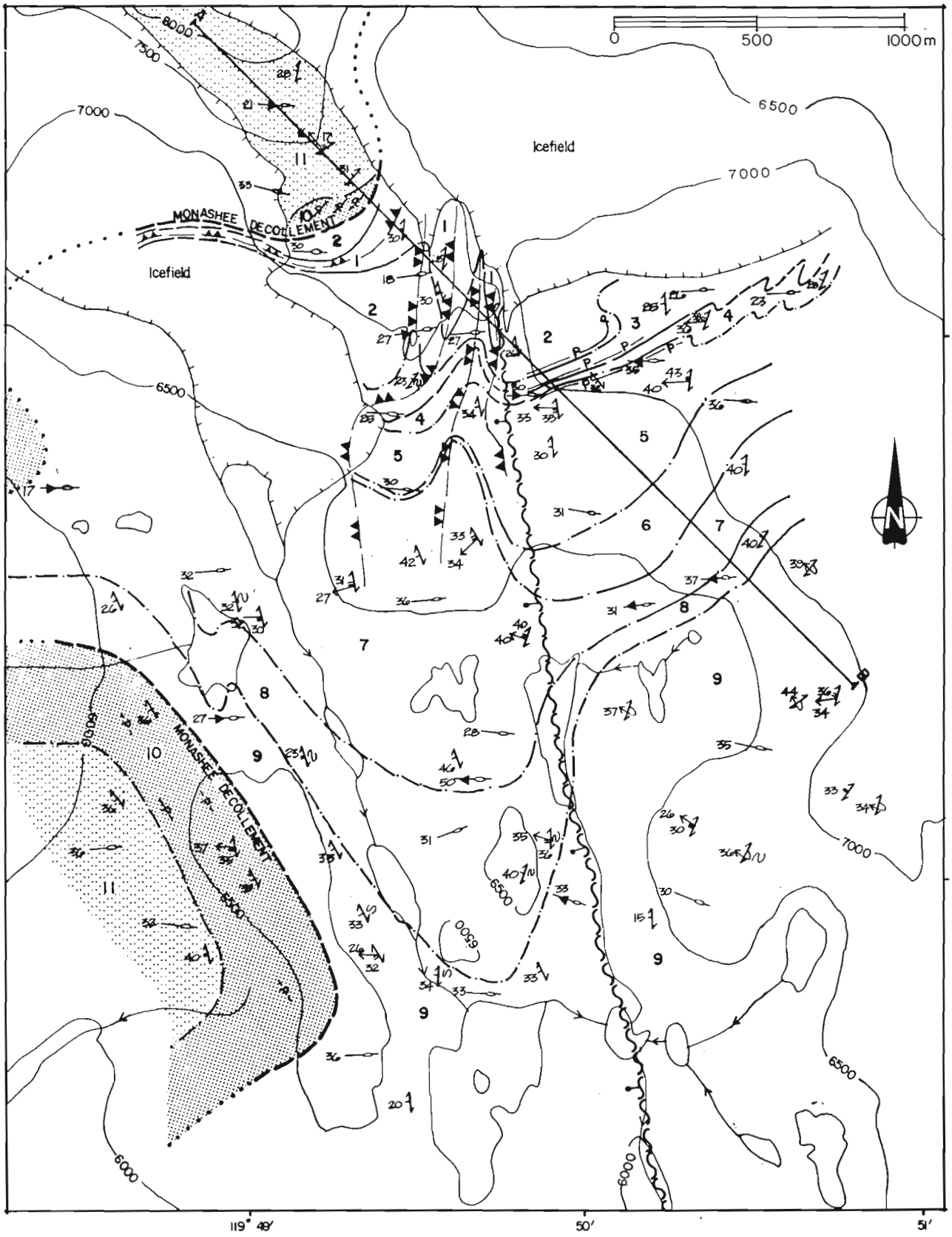

Figure 40.2. *Map of stratigraphy and structure on the northwestern flank of Frenchman Cap dome.*

LEGEND

ALLOCHTHONOUS ROCKS

11 Interbedded sillimanite-bearing pelites, quartzites & psammites.

10 Amphibolite locally interbedded with kyanite-sillimanite-garnet-bearing pelite; extensively invaded by concordant & discordant pegmatite.

AUTOCHONOUS ROCKS

9 Quartzite locally interbedded with amphibolite & minor pelite.

8 Amphibolite locally interbedded with hornblende-bearing quartzite.

7 Mixed gneisses-amphibolites, psammites, quartzite & minor pelite.

6 Pelite & semipelite.

5 Mixed gneisse-amphibolilites, psammites, quartzite & minor pelite.

4 Biotite-kyanite-garnet-sillimanite-bearing pelite.

3 Diopside-bearing psammitic marble & calc-silicate locally interbedded with quartzite.

2 Thinly layered hornblende-garnet-bearing gneiss & minor pelite.

1 Quartzite.

-P- Pegmitite.

SYMBOLS

Lithologic contact: sharp- definite, interpreted.

: gradational- definite, interpreted.

Attitude of compositional layering (S1): tops unknown.

: beds overturned.

Attitude of axial plane (S2) & fold hinge (F2) for phase 2 folding.

S 2 Vergence.

Phase 2 axial surface traces (approx.): overturned anticline.

: overturned syncline.

Stretching lineation.

Stretching lineation with motion of upper plate indicated.

Fault with down thrown block indicated.

Monashee Decollement: definite, interpreted.

Lake stream with flow indicated.

Edge of ice field.

6000 Contour. (feet a.m.s.l.)

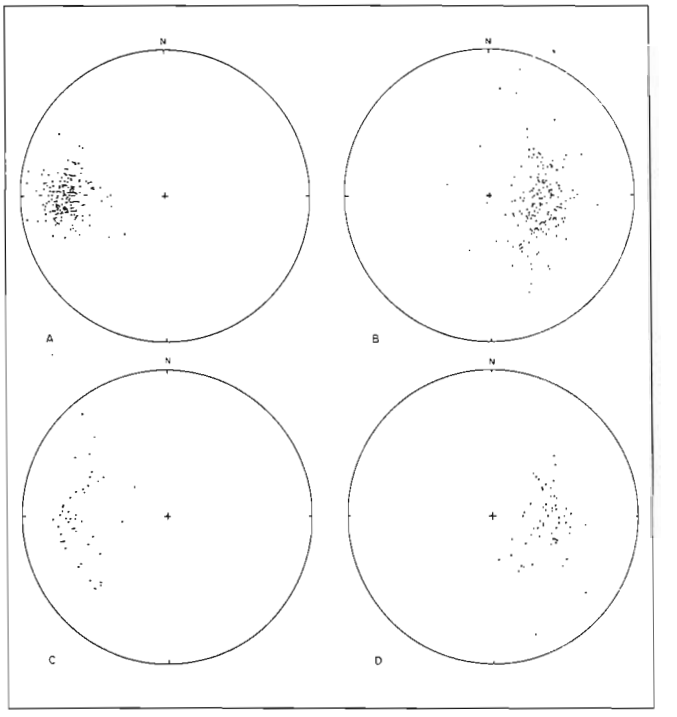

Figure 40.3. *Equal area stereonet compilation of planar and linear fabric element data:*

A. Stretching lineation (LS)

B. Poles to compositional layering (SO)

C. Phase 2 fold hinges (F_2)

D. Poles to phase 2 axial planes (S2)

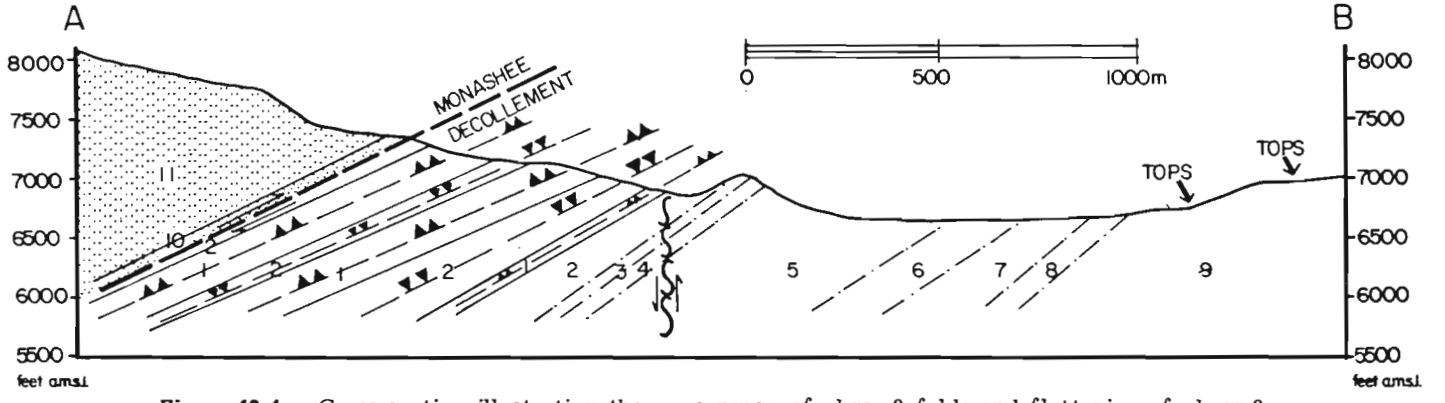

Figure 40.4. *Cross-section illustrating the appearance of phase 2 folds and flattening of phase 2 axial planes (S_2) and compositional layering (S0) as the décollement is approached from B to A located in Figure 40.3.*

Most pegmatite at the décollement is sheared and parallel or subparallel to the compositional layering in both hanging wall and footwall rocks. It is presently thought that pegmatite played a significant role in the accommodation of strain during motion on the décollement. The presence of fluid phases at the décollement would most certainly facilitate major displacement along the décollement. A study of metamorphic mineral assemblages and textures presently in progress may also provide evidence of a significant metamorphic discordance across the décollement.

Conclusions

1. High grade metamorphic autochthonous cover rocks which comprise an assemblage of clastics, carbonates and volcanics, form the overturned limb of the Sibley Syncline and record two phases of synmetamorphic deformation.
2. As the Monashee Décollement is approached within the autochthonous cover, phase 2 folds become tighter, their fold hinges become subparallel to the stretching lineation and their axial planes flatten to parallel the décollement.
3. High grade metamorphic allochthonous cover rocks comprise a sequence of amphibolite with extensive pegmatite, pelite, quartzite and psammite which record one phase of synmetamorphic deformation.
4. A well-developed penetrative east trending stretching lineation is present throughout the map area.
5. North trending, possibly Tertiary, minor normal faults with down-side to the west crosscut the area.
6. Kinematic indicators in local shear zones give both westward and eastward senses of shear.
7. The Monashee Décollement truncates the stratigraphic succession in lower plate rocks.

Acknowledgments

The project is part of an M.Sc. thesis in progress at Carleton University, under the supervision of Richard L. Brown, whose guidance is most appreciated. The author expresses his gratitude to Donald C. Murphy for providing a start on the right foot, and David Bethune for assistance in the field.

Funding of this project is in part provided by NSERC operating grant A2693 to Richard L. Brown.

References

Brown, R.L.
1980: Frenchman Cap Dome, Shuswap Complex, British Columbia; in Current Research, Part A, Geological Survey of Canada, Paper 80-1A, p. 47-51.

1981: Metamorphic complex of southeast Canadian Cordillera and relationships to foreland thrusting; in Thrust and nappe tectonics, Geological Society of London Special Publication 9, p. 463-474.

Brown, R.L., Journeay, M.J., Lane, L.S., Murphy, D.C., and Rees, C.J.
– Obduction, back-folding and piggyback thrusting in the metamorphic hinterland of the southeastern Canadian Cordillera; Journal of Structural Geology. (in press)

Brown, R.L. and Read, P.B.
1983: Shuswap terrane of British Columbia: A Mesozoic "core complex"; Geology, v. 11, p. 164-168.

Hoy, T. and Brown, R.L.
1980: Preliminary map 43, geology of the eastern margin of Shuswap complex, Frenchman Cap area; British Columbia Ministry of Energy, Mines and Petroleum Resources.

Read, P.B. and Brown, R.L.
1981: Columbia River fault zone: Southeastern margin of the Shuswap and Monashee Complexes, southern British Columbia; Canadian Journal of Earth Sciences, v. 18, p. 1127-1145.

DEVELOPMENT-INDUCED TIDAL FLAT EROSION, FRASER RIVER DELTA, BRITISH COLUMBIA

Project 790006

D.M. Duggan[1] and J.L. Luternauer[2]
Cordilleran Geology Division, Vancouver

Duggan, D.M. and Luternauer, J.L., Development-induced tidal flat erosion, Fraser River delta, British Columbia; in Current Research, Part A, Geological Survey of Canada, Paper 85-1A, p. 317-326, 1985.

Abstract

*Dendritic creeks, produced by the concentration of ebb tidal flows towards a dredged ship basin on southern Roberts Bank, have denuded part of an ecologically important eelgrass bed adjacent to the basin. Our investigations indicate that: (a) this loss of eelgrass (**Zostera marina** L.) has been accompanied by the continuous extension of the inshore limits of the northwest part of the eelgrass field since the port was constructed; (b) decrease in the rate of growth of the channels cannot be linked to construction of the crest protection wall (c.p.w.) (a shallow dyke); (c) the c.p.w. did not prevent an erosional response to the truncation of the lower reaches of the earlier established channels by the expansion of the original dredged basin; (d) the study area is still adjusting to the initial and subsequent development of the coal port site but creeks have approached a dynamic equilibrium under prevailing conditions; (e) areas where flows are slower and sediments are finer. Other favourable conditions for re-establishing eelgrass.*

Résumé

*Les cours d'eau dendritiques, produits de l'écoulement des marées descendantes vers un bassin dragué dans la partie sud du banc Roberts, ont dénudé une partie de la prairie de zostères qui est contiguë au bassin. Cette prairie revêt une importance écologique considérable. Les études révèlent que: (a) la perte de zostères (**Zostera marina** L.) a été accompagnée par l'extension continue des limites littorales de l'extrémité nord-ouest de la prairie depuis la construction du port; (b) le ralentissement de la croissance des chenaux ne peut pas être reliée à la construction du brise-lames (une digue peu profonde); (c) le brise-lames n'a pas empêché l'érosion à la suite du retranchement des cours inférieurs des chenaux plus anciens d'agrandir le bassin original; (d) la région étudiée est encore en train de s'adapter à l'aménagement initial et subséquent du port charbonnier, mais les cours d'eau ont presque atteint un état d'équilibre dynamique dans les conditions actuelles; (e) les cours d'eau de la région I présentent des conditions plus favorables au rétablissement des zostères que la région II puisque les courants y sont plus lents et les sédiments plus fins.*

[1] Department of Geological Sciences (Geological Engineering), University of British Columbia, Vancouver, B.C. V6T 2B4
[2] Pacific Geoscience Centre, Sidney, British Columbia

Introduction

This report evaluates the impact of the Roberts Bank Coalport and associated structures on the stability of the surface of the tidal flats at the head of the ship turning basin on the southern Fraser River Delta (Fig. 41.1, 41.2). Specifically, it assesses the effects of the manmade features on the flow regime, growth of eelgrass, erosion of channels and sediment transport during the falling tide. This study is based on field and laboratory investigations undertaken in 1983 and 1984 and previously available reports including a preliminary report by Luternauer et al. (1984).

General Background

Initial construction of the Roberts Bank Coalport (Pod site 1; Fig. 41.2) and the associated causeway took place in 1969 (McKenzie, 1983). Material extracted to form the adjacent ship basin was used as core material for the port facility. The basin lies between the Coalport and the Tsawwassen Ferry Terminal to the southeast (Fig. 41.1), within a 400 ha, ecologically valuable, bed of eelglass (Beak Consultants Ltd., 1977a, b; Wiebe and Moody, 1983). The two types of eelgrass in the intercauseway area are **Zostera marina** L (large frond eelgrass) and **Zostera japonica** Aschers and Graebn (dwarf frond eelgrass) (P. Harrison, personal communication, 1984) growing on silty sand and sand substrate (Luternauer, 1976, 1980; Beak Consultants Ltd., 1977a). Ebb tidal flow concentration near the ship-turning basin and a probable associated increase in current velocity over the neighbouring tidal flats is considered to have caused the formation of dendritic creeks at the head of the basin (Beak Consultants Ltd., 1977b). By 1975, a well developed intertidal drainage system had concentrated into two main channels, herein referred to as Channel Areas I and II (Fig. 41.2). Three pods were added from September 1981 to June 1983 (M. Tarbotton, personal communication, 1983) (Fig. 41.2). Material for the fill was again obtained from the ship-turning basin in the course of deepening and enlarging it from September 1981 to June 1983 (Ekstrom, 1983). To combat the seaward flow of sediment within the channels (Hawley, 1979; Wiebe and Moody, 1983), a riprap crest protection wall (c.p.w.) or dyke approximately 6 m wide by 0.5 to 1 m high was constructed around the perimeter of the ship basin in the spring of 1983 (Fig. 41.3). The riprap covers a trench, approximately 0.5 m deep, filled with gravel. Sand removed to form this trench was dumped immediately inshore of the trench in an attempt to replace some of the sediment eroded by the creeks and raise the tidal flat surface (M. Tarbotton, personal communication, 1983). Construction took place while the area was submerged and the dumped sand was not entirely contained within the channels; some remains as sand mounds visible at low tide (Fig. 41.4). As well, it was difficult to maintain a consistent c.p.w. elevation along its length and at several locations the crest is lower where channels intersect the wall (Fig. 41.3). The height of the c.p.w. was kept to a minimum to discourage a transfer of erosion to other locations on the tidal flats (M. Tarbotton, personal communication, 1983). At present, Coalport construction-related erosion of the tidal flat surface tends to be confined to the west half of the intercauseway area northeast of the ship-turning basin.

Concurrent field investigations were undertaken by P.G. Harrison and associates of the University of British Columbia to establish the requirements for successful transplantation of eelgrass within the denuded area. Channel Area I was selected as a test site for this experiment which included construction of a sand-bag weir in 1983 to slow ebb flows and induce accretion (Luternauer et al., 1984).

Field techniques

Channel morphology and height of crest protection wall

Nine representative locations (four in Channel Area I and five in Channel Area II) were selected in June 1983 for monitoring of the stability of channel cross-sections (Fig. 41.4). They were identified by placing 6 mm (1/4 inch) rebar 5 to 10 m beyond the channel flanks on the adjacent banks. Rebar was driven 0.5 m into the sediment and protruded 0.75 to 1.0 m above the exposed tidal flats. Initially, each cross-section was surveyed to determine the elevation at well-defined inflection points along the bed or at 5 m intervals (whichever length was shorter) using a Zeiss Auto Level, rod and a measuring tape extended between the two end points. Four benchmarks (IP) established on the c.p.w. by Swan Wooster Engineering Ltd., were used for backsites (Fig. 41.2). Subsequent surveys of the cross-sections during 1983 and 1984 recorded the current elevation of the previously established points along the profile and any new inflection points. Vertical precision of the surveyed elevations is ±5 cm. Four baselines marked by rebar were established in 1983 near the heads of several channels to measure headward erosion (Fig. 41.4). The distance from the baseline (measured along a normal to the baseline) to the heads of the channels as determined by a break in slope and eelgrass denudation was recorded in June 1983 and June 1984. This information offers ground truth against which measurements made from airphotos can be checked. Selected points at regular intervals on the c.p.w. also were surveyed in 1983 to establish a datum against which degradation of the wall can be documented (Fig. 41.3).

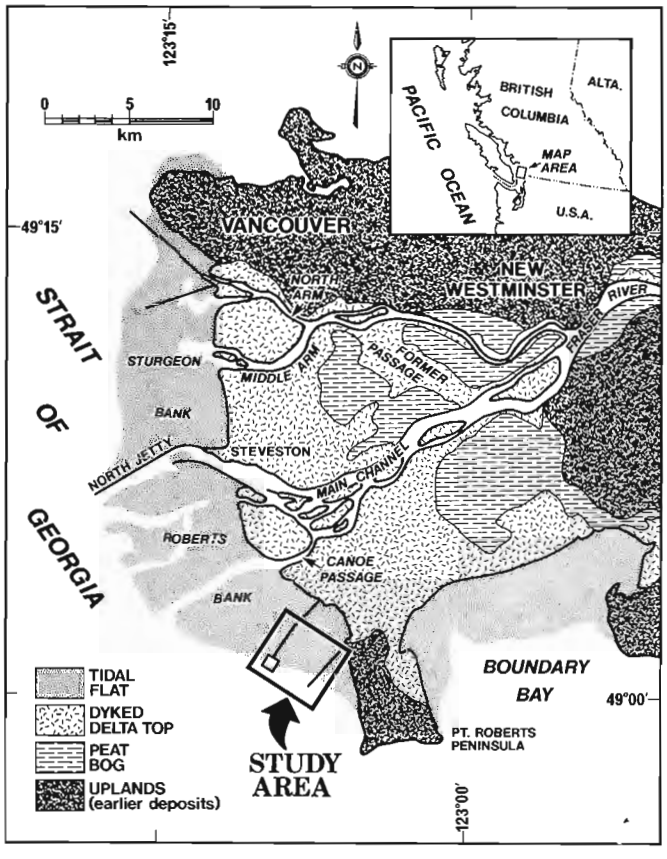

Figure 41.1. *Sedimentary setting and location of study area.*

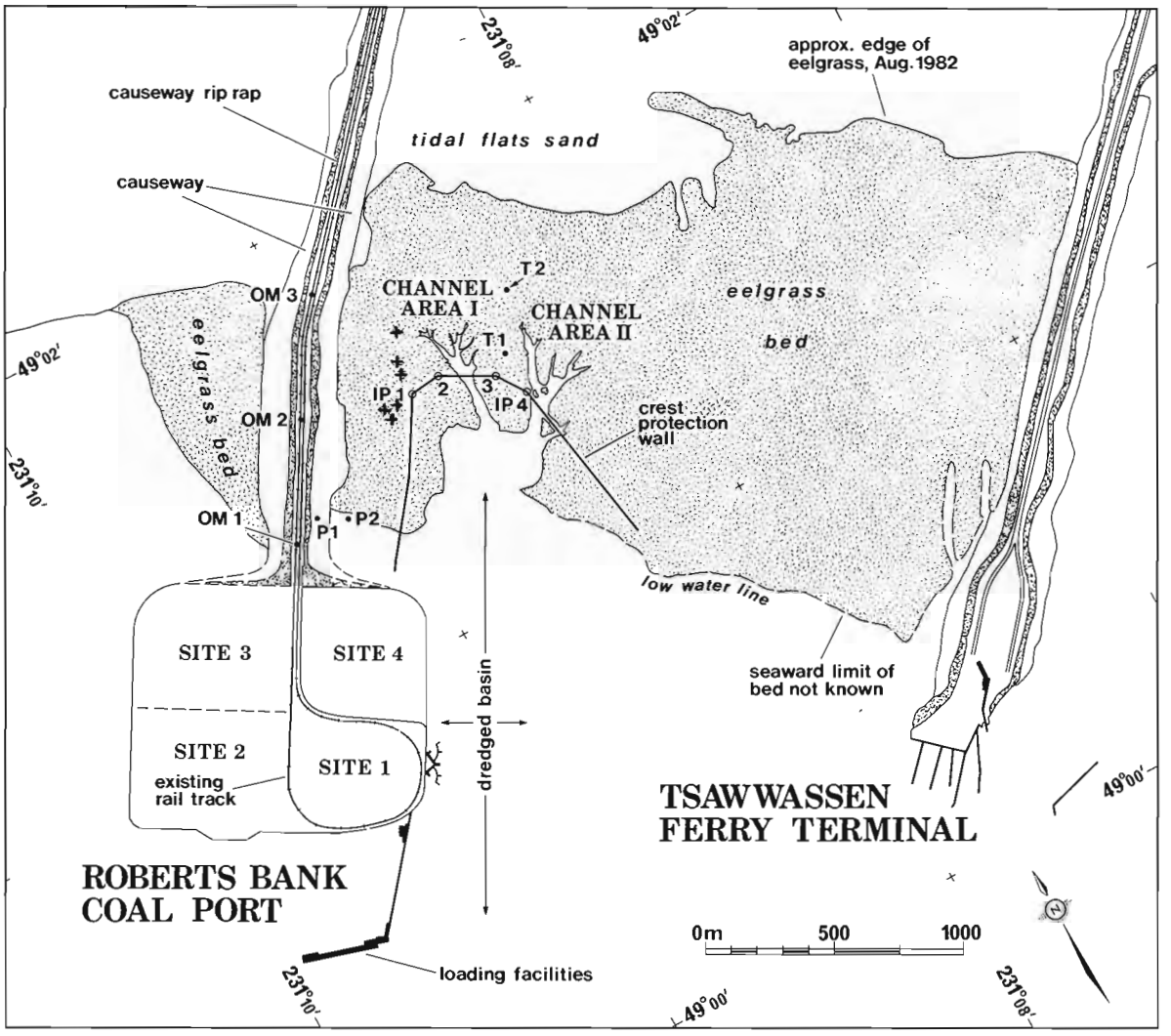

Figure 41.2. *Major features within study area including dendritic channels at head of dredged ship basin. OM, P, IP represent survey marker locations. T = navigation towers. Base map adapted from National Airphoto Library imagery (Roll # A37849) and Swan Wooster Engineering Ltd. blueprint drawings. Crosses (+) by IP1 indicate locations of coring sites.*

Sediment distribution

Thirty-four grab samples consisting of the top 2 to 3 cm of sediment were collected in the study area in 1983 and 38 in 1984 (Fig. 41.5). Position was fixed with a sextant (survey accuracy: ±10 m). Eight of the 1983 sampling positions were re-occupied in 1984 to establish whether the finer surface deposits are becoming coarser because of wave and current washing. Hand-driven cores up to 100 cm long collected at six stations (Fig. 41.2) between the Coalport causeway and c.p.w. in 1983 were re-occupied in 1984 to define the thickness and stability of the mud layer formed from the silt and clay discharged onto the flats during the pod land-filling operations which required only the coarser fraction of dredge spoil.

Channel flow metering

Flow velocities at several sites within the channels were measured with OTT C1 and Swoffer Model 2100 STD meters. A current metering program was established in 1984 to a) measure velocities in Channel Area II at cross-section 3 (Fig. 41.4) on an ebbing tide to establish a representative velocity profile and study the effect on the flow regime of the onset of channelized flow through the dendritic channels and b) acquire preliminary synoptic observations at comparable locations in both channel systems.

Tidal flat ebb tidal flow directions

The orientation of the eelgrass fronds at low tide was measured at 50 sites on the exposed tidal flats. Brunton compass measurements of the direction of last water flow as represented by the eelgrass orientation defined possible drainage paths and drainage basin sizes.

Effect of a flow obstruction in a channel

An experimental dam composed of sand filled plastic bags was placed near the head of one of the channels in Area II to study the effect on flow of water around the obstruction at low tide. The dam bridged the distance between the edges of the channel and was approximately the same elevation as the tidal flats on either side.

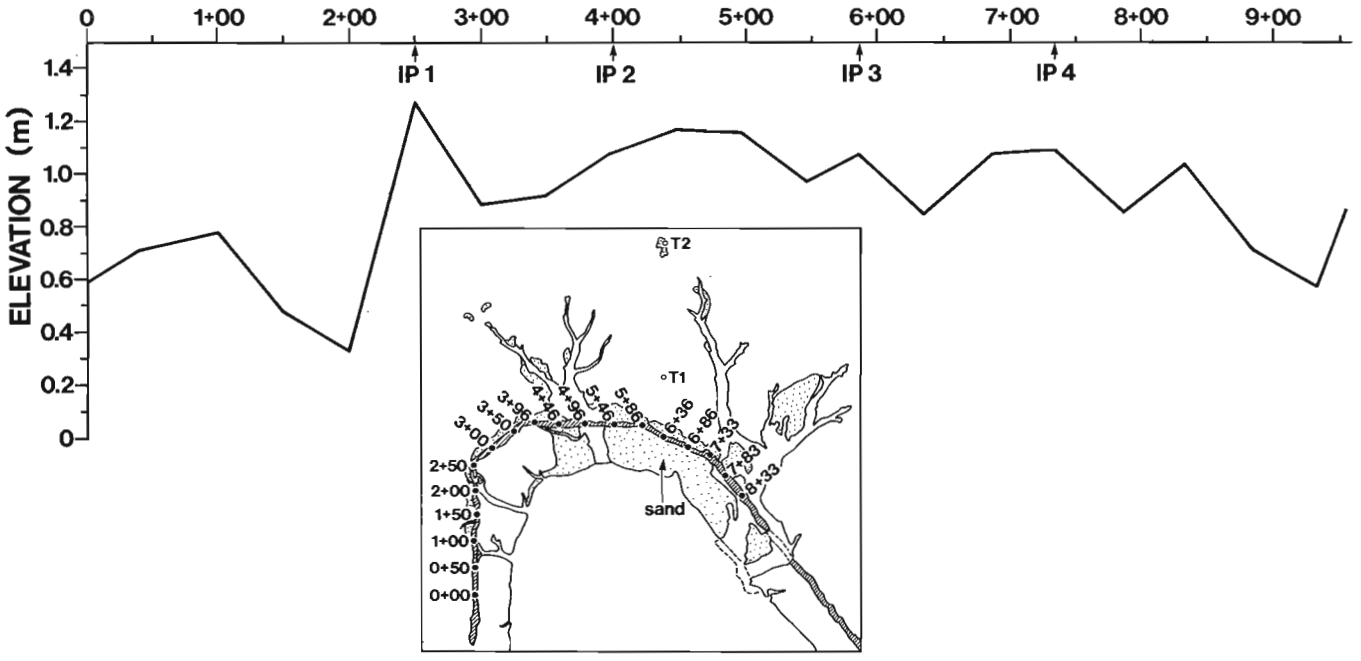

Figure 41.3. *Elevations along ship basin crest-protection wall surveyed in 1983. IP = Survey marker locations.*

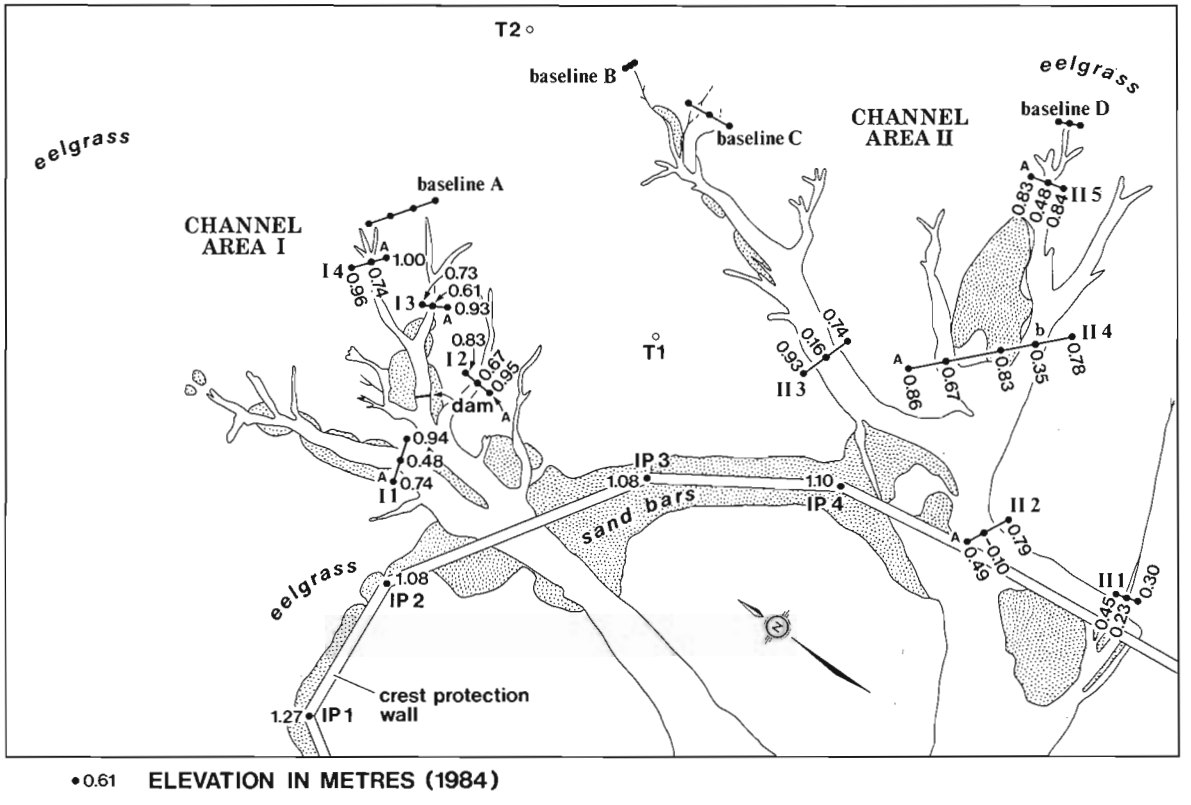

•0.61 **ELEVATION IN METRES (1984)**

Figure 41.4. *Locations of reference (or base) lines at heads of channels and transects where channel profiles were surveyed (lines along which selected elevations are noted). Note higher relief in Channel Area II.*

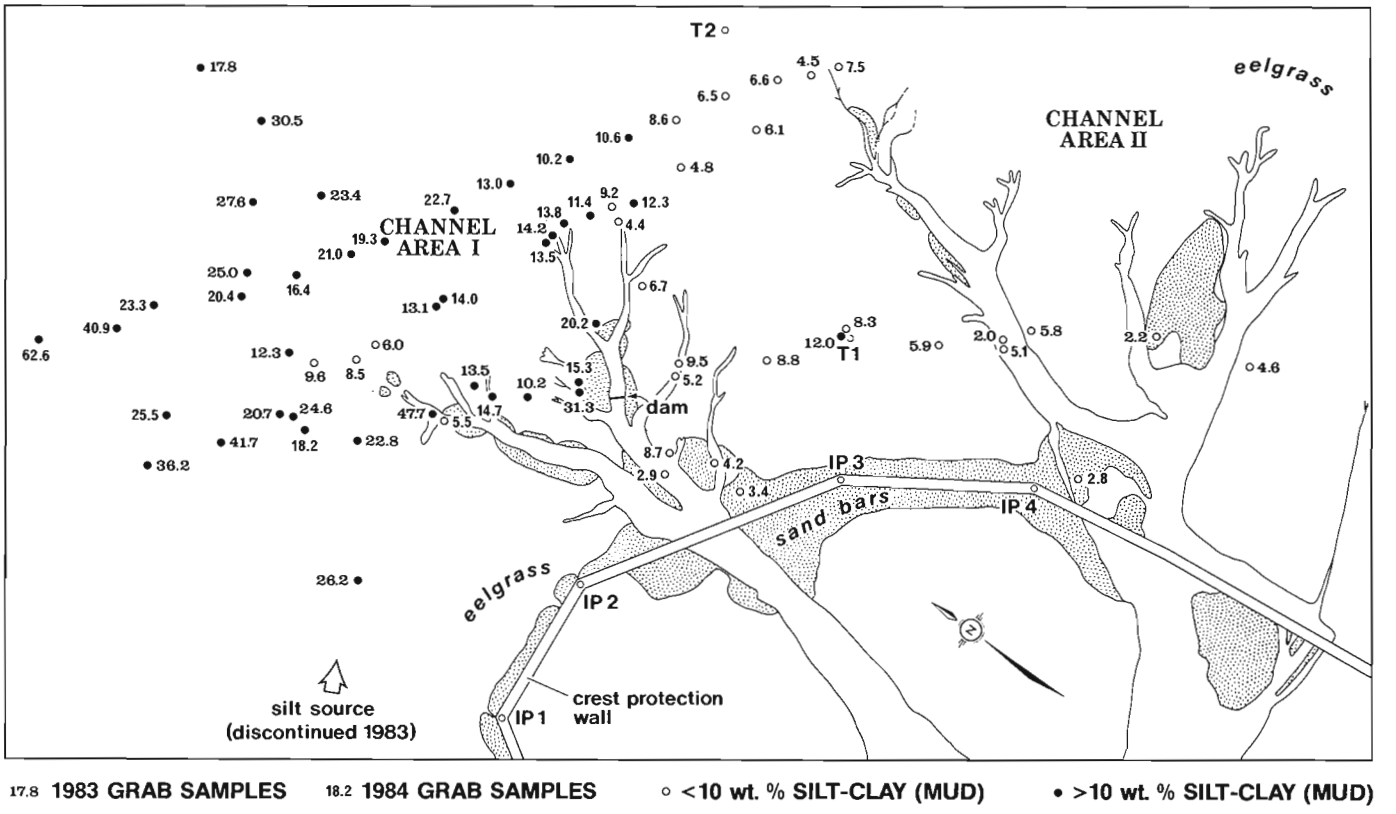

Figure 41.5. *Grab sample locations indicating weight per cent mud. Silt (mud) Source refers to construction operations for Pod 4 during which fine material was pumped onto flats.*

Laboratory techniques

Grain size analysis

Grab samples and subsamples from cores were split, washed to remove salt, dried, weighed, and wet sieved through a 63 m sieve to determine the dry weight proportion of sand to mud. The thickness of the mud layer was measured from the split cores.

Airphoto analysis

The rate of advance of the channel system was determined by: 1) measuring along the centreline of a main trunk in each of the two channel areas from 11 airphotos spanning the years 1969 to 1984 (Fig. 41.6A, 41.6B). Accuracy of these measurements is assumed to be ±20 m. 2) measuring from 8 airphotos, covering the period 1970 to 1984, the area of the channels using a planimeter. Recorded values represent the mean of three repeat determinations. Allowance was made for the area lost by the enlargement of the ship-turning basin to ensure a consistent base of measure (Fig. 41.6A). The linear rate of growth of the limit of the eelgrass (**Zostera marina**) field shoreward was measured normal to a fixed baseline in 14 airphotos from 1969 to 1984 (Fig. 41.6A, 41.6B). Accuracy is estimated to be ±20 m. Measurements of the rate of erosion of the channel system and the shoreward growth of the eelgrass were taken to determine if there is a correlation between these rates and Coalport construction activities.

Results

Grab sample analysis indicates that the weight per cent mud in the top 2-3 cm of sediment within the eelgrass beds remained relatively constant (±5%) for sites resampled in 1984. Samples obtained in the channels varied by up to 42%. Localized silt patches may be responsible for this extreme variation. The percentage of mud from the 1984 samples confirms the location of a 10% mud boundary established in 1983 (Luternauer et al., 1984). It is apparent, therefore, that sediments in Channel Area I are consistently and persistently finer than those in Channel Area II. Furthermore, sediment in cores revealed no significant change in the thickness of the surface mud layer between 1983 and 1984. Channel profiles for Area I show no significant fluctuations from 1983 to 1984 (Fig. 41.7A). Channel Area II, cross-sections 1, 4 and 5 likewise display no significant change (Fig. 41.7B, 41.7C). Several of these channels have begun to be colonized with eelgrass. Only cross-sections 2 and 3 in Area II continue to display fluctuations in the elevation of the bed up to 25 cm. Channel heads at the baselines in Area I did not advance from 1983 to 1984, rather, the channels showed signs of new eelgrass growth, likely by vegetative propogation whereby a subsurface rhyzome of the plant grows horizontally and produces new fronds which extend above the sediment surface. Area II channel heads advanced 1 m or less but the eelgrass beds immediately adjacent to the channel heads were noticeably less dense than in the previous year, suggesting that gradual eelgrass denudation is still proceeding there.

The flow of water at low tide as defined by the orientation of the eelgrass fronds is illustrated in Figure 41.6A. These data show that water farther up the flats is deflected toward the eastern half of the intercauseway area. Nearer the c.p.w. the water is focused toward the dredged ship basin within two broad and shallow drainage basins separately encompassing Channel Areas I and II (Fig. 41.6A). A muted topographic rise, a matter of centimetres high, between Area I and Area II separates the channel systems.

The sandbag dam constructed near the head of one of the channels demonstrated the effect of a flow obstruction on creek erosion. Water which previously flowed in the channel overcame the resistance to flow in the adjacent eelgrass bed, eroded sediment from the sides of the dam and formed plunge pools behind and in front of the dam. The removal of sediment continued until a new equilibrium (with adjusted velocity and cross-sectional area) was established. This likely mimics the effect that the c.p.w. had on flows in Channel Areas I and II which it obstructed.

Velocity measurements were not entirely successful because the Ott meter malfunctioned and eelgrass in suspension repeatedly jammed the meter propeller. The data that were collected do suggest, however, that at the

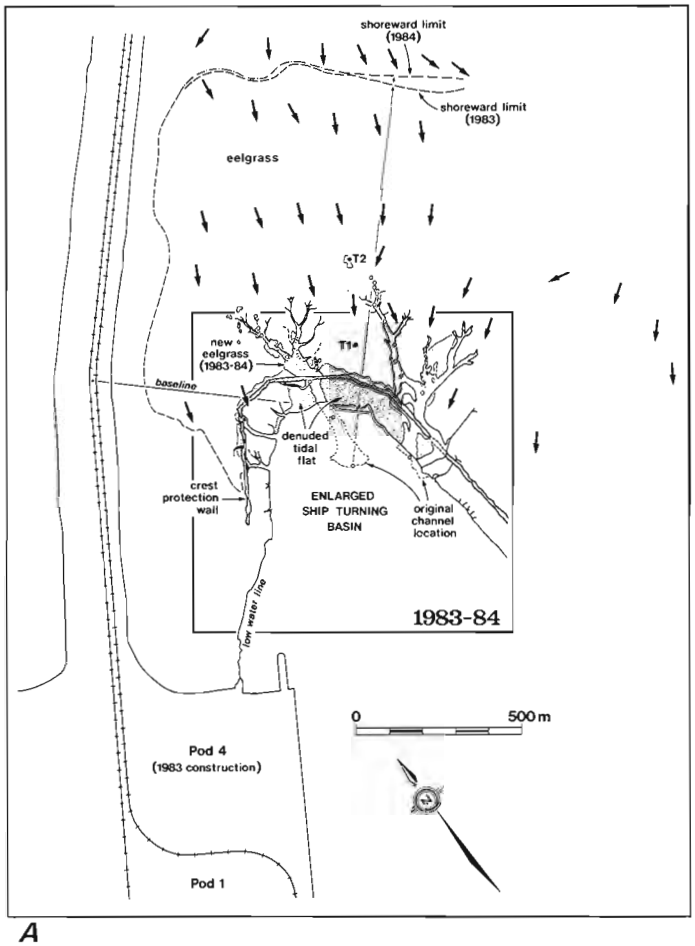

A

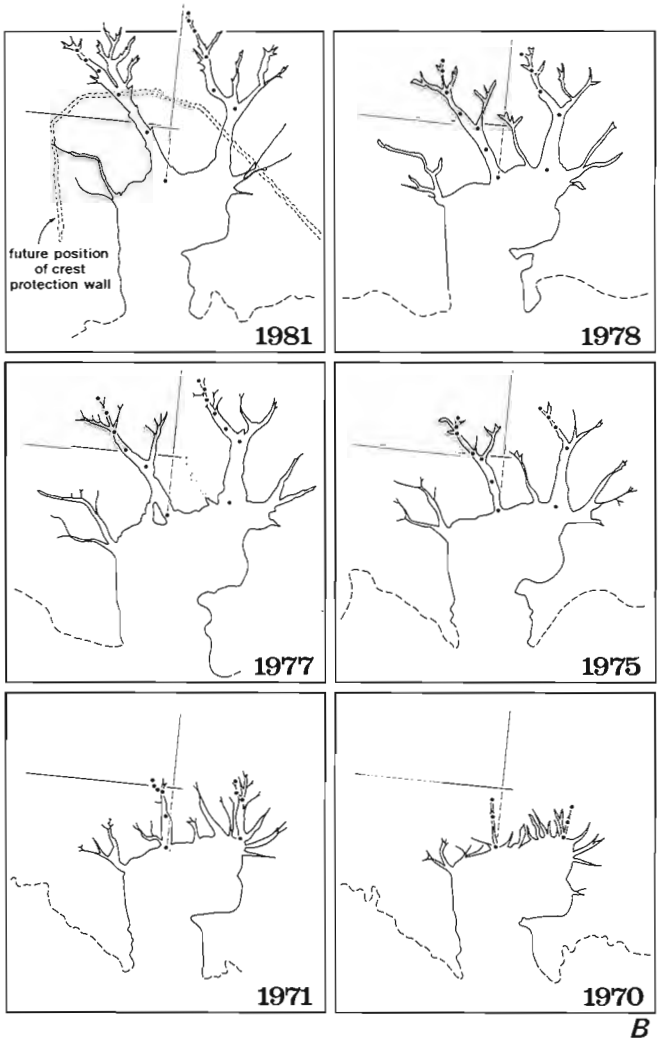

B

Figure 41.6A, 6B

A – Physical and biological features adjacent to Coalport 1983-1984. Square encloses area also represented in Figure 41.6B. Heavy arrows represent average orientation of eelgrass fronds at low water. Eelgrass fronds farther inshore tend to be oriented north-south. These arrows suggest the drainage basins at low water for the two Channel Areas I and II are divided approximately along a line which extends from navigation tower T1 to T2 and from there due north. Thus, the drainage basin for Channel Area I is probably considerably smaller than that for Channel Area II. The fine line extending from the bend in the Coalport causeway is the baseline from which the 1983 and 1984 shoreward limit of the eelgrass bed was measured from airphotos. Fine stippling in dendritic creeks indicates sites of local eelgrass recolonization. Original channel location represents position of channels on the tidal flats prior to enlargement of the ship basin. Open circles indicate segments along which linear growth of channels was measured (Fig. 41.8).

B – Successive stages in the evolution of the dendritic creeks. Solid circles indicate segments along which linear growth of channels was measured (Fig. 41.8). Fine lines at right angles to each other represent baseline and line along which shoreward limit of eelgrass at the time was measured.

inception of channelled flow on a falling tide, velocities temporarily rise before gradually declining again as the tide continues to ebb. This velocity peak, however, is not as high as that achieved at mid-phase of an ebbing tide. A typical velocity profile could not be established due to periodic turbulent flow in places, however, measurements show that near-bottom velocities exceeding the threshold velocity for initiation of sand movement (cf. Sternberg, 1971) are achieved during channelled flow up to 2 hours prior to low tide. Mean velocity measured at 4/10 of the water depth from the channel floor at comparable locations in the two channel systems was up to 45 cm/s higher in Area II. Maximum velocities up to 90 cm/s within 0.5 hr of low water were recorded in Area II, but were approximately half this velocity in Area I.

Estimates of the linear growth of channels and the change in area of channels measured from airphotos, indicate a general slowing of growth, with the exception of the linear growth rate from 1982-1983, which rose significantly (Fig. 41.8). The rates of growth between 1983-1984 are neglible (Tables 41.1 and 41.2). Estimates of the linear growth of the shoreward limit of eelgrass as measured from airphotos indicate a disproportionately high rate of growth occurred between 1979 and 1983 (Table 41.3) that cannot be directly related to any Coalport construction activity. The 18 m growth of the eelgrass limit from 1983-1984 (Fig. 41.6A) may represent the final extension of the **Zostera marina** field, i.e., it may have reached the limit of the habitat to which it is suited.

Discussion and conclusions

It is readily apparent that the focusing of flow towards the ship basin had led to creek formation and consequent denudation of part of the eelgrass bed. The influence of engineering structures on the slowing of creek erosion and the shoreward extension of the eelgrass bed is, however, not as clearly discernible.

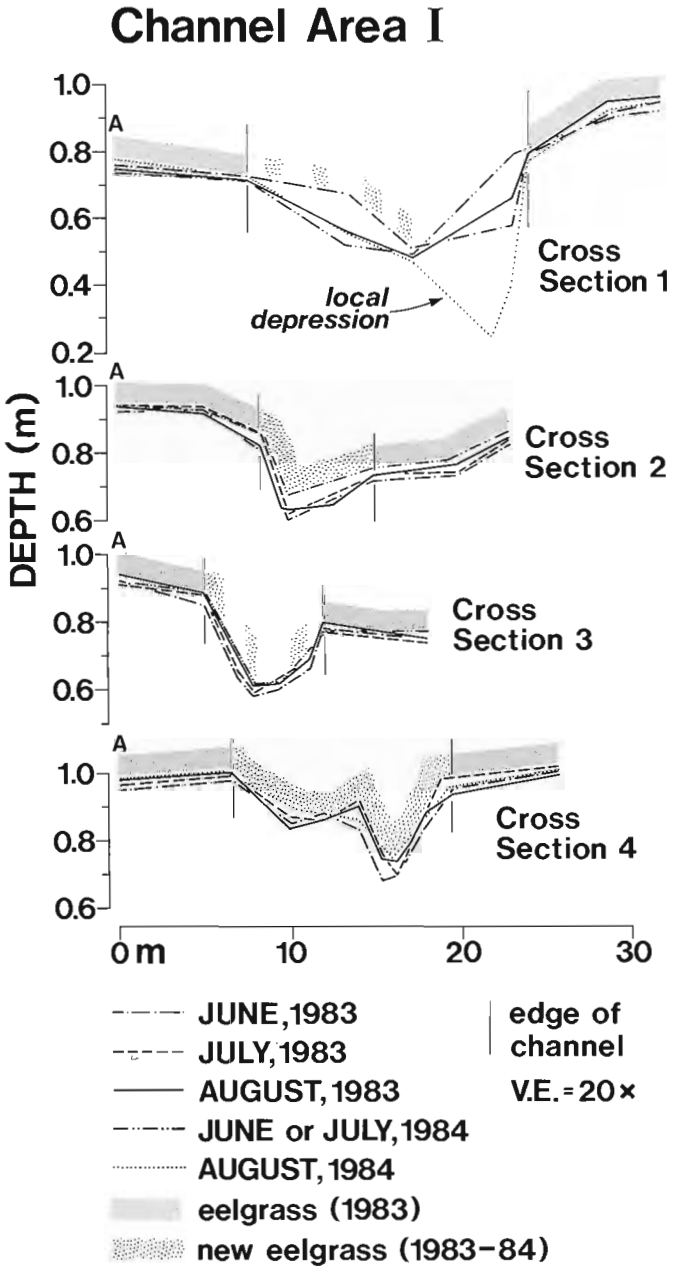

Figure 41.7A. *Comparison of channel profiles surveyed in Channel Area I (Fig. 41.4).*

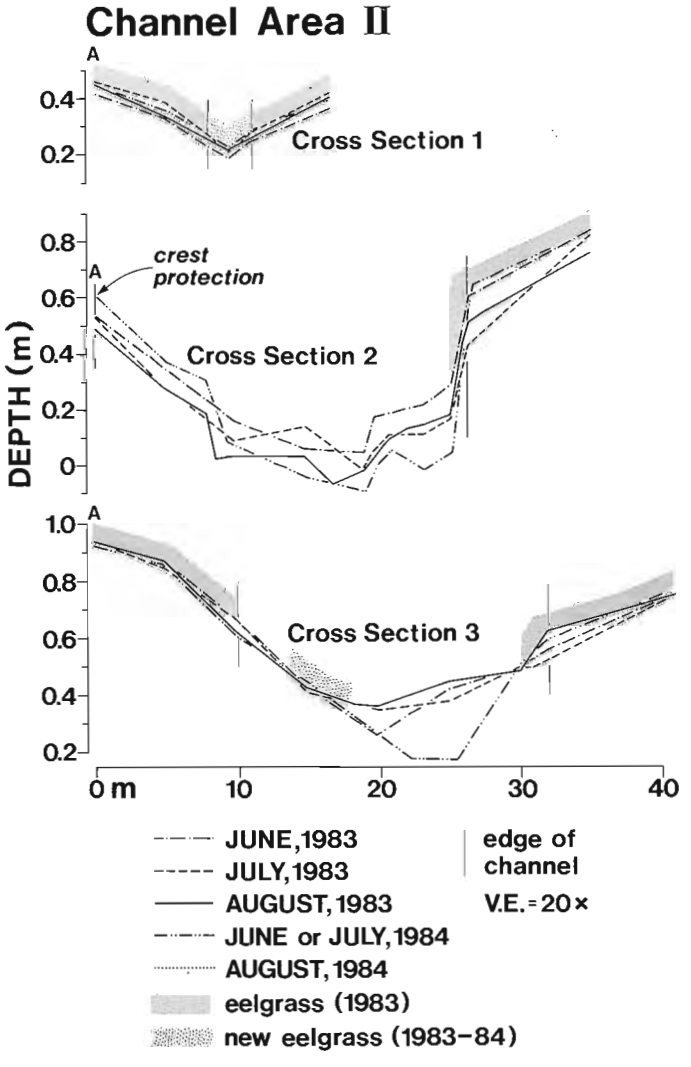

Figure 41.7B. *Comparison of channel profiles surveyed in Channel Area II (Fig. 41.4).*

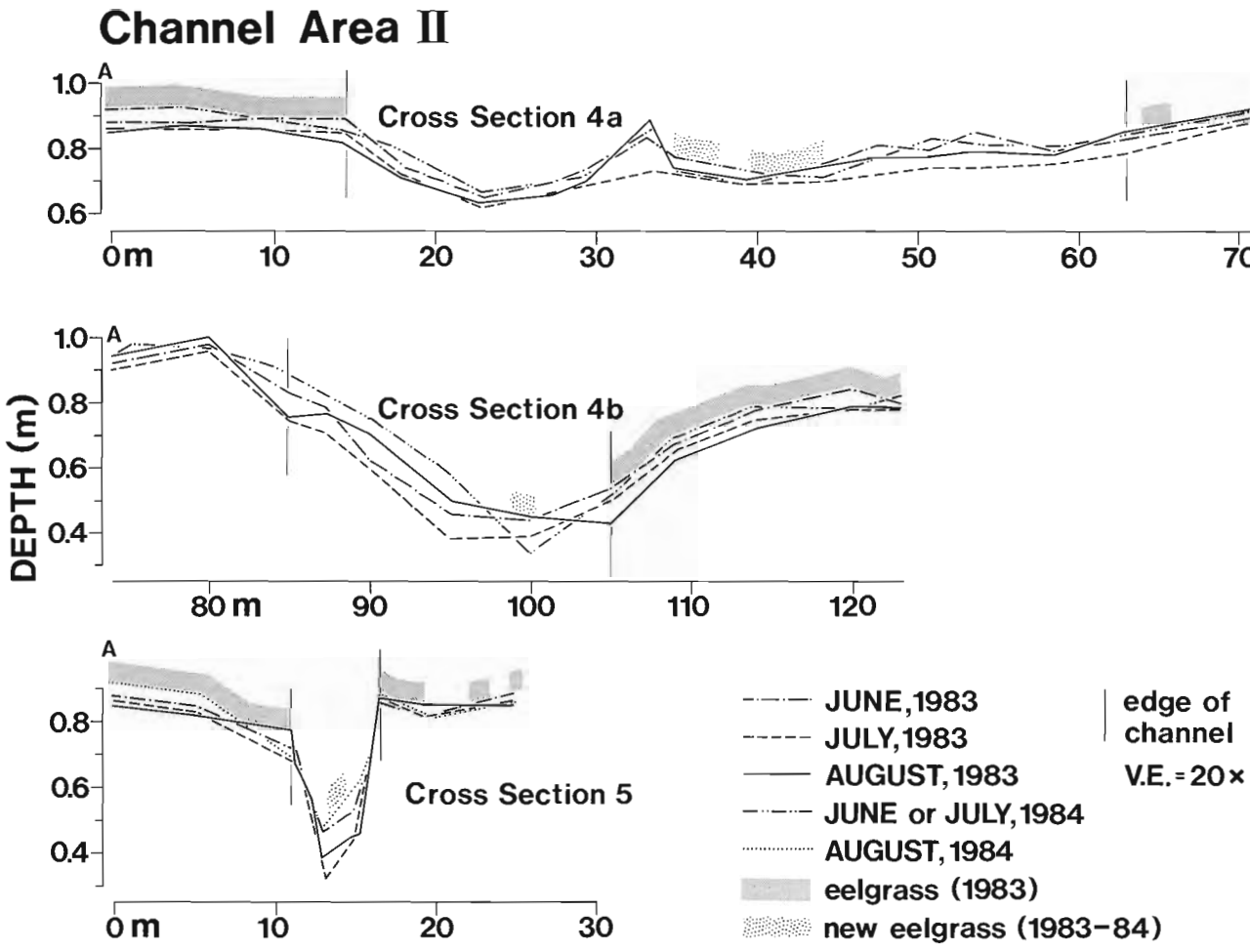

Figure 41.7C. *Comparison of channel profiles surveyed in Channel Area II (Fig. 41.4).*

Table 41.1. Estimate of linear channel growth calculated from airphotos (±20 m)

Airphoto			Channel Area I		Channel Area II	
Year	Roll No.	Exposure	Length (m)	Rate of growth; avg. (m/a)	Length (m)	Rate of growth; avg. (m/a)
1969 May	BC5332	009	0		0	
				140		104
1970 May	BC5371	109	140		104	
				70		91
1971 Aug	BC5431	218	210		195	
				24		29
1975 June	A37169	39	308		312	
				75		55
1977 June	A31164	28	457		421	
				20		30
1979	BC79207	139	496		451	
				21		22
1980	A37779IR	13	517		483	
				1		20
1981	A37817	344	518		503	
				11		6
1982	BC5332	009	529		509	
				56		91
1983 July	BR83076	L2-59	585		600	
				0		3
1984 July	BR84036	L2-41	585		603	

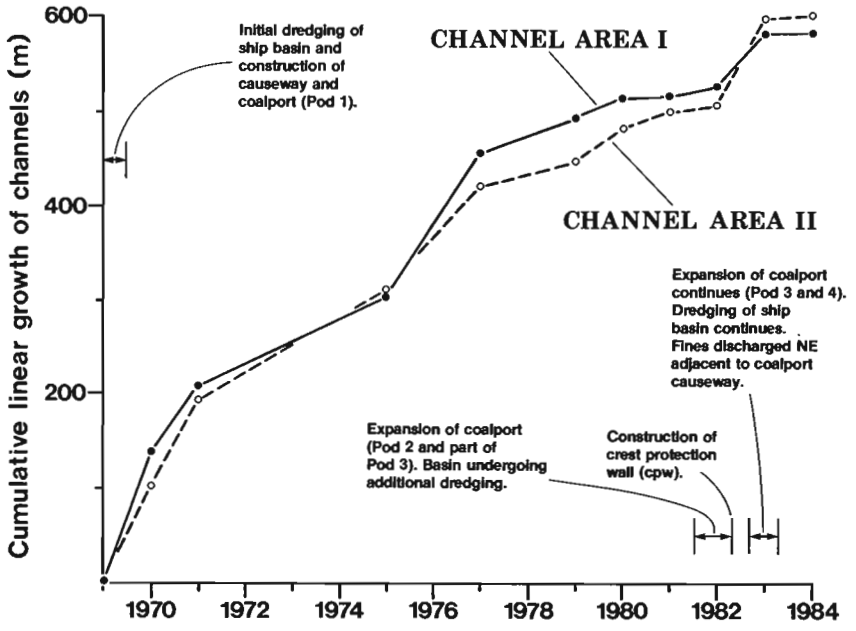

Figure 41.8

Plots of the historical changes in the linear growth of major creeks within each of the channel areas (see Fig. 41.6).

Increase in the erosion rate of the creeks had ceased by the spring of 1982 when the crest protection wall was erected. Therefore, ordinarily, it would be difficult to recognize, what, if any effect the c.p.w. has had on the rate of channel extension. But by 1982 dredging to expand the ship basin had truncated the lower reaches of the creeks and an expected surge in the rate of erosion occurred between the summer of 1982 and 1983. It is evident, then, that although the wall may have temporarily forestalled this erosional response (imagery obtained during the summer of 1982 indicates no unusual change in erosion rate), ultimately, it could not prevent it.

Shoreward extension of the west side of the eelgrass bed since the construction of the Coalport causeway was probably promoted by deflection of the turbid water of the Fraser River away from the southern flats by the causeway. This is suggested by the higher shoreward limit of the eelgrass bed on the eastern side of the intercauseway area – the side farthest from the plume. The sharp rise in the rate of shoreward colonization of **Zostera marina** on the west side during the period 1979-1983 followed by a marked reduction probably reflects both the presence of the clearer water which permits greater light penetration and a period of high seed production and successful germination which persisted for several years. Ponding of water by the c:p.w. at low tide might also be considered to have influenced shoreward eelgrass colonization by maintaining higher parts of the tidal flats submerged longer. However, the c.p.w. was erected only during the latter stage of the rapid growth period. Furthermore, a cursory check, at low tide, of water depths within the eelgrass bed shoreward of the c.p.w. and at equivalent locations towards the eastern side of the bed suggested water was not higher on average behind the c.p.w. The wall must interfere with the direct seaward movement of non-channel surface wash in the broad shallow depressions within which the channels systems lie, but this probably does not contribute as much to the ponding of water as the resistance to flow presented by the eelgrass.

However, the c.p.w. may have somewhat sheltered Channel Area I from wave attack and encouraged ponding and retention of silt and clay pumped onto this area. This mud is more resistant than sand to ambient tidal current wash on the tidal-flat surface outside the creeks. Thus, it offers a stable substrate for the recolonization of **Zostera marina** in that area.

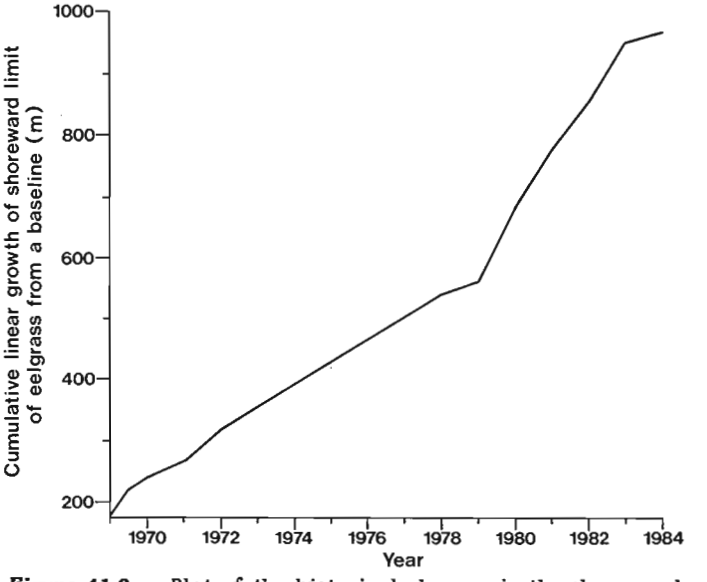

Figure 41.9. *Plot of the historical changes in the shoreward advance of the western side of the* ***Zostera marina*** *bed.*

In the creeks of Channel Area I, which are floored primarily by sand, eelgrass has re-established itself because currents have slowed sufficiently as the creeks approach a dynamic equilibrium and channel morphology is stablized. Recolonization within the creeks of Channel Area II has not proceeded as far because flows in those creeks are faster and their morphology less stable. Those conditions are a reflection of the larger low-water drainage area of Channel Area II.

To the extent that the c.p.w. may inhibit the resuspension of the silt by waves and seaward transport of sediment by the creeks (although there is no evidence of the latter), it should be maintained. In addition, it is advisable to infill the depressions along the c.p.w. to a uniform height above the flats as continued concentration of flow will promote degradation of the wall and diminish any capacity it may have to trap sediment.

Table 41.2. Estimated changes in areal extent of dendritic channels calculated from airphotos

Year	Airphoto Roll no.	Exposure	Area (m^2)	Change in area per year ave. (%)
1969	BC5332	009	0	-
1970	BC5371	109	10370	92.4
1971	BC5431	218	19955	8.0
1975	A37169	39	26355	12.9
1977	A31164	28	33157	8.7
1978	A37597	146	36058	6.9
1981	A37817	344	43500	4.4
1983	BR83076	L2-59	47347	0
1984	BR84036	L2-41	~47347	

Table 41.3. Estimated Linear Growth of Shoreward Eelgrass Limit calculated from airphotos

Year	Airphoto Roll no.	Exposure	Distance from baseline (m)	Rate of growth ave. (m/a)
1969 May	BC5332	009	175	
1969 July	38516(B)	W 1295	220	65
1970 May	BC5371	109	240	25
1971 Aug.	BC5431	218	265	55
1972	A30518	61	320	37
1975 June	A37169	39	430	37
1977 July	A31164	28	503	37
1978	A37597	146	540	21
1979	BC79207	139	561	119
1980	A37778IR	55	680	82
1981	A37817IR	331	762	88
1982	BC5332	009	850	100
1983 July	BR83076	L2-59	950	18
1984 July	BR84036	L2-41	968	

Acknowledgments

Special thanks are due to R. Moody (Port of Vancouver), and P.G. Harrison (Botany Department, University of British Columbia) and M. Quick (Department of Civil Engineering, University of British Columbia) for helpful advice and general assistance during the 1984 field season. The authors are also grateful for the use of the hovercraft and for the assistance of the personnel from the Canadian Coast Guard Hovercraft Base, Vancouver during field mapping operations

References

Beak Consultants Ltd.
1977a: The existing physical environment; in Environmental Impact Assessment of Roberts Bank Port Expansion; National Harbours Board, Port of Vancouver, v. 3 (Appendix A), 91 p.

1977b: The existing biological environment; in Environmental Impact Assessment of Roberts Bank Port Expansion; National Harbours Board, Port of Vancouver, v. 4 (Appendix B), 140 p.

Ekstrom, B.A.
1983: Roberts Bank Port expansion – an engineering overview in Proceedings of the 13th International Association of Ports and Harbours Conference, June 4-11, 1983, Vancouver, British Columbia, p. 39-55.

Hawley, P.M.
1979: Erosional stability of a dredged burrow pit on southern Roberts Bank, Fraser Delta, B.C.; unpublished B.A. Sc. thesis, University of British Columbia, Vancouver, 65 p.

Hinton, B.R. & Associates Ltd.
1977: Main report; in Environmental Impact Assessment of Roberts Bank Port Expansion; National Harbours Board, Port of Vancouver, 201 p.

Luternauer, J.L.
1976: Fraser Delta sedimentation, Vancouver, British Columbia; in Report of Activities, Part A, Geological Survey of Canada, Paper 76-1A, p. 213-219.

1980: Genesis of morphologic features on the western delta front of the Fraser River, British Columbia – status of knowledge; in The Coastline of Canada, ed. S.B. McCann; Geological Survey of Canada, Paper 81-10, p. 381-396.

Luternauer, J.L., Duggan, D., and Hendry, M.
1984: Development – induced tidal flat erosion, Fraser River Delta, B.C.; in Current Research, Part A, Geological Survey of Canada, Paper 84-1A, p. 75-80.

McKenzie, W.C.
1983: Expansion of the Roberts Bank Coal Export Port, B.C.; Professional Engineer, February, p. 7-11.

Sternberg, R.W.
1971: Measurements of incipient motion of sediment particles in the marine environment; Marine Geology, v. 10, p. 112-119.

Weibe, J.D. and Moody, R.
1983: Roberts Bank: an environmental overview; in Proceedings of the 13th International Association of Ports and Harbours Conference, June 4-11, 1983, Vancouver, British Columbia, p. 106-115.

POSTMETAMORPHIC THRUST FAULTING ON THE NORTHEASTERN MARGIN OF THE SHUSWAP METAMORPHIC COMPLEX, WELLS GRAY PROVINCIAL PARK, BRITISH COLUMBIA

Project 820014

M.D. Gerasimoff[1]
Cordilleran Geology Division, Vancouver

Gerasimoff, M.D., Postmetamorphic thrust faulting on the northeastern margin of the Shuswap Metamorphic Complex, Wells Gray Provincial Park, British Columbia; in Current Research, Part A, Geological Survey of Canada, Paper 85-1A, p. 327-331, 1985.

Abstract

Three phases of deformation are recognized within the cover sequence of the northeastern margin of the Shuswap Metamorphic Complex south of Twin Spires. First-phase deformation was accompanied by regional metamorphism and produced large-scale, tight to isoclinal, southwest-verging folds which plunge to the northwest. Second-phase deformation was brittle-ductile and postdated regional metamorphism. It produced large-scale kink folds and thrust faults which verge southwesterly. Thrust faults of this generation are believed to be responsible for the juxtaposition of the lower grade cover of Cariboo Group strata and the underlying Shuswap Metamorphic Complex south of Twin Spires. Field relationships suggest that these faults are younger than a Jura-Cretaceous granitoid pluton to the south. The third phase of deformation was brittle and resulted in steep north-northwest and northeast trending normal faults.

Résumé

On observe trois phases de déformation dans la séquence de couverture de la marge nord-est du complexe métamorphique de Shuswap au sud de Twin Spires. La première phase de déformation a été accompagnée d'un métamorphisme régional et a produit de grands plis fermés à isoclinaux qui sont détournés vers le sud-ouest et qui plongent vers le nord-ouest. La deuxième phase de déformation a été cassante et ductile et postérieure au métamorphisme régional. Elle a produit de grands plis en chevrons et des failles chevauchantes en direction sud-ouest. Les failles chevauchantes de cette phase tectonique sont vraisemblablement responsables de la juxtaposition de la couverture moins métamorphisée du groupe de Cariboo et du complexe métamorphique sous-jacent de Shuswap au sud de Twin Spirs. L'orbservation sur le terrain portent à croire que ces failles sont plus récentes qu'un pluton granitoïde jurassique-crétacé qui est situé au sud. La troisième phase de déformation a été cassante et a produit des failles normales abruptes à orientations nord-nord-ouest et nord-est.

[1] Department of Geological Sciences, Queen's University, Kingston, Ontario K7L 3N6

Introduction

A study of structure, stratigraphy, and metamorphism in the cover sequence and subjacent rocks on the northeastern margin of the Shuswap Metamorphic Complex was initiated during July and August of 1984 near Hobson Lake in Wells Gray Provincial Park (Hobson Lake map area 93A/9).

The study area (Fig. 42.1) includes strata of the Cariboo Group (Table 42.1, see Campbell et al., 1973; Pigage, 1978; and Campbell, 1978) and Snowshoe Formation, although rocks of the latter were not examined extensively. The Cariboo Group ranges from Hadrynian to Cambrian.

Structure, Metamorphism

The Shuswap Metamorphic Complex and adjacent cover sequence near Wells Gray Provincial Park are polydeformed as recognized by Pigage (1978) and Fletcher and Greenwood (1979).

In the study area three phases of deformation are recognized. First-phase deformation was ductile and is characterized by large southwesterly-verging tight to isoclinal folds (F_1) with pervasive axial-planar foliation (S_1) defined by phyllosilicates. South of Twin Spires, bedding in the Isaac Formation is commonly transposed parallel to the axial-planar foliation (S_1). Minor F_1 folds in this area plunge to the northwest at 20° to 50°.

Second-phase deformation is transitional between brittle and ductile and consists of megascopic kink folds which plunge gently to either the northwest or southeast. Minor features include kink bands, box folds (conjugate kink bands), crenulation cleavage, and chevron folds (Fig. 42.2, 42.3). Second-phase structures deform bedding (S_0) and first-phase axial planar foliation (S_1), but no metamorphic mineral growth is associated with this phase. The second-phase deformation is interpreted as produced at upper crustal levels and postmetamorphic because of its semiductile nature and the lack of metamorphic mineral growth, respectively.

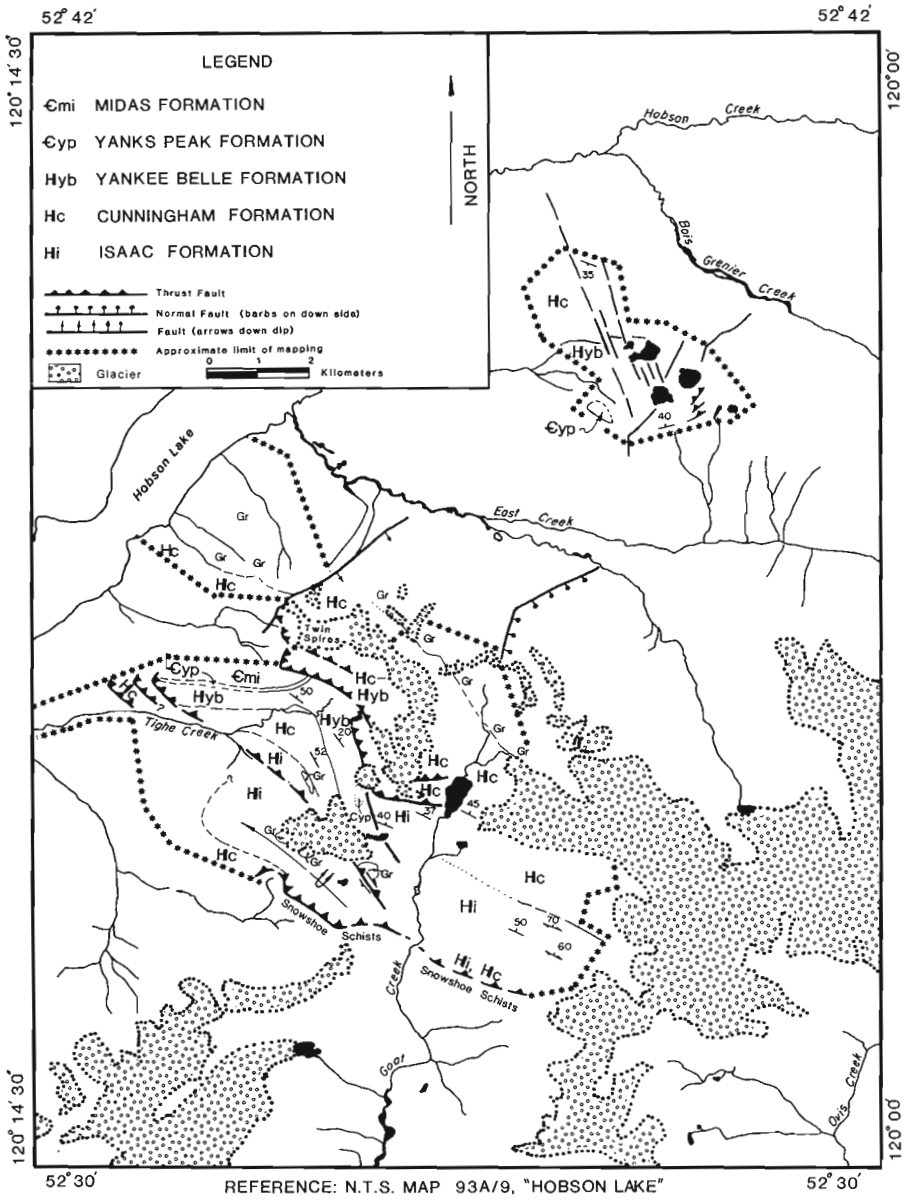

Figure 42.1. *Geological sketch map of the study area, Wells Gray Provincial Park.*

Thrust faults that verge southwestward and dip 50° to 60° to the northeast are a significant feature of second-phase deformation near Twin Spires (Fig. 42.4, 42.5). The orientation of the thrust faults appears to be controlled by a pre-existing anisotropy, the axial plane orientation of the large first-phase folds. The juxtaposition of Cariboo Group strata of the cover sequence with schists and gneisses of the Snowshoe Formation south of Twin Spires is the result of thrust faulting during second phase deformation (Fig. 42.6).

Third-phase deformation is marked by brittle normal faults trending north-northwest and northeast. The north-northwest-trending set is well developed north of East Creek, and the northeast-trending set is represented by two faults north and east of Twin Spires (Fig. 42.1). Displacement on the faults north of East Creek appears to be on the order of a few hundred metres or less; lack of marker horizons in the offset strata makes more precise determinations impossible. The large northeast trending faults are very persistent vertically; displacements may range up to a kilometre.

Granitoid intrusives

A granitoid pluton, here informally called the Hobson Lake pluton, is exposed north of Twin Spires. It is bounded locally on its northern side by East Creek, which probably marks the trace of a steep fault. Rb-Sr dates obtained by Pigage (1978) from stocks in the Azure Lake area to the south indicate a Jura-Cretaeous age. Pigage (1978) noted that these plutons cut across structural trends of his first- and second-phase deformations and impose a contact metamorphic aureole on regionally metamorphosed country rock. It follows from these observations that folding and metamorphism were complete by Jura-Cretaceous time. East of Goat Creek, there are minor granitoid intrusives, mainly sills and dykes, which are well foliated and locally garnetiferous. These are obviously premetamorphic, and field relationships to folded bedding in the country rock suggest that they are synkinematic to postkinematic with respect to first-phase deformation.



Figure 42.2. *A second-phase kink fold in a sandy horizon of Isaac Formation is outlined in white. In phyllites above and below, note progression from widely spaced kink bands on right to closely spaced kink bands and chevron folds in the core of the large kink fold. About 5 km south of Twin Spires; viewed to southeast; ice axe is 75 cm long.*



Figure 42.3. *Macroscopic second-phase conjugate box folds in calcareous phyllites of Isaac Formation south of Twin Spires. White line indicates trace of plane of symmetry of conjugate box folds, and probable plane of partial décollement.*

Table 42.1. Table of formations of the Cariboo Group

CARIBOO GROUP	UPPER AND LOWER CAMBRIAN (MIDDLE CAMBRIAN MAY BE ABSENT)	Dome Creek Formation *Shale, silstone, argillite, minor limestone*
	LOWER CAMBRIAN	Mural Formation *Limestone, dolostone, shale, minor siltstone*
	LOWER CAMBRIAN AND HADRYNIAN	Midas Formation *Shale, siltstone, minor sandstone*
		Yanks Peak Formation *Grey, white, pink quartzite, minor silty shale*
	HADRYNIAN	Yankee Belle Formation *Interbedded shale, siltstone, limestone, minor sandstone and dolostone*
		Cunningham Formation *Limestone, minor grey shale*
		Isaac Formation *Grey to black phyllite and shale, minor siltstone, sandstone and limestone*

After Campbell *et al*, 1973



Figure 42.4. *Two northeast dipping thrust fault traces exposed on south side of Twin Spires massif; Twin Spires are peaks on ridge at centre. Resistant strata of Yanks Peak Formation at lower left, and to right of Twin Spires were formerly mapped (Campbell, 1978) as forming a continuous asymmetric syncline.*



Figure 42.5. *Continuation of the lower thrust of Figure 42.4 has been mapped to the lake at the head of Goat Creek. here it places dolomitic marbles of Cunningham Formation and Yankee Belle Formation in the core of an overturned syncline, over grey platy and massive marbles of Cunningham Formation. At lower left, another thrust fault places these grey marbles over Isaac Formation.*

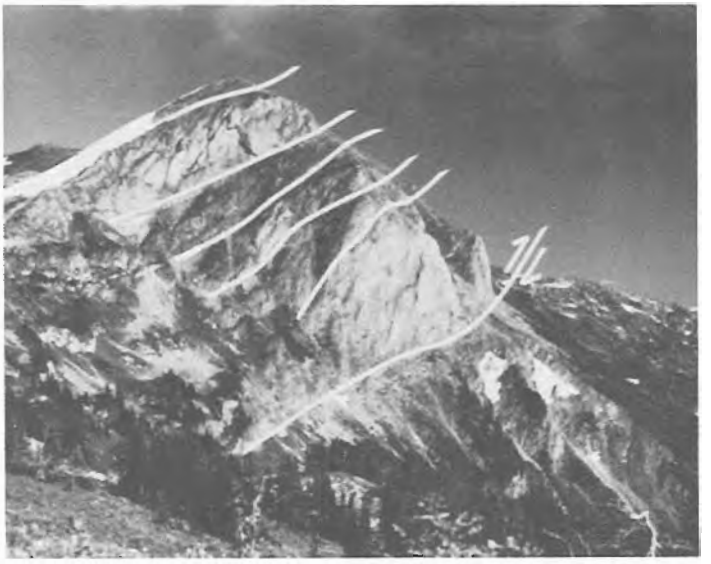

Figure 42.6. *Six thrust faults imbricate Isaac and Cunningham formations south of Twin Spires. Figures 42.2 and 42.3 from outcrops exposed near left margin of the photograph. View is towards the southeast. These rocks are interpreted to lie on the lower limb of a large overturned first-phase anticline; i.e., the sequence seen here would be upside-down. The lowest exposed thrust fault places Cunningham Formation marble over mylonitic biotite-garnet schists of the Snowshoe Formation.*

Discussion

Pigage (1978) believed that the Shuswap Metamorphic Complex is separated from the adjacent cover sequence of Cariboo Group strata by a first-phase "tectonic slide" (cf. Fleuty, 1964). This slide was thought to have been re-activated during his second-phase of deformation, causing offsets of structural trend and metamorphic isograds.

At Hobson Lake, the Hobson Lake pluton is a crudely foliated plagioclase-K-feldspar-quartz-biotite granitoid. A plug of similar composition and texture is exposed south of Twin Spires where it is crosscut by a shear zone (Fig. 42.1). Shear zone fabrics indicate dextral strike slip with a component of northeast side upwards thrust motion. Along strike to the northwest, this shear zone appears to pass upward into a series of thrust faults exposed north of Tighe Creek. If the Hobson Lake pluton is of Jura-Cretaceous age, then these second-phase thrust faults and the juxtaposition of the cover sequence with the Shuswap Metamorphic Complex may be much younger than previously assumed. It may be related to the Eocene "thermal event" which caused the re-setting of both the Rb-Sr and K-Ar isotopic systems (Pigage, 1978).

Acknowledgments

The author would like to acknowledge the permission of the Ministry of Lands, Parks, and Housing, Parks and Outdoor Recreation Division, Province of British Columbia, for access to Wells Gray Provincial Park during the 1984 field season. Many thanks go to L.C. Struik and R.B. Campbell of the Cordilleran Geology Division, who suggested and provided the means for this study.

The author would like to acknowledge personal financial support in the form of a Natural Sciences and Engineering Research Council Postgraduate Scholarship awarded for the 1983/84 and 1984/85 academic years.

References

Campbell, R.B.
1978: Quesnel Lake (93A) map area; Geological Survey of Canada, Open File Map 574.

Campbell, R.B., Mountjoy, E.W., and Young, F.G.
1973: Geology of McBride map area, British Columbia; Geological Survey of Canada, Paper 72-35.

Fletcher, C.J.N. and Greenwood, H.J.
1979: Metamorphism and structure of Penfold Creek area, near Quesnel Lake, British Columbia; Journal of Petrology, v. 20, pt. 4, p. 743-794.

Fleuty, M.J.
1964: Tectonic slides; Geological Magazine, v. 101, p. 452-456.

Pigage, L.C.
1978: Metamorphism and deformation on the northeastern margin of the Shuswap Metamorphic Complex, Azure Lake, B.C.; unpublished Ph.D. thesis, University of British Columbia.

-43-

THE KELOWNA DETACHMENT ZONE, OKANAGAN VALLEY, SOUTH-CENTRAL BRITISH COLUMBIA

Marc Bardoux[1]
Cordilleran Geology Division

Bardoux, M., The Kelowna detachment zone, Okanagan Valley, south-central British Columbia; in Current Research, Part A, Geological Survey of Canada, Paper 85-1A, p. 333-339, 1985.

Abstract

The Okanagan metamorphic and plutonic complex is defined as a basement assemblage composed, in the Kelowna area, of mylonitic high-grade para- and orthogneisses, possibly intruded by Cretaceous felsic plutonic rocks. The mylonitic rocks are structurally overlain by weakly deformed Tertiary sediments and volcanics.

Mylonitic fabrics within the basement extend at least one kilometre below the basement-cover boundary. Kinematic indicators in the mylonites demonstrate that shearing was predominantly in the direction of the upper member to the west.

Ductile shear occurred primarily before the Eocene; volcanic dykes of that age cut the mylonitic fabric and are only slightly deformed. Pre-Eocene rocks that originally formed the hanging wall of this shear zone are presumed to have been removed by tectonic denudation. Retrogression and intense fracturing of the uppermost parts of the mylonitic basement suggest that, before or after Eocene time, brittle reactivation of the shear zone occurred along the basement-cover boundary.

Résumé

Le complexe métamorphique et plutonique d'Okanagan est un socle métamorphique qui dans la région de Kelowna, se compose de paragneiss et d'orthogneiss mylonitiques fortement métamorphisés dans lesquels des roches plutoniques felsiques crétacées ont peut-être pénétrées. Les roches mylonitiques sont structuralement recouvertes de sédiments et de roches volcaniques tertiaires faiblement déformés.

Les éléments structuraux mylonitiques dans le socle se prolongent au moins à un kilomètre sous le contact socle-couverture. Les indicateurs cinématiques observés dans les mylonites montrent que le cisaillement s'est produit principalement en direction du terme supérieur vers l'ouest.

Le cisaillement ductile s'est produit surtout avant l'Eocène; des filons volcaniques légèrement déformés de cet âge recoupent les éléments structuraux mylonitiques. Les roches pré-éocènes qui avaient à l'origine formé la lèvre supérieure de cette zone de cisaillement ont vraisemblablement été enlevées par dénudation tectonique. La régression et l'intense fracturation des parties supérieures du socle mylonitique laissent croire qu'il y a eu réactivation cassante, avant ou après l'Eocène, de la zone de cisaillement le long du contact entre le socle et la couverture.

[1] Ottawa-Carleton Centre for Geoscience Studies, Department of Geology, Carleton University, Ottawa, Ontario, K1S 5B6

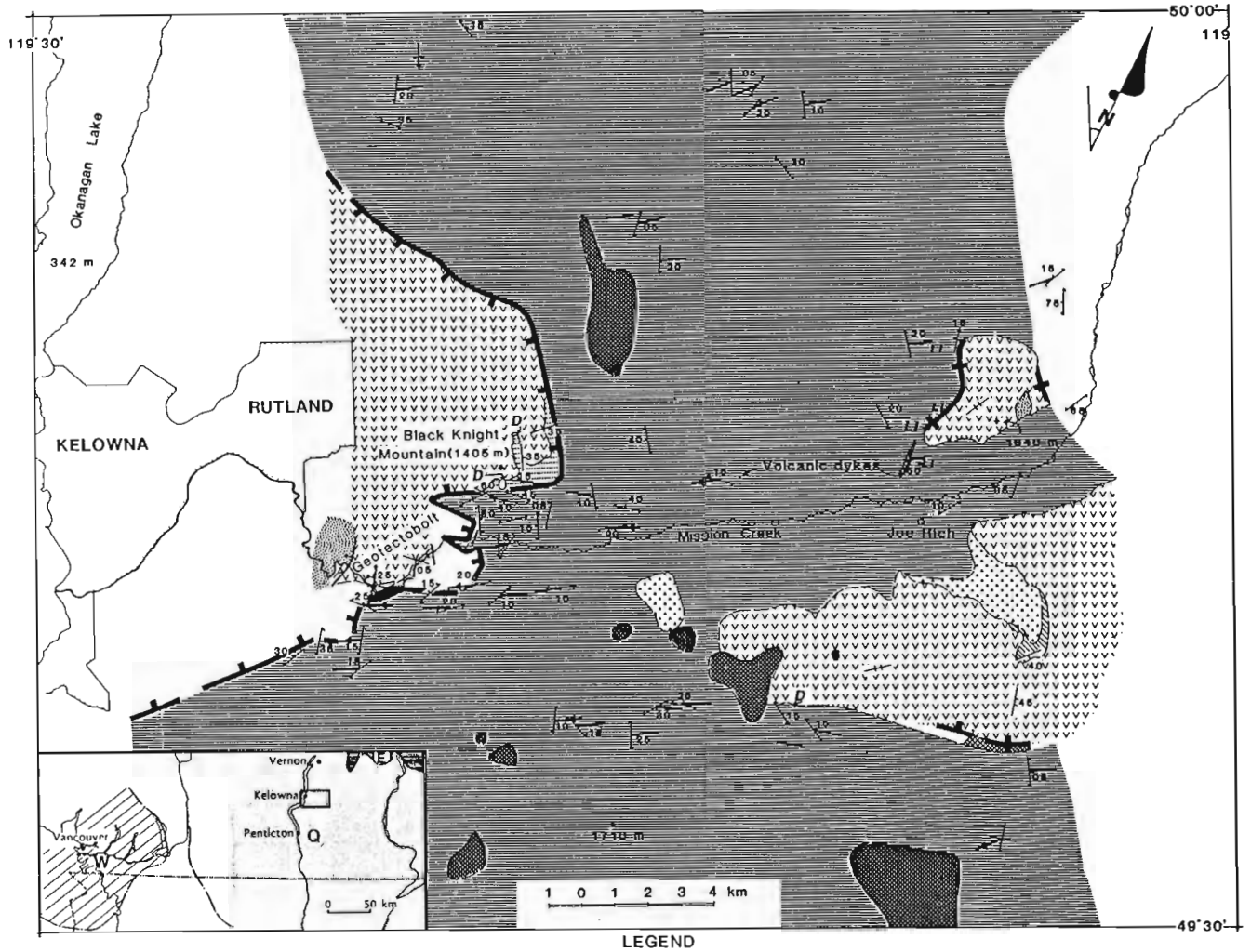

Figure 43.1. *Detailed geological map of the area east of Kelowna. The contact between cover and basement is outlined by the heavy line. This contact is warped gently to the west at Black Knight Mountain but appears to be much steeper (near vertical) around Joe Rich village. Foliation in the basement dips generally gently to the west around Black Knight Mountain but becomes more easterly dipping farther east. The foliation attitudes show many local flexures. Deformation of Cache Creek Group rocks (open triangles) was brittle not ductile; those rocks might represent upper plate relicts of a pre-Eocene extensional event that were later welded, in situ, by Eocene volcanics. Stretching lineations consistently trend northeast. Local kinematic indicators suggest top to the west (arrows on stretching lineation symbols).*

Introduction

The Okanagan metamorphic and plutonic complex, named by Okulitch and Woodsworth (1977) for gneissic rocks along the east side of Okanagan Valley, consists of various granitoid rocks and metasediments. Bostock (1941), Little (1961) and Okulitch and Woodsworth (1977) suggested a Precambrian or early Paleozoic age for these gneissic rocks which are considered by Monger et al. (1982) to be part of the accreted Quesnellia terrane (Fig. 43.1). Mathews (1981) pointed out that similar rocks may be found farther east within the Omineca belt. He also published Cretaceous and minimum late Eocene K-Ar isotopic ages for these rocks. The gneisses generally dip gently to the west under the Okanagan Valley. They are thought to be cut by numerous normal faults trending parallel to this valley (Bostock, 1941; Little, 1961) which, interestingly, is the lowest geomorphologic feature between the west coast and Saskatchewan.

The west side of the Okanagan Valley is composed of discontinuous thick sequences of Carboniferous to Triassic metasedimentary and metavolcanic rocks (Little, 1961; Okulitch and Woodsworth, 1977) which have been intruded by Jurassic and Cretaceous plutons associated with the Nelson and Valhalla plutonic suites (Little, 1961). Similar intrusions are also found within the basement complex to the east.

Early in the Tertiary, thick sedimentary and volcanic sequences, which remain unmetamorphosed and only weakly deformed, were deposited unconformably upon these older rocks (Little, 1961; Church, 1973).

In the Kelowna area, the Okanagan metamorphic and plutonic complex primarily consists of a thick (>1 km) assemblage of gently warped mylonitic gneisses. The pervasive mylonitic fabric implies large scale ductile shearing. Superimposed on the ductile fabric is a zone of brittle fracturing and retrogression which is located discontinuously along the basement-cover boundary.

The model to be tested (Tempelman-Kluit, personal communication, 1984) is that Okanagan Valley marks a large, low angle, west dipping, Eocene extensional detachment between upper and lower plates. Gneiss at the top of the lower plate formed at mid-crustal depths; the brittle fabrics superposed on the ductile fabric of the gneiss formed progressively as the lower plate was tectonically unroofed. Data detailed here support the model generally and agree with the west over east sense of shear and mid-crustal level of deformation demanded by it. The continuum from ductile to brittle fabrics envisaged by Tempelman-Kluit is contested. Instead the ductile fabric may have formed at depth before the Eocene while the brittle fabric was imposed during a separate event, after the gneiss was denuded and Eocene rocks had been deposited.

The writer initiated a Ph.D. thesis under the supervision of R.L. Brown of Carleton University and guidance of D.J. Tempelman-Kluit of the Geological Survey of Canada. Two months of the summer of 1984 were spent mapping in the Kelowna region. This is a summary of the preliminary results.

Mylonitic basement

The basement rocks forming the Okanagan complex east of Kelowna and as far as Joe Rich (Fig. 43.1) comprise high-grade hornblende-feldspar-bearing mylonitic orthogneisses, and locally structurally high in the complex, lenses of paragneiss, chloritic schist, and limestone. The paragneisses commonly contain garnet (?almandine), hornblende, feldspar, quartz, and pyrite. One lens of kyanite with garnet and muscovite was found as were five occurrences of diopside with garnet and scapolite. The gneisses are commonly cut by mafic dykes and sills which have generally been transposed to nearly parallel to the mylonitic fabric (Fig. 43.3).

Within the map area the mylonitic section of the Okanagan metamorphic complex is at least 1 km thick. Foliation commonly dips less than 20 degrees though there are sharp local flexures (Fig. 43.1). Most of these flexures occur near the contact with Tertiary rocks, especially in the vicinity of Black Knight Mountain and at a locality 12 km to the east where isoclinal folding of the mylonitic foliation was also observed. Similarly folded ultramylonitic paragneisses also occur 12 km north-northwest of Black Knight Mountain. Though the ductile fabric appears to die out downward, well preserved protolithic textures have yet to be found.

Mesoscopic fabrics

Mesoscopic fabrics have been observed in the basement mylonites on planes parallel and perpendicular to a consistent northeast-trending stretching lineation (Fig. 43.2) which is commonly defined by aligned hornblende in the flattening foliation as well as elongate quartz and feldspar grains. Boundinaged mylonitic bands have vertical quartz-filled pull-aparts that trend perpendicular to the lineation, also suggesting northeast-southwest extension. Disrupted sheath folds with curvilinear northeast fold axes have been recorded (Fig. 43.3); and minor, west verging, cylindrical reclined folds are also present.

Four kinematic indicators were analyzed in the field: 1) Asymmetrically aligned feldspar megacrysts (Simpson and Schmid, 1983) are the most diagnostic mesoscopic kinematic indicators of the mylonitic gneisses (Fig. 43.3). Their long axes are parallel with? the stretching lineation and their tails indicate sense of shear. This indicator has been observed in most of the mylonitic exposures and generally gives a consistent sense of shear. 2) C and S surfaces: 30 unambiguous examples of these planar features (cf. Berthe et al., 1979) were observed in various deformed bands. In most cases the angle between the two sets of surfaces is near 10 to 15 degrees. Ultra mylonitic stages where both surfaces are parallel are frequently encountered (Fig. 43.4). 3) Six good examples of disrupted minor west verging folds were found.

These fabrics predominantly convey an upper-plate-to-the-west-sense of shear. Even where the foliation dips east the shear sense is to the west. Microfabrics will be systematically analyzed to verify these mesoscopic observations.

Two distinct generations of small-scale extensional structures of different ages are superimposed on the ductile fabrics previously described. The first generation, and probably oldest, consists of shear bands and shear fractures (Fig. 43.5) as well as asymmetric and symmetric foliation boundinage (Fig. 43.6) (Platt and Vissers, 1980). These features can be observed throughout the basement mylonites as opposed to the second class of younger shear fractures which are restricted to the uppermost parts of the basement. Most first generation shear fractures dip steeply west (Fig. 43.5) and have normal down-dip displacement. However, reverse movements were also observed.

These superimposed structures are kinematically compatible with those developed during the early ductile phase, suggesting that deformation was progressive from ductile to brittle.

Discussion

The metamorphic grade of the basement gneisses and the ductile fabrics indicate that most deformation occurred at mid-crustal depths; however, during later deformation,

the ductile fabrics gave way to brittle features. It appears that the originally deeply buried shear zone was synkinematically exhumed as the upper plate moved westward. This appears to have been followed by erosion prior to deposition of the Eocene volcanics.

Dykes similar in composition to the Eocene and Miocene volcanics covering the gneisses have been found to cut and locally brecciate the mylonites (Fig. 43.1). They are weakly deformed with chilled margins and vertical lineations at contacts. If these are indeed feeder dykes to nearby Eocene and Miocene volcanics, then large displacements in post-Eocene time involving the basement shear zone, can be ruled out.

One Cache Creek Group outlier might be a relict of the detached upper plate. It presumably lies between basement and Eocene rocks. Little (1961) classified it as an equivalent to the Cache Creek Group of Permian age (Fig. 43.1). It consists of a non-mylonitic, black, cherty argillite that outcrops around Joe Rich settlement and at a locality (not visited) 9 km to the west (from Little's map, 1961). At the former locality the metasediments are extremely fractured and faulted and do not appear to have been ductilely deformed. Their contact with the mylonitic basement was not observed but they are welded by undeformed Eocene dacitic rocks at the top. Because they are so fractured (much more than any of the Eocene rocks across the area) but not ductilely deformed and overlain by undeformed Tertiary rocks, it is suggested that this unit may be a relict of the upper plate.

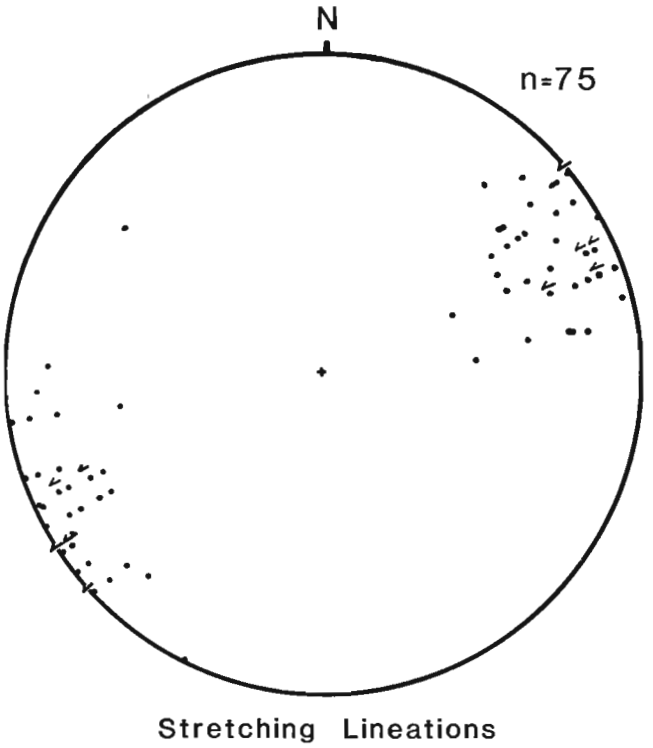

Figure 43.2. *Stereogram showing orientation of stretching lineations in mylonite gneisses. Arrows indicate sense of shear of upper member of shear couple at various localities. Equal-area, lower hemisphere projections.*

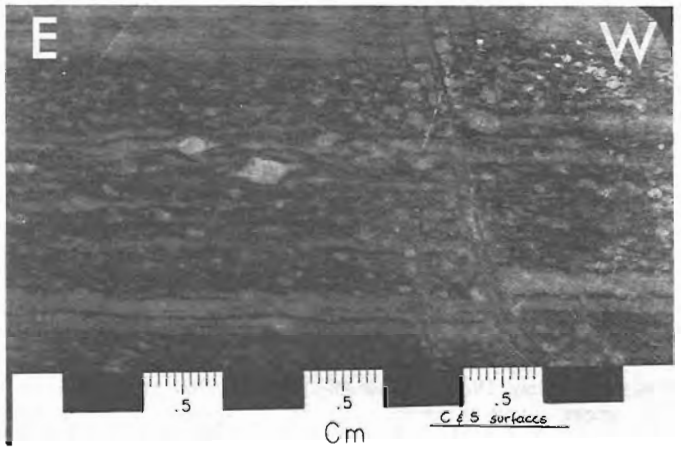

Figure 43.4. *Close-up of slab of mylonite sample collected near uppermost contact, 0.5 km south of "Geotectobolt". The shear plane moderately dips from left to right. Inclination of most megacrysts indicate upper-member-to-the-west sense of shear. A small shear fracture filled with epidote can also be seen (view looking south).*



Figure 43.3. *Sheath folding in mylonite gneiss along highway 33, approximately 8 km southeast of Joe Rich. Pegmatitic and mafic gneissic bands can also be recognized.*



Figure 43.5. *West dipping shear band and asymmetric boundiage in mylonitized hornblende-bearing orthogneiss. Looking south.*

Cover rocks

Eocene sediments and volcanics

Three occurrences of Eocene rocks (Little, 1961; Church, 1973, 1981) were recognized in the present study area.

Black Knight Mountain area. Around Black Knight Mountain, unmetamorphosed terrestrial lake sediments composed mostly of interbedded mudstones and sandstones with a few conglomeratic lenses outcrop at the base of the section. Bedding is well preserved and plant remains are common; however, most outcrops are thoroughly altered. In general, the sediments are only gently folded, but one case of overturned beds was discovered. Small syndepositional faults are common. The unit has a maximum thickness of 50 m and appears to be truncated by overlying dacitic lavas on the north and south sides of Black Knight Mountain. The sediments reappear along Mission Creek immediately east of the "Geotectobolt" of Church (1981) (Fig. 43.1). At this locality, there is a thick sandstone with excellent graded bedding. Approximately 20 m of weakly deformed and horizontally bedded, fossiliferous mudstone overlies the sandstone. The contact between the Eocene terrestrial sediments and the underlying mylonitic gneiss is not exposed. An east trending normal fault was mapped at that locality (Little, 1961; Church, 1981) because of the apparent juxtaposition of mylonitic gneiss interpreted as outcrop across Mission Creek. However, this interpretation is probably not correct since the gneiss is found on the north shore of Mission Creek where it may be projected underneath the Eocene sediments and volcanics. It is true that steep dippng normal faults occur in this area but they generally trend northerly (Fig. 43.1) and clearly truncate Tertiary rocks.

Dacitic and rhyodacitic lavas containing hornblende, biotite, quartz and feldspar phenocrysts overlie the terrestrial sediments at Black Knight Mountain (Fig. 43.7). The volcanic rocks have columnar joints and regularly layered flow bands. The flow banding is generally steep and flow folds were observed at Black Knight Mountain. At the "Geotectobolt" at least 30 beds, each 3 m thick, ring the hillside nearly horizontally; hence, its name. The contact with underlying sediments is observed farther east. The lowermost 0.5 m of the volcanics are brecciated and underlain by a black shaly layer approximately 10 cm thick. It is questionable whether this is a depositional or structural contact. At Black Knight Mountain the dacite is altered near the contact with the gneiss.



Figure 43.6. Mylonitized hornblende-bearing orthogneiss with synkinematic minor listric normal faults dropping west. Faults die out within the foliation. Offsets are approximately 15 cm (arrows). Section is located 2 km southeast of Black Knight Mountain along highway 33. Looking north.

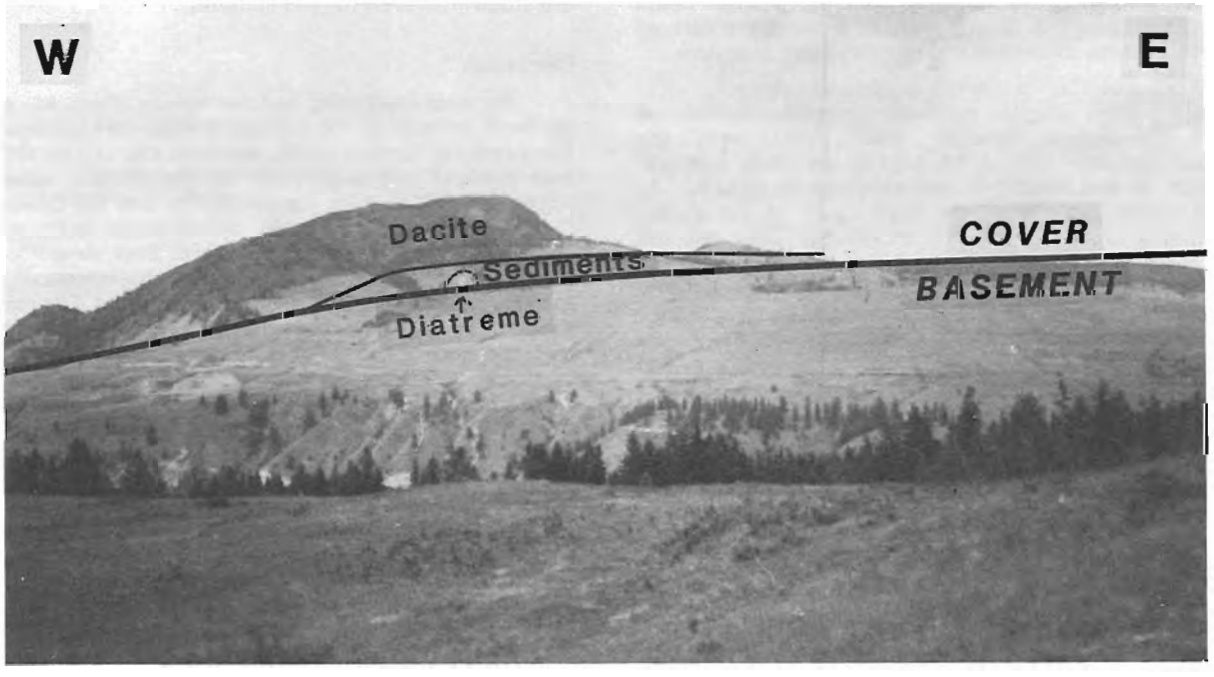

Figure 43.7. View looking north at Black Knight Mountain from the south side of Mission Creek. Contact between Tertiary cover and mylonitic basement warps gently to the west. Diatreme cutting terrestrial sediments could possibly be a feeder to the dacitic lavas forming Black Knight Mountain. The diatreme is not well exposed but appears to be cylindrical and is probably truncated by the displacement along the basement-cover contact.

A small diatreme was discovered immediately below the south cliff of Black Knight Mountain (Fig. 43.1). This body has a circular surface of approximately 900 m^2 and contains a large percentage of metasomatized dacitic clasts and a few sandstone pebbles and other volcanic clasts of unknown origin. The matrix of this brecciated rock is vitrified and commonly vertically banded. The absence of mylonitic clasts in the diatreme suggests that it does not truncate the basement. The terrestrial sediments cut by this diatreme are extremely indurated due to contact metamorphism. Two similar occurrences of diatreme material, which are not as well preserved, are outlined in Figure 43.1.

Isoclinally folded and slightly faulted sedimentary beds equivalent to the White Lake Member (Church, 1981) are mapped along Mission Creek west of the "Geotectobolt". These units are stratigraphically younger than the dacitic lavas (Church, 1973), but here are clearly juxtaposed against these lavas by a north trending normal fault of unknown extent (Fig. 43.1).

North of Joe Rich. Here another body of light grey dacite is also flow banded, columnar jointed and caps the top of a ridge. This body could be a klippe; however, there are two observations which argue against this. Firstly, a long winding, northerly trending dyke of the same dacitic composition truncates and brecciates the mylonite. This dyke also extends towards the main dacite body suggesting that it might be one of its feeders. Secondly, the mylonitic foliation is flexured all around the dacite body and dips towards it. The mylonites are also faulted and extremely altered and this is interpreted as being caused by the massive emplacement of the volcanic rocks.

Carbonaceous sediments, mapped as equivalents to the White Lake Member (Little, 1961), are found on the east side of this body. They are composed of immature conglomerate and sandstone beds containing numerous plant remnants of unknown age. These sediments are believed to be younger than the volcanics because 90 per cent of the pebbles found in the conglomerates are dacitic. Other pebbles are derived from cherts, basalts, mudstone and possibly from gneisses.

Joe Rich area. Dacitic volcanics containing biotite and hornblende phenocrysts (smaller than 1 cm) form the predominant Cenozoic unit in this part of the study area and are identical to the dacitic bodies at other localities. As mentioned, these rocks weld the upper part of the Cache Creek argillites as seen near Joe Rich village. They also cut a boulder conglomerate which appears to be different from any of the other sedimentary units. The boulder conglomerate (clasts up to 0.5 m across), with interbedded sandstone lenses, lies between the Tertiary dacites to the south and the postulated Permian argillites to the north, and dips 40 degrees to the southeast (Fig. 43.1). The boulders within the conglomerate are mostly derived from undeformed salt and pepper hornblende granite, biotite and feldspar basalts, and fine grained pink biotitic granite. A few small chert grains are also scattered throughout the unit. No mylonitic or dacitic boulders have been identified in the conglomerate. The unit is possibly equivalent to the Springbrook Formation (Fig. 43.1) (Bostock, 1941; Church, 1973).

A last unit of interest in this area lies south of this third dacitic body. It consists of an extremely chloritized breccia (Fig. 43.1) containing approximately 30 per cent fragments, most being about 15 cm across. These angular fragments are either derived from adjacent mylonites or from granodiorites of the Valhalla suite of which the closest outcrop is 9 km to the south (Little, 1961). The significance of the breccia is unknown though it appears to be truncated almost vertically by the dacitic volcanics to the north and overlies the mylonite to the south.

Miocene Plateau Basalts

Miocene plateau basalts, like the Eocene volcanics, occupy high topographic positions. Most are columnar jointed and appear to be flat lying over both basement gneiss and early Tertiary rocks (Fig. 43.1). Thick iron-stained hydrothermally altered zones occur at the contacts of the basalts. Published K-Ar isotopic dates for these basalts are 14.9 Ma (Church, 1981).

Basement and cover contact

The contact has not been observed although rocks within a few metres of it are exposed at Black Knight Mountain (Fig. 43.7) and north of Joe Rich. Two features are frequently observed near the contact. The mylonites are commonly intensely fractured or brecciated, and epidotized, chloritized or leached. Shear fracturing seems to be concentrated in the uppermost 50 m of the basement and does not much affect the Tertiary cover, although locally, sediments are completely shattered. Westerly dipping listric normal faults are observed along Mission Creek where the contact dips gently to the west (Fig. 43.1, 43.7). It is believed that these faults are responsible, in part, for the tilting of east-dipping mylonitic foliations around Black Knight Mountain.

Locally, retrograde alteration of the mylonites completely obliterated all textures leaving only a soapy, chloritized, green rock. Alteration also affects the lower parts of the Eocene section but less intensely.

Where fracturing is not too dense in the gneisses, en echelon fracture patterns are observed. The fracture planes are generally steep and trend north-northwest which is also the orientation of the normal faults mapped along Mission Creek (Fig. 43.1). Normal displacements with the hanging wall down to the west are most commonly seen although reverse offsets exist as well (Fig. 43.4). A few gypsum-filled fractures were seen in a quarry approximately 2 km south of the "Geotectobolt"; however, most fractures are filled with chlorite and epidote.

Discussion

Because fracturing and retrograde alteration appears to be more intense in the mylonitic basement gneisses than in the overlying Eocene rocks, much of this brittle deformation may predate the deposition of the Eocene cover. This suggestion leaves open the possibility that pre-Eocene ductile strain gave way to brittle deformation with progressive unroofing; the Eocene rocks were then deposited on the exhumed, denuded and weathered basement. Renewed faulting in post-Eocene time or during the Eocene volcanic episode would explain the weaker deformation associated with the Eocene cover rocks. Alteration of the bottom of the overlying Eocene rocks could have been generated during a reactivation of the shear zone permitting fluid circulation through this zone of weakness.

Conclusions

A four-stage structural history is envisaged to explain the various geological features of the Kelowna shear zone as mapped east of Kelowna:

1. A gently dipping, west-verging, ductile shear zone developed within a block composed of pre-Eocene metamorphic and plutonic rocks (Okanagan complex). The zone was initiated at a crustal depth compatible with amphibolite metamorphic grade.
2. Uplift of the upper boundary of the shear zone carried it through a ductile-brittle transition and simultaneously erosion of the upper plate took place.

3. Deposition in the Eocene of terrestrial sediments and extrusion of volcanic rocks onto the exhumed mylonitic basement. Intrusion of the feeder dykes through the mylonitic basement caused extensive alteration.

4. Brittle reactivation of the contact surface between the Eocene cover and the pre-Eocene ductile zone localized fluids which caused alteration at the basement-cover boundary. Pre-existing brittle zones within the lower plate may have been reactivated in the Eocene or later.

Acknowledgments

This project is part of a Doctorate thesis in progress at Carleton University. Richard L. Brown is gratefully acknowledged for his support and advice during the field season and the writing of this report. Dirk Tempelman-Kluit of the Geological Survey of Canada in Vancouver proposed the field area and offered great hospitality throughout the season. Thanks are also expressed to Sharon Carr for helpful recommendations. Funding of this project is in part provided by NSERC operating grant A2693 to Richard L. Brown.

References

Berthe, D., Choukroune, P., and Gapais, D.
1979: Orientations preferentielles du quartz et orthogneissification progressive en regime cisaillant: l'exemple du cisaillement sud-armoricain; Bulletin of Mineralogy v. 102, p. 265-272.

Bostock, H.S.
1941: Okanagan Falls, B.C.; Geological Survey of Canada, Map 627A.

Church, B.N.
1973: Geology of the White Lake basin; British Columbia Department of Mines and Petroleum Resources, Bulletin 61, 120 p.

Church, B.N. (cont.)
1981: Geology of the Kelowna Tertiary Outlier (East Half), Preliminary map 45; Province of British Columbia, Ministry of Energy, Mines and Petroleum Resources.

Little, H.W.
1961: Kettle River (West Half), B.C.; Geological Survey of Canada, Map 15-1961.

Mathews, W.H.
1981: Early Cenozoic resetting of potassium-argon dates and geothermal history of north Okanagan area, British Columbia; Canadian Journal of Earth Sciences, v. 18, p. 1310-1319.

Monger, J.W.H., Price, R.A., and Tempelman-Kluit, D.J.
1982: Tectonic accretion and the origin of the two major metamorphic and plutonic welts in the Canadian Cordillera; Geology, v. 10, p. 70-75.

Okulitch, A.V. and Woodsworth, G.J.
1977: Kootenay River, B.C.; Geological Survey of Canada, Open File 481.

Platt, J.P. and Vissers, R.L.M.
1980: Extensional structures in anisotropic rocks; Journal of Structural Geology, v. 2, no. 4, p. 397-410.

Simpson, C. and Schmid, S.M.
1983: An evaluation of criteria to deduce the sense of movement in sheared rocks; Geological Society of America Bulletin, v. 94, p. 1281-1288.

THE YELLOWHEAD AND ASTORIA CARBONATE PLATFORMS IN THE LATE PROTEROZOIC UPPER MIETTE GROUP, JASPER, ALBERTA

Martin Teitz[1] and Eric W. Mountjoy[1]
Cordilleran Geology Division

Teitz, M. and Mountjoy, E.W., The Yellowhead and Astoria carbonate platforms in the late Proterozoic Upper Miette Group, Jasper, Alberta; in Current Research, Part A, Geological Survey of Canada, Paper 85-1A, p. 341-348, 1985.

Abstract

The platforms reach a maximum thickness of 400 m and consist of thin to thick beds of buff to grey weathering dolomite, and grey to brown weathering sandstone and pelite. The Yellowhead Platform contains stromatolitic mounds, allochthonous blocks, crinkly laminated and pisolitic dolomite. The Yellowhead Platform thins markedly, mainly from the base, and interfingers with siliciclastic sediment. The Astoria Platform contains stromatolitic mounds, and intraclastic dolomite composed of aggregate peloidal and oolitic grains. The presence of stromatolites, pisolites, and other textures indicates that the platforms formed in shallow water, under low to moderately high current energy conditions, during a period of reduced siliciclastic influx. The Yellowhead Platform was exposed and karstified prior to the deposition of the overlying Gog Group.

Résumé

Les plates-formes calcaires de Yellowhead et d'Astoria sont présentes par endroits dans la zone la plus élevée de la partie supérieure du groupe tardiprotérozoïque de Miette dans le chaînon Main du parc national de Jasper et du parc provincial du mont Robson. Les plates-formes ont une épaisseur maximale de 400 m et se composent de couches minces à épaisses de dolomies, de grès et pélite. La surface altérée de la dolomie varie de chamois à gris et celle du grès et de la pélite, de gris à brun. La plate-forme de Yellowhead contient des monticules stromatolitiques, des blocs allochtones et de la dolomie feuilletée plissotée et pisolitique. Elle s'amincie de façon marquée surtout à partir de sa base, et est interstratifiée avec des sédiments silicoclastiques. La plate-forme d'Astoria contient des monticules stromatolitiques et de la dolomie intraclastique composée d'agrégats de grains allochimiques et oolitiques. La présence de stromatolites, de pisolites et d'autres structures indique que ces plates-formes se sont formées en eau peu profonde, dans des milieux à courant énergétique faible ou moyennement élevé, au cours d'une période d'apport réduit de matériau silicoclastique. La plate-forme de Yellowhead a été d'écouverte et karstifiée avant la dépositon du groupe sus-jacent de Gog.

[1] Department of Geological Sciences, McGill University, 3450 University Street, Montreal, Quebec H3A 2A7

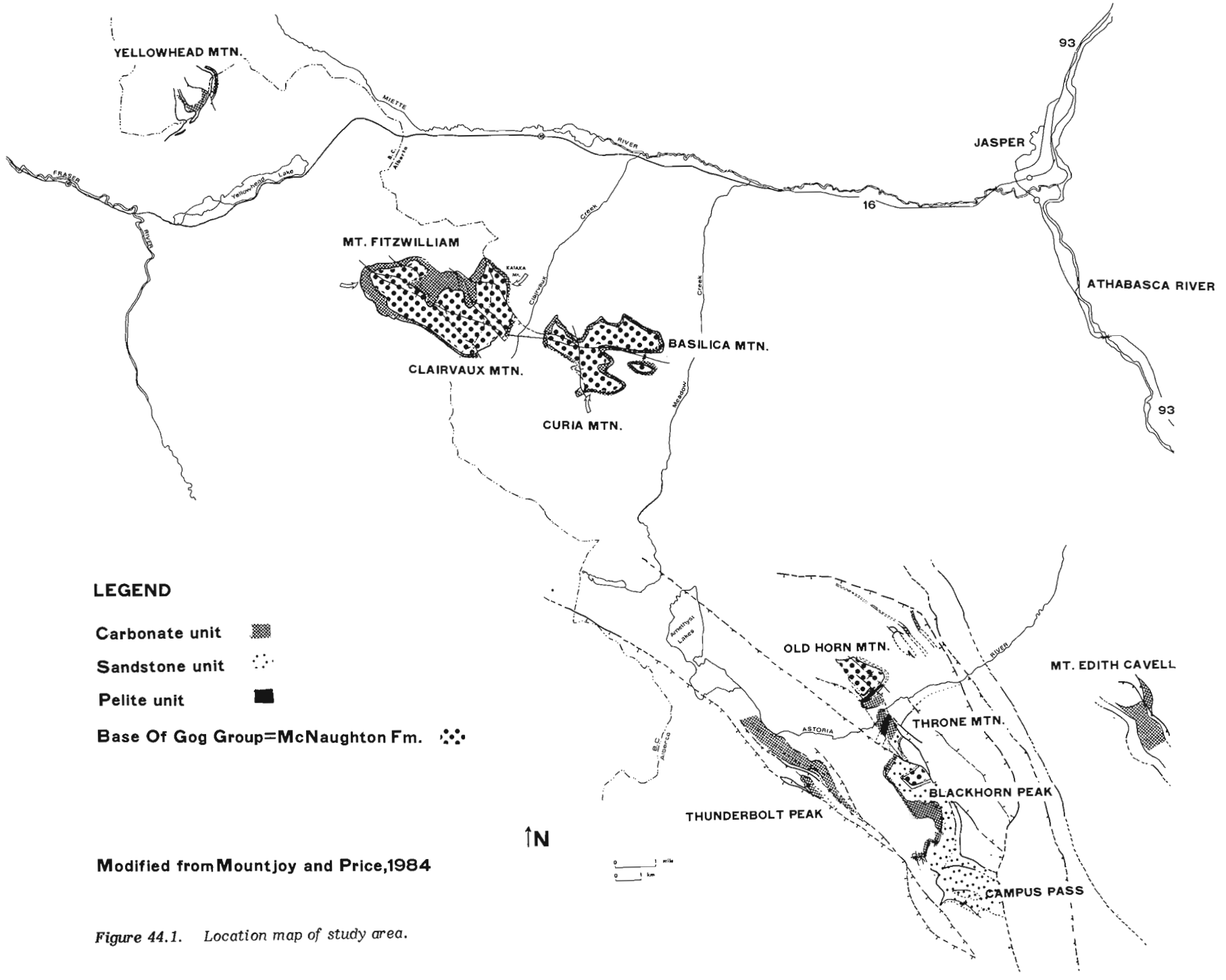

Figure 44.1. Location map of study area.

Introduction

In western Jasper National Park and adjacent eastern portions of Mount Robson Provincial Park, two carbonate platforms, Yellowhead and Astoria (Mountjoy, 1983; Mountjoy and Price, 1984a, b), are well exposed and were investigated during the 1983 and 1984 field seasons (Fig. 44.1). Fieldwork included measurement of stratigraphic sections and detailed mapping of lateral facies variations.

Stratigraphy

The Miette Group, part of the Hadrynian Windermere Supergroup, forms a thick succession of fine to coarse clastic rocks in the Jasper region. The Miette Group was mapped in the Mount Robson area by Mountjoy (1962, 1980) who raised the Miette Formation of Walcott (1913) to group status. Charlesworth et al. (1967) mapped the Miette Group and subdivided it into three formations, during detailed structural mapping of the lower Miette valley around Jasper. During the course of mapping (Price and Mountjoy, 1970; Mountjoy, 1976b; Mountjoy and Price, 1984a, b) Mountjoy did not find the formations recognized by Charlesworth et al. (1967) to be useful mappable units, except for the lowest Old Fort Point Formation. The rest of the Miette Group was subdivided into informal units: an upper Miette consisting predominantly of pelites with subordinate sandstone and carbonate in the upper part, and a middle Miette of cliffs of coarse grained and conglomeratic sandstone (grit) in composite units, alternating with recessive dark pelites (Mountjoy, 1970, 1976a). Recent mapping has confirmed the usefulness of these units in the Jasper region and the Selwyn Range. In addition mapping in the Selwyn Range by Mountjoy, Forest and Leonard (1985) indicated that the middle Miette grits are underlain by two additional units both assigned to the lower Miette, a lower Miette pelite 2000 to 3000 m thick, underlain by a lower Miette grit more than 1500 m thick.

Carbonate Unit

In the study area, the carbonate unit is developed into small distinct carbonate platforms, stratigraphically equivalent to but separate from the Byng Formation of the Mount Robson area (Slind and Perkins, 1966; Mountjoy, 1980).

Two platforms were investigated, one in the Yellowhead Pass area, and the other in the Astoria River drainage area (Fig. 44.1). They are informally named the Yellowhead and Astoria platforms, respectively. They consist of cliff-forming, grey-buff-red weathering, thin to thick bedded dolomite, intercalated with minor thin to medium bedded sandstone and siltstone. The carbonate unit (Yellowhead Platform) reaches a maximum thickness of 400 m and is flanked by stratigraphically equivalent but lithologically distinct siliciclastic sediments of the upper Miette Group.

Yellowhead Platform

The Yellowhead Platform extends for about 21 km from Yellowhead Mountain, into Mount Fitzwilliam and Clairvaux Mountain, to Basilica Mountain (Mountjoy and Price, 1984a). It is well exposed as cliff-forming, buff-red weathering dolomite. The platform is best displayed on Mt. Fitzwilliam where sediments reach a maximum thickness of 400 m. From here the platform thins markedly, mainly from the base, grading into siliciclastic sediments (Fig. 44.2). To the northwest at Yellowhead Mountain, the platformal dolomite is 50 m (maximum) thick and can be traced westward along the mountainside where it thins and interfingers with siliciclastic sediments.

The Yellowhead Platform is composed of four sedimentary facies: pisolite, stromatolite mound, allochthonous block, and siliciclastic (Fig. 44.3). The pisolite facies is the dominant facies and forms most of the platform; the stromatolitic mound and allochthonous – block facies are present in western outcrops and are restricted to the lower third of the platform. The siliciclastic facies consists of mudstone and fine- to medium-grained sandstone, and is present as laterally continuous (on outcrop scale) interbeds in the pisolite facies, and as discontinuous beds and lenses in the mound facies. Eastward siliciclastic sediments increase in amount and grainsize.

Pisolite facies

The pisolite facies consists primarily of medium to thick tabular units of buff and red weathering, grain-supported, mostly cross-stratified, pisolitic dolomite. Beds are dominated by pisoids, but commonly contain a high proportion of irregularly laminated stromatolites and intraclasts.

Pisoid grains are present as single or more commonly as composite grains. These are well rounded and sorted, spherical to elongate in shape, and vary in size from 2 to 10 mm, but some range up to 40 mm. Pisoids consist of a nucleus, most often sparry or micritic, coated by smooth alternating red, grey, and white micritic laminations.

The pisolite facies is the thickest and most extensive facies of the Yellowhead Platform. This facies varies considerably from northwest to southeast (Fig. 44.3). In northwestern exposures at Mt. Fitzwilliam where the platform is thickest, this facies overlies the mound facies and comprises the upper 380 m of the platform. Approximately 9 km southeast at Basilica Mountain the pisolite facies thins to 60 m where it is interbedded with coarse grained sandstone.

Stromatolitic Mound facies

This facies varies in thickness from 0-150 m and is developed on the north and west faces of Mt. Fitzwilliam (Fig. 44.3). It forms the base of the platform, where it overlies and interfingers laterally with siliciclastic sediments.

Mounds are buff weathering, domal to lenticular in shape and are most commonly 0.5 to 2 m thick, but thicknesses over 30 m occur (Fig. 44.4A). Mound thickness to length ratio usually varies from 1:3 to 1:6.

Internally, the mounds are composed of undifferentiated subcentimetre-scale crinkly laminated dolomite, probably constructed in part by stromatolites. Laminations are formed by grey and white alternations or medium crystalline dolomite. In some mounds the crinkly laminations conform to mound shape, in others, laminations are poorly developed. Centimentre scale unwalled, partly latterally linked columnar stromatolites are present at the perimeter of some mounds. Dolomitic sandstone and siltstone are commonly present as internal sediment between columns and as lenses in crinkly laminations.

The largest stromatolite mounds occur near the base of the platform and in most places are interbedded with siltstone and fine grained sandstone. Mounds are generally closely spaced, coalescing, and many are overturned. Intermound sediment consists of intraclastic sandy dolomite, and green to purple mudstone. The latter commonly drapes mounds. The mudstone drape on some mounds gives a good indication of synoptic relief which varies from 0.25 to over 20 m.



Figure 44.2. *View of west face of Mount Fitzwilliam illustrating part of the Yellowhead Carbonate Platform. Light weathering carbonate unit, overlain by dark weathering basal Gog Group. Carbonate thins to right (southeast) from base. 1 locates Figure 44.4.*

The crinkly laminated dolomite subfacies of the stromatolitic mound facies occurs locally on the west face of Mt. Fitzwilliam (Fig. 44.3, 44.4C). This subfacies is approximately 75 m thick and gradationally overlies the stromatolitic mound facies. It consists of thick, tabular, crinkly to wavy laminated dolomite units, probably constructed in part by stromatolites. Subcentimetre grey laminations of medium crystalline dolomite alternate with buff-brown laminations of silty dolomite. Some units contain centimetre-scale unwalled, partly laterally linked columnar stromatolites.

The crinkly laminated dolomite subfacies can be traced laterally north and south for 1.5 km on the west face of Mt. Fitzwilliam. In a southward direction this facies thins and is interbedded with pisolitic grainstones and stromatolitic mounds. Northward, tabular units of crinkly laminated dolomite curve abruptly with northwest dips up to 90 degrees (Fig. 44.5). When traced down dip, these crinkly laminated dolomite units maintain a relatively constant dip-angle for variable distances (10-200 m), and occur over a lateral distance of 300 m. They mark a local margin of the platform, with allochthonous blocks and stromatolitic mounds occurring next to them (Fig. 44.4). These steeply dipping units are internally similar to the flat-lying ones, except they lack columnar stromatolites.

Allochthonous blocks

The allochthonous-block facies occurs along the west face of Mt. Fitzwilliam in the basal 100 m of the platform, adjacent to steeply dipping crinkly laminated dolomite and stromatolitic mounds (Fig. 44.3, 44.4B, 44.6). The blocks consist of buff weathering, angular to subrounded dolomite up to 5 m across (Fig. 44.6). They contain subcentimetre scale crinkly laminations, and are identical to those that occur in the stromatolitic mound and the steeply dipping crinkly laminated textures.

Siliciclastic facies

The siliciclastic facies shows considerable variation in terms of siliciclastic sediment percentage and composition across the Yellowhead Platform (Fig. 44.3). In general, siliciclastic sediment within the platform increases from less than 20% to over 60% from northwest to southeast. At Mt. Fitzwilliam, siliciclastic sediment consists of siltstone and fine- to medium-grained sandstone. These beds occur only at certain stratigraphic levels in the basal and upper parts of the platform. In upper parts, they form marker beds that, because of their distinctive red weathering can be traced along the mountainside for several kilometres (Fig. 44.2). To the southeast the sand increases in amount and grain size. At Basilica Mountain dolomite units contain over 60% medium- to coarse-grained quartz sand and are interbedded with thick, coarse grained quartzose sandstone units.

Astoria Carbonate Platform

The Astoria Carbonate Platform consists of resistant grey to dark brown weathering dolomite, sandstone, and pelite. It extends for about 12 km southward from Old Horn Mountain, into Throne Mountain and Blackhorn Peak to Campus Pass (Fig. 44.1, 44.7). It also outcrops on Thunderbolt Mountain to the west and Mt. Edith Cavell to the east over a distance of 10 km (Mountjoy and Price, 1984b). Platform sediments are best preserved and exposed on the west face of Blackhorn Peak and Throne Mountain, where they reach a maximum thickness of 30 m. Northward, over a distance of 2 km carbonate sediments thicken to over 350 m at Old Horn Mountain.

The Astoria Carbonate Platform consists of three sedimentary facies: intraclast, stromatolitic mound, and siliciclastic. In contrast to the Yellowhead Platform, pisoids are rare and allochthonous blocks are not observed. The intraclast facies comprises most of the platform and is commonly cyclically interbedded with sandstone (Fig. 44.7). The stromatolitic mound facies occurs mainly in the basal 200 m of the carbonate platform at Old Horn Mountain. The siliciclastic facies includes sandstone and pelite. The sandstone, present at Blackhorn Peak, occurs as 10 to 50 m units above and below the intraclast facies. The pelite is observed as 50 to 150 m thick units at the top of the platform, and is interbedded with the sandstone.

The Intraclast facies

The intraclast facies is the most prominent facies of the Astoria Carbonate Platform (Fig. 44.7). This facies is present at most platform exposures, and consists of grey weathering, thin to thick, wavy to tabular bedded, clast-supported intraclastic dolomite. Some beds also contain subcentimetre-scale planar and crinkly laminated dolomite, pisoids, and small stromatolitic mounds. Intraclast grains are lenticular to globular in shape, vary between 1 and 3 cm across, are angular to subrounded, and have their long axis oriented parallel to bedding. Internally, intraclasts are

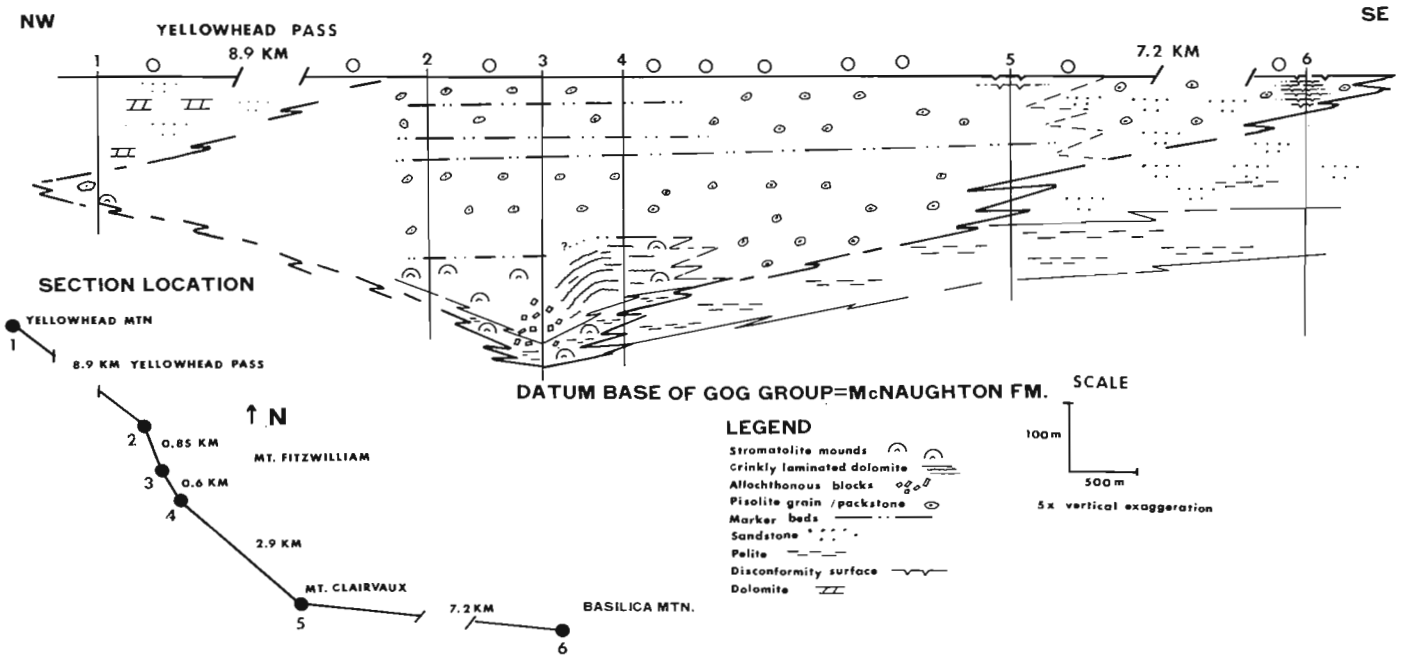

Figure 44.3. Schematic cross-section of Yellowhead Carbonate Platform. Marker beds in upper part of carbonate parallel the base of the Gog Group.

composed of medium- to coarse-grained peloidal and oolitic(?) allochems, which are truncated at the intraclast margin. These would be termed lumps by Leighton and Pendexter (1962).

The intraclast facies thins southward from 120 m on the west face of Throne Mountain to 80 m at Blackhorn Peak. Thinning to the south is accompanied by an increase in sandstone interbeds resulting in distinct cycles between these two facies. This is well displayed on the southwest ridge of Blackhorn Peak (Fig. 44.8B). The cycles vary in thickness from 1 to 6 m. An ideal cycle consists of a basal 0.25 to 3 m bed of intraclastic dolomite commonly planar or crosslaminated, overlain by medium- to coarse-grained, well sorted and rounded sandstone. Primary sedimentary structures in the sandstone include planar, bidirectional low angle, and trough cross-laminations.

Stromatolitic Mound facies

Stromatolitic mounds are restricted to the south side of Old Horn Mountain (Fig. 44.7). They form the basal 200 m of the platform, but are poorly exposed and preserved. Mounds are domal to lenticular and are most commonly 1 to 3 m thick. Most are closely spaced and coalesce. Intermound sediment consists of thin, wavy bedded dolomite; pisolites and intraclasts are occasionally observed. Mound are composed of subcentimentre-scale, crinkly dolomitic laminations that conform to mound shape.

Small stromatolite mounds also occur locally throughout the platform. They are less than 1 m thick and are interbedded with intraclastic and sandy dolomite.

Siliciclastic facies

The siliciclastic facies consists of sandstone and pelite. Sandstone is present within the upper portions of the platform on the western faces of Throne Mountain and Blackhorn Peak (Fig. 44.7, 44.8C). The sandstone is quartzose, medium- to very coarse-grained, and moderate to well sorted and rounded. Primary sedimentary structures are

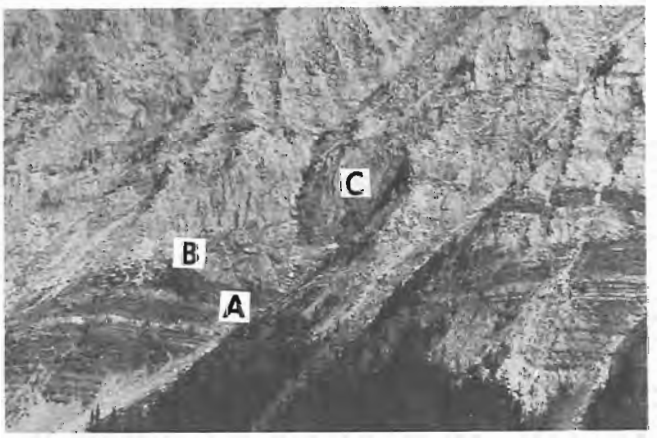

Figure 44.4. View of west face of Mount Fitzwilliam showing relationships at base of Yellowhead Platform. See Figure 44.2 for location. Above A is a large mound approximately 30 m thick. B is location of allochthonous blocks shown in Figure 44.6. C is location of steeply dipping units of the crinkly laminated dolomite subfacies, see Figure 44.5.

well preserved and include small to large-scale trough crossbeds, and planar to low angle crosslaminations. Shale clasts, quartz pebbles, and erosional scours are present in lower parts of some beds.

The sandstone thickens from approximately 50 m to 130 m southeastward from Throne Mountain to Campus Pass.

The pelite consists of grey-green-purple weathering shale, siltstone, and fine grained sandstone in units 3 to 40 m thick. It is generally restricted to the upper parts of the platform (Fig. 44.7). Siltstone and fine grained sandstone together comprise over 50% of the facies and commonly preserve isolated, internally crosslaminated thin lenses. This facies is in many places interbedded with the sandstone facies. At Old Horn and Throne mountains the pelite facies forms the topmost unit of the platform.

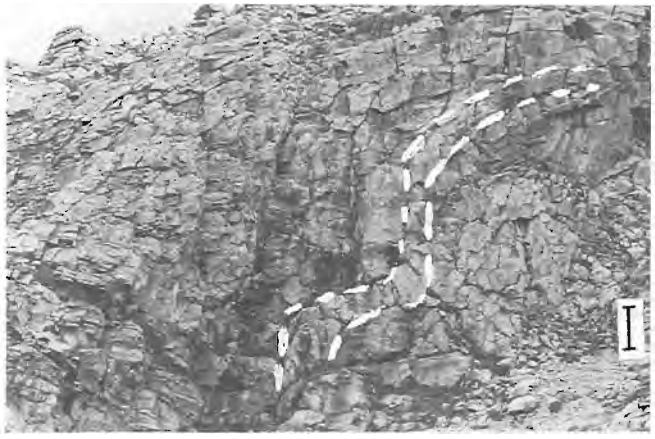

Figure 44.5. Steeply dipping crinkly laminated dolomite layers, scale bar 2 m. For location see Figures 44.3 and 44.4C.



Figure 44.6. Allochthonous blocks up to 4 m long, scale bar 2 m. For location see Figures 44.3 and 44.4B.

Disconformity at the base of the Gog Group (McNaughton Formation)

In the study area, the contact between the carbonate unit and the Gog Group is disconformable. The disconformity is most obvious on the Yellowhead Platform. The contact is well exposed at Mt. Fitzwilliam, where buff to red weathering dolomite is in sharp contact with the overlying dark grey, cliff-forming quartzose sandstones of the Gog Group (Fig. 44.2). In outcrop, the contact is irregular with relief up to about 3 m. East of section 5 (Fig. 44.3) on Mount Fitzwilliam irregular lenses and crosscutting beds of coarse to conglomeratic quartzose sandstone fill solution features in pisolitic dolomite up to 3 m below the base of the Gog. These quartz sandstones, are commonly graded and crosslaminated, and are texturally and mineralogically similar to the overlying basal Gog Group. The crosscutting sandstones can be traced upward into the basal Gog. Approximately 6 km to the southeast at Basilica Mountain seven disconformity surfaces are present in the upper 60 m of the platform (Fig. 44.9).

On Astoria Platform the disconformity between the carbonate unit and the Gog Group is difficult to recognize, mainly due to the general absence of platformal dolomites below the contact (Fig. 44.7, 44.8C). Over most of the platform, crossbedded sandstone and pelite are present beneath the contact. Pelites overlie the top of the platform at Old Horn Mountain, and are in sharp contact with the basal Gog Group. At Blackhorn Peak, a crossbedded quartzose sandstone, similar in weathering colour, bedding thickness and lithology to the basal Gog Group occurs at the top of the upper Miette, making recognition of a disconformity surface difficult. Only the higher proportion of pelite interbeds distinguishes the crossbedded sandstone from the sandstones of the basal Gog Group.

Southeast of Campus Pass a thin 12 m dolomite unit overlies the sandstone facies. It consists of buff to red weathering tabular beds of sandy dolomite, and irregular lenses and crosscuttig beds of coarse grained, quartzose sandstone. This dolomite is overlain by thick bedded quartz sandstones of the basal Gog Group (McNaughton Formation) (Fig. 44.7).

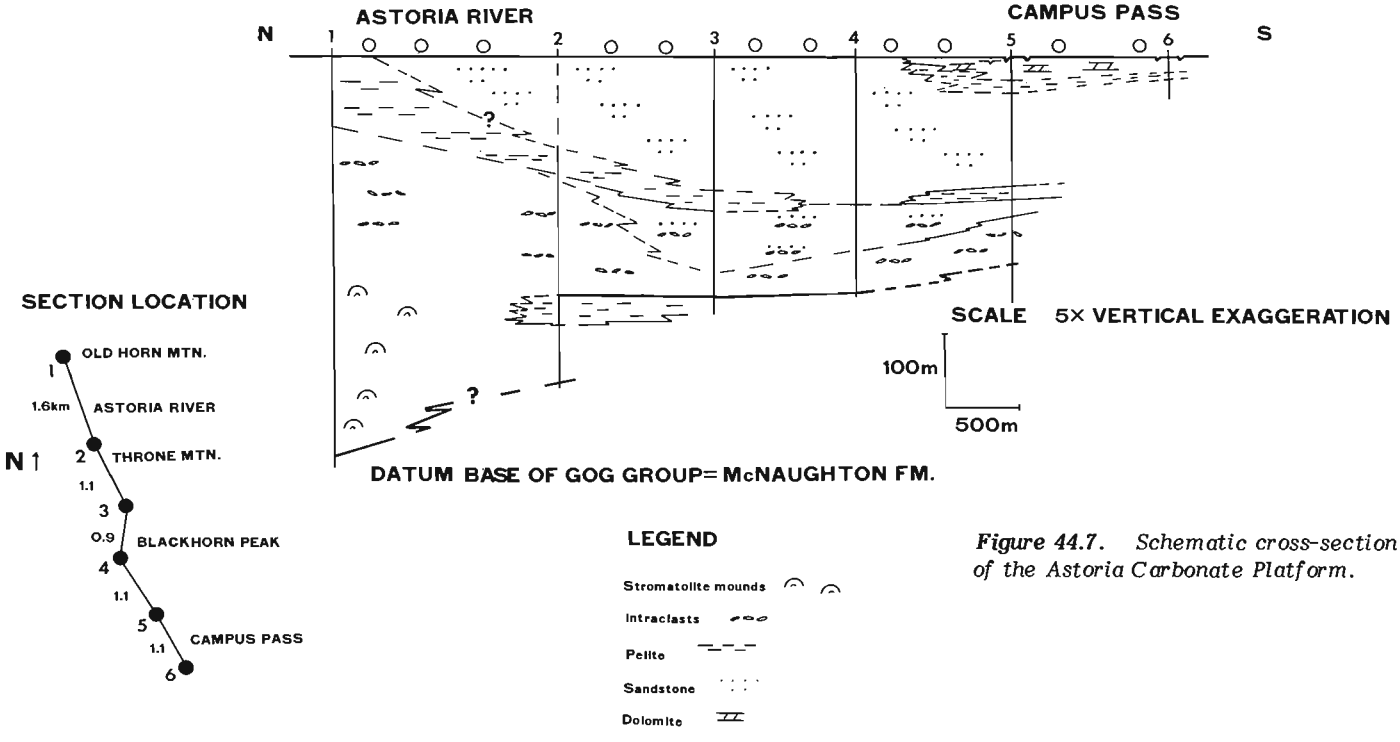

Figure 44.7. Schematic cross-section of the Astoria Carbonate Platform.

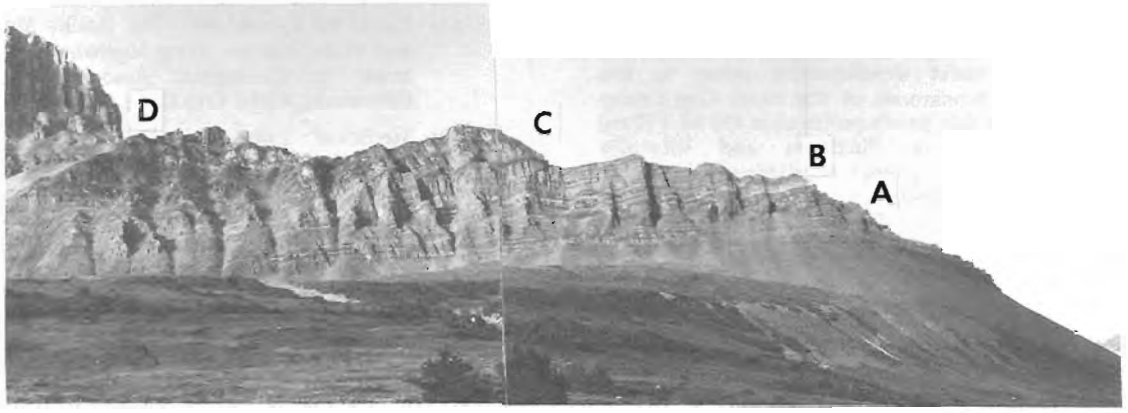

Figure 44.8. View of southwest face of Blackhorn Peak. A – intraclastic dolomite units. B – interbedded dolomite and sandstone units. C – sandstone units. D – base of Gog Group at base of cliff.



Figure 44.9. Solution enlarged fractures and solution holes in upper 3 m of Yellowhead Carbonate Platform, developed beneath the sub Gog unconformity. Cross-laminated, medium- to coarse-grained, quartzose sandstones (light) of the basal McNaughton Formation fill solution features in sandy, cross-laminated, pisolitic dolomite (dark). Scale bar 20 cm.

The presence of disconformity surfaces in carbonate sediments near the top of both platforms suggests early lithification and periods of exposure. The uppermost solution and karst surface indicates a long period of exposure and nondeposition, solution, and subsequent filling of solution features by quartzose sandstone.

Interpretation

In each platform a general shallowing-upward sequence occurs. The carbonate platform begins with up to 30 m thick stromatolite mounds, gradationally overlain by allochthonous blocks, and ending with crosslaminated pisolite and intraclast grainstone to packstone. The steeply dipping crinkly laminated dolomites occur adjacent to and overlie the allochthonous blocks.

The stromatolite mounds appear to have had a maximum synoptic relief of about 20 m, and their tops did not reach sea level. The mounds are overlain by siliciclastic mudstone, allochthonous blocks, or steeply inclined crinkly laminated dolomite (Fig. 44.3). The mounds appear to have grown in relatively tranquil waters in depths ranging from a few metres to 20 or 30 metres.

The allochthonous blocks are angular to subrounded and consist predominantly of crinkly laminated dolomite and rare columnar stromatolites. The origin of the blocks is uncertain but they probably represent material derived from the carbonate platform margin, possibly stromatolite mounds or heads that were broken off the margin (during storms?). The blocks accumulated below steeply inclined crinkly laminated dolomite at the edge of the carbonate platform, or were transported a short distance down slope (Fig. 44.3). Locally the blocks were incorporated in small debris flows that transported material a short distance into the basin.

Shallow water crinkly laminated dolomite accumulated over the underlying foundation formed by stromatolite mounds and associated fill of allochthonous blocks and basin shales. The crinkly dolomites do not occur in Astoria Platform. At Mt. Fitzwilliam the crinkly dolomites built out laterally and extended down the northwest margin of the platform on slopes of 30 to 90 degrees, into water depths of about 20 to 40 m. This indicates that the platform margins had a relief of about 40 m, at least locally.

The upper two thirds of the Yellowhead and most of the Astoria Carbonate Platform consist of crosslaminated, grain supported pisolitic and intraclastic dolomite. The intraclastic dolomite internally consists of grain-supported peloidal and oolitic grains similar in shape but not in size to the pisoids. These rocks are gradational to and interfinger with the underlying stromatolitic mounds and crinkly laminated dolomite. The grain-supported textures, paucity of micrite, and low angle crosslaminations reflect moderate to highly agitated subtidal conditions. Deposition likely took place on shoals. The interclasts were formed by cementation of the peloidal and oolitic grains which took place in local sheltered subtidal areas, or possibly during exposure. They were subsequently ripped-up and reworked to form angular to subrounded intraclasts during high energy events.

The southeastern parts of both platforms interfinger with fine- to coarse-grained quartz sandstone (Fig. 44.3, 44.7). The planar, bidirectional low angle crosslaminations, and trough crossbeds suggest depositon by tidal currents in a shallow subtidal environment.

Conditions for carbonate deposition continued longer on the Yellowhead Platform and it presumably built up to sea level. During a slight lowering of sea level it was subjected to solution and minor karst development prior to the deposition of the quartz sandstones of the basal Gog Group (Fig. 44.9). By contrast, a thin sandy pelite unit (50 to 150 m) overlies portions of Astoria Platform and laterally interfingers (?) with adjacent quartz sandstone (Fig. 44.7). The pelite reflects a shallow, relatively tranquil lagoon. This pelite is abruptly and disconformably overlain by the basal Gog Group.

Acknowledgments

M. Teitz was ably assisted in the field by B. Maynes and C. Wisse. We are grateful for the permission from Parks Canada and Mount Robson Provincial Park to collect specimens. Phil Laurie at Lucerne is gratefully recognized for his support. In addition to EMR support, financial support for field work and laboratory analyses came from Mountjoy's NSERC grant A2128.

References

Charlesworth, H.A.K., Weiner, J.L., Akehurst, A.J., Bielenstein, H.U., Evens, C.R., Griffiths, R.E., Remington, D.B., Stauffer, M.R., and Steiner, J.
1967: Precambrian geology of the Jasper region, Alberta; Research Council of Alberta, Bulletin 23.

Leighton, M.W. and Pendexter, C.
1962: Carbonate rock types; in Classification of carbonate rocks, ed. W.E. Ham; American Association of Petroleum Geologists, Memoir 1, p. 33-60.

Mountjoy, E.W.
1962: Mount Robson (southeast) map area; Geological Survey of Canada, Paper 61-31.

1970: Geology of the Main Ranges between Tete Jaune Cache and Jasper; in Edmonton Geological Society 1970 Field Conference, p. 94-107.

Mountjoy, E.W. (cont.)
1976a: Edson to Valemount – The Rocky Mountain Front and Main Ranges along highway 16 in the Jasper area; in Geological Association of Canada, Edmonton, Field Trip C-11 Guidebook, p. 4-42.

1976b: Medicine Lake map area 83C/13 (E and W); Geological Survey of Canada, Open File 371.

1980: Mount Robson map and cross-section 1:250 000 scale; Geological Survey of Canada, Map 1499A.

1983: Late Proterozoic carbonate platforms near Jasper, Alberta; Geological Association of Canada and Mineral Association of Canada, Program with abstracts, v. 8, p. A49.

Mountjoy, E.W. and Price, R.A.
1984a: Jasper 83D/16 geologic map and cross-sections 1:50 000 scale; Geological Survey of Canada, Open File Report 1038.

1984b: Amethyst Lakes 83D/9 geologic map and cross-sections 1:50 000 scale; Geological Survey of Canada, Open File Report 1075.

Mountjoy, E.W., Forest, R., and Leonard, R.
1985: Structure and stratigraphy of the Miette Group, Selwyn Range, between Ptarmigan and Hugh Allan creeks, British Columbia; Geological Survey of Canada, Paper 85-1A, report 58.

Price, R.A. and Mountjoy, E.W.
1970: Geologic structure of the Canadian Rockies between Bow and Athabasca rivers – A progress report; in Structure of the Southern Canadian Cordillera, Geological Association of Canada, Special Pub. No. 6, p. 7-25.

Slind, O.L. and Perkins, G.D.
1966: Lower Paleozoic and Proterozoic sediments of the Rocky Mountains between Jasper, Alberta and Pine River, British Columbia; Canadian Petroleum Geology Bulletin, v. 14, no. 4, p. 442-468.

Walcott, C.D.
1913: Cambrian formations of the Mount Robson Peak district, British Columbia and Alberta, Canada; Smithsonian Miscellaneous Collections, v. 57, p. 327-343.

STRUCTURAL EVOLUTION OF THE SOUTHWESTERN INTERMONTANE BELT, ASHCROFT AND HOPE MAP AREAS, BRITISH COLUMBIA

Project 800029

J.W.H. Monger
Cordilleran Geology Division, Vancouver

Monger, J.W.H., Structural evolution of the southwestern Intermontane Belt, Ashcroft and Hope map areas, British Columbia; in Current Research, Part A, Geological Survey of Canada, Paper 85-1A, p. 349-358, 1985.

Abstract

Four episodes of regional deformation have been recognized in the southwestern Intermontane Belt. (1) Post-Permian, pre-Middle Jurassic structure and metamorphism is developed in rocks in the northern part of the Mount Lytton Plutonic Complex. (2) In the northeastern part of the region, southwestward overturned folds and metamorphism may be related to Lower and Middle Jurassic deformation to the east in the Omineca Crystalline Belt. (3) In the southwestern part of the region, congruent southwest dipping foliation that characterizes both the southern part of the Mount Lytton Plutonic Complex, and western parts of the Nicola Group, is probably of Late Jurassic(?) to early Early Cretaceous age, and its development is followed by uplift of the Mount Lytton Plutonic Complex and coeval broad warping of the Spences Bridge and Kingsvale groups. (4) Pervasive, "transtensional" block faulting of Eocene age is related to the dextral wrench faulting of the Fraser River Fault System.

Résumé

Quatre phases de déformation régionale sont reconnues dans la partie sud-ouest de la zone Intermontagneuse. Des structures et du métamorphisme qui se sont produits après le Permien et avant le Jurassique moyen ont été identifiés dans les roches de la partie nord du complexe plutonique de Mount Lytton. (2) Dans la partie nord-est de la région, le métamorphisme et les plis déversés vers le sud-ouest pourraient être reliés à une déformation qui a eu lieu au cours du Jurassique inférieur et moyen dans la zone cristalline d'Ominéca à l'est. (3) Dans la partie sud-ouest de la région, une foliation conforme, à pendage sud-ouest, caractéristique à la fois de la partie sud du complexe plutonique de Mount Lytton et des parties ouest du groupe de Nicola, s'est vraisemblablement développée entre le Jurassique récent(?) et le début du Crétacé inférieur; elle a été suivie par le soulèvement du complexe plutonique de Mount Lytton et le gauchissment contemporain des groupes de Spences Bridge et de Kingsvale. (4) La formation, par extension et par décrochement, de blocs faillés, au cours de l'Eocène, est liée à la formation de failles de basculement dextres du réseau de failles du fleuve Fraser.

Introduction

Field work in 1984 in the east half of Hope map area (92 H E/2; bounded by latitudes 49 and 50 degrees and longitudes 120 and 121 degrees) resulted in revision of the earlier reconnaissance map of this area by Rice (1947). This revision is combined with data from Ashcroft map area (92 I; Monger and McMillan, 1984) to the north, to make the following preliminary structural synthesis of the region. It should be noted that the sketch maps of the east half of the Hope area incorporate, in modified form, the detailed studies of Preto (1972, 1979) and McMechan (1983).

The writer was ably assisted in the field by A.J. Arthur and J.A. O'Brien. Field work funded by Project 800029, carried out by D.J. Thorkelson on Cretaceous volcanics near Kingsvale, north-central Hope map area, is towards an M.Sc. degree at the University of British Columbia.

Ashcroft map area spans the Intermontane Belt, from greenschist-grade metamorphic rocks in the northeastern corner of the sheet which are marginal to the predominantly metamorphic Omineca Crystalline Belt, to the eastern part of the Coast Plutonic Complex and its southeasterly extension, the Cascade Fold Belt (Roddick et al., 1979) west of the Fraser and Pasayten faults. The typically unmetamorphosed or low grade metamorphic strata in this part of the Intermontane Belt range from latest Devonian to Recent (Fig. 45.1). The oldest strata belong to the Harper Ranch Group, complexly deformed sedimentary and volcanic rocks, exposed in the northeast corner of the map area. Volcanic and sedimentary Triassic strata, the most widespread in the region, include three units: the Bridge River (within the Coast Plutonic Complex), Cache Creek and Nicola groups. The Nicola Group is associated with plutonic rocks, some of which are probably comagmatic with the volcanics, and some possibly slightly younger on the basis of isotopic dates; both are overlain unconformably by clastic rocks of the Lower and Middle Jurassic Ashcroft Formation. The Cretaceous record is one of largely continental volcanic rocks of the Spences Bridge and Kingsvale groups and possible comagmatic granitic rocks. These were flanked, west of the Pasayten and Fraser faults, by continental and marine clastics of the Jackass Mountain Group and underlying sedimentary rocks. Early Tertiary volcanic and sedimentary rocks are entirely continental, commonly occur in downfaulted areas, and are overlain by flat-lying Miocene and younger basalt.

Early Tertiary "transtensional" block faulting, associated with wrench faulting along the Fraser River, is largely responsible for the present map pattern and obscures pre-Tertiary stratigraphic and structural relationships. To emphasize the difficulty of "seeing through" the latest structures, the deformational history is summarized below, from youngest to oldest structural events, concentrating on the early Tertiary, Early Cretaceous and Late Triassic intervals.

Tertiary structures

The structural geology of the southern Intermontane Belt is dominated by early Tertiary faults, regionally related by Price (1979) and Ewing (1980) to right-lateral transform motions and crustal extension.

Fraser River Fault System

The major Tertiary structure in this area is the Fraser River Fault System (Fig. 45.2). Between latitudes 50 and 51 degrees it bounds the western margin of the Intermontane Belt, but to the north cuts obliquely across the Intermontane Belt, and to the south passes through the town of Hope and southwards along the central part of the Cascade Fold Belt into Washington State, where it is known as the Straight Creek Fault (Misch, 1966).

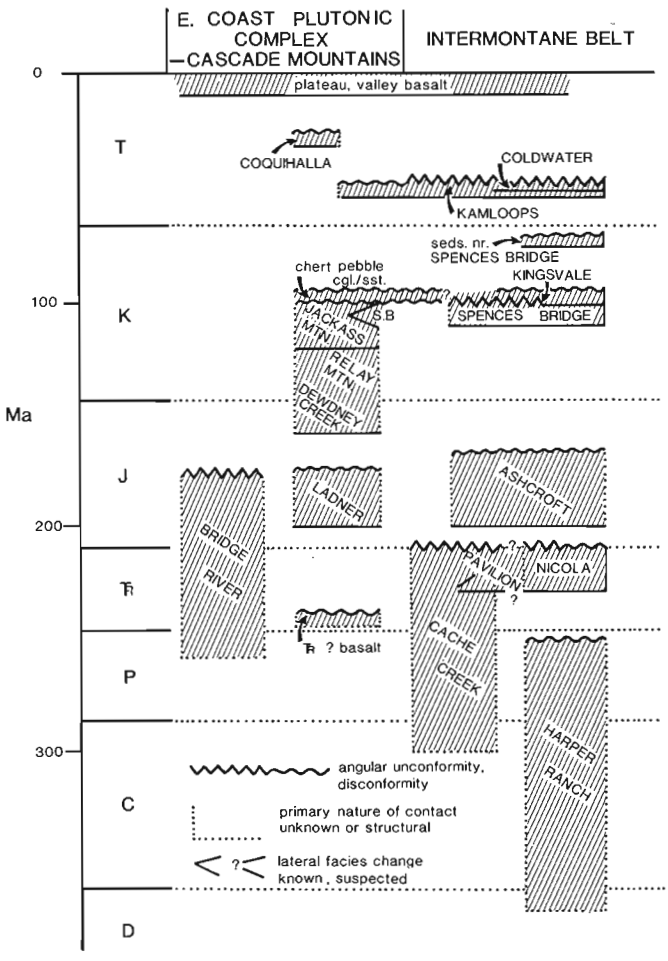

Figure 45.1. Correlation chart of rock-units in the southwestern Intermontane Belt, and adjacent parts of the Coast Plutonic Complex and Cascade Fold Belt.

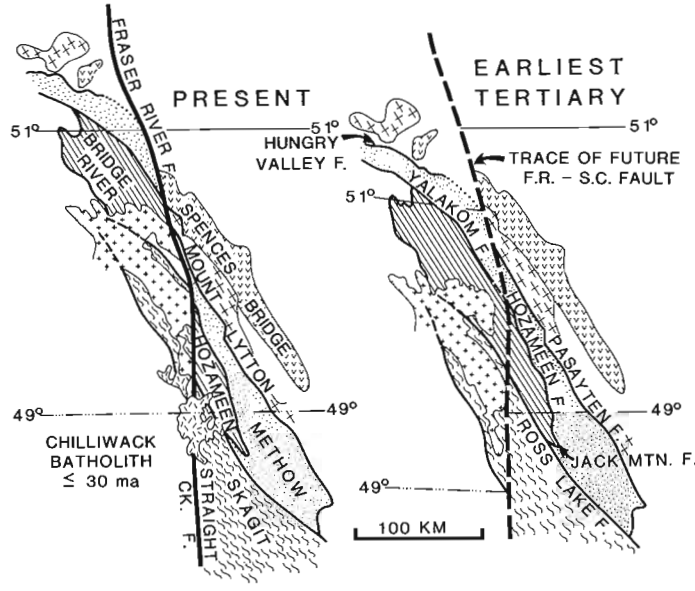

Figure 45.2. Present and pre-Eocene configurations of major lithological units and bounding faults with respect to the Fraser River Fault System.

The Fraser River Fault System possesses the features of a right-lateral wrench fault system, as described by Wilcox et al. (1973; Fig. 45.3). These features are particularly well displayed near the town of Lillooet, where north-northwest trending thrust faults (Phair Creek Fault), small folds with north-northwest trending axial traces (Monger and McMillan, 1984), northeast trending normal faults, and north trending, possible synthetic strike-slip faults (Botanie Creek Fault) fit the strain ellipse pattern oriented with respect to the average trend of the Fraser River Fault System. The direction of maximum compression necessary to produce these structures is north 30 degrees east.

The right-lateral offset on the Fraser River Fault System in this area is probably between 70 and 110 km with the lower figure more likely (Fig. 45.2). More precise estimates of offset are difficult to arrive at, because the rock units and their bounding faults near the main fault system "smear" into alignment with it. Earlier estimates of offsets range between 200 and 100 km (Misch, 1977; Davis et al., 1978; Vance and Muller, 1981; Kleinspehn, 1982). Present estimates are 90 km on the Straight Creek Fault in Washington (J.A. Vance, personal communication), and 70 km on the Fraser River Fault System north of latitude 51 degrees (Mathews and Rouse, in prep.).

In this area, three rock units and the faults which bound them on their northeastern boundaries are matched across the Fraser River Fault Zone (Fig. 45.2). High grade metamorphic rocks in the Coast Plutonic Complex and their northeastern contact with low grade metamorphic rocks of the Bridge River Group, exposed near Kwoiek Creek northwest of Boston Bar, are matched with the Custer (Skagit) gneiss and its boundary, the Ross Lake Fault, near Hope (Hollister, 1969; Monger, 1970; Monger and McMillan, 1984). This offset is about 70 km. Secondly, the Bridge River Group and the Hozameen Group, of similar lithology and age range, are correlated; their northeastern boundaries, respectively the Yalakom and Hozameen faults, are offset approximately 90 km. Thirdly, the Jackass Mountain Group, and its northeastern boundary, marked by the Pasayten and Hungry Valley faults (Tipper, 1978) is offset by about 110 km. It may be erroneous to match the Pasayten and Hungry Valley faults, for the last(?) movements on them are different. The Pasayten Fault probably has mid-Tertiary, west-side-down, normal displacement, whereas the Hungry Valley Fault is a post-Eocene thrust (Tipper, 1978; Mathews and Rouse, in preparation), that is probably complementary to dextral wrench faulting on the Fraser River Fault System. For this reason, the lower figures of 70 to 90 km are favoured.

The Fraser River Fault System appears to have been active as a wrench fault system in Late Cretaceous and/or Early Tertiary time, with the latter favoured by the writer. Although only rock units and their bounding faults that are as young as mid-Cretaceous are offset by 70 km or more, Eocene rocks along the fault system are internally highly deformed and are involved in structures complementary to the wrench fault system. On the Phair Creek Fault, southwest of Lillooet, Triassic Bridge River strata are thrust over Cretaceous clastic rocks and a granitic intrusion that gives a U-Pb date of 47 Ma. North of the area, Eocene strata on the west side of the Fraser River Fault Zone were probably overridden by Cretaceous strata on the Hungry Valley Fault (Mathews and Rouse, in preparation; Fig. 45.2). A minimum age for strike-slip displacement on the fault system is given by the Oligocene Chilliwack batholith, which clearly crosscuts the fault near latitude 49 degrees.

Tertiary faults of the Intermontane Belt

A prominent system of north, northeast and northwest trending faults underlies the southern Intermontane Belt, clearly disrupts Eocene and older strata, and is overlain by flat-lying, unfaulted Miocene plateau basalt with K-Ar dates ranging from 2 to 14 Ma (Fig. 45.3). The structure appears to reflect both regional early Tertiary clockwise rotation related to dextral wrench faulting on the Fraser River Fault System and crustal extension, and is manifested by pervasive normal and local reverse faulting, minor folding and dextral strike-slip faulting with small displacements.

As recognized by Ewing (1980), the key to the Tertiary fault pattern is provided by the Nicola Batholith and associated metamorphic rocks, which are exposed in a horst flanked by the Coldwater and Quilchena faults, and truncated at the north end by the Cherry Creek Fault (Fig. 45.3). Parts of the Nicola Batholith appear to be of early Mesozoic age and their K-Ar isotopic systems were re-set in the early Tertiary. The development of this horst can be linked with wrench faulting on the Fraser River Fault System, since both appear to be about the same age, and the orientation of the north-northwest-trending Coldwater and Quilchena faults is parallel to the direction of maximum stress deduced from the fault geometry near Fraser River. The structural pattern predicts that the Cherry Creek Fault has both dextral strike-slip and north-side-down reverse fault movements, and that the northwest-trending (relative) structural depression containing Eocene volcanics northwest of Kamloops is probably the result of regional compression.

Other structures in this region show similar combinations of dip-slip and strike-slip fault motions. McMechan (1983) proposed that the Princeton basin was a half graben, bounded on the east by the listric Boundary Fault. Northeast to southeast trending folds within the basin were produced by transfer of right-lateral offset from the Asp Creek Fault to the Boundary Fault (Fig. 45.3). Dextral displacements on the Highland Valley and Lornex faults, which cut the Guichon Batholith, have long been recognized (McMillan, 1976; Hollister et al., 1975). Early Mesozoic movements on those faults were deduced from relationships of the faults to well-dated early Mesozoic granitic intrusions and hydrothermal veins, but the faults clearly involve Eocene strata. In particular the 'flattened-S' pattern of the Highland Valley Fault is characteristic of regions of wrench faulting (Wilcox et al., 1973). Possibly old, early Mesozoic, structures were re-activated in this area in Tertiary time. Church (1975) proposed that the fault pattern of the Hat Creek graben was due to maximum north-south directed compression. The Botanie Creek Fault, which lies south of the Hat Creek Graben, may be an example of a dextral synthetic strike-slip fault (Wilcox et al., 1973), that is complementary to the Fraser River Fault zone. Movement on this fault produced the stress orientation proposed by Church.

Late Mesozoic deformation

There are three main Cretaceous rock units in the southwestern Intermontane Belt, namely (1) the late Early Cretaceous to mid(?) Cretaceous rhyolitic-andesitic-basaltic volcanic and associated clastic rocks of the Spences Bridge and Kingsvale groups, (2) mid-Cretaceous granitic rocks in the Cathedral Lakes-Summers Creek areas, and (3) granitic and gneissic rocks at the south end of the Mount Lytton Plutonic Complex (Fig. 45.4). In addition, late Early Cretaceous clastic rocks of the Jackass Mountain Group overlie older Cretaceous and Jurassic clastic strata west of the Pasayten Fault and along the Fraser River Fault System, and are a facies equivalent of the Spences Bridge Group.

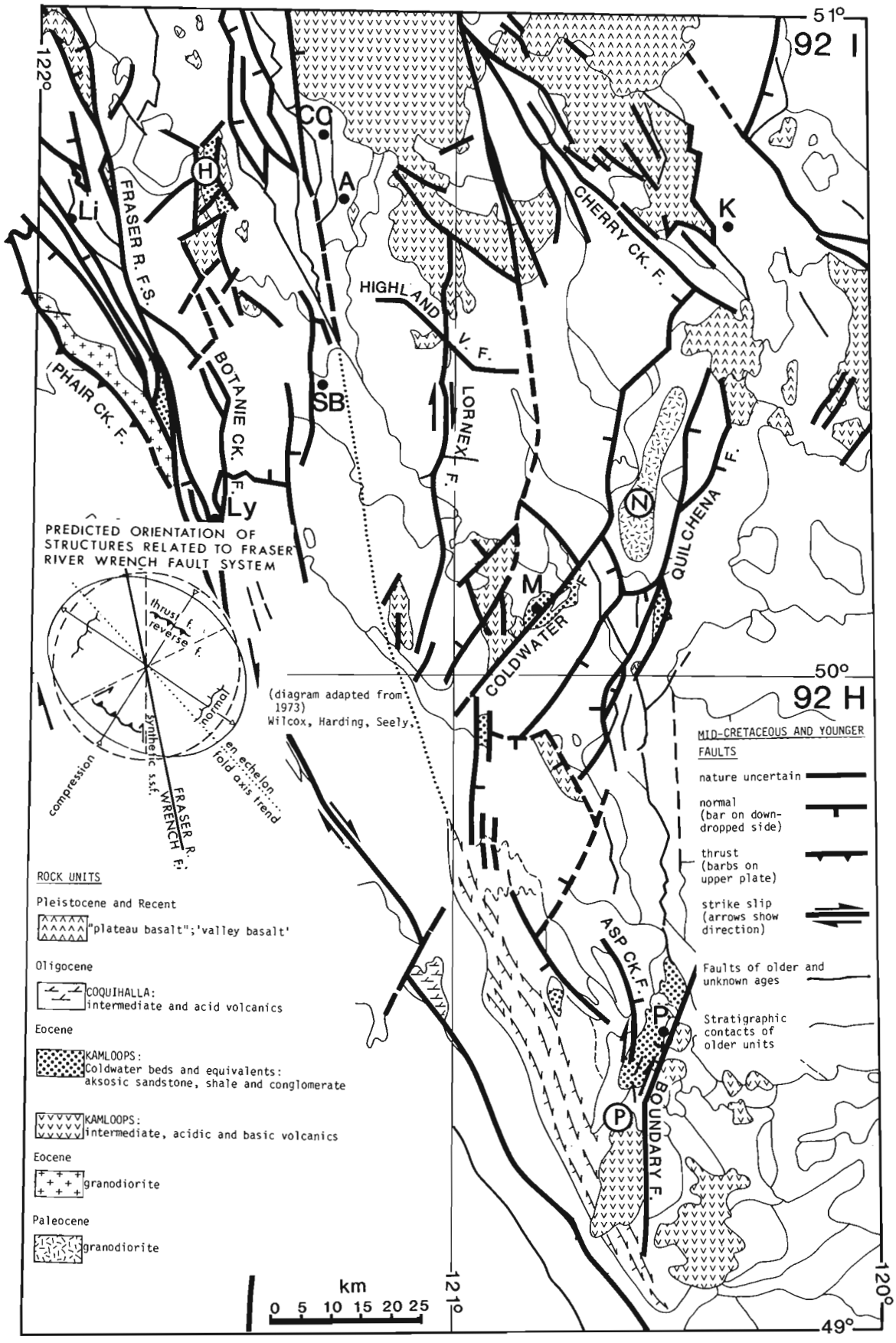

Figure 45.3. *Distribution of early Tertiary rocks and post-mid-Cretaceous faults in the southwestern Intermontane Belt, and adjacent parts of the Coast Plutonic Complex. Note the near-parallelism of the maximum direction of compression deduced from the fault pattern near Fraser River with faults such as the Coldwater Fault.* ***H:*** *Hat Creek graben;* ***N:*** *Nicola horst;* ***P:*** *Princeton Basin. Settlement locations on Figure 45.3 and Figures 45.4, 45.5 shown by* ***A:*** *Ashcroft;* ***CC:*** *Cache Creek;* ***Li:*** *Lillooet;* ***Ly:*** *Lytton;* ***K:*** *Kamloops;* ***M:*** *Merritt;* ***P:*** *Princeton;* ***SB:*** *Spences Bridge.*

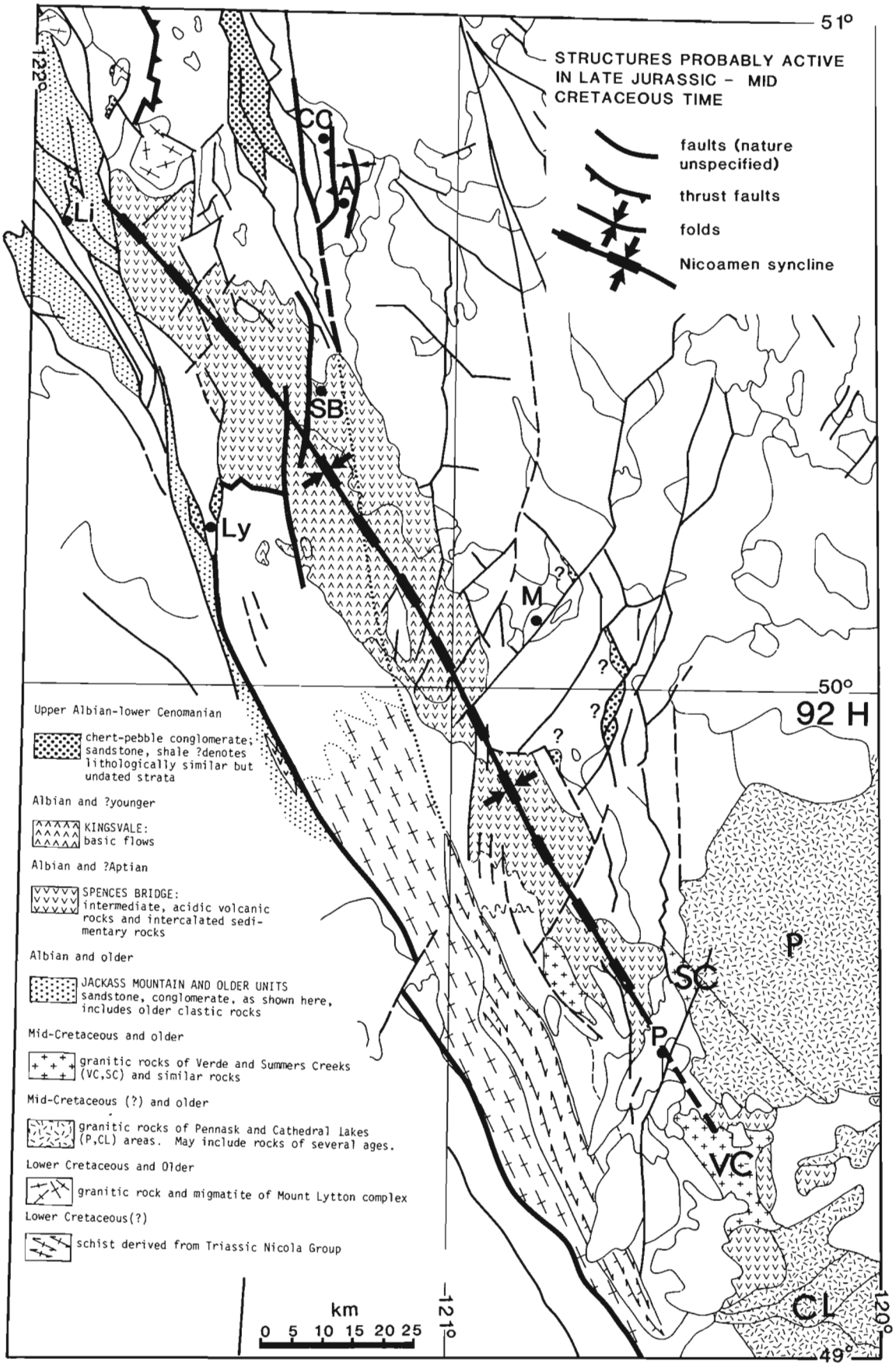

Figure 45.4. *Distribution of Cretaceous rocks and Late Jurassic(?) to mid-Cretaceous structural features. The dotted line speculatively connects the eastern boundary of the southern Mount Lytton Complex, with its southwest dipping gneissosity and adjacent concordant schist belt, with the east-verging structures near Ashcroft, described by Travers (1978, 1982).*

Associated both with the Jackass Mountain Group and forming small isolated outliers scattered across the Intermontane Belt, are sandstones, conglomerates and shales, notably with a high percentage of chert detritus, that contain mid- to Late Cretaceous fossils in the northwestern part of the area.

Deformation related to Spences Bridge and Kingsvale groups

Field work in 1984 showed that the Spences Bridge Group in the east half of Hope map area is more extensive than shown by Rice (1947). Both Preto (1979) and McMechan (1983) reported the presence of Cretaceous volcanics, which they called Kingsvale Group, near Princeton; the writer feels that these rocks are more properly correlated on lithological grounds with the Spences Bridge Group. The Cretaceous volcanics extend, more or less continuously, from the northwestern part of Ashcroft map area, where they are cut off by the Fraser River Fault System, to the southeastern corner, where they are intruded by Cretaceous granite.

Both the Spences Bridge and the overlying Kingsvale Group lie in the major north-northwest-trending Nicoamen syncline, which is named herein from the Nicoamen Plateau, southeast of Spences Bridge. Stratigraphic relationships suggest that the syncline was forming during deposition of the Spences Bridge and Kingsvale groups. South of Spences Bridge, the Kingsvale Group lies with angular unconformity on the Spences Bridge Group (Devlin, 1981), and also the latter thins and pinches out against the northern part of the Mount Lytton Plutonic Complex, so that the Kingsvale Group lies nonconformably on the complex (Duffell and McTaggart, 1952; Monger and McMillan, 1984). Mapping in 1984 by D.J. Thorkelsen showed that near Kingsvale the Spences Bridge Group grades upwards into the Kingsvale Group. This suggests that the syncline was subsiding and the Mount Lytton Plutonic Complex was rising during late Early Cretaceous and(?) mid-Cretaceous deposition of the Cretaceous volcanics.

Deformation related to Mount Lytton Plutonic Complex

The Mount Lytton Plutonic Complex can be divided into two parts, with a boundary whose nature is not clear at present (Fig. 45.4, 45.5). The northern part, discussed below, is older, and does not have the relatively uniformly oriented fabric of the southern part. The latter, known as the Eagle Granodiorite (Rice, 1947; Anderson, 1984), comprises granodiorite, granodiorite and hornblende gneiss, or migmatite, and local pegmatitic quartz monzonite. Its foliation in most places strikes north-northwest and dips steeply to the west. On the east side it grades into, interfingers with, and locally crosscuts biotite hornblende schist, biotite schist, and minor marble, whose foliation is generally concordant with that of the granitic rock. Eastwards the schist decreases in metamorphic grade, the foliation becomes less regular, and 5 to 10 km west of the contact with the Eagle Granodiorite, the schist grades into non- or poorly-foliated, mainly subgreenschist grade metamorphic rocks of the Nicola Group. Because of the gradational contacts, and similarly oriented fabric, the formation of the schist and the granodiorite intrusion appear to be genetically related. If so, a U-Pb date of 135 Ma, obtained by P. Van der Heyden from migmatite in the Eagle Granodiorite (near longitude 121°, latitude 49°38') indicates that the fabric is of earliest Cretaceous age.

There is no evidence that this deformation affected the Spences Bridge and Kingsvale groups, although as noted earlier, the northern part of the Mount Lytton Plutonic Complex appears to have been actively rising during their deposition. North of the Cretaceous volcanic belt, on the Trans-Canada Highway north of Spences Bridge and near Ashcroft, are low metamorphic grade schists of the Nicola Group, and west-dipping thrust faults which bring the Cache Creek and Nicola groups over the Lower and Middle Jurassic Ashcroft Formation (Travers, 1978, 1982; Monger and McMillan, 1984). On the basis of the style of deformation of the Ashcroft Formation, Travers (1982) proposed that deformation took place in the Late Jurassic not long after deposition when the formation was only partly dewatered. Speculatively, as indicated by the dotted line in Figure 45.4, connecting the east side of the Mount Lytton Plutonic Complex with the Ashcroft area, all these structures are related, with that of the Eagle Granodiorite and its associated schist belt being the deep structural equivalent of Ashcroft deformation.

There thus seems to be ample evidence in this area of a period or periods of compression affecting the western part of the Intermontane Belt from Late Jurassic(?) to mid-Cretaceous time.

Early Mesozoic deformation

Jurassic deformation

Jurassic strata of the Ashcroft Formation are restricted to scattered outcrops of shale, sandstone and conglomerate, which contain fossils ranging from Sinemurian to Callovian (Monger and McMillan, 1984). The sources of clasts in many of the conglomerates appear to be mainly local, with an abundance of volcanic, subvolcanic and granitic detritus derived mainly from the Nicola Group and Early Jurassic granitic plutons. Quartzite clasts, perhaps derived from Paleozoic miogeoclinal strata to the east occur in conglomerate north of Kamloops Lake. Possibly they reflect late Early to Middle Jurassic uplift and erosion of rocks now in the Omineca Crystalline Belt.

In the northeastern part of the map area, rocks of the late Paleozoic Harper Ranch Group are deformed and metamorphosed up to greenschist grade. Deformation has resulted in southeastward overturned structures (Smith, 1974). This metamorphism is continuous with metamorphism in rocks of the Omineca Crystalline Belt to the east that is probably of Early to Middle Jurassic age (Monger et al., 1982).

Triassic-Jurassic deformation

Triassic strata (Fig. 45.5) are the most extensive of those of any age in the southwestern Intermontane Belt; they include three main units: Bridge River and Cache Creek complexes and Nicola Group. The first two units have been interpreted as being of oceanic origin, the last as an intra-oceanic volcanic arc (e.g. Monger and Price, 1979).

The Bridge River Group (1 of Fig. 45.5, 45.6) lies west of the Fraser River Fault System and probably is not stratigraphically related to strata to the east since stratigraphic linkages between strata west and east of the Fraser River Fault System cannot be made until Cretaceous time.

The Cache Creek Group comprises three main belts. A western belt (2 of Fig. 45.5, 45.6), mainly chert and argillite of Triassic age, locally contains a volcanic facies, the "Pavilion Beds", which lithologically are similar to western parts of the Nicola Group. The central belt (3) includes the Marble Canyon Formation, which is massive carbonate containing a fusulinid fauna that is exotic with respect to the North American craton, overlain by tuffaceous and cherty carbonates of Triassic age. The exotic fauna is critical to the structural discussion, since the eastern part of the Nicola Group lies stratigraphically on the Paleozoic Harper

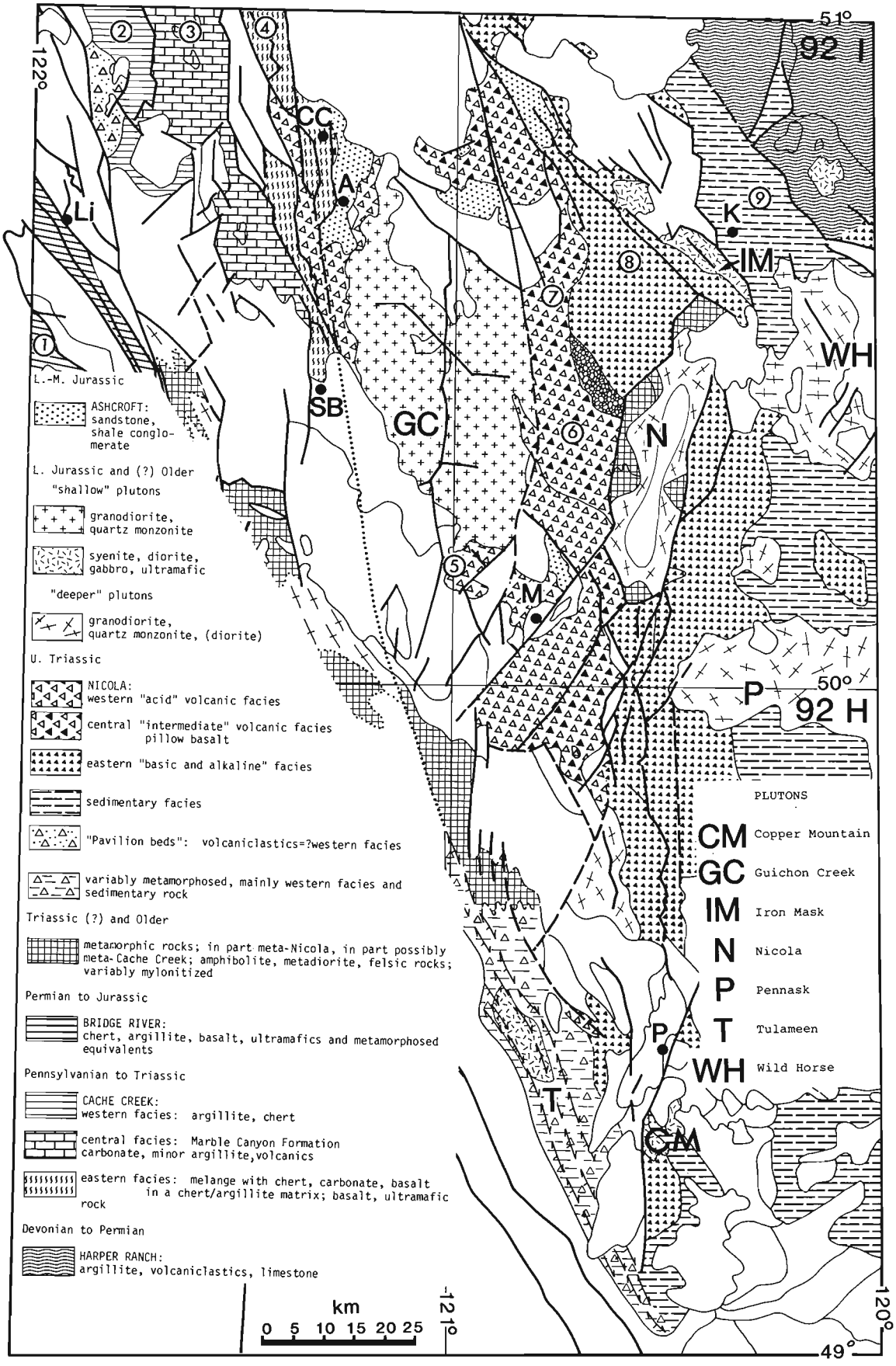

Figure 45.5. *Distribution of early Mesozoic and late Paleozoic rocks. Numbers 1 to 9 refer to approximate locations of schematic sections shown in Figure 45.6.*

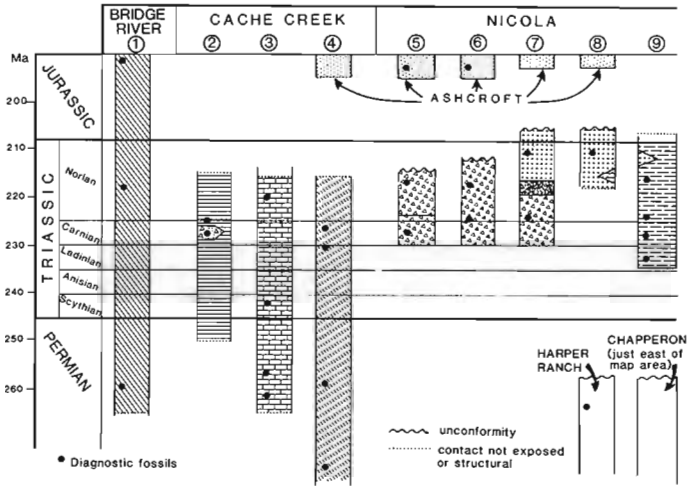

Figure 45.6. *Time-stratigraphic correlation chart of major rock units in the southwestern Intermontane Belt and adjacent parts of the Coast Plutonic Complex. The diagnostic fossils are mainly conodonts identified by M.J. Orchard.*

Ranch Group, which has a different, more normal, North American fusulinid fauna (Ross and Ross, 1983). If the Cache Creek Group were contiguous with the Nicola Group by Triassic time, for which there is some stratigraphic evidence (e.g. Shannon, 1982), then very different Permian faunal provinces, perhaps originating great distances apart, were together by Late Triassic time. The eastern belt (4) is in large part a disrupted mélange containing blocks of Pennsylvanian and Early Permian limestone, together with chert, basalt, ultramafics and local blocks of acid volcanics that resemble rocks in the western part of Nicola Group. The age of the chert and argillite matrix enclosing these blocks is Late Permian to Late Triassic (Orchard, 1984).

The lithological subdivisions of the Nicola Group made herein are similar, but not identical, to those of Preto (1975, 1979) and Morrison (1980). It is subdivided into three main volcanic facies and a sedimentary one. Westernmost (5) is a belt of Carnian and lower Norian acidic to intermediate volcaniclastics and carbonate. Above and east of those rocks is a central facies (6) of feldspar porphyry and feldspar augite porphyry volcaniclastics, volcanic conglomerate and sandstone of mainly early Norian age. They are overlain locally by aphanitic pillowed basalt (7) and the eastern facies of augite porphyry volcaniclastics and alkaline flows (8) of latest Triassic and (?) earliest Jurassic age. This facies lies stratigraphically on the Paleozoic Harper Ranch Group, in the northeastern part of the area (Read and Okulitch, 1977; Monger and McMillan, 1984). It grades eastwards into Middle and Upper Triassic, locally tuffaceous, black argillites and siltstones (9). The rocks show a general progression from oldest on the west to youngest on the east, which may be a function of Early Jurassic erosion prior to deposition of the overlying Ashcroft Formation.

Plutonic rocks associated with the Nicola Group include the probably subvolcanic Iron Mask Batholith, associated with the eastern, augite porphyry facies, and the earliest Jurassic Guichon Creek batholith, emplaced within the western facies. If the Guichon Creek batholith is comagmatic with an eroded western facies, then the Nicola Group shows a chemical progression from calc-alkaline in the west to alkaline in the east. This observation, together with the character of the Cache Creek rocks, the structural and stratigraphic intermixing of Cache Creek and Nicola rocks (Monger, 1981; Shannon, 1982), and the coming-together of different Permian faunas in Late Triassic time, suggests that the Cache Creek is the accretionary prism/subduction complex associated with the Nicola volcanic arc, and that the sedimentary eastern Nicola represents a backarc basin.

Upper Triassic-Lower Jurassic deformation

Other intrusive rocks, called "deeper plutons" on Figure 45.5, occur in the northern part of the Mount Lytton Plutonic Complex and in the Nicola Batholith. In part, these plutons crosscut associated metamorphic rocks, but in part they are foliated, with the foliation concordant with that of associated foliated, locally mylonitic, amphibolite, metadiorite, meta-augite porphyry and felsite that is particularly well exposed along the Thompson River near Lytton. A U-Pb date of 250 Ma was obtained by P. van der Heyden from metamorphic rocks of this complex exposed along the Fraser River, north of Lytton. Crosscutting, nonfoliated granitic rocks near Mount Lytton yield K-Ar dates of 186 Ma. These data suggest post-Permian deformation and metamorphism, and Early Jurassic uplift for the northern part of the Mount Lytton Complex. Speculatively the metamorphic rocks and associated plutons, exposed in the northern part of the Mount Lytton Complex and(?) in the horst containing the Nicola Batholith represent a lower structural storey, possibly derived in part from the Cache Creek and in part from the Nicola. This storey may have formed during Late Triassic subduction of the Cache Creek Group beneath the Nicola arc, and is derived from these units by subcrustal erosion and underplating. The western part of the Nicola Group may thus lie on a thrust fault, beneath which are those metamorphic and granitic rocks, whereas the eastern part lies stratigraphically on the Harper Ranch Group. Much more isotopic and structural data are needed to substantiate this speculation.

Other early Mesozoic structures include faults in the Nicola Group and in the Guichon Creek batholith. Detailed studies of the petrology and mineral deposits of these rocks showed that faulting took place in early Mesozoic time (Preto, 1975; Hollister et al., 1975; McMillan, 1976). It is not possible at present to identify any regional pattern to this early Mesozoic faulting.

Conclusions

The following episodes of deformation were recognized in the southwestern Intermontane Belt.

1. The pre-Middle Jurassic, post-Permian fabric of metamorphic rocks preserved in the northern part of the Mount Lytton Plutonic Complex, and possibly around the Nicola Batholith, is speculatively linked to subduction of Cache Creek strata beneath the partly coeval Nicola volcanic arc in Late Triassic time. The fabric may have formed in rocks that were tectonically eroded from the western edge of the upper, Nicola plate and underplated farther east. Evidence for contemporaneous faulting in the upper plate rocks was discussed by Preto (1975), Hollister et al. (1975) and McMillan (1976).

2. Southwesterly overturned structures and greenschist grade metamorphism in the northeastern part of the map area may be related, by continuity, to structure and metamorphism in the Omineca Crystalline Belt.

3. In Late Jurassic(?) to mid-Cretaceous time, west-dipping schistosity in Nicola rocks, in the southern part of the area, and congruent gneissosity in the southern, early Early Cretaceous, part of the Mount Lytton Plutonic Complex is speculatively linked with the high-level, eastward overthrusting of Cache Creek rocks on to Nicola and Ashcroft strata to the east, that was reported by Travers (1978, 1982). Overlap-unconformable-conformable relationships between Spences Bridge and Kingsvale groups suggest that the north-northwest-trending Nicoamen syncline was forming during deposition of those groups, together with uplift of the Mount Lytton Plutonic Complex.

4. In Late Cretaceous(?)-Early Tertiary time, the region underwent dextral shear concentrated along the Fraser River Fault System, where 70 to 90 km of offset are recorded. As discussed by Ewing (1980), this shear was distributed through the southwestern Intermontane Belt. It accompanied regional extension, and produced a complex system of horsts, exposing older, deep structural level rocks, and grabens, within which Eocene volcanic and sedimentary strata were deposited. An upper limit to this deformation is provided by middle Miocene and younger strata, which overlap those structures.

References

Anderson, P.
1984: Geology, petrology, origin and metamorphic history of the Eagle Granodiorite and Nicola Group, Whipsaw Creek, Princeton area, southern British Columbia; unpublished B.Sc. thesis, University of British Columbia, 201 p.

Church, B.N.
1975: Geology of the Hat Creek Coal Basin; British Columbia Ministry of Mines and Petroleum Resources, "Geology in British Columbia", p. G99-G118.

Davis, G.A., Monger, J.W.H., and Burchfiel, B.C.
1978: Mesozoic construction of the Cordilleran "collage", central British Columbia to central California; in Mesozoic paleogeography of the western United States, ed. D.G. Howell and K.A. McDougall; Society of Economic Paleontologists and Mineralogists, Pacific Section, Pacific Coast Paleogeography Symposium 2, p. 1-32.

Devlin, B.D.
1981: The relationships between the Cretaceous Spences Bridge and Kingsvale Groups; unpublished B.Sc. thesis, University of British Columbia, 57 p.

Duffell, S. and McTaggart, K.C.
1952: Ashcroft map area, British Columbia; Geological Survey of Canada, Memoir 262.

Ewing, T.E.
1980: Paleogene tectonic evolution of the Pacific Northwest; Journal of Geology, v. 88, p. 619-638.

Hollister, L.S.
1969: Metastable paragenetic sequence of andalusite, kyanite and sillimanite, Kwoiek area, British Columbia; American Journal of Science, v. 267, p. 352-370.

Hollister, V.F., Allen, J.M., Anzalone, S.A., and Seraphim, R.H.
1975: Structural evolution of porphyry mineralization at Highland Valley, British Columbia; Canadian Journal of Earth Sciences, v. 12, p. 807-820.

Kleinspehn, K.L.
1982: Cretaceous sedimentation and tectonics, Tyaughton-Methow Basin, southwestern British Columbia; unpublished Ph.D. thesis, Princeton University, 184 p.

McMechan, R.D.
1983: Geology of the Princeton Basin; British Columbia Ministry of Energy, Mines and Petroleum Resources, Paper 1983-3, 52 p.

McMillan, W.J.
1976: Geology and genesis of the Highland Valley ore deposits and the Guichon Batholith; in Porphyry deposits of the Canadian Cordillera, ed. A. Sutherland-Brown; Canadian Institute of Mining and Metallurgy Special Volume 15, p. 85-104.

Mathews, W.H. and Rouse, G.E.
– The Gang Ranch-Big Bar area, south central British Columbia: stratigraphy, geochronology and palynology of the Tertiary beds and their relationship to the Fraser Fault. (in preparation)

Misch, P.
1966: Tectonic evolution of the Northern Cascades of Washington State; in Tectonic history and mineral deposits of the western Cordillera, sen. ed. H.C. Gunning; Canadian Institute of Mining and Metallurgy, Special Volume 8, p. 101-148.

1977: Dextral displacements at some major strike faults in the northern Cascades; Geological Association of Canada, Program with Abstracts, v. 2, p. 37.

Monger, J.W.H.
1970: Hope map area, west half, British Columbia; Geological Survey of Canada, Paper 69-49, 75 p.

1981: Geology of parts of western Ashcroft map area, southwestern British Columbia; in Current Research, Part A, Geological Survey of Canada, Paper 81-1A, p. 185-189.

Monger, J.W.H. and McMillan, W.J.
1984: Bedrock geology of Ashcroft (92 I) map area; Geological Survey of Canada, Open File 980.

Monger, J.W.H. and Price, R.A.
1979: Geodynamic evolution of the Canadian Cordillera – progress and problems; Canadian Journal of Earth Sciences, v. 16, p. 770-791.

Monger, J.W.H., Price, R.A., and Tempelman-Kluit, D.J.
1982: Tectonic accretion and the origin of the two major metamorphic and plutonic welts in the Canadian Cordillera; Geology, v. 10, p. 70-75.

Morrison, G.W.
1980: Stratigraphic control of Cu-Fe skarn ore distribution and genesis at Craigmont, British Columbia; Canadian Institute of Mining Bulletin, August, 1980, p. 109-123.

Orchard, M.J.
1984: Pennsylvanian, Permian and Triassic conodonts from the Cache Creek Group, southern British Columbia; in Current Research, Part B, Geological Survey of Canada, Paper 84-1B, p. 197-206.

Preto, V.A.
1972: Geology of Copper Mountain; British Columbia Department of Mines and Petroleum Resources, Bulletin 59, 87 p.

1975: The Nicola Group: Mesozoic volcanism related to rifting in southern British Columbia; in Volcanic regimes in Canada, ed. W.R.A. Baragar, L.G. Coleman, and J.M. Hall; Geological Association of Canada, Special Paper 16, p. 38-57.

1979: Geology of the Nicola Group between Merritt and Princeton; British Columbia Ministry of Energy, Mines and Petroleum Resources, Bulletin 69, 90 p.

Price, R.A.
1979: Intracontinental ductile spreading linking the Fraser River and Northern Rocky Mountain Trench transform fault zones, south-central British Columbia and northeast Washington; Geological Society of America, Abstracts with Programs, v. 11, p. 499.

Read, P.B. and Okulitch, A.V.
1977: The Triassic unconformity of south central British Columbia; Canadian Journal of Earth Sciences, v. 14, p. 1127-1145.

Rice, H.M.A.
1947: Geology and mineral deposits of Princeton map area, British Columbia; Geological Survey of Canada, Memoir 243.

Roddick, J.A., Muller, J.E., and Okulitch, A.V.
1979: Fraser River, British Columbia-Washington; Geological Survey of Canada, Map 1386A, 1:1,000,000 scale.

Ross, C.A. and Ross, J.R.P.
1983: Late Paleozoic accreted terranes of western North America; in Pre-Jurassic rocks in western North American suspect terranes, ed. C.H. Stevens; Society of Economic Geologists and Paleontologists, Pacific Section, p. 7-22.

Shannon, K.R.
1982: Cache Creek Group and contiguous rocks, near Cache Creek, B.C.; unpublished M.Sc. thesis, University of British Columbia, 72 p.

Smith, R.B.
1974: Geology of the Harper Ranch Group (Carboniferous-Permian) and Nicola Group (Upper Triassic), northeast of Kamloops, British Columbia; unpublished M.Sc. thesis, University of British Columbia, 211 p.

Tipper, H.W.
1978: Taseko Lakes (92 O) map area; Geological Survey of Canada, Open File 534.

Travers, W.B.
1978: Overturned Nicola and Ashcroft strata and their relation to the Cache Creek Group, southwestern Intermontane Belt, British Columbia; Canadian Journal of Earth Sciences, v. 15, p. 99-109.

1982: Possible large-scale overthrusting near Ashcroft, British Columbia: implications for petroleum prospecting; Bulletin of Canadian Petroleum Geology, v. 30, p. 1-8.

Vance, J.A. and Muller, R.E.
1981: The movement history of the Straight Creek Fault in Washington State; Geological Association of Canada, Cordilleran Section, Programme and Abstracts, p. 39-41.

Wilcox, R.E., Harding, T.P., and Seely, D.R.
1973: Basic wrench tectonics; American Association of Petroleum Geologists, v. 57, p. 74-96.

GEOLOGY OF THE ARTILLERY LAKE PB-ZN-CU DISTRICT, DISTRICT OF MACKENZIE

Project 770024

S.S. Gandhi
Economic Geology and Mineralogy Division

Gandhi, S.S., Geology of the Artillery Lake Pb-Zn-Cu district, District of Mackenzie; in Current Research, Part A, Geological Survey of Canada, Paper 85-1A, p. 359-363, 1985.

Abstract

Aphebian dolomitic beds of Artillery Lake formation were deposited on Archean granitic terrain of low relief. They were gently folded and down-faulted with respect to gneissic rocks to the southeast along a fault trending 055°. Associated quartz-carbonate veins carrying coarse galena, sphalerite, chalcopyrite and pyrite, have a regional northeasterly trend approximately parallel to that of the folds.

Résumé

La mise en place des couches dolomitiques d'âge aphébien de la formation d'Artillery Lake s'est produite sur un terrain archéen de nature granitique et peu accidenté. Une faille d'orientation 055° a causé l'affaissement de ces couches légèrement plissées par rapport aux roches gneissiques au sud-est. Les couches sont associées à des veines de quartz et carbonate qui renferment des grains grossiers de galène, de sphalérite, de chalcopyrite et de pyrite et qui présentent une direction régionale nord-est à peu près parallèle à celle des plis.

Introduction

Fieldwork done during 1984 in the Artillery Lake Pb-Zn-Cu district as a follow-up of its discovery in 1983, revealed some aspects of regional geology, 10 new Pb-Zn-Cu occurrences and additional mineralization near some of the 11 similar occurrences reported earlier (Gandhi, 1984). These field observations are briefly summarized here.

The area is part of a proposed National Park withdrawn from staking in 1971, and the present work is an extension of the mineral resource assessment undertaken by the Geological Survey of Canada.

Regional Geology

The dolomitic Artillery Lake formation[1] was deposited during Aphebian time on Archean basement. Basement is predominantly granitic and includes a narrow southeast extension of the Walmsely Lake greenstone belt (Fig. 46.1; Folinsbee, 1952; Gandhi, 1984). The basement granitic rocks are mainly porphyritic to megacrystic, and biotite-muscovite-bearing. They are referred to here as Artillery granite. Related muscovite-bearing pegmatite have yielded Archean dates (Gandhi, 1984). The Artillery Lake formation was gently folded about north-northeast axes, and is truncated on the southeast side by Artillery Fault, which trends 055° and appears to be nearly vertical. The fault is well defined for a 25 km strike length northeast from longitude 108°00'W, beyond which it is concealed by overburden and lakes and can be inferred from topographic, geological and magnetic data. It continues northeast of the present study area, and most probably links up with a fault at the west end of Deville Lake, 40 km from Artillery Lake, mapped by Henderson and Macfie (1985). The uplifted southeast side of Artillery fault is a complex of banded amphibolitic, quartzofeldspathic and micaceous gneisses and schists, granodioritic gneiss, migmatite with small bodies and dykes of granite and pegmatite. The gneissic rocks have a regional east-northeast trend approximately parallel to the fault, although locally they are highly contorted.

The boundary of the gneissic rocks with Artillery granite to the west, including a stretch along Artillery Fault, is marked by a distinctive change in regional total magnetic intensity, from moderate over the Artillery granite to low over the gneissic terrain (Geological Survey of Canada, 1981). This magnetic low east of Artillery Lake extends well beyond the present study area and is approximately 100 km long in a north-south direction and up to 30 km wide. It is bounded on the south by Ford-Larocque Fault which is marked by a topographic linear (Fig. 46.1). To the southwest the magnetic low extends discontinuously between Artillery and McDonald faults. Variations in magnetic pattern here are attributable to the presence of relatively more magnetic amphibolitic bands and lenses, and of Mackenzie diabase dykes in the gneissic rocks. The area south of Ford-Larocque and McDonald faults, which is also underlain largely by a variety of gneissic rocks, is however characterized by pronounced magnetic anomalies trending northeast and east-northeast.

The boundary between Artillery granite and gneissic rocks in the study area north of 63°15'N is close to what Wright (1967) regarded as 'Thelon Front' separating the Slave and Churchill structural provinces. The front extends for 700 km to the north and northeast. Recent work by Henderson et al. (1982) in the Healey Lake map area 90 km northeast of Artillery Lake, indicates that a better candidate for the front in that area is a mylonitic 'straight zone' 20 km or more to the east of the one defined by Wright (1967). This mylonitic zone trends south-southwest. Its continuation southwards (from 64°00'N, 106°30'W) is evident from its geomorphological and magnetic expression and lies east of the low magnetic gneissic terrane north of Ford-Larocque Fault in the present study area. Hence this terrane is regarded tentatively here as part of the Slave Structural Province. The Ford-Larocque and other related faults of the McDonald Fault system transected and shifted the boundary between the Slave and Churchill structural provinces during late Aphebian time. Much of the displacement due to this fault-system is right lateral (Reinhardt, 1969; Hoffman et al., 1977). Wright (1967) reported a K-Ar date of 1680 Ma on paragneiss near Ford Lake south of Ford-Larocque Fault (Fig. 46.1), and in contrast to the present interpretation regarded most of the area between this fault and Artillery Lake to be in the Churchill Structural Province.

Dolomitic veins and dykes of sedimentary origin, formed by infilling along fractures (neptunian dykes) or by abnormal pressure (injection dykes), occur in Archean basement as far as 7 km northwest of the present outline of Artillery Lake formation. They indicate that dolomitic Artillery Lake formation formerly extended over a much greater area, and that subsequent erosion here has not penetrated far below the basement-Artillery Lake formation unconformity. To the southeast, similar dykes as well as Pb-Zn-Cu occurrences occur in Artillery granite but none have yet been found in gneissic rocks to the east and south, or south of Artillery Fault. This implies that the gneissic rocks are uplifted relative to the Artillery Lake formation and Artillery granite. Shear zones subsidiary to Artillery Fault occur in the granite 7 km northeast of Trout Creek and they contain some stretched out remnants of dolomite dykes. The fault is probably a part of the Aphebian McDonald Fault system. Isotopic data on galenas from the Pb-Zn-Cu occurrences indicate a probable age of 1890 to 1950 Ma (Roscoe, 1984; Gandhi, 1984). The veins are believed to have formed prior to the late stages of movements along the McDonald Fault system.

Artillery Lake formation

This predominantly dolomitic unit was deposited during marine transgression over largely granitic terrane of low relief and is more than 300 m thick.

The unconformity is exposed along the northwest shore of Artillery Lake, and is characterized by intense dolomitization of the basement and the presence in it of numerous dolomitic veins and dykes of sedimentary origin. Cherty veinlets of sedimentary or diagenetic origin are common in and near the dolomitic dykes. Patches of breccia containing basement fragments and grit in dolomitic matrix occur on the basement exposures near the unconformity.

The basal beds of Artillery Lake formation are exposed along the northwest shore of the lake, and are up to a few metres thick. They are mostly massive buff dolomite, and include lenses of grit and quartz pebble conglomerate up to 0.5 m thick and a few tens of metres long, with a dolomitic matrix, and also lenses of chert and chert-pyrite. The pyritic lenses contain pyrobitumen and some are associated with small colonies of columnar stromatolites a few centimetres high and few millimetres in diameter. The basal beds are of interest because the majority of the veins carrying Pb, Zn, and Cu sulphides found to date occur here or in the basement near the unconformity, or both.

A minimum thickness of 300 m for Artillery Lake formation is estimated from exposures on the southeast shore near longitude 107°52'W, in a 2 km strike zone near Artillery Fault. Here, the beds are vertical to steeply dipping and face northwest. This is the thickest observed section of the formation, but it is not considered complete because the base and top of the formation are not exposed. The lower part of the section has massive and thick to thin bedded dolomite with numerous cherty layers and lenses up to a few centimetres thick. It is lithologically similar to and probably

[1] Informal designation (Gandhi, 1984).

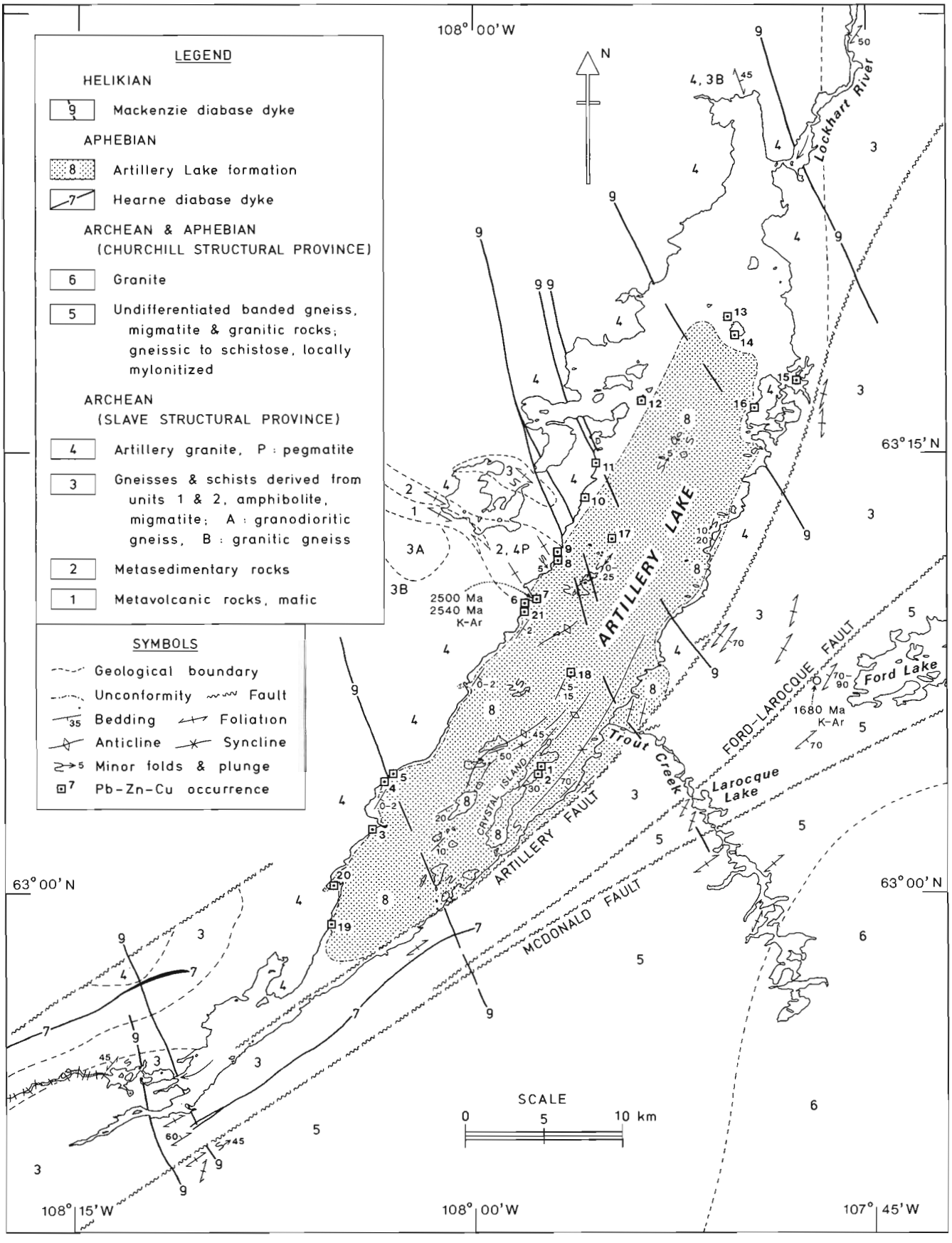

Figure 46.1. *Geology and Pb-Zn-Cu occurrences of Artillery Lake area.*

stratigraphically equivalent to that found along the chain of islands trending north-northeast in Artillery Lake. There are however no marker units to make reliable correlations in different parts of the 50 X 10 km exposure area of the formation. On the islands, the lower part of the formation also includes beds showing polygonal mudcracks filled with chert, and some beds and lenses of intraclast breccia, argillite, and grit.

The upper part of the section has abundant dolomitic sand and grit beds, thick and thin bedded dolomite and a few breccia beds. At the top of the section, closely packed, well rounded quartz pebble conglomerate occurs in a lens over 15 m thick and 50 m in strike length, the largest of its kind found in the formation. It has a dolomitic matrix, carries rare dolomite fragments, and appears to be a channel-fill.

Stromatolitic beds are common in exposures 2 km northeast of the 300 m thick section, as well as on the north shore of Crystal Island and on nearby islands to the south. They may in part be lateral equivalents of beds in the section mentioned above, but some may be stratigraphically above or below them. The most common variety of stromatolite is columnar, up to a few centimetres in diameter and 2 m in height. The stromatolites are partially silicified. Some flat laminated beds and others showing laterally linked hemispherical forms are probably of algal origin. Such beds and lenses are aerially widely distributed in Artillery Lake formation.

A lithologically distinctive sequence of interbedded grey and red shales (argillite) and dolomite, approximately 20 m thick, is exposed over a 1.5 km strike length on the southeast shore of Artillery Lake near longitude 107°41'W. This gently to moderately folded sequence lies near the outcrops of Artillery granite indicating close proximity to the basal unconformity.

The lithological characteristics of Artillery Lake formation are indicative of deposition largely in transgressive intertidal to supratidal environments. The presence of argillite suggests subtidal deposition, and is a favourable geological feature in terms of possibility for stratabound Mississippi Valley type Pb-Zn deposits in the basin as suggested by Gandhi (1984). Irregular patches of tan-weathering dolomite as well as numerous dolomitic and cherty veins are interpreted as synsedimentary to diagenetic. Later deformation has produced breccia along hinge zones of some folds.

Pb-Zn-Cu occurrences

Veins carrying galena, sphalerite, chalcopyrite and pyrite in quartz-carbonate matrix are widely distributed in the Artillery basin (Fig. 46.1). Eleven of the occurrences were discovered in 1983 and were reported by Gandhi (1984), and 10 others were found in 1984. Most are at or close to the unconformity at the base of Artillery Lake formation but a few occur at stratigraphically higher levels. They postdate dolomitic and cherty veins, and folding of the formation. They range in size from stringers and small veins to larger veins up to a metre thick and several tens of metres long. The larger veins are quartz-rich, and contain aggregates of chalcopyrite, pyrite and less commonly of galena and sphalerite. These veins are steep and have a regional northeasterly trend approximately parallel to the main trend of the folds. The smaller, more numerous veins contain up to 75 per cent galena and sphalerite in coarse aggregates, are more variable in attitude, and commonly occur in stockworks and anastomosing clusters. The mineralization is believed to be low temperature hydrothermal, controlled by tensional fractures that are related to gentle warping of Artillery Lake formation along northeast trending axes, accompanied by structural adjustments in the basement (Gandhi, 1984).

Further examination of some of the previously reported showings (no. 1 to 11, Gandhi, 1984) revealed that the veins are significantly longer and that additional veins occur in their vicinity. Thus at showing 1, veins occur discontinuously along a 350 m strike length along the shore of Crystal Island. Others were observed as far as 30 m offshore from showings 1 and 2, by snorkling in water up to 3 m deep. Showing 7 has veins distributed widely on the shore of a peninsula 500 m long and up to 400 m wide. It is essentially a group of showings. The adjacent showing 6 and newly discovered showing 21 are similar in character, and it is apparent that more such veins can be expected to be found under the extensive overburden and water cover in the area of these showings (over 1500 m long and 500 m wide). Furthermore, showings 8 and 9, 3 km to the northeast, are also similar to them, and the intervening area may contain more such veins. In contrast to these groups of veins that contain coarse aggregates of minerals, the vein seen at showing 11 has a layered agate-pyrite-sphalerite-quartz structure (Gandhi, 1984). It is up to 25 cm thick, dips 5 to 35° to the southeast and is exposed discontinuously over a strike length of 170 m.

Showings 12 to 21 (Fig. 46.1) were discovered during 1984. Five of these (no. 12 to 16) are hosted by Artillery granite. Proximity to the unconformity is indicated by the presence of numerous dolomite dykes, remnants of dolomite beds and dolomite cemented breccia carrying fragments of granite, that are present in the vicinity of the showings. Showings 12, 13 and 16 have galena-rich viens up to 3 cm thick. Showing 14 has two nearly vertical quartz veins which are up to 30 cm wide, trend 045° and 010°, and are 20 m apart on the shore. They carry some chalcopyrite and pyrite. Galena and sphalerite are not found in these veins, but it may be noted that similar large quartz-pyrite-chalcopyrite veins occur in close association with, and a few grade into, galena-sphalerite-bearing veins at showing 4 (Gandhi, 1984). Showing 15, on the northwest tip of an unnamed small island, has an unusually rich concentration of coarse galena and sphalerite in a lens 2 m long and 0.3 m wide, within a steep north-northeast striking vein.

Showings 17 and 18 occur in beds that are stratigraphically considerably above the unconformity, and in this respect they resemble showings 1 and 2 and differ from the other occurrences. At showing 17, there are several nearly vertical veins that trend atypically north-northwest across an island 30 m in diameter. Galena and sphalerite are restricted to a few of the veins whereas chalcopyrite is more widely distributed throughout. Showing 18 is on the north tip of an island where sulphide-rich veins and stringers occur in a 40 X 10 m area. They include a few lensoid aggregates, up to 25 cm in diameter, of very coarse sphalerite and galena.

Showing 19 has one gently dipping quartz vein which occurs in basement granite and carries pyrobitumen in addition to the sulphides, and several other quartz-pyrite-chalcopyrite veins that occur in basal beds of Artillery Lake formation. The latter veins are vertical and trend north-northeast. Similar quartz-pyrite-chalcopyrite veins occur at showing 20. These are also vertical and trend northeast for over 100 m.

Showing 21, near showing 6 at the unconformity, has galena-sphalerite-rich veins up to 20 cm wide, in dolomite beds with chert and chert-pyrite lenses.

Concluding remarks

The Artillery Lake Pb-Zn-Cu district is known to contain numerous vein-type occurrences that are structurally controlled by tensional fractures related to deformation of

dolomitic Artillery Lake formation. Most of the veins are in basal beds of these Aphebian formation and/or in Archean basement near the unconformity. They differ morphologically from the larger, economically important stratabound Mississippi Valley-type Pb-Zn deposits. They are however believed to be similar to these deposits in terms of genetic processes and general geological setting, and they are comparable to veins associated with some of the deposits. Hence the Artillery Lake metallogenic district is considered to have some interesting exploration potential for larger vein-type as well as stratabound Pb-Zn deposits.

Acknowledgments

The writer was ably assisted in the fieldwork by Gregory Philpott. S.M. Roscoe took a keen interest in the work and provided some logistic support during the field season.

The manuscript was critically read by S.M. Roscoe and R.T. Bell of the Geological Survey of Canada.

References

Folinsbee, R.E.
1952: Walmsley Lake, District of Mackenzie, Northwest Territories; Geological Survey of Canada, Map 1013A.

Gandhi, S.S.
1984: Galena-sphalerite-chalcopyrite veins in Aphebian dolomite and Archean basement at Artillery Lake, Northwest Territories; in Current Research, Part B, Geological Survey of Canada, Paper 84-1B, p. 33-40.

Geological Survey of Canada
1981: Magnetic anomaly map of Lockhart River, Northwest Territories; Map 1566A, scale 1:1 000 000.

Henderson, J.B. and Macfie, R.I.
1985: Northern Artillery Lake map area: a transect across the Thelon Front, District of Mackenzie; in Current Research, Part A, Geological Survey of Canada, Paper 85-1A, report 54.

Henderson, J.B., Thompson, P.H., and James, D.T.
1982: The Healey Lake map area and the Thelon Front problem, District of Mackenzie; in Current Research, Part A, Geological Survey of Canada, Paper 82-1A, p. 191-195.

Hoffman, P.F., Bell, I.R., Hildebrand, R.S., and Thorstad, L.
1977: Geology of the Athapuscow Aulacogen, East Arm of Great Slave Lake, District of Mackenzie; in Report of Activities, Part A, Geological Survey of Canada, Paper 77-1A, p. 117-129.

Reinhardt, E.H.
1969: Geology of the Precambrian rocks of Thubun Lakes map-area in relationship to the McDonald Fault system, District of Mackenzie; Geological Survey of Canada, Paper 69-21, 29 p.

Roscoe, S.M.
1984: Lead-isotope dating of galena-bearing veins in dolomite at Artillery Lake, Northwest Territories and Mistassini Lake, Quebec; Geological Association of Canada – Mineralogical Association of Canada, Program with abstracts, v. 9, p. 101.

Wright, G.M.
1967: Geology of the southeastern barren grounds, parts of the District of Mackenzie and Keewatin (Operations Keewatin, Baker, Thelon); Geological Survey of Canada, Memoir 350, 91 p.

-47-

THE STRATIFIED NATURE OF DEPOSITS IN STREAMLINED GLACIAL LANDFORMS ON SOUTHERN VICTORIA ISLAND, DISTRICT OF FRANKLIN

Project 830018

D.R. Sharpe
Terrain Sciences Division

Sharpe, D.R., The stratified nature of deposits in streamlined glacial landforms on southern Victoria Island, District of Franklin; in Current Research, Part A, Geological Survey of Canada, Paper 85-1A, p. 365-371, 1985.

Abstract

The structure of streamlined landforms near Cambridge Bay, Northwest Territories, suggests that these major glacial deposits may be produced by deposition from subglacial meltwater. Fluted landscapes are spatially gradational to drumlin features, which in turn are transitional to large eskers, all comprising stratified deposits including interbedded sand and diamicton. These sediments are intact, interbedded, and conformable with the landform, and they probably represent accumulation in a subaqueous environment. Both drumlinoid and fluted forms could result from meltwater eroding subglacial cavities that were subsequently filled with sediment from the meltwater and from the glacier.

The implications of the proposed meltwater origin of streamlined landforms are that landform-sediment descriptions are crucial to mapping glacial sediments and that interpretation of the glacial geology and sediments of many areas needs to take into account the significance of subglacial meltwater deposition.

Résumé

La structure des formes de relief fuselées que l'on trouve près de Cambridge Bay, dans les Territoires du Nord-Ouest, semble indiquer que ces importants dépôts glaciaires sont, peut-être dus aux apports des eaux de fonte sous-glaciaires. Un modelé en cannelures passe horizontalement à des drumlins, puis à de larges eskers; toutes ces formes sont constituées de dépôts stratifiés qui renferment du sable et du diamicton interstratifiés. Ces sédiments sont intacts, interstratifiés et conformes, et ils résultent probablement d'une accumulation de matériaux dans un milieu subaqueux caractérisé par de faibles tensions. Pour expliquer les formes drumlinoïdes et cannelées des dépôts, on pourrait émettre l'hypothèse que les eaux de fonte ont érodé des cavités sous-glaciaires qui ont par la suite été remplies de sédiments déposés par les eaux de fonte et par les glaciers.

Si les eaux de fonte sont effectivement à l'origine des formes de relief fuselées, les descriptions des modelés et des sédiments assument alors une importance capitale pour l'étape de cartographie des dépôts glaciaires et les interprétations de la géologie et des sédiments glaciaires de nombreuses régions doivent tenir compte du rôle important des eaux de fonte glaciaires dans le dépôt des sédiments.

Introduction

Fieldwork carried out to map the glacial geology on southern Victoria Island, Northwest Territories, during the summers of 1983 and 1984 has concentrated on understanding the origin of distinct glacial landforms (Sharpe, 1984). Relationship between form and the enclosed sediments has been investigated for till plains, hummocky moraine, end moraine, drumlins, and fluted surfaces. As measured sections in drumlins and fluted terrain were obtained around Cambridge Bay, Victoria Island, these two landforms will be emphasized in the present report.

Much of Victoria Island is covered by streamlined glacial landforms (Fig. 47.1).

This report describes the measured sections from fluted terrain and drumlinoid features mapped in southern Victoria Island. Data from measured sediment sequences are used to show that current views on the origin of streamlined glacial forms do not explain the landforms studied in this report. An origin of deposition that considers stratified and interbedded sequences in drumlins (Shaw, 1983) and fluting to have been deposited by subglacial meltwater is tested using field mapping from the Cambridge Bay area, Victoria Island.

The geomorphic setting

The sections studied are located 50 km north of Cambridge Bay (Fig. 47.1). One set (field sites 76, 78, and 79) lies in a field of longitudinal ridges described as drumlinoid features (Fig.47.2). Most of the drumlinoid ridges are straight crested, 10 to 25 m high, and 500 to 2000 m long. Slightly sinuous ridges (esker or drumlinoid) intersect a large main esker system at right angles. Thaw erosion of the landscape has modified up to a third of the terrain, and this is now largely covered by lakes. In addition, it appears that chains of low-lying areas, which cut across the fluted landscape and terminate at the large esker, are former tunnel valleys. Much of the remaining landscape consists of a poorly formed ridged surface that has been thaw eroded. The transitional relationship between the drumlinoid landscape, eskers, and a field of drumlins can be seen in Figure 47.3.

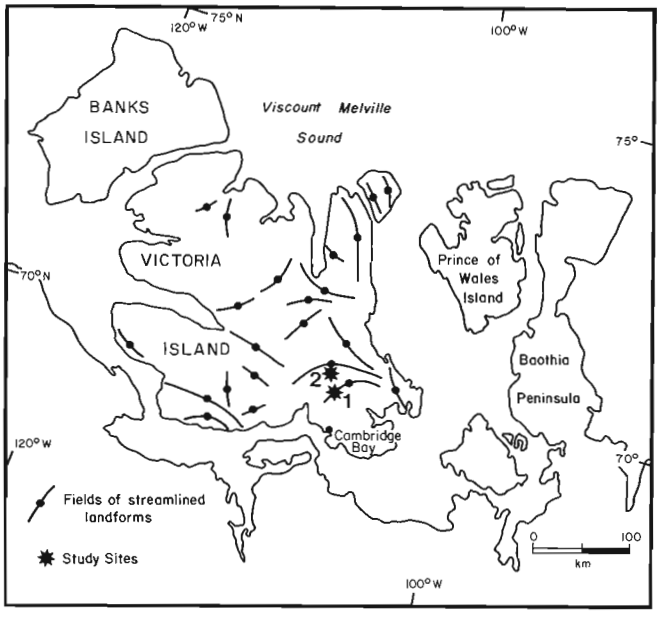

Figure 47.1. Location of study sites (1, 2) and fields of streamlined landforms on Victoria Island.

The geomorphic setting for the second set of sites (115, 118) is an overall level upland on which longitudinal ridges occur (Fig. 47.4). One third of this terrain has also been eroded by thaw slumping. The pattern of ridges and the longitudinal ridges themselves, are more clearly defined than at study site 1 and almost all are straight crested. The fluted ridges are 5-8 m high whereas the underlying glacial sediments are 40-50 m thick in places, with the inter-ridge area comprising a level upland plain. Many other excellent exposures, besides the measured ones, (110, 111, 115A, 118, 118B, and 119; Fig. 47.4) occur on the margins of the thaw eroded terrain. The relationship between the fluted terrain, esker system, and drumlin field is shown in Figure 47.5.

The exposures in drumlinoid forms (76, 78, 79) have diamicton facies associated with them whereas the exposures in fluted forms (115, 118) are dominated by sand strata and contain little or no diamicton. Most of the diamictons are considered to be glacial drift deposited as debris flows.

Drumlinoid landscape

Section 76

This sequence of sediments consists of three major units exposed in the end of a drumlinoid ridge (Fig. 47.6). The lower diamicton (A) comprises sandy silt pebbly beds 10-25 cm thick, interbedded with the overlying sand. The contacts between diamicton and sand units are conformable. The lower part of unit B consists of rippled, medium sand (B1) overlain by irregularly crossbedded pebbly sand (B2). Massive sand units (B3), including several normally graded sand strata 15-20 cm thick, occur next, overlain by ripple-bedded sand near the top of the unit (B4). Minor faulting (possibly related to thaw erosion) has resulted in small displacements. The sand is capped by a 1.5 m-thick massive cobbly sandy silt diamicton (C) that has a nonerosional interbedded contact with the underlying sand unit. The section represents the upper 9 m of a drumlinoid ridge that stands about 20 m at its crest, sloping to 15 m near the flank; thus the section represents a significant part of the total landform thickness.

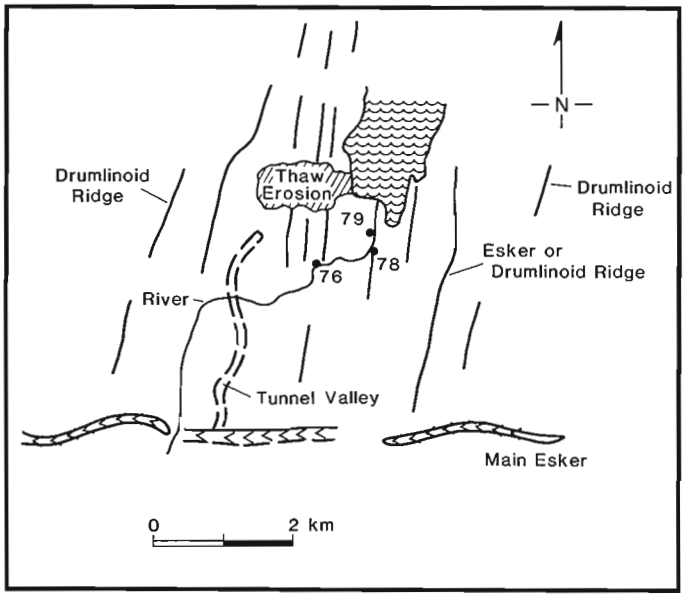

Figure 47.2. Location of sites (76, 78, 79) in drumlinoid landscape. See Figure 47.1 (study site 1) for location on Victoria Island and Figure 47.3 for aerial view of adjacent landforms including main esker and drumlin field in the distance.

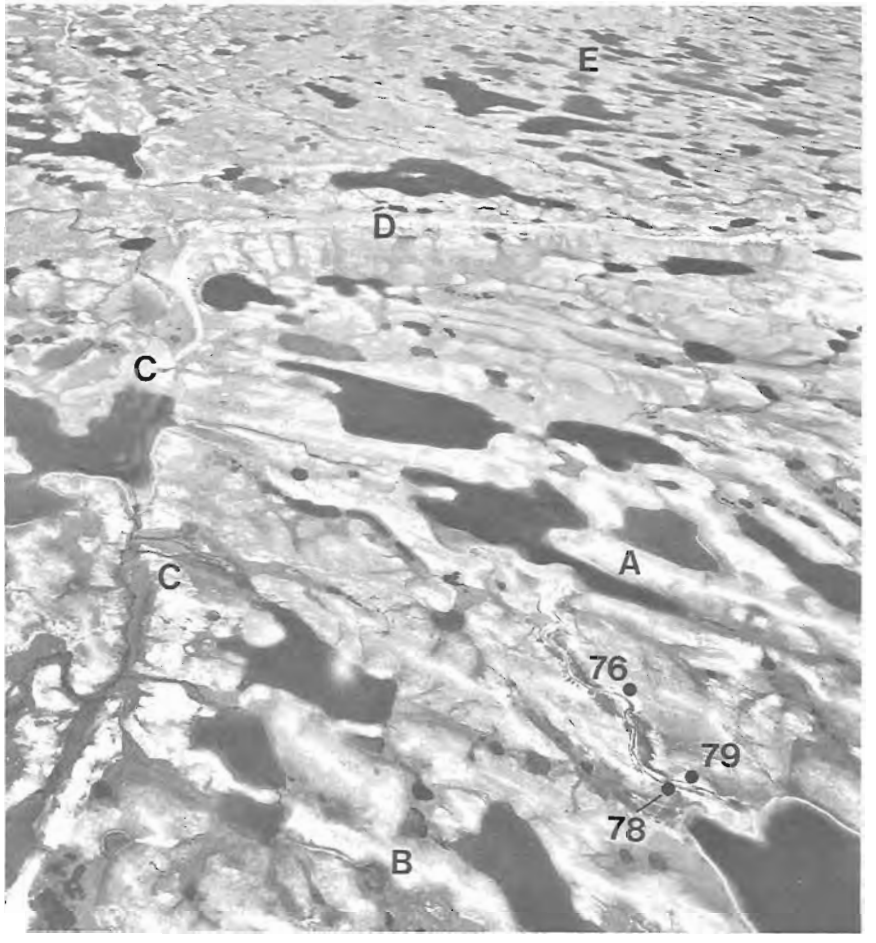

Figure 47.3

Aerial view (oblique) of drumlinoid landscape (A), drumlinoid or esker (B), trunk esker (C) and main esker (D) and relationship to field of drumlins (E), near study site 1, Figure 47.1. (NAPL T466L-120)

There are adjacent exposures in this landscape although they are not part of the same drumlinoid ridge in which section 76 was recorded, but they are in similar and contiguous features.

Section 78

This section is exposed on a drumlinized ridge or on the flanks of the drumlinized terrain, adjacent to section 76. Section 78 reveals predominantly massive sand (A,C_3), interrupted by a series of minor debris flow units (Fig. 47.7). The bedding in the section is inclined at 5-10° to the south indicating some postdepositional settlement of all the strata. The lowest unit (A) consists of sand with minor pebbly sediment and the unit is faulted. The faults, however, are bounded by the next unit of interbedded sand and debris flow diamictons (B). This is followed by a fining-upwards pebbly sand (C_1 and C_3). The upper part of the unit consists of a series of (pebbly) sand beds, massive to faintly bedded and stratified, and interbedded with these are fine textured diamictons. A cryoturbated colluvial sand unit (D) forms the top metre of sediment exposed in this 7 m section.

Section 79

This section was measured in a river bank cut into drumlinoid landscape eroded by a lake-drainage event. The section consists of eight units: stratified diamicton and sand, massive to banded sand, gravelly sand, rippled sand, gravelly sand, massive diamicton, soil, and slope debris (Fig.47.8).

The lowest unit (A) is a stratified diamicton with a graded sand bed separating the two massive segments; the contact is conformable and possibly gradational with the

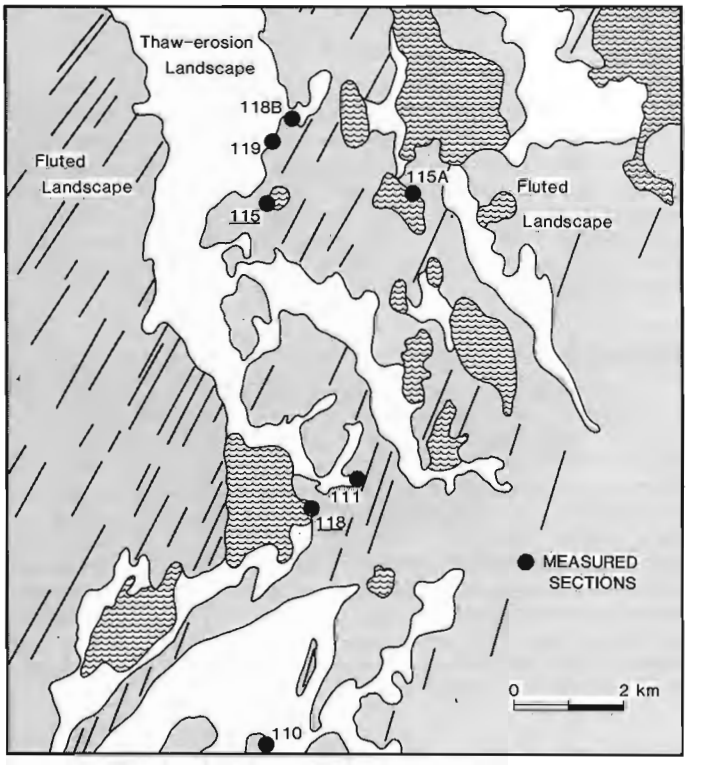

Figure 47.4. *Location of reported sites (115, 118) and other measured sections in fluted landscape. See Figure 47.1 (study site 2) for location on Victoria Island and Figure 47.5 for aerial view of adjacent landforms.*

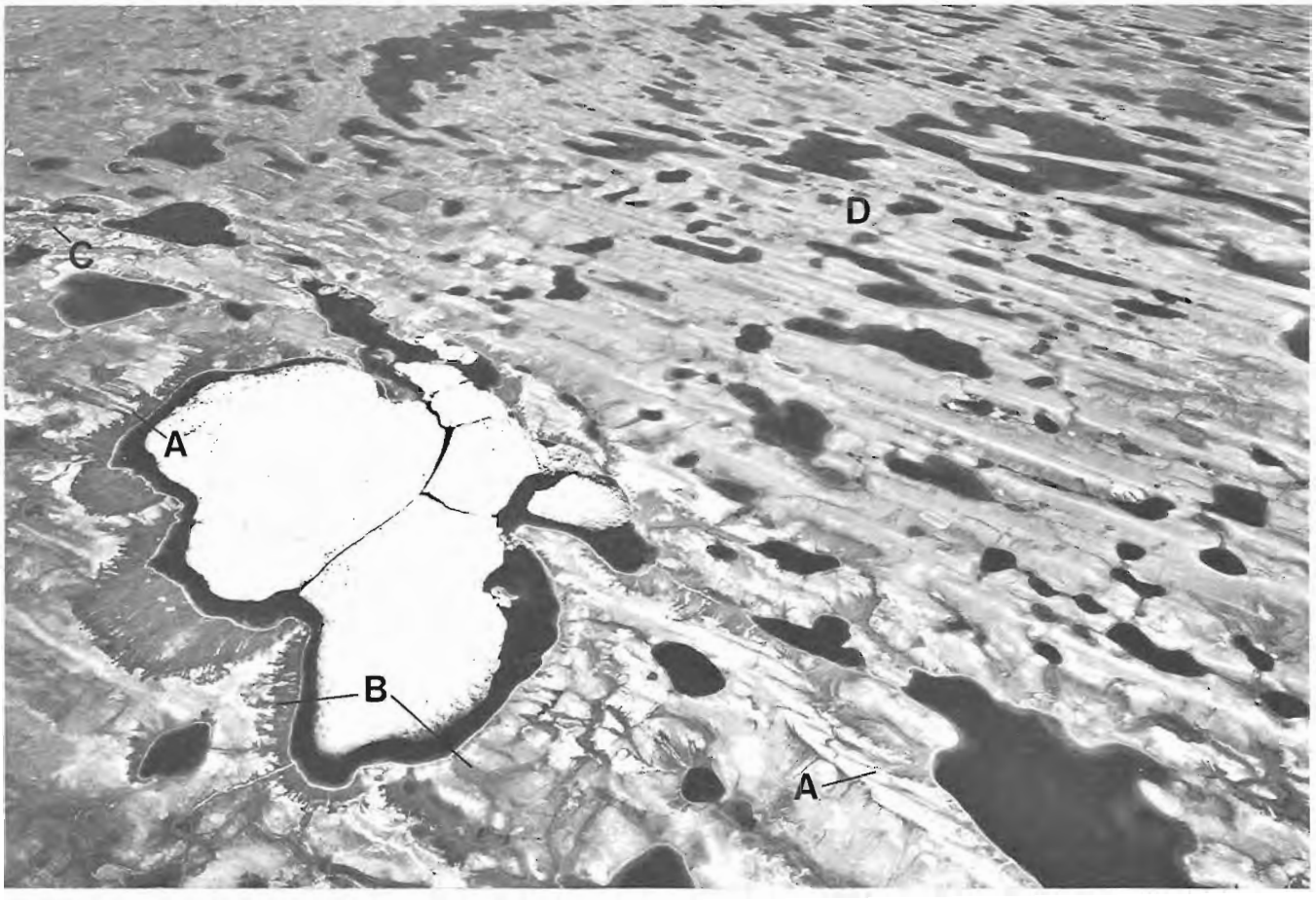

Figure 47.5. *Aerial view (oblique) of fluted landscape (A), thaw-eroded landscape (B), esker complex (C), and drumlin field (D) near study site 2, Figure 47.1. (NAPL T466L-126)*

overlying diamicton. There is a sharp contact to the overlying massive to weakly banded sand (B). This sand coarsens upwards to gravelly sand (C) and is overlain by a rippled sand (D_1). A sharp, erosional contact marks the pebbly, massive and unsorted sand (D_2). This is overlain by a sandy silt diamicton (E) with an irregular contact and by a soil horizon consisting of organic-rich sand and silty sand. The top of the sequence is a slope deposit (F) consisting of a greenish marine silt with clasts included in the unit.

Summary and comments

In summary, the strata in sections 76, 78 and 79 represent a conformable, intact unfolded set of beds that probably represent essentially continuous deposition with minor current erosion. All the contacts are conformable as there are no angular unconformities nor apparent hiatuses in the sequence. All the strata are intact, with the exception of some minor faulting in section 78; similarly no evidence exists for deformation except in the top unit (D). There are many graded sand and massive sand units suggestive of rapid subaqueous deposition. The paucity of ripple structures indicates mass flow deposition of the sand. Therefore, an episodic but continuous subaqueous deposition of (pebbly) sand and unsorted debris is suggested.

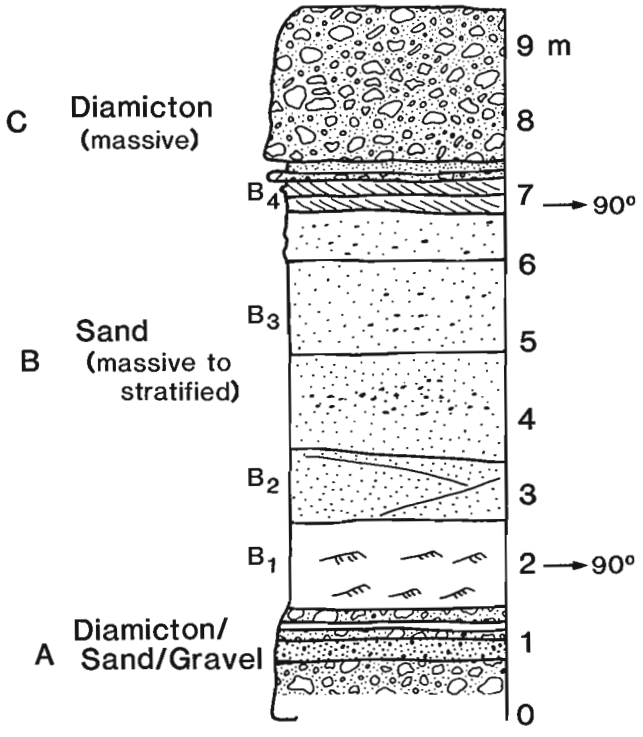

Figure 47.6. *Measured end section (76) in a drumlinoid ridge.*

Fluted landscape

Section 115

Section 115 is in a fluting occurring at the edge of a thaw lake on a level upland surface that has abundant longitudinal ridges or flutings (Fig. 47.4). The 7 m-high section exposes the sediments of this landscape (Fig. 47.9). One third of the area has been thaw eroded, exposing sandy sediments that have been wind eroded.

The lowest and thickest unit (A) is a sand sequence that comprises inclined, weakly to strongly bedded to massive sand and pebbly sand. In places the unit comprises 30-40 cm-thick beds of normally graded coarse to medium sand (A_1). The contacts appear to be gradational or at least they are not indicative of major erosion where they are not gradational. These sand beds are inclined about 15° to the north, and minor normal faulting affects the lowest unit (A_0).

A stone line (B) represents a lag from water or wind that winnowed a coarse layer which has subsequently been buried by slope and wind deposits. The top unit (C) has stones at the surface and organic material throughout the massive silty sand; the unit is interpreted as a combined slope movement and windblown deposit that forms a thin capping on the lower sand.

A similar sequence was observed in similar terrain about 5 km south of site 115.

Section 118

Much of the sequence comprises a sand unit (7+ m) that displays massive horizontally bedded, well sorted to pebbly sand and common normal grading (Fig. 47.10). Fine pebbly gravel is also common and it occurs as massive to well sorted or banded beds. Several striated clasts occur on the fluted upper surface. There are no major breaks in this sequence of

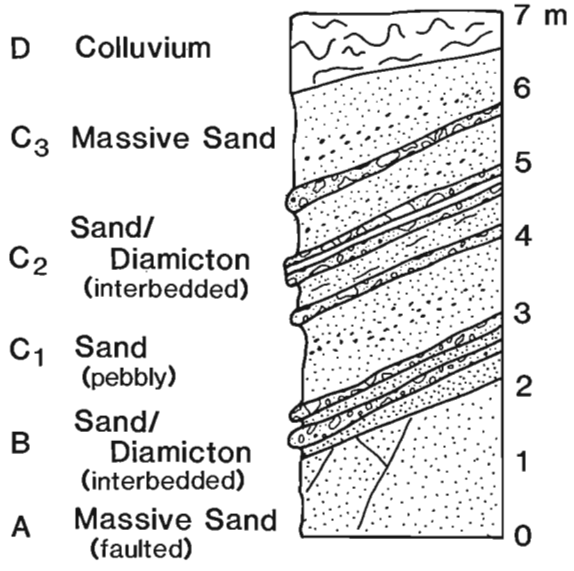

Figure 47.7. *Measured side section (78) in a drumlinoid ridge.*

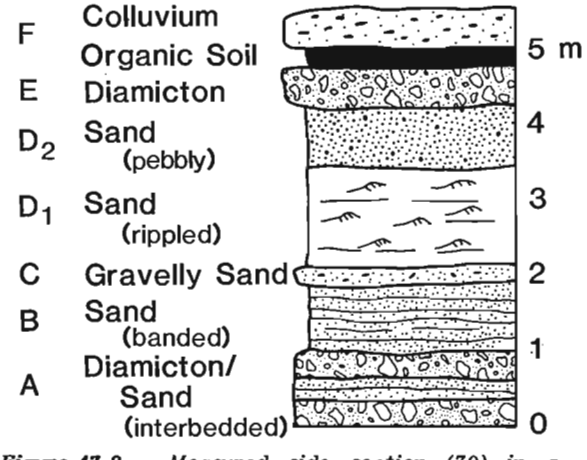

Figure 47.8. *Measured side section (79) in a drumlinoid ridge.*

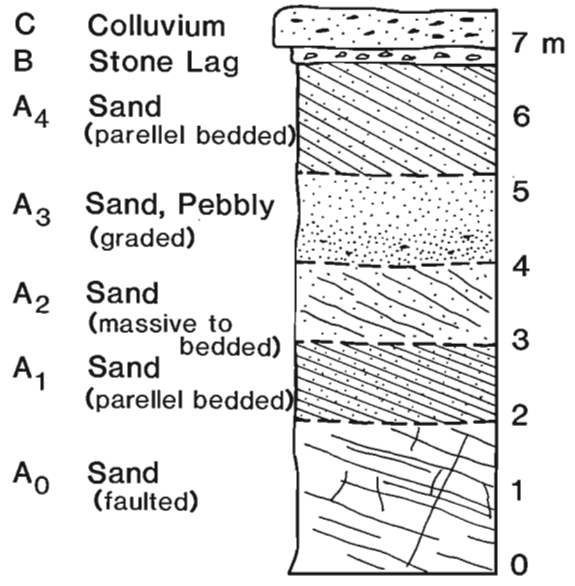

Figure 47.9. *Measured section (115) in fluted landscape.*

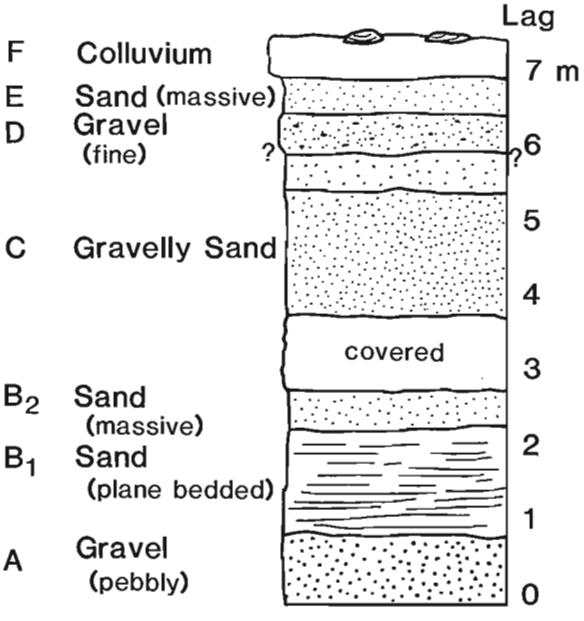

Figure 47.10. *Measured section (118) in fluted landscape.*

sand and gravel and this seems to indicate continuous sedimentation. Few structures occur in the sequence but no deformation is evident in the structures that are present.

Summary and comments

Additional sections were measured within the fluted terrain (sites 110, 111, 115A, 118B, 119, Fig. 47.4). Except for section 110 these sequences, together with 115 and 118, consist almost entirely of sand with pebbles. The sand is massive with conformable and gradational contacts and common graded bedding. There are no or few traction current structures. Thus the most likely depositional environment is one with high rates of sedimentation from suspension. This can explain the occurrence of both graded and massive sand. A mass of sediment flowing by gravity into a subaqueous environment could also form the massive sand. In places (site 110) the sandy facies is interbedded with diamictons that are probably debris flow units. The fact that the above sections have clearly marked colluvial deposits on top rules out the possibility that the lower deposits were emplaced by slope failure.

The interpretation of the sediments exposed in the drumlinoid landscape and the fluted landscape is that they represent mainly aqueous deposition with little erosion or wholesale deformation. Debris units are taken to represent slumping in this subaqueous environment, from the accumulating sediments or directly from the glacier. These descriptions will be compared with the common views on the origin of drumlinized and fluted terrain.

Discussion of streamlined landforms

Current views on the origin of drumlins

Drumlins are commonly described as being composed of basal till, generally lodgment in origin (Smalley and Unwin, 1968; Menzies, 1979; Boulton, 1982). Various mechanisms of deposition have been proposed for a lodgment till including mechanisms of formation initiated by a pre-existing obstacle (Gillberg, 1976), deformation of subglacial material (Smalley and Unwin, 1968; Menzies, 1979), or englacial agglomeration (Gravenor and Meneley, 1958; Evenson, 1971; Shaw and Freschauf, 1973; Aario, 1977). Many of these mechanisms require deposition of debris under high glacially applied stresses. This is said to result in accumulation of massive, dense, thick subglacial till. One key test of these modes of emplacement would be evidence of high shear stress, deformation, flame or load structures, and drag folds (Whittecar and Mickelson, 1979). In the apparent absence of these features other modes of deposition should be explored.

Stratified sediment has been noted as a component of drumlins and is normally explained as a pre-existing sediment that has been overridden (Gravenor, 1953; Lemke, 1958; Goldthwait, 1974). While folding and faulting of some stratified cores (Slater, 1929; Whittecar and Mickelson, 1979) may attest to overriding, many stratified cores are not deformed (DeJong et al., 1982, Fig. 7) and therefore may not have formed in a high stress subglacial environment.

Dardis and McCabe (1983) have studied three sand-cored drumlins in Ireland and they concluded that sediment gravity flows filled subglacial cavities. The sands are undisturbed and they are overlain by various diamictons that appear to have been deposited at the same time as the adjacent sands.

This discussion indicates that drumlins are not necessarily or demonstratively produced by strong glacier flow. In fact, it may be that drumlin sedimentation occurred in stagnating ice where there was no sediment in the upper portions of the ice and where no ice marginal moraines were formed. Thus, a sequence of conformable, nondeformed stratified sediments may have aggraded beneath the glacier in water-eroded and sediment-filled cavities.

The meltwater origin of drumlins

An alternative hypothesis of drumlin formation by meltwater has been proposed by Shaw (1983) based on the analogy between the shape of drumlins and strikingly similar forms created by water erosion called flutes (Allen, 1969, 1971). Erosion marks are considered to form on the underside of glaciers by subglacial meltwaters that ultimately filled in the eroded cavity. An expected sediment sequence would consist of undisturbed stratified beds conformable with the landform. Deposition by water current and/or mass flows would result in interbeddded massive or stratified units and diamictons. These types of features were found in measured sections from a drumlin at Camden East, Ontario (Shaw, 1983). Muller (1974) considered that stratified sediment accumulated as an integral part of drumlin formation deposited within a cavity. Dardis and McCabe (1983) described complex drumlin sediments from Ireland that they consider to have formed in water-filled cavities associated with a major subglacial meltwater escape route. However, Muller concluded that it was difficult to explain the origin of the cavity, whereas Dardis and McCabe (1983) concluded that the sand cores and melt-out till facies were deposited before the drumlins were streamlined. Shaw (1983) has provided a mechanism for subglacial cavity formation and filling. This report discusses sediment sequences that were not deformed by a "streamlining" glacier, but more probably accumulated in place beneath an ice sheet.

The origin of fluted terrain

Hoppe and Schytt (1953) and Boulton (1976) believed that small-scale fluted terrain develops when till intrudes into tunnels that open up in the lee of an obstruction. Boulton considered that all true fluted terrain consists of lodgment till, particularly small-scale fluted forms related to boulder obstructions. Shaw and Freschauf (1973), however, considered that larger fluting formed by the redistribution of subglacial sediment by secondary flow cells. Jones (1982) combined a thrusting and streamlining concept (Moran et al., 1980) and secondary flow cells to explain glacial flutings in Alberta. Paul and Evans (1974) described flutes in stratified sands and considered them to possess bedded inclined structures that indicate upward movement of sediment within the flute.

None of the above features are found in the fluted terrain north of Cambridge Bay, Victoria Island. Here fluted terrain comprises undeformed sandy sediments (massive to graded) that apparently represent continuous sedimentation in a subaqueous environment.

It is speculated that inverted meltwater erosion marks (Shaw, 1983) may explain the Victoria Island fluted terrain by analogy to the water-eroded forms of Allen (1969, 1971). Allen showed experimentally that at lower discharges (than needed to form meandering, flute, or transverse marks), turbulent flow produces longitudinal erosion marks on clay beds. Thus it is possible that subglacial meltwater erosion of the glacier base produced a linear form that is filled with sands to obtain the fluted forms on Victoria Island.

Summary

The observed internal structure of drumlinoid and fluted landforms on Victoria Island does not correspond to the predictions of commonly presented theories on the origin of these forms. These theories hold that both drumlin and fluted forms develop when stress at the base of the glacier exerts enough pressure to deform pre-existing or basal sediment (till or stratified drift) into these streamlined forms. The observed strata on Victoria Island comprise intact, conformable, and interbedded massive sand, stratified sand, and diamictons that form sediment accumulations in subaqueous environments without deformation by high shear stresses. Shaw (1983) has proposed that meltwater-eroded subglacial cavities are probable sites for this deposition.

The implication of the stratified nature of streamlined landforms on Victoria Island is that current mapping techniques may provide misleading results if they do not include sediment descriptions of the landforms. The implication of the potential meltwater origin of streamlined landforms is that the apparent cross-cutting relationship of fields of streamlined landforms on Victoria Island (Fig. 47.1), which are located in depressional areas, may be more readily explained as subglacial drainage events (transverse forms of Allen, 1969) related to stagnating ice. Furthermore, our understanding of the glacial history of Victoria Island, and other similar glaciated areas, may need to be amended to take account of the significance of subglacial meltwater deposition.

Acknowledgments

Field logistics were well managed and supplied by Polar Continental Shelf Project and the DEW Line station at Cambridge Bay. Appreciation is extended to Adlair Aviation for air services and Terry Snelgrove and Wanda Sheldrick for helpful field assistance. I thank D.A. Hodgson, D.A. St-Onge and J. Shaw for their helpful comments on this paper.

References

Aario, R.
1977: Classification and terminology of morainic landforms in Finland; Boreas, v. 6, p. 87-100.

Allen, J.R.L.
1969: Erosional current marks of weakly cohesive mud beds; Journal of Sedimentology, v. 39, no. 2, p. 607-623.

1971: Transverse erosional marks of mud and rock: their physical basis and geological significance; Sedimentary Geology, v. 5, Special Issue No. 3-4, p. 167-385.

Boulton, G.S.
1976: The origin of glacially fluted surfaces – observations and theory; Journal of Glaciology, v. 17, no. 76, p. 287-309.

1982: Subglacial processes and the development of glacial bedforms; in Research in glacial, glaciofluvial and glaciolacustrine systems, ed. R. Davidson-Arnott, W. Nickling, and D.B. Fahey; Proceedings of the 6th Guelph Symposium on Geomorphology, 1980, Geo Books, Norwich, p. 1-33.

Dardis, G.F. and McCabe, A.R.
1983: Facies of subglacial channel sedimentation in late-Pleistocene drumlins, northern Ireland; Boreas, v. 12, p. 263-278.

De Jong, M.G.G., Rappol, M., and Rupke, J.
1982: Sedimentology and geomorphology of drumlins in western Algara, south Germany; Boreas, v. 11, p. 37-45.

Evenson, E.B.
1971: The relationship of macro- and micro-fabrics in till and the genesis of glacial landforms in Jefferson County, Wisconsin; in Till: A Symposium, ed. R.P. Goldthwait; Ohio State University Press, p. 345-364.

Gillberg, G.
1976: Drumlins in southern Sweden; Bulletin of the Geological Institutions of the University of Uppsala, New Series, v. 6, p. 125-189.

Goldthwait, R.P.
1974: Rates of formation of glacial features in Glacier Bay, Alaska; in Glacial Geomorphology, ed. D.R. Coates; State University of New York, Binghampton, New York, p. 163-185.

Gravenor, C.P.
1953: The origin of drumlins; American Journal of Science, v. 251, no. 9, p. 614-684.

Gravenor, C.P. and Meneley, W.A.
1958: Glacial fluting in central and northern Alberta; American Journal of Science, v. 256, no. 10, p. 715-728.

Hoppe, G. and Schytt, V.
1953: Some observations on fluted moraines surfaces; Geografiska Annaler, v. 35, no. 2, p. 105-115.

Jones, N.
1982: The formation of glacial flutings in east central Alberta; in Research in Glacial, Glaciofluvial and Glaciolacustrine Systems, ed. R. Davidson-Arnott, W. Nickling, and B.D. Fahey; Proceedings of the 6th Guelph Symposium on Geomorphology, 1980, Geo Books, Norwich, p. 49-70.

Lemke, R.W.
1958: Narrow linear drumlins near Velva, North Dakota; American Journal of Science, v. 256, no. 4, p. 270-283.

Menzies, J.
1979: A review of the literature on the formation and location of drumlins; Earth Science Reviews, v. 14, no. 4, p. 315-359.

Moran, S.R., Clayton, L., Hooke, R.L., Fenton, M.M., and Andriashek, L.D.
1980: Glacier-bed landforms of the Prairie Region of North America, Journal of Glaciology, v. 25, no. 93, p. 457-476.

Muller, E.H.
1974: Origin of drumlins; in Glacial Geomorphology, ed. D.R. Coates; State University of New York, Binghampton, New York, p. 187-209.

Paul, M.A. and Evans, H.
1974: Observations on the internal structure and origin of some flutes in glaciofluvial sediments, Blomstrandbreen northwest Spitsbergen; Journal of Glaciology, v. 13, no. 69, p. 393-400.

Sharpe, D.R.
1984: Late Wisconsinan glaciation and deglaciation of Wollaston Peninsula, Victoria Island, Northwest Territories; in Current Research, Part A, Geological Survey of Canada, Paper 84-1A, p. 259-269.

Shaw, J.
1983: Drumlin formation related to inverted melt-water erosional marks; Journal of Glaciology, v. 29, no. 103, p. 461-479.

Shaw, J. and Freschauf, R.C.
1973: A kinematic discussion of the formation of glacial flutings; Canadian Geographer, v. 17, p. 19-35.

Slater, G.
1929: Structure of drumlins on southern shore of Lake Ontario; New York State Bulletin of the New York State Museum, no. 281, p. 3-19.

Smalley, I.J. and Unwin, D.J.
1968: The formation and shape of drumlins and their distribution and orientation in drumlin fields; Journal of Glaciology, v. 7, no. 51, p. 377-390.

Whittecar, G.R. and Mickelson, D.M.
1979: Composition, internal structures and an hypothesis of formation for drumlins, Waukesha County, Wisconsin, U.S.A.; Journal of Glaciology, v. 22, no. 87, p. 357-371.

GEOLOGY OF THE RIVIÈRE GRANDIN MAP AREA (HOTTAH TERRANE AND WESTERN GREAT BEAR MAGMATIC ZONE), DISTRICT OF MACKENZIE

Project 820009

R.S. Hildebrand and C.F. Roots[1]
Precambrian Geology Division

Hildebrand, R.S. and Roots, C.F., Geology of the Rivière Grandin map area (Hottah Terrane and western Great Bear Magmatic Zone), District of Mackenzie; in Current Research, Part A, Geological Survey of Canada, Paper 85-1A, p. 373-383, 1985.

Abstract

Hottah Terrane comprises deformed metasedimentary and metavolcanic rocks cut by two distinct suites of plutons: a deformed suite of intermediate bodies (1.914-1.9 Ga) and a suite of undeformed leucogranites (1.9-1.875 Ga). Sedimentary and volcanic rocks of the Bell Island Group, a basal unit of the Great Bear Magmatic Zone, unconformably overlie rocks of Hottah Terrane and are intruded by swarms of granitoid plutons and porphyries. One of the plutons, the Yen, has large areas of associated intrusion breccias of problematic origin. Both Hottah Terrane and Great Bear Magmatic Zone are cut by swarms of transcurrent faults. At least two of the faults had a component of vertical extension, as indicated by the existence of associated thrust faults similar to positive flower structures found in other wrench zones. The recognition of a deformed arc-like plutonic suite generated between 1.914-1.9 Ga in the Hottah Terrane supports the interpretation that Coronation Margin developed in a back-arc setting.

Résumé

Le terrain de Hottah se compose de roches métasédimentaires et métavolcaniques déformées que traversent deux suites distinctes de plutons: une suite déformée de massifs intermédiaires (1,914 à 1,9 Ga) et une suite de leucogranites non déformés (1,9 à 1,875 Ga). Les roches sédimentaires et volcaniques du groupe de Bell Island, unité basale de la zone magmatique de Great Bear, reposent en discordance sur des roches du terrain de Hottah et sont traversées par des essaims de plutons granitoïdes et de porphyres. Un des plutons, le Yen, comporte de vastes étendues de brèches d'intrusion dont l'origine est énigmatique. Le terrain de Hottah et la zone magmatique de Great Bear sont tous deux traversés par des essaims de décrochements. Au moins deux de ces failles avaient une composante d'extension verticale, ainsi qu' en témoigne la présence de failles de chevauchement semblables aux structures << en fleurs>> positives observées dans d'autres zones de décrochements à rejet vertical. On a reconnu, dans le terrain de Hottah, la présence d'une suite plutonique déformée en arc qui aurait été produite entre 1,914 et 1,9 Ga; cette observation appuie l'interprétation selon laquelle la formation de la marge du Couronnement aurait eu lieu à l'arrière d'un arc.

[1] Department of Geology, Carleton University, Ottawa, Ontario, K1S 5B6

Introduction

Detailed geological mapping of the early Proterozoic rocks occurring in the Rivière Grandin map area (86 D) was completed during the summer of 1984. This mapping is part of a continuing project in western Wopmay Orogen to understand the geology and tectonic significance of Hottah Terrane as well as the western part of the Great Bear Magmatic Zone in map areas 86 D and 86 E (Hildebrand et al., 1983, 1984; see Fig. 48.1).

The first geological examination of the area was that of Kidd (1936) who mapped a strip from Great Bear Lake to Great Slave Lake. Later, a detailed study of Beaverlodge Ridge by Henderson (1949) focused on low tonnage uranium showings found there in the early 1930s. More recently, McGlynn (1979) mapped the areas in reconnaissance fashion and was the first to recognize a complex of tectonized metamorphic rocks (Hottah Terrane of Hildebrand, 1981) unconformably beneath rocks of the Great Bear Magmatic Zone. Hildebrand et al. (1983) suggested, on the basis of geochronological and geological data collected during 1982, that Hottah Terrane is exotic with respect to Coronation Margin (eastern Wopmay Orogen) and was accreted to it between about 1.9 and 1.89 Ga. This paper reports the results of 1:50 000 scale mapping of those parts of the Rivière Grandin map area not mapped during 1982 and presents a revised tectonic model for the evolution of Wopmay Orogen.

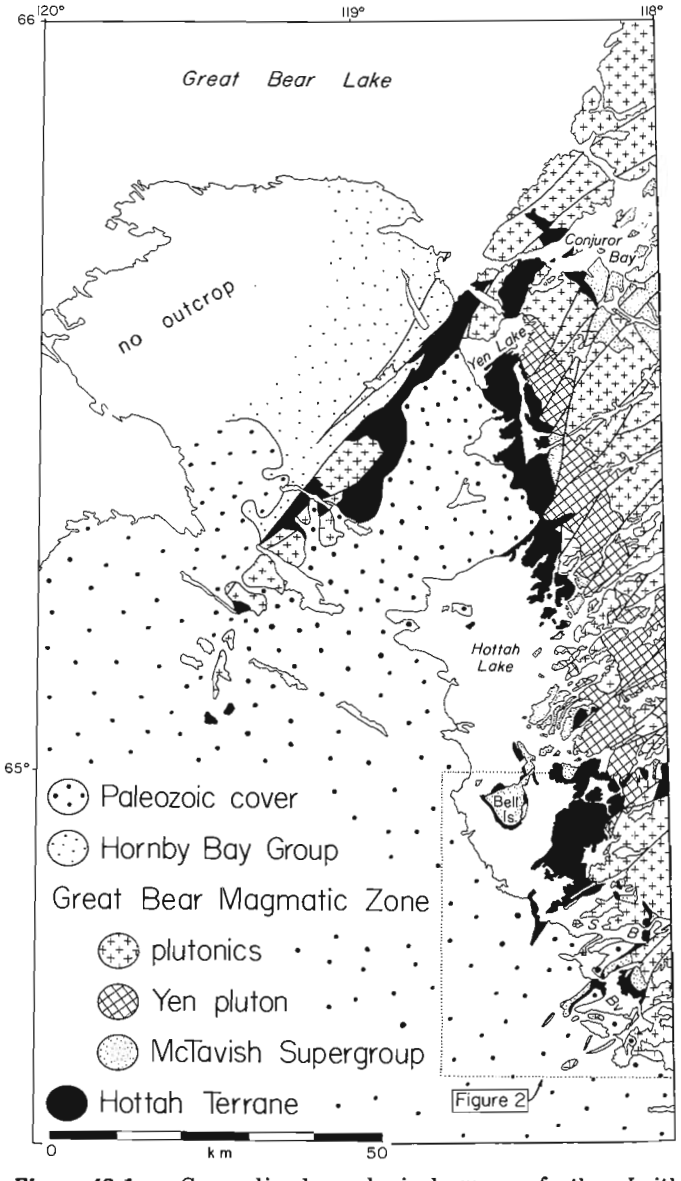

Figure 48.1. *Generalized geological map of the Leith Peninsula (86E) and the north half of the Rivière Grandin (86D) map areas showing distribution of Hottah Terrane, McTavish Supergroup, and Great Bear plutonic rocks. SB = Stairs Bay; Bv = Beaverlodge Lake.*

Acknowledgments

We would like to thank Dianne Paul and Andrew Muirhead for their cheerful, pleasant, and able assistance; Martin Irving (GSC) and Craig Robinson (DIAND) for their superb job of expediting; and Mike Hogan (Latham Island Airways) for careful air support. Peter Lipman and Roy Bailey, both of the USGS, spent a week with us in the field and provided stimulating discussions on the outcrop. As usual, R. Tirrul and S. Hanmer contributed greatly to our understanding of various aspects of structural geology. Many of the ideas related to the back-arc setting of Coronation Margin originated during discussion with P.F. Hoffman. I.G. Reichenbach and P.F. Hoffman critically read the manuscript and suggested many ways to improve it.

Hottah Terrane

In the map area, rocks of the Hottah Terrane can be divided into 3 main groups, based on lithology and degree of deformation. The oldest rocks are deformed metasedimentary and metavolcanic rocks. They are intruded by a suite of tectonized plutons, mainly intermediate in composition. Both the tectonized plutons and the supracrustal rocks are cut by a number of undeformed leucocratic granites.

Supracrustal rocks (Holly Lake metamorphic suite)

Rocks included under this heading are psammites, pelitic schists, probable volcaniclastic rocks, minor hematite beds, and mafic to intermediate lava flows. They are metamorphosed to assemblages typical of the amphibolite facies and sedimentary bedding is in many places completely transposed. Metasedimentary rocks are commonly cut by sheets of fine- to medium-grained leucocratic syenogranite.

The lava flows mapped this year occur east of Hottah Lake (Fig. 48.2) and are mostly fine grained dark rocks, probably andesite, containing 10-30% plagioclase phenocrysts up to 1.5 cm (Fig. 48.3) and quartz amygdules up to 5 mm. The groundmass is now recrystallized to mixtures of quartz, biotite, plagioclase, and amphibole(?). The flows are variably strained and in places there is no visible deformation. In other areas plagioclase phenocrysts are strongly lineated, measuring 2 x 10 mm in cross-section and several centimetres long, or only slightly stretched but strongly flattened.

Deformed plutonic rocks

Large expanses of exposed Hottah Terrane are composed of deformed granitoid plutons of mainly dioritic, quartz dioritic, granodioritic, and monzogranitic composition (McGlynn, 1979; Hildebrand et al., 1983; 1984). Hornblende or biotite + hornblende generally constitute the ferromagnesian assemblage. U-Pb ages from zircons in these bodies range from 1.914-1.90 Ga (Hildebrand et al., 1983; Bowring, in prep.).

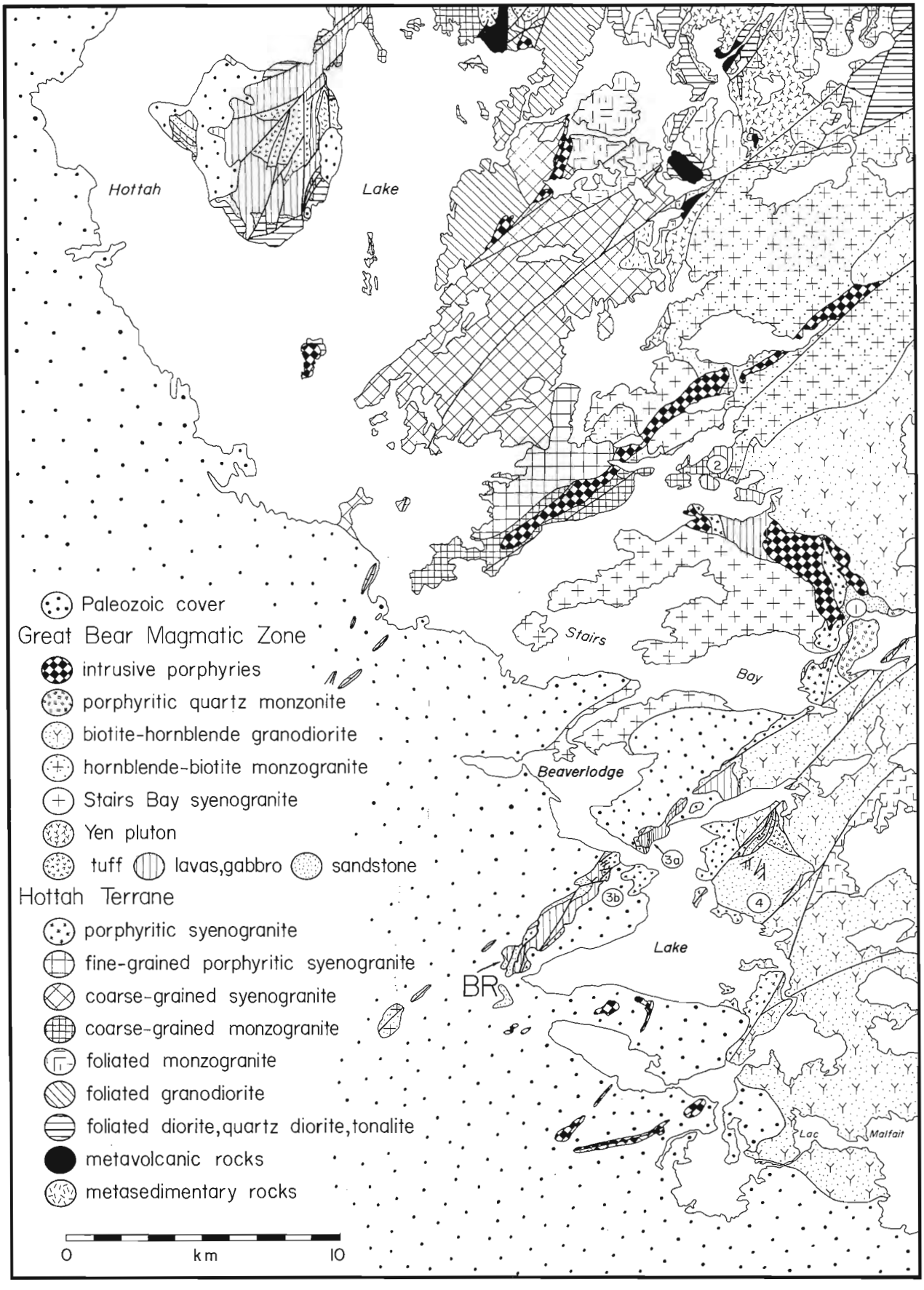

Figure 48.2. *Generalized geological map of the northeast corner of the Rivière Grandin map area. Numbers in ellipses refer to localities discussed in text. Beaverlodge Ridge is a prominent ridge that extends from BR in a northeasterly direction to the southeast corner of Stairs Bay.*

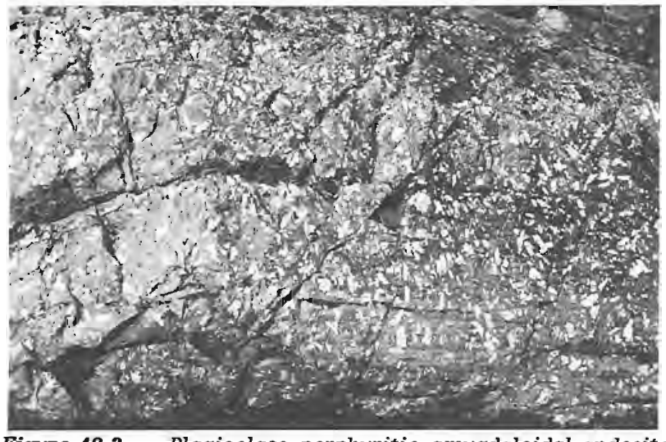

Figure 48.3. *Plagioclase porphyritic amygdaloidal andesite of the Hottah Terrane. Penny in centre for scale. (GSC 204113-A)*

During the past field season, several small plutons of deformed hornblende diorite, quartz diorite, and tonalite were mapped east of Hottah Lake (Fig. 48.2). Penetrative deformation ranges from slight to intense, but overall, quartz-bearing rocks are more deformed (Fig. 48.4). Intrusive relations between bodies are sufficiently complex that maps at 1:16 000 scale fail to portray them accurately.

The overall intermediate nature of the entire suite of deformed plutons mapped in Hottah Terrane during the current project is very similar to plutonic suites characteristic of continental margin arcs in younger terranes, as well as in the Great Bear Magmatic Zone. This suggests that Hottah Terrane may represent a 1.914-1.9 Ga magmatic arc.

Undeformed plutonic rocks

Several plutons of relatively undeformed granitic rock considered to belong to Hottah Terrane were mapped in the Stairs Bay-Beaverlodge Lake area. We have used several criteria in order to differentiate undeformed plutons of the Hottah Terrane from those of Great Bear Magmatic zone: (1) several bodies lie unconformably beneath rocks of the Bell Island Group; (2) they are cut by numerous glomeroporphyritic diabase and gabbro dykes identical to sills related to volcanism in the Bell Island Group (see Hildebrand et al., 1983); (3) the original ferromagnesian minerals are often recrystallized to clots of tiny biotite and/or chlorite flakes; (4) in places they have suffered severe cataclastic deformation; (5) they are often extremely leucocratic (<5% ferromagnesian minerals); and (6) they may contain blue quartz, a feature which we have not noticed in Great Bear granites. In general, most bodies show two or more of the above features.

A large body of medium grained chlorite syenogranite to alkali-feldspar granite lies unconformably beneath sandstone northeast of Stairs Bay and on Beaverlodge Ridge (Fig. 48.2). The body is variably porphyritic (20-40%) with spherical phenocrysts or snowflake clots of potassium feldspar to 3 cm in a groundmass of anhedral blue quartz (2-3 mm), anhedral-subhedral plagioclase (3 mm), potassium feldspar and 10-20% chlorite. In many places, most notably at the northeast end of Stairs Bay, the rock has suffered severe cataclasis. The granite is riddled with brittle fractures and potassium feldspar phenocrysts were crushed into tiny angular chips, which are in a dark chloritic matrix.

Another body, one of the largest plutons mapped in Hottah Terrane, occurs northwest of Stairs Bay. It is a medium- to coarse-grained leucocratic syenogranite that generally contains less than 5% mafic minerals, mostly chlorite. Anhedral grey quartz ranges from 1-4 mm and plagioclase is subhedral (<2 mm). The pluton weathers various shades of white, pink and red.

A smaller pluton of fine grained porphyritic syenogranite cuts the above pluton along its southern margin at the west end of Stairs Bay. It contains subhedral-euhedral potassium feldspar phenocrysts (1-5 cm long) and anhedral-subhedral blue quartz (3-5 mm) sitting in a much finer grained groundmass of anhedral plagioclase, quartz, potassium feldspar, and tiny biotite flakes. The pluton is cut by numerous diabase dykes.

Coarse grained monzogranite outcrops along the east side of the above body. The age relationship with its western neighbour is unknown as the contact was not seen due to poor outcrop. The pluton is characterized by its coarse grained, non-porphyritic, leucocratic nature. It is similar to leucocratic monzogranite mapped directly beneath the Hottah Great Bear unconformity on eastern Bell Island (Hildebrand et al., 1983).

The leucocratic plutons clearly postdate ductile deformation in Hottah Terrane and are, in several instances, unconformably overlain by rocks of the Great Bear Magmatic Zone. Thus, their age of emplacement is constrained by the youngest deformed pluton in Hottah Terrane (1.90 Ga) and the oldest dated rock in Great Bear Magmatic Zone (1.875 Ga). We suggest that the granites of the leucocratic suite were generated during collision of Hottah Terrane with Coronation Margin. If true, their U-Pb ages should fall close to 1.88 Ga, the approximate age of post-tectonic plutons in Hepburn batholith (Hoffman and Bowring, 1984; Bowring, in prep.).

Great Bear magmatic zone

McTavish Supergroup

At locale 1 (Fig. 48.2) the unconformity between rocks of the Great Bear Magmatic Zone and Hottah Terrane is well exposed. There, crossbedded cobbly to granular arkose fills paleovalleys cut into granitoid rocks. The best exposed paleovalley has a steep scarp, interpreted as an east side down normal fault and preserved as a buttress unconformity about 15 m high along its western margin. In the lowest part of the paleovalley a thin (<1 m) conglomerate containing subrounded to subangular clasts of granite and quartz porphyry overlies a relatively low relief surface of bleached

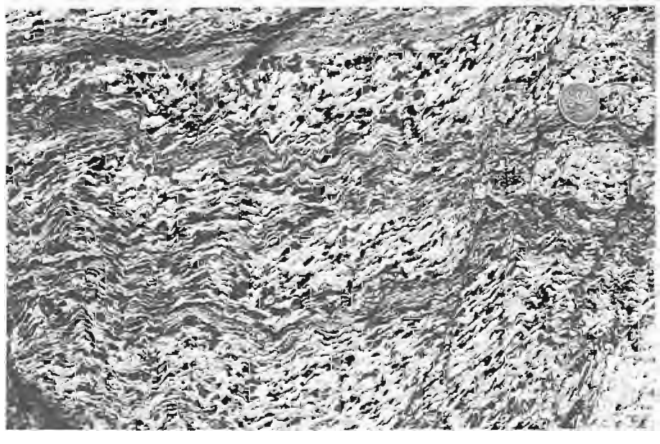

Figure 48.4. *Deformed hornblende quartz diorite of the Hottah Terrane. (GSC 204112-E)*

and altered granite. The rest of the paleovalley is filled with crossbedded granular to pebbly arkose, except adjacent to the scarp where angular blocks of granite up to 4 m across were found in the arkose. Apparently, the blocks spalled from the steep escarpment during sedimentation. The arkose occurs only within the paleovalleys and out of them the granite is overlain, as is the arkose within them, by 30-40 m of crossbedded and rippled quartz arenite in beds varying in thickness up to 1 m. The quartz arenite is, in turn, overlain by thinly bedded to laminated tuff, siltstone, and mudstone. The total thickness of these units is unknown due to cover and younger plutons, but 50 m are exposed. The tuffs are white to pink fine grained beds up to 0.3 m thick. They are interpreted as waterlain airfall tuff because they are intercalated with siltstone and mudstone. In general, the siltstones are well-layered rocks with interbedded 1-3 mm greenish, fine sandy layers and 2 cm limy beds. In some places there are abundant slump folds and synsedimentary breccias.

Amygdaloidal basalt directly overlies intensely weathered granite at locale 2 (Fig. 48.2). The buried erosional surface has up to 1 m of relief and the granite is hematized and more strongly weathered in hollows. The lowermost basalt flow has a 0.5 m thick basal flow breccia containing sparse elongate granite clasts. Locally, basaltic magma flowed down into v-shaped open fractures within the uppermost 0.3 m of basement. The basalt flows are cut by abundant gabbro intrusions, probably sills. Overlying the basalt flows is a complex of siliceous ash-flow tuff and lava. The lava flows have abundant associated flow and talus breccias and the ash-flow tuff is strongly eutaxitic with lineated pumice fragments and minor flow folds.

At location 3a (Fig. 48.2) at least 50 m of well bedded sandstone unconformably overlies granite of the Hottah Terrane, but a complete section is not present due to complex faulting. The granite is generally altered and bleached such that few ferromagnesian minerals remain unaltered. The unconformity itself is generally planar with only minor local relief. The overlying sandstone is mostly fine to coarse quartz arenite with sparse granules and pebbles of vein quartz. Bedding ranges in thickness from 1 or 2 cm to about 2 m. Some bedding surfaces are rippled and many beds are internally crossbedded. Interbedded with the sandstone are discontinuous lenses of laminated, greenish-weathering tuff and minor beds of siltstone and mudstone. The sedimentary section is overlain by stubby quartz-phyric dacite lava flows with well developed basal breccias and locally by thin basalt flows. In some areas there is a thin volcanic cobbly conglomerate between the sandstones and lavas. This section is cut by gabbro sills and intermediate porphyry bodies that, in some cases, are similar in modal mineralogy to the dacite lavas.

Examination of the unconformity at 3b (Fig. 48.2) reveals only minor pebbly sandstone and conglomerate, such that intermediate lavas lie, for the most part, directly on granitic basement. The pebbly sandstone fills local depressions up to 1 m deep and is a massive unsorted rock that weathers maroon to dark purple. The lava flows are probably dacitic and weather various shades of purple, steel grey, and brown. They are generally amygdaloidal and in places have well developed devitrification features and flow banding. Intercalated with the dacites are thin aphyric basalt(?) flows. These flows are generally amygdaloidal and weather shades of blue-grey. At the south end of Beaverlodge Ridge minor lenses of sandstone and conglomerate are intercalated with the lava flows. The conglomerates are polymictic aggregates of volcanic and sedimentary clasts, mostly subrounded, in a sandy hematitic matrix. The sandstones vary from quartz arenites to feldspathic wackes. Overlying the sequence of lava flows are thin tuff beds of unknown composition and provenance. Locally, polymictic bouldery conglomerate and gritstone fills channels cut into the tuff and underlying lava flows. Capping the entire section is at least 60 m of white to pink weathering arkose and quartz arenite. The top of the sandstone is not exposed. The sandstones are well bedded rocks in beds up to 1 m thick. In the few places where there are bands of heavy minerals crossbedding is seen, but in most outcrops there was no visible internal stratification, perhaps because the sands are very clean and there is little size variation among grains.

The unconformity at location 4 (Fig. 48.2) is only locally well exposed; where quartz arenite and arkosic conglomerate overlie an irregular surface eroded into quartz-potassium feldspar porphyry. Angular to subangular clasts of the porphyry, ranging up to 70 cm across, occur in the sandstone within a metre or so of the unconformity. In addition, a few pebbles of jasper, vein quartz, and fine grained plagioclase porphyritic lava were found. The overlying sandstones are mostly fine-to medium-grained, light-coloured rocks with minor quartz pebbly lenses. Near the top of the sandstone section, beds of fine grained, crossbedded, red to brown weathering lithic arkose occur. The sandstones are overlain by a succession of welded tuffs with locally well developed eutaxitic foliation. They are mostly intermediate in composition and contain broken phenocrysts of plagioclase, alkali feldspar and quartz, as well as tiny lithic fragments, in a dark green to grey groundmass. The top of the section is not exposed as it is intruded by a younger granodiorite-monzogranite pluton. Both the sandstone and the tuffs are intruded by myriads of hornblende-plagioclase porphyry dykes and sills.

Additional exposures of the unconformity and overlying basal sandstone were found east of Hottah Lake. Most of those exposures are large pendants or enclaves in younger granitoid plutons of the Great Bear Zone. In general, only a few metres of sandstone are exposed and they are arkosic, similar to outcrops of the basal sandstone found elsewhere. The overlying lava flows are not present due to the intrusion of Great Bear plutons.

All of the above sections are similar to those described by Hildebrand et al. (1983) on Bell Island and to the north. They are all characterized by a basal sandstone or conglomerate above the Hottah unconformity and are in turn overlain by a wide variety of mafic to intermediate lava flows and ash-flow tuff. Therefore, the supracrustal rocks described above are included in the Bell Island Group of Hildebrand et al. (1984).

Great Bear plutons

Several large plutons compositionally and texturally typical of those found elsewhere in the Great Bear Magmatic Zone were mapped during the field season (Fig. 48.2). We provide descriptions for only two of the more interesting bodies, the Yen pluton and the Stairs Bay syenogranite.

Yen pluton. This pluton is the largest magmatic body mapped during the current project. It extends from Yen Lake southward to just north of Stairs Bay (Fig. 48.1), a distance of about 60 km. Because it is intruded by younger granite plutons its original extent is unknown, but presumably it was even larger. The pluton was informally called the Zebulon pluton by Hildebrand et al. (1983) but subsequent mapping has demonstrated that it is continuous with a pluton that Hildebrand (1983) named the Yen pluton after its occurrence east of Yen Lake. Because the name Yen pluton has precedence, the term Zebulon is abandoned and the entire mass is now referred to as the Yen pluton.

Throughout most of its area of outcrop, the Yen pluton is a homogeneous body of medium grained biotite-hornblende granodiorite to monzogranite with ferromagnesium content varying between 10 and 25%. Characteristic of the pluton is the presence of euhedral prisms of hornblende up to 1 cm long. Biotite is mostly fresh, forms plates up to 5 mm across, and often occurs as clots or aggregates up to 1 cm in diameter. Plagioclase is slightly greenish on the fresh surface, subhedral to euhedral, and ranges up to 8 mm long. Quartz and potassium feldspar are mostly interstitial. However, in some areas potassium feldspar phenocrysts up to 2 cm long occur, but they never constitute a large enough percentage to shift the modal composition into the syenogranite field.

The contact of the pluton with its wall rocks is very irregular and there is a narrow metamorphic aureole of hornblende hornfels developed in the country rocks. In places adjacent to the outer contacts the hornblende crystals define a lineation, but it is not consistent, even over a single outcrop. It probably originated during convective flow within the magma body and the variability of the lineation may reflect turbulent eddies adjacent to the chilled marginal zone. Occurring locally at the contact are discontinuous layers, 1-10 cm thick, of variable composition (Fig. 48.5). They are more or less parallel to the margin and truncations by successive layers are common. Another characteristic feature of the margin of the Yen pluton is the occurrence of zones of intrusion breccia that range up to 1 km wide. Figure 48.6 depicts somewhat typical relationships found along much of the western margin of the pluton, where there are large areas of intrusion breccia. Continuous north-south strips, or zones, of breccia are made up of blocks of similar rock type, such as schist or diorite, with little or no rotation of individual enclaves. That is, the foliation varies little in direction from block to block, yet in the two-dimensional view seen on the outcrops each block is surrounded by granodiorite. In general, diorite and quartz diorite enclaves are angular (Fig. 48.7), while schist enclaves are elongate and irregular in shape (Fig. 48.8). Where the pluton intrudes older gabbro, veins of granodiorite fill fractures, and enclaves occur only immediately next to the contact (Fig. 48.9). Large tongues of granodiorite with sparse, partly digested xenoliths, intrude the zones of intrusion breccia (Fig. 48.6). They probably represent pulses of magma that migrated upwards after the intrusion breccias had formed. Similar features, but on a smaller scale, are seen where younger granites intrude the Yen. Figure 48.10 shows a large enclave of Yen granodiorite veined by aplite and included in a younger granite. Close inspection (Fig. 48.11) shows that the younger granite cuts the aplites. This suggests that either



Figure 48.5. *Discontinuous compositional banding in marginal facies of Yen pluton. Pen in upper right for scale. (GSC 204112-P)*

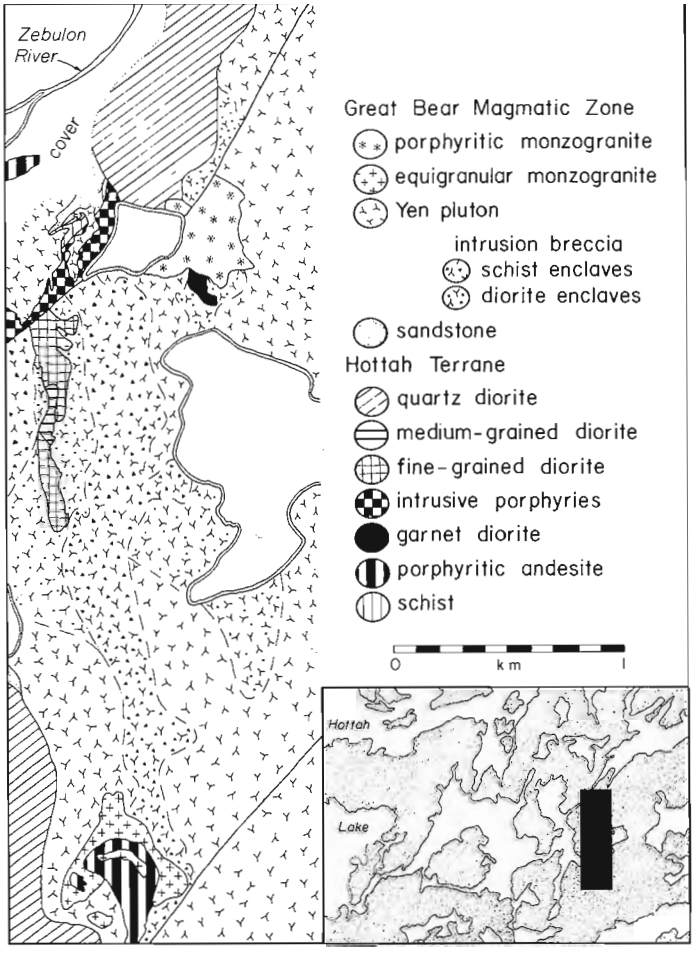

Figure 48.6. *Geological sketch map of part of the west margin of the Yen pluton showing distribution of intrusion breccias and "ghost stratigraphy".*

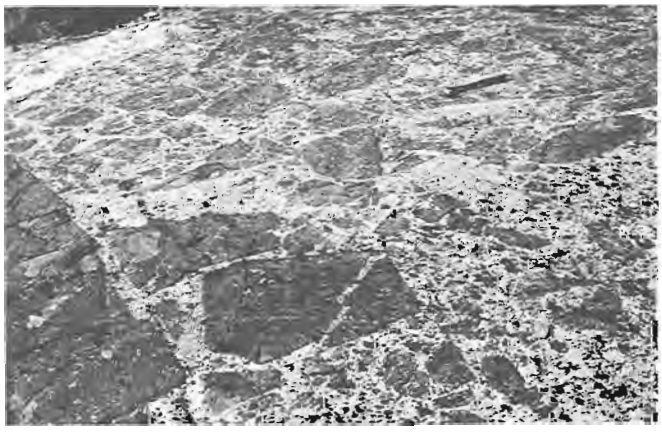

Figure 48.7. *Intrusion breccia of diorite blocks in granodiorite near margin of Yen pluton. (GSC 204112-H)*

the aplites and the younger granite are unrelated or that the aplites represent an earlier pulse of magma from the same body as the younger granite. Because aplites are not known to cut the Yen, except where it is in contact with younger granitoid bodies, the second possibility is favoured.

Where the Yen pluton intrudes quartz arenite, the sandstone is disaggregated and individual grains of quartz are included in the granodiorite. The net effect is to make the granodiorite in the immediate vicinity richer in quartz.

Where the pluton cuts other rock types, xenoliths become smaller, more irregular and more diffuse away from the contact. Ultimately, the xenoliths either sink or are completely digested and the only evidence of their former existence are small clots of biotite.

The above evidence suggests that the Yen pluton intruded, at least in its final stages, by block stoping. Inclusion of different rock types may affect the chemical, and hence modal, composition of the pluton, but without knowing the composition of the original magma we are unable to evaluate the changes quantitatively.



Figure 48.8. *Intrusion breccia of schist blocks in granodiorite near margin of Yen pluton. Compare the shape of these blocks with those in Figure 48.7. (GSC 204112-L)*

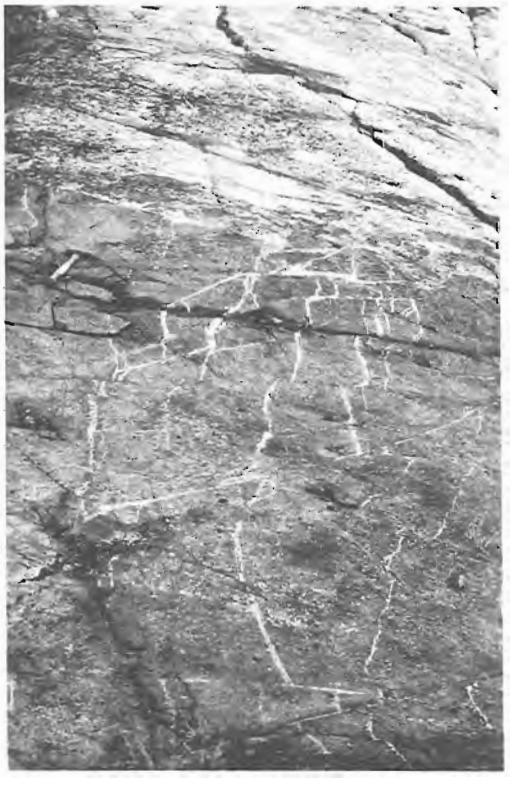

Figure 48.9. *Yen granodiorite intruding Great Pear gabbro. (GSC 204112-D)*



Figure 48.10. *Large block of Yen granodiorite in younger monzogranite. Pen in centre for scale. (GSC 204112-F)*

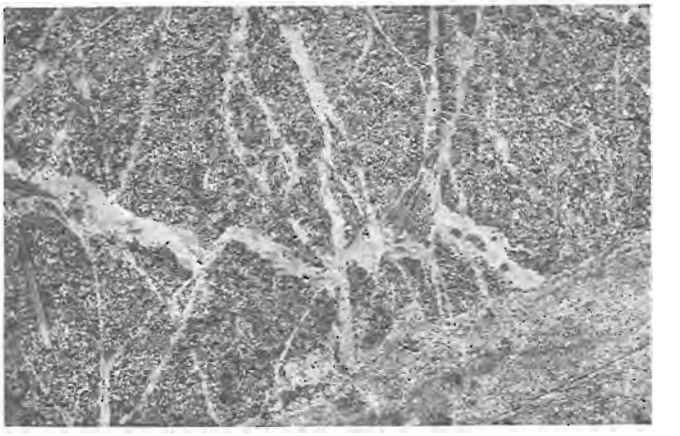

Figure 48.11. *Detailed view of contact between Yen granodiorite (top) and younger monzogranite (bottom right). Note that the monzogranite intrudes the aplite veins in the granodiorite. (GSC 204113-D)*

Stairs Bay syenogranite. This pluton (Fig. 48.2) is a massive porphyritic biotite syenogranite. Phenocrysts of potassium feldspar are 1-3 cm long and are subhedral to euhedral. Subhedral crystals of plagioclase range up to 1.5 cm. Both feldspars occur in a fine- to medium-grained matrix of anhedral quartz, feldspar and tiny flakes of biotite. The pluton is cut by swarms of even finer grained porphyritic and nonporphyritic granite bodies. They are probably derived from the same magma body as the Stairs Bay since they only occur within the pluton and are cut by and cut the main body of granite. The outer contact of the pluton is well exposed northeast of Stairs Bay where it dips shallowly beneath Hottah Terrane granite (Fig. 48.12). The contact is razor sharp, very irregular in detail, and has a 1-3 cm thick border phase of very fine grained granite. Inward from this zone there are several metres of quartz-plagioclase-potassium feldspar porphyry with potassium feldspar phenocrysts to 2 cm. This zone contains abundant miarolitic cavities, 10-15 cm across, filled with pegmatitic quartz and potassium feldspar. Most are mineralogically zoned with quartz cores, as are numerous pegmatitic stringers which occur in the more interior parts of the pluton.

Intrusive porphyries

Two northeast-trending porphyries were mapped east of Hottah Lake. They are generally pink-weathering bodies, except at their margins where they weather red. The border



Figure 48.12 *(opposite). Shallowly dipping contact between Stairs Bay syenogranite (bottom) and porphyritic granite of the Hottah Terrane. (GSC 204112-O)*

Figure 48.13 *(below). (a) Geological sketch map showing the geology of the southwestern corner of Beaverlodge Ridge; (b) Geological sketch map illustrating the geology of the thrust faults at the southwestern end of (a), numbers in ellipses refer to individual tectonic slices discussed in the text; (c) schematic stratigraphic sections in the various slices.*

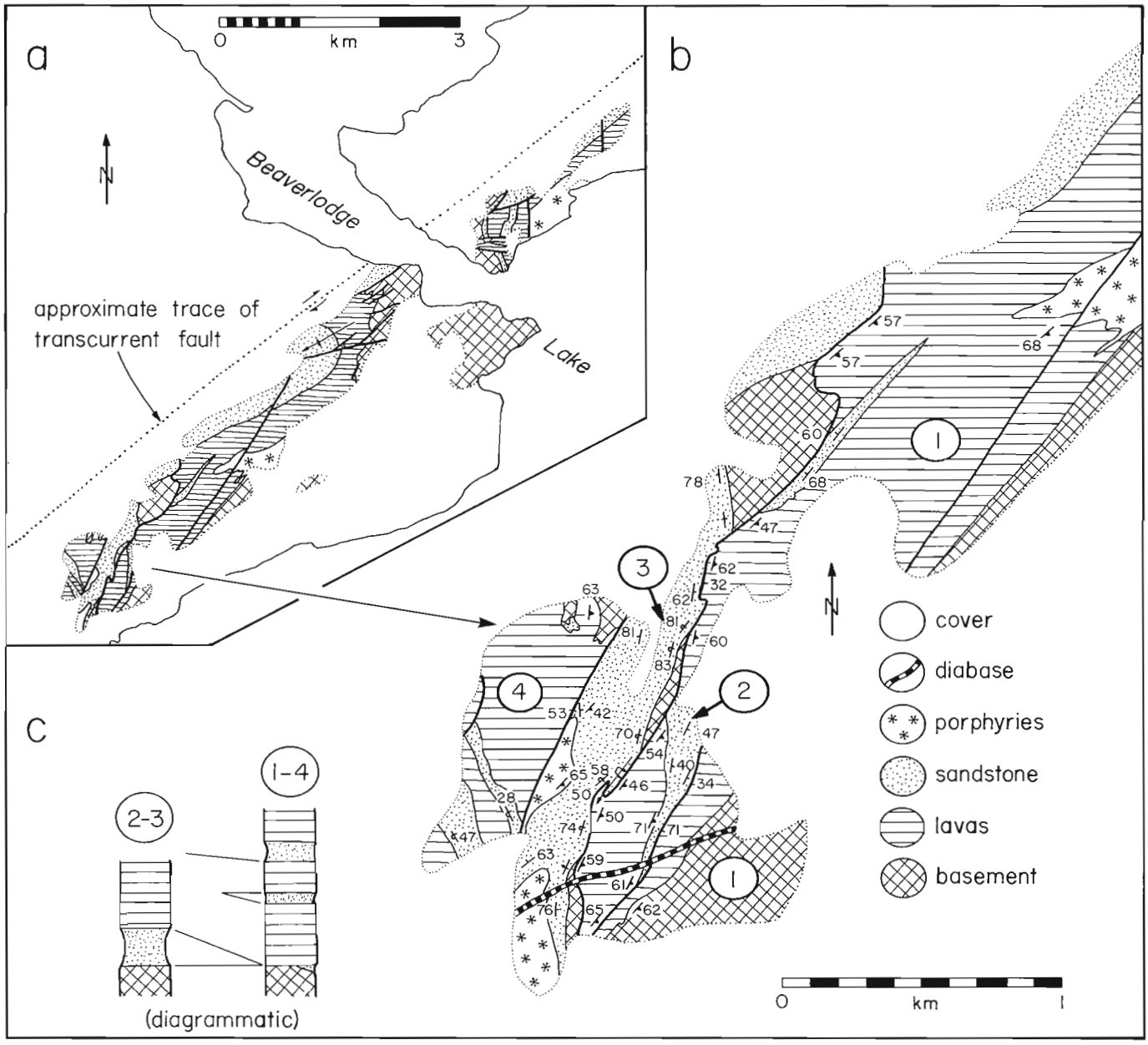

phase comprises about 10% anhedral-subhedral phenocrysts of quartz (1 mm) in a dark red aphanitic matrix that is locally flow-banded. The cores of the bodies contain up to 20% clear, greyish quartz phenocrysts ranging from 2-4 cm across, 5-30% subhedral to euhedral potassium feldspar crystals (2-5 mm), and less than 5% greenish subhedral plagioclase phenocrysts up to 3 mm long.

Two more porphyry bodies occur northeast of Stairs Bay where they intrude Hottah Terrane syenogranite, Great Bear volcanic and sedimentary rocks, and the Stairs Bay syenogranite. Age relations between the two bodies are unknown. In general, the porphyries weather grey or brown and contain mostly anhedral quartz (1-3 mm) and subhedral plagioclase (3 mm) phenocrysts in a dark aphanitic matrix. In places the eastern body also contains phenocrysts of hornblende and potassium feldspar.

Various small porphyry bodies cut volcanic and sedimentary rocks on Beaverlodge Ridge. They generally weather orange-red or green unless they are altered when they weather white. Total phenocryst abundance reaches 30-35%. The phenocrysts are mostly subhedral to euhedral laths of plagioclase (3 mm), in places flow-aligned, 1 mm prisms of amphibole, tiny clots of biotite, resorped subhedral potassium feldspar, and blue-grey to purple anhedral quartz phenocrysts.

Many other porphyries, mainly dykes and sills too small to show on the map, occur throughout the area. They are most common east of the southern half of Beaverlodge Lake, where they range from hornblende-plagioclase to quartz-potassium feldspar-plagioclase porphyritic.

Structure

Normal faults. Numerous normal faults that cut the oldest rocks of the Great Bear Magmatic Zone were mapped during the field season. The faults do not, for the most part, cut all of the supracrustal rocks but either die out upsection or are overstepped by younger rocks. Therefore, the faults are considered to be synvolcanic. The best examples occur on Beaverlodge Ridge just south of the narrows in Beaverlodge Lake, east of Beaverlodge Lake, and bounding paleovalleys northeast of Stairs Bay. They are similar to the swarm of normal faults mapped on Bell Island (Hildebrand et al., 1983) and may be related to those postulated to exist in the Conjuror Bay area (Hildebrand, 1983). Since in each area the faults cut correlative rocks that sit unconformably on the Hottah Terrane, a period of widespread extension was likely during the initial stages of Great Bear magmatism.

Transcurrent faults, folds, and flower structures. All of the early Proterozoic rocks of the area except younger diabase and gabbro are cut by northeast-trending transcurrent faults, most of which have right lateral separation (Fig. 48.2). They are part of a much larger swarm that occurs not only throughout the Great Bear Magmatic Zone but throughout Wopmay Orogen. They are thought to have been generated by east-west compression during plate collision west of Hottah Terrane (Hoffman et al., 1982).

Rocks of the Great Bear Magmatic Zone and Hottah Terrane (Fig. 48.13a) are folded into a large southwesterly trending and plunging syncline located on southwest Beaverlodge Ridge. The southwest trend of this fold is markedly different than the northwest trend typical for folds in the Great Bear Zone. North-northeast-trending thrust or reverse faults truncate the southeast limb of the fold in the southwest (Fig. 48.13b). The fault separating slice 1 from slice 2 (lower part, Fig. 48.13b) dips steeply (50-70°) to the southeast. Rocks in slice 1 dip approximately 50-60° to the northwest and those in slice 2 define a reclined isoclinal fold in the sandstone too tight to show on Figure 48.13b. Both limbs of the fold are roughly coplanar with the fault. The fault between slices 1 and 3 also dips to the southeast, but more gently (30-60°) than the fault between 1 and 2. The fault itself is tightly folded into southwest-trending reclined folds that plunge about 50° to the southwest. The rocks in slice 3 are, for the most part, overturned such that Hottah basement structurally overlies basal Great Bear sandstone. Rocks within a few metres of both of the above faults have a strong cleavage (Figs. 48.14, 48.15) that is approximately coplanar with the fault zones. However, the actual fault zones are marked by a few centimetres of vein quartz containing angular fragments of country rocks. The fault between slices 3 and 4 is not exposed, but rocks in slice 4 are overturned to the northeast.

The southwest-trending syncline and the reverse or thrust faults occur just south of a major transcurrent fault, as shown in Figure 48.13a. East of Beaverlodge Lake there are more reverse faults that occur along the south side of another transcurrent fault (Fig. 48.16). The strata in those slices dip steeply to the northwest and are overturned. The faults in that area appear to join, or climb out of, the transcurrent fault zone. The origin of the reverse faults is problematic but because they seem to be spatially related to the transcurrent faults they may be another manifestation of east-west shortening like the transcurrent faults and have been active synchronously with them. The geometry and relationships of the reverse faults to the transcurrent faults are remarkably similar to thrust and reverse faults thought to occur in wrench zones elsewhere (Harding et al., 1983). They call such faults "positive flower structures", presumably

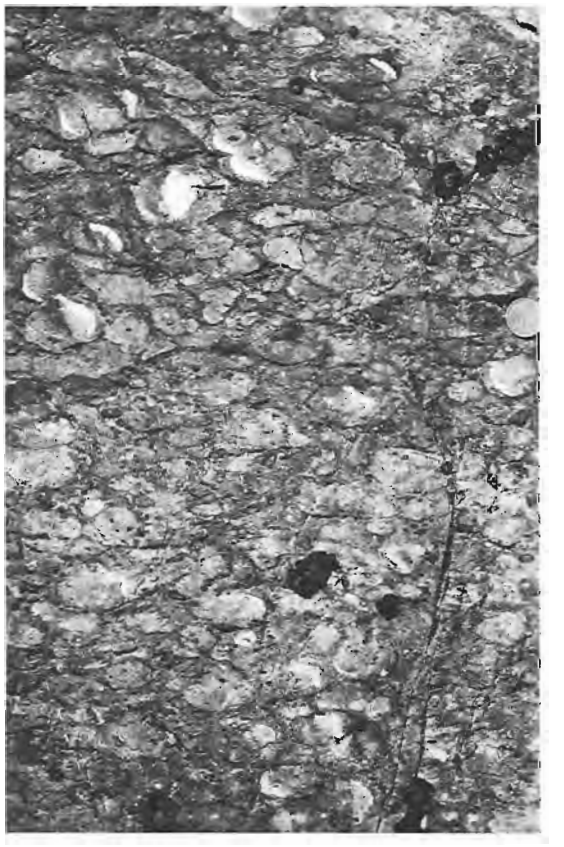

Figure 48.14. *Spherulites and crescent-shaped amygdules in Great Bear lava flow. The spherulites are slightly flattened in this photo. Photo taken 20 m from fault between slices 2 and 3. (GSC 204112-X)*

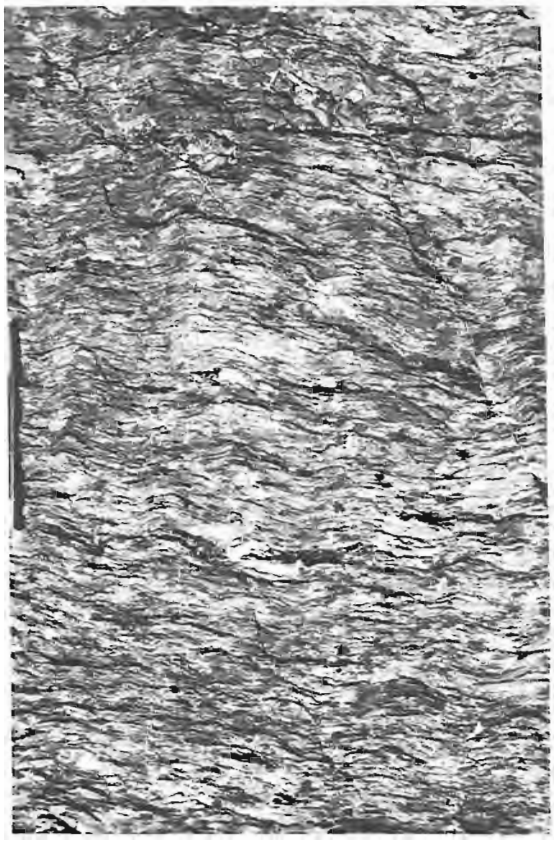

Figure 48.15. *Strongly flattened spherulites in Great Bear lava flow. Photo taken 2 m from fault separating slice 2 from slice 3. This is the same lava flow as that shown in Figure 48.14. (GSC 204112-W)*

because they grow up and blossom out of transcurrent faults. Faults of this type develop in order to accommodate a component of vertical extension. Thus, there can be considerable thickening, at least locally, during deformation. This is somewhat different than transcurrent faulting in the externides of Wopmay Orogen where Tirrul (1984) has shown that transcurrent deformation closely approximates plane strain, except in areas of extreme fault rotation where there is minor thickening by reverse faulting.

When the deformation deviates from plane strain then the fault patterns and separations may be very complex, for as shortening progresses new faults are born, some lock and die, and others continue to have slip along them. Ultimately this leads to a pattern of braided strike, reverse, and oblique slip faults whose kinematic history may be exceedingly difficult, if not impossible, to unravel.

Tectonic implications. The recognition of a suite of deformed intermediate plutons in Hottah Terrane has important implications for the tectonic evolution of Wopmay Orogen. The suite is compositionally similar to plutonic suites of continental magmatic arcs and was emplaced between 1.914-1.90 Ga (Hildebrand et al., 1983; Bowring, in prep.). Since the age of initial rifting in Coronation Margin is 1.90 Ga (Hoffman and Bowring, 1984), Hottah Terrane could not represent an active arc beneath which Coronation Margin was subducted, but the constraints on the ages of deformation in Hottah Terrane and Coronation Margin suggest that deformation in both areas was synchronous (Hildebrand et al., 1983). This, coupled with the overall eastward vergence of Calderian structures throughout

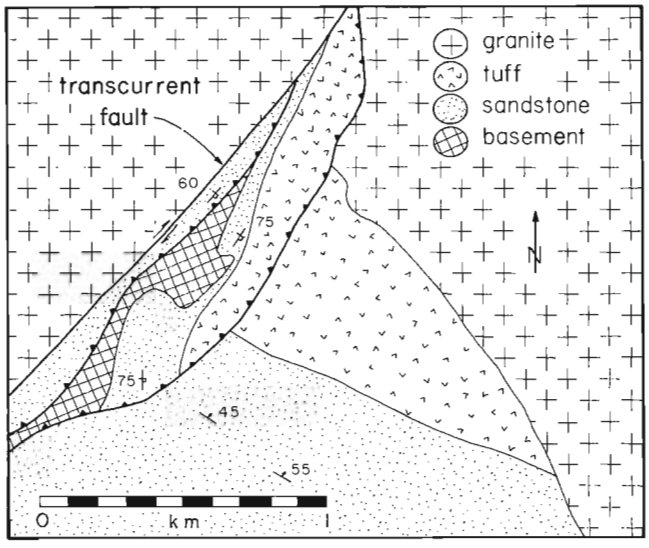

Figure 48.16. *Geological sketch map, east side of Beaverlodge Lake, showing reverse, or thrust, faults merging into transcurrent fault.*

the foreland (Tirrul, 1983) and hinterland (King, 1984) of Wopmay Orogen, suggest that the Hottah Terrane collided with and partly overrode the Coronation Margin. We had originally favoured a model in which Hottah Terrane was exotic with respect to Coronation Margin because of the absence, in Hottah Terrane, of Archean basement (Hildebrand et al., 1983). To date, however, we have not found basement of any age in Hottah Terrane and therefore the possibility exists that Hottah Terrane was rifted from Slave Craton at about 1.90 Ga.

If one accepts the possibility that Hottah Terrane was an arc between 1.914-1.9 Ga, and that it was contiguous with Slave Craton before 1.90 Ga, then subduction must have been easterly because rifting in Coronation Margin did not begin until 1.90 Ga. This implies that Coronation Margin developed in a back arc setting. The principal objection to a back arc model is that there is no arc-derived airfall tuff in the Coronation passive margin (Hoffman and Bowring, 1984) as expected for an active arc located to the west, for paleowind directions were from the southwest toward Coronation Margin (Hoffman et al., 1983). The key word here is active, for if, as the geochronology suggests, arc volcanism in Hottah Terrane shut down coincident with rifting in Coronation Margin then there would be no tuff deposited on the margin and the major objection to a back arc setting would be removed. Arc magmatism may have stopped due to a change in interplate slip vector (e.g. oblique convergence to oblique divergence), which could possibly lead to back arc extension. When convergence resumed, the back arc basin closed and the Hottah Terrane was thrust back against the Coronation Margin.

There need not have been an active arc related to closure of the back-arc basin for there may have been no oceanic crust between the older rifted Hottah Terrane arc and Coronation Margin. Alternatively, if there was oceanic crust between them, the ocean may not have been wide enough for the descending slab to reach the 100 km depth necessary for the generation of arc magmatism (Marsh, 1979). Quite simply, for a slab dipping at 30° the ocean would have to be at least 200 km wide for the leading edge to even reach 100 km depth, and for a 15° dipping slab it would have to be nearly 400 km. In the case of Coronation Margin the ocean would have been floored by young, buoyant

oceanic lithosphere or thinned continental lithosphere and the dip of the slab would probably have been very shallow (Molnar and Atwater, 1978).

Furthermore, if the resumption of east-dipping subduction is linked to the closure of the back-arc basin, then one would expect arc magmatism to resume 5-15 Ma later. This is because it would take 20 Ma for a 30° dipping slab converging at 1 cm/year to reach 100 km depth and nearly 8 Ma for a 15° dipping slab converging at 5 cm/year to reach the same depth. This prediction is consistent with the observed onset of Great Bear arc magmatism at about 1.875 Ga (Hoffman and Bowring, 1984), 10-15 Ma after the onset of Calderian Orogeny. Thus, the geology and geochronology are compatible with the Coronation Margin evolving due to opening and closing of a back-arc basin synchronous with a magmatic lull in the arc.

References

Bowring, S.A.
– U-Pb zircon geochronology of Wopmay Orogen, N.W.T., Canada: an example of rapid crustal growth; Tectonics. (in prep.)

Harding, T.P., Gregory, R.F., and Stephens, L.H.
1983: Convergent wrench fault and positive flower structure, Ardmore Basin, Oklahoma; in Seismic Expression of Structural Styles, Volume 3, ed. A.W. Balley; American Association of Petroleum Geologists, Studies in Geology Series No. 15, p. 4.2-13-4.2-17.

Henderson, J.F.
1949: Pitchblende occurrences between Beaverlodge and Hottah Lakes, Northwest Territories; Geological Survey of Canada, Paper 49-16, p. 1-17.

Hildebrand, R.S.
1981: Early Proterozoic LaBine Group of Wopmay Orogen: remnant of a continental volcanic arc developed during oblique convergence; in Proterozoic Basins of Canada, ed. F.H.A. Campbell; Geological Survey of Canada, Paper 81-10, p. 133-156.

1983: Geology of the Rainy Lake and White Eagle Falls map areas, District of Mackenzie: Early Proterozoic cauldrons, stratovolcanoes and subvolcanic plutons; Geological Survey of Canada, Paper 83-20, 42 p.

Hildebrand, R.S., Bowring, S.A., Steer, M.E., and Van Schmus, W.R.
1983: Geology and U-Pb geochronology of parts of the Leith Peninsula and Rivière Grandin map areas, District of Mackenzie; in Current Research, Part A, Geological Survey of Canada, Paper 83-1A, p. 329-342.

Hildebrand, R.S., Annesley, I.R., Bardoux, M.V., Davis, W.J., Heon, D., Reichenbach, I.G., and Van Nostrand, T.
1984: Geology of the Early Proterozoic rocks in parts of the Leith Peninsula map area, District of Mackenzie; in Current Research, Part A, Geological Survey of Canada, Paper 84-1A, p. 217-221.

Hoffman, P.F., McGrath, P.H., Bowring, S.A., Van Schmus, W.R., and Thomas, M.D.
1982: Plate tectonic model for Wopmay Orogen consistent with zircon chronology, gravity and magnetic anomalies, east of Mackenzie Mtns.; Canadian Geophysical Union Meeting, Toronto.

Hoffman, P.F. and Bowring, S.A.
1984: Short-lived 1.9 Ga continental margin and its destruction, Wopmay Orogen, northwest Canada; Geology, v. 12, p. 68-72.

Hoffman, P.F., Tirrul, R., and Grotzinger, J.P.
1983: The externides of Wopmay Orogen, Point Lake and Kikerk Lake map areas, District of Mackenzie; in Current Research, Part A, Geological Survey of Canada, Paper 83-1A, p. 429-435.

Kidd, D.F.
1936: Rae to Great Bear Lake, Mackenzie District, N.W.T.; Geological Survey of Canada, Memoir 187, 44 p.

King, J.E.
1984: Eastward transport of the marginal prism in a ductile décollement, and basement involvement, within the internal metamorphic zone of Wopmay Orogen, N.W.T.; in Geological Association of Canada, Programs with Abstracts, v. 9, p. 78.

Marsh, B.D.
1979: Island-arc volcanism; American Scientist, v. 67, p. 161-172.

McGlynn, J.C.
1979: Geology of the Precambrian rocks of the Rivière Grandin and in part of the Marion River map areas, District of Mackenzie; in Current Research, Part A, Geological Survey of Canada, Paper 79-1A, p. 127-131.

Molnar, P. and Atwater, T.
1978: Interarc spreading and Cordilleran tectonics as alternates related to the age of subducted oceanic lithosphere; Earth and Planetary Science Letters, v. 41, p. 330-340.

Tirrul, R.
1983: Structure cross-sections across Asiak Foreland Thrust and Fold Belt, Wopmay Orogen, District of Mackenzie; in Current Research, Part B, Geological Survey of Canada, Paper 83-1B, p. 253-260.

1984: Regional pure shear deformation by conjugate transcurrent faulting, externides of Wopmay Orogen, N.W.T.; in Geological Association of Canada, Programs with Abstracts, v. 9, p. 111.

-49-

REGIONAL GEOLOGICAL SYNTHESIS OF WESTERN SUPERIOR PROVINCE, ONTARIO

Project 820006

John A. Percival, Richard A. Stern[1], and Mark R. Digel[2]
Precambrian Geology Division

Percival, J.A., Stern, R.A., and Digel, M.R., Regional geological synthesis of western Superior Province, Ontario; in Current Research, Part A, Geological Survey of Canada, Paper 85-1A, p. 385-397, 1985.

Abstract

In the central Quetico belt, metamorphism in marginal metasedimentary schist grades from greenschist to amphibolite facies toward an interior unit of schists, gneisses, small biotite leucogranite bodies, and the peraluminous Sturgeon Lake granite batholith. Across the belt the metamorphic zonation is symmetrical; from west to east along its strike, pelitic assemblages indicate pressure increase from bathozone 2 of Carmichael to bathozone 3 and possibly higher.

Four intermediate crescentic plutons of the Wawa and Wabigoon subprovinces have wide-ranging composition (clinopyroxenite to granite) and textures (massive, megacrystic to strongly foliated and lineated). Bulk composition of the Sleigh Lake and Floranna Lake bodies are diorite, the Colwill Lake pluton is monzonite and the Kekekuab Lake pluton is granite.

The Whitewater-Mojikit lakes area, in the English River subprovince, is underlain mainly by metasedimentary metatatexite, with intrusive tonalite, gneissic biotite granite, peraluminous granite and late, locally andalusite-bearing granite. Orthopyroxene occurs in gneissic and foliated tonalite, in rare mafic gneiss and locally in peraluminous granite, whereas garnet-cordierite-sillimanite assemblages characterize diatexite paleosome.

Résumé

La zone de Quetico comprend une unité marginale de schistes métasédimentaires où le degré de métamorphisme passe du faciès de schiste vert au faciès amphibolite vers une unité interne qui contient des schistes, des gneisses, des petits plutons de granite leucocrate à biotite et la batholithe à granite peralumineux de Sturgeon Lake. D'un bout à l'autre de la zone la zonation métamorphique est symétrique; de l'ouest à l'est, suivant la direction principale, les assemblages pélitiques indiquent un accroissement de pression allant du bathozone 2 de Carmichael au bathozone 3.

Quatre plutons de composition intermédiaire dans les sous-provinces de Wawa et Wabigoon consistent en unités intrusives diverses (clinopyroxénite à granite), avec textures variables, massives et mégacrystiques à foliées avec linéation prononcée. Les plutons de Sleigh Lake et Floranna Lake sont grossièrement dans l'ensemble dioritiques, alors que les plutons de Calwill Lake et de Kekekuab sont respectivement monzonitique et granitique.

Dans la région des lacs Whitewater et Mojikit de la sous-province d'English River, il y a surtout de la diatexite métasédimentaire, avec intrusions de tonalite, de granite gneissique à biotite, de granite peralumineux et de granite tardif avec très localement de l'andalousite. On trouve de l'orthopyroxène dans la tonalite gneissique foliée, dans le rare gneiss mafique et localement dans le granite peralumineux, tandis que l'assemblage grenat-cordiérite-sillimanite caractérise la diatexite (paléosome).

[1] Department of Earth & Space Sciences, State University of New York at Stony Brook, New York 11794, U.S.A.
[2] Department of Geology, University of Ottawa, Ottawa, Ontario, K1N 6N5

Introduction

Geological compilation of part of the Superior Province of northwestern Ontario and eastern Manitoba (IMW NM-15) is underway at a scale of 1:1 000 000. Part of the program involves field studies at various scales aimed at improving our understanding of relatively poorly known areas. Many of the greenstone belts of the Superior Province have been mapped in detail and thus most of the field work for this project concerns the geology of granitoid rocks in greenstone-granite terranes and of metasedimentary belts (Percival, 1983; Percival and Stern, 1984).

Descriptions of three areas are presented. Part I deals with regional aspects of the igneous and metamorphic petrology of the central Quetico belt in western Ontario. The second part describes the geology of four crescentic plutons of intermediate composition of the Wawa and Wabigoon subprovinces. Petrogenesis of the suite of plutons is the subject of R.A. Stern's M.Sc. thesis at the State University of New York at Stony Brook. In Part III, the geology of the Whitewater-Mojikit lakes area of the northern metasedimentary domain of the English River subprovince is described. The petrology of this region, characterized by granulite-facies metamorphism, will be the focus of M.R. Digel's M.Sc. thesis at the University of Ottawa.

Acknowledgments

Capable field assistance was provided by S. Van Sickle. For access to Quetico Park, the co-operation of D. Elder and A. Harjula (M.N.R. Atikokan) is gratefully acknowledged. K.H. Poulsen (G.S.C.) and J. Wood (O.G.S.) are thanked for field guidance. M.R. St-Onge made helpful comments on Part I.

PART I. CENTRAL QUETICO BELT

J.A. Percival

Reconnaissance studies were completed on 350 km of strike length of the Quetico belt between Lake Nipigon in the east and the international boundary in the west (Percival, 1983; Percival and Stern, 1984). Results of previous compilations (Mackasey et al., 1974; Pirie and Mackasey, 1978) showed that the 10-100 km wide, broadly symmetrical belt consists of marginal low-grade metasedimentary rocks and interior higher-grade schists, gneisses and plutonic rocks over a strike length of some 1200 km. Metamorphic grade in the marginal pelitic schists varies from a chlorite-muscovite zone at the outer margin to a garnet-sillimanite-biotite zone toward the interior (Pirie and Mackasey, 1978).

On the basis of metamorphic assemblage data, Percival (in Percival and Stern, 1984) concluded that metamorphism in the marginal metasedimentary schists of the Quetico Park area (Fig. 49.1) occurred under overburden less than 10 km thick as a result of heat transported to the higher structural levels by granitic plutons. In addition to the cross-strike thermal gradient, assemblages developed in pelitic rocks can be used in the bathozone scheme of Carmichael (1978) to document a variation in along-strike depth of exposure.

Sedimentary protoliths of the belt margin consist of interbedded greywacke and shale with grain-size gradation, scour marks and rip-up clasts, interpreted to represent a turbidite sequence. At least two (Borradaile, 1982; Kehlenbeck, 1984) and as many as three (Sawyer, 1983) sets of recumbent and upright folds are recognized in the marginal schists; however, easterly bedding and cleavage generally dip steeply to moderately northward (Pirie and Mackasey, 1978). Marginal schists are variably metamorphosed and recrystallized to assemblages characteristic of the greenschist and amphibolite facies. In the Quetico Park area, biotite-plagioclase-quartz ± garnet schist is the common rock type adjacent to granitic plutons and in enclaves within granite bodies.

Field work in 1984 focused on the western Quetico Park complex (Percival and Stern, 1984) and the area underlain by metasedimentary rocks to the west, between the Quetico Park complex and Vermilion granitic complex (Southwick, 1972) of Minnesota.

Two distinct granite types make up most of the interior of the Quetico belt in the Quetico Park complex (Percival and Stern, 1984). The Sturgeon Lake batholith (Fig. 49.1) is a white-weathering, muscovite-bearing granite with associated pegmatite that occurs in the central part of the interior of the belt. It is medium grained to pegmatitic and contains subequal amounts of quartz, plagioclase and K-feldspar with 5-10 per cent muscovite as well as biotite and/or garnet and/or sillimanite, and some apatite, tourmaline and rare fluorite. Dykes of white granite pegmatite with mineral assemblages similar to those in the Sturgeon Lake batholith are common in biotite schist country rock and occur up to 60 km away from the batholith. Elongate inclusions of biotite schist are common in granite. A gradational contact characterizes the inclusion-rich western end of the batholith, where pegmatite dykes intrude schists parallel to the regional east-northeast foliation.

Common to both pegmatite and granite in the western Sturgeon Lake batholith are feather-like sillimanite-quartz ± muscovite aggregates on the 1-10 cm scale (Fig. 49.2), constituting up to 15 per cent of the rock. Subhedral garnet is overgrown by the aggregates locally. Plumose structure in the aggregate suggests in situ crystallization rather than xenocrystic origin. The composition of the magma must therefore have been very aluminous, suggesting a high liquidus temperature (Schairer and Bowen, 1955).

A second distinct granite type is medium- to coarse-grained, equigranular to K-feldspar megacrystic biotite ± magnetite leucogranite, readily distinguished from white granite of the Sturgeon Lake batholith by its pink weathering colour. Several bodies of leucogranite (Fig. 49.1) occur near the contact between biotite schist and the Sturgeon Lake batholith.

Rocks of the Sturgeon Lake batholith have many characteristics in common with S-type granites of Chappell and White (1974). These include peraluminous compositions, as evidenced by the presence of muscovite, sillimanite and garnet, and association with metasedimentary rocks. Biotite-magnetite leucogranite has some characteristics of I-type granites but has no hornblende. Because both granite types intrude the same metasedimentary sequence, the difference in colour cannot be related to emplacement conditions. Rather, it may be ascribed to a more oxidized state for the source region of pink granite and more reduced state, possibly buffered by graphite, for the source terrane of white granite. White and Chappell (1983) deduced a more reduced source for the commonly ilmenite-bearing S-granites and more oxidized source for the magnetite-bearing I-type granitoids (cf. Ishihara, 1981).

Muscovite-bearing plutons occur inland from less aluminous, more typical continental margin granitic rocks in the North American Cordillera (Miller and Bradfish, 1980), the Appalachians of Newfoundland (Strong and Dickson, 1978) and several other areas (e.g. Pitcher, 1979). To account for their location, composition and timing of emplacement, Miller and Bradfish (1980) postulated the existence of a regional structural control localizing heat flow or fluid transport to generate peraluminous magma in the middle or

upper crust. Asthenospheric upwelling beneath a back-arc environment could have given rise to high heat flow and possible crustal melting during the development of the Quetico belt (Percival and Stern, 1984).

Many parts of the marginal metasedimentary unit have medium-grade metamorphic mineral assemblages (Pirie and Mackasey, 1978; Kehlenbeck, 1976; Birk, 1971). In the Lac La Croix area (Fig. 49.1), between the Quetico Park and Vermilion granitic complexes, the marginal schist unit attains its maximum width of 42 km and metamorphic porphyroblasts are common. Most assemblages include staurolite, quartz and plagioclase as well as some combination of muscovite, biotite, garnet, cordierite, andalusite and sillimanite. Assemblages are numbered in order of increasing grade in Table 49.1 and keyed in to their geographic location in Figure 49.1. A patch of biotite-grade schist forms a low-grade "island" within the staurolite zone and higher grade is indicated to the north and south by occurrences of garnet-sillimanite. Metasedimentary rocks adjacent to granite contacts are typically biotite-plagioclase-quartz ± muscovite schist, devoid of aluminous phases such as staurolite and aluminosilicates.

Migmatites in the area west of Shebandowan Lake (Fig. 49.1) consist of homogeneous biotite schist with sharp-walled concordant sills of coarse grained granite and pegmatite on the 10-100 cm scale. Evidence for the process of in situ anatexis in the development of migmatites has not been observed, although Sawyer (1983) reported diatexite migmatite from the Huronian Lake area, 20 km northwest

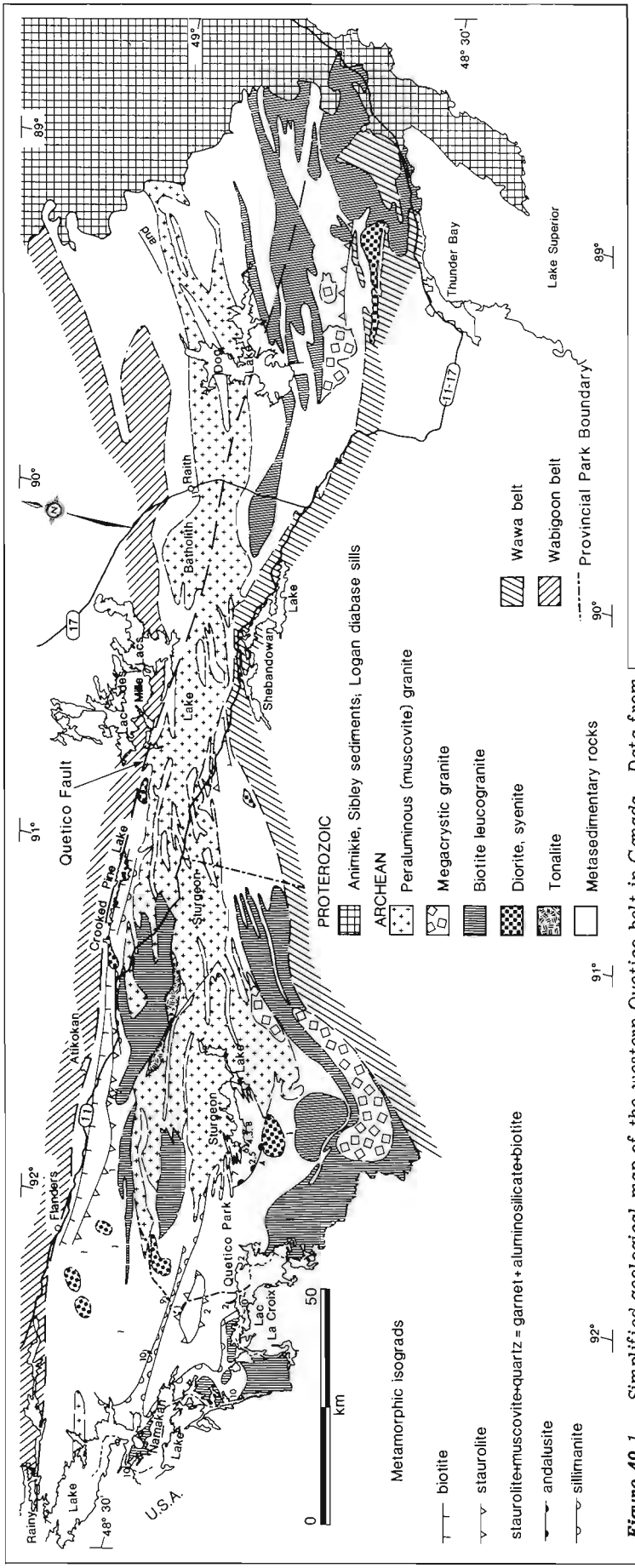

Figure 49.1. *Simplified geological map of the western Quetico belt in Canada. Data from Kehlenbeck (1976), Lehto (1975), Percival (1983), Percival and Stern (1984) and Pirie and Mackasey (1978). Numbered assemblages are listed in Table 49.1 and positioned in P-T space in Figure 49.3. Ornaments on isograd symbols indicate high-grade side.*



Figure 49.2. *Radiating sillimanite clusters in sillimanite, garnet, muscovite-bearing white granite pegmatite, Vague point, Rainy Lake. Sillimanite comprises up to 15 per cent of some outcrops. (GSC 203840-X)*

Table 49.1. Metamorphic assemblages in pelitic rocks of the Quetico belt, numbered in order of increasing grade. See Figure 49.1 for location of occurrences and Figure 49.3 for P-T relationships among assemblages. Most occurrences of assemblage 1 do not contain chlorite, making the staurolite-garnet assemblage divariant

	Gt	And	Sl	Ky	St	Cd	Ms	Bt	Pl	Qz
1	x				x		x	x	x	x
2	x				x	x	x	x	x	x
3	x					x	x	x	x	x
4		x			x	x	x	x	x	x
5	x	x			x	x	x	x	x	x
6	x	x			x		x	x	x	x
7	x	x					x	x	x	x
8	x	x				x	x	x	x	x
9	x		x		x		x	x	x	x
10	x		x				x	x	x	x
11	x		x	x				x	x	x

Gt: garnet; And: andalusite; Sl: sillimanite; Ky: kyanite; St: staurolite; Cd: cordierite; Ms: muscovite; Bt: biotite; Pl: plagioclase; Qz: quartz.

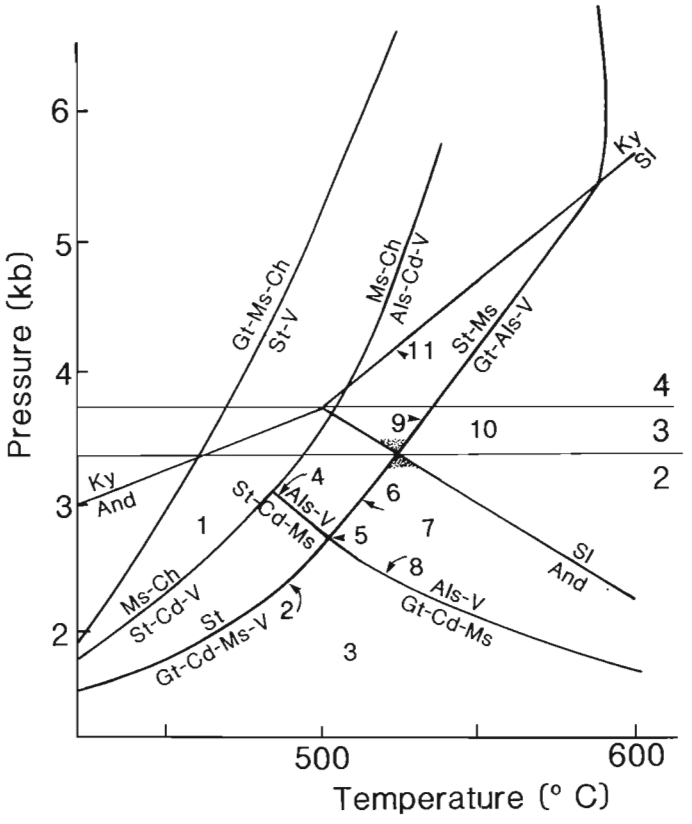

Figure 49.3. *P-T petrogenetic grid showing stability fields of mineral assemblages in pelitic rocks at medium grade (modified after Carmichael, 1978 according to Archibald et al. (1983)). Note that bathozone 2 is defined by the assemblage garnet-andalusite and bathozone 3 by staurolite-sillimanite. Bathozone 4 is characterized by the coexistence of kyanite and sillimanite. Numbers refer to assemblages from the western Quetico belt, listed in Table 49.1. Mineral abbreviations as in Table 49.1, except Ch (chlorite), Als (aluminosilicate), and V (vapour).*

of Shebandowan Lake. Most migmatite in the Crooked Pine Lake area is a mixture of schist and "intrusive mobilizate" (Pirie, 1978).

Post-metamorphic regional uplift can be estimated provided that appropriate mineral assemblages are present in pelitic rocks (Carmichael, 1978). Garnet-andalusite assemblages, characteristic of bathozone 2 (<3.4 kb; Fig. 49.3) have been reported from many areas in the marginal metasedimentary unit (Pirie and Mackasey, 1978), thus indicating less than 10 km of erosion since metamorphism at the belt margins. The occurrence of garnet-andalusite in the Sturgeon Lake area, in the central part of the belt along strike with interior granites to the east, indicates that low pressure metamorphism also characterizes the interior of the belt in this area and that granites of the Quetico Park complex have risen to high structural levels.

On the regional scale, the width of the prograde sequence of isograds is proportional to the width of the marginal metasedimentary belt. For example, in the Crooked Pine Lake area, where the belt is about 6 km wide, the chlorite to garnet-sillimanite isograd sequence is less than 4 km wide (Pirie, 1978). In the Flanders-Lac La Croix area (Fig. 49.1), the metasedimentary belt and isograd sequences are 40 km wide. The association between intrusive contacts and the highest metamorphic grade in schists suggests that metamorphic heat was supplied by the granites. Isograd dips can not be observed owing to lack of topographic relief, however they are probably steep where isograds are closely spaced and more moderate where widely spaced (see Fig. 53.3, Percival and Stern, 1984).

Regional differences in mineral assemblages in metamorphic and igneous rocks are evident over the 350 km of strike length of the Quetico belt under consideration. Evidence for low metamorphic pressure (less than 3.4 kb) has been cited for the Sturgeon Lake area and for parts of the marginal metasedimentary belt. Some 60 km to the east, assemblages in the Crooked Pine Lake area include garnet-staurolite-andalusite-sillimanite, suggesting a transition from bathozone 2 to bathozone 3 (sillimanite-staurolite diagnostic of bathozone 3, corresponding to pressure above ~3.4 kbars (Carmichael, 1978)). Staurolite is also present with garnet and sillimanite at one locality 20 km north of Lac La Croix. This occurrence may reflect higher pressure or a staurolite composition (Zn-rich?) which expands its stability field. Farther east, in the Raith area (Fig. 49.1), relict kyanite is present locally in plagioclase in garnet-sillimanite-biotite-plagioclase-quartz schist. Although kyanite and sillimanite are not in textural equilibrium, the presence of kyanite suggests relatively higher pressure in this area than farther west at some early stage in the metamorphic history. Kyanite occurs at Abbess Lake (Fig. 49.1; Moore, 1940) without a petrographic description or assemblage data. Ayres (1978) ascribed most kyanite occurrences in the western Superior Province to local high pressures imposed during deformation.

Sillimanite knots are common in granite only in the western part of the Sturgeon Lake batholith. Its presence is probably a function of both bulk magma composition and crystallization conditions.

Migmatites originating by in situ partial melting are recognized by fine-scale (<1 cm) layering of leucosome and melanosome, mafic selvages in paleosome adjacent to leucosome and by isolated patches of leucosome (e.g. Kenah and Hollister, 1982). Migmatites of this type are not present west of Shebandowan Lake (Fig. 49.1). Rather, mixed rocks in the west occur in the form of inclusions of schist in granite, or dykes of granite and pegmatite in schist. Despite the presence of large intrusive granite bodies in the west, metamorphic temperature in country rocks and inclusions apparently did not exceed the granite solidus. Therefore, either the granites were not superheated, or the country rocks had a low ambient temperature before granite intrusion. The presence of sillimanite in granite in the west, suggesting highly aluminous magma with a high liquidus temperature, argues in favour of cool country rocks.

Cordierite is common in granite, pegmatite and migmatite leucosome, in association with garnet and muscovite, in the area east of Dog Lake. It is absent in these rocks farther west, although "low-grade" cordierite in schists is common. East of the present map area, granulite-facies rocks of the Quetico belt in the Stevens-Kagiano Lake area (Coates, 1968) and Mattagami River area (Percival, 1985), have cordierite associated with garnet, sillimanite and K-feldspar.

To summarize, in addition to the across-strike metamorphic gradient in the marginal metasedimentary unit, along-strike variation is also evident. In the Sturgeon Lake area in the west, metamorphic pressure was low (bathozone 2) in the centre of the belt and the temperature of marginal schists did not exceed that of the granite solidus (~650°C). At Crooked Pine Lake, and north of Lac La Croix, temperature was also low, but pressure was slightly higher, at bathograd 2/3. Near Raith to the east, pressure was higher at some time during the metamorphic history, as evidenced by the presence of relict kyanite. East of Shebandowan Lake, in situ migmatites are common, suggesting that the temperature of country rock schists exceeded that of the granite solidus. In the same region, cordierite is common in leucosome as well as granite plutons and pegmatite.

On a regional scale, these facts suggest a relatively shallow erosion level for the interior of the belt in the west (<10 km) and deeper level in the east (>12 km), however, pressure-sensitive assemblages are scarce in the mainly granitoid interior. It is interesting that both temperature and pressure appear to be higher in the east as this suggests a gentle westerly post-metamorphic regional plunge. The occurrence of regional granulite-facies metamorphism in the interior of the Quetico belt at its far eastern end (Percival, 1985), suggests the possibility that the regional plunge may be consistent for some 800 km.

PART II. FIELD SETTING OF CRESCENTIC INTERMEDIATE PLUTONS

R.A. Stern

Introduction

This section describes the preliminary results of mapping of four intermediate plutons in the Wawa and Wabigoon subprovinces of the Superior Province. The purpose of the study is to identify compositional and textural variations in the plutons as a first step in a petrological and geochemical evaluation. Recently, Shirey and Hanson (1984) have shown that intermediate plutons in the western Wabigoon subprovince bear chemical similarities to primitive Miocene andesites, called sanukitoids, of the Setouchi Volcanic Belt, Japan. They recommend that Archean rocks with these characteristics also be called "sanukitoids". Silica-saturated to oversaturated Archean sanukitoids are a potentially important group of crust-forming rocks because they indicate that it is possible for much of the crust to be derived directly from the mantle.

Colwill-Empire lakes area

The Colwill Lake pluton and the Empire Lake gabbro (Percival, 1983; Fig. 49.4a) are a spatially-related suite of rocks ranging from gabbro to quartz monzonite. They intrude amphibolite, mafic gneiss, foliated to gneissic tonalite, and granodiorite, and are themselves cut by late leucogranite. The Colwill Lake pluton is a crescent-shaped body measuring 50 km by 1 to 5 km. Mineral foliations, produced by alignment of biotite and hornblende, are concordant to the margins of the pluton and define an antiformal structure plunging steeply to the southeast. Most of the pluton is composed of massive to well-foliated or lineated clinopyroxene-biotite-hornblende monzonite to quartz monzonite (terminology after Streckeisen, 1974). Small bodies of clinopyroxene-hornblende gabbro to diorite occur throughout the pluton, mainly as marginal phases, and are cut by late monzonitic rocks. Numerous hornblendite to diorite xenoliths occur throughout the monzonite. Cumulate layers of hornblende and clinopyroxene are a characteristic feature of the gabbros. Monzonitic rocks grade laterally into diorite and gabbro near Allely Lake at the western end of the Colwill Lake pluton.

Although the Empire Lake gabbro is separated from the Colwill Lake pluton by tonalitic gneiss, the two are similar in age, judging by contact relations with adjacent units. They may also be genetically related, on the basis of common rock types and textures. Three phases of the Empire Lake gabbro were recognized: (1) an early marginal phase of massive, fine grained gabbro with orthopyroxene, biotite, hornblende, and clinopyroxene; (2) medium- to coarse-grained, massive to foliated gabbro with magnetite, biotite, orthopyroxene, clinopyroxene, and hornblende, abundant centimetre-wide cumulate layers of these mafic minerals, and plagioclase with trachytoidal textures; (3) late diorite to quartz diorite with up to 10 per cent quartz.

Sleigh Lake pluton

The Sleigh Lake pluton (Percival, 1983; Fig. 49.4b) lies within the Northern Light-Perching Gull lakes plutonic terrane of the western Wawa subprovince. It is a mafic body characterized by tentacle-like arms of diorite, gabbro, hornblendite, pyroxenite and mafic monzonitic rocks. The southern, dioritic arm of the pluton intrudes between a thin unit of mafic gneiss-amphibolite and tonalitic gneiss, where it has a southwesterly-dipping foliation concordant to layering in adjacent rocks. A 0.5 km circular clinopyroxenite body is along strike from this arm to the south and is associated with smaller bodies of serpentinized ultramafic rocks with orbicular textures. The two easterly-trending arms of the pluton are composed of massive, coarse grained, clinopyroxene-biotite-hornblende diorite and gabbro, hornblendite and clinopyroxenite. These rocks display a wide range of igneous textures such as glomeroporphyritic plagioclase aggregates that have a "snowflake" appearance. Dioritic rocks grade into monzonite and quartz monzonite with 30 to 40 per cent hornblende in the westerly arms of the pluton. The tentacle-like appearance of the pluton is caused, in part, by the presence of late biotite leucogranite that separates the two east-west trending limbs of the body. Leucogranite appears to have dismembered diorite in the

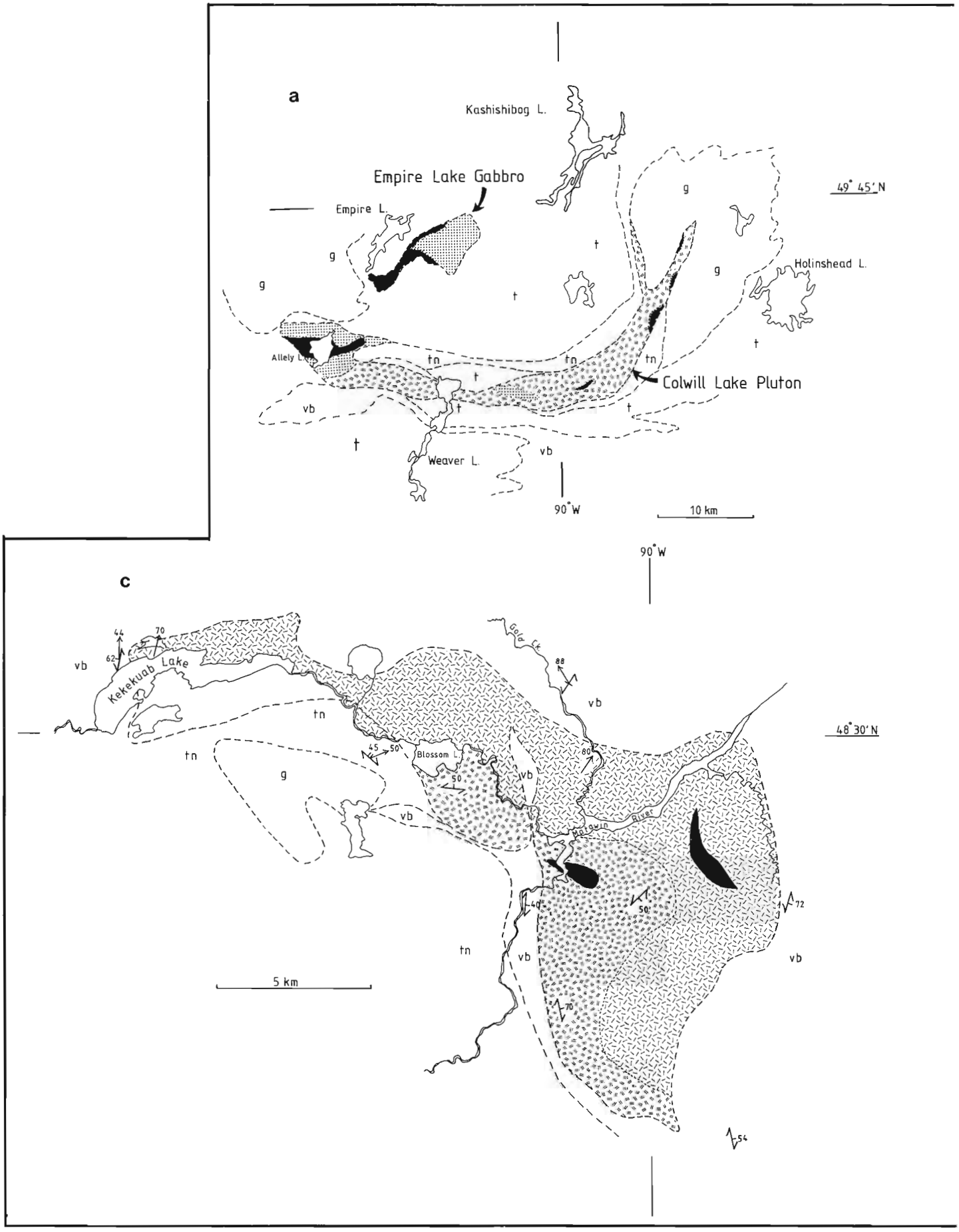
a
Kashishibog L.
Empire Lake Gabbro
Empire L.
49° 45' N
Holinshead L.
Allely L.
Colwill Lake Pluton
Weaver L.
90° W
10 km
c
90° W
Kekekuab Lake
Gold Ck
48° 30' N
Blossom L.
Berguin River
5 km
vb
tn
g
t

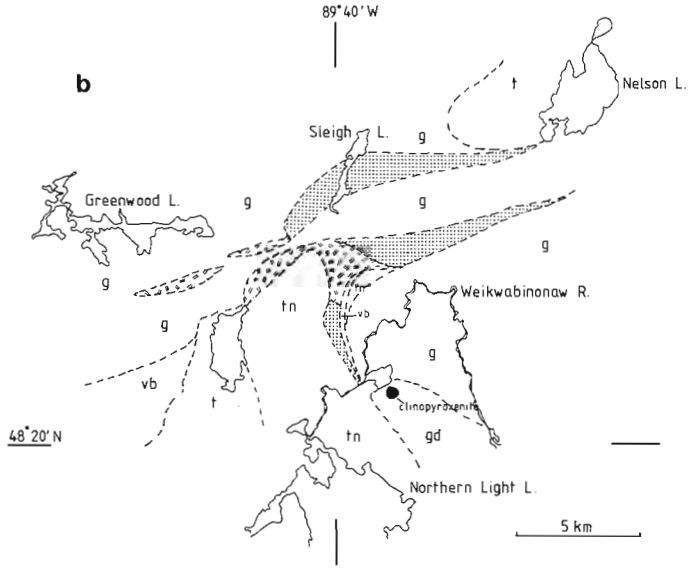

LEGEND

Intermediate Plutons

- hornblende-quartz monzonite, granite
- cpx-hb monzonite, qtz monzonite, syenite, monzodiorite
- cpx-hb diorite
- bi-hb-cpx (mag-opx) gabbro

Surrounding Rocks

g	biotite leucogranite
t, tn	foliated, gneissic tonalite-granodiorite
vb	mafic metavolcanic rocks
nm	gar-cpx-hb mafic gneiss
ns	metasedimentary gneiss

mineral foliation, lineation

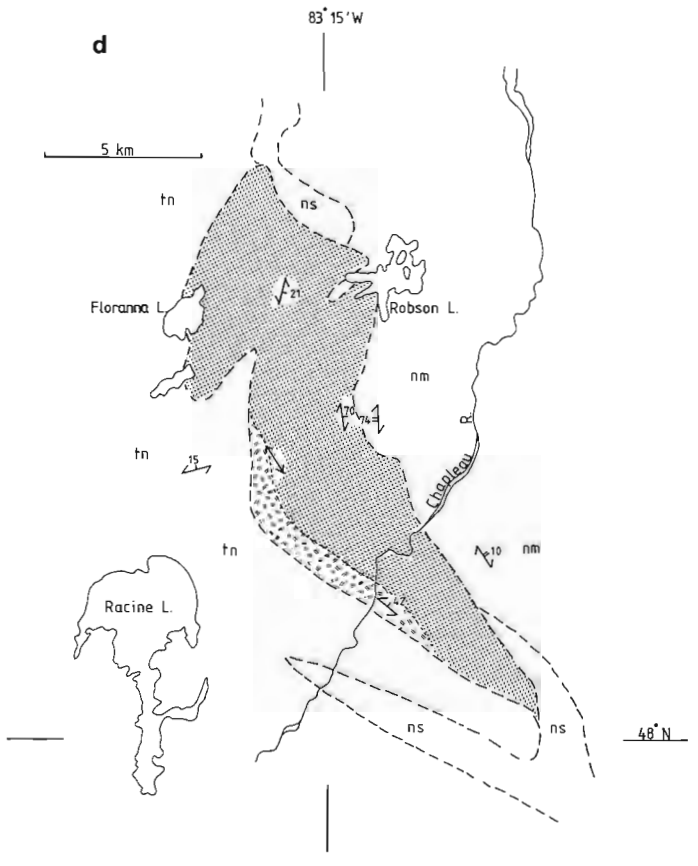

Figure 49.4

a) *Geology of the Colwill Lake pluton and Empire Lake gabbro of the Wabigoon subprovince.*

b) *Geology of the Sleigh Lake pluton of the western Wawa subprovince.*

c) *Geology of the Kekekuab Lake pluton of the western Wawa subprovince.*

d) *Geology of the Floranna Lake pluton in the eastern Wawa subprovince (modified after Percival, 1981).*

area between the arms of the pluton, where complex mixtures of diorite and hornblendite xenoliths occur in a granitic matrix. Late northeast-trending faults cut all rock types and indicate dextral slip motions on a local scale.

Kekekuab Lake pluton

The Kekekuab Lake pluton (Fig. 49.4c), also within the Northern Light-Perching Gull Lakes plutonic terrane, cuts mafic to felsic metavolcanic rocks of the Shebandowan belt to the north, and tonalitic gneiss, amphibolite and mafic gneiss to the south. It is a crescent-shaped body measuring 25 to 30 km long and 3 to 7 km wide. Most of the pluton is composed of medium- to coarse-grained biotite-hornblende quartz monzonite to granite, commonly with 1 to 3 cm K-feldspar megacrysts. Rocks with greater than 15 per cent modal quartz grade into less siliceous monzonites and quartz monzonites at the western margin of the pluton. Two diorite-gabbro bodies with biotite, clinopyroxene and hornblende occur within the pluton and are cut by granite. Diorite cuts amphibolitic rocks at the western margin and is probably the earliest intrusive phase. Most of the pluton is massive except adjacent to metavolcanic or tonalitic rocks where foliations are concordant to the margin and define an antiformal structure plunging to the northeast. A steep, northeasterly plunging mineral lineation is present in marginal phases of the pluton as well as in the adjacent Shebandowan belt. Mafic xenoliths in foliated monzonitic rocks are elongated and flattened parallel to their host. A body of white-weathering biotite leucogranite cuts tonalite gneiss adjacent to the pluton and may be the source of ubiquitous aplitic dykes in the Kekekuab Lake Pluton.

Floranna Lake pluton

The Floranna Lake pluton (Fig. 49.4d) is a dioritic body intruding upper amphibolite to granulite facies rocks in the eastern Wawa subprovince (Percival et al., 1983). It occurs between garnet-clinopyroxene-hornblende gneiss of the Robson Lake Dome to the east and clinopyroxene-hornblende tonalite gneiss of the Racine Lake Dome to the west. Unlike the plutons discussed previously, which show well preserved igneous textures, this pluton has strong mineral foliation and lineation, granoblastic textures, and areas with concordant granitic leucosome and gneissic layering. It measures 20 km by 3 to 6 km and is composed mainly of foliated or lineated, magnetite-biotite-clinopyroxene-hornblende diorite. The composition grades from diorite through monzodiorite, monzonite, and granite from east to west across the central portion of the pluton. Dioritic phases commonly contain centimetre-wide gabbroic layers with clinopyroxene, hornblende and plagioclase, interpreted as relict igneous layers. The eastern contact with the Robson Lake Dome is a zone several hundred metres wide, characterized by complex folds of diorite, gabbro and mafic gneiss layers, and by numerous massive, crosscutting pegmatitic granite and tonalite dykes. Folds plunge to the south and southwest at moderate angles. Pegmatitic and gneissic hornblende tonalite characterizes a 50 m-wide contact zone with the Robson Lake mafic gneiss. The origin of these massive tonalites is unclear, but they do not appear to be cogenetic with the strongly foliated rocks of the Floranna Lake pluton. Foliation within the body is generally concordant to the margins and dips easterly at moderate angles. Mineral lineations are most pervasive in the central part of the pluton where they trend north-south and are subhorizontal.

Conclusions

Four intermediate plutons within the Wawa and Wabigoon subprovinces have a wide range in composition, from clinopyroxenite to granite, and textures ranging from massive and megacrystic to strongly recrystallized and lineated. Several features are common to the suite as a whole. All plutons have small gabbro bodies as inclusions within dioritic to monzonitic rocks. Gabbro commonly displays cumulate igneous layers of hornblende, clinopyroxene, plagioclase, orthopyroxene, and magnetite. Crystal fractionation may thus have been an important genetic process. Possible initial liquid compositions for the suite, deduced from mafic dykes and marginal phases, are gabbro and diorite.

The main rock type of the plutons is diorite to quartz monzonite with 0 to 10 per cent modal quartz. In most of the plutons, gabbro and quartz-rich phases are not gradational. Rather, gabbro grades into diorite, diorite into monzonite, and monzonite into granite.

The plutons have a characteristic crescentic shape and intrusive style (Schwerdtner et al., 1979, 1983), occurr at the contact between gneissic and metavolcanic rocks, and possess mineral fabrics that suggest they were acquired during intrusion. Plutons in the western Superior Province have preserved igneous textures and mineralogy, whereas the Floranna Lake pluton in the east is deformed and metamorphosed and its mineralogy may not be igneous.

A noteworthy feature of the suite is that each body has a narrower compositional range than the group of plutons as a whole. For example, plutons can be termed gabbroic Empire Lake gabbro, dioritic Sleigh and Floranna lakes plutons, monzonitic Colwill Lake pluton, and granitic Kekekuab Lake pluton after their most prominent rock type. Genetic models for the suite must accommodate this large compositional diversity.

PART III. GEOLOGY OF THE WHITEWATER-MOJIKIT LAKES AREA

M.R. Digel

Introduction

The English River subprovince of the Superior Province is a 25-100 km wide belt of metasedimentary and intrusive granitoid rocks, that extends some 750 km eastward from Lake Winnipeg to the Moose River basin. It is bounded by the Uchi subprovince to the north and the Wabigoon subprovince to the south, both of which are dominated by metavolcanic and granitoid rocks. The English River subprovince has been subdivided into two domains of contrasting lithology (Beakhouse, 1977; Breaks et al., 1978), namely a northern metasedimentary domain, and a southern gneissic and granitic intrusive domain.

The Whitewater-Mojikit Lakes area (Fig. 49.5) (Thurston et al., 1969; Sage et al., 1974; Stott, 1984) is located within the northern metasedimentary domain, and represents the easternmost zone of granulite facies metamorphism in the English River subprovince (Percival, 1983). Migmatitic metasedimentary rocks, locally interlayered with mafic gneiss, are the dominant rock type and represent the oldest unit in the study area, followed by foliated to gneissic granitic and tonalitic intrusive bodies, S-type granites, late granite dykes and Proterozoic gabbro sills and dykes.

Metasedimentary and associated rocks

Migmatitic metasedimentary rocks within the Whitewater-Mojikit lakes area can be subdivided according to the classification of Breaks et al. (1978) into metatexite, inhomogeneous diatexite and homogeneous diatexite. Metatexite is the most abundant rock type and consists of medium grained garnet-biotite-plagioclase-quartz ±

sillimanite ± cordierite paleosome, and thin (average 1.5 cm wide) concordant lenses and pods of leucosome of medium- to coarse-grained, white biotite-plagioclase-K-feldspar-quartz ± garnet ± cordierite granite, giving the rock a gneissic appearance. Contacts between leucosome and paleosome are generally diffuse and biotite-rich selvages are common. The amount of leucosome varies with the composition of the paleosome; in outcrops with intercalated pelite and wacke layers, leucosome is restricted to or occurs in a higher proportion in the more pelitic layers. This relationship has been documented farther west in the English River subprovince by Breaks et al. (1978). The volume of leucosome in metatexite varies from 0-70 per cent but is generally less than 25 per cent in the more abundant wacke layers and is 50 per cent or greater in pelitic layers. Metatexites are cut by variable amounts of medium- to coarse-grained, white biotite-garnet-K-feldspar-quartz ± cordierite leucogranite, which is interpreted to be injected rather than produced in situ because: 1) it is relatively homogeneous, 2) it exhibits sharp discordant contacts with the metatexite, 3) where abundant, it includes angular metatexite xenoliths, 4) it occurs in highly variable amounts (10-90 per cent of an outcrop) in areas of similar composition and metamorphic grade, and 5) it locally cuts earlier intrusive tonalite bodies. Megacrysts of K-feldspar are common locally in biotite-garnet ± cordierite leucogranite.

Inhomogeneous diatexites are medium- to coarse-grained garnet-biotite-plagioclase-K-feldspar-quartz mafic granites with abundant (10-20 per cent) evenly distributed xenoliths of metatexite and garnet and biotite-rich schlieren. Megacrysts of plagioclase and K-feldspar are common. Rare homogeneous diatexites are non-xenolithic garnet-biotite mafic granites.

Migmatitic mafic gneiss consisting of orthopyroxene-hornblende - plagioclase ± clinopyroxene ± garnet ± quartz occurs locally as layers and blocks in metatextite and as xenoliths within inhomogeneous diatexite. Thin concordant layers of orthopyroxene-clinopyroxene-plagioclase-quartz leucosome give the rock its gneissic character. Thin reaction zones (average 3 cm thick) are locally developed at the contact between mafic gneiss and metasedimentary or tonalitic rocks. Reaction zones are richer in orthopyroxene and poorer in hornblende than the interior of the mafic gneiss. Layers of garnet-rich meta-banded iron formation and blocks of metagabbro and ultramafic rock occur locally within metasedimentary migmatites. Coarse grained to pegmatitic white biotite-K-feldspar-plagioclase-quartz ± andalusite granite dykes cut all components of the metasedimentary migmatites.

Metasedimentary rocks at Whitewater Lake (Fig. 49.5) generally have less leucosome than rocks in the eastern part of the area, have a lower proportion of biotite-garnet ± cordierite leucogranite, and cordierite and sillimanite are only present locally. Mafic layers rarely contain orthopyroxene, in contrast to mafic rocks in the east which invariably have some orthopyroxene.

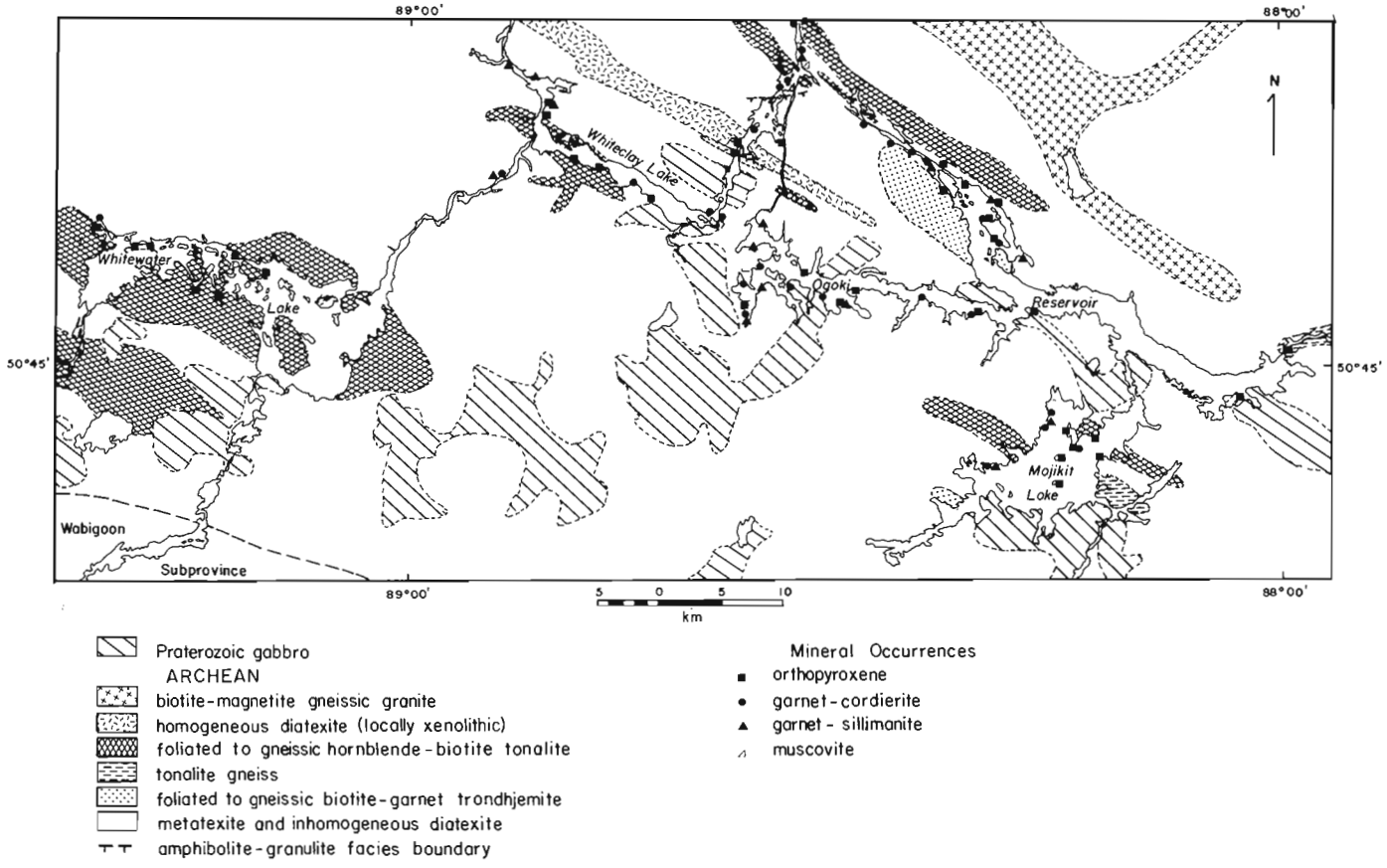

Figure 49.5. *Geology of the Whitewater–Mojikit lakes area, with metamorphic mineral occurrences (modified after Thurston et al. (1969), Sage et al. (1974), Stott (1984) and Percival (1983)).*

Table 49.2. Mineral analyses and derived pressure-temperature conditions for mafic gneiss (sample 1) and pelitic gneiss (sample 2) from Ogoki Reservoir. In addition to garnet (1-1) orthopyroxene (1-2), clinopyroxene (1-3) and plagioclase (1-4), sample contains hornblende, cummingtonite and quartz. Sample 2 contains garnet (2-1), biotite (2-2), cordierite (2-3), and plagioclase (2-4), as well as sillimanite, quartz and gahnite spinel.

	1-1	1-2	1-3	1-4	2-1	2-2	2-3	2-4
SiO_2	36.93	47.99	50.15	45.91	37.46	34.58	47.43	60.94
TiO_2	0.00	0.14	0.12		0.00	3.99	0.00	
Al_2O_3	20.98	0.70	1.29	34.30	20.48	17.43	32.94	24.16
FeO	29.64	39.63	19.38	0.19	36.45	20.11	8.78	0.07
MnO	2.78	1.27	0.57		1.33	0.00	0.14	
MgO	2.06	10.00	8.51		3.67	8.65	8.88	
CaO	7.73	0.77	19.92	17.93	0.91	0.19	0.00	5.52
Na_2O	0.00	0.00	0.00	1.26	0.00	0.23	0.00	9.12
K_2O	0.00	0.00	0.06	0.10	0.00	9.65	0.00	0.25
Total	100.12	100.56	100.11	99.69	100.3	95.14	98.17	100.06
(0)	(12)	(6)	(6)	(8)	(12)	(10)	(18)	(8)
Si	2.921	1.942	1.958	2.120	3.012	2.745	4.878	2.687
Al^{iv}		.003	.042			.255	1.122	
Al^{vi}	1.956	.033	.017	1.867	1.941	1.375	2.871	1.255
Ti		.004	.004			.238	0.000	
Fe^{3+}	.044	.074	.018	.007	.059		.250	.003
Fe^{2+}	1.916	1.266	.614		2.391	1.335	.505	
Mn	.186	.044	.019		.091		.012	
Mg	.243	.603	.495		.440	1.023	1.361	
Ca	.655	.033	.833	.887	.078	.016	0.000	.261
Na				.113		.035	0.000	.780
K				.006		.977	0.000	.014
Temperature (°C):	(a) 730					(b) 680		
Pressure (kb):	(c) 4.4 (f) 5.8	(d) 3.0 (g) 3.0	(e) 8.1			(h) 4.0	(i) 4.2	(j) 2.1

Notes: 1: Total iron as FeO; 2: Fe^{3+} from stoichiometry
(a) garnet-clinopyroxene thermometer (Ellis and Green, 1979)
(b) garnet-biotite thermometer (Ferry and Spear, 1978)
(c) pyrope-grossular-anorthite-enstatite-quartz barometer (Newton and Perkins, 1982)
(d) almandine-grossular-anorthite-ferrosilite-quartz barometer (Bohlen et al., 1982)
(e) Perkins and Chipera (in press) version of (c)
(f) Perkins and Chipera (in press) version of (d)
(g) pyrope-grossular-anorthite-diopside-quartz barometer (Newton and Perkins, 1982)
(h) grossular-anorthite-aluminosilicate-quartz barometer (Ghent, 1976) with activity coefficient ratio from Ghent et al. (1979)
(i) Newton and Haselton (1981) version of (h).
(j) same as (i) but with interaction parameters of Ganguly and Saxena (1984)

Early intrusive rocks

Early intrusive rocks occur as elongate (16-38 km long) concordant bodies and include: foliated to gneissic hornblende-biotite tonalite; foliated to gneissic biotite-garnet trondhjemite; tonalite gneiss and biotite-magnetite gneissic granite (Percival, 1983).

Foliated to gneissic tonalites are grey, medium grained rocks with hornblende-biotite-plagioclase-quartz ± orthopyroxene ± clinopyroxene assemblages. They are sparsely to moderately xenolithic with mafic tonalite and mafic rocks with assemblages of hornblende-plagioclase ± orthopyroxene ± clinopyroxene. Orthopyroxene and clinopyroxene were noted only in tonalites at Mojikit Lake. Small isolated pods of coarse grained leucosome of orthopyroxene-clinopyroxene-plagioclase-quartz with igneous appearance also occur in tonalites at Mojikit Lake. Tonalitic gneiss consists of thin alternating layers of medium grained, grey, foliated biotite ± hornblende tonalite and medium grained, pink foliated biotite granite. Xenoliths of metasedimentary rock within both foliated and gneissic tonalite indicate that metasedimentary rocks predate the tonalites.

Foliated to gneissic trondhjemitic rock is fine- to medium-grained, white, and has a biotite-garnet-plagioclase-quartz assemblage. Biotite-garnet trondhjemitic rock is locally interlayered with or occurs as blocks in metatexite, suggesting that it may represent more siliceous sedimentary compositions.

All tonalitic bodies are cut by medium grained pink biotite leucogranite, consisting of a biotite-plagioclase-K-feldspar-quartz ± garnet assemblage. Garnet occurs locally as large poikiloblasts. Pink, biotite leucogranite is distinguished from white biotite-garnet ± cordierite leucogranite found in metatexites by its colour, the absence of cordierite and its poikiloblastic garnet.

Structure and metamorphism

Foliation and gneissosity trend east to southeast and dip generally 40-85° N. Small scale structures such as folds, shear zones and faults are common in metasedimentary rocks, particularly where injected biotite-garnet ± cordierite leucogranite is the dominant rock type, suggesting that these structures developed on intrusion.

The occurrence of orthopyroxene in the leucosome of hornblende-biotite tonalite and mafic gneiss, in reaction zones between mafic blocks and metatexite and rarely in biotite-garnet ± cordierite leucogranite, indicates prograde metamorphism of all major rock types to the granulite facies. The granulite-amphibolite facies transition was observed in the northernmost part of the map area at Whiteclay Lake (Fig. 49.5) and is characterized by the disappearance of orthopyroxene from mafic rocks and the appearance of muscovite in metasedimentary and derived rocks. The patchy occurrence of orthopyroxene and the lower quantity of leucosome in metatexites at Whitewater Lake indicate that it may be near the western extent of granulite facies metamorphism in the Whitewater-Mojikit lakes area.

Preliminary thermometry and barometry based on garnet-sillimanite-plagioclase-quartz assemblages in metasediments and garnet-pyroxene-plagioclase-quartz assemblages in mafic rocks is summarized in Table 49.2.

Discussion

Temperatures of 680 to 720°C and pressures on the order of 4 to 5 kb (Table 49.2) indicate equilibration at relatively low pressure in the granulite facies. These values are similar to those derived from granulites farther west in the English River subprovince (Perkins and Chipera, in press) and are consistent with the model of metamorphism in an environment with an elevated geothermal gradient caused by high-level synmetamorphic plutonism (Breaks et al., 1978).

Biotite-garnet ± cordierite leucogranite and garnet-biotite mafic granite (diatexite) have many characteristics of S-type granites (Chappell and White, 1974; Pitcher, 1983), suggesting that both are derived by partial melting of metasedimentary rocks. The mafic composition of the garnet-biotite mafic granite implies a high degree of partial melting, whereas biotite-garnet ± cordierite leucogranite is closer to a minimum melt composition. Late biotite ± andalusite granite dykes postdate the peak of granulite facies metamorphism. It is hoped that current studies involving major and trace element chemistry of all major rock types and more detailed barometry and thermometry will provide a better understanding of the genetic relationships between the various granite types and the metasedimentary and tonalitic rocks.

References

Archibald, D.A., Glover, J.K., Price, R.A., Farrar, E., and Carmichael, D.M.
1983: Geochronology and tectonic implications of magmatism and metamorphism, southern Kootenay Arc and neighbouring regions, southeastern British Columbia. Part I. Jurassic to mid-Cretaceous; Canadian Journal of Earth Sciences, v. 20, p. 1891-1913.

Ayres, L.D.
1978: Metamorphism in the Superior Province of northwestern Ontario and its relationship to crustal development; in Metamorphism in the Canadian Shield, Geological Survey of Canada, Paper 78-10, p. 25-36.

Beakhouse, G.B.
1977: A subdivision of the western English River subprovince; Canadian Journal of Earth Sciences, v. 14, p. 1481-1491.

Birk, D.
1971: Progressive metamorphism of the Kashabowie Group at Shebandowan, Ontario, with special reference to zoning in garnets; unpublished B.Sc. thesis, Queen's University, Kingston, Ontario.

Bohlen, S.R., Wall, V.J., and Boettcher, A.L.
1983: Experimental investigation and application of garnet granulite equilibria; Contributions to Mineralogy and Petrology, v. 83, p. 52-61.

Borradaile, G.J.
1982: Comparison of Archean structural styles in two belts of the Canadian Superior Province; Precambrian Research, v. 19, p. 179-189.

Breaks, F.W., Bond, S.D., and Stone, D.
1978: Preliminary geological synthesis of the English River subprovince, northwestern Ontario and its bearing upon mineral exploration; Ontario Geological Survey, Miscellaneous Paper 72, 55 p.

Carmichael, D.M.
1978: Metamorphic bathozones and bathograds: a measure of the depth of post-metamorphic uplift and erosion on the regional scale; American Journal of Science, v. 278, p. 769-797.

Chappell, B.W. and White, A.J.R.
1974: Two contrasting granite types; Pacific Geology, v. 8, p. 173-174.

Coates, M.E.
1968: Stevens-Kagiano Lake area; Ontario Department of Mines, Geological Report 68, 22 p.

Ellis, D.J. and Green, D.H.
1979: An experimental study of the effect of Ca upon garnet-clinopyroxene Fe-Mg exchange equilibria; Contributions to Mineralogy and Petrology, v. 71, p. 13-22.

Ferry, J.M. and Spear, F.S.
1978: Experimental calibration of the partitioning of Fe and Mg between biotite and garnet; Contributions to Mineralogy and Petrology, v. 66, p. 113-117.

Ganguly, J. and Saxena, S.K.
1984: Mixing properties of aluminosilicate garnets: constraints from natural and experimental data, and application to geothermobarometry; American Mineralogist, v. 69, p. 88-97.

Ghent, E.D.
1976: Plagioclase-garnet-Al_2SiO_5-quartz: a potential geobarometer-geothermometer; American Mineralogist, v. 61, p. 710-714.

Ghent, E.D., Robbins, B., and Stout, M.Z.
1979: Geothermometry, geobarometry and fluid compositions of metamorphosed calc-silicates and pelites, Mica Creek, British Columbia; American Mineralogist, v. 64, p. 874-885.

Ishihara, S.
1981: The granitoid series and mineralization; Economic Geology, 75th Anniversary Volume, p. 458-484.

Kehlenbeck, M.M.
1976: Nature of the Quetico-Wabigoon boundary in the de Courcey-Smiley Lakes area, northwestern Ontario; Canadian Journal of Earth Sciences, v. 13, p. 737-748.

1984: Use of stratigraphic and structural-facing directions to delineate the geometry of refolded folds near Thunder Bay, Ontario; Geoscience Canada, v. 11, p. 23-32.

Kenah, C. and Hollister, L.D.
1982: Anatexis in the Central Gneiss Complex, British Columbia; in Migmatites, Melting and Metamorphism, ed. M.P. Atherton and C.D. Gribble; Shiva Geology Series, p. 142-162.

Lehto, D.A.W.
1974: Structural and petrological evolution of the Quetico gneiss belt in the Dog-Hawkeye Lakes area; unpublished B.Sc. thesis, Lakehead University, Thunder Bay, Ontario, 92 p.

Mackasey, W.O., Blackburn, C.E., and Trowell, N.F.
1974: A regional approach to the Wabigoon-Quetico belts and its bearing on exploration in northwestern Ontario; Ontario Division of Mines, Miscellaneous Paper 58, 30 p.

Miller, C.F. and Bradfish, L.J.
1980: An inner Cordilleran belt of muscovite-bearing plutons; Geology, v. 8, p. 412-416.

Moore, E.S.
1940: Geology and ore deposits of the Atikokan area; Ontario Department of Mines, 48th Annual Report, part II, p. 1-34.

Newton, R.C. and Haselton, H.T.
1981: Thermodynamics of the plagioclase-Al_2SiO_5-quartz geobarometer; in Thermodynamics of Minerals and Melts, ed. R.C. Newton, A. Navrotsky, and B.J. Wood; Springer-Verlag, p. 131-148.

Newton, R.C. and Perkins, D.
1982: Thermodynamic calibration of geobarometers based on the assemblages garnet-plagioclase-orthopyroxene (clinopyroxene)-quartz; American Mineralogist, v. 67, p. 203-222.

Percival, J.A.
1981: Geology of the Kapuskasing structural zone in the Chapleau-Foleyet area; Geological Survey of Canada, Open File Map 763.

1983: Preliminary results of geological synthesis in the western Superior Province; in Current Research, Part A, Geological Survey of Canada, Paper 83-1A, p. 125-131.

1985: The Kapuskasing structure in the Kapuskasing-Fraserdale area, Ontario; in Current Research, Part A, Geological Survey of Canada, Paper 85-1A, Report 1.

Percival, J.A. and Stern, R.A.
1984: Geological synthesis in the western Superior Province, Ontario; in Current Research, Part A, Geological Survey of Canada, Paper 84-1A, p. 397-408.

Percival, J.A., Card, K.D., Sage, R.P., Jensen, L.S., and Luhta, L.E.
1983: The Archean crust in the Wawa-Chapleau-Timmins Region; in A Cross Section of Archean Crust, ed. L.D. Ashwal and K.D. Card; Lunar and Planetary Institute Technical Report 83-03, p. 99-169.

Perkins, D. and Chipera, S.J.
– Garnet-orthopyroxene-plagioclase-quartz barometry: refinement and application to the English River subprovince and the Minnesota River Valley; Contributions to Mineralogy and Petrology. (in press)

Pirie, J.
1978: Geology of the Crooked Pine Lake area, District of Rainy River; Ontario Geological Survey Report 179, 73 p.

Pirie, J. and Mackasey, W.O.
1978: Preliminary examination of regional metamorphism in parts of Quetico metasedimentary belt, Superior Province, Ontario; in Metamorphism in the Canadian Shield, Geological Survey of Canada, Paper 78-10, p. 37-48.

Pitcher, W.S.
1979: The environmental control of granitic emplacement in orogenic belts; Geological Society of America, Abstracts with Programs, v. 11, p. 496.

1983: Granite type and tectonic environment; in Mountain Building Processes, ed. K.J. Hsu; Academic Press Inc., London, p. 19-40.

Sage, R.P., Breaks, F.W., Stott, G., McWilliams, G., and Bowen, R.P.
1974: Operation Ignace-Armstrong, Pashkokogan-Caribou Lakes Sheet, District of Thunder Bay; Ontario Department of Mines, Map P.962.

Sawyer, E.W.
1983: The structural history of a part of the Archaean Quetico metasedimentary belt, Superior Province, Canada; Precambrian Research, v. 22, p. 271-294.

Schairer, J.F. and Bowen, N.L.
1955: The system K_2O-Al_2O_3-SiO_2; American Journal of Science, v. 253, p. 681-746.

Schwerdtner, W.M., Stone, D., Osadetz, K., Morgan, J., and Stott, G.M.
1979: Granitoid complexes and the Archean tectonic record in the southern part of northwestern Ontario; Canadian Journal of Earth Sciences, v. 16, p. 1965-1977.

Schwerdtner, W.M., Stott, G.M., and Sutcliffe, R.H.
1983: Strain patterns of crescentic granitoid plutons in the Archean greenstone terrain of Ontario; Journal of Structural Geology, v. 5, p. 419-430.

Shirey, S.B. and Hanson, G.N.
1984: Mantle-derived Archean monzodiorites and trachyandesites; Nature, v. 310, p. 222-224.

Southwick, D.L.
1972: Vermilion granite-migmatite massif; in Geology of Minnesota: A Centennial Volume, ed. P.K. Sims and G.B. Morey; Minnesota Geological Survey, p. 108-119.

Stott, G.M.
1984: Mojikit Lake Sheet, District of Thunder Bay, Ontario; Ontario Geological Survey, Map P.267 (rev.).

Streckeisen, A.L.
1974: Classification and nomenclature of plutonic rocks; Geologisches Rundschau, v. 63, p. 773-786.

Strong, D.F. and Dickson, W.L.
1978: Geochemistry of Paleozoic granitoid plutons from contrasting tectonic zones of northeast Newfoundland; Canadian Journal of Earth Sciences, v. 15, p. 145-156.

Thurston, P.C., Carter, M.W., and Riley, R.A.
1969: Operation Fort Hope, Attwood-Caribou Lakes Sheet, Districts of Kenora, Patricia Portion, and Thunder Bay, Ontario; Ontario Department of Mines, Map P.564.

White, A.J.R. and Chappell, B.W.
1983: Granitoid types and their distribution in the Lachlan Fold Belt, Southeastern Australia; Geological Society of America, Memoir 159, p. 21-34.

HUMBER ARM ALLOCHTHON AND NEARBY GROUPS BETWEEN BONNE BAY AND PORTLAND CREEK, WESTERN NEWFOUNDLAND

EMR Research Agreement 259/04/84

Harold Williams[1], N.P. James[1], and R.K. Stevens[1]
Precambrian Geology Division

Williams, H., James, N.P., and Stevens, R.K., Humber Arm Allochthon and nearby groups between Bonne Bay and Portland Creek, western Newfoundland; in Current Research, Part A, Geological Survey of Canada, Paper 85-1A, p. 399-406, 1985.

Abstract

Precambrian rocks of the Grenvillian Long Range complex are overlain by a shallow water Cambro-Ordovician, mainly carbonate sequence (Forteau and Hawke Bay formations, St. George and Table Head groups) with Middle Ordovician clastics at its top (Norris Point Formation). At Bonne Bay these rocks are autochthonous but farther north they are parautochthonous where affected by thrusts and steep reverse faults at the Long Range structural front.

Cambro-Ordovician rocks of the Humber Arm Allochthon structurally overlie the shallow water sequence. The basal mélange is gradational with the underlying Norris Point Formation. Most of the Humber Arm Allochthon comprises northeast-trending belts of limestone breccia, platy limestone, dolomitic shales and cherts (Cow Head Group) which indicate a proximal to distal facies change from northwest to southeast. The overlying Ordovician Lower Head Formation contains Cow Head clasts in conglomerates. On the south side of Bonne Bay, feldspathic sandstones, probably of Lower Cambrian age, overlie the basal mélange of the allochthon. A mélange with sandstone and pillow lava blocks separates these sandstones from the overlying ophiolitic gabbros of the Little Port complex.

Structures in the area are dominated by assembly and emplacement of the Humber Arm Allochthon which involved Ordovician imbrication, and later, probably Devonian deformation at the Long Range structural front.

Résumé

Sur les roches précambriennes du complexe grenvillien de Long Range repose une séquence cambro-ordovicienne d'eau peu profonde constituée essentiellement de carbonate (formations de Forteau et de Hawke Bay, groupes de St. George et de Table Head) et coiffée de roches clastiques de l'Ordovicien moyen (formation de Norris Point). À la baie Bonne, ces roches sont autochtones mais, plus au nord, elles sont parautochtones et subissent l'influence de failles de chevauchement et de failles inverses très inclinées au front structural du complexe de Long Range.

Des roches cambro-ordoviciennes du terrain allochtone de Humber Arm reposent structuralement sur la séquence mise en place en eau peu profonde. Le mélange basal passe progressivement à la formation sous-jacente de Norris Point. La majeure partie de l'allochtone de Humber Arm comprend des zones à orientation nord-est de brèches de calcaire, de calcaires lités, de schistes dolomitiques et de cherts (groupe de Cow Head); elles indiquent le passage d'un faciès proximal à un faciès distal du nord-ouest en direction du sud-est. Les conglomérats de la formation susjacente de Lower Head, d'âge ordovicien, contient des clastes de Cow Head. Du côté sud de la baie Bonne, des grès feldspathiques, qui datent probablement du Cambrien inférieur, reposent sur le mélange basal de l'allochtone. Un mélange comprenant des grès et des blocs de lave en coussins sépare ces grès des gabbros ophiolitiques susjacents du complexe de Little Port.

Les structures de la région sont dominées par l'assemblage et la mise en place de l'allochtone de Humber Arm survenus au front structural du complexe de Long Range suite à un épisode d'imbrication durant l'Ordovicien et probablement d'un épisode de déformation au cours du Dévonien.

[1] Department of Earth Sciences, Memorial University of Newfoundland, St. John's, Newfoundland, A1B 3X5

Introduction

During 1984, the Humber Arm Allochthon, and autochthonous to parautochthonous rocks of the Paleozoic carbonate sequence and its underlying basement, were mapped across the Gros Morne area (12 H/12) with reconnaissance studies extended northward to St. Pauls Inlet (12 H/13) and into the Portland Creek area (12 I/4). This work is a continuation of a field investigation to cover the entire Humber Arm Allochthon and nearby groups (Williams, 1973, 1981; in press; Schillereff, 1979; Schillereff and Williams, 1979; Kennedy, 1980; Williams and Godfrey, 1980; Godfrey, 1982; Williams et al., 1982, 1983; Quinn and Williams, 1983; Williams et al., 1984; Nyman et al., 1984).

The Humber Arm allochthonous rocks occupy the coastal lowland between Bonne Bay and Portland Creek, so that exposure is generally poor. Toward the east, the Paleozoic carbonate sequence forms rolling hills and discrete sharp summits. Precambrian granites farther east form the morphologic front of the Long Range Mountains. The coastal lowland is covered by swamps and stunted spruce. This also has bedrock-controlled, wooded, northeast-trending ridges, but these lack exposures in most cases. The carbonate sequence is tree covered in most places but there are local bare hills and cliff faces. The Precambrian rocks are barren and well exposed. Ponds that resemble fiords trend east-west across the Long Range morphologic front and geologic structural grain. From south to north these are Bakers Brook Pond, Western Brook Pond, St. Pauls Inlet, Parsons Pond and Portland Creek Pond. They provide access and display important shoreline exposures across the allochthonous rocks. Coastal exposure varies from poor to excellent with points and headlands separated by long intervals of sand or boulder beaches. Streams provide the only other outcrops in lowland areas.

Some rocks of the area such as those at Cow Head have been studied in detail and they are well known for their coarse limestone breccias, stratigraphy and faunas (Kindle and Whittington, 1958; Whittington, 1963; James, 1981; Fortey et al., 1982; Kindle, 1982). Rocks at other localities, especially inland, are relatively unknown and there have been few attempts to combine stratigraphic studies with regional structural analyses.

The classic work of Schuchert and Dunbar (1934) forms the basis of all later studies in western Newfoundland. Troelsen (1947) mapped the southern part of the study area at Bonne Bay. Oxley (1953) mapped the area between Western Brook Pond and Portland Creek, and the area between Parsons Pond and Bonne Bay forms part of a reconnaissance map by Baird (1960). Detailed stratigraphic studies of coastal exposures augmented by shoreline sections at Parsons Pond, St. Pauls Inlet and Western Brook Pond were conducted by James and Stevens (1982). Stratigraphy and faunas at Rocky Harbour were studied by Gonzalez-Bonorino (1979) and a detailed structural study of the same area is in progress by Nicholas Vermuellen of the University of Utrecht. The peninsula opposite Norris Point is being mapped by L. Quinn, and the Precambrian rocks and their cover are being mapped on the north side of Bonne Bay by M. Nyman.

General geology

Rocks of the study area are of Precambrian to Middle Ordovician age (Fig. 50.1). The oldest rocks are Precambrian granites of the Long Range Complex that form part of the Grenvillian Long Range Inlier. Two Paleozoic sequences, largely coeval, present problems in stratigraphic and structural interpretation. A shallow-water mainly carbonate sequence (Forteau, Hawke Bay, St. George, Table Head) with clastics at its top (Norris Point) can be linked stratigraphically to Long Range basement rocks. A deeper water limestone breccia-shale-chert sequence (Cow Head), also with clastics at its top (Lower Head), occurs in repeated belts structurally above the carbonate sequence. The present juxtaposition of the coeval contrasting sequences demands tectonic transport. Structural polarity and paleogeographic considerations indicate that the deeper water sequence was transported westward across the shallow water carbonate sequence (Rodgers and Neale, 1963; Stevens, 1970; Williams and Stevens, 1974). Toward the south the coeval sequences are separated by mélange (Rocky Harbour), which surrounds discrete blocks or olistoliths of the Cow Head-Lower Head section, grey shale, quartz sandstone and polymictic conglomerate (Irishtown), limestone breccia (Cape Cormorant) and shale and sandstone (Norris Point). A structural slice of thick feldspathic sandstones (Sellars) occurs above the mélange opposite Norris Point and it is overlain in turn by a structurally higher mélange (Crolly Cove) and an uppermost ophiolitic slice (Little Port Complex). All of the transported rocks above the carbonate sequence are part of the Humber Arm Allochthon.

At Gros Morne and southward, basement granites of the Long Range Complex are overlain with profound unconformity by gently south-dipping beds of the Lower Cambrian Forteau and Hawke Bay formations. The same unconformity, although poorly exposed, occurs between basement and cover northward between St. Pauls Inlet and Parsons Pond. It is present also at the east end of Parsons Pond, and between Parsons Pond and Portland Creek Pond. Elsewhere the basement is faulted against Upper Cambrian to Middle Ordovician rocks of the St. George and Table Head groups, and at Western Brook Pond, granites abut rocks of the Humber Arm Allochthon. This phase of structural development that involved the basement rocks followed the emplacement of the Humber Arm Allochthon.

North of Bonne Bay, rocks of the Humber Arm Allochthon are all sedimentary and they are of different facies compared to coeval rocks to the south. Structural relationships in the north between allochthonous and autochthonous rocks, and the notion of an allochthonous Long Range basement complex have never been properly addressed by work in the field. Since the lithology and stratigraphy of most rocks in the area north of Bonne Bay have been described elsewhere (Schuchert and Dunbar, 1934; Kindle and Whittington, 1958; Levesque, 1977; James et al., 1980; James and Stevens, 1982; Nyman et al., 1984), structural relationships and regional lithological patterns are emphasized in the following brief account.

Autochthonous and parautochthonous rocks

The gently southward-dipping cover sequence that overlies the Long Range Inlier at Bonne Bay is complete and essentially uninterrupted structurally from base to top (Nyman et al., 1984). It is overlain in turn by transported rocks of the Humber Arm Allochthon. North of Bonne Bay to Western Brook Pond, more and more of the stratigraphy of the autochthonous sequence is absent and the entire sequence is missing at Western Brook Pond where the Precambrian basement abuts the Humber Arm Allochthon. This implies increasing transport of the Long Range Complex from Bonne Bay to Western Brook Pond. Structural slivers of St. George and Table Head limestones that occur between the Humber Arm Allochthon and Long Range Complex, such as the example at St. Pauls Inlet, have also been moved unknown distances. The Long Range Complex and its cover sequence therefore are autochthonous in some places and parautochthonous in others.

Basement rocks

The Long Range Complex (Baird, 1960) is pink, medium to coarse grained, massive to foliated granite, where observed between Bakers Brook Pond and Parsons Pond. Near structural contacts with the Paleozoic carbonate sequence, the rocks are sheared and broken. Examples of reddish, crushed rocks occur at St. Pauls Inlet, and greenish chloritic zones occur in pink granites where they are structurally above nearby carbonates four kilometres south of Parsons Pond.

The unconformable relationship between the Long Range Complex and overlying gently dipping beds of the Lower Cambrian Forteau Formation is easily mapped at Gros Morne and southward but the actual contact is nowhere well exposed. Northeast-trending high-angle faults that cut the unconformity are downthrown on their northwest sides.

North of Bakers Brook Pond, Paleozoic rocks of both the carbonate sequence and Humber Arm Allochthon are commonly overturned to the west near the Long Range morphologic front, implying thrusts or reverse faults that bring the Long Range Complex westward and structurally above the Paleozoic rocks. In a few places north of St. Pauls Inlet, Lower Cambrian rocks rest unconformably upon basement granites. Where this occurs the Long Range structural front lies west of the basement granites and separates the carbonate sequence from the Humber Arm Allochthon.

A structural contact between the Long Range Complex and carbonate sequence can be observed in several places. An obvious faulted contact is well exposed 4 km south of Parsons Pond in the bed of a brook that drains westward and then northward into Parsons Pond (West Brook). At the contact, Long Range granites are chloritized, crushed and broken, and overlie recrystallized limestones that have a tectonic banding and numerous calcite stringers. The fault contact dips 30 degrees eastward and tectonic banding in the carbonates is parallel to the fault. Downstream and toward the west, bedding in the carbonates dips moderately eastward toward the basement rocks.

Where exposed at St. Pauls Inlet, the contact has less morphologic expression and is steeper. There, an outlier of Precambrian granite is in contact with carbonates to the east. The contact is marked by crushed granite and recrystallized limestone, and steep quartz veins mark the contact just north of the pond. Small patches of reddish quartzite that occur at the contact may represent the Lower Cambrian Hawke Bay Formation, structurally comingled in the contact zone.

Three kilometres south of Western Brook Pond at Stag Brook, intensely deformed grey to black shales of unknown affinity occur along the projection of the Long Range morphologic front and between limestones downstream and granites upstream.

On the south side of St. Pauls Inlet and north side of Bakers Brook Pond, shear zones or faults in the Long Range Complex dip moderately southeastward or eastward and these may represent subsidary faults that parallel the major tectonic contact between granites and carbonates to the west.

Paleozoic carbonate cover sequence

The Forteau and Hawke Bay formations (Schuchert and Dunbar, 1934) vary from essentially undeformed and gently dipping at Gros Morne to openly folded at Deer Arm and southeastward. A single prominent cleavage trends northeast and dips steeply southeast. A fault is inferred between the Lower Cambrian rocks to the east of Deer Arm and carbonates of the St. George and Table Head groups to the west. The inference is based on stratigraphic omission, and westward overturning in the carbonate sequence.

In the small area of cover rocks above the basement to the north of St. Pauls Inlet, bedding varies from upright and moderately west-dipping in the south to overturned and east-dipping in the north. The overturned section is exposed in a stream bed where Hawke Bay quartzites are overlain by dolomites and limestones.

East of Parsons Pond, another local occurrence of Lower Cambrian rocks shows a similar structural style, with steeply west-dipping beds in the south and overturned beds with stratigraphic omission to the north. An occurrence of the Forteau Formation farther north dips gently westward and away from the Precambrian basement, but the implied unconformity is not exposed.

Limestones and dolomites that occur along the front of the Long Range Inlier are assigned collectively to the St. George and Table Head groups (Schuchert and Dunbar, 1934). South of Norris Point, the section dips moderately southwestward and is upright with Table Head limestones overlain by shales and sandstones, in turn overlain by mélange and transported rocks of the Humber Arm Allochthon. At Norris Point and northward, the same section is steep and in places overturned. Overturning is also common in isolated exposures to the north of St. Pauls Inlet, but farther north opposite Portland Hill the carbonate sequence dips gently to moderately westward and the beds are upright.

Shales and graded sandstones that overlie the Table Head limestones are assigned informally to the Norris Point formation. Stratigraphic contacts can be seen on both sides of Bonne Bay at Norris Point and a similar relationship between Table Head limestones and overlying shales occurs on the west limb of an anticline exposed on the north shore of Portland Creek Pond. The informal name, Sandbar formation (Williams et al., 1984), used for these rocks south of Bonne Bay is now dropped.

A prominent ridge of carbonate breccia between Bakers Brook and Western Brook Pond is assigned to the Cape Cormorant Formation (Klappa et al., 1980). Similar breccias occur at Berry Hill and southward where they are interpreted as large olistoliths structurally incorporated in mélange. North of Bakers Brook, the Cape Cormorant breccias are overlain by the Norris Point formation, implying that they are equivalent to Table Head limestones at Bonne Bay. Dips are generally to the east, indicating an overturned section or more likely a thrust contact between the Cape Cormorant to the west and carbonates to the east. Another large area of Cape Cormorant breccia occurs north of Portland Creek but stratigraphic relationships there are unknown. The Cape Cormorant breccia is not represented in nearby continuous stratigraphic sections of the carbonate sequence, suggesting that all occurrences are parautochthonous with respect to nearby sections of the Table Head Group.

The Norris Point formation is everywhere strongly cleaved and two generations of cleavage are recognized locally. A prominent cleavage at Norris Point is at high angles to bedding and its easterly strike contrasts with a northeast-trending cleavage in rocks farther east. The Norris Point formation at the top of the autochthonous section is everywhere more deformed than the Forteau and Hawke Bay formations, even though the Norris Point occurs farther west and in the general direction of decreasing intensity of deformation in western Newfoundland.

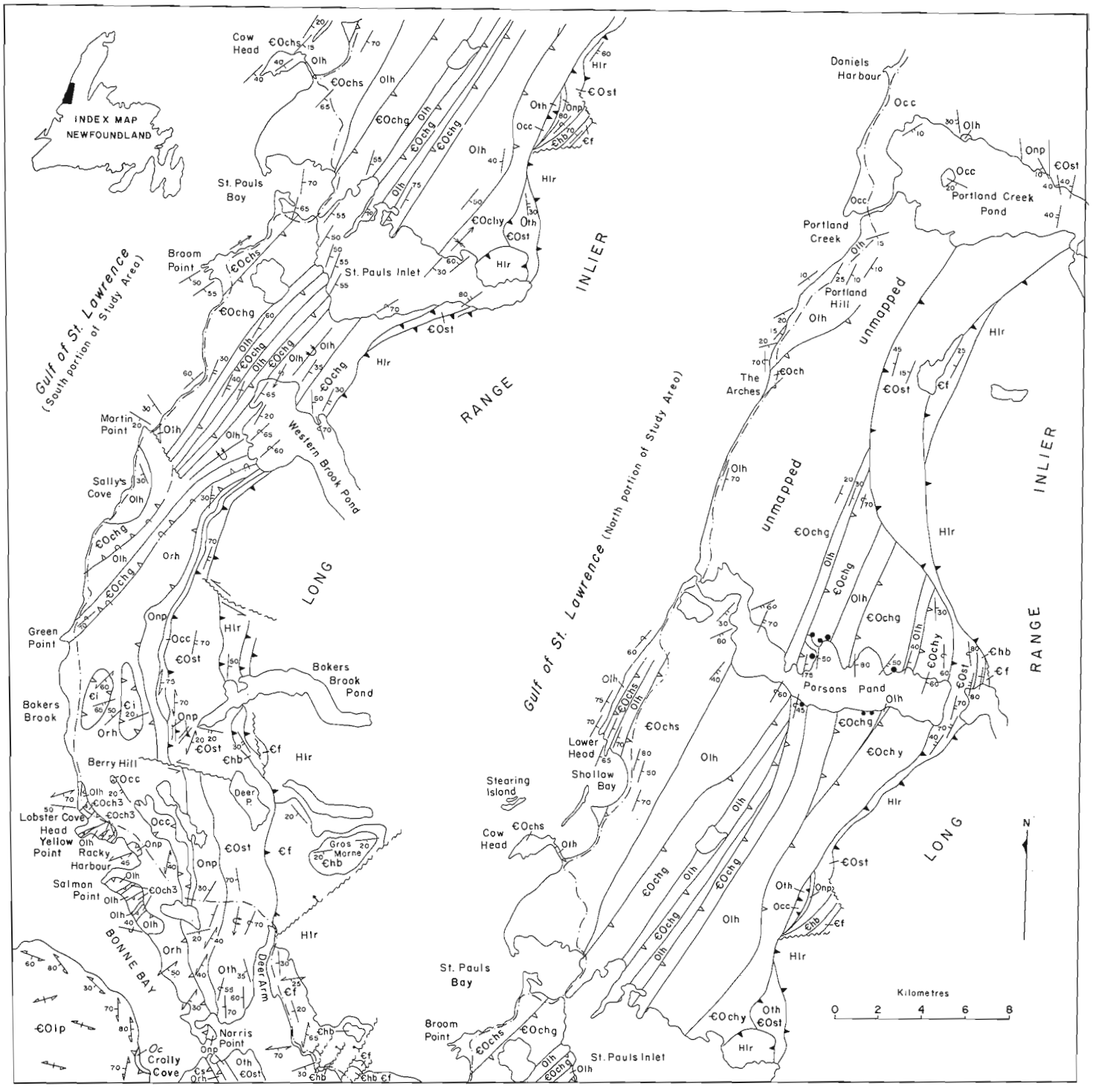

Figure 50.1. *General geology of the area between Bonne Bay and Portland Creek, western Newfoundland.*

Humber Arm Allochthon

Rocks and structural styles of the Humber Arm Allochthon show significant differences north of Bonne Bay compared with those farther south. The Cow Head Group (Kindle and Whittington, 1958) and overlying sandstones dominate the allochthon and their occurrence in northeast-trending repeated belts represents a structural style that is not well developed among allochthonous rocks south of Bonne Bay. The occurrence of imbricated structural slices surrounded by mélange, as at Lobster Cove Head and Salmon Point, and occurrences of Cape Cormorant breccia as large blocks within mélange are also of special interest.

The extensively developed mélange that directly overlies the Norris Point formation is referred to informally as the Rocky Harbour mélange. Correlatives to the south (Williams et al., 1984) were informally designated Gadds Point mélange, but the Rocky Harbour exposures are superior, and the mélange there is more extensive and

HUMBER ARM ALLOCHTHON (Structural Succession)

Upper Cambrian to Lower Ordovician

Little Port Complex (overlies Crolly Cove melange)

-Olp Massive to banded and foliated grey gabbro, massive to foliated black mafic dykes, minor grey trondhjemite.

Middle Ordovician

Crolly Cove melange*

Oc Grey to black scaly shale with blocks of Sellars sandstone and green pillow lava.

Lower Cambrian

Sellars formation* (overlies Rocky Harbour melange)

-Cs Thick bedded grey to pink coarse feldspathic sandstone, graded beds with pebbly bases, minor red and green shale.

Lower to Middle Ordovician

Lower Head formation* (overlies Cow Head Group)

Olh Medium to thick bedded grey to green sandstone, pebble to boulder conglomerate with clasts of red argillite, chert, limestone and minor limestone breccia.

Middle Cambrian to lower Middle Ordovician

Cow Head Group (overlies Rocky Harbour melange)

-COch Coarse boulder to cobble and pebble limestone breccia and conglomerate, lime sandstone, thin bedded platy limestone, grey to black shale, green to black chert, buff dolomitic shale, includes undated dolomitic limestone breccia of unknown affinity at 'The Arches'. Shallow Bay formation* (-COchs) contains abundant thick units of coarse limestone breccia and conglomerate; Green Point formation* (-COchg) has few and thinner units of mainly cobble to pebble limestone breccia with more shale; Yellow Point formation (-COchy) has buff dolomitic shale, grey to black shale, chert, thin bedded platy limestone, minor thin units of pebble limestone breccia.

Middle Ordovician

Rocky Harbour melange* (gradational above Norris Point formation)

Orh Mainly grey scaly shale with blocks of grey to buff sandstone. Surrounds imbricated sections of Yellow Point (-COchy) and Lower Head (Olh) formations at Salmon Point and Lobster Cove Head, includes Norris Point formation (Onp) at Rocky Harbour, surrounds Irishtown Formation (-Ci) of shale, quartz sandstone and polymictic conglomerate with fossiliferous Cambrian limestone clasts at Bakers Brook, and interpreted to surround areas of Cape Cormorant Formation (Occ) at Berry Hill and southward.

AUTOCHTHONOUS AND PARAUTOCHTHONOUS ROCKS

Middle Ordovician

Norris Point formation*

Onp Medium to thin bedded grey shale and graded beds of sandstone and siltstone.

Cape Cormorant Formation

Occ Medium to coarse limestone breccia with clasts of mainly Table Head limestone.

Upper Cambrian to Middle Ordovician

St. George and Table Head Groups

-COst Medium to thick bedded grey limestone, dense fine-grained white limestone, grey to buff dolomite, minor shale, grey to white marble near Long Range structural front; includes medium to thin bedded dolomite, shale and limestone of possible Middle Cambrian age; Oth, thick bedded grey limestone of Table Head Group.

Lower Cambrian

Hawke Bay Formation

-Chb Thick bedded massive to crossbedded white and pink quartzite.

Forteau Formation

-Cf Medium to thin bedded grey, green to buff shale and grey to buff limy siltstone and limestone, local thick limestone beds; includes a thin unit of green sandstone and arkosic sandstone at base.

Precambrian (Helikian)

Long Range Complex

Hlr Foliated to massive pink granite, sheared pink to reddish and greenish granite.

* New stratigraphic names are informal

Stratigraphic contact, assumed in areas of poor exposure that are identifiable by a lack of structural symbols in Figure 1.

Early thrust fault or tectonic contact beneath allochthonous slice or around large olistolith

Overturned thrust or tectonic contact . . . . . .

Late or out-of-sequence thrust fault or high angle reverse fault . .

High angle fault with sense of offset, dot indicates downthrown side . . . . .

Bedding, tops known, inclined, overturned, vertical . . . . .

Bedding, tops unknown, inclined, vertical . . . . . .

Dominant cleavage in sedimentary rocks, inclined, vertical . .

Foliation in plutonic rocks, inclined, vertical . . . . . .

Axes of minor folds with direction of plunge . . . . . .

Synclinal axis with plunge . . . . . .

Axis of overturned syncline . . . . . .

Axis of overturned anticline with plunge . . . . . .

Petroleum exploratory well . . . . . .

Main highway . . . . . .

more accessible. The name Gadds Point is therefore dropped. The Rocky Harbour mélange extends along the east side of the allochthon from Bonne Bay to Western Brook Pond and it is widest in the vicinity of Rocky Harbour and southward. The mélange forms a uniformly narrow zone on the south side of Bonne Bay and southward.

The Rocky Harbour mélange has a scaly grey shale matrix with several generations of cleavage. Most blocks are sandstone and siltstone but buff dolomite, limestone and limestone breccia are common in places. Blocks range from pebbles to hillside outcrops a kilometre in width. The largest blocks contained in or surrounded by shales are the Cape Cormorant breccias at Berry Hill and southward, the Irishtown Formation at Bakers Brook, and the imbricated slices at Lobster Cove Head and Salmon Point. Well developed mélange occurs between intact rock slices to the north of Lobster Cove and along tectonic boundaries between the imbricated slices to the south of Salmon Point. In the vicinity of Norris Point, the Norris Point formation clearly grades upwards into the Rocky Harbour mélange. Shales and sandstones of the Norris Point formation are progressively disrupted at the contact with the bedded section passing into disturbed shales and sandstones and then into shales with sandstone blocks. Farther from the contact, blocks that are exotic to the carbonate sequence appear in the grey shaly matrix. The Rocky Harbour mélange is unknown north of Western Brook Pond and it is absent or unexposed between repeated belts of the Cow Head Group north of Green Point.

Between Green Point and Portland Creek, the Humber Arm Allochthon consists of Cambrian-Ordovician limestone breccias, platy limestones, dolomitic shales and cherts that are overlain by green sandstones. The rocks occur in northeast-trending belts with separate sections dipping southeast and facing southeast, except where locally folded and overturned especially at the Long Range structural front. The breccias exhibit rapid facies changes, even within local sections, and they are lenticular, commonly thinning northeastward. Synsedimentary erosion and recycled breccia blocks are common.

At Cow Head and vicinity, the rocks were assigned to the Cow Head Series (Schuchert and Dunbar, 1934) or the Cow Head Group (Kindle and Whittington, 1958). Finer and shalier equivalents to the east or south across the structural grain were called the Green Point Series or Green Point Formation (Schuchert and Dunbar, 1934), or the Green Point-St. Pauls Group (Oxley, 1953). Overlying sandstones were assigned to the Long Point sandstone (Schuchert and Dunbar, 1934) or were purposely unnamed (Kindle and Whittington, 1958).

The Cambrian-Ordovician limestone breccia, platy limestone, shale and chert sections are essentially coeval and related stratigraphically. All are assigned to the Cow Head Group. The overlying sandstones are unrelated depositionally and are named the Lower Head sandstone. Regional mapping indicates that the Cow Head Group can be divided into three gradational facies. The coarsest, thickest and most abundant limestone breccias occur toward the west in the vicinity of Cow Head (COchs, Fig. 50.1). Toward the east the breccias are progressively finer, thinner and less frequent in local stratigraphic sections that contain more platy limestone and shale (COchg). Sections farther east are mainly shaly with dolomitic buff shales, platy limestone and only minor limestone breccia (COchy). The divisions are equivalent to formations and informal names from west to east are, Shallow Bay (COchs), Green Point (COchg) and Yellow Point (COchy). This practical threefold division of the Cow Head Group shows that the arrangement of lithic belts records a proximal to distal facies change from west to east. Depositional contacts between the Cow Head Group and overlying Lower Head sandstones are exposed at Western Brook Pont, St. Pauls Inlet, Lower Head, Lobster Cove Head and Salmon Point. Lower Head sandstones are interlayered with the highest limestone breccia units of the Green Point formation at St. Pauls Inlet, and here and elsewhere the base of the Lower Head is taken as the lowest sandstone bed in the section.

Sandstones of the Lower Head formation range in age from upper Lower Ordovician to lower Middle Ordovician and possibly record a westward transgression across the repeated Cow Head sections. Rocks of similar aspect occur above the Middle Ordovician Table Head Group just north of the study area, so that the entire Cow Head Group and carbonate sequence toward the west were transgressed by sands of Lower Head type. In the study area, coarser varieties of the Lower Head and its conglomeratic units are quartz-feldspar sandstones with common red shale, chert, limestone and limestone breccia clasts. The largest clasts are an obvious sampling of Cow Head Group lithologies. Conglomeratic varieties occur at Portland Hill, at the southwest shore of St. Pauls Inlet, and south of Martin Point. At Portland Hill, limestone conglomerates increase in abundance and coarseness upward in the stratigraphic section. A cross-bedded quartz sandstone that is whitish and cleaner than other varieties of the Lower Head occurs on the coast 4 km north of Parsons Pond.

The repetition of northeast-trending belts of Cow Head-Lower Head rocks is interpreted as thrust imbrication of the southeast-facing southeast-dipping sections. The actual structural contacts are exposed in only a few places, but the evidence for their presence elsewhere is strong. On the southwest side of St. Pauls Inlet, Lower Head sandstones dip southeastward beneath rocks of the Green Point formation. The contact is marked by disruption of both rock units and a narrow zone of shaly mélange. Minor folds are inclined westward. Similarly at Lower Head, southeast-dipping sandstones are in structural contact with Shallow Bay limestone and limestone breccias. The contact there is marked by tight minor folds in shales and a large disrupted limestone breccia block is surrounded by shales in the contact zone. An obvious repetition of Yellow Point-Lower Head sections with tectonic contacts between structural blocks and local mélange development occurs at Lobster Cove Head and south of Salmon Point. Perhaps the strongest evidence for thrust repetition of the Cow Head Group is provided by the log of a petroleum exploration well at Parsons Pond (Fleming, 1970). Over its 4200 foot (1300 m) vertical length the well penetrated two intervals of the Green Point formation separated by, and each structurally above, Lower Head sandstones.

The number of repeated belts shown in Figure 50.1 is interpreted from existing exposures and air photo expression. The drillhole data imply that the number of belts depicted is minimal and that the actual number of imbricates is far greater.

The timing of imbrication is difficult to ascertain. At Lobster Cove Head and Salmon Point, the structural slices are separated in places by mélange and they are surrounded by the Rocky Harbour mélange. Since the mélanges relate to the assembly and transport of structural slices, the imbrication here is reasonably interpreted as Ordovician. Farther north between Green Point and Parsons Pond, the imbrication is also thought to be Ordovician and related to the assembly and emplacement of the Humber Arm Allochthon. However overturning of the Cow Head Group, such as that exhibited at Green Point and northeastwards at the Long Range structural front, and the formation of steep westerly inclined folds that increase in abundance from west to east across the group at St. Pauls Inlet and Parsons Pond are interpreted as later structural features. These were superposed on an already imbricated structural pile, most reasonably in response to faulting at the Long Range structural front. Relationships across the Humber Arm Allochthon at its southern end in the Stephenville area suggest a Devonian age for this latest deformation (Williams, in press).

On the south side of Bonne Bay, coarse feldspathic sandstones of the Sellars formation (Williams et al., 1984) that are graded with pebbly bases, occur above the Rocky Harbour mélange. The sedimentology of these rocks is the subject of a continuing study. Preliminary results indicate that the rocks are unrelated to the Lower Head and that they are older and derived entirely from a Grenvillian source.

At Crolly Cove, a locally spectacular mélange separates the Sellars formation from the overlying Little Port Complex. Blocks of Sellars sandstone and resistant green pillow lava occur in a black shale matrix.

The Little Port Complex consists mainly of foliated gabbros. Within the complex, mafic dykes and trondhjemites cut the foliated gabbros and the younger rocks are themselves locally foliated and almost everywhere sheared and broken.

Structure

Structures in the area are dominated by the assembly and emplacement of the Humber Arm Allochthon and by later deformation at the Long Range structural front. Several important observations in the study area bear on the question of an allochthonous Long Range Inlier. At Bonne Bay and southward, the Long Range Complex is unconformably overlain by Lower Cambrian strata which continue upward into the Table Head Group and overlying Norris Point formation without a major break. Eastward toward Wiltondale, the intensity of deformation in cover rocks increases profoundly with different structural styles and complex basement-cover relationships. However at Bonne Bay, the Long Range Complex is autochthonous with respect to its carbonate cover sequence.

From Bonne Bay to Western Brook Pond, more and more of the carbonate sequence is absent and at Western Brook Pond the Long Range Complex is in contact with rocks of the Humber Arm Allochthon. Overturning of local stratigraphic sections to the north of Bonne Bay and repetitions of stratigraphy at the western end of Bakers Brook Pond all favour an overthrust or allochthonous Long Range Inlier. A similar situation prevails at least as far as Parsons Pond and the truncation of Cow Head-Lower Head belts implies overthrusting still farther northward. A more complete stratigraphy in cover rocks that dip uniformly westward and away from the basement rocks near Portland Creek Pond suggests a basement-cover situation like that at Bonne Bay. Overturning of the Green Point formation from Green Point to Parsons Pond appears to define a westerly-overturned footwall-syncline in response to an overthrust Long Range Inlier.

Between Bakers Brook Pond and Western Brook Pond the Long Range Complex is offset westward by a left lateral tear fault. A marked air photo lineament may represent a similar fault at Deer Pond. The overall situation suggests increasing westward transport of the Long Range Inlier between Bakers Brook Pond and Western Brook Pond with the Precambrian rocks advancing northwestward with respect to cover rocks along left lateral tear faults. Steep northwest-trending faults with left lateral displacement also affect Cow Head sections in many places.

An allochthonous Long Range Inlier at the structural salient between Bakers Brook Pond and St. Pauls Inlet explains the omission of several northeast-trending lithic belts as follows: (a) the Paleozoic carbonate sequence at Western Brook Pond, (b) the Rocky Harbour mélange north of Western Brook Pond, and (c) the Yellow Point formation south of St. Pauls Inlet and its reappearance along strike at Rocky Harbour. Furthermore a wide zone of relatively intense deformation in the Paleozoic autochthonous sequence and nearby parts of the Humber Arm Allochthon coincides with the Long Range morphologic front from Bonne Bay to Portland Creek Pond.

The occurrence of the Paleozoic carbonate sequence between the Humber Arm Allochthon and Long Range Complex almost everywhere along the structural front and the occurrence of local complete autochthonous sections stratigraphically upon the Long Range Complex speak against a highly allochthonous Long Range Inlier. Transport may be in the order of only a few kilometres on steep reverse faults or a few tens of kilometres on moderately dipping thrusts at structural salients.

The Parsons Pond area has been of interest for its petroleum seepages since early in the last century. A number of exploration wells were drilled along the shores of Parsons Pond and at St. Pauls Inlet. A complete history of petroleum exploration is given by Fleming (1970).

Acknowledgments

The authors wish to thank Alvin Crocker for his cheerful field assistance and canoe expertise. Thanks are also extended, to Daniel Lesauteur and his staff at Gros Morne National Park for their help with field work, to L.M. Cumming and J.A. Karson for the use of compilation maps, to P.A. Cawood and J.W. Botsford for work carried out in the field, and to J.W. Botsford and L. Quinn for critically reading this paper. Excellent flying service was provided by Viking Helicopters.

Our work in western Newfoundland is supported by operating grants from the Natural Sciences and Engineering Research Council of Canada, Research Agreements with the Department of Energy, Mines and Resources through the Geological Survey of Canada, and fellowships to graduate students from Memorial University of Newfoundland. We thank all of these institutions for their continued support.

References

Baird, D.M.
1960: Sandy Lake (west half), Newfoundland; Geological Survey of Canada, Map 47-1959.

Fleming, J.M.
1970: Petroleum Exploration in Newfoundland and Labrador; Newfoundland Department of Mines, Agriculture and Resources, Mineral Resources Report No. 3, 118 p.

Fortey, R.A., Landing, E., and Skevington, D.
1982: Cambrian-Ordovician boundary sections in the Cow Head Group, western Newfoundland; in The Cambrian-Ordovician boundary: sections, fossil distributions and correlations, ed. M.G. Bassett and W.G. Dean; National Museum of Wales, Geological Series No. 3, Cardiff, p. 95-129.

Godfrey, S.C.
1982: Rock groups, structural slices and deformation in the Humber Arm Allochthon at Serpentine Lake, western Newfoundland; unpublished M.Sc. thesis, Memorial University of Newfoundland, 182 p.

Gonzalez-Bonorina, G.
1979: Sedimentology and Stratigraphy of the Curling Group (Humber Arm Supergroup), central western Newfoundland; Ph.D. thesis, McMaster University, 294 p.

James, N.P.
1981: Megablocks of calcified algae in the Cow Head Breccia, western Newfoundland: vestiges of a Cambro-Ordovician platform margin; Geological Society of America Bulletin, v. 92, p. 799-811.

James, N.P. and Stevens, R.K.
1982: Anatomy and evolution of a Lower Paleozoic continental margin; International Association of Sedimentologists Guidebook, Excursion 2B, 75 p.

James, N.P., Klappa, C.F., Skevington, D., and Stevens, R.K.
1980: Cambro-Ordovician of west Newfoundland – Sediments and Faunas; Guidebook, Trip 13, Geological Association of Canada, 88 p.

Kennedy, D.P.
1980: Geology of the Corner Brook Lake area, western Newfoundland; in Current Research, Part A, Geological Survey of Canada, Paper 80-1A, p. 235-240.

Kindle, C.H.
1982: The C.H. Kindle Collection: Middle Cambrian to Lower Ordovician trilobites from the Cow Head Group, western Newfoundland; in Current Research, Part C, Geological Survey of Canada, Paper 82-1C, p. 1-17.

Kindle, C.H. and Whittington, H.B.
1958: Stratigraphy of the Cow Head region, western Newfoundland; Geological Society of America Bulletin, v. 69, p. 315-342.

Klappa, C.F., Opalinski, P.R., and James, N.P.
1980: Ordovician Table Head Group of western Newfoundland: a revised stratigraphy; Canadian Journal of Earth Sciences, v. 17, p. 1007-1019.

Levesque, R.J.
1977: Stratigraphy and sedimentology of the Middle Cambrian to Lower Ordovician shallow water carbonate rocks, western Newfoundland; unpublished M.Sc. thesis, Memorial University of Newfoundland, 276 p.

Nyman, M., Quinn, L., Reusch, D.N., and Williams, H.
1984: Geology of Lomond map area, Newfoundland; in Current Research, Part A, Geological Survey of Canada, Paper 84-1A, p. 157-164.

Oxley, P.
1953: Geology of Parsons Pond-St. Pauls area, west coast, Newfoundland; Newfoundland Geological Survey Report No. 5, 53 p.

Quinn, L. and Williams, H.
1983: Humber Arm Allochthon at South Arm, Bonne Bay, west Newfoundland; in Current Research, Part A, Geological Survey of Canada, Paper 83-1A, p. 179-182.

Rodgers, J. and Neale, E.R.W.
1963: Possible "Taconic" klippen in western Newfoundland; American Journal of Science, v. 261, p. 713-730.

Schillereff, H.S.
1979: Relationships among rock groups within and beneath the Humber Arm Allochthon at Fox Island River, western Newfoundland; unpublished M.Sc. thesis, Memorial University of Newfoundland, 166 p.

Schillereff, H.S. and Williams, H.
1979: Geology of Stephenville map area, Newfoundland; in Current Research, Part A, Geological Survey of Canada, Paper 79-1A, p. 327-332.

Schuchert, C. and Dunbar, C.O.
1934: Stratigraphy of western Newfoundland; Geological Society of America, Memoir 1, 123 p.

Stevens, R.K.
1970: Cambro-Ordovician flysch sedimentation and tectonics in west Newfoundland and their possible bearing on a Proto-Atlantic Ocean; in Flysch Sedimentology in North America, ed. J. Lajoie; Geological Association of Canada, Special Paper No. 7, p. 165-177.

Troelsen, J.C.
1947: Stratigraphy and structure of the Bonne Bay-Trout River area; unpublished Ph.D. thesis, Yale University.

Whittington, H.B.
1963: Middle Ordovician trilobites from Lower Head, western Newfoundland; Bulletin Museum Comparative Zoology, Harvard College, v. 129, p. 1-118.

Williams, H.
1973: Bay of Islands map area, Newfoundland; Geological Survey of Canada, Paper 72-34, 7 p.

1981: Geology of the Stephenville map area, north half, Newfoundland; Geological Survey of Canada, Open File 726.

– Stephenville map area, north half, Newfoundland; Geological Survey of Canada, Map 1579A. (in press)

Williams, H. and Godfrey, S.C.
1980: Geology of the Stephenville map area, Newfoundland; in Current Research, Part A, Geological Survey of Canada, Paper 80-1A, p. 217-221.

Williams, H. and Stevens, R.K.
1974: The ancient continental margin of eastern North America; in The Geology of Continental Margins, ed. C.A. Burk and C.L. Drake; Springer-Verlag Publisher, p. 781-796.

Williams, H., Gillespie, R.T., and Knapp, D.A.
1982: Geology of Pasadena map area, Newfoundland; in Current Research, Part A, Geological Survey of Canada, Paper 82-1A, p. 281-288.

1983: Geology of the Pasadena map area, western Newfoundland; Geological Survey of Canada, Open File 928.

Williams, H., Quinn, L.A., Nyman, M., and Reusch, D.
1984: Geology of Lomond map area, 12H/5, western Newfoundland; Geological Survey of Canada, Open File 1012.

NAPPES IN THE KILOHIGOK BASIN, AND THEIR RELATION TO THE THELON TECTONIC ZONE, DISTRICT OF MACKENZIE

Project 830010

Rein Tirrul
Precambrian Geology Division

Tirrul, R., Nappes in the Kilohigok Basin and their relation to the Thelon Tectonic Zone, District of Mackenzie; in Current Research, Part A, Geological Survey of Canada, Paper 85-1A, p. 407-420, 1985.

Abstract

A thin-skinned thrust and fold belt involving Goulburn Group rocks is exposed in oblique cross-section in the Bear Creek Hills area of Bathurst Inlet. Upright, northwest-verging folds at high structural level pass downward into recumbent tight folds and thrusts near the basement/cover contact, reflecting increasing shear strain. On the basis of style, orientation, amount of strain, and relative timing, it is clear that this structural belt is unrelated to Bathurst Fault, and is tentatively interpreted to be a remnant of the highest Proterozoic structural level of the Thelon Tectonic Zone. Absence of the belt south of Bathurst Fault indicates that the latter has a minimum of 100 km of left-slip with 4 km north-side down movement.

Résumé

Une mince zone de charriage et de plissement intégrant les roches du groupe de Goulburn est exposée suivant une coupe oblique, dans la région des collines Bear Creek, dans l'inlet Bathurst. Les plis droits et faisant face au nord-ouest en altitude passent plus bas à des plis renversés et serrés et à des chevauchements près du contact entre le soubassement et la couverture, ce qui indique une augmentation des déformations par cisaillement. D'après le style, l'orientation, l'importance de la déformation, et sa chronologie relative, il est évident que cette zone structurale n'est pas apparentée à la faille de Bathurst, et de façon provisoire, on la considère comme un vestige du niveau structural le plus élevé du Protérozoïque dans la zone tectonique de Thelon. L'absence de la zone au sud de la faille de Bathurst, indique que cette dernière présente un glissement directionnel sénestre d'au moins 100 km et un rejet de 4 km de sa paroi nord.

Introduction

The complex structure of the Bear Creek Hills area (Fig. 51.1) of Kilohigok Basin was first identified during the regional studies of Campbell and Cecile (1975, 1976b). In contrast to the rest of the basin, strata here are both tightly and multiply folded. Although late north-trending folds were interpreted to be related to Bathurst Fault (Fraser, 1964; and subsequent workers), older structures of more variable trend were difficult to interpret. The recognition of highly deformed structural outliers of probable Western River Formation equivalents adjacent to the Thelon Tectonic Zone to the east (Fraser, 1968; and especially Thompson and Ashton, 1984) invited speculation that the Bear Creek Hills might preserve Proterozoic foreland structures of the Thelon Tectonic Zone. To test this idea, the structure of two areas (NTS 76 J/11 and 76 G/15) on either side of Bathurst Fault (Fig. 51.1) was studied during a six week visit to the region. The field data are summarized and interpreted in this report, and a 1:50 000 scale geological map will be available on Open File.

Stratigraphy

In both the northern Beechey Lake area and the Bear Creek Hills, deformed Archean metasedimentary rocks intruded by a few bodies of leucogranite are unconformably

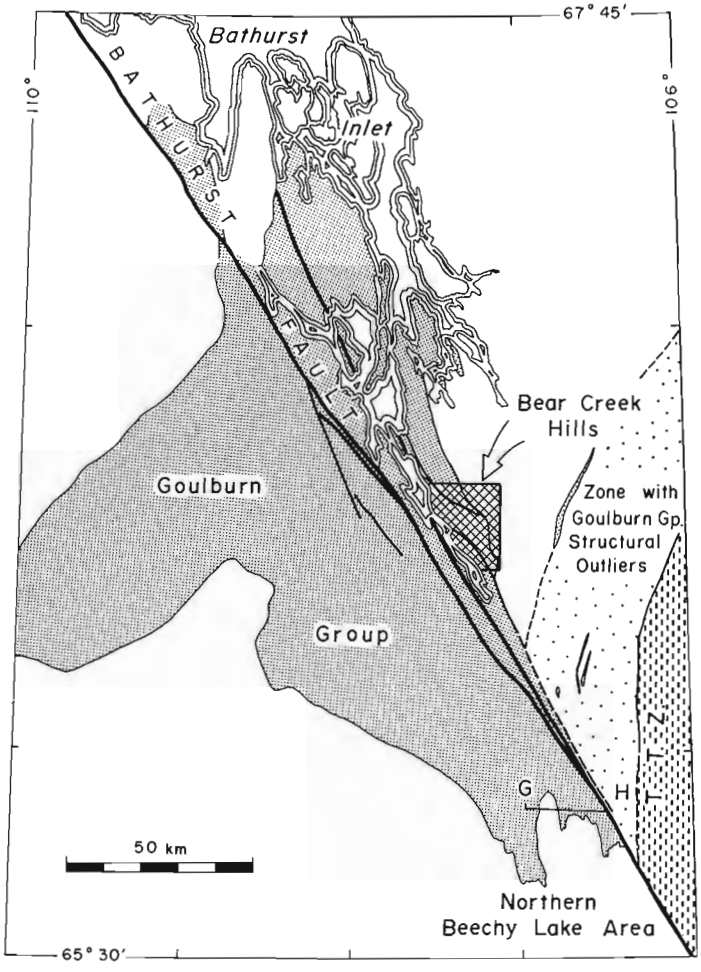

Figure 51.1. *Location map showing studied areas. T.T.Z. is Thelon Tectonic Zone.*

overlain by the Western River Formation of the Goulburn Group. The formation has been described and interpreted by Tremblay (1967, 1968, 1971) and Campbell and Cecile (1975, 1976a, 1981). Although the emphasis in this report is structural, some aspects of the stratigraphy in the Bear Creek Hills (Section 5, Fig. 51.2) can now be clarified, so a brief stratigraphic review is in order. Unit designations follow those of Campbell and Cecile (1976a,b) as much as possible.

Unit 1 (Lower Member of Campbell and Cecile, 1981) is characterized by a distinctive, diverse lithology with abundant carbonate, all of generally shallow water facies. Quartz pebble conglomerate and crossbedded orthoquartzite (Unit 1a) are everywhere present in unconformable contact with basement rocks in the Bear Creek area. Thinly interbedded psammite and pelite with minor carbonate (Unit 1b) in the Kenyon Lake area is apparently a facies of the upper part of 1a. Unit 1c consists mostly of argillite with subordinate stromatolitic and nonstromatolitic carbonate interbeds which increase upwards into Unit 1d, dominated by stromatolite mounds. Interbedded, crossbedded quartzite and dolarenite distinguish Unit 1e; it is capped by a bed up to 15 m in thickness of stromatolitic dolomite. This bed is sharply overlain by 50 m of carbonate-mudstone rhythmites (Unit 1g), indicating an abrupt increase in water depth. In the highly deformed area around Forgetit Lake, the contact between Units d and e was not mapped; together they comprise Unit 1f in Figure 51.4. Unit 1h (Fig. 51.4) is everywhere highly strained. It consists of thinly interbedded carbonate psammite and pelite, interpreted to be deeper-water equivalents of Units 1d-g (Campbell and Cecile, 1981).

An interesting feature, shown in Figure 51.3, interpreted to be a synsedimentary detachment fault scar, occurs in the core of the overturned syncline at the south end of Peg Lake. In this area stromatolitic dolomite of Unit 1d is directly overlain by argillite of Unit 2a, with interbedded matrix-supported block breccia beds at and near the basal contact. Units 1e and g are missing. They reappear, in very similar facies to that seen on the north shore of Peg Lake, south of Bro Lake thrust. Blocks within the breccia beds, up to 2 m in diameter, include abundant stromatolitic dolomite and crossbedded dolomitic quartzite. The structure is not a simple paleosubmarine channel, because deeper-water equivalents of Unit 1e (quartzose turbidites, for example) are not present in the lower argillite of Unit 2a. The absence of Units 1e and g at this locality is interpreted to be due to their removal by a gravity-driven slide. This could be related to the inferred drowning of Unit 1e and possible increase of paleoslope at that time.

Unit 2 (Fig. 51.2) is dominated by pelite (Unit 2a) in the lower half and subarkose in the upper half, at least in the southern Bear Creek Hills. A few thick beds of ferruginous subarkose with normally graded carbonate clasts are interbedded near the base; otherwise, pelite at various stratigraphic levels cannot generally be distinguished on lithological characteristics. Intervals with discontinuous sandy laminations and starved ripples alternate with zones containing very continuous laminations of fine greywacke, showing both normal and reverse grading.

Southwest of Peg Lake, Unit 2b consists of 250 m of thickly bedded subarkose turbidites, commonly containing normally graded dolomite clasts. To the north, these beds interfinger and pinch out within Unit 2a above Unit 1g. Their northern exposed limit is in the islands of Peg Lake. Similarly, the unit is represented by only a few beds south of Bro Lake fault. The position of this sandstone lens in the region of the proposed detachment scar, but 200 m or more above it, suggests that the scar persisted as a bathymetric depression during the deposition of Unit 2b.

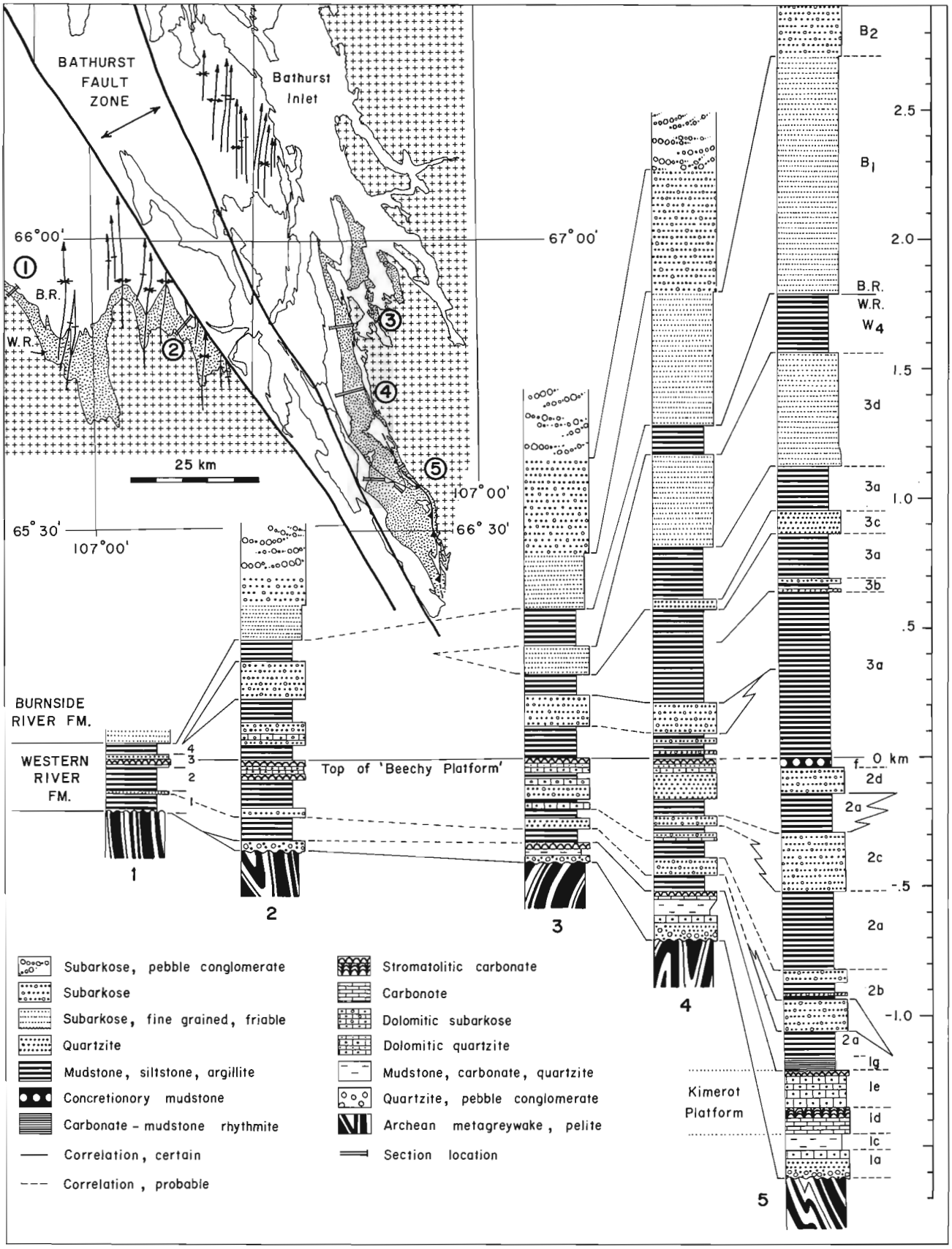

Figure 51.2. Proposed correlation of Western River Formation stratigraphic sections, southern Kilohigok Basin, with 130 km of restored strike-slip on Bathurst Fault zone. Section 1 is from Tremblay (1971), section 3 compiled from P.F. Hoffman (1975, unpublished), section 4 from M.P. Cecile (1974, unpublished) and sections 2 and 5, this report. Numbers on section 1 refer to Tremblay's members.

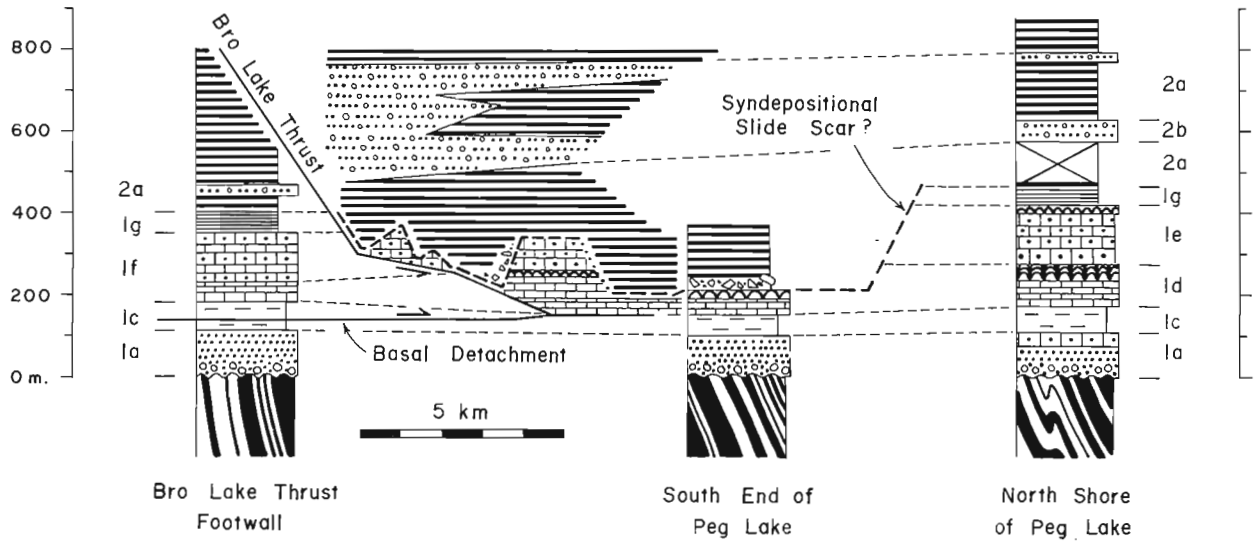

Figure 51.3. *Stratigraphic relations in the lower Western River Formation, as observed adjacent to Bro Lake thrust and on the autochthon showing the position of a syndepositional slide scar(?) and younger thrust trajectories. Ornamentation follows that of Figure 51.2.*

Unit 2e is greater than 50% subarkose interbeds, commonly crossbedded, especially near the top. It interfingers with 2a to the north, where it is divided into lower (Unit 2c) and upper (Unit 2d) intervals. The lower one very nearly pinches out completely south of Starvin Lake.

Unit 3 begins with more than 600 m of argillite with no sandstone beds. Red argillite at the base of the unit shares an interbedded lower contact with subarkose of Unit 2. In the central Bear Creek Hills this 50 m interval is marked by carbonate concretions (Unit 2f). The same stratigraphic level can be traced to Starvin Lake, and north of the lake to where Beechey platform stromatolite beds occur. Unit 3b is a 200 m interval containing a few thick greywacke beds. Unit 3c consists of white, crossbedded orthoquartzite and subarkose. Unit 3d consists of mostly fine grained, poorly indurated red subarkose thickly bedded and with abundant reduction spots. It is identical in appearance to the subarkose which has been mapped in the past as the base of the Burnside River Formation, but separated from it by a 250 m interval dominated by red mudstone (Unit 4).

Suggestions for future work

Unit 1 (Lower Argillite Member of Campbell and Cecile, 1976a,b; Lower Member of Campbell and Cecile, 1981) should be elevated to a formation (Kimerot Formation?). It has little argillite, distinctive lithology, clearly definable upper and lower limits, and pinches out beneath the classic Lower Argillite Member of Tremblay (1971; see Fig. 51.2). As recognized by Tremblay (1971) and Campbell and Cecile (1975), quartzite intervals in the Western River are discontinuous. The only stratigraphic level between Unit 1 and the Burnside River Formation that can be confidently traced throughout the entire region is the top of the Beechey platform. Perhaps the uppermost stromatolite bed, or its lateral equivalent, could be defined as a formal boundary. The use of this datum would not conflict with previous work because it is very near the top of the Quartzite Member, as mapped by Tremblay in the Beechey Lake area. It would be difficult to project the contact between the Lower Argillite and Red Siltstone members of Tremblay (1971) into the Bear Creek Hills because criteria to map such a contact in Unit 2a could not be identified. Similarly, if the base of Unit 2e were taken to be the base of the Quartzite Member, then the latter is in part a facies equivalent of a lower member(s).

Also, a cautionary note should be made about the use of colour for stratigraphic descriptions and subdivisions. As Unit 2f is traced from Peg Lake to Bathurst Inlet, up more than 2 km of structural relief (see Fig. 51.4, 51.6), its colour changes progressively from purple-grey to bright red with no change of sedimentary facies. There is a general tendency for sandstones at lower structural levels to be white or greenish, and those higher up to be pink, regardless of composition, and for red argillite to dominate at high levels. Similar changes in the Externides of Wopmay Orogen were documented and demonstrated to be related to metamorphic grade (Lucas, 1984). Thus, the colour of sedimentary rock of the Goulburn Group is probably also partly controlled by metamorphic grade, in addition to bulk composition and environment of deposition. The complete results of a study of metamorphism of the Goulburn Group, including the Bear Creek Hills, undertaken by Martin Frey, will be forthcoming.

Structure

The structural elements of the region studied can be grouped into two major associations, corresponding to the main deformational phase (D_2) and a younger event (D_3). The main phase is characterized by asymmetric folds, thin-skinned thrusts, and by a well developed, commonly continuous cleavage, with an overall northwest vergence. This phase is interpreted to relate to the evolution of the Thelon Tectonic Zone. D_3 structures include high-angle faults, upright, basement involved folds, crenulation cleavage and kink bands, collectively compatible with subhorizontal, E-W-shortening. These structures are thought to be associated with the development of Bathurst Fault. An older fold set (D_1) is difficult to interpret.

D_1 structures

The intersection of 355 and 015° trending folds of leucogranitic basement and cover rocks on the east side of Kenyon Lake (Fig. 51.4) define a Type 1 (Ramsay, 1967) interference pattern. The NNW-trending folds are open to

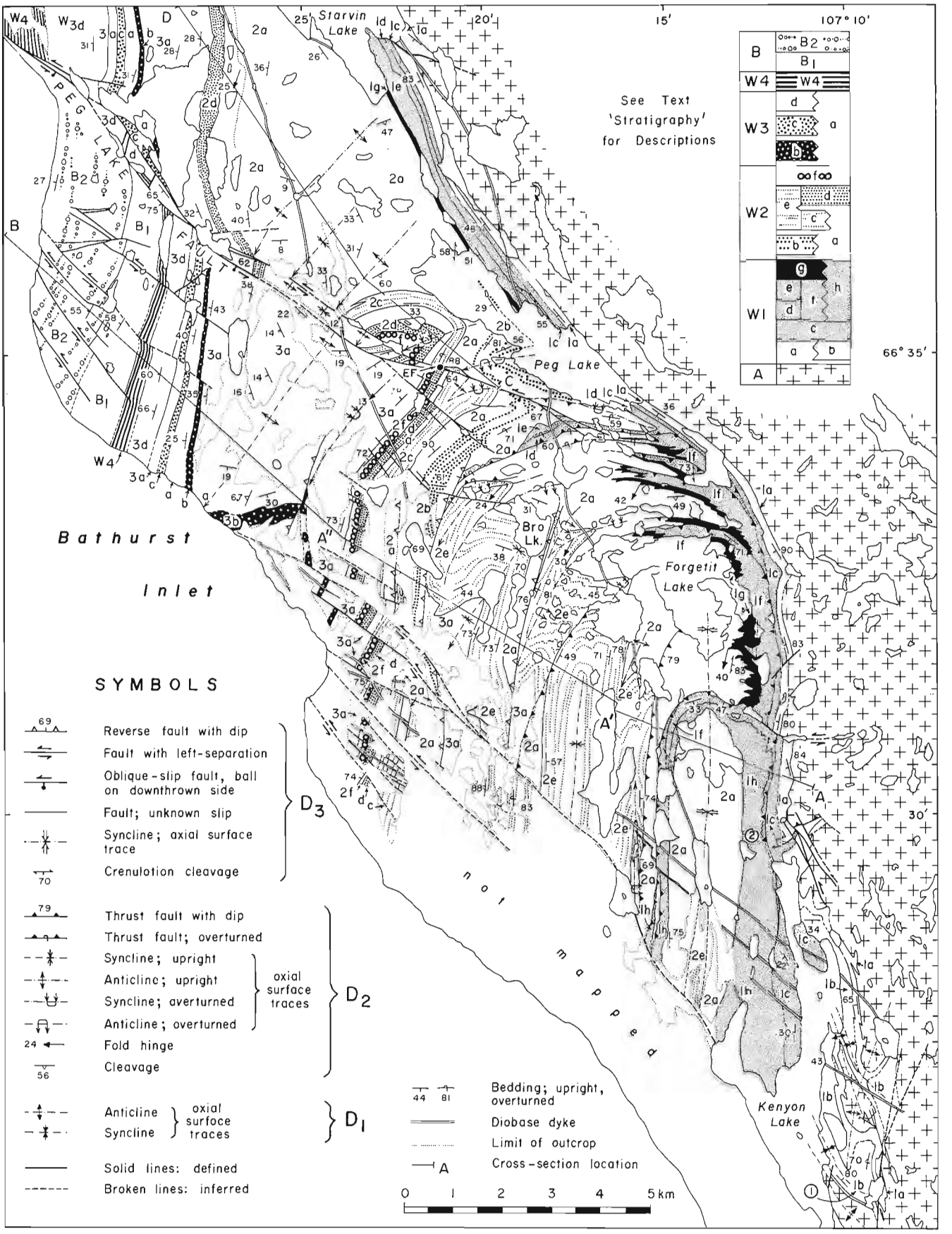

Figure 51.4. *Geological map of the Bear Creek Hills area.*

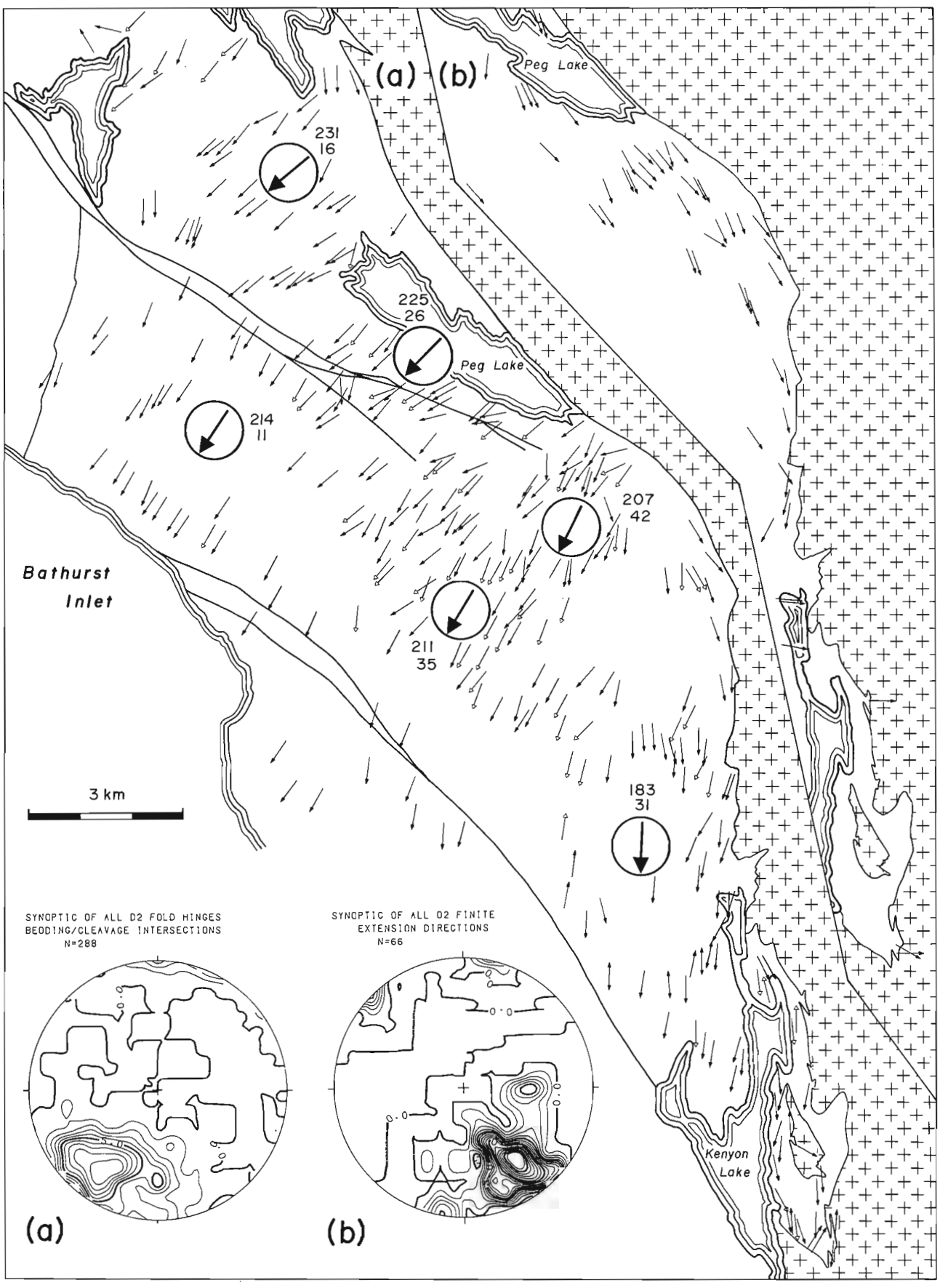

Figure 51.5. *D_2 lineations in the Rear Creek Hills. On the map: (a) trend of fold hinges (open arrowheads) and bedding/cleavage intersections (closed arrowheads). Circled measurements are concentration peaks for data from domains centred on those points. (b) trend of finite extension lineations. Equal-area net contours are in per cent per 1% area.*

close with steep (up to 90°) NE-dipping flanks; the other set is upright. The main phase cleavage in this region has a variable easterly dip, and transects northwest-trending minor folds at localities 1 and 2 (Fig. 51.4). On this basis, the NNW fold set is interpreted to be the oldest to affect the Goulburn Group. Fold orientation prior to D_2 and D_3 is not known, and it is not clear how they should be interpreted.

D_2 structures

Most of the structural geometry of the Bear Creek Hills can be ascribed to the main phase of deformation (D_2). The key to understanding these structures is their consistently steep (circa 30°) SW plunge. Thus, the map itself (Fig. 51.4) is a cross-section of D_2 structure with 2 x vertical exaggeration. At a relatively deep structural level, to the northeast, the basement/cover contact and immediately overlying units have a comparatively straight trace; to the southwest, at high levels, the cover is tightly folded and imbricated, establishing that the D_2 involves detachment and shortening of the cover relative to the basement.

Main phase fold hinges, both minor and major, as well as bedding/cleavage intersection lineations ($S_0 \times S_2$) are plotted on map view and, with a more complete data set, on equal-area projection in Figure 51.5. Because of areal differences in trend and plunge, and because some structures are demonstrably noncylindrical, it is not possible to draw a single, 'undistorted' down-plunge view of the entire area. The data were used to divide the area into domains that were projected separately along slightly different directions, and then assembled into a composite (Fig. 51.6) such that distortion is minimized along Units 2c-d. To key from the map (Fig. 51.4) to the projection, two reference levels, A-B and C-D are located on both. Bro Lake thrust and adjacent bedding intersect the projection plane obliquely; the fault has true average dip of 60°. The geometry of structures at high level from A" to B does not mesh with that observed to the north. Also, faults 9-12 are D_3 structures oblique to the projection plane, with separation that increases to the south. They appear on the projection because I could not restore them with confidence. Despite these shortcomings, the essential features of D_2 are well displayed.

At high structural levels, folds in Units 2c-d have aggregate profiles which approach chevron geometry, are upright or steeply inclined toward the northwest, and have interlimb angles which generally exceed 90°. Cleavage is not strong, especially to the northwest, where it is spaced, even in pelitic units. Cleavages in pelite describe divergent upright fans, except for the broad anticline northwest of fault 9, which is convergent.

Where axial surfaces are traced to deeper levels, their dip progressively decreases, and in the case of some major anticline-syncline pairs, meet thrust faults which accommodate buckling strain. Concomitant with this change is the flattening and intensification of associated cleavage, and a general decrease in the interlimb angle of folds (Fig. 51.7a). Even the most competent dolomite layers in Unit 1f are commonly tightly folded.

Conspicuous extension lineations also develop with increasing structural depth. Two kinds were measured. The most prominent lineations are defined by streaks of mineral aggregates in very fine grained pelitic dolomite L-S tectonite adjacent to thrusts 2-8, and immediately above the basal detachment (Fig. 51.7b,c). Quartz fibres in extensional veins in Unit 1 and in sandy layers near the base of Unit 2, comprise the second type. They record a small rotational strain component, and their orientation is not statistically different than lineations on S_2, so they have not been distinguished from them in Figure 51.5. The average extension lineation orientation is at a high angle to $S_0 \times S_1$ intersection lineations, so the projection surface of Figure 51.6 is nearly parallel to the transport direction.

The basal detachment can be traced from the north end of Kenyon Lake to the axial plane of Peg Lake syncline, southeast of Peg Lake, where both terminate. It is situated within pelite of Unit 1c, and although poorly exposed, is easily mapped because it separates rocks which are ubiquitously and tightly folded from beds beneath, which are either not folded, or buckled into minor folds of low amplitude. The succession beneath the detachment, which was everywhere observed to be intact, consists of a basal quartz pebble conglomerate and overlying orthoquartzite about 100 m thick (Unit 1a) followed by a few tens of metres of argillite with interbeds of orange dolomite, in places stromatolitic (Unit 1c). These rocks all display the main phase cleavage (Fig. 51.7d) and are locally strongly strained, but not imbricated. The cleavage can be traced into basement rocks, where it is difficult to distinguish from older fabrics, and the unconformity is an irregular surface where it underlies the detachment, indicating that D_2 was not strictly thin-skinned.

A part of the structural sequence can be deduced from the unusual geometry of Bro Lake thrust and the next fault (2, Fig. 51.6) to the southeast. Both faults have a similar orientation (Bro Lake thrust has a steeper dip, about 60°) to thrusts farther southeast, which carry older rocks on hanging walls. However, in their present configuration, younger rocks rest on older ones along both Bro Lake thrust and thrust 2. They cannot be northwest-directed thrusts because no amount of back slip will restore them. They also cannot be extensional normal faults because they stack stratigraphy. The only reasonable interpretation is that they are early SE-directed back thrusts which have been rotated through the vertical to their present overturned position. Furthermore, because they do not root in the basement farther to the northwest, they must have originally formed the roof to a NW-directed tectonic wedge or 'triangle zone' riding on the basal décollement. The evolution of these structures is shown schematically in Figure 51.8. Similar structures, although not as severely rotated, are found in the southern Asiak thrust and fold belt (Tirrul, 1983) and in the Porcupine Creek and Selkirk structural fans of the Southern Canadian Rockies (Price, in press).

The relative orientation of the back thrusts and adjacent cleavage is compatible with cleavage formation during back thrust emplacement, and subsequent rotation through the vertical along with the faults, but this is not the preferred interpretation. This would predict the occurrence of multiple D_2 cleavages, since the cleavage developed during back thrusting would have rotated through the shortening direction of subsequent strain. Because such fabrics are not observed, the earliest stage (2, Fig. 51.8) is interpreted to have been relatively brittle, with cleavage development mainly during the forward (NW) rotation of the back thrusts. Many discrete forward thrusts have apparently developed from zones of ductile strain because they truncate tight NW-verging folds (thrusts 3 and 4, Fig. 51.6, for example). The disharmonic synclinorium northwest of Bro Lake thrust originated as a fault-bend syncline whose hinge migrated northwestward (Stage 2, Fig. 51.8). The shear required on the limbs of this fold between Units 2c-d and Unit 1 is distributed throughout Unit 2a, and may die out at

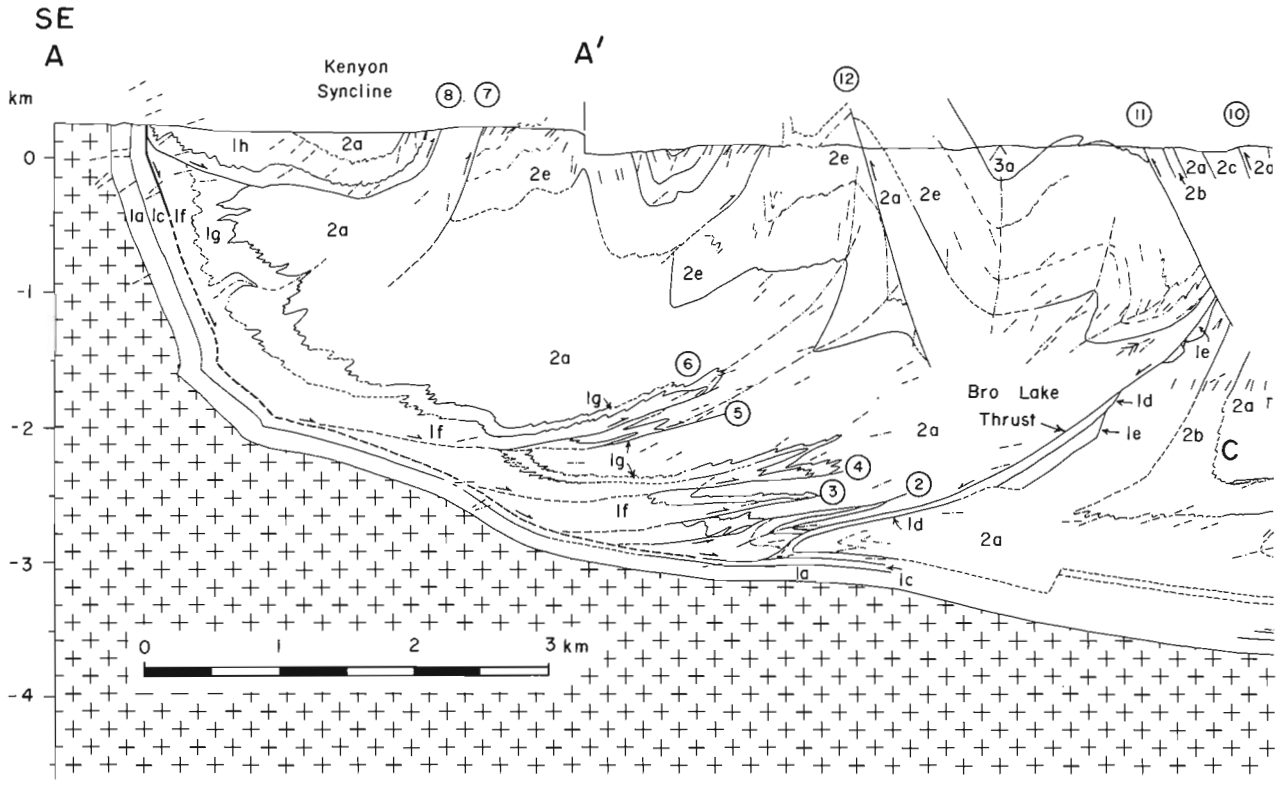

Figure 51.6. *Down-plunge projection of Pear Creek Hills structure. Levels A-B and C-D are located on Figure 51.4. Due to marked deviations from cylindricity, higher levels from A" to B are not compatible with C-D. Bro Lake thrust also appears in oblique view; it has an average dip closer to 60°. Contacts dashed when surface data are unavailable. D_2 cleavage, F_2 axial traces in dot-dash line; miscellaneous bedding in double dot-dash line.*

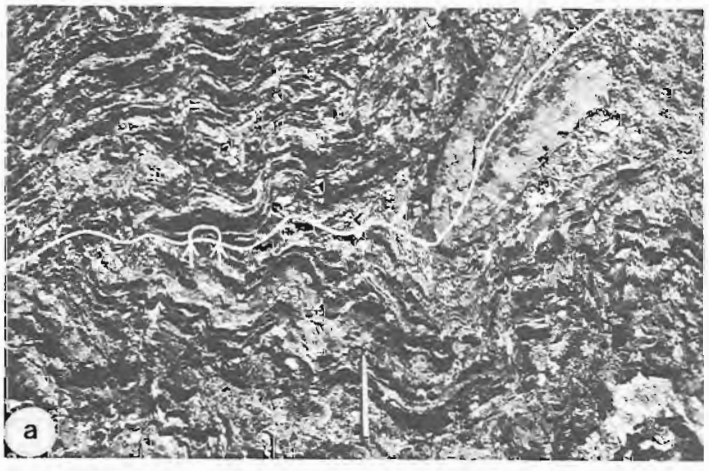





Figure 51.7a. *D_2 recumbent, NW-verging tight folds in carbonate-mudstone rhythmite of Unit 1g, southeast of Bro Lake thrust, refolded across upright D_3 axial planes. Pen points south.*

Figure 51.7b. *Fine grained pelitic dolomite LS tectonite of Unit 1f thrust over argillite of Unit 2a (thrust 3, Figure 51.4). The foliation is at a very low angle to the thrust trace. View is to the northwest.*

Figure 51.7c. *Strongly lineated foliation surfaces, 0.5 m above thrust 3, same locality as Figure 51.7b. Higher in the hanging wall the same fabric, although more weakly developed, is axial planar to tight D_2 folds. Lineations trend 150°, plunge 36°.*

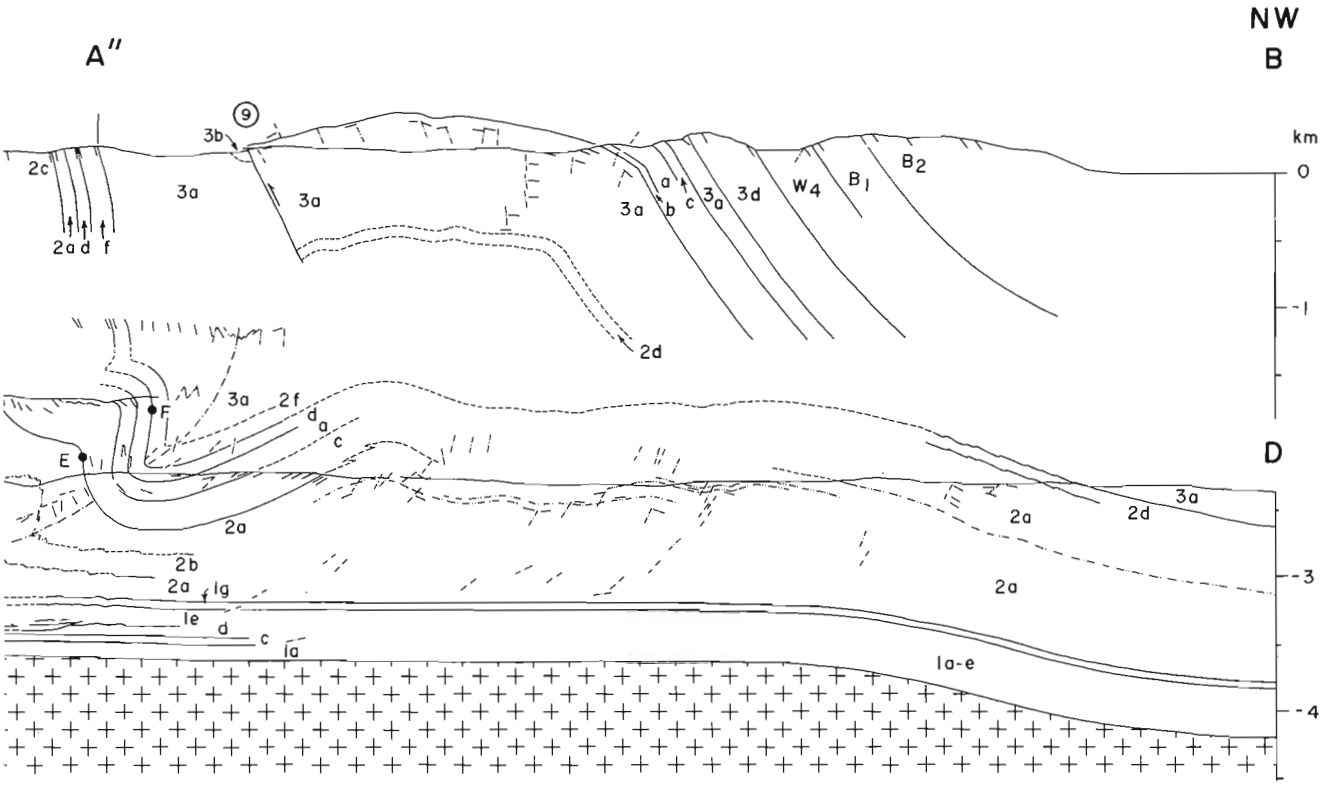



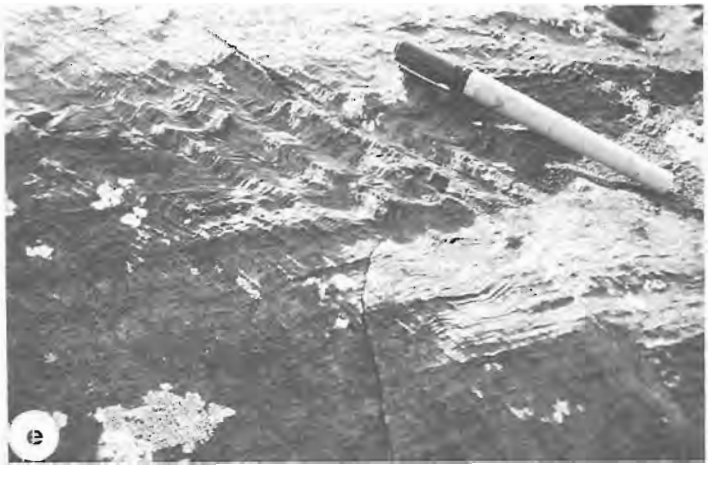

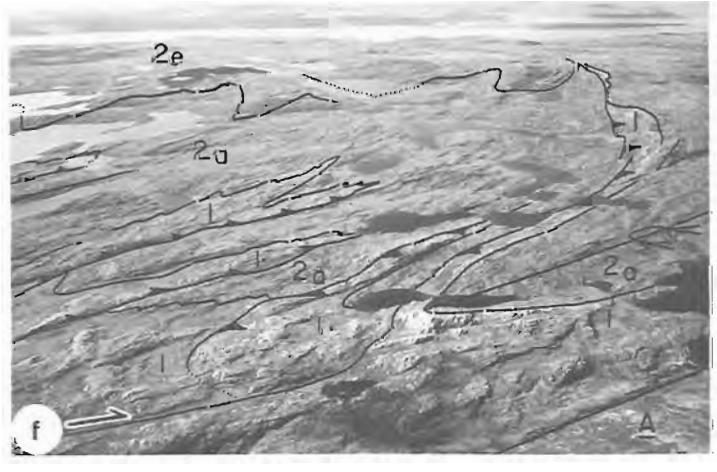

Figure 51.7d. *Main phase cleavage, in interbedded argillite and dolomite of Unit 1c on the autochthon north of Kenyon Lake. View is to the south and bedding faces west. Note that vergence is 'downhill'.*

Figure 51.7e. *Well developed S_3 crenulation cleavage (S_3) with a 50° west dip, overprinting S_2 continuous cleavage in pelitic dolomite of Unit 2d, on the autochthon at the south end of Peg Lake.*

Figure 51.7f. *Down-plunge areal view showing structures south of Peg Lake.*

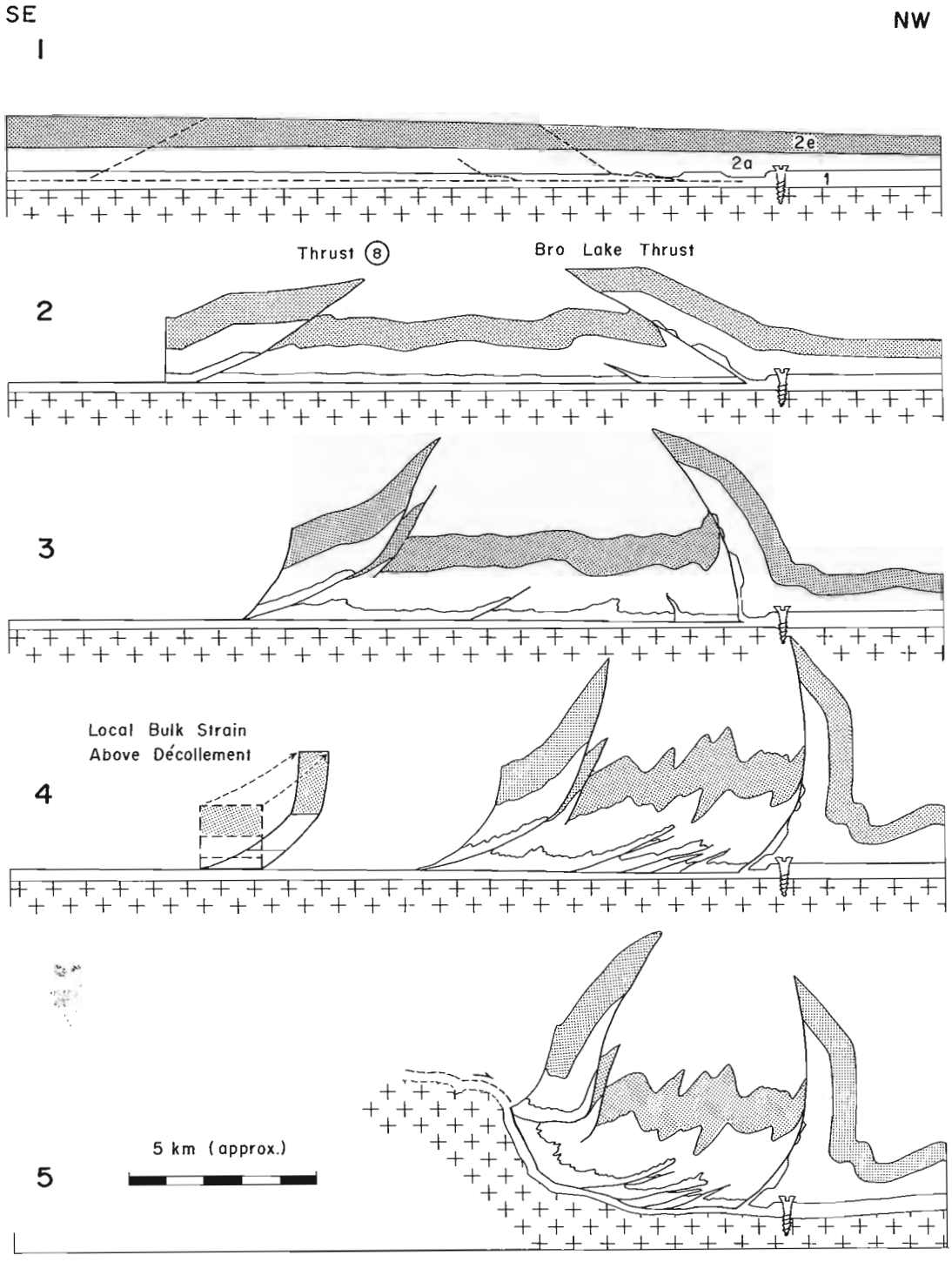

Figure 51.8. *Schematic structural evolution of the Bear Creek Hills. See text for discussion.*

the axial surface of the synclinorium. There is no requirement for a basal detachment here to link with the décollement to the southeast.

The progressive change in structural style with depth observed in the Bear Creek Hills is common to many orogens. In the Variscan fold belt of southwest England (Sanderson, 1979) and in the Helvetic nappes of Switzerland (Ramsay, 1981; Ramsey et al., 1983) most structures are attributed to simple shear, and the vertical change to increasing shear with depth. In the Bear Creek Hills, the tight, upright fold train of Unit 2e is compatible only with large subhorizontal compressive strain, with subvertical extension. The lower units must have suffered large ductile shear because the back thrusts have rotated through the finite shortening direction marked by regional cleavage. A qualitative picture of this strain regime is shown at the left of Figure 51.8(4).

D_3 structures

Main phase recumbent, reclined folds are refolded across upright or steeply inclined north-trending axial surfaces, most conspicuously in the area between Peg Lake and Kenyon Lake (Fig. 51.6, 51.7a). These folds have a weakly fanning crenulation cleavage, which is also commonly developed where there are no D_3 folds (Fig. 51.7e), but is restricted to low structural levels where D_2 continuous cleavage is well developed. The crenulations and axial planes are plotted in Figure 51.9, which reveals a weak overall easterly vergence. Thrust 7 is folded about a north-trending axis (Kenyon syncline), and the basement in that region has been rotated to vertical. Both effects are interpreted to relate to D_3. The high angle which is commonly (Fig. 51.6), but not exclusively (Fig. 51.7d) observed between bedding and S_2 along the steeply dipping basement flank, is problematical. It may be due to relative rotation of bedding and S_2 cleavage as a result of D_3 flexural shear in the manner proposed by Gray (1981).

North-trending folds are common astride Bathurst Fault throughout Kilohigok Basin (Campbell and Cecile, 1976b). In the northern Beechey Lake area (Fig. 51.1) they are well developed and exposed at the level of the basal unconformity. A cross-section (shown in Figure 51.10 and located in Figure 51.1) illustrates the harmonic folding of basement and cover. There is no décollement here. The unconformity is not folded into a cuspate-lobate geometry, as documented in the Tree River Fold Belt (Hoffman et al., 1984), presumably because the strength of rocks above and below it were similar at the time of folding.

Basement (Fig. 51.10) consists of interbedded Archean metagreywacke and pelite at sub-biotite grade (Frith, 1982), tightly folded prior to deposition of the Goulburn Group. These folds have axial surfaces with a mean 340° strike and steep northeast dip. The data are sparse, but the sense of fanning of the Archean axial surfaces is consistent with active buckling of the upper part of the basement. Although less precise, bedding attitudes in the basement near the unconformity also describe a convergent fan. A crenulation cleavage related to the Proterozoic folds is very well developed in basement pelite, and passes upward into a continuous or spaced cleavage, depending on lithology, in the cover. This fabric has a consistent, steep easterly inclination in both basement and cover, suggesting that it was to a large degree superimposed onto the folds.



Figure 51.9. *Poles to D_3 planar fabric elements. Equal-area net contours are in per cent per 1% area.*

The folds of the northern Beechey Lake area are correlated with F_3 in the Bear Creek Hills on the basis of orientation. They are interpreted to be related to Bathurst Fault on the basis of compatible orientation and proximity to the fault. North-trending folds are not present beyond 30 km west from the fault.

Peg Lake fault and other faults of similar orientation in the Bear Creek Hills are almost certainly a part of Bathurst Fault system. Slip on Peg Lake fault is comparatively well constrained. West of Peg Lake, its strike-slip component is 570 m, indicated by the offset of Units 2d-f, which have a vertical dip. The dip-slip is constrained by noting that the gently dipping fold limb above E (Fig. 51.6) is not preserved at the level of Unit 2c on the north side of Peg Lake. This requires a minimum 330 m south-side-down component. Thus, E-F on Figure 51.6 is the net slip on this fault since these points are now coincident (Fig. 51.4). To the northwest, the absence of an anticlinal closure in Units 2d and f south of the fault also requires a minimum of 300 m south-side-down slip. Dips of well exposed fault planes (either the main strand or its splays) vary from 75 to 64° S, indicating the dip slip component to be normal. To the north, slip must increase because separation on west-dipping contacts increases to 4 km.

Faults 9-12 are well exposed, steeply west-dipping faults that sharply truncate D_2 structures along narrow zones of cataclasite. They consistently have a reverse separation that increases southward. To the north, they die out in 'soft' pelite of Unit 2a. Their orientation, character and location on the compressional side of the termination of Peg Lake fault suggests a genetic link, so they have been classified as D_3 structures. Variably northwest-trending subvertical left-kinks, extremely common in the corner zones between these faults and Peg Lake fault, also suggest a mechanism for slip transfer.

Regional tectonic considerations

Because of important regional implications, it is worth reviewing the reasons why D_2 cannot be related to slip on the Bathurst Fault system:

a. Structural style: D_2 is characteristically thin-skinned. Compressional structures associated with major strike-slip faults are typically steeply dipping reverse or oblique slip faults that involve basement (see Sylvester and Smith, 1976, for example).

b. Crosscutting and overprinting relationships: Steeply dipping faults subparallel to Bathurst Fault clearly truncate D_2 structures, and north-trending upright folds compatible with left-slip on Bathurst Fault refold D_2 structures.

c. Fault character: All D_3 faults are marked by cataclastic breccia, and some by quartz-carbonate stockworks. Adjacent D_2 shears are associated with recumbent folds, strong continuous cleavage and LS tectonite, indicating a dutile, higher P-T strain regime.

d. Orientation: The main trend of D_2 fold hinges (216°, Fig. 51.5) is at a high angle to the strike of Bathurst Fault (148°). Peg Lake fault is perpendicular to D_2 folds it intersects. Folds genetically related to major strike-slip faults initiate at angles less than 45° and are observed at about 30° to the shear direction (Wilcox et al., 1973). The difference cannot be an effect of fault termination because folds near the end of Peg Lake fault have a similar orientation on either side of it.

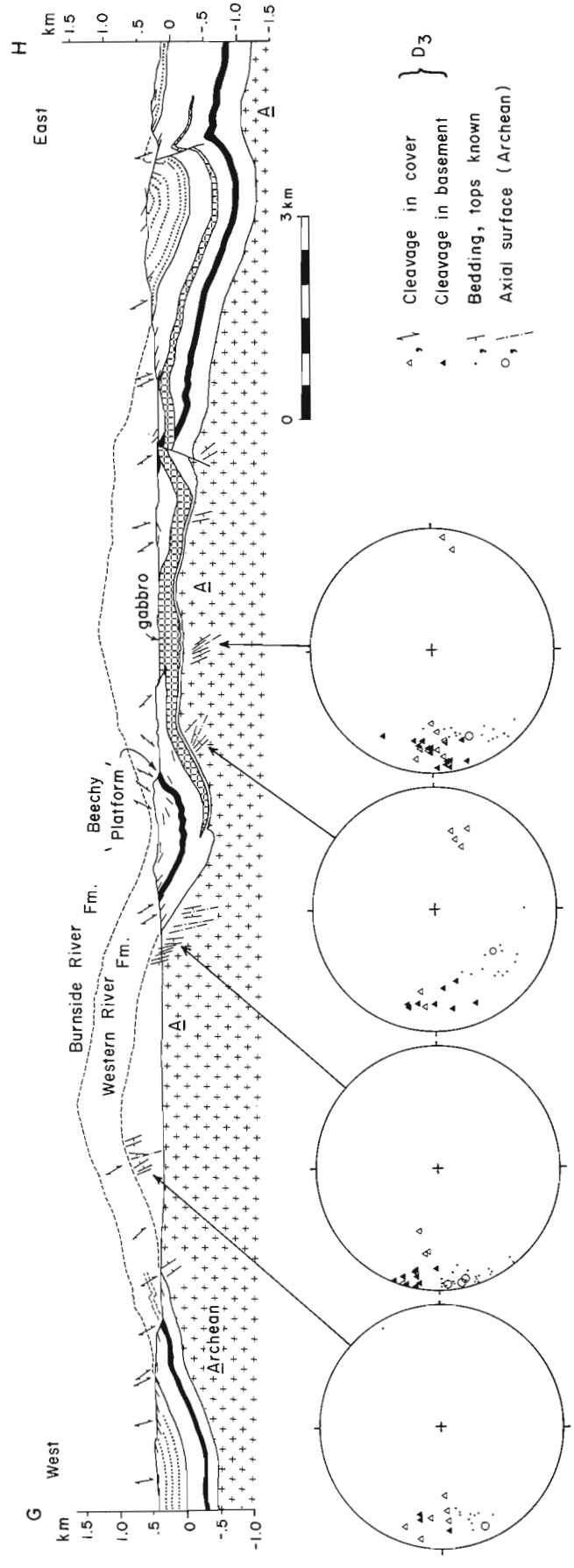

Figure 51.10. Structure cross-section across the northern part of Beechey Lake area. See text for discussion, and Figure 51.1 for location.

e. Amount of slip: Peg Lake fault has about 600 m of oblique slip west of Peg Lake. South of this area, the thin-skinned structures represent at least 5 km of transport, so shortening in the cover is not transferred to strike-slip on this fault.

f. Regional correlations: D_2 structures have the same relative timing and an orientation comparable to the nappes of Athapuscow Aulacogen and Tree River folds (see below). All predate regional strike-slip faulting.

Slip on Bathurst Fault system

Recent estimates of slip on Bathurst Fault system are contradictory. Thomas et al. (1976) suggested 48 km of cumulative left-slip based on apparent offset of prominent magnetic anomalies along discrete discontinuities where the fault projects into the Thelon Tectonic Zone. Campbell and Cecile (1979, 1981) suggested 140 km of left-slip on the fault zone, based on facies variations in several formations, including the Western River, of the Goulburn Group.

Structural data in this report independently support the higher estimate of Campbell and Cecile. Since evidence for large (≈10 km) pre-transcurrent, northwest transport of cover on the basal detachment is preserved in the Bear Creek Hills, the detachment must have existed south of Bathurst Fault. Any reconstruction less than 100 km juxtaposes thin-skinned Bear Creek structures against gently folded autochthonous cover. More than 100 km of slip simply requires that these structures have been erosionally removed from the south side. In either case, a large north-side-down slip component (4 km minimum for left slip of 100 km or more), is required to preserve Bear Creek Hills structures.

Additional support for large slip comes from deciphering the stratigraphy of the Bear Creek Hills. Proposals of less than 130-140 km make progressively poorer matches of Western River Formation thickness and facies. Limiting slip to 75 km would juxtapose section 3 (850 m, Fig. 51.2) with section 5 (3.4 km).

How can the apparent discrepancy between 140 and 48 km of left-slip be resolved? One source of error concerns the treatment of magnetic anomalies as piercing points. They can only be used to determine strike-slip if the magnetic carriers (which have not been mapped) are steeply dipping – otherwise a small normal component can greatly increase or decrease the separation on the fault. Potentially more important is the proposal that to the south the fault system becomes increasingly ductile (Frith, 1982), so that discrete large scale offsets record only a small part of the total slip. The existence of north-trending folds and associated cleavage requires some ductile strain, even in the north. To produce a continuous cleavage in pelite, 30% shortening is required (Ramsay 1967, p. 180); even pencil cleavage requires 9-26% shortening (Simon and Gray, 1982). If a modest 20% shortening is assumed to produce the cleavage and folds in the northern Beechey Lake area, and if these folds were produced by simple shear, then the corresponding shear strain (0.5) converts to 15 km of total ductile left-slip (Ramsay, 1967, Eqn. 3-67) integrated across the width of the folded zone (30 km). Clearly, in the absence of detailed strain analysis, one cannot rule out very large ductile strain in the basement rocks to the southeast.

Regional correlations

This work supports the inference by Thompson and Ashton (1984) that D_2 structures in the Bear Creek Hills are genetically linked to Proterozoic deformation along

the Thelon Tectonic Zone. The basal décollement in the Bear Creek Hills should root in the basement rocks southeast of Kenyon Lake. Proterozoic outliers mapped by them have an identical trend, are involved in northwest-directed thrusting, and together with the Bear Creek Hills, define a general outward progression from higher grade, basement-involved structure to a low grade thin-skinned foreland.

On the basis of timing constraints (pre-transcurrent faulting, post-Burnside River Formation), correlations with Tree River deformation or thrusting in Athapuscow Aulacogen is permissive (see discussion by Hoffman et al., 1983, 1984), but these structures have a different mean trend (240 vs 215°). Until the character of the strain along Thelon Tectonic Zone is better known, and until the scale over which this difference is maintained is determined, the significance of the deviation will be debatable.

Acknowledgments

It is a pleasure to thank Norman Begin, Marlene Charland, and Dave Scott for mapping assistance. Jack Henderson and Paul Hoffman reviewed the manuscript. Fred Campbell and Peter Thompson have been very generous with their ideas, data and time.

References

Campbell, F.H.A. and Cecile, M.P.
1975: Report on the geology of the Kilohigok Basin, Goulburn Group, Bathurst Inlet, N.W.T.; in Report of Activities, Part A, Geological Survey of Canada, Paper 75-1A, p. 297-306.

1976a: Geology of the Kilohigok Basin, Goulburn Group, Bathurst Inlet, N.W.T.; in Report of Activities, Part A, Geological Survey of Canada, Paper 76-1A, p. 369-377.

1976b: Geology of the Kilohigok Basin; Geological Survey of Canada, Open File Map 332, 1:500 000 Scale.

1979: The northeastern margin of the Kilohigok Basin, Melville Sound-Victoria Island, District of Franklin; in Current Research, Part A, Geological Survey of Canada, Paper 79-1A, p. 91-94.

1981: Evolution of the early Proterozoic Kilohigok Basin, Bathurst Inlet-Victoria Island, Northwest Territories; in Proterozoic Basins of Canada, ed. F.H.A. Campbell; Geological Survey of Canada, Paper 81-10, p. 103-131.

Fraser, J.A.
1964: Geological notes on northeastern District of Mackenzie, Northwest Territories (Report and Map 45-1963); Geological Survey of Canada, Paper 63-40, 16 p.

1968: Geology across Thelon Front, District of Mackenzie (76I,J); in Report of Activities, Part A, Geological Survey of Canada, Paper 68-1A, p. 134.

Frith, R.A.
1982: Second preliminary report on the geology of the Beechey Lake-Duggan Lakes map areas, District of Mackenzie; in Current Research, Part A, Geological Survey of Canada, Paper 82-1A, p. 203-311.

Gray, D.R.
1981: Cleavage-fold relationships and their implications for transected folds:' an example from southwest Virginia, U.S.A.; Journal of Structural Geology, v. 3, p. 265-277.

Hoffman, P.F., Tirrul, R., and Grotzinger, J.P.
1983: The externides of Wopmay Orogen, Point Lake and Kikerk Lake map areas, District of Mackenzie; in Current Research, Part A, Geological Survey of Canada, Paper 83-1A, p. 429-435.

Hoffman, P.F., Tirrul, R., Grotzinger, J.P., Lucas, S.B., and Eriksson, K.A.
1984: The externides of Wopmay Orogen, Takijuq Lake and Kikerk Lake map areas, District of Mackenzie; in Current Research, Part A, Geological Survey of Canada, Paper 84-1A, p. 383-395.

Lucas, S.B.
1984: Low-grade metamorphism in the externides of Wopmay Orogen, N.W.T.; Geological Association of Canada, Program with Abstracts, v. 9, p. 85.

Price, R.A.
– The southeastern Canadian Cordillera: thrust faulting, tectonic wedging and delamination of the lithosphere; Journal of Structural Geology. (in press)

Ramsay, J.G.
1967: Folding and Fracturing of Rocks; McGraw-Hill, New York.

1981: Tectonics of the Helvetic Nappes; in Thrust and Nappe Tectonics, ed. K. McClay and N.J. Price; Geological Society of London, Special Publication, v. 9, p. 293-304.

Ramsay, J.G., Casey, M., and Kligfield, R.
1983: Role of shear in development of the Helvetic fold-thrust belt of Switzerland; Geology, v. 11, p. 439-442.

Sanderson, D.J.
1979: The transition from upright to recumbent folding in the Variscan fold belt of southwest England: a model based on the kinematics of simple shear; Journal of Structural Geology, v. 1, p. 171-180.

Simon, R.I. and Gray, D.R.
1982: Interrelations of mesoscopic structures and strain across a small regional fold, Virginia Appalachians; Journal of Structural Geology, v. 4, p. 271-289.

Sylvester, A.G. and Smith, R.R.
1976: Tectonic transpression and basement controlled deformation in the San Andreas fault zone, Salton Trough, California; American Association of Petroleum Geologists, Bulletin, v. 60, p. 2081-2102.

Thomas, M.D., Gibb, R.A., and Quince, J.R.
1976: New evidence from offset aeromagnetic anomalies for transcurrent faulting associated with the Bathurst and McDonald faults, Northwest Territories; Canadian Journal of Earth Sciences, v. 13, p. 1244-1250.

Thompson, P.H. and Ashton, K.
1984: Preliminary report on the geology of the Tinney Hills-Overby Lake (W 1/2) map area - a look at the Thelon Tectonic Zone northeast of the Bathurst Fault; in Current Research, Part A, Geological Survey of Canada, Paper 84-1A, p. 415-423.

Tirrul, R.
1983: Structure cross-sections across Asiak Foreland Thrust and Fold Belt, Wopmay Orogen, District of Mackenzie; in Current Research, Part B, Geological Survey of Canada, Paper 83-1B, p. 253-260.

Tremblay, L.P.
1967: Contwoyto Lake area (north half) District of Mackenzie; Geological Survey of Canada, Paper 67-28, 63 p.

Tremblay, L.P. (cont.)
1968: Preliminary account of the Goulburn Group, N.W.T.; Geological Survey of Canada, Paper 67-8, 37 p.

1971: Geology of Beechey Lake map area, District of Mackenzie; Geological Survey of Canada, Memoir 365, 56 p.

Wilcox, R.E., Harding, T.P., and Seely, D.R.
1973: Basic wrench tectonics; American Association of Petroleum Geologists, Bulletin, v. 57, p. 74-96.

AN INTERPRETATION METHOD FOR GRAVITY AND MAGNETIC DATA FOR AREAS PERIPHERAL TO THE CANADIAN SHIELD

Project 840057

B.S. Daudier and E.J. Schwarz
Resource Geophysics and Geochemistry Division

Daudier, B.S. and Schwarz, E.J., An interpretation method for gravity and magnetic data for areas peripheral to the Canadian Shield; in Current Research, Part A, Geological Survey of Canada, Paper 85-1A, p. 421-430, 1985.

Abstract

A computer based interpretation system for the cheap and rapid inversion of magnetic and/or gravity data is being developed. Initially, anomaly sources are supposed to be due solely to relief (approximated by horizontal sheets) on the interfaces between layers of different density or magnetization (e.g. sediments with intercalated volcanics and underlying Precambrian rocks). Eventually, working from the surface downwards and using surface geology, excessive relief on the interfaces as anomaly sources may be replaced by more likely sources within the layer immediately above the interface. A synthetic example is discussed which shows that the system can be made to yield rapidly converging and accurate solutions for the depth to causative sources. Bouguer gravity data along an east-west profile in the Gaspé may be explained in a preliminary fashion by a weakly west dipping layered crust.

Résumé

La mise au point d'une méthode d'interprétation rapide et semi-automatique de données gravimétriques ou magnétiques, ou les deux, se poursuit présentement et repose essentiellement sur des calculs dans le domaine de Fourier. Dans un premier temps, on considère que les anomalies sont dues uniquement à la topographie d'interfaces séparant des couches à densité ou magnétisation différentes. Puis, à l'aide de données géologiques recueillies sous la surface, une variation en apparance anormale dans le relief d'une interface pourra être remplacée par des sources plus probables localisées à l'intérieur de couches susjacentes. L'exemple synthétique utilisé dans le présent document montre que le système est capable de produire rapidement des solutions précises. Il est ensuite appliqué à des données gravimétriques de Bouguer relevées le long d'un profit est-ouest effectué dans la région de Gaspé et, à ce stade du développement, en fournit une interprétation préliminaire.

Introduction

In areas peripheral to the Precambrian Shield, such as the Gaspé and the Eastern Townships, gravity and magnetic anomalies can be expected to arise from sources in (1) an upper layer of late Proterozoic and younger sediments and volcanics, (2) the underlying southwards-dipping extension of the Precambrian Shield and (3) sources due to irregularities of the interface between the upper layer and the underlying Shield rocks. A large quantity of gridded digitized data, in particular aeromagnetic data from the Geological Survey of Canada, and also Bouguer gravity data from the Earth Physics Branch, both of Energy, Mines and Resources Canada, is now available. It is clearly an impossible task to quantitatively interpret these data by inversion of individual anomalies. Therefore, an attempt is being made to determine the characteristics such as depth, depth extent and general shape of anomaly sources in a large area by computer-assisted calculations. Surface geology must provide a significant input and so must relevant physical properties determined for the outcropping rocks. The aim is to arrive at a fast and cheap method for a simultaneous inversion of gravity and magnetic data distributed two-dimensionally. More detailed interpretation can then be carried out on individual anomalous features of prime interest. The presently proposed system offers substantial advantages over earlier ones (e.g. that proposed by Peters, 1949, for layered structures) in that (1) the expression for the anomaly source field is simple, (2) most of the calculations are based on once to be determined Fourier coefficients, (3) rapid convergence is easily obtained, and (4) provides for anomaly sources within lithologically distinct layers as well as on their interfaces.

Simultaneous interpretation of gravity and magnetic data is advantageous where gravity and magnetic anomalies can be ascribed to the same source geometry. This will in general be the case for sources of types (1) and (3) in the described two-layer crustal model, but will be more questionable for sources in the basement layer. Another difficulty that will be encountered in many cases is that the detail at which the Bouguer gravity and the magnetic fields were mapped varies strongly. In the present case, the short wavelength information in the mapped magnetic field cannot be used as there is no equivalent in the mapped gravity field due to the large, up to about 10 km distance, between the successive gravity stations.

Another difference between the IGRF corrected magnetic and Bouguer gravity anomalies is the maximum depth to the causative sources. For the magnetic sources, this depth is the Curie point isotherm at 20 to 40 km depth depending on the regional geothermal gradient. For the Bouguer gravity sources, the maximum depth is rather the depth at which noticeable lateral density contrasts disappear which may be at the MOHO or even deeper. Furthermore, the change in magnetization with depth is probably much more complicated than that of the density. Consequently, extrapolation of the surface susceptibility and remanent magnetization of both the upper and the lower layer (in this application the Grenville rocks to the north) will be uncertain although viscosity effects may be estimated.

Notations

NS : Number of samples available
NS1 : Number of samples after periodisation
NS2 : Number of samples after doubling the sampling interval
NS4 : Number of samples after quadrupling the sampling interval
PY : Sampling interval
PY2 : Sampling interval where PY2 = 2 PY
PY4 : Sampling interval where PY4 = 4 PY
$G(j)$: Bouguer gravity value for sample j (NS samples)
$G^1(j)$: Bouguer gravity value for sample j (NS1 samples)
$G^2(j)$: Bouguer gravity, upward continuated by PY2, for sample j (NS2 samples)
$G^4(j)$: Bouguer gravity, upward continuated by PY4, for sample j (NS4 samples)
G^*_i : Bouguer gravity function computed at iteration i using Fourier transform according to interface depth B_i (* = 2) or Ci (* = 4)
g : Fourier transform of Bouguer gravity function
N : Number of harmonic
f : Frequency where $f = \frac{N}{NS\ PY}$
ΔG^*_i : Difference between actual and computed gravity functions at iteration i (* = 2 or 4). $\Delta G^*_i(j) = G^*(j) - G^*_i(j)$
A : Horizontal plane at which potential field data were measured
B : Depth of bottom surface for first layer (density ρa)
C : Depth of bottom surface for second layer (density ρb)
D : Depth of bottom surface for third layer (density ρc)
γ : Universal gravity constraint ($\gamma = 6.67.10^{-8}$ c.g.s.)
π : 3.14159...

Method and theoretical example

The present discussion is on the inversion of Bouguer gravity data (G_o) to obtain the depth and geometry of the sources of Bouguer anomalies. The method can be used for the interpretation of magnetic anomalies as well, either separately or simultaneously with gravity data.

Model

The interpretation method is based on a layered model. In the theoretical example a two-layer model with different densities (ρa, first layer and ρb, second layer) is used (Fig. 52.1). Furthermore, the depth (C) must be evaluated below which no important lateral density variations occur. The depth (B) to the interface between the layers is variable and is supposed to cause the anomaly field.

Method

In the theoretical example NS values for the interface depth (B_o) between the two homogeneous layers are chosen. The procedure is shown on Figure 52.2. By forward calculation in the frequency domain a Bouguer gravity function (G_o) is obtained. Then, using different hypotheses (infinite horizontal slabs, vertical prisms, finite horizontal sheets) and an iterative system, experimental values for the depth (B_n) will be calculated. To evaluate the accuracy of the method B_n is then compared to the original B_o.

Step 1: Infinite horizontal slabs hypothesis. This single hypothesis allows easy and fast calculation of the initial values for the depth (B_1, NS values) prior to initiating the iterative process. The jth sample of the gravity field is supposed to be due only to two horizontal infinite layers of respective thickness and density B_1-A, ρa and C-B_1, ρb yielding:

$$B_1(j) = \left(\frac{G_o(j)}{2\pi\gamma} + A\,\rho a - C\,\rho b\right)/(\rho a - \rho b).$$

Thus, the jth value of the interface depth ($B_1(j)$) vertically below the jth point is obtained. This depth is considered constant along the profile for one horizontal sampling interval (PY) centered on the jth sample location (Fig. 52.3).

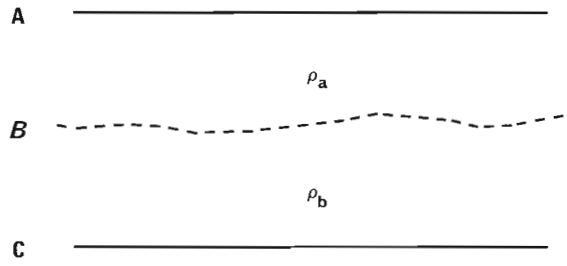

Figure 52.1. Schematic representation of a two layer crust with densities ρa and ρb. A, B, and C indicate depth to interfaces between layers. Unknown depths are indicated by Italic lettering.

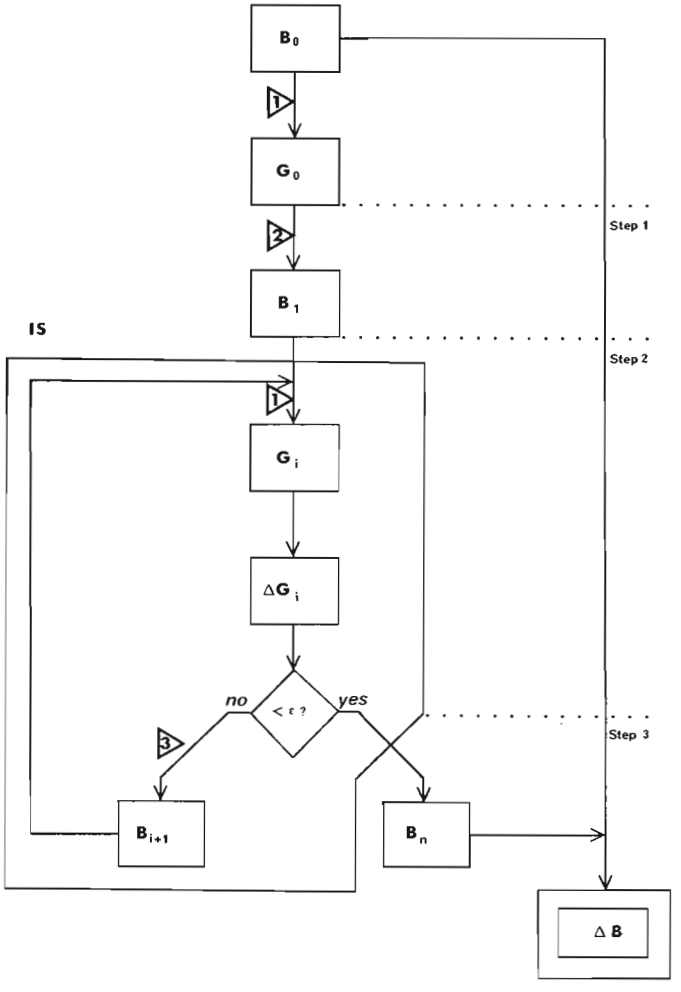

Figure 52.2. Flow chart giving sequence of procedures used in the theoretical studies. G and B indicate respectively the gravity function and interface depth. The operations 1, 2 and 3 (symbols within triangles) indicate respectively Fourier calculation, infinite horizontal slab approximation, and matrix method according to finite horizontal sheet representation. Steps 1, 2, and 3 are discussed in the text. The large box IS indicates the Iterative System.

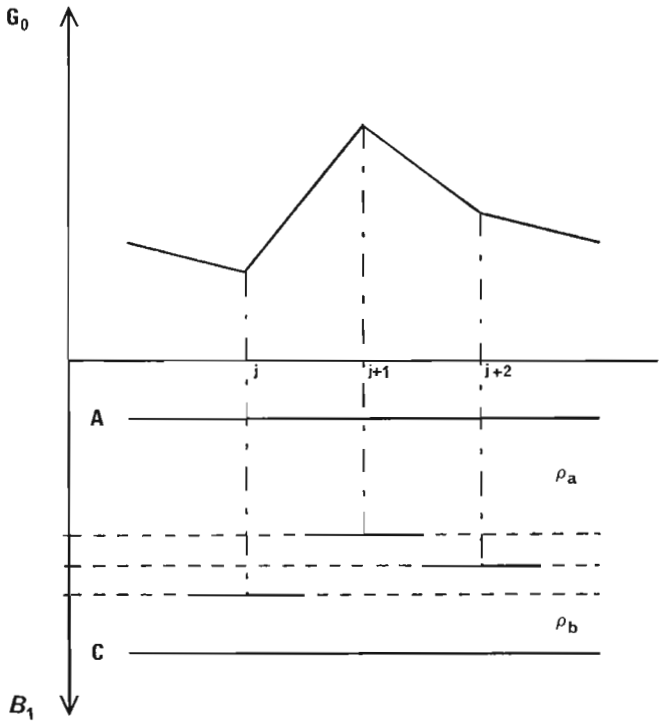

Figure 52.3. Infinite horizontal slab model. G_0 is observed Bouguer data and B_1 is interface depth calculated using this model.

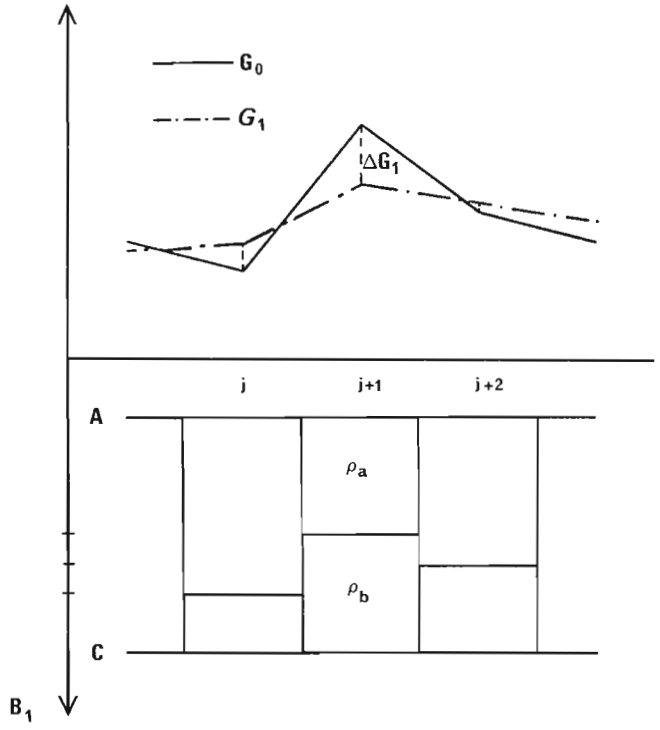

Figure 52.4. Two-layer vertical prism model. B_1 is initial depth (see Fig. 52.3), G_1 is Bouguer function calculated using this prism model and ΔG_1 is the difference between G_0 (see Fig. 52.3) and G_1.

Step 2: Vertical prism model. This procedure described in step 1 leads to a vertical prism model (Fig. 52.4). At each point j we have two vertical prisms (respective density ρa and ρb) separated by an interface situated at depth $B_1(j)$. Using a frequency domain calculation (see Appendix) the gravity function G_1 is obtained, created by the NS layered prisms making up this model. Usually G_1 and G will not match. Consequently, in the theoretical example, ΔG_1 is compared to a chosen error limit value (E). If ΔG_1 is small enough, we settle on the values of the depth (B_1) otherwise we proceed to step 3.

Step 3: Finite horizontal sheets. To progressively eliminate the differences ΔG_j the hypothesis of a horizontal sheet of length PY and density $\Delta\rho = \rho a - \rho b$ is used at each interface j within each prism (Fig. 52.5). The thickness ΔB_j of these layers is calculated in the following manner.

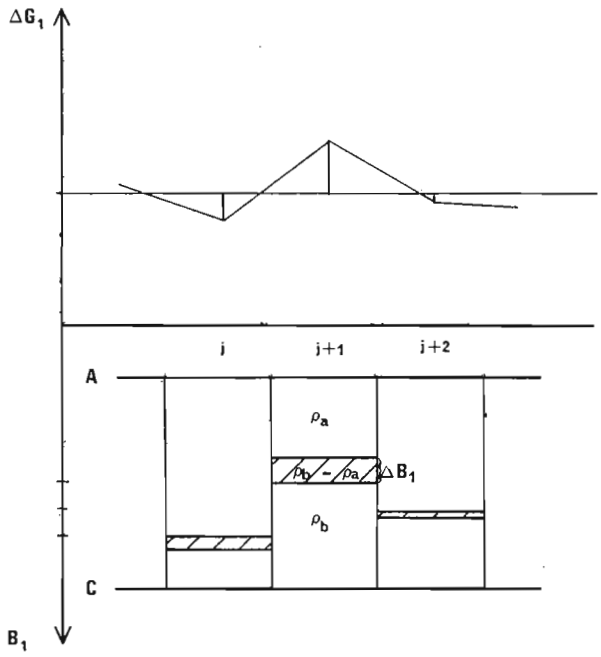

Figure 52.5. Finite horizontal sheet model. ΔB_1 is correction of depth obtained by matrix calculation using this model.

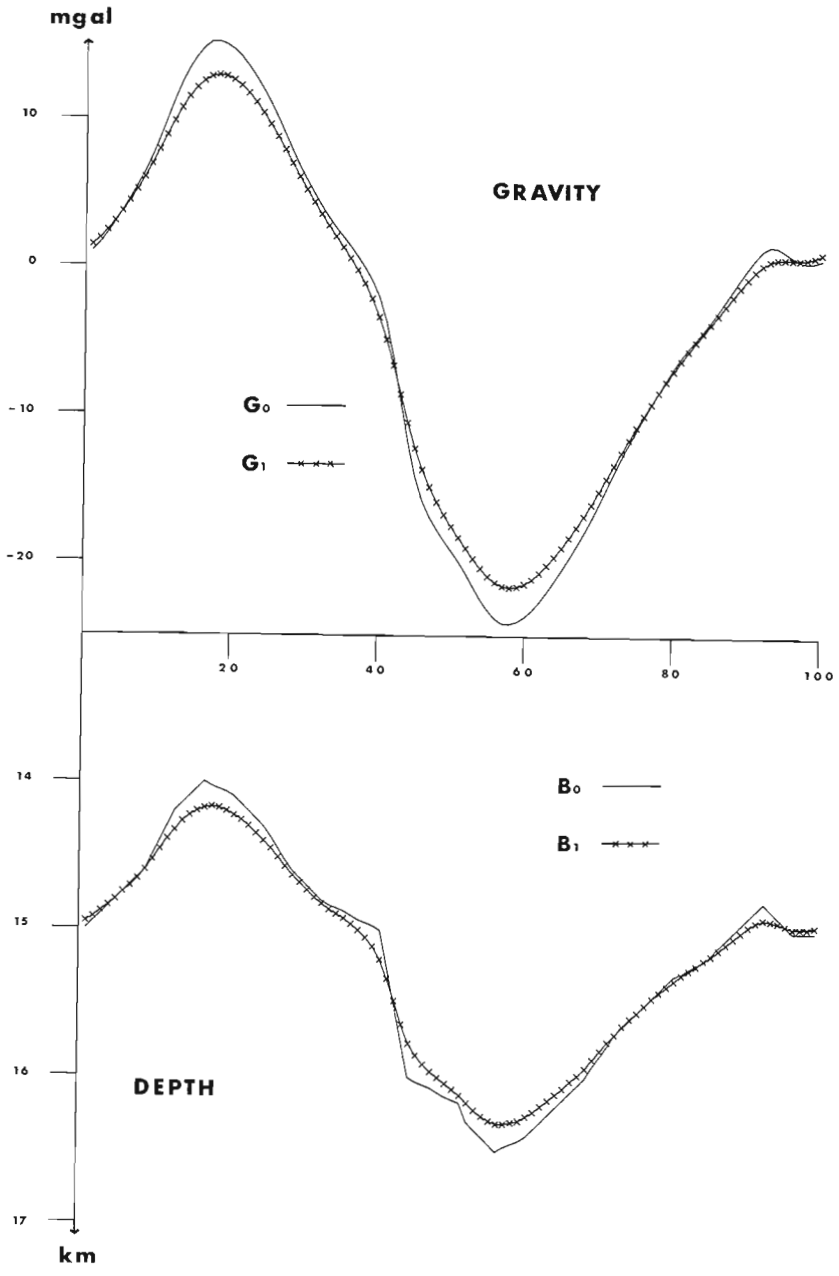

Figure 52.6. Theoretical example where the interface given by B_0 was chosen. G_0 is obtained by forward calculation from the model values, B_0 and B_1 are the initial values using the infinite horizontal slab model which gives rise, again by forward calculation, to gravity field G_1.

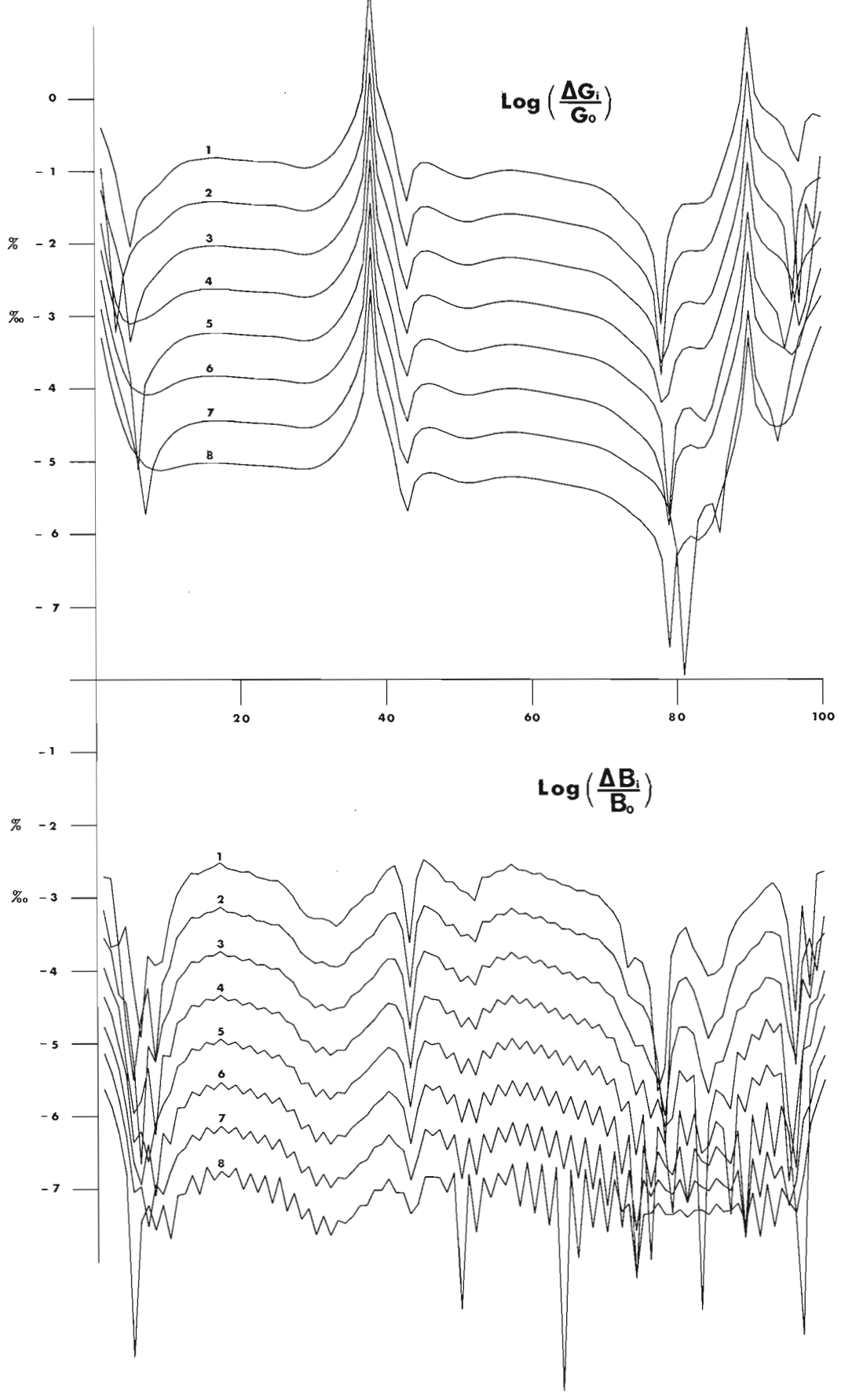

Figure 52.7. Convergence within the first 8 iterations of the calculated gravity (G) and depth (B) values, for the same example as Fig. 52.6. A logarithmic expression for the relative errors on G and B is used and the horizontal indicates the length of the profile. The change in this expression during the iterative procedure is essentially linear during the first 8 iterations. The relative error for G is less than 1% after the third iteration and that for B is less than 1‰ after the second iteration.

The gravity field created at observation point k by the NS horizontal sheets of length PY and of thickness $\Delta B(j)$ is:

$$\Delta G(k) = \sum_{j=1}^{NS} (-2\gamma \rho b (\tan^{-1}(\frac{PY}{B(j)}(\tfrac{1}{2} - |k-j|)) + \tan^{-1}(\frac{PY}{B(j)}(\tfrac{1}{2} + |k-j|))) \Delta B(j))$$

which is of the form $\Delta G(k) = \sum_{j=1}^{NS} M(k,j).\Delta B(j)$. Thus we have the matrix relation $M.\Delta B = \Delta G$, where ΔB is the unknown vector of length NS and M is an NS x NS matrix. ΔG and M are calculated during each iteration. Once determined, ΔB_i is applied to B_i to find an "improved" depth B_{i+1}. In practice, it was found that due to problems of numeric stability it is better to apply only a part of the correction. The best overall results were obtained setting $B_{i+1} = B_i + 0.75\ \Delta B_i$. The procedure is repeated following step 2 and step 3 until either ΔG_n is smaller than a set value E or a specified number of iterations has been performed. The resulting depth B_n is retained as the solution.

Results

Tests were conducted on many different parameters for several chosen models for which the Bouguer gravity field has been calculated.

Figure 52.6 shows the following parameters and results:

- the "actual" depth of the interface (B_o)
- the gravity "data" deduced from depth B_o (G_o)
- the initial depth calculated according to step 1 (B_1)
- the gravity function calculated in step 2 (G_1).

The result of the first 8 iterations is shown on Figure 52.7, especially the decrease of the error on both the gravity field (ΔG_i) and the depth ($\Delta B_i = |B_o - B_i|$). In this example the values for G_i, B_i are converging rapidly.

Exact values for ρa and ρb were taken in this example but other tests were conducted with density contrasts for the model up to 30% different from the original model values. In many cases the calculated depths to the interface were not strongly affected. The best convergence and stability were obtained for a sampling step superior or equal to the expected value of the interface depth ($PY \geq B$). It was also found that instead of applying at each iteration the full variation ΔB_i, applying only 75% of this value gives better convergence ($B_{i+1} = B_i + 0.75\ \Delta B_i$). Coefficients of less than 75% result in slower convergence while using coefficients from 75% to 100% may cause numeric instability. Therefore a coefficient of 75% was adopted for the example using real data.

Application to Gaspé and Eastern Townships

Taking into account the results of the theoretical examples the system was applied to real data in the Gaspé and Eastern Townships.

Model

The crust was considered to consist of the following three layers (Fig. 52.8):

- First layer: Paleozoic sediments and volcanics (ρ = 2.44)
- Second layer: Precambrian migmatite (ρ = 2.90)
- Third layer: Precambrian mafic granulite (ρ = 3.31)

It is also supposed that there is no important anomaly caused by lateral density variations below a depth of 40 km (D) so that the Bouguer field is caused entirely by relief on the interfaces B and C.

The first interface studied is C between the lower layer and an upper layer consisting of both layers 1 and 2 (ρ_{a+b} = mean value of ρa and ρb, Fig. 52.9). Then, knowing C, the depth of interface B is calculated (Fig. 52.10). The calculations are performed with NS1 = 100 samples and NS=85 samples are retained for plotting and interpretation (i.e. 15 samples were added for the periodisation, see below).

Method

The procedure is shown on a flow chart (Fig. 52.11). First the Bouguer gravity (G_o, sample interval of 5 km, 85 samples) must be made periodic by interpolation between $G_o(NS)$ and $G_o(1)$ to obtain $G_1(NS+1)$ to $G_1(NS1)$. Then the obtained function (G_o^1) is upward continued and the sampling interval is increased yielding G_o^2 (gravity function upward continued by 10 km using a sampling interval PY2 = 10 km), and G_o^4 (gravity function upward continued by 20 km using a sampling interval PY4 = 20 km). Subsequently, the treatments described for the theoretical example in steps 2 and 3 are applied, first to G_o^4 (yielding C), and, knowing that interface, to G_o^2 (yielding B).

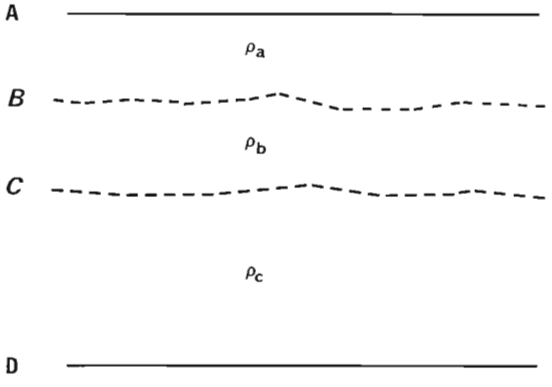

Figure 52.8. *Three-layer model down to depth of gravitational compensation D. Depths B and C are to be evaluated.*

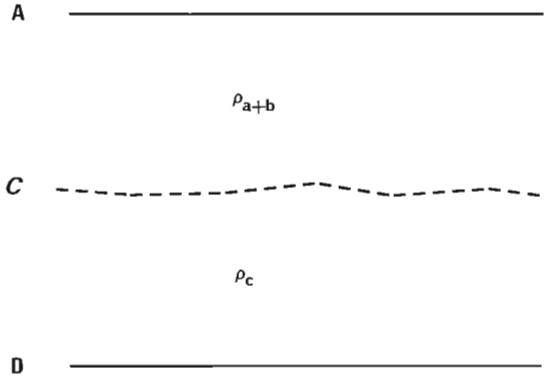

Figure 52.9. *Model when uppermost two layers are taken together i.e. sedimentary-volcanic and gneiss-migmatite. Layer 3 may correspond to a granulite layer down to the MOHO. Depth C is to be calculated.*

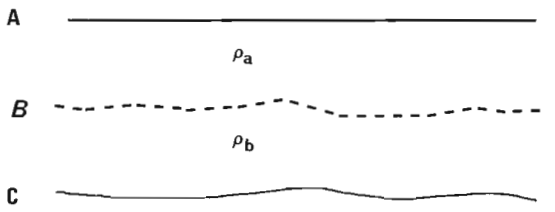

Figure 52.10

A two-layer model in which the depth of compensation is below interface C but unspecified. Depth B is to be calculated.

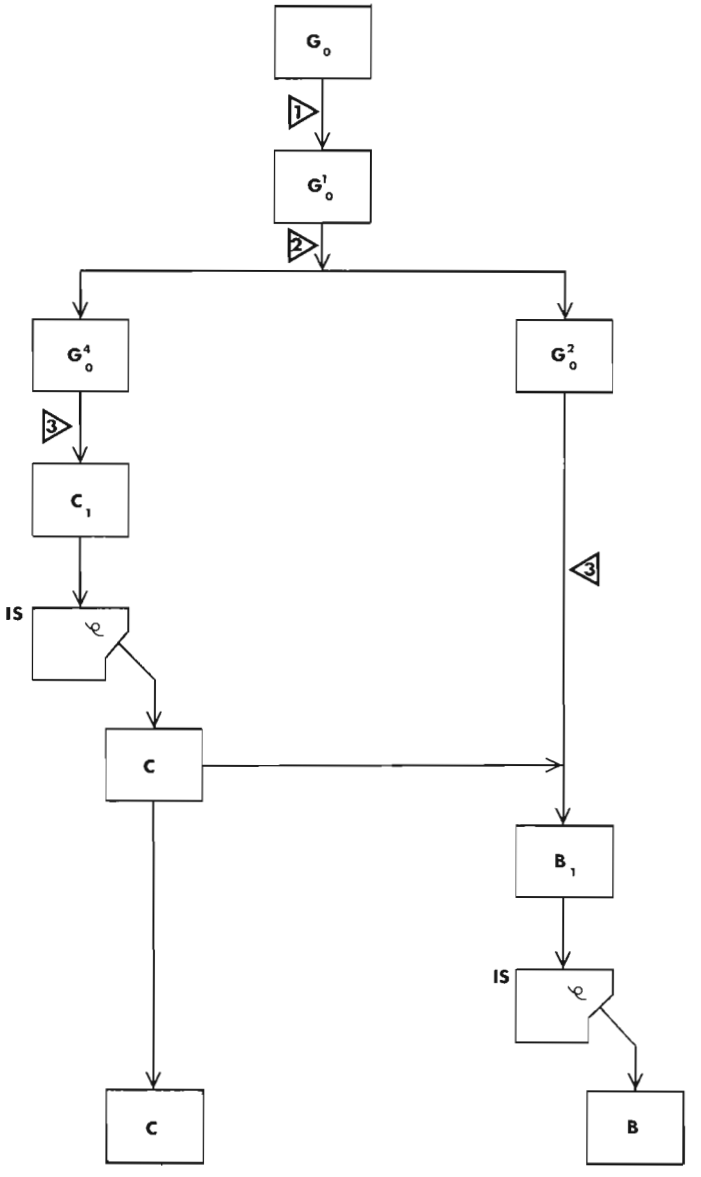

Figure 52.11. Flow chart giving the followed procedure used in the Gaspé study. Operations 1, 2, and 3 are respectively periodization of G (padding by extrapolation of known data to arrive at complete fundamental period), upward continuation and reduction of number of basic datum, and application of infinite horizontal slab model. The two boxes IS indicate the Iterative System shown in detail on Fig. 52.2.

Upward continuation of the gravity and magnetic field is used to relatively strongly decrease the effect of near-surface anomaly sources in order to optimize the data for interpretation of the deeper interfaces. The theoretical examples showed that it was advantageous to have a sampling interval close to the expected depth of the interface to be studied for a fast converging solution. Therefore it was decided to have a step of PY4 (20 km) in the Gaspé study to obtain interface depth C and a step of PY2 (10 km) to obtain interface depth B. As the data were gridded at 5 km x 5 km (PY x PY) it was necessary to reduce the number of samples. The required number of high frequencies is skipped in the Fourier domain to achieve this result. In an attempt to discriminate between anomaly sources at different depths, the selected data were upward continued by PY4 km for C and PY2 km for B. Upward continuation is a simple operation using the already available Fourier coefficients:

$$g_{alt\ (Z+A)}(N) = g_{alt(A)}(N)\, e^{-2\pi f(Z-A)}.$$

Preliminary results and interpretation

Figures 52.12 and 52.13 show respectively ground and upward continued Bouguer values and an interpretation along an east-west profile at 47°N spanning the area between 64° and 69°30'W (Gaspé). The increase in sampling interval is shown, and the increase in smoothing of the field with upward continuation is noted. The interpretation given here is one extreme solution where the upward continued data at 10 km is considered due solely to topography on interface B while that at 20 km is due to topography on interface C. A more acceptable interpretation will be achieved using the other extreme of considering B and C as west dipping planes, and, guided by surface geology, explain the residuals by inter-layer prisms using either the method described here or a modelling program such as MAGRAV (e.g. McGrath et al., 1983).

The principal difficulty is to decide where the relief on interface B is unreasonably strong. This relief can then be smoothed and the difference between the smoothed (or acceptable relief on B) and the calculated relief on B can be taken as representing sources that are in fact present in the first layer. With the help of the surface geology, these sources could then be modelled and their effect at 20 km calculated. These effects may be subtracted from the upward continued field at 20 km allowing interface depth C to be calculated. Smaller wavelength topography on C can again be considered as in fact due to sources in the second layer and the process may be repeated.

The above procedure can be applied to each of mutually perpendicular profiles so that a 3-dimensional picture of the crust above the depth of compensation would emerge. The proposed method is presently being applied first on gravity data alone to evaluate its usefulness.

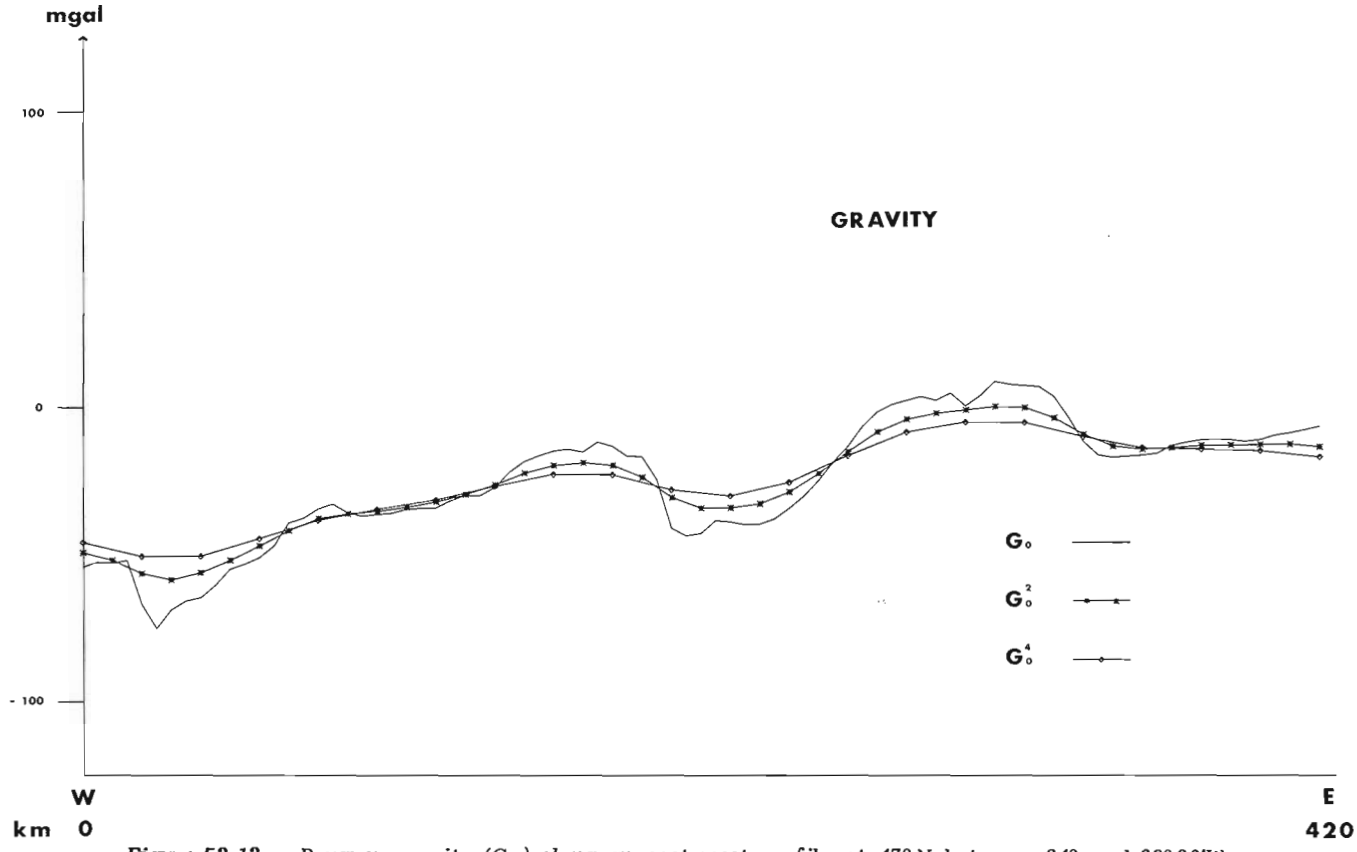

Figure 52.12. Bouguer gravity (G_o) along an east-west profile at 47°N between 64° and 69°30'W, sample interval is 5 km. G_o^2 and G_o^4 are the upward continued G_o surface data to respectively 10 and 20 km with sampling intervals increased to 10 and 20 km.

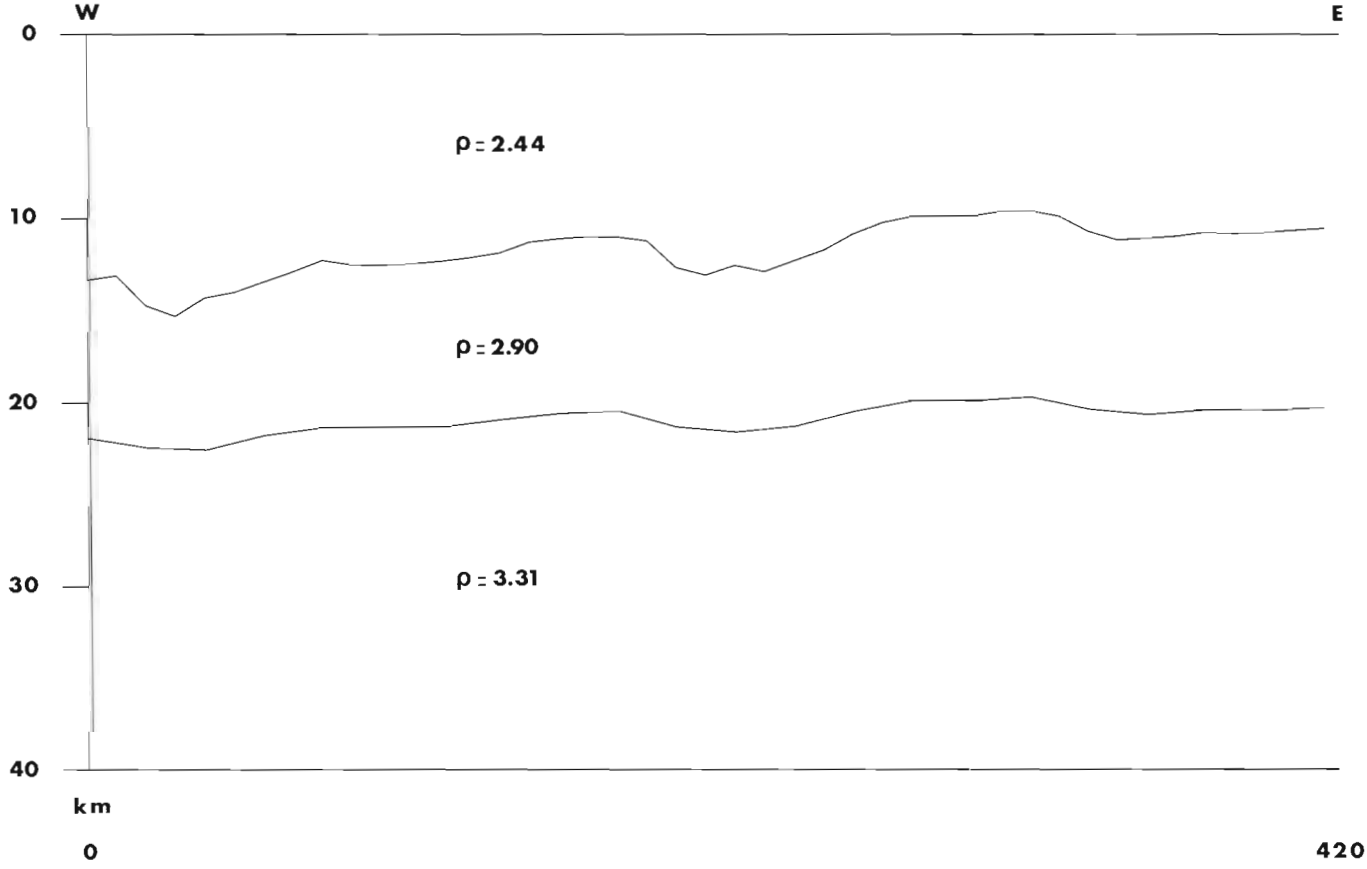

Figure 52.13. Depth to the interfaces B and C for density distribution as shown when G_o^2 (Fig. 52.12) is taken to be due entirely to relief on B and G_o^4 is due to relief on C.

Magnetic data can be treated in a similar fashion. For simultaneous inversion with the gravity data, the magnetic data must be reduced to the pole i.e. calculation of the anomaly field for vertical magnetic induction. The magnetic data must also be integrated – or the gravity data be differentiated with respect to the vertical – before it can be equated to the gravity data multiplied by a constant which depends on the density of the source and its total magnetic intensity. The proposed method has been tested on a synthetic example and the results agreed with the above mentioned equality.

Acknowledgments

This study is being carried out during BSD's term as a "co-opérant" under a French-Canadian cultural agreement. Bouguer gravity data were obtained from the Gravity Data Centre of the Earth Physics Branch. D. Teskey critically read the manuscript.

References

Gérard, A. and Debeglia, N.
1975: Automatic three-dimensional modeling for the interpretation of gravity or magnetic anomalies; Geophysics, v. 40, no. 6, p. 1014-1034.

McGrath, P.H., Henderson, J.B., and Lindia, F.M.
1983: Interpretation of a gravity profile over the contact zone between Archean granodiorite and the Yellowknife Supergroup using an interactive computer program with partial automatic optimization; in Current Research, Part B, Geological Survey of Canada, Paper 83-1B, p. 189-194.

Peters, L.J.
1949: The direct approach to magnetic interpretation and its practical application; Geophysics, v. 14, p. 290-320.

Appendix

The Fourier transform of the gravity field due to the jth two-layer vertical prism with an interface depth B(j) can be written as (Gérard and Debeglia, 1975):

$$g_j(N) = \frac{1}{NS}\frac{1}{2\pi f} 2\pi\gamma \left((\rho_a^* (e^{-2\pi fA} - e^{-2\pi fB(j)}) + \rho_b^* (e^{-2\pi fB(j)} - e^{-2\pi fC})\right) e^{\frac{-2\pi iNj}{NS}}, \quad (i^2=-1),$$

which, when summed over the NS two-layer prisms yields:

$$g_j(N) = \frac{1}{NS}\frac{1}{2\pi f} 2\pi\gamma \sum_{j=0}^{NS-1} \left((\rho_a^* (e^{-2\pi fA} - e^{-2\pi fB(j)}) + \rho_b^* (e^{-2\pi fB(j)} - e^{-2\pi fC})\right) e^{\frac{-2\pi iNj}{NS}}$$

Simplification: rather than using actual values for density (ρ_a^*, ρ_b^*), density contrasts are used: $\rho a = \frac{\rho_a^* - \rho_b^*}{2}$, $\rho b = \frac{\rho_b^* - \rho_a^*}{2}$ so that $\rho a = -\rho b$. Thus,

$$g_j(N) = \frac{1}{NS}\frac{1}{2\pi f} 2\pi\gamma\, \rho b \sum_{j=0}^{NS-1} \left((2e^{-2\pi fB(j)} - e^{-2\pi fA} - e^{-2\pi fC})\, e^{\frac{-2\pi iNj}{NS}}\right)$$

Where the real and imaginary components are considered i.e.

$$g(N) = g_R(N) + i\, g_I(N)$$

There is an obvious numeric problem for N=0 (f=0), which is circumvented in the following manner:

$N \to 0 \quad (f \to 0)$

$$e^{-2\pi fA} = 1 - 2\pi fA + 4\pi^2 f^2 A^2 + E_3$$

$$\cos\frac{2\pi Nj}{NS} = 1 - \frac{4\pi^2 N^2 j^2}{2\,NS^2} + E_4$$

$$\sin\frac{2\pi Nj}{NS} = \frac{2\pi Nj}{NS} + E_3$$

where E_b is a function of type αf^b

Consequently,

$$g_R(N) = \frac{1}{NS}\frac{1}{2\pi f} 2\pi\gamma\, \rho b \sum_{j=0}^{NS-1} \left((2\pi f\,(A + C - 2B(j)) - 4\pi^2 f^2 (A^2 + C^2 - 2B^2(j)) + E_3)\,(1 - \frac{4\pi^2 N^2 j^2}{2NS^2} + E_4)\right)$$

$$g_R(N) = \frac{1}{NS} 2\pi\gamma\, \rho b \sum_{j=0}^{NS-1} \left((A + C - 2B(j)) - 2\pi^2 f\,(A^2 + C^2 - 2B^2(j)) + E_2\right)$$

$$g_R(N) = 4\pi\gamma\ \rho b\ \left(\left(\frac{A + C}{2}\right) - \bar{B}\right) - 2\pi^2 f\ \left(\left(\frac{A^2+C^2}{2}\right) - \bar{\bar{B}}\right) + E_2)$$

where $\bar{B}$ is the mean value of B(j) and $\bar{\bar{B}}$ is the mean value of $B^2(j)$.

The imaginary component is expressed as:

$$g_I(N) = \frac{1}{NS}\ \frac{1}{2\pi f}\ 2\pi\gamma\ \rho b \sum_{j=0}^{NS-1} ((2\pi f\ (A + C - 2\ B(j)) - 4\pi^2 f^2\ (A^2+C^2 - 2B^2(j)) + E_3)\ (\frac{2\pi Nj}{NS} + E_3),$$

$$g_I(N) = \frac{1}{NS}\ 2\pi\gamma\ \rho b\ 2\pi f\ PY \sum_{j=0}^{NS-1} ((A + C - 2\ B(j)) - 2\pi f\ (A^2+C^2 - 2B^2(j)) + E_2)\ j),$$

$$g_I(N) = 2\pi\gamma\ \rho b\ 2\pi f\lambda\ \left(\left(\frac{A + C}{2}\right) - \frac{2}{NS(NS-1)} \sum_{j=0}^{NS-1} jB(j)\right) - 2\pi f\ \left(\left(\frac{A^2+C^2}{2}\right) - \frac{2}{NS(NS-1)} \sum_{j=0}^{NS-1} jB^2(j)\right) + E_2)$$

where λ is the spatial period (λ = (NS-1) PY)

The expressions for $g_R(N)$ and $g_I(N)$ give use to the following general conditions:

if $\bar{B} \neq \frac{A+C}{2}$ $\quad g_R(0) = 4\pi\gamma\ \rho b\ \left(\frac{A+C}{2} - \bar{B}\right)$

if $\sum_{j=0}^{NS-1} jB(j) \neq \frac{NS(NS-1)}{2}\ \left(\frac{A+C}{2}\right)$ $\quad g_I(0) = 0$ $\quad (g_I(0) \curvearrowleft E_1)$

if $\bar{B} = \frac{A+C}{2}$ $\quad g_R(0) = 0$ $\quad (g_I(0) \curvearrowleft E_1)$

if $\sum_{j=0}^{NS-1} jB(j) = \frac{NS(NS-1)}{2}\ \left(\frac{A+C}{2}\right)$ $\quad g_I(0) = 0$ $\quad (g_I(0) \curvearrowleft E_2)$

AN ELECTROMAGNETIC SURVEY OVER THE GLOUCESTER LANDFILL SITE FOR THE DETECTION OF CONTAMINATED GROUNDWATER

Project 790034

L.E. Stephens and B.W. Graham[1]
Resource Geophysics and Geochemistry Division

Stephens, L.E. and Graham, P.W., An electromagnetic survey over the Gloucester Landfill Site for the detection of contaminated groundwater; in Current Research, Part A, Geological Survey of Canada, Paper 85-1A, p. 431-440, 1985.

Abstract

Electromagnetic and magnetic surveys were conducted over a former landfill site near Gloucester, Ontario, 10 km south of Ottawa to delineate zones of groundwater contamination derived from buried municipal and chemical wastes. Electromagnetic detection of contaminated groundwater resulting from the presence of dissolved chemicals relies on an increase in electrical conductivity above that of the surrounding uncontaminated groundwater. At the Gloucester Landfill Site, two electromagnetic conductors were detected. Correlation of borehole conductivity and chemical data with the conductors shows that contamination and electromagnetic ground conductivity are related and that electromagnetic surveying is a viable means of delineating groundwater contamination.

A magnetic survey was conducted over the landfill site to distinguish conductivity anomalies caused by buried metallic waste.

Résumé

On a effectué des levés électromagnétiques et magnétiques au-dessus d'un ancien terrain de remblayage situé près de Gloucester en Ontario à 10 km au sud d'Ottawa, afin de délimiter les zones de contamination des eaux souterraines par des déchets urbains et chimiques enfouis. La détection électromagnétique des eaux souterraines contaminées par des produits chimiques dissous est basée sur l'augmentation de leur conductivité électrique par rapport aux eaux souterraines environnantes non contaminées. Sur le site de remblayage de Gloucester, on a décelé deux conducteurs électromagnétiques. La corrélation établie entre la conductivité mesurée dans les sondages et les données chimiques d'une part, et les conducteurs d'autre part, montre que la contamination et la conductivité électromagnétique du sol sont liées, et que les levés électromagnétiques constituent une méthode valable pour délimiter la zone de contamination par les eaux souterraines.

On a réalisé un levé magnétique au-dessus du site de remblayage, de façon à reconnaître les anomalies de conductivité résultant de l'enfouissement de déchets métalliques.

[1] National Hydrology Research Institute, Inland Waters Directorate, Environment Canada, Ottawa

Introduction

During the period 1979 to 1982, drilling and chemical testing by the National Hydrology Research Institute (NHRI, Environment Canada) had detected groundwater contamination at a landfill site near Gloucester, Ontario, 10 km southeast of Ottawa (Fig. 53.1). In 1983, the Geological Survey of Canada (GSC) carried out electromagnetic and magnetic surveys in an attempt to outline the contamination. The survey was part of a cooperative effort between the GSC, NHRI (Inland Waters Directorate) and the Ontario Ministry of the Environment to study the extent and environmental impact of pollution emanating from the site previously used for domestic waste from 1956 to 1973. A special compound located within the domestic waste site, had been used from 1969 to 1980 for the disposal of industrial toxic and organic chemical wastes.

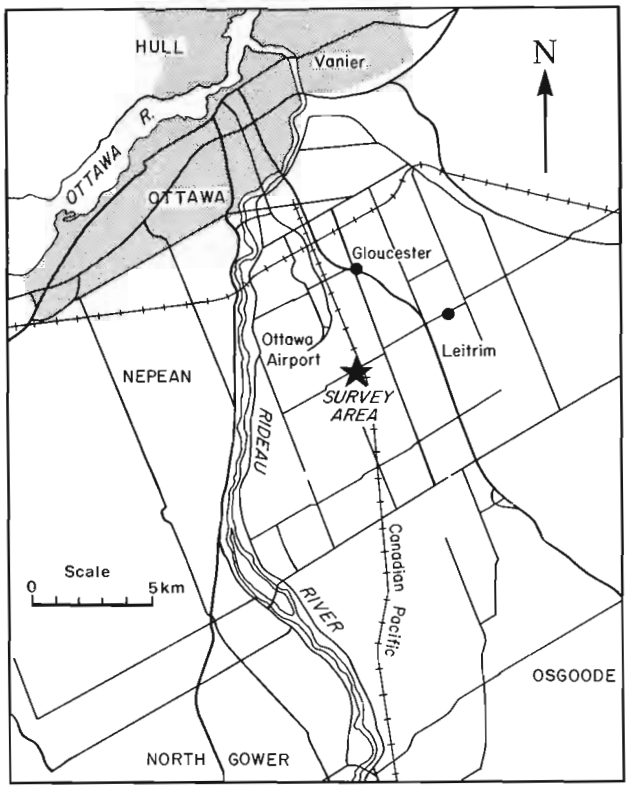

Figure 53.1. Location map for Gloucester Landfill Site.

Statement of the problem

Flowing groundwater carried dissolved contaminants out of the landfill site thereby causing a contaminant "plume"; in fact, two plumes have been detected by chemical analyses of water samples taken from different depths in various boreholes: 1) an upper plume (3 to 8 m deep) stretching north and northeast from the general waste site, and 2) a deeper plume (19 to 25 m deep) moving eastward from the special waste compound (Fig. 53.2).

The source of the shallow plume is surficial municipal waste which covers most of the landfill area outlined in Figure 53.3. The top stratigraphic unit containing this plume consists of 4 to 9 m of medium to fine sand with imbedded gravel underlain by 3 to 4 m of well compacted clayey silt (French and Rust, 1981). The clayey silt layer is impervious to water flow and is a confining boundary between the upper and lower plumes.

The lower contamination plume resides in a highly permeable gravel layer below the clayey-silt layer. Borehole data have shown the clayey-silt layer beneath the special waste compound to pinch out, and that "holes" in this layer which is generally uniform throughout the remainder of the

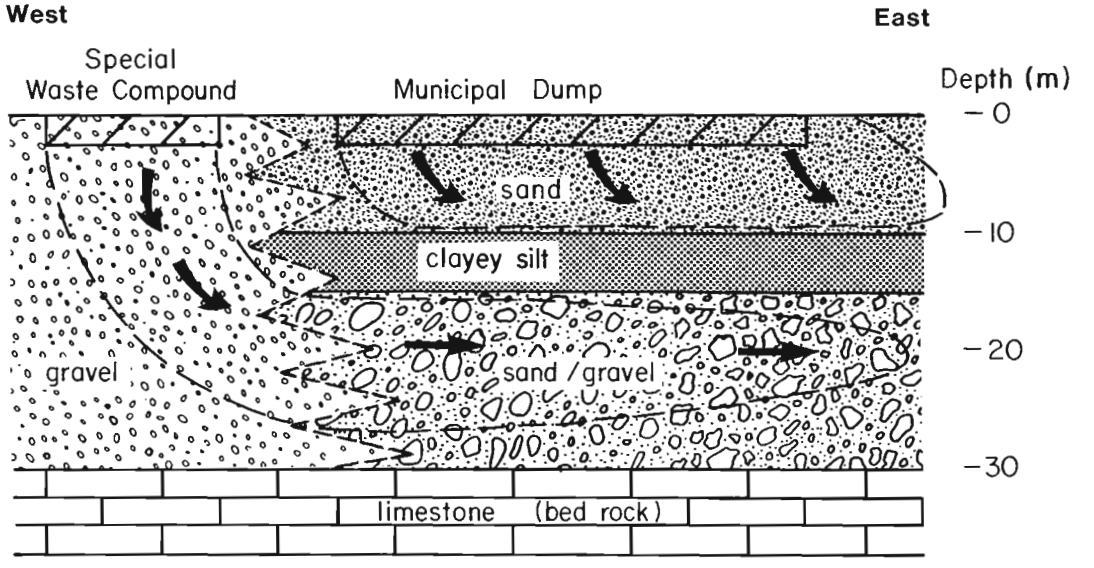

Figure 53.2. Diagrammatic cross-section of geology structure and contamination plume migration (geology after Jackson et al., in press).

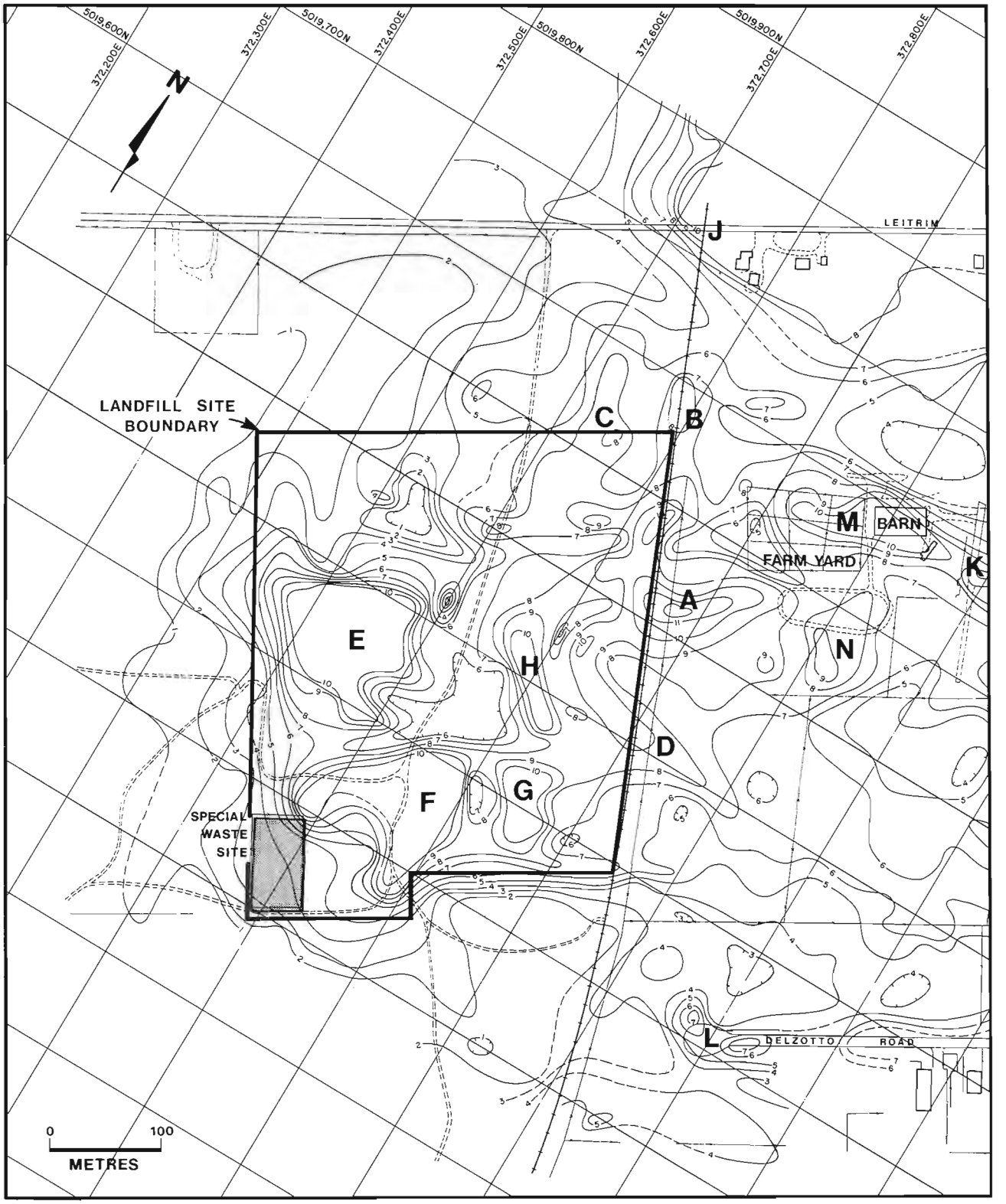

Figure 53.3. *Shallow surface electrical conductivity mapping using the Geonics EM31 at the Gloucestor Landfill Site. Contours are apparent conductivity values in mS/m.*

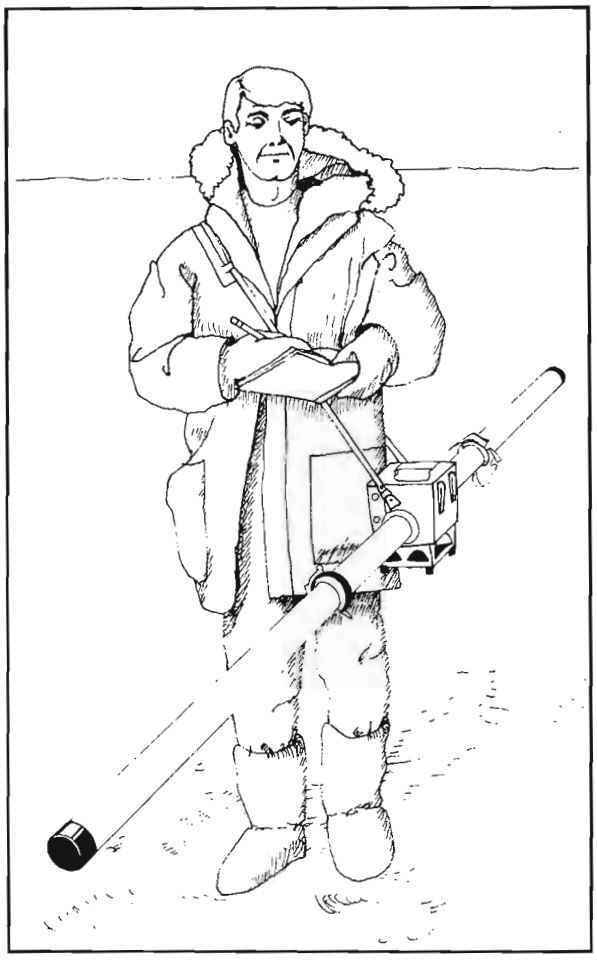

Figure 53.4. *Geonics EM31 in operation.*

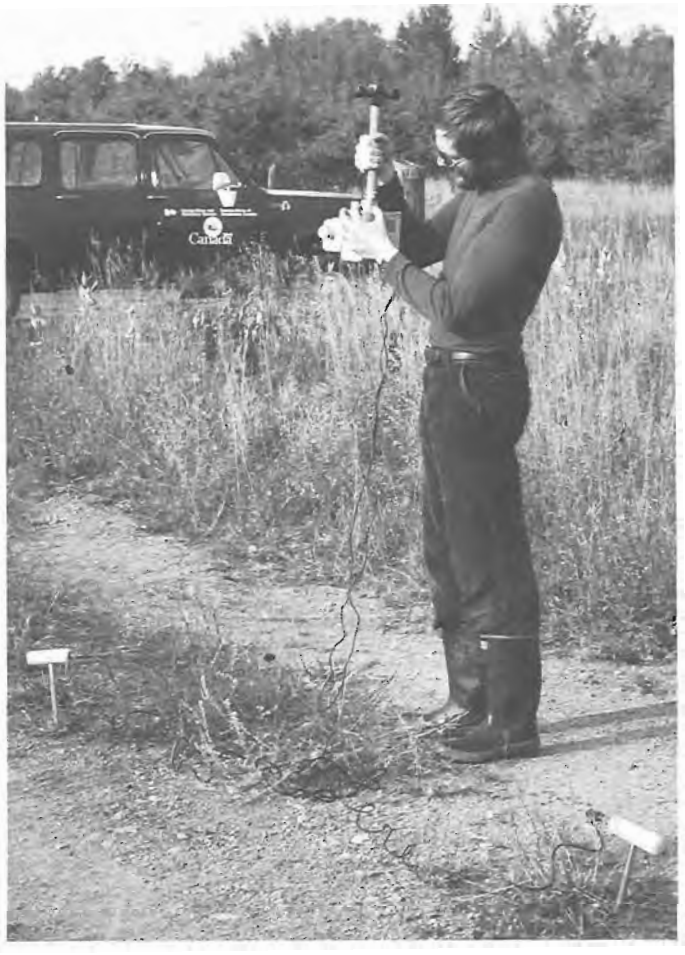

Figure 53.5. *Geonics EM16R VLF receiver.*

landfill site, have permitted contamination to seep through gravel into the lower acquifer (Fig. 53.2). On the site, the base of the lower plume is confined to a maximum depth of about 30 m by limestone bedrock which rises and eventually outcrops 1 km to the east of the site.

Geophysical survey plan

For electromagnetic studies of groundwater contamination to be successful, the contaminated water must be electrically more conductive than the "clean" water surrounding it. Active groundwater bearing dissolved salts would carry contamination out of the site. If there were sufficient electrical conductivity contrast with adjacent cleaner water having lower electrical conductivity, electromagnetic equipment might be able to detect contamination within the depth range of detectability for the equipment. A decrease in apparent conductivity towards the edges of the anomaly may be caused by the contamination plume descending and thinning or by diffusion into the surrounding cleaner water.

Electromagnetic surveying was carried out with Geonics EM31 and EM16R instruments throughout the landfill site and eastward in the direction of contaminant migration determined by chemical sampling from boreholes. A magnetic survey with a Scintrex MP-2 was conducted over the same area in order to delineate areas of buried metallic waste which would cause EM anomalies masking the more subtle anomalies associated with contaminated groundwater.

Instruments and results

Geonics EM31

The Geonics EM31 is a continuous reading, one-man instrument capable of measuring apparent conductivity of the ground to a depth of 6 m (Fig. 53.4) (McNeill, 1980). The EM31 has a transmitter and receiver fixed to each end of a rigid 3.7 m pole. The transmitter emits a 9.8 kHz electromagnetic signal. The transmitted electromagnetic field induces electrical currents in nearby conductive structures and surrounding ground which are sensed by the receiving coil.

The EM31 instrument weighs about 9 kg and is very portable. An operator can traverse between stations at walking speed and take about 5 seconds for each measurement. The EM31 is an inductive electromagnetic instrument and unlike a DC resistivity instrument which requires electrodes to be pushed into the ground, the EM31 output is a direct reading of ground conductivity in milli-Seimens/metre (mS/m). If the ground is laterally and vertically homogeneous within about 6 m of the instrument, true ground conductivity will be measured (McNeil, 1980). If, however, there are sufficiently massive metallic objects, contaminated water or layers of sediments with different electrical conductivities (e.g. clay, silt and sand) beneath the ground, the EM31 will measure the apparent conductivity which is the cumulative effect of these conductors and the surrounding ground. EM31 measurements are strongly

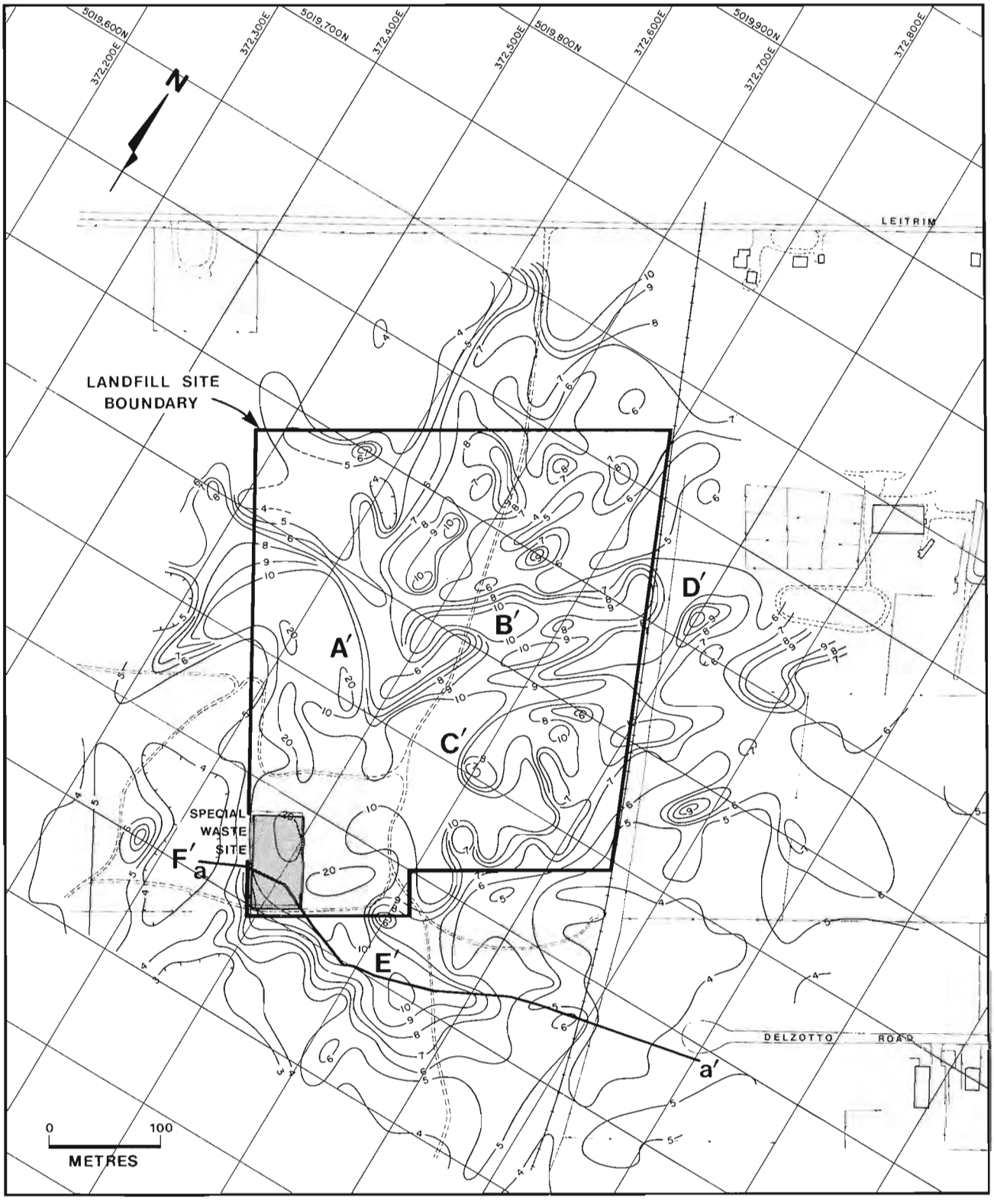

Figure 53.6. *Electrical conductivity mapping using the Geonics EM16R at the Gloucester Landfill Site. Contours are apparent conductivity values in mS/m.*

affected by metallic structures such as metal barns and railways and also by electrical noises from powerlines. Measurements at stations within 25 m of buildings, railways and powerlines were avoided.

Initially, the EM31 was used for a reconnaissance survey at 25 m intervals on east-west and north-south grid lines 100 m apart (Fig. 53.3). Highly anomalous features discovered during this reconnaissance survey were later surveyed in greater detail by measurements within the 100 m grid squares. EM31 measurements at 695 stations were done in 9 days. Measurement accuracy was assessed by repeated readings at 36 randomly selected stations. The standard deviation of the differences was ± 0.47 mS/m.

Apparent conductivity values over the survey area vary from 1 to more than 10 mS/m (Fig. 53.3). Values greater than 10 mS/m which occur within the landfill site boundaries are believed to be associated with metallic waste (anomalies E,F,G and H). The northern one third of the landfill site has only moderately high anomalies, apparently because of the lower metallic waste content of the landfill than in the southern part of the site.

Apparent conductivity values lower than 3 mS/m west and south of the landfill site (anomaly I) are caused by a less conductive layer of gravel adjacent to more conductive clayey silt under the remainder of the landfill site. Gravel was found in boreholes west of the special waste compound. At the northeast corner of the landfill site, two anomalies (B and C) extend northward while two other anomalies (A and D) suggest that contamination may have also progressed eastward across the railway tracks. Chemical analyses from a borehole off the east end of anomaly "A" have detected contaminants at shallow depths (Jackson et al., in press).

Two high conductivity anomalies on a farm (anomalies M and N) could be caused by increased nitrates and sulphates from farm animal wastes and not by landfill site contamination. Detailed traversing in the vicinity of anomaly N shows the extent of the anomaly to be coincident with the farm yard; skewness of the anomaly to the north seems to correspond to surface drainage. Anomaly M occurs in a wooden holding pen for farm animals.

Anomalies in excess of 10 mS/m (anomalies J, K and L) coincide with roads (Leitrim, Quinn and Delzotto). These linear anomalies could be caused by road salt applied during winter months which would permeate the near surface sediments in the vicinity of the roads. The presence of salt could be proven by chemical analyses of surface soil samples. Since residential houses are proximate to the roads, an alternate source of these "road anomalies" might also be effluent from septic tile beds. The "road anomalies" do not appear related to powerlines since the EM effect of powerlines along Leitrim Road west of the railway tracks is less than 25 m from the powerlines and the high conductivity values associated with the roads extends almost 100 m from the roads. Also, no "road anomaly" occurs on Leitrim Road west of the railway tracks where powerlines still exist.

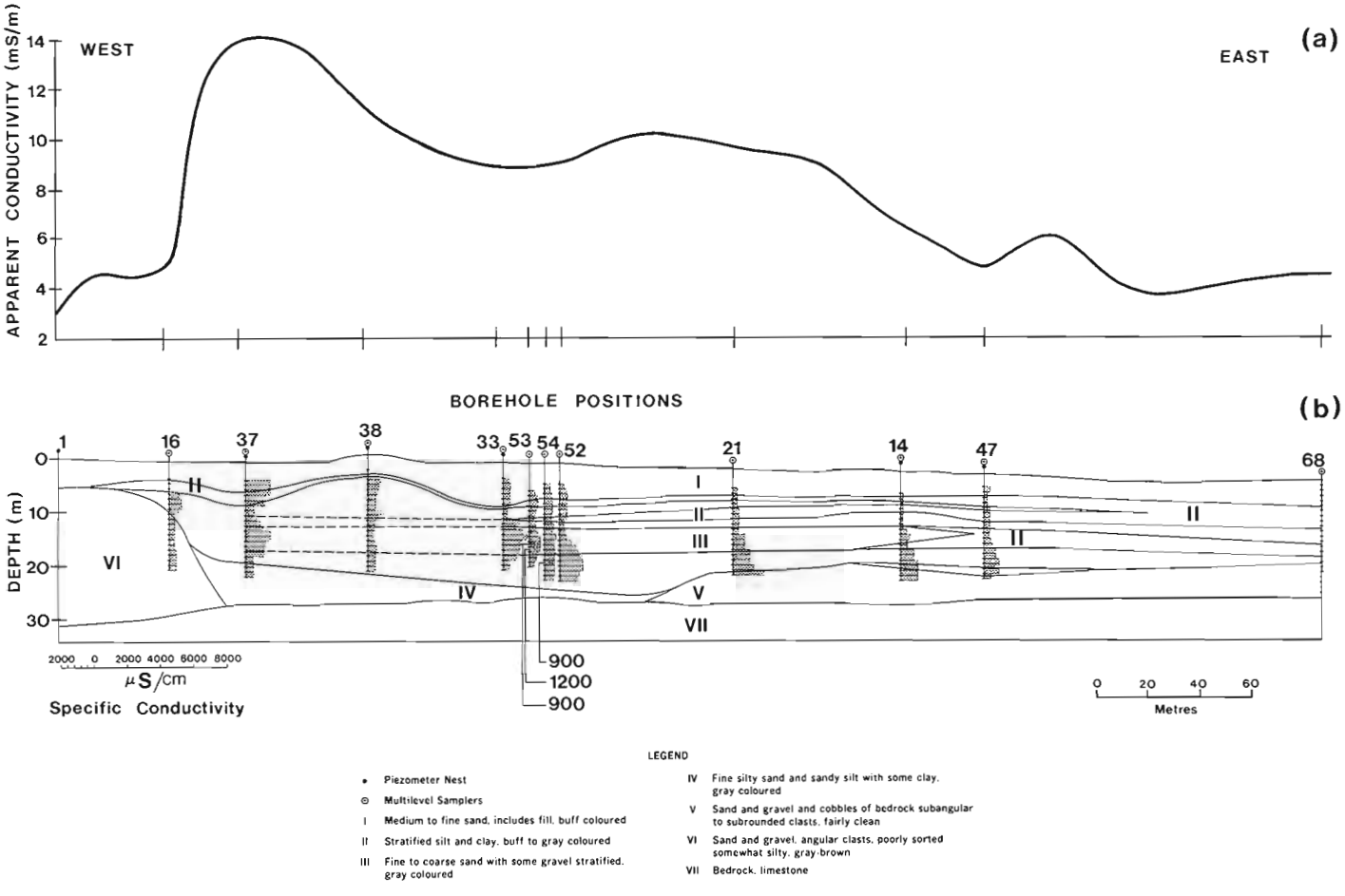

Figure 53.7. *Profile a-a' (see Fig. 53.6, 53.8) showing a) Geonics EM16R apparent conductivity; b) Specific conductivity in borehole water and stratigraphy (Fig. 53.7b from Jackson et al., in press).*

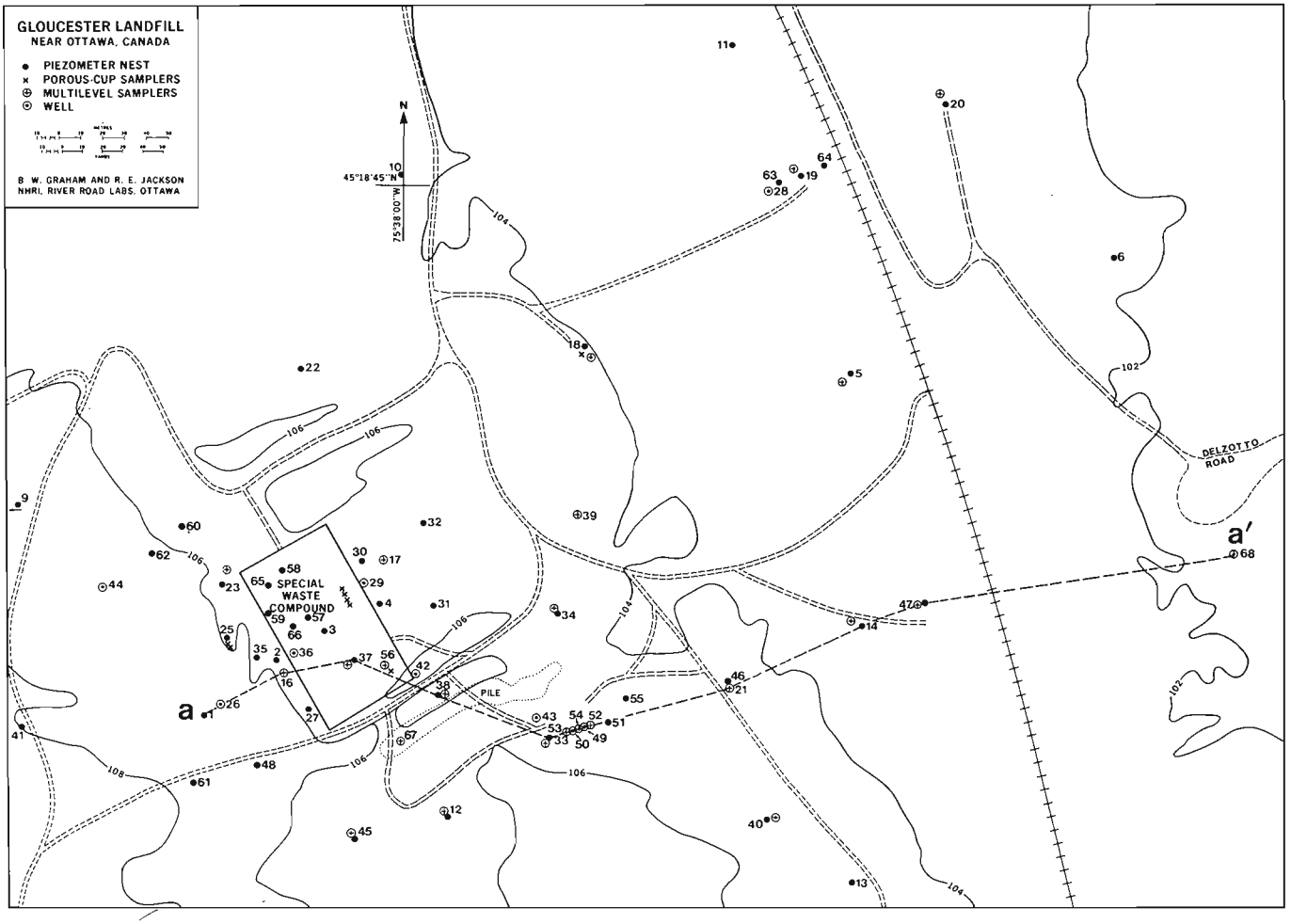

Figure 53.8. *Distribution of boreholes in the vicinity of the Special Waste Compound (from Jackson et al., in press).*

Geonics EM16R

The Geonics EM16R (Fig. 53.5) is a 1.5 kg receiver which uses 15 to 25 kHz signals from military VLF radio transmitters. The receiver measures the horizontal magnetic component of the VLF signal through a coil in the hand-held unit while the horizontal electric field is measured across two probes that are inserted into the ground 10 m apart. Output from the EM16R is apparent resistivity (ie. inverse of apparent conductivity) in ohm-metres and phase angle between the horizontal quadrature and inphase electric field, the electric field being compared with the horizontal magnetic field for phase reference. A phase angle of 45 degrees signifies homogeneous ground while any departure from 45 degrees indicates a layered subsurface. Lateral changes in ground conductivity may also affect the phase angle. The EM16R, having an effective depth of penetration of 50 m, was used to detect contamination in the lower aquifer and to complement the EM31 measurements whose 6 m maximum depth penetration was suitable for detecting contamination in the upper aquifer.

The EM16R survey can be carried out by one person but is facilitated by a crew of 3 – one for handling each of the two probes and the third for holding the main unit during the measurement. Each measurement takes about one minute. Although not all measurement locations for the EM16R were identical to those for the EM31, a survey plan similar to that for the EM31 was followed; measurements were made at 25 m intervals along east-west and north-south grid lines spaced 100 m apart. This reconnaissance coverage was followed up with readings on a 25 m square grid at locations selected for more detailed coverage.

Although the EM16R measures resistivity, the results in Figure 53.6 have been converted to conductivity values for comparison with the EM31 results. The EM16R results vary from 3 to 30 mS/m and generally show high and erratic results in the disposal area because of high concentrations of metallic wastes (A',B' and C'). A comparison between EM16R anomalies A', B' and C' (Fig. 53.6) and EM31 anomalies E, F and H (Fig. 53.3), respectively, shows similarities in distribution and shape.

Anomaly D' is coincident with EM31 anomaly A but is much reduced in width and amplitude. The sphere of influence for the EM16R is much broader than for the EM31 yet near-surface conductors have some contribution to EM16R measurements. EM31 anomalies with relative amplitudes less than 2 or 3 mS/m do not have corresponding EM16R equivalents.

The most important EM16R anomaly related to contamination, trends easterly from the special waste site (anomaly E') and is about 6 mS/m above the background level of 4 mS/m (Fig. 53.6). Chemical analyses of borehole water

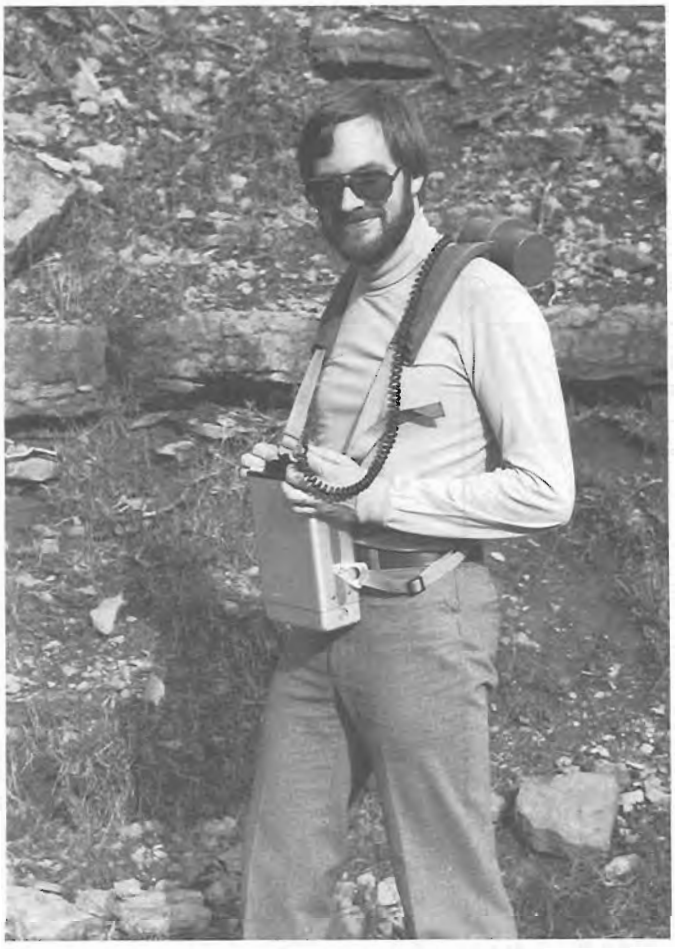

Figure 53.9. *Scintrex MP-2 total field magnetometer in operation.*

for sulphate and chloride ion concentrations and specific conductivity (Fig. 53.7) indicate this anomaly is caused by contamination in the lower aquifer (Jackson et al., in press). Furthermore, the anomaly trend is in agreement with the hydrologic gradient measurements. Cross section a-a' (Fig. 53.6, 53.8) shows that high specific conductivity in boreholes corresponds to high apparent conductivity from EM16R surface results (Fig. 53.7). The EM31 anomalies indicate a contaminant migration of about 100 m (Fig. 53.3, anomaly A) while the EM16R indicates a migration of about 250 m (Fig. 53.6, anomaly E'). This is consistent with borehole chemical analyses of contaminants and with flow velocities in the upper and lower aquifers (Jackson et al., in press). Lower apparent conductivity values at F' (Fig. 53.6), correspond to gravel deposits which appear in boreholes near the special waste site. This gravel layer has allowed contaminants to percolate from the special waste site into the lower aquifer (Jackson et al., in press).

Borehole stratigraphic data suggest that clay does not blanket the entire area and occurs as a minor constituent of the clayey silt layer (Jackson et al., in press). The borehole data also show the clay bearing layers (unit II, Fig. 53,7) pinch out gradually rather than terminate abruptly. Near-surface clay layers pinching out should cause broad anomalies quite different from the discrete anomalies associated with contaminated groundwater.

Regional geological mapping of the underlying limestone/dolomite of the Oxford Formation show this particular geological formation to be laterally uniform. It is, therefore, not likely causing apparent conductivity anomalies in the survey area.

Scintrex MP-2 magnetometer

A Scrintrex MP-2 total field proton precession magnetometer (Fig. 53.9) was used to detect magnetic objects. The sensor is strapped to the back of the operator while the operating console is on his front. Each reading took about 5 seconds and measurements were made every 25 m throughout the landfill site and beyond. A base station recording magnetometer was used to monitor diurnal fluctuations during the two days required to do the survey. Diurnal corrections were not applied to the data since the diurnal fluctuations were less than the accuracy of the magnetometer (± 1 nT). For the convenience of plotting magnetic data (Fig. 53.10), mapping values were determined by subtracting 56 000 nT from the observed data and dividing the result by 10.

Landfill at the Gloucester Waste Site incorporated a considerable amount of metallic waste. Some metallic debris is visible on the ground surface but much of it has been covered by sand backfill. Areas of metallic waste where the EM effects of contaminated groundwater and metallic waste could not be discriminated, were delineated by means of a magnetic survey. These areas were avoided for interpreting the presence of contaminated groundwater from EM data. Although some metallic waste might be non-magnetic aluminum and copper which are electrically conductive, the metallic waste most likely encorporates a mixture of iron, copper and aluminum.

The majority of magnetic anomalies greater than 2000 nT above a background of 56 000 nT, lie within the southern two thirds of the landfill site except for anomalies A" and B" which are caused by isolated surficial metallic waste (Fig. 53.10). The northern one third of the landfill site consists of low amplitude anomalies while the southern two thirds of the site contains the highest anomalies. The southern two thirds of the site containing many magnetic anomalies is also an area with many EM anomalies. Interpretation of EM anomalies in terms of contaminated groundwater was avoided in this magnetically anomalous area. EM31 anomalies A, B, C and D (Fig. 53.3) and EM16R anomaly E' (Fig. 53.6) are not associated with magnetic anomalies and so were considered to be a result of non-metallic origin, ie. chemical contaminants within the groundwater.

Summary and conclusions

Ground conductivity measurements with Geonics EM31 and EM16R instruments proved to be successful in mapping the extent of groundwater contamination at the Gloucester Landfill site. Since each instrument could measure ground conductivities to different depths, contamination plumes in an upper and a lower aquifer could be mapped separately. Conductivity measurements to a depth of 6 m suggest that contamination in the upper aquifer has progressed 100 m northwest and northeast of the landfill site while measurements to a depth of 30 m show that contamination in the lower aquifer has extended 250 m eastward from the special waste site. These results are compatible with contamination determined by borehole chemical and conductivity data.

Since boreholes are expensive and time-consuming to drill, they are placed at widely-spaced intervals. EM measurements could be used cost-effectively to interpolate contamination between boreholes as well as to locate contamination drilling targets beyond the survey area.

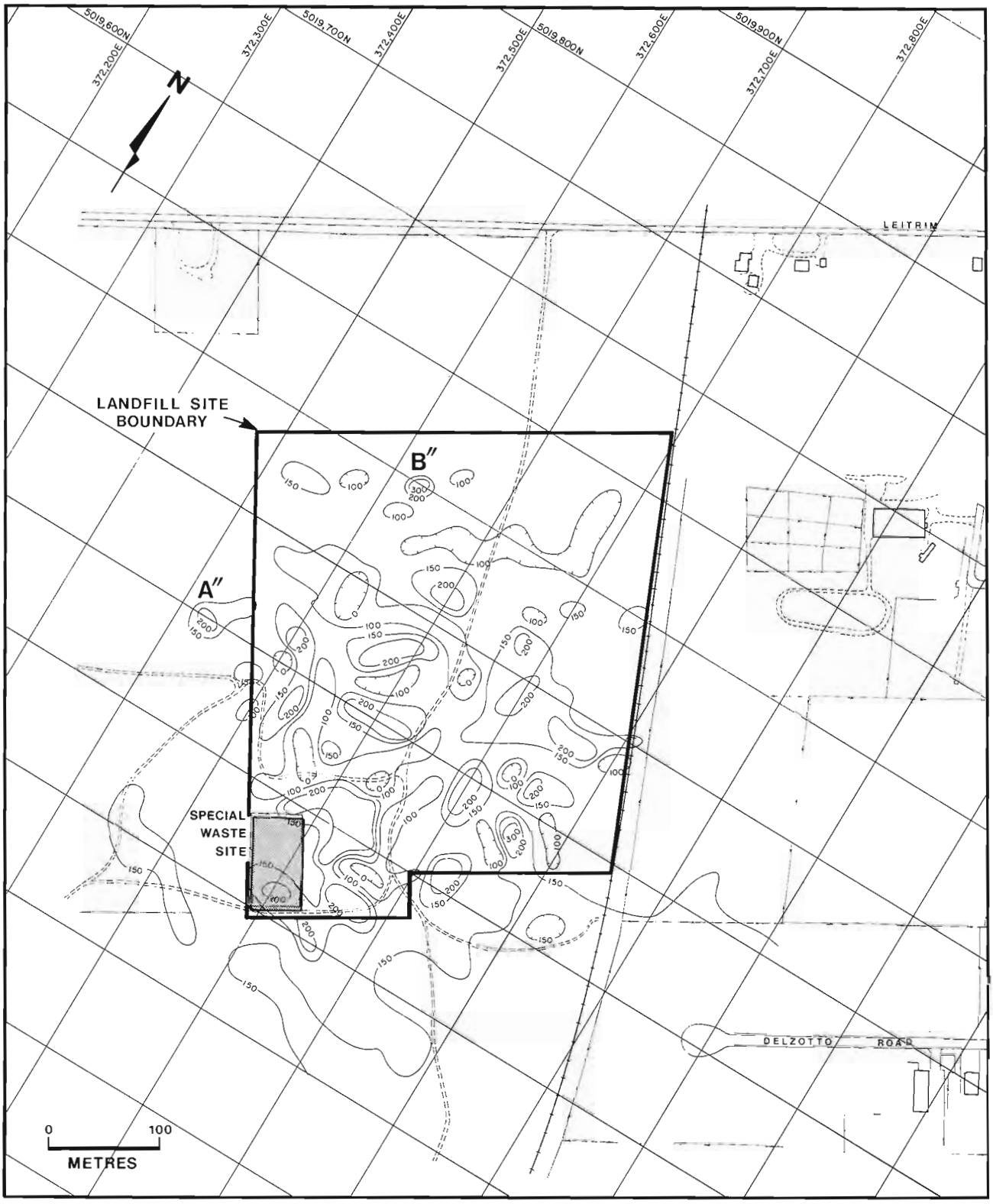

Figure 53.10. *Total magnetic field mapping using the Scintrex MP-2 at Gloucester Landfill Site. Contour values in nT/10 above a background of 56 000 nT.*

It is recommended the EM surveying should be an essential of a landfill contamination study and that it should be implemented in the initial stages of a program before drilling commences. EM measurements should be repeated annually to monitor contaminant movement. In areas where ground conductivity is moderately anomalous, groundwater contamination can be estimated by a comparison of EM data from surveys before and after a landfill site is initiated.

Acknowledgments

The authors wish to thank Jim Hunter for initiating this electromagnetic study and Jean Bahr, PhD student, Stanford University for her support and helpful suggestions for this program.

References

French, H.M. and Rust, B.R.
1981: Stratigraphic Investigation – South Gloucester Special Waste Disposal Site; Contract Submission to National Hydrological Research Institute, Environment Canada, 562 Booth Street, Ottawa, April 1982.

Greenhouse, J.P. and Slaine, D.D.
1983: The use of reconnaissance electromagnetic methods to map contaminant migration; Groundwater Monitoring Review, v. 3, no. 2, p. 47-59.

Jackson, R.E., Graham, B.W., Bahr, J., Belanger, D., Lockwood, J., and Priddle, M.
– Contaminant Hydrogeology of Toxic Organic Chemicals in an Outwash Aquifer, *Phase I Report of the Gloucestor Project*; National Hydrology Research Institute Paper, Inland Waters Directorate Scientific Series, Environment Canada, Ottawa. (in press)

McNeill, J.D.
1980: Electromagnetic terrain conductivity measurement at low induction numbers; Technical Note TN-6, Geonics Ltd., Mississauga, Ontario.

1982: Electromagnetic Resistivity Mapping of Contaminant Plumes; Proceedings of 1982 National Conference on Management of Uncontrolled Hazardous Waste Sites.

THE NORTHERN ARTILLERY LAKE MAP AREA: A TRANSECT ACROSS THE THELON FRONT, DISTRICT OF MACKENZIE

Project 840005

John B. Henderson and Robert I. Macfie[1]
Precambrian Geology Division

Henderson, J.P. and Macfie, R.I., The northern Artillery Lake map area: a transect across the Thelon Front, District of Mackenzie; in Current Research, Part A, Geological Survey of Canada, Paper 85-1A, p. 441-448, 1985.

Abstract

The transect consists of three structural domains. The western domain is typical of the Slave Province with curvilinear structural trends, abundant Yellowknife supracrustal rocks and low to intermediate grade metamorphic gradients. The eastern domain is characteristic of the Thelon Tectonic Zone of the western Churchill Province with linear structural trends, abundant mylonitic shear zones and high metamorphic grades. The central domain is separated from the other two by shear zones and is transitional between them, representing an intermediate structural level. The Thelon Front is recognized in the Healey Lake area to the north as a wide shear zone. In the Artillery Lake area, where the same shear zone represents the boundary between the central and eastern domains, it narrows, and to the south, possibly dies out. The 'Front' then may well translate across the central domain to the western domain boundary shear zone which appears to be increasing in importance to the south.

Résumé

Le profil transversal comprend trois domaines structuraux. Le domaine occidental est typique de la province des Esclaves, caractérisée par des alignements structuraux curvilignes, les roches supracrustales abondantes de Yellowknife, et des gradients de métamorphisme faibles à intermédiaires. Le domaine oriental est caractéristique de la zone tectonique de Thelon qui fait partie de l'ouest de la province de Churchill; on y trouve en effet des alignements structuraux linéaires, d'abondantes zones de cisaillement mylonitique et des gradients de métamorphisme élevés. Le domaine central est séparé des deux autres par des zones de cisaillement et représente une transition entre celles-ci, c'est-à-dire un niveau structural intermédiaire. Le front de Thelon est identifié dans la zone du lac Healey, au nord, comme une vaste zone de cisaillement. Dans la région du lac de l'Artillerie, où la même zone de cisaillement représente la limite entre les domaines central et oriental, le front se rétrécit et s'amincit peut-être jusqu'à disparaître au sud. Il est donc bien possible que le "front" se transporte à travers le domaine central jusqu'à la zone de cisaillement qui constitue la limite du domaine occidental, et semble prendre plus d'importance au sud.

[1] Department of Geology, University of Western Ontario, London, Ontario

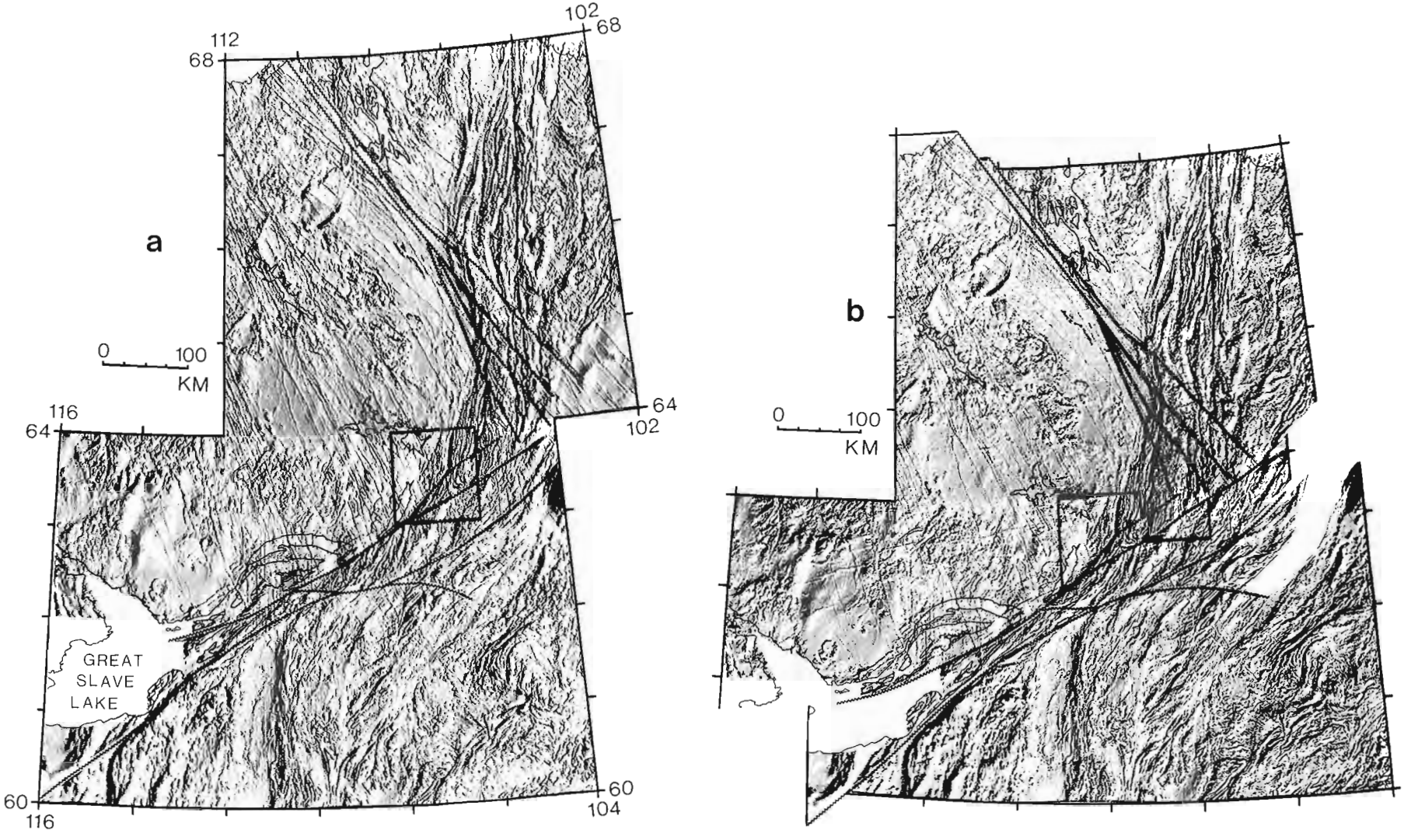

Figure 54.1. *Shaded magnetic relief maps of the relatively flat eastern Slave Province and the magnetically rugged, linear terrane of the Thelon Tectonic Zone of the western Churchill Province (see Teskey and Broome, 1984, for a discussion of the shaded relief technique). With sufficient magnetic contrast among units, such maps commonly result in a spectacular representation of structural trends. In 'a' the location of the Artillery Lake area is indicated by a square on the boundary between the two provinces, while the wavy lines represent the traces of major Proterozoic faults and include the northeasterly trending McDonald and Laloche faults and the northwesterly trending Bathurst system. In 'b' the displacement along the major faults of the two systems is replaced by matching aeromagnetic anomalies across the fault traces. This has the effect of 'straightening' the Thelon Tectonic Zone to some degree and clarifies its continuity with the highly deformed rocks south of the east arm of Great Slave Lake. It is also evident that the southestern part of the Artillery Lake area is geologically out of context with the main part of the area, in that it represents a much more easterly sample of the Thelon Tectonic Zone than that in the main part of the area. While the match across the faults is reasonably satisfactory over most of the Thelon Tectonic Zone, there is serious difficulty in the area east of the intersection of the two fault systems where extensive areas of overlap and open space are generated. This is in part a geometric consequence of considering only a few of the major faults at high angle to the structure and then only the strike-slip component.*

Introduction

The Artillery Lake area is approximately bisected by the north-northeasterly trending Thelon Front, the boundary between the Slave and Churchill structural provinces in the northwestern Canadian Shield (Fig. 54.1). Geological mapping of the Artillery Lake area at 1:250 000 scale which was started during the 1984 field season is part of an ongoing program looking into the nature and significance of the boundary area between the two provinces. The Thelon Front was originally recognized, defined and named during 1:1 000 000 scale reconnaissance mapping of parts of the northwestern Shield (Wright, 1957, 1967; Fraser, 1964) and recently has been the subject of somewhat more detailed study (1:250 000 scale mapping) in the Healey Lake area (Henderson et al., 1982; Henderson and Thompson, 1982), the Beechey Lake-Duggan Lakes area, north-northeast of Healey Lake area (Frith, 1982a,b) and the Tinney Hills-Overby Lakes area east of Bathurst Inlet (Thompson et al., 1985). In addition, a structural metamorphic study across the boundary at 1:50 000 scale is being undertaken immediately north and north-northeast of the Artillery Lake area (James, 1985). Ground geophysical surveys, including both magnetic and VLF electromagnetic methods, were undertaken in part of the Artillery Lake area mapped this past field season (McGrath and Henderson, 1985).

The Artillery Lake area was originally mapped at 1:1 000 000 scale as part of Operation Thelon (Wright, 1957, 1967). The eastern half of the area was subsequently mapped at 1:250 000 scale by Fraser (1972). An examination of the geology and mineral deposits of Artillery Lake itself in the southwest part of the map area is currently being undertaken by Gandhi (1984, 1985).

Work in the Artillery Lake area in 1984 concentrated on the northern third of the area and so represents a continuation of the geology of the Healey Lake area (Henderson et al., 1982; Henderson and Thompson, 1982). There the boundary represents the change from typical Slave Province geology of low to intermediate grade metavolcanic and metasedimentary rocks with curvilinear trends, intruded by massive granitoid rocks, to the higher grade gneisses, foliated granitoids and linear structural pattern of the Queen Maud Block of the Churchill Province. Archean low pressure series metamorphic gradients increase from greenschist to upper amphibolite to the boundary area, while granulite grade rocks occur to the east of it. There is a high pressure zone in the vicinity of the boundary itself. Superimposed on the Archean gradient is a second intermediate pressure facies metamorphic gradient. It was suggested that if a single feature to mark the boundary were necessary, a good candidate would be the shear zone that is coincident with a prominent linear low magnetic anomaly and in part with the line of inflection between the prominent negative and positive gravity pair that underlies a significant part of the Slave Province between the Bathurst and McDonald fault systems and the immediately eastern Churchill Province. The shear zone is up to 4.5 km wide and occurs within migmatitic metasediments. The geology of the northern part of the Artillery Lake area mapped in 1984 is broadly similar to that seen to the north, although differing in detail to some degree.

General geology

The area mapped represents a transect across the boundary between the two provinces and can be divided into three domains with their boundaries defined by shear zones or faults (Fig. 54.2). These are based mainly on structural criteria, as in many cases individual rock units can be recognized in two or in some cases all three domains, albeit having undergone differing degrees of deformation and metamorphism. In general, the degree of deformation and metamorphism increases from west to east, although within any one domain there can be considerable variation. The domain boundaries occur at a fault near the east end of Clinton-Colden Lake and in the wide shear zone west of Sifton Lake that represents the continuation of the straight zone previously mapped in the Healey Lake area.

Yellowknife Supergroup

Rocks of the Yellowknife Supergroup are particularly abundant in the vicinity of Clinton-Colden Lake and Lac de Charloit in the western domain. There, as is normally the case throughout the Slave Province, metasedimentary rocks consisting primarily of metamorphosed greywacke-mudstone turbidites are more abundant than the dominantly mafic metavolcanic rocks. In most places the metamorphic grade is in the amphibolite facies and most sedimentary structures other than bedding and grading have not been preserved. North of Lac de Charloit the metasediments appear to be more iron-rich than is normally the case, as shown by the common occurrence and in some places spectacular development of staurolite in the metamorphic assemblage. No iron formations as such were recognized. Small areas of greenschist grade rocks occur in both the north and south-central part of the lake. The metasediments become migmatitic between the lobes of the intrusive plutons, in particular south of Lac de Charloit.

A major unit of mafic metavolcanics occurs along the northeast side of Clinton-Colden Lake and extends northwesterly into the Healey Lake area. Both pillowed and massive flows are common, along with carbonate-cemented volcanic breccias and finer volcaniclastic units. Amygdaloidal flows are also common. Much of the unit appears to be at greenschist grade. Although pillow structures are common there has been sufficient deformation that top determinations are difficult. As a result, the structure of the unit is not clear. Nevertheless, the rather unusual, almost dumbell-shaped outcrop pattern of the whole unit, including that part of it in the Healey Lake area, and the fact that it is partially surrounded by metasediments, may suggest it represents a pair of mafic volcanic centres within, as opposed to at the margin of, a sedimentary basin, as is commonly the case with mafic volcanic sequences elsewhere in the Slave Province (Henderson, 1981). A small dacitic volcaniclastic unit occurs with the mafic sequence in north-central Clinton-Colden Lake.

Amphibolitic and pelitic to psammitic supracrustal rocks occur in the central and eastern domains, as previously reported by Fraser (1972). Both the metasediments and the metavolcanics are everywhere migmatitic, commonly with a high proportion of leucosome in the case of the metasedimentary migmatites. Irregular areas of metasedimentary migmatite occur in the vicinity of Deville Lake in the central domain, but in the eastern domain the migmatitic supracrustal rocks are always in long linear units and in many cases represent tectonic slices. The major belt of supracrustal rocks that occurs west of Sifton Lake is continuous into the Healey Lake area and contains within it the major shear zone or 'straight zone' of the region. The bulk of the zone as mapped consists of migmatitic metasediments but differs from most metasedimentary terranes in that it contains abundant migmatitic mafic sills a few metres to a few tens of metres thick. In the shear zone the coarser leucosome lenses are completely disrupted, resulting in a relatively homogeneous porphyroclastic rock with local scattered lenses of amhibolite. The shear zone appears to narrow significantly to the south as it passes Sifton Lake.

106°00'
64°00'
45'
63°30'
106°00'
MORAINE LAKE
HANBURY RIVER
EASTERN DOMAIN
CENTRAL DOMAIN
WESTERN DOMAIN
5 0 5 10
KM
SIFTON LAKE
SMART LAKE
DEVILLE LAKE
PTARMIGAN LAKE
CLINTON-COLDEN LAKE
LAC DE CHARLOIT
108°00'
64 00'
107°00'
108 00'

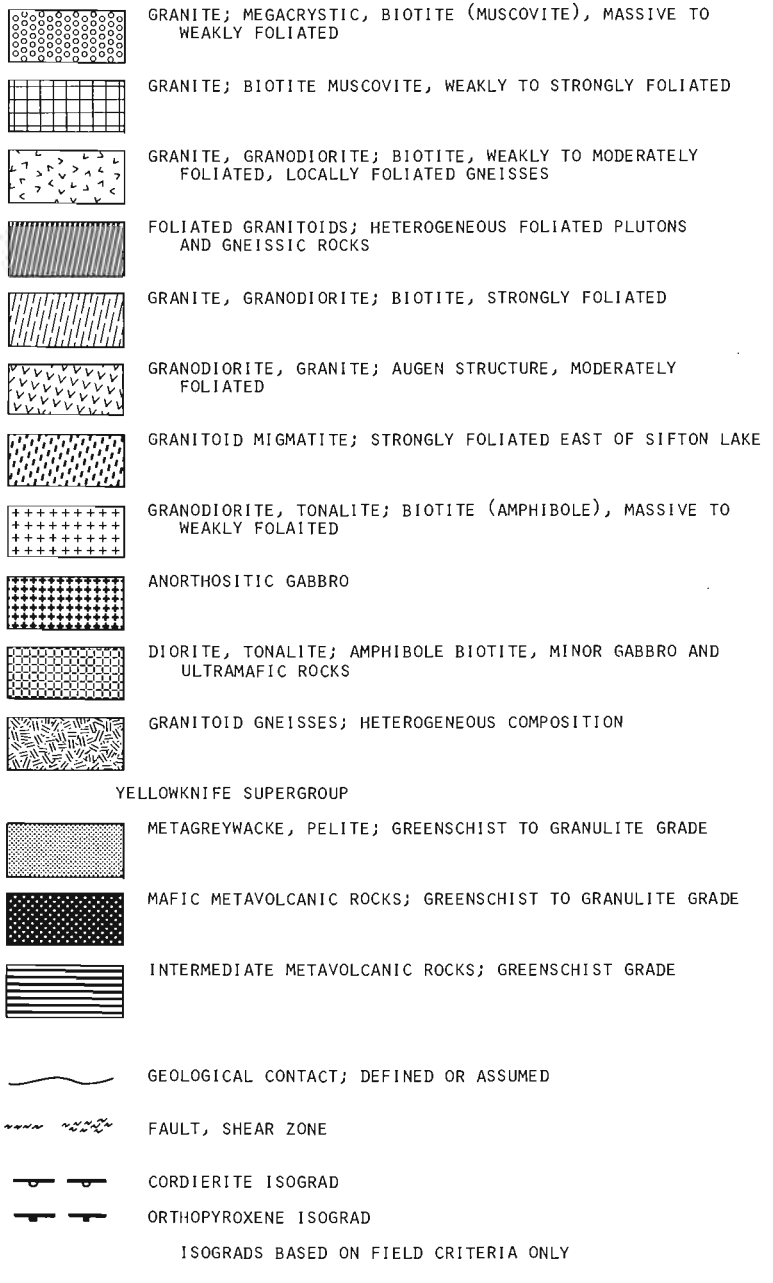

Figure 54.2. *General geology of parts of the northern Artillery Lake area. The transect across the Thelon Front, the boundary between the Slave and Churchill provinces, is represented by three structural domains. The western domain in the vicinity of Clinton-Colden Lake is typical of the geology of the Slave Province with abundant, well preserved metasediments and metavolcanics of the Yellowknife Supergroup that have been intruded by massive, lobate granitoid to diorite intrusions. Structural trends are generally northwesterly but locally conform to the outline of the intrusions. Dips are generally steep. Metamorphic grade is in a low pressure facies series and ranges from greenschist in the central part of Clinton-Colden Lake to migmatite in the septa between plutonic lobes. The central domain, east of Clinton-Colden Lake and west of Sifton Lake, is a transitional zone. Structural trends are generally northerly with local variations. Dips continue to be steep. Also present are a few northerly trending shear zones, two of which define the margins of the domain. This terrane represents a significantly deeper structural level with rock units consisting primarily of heterogeneous, ill-defined granitoid units, augen and migmatitic granitoids, and a heterogeneous gneissic unit. Yellowknife metasedimentary units are present but greatly reduced in proportion and are everywhere highly migmatitic. The largest area of these metasedimentary rocks occurs west of Sifton Lake and contains within it the major shear zone that is a continuation of the 'straight zone' previously recognized in the Healey Lake area to the north and so extends over a distance of 100 km. The easternmost domain is characterized by a higher degree of deformation and, at least in the central part of the zone, higher grades of metamorphism, and is more characteristic of the Thelon Tectonic Zone. The rock units are similar to many seen in the central zone and include units of preserved Yellowknife migmatitic metasediments and metavolcanic rocks. All units have a pronounced north-northeasterly trend, with generally steep easterly dips. Superimposed are a series of discrete, steep, mylonite zones of similar trend. The metamorphic grade rises to granulite grade in the central part of the domain but drops back to amphibolite grade farther to the east. The rock units are all considered to be Archean. The regional straightening of the units in the eastern part of the transect is also considered to be Archean, while the higher-level mylonitic shears may well be significantly younger. The pronounced metamorphic gradients are also considered to be Archean. A second metamorphic event affects sets of only weaky deformed diabase dykes of presumed Proterozoic age. Structural trends in all three parts of the area are offset by the northeasterly trending dextral faults that parallel the McDonald fault.*

Because of their lithological similarity with similar rocks in the Slave Province, these rocks are all considered to be correlative with the Yellowknife Supergroup. This is clearly the case with the rocks west of Sifton lake, which can be traced north continuously, without a break, into the Slave Province proper. The Yellownife Supergroup was originally defined "to designate any Archean volcanic and sedimentary assemblages within the Slave Province" (Henderson, 1970, p. 3), but it was not stated that clearly correlative rocks from beyond the Slave Province should necessarily be excluded. In this context then it would appear useful to include these metasedimentary and metavolcanic rocks as part of the Yellowknife Supergroup even though they may in part occur beyond what is normally considered the Slave Province.

Intrusive and gneissic rocks

The greater part of the area is underlain by a varied assemblage of plutonic to gneissic rocks. The least deformed bodies occur in the west. Those to the east are, in general, increasingly more foliated, with gneissic phases more abundant in the more deeply exposed levels of the eastern domains. All the units are considered to be Archean but some of the metamorphic and deformational events that have affected them are post-Archean. In the western domain southwest of Clinton-Colden Lake, the most dominant intrusive phase is a typically massive, leucocratic, medium grained, even grained, biotite (amphibole) granodiorite to tonalite. The suite is morphologically, compositionally and texturally identical to the granodiorites west and southeast of Yellowknife in the south-central Slave Province. The other major plutonic unit is a melanocratic suite of massive, medium- to coarse-grained, even grained, amphibole biotite, mainly diorite, but whose composition ranges from tonalite through gabbro to local ultramafic phases. These plutons are thought to be a more mafic variation of the series of more felsic tonalite plutons that occur in the western Healey Lake area. East of the southeast end of Clinton-Colden Lake is a heterogeneous unit of anorthositic gabbro. It ranges from relatively rare, coarse grained anorthosite through anorthositic gabbro to medium grained gabbro. Commonly the coarser phases are recrystallized, but the outline of the original coarse plagioclase is evident. A similar but much smaller anorthositic gabbro body occurs east of the Hanbury River in the eastern domain. Northeast of Clinton-Colden Lake is a megacrystic, biotite, locally muscovite-bearing, granite that continues north into the Healey Lake area. A smaller body of similar granite occurs southwest of the lake as well. A leucocratic, medium grained, even grained biotite-muscovite granite occurs east of Clinton-Colden Lake and extends eastward into the central domain where it becomes moderately to strongly foliated. Muscovite-bearing pegmatites are locally associated with the unit but also occur elsewhere in the domain. In particular, spodumene-bearing muscovite pegmatites, one over 800 m in length, occur in the small diorite pluton at 63°51'N, 107°31'W.

In the central domain the granitoid bodies are generally moderately to well foliated and tend to have more irregular, poorly defined outlines as compared with the more bulbous, sharply defined units to the west. Gneissic units are also present. That west of Sifton Lake consists of a complex, heterogeneous assemblage that ranges in composition from mafic amphibolite gneiss to granitic gneiss and includes as well small foliated granitoid plutons. It is similar in many respects to the heterogeneous granitoid gneiss unit of the Healey Lake area that is considered to be at least in part basement to the Yellowknife supracrustal rocks. Southwest of the gneisses is a rather heterogeneous migmatitic granitoid consisting for the most part of grey, finer grained, biotite amphibole, abundant granodiorite to tonalite with wisps and lenses of pink, coarser grained, more mafic-poor, granitic leucosome. The unit is moderately foliated with local protomylonitic zones. Its much more highly deformed equivalent occurs at, and east of, Sifton Lake in the eastern domain. The western part of the central domain in the vicinity of Deville Lake consists of a varied assemblage of pink, generally medium- to even-grained, massive to moderately foliated, granodiorite to granite with local gneissic phases. To the north is a more homogeneous foliated granite that is augen textured, pink to red, with black biotite-rich matrix. Its equivalent also occurs in the eastern domain.

Rocks in the easternmost domain are in general more intensely deformed due to the imposition of a set of mylonitic shears parallel to the trend of the regional foliation. Several units previously described to the west are present. The largest of these is the granitoid migmatite unit in the vicinity of Sifton Lake which commonly takes on the appearance of a thinly layered pink and grey gneiss due to the drawing out of the leucosome in the foliation. In places, however, the unit is preserved in an almost undeformed state. Locally, thin amphibolitic layers are present. At granulite grade the more mafic phases of the unit become rusty and the more felsic phases commonly contain coarse garnet. An augen textured granite, similar to that north of Deville Lake, is present in several linear zones in the eastern part of the domain. There the rocks are in general more strongly foliated, with local zones where the augen are totally recrystallized into elongate lenses and wispy structures. In the central part of the domain is a heterogeneous unit of foliated granitoids and granitoid gneisses with wavy to irregular layering but with overall consistently north-northeasterly trends. Small bodies and inclusions of Yellowknife metasediments and metavolcanics are common within this unit. A rather large, fairly homogeneous, well foliated, biotite-poor, granite to granodiorite is present in the eastern part of the domain. It appears to be largely contained by migmatitic metsediments.

In addition to the granitoid and gneissic rocks, several sets of post-Archean diabase dykes are present within the area mapped. These include an east-west set which, as in the Healey Lake area, becomes increasingly metamorphosed and weakly foliated towards the east. These have not been recognized east of the major shear zone west of Sifton Lake. A less abundant, northeasterly trending set is also present and in some cases is similarly metamorphosed and foliated, suggesting perhaps more than one age of emplacement. North-northeasterly trending sills parallel to the foliation also occur in the migmatitic granitoid at Sifton Lake. A few north-northwesterly trending Mackenzie dykes are also present.

Structural geology

The three domains for which the geology of the area has been discussed thus far are based primarily on structural criteria. The western domain has the structural style of the Slave Province. The overall structural trends are northwesterly to north-northwesterly, shown by the overall orientation of supracrustal units, the distribution of many plutonic bodies and the general foliation trend, particularly in the northwestern part of the domain. Deviations from this general trend are common and are particularly evident in the supracrustal units near the bulbous intrusive bodies with which they are generally structurally conformable. Southeast of the large island in Clinton-Colden Lake, however, a weak, northerly to northeasterly trending foliation is present that becomes increasingly stronger towards the margin of the domain. The domain boundary is taken as the narrow north-northeasterly trending mylonitic shear zone or its easterly splay, that is approximately parallel to the structural grain of

the Thelon Tectonic Zone (Fig. 54.1). This shear zone also corresponds to a sharp 200 nanotesla change in the magnetic base level of the terrane in this region (Geological Survey of Canada, 1968).

In the central domain, the northerly to north-northeasterly foliation is dominant and the various lithological units, although generally rather irregular in outline, tend to show a preferred orientation in this direction. Foliations still show considerable variation within the northeast quadrant, and their dip directions, while typically steep, show no particular preference for east or west. Narrow mylonitic shears parallel to the domain boundary fault are also present. The rocks within this domain appear to represent a lower structural level as the sparse metasedimentary rocks are migmatitic with a high proportion of leucosome, the granitoid rock units are heterogeneous and diffusely bounded, and gneissic units are more common. The eastern boundary of the domain is the shear zone, up to 3 km wide, within the belt of migmatitic metasedimentary rocks west of Sifton Lake. This major shear zone is the southerly extension of the 'straight zone' in similar rocks in the Healey Lake area (Henderson et al., 1982; James, 1985) and was considered as likely a single feature for demarcating the Thelon Front. Although still a dominant feature, it becomes significantly narrower as it passes to the south of Sifton Lake.

In the eastern domain the north-northeasterly foliation is increasingly prominent, particularly in the western part. The foliation trend shows much less variation and typically dips steeply east. Small scale fold axes, rod and mullion structures in the foliation have a steep to moderate plunge. Superimposed on the foliated rocks are similar, north-northeasterly trending mylonitic shears similar to those seen to the west, but in this domain they are much more abundant and more closely spaced. They are prominent linear features on air photos of the region and strongly control the shape of long narrow lakes. These relatively higher level shears contrast strongly with the more plastic, although similarly trending regional foliation. Glassy looking, mylonite to pseudotachylyte veins are commonly present in these structures. Lineations associated with these shears are steeply plunging, while fine muscovitic crenulations are close to horizontal. VLF electromagnetic ground surveys over these structures suggest they are vertical to very steeply dipping to a depth of at least 300 m (McGrath and Henderson, 1985).

All structures in the area mapped are offset by northeast-trending faults. Some of the larger ones are noted in Figure 54.2 but many smaller faults are present in addition. They have a trend and sense of offset similar to that of the McDonald fault system (Fig. 54.1).

Metamorphism

The metamorphic patterns seen in the Healey Lake area appear to be present as well in the Artillery Lake area although the broad regional southeasterly increasing metamorphic gradient is less evident in the transect across the northern Artillery Lake area. Lower grade rocks occur in the western domain. In the north-central part of Clinton-Colden Lake is an area of greenchist grade rocks that include both biotite-chlorite-bearing metasediments as noted in Figure 54.2 and a fairly high proportion of the chloritic mafic metavolcanics. A second smaller greenschist zone occurs to the south of the large island in the lake. Most of the Yellowknife metasediments in the domain are at amphibolite grade, with assemblages made up from quartz, plagioclase, biotite, muscovite, andalusite, cordierite, staurolite and garnet, reflecting a low pressure facies series. Sillimanite was recognized close to the plutons and migmatitic rocks are present in metasedimentary septa between plutons. In the central domain the metasedimentary rocks are all migmatitic, containing biotite, sillimanite, garnet assemblages with a very high proportion of leucosome. Coarse kyanite was recognized in the migmatites east of the major shear zone in the eastern domain, which corresponds to the zone of kyanite found in the boundary area in the Healey Lake area (Henderson and Thompson, 1981; James, 1985). East of Sifton Lake the granitoid migmatites and gneisses are at granulite grade, as indicated by the presence of orthopyroxene. The orthopyroxene zone, however, is relatively narrow as the migmatitic supracrustal and granitoid rocks in the eastermost part of the domain appear to be at amphibolite grade and do not seem to have been at significantly higher grades. Fraser (1972) has presented some assemblage data and discussed the metamorphism in the eastern half of the Artillery Lake map area which is relevant to the eastern two domains considered here.

As in the Healey Lake area, a second, Proterozoic metamorphic gradient is recognized west of the major shear zone, west of Sifton Lake, due to the alteration of the Proterozoic diabase dyke sets. Although difficult to judge by field criteria alone, the extent of this metamorphism west of the shear zone appears to be less than that to the north.

Discussion

Although the transect across the boundary between the two provinces in the Artillery Lake area is only a few kilometres south of the Healey lake area, the perspective on the Thelon Front from the two areas is somewhat different. In the Artillery Lake area, the transect can be divided into three structural domains. The westernmost domain has relatively low metamorphic grades and the curvilinear structural style of the Slave Province, whereas the easternmost domain has the linear structural style and high metamorphic grades characteristic of the Thelon Tectonic Zone of the western Churchill Province. The central domain is a transitional zone between the high and low structural levels of the eastern and western domains. In the Healey Lake area the major shear zone, whose southerly continuation marks the boundary between the eastern and central domains of the Artillery Lake transect, was considered a good candidate for a single feature to mark the Thelon Front, the western margin of the Thelon Tectonic Zone (Henderson et al., 1982; Thompson and Henderson, 1983). Although it was recognized that the terrane to the west of the major shear zone in the Healey Lake area was gradational in structural style to the curvilinear style of the western half of the area, no distinct intermediate domain with a discrete western boundary was recognized. A few narrow shear zones, including the one that defines the western boundary of the central domain in the Artillery Lake area, were mapped, but there appears to be no significant change across them. Furthermore, the increase in magnetic base level, one of the characteristic features of the central domain, fades away near the boundary between the two areas.

While the boundary on the west side of the central domain appears to be increasing in importance to the south, the eastern boundary seems to be decreasing in importance. The major shear zone of the Healey Lake area becomes much thinner in the Artillery Lake area and, as it passes Sifton Lake and swings more southerly, its width continues to decrease. In conjunction with this, the inflection between the major paired Bouguer gravity anomalies that is coincident with the shear zone in the southern half of the Healey Lake area and in the Artillery Lake area south to Sifton Lake, shifts southwesterly through Deville Lake and then continues southerly, close to the narrow shear zone that marks the boundary of the central domain (Earth Physics Branch, 1969a, b). This shear zone may well continue as far south as

Artillery Lake itself, where Gandhi (1985) reported a similarly trending structure which separates relatively massive Archean granites that are unconformably overlain by gently folded early Proterozoic carbonates in the west from a complex of amphibolitic to granitoid gneisses and migmatites to the east. The Thelon Front then may not be represented by a single structure.

In the Artillery Lake area at least, the Front may well shift laterally in an en echelon fashion. Continued mapping to the south should shed further light on this. A similar pattern may be seen to the north where in the east-central Healey Lake area, a relatively narrow, northerly trending splay leaves the major shear zone and continues north into the Beechey Lake area where Frith (1982) reported a significant change in deformational style which he considers to be the location of the Front in that area. The line of inflection between the paired gravity anomalies also follows this northerly trending structure.

Acknowledgments

Pierre Blais, David Corrigan, Mark Newman, Jim Shaver and James Mackintosh greatly facilitated the field work with their enthusiastic assistance and good company. Martin Irving and Craig Robinson provided excellent expediting services, using the facilities of the Geology Office, Indian and Northern Affairs Canada, Yellowknife. P.H. McGrath and Regional Geochemistry and Geophysics Division provided the computer plots used in Figure 54.1. The report was critically read by J.A. Fraser.

References

Earth Physics Branch
1969a: Artillery Lake, Northwest Territories; Earth Physics Branch, Department of Energy, Mines and Resources, Canada, Gravity Map Series No. 89.

1969b: Upper Back River, Northwest Territories; Earth Physics Branch, Department of Energy, Mines and Resources, Canada, Gravity Map Series No. 92.

Fraser, J.A.
1964: Geological notes on northeastern District of Mackenzie, N.W.T.; Geological Survey of Canada, Paper 63-40 (Map 45-1963).

1972: Artillery Lake map-area, District of Mackenzie; Geological Survey of Canada, Paper 71-38, 17 p.

1978: Metamorphism in the Churchill Province, District of Mackenzie; in Metamorphism in the Canadian Shield, ed. J.A. Fraser and W.W. Heywood; Geological Survey of Canada, Paper 78-10, p. 195-202.

Frith, R.A.
1982a: Second preliminary report on the geology of the Beechey Lake-Duggan Lakes map areas, District of Mackenzie, N.W.T.; in Current Research, Part A, Geological Survey of Canada, Paper 82-1A, p. 203-211.

1982b: Geology of Beechey Lake-Duggan Lake map area; Geological Survey of Canada, Open File 851.

Gandhi, S.S.
1985: Geology of the Artillery Lake Pb-Zn-Cu District, Northwest Territories; in Current Research, Part A, Geological Survey of Canada, Paper 85-1A, report 46.

Geological Survey of Canada
1968: Artillery Lake, District of Mackenzie, Northwest Territories; Geological Survey of Canada, Aeromagnetic Series, Map 7192G, Geophysics Paper 7192.

Henderson, J.B.
1970: Stratigraphy of the Archean Yellowknife Supergroup, Yellowknife Bay-Prosperous Lake area, District of Mackenzie; Geological Survey of Canada, Paper 70-26, 12 p.

1981: Archean basin evolution in the Slave Province, Canada; in Precambrian Plate Tectonics, ed. A. Kroner; Elsevier, Amsterdam, p. 213-235.

Henderson, J.B. and Thompson, P.H.
1982: Geology, Healey Lake, District of Mackenzie, Northwest Territories; Geological Survey of Canada, Open File 860.

Henderson, J.B., Thompson, P.H., and James, D.T.
1982: The Healey Lake map area and the Thelon Front problem, District of Mackenzie; in Current Research, Part A, Geological Survey of Canada, Paper 82-1A, p. 191-195.

James, D.T.
1985: Geology of the Moraine Lake area and the Thelon Front, District of Mackenzie; in Current Research, Part A, Geological Survey of Canada, Paper 85-1A report 55.

McGrath, P.H. and Henderson, J.B.
1985: Reconnaissance ground magnetic and VLF profile data in the vicinity of the Thelon Front, Artillery Lake area, District of Mackenzie; in Current Research, Part A, Geological Survey of Canada, Paper 85-1A, report 56.

Teskey, D. and Broome, J.
1984: Computer programs for production of shaded relief and stereo shaded relief maps; in Current Research, Part B, Geological Survey of Canada, Paper 84-1B, p. 375-389.

Thompson, P.H. and Henderson, J.B.
1983: Polymetamorphism in the Healey Lake map area – implications for the Thelon Tectonic Zone; in Current Activities Forum 1983, Program with Abstracts, p. 2-3 (abstract).

Thompson, P.H., Culshaw, N., Thompson, D., and Buchanan, R.
1985: Geology across the western boundary of the Thelon Tectonic Zone in the Tinney Hills – Overby lake area (west half), District of Mackenzie; in Current Research, Part A, Geological Survey of Canada, Paper 85-1A, report 68.

Wright, G.M.
1957: Geological notes on eastern District of Mackenzie, Northwest Territories; Geological Survey of Canada, Paper 56-10.

1967: Geology of the southeastern barren grounds, parts of the Districts of Mackenzie and Keewatin (Operations Keewatin, Baker, Thelon); Geological Survey of Canada, Memoir 350.

-55-

GEOLOGY OF THE MORAINE LAKE AREA AND THE THELON FRONT, DISTRICT OF MACKENZIE

Project 840005

Donald T. James[1]
Precambrian Geology Division

James, D.T., Geology of the Moraine Lake area and the Thelon Front, District of Mackenzie; in Current Research, Part A, Geological Survey of Canada, Paper 85-1A, p. 449-454, 1985.

Abstract

Upper-amphibolite facies supracrustal gneisses and granitoid/magmatite gneisses typical of the eastern part of the Slave Province are separated from a compositionally heterogeneous group of granulte gneisses across a 6 km boundary shear zone. The granulite gneisses to the east of the zone have a significant supracrustal component, a linear structural pattern and are deformed by a series of smaller shear zones parallel to the boundary zone. The major element, a 4.5 km wide shear zone, has a dextral, strike slip sense of shear. The shearing is preceded by an intermediate pressure facies Proterozoic metamorphism which overprints low pressure facies Archean assemblages in the western and eastern terranes. The differences between the two terranes and the coincidence of major geophysical anomalies with the boundary zone suggests that this feature may be the main element of the Thelon Front, the boundary between the Slave and Churchill structural provinces.

Résumé

Les gneiss supracrustaux du faciès supérieur des amphibolites, et les gneiss granitoïdes ou migmatitiques typiques de la partie est de la province des Esclaves, sont séparés d'un groupe de gneiss granulitiques de composition hétérogène à travers une zone de cisaillement limitrophe de 6 km. A l'est de la zone, les gneiss granulitiques présentent une composante supracrustale significative, une configuration structurale linéaire, et sont déformés par une série de petites zones de cisaillement parallèles à la zone limitrophe. L'élément principal, une zone de cisaillement de 4,5 km de large, est caractérisé par des mouvements de décrochement dextres. Le cisaillement a été précédé d'un métamorphisme protérozoïque qui a produit des faciès typiques des pressions moyennes, répris par des assemblages métamorphiques archéens à faciès typiques de basses pressions dans les terrains ouest et est. Les différences entre les deux terrains et la coïncidence des principales anomalies géophysiques avec la zone limitrophe, semblent indiquer que cette structure pourrait être le principal élément du front de Thelon, limite entre les provinces structurales des Esclaves et de Churchill.

[1] Department of Geological Sciences, Queen's University, Kingston, Ontario K7L 3N6

Introduction

The most striking feature of the Moraine Lake area is a 6 km wide north-northeasterly trending boundary zone which is coincident with the inflection between major, paired negative (Slave side) and positive (Churchill side) gravity anomalies and a magnetic low. The western margin of the boundary zone is along a 4.5 km wide shear zone called the straight zone by Henderson and Thompson (1981). The eastern margin is placed along a narrow shear zone that is 1.5 km east of the straight zone. The boundary zone separates upper amphibolite facies equivalents of Archean Yellowknife Supergroup volcanics and sediments and presumed pre-Yellowknife basement gneisses in the west from granulite facies gneisses of uncertain origin in the east. Structural trends west of the boundary zone are gradational towards the west into typical curvilinear structural patterns of the Slave Province (Henderson and Thompson, 1981). East of the boundary zone the granulite gneisses have consistent north-northeasterly structural trends and are subdivided into distinct, lesser deformed blocks, separated by north-northeasterly trending shear zones. These east to west changes mark the Thelon Front as expressed in the Moraine Lake area.

This preliminary report summarizes the 1984 field season. The objectives of this study are to examine in detail the geology on either side of and within the boundary zone; explain the time relationships between Archean and Proterozoic metamorphisms and the deformation; and discuss the significance of the Thelon Front in the Moraine Lake area. This study is part of a continuing program to map and gain a better understanding of the nature and significance of the 850 km long Thelon Front Tectonic Zone. Mapping for this study is being carried out as a transect across part of the Thelon Front (Fig. 55.1) at 1:50 000 scale. This is in contrast to the 1:250 000 scale projects at Artillery Lake (Henderson and Macfie, 1985), Healey Lake (Henderson et al., 1982), the Beechey-Duggan Lakes area (Frith, 1982) and the Tinney Hills-Overby Lake area (Thompson and Ashton, 1984). Most of the area mapped is contained within the Healey Lake map sheet (NTS 76 B) although portions of the Baillie River (NTS 76 A), Artillery Lake (NTS 75 O) and Hanbury River (NTS 75 P) map sheets are also covered.

Lithology

Granulite gneisses and intrusive rocks

A diverse group of granulite gneisses and intrusive rocks is present east of the boundary zone (Fig. 55.2). The granulites are divided into four map units. These are: biotite-garnet migmatite gneisses; interlayered pink and grey gneisses; garnet-orthopyroxene gneisses; and a heterogeneous, unsubdivided group of gneisses composed of the first three types together with granitoid gneisses, mafic gneisses, K-feldspar augen gneisses and, rusty coloured quartzo-feldspathic gneisses. These gneisses are intruded by small bodies of white to pink, strongly foliated leucogranite which locally contains garnet.

The biotite-garnet migmatite gneisses are brown, rusty brown or tan weathering rocks which occur in narrow belts in the central and eastern parts of the map area. They are well foliated and migmatitic. The percentage of leucosome is generally less than 40% although near the south end of Moraine Lake outcrops of 100% leucosome/diatexite exist. Biotite-rich portions of these gneisses do not contain K-feldspar but small amounts are contained in some diatexites. Garnet is present in the restite and leucosome. The age of this unit is not known although the composition suggests that these gneisses may be equivalent to the pelitic and psammitic gneisses and migmatites derived from the Yellowknife Supergroup.

Interlayered pink and grey gneisses are present in the eastern part of the area. This unit is composed of intimately interlayered quartzo-feldspathic and mafic gneisses where individual layers are most commonly less than 20 cm thick. Mineralogy is simple with quartz, plagioclase and K-feldspar present in the felsic portions and hornblende, plagioclase and clinopyroxene present in the mafic parts. Orthopyroxene appears to be relatively common in mafic and felsic portions. A prominent feature of these gneisses is that the compositional layering is folded into outcrop scale, open to tight structures with highly variable attitudes of axial surfaces. This is in contrast to the other granulite units which have consistent north-northeasterly structural trends.

Garnet-orthopyroxene gneisses that weather pink, rusty-tan and grey are present in a narrow belt in the central part of the map area. These rocks are most commonly finely foliated and have a gneissosity defined by alternating, thin quartzo-feldspathic-rich and hornblende-rich layers. Quartzo-feldspathic layers may contain coarse K-feldspar augen. Medium- to coarse-grained porphyroblasts of garnet and orthopyroxene are common.

The most extensive gneiss unit in the area is a complex and heterogeneous unit that cannot be subdivided at 1:50 000 scale. This unit is highly variable in texture and composition. This unit includes granulite gneisses that resemble those of the three units described above, together with quartzo-feldspathic gneisses similar to the migmatitic and granitoid gneisses west of the boundary zone; foliated and gneissic granitoid rocks; K-feldspar augen gneisses; rusty coloured quartzo-feldspathic gneisses; and mafic gneisses. Most rocks within this heterogeneous unit are layered and all are foliated with structural trends consistently to the north-northeast. Highly sheared equivalents of all rock types may

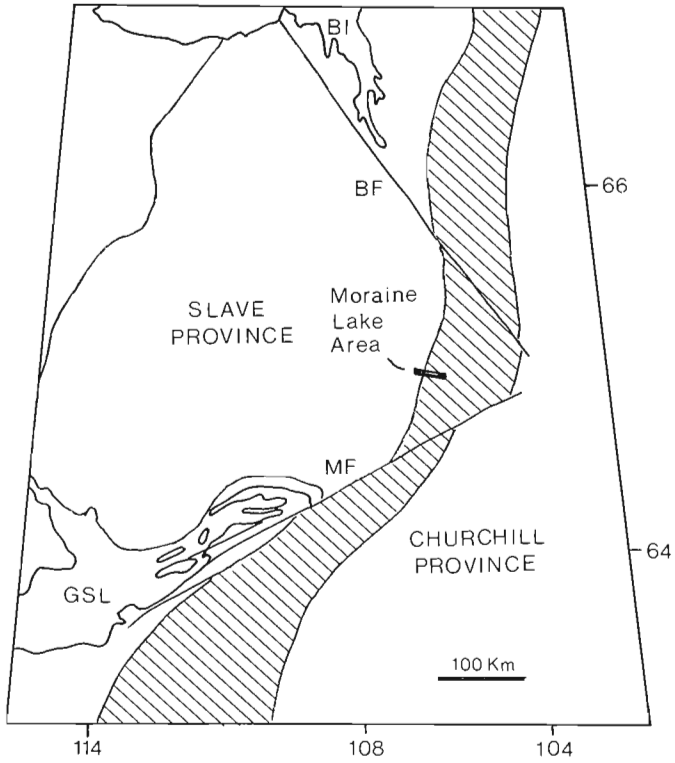

Figure 55.1. *Location Map. The tentative width of the Thelon Tectonic Zone is shown in the hatched area (Thompson and Ashton, 1984). BI = Bathurst Inlet, GSL = Great Slave Lake, BF = Bathurst Fault, MF = MacDonald Fault.*

be found. Many outcrops contain an abundance of mafic inclusions and portions of deformed dykes. Unlike the lower grade gneisses to the west of the boundary zone no dyke swarms exist in any of the granulitic region. Locally the compositional layering is cut by narrow, discordant, coarse grained pink pegmatite veins.

Intrusive to the granulite gneisses are white to pink to tan leucogranites which locally contain garnet. These rocks are fine grained, strongly foliated and commonly highly sheared. Garnet is a common constituent and sillimanite has been found in one outcrop east of Moraine Lake. Although the unit contains no biotite-rich xenoliths the close field association of these granites with the biotite-garnet migmatite gneisses at Moraine Lake and the presence of garnet and sillimanite suggests that they may be derived from the complete anatexis of metasedimentary rocks.

Very small, foliated intrusive bodies ranging in composition from granite to diorite outcrop west of Moraine Lake.

Migmatitic and granitoid gneisses

Pink, white and tan quartzofeldspathic migmatitic gneisses and granitoid gneisses are common in the western part of the area. Previously described by Henderson and Thompson (1981) these gneisses are believed to be basement to the Yellowknife Supergroup. This unit is characteristically variable in its texture, however, mineralogical variations are slight. Textural changes may be quite local with gradations from granitoid gneiss to migmatite gneiss to a foliated granitoid rock occurring over several metres. Poorly layered phases are common along the western margin of the area although in most cases the unit has a gneissic or migmatitic texture. Foliations and gneissosities are commonly tightly folded with axial traces variable in attitude over the region.

The proportions of quartz, plagioclase, K-feldspar biotite and/or hornblende are never constant but these minerals are always present. Composition is variable from quartz-diorite to granite. Garnet and aluminosilicate were not recognized megascopically in these gneisses. The mineralogy and texture indicate an upper amphibolite facies metamorphic grade. No evidence of any retrogressed granulite facies mineralogy has been recognized to date.

Yellowknife Supergroup gneisses

Brown, rusty brown to grey-brown weathering pelitic and psammitic gneisses of the Yellowknife Supergroup are present in the western part of the map area. More highly deformed equivalents of this unit occur within the straight zone. West of the straight zone these gneisses are fine grained, well foliated and commonly have a migmatitic texture. Outcrops contain up to 70% concordant lenses and layers of medium- to coarse-grained white leucosome. There are small areas in the northwest part of the map where the percentage of leucosome exceeds 70%. The assemblage biotite-garnet-sillimanite is present throughout this region. Within the straight zone these gneisses are strongly foliated but not well layered. Protomylonitic textures such as medium- to coarse-grained plagioclase porphyroclasts in a fine grained biotite-rich matrix are common. In the field, kyanite and less commonly staurolite appear to overprint the assemblage biotite-garnet-sillimanite in the straight zone. Within the area mapped no kyanite was observed west of the straight zone. Pelitic and psammitic gneisses within the straight zone commonly contain thin (several metres), foliation parallel, amphibolite sheets.

Mafic to intermediate composition gneisses derived from metavolcanic rocks of the Yellowknife Supergroup are present in narrow belts within the west of the straight zone. Most commonly these metavolcanics are black, tan or grey, medium grained, well layered hornblende-plagioclase amphibolites. Garnet-biotite-bearing assemblages are common. Locally rocks may have a migmatitic texture with less than 25% leucosome. Protomylonitic to mylonitic metavolcanics in the straight zone are composed of fine- to coarse-grained plagioclase porphyroclasts set in a characteristically grey coloured, very fine grained matrix. The unit also contains a few outcrops of interlayered amphibolites and pelitic gneisses and scattered occurrences of marble. Felsic metavolcanics are rare.

The Yellowknife Supergroup gneisses within the straight zone also contain concordant bodies of pink to grey, strongly foliated leucogranite. These bodies are lens shaped and may be as large as 200 m wide and 6 km long.

Metamorphosed mafic dykes

Three sets of mafic dykes are recognized in the area. Attitudes of these sets are 000-025°, 040-060°, and 085-110°. No dykes of the Mackenzie swarm are present in the area mapped. The northeast and east-west sets of dykes cross-cut Archean structures and are therefore assumed to be Proterozoic in age. North-northeasterly trending dykes are parallel to the Archean gneissosity. West of the boundary zone the three dyke sets are present in abundance, however, east of the zone none are present. Within the boundary zone only the north-northeasterly set is present where it is confined to a narrow, 1.5 km wide, zone adjacent to the eastern margin of the straight zone.

All dykes are metamorphosed and contain the assemblage hornblende-plagioclase with garnet common. Dykes may be foliated or massive.

Structural geology

A tentative chronology of deformational episodes has been determined using observed field relationships between structures and metamorphic events.

Folding of the Archean gneissosity and the development of a regional foliation is the expression of the oldest observed deformational event. These structures are believed to have been developed synchronous with the peak of the Archean metamorphism. East of the boundary zone foliations dip moderately to the east and west and for the most part have consistent north-northeasterly trends. Fold axes plunge to the southeast. West of the boundary zone foliation trends are variable from north-northwesterly to north-northeasterly. Dips are moderate to steep and are predominantly to the east with very few exceptions. Henderson and Thompson (1981) have observed that to the west of the map area structural trends become less consistent in attitude and their orientation defines a curvilinear structural pattern. They believed this variation to be Archean.

Four, north-northeasterly trending ductile shear zones which deform the Archean metamorphic layering dominate the structure of the map area. The development of these shear zones is believed to postdate the intrusion of the mafic dykes and predate the Proterozoic metamorphism. All four zones include protomylonitic to mylonitic to ultramylonitic rocks and have shear fabrics which dip steeply towards the east. The shear zones are also marked by aeromagnetic lows (Geological Survey of Canada, Maps 356G, 3565G, 3568G, 3576G, 1966).

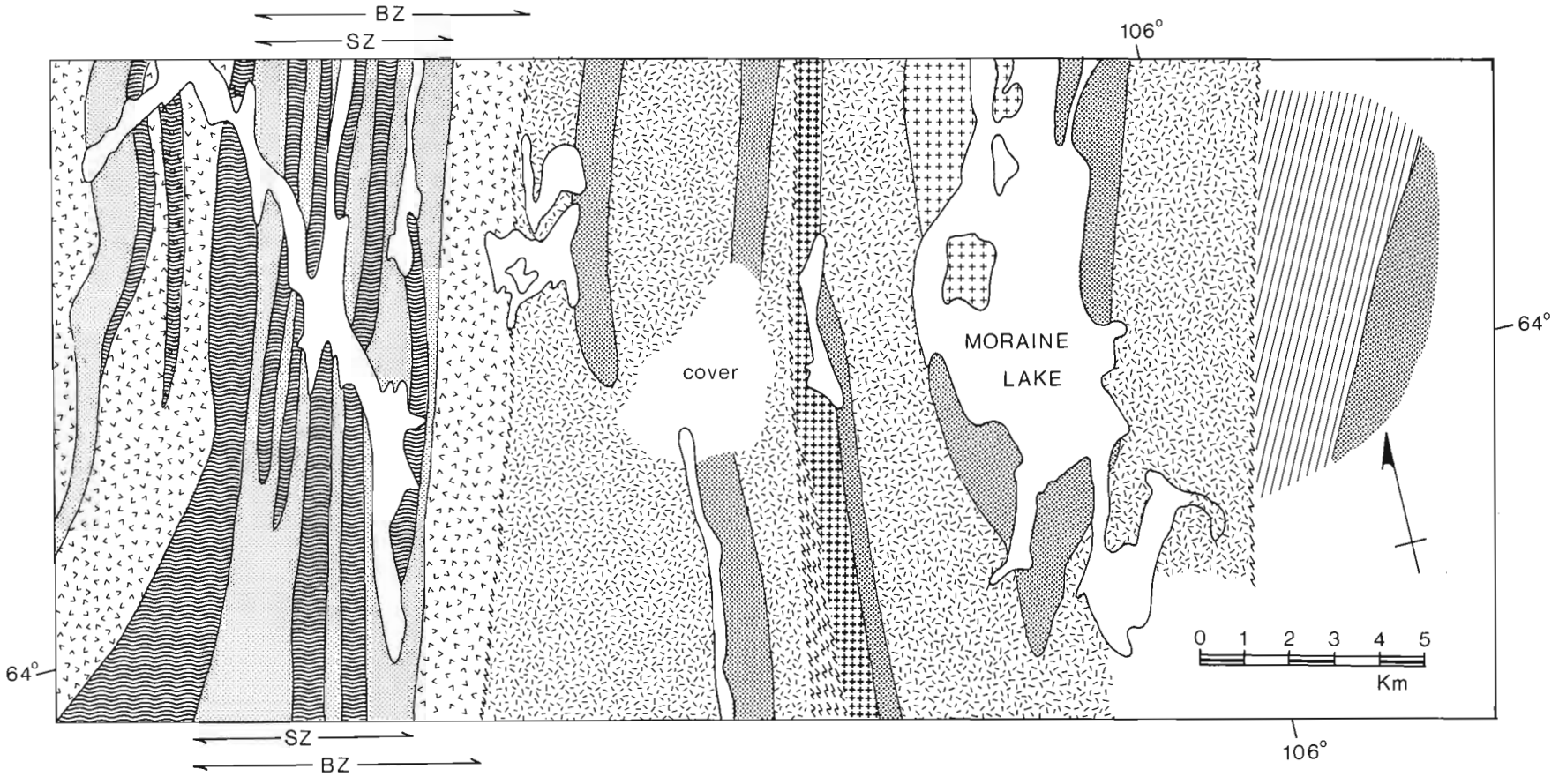

LEGEND

YELLOWKNIFE SUPERGROUP

- PELITIC - PSAMMITIC GNEISS, MIGMATITE
- AMPHIBOLE GNEISS
- MIGMATITE AND GRANITOID GNEISS
- BIOTITE - GARNET MIGMATITE GNEISS
- LEUCOGRANITE LOCALLY WITH GARNET
- INTERLAYERED PINK AND GREY GRANULITE GNEISS
- GARNET - ORTHOPYROXENE GNEISS
- HETEROGENEOUS GRANULITE GNEISS
- BZ — BOUNDARY ZONE WIDTH INDICATED
- SZ — STRAIGHT ZONE WIDTH INDICATED
- SHEAR ZONE

Figure 55.2

General geology of the Moraine Lake area.

The widest and most western of the four zones within the area mapped is the straight zone. It has a distinctive topographic expression with lakes within it being long and narrow. Narrow shear zones with the same orientation as the straight zone occur in the region south of Healey Lake, 15 km west of the map area. The straight zone is developed in pelitic and psammitic, and amphibolite gneisses of the Yellowknife Supergroup although very minor bodies of foliated, pink leucogranite are also present. Strain across the zone is not homogeneous resulting in highly sheared rocks being in relative close contact with rocks of lower strain. Protomylonitic/porphyroclastic gneisses are most common with lesser amounts of mylonite and ultramylonite. Pseudotachylite occurs in several outcrops. The western boundary of the straight zone is gradational in that from the west amphibolite gneisses of low strain are at first boudinaged and then are progressively sheared towards the east. The eastern boundary of the zone on the other hand is sharp with protomylonitic to ultramylonitic rocks against migmatitic and granitoid gneisses of low strain. Rotated porphyroclasts, deformed boudins, C-S fabrics and mineral lineations indicate a dextral, strike slip sense of shear. The shear fabric in the straight zone is locally folded into small scale, closed to tight and inclined structures that plunge very shallowly towards the north and south.

The three shear zones to the east of the straight zone are generally less than a few hundred metres wide and are marked by sporadic occurrences of protomylonitic to ultramylonitic rocks. Kinematic indicators are limited to a small number of mineral elongation lineations. In the western and central shear zones lineations plunge shallowly towards the north. In the most easterly zone the lineations plunge steeply towards the east. In addition to these larger through going shear zones many outcrops display mylonitic fabrics which define minor shear zones that cannot be traced for significant distances along strike.

Late brittle structures are found throughout the map area. The largest brittle structures are two northeast trending faults which can be traced for 1.5 km across part of the straight zone. Apparent offsets are less than 5 m on both faults. Sets of conjugate shear fractures which trend approximately 270° and 300° are the most common brittle structures. Generally, fractures are vertical and extend for less than 1 m.

Metamorphism

Field observations and a limited amount of petrography confirm that the region has undergone two phases of metamorphism. This is in agreement with the findings of Henderson and Thompson (1981). The main metamorphic event is an Archean low pressure type metamorphism typical of the Slave Province (Thompson, 1978). Superimposed on the Archean event is a medium pressure Proterozoic metamorphism (Henderson and Thompson, 1981; Henderson et al., 1982).

The Archean metamorphic gradient is from upper amphibolite facies in the west to granulite facies in the east. The boundary between the facies, the orthopyroxene isograd, has been placed from field observations along the north-northeasterly trending shear zone that is 1.5 km east of the eastern margin of the straight zone. West of this line pelitic and semi-pelitic gneisses contain the assemblage biotite-garnet-sillimanite. These gneisses are migmatitic with a K-feldspar-absent leucosome. Hornblende-biotite and hornblende-clinopyroxene assemblages are common in mafic rocks. East of the orthopyroxene isograd the biotite-garnet migmatite gneisses commonly contain the assemblage biotite-garnet-orthopyroxene with K-feldspar-bearing leucosome. Biotite-garnet-sillimanite assemblages are less common. Hornblende-orthopyroxene-clinopyroxene is the predominant assemblage in mafic rocks. Quartzofeldspathic gneisses may also contain orthopyroxene or orthopyroxene-garnet. Retrogression of orthopyroxene to hornblende or hornblende-biotite is extensive. From field observations it appears that the deformation of the Archean gneissosity outlasted mineral growth although Henderson and Thompson (1981) have observed that porphyroblastic growth outlasted the main phases of deformation in some cases.

The second phase of metamorphism is evident in the Proterozoic mafic dykes and in the pelitic gneisses which outcrop in the straight zone. The mafic dykes are composed primarily of hornblende and plagioclase with garnet common in the northeast and east-west sets. Kyanite and kyanite-staurolite overprint Archean assemblages in pelitic gneisses within the straight zone. Although neither kyanite nor staurolite has been found west of the straight zone in the area mapped, kyanite-staurolite has been recognized to overprint Archean andalusite in the Healey Lake area 20 km to the northwest. Preliminary field observations indicate that kyanite growth outlasted the shearing event that formed the straight zone. Kyanite blades are randomly oriented on foliation surfaces in highly sheared prophyroclastic gneisses within the straight zone. The retrogression of the granulite gneisses may be part of this same Proterozoic event.

The Thelon Front

Wright (1967) defined the Thelon Front as a feature which marked changes in lithology, metamorphic grade and structural style. He described this feature as being "...gradational, probably over some miles..." although "...on the present regional scale it appears as an abrupt, clearly defined feature...". Henderson and Thompson (1981) and Henderson et al. (1982) speculated that the straight zone might perhaps be the best candidate for the Thelon Front if a single boundary feature was to be selected. On the basis of the 1984 mapping does the straight zone correspond to a boundary marking changes in lithology, metamorphic grade and structural style?

The straight zone does not appear to be a metamorphic boundary. Upper amphibolite facies rocks west of the straight zone and granulite facies rocks to the east form part of an apparently continuous Archean gradient. However, the orthopyroxene isograd is coincident with the shear zone that is 1.5 km east of the straight zone. This suggests that there may be a metamorphic break along this shear zone.

West of the straight zone structural fabrics have a somewhat variable trend with lineations plunging to the southeast. Henderson and Thompson (1981) have recognized that these trends grade westerly into curvilinear structural patterns characteristic of the Slave Province. Structural trends east of the straight zone are consistently north-northeasterly and the structural pattern is dominated by a set of relatively closely spaced north-northeasterly trending shear zones that deform Archean structures. Aeromagnetic patterns suggest that this structural style continues to the east.

The relationships between lithologic units on either side of the straight zone are unclear. The biotite-garnet migmatite gneisses in the eastern part of the area may be higher grade equivalents of Yellowknife pelitic and psammitic gneisses although there is nothing to preclude the eastern gneisses from being pre-Yellowknife Supergroup. There are definite compositional differences between the

migmatitic and granitoid gneisses in the west and the heterogeneous group of granulite gneisses in the east. The presence of garnet-bearing gneisses, garnetiferous leucogranites and rare sillimanite-garnet migmatites suggests that the eastern gneisses contain a significant supracrustal component. Perhaps the most striking lithologic difference between the eastern and western parts of the area occurs across the shear zone that is 1.5 km east of the eastern margin of the straight zone. West of this line there is an abundance of mafic dykes although to the east of this shear zone there is a complete absence of dykes.

From these observations it appears that the straight zone by itself is not the best candidate for the Thelon Front in the Moraine Lake area. A better boundary feature is defined by the zone bounded by the straight zone in the west and to the east by the shear zone that is 1.5 km to the east of the straight zone. This 6 km wide boundary zone marks discontinuities in structural style, lithology and metamorphic grade, and is coincident with major geophysical anomalies. It is suggested that this boundary zone is the main element of the Thelon Front in the Moraine Lake area.

Acknowledgments

I would like to acknowledge the able assistance of Jamie Macintosh, Mark Newman, and Pierre Blais. John Dixon, Dugald Carmichael, John Henderson and Otto van Breeman made visits to the field area. The field work for this study is supported as part of the adjacent and concurrent mapping of the Artillery Lake area by John B. Henderson. Expediting was provided by Martin Irving and Craig Robinson with the support of the Geology Office, Indian and Northern Affairs Canada in Yellowknife and the Geological Survey of Canada. John B. Henderson read an earlier version of this report.

References

Frith, R.A.
1982: Second preliminary report on the geology of the Beechey Lake-Duggan Lake map areas, District of Mackenzie, N.W.T.; in Current Research, Part A, Geological Survey of Canada, Paper 82-1A, p. 203-211.

Henderson, J.B. and Macfie, R.
1985: The northern Artillery Lake map area: a transect across the Thelon Front, District of Mackenzie; in Current Research, Part A, Geological Survey of Canada, Paper 85-1A, report 54.

Henderson, J.B. and Thompson, P.H.
1981: The Healey Lake map area and the enigmatic Thelon Front, District of Mackenzie; in Current Research, Part A, Geological Survey of Canada, Paper 81-1A, p. 175-180.

Henderson, J.B., Thompson, P.H., and James, D.T.
1982: The Healey Lake map area and the Thelon Front problem, District of Mackenzie; in Current Research, Part A, Geological Survey of Canada, Paper 82-1A, p. 191-195.

Thompson, P.H.
1978: Archean regional metamorphism in the Slave Structural Province – a new perspective on some old rocks; in Metamorphism in the Canadian Shield, ed. J.A. Fraser and W.W. Heywood; Geological Survey of Canada, Paper 78-10, p. 85-102.

Thompson, P.H. and Ashton, K.E.
1984: Preliminary report on the geology of the Tinney Hills-Overby Lake (W½) map area, District of Mackenzie: a look at the Thelon Tectonic Zone northeast of the Bathurst Fault; in Current Research, Part A, Geological Survey of Canada, Paper 84-1A, p. 415-423.

Wright, G.M.
1967: Geology of the southeastern barren grounds, parts of the Districts of Mackenzie and Keewatin (Operations Keewatin, Baker, Thelon); Geological Survey of Canada, Memoir 350.

RECONNAISSANCE GROUND MAGNETIC AND VLF PROFILE DATA IN THE VICINITY OF THE THELON FRONT, ARTILLERY LAKE MAP AREA, DISTRICT OF MACKENZIE

Project 840005

Peter H. McGrath and John B. Henderson[1]
Resource Geophysics and Geochemistry Division

McGrath, P.H. and Henderson, J.P., Reconnaissance ground magnetic and VLF profile data in the vicinity of the Thelon Front, Artillery Lake map area, District of Mackenzie; in Current Research, Part A, Geological Survey of Canada, Paper 85-1A, p. 455-462, 1985.

Abstract

Reconnaissance ground magnetic and VLF data were collected along profiles over a high grade metamorphic terrane in the Sifton Lake area. Unusually high magnetic response in this area is related to granitoid migmatite terranes, whereas low magnetic signature occurs over metasedimentary and metavolcanic units. The resistivity of the bedrock is higher (>9000 ohm-m) than normal Shield values, but is typical of permafrost areas. Several linear north-northeasterly trending conductors occur in narrow linear topographic depressions, are modelled as planar vertical sheet conductors, and are probably related to graphitic zones within the metasedimentary gneisses.

Résumé

On a effectué des levés de reconnaissance magnétique au sol et des levés VLF le long de profils traversant un terrain fortement métamorphisé dans la région du lac Sifton, (Territoires du Nord-Ouest). Dans ce secteur, la signature magnétique inhabituellement prononcée est liée à la présence de terrains migmatitiques et granitoïdes, tandis que les unités métasédimentaires à métavolcaniques sont caractérisées par une faible signature magnétique. La résistivité du soubassement est plus élevée (>9000 ohm-m) que les valeurs normales pour le Bouclier, mais est typique des zones de pergélisol. Plusieurs conducteurs linéaires d'orientation nord-nord-est, présents dans d'étroites dépressions topographiques linéaires, ont l'aspect de conducteurs parallèles multiples situés dans des plans verticaux, et son probablement associés à des zones graphiteuses à l'intérieur des gneiss métasédimentaires.

[1] Precambrian Geology Division

Introduction

During June 1984, a pilot project was undertaken in the Artillery Lake area (NTS 75O, Fig. 56.1) to collect ground geophysical data 1) to test the usefulness of such data to enhance active geological mapping (Henderson and Macfie, 1985), and 2) as ground truth for the interpretation of the regional aeromagnetic survey which was flown over the area in 1966 by Spartan Air Services, and published at scales of one inch to one mile and one inch to four miles by the Geological Survey of Canada (for example see Geological Survey of Canada maps 3563G and 7192G). Also published in 1981 was a coloured, one to one million magnetic map (1566A).

Oriented drill-core rock specimens were collected at twelve sites for laboratory measurement of their magnetic susceptibility and the intensity and direction of any natural remanent magnetization. The report describes the collection of geophysical data, and preliminary attempts to relate these data to geological features.

General geology

The Artillery Lake area encompasses part of the Thelon Front, the 700 km long boundary between the Slave and Churchill structural provinces (Fig. 56.1) which represents the western margin of the Thelon Tectonic Zone (Thompson and Henderson, 1983). The Front was originally described by Wright (1957, 1967) and Fraser (1964) as an abrupt change, at least on a regional scale, in lithology, structural style and metamorphic grade that reflected the farthest westward extent of the 'Hudsonian orogeny'. In the Healey Lake area immediately north of the Artillery Lake area, Henderson et al. (1982) described an Archean low pressure metamorphic gradient from low to intermediate grade metavolcanic and metasedimentary rocks in the Slave Province to high grade granitoid gneiss in the Churchill Province with a local higher pressure zone immediately west of the boundary. The characteristic curvilinear structural trends of the Slave Province, brought about by warping of supracrustal units around intruded massive granitoid rocks, changes within the Thelon Tectonic Zone to the strongly linear structural style of the foliated granitoids and gneisses of the adjacent Queen Maude block (Heywood and Schau, 1978) of the Churchill Province. Imposed on the highly metamorphosed and deformed rocks are a set of cataclastic to mylonitic shear zones, the largest of which is the up to 4.5 km wide north-northeasterly trending 'straight zone' in the southeast corner of the Healey Lake area. It is the most prominent of several mylonite zones of similar trend, most of which occur to the east. As suggested by Henderson and Thompson (1981), this 'straight zone' is perhaps the best candidate for a single boundary feature to represent the Thelon Front in this region if a single feature is required.

The 'straight zone' has a strong geomorphological expression characterized by many linear lakes of the same trend. It also corresponds to two pronounced geophysical features: 1) A linear magnetic low anomaly (Geological Survey of Canada, Map NQ 12-13-14-AM), traceable for at least 200 km along strike, and 2) the loci of points of inflection between a negative Bouguer gravity anomaly (-35 mGal) over the eastern Slave Province and a paired positive anomaly (+30 mGal) over the adjacent Churchill Province correspond in part to the 'straight zone'. Gibb and Thomas (1977) suggested the paired gravity anomaly indicates a fundamental change in crustal structure in the vicinity of the Thelon Front, and is an edge effect produced by juxtaposing crustal blocks of different mean density and thickness. They proposed that the density discontinuity extends through the entire crust and may correspond to a cryptic suture between the Slave craton and rocks of the Churchill Province.

The bedrock, where not exposed, is mantled by a thin veneer of overburden which is frozen below a depth of about 30 cm.

Geophysical data collection

Ground geophysical data were collected along lines in the vicinity of Sifton Lake in the northeast quadrant of the Artillery Lake area. The geology in the region of the test site is broadly similar to that in the vicinity of the 'straight zone' in the southeastern part of the Healey Lake area (Henderson and Macfie, 1985). The southern extension of the 'straight zone' occurs about 3 km west of Sifton Lake. Figure 56.2 shows the location of the 50 km of survey lines which cross the 'straight zone', and a part of the high grade metamorphic terrane to the east. Offsets in the lines were required to bypass bodies of water.

Each of the survey lines was laid out by a two-man team with a Brunton compass. In general, magnetic measurements were taken at the time the survey line was laid out and VLF data were recorded at the same stations while returning. The recording interval was 25 m.

Ground magnetometer data

Ground magnetometer data were collected to map contrasts in the intensity and/or direction of magnetization of the underlying rocks. Two magnetometers were used in the survey: a Sharpe MP-4 proton precession instrument was utilized as a base station, and a Sharpe MF-1 fluxgate instrument as the traversing magnetometer. Because the main geomagnetic field has an inclination of 84.6 degrees in the Sifton Lake area, the difference between the total field and vertical field magnetometers used in the survey was

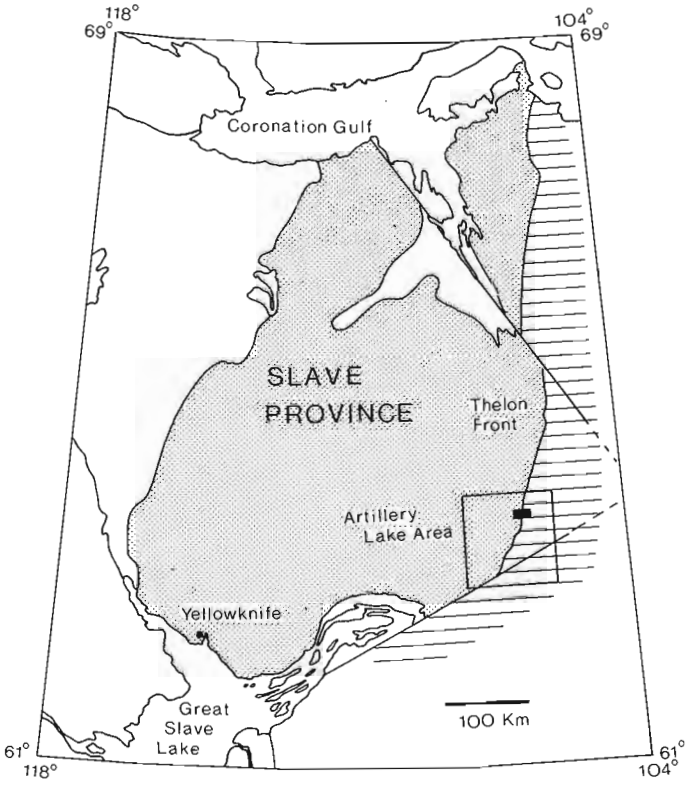

Figure 56.1. Map showing location of the Artillery Lake map area on the boundary between the Slave and Churchill structural provinces. The black rectangle shows the location of Figure 56.2.

considered to be negligible. A base station (Fig. 56.2) at Sifton Lake (68°45.5'N, 106°33.5'W) was assigned a value of 60 440 nanotesias (nT), a normal base station reading in times of low geomagnetic field activity. Magnetic readings taken with the traversing magnetometer were tied to this value by taking readings at the base station with the fluxgate magnetometer at the beginning and end of each day's work. During the day, base station readings were recorded every half hour. To correct the profile data for diurnal variations in the magnetic field, the base station readings were linearly interpolated to the observation times of the traversing magnetometer and the interpolated base station readings were subtracted from the appropriate traversing magnetometer readings. A value of 60 440 nT (base station value) was added to the corrected data. In tieing the traversing magnetometer readings to the base station, any closure differences between the two magnetometers was assumed to be the result of instrument drift and arbitrarily assigned to the traversing magnetometer. Instrument drifts in the order of 50 nT per day were common and a correction was calculated assuming the drift was constant during the day. Although errors in the order of tens of nanotesias probably remain in the diurnally corrected profile data, the survey procedure proved to be satisfactory because of the large variation in amplitude of the magnetic anomalies in the area. It was, however, necessary to discontinue magnetic surveying between 18 and 22 June because of very large random variations in the geomagnetic field; excursions as large as 600 nT with a rate of change as rapid as 70 nT per minute were recorded at the base station.

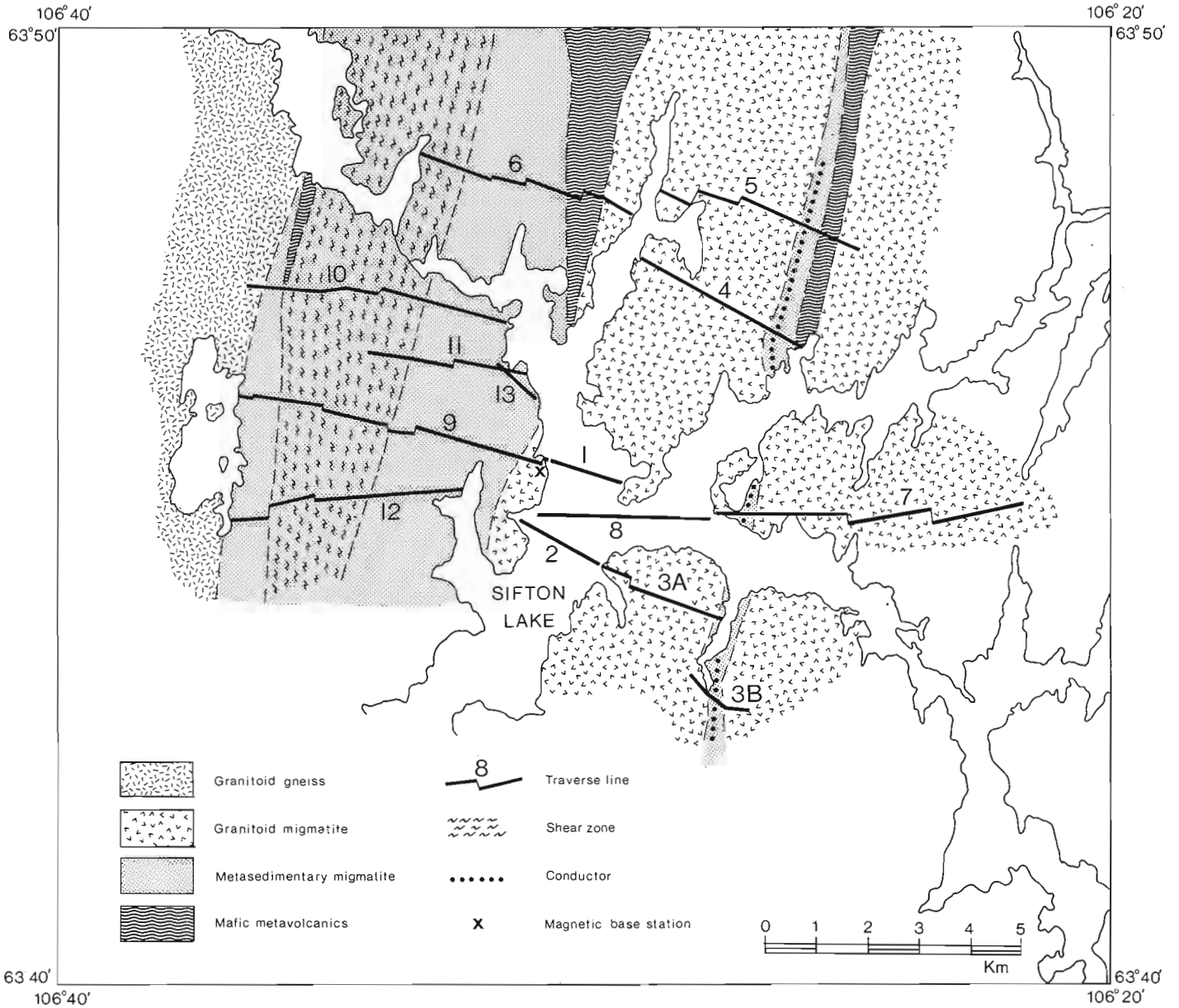

Figure 56.2. *Map of geophysical traverse lines. Offsets in the lines were required to bypass small bodies of water. Also shown is the location of a good conductor which is probably related to a graphitic zone within the high grade metasedimentary gneisses. X-Location of the magnetic base station.*

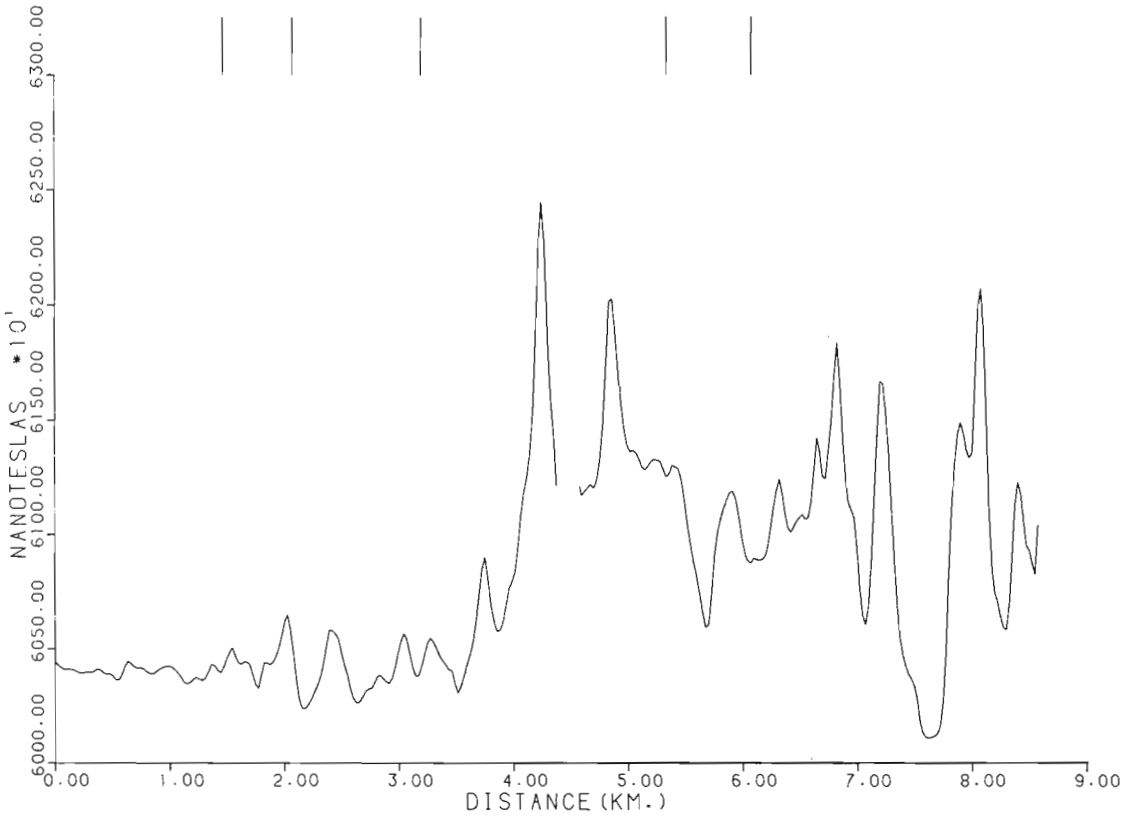

Figure 56.3. *Diurnally corrected magnetic data for traverses 5 and 6 with data along offsets deleted. The small vertial lines at the top of the figure indicate the positions of the offsets. The magnetic low area left of 4 km corresponds with metasedimentary and metavolcanic units, whereas the magnetic high area to the right is related to a granitoid migmatite terrane.*

Ground VLF data

The VLF technique is a useful method to map geological structures and rock units (Telford et al., 1977; Cameron, 1972). It uses electromagnetic energy radiated by a very low frequency (VLF) transmitter located at a remote site (for example, a military transmitter operated to communicate with submarines) to provide information about the electrical conductivity of the surface layer of the earth. This electrically responsive layer, which includes water and overburden materials, varies in thickness from a few metres for highly conductive materials such as graphitic schists and marine clays, to approximately 300 m for more resistive rocks.

The transmitted wave is sinusoidal, osciliates with a frequency between 15 and 25 kHz (wavelengths between 20 and 12 km), and travels in a wave guide bounded by the ionosphere and the surface of the earth. It consists of an electrical component which osciliates in a vertical plane, and a magnetic component which osciliates in a horizontal plane. When this planar electromagnetic wave is propagated along the earth's surface, it induces currents to flow in conductive inhomogeneities which in turn radiate secondary fields. Normally, in the absence of anomalous conductors, the magnetic wave being horizontal has a zero tilt (dip) angle. However, with the addition of vertical magnetic components due to the presence of currents in local conductors, the net effect is a non zero tilt in the magnetic field in the vicinity of the conductor. Hence by measuring tilt (dip) angles of the magnetic field it is possible to map conductors. In addition, the secondary magnetic fields are often not in phase with the primary field. The degree by which the secondary field is out of phase with the primary field, it's quadrature, can often be used to make inferences about the conductor. For example, the primary wave undergoes a phase shift when penetrating a conductive medium such as the earth, hence the amount of quadrature associated with a secondary field may be useful in separating conductors lying at depth from those at the surface.

The present survey was carried out using a Geonics EM-16 instrument which is little more than a sensitive receiver with two orthogonal receiving coils. Tilt angles and quadrature measurements were taken following the field procedure described by Paterson and Ronka (1971). The VLF station used was NLK, Seattle, Washington which transmits at a frequency of 24.8 kHz with a power of 125 kW. This VLF station was selected for the survey because it is approximately along strike with the regional structural trends in the Sifton Lake area, hence assuring maximum coupling between the magnetic component of the transmitted wave and conductors with a north-northeasterly orientation. At each measuring site the apparent azimuth of the transmitter was determined by holding the EM-16 in a horizontal position and rotating the instrument about a vertical axis until a null was located. Then the tilt angle and quadrature measurements were taken in a perpendicular direction to the azimuth direction. By convention the observer always faces in a westerly direction when measuring along E-W survey lines so that conductors to the west of the observer produce a positive (upward) tilt angle whereas for those to the east the tilt angle is negative (downward).

A VLF resistivity survey was also carried out on lines 10, 11, 12 and 13 (Fig. 56.2). Resistivity, like density, is a physical property of a material, and is defined as the resistance in ohms to the flow of current between opposite

faces of a unit cube of a given material. Conductivity is defined as the reciprocal of resistivity. In the MKS system, the unit of resistivity is the ohm-metre, and of conductivity is mhos/metre. Resistivities of natural materials vary from approximately 0.1 ohm-metres for good conductors such as graphitic schist, to 5000 ohm-metres for igneous and metamorphic rocks in a field environment (Dennis Woods, personal communication, 1984).

The resistivity survey was conducted using the Radiohm method (Collett and Becker, 1968), and the signal transmitted by NLK, Seattle, Washington. The instrument was a Geonics EM16R, and the field procedure employed is described by Scott (1975).

With the EM16R the horizontal component of the electric field in the direction of the transmitter is measured using two electrodes which are spaced 10 m apart. Also measured is the horizontal magnetic component perpendicular to the azimuth of the transmitting station which is a measure of the current flowing between the electrodes. Using the Cagniard (1953) equation, the apparent resistivity of the earth is determined from these two quantities and read directly from a dial on the EM16R. Also measured with the EM16R is the phase angle between these two orthogonal components. Over an electrically homogeneous half-space (idealized earth) the electrical component leads the magnetic component by a phase angle of 45 degrees, and the resistivity measured is the true resistivity of the ground. In the case of a layered earth where a more (less) resistive lower layer is present, the phase angle generally decreases (increases) and the measured resistivity is an apparent resistivity being a net effect of the resistivities of both the upper and lower layers.

Filtering of geophysical obervations

The 25 m sampling interval used in the survey is inadequate to properly define small scale variations, and as a consequence the profile data contain some sampling noise (one station anomalies). In order to limit this degrading influence in the data and to enhance anomalies produced by larger scale features, all of the field data, except the VLF resistivity results, were filtered before plotting using a three point recursive smoothing operator (Shanks, 1967) following a procedure described by McGrath and Cameron (1975).

In addition, the VLF dip-angle data were filtered using the Fraser filter (Fraser, 1969, 1981). This is a simple derivation and smoothing process which transforms zero-crossings (the change from a positive to a negative dip angle which occurs over a conductor) into peaks, thus providing a more convenient form of the data for interpretation purposes.

Preliminary results

Figure 56.3 illustrates the diurnally corrected magnetic data measured along traverses 5 and 6 (Fig. 56.2) with data from offsets deleted. The position of the offsets is indicated at the top of the figure by the small vertical lines. The magnetically active area right of 4 km is related to strongly foliated granitoid migmatite (Fig. 56.2, Henderson and Macfie, 1985). The areas between zero and 1.5 km and between 1.5 and 4 km appear to be a reflection of the underlying metasedimentary and metavolcanic rocks. The prominent magnetic low at 7.6 km is related to a north-northeasterly trending unit of metasedimentary and metavolcanic rocks within the granitoid migmatite. Figures 56.4 and 56.5 represent the filtered dip angle and quadrature measurements recorded along traverses 5 and 6

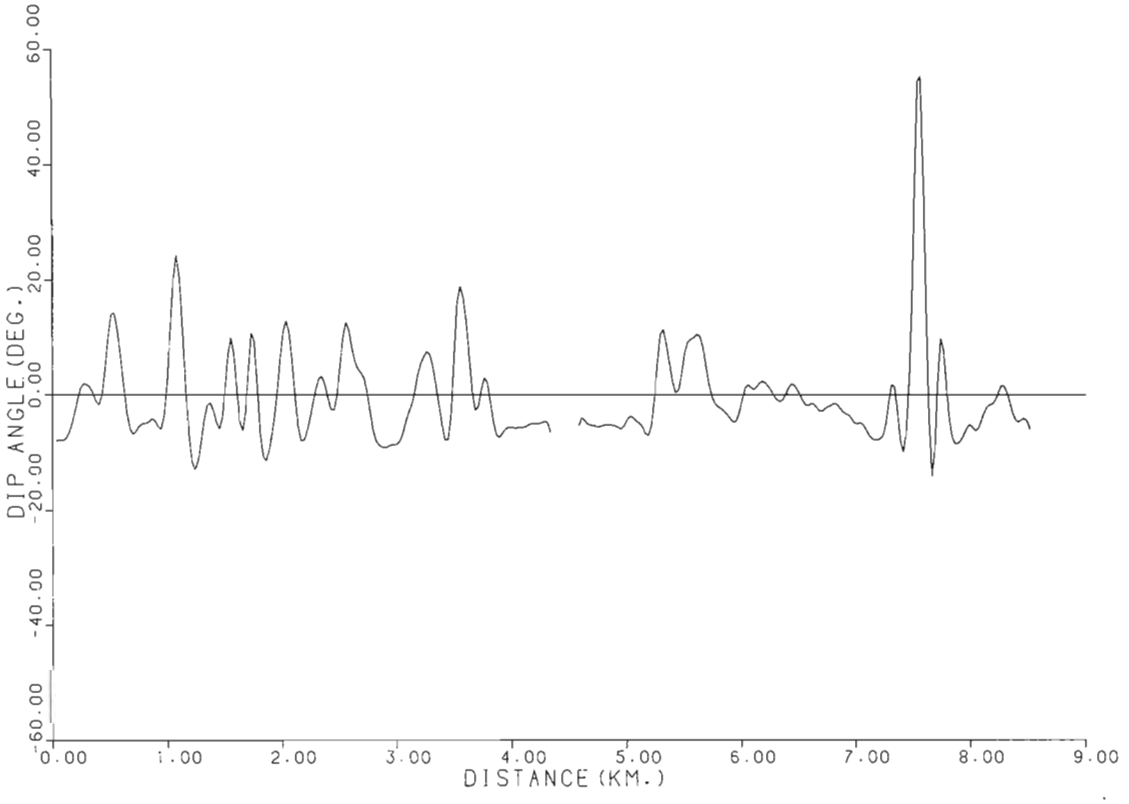

Figure 56.4. *Fraser-filtered VLF dip-angle data for traverses 5 and 6 with data along offsets deleted. The facing direction of the survey is to the left. Note the very large anomaly at 7.6 km. The location of this conductor is shown in Figure 56.2.*

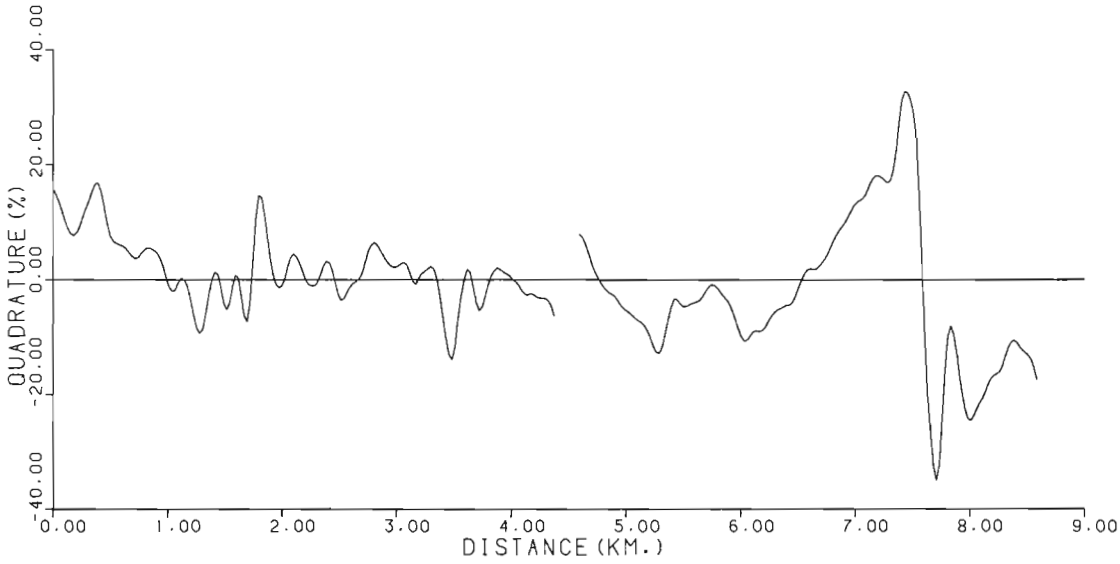

Figure 56.5. *Quadrature data for traverses 5 and 6 with data along offsets deleted. The facing direction of the survey is to the left. Note the reversed polarity of the quadrature anomaly over the conductive zone.*

with the offset data deleted. In general, the metasedimentary and metavolcanic rocks between zero and 4 km contain many more conductive zones than the granitoid migmatite to the right. The very large dip angle anomaly at 7.6 km is caused by the aforementioned linear metasedimentary-volcanic unit traversed by the profile at this location. This linear unit produces a large quadrature anomaly, the polarity of which is opposite to the associated dip angle polarity (the sign of the quadrature angle is opposite to the sign of the dip angle). This suggests that the metasedimentary-volcanic unit contains a good conductor. Wagg (1969), based on an interpretation of an airborne EM survey flown at 200 m by Geoterrex Limited using a Rio Tinto type in-phase/out-phase electromagnetometer, suggested that the cause of this conductor is a carbonaceous zone in metasedimentary rocks. This condutive zone was also intersected on traverses 4, 7, 3A and 3B (see Fig. 56.2).

Figure 56.6 illustrates the results of the VLF dip angle, quadrature and resistivity surveys along traverse 11. The generally high average apparent resistivity values (10 000 ohm-metres) is typical of permafrost regions (Saydam, 1981). Two prominent zones of low resistivity at 0.9 and 1.4 km also produce dip angle and quadrature anomalies, and occur over narrow north-northeasterly trending topographic depressions. Within these linear depressions, disseminated iron sulphides were observed in a highly weathered, sheared sericitic rock. It is also probable that graphite occurs in these conductive zones although none was observed.

If it is assumed that the VLF data can be modelled with vertical sheet conductors, which is geologically reasonable, it is possible to make the following inferences using the method of Saydam (1981). The interpreted depths to the top of the conductive zones are at the most a few metres, hence it is unlikely that any significantly larger conductors, such as a zone of massive sulphides, exist in these shear zones at a greater depth. The interpreted conductivity-thickness product for the conductors is in the order of 150 Siemens (mhos), which is indicative of a good conductor such as a graphitic schist.

Figure 56.7 is an interpretation of the dip-angle anomaly at 7.6 km (Fig. 56.4). This section was derived from a Karous and Hjelt (1983) inverse filter which uses the dip angle data to derive a possible causative current density. These data indicate that the anomalously high conductive zone is near vertical – which is in agreement with observed foliation inclinations.

Summary of preliminary results

1. The strongly foliated granitoid gneisses are mainly responsible for the high magnetic values.
2. More shear zones are apparent in the strongly magnetic granitoid migmatite east of Sifton Lake than in the less magnetic metasedimentary rocks to the west suggesting that shearing probably plays a minor role in the destruction of rock magnetization. Hence the major magnetic contrasts seem to be mainly lithologically controlled.
3. The reversed polarity of the quadrature with respect to the dip-angle polarity indicates the presence of several good conductors which typically occur in linear topographic depressions. These may be related to zones of graphitic schist.
4. Interpretations of the VLF data using the Karous-Hjelt filter and a technique developed by Saydam (1981) indicate that the conductors are vertical, and that the tops of the conductive zones are shallow and have large conductivity-thickness products.
5. The large bedrock resistivities measured are typical of permafrost regions, and the presence of good conductors within the bedrock make this an ideal type of terrain for VLF surveys.

Acknowledgments

We wish to thank Pierre Blais, David Corrigan, Mark Newman and Jim Shaver for their enthusiastic assistance in the field. We also wish to acknowledge A.K. Sinha for the loan of the VLF instruments, John Hayles and A.V. Dyck for their helpful discussions concerning field procedures and interpretation of the VLF data, and J.A. Percival and D.V. Woods for their constructive comments on the paper.

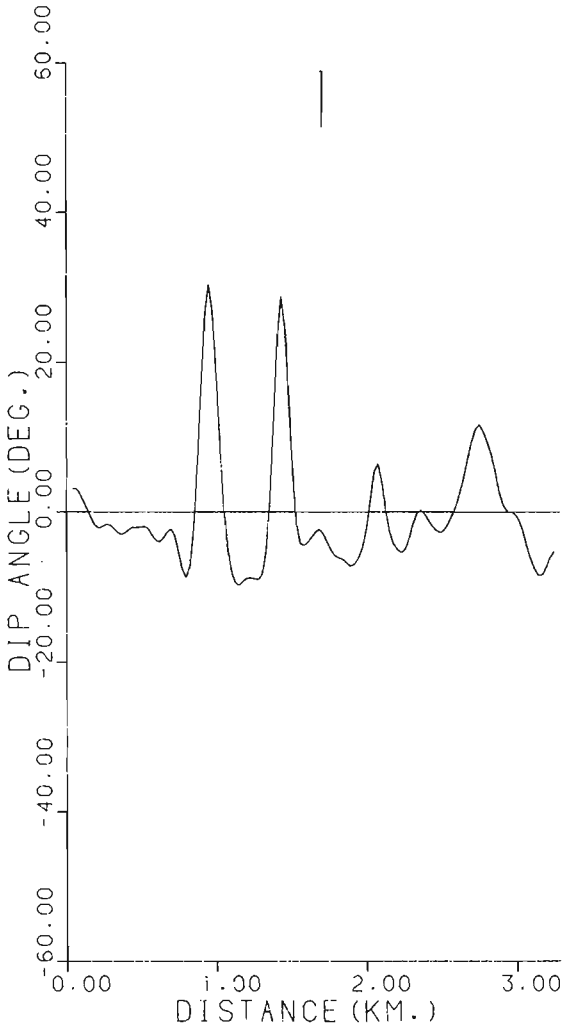

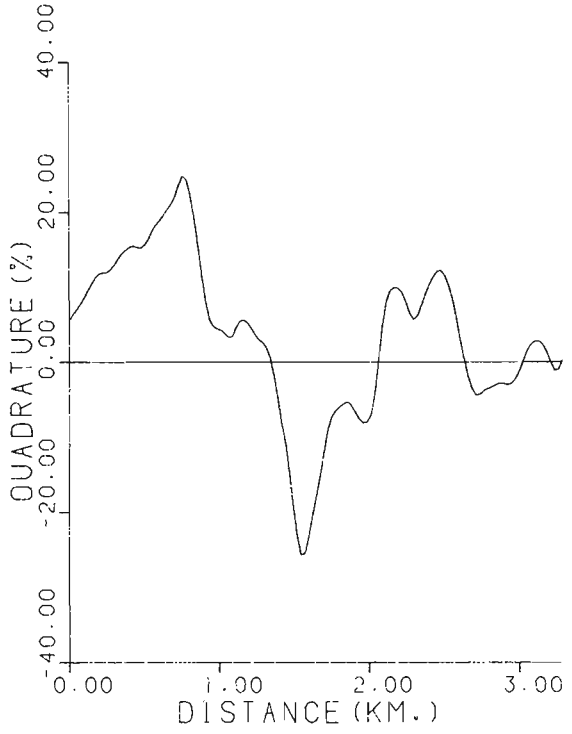

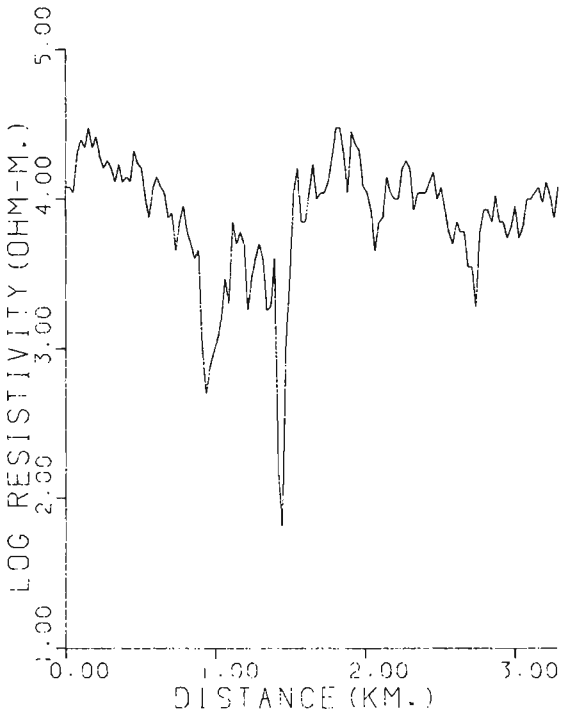

Figure 56.6. *Dip angle, quadrature and resistivity data for traverse 11 with data along offsets deleted. The facing direction of the survey is to the left. Note the high background resistivity values for the bedrock which is typical of permafrost regions. Note also the low resistivities at 0.9 and 1.4 km which are associated with north-northeasterly trending conductive zones in metasedimentary rocks.*

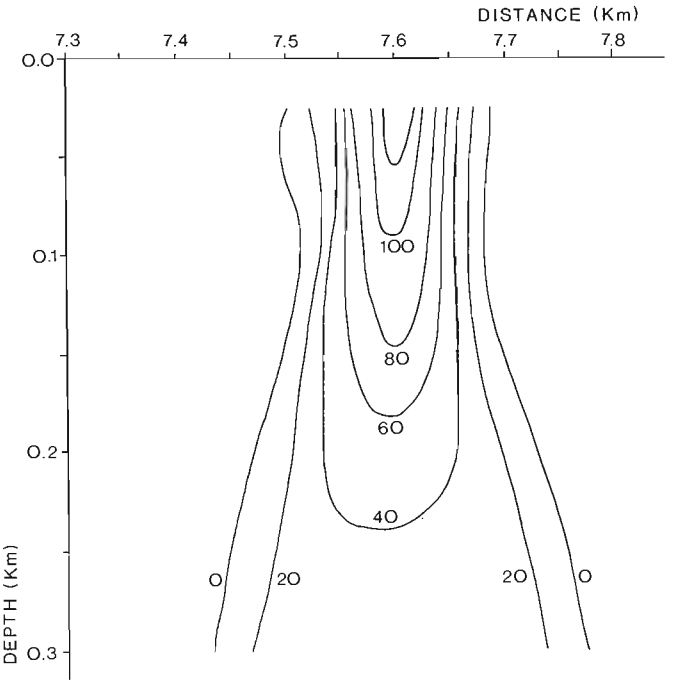

Figure 56.7. *A current density section derived from the dip-angle data over the anomaly located at 7.6 km in Figure 56.4 using a Karous-Hjelt filter. This section indicates that the conductive zone is near vertical which is in general agreement with observed foliation inclinations.*

References

Cagniard, L.
1953: Basic theory of the magneto-telluric method of geophysical prospecting; Geophysics, v. 18, no. 3, p. 605-635.

Cameron, G.W.
1972: Magnetic, electromagnetic, radiometric and geologic surveys and interpretations in Cavendish and Lavant Townships, Ontario; B.Sc. Thesis, Carleton University.

Collett, L.S. and Becker, A.
1968: Radiohm method for earth resistivity mapping; Canadian Patent 795919.

Fraser, D.C.
1969: Contouring of VLF-EM data; Geophysics, v. 34, no. 6, p. 958-967.

1981: A review of some useful algorithms in geophysics; Canadian Institute of Mining and Metallurgy Bulletin, v. 74, no. 828, p. 76-83.

Fraser, J.A.
1964: Geological notes on northeastern District of Mackenzie, N.W.T.; Geological Survey of Canada, Paper 63-40.

Geological Survey of Canada
1967: Aeromagnetic map 3563G, Musclow Lake, scale – one inch to one mile.

1968: Aeromagnetic map 7192G, Artillery Lake, scale – one inch to four miles.

1981: Coloured Magnetic Anomaly Map 1566A, Lockhart River, scale – one to one million.

1983: Coloured Magnetic Anomaly Map NQ 12-13-14-AM, Thelon River, scale – one to one million.

Gibb, R.A. and Thomas, M.D.
1977: The Thelon Front: a cryptic suture in the Canadian Shield?; Tectonophysics, v. 38, p. 211-222.

Henderson, J.B. and Macfie, R.I.
1985: The northern Artillery Lake area and the Thelon Front, District of Mackenzie; in Current Research, Part A, Geological Survey of Canada, Paper 85-1A, report 54.

Henderson, J.B. and Thompson, P.H.
1981: The Healey Lake map area and the enigmatic Thelon Front, District of Mackenzie; in Current Research, Part A, Geological Survey of Canada, Paper 81-1A, p. 175-180.

Henderson, J.B., Thompson, P.H., and James, D.T.
1982: The Healey Lake map area and the Thelon Front problem, District of Mackenzie; in Current Research, Part A, Geological Survey of Canada, Paper 82-1A, p. 191-195.

Heywood, W.W. and Schau, M.
1978: A subdivision of the northern Churchill Structural Province; in Current Research, Part A, Geological Survey of Canada, Paper 78-1A, p. 139-143.

Karous, M. and Hjelt, S.E.
1983: Linear filtering of VLF dip-angle measurements; Geophysical Prospecting, v. 31, p. 782-794.

McGrath, P.H. and Cameron, G.W.
1975: Ground magnetic survey, Roberts Arm, Newfoundland; in Report of Activities, Part A, Geological Survey of Canada, Paper 75-1A, p. 117-119.

Paterson, N.R. and Ronka, V.
1971: Five years of surveying with the very low frequency-electromagnetic method; Geoexploration, v. 9, p. 7-26.

Saydam, A.S.
1981: Very low-frequency electromagnetic interpretation using tilt angle and ellipticity measurements; Geophysics, v. 46, no. 11, p. 1594-1605.

Scott, W.J.
1975: VLF resistivity (radiohm) survey, Agricola Lake area, District of Mackenzie; in Report of Activities, Part A, Geological Survey of Canada, Paper 75-1A, p.. 223-225.

Shanks, J.L.
1967: Recursion filters for digital processing; Geophysics, v. 32, no. 2, p. 33-51.

Telford, W.M., King, W.F., and Becker, A.
1977: VLF mapping of geological structure; Geological Survey of Canada, Paper 76-25.

Thompson, P.H. and Henderson, J.B.
1983: Polymetamorphism in the Healey Lake map area – Implications for the Thelon Tectonic Zone; in Current Activities Forum, 1983 Progam with Abstracts, Geological Survey of Canada, Paper 83-8.

Wagg, D.M.
1969: Assessment report N 060311; Department of Indian and Northern Affairs.

Wright, G.M.
1957: Geological notes on eastern District of Mackenzie, Northwest Territories; Geological Survey of Canada, Paper 56-10.

1967: Geology of the southeastern barren grounds, parts of the District of Mackenzie and Keewatin (Operations Keewatin, Baker, Thelon); Geological Survey of Canada, Memoir 350.

-57-

STUDIES IN THE GRENVILLE PROVINCE OF ONTARIO

Project 760061

A. Davidson, L. Nadeau[1], S.M. Grant[2], and L.L. Pryer[3]
Precambrian Geology Division

Davidson, A., Nadeau, L., Grant, S.M., and Pryer, L.L., Studies in the Grenville Province of Ontario; in Current Research, Part A, Geological Survey of Canada, Paper 85-1A, p. 463-483, 1985.

Abstract

Recent geological reconnaissance in the southwestern Grenville Province of Ontario has raised many questions pertaining to the interpretation of this region. This paper contains interim reports on three studies aimed at answering some of these questions, being concerned with (1) the nature and origin of lithotectonic units and their boundaries in the Central Gneiss Belt, (2) coronitic metagabbro and meta-anorthosite occurrences in the Central Gneiss Belt and their tectono-metamorphic history, and (3) the nature and kinematic history of the Grenville Front Tectonic Zone.

Résumé

De nombreuses questions concernant l'interprétation de la partie sud-ouest de la province de Grenville en Ontario ont été soulevées à la suite d'une reconnaissance géologique récente. Cette contribution comprend les rapports préliminaires de trois études qui ont pour but de répondre à quelques unes de ces questions. Ces travaux traitent respectivement (1) de la nature et de l'origine de certaines unités lithotectoniques et de leurs limites qui divisent la zone gneissique centrale, (2) de l'histoire tectonométamorphique des masses de métagabbro coronitiques ainsi que des lambaux de méta-anorthosite qui affleurent dans la zone gneissique centrale, (3) de la nature et de l'histoire cinématique de la zone tectonique du front de Grenville.

[1] Ottawa-Carleton Centre for Geoscience Studies, Ottawa K1S 5B6
[2] Department of Geology, University of Leicester, Leicester LE1 7RH, England
[3] Department of Geology, McMaster University, Hamilton, Ontario L8S 4M1

Introduction

Reconnaissance work in the southwestern part of the Grenville Province in Ontario during the past few years (Davidson and Morgan, 1981; Davidson et al., 1982; Schwerdtner and Mawer, 1982; Culshaw et al., 1983; Davidson, 1984), in addition to outlining a tectonic framework, has raised many questions concerning both large- and small-scale topics. Some of these centre on the actual nature of the rocks themselves, and are bound up with the age-old questions of what gneisses are, how they were formed, and whether or not interpretation of certain tracts of well-layered gneiss as paragneiss belts is correct. Others concern correlation of rocks, both across tectonic boundaries in this region and also within lithotectonic domains where rock types change drastically from place to place on account of variation in strain and degree of metamorphic recrystallization. Although it has been shown that, for example, particular bodies of massive gabbroic anorthosite have given rise, through deformation, to 'drawn-out tails' of highly attenuated and in places mylonitized equivalent rock, totally different in aspect to the parental rock (Nadeau, 1984), controversy remains about the nature and interpretation of thin, isolated anorthositic gneiss layers, concordant within layered, migmatitic quartzofeldspathic gneisses, that can be traced for tens of kilometres. Another concern is that geochronological studies in this area, although within the Grenville Province and considered to have undergone severe orogeny at approximately 1 Ga, are proving the common presence of older plutonic rocks and metamorphism (1.3 to 1.5 Ga and older) that a) are not related to the Grenville Orogeny sensu stricto, and b) do not correlate with any known events exposed in the older Shield provinces to the north. In addition, igneous activity synplutonic with respect to the Grenvillian Orogeny is apparently lacking, known exceptions being restricted to the Central Metasedimentary Belt of southeast Ontario and western Quebec. What, then, is the expression of the Grenvillian Orogeny in the region between the Metasedimentary Belt and the Grenville Front? Do the linear and curved tracts of enigmatic gneiss really represent zones of deep-seated ductile shear along which lateral translation has caused stacking of slices and thickening of the crust? Is it possible that these rocks have undergone enormous strain for which evidence has been partly or wholly obliterated, or was never recorded, through the agency of syn- or post-deformation recrystallization? Can the map patterns be interpreted in any other way? What conditions are recorded by the metamorphic mineral assemblages, and is there evidence for inversion through tectonism of metamorphic isograds? Why, despite high metamorphic grade and migmatization, is there no evidence for widespread Grenvillian plutonism? How does the internal history of this part of the Grenville Province relate to the Grenville Front? And what is the nature and age-span of the Grenville Front as a tectonic entity?

Studies confronting aspects of these and other questions are already bearing fruit (Nadeau, 1984; Davidson, in press; van Breemen et al., in press; Hanmer, 1984; Hanmer and Ciesielski, 1984). This report outlines the progress made to date in three current studies, two in the Central Gneiss Belt and one in the Grenville Front Tectonic Zone; the study areas are located in Figure 57.1.

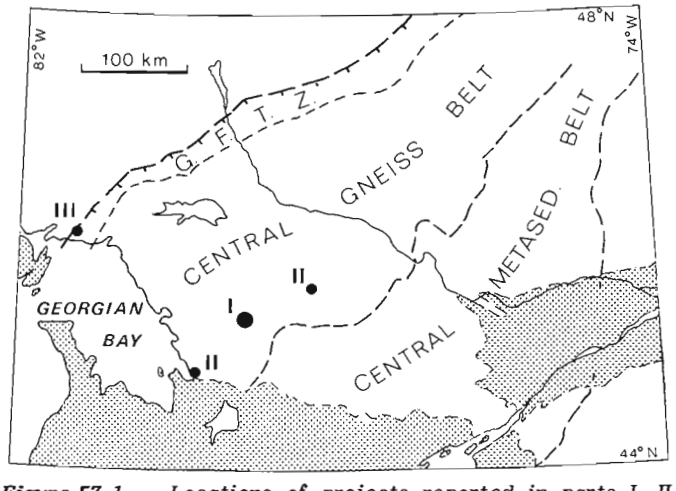

Figure 57.1. *Locations of projects reported in parts I, II and III. GFTZ – Grenville Front Tectonic Zone; shaded area is Paleozoic cover.*

PART I: CHARACTERIZATION OF LITHOTECTONIC UNITS AND THEIR BOUNDARIES IN THE HUNTSVILLE REGION, CENTRAL GNEISS BELT

L. Nadeau

Introduction

Reconnaissance mapping in the southwestern Grenville Province between the Grenville Front and the Central Metasedimentary Belt (Davidson and Morgan, 1981; Davidson et al., 1982; Culshaw et al., 1983) has revealed that the southwest part of the Central Gneiss Belt (Wynne-Edwards, 1972) is composed of several domains and subdomains that are distinguished on the basis of their geophysical characteristics, rock assemblages, structural styles, and metamorphic overprints. These lithotectonic units lie within a large scale network of continuous curved zones of highly strained rocks interpreted as tectonic zones formed during deep crustal ductile shearing. The overall tectonic polarity of the various domains and subdomains, as deduced from the geometry of truncations of structure along their bounding shear zones, together with consistent shear sense deduced from various kinematic indicators, suggest that the development of this terrane resulted from northwesterly-directed crustal stacking. A similar scenario is envisaged for the Grenville Front Tectonic Zone and for the northwestern boundary of the Central Metasedimentary Belt. Although limited, U-Pb zircon geochronological data obtained from orthogneisses, originally emplaced as plutons in previously metamorphosed and deformed rocks, suggest major igneous activity in the age range 1350 to 1500 Ma, and that ductile deformation took place at about 1150 Ma (van Breemen et al., in press).

In Huntsville area (Fig. 57.2, inset) rocks and structures of Muskoka domain have been shown to contrast with and structurally overlie those of Algonquin domain, whose structures they truncate. Both domains have been internally subdivided into smaller lithotectonic units. Rocks of Huntsville subdomain in southwestern Algonquin domain structurally overlie and truncate those of Novar subdomain, whereas Seguin subdomain, characterized by its southeasterly-plunging synformal structure, is separated from the southeastern undivided part of the Muskoka domain, where structure is far from regular (Culshaw et al., 1983).

This study will form the core of a Ph.D. thesis under the supervision of J.M. Moore and G. Ranalli of Carleton University. Its purpose is to examine in greater detail the geology of the Huntsville region in an attempt: 1) to highlight and contrast the distinctive lithological, petrological and structural characteristics of the subdomains mentioned above and to unravel their geological history;

2) to document the macro-, meso- and microstructural features exhibited by the bounding tectonites, and to discuss these features in terms of physiochemical conditions of metamorphism, deformation mechanism, kinematic and tectonic models; and 3) to test the model developed during reconnaissance mapping.

Seguin subdomain

Seguin subdomain (Fig. 57.2, 57.3) has been described as a gently southeast-plunging synformal structure bounded by a continuous inward-dipping tectonite zone (Davidson et al., 1982; Culshaw et al., 1983). It is underlain by vaguely layered, medium grained, migmatitic gneiss that encloses, in the constricted part of the synform, charnockitic, granitic and granodioritic orthogneiss masses. Small blocks and slivers of metamorphosed mafic rock occur throughout this terrane. Muskoka domain to the southeast contains similar rocks but with less regular distribution. Except for orthogneiss masses, protoliths in this domain are usually indecipherable.

The surface outline of Seguin subdomain is shaped rather like the end of a dog bone. For the purpose of description the closed end is referred to as the lobe, and the narrow part as the neck.

Migmatitic gneisses of the lobe

Within the abundant, dominantly quartzofeldspathic migmatitic gneiss (Fig. 57.4A) that occurs in this lobe, no evidence of primary layering or metasedimentary parentage has been found, and although of varying appearance at small scale, these rocks are compositionally fairly homogeneous at exposure and map scale. A leucosome commonly forms 25 to 30 per cent of the rocks, no parts of which can be assumed unchanged and identified as protolith or paleosome. For this reason Johannes' (1983) migmatite nomenclature is preferred to that of Mehnert (1968). The mesosome is commonly medium grained, equigranular, medium grey, granodioritic in composition and contains 15 to 25 per cent hornblende and biotite with or without minor red garnet. Small masses of pink, leucocratic biotite granitoid mesosome also occur in places forming a small scale mappable unit. The quartzofeldspathic leucosome is typically pink, granular, medium- to coarse-grained and contains markedly less biotite and hornblende than the mesosome. Seen in sections parallel to the stretching lineation, the dominant mesostructures would be described as schlieren and stromatic in the sense of Mehnert (1968), whereas in sections perpendicular to the lineation they invariably show phlebitic or folded forms.

Geology of the neck

To the southeast, in the necked part of the structure east of Skeleton Lake (Fig. 57.2), these monotonous migmatites merge into compositionally similar but locally less migmatitic gneisses which commonly exhibit dichtyonitic meso-structures (Mehnert, 1968) and, in places, grade into pink and grey granitic to granodioritic augen orthogneisses. This indicates that part of the rocks of the lobe resulted from the remobilization of plutonic masses. These orthogneisses typically exhibit a strong stretching lineation but much less complex small-scale folded structures than the adjacent migmatites, suggesting that the migmatite development resulted in a marked increase of the ductility of the material. These migmatites and orthogneisses are juxtaposed and enclose wedge-shaped masses of waxy, buff-brown to dark green, medium grained, hypersthene-bearing charnockitic orthogneiss that carries up to 15 per cent mafic minerals. In blasted road sections and on weathered exposures these rocks show little evidence of deformation, exhibiting a granular or a ribbon texture typically hard to measure. Locally, however, clean glacial polished surfaces reveal that this first foliation is transected by small ductile shear zones and outlines folds and crenulations with axial surfaces parallel to typical Seguin planar fabric (Fig. 57.4B). Accordingly, granulite facies metamorphism and the final foliation may predate the development of the Seguin structure. Moreover, small leucosome stringers are, in places, developed along the crenulation plane, suggesting that part of the Seguin migmatites may also be derived from remobilization of these charnockitic bodies.

Structure

Planar structures, namely preferred orientation leucosome and mineral foliation, are well developed in the neck, where they are parallel to lithologic contacts, and better developed along the margin of the lobe than in its core where the shallow southeasterly-dipping enveloping surfaces of complex folds, including sheath folds (Fig. 57.4C), with axes nearly parallel to the mineral and stretching lineations are common. In the neck, however, shallow northeasterly-plunging linear features are locally developed.

Huntsville subdomain

Shallow south-southeasterly-dipping, thin, sheet-like masses of orthogneiss interleaved with various types of fine to very fine grained, well lineated, flaggy, in part layered, high grade gneiss and tectonite that includes mafic lenses characterize this subdomain. Flaggy gneiss is developed from both plutonic and sedimentary protoliths. Most of these rocks have a well developed mylonitic fabric and metre scale recumbent tight to isoclinal folds with axes subparallel to a southeast-plunging stretching lineation.

Major rock groups

All the rocks in Huntsville subdomain have been subjected to high grade regional metamorphism which resulted in the extensive obliteration of the primary structures and textures of the metaplutonic rocks and in the complete destruction of those of the supracrustal-derived gneisses. A large proportion of the fine grained gneisses have demonstrably experienced extensive deformation-induced grain size reduction and exhibit textures and structures indicative of high shear strain. As a rule, lithologic contacts and mineral foliation are conformable. Where present, compositional layering in the bounding rocks shows abundant evidence of tectonic modification, such as well developed mylonitic structures. Contacts of metaplutonic masses lack associated metamorphic effects and intrusive character. For these reasons no lithologic contact can be assumed primary. This together with the limited thickness and repetition across strike of the rock units within the succession, and the widespread occurrence of recumbent isoclinal and rootless intrafolial folds, indicate that the lithologic succession resulted largely from transposition and slicing. It is emphasized that the strongly developed fabric overwhelms almost all pre-existing structures. Presence of highly attenuated granitoid stringers in amphibolite facies rocks suggests a period of high grade metamorphism before flattening. Granulite facies rocks may also retain evidence of earlier metamorphism.

Most of the orthogneiss which outcrops in the southern and western part of Huntsville subdomain is granitic to granodioritic in composition, pink to medium grey, and contains up to 20 per cent biotite with or without hornblende and/or garnet. Locally, as between Lake of Bays and

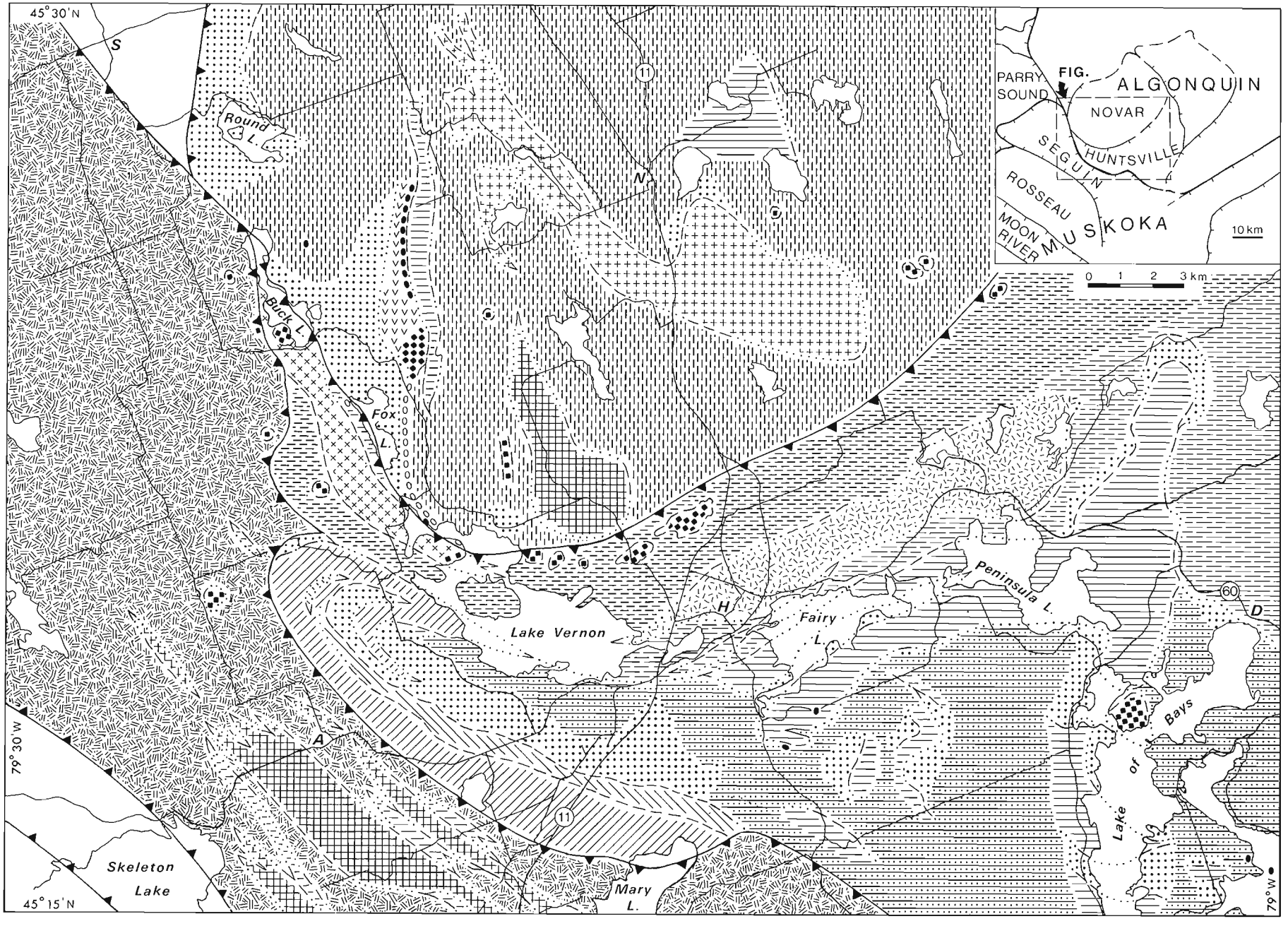

Figure 57.2. *Sketch map of the geology, Huntsville area.*

LEGEND

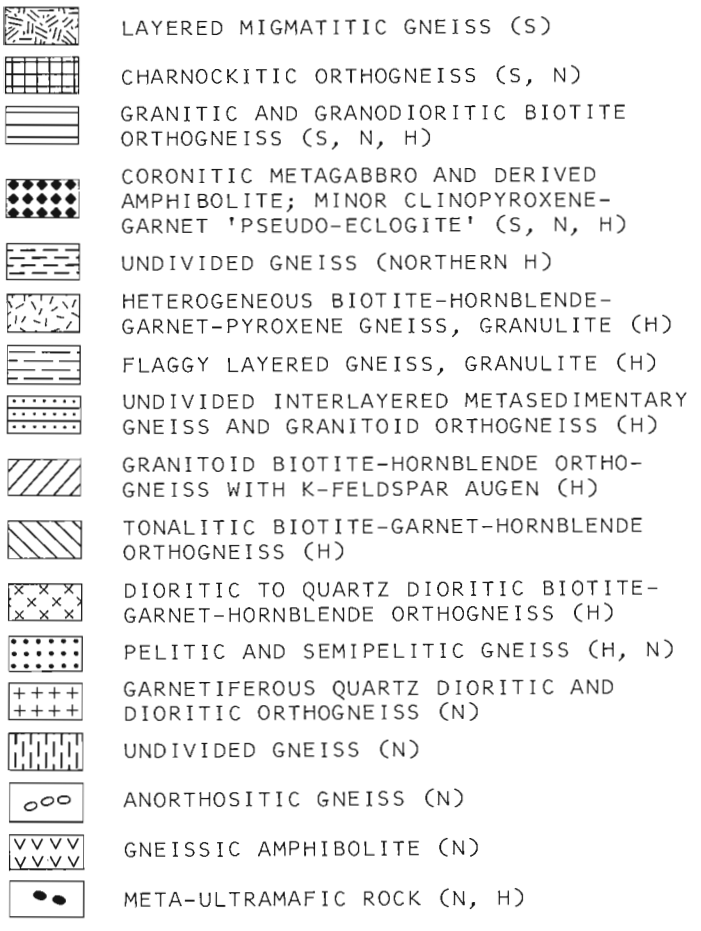

S - SEGUIN, H - HUNTSVILLE, N - NOVAR SUBDOMAINS

Fairy Lake, it grades into compositionally similar dark waxy brown hypersthene-bearing gneiss. In the least deformed parts this orthogneiss contains coarse K-feldspar augen (Fig. 57.5A). Where more highly deformed, this structure is commonly obliterated, the augen gneiss grading locally, with increasing strain, into fine grained, equigranular, strongly lineated, flaggy tectonites bearing no textural resemblence to the parental rock. The K-feldspar augen are recrystallized into flat, sugary aggregates, or even disappear altogether, and quartz forms well developed blades. A preferentially oriented and variably attenuated leucosome is commonly present.

Along the southwestern edge of this subdomain, a pink biotite augen granite sheet is juxtaposed with a recrystallized, medium grey, homogeneous quartz dioritic to granodioritic orthogneiss outlining a broad, moderately dipping hook-shaped structure. The grey gneiss carries up to 25 per cent hornblende and red garnet, minor biotite and, in places, retains relict pyroxene. North of Lake Vernon these metaplutonic rocks enclose a few decametre thick lenses of fine grained, sugary, pinkish cream, leucocratic, biotite- and/or garnet-studded monzonitic orthogneiss. Collectively these rocks constitute a deformed plutonic suite informally referred to as the Lake Vernon suite (Fig. 57.2). The lobe of granitic orthogneiss exposed north of Peninsula Lake structurally overlies concordant shallow dipping metasedimentary gneiss and, along its upper margin south of the lake, projects beneath other metasediments defining a gently dipping, relatively thin, sheet-like body. Granitic and granodioritic sheets are also present in the area extending southeasterly from Fairy Lake to Lake of Bays. They are again very shallow dipping, decametre-thick and, as seen in several small bluffs, enclosed by structurally concordant metasedimentary gneisses. Their shape and attitude coupled with a hilly topography result in a complicated outcrop pattern.

Although particularly abundant in the southern and western parts of Huntsville subdomain, small occurrences of pelitic and semipelitic gneisses are widespread throughout this terrane. These rocks are typically well foliated, fine- to medium-grained, garnet porphyroblastic and exhibit an attenuated planar leucosome, and a crude layering (Fig. 57.5B). They contain abundant plagioclase, quartz and up to 40 per cent garnet and biotite with or without a little hornblende. Minor to trace amounts of graphite and pyrite, the latter causing distinctive rusty weathering, are almost invariably present. As a whole, the semipelitic gneisses are richer in mafic minerals than the pelitic rocks. The former are medium grey and carry deep red garnet and small amounts of hornblende, whereas the pelitic rocks are lighter grey and typically exhibit pale pinkish to mauve garnets, biotite with a bronzy hue, and sillimanite needles and rosettes lying in the foliation plane. Cordierite, a common mineral in low and moderate pressure amphibolite facies pelitic gneisses, is absent. A distinctive, milky white, fine grained, granular quartz plagioclase gneiss peppered with garnet neoblasts, invariably associated with pelitic and semipelitic gneisses, is present locally. This gneiss forms centimetre- to metre-scale discontinuous lenses and layers but, although likely diagnostic of sedimentary parentage, does not constitute a mappable unit.

The following associated gneisses, in part demonstrably of sedimentary origin, are found locally: muscovite-biotite-sillimanite quartzofeldspathic gneiss of granitoid aspect; leucocratic, cream to pink, vaguely layered, quartz-rich feldspathic gneiss; calc-silicate gneiss (diopside-grossularite-scapolite-Ca-plagioclase) enclosing thin marble layers; pink to grey nondescript biotite and/or hornblende quartzofeldspathic gneisses; and dark waxy green garnet-studded charnockitic gneiss.

Structurally beneath the granitic orthogneiss sheets, the northern and eastern parts of this subdomain are characterized by a crescent-shaped planar succession of thin and highly flattened typically dark granulite facies flaggy tectonites of both metasedimentary and meta-igneous origin. Intercalated within this succession, north of Fairy lake, is a sheet of heterogeneous appearing medium grey to dark waxy green upper amphibolite and granulite facies gneisses which grade in composition from diorite to granodiorite and contain up to 30 per cent mafic minerals. These fine grained gneisses contain biotite, hornblende and red garnet in variable proportions with or without minor pyroxene and, although commonly migmatitic (Fig. 57.5C), they exhibit, here and there, the uniform appearance and the streaky texture typical of metaplutonic rocks. These gneisses, as the flaggy tectonite succession, enclose discontinuous folded and pulled-apart amphibolite and mafic granulite layers, in places likely derived from dykes, and metre- to outcrop-size lenses (Fig. 57.5F) which locally retain coarse grained relict igneous texture in their cores. Northeast of Dwight, sheets of charnockitic orthogneiss and of metagabbro associated with garnet clinopyroxenite (pseudo-eclogite of Culshaw et al., 1983) are also present within the flaggy tectonite.

At mesoscopic scale, this sequence of fine- to medium-grained flaggy tectonites is very heterogeneous in its make up. At map scale, however, the sequence retains the same lithological and structural characteristics. Rock units commonly form decametre-thick sheets which are difficult to trace along strike, especially where outcrop is discontinuous,

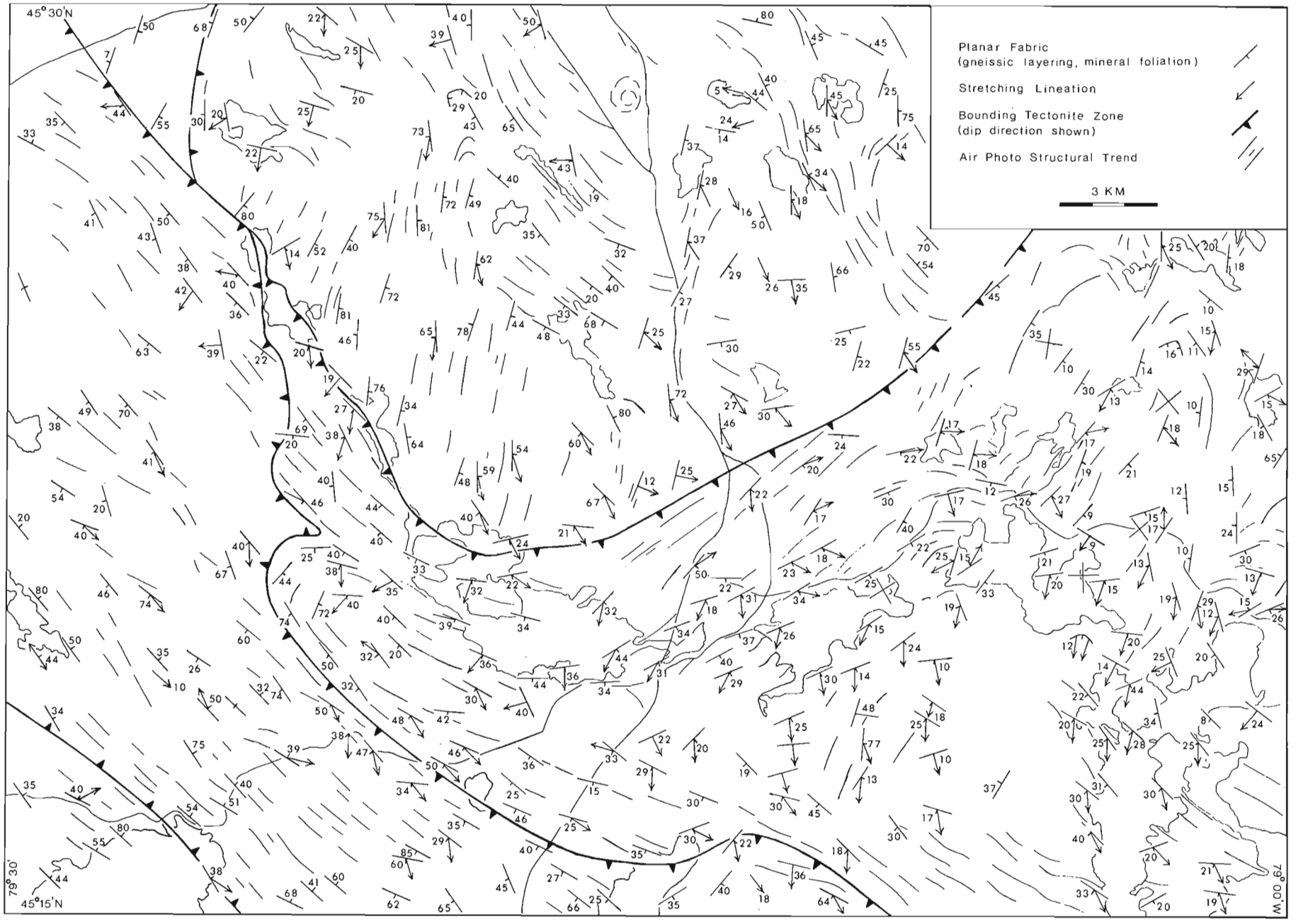

Figure 57.3. *Planar and linear structures, Huntsville area.*



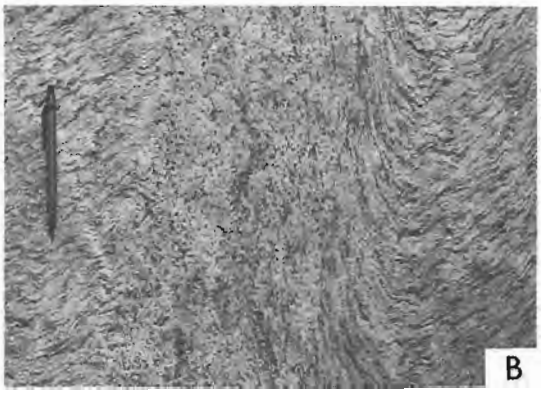









A. *Migmatitic gneiss with disrupted mafic layers, Seguin subdomain.*
B. *Folded charnockitic gneiss showing recrystallization in core of shear zone, Seguin subdomain.*
C. *Sheath fold in migmatitic gneiss, Seguin subdomain; sheath axis plunges away from viewer in direction indicated by pencil.*
D. *Deformed migmatitic gneiss, Seguin-Huntsville boundary zone.*
E. *Gently dipping extensional ductile shear in granulite gneiss, Huntsville subdomain.*
F. *Steep extensional ductile shear with associated pegmatite, Huntsville subdomain.*

Figure 57.4

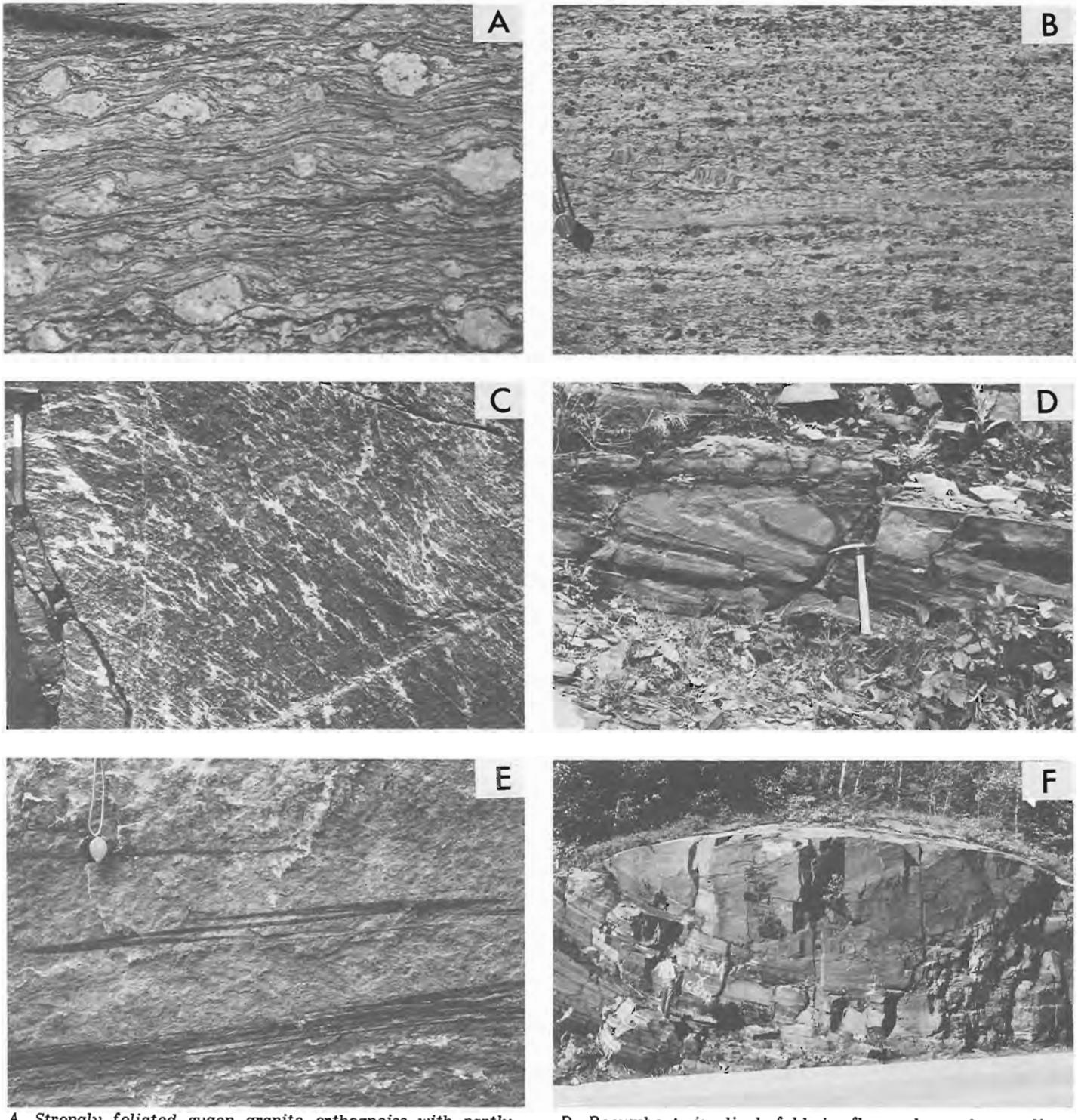

A. Strongly foliated augen granite orthogneiss with partly recrystallized K-feldspar megacrysts, Huntsville subdomain.

B. Highly strained pelitic gneiss with garnet and plagioclase augen, Huntsville subdomain.

C. Development of quartz-plagioclase leucosome in garnet-biotite-hornblende orthogneiss, Huntsville subdomain.

D. Recumbent isoclinal fold in flaggy layered granulite, Huntsville subdomain.

E. Rootless isoclinal folds displayed by highly attenuated metamorphosed mafic dyke in charnockitic orthogneiss, eastern Huntsville subdomain.

F. Large lens of mafic granulite in well layered flaggy granulite gneiss, Huntsville subdomain.

Figure 57.5

and are repeated at different structural levels within the succession. Rocks of sedimentary and igneous parentage alternate with gneiss of undecipherable protolith. Dark-coloured granulite facies rocks of felsic and intermediate composition predominate over grey hornblende and biotite quartzofeldspathic gneiss. Centimetre- to metre-scale mafic layers are widespread, and some, although extremely thin, are remarkably continuous along strike. In other exposures the mafic layers are disrupted, isoclinally or more complexly folded and the folds may themselves be pulled apart. Highly attenuated felsic streaks are present in most of these gneisses, suggesting a predeformation episode of migmatization.

Structure

In the western part of Huntsville subdomain the planar fabric (mineral foliation, compositional layering and preferred orientation of leucosome) is parallel to the lithologic contacts and dips shallowly to moderately southwesterly; to the east, the strike of planar fabric swings progressively northeastward. Southeast dips become much shallower, in places even horizontal, to the south away from the Novar subdomain boundary (see Fig. 28.5, Culshaw et al., 1983). Mineral and stretching lineations are variably oriented: in a zone parallel to the Novar boundary they plunge gently north-northeast; to the south they plunge gently southward, but swing to the southeast as the Muskoka domain boundary is approached. Much of this variation in lineation attitude, as well as local complex structures and widespread outcrop-scale warping of the planar fabric, are caused by deflections around abundant mafic lenses (Fig. 57.5F) and by steep late extensional shears (see below).

Although easily recognizable in layered rocks, tight to isoclinal recumbent folds showing up to decimetre-scale interlimb separations are developed in all types of gneisses and are widespread throughout the subdomain (Fig. 57.5D, E). Layering and mineral foliation are concordant along the fold limbs but the latter crosscuts layering in fold hinges. Fold axes plunge shallowly and are invariably virtually parallel to the local stretching lineation.

Novar subdomain

Previous reconnaissance mapping has shown that metaplutonic rocks, ranging widely in composition and separated by septa of supracrustal gneisses, underlie a large proportion of Novar subdomain, in places forming thick sheets folded around southeast-plunging axes (Culshaw et al., 1983).

Major rock units

The largest orthogneiss body of this subdomain, which outcrops in the vicinity of Novar, defines a broad southeast oriented Z-shaped structure (Fig. 57.2). This body is composed mainly of homogeneous hornblende-rich garnetiferous meta-quartz diorite, commonly carrying trace amounts of biotite and magnetite, which locally grades into more mafic dioritic to gabbroic phases. These dioritic rocks are fine- to medium-grained, well foliated and, although thoroughly recrystallized, locally retain relict igneous texture and rare plagioclase phenocrysts. Such dioritic rocks also form small satellitic or possibly interconnected masses, forming extensions of the main body. A weakly migmatitic, pink, granitic augen gneiss is locally associated with these meta-quartz dioritic rocks.

Charnockitic orthogneiss is present here and there throughout Novar subdomain. It appears to form kilometre-size isolated masses enclosed in pink and grey, commonly migmatitic granitoid or quartzofeldspathic gneiss. This peculiar distribution results, in part at least, from the fact that charnockitic rocks grade into compositionally similar and commonly migmatitic pink and grey gneiss, with or without the development of leucosome, and the latter merges, with increasing strain, into highly migmatitic gneissic tectonite of indecipherable parentage. These bodies are, consequently, heterogeneous in their make up and particularly difficult to map because the relationships between the various phases cannot everywhere be unequivocally established. The largest of them, exposed north of Lake Vernon (Fig. 57.2), exhibits a core composed of equigranular, fine- to medium-grained, dark waxy green, weakly migmatitic garnet-, magnetite- and pyroxene-bearing charnockite. In places, this rock grades into varieties of compositionally and texturally similar, light pinkish grey hornblende and biotite granite. These rocks locally contain K-feldspar megacrysts and exhibit augen structure which, together with their local intimate spatial association, reveal their parentage and allow their identification in remote exposures. As the boundary with Huntsville subdomain is approached, rocks become more severely tectonized, finer grained and exhibit a well developed linear and planar fabric, whereas along the northern and eastern sides of the body the rocks appear to merge into more severely migmatitic hornblende biotite granitic gneiss.

Several exposures of anorthositic gneiss have been discovered in the northwest part of Lake Vernon and farther north, east of Fox Lake (Fig. 57.2). These occurrences define a narrow (metres to decametres) seam-like body that has been traced for more than 7 km along strike and appears to connect northward to a larger mass of foliated garnet amphibolite, medium- to coarse-grained metagabbro and garnet clinopyroxenite that also encloses a few metre-thick, discontinuous meta-anorthosite layers. Farther north, along strike, a thin sheet of very deeply weathered meta-ultramafic rock has been traced discontinuously for more than 3 km. This meta-ultramafic rock occurs in contact with well foliated, homogeneous garnet amphibolite, likely derived from metagabbro.

In its least deformed parts, the anorthositic gneiss in the Lake Vernon area is milky white, thoroughly recrystallized, medium grained, granoblastic, contains less than 10 per cent hornblende with or without biotite and garnet, and only locally retains relict igneous texture. This rock is usually well foliated and, in places, grades into fine grained, grey, mylonitic gneiss. East of Fox Lake, this anorthositic rock lies within metasedimentary gneiss and displays a tectonic fabric concordant with that of its host. To the south, the seam is deflected toward parallelism with the Novar-Huntsville subdomain boundary. This meta-anorthosite is similar in appearance to those forming seams and inclusion trains tens of kilometres long within tectonite zones in Rosseau and Go Home subdomains, and along the outer margin of Moon River subdomain (Davidson et al., 1982; see also Grant, part II of this report).

Small masses of granitic and granodioritic orthogneiss are widespread within Novar subdomain; most of these are not distinguished in Figure 57.2. This orthogneiss is typically well foliated, light to medium grey, biotite-rich, and carries centimetre-size K-feldspar megacrysts. It is inhomogeneously strained, commonly ranging from augen gneiss to fine grained tectonite. Although less than a kilometre wide, one of these masses extends for more than 10 km along strike, suggesting a sheet-like shape.

Novar subdomain metasedimentary gneisses are indistinguishable in outcrop and hand sample from those of Huntsville and Seguin subdomains. Semipelitic and pelitic varieties are the most widespread, but the proportion of semipelitic to pelitic gneiss is distinctly greater in Novar subdomain. Leucocratic, quartz-rich feldspathic gneiss

(meta-arkose?) is also more widespread, though forming small outcrops, whereas calc-silicate gneiss and marble were not identified. A common rock type, nondescript quartzofeldspathic biotite gneiss with or without garnet, may be in part supracrustal in origin, but has no characteristics that allow inference of protolith.

Structure

The structure of Novar subdomain differs distinctly in both style and orientation from those of Huntsville and Seguin subdomains. North-northwest strikes prevail throughout much of the southern half of this terrane but swing to northeast along its west edge. Dips vary from moderate to vertical. Lineation attitudes vary widely, reflecting the variability of the structure. Considered as a whole, Novar subdomain structure is highly discordant with the continuous wrap-around structure at its boundary, suggesting that it is inherited from an earlier phase of deformation.

Distinctions between subdomains

The most important distinctions between the Seguin, Huntsville and Novar subdomains can be summarized from the foregoing as follows. Gneisses of recognizable sedimentary origin, dominantly of pelitic affinity and characterized by their graphite content (Davidson, 1982), are abundant in Huntsville subdomain and in the western part of Novar subdomain, but are absent in Seguin subdomain. Although migmatitic rocks are present in Huntsville and Novar subdomains, they are characteristic of Seguin subdomain where they commonly have a disrupted mafic component. The Seguin migmatitic rocks, although varied at any one place, are much the same throughout this subdomain, making arbitrary separation of map units difficult to justify, in distinction to Huntsville and Novar subdomains where contrasting lithologies can be mapped. Orthogneissic rocks in Huntsville subdomain are dominantly granitic or granodioritic; those in Novar subdomain are more varied in composition. In both these subdomains orthogneiss occurs in sharp, concordant contact with metasedimentary gneiss in places. In Seguin subdomain, orthogneiss is restricted to lenticular relics of charnockite and megacrystic granodiorite that grade to equivalent migmatitic rocks. Metamorphic grade in Huntsville and Novar subdomains ranges from amphibolite to granulite facies; except for the charnockitic relics, amphibolite facies prevails in Seguin subdomain. Huntsville subdomain is characterized by highly flattened and generally very fine grained rocks whose units form sheets folded together. In contrast the orthogneissic rocks of Novar subdomain, although deformed, appear somewhat less strained. Planar and linear mineral fabrics are well developed in Huntsville and Novar subdomains, but are less obvious in most of the more highly and coarsely recrystallized migmatitic rocks of Seguin subdomain. Planar structures and rock units in Novar subdomain are oriented northwest and dip moderately; those in Huntsville subdomain are shallowly southward-dipping, and in Seguin subdomain they define a synform plunging gently southeast and having steep attitudes in its core.

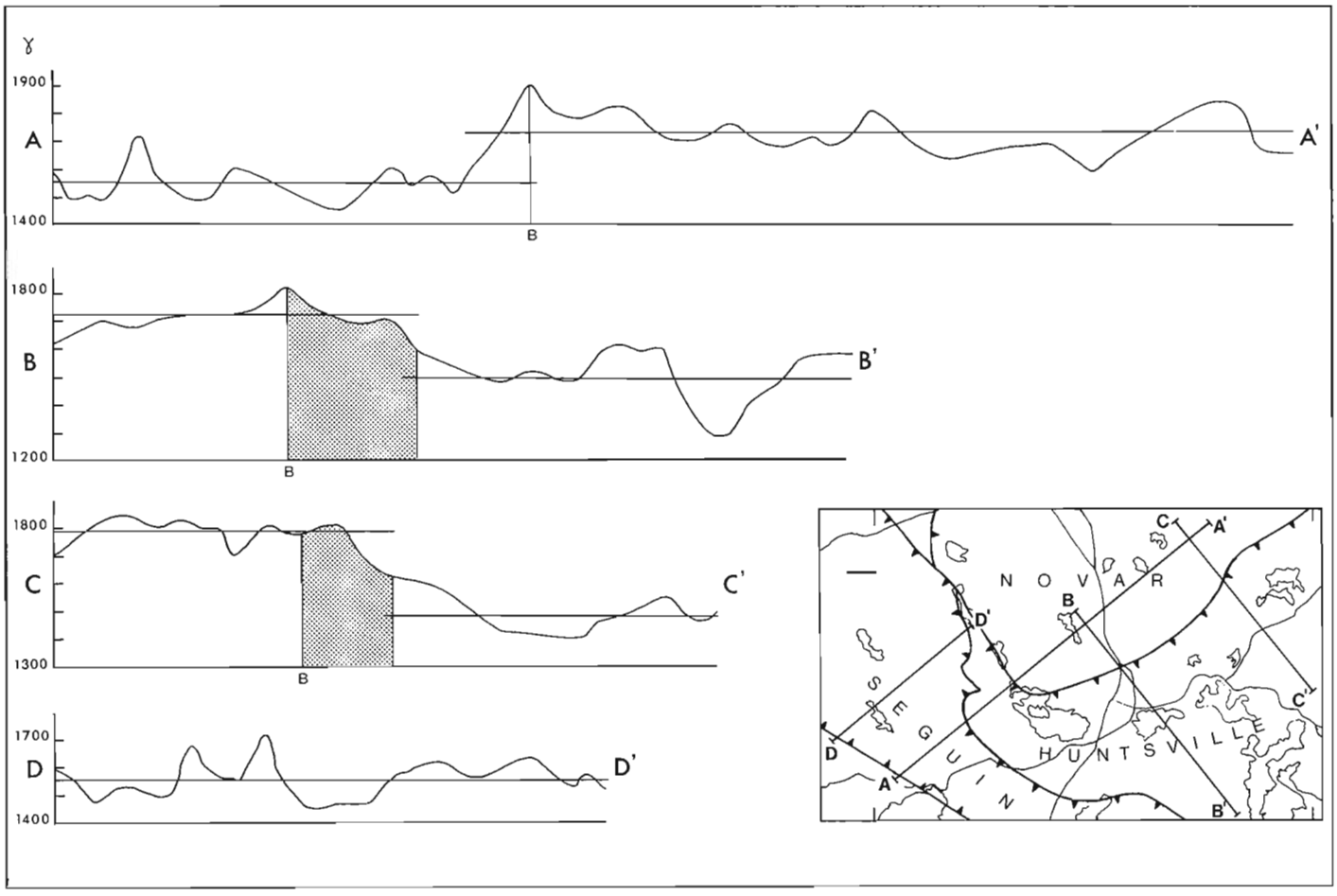

Figure 57.6. *Aeromagnetic profiles across subdomains and their boundaries (B) in the Hunstville area. Shaded areas denote extension of Novar subdomain signature within Huntsville subdomain.*

Aeromagnetic signature

Examination of aeromagnetic maps of the area studied (Geological Survey of Canada, Aeromagnetic Series, Maps 1026 G, 1126 G and 1276 G) allows further characterization of the lithotectonic units previously described (Fig. 57.6). Magnetic anomalies are relatively broad and smooth, and outline only map scale features. Huntsville subdomain shows the lowest background (c. 1500 gammas) and negative anomalies (less than 1200 gammas). The shallow-dipping structure of much of this terrane results in erratically distributed rounded anomalies which merge to the northwest into a broad, hook-shaped pattern that mimics the folded outline of the Lake Vernon plutonic complex. The southern part of Novar subdomain exhibits the highest magnetic background (c. 1700 gammas); positive anomalies (more than 1900 gammas) as well as a north-northwest-oriented pattern conform to its internal structure. Its positive aeromagnetic signature is also seen to extend a few kilometres farther south than the Huntsville-Novar lithotectonic boundary, independently suggesting a southern extension of Novar rocks underneath Huntsville subdomain. The magnetic background of Seguin subdomain (c. 1560 gammas) is slightly above that of the latter terrane, but remains markedly low relative to that of Novar subdomain. It faithfully reflects the bone-shaped closure of the Seguin structure.

Subdomain boundary zones

The boundaries between subdomains are marked by continuous, curved zones of highly deformed gneiss and even mylonitic gneiss. Davidson et al. (1982) have suggested that these are tectonic zones marking the boundaries between crustal blocks and slices that were involved in deep-seated, northwest-directed ductile thrusting. Culshaw et al. (1983, Fig. 28.11) proposed that the Huntsville and Novar subdomains, and Rosseau subdomain to the southwest, form a lower tectonic unit over which the Seguin migmatite lobe was emplaced, riding up on to Parry Sound domain to the northwest. It is suggested in this report that Huntsville subdomain represents a slice that has overridden the Novar block prior to the formation of the Seguin lobe.

Northwest of Buck Lake (Fig. 57.3), the boundary between Seguin and Novar subdomains is marked, at map scale, by a structural truncation that corresponds with a change in lithologic assemblage. The Seguin migmatitic gneiss does not share the sedimentary parentage of the Novar rocks. The north to northeast structural grain of the west side of Novar subdomain is truncated by the northwest-striking, southwesterly-dipping northeast limb of the Seguin synformal structure. Local development of a down-dip lineation at the margins suggests lateral spreading of the lobe during its emplacement. Southeast of Sprucedale, Novar metasedimentary gneisses swing into concordance with flattened Seguin migmatites, suggesting involvement of Novar marginal gneisses in the bounding shear zone. These gneisses are followed up section by a zone of fine grained, equigranular, granoblastic, medium grey, flaggy and lineated tectonites derived from Seguin migmatitic gneisses. They show weak to moderately contrasting centimetre-thick straight layering, scattered coarse grained hornblende porphyroblasts, tight to isoclinal folds, and carry mafic and, locally, anorthositic boudins, disaggregated and transposed pegmatites and isolated mineral augen.

To the south, in Buck Lake-Fox Lake area, Novar subdomain is separated from the Seguin structure by a wedge-shaped extension of Huntsville subdomain. Adjacent rocks on either side of the Seguin-Huntsville boundary are structurally conformable. Farther south, the upper granitoid orthogneiss sheet of Huntsville subdomain projects beneath the migmatitic gneiss of Muskoka domain, but their mutual contact is hidden by a narrow, continuous topographic depression. Near the boundary, the rocks of both terranes are highly flattened, locally flaggy, and exhibit concordant planar fabric and a shallow south-southeasterly lineation in relation to which the shear sense, deduced from rotated mineral augen and from the orientation of shear band foliation, is one of north-northwesterly directed displacement of Muskoka domain. East of Aspdin, tectonites (Fig. 57.4D) very similar to those described southeast of Sprucedale are present, but they are less strongly lineated and may lack the scattered hornblende porphyroblasts. They grade within 50 m up structural section into medium grained, grey, granodioritic, migmatitic gneisses typical of the Seguin subdomain.

East of Mary Lake, however, in the southeastward transition of Seguin subdomain into an area of highly heterogeneous gneisses, the bounding tectonites of Muskoka domain change composition but keep the same tectonic signature. Fine grained, layered, pink and grey quartzofeldspathic tectonites, flaggy, well lineated and carrying centimetre-scale discontinuous amphibole layers and metre- to exposure-size mafic lenses, lie along the edge of and merge southward with highly migmatitic heterogeneous pink and grey granitic and granodioritic gneiss.

Truncation of lithologic units and progressive southeastward deflection of north-trending structure of Novar subdomain into parallelism with the fabric of overlying Huntsville subdomain marks, in Lake Vernon-Buck Lake area, the boundary between these terranes. A layer of fine grained layered flaggy L/S tectonite, tens of metres thick and structurally and texturally similar to those present along the boundary of the Seguin structure, has been traced from Lake Vernon to Buck Lake. Metre-size tectonic fragments of anorthositic gneiss are present within this zone in Lake Vernon area and north of Fox Lake. Northeast of Lake Vernon the Novar-Huntsville boundary follows the topographic break of the Big East River along which Novar lithology and structural grain are truncated at 90 degrees by overriding, northeasterly-striking, shallow southeasterly-dipping Huntsville subdomain tectonites.

Metagabbroic rocks

Metagabbroic rocks occur within all three subdomains as several bodies up to 2 km in maximum map dimension. Many smaller bodies are also present, particularly within the Seguin migmatitic rocks, but are too small to be shown on the accompanying map (Fig. 57.2). Several of the larger masses are concentrated along the boundary between Huntsville and Novar subdomains. It is not known at present whether these were once part of a single mass, now disrupted, or whether they represent separate intrusions.

Where exposed, contacts of the metagabbro bodies are seen to be strongly deformed, the gabbro having been changed to foliated amphibolite. The cores of these masses, however, even those as small as a few metres in diameter, are massive, composed of medium- to coarse-grained metagabbro with relict ophitic texture. In the least altered rocks, primary igneous minerals, particularly olivine and iron oxide grains, are rimmed with secondary reaction products (clinopyroxene, amphibole, garnet, biotite) that form a corona structure (see Davidson et al., 1982). In more highly altered but still massive metagabbro, original plagioclase laths are recrystallized to diffuse aggregates and the secondary minerals are widely dispersed, although a fuzzy relict igneous texture can still be discerned. Lack of stable pyroxene in the sheared marginal envelopes suggests equilibration under amphibolite facies conditions during shearing.

Late extensional shears and pegmatite

Late metre-wide shears geometrically similar to ductile and brittle-ductile shears described by Ramsay (1980) are common throughout the area and are locally responsible for major disturbances of the pre-existing structures (Fig. 57.4E, F). These shears typically show well developed deflection folds with gently plunging axes and steep shear planes. They can rarely be traced for more than a few tens of metres, and show offsets of a metre or so. Late granitic pegmatites are commonly emplaced along the shear plane and exhibit, in places, wedge-shaped terminations. Where these shears transect granulite facies rocks, they are invariably associated with zones of retrogression to amphibolite facies up to ten metres wide. Although locally cutting fairly massive gneisses such as metagabbro, they are preferentially developed in well layered rocks.

Several subparallel shears are commonly developed in large exposures. Locally, more than one set of such shears is present, one of which is the most prominent; these various sets are oriented at high angle to each other. Although movement vectors can seldom be accurately determined, they appear in most cases to be steep and normal. Shears with a reverse fault geometry are rare and appear to be developed only where more than one set of shears is present.

These shears are found throughout the area studied, but they are particularly abundant in Huntsville subdomain and rather rare in Seguin subdomain. Similar shears have been described by Nadeau (1984) in Parry Sound area. They are locally present throughout Muskoka and the southern part of Algonquin domain. To the east, Lumbers (1982) described abundant late pegmatite dykes occurring in the same context in all gneissic rocks throughout Renfrew County. The regional distribution and orientation of these shears remain to be studied and their regional kinematic significance determined. East-northeasterly-striking and steep southerly-dipping shears appear to dominate in both Huntsville and Parry Sound areas, suggesting that southeasterly-directed relaxation may postdate northwesterly-directed overthrusting.

Summary and working hypothesis

Novar subdomain is underlain by a large variety of amphibolite and granulite facies supracrustal and metaplutonic gneisses. These rocks form relatively extensive units which define broad, northwesterly- to northeasterly-oriented, moderately to steeply dipping structures that give this terrane a structural grain highly discordant with that of Grenvillian structures. It is suggested that this lithotectonic unit represents an allochthonous slice which carries an internal metamorphic and structural signature inherited from an earlier, possibly pre-Grenvillian deformation, and which has been reworked subsequently in narrow zones along its margin during emplacement of the overlying Huntsville and Seguin subdomains.

The Huntsville subdomain is characterized by a succession of thin, interleaved, shallowly southward-dipping sheets of fine grained, high grade, flaggy, strongly lineated gneisses, in part mylonitic, of both supracrustal and plutonic origin. Although dipping more shallowly, the attitude of the overall planar structure of this terrane is oriented similarly to those of other shear zones between the Grenville Front and the Central Metasedimentary Belt. Consequently, this terrane is viewed as a deep crustal slice composed of several stacked sheets of interleaved supracrustal and metaplutonic tectonites developed under a highly ductile, northwest-directed shear regime.

The overlying shallow southeast-plunging Seguin synformal subdomain is composed, in large part, of highly migmatitic, dominantly granodioritic gneisses that lack evidence of sedimentary parentage. These migmatitic gneisses are associated and locally grade into non-migmatitic amphibolite and granulite facies orthogneiss, in places exhibiting small scale structures that likely predate migmatization and development of the structure. The migmatitic gneisses also host erratically distributed metre- to kilometre-size mafic inclusions, dominantly metagabbroic, that are invariably deformed and amphibolitized along their margins. This terrane merges southeastward with an area of migmatites of obscure origin associated with metaplutonic rocks that are in part in granulite facies. The Seguin structure is, accordingly, interpreted as a northwest-directed migmatite nappe (sensu lato) derived through remobilization from a deformed and highly metamorphosed plutonic complex.

PART II: CORONITIC GABBRO AND META-ANORTHOSITE IN THE CENTRAL GNEISS BELT, GRENVILLE PROVINCE OF ONTARIO

S.M. Grant

Introduction

Small masses of coronitic gabbro are reported to occur in many parts of the Central Gneiss Belt in Ontario (Davidson et al., 1982). In some places they seem to be restricted to zones of high strain that mark the boundaries of lithotectonic domains. In others they occur in clusters of small bodies scattered throughout the enclosing gneiss or granulite. Some gabbro masses retain traces of discontinuous primary igneous layering. A few have narrow, fine grained zones along parts of their margins, but most contacts have been tectonically modified. Massive, well preserved gabbro, containing primary olivine and only minor development of corona reactions, is commonly associated with and grades into amphibolite with or without garnet porphyroblasts on the one hand, and granulite rich in garnet and pyroxenes (pseudo-eclogite) on the other (Culshaw et al., 1983). It is hoped that study of the mineral chemistry in this suite of rocks, taken from different environments (amphibolite facies, granulite facies, shear zones), will elucidate the nature of the reactions that produced the various assemblages encountered, and that estimates can be made of pressure and temperature and their variation in time and space.

Anorthositic rocks, as well as occurring in large ovoid masses, as at the west side of Parry Sound domain (Davidson et al., 1982), form narrow, concordant layers that can be traced within quartzofeldspathic gneisses for many kilometres. Primary mineral relics intimating igneous origin (large plagioclase crystals, ophitic intergrowth of plagioclase and clinopyroxene) are preserved very locally, but most of the anorthositic rocks are gneisses, having been completely recrystallized to fine aggregates of granular plagioclase and hornblende, in places with garnet, biotite and scapolite. The anorthositic gneiss layers are commonly strongly foliated and lineated, and appear to have been tectonically derived. Their ultimate origin is not known, but it appears on petrological grounds unlikely that they were once relatively narrow dykes or sills. Their association with high strain zones suggests extreme attenuation of tectonic slivers derived from larger masses. It is hoped that careful study of some of these bodies will demonstrate retention of former igneous layering or differentiation of the type documented for some tectonically attenuated Archean anorthosites, such as the Fiskenaesset complex in Greenland (Weaver et al., 1981; Windley et al., 1981). Whatever their origin, metamorphic reactions recorded in these rocks may give estimates of the conditions under which they were deformed.

Field work in 1984 involved mapping and sampling within two areas in which these rocks occur (Fig. 57.1). Near Port Severn in Go Home domain, several lenses of 'anorthositic metagabbro and gabbroic metaanorthosite' mapped by Schwerdtner and Mawer (1982) were located and traced in detail. One of these bodies, formed of anorthositic gneiss, was followed for a strike length in excess of 8 km. Another body proved to be composed of coronitic gabbro in two, possibly three, separate masses, equant in plan. The second area is located in Algonquin Park astride Highway 60 in the vicinity of Costello Lake, where coronitic gabbro is exposed in roadcuts (Guillet, 1969). Detailed mapping revealed at least 30 gabbro masses in a 30 km^2 area, ranging in size from a few metres to as much as 1 km in maximum surface dimension. Other masses may occur beyond the area mapped; a substantial body is exposed at Whitney, 13 km to the southeast.

This study is being undertaken as a Ph.D. thesis project at the University of Leicester under the supervision of B.F. Windley.

Port Severn area

The area studied lies along the coast of Georgian Bay from the vicinity of Port Severn northwest to Honey Harbour (Fig. 57.7), and is underlain by Precambrian crystalline rocks

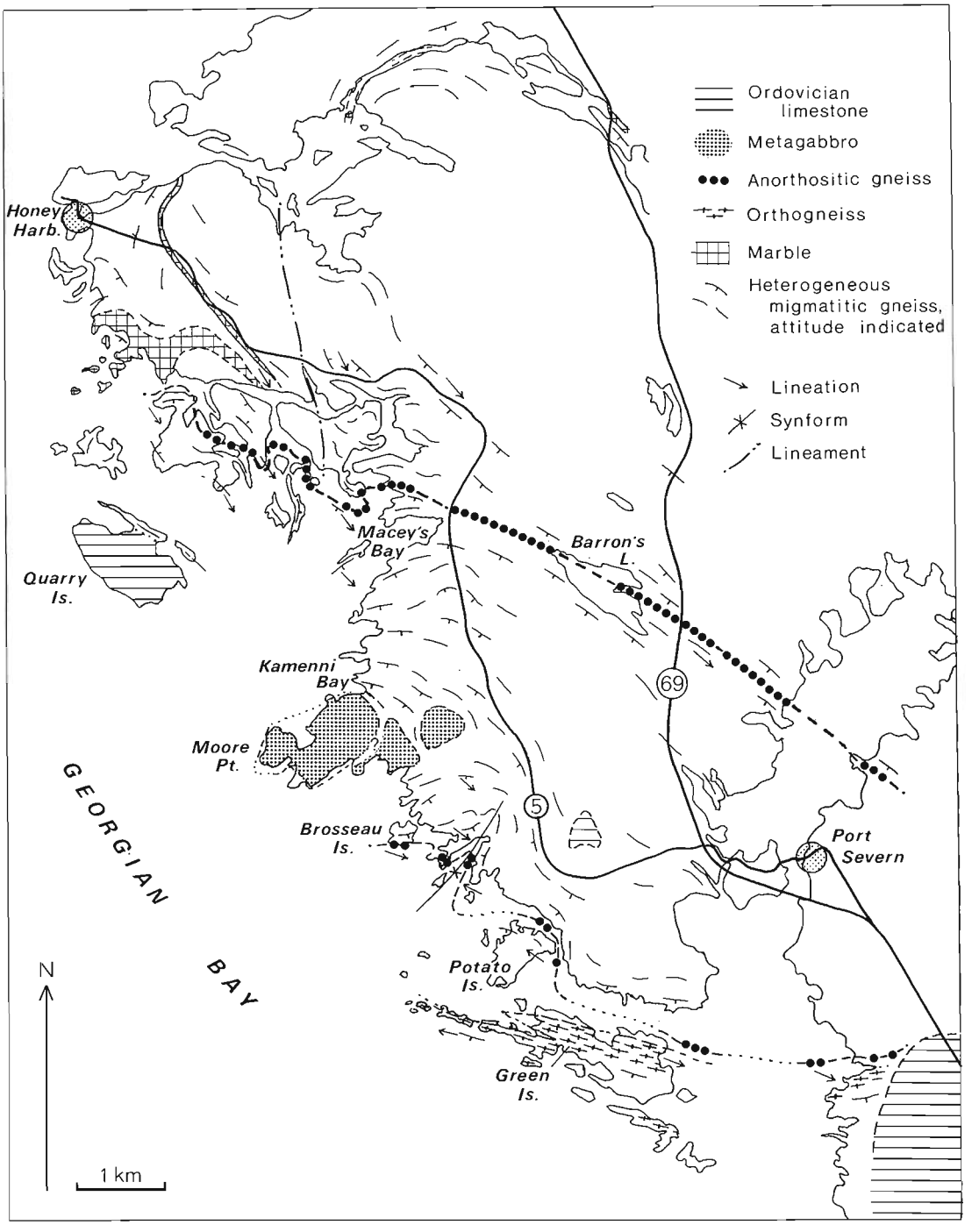

Figure 57.7. *Map of the coast of Georgian Bay between Port Severn and Honey Harbour showing location of metagabbro bodies and anorthositic gneiss layers.*

except for small areas covered by Ordovician limestone on Quarry Island and west and southeast of Port Severn. Most of the area is underlain by heterogeneous grey migmatitic gneiss with pink leucosomes. Biotite and hornblende are the mafic minerals in these rocks, in keeping with amphibolite facies metamorphism; a few kilometres north of the mapped area, however, garnet and hypersthene in rocks with dark feldspars suggest that granulite facies was attained there. In the south, on Green Island and the mainland shore to the east, the rock is more homogeneous, and is a pink, garnet bearing orthogneiss. It has a strong linear fabric defined by aligned feldspar megacrysts or polycrystalline aggregates. The contact between these two units, exposed on the north side of Green Island, is isoclinally folded. Similar garnetiferous orthogneiss outcrops along Highway 69 north of Barron's Lake.

There is a pronounced structural 'break' along the channel north of Green Island. On the island itself the foliation is regular and dips moderately to the south, whereas on the mainland and islands to the north the gneisses have a disrupted appearance, containing wedges and slivers of other rock types in a highly folded, migmatitic matrix. To the north, the dominant trend of gneissosity is northwesterly with southwest dip. Attitudes are regular around Barron's Lake, but become progressively variable in orientation near the shore of Georgian Bay. Lineations generally plunge shallowly to the southeast.

Marble is exposed in the area around Honey Harbour and to the east. It has a sugary, granular texture with 1-2 mm grain size. Other than calcite, the marble contains dispersed grains of feldspar, pale green diopside, brown scapolite and some wollastonite; grossularite is locally associated with bright green diopside in calc-silcate pods. In outcrops along the road to Honey Harbour, marble is associated with pale cream-coloured granite and pegmatite containing amphibole and some pyroxene, with which it forms a thin unit that can be traced for several kilometres. A thicker marble unit to the southwest is characterized by many lensoid inclusions of folded mafic rock, and porphyroclasts of feldspar and pyroxene. It is not associated with the pegmatite of the thin unit, and is in direct contact with the regional migmatitic gneiss. It thins abruptly to the southeast where it may either pinch out or be isoclinally folded to link with the band on the Honey Harbour road. If this marble can be traced on islands to the west, it will make a useful marker for outlining the regional fold pattern.

Two, possibly three bodies of medium- to coarse-grained gabbro with relict ophitic texture are exposed at Moore Point. At contacts with the enclosing migmatitic gneiss this rock is generally highly strained and converted to amphibolite. At Moore Point itself metagabbro occurs within the gneissic envelope as boudins with highly strained marginal zones up to 2 m thick. At the northeast contact of the largest body at Kamenni Bay, the gneisses enclose lenses of metagabbro sheared off the main body in a vertical high strain zone showing marked grain size reduction, thinned and fragmented pegmatite, and possible sheath folds. To the west of here, however, the gabbro is massive and fine grained at its contact with indurated country rock. The smaller body northeast of Musky Bay is relatively finer grained; its texture and mineralogy suggest that it may differ somewhat from the larger mass to the west.

Anorthositic gneiss outcrops in long, linear ridges. It is commonly associated with a more mafic phase. Both types are fine grained and highly strained, as evidenced by foliation defined by elongate aggregates and dispersed streaks of dark mineral grains. The anorthositic phase commonly shows internal boudinage in which blocks have internal foliation turned with respect to that in the enclosing, finer grained anorthositic matrix. The most prominent ridge extends from north of Port Severn northwest to the shore and islands of Georgian Bay south of Honey Harbour, a distance in excess of 8 km. The unit's continuity is remarkable in that nowhere does it attain a thickness of more than 8 m. In two places, two anorthositic layers are separated by more mafic material, possibly reflecting an original igneous stratigraphy, now extremely attenuated. These rocks range in composition from anorthosite (CI less than 10) to leucogabbro (CI ± 25). This unit follows a straight course northwest to Macey's Bay, where it becomes folded. In a hinge zone exposed on a small island there is a patch of well preserved coronitic leucogabbro (amphibole-garnet rims around orthopyroxene) that passes rapidly into foliated leucogabbroic gneiss on the south limb of the fold. Farther west the anorthositic gneiss unit becomes discontinuous on account of large scale boudinage. A similar mechanism may explain the isolated occurrences of anorthositic gneiss to the south, around Brousseau Island, again in an area where the gneisses are strongly folded. Lack of outcrop precludes confirmation, but this second unit may extend, parallel to the regional gneissosity, past Potato and Green islands to connect with outcrops on the mainland shore south of Port Severn. It may be important to note that occurrence of marble is limited to the area north of the northernmost anorthositic band, but that calc-silicate and other metasedimentary gneisses occur southwest of the anorthositic gneiss at Brousseau Island. It is thus possible that all the anorthositic gneiss is the same unit, repeated on either side of a migmatite-cored antiform that plunges gently to the southeast, is overturned to the northeast, and has been refolded to the west.

It is difficult to explain the occurrence of anorthositic rocks in such narrow yet laterally continuous bodies. If they are tectonic slices originally derived from a larger mass, they have been subsequently highly flattened and drawn out. The associated mafic phases appear to have behaved in a more ductile fashion, allowing the more competent plagioclase-rich rocks to rupture internally.

Costello Lake gabbro, Algonquin Park

This region has experienced granulite facies metamorphism. The rocks include mafic and feldspathic granulites, minor occurrences of quartzofeldspathic orthogneiss, and coronitic gabbro. The orthogneiss was recognized in small patches along Highway 60 in the southeast part of the area mapped (Fig. 57.8), and contains pink feldspar megacrysts that define a strong southeast-plunging lineation. At one locality it is adjacent to hypersthene-bearing granulite and reconstituted mafic metagabbro and thus seems to be a separate lithology, not a preserved precursor of granulite. Varying degree of deformation is documented by the passage of megacrystic orthogneiss into well foliated grey gneiss that retains no megacrysts and has a fabric defined by narrow, pink leucosomes.

Several small metagabbro bodies outcrop along Highway 60 in the vicinity of Costello Lake. This rock resists weathering and tends to be exposed on hilltops and knolls, although some smaller masses occur lower down in cliff sections and in valleys. Some 30 separate bodies have been identified to date. The larger bodies have both tectonic and intrusive contacts, the latter characterized by finer grained margins, preserved despite metamorphic recrystallization. A tectonic mechanism is preferred to explain foliated margins of parts of some bodies, where porphyroclasts of mafic minerals (clinopyroxene, hornblende) up to 3 cm in diameter commonly show evidence of rotation.

Where not strongly deformed, the metagabbros retain a coarse ophitic texture, and primary twinning in large, dark plagioclase laths can be recognized. Olivine is locally preserved, even though garnet is present as narrow rims around opaque oxide grains (ilmenite) and other mafic silicate aggregates, and in the cores of recrystallized plagioclase laths. Large, primary clinopyroxene grains, however, are not rimmed by garnet in the least altered gabbros.

Some metagabbro bodies occurring on adjacent hilltops may be eroded remnants of larger ones. Others seem to be tectonic slices of larger masses; south of Lake St. Anthony, for example, gabbro has a highly foliated and folded contact with underlying granulite.

The dominant regional foliation strikes north-northeast and dips easterly, but swings to southeast with northeast dip toward the southeast. Lineations plunge consistently southeast. The metagabbro is not foliated except where locally sheared. Within both gabbro and the enclosing granulites there are several narrow, minor shear zones, generally trending northwest. Curvature of associated foliation shows a consistent sense of tectonic transport, with the northeast sides having moved down-lineation (southeast) relative to the southwest sides. In the metagabbros, shearing has resulted in amphibole formation and grain size reduction, locally to mylonite.

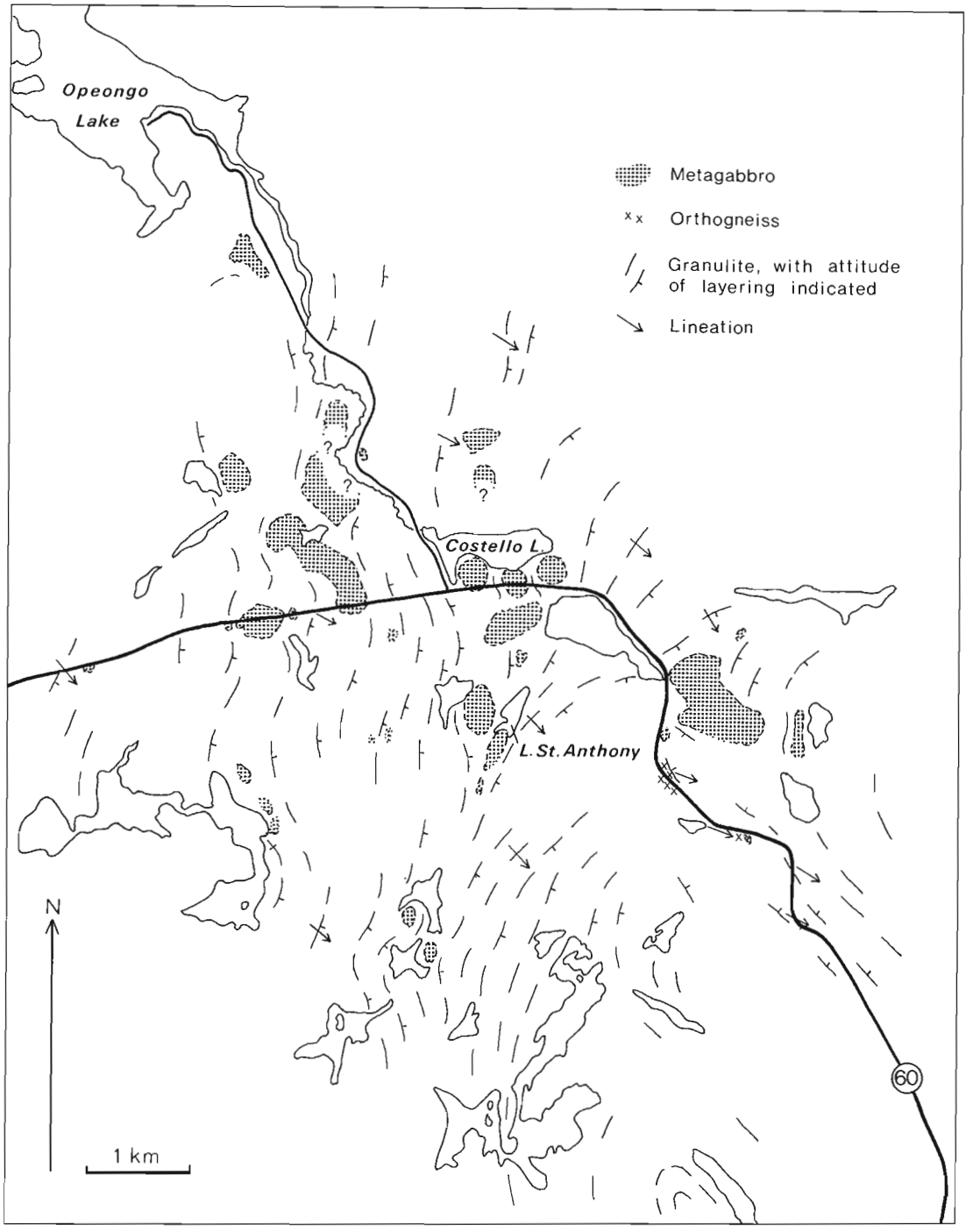

Figure 57.8. *Map of the area around Costello Lake, Algonquin Park, showing distribution of metagabbro bodies.*

Within the granulites there are thin mafic lenses and layers, usually complexly folded or boudined. These may have been mafic dykes associated with the larger gabbro masses, or an earlier, pre-gabbro phase of intrusive activity. Some mafic clots, however, could be the restite from differentiation metasomatism that has resulted in the formation of orthopyroxene- and clinopyroxene-bearing neosomes in most of the granulites.

PART III: PRELIMINARY REPORT ON THE GRENVILLE FRONT TECTONIC ZONE, CARLYLE TOWNSHIP, ONTARIO

L.L. Pryer

Introduction

The study area is located within the Grenville Front Tectonic Zone approximately 25 km northeast of Killarney, Ontario (Fig. 57.9). The northwest boundary of the area

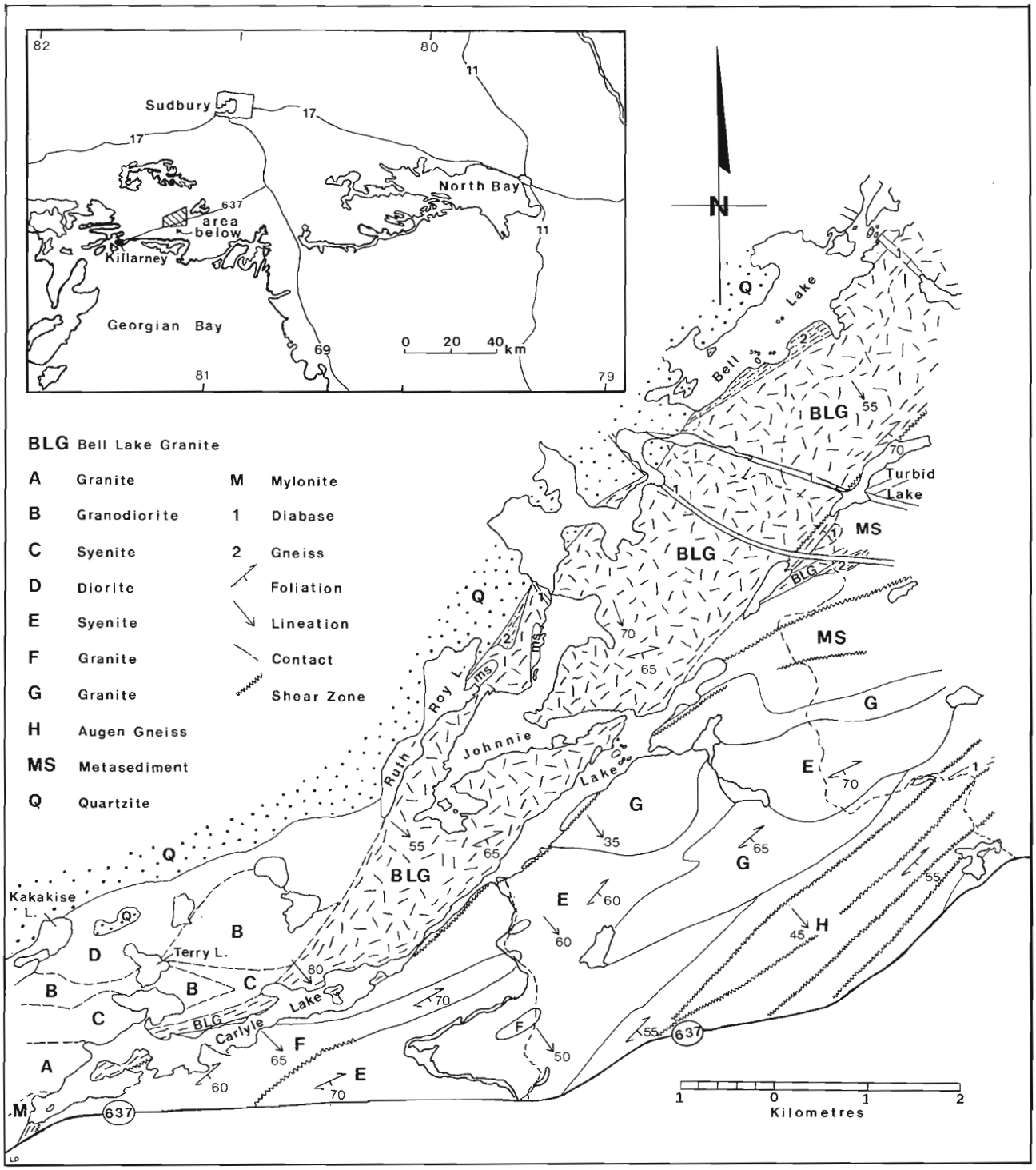

Figure 57.9. Geological map of part of Carlyle Township.

mapped is defined by the contact between Huronian sedimentary rocks, to the northwest, and granitoid rocks that form a number of northeast-elongate bodies referred to as the 'Grenville Front Granites' by Frarey and Cannon (1969). This contact follows a line connecting Kakakise, Ruth-Roy and Bell lakes, and according to Frarey and Cannon separates the Southern and Grenville provinces, characterized respectively by east-trending, steeply folded Huronian strata and adjacent northeast-trending, southeast-dipping gneissic rocks. Card and Lumbers (1977), however, place the Grenville Front farther east, passing through Carlyle Lake and the southeast part of Johnnie Lake; this is within the Grenville Front Tectonic Zone of Lumbers (1978). The Grenville Front is generally acceded to be the locus of reverse faulting (e.g. Wynne-Edwards, 1972). Deformation associated with this displacement, however, is not restricted to a single fault plane, but becomes increasingly penetrative southeastward from the Grenville Province boundary, and is associated with several zones of sheared and mylonitized rocks.

The purpose of this study is to document the nature of this deformation within part of the Tectonic Zone adjacent to the Southern Province. It is being undertaken as a M.Sc. thesis project at McMaster University under the supervision of P.M. Clifford. The area is underlain by various granitoid phases and metasedimentary xenoliths and screens, all cut by dykes of diabase, pegmatite and fine grained granite. The state of strain recorded in the rocks is highly variable, ranging from essentially zero to that required to produce ultramylonite. Deformation ranges from ductile to brittle, the latter commonly being superimposed on the former.

Map unit descriptions

The following units have been defined on field observations and hand sample analysis. Subsequent thin section analysis may bring modification to the field nomenclature applied here to the granitoid rocks. The units are described in two sections, corresponding to the areas on either side of a major northeast-trending structure, the Johnnie Lake shear zone.

Grenville Front granites northwest of the Johnnie Lake shear zone

The Bell Lake Granite (BLG) is the most distinctive unit in the area and was first described by Brooks (1967). This granite is a lenticular unit occupying approximately one third of the study area. It has a characteristic megacrystic texture formed by subhedral to euhedral microcline crystals averaging 2 cm in length where the granite is not deformed. The abundance of megacrysts varies widely, from 20 to 70 per cent of the rock. The groundmass is phaneritic, hypidiomorphic-granular, and is composed essentially of K-feldspar, plagioclase, biotite and quartz. Visible accessory and secondary minerals include muscovite, epidote, iron oxides and sulphides.

An intrusive contact between Bell Lake granite and Huronian sedimentary rocks extends from beyond the northeast tip of the area southwest for approximately 8 km to the south tip of Ruth-Roy Lake. In places the contact is marked by a zone a few tens of metres wide (unit 2, Fig. 57.9) in which the granite has intruded between bedding planes of the adjacent quartzite (Fig. 57.10A). Southeastward across these zones the proportion of granite to quartzite gradually increases until the metasediments occur as definable xenoliths in granite. Xenoliths of quartzite, quartz arenite, arenite and argillite occur throughout the granite and vary in size from a few centimetres to tens of metres.

From Ruth-Roy to Carlyle lakes the body of Bell Lake granite tapers until, in the western half of Carlyle Lake, it is only 200 m wide; here it has a pronounced augen structure and is interlayered with equigranular granite as well as pegmatite and felsite sheets. The southeast boundary of the granite follows a major shear zone (Johnnie Lake shear zone) that extends northeasterly across the whole map area.

Between Carlyle Lake and the Huronian sedimentary rocks lie three other granitoid units included in the 'Grenville Front granites'. The Terry Lake diorite (unit D) occurs in contact with the Huronian from the southern tip of Ruth-Roy Lake to the edge of the area studied at Kakakise Lake. The texture of the diorite is phaneritic, hypidiomorphic-granular. The rock appears to have a uniform composition of plagioclase, biotite and amphibole, though it contains minor quartz in places. The contact with the Huronian is again an intrusive one, with large xenoliths of quartzite occurring in the diorite near the contact. The southern contact with other granitoid units is not exposed.

To the south is a large-scale mixture of granodiorite and syenite (units B and C). Both have similar grain size and phaneritic, hypidiomorphic-granular texture, but vary in type of feldspar and quartz content. The granodiorite contains minor amounts of light pink K-feldspar and has a quartz component as high as 30 per cent. Other minerals are plagioclase, biotite and accessory magnetite and sulphide. The syenite is composed essentially of K-feldspar, biotite and magnetite. Contacts between these two units are not exposed. South of these two units lies a small area of alkali-feldspar granite (unit A) composed of deep red feldspar, biotite and quartz; accessory minerals include allanite, magnetite and sulphide.

Area southeast of the Johnnie Lake shear zone

Southeast of the Johnnie Lake shear zone, the area can be further divided into three parts on the basis of differing rock assemblages, namely pink and purple granite and syenite (units E, F and G), gneissic granodiorite (unit H), and metasedimentary gneiss (unit MS) (Fig. 57.9). Immediately southeast of Carlyle and Johnnie lakes, the most distinctive rock is a fine grained purple syenite or monzonite (unit E). This unit invariably contains pegmatite as well as small, thin quartzofeldspathic lenticles ('sweat-outs'). Quartz may be present, but its content could not be ascertained in the field on account of the fine grain size. The mafic mineral is biotite. Southeast of Carlyle Lake, a coarser unit of alkali-feldspar granite (unit F) occurs partly within the purple syenite. This rock is similar in appearance and composition to unit A, differing only in its obvious lack of allanite. A third granitoid rock (unit G) is medium- to fine-grained and equigranular. It is light pink to orange and composed of feldspars, quartz, biotite and magnetite.

The majority of the southeasternmost part of the study area is underlain by a medium grained, light pink to dark grey granodiorite (unit H). It possesses a well developed fabric wherever observed, usually associated with an augen gneissic structure. The unit contains rounded K-feldspar and plagioclase augen that commonly include biotite grains. The foliated groundmass is relatively fine grained and is composed of feldspars, quartz, biotite, magnetite and allanite.

The east-central section of the map area is occupied by a large block of metasedimentary rocks that may be equivalent to Huronian strata northwest of the Bell Lake granite. These include quartzite ('Lorrain-type' of Frarey and Cannon, 1969), and schists and gneisses derived from quartz arenite, arenite and argillite. One outcrop of metaconglomerate probably derived from the Gowganda

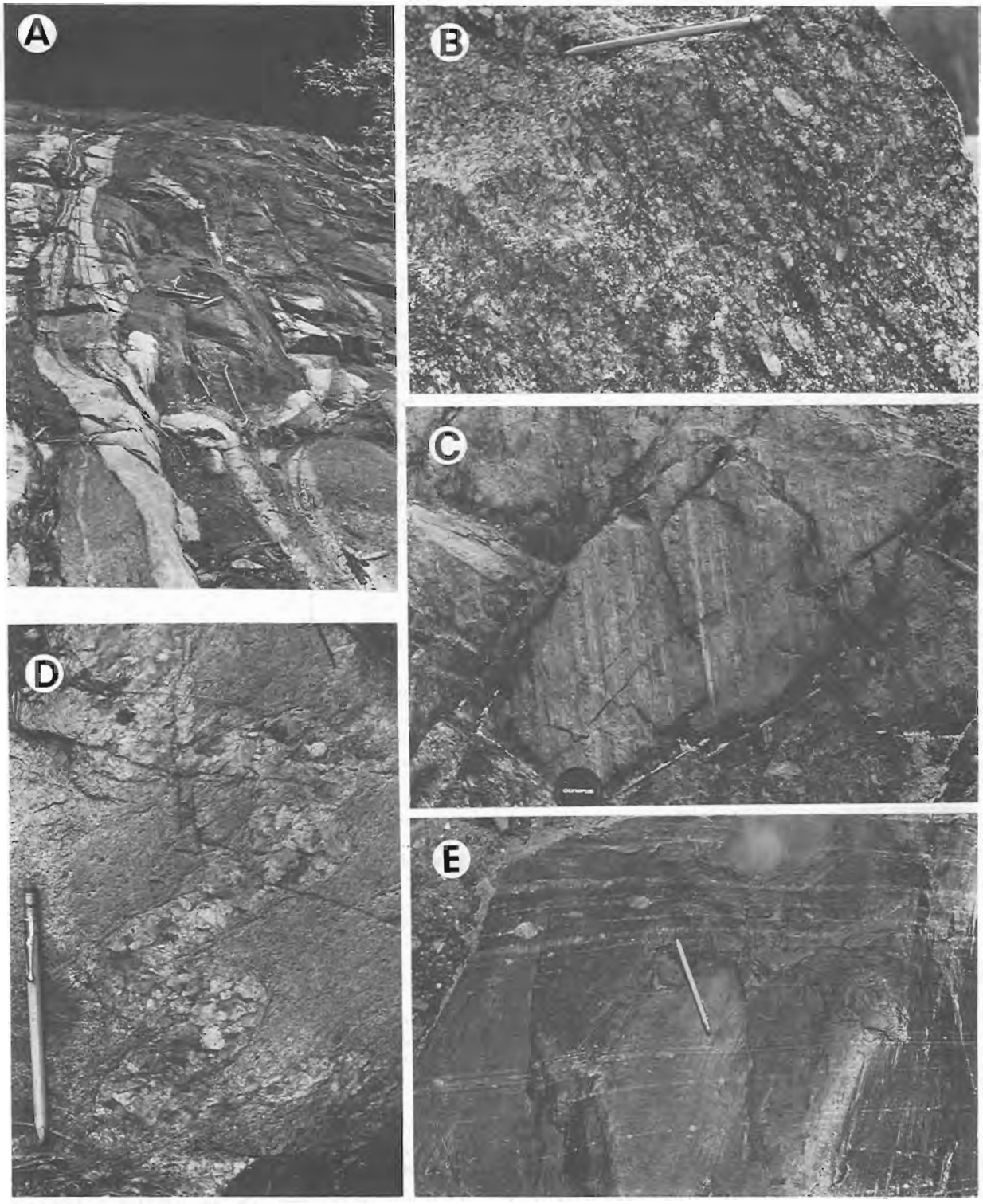

A. *Interlayering of quartzite and Bell Lake granite along the northwest contact at Johnnie Lake.*
B. *Well developed foliation in Bell Lake granite with blocky K-feldspar augen.*
C. *Pronounced stretching lineation on foliation surface.*
D. *Folded pegmatite vein in foliated syenite (unit E).*
E. *Plan view of mylonite developed from syenite (unit E); note trains of single feldspar augen.*

Figure 57.10

Formation is exposed on the road to Bell Lake. All the metasediments are deformed and, where bedding surfaces can be identified, are severely folded.

Structural framework

Planar elements and stretching lineations for the entire area are plotted on lower hemisphere, equal area stereonets (Fig. 57.11). It can be seen from these plots that both planar and linear elements are moderately to steeply inclined to the southeast. Most of the scatter occurring in the plots results from measurements recorded northwest of the Johnnie Lake shear zone; attitudes southeast of this structure are much more consistent.

The amount of strain recorded in the rocks is inhomogeneously distributed in northeast-trending zones, but in general increases southeast from the Huronian contact. It is shown by penetrative mica foliation and, southeastward, by flattened quartz in the form of elongate plates that define a stretching lineation. Within this regime, spaced zones of more intense shear deformation are manifest as mylonite zones.

Much of the core of the thicker part of Bell Lake granite appears little deformed; biotite foliation is, at the most, weakly developed, and xenoliths are equant to only slightly flattened in the plane of this foliation. Severe deformation is restricted to thin (less than 10 cm) bands of protomylonite and mylonite that occur at irregular intervals. At their margins well foliated granite passes within a few centimetres to comparatively non-deformed equivalent rock. The mylonitic zones trend northeast and in places are at a high angle to the weak regional foliation in the Bell Lake granite. Parts of the granite are more strongly and regularly foliated (Fig. 57.10B), particularly along the north side of Carlyle Lake and west of Turbid Lake; K-feldspar megacrysts have become blocky augen and the rock has a 'cataclastic' aspect. At its southwest end, the Bell Lake granite is represented entirely by a dark augen protomylonite.

Southeast of the Johnnie Lake shear zone the granitoid rocks exhibit a more uniformly distributed foliation parallel to the mylonite zones, and contain an increasingly strong and persistent stretching lineation defined primarily by quartz (Fig. 57.10C) that, at higher levels of strain, is accompanied by 'rolling and crushing' of feldspars. Even in this region, however, there are lenticular areas of weakly foliated rock in which foliation attitude is at an angle to the mylonitic shears.

The relatively narrow mylonitic zones in the northwest part of the area commonly have cores of flinty ultramylonite, generally containing very small feldspar augen. Ultramylonite locally forms a small-scale vein structure penetrating less mylonitic rock. Mylonite zones are wider and more closely spaced to the southeast, particularly in unit H (Fig. 57.9). Mylonite in these zones is light pink or grey, very fine grained, and characterized by planar foliation commonly containing trains of feldspar augen along thin seams (Fig. 57.10E).

The variable development of strain fabrics is best displayed by dykes within the rocks northeast of unit H. Many parts of dykes appear non-deformed, but when followed along strike invariably become strained. This behaviour is well illustrated by a large pegmatite mass that occurs within metasedimentary schist along the road to Bell Lake, and by a coarse olivine diabase located at the northern narrows of Johnnie Lake (described by Brooks, 1976). Along the Johnnie Lake shear zone and to the southeast all observed pegmatites have undergone deformation, ranging from folded forms within foliated granitoid rocks (Fig. 57.10D) to strings of feldspar augen in mylonite (Fig. 57.10E). Some of the mylonite zones seem to have been initiated along, or guided by, pegmatites. Mylonite has not been observed to have been cut by pegmatite dykes. The diabase dykes (unit 1) that cut the Bell Lake granite and the Johnnie Lake shear zone in the vicinity of Bell Lake are not deformed, and belong to a swarm that extends across the Grenville Province almost as far as Montreal, 500 km to the east. Diabase dykes that are deformed in the Grenville Front Tectonic Zone are likely correlative with the northwest-trending Sudbury swarm that is prevalent in the Huronian rocks to the northwest.

An outline of the general trend of fabric development is as follows: the first fabric to appear is a single foliation (schistosity); this is followed by the development of a C-and-S fabric that, in turn, is replaced (or accompanied) by an augen structure. In the southeast part of the map area augen gneiss with augen mylonite is developed in a band more than 1 km wide.

The same trend of fabric development also occurs on a local scale immediately adjacent to individual mylonite zones. The distance across which this sequence is observed is

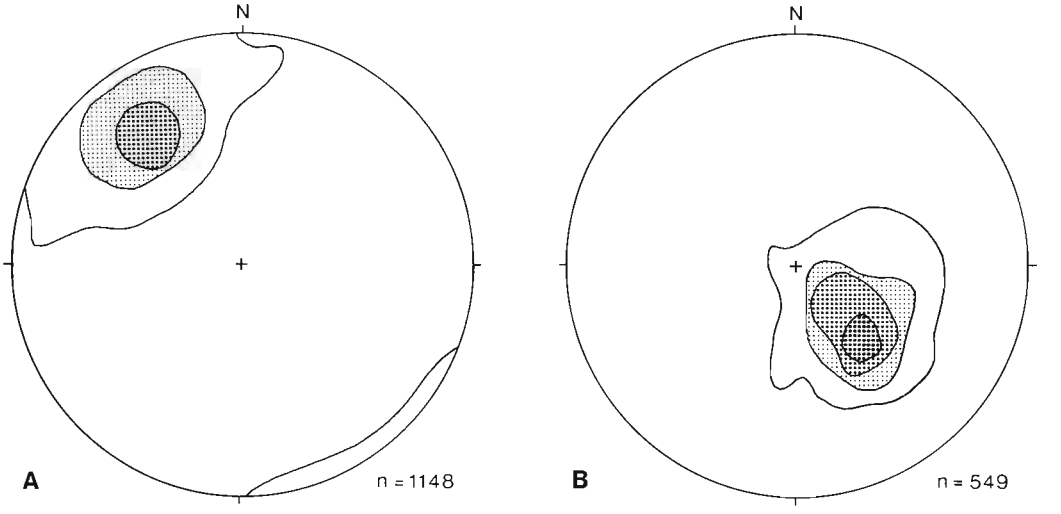

Figure 57.11. *Contoured lower hemisphere stereoplots of planar element (A) and stretching lineations (B). Contour intervals are 1, 5, 10 and 20 per one per cent area.*

dependent on the location of the mylonite with respect to the Huronian contact. Generally the effect of mylonitization on the surrounding rocks increases, and thus the width of the zones increases southeast from the Huronian contact.

Kinematic indicators

The most abundant and probably most reliable kinematic indicator in the area is C-and-S fabric. This may occur in association with development of shear band foliation. Another useful kinematic indicator is provided by rolled feldspar augen with 'tails' (Fig. 57.12). Where sense of shear could be determined, the vast majority (95 per cent) of indicators imply southeast-side-up sense, when observed in a plane parallel to the stretching lineation and normal to the foliation (X-Z sections).

The total amount of displacement across this part of the Grenville Front Tectonic Zone cannot be estimated. Occurrence of Lorrain Formation on either side of the Bell Lake granite, separated by the Johnnie Lake shear zone, suggests at first that displacement may not be very great. The presence of Gowganda Formation rocks on the east side, opposite middle Lorrain Formation on the west (Frarey and Cannon, 1969), is compatible with the sense of displacement deduced from the deformation fabrics. However, as the Lorrain Formation in the Southern Province to the west is almost isoclinally folded about east-west vertical axial planes with unknown axial attitude, it cannot be estimated how deep below the surface the Gowganda Formation may be on the west side.

Age considerations

The Bell Lake granite has been dated by both U-Pb zircon and Rb-Sr whole rock methods at about 1550 Ma, and granitoid rocks southeast of the Johnnie Lake shear zone at about 1730 Ma (Krogh et al., 1971). Other 'Grenville Front Granites' have given similar ages (Stockwell, 1982). The supposition is made that the emplacement of these granites had something to do with the existence of a Grenville Front (thus implying the existence of the Grenville Province) at that time. Stockwell (1982) ascribed this event to the Killarnean Orogeny. Apparently because the older granitoid rocks southeast of the Bell Lake granite are more highly deformed than the Bell Lake granite itself, deformation in the Tectonic Zone was interpreted to have occurred considerably earlier than the usually accepted age (about 1 Ga) of Grenvillian Orogeny. Nothing observed within this project's area, however, dictates that the intense deformation producing augen gneiss and mylonite is other than a Grenvillian event sensu stricto, although possible relics of an earlier foliation (Killarnean?) may be preserved in the least deformed parts of the granitoid rocks. Pegmatites in the Grenville Front region give ages similar to or somewhat younger than those obtained from the 'Grenville Front Granites', but the younger ages may be updated (Krogh and Davis, 1970). The fact that pegmatites are all deformed southeast of the Johnnie Lake shear zone suggests that the bulk of the deformation postdates pegmatite formation.



Figure 57.12. *Rolled feldspar augen with 'tails' in mylonite derived from pegmatite and syenite (unit E). Plane of photograph is X-Z section. Reverse displacement is indicated.*

Davidson (in press) has shown that the Killarney Granite, lying to the southwest of Carlyle Lake (possibly represented by unit A), has a steep northeast trending foliation that is cut by non-deformed pegmatite dykes, and that along the southwest extension of the Johnnie Lake shear zone these pegmatites are clearly older than mylonitization, as are diabase dykes equated with the Sudbury swarm (1250 ± 50 Ma; Palmer et al., 1977). Again, pegmatites do not cut this shear zone. The pre-pegmatite foliation in the Killarney Granite and associated hypabyssal and felsic volcanic rocks (which postdate deformation of Huronian strata to the northwest) is associated with an east to northeast plunging lineation. This contrasts with southeast plunging linear structures associated with foliation and mylonite development at and southeast of the Johnnie Lake shear zone and its southwest extension. It is possible that this earlier deformation, and indeed the 'Grenville Front Granites' themselves, are related to a continent-wide Middle Proterozoic event (Van Schmus and Bickford, 1981) that has nothing to do with the Grenvillian Orogeny. It is also possible that the granitoid rocks southeast of the Johnnie Lake shear zone within the study area, certainly related in age, retain relics of this earlier deformation, now modified (re-oriented) and for the most part attenuated beyond recognition by orogeny of Grenvillian age.

Summary

The Grenville Front Tectonic Zone in Carlyle Township exhibits an inhomogenously developed, large-scale strain gradient, marked by foliation and mylonitization, whose effects intensify southeastward. All rocks except post-Grenvillian diabase dykes were involved in this deformation. Related planar features strike northeast, dip moderately to steeply southeast, and carry a well developed, consistently down-dip stretching lineation. Kinematic indicators imply reverse displacement throughout the study area. It is possible that the 'Grenville Front Granites' were deformed during an earlier event, unrelated to the Grenvillian Orogeny to which the development of the strain gradient is ascribed.

References

Brooks, E.R.
1967: Multiple metamorphism along the Grenville Front north of Georgian Bay, Ontario; Geological Society of America, Bulletin, v. 78, p. 1267-1280.

1976: The Sudbury Basin, the Southern Province, the Grenville Front, and the Penokean Orogeny: discussion; Geological Society of America, Bulletin, v. 87, p. 954-958.

Card, K.D. and Lumbers, S.B.
1977: Sudbury - Cobalt; Ontario Geological Survey, Geological Compilation Series, Map 2361.

Culshaw, N.G., Davidson, A., and Nadeau, L.
1983: Structural subdivisions of the Grenville Province in the Parry Sound – Algonquin region, Ontario; in Current Research, Part B, Geological Survey of Canada, Paper 83-1B, p. 243-252.

Davidson, A.
1982: Graphite occurrences in the Algonquin region, Grenville Province, Ontario; Geological Survey of Canada, Open File 870.

1984: Identification of ductile shear zones in the southwestern Grenville Province of the Canadian Shield; in Precambrian Tectonics Illustrated, ed. A. Kroner and R. Greiling; E. Schweizerbart'sche Verlagsbuchhandlung, p. 263-279.

– The Killarney Granite and its relationship to the Grenville Front; in New Perspectives on the Grenville Problem, Geological Association of Canada Special Paper. (in press)

Davidson, A. and Morgan, W.C.
1981: Preliminary notes on the geology east of Georgian Bay, Grenville Structural Province, Ontario; in Current Research, Part A, Geological Survey of Canada, Paper 81-1A, p. 291-298.

Davidson, A., Culshaw, N.G., and Nadeau, L.
1982: A tectono-metamorphic framework for part of the Grenville Province, Ontario; in Current Research, Part A, Geological Survey of Canada, Paper 82-1A, p. 175-190.

Frarey, M.J. and Cannon, R.T.
1969: Notes to accompany a map of the geology of the Proterozoic rocks of the Lake Panache – Collins Inlet map-areas, Ontario; Geological Survey of Canada, Paper 68-63, 5 p.

Guillet, G.R.
1969: A geological guide to Highway 60, Algonquin Provincial Park; Ontario Department of Mines, Miscellaneous Paper 29, 44 p.

Hanmer, S.K.
1984: Structure of the junction of three tectonic slices; Ontario Gneiss Segment, Grenville Province; in Current Research, Part B, Geological Survey of Canada, Paper 84-1B, p. 109-120.

Hanmer, S.K. and Ciesielski, A.
1984: Structural reconnaissance of the northwest boundary of the Central Metasedimentary Belt, Grenville Province; in Current Research, Part B, Geological Survey of Canada, Paper 84-1B, p. 121-131.

Johannes, W.
1983: On the origin of layered migmatites; in Migmatites, Melting and Metamorphism, ed. M.P. Atherson and C.D. Gribble; Shiva Publishing Company, Nantwich, Cheshire, U.K., p. 234-248.

Krogh, T.E. and Davis, G.L.
1970: Isotopic ages along the Grenville Front in Ontario; Carnegie Institute of Washington, Yearbook 68, p. 309-313.

Krogh, T.E., Davis, G.L., and Frarey, M.J.
1971: Isotopic ages along the Grenville Front in the Bell Lake area, southwest of Sudbury, Ontario; Carnegie Institute of Washington, Yearbook 69, p. 337-339.

Lumbers, S.B.
1978: Geology of the Grenville Front Tectonic Zone in Ontario; in Toronto '78, Field Trips Guidebook, ed. A.L. Currie and W.O. Mackasey; Geological Association of Canada, p. 347-371.

1982: Summary of metallogeny, Renfrew County area; Ontario Geological Survey, Report 212, 59 p.

Mehnert, K.R.
1968: Migmatites and the origin of granitic rocks; Elsevier, Amsterdam, 405 p.

Nadeau, L.
1984: Deformation of leucogabbro at Parry Sound, Ontario; unpublished M. Sc. thesis, Carleton University, Ottawa.

Palmer, H.C., Merz, B.A., and Hayatsu, A.
1977: The Sudbury dikes of the Grenville Front region: paleomagnetism, petrochemistry, and K-Ar age studies; Canadian Journal of Earth Sciences, v. 14, p. 1867-1887.

Ramsay, J.G.
1980: Shear zone geometry: a review; Journal of Structural Geology, v. 2, p. 83-99.

Schwerdtner, W.M. and Mawer, C.K.
1982: Geology of the Gravenhurst region, Grenville Structural Province, Ontario; in Current Research, Part B, Geological Survey of Canada, Paper 82-1B, p. 195-207.

Stockwell, C.H.
1982: Proposals for time classification and correlation of Precambrian rocks and events in Canada and adjacent areas of the Canadian Shield; Part 1: a time classification of Precambrian rocks and events; Geological Survey of Canada, Paper 80-19, 135 p.

van Breemen, O., Davidson, A., Loveridge, W.D., and Sullivan, R.W.
– U-Pb zircon geochronology of Grenville tectonites, granulites and igneous precursors, near Parry Sound, Ontario; in New Perspectives on the Grenville Problem, ed. J.M. Moore; Geological Association of Canada, Special Paper. (in press)

Van Schmus, W.R. and Bickford, M.E.
1981: Proterozoic chronology and evolution of the midcontinent region, North America; in Precambrian Plate Tectonics, ed. A. Kroner; Elsevier, Amsterdam, p. 261-296.

Weaver, B.L., Tarney, J., and Windley, B.
1981: Geochemistry and petrogenesis of the Fiskenaesset anorthosite complex, southern West Greenland: nature of the parent magma; Geochimica et Cosmochimica Acta, v. 45, p. 711-725.

Windley, B.F., Bishop, F.C., and Smith, J.V.
1981: Metamorphosed layered igneous complexes in Archean granulite-gneiss belts; Annual Review of Earth and Planetary Sciences, v. 9, p. 175-198.

Wynne-Edwards, H.R.
1972: The Grenville Province; in Variations in Tectonic Styles in Canada, ed. R.A. Price and R.J.W. Douglas; Geological Association of Canada, Special Paper 11, p. 263-334.

STRUCTURE AND STRATIGRAPHY OF THE MIETTE GROUP, SELWYN RANGE, BETWEEN PTARMIGAN AND HUGH ALLAN CREEKS, BRITISH COLUMBIA

EMR Research Agreement 53/04/83

Eric W. Mountjoy[1], Richard Forest[1], and Richard Leonard[1]
Cordilleran Geology Division

Mountjoy, E.W., Forest, R., and Leonard, R., Structure and stratigraphy of the Miette Group, Selwyn Range, between Ptarmigan and Hugh Allan creeks, British Columbia; in Current Research, Part A, Geological Survey of Canada, Paper 85-1A, p. 485-490, 1985.

Abstract

A thick sequence of pelites and grits is recognized for the first time in the Selwyn Range beneath the more than 3000 m thick middle Miette Group. They are assigned to the lower Miette which is divisible into an upper 2000 to 3000 m thick pelite (lower Miette Pelite), and an underlying grit sequence (lower Miette grits) more than 1500 m thick. Thus the total Miette Group is more than 8000 m thick.

Four major thrust faults duplicate the Miette Group. From northeast to southwest these are Chatter Creek, Ptarmigan, Blackman, and Purcell thrusts. The Mount Blackman Gneiss and its Hadrynian Horsethief Creek Group(?) cover form the Purcell thrust sheet.

Two episodes of deformation are recognized: the first, southwest of Blackman thrust, produced southwest verging folds; the second, produced a set of northeast verging folds southwest of Blackman thrust and two sets of northeast verging folds in the Ptarmigan and Chatter Creek thrust sheets.

Metamorphic grade increases southwestward from greenschist in the Chatter Creek thrust sheet, to lower amphibolite in the Ptarmigan, to upper amphibolite in the Purcell thrust sheet.

Résumé

On a pour la première fois identifié une épaisse séquence de grès grossiers dans la chaîne de Selwyn, au-dessous du groupe intermédiaire de Miette, dont la puissance dépasse 3000 m. On a attribué cette séquence à la partie inférieure du groupe de Miette, que l'on a subdivisée en une pélite sus-jacente de 2000 à 3000 m de puissance (pélite inférieure de Miette), et une séquence de grès grossiers sous-jacents (grès grossiers inférieurs de Miette), de plus de 1500 m de puissance. Ainsi, la puissance totale du groupe de Miette dépasse 8000 m.

Quatre grandes failles de chevauchement sont la cause de la répétition du groupe de Miette. Du nord-est au sud-ouest, il s'agit des failles de chevauchement de Chatter Creek, Ptarmigan, Blackman et Purcell. Le gneiss de Mount Blackman et sa couverture constituée du groupe Hadrynien de Horsethief Creek (?) constituent la nappe de charriage de Purcell.

On a identifié deux épisodes de déformation. Le premier, au sud-ouest de la faille chevauchante de Blackman, a produit des plis d'inclinaison sud-ouest; le second a produit un ensemble de plis inclinés vers le nord-est, au sud-ouest de la faille chevauchanze de Blackman, et deux ensembles de plis inclinés vers le nord-est dans les nappes de charriage de Ptarmigan et Chatter Creek. La déformation fragile est associée au faillage normal d'âge tertiaire(?). Une faille normale présumée, située le long du ruisseau Hugh Allan, crée une dénivellation de plus de 5000 m par rapport à la paroi sud-est.

Le degré de métamorphisme augmente vers le sud-ouest, du faciès des schistes verts dans la nappe de charriage de Chatter Creek, jusqu'à celui des amphibolites inférieures dans la nappe de charriage de Ptarmigan, et à celui des amphibolites supérieures dans la nappe de charriage de Purcell.

[1] Department of Geological Sciences, McGill University, 3450 University Street, Montreal, Quebec, H3A 2A7

Introduction

Field work was carried out during the summers of 1983 and 1984 in the Selwyn Range, in the western Main Ranges of the Rocky Mountains. The study area is bounded by the Chatter Creek thrust on the northeast and the Mount Blackman and Hugh Allan gneisses on the southwest, and between the north fork of Hugh Allan Creek on the southeast to northwest of Ptarmigan Creek (52°20' to 52°45'N), about 60 km southeast of Valemount, British Columbia (Fig. 58.1). The project includes M.Sc. thesis projects by Forest and by Leonard who prepared maps on a scale of 1:25 000 and who studied the stratigraphy, structure and metamorphism to elucidate the tectonic relationships between the Mount Blackman Gneiss and the rocks to the east.

Previous work includes reconnaissance scale mapping of Canoe River (83 D) by Campbell (1968) and Price and Mountjoy (1970) and more detailed study of the gneisses by Chamberlain et al. (1979), and Oke and Simony (1981). The geology of the area to the northwest around Bulldog Creek was outlined by McDonough and Simony (1984). The metamorphism of the southwest part of the area, north of Mount Blackman, was described by Leonard (1984). We have used unpublished information from the Geological Survey of Canada's Bow-Athabasca project (Price and Mountjoy, 1970).

Major structural features

Four major thrust faults are recognized in the area, from northeast to southwest, the Chatter Creek, Ptarmigan, Blackman, and Purcell thrust faults (Fig. 58.1). The gneisses and their cover of Hadrynian strata of Horsethief Creek Group(?) form the most westerly Purcell thrust sheet (Leonard, 1984). The Fraser River anticlinorium dominates the Chatter Creek thrust sheet (Fig. 58.1, 58.2) at the head of Ptarmigan Creek. Details of these structures are outlined below.

Stratigraphy

The area is underlain by the strata of the Hadrynian Miette Group. The Miette Group is divisible into three informal mappable units; upper, middle and lower on the basis of stratigraphy established on 1:50 000 scale maps in the Jasper area (Mountjoy, 1976; Mountjoy and Price, 1984a, b). The upper Miette consists of a predominantly pelitic sequence up to 2000 m thick. The middle Miette is more than 2500 m thick and consists of a composite series of graded, pebbly sandstones (grits) in cliff-forming units 50 to 100 m thick which alternate with somewhat thicker dark grey to greenish grey pelites. The lower Miette comprises two distinct units, an upper dark grey to black pelite, 2000 to 3000 m maximum thickness (not true thickness due to folding), and a lower grit sequence more than 1500 m thick. The upper black pelite is similar to the lower Miette of the McBride area (Carey and Simony, 1984), but lacks black carbonate in its upper part. In the Jasper area the lower Miette is represented by the distinctive red and green pelites and limestones of the Old Fort Point Formation found along the bases of some thrust sheets. Old Fort Point Formation lithologies are not found west of the continental divide.

The upper Miette Group outcrops only in the Ptarmigan thrust sheet. It consists predominantly of pelite, some quartzite, rare pink calcareous sandstone and rare thin grits. The pelites are green and lustrous. Minimum thickness is 1000 m.

Middle Miette strata in the Chatter Creek thrust sheet are similar to those to the east in the Amethyst Lakes and Jasper areas (Mountjoy and Price, 1984a, b) in terms of sedimentary lithologies and textures, except that the pelites are thicker. The bases of the grit units are often conglomeratic with pebbles of quartz and carbonate reaching 4 to 6 cm in diameter. Rare boulders are 30 to 50 cm and a few reach a few metres in length. These larger clasts and boulders are generally brown weathering dolomites. The middle Miette Group has a minimum thickness of 3000 m on the east limb of the Fraser River anticlinorium. The middle Miette conformably overlies pelites of the lower Miette. The base is arbitrarily chosen at the base of the lowest mappable thick composite grit unit. This contact is well exposed on several of the ridges that form the east limb of the Fraser River anticlinorium.

Two older stratigraphic units, exposed below the middle Miette, are recognized for the first time in the Miette Group in the Selwyn Range of the western Main Ranges. A 2000 to 3000 m sequence of dark brown and rusty weathering pelites, here termed lower Miette pelite, outcrops beneath the middle Miette at the head of Ptarmigan Creek in the core of the Fraser River anticlinorium (Fig. 58.1, 58.2). These pelites form a monotonous sequence of dark grey to rusty weathering outcrops with rare silty and sandy intervals. Thin quartzite units occur near the top of the lower Miette pelite in the Ptarmigan thrust sheet. Discontinuous pods and lenses of composite grits up to 100 m thick occur in the lower half. Generally these lenses of grit extend laterally for less than 1 km but a few extend up to 2 km. They probably represent distal submarine fan channel deposits. Dark grey to black micritic limestones in units 10 to 30 m thick occur in the lower part of the lower Miette pelite. During the summer of 1983 some of these pelites in the Ptarmigan thrust sheet were confused with and mapped as upper Miette.

A lower grit sequence, the lower Miette grits, lies conformably beneath the lower Miette pelites. The base is not observed. About 800 m is exposed within the Fraser River anticlinorium and approximately 1500 m in the hanging wall of the Ptarmigan Creek thrust (Fig. 58.2). The lower Miette grits are superficially similar to the grits in the middle Miette, except that the composite grit units are generally thinner and the thickness of the interbedded pelite sequences is more variable. The lower Miette grits are more calcareous and contain brown weathering carbonate units throughout, with some up to 50 m thick. Dark grey to black carbonates also occur in the lower part of these grits. This more carbonate-rich sequence is similar to strata tentatively assigned to the Horsethief Creek Group(?) in the Purcell thrust sheet, that overlie the Mount Blackman Gneiss (Leonard, 1984). Similar strata occur in both the Horsethief Creek Group and in the overlying lower Kaza Group to the west (Pell and Simony, 1982, 1984). The suggested correlation of Oke and Simony (1981) of the strata above the gneisses in the hanging wall of the Purcell thrust with similar pelites, quartzites and carbonates beneath the Gog Group in the Park Ranges 30 km to the southeast observed by Craw (1977, 1978) in the footwall of the Purcell thrust is, in our view, incorrect. We contend that the middle and upper Miette are <u>not</u> missing south of Hugh Allan Creek, but rather that the Gog Group rests on the upper Miette like it does everywhere in the Rocky Mountains to the northwest and northeast. Thus the upper clastic, carbonate, and slate units of Simony et al. (1980) and Oke and Simony (1981) are not equivalents of the Horsethief Creek Group west of the Rocky Mountain Trench but rather are the equivalents of the stratigraphically higher Isaac, Cunningham, and Yankee Belle formations of the Cariboo Mountains or upper Miette as Price and Mountjoy (1970) and Craw (1977) originally suggested.

In the region mapped the total composite thickness of the Miette Group is a minimum of 8000 m (upper Miette 1000 m+, middle Miette 3000 m+, and lower Miette 4000 m).

Between 5000 and 6000 m of Miette Group strata outcrop in an unfaulted sequence on the east limb of the Fraser River anticlinorium (Fig. 58.3). East of the Chatter Creek thrust the upper Miette is about 1500 m thick (Mountjoy and Price, 1984a, b) thus the total thickness of the Miette Group is more than 8500 m.

Structure

Chatter Creek thrust sheet

The Chatter Creek thrust sheet mainly consists of the middle Miette northeast dipping limb of the Fraser River anticlinorium. The Chatter Creek thrust is covered in the upper Fraser River valley. It places middle Miette strata against east-dipping Gog Group and upper Miette strata of the Simon syncline to the northeast (Mountjoy and Price, 1984b).

The doubly plunging Fraser River anticlinorium, a second phase open anticlinal structure, reaches a culmination at the head of Ptarmigan Creek which brings the lower Miette sequence to the surface (Fig. 58.2, 58.3). The lower Miette pelite is thickened considerably in the core of this structure by tight inclined to recumbent F1 folds. These F1 folds are not clearly observable because of the homogeneity of the pelite. Careful examination of facing direction indicates several reversals, suggesting an extensive development of F1 folds. Rare thin sandstone beds intercalated with pelite form markers that can be traced to delineate F1 folds with wavelength up to 10 m. Upright open F2 folds are coaxially developed on the limbs of F1 folds. Because F1 folds are not obvious in the pelite, only a folded primary schistosity was generally observed. A zonal and discrete crenulation cleavage is axial planar to F2 folds. The middle Miette grits of the east limb are disrupted by small scale southwest verging parasitic folds, and by small scale northeast dipping thrusts and normal faults.

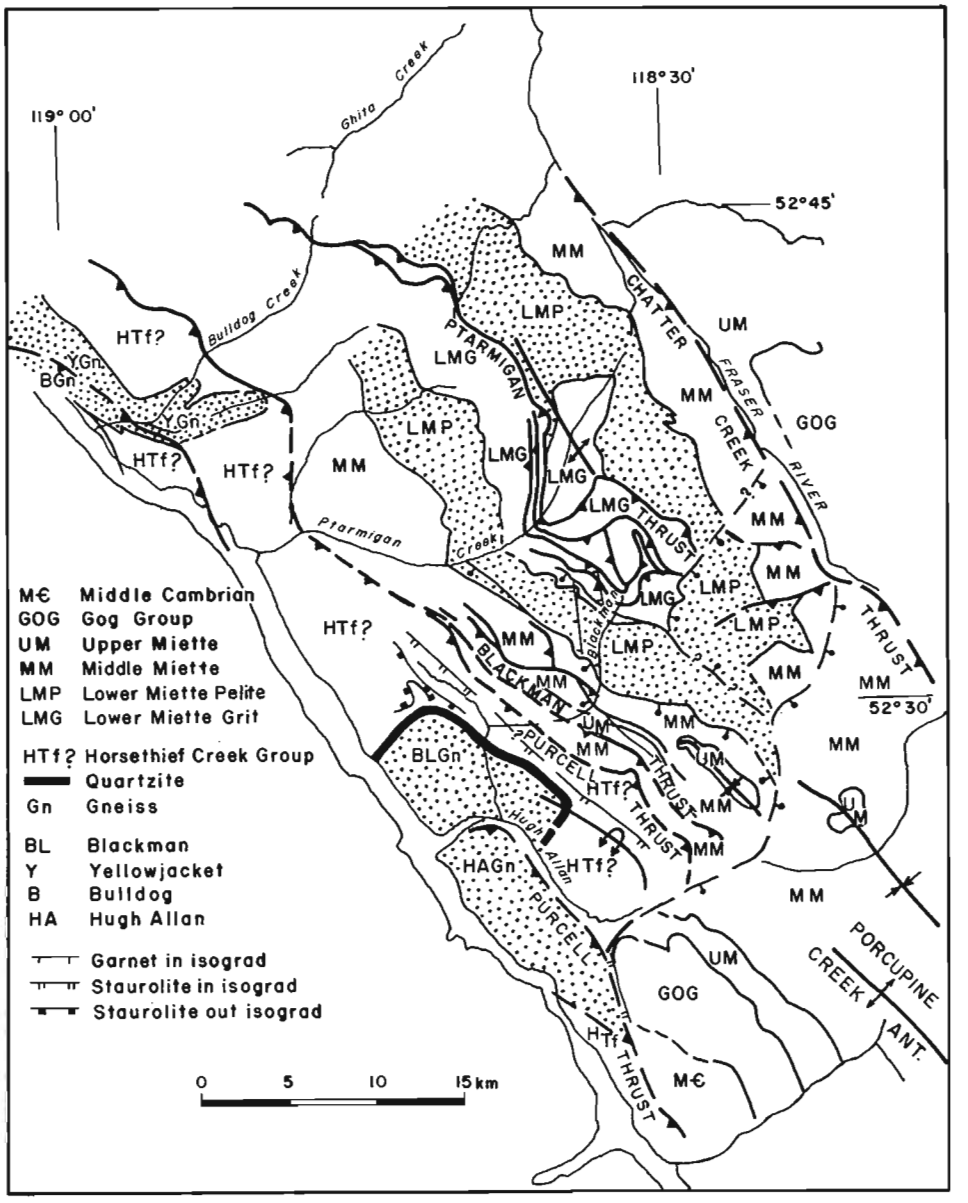

Figure 58.1

Geological map of the Ptarmigan-Hugh Allan Creek region, Selwyn Range. Geology around Pulldog Creek from McDonough and Simony (1984).

Ptarmigan thrust sheet

The Ptarmigan thrust sheet is the major structure in the area and outcrops over a width of about 13 km (Fig. 58.1, 58.2). It comprises a southwest dipping panel of lower and middle Miette strata divisible into two major zones; a narrow northeastern imbricate zone, and a wide southwestern part broken by two southwest-dipping normal faults.

The Ptarmigan thrust outcrops on both sides of the head of Ptarmigan Creek. It is especially evident where lower Miette grits are faulted above lower Miette pelites on the west flank of the Fraser River anticlinorium (Fig. 58.2, 58.3). The Ptarmigan thrust continues northwest at least as far as Yellowjacket Creek. In the vicinity of Ptarmigan Creek the

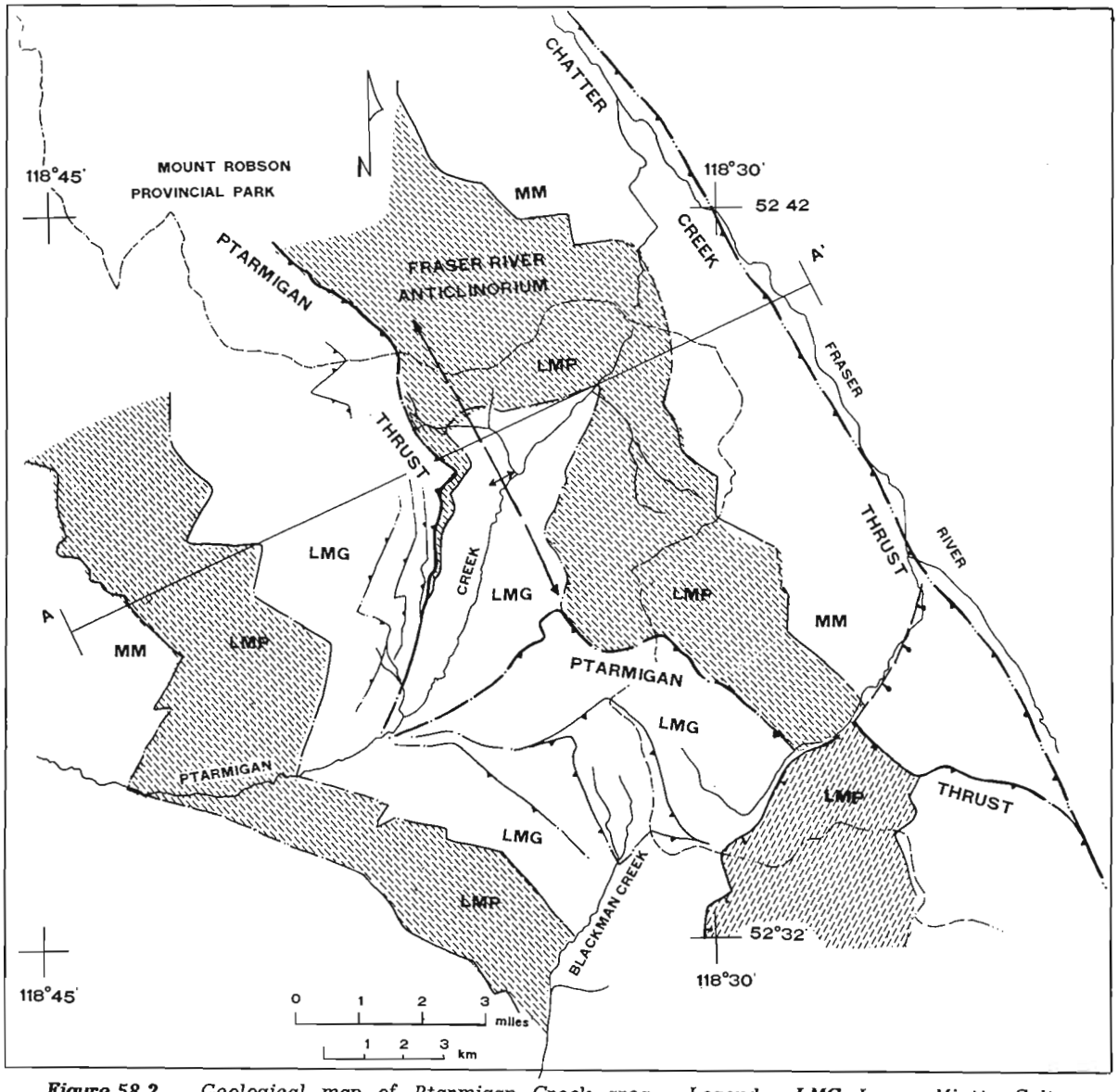

Figure 58.2. *Geological map of Ptarmigan Creek area. Legend:* ***LMG:*** *Lower Miette Grits,* ***LMP:*** *Lower Miette Pelite,* ***MM:*** *Middle Miette Grits.* ***AA'*** *shows location of cross-section shown in Figure 58.3.*

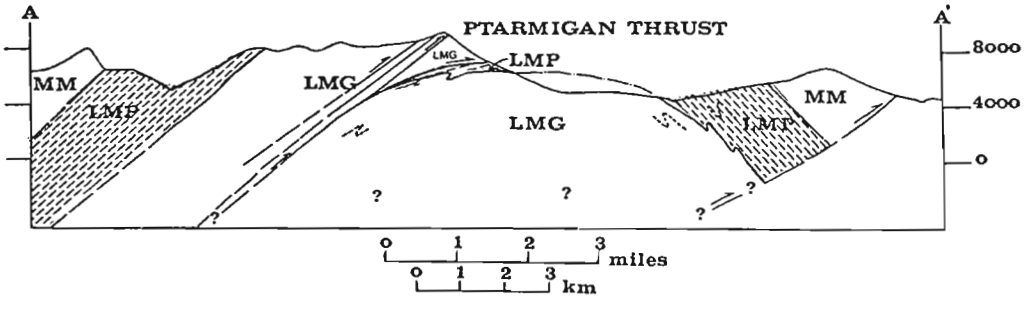

Figure 58.3. *Cross-section AA' of the Fraser River Anticlinorium (for symbols refer to Fig. 58.2).*

thrust dips southwest between 25 and 35 degrees and flattens northeastward towards the crest of the Fraser River anticlinorium (Fig. 58.3). North of Ptarmigan Creek the metamorphism changes across the Ptarmigan thrust from muscovite-chlorite assemblage to biotite-garnet assemblage. South of Ptarmigan Creek the garnet isograd trends southward to the immediate hanging wall of the Blackman thrust and is offset by a normal fault (Fig. 58.1).

Southeastwards the Ptarmigan thrust splits into 5 or more fault splays or imbricates forming a complex, southeast plunging schuppen or duplex structure between the Ptarmigan sole thrust and the highest thrust splay (Fig. 58.2). This imbricate zone with associated numerous first phase northeast verging recumbent folds is about 2 km wide north of Ptarmigan Creek increasing in width and structural complexity southeastward. One of the thrust splays is sheared and broken into a complex tectonic mélange about 300 m thick. Southeastward some of the thrust splays merge but most are truncated by a north-south trending, east-dipping Tertiary(?) normal fault at the head of the east fork of Hugh Allan Creek. Farther southeast the Ptarmigan thrust overlaps and joins the Chatter Creek thrust at the head of the Fraser River near 52°35'N.

Thrusting and two phases of folding related to the same progressive deformational event occur throughout most of the Ptarmigan thrust sheet. First phase folds are tighter and vary from shallowly inclined to isoclinal, compared to the more open and upright second phase folds. These two sets of folds occur throughout the Ptarmigan thrust sheet and are associated with a single deformation event related to thrusting.

First phase folds have fold amplitudes of 20 to 150 m. The strong southwest shallow-dipping schistosity reflects northeast vergence of first phase isoclinal folds to which the schistosity is axial planar. Minor thrusts truncate the inverted limbs of these folds near Ptarmigan thrust and associated splays. First phase fold structures are overprinted by a shallow, southwest dipping crenulation cleavage. First phase folds are considered to have developed early, during initial movements of the Ptarmigan thrust.

Second phase folds are open and upright, with amplitudes of about 5 to 50 m, and have axial planar crenulation cleavage. They are most common in the middle of the Ptarmigan thrust sheet near the top of the middle Miette. Crenulation cleavage is the most common microstructure in the pelitic rocks of the central and western part of the Ptarmigan thrust sheet. The development and steepness of the axial planes of these folds is controlled by the stratigraphic level and the proximity to Ptarmigan thrust and splays. Second phase folds are usually better developed and more upright in the upper part of the middle Miette strata. These folds are more inclined at lower stratigraphic levels and are absent or rare near the Ptarmigan thrust and associated thrust splays. Where the Ptarmigan thrust splays disappear north of Ptarmigan Creek more upright second phase folds are present. Hence second phase upright folds are more common in areas some distance from the Ptarmigan thrust and splays. The associated crenulation cleavage also reflects this change having shallower dips near the Ptarmigan thrust (but is also poorly developed) and steeper dips at higher stratigraphic levels. This means that the crenulation cleavage is asymptotic to Ptarmigan thrust and that second phase structures are also related to the major episode of thrusting. This supports the model of Sanderson (1982).

Locally a second crenulation cleavage is present. It strikes northeast and has a steep dip. Its origin is uncertain.

In the upper part of the Ptarmigan thrust sheet tight and chevron third phase folds occur on the limbs of some second phase folds. They have the same orientation and geometry as kinks in the crenulation cleavage. They represent a brittle type of deformation. The proximity of these structures to normal faults and their southwestward and downward vergence suggests that they were produced by these Tertiary(?) faults. A normal fault offsets and downdrops garnet isograd to the west. The normal faults trend northwestward and dip about 40 degrees southwest.

Blackman thrust sheet

The Blackman thrust sheet is a narrow panel of middle Miette grits that dips 30 to 40 degrees southwest. Interbedded grits and rare pelites form upright, slightly inclined, northeast verging, tight folds with amplitudes of 3 to 40 m. The schistosity in the pelites and the pervasive fractures in the grits are folded along with bedding and are not axial planar. The schistosity is axial planar to very rare, earlier, southwest verging, isoclinal small folds with up to 10 cm amplitudes. These microstructures are similar to ones that occur to the southwest in the Purcell thrust sheet. Metamorphism is at garnet-biotite grade throughout this thrust sheet.

Purcell thrust sheet

The Purcell thrust fault has been traced northwards from the Purcell Mountains along the west side of the Rocky Mountain Trench (Price and Mountjoy, 1970; Oke and Simony, 1981). Near Wood River it emerges on the east side of the Trench, and south of Hugh Allan Creek it brings "basement" gneisses to the surface. Hence the eastern surface trace of the Purcell thrust is the fault that occurs east of the easternmost gneisses. Thus the Purcell thrust must connect with the unnamed thrust fault that Leonard (1984) mapped east of the Mount Blackman Gneiss. This thrust appears to be offset to the east along Hugh Allan Creek by a normal fault that downdrops the south side (Fig. 58.1, see below) and may also have some transcurrent movement. The structure and metamorphism of this thrust sheet was outlined by Leonard (1984). These rocks have been affected by at least two phases of deformation. Second phase, northeast verging folds, overprint first phase southwest verging structures. The structure is dominated by the second phase large, northeast verging overturned gneiss-cored anticline (Fig. 58.1). Rocks close to the basement cover contact are more highly sheared by an earlier southwest directed shear of the cover rocks. Second phase folding and crenulation cleavage are more common near the hinge of the anticline. Upper amphibolite facies metamorphism in these rocks has been outlined and discussed in detail by Leonard (1984).

Hugh Allan Fault

As pointed out previously the stratigraphic sequence beneath the Gog south of Hugh Allan Creek corresponds very closely to that of the upper and middle Miette of the Main Ranges east of the Chatter Creek thrust (see Teitz and Mountjoy, 1985). Therefore the Windermere of this region is correlated with the upper and middle Miette of the Jasper Main Ranges rather than the Horsethief Creek Group of the Selkirks and Purcell mountains as suggested by Simony et al. (1980). A major normal fault is inferred to occur along much of Hugh Allan Creek and bifurcates in the upper part of Hugh Allan Creek. This fault appears to truncate both the Blackman and Ptarmigan thrusts (Fig. 58.1) and merges with the Chatter Creek thrust. This interpretation is based on the following observations:

1. If these stratigraphic assignments are correct, Lower Miette Group (Horsethief Creek(?) equivalent) on the north side of the Hugh Allan Creek is juxtaposed by the fault opposite Lower Cambrian quartzose sandstones and upper Miette pelites on the south side of the creek. Thus the Hugh Allan Fault has a normal fault displacement of more than 5000 m, down thrown on the east side.

2. On the west side of the fault the Purcell thrust and associated overturned gneiss cored anticline is shifted some 4 to 6 km to the east (Fig. 58.1) relative to the south side. The Blackman thrust does not appear to continue to the southeast.
3. It is difficult to match Miette stratigraphy across the head of Hugh Allan Creek.
4. The Ptarmigan thrust is truncated by the west branch of this normal fault.
5. The axes of the Porcupine Creek anticline and syncline do not continue northwest across Hugh Allan Creek.
6. The northern Rocky Mountain Trench transcurrent fault splays southeastwards and apparently dies out in the northern Cariboo Mountains (Price et al., 1981, Fig. 14). Some east-west extension along with some transcurrent movement can be reasonably expected in the Selwyn Range.

Obviously additional mapping needs to be done south of Hugh Allan Creek to obtain more information on the Miette Group to determine: 1) if the Horsethief Creek(?) equivalents extend southeastward beneath the Gog, 2) whether the Blackman thrust continues southeastward, and 3) the nature of the Porcupine Creek anticlinorium.

Acknowledgments

Forest and Leonard are supported by National Science and Engineering Research Council postgraduate scholarships. In addition to EMR research support, financial support for field work and laboratory analyses came from Mountjoy and Hynes' NSERC grants A2128 and A7983. The authors are grateful to A. Hynes for counsel and helpful discussions.

References

Campbell, R.B.
1968: Canoe River, British Columbia; Geological Survey of Canada, Map 15-1967.

Carey, A. and Simony, P.S.
1984: Structure and stratigraphy of the late Proterozoic, Miette Group, Cushing Creek area, Rocky Mountains, British Columbia; in Current Research, Part A, Geological Survey of Canada, Paper 84-1A, p. 425-428.

Chamberlain, V.E., Lambert, R., St. J., Baadsgaard, H., and Gale, N.H.
1979: Geochronology of the Malton Gneiss complex of British Columbia; in Current Research, Part B, Geological Survey of Canada, Paper 79-1B, p. 45-50.

Craw, D.
1977: Metamorphism, structure and stratigraphy of the Southern Park Ranges (Western Rocky Mountains) British Columbia; unpublished M.Sc. thesis, University of Calgary, Calgary.

1978: Metamorphism, structure and stratigraphy in the Southern Park Ranges, British Columbia; Canadian Journal of Earth Sciences, v. 15, p. 86-98.

Leonard, R.
1984: Metamorphism, structure and stratigraphy around the Mount Blackman Gneiss, British Columbia; in Current Research, Part A, Geological Survey of Canada, Paper 84-1A, p. 121-124.

McDonough, M.R. and Simony, P.S.
1984: Basement gneisses and Hadrynian Metasediments near Bulldog Creek, Selwyn Range, British Columbia; in Current Research, Part A, Geological Survey of Canada, Paper 84-1A, p. 99-102.

Mountjoy, E.W.
1976: Edson to Valemount – The Rocky Mountain Front and Main Ranges along highway 16 in the Jasper area; in Geological Association of Canada Edmonton meetings Field Trip C-11 Guidebook, p. 4-42.

1980: Mount Robson map and cross-section 1:250,000 scale; Geological Survey of Canada, Map 1499A.

Mountjoy, E.W. and Price, R.A.
1984a: Jasper (83 D/16) geological map and cross-sections, 1:50 000 scale; Geological Survey of Canada, Open File 1038.

1984b: Amethyst Lakes 83 D/9 geological map and cross-sections 1:50 000 scale; Geological Survey of Canada, Open File 1075.

Oke, C. and Simony, P.S.
1981: Basement gneisses of the Western Rocky Mountains, Hugh Allan Creek area, British Columbia; in Current Research, Part A, Geological Survey of Canada, Paper 81-1A, p. 181-184.

Pell, J. and Simony, P.S.
1982: Hadrynian Horsethief Creek Group/Kaza Group correlations in southern Cariboo Mountains, British Columbia; in Current Research, Part A, Geological Survey of Canada, Paper 82-1A, p. 305-308.

1984: Stratigraphy of the Hadrynian Kaza Group between the Azure and North Thompson Rivers, Cariboo Mountains, British Columbia; in Current Research, Part A, Geological Survey of Canada, Paper 84-1A, p. 95-98.

Price, R.A. and Mountjoy, E.W.
1970: Geologic structure of the Canadian Rocky Mountains between Bow and Athabasca Rivers, a progress report; Geological Association of Canada, Special Paper 6, p. 7-26.

Price, R.A., Monger, J.W.H., and Muller, J.E.
1981: Cordilleran Cross-section – Calgary to Victoria; in Field Guides to Geology and Mineral Deposits, Calgary, ed. Cook and Thompson; Geological Association of Canada and Mineralogical Association of Canada, p. 261-334.

Sanderson, D.J.
1982: Models of strain variation in Nappes and Thrust Sheets: a review; Tectonophysics, v. 88, p. 201-233.

Simony, P.S., Ghent, E.D., Craw, D., Mitchell, W., and Robbins, D.B.
1980: Structural and metamorphic evolution of Northeast flank of Shuswap complex, southern Canoe River area, British Columbia; Geological Society of America, Memoir 153, p. 445-461.

Teitz, M. and Mountjoy, E.
1985: The Yellowhead and Astoria carbonate platforms in the Late Proterozoic Upper Miette Group, Jasper, Alberta; in Current Research, Part A, Geological Survey of Canada, Paper 85-1A, Report 44.

ACQUISITION AND PROCESSING OF HIGH RESOLUTION REFLECTION SEISMIC DATA FROM PERMAFROST AFFECTED AREAS OF THE CANADIAN PART OF THE BEAUFORT SEA

Project 700092

D.F. Poley[1] and D.C. Lawton[1]
Atlantic Geoscience Centre

Poley, D.F. and Lawton, D.C., Acquisition and processing of high resolution reflection seismic data from permafrost affected areas of the Canadian part of the Beaufort Sea; in Current Research, Part A, Geological Survey of Canada, Paper 85-1A, p. 491-498, 1985.

Abstract

Interpretation of the shallow stratigraphy and permafrost distribution in the Beaufort Sea continental shelf sediments is based mainly on high resolution reflection seismic data. An assessment of the acquisition and processing techniques applied to this type of data has been undertaken. Source signature tests and studies of an existing data set, as well as development and implementation of a raytracing – amplitude analysis program have been undertaken. Current acquisition and processing techniques, particularly the use of long arrays and standard common-depth-point stacking techniques, are inappropriate for areas with severe shallow velocity anisotropy.

Résumé

L'interprétation de la stratigraphie à faible profondeur et de la distribution du pergélisol dans les sédiments de la plate-forme continentale de la mer de Beaufort est essentiellement fondée sur les données de sismique-réflexion à haute résolution. On a entrepris d'évaluer les techniques d'acquisition et de traitement appliquées à ce type de données. On a aussi entrepris des expériences relatives à la signature des sources et à l'étude d'un ensemble de données existantes, ainsi que la mise au point et l'application d'un programme d'analyse de l'amplitude et de la direction de propagation des ondes sismiques. Les techniques actuelles d'acquisition et de traitement des données, en particulier l'utilisation de longs alignements d'appareils et de techniques standard CDP, ne conviennent pas aux secteurs caractérisés par une forte anisotropie des vitesses de propagation des ondes sismiques à faible profondeur.

[1] Department of Geology and Geophysics, University of Calgary, Calgary, Alberta T2N 1N4

Introduction

High resolution reflection seismic surveys and shallow boreholes have provided most information about the shallow (0-600 m) stratigraphy of the Beaufort Sea continental shelf. However, the seismic data are of variable quality, mainly due to severe seismic velocity variations caused by discontinuous sub-sea permafrost. The objective of this research is to improve knowledge about the shallow stratigraphy of the area by re-evaluating seismic data acquisition, processing and interpretation techniques. In particular, the nature and distribution of sub-sea acoustically defined permafrost (APF) as delineated by O'Connor (1980, 1981), is very important because of its effect on engineering development and its implications on the recent geological history of the shelf. Hydrocarbon production facilities such as pipelines, artificial islands, conductor pipes and present exploration drilling are all affected by the distribution and behavior of shallow permafrost.

Permafrost distribution

At best, limited shallow well log and borehole data provide only a one dimensional picture of the permafrost occurrence with depth and lateral distribution can only be investigated using high resolution seismic techniques. The spatial extent and degree of ice bonding of shelf sediments is highly variable, and consequently, bulk physical properties such as density, resistivity and acoustic velocity show wide variations. For example, the velocity of sound in sediments in which permafrost has been delineated acoustically is generally much higher (2000-4000 m/s) than that of the non-frozen sediments (1500-2500 m/s).

The nature of ice bonding depends on lithology, porosity, grainsize, pore water salinity, stratigraphy and the thermal history of the sediments. Shallow sediments of the Beaufort Sea comprise mainly unconsolidated sands, gravels, muds and clays which were deposited in complex deltaic/shelf environments (O'Connor, 1981). Consequently the degree and extent of ice bonding varies both laterally and vertically with contacts which may be abrupt or gradational. Ice bonding is generally considered to extend to a maximum depth of about 600 m. Shallow permafrost can occur in spatially continuous or discontinuous layers, in lenses, or in a cyclic pattern with depth. This irregular interlayered distribution of permafrost causes acoustic masking and also results in inaccurate velocity/depth calculations. Consequently, the estimation of pre-drill depths to markers, or delineation of shallow drilling hazards such as gas, faults and hydrates may not be reliable. As well, the stratigraphy in the affected zone is generally not discernible.

The seismic problem

Broad bandwidth seismic sources (100-10 000 Hz) with high central frequencies, and analogue single channel recorders trade off acoustic penetration for superior resolution and are therefore inadequate for the determination of acoustically defined permafrost distribution at greater depth. To investigate the stratigraphy below the shallow acoustically defined permafrost, we rely on multichannel data recorded using more energetic but lower central frequency sources (10-200 Hz). This research program is directed primarily at assessing the quality of existing multichannel reflection seismic data, determining the problems with the current acquisition and processing techniques and proposing feasible methods of improving the data such that more confident interpretations can be made in the range 0 to 600 m. Studies have included some research into and experimentation with source array design.

Observations from current investigation

Six multichannel seismic lines acquired over two acoustically defined permafrost affected areas and using three different acquisition systems have so far been reprocessed. The three acquisition systems differ in source, cable length, near offset, group interval and number of hydrophones per group. Notable features on the 24-fold sections are reverberations, signal attenuation, and static shifts below shallow, high-amplitude reflectors (Fig. 59.1). Probably the most profound observation has been that reflectors in the zone of interest can seldom be correlated at the tie points of intersecting sections. Also, sections created from using the 12 traces nearest to the shot point (57 to 332 m offset) showed little comparison to those

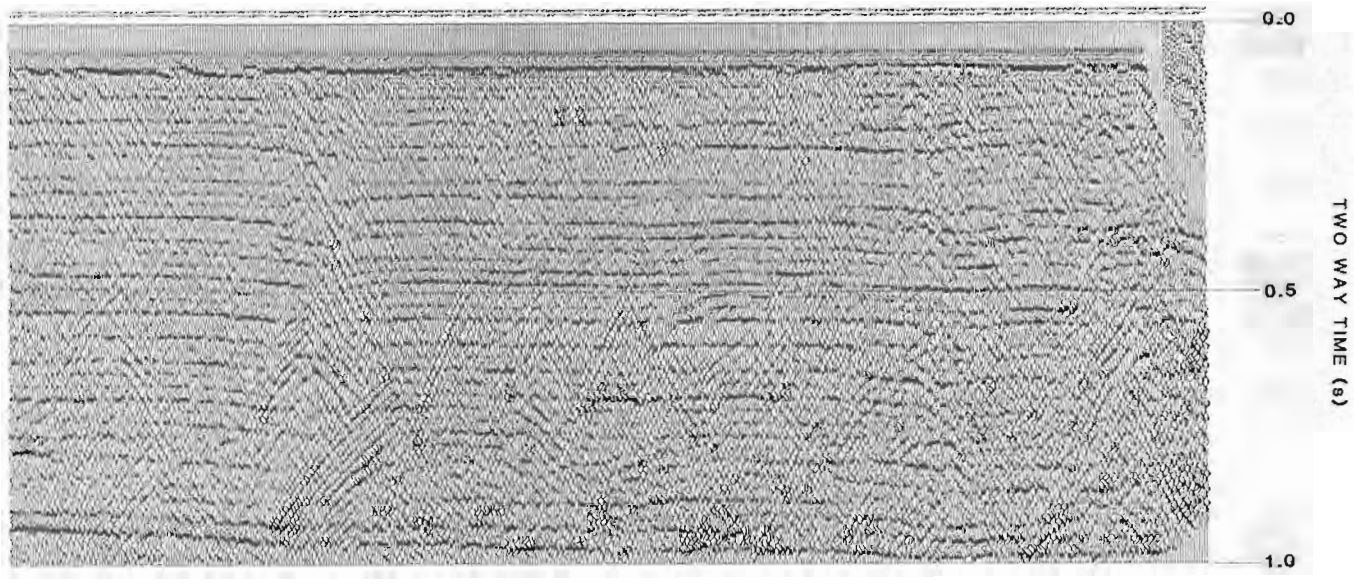

Figure 59.1. *A 24-fold brute stack showing acoustic linear noise, diffractions and severe static shifts caused by shallow acoustically defined permafrost.*

created from using the far 12 traces, (357 to 632 m offset) of common 24 trace records (Fig. 59.2). It was found that an understanding of the causes of these problems could best be achieved by studying the shot and common-depth-point (CDP) records. Figure 59.3 shows a shot record with refraction reverberation and a diffraction hyperbola (arrowed). Multiple reflection events and terminating reflectors are evident on the shot record shown in Figure 59.4. Generally, large amplitude and phase differences were noted along many reflection hyperbola. Furthermore, the curvature (move-out) of reflections on shot records is distorted by the complex velocity structure and conventional processing techniques are obviously inadequate. Stacking these data with poorly determined dynamic and static corrections often results in serious degradation of reflection amplitude and the high frequency content of the stacked trace.

Diffractions observed on the shot records (Fig. 59.3), were found to cause the severe linear noise (Fig. 59.1) on the stacked sections. The apex of the diffractions were often seen to lie other than at the near offset trace indicating that the diffractors occur off the line of the survey. In addition, the periodicity of multiple events indicates that both 'water surface-water bottom' and 'water bottom-top of acoustically defined permafrost', reverberations are prevalant in these data. Both overall signal attenuation and degradation of the high frequency component of the reflection spectrum cause major problems in delineating the stratigraphy and acoustically define permafrost distribution below the shallow permafrost. Much of the attenuation observed can be accounted for simply by transmission losses since a large percentage of the acoustic energy is reflected off the top of the shallowest permafrost.

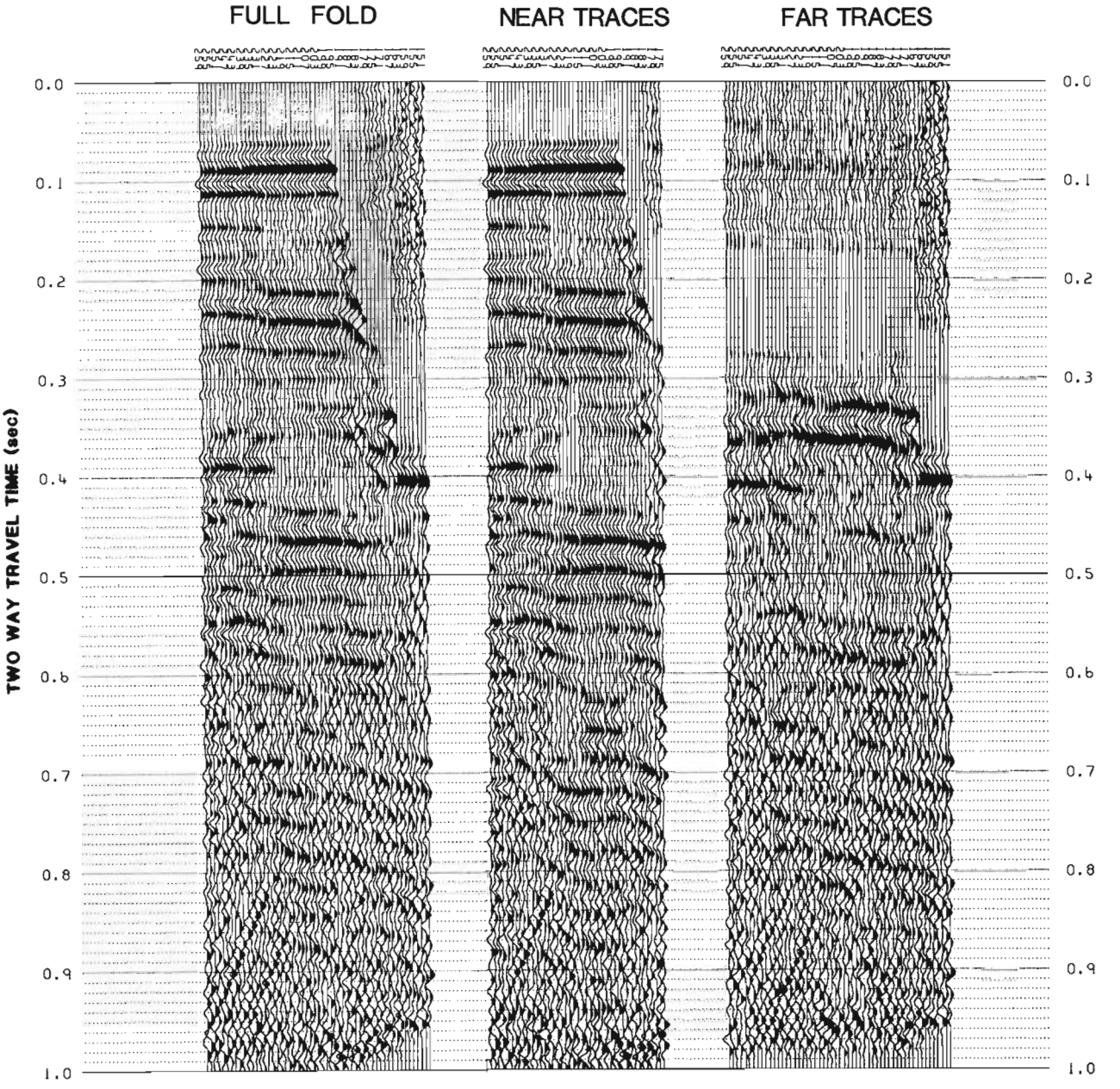

Figure 59.2. *Comparison of full 24-fold section with near and far offset 12-fold stacks.*

Modelling studies

A program was developed (called OFFSET), to investigate the problems outlined. The program can be used for numerical modelling and evaluating the angular dependence of the reflection and transmission coefficients at the acoustic boundaries. Three types of observed acoustically defined distributions have been examined in modelling studies: a continuous permafrost layer, laterally terminating permafrost lenses, and thin permafrost layers (about 10 m), cyclicly layered with non-frozen sediments.

Static shifts occurring in shot records can often be explained by the fact that rays for different source-receiver offsets travel along paths with distinctly different velocities. This is true, particularly where the lateral distribution of the acoustically defined permafrost is variable. Even in the case of laterally continuous layers of permafrost (Fig. 59.6), reflections can no longer be approximated as hyberbolic on shot records. The timing of arrivals from the base of the permafrost layer can be seen in Figure 59.5 with those calculated using the stacking velocity and Dix's expanding spread approximation. The true and calculated arrival times differ by as much as 30 ms at 650 m offset. Application of the standard normal-move-out (NMO) corrections in this case would 'over-correct' the true arrivals such that the reflector energy would be smeared over at least 15 ms on the stacked trace. The common-depth-point stacking technique is only successful in this environment if the range of angles of incidence is small and near vertical (<5°). For the models studied, the angles of incidence on the basal interface of the permafrost range from about 10 to 60 degrees. These timing and amplitude effects are then accentuated if the length of the receiver array or aperature window is in the order of the depths of interest. Figures 59.7 and 59.8 illustrate Knott energy coefficients as a function of angle of incidence for a single interface. They demonstrate the large range in reflection coefficients and mode conversion which is likely to occur at the boundaries of acoustically defined permafrost. Critical angles as low as 25 degrees can occur at the top of the permafrost, resulting in severe limitations to the offset distance at which deeper reflectors can be successfully imaged. Changes of phase with incidence angle are also significant and can result in cancellation of reflection energy along a normal-move-out – corrected event when a common-depth-point record is stacked. Where lenses are laterally discontinuous, upgoing energy may be critically refracted along the base. Another consequence of the large velocity contrasts is that refraction (bending) of rays at the interfaces is extreme. Consequently, a longer ray path to a given depth through permafrost affected sediments is realized than the equivalent raypath in non-frozen sediments. A higher degree of spherical spreading losses and inelastic absorption occurs in layered frozen and unfrozen sediments. Consideration of the raypaths in a cyclic frozen and non-frozen layered sequence also reveals another form of frequency attenuation. First order multiples within the layers can constructively add to the down going energy with small time lags having the effect of broadening the source pulse (Waters, 1981). Where high velocity layers are thin and exhibit gradational lower contacts, further pulse broadening and subsequent high frequency attenuation can occur.

Source tests

As stated previously, the depths to tops of acoustically defined permafrost have been interpreted mainly from analogue single-channel data acquired using sources such as the airgun and boomer. The Geological Survey has generally employed a single airgun (usually 5 cu. in.), for acquisition of this type of data. Source 'ringing', offline source-generated noise and poor penetration are the major problems with

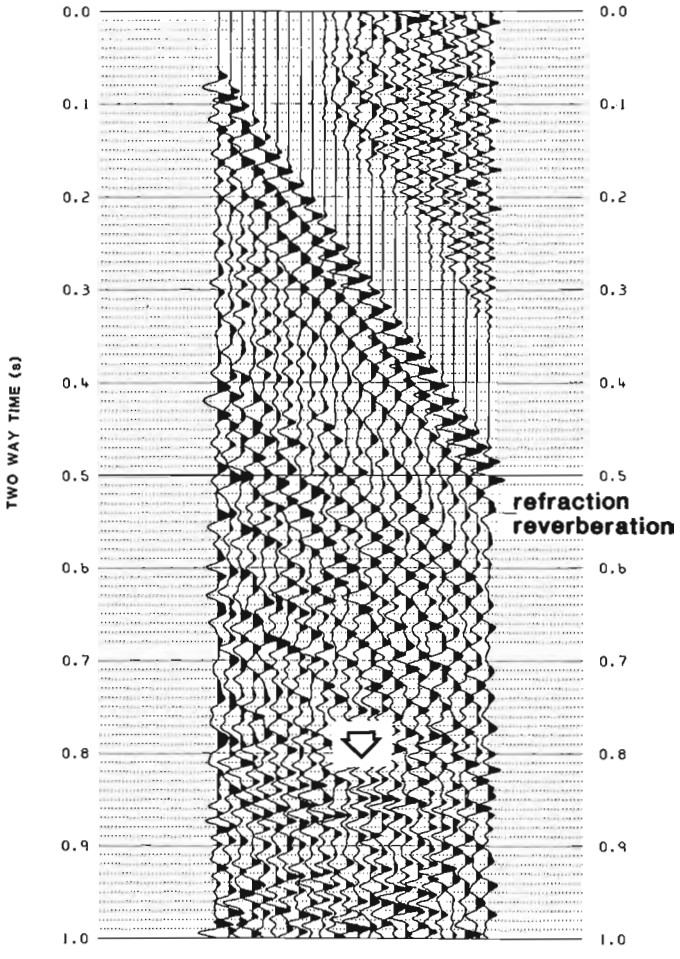

Figure 59.3. *Shot record demonstrating refraction reverberation and event from an offline diffractor.*

these data. A need to improve the power and bandwidth of the source signature is recognized and source directivity is required to suppress offline diffractions.

A study of airgun arrays was undertaken, followed by field testing of various combinations of two airguns with 5 and/or 10 cu in chambers. An increase in source strength is better achieved by grouping several small airguns than by increasing the volume of individual guns (Johnston, 1982). Figure 59.8 is a typical single airgun signature. An optimum signature is one with a high amplitude, narrow primary pulse and little energy in the secondary bubble oscillations, i.e. it is desirable to optimize the primary pulse to bubble pulse ratio (BPR). To achieve this, sources are often grouped in arrays. The primary to bubble period (T_b in Fig. 59.9), is directly related to an airgun's chamber size. Airguns of increasing chamber size and thus bubble period are often strung juxtaposed in a manner such that the bubbles generated do not coalesce. When the guns are fired simultaneously, the primary peaks add in phase whereas the secondary bubble oscillations tend to be slightly out of phase between adjacent airguns, causing a cancelling effect and minumum reverberations in the signature tail. A second approach is to coalesce small airguns to make the equivalent volume of a larger gun. Improvement in the primary to bubble ratio from that of the

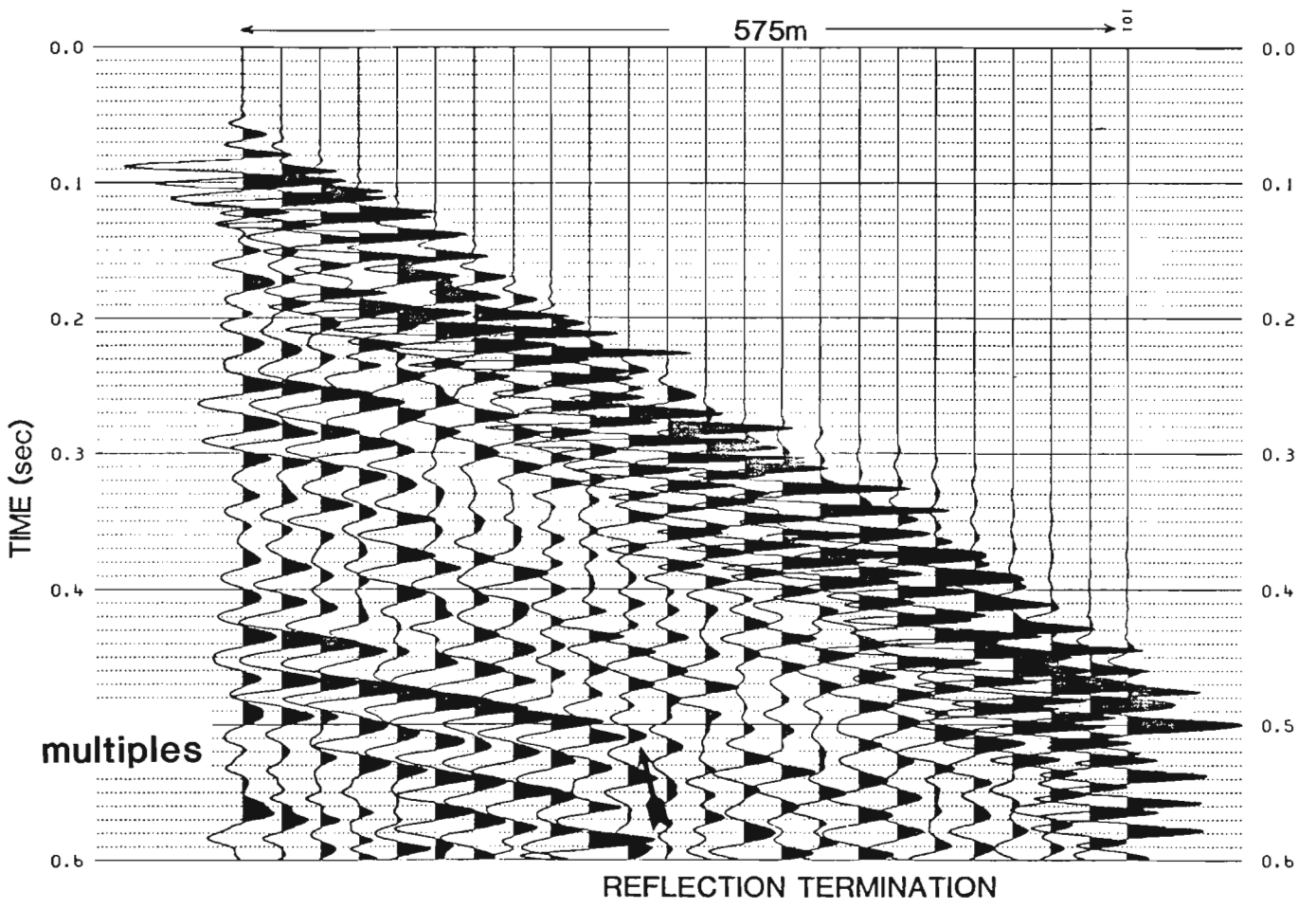

Figure 59.4. *Shot record demonstrating multiple reflection events and terminating reflectors.*

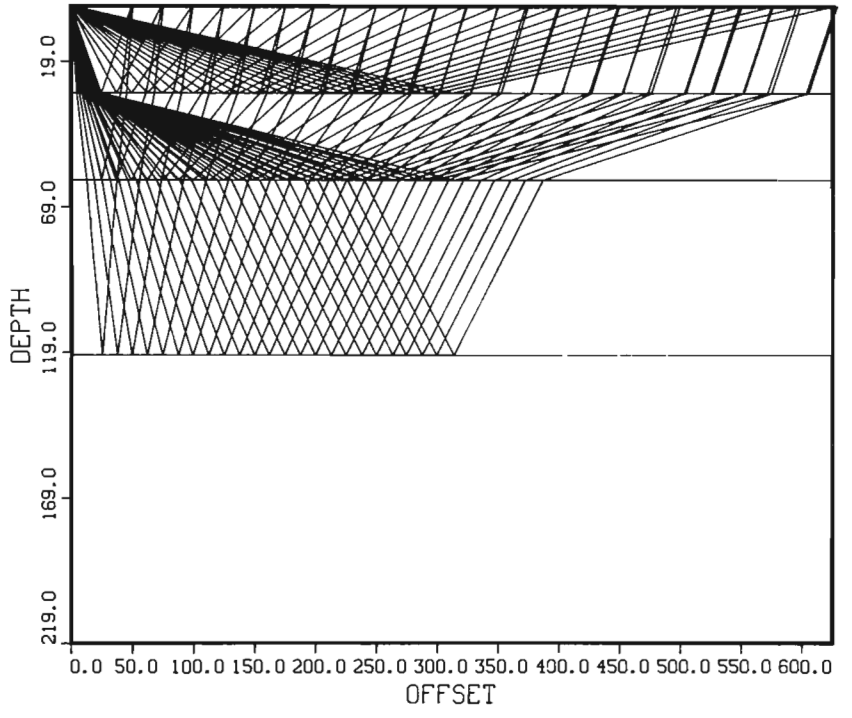

LAYER PARAMETERS

LYR	VP	VS	RHO	H
1	2000.	1400.	1.5	30.0
2	3200.	2300.	1.5	30.0
3	2500.	1800.	1.5	60.0
4	2800.	2000.	1.5	99.0

Figure 59.5

Raypaths through a continuous layer of acoustically defined permafrost. VP = P wave velocity, VS = S wave velocity, and RHO = density.

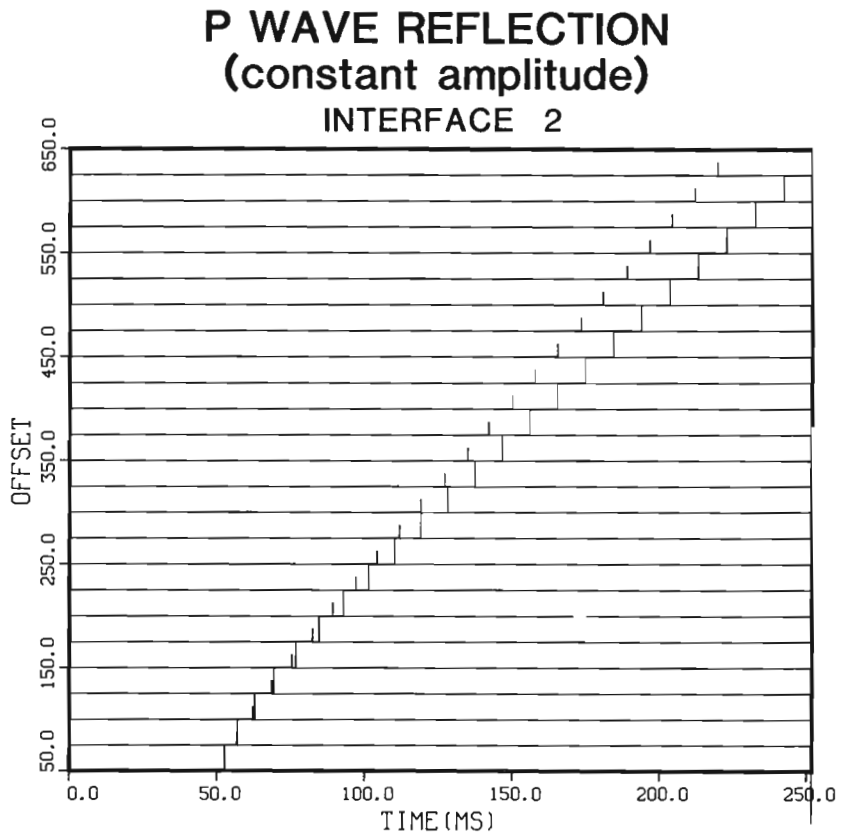

LAYER PARAMETERS

LYR	VP	VS	RHO	H
1	2000.	1400.	1.5	30.0
2	3200.	2300.	1.5	30.0
3	2500.	1800.	1.5	60.0

– actual arrival time

— calculated arrival time (rms)

Figure 59.6

Comparison of correct arrival times with those calculated from the rms velocity for the base of the acoustically defined permafrost layer in Figure 59.5.

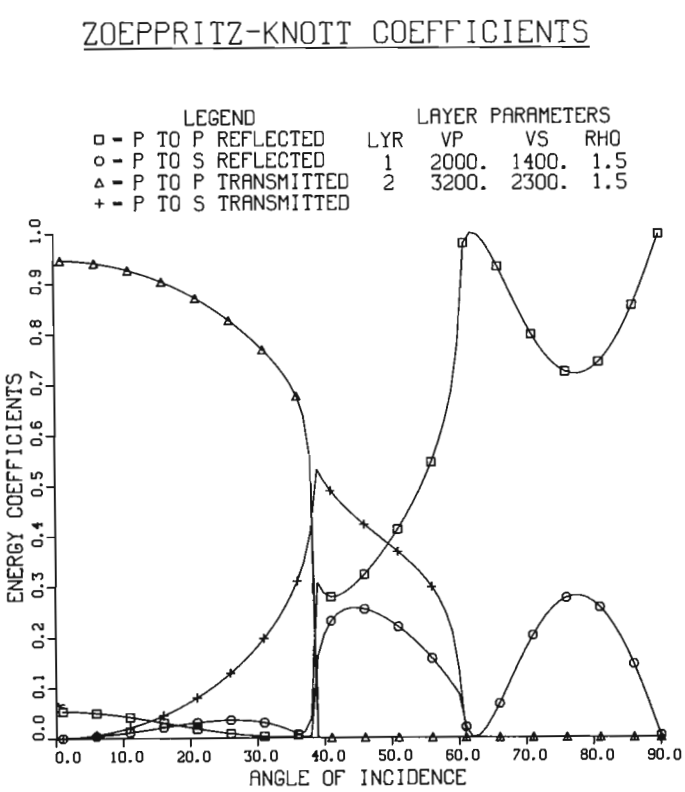

Figure 59.7. *Knott energy coefficients as a function of angle of incidence for the top of an acoustically defined permafrost layer.*

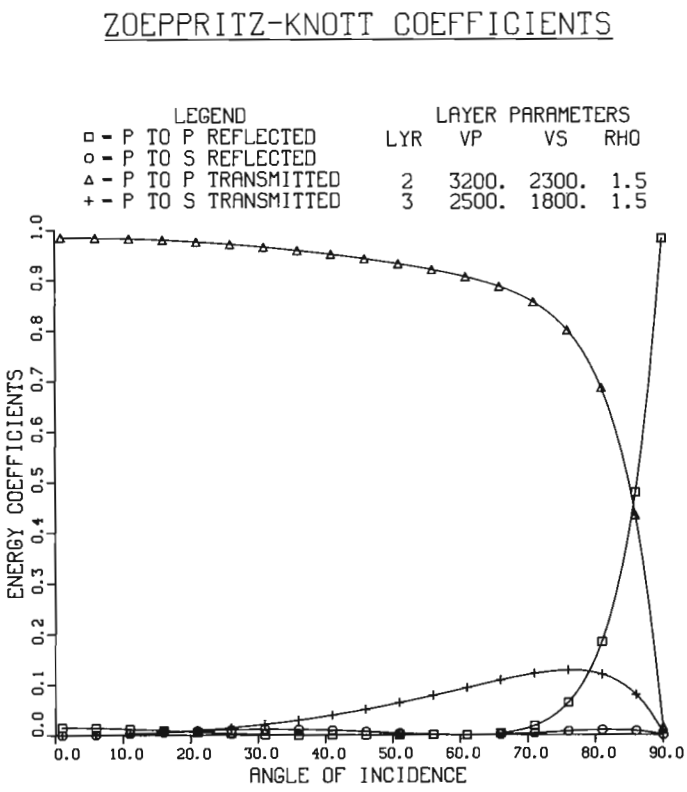

Figure 59.8. *Knott energy coefficients as a function of angle of incidence for the base of the acoustically defined permafrost layer.*

equivalent large gun results. Johnston (1982) concluded that better primary to bubble pulse ratio enhancement could be achieved by using a group of interacting guns of different volumes than by coalescing the same number of guns of the same volume. It was not known if this is true for as few as two airguns.

Acoustic signatures in the near and far field were recorded for various combinations of two airgun array geometries. Chamber volume, gun spacing, and water depths were varied. Single and two gun shots were fired for each configuration. Spectral analysis of all signatures recorded were run to determine the frequency content. Table 59.1 lists the test geometries and parameters measured. Several observations can be made from the measured signatures:

1. Firing of the airguns 1 m below the surface provided the best primary to bubble pulse ratio and the broadest frequency bandwidth because the bubble broke at the surface, though a strong reduction in power output was a consequence.
2. Most signatures were recorded at a depth of 1/4 wavelength of the dominant frequency to provide constructive interference between the downgoing and surface reflected (ghost) pulse at this frequency. Of these, two 10 cu. in. airguns coalesced and fired at 14 m produced the highest primary to bubble pulse ratio.
3. Poor synchronization of two airguns of different volumes, with 1.2 m separation, resulted in broadening of the pulse, narrowing of the bandwidth and decrease in primary to bubble pulse ratio.
4. Leaking guns produced a lower power output but, surprisingly, an increase in primary to bubble pulse ratio and bandwidth.
5. Repeatability of signatures was excellent, at ±4 ms in bubble period and ±5 mV in amplitude.
6. From comparison of near and far field signatures it is concluded that use of the nearfield signature for design of a signature deconvolution operator would probably result in significant improvement of the source wavelet during data acquisition.
7. Comparison of the manufacturers (Bolt Associated Inc.) signatures was fair. Values of T_b were within 1% and primary to bubble pulse ratio within 10%.
8. The difference between the sum of individual signatures of two guns, from that recorded for the same two guns (at 1.2 m separation), fired simultaneously, should be a measure of the degree of acoustic energy interaction when the bubbles do not physically coalesce. Signatures from a single 10 cu. in. airgun and a single 5 cu. in. gun fired independently at 12 m water depth (FF13(990) and FF14(1000) in Table 59.1) were summed and compared with the signature recorded for the same two airguns fired simultaneously (FF2C(930)). Primary to bubble pulse ratio, T_b, and P_a agree to within 5%.

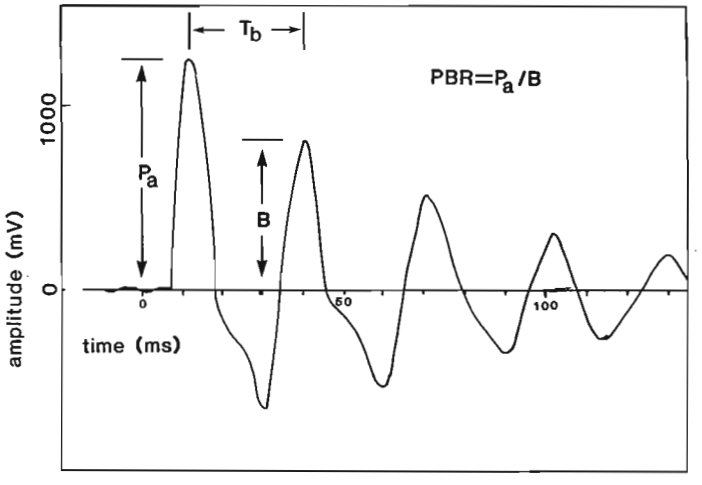

Figure 59.9. *A conceptual 'typical' airgun signature. Pa = primary acoustic amplitude, B = 1st bubble oscillation amplitude and PBR = primary to bubble pulse ratio.*

Discussion

1. Current multi-channel high resolution data acquisition and processing techniques are indequate in areas with shallow sediments which exhibit strong velocity anisotropy. In particular, the use of long arrays in acquisition and standard common-depth point stacking techniques in processing degrade reflection integrity.
2. Shorter arrays (<300 m) would provide less amplitude and phase distortion across the receiver array length. As well, error in the expanding spread approximation (during normal-move-out correction) would be reduced.

Table 59.1. Airgun signature measurements

Geometry	Depth (m)	Shot	P(V)	PBR	T_b(ms)
Single 5	11.7	FF8(1160)	.93	1.16	17.4
		FF8B(1170)	.90	1.06	16.8
		FF8C(1180)	.90	1.13	16.8
	12.0	FF14(1000)	1.00	1.33	16.8
	9.4	FF7(1070)	1.10	1.38	19.6
		FF7B(1080)	1.05	1.20	19.1
	1.0	FF1A((850)	.25	4.43	26.7
		FF1B(860)	.25	4.41	25.8
Single 10	14.0	FF12A(1510)	.58	1.64	18.5
		FF12B(1540)	.60	1.85	18.5
		FF12C(1500)	.63	1.79	17.9
		FF12D(1550)	.60	1.71	18.5
	12.0	FF13(990)	1.08	1.08	19.1
		FF13B(980)	1.10	1.10	19.1
	9.4	FF6(1050)	1.15	1.21	23.5
		FF6B(1060)	1.13	1.29	22.9
2 Coalesced 10's	14.0	FF11C(1440)	0.90	3.60	22.9
		FF11A(1450)	1.03	3.41	21.3
		FF11B(1470)	1.00	3.33	22.4
2 Coalesced 5's	13.0	FF10A(1320)	1.35	2.25	23.5
		FF10B(1330)	1.33	2.21	22.4
	11.7	FF9D(1300)	1.70	2.06	23.5
		FF9C(1280)	1.63	1.86	23.5
		FF9E(1290)	1.65	1.83	23.5
		FF9A(1270)	1.50	1.71	23.5
Interacting 5 and 10 out of synchronization	12.0	FF2F(900)	1.53	1.17	21.3
		FF2(910)	1.48	1.23	20.2
Interacting 5 and 10 synchronized	12.0	FF2C(930)	2.03	1.59	19.6
		FF2E(950)	2.03	1.82	19.6
	9.4	FF5(1030)	1.95	1.90	24.7
		FF5B(1040)	1.78	1.65	24.7
Bolt Signature for single 5	9.14	Bolt 5		1.36	19.0
Bolt Signature for single 10	9.14	Bolt 10		1.33	24.0

Single channel data are recorded at near zero offset but provide insufficient multiplicity for adequate signal to noise ratios or velocity discrimination. Better acquisition techniques which provide high multiplicity at shorter offsets, such as split spread or two towed receiver arrays, must be considered.

3. Single channel zero offset data must be recorded digitally with implementation of digital filtering (including signature deconvolution) during data acquisition.
4. Both digital multi-channel and analogue single-channel data would benefit from improvement in source signature and source directivity at the acquisition stage.
5. Field tests showed that a 5 cu. in. airgun fired at 1 m water depth provided the broadest bandwidth and highest primary to bubble pulse ratio of those measured though a severe power reduction from all other source configurations tested was noted. Two 10 cu. in. airguns coalesced and fired at 14 m produced higher power output, better power efficiency and a significant improvement in primary to bubble pulse ratio from that of a single gun.
6. A raytracing program, called OFFSET, has been developed using the Zoeppritz and Knott equations to study reflection amplitude and phase characteristics with offset. It is anticipated that this program will provide a powerfull means for evaluating current acquisition and processing techniques.

Continuing studies

1. Various acoustically defined permafrost models are being studied using the program OFFSET in collaboration with the physical modelling studies by Cheadle et al. (1985).
2. The program OFFSET will be further developed to include absorption and spreading losses (including fresnel zone), as well as array response. Also, an option to write the output to a formatted tape (SEGY) will be incorporated for testing processing algorithms on the department's Perkin Elmer 3240 seismic processing facility.
3. New processing algorithms are being developed for improved stacking and velocity analysis of multi-channel data.
4. Algorithms for the DMAPS system: a new digital marine seismic reflection system, are being developed to facilitate broad band data acquisition with real time processing capabilities (Bays et al., 1985).

Acknowledgments

The authors thank Dome Petroleum for providing the primary data set and the Panel on Energy Research and Development (PERD) Task 6: Conventional Energy Systems, for funding these studies. This work is co-ordinated through the Beaufort Sea Project under S.M. Blasco at the Atlantic Geoscience Centre.

References

Bays, A.R., Poley, D.F., and Blasco, S.M.
1985: DMAPS: A new experimental digital marine reflection seismic acquisition and processing system; in Current Research, Geological Survey of Canada, Paper 85-1A, report 64.

Cheadle, S.P., Bertram, M., and Lawton, D.C.
1985: Development of a physical seismic modelling system, University of Calgary; in Current Research, Part A, Geological Survey of Canada, Paper 85-1A, report 60.

Johnston, R.C.
1982: Development of more efficient air gun arrays: theory and experiment; Geophysical Prospecting v. 30, p. 752-773.

O'Connor, M.J. and Associates Ltd.
1980: Development of a proposed model to account for the surficial geology of the southern Beaufort Sea; Geological Survey of Canada, Open File 954.

1981: Distribution of shallow permafrost in the southern Beaufort Sea; Geological Survey of Canada, Open File 953.

Waters, K.H.
1981: Reflection Seismology: A Tool for Energy Resource Exploration. John Wiley & Sons Inc., Toronto, 453 p.

-60-

DEVELOPMENT OF A PHYSICAL SEISMIC MODELING SYSTEM, UNIVERSITY OF CALGARY

Project 700092

S.P. Cheadle, M.B. Bertram, and D.C. Lawton[1]
Atlantic Geoscience Centre, Dartmouth

Cheadle, S.P., Bertram, M.B., and Lawton, D.C., Development of a physical seismic modeling system, University of Calgary; in Current Research, Part A, Geological Survey of Canada, Paper 85-1A, p. 499-504, 1985.

Abstract

A seismic scale-modeling system is currently under development in the Department of Geology and Geophysics at the University of Calgary. The system incorporates physical models in a water filled tank, ultrasonic piezoelectric transducers and a high speed digital data recorder. Scaled geological models are submerged in the tank, and synthetic seismic studies are conducted. The system is being used to model the acoustic response of a variety of assumed permafrost structures and to test developments in the aquisition and processing of high resolution seismic reflection data from permafrost-affected areas of the Canadian part of Beaufort Sea.

Résumé

Actuellement, au Département de géologie et de géophysique de l'université de Calgary, est mis au point un système de modélisation sismique à échelle réduite. Ce système comporte des modèles réduits installés dans un réservoir rempli d'eau, des transducteurs piézoélectriques ultrasonores, et un enregistreur rapide de données numériques. Les modèles géologiques à échelle réduite sont submergés dans le réservoir, et font l'objet d'études sismiques synthétiques. On emploie ce système pour modéliser la réponse acoustique de diverses structures pergélisolées hypothétiques, pour mettre à l'épreuve les derniers développements relatifs à l'acquisition et au traitement des données de sismique-réflexion à haute résolution obtenues dans les zones pergélisolées du secteur canadien de la mer de Beaufort.

[1] Department of Geology and Geophysics, University of Calgary, Calgary, Alberta T2L 2A7

Introduction

In many areas of seismic research, determination of the acoustic response of a particular structure is of interest. A variety of numerical methods such as wave equation modeling and ray tracing provide one theoretical approach, but these are constrained to approximations of the full wave field to avoid excessive computational requirements. Physical scale modeling exploits the natural interaction of acoustic energy with the model. The contribution of physical seismic modeling is limited only by the care taken in the design of the experiment and in the constraints of scaling factors.

The physical modeling system in the Department of Geology and Geophysics, University of Calgary, will be used to study problems related to reflection seismic imaging in areas affected by subsea permafrost in the Beaufort Sea. The specific aims of the program are twofold. Firstly, it is to gain some basis understanding of the acoustic response of models which represent the assumed distribution of permafrost. Secondly, the tank system will be used to evaluate shallow high resolution seismic acquisition techniques for the improved detection and delineation of acoustically defined permafrost (APF). An outline of the problems related to APF and potential improvements in the acquisition of seismic data in affected areas is given by Poley and Lawton (1985).

The study involves testing the concepts of reflection seismic imaging and array designs intended to minimize the effects of severe lateral velocity variations. As an example, Poley (1984, personal communication) is currently exploring the optimization of marine air gun arrays for the purpose of improving seismic resolution in APF-affected areas. Such arrays can be simulated in the tank with either piezoelectric transducers or with 0.5 cu. in. air guns. The physical modeling system will also be used in conjunction with Sierra 3-D ray tracing software to compare the results of numerical techniques with data recorded over a model with a known velocity structure. In turn these results can be compared with seismic reflection sections recovered from the field.

The modeling tank

A schematic view of the tank is shown in Figure 60.1. The tank dimensions are approximately 4 m x 3 m x 2 m, and it is operated while filled with water. A water pump and filter cartridge have been installed and chlorine is added to

MODELING TANK SCHEMATIC

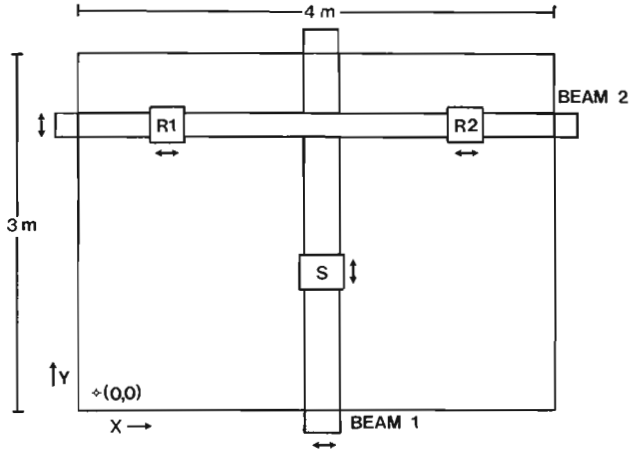

Source and Receiver Elements
ITC-1089C spherical piezoelectric transducers
frequency range 1Hz - 350KHz

Tank Control Motors
Sigma 4 volt D.C. 1.8° stepping motors
200 steps/revolution geared to 40 steps = 1cm.
positional accuracy better than ±1 step

Element	Direction	Motor
R1 Receiver #1	X	1
Beam 2	Y	2 & 3
Beam 1	X	4 & 5
S Source	Y	6
R2 Receiver #2	X	7

Figure 60.1. *Schematic outline of the arrangement of the beams and carriages which constitute the transducer positioning system. Software control of the system permits the simulation of a wide variety of survey spreads and arrays.*

PHYSICAL MODELING SYSTEM FLOWCHART

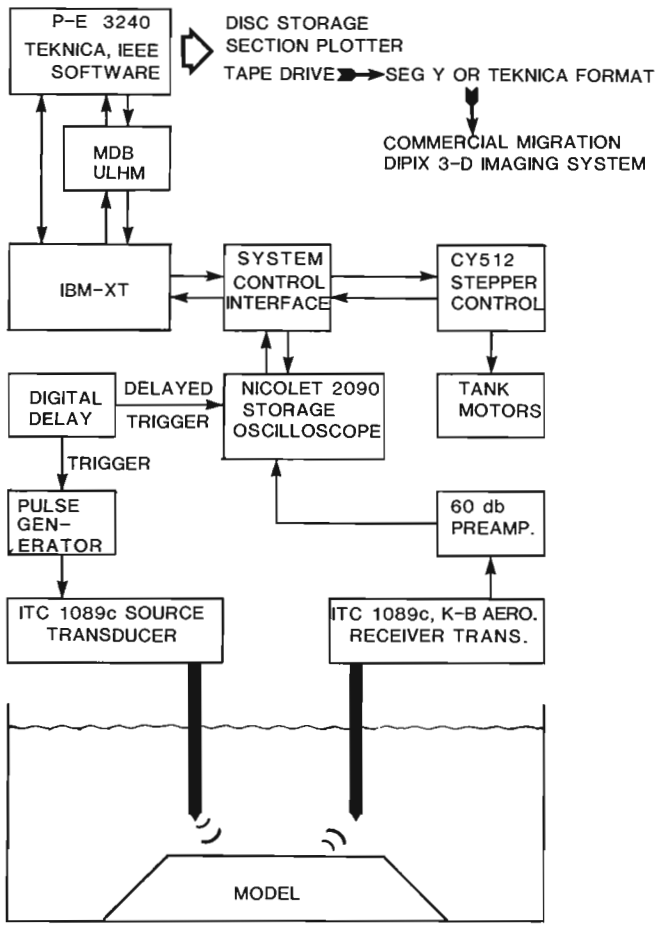

Figure 60.2. *Flowchart outlining the operational cycle of the physical modeling system.*

the water to prevent stagnation. Two mutually orthogonal beams move along aluminum tracks that surround the top of the tank. Rails along the length of the beams support the carriages that carry the transducers. The beam mounts, tracks and carriage rails are designed to be adjustable for levelling and squaring of the transport assembly. The carriages themselves and the rail supports are made of plexiglas. Figure 60.4 shows the beam and carriage system.

Positioning system

The beams and transducer carriages are moved by 4 volt D.C. Sigma stepping motors controlled from an IBM-XT computer interfaced to Cybernetics CY512 motor control microchips. The beams are driven by synchronized motor and gear wheel assemblies mounted at both ends of the beams. The carriages are controlled by nonstretching pulley cables operated by single motors fixed at one end of the beams. In all, seven motors control the transducer positioning system, which has a positional accuracy of 1 mm, based on repeated tests.

Computer programs have been written to generate coordinate data files for executing common seismic survey patterns such as split spreads, normal incidence and walkaways. Coordinate data are transmitted from the computer to the motor control boards which then move the beams and carriages relative to an initialized zero or home position. When the controllers have properly positioned the transducers, a handshake line returns a signal to the computer which then activates the data aquisition cycle.

Data acquisition

The present data acquisition system includes a variable pulse generator, a digital delay, a receiver preamplifier and a digital storage oscilloscope. A Nicolet 2090 storage oscilloscope is presently configured with a 20 MHz 8 bit sampling module and a 4k byte memory capacity. The pulse generator and the Nicolet are triggered from the digital delay. Upon receiving the start trigger, the pulse generator outputs up to three pulses of variable polarity, amplitude, pulse width and delay time. The first pulse to the source transducer generates the primary wavelet while the second and third pulses are adjusted to attenuate ringing or side lobe energy of the primary pulse. The resulting output from the source is a broad band wavelet with a frequency spectrum centred between 100 kHz and 400 kHz. The pulse generator is powered by an amplifier capable of ±50 volts output and tracking at up to 2 MHz. Plans include the implementation of a digital to analogue output from the computer to enable the generation of more complex signals.

The digital delay was installed because of the limited memory capacity of the storage oscilloscope. Initial tests with the system indicated that a 2 MHz sampling rate and a 2 millisecond record length provides the necessary resolution and time window for reflection events of interest. Sampling by the oscilloscope is initiated after receiving a trigger from the digital delay that lags behind the trigger to the pulse generator. Typically, a 60-100 microsecond delay between the pulse trigger and the start of digital sampling eliminates high amplitude direct arrivals and surface ghosts while better centring the sampling interval over the reflection interval. The digital delay has a 1 microsecond resolution from 0 to 9999 microseconds.

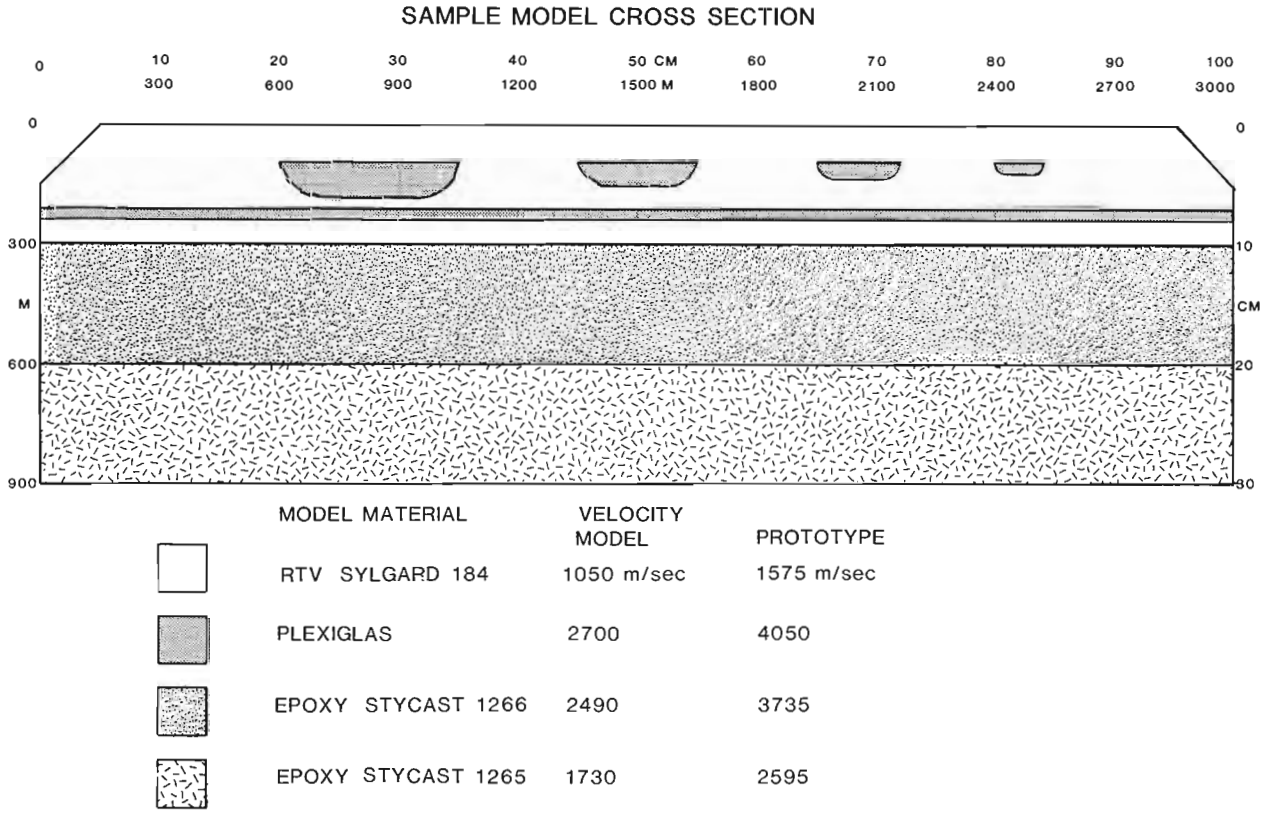

Figure 60.3. *Cross sectional view of a model incorporating three assumed distributions of APF. These include frozen channel like features shallow in the sequence underlain by a thin stratigraphically controlld horizon of permafrost and a more massive APF unit deeper in the section.*

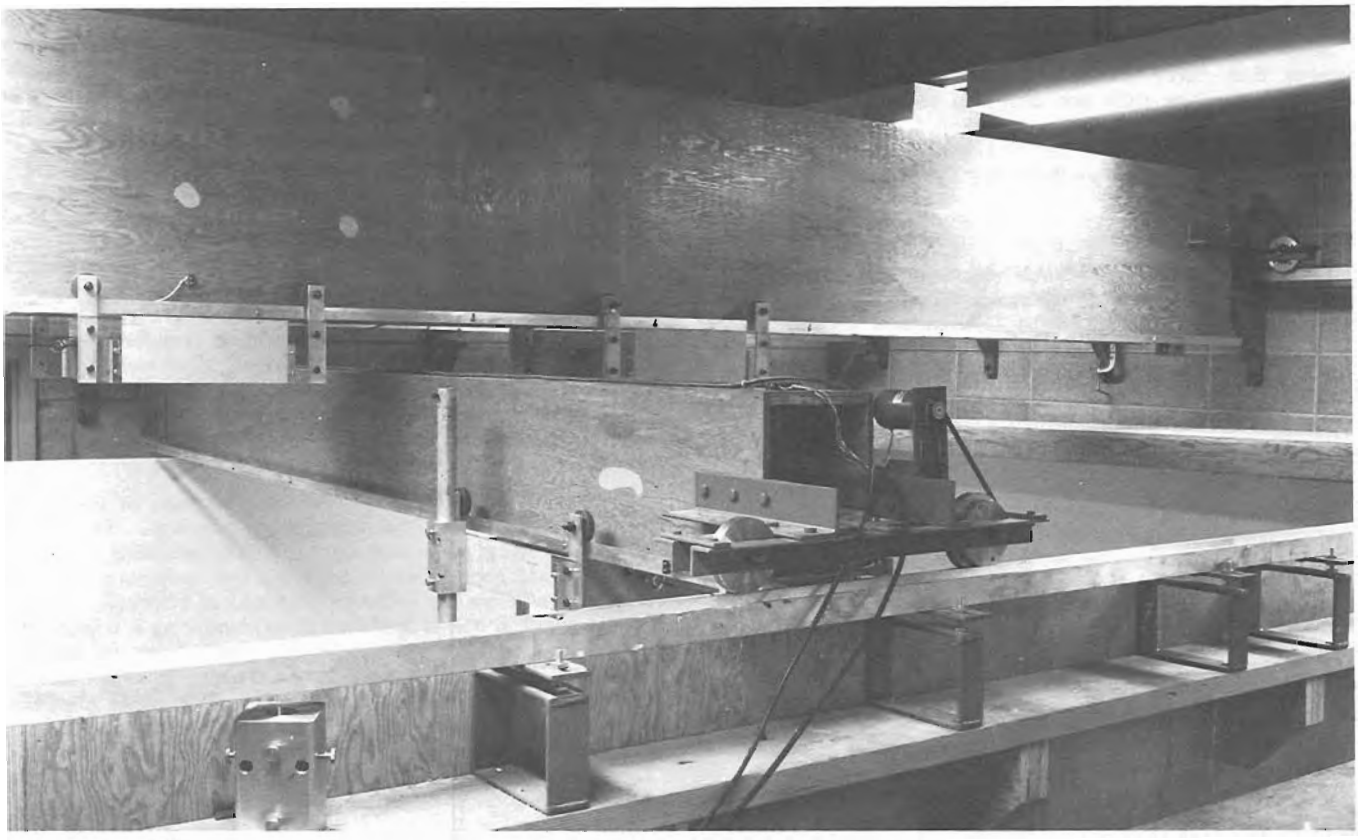

Figure 60.4. *A view of the tank system showing the beam, carriage and motor drive assemblies.*

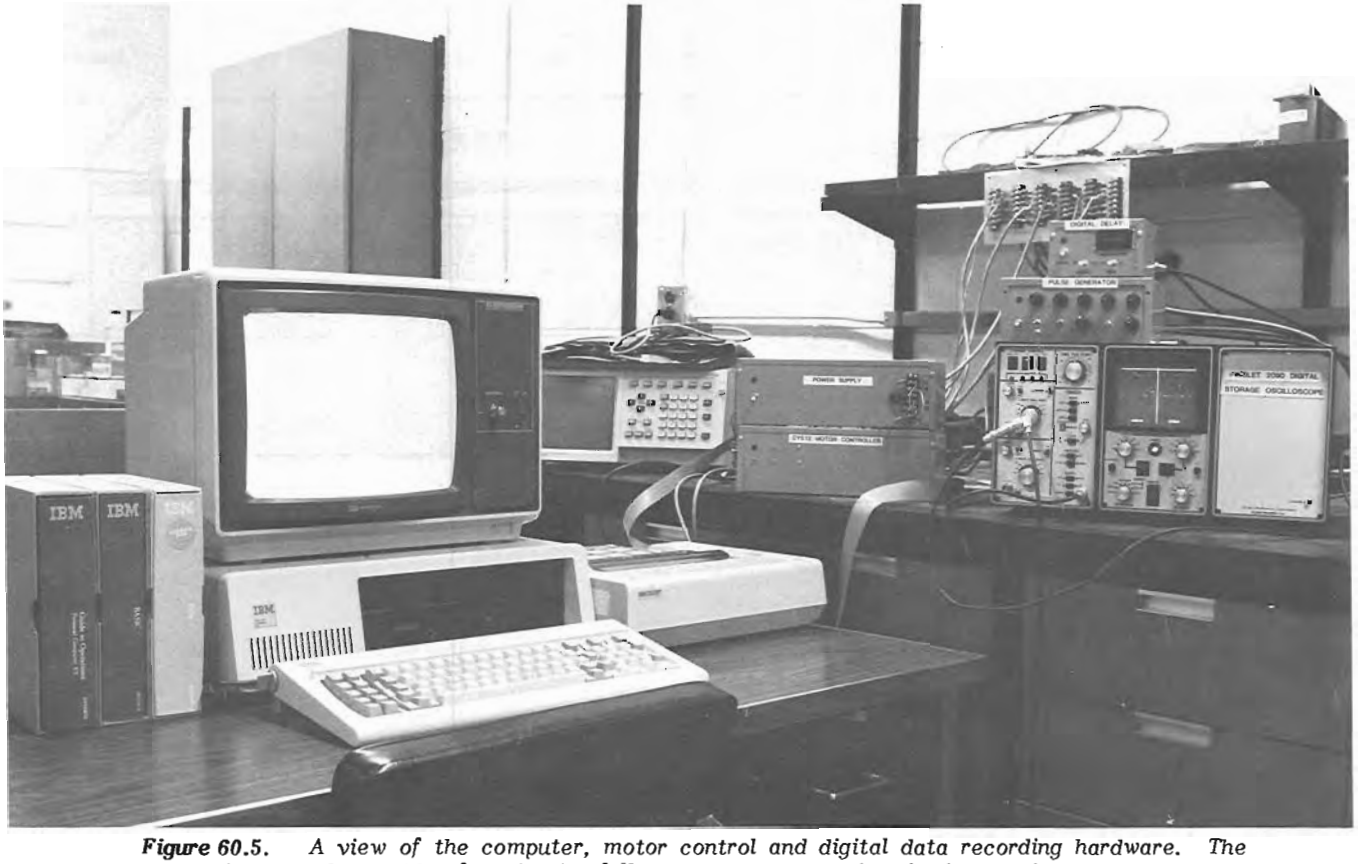

Figure 60.5. *A view of the computer, motor control and digital data recording hardware. The system is currently capable of conducting fully automated synthetic seismic experiments.*

The interface between the oscilloscope and the computer includes direct memory access (DMA), which allows a trace of 4096 samples to be transferred in 30 milliseconds. At present the data are stored on the IBM 10 megabyte hard disc. A high speed communications interface, MDB Systems Universal Logic Half Module (ULHM), is currently being installed which will enable data to be transferred to the Perkin-Elmer 3240 seismic processing facility operated by the Department of Geology and Geophysics at the University of Calgary. It is anticipated that the total acquisition and transfer time will be less than 0.2 seconds per trace. A flowchart of the modeling tank system is shown in Figure 60.2. The tank facility and the control hardware are shown in Figures 60.4, 60.5.

Transducers

Piezoelectric transducers are currently being used as source and receivers in the tank system. Transducers with spherical and hollow cylindrical crystal elements have been tested. These are shown in Figure 60.6. The spherical ITC 1089c transducers have a diameter of 1 cm and operate omnidirectionally over a frequency range from 1-350 kHz. When two of these elements are used as a source-receiver pair, they resonate near 300 kHz, although this response can be damped. The hollow cylindrical elements are manufactured by KB-Aerotech, and are 0.6 cm in length with a diameter of 0.3 cm. These crystals have a useable frequency response from 1-600 kHz, and have a radial omnidirectional response. Due to their smaller size and power handling capability these units have been most useful as receivers for a 1089c source, since the mismatch of their resonance peaks results in a visible improvement in the observed reflections. These elements may be used in combination to form a source array.

Modeling materials and scale factors

The success of physical modeling is directly dependent on the choice of the modeling materials and scaling factors chosen for the simulation. The modeling materials used must have acoustic velocities appropriate for scaling with respect to the velocity of water (1500 m/s) and must be readily formable into complex shapes. The experience of the seismic modeling group at the University of Houston (McDonald, 1983) indicates that RTV (room temperature vulcanizing) rubber compounds, epoxy resins and plexiglas make the most suitable modeling media. The RTV rubbers and the epoxy resins can be readily molded without the inclusion of air bubbles which tend to scatter acoustic energy at the wavelengths typical of ultrasonic modeling. Plexiglas sheets and tubes are suitable for modeling features such as frozen layers or channel sands.

Scale factors are chosen for the model experiments such that the value of a model parameter multiplied by the appropriate scale factor results in the dimensions of the field prototype. Table 60.1 shows a typical set of scale factors which will be used for permaforst models. Model layers are constructed by forming a clay model of the desired structure,

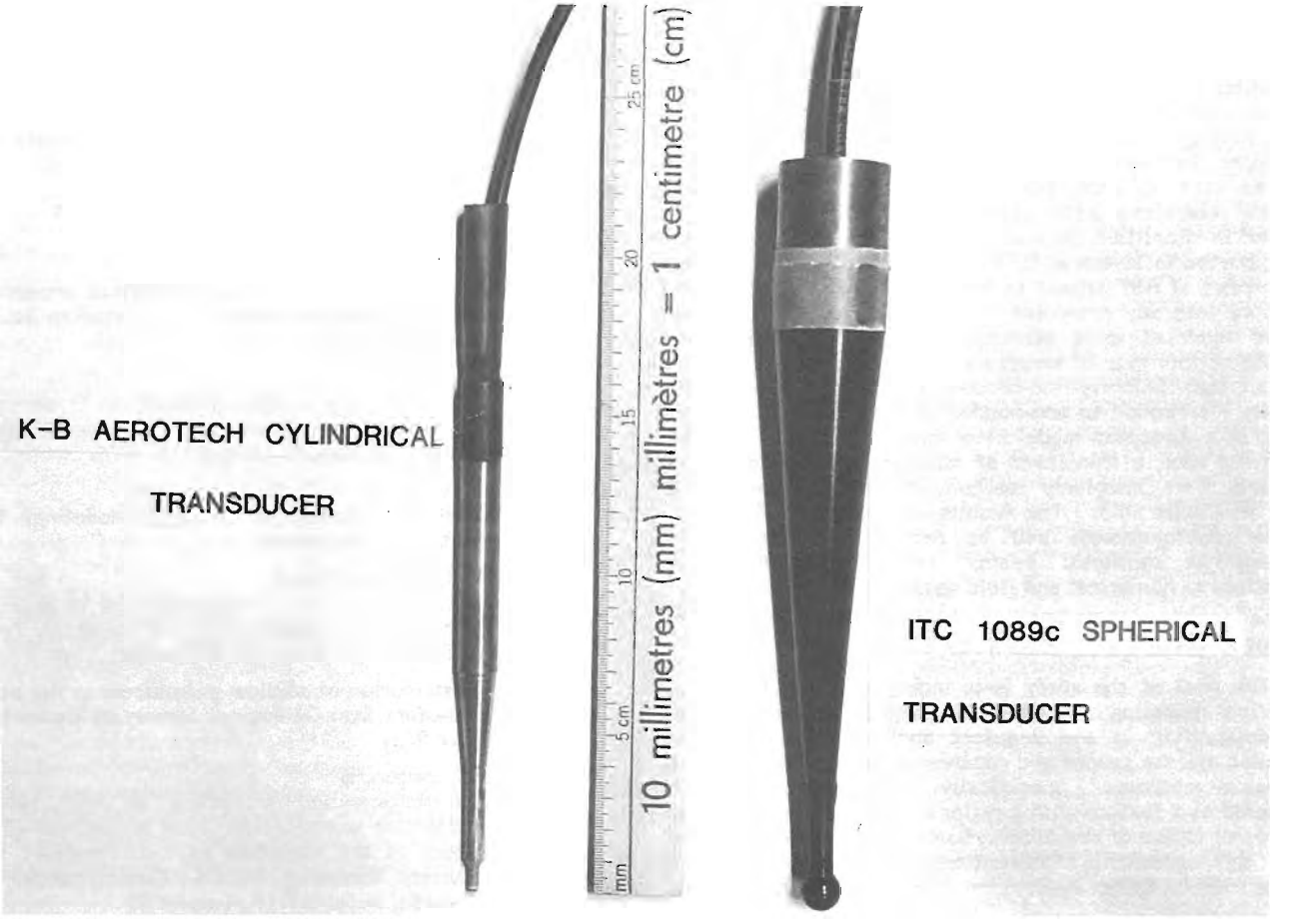

Figure 60.6. The two piezoelectric transducer types are shown. The actual crystal elements are watersealed in the small cylindrical (at left) or spherical (at right) tips of the units.

Table 60.1. Scaling Factors

Dimension	Prototype		Model	Scale Factor	
Distance	30 m		1 cm	3000	
Time	1 msec.		0.5 μsec.	2000	
Velocity	1500 m/sec		1000 m/sec	1.5	
Frequency	60-240 Hz		12-480 kHz	1/2000	
Wavelength Velocity	Metres		Velocity	Centimetres	
	60 Hz	240 Hz		12 kHz	480 kHz
1500 m/sec	25	6.25	1000 m/sec	8.3	0.2
3600 m/sec	60	15	2400 m/sec	20	0.5

making a plaster mold of the clay model and then filling the mold with the pourable RTV or epoxy resin. A sample of any individual pour is retained for measurement of velocity. Once constructed the models are placed on a plexiglas pallet that is lowered into the tank. The legs of the pallet fit into sockets in a larger plexiglas table fixed on the floor of the tank, providing both a stable platform and a flat reference reflector beneath the model.

Initial permafrost model

The strongest velocity anomalies in the shallow Beaufort seabottom are associated with the coarser lithologies since these appear to be more readily icebonded (O'Connor, 1980, 1981). These sediments also show the greatest increase in velocity even at temperatures just below the freezing point (King, 1977; Kurfurst, 1976). These lithologies may be associated with deltaic and shallow shelf features such as bars, ridges, spits and channels. They probably correlate with discontinuous APF and will be modeled in simplified form as molded epoxy or cut plexiglas tubing hosted in layers of RTV with a lower velocity. Some occurrences of APF appear to be stratigraphically controlled and more laterally extensive (O'Connor, 1980, 1981). These will be modeled using plexiglas sheets. One important example of this type of structure is the alternation of layers between high velocity ice-bonded sands and low velocity partially ice-bonded to non-bonded silts and clays. A cross-section of a proposed model incorporating "frozen" channels of varying size, a thin layer of stratigraphically controlled APF and more massively ice-bonded deeper sediments is shown in Figure 60.3. The results of a variety of source-receiver configurations will be recorded, processed and displayed as synthetic seismic reflection sections for comparison to numerical and field data.

Acquisition simulation

The goal of the study is to incorporate the results of permafrost modeling into a broader investigation to optimize APF delineation in the Beaufort Shelf. Two aspects in particular are the source and receiver array designs and data processing methods. Specifically, a diffractor may be considered as a feature with a reflecting surface smaller than the Fresnel radius of resolution. Some APF structures appear to fit this criterion. Conventional seismic methods are capable of imaging reflectors better than diffractors. Consequently, source wavelet wavelengths must be shortened and arrays designed to preferentially record or spatially filter those wavelengths of interest. Beam steering techniques may be simulated by source array methods and during data processing. The effect of conventional CDP stacking of this type of data will also be assessed and compared with other available methods of displaying the records such as the offset panel and the slant stack technique. While the initial efforts will be 2-D profiles, 3-D methods will also be explored as processing capacity permits.

Acknowledgments

This project is jointly funded by the University of Calgary and the Panel on Energy Research and Development (PERD) Task 6: Conventional Energy Systems and is coordinated through the Beaufort Sea project under Steve M. Blasco at the Atlantic Geoscience Centre.

References

King, M.S.
1977: Acoustic velocities and electrical properties of frozen sandstones and shales; Canadian Journal of Earth Sciences, v. 14, p. 1004-1013.

Kurfurst, P.J.
1976: Ultrasonic wave measurements on frozen soils at permafrost temperatures; Canadian Journal of Earth Sciences, v. 13, p. 1571-1576.

McDonald, J.A., ed.
1983: Seismic Studies in Physical Modeling; IHRDC Publ., Boston, Mass.

O'Connor, M.J. and Associates
1980: Development of a proposed model to account for the surficial geology of the southern Beaufort Sea; Geological Survey of Canada, Open File 954.

1981: Distribution of shallow permafrost in the southern Beaufort Sea; Geological Survey of Canada, Open File 953.

Poley, D. and Lawton, D.
1985: Acquisition and processing of high resolution reflection seismic data from permafrost-affected areas of the Canadian part of Beaufort Sea; in Current Research, Part A, Geological Survey of Canada, Paper 85-1A, Report 59.

RECONNAISSANCE STUDY OF PROGLACIAL STEWART LAKES, BAFFIN ISLAND, DISTRICT OF FRANKLIN

Project 810042

Robert Gilbert[1], James P.M. Syvitski, and Robert B. Taylor
Atlantic Geoscience Centre, Dartmouth

Gilbert, R., Syvitski, J.P.M., and Taylor, R.B., Reconnaissance study of proglacial Stewart Lakes, Baffin Island, District of Franklin; in Current Research, Part A, Geological Survey of Canada, Paper 85-1A, p. 505-510, 1985.

Abstract

Stewart Lakes are dammed by neoglacial moraines in a through-valley between Gibbs and Sam Ford fiords in northeastern Baffin Island. Maximum water depth on the basis of spot soundings is 108 m. Glaciers are retreating at rates between 19 and 34 m/a, and the lake level has lowered from 69 m above sea level to 55 m as a result of ice retreat and downcutting of the moraines. On 13 September 1983, suspended sediment concentrations in Stewart Lakes varied from 66 to 109 mg/L. In Refuge Harbour (Gibbs Fiord) the concentration in overflowing fresh water was 135 mg/L. These values are signficantly higher than those measured in most other ice-proximal lakes and fiords.

Résumé

Des moraines néoglaciaires servent de retenue aux lacs Stewart, dans une vallée glaciaire située entre les fjords Gibbs et Sam, dans la partie nord-est de l'île Baffin. D'après des sondages ponctuels, la profondeur maximum de l'eau est de 108 m. Les glaciers reculent à des vitesses comprises entre 19 et 34 m/a, et le niveau limnimétrique est passé de 69 m à 55 m au-dessus du niveau de la mer, par suite du recul des glaces et de la dissection des moraines. Le 13 septembre 1983, les concentrations de sédiments en suspension ont varié dans les lacs Stewart entre 66 et 109 m/l. À Refuge Harbour (fjord Gibbs), la concentration des sédiments en suspension dans les eaux douces de trop-plein était de 135 m/l. Ces valeurs sont nettement plus élevées que celles mesurées dans la plupart des autres lacs et fjords les plus proches des glaces.

[1] Department of Geography, Queen's University, Kingston, Ontario K7L 3N6

Introduction

During the shore-based portion of the Sedimentology of Arctic Fiords Experiment in 1983 (Syvitski and Schafer, in press), there was an opportunity on September 13 for a brief reconnaissance by helicopter of proglacial Stewart Lakes. The lakes are located on the floor of a glacial trough between Gibbs and Sam Ford fiords in northeastern Baffin Island (Fig. 61.1). The geomorphology and hydrology of this remote area are uninvestigated, although studies were made by the Geographical Branch of the glacial geomorphology of the upper regions of Sam Ford Fiord (Smith, 1966) and of the peninsula to the northeast of Stewart Lakes (Ives and Buckley, 1969). The results presented here provide a background for proposed detailed study of the sedimentology of these lakes.

Physical setting

The lakes are dammed on the north at 55 m above sea level by the neoglacial moraine of a large glacier, and to the southwest, a large calving glacier terminates in the lake (Fig. 61.2). A moraine from one of the side-entry glaciers separates the lakes (here referred to as North and South Stewart Lakes). Flow of water in the lakes is from south to north, and thence into Refuge Harbour. Summary statistics of the characteristics of the drainage basins and the lakes are presented in Table 61.1.

Although the valley is a major glacial trough with cliffs rising to 1600 m in the vicinity of the lakes, the spot observations of water depth shown in Figure 61.2 indicate that the lakes are relatively shallow, attaining a maximum depth of 108 m.

Glacier fronts around the shores of Stewart Lakes are retreating rapidly from their neoglacial moraines (Fig. 61.3). Between 1961 and 1983 the large glacier at the south (Fig. 61.3a, b) has retreated about 750 m (34 m/a on average). The profile of the lower section of the glacier has also changed significantly in that period. At present a large area appears to have detached from the active glacier, possibly as a result of the ice thinning and then floating to allow lake water beneath. This section now forms a nearly flat-lying, floating ice sheet (Fig. 61.4), the outer edge of which is less than 1 m above lake level.

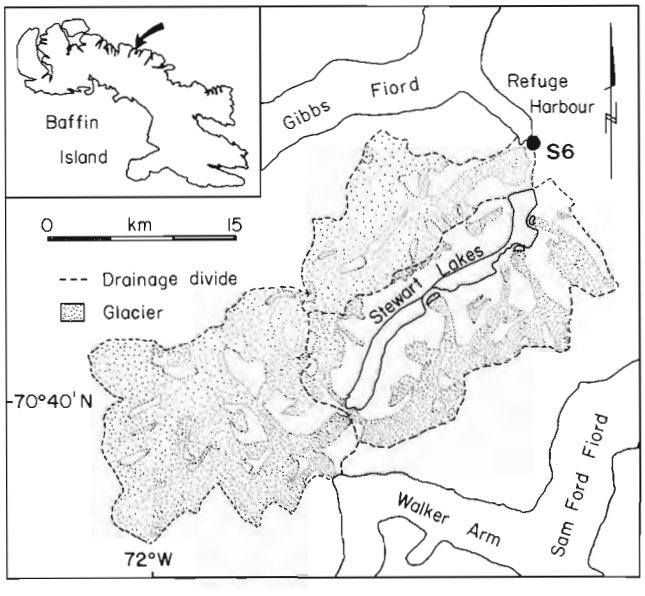

Figure 61.1. Drainage basins tributary to Stewart Lakes and glaciers to the north and west (from NTS map 27F).

Ice cored mounds of sediment stand up to 5 m above the present surface (Fig. 61.4, 61.5). The thin veneer of glaciofluvial sand and silt (samples 1 and 2, Fig. 61.6) protects the ice beneath from melt. These are thought to be remanent pockets of deposition in a formally active meltwater drainage system within the ice. Since only a thin floating sheet remains, it is probable that the ice tongue is melting both from above and below. Because the water level in the lakes changes only about 1 m from winter to summer, this sheet has not been calved and broken up, although it is probable that it is unstable, and rapid retreat, at least to the active ice front, will continue.

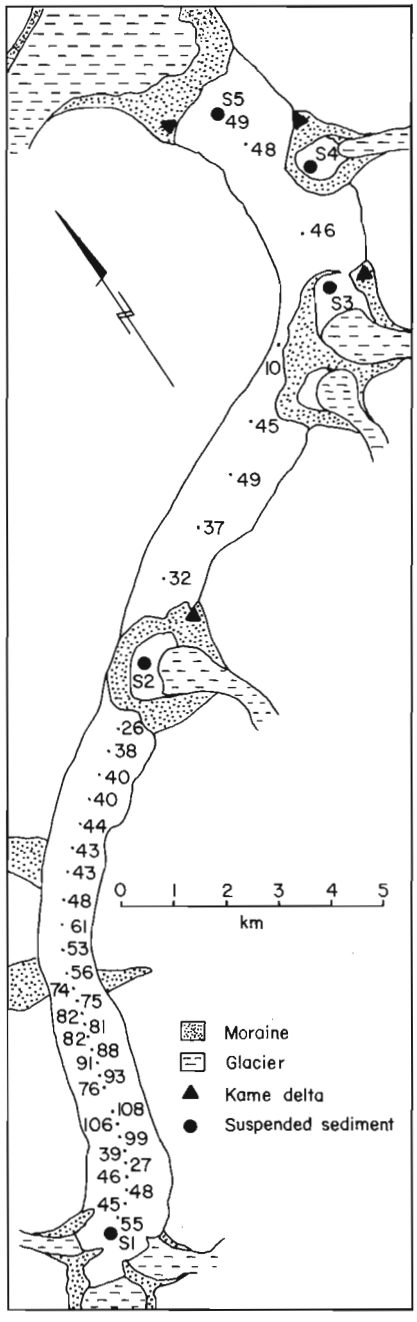

Figure 61.2. Outline of Stewart Lakes showing bathymetry in metres, location of suspended sediment sampling sites (S1 to S5) and kame deltas. The shoreline indicates ice front locations in 1983.

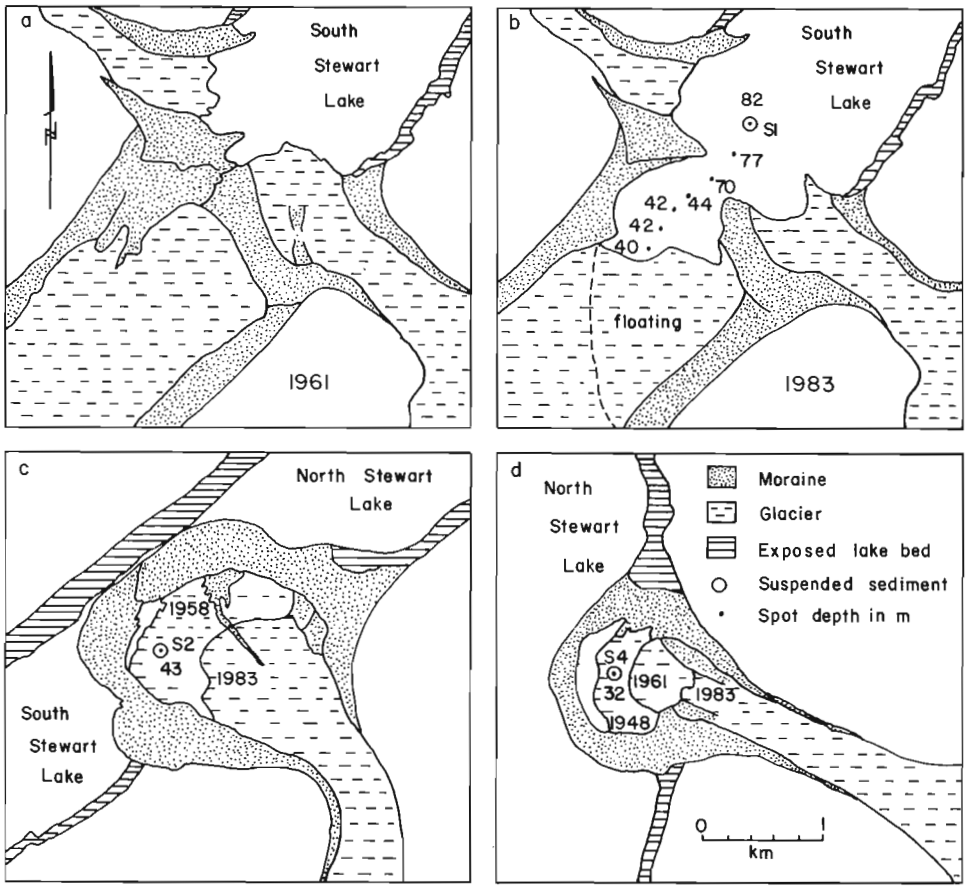

Figure 61.3. *Maps showing the retreat of glaciers around Stewart Lakes; at the south end (a and b), between North and South Stewart Lakes (c) and at the northeast end of North Stewart Lake (d). Ice fronts are mapped from air photos from The National Air Photo Library taken in 1948 (T215R-91), 1958 (A16218-34 and A16300-106), and 1961 (A17045-18,20,33). Ice fronts in 1983 are estimated from photographs taken in the field.*



Figure 61.4

View looking west showing the floating ice tongue and the active glacier at the south end of Stewart Lakes (Fig. 61.3b). Human figures (circled) indicate scale.

During the same period of 1961 to 1983, the side entry glacier shown in Figure 61.3c has retreated 530 m (24 m/a). In air photographs on 22 June and 30 August 1958 a small lake appears at the toe of the glacier (Fig. 61.3c). In photographs on 16 and 27 July 1961 the position of the toe of the glacier is nearly the same, but the lake has disappeared. This may have occurred as the outlet cut down or as water percolated through the moraine. At the present time a lake of 0.88 km^2 and at least 43 m deep exists inside the moraine. The glacier shown in Figure 61.3d has retreated 250 m between 1948 and 1961 (19 m/a) and 480 m between 1961 and 1983 (22 m/a). The present lake inside its moraine has an area of 0.70 km^2 and is at least 32 m deep.

Sometime before the first air photographs were taken in 1948, the level of Stewart Lakes dropped from about 69 m above sea level to the present level of 55 m, and North and South Stewart Lakes became separated by the moraine between them. It is probable that this process occurred slowly over a period of years, as a number of distinct beaches appeared between these two levels. The lowering apparently resulted from downcutting of the moraine dam at the north end of the lakes as the glacier there retreated.

Sedimentary environments

Suspended sediments

Six one litre surface water samples were recovered from Stewart Lakes, the smaller lakes behind the side-entry moraines (Fig. 61.1, 61.2), and the overflowing plume of fresh water in Refuge Harbour. The results of analysis of sediment concentration and grain size are presented in Table 61.2 and Figure 61.7.

The concentrations of suspended sediment are high in comparison to other glacial lakes which range from about 5 to 50 mg/L (Gilbert, 1975; Pickrill and Irwin, 1982; Smith and Syvitski, 1982; Smith et al., 1982). Only in the very high energy environment of Malaspina Lake, Alaska where sediment concentrations reach 700 mg/L (Gustavson, 1975) are reported values higher than those measured in Stewart Lakes. The values from Stewart Lakes are even more remarkable because arctic glacial streams normally carry significantly less suspended sediment than their temperate alpine counterparts (Østrem et al., 1967; Church, 1972; Lemmen, 1984). In addition, the samples were collected from Stewart Lakes in mid-September, well after the period of highest sediment input during mid-summer.



Figure 61.5. Ice-cored debris cone on the floating ice tongue at the south end of Stewart Lakes.

Table 61.1. Characteristics of the drainage basins of Stewart Lakes

Basin	Area km^2 Total	Lakes	Per cent glacier covered	Maximum elevation m
North basin	128	0	80	1870
West basin	260	0	85	1740
Stewart valley	268	27	45	1810

Lake	Area km^2	Length km	Mean width km	Maximum recorded depth m
North Stewart	12.5	10.6	1.18	108
South Stewart	14.4	10.9	1.32	49

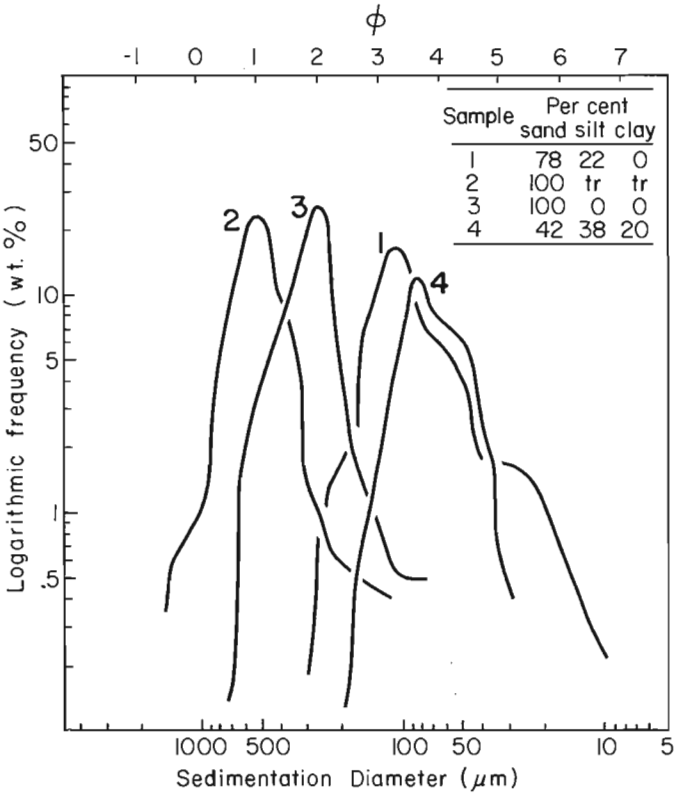

Figure 61.6. Grain size distribution of sediment samples collected from Stewart Lakes. Samples 1 and 2 are from the fine and coarse sediments respectively on the debris cone shown in Figure 61.5. Sample 3 is from the beach on the alluvial fan at the base of the raised kame delta at the south end of North Stewart Lake (Fig. 61.2) and sample 4 is from the topset beds of that delta (Fig. 61.8).

Table 61.2. Summary statistics of suspended sediment samples from Stewart Lakes and Refuge Harbour

		Grain size moment measures			
Sample No*	Concentration mg/L	Mean ϕ	Standard deviation ϕ	Skewness	Kurtosis
1	109	9.43	1.03	-1.1	3.6
2	24	9.40	1.01	-0.9	3.4
3	94	9.19	1.11	-0.8	2.8
4	73	9.20	1.07	-0.7	2.9
5	66	9.67	0.92	-1.4	4.5
6	135	9.20	1.22	-0.7	2.3

*for sample locations see Figures 61.1-61.3

The major source of sediment is the large glacier to the southwest. The sediment concentration remains high throughout the length of the lakes, suggesting efficient mixing of the lake waters and significant throughput of suspended sediment. The side entry glacier dividing North and South Stewart Lakes has a much lower input of fine sediment than the other glaciers, and the water colour is a light grey in comparison to the dark brown of Stewart Lakes.

In Refuge Harbour the sediment concentration is the highest of all sites measured, and is significantly higher than that in other fiords on Baffin Island, even at the height of the melt season (Gilbert, 1978; 1982). The high concentration reflects the input from Stewart Lakes, glaciofluvial input from the large glacier nearby, and the restricted mixing in the overflowing fresh water.

The size range (Fig. 61.7) is typical of glacial 'rock flour' (0.25-12 μm; Keller and Reesman, 1963). In all samples, less than about 2% of the material is greater than 10 μm, indicating the settling of coarser particles. This loss of the coarse tail is most apparent in surface sample 5 from the north end of Stewart Lakes.

Deltaic environments

At the sides of some of the moraines in Stewart Lakes are kame deltas which built into the lakes at the older 69 m water level (Fig. 61.2). The most southerly of these was examined briefly. Sections up to 14 m high have been exposed by downcutting streams as the lake level lowered (Fig. 61.8). The delta consists of foreset beds dipping at 20° to 27°. Above are topset beds of rippled sands and silts (sample 4, Fig. 61.6) from a small sandur which built over the delta. The sediments that were eroded as the lake level lowered and streams cut through the delta, were deposited in lower angle (15° to 19°) alluvial fans in front of the delta. These fans are currently being modified by wave action to form beaches (sample 3; Fig. 61.6) as the lake level varies about 1 m between summer and winter.

Discussion

Stewart Lakes are an excellent field site for detailed study of glaciolacustrine processes in an arctic environment. Recent, rapid glacier retreat has created new lakes and exposed portions of the main lakes, so that ice-proximal lacustrine processes can be assessed above a known ice-contact base. High sediment concentration in the lake water indicates large rates of deposition. Processes such as turbidity current flow and redistribution of sediment by slope failure probably predominate. Instability caused by glacier

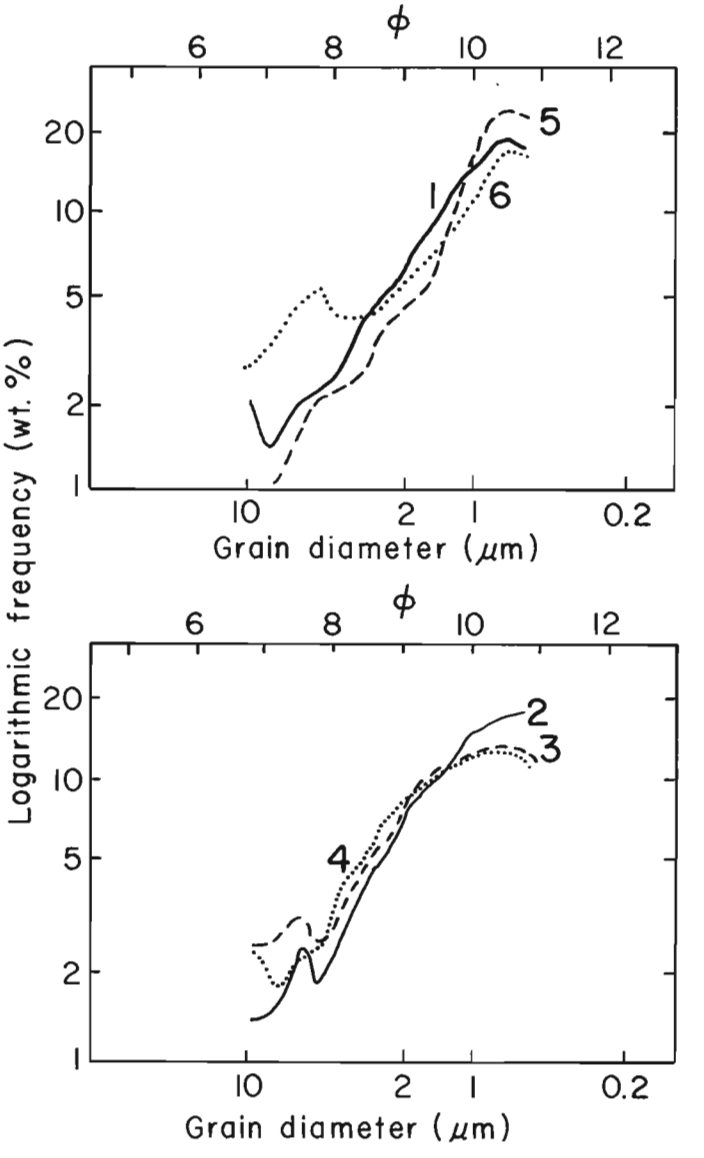

Figure 61.7. Histograms of grain size distribution of suspended sediment samples collected from Stewart Lakes and Refuge Harbour. Sample locations are shown in Figures 61.1-61.3.



Figure 61.8. *Upper section of the raised kame delta at the south end of North Stewart Lake (Fig. 61.2). The topset beds of rippled sands and silts were sampled and analyzed (sample 4, Fig. 61.6).*

ice-push and the melting of ice-cored moraines also may be significant sources of disturbance to lake sediments. The different rates of sediment input from the side entry glaciers as compared to those in the main valley provide opportunity to assess different sedimentary processes in a similar climatic setting, and to assess varying sediment yield from a variety of glaciers in the same area.

The sedimentology of the abundantly dissected raised deltas can be investigated in the presence of the glaciers and their sediments that created these features, so that the amount and distribution of water and sediment involved can be estimated reasonably. Such is not the case for most of the Quaternary glacial landforms available for study in section.

The valley of Stewart Lakes may have been occupied by sea water at various times during the Holocene. Long cores and continuous seismic survey through the lake sediments may provide information on the sea level and glacial history of the area.

Finally, the proximity of Stewart Lakes to Gibbs Fiord and Walker Arm will also allow comparison of glaciolacustrine and glaciomarine sedimentology of these areas where conditions of sediment input are similar. It should be possible to compare the quality of a climatic and hydrologic record and the processes of deposition in both the freshwater and marine environment.

Acknowledgments

The authors gratefully acknowledge the invaluable logistics support of Polar Continental Shelf Project. We thank G. Vilks for his comments on the draft manuscript.

References

Church, M.
1972: Baffin Island sandurs: a study of arctic fluvial environments; Geological Survey of Canada, Bulletin 216, 208 p.

Gilbert, R.
1975: Sedimentation in Lillooet Lake, British Columbia; Canadian Journal of Earth Sciences, v. 12, p. 1697-1711.

1978: Observations on oceanography and sedimentation at Pangnirtung Fiord, Baffin Island; Maritime Sediments, v. 14, p. 1-9.

1982: Contemporary sedimentary environments on Baffin Island, N.W.T., Canada: glaciomarine processes in fiords of eastern Cumberland Peninsula; Arctic and Alpine Research, v. 14, p. 1-12.

Gustavson, T.C.
1975: Sedimentation and physical limnology in proglacial Malaspina Lake, southeastern Alaska; in Glaciofluvial and Glaciolacustrine Sedimentation, ed. A.V. Jopling and B.C. McDonald; Society of Economic Paleontologists and Mineralogists, Special Publication 23, p. 248-262.

Ives, J.D. and Buckley, J.T.
1969: Glacial geomorphology of Remote Peninsula, Baffin Island, N.W.T., Canada; Arctic and Alpine Research, v. 2, p. 83-96.

Keller, W.D. and Reesman, A.L.
1963: Glacial milks and their laboratory-simulated counterparts; Geological Society of America Bulletin, v. 74, p. 61-76.

Lemmen, D.S.
1984: Sedimentation in a glacially-fed arctic lake: Tasikutaak Lake, Cumberland Peninsula, Baffin Island, N.W.T.; unpublished M.Sc. thesis, Department of Geography, Queen's University, 157 p.

Østrem, G., Bridge, C.W., and Rannie, W.F.
1967: Glaciohydrology, discharge and sediment transport in the Decade Glacier area, Baffin Island N.W.T.; Geografiska Annaler, v. 49A, p. 268-282.

Pickrill, R.A. and Irwin, J.
1982: Predominant headwater inflow and its control of lake-river interactions in Lake Wakatipu; New Zealand Journal of Marine and Freshwater Research, v. 16, p. 201-213.

Smith, J.E.
1966: Sam Ford Fiord: a study in deglaciation; unpublished M.Sc. thesis, Department of Geography, McGill University, 93 p.

Smith, N.D. and Syvitski, J.P.M.
1982: Sedimentation in a glacier-fed lake: the role of pelletization on deposition of fine-grained suspensates; Journal of Sedimentary Petrology, v. 52, p. 503-513.

Smith, N.D., Vendl, M.A., and Kennedy, S.K.
1982: Comparison of sedimentation regimes in four glacier-fed lakes of western Alberta; in Research in Glacial, Glaciofluvial and Glaciolacustrine Systems, ed. R. Davidson-Arnott, W. Nickling, and B.D. Fahey; Proceedings of the 6th Guelph Symposium on Geomorphology, 1980, p. 203-238.

Syvitiski, J.P.M. and Schafer, C.T.
– Sedimentology of Arctic Fjords Experiment (SAFE): 1. Project introduction; Arctic. (in press)

-62-

METAMORPHIC PROCESSES IN THE KISSEYNEW METASEDIMENTARY GNEISS BELT, MANITOBA

Project 830014

T.M. Gordon, S.L. Jackson[1], and E. Zaleski[1]
Precambrian Geology Division

Gordon, T.M., Jackson, S.L., and Zaleski, E., Metamorphic processes in the Kisseynew metasedimentary gneiss belt, Manitoba; in Current Research, Part A, Geological Survey of Canada, Paper 85-1A, p. 511-516, 1985.

Abstract

On the south flank of the Kisseynew sedimentary gneiss belt the transition between pelitic paragneiss and migmatite is often marked by an increasing abundance of intrusive rocks. The effects of these intrusions have obliterated much of the record of the initial stages of migmatite formation. Metapelites in the Flin Flon belt contain abundant sillimanite and garnet while similar rocks in the core of the Kisseynew belt commonly contain garnet and cordierite. An intervening zone of metapelites is notably devoid of sillimanite and cordierite. Differences in bulk composition as well as metamorphic grade are required to explain these observations.

Résumé

Sur le versant sud de la zone gneissique sédimentaire de Kisseynew, la transition entre les paragneiss pélitiques et les migmatites est souvent marquée par une augmentation de l'abondance des roches intrusives. Ces intrusions ont réussi à oblitérer en majeure partie les traces des premières phases de formation des migmatites. Les métapélites de la zone de Flin Flon contiennent des quantités abondantes de sillimanite et de grenats, tandis que des roches similaires situées au coeur de la zone de Kisseynew contiennent généralement des grenats et de la cordiérite. Une zone intermédiaire de métapélites est manifestement dépourvue de sillimanite et de cordiérite. Les détails observés ne peuvent s'expliquer que par des différences de la composition globale des roches, et aussi de l'intensité du métamorphisme.

[1] Department of Geological Sciences, Queen's University, Kingston, Ontario K7L 3N6

Introduction

The Kisseynew metasedimentary gneiss belt lies between the Lynn Lake greenstone belt and the Flin Flon-Snow Lake greenstone belt at the southwest margin of the Churchill Structural Province. This project is aimed at an improved understanding of the timing and physical conditions of metamorphism of the Kisseynew belt. Previously, a tentative sequence of metamorphic and deformational events was established for the Noble Lake region (Gordon, 1984). This summer's work involved three separate problems:

1. S.L. Jackson began a detailed study of the metamorphism and deformation at Laurie Lake on the north flank of the belt. Preliminary results of this work are reported elsewhere (Jackson and Gordon, 1985) and will not be repeated here.
2. A reconnaissance was made of the southern flank of the Kisseynew belt to select areas suitable for future studies on the prograde migmatization of pelitic rocks.
3. A 120 km north-south transect through the central part of the belt was traversed to obtain samples of mineral assemblages suitable for geothermometry and geobarometry, to obtain material for geochronological investigations, and to assess the area for further geochemical work.

Acknowledgments

A.H. Bailes and H.V. Zwanzig of Manitoba Mineral Resources Division provided invaluable advice during the field work. Special thanks are due Julie Jackson for able field assistance and inspired cuisine.

Migmatization of pelitic rocks

The transition between the Flin Flon volcanic belt and the migmatitic Kisseynew sedimentary gneiss belt is in part the result of increasing metamorphic grade (Froese, 1984; Froese and Moore, 1980; Bailes, 1980). An understanding of the metamorphic conversion of paragneiss to migmatite is thus important for understanding the thermal evolution of the area.

Possible mechanisms of migmatite formation have been classified according to whether the rock has behaved as an open or closed system and whether a silicate melt or a hydrothermal fluid was involved (Yardley, 1978). Recent studies suggest that more than one mechanism may be involved in any one migmatite occurrence (Olsen, 1983; Johannes, 1983).

Attempts to decipher physical conditions of metamorphism will be hampered if open system mechanisms have dominated. Theoretical studies (Thompson, 1982; Grant, 1983) have not dealt with the effects of externally imposed ionic activities that hydrothermal fluids might introduce. On the other hand, migmatites formed by igneous injection may contain mineral assemblages that crystallized at separate times under different physical conditions.

Migmatites in the Kisseynew belt are almost exclusively derived from pelitic rocks of the Burntwood Metamorphic Suite (Lenton, 1981; Baldwin et al., 1979). Psammitic rocks of the Sickle Metamorphic Suite, on the other hand, are less widespread and generally have not undergone migmatization. This, coupled with the fact that most theoretical work on migmatization deals with model pelitic systems, suggests that the most productive study area would be one in which closed system behaviour can be inferred for pelitic rocks that can be mapped across the paragneiss-migmatite boundary. Existing maps of the southern flank of the gneiss belt indicate that only two areas contain pelitic rocks at the appropriate metamorphic grade: the Duval Lake area and the File Lake area.

Duval Lake area

The Duval Lake area lies 40 km north of Flin Flon, immediately west of Kississing Lake. It has been mapped at a scale of 1:63 360 by Pollock (1964) and part of the area has been investigated by Manitoba Mineral Resources Division (Zwanzig, 1983). Recent logging has provided new access roads and rock exposures which were examined this summer.

The lowest grade pelitic rocks are the Duval Lake Schists, exposed in an east-west trending synclinal structure at the south margin of the map sheet. They consist of metamorphosed greywacke-mudstone turbidites lithologically identical to the File Lake Formation of Bailes (1980). Assemblages observed in the field include both quartz-feldspar-muscovite-biotite-garnet-staurolite and quartz-feldspar-biotite-garnet-sillimanite. Pollock (1964) reported that sillimanite occurs sporadically at the northern boundary of the unit, and that the staurolite-out isograd lies within the area mapped as Duval Lake Schist with metamorphic grade increasing towards the north.

Boudinaged quartz and quartz-feldspar pods, in part with sillimanite selvages, were observed in some paragneiss exposures. Secondary muscovite has a coarser grain size than other minerals cross cuts the foliation.

North of the Duval Lake Schists are rocks mapped as Nokomis paragneiss and Nokomis migmatite. The contact between the two map units is gradational and somewhat arbitrary. Where these rocks were observed, the paragneiss assemblages are mainly quartz-plagioclase-K-feldspar-biotite-muscovite with and without garnet and sillimanite. Grain size of the paragneiss is distinctly coarser than that of the Duval Lake Schists.

The migmatite is a mixed rock consisting of paragneiss with variable proportions of concordant and discordant veins and pods of muscovite-biotite pegmatitic granite. Accessory minerals in the granite include garnet and tourmaline, while sillimanite and possible andalusite were seen in cross cutting fractures. Muscovite was observed in both granite and paragneiss at most localities, with the muscovite/biotite ratio of granite generally greater than that of adjacent rocks. A limited number of observations suggest that the muscovite content of the paragneiss component of migmatite increases with the amount of granitic material present.

The contact between Duval Lake Schists and Nokomis paragneiss and migmatite was not seen in outcrop. The minimum (covered) transition interval observed was 300 m. As mapped by Pollock, the boundary is conformable with the foliation and layering in the adjacent map units. All outcrops of migmatite examined near the boundary contained crosscutting veins of pegmatitic granite.

These observations lead us to the conclusion that, in the Duval Lake area, formation of Nokomis migmatite is due in part to the introduction of granitic melts. The apparent relationship between muscovite content of paragneiss and presence of granite, as well as the late development of aluminosilicates in fractures in granite, further suggests that there was material transport between granite and country rock, possibly involving hydrothermal solutions. Thus, although the area contains ample material for a fascinating metamorphic study, it is unlikely to provide insight into the phenomenon of closed system migmatite formation.

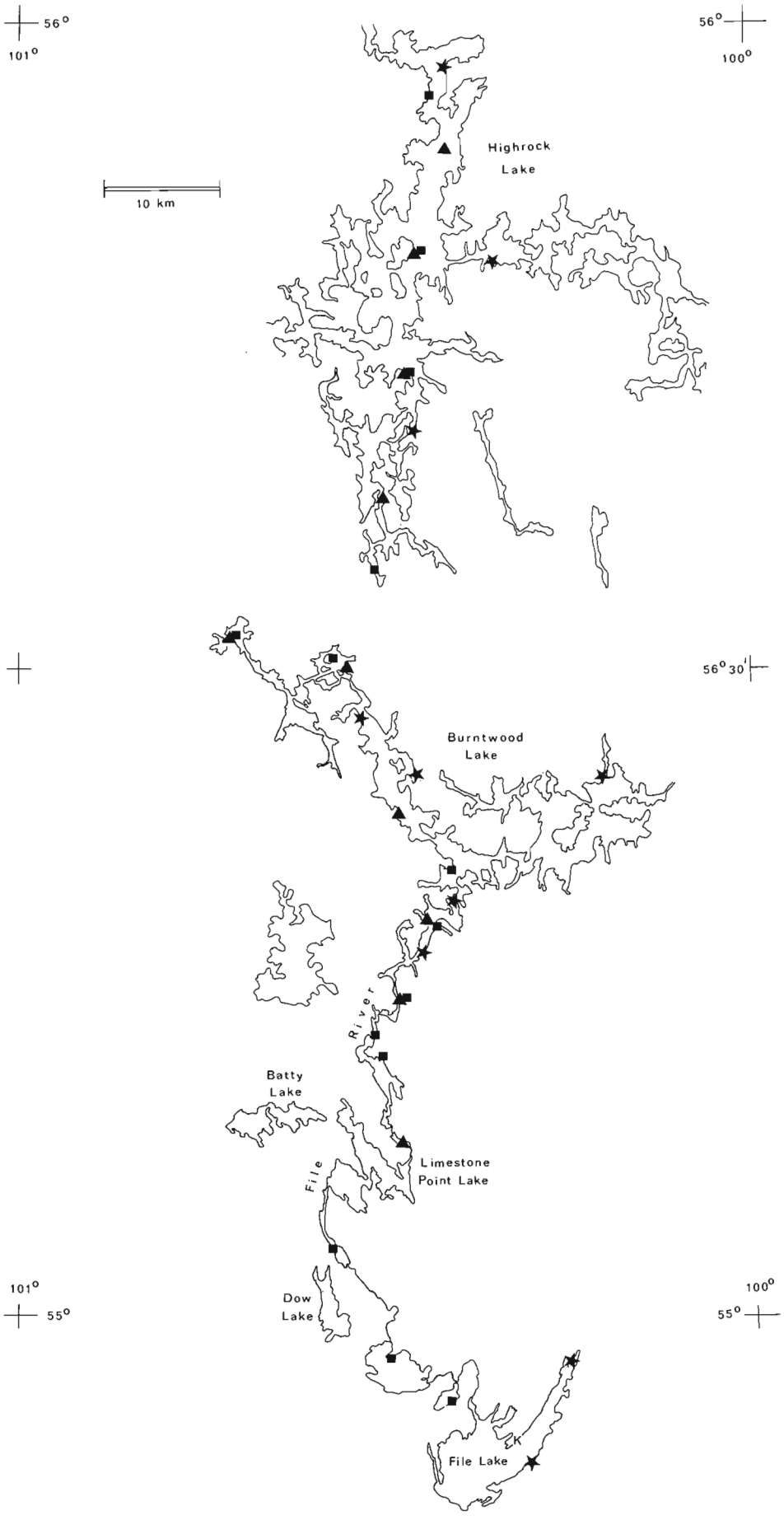

Figure 62.1. *Location of samples collected on Kisseynew transect. stars – geochronological samples; squares – garnet-sillimanite-biotite assemblages; triangles – garnet-cordierite-biotite assemblages.*

File Lake area

The File Lake area lies immediately west of Snow Lake. It was originally mapped at a scale of 1:63 360 by Harrison (1949) and has been the subject of recent metamorphic studies (Bailes, 1980; Froese and Moore, 1980). Metamorphosed greywacke-mudstone turbidites of the File Lake Formation display a sequence of isograds culminating in the disappearance of muscovite and the appearance of tonalite and granodiorite veins and lit. While attributing this isograd to the reaction:

$$\text{muscovite} + \text{plagioclase} + \text{quartz} + H_2O = \text{melt} + \text{sillimanite} \quad (1)$$

Bailes described two phenomena that are inconsistent with this interpretation. Firstly, although sillimanite is a product of the reaction, it was not observed above the isograd in rocks of the File Lake Formation. Secondly, the assemblage muscovite-plagioclase-quartz is present above the isograd in metamorphosed psammitic rocks of the Missi Group. Observations made this summer lead to alternative interpretations. In the File Lake area, staurolite and quartz persist in rocks above the isograd corresponding to the reaction:

$$\text{staurolite} + \text{muscovite} + \text{quartz} = \text{garnet} + \text{biotite} + \text{sillimanite} + H_2O \quad (2)$$

This suggests that muscovite may be the least abundant reactant in many rocks, and hence its prograde disappearance may be due to reaction (2) rather than reaction (1). Secondly, many granitic veins are ptygmatic and discordant possibly due to igneous injection. Thirdly, although garnet and sillimanite are common in rocks below the sillimanite-melt isograd, they are remarkably rare in many outcrops in the higher grade zone. This latter observation suggests that some of the higher grade rocks may have a different bulk composition. One explanation for such a change in composition is metasomatism. The source of metasomatic material could be the pegmatites and sheeted sill and dyke complexes of granodiorite noted by Bailes to be particularly abundant above the melt isograd.

Fortunately, an inland outcrop area of File Lake Formation appears to be at the required metamorphic grade and sufficiently distant from intrusions to provide a control for testing the metasomatic hypothesis. Although moss and lichen cover is extensive, field examination revealed some conformable granitoid segregations that appear to have developed in situ. This area will be studied in subsequent years.

Conclusions

The transition between metasedimentary pelites and migmatites in both the Duval Lake and File Lake areas is marked by an increasing abundance of intrusive granite and pegmatite. There is circumstantial evidence of metasomatic activity related to these igneous bodies. Although the intrusive rocks probably originated as anatectic melts, it has not yet been possible to identify an area with unequivocal in situ anatectic material. We speculate that melts generated in the core of the Kisseynew Belt have intruded and altered the adjacent rocks, hence destroying much of the record of the initial stages of migmatite formation. Part of the File Lake area may have escaped this alteration and will be studied further.

Kisseynew Transect

The File River, Burntwood Lake, and Highrock Lake provide excellent access to a north-south transect extending from the Flin Flon-Snow Lake volcanic belt through the core of the Kisseynew metasedimentary gneiss belt (Fig. 62.1). Previous work in the area includes that of McGlynn (1959), Harrison (1940), Bailes (1980), Robertson (1953), Kornik (1968), Baldwin et al. (1979), and Bailes and McRitchie (1978). This summer's efforts were concentrated on sampling pelitic mineral assemblages for geothermometry and geobarometry and collecting material for geochronological studies. Some general observations relating to this work are reported here.

At the south end of the transect, in the File Lake area, a recent forest fire has exposed several kyanite-bearing quartz-feldspar veins. These veins are discordant to the foliation in sillimanite-bearing rocks in the sillimanite-biotite zone. The veins can be traced north towards higher grade rocks where the kyanite is partially to completely replaced by sillimanite. Kyanite also occurs in schists 20 km east in the Snow Lake area (Froese and Moore, 1980).

Within the File Lake area, Bailes (1980) has shown that greywacke-mudstone turbidites of the File Lake Formation extend northwards through zones of increasing metamorphic grade to become biotite-garnet paragneisses. North of File Lake these rocks can be traced into paragneisses of the Kisseynew metasedimentary gneiss belt that have been assigned to the Nokomis Group. Quartzofelspathic psammites of the Missi Group can also be traced north and may be equivalent to quartz-rich gneisses of the Sherridon Group. Froese (1984) has recently summarized these correlations.

Robertson (1953) mapped a strip of Nokomis quartz-plagioclase-biotite gneiss extending across Dow Lake northwest to Batty Lake. On the northeast shore of Dow Lake this rock is a medium to coarse grained, strongly foliated, biotite-garnet gneiss with conspicuous feldspar augen. No sillimanite or cordierite was detected in these outcrops. These rocks are mineralogically similar to the highest grade File Lake Formation rocks seen along strike to the southeast, but are coarser grained and much more intensely deformed.

North of Dow Lake on the File River the same map unit includes well layered, garnetiferous, quartz-rich gneiss, garnet-biotite-anthophyllite gneiss and hornblende- and magnetite-bearing quartzofeldspathic gneisses. These outcrops match descriptions of the Sherridon Group rather than the Nokomis Group and should probably be reassigned.

A belt of Sherridon Group rocks extends through Limestone Point Lake. No pelitic assemblages were found in this area. Our observations suggest that much of the area mapped as 'granitized' Sherridon Group metasedimentary gneiss is orthogneiss. Froese (1984) and Zwanzig (1983) have emphasized the importance of separating orthogneiss from paragneiss within the Kisseynew belt.

North of Limestone Point Lake, the Nokomis Group consists of fine to medium grained paragneiss. Alternating layers of garnetiferous metapsammite and biotite-sillimanite-garnet metapelite suggest that the protolith was an aluminous turbidite. Concordant quartz-feldspar pods and garnet-cordierite-bearing pegmatitic segregations form 5 to 20 per cent of the outcrop. This lithology, common throughout the central part of the Kisseynew belt, is characteristic of the Burntwood Metamorphic Suite (Lenton, 1981; Baldwin et al., 1979).

Although sillimanite is common in metapelites immediately north of Limestone Point Lake, it becomes increasingly scarce towards Highrock Lake. Cordierite and cordierite pseudomorphs are relatively common throughout the northern portion of the transect.

An increase in abundance of granitic and pegmatitic dykes towards the core of the Kisseynew belt culminates in a granitic to tonalitic plutonic complex at Highrock Lake.

Most of the granitoid rocks are characteristically heterogeneous in grain size and mineralogy. Biotite and garnet are common, while cordierite occurs sporadically. Pegmatite veins in the central Kisseynew belt contain rare 2 by 10 mm euhedral andalusite crystals, often with sericitic margins. The same veins usually contain 10 to 40 mm wispy sprays of sillimanite in thin crosscutting fractures. Metasedimentary inclusions and screens can be found in most parts of the complex.

Secondary alteration has affected both gneisses and granitoid rocks from the north end of Burntwood Lake to the north end of Highrock Lake. This alteration is manifested by conspicuous biotite rims aroung garnet and pinitization of cordierite.

Conclusions

Pelitic rocks in the transect area can be divided into three mineralogically distinct groups. In the File Lake area porphyroblasts of garnet and sillimanite are conspicuous, while apparently stratigraphically equivalent rocks immediately to the north are notably free of sillimanite and relatively poor in garnet. In the core of the Kisseynew belt pelitic gneisses are characterized by abundant garnet and cordierite while sillimanite is rare.

It was previously speculated that the bulk composition of the sillimanite free rocks might differ from that of the lower grade aluminous metasediments. No such explanation is required for the sillimanite poor, garnet-cordierite rocks in the core of the complex. As pointed out by Bailes and McRitchie (1978) the reaction:

biotite + sillimanite + plagioclase + quartz = garnet + cordierite + melt (3)

consumes sillimanite while producing the common assemblage of the highest grade rocks.

The aluminum silicate minerals are notorious for metastability, making risky any interpretation of the occurrences reported here. With this in mind, we offer the following speculations. The preservation of kyanite may be more significant than its conditions of crystallization. It may indicate that uplift on the margin of the Kisseynew belt was more rapid than in the core, so that kyanite that initially crystallized metastably was quenched rather than inverting to sillimanite. Slower uplift of rocks in the core could also account for the observed retrogression of garnet and cordierite.

The textures of the andalusite-sillimanite pegmatites suggest that the andalusite was a primary mineral, while the sillimanite formed after crystallization was complete and the pegmatites were experiencing minor brittle deformation. If the polymorphs crystallized within their stability fields, this requires that the rocks experienced an increase in pressure and/or temperature after emplacement of the pegmatite. Increasing temperature during uplift is a characteristic feature of the overthrust model of metamorphism (England and Richardson, 1977) and such a model may apply to the evolution of the Kisseynew belt.

References

Bailes, A.H.
1980: Geology of the File Lake area; Manitoba Mineral Resources Division, Geological Report 78-1.

Bailes, A.H. and McRitchie, W.D.
1978: The transition from low to high grade metamorphism in the Kisseynew sedimentary gneiss belt, Manitoba; in Metamorphism in the Canadian Shield, ed. J.A. Fraser and W.W. Heywood; Geological Survey of Canada, Paper 78-10, p. 155-177.

Baldwin, D.A., Frohlinger, T.G., Kendrick, G., McRitchie, W.D., and Zwanzig, H.V.
1979: Geology of the Nelson House-Pukatawagan region (Burntwood Project); Manitoba Mineral Resources Division, Geological maps 78-3-1 to 78-3-2.

England, P.C. and Richardson, S.W.
1977: The influence of erosion upon the mineral facies of rocks from different metamorphic environments; Journal of the Geological Society of London, v. 134, p. 201-213.

Froese, E.
1984: Geology of the Weldon Bay-Fay Lake area, Manitoba; in Current Research, Part B, Geological Survey of Canada, Paper 84-1B, p. 355-358.

Froese, E. and Moore, J.M.
1980: Metamorphism in the Snow Lake area, Manitoba; Geological Survey of Canada, Paper 78-27.

Gordon, T.M.
1984: Metamorphic processes in the Kisseyenew sedimentary belt. 1. Initial stages of migmatite formation in the Noble Lake area, Manitoba; in Current Research, Part A, Geological Survey of Canada, Paper 84-1A, p. 307-312.

Grant, J.A.
1983: Equilibria in low-pressure melting of pelitic rocks; in Migmatites, Melting and Metamorphism, ed. M.P. Atherton and C.D. Gribble; Shiva Publishing Limited, p. 292-293.

Harrison, J.M.
1949: Geology and mineral deposits of the File-Tramping Lakes area, Manitoba; Geological Survey of Canada, Memoir 250.

Jackson, S.L. and Gordon, T.M.
1985: Metamorphism and structure of the Laurie Lake region, Manitoba; in Current Research, Part A, Geological Survey of Canada, Paper 85-1A, mineral development agreement.

Johannes, W.
1983: On the origin of layered migmatites; in Migmatites, Melting and Metamorphism, ed. M.P. Atherton and C.D. Gribble; Shiva Publishing Limited, p. 234-248.

Kornik, L.J.
1968: Guay Lake area (West Half); Manitoba Mines Branch, Publication 64-6.

Lenton, P.G.
1981: Geology of the McKnight-McCallum Lakes area; Manitoba Mineral Resources Division, Geological Report GR79-1.

McGlynn, J.C.
1959: Elbow-Heming Lakes area, Manitoba; Geological Survey of Canada, Memoir 305.

Olsen, S.N.
1983: A quantitative approach to local mass balance in migmatites; in Migmatites, Melting and Metamorphism, ed. M.P. Atherton and C.D. Gribble; Shiva Publishing Limited, p. 201-233.

Pollock, G.D.
1964: Geology of the Duval Lake area; Manitoba Mines Branch, Publication 61-6.

Robertson, D.S.
1953: Batty Lake map-area, Manitoba; Geological Survey of Canada, Memoir 271.

Thompson, A.B.
1982: Dehydration melting of pelitic rocks and the generation of H_2O-undersaturated granitic liquids, American Journal of Science, v. 282, p. 1567-1595.

Yardley, B.W.D.
1978: Genesis of the Skagit Gneiss migmatites, Washington, and the distinction between possible mechanisms of migmatisation; Geological Society of America, Bulletin, v. 89, p. 941-951.

Zwanzig, H.V.
1983: Kisseynew project: Lobstick Narrows (parts of 63K/13,14 and 63N/3,4); Manitoba Mineral Resources Division, Report of Field Activities 1983, p. 15-22.

DIRECT GEOPHYSICAL EVIDENCE FOR DISPLACEMENT ALONG NARES STRAIT (CANADA-GREENLAND) FROM LOW-LEVEL AEROMAGNETIC DATA: A PROGRESS REPORT

Project 650007

P.J. Hood, M.E. Bower, C.D. Hardwick[1], and D.J. Teskey
Resource Geophysics and Geochemistry Division

Hood, P.J., Power, M.E., Hardwick, C.D., and Teskey, D.J., Direct geophysical evidence for displacement along Nares Strait (Canada-Greenland) from low-level aeromagnetic data: a progress report; in Current Research, Part A, Geological Survey of Canada, Paper 85-1A, p. 517-522, 1985.

Abstract

A low level aeromagnetic reconnaissance of Nares Strait shows a sinistral offset of approximately 25 km in a band of 500-gamma anomalies extending from Bache Peninsula on Ellesmere Island to the southern side of the Humboldt Glacier on Greenland.

A line of isolated 200 gamma anomalies extends north from Judge Daly Promontory along Robeson Channel to the Arctic Ocean. These anomalies, which appear to be due to a swarm of closely spaced dykes, line up with the prominent fault zone on Judge Daly Promontory, which has been mapped with a 19 km sinistral displacement. Volcanic fragments with an olivine-basaltic composition have been found in Tertiary rocks along the fault zone and the aeromagnetic evidence also suggests that the dyke system extends across Judge Daly Promontory.

Thus it is concluded that at least 19 km of sinistral strike-slip displacement has occurred along the Strait itself, supporting Wegener's 1912 hypothesis.

Résumé

Un levé aéromagnétique de reconnaissance à faible altitude effectué au-dessus du détroit de Nares montre un décalage sénestre d'environ 25 km dans une bande d'anomalies de 500 gammas comprise entre la péninsule de Bache sur l'île Ellesmere et le versant sud du glacier Humboldt au Groenland.

Une ligne d'anomalies isolées de 200 gammas s'étend du promontoire Judge Daly au nord jusqu'à l'océan Arctique, en passant par le détroit de Robeson. Ces anomalies, qui semblent résulter de la présence d'un faisceau de dykes très rapprochés, s'alignent avec la zone faillée bien visible du promontoire Judge Daly, que l'on a représenté sur la carte avec un déplacement sénestre de 19 km. On a découvert dans des roches tertiaires des fragments volcaniques de type basalte à olivine, le long de la zone faillée; les indices aéromagnétiques suggèrent aussi que le réseau de failles se prolonge à travers le promontoire Judge Daly.

Ainsi, on conclut qu'il s'est produit un décrochement sénestre d'au moins 19 km le long du détroit lui-même, ce qui semble confirmer l'hypothèse de Wegener formulée en 1912.

[1] National Aeronautical Establishment, Ottawa

Introduction

The question of whether there has been significant relative movement along the Nares Strait between Ellesmere Island and northern Greenland has been a contentious issue since Alfred Wegener first published his famous book on continental drift more than seventy years ago. In 1982, the available geological and geophysical evidence for and against such movement was well summarized in a volume published by the Geological Survey of Greenland edited by Peter Dawes of the Greenland Survey and William Kerr formerly of GSC (Dawes and Kerr, 1982). This was the proceedings of a symposium held in Halifax by the Geological Association of Canada in 1980. In the volume, one of the pieces of published geophysical evidence cited for minimal relative displacement was a vertical component magnetic anomaly which extended right across the Kane Basin (Riddihough et al., 1973). The anomaly in question was obtained by a high level (11 500 feet) airborne magnetic survey flown by the Earth Physics Branch. The flight line spacing for the survey was 75 km, which resulted in two lines being flown in a northeasterly direction across Kane Basin. The contoured magnetic data were the vertical component values averaged over a 60 second time period which represented a distance of 7.3 kilometres on the ground. Thus the ability of the data to resolve the underlying geology was not very high and indeed the main objective of the survey was to map the various components of the main earth's field.

Accordingly a low-level aeromagnetic reconnaissance of the Kane Basin was planned to be undertaken as part of the co-operative project between the National Aeronautical Establishment and the Geological Survey of Canada. A series of parallel flight lines were laid out at a 10 nautical mile line spacing to cross the inferred elongated anomaly at right angles. The first aeromagnetic field operation was carried out in April 1981 using the NAE Convair 580 aircraft (Hardwick, 1978) which was equipped with a high-sensitivity

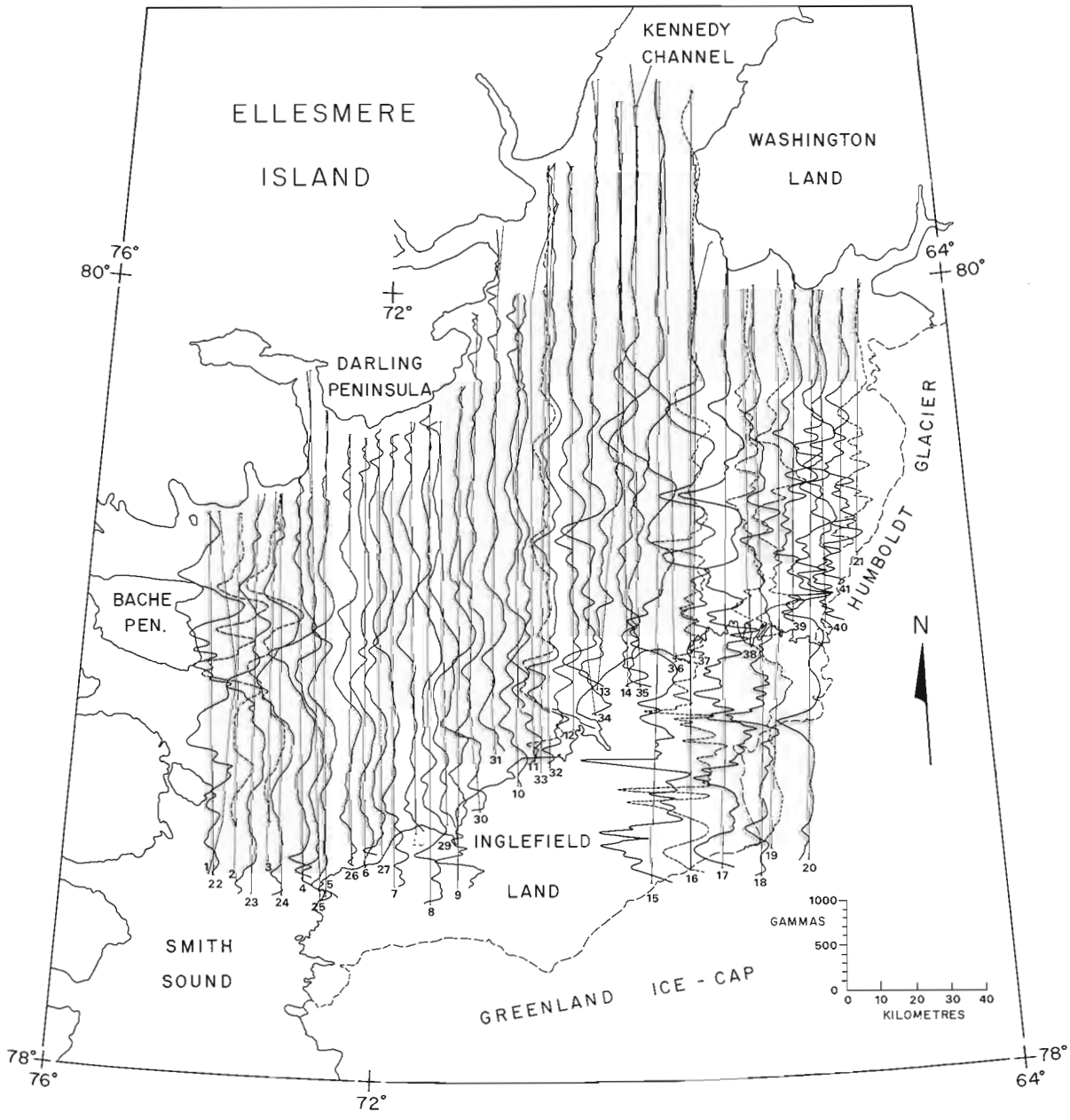

Figure 63.1. Filtered aeromagnetic profiles in the Kane Basin, NWT.

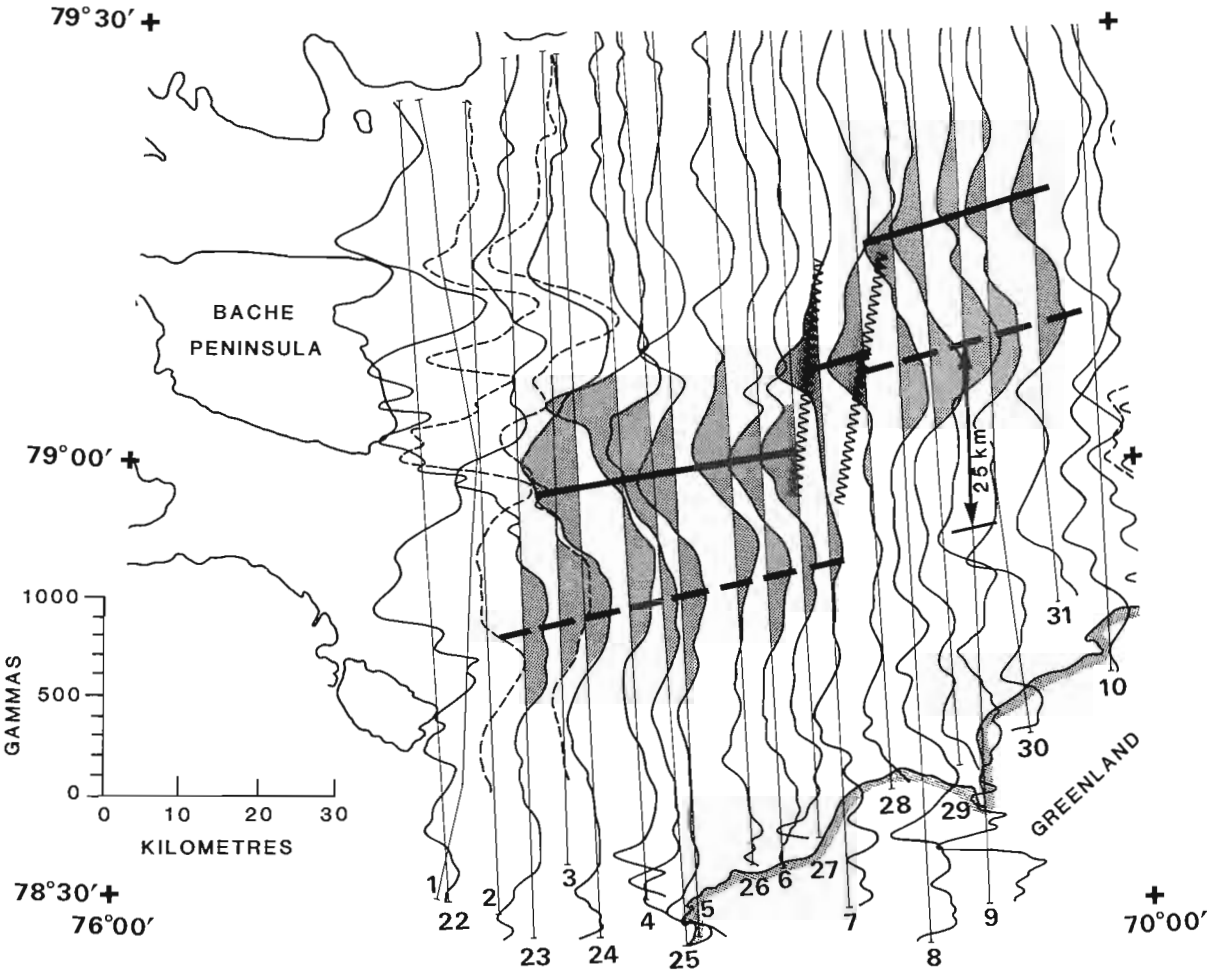

Figure 63.2. *Enlarged portion of Figure 63.1 showing 25 km offset in the magnetic anomalies which strike in an east-west direction from Bache Peninsula on Ellesmere Island.*

cesium-vapour magnetometer system. The US Air Force Base at Thule, Greenland was used as a base of operations. The lines were flown at a height of 305 m using the VLF Global Navigation System as the prime navigation aid. The results of the 1981 aeromagnetic reconnaissance indicated that the elongated anomaly did not extend right across Kane Basin but it was decided that the flight line spacing was too great to be sure of the continuity of the anomalies between the flight lines. Accordingly additional work was carried out in Kane Basin in April 1982 to fill in between the flight lines so that the spacing was reduced to 5 nautical miles. In 1982, it was decided to extend the reconnaissance to the north to obtain orthogonal aeromagnetic profiles across the Kennedy and Robeson channels and additional work was also carried out in 1983.

Results

Figure 63.1 shows the 40 stacked magnetic profiles in the Kane Basin which resulted from the 1981 and 1982 field operations filtered to eliminate the long wavelength component including the core field. This procedure enables both the profile and its associated flight line to be more easily recognized. The typical magnetic response of the Precambrian rocks in the southeast part of the Kane Basin is readily apparent. The smooth nature of the profiles in the northeast part of the Kane Basin is indicative of a sedimentary basin which appears to extend under the Paleozoic rocks of Washington Land. There is a disruption in the trends of the line of highs and lows some 500 gammas or so in amplitude which extend from Bache Peninsula in an easterly direction across Kane Basin. These offsets which occur about 60 km east of Bache Peninsula are shown in greater detail in Figure 63.2. The total offset is about 25 km in a sinistral sense and is best seen by tracing the dominant low across the lines. Presumably the rocks in the Bache Peninsula which produce the anomalies are the diabase sills of Late Proterozoic age mapped by Christie (1967). Thus the age of the diabase sills, which have been dated by potassium-argon techniques (see Peel et al., 1982) at about 1200 Ma, predate the onset of continental drift in the Mesozoic.

Figure 63.3 shows the 34 profiles flown north of Kane Basin between the high cliffs which bound either side of the Kennedy and Robeson channels. In Kennedy Channel, the profiles are mostly flat but striking north of Judge Daly Promontory are a series of distinctive isolated anomalies 200 gammas or so in amplitude. From the continuity of the anomalies, they appear to be due to parallel dyke-like intrusions which extend a distance of 107 km from Judge Daly Promontory to the Arctic Ocean.

Interpretations of the anomalies on lines 61 and 64 were carried out using an interactive least-squares modelling program (Teskey, 1982). Figure 63.4 shows an interpretation of the results on line 61 which is about 13 km north of Judge Daly Promontory. The depth of water at the prominent

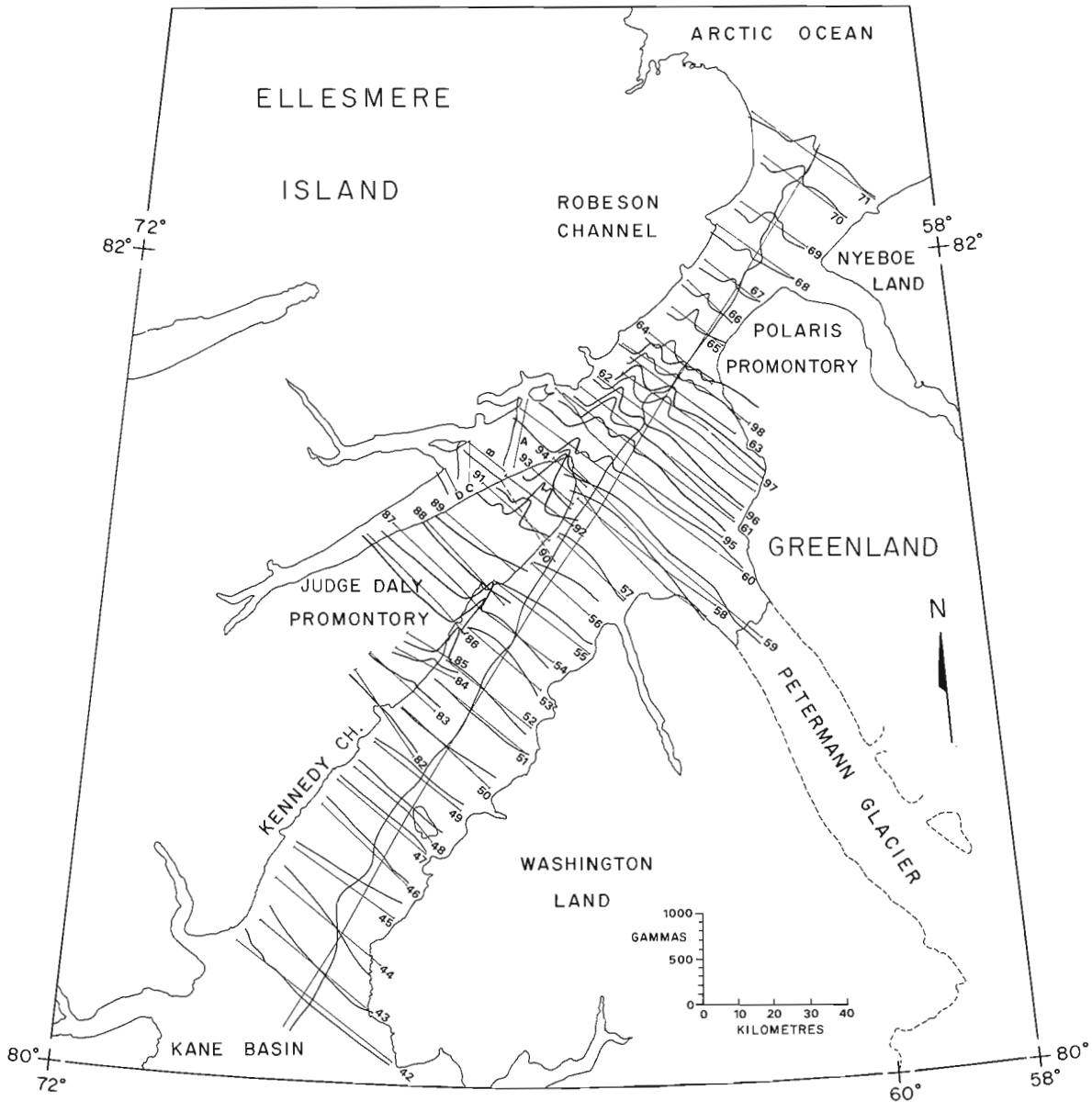

Figure 63.3. *Aeromagnetic profiles obtained in Kennedy and Robeson Channels, NWT.*

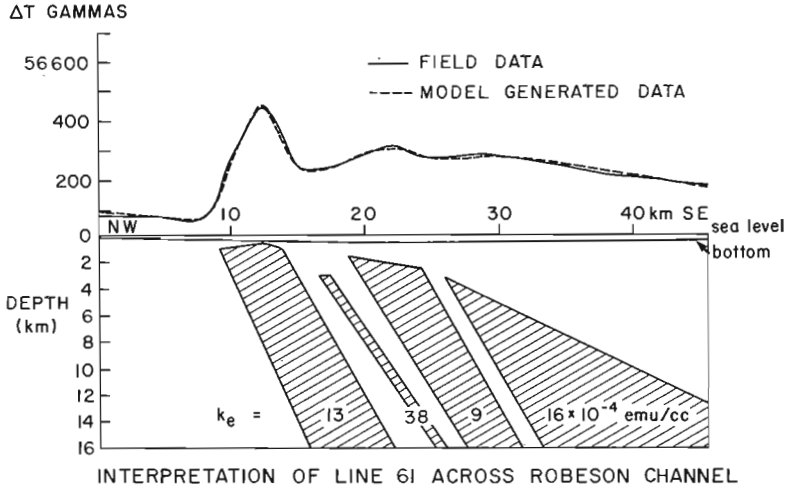

Figure 63.4

Interpretation of the total field data along line 61 across Robeson Channel, 13 km north of Judge Daly Promontory.

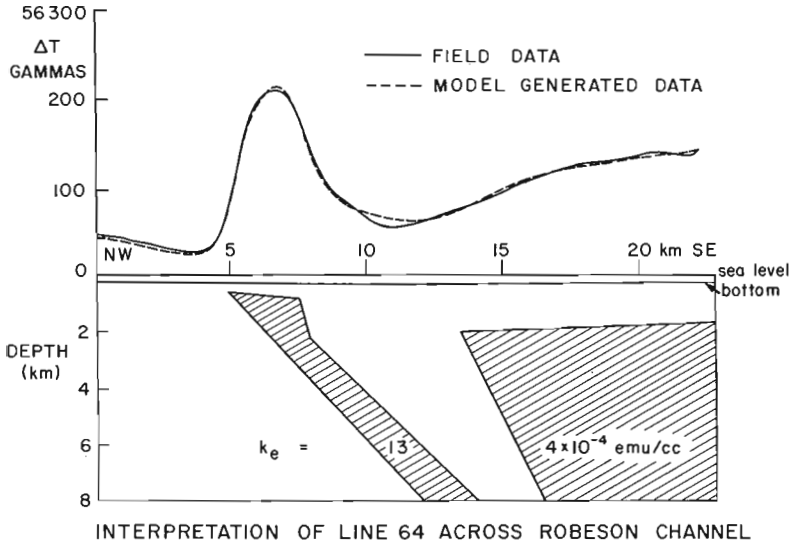

Figure 63.5

Interpretation of the total field data along line 64 across Robeson Channel, 40 km north of Judge Daly Promontory.

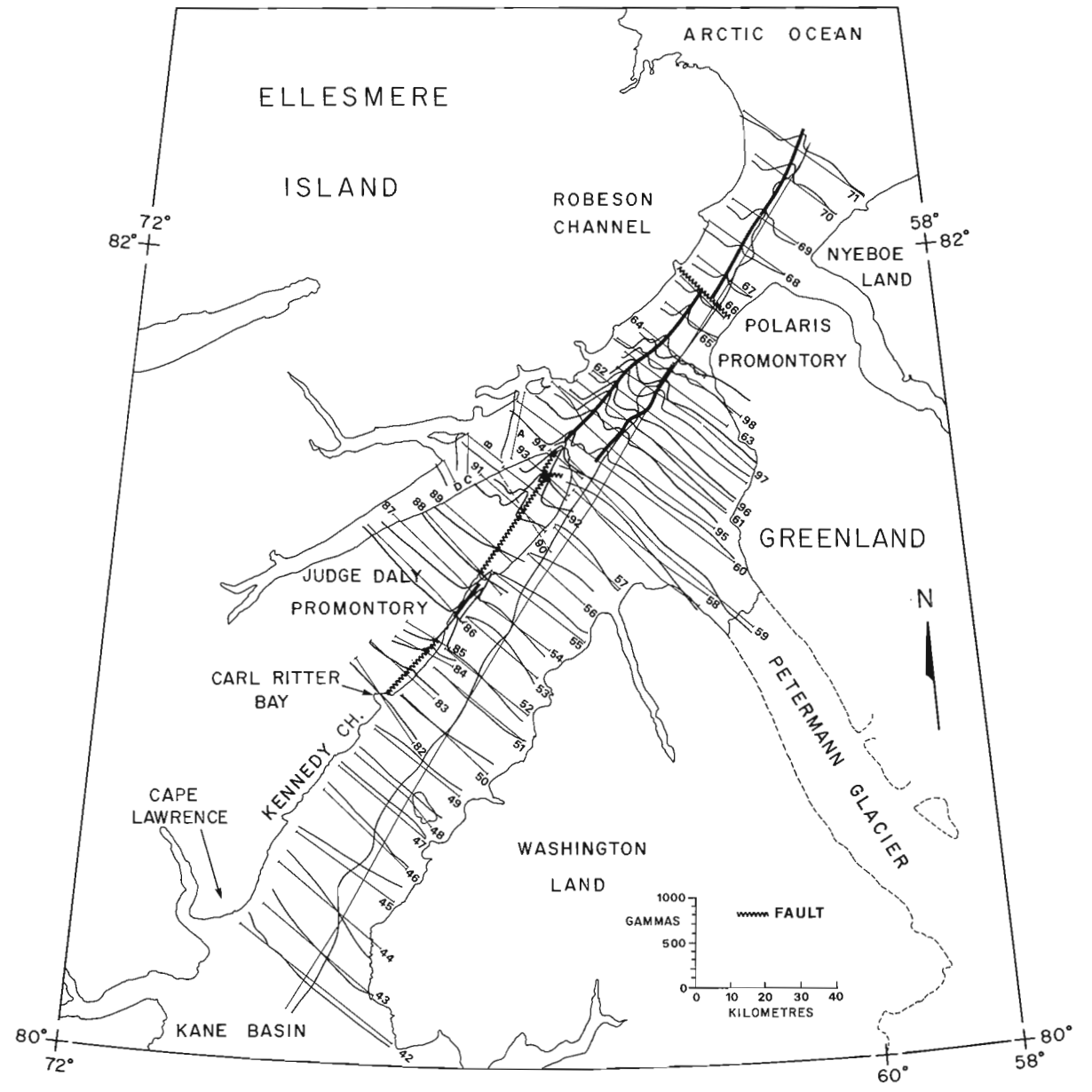

Figure 63.6. *Inferred correlation of the anomalies between the flight lines in Robeson Channel and with the mapped fault in Judge Daly Promontory.*

400-gamma anomaly approximately 12 km from the northwest end of line 61 is approximately 700 m. The computer program has calculated that the causative dyke which dips at 65° to the southeast is at no great distance below the bottom of the strait so the distance from the survey aircraft to the top of the dyke is approximately 1000 m. The dyke has a thickness of 4.5 km but in reality it may be a swarm of thin dykes which cannot be resolved at that height and that may also be the case for the causative bodies to the southeast.

Figure 63.5 shows an interpretation of the aeromagnetic data on line 64 which is approximately 40 km north of Judge Daly Promontory. The causative body also dips at a high angle to the southeast indicating that the fault plane also dips to the southeast; and again its top is at no great distance below the bottom of the strait. The effective susceptibility (which would include any remanent magnetism contribution) has been calculated by the program to be 13×10^{-4} emu/cc which is equivalent to about 0.5% magnetite content and is exactly the same as the value for the same anomaly on line 61. Its thickness is however somewhat smaller being only about 1000 m.

Figure 63.6 shows the inferred correlation of the anomalies in Robeson Channel. It transpires that the dyke anomalies line up with a prominent fault on Judge Daly Promontory that has been mapped by Christie (1964), and others appropriately called the Judge Daly fault. The fault appears to extend to the south as far as Carl Ritter Bay according to Miall (1982) and is associated with a Tertiary inlier. Volcanic rock fragments with an olivine-rich basaltic composition have been found along the fault system and Miall concluded that it was derived from a volcanic source under the waters of Nares Strait. Sinistral displacement along the fault has been estimated by Mayr and DeVries (1982) to be 19 km.

We concluded from this evidence in a paper presented at the GSC Current Activities Forum in Ottawa in January 1984 that the dyke system north of the Promontory had been injected into an existing fault system, and that the dyke probably extended across the Judge Daly Promontory.

Accordingly to prove this inference we flew 13 additional low-level aeromagnetic profiles (lines 82 to 94 in Fig. 63.3) across the rugged topography of the Promontory in April 1984. Four additional lines were also flown to fill in between the lines in the Robeson Channel immediately to the north (lines 95 to 98). The results from these lines are also included in Figure 63.3. The dyke had a recognizable expression on ten of the profiles flown in 1984. The dyke anomaly was not present on two of the lines in the central part of Judge Daly Promontory so it may be confined to the Tertiary outliers mapped by Miall (1982). Nor does the dyke appear to extend into Carl Ritter Bay; it may however be present farther south. Further work across the Ellesmere Island shoreline of southern Kennedy Channel is required to check this possibility especially in the vicinity of Cape Lawrence.

Conclusion

The low-level aeromagnetic reconnaissance has been able to define a fault system that runs parallel to the Nares Strait for approximately 200 km, and which from geological evidence on Judge Daly Promontory has had at least 19 km of movement along it. This evidence coupled with corroborating evidence in Kane Basin appears to be the first direct geophysical evidence that there has been some relative motion along the Nares Strait in a left-handed sense. We hope that we have also demonstrated that it is necessary to fly low-level reconnaissance surveys to obtain diagnostic magnetic data that can detect the rather subtle features that are important in elucidating the Nares Strait problem.

We believe there has been substantial differential movement between Ellesmere Island and Greenland with only part of the movement being confined to Nares Strait itself. This view has been strengthened during the survey flights by visual impressions of the topography on either side of the Nares Strait. The topography of the land on either side of the Strait is markedly different in spite of the apparent continuity of the geology across the strait. On the Canadian side the topography is quite rugged due no doubt to the influence of the middle Tertiary Eurekan orogeny whereas on the Greenland side the topography is relatively flat except for incised valleys indicative of a rather mature topography. The photograph on the title page of the volume edited by Dawes and Kerr (1982) which is a view across the Nares Strait near Franklin Island illustrates this fact very well indeed.

References

Christie, R.L.
1964: Geological reconnaissance of northeastern Ellesmere Island, District of Franklin; Geological Survey of Canada, Memoir 331, 79 p.

1967: Bache Peninsula, Ellesmere Island, Arctic Archipelago; Geological Survey of Canada, Memoir 347, 63 p.

Dawes, P.R. and Kerr, J.W.
1982: Nares Strait and the drift of Greenland: a conflict in plate tectonics; Meddelelser om Gronland, Geoscience 8, 392 p.

Hardwick, C.D.
1978: The NAE Convair 580 research aircraft – an update for potential users; National Aeronautical Report, LTR-FR-64, 23 p.

Mayr, U. and de Vries, C.D.S.
1982: Reconnaissance of Tertiary structures along Nares Strait, Ellesmere Island, Canadian Arctic Archipelago; in Nares Strait and the Drift of Greenland: A Conflict in Plate Tectonics, ed. P.R. Dawes and J.W. Kerr; Meddelelser om Gronland, Geoscience 8, p. 167-175.

Miall, A.D.
1982: Tertiary sedimentation and tectonics in the Judge Daly Basin, northeast Ellesmere Island, Arctic Canada; Geological Survey of Canada, Paper 80-30, 17 p.

Peel, J.S., Dawes, P.R., Collinson, J.D., and Christie, R.L.
1982: Proterozoic-basal Cambrian stratigraphy across Nares Strait: correlation between Inglefield Land and Bache Peninsula; in Nares Strait and the Drift of Greenland: A Conflict in Plate Tectonics, ed. P.R. Dawes and J.W. Kerr; Meddelelser om Gronland, Geoscience 8, p. 105-115.

Riddihough, R.P., Haines, G.V., and Hannaford, W.
1973: Regional magnetic anomalies of the Canadian Arctic; Canadian Journal of Earth Sciences, v. 10, p. 157-163.

Teskey, D.J.
1982: An interactive program for estimating the parameters of magnetic anomaly sources; in Current Research, Part A, Geological Survey of Canada, Paper 82-1A, p. 51-53.

DMAPS: A NEW EXPERIMENTAL DIGITAL MARINE REFLECTION SEISMIC ACQUISITION AND PROCESSING SYSTEM

Project 700092

A.R. Bays[1], D.F. Poley[1], and S.M. Blasco
Atlantic Geoscience Centre, Dartmouth

Bays, A.R., Poley, D.F., and Blasco, S.M., DMAPS: a new experimental digital marine reflection seismic acquisition and processing system; in Current Research, Part A, Geological Survey of Canada, Paper 85-1A, p. 523-526, 1985.

Abstract

A new microcomputer based digital seismic reflection data acquisition and processing system (DMAPS) has been designed to replace existing analogue equipment for use in high-resolution, shallow marine seismic reflection surveys in the Beaufort Sea. DMAPS is based on an IBM-PC microcomputer and is constructed largely using commerically available components. The system is capable of sampling rates of up to 14 kHz for each of two channels. Data may be digitally filtered, deconvolved and summed during acquisition and can also be stored on digital magnetic tape for subsequent processing and analysis.

Résumé

On a conçu un nouveau système d'acquisition et de traitement des données numériques de sismique-réflexion basé sur l'emploi d'un microordinateur (DMAPS), capable de remplacer le matériel analogique existant, pour effectuer dans la mer de Beaufort des levés marins détaillés de sismique-réflexion à faible profondeur. Le DMAPS fait appel à un microordinateur IBM-FC et a largement été construit avec des éléments disponibles dans le commerce. Ce système est équipé pour des fréquences d'échantillonnage pouvant atteindre 14 kHz sur chacun des deux canaux. On peut filtrer, décrypter et additionner numériquement les données pendant leur acquisition, et aussi les enregistrer sur bande magnétique numérique, afin d'effectuer plus tard leur traitement et leur analyse.

[1] Department of Geology and Geophysics, University of Calgary, Calgary, Alberta T2L 2A7

Introduction

Digital technology is widely used in conventional multi-channel seismic data acquisition equipment. The advantages of digital acquisition include the capacity for processing data, the possibility of automating the acquisition process, and the capability to interface with other digital electronic equipment (e.g. navigation systems). Most single or dual channel, high resolution seismic systems currently in use, however, are based on analogue equipment. The need to update the acquisition of high resolution seismic data has stimulated the development of DMAPS, a new digital system by the Geological Survey in conjunction with the University of Calgary.

The main justification for developing a data acquisition unit rather than purchasing one, is that the specifications and capabilities of the system can be tailored to the specific operational requirements of the experiment. Also, because of the recent availability of powerful yet inexpensive micro-computers, it is presently possible to construct a flexible, easily reconfigured data acquisition system from commercially available components at a considerably lower cost than would be involved if such a system were to be custom built. By making the new system modular in design, it may be enhanced and upgraded as new components become available. As an additional benefit, the experience gained during the construction and evaluation of the prototype system will be applicable to future projects of a similar nature.

System concept

The initial requirements for the DMAPS were that it should be a microcomputer based, 2 channel marine seismic data acquisition and processing unit, suitable for use on ocean-going survey vessels. Before drawing up a detailed specification for the new system, several general requirements were established which had to be met by any equipment destined for shipboard use in the Beaufort Sea. Amongst the most important of these were that:

1. The system must be rugged enough for reliable, long-term field use under arctic conditions.
2. The equipment must be compact to allow installation in confined spaces, and isolated from external electrical interference.
3. The instrumentation should be simple to install, operate, service and maintain.
4. Wherever possible, commercially available equipment and components should be utilized.
5. The system should be modular in design to allow for easy modification and improvement and to permit economical updating in the future.

In addition, a number of other factors were also considered prior to drawing up a detailed specification for the new equipment. These included: the cost and availability of components, compatibility with existing instrumentation, and possible future applications for the equipment. With these constraints in mind, a detailed list of necessary system characteristics was compiled based upon geophysical requirements.

System outline

Some of the more important features of DMAPS are:

1. A minimum of 2 channels of data acquisition with a provision for expansion at a later date.
2. The capability to sample frequencies of up to 14 kHz (28 kHz single channel sampling rate).
3. A digitizing precision of 12 bits plus gain word.
4. Provision for analogue first-stage amplification and filtering.
5. The capability to acquire, process, display and record a seismic trace (1/10-1/2 second in length and consisting of at least 2000 data points) at repetition rates up to one per second.
6. Signal processing capabilities including: real time, on-line deconvolution, filtering, trace summing and water column removal; real-time, off-line spectral analysis and stacking.
7. The capability to interface with an electronic navigation system.
8. The provision for shot timing based on time or distance.
9. Data storage capabilities to include a permanent, machine-readable record as well as a floppy disk drive for temporary storage.
10. Record annotation – location, time, line ID, instrument settings, etc.
11. Versatile data display options – CRT monitor and paper record – variable area or variable density display.
12. Real-time, on-line and/or off-line generation of seismic sections.

The seismic system has to be capable of acquiring at least two channels of data simultaneously. This is to allow the recording of both the reflected seismic pulse and the source signature. The provision of extra channels will permit additional hydrophones and other geophysical devices that may be required in the future to be monitored and recorded simultaneously with the seismic data.

Current studies of airgun sources at the University of Calgary suggest that there may be useful information content in frequencies in excess of 2000 Hz. For the system to acquire accurate data in this band, a minimum digitizing rate of 4000 samples per second is necessary. In order to minimize the volume of data to be processed and stored, however, it must be possible to reduce this acquisition rate if desired. If high frequency profiling devices are used, even greater digitizing rates may be required and, for this reason, the system has been designed to acquire up to 28 000 samples per second.

The analogue to digital conversion process must handle a signal with a large dynamic range. To accommodate this large variation in signal amplitude, a minimum of 12 Bits (72 dB) of A-D range is required. In addition, some programmable amplifier gain is necessary in order to permit the amplitude of the incoming signal to be matched to the voltage range of the A-D converter. An analogue pre-amplifier is used to increase the hydrophone signal up to a level suitable for the programmable gain stage. This device also provides some filtering capability to prevent aliasing.

Signal processing

One of the justifications for using a digital data acquisition system is that it provides the ability to perform digital signal processing. The real-time processing capabilities of the new system may be divided into:

a. On-line operations which are performed at the time of acquisition of the signal and before it is printed; e.g. time variable gain, digital filtering, trace summing and deconvolution with the source signature.

b. Off-line processing which may be performed at any time after the signal has been stored; e.g. stacking, filtering and frequency analysis.

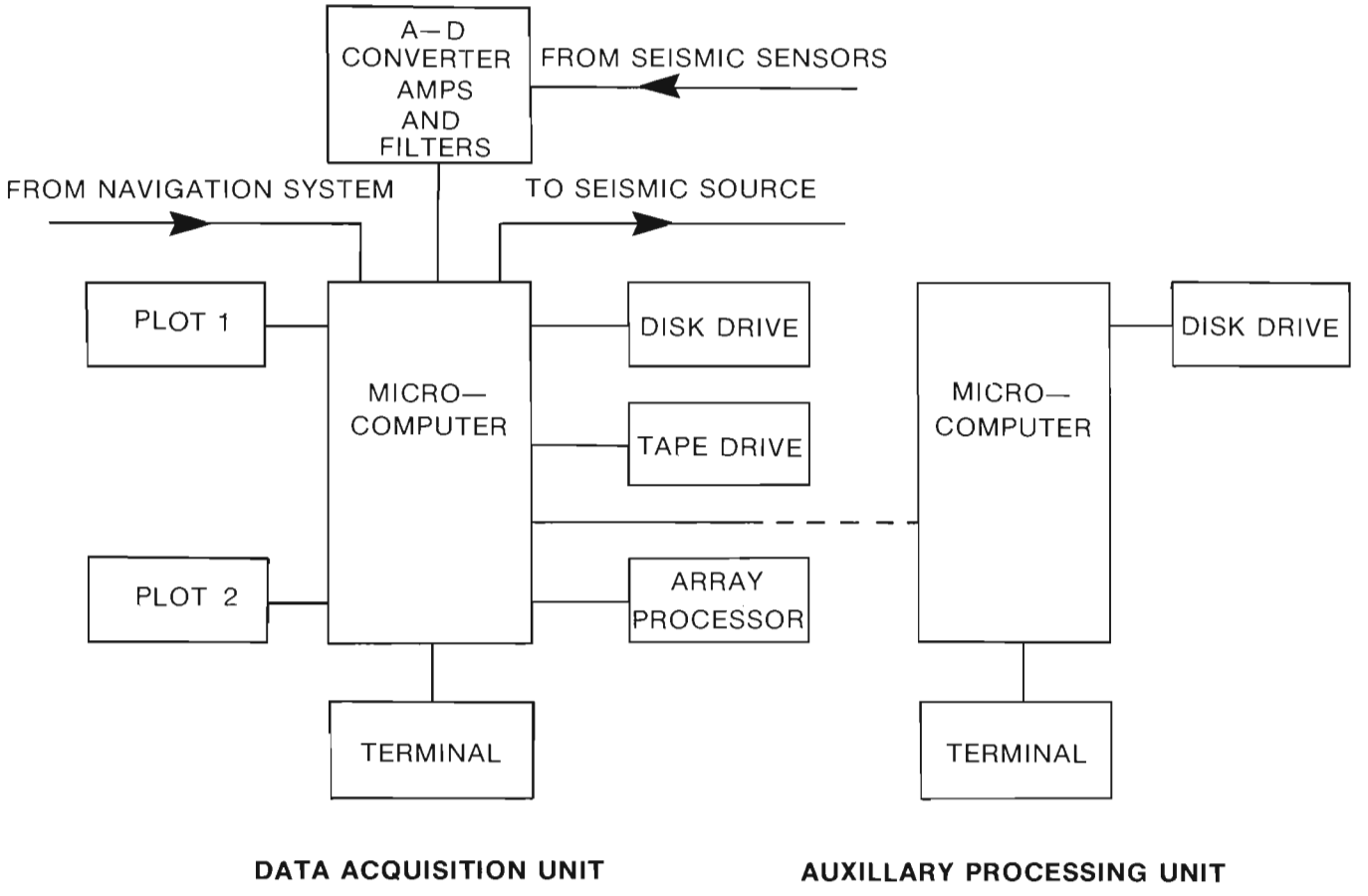

Figure 64.1. *Schematic diagram of the digital marine seismic reflection data acquisition and processing system (DMAPS).*

The host microcomputer can be used for both a and b functions, however, the time required to perform necessary operations is prohibitive for most applications. For real-time processing requirements, a separate hardware array processor is employed. This relieves the host computer of some of the more demanding numerical manipulation and leaves it free for other tasks. Coded algorithms for numerical filtering, trace summing and deconvolution can be downloaded into the array processor program memory prior to the commencement of data acquisition. The array processor then acts as an extremely fast, independent computer to implement these algorithms on the data immediately following acquisition and prior to display.

The existing analogue system which DMAPS is designed to improve upon, suffers from three major drawbacks including long oscillatory source pulse problems, multiple reverberations and low signal to noise ratio beyond 100 ms. Digital acquisition of seismic data will allow real-time and post acquisition processing aimed at resolving these drawbacks. The following processes are currently under development:

1. Programmable linear or time variable gain – both pre-amplifier gain and post-processing trace scaling capabilities.
2. Digital filtering – band pass filters will improve signal to noise ratio over the spectrum of the recorded data. Programmable, narrow band reject filters will be designed to eliminate monochromatic noise (including electrical interference and harmonics).
3. Two or more tracing summing – presently, single channel reflection data are acquired at a ship speed of about 8.3 km/h (4.5 knots) with a firing rate of 1 to 3 seconds. Spatial sampling between shots is generally less than 5 m. Summing of two or more traces from successive shots will increase the signal to noise ratio approximately 1.4 times without significant loss of lateral resolution.
4. Signature deconvolution – Airguns are commonly used with the present Geological Survey marine system. Duration of the source signature is generally greater than 200 ms for a high resolution airgun source. This causes masking of returning reflection data, especially below a high amplitude event such as the reflection from the top of permafrost. Knowledge of the source wavelet and the process of deconvolution will compensate for some of the undesirable signature characteristics hence improving the acquired data. Important considerations are: (a) ability of the 'known' signature to approximate that travelling through the earth; (b) choice of deconvolution operator length; (c) source wavelet and therefore operator phase; and (d) system capabilities (time constraints).

An auxilliary processing unit, comprising a second, independent computer, is used specifically for data analysis and allows for real-time, off-line processing and hence the generation of real-time processed seismic sections. This approach offers some logistic advantages, because the data analysis machine and its operator need not be located near the acquisition equipment. An additional benefit is that the two computers can be of the same type, thereby allowing interchange of parts in case of a breakdown of the acquisition unit in the field.

Data acquisition, storage and display

One of the most important reasons for constructing a new seismic system is to allow the data acquisition system to be linked to the computer-controlled navigation equipment presently in use. This feature permits survey data to be obtained at regular spatial intervals rather than on a time increment basis as is currently the most common practice. The seismic system computer communicates with the navigation system via a digital interface and computes the ship's current position by using the most recent navigation fix and the ship's velocity. The seismic source can then be triggered by the computer at a subsequent time, calculated to correspond with the required shot location.

Data recording and storage requirements are threefold: firstly, an immediate paper record is needed to allow for data quality assessment and preliminary data interpretation to be performed; secondly, data stored on floppy disks in digital format are needed for frequency analysis, source comparisons and other real-time data analysis; and finally, some form of long-term, machine-readable record is required for archiving and so that subsequent data processing may be performed if required.

During the course of a survey line requiring 16 hours to complete, up to 60 000 seismic traces may be acquired. Assuming that 2000 samples are acquired in each trace, this data would require 240 000 000 bytes of long-term storage space which is the equivalent of about 6 reels of half-inch magnetic tape. At present, digital magnetic tape records are the most commonly used medium for long-term data storage and will be utilized in the new system initially. It is likely, however, that another storage method such as optical recording will eventually prove to be superior and may be adopted in the future.

The paper record has to be able to display the individual traces, each comprising approximately 2000 samples. Display resolution is 4 bits using the EPC 3200 (equivalent to a 16 shade, variable density scale), however this resolution may be increased by choosing a variable area type of presentation when greater precision is required. Both the paper plot and the magnetic tape record can be annotated to show the location, line number, time and details of the survey parameters. Facilities for plot scaling and water column delay are provided by the host computer.

Hardware specifications

A schematic diagram of the new system is given in Figure 64.1. The microcomputer used in the data acquisition unit is an IBM-PC with two, 360 kbyte capacity disk-drives, 256 kbytes of random access memory and an Intel 8087 numeric co-processor. Internally mounted accessories include a Plantronics Colorplus graphics card with parallel port (driving an IBM colour monitor), an expansion chassis adaptor card and a Marinco APB-3024PC array processor.

Peripheral interfaces and extra hardware are contained in an external expansion chassis (Anrok PCX-6) and include an Overland Data TC-PC 1/2" tape controller card, a Data Translation DT-2801A analogue/digital interface board, a real time clock, a Sritek iAPX-286 Microcard auxiliary processor which is used to control printed output and an additional parallel port. Analog signal conditioning is provided by a custom made, time-varient-gain pre-amplifier. Digital data storage is provided by a Cypher F880 1/2" tape drive whilst paper records are produced on an EPC-3200 recorder and Epson FX-80 matrix printer.

The auxiliary processing unit comprises a similarly equipped IBM-PC without the expansion chassis and other peripheral interfaces. Data are transferred from one computer to the other either by means of floppy disks or via a serial communications link.

Because of the rapid developments in microelectronic technology, it is not practical to construct instrumentation that is fully 'state of the art'. For this reason the new seismic system has been designed to facilitate continual improvement and expansion and the hardware has been selected to be as compatible as possible with anticipated new developments in the microelectronics field. Some examples of future upgrading which are currently under consideration include: a more powerful Intel 80286 based microcomputer, a laser printer to replace the EPC-3200 and an optical disk data storage system.

Software requirements

The real-time operating constraints of the acquisition and processing system required that the software be efficient, so as to take maximum advantage of the hardware capabilities. Another important requirement was that software development should proceed as rapidly as possible and for this reason, the software has been designed to be modular so that several programmers can work simultaneously. This approach also facilitates the inevitable program modifications and improvements that will be required from time to time.

The system control and data processing programs are written in the C language working under the PC-DOS 2.1 operating system. Assembler language device drivers are used to control peripheral devices and assembler language is also used for coding some critical operations requiring maximum speed and for programming the array processor.

Because of the necessity to quickly transfer large amounts of data between the components of the system, direct memory access (DMA) techniques have been used extensively to permit maximum data transfer rates between the computer and the other devices (i.e. A-D board, array processor and tape drive). Communications with external devices such as the navigation system and the control console are all interrupt driven to minimize the overhead requirements of the IBM-PC. The bandwidth limitations of the IBM bus structure have made it necessary to employ parallel processing to permit maximum data throughout. This has been implemented by making use of intelligent peripheral devices such as the APB-3024PC array processor for signal processing and the Sritek Microcard for data output.

Acknowledgments

This project is funded by the Panel on Energy Research and Development (PERD) Task 6: Conventional Energy systems.

HIGH GRADE METAMORPHIC ROCKS OF NORTHWESTERN MELVILLE PENINSULA, DISTRICT OF FRANKLIN

Project 840013

Mikkel Schau and K.E. Ashton[1]
Precambrian Geology Division

Schau, M. and Ashton, K.E., High grade metamorphic rocks of northwestern Melville Peninsula, District of Franklin; in Current Research, Part A, Geological Survey of Canada, Paper 85-1A, p. 527-532, 1985.

Abstract

High grade metamorphic rocks are exposed in the Encampment Bay area on Melville Peninsula. Preliminary results indicate that a tonalitic-granodioritic suite was intruded by granite and mafic dykes and later unconformably(?) overlain by sediments correlated with the 2.9 Ga Prince Albert Group and was then metamorphosed to granulite (in the west) and upper amphibolite (in the east) grade probably during late Archean time. Steep, east-west faults of Proterozoic age cut the region into blocks prior to the mid-Devonian uplift of the Melville Peninsula horst. Small showings of pyrite and rare molybdenite are associated with quartz, hematite, and/or epidote alteration associated with faults.

Résumé

Des roches fortement métamorphisées affleurent dans la région de la baie Encampment sur la péninsule de Melville. Les résultats préliminaires indiquent qu'une série tonalitique et granodioritique a été traversée par des dykes granitiques et fémiques, et plus tard recouverte en discordance(?) par des sédiments qui présentent une corrélation avec le groupe de Prince Albert (2,9 Ga) et que par la suite, cette série a été transformée par un métamorphisme du faciès des granulites (à l'ouest) et du faciès supérieur des amphibolites (à l'est), probablement pendant l'Archéen supérieur. Pendant le Protérozoïque, des failles orientées est-ouest et de fort pendage ont partagé la région en blocs, avant le soulèvement du horst de la péninsule de Melville survenu pendant le Dévonien moyen. De petites manifestations de pyrite et d'un peu de molybdénite sont associées à du quartz et à de l'hématite, et à des altérations en épidote associées à la présence des failles.

[1] Department of Geological Sciences, Queen's University, Kingston, Ontario K7L 3N6

Introduction

Granulites were reported in the Encampment Bay map area (47C) by W.W. Heywood (1974) and their distribution shown on the Metamorphic Map of Canada (Fraser and Heywood, 1978). A preliminary compilation of the 1973 results is available (G.S.C. Open File 1046) which presents a slightly modified version of granulite distribution. A positive gravity anomaly underlying the northwestern part of the Melville Peninsula can be modelled as a tilted slab of more dense (+0.1 g/cm^3) material with a southerly dip underlying less dense material. According to the model the more dense material should be exposed in the Encampment Bay area. This paper reports on 1984 field work in parts of 47C and focuses on the high grade metamorphic rocks. The granulites may be interpreted as exposures of middle crust or alternately as the product of a late Archean thermal dome such as those postulated for an area a hundred kilometres to the southwest in rocks of similar age and provenance (Schau, 1978).

The map area contains many glacial features which in part obscure the bedrock geology. The amphibolite grade rocks occur at the higher elevations but are largely covered by felsenmeer, till, and other glacial debris. Granulites occur at lower elevations but are better exposed and present a more rugged topography since dykes, joints, and minor fractures have been preferentially excavated. The map sheet is within the barren lands and there is only a sparse vegetational cover. Large lakes were ice covered until mid-July. The weather in July was clear but extensive sweeping fog banks covered the area in August.

Method of mapping was by foot traverses originating from a main camp and later subsidiary camps. A helicopter was available for ten days in August. The region is very close to the magnetic north pole and suncompasses were used when possible. Brunton compasses were calibrated against the suncompasses to provide a means of measuring orientations during cloudy periods. Daily drift of magnetic declination in excess of 20 degrees was noted but on most days the drift was only a few degrees.

Description of units

Unit 1 (tonalite-granodiorite suite)

Unit 1, which underlies most of the area, consists of granodioritic to tonalitic members of a metaplutonic suite (orthogneiss) which in the west and in smaller irregular areas to the east has been metamorphosed to granulite grade. Elsewhere the unit is at amphibolite grade.

At granulite grade the outcrops are smooth weathering in various shades of olive. The rocks have a low colour index and variable textures made up of both linear and planar elements defined by biotite, orthopyroxene, and locally, hornblende. At amphibolite grade the outcrops are smooth weathering in various shades of white to grey and pink. The rocks have a low colour index and a mix of planar and linear elements defined by biotite, hornblende, and opaques.

Local, poorly defined layers and aggregates of mafic minerals are tightly folded about horizontal axial planes defined by mafic clots and flattened quartz. Two poorly defined sets of subhorizontal foliations that intersect at small angles were noted in several localities. Some of the folded layers are granite that may be part of unit 2. In contrast to the mesoscopic folds noted above a thin linear zone of garnet-sillimanite-biotite-quartz-feldspar gneiss with locally developed rusty patches stretches for 20 km in a north-south direction. The zone is a thin aluminous unit formed after folding but prior to metamorphism. A working hypothesis is that it represents a metamorphosed gouge or fault zone. Unit 1 consisted of a plutonic suite of tonalite to granodiorite composition prior to metamorphism and deformation. Unit 1 is cut by all other units in the area. No radiometric data are available for it. In NTS area 47 B to the south Frisch (1982) described a tonalite unit which he speculated was older than the Prince Albert Group. Perhaps unit 1 is correlatable with this unit.

Unit 2 (lineated granite)

Stocks, sheets, and dykes of unit 2 cut the granulite grade country rock in the western part of the region. Large bodies are slightly less resistant to erosion than the granulite host. The sheets have a shallow dip and are interleaved with the host in an intricate manner. Some of the smaller sheets have been omitted from Figure 65.1 for clarity.

Unit 2 consists of orange to pink weathering, pink to white, medium or coarse grained, homogeneous granite with foliation or lineation. It has a low colour index with only a few per cent biotite altered to chlorite and a trace of magnetite. Feldspars are locally sugary in texture and quartz is smoky. In thin section the rock is seen to be a perthite rich granite with a trace of biotite partly altered to chlorite and a trace of magnetite.

The mineral assemblage quartz-alkali-feldspar-biotite-opaque is not characteristic of, but is stable at, granulite grade. Dykes of unit 3 cut unit 2 and since unit 3 is locally metamorphosed to granulite grade the granite is likewise interpreted to have been affected by granulite metamorphism even though, as yet, no orthopyroxene has been identified from the granite. Quartz grains are linear or pancake shaped and feldspars have been polygonitized and flattened. Poorly defined foliations are flat and lineations have shallow plunges. The age of the granite is younger than unit 3 and older than unit 1 but correlatives are not currently known.

Unit 3 (lineated metabasic dykes)

Foliated, lineated metadiabase dykes are well exposed in the cleared area southeast of the lake at the head of Brevoort River but are found in unit 1, and less abundantly in unit 2, throughout the area.

The dykes are 10 cm to 30 m wide and extend along strike for up to 6 km, but poor exposure and tectonic disruption combine to make most mapped dyke segments short. The dykes are black weathering, black, fine to medium grained and consist of lineated hornblende and minor plagiclase. Thinner dykes are finer grained and occur as satellites to nearby thicker medium grained dykes. The latter generally contain fist sized medium to coarse grained, feldspar rich, pyroxene and hornblende bearing aggregates referred to as sweats. The dykes are folded along with internal lineation defined by hornblende elongation. The folds are upright, open and have a moderate plunge to the northeast. Dykes from the west of the orthopyroxene line (Fig. 65.1) consist of hornblende-orthopyroxene-clinopyroxene-plagioclase-quartz-biotite-opaque which is consistent with granulite grade. In contrast, dykes from amphibolite grade country rocks are lineated, medium grained and contain sweats which, on the basis of one thin section, consist of hornblende-clinopyroxene-plagioclase-quartz-biotite-opaque-alkali feldspar which is consistent with the amphibolite grade of the country rock. We conclude that the dykes were emplaced prior to the high grade metamorphism which has affected the region.

The dykes cut units 1 and 2 and predate unit 5 granite which cuts it and which contains inclusions of unit 3 (Fig. 65.2, 65.3). The contact relations between units 3 and 4 have not been seen. There are three sets of deformed Archean dykes exposed to the southeast (GSC Open File 1046); the correlation of unit 3 with one of these three sets may be possible with further knowledge of field relationships and geochronological results.

Unit 4 (metasedimentary suite)

Small areas in the northern part of the map area are underlain by metasedimentary gneiss. Resistant units such as metaquartzite characteristically form hills whereas units such as sillimanite schist are recessive.

Rock types of the suite include gneiss, amphibolite, quartzites, sillimanite schist, and metapyroxenite. Hornblende- and biotite-bearing quartzofeldspathic gneisses grade into biotite-bearing quartzofeldspathic gneisses. The amphibolites are thin layers composed of hornblende and plagioclase and are locally garnetiferous. The quartzites are generally white but are locally red or green. They contain scattered muscovite and locally, chromiferous muscovite. They are fine to medium grained with abundant quartz veins and thin interbeds containing mica and sillimanite. Near the base, thin layers of strongly foliated quartzite pebble conglomerate and biotite-muscovite-feldspar-bearing quartzite are interbedded with relatively pure quartzite and sillimanite schist. The schists generally contain muscovite-biotite-sillimanite and on occasion garnet and/or cordierite. Metre thin metapyroxenite dykes cut quartzites.

In general, the foliations are shallow dipping and lineations have shallow plunges. The relationship of unit 4 with structurally underlying units is locally gradational, although crosscutting pods of unit 5 granite occur throughout the contact region complicating relationships. The metasediments in contact with unit 1 are aluminous and grade into unit 1 since sillimanite decreases and hornblende increases. Nowhere is there an intrusive relation recognized between units 1 and 4. Instead we postulate that the aluminous metasediments are pelites and that the gradational part constitutes a metaregolith formed over an unconformity between units 1 and 4.

The metamorphic grade of the metasediment is upper amphibolite based on the coexistence of garnet and hornblende in the amphibolites and quartz and muscovite in the schist. An occurrence of garnet-cordierite-boitite-sillimanite in schist suggests that metamorphic conditions were near highest amphibolite grade (Froese, 1978; Perara, 1984). Metasedimentary rocks of unit 4 overlie unconformably(?) granodiorite of unit 1 and are cut by granite of unit 5. The association of chromiferous quartzites

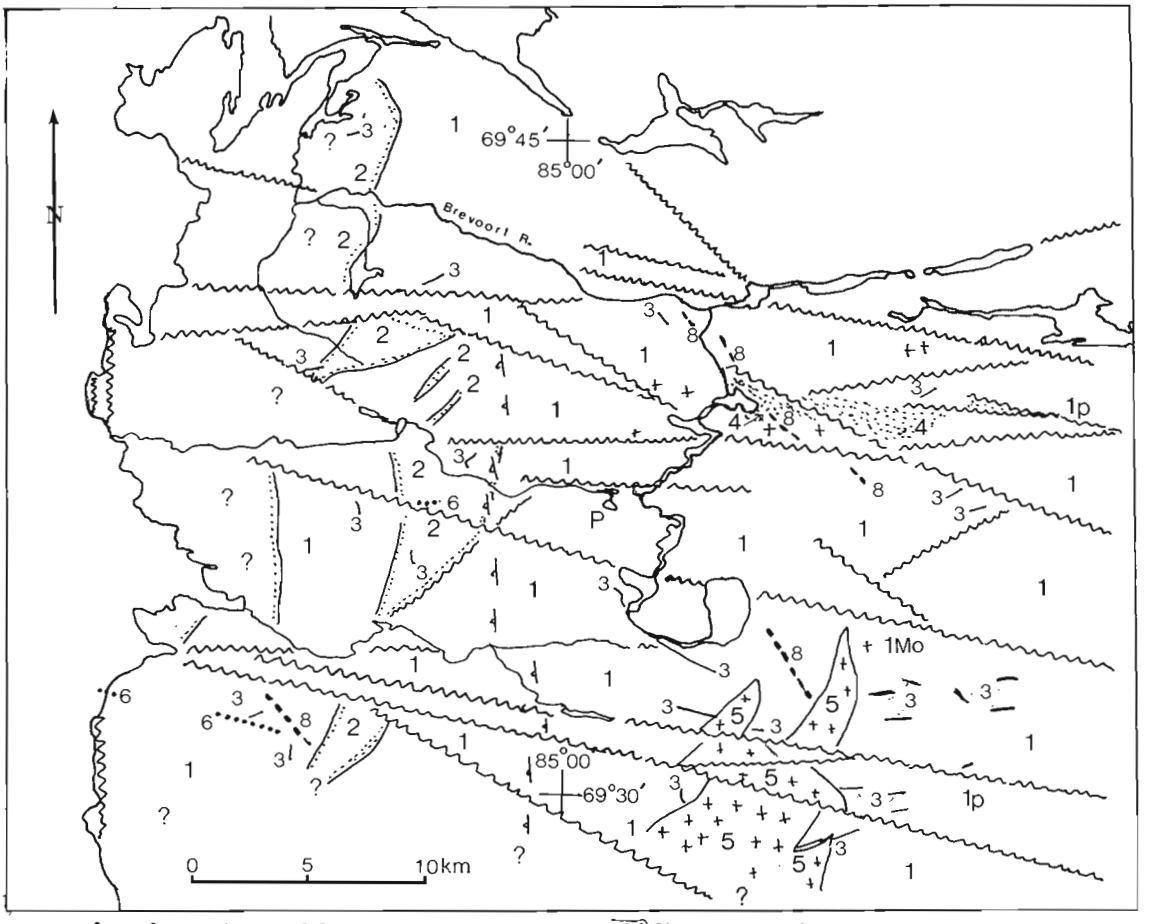

8 *fresh diabase dykes*

~7~ *fault rocks*

···6·· *massive metagabbro dykes*

+ 5 + *massive hornblende biotite granite*

4 *metasedimentary suite*

~3~ *lineated metabasic dykes*

2 *lineated granite*

1 *tonalite-granodiorite suite*

P *location of fig 3*

Mo *molybdenite showing*

orthopyroxene on tooth side

1p *local orthopyroxene in amphibolite grade*

Figure 65.1. *Geological sketch map of parts of NTS 47C map 1.*

and iron rich (=garnetiferous) sediments is similar in lithology to the Prince Albert Group as described in adjacent areas (Frisch, 1982; Schau, 1977). We postulate that unit 1 can be correlated with the 2.9 Ga Prince Albert Group.

Unit 5 (massive hornblende-biotite granite)

Irregular stocks of fresh granite and dykes of pegmatite and aplite occur in areas underlain by amphibolite grade country rock. The granite is pink weathering, white to grey, medium grained, massive hornblende biotite granite. The aplites are pink and white with only a small amount of biotite. The pegmatites are coarse grained with large books of biotite, graphic granite intergrowths, magnetite, and an accessory tentatively identified as allanite. Most outcrops of amphibolite grade contain about 15% leucosome fraction of granite veins or pods. The granite cuts and contains inclusions of units 3 and 1. Gneissic rocks occur locally where sheets of granite intrude lit-par-lit into tonalite of unit 1. Elsewhere, decimetre long, massive, unconnected pods of granite are set in tonalite and granodiorite cut by aplite and pegmatite dykes. The composition of this leucosome is similar to larger bodies of granite. A clockwise sense of rotation of small elongate blocks of unit 1 separated by massive granite or pegmatite indicates that granite emplacement was coeval with some bulk strain. A working hypothesis is that the granite results from partial melting of tonalite granodiorite suite which occurred at deeper levels and, possibly, at the currently exposed structural level. Perhaps partial melting and the high grade metamorphism are coeval and/or cogenetic. The location of granite bodies in the lower-grade part of unit 1 may indicate that higher partial pressures of water occurred in the lower grade rocks. Pegmatites of unit 5 are also widespread in amphibolite grade unit 1 and are present locally in unit 1 at granulite grade.

8 *fresh diabase dykes*

7 *fault rocks*

5 *massive hornblende biotite granite*

3 *lineated metabasic dykes*

1 *tonalite-granodiorite suite*

foliation

lineation

Figure 65.2. *Geological sketch map of region showing relations of units 1, 3, and 5.*

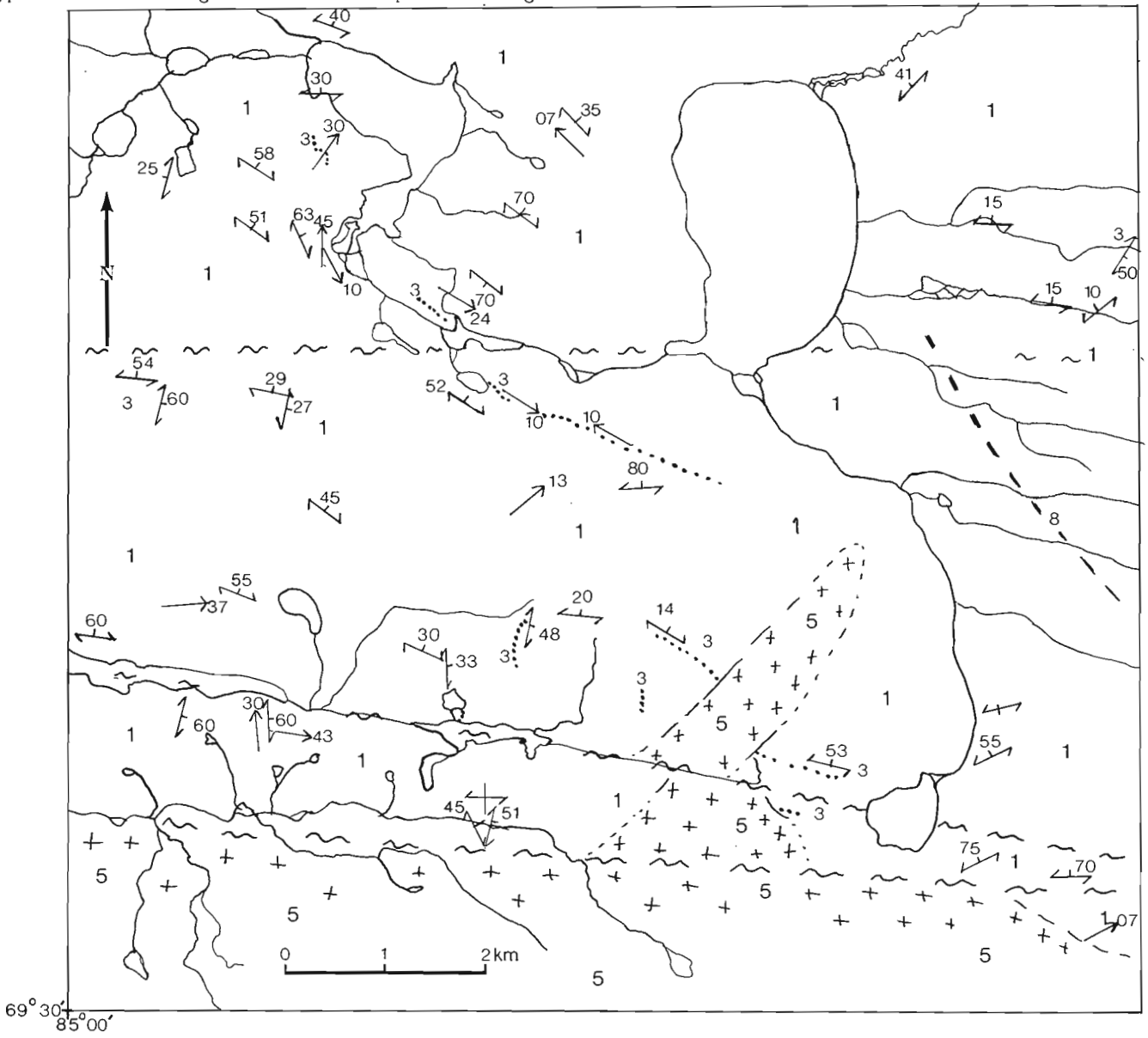



Figure 65.3. *Photograph of unit 3 dyke which cuts deformed rocks of unit 1 and is cut by undeformed unit 5. (GSC 203176-Y)*

The age of the granite is uncertain. Massive granites of both early to middle Proterozoic and late Archean age occur on the peninsula to the south (G.S.C. Open File 1046). A working hypothesis is that the granite emplacement and the high grade metamorphism was coeval with the late Archean metamorphic event that affected the Prince Albert Group elsewhere on the peninsula.

Unit 6 (massive metagabbro dykes)

West-trending, steeply dipping dykes of black weathering, fine to medium grained metagabbro cut granulite terrane. The dykes are less resistant to erosion than the country rock and are poorly exposed at edges of canyons or as small bumps in the canyon floor. It is not known whether these dykes cut amphibolite grade rocks, their recessive weathering characteristics would appear to preclude their exposure in these felsenmeer rich regions.

The dykes are hornblende-plagioclase rocks with white plagioclase suggesting that the dykes are metamorphosed. The age and assignment of the dykes is not known. Other dyke swarms of similar appearance to the south on Melville Peninsula are Proterozoic in age.

Unit 7 (fault rocks)

Late faults are marked by linear zones of intensely altered rocks. The alteration is commonly quartz and hematite impregnation but epidosites are also abundant. In a few localities argillic alteration has reduced the rock to a poorly coherent mass of clay. Rusty patches are found as well. In a few, pyrite and less frequently molybdenite was found. Where rare fabrics were observed, slickensides are nearly horizontal. The faults contain disrupted veins and have several episodes of movement and hence the fault rocks were probably formed at different times after the metamorphism. The east west faults and included fault rocks are part of a peninsula wide fault set of middle Proterozoic age (GSC Open File 1046).

Unit 8 (fresh diabase dykes)

Brown weathering, black to greenish brown, very fine to medium grained diabase dykes with steep dips and a northwesterly trend and width of 5 cm to 45 m cut all units. The dykes are more resistant to weathering than the country rock but are more poorly exposed in the felsenmeer covered amphibolite grade country rock. There, linear magnetic anomalies (from GSC Aeromagnetic Map 8304G) with similar trends and marked by diabase boulder trains probably indicate additional diabase dykes to those located in outcrop.

Although the dykes are linear on a map scale in detail the contacts are irregular and metre long blocks of country rock have spalled from walls of the dykes. The thinner dykes have irregular and angular shapes. At one locality an east-west trending steeply dipping fault offsets a fresh dyke with an apparent dextral offset of a few metres. Assignment of the fresh dykes to either of the major late Proterozoic north-west trending dyke swarms (ie. the Franklin or Mackenzie sets), must await further work.

Special problems

Age relationships in multiply deformed and metamorphosed high grade terranes are notoriously difficult to establish. In this work we have used metamorphosed and deformed basic dykes which contain sweats of leucosome (unit 3) as the principal marker. Granites can be divided according to whether they predate or postdate dykes of unit 3 (Fig. 65.2, 65.3).

What is not clear, however, is the relationship between the metasediments (unit 4) and the plutonic suite (unit 1). Most of the contacts between the two units are faults but in a few locations nontectonic contacts were found. If the contact is, in fact, unconformable and the sediments are correlative with the Prince Albert Group then unit 1 would be of middle Archean age. North of the mapped area there is another small outcrop area of metasediments (Heywood, personal communication, 1981); perhaps clear contact relationships will be established when it is mapped.

The sequence of events as implied by the order of the units in their description is considered the most likely but as contacts between unit 3 and unit 4 have not been observed and the sediments are not seen at granulite grade other possible sequences are also under consideration. More field work coupled with radiometric geochronology should allow selection among competing hypotheses.

Nomenclature of high grade rocks is not standardized (Mehnert, 1972). For instance, a time honoured definition of granulite was recently restated by Othman et al. (1984):

> "In a strict petrological sense, granulite facies rocks correspond to regional high grade metamorphism with rare hydrous minerals, high rock densities (3.0 g/cm^3), and high temperature high pressure paragenesis. Common features are the presence of hypersthene and clinopyroxene in calcic assemblages, the presence of myrmekite, greyish blue quartz and pleochroic hypersthene in acidic assemblages, with plagioclase and potash feldspar."

This definition is not applicable in this region. Only a few of the rocks in this region have densities as high as 3.0 g/cm^3 yet they would be called granulites by most petrologists. In this paper we use Reinhardt and Skippen's 1970 definition, one which has proven to be useful in field and compilation work (Fraser and Heywood, 1978): "Granulites may be regarded as high grade metamorphic rocks that characteristically contain pyroxene and that exhibit distinctive olive green or brown colours on weathering".

Whether one can say that the granulites of unit 1 in the area are of 'higher' grade than the amphibolites and the associated partial melts (unit 5) is not clear. Petrochemical methods may demonstrate instead that the two 'grades' differ only in partial pressure of fluids rather than temperature or total pressure. Johannes (1984) recently conluded that "high grade metamorphic rocks were probably dry and anatectic magmas of granitic or granodioritic composition are generally not saturated with water." and that the amount of leucosome may be even lower in areas of higher metamorphic grade which is concordant with our observations.

In a study of high grade metamorphic rocks in the Chapleau-Foleyet area of northern Ontario, Percival (1983) estimated the water pressure using relations derived from the mineral reaction below:

1 biotite + 3 hornblende = 9 orthopyroxene + 6 clinopyroxene + 1 potash feldspar + 1 water

Rocks which contain all the above mineral phases (seemingly at equibrilibrium with each other) are present in the map area and will be analyzed to estimate fluid pressure during metamorphism. Percival (1983) found no correlation between calculated water activity and the presence or absence of orthopyroxene in his area. Whether this result will also be found on Melville Peninsula awaits further work.

Future work

The major question facing the investigators prior to the field season was the age of the granulite metamorphism. Now that seems to favour the hypothesis that high grade metamorphism has affected units older than unit 6.

At the outcrop scale one can show that a mineral lineation (probably indicating direction of extension) is folded. If unit 4 is correlative with Prince Albert Group and metamorphism is late Archean then it is possible to speculate about a tectonic model in which units 1 to 4 were rapidly moved from surface to depth by tectonic thickening (marked by lineation?) and then folded and metamorphosed to high grades and locally partially melted as thermal equilibration of the overthickened pile took place. A scenario has been suggested for the Prince Albert Group some hundred kilometres to the southwest (Schau, 1978). The speculation will require much work to substantiate on Melville Peninsula and as such will act as a guide as to the direction of future work. The following questions need answers:

Is unit 4 same as Prince Albert Group?

Is unit 4 underlain by an unconformity?

Is there evidence for lateral movement on flat surfaces?

Was horizontal tectonic transport important in the history of the granulites?

Can mineral assemblages and their petrochemistry be used to trace the route of the rocks through temperature, pressure, fluid pressure space or is disequilibrium beyond unravelling?

Is unit 5 of a composition consistent with an origin of partial melting?

Is unit 5 coeval with metamorphism? The granulites probably formed in a thermal dome environment and whether the gravity anomaly associated with the granulites is a metamorphic effect or is a characteristic of unit 1, whatever its metamorphic grade, will be actively pursued in upcoming seasons.

Acknowledgments

We thank J. Grant, L. Madore, and S. Prevec for their assistance in the field and the staff of the Hudson Bay Company and First Air for their assistance and service. J. Percival suggested improvements to an earlier version of the manuscript.

References

Fraser, J.A. and Heywood, W.W.
1978: Metamorphism in the Canadian Shield; Geological Survey of Canada, Paper 78-10.

Frisch, T.
1982 Precambrian geology of the Prince Albert Hills, Western Melville Peninsula, Northwest Territories; Geological Survey of Canada, Bulletin 346, 70 p.

Froese, E.
1978: The graphical representation of mineral assemblages in biotite bearing granulites; in Current Research, Part A, Geological Survey of Canada, Paper 78-1A, p. 323-325.

Heywood, W.W.
1974: Geological reconnaissance of Northern Melville Peninsula, District of Franklin (Parts of 47A, B, C, D); in Report of Activities, Part A, Geological Survey of Canada, Paper 74-1A, p. 381.

Johannes, W.
1984: Beginning of melting in the granite system Qz-Or-Ab-An-H_2O; Mineralogy and Petrology, Volume 86, p. 264-273

Mehnert, K.R.
1972: Granulites-Results of a discussion II; Neues Jahrbuch fur Mineralogie, Monatshefte, v. 4, p. 139-150.

Othman, D., Polve, M., and Allegre, C.J.
1984: Nd-Sr isotopic composition of granulites and constraints on the evolution of the lower continental crust; Nature, v. 307, p. 510-515.

Perara, L.R.K
1984: Co-existing cordierite-almandine: A key to the metamorphic history of Sri-Lanka; Precambrian Research, v. 25, p. 349-364.

Percival, J.A.
1983: High grade metamorphism in the Chapleau-Foleyet area, Ontario; American Mineralogist, v. 68, p. 667-686.

Reindhardt, E.W. and Skippen, G.
1970: Petrochemical study of Grenville granulites; in Report of Activities, Part B, Geological Survey of Canada, Paper 70-1B, p. 48-54.

Schau, M.
1977: "Komatiites" and quartzites in the Archean Prince Albert Group; in Volcanic Regimes in Canada, ed. W.R.A. Baragar, L.C. Coleman, and J.M. Hall; Geological Association of Canada, Special Paper 16, p. 341-354.

1978: Metamorphism of the Prince Albert Group, District of Keewatin; in Metamorphism of the Canadian Shield; Geological Survey of Canada, Paper 78-10, p. 203-213.

LARGE-SCALE ELECTROMAGNETIC INDUCTION INVESTIGATION OF THE KAPUSKASING STRUCTURAL ZONE, NORTHERN ONTARIO

Dennis V. Woods[1]
Precambrian Geology Division

Woods, D.V., Large-scale electromagnetic induction investigation of the Kapuskasing Structural Zone, northern Ontario; in Current Research, Part A, Geological Survey of Canada, Paper 85-1A, p. 533-542, 1985.

Abstract

A large-scale electromagnetic induction investigation of the Kapuskasing Structural Zone has been carried out using an array of 30 recording magnetometers. From a preliminary examination of the three-component geomagnetic fluctuation data recorded by the magnetometer array, it is tentatively concluded that the zone is not significantly anomalously conductive. No anomalies in the variation field are observed in the vicinity of the zone even though the events examined have optimal horizontal polarization and as high frequency as possible for a magnetometer array (1-2 minutes period). Since it can be demonstrated that the lower crust in this region of the Superior Province is highly conductive and that the Kapuskasing zone is a section of this lower crust thrust to surface along the Ivanhoe Lake cataclastic zone, it is further concluded that high conductivity of the lower crust must be due to special conditions at lower crustal depths rather than a special mineralogical composition. This rules out explanations of lower crustal conductivity such as the presence of graphite, magnetite or hydrous silicates (amphibole, serpentine). The most favoured explanation of high conductivity in the lower crust of stable cratonic interiors is trapped pore fluids (water) with suitable ionic concentrations.

Résumé

On a réalisé un levé d'induction électromagnétique à grande échelle, dans la zone structurale de Kapuskasing, en employant un ensemble de 30 magnétomètres pourvus d'un dispositif d'enregistrement. Après un examen préliminaire des données de fluctuation géomagnétique de trois composantes, enregistrées par l'ensemble de magnétomètres, on a conclu de façon provisoire que la zone ne présentait pas d'anomalies de conductivité significatives. On n'a observé aucune anomalie du champ de variation à proximité de la zone, même si les secteurs examinés étaient caractérisés par une polarisation horizontale optimale, et même si l'on employait une fréquence aussi élevée que possible pour le dispositif magnétométrique (période d'une à 2 minutes). Étant donné que l'on a pu démontrer que dans cette région de la province du lac Supérieur, la croûte inférieure est fortement conductrice et que la zone est une portion de celle-ci repoussée à la surface le long de la zone cataclastique du lac Ivanhoe, on en a conclu que la forte conductivité de la croûte inférieure est sans doute régie par des conditions particulières en profondeur, plutôt que par une composition minéralogique particulière. Ceci exclut les explications suivant lesquelles la conductivité de la croûte intérieure résulterait de la présence de graphite, de magnétite ou de silicates hydratés (amphibole, serpentine). L'hypothèse la plus vraisemblable pour expliquer la conductivité élevée de la croûte inférieure des plates-formes cratoniques stables, est la présence de fluides interstitiels (eau) piégés dans la croûte et contenant des concentrations ioniques appropriées.

[1] Visiting scientist from the Department of Geological Sciences, Queen's University, Kingston, Ontario K7L 3N6

Introduction

The Kapuskasing Structural Zone has long been recognized as a major geological and structural discontinuity in the Superior Province of the Canadian Shield. It comprises a linear north-northeast trending zone of high-grade metamorphic rocks which transects the general east-west structural grain of this part of the Superior Province: separating the Wawa and Abitibi greenstone belts, and the Quetico and Opatica gneissic domains (Fig. 66.1). The high-grade metamorphic rocks of this zone are interpreted to have formed at mid- to lower-crustal depths (20-25 km) on the basis of their metamorphic mineral assemblages (Percival, 1983). In addition, the metamorphic grade is observed to increase gradually from greenschist facies in the Wawa subprovince through amphibolite to granulite facies in the Kapuskasing zone proper and then drop abruptly to greenschist facies in the Abitibi subprovince east of the Ivanhoe Lake cataclastic zone. This latter zone has been interpreted as a reverse or thrust fault which cuts through the entire crust, and indeed, preliminary results from a short seismic reflection experiment in July 1984 indicate a westward dipping reflector coincident with the fault (F. Cook, personal communication, 1984).

The above geologic evidence taken together with the prominent gravity and magnetic geophysical signature of the Kapuskasing Structural Zone, observable on regional gravity and magnetic maps, are cited by Percival and Card (1983) in their interpretation of the Kapuskasing zone as a section of the lower continental crust thrust to surface along the Ivanhoe Lake cataclastic zone. This significant finding is to be the focus of an integrated geophysical and geological investigation as part of the Canadian LITHOPROBE geoscience program (Clowes, 1984), combining large-scale seismic refraction, deep-sounding seismic reflection and ancilliary geophysical and geological studies, such as geochronology, geochemistry, paleomagnetism, structural geology and electromagnetic induction studies; the objective of the latter being to investigate the electrical conductivity structure of the Kapuskasing Structural Zone.

The continental lower crust in many areas of the world is known to have anomalously high electrical conductivity as compared with the upper crust and the upper mantle. Magnetotelluric (MT), controlled source electromagnetic (EM) and resistivity soundings have discovered a layer of increased conductivity, by one or two orders of magnitude, at depths ranging from 10 to 30 km and thickness of 5 to 20 km. This conductive layer, although not universal, is found in a number of different tectonic settings around the world. As Hermance (1983) pointed out in a recent review, it appears to be ubiquitous in zones of crustal extension such as the Basin and Range Province and Rio Grande Rift, presumably due to increased temperature effects on pore fluid ionic mobility, partial melting or thermal alterations (Jiracek et al., 1979). High conductivity in the lower crust has also been interpreted in regions of continental collision and subduction zones such as the western Canadian Cordillera (Caner et al., 1971) and the Canadian Appalachians (Cochrane and Hyndman, 1974), perhaps due to increased water content carried down by subducting lithosphere or released by dehydration processes (Hyndman and Hyndman, 1968).

Most significant to the present study, however, are the reports of conductive lower crust in the interiors of stable cratons. A conducting layer at lower crustal depths has been observed beneath both shield and platform areas of central Asia (Berdichevsky et al., 1976), and beneath both cratons and mobile belts in southern Africa (van Zijl, 1977). In North America, evidence for a conductive lower crust has been obtained beneath the western Great Plains (Chaipayungpun and Landisman, 1977), and beneath the Southern Province (Dowling, 1970; Sternberg, 1979), the Grenville Province (Connerney et al., 1980; Kurtz, 1982) and the Superior Province (Koziar and Strangway, 1978; Duncan et al., 1980) of the Canadian Shield.

The results of the controlled source EM experiment by Duncan et al. (1980) in the Abitibi greenstone belt just east of the Kapuskasing Structural Zone, indicate a lower crustal layer almost two orders of magnitude more conductive than the upper crust (the conductivity of the upper mantle was not resolved by this relatively high frequency sounding technique) at depths ranging from 17 to 29 km and apparently deepening to the west. The existence of the high conductivity lower crust in this area has recently been confirmed by an MT traverse across the Abitibi belt in western Quebec (M. Chouteau, personal communication, 1984) and an MT sounding 100 km west of Sudbury (R. Kurtz, personal communication, 1984). These results, in combination with the controlled source EM and resistivity soundings in Wisconsin (600 km to the southeast) by Sternberg (1979), who interpreted a three order of magnitude increase in conductivity at a depth of approximately 20 km, and the audio-magnetotelluric results of Koziar and Strangway (1978) from the English River area in northwestern Ontario (600 km to the northwest), who interpreted a similar increase in conductivity at a depth in excess of 7 km, indicate that the lower crust underlying the entire region of the central Superior Province in the vicinity of the Kapuskasing Structural Zone is anomalously conductive.

Reasons for high conductivity of the lower crust in stable cratonic interiors abound in the literature; however none is conclusive and all are contentious. Fundamentally they can be divided into those which require the presence of special mineralogical compositions such as graphite, magnetite or hydrous silicates, and those which rely on the special conditions found at lower crustal depths such as partial melting or trapped pore water. An electromagnetic induction investigation of the Kapuskasing Structural Zone provides a unique opportunity to test these compositional versus positional explanations of high conductivity in the lower continental crust. A positive result (i.e. the Kapuskasing zone is anomalously conductive) would indicate that the mineralogical constituents of lower crust cause its increased conductivity. A negative result (i.e. layered conductivity structure only) would suggest that the lower crust is more conductive due to its unique position.

Magnetometer array studies

The electromagnetic induction technique used in this investigation consists of monitoring temporal fluctuations of the geomagnetic field over a large 2-D area with a set of 30, three-component, recording magnetometers. The technique is referred to as geomagnetic deep sounding (GDS) using magnetometer arrays. Time variations of the geomagnetic field strength, due to magnetospheric and ionospheric disturbances and electric currents, are in fact electromagnetic source fields which will induce electric currents within the earth. The telluric currents will generate magnetic fields of their own and by measuring the total (externally plus internally derived) magnetic fluctuations, the electrical current and hence conductivity of the interior of the earth can be deduced.

In the magnetotelluric method, horizontal geomagnetic field fluctuations are measured along with the orthogonal, horizontal telluric fields. The ratio of the two fields gives an apparent resistivity parameter which can be interpreted in terms of one-dimensional (layered) conductivity structure of the earth from one station, or two- and sometimes three-dimensional conductivity structures if more than one station is occupied in a certain area. In the geomagnetic deep sounding method using large magnetometer arrays,

the horizontal and vertical magnetic fluctuations are measured simultaneously from a large number of recording magnetometers in a 2-D areal pattern. The spatial configuration of magnetic fluctuations can be observed from this data and the gross conductivity structure of the area, whether one-, two-, or three-dimensional, can be immediately assessed. In addition, the ratio of the vertical component, which is largely due to the internal telluric currents, to the horizontal components can be used to quantify the conductivity structure.

Magnetometer array studies have previously been carried out in many parts of North America by the University of Texas at Dallas, the University of Alberta and the Earth Physics Branch. Initial studies were conducted in the western United States and Canada during the late sixties (Reitzel et al., 1970; Porath and Gough, 1971; Camfield et al., 1971) and resulted in the discovery of anomalous conductivity beneath the southern Rocky Mountains and the Wasatch Front (Porath et al., 1970), and beneath the Black Hills in the western Great Plains (Porath et al., 1971; Gough and Camfield, 1972). This last conductivity anomaly, referred to as the North American Central Plains anomaly, was extended north to the Canadian Shield by a subsequent array study (Alabi et al., 1975). Other array studies carried out in the mid-seventies investigated the conductivity anomaly south of the Rio Grande rift (D. Bennett, personal communication, 1978) and in the southern Grenville Province (Camfield, 1981). Recently Gough et al. (1982) carried out a number of magnetometer array studies in western Canada and discovered conductivity anomalies beneath the Rocky Mountain Trench and in the foothills of southwestern Alberta.

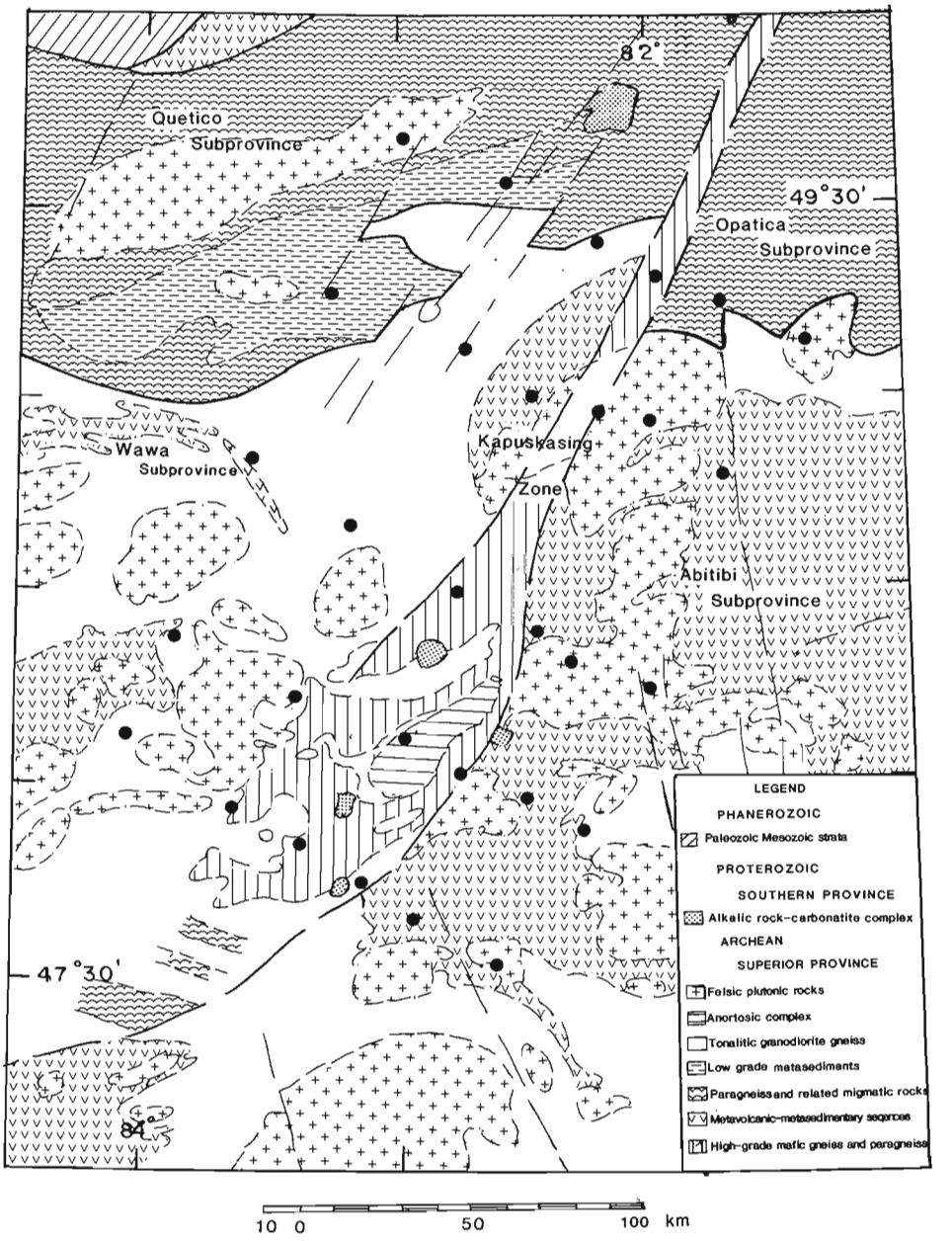

Figure 66.1. *Geological map of the Kapuskasing Structural Zone and surrounding areas (after Percival and Card, in press). Black dots are station locations of the Kapuskasing magnetometer array.*

Table 66.1. Station codes, names and locations for the 1984 Kapuskasing magnetometer array

Code	Station name	Abbreviation	Latitude	Longitude	Declination
A1	Raft Lake	RAF	49°42'N	82°58'W	8°54'W
A2	Lost River	LOS	49°34'N	82°33'W	9°36'W
A3	Remi Lake	RMI	49°24'N	82°12'W	10°07'W
A4	Grégoires Mill	GRE	49°19'N	81°58'W	10°27'W
A5	Muskego River	MUS	49°16'N	81°42'W	10°42'W
A6	Driftwood	DRI	49°08'N	81°22'W	10°56'W
B1	Rykerk Creek	RYK	49°17'N	83°16'W	8°06'W
B2	Kapuskasing River	KAP	49°08'N	82°46'W	8°48'W
B3	Keenoa Lake	KEE	49°00'N	82°28'W	9°14'W
B4	Groundhog River	GHG	48°58'N	82°13'W	9°39'W
B5	South Creek	STH	48°57'N	81°58'W	10°04'W
B6	Thorburn Lake	THR	48°47'N	81°40'W	10°13'W
C1	Puskuta Lake	PUS	48°51'N	83°35'W	7°27'W
C2	Stefansson Lake	STF	48°40'N	83°12'W	7°54'W
C3	Lougheed Lake	LGH	48°29'N	82°47'W	8°23'W
C4	Ivanhoe River	IVA	48°23'N	82°28'W	8°47'W
C5	Beattie Lake	BEA	48°18'N	82°19'W	8°55'W
C6	Sewell Lake	SEW	48°14'N	82°02'W	9°14'W
D1	Renabie Mine	REN	48°23'N	83°53'W	7°05'W
D2	Hay Lake	HAY	48°13'N	83°25'W	7°33'W
D3	Nemegosenda River	NEM	48°07'N	82°59'W	7°57'W
D4	Birch Lake	BIR	48°02'N	82°46'W	8°10'W
D5	Marta Lake	MAR	47°57'N	82°30'W	8°26'W
D6	Horwood Lake	HOR	47°52'N	82°18'W	8°38'W
E1	Shikwamkwa Lake	SHK	48°08'N	84°04'W	6°56'W
E2	Windermere Lake	WIN	47°56'N	83°40'W	7°18'W
E3	Chapleau	CHA	47°50'N	83°23'W	7°32'W
E4	Halsey Lake	HAL	47°44'N	83°10'W	7°42'W
E5	Kormak	KOR	47°38'N	82°57'W	7°52'W
E6	Woman River	WOM	47°32'N	82°38'W	8°10'W

Experimental procedure

The 30 magnetic variometers used in this study are based on a design by Gough and Reitzel (1967) and consist of three sensor magnets suspended by torsion wires in three orthogonal orientations to measure the magnetic east-west (D), magnetic north-south (H), and vertically down (Z) components. Minute rotations of the sensor magnets, which are directly related to changes in magnetic field strength, are recorded by an optical lever which consists of a lamp filament, an achromatic lens, reflecting mirrors (and the polished surface of the magnets), and a 35 mm camera with a fine slit aperture. Magnetic field variations result in displacement of the light dot images on the film. The 35 mm film is capable of recording fluctuations of up to 500 nT and, by enlarging the images, to a precision of better than 1 nT. The instruments are calibrated by applying a known magnetic field with a permanent magnet at the beginning and end of a recording period. Temperature fluctuation effects are eliminated by burying the instruments in 2 m auger holes. This installation procedure also provides security.

The instruments are powered by a high-capacity, 6 volt lead-acid battery, and are capable of about 300 000 recordings on a single 150 foot roll of film. The timing interval between recordings can be set anywhere between 8 and 99 seconds providing up to almost one year of record if required. For the Kapuskasing array study, the timing interval was set to 10 seconds; however, a problem with the film advance mechanism reduced the recording period to about four weeks instead of the expected 35 days. The instruments recorded in two separate sessions during July and August 1984. Installation and switch-on was carried out in June and the instruments were retrieved in early September. A service trip was required in late July to change film and recalibrate the instruments.

Recording efficiency was quite high, especially in light of the fact that these particular instruments were being used for the first time in 10 years and after a complete overhaul and modification. During the first recording session, one instrument completely malfunctioned due to an improperly installed camera drive motor and one other instrument lost a few days record due to an electronic malfunction. Such 95% efficiency for a magnetometer array study is not routinely attained. More problems were encountered during the second recording session primarily due to difficulties in reloading the camera in adverse weather conditions. Other operational mistakes may have occurred during the second recording session to further reduce the recording efficiency, although details are not known at the time of writing because the second set of films has yet to be processed.

A map of the Kapuskasing magnetometer array is shown in Figure 66.2 and the station names and locations are listed in Table 66.1. The array consists of five east-west lines of six stations each, crossing the Kapuskasing Structural Zone at right angles. The stations were concentrated over the zone and spaced out on either side, with somewhat greater spacing downdip to the west. Station locations were also chosen close to main highways and major logging roads to ease the logistics of visiting all instruments in the shortest

time possible. Due to a lack of suitable roads in some areas, regular station spacing was maintained by servicing three stations (C1, C2 and C3) by float plane and one station (D6) by boat. At each station, the instruments were installed at sites remote from cultural magnetic disturbances and where augering was easiest.

The Kapuskasing magnetometer array is shown relative to regional geologic features in Figure 66.1. The third or fourth station on each line was located either within the Kapuskasing zone or close to the Ivanhoe Lake cataclastic zone. Note that the array also straddles some other major geological subprovinces in the region, most notably the Abitibi greenstone belt to the east.

Data analysis procedures

The analysis procedures of magnetometer array data have developed over the past fifteen years to the point where they are now fairly routine (Gough and Ingham, 1983):

1. Out of the entire film record, a number of isolated geomagnetic fluctuation events are selected for digitization and numerical analysis.
2. Each individual event is digitized from all operative stations and the data are compiled and displayed in the form of magnetograms (magnetic field strength versus time for each component) and hodographs (traces of horizontal magnetic field fluctuation in map form).

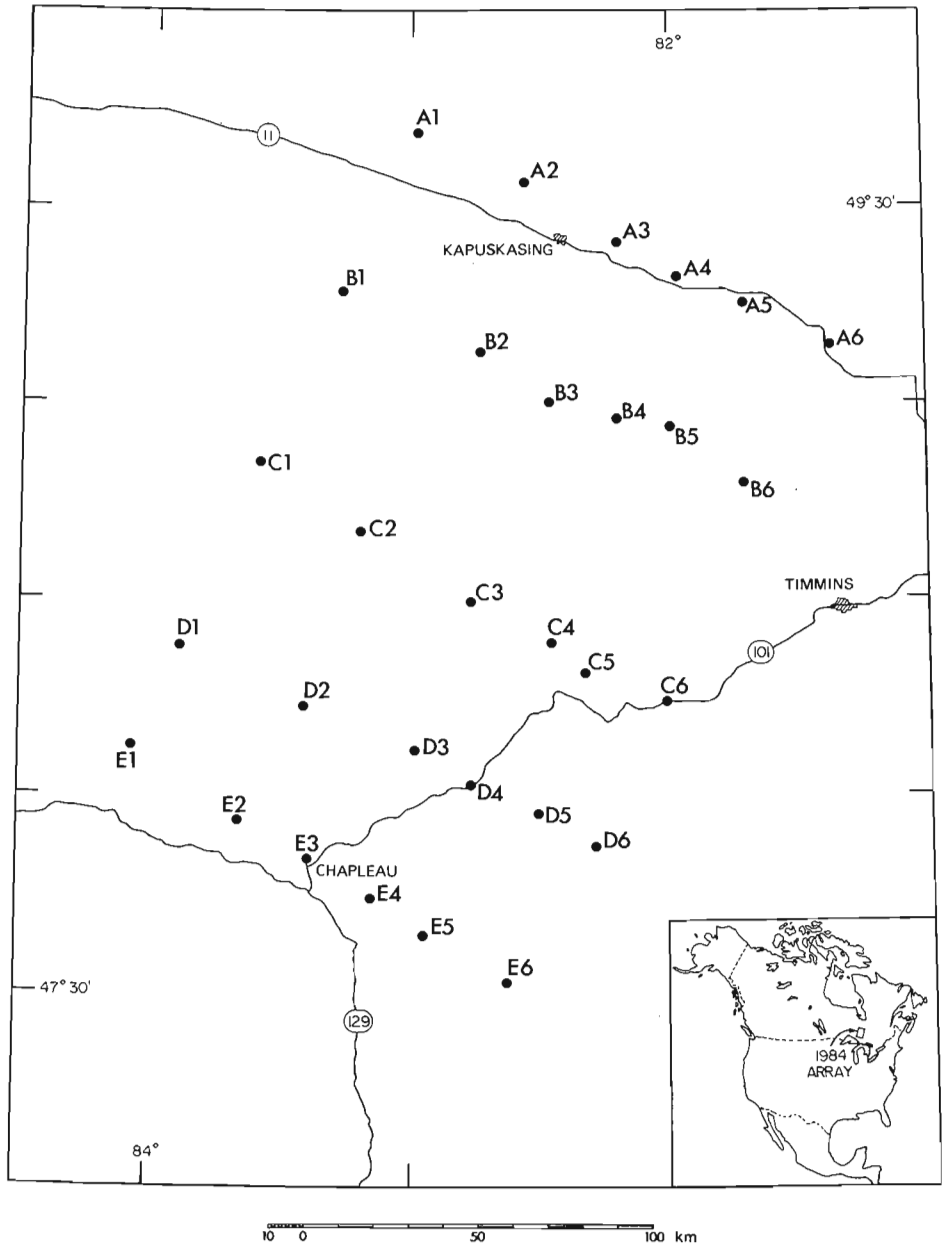

Figure 66.2. *Map of the Kapuskasing magnetometer array showing station locations in relation to the highway network in north-central Ontario.*

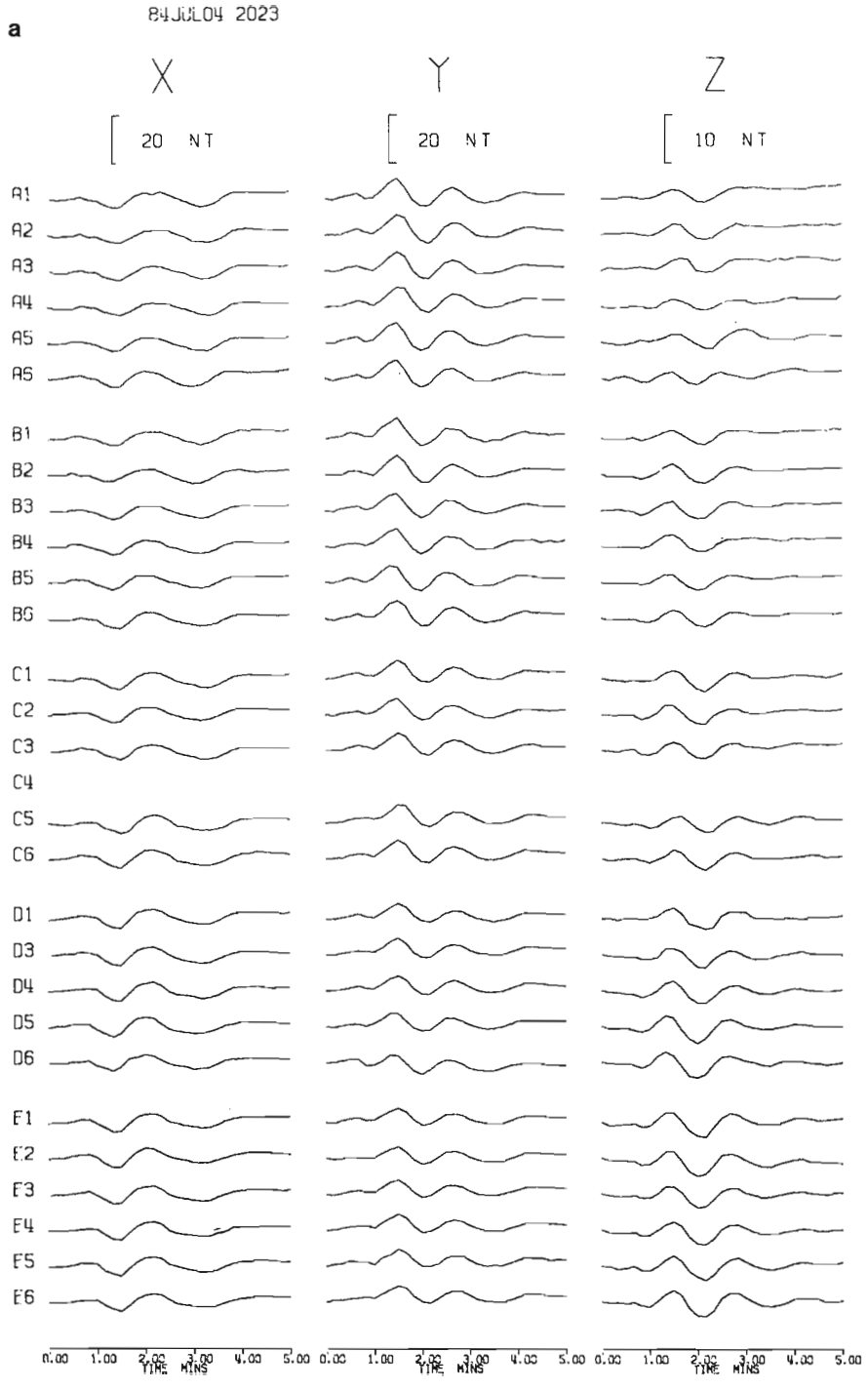

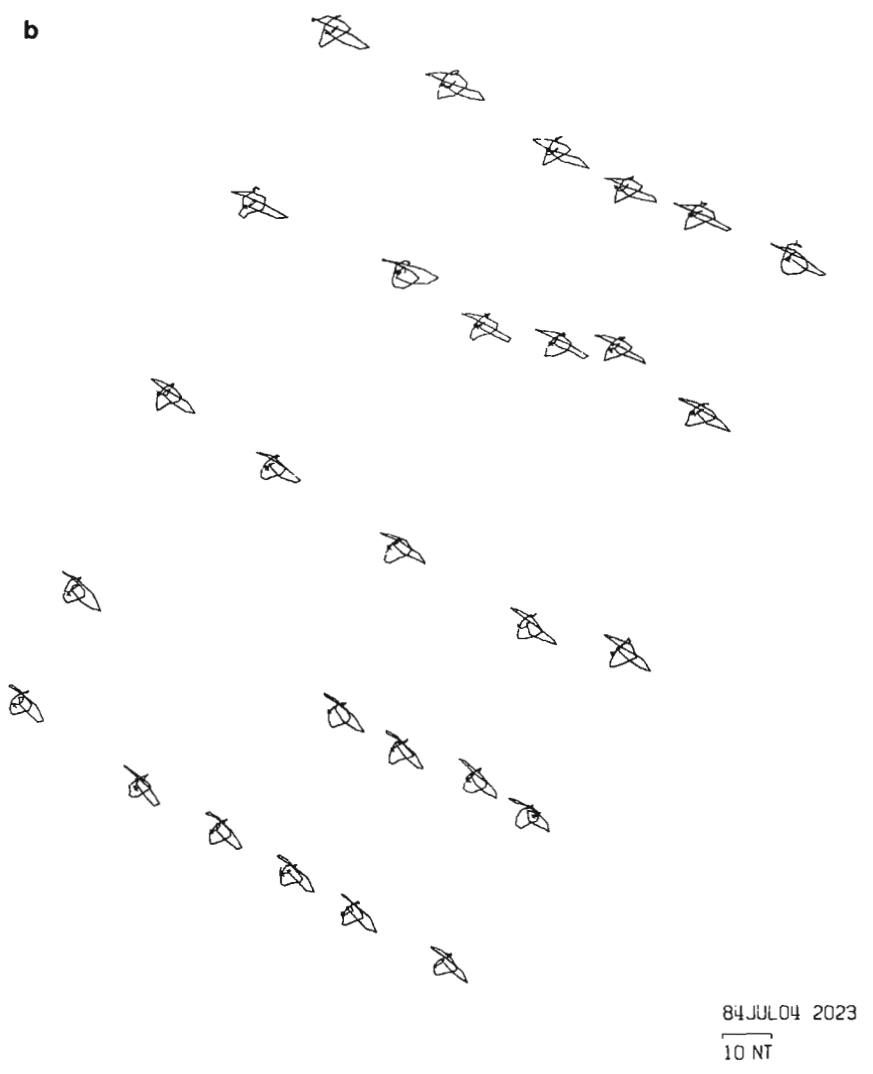

Figure 66.3. *a) Stacked magnetograms of a geomagnetic pulsation event which commenced at 2023 UT on 4 July 1984. Magnetic fluctuation components are: X-geographic north, Y-geographic east, and Z-vertically down. Station D2 was not operating during the event and data from station C4 has yet to be processed. b) Hodographs (traces of the horizontal fluctuation vector) of the pulsation event.*

3. Events are then Fourier transformed so that the data can be displayed and analyzed as a function of frequency.
4. Maps and profiles of the Fourier components are constructed, and the relationship (i.e. transfer functions) between the vertical component and the horizontal components or the horizontal gradients is calculated.

Further interpretation depends on the nature of the observed data and results from step 4.

Smoothly varying, isolated events in otherwise quiet geomagnetic sections of record are selected to facilitate frequency dependent EM induction analysis by Fourier transformation. Events thus selected can be considered complete recordings of separate and independent EM source fields generated in the ionosphere or magnetosphere. Each event will have its own characteristic spatial geometry, expressed principally by the polarization of horizontal components, and temporal morphology with some dominant period. Hence, complete EM induction investigation of the array area is accomplished by the analysis of a compendium of such separate events, each with different horizontal polarization and dominant period.

At the time of writing, only films from the first recording session in July have been processed and only three events have been digitized. Since the possibility of near-surface conductivity features is under investigation, it was decided to concentrate initial analysis on the highest frequencies possible. Hence short-period fluctuations due to magnetospheric pulsations were identified from the film record and an event, with a horizontal magnetic field which appeared to be linearly polarized in a northwest-southeast direction (i.e. perpendicular to the Kapuskasing Structural Zone), was selected for digitization. Subsequently, a pair of pulsation-like events with northeast-southwest polarization were selected for digitization. These two events are separated in time by 5 minutes but they have essentially the same polarization. They were digitized together for expediency, but later will be split into separate events before further analysis.

Results

Results presented here are tentative as they are based solely on visual examination of the magnetograms and hodographs of the three events digitized to date. Further analysis will be performed on these and other events by applying the Fourier transform, however the overall conclusions based on the present data are not likely to be altered substantially by future study – only refined. This is because the events selected and presented here are optimal for illuminating conductivity features associated with the Kapuskasing Structural Zone and surrounding geological structures.

Magnetograms of the first event digitized from the July recording session are shown in Figure 66.3a and hodographs of this event are shown in Figure 66.3b. The event occurred at 2023 UT on 4 July 1984 and is typical of short-period daytime pulsations. It has a dominant period of about 1 to 1.5 minutes and a horizontal polarization which can be seen by the hodographs in Figure 66.3b to be aligned perpendicular to the structural zone. Such an event should have maximum EM inductive effect on the Kapuskasing Structural Zone.

As can be seen by the magnetograms in Figure 66.3a the variation fields are entirely uniform over the array area except for some slight irregularities in the Z component at stations A5 and A6. There is no enhancement of the horizontal components over the Kapuskasing Structural Zone (stations 3 and 4 on each line) and no change in the Z components from the east side of the array to the west as would be expected if the zone was anomalously conductive. The Z component variation, being of relative large amplitude, is probably due to the external source field structure of the event and this may tend to mask subtle, anomalous Z variation. This appears to be the case for the irregularities mentioned above at stations A5 and A6.

In order to examine this Z response more clearly, the next event to be digitized (actually a pair of events) was selected with noticeably flat Z response and dominant north-south horizontal polarization to illuminate any conductive features with east-west trends. These events commenced at 2055 UT and 2105 UT on 4 July 1983. As can be seen by the magnetograms in Figure 66.4a and the hodographs in Figure 66.4b, the events have somewhat longer dominant period than the previous event (2-3 minutes) and linear polarization perpendicular to the previous event. Again the variation fields are essentially uniform over the array area except for the response near stations A5 and A6. The Z component shows somewhat more character than the first event because the external Z field is reduced, however still no response is observed in the vicinity of the Kapuskasing Structural Zone. Interestingly, the Z component displays a gradually increasing response to the west on lines C, D and E, and a greatly reduced response on line B. This type of second order variation may be defined more explicitly with further detailed analysis using additional events.

The anomaly at the east end of line A shows quite clearly in this pair of events. The Z response at station A5 is reversed with respect to the Z variations at the other A-line stations. The anomalous response is also quite large at stations A5 and A6 and gradually weakens at stations A4 and A3. In addition, there is a pronounced enhancement of the X (north) component at station A6. These results taken together suggest an anomalous east-west concentration of telluric current beneath the stations at the east end of line A, and in fact running between station A5 and the other stations.

An examination of the geological and topographical maps of the area led immediately to the cause: the trans-Canada gas pipeline which is buried along the Highway 11 transportation corridor which runs between stations A4, A5 and A6. Other man-made conductive structures along the corridor (high-voltage power transmission lines and the Canadian National railway line) were ruled out because the distance from these features to the anomalous stations did not fit the pattern of observed response. As summarized in Table 66.2, the anomalous Z response appears to be directly related to the distance from each station to the buried pipeline.

Although this anomalous geomagnetic variation is apparently not associated with a real geological feature, the anomaly is nevertheless interesting and warrants further study for the following reasons:

1. It provides a test case for the efficiency of magnetometer array data analysis and interpretation procedures.
2. It may represent a quantified example of the relative effect of current channelling versus EM induction, a contentious issue in geomagnetic deep sounding studies (Jones, 1983).
3. Naturally induced electrical current in buried pipelines is an engineering problem, and possibly a hazard, which is gaining increased attention (Campbell, 1982).

Discussion

The tentative result of the Kapuskasing magnetometer array study after visual inspection of three pulsation events is that the Kapuskasing Structural Zone is not anomalously

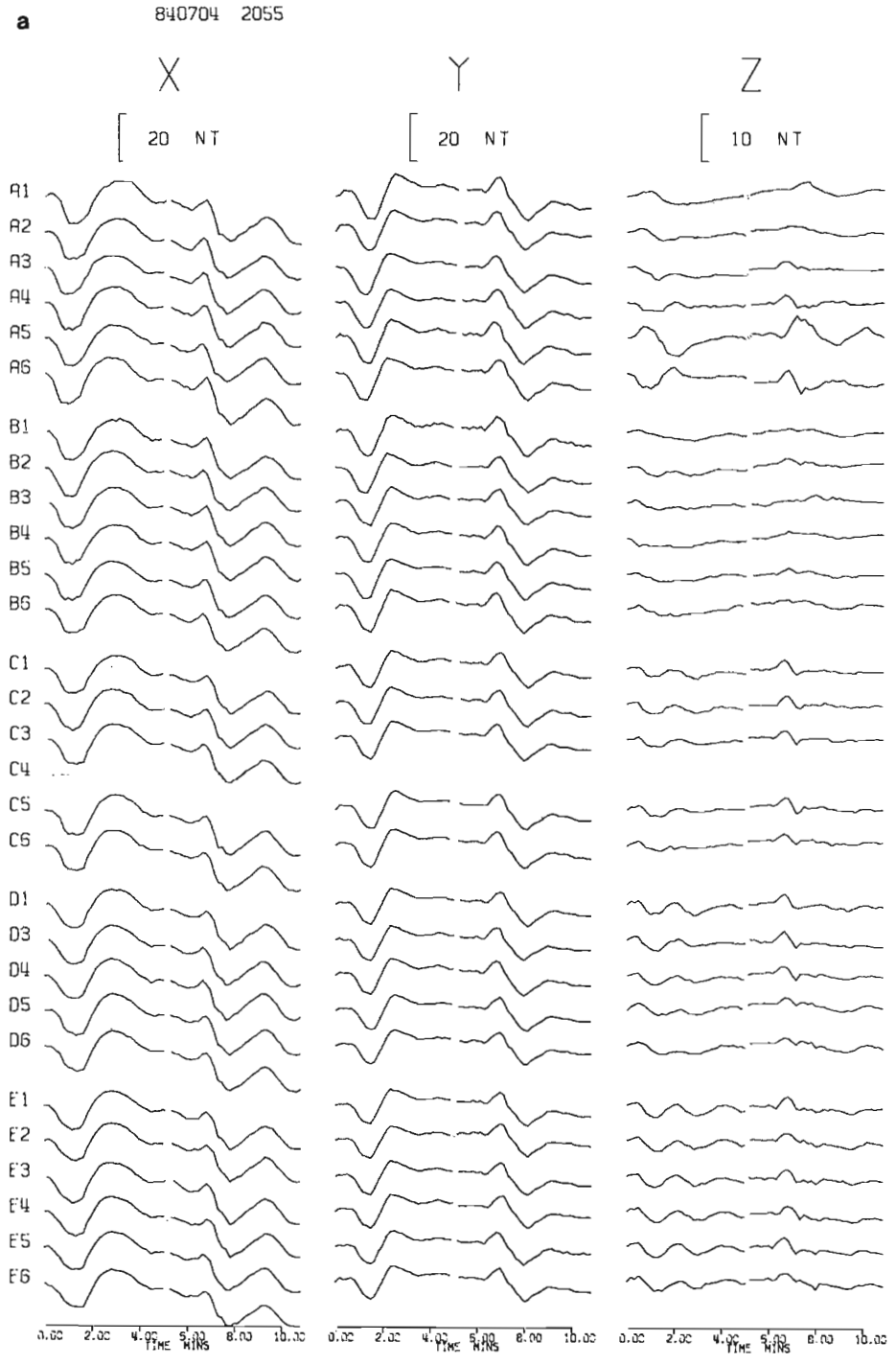

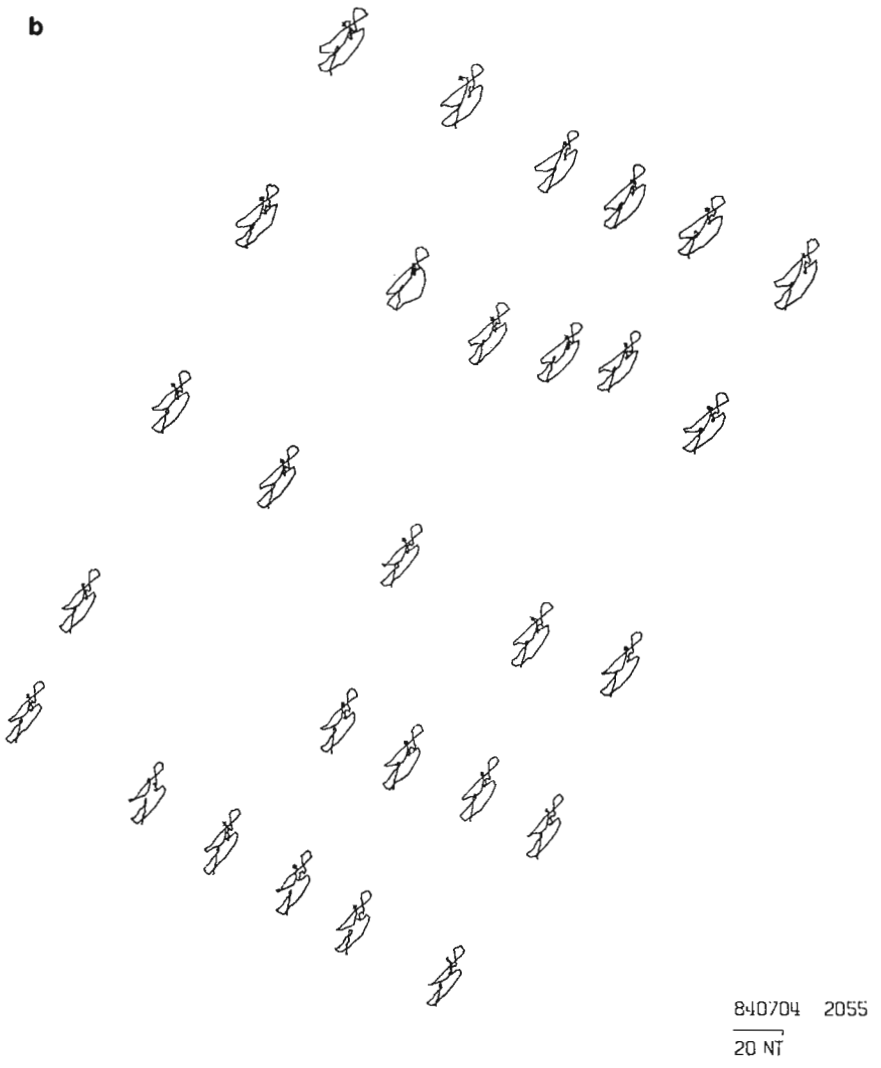

Figure 66.4. *a) Stacked magnetograms of a pair of pulsation-like magnetic fluctuation events which commenced at 2055 and 2105 on 4 July 1984. There is a 5 minute section of quiet magnetic field missing from between the two events at 2100 UT (5 minutes after the start of the first event). Other comments as in Figure 66.3. b) Hodographs of the pair of pulsation-like events.*

Table 66.2. Distances from the trans-Canada gas pipeline to stations A3, A4, A5 and A6 of the Kapuskasing magnetometer array compared with the anomalous vertical response measured at 2056 UT, 4 July 1984.

Station	Distance (km)	Anomalous Z Response (nT)
A6	1.4 N	- 3.0
A5	1.6 S	+ 3.0
A4	3.3 N	- 1.5
A3	6.1 N	- 1.0

conductive and that the region, to first order, is laterally uniform. This conclusion is drawn from the result that no variation anomalies are observed over the zone, even for an optimally polarized EM source field at as high frequency as possible for magnetometer array studies – periods of 1-2 minutes. Forward modelling of the zone with a conductivity contrast of only 10 to 1 produced a variation anomaly in the horizontal components of more than 15% and a complete reversal of the vertical components across the structure.

The implication of this result, as outlined in the Introduction, is that if the Kapuskasing Structural Zone is composed of lower crustal material thrust to surface, then the lower crust in the central Superior Province is conductive because of its intrinsic conditions and not because of its mineralogical composition. This would appear to rule out explanations of lower crustal conductivity such as: 1) interstitial graphite or carbon coating on grain boundaries, 2) interconnecting magnetite, and 3) hydrous silicates such as serpentine, amphibole, chlorite and clay minerals. Graphite, magnetite and amphibole have been observed in the high-grade metamorphic rocks of the zone (Percival, 1983), however they must either not be in sufficient abundance (graphite, magnetite) or they do not have high enough conductivity (amphibole) to increase the bulk conductivity of the Kapuskasing Structural Zone. Although it has been argued that lower crustal conductivity is due to the presence of amphibolite or serpentinite rocks (Jones, 1981), as Shankland and Ander (1983) pointed out, these hydrous minerals are not always conductive and their measured high conductivity may in some cases be due to presence of free water during the measuring process.

Explanations of high conductivity in the lower crust which require special conditions at lower crustal depths are partial melting, and trapped pore water with suitable ionic content. Although partial melting is an acceptable explanation of high conductivity in the lower crust beneath zones of crustal extension, the high temperatures required are inconsistent with the low heat flow values observed in stable cratonic interiors. Therefore the most likely explanation of high conductivity in the lower crust is the presence of water.

Meteoric water in the pore spaces of near-surface rocks, particularly sedimentary rocks, is well known to be the primary mechanism of the conduction of electricity at shallow depths (Keller and Frischknetch, 1966). However, it is also held that with increased depth of burial, the effect of increased lithostatic pressure is to close the pore spaces and hence reduce electrical conductivity (Brace, 1971). At depths greater than a few kilometres, conduction is probably controlled by water-filled microfractures and at depths greater than about 7 km these microfractures are expected to be closed or sealed by secondary minerals (Richter and Simmons, 1977). Beyond this depth, conduction is presumably due to electronic semiconduction in the silicate minerals. It has been observed (e.g. Sternberg, 1979) that conductivity decreases rapidly with depth and assumes low values (10^{-4}-10^{-5} S/m) in the upper crust, in agreement with the above model. However, conductivity in the lower crust is too high to be explained by electronic semiconduction at the temperatures to be expected at lower crustal depths (400-600°C). The pronounced increase in conductivity at lower crustal depths may be due to increased water content under sufficiently high pore pressure to keep micro-porosity open (Walder and Nur, 1982). Shankland and Ander (1983) presented evidence that only 0.1% free water is required at lower crustal conditions to account for the observed high conductivity of the lower crust in stable cratonic interiors. Recent results from the Soviet crustal drilling program on the Kola Peninsula have indicated the presence of brine solutions at depths greater than 11 km (Kozlovsky, 1982).

Acknowledgments

Significant contributions to the preparation of instruments were made by Hugh Geiger and Robert Renaud. Field operations were primarily carried out by Michel Allard with the assistance of Mr. Geiger and Mr. Renaud. Mr. Allard digitized the film records and prepared the figures. All contributions are gratefully acknowledged.

References

Alabi, A.O., Camfield, P.A., and Gough, D.I.
1975: The North American central plains conductivity anomaly; Geophysical Journal Royal Astronomical Society, v. 43, p. 815-833.

Berdichevsky, M.N., Fainberg, E.B., Rotanova, N.M., Smirnov, J.B., and Vanyan, L.L.
1976: Deep electromagnetic investigations; Annales de Geophysique, v. 32, p. 143-155.

Brace, W.F.
1971: Resistivity of saturated crustal rocks to 40 km based on laboratory measurements; in The Structure and Physical Properties of the Earth's Crust, ed. J.G. Heacock; American Geophysical Union Geophysical Monograph Ser., v. 14, p. 243-255.

Camfield, P.A.
1981: Magnetometer array study in a tectonically-active region of Quebec, Canada; Geophysical Journal of Royal Astronomical Society, v. 65, p. 553-570.

Camfield, P.A., Gough, D.I., and Porath, H.
1971: Magnetometer array studies in the northwestern United States and southwestern Canada; Geophysical Journal of Royal Astronomical Society, v. 22, p. 201-221.

Campbell, W.H.
1982: Observation of electric currents in the Alaska oil pipeline resulting from auroral electrojet current sources; Geophysical Journal of Royal Astronomical Society, v. 61, p. 437-449.

Caner, B., Auld, D.R., Dragert, H., and Camfield, P.A.
1971: Geomagnetic depth-sounding and crustal structure in western Canada; Journal of Geophysical Research, v. 76, p. 7181-7201.

Chaipayungpun, W. and Landisman, M.
1977: Crust and upper mantle near the western edge of the Great Plains; in The Earth's Crust: Its Nature and Physical Properties, ed. J.G. Heacock; America Geophysical Union Geophysical Monograph Ser., v. 20, p. 553-576.

Clowes, R.
1984: Phase I Lithoprobe: A coordinated national geoscience project; Geoscience Canada, v. 11, no. 3, p. 122-126.

Cochrane, N.A. and Hyndman, R.D.
1974: Magnetotelluric and magnetovariational studies in Atlantic Canada; Geophysical Journal of Royal Astronomical Society, v. 39, p. 385-406.

Connerney, J.E.P., Nekut, A., and Kuckes, A.F.
1980: Deep crustal electrical conductivity in the Adirondacks; Journal of Geophysical Research, v. 85, p. 2603-2614.

Dowling, F.L.
1970: Magnetotelluric measurements across the Wisconsin Arch; Journal of Geophysical Research, v. 75, p. 2683-2698.

Duncan, P.M., Huang, A., Edwards, R.N., Bailey, R.C., and Garland, G.D.
1980: The development and applications of a wide band electromagnetic sounding system using a pseudo-noise source; Geophysics, v. 45, p. 1276-1296.

Gough, D.I. and Reitzel, J.S.
1967: A portable three-component magnetic variometer; Journal of Geomagnetism and Geoelectricity, v. 19, p. 203-215.

Gough, D.I. and Camfield, P.A.
1972: Convergent geophysical evidence of a metamorphic belt through the Black Hills of South Dakota; Journal of Geophysical Research, v. 77, p. 3168-3170.

Gough, D.I. and Ingham, M.R.
1983: Interpretation methods for magnetometer arrays; Reviews of Geophysics and Space Physics, v. 21, p. 805-827.

Gough, D.I., Bingham, D.K., Ingham, M.R., and Alabi, A.O.
1982: Conductive structures in southwestern Canada: A regional magnetometer array study; Canadian Journal of Earth Sciences, v. 19, p. 1680-1690.

Hermance, J.F.
1983: Electromagnetic induction studies; Review of Geophysics and Space Physics, v. 21, p. 652-665.

Hyndman, R.D. and Hyndman, D.W.
1968: Water saturation and high electrical conductivity in the lower continental crust; Earth Planetary Science Letters, v. 4, p. 427-432.

Jiracek, G.R., Ander, M.E., and Holcombe, H.T.
1979: Magnetotelluric soundings of crustal conductive zones in major continental rifts; in Rio Grande Rift: Tectonics and Magmatism, ed. R.E. Ricker; American Geophysical Union, Washington, p. 209-222.

Jones, A.G.
1981: On a type classification of lower crustal layers under Precambrian regions; Journal of Geophysics, v. 49, p. 226-233.

1983: The problem of current channelling: A critical review; Geophysical Surveys, v. 6, p. 79-122.

Keller, G.V. and Frischknecht, F.C.
1966: Electrical Methods in Geophysical Prospecting; Pergamon, Oxford, 526 p.

Koziar, A. and Strangway, D.W.
1978: Shallow crustal sounding in the Superior Province by audio frequency magnetotellurics; Canadian Journal of Earth Sciences, v. 15, p. 1701-1711.

Kozlovsky, Y.A.
1982: Kolo Super-Deep: Interim results and prospects; Episodes, no. 4, p. 9-11.

Kurtz, R.D.
1982: Magnetotelluric interpretation of crustal and mantle structure in the Grenville Province; Geophysical Journal of Royal Astronomical Society, v. 70, p. 373-397.

Percival, J.A.
1983: High-grade metamorphism in the Chapleau-Foleyet area, Ontario; American Mineralogist, v. 68, p. 667-686.

Percival, J.A. and Card, K.D.
1983: Archean crust as revealed in the Kapuskasing uplift, Superior Province, Canada; Geology, v. 11, p. 323-326.

– Structure and evolution of Archean crust in central Superior Province, Canada; in Archean Supracrustal Sequences, ed. L.D. Ayres and P.C. Thurston; Geological Association of Canada, Special Paper. (in press)

Porath, H. and Gough, D.I.
1971: Mantle conductive structures in the western United States from magnetometer array studies; Geophysical Journal of Royal Astronomical Society, v. 22, p. 261-275.

Porath, H., Oldenburg, D.W., and Gough, D.I.
1970: Separation of magnetic variation fields and conductive structures in the western United States; Geophysical Journal of Royal Astronomical Society, v. 19, p. 237-260.

Porath, H., Gough, D.I., and Camfield, P.A.
1971: Conductivity structures in the northwestern United States and southwest Canada; Geophysical Journal of Royal Astronomical Society, v. 23, p. 387-398.

Reitzel, J.S., Gough, D.I., Porath, H., and Anderson, C.W.
1970: Geomagnetic deep sounding and upper mantle structure in western United States; Geophysical Journal of Royal Astronomical Society, v. 19, p. 213-235.

Richer, D. and Simmons, G.
1977: Microcracks in crustal igneous rocks; in The Earth's Crust: Its Nature and Physical Properties, ed. J.G. Heacock; American Geophysical Union Geophysics Monograph Ser., v. 20, p. 149-181.

Shankland, T.J. and Ander, M.E.
1983: Electrical conductivity, temperatures, and fluids in the lower crust; Journal of Geophysical Research, v. 88, p. 9475-9484.

Sternberg, B.K.
1979: Electrical resistivity structure of the crust in the southern extension of the Canadian Shield – layered earth models; Journal of Geophysical Research, v. 84, p. 212-228.

van Zijl, J.S.V.
1977: Electrical studies of the deep crust in various tectonic provinces of southern Africa; in The Earth's Crust: Its Nature and Physical Properties, ed. J.G. Heacock; American Geophysical Union Geophysics Monograph Ser., v. 20, p. 470-500.

Walder, J. and Nur, A.
1982: Water and pore pressure in the crust: Some simple models (abstract); EOS Transactions American Geophysical Union, v. 63, p. 1123.

LITHOPROBE - PHASE 1: SOUTHERN VANCOUVER ISLAND: PRELIMINARY ANALYSES OF REFLECTION SEISMIC PROFILES AND SURFACE GEOLOGICAL STUDIES

C.J. Yorath, R.M. Clowes, A.G. Green, A. Sutherland-Brown, M.T. Brandon, N.W.D. Massey, C. Spencer, E.R. Kanasewich, and R.D. Hyndman

Yorath, C.J., Clowes, R.M., Green, A.G., Sutherland-Brown, A., Brandon, M.T., Massey, N.W.D., Spencer, C., Kanasewich, E.R., and Hyndman, R.D., LITHOPROBE – Phase 1: southern Vancouver Island: preliminary analyses of reflection seismic profiles and surface geological studies; in Current Research, Part A, Geological Survey of Canada, Paper 85-1A, p. 543-554, 1985.

Abstract

Seismic reflection and geological studies conducted on southern Vancouver Island during 1984 show that the region has sustained considerable shortening above a widespread décollement zone. Beneath Wrangellia, a thick interval of possibly underplated pre-Upper Miocene oceanic crust overlies the modern subducting Juan de Fuca Plate. The latter is clearly seen on all record sections and comprises an undeformed layered sequence resting upon presumed oceanic crust. The Leech River Fault is identified as a surface dipping towards the north at 35°. Beneath the fault the Eocene Metchosin Volcanics and Sooke Gabbro are seen to overlie a succession that may have its correlatives in the core zone Olympic Mountains of northern Washington.

Résumé

Des levés de sismique-réflexion et géologiques effectués dans le sud de l'île de Vancouver en 1984 montrent que cette région a subi un rétrécissement considérable au-dessus d'une vaste zone de décollement. Au-dessous de Wrangellia, un épais intervalle de croûte océanique, peut-être sus-jacent à une plaque et formé avant le Miocène supérieur, recouvre l'actuelle plaque de subduction de Juan de Fuca. On voit clairement cette dernière dans tous les diagrammes basés sur les enregistrements; elle est constituée d'une séquence stratifiée non déformée, reposant sur la croûte océanique hypothétique. On a identifié la faille de Leech River comme étant une faille superficielle dont le pendage est de 35° vers le nord. Au-dessous de la faille, les roches volcaniques de Metchosin et le gabbro de Sooke d'âge Eocène recouvrent une succession dont les éléments corrélatifs se trouvent sans doute dans la zone centrale des monts Olympiques, dans le nord de l'Etat de Washington.

Pacific Geoscience Centre,
Sidney, B.C.
V8L 4B2

Introduction

LITHOPROBE is a collaborative geoscientific project involving the co-ordination of geophysical, geological and geochemical techniques to elucidate the geology of the lithosphere in Canada by extending and relating surface geology to structures at depth. The project is spearheaded by the use of the Vibroseis[1] technique which permits deep seismic sounding to depths of as much as 16 seconds (two way-time, ca 50 km). In conjunction with the reflection profiling other important avenues of research are being conducted so as to facilitate the interpretation of the record sections and to help answer important questions about the nature and processes affecting the deep crust. The project is funded jointly by NSERC and the Department of Energy, Mines and Resources and involves university, government and industrial geoscientists in all phases from initial planning to final interpretation. For further details on the history of development of the project the reader is referred to Fyfe and Rust (1981), CANDEL (1981) and Clowes (in press).

Phase 1 of LITHOPROBE comprised field components in two areas: southern Vancouver Island (this report) and the Kapuskasing structural zone of Ontario (Woods, 1985). Veritas Geophysical Ltd. of Calgary was the company chosen to conduct the reflection seismic program which was completed during late May and June. It is to the credit of this young and vigorous company that it did an outstanding job and with such cooperative personnel. Supporting geoscience studies were carried out by many scientists. This report presents preliminary interpretations of the seismic reflection data and new suurface geological studies. It also lists other studies which have been completed or are in progress.

Regional geological and tectonic setting

The regional geological setting of southern Vancouver Island is largely known through the work of Muller (1977, 1980a) and his co-workers. During the past three decades other authors, eg. Fyles (1955) and Yole (1969) have discussed various aspects of the geology of the region. Numerous university postgraduate research theses have been devoted to both topical and regional studies.

The Tofino Basin, underlying the continental shelf off western Vancouver Island, received considerable attention during and following the exploration program in that region by Shell Canada Resources Ltd. in the late 1960s (Shouldice, 1971; MacLeod et al., 1977; Tiffin et al., 1972 and Yorath, 1980). Recently several geophysical studies have focused on the plate tectonic regime of the convergent margin (Keen and Hyndman, 1979; Riddihough, 1977, 1979, 1982).

A wide range of data was previously available (although of variable density and quality) to constrain models of deep crustal structure (notably those of Riddihough, 1979 and Spence, 1984). These include magnetotellurics studies in the Victoria and Buttle Lake areas, gravity data at 5 to 15 km spacing, repeated geodetic levelling and positioning for vertical movements, seismicity data, aeromagnetic surveys over the southernmost part of Vancouver Island, geothermal cross-sections and crustal temperatures and paleomagnetic studies.

A series of seismic refraction, reflection and surface-wave experiments have progressively defined the structure beneath the Island (White and Savage, 1965; Tseng, 1968; Wickens, 1977; McMechan and Spence, 1983; Ellis et al., 1983; Spence, 1984). The most recent of these references described aspects of the VISP experiment which involved four reversed refraction profiles across and parallel to the island, and two short reflection lines near the southwestern end of LITHOPROBE line 1. It was the success of these lines in identifying deep crustal reflectors that gave strong support to Vancouver Island being chosen as the first LITHOPROBE study area. Previously acquired data, particularly refraction, gravity and seismicity, have been interpreted in terms of a shallowly dipping subducting slab from beneath the edge of the continental shelf to beneath central Vancouver Island; beyond there the dip is believed to increase. Several authors have pointed out the requirement for a discontinuity or bend in the subducted slab in the area of Juan de Fuca Strait and the south end of the Island.

The regional geology of southern Vancouver Island and the location of the four multichannel seismic reflection profiles is shown in Figure 67.1. The island is made up of Paleozoic, Mesozoic and Cenozoic volcanic, plutonic, sedimentary and metamorphic rocks, which are complexly partitioned by a dominant northwesterly aligned structural grain. The main stratigraphic and structural unit is the Karmutsen Formation, a thick, relatively uniform basaltic lava sequence of Late Triassic age that separates middle and upper Paleozoic from Jurassic and younger volcanic, sedimentary and plutonic units. Along its axis and eastern margin, northwesterly aligned structural culminations expose the island's oldest rocks, the Sicker Group, in the Cowichan, Buttle and Nanoose uplifts and in the Victoria Arch. On the west coast and beneath the continental margin an apron of Cenozoic clastic rocks (Carmanah Group) overlies complexly deformed Upper Triassic to Cretaceous slope and trench deposits (Pacific Rim Complex) and Eocene oceanic basalts. The latter unit represents the structurally highest slice within the modern subduction complex. On the east coast the Nanaimo Group of Late Cretaceous age comprises cyclical graded sequences of conglomerate, sandstone and shale that developed within a successor basin occupying a forearc setting adjacent to the Coast Plutonic Complex. Beneath the Strait of Georgia, Nanaimo strata are overlain by a thick succession of dominantly nonmarine Tertiary clastics and subordinate Pleistocene sediments. The stratigraphy of the region is partly illustrated by the legend of Figure 67.1.

Objectives

The primary crustal architecture of Vancouver Island is thought to comprise an underthrusting oceanic plate overlain by a complex of accreted terranes. During the past several years many workers have identified Vancouver Island as part of Wrangellia, a terrane known to be allochthonous by virtue of paleomagnetic studies on Triassic and Jurassic volcanics (Yole and Irving, 1980; Irving and Yole, 1983). The manner of assembly of this and other adjacent terranes and their accretion to the ancient continental margin is largely unknown. However, a reasonable model has recently been proposed by Monger et al. (in press) which shows the various terranes of the Cordillera as having underthrust one another during accretion such that they are presently vertically juxtaposed, one above the other. Part of this model is shown in Figure 67.2b, which portrays Wrangellia as having been underplated by later accretionary terranes such as the Pacific Rim Complex along with the Crescent volcanics and Hoh and Ozette mélanges. Beneath these ancient terranes, the modern Juan de Fuca Plate is thought to decend beneath the margin, first at a relatively shallow angle beneath the continental shelf and then more steeply beneath the Island. LITHOPROBE was designed to test this terrane accretion and subduction model.

In order to accomplish the above objective a number of specific studies are being carried out by EMR. Geological projects include:

a. The construction of detailed corridor maps at 1:50 000, each of which is to contain one or more of the seismic profiles.

[1] Registered trademark of Continental Oil Company.

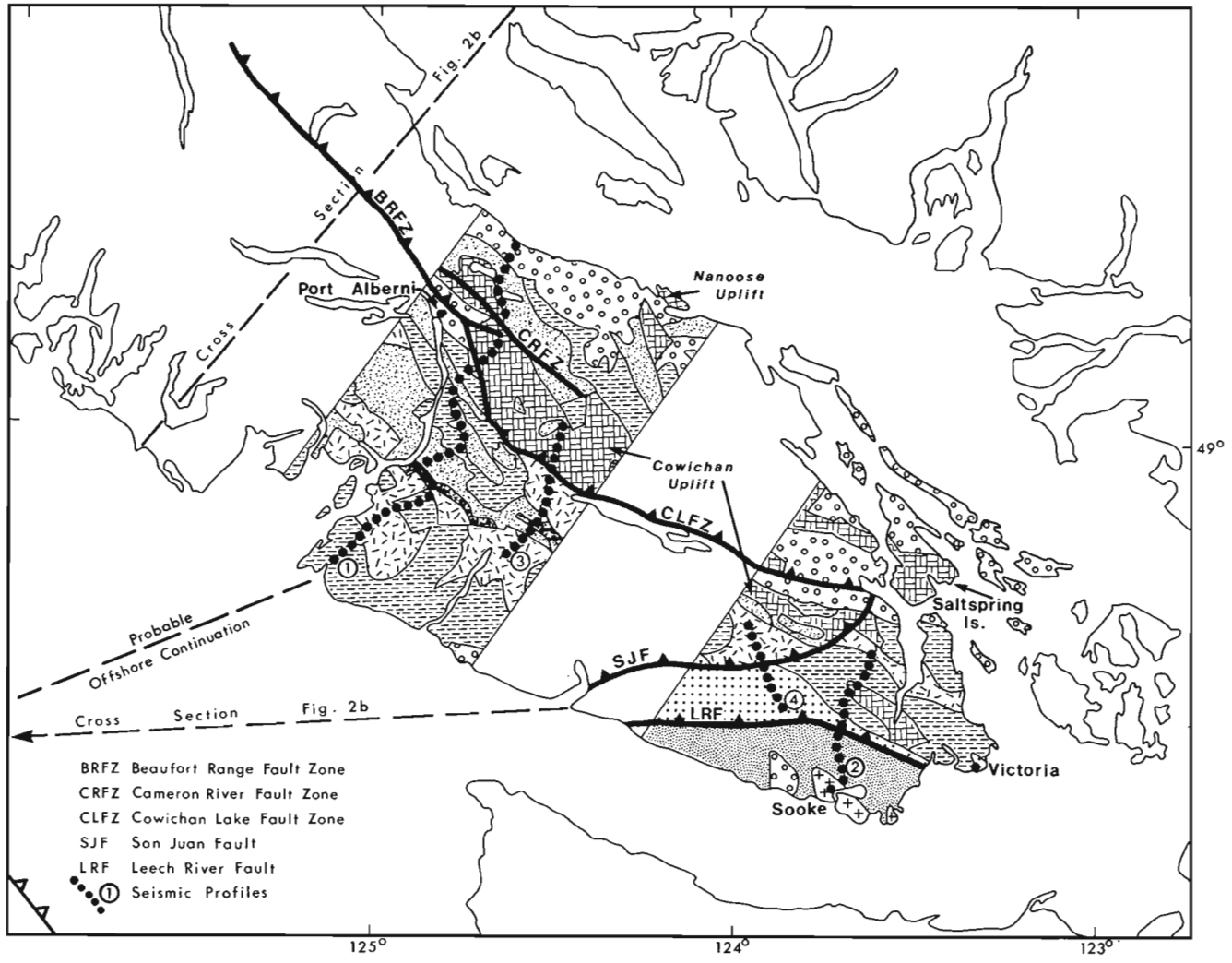

Figure 67.1. Partial geological map of southern Vancouver Island showing the locations of the four seismic profiles.

LEGEND

LOWER TERTIARY

Metchosin Volcanics and Sooke Gabbro.

TERTIARY AND UPPER CRETACEOUS

Carmanah Gp. and Nanaimo Gp. - Sediments. uKn

JURASSIC - CRETACEOUS

Leech River Fm. - metasediments.

MIDDLE JURASSIC

Island Intrusions and West Coast Crystalline Complex - plutonic and metamorphic rocks.

LOWER JURASSIC

Bonanza Gp. - Volcanics, sediments.

UPPER TRIASSIC

Quatsino Limestone

Karmutsen Fm. - Volcanics. uTrk

MID TO UPPER PALEOZOIC

Sicker Gp. - Volcaniclastics, epiclastics, lavas, limestone, chert. Ps

b. The identification of major structures and stratigraphic relationships which could be recognized on the record sections and traced to depth.

c. The examination of the differences in structural style of various units so as to be able to identify their seismic signatures on the reflection profiles.

d. Conducting stratigraphic and biostratigraphic studies of the middle to upper Paleozoic Sicker Group in the Cowichan and Nanoose uplifts and adjacent areas in order to identify stratigraphic units that may be identifiable on the seismic sections.

e. The determination of the uplift history of eastern Vancouver Island through studies of the Upper Cretaceous Nanaimo Group and Tertiary Chuckanut Formation, thus permitting the construction of mechanical and thermal models.

Geophysical studies include:

a. Magnetotelluric studies – a Phoenix Geophysics Ltd. system was used at several stations along line 1 and at several other sites to obtain information on the electrical conductivity structure of the crust and of the upper mantle, particularly of conductive layers associated with the underthrusting Juan de Fuca Plate. (J.M. DeLaurier, R.D. Kurtz)

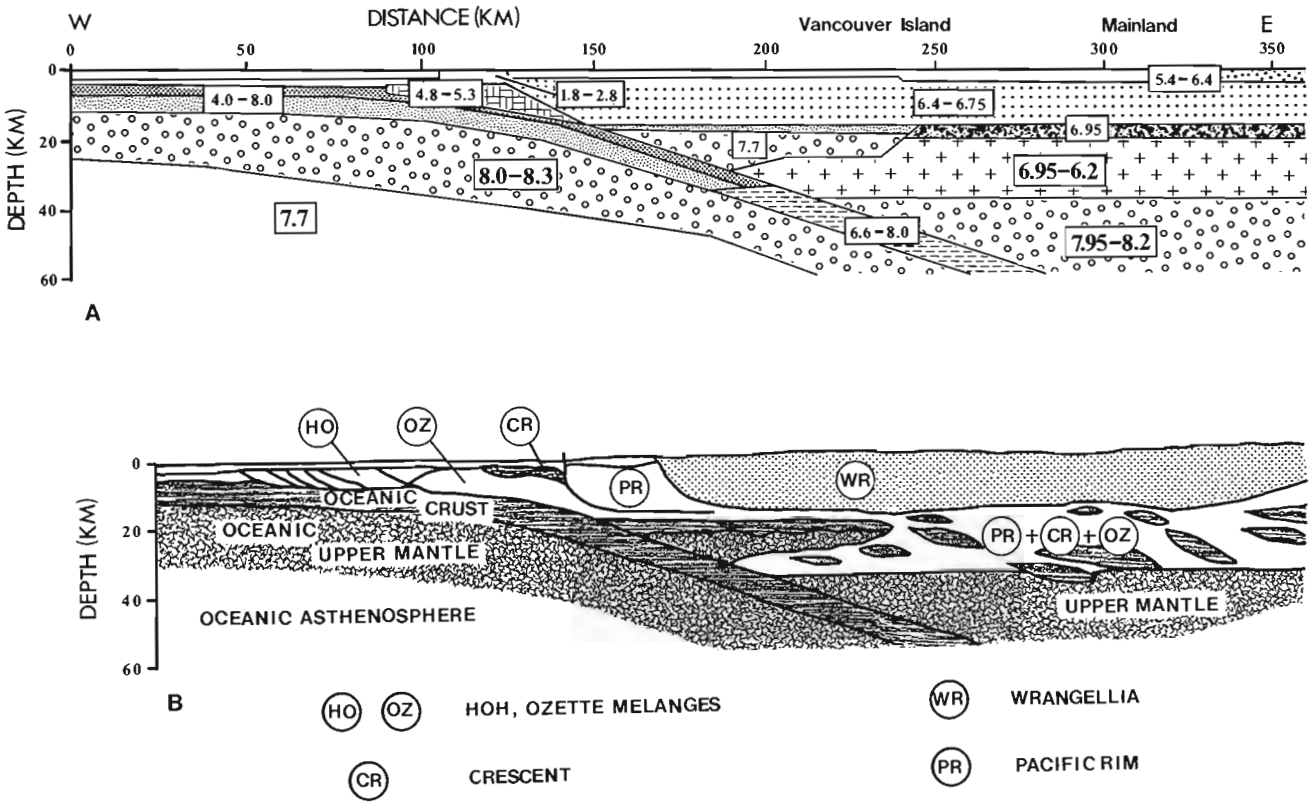

Figure 67.2. *(a) Velocity model across the continental margin (from Spence, 1984); (b) Tectonic cross-section across the continental margin (location shown in Fig. 67.1) (modified from Monger et al., in press).*

b. Gravity profiles were conducted along line 1 and along the east coast of the Island to improve the previous data density. These will further constrain the interpretation of the deep structure of the crust and upper mantle. (J. Sweeney, D. Seemann, J.B. Boyd, H. Dragert)

c. Geodetic levelling and positioning – a levelling profile was carried out by the Surveys and Mapping Branch that will be combined with previous and future Vancouver Island data to determine contemporary uplift and subsidence rates in the region.

d. Seismicity cross-section – this section is being constructed along a corridor which includes line 1 and is to be integrated with the reflection profiles so as to enhance deep crustal and tectonic models. (G.C. Rogers)

e. Aeromagnetic surveys – existing aeromagnetic coverage of southern Vancouver Island was expanded so as to include all of the area traversed by the seismic profiles. (P.J. Hood)

f. Geothermal measurements – a profile of heat flow and crustal radioactive heat production measurements and implied crustal temperatures is being constructed. (T. Lewis)

g. Paleomagnetic studies of Tertiary and Paleozoic rocks are being undertaken in cooperation with R.W. Yole of Carleton University. (E. Irving)

A number of supporting geoscientific studies are being conducted by university professors and their students. R.L. Armstrong and C.E. Isachsen of the University of British Columbia are further refining the geochronological relationships between the Early and Middle Jurassic Island Intrusions and the West Coast Crystalline Complex. Results to date suggest that the two are closely related in time but originated at different crustal levels (R.L. Armstrong, personal communication). R.M. Bustin and G.E. Rouse, also of U.B.C., are carrying out stratigraphic, biostratigraphic, thermal maturation and clay mineralogical studies on parts of the Upper Cretaceous Nanaimo Group. C.M. Scarfe along with K. Muehlenbachs at the University of Alberta are undertaking detailed geochemical studies on volcanic and plutonic rocks so as to help determine depths of emplacement, source materials and alteration history. H. Dosso of the University of Victoria is studying electromagnetic induction models of Vancouver Island and the adjacent sea to facilitate the interpretation of the magnetotelluric data. It is reported that W.S. Fyfe of the University of Western Ontario has found evidence of dewatering of the subducting Juan de Fuca Plate.

A few results

Surface geology

A. The dominant structural style of southern Vancouver Island is one of horizontal shortening across the northwesterly trending axis of the Island. All rock units have sustained at least moderate folding subparallel to the axis although penetrative deformation is relatively rare except in the Mt. Sicker – Saltspring Island area. Fold axes and the trends of major faults are subparallel and the latter appear to combine significant thrust as well as dextral separation. Two structural culminations, the Cowichan and Nanoose uplifts (Fig. 67.1), expose Paleozoic Sicker Group rocks and each are thought to have been elevated during the Late Cretaceous by uplift along easterly dipping faults. The Cowichan Uplift and its colinear expression in the Beaufort Range are bounded on the southwest by two fault zones that are believed to be dynamically linked. These are the Cowichan Lake Fault Zone (Fig. 67.3) and the Beaufort Range Fault Zone (Fig. 67.4), the latter is thought to have been the locus of the 1946 earthquake that caused significant damage to several communities in central Vancouver Island (Rogers and Hasegawa, 1978).



Figure 67.3. View looking southeast along Cowichan Lake. The trace of the Cowichan Lake Fault Zone occurs along the lower slopes of the ridge on the north side of the lake.



Figure 67.5. Upper strand of the Beaufort Range Fault Zone on Highway 4 near Port Alberni. The man (K. Dom) has his hand on the breccia zone immediately adjacent to the fault which dips easterly at 45°. Ps = Paleozoic Sicker Group. uKn = Upper Cretaceous Nanaimo Group.



Figure 67.4. View looking northwesterly along the west flank of the Beaufort Range and the Alberni Valley. The trace of the Beaufort Range Fault Zone occurs near the base of the steeper slope of the range.



Figure 67.6. Assymetric fold in interbedded limestone and siliceous mudstone. View looking northwesterly down plunge. Copper Canyon, Chemanus River. ls = limestone; S_1 = trace of axial plane cleavage.

The Beaufort Range Fault Zone juxtaposes upper Paleozoic Sicker Group and Upper Triassic Karmutsen Formation rocks in the hanging wall above the lowermost units of the Upper Cretaceous Naniamo Group (Comox and Haslam formations) which underlies the floor of the Alberni Valley. The fault zone comprises at least two strands, each about 40 km long; one dips eastward at about 45° (Fig. 67.5) and the other is nearly vertical. The zone is thought to connect with either the Cameron River Fault Zone (35 km) or the Cowichan Lake Fault Zone (85 km +) although the latter is considered more likely because of the close similarity in relative stratigraphic separation and structural style as well as physiographic expression. The Cowichan Lake Fault zone comprises two to three strands, each of which dip steeply easterly and which separate Sicker and Karmutsen rocks in the hangingwall from Nanaimo Group strata in the footwall.

The Cowichan Uplift is a gently northwesterly plunging structure within which Sicker Group sedimentary and pyroclastic rocks are typically folded into tight to isoclinal folds. More massive volcanic and intrusive rocks are penetratively deformed, and are flattened to varying degrees; the resulting foliation is coplanar with the vertical axial planes of the folded rocks. Locally these rocks are converted to quartz-mica and chlorite-epidote schists. Bedded limestones, perhaps correlative with the Buttle Lake Formation, also are involved in this deformation (Fig. 67.6) and hopefully will provide some useful age control for the folding.

The timing and tectonic significance of deformational events that affected Sicker rocks are poorly understood, in part due to the paucity of reliable age control and the lack of distinctive and widely recognizable stratigraphic units. It may be that in the southeastern Cowichan Uplift more highly deformed rocks represent an older part of the group that sustained deformation prior to the deposition of younger Sicker units. Previously reported radiometric dates (Muller, 1980a, b; Eastwood, 1983) lend some support to this view. The Tyee quartz porphyry and hornblende porphyry intrusions in the Mt Sicker – Saltspring Island area yielded Devonian ages thus suggesting a pre-Devonian age for the host rocks. Conclusive intrusive contacts are rare; however, one occurs in the Duncan area (Fig. 67.7). It is noted, however, that if the folded limestones in this region belong to the Buttle Lake Formation, a post Permian age of deformation would be indicated.

In the Nanoose Uplift most Sicker rocks are isoclinally folded about vertical axial planes; penetrative strain occurs in argillites. Some support for the presence of thrust faults is suggested by the apparent position of the Campanian Extension-Protection Formation above the Santonian Comox Formation, however, the principal Paleozoic packages within the uplift are separated by faults of unknown type.

B. The stratigraphy of the Sicker Group has been the subject of much study. Muller (1980a) divided the sequence beneath the Buttle Lake Limestone into an informal "Sediment-Sill Unit" and two formal units, the Myra and Nitinat formations, all in descending stratigraphic order. Our preliminary work indicates that these units are not useful since their relative position and continuity are poorly understood. We have resorted to the establishment of local, informal units, and hope to resolve their stratigraphic relationships after more extensive detailed studies and dating.

In the Cowichan Uplift only the uppermost stratigraphic succession is known with confidence. The top of the group is represented by an unnamed unit, some 50 to 100 m thick, of turbiditic sandstones, shales and intercalated basaltic intrusions or flows (Fyles, 1955; Yole, 1969). This unit rests conformably upon the Buttle Lake Limestone which comprises about 500 m of bioclastic, locally tuffaceous and cherty calcarenite and minor interbedded argillite and volcanic sandstone (Fig. 67.8). The formation has yielded fossils ranging in age from Middle Pennsylvanian to Early Permian (Yole, 1969; Muller, 1980a). Both the uppermost unnamed unit and much of the Buttle Lake Limestone are widely truncated by the unconformity at the base of the Upper Triassic Karmutsen Formation.

Beneath the Buttle Lake Formation is a homogeneous succession, about 1000 m thick, of dominantly epiclastic strata consisting of massive, well bedded volcanic sandstones, lithic tuffs with lesser amounts of pyroxene-bearing agglomerate and volcanic conglomerate. This succession is underlain by a much thicker sequence of mainly pyroclastic rocks dominated by pyroxene-bearing agglomerate (Fig. 67.9), tuff, volcanic sandstone and minor green chert. This sequence includes some pillow lavas, commonly in relatively thin flow units but at least 200 m are exposed at one locality. These pillow lavas are of different character than those of the Upper Triassic Karmutsen Formation; individual pillows tend to be much larger, richly pyroxene-bearing and with jasper as interpillow material.

In the Nanoose Uplift, which includes the Nanoose Peninsula and adjacent offshore islands, the Sicker Group is dominated by epiclastic strata with lesser amounts of volcanic and pyroclastic rocks. Calcarenite and quartz arenite grain flows, chert and argillite breccia, volcanic sandstones, turbidites, tuffs and pillow basalts characterize the uppermost part of the succession. On the offshore islands this unit is underlain by rocks thought to be equivalents of the Buttle Lake Formation comprising bioclastic limestone, chert, volcanic sandstone and conglomerate. On the peninsula, rocks in a structurally equivalent position include olistostromes (Fig. 67.10) and tectonic mélange made up of bioclastic limestone, argillite, basalt breccia and quartzite. The lowermost unit in both areas comprises rhythmite, turbidite, orthoquartzite and argillite, the latter enclosing pods of limestone; on the peninsula these rocks are underlain by green and white banded tuffaceous chert and minor interbedded argillite. The Paleozoic rocks are overlain with spectacular unconformity by massive, resedimented conglomerate of the Upper Cretaceous Nanaimo Group (Fig. 67.11).

C. The Nanaimo Group of the Alberni, Cowichan and Comox valleys received much attention. Extensive sampling of coals and shales for vitrinite reflectance, as well as biostratigraphic data and sandstones for porosity and thermal conductivity values, was carried out to obtain input data for the calculation of mechanical and thermal models of basin formation. The coarse sandstones and conglomerates of the Extension-Protection Formation contain significant quantities of white quartz, unlike other conglomerate members of the Nanaimo Group. This quartz was sampled as was the interpillow quartz ("dallasite") of the Karmutsen Formation to determine through fluid inclusion and oxygen ratio studies if the latter was the source for the former. The significance of this lies in its relationship to the timing of uplift of the Beaufort Range, much of which is underlain by Karmutsen pillow basalts.

D. In at least two areas west of the Beaufort Range Fault zone, well indurated and lithified marine sandstones of the Comox Formation, the lowermost formation of the Nanaimo Group, rest upon deeply weathered quartz diorite of the Lower to Middle Jurassic Island Intrusions. The weathering has resulted in a soft quartz diorite grus which can be mined by hand from beneath the sandstones, the lowermost levels of which contain clasts of the weathered granitic rocks (Fig. 67.12). Moreover, the weathered granitic rocks provide

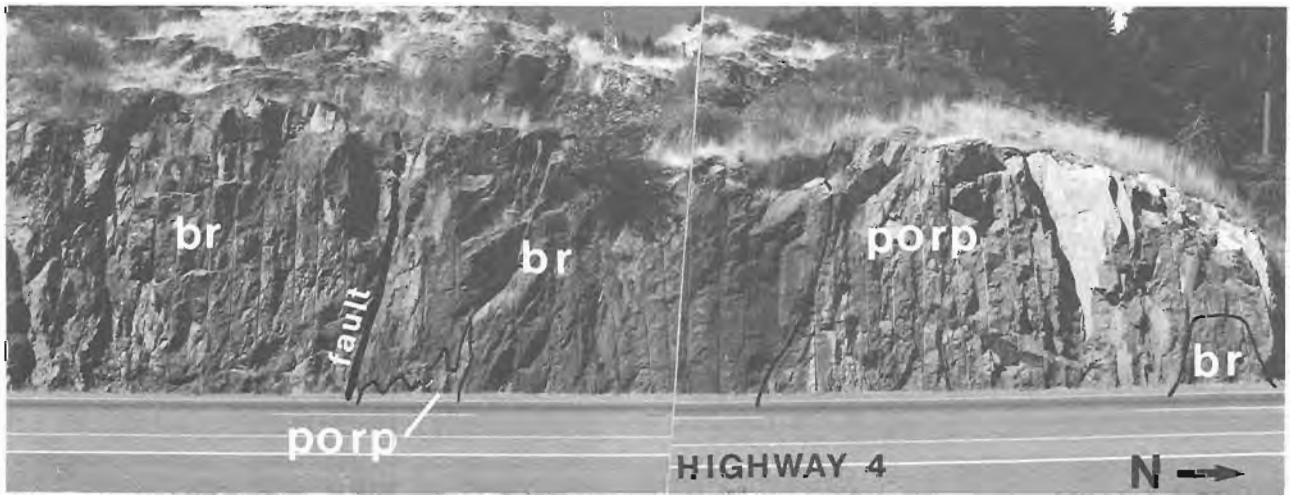

Figure 67.7. *Intrusive contacts between quartz porphyry (porp) and older fragmental rocks (br) consisting of rounded volcanic clasts within a tuffaceous matrix. The volcanic rocks typically contain abundant mafic phenocrysts and have been strongly epidotized. Highway 1, north of Duncan, British Columbia.*

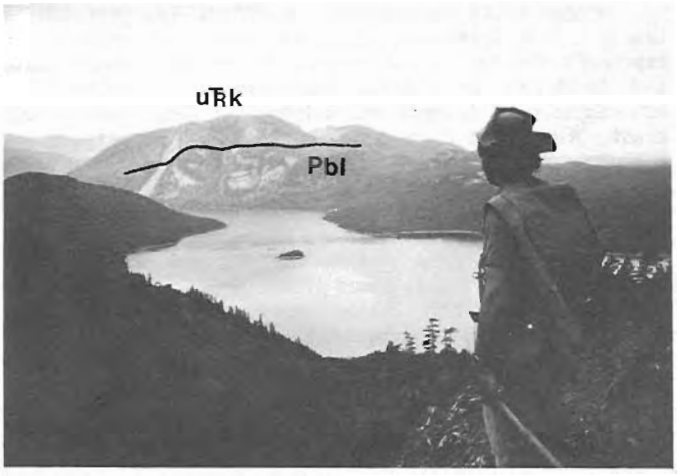

Figure 67.8. View looking northwesterly across Horne Lake at Mount Mark. Pbl = Paleozoic Buttle Lake Limestone; uTRk = Upper Triassic Karmutsen Formation.



Figure 67.9. Pyroxene-bearing agglomerate in the upper part of the pyroclastic unit, upper Sicker Group; Upper Cameron River.



Figure 67.10. Olistostrome in upper Paleozoic Sicker Group, Nanoose Peninsula. Outlined blocks are mainly limestone, turbidites and quartzite in an argillite matrix.



Figure 67.11. Resedimented conglomerate of the upper Cretaceous Nanaimo Group (uKn) resting on sheared argillites of the upper Paleozoic Sicker Group (Ps); Nanoose Peninsula.

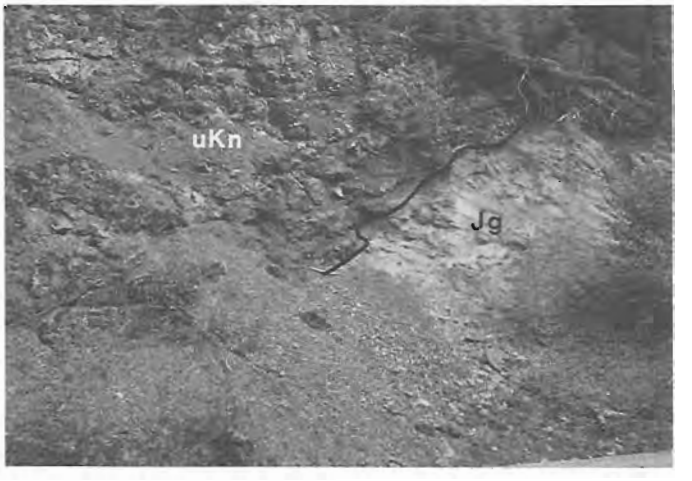

Figure 67.12. Upper Cretaceous Nanaimo Group (uKn – Comox Formation) resting upon deeply weathered quartz diorite (Jg); Bainbridge Lake.

an ^{18}O value of 14.1‰ which suggests low temperature weathering with relatively high ^{18}O water, perhaps in a different climate and location than at present (K. Muehlenbachs, personal communication, 1984). In other areas to the east of the fault zone basal nonmarine Nanaimo sandstones and conglomerates likewise rest upon plutonic rocks but no evidence of deep chemical weathering is evident. This and other criteria, such as the difference in relative size and distribution of plutonic rocks on either side of the "Beaufort Range – Cowichan Valley Fault System" suggests that the plutonic rocks in the two regions are different in some way and, moreover, that those on the west side sustained different chemical weathering conditions than those on the east side. Detailed chemical analyses and geochronology may resolve this question.

E. The early Eocene Metchosin Volcanics and Sooke Gabbro, south of the Leech River Fault (Fig. 67.1) show a pseudo-ophiolitic stratigraphy. Massive and layered gabbros (Fig. 67.13) pass upward into and are intruded by a well developed sheeted dyke complex. This in turn is succeeded by subaqueous pillow and sheet flow basalts with minor pyroclastics which in turn are overlain by subaerial(?) amygdaloidal flows. The general stratigraphy suggests that the succession developed as seamounts, probably in a marginal basin setting, close to a continental edge. Muller (1980b) came to a similar conclusion on the basis of chemical studies.

Reflection seismic profiles

Approximately 205 km of reflection seismic profiling was conducted along the four lines illustrated in Figure 67.1. The instrumentation employed was a 120 channel DFS 5 system employing up to four synchronized vibrator sources (Fig. 67.14) along a geophone layout with a 90 m group spacing. The data were digitally recorded to 16 s using a 4 ms sampling rate and stacked to 3000%. Processing included crooked line correction, demultiplexing, AGC, filtering, automatic static correction and stacking. Figures 67.15, 67.16 and 67.17, selected from lines 1 and 4, provide good examples of the excellent data quality achieved (horizontal exaggeration approximately 1.5 to 1.7; original display = 24 traces/inch). The illustrated line drawings (Fig. 67.18, 67.19) represent preliminary coarse interpretations of lines 1 and 4. Some structural boundaries pass through groups of dipping reflectors; these will ultimately shift in position and increase in dip when the sections are migrated.

Figure 67.18 summarizes the initial interpretation of line 1. The lowermost reflector zone is considered to represent the top of the present descending oceanic plate, and comprises an interval (approximately 3 km thick) of interdigitated sediments and volcanics resting upon oceanic crust. Within this lower group some reflectors suggest that the upper part of the interval may have been accreted to the overriding upper plate. Widely scattered reflectors, possibly within the mantle, occur below this zone. The depth to the deepest zone of strong reflectors is remarkably close to that postulated in previous models for the top of the underthrusting oceanic crust; about 20 km beneath the west coast of the island and 30 km beneath the east coast (Riddihough, 1979; Spence, 1984). These models were constrained by the depth to the top of the oceanic crust beyond the continental slope where it can be seen in single channel seismic reflection profiles, and, by seismic refraction data obtained on Vancouver Island. The reflectors show some indication of an increase in dip towards the eastern end of the line, beyond which continuity is lost. At about this location, previous models have shown a change in dip from about 10° to at least 30°. A change to steeper dips is a common feature of many models of subducting plates (e.g. Karig et al., 1976); Rogers (in press) has suggested that this is due to the initiation of high density phase changes at those depths. It is possible that at these depths, the underthrust slabs become decoupled from the base of the overlying lithosphere and penetrate the aesthenosphere (Riddihough, 1984).

Above the lower zone is a thick layer with few coherent reflectors which may be an older oceanic slab now accreted to the overlying continental crust (the underplated zone). A seaward jump in the locus of subduction prior to the Late Miocene that might leave such an underplated slab was proposed by Keen and Hyndman (1979). Above this is another layered zone within which groups of reflectors show dip divergence at several localities. This interval, like the one below, may represent oceanic sediments that were underplated beneath Wrangellia when the older oceanic slab (the underplated zone) was being underthrust. This sediment zone may since have acted as a zone of décollement for listric faults that extend upwards into the Sicker Group. The uppermost prominent band of reflectors is considered to represent the Buttle Lake Limestone which is unconformably overlain by the Upper Triassic Karmutsen Formation and younger Mesozoic rocks. It should be noted that the thick dashed lines roughly defined the limits of similarity of reflector type and geometry; they do not necessarily have

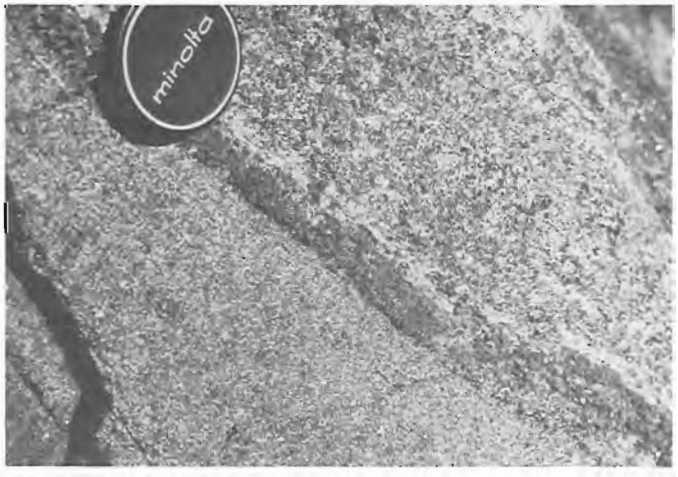

Figure 67.13. *Size-graded layering in the Rocky Point Gabbro.*



Figure 67.14. *Vibrator trucks at the beginning of line 1 near Bamfield.*

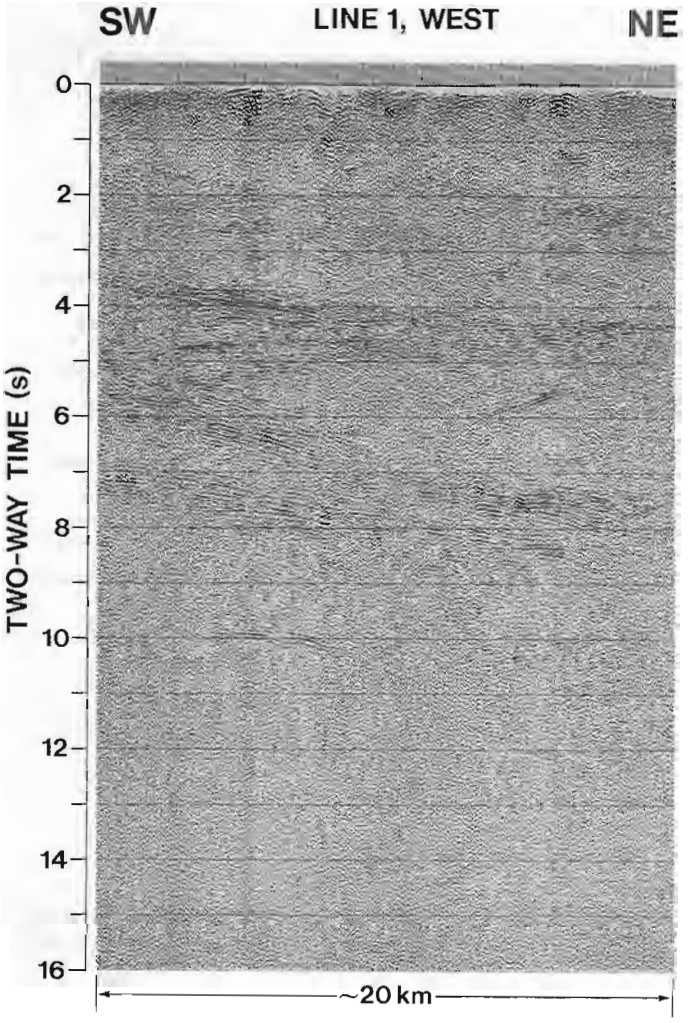

Figure 67.15. Example of record section selected from the southwestern end of line 1. Horizontal exaggeration approximately 1.7 x.

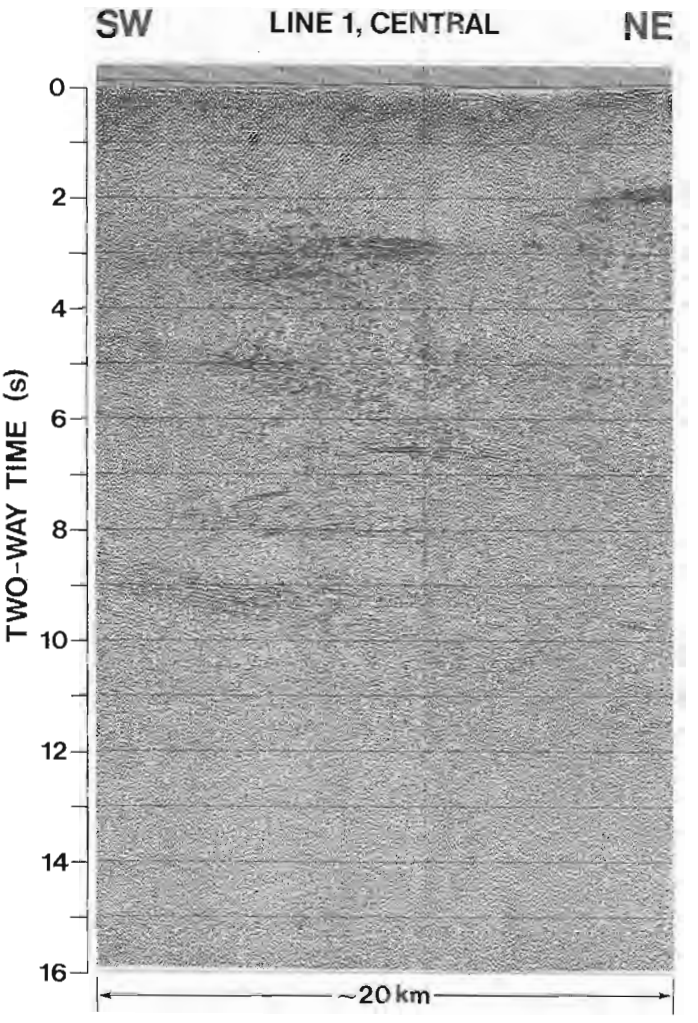

Figure 67.16. Example of record section selected from the central portion of line 1. Horizontal exaggeration approximately 1.7 x.

precise stratigraphic significance. The lack of good reflectors in the uppermost part of the record is a function of velocity and processing parameters chosen; future processing of the higher frequencies within the first 4 s should enhance the data in this interval. It is hoped that migrated sections with enhanced data quality in the upper section will permit some degree of palinspastic restoration along the arcuate faults. Note the apparent near doubling in thickness of the décollement zone where each of these becomes listric. This suggests that these faults are thrusts, however, there is an apparent normal displacement to the Sicker/Karmutsen contact.

The westernmost fault is thought to be a surface along which Eocene volcanic rocks have been emplaced beneath the western edge of Wrangellia (Brandon, 1984). These volcanics have been recognized in offshore seismic profiles to the south where they were penetrated by three offshore wells drilled in the late 1960s (Snavely and Wagner, 1981, Shouldice, 1971; MacLeod et al., 1977; Yorath, 1980). Assuming that the underplated and décollement zones are younger than the early Tertiary volcanics, then considerable material may have been removed from the base of Wrangellia prior to or concurrently with the emplacement of the underplated zone. Also, the necessary uplift as a consequence of underthrusting and underplating would have resulted in considerable erosion of westernmost Vancouver Island; this may be reflected in the geochronological and geochemical studies of the Island Intrusions and Westcoast Crystalline Complex described above. The easternmost faults are the high angle reverse faults identified as the Beaufort Range and Cameron River fault zones. At the northernmost end of the Cowichan Uplift these faults bound a large and broad, internally disrupted anticlinorium, thus reflection quality in this region is poor.

Figure 67.19 shows our initial interpretation of line 4 which crossed the San Juan Fault and terminated close to the Leech River Fault on southern Vancouver Island (Fig. 67.1). The San Juan Fault has been interpreted as a high angle reverse fault and/or sinistral fault (Muller, 1977) separating the Lower and Middle Jurassic Bonanza volcanics to the north from Jura-Cretaceous Leech River schist and Wark and Colquitz gneiss to the south. The Leech River Fault, with both high angle reverse and sinistral separation, bounds the Leech River Formation to the north and the Eocene Metchosin volcanics and Sooke gabbro to the south (Muller, 1977, 1983; Fairchild and Cowan, 1982).

The San Juan Fault (outcrop location shown) is not evident on line 4, (Fig. 67.19) probably due to its very steep dip and/or to processing parameters and velocity choices employed. Reprocessing of the uppermost part of the record section might reveal the geometry of the fault. The Leech River Fault is clearly shown with an apparent dip of 28° (true dip about 35°) towards the north. Beneath the fault the Metchosin Volcanics and underlying layered Sooke Gabbros

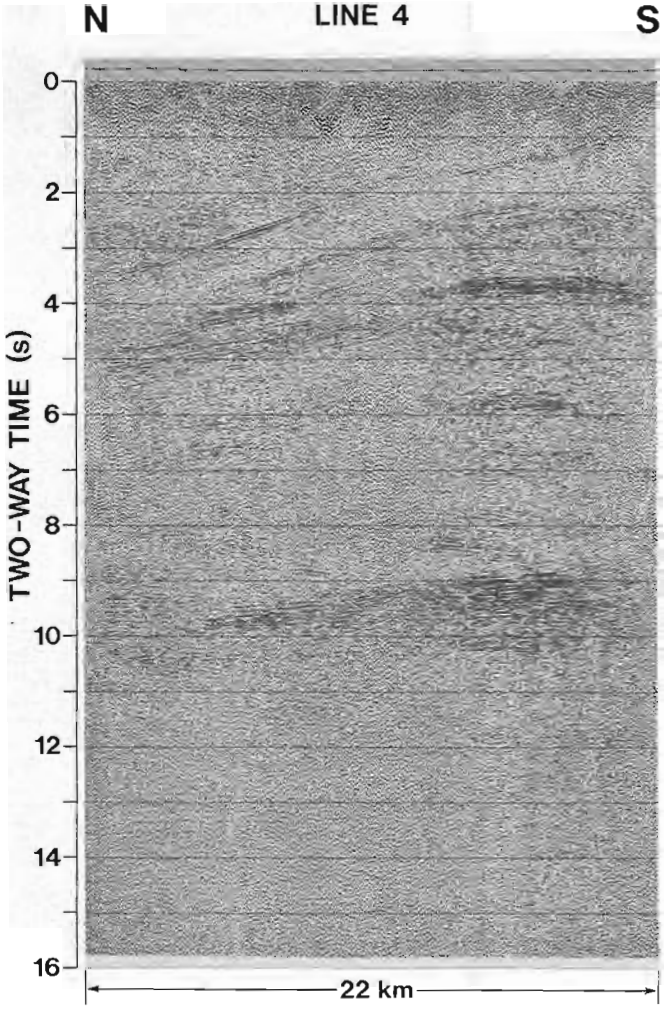

Figure 67.17. Complete record section of line 4. Horizontal exaggeration approximately 1.7 x.

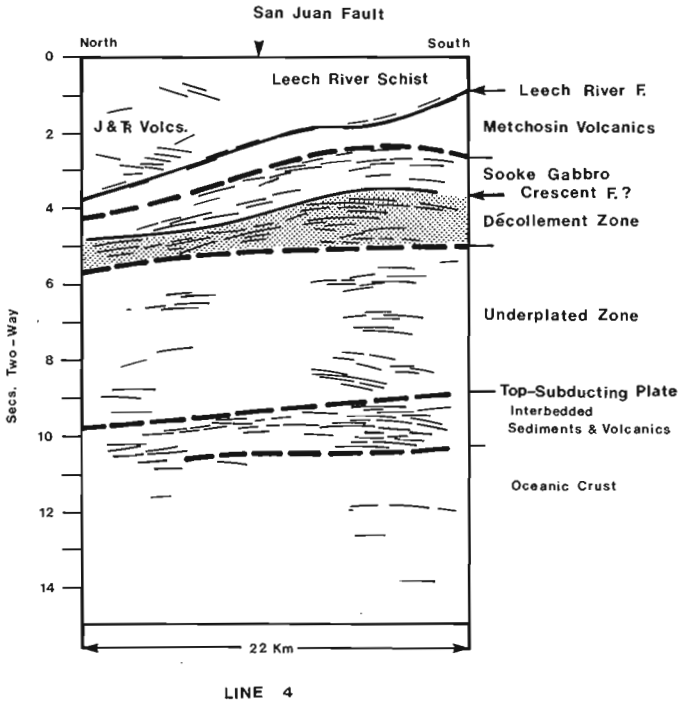

Figure 67.19. Preliminary interpretation of line 4. See text.

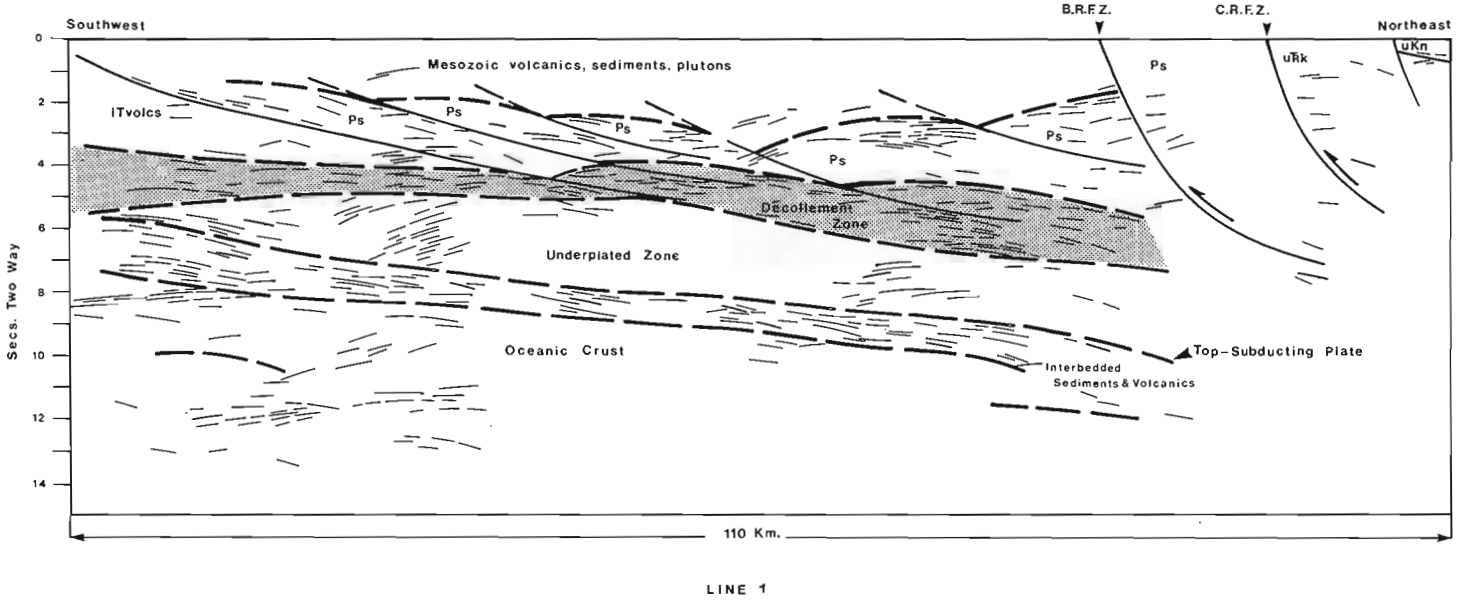

Figure 67.18. Preliminary interpretation of line 1. See text.

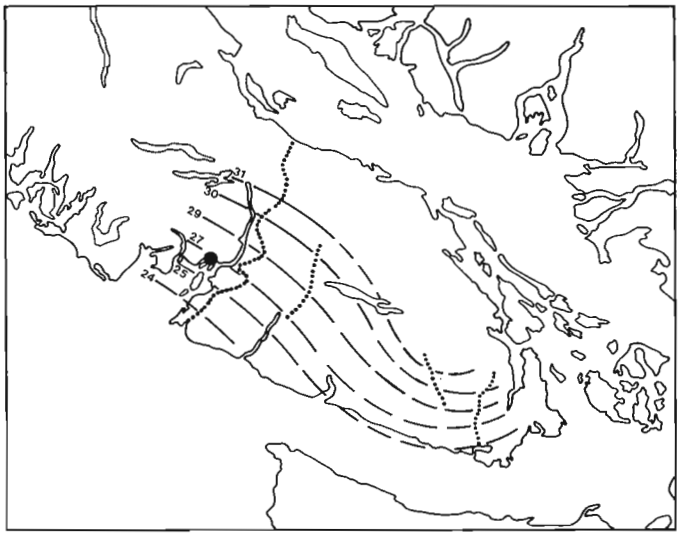

Figure 67.20. *Isochron surface, converted to depth in kilometres, drawn on the top of the subducting plate. Black dot is the epicentre of an earthquake with an estimated focal depth of 37 km.*

are displayed in a broad anticline, floored by the Crescent thrust, above layered sequences (Décollement Zone and Underplated Zone) which possibly have their surface expressions in the sedimentary rocks of the core zone of the Olympic Mountains in northwestern Washington. The modern descending Juan de Fuca Plate again comprises layered interbedded sediments and volcanics resting upon oceanic crust.

One of the principal features of all four seismic profiles is the uniformity and consistency of major reflecting horizons and zones. Both the décollement zone and the descending Juan de Fuca Plate are seen on all lines and show remarkably similar character throughout the southern half of Vancouver Island. Figure 67.20 is an approximation of the isochron surface, converted to depth in kilometres drawn on the surface of the subducting plate. The slope of the plate descends from about 24 km near the coast at line 1 to about 30 km beneath the centre of the island (Slope = 9°). Towards the south there is a bend or discontinuity in the plate, as predicted by Keen and Hyndman (1979) based on geometrical arguments and by Rogers (1983) on the basis of seismicity studies. Because of differences in input velocities for processing purposes between the northern two and southern two lines, the degree of plate curvature in the south may be either more or less than shown, but not significantly. The large black dot at the head of Barkley Sound is the epicentre of an earthquake that occurred on 18 October 1984. Its focal depth was estimated at 37 km which suggests that it occurred at or near the base of the descending plate.

Conclusions

The Vancouver Island component of Phase 1 of LITHOPROBE, to date has been extraordinarily successful. The quality of the seismic record sections far exceeded expectations. The modern underthrusting oceanic plate is clearly seen on all profiles as is an apparently older slab, now accreted to the overlying crust. Although the seismic data have not yet been processed to enhance reflections in the uppermost portions of the record sections, the profiles clearly show the major structural and stratigraphic features recognized in the surface geology. Geological field studies will continue through 1985 with the object of producing corridor maps for each profile as well as additional stratigraphic and structural control information for more detailed interpretations of the record sections. Furthermore, as indicated in Figure 67.1, an offshore extension of the seismic profile of line 1 is planned for the summer of 1985. This report describes the preliminary results only of the reflection seismic and part of the geological work. A wide variety of other studies are in progress. Most important will be the synthesis resulting from the integration of all aspects of the LITHOPROBE project on southern Vancouver Island.

Acknowledgments

The writers would like to thank R.W. Yole, R.L. Brown and J.M. Moore of Carleton University for helpful discussions and visits in the field. Thanks are expressed to the companies and personnel of Crown Forest Products and McMillan Bloedell Ltd. for access to logging areas and for their assistance in providing logging road maps. The co-operation of the Greater Victoria Water District is greatly appreciated. Gratitude is expressed to the British Columbia Ministry of Transportation and Highways and the Ministry of Finance as well as the Royal Canadian Mounted Police for their assistance and co-operation with regard to seismic field operations.

References

Brandon, M.T.
1984: Deformational processes affecting unlithified sediments at active margins: a field study and a structural model; unpublished Ph.D. thesis, University of Washington.

Candel
1981: Lithoprobe: Geoscience studies of the third dimension – A co-ordinated national geoscience project for the 1980s; Geoscience Canada, v. 8, p. 117-125.

Clowes, R.M.
– Phase 1 Lithoprobe – A co-ordinated national geoscience project; Geoscience Canada. (in press)

Eastwood, G.E.P.
1983: Sicker Project (92B/13); British Columbia Ministry of Energy, Mines and Petroleum Resources; Geological Fieldwork, 1983. Paper 1983-1, p. 46.

Ellis, R.M., et al.
1983: The Vancouver Island seismic project: CO-CRUST onshore-offshore study of a convergent margin; Canadian Journal of Earth Sciences, v. 20, p. 719-741.

Fairchild, L.H. and Cowan, D.S.
1982: Structure, petrology and tectonic history of the Leech River complex northwest of Victoria, Vancouver Island; Canadian Journal of Earth Sciences, v. 19, p. 1817-1835.

Fyfe, W.S. and Rust, B.R.
1981: The next decade of earth science research in Canadian universities: Proceedings of the earth science workshop, 1981; Geoscience Canada, v. 8, p. 113-116.

Fyles, J.T.
1955: Geology of the Cowichan Lake area, Vancouver Island, British Columbia; British Columbia Department of Mines, Bulletin No. 37.

Irving, E. and Yole, R.W.
1983: Paleolatitudes, apparent displacements and internal rotations of the Bonanza Volcanics (Early Jurassic) of Vancouver Island, B.C.; in program with Abstracts, Geological Association of Canada/Mineralogical Association of Canada/Canadian Geophysical Union, Joint Annual Meeting, Victoria, v. 8.

Karig, D.E., Caldwell, J.G., and Parmentier, E.M.
1976: Effects of accretion on the geometry of the descending lithosphere; Journal of Geophysical Research, v. 81, p. 6281-6291.

Keen, C.E. and Hyndman, R.D.
1979: Geophysical review of the continental margins of eastern and western Canada; Canadian Journal of Earth Sciences, v. 16, p. 712-747.

MacLeod, N.S., Tiffin, D.L., Snavely, P.D., Jr., and Currie, R.G.
1977: Geologic interpretation of magnetic and gravity anomalies in the Strait of Juan de Fuca, U.S. – Canada; Canadian Journal of Earth Sciences, v. 14, p. 223-238.

McMechan, G.A. and Spence, G.D.
1983: P-wave velocity structure of the Earth's crust beneath Vancouver Island; Canadian Journal of Earth Sciences, v. 20, p. 742-752.

Monger, J.W.H., Clowes, R.M., Price, R.A., Riddihough, R.P., and Woodsworth, G.J.
– Continent: Ocean Transect B2, Juan de Fuca Plate to Alberta Plains; International Geodynamics Transect Program, Geological Society of America. (in press)

Muller, J.E.
1977: Evolution of the Pacific margin, Vancouver Island and adjacent regions; Canadian Journal of Earth Sciences, v. 9, p. 2062-2085.

1980a: The Paleozoic Sicker Group of Vancouver Island, British Columbia; Geological Survey of Canada, Paper 79-30.

1980b: Chemistry and origin of the Eocene Metchosin Volcanics, Vancouver Island, British Columbia; Canadian Journal of Earth Sciences, v. 17, p. 199-209.

1983: Geology, Victoria, British Columbia; Geological Survey of Canada, Map 1553A.

Riddihough, R.P.
1977: A model for recent plate interactions off Canada's west coast; Canadian Journal of Earth Sciences, v. 14, p. 384-396.

1979: Gravity and structure of an active margin – British Columbia and Washington; Canadian Journal of Earth Sciences, v. 16, p. 350-363.

1982: Contemporary movements and tectonics on Canada's west coast: a discussion; Tectonophysics, v. 86, p. 319-341.

1984: Recent movements of the Juan de Fuca plate system; Journal of Geophysical Research, v. 89, p. 6980-6994.

Rogers, G.C.
1983: Some comments on the seismicity of the northern Puget Sound – southern Vancouver Island region; in Earthquake hazards of the Puget Sound region, Washington State, ed. J.C. Yount and R.S. Crossan; United States Geological Survey, Menlo Park, California, Open File Report 1983-19, p. 19-39.

Rogers, G.C. (cont.)
– Variation in Cascade volcanism with margin orientation; Geology. (in press)

Rogers, G.C. and Hasegawa, H.S.
1978: A second look at the British Columbia earthquake of June 23, 1946; Bulletin of the Seismological Society of America, v. 68, p. 653-675.

Shouldice, D.H.
1971: Geology of the western Canadian continental shelf; Canadian Society of Petroleum Geologists Bulletin, v. 19, p. 405-424.

Snavely, P.D., Jr. and Wagner, H.C.
1981: Geologic cross section across the continental margin off Cape Flattery, Washington, and Vancouver Island, British Columbia; United States Geological Survey, Menlo Park, California, Open File Report 81-978.

Spence, G.D.
1984: Seismic structure across the active subduction zone of western Canada; unpublished Ph.D. thesis, University of British Columbia.

Tiffin, D.L., Cameron, B.E.B., and Murray, J.W.
1972: Tectonics and depositional history of the continental margin off Vancouver Island, British Columbia; Canadian Journal of Earth Sciences, v. 9, p. 280-296.

Tseng, K.H.
1968: A new model for the crust in the vicinity of Vancouver Island, M.Sc. thesis, University of British Columbia.

White, W.R.H. and Savage, J.C.
1965: A seismic refraction and gravity study of the Earth's crust in British Columbia; Bulletin of the Seismological Society of America, v. 55, p. 463-486.

Wickens, A.J.
1977: The upper mantle of southern British Columbia. Canadian Journal of Earth Sciences, v. 14, p. 1100-1115.

Woods, D.V.
1985: Large scale electromagnetic induction investigation of the Kapuskasing Structural Zone; in Current Research, Part A, Geological Survey of Canada, Paper 85-1A, report 66.

Yole, R.W.
1969: Upper Paleozoic stratigraphy of Vancouver Island, British Columbia; Proceedings of the Geological Association of Canada, v. 20, p. 30-40.

Yole, R.W. and Irving, E.
1980: Displacement of Vancouver Island, paleomagnetic evidence from the Karmutsen Formation; Canadian Journal of Earth Sciences, v. 17, p. 1210-1228.

Yorath, C.J.
1980: The Apollo structure in Tofino Basin, Canadian Pacific continental shelf; Canadian Journal of Earth Sciences, v. 17, p. 758-775.

GEOLOGY ACROSS THE WESTERN BOUNDARY OF THE THELON TECTONIC ZONE IN THE TINNEY HILLS-OVERBY LAKE (WEST HALF) MAP AREA, DISTRICT OF MACKENZIE

Project 830010

Peter H. Thompson, Nicholas Culshaw, D.L. Thompson[1], and J.R. Buchanan[2]
Precambrian Geology Division

Thompson, P.H., Culshaw, N., Thompson, D.L., and Buchanan, J.R., Geology across the western boundary of the Thelon Tectonic Zone in the Tinney Hills-Overby Lake (west half) map area, District of Mackenzie; in Current Research, Part A, Geological Survey of Canada, Paper 85-1A, p. 555-572, 1985.

Abstract

The Bathurst Terrane (predominantly Yellowknife Supergroup metasediments) is separated from the Ellice River Terrane (amphibolite and granulite facies gneisses, linear granitoid complexes and subordinate medium and high grade supracrustal rocks) by an abrupt north-northeast-trending boundary marked by a metadiabase dyke swarm and a low grade transcurrent shear zone. Bathurst Terrane is characterized by Archean high to medium grade metamorphism which accompanied postulated tectonic thickening by thrusting perpendicular to the present main boundary. Basement thrusting at lower grade accompanied infolding of Goulburn Group (about 1900 Ma) sediments synchronous with a thin-skinned event to the west and approximately contemporaneous with transcurrent shearing within Ellice River Terrane. The ages of early high grade metamorphism and late stage granites in Ellice River Terrane, although not known, are crucial for discriminating between predominantly Archean or Proterozoic histories of the Thelon Tectonic Zone.

Résumé

La formation de Bathurst (principalement composée de métasédiments du supergroupe de Yellowknife) est séparée de la formation d'Ellice River (gneiss des faciès à amphibolites et à granulites, complexes granitoïdes linéaires et roches supracrustales subordonnées, moyennement et fortement métamorphisées) par une limite abrupte d'orientation nord-nord-est, marquée par un faisceau de dykes de métadiabase, et une zone de cisaillement avec failles de décrochement horizontales, faiblement métamorphisée. La formation de Bathurst est caractérisée par un métamorphisme archéen d'intensité élevée à moyenne, qui a accompagné l'épaississement tectonique postulé, causé par un chevauchement perpendiculaire à la principale limite actuelle. Un charriage du soubassement, accompagné d'un métamorphisme léger, a accompagné le plissement des sédiments du groupe de Goulburn (1900 Ma), synchrone par rapport à une phase de plissement superficiel à l'ouest et approximativement contemporain d'un cisaillement avec décrochements horizontaux, à l'intérieur du groupe d'Ellice River. Bien que l'on ne connaisse ni la date du métamorphisme initial d'intensité élevée ni l'âge des granites apparus pendant les phases finales du métamorphisme dans la formation d'Ellice River, ces dates sont cruciales pour distinguer les phases d'évolution, surtout archéennes ou protérozoïques, de la zone tectonique de Thelon.

[1] Department of Geology, Princeton University, Princeton, New Jersey 08540
[2] Department of Geology, University of Ottawa, Ottawa, Ontario K1N 6N5

Introduction

The map area includes 120 km of the western boundary of the Thelon Tectonic Zone (TTZ), a 75-100 km wide feature having variable but distinctive topographic, geophysical and geological characteristics, that occurs along the boundary between the Slave and Churchill provinces of the northwestern Canadian Shield (Fig. 68.1). To determine the history and tectonic significance across 11 000 km^2 of this part of the Thelon Tectonic Zone, bedrock mapping, petrography, structural analysis, and geochronology, and several detailed petrologic and structural studies are in progress. This year, the second field season, 5500 km^2 were mapped at 1:250 000 scale and a detailed study of the structure of the Proterozoic cover sequence, the Goulburn Group east of the south end of Bathurst Inlet (see R. Tirrul, 1985), was completed. Work began on metamorphism of Goulburn Group (M. Frey, Basel), petrology of basic dykes (R.B.), geothermobarometry of migmatites (M. Brown, Kingston, U.K.), and a Ph.D. project across the main boundary at Ragged Lake (D.L.T.). The structural geology of the map area is primarily the responsibility of N. Culshaw, a visiting fellow associated with the project. As rapidly as important parts of a complex history spanning more than one billion years are revealed by this work, new questions are raised about the origin and significance of the Thelon Tectonic Zone.

Geological setting

The first geological reconnaissance map of the northwestern Canadian Shield (Wright, 1957) showed marked changes in lithology, structural style and orientation, and metamorphic grade across a zone a few kilometres wide that was traced from the East Arm of Great Slave Lake to Bathurst Fault (Fig. 68.1). The transition was named the Thelon Front (Wright, 1967), the boundary between the Slave and Churchill structural provinces (Stockwell, 1961) and was interpreted as the western limit of high grade metamorphism and deformation related to the middle Proterozoic "Hudsonian orogeny". More recent work in the Healey Lake map area (Henderson, 1979; Henderson and Thompson, 1980, 1981; Henderson et al., 1982) led to the conclusions that the change in structural style and the increase in grade of the main metamorphism eastward across the Thelon Front are Archean rather than Proterozoic and that the western edge of a straight zone of highly strained rocks 20-30 km east of the front is a more appropriate structural province boundary. These observations, together with 1:1 000 000 scale coloured aeromagnetic anomaly maps (Geological Survey of Canada, Maps 1566A, 1567A, NQ-12-13-14-AM) and unpublished compilations of lithology, structure and metamorphism in the area between 62° and 68°30'N and 102° and 112°W, were the basis for the suggestion by Thompson and Henderson (1983) that the Slave Province is bounded to the east by a distinctive linear zone 75-100 km wide which they named the Thelon Tectonic Zone.

The Thelon Tectonic Zone has a characteristic linear aeromagnetic anomaly pattern with highly variable relief that contrasts with the relatively flat pattern to the west and the irregular pattern of variable relief to the east. Generally, rocks within the zone north of McDonald Fault are more highly strained than those in adjacent terranes and they have a well-defined north-northeast-oriented structural fabric that contrasts with the irregular structures to the east and the north to northwest structures to the west. Anorthosite and granulites, absent to the west, are present in the zone and to the east. The zone is defined on the basis of the coincidence of a number of characteristics; for example, granulites are widespread to the east but north-northeast-oriented granulites associated with mylonites are limited to the zone. In view of the fact that only a small proportion of the Thelon Tectonic Zone has been mapped at 1:250 000, the boundaries indicated in Figure 68.1 are tentative and the idea (Thompson and Henderson, 1983) that the Thelon Tectonic Zone formed in the Archean and was a locus for intracratonic thrusting during the Proterozoic is one of several working hypotheses that are being tested in the Tinney Hills-Overby Lake map area.

In the current map area, the Thelon Front (Fraser, 1968; Stockwell, 1969) originally followed the northwesternmost limit of prominent north-northeast structural trends. More recently, Stockwell (1982) altered this segment of the boundary to a more northerly trend parallel to a prominent change in the aeromagnetic map that was the basis for the tentative western boundary of the Thelon Tectonic Zone (Fig. 68.1).

General geology

J.A. Fraser (1964) subdivided the crystalline rocks into metasedimentary and metavolcanic rocks correlated with Archean supracrustal rocks (Yellowknife Supergroup) of the Slave Province, various small plutonic bodies, and a heterogeneous unit of migmatite, quartzofeldspathic gneisses, granulite and mylonite, derived in part from the Yellowknife Supergroup. Archean rocks were recognized as continuous across a line marking a prominent change in structural orientation (Fraser, 1968) but the predominance of high grade metamorphic rocks and a north-northeast structural grain distinguished most of the area from the Slave Province to the north and west. The predominant metamorphism in the western Churchill (Fraser, 1978) and Slave (Thompson, 1978) Provinces occurred in Late Archean but Fraser suggested the granulite facies assemblages may predate the Yellowknife Supergroup and noted variable development of relatively low grade retrogressive Proterozoic overprint.

Fraser (1964) also outlined the stratigraphy of the Goulburn Group, a sequence of clastic and carbonate rocks that overlies unconformably the Archean near Bathurst Inlet and occurs as outliers within the Archean terrane to the east. The Goulburn Group occupies the Kilohigok Basin, an intracratonic feature with a tectonodepositional history that can be linked to events associated with the 1.9 Ga Wopmay Orogen 500 km to the west (Campbell and Cecile, 1981). Hoffman et al. (1984) altered somewhat earlier correlations (Fraser and Tremblay, 1969; Campbell and Cecile, 1981) between the Goulburn Group and rocks of the Coronation Supergroup in Wopmay Orogen and suggested the thickening of the Goulburn Group eastward to Bathurst Inlet may represent a clastic wedge derived from uplift of a source terrane in the region of the Thelon Tectonic Zone.

The past summer's mapping confirmed an observation made the previous year (Thompson and Ashton, 1984) that the map area can be divided into two terranes along the western contact of the pink gneiss/migmatite/granitoid unit. Within the Bathurst Terrane, west of the main boundary, alumino-silicate-bearing migmatites and related pelitic schist and metagreywacke of the Yellowknife Supergroup underlie 80 per cent of the area. Muscovite-biotite leucogranite/granodiorite is the next most widespread unit. More mafic plutonic rocks occur east of Gordon Bay and as small bodies in the migmatite or along the main boundary. The highly variable lithologic package comprising mafic schist, banded amphibolite, felsic gneiss, marble and psammitic/pelitic metasedimentary rocks may be significant in that it is thought to be, at least in part, of volcanic origin and that it is most prominent in the vicinity of the main boundary.

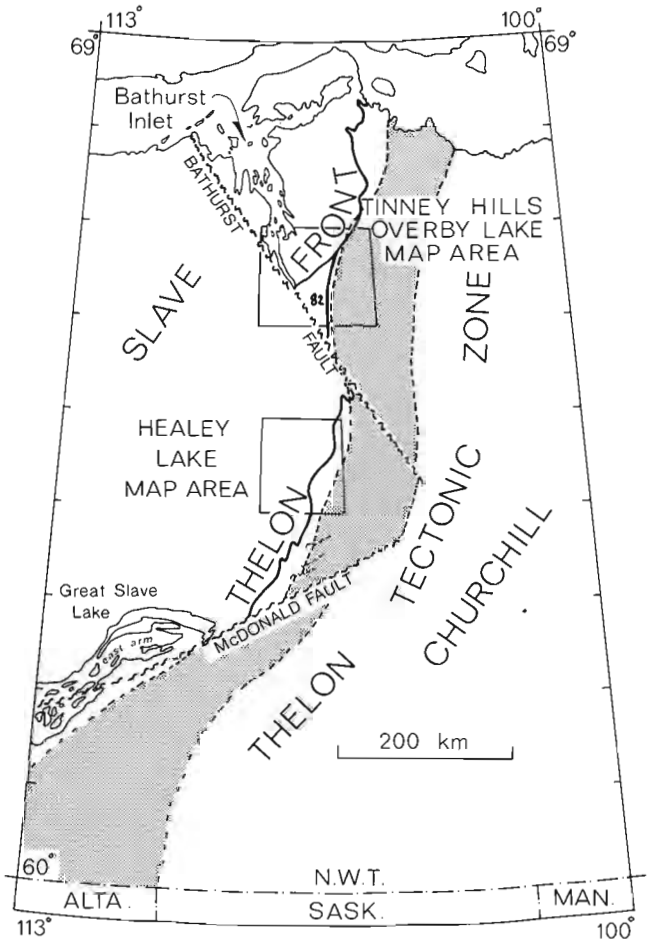

Figure 68.1. *Location map. The width of the tentative outline of the Thelon Tectonic Zone south of the Macdonald Fault is an indication of the uncertainty of its position there. Position of Thelon Front is after Wright (1967), Fraser (1968), and Stockwell (1969, 1982).*

East of the boundary, in the Ellice River Terrane, sillimanite- garnet/cordierite gneisses and migmatites are also present but they are subordinate to wide expanses of hornblende/biotite gneiss and migmatite and granulites of both gneissic and charnockitic character. It still is not clear if the high grade rocks of supracrustal origin in this terrane are Yellowknife Supergroup equivalent (Fraser, 1964) or part of an older basement complex (Thompson and Ashton, 1984) or Proterozoic in age. Two major batholiths, one a megacrystic biotite granodiorite/quartz tonalite, and the other a garnet granite are present. The latter clearly postdates granulite facies metamorphism and a period of high strain in these rocks. The sequence of medium grade supracrustal rocks east of Ragged Lake is very similar to the heterogeneous schist/amphibolite unit to the west.

Preliminary structural analysis of the Archean rocks indicates a complex polyphase history involving nappe style tectonics and, possibly, transcurrent shearing at relatively high grade. Further work on the Goulburn Group near Bathurst Inlet and in the outliers to the east has produced more evidence of basement involved thrusting and folding of the cover sequence that predates movement on the Bathurst Fault (Thompson and Ashton, 1984).

Lithology

Goulburn Group

Regional mapping of the Goulburn Group in 1984 was limited to that part of the sequence immediately west of Gordon Bay and to the outliers folded into and overthrust by the Archean basement in the western half of the area. New information on the structure and metamorphism of these rocks is presented in the appropriate sections of this paper. The exposed limits of Outlier I were determined and Outliers II and III traced along strike for 10 km (Fig. 68.2). A Goulburn Group locality near the Western River on Fraser's map was found to be a fourth outlier (Fig. 68.2) in the form of a Y-shaped infold of quartzite, thinly interlayered chlorite-white mica phyllite and carbonate, brown weathering marble and pelitic phyllite. The basal quartzite is upside down and dipping 35° eastward under severely retrograded Archean knotted schists and white pegmatite along the east contact of the outlier. The western contact dips moderately in the same direction but the brown marble sits directly on quartzite which is on top of a shattered pegmatite.

Leucogranite/granodiorite

White weathering, relatively unfoliated masses of fine- to medium-grained muscovite-biotite granite/granodiorite ranging in size from sills one metre thick to plutons several kilometres across and one batholith-sized body east of Quasiok Lake are associated with white pegmatite, sillimanite zone metsediments, and adjacent migmatites in the Bathurst Terrane (Fig. 68.2). In addition to quartz, plagioclase, potassium feldspar, muscovite, and biotite, accessory cordierite, garnet and/or sillimanite are common. Contacts of the larger plutons in the Bathurst Terrane are locally diffuse with a transition from metasediments laced with leucogranite to leucogranite full of sillimanite schist or migmatite inclusions. These intrusive granites have weakly to moderate foliation that is approximately concordant with the regional foliation, even where the foliation is only gently dipping, east of Gambit Lake. Regional foliation wraps around plutons or boudinaged sills in many localities. The structural and metamorphic setting and mineralogy of these granites suggest that in the Bathurst Terrane they were derived from Yellowknife Supergroup metasedimentary rocks by anatexis during the metamorphism that produced the regional isograd pattern. They intruded to their present level during main phase deformation.

Garnet granite

Medium grained, moderately to strongly foliated granite accompanied by biotite-clinopyroxene monzodiorite along its western border, occupies most of the southeast corner of the map area east of the Ellice River. Garnet, a common accessory, is almost invariably rimmed by biotite, suggesting an incompatibility between garnet and K-feldspar at some time during or after the crystallization of the granite. Cut by high strain zones and containing strongly deformed granulite inclusions of high grade, this unit is an important marker in the history of deformation in the Ellice River Terrane.

Megacrystic granodiorite

This unit comprises megacrystic biotite granodiorite, tonalite, and minor quartz diorite that is associated with pink gneiss/migmatite in a belt between two granulite facies zones east of Ragged Lake. Contact relations with the latter unit are not clearcut, but small dykes of relatively undeformed granodiorite cut the gneiss complex and there is no evidence that the pluton has itself ever been in the

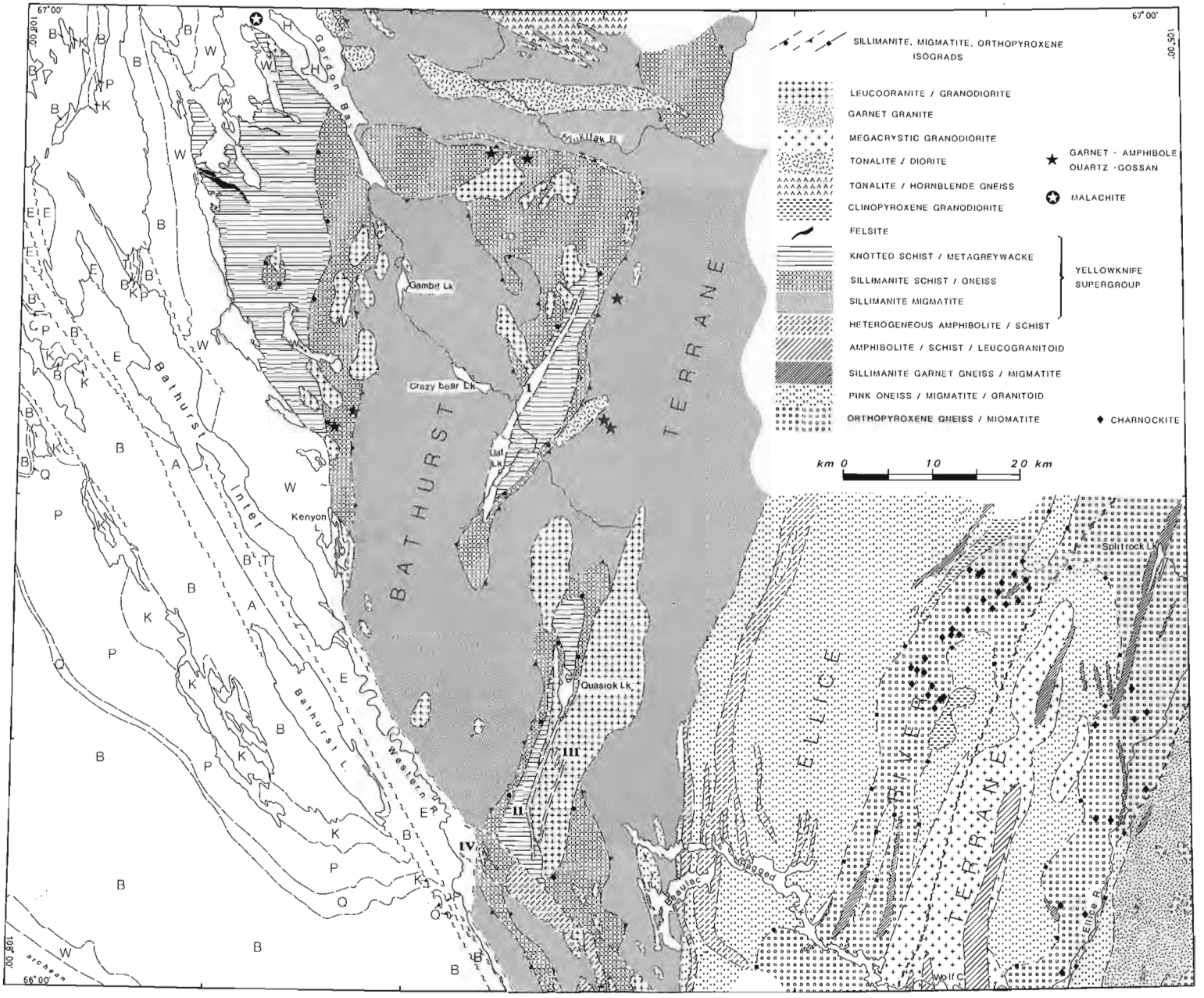

Figure 68.2. *Lithology in parts of the Tinney Hills-Overby Lake map area. Subdivision of Goulburn Group (not patterned) after Campbell and Cecile (1976); Western River (W), Burnside (B), Quadyuk (Q), Peacock Hills (P), Kuuvik (K), Brown Sound (B) and Amagok (A) formations; also late Proterozoic Ellice Formation (E) and undifferentiated late Proterozoic sediments and volcanics (H). Outliers I-IV are correlated with the Western River Formation.*

granulite facies. The sequence is deformed in one of the high strain zones that reduce the granodiorite to augen and a pink mylonitic gneiss. Younger than the pink gneiss/migmatite/granitoid, the pluton may be Proterozoic, but Frith (1982) described a megacrystic granodiorite batholith along strike in the map area to the south that he considers to be late Archean.

Tonalite/diorite

Several foliated plutons of dark hornblende-biotite granodiorite, tonalite and quartz diorite containing rare mafic granitoid or amphibolite inclusions occur east of Gordon Bay where structural trends are mainly east-west. The thin tonalitic body that parallels the migmatite isograd south of the Hiukitak River seems to be the extension of a line of small plutons of similar composition that occurs east of outlier I (Fig. 68.2). Several small plutons of quartz diorite occur west of Ragged Lake near the western contact of the pink gneiss/migmatite/granitoid unit. Leucogranite and granodiorite intrude the quartz diorite.

Tonalite/hornblende gneiss

North of Hiukitak River biotite and hornblende-bearing tonalite to quartz diorite gneiss commonly associated with amphibolite, is infolded with the sillimanite migmatites of the Yellowknife Supergroup. It is probably an orthogneiss possibly related to the tonalite/quartz diorite metaplutonic suite but the variability and mineralogy of these rocks is similar to that in the pink gneiss/migmatite/granitoid unit of the Ellice River Terrane.

Clinopyroxene granodiorite

This unit occurs as small bodies in the north-central part of the Ellice River Terrane on the boundary between orthopyroxene-bearing rocks and the pink gneiss/migmatite/granitoid. This weakly foliated fine- to medium-grained granodiorite is characterized by centimetre-size green clinopyroxene phenocrysts rimmed by black hornblende.

Felsite

Southwest of Gordon Bay a very tough, white-weathering fine grained to aphanitic rock of uncertain origin forms layers in knotted schist of the Yellowknife Supergroup (Fig. 68.2). At one outcrop of the northernmost occurrence, the rock has ghostly lenticles, suggestive of ignimbritic texture. Feathery, colourless to pale green amphiboles a few millimetres long occur on the foliation where it is developed or on fracture surfaces in more massive rocks. Pyrite cubes are usually present. The larger, southernmost body is aplitic and has a small dyke offshoot that cuts across bedding in the metasediment.

A felsic dyke intrudes the cordierite knotted schists on the small island near the tip of the peninsula west of Gordon Bay. The dyke contains clots of pyrite/chalcopyrite associated with malachite stains; knotted schists and dark grey to black phyllites (graphitic?) several metres from the dyke also contain malachite.

Knotted schist/metagreywacke

Grey- to brown-weathering biotite-rich schist and metagreywacke containing knots of cordierite, staurolite and/or andalusite occur in the northwest part of the area and in narrow belts associated with outliers of Goulburn Group to the southeast (Fig. 68.2). These rocks are typical of the metamorphosed Yellowknife Supergroup elsewhere in the Slave Province (Thompson, 1978). A small area of sub-cordierite grade rocks near the unconformity at the base of the Goulburn Group 25 km west of Gordon Bay and the sub-cordierite grade Yellowknife Supergroup rocks in the extreme southwestern corner of the map area have been included in the knotted schist unit on Figure 68.2. Southwest of easternmost Goulburn Group west of Gordon Bay iron formation is present in the unit at several localities. In knotted schist and metagreywacke bedding/cleavage relations are often clear and graded bedding, sometimes reversed by metamorphic recrystallization, provides scattered top determinations. Petrography shows that poikiloblasts, generally, have overgrown the main foliation in the rock, but continuing deformation has warped the foliation around the poikiloblasts. A late retrogressive event has produced very fine grained white mica-chlorite aggregates after cordierite and andalusite and altered biotite, and imposed a low grade fabric on some knotted schists near the outliers of Goulburn Group and north of Kenyon Lake east of the conformity.

Sillimanite schist and gneiss

Sillimanite-bearing rocks with or without cordierite occupy an inverted U-shaped zone in the northern half of the Bathurst Terrane and separate knotted schist from migmatites in the vicinity of Goulburn outliers I and II (Fig. 68.2). Sillimanite first appears as ellipsoidal knots a few millimetres long which stand out on the weathered surface of pelitic schist and psammite/metagreywacke. The variable width of the zone is unlikely to be primary as its present form has been influenced by main phase Archean and post-Goulburn deformation. Sillimanite aggregates parallel the main foliation in these rocks or, at some localities, a later fabric, and usually define a lineation that can be related to the main phase of deformation. The common occurrence of garnet rimmed by cordierite and/or plagioclase in the sillimanite zone rocks south of the Hiukitak River contrasts with its relative scarcity elsewhere.

Sillimanite migmatite

The most extensive unit in the western half of the map area is a biotite-rich, aluminosilicate-bearing migmatite derived from Yellowknife Supergroup metasediments. The migmatite isograd marks the appearance of more than 5-10 per cent leucosome. Using the terminology of Brown (1973), there is a transition up grade of the migmatite isograd from metatexite in which layering is still preserved with sillimanite biotite melanosomes and leucosome concentrated in pelitic layers, to irregular patches of diatexite, a homogeneous rock with wisps of melanosome scattered through a granitoid matrix. While biotite and sillimanite are almost ubiquitous in the migmatites, cordierite and garnet are irregularly distributed. In some areas they are mutually exclusive and where they occur together garnet is usually rimmed by cordierite or plagioclase. Cordierite is common in migmatite west of Quasiok Lake and west of a line extending northeast from the north end of the lake. The presence of kyanite in the southern part of the cordierite-absent zone east of the line suggests that higher pressures rather than more Fe-rich compositions may be the reason for the lack of cordierite. At several localities within the zone west of the cordierite-absent zone cordierite grains have been partially replaced by tiny euhedral staurolites, green biotite and, possibly, andalusite. East of the Hiukitak River late kyanite coexists with the new staurolite. Late chlorite and white mica are common throughout the unit.

Garnet-quartz-amphibole rocks associated with gossans occur in the migmatite unit, commonly as boudin-like zones a few tens of metres long. Some localities are indicated in Figure 68.2.

A comparison of the metamorphic and structural maps (see Fig. 68.5, 68.6) shows that much of the migmatite is sufficiently highly strained that it forms straight zones. The strain has occurred at both high and low grades of metamorphism. North and south of the Hiukitak River gently dipping ductile shear zones in cordierite-garnet-sillimanite-biotite migmatite (Fig. 68.3a, b, c) contain prominent sillimanite. Sillimanite grade high strain also occurs within straight zones northwest of Quasiok Lake and west of the boundary between the Bathurst and Ellice River terranes. East of J.A.F. Lake cordierite-garnet-sillimanite-biotite diatexite has been transformed to chlorite-white mica-biotite schist in north-northeast shear zones tens of metres wide.

Heterogeneous amphibolite/schist

Narrow belts of an extremely variable lithologic package comprising banded amphibolite, felsic gneiss, fine grained metagabbro, marble, rusty schist, and, locally, pelitic schist/migmatite occurs on both sides of the boundary between the Bathurst and Ellice River terranes (Fig. 68.2). Smaller masses (lenses?) are present west of Beaulac and another west of Gambit Lake. A rock comprising amphibolite lenses in a carbonate matrix, is part of the unit at several localities. Pegmatites and granitic sills are common in the sequence west of Ragged Lake. Contacts with the pink gneiss/migmatite/granitoid are sheared or covered, while those with sillimanite migmatite and sillimanite schist are transitional across several metres. More detailed mapping is

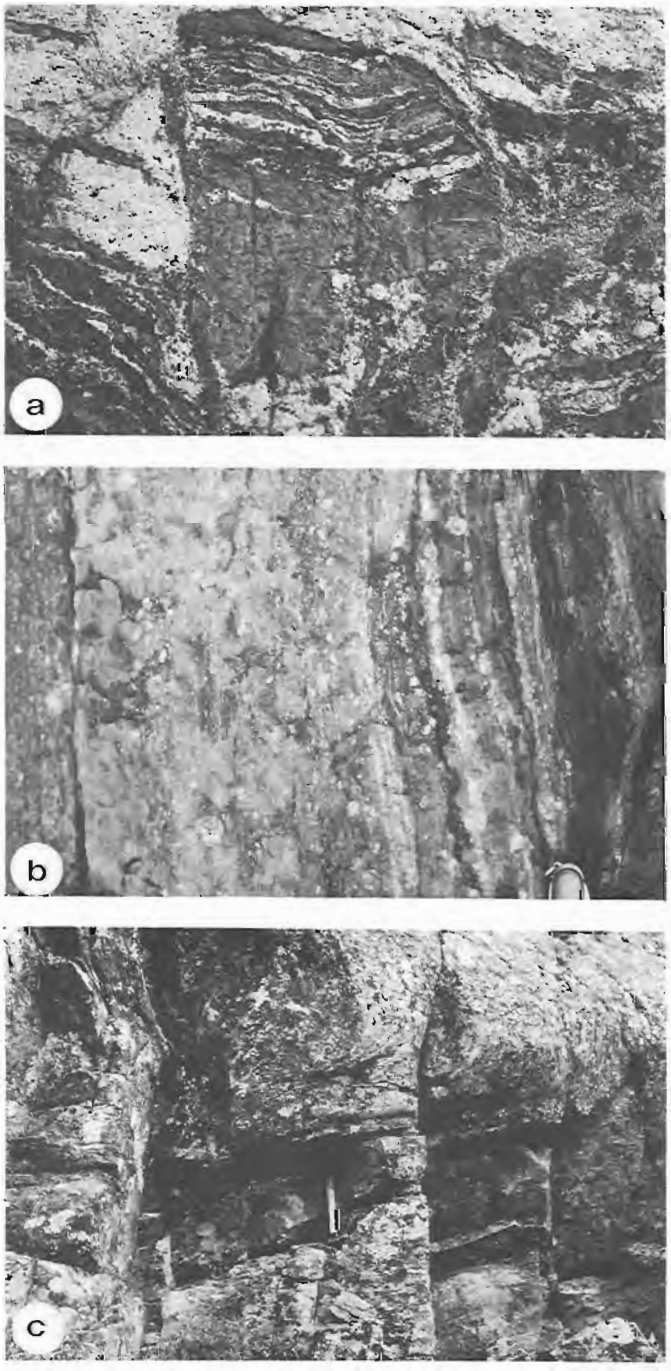

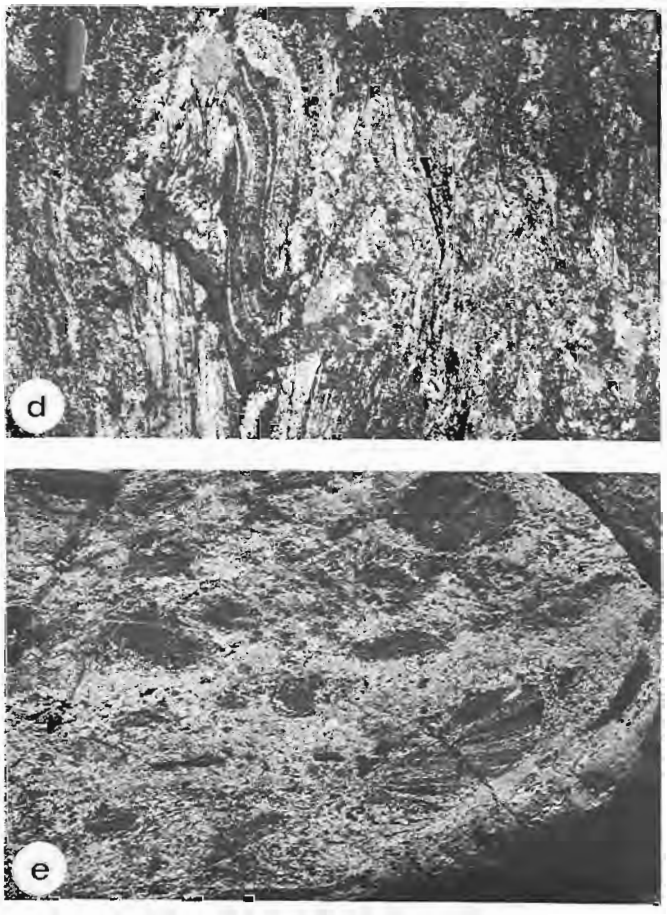

Figure 68.3

a) Garnet-cordierite-sillimanite biotite metatexite from north of Hiukitak River. (GSC 204131-M)

b) Tectonite derived from (a). (GSC 204131-L)

c) Gently north-dipping sillimanite grade shear zone in biotite-cordierite-sillimanite diatexite. (GSC 204131-K)

d) Pink gneiss/migmatite/granitoid. (GSC 204131-G)

e) Agmatitic orthopyroxene hornblende migmatite from orthopyroxene gneiss/migmatite unit. (GSC 204131-H)

required to determine if these rocks are equivalent to the thin sequences of Yellowknife Supergroup metavolcanic rocks that separate the metasediments from a possible basement unit in the Healey Lake area (Fig. 68.1) (Henderson and Thompson, 1981). North of Ragged Lake layers of tectonoclastic schist derived at least in part from metasedimentary migmatite are included in this unit even where they are not associated with amphibolite.

Sillimanite garnet gneiss/migmatite

With a more restricted distribution the aluminous gneisses and diatexitic migmatites in the Ellice River Terrane are less well known than those to the west. Narrow zones a few hundred metres to several kilometres wide and from a few to 25 km long are scattered across the eastern part of the map area. Not all occurrences are large enough to show in Figure 68.2. Normally these rocks are associated with hornblende-pyroxene-bearing and rusty pyritic quartzofeldspathic gneisses that leave little doubt the lithologic package is a sequence of supracrustal rocks. The lower proportion of biotite, finer grain size, abundance of purplish garnet and absence of retrogressive white mica distinguish these rocks from the migmatites of the Yellowknife Supergroup. These rocks could be high metamorphic grade equivalents of the heterogeneous amphibolite/schist unit of the supergroup, but without geochronology a firm correlation cannot be made.

Amphibolite/schist/leucogranitoid

Between Ragged Lake and Ellice River, surrounded almost entirely by the megacrystic granodiorite, a belt of relatively low grade metamorphosed supracrustal rocks exhibits the same sort of lithologic variation that occurs in the heterogeneous amphibolite/schist unit in the Bathurst Terrane. Staurolite-biotite-chlorite and staurolite-biotite-sillimanite muscovite schists, amphibolite, amphibolite "breccia" with carbonate matrix, calc-silicate gneiss and pink-grey psammitic rocks are present in the belt. Along the west contact, muscovite-biotite leucogranitoid similar to the leucogranite suite in the Bathurst Terrane separates the metasedimentary rocks from the megacrystic granodiorite. On the other hand, the pelitic schists are not typical knotted schists and, although serpentine (after forsterite) marbles occur in the heterogeneous amphibolite/schist unit, there is nothing quite like the lens of tremolite-serpentine-olivine-carbonate rocks that is interlayered with the amphibolites in the eastern belt. It resembles a metamorphosed ultramafic rock. Like the heterogeneous amphibolite/schist unit to the west, these supracrustal rocks are considered to be at least in part volcanic in origin. The continuation of this belt to the south was mapped as Yellowknife Supergroup (Frith, 1982).

Pink gneiss/migmatite/granitoid

This unit, referred to as "homogeneous in its heterogeneity" by Thompson and Ashton (1984), is an important though enigmatic part of the Ellice River Terrane. The complex mix of hornblende-biotite gneiss, migmatite and granitoid present at Ragged Lake (Fig. 68.2) continues north and northeastward to the limit of this year's mapping (e.g. Fig. 68.2). The colour, however, is not everywhere pink: shades of grey are common, and in some zones of shearing and retrogression it is greenish white. The heterogeneity in the unit is more textural than mineralogical or compositional: quartz, plagioclase, K-feldspar, biotite and/or hornblende are present in most variations. Except for the boundary with the orthopyroxene-bearing gneisses and migmatites, contacts with other units are sharp and usually tectonized. Sporadic occurrences of orthopyroxene in the pink gneiss/migmatite/granitoid unit and localized retrogression in the granulites, together with a similarity in degree and type of textural heterogeneity in large parts of the granulite terrane, are the basis for designating the boundary as a metamorphic feature. Systematic petrography will help to determine the nature of the transition and the extent to which it represents a prograde change from hornblende to pyroxene-bearing rocks or the limit of a retrogressive overprint that transformed large tracts of granulite to pink gneiss/migmatite/granitoid. The partial melting of hornblende gneiss with hornblende produced in the leucosome requires high temperatures that would be compatible with a mid-crustal origin for this unit. Aside from the striking similarity of this unit to the proposed basement to the Yellowknife Supergroup in the Healey Lake area, no further evidence that the pink gneiss/migmatite/granitoid is basement to the supergroup in this map area was found.

Orthopyroxene gneiss/migmatite

The orthopyroxene gneiss/migmatite unit includes a variety of rock types that cannot be subdivided at the scale of Figure 68.2: mafic and leucocratic-gneisses, migmatite, and charnockite (orthopyroxene granite), make up most of the unit with small lenses of aluminous gneiss/migmatite and calc-silicate marble also present. These rocks form two north-northeast-oriented belts in the Ellice River Terrane. The contacts of the unit have not been observed directly but the transition from pink gneiss/migmatite/granitoid to orthopyroxene gneiss/migmatite does occur from one outcrop to the next in many cases. At some localities the two units alternate for several hundred metres, suggesting some sort of transitional zone. West of Splitrock Lake, steeply dipping shear zones transform the granulites to biotite-blue-green amphibole grade mylonites or mylonitic gneiss within several metres.

Figure 68.3d is an agmatitic phase of an outcrop on the Ellice River that is made up of gneiss, layered migmatite, and charnockite. In general, these rocks are orange-brown or greyish brown rounded weathering outcrops with the classic greasy green fresh surface. Pinkification of feldspar and replacement of pyroxene by hornblende and biotite, appears to accompany a change to the pink gneiss/migmatite granitoid in some cases. Elsewhere, the change from hornblende in the leucosome to pyroxene looks like a prograde change from upper amphibolite to granulite facies conditions. Preliminary petrography of relatively low strain rocks has revealed that many of the granulite facies assemblages are fresh. Orthopyroxene-plagioclase, clinopyroxene-plagioclase-garnet, and orthopyroxene-garnet-plagioclase rocks, for example, are free of coronas and reaction rims.

Mafic intrusions

Basic dykes (Fig. 68.4a) in the area can be grouped into three associations: (1) late, relatively fresh, orange-brown weathering Mackenzie(?) dykes; (2) metamorphosed dykes ranging in grade from altered diabase to amphibolite that are discordant to the principal foliation and layering in the country rock; and (3) garnet amphibolite and metagabbro/diabase bodies that are mainly conformable with the structure in the country rock. The youngest, Mackenzie type dykes, are compositionally and texturally uniform and the only ones known to intrude the Goulburn Group. Their high magnetite content is evident from the aeromagnetic map. The other two associations (Fig. 68.4) have more interesting tectonic implications and will be discussed in more detail.

Discordant metamorphosed dykes are widely but irregulary distributed across the map area with a higher density of occurrences west of the main boundary than in the Ellice River Terrane and in the western part of the Bathurst Terrane (Fig. 68.4). Their orientations range from 320 to 060° but most are between 320 and 000°. At several localities, northwest dykes split off toward the northeast. Porphyritic and amygdaloidal varieties seem to be most common in the western parts of the map area. Porphyritic phase dykes cut the more massive dykes such as the metagabbro east and west of Gambit Lake (Fig. 68.4). In general, the degree of alteration or metamorphism increases eastward toward and into the Ellice River Terrane. Dykes east of Ellice River are less amphibolitized than those near the western boundary of the terrane. At low grade the metamorphism is discontinuous; typically, there is a complete transformation to chlorite schist in a shear zone, striking north to northeast, while the rest of the dyke suffers a partial static retrogression (e.g. Buchanan, 1984). Farther east, recrystallization is more pervasive, particularly in small dykes, and the new amphibolite may be lineated and/or foliated. These dykes cut across deformed country rocks where the foliation is oriented north-northeast as well as other orientations. Nowhere have the dykes been observed to intrude the Goulburn Group; in fact, at two localities, Kenyon Lake and west of Gordon Bay, the dykes appear to be unconformably overlain by the cover sequence. These relations suggest that at least part of the strain in north-northeast straight zones predates the deposition of the Goulburn Group.

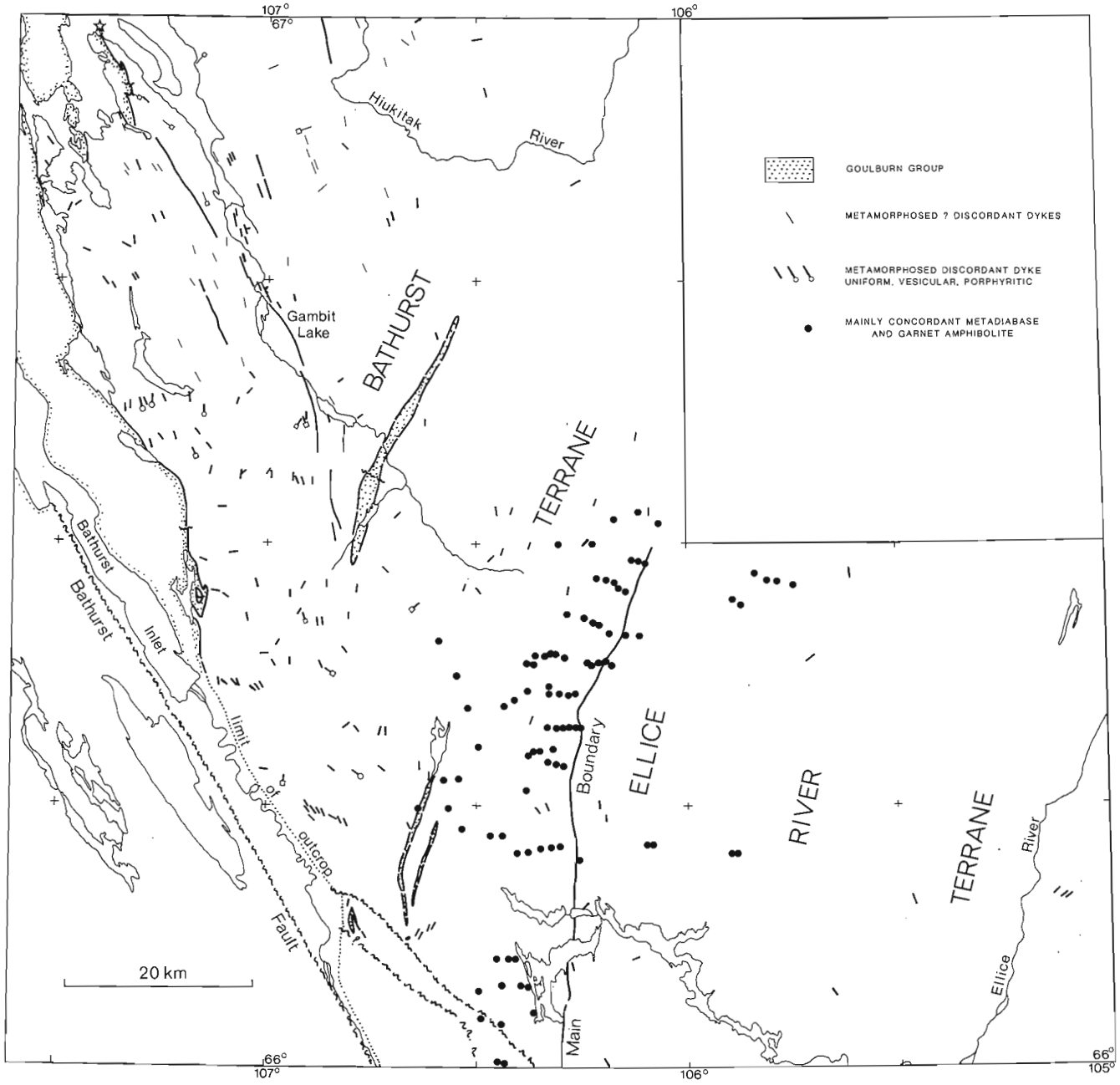

Figure 68.4. *Preliminary map showing distribution of dykes in part of the Tinney Hills-Overby Lake map area. Mackenzie dykes are not shown. The main boundary between the Bathurst and Ellice River terranes is shown as a heavy continuous line; outliers of Goulburn Group are stippled.*

The garnet amphibolite-metagabbro/diabase association is more problematic. There appear to be two groups making up the high density of dykes/sills at the main boundary, one older and the other younger than the main phase metamorphism. The older group includes conformable layers and boudins of garnet amphibolite, variably foliated and lineated, that look like they have been metamorphosed and deformed with the main phase events in the outcrop. Similar garnet amphibolites occur in the kyanite migmatites in the eastern part of the Healey Lake area (Henderson and Thompson, 1980) and south of Bathurst Fault (Frith, 1982). The group of mainly conformable metagabbro/diorite dykes/sills considered to be younger shows much more variable degrees of deformation and metamorphism. In single outcrops textures commonly range from recrystallized but weakly deformed primary textures to amphibolite. The concentration of both types of dykes at the boundary between the Bathurst and Ellice River terranes (Fig. 68.4) may be significant. A high density of basic dykes and sills is prominent near the unconformity between the Yellowknife Supergroup and underlying basement east of Yellowknife (Baragar, 1966) and major tectonic boundaries associated with ductile shearing, sedimentation and volcanism, such as the Nelson Front (Baragar and Scoates, 1981).

Metamorphism

As a record of the variations of temperature and pressure in the crust during the major tectonic events that have occurred in the map area, the isograd patterns and mineral assemblages impose useful constraints on the scale and timing of the events and on the processes involved.

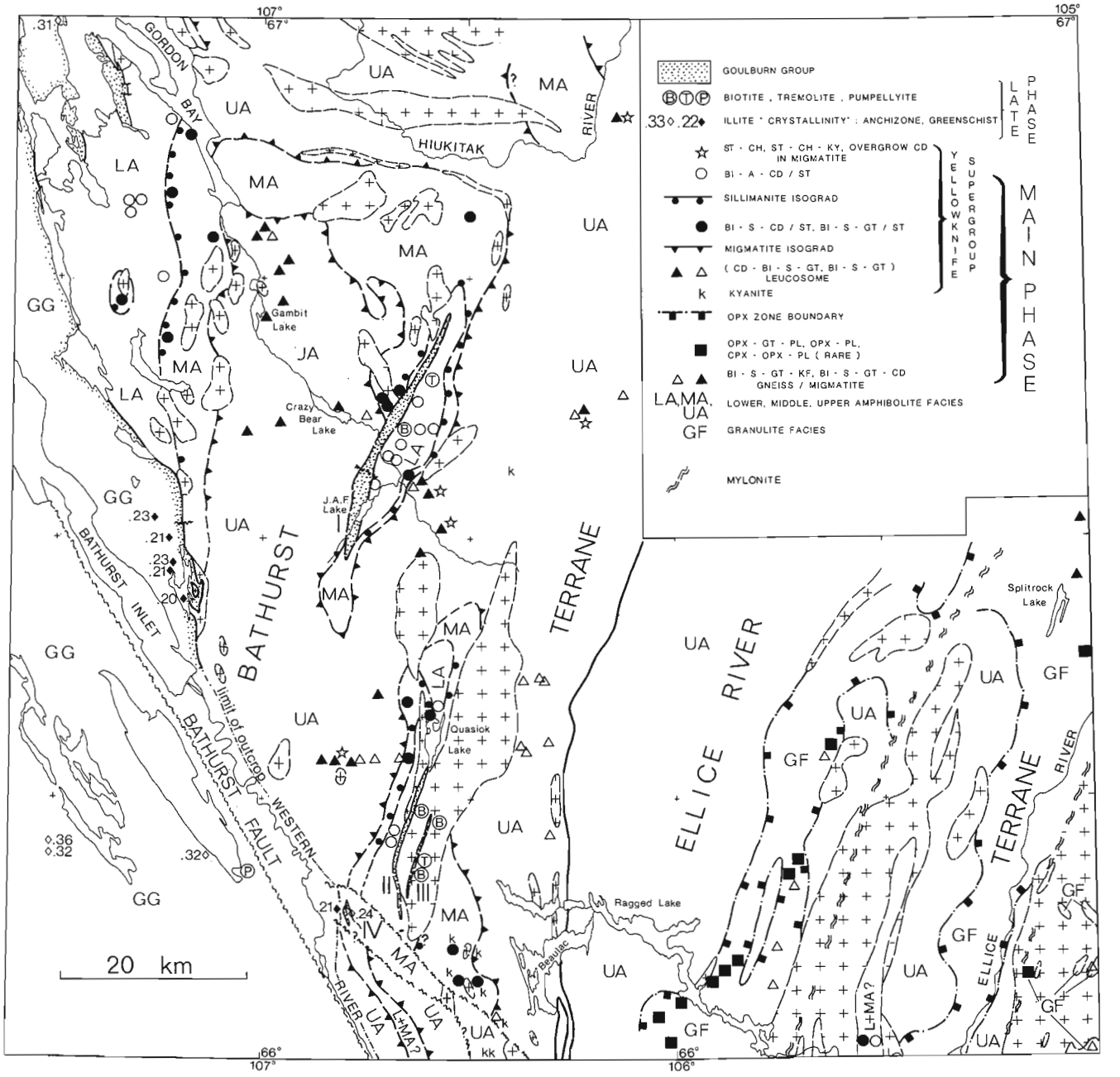

Figure 68.5. Preliminary metamorphic map of part of the Tinney Hills-Overby Lake map area. Illite crystallinity data from Martin Frey (personal communication, 1984).

At this time, in the absence of comprehensive petrography, only general observations can be made about the nature of metamorphism in these polymetamorphic rocks. Generally, field observations and preliminary petrography indicate two major phases of regional metamorphism (Fig. 68.5). The earlier event (main phase) produced the predominant metamorphic pattern and mineral assemblages under conditions ranging from upper greenschist facies through amphibolite to granulite facies. The later event (late phase) was less pervasive, ranging from anchizone (subgreenschist) to upper greenschist/lower amphibolite facies.

In the Bathurst Terrane the two phases are separated by intrusion of a set of basic dykes and deposition of the Goulburn Group. Coarse grained muscovite from pegmatites in the sillimanite zone north of Kenyon Lake and in diatexitic migmatite east of Gambit Lake yield Rb-Sr ages of 2556 and 2566 Ma respectively (van Breemen, personal communication, 1984), confirming that the main phase metamorphism is Late Archean. Ages of 2300 and 2007 Ma from similar pegmatites and 1898 Ma from finer grained muscovite (van Breemen, personal communication, 1984) together with K-Ar muscovite and biotite ages from 1765 to 1948 Ma by previous workers (see Thompson and Frey, 1984 for a compilation of this data) reflect the later metamorphism and deformation.

Main phase metamorphism is associated with the early phase of deformation that produced a complex structural pattern, including northwest and north- northeast oriented structures that are interpreted to be the result of Archean high grade thrusting. The widespread retrogressive effects of late phase metamorphism are associated with a late phase of deformation that formed and possibly reactivated north-northeast-oriented zones of high strain related to northwest directed thrusting of basement and Goulburn Group (Bathurst Terrane) and transcurrent movement (Ellice River Terrane).

The cordierite-biotite-andalusite and sillimanite schist, commonly containing staurolite, of the lower and middle amphibolite facies in the map area are typical of the late Archean low pressure type metamorphism that has transformed the Yellowknife Supergroup throughout the Slave Province (Thompson, 1978). The widespread cordierite-sillimanite-biotite migmatites with or without garnet or potassium feldspar are the higher grade equivalents of these rocks. West of Beaulac (Fig. 68.5) sillimanite-kyanite-staurolite schist and migmatite are present. Transformation of migmatite and pink gneiss to tectonoclastic schist and straight gneiss has obscured relations along sections of the boundary but there does not appear to be a major difference in metamorphic grade between Bathurst and Ellice River terranes. In the granulite facies zones main phase orthopyroxene-plagioclase and sillimanite-potassium feldspar are compatible with low to intermediate pressures and cordierite reappears near Splitrock Lake. Contacts between lower and middle amphibolite facies rocks east of Ragged Lake and other rock units are strongly deformed or mylonitic. As yet, there is no evidence against the assumption main phase metamorphism has affected these rocks.

Although main phase kyanite is rare in the Slave Province generally, near the western boundary of the Thelon Tectonic Zone, it is quite common in migmatites derived from the Yellowknife Supergroup (Henderson and Thompson, 1980, 1981; Frith, 1982). Henderson and Thompson concluded these rocks represent a more deeply eroded part of the Archean crust than that elsewhere in the Slave Province. The occurrence of sub-migmatite grade staurolite-kyanite-bearing rocks west of Beaulac suggests that a P-T-time curve whereby the kyanite forms in staurolite-kyanite zone and persists unstably into the migmatite zone (Curve 2, Fig. 26.4, Henderson and Thompson, 1980) would be appropriate for the kyanite migmatites nearby to the east and south. North-northeast along strike from the kyanite-bearing rocks and west of the west-dipping boundary of the Ellice River Terrane, a zone of sillimanite-garnet-biotite migmatites that do not contain cordierite contrasts with the extensive cordierite migmatites to the west. The possibility that the absence of cordierite indicates relatively higher pressure is supported by another kyanite occurrence (Fraser, personal communication, 1978) not far to the west that appears to be a main phase assemblage. This zone of kyanite-bearing, relatively deeply eroded Archean rocks parallels the western boundary of the Thelon Tectonic Zone for at least 150 km.

The correlation between metamorphism and deformation shown by the marked correspondence between the isograd pattern and structural trends (compare Fig. 68.5 and 68.6) is also seen on single outcrops where, for example, sillimanite knots define a fabric oblique to bedding, leucosomes and sillimanite-bearing melanosomes in schlieric migmatites define a strong foliation, and ductile shear zones (Fig. 68.3) contain a prominent sillimanite lineation. In thin section, well-foliated rocks at all grades have textures indicating the synkinematic nature of the main phase mineral assemblages. In addition to the spatial and temporal relations between main phase metamorphism and the early phase structural events, the occurrence of high grade rocks over low grade east and southeast of Gordon Bay and the correspondence between the sillimanite lineations and the expected northwest-southeast transport direction in the area derived from the structural geometry are compatible with synmetamorphic thrusting. Tectonic thickening by high grade thrusting would help to account for the discrepancy between the volume of Yellowknife Supergroup metasedimentary rocks in the map area and the estimate of 5 km for the original thickness of these rocks at at least one locality in the Slave Province (Henderson, 1975).

Evidence of the late phase metamorphism is found in the Goulburn Group, in metadiabase dykes younger than main phase metamorphism, and as a retrograde overprint on main phase assemblages (Fig. 68.5). Preliminary illite crystallinity data from samples collected this summer (Martin Frey, personal communication, 1984) indicate the lowest grade in the area is in middle anchizone Goulburn rocks west of Bathurst Fault and west of Gordon Bay. This information, along with a new occurrence of pumpellyite in Brown Sound basalt and of stilpnomelane in Kuuvik Formation, indicates the metamorphism of the Goulburn Group (Thompson and Frey, 1984) affects the entire sequence and not just the basal Western River Formation. New data, together with that already published, show that southward and eastward in the direction of increasing degree of deformation of the Goulburn and of increasing basement involvement the grade increases to lowermost greenschist facies. Chlorite and white mica are well recrystallized but biotite, phlogopite and tremolite are rare in outlier I, only becoming more common in outlier III. The westernmost occurrence of late biotite is in sheared metadiabase east (Buchanan, 1984) and southeast of Gambit Lake. The grade of metamorphism increases eastward in metadiabase dykes with most of them transformed to amphibolite in the vicinity of the boundary between the Bathurst and Ellice River terranes and to the east. Late phase replacement of main phase Archean assemblages in associated pelitic rocks, however, is limited to the growth of chlorite and white mica except as noted below. The amphibolitization of basic dykes in the Healey Lake area (Henderson and Thompson, 1981, 1982) is also associated with greenschist facies assemblages in pelitic country rock. Higher grade late phase assemblages occur at several localities along a northeast line between outliers I and II. Very fine grained staurolite, green biotite and chlorite aggregates have partially replaced cordierite in the migmatite. The southwesternmost samples appear to have andalusite as well, while aggregates at one locality to the

northeast contain kyanite. Whether these assemblages are early late phase or, possibly, late main phase, remains a problem. Fifty metres to the west of one locality, migmatite containing staurolite-chlorite aggegates is completely transformed to chlorite-muscovite schist in a north-south shear zone 80 m wide. Steep high strain zones in the Ellice River Terrane are also relatively low grade, with formations of blue-green amphibole coronas on granulated pyroxene and growth of epidote, muscovite and chlorite evident.

Structural geology

Two major sets of events have occurred which correspond to the two metamorphic events described in the previous section. The first, only clearly distinguished in the Bathurst Terrane, is characterized by low plunging structures with a trend approximately perpendicular to those of the Ellice River Terrane, is most easily recognizable from the northwest trending foliations in the northern and western parts of the Bathurst Terrane (Fig. 68.6) and is interpreted as

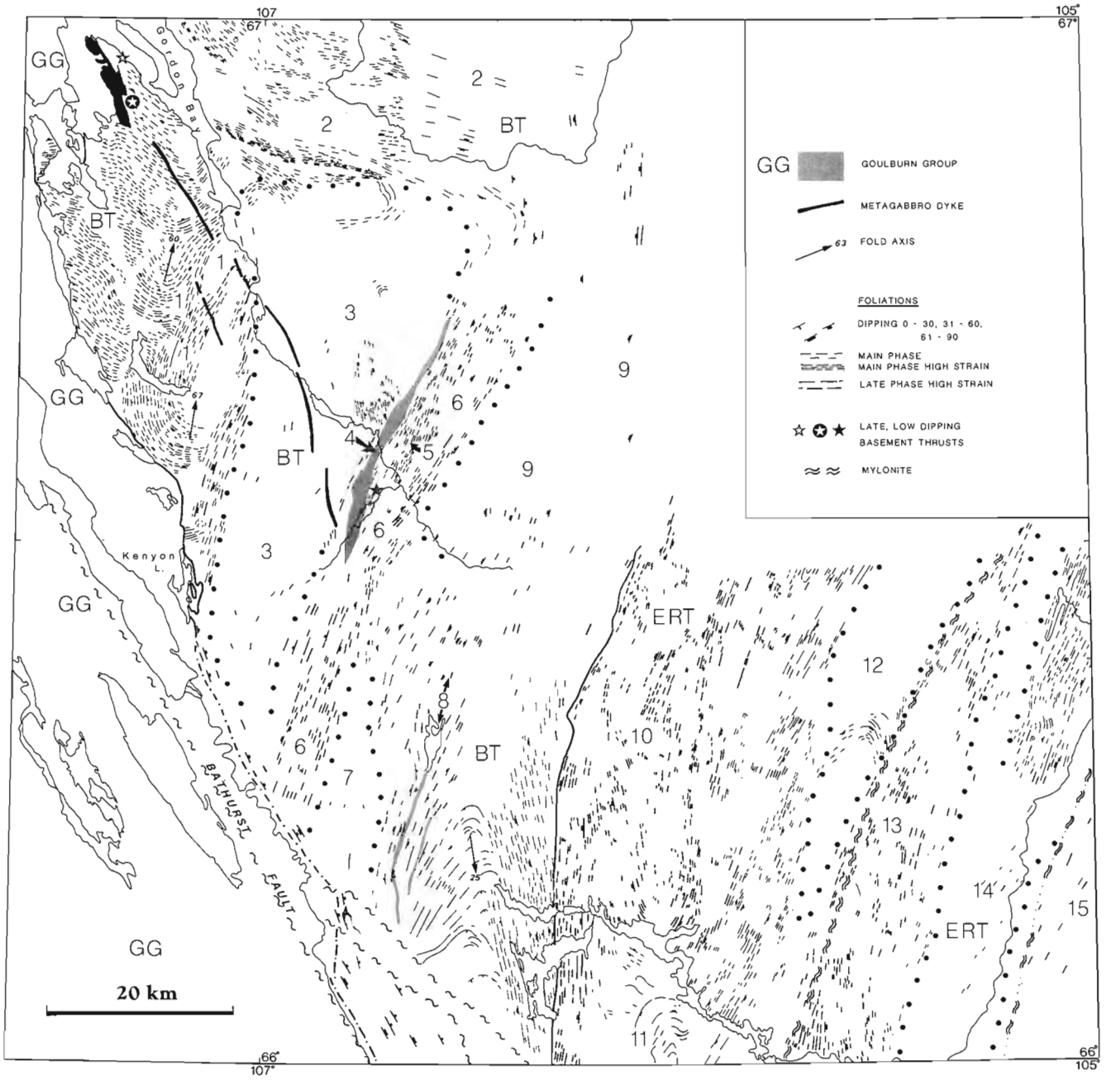

Figure 68.6. *Structural form line map of parts of the Tinney Hills-Overby Lake map area, compiled from air-photo interpretation with some observed dip values indicated. Numbers denote areas which are homogeneous with respect to a structural pattern and referred to as "domains". Approximate boundaries of domains with irregular foliation trends are dotted. Starred locations are those of small basement thrusts referred to in the text. The boundary between the Ellice River Terrane (ERT) and Bathurst Terrane (BT) shown as a heavy continuous line.*

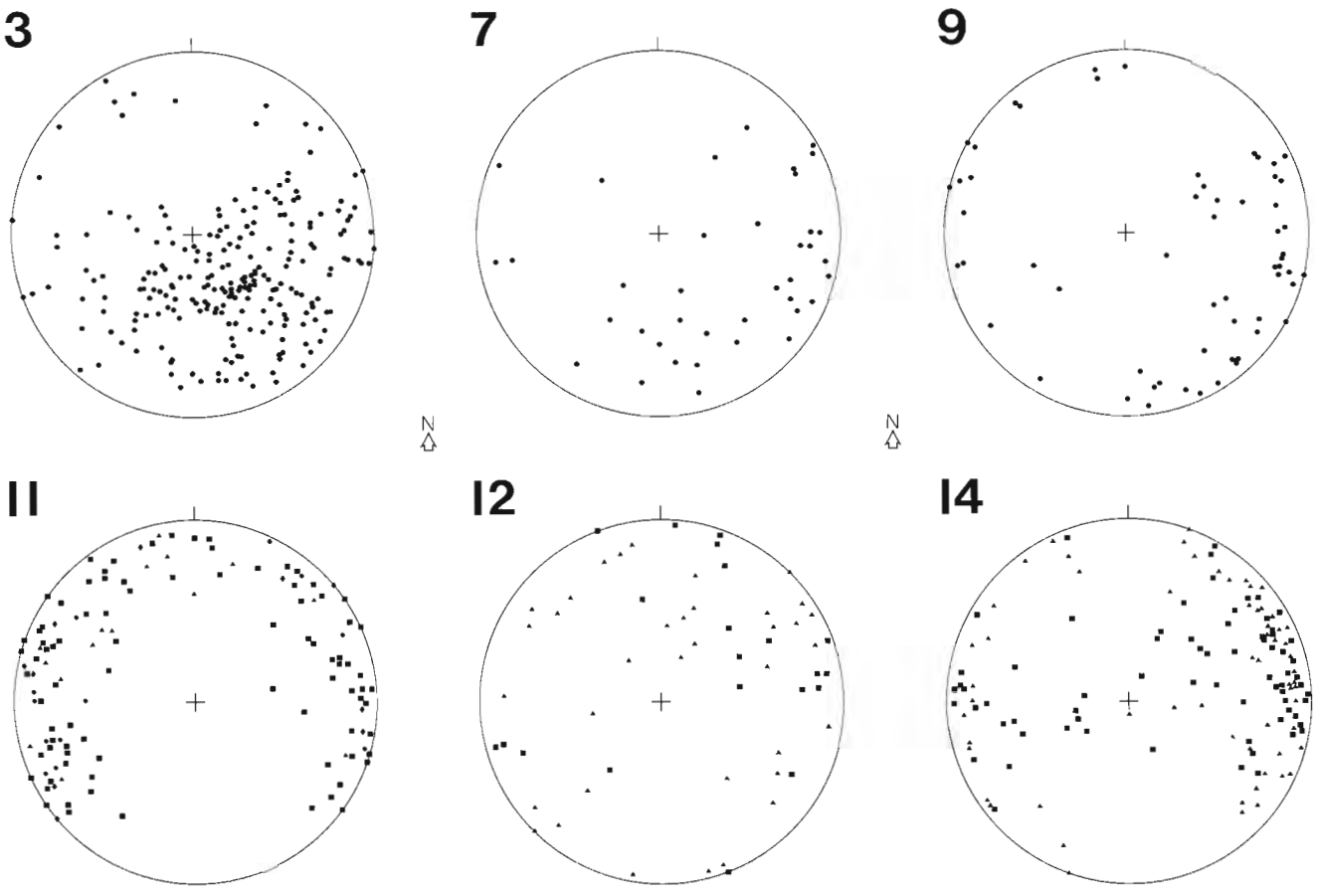

Figure 68.7. *Equal area plots of poles to foliations in domains with irregular trends; in 3, 7 and 9* ● *migmatite layering; in 11, 12 and 14,* ■ *amphibolite facies,* ▲ *granulite facies; in 11* ◆ *mylonite; equal area plot. Numbers refer to the domains indicated in Figure 68.6.*

an episode of Archean synmetamorphic thrusting. There is also at least one major probable first phase structure which parallels the straight zones that are typical of much of the Ellice River and eastern Bathurst terranes where there is a pattern of straight zones and large scale augen of irregular foliation trends (Figs. 68.7 and 68.8). Second phase deformation and metamorphism is mainly restricted to these zones, although they may be reworked first phase structures (cf. Watterson, 1975), as suggested by their parallelism with main phase metamorphic zonation and north-northeast-trending main phase structures (domain 1, Fig. 68.6). Throughout the map sheet these steep belts display a remarkable geometric similarity (Fig. 68.8). Whereas in the Ellice River Terrane these steep belts appear to be primarily related to a dextral transcurrent shear, in the Bathurst Terrane they are associated with tight infolding of Goulburn Group sediments, most probably formed in a thrust regime. This event therefore represents the thick-skinned counterpart to the thin-skinned fold and thrust event in the Goulburn sediments east of Bathurst Inlet (Tirrul, 1985).

No ductile equivalents of the Bathurst Fault have been recognized with certainty in the crystalline rocks, although several brittle splays are postulated.

The first event - Archean thrusting?

The areas of foliation, migmatites and knotted schist which strike regularly northwest in the north and northwest-southeast of the Bathurst Terrane are first phase structures (domain 2 and that to west of domain 1, Fig. 68.6). Variable dips indicate that these are zones of folding about low plunging northwest-southeast trending axes. In the west, the northwest-southeast foliation is deflected at the boundary of the migmatite core of domain 3, such that it dips steeply west (domain 1, Fig. 68.6). These structures are inferred to be main phase since they are cut by a metagabbro (pre-Goulburn) dykes and parallel the main phase metamorphic zonation. The foliation also follows the northern boundary of domain 3 along a belt of high strain which dips shallowly north-northeast and has sillimanite grade low rake stretching lineations which can locally be related to dextral transport (Fig. 68.6). Although the eastern boundary of domain 3 is overprinted by second phase structures, it is inferred to grossly retain its original orientation since, like the western boundary, it parallels the main phase metamorphic zonation. The north-northeast-trending structures formed at the deflection in domain 1 are not yet well understood. These are steeply plunging folds with hinges which appear to be truncated by west dipping limbs of structurally lower folds (Fig. 68.6). Domain 1 is tentatively interpreted as a zone of main phase high strain marked by thrust disrupted folds. The migmatites of domain 3 themselves display north-northwest-plunging fold structures (Fig. 68.7), although they must be internally modified both by second phase structures within and on the eastern boundary of the domain. Throughout domains 2 and 3, a hallmark of the main phase event is the northwest-southeast-trending stretching lineation (Fig. 68.9b). Its most spectacular development is in

low dipping high strain foliations developed along the boundary between domains 2 and 3 and at places in similar strongly deformed shallow dipping foliations at the base of granites in the northeast of domain 3.

The evidence presented supports the idea of a main phase deformation with a low angle direction of transport parallel to the northwest-southeast-trending stretching lineation. It is worth remarking that such a thrusting event is compatible with the production during a progressive deformation of structures with orthogonal trends (Culshaw, 1983) comparable with structures illustrated from the high grade thrust environment in the Grenville Province (Davidson et al., 1982; Rivers, 1983; Davidson, 1984; Nunn et al., 1984). We further speculate that the migmatites of domain 3 are overlain by a nappe of metasediments of varied metamorphic grade emplaced during this event, which is floored by a high strain zone. Finally, it is notable that in a regional sense the main phase trends are roughly perpendicular to the trends of the Ellice River Terrane.

The second event(s) - shear belts and basement thrusting

As noted, despite the geometric similarity of second phase foliation belts in the Bathurst and Ellice River terranes, they may have different kinematic significance in either terrane. Accordingly, the terranes are treated below as separate entities.

The Ellice River Terrane is dominated by two zones of dominantly lower grade high strain and transcurrent shearing (domains 10 and 13). The high strain is manifested in all rocks by strongly developed regular tectonic fabrics, in quartzofeldspathic gneiss by a fine to very fine grain size, in micaceous rocks by porphyroclastic textures and in some granitoids by augen textures in a wide variety of recrystallization states. The transcurrent shearing is evinced both by the widespread subhorizontal stretching lineation (Fig. 68.9a) and by a variety of mesoscopic kinematic indicators – particularly shear band foliations (White et al., 1980) "surf and turf" (Hanmer, 1984) and other extension structures (Platt and Vissers, 1980) which indicate a dextral sense.

The shear belts lie parallel to elongate domains of more irregular structure in which granulite facies rocks are generally dominant (domains 12 and14; Fig. 68.6, 68.7). It is interesting that, especially in domain 14, north-northwest-trending foliations are common, perhaps a vestige of main phase structures.

Several problems remain within the Ellice River Terrane. For example, the role of the steep folding in domain 11 (Fig. 68.6) is not understood. It appears to be at least synchronous with the shear belts since high strain foliations are folded (Fig. 68.7). A second problem is whether the regionally straight high grade gneisses which are not obviously deformed and retrogressed in the second

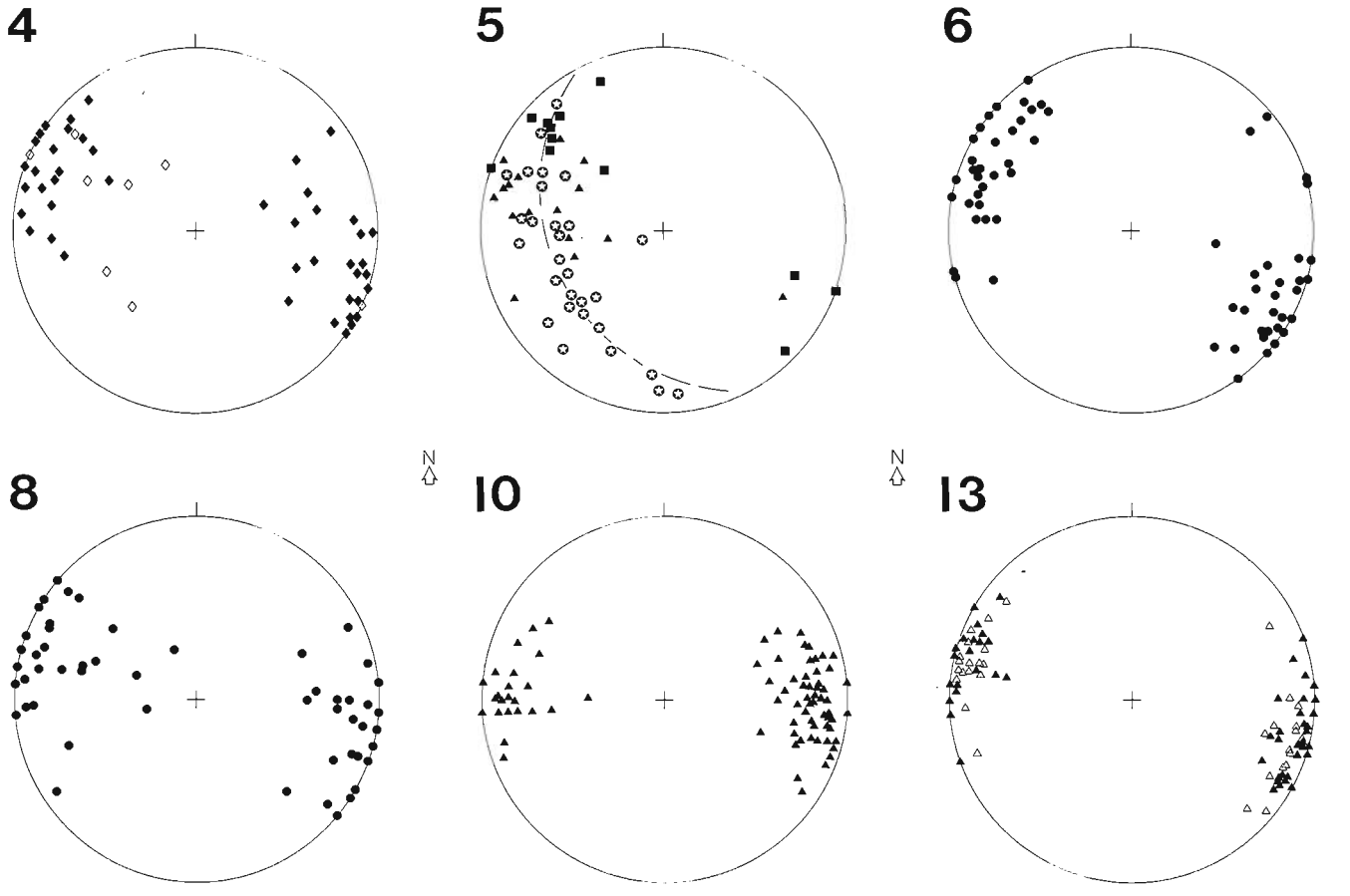

Figure 68.8. *Equal area plots of poles to foliations in zones deformed in the second phase event; 4, ◆ layering transposed parallel to cleavage; ◇ layering; 5, ✪ layering; ■ cleavage; △ unclassified foliation. In 6 and 8 ● are second phase foliations; in 10 and 13 ▲ are second phase foliations and △ are foliations in the granitoid of domain 13.*

metamorphic event (e.g. that between domains 10 and 12, and that north-northeast of domain 14) were formed in a transcurrent- or thrust-fault environment during the first or second phases. Thirdly, and probably related to the last point, a gross variation in dip direction is evident across the terrane, changing from steeply westward on the western margin through steep southeastward in the straightened gneisses east of domains 10 and 11 to westward in the north-northeast of domain 14. The development of the latter belt may be related to the formation of both mylonites on the western boundary of the Ellice River granite (domain 15) and fabrics within the granite itself which lie parallel to those in the gneiss belt. In both cases, steeply west dipping foliations carry near down-dip stretching lineations (Fig. 68.9). The possibility of thrusting implied by these fabrics will be tested with petrofabric analysis.

Within the Bathurst Terrane there are two prominent zones of retrogression and straightening of main phase fabrics (domains 8 and 6), which are associated with linear belts of deformed Goulburn Group sediments. Domain 8, which contains Goulburn outliers II and III, is separated from the boundary shear of the Ellice River Terrane by a fold plunging gently to the south, which is interpreted as a flat Archean structure deformed at the boundary shear (Fig. 68.6). Domain 8 is separated from the interpolated extension of domain 6 by an augen of earlier structures, reminiscent of both domain 3 and those within the Ellice River Terrane. The second phase belts of domains 6 and 8 are similar in geometry (Fig. 68.8) and in their relation to the main phase metamorphic pattern (Fig. 68.5) and consequently are in all likelihood essentially similar in their development. Thus the relations established across domain 6 to the Goulburn outlier are assumed to be valid for both.

Domain 6 comprises partially retrograde straightened main phase migmatites and less common schists in which the rocks contain a much higher proportion of second phase mica. The regular trends contrast with those in the main phase migmatites to the east (Fig. 68.7, 68.8). It displays two features indicating its possible origin as a belt of high second phase strain associated with thrusting. Firstly, within the belt some of the schists have shear band foliations which indicate a thrusting of eastern over western blocks with a small component of oblique slip consistent with a northwest-southeast transport direction. Secondly, the western boundary of the retrograde migmatites with the sillimanite zone is in many places markedly abrupt across a belt of strong deformation, suggestive of a tectonic telescoping.

In the knotted schists of domain 5, retrogression is obvious only immediately adjacent to their contact with the Goulburn Group, elsewhere it is not evident on the outcrop. Poles to bedding define moderately northeast plunging fold axes associated with foliations which are subparallel to the second phase foliations in domains 4 and 6 (Fig. 68.8). These bedding folds in the knotted schists may be either first phase folds or reoriented first phase folds depending on whether the postulated second phase thrusting had simply followed narrow zones parallel to first phase foliations or whether second phase deformation had reoriented first phase structures without macroscopically retrograding the rocks. Although we note that the orientation of these bedding folds is quite close to those in and adjacent to domain 1, it is difficult to conceive that the knotted schists of domain 5, in which foliations are parallel to those in rocks on either flank which were penetratively deformed in the second phase, were not themselves deformed (Fig. 68.8). A tentative explanation of this may be that the folds were once first phase folds similar in orientation to those in domain 1, but were moderately reoriented by penetrative ductile flow in the second phase event. This is compatible with the hypothesis that the second phase belts (domains 5 and 6) are first phase belts accompanied by a minimum reorientation of internal structures.

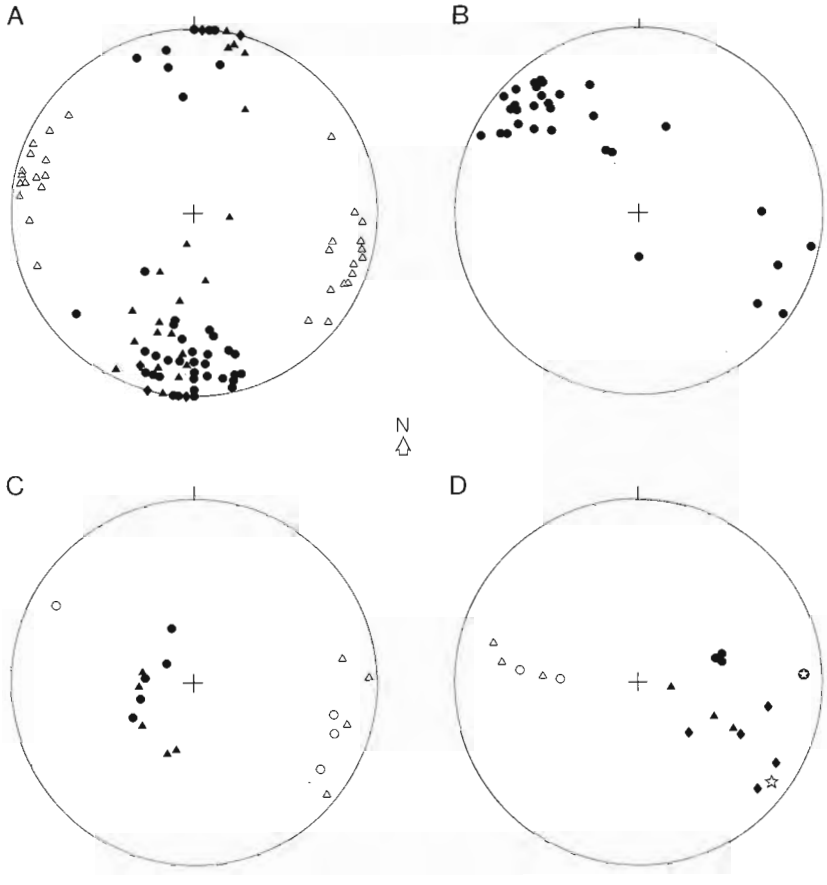

Figure 68.9

Equal area plots of stretching lineations. A, ◆ domain 1; ● domain 10; ▲ domain 13 and △ poles to foliation in LS fabric. In B, ● are lineations formed in the first phase in domains 2 and 3. C, ● lineation in mylonite and ○ pole to mylonitic foliation; ▲ lineation in Ellice River granite and △ pole to foliation in LS fabric of Ellice River granite. D, data from locations of basement/Goulburn Group interaction; ▲ lineation and △ pole to foliation in basement thrust at solid star (★) in Figure 68.6; ● , lineation and ○ pole to foliation in basement thrust at circled star (✪) in Figure 68.6; ◆ lineation in Goulburn Group argillite near thrust at open star in Figure 68.6; open (☆) and circled stars (✪) are bulk stretching directions for Goulburn Group and basement, respectively, at locations with matching symbols in Figure 68.6; these stretching directions are deduced from orientation data of syntectonic veins and fibres according to the method of Arthaud (1969). All on equal area net.

Within the Goulburn sediments themselves (domain 4), both minor folds and major folds – the latter affording a spectacular sight from the air – have subhorizontal axes trending parallel to the belt. However, in the largest proportion of the material deformation is very strong, with bedding transposed parallel to cleavage, such that the dominant foliation is steep (Fig. 68.8) parallel to other second phase foliations. This foliation is often marked by a down dip intersection and stretching lineation and, more rarely, by a subhorizontal crenulation lineation.

A remarkable feature of the western contact of the Goulburn outlier and one which may prove relevant to the understanding of the zone (domain 4, Fig. 68.6) is the truncation of both lithological contacts and foliations of the underlying domain 3 by the overlying lithological contacts and foliations. This may be either a first or second phase feature, or both. It is very similar to truncations along deep seated thrust contacts in gneisses of the western Grenville Province (Davidson, 1984) and may have similar significance.

It is reasonable to tentatively explain the strong second phase ductile strain of the Goulburn Group outlier and adjacent basement by reference to thrusting such as that postulated in domain 6. A caveat is appropriate here, since although little evidence can be adduced to support the notion of strike-slip motion along this zone, we feel it cannot yet be discounted. It is probable that this event correlates with the thin-skinned thrusting in the Goulburn Group east of Bathurst Inlet (Tirrul, 1985), however the picture is complicated by the discovery of three localities where low dipping rather narrow thrust zones in the basement demonstrably affect the cover and have a similar transport direction to thrusts described by Tirrul in the main outcrop of cover (Fig. 68.6). It is remarkable that these localities were discovered during the only two specifically structurally oriented transverses conducted this season, it is likely therefore that such features are more common than indicated on the map (Fig. 68.6). All three examples have in common a relatively shallow easterly dipping thrust plane, contrasting with the generally steep dips of most second phase structures, and a northwest-southeast or east-west transport direction (Fig. 68.9).

The first example is located at the southeast end of Goulburn outlier I (domain 9). A 2 to 3 m wide zone of intense schistosity with a strong down dip lineation cuts northward obliquely across bedding and cleavage of knotted schists in domain 5. At the projected point of intersection of the zone with the basement-cover contact, Goulburn dolomites are strongly transposed with foliations dipping to the southeast (Fig. 68.10a). The cover rocks, which farther south are vertical, have evidently been overturned where the basement thrust intersected the steep basement-cover contact.

The second locality is the most southerly of the two on the west side of Gordon Bay (Fig. 68.6). Here, near the contact with subvertical layering in the Goulburn, both the stretching lineation within a moderately southeast dipping basement schistosity which transposes older foliations and quartz fibres in syntectonic quartz veins in untransposed basement indicate an east-west direction of transport (Fig. 68.9). Here, perhaps the steepening of the basement-cover contact is caused by these basement structures.

Several kilometres to the north of this locality basement is unequivocally thrust over the cover (Fig. 68.6, 68.10b). The key relationships are depicted in Figure 68.11. Stretching lineations, quartz fibres and shear band foliations in the argillite underlying the thrust indicate a thrusting toward the northwest (Fig. 68.9). It is significant that displacement on the thrust is preceded by steepening of the basement-cover contact. This supports the contention that this steepening is the product of basement thrusting in accord with the model of Ramsay (1980) where the initial result of impingement of ductile basement thrusts into the cover is folding of the cover.

A third set of second phase fabrics of distinct orientation form a narrow strip along the western margin of the basement outcrop, south of Kenyon Lake, and make up a fault bound block in the extreme southwest corner (Fig. 68.6). Here the foliations dip moderately to steeply northeast and, like the local main phase metamorphic zonation,

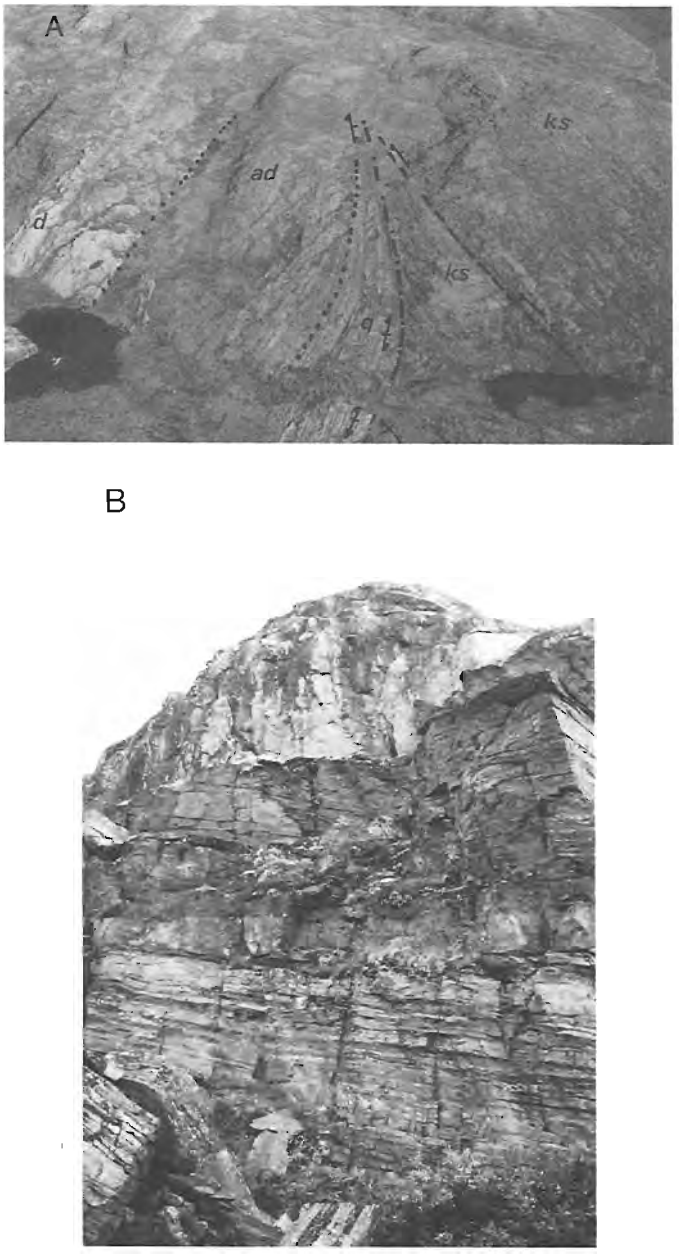

Figure 68.10. *Relations of Goulburn Group to basement. (a) Basement thrust (dashed line) at solid star in Figure 68.6, looking north; basement-cover contact, dot-dash line; moderate and steep dips indicated; KS, Archean knotted schists; Q, AD, D, Goulburn Group quartzite, argillite with dolomite and dolomite; a Mackenzie dyke cuts all lithologies in foreground. (GSC 204131-I). (b) Thrust of basement granite over dark Goulburn Group argillite and quartzites. (GSC 204131-H)*

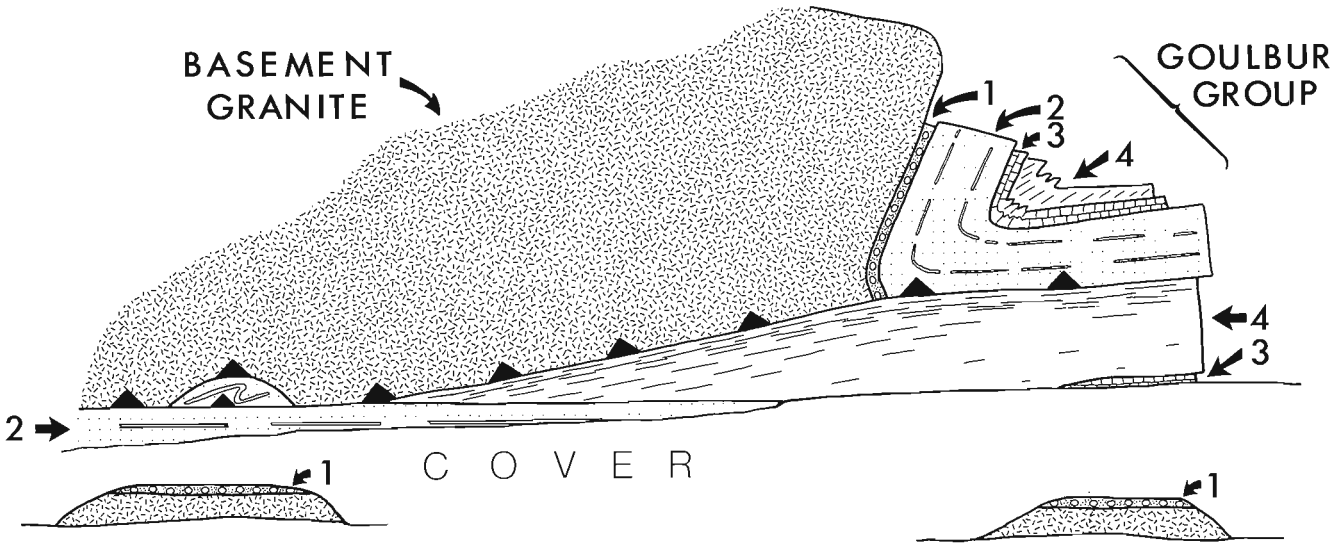

Figure 68.11. *Diagram of relations at thrust of basement granite onto Goulburn Group, open star in Figure 68.6. 1, conglomerate; 2, quartzite; 3, dolomite; 4, argillite. Horizontal length is approximately 300 m; vertical exaggeration about 3x. The outcrops depicted in the foreground are approximately 150 m north of the cliff.*

strike parallel to the Bathurst Fault. The origin of these zones – whether they are thrust related or ductile variants of the Bathurst Fault or both – is a pressing question.

Thelon tectonic zone

The boundary between the Bathurst and Ellice River terranes corresponds quite closely to the tentative western limit of the Thelon Tectonic Zone as derived from 1:1 000 000 scale compilation and aeromagnetic anomaly maps. If "tectonic" is taken to mean "structural", however, a better zone boundary would be the northwestern limit of the development of major north-northeast-oriented structures, a parallel line 35 km farther northwest, Fraser's Thelon Front. The difficulty with single parameter boundaries is that their position depends on the parameter chosen (Gower et al., 1980; Henderson and Thompson, 1981). The Thelon Tectonic Zone is an entity defined by the coincidence of lithologic, structural, metamorphic and geophysical characteristics. Therefore, the boundary between the Bathurst and Ellice River terranes which coincides with a fundamental llthologic change, a high concentration of basic dykes, a major shear zone and, to the west, the occurrence of anomalously high pressure rocks, is an appropriate western limit of the Thelon Tectonic Zone.

To the west there is a relatively homogeneous terrane made up mainly of Yellowknife Supergroup metamorphosed, deformed, and probably tectonically thickened during a northwest-southeast directed, synmetamorphic thrusting event at about 2600 Ma. These rocks were intruded by basic dykes and, later, unconformably overlain by the Goulburn Group (about 1900 Ma). A later event metamorphosed the cover, retrogressed the basement, and caused the Goulburn rocks to be folded into and overthrust by the Archean along steeply-dipping north-northeast low grade shear zones. Whether the regional structural fabric of alternating straight zones with strong Proterozoic retrogression and large scale augen within the 30 km wide zone west of the boundary is originally Archean or Proterozoic has yet to be determined.

East of the boundary in the Ellice River Terrane, there is a much more heterogeneous domain of gneisses, migmatites and plutonic rocks, for which the ages are not known but a two-stage history is evident. Supracrustal gneisses and granitoids were involved in a major phase of deformation and metamorphism that culminated in the granulite facies. Later plutons in the interior of the Ellice River Terrane have been strongly deformed at relatively low grade in steeply-dipping north-northeast shear zones which are parallel to the contemporaneous shear at the main boundary.

A Proterozoic age for the main phase high grade metamorphism, deformation and plutonism in the Ellice River Terrane would support the hypothesis that the Thelon Tectonic Zone is the eroded internal zone of a Proterozoic collisional orogen. As suggested by Tirrul (1985), the Goulburn Group east of Bathurst Inlet would be the corresponding external zone. According to this model, Gibb and Thomas (1977) would have the right concept but the wrong position for the suture. On the other hand, Archean ages for the main phase events in the Ellice River Terrane would confirm the idea that the Thelon Tectonic Zone is part of an Archean mobile belt or orogen that was a locus for thrusting and transcurrent movement after deposition of the Goulburn Group. In this case the external zone at Bathurst Inlet would reflect the westward limit of the reactivation. A thin skin of Proterozoic cover derived from and overridden by basement thrusts rooted in reactivated Archean straight zones is the preferred hypothesis, but the possibility the Thelon Tectonic Zone includes a record of a Proterozoic orogenic event of Wopmay age or older has not been eliminated.

Acknowledgments

We would like to thank Norman Begin, Marlene Charland, Nicole St-Onge and Dave Scott for their enthusiastic assistance in the field. Martha Fahrig performed wonders in the cook tent, that were enjoyed by us all, and at least one other crew in the District of Mackenzie. Martin Irving and Craig Robinson, using the facilities of the Department of Indian Affairs and Northern Development, handled the expediting out of Yellowknife with the usual panache. Lakeland Helicopters provided an excellent crew, with pilot Mike Laughlin and engineer Keith Comyn.

Ptarmigan Airways provided excellent fixed wing support. We would like to acknowledge stimulating discussions and special expertise of visitors Martin Frey (Basel) and Mike Brown (Kingston, U.K.). In agreeing to do a detailed study of structure of the Goulburn Group, Rein Tirrul provided us with a Proterozoic benchmark that has helped us to deal with the complexities of the polymetamorphic basement and basement-cover relations in the map area. Maurice Lambert's comprehensive and constructive review was much appreciated, as were John McGlynn's comments.

References

Arthaud, F.
1969: Méthode de la détermination graphique des direction d'allongement, de raccourscissement et intermediaire d'une population de failles; Bulletin de la Societé geologique de France, v. 11, p. 729-737.

Baragar, W.R.A.
1966: Geochemistry of the Yellowknife volcanic rocks; Canadian Journal of Earth Sciences, v. 3, p. 9-30.

Baragar, W.R.A. and Scoates, R.F.J.
1981: The Circum-Superior Belt: A Proterozoic Plate Margin; in Precambrian Plate Tectonics, ed. A. Kroner; p. 297-330.

Brown, M.
1973: The definition of metatexis, diatexis, and migmatite; Proceedings of the Geological Association, v. 84, p. 371-382.

Buchanan, J.R.
1984: Dynamic metamorphism in a basic dyke near Gordon Bay, Bathurst Inlet, N.W.T.; unpublished B.Sc. thesis, University of Ottawa, 111 p.

Campbell, F.H.A. and Cecile, M.P.
1976b: Geology of the Kilohigok Basin; Geological Survey of Canada, Open File Map 332, 1:500 000 scale.

1981: Evolution of the early Proterozoic Kilohigok Basin, Bathurst Inlet-Victoria Island, Northwest Territories; in Proterozoic Basins of Canada, ed. F.H.A. Campbell; Geological Survey of Canada, Paper 81-10, p. 103-131.

Culshaw, N.G.
1983: Northeast and northwest trends in the Grenville Province-Expressions of propagating shear zones? Abstract, Report of the Second Meeting of the Canadian Tectonics Group held on 23-24 October, 1982 at Gravenhurst, Ontario, ed. W.M. Schwerdtner; in Journal of Structural Geology, v. 5, p. 549-554.

Davidson, A.
1984: Identification of ductile shear zones in the southwestern Grenville Province of the Canadian Shield; in Precambrian Tectonics Illustrated, ed. A. Kroner and R. Greiling; E. Schweizerbart's Verlags Buchhandlung (Nagele u. Obermiller), Stuttgart, p. 263-279.

Davidson, A., Culshaw, N.G., and Nadeau, L.
1982: A tectono-metamorphic framework for part of the Grenville Province, Parry Sound region, Ontario; in Current Research, Part A, Geological Survey of Canada, Paper 82-1A, p. 175-190.

Fraser, J.A.
1964: Geological notes on northeastern District of Mackenzie, Northwest Territories (Report and Map 45-1963); Geological Survey of Canada, Paper 63-40, 16 p.

Fraser, J.A. (cont.)
1968: Geology across Thelon Front, District of Mackenzie (76I, J); in Report of Activities, Part A, Geological Survey of Canada, Paper 68-1A, p. 134.

1978: Metamorphism in the Churchill Province, District of Mackenzie; in Metamorphism in the Canadian Shield, ed. J.A. Fraser and W.W. Heywood; Geological Survey of Canada, Paper 78-10, p. 195-202.

Fraser, J.A. and Tremblay, L.P.
1969: Correlation of Proterozoic strata in the northwestern Canadian Shield; Canadian Journal of Earth Sciences, v. 6, p. 1-9.

Frith, R.A.
1982: Second preliminary report on the geology of the Beechey Lake-Duggan Lakes map areas, District of Mackenzie; in Current Research, Part A, Geological Survey of Canada, Paper 82-1A, p. 203-211.

Geological Survey of Canada
1981a: Magnetic anomaly map of Lockhart River, N.W.T., NP 12/13 (1:1 000 000); Geological Survey of Canada, Map 1566A.

1981b: Magnetic anomaly map of Dubawnt River, N.W.T., NP 13/14 (1:1 000 000); Geological Survey of Canada, Map 1567A.

1982: Magnetic anomaly map Thelon River, (1:1 000 000); Geological Survey of Canada, Map NQ 12-13-14-AM

Gibb, R.A. and Thomas, M.D.
1977: The Thelon Front: a cryptic suture in the Canadian Shield?; Tectonophysics, v. 38, p. 211-222.

Gower, C.F., Ryan, A.B., and Bailey, D.G.
1980: The position of the Grenville Front in eastern and central Labrador; Canadian Journal of Earth Sciences, v. 17, p. 784-788.

Hanmer, S.K.
1984: The potential use of planar and elliptical structures as indicators of strain regime and kinematics of tectonic flow; in Current Research, Part B, Geological Survey of Canada, Paper 84-1B, p. 133-142.

Henderson, J.B.
1975: Sedimentology of the Archean Yellowknife Supergroup at Yellowknife, District of Mackenzie; Geological Survey of Canada, Bulletin 246.

1979: Healey Lake map area, District of Mackenzie; in Current Research, Part A, Geological Survey of Canada, Paper 79-1A, p. 400.

Henderson, J.B. and Thompson, P.H.
1980: The Healey Lake map area (northern part) and the enigmatic Thelon Front, District of Mackenzie; in Current Research, Part A, Geological Survey of Canada, Paper 80-1A, p. 165-169.

1981: The Healey Lake map area and the enigmatic Thelon Front, District of Mackenzie; in Current Research, Part A, Geological Survey of Canada, Paper 81-1A, p. 175-180.

1982: Geology of Healey Lake map area (1:125 000 scale map and marginal notes); Geological Survey of Canada, Open File 860.

Henderson, J.B., Thompson, P.H., and James, D.T.
1982: The Healey Lake map area and the Thelon Front problem, District of Mackenzie; in Current Research, Part A, Geological Survey of Canada, Paper 82-1A, p. 191-195.

Hoffman, P.F., Tirrul, R., Grotzinger, J.P., Lucas, S.B., and Eriksson, K.A.
1984: The externides of Wopmay Orogen, Takijuq Lake and Kikerk Lake map areas, District of Mackenzie; in Current Research, Part A, Geological Survey of Canada, Paper 84-1A, p. 383-395.

Nunn, G.A.G., Noel, N., and Culshaw, N.G.
1984: Geology of the Atikonak area, Grenville Province, Western Labrador; in Current Research, Newfoundland Department of Mines and Energy, Mineral Development Division, Report 83-1, p. 30-41.

Platt, J.P. and Vissers, R.L.M.
1980: Extensional structures in anisotropic rocks; Journal of Structural Geology, v. 2, p. 397-410.

Ramsay, J.G.
1980: Shear zone geometry: a review; Journal of Structural Geology, v. 2, p. 83-99.

Rivers, T.
1983: The northern margin of the Grenville Province in western Labrador – anatomy of an ancient orogenic front; Precambrian Research, v. 22, p. 41-73.

Stockwell, C.H.
1961: Structural provinces, orogenies, and time classification of rocks of the Canadian Precambrian Shield; in Age determinations by the Geological Survey of Canada (compiled by J.A. Lowdon), Report 2, Isotope Ages; Geological Survey of Canada, Paper 61-17.

1969: Tectonic map of Canada (1:5 000 000); Geological Survey of Canada, Map 1251A.

1982: Proposals for time-classification and correlation of Precambrian rocks and events in Canada and adjacent areas of the Canadian Shield Part I: A time classification of Precambrian rocks and events; Geological Survey of Canada, Paper 80-19, 135 p.

Thompson, P.H.
1978: Archean regional metamorphism in the Slave Province - A new perspective on some old rocks; in Metamorphism of the Canadian Shield, ed. J.A. Fraser and W.W. Heywood; Geological Survey of Canada, Paper 78-10, p. 85-102.

Thompson, P.H. and Ashton, K.
1984: Preliminary report on the geology of the Tinney Hills-Overby Lake (west half) map area - a look at the Thelon Tectonic Zone northeast of the Bathurst Fault; Geological Survey of Canada, Paper 84-1A, p. 415-423.

Thompson, P.H. and Frey, M.
1984: Illite "crystallinity" in the Western River Formation and its significance regarding the regional metamorphism of the early Proterozoic Goulburn Group, District of Mackenzie; in Current Research, Part A, Geological Survey of Canada, Paper 84-1A, p. 409-414.

Thompson, P.H. and Henderson, J.B.
1983: Polymetamorphism in the Healey Lake map area - implications for the Thelon Tectonic Zone; in Current Activities Forum, 1983, Program with Abstracts, Geological Survey of Canada, Paper 83-8, p. 2.

Tirrul, R.
1985: Nappes in the Kilohigok Basin and their relation to the Thelon Tectonic Zone; in Current Research, Part A, Geological Survey of Canada, Paper 85-1A, report 51.

Watterson, J.
1975: Mechanism for the persistence of tectonic lineaments; Nature, v. 253, p. 520-521.

White, S.H., Burrows, S.E., Carreras, J., Shaw, N.D., and Humphreys, F.J.
1980: On mylonites in ductile shear zones; Journal of Structural Geology, v. 2, p. 175-187.

Wright, G.M.
1957: Geological notes on eastern District of Mackenzie, Northwest Territories; Geological Survey of Canada, Paper 56-10.

1967: Geology of the southeastern barren grounds, parts of the Districts of Mackenzie and Keewatin (Operations Keewatin, Baker, Thelon); Geological Survey of Canada, Memoir 350.

-69-

BASE METALS IN UPPER WINDSOR (CODROY) GROUP OOLITIC AND STROMATOLITIC LIMESTONES IN THE ATLANTIC PROVINCES

Project 700059

R.V. Kirkham
Economic Geology and Mineralogy Division

Kirkham, R.V., Base metals in upper Windsor (Codroy) Group oolitic and stromatolitic limestones in the Atlantic Provinces; in Current Research, Part A, Geological Survey of Canada, Paper 85-1A, p. 573-585, 1985.

Abstract

This is a preliminary report on numerous minor base metal occurrences in Late Viséan upper Windsor (Codroy) Group limestones in the Atlantic Provinces. Minor base metal occurrences and a few significant deposits have long been known to exist near the base of the Windsor Group but little has been written about base metal occurrences in upper Windsor Group limestones. Chalcopyrite, sphalerite, galena and, at one locality, tetrahedrite are widely dispersed in upper Windsor Group brown, grey and black oolitic and stromatolitic limestones interlayered with red clastic sedimentary rocks, lesser amounts of grey and green limy shales and pale evaporites.

These metal concentrations are of a sedimentary copper type that is economically important in other parts of the world. Base metal sulphides described here occur over several metres of section and display evidence of stratigraphic continuity, although metal contents found to date are too low to be of economic interest.

The occurrences probably formed during early diagenesis by infiltration of metalliferous brines from the adjacent redbeds into the relatively permeable, anoxic, sulphurous oolitic and stromatolitic limestones where the metals were precipitated.

Résumé

Ce rapport est un rapport préliminaire sur les nombreuses manifestations peu importantes de métaux communs dans les calcaires du groupe supérieur de Windsor (Codroy) d'âge vissséen supérieur dans les provinces Atlantiques. On connaît depuis longtemps des manifestations mineures de métaux communs et l'existence de quelques gisements significatifs, proches de la base du groupe de Windsor, mais peu de rapports ont été rédigés sur les manifestations de métaux communs dans les calcaires de la partie supérieure du groupe de Windsor. De la chalcopyrite, de la sphalérite, de la galène, et en un endroit, de la tétrahédrite sont largement dispersées dans les calcaires oolitiques et stromatolitiques bruns, gris et noirs de la partie supérieure du groupe de Windsor, interstratifiés avec des roches sédimentaires clastiques de couleur rouge, et des couches moins importantes d'argiles litées et carbonatées de couleur grise et verte et d'évaporites pâles.

Ces concentrations de métaux sont du type cuprifère sédimentaire, et sont économiquement importantes dans d'autres parties du globe. Les sulfures de métaux communs décrits ici apparaissent sur plusieurs mètres dans les coupes et montrent une continuité stratigraphique, mais les teneurs en métaux observées jusqu'à présent sont trop faibles pour présenter un intérêt économique.

Ces manifestations se sont probablement formées pendant les premières phases de diagénèse, par infiltration de saumures métallifères provenant des formations rouges (red beds) adjacentes, dans les calcaires oolitiques et stromatolitiques relativement perméables, déposés en milieu réducteur, riches en sulfures, dans lesquels les métaux ont précipité.

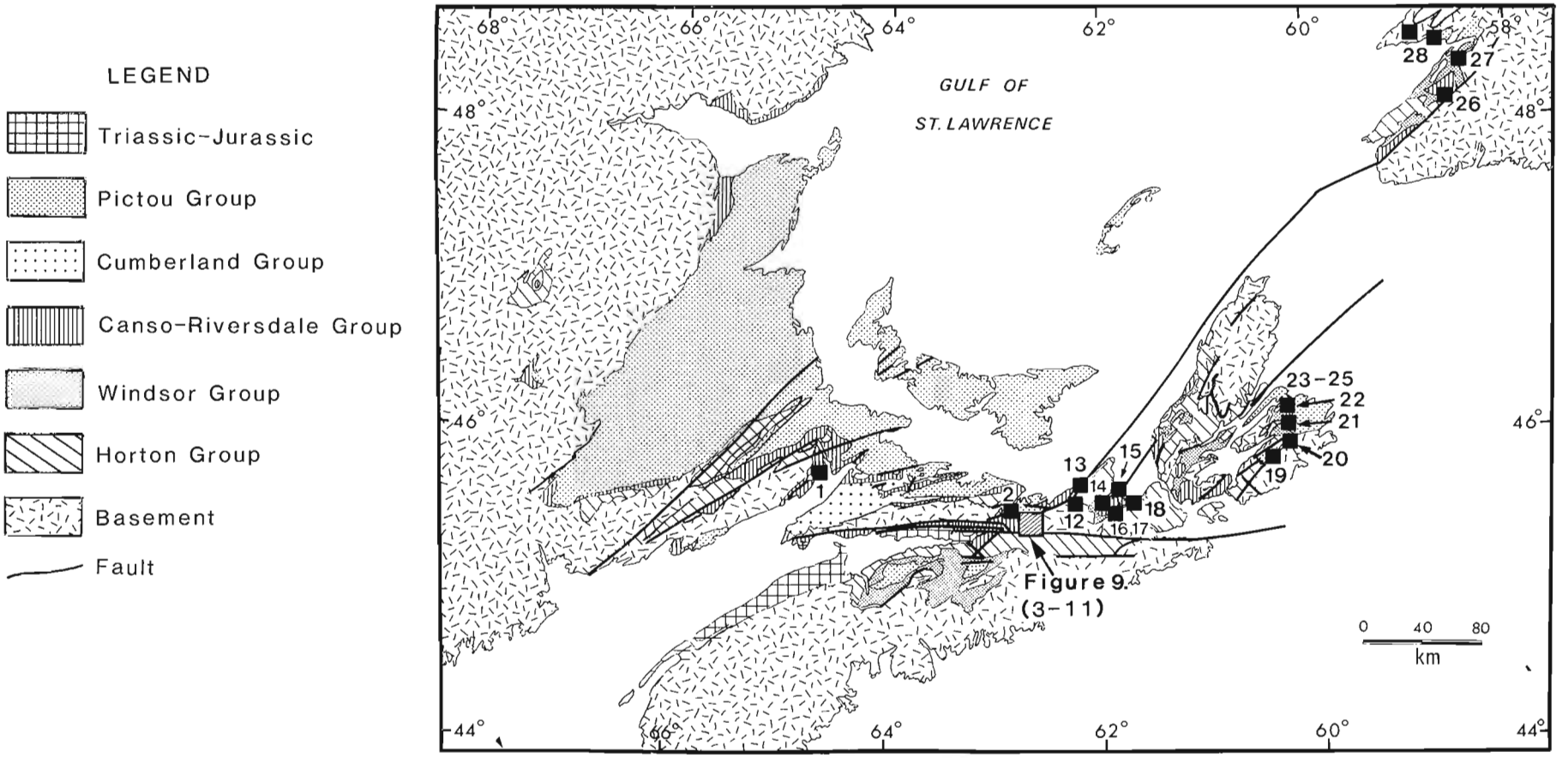

1) *Hopewell Cape (The Rocks) – Cu, Zn*
2) *Limerock – Cu (Pb)*
3) *Centerdale – Zn*
4) *Springville – Zn*
5) *The Island roadcut – Cu*
6) *Eureka Hole 1 – N.S. reference hole – Zn, Cu*
7) *East River near The Island – Pb, Zn, Cu*
8) *Eureka (Ferrona Junction) – Cu(Zn, Ag)*
9) *Churchville Road – Zn, Cu*
10) *McLellan Brook Holes 1, 2, & 3 – Cu*
11) *McLellan Brook (Stewart Brook) – Cu*
12) *Bailey's Brook – Ardness Limestone – Cu*
13) *Ardness Limestone (coastal outcrop) – Zn*
14) *Lower South River – Pb*
15) *Pomquet Harbour – Pb*
16) *Pomquet River – Cu*
17) *Kennco Hole 6 (Meadow Green) – Cu*
18) *Monastery Brook – Cu*
19) *Rig Glen (Rig Barren) – Pb*
20) *Woodbine Hole 1 – N.S. reference hole – Zn(Cu, Pb)*
21) *Portage East Bay roadcut – Zn*
22) *Sydney River – Zn*
23) *Limestone Point Limestone – roadcut – Pb*
24) *Crawley Creek – Crawley Limestone – Cu*
25) *Opposite Amelia Point – Rudderham Point Limestone – Pb, Zn*
26) *Bald Mountain – Black Point Limestone – Cu*
27) *Shallop Cove – Pb*
28) *Lead Cove, Belmans Cove, Boswarlos (Port au Port Peninsula) – Pb (Zn, Cu)*

Figure 69.1. *Location map with generalized Carboniferous geology of the Atlantic Provinces modified after Howie (personal communication, 1979).*

Introduction

Minor concentrations of base metals are widely distributed in Late Viséan upper Windsor Group[1] limestones in the Atlantic Provinces. This paper is a preliminary report on their nature, distribution and genesis. Many of the occurrences mentioned in this paper were located during the course of this study and have not been described previously. This type of occurrence and metallogenetic setting are relatively undocumented and have received only limited attention from exploration companies.

The nature and distribution of base metals in Carboniferous sequences in eastern Canada have been documented intermittently by the author and colleagues (e.g. Binney and Kirkham, 1975; Binney, 1975; Kirkham, 1978, 1980). Emphasis has been on occurrences in rocks near the Windsor-Horton contact, long known to be a site of base metal accumulation. In 1978, however, John MacLeod of Esso Minerals Canada brought to my attention minor, disseminated chalcopyrite in an upper Windsor oolitic limestone. This limestone was intersected in a hole drilled to test a geochemical anomaly near McLellan Brook southeast of Stellarton, Nova Scotia (Fig. 69.1, loc. 10). Similar chalcopyrite occurrences in oolitic limestone had been reported previously in an outcrop on the Pomquet River (loc. 16) and in a hole drilled in 1966 by Kennco Limited near Meadow Green (loc. 17) in the Antigonish basin to the northeast. Based on this information and the similarities of these occurrences with typical sedimentary copper deposits, I attempted to locate and document as many such occurrences as possible. This report presents some of the main findings to date.

General geology

The Windsor Group (Fig. 69.1) was the focus of considerable exploration and study through most of the 1970s and numerous papers have been published on it. For general background information the reader is referred to Giles (1981), Knight (1983) and McCutcheon (1981). As outlined by Giles (1981) the Windsor Group comprises essentially five major marine transgressive carbonate-evaporite (mudstone) cycles interlayered with continental redbeds. The lowest cycle, the thickest and most widely distributed, corresponds with the A faunal subzone of Bell (1929). This cycle plus the second cycle, which corresponds roughly with the B faunal subzone of Bell, constitutes the lower macro- and microfaunal zones (Mamet, 1970; von Bitter and Plint-Geberl, 1982) of the Windsor Group. The last three major cycles, according to Giles (1981), correspond to the upper Windsor macrofaunal zones C, D and E of Bell (1929) and the microfaunal zones (Mamet, 1970; von Bitter, 1976; von Bitter and Plint-Geberl, 1982).

These last three major cycles are characterized by a basal limestone, and/or limy shale overlain by gypsum or gypsiferous mudstone which is in turn overlain by red siltstone and/or sandstone. In the marginal parts of basins, the limestones at many localities are overlain directly by red clastic sedimentary rocks without intervening evaporites. In the deeper parts of the basins several minor cycles are present in addition to the major cycles. Fewer redbeds are present in the deeper parts of the basins and the proportion of evaporites and reduced clastic sedimentary rocks is greater than in marginal areas. At some localities, such as exposures of the Ardness Limestone along the coast at Knoydart, Nova Scotia (Fig. 69.1, loc. 13), the oolitic limestone is both overlain and underlain by typical fining-upward red fluvial sandstones. At Hopewell Cape in New Brunswick (loc. 1) sandy oolitic and argillaceous stromatolitic limestones are both under- and overlain by red immature, proximal, braided-stream and mass flow, alluvial fan conglomerates.

Upper Windsor limestone units vary greatly from one locality to another. Most range from tan, through medium brown and grey to black in colour, but some have been oxidized and are reddish or cream coloured. Oxidized limestones are most prevalent near the margins of the basins and near the tops and bottoms of marine sections immediately adjacent to redbeds. Some limestones, even dark reduced units, contain well developed calcretes and/or pisolites indicating that during deposition they were exposed periodically, possibly due to evaporitic draw-down. Many of



Figure 69.2. *Typical large ripple marks in ooid grainstone, Ardness Limestone, Knoydart Point, Nova Scotia (loc. 13). (GSC 203633-X)*

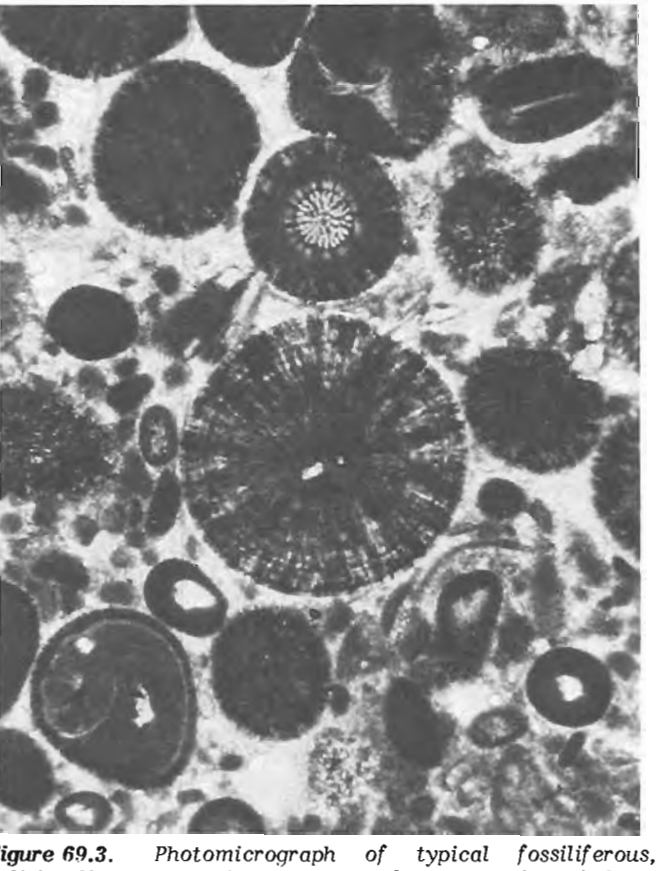

Figure 69.3. *Photomicrograph of typical fossiliferous, oolitic limestone with sparry calcite matrix, Ardness Limestone, Knoydart Point, Nova Scotia (loc. 13). Large ooid in centre is about 5.3 mm in diameter. KQ-78-81B*. (GSC 204076-U)*

[1] Codroy Group in Newfoundland is equivalent to the Windsor Group on the mainland

the carbonate units range from a few centimetres to greater than 10 metres thick and several average about 2 to 5 metres thick, although detailed thickness and facies variations of individual carbonate units are not well known.

The limestones include a spectrum of lithologies ranging from very fine-grained, argillaceous micrite and biomicrite, through well-sorted grainstones and algal bindstones to somewhat crystalline sparites. Based on field observations, the ooid grainstones and stromatolitic units at most localities apparently contain more base metal sulphides than the micritic and crystalline (sparite) units. Well-developed oncolites or algal biscuits are present at a few localities. At a number of localities the ooid grainstones contain large ripple marks (Fig. 69.2, loc. 13) and crossbeds indicative of high energy, marine shoals. The oolites exhibit both well developed radial and concentric structures (Fig. 69.3, loc. 13). Limestones have been dolomitized at some localities. For example, at locality 8, near Eureka, Nova Scotia, dolomite occurs along fractures that are probably related to large fault systems in the area.

At most localities beds dip gently and are not strongly folded. But overturned beds and recumbent folds in Carboniferous sequences in parts of Nova Scotia might be related to gravity slump structures and/or thrust faults. Nevertheless, rocks in the areas examined have not been metamorphosed or subjected to penetrative deformation.

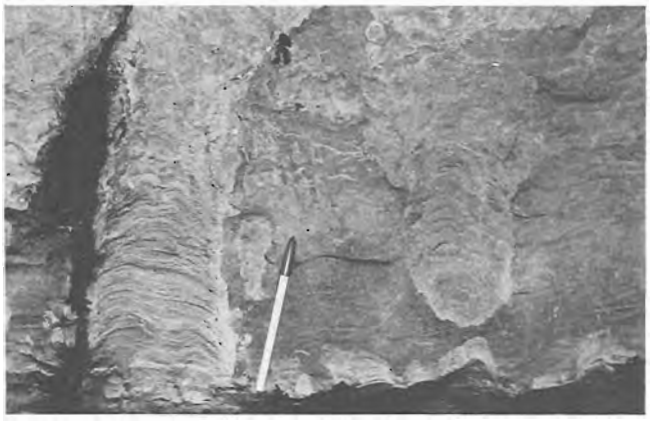

Figure 69.4. *Columnar stromatolites in crossbedded, siliceous ooid grainstones, Hopewell Cape, New Brunswick (loc. 1). (GSC 203633-W)*

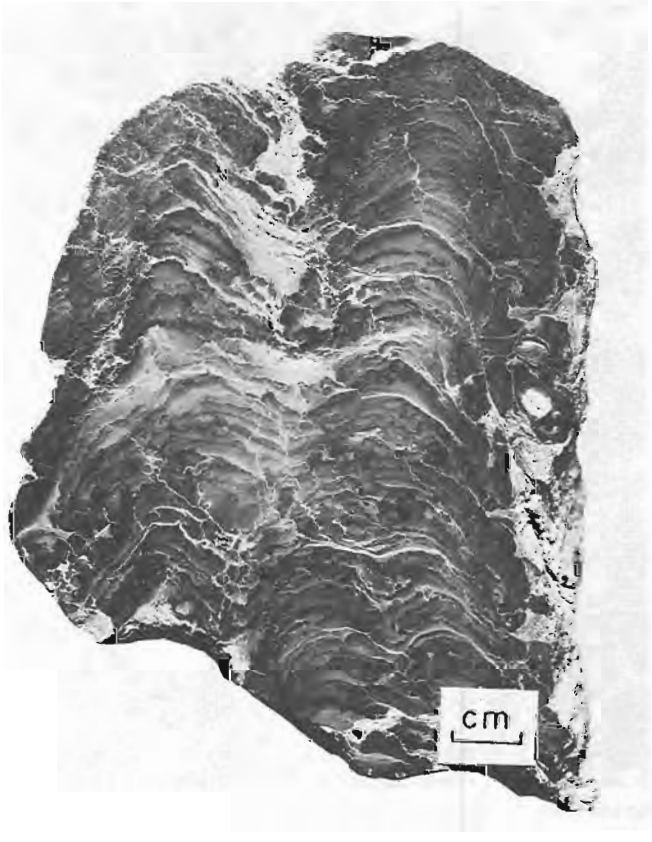

Figure 69.5. *Smooth mat, laterally linked, columnar stromatolites with disseminated chalcopyrite, Stewart Brook, Nova Scotia (loc. 11). KQ-78-75G*. (GSC 204076-S)*

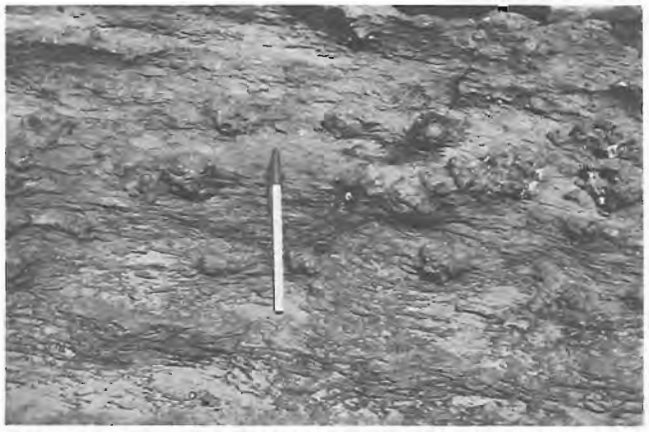

Figure 69.6. *Small bulbous, fenestral stromatolites in argillaceous limestone containing minor disseminated chalcopyrite and sphalerite, Hopewell Cape, New Brunswick (loc. 1). (GSC 203633-Z)*



Figure 69.7. *Dark grey fenestral algal limestone with sparry white calcite and disseminated chalcopyrite and pyrite in the fenestrae, Limerock, Nova Scotia (loc. 1). KQ-77-26. (GSC 204076-V)*



Figure 69.8

Dark grey limestone with algal biscuits and disseminated galena, Limestone Point, Point Edward, Nova Scotia (loc. 23). KQ-78-93. (GSC 203561-P)*

However, gash veins, minor faults, stylolites and other dissolution features are common. Gash veins (mostly white sparry calcite) are most abundant near major faults and apparently postdate base metal sulphides. Diagenetic sparry calcite cement is widely distributed and is probably closely related to base metal sulphide deposition.

Fossils in the limestones suggest restricted, hypersaline environments. For instance, large robust brachiopods and colonial corals were not observed at the localities examined. Instead small scattered brachiopods, gastropods, ostracods, bryozoans, crinoid stems, calcareous algae, foramanifera and cyanobacteria (in stromatolites) are characteristic. Stromatolites include discrete columns within crossbedded, siliceous ooid grainstones (Fig. 69.4, loc. 1); laterally linked, and partially walled smooth layered columns (Fig. 69.5, loc. 11); small, bulbous stromatolites contained within argillaceous limestone (Fig. 69.6, loc. 1); pustular algal mats (Fig. 69.7, loc. 2) and algal biscuits (Fig. 69.8, loc. 23) and oncolites. Obviously the sedimentary environments involved were conducive to the growth of micro-organisms, principally cyanophytes, that produce stromatolites.

Mineral distribution

Figures 69.1 and 69.9 show the distribution of base metal occurrences and some metal contents; lithological features of the occurrences are listed in Table 69.1. The distribution of occurrences should be viewed as preliminary as it is based on incomplete field examinations and limited drill core. The occurrences consist of variable amounts of chalcopyrite, sphalerite, pyrite and galena. Tetrahedrite was found at locality 3 in the Eureka area, Nova Scotia (Fig. 69.9) but significant amounts of bornite and chalcocite have not been observed except in associated red bed copper occurrences (i.e. hosted by continental sedimentary rocks) (Kirkham, 1973) in grey fluvial sandstones. Chalcopyrite and/or sphalerite appear to be more abundant than galena, although quantitative chemical information is limited.

A characteristic feature of the sulphides is their disseminated nature, especially in the sparry calcite matrix of oolitic limestones (Fig. 69.3). Most of the base metal sulphides are concentrated preferentially in what were originally the most permeable beds in the sequence, such as ooid grainstone, fenestral algal limestone, and interbedded quartzofeldspathic sandstone and siltstone. In places, the sulphides are concentrated along stylolites. The concordant, disseminated nature of the sulphides and their association with redbeds and evaporites are characteristic features of sedimentary copper deposits.

At some localities, such as the coastal exposures at Knoydart Point (loc. 13) in Nova Scotia and Hopewell Cape (loc. 1) in New Brunswick, redbed copper occurrences are present in proximity to the base metal occurrences in Windsor limestones. Most of the redbed occurrences consist of chalcocite, bornite and/or chalcopyrite associated with wood trash and early diagenetic pyrite.

Unlike the base metal sulphides along the Windsor-Horton contact (Kirkham, 1978), those in the upper Windsor limestone, tend to be widely distributed throughout the oolitic and stromatolitic limestones rather than concentrated only along the basal contact. Although metal contents tend to be low, at some localities base metal sulphides occur over significant stratigraphic intervals (e.g., 17.7 m in McLellan Brook Hole No. 1 at locality 10, Fig. 69.10, and 5.5 m at locality 16 on the Pomquet River). At other localities, such as Shallop Cove in Newfoundland (loc. 27) and Limestone Point at Point Edward in Nova Scotia (loc. 23), base metal sulphides appear to be concentrated in 1 to 2 m intervals within limestone units that are several metres thick. In these localities more permeable zones were probably a key factor in localizing the sulphides. Micritic, slightly crystalline and argillaceous limestones, in general, appear to be less favourable hosts than more permeable oolitic and fenestral, algal limestones (Fig. 69.11).

Chemical analyses

Many samples from outcrop and drill core were collected for chemical analyses. Most analyses remain to be done but available results are presented in Table 69.1. The purpose of the analyses is to determine accurately the metal contents of representative samples and document vertical and lateral changes in metal contents. This work is part of a broader study of metal distribution and zonation in Carboniferous basins of eastern Canada.

Samples selected were representative and not atypical, local higher grade material. Weathered surfaces and secondary veins were avoided where possible. Samples from outcrop and drill core were collected in profiles to document vertical variations in metal contents. The position (feet or metres) recorded for drill core samples is for the mid-point of the specimen and the length of the specimen has been reported to record the sample interval. For outcrop samples the stratigraphic positions are mostly visual estimates except for samples collected in 1984 which were measured. In the laboratory most specimens were cut with a diamond saw and any weathered material and gash veins were removed.

Samples were crushed and ground carefully keeping barren redbeds separate from samples containing base metal sulphides. Pure quartz was passed through the equipment and the equipment was washed between samples. All of these procedures are viewed as necessary to avoid inter-sample contamination and erroneous trace element analyses.

The analyses quoted here were done in the laboratories of the Analytical Chemistry Section of the Survey by atomic absorption spectrometry. The validity of results are estimated to be: Cu, ± 7 ppm; Pb, ± 20 ppm; Zn, ± 7 ppm; Ni, ± 15 ppm; Co, ± 10 ppm; Ag, unknown, and for all elements, ±10% of the value quoted. Values below these limits have been included but they are of questionable reliability. Replicate samples included in each batch of samples suggest, however, that the analytical precision is better than these limits.

Table 69.1. Chemical analyses

Locality[1]	Sample No.[2]	Length[3]	Cu[4]	Pb[4]	Zn[4]	Ag[4]	Co[4]	Ni[4]	Description
2) Limerock	KQ-77-26	10(+)	2250	13	20	1	-	-	black fenestral algal ls; sparry cal, cp, py
	LR-1-16'	4.3	69	16	31	-	-	-	dark grey limy ark(?); py
	LR-1-47'	5.7	33	29	44	-	-	-	dark grey limy fos siltst; py
	LR-1-73'	7(?)(chips)	22	46	57	-	-	-	black silty fos ls; py
	LR-1-83'	7(?)(chips)	120	29	65	-	-	-	black fos ls; py
	LR-1-89'	5(?)(chips)	2070	68	140	<1	-	-	black fos ls; cp
	LR-1-92'	8(?)(chips)	2410	58	170	<1	-	-	black fos ls; cp
	LR-1-94'	7(?)(chips)	550	60	160	<1	-	-	dark grey fos ls; cp
	LR-1-97'	8(?)(chips)	690	50	86	nd	-	-	dark grey fos ls; cp
	LR-1-103'	8(?)(chips)	870	20	85	<1	-	-	grey fenestral ls; py, cp
	LR-1-106'	7(?)(chips)	530	38	63	-	-	-	grey fenestral ls; py, cp
	LR-1-107'	5	280	5	58	-	-	-	mottled grey fenestral ls; py, cp
	LR-1-112'	5	110	nd	10	-	-	-	mottled grey fenestral ls; py, tr cp
	LR-1-116'	6.8	49	nd	5	-	-	-	mottled grey fenestral ls; py
	LR-3-97'[5]	5.7	5	16	19	-	-	-	pale green-grey limy shale; py
	LR-3-101'	5	33	8	62	-	-	-	green limy shale; py
	LR-3-106'	6	66	5	55	-	-	-	green fos shale; py, tr cp
	LR-3-108'	4.8	41	24	48	-	-	-	mottled green shale; py
	LR-3-111'	5.8	180	10	47	-	-	-	mottled green fos shale; py, tr cp
	LR-3-119.5'	5	80	10	41	-	-	-	grey shaly algal ls; py
	LR--3-122'	5.2	270	20	61	-	-	-	grey shaly algal ls; cp, py
	LR-3-124'	4.1	1480	37	73	-	-	-	grey shaly algal ls; cp, py
	LR-3-128'	6.6	910	24	115	nd	-	-	mottled grey fenestral ls; cp, py
	LR-3-130'	5.4	400	4	26	nd	-	-	mottled grey fenestral ls; py, cp
	LR-3-132'	5	620	4	67	-	-	-	mottled dark grey fenestral ls; py, cp
	LR-3-135'	3.2	210	nd	23	-	-	-	mottled dark grey fenestral ls; py, cp
	LR-3-137.5'	4.8	26	17	15	-	-	-	mottled dark grey fenestral ls; py
	LR-3-139.8'	3	17	19	14	-	-	-	mottled pale grey fenestral ls; py
	LR-3-141'	4.3	42	56	23	-	-	-	pale green-grey limy siltst; py
	LR-3-147.5'	7.5	8	nd	8	-	-	-	pale grey crystalline gyp and green silty ls; py
5) The Island Roadcut	KQ-84-69A +10 cm	9	160	22	35	nd	6	6	dark grey oolitic and micritic ls; tr cp
	KQ-84-69B +25-30 cm	5.3	51	20	53	1	7	1	dark brown-grey oolitic ls; tr cp
	KQ-84-69C +45 cm	5.9	310	22	25	2	11	10	dark grey oolitic and micritic ls; py, cp
	KQ-84-69D +95 cm	7	470	15	24	2	18	5	black oolitic and micritic ls; py, cp
6) Eureka Hole 1	E1-78-1559'	7.6	1	nd	33	-	-	-	medium red-grey siltst
	E-1-78-1566'	8.8	2	5	32	-	-	-	medium red-grey siltst
	E-1-78-1574'	8.1	1	nd	27	-	-	-	medium red-grey fg ark
	E-1-78-1579'	6.4	1	nd	32	-	-	-	medium red-grey fg ark
	E-1-78-1583'	6.0	2	nd	22	-	-	-	medium red-grey fg ark
	E-1-78-1588.5'	10.5	1	nd	27	-	-	-	medium red-grey siltst
	E-1-78-1593'	7.6	1	nd	34	-	-	-	medium red-grey fg ark
	E-1-78-1594'	7	14	8	46	-	-	-	pale to medium green-grey siltst
	E-1-78-1595.3'	10.7	290	32	29	1	-	-	pale grey siltst; py, cp
	E-1-78-1596'	8.5	150	24	50	-	-	-	medium to dark grey, oolitic, fos ls and mudst; py cp
	E-1-78-1596.7'	7	20	3150	160	-	-	-	medium grey mudst
	E-1-78-1598.5'	8.8	6	42	86	-	-	-	pale to dark grey limy siltst
	E-1-78-1599.3'	6.5	160	8	320	-	-	-	medium grey and green-grey oolitic-strome(?) ls; cp
	E-1-78-1600.4'	8.9	1510	90	360	1	-	-	dark grey argillaceous stromatolitic ls; py, cp
			1490	85	370	-	-	-	
	E-1-78-1601.6'	6.5	94	52	360	-	-	-	dark grey stromatolitic ls
	E-1-78-1603'	7.9	160	58	360	-	-	-	dark grey stromatolitic ls; py, tr cp
	E-1-78-1603.6'	8.8	18	46	3120	-	-	-	dark grey stromatolitic ls; py
	E-1-78-1604.4'	9.5	22	54	2090	-	-	-	dark grey stromatolitic ls; py
	E-1-78-1605.7'	11.1	22	64	1760	nd	-	-	dark grey, drusy stromatolitic ls; py
	E-1-78-1607.3'	6.8	96	58	4540	-	-	-	medium to dark grey oolitic ls; sparry cal, sp
	E-1-78-1608.3'	10.2	52	74	5660	-	-	-	medium to dark grey oolitic ls; sparry cal, sp, tr py
	E-1-78-1609'	4.3	78	210	5720	-	-	-	medium to dark grey oolitic ls; sparry cal, sp
	E-1-78-1610.4'	9.8	13	79	4810	nd	-	-	medium to dark grey oolitic ls; sparry cal, sp
	E-1-78-1611.6'	13.5	6	50	3780	-	-	-	medium to dark grey oolitic-strome ls; sparry cal, sp
	E-1-78-1613'	11.4	24	78	5080	-	-	-	medium grey, drusy oolitic ls; sparry sp, tr py
	E-1-78-1613.4'	7.8	390	100	610	-	-	-	dark grey oolitic-strome ls; tr py and cp
	E-1-78-1613.6'	2.2	530	200	650	-	-	-	dark grey to black silty ls; py, cp
	E-1-78-1613.9'	6.3	910	320	510	-	-	-	medium grey argillaceous oolitic ls; sparry cal, py, cp
	E-1-78-1614.8'	6	160	160	450	2	-	-	medium grey limy siltst; py
	E-1-78-1615.3'	3.5	520	72	670	-	-	-	dark grey ls and limy mudst; py, tr cp
	E-1-78-1616.2'	4	2800	58	490	-	-	-	dark grey strome ls and limy mudst; py, cp
	E-1-78-1616.7'	5	470	18	220	-	-	-	medium green-grey limy siltst; py, cp
	E-1-78-1617.4'	6.4	150	110	280	-	-	-	dark grey, fenestral strome ls and mudst; py, tr cp
	E-1-78-1618.2'	6.5	920	210	170	-	-	-	medium green-grey shale; py, cp
	E-1-78-1619.4	6.5(?)	1570	400	180	2	-	-	medium green-grey shale and algal(?) ls; py, cp
			1500	400	180	-	-	-	
	E-1-78-1621'	7.2	350	20	88	-	-	-	medium green-grey shale; py, cp
	E-1-78-1622.1'	7	38	18	70	-	-	-	medium green-grey shale and limy siltst; py
	E-1-78-1623.5'	6	7	nd	42	-	-	-	mottled medium green-grey and grey (red) siltst and mudst
	E-1-78-1625'	6.4	1	nd	26	-	-	-	medium (red) grey siltst
	E-1-78-1627.5'	6	1	nd	49	-	-	-	medium maroon-grey siltst
	E-1-78-1630'	8.3	2	5	49	-	-	-	medium maroon-grey siltst
	E-1-78-1632'	6.3	1	3	23	-	-	-	medium maroon-grey siltst
	E-1-78-1635'	8	1	3	38	-	-	-	medium maroon-grey siltst
	E-1-78-1640'	6.7	3	8	59	-	-	-	medium maroon-grey siltst
	E-1-78-1645'	6.5	2	3	22	-	-	-	medium red-grey siltst
	E-1-78-1650'	8.4	2	nd	32	-	-	-	medium red-grey siltst
	E-1-78-1655'	7.5	2	4	38	-	-	-	medium maroon-grey siltst
	E-1-78-1660'	7	2	3	30	-	-	-	medium red-grey siltst
	E-1-78-1665'	8.5	2	nd	32	-	-	-	medium red-grey siltst; lime nodules
	E-1-78-1670'	8	5	nd	120	-	-	-	medium red-grey siltst
8) Eureka (Ferrona Junction)[6]	KQ-84-65A -2.5 m	4.9	310	93	46	3	42	60	dark grey dol shale; cp
	KQ-84-65B -2.5 m	6.5	420	57	62	2	28	47	dark grey shaly dol; py, cp
	KQ-84-65C -10 cm	2	75	47	33	4	56	61	dark grey shale
	KQ-84-650 +0 to 9 cm	7.5	410	4	40	1	64	69	dark brown-grey crystalline dol; cp
	KQ-84-65E +20 cm	8.5	1300	13	55	2	150	120	dark brown-grey crystalline dol; cp, py
	KQ-84-65F +60 cm	4	560	3	43	1	61	59	dark brown-grey, crystalline dol; cp
	KQ-84-66A -3 to 10 cm	5	130	25	490	1	38	41	medium brown-grey dol shale; tr cp
	KQ-84-66B +0 to 15 cm	9	1600	3	57	nd	280	260	dark grey, crystalline dol; cp
	KQ-84-66BB +0 to 15 cm	10.5	1200	24	90	nd	120	57	black, oolitic, brachiopod ls; cp, tr py and tetrah
	KQ-84-66C +15 to 30 cm	9	4100	16	60	1	190	270	black crystalline dol; cp
	KQ-84-66D +25-35 cm	8.4	890	8	63	nd	280	190	black crystalline dol; cp
	KQ-84-66E +45 to 55 cm	7	1100	3	72	1	210	170	black crystalline dol; cp
	KQ-84-66F +70 to 80 cm	5.5	840	2	52	4	72	130	black crystalline dol; cp
	KQ-84-66FT +70 to 80 cm[7]	4.4	2500	7	290	5	84	110	black crystalline dol; tetrah, cp
	KQ-84-66G +90 to 105 cm	11	630	12	110	nd	93	130	black crystalline dol; sp(?)

Locality[1]	Sample No.[2]	Length[3]	Cu[4]	Pb[4]	Zn[4]	Ag[4]	Co[4]	Ni[4]	Description
9) Churchville Road	KQ-84-67	11.8	950	33	280	3	44	6	black oolitic ls; cp
	KQ-84-68A	8	23	78	1700	2	8	3	black micritic ls
	KQ-84-68B-1	3	140	280	26000	4	5	6	dark grey oolitic ls; sp, py, tr cp
	KQ-84-68B-2	8.7	80	850	17000	1	10	10	dark grey oolitic ls; sp, py(?)
10) McLellan Brook	MB-1-30'	6.9	4	nd	43	-	-	-	medium red-grey fg ark
	MB-1-53'	4.3	4	nd	72	-	-	-	maroon siltst
	MB-1-58'	3.4	7	nd	62	-	-	-	mottled red and green siltst
	MB-1-64'	6	1220	14	1200	-	-	-	mottled grey-green silty(?) stromatolitic ls; py, tr sp and cp
	MB-1-68'	5.8	660	31	650	-	-	-	mottled grey-green silty stromatolitic ls; py, tr cp
	MB-1-72'	8.5	330	14	420	-	-	-	mottled pink and grey-green silty stromatolitic ls; py
	MB-1-75'	5.5	86	21	710	-	-	-	dark brown-grey oolitic ls; py
	MB-1-85'	5.6	1110	7	84	nd	-	-	dark brown-grey oolitic ls; cp
	MB-1-94'	4.6	3940	92	74	nd	-	-	dark brown-grey oolitic ls; cp
	MB-1-112'	5.4	1360	77	240	nd	-	-	dark crystalline oolitic ls; cp, py
	MB-1-115'	10.7	1280	26	280	nd	-	-	dark crystalline oolitic ls; cp, py
	MB-1-121'	5	6	nd	54	-	-	-	medium red-grey siltst
	MB-1-126'	4.3	4	nd	39	-	-	-	medium red-grey siltst
	MB-1-149'	7.5	4	nd	36	-	-	-	medium red-grey fg ark
	MB-1-166'	4	5	4	54	-	-	-	medium maroon siltst and fg ark
	MB-1-215'	7.3	2	nd	34	-	-	-	dark maroon siltst and fg ark
10) McLellan Brook (Stewart Brook)	KQ-78-74*	4.3	3	nd	33	-	-	-	medium red-grey, fg ark
	KQ-78-75A* -1.5 m(?)	9.6	4	nd	39	nd	-	-	medium red-grey siltst
	KQ-78-75B* +20 cm(?)	10(?)	410	46	110	nd	-	-	dark grey oolitic ls; sparry cal, py, cp
			390	58	100	2	110	3	
	KQ-78-75C* +1m(?)	5.1	170	30	33	nd	-	-	dark grey oolitic ls; sparry cal, cp, py
	KQ-78-75G* +4m(?)	12	810	33	110	nd	-	-	dark grey micritic stromatolitic ls; cp
			800	29	240	1	18	6	
12) Bailey's Brook	KQ-78-80A* +5cm	4.1	280	40	130	-	-	-	dark grey oolitic ls; sparry cal, tr cp
	KQ-78-80B* +25cm	9.2	130	8	45	-	-	-	dark grey oolitic ls; sparry cal, cp
	KQ-78-80C* +40 cm	19.5	220	11	46	nd	-	-	dark grey oolitic ls; sparry cal, cp
	KQ-78-80D* +70 cm	22.5	76	3	62	nd	-	-	medium grey, crystalline ls; tr cp
	KQ-78-80F* +95 cm	8.3	71	13	27	-	-	-	medium grey, crystalline ls; tr cp
	KQ-78-80G* +1.4 m	14	14	11	63	-	-	-	dark micritic ls
	KQ-78-80H* +1.9 m	8	350	33	55	-	-	-	dark grey, crystalline oolitic ls; cp
	KQ-78-80I* +2.1 m	7.6	120	110	53	-	-	-	medium grey, crystalline oolitic ls; cp
13) Ardness Limestone	KQ-78-81A* +30 cm	4.6	8	260	2900	-	-	-	medium grey oolitic ls; sparry cal, py
	KQ-78-81B* +60 cm	12.8	14	25	4000	nd	-	-	dark grey oolitic ls; sparry cal
	KQ-78-81C* +1.2 m	9(?)	10	130	2800	nd	-	-	medium grey oolitic ls; sparry cal, sp
	KQ-78-81D* +3 m	7	67	320	170	-	-	-	medium grey oolitic ls, sparry cal, py
	KQ-78-81E* +4.2 m	8.8	2	6	57	-	-	-	medium to pale grey crystalline oolitic ls; sparry cal, tr py
16) Pomquet River	KQ-79-1A 0	13	52	15	220				medium brown-grey, crystalline dol ls
	KQ-79-1B +90 cm	6.2	41	20	210				medium brown-grey, crystalline dol ls
	KQ-79-1C +2.1 m	7	220	32	120				medium brown-grey, crystalline dol ls; tr cp
	KQ-79-1D +2.7 m	9	740	29	110	nd	-	-	mottled medium brown oolitic ls; cp
	KQ-79-1E +3 m	7	1040	25	120	nd	-	-	pale brown, crystalline dol ls; sparry cal, cp
	KQ-79-1F +3.5 m	4	370	15	68	-	-	-	medium brown, crystalline dol ls; tr cp
	KQ-79-1G +3.6 m	5.7	850	20	82	-	-	-	medium brown, crystalline oolitic ls; cp
	KQ-79-1H +3.9 m	5.8	570	15	63	nd	-	-	medium brown, crystalline ls; sparry cal, tr cp
	KQ-79-1I +4.5 m	3.6	630	10	78	-	-	-	medium brown, crystalline ls, sparry cal, tr mala
	KQ-79-1J +6 m	9	470	46	47	-	-	-	medium brown-grey, crystalline oolitic ls; cp
	KQ-79-1K +6.1 m	12	330	32	62	nd	-	-	medium brown-grey, crystalline oolitic ls; cp
	KQ-79-1L +6.5 m	6	310	49	26	-	-	-	medium brown-grey, crystalline oolitic ls; cp
	KQ-79-1M +7.2 m	6	270	10	68	-	-	-	pale brown, crystalline dol; sparry cal, cp
	KQ-79-1N +7.5 m	12.5	360	22	49				medium brown-grey, crystalline dol ls; cp
	KQ-79-1O +7.8 m	15(?)	1030	20	120				medium brown-grey, crystalline oolitic ls; cp
	KQ-79-1P +8.5 m	5.5	6	nd	33				mottled pink and pale green fg ss
18) Monastery Brook	KQ-78-88A* -10 m	4.1	3	nd	25	-	-	-	mottled pale and medium red-grey, fg ark
	KQ-78-88B* -7 m	2	2	nd	23	-	-	-	medium red-grey ark
	KQ-78-88C* -60 cm	4.5	480	25	120	-	-	-	pale to medium grey and red-grey ark; py
	KQ-78-88D* +5 cm	11.5	530	60	7	<1	-	-	black, slightly fenestral micritic ls; cp
	KQ-78-88DD* +5 cm	8	230	13	7	nd	-	-	black, slightly fenestral ls; cp
	KQ-78-88E* +25 cm	7	620	18	12	-	-	-	dark grey slightly fenestral ls; cp
	KQ-78-88F* +40 cm	12	700	13	13	-	-	-	black, crystalline micritic ls; cp
	KQ-78-88G* +50 cm	7	360	nd	16	nd	-	-	black, crystalline micritic ls; cp
	KQ-78-88H* +1.3 m	9.2	20	nd	13	-	-	-	dark grey, crystalline bioclastic ls; tr cp
	KQ-78-88I* +1.5 m	11	12	7	6	-	-	-	medium brown-grey, crystalline oolitic ls
	KQ-78-88J* +2 m	11.5	7	nd	8	nd	-	-	dark grey, crystalline micritic ls; tr cp
	KQ-78-88K* +4.2 m	4.4	6	nd	18	-	-	-	medium to dark grey, crystalline micritic ls
	KQ-78-88L* +6.6 m	9.4	41	10	11	nd	-	-	medium grey, crystalline micritic ls; tr cp
23) Limestone Point Limestone - roadcut quarry south of church	KQ-78-93* -1	2.5?	8	3250	1310	nd	-	-	dark grey bioclastic ls; gn, sp
	KQ-78-93*-2	6.5	8	3300	520	1	-	-	dark grey to black bioclastic micritic ls; gn
	KQ-78-93*-3	6.3	6	3720	580	nd	-	-	dark grey to black micritic ls; algal balls, gn, sp
- inland quarry	KQ-78-99A*	9.1	14	7	11	-	-	-	pale oolitic ls; tr py
	KQ-78-99B*	13.4	53	38	35	-	-	-	pale oolitic ls; tr cp
	KQ-78-99O*	5.3	12	19	54	-	-	-	pale onocolitic-bioclastic ls
- roadcut opposite church	KQ-78-100A* 0	4.4	33	2020	970	1	-	-	dark grey to black oolitic ls; gn, sp
	KQ-78-100B* +30 cm	4.4	14	2430	520	1	-	-	dark grey oolitic ls; gn, sp
	KQ-78-100C* +60 cm	4.3	560	350	170	nd	-	-	medium to dark grey oolitic ls; sparry cal, cp, py
	KQ-78-100D* +90 cm	6.5	12	36	56	-	-	-	medium to dark grey oolitic ls; sparry cal
	KQ-78-100E* +1.8 m	5.5	4	94	32	-	-	-	dark grey oolitic ls; sparry cal
	KQ-78-100F* +2.1 m	4.3	2	42	30	-	-	-	medium brown-grey oolitic ls; sparry cal

[1] Localities are shown on Figures 1 and 9.

[2] Measurements are either depths in drill holes, distances above or below basal contacts of limestones or distances above bases of outcrops where the basal contacts of the limestones are not exposed.

[3] Length of sample in centimetres.

[4] Values are expressed in parts per million.

[5] D. Murray (1975, p. 140) stated that disseminated galena occurred in brecciated siltstone from 59 to 62.4 feet, but no core from this interval was available for the writer to sample.

[6] KQ-84-65 and 66 are from faulted segments of the same limestone a few 10s of metres apart.

[7] "FT" indicates sample with abundant tetrahedrite.

Abbreviations: ark = arkose; cal = calcite; cg = conglomerate; cm = centimetre; cp = chalcopyrite; dol = dolomite; fg = fine-grained; fos = fossiliferous; gn = galena; gyp = gypsum; ls = limestone; m = metre; mala = malachite; mudst = mudstone; nd = not detected; py = pyrite; siltst = siltstone; sp = sphalerite; ss = sandstone; tetrah = tetrahedrite, and tr = trace.

The results indicate that, although metal values are low, base metals in anomalous amounts are widely distributed in upper Windsor Group limestones. Locality 8 near Eureka, Nova Scotia (Fig. 69.9) contains elevated levels of Co and Ni and locally slightly elevated concentrations of Ag (Table 69.1). Faint pink stains on limestone outcrops in the Eureka area were amphorous to X-ray diffraction and no cobalt was identified with the Energy Dispersive System of an Electron Microscope.

Mineral genesis

Early infiltration of oxidized metalliferous brines into anoxic limestones before they lost their permeability best fits the data for these occurrences. The brines were probably derived from evaporites in the basins, extracted metals from the redbeds, migrated through the permeable parts of the limestones and precipitated their metals either by reacting with H_2S gas or early-formed pyrite.

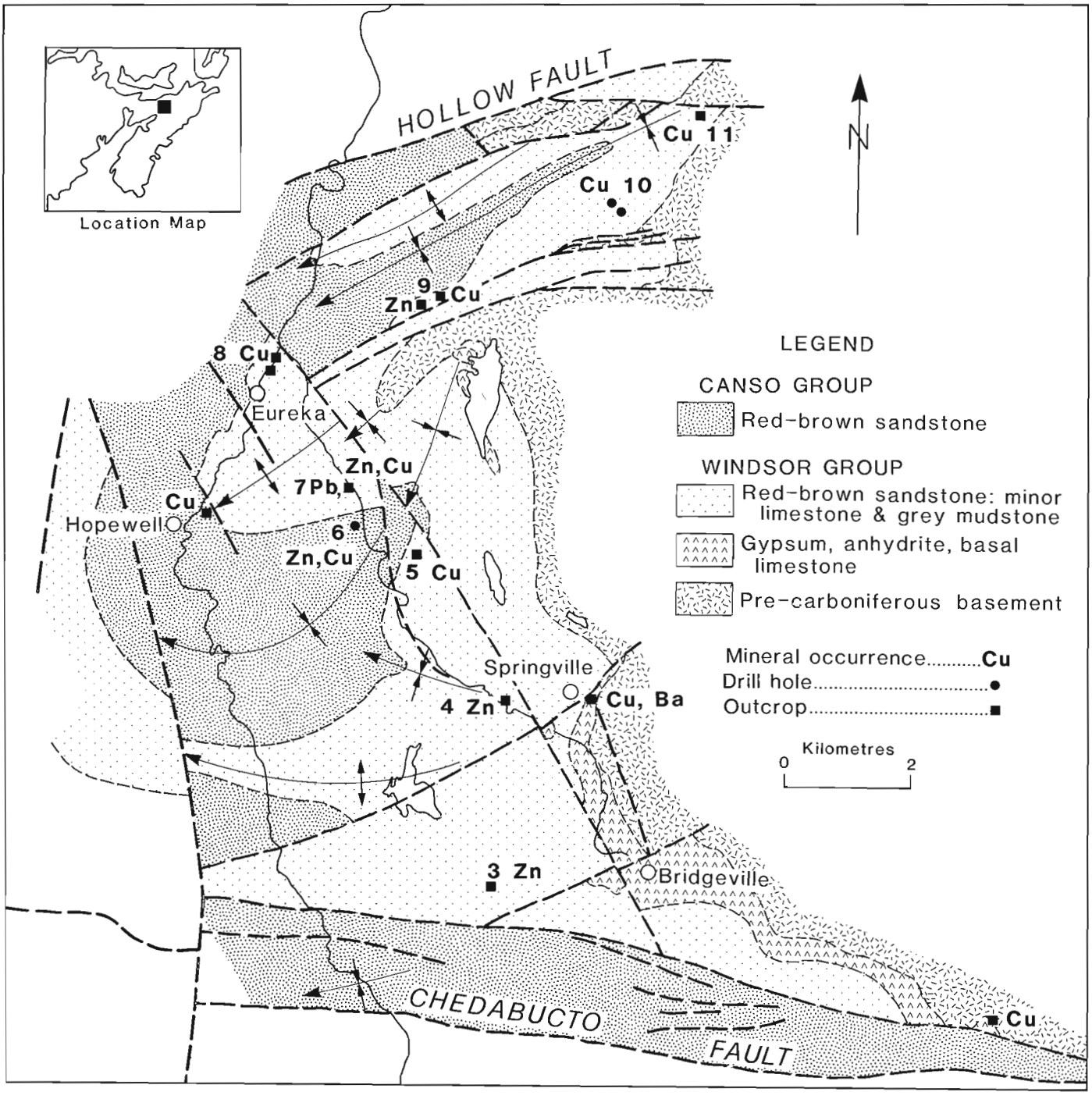

Figure 69.9. *Geology of the Eureka area Nova Scotia (generalized after Giles, 1982, and Benson, 1967), and base metal occurrences.*

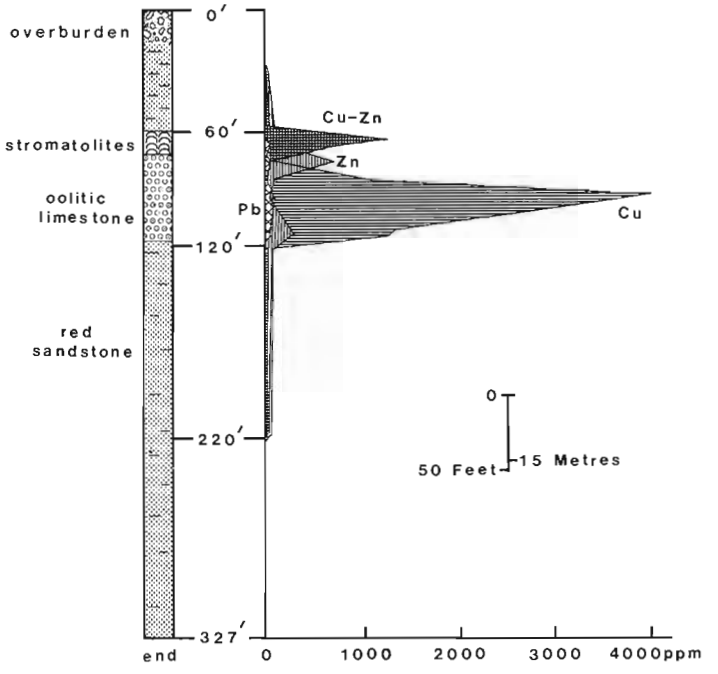

Figure 69.10. *Geological section and base metal distribution in McLellan Brook Hole 1, Nova Scotia (loc. 10, Fig. 69.9).*

Some limestones, such as those at Hopewell Cape in New Brunswick (loc. 1), show evidence of high energy intertidal environments with well-developed, columnar stromatolite colonies in crossbedded, siliceous oolitic grainstones. Others such as the Ardness Limestone at Knoydart Point (loc. 13) and The Island roadcut (loc. 5) in Nova Scotia show evidence of high energy shoals with large, well-formed ripples in ooid grainstones, and others such as the Crawley Limestone near Sydney, Nova Scotia (loc. 24) and at Shallop Cove, Flat Bay, Newfoundland (loc. 27) contain calcretes and pisolitic units indicative of periodic subaerial exposure. None of these environments would have been conducive to syngenetic metal precipitation. On the other hand, sub-tidal argillaceous limestones, in which one might expect syngenetic sulphides, tend to be low in base metals. The calcretes, pisolites and other subaerially exposed units would have retained little primary organic matter, as they would have been oxidized. Therefore, much of the organic matter and sulphides in some of these dark limestones must have been added after the limestones were buried. The carbonaceous material was probably derived from deeper in the basins from the same limestones, because in many areas these limestones are under- and overlain by redbeds with no other obvious source of organic material.

An important factor in understanding the distribution of lithofacies is the distinct possibility that the basins were below sea level. This is a similar model to that proposed for the basal Windsor transgression (Kirkham, 1978; Geldsetzer, 1978) and discussed by Giles (1981), in conjunction with eustatic changes in sea level, to explain all

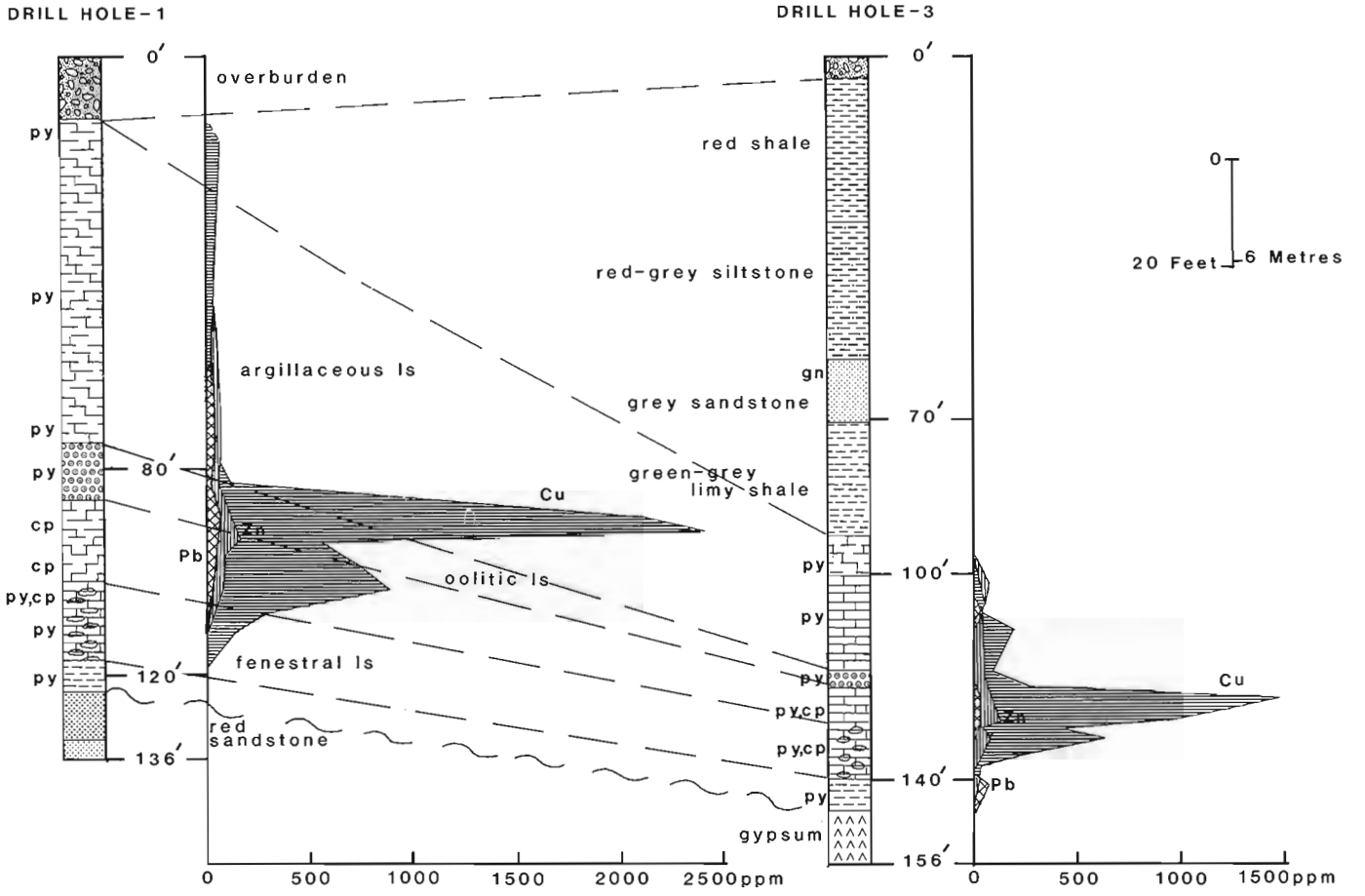

Figure 69.11. *Sketched sections of hole 1 and 3, Limerock, Nova Scotia (loc. 2) showing base metal distribution. Locations of holes and additional geological information is given by Giles (1979) and Murray (1975).*

Windsor transgressions. These were probably low-latitude desert basins that were invaded periodically by the sea. This feature is strongly supported by the fact that at several localities essentially identical fluvial lithofacies both underlie and overlie the marine limestones indicating that as soon as the sea retreated very similar continental sedimentary environments returned. The major exception is the initial Windsor transgression that was of a much greater magnitude than subsequent transgressions. The first Windsor transgression filled the desert basins to considerable depth and overstepped their margins onto adjacent basement areas completely drowning the continental sediment source areas (Kirkham, 1978; Giles et al., 1979).

In extreme marginal areas the limestones tend to be barren, reddish and oxidized. In adjacent, more basinal positions they are reduced and contain chalcopyrite and in the deeper parts of the basins, where they are part of a thicker marine sequence with mudstones and evaporites, they contain sphalerite or pyrite as the dominant sulphide. Galena possibly occurs intermediate between chalcopyrite and sphalerite at some localities but from preliminary examinations it does not seem to be as abundant as either chalcopyrite or sphalerite.

The vertical distribution of sulphides was probably dependent on several depositional and diagenetic factors, including availability of reductants, fluid flow, with both lateral and vertical components, and original permeability. The dark, carbonaceous, sulphurous limestones and associated marine mudstones were probably the main reduced units in the sequence. However, the distribution of reduced units is complicated by the presence of grey fluvial sandstones containing wood trash and early pyrite, and by the repetition of several reduced marine units of variable thicknesses interlayered with the redbeds. These reduced units, probably acted as "chemical filters", to varying degrees, which extracted metals en route before they reached the main reduced units. A number of minor redbed copper occurrences below and above the Ardness Limestone near Knoydart Point (loc. 13) may explain why zinc is prevalent and copper is subordinate in the oolitic limestone at this locality (Fig. 69.12).

If fluid flow had a significant vertical component, then in areas containing several reduced limestones, the lower limestones should contain more copper and higher limestones should contain more lead and zinc. Analyses for the limestone sampled in the Eureka reference diamond drill hole (loc. 6) indicate anomalous copper values near the top and bottom of the limestone with higher zinc values in the central part of the unit (Fig. 69.13). This feature is compatible with the metal-bearing fluids entering the limestone from both sides and not solely from the bottom. One limestone examined in the Woodbine reference diamond drillhole (loc. 20), is underlain by dark pyritic shale yet contains traces of chalcopyrite for 10 to 20 cm above the shale and minor sphalerite scattered throughout the limestone for a few metres above. Such occurrences well within the evaporite basin could suggest lateral rather than vertical migration of base metal-bearing fluids through more permeable parts of the limestones. The preference of base metal sulphides for oolitic and stromatolitic limestones instead of micritic and argillaceous limestones was probably mainly a function of original permeability. With these factors in mind, each locality probably has somewhat different controls on metal distribution and zoning.

Figure 69.14 illustrates the general geological settings of the occurrences. Several marine transgressive carbonate-evaporite cycles in basins below sea level are shown. The Antigonish Highlands horst block is depicted to indicate tectonic activity during deposition of the Windsor Group probably during approximately B or C subzone time. The

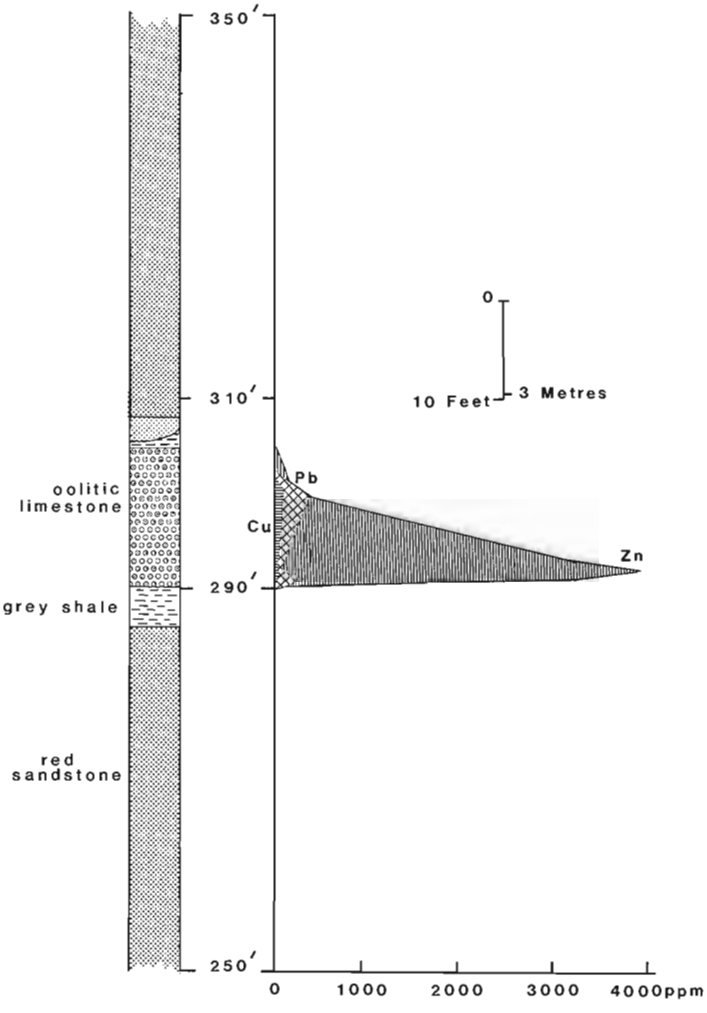

Figure 69.12. *Geological section and preliminary base metal distribution in Ardness Limestone, coastal exposure, Knoydart Point, Nova Scotia (loc. 13).*

reference area to document this uplift is the Antigonish Highlands block from the west side of the main Antigonish basin (Boehner and Giles, 1982) to southwest of Eureka, Nova Scotia. Possibly the Port au Port Peninsula block in western Newfoundland was also active at this time or slightly later.

General patterns of metal distribution are illustrated with copper dominant in grey fluvial sandstone in the redbeds and marginal marine sediments in close contact with redbeds. Lead and zinc tend to prevail farther out in the basins and only barren pyritic units occur in the central parts of the basins where most of the section is reduced. Although certain elements of this distribution such as the close association of copper with redbeds, are well documented, the general model is preliminary and speculative. Factors, such as the precise timing and duration of the mineralizing event(s), the amount of fluids involved and their metal contents, the source(s) of the metals and the processes that cause fluids to migrate, are poorly known. However, such factors are critical for developing predictive models that would be useful in exploration.

Oolitic limestones have not generally been identified as common hosts for sediment-hosted stratiform copper deposits. However, Perty and Wazny (1980) described low-grade copper in oolitic, bioclastic and stromatolitic shoals near higher grade copper which occurs in argillaceous,

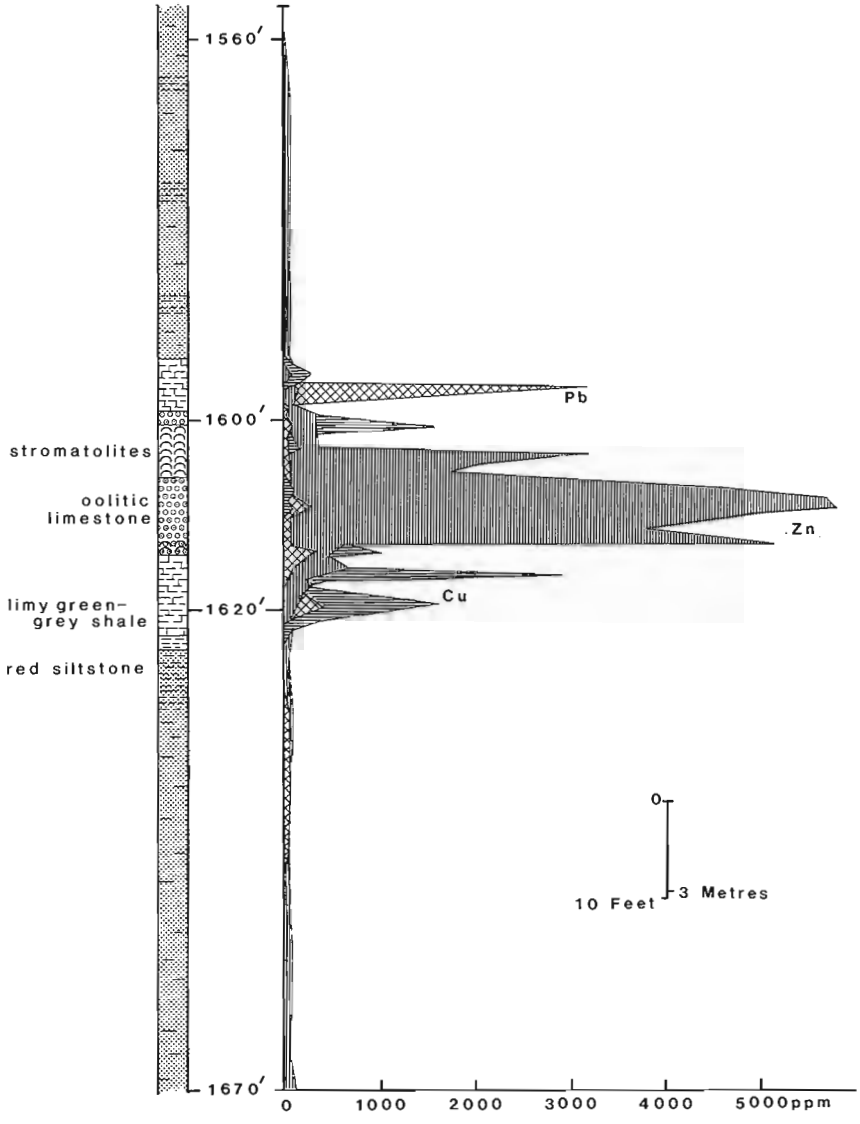

Figure 69.13. *Geological section and base metal distribution in part of Eureka Hole 1, Nova Scotia (loc. 6, Fig. 69.9).*

micritic limestone occupying depressions near the base of the Upper Permian Zechstein sequence in Poland. In addition, Lange and Eby (1981) have described minor copper-silver occurrences in oolitic beds in the Proterozoic Belt Supergroup in Montana, and Nishioka et al. (1984) have described minor amounts of native copper in thin oolitic beds associated with stromatolites in the Late Precambrian Copper Harbour Conglomerate redbed sequence in Michigan. Furthermore, Bottrill in 1980 and Kavanaugh in 1982 (personal communications) have informed the writer of copper and silver associated with minor lead and zinc in Cretaceous(?) oolitic limestones interlayered with redbeds in Salta Province, northern Argentina. These examples suggest that oolitic limestones and associated lithofacies are not uncommon hosts for sedimentary copper occurrences.

Conclusions

Minor amounts of base metal sulphides are widely distributed in upper Windsor (Codroy) Group limestones. The base metal sulphides tend to be disseminated in the matrix and voids and are probably products of early diagenetic infiltration of metalliferous, oxidized brines which reacted with H_2S gas and/or early diagenetic pyrite in anoxic units within red bed sequences. These features and general settings are consistent with a sedimentary copper environment of formation which has produced many economically important deposits in other parts of the world.

Some of the showings studied to date have reasonable thicknesses ranging up to 10 m or more and evidence of significant lateral continuity, such as in the Eureka area, Nova Scotia (Fig. 69.9), but none of the occurrences have grades that approach economic concentrations (i.e. assuming that about 1 to 2% Cu equivalent would be necessary in large deposits amenable to highly mechanized, low-cost mining in Atlantic Canada). Although the low metal contents of the occurrences are discouraging, so little is known about their overall nature and metal variations that more work is required before their potential can be assessed properly. Chalcocite and bornite are noteworthy by their absence. Perhaps if chalcocite and/or bornite-dominated sulphide assemblages could be found, they might be of higher grade. A well documented feature of economic sedimentary copper deposits is that chalcocite and/or bornite are essential minerals, even though chalcopyrite might also be important.

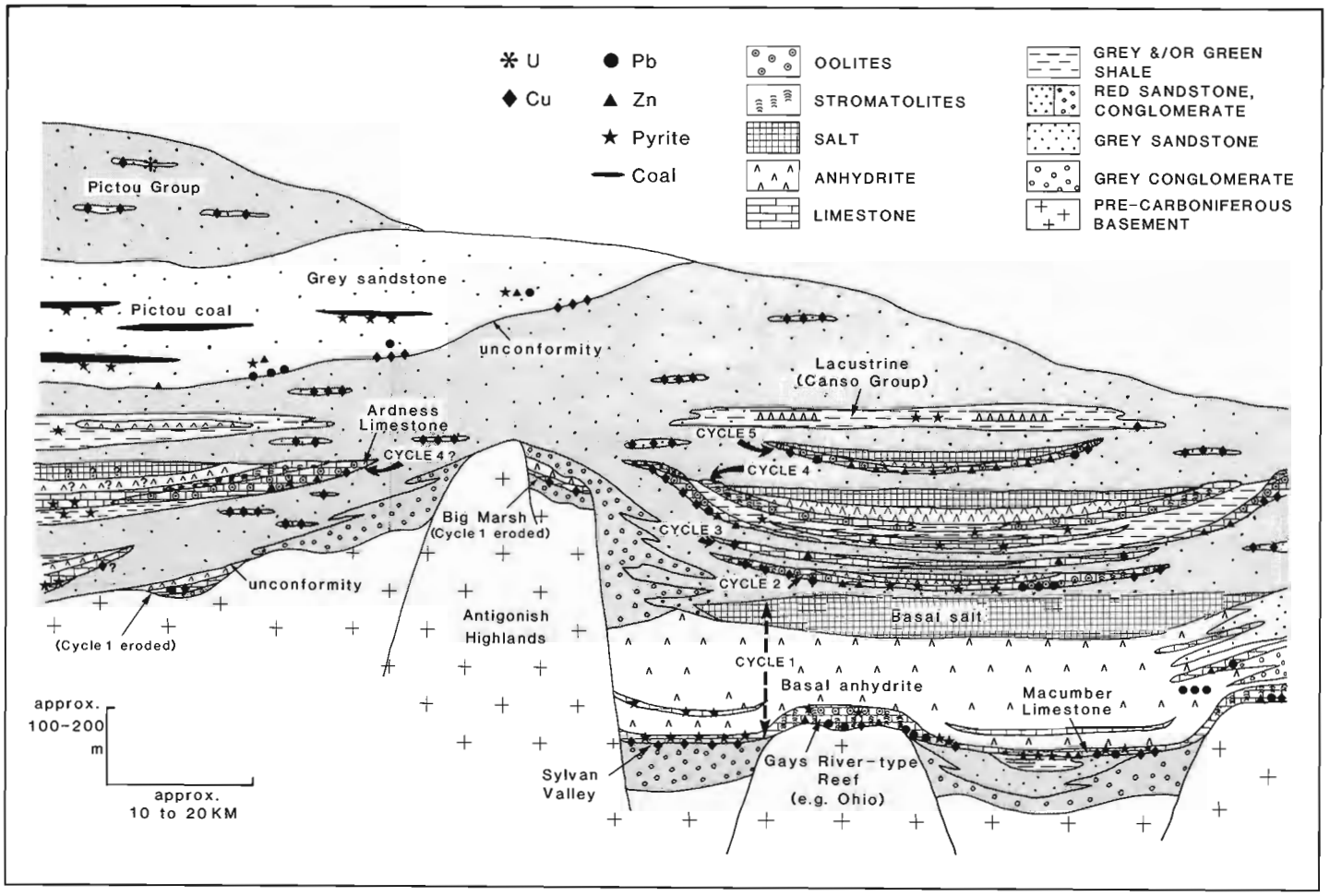

Figure 69.14. *Generalized, speculative geological section through typical Carboniferous basin depicting general stratigraphic setting and typical sites of base metal accumulation. Cycles refer to carbonate-evaporite cycles referred to in text.*

At this time moreover, insufficient data are available to eliminate the possibility that nearby lithofacies might be more favourable hosts for copper than the oolitic and stromatolitic units emphasized in this paper. Such facies relationships evidently have been established for the very large Lubin deposit in Poland (Peryt and Wazny, 1980).

Acknowledgments

This study would not have been possible without the help and cooperation of many people. J. MacLeod of Esso Minerals Canada, L. Decker of Chevron Canada Resources, P. Giles and R. Boehner of the Nova Scotia Department of Mines and Energy, I. Knight of the Newfoundland Department of Mines and Energy, and H. Geldsetzer of the Geological Survey of Canada all provided information on mineralized localities. P. Giles and R. Boehner also provided stimulating discussions on the geology of the Windsor Group. G. Darcy, for many years, has helped the writer by very efficient processing of samples. G. Young, S. Green, J.J. Carriere and K. Nguyen kindly helped draft the diagrams.

C.W. Jefferson and W.D. Sinclair reviewed the manuscript and made many useful comments.

References

Bell, W.A.
1929: Horton-Windsor district, Nova Scotia; Geological Survey of Canada, Memoir 155, 268 p.

Benson, D.G.
1967: Geology of Hopewell map-area, Nova Scotia; Geological Survey of Canada, Memoir 343, 58 p.

Binney, W.P.
1975: Copper occurrences in Lower Carboniferous sedimentary rocks of the Maritime Provinces; Geological Survey of Canada, Open File 281, 156 p.

Binney, W.P. and Kirkham, R.V.
1975: A study of copper mineralization in Mississippian rocks of the Atlantic Provinces; in Report of Activities, Part A, Geological Survey of Canada, Paper 75-1A, p. 245-248.

Boehner, R.C. and Giles, P.S.
1982: Geological map of the Antigonish Basin, Nova Scotia; Nova Scotia Department of Mines and Energy.

Geldsetzer, H.H.J.
1978: The lower Windsor of Cape Breton Island, Nova Scotia, Canada: An early Carboniferous basin of a Zechstein-type? (abstract); Geological Society of America, Abstracts with Programs, Northeast Section, p. 43.

Giles, P.S.
1979: Upper Windsor limestone at Limerock, Pictou County; in Report of Activities 1978, Nova Scotia Department of Mines, Report 79-1, p. 79-80.

1981: Major transgressive-regressive cycles in Middle to Late Viséan rocks of Nova Scotia; Nova Scotia Department of Mines and Energy, Paper 81-2, 27 p.

1982: Geological map of the Eureka area, central Nova Scotia, Nova Scotia Department of Mines and Energy.

Giles, P.S., Boehner, R.C., and Ryan, R.J.
1979: Carbonate banks of the Gays River Formation in central Nova Scotia; Nova Scotia Department of Mines and Energy, Paper 79-7, 57 p.

Kirkham, R.V.
1973: Environments of formation of concordant and peneconcordant copper deposits in sedimentary sequences (abstract); Canadian Mineralogist, v. 12, pt. 2, p. 145-146.

1978: Base metal and uranium distribution along the Windsor-Horton contact, central Cape Breton Island, Nova Scotia; in Current Research, Part B, Geological Survey of Canada, Paper 78-1B, p. 121-135.

1980: Copper occurrences in Carboniferous sedimentary sequences of the Atlantic Provinces (abstract); Geological Association of Canada-Mineralogical Association of Canada, Annual Meeting, Program with Abstracts, v. 5, p. 66.

Knight, I.
1983: Geology of the Carboniferous Bay St-George subbasin, western Newfoundland; Newfoundland and Labrador Department of Mines and Energy, Mineral Development Division, Memoir 1, 358 p.

Lange, I.M. and Eby, D.E.
1981: Stratabound copper-silver-bearing oolitic deposits in the Belt Supergroup of Montana; Economic Geology, v. 76, p. 933-937.

Mamet, B.L.
1970: Carbonate microfacies of the Windsor Group (Carboniferous), Nova Scotia and New Brunswick; Geological Survey of Canada, Paper 70-21, 121 p.

McCutcheon, S.R.
1981: Stratigraphy and paleogeography of the Windsor Group in southern New Brunswick; New Brunswick Department of Natural Resources, Mineral Resources Division, Open File Report 81-31, 210 p.

Murray, D.A.
1975: Limestones and dolomites of Nova Scotia. Part II – Antigonish, Guysborough, Pictou and Cumberland Counties; Nova Scotia Department of Mines, Bulletin No. 2, 155 p.

Nishioka, G.K., Kelly, W.C., and Elmore, R.D.
1984: Copper occurrences in stromatolites of the Copper Harbor Conglomerate, Keweenaw Peninsula, northern Michigan; Economic Geology, v. 79, p. 1393-1399.

Peryt, T.M. and Wazny, H.
1980: Microfacies and geochemical development of the basin facies of the Zechstein Limestone (Ca 1) in western Poland; Contributions to Sedimentology, p. 279-306.

von Bitter, P.H.
1976: Paleoecology and distribution of Windsor Group (Viséan-?early Namurian) conodonts, Port Hood Island, Nova Scotia, Canada; Geological Association of Canada, Special Paper 15, p. 225-241.

von Bitter, P.H. and Plint-Geberl, H.A.
1982: Conodont biostratigraphy of the Codroy Group (Lower Carboniferous), southwestern Newfoundland, Canada; Canadian Journal of Earth Sciences, v. 19, p. 193-221.

-70-

LOWER DEVONIAN RUGOSE CORALS OF LOCHKOVIAN AGE FROM YUKON TERRITORY

Project 680093

A.E.H. Pedder
Institute of Sedimentary and Petroleum Geology, Calgary

Pedder, A.E.H., Lower Devonian rugose corals of Lochkovian age from Yukon Territory; in Current Research, Part A, Geological Survey of Canada, Paper 85-1A, p. 587-602, 1985.

Abstract

The mucophyllid genus ***Stylopleura*** *and the spongophyllid genus* ***Carlinastraea*** *are revised. In western and arctic North America, the temporal ranges of these genera overlap in Lochkovian time.* ***Stylopleura julli*** *and* ***Carlinastraea pygmaea*** *are established as new species.* ***Carlinastraea halysitoides*** *(Etheridge) is revised, and is shown to have had a remarkable geographic range, that, in Lochkovian time, extended from eastern Australia, through China, Mongolia, Asiatic Russia, the Urals, Yukon Territory and British Columbia, to Nevada. An early Pragian coral from Victoria and New South Wales, eastern Australia, is discussed and figured under the name of* ***Carlinastraea*** *sp. cf.* ***C. halysitoides*** *(Etheridge).*

Résumé

Les genres mucophyllide ***Stylopleura*** *et spongophyllide* ***Carlinastraea*** *sont révisés; au cours du Lochkovien, leurs extensions géochronologiques se chevauchent dans les parties ouest et arctique de l'Amérique du Nord. Deux espèces nouvelles,* ***Stylopleura julli*** *et* ***Carlinastraea pygmaea****, sont fondées, tandis que la révision de* ***Carlinastraea halysitoides*** *(Etheridge) met en évidence sa remarquable répartition géographique pendant le Lochkovien: est de l'Australie, Chine, Mongolie, Russie d'Asie, Oural, Territoire du Yukon, Colombie-Britannique, Nevada. Un corail du début du Pragien des États de Victoria et de Nouvelle-Galles du Sud, dans l'est de l'Australie, est discuté et figuré sous le nom de* ***Carlinastraea*** *sp. cf.* ***C. halysitoides*** *(Etheridge).*

Introduction

Stylopleura and **Carlinastraea** are late Silurian to early Devonian coral genera that are known from most of the regions comprising the Devonian Old World Faunal Realm. In western North America, they range from Nevada, through Yukon Territory, to the Canadian Arctic Archipelago. Their temporal ranges overlap in the earliest Devonian stage, that is in Lochkovian time, so that co-occurrences of the two genera, in any fauna from these regions, is good evidence of Lochkovian age.

The present paper is a contribution toward the understanding of **Stylopleura** and **Carlinastraea** (see Plate 70.1). Three species are described, and two forms are discussed informally. Two of the described species, **Stylopleura julli** and **Carlinastraea halysitoides**, hold exceptional promise as index fossils.

Systematic paleontology

Family MUCOPHYLLIDAE Hill, 1940

Remarks. The family Mucophyllidae was proposed by Hill (April, 1940a, p. 156-157) for **Mucophyllum**, **Pseudamplexus** and several possible synonyms of **Pseudamplexus**. The proposal was accompanied by a thorough discussion of the new family, including the designation of **Mucophyllum** as the type genus. Five months later, Hill (September, 1940b, p. 399) had occasion to refer to the family again, but, in response to Lang, Smith and Thomas' (1940, p. 87) emendation of Etheridge's generic name of **Mucophyllum** to **Mycophyllum**, cited it as Mycophyllidae Hill, 1940. Although both emendations were illegal, they have been upheld by many subsequent authors. In the revised Kansas treatise on corals (Hill, 1981, p. 175), the family name of Mycophyllidae Hill, 1940, is rejected on the grounds that it was based on an invalid junior synonym. However, the reinstated name of Mucophyllidae is attributed erroneously to Soshkina (1947, p. 761). The correct authorship is Hill, 1940.

Genus **Stylopleura** Merriam, 1974

Stylopleura Merriam, 1974, p. 34-35.

Type species. **Stylopleura berthiaumi** Merriam, 1974, p. 35, Pl. 3, figs. 6-20. Most of the original material, including the holotype, came from the upper part of Unit 3 of the Roberts Mountains Formation on upper Pete Hanson Creek, northwestern side of Roberts Creek Mountain, central Nevada. Merriam believed the type horizon to be Silurian ("Silurian coral zone D"). In fact, it is very near the top of the Roberts Mountains Formation, and is Lochkovian (Klapper and Murphy, 1975).

Additional species. **Calophyllum phragmoceras** Salter, 1852, p. ccxxx, Pl. 6, figs. 4, 4a (provisional assignment). **Amplexus (Coelophyllum) eurycalyx** Weissermel, 1894, p. 634-638, text-figs. 1, 2, Pl. 50, figs. 8, 9; Pl. 51, fig. 1. **Tryplasma liliiforme** Etheridge, 1907, p. 95-97, Pl. 14, figs. 2, 3; Pl. 15, figs. 2, 3; Pl. 17, figs. 7, 8; Pl. 24, fig. 1; Pl. 25, fig. 8; Pl. 27, figs. 1, 2 (also Hill, 1940b, p. 401, Pl. 11, figs. 18, 19; Pl. 12, figs. 3-6). **Zelophyllum subdendroideum** Zheltonogova, 1961, p. 84, 162, Pl. S-21, figs. 2a, b. **Stylopleura nevadensis** Merriam, 1974, p. 35-36, Pl. 2, figs. 11, 12, 15, 16; Pl. 15, figs. 1-4 (also Merriam and McKee, 1976, Pl. 2, figs. 3-6). **S. julli** sp. n.

Distribution. Ludlow of New South Wales and Devon Island (Canadian Arctic Archipelago); Pridolian of Yukon Territory; Lochkovian of New South Wales, Salair, Baillie Hamilton Island (Canadian Arctic Archipelago), Yukon Territory, western District of Mackenzie and Nevada; early Pragian of New South Wales; glacial drift of northern Germany.

G.M. Bradley (in Pickett, 1982, p. 180) listed **Mucophyllum liliiforme** in the fauna of the Tanwarra Shale of New South Wales. The age of the Tanwarra Shale is regarded as late Llandovery to Middle Wenlock. If the species identification is correct, this is the earliest known occurrence of **Stylopleura**.

Description. In early stages, the protocorallite is subcylindrical to ceratoid; at maturity, it develops a flaring, trumpet-like calice, around which as many as 11 offsets may develop simultaneously. Corallum increase is tabularial, although offsets inherit very little skeletal tissue from the parent, and is invariably parricidal. The change from subcylindrical, or ceratoid, to trochoid form is accompanied by, and directly related to, a change in trabecular structure from simple holacanthine (secondary?, originally monacanthine?) to compound rhabdacanthine. Both the protocorallite and offsets typically produce long support talons. The short septa are radially arranged and undifferentiated. In the narrow part of the corallite, the septa are commonly acanthine; in the expanded calice, they are low, convex, contiguous ridges. There are no dissepiments. Tabulae are more or less flat and are usually widely spaced. Many of them are complete.

Remarks. **Stylopleura** has been discussed previously by the present author (Pedder, 1976, p. 289-290). At that time, all of the material assigned to the genus was either silicified or inadequately described. Description of the microstructure given here is based on newly sectioned material.

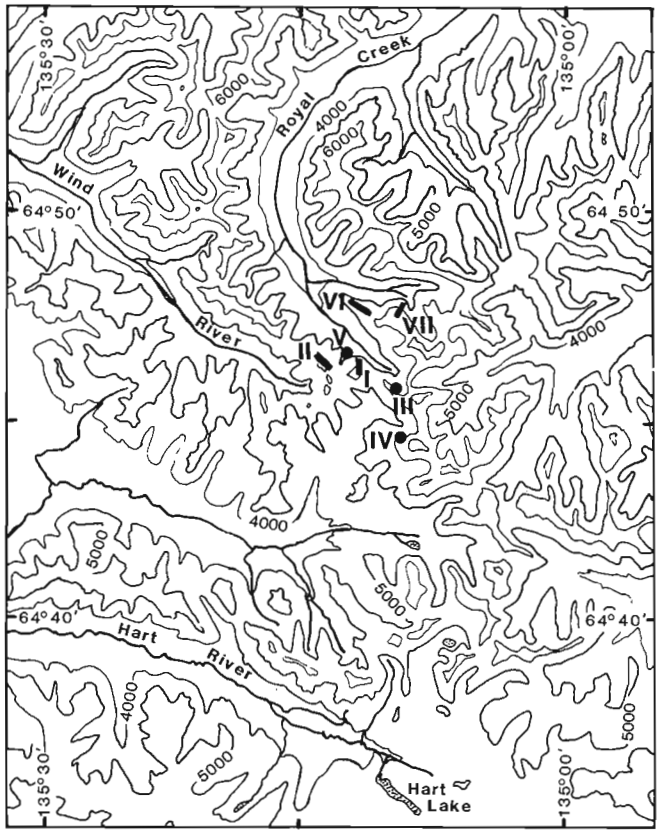

PLATE 70.1

Figure 1. Map of the Royal Creek headwaters area showing locations of the author's Royal Creek sections 1 to 7. Edition 3 of the Nash Creek 106D, 1:250 000, map sheet served as a base for this figure.

Stylopleura julli sp. n.

Plate 70.1, figures 2-7, 9, 11-23

Stylopleura sp., Pedder in Jackson and others, 1978, p. 38, Pl. 27, figs. 1-5.

Type series. Holotype, GSC 46091, from GSC loc. 69300. Four paratypes, GSC 75883 from GSC loc. 69300; GSC 75884-75886, all from GSC loc. C-6386.

Diagnosis. Species of **Stylopleura** with a maximum mean subcalicular diameter of about 30 mm, and a maximum mean calicular diameter of about 40 mm. Septal count in calicular region 60 to 68.

Description. The type material is embedded in matrix, and it is not known whether clusters of corallites are dendroid colonies, initiated by a single protocorallite, or pseudocolonies, formed from more than one protocorallite. Mature corallites are estimated to be about 6 cm long. The lower 3 to 4 cm is subcylindrical to ceratoid; the remaining calicular region is trochoid. In transverse section, most corallites are somewhat elliptical. The largest diameter at the base of the calice is 2.2 to 3.3 cm, and at the rim of the calice, 4 to 5 cm. Well preserved exteriors bear low, but sharp, interseptal ridges and broad, gently concave septal grooves. Growth ridges are faint, and there is no evidence of rejuvenescense in any of the corallites. Hollow talons are abundant, although most have been broken off close to the corallite. They are 2.0 to 2.9 mm in diameter and may be more than 3 cm long. They tend to be directed horizontally, and probably were attached to nearby organisms, rather than the substrate.

Typically, four or five offsets arise simultaneously from the inner surface of the distal region of a parental calice. Despite the marginal position of the offsets in respect to the parent, the mode of increase is tabularial, not marginarial.

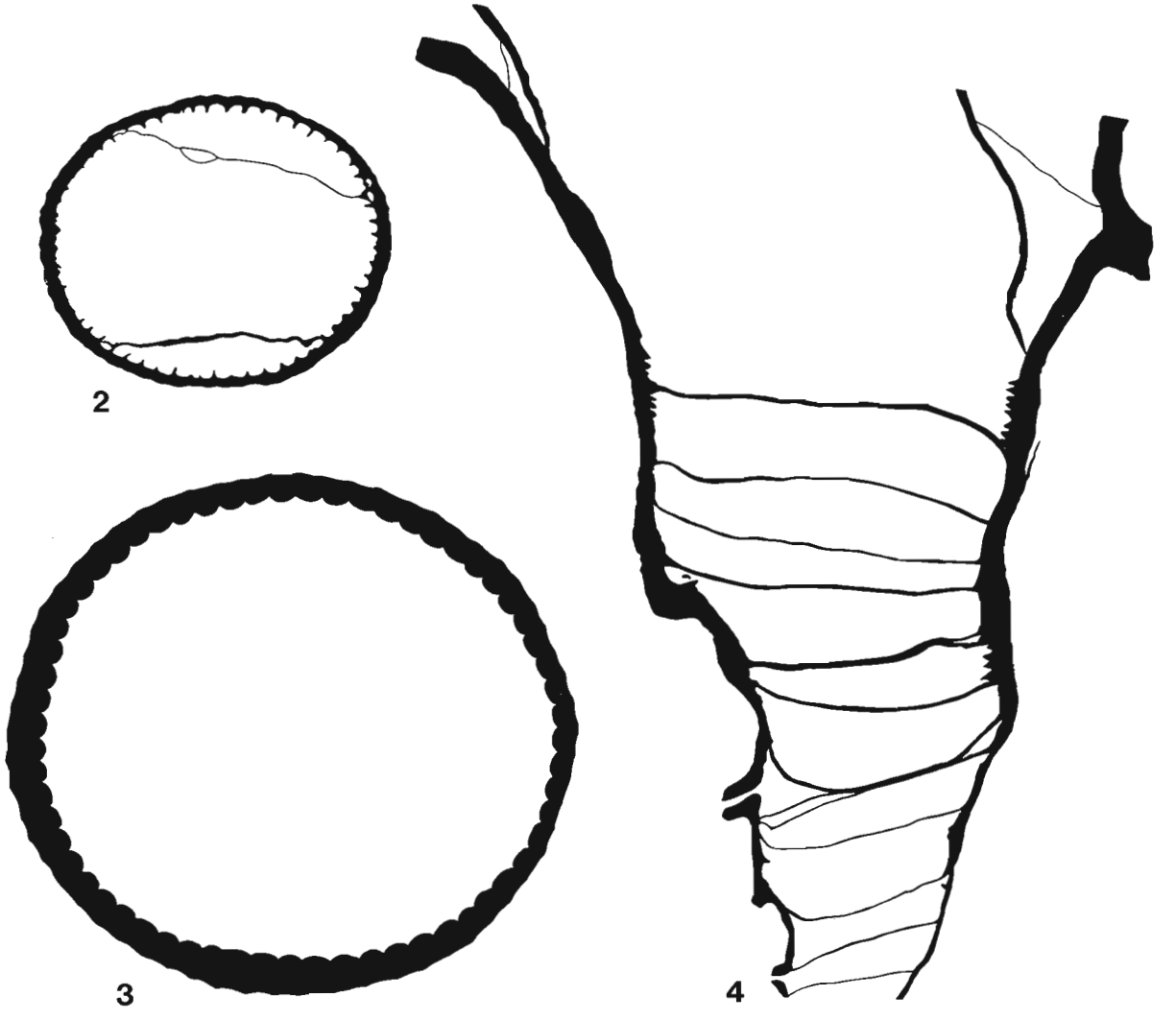

PLATE 70.1

Figures 2-4. **Stylopleura julli** sp. n., all x2.5.

2. Subcalicular transverse section of the holotype, GSC 46091.
3. Partly reconstructed calicular transverse section based on GSC 75886.
4. Longitudinal reconstruction based on GSC 46091 and 75884.

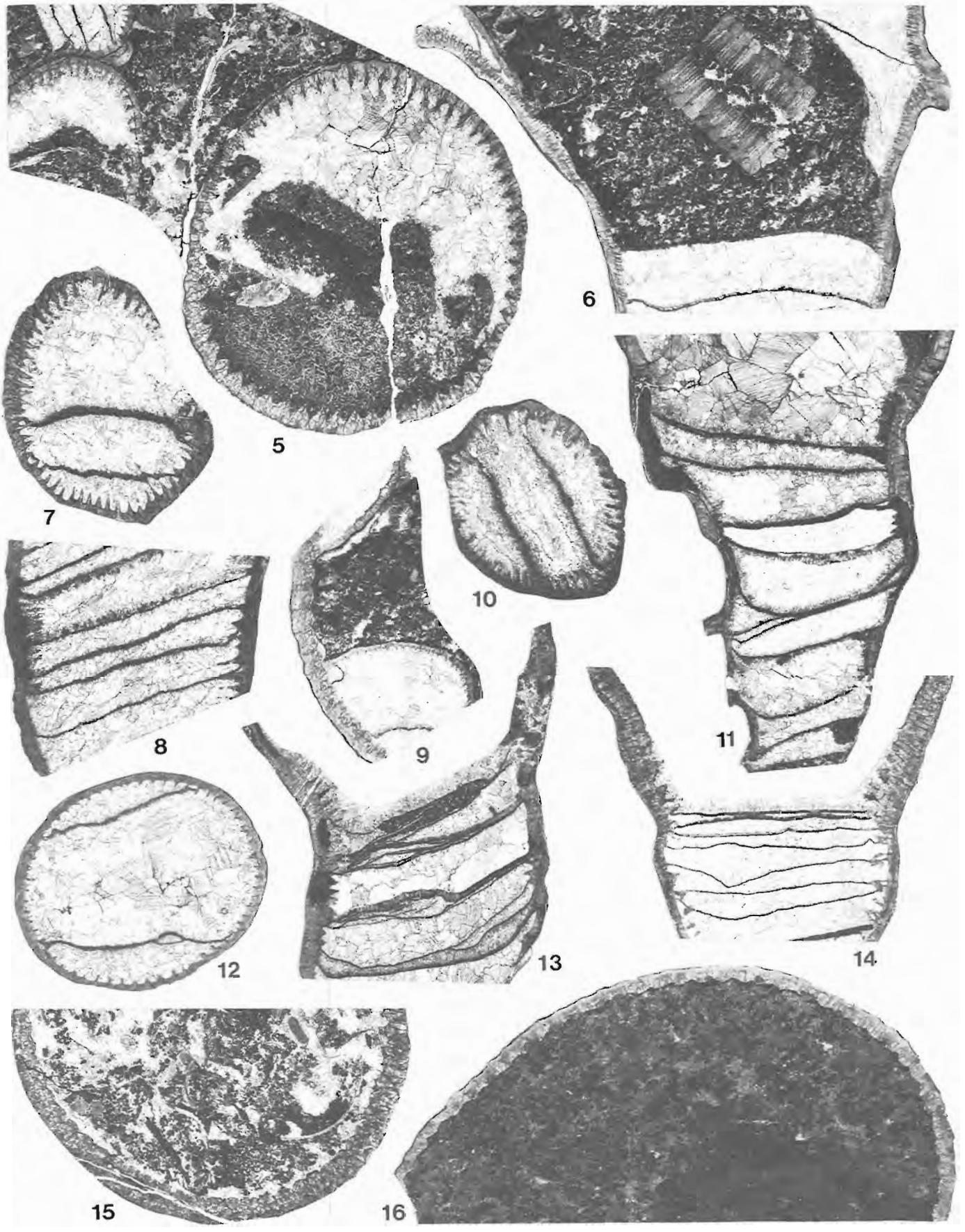
5
6
7
8
9
10
11
12
13
14
15
16

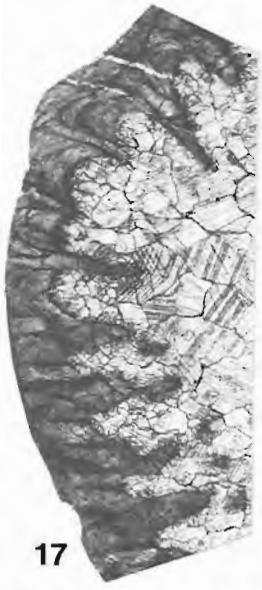



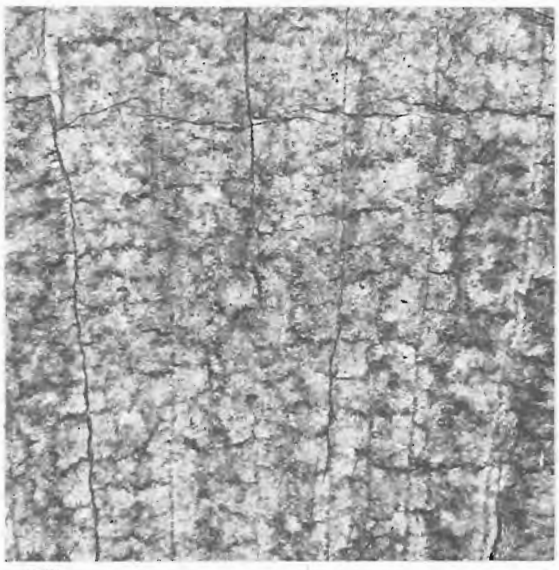





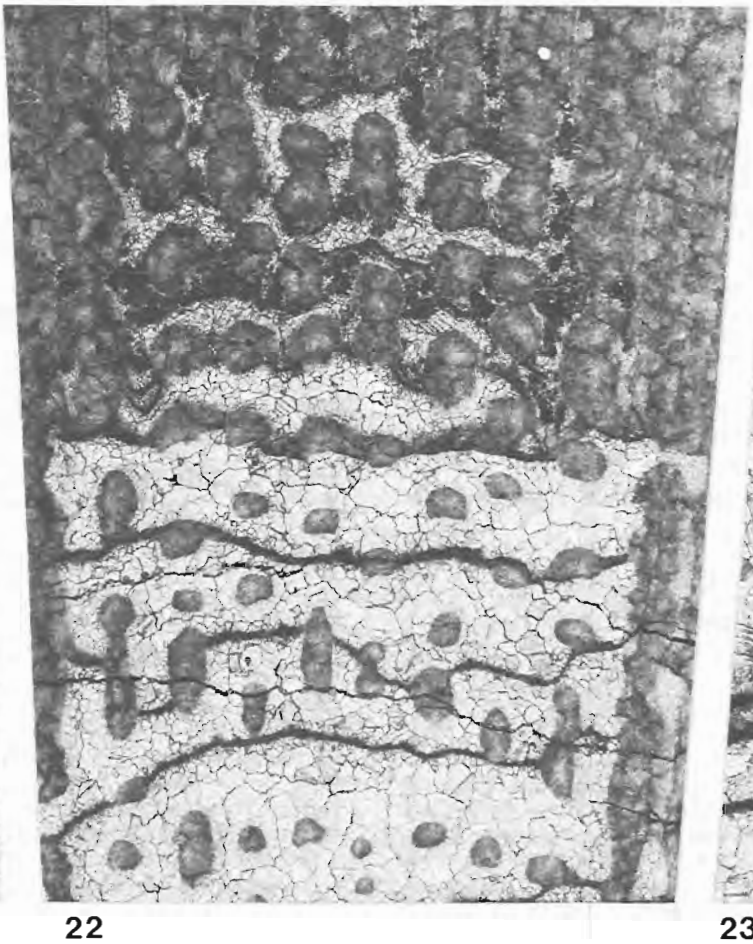



PLATE 70.1

Figures 5-7, 9, 11-16. **Stylopleura julli** sp. n., all x2.5

5, 11. Paratype, GSC 75884, transverse and longitudinal sections.

6, 9, 12. Holotype, GSC 46091, longitudinal section of calicular region cutting two offsets, transverse section of part of the calice also showing two offsets, and a subcalicular transverse section.

7, 13. Paratype, GSC 75885, transverse and longitudinal sections.

14, 15. Paratype, GSC 75886, longitudinal thin section, and part of a transverse section through the expanded calice.

16. Paratype, GSC 75883, part of a calicular section.

Figures 8, 10. **Stylopleura** sp. n. cf. **S. julli** sp. n., both x2.5.

8, 10. Figured specimen, GSC 53085.

Figures 17-23. **Stylopleura julli** sp. n., all x10.

17. Paratype, GSC 75885, part of a transverse section from below the expanded calice showing short holacanthine septal spines.

18. Holotype, GSC 46091, part of a transverse section from the unexpanded region of the corallite.

19. Paratype, GSC 75886, tangential section through part of the expanded calice showing rhabdacanthate septal structure.

20. Holotype, GSC 46091, part of a transverse section through the expanded calice showing rhabdacanthate septal structure.

21, 23. Paratype, GSC 75886, transverse sections through the wall in the lower calicular and subcalicular regions, showing transition from spinose septal structure below the calice, to nonspinose rhabdacanthate septal structure in the more distal and expanded part of the calice.

22. Paratype, GSC 75886. Tangential section of the same transition in septal morphology depicted in figures 21 and 23.

It is also parricidal. The only skeletal tissue inherited by an offset are a few septa that previously formed part of the calicular wall of the parent.

In the lower subcylindrical or ceratoid part of the corallite, septa consist of short (free protruding part rarely more than 1.0 mm long), vertically aligned holacanths, embedded in the narrow (normally 0.5 to 1.0 mm thick) corallite wall. Near the base of the expanded trochoid part of the corallite, the trabecular structure changes from simple holacanthine to compound rhabdacanthine, the septa become broad, convex, contiguous ridges, and the width of the marginarium enlarges to between 1.1 and 1.9 mm. In early stages, when the mean corallite diameter is 10 to 12 mm, there are about 50 septa. Later, when the mean corallite diameter has increased to between 20 and 30 mm, there are 60 to 63 septa. Because the septa are much broader in the expanded calice, the number of septa there is not significantly greater than in the immediate subcalicular part of the corallite. The largest calice seen has a mean diameter of about 40 mm, and yet has only 68 septa. The septal arrangement is radial, and at no stage are the septa differentiated into major and minor orders.

There are no dissepiments. Most of the tabulae are complete. Many are more or less flat, others are gently undulative or convex, a few are slightly convex. Some tabularial surfaces bear a layer of sclerenchyme, as much as 0.6 mm thick. Spacing of the tabulae varies from three to eight over a vertical distance of 10 mm.

Remarks. The two named species most resembling the new species are **Stylopleura berthiaumi** Merriam and **S. eurycalyx** (Weissermel). The latter is presumed to be derived from the Upper Silurian of the Baltic region, but is known only from glacial drift in northern Germany. **S. berthiaumi** is smaller (subcalicular diameter about 8 to 16 mm) and has fewer septa (44 to 60) than **S. julli**. Its tabulae are also more widely spaced (3 to 5 per 10 mm) than those of **S. julli**, but this may not be taxonomically important. **S. eurycalyx** is also smaller (according to Weissermel the largest subcalicular diameter is 18 mm) than **S. julli**, and appears to have only slightly more than 50 septa.

The trivial name of the new species is a patronym for the late R.K. Jull.

Stylopleura sp. n. cf. **S. julli** sp. n.

Plate 70.1, figures 8, 10

?**Pseudamplexus** sp., Pedder in Jackson and others, 1978, Pl. 27, figs. 7, 9 only.

Tryplasma (s.l.) sp., Pedder in Jackson and others, 1978, Pl. 31, figs. 2, 3.

Remarks. It is possible that two previously figured corals from the Lochkovian (probable **eurekensis** Zone equivalent and **pesavis** Zone) of the Royal Creek headwaters area (GSC loc. 69301 and C-12887) are subcalicular and calicular fragments of the same species of **Stylopleura**. If this is so, the species is similar to **Stylopleura julli**, but differs in having longer septal spines (free ends projecting by as much as 1.6 mm) and a thicker (4.0 mm thick) calicular marginarium.

Family SPONGOPHYLLIDAE Dybowski, 1873
Genus **Carlinastraea** Merriam, 1976

Carlinastraea Merriam in Merriam and McKee, 1976, p. 32-33.

Type species. **Carlinastraea tuscaroraensis** Merriam in Merriam and McKee, 1976, p. 33-34, Pl. 6, figs. 5-7; Pl. 7, figs. 1-4. The holotype is from 385 to 400 m above the base, and 55 to 70 m below the top, of the Roberts Mountains Formation on Bootstrap Hill, southern Tuscarora Mountains, northern Nevada. Merriam considered the type horizon to be Silurian ("Silurian coral zone D or E"), but it is about 215 m stratigraphically above the Devonian graptolite zone of **Monograptus uniformis** (W.B.N. Berry in Merriam and McKee, 1976, p. 18), and its age is considered to be late Lochkovian. Other specimens figured in support of the original description of the species came from what Merriam and McKee (1976, p. 13) termed the upper 120-m unit of the Roberts Mountains Formation, on the western side of Coal Canyon, in the northern Simpson Park Mountains, central Nevada. This unit is the part of the type Windmill Formation section (Johnson, 1965, p. 369-372) that is exposed to the west of Coal Canyon Fault (Berry and Murphy, 1975, Fig. 14; Merriam and McKee, 1976, Fig. 2). Faunas of the Windmill Formation in the Coal Canyon area include **Quadrithyris** Zone brachiopods (Johnson, Penrose and Wise, 1978), **delta** Zone and **pesavis** Zone conodonts (Klapper and Murphy, 1980), and graptolites of the **praehercynicus** and **hercynicus** Zones (Berry and Murphy, 1975; Murphy and Berry, 1983). In the light of this evidence, the age of the **Carlinastraea tuscaroraensis** occurrence at Coal Canyon is unequivocally late Lochkovian.

Additional species. **Spongophyllum halysitoides** Etheridge, 1918, p. 49, Pl. 7, figs. 1-3. **S. sugiyamai** Yabe and Eguchi, 1945, p. 432-434, text-figs. 1-4 (also Guo, 1980, p. 139, Pl. 43, figs. 6a, b) (provisional assignment). **S. originale** Zhmaev in Kraevskaya, 1955, p. 214, Pl. 41, figs. 3a, b. **Neomphyma rosiformis** Zheltonogova, 1961, p. 81-82, Pl. S-20, figs. 3a-b. **Neomphyma pseudofritchi** Soshkina in Soshkina and Dobrolyubova, 1962, Pl. 19, figs. 1a, b (improperly founded name). **S. halysitoides minor** Strusz, 1966, p. 575 (elevation of **S. halysitoides** var. **minor** Hill, 1940a, p. 162-163, Pl. 3, figs. 3a, b, to species-group rank). **S. pseudohalysitoides** Lavrusevich, 1968, p. 114-115, Pl. 9, figs. 3a, b. **S.** (?) **neomphymoides** Zhavoronkova in Tyazheva and others, 1976, p. 76-77, Pl. 26, figs. 4a-5; Pl. 27, fig. 1. **Neomphyma crassa** Zhavoronkova in Tyazheva and others, 1976, p. 78, 79, Pl. 27, figs. 2a-d. **Carlinastraea martinae** Galle, 1983, p. 118-120, text-fig. 2, Pl. 3, figs. 1-3, Pl. 4, fig. 3. **C. pygmaea** sp. n.

Doubtful species. **Spongophyllum kettneri** Prantl, 1951, p. 235-237, text-fig. 3, Pl. 2, figs. 1, 2 (also Galle, 1983, p. 116-118, text-fig. 1, Pl. 1, figs. 1-3; Pl. 2, figs. 2, 3). **S. maikottaense** Lavrusevich, 1968, p. 114, Pl. 8, figs. 6a-7b. A Lower Devonian coral from the Ural Mountains, listed by Chodalewitsch (1960, p. 232) as **Neomphyma cerioides** Vaganova (in litt.), may be a species of **Carlinastraea**. However, no description has been traced and the name is probably a nomen nudum.

Distribution. Pridolian of Tadzhikistan and Inner Mongolia (Xibiehe Formation), and possibly Jilin Province of northeastern China (S_3^2 horizon of Guo, 1980). Lochkovian of New South Wales, Yunnan, Inner Mongolia, Tadzhikistan, Gornoy Altai, Salair, southern and northern Ural Mountains, Yukon Territory, British Columbia, Nevada, and possibly Czechoslovakia and Alaska. Pragian of Victoria (Australia), New South Wales, Queensland, Tadzhikistan, Gornoy Altai, southern and northern Ural Mountains and Alaska. Early Zlichovian of Czechoslovakia, Austria, and possibly the northern Ural Mountains (Toshemka Horizon) and Alaska (basal McCann Hill Chert).

Description. Corallum cerioid, increase marginarial and nonparricidal. Corallites slender; intercorallite wall commonly moniliform. Septa much reduced in the dissepimentarium. Relatively large presepiments dominate the marginarium. Tabularium narrow with numerous, typically complete, flat to concave tabulae.

Remarks. **Carlinastraea** resembles both **Spongophyllum** Milne Edwards and Haime and **Australophyllum** Stumm. It differs from **Spongophyllum** by having a marginarium dominated by

presepiments rather than dissepiments. Species of **Australophyllum** have relatively broader tabularia with closer spaced and distinctly sagging tabularial surfaces.

Carlinastraea halysitoides (Etheridge, 1918)

Plate 70.1, figures 24-33

Spongophyllum halysitoides Etheridge, 1918, p. 49, Pl. 7, figs. 1-3.

Spongophyllum halysitoides Etheridge; Jones, 1932, p. 56-57 (in part; includes **Carlinastraea minor**).

Spongophyllum halysitoides Etheridge; Hill, 1940a, p. 162.

Spongophyllum halysitoides Etheridge; Hill, 1942, p. 161, Pl. 2, figs. 5a, b.

Spongophyllum halysitoides Etheridge var. **minor** Hill; Soshkina, 1949, p. 123-124 (in part, not var. **minor** Hill), Pl. 47, figs. 1a, b only (not Pl. 47, figs. 2-4; Pl. 48, figs. 1a-d; ?Pl. 58, fig. 3, which are other species of **Carlinastraea, Kozlowiaphyllum** or **Australophyllum**).

Spongophyllum halysitoides Etheridge; Soshkina, 1952, p. 93 (in part), upper and lower right figs. of Pl. 30, fig. 106 only (not others, which are **Kozlowiaphyllum**(?) **medium** and **Carlinastraea** sp.).

?**Spongophyllum halysitoides** Etheridge; Spasskiy, 1955, p. 127-128 (in part; includes indeterminate forms).

Neomphyma rosiformis Zheltonogova, 1961, p. 81-82, Pl. S-20, figs. 3a, b.

Neomphyma pseudofritchi Soshkina in Soshkina and Dobrolyubova, 1962, Pl. 19, figs. 1a, b.

Spongophyllum originale Zhmaev; Shurygina, 1968 (not Zhmaev), p. 134, Pl. 59, figs. 3a, b.

Spongophyllum halysitoides Etheridge; Lavrusevich, 1971, p. 44-45, Pl. 8, figs. 2a-3.

Neomphyma rosiformis Zheltonogova; Cherepnina, 1971, Pl. 25, figs. 1a, b.

?**Spongophyllum halysitoides**; Wright, A.J. in Strusz, 1972, p. 445.

Neomphyma rosiformis Zheltonogova; Zavoronkova in Tyazheva and Zhavoronkova, 1972, p. 40-41, Pl. 19, figs. 4a-5b; Pl. 20, fig. 1.

Spongophyllum(?) sp. ex gr. **S.**(?) **halysitoides** Etheridge; Pedder in Campbell and others, 1973, p. 57.

Spongophyllum pseudofritchi (Soshkina); Guo, 1976, p. 92, Pl. 28, figs. 3a, b.

Carlinastraea tuscaroraensis Merriam in Merriam and McKee, 1976, p. 33-34, Pl. 6, figs. 5-7; Pl. 7, figs. 1-4.

Carlinastraea sp. cf. **C. tuscaroraensis** Merriam in Merriam and McKee, 1976, Pl. 8, figs. 1, 2.

Spongophyllum pseudofritchi (Soshkina); Guo, 1978, p. 62, Pl. 19, figs. 1a, b.

Spongophyllum pseudofritchi (Soshkina); Yu and Liao, 1978, p. 259-260, Pl. 3, figs. 6a, b.

?**Spongophyllum cyathophylloides** Etheridge; Yu and Liao, 1978 (not Etheridge), p. 260, Pl. 3, figs. 4a, b.

Carlinastraea sp.; Pedder in Jackson and others, 1978, p. 38, Pl. 25, figs. 8, 10; Pl. 28, figs. 1, 4.

Spongophyllum originale Zhmaev; Tsyganko, 1981 (not Zhmaev), p. 50-51, Pl. 14, figs. 1a, b.

not **Spongophyllum halysitoides** Etheridge; Spasskiy, 1960, p. 55-56, Pl. 29, figs. 3, 4 (=**Xystriphyllum** sp.).

not? **Spongophyllum halysitoides halysitoides** Etheridge; Strusz, 1966, p. 573-575, Pl. 90, figs. 2-3b (=**Carlinastraea** sp. cf. **C. halysitoides** and **Xystriphyllum** sp. from Attunga).

not **Spongophyllum halysitoides** Etheridge; Churkin in Churkin and Brabb, 1968, Pl. 3, figs. 4a, b (=**Carlinastraea** sp.).

not? **Spongophyllum halisitoides** n. ssp.; Kodsi, 1971, p. 586-587, Pl. 3, figs. 1, 2 (=**Carlinastraea** sp.).

not **Spongophyllum rosiforme** (Zheltonogova); Guo, 1978, p. 62, Pl. 19, figs. 3a, b (=**Carlinastraea** sp.).

not **Spongophyllum halysitoides** Etheridge; Shurygina, 1977, p. 47-48, Pl. 19, figs. 3a, b (=?**Carlinastraea** sp. n.).

Holotype of **Carlinastraea halysitoides** (Etheridge). Australian Museum, Sydney, F16453; figured by Etheridge, 1918, Pl. 7, figs. 1-3 and by Hill, 1942, Pl. 2, figs. 5a, b. Etheridge recorded its occurrence as Middle Devonian(?), road near Beedle's Farm, Moonbi, County Inglis, New South Wales. The type stratum is apparently in one of the limestone lenses that comprise the Nemingha Limestone Member of the Drik Drik Formation (Crook, 1961, p. 182-183). According to Philip and Jackson (1973), all of the Nemingha limestone lenses lie within the **Icriodus woschmidti** Zone, and are of early Lochkovian age. The Beedle's Farm locality, however, is not known to have yielded conodonts, and is probably more safely regarded as Lochkovian, undivided.

Holotype of **Carlinastraea rosiformis** (Zheltonogova). West-Siberian Geological Administration Collection, Novokuznetsk, 7035-a; figured by Zheltonogova, 1961, Pl. S-20, figs. 3a, b. Tom'-chumysh Horizon, Uksunay River, Salair, U.S.S.R. When this species was proposed, the Tom'-chumysh Horizon was considered to be Silurian. However, it has yielded **Icriodus woschmidti** recently (E.A. Yelkin, personal communication, 1983), and is early Lochkovian.

Holotype of **Carlinastraea pseudofritchi** (Soshkina). T.I. Vaganova Collection, Urals Geological Research Administration, Sverdlovsk, catalogue number not published; figured by Soshkina and Dobrolyubova, 1962, Pl. 19, figs. 1a, b. Stratum and locality cited only as Gedinnian Stage of the Urals. This name does not satisfy Article 13 of the International Code of Zoological Nomenclature and is invalid.

Holotype of **Carlinastraea tuscaroraensis** Merriam. United States National Museum, Washington, 166482; figured by Merriam and McKee, 1976, Pl. 6, figs. 6, 7; Pl. 7, figs. 1-3. For further details see above under type species of **Carlinastraea**.

Figured Hypotypes from Yukon Territory. GSC 46086, from GSC loc. C-64089. GSC 46094, from GSC loc. 69300. GSC 75887, from GSC loc. C-4269. GSC 75888, from GSC loc. C-6386. GSC 75889, from GSC loc. C-12877. GSC 75890, 75891, both from GSC loc. C-12887.

Description of Yukon material. All of the material from Royal Creek probably derives from debris flows. Certainly, none of the specimens is complete. GSC 75889, which is the largest fragment available, is from a cerioid corallum that would have been at least 30 cm high, 25 cm wide, and would have comprised several hundred prismatic corallites. Mean adult corallite diameters, in the Yukon material, range from 2.9 to 5.0 mm; most are between 3.8 and 4.2 mm.

Increase of the corallum is marginarial and non-parricidal. Normally, only one new corallite is budded at a time, but locally, two, or rarely as many as three offsets are produced simultaneously from the same parent. Although the vertical and horizontal skeletal elements of the daughter corallites develop rapidly, and an intercorallite wall, separating parent from daughter, appears soon after the inception of hystero-ontogeny, daughter corallites enlarge slowly. Normally, their full diameter is not attained until they have achieved a vertical growth of 30 mm.

Intercorallite walls vary considerably. Some are as thin as 0.1 mm and are only slightly wavy. Others have prominent septal ridges. Where ridges of adjacent corallites are back to back, the maximum thickness of the intercorallite wall is as much as 0.7 mm. Short septal spines, of unknown original

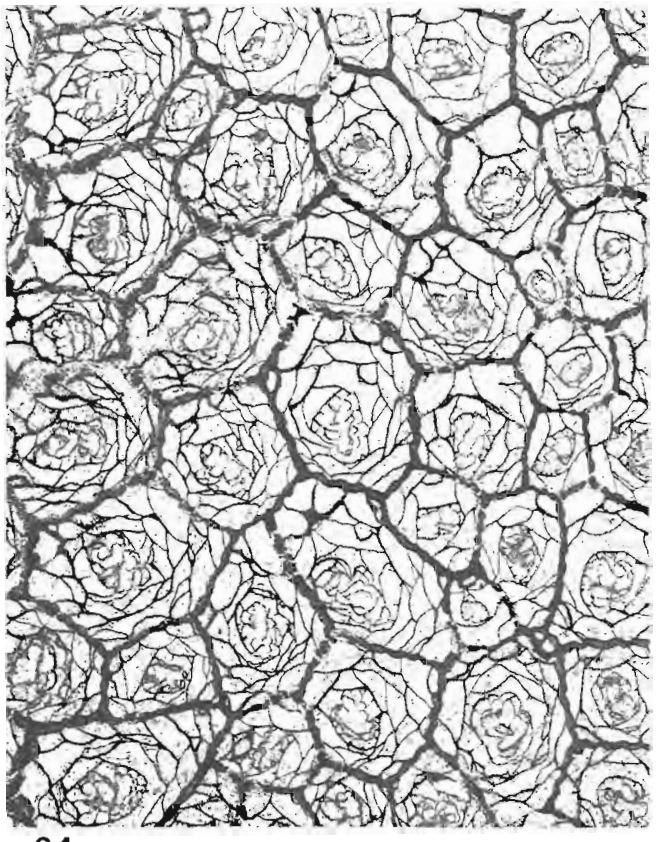

24

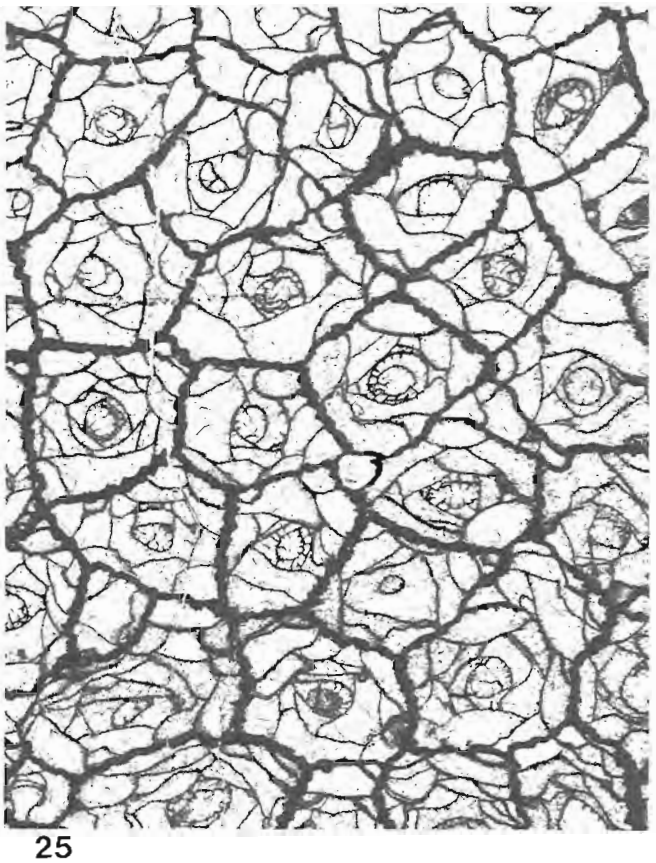

25

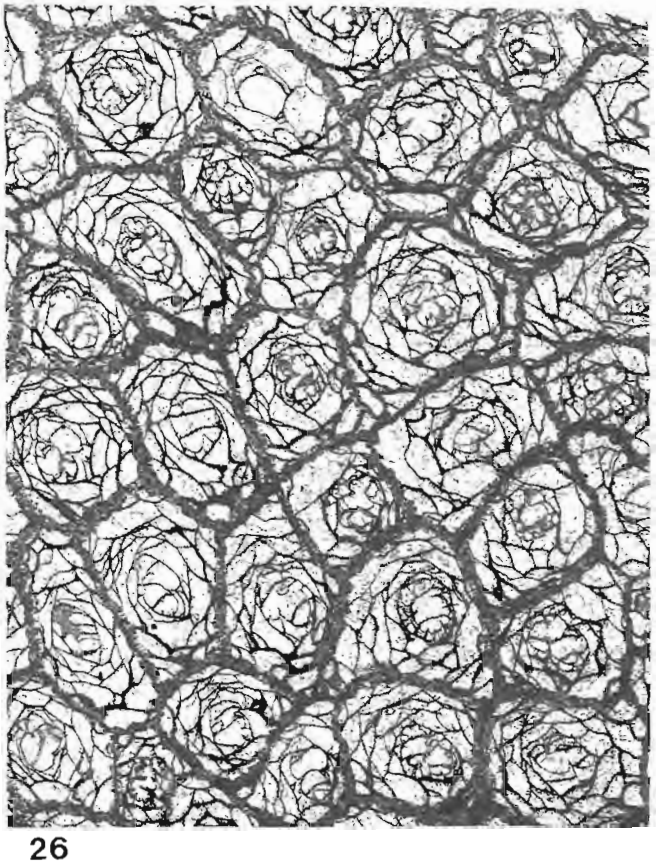

26

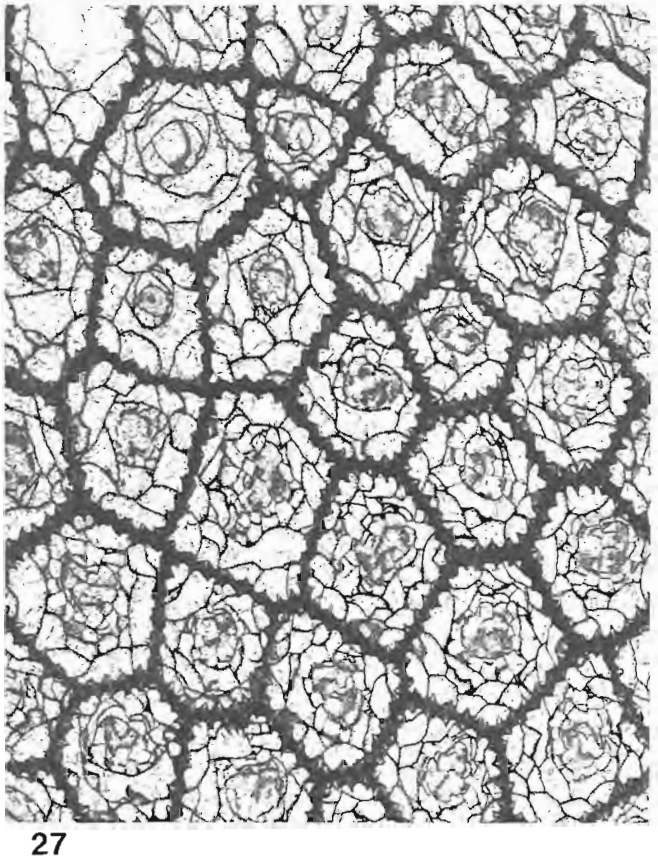

27

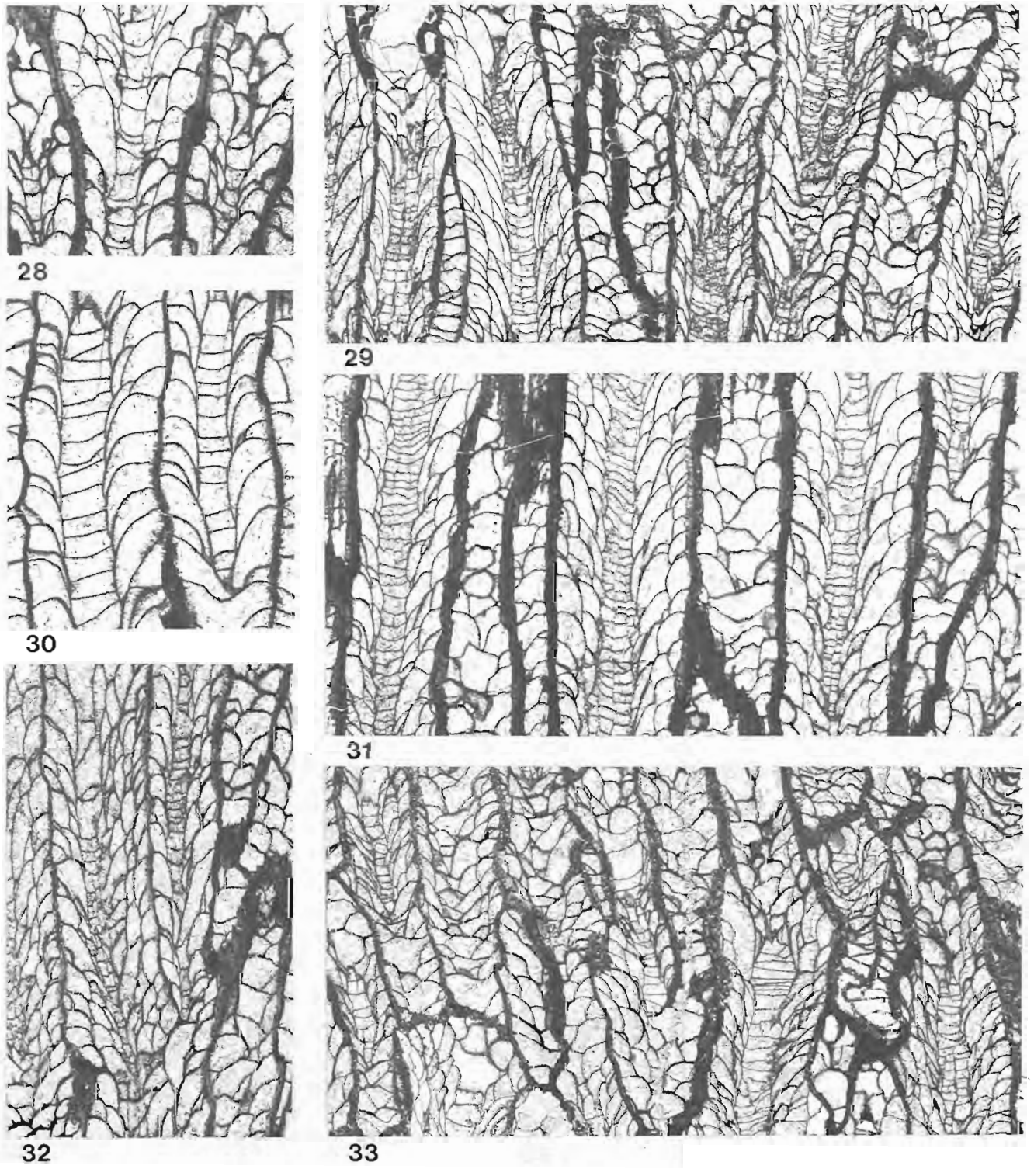

PLATE 70.1

Figures 24-27. **Carlinastraea halysitoides** (Etheridge), transverse sections, all x5.

24. Hypotype, GSC 75891.
25. Hypotype, GSC 75887.
26. Hypotype, GSC 75890.
27. Hypotype, GSC 75889.

Figures 28-33. **Carlinastraea halysitoides** (Etheridge), longitudinal sections, all x5.

28. Hypotype, GSC 46086.
29. Hypotype, GSC 75891.
30. Hypotype, GSC 46094.
31. Hypotype, GSC 75889.
32. Hypotype, GSC 75887.
33. Hypotype, GSC 75890.

microstucture, are present in some of the intercorallite walls. Locally, especially in GSC 75889, these spines project from the septal ridges. In other specimens, they are much less evident, and are either absent, or are confined to the septal bases.

Septa are much reduced or totally suppressed in the dissepimentarium. Adaxially from the septal bases, most of the septa are short, smooth and based on adaxial surfaces of the inner presepiments. They vary in length, but are not consistenly differentiated into two orders. There are 24 to 32 undifferentiated septal ridges around the periphery of the corallite. Adaxially, septal development varies greatly, even within a single colony. In extreme cases, there are none, or as many as 24 septa around the tabularium; the normal range is 5 to 12.

Despite the narrow diameter of the corallites, a dissepimentarium is invariably present. It consists of one to four, rarely five, ranks of relatively large, elongate presepiments. The diameter of the tabularium, which is commonly somewhat excentric, is about one third that of the corallite. Most of the tabulae are complete, and are either flat or slightly concave. Their spacing ranges from 24 to 50 over a vertical distance of 10 mm.

Remarks. The taxonomically conservative attitude, adopted first by Lavrusevich (1971), towards **Spongophyllum halysitoides** and similar species, is entirely justified by the range of morphology expressed in large collections of **Carlinastraea halysitoides** from Royal Creek, Yukon Territory.

In addition to the holotype occurrences given above, **Carlinastraea halysitoides** is known from the following Lochkovian strata: Shanjiang Formation, Lijiang region of Yunnan (Yu and Liao, 1978); upper member of the Chaganhebu Formation, northern Bailingmiao, Inner Mongolia (Guo, 1976, 1978); Remnev Beds, Kamyshenki region, Gornoy Altai (Cherepnina, 1971); Shishkat Horizon, Zeravshan and Turkestan Ranges, Tadzhikistan (Lavrusevich, 1971); Siyak Beds, Irgizly River and tributaries, western slope of the southern Urals (Zhavoronkova, 1972); Saraynaya Horizon, Sauna River, eastern slope of northern Urals (Shurygina, 1968); Ovinparmskiy Horizon, Ilych River, western slope of the northern Urals (Tsyganko, 1981); Lochkovian part of the Road River Formation, central Yukon Territory (Pedder in Jackson and others, 1978 and this work); lower part of the Black Stuart Formation, Quesnel Lake map area, British Columbia (Pedder in Campbell et al., 1973). It has been listed, also, from the lower (Lochkovian) fauna of the Mullamuddy Formation of New South Wales (Wright in Strusz, 1972), and the early Pragian part of the Rosenthal Creek Formation of Queensland (Lomas North locality of Hill, 1940a, p. 163).

Carlinastraea sp. cf. **C. halysitoides** (Etheridge)

Plate 70.1, figures 34-37

Spongophyllum halysitoides halysitoides Etheridge; Strusz, 1966, p. 573-575 (in part), Pl. 90, figs. 2-3b (not specimen from Attunga, which is **Xystriphyllum** sp.).

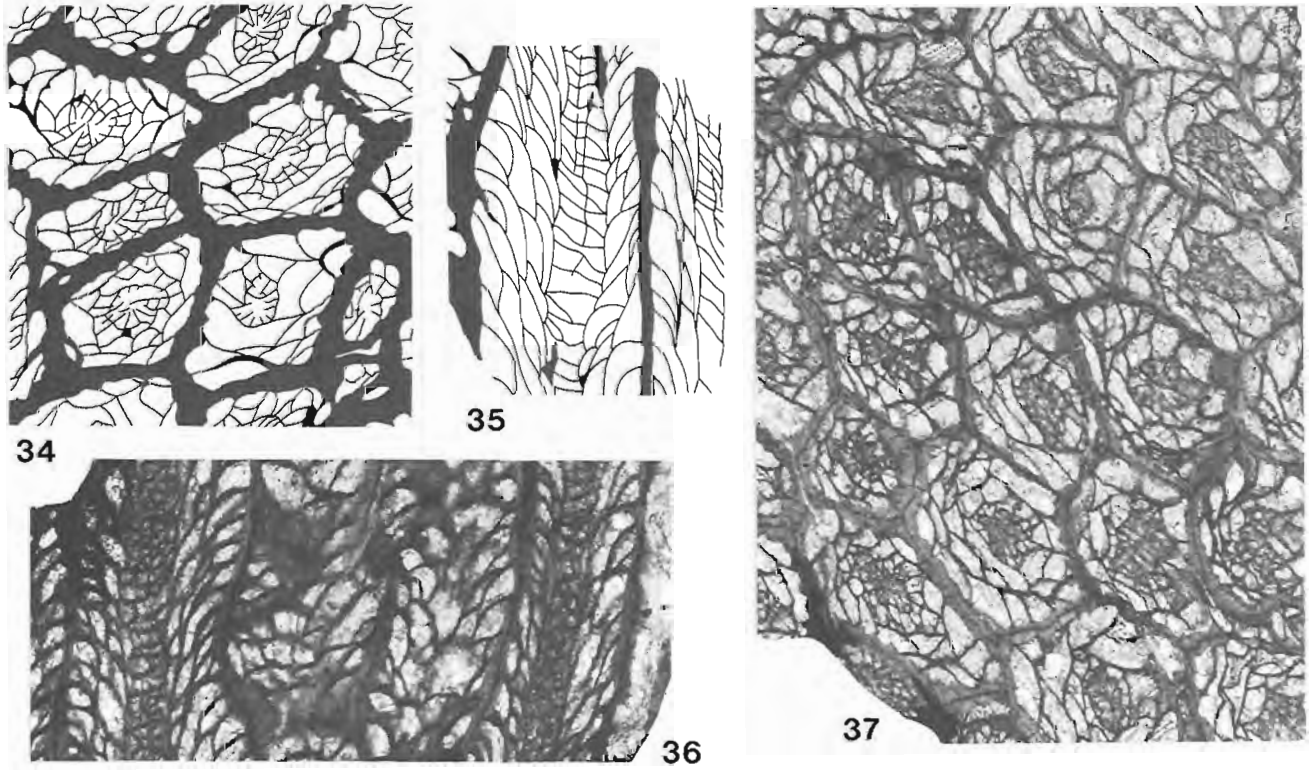

PLATE 70.1

Figures 34-37. **Carlinastraea** sp. cf. **C. halysitoides** (Etheridge), all x5. University of New England, Armidale, Australia, Geological Department Collections F8991. Early Pragian limestone lens or megaclast in the Coopers Creek Formation; Coopers Creek, Victoria, Australia.

34, 37. Transverse sections.
35, 36. Longitudinal sections.

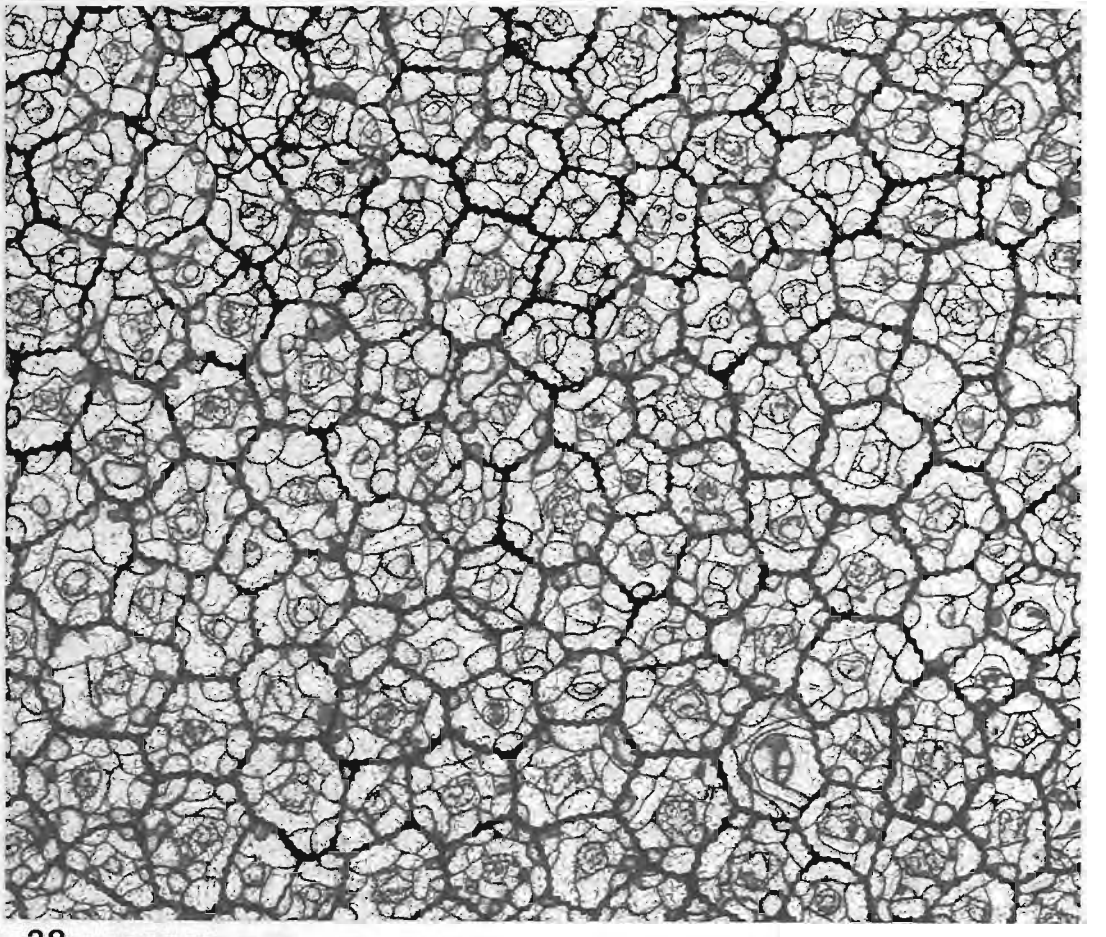

38

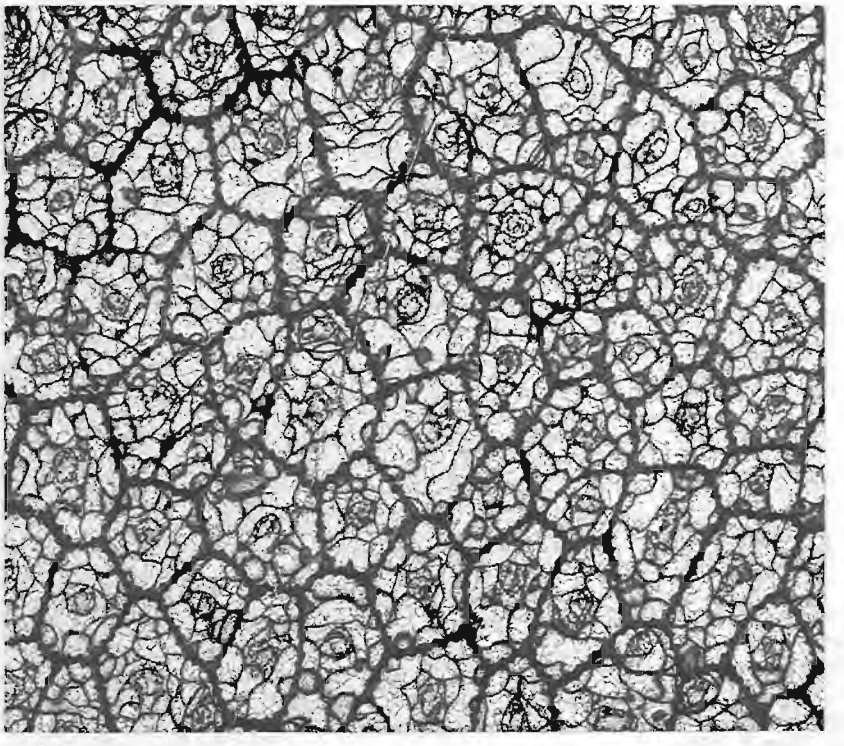

39

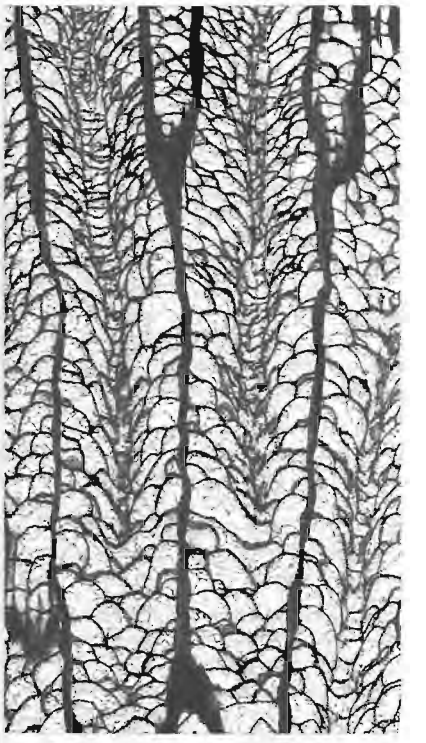

40

PLATE 70.1

Figures 38-40. **Carlinastraea pygmaea** sp. n., all x5.

38. Paratype, GSC 75892, transverse section.
39, 40. Holotype, GSC 42566, transverse and longitudinal sections.

Figured specimens. The University of Sydney, Department of Geology and Geophysics Collection 16223, 16224; lower part of the Garra Formation; Portion 80 (grid reference Dubbo 180.925), Parish of Eurimbula, County Gordon, New South Wales; collected by D.L. Strusz. The University of New England, Armidale, Department of Geology Collection F8991; limestone in the Coopers Creek Formation, Coopers Creek, Victoria; collected by G.M. Philip. The Devonian stratigraphy at Coopers Creek has been summarized by VandenBerg and others (1976, Fig. 4.5, p. 53-54).

Remarks. These early Pragian specimens from eastern Australia are similar to typical Lochkovian specimens of **Carlinastraea halysitoides**, but have irregularly thickened walls. They are probably conspecific with **C. halysitoides**, but may represent a distinct subspecies.

Carlinastraea pygmaea sp. n.

Plate 70.1, figures 38-42

Spongophyllum sp. cf. **S. rosiforme** (Zheltonogova), Pedder, 1975, p. 290, figs. 2, 5.
Carlinastraea sp. cf. **C. rosiformis** (Zheltonogova), Pedder in Jackson and others, 1978, p. 39, Pl. 31, figs. 5, 6.

Type series. Holotype, GSC 42566, paratype, GSC 75892, both from GSC loc. 69301.

Diagnosis. Small species of **Carlinastraea** with mean adult corallite diameters of 2.5 to 3.0 mm; intercorallite wall narrow (0.1 to 0.2 mm thick between back to back septal bases); septal bases short but well defined, 27 to 34 in number in adult corallites.

Description. Both specimens in the type series are fragments of cerioid coralla that originally were at least 10 cm high and 8 cm in diameter. Corallites are prismatic in transverse section and have adult mean diameters of 2.5 to 3.0 mm.

Corallum increase is marginarial and nonparricidal. Normally, only one offset is produced at a time; rarely two develop simultaneously from a parent, and in one, of nearly three hundred corallites studied, three offsets were budded simultaneously. Although the horizontal skeletal elements of the daughter corallite, and the intercorallite wall that separates the offset from the parent, both develop rapidly in hystero-ontogeny, daughter corallites enlarge very slowly.

Intercorallite walls are 0.1 to 0.2 mm thick between back to back septal bases. Septal bases, which are low, wedge-shaped ridges, number from 28 to 34 in adult corallites. Throughout most of the dissepimentarium, septa are reduced to rare, extremely short septal crests. From zero to thirteen short and vertically discontinuous septal lamellae are present around the region of the inner dissepimentarium and outer tabularium. In no part of the corallite are the septa differentiated into major and minor orders.

The dissepimentarium consists of one to three, locally four, ranks of generally elongate and inwardly inclined presepiments. Diameters of the tabularia vary from 0.4 to 0.7 mm. Most of the tabulae are complete and concave; their spacing is such that from 25 to 35 are present over a vertical distance of 10 mm.

Remarks. **Carlinastraea halysitoides minor** (Strusz) is based on a weathered and inadequately figured fragment from a limestone lens, or megaclast, in the early Pragian (Strusz, 1972, chart) Connolly Volcanics (Olgers and others, 1974, p. 27), at a locality known as Limestone Siding in southeastern Queensland. As far as can be ascertained from Hill's (1940a, p. 162) description, and the best illustrations available (Richards and Bryan, 1924, Pl. 17, figs. 1, 2), it differs from the new species, in having fewer (22 to 26) septal bases, better developed septa, and a dissepimentarium that has only one or two ranks of presepiments, but includes some dissepiments. Compared with **C. halysitoides** (Etheridge), **C. pygmaea** is smaller (corallite diameter typically 3.8 to 4.2 mm in **C. halysitoides**), but has as many, or more (24 to 32 in **C. halysitoides**) septal bases.

The trivial name is the Latin adjective, **pygmaeus**, meaning dwarf.

Locality Register

GSC loc. 69300. Road River Formation; probable **eurekaensis** Zone equivalent, between the local ranges of **Icriodus woschmidti hesperius**, below, and **Ozarkodina delta**, above; 67.4 to 72.6 m above base of section. Royal Creek headwaters, Section 1, Yukon Territory; 64°46'20"N latitude, 135°12'00"W longitude. Collected by A.C. Lenz, 1965. **Cladopora** sp., **Kodonophyllum** sp., **Stylopleura julli** Pedder, **Carlinastraea halysitoides** (Etheridge). Lenz (1977) recorded the following brachiopods from 67.1 m above the base of this section: **Skenidioides variabilis** Lenz, **Isorthis (Isorthis)** sp., **Resserella** sp., **Schizophoria** sp. cf. **S. paraprima** Johnson, Boucot and Murphy, **Salopina submurifer** Johnson, Boucot and Murphy, **Leptagonia** sp., **Aesopomum varistriata** Johnson.

GSC loc. 69301. Road River Formation; **pesavis** Zone; 114.4 to 120.5 m above base of section (mistakenly said to be 105.5-108.9 m above base by Jackson, Lenz and Pedder, 1978, p. 65). Royal Creek headwaters, Section 1, Yukon Territory; 64°46'20"N latitude, 135°12'00"W longitude. Collected by A.C. Lenz, 1965. **Favosites** sp., **Loboplasma multilobatum** (Spasskiy), **Stylopleura** sp. n. cf. **S. julli** Pedder, **Carlinastraea pygmaea** Pedder, **Lyrielasma** sp., **"Dolerorthis" borealis** Lenz, **Skenidioides variabilis** Lenz, **Protocortezorthis carinatus** Smith, **Cortezorthis norfordi** Lenz, **Dalejina** sp., **Schizophoria** sp. cf. **S. paraprima** Johnson, Boucot and Murphy, **S.** sp., **Muriferella** sp. aff. **M. masurskyi** Johnson and Talent, **Leptagonia** sp., **"Nervostrophia"** sp., **Mesodouvillina (Protocymostrophia)** sp., nov. stropheodontid aff. **Mesodouvillina** sp., **Mclearnites (Mclearnitesella)** (?) sp., **Gorgostrophia** (?) sp., **Phragmostrophia mucronata** Lenz, **Clorinda** sp., **Sieberella** (?) sp., **Gypidula thorsteinssoni** Johnson, **Gypidula** spp., **Machaeraria** sp., **Ancillotoechia** sp., **"Linguopugnoides"** sp., **Nymphorhynchia nympha** (Barrande), **Werneckeella hartensis** Lenz, **Nemesa** (?) sp., **Atrypa aspiformis** Lenz, **A.** sp. cf. **A. aspiformis** Lenz, **Reticulariatrypa** (?) sp. aff. **R. granulifera** (Barrande), **Cryptatrypa** sp., **Nucleospira laevigata** Lenz, **Ambocoelia** sp. aff. **A. praecox** Kozlowski, **Plicoplasia acutiplicata** Lenz, **Cyrtina** sp., **Cyrtinaella** sp., **Reticulariopis** sp., **Pandorinellina optima** (Moskalenko), **P.** (?) **boucoti** (Klapper), **Pedavis pesavis pesavis** (Bischoff and Sannemann).

GSC loc. C-4269. Road River Formation; probable **eurekaensis** Zone equivalent, between the local ranges of **Icriodus woschmidti hesperius**, below, and **Ozarkodina delta**, above; 63.7 to 66.5 m above base of section. Royal Creek headwaters, Section 1, Yukon Territory; 64°46'20"N latitude, 135°12'00"W longitude. Collected by A.E.H. Pedder, 1969. **Carlinastraea halysitoides** (Etheridge).

GSC loc. C-6386. Road River Formation; estimated to be approximately from the **delta** Zone; 341 m above top of Ordovician carbonate. Royal Creek headwaters, A.W. Norris' Section 106D-2, which is partly Section 6 and partly between sections 6 and 7 of the present author, Yukon Territory; 64°47'30"N latitude, 135°10'30"W longitude. Collected by A.W. Norris, 1970. **Favosites** sp., **Stylopleura julli** Pedder, **Carlinastraea halysitoides** (Etheridge).

GSC loc. C-12877. Road River Formation; probable **eurekaensis** Zone equivalent, between the local ranges of **Icriodus woschmidti hesperius**, below, and **Ozarkodina**

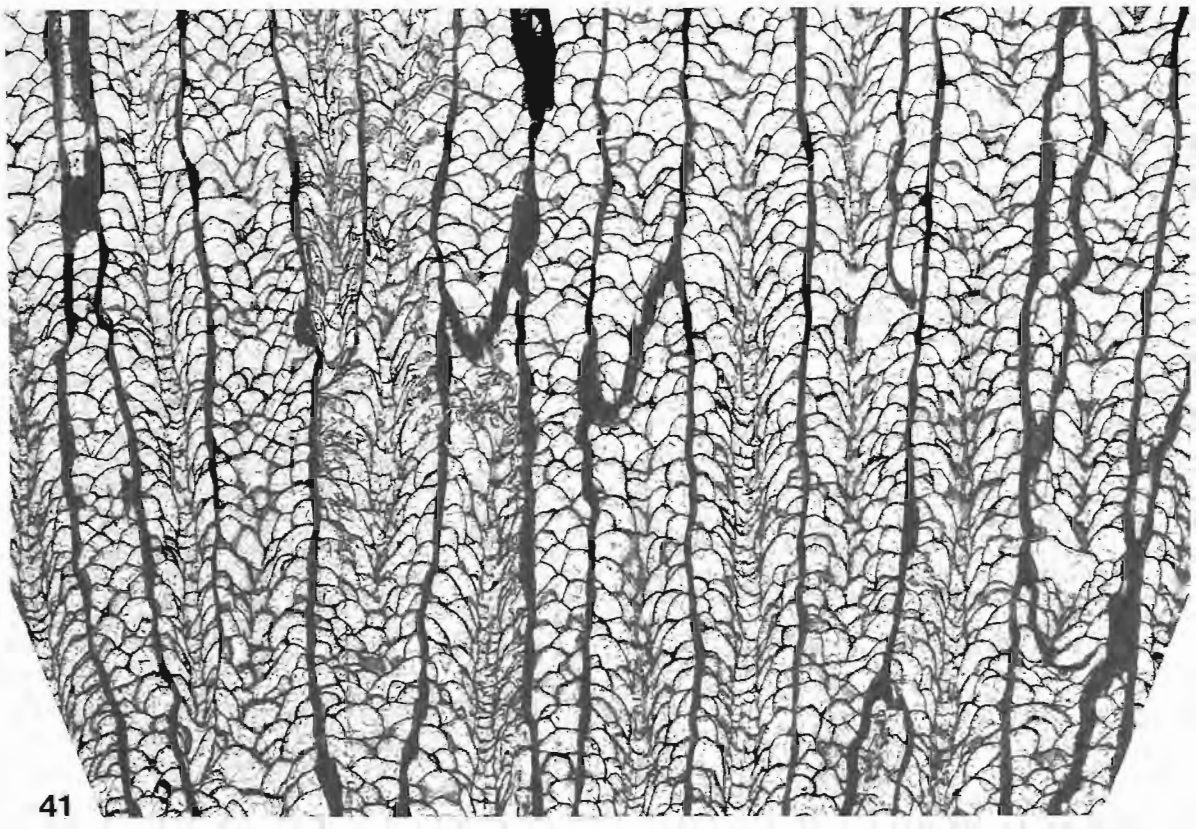

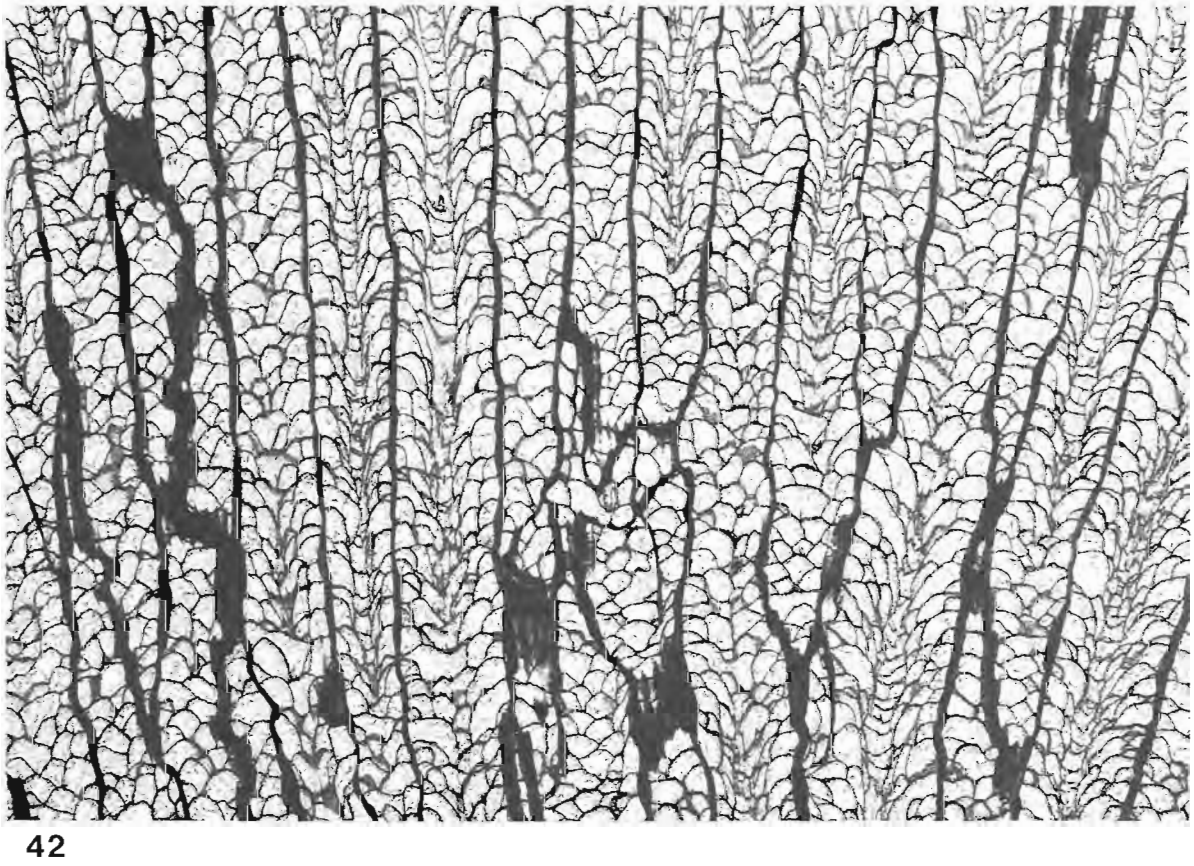

PLATE 70.1

Figures 41, 42. **Carlinastraea pygmaea** sp. n., longitudinal sections, both x5.

41. Holotype, GSC 42566.
42. Paratype, GSC 75892.

delta above; 65.0 m above base of section. Royal Creek headwaters, Section 1, Yukon Territory; 64°46'20"N latitude, 135°12'00"W longitude. Collected by A.E.H. Pedder, 1971. **Carlinastraea halysitoides** (Etheridge).

GSC loc. C-12887. Road River Formation; probable **eurekaensis** Zone equivalent, between the local ranges of **Icriodus woschmidti hesperius**, below, and **Ozarkodina delta**, above; 160.1 to 166.2 m above base of section. Royal Creek headwaters, Section 2, Yukon Territory; 64°46'30"N latitude, 135°14,10"W longitude. Collected by A.E.H. Pedder, 1971. **Stylopleura** sp. n. cf. S. **julli** Pedder, **Carlinastraea halysitoides** (Etheridge), **Kozlowiaphyllum** sp., **Ozarkodina remscheidensis remscheidensis** (Ziegler), **Pandorinellina optima** (Moskalenko).

GSC loc. C-64089. Road River Formation; probable **delta** Zone equivalent; 63.0 to 64.0 m above base of section. Royal Creek headwaters, Section 7, Yukon Territory; 64°47'45"N latitude, 135°09'30"W longitude. Collected by A.E.H. Pedder, 1976. **Carlinastraea halysitoides** (Etheridge). Lenz (1982, p. 366) recorded the following brachiopods from 60 m above the base of this section: **Skenidioides** sp., **Protocortezorthis** sp., **Schizophoria** sp., **Salopina submurifer** Johnson, Boucot and Murphy, **Parapholidostrophia** (?) sp., **Machaeraria paraformosa** Lenz, **Atrypa** sp., **Spirigerina supramarginalis** (Khalfin), **Cryptatrypa** sp., **Howellella** sp., **Cyrtina** spp.

References

Berry, W.B.N. and Murphy, M.A.
1975: Silurian and Devonian graptolites of central Nevada; University of California Publications in Geological Sciences, v. 110, 109 p.

Campbell, R.B., Mountjoy, E.W., and Young, F.G.
1973: Geology of McBride map-area, British Columbia; Geological Survey of Canada, Paper 72-35, 104 p.

Cherepnina, S.K.
1971: Rugozy zhedinskikh otlozheniy Gornogo Altaya (remnevskie sloi); in Rugozy i stromatoporoidei paleozoya SSSR, ed. A.B. Ivanovskiy; Trudy II Vsesoyuznogo simpoziuma po izucheniyu iskopaemykh korallov SSSR, vyp .2, p. 89-91, 143.

Chodalewitsch (Khodalevich), A.N.
1960: Grundsätz der biostratigraphischen Gliederung der unterdevonischen und mitteldevonischen Sedimente des Osthangs des Urals nach der Brachiopoden; in Prager Arbeitstagung über die Stratigraphie des Silurs and des Devons (1958), ed. J. Svoboda; Ústredni Ústav Geologický, Praha, p. 231-243.

Churkin, M., Jr. and Brabb, E.E.
1968: Devonian rocks of the Yukon-Porcupine Rivers area and their tectonic relation to other Devonian sequences in Alaska; in International Symposium on the Devonian System, Calgary, 1967, ed. D.H. Oswald; Alberta Society of Petroleum Geologists, Calgary, v. II, p. 227-258.

Crook, K.A.W.
1961: Stratigraphy of the Tamworth Group (Lower and Middle Devonian), Tamworth-Nundle district, N.S.W.; Royal Society of New South Wales, Journal and Proceedings, v. 94(5), p. 173-188.

Etheridge, R., Jr.
1907: A monograph of the Silurian and Devonian corals of New South Wales: with illustrations from other parts of Australia. Part II. - The genus **Tryplasma**; Geological Survey of New South Wales, Memoirs, Palaeontology, no. 13, 102 p.

Etheridge, R., Jr.
1918: Two remarkable corals from the Devonian of New South Wales; Australian Museum, Records, v. 12(4), p. 49-51.

Galle, A.
1983: Spongophyllidae (Rugosa) of Bohemian Silurian and Devonian; Sbornik Narodniho Muzea v Praze, v. 39B(2), p. 115-126.

Guo Sheng-zhe
1976: Tetracoralla; in Atlas of Paleontology of the North China region, Inner Mongolia (Chinese), Research Institute of Geological Sciences of the Northeast, Bureau of the Inner Mongolian Autonomous Region (ed.); Geological Publishing House, Peking, v. 1, p. 63-101.

1978: Late Silurian tetracorals from northern Bailingmiao of the Autonomous Region of Inner Mongolia (Chinese); Professional Papers of Stratigraphy and Palaeontology, no. 6, p. 50-68.

1980: Tetracoralla; in Paleontological atlas of northeast China, Paleozoic volume (Chinese), Shenyang Institute of Geology and Mineral Resources (ed.); Geological Publishing House, Beijing, p. 106-153, 641-646.

Hill, D.
1940a: The Middle Devonian rugose corals of Queensland, II. The Silverwood-Lucky Valley area; Royal Society of Queensland, Proceedings, v. 51(9), p. 150-168.

1940b: The Silurian Rugosa of the Yass-Bowning district, N.S.W.; Linnean Society of New South Wales, Proceedings v. 65(3-4), p. 388-420.

1942: The Devonian rugose corals of the Tamworth district, N.S.W.; Royal Society of New South Wales, Journal and Proceedings, v. 76(3), p. 142-164.

1981: Treatise on invertebrate paleontology. Part F. Coelenterata. Supplement 1. Rugosa and Tabulata, ed. C. Teichert; Geological Society of America and University of Kansas Press, Boulder and Lawrence, xl+762 p. (2 v.).

Jackson, D.E., Lenz, A.C., and Pedder, A.E.H.
1978: Late Silurian and Early Devonian graptolite, brachiopod and coral faunas from northwestern and arctic Canada; Geological Association of Canada, Special Paper, no. 17, 160 p.

Johnson, J.G.
1965: Lower Devonian stratigraphy and correlation, northern Simpson Park Range, Nevada; Bulletin of Canadian Petroleum Geology, v. 13(3), p. 365-381.

Johnson, J.G., Penrose, N.L., and Wise, M.T.
1978: Biostratigraphy, biotopes and biogeography in the Lower Devonian (Upper Lochkovian, Lower Pragian) of Nevada; Journal of Paleontology, v. 52(4), p. 793-806.

Jones, O.A.
1932: A revision of the Australian species of the coral genera **Spongophyllum** E. and H. and **Endophyllum** E. and H. with a note on **Aphrophyllum** Smith; Royal Society of Queensland, Proceedings, v. 44(4), p. 50-63.

Klapper, G. and Murphy, M.A.
1975: Silurian-Lower Devonian conodont sequence in the Roberts Mountains Formation of central Nevada; University of California Publications in Geological Sciences, v. 111, 62 p. (imprint 1974).

Klapper, G. and Murphy, M.A. (cont.)
1980: Conodont zonal species from the **delta** and **pesavis** Zones (Lower Devonian) in central Nevada; Neues Jahrbuch für Geologie und Paläontologie, Monatshefte, Jahrgang 1980, Heft 8, p. 490-504.

Kodsi, M.G.
1971: Korallen aus dem Unterdevon des Karnischen Alpen; Geologischen Bundesanstalt, Verhandlungen, Jahrgang 1971, Heft 3, p. 576-607.

Kraevskaya, L.N.
1955: Podklass Zoantharia. Otryad tetracoralla ili rugosa. Tetrakorally (nizhniy i sredniy devon); in Atlas rukovadyashchikh form iskopaemykh fauny i flory zapadnoy Sibiri. Tom 1, ed. L.L. Khalfin; Gosudarstvennoe Nauchno-Tekhnicheskoe Izdatel'stvo Literatury po Geologii i Okhrane Nedr, Moskva, p. 206-228.

Lang, W.D., Smith, S., and Thomas, H.D.
1940: Index of Palaeozoic coral genera; British Museum (Natural History), London, vii+231 p.

Lavrusevich, A.I.
1968: Rugozy postludlovskikh otlozheniy doliny r. Zeravshan (Tsentral'nyy Tadzhikistan); in Biostratigrafiya pogranichnykh otlozheniy silura i devona, ed. B.S. Sokolov and A.B. Ivanovskiy; Izdatel'stvo "Nauka", Moskva, p. 102-130.

1971: Nekotorye rugozy iz pozdnesiluriyskikh i rannedevonskikh otlozheniy Tsentral'nogo Tadzhikistana; Upravleniya Geologii Soveta Ministrov Tadzhikskoy SSR, Trudy, Paleontologiya i Stratigrafiya, vyp. 4, p. 33-52, 123-135.

Lenz, A.C.
1977: Upper Silurian and Lower Devonian brachiopods of Royal Creek, Yukon, Canada, Part 1. Orthoida, Strophomenida, Pentamerida, Rhynchonellida; Palaeontographica, Abt. A, Band 159, p. 37-109.

1982: New data on Late Silurian and Early Devonian brachiopods from the Royal Creek area, Yukon Territory; Canadian Journal of Earth Sciences, v. 19(2), p. 364-375.

Merriam, C.W.
1974: Silurian rugose corals of the cental and southwest Great Basin; United States Geological Survey, Professional Paper 777, 66 p. (imprint 1973).

Merriam, C.W. and McKee, E.H.
1976: The Roberts Mountains Formation, a regional stratigraphic study with emphasis on rugose coral distribution; United States Geological Survey, Professional Paper 973, 51 p.

Murphy, M.A. and Berry, W.B.N.
1983: Early Devonian conodont-graptolite collation and correlations with brachiopod and coral zones, central Nevada; American Association of Petroleum Geologists, Bulletin, v. 67(3), p. 371-379.

Olgers, F., Flood, P.G., and Robertson, A.D.
1974: Palaeozoic geology of the Warwick and Goondiwindi 1:250 000 sheet areas, Queensland and New South Wales; Bureau of Mineral Resources, Geology and Geophysics (Australia), Report 164, iv+109 p.

Pedder, A.E.H.
1975: Sequence and relationships of three Lower Devonian coral faunas from Yukon Territory; in Report of Activities, Part B, Geological Survey of Canada, Paper 75-1B, p. 285-295.

Pedder, A.E.H. (cont.)
1976: First records of five rugose coral genera from Upper Silurian rocks of the Canadian Arctic Islands; in Report of Activities, Part B, Geological Survey of Canada, Paper 76-1B, p. 287-293.

Philip, G.M. and Jackson, J.H.
1973: Posledovatel'nost' konodontovykh kompleksov v nizhnem i srednem devone vostochnoy Avstralii; in Stratigrafiya nizhnego i srednego devona, ed. D.V. Nalivkin and others; Trudy III Mezhdunarodnogo simpoziuma po granitse silura i devona i stratigrafii nizhnego i srednego devona (Leningrad, 1968 g.), tom 2, p. 248-254.

Pickett, J.
1982: The Silurian System in New South Wales; Geological Survey of New South Wales, Bulletin 29, 264 p. and separate plates.

Prantl, F.
1951: Rod **Endophyllum** Edwards a Haime a **Spongophyllum** Edwards a Haime v českém siluru a devonu; Sborník Ústředního Ústavu Geologického Československé Republiky, svazek 18, p. 221-240.

Richards, H.C. and Bryan, W.H.
1924: The geology of the Silverwood-Lucky Valley area; Royal Society of Queensland, Proceedings, v. 36(6), p. 44-108.

Salter, J.W.
1852: Geology; in Journal of a voyage in Baffin's Bay and Barrow Straights, in the years 1850-1851, performed by H.M. ships "Lady Franklin" and "Sophia"---, P.C. Sutherland; Longman, Brown, Green and Longmans, London, v. 2, p. ccxvii-ccxxxiii.

Shurygina, M.V.
1968: Pozdnesiluriyskie i rannedevonskie rugozy vostochnogo sklona severnogo i srednego Urala; in Korally pogranichnykh sloev silura i devona Altae-Sayanskoy gornoy oblasti i Urala, ed. A.B. Ivanovskiy; Izdatel'stvo "Nauka", Moskva, p. 117-150, 161-164.

1977: Rugozy; in Biostratigrafiya i fauna rannego devona vostochnogo sklona Urala, ed. E.S. Sycheva and L.N. Shimanova; Moskva "Nedra", p. 43-51, 161-163.

Soshkina, E.D.
1947: O sistematike siluriyskikh i devonskikh korallov Rugoza; Akademii Nauk SSSR, Doklady, nov. ser., tom 55(8), p. 761-764.

1949: Devonskie korally Rugosa Urala; Akademiya Nauk SSSR, Paleontologicheskogo Instituta, Trudy, tom 15, vyp. 4, 160 p.

1952: Opredelitel' devonskikh chetyrekhluchevyk korallov; Akademiya Nauk SSSR, Paleontologicheskogo Instituta, Trudy, tom 39, 127 p.

Soshkina, E.D. and Dobrolyubova, T.A.
1962: Otryad Evenkiellida; in Osnovy paleontologii, tom 2. Gubki, arkheotsiaty, kishechnopolostnye, chervi, ed. B.S. Sokolov; Izdatel'stvo Akademii Nauk SSSR, Moskva, p. 333-339.

Spasskiy, N.Ya.
1955: Korally Rugosa i ikh znachenie dlya stratigrafii srednego devona zapadnogo sklona Urala; in Stratigrafiya paleozoyskikh otlozheniy Timana i zapadnogo sklona Urala (sbornik statey), ed. M.V. Kulikov; Vsesoyuznogo Neftyanogo Nauchno-Issledovatel'skogo Geologo-Razvedochnogo Instituta (VNIGRI), Trudy, nov. ser., vyp. 90, p. 91-224.

1960: Devonskie chetyrekhluchevye korally Rudnogo Altaya; Paleontologicheskoe obosnovanie stratigrafii paleozoya Altaya, vyp. 3, 143 p.

Strusz, D.L.
1966: Spongophyllidae from the Devonian Garra Formation, New South Wales; Palaeontology, v. 9(4), p. 544-598.

1972: Correlation of the Lower Devonian rocks of Australasia; Geological Society of Australia, Journal, v. 18(4), p. 427-455.

Tsyganko, V.S.
1981: Devonskie rugozy severa Urala; "Nauka" Leningradskoe Otdelenie, 220 p.

Tyazheva, A.P. and Zhavoronkova, R.A.
1972: Korally i brakhiopody pogranichnykh otlozheniy silura i nizhnego devona Yuzhnogo Urala; Izdatel'stvo "Nauka", Moskva, 183 p.

Tyazheva, A.P., Zhavoronkova, R.A., and Garifullina, A.A.
1976: Korally i brakhiopody nizhnego devona Yuzhnogo Urala; Izdatel'stvo "Nauka", Moskva, 226 p.

VandenBerg, A.H.M., Garratt, M.J., and Spencer-Jones, D.
1976: Silurian-Middle Devonian; in Geology of Victoria, ed. J.G. Douglas and J.A. Ferguson; Geological Society of Australia, Special Publication no. 5, p. 45-76.

Weissermel, W.
1894: Die Korallen des Silurgeschiebe Ostpreussens und des östlichen Westpreussens; Deutschen Geologischen Gesellschaft, Zeitschrift, Band 46, p. 580-674.

Yabe, H. and Eguchi, M.
1945: **Spongophyllum** from the Middle Gotlandian Limestone of Erhtaokou near Kiturin, Mansyu; Japan Academy, Proceedings, v. 21(9), p. 431-434.

Yu Chang-ming and Liao Wei-hua
1978: Lower Devonian rugose corals from Alengchu, Lijiang, northwestern Yunnan (Chinese with English abstract); Acta Palaeontologica Sinica, v. 17(3), p. 245-266.

Zheltonogova, V.A.
1961: Siluriyskaya Sistema. Podklass Tetracoralla (Rugosa). Tetrakorally; in Biostratigrafiya paleozoya Sayano-Altayskoy gornoy oblasti. Tom II. Sredniy paleozoy, ed. L.L. Khalfin; Sibirskogo Nauchno-Issledovatel'skogo Instituta Geologii, Geofiziki i Mineral'nogo Syr'ya (SNIGGIMS), Trudy, vyp. 20, p. 33-36, 74-88, 152-169 (imprint 1960).

PRECAMBRIAN-CAMBRIAN BOUNDARY SEQUENCE, WERNECKE MOUNTAINS, YUKON TERRITORY

Project 730058

G.M. Narbonne[1], H.J. Hofmann[2], and J.D. Aitken
Institute of Sedimentary and Petroleum Geology, Calgary

Narbonne, G.M., Hofmann, H.J., and Aitken, J.D., Precambrian-Cambrian boundary sequence, Wernecke Mountains, Yukon Territory; in Current Research, Part A, Geological Survey of Canada, Paper 85-1A, p. 603-608, 1985.

Abstract

Uppermost Proterozoic and Lower Cambrian strata of the Wernecke Mountains comprise a thick succession of alternating carbonate and siliciclastic formations. Fieldwork in 1984 revealed several distinctive units that permit greater precision in lithostratigraphic correlation. Ediacaran megafossils, simple and complex trace fossils, vendotaenid algae, and small shelly fossils occur sporadically throughout this succession, and are useful in regional and global biostratigraphic correlation.

Résumé

Dans les monts Wernecke, les strates du sommet du Protérozoïque et les strates du Cambrien inférieur constituent une épaisse succession de formations carbonatées et silicoclastiques alternées. Les études faites sur le terrain en 1984 ont révélé l'existence de plusieurs unités distinctives, qui permettent des corrélations lithostratigraphiques de grande précision. Dans toute cette succession, on rencontre sporadiquement des mégafossiles de l'Édiacarien, des ichnofossiles simples et complexes, des algues du type vendotaenidé, et de petits fossiles à coquille; ces fossiles sont utiles pour établir des corrélations biostratigraphiques régionales et globales.

[1] Department of Geological Science, Queen's University, Kingston, Ontario K7L 3N6
[2] Department of Geology, University of Montreal, Montreal, Québec H3C 3J7

Introduction

The Wernecke Mountains are unique in that they contain abundant, well-preserved specimens of all the fossil groups commonly used to recognize the Precambrian-Cambrian boundary (Narbonne et al., 1984). A preliminary description of the stratigraphy and trace fossils in the Precambrian-Cambrian boundary interval (Fritz et al., 1983) has served as a foundation for subsequent studies of the Ediacaran fossils (Hofmann et al., 1983), organic-walled microfossils (Hofmann, 1984), and small shelly fossils (Nowlan et al., in press) in this succession. More detailed studies of these fossil groups are now in progress.

Recently, a discussion by Aitken (1984) and a reply by Fritz et al. (1984) have raised questions about some aspects of the stratigraphic framework proposed by Fritz et al. (1983). Because of the economic potential of these strata (Reeve, 1977) and their importance in global biostratigraphic correlation of the Precambrian-Cambrian boundary, it is important that these stratigraphic problems be resolved. In June of 1984, we jointly investigated two of the critical sections described by these authors. The new data collected have elucidated several of the lithostratigraphic and biostratigraphic problems discussed by these authors.

Lithostratigraphy

Fritz et al. (1983, 1984) based their interpretations on sections in the Corn Creek/Goz Creek areas, whereas Aitken (1984) studied sections slightly to the north (Fig. 71.1). A key section in Aitken's area is Section A, where his reconnaissance (1984) revealed a thick succession of Upper Proterozoic and Lower Cambrian strata. The most richly fossiliferous section in the Corn Creek/Goz Creek area is Section 8 of Fritz et al. (1983). These two sections were therefore chosen by the authors for further detailed study in 1984.

Section 8

The following description of Section 8 (Fig. 71.2 (1-2), 71.3) is based primarily on that of Fritz et al. (1983), but has been supplemented by our observations of strata below the base of their published section. Several minor faults are present, but marker beds allow the section to be established, from top to bottom:

7. The Vampire Formation (296.5 m thick), consisting of sandstones, siltstones and minor carbonates that bear Cambrian-type complex trace fossils. Small shelly fossils such as **Anabarites trisulcatus** and **Protohertzina anabarica** occur in phosphatic limestone at the base of the formation.
6. A resistant formation (125.5 m thick) consisting of thick bedded dolostone that weathers to a light orange-pink. Fritz et al. (1983) correlated this unit with Map unit 11 of Blusson (1971) in the Mackenzie Mountains to the east.
5. A recessive formation (147.5 m thick) consisting of shale, fine grained quartzarenite and siltstone. Ediacaran megafossils and simple trace fossils occur sporadically. These strata are the Unnamed siltstone unit 1 of Fritz et al. (1983).
4. A resistant formation (69 m thick) of thick bedded dolostone and fine grained quartzarenite that weathers to light orange and pink hues. These strata are the Unnamed dolostone unit of Fritz et al. (1983).
3. A recessive formation (approx. 350 m thick) of siltstone, shale, fine grained quartzarenite and minor carbonate. Ediacaran megafossils, including **Beltanelliformis brunsae**, occur near the top of this unit; vendotaenid algae occur in the lower part. Fritz et al. (1983) referred to these strata as "Unnamed siltstone unit 2".
2. A resistant formation (approx. 60 m thick) of grey weathering dolostone. Dolostone breccia and laminated dolostone are common; stromatolitic dolostone is rare. "Zebra dolostone", in which thin, rhythmically spaced seams of coarse, white dolomite spar occur in fine grained, grey dolostone (Fig. 71.2 (3)), is a conspicuous rock type in this formation. These strata lie below the base of Fritz et al.'s (1983) Section 8.
1. A recessive formation of light grey, thin bedded siltstone that weathers grey-buff (Fig. 71.2 (4)). Channelized, graded grit units occur in the upper part of the formation. These strata will be referred to as "Unnamed siltstone unit 3" throughout the rest of this report.

Section A

In a reconnaissance section at locality A, Aitken (1984, Fig. 71.2 (5)) documented a succession of alternating siliciclastic and carbonate formations in the Precambrian-Cambrian boundary interval. This section was examined in greater detail in 1984, at which time additional fossils were collected, and the thicknesses of the units were measured. The section is described from the top downwards:

5. A 177 m thick succession of sandstone and siltstone that contains Cambrian-type complex trace fossils. Aitken correlated these strata with the Vampire/Backbone Ranges Fromation.
4. A tripartite unit that Aitken correlated with Map unit 11 of Blusson (1971). Our subsequent investigation has revealed that the unit as a whole, and the clastic middle division in particular, are much thicker than Aitken's (1984) estimate. Furthermore, we have determined that each of the three divisions is a mappable unit. These units are:

   c. A resistant formation (28.5 m thick) of thick bedded dolostone that weathers light orange and pink. This unit is lithologically equivalent to the entire Map unit 11 as recognized by Fritz et al. (1983, 1984) in the Corn Creek/Goz Creek area, but is considerably thinner.

   b. A recessive formation (125 m thick) of shale, siltstone and fine grained sandstone. Ediacaran megafossils and simple trace fossils occur sporadically throughout the unit. The rock types, fossils and stratigraphic position are the same as those of Unnamed siltstone unit 1 at Section 8.

   a. A resistant formation (62.5 m thick) of thick bedded dolostone that weathers light orange and pink. Sandstone is abundant, and occurs as thin to thick beds and as sedimentary sills. This unit is lithologically equivalent to the Unnamed dolostone unit at Section 8.
3. A resistant formation of grey weathering dolostone. "Zebra dolostone" and dolostone breccia pass upwards into thick bedded and stromatolitic dolostone. A karstic erosion surface caps the unit. Aitken (1984) correlated this formation with the "Sheepbed carbonate" of the Mackenzie Mountains (Aitken, 1982), and tentatively suggested that the Unnamed dolostone unit of Fritz et al. (1983) was a lithologic correlative of this unit. However, our new data suggest that the dolostone unit near the base of Section 8 is the correlative unit.
2. A recessive formation composed of fissile black shale. Blusson (1974), Eisbacher (1981) and Aitken (1984) regarded this unit as the Sheepbed Formation.
1. The Keele Formation, composed of quartzose beds that pass upwards into a "teepee dolostone". This distinctive formation is widely traceable throughout the northern Canadian Cordillera (Eisbacher, 1981).

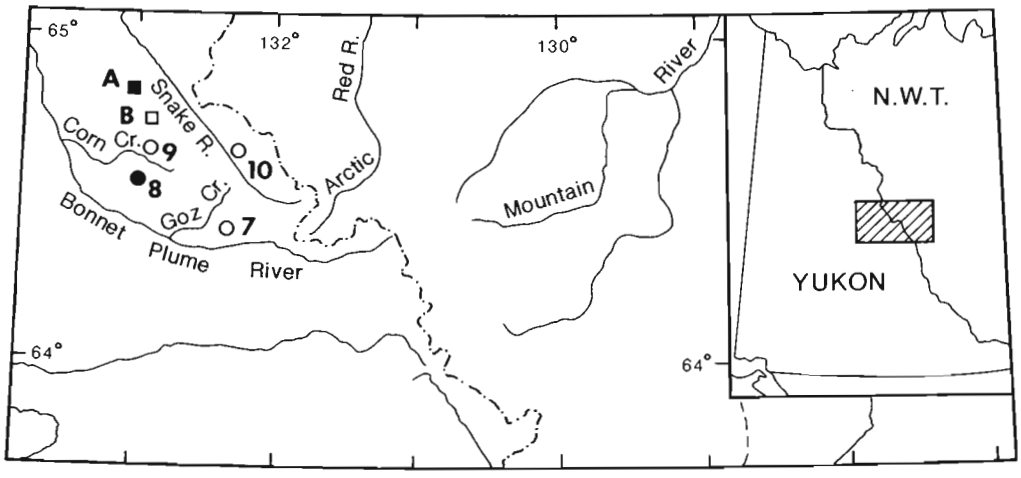

Figure 71.1
Location of sections.

□ Section studied by Aitken (1984).

○ Section studied by Fritz et al.(1983).

●■ Sections re-examined in 1984

kilometres
0 20 40 60 80 100
0 10 20 30 40 50 60
miles

Correlation

A revised correlation is presented in Figure 71.3. The major difference from Aitken's (1984, Fig. 2) previous correlation is our correlation of the Unnamed dolostone unit at Section 8 with strata immediately overlying the "Sheepbed carbonate" at Section A. The implication of this correlation is that Unnamed siltstone unit 2 at Section 8 is not equivalent to strata assigned to the Sheepbed Formation of Section A but is, in fact, considerably younger. At Section A, Unnamed siltstone unit 2 apparently has been removed by erosion prior to the deposition of the Unnamed dolostone unit.

Correlation of Unnamed siltstone unit 3 beyond Section 8 is difficult. It underlies the "Sheepbed carbonate", but differs lithologically from the Sheepbed Formation at Section A. On the other hand, the Sheepbed Formation in Sekwi Mountain and Mount Eduni map areas is lithologically variable and includes channelized grit beds and buff weathering siltstone beds. Further study is required to determine whether Unnamed siltstone unit 3 is a facies of the Sheepbed Formation or whether it is a formation restricted to the Corn Creek/Goz Creek area.

Biostratigraphy

The Wernecke Mountains contain well preserved specimens of a wide variety of fossil groups throughout the Precambrian-Cambrian boundary interval. The distribution of megafossils and trace fossils has been summarized by Fritz et al. (1983) and Narbonne et al. (1984); Hofmann (1984) has outlined the distribution of the microfossils. These data indicate that in this area, the Precambrian-Cambrian boundary lies within the Vampire Formation.

Hofmann et al. (1983) reported the occurrence of Ediacaran megafossils in Unnamed siltstone unit 1 and Unnamed siltstone unit 2. Aitken (1984) questioned the supposed occurrence of Ediacaran fossils in Unnamed siltstone 2, as all the material was from loose blocks. He pointed out that Ediacaran fossils had been found in strata equivalent to "Unnamed siltstone unit 1" in the Mackenzie Mountains (e.g. Hofmann, 1981), but that the underlying strata were barren. Because of this uncertainty concerning the position of these potentially significant fossils, both localities that had yielded Ediacaran fossils in Unnamed siltstone unit 2 were re-examined in 1984.

At Locality 8, we discovered numerous specimens of **Beltanelliformis brunsae** and other Ediacaran megafossils in outcrop and float of Unnamed siltstone unit 2. This confirms that Ediacaran fossils do occur in this unit.

Hofmann et al. (1983) described specimens of the Ediacaran megafossil **Cyclomedusa davidi**? from float of Unnamed siltstone unit 2 along the east side of Goz Creek (GSC loc. 99093; 2.5 km northwest of Section 7). We have now collected additional specimens from outcrops of siltstone at this locality, confirming that the material was locally derived. However, subsequent investigations revealed that the siltstone outcrops are part of an isolated fault block of undetermined stratigraphic position. The absence of similar strata above the Unnamed dolostone unit strongly suggests that these strata predate it. The fossil-bearing siltstone unit, herein informally referred to as the "Goz siltstone", consists predominantly of thin bedded, grey to grey-green siltstone that weathers grey-buff. Channelized, graded grit beds and slumped beds of siltstone are common. These strata do not resemble Unnamed siltstone unit 2 at Section 8, but are lithologically similar to Unnamed siltstone unit 3 at that locality. However, the apparent absence of Ediacaran fossils from Unnamed siltstone unit 3 at Section 8 suggests that correlation between this unit and the "Goz siltstone" must remain tentative at this time.

Ediacaran megafossils and simple trace fossils occur sporadically throughout Unnamed siltstone unit 1 at localities A, B, 9 and 8. Small shelly fossils of latest Precambrian age occur at the base of the Vampire Formation at Locality 8 (Nowlan et al., in press). The occurrence of complex trace fossils in the Vampire Formation and vendotaenid algae in Unnamed siltstone unit 2 also help to date this succession.

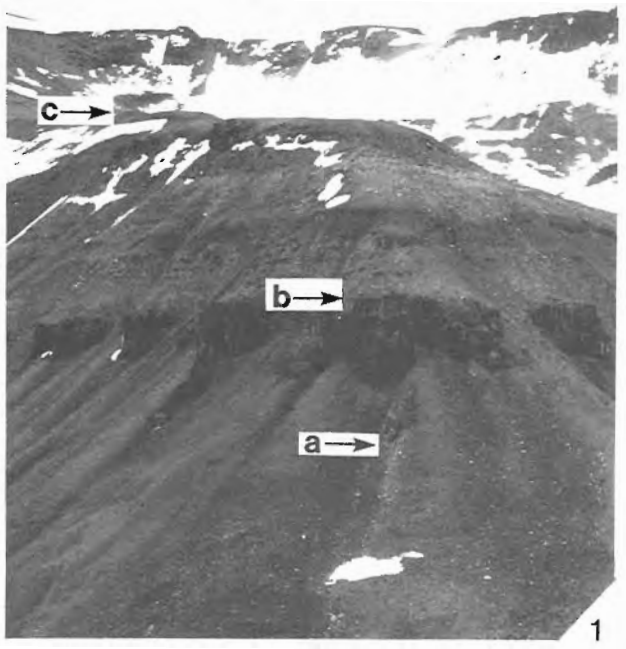
c
b
a
1

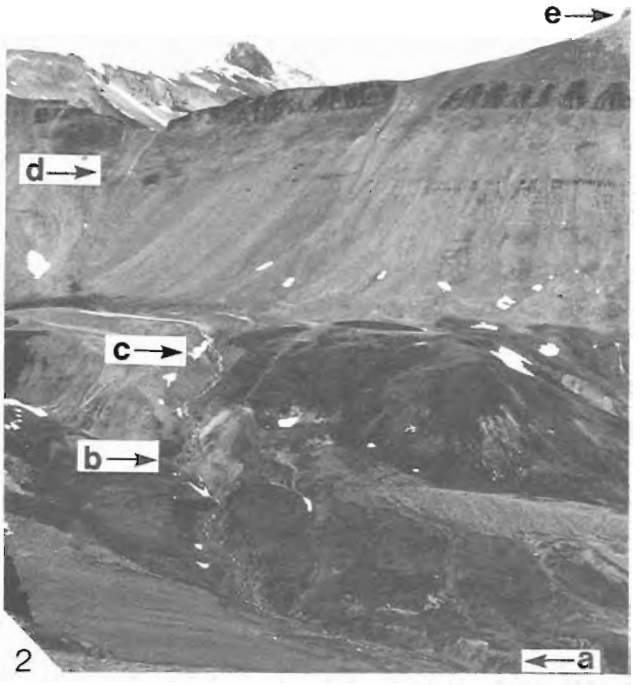
e
d
c
b
2
a


3

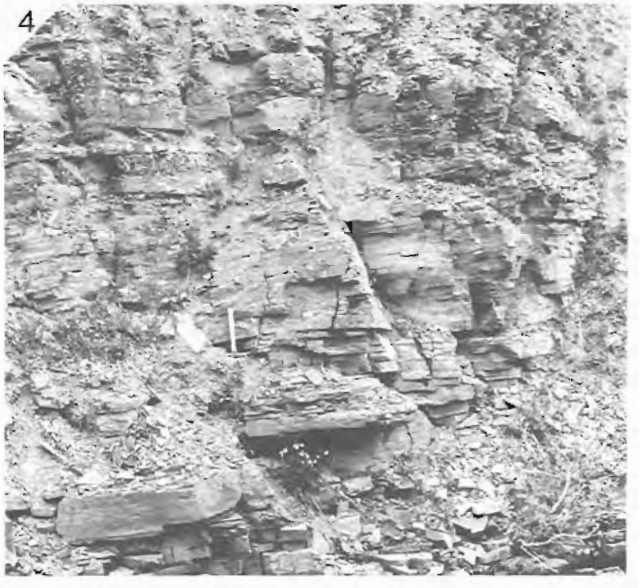
4

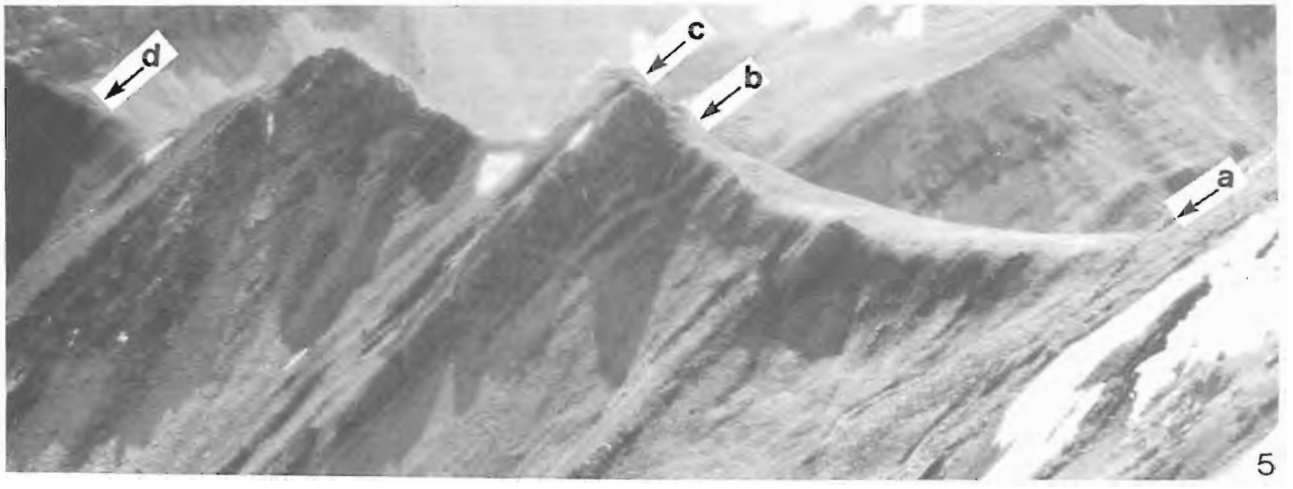
d
c
b
a
5

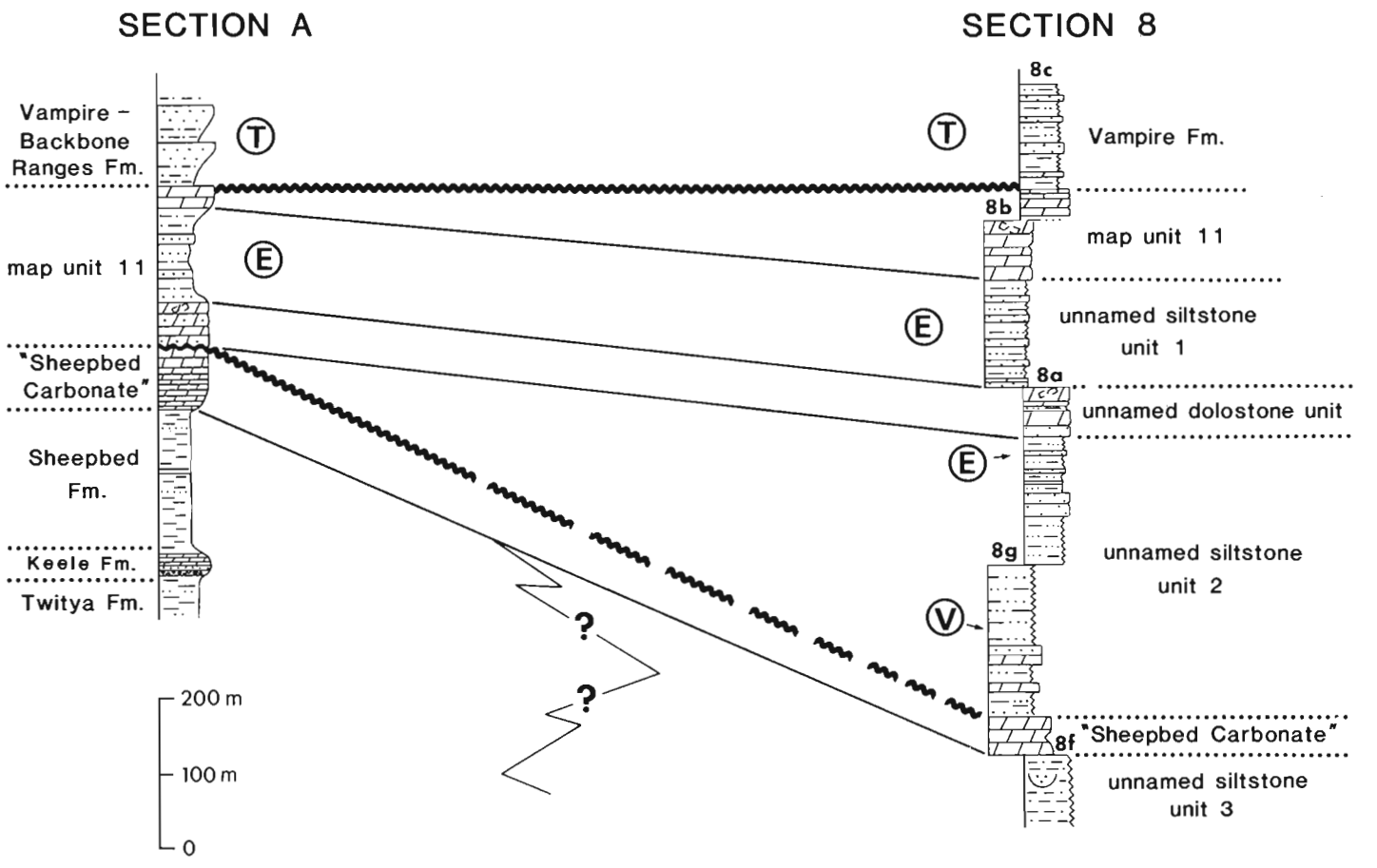

Figure 71.3. *Correlation of uppermost Precambrian strata in the Corn Creek/Goz Creek area. Terminology in Section A is from Aitken (1984, Fig. 2), in sections 8a-c is from Fritz et al. (1983, Fig. 44.2a), and sections 8f and g is by the present authors. Sections 8d and e (not shown) are as yet unpublished sections measured by W.H. Fritz; sections 8f and g are new. Thicknesses in sections 8f, 8g, and in the lower part of A are approximate.*

Figure 71.2 *(opposite)*

(1) View looking east to Section 8g (new), 1.5 km southeast of 8a at 64°31'45"N, 132°54'45"W. The base of the section and the "Sheepbed carbonate" are at "a"; the base of Unnamed siltstone unit 2 is at "b"; the top of the section is at "c".

(2) View looking west of sections 8a and b (Fritz et al., 1983) and Section 8f (new). The base of 8f is at "a"; the top of 8f and Unnamed siltstone unit 3 is at "b"; the top of the "Sheepbed carbonate" is at "c"; the base of 8a is at "d"; the top of Unnamed siltstone unit 2 is at "e". For strata above the base of the Unnamed dolostone unit see Fritz et al. (1983, Pl. 44.2, Fig. 3).

(3) "Zebra dolostone" in the "Sheepbed carbonate" at 8g. Scale in decimetres.

(4) Platy and blocky weathering siltstone in Unnamed siltstone unit 3 near the base of 8f. Hammer handle is 30 cm long.

(5) View east of the upper part of Section A of Aitken (1984). The top of the Unnamed dolostone unit is at "a"; the top of Unnamed siltstone unit 1 is at "b"; the top of Map unit 11 is at "c"; and the top of the Vampire/Backbone Ranges Formation is at "d". Photo by J. Carrick.

Conclusions

1. Unnamed siltstone unit 2 of Fritz et al. (1983) at Section 8 is younger than the Sheepbed Formation at Section A and is not correlative with it. The "Goz siltstone" also differs significantly from Unnamed siltstone unit 2, but its precise stratigraphic position is presently uncertain. Detailed mapping of the Nadaleen River map area would greatly elucidate correlation of these Upper Proterozoic strata.
2. Ediacaran megafossils occur in Unnamed siltstone unit 1, Unnamed siltstone unit 2, and the "Goz siltstone". Further systematic study of these fossils is under way, and should aid correlation of these strata.

Acknowledgments

We gratefully acknowledge a grant from the Canadian National Committee of the International Geologic Correlation Project (I.G.C.P., Project 29) that enabled the three of us to jointly examine the strata in question. We would like to thank W.H. Fritz for arranging this grant and for reviewing this paper. Narbonne also acknowledges

support from the Natural Sciences and Engineering Research Council of Canada (N.S.E.R.C., Grants A2648 and N0108) and the Queen's University Advisory Research Committee. Hofmann received support through N.S.E.R.C., Grant A7484. C. Peck prepared the illustrations. D.T. Osborne and J. Carrick assisted in the field, contributing significantly to the success of the project.

References

Aitken, J.D.
1982: Precambrian of the Mackenzie Fold Belt – a stratigraphic and tectonic overview; Geological Association of Canada, Special Paper 25, p. 149-161.

1984: Strata and trace fossils near the Precambrian-Cambrian boundary, Mackenzie, Selwyn and Wernecke Mountains, Yukon and Northwest Territories: Discussion; in Current Research, Part B, Geological Survey of Canada, Paper 84-1B, p. 401-407.

Blusson, S.L.
1971: Sekwi Mountain map area, Yukon Territory and District of Mackenzie; Geological Survey of Canada, Paper 71-22, 17 p.

1974: Geology, northern Selwyn Basin (Operation Stewart), Yukon and Northwest Territories; Geological Survey of Canada, Open File 205.

Eisbacher, G.H.
1981: Sedimentary tectonics and glacial record in the Windermere Supergroup, Mackenzie Mountains, northwestern Canada; Geological Survey of Canada, Paper 80-27, 40 p.

Fritz, W.H., Narbonne, G.M., and Gordey, S.P.
1983: Strata and trace fossils near the Precambrian-Cambrian boundary, Mackenzie, Selwyn and Wernecke Mountains, Yukon and Northwest Territories; in Current Research, Part B, Geological Survey of Canada, Paper 83-1B, p. 365-375.

Fritz, W.H., Narbonne, G.M., and Gordey, S.P. (cont.)
1984: Strata and trace fossils near the Precambrian-Cambrian boundary, Mackenzie, Selwyn and Wernecke Mountains, Yukon and Northwest Territories: Reply; in Current Research, Part B, Geological Survey of Canada, Paper 84-1B, p. 409-412.

Hofmann, H.J.
1981: First record of a Late Proterozoic faunal assemblage in the North American Cordillera; Lethaia, v. 14, p. 303-310.

1984: Organic-walled microfossils from the latest Proterozoic and earliest Cambrian of the Wernecke Mountains, Yukon; in Current Research, Part B, Geological Survey of Canada, Paper 84-1B, p. 285-297.

Hofmann, H.J., Fritz, W.H., and Narbonne, G.M.
1983: Ediacaran (Precambrian) fossils from Wernecke Mountains, northwestern Canada; Science, v. 221, p. 455-457.

Narbonne, G.M., Fritz, W.H., Nowlan, G.S., and Hofmann, H.J.
1984: Faunal evolution across the Precambrian-Cambrian boundary, Yukon Territory, Canada; S.E.P.M. Annual Midyear Meeting, Abstracts, p. 59.

Nowlan, G.S., Narbonne, G.M., and Fritz, W.H.
– Small shelly fossils and trace fossils near the Precambrian-Cambrian boundary in the Yukon Territory, Canada; Lethaia, v. 18. (in press)

Reeve, A.F.
1977: The Goz Creek zinc deposit, Yukon Territory; in North of 60, Mineral Industry Report, Yukon Territory, 1976; Department of Indian and Northern Affairs, EGS 1977-1, p. 6-19.

-72-

VOLCANIC BRECCIAS IN THE ISACHSEN FORMATION NEAR STRAND FIORD, AXEL HEIBERG ISLAND, DISTRICT OF FRANKLIN

Project 770047

B.D. Ricketts
Institute of Sedimentary and Petroleum Geology, Calgary

Ricketts, B.D., Volcanic breccias in the Isachsen Formation near Strand Fiord, Axel Heiberg Island, District of Franklin; in Current Research, Part A, Geological Survey of Canada, Paper 85-1A, p. 609-612, 1985.

Abstract

An 80 m thick sequence of volcanic breccia occurs in the upper Isachsen Formation at the northeast end of Strand Fiord. Most of the sequence consists of nonstratified, angular, nonsorted basalt breccia. These massive breccias originated when rising magma reacted with meteoric water at very shallow burial depths, and were subsequently extruded as breccia onto the Isachsen delta plain. A different origin is envisaged for the crudely stratified and matrix-supported breccias that occur in the upper few metres of the sequence. They are probably lahars that reworked the extruded breccia and small amounts of included bedrock.

Résumé

Dans la partie supérieure de la formation d'Isachsen, à l'extrémité nord-est du fjord Strand, on rencontre une épaisse séquence (80 m) de brèches volcaniques. La majeure partie de cette séquence est constituée de brèches basaltiques non stratifiées, à éléments anguleux, non triés. Ces brèches massives se sont formées lorsque le magma ascendant a réagi avec les eaux météoriques à très faible profondeur, et s'est déversé ensuite sous forme de brèches sur la plaine deltaique d'Isachsen. On a envisagé une origine différente pour les brèches grossièrement stratifiées et englobées dans une matrice, que l'on rencontre dans les premiers mètres supérieurs de la séquence. Il s'agit probablement de coulées de boue (lahars) qui ont remanié les brèches extrudées, et de petits volumes de roche de fond incluse.

Stratigraphic setting

During field studies on western Axel Heiberg Island in 1983, some unusual volcanic breccias occurring in the Isachsen Formation were examined. The breccias, first described by Souther (1963), are exposed in two dip-slopes; one that forms a prominent ridge at the northeast end of Strand Fiord, and the other between Monkhead Mountain and a small glacial lobe of Hidden Icefield (Fig. 72.1). Stratigraphically, the breccias occur in the upper part of the Isachsen Formation, and therefore are probably Barremian-Aptian in age (A.F. Embry, personal communication, 1984).

Both upper and lower contacts appear to be conformable. Where breccias overlie typical Isachsen lithologies of interbedded sandstone, grey shale and thin coal seams, the lower bounding surface is abrupt. Diabase sills, some with prominent jointing, intrude the lower breccias and clastic Isachsen strata. In addition, Souther (1963, p. 439) also noted the presence of tuff beds near this contact.

The upper contact of the breccias is in most places faulted against dark grey shale of the Christopher Formation. However, a stratigraphic contact is exposed in a small saddle 5 km due north of the head of Strand Fiord. Here, the breccias are overlain by a 3 m interval of thin quartz arenites and interbedded shale (Fig. 72.2); the lowermost sandstone beds contain fine basalt pebbles and granules. This interval in turn is overlain by Christopher shale.

The maximum thickness of breccia exposed at these localities is about 80 m. In adjacent areas, the breccia appears to have pinched out completely. Upper Isachsen strata that outcrop near Strand Diapir contain only isolated

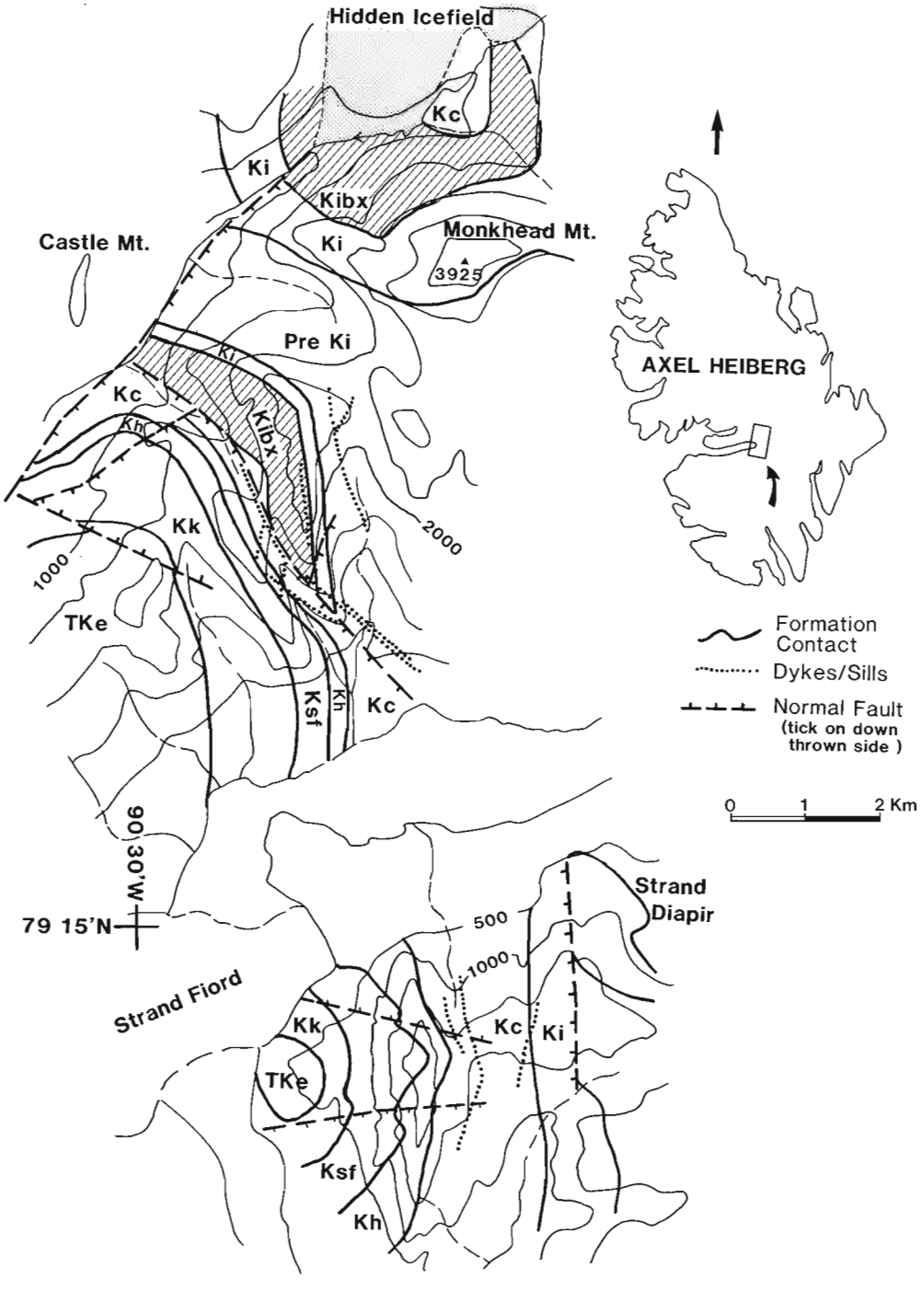

Figure 72.1

Locality map of the Isachsen breccias, western Axel Heiberg Island. Area of exposure is delineated by the diagonal pattern (Kibx). Other stratigraphic units are:

(oldest) Pre-Ki = pre-Isachsen strata;
Ki = Isachsen;
Kc = Christopher Fm;
Kh = Hassel Fm;
Ksf = Strand Fiord Fm;
Kk = Kanguk Fm;
TKe = Eureka Sound Fm.

Geology modified after Thorsteinsson (1971a).



Figure 72.2. *Stratigraphic contact between the crudely stratified breccia and interbedded sandstone and shale at the top of the Isachsen Formation. Located approximately 5 km due north of Strand Fiord. (ISPG 2045-382)*



Figure 72.3. *Matrix supported breccia containing large basalt blocks. The lower part of this unit is ice covered. Hammer is 33 cm long. Same locality as Figure 72.2. (ISPG 2045-383)*

diabase sills, the breccias having disappeared over a distance of less than 5 km. Similarly, Fricker (1963) noted the presence of sills and a few basalt flows in the Isachsen Formation near Wolf Mountain some 12 km to the northwest, but no breccias. Thus, distribution of the breccias seems to be restricted to an area having a radius of 10 to 15 km about Monkhead Mountain.

Many of the diabase and gabbro dykes and sills that intrude the breccias also intrude overlying Christopher shale and Hassel sandstone, and are probably associated with the Upper Cretaceous extrusive event represented by the Strand Fiord volcanics.

Internal organization of the breccias

Crude sedimentary layering occurs at the top of the breccia sequence, and bedding, although vague, can be discerned by grain size contrasts. In contrast, breccia in the middle and lower part of the sequence is more massive. Two types of breccia are recognized:

a. Crudely bedded, poorly sorted pebble and cobble breccia layers in the upper few metres of the sequence, having a matrix-supported framework consisting mostly of basalt (90%) and subordinate clasts of shale, rare pebbles of andesite and dacite, and reworked lapillistone breccia. Clast size averages 20 cm. Some of the clasts show a moderate degree of rounding. The matrix is composed of shale, fine sand-sized basalt, and some rounded epiclastic quartz grains with abraided quartz overgrowths. One bed near the top of the sequence contains blocks of basalt that appear to float in a matrix of dark grey shale (Fig. 72.3).

b. Nonstratified and nonsorted breccias, some of which contain matrix-supported and others clast-supported frameworks (Fig. 72.4). Here, blocks consist almost exclusively of basalt that ranges from aphanitic to coarse grained, and up to 15% (by volume) amygdules. All fragments are extremely angular and range in size up to 2 m, averaging 50 cm. Occasional fragments show evidence of multiple brecciation.

Interpretation

A nonstratified and nonsorted breccia that bears some resemblance to the Isachsen breccia at Strand Fiord is found in the upper Cretaceous Hassel Formation on Amund Ringnes



Figure 72.4. *Massive, nonstratified breccia composed of a chaotic jumble of basalt blocks. Hammer is 33 cm long. (ISPG 2045-385)*

Island (Balkwill, 1983). Balkwill was able to trace the brecciated flows laterally to nonbrecciated, aphanitic basalt flows. The Hassel breccia was interpreted to be the product of phreatomagmatic fracturing of magma that had been intruded into water-saturated sediment at shallow depths, and subsequently extruded as breccia.

The Isachsen breccia however, is different from the Hassel example in a number of ways:

- crude stratification is present in the upper few metres of the Isachsen breccia;
- matrix and clast-supported frameworks occur, the matrix-supported varieties containing reworked shale and sandstone;
- no massive (nonbrecciated) lava flows occur in the eastern Strand Fiord area.

In regional stratigraphic considerations (Balkwill, 1978), the Isachsen Formation represents a major stage of delta construction in Sverdrup Basin. Isachsen strata immediately underlying the breccia at Strand Fiord are thin bedded sandstone, shale and coal, suggesting a delta plain setting, upon which the breccias accumulated.

A mechanism involving autobrecciation of massive lava flows cannot be completely dismissed, although one might expect to see at least some relics of massive lava preserved. The mechanism of brecciation suggested by Balkwill is considered feasible here, but with some modification. The Isachsen breccias probably originated in two ways. In the first case, rising magma reacted with meteoric water at very shallow depths beneath the delta plain, and was subsequently extruded as breccia. Some autobrecciation may also have occurred. Once a significant pile of breccia had accumulated on the delta plain (producing the bulk of the breccia sequence) reworking of basalt debris and included fragments of bedrock took place as a result of lahars that flowed down the flanks of the breccia pile, giving rise to the upper, stratified part of the sequence.

The Isachsen breccias are part of an intermittent but locally significant period of Lower Cretaceous volcanism in central and eastern Sverdrup Basin, represented by minor basic flows and volcaniclastics at Li Fiord (Fortier, 1963, p. 514) and the southwest shore of Strand Fiord (Tozer, 1963, p. 453), and felsic tuffs on Amund Ringnes (Balkwill, 1983). Map unit Kv, at the top of the Isachsen south of Hare Fiord, contains basalt flows (Thorsteinsson, 1971b).

Acknowledgments

A.F. Embry and K.G. Osadetz are gratefully acknowledged for their constructive criticism of the manuscript, and numerous discussions during the course of the field season.

References

Balkwill, H.R.
1978: Evolution of Sverdrup Basin, Arctic Canada; American Association of Petroleum Geologists, Bulletin, v. 62, p. 1004-1028.

1983: Geology of Amund Ringnes, Cornwall, and Haig-Thomas Islands, District of Franklin; Geological Survey of Canada, Memoir 390.

Fortier, Y.O.
1963: South side of Strand Fiord; in Geology of the North-Central part of the Arctic Archipelago, Northwest Territories (Operation Franklin), Fortier et al.; Geological Survey of Canada, Memoir 320, p. 513-515.

Fricker, P.E.
1963: Geology of the Expedition area, western central Axel Heiberg Island, Canadian Arctic Archipelago; Axel Heiberg Island Research Reports, McGill University, Montreal, Geology No. 1.

Souther, J.G.
1963: Geological traverse across Axel Heiberg Island from Buchanan Lake to Strand Fiord; in Geology of the North-Central part of the Arctic Archipelago, Northwest Territories (Operation Franklin), Fortier et al.; Geological Survey of Canada, Memoir 320, p. 426-448.

Thorsteinsson, R.
1971a: Geology, Strand Fiord, District of Franklin; Geological Survey of Canada, Map 1301A.

1971b: Geology, Greely Fiord west, District of Franklin; Geological Survey of Canada, Map 1311A.

Tozer, E.T.
1963: South side of Strand Fiord; in Geology of the North-Central part of the Arctic Archipelago, Northwest Territories (Operation Franklin), Fortier et al.; Geological Survey of Canada, Memoir 320, p. 448-456.

SEQUENCE ANALYSIS AND NOMENCLATURE OF UPPER CRETACEOUS TO HOLOCENE STRATA IN THE BEAUFORT-MACKENZIE BASIN

Project 790031

J.R. Dietrich, J. Dixon, and D.H. McNeil
Institute of Sedimentary and Petroleum Geology, Calgary

Dietrich, J.R., Dixon, J., and McNeil, D.H., Sequence analysis and nomenclature of Upper Cretaceous to Holocene strata in the Beaufort–Mackenzie Basin; in Current Research, Part A, Geological Survey of Canada, Paper 85-1A, p. 613-628, 1985.

Abstract

Eleven sequences, recognized in part from reflection seismic data, are present in Cenomanian to Holocene strata of the Beaufort-Mackenzie Basin. From youngest to oldest they are named: Shallow Bay, Iperk, Akpak, Mackenzie Bay, Kugmallit, Kopanoar, Richards, Reindeer, Fish River, Smoking Hills, and Boundary Creek. The last two units are of formational rank. Most of the sequences were deposited during times of delta progradation, with the exception of the Kopanoar sequence, which was deposited mostly in a deep water, turbidite fan-complex.

Résumé

On rencontre onze séquences, partiellement identifiées à l'aide des données de sismique-réflexion, dans les strates d'âge cénomanien à holocène, dans le bassin de la mer de Beaufort et du delta du Mackenzie. De la plus récente à la plus ancienne, il s'agit de: Shallow Bay, Iperk, Akpak, Mackenzie Bay, Kugmallit, Kopanoar, Richards, Reindeer, Fish River, Smoking Hills et Boundary Creek. Les deux dernières unités sont considérées comme des formations. La plupart de ces séquences ont été mises en place lors de phases de progradation du delta, à l'exception de la séquence de Kopanoar dont la mise en place a principalement eu lieu dans un complexe de cône de déjection à turbidites gisant en eaux profondes.

Introduction

A number of informal and formal stratigraphic nomenclature schemes for the Upper Cretaceous to Holocene succession in the Beaufort-Mackenzie Basin exist (e.g. Young et al., 1976; Hea et al., 1980; Lane and Jackson, 1980; Jones et al., 1980; Young and McNeil, 1982; Willumsen and Coté, 1982; Table 1, this paper). As a result, some successions have several names, or similar terms are employed for different stratigraphic intervals. Formal lithostratigraphic nomenclature has been proposed for the area under the modern Mackenzie Delta (Young and McNeil, 1982), but the identified units have limited use basin-wide. Interpretation of reflection seismic profiles and well data in terms of sequences (Mitchum et al., 1977) has become a commonly accepted method of analysing the stratigraphy of offshore basins. The formal naming and criteria for recognizing seismic/depositional sequences as stratigraphic units has not been incorporated into the principles of any code or guide to stratigraphic nomenclature. The recognition of sequences, however, is the most practical method for dividing the succession in the Beaufort-Mackenzie Basin, and in lieu of formal guidelines, the method is applied on an informal basis using the criteria as outlined by Mitchum et al. (1977). In effect, sequences are operational or parastratigraphic units (Bates and Jackson, 1980, p. 437).

Late Cretaceous to Recent sedimentation was, and still is, dominated by deltaic processes, resulting in a series of thick, generally northward prograding, delta-complexes. In the vicinity of the deltaic sediments the strata can be divided into sandstone and mudstone dominant successions, to which lithostratigraphic terminology can be applied (Young and McNeil, 1982). However, basinward, lithological differentiation is less apparent, and much of the offshore succession is lithologically similar over considerable thicknesses of strata. These offshore successions contain strata that may be equivalent to more than one lithostratigraphic unit of the basin margin. The sequence concept is well suited to overcoming some of these problems, and there have been some attempts to identify sequences in the past (Lane and Jackson, 1980; Willumsen and Coté, 1982). However, these earlier studies have not been exacting in their definitions and different terminology was used for similar sequences. Jones et al. (1980) tried to overcome the

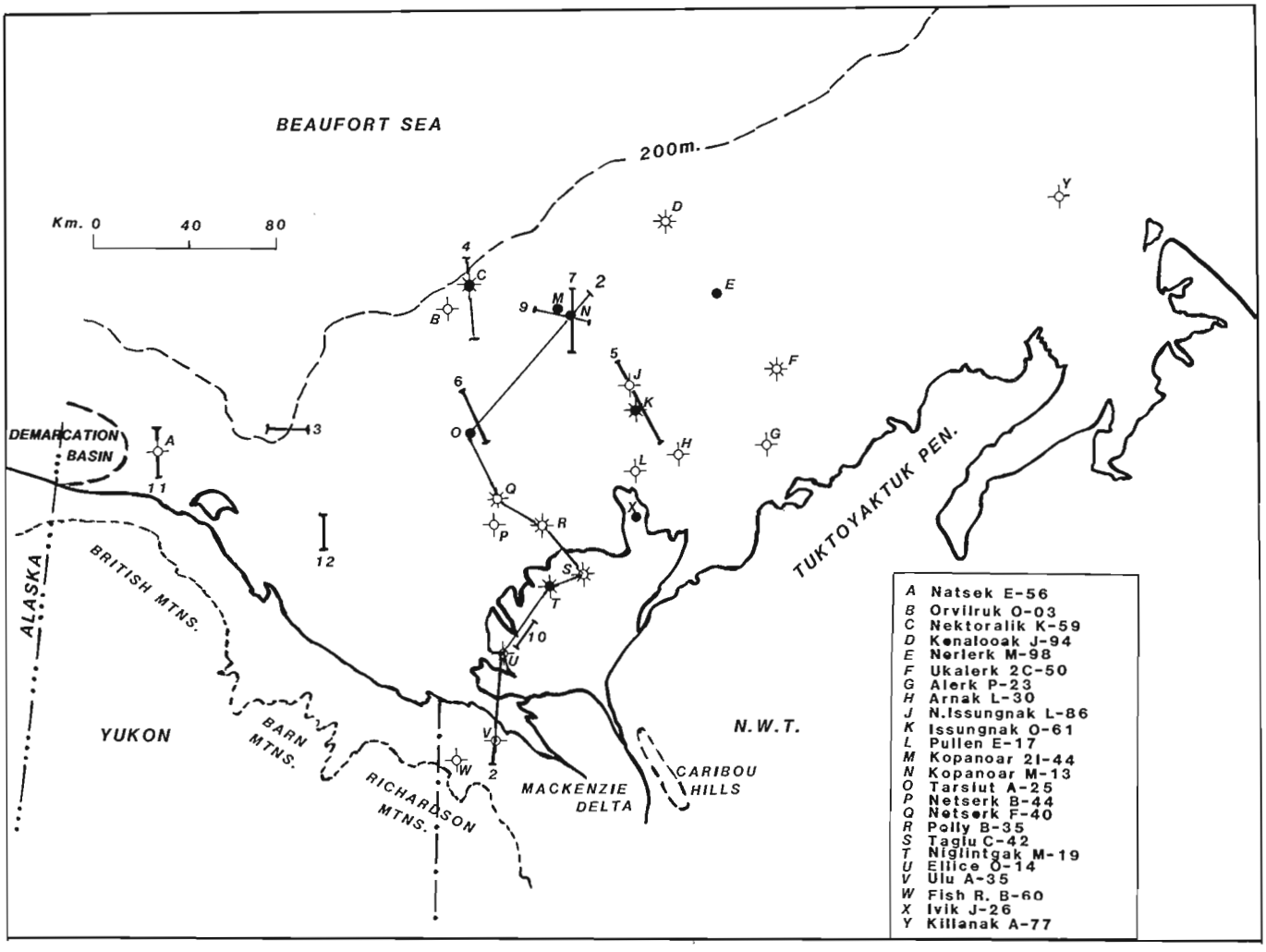

Figure 73.1. Location of wells, cross-section (Fig. 73.2) and seismic profiles (Fig. 73.3-73.7, 73.9-73.12).

nomenclature problem in the Pliocene-Pleistocene sequence by naming it the Iperk Group, allowing future workers the opportunity of subdividing it into formations.

In order to minimize the number of stratigraphic names used in the Beaufort-Mackenzie Basin it is proposed that the identified sequences bear the same name as the dominant formation within the sequence. For example, the Reindeer sequence contains the Reindeer Formation, as well as all other coeval facies. However, it should be noted that sequence and formational boundaries do not necessarily coincide. For example, the base of the Reindeer sequence is recognized as the base of the Ministicoog Member of the Moose Channel Formation.

The eleven sequences have been identified using reflection seismic profiles, well data, and, to a limited extent, outcrop data. The most important aspect of the analysis is the recognition of the sequence boundaries. At the basin margins, the sequence boundaries are usually subaerial unconformities, commonly exhibiting pronounced angular relationships on seismic data. Basinward, where the strata become more conformable, the boundaries represent, in part, submarine unconformities (?hiatal surfaces of Frazier, 1974). Whether the two surfaces are stratigraphically contiguous is debatable (Embry, 1983). The submarine unconformities have been identified either from seismic data (as conformable but abrupt changes in reflection character across the boundary) or from well data (using such criteria as abrupt changes in velocity gradients and lithofacies). Pronounced submarine erosion is locally developed at sequence boundaries, especially along paleo-shelf edges and slopes.

Biostratigraphic studies of selected wells have allowed for dating of the sequences as well as providing additional control for the sequence correlations. Most of the well

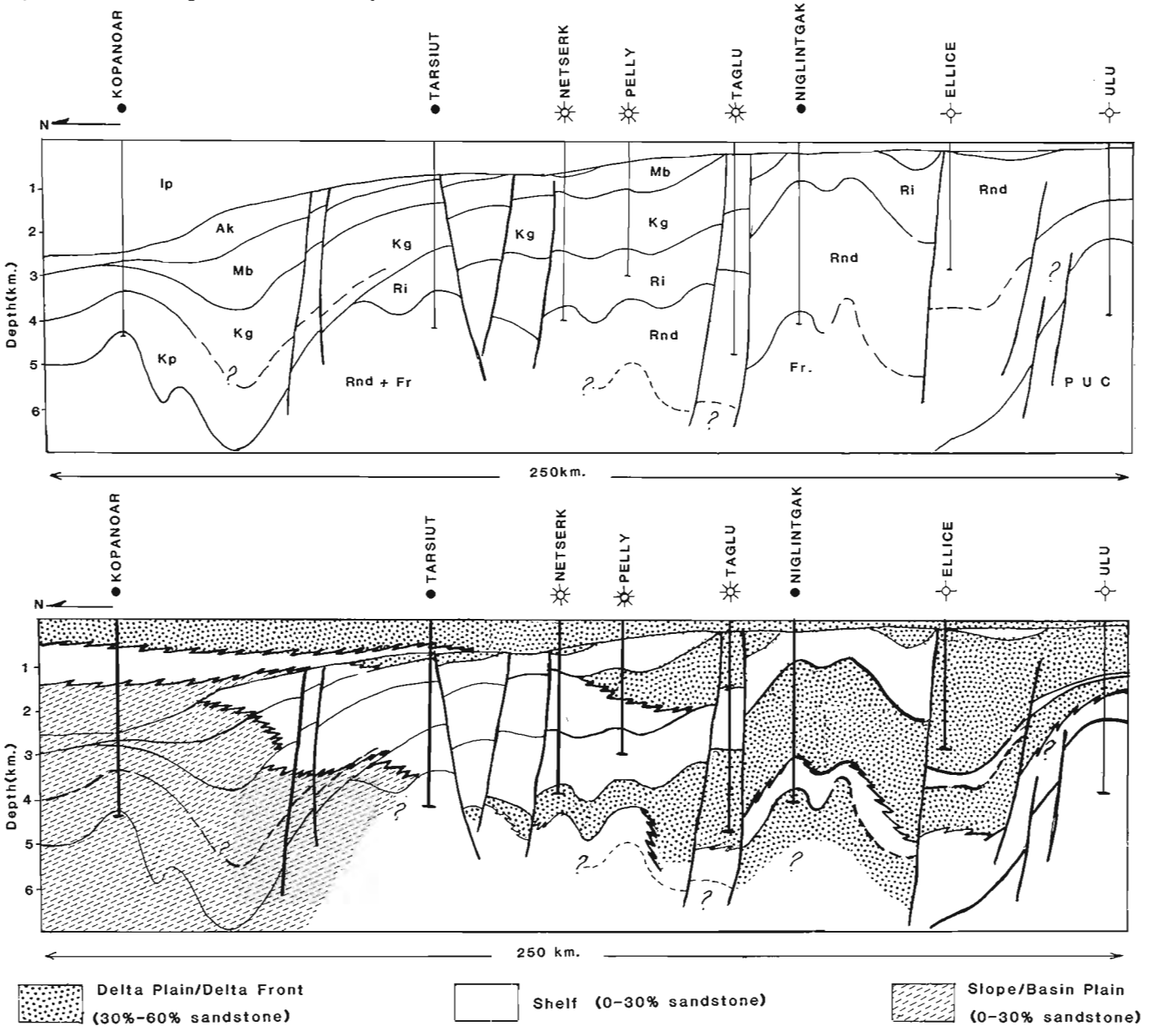

Figure 73.2. *Schematic structural-stratigraphic cross-section through the Beaufort-Mackenzie Basin. A. Distribution of sequences, Ip - Iperk; Ak - Akpak; Mb - Mackenzie Bay; Kg - Kugmallit; Kp - Kopanoar; Ri - Richards; Rnd - Reindeer; Fr - Fish River; PUC - Pre-Upper Cretaceous. B. Facies distribution within the sequences.*

control is from the Mackenzie Delta and the offshore areas immediately north of the Delta (Fig. 73.1). In the western and eastern Beaufort Sea well control is minimal (Fig. 73.1), and the character and identity of the sequences have not been confirmed with direct evidence. Nevertheless, it has been possible to correlate many of the sequences into areas of less control because of the generally good quality seismic data. Regional cross-sections, constructed from seismic and well data (Fig. 73.2a,b), illustrate the general distribution and lithofacies for the central portion of the basin. Much of the following discussion will tend to concentrate on the character of the sequences as determined in the area of better control.

Shallow Bay sequence

The Shallow Bay sequence is the youngest identifiable seismic sequence. It is best developed in the Mackenzie Trough (formerly Mackenzie Canyon), where it reaches a thickness estimated to be about 400 m (Fig. 73.3). Within the trough, the sequence rests erosionally on older strata; on the shelf areas, the sequence is thinner and is not detectable on most conventional CDP seismic data and therefore is not readily separated from the underlying strata (mostly the Iperk sequence). In the boreholes, samples are usually not available from these shallow depths, but from our knowledge of seabed samples in the offshore, the sediments consist of mud, silt, sand and gravel (Vilks et al., 1979). The Shallow Bay sequence includes sediments of the modern delta.

Reflections within the Shallow Bay sequence at its type area are generally low amplitude, discontinuous and subparallel (Fig. 73.2).

It is assumed that deposition of the Shallow Bay sequence began after the last major glaciation and was mostly Holocene, however, sediments as old as latest Pleistocene may be included.

Iperk sequence

The Iperk sequence is named after the Iperk Group (Jones et al., 1980). The Iperk Group has its type section in the Ukalerk C-50 well, between the base of the glory hole and 1568 m (5144 ft) below KB (Kelly Bushing), where a regional unconformity forms the base of the group. McNeil et al. (1982, p. 2) placed the base of the group (i.e. the unconformity) at 1571.5 m (5156 ft). As originally defined, the Iperk Group includes strata equivalent to the Shallow Bay sequence, however, the Iperk sequence excludes such strata. Unfortunately, an accurate estimate of the thickness of Shallow Bay strata at Ukalerk C-50 is not possible because control is inadequate, but it is guessed to be only a few metres thick.

The Iperk sequence forms a distinct, thick, lens-shaped deposit in which there is very little seismically visible structure (Fig. 73.4). It is a relatively simple progradational sequence in which parallel and divergent reflections on the basin margin grade laterally into continental-slope clinoform reflections. Thickness of the sequence varies from a few tens of metres at the basin margin to about 5000 m at its depocentre northeast of the Kenalooak J-94 well. Rapid thickening of the sequence begins just north of the Tarsiut-Issungnak areas, and can be traced eastward through the Tingmiark-Ukalerk area, then northeastward across the Amundsen Gulf. In the western Beaufort Sea, the Iperk sequence is relatively thin.

At the basin margin, and forming the topset portion of the sequence, are parallel, discontinuous reflections of low to moderate amplitude. The basin margin sediments consist of sand and gravel. These sediments are predominantly nonmarine to marginal marine near the Tuktoyaktuk Peninsula, grading laterally into marine sediments. The foreset reflections have moderate to high amplitudes and are discontinuous (Fig. 73.4). The sediments of the foreset beds are predominantly mud and silt. The bottomset reflections have low to moderate amplitudes, are discontinuous and subparallel to hummocky. Sediments in the bottomset beds consist of interbedded mud, silt, and sand.

The Nuktak Formation (Young and McNeil, 1982) is the correlative unit on the Mackenzie Delta (Table 73.1). However, the term Iperk has precedence and also incorporates all facies within the sequence. The term Beaufort (both as a formation and a sequence) has been used

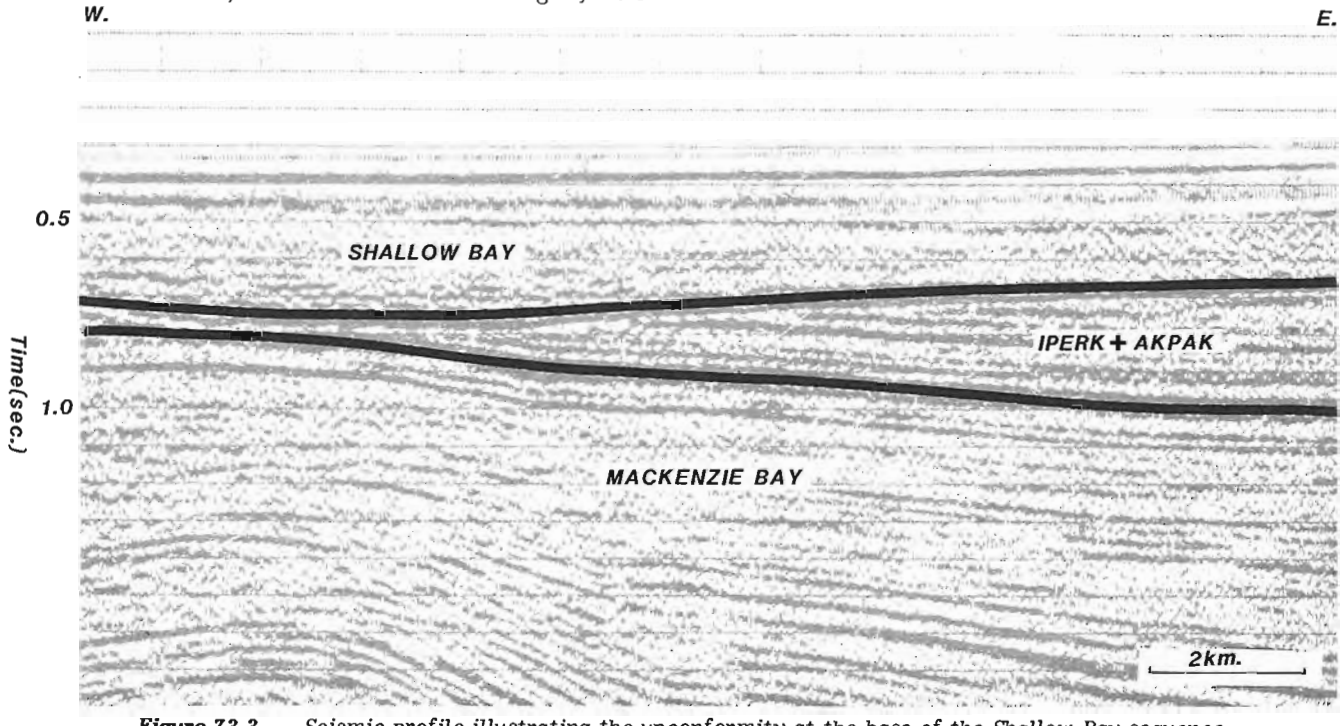

Figure 73.3. Seismic profile illustrating the unconformity at the base of the Shallow Bay sequence.

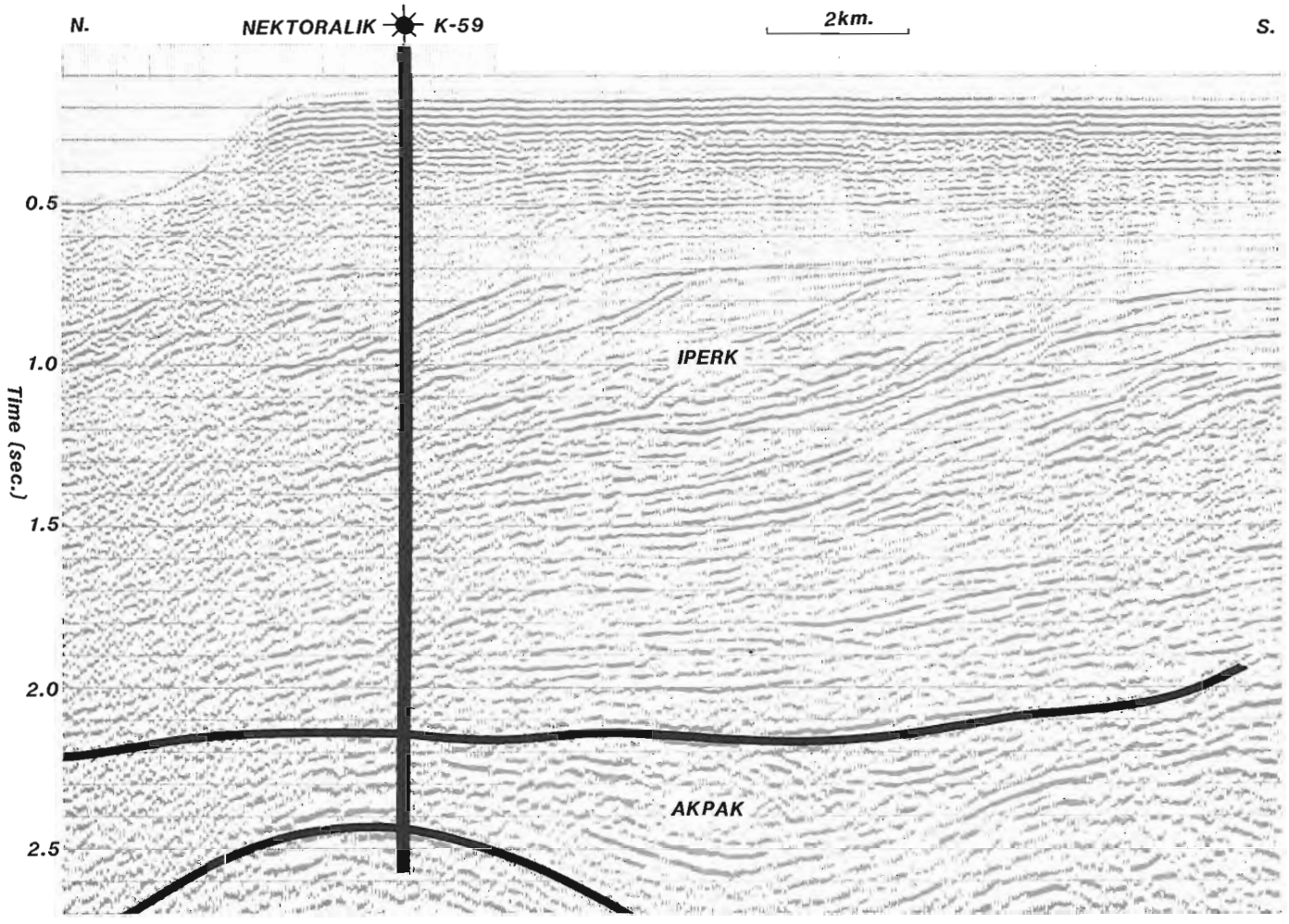

Figure 73.4. *Well-developed continental-slope clinoforms in a thick Iperk sequence.*

to name strata equivalent to the Iperk (Table 73.1; Hea et al., 1980; Lane and Jackson, 1980; Willumsen and Coté, 1982). However, the use of this term is fraught with numerous problems. Beaufort Formation was used originally to identify the youngest sands and gravels on Prince Patrick Island in the Arctic Archipelago (Tozer, 1956). Unfortunately, no definitive ages have ever been determined at the type section. Lithologically similar strata on Banks Island have been identified as Beaufort Formation and dated as Early to Late Miocene, and possibly as young as Pliocene, although an Early to Middle Miocene age seems to be most commonly accepted (Hills and Fyles, 1973; Hills et al., 1974; Hopkins, in Miall, 1979). In the Caribou Hills, on the southeast margin of the Mackenzie Delta, gravels overlying the Reindeer Formation have been tentatively correlated with the Beaufort Formation (Doerenkamp et al., 1976; Young et al., 1976, p. 36; Price et al., 1980). The floral assemblages from the Banks Island and Caribou Hills successions contain similar elements (Doerenkamp et al., 1976). The flora from these two localities are also similar to those of the pre-Iperk Miocene under the Mackenzie Delta and Beaufort Sea (Young and McNeil, 1982; McNeil et al., 1982; Dixon et al., 1984). It would appear that the Beaufort Formation of Banks Island and the Caribou Hills is older than the Iperk sequence and not coeval, as implied by some authors. Young et al. (1976, p. 38) suggested that the Beaufort Formation may be older than Pliocene-Pleistocene but still retained it as such in their table of formations (op. cit., Table 1, p. 8-9). In a later publication Young and McNeil (1982) redefined the Beaufort Formation as used in the Mackenzie Delta area, and identified it as a Miocene unit. However, the validity of their "Beaufort Formation" as a mappable entity, separate from the upper beds of the Kugmallit Formation/sequence is debatable. From the preceding discussion it would be reasonable to assume that some, or the whole of the Beaufort Formation on Banks Island is equivalent to the Mackenzie Bay and/or Akpak sequences of the Beaufort-Mackenzie Basin. The relationship between the Banks Island Beaufort and that of the type section remains obscure.

The age of the Iperk sequence is Pliocene-Pleistocene, and possibly as old as latest Miocene (Young and McNeil, 1982 – their Nuktak Formation; McNeil et al., 1982; Dixon et al., 1984 – their Sequence 1).

Akpak sequence

Willumsen and Coté (1982) introduced the term Akpak Delta for a succession between the top of the Kugmallit (their Pullen) and the base of the Iperk. It is proposed that the Akpak sequence be restricted to the upper half of Willumsen and Coté's Akpak Delta, corresponding approximately to the hachured interval on their Figure 13 (op. cit.). The lower part of the Akpak Delta is equivalent to the Mackenzie Bay sequence.

The Akpak sequence is present throughout most of the basin. It is about 700 to 800 m thick in the vicinity of North Issungnak L-86, but is thickest in the west Beaufort, where it

Table 73.1. Comparison of stratigraphic terminology used by various authors for Upper Cretaceous-Holocene strata in the Beaufort-Mackenzie Basin. Note that although similar physical units have been recognized by many authors, ages vary quite markedly. Non-hachured sequence boundaries imply contact is a submarine unconformity.

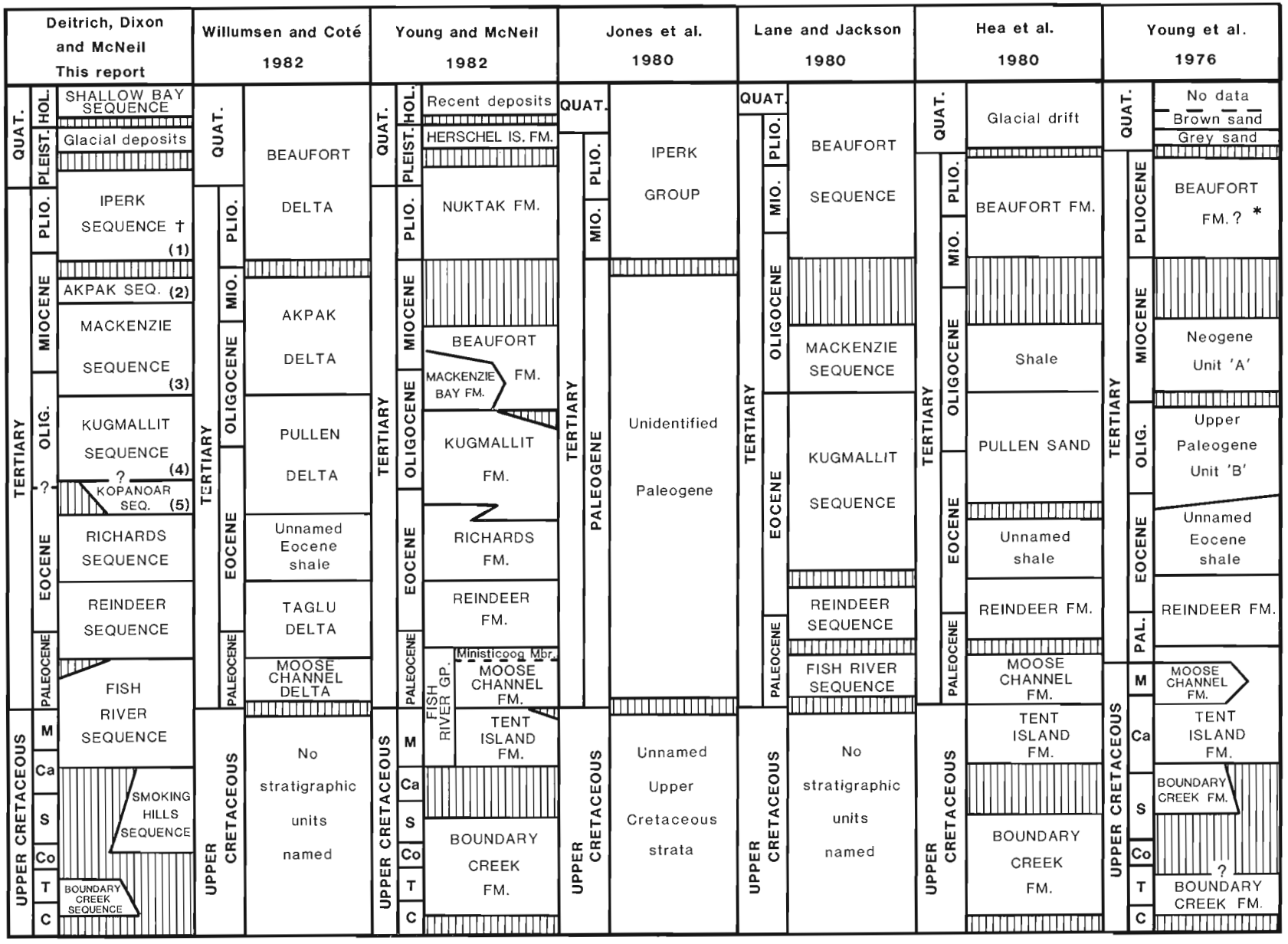

\+ Numbers refer to sequences identified in the Kopanoar M-13 well (Dixon et al., 1984).

* Young et al. (1976, p. 38) also tentatively suggested an older age, and that the Beaufort may be the same as their Neogene Unit "A".

is estimated to be 2500 m thick. Some of the strata in the Demarcation Basin (also known as the Jago Basin) appear to be Akpak strata. Its southern limit is a truncation edge under the sub-Iperk unconformity and is located just north of the Netserk B-44 and Pullen E-17 wells. In the areas where the Akpak has been penetrated, it is predominantly mud and silt, with a few thin sand beds. In the Tarsiut wells and Netserk F-40 there are several thick sand units, although mud and silt are the predominant lithotypes.

On seismic profiles, the Akpak sequence is characterized by a reflection-free interval in the central part of the basin (Fig. 73.5), grading laterally into an interval of discontinuous reflections of low amplitude in the west Beaufort area. Continental slope clinoform reflections are present within the sequence. The bottomset reflections commonly have a hummocky appearance, grading northward into sub-parallel reflections.

The age of the Akpak sequence is probably Middle to early Late Miocene (unpublished work of D.H. McNeil).

Mackenzie Bay sequence

Underlying the Akpak sequence is the Mackenzie Bay sequence (Fig. 73.5). It is named after the Mackenzie Bay Formation (Young and McNeil, 1982), to which it is essentially equivalent. However, unlike Young and McNeil (1982) we do not recognize the interdigitation of their Beaufort Formation with the Mackenzie Bay, but rather suggest that the Mackenzie Bay rests abruptly on Kugmallit strata. In fact, Young and McNeil's Beaufort Formation does not appear to be a mappable unit. Their so-called Beaufort sands and gravels are the uppermost beds of the Kugmallit Formation/sequence.

The Mackenzie Bay sequence is present under most of the Beaufort shelf. The southern limit is a truncation edge under the sub-Iperk unconformity and consequently is rarely preserved under the modern delta. The sequence is about 362 m thick at Netserk B-44 (this is the type section of Young and McNeil's (1982) Mackenzie Bay Formation), thickening northward to about 1000 m in the vicinity of North Issungnak L-86. However, its thickest development is in the western Beaufort, where it is estimated to be as thick as 2500 m in areas where correlations are reasonably certain. The Demarcation Basin is believed to be filled, in large part, by Mackenzie Bay and Akpak strata, estimated to be 5000-6000 m thick.

Where penetrated, the Mackenzie Bay sequence is dominated by mud and silt, although some thin sand units are present in the Netserk-Tarsiut area.

Reflections vary from moderate to high amplitude and are generally continuous in topset and foreset strata (Fig. 73.5). Bottomset bed reflections have low to moderate amplitude, and are hummocky to subparallel.

The age of the Mackenzie Bay sequence is Late Oligocene to Middle Miocene (Young and McNeil, 1982; Dixon et al., 1984).

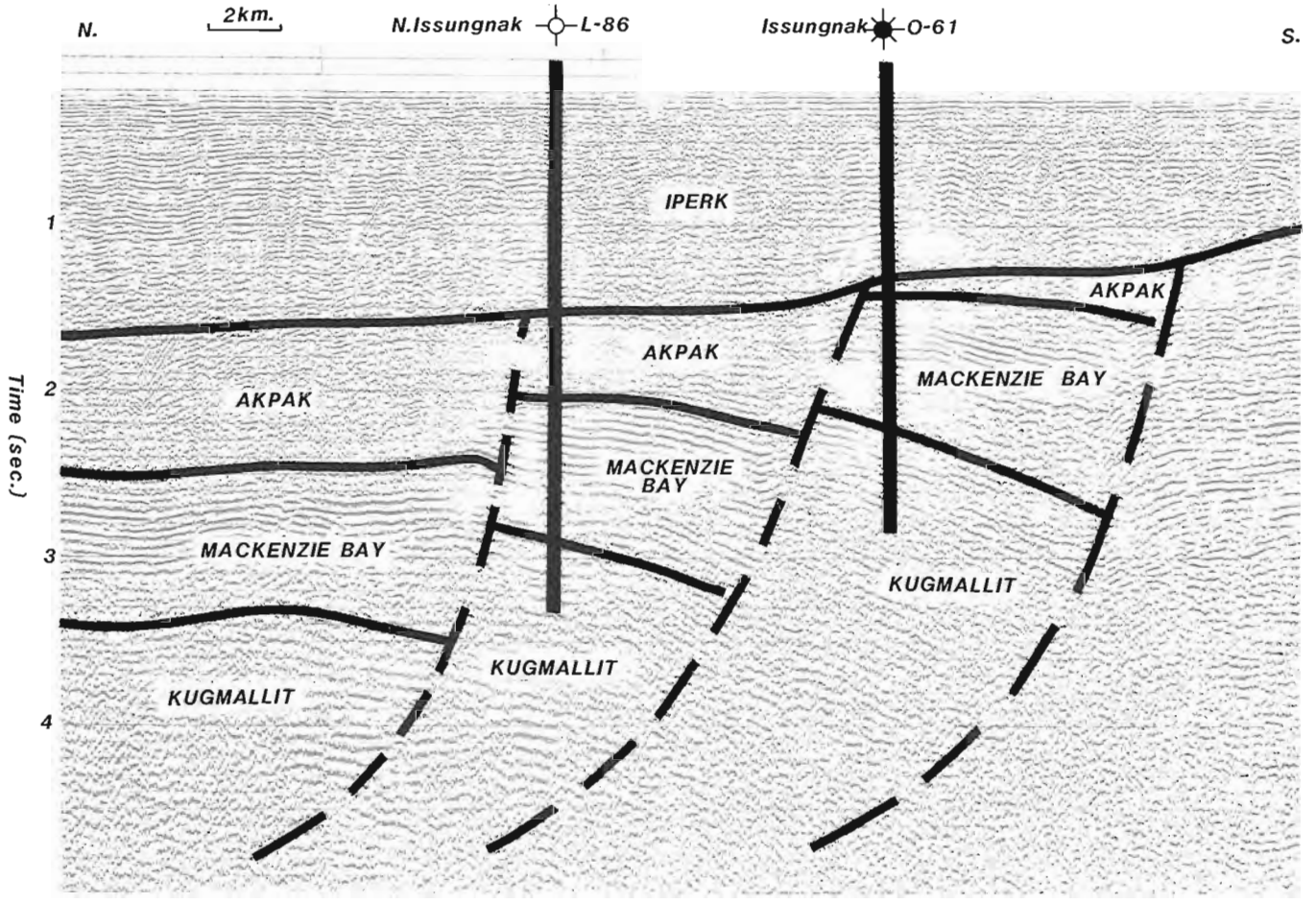

Figure 73.5. *Correlation of sequences across the listric fault zone.*

Kugmallit sequence

The Kugmallit sequence is named after the Kugmallit Formation (Young and McNeil, 1982), which forms the deltaic facies of the sequence. It underlies conformably, but abruptly, the Mackenzie Bay sequence. The basal contact of the sequence is apparently conformable over many parts of the shelf, but correlations indicate major shelf-edge erosion and an erosional unconformity. This sub-Kugmallit unconformity is apparent on dip-oriented seismic profiles located north of the Tarsiut area (Fig. 73.6).

The Kugmallit sequence is present under much of the Beaufort shelf and part of the Mackenzie Delta. It is up to 3000 m thick at its depocentre in the vicinity of North Issungnak L-86. Northward and westward from the depocentre there is depositional thinning, but its southern and southeastern limits are erosional. It extends onto the northern edge of the Mackenzie Delta and subcrops under the Iperk sequence between the Taglu and Kumak areas.

Reflections from the topset strata of the Kugmallit sequence are of low to moderate amplitude, parallel and subparallel and discontinuous (Fig. 73.5). Reflections from foreset and proximal bottomset beds have variable amplitude and are hummocky to subparallel. Reflections from distal bottomset beds have low to moderate amplitude, and are parallel and subparallel.

Interbedded sand and mud of delta front origin occupy the depocentre in the Isserk-Issungnak area; to the south, the succession becomes sandier as delta plain deposits become more prevalent. East and west of the delta plain deposits, shelf and prodelta muds are dominant in the sequence, although local, isolated sand bodies are present (e.g. at Tarsiut and Ukalerk). North of the deltaic and shelf deposits are deep water muds and silts deposited as slope and submarine fan deposits. These deep water beds are mainly mud, but contain some interbedded sands, presumably of turbidite origin.

Willumsen and Coté's (1982) Pullen Delta and Young et al's. (1976) Upper Paleogene Unit B correspond, approximately, to the Kugmallit sequence (Table 73.1). The Kugmallit Formation of Young and McNeil (1982) is part of the Kugmallit sequence. It is also recognized that much of their Beaufort Formation cannot be differentiated from the uppermost strata of the Kugmallit Formation/sequence. Consequently, most of the sands and gravels identified as Beaufort by Young and McNeil are now regarded as Kugmallit beds.

The age of the Kugmallit sequence is believed to be Late Eocene to Middle or earliest Late Oligocene, and the oldest part of the sequence may be as young as Early Oligocene (Young and McNeil, 1982; Dixon et al., 1984; unpublished data by D.H. McNeil).

Kopanoar sequence

The Kopanoar sequence has been identified only in the farthest offshore wells, such as in the Kopanoar M-13 and 2I-44 boreholes (in M-13 between log depths 3339 m and 4288.5 m; in 2I-44 between log depths 3160-3915 m). It is separated from older strata by a major erosional unconformity and overlain conformably, but abruptly, by the Kugmallit sequence. The basal boundary is not difficult to identify on seismic profiles, but the upper boundary is not as apparent (Fig. 73.7). In the wells, the upper boundary is marked by a distinct change in the character of the sonic and resistivity log traces. In both log types there is a ragged trace through the Kugmallit sequence that changes to a very uniform trace at the top of the Kopanoar sequence (Fig. 73.8). Also, the velocity gradient changes at the

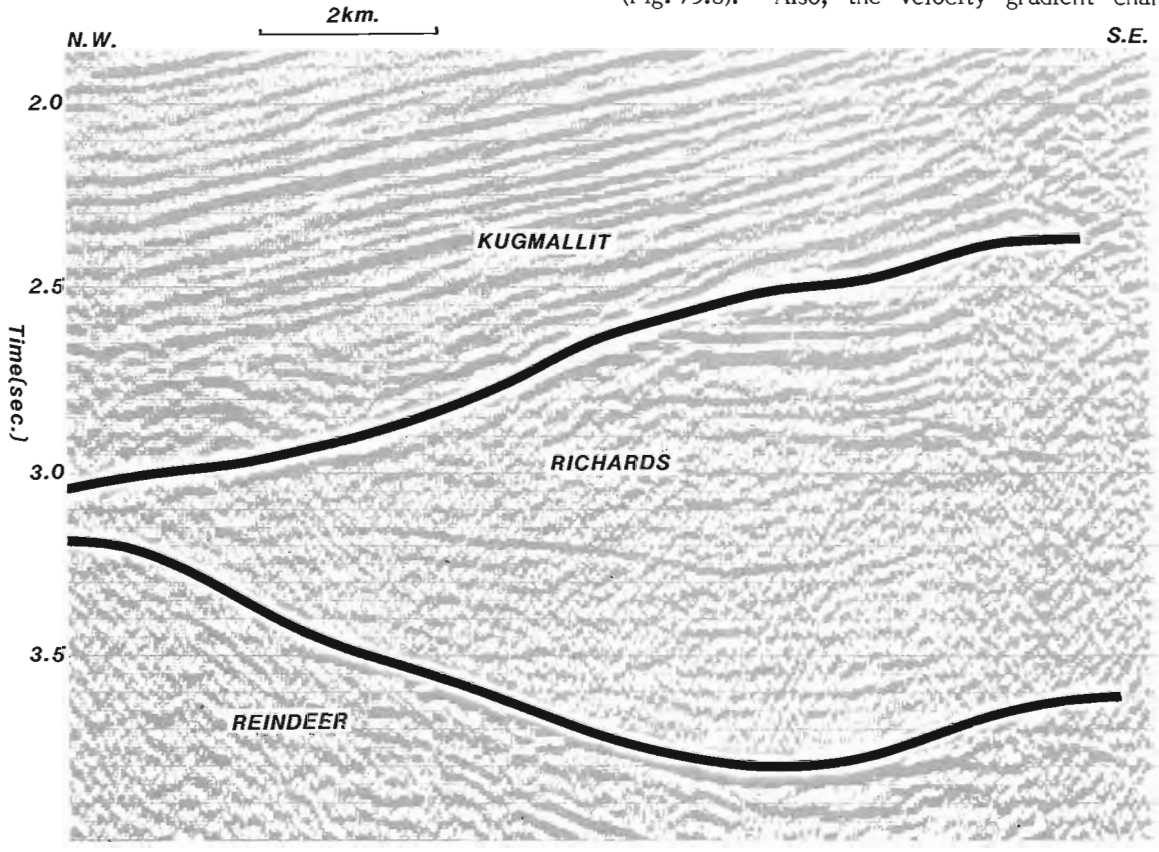

Figure 73.6. Portion of a seismic profile illustrating the unconformity at the base of the Kugmallit sequence.

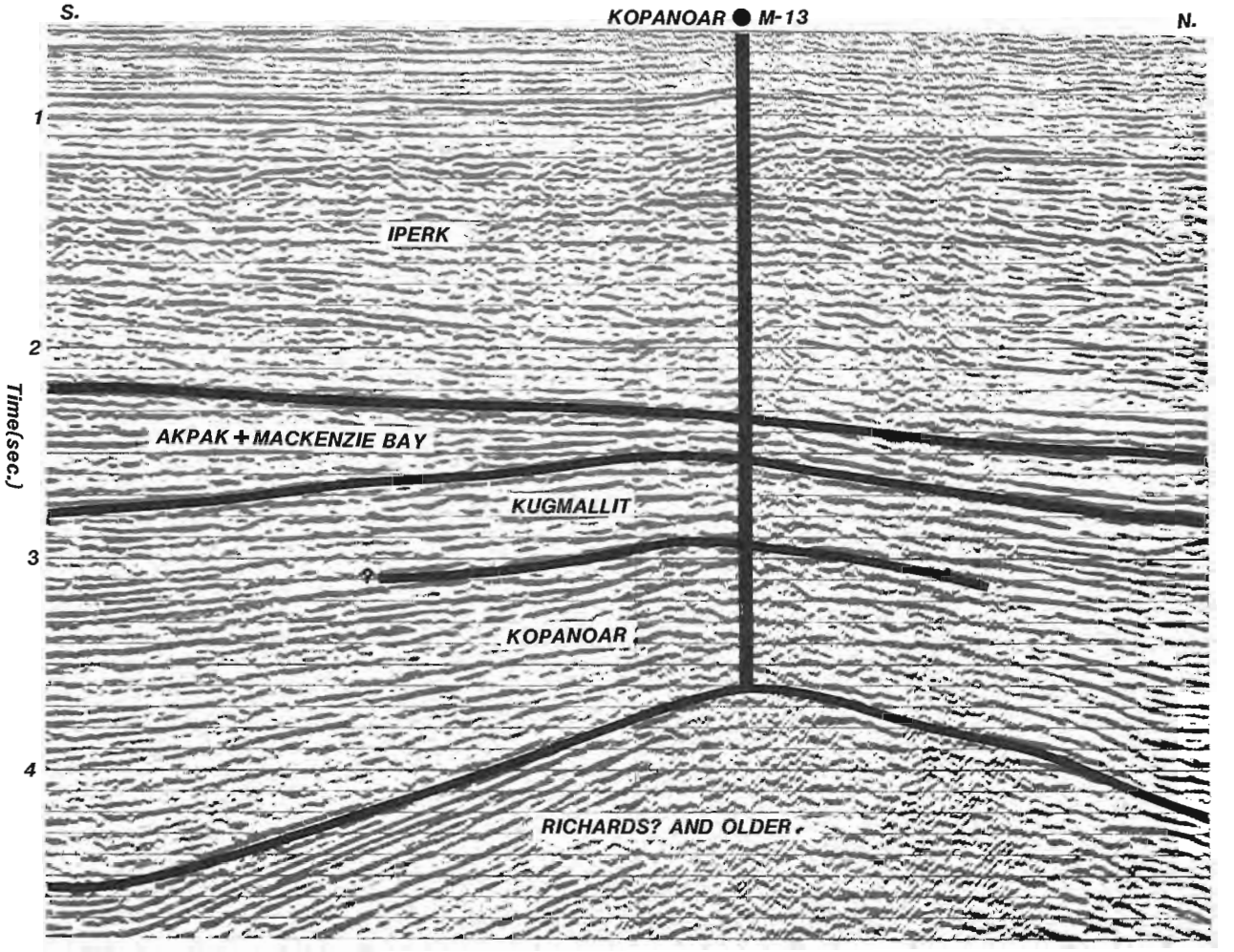

Figure 73.7. *Correlation of sequences across the Kopanoar structure. Note the well-defined sequence boundary at the base of the Kopanoar sequence.*

Kopanoar-Kugmallit contact (see Fig. 3 in Dixon et al., 1984) The Kopanoar-Kugmallit contact is interpreted to be a regional submarine unconformity (?hiatal surface of Frazier, 1974).

The Kopanoar sequence rarely exceeds 1000 m where penetrated, but seismic data indicate it may be up to 2500 m thick. Its extent south of the most northerly large-scale listric fault is uncertain, because of the difficulty in correlating reflections across the faulted area. Seismic reflection and well log correlations in the Alerk-Arnak area indicate that a thin representative of the Kopanoar sequence may extend south of the listric fault zone.

In the Orvilruk to Nerlerk area, the Kopanoar sequence consists mainly of silt and mud, but scattered throughout are sand-rich zones. The bulk of the Kopanoar sequence is interpreted to be of deep-water origin, and the sand beds were probably deposited on submarine fans (Dixon et al., 1984).

From the listric fault zone, north to the Kopanoar-Nerlerk trend, the sequence is dominated by reflections of variable amplitude, that are divergent to hummocky (similar to the overlying Kugmallit sequence). Strike oriented profiles clearly illustrate the mounded and chaotic nature of this seismic facies (Fig. 73.9). Farther north, the Kopanoar sequence grades into an interval of more continuous, subparallel reflections, probably representing deposition on the outer portions of the submarine fan complexes.

The age of the Kopanoar sequence is based principally on its stratigraphic position between two better dated units – the Richards and Kugmallit sequences. A Late Eocene and/or Early Oligocene age is indicated.

Although it is recognized that the Kopanoar sequence is not readily differentiated from the overlying Kugmallit sequence on seismic profiles, the log correlations indicate that a distinct mappable unit is present.

Richards sequence

The Richards sequence is named after the Richards Formation (Young and McNeil, 1982), which forms the bulk of the sequence. An unconformity separates the Richards and younger strata. In the west Beaufort, pre-Kugmallit shelf-edge erosion removed much of the Richards (Fig. 73.9). The lower boundary with the Reindeer sequence is conformable, but abrupt, and represents a submarine unconformity.

The Richards sequence is estimated to be 1200-1500 m thick in the Ivik area, and up to 2000 m thick in fault bounded synclines in the Ellice area. Under the Mackenzie Delta it subcrops beneath the Iperk sequence; in the offshore areas it subcrops under the Kugmallit sequence, and it appears to be absent in the farthest offshore wells.

Mud and silt are the dominant sediments, although some local sand and gravel beds are present. In the Ivik area, some of the lower, coarsening-upward cycles of the Kugmallit

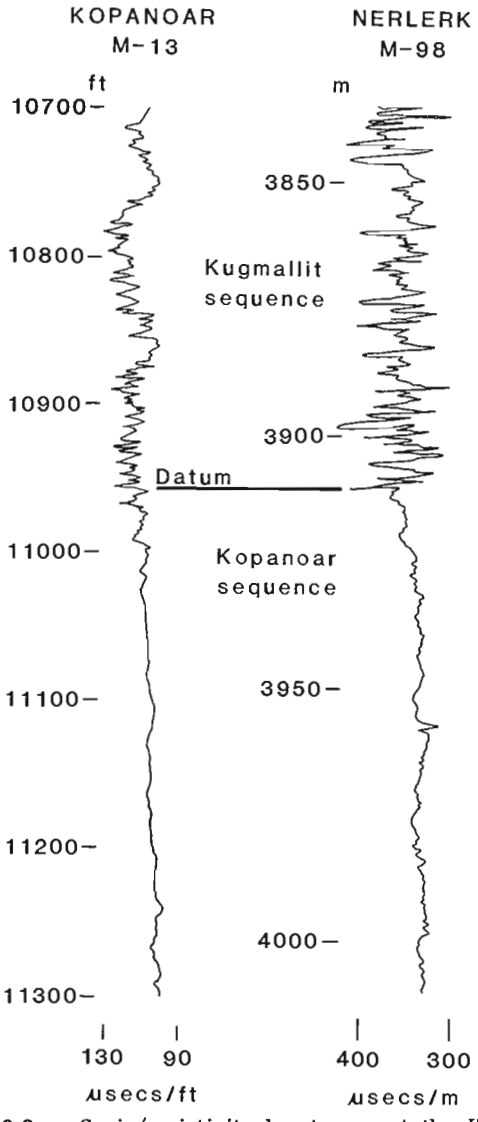

Figure 73.8. *Sonic/resistivity log traces at the Kugmallit-Kopanoar contact through two wells.*

Formation (Ivik Member of Young and McNeil, 1982) are interpreted to be part of the uppermost beds of the Richards sequence. These beds in the Ivik area would represent the only preserved part of a Richards subaerial delta.

Reflections in the Richards sequence are parallel, have a high degree of continuity and have low to moderate amplitude. A low-velocity mudstone section in the lower portion of the Richards sequence forms a distinct low amplitude reflection interval on several seismic profiles (Fig. 73.10). Where foreset beds have been identified in the Richards the reflections are discontinuous, and of low amplitude.

The age of the Richards sequence is Middle to Late Eocene (Young and McNeil, 1982).

Reindeer sequence

The Reindeer sequence is named after the Reindeer Formation (Mountjoy, 1967; Young et al., 1976; Price et al., 1982; Young and McNeil, 1982), which represents the delta plain and delta front facies of the sequence. Included in the Reindeer sequence is the Ministicoog Member of the Moose Channel Formation. The member is interpreted to represent the earliest phase of progradation, during which prodelta/shelf muds were deposited. In the Richards Island and nearshore areas the Reindeer-Richards contact is conformable but abrupt, and is readily recognized on seismic profiles (Fig. 73.10) and on geophysical well logs. The basal boundary is less readily recognized on seismic profiles, largely because it occurs within a thick, conformable succession of uniform seismic response that includes the Fish River sequence. Consequently, the basal contact has been identified in some wells and then correlated to a seismic profile. In the Caribou Hills and along most of the Tuktoyaktuk Peninsula, the Reindeer sequence rests unconformably on the lower part of the Fish River sequence (i.e. Mason River Formation) and, in places, Smoking Hills strata. In the west Beaufort, in the Natsek E-56 well and in the surrounding areas, seismic and well data indicate that the Reindeer sequence rests unconformably on the Fish River sequence, specifically the Moose Channel Formation of the sequence (Fig. 73.11, 73.12).

The main delta depocentre of the Reindeer sequence appears to have been centred in the Ellice area. Upwards of 4000 m of strata may be present in this area. Nonmarine and marginal marine sands and gravels are present along the Tuktoyaktuk Peninsula. North and northwest of the delta depocentre, the sequence is represented by prodelta/shelf muds and silts (Tarsiut to Natsek). Northeast of the Taglu area, the Reindeer sequence has not been penetrated, or at least not identified. However, on the basis of the known facies distribution, it is speculated that these unknown areas will contain prodelta muds and silts, and further northward will grade into deep water deposits.

Where identified, the Reindeer sequence is characterized by parallel to subparallel, continuous reflections of moderate to high amplitude. The reflection character of both the Reindeer and underlying Fish River strata is highly variable in areas where the sediments have been uplifted in large diapiric anticlines. In the far offshore areas, the pre-Kopanoar strata are presumed to be Reindeer sequence, in part at least, and these are characterized by discontinuous, parallel to divergent reflections of moderate to high amplitude.

The age of the Reindeer sequence is Paleocene to Early Eocene (Young and McNeil, 1982).

Fish River sequence

The Fish River sequence is named after the Fish River Group (Young, 1975), strata of which form the bulk of the sequence. Formational units within the sequence include the Moose Channel (exclusive of the Ministicoog Member), Tent Island and Mason River. The sequence rests abruptly, and commonly unconformably, on older strata. The Fish River sequence can only be identified with certainty on the basin margins, where the sequence occurs within the first few thousand metres below the surface. Throughout most of the central part of the basin, reflection character is lost at depth and the identification of the sequence is difficult. Some of the pre-Kopanoar strata in the far offshore areas almost certainly include equivalents of the Fish River strata. In the west Beaufort, including the Natsek area, the top of the Fish River sequence is very distinct on seismic profiles but its base is difficult to locate (Fig. 73.11, 73.12).

In the northern Richardson Mountains and southwestern Mackenzie Delta, the sequence is 1800-2000 m thick. At Natsek E-56 an incomplete section, 1951 m thick, was penetrated. The sequence is probably 4000-6000 m thick in the Natsek area. It appears from seismic data that the Fish River depocentre was located in the west Beaufort-Mackenzie Bay area.

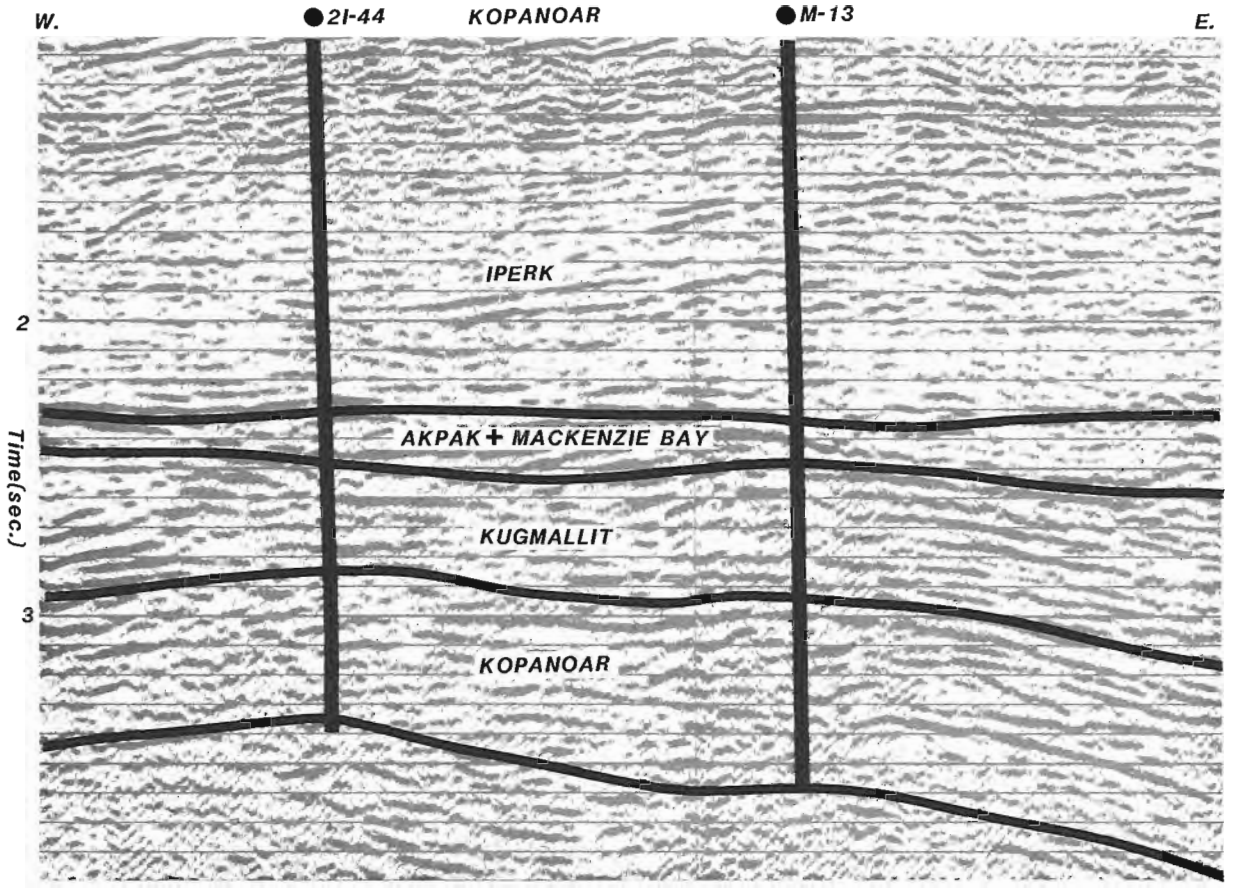

Figure 73.9. *Strike oriented seismic profile through the two deep Kopanoar wells, illustrating correlations and the mounded character of the reflections through much of the section.*

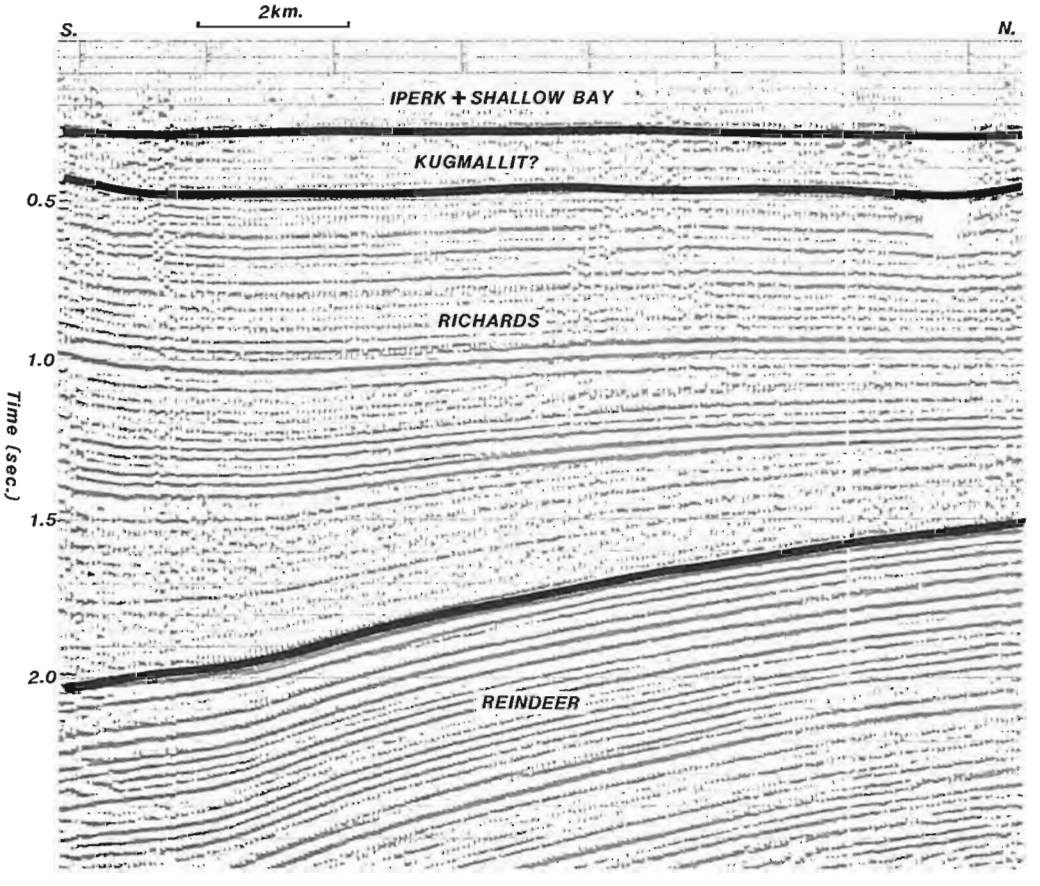

Figure 73.10. *Relatively conformable but abrupt contact between the Richards and Reindeer sequences.*

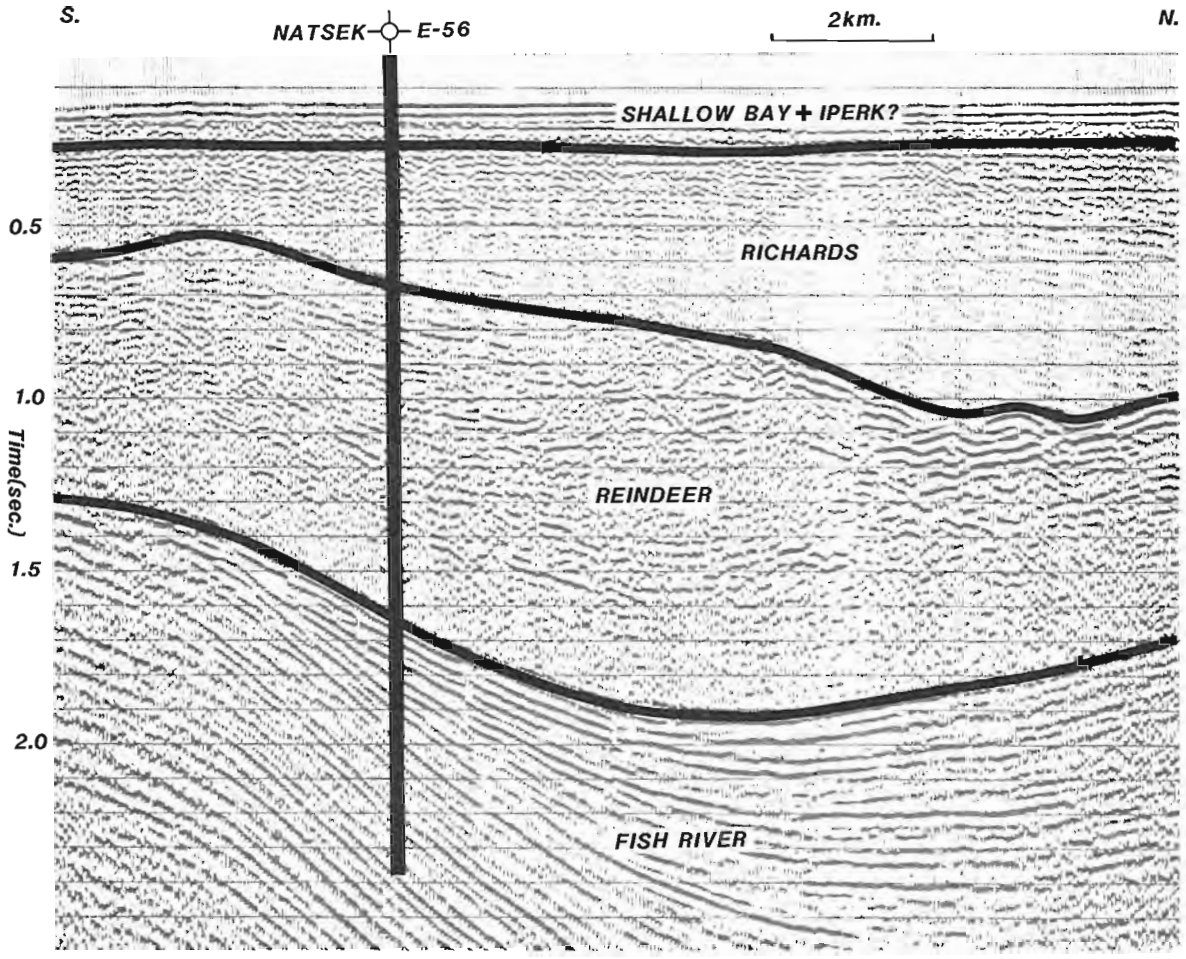

Figure 73.11. *Seismic profile through the Natsek E-56 well.*

The Fish River sequence is characterized by prodelta mud and silt in its lower part (Tent Island-Mason River formations), overlain by a thick succession of delta plain and delta front rocks, which in the Natsek area contain some of the thickest coal seams known in the basin. Throughout most of the basin, Fish River strata have not been penetrated.

In areas where Fish River strata are relatively unstructured (as seen in seismic profiles), the lower part of the sequence is characterized by discontinuous reflections of low amplitude, whereas the delta plain – delta front rocks of the sequence have subparallel to divergent reflections of high amplitude.

The age of the Fish River sequence is Late Campanian to Paleocene (Young et al., 1976).

Cenomanian-Campanian sequences

Below the Fish River sequence and above Albian strata are at least two unconformity-bounded units of formational rank, the Boundary Creek and Smoking Hills formations. These two units are relatively thin – only a few hundred metres or less – and can only be identified with certainty on the basin margins. Their thinness makes them difficult to separate from Fish River strata on most seismic profiles.

The Boundary Creek sequence consists of organic-rich shale with bentonites and concretionary layers. It is present in the northern Richardson Mountains, the northern flank of the Barn Mountains, and has been identified in a few wells on the northernmost edge of the Richardson Mountains (e.g. Fish River B-60). It is overlain unconformably by Fish River strata, and unconformably overlies a variety of Lower Cretaceous units. A Cenomanian to Turonian age is indicated by the contained microflora (D. McIntyre, personal communication).

On the east side of the delta, in the subsurface of the Tuktoyaktuk Peninsula, and in the Anderson Plains, the Smoking Hills Formation forms another, younger, unconformity-bounded sequence. It rests unconformably on a variety of Paleozoic and Lower Cretaceous units, and is overlain abruptly, and probably disconformably, by Mason River shale of the Fish River sequence. The Smoking Hills unit is a bituminous shale. It is probably the highly radioactive shale seen in the subsurface of the Tuktoyaktuk Peninsula. A Coniacian to Campanian age is indicated for the Smoking Hills Formation/sequence (McIntyre, 1974; Yorath et al., 1975).

The Boundary Creek and Smoking Hills sequences represent the basal beds of the Upper Cretaceous to Holocene sequences. However, from the limited data available, their extent throughout the basin is not well known. They may form a thin, but discontinuous veneer at the base of the sequences, or be present in only a few local areas because of widespread, pre-Fish River erosion.

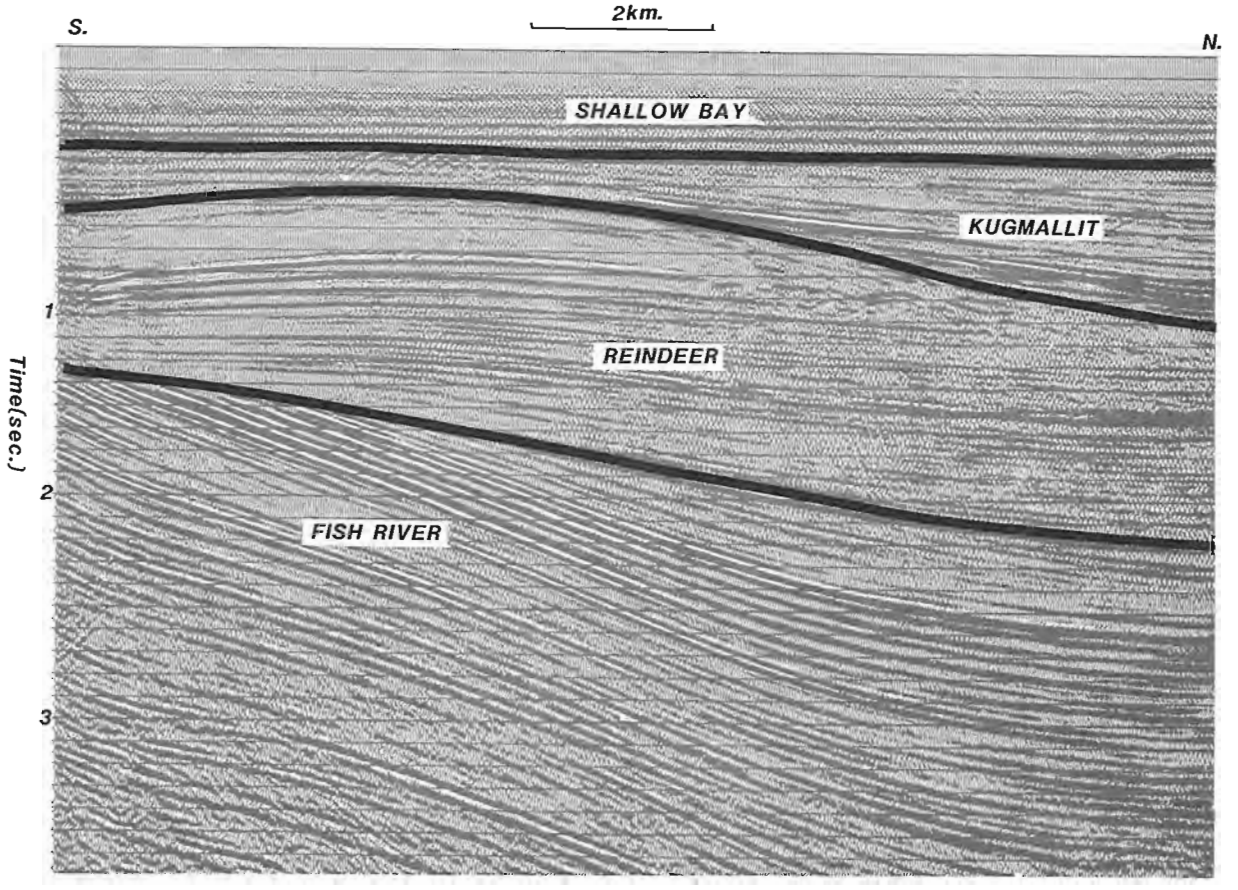

Figure 73.12. *Seismic profile illustrating three unconformities: between the Shallow Bay and Kugmallit; the Kugmallit and Reindeer, and the Reindeer and Fish River.*

References

Bates, R.L. and Jackson, J.A.
1980: Glossary of Geology; American Geological Institute, Falls Church, Virginia.

Dixon, J., McNeil, D.H., Dietrich, J.R., Bujak, J.P., and Davies, E.H.
1984: Geology and biostratigraphy of the Dome Gulf et al. Hunt Kopanoar M-13 well, Beaufort Sea; Geological Survey of Canada, Paper 82-13.

Doerenkamp, A., Jardine, S., and Moreau, P.
1976: Cretaceous and Tertiary palynomorph assemblages from Banks Island and adjacent areas (NWT); Bulletin of Canadian Petroleum Geology, v. 24, p. 372-417.

Embry, A.F.
1983: Depositional sequences – impractical lithostratigraphic units; Geological Society of America. Program with Abstracts, v. 15, no. 6, p. 567.

Frazier, D.E.
1974: Depositional-episodes: Their relationship to the Quaternary stratigraphic framework in the northwestern portion of the Gulf Basin; Bureau of Economic Geology, The University of Texas at Austin, Austin, Texas, Geological Circular 74-1.

Hea, J.P., Arcuri, J., Campbell, G.R., Fraser, I., Fuglem, M.O., O'Bertos, J.J., Smith, D.R., and Zayat, M.
1980: Post-Ellesmerian basins of Arctic Canada: their depocentres, rates of sedimentation and petroleum potential; in Facts and Principles of World Oil Occurrence, ed. A.D. Miall; Canadian Society of Petroleum Geologists, Memoir 6, p. 447-488.

Hills, L.V. and Fyles, J.G.
1973: The Beaufort Formation, Canadian Arctic Islands (abs.); in Program and Abstracts, Symposium on the Geology of the Canadian Arctic, Saskatoon, May 1973, Canadian Society of Petroleum Geologists and Geological Association of Canada, p. 11.

Hills, L.V., Klovan, J.E., and Sweet, A.R.
1974: *Juglans eocinera* N. sp. Beaufort Formation (Tertiary), southwestern Banks Island, Arctic Canada; Canadian Journal of Botany, v. 52, p. 457-464.

Jones, P.B., Brache, J., and Lentin, J.K.
1980: The geology of the 1977 offshore hydrocarbon discoveries in the Beaufort-Mackenzie Basin, N.W.T.; Bulletin of Canadian Petroleum Geology, v. 28, p. 81-102.

Lane, F.H. and Jackson, K.S.
1980: Controls on occurrence of oil and gas in the Beaufort-Mackenzie Basin; in Facts and Principles of World Oil Occurrences, ed. A.D. Miall; Canadian Society of Petroleum Geologists, Memoir 6, p. 489-507.

McIntyre, D.J.
1974: Palynology of an Upper Cretaceous section, Horton River, District of Mackenzie, N.W.T.; Geological Survey of Canada, Paper 74-14.

McNeil, D.H., Ioannides, N.S., and Dixon, J.
1982: Geology and biostratigraphy of the Dome Gulf et al. Ukalerk C-50 well, Beaufort Sea; Geological Survey of Canada, Paper 80-32.

Miall, A.D.
1979: Mesozoic and Tertiary geology of Banks Island, Arctic Canada; Geological Survey of Canada, Memoir 387.

Mitchum, R.M., Jr., Vail, P.R., and Thompson, S. III.
1977: Seismic stratigraphy and global changes of sea level, part 2: the depositonal sequence as a basic unit for stratigraphic analysis; in Seismic Stratigraphy - Applications to Hydrocarbon Exploration, ed. C.E. Payton; American Association of Petroleum Geologists, Memoir 26, p. 53-62.

Mountjoy, E.W.
1967: Upper Cretaceous and Tertiary stratigraphy, northern Yukon and northwestern District of Mackenzie; Geological Survey of Canada, Paper 66-16.

Price, L.L., McNeil, D.H., and Ioannides, N.S.
1980: Revision of the Tertiary Reindeer Formation in the Caribou Hills, District of Mackenize; Geological Survey of Canada, Paper 80-1B, p. 179-184.

Tozer, E.T.
1956: Geological reconnaissance, Prince Patrick, Eglinton and western Melville Islands, Arctic Archipelago, Northwest Territories; Geological Survey of Canada, Paper 55-5.

Vilks, G., Wagner, F.J.E., and Pelletier, B.R.
1979: The Holocene marine environment of the Beaufort Shelf; Geological Survey of Canada, Bulletin 303.

Willumsen, P.S. and Coté, R.P.
1982: Tertiary sedimentation in the southern Beaufort Sea, Canada; in Arctic Geology and Geophysics, ed. A.F. Embry and H.R. Balkwill; Canadian Society of Petroleum Geologists, Memoir 8, p. 43-53.

Yorath, C.J., Balkwill, H.R., and Klassen, R.W.
1975: Franklin Bay (97C) and Malloch Hill (97F) map-areas, District of Mackenzie; Geological Survey of Canada, Paper 74-36.

Young, F.G. and McNeil, D.H.
1982: Cenozoic stratigraphy of Mackenzie Delta, Northwest Territories, NTS 107B, 107C; Geological Survey of Canada, Open File 872.

Young, F.G., Myhr, D.W., and Yorath, C.J.
1976: Geology of the Beaufort-Mackenzie; Geological Survey of Canada, Paper 76-11.

Appendix 1

Sequence tops for selected wells in the Beaufort-Mackenzie Basin

All depths are in metres (feet, in parentheses) and were obtained principally from the sonic/gamma logs. In most of the wells listed below the Shallow Bay sequence cannot be differentiated from the Iperk sequence because of inadequate data.

		metres	feet
Esso Pex Alerk P-23			
Shallow Bay/Iperk		seabed	
Mackenzie Bay		845.0 or 900?	
Kugmallit		1033.0	
Kopanoar		2665.0?	
	TD	3223.0	
IOE Ellice O-14			
Shallow Bay/Iperk		surface	
Reindeer		228.6?	(750?)
	TD	2905.0	(9531)
Chevron Canada Pex et al. Fish River B-60			
Surficial sediments		surface	
Reindeer		15.2?	(50?)
Fish River		497.4?	(1632?)
(Tent Island Fm., 1364 m: 4475 ft)			
Boundary Creek		2199.0	(7214)
Pre-Upper Cretaceous		2430.5	(7974)
	TD	3502.2	(11 490)
Esso et al. Issungnak O-61			
Shallow Bay/Iperk		seabed	
Akpak		1340.0	
Mackenzie Bay		1428.0?	
Kugmallit		2254.0	
	TD	3583.0	
Imperial Oil Ivik J-26			
Shallow Bay/Iperk		surface	
Kugmallit		518.2	(1700)
Richards		2462.8?	(8080?)
	TD	3648.2	(11 969)
Dome Hunt Gulf Kopanoar 2I-44			
Shallow Bay/Iperk		seabed	
Akpak/Mackenzie Bay undifferentiated		2489.0	
Kugmallit		2655.0	
Kopanoar		3160.0	
Unknown sequence		3915.0	
	TD		
Dome Gulf et al. Hunt Kopanoar M-13			
Shallow Bay/Iperk		seabed	
Akpak		2557.0	(8390)
Mackenzie Bay		2682.0?	(8800?)
Kugmallit		2785.0	(9138)
Kopanoar		3339.0	(10 956)
Unknown sequence		4288.5?	(14 070?)
	TD	4320.2	(14 174)
Dome Pacific et al. Pex Natsek E-56			
Shallow Bay/Iperk		seabed	
Richards		216 or 298	
Reindeer		550 or 600	
Fish River		1950.7	
	TD	3520.0	
Dome Hunt Nektoralik K-59			
Shallow Bay/Iperk		seabed	
Akpak		2258.6	(7410)
Mackenzie Bay		2640.0?	(8660?)
	TD	2790.1	(9154)

Appendix 1 (cont.)

		metres	feet
Dome Nerlerk M-98			
Shallow Bay/Iperk		seabed	
Akpak		2843.0	
Kugmallit		3137.0	
Kopanoar		3910.0	
Unknown sequence		4350.0 or 4420.0	
	TD	4940.0	
Imperial Netserk F-40			
Shallow Bay/Iperk		seabed	
Akpak		719.3	(2360)
Mackenzie Bay		816.9?	(2680?)
Kugmallit		1422.9	(4668)
Richards		2426.2?	(7960?)
Reindeer		3772.8	(12 378)
	TD	4370.2	(14 338)
Shell Niglintgak M-19			
Shallow Bay/Iperk		surface	
Richards		252.1	(827)
Reindeer		796.1	(2612)
Fish River		3822.8	(12 542)
	TD	4025.2	(13 206)
Gulf et al. North Issungnak L-86			
Shallow Bay/Iperk		seabed	
Akpak		1615.0	
Mackenzie Bay		2392.0	
Kugmallit		3390.0	
	TD	4771.0	
Sun BVX et al. Pelly B-35			
Shallow Bay/Iperk		seabed	
Mackenzie Bay		652.3	(2140)
Kugmallit		1115.6	(3660)
Richards		2478.0?	(8130?)
	TD	3328.1	(10 919)
IOE Taglu C-42			
Shallow Bay/Iperk		surface	
Kugmallit		353.6?	(1160?)
Richards		1625.2	(5332)
Reindeer		2835.2	(9302)
	TD	4895.1	(16 060)
Dome Gulf Tarsiut A-25			
Shallow Bay/Iperk		seabed	
Akpak		749.0?	
Mackenzie Bay		900.0?	
Kugmallit		1325.0	
Richards		2270.0	
	TD	4434.0	
Dome Gulf et al. Ukalerk 2C-50			
Shallow Bay/Iperk		seabed	
Mackenzie Bay		1587.4	(5208)
Kugmallit		2001.9	(6568)
?Richards		3407.7	(11 180)
	TD	4953.0	(16 250)
Shell Ulu A-35			
Shallow Bay		surface	
Iperk		24.4?	(80?)
Reindeer		280.4	(920)
Fish River		1423.4	(4670)
(Tent Island Fm., 1661.2 m: 5450 ft)			
Smoking Hills (?)		2063.5	(6770)
Pre-Upper Cretaceous		2188.5	(7180)
	TD	3919.7	(12 860)

STRATIGRAPHIC AND STRUCTURAL STUDIES ON MELVILLE ISLAND, DISTRICT OF FRANKLIN

Project 840048

J.C. Harrison, Q.H. Goodbody[1], and R.L. Christie
Institute of Sedimentary and Petroleum Geology, Calgary

Harrison, J.C., Goodbody, Q.H., and Christie, R.L., Stratigraphic and structural studies on Melville Island, District of Franklin; in Current Research, Part A, Geological Survey of Canada, Paper 85-1A, p. 629-637, 1985.

Abstract

Melville Island is a key area in the Arctic Islands for understanding the Middle to Upper Devonian clastic wedge, the Ellesmerian Orogeny, the Melvillian Disturbance, and the evolution of Carboniferous to Tertiary tectonics and sedimentation of the Sverdrup Basin margin.

A mapping project to produce new 1:250 000 scale maps and cross-sections of Melville Island was begun in 1984, and some preliminary stratigraphic and structural results are presented in this paper. Various refinements to the stratigraphy proposed by Embry, Nassichuk, Kerr and others were found to be useful in the current studies. Middle Devonian shales have acted as a regionally significant décollement horizon during the Upper Devonian Ellesmerian Orogeny; we also suggest that the Permian Melvillian Disturbance, previously interpreted as a mild orogenic pulse on northwestern Melville Island, was a period during which drape folding and extensional tectonics related to the development of the margin of Sverdrup Basin occurred.

Résumé

Pour une meilleur compréhension du prisme clastique d'âge dévonien moyen à supérieur, de l'orogenèse de l'Ellesmérien, de l'accident du Melvillien, de l'évolution tectonique des roches carbonifères à tertiaires, et de la sédimentation de la marge du bassin de Sverdrup, l'île Melville représente une région clé dans l'étude de l'archipel Arctique.

En 1984, a été entrepris un projet de cartographie consistant à produire de nouvelles cartes à 1/250 000 et des coupes de l'île Melville; certains résultats préliminaires des études tectoniques et stratigraphiques sont donnés dans la présente étude. On a constaté que dans les études en cours, diverses améliorations de la stratigraphie proposées par Embry, Nassichuk, Kerr et d'autres auteurs se sont avérées utiles. Les schistes argileux du Dévonien moyen ont agi à titre d'horizon de décollement important à l'échelle régionale pendant l'orogenèse de l'Ellesmérien au Dévonien supérieur; les auteurs suggérent aussi que l'accident du Melvillien survenu au Permien et autrefois interprété comme une phase modérée d'orogenèse dans le nord-ouest de l'île Melville, a correspondu à une période de plissement moulant et de tectonique d'extension liée au développement de la marge du bassin de Sverdrup.

[1] Department of Geology, University of Alberta, Edmonton, Alberta T6G 2E3

Introduction

Melville Island and the nearby offshore region has been the site of considerable petroleum exploration since the early 1960s. Both seismic exploration and drilling have been carried out, with a well spudded as recently as 1983. The aim of the present project, a restudy of the geology of the island, is to obtain an improved understanding of the stratigraphy and structure. Further field work will be carried out in 1985. This report is a brief 'update' of the surface stratigraphy of Melville Island. Included are some notes on highlights of the 1984 field season.

Earlier geological work

Tozer and Thorsteinsson (1964, p. 2-17) provided a full account of both early geographical and geological exploration of the Melville Island region. Up until 1964, what was known of the geology of Melville Island was mainly due to the work of McMillan (1910), geologist on Captain J.E. Bernier's 1908-09 expedition in the D.G.S. Arctic, and Tozer (1956, 1963). Tozer and Thorsteinsson's (1964) account and reconnaissance mapping of Melville and other islands of the western Queen Elizabeth Islands has provided a basic stratigraphic and structural framework for the present studies.

Geological and geophysical exploration of Melville Island continued throughout the 1960s and 1970s. In 1964, H.P. Trettin studied the tar sands of Sproule Peninsula (Trettin and Hills, 1966, 1967) and W.W. Nassichuk studied and collected ammonoids from Permian beds. Nassichuk (1975) made further collections in 1967 at Barrow Dome, a site from which a large collection had earlier been obtained by B.P. Exploration Limited. Stratigraphic sections of Middle Devonian beds were measured in 1968 by D.C. McGregor and T.T. Uyeno, and samples for miospore studies were collected. The results of this study (see McGregor and Camfield, 1982) completed one phase of a broader study, by these and other authors, aimed at both interfacies correlation and correlation of marine and nonmarine biozones. Seismic exploration began on Melville Island in 1968, a year that also saw the announcement of the giant oil strike at Prudhoe Bay, Alaska (see Jones, 1981).

Five wells were drilled on Melville Island in 1969 and 1970. Two wells were completed in Ordovician and three in Pennsylvanian-Permian units. In 1970 the first successful well was completed, by Panarctic Oils Limited, in Triassic sandstone. This well, Panarctic Drake Point L-67, blew out of control (control was later recovered by drilling a relief hole). Panarctic Oils has since outlined the Drake Point gas field, one of the largest in Canada (Jones, 1981). About 45 exploratory wells have been drilled on Melville Island and in the nearby offshore area since 1960.

Seismic surveys were extended to offshore areas in the early 1970s. A considerably improved picture of the subsurface structure has been obtained from the seismic data, and is reported on and illustrated by Fox (1983) and Texaco Canada Resources Limited (1983).

Stratigraphic sections of Lower Paleozoic beds on Melville Island formed a major component of a wide-ranging study by Embry and Klovan (1976) of the Middle and Upper Devonian 'clastic wedge' of the Arctic Islands. This study, carried out between 1972 and 1975, resulted in refinements of the nomenclatural framework and understanding of the sedimentary environments of the several Middle and Upper Devonian facies. More recently, Embry (1983; 1984a, b, c) erected new stratigraphic divisions for the Middle Triassic to Middle Jurassic beds, based on the extensive subsurface information now available.

The surficial deposits and glacial features of Melville Island have been studied and reported on by several field parties. In 1980, D.A. Hodgson, J-S. Vincent, and S.A. Edlund carried out an airphoto and ground mapping study of Dundas Peninsula and central parts of the island (see Hodgson et al., 1984; Edlund, 1982, in press). These authors note that uplands of the island sustained local ice caps, but that the south coast and parts of the coasts of Liddon Gulf were impinged upon by continental ice approaching from the south. Evidence has been found for at least three advances of continental ice over parts of Dundas Peninsula, the southernmost extension of Melville Island.

Fieldwork in 1984

The field program of 1984 was carried out between late June and mid-August by a party of 13, with air support by Bell 206B Jet Ranger helicopter (Quasar Helicopters) and by de Havilland Twin Otter (Bradley Air Services), both provided by the Polar Continental Shelf Project (PCSP). Fuel and other support was obtained from the Panarctic Oils Limited camp at Rea Point, eastern Melville Island, and through the PCSP at Resolute, Cornwallis Island.

Stratigraphic studies were carried out by M. Jennifer Robson, University of Western Ontario, Q.H. Goodbody, University of Alberta, and R.L. Christie. J.C. Harrison was responsible for structural-stratigraphic mapping, and Sylvia Edlund (Ottawa), for geobotanical studies. Other fieldwork supported by the project included: Jurassic biostratigraphy, T. Poulton; Pennsylvanian-Permian biostratigraphy, J. Utting, A.C. Higgins, and P. Von Bitter (Royal Ontario Museum). Louise Journault and David Christensen, cook and camp manager, respectively, contributed considerably to the morale of the party by keeping both base and 'fly' camps well supplied. Able and cheerful field assistance was provided by Jane Bracken, Sabine Fuelgen, Kathi Higgins, and Todd Cross. The helicopter was skilfully piloted, frequently in trying conditions, by G. Dionne; engineering support by K. Mahoney, S. Long, and D. Tranelis also was appreciated.

Revisions to surface stratigraphic nomenclature since 1964

Significant revisions to the surface stratigraphic nomenclature of Melville Island have occurred since the 1:500 000 scale reconnaissance mapping in the area by Tozer and Thorsteinsson (1964). These changes have resulted from regional stratigraphic refinements introduced by A.F. Embry, W.W. Nassichuk, J.Wm. Kerr, H.R. Balkwill and others of the Geological Survey of Canada, working on Melville Island and throughout the Arctic Islands over the last twenty years.

All accepted modifications to the surface stratigraphy of Melville Island are shown in Tables 74.1 and 74.2. Selective comments on these changes follow.

1. Thumb Mountain and Irene Bay formations

   Tozer and Thorsteinsson (1964) assigned the Middle Ordovician limestone, argillaceous limestone and dolomite unit underlying the Cape Phillips Formation on McCormick Inlet to the upper two members of the Cornwallis Formation. [The Cornwallis Formation was later (Kerr, 1967) raised to group status to include the Bay Fiord, Thumb Mountain and Irene Bay formations]. The Thumb and Irene Bay formations are both exposed around McCormick Inlet, and evaporites of the underlying Bay Fiord Formation were intersected below 3270 m in the Panarctic et al. Sabine Bay A-07 wildcat well, drilled on central Melville Island.

Table 74.1. Nomenclature of Carboniferous to Quaternary surface formations, Melville Island, District of Franklin. Sources: Tozer and Thorsteinsson (1964), Nassichuk, (1956), Balkwill et al. (1977), Embry (1984a), Thorsteinsson (1974), Balkwill (1983), and Tozer (1970).

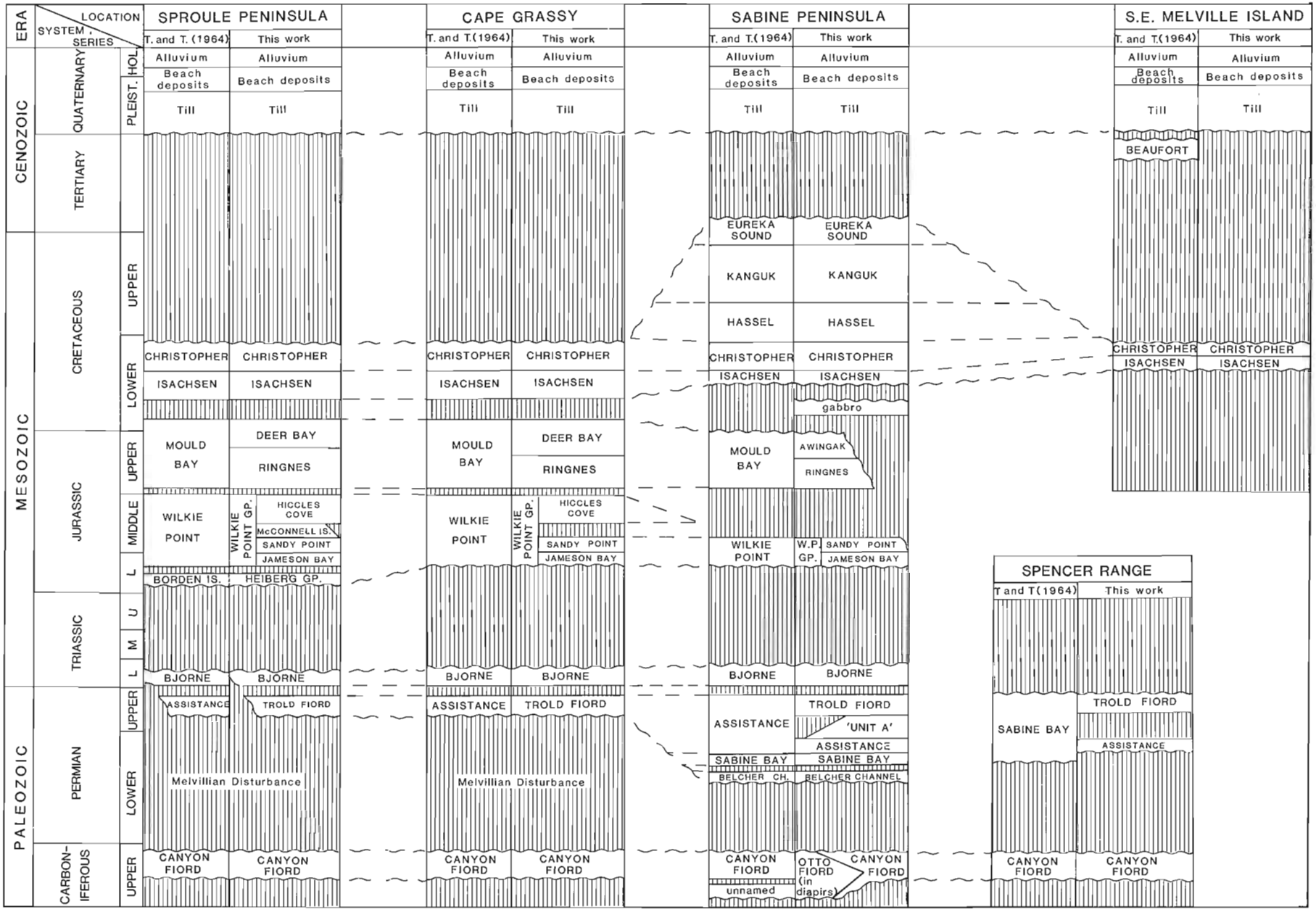

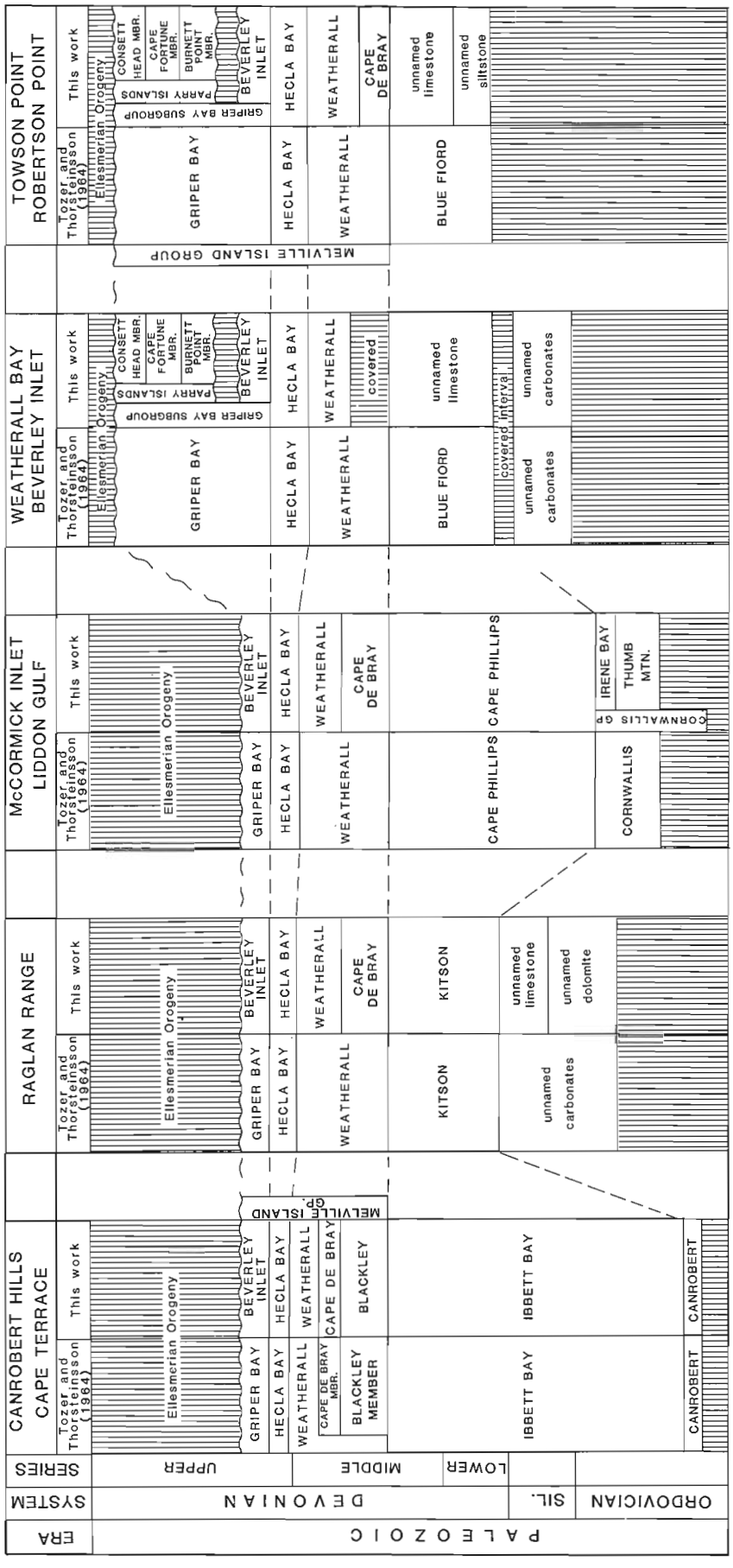

Table 74.2. Nomenclature of Lower Ordovician to Upper Devonian surface formations, Melville Island, District of Franklin. Sources: Tozer and Thorsteinsson (1964), Embry and Klovan (1976), and Kerr (1967).

2. Silurian and Devonian carbonate units

Silurian and Lower Devonian limestones, dolomite and minor siltstone units are exposed at four widely scattered localities on Melville Island. These units can not be correlated with equivalent strata in the eastern Arctic Islands. Stratigraphic revisions based on combined outcrop and drillhole information are being planned.

3. Subdivision of the Weatherall Formation

Tozer and Thorsteinsson (1964) recognized two distinct units at the base of the Weatherall Formation in Canrobert Hills and called them the Blackley and Cape de Bray members. These members were later raised to formational status by Embry and Klovan (1976). While the Blackley Formation is only exposed in the Canrobert Hills, the overlying Cape de Bray Formation is exposed in the cores of anticlines as far east as Weatherall Bay, and is suspected to gradationally underlie the Weatherall Formation everywhere in the subsurface of Melville Island. East of the Canrobert Hills, the Cape de Bray Formation lies conformably on the Kitson, Cape Phillips or Devonian carbonate formations (Embry and Klovan, 1976, Fig. 20).

4. Facies changes in the Middle and Upper Devonian clastic wedge

Stratigraphic studies of the Weatherall and Hecla Bay formations confirm the westward change of massive Hecla Bay Formation sandstone across Melville Island, as was suggested by Embry and Klovan (1976). On eastern Melville Island, two informal members of the Hecla Bay Formation are distinguished: (1) a thin, lower unit of white quartzose sandstone and interbedded green lithic siltstone and shale, and (2) a massively bedded, white quartzose sandstone that dominates the formation. The upper member becomes progessively thinner westwards and is entirely missing above a proportionately thicker lower member in the vicinity of Murray Inlet and the head of Purchase Bay. Marine to brackish conditions of sedimentation within the lower member of the Hecla Bay Formation are indicated by the occurrence of lingulid brachiopods.

5. Griper Bay Subgroup

Embry and Klovan (1976) demonstrated that a disconformity exists within the Griper Bay Formation and raised it to the status of a subgroup. On eastern

Melville Island, the Griper Bay Subgroup includes the Beverley Inlet Formation and three formal members of the Parry Islands Formation. All these units are mappable and can even be distinguished on 1:1 000 000 scale Landsat imagery (see Fig. 74.1).

On central Melville Island the Beverley Inlet Formation comprises three members, which are indicative of alternating marine and nonmarine conditions.

6. Otto Fiord Formation

Tozer and Thorsteinsson (1964) mapped Pennsylvanian anhydrite and limestone in two piercement diapirs on northern Sabine Peninsula. Based on the ammonoid collections of Nassichuk (1968), Thorsteinsson (1974) assigned the diapiric evaporite rocks to the Otto Fiord Formation.

7. Permian formations

Tozer and Thorsteinsson (1964) mapped two Permian formations in the Tingmisut Lake area, but recognized three: the Belcher Channel, Sabine Bay, and Assistance formations. Later, Nassichuk (1965) observed that the Assistance Formation of Tozer and Thorsteinsson included three readily mappable units. He restricted the name Assistance Formation to the lowest unit, and the upper two he called Unit A and Unit B. Thorsteinsson and Tozer (1970) eventually correlated Unit B with the Trold Fiord Formation.

8. Wilkie Point Group

Embry (1984b) raised the Wilkie Point Formation to group status and proposed four new formations: the Jameson Bay, Sandy Point, McConnell Island and Hiccles Cove formations. These new formations are defined in well sections and can also be recognized in surface exposures.

The Jameson Bay Formation consists of recessive, grey to light green weathering siltstone, and is gradationally overlain by the glauconitic sandstone of the Sandy Point Formation. These two formations have an aggregate thick-ness of about 100 m, and are not easily distinguishable at the scale of mapping. Castellate weathering, quartzose sandstone of the Hiccles Cove Formation is mappable across northwestern Melville Island, and brown shale of the underlying McConnell Island Formation appears to be present only north of Marie Bay. Skeletal remains of a Middle Jurassic vertebrate were found in the upper Hiccles Cove Formation south of Cape Grassy on northwestern Melville Island. They have been tentatively identified (from photographs) to be those of a plesiosaur (D. Russell, personal communication, 1984).

Locally, the Wilkie Point Group is unconformably underlain by Pleinsbachian and possible Sinemurian sandstone, which Tozer and Thorsteinsson (1964) assigned to the Borden Island Formation. These strata correlate with the Heiberg Group of Embry (1983).

9. Deer Bay, Awingak and Ringnes formations

Regional mapping and stratigraphic studies throughout central and western Sverdrup Basin by Balkwill (1983), A.F. Embry and others indicate that the Mould Bay Formation of Melville Island includes the Ringnes, Awingak and Deer Bay formations. On Sproule Peninsula, the Ringnes Formation is composed of black shale containing large, calcareous, siltstone concretions. The formation also includes underlying, non-concretionary, black shale strata above the Hiccles Cove Formation. The Ringnes is gradationally overlain by pale green siltstone and grey shale of the Deer Bay Formation. The Ringnes Formation thins eastward and lacks its distinctive concretions in the Cape Grassy area. Poorly exposed sandstone overlying a thin Ringnes shale on southern Sabine Peninsula is assigned to the Awingak Formation (Embry, personal communication, 1984).

10. Beaufort Formation

Poorly consolidated gravels containing uncompressed wood are exposed on hilltops in the Bridport Inlet area. These gravels were assigned to the Beaufort Formation by Tozer and Thorsteinsson (1964) and later were mapped by Hodgson and Vincent (1980) (and see Barnett et al., 1975). Fieldwork this year revealed that uncompressed wood is rare and that marine shell fragments are ubiquitous in these conglomeratic deposits. We believe that this is consistent with a glacial or glaciomarine origin. The unit is therefore probably Pleistocene in age and not assignable to the Beaufort Formation. Age determinations and palynological studies on these deposits are planned.

Highlights of regional mapping

1. A detachment in Middle Devonian shale

The convincing observations put forth by Workum (1965), and more recently, the evidence from seismic profiles published by Fox (1983), indicate that anticlines in the Parry Islands Foldbelt are the result of flexural flow deformation of evaporites in the Middle Ordovician Bay Fiord Formation and coincident thrust faulting in overlying Ordovician to Devonian strata. Tozer and Thorsteinsson (1964) suggested that the absence of the Bay Fiord Formation in the Lower Paleozoic strata of Canrobert Hills required the presence of a second (Cambrian or Precambrian) detachment level somewhere in the subsurface.

From the 1984 fieldwork it appears that a third detachment, in Middle Devonian shale, may be present. Below the Cape de Bray Formation, the radii of curvature of folds increase upward in anticlines and decrease upward in synclines. In contrast, folded beds above the Cape de Bray Formation have radii that decrease upward in anticlines and increase upward in synclines. Rare, resistent beds in the Cape de Bray Formation display brittle failure, and the dominant, clay-rich, micaceous mudstone lacks primary bedding and appears to have deformed in a semi-viscous fashion. Mesoscopic, and in many cases disharmonic, folds are common in the overlying Weatherall Formation and underlying Blackley Formation. These observations are consistent with a zone of flexural flow within the Cape de Bray Formation.

Flexural flow deformation in the Cape de Bray shale would explain the rarity of thrust faults and listric reverse faults at the surface on southeastern Melville Island. The appearance of fold-parallel reverse faults east of Sabine Bay could result from northward thinning of the Cape de Bray shale (as indicated on the seismic sections of Fox, 1983).

2. Observations on the Melvillian Disturbance

Thorsteinsson and Tozer (1964) observed that compressional fold structures in Ordovician to Devonian strata in the Canrobert Hills could be traced into the unconformably overlying Carboniferous strata, and interpreted these tectonic features as refolded folds. This post-Ellesmerian deformation, which they named



Figure 74.1. *Vertical satellite image of the Parry Islands Foldbelt on eastern Melville Island (part of C.C.R.S. image 415-45-7, 6 Aug., 1974). 1. unnamed Devonian limestone, 2. Weatherall Formation, 3. Hecla Bay Formation, 4. Peverley Inlet Formation, 5, 6, 7. Parry Islands Formation (5. Burnett Point Member, 6. Cape Fortune Member, 7. Consett Head Member), 8. Canyon Fiord Formation, 9. Permian formations (undivided), 10. Pjorne Formation.*

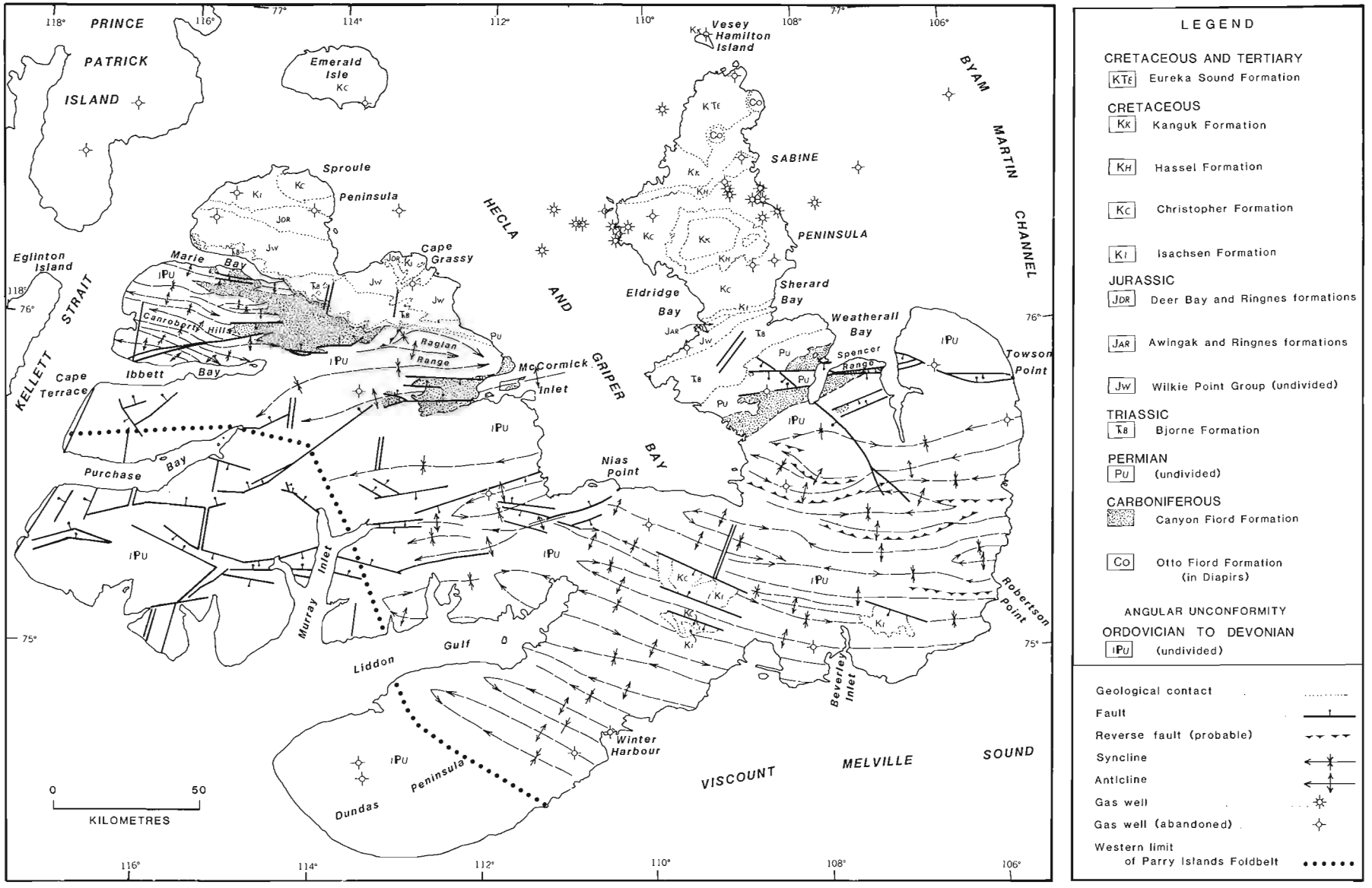

Figure 74.2. *Simplified geology of Melville Island. Information compiled from unpublished field observations and air photo interpretation by Balkwill (1976, 1978) on Sabine Peninsula, Harrison (1984), and from Tozer and Thorsteinsson (1964; Map 1142A).*

the Melvillian Disturbance, was observed to predate unconformably overlying Upper Permian strata (Thorsteinsson and Tozer, 1970).

We have confirmed that the Melvillian folds are broad, gently-dipping structures. The fold axes of both anticlines and synclines are short and tend to be associated with the termination of fault segments. Some Melvillian synclines can be described as small, circular, basin-like structures, and anticlines are asymmetric, with one limb gently dipping to flat.

Normal faults, cutting Carboniferous and older strata, strike mainly east-northeast. Oblique faults strike east and northeast. Across northwestern Melville Island, where Canyon Fiord Formation lies unconformably on shale of the Cape de Bray Formation, the unconformity is often marked by a moderate- to shallow-dipping normal fault that is probably listric in the subsurface. These faults, like most east-northeast striking faults in this area, apparently do not cut the Upper Permian strata, and are therefore probably Melvillian in age.

We suggest that the deformation style within Carboniferous strata on northwestern Melville Island is representative of horst and graben tectonics. The Melvillian 'folds' could be due to the drape of beds over normal faulted blocks in Lower Paleozoic "basement". Local angular unconformities beneath the Trold Fiord Formation could be accounted for by pre-Trold Fiord erosional truncation following the development of horst and graben structures.

3. Permian faults and drape folds

On southern Sabine Peninsula, en echelon, curvilinear, normal faults striking east are particularly common in the Lower Permian formations, and tend to die out upsection below the Bjorne Formation. Reverse drag of bedding is common in the hanging walls of these faults, suggesting that the faults are listric in the subsurface. Stratigraphic offset at the surface ranges from a few tens of metres to about 100 m.

An important en echelon fault system (on southern Sabine Peninsula) is exposed along the main southern boundary of outcrop of Permian strata. These north-dipping normal faults can be traced from western Spencer Range to the southwest across the west arm of Weatherall Bay as far as the lowlands east of Sabine Bay. A condensed Permian section is exposed in flat-lying outliers south of this fault system. A reflection seismic survey line crosses this fault in the vicinity of the Dome Panarctic Texex Weatherall O-10 wildcat well, and interpretation indicates a rapid thickening of the Canyon Fiord Formation on the north side. This structure may have been an important boundary fault on the southern margin of Sverdrup Basin.

It seems likely that many of the east- to east-northeast striking faults, related oblique faults, and drape structures that offset the Canyon Fiord Formation on northwest Melville Island, and the Permo-Carboniferous formations on southern Sabine Peninsula, represent a rifting event that affected the margin of the Sverdrup Basin prior to the Late Permian or Early Triassic.

4. Northeast-striking faults

North-northeast to northeast-striking faults and keystone grabens occur throughout Melville Island. Faults and other linear tectonic elements of this orientation are particularly common in the Blue Hills of southwestern Melville Island, along Kellet Strait, along a line joining Cape Grassy and western Dundas Peninsula, and throughout southern Sabine Peninsula. A prominent keystone graben cuts Hecla Bay Formation north of Bridport Inlet and apparently does not offset outliers of the Isachsen and Christopher formations in this area.

Average displacement on northeast-striking faults ranges up to to a few tens of metres. The faults are subparallel to Hauterivian gabbro dykes near Tingmisut Lake (Balkwill and Haimila, 1978) and in some cases are exactly coincident with linear magnetic anomalies as described by Balkwill and Fox (1982, see Fig. 2). These authors suggested that the northeast striking fault array resulted from the emplacement of gabbro sills in the subsurface and from simultaneous doming and fracturing of overlying strata. Although isotopic ages on the intrusive rocks range from 190 Ma to 86 Ma (Early Jurassic to Late Cretaceous; Balkwill and Fox, 1982), our observation that associated faults fail to penetrate the Isachsen Formation indicates that the most active period of northwest-southeast extension in the Melville Island area was complete by mid-Early Cretaceous time.

5. Post-Lower Cretaceous faults

Normal faults striking west-northwest offset Christopher Formation (Albian) and older strata on Sproule Peninsula, and in the Bridport Inlet area.

Outliers of the Isachsen and Christopher formations near Bridport Inlet are bounded by faults, the offsets on which must be at least 65 m, or the thickness of Lower Cretaceous strata preserved within the outliers. The regional extent of these post-Lower Cretaceous structures is unknown. It seems likely that some faults in the Blue Hills were active during this period, as was suggested by Tozer and Thorsteinsson (1964, p. 188).

References

Balkwill, H.R.
1983: Geology of Amund Ringnes, Cornwall, and Haig-Thomas islands, District of Franklin; Geological Survey of Canada, Memoir 390, 76 p.

Balkwill, H.R. and Fox, F.G.
1982: Incipient rift zone, western Sverdrup Basin, Arctic Canada, in Arctic Geology and Geophysics, ed. A.F. Embry and H.R. Balkwill; Canadian Society of Petroleum Geologists, Alberta, p. 171-187.

Balkwill, H.R. and Haimila, N.E.
1978: K/Ar ages and significance of mafic rocks, Sabine Peninsula, Melville Island, District of Franklin; in Current Research, Part C, Geological Survey of Canada, Paper 78-1C, p. 35-38.

Balkwill, H.R., Wilson, D.G., and Wall, J.H.
1977: Ringnes Formation (Upper Jurassic), Sverdrup Basin, Canadian Arctic Archipelago; Bulletin of Canadian Petroleum Geology, v. 25, p. 1115-1144.

Barnett, D.M., Edlund, S.A., Dredge, L.A., Thomas, D.C., and Prevett, L.S.
1975: Terrain classification and evaluation, Melville Island, Northwest Territories; Geological Survey of Canada, Open File 252.

Edlund, S.A.
1982: Vegetation of Melville Island, District of Franklin, Northwest Territories; Geological Survey of Canada, Open File Report 852, scale 1:250 000.

Edlund, S.A. (cont.)
– Vegetation of Central Melville Island, Northwest Territories; Geological Survey of Canada, Paper. (in press)

Embry, A.F.
1983: The Heiberg Group, western Sverdrup Basin, Arctic Islands; in Current Research, Part B, Geological Survey of Canada, Paper 83-1B, p. 381-389.

1984a: Stratigraphic subdivision of the Roche Point, Hoyle Bay and Barrow formations (Schei Point Group), western Sverdrup Basin, Arctic Islands; in Current Research, Part B, Geological Survey of Canada, Paper 84-1B, p. 275-283.

1984b: The Wilkie Point Group (Lower-Upper Jurassic) Sverdrup Basin, Arctic Islands; in Current Research, Part B, Geological Survey of Canada, Paper 84-1B, p. 299-308.

1984c: The Schei Point and Blaa Mountain groups (Middle-Upper Triassic) Sverdrup Basin, Canadian Arctic Archipelago; in Current Research, Part B, Geological Survey of Canada, Paper 84-1B, p. 327-336.

Embry, A.F. and Klovan, J.E.
1976: The Middle-Upper Devonian clastic wedge of the Franklinian Geosyncline; Bulletin of Canadian Petroleum Geology, v. 24, p. 485-639.

Fox, F.G.
1983: Structure sections across Parry Islands Fold Belt and Vesey Hamilton Salt Wall, Arctic Archipelago, Canada, in Seismic expression of structural styles, v. 3, ed. A.W. Bally; American Association of Petroleum Geologists, p. 3.4.1-54 to 3.4.1-72.

Hodgson, D.A. and Vincent, J-S.
1980: Surficial geology, central Melville Island; Geological Survey of Canada, Open File 874 (map with legend).

Hodgson, D.A., Vincent, J-S., and Fyles, J.G.
1984: Quaternary geology of central Melville Island, Northwest Territories; Geological Survey of Canada, Paper 83-16.

Jones, G.H.
1981: Economic development – oil and gas; in A Century of Canada's Arctic Islands, 1880-1980, ed. M. Zaslow; Royal Society of Canada.

Kerr, J.Wm.
1967: New nomenclature for Ordovician rock units of the eastern southern Queen Elizabeth Islands, Arctic Canada; Bulletin of Canadian Petroleum Geology, v. 15, p. 91-113.

McGregor, D.C. and Camfield, M.
1982: Middle Devonian miospores from the Cape de Bray, Weatherall, and Hecla Bay formations of northeastern Melville Island, Canadian Arctic; Geological Survey of Canada, Bulletin 348.

McMillan, J.G.
1910: Geological Report; in Report on the Dominion of Canada Government Expedition to the Arctic Islands and the Hudson Strait on board the D.G.S. Arctic (1908-09), by J.E. Bernier; Ottawa, Queen's Printer.

Nassichuk, W.W.
1965: Pennsylvanian and Permian rocks in the Parry Islands group, Canadian Arctic Archipelago, in Report of Activities: Field 1964; Geological Survey of Canada, Paper 65-1, p. 9-12.

1968: Upper Paleozoic studies in the Sverdrup Basin, District of Franklin (49C, F; 59B; 79B), in Report of Activities, 1967; Geological Survey of Canada, Paper 68-1, Part A, p. 204-106.

1975: Carboniferous ammonoids and stratigraphy in the Canadian Arctic Archipelago; Geological Survey of Canada, Bulletin 237.

Texaco Canada Resources Ltd.
1983: Melville Island – Northwest Territories, Canada: Line No. 7; in Seismic expression of structural styles, v. 3, ed. A.W. Bally; American Association of Petroleum Geologists, p. 3.4.1-73 to 3.4.1-78.

Thorsteinsson, R.
1974: Carboniferous and Permian stratigraphy of Axel Heiberg Island and western Ellesmere Island, Canadian Arctic Archipelago; Geological Survey of Canada, Bulletin 224, 115 p.

Thorsteinsson, R. and Tozer, E.T.
1970: Geology of the Arctic Archipelago, in Geology and Economic Minerals of Canada, ed. R.J.W. Douglas; Geological Survey of Canada, Economic Geology Report No. 1, Fifth edition, p. 548-589.

Tozer, E.T.
1956: Geological reconnaissance, Prince Patrick, Eglinton, and western Melville Islands, Arctic Archipelago, Northwest Territories; Geological Survey of Canada, Paper 55-5.

1963: Southeastern Sabine Peninsula, Melville Island; in Geology of the north-central part of the Arctic Archipelago, Northwest Territories (Operation Franklin); Geological Survey of Canada, Memoir 320, p. 645-655.

1970: Mesozoic and Cenozoic; in Geology of the Arctic Archipelago, by R. Thorsteinsson and E.T. Tozer, Chapter X, in Geology and Economic Minerals of Canada, ed. R.J.W. Douglas; Geological Survey of Canada, Economic Geology Report No. 1, 5th ed., p. 548-590.

Tozer, E.T. and Thorsteinsson, R.
1964: Western Queen Elizabeth Islands, Arctic Archipelago; Geological Survey of Canada, Memoir 332, 242 p.

Trettin, H.P. and Hills, L.V.
1966: Lower Triassic tar sands of northwestern Melville Island, Arctic Archipelago; Geological Survey of Canada, Paper 66-34.

1967: Triassic "tar sands" of Melville Island, Canadian Arctic Archipelago; Proceedings of the 7th World Petroleum Congress, Mexico City, v. 3, p. 773-787.

Workum, R.H.
1965: Lower Paleozoic salt, Canadian Arctic Islands; Bulletin of Canadian Petroleum Geology, v. 13, p. 181-191.

NEOHELIKIAN BYLOT SUPERGROUP OF BORDEN RIFT BASIN, NORTHWESTERN BAFFIN ISLAND, DISTRICT OF FRANKLIN

Project 770013

G.D. Jackson, T.R. Iannelli[1], R.D. Knight[2], and D. Lebel[3]
Precambrian Geology Division

Jackson, G.D., Iannelli, T.R., Knight, R.D., and Lebel, D., Neohelikian Bylot Supergroup of Borden Rift Basin, northwestern Baffin Island, District of Franklin; in Current Research, Part A, Geological Survey of Canada, Paper 85-1A, p. 639-649, 1985.

Abstract

About 6100 m of sandstones, shales, conglomerates and stromatolitic carbonates were deposited during a 1200-1250 Ma Mackenzie rifting episode and are separated into three groups: a lower and an upper sequence, each of which grades from predominantly alluvial up into basinal and/or subtidal strata, and a middle shelf carbonate sequence. Thick coastal sabkha evaporites occur in the middle carbonates, and tholeiitic subaerial basalts occur near the base of the lower group.

Episodic syndepositional faulting in northern Borden Basin was coincidental with, but less intense than that in southern Borden Basin. An uplifted western source area existed during lower Elwin and a northern source area during upper Elwin sedimentation. Some separation of Greenland from North America probably occurred during Bylot Supergroup sedimentation.

Postdepositional faulting increases in intensity northward and may be related largely to formation of Lancaster Aulacogen in the Cretaceous.

Résumé

Environ 6 100 m de grès, schistes argileux, conglomérats et carbonates stromatolitiques ont été mis en place pendant un épisode de formation d'un fossé tectonique dans le bassin du Mackenzie il y a 1200 à 1250 Ma. On subdivise ces dépôts en trois groupes: une séquence inférieure et une séquence supérieure, dont chacune passe progressivement de strates principalement alluviales à des strates de type sédimentaire profond ou subtidal, ou aux deux à la fois, et une séquence carbonatée de plate-forme médiane. Dans les carbonates de la séquence médiane, on rencontre d'épaisses couches d'évaporites de sebkha littorales, et des basaltes tholéiitiques d'origine subaérienne, près de la base du groupe inférieur.

Les épisodes de formation de failles synsédimentaires dans le nord du bassin de Borden, ont coincidé avec un épisode du même type dans le sud de ce bassin, toutefois moins intense. Il existait dans la partie ouest une région source soulevée pendant la sédimentation ancienne d'Elwin, et une région source au nord pendant la sédimentation récente d'Elwin. Durant la sédimentation du supergroupe de Bylot, a probablement eu lieu un mouvement de séparation entre le Groenland et l'Amérique du Nord.

L'intensité des épisodes de formation de failles postsédimentaires augmente vers le nord, phénomène peut-être dû largement à la formation de l'aulacogène de Lancaster survenue au cours du Crétacé.

[1] Department of Geology, University of Western Ontario, London, Ontario N6A 5B7
[2] Department of Geology, Carleton University, Ottawa, Ontario K1S 5B6
[3] Université de Montréal, Montréal, Québec H3C 3J7

Introduction

The 1984 field season was oriented toward filling gaps in the field coverage remaining from previous field seasons, and in investigating some aspects of the Bylot Supergroup in more detail (Fig. 75.1).

This preliminary report deals chiefly with the data gathered during the 1984 field season, and the reader is referred to previous publications for additional data on the Bylot Supergroup and Nanisivik mine (Blackadar, 1970; Clayton and Thorpe, 1982; Geldsetzer, 1973a, b; Iannelli, 1979; Jackson and Davidson, 1975; Jackson and Iannelli, 1981; Jackson et al., 1975, 1978, 1980; Olson, 1977, 1984). All previous data for the Elwin Formation, and selected data for the other map units within the 1984 field area, have been incorporated into the figures of this paper. Iannelli is completing a Ph.D thesis on the Arctic Bay and Fabricius Fiord Formations; the Elwin Formation is the subject of a master's thesis by Knight. Lebel provided a résumé and an interpretation of his observations during the summer for this paper.

The regional distribution of formations is essentially as shown by Blackadar (1968a, b), Jackson and Davidson (1975), and by Jackson and Iannelli (1981, Fig. 16.2).

The Bylot Supergroup (up to 6100 m, Table 75.1) is spectacularly exposed throughout much of the map area (Fig. 75.2), unconformably overlies an Archean-Aphebian gneiss complex and is intruded by northerly to northwesterly trending 750 Ma Hadrynian Franklin diabase dykes. Christie and Fahrig (1983) have concluded that an older swarm – the 950 Ma Borden dykes – and a few Mackenzie dykes are also present.

Bylot Supergroup is overlain unconformably by Cambro-Silurian strata (Blackadar, 1968a,b) in northern Borden Peninsula, and rests directly on the gneiss complex of the Navy Board High.

Bylot Supergroup strata are overlain unconformably by Cretaceous-Eocene Eclipse Group strata on northern Bylot Island (Jackson and Davidson, 1975).

The Eqalulik and Uluksan groups (Table 75.1) occur in a narrow belt along the north side of Navy Board High from Elwin Inlet eastward to about 20 km west of Navy Board Inlet (Fig. 75.1, 75.2). On Bylot Island the strata floor North Bylot Trough, and Eclipse Trough north and east of Canada Point. Eqalulik strata also outcrop around the northwest nose of Byam Martin High. Nunatsiaq Group strata underlie most of northern Borden Peninsula north of the Hartz-Mounlain Fault Zone. Strathcona Sound strata also occur north of Canada Point on Bylot Island.

Basement complex

A cursory examination of the basement complex of Navy Board High indicated that the gneisses are highly sheared. Remnants of supracrustal strata and mafic rocks are common, and late granitic intrusions, although abundant, are rarely more than 500 m in diameter.

An east-west trending belt of partially migmatized high-grade supracrustals extends southward for at least 20 km across the Navy Board High just west of Navy Board Inlet and may be the western extension of a similar belt southwest of Pond Inlet (Jackson et al., 1975). Amphibolite is the predominant lithology. Greywacke-type paragneiss, intermediate metavolcanics and quartzose metasandstones occur chiefly on the southern side of the belt. A coarse grained to pegmatitic, differentiated metamorphosed basic-ultrabasic intrusion, some 600 m in diameter, occurs about 5 km west of the coast. Anorthositic gabbro and gabbro occur in layers up to 100 m thick and bronzite-bearing ultrabasics in layers up to 25 m. Some metagabbro layers up to 2 m thick are internally thinly banded.

A preliminary Rb-Sr age of 2330 ± 49 Ma (M.S.W.D. = 2.0) has been determined by the Survey's Geochronological Laboratory for a migmatite on the east coast of Admiralty Inlet a few kilometres south of Arctic Bay (Fig. 75.1). In comparison granite gneiss from southern Devon Island has yielded a U-Pb age of 2426 Ma (Frisch, 1983). K-Ar ages for basement gneisses about Borden Basin range from 1525-2011 Ma.

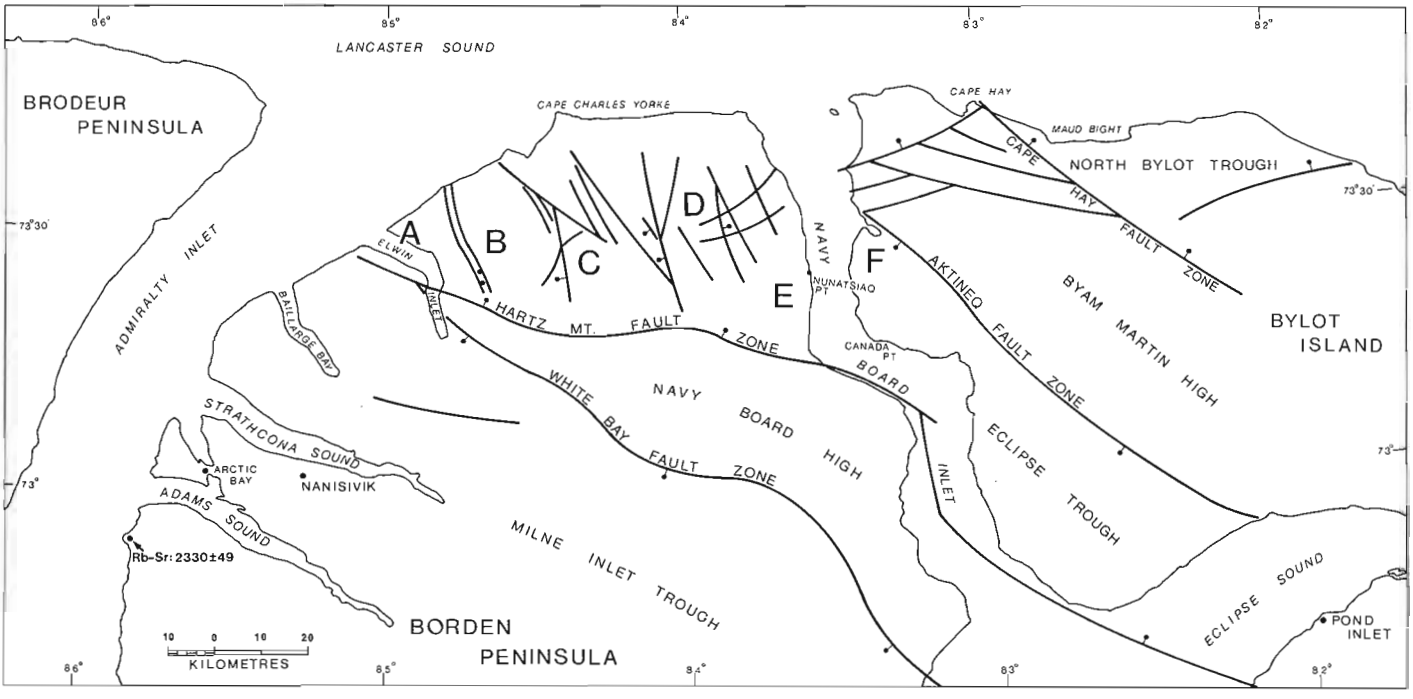

Figure 75.1. Location map and distribution of major structural elements. Thick lines indicate faults and dots the downthrown side.

Table 75.1. Table of formations

HADRYNIAN		Franklin Intrusions: Diabase	
	GP	Intrusive Contact	
NEOHELIKIAN	BYLOT SUPERGROUP	NUNATSIAQ	Elwin Fm. (470-1220 m):	EL_1: Quartzarenite, siltstone EL_2: Sandstone, siltstone, dolostone
		Gradational	
			Strathcona Sound Fm: (430-910 m+)	SS_6: SS_{1-5} lithologies interbedded SS_5: Polymictic conglomerate SS_4: Siltstone, greywacke SS_3: Arkose-greywacke, shale SS_2: Dolostone, dolostone conglomerate SS_1: Shale, siltstone
		Gradational	
			Athole Point Fm: (0-585 m) Limestone, sandstone, shale	
		Gradational	Gradational to Unconformable
		ULUKSAN	Victor Bay Fm: (156-735 m)	VB_2: Limestone, dolostone, flat pebble conglomerate VB_1: Shale, siltstone, sandstone, limestone
		Conformable, Abrupt to Gradational	
			Society Cliffs Fm: (263-856 m)	SC_2: Stromatolitic & massive dolostones
		Chiefly Unconformable?	
		EQALULIK	Fabricius Fiord Fm: (400-2000 m+)	SC_1: Stromatolitic dolostone, shale, sandstone, gypsum
			FF_4: Arkose, conglomerate, dolostone	Gradational to Unconformable
			FF_3: Subarkose, conglomerate	Arctic Bay Fm: (180-770 m) AB_4: Shale, dolostone
			FF_2: Shale, quartzarenite	AB_3: Shale, siltstone AB_2: Shale, quartzarenite
			FF_1: Quartzarenite, shale	AB_1: Siltstone, quartzarenite
		Conformable, Abrupt to Gradational	
			Adams Sound Fm: (0-610 m)	
			AS_3: Quartzarenite, conglomerate, shale	AS_U: Quartzarenite
			AS_2: Quartzarenite	AS_L: Quartzarenite, conglomerate
			AS_1: Quartzarenite, conglomerate	
		Conformable	
			Nauyat Fm: (0-430 m)	NA_2: Plateau basalt NA_1: Quartzarenite, subarkose, basalt
Nonconformity			
ARCHEAN-APHEBIAN		Granitic gneiss basement complex: Migmatite, foliated granitic rocks, granite, charnockite, supracrustal relics	

Nauyat Formation

The Nauyat Formation is the basal formation of the Bylot Supergroup. It consists of two conformable members: a lower NA_1 member composed chiefly of quartzarenite, and an upper NA_2 member of basalt flows. The formation is about 100 m thick east of Elwin Inlet (Fig. 75.2).

NA_1 member

The lower (NA_1) member (40-45 m) consists of very thin- to medium-bedded buff to reddish brown and pink quartzarenite, with thin quartz-pebble conglomerate layers in the basal part. Crossbeds indicate unimodal northwesterly directed paleocurrents east of Elwin Ice Cap.

NA_2 member

The NA_2 member consists of at least 4 massive columnar jointed tholeiitic basalt flows conformably overlying the NA_1 member. Amygdules are abundant in most of the flow tops and are commonly filled with agate, quartz, carbonate minerals, and chlorite. Thin units of quartzarenite, chert, and varicoloured siltstone occur between the flows. The NA_2 member is about 60 m thick east of Elwin Inlet.

Interpretation

The Nauyat flows (NA_2) were probably extruded along the major fault zones into a subaerial environment on a fluvial braidplain (NA_1), and were burried by quartzarenite before significant erosion could take place (Jackson and Iannelli, 1981). Absence of Nauyat flows below the Adams Sound Formation on eastern Borden Peninsula and northwestern Bylot Island probably reflects an absence of an eruption centre. No evidence has been found anywhere for significant erosion of flows during the filling of Borden Basin. Absence of the lower Adams Sound member in most of these localities suggests a local topographic control.

Adams Sound Formation

The Adams Sound east of Elwin Inlet (Fig. 75.2) and at several places on Bylot Island consists of thin- to thick-bedded quartzarenites. Sedimentary structures are varied and abundant throughout the unit (eg. Jackson and Iannelli, 1981).

The formation is more than 300 m thick east of Elwin Inlet. On Bylot Island it is about 210 m thick along the northeast side of Eclipse Trough (Fig. 75.1) but may be as much as 490 m thick to the north where partial sections of 367-414 m are exposed. More than 160 m of Adams Sound strata are exposed in North Bylot Trough. The Adams Sound Formation is conformable with the underlying Nauyat Formation, and also overlies basement gneisses nonconformably. At one locality on Bylot Island, adjacent to the Aktineq Fault Zone, 10 cm-1 m of grey greywacke regolith in the basement grades upward into 1 m of grey impure sandstone which in turn to grades into quartzarenite of the upper member of the Adams Sound. The contact with the overlying Arctic Bay Formation is gradational. Adams Sound strata have been divided into two intergradational members (AS_L, AS_U), as detailed below.

AS_L member

The AS_L member consists of pink, to light brown and purple-red quartzarenite with some siltstone and shale in the upper part. Thin quartz-pebble- to cobble-conglomerate beds occur at the base of fining upward cycles. The AS_L member is up to 130 m thick east of Elwin Inlet, 171-262 m thick in northern Byam Martin Mountains, 100 m at Cape Hay and 20-100 m in North Bylot Trough, but is absent in most of northern Borden Peninsula area, and along much of the north edge of Eclipse Trough on Bylot Island.

AS_U member

White to grey, buff and pink quartzarenite dominate this member. Thin interlayers of quartz-pebble conglomerate occur locally, and minor green siltstone and shale beds in the upper part increase in abundance adjacent to the contact

with the Arctic Bay Formation. Fining- and thinning-upward cycles are present. Needle shaped cavities, common east of Elwin Inlet, may represent gypsum molds. The member is more than 170 m thick east of Elwin Inlet, about 210 m on Bylot Island in Eclipse Trough, 146-270 m in northern Byam Martin Mountains and 160 m in North Bylot Trough (Fig. 75.1).

Interpretation

Adams Sound strata in the field area have been interpreted to have been deposited in mixed fluvial marine environments (Jackson and Davidson, 1975; Jackson et al., 1978; Jackson and Iannelli, 1981).

Paleocurrent patterns for individual units range from unimodal to bimodal, bimodal-bipolar, and polymodal (Jackson et al., 1980; Jackson and Iannelli, 1981). Cumulative roses (Fig. 75.3) indicate similar features, and show that westerly to northeasterly trends predominante, except at the extreme west where a south-southwest direction is indicated for one unit and at the extreme east where a northeast direction is indicated for another unit.

Arctic Bay Formation

The Arctic Bay Formation was examined at one locality a few kilometres east of Elwin Inlet (Fig. 75.1, 75.2) and at several localities on Bylot Island. It consists of dark grey to black, commonly micaceous, locally pyritiferous shale,

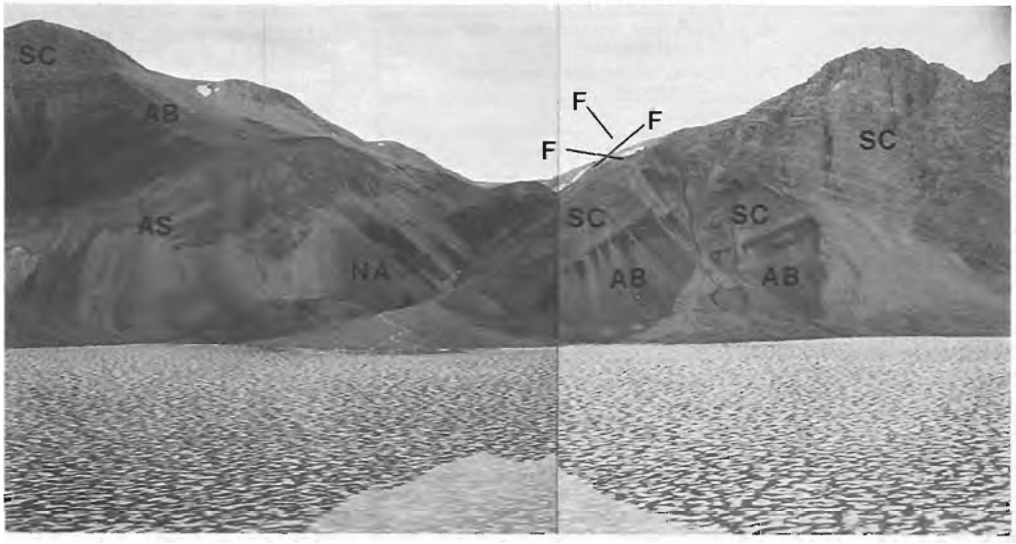

Figure 75.2. Looking east at Elwin Inlet toward splay from Hartz Mountain Fault Zone. NA = Nauyat Fm., AS = Adams Sound Formation, AB = Arctic Bay Formation, SC = Uluksan Group, F = faults. The highest elevations are about 620 m. Photo by G.D. Jackson.

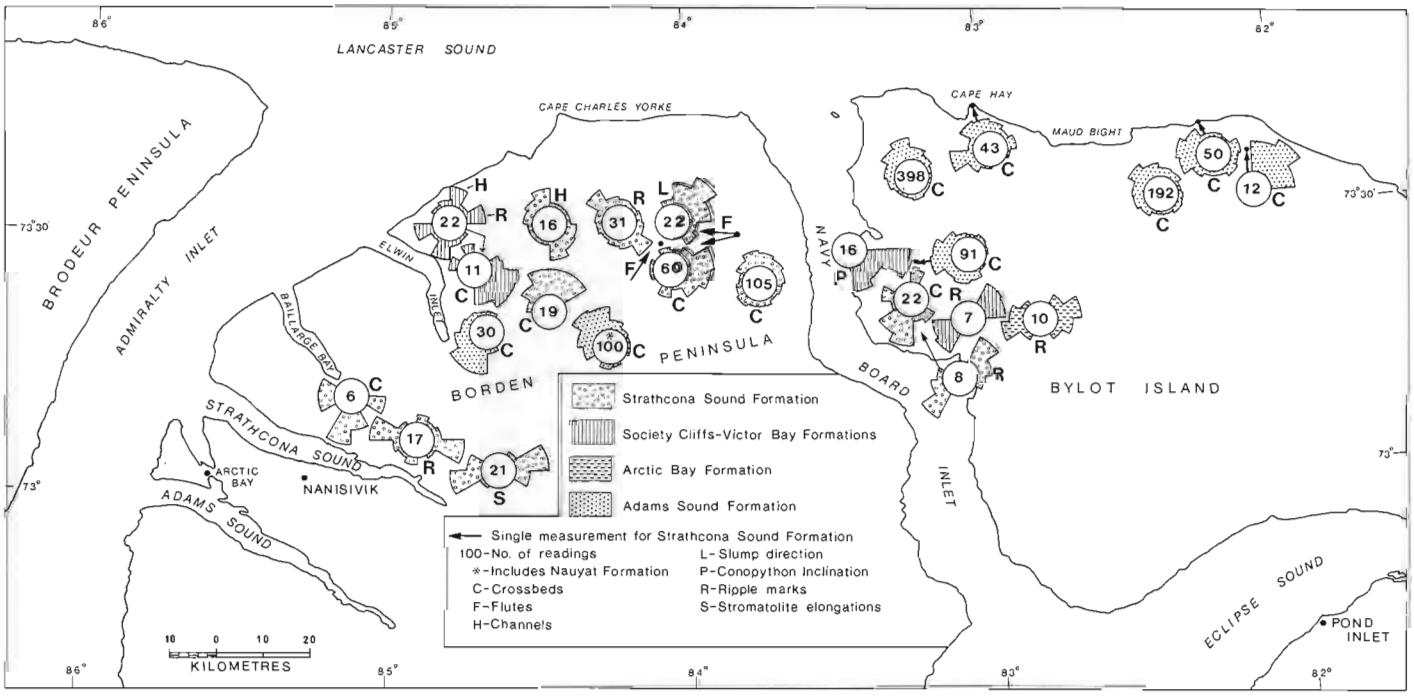

Figure 75.3. Paleocurrent data for some of Bylot Supergroup strata. Radius of circle in centre of rose is 20 per cent. Readings start on the circumference.

similar to the Arctic Bay of Milne Inlet Trough. Siltstone, quartzarenite and subarkose are interbedded with shale throughout the Formation and dolostones form interbeds in the upper part. Thickness of 520 to more than 600 m occur east of Elwin Inlet and 604 m were measured in Eclipse Trough on Bylot Island. Comparable thicknesses appear to be present west of Cape Hay and in North Bylot Trough. Sedimentary structures are common (Jackson and Iannelli, 1981; Jackson et al., 1978, 1980). The same four intergradational members distinguished farther south (Table 75.1; Iannelli, 1979) are also present throughout the area.

AB_1 member

Greyish green to grey white and brownish thinly interbedded fine grained quartzarenite, siltstone and minor shale make up this member. Black shale increases upward. Some beds contain shale intraclasts similar to Fabricius Fiord strata. The member is 10-44 m east of Elwin Inlet and up to 24 m in Eclipse Trough.

AB_2 member

This member is composed of shale dominated shale-siltstone-sandstone coarsening-upward cycles. The shale is grey to black and the coarser lithologies grey-green to grey and brown. The sandstones are predominantly quartzarenite but some are subarkose and resemble Fabricius Fiord strata. The AB_2 member is 120-146 m thick east of Elwin Inlet where about twenty 5-15 m thick cycles are present. However, the total AB_2 may be no more than 25 m thick in Eclipse Trough.

AB_3 member

The AB_3 member consists predominantly of planar to lenticular bedded grey to black shale with up to 25% siltstone and quartzarenite. A few coarsening up sequences occur in Eclipse Trough where a 20 m unit in the upper part of the member consists of alternating red and green shale dominated units with some thin concretion-rich layers and conglomerate composed of concretions. AB_3 strata range from 142-400 m east of Elwin Inlet, and are 195 m in Eclipse Trough.

AB_4 member

Grey or black shale is typically the chief lithology of this member which is 372 m thick in the Eclipse Trough, and more than 30 m thick east of Elwin Inlet, where the member consists of coarsening up shale-siltstone cycles. Sandstones are generally lacking in this member in North Bylot Trough and carbonates are relatively abundant. In Eclipse Trough on Bylot Island the shale is interbedded with several other lithologies. There, grey to greenish grey subarkose is the major lithology in the basal 135 m, whereas grey quartzarenite is prominent in the middle 50 m. Grey, buff to orange-brown weathering dolostones increase in abundance in the upper part of the sequence which is capped by 23 m of the carbonates. The carbonates include dolosiltite, dololutite, stromotalitic to biohermal dolostone and dolostone conglomerate. Grey siltstones are common throughout the section.

Most of the strata in Eclipse Trough are arranged in shale-subarkose, or shale-quartzarenite coarsening up cycles and much of the strata are reminiscent of Fabricius Fiord strata. Interbedded shale-dolostone sequences are common in the middle and upper parts of the section.

Interpretation

AB_1 member has been interpreted to have been deposited in a mixed intertidal-shallow subtidal environment (Jackson and Iannelli, 1981). Clastic shoreline and muddy shelf regimes persisted during deposition of the AB_2 member, and shallow to deep subtidal or basinal during AB_3 sedimentation. The AB_4 member east of Elwin Inlet and on western Bylot Island were probably deposited in marine-influenced delta complexes while shallow shelf carbonate environments persisted farther out in the basin and on northern Bylot Island.

Uluksan Group

The Uluksan Group was examined in one area east of Elwin Inlet and in several localities on Bylot Island (Fig. 75.1, 75.2). Although these strata have been examined at several other localities previously in this region, a satisfactory way of dividing these strata on a regional basis north of Navy Board High has not yet been determined (see also Blackadar, 1968a). The lower Victor Bay shaly member (VB_1) is absent on northern Borden Peninsula and there has been a "telescoping" of facies, so that Victor Bay lithologies and structures are identical to those in the Society Cliffs. Subdivisions can be made adjacent to Byam Martin High on Bylot Island, but the relation of these boundaries to the Society Cliffs-Victor Bay boundary in Milne Inlet Trough is not known. The Uluksan Group is probably about 900 m thick east of Elwin Inlet and at least 1000 m thick on Bylot Island.

The contact with the underlying Arctic Bay Formation is either drift covered or faulted. The contact with the overlying Strathcona Sound Formation is disconformable east of Elwin Inlet, but gradational on Bylot Island where varicoloured shale, siltstone quartzarenite and arkose increase upward in abundance adjacent to the Strathcona Sound Formation.

Victor Bay strata were examined north of eastern Strathcona Sound in Milne Inlet Trough. The thickness and composition of the formation is similar to that at Nanisivik but there is considerably more limestone and the VB_2 member is at least 50 m thicker than at Nanisivik.

On Borden Peninsula and on much of Bylot Island, the Uluksan Group is composed almost entirely of grey to buff and light brown dolostones similar in composition and contained structures to those of the Society Cliffs Formation in Milne Inlet Trough (Jackson and Iannelli, 1981). Uluksan Group strata emit a petroliferous odour and locally contain flecks of bitumen and may be classified as: thick bedded to massive dolostone, laminated to thin bedded dolostone, nodular to ellipsoidal dolostone, and dolostone conglomerate and breccia. Each of these categories is locally predominant in units up to 25 m thick. Cyclic deposition is similar to that in Milne Inlet Trough, but is less obvious. Several types of stromatolites are common and include conophyton. Biohermal mounds seem less common than in Milne Inlet Trough and are less than 15 m in diameter. Local chert replacement of dolostone is common. Shale and sandstone beds are relatively rare except adjacent to Byam Martin High (Fig. 75.1). East of Elwin Inlet 15-25 m of basal brown-weathering dolostones closely resemble the Society Cliffs in western Milne Inlet Trough.

Evaporitic sequences in the Uluksan Group are abundant adjacent to Byam Martin High on Bylot Island but may die out completely within 20 km from the High. These sequences consist of grey, brown, green, and pink dolostones interbedded with grey to black green and red shales and gypsum in units up to 66 m thick. Abundant salt casts occur at several positions in the sequence, and oncolites and oolites occur locally. Depositional sequences include those

previously described, but also include numerous thinning-upward cycles and intergradational dolostone to shale up to gypsum units to 6 m thick with abrupt contacts at the tops. Adjacent to Byam Martin High shale bearing zones alternate with shale-free zones 50-140 m thick. Zones containing red shale units range from 100 to 190 m thick and occur primarily in the middle and upper parts of the Group.

At one locality the lower 610 m of the Uluksan Group is gypsiferous, contains at least 60 gypsum beds that range from 10 cm to 3 m, innumerable beds and lenses less than 10 cm thick, and a large amount of nodular gypsum and gypsum interlaminated with shale and dolostone (Fig. 75.4). Most of the gypsum is white and ranges from impure to pure, and granular to dense and massive.

Interpretation

Uluksan Group strata on Borden Peninsula were deposited in shallow subtidal to intertidal environments. Adjacent to Byam Martin High the strata, which include coastal gypsiferous sabkha sequences, were deposited in a variety of environments ranging from alluvial plain to supratidal and intertidal including lagoons and ephemeral ponds. While Byam Martin High must have been uplifted somewhat, the north side of Navy Board High seems to have been stable.

Strathcona Sound Formation

The formation, as noted previously (Jackson and Iannelli, 1981), comprises a wide variety of complexly interfingering laminated to thin-bedded shales and siltstones, thin- to very thick-bedded sandstones, dolostones and dolostone breccia-conglomerates which occur interbedded in units up to 75 m. The shales-sandstones commonly contain white mica.

This formation occurs throughout an irregular narrow belt that broadens eastward from Elwin Inlet to a width of 20 km west of Navy Board Inlet. It also underlies a few small areas north of Canada Point (Fig. 75.1). The Strathcona Sound Formation is 493 m thick east of Elwin Inlet in a complete section, and sections of 400-520 m have been measured to the east (Fig. 75.2). It is, however, much thinner north of Navy Board High than to the south. The contact between the Strathcona Sound and underlying Uluksan Group



Figure 75.4. *Deformed gypsum bed in Uluksan Group, northwest Bylot Island. The lens cap is about 5 cm. Photo by G.D. Jackson. (GSC 204194)*

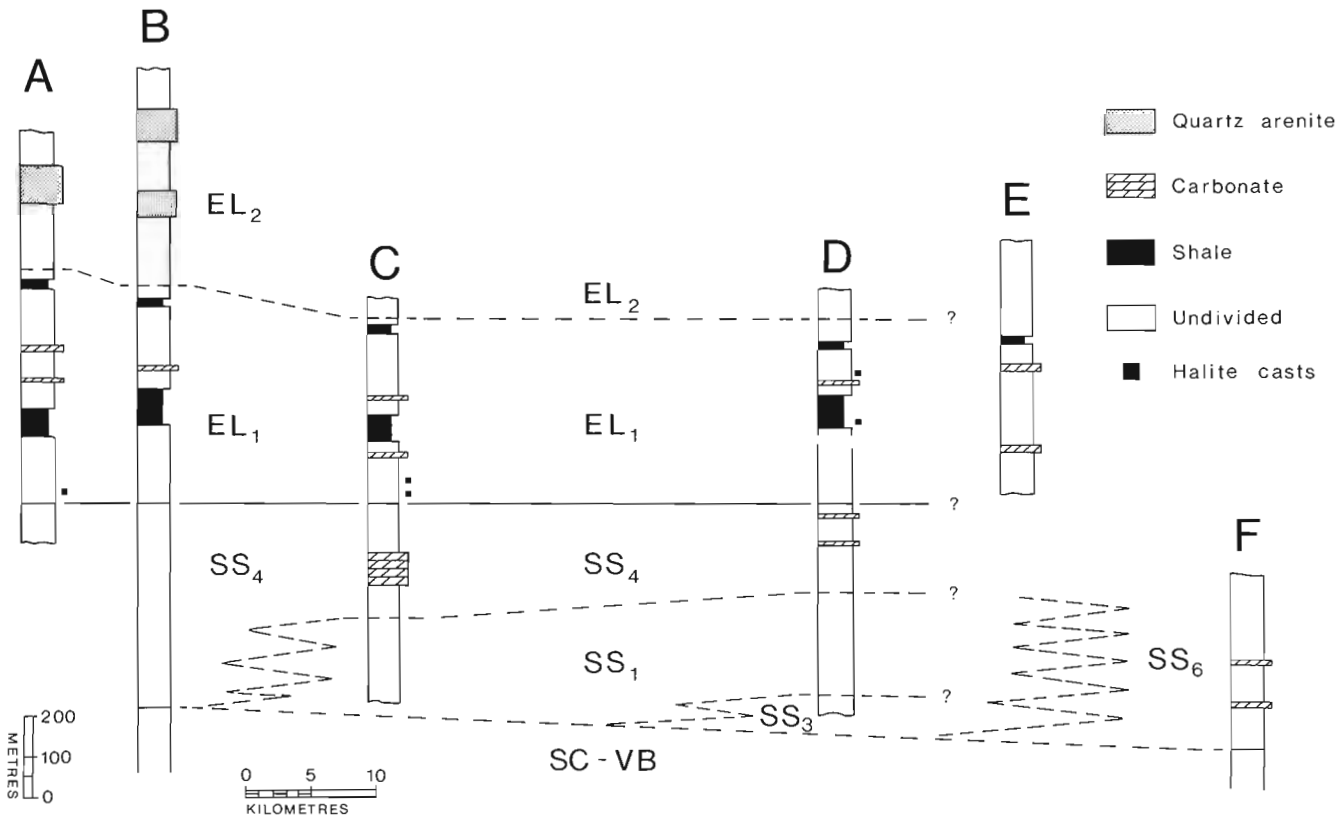

Figure 75.5. *Generalized stratigraphy of Strathcona Sound Formation ($SS_{1,3,4,6}$) and Elwin Formation ($EL_{1,2}$), northern Borden Basin.*

on northern Borden Peninsula is disconformable, but gradational on Bylot Island. The contact with the overlying Elwin Formation is everywhere conformable, and in places gradational.

The Strathcona Sound Formation has been divided into 6 members by Jackson and Iannelli (1981). These members grade into one another vertically and laterally, but locally are disconformable with one another. Five of the six (SS_{1-4}, SS_6) members were examined during the past season and four of these (SS_1, SS_3, SS_4, SS_6), occur in Eclipse Trough (Fig. 75.5). Fining- and thinning-upward cycles predominate in these four members, but coarsening- and thickening-upward cycles also occur. Dolostone breccia-conglomerate lenses up to a few metres thick are common in the basal parts of SS_3 and SS_4 members with as many as 6 lenses locally. Some are probably debris flows. Structures were noted previously (Jackson and Iannelli, 1981) although crossbeds, ripple marks, and dissication cracks are rare in SS_1 and SS_4 members, in which the most common structures are slumps, channels, load structures, flutes, and graded bedding. The Strathcona Sound Formation comprises chiefly the SS_1 and SS_4 members on northern Borden Peninsula (Fig. 75.5).

Red Arkose member (SS_3)

This member is composed chiefly of red arkose and subarkose with minor siltstone, shale, dolostone, stromatolitic dolostone, and dolostone breccia-conglomerate. Crossbeds are common and some sandstone-to-dolostone cycles are present. The SS_3 member has been recognized only in eastern Borden Peninsula immediately north of Navy Board High where at least 100 m is present, and it is overlain by SS_1 member (Fig. 75.5).

Red Shale-Siltstone member (SS_1)

Red shales and calcareous siltstones predominate in this member and are interbedded with green to grey and red arkose, subarkose, and quartzarenite. Some 115 m of dark grey sandstone occurs locally near the top of SS_1 member, and slump features up to several metres across are common (Fig. 75.6).

The SS_1 member is at least 300 m thick in east-central Borden Peninsula. It probably interfingers laterally eastward with the SS_6 member on Bylot Island. It dies out to the west where it interfingers laterally with the SS_4 member (Fig. 75.6).



Figure 75.6. *View looking west at slumps in red shale and subarkose beds of SS_1 member of Strathcona Sound Formation. Slump moved from left to right. Base of an overriding slump occurs in the top of the picture. The hammer is 30 cm long. Photo by G.D. Jackson. (GSC 201952-S)*

Green-Grey Siltstone member (SS_4)

Most of this member is a monotonous sequence of shales and calcareous siltstones interbedded with minor arkose and subarkose. Fine grained quartzarenite is abundant in the upper part adjacent to the Elwin contact and dolostone and limestone units to 15 m thick are common in Central Borden Peninsula. Dolostone breccia-conglomerate lenses occur in the basal part. Slump structures are abundant. The SS_4 member constitutes the entire Strathcona Formation in the Elwin Inlet area where it is 492 m thick. About 220 m of SS_4 strata overlie SS_1 strata in east-central Borden Peninsula (Fig. 75.5).

Interbedded member (SS_6)

This member contains a variety of thinly interbedded lithologies including dolostone, and has been described previously. Only the strata on Bylot Island (400-450 m) are now considered to belong to this member (see Jackson and Iannelli, 1981).

Dolostone member (SS_2)

The SS_2 member, about 250 m thick, extends from the head of Strathcona Sound northward to White Bay Fault Zone (Jackson and Iannelli, 1981). It is a biohermal platform complex composed chiefly of grey stromatolitic dolostone bioherms and dolostone conglomerates and breccias that have



Figure 75.7. *Strathcona Sound (SS_2) bioherm overlying horizontal Victor Bay strata. Smaller domal structures are faintly visible. Height of the dome is about 150 m above Victor Bay beds. Photo by G.D. Jackson. (GSC 201952-V)*



Figure 75.8. *Strathcona Sound (SS_2) conglomerate. Dolostone clasts in red calcareous siltstone matrix. Hammer is 30 cm long. Photo by G.D. Jackson. (GSC 201952-Y)*



Figure 75.9. *Conophyton in SS_2 dolostone, grading into a hemispheroidal stromatolite at the top. Small stromatolites also present. The lens cap is about 4 cm in diameter. Photo by G.D. Jackson.*

in part slumped off the bioherms to form aprons which interfinger with the interbiohermal SS_1, SS_3, and SS_4 strata (Fig. 75.7, 75.8, 75.9). Locally, SS_1 red shale and siltstone interfinger with, underlie and overlie the Strathcona Sound bioherms. Some bioherms began growing during deposition of the Victor Bay and continued growing throughout Strathcona Sound accumulation. Elsewhere in the same area, a disconformity separates Victor Bay strata from the overlying Strathcona Sound bioherms. The present topography is in part exhumed.

Interpretation

Most of the paleocurrent data for Strathcona Sound strata north of Navy Board High indicate northerly to easterly transport (Fig. 75.3). Slumps and channels, abundant throughout the formation, are especially common in central and eastern Borden Peninsula. These data, the relative abundance of carbonates adjacent to Navy Board High, and the general absence of alluvial fan conglomerates (SS_5) adjacent to the eastern part of the High indicate that Navy Board High was uplifted to the east and south relative to the west and north. The southern and eastern sides of the Eclipse Block west of Navy Board Inlet probably dropped down slightly and Byam Martin High rose. Principal depositional environments for the various members were probably as follows:

- SS_3 - mixed alluvial, intertidal (northeast Borden P.)
- SS_1 - alluvial plain (north central Borden P.)?
- SS_4 - intertidal-shallow subtidal (northwest Borden P.)
- SS_6 - mixed alluvial plain, supratidal to intertidal (west Bylot I.)
- SS_2 - shallow subtidal to intertidal carbonate platform. Bioherms "drowned" by encroaching SS_1 strata (south central Borden P.).

Elwin Formation

The Elwin, the uppermost formation of the Bylot Supergroup, outcrops solely on northern Borden Peninsula where the type section is on Elwin Inlet (Lemon and Blackadar, 1963). It consists of laminated to thick bedded, and massive varicoloured micaceous (white) sandstones and siltstones with minor shales and rare dolostones. The latter commonly contain planar to low domal and laterally linked hemispheroidal stromatolites and serve as key (traceable) beds. The strata are variously interbedded in units up to 50 m thick, but most are 10 m or less.

The Elwin Formation is conformable and locally gradational with the underlying Strathcona Sound Formation. The base of the Elwin is taken at the base of a thick (± 15 m) distinctive white quartzarenite, below which the drab shales and siltstones of the Strathcona Sound SS_4 member contain minor thin quartzarenite beds. Above it are chiefly grey, green to red or white subarkose-quartzarenite. The basal quartzarenite contains crossbeds and, except in the Elwin Inlet area, also contains slumps, basal loads, and rip-up clasts. Elwin strata are 1070 m thick in the Elwin Inlet region, which is probably close to the maximum thickness present. The strata have been truncated by lower Paleozoic strata and by the present erosion surface. The formation has been divided into two intergradational members, lower (EL_1) and upper (EL_2).



Figure 75.10. *Buff and red fluvial subarkoses of lower Elwin (EL_1) member. Cross beds are unimodal and indicate eastward transport. The rod is 1.5 m. Photo by R.D. Knight. (GSC 201952-T)*

Planar and trough crossbeds, symmetrical and assymetrical ripples, synaeresis and dessication cracks, slumps, and small scour channels are common throughout the formation. Rip-up clasts and mud chips are common and rare quartz and dolostone clasts occur locally.

Lower member (EL_1)

EL_1 strata outcrop throughout northern Borden Peninsula. The lithofacies are similar throughout and consist of interbedded quartzarenite, lithic arenite, subarkose, siltstone, and dolostone (dolosiltite, intraformational dolorudite; minor dololutile, stromatolitic dolostone). However, whereas colours in northwest Borden Peninsula are red, grey-green, white, and buff, northeastern Broden strata are chiefly buff brown to brown. Basal strata in the latter area also commonly contain large (2 m diameter) ball and pillow structures and numerous slumps.

Several submembers are present in the western two thirds of Borden Peninsula. The lower 150 m of the EL_1 member is a distinctive unit of fining- and shallowing-upward cycles, the lower parts of which are crossbedded, and ripple-marked medium- to coarse-grained thin- to medium-bedded buff-pink subarkose. Upper parts are fine grained laminated to very thin-bedded subarkose to quartz arenite with ripples, dessication cracks and halite casts. Some cycles are overlain by dolostone with red shale below and/or above. Several 2-20 m thick green to minor red siltstone-shale units also occur within the lower submember.

The basal submember is overlain by 60-90 m of strata that consist of two shale-siltstone units separated by 5-15 m of thin- to medium-bedded grey subarkose. The lower thicker shale unit itself contains a lower red and an upper green unit in the west but is entirely green in the east. The upper shale unit is predominantly green.

The remainder of the EL_1 member is commonly cyclical, and is chiefly subarkoses and quartzarenites with the minor vari-coloured lithologies (Fig. 75.10). A few 50-100 m thick sand dominated units contain few minor lithologies and are relatively resistant.

The contact between the EL_1 and EL_2 members is gradational and taken at the top of a 10 m thick unit of thin-bedded red subarkose containing minor interbedded shale. EL_1 member is 525-536 m in the Elwin Inlet region and thins to about 450 m in eastern Borden Peninsula.

Several structures and cycles have been documented previously (Jackson and Iannelli, 1981). Halite casts are common in the lower part of the member, a few gypsum casts may occur locally, and "rain-drop" imprints were noted in several places.

Upper member (EL_2)

Elwin strata undergo an abrupt colour change at the EL_1-EL_2 contact, as the EL_2 strata are predominantly white to light grey, and buff to orange brown quartzarenites. Minor interbedded siltstones and shales are green to grey and black, occur in beds up to 3 m thick, and locally are as much as 60 per cent of a few thicker units. Subarkose and sublitharenite occur rarely in the lower part of the member and red beds are rare or absent (Fig. 75.11).

EL_2 strata occur only in northwestern Borden Peninsula where 534 m are present. Upper member strata are thicker bedded, and more mature than lower member strata. Coarsening-up cycles are common in the EL_2 member and are defined by an upward decrease of shale interbedded in quartzarenite, which grades upward into thick "clean" units up to 70 m thick.

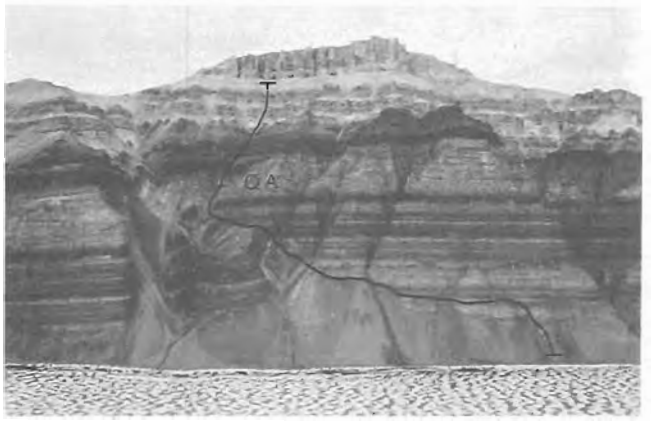

Figure 75.11. *Upper Elwin (EL_2) strata on the north side of Elwin Inlet, capped by vertically jointed lower Paleozoics. QA = thick quartzarenite unit in section A of Fig. 5. The measured section is indicated by the black line. The peak is 582 m high. Photo by G.D. Jackson. (GSC 201952-N)*

Fewer and lesser varieties of sedimentary structures occur in EL_2 strata as compared with EL_1. Synaeresis and dessication cracks are abundant locally. Channels (both shale and sandstone infilled), slumps and current lineations are present.

Interpretation

The various lithologies, depositional cycles, sedimentary structures, and presence of halite casts and gypsum molds indicate the EL_1 member accumulated in an intertidal to predominantly supratidal and alluvial braidplain environments. Evaporitic strata probably accumulated in ephemeral tidal flat pools or in lagoons. The basal (150 m) submember was probably deposited in a relatively low-energy subaerial, semi arid to arid environment. The shaly submember is probably intratidal for the most part, whereas the overlying thick quartzarenite units are probably braidplain deposits (Jackson and Iannelli, 1981). El_2 strata accumulated chiefly in an intertidal to subtidal shelf environment.

An abatement of tectonic activity in the immediate area is suggested for deposition of most El_1 strata (Jackson and Iannelli, 1981). Cumulative roses for crossbeds (Fig. 75.12) indicate predominance of easterly directed currents on western Borden Peninsula, northerly-directed on central Borden and easterly directed on eastern Borden. The paleocurrent data, the easterly thinning of El_1 member, and the slump features and increased dolostone content and facies changes in eastern Borden, indicate a western source area such as Brodeur Peninsula may have been uplifted about this time. Byam Martin High also probably rose slightly while the floor of Eclipse Trough on Borden Peninsula was down tilted eastward toward Navy Board Inlet.

A period of relative stability prevailed during El_2 sedimentation and northwesterly-directed paleocurrents (dominant in Borden Basin) again prevailed. Southerly-directed paleocurrents in north-central Borden Peninsula may be related to the Devon High (Fig. 16.35, Jackson and Iannelli, 1981).

Economic geology

Little of economic interest was seen in the field area. Gypsum is abundant on northern Bylot Island, traces of malachite staining and pyrite, marcasite, chalcopyrite and galena occur locally, and a few manganiferous goethite pods occur in uppermost Uluksan Group strata east of Elwin Inlet.

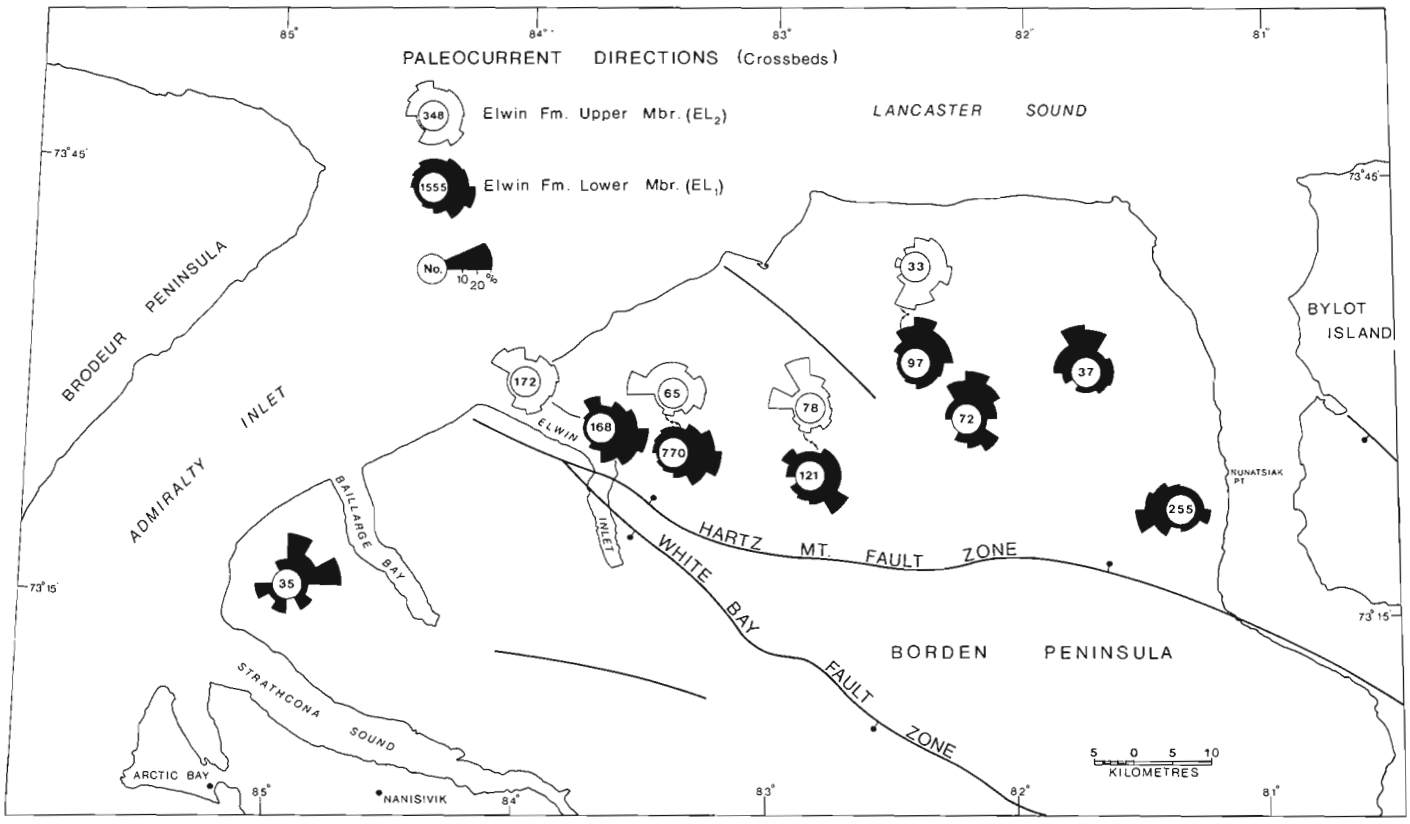

Figure 75.12. *Crossbed measurements in the Elwin Formation.*

Lower Victor Bay (VB_1) shales are thickest in the Nanisivik mine area, and may have acted as a cap rock to ore solutions percolating upward. If northwest trending faults have played any part in emplacement of zinc-lead orebodies on Little Cornwallis Island and at Nanisivik, then the intervening Brodeur Peninsula and Somerset Island carbonates should be considered as possible exploration areas.

Regional tectonics

The lower Eqalulik and upper Nanatsiaq groups grade upward from predominantly alluvial into subtidal strata. They are separated by the Ulukson Group shelf carbonates.

Syndepositional faulting was episodic throughout Borden Basin with culminations during lower Arctic Bay and Strathcona Sound sedimentation. Tilting of adjacent grabens was toward the Navy Board High on both sides of the High and faulting was less intense to the north of it.

Formation of Borden Basin and deposition of Bylot Supergroup has been related by Jackson and Iannelli (1981) to rifting during the Mackenzie Igneous events, and the opening of the Poseidon Ocean to the northwest at 1200-1250 Ma. Bylot Supergroup strata formerly extended much farther to the east and southeast than their present distribution. Thus it seems likely that Borden and Thule basins were either connected during contemporaneous sedimentation or part of a single larger sedimentary basin. This is even more likely if Greenland is brought closer to Baffin Island by using any one of several available reconstructions (e.g. Le Pichon et al., 1977).

Lithofacies distributions indicate north-south faulting was active along Milne Inlet-Navy Board Inlet during Bylot Supergroup sedimentation. Also paleomagnetic results of Marcussen and Abrahamsen (1983) indicate Greenland probably has moved away from North America during the Neohelikian. Significant movement in the Phanerozoic is debatable (Dawes and Kerr, 1982), and it seems likely that some separation of Greenland from North America was a result of Navy Board Inlet-Nares Strait fault movement during the Neohelikian rifting.

Phanerozoic block faulting is most abundant in northern Borden Basin adjacent to Lancaster Sound (Fig. 75.1), and is probably related to the Cretaceous Lancaster Aulacogen (Kerr, 1980). Although most faults are northerly, movement has also occurred along and parallel to the major southeast-trending faults (Fig. 75.2).

Acknowledgments

The authors are grateful to Polar Continental Shelf Project for excellent helicopter, fixed wing and other logistical support, which made the project possible. Ron Sutherland, chief geologist for Nanisivik Mines Limited, and his staff provided an informative tour of the mine area and additional data on the mineralization. Harry Finnis, government field officer at Nanisivik was most helpful in many ways throughout the summer. Jack Markle and Gordon Darcy, of Nanisivik Mines, helped with local transportation and the sealift. F.H.A. Campbell critically read the manuscript and made many improvements.

References

Blackadar, R.G.

1968a: Navy Board Inlet, District of Franklin (map with marginal notes); Geological Survey of Canada, Map 1236A.

1968b: Arctic Bay-Cape Clarence, District of Franklin (map with marginal notes); Geological Survey of Canada, Map 1237A.

Blackadar, R.G. (cont.)
1970: Precambrian geology northwestern Baffin Island, District of Franklin; Geological Survey of Canada, Bulletin 91, 89 p.

Christie, K.W. and Fahrig, W.F.
1983: Paleomagnetism of the Borden dykes of Baffin Island and its bearing on the Grenville Loop; Canadian Journal of Earth Sciences, v. 20, p. 275-289.

Clayton, R.H. and Thorpe, L.
1982: Geology of the Navisivik Zinc-lead deposit; in Precambrian sulphide deposits, ed. R.W. Hutchinson, C.D. Spence and J.M. Franklin; Geological Association of Canada, Special Paper 25, p. 739-758.

Dawes, P.R. and Kerr, J.W. (editors)
1982: Nares Strait and the drift of Greenland: a conflict in plate tectonics; Meddelelser Om Grønland, Geoscience 8, Copenhagen, 392 p.

Frisch, T.
1983: Reconnaissance geology of the Precambrian Shield of Ellesmere, Devon and Coburg Islands, Arctic Archipelago: a preliminary account; Geological Survey of Canada, Paper 82-10, 11 p.

Geldsetzer, H.
1973a: Syngenetic dolomitization and sulfide mineralization; in Ores in Sediments, ed. G.G. Amstutz and A.J. Bernard; Springer-Verlag, p. 115-127.

1973b: The tectono-sedimentary development of an algal-dominated Helikian succession on norther Baffin Island, N.W.T.; in Symposium on Arctic Geology, Geological Association of Canada, Memoir 19, p. 99-126.

Iannelli, T.R.
1979: Stratigraphy and depositional history of some upper Proterozoic sedimentary rocks on northwestern Baffin Island, District of Franklin; in Current Research, Part A, Geological Survey of Canada, Paper 79-1A, p. 45-56.

Jackson, G.D. and Davidson, A.
1975: Bylot Island map-area, District of Franklin; Geological Survey of Canada, Paper 74-29, 12 p.

Jackson, G.D. and Iannelli, T.R.
1981: Rift-related cyclic sedimentation in the Neohelikian Borden Basin, norther Baffin Island; in Proterozoic Basins of Canada, ed. F.H.A. Campbell; Geological Survey of Canada, Paper 81-10, p. 269-302.

Jackson, G.D., Davidson, A., and Morgan, W.C.
1975: Geology of the Pond Inlet map-area, Baffin Island, District of Franklin; Geological Survey of Canada, Paper 74-25, 33 p.

Jackson, G.D., Iannelli, T.R., Narbonne, G.M., and Wallace, P.J.
1978: Upper Proterozoic sedimentary and volcanic rocks of northwestern Baffin Island; Geological Survey of Canada, Paper 78-14, 15 p.

Jackson, G.D., Iannelli, T.R., and Tilley, B.J.
1980: Rift-related late Proterozoic sedimentation and volcanism on northern Baffin and Bylot Islands, District of Franklin; in Current Research, Part A, Geological Survey of Canada, Paper 80-1A, p. 319-328.

Kerr, J.W.
1980: Structural framework of Lancaster Aulacogen, Arctic Canada; Geological Survey of Canada, Bulletin 319, 24 p.

Lemon, R.R.H. and Blackadar, R.B.
1963: Admiralty Inlet area, Baffin Island, District of Franklin; Geological Survey of Canada, Memoir 328, 84 p.

Le Pichon, X., Sibnet, J.C., and Francheteau, J.
1977: The fit of the continents around the North Atlantic Ocean; Tectonophysics, v. 38, p. 169-209.

Marcussen, C. and Abrahamsen, N.
1983: Palaeomagnetism of the Proterozoic Zig-Zag Dal basalt and the Midsommers dolerites, eastern north Greenland; Geophysical Journal of Royal Astronomical Society, v. 73, p. 367-387.

Olson, R.A.
1977: Geology and genesis of zinc-lead deposits within a late Precambrian dolomite, northern Baffin Island, N.W.T.; unpublished Ph.D. thesis, University of British Columbia, 371 p.

1984: Genesis of paleokarst and strata-bound zinc-lead sulfide deposits in a Proterozoic dolostone, northern Baffin Island, Canada; Economic Geology, v. 79, p. 1059-1103.

A GENERAL GENETIC MODEL FOR STRATIFORM BARITIC DEPOSITS OF THE SELWYN BASIN, YUKON TERRITORY AND DISTRICT OF MACKENZIE

Projects 770063, 790033, 740081

John W. Lydon[1], Wayne D. Goodfellow[2], and Ian R. Jonasson[2]

Lydon, J.W., Goodfellow, W.D., and Jonasson, I.R., A general genetic model for stratiform baritic deposits of the Selwyn Basin, Yukon Territory and District of Mackenzie; in Current Research, Part A, Geological Survey of Canada, Paper 85-1A, p. 651-660, 1985.

Abstract

Stratiform baritic deposits of the Selwyn Basin can be divided into three main types:

Type A: localized lensoidal deposits of sphalerite-galena-barite-quartz ± pyrite ± siderite,

Type B: localized lensoidal deposits of barite + quartz ± calcite,

Type C: laterally extensive low grade baritic shale (5-20% $BaSO_4$) member(s).

Consideration of the differences in the geological setting and geochemistry of the three types coupled with their relationship to the geological evolution of the Selwyn Basin, indicates that:

Type A deposits were formed by the exhalation of >200° C formational waters from the Upper Proterozoic Grit Unit, through deeply penetrating faults.

Type B deposits were formed by the exhalation of about 100° C formational waters from the Ordovician-Silurian Road River Group carbonaceous shales by shallow listric faults.

Type C deposits represent anomalously high depositional rates of barium dispersed in Selwyn Basin ocean water, during periods of exceptionally high dewatering rates of the substrate and perhaps periods of basinal ventilation.

Résumé

On peut subdiviser les gisements stratiformes de barytine du bassin de Selwyn en trois types principaux:

Type A: gîtes constitués de lentilles localisées de sphalérite, galène, barytine, quartz, ± pyrite, ± sidérite;

Type B: gîtes constitués de lentilles localisées de barytine + quartz ± calcite;

Type C: membre(s) latéralement étendu(s), à faible teneur en schistes argileux à barytine (5 à 20 % de $BaSO_4$).

L'examen des différences existant du point de vue du cadre géologique et de la géochimie des trois types de gisements liées à l'évolution géologique du bassin de Selwyn, indique que:

Les gîtes de type A ont été formés par exhalation, à une température supérieure à 200° C, d'eaux de formation provenant de l'unité de grès grossiers d'âge protérozoique supérieur, à partir de failles profondes.

Les gîtes de type B ont été formés par exhalation, à une température d'environ 100° C, d'eaux de formation provenant des schistes argileux charbonneux du groupe de Road River, d'âge ordovicien-silurien, à partir de failles listriques peu profondes.

Les gîtes de type C correspondent à des périodes de mise en place anormalement rapide du baryum dispersé dans les eaux océaniques du bassin de Selwyn, à des époques d'assèchement exceptionnellement rapide du substrat et peut-être d'assèchement total du bassin.

---

[1] Economic Geology and Mineralogy Division
[2] Resource Geophysics and Geochemistry Division

Introduction

For the last six years personnel from the Economic Geology and Mineralogy (EGM) and the Resource Geophysics and Geochemistry (RGG) Divisions have participated in activities aimed at the documentation and understanding the genesis of stratiform baritic deposits in the Selwyn Basin. Although the systematic collection of samples from these deposits for these current studies had been initiated earlier (e.g., Dawson, 1977; Lydon et al., 1979), field and laboratory studies of these deposits since 1979 were incorporated into the Nahanni Integrated Multidisciplinary Pilot Project under the general direction of J.E. Reesor. Under the auspices of this program, naturally exposed sections and available drill core of selected deposits were measured and sampled in detail. Chemical analyses of collected samples are nearly complete, via the resources and facilities of RGG Division. Parallel to this detailed geological and geochemical documentation of selected deposits, K.M. Dawson of EGM Division has studied the regional metallogenetic significances of these deposit types, and together with M.H. Orchard of the Cordilleran Geology Division, continues to establish their stratigraphic ages and geological settings via conodont dating (Dawson, 1977; Dawson and Orchard, 1982).

This article briefly summarizes some of the major results of these collective studies pending publication of the detailed results, in the form of a general genetic model, and to provide background information necessary to the accompanying article (Lydon et al., 1985).

Geological setting and distribution of stratiform baritic deposits

The locations of the stratiform deposits mentioned in this article are shown in Figure 76.1. Bedrock geology in this area is summarized in the simplified stratigraphic column shown in Figure 76.2, which refers to the central part of the Selwyn Basin.

The Selwyn Basin has been described as an epicratonic marine basin that formed due to subsidence accompanying rifting, and the development of an aulacogen that was tectonically active through Paleozoic time (Tempelman-Kluit, 1981; Cecile, 1982). Extensional tectonics during the Cambrian affected a thick Proterozoic sequence of turbiditic subarkoses, siltstones, shales and minor quartz arenite (Grit Unit) and conformably overlying Lower Cambrian siltstones, mudstones, and carbonates that together form a dominantly arenaceous-argillaceous marine sequence over 4000 m thick (Gordey, 1981). Transitional transgression of shelf-edge limestone over basinal carbonaceous mudstone and chert appears to be diachronous throughout the Selwyn Basin, occurring as early as latest Early Cambrian in the Misty Creek Embayment to the north (Cecile, 1982) to as late as Middle Ordovician near Howards Pass (Norford and Orchard, 1983). Throughout its existence from Cambrian to Mississippian time, the Selwyn Basin was bounded by the Mackenzie Carbonate Platform to the north and east, and by the Cassiar Platform to the southwest.

Within the Selwyn Basin, siliceous and carbonaceous shales and cherts were deposited at rates of less than 0.4 cm/1000 years (Goodfellow et al., 1983). Sulphur isotope evidence from disseminated pyrite indicates that throughout its existence the water column of the Selwyn Basin oscillated from stratified, anaerobic bottomed, restricted circulation conditions to well-mixed, oxygenated, open circulation conditions (Goodfellow and Jonasson, in press). The prime factor causing these oscillations was continued tectonic activity, which caused both regional uplift and subsidence, and localised vertical movements along synsedimentary faults (Cecile, 1982; Goodfellow and Jonasson, 1984).

One of the most obvious expressions of one of these tectonic disturbances resulting in the oxygenation of bottom waters, is the regionally extensive orange weathering, bioturbated silty mudstone (Unit Sp[1]; Gordey, 1981) at the top of the Road River "Group". In this unit the high carbon content typical of the carbonaceous basinal facies rocks occurs as carbonate in ferruginous dolomite (Fig. 76.2).

Beginning about Middle Devonian localized, rapid, differential vertical movements resulted in basin-derived debris flows, conglomerates and related rock types as fan

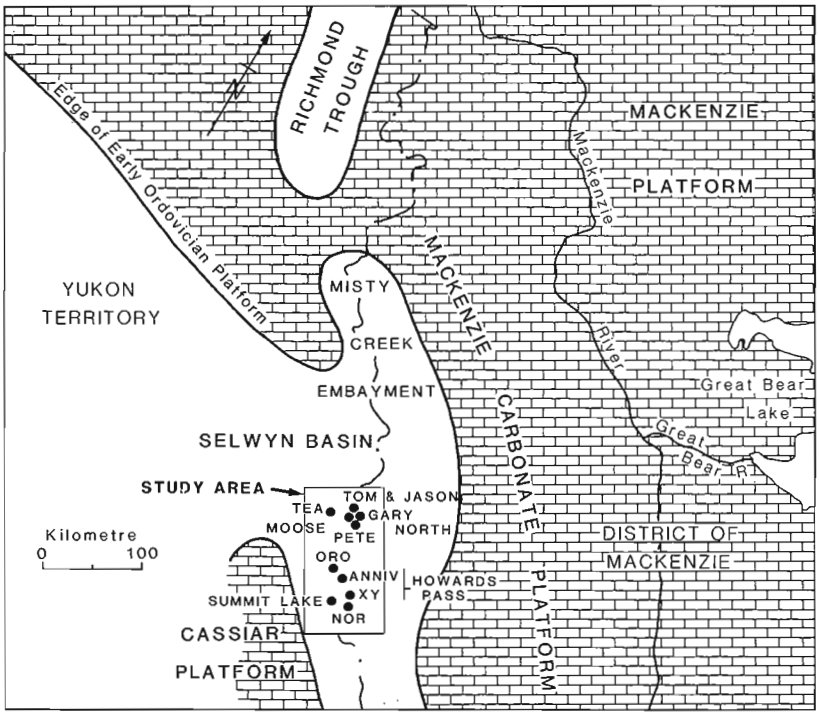

Figure 76.1

Location of study area and baritic deposits sampled. Geological elements after Cecile (1982).

[1] All stratigraphic age notations used in this article are those of Gordey (1981).

complexes, within the Lower Earn Group (Gordey et al., 1981; Gordey et al., 1982). Presumably, these "black clastic" fan complexes originated by erosion of fault scarps or topographically elevated parts of the horst blocks, and were deposited in the intervening graben structures. In the Macmillan Pass area, the age of the oldest coarse clastic unit has been loosely estimated as post-early Givetian (Gordey et al., 1982). Sulphur isotope evidence from pyrite suggests that tectonic activity led to a temporary ventilation of the Selwyn Basin during the Emsian-Eifelian, but stratified, anoxic conditions returned during Givetian and perhaps early Frasnian.

The Upper Earn Group consists of brown weathering shales, sandstone and conglomerate (Gordey et al., 1982). Although small, local anoxic basins may have survived up to Osagean time, the widespread deposition of up to 200 m of clean quartz sandstone unconformably upon Upper Earn Group, indicates that by Visean time, the site of the Selwyn Basin had become an environment of shallow marine clastic sedimentation (Gordey et al., 1982).

Most of the stratiform baritic deposits of the Selwyn Basin are hosted by rocks of the Lower Earn Group. Current information indicates that the oldest host rocks are Eifelian age, with perhaps the majority of known major deposits occurring in rocks of Frasnian age (Dawson and Orchard, 1982). The TEA deposit, with a currently attributed Osagean age, may be the youngest major stratiform barite deposit of the area, although detailed studies are still in progress to verify that the previously dated conondont-bearing unit correlates with the main baritic members on the property (Lydon et al., 1985).

Generalized geological and geochemical description of stratiform baritic deposits

Stratiform baritic deposits of the Selwyn Basin may be divided into three main types (Lydon et al., 1982):

Type A: localized lensoidal deposits of sphalerite-galena-barite-quartz ± pyrite ± siderite,

Type B: high grade (up to 90% $BaSO_4$) localized lensoidal deposits of barite + quartz ± calcite,

Type C: low grade (5-20% $BaSO_4$) laterally extensive baritic member(s) within siliceous Lower Earn Group sediments.

The TOM and JASON deposits of the Macmillan Pass area are the major representatives of Type A. The NOR deposit near Howards Pass contains both barite and base metal sulphides, but galena and sphalerite may have been epigenetically emplaced into a Type B deposit. The Tom and Jason deposits each contain about 10^7 tonnes in a concordant lens or lenses of bedded and laminated barite-rich, sphalerite

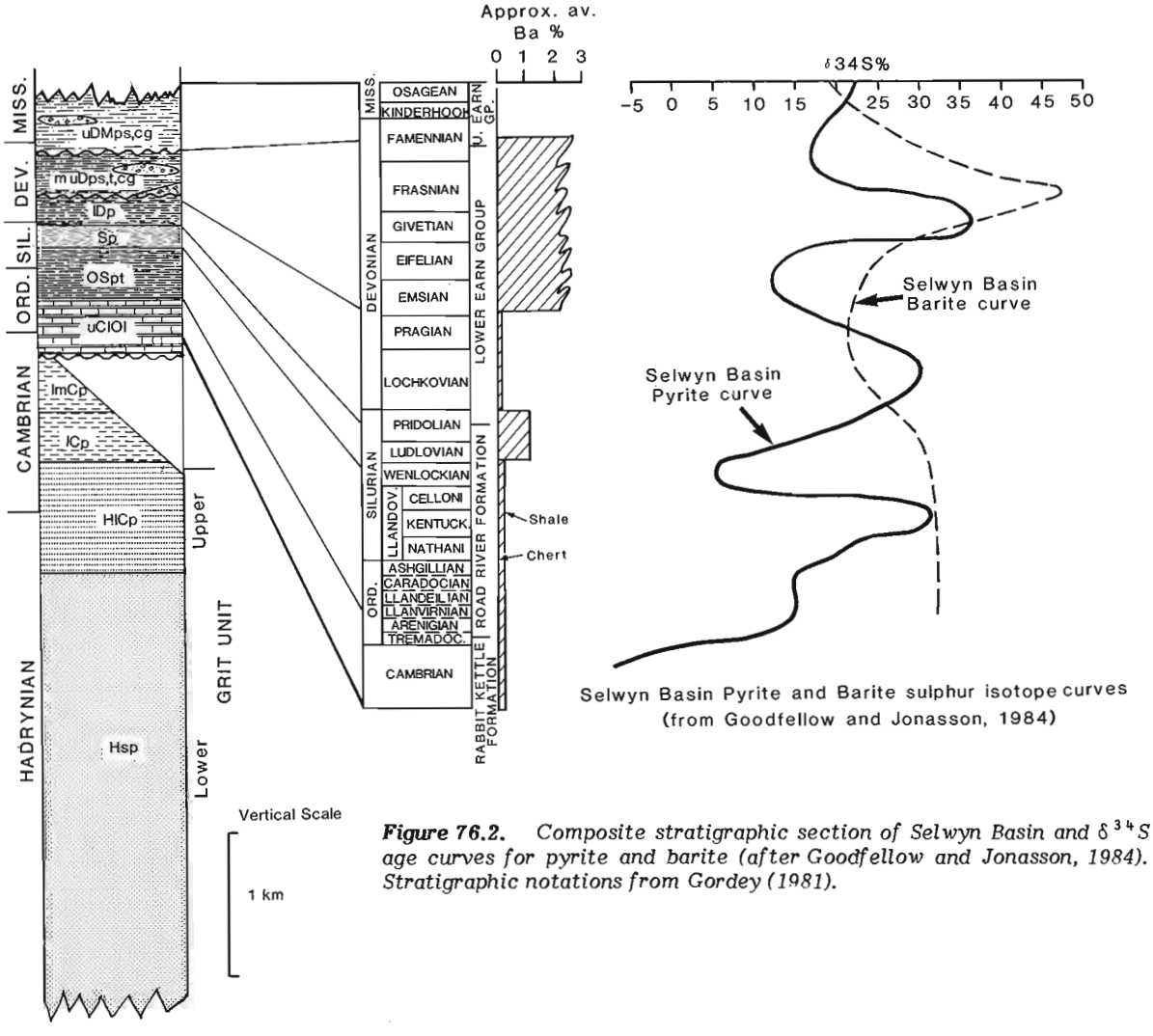

Selwyn Basin Pyrite and Barite sulphur isotope curves (from Goodfellow and Jonasson, 1984)

Figure 76.2. *Composite stratigraphic section of Selwyn Basin and $\delta^{34}S$ age curves for pyrite and barite (after Goodfellow and Jonasson, 1984). Stratigraphic notations from Gordey (1981).*

and galena ore. The barite, sulphide or chert laminae are typically 1 mm in thickness, and are commonly monomineralic. The morphology of the TOM deposit and the distinctive mineralogical zonation away from a footwall stockwork zone along a synsedimentary fault zone, led to its classification as a sedimentary-exhalative type of deposit, formed from hydrothermal solutions that arose along an active fault system and discharged onto the ocean floor (Carne, 1979).

From naturally exposed sections Type B deposits are estimated to contain between 10^5 and 10^6 tonnes of barite, and are thus at least an order of magnitude smaller than Type A deposits. Like Type A deposits, the barite-quartz deposits comprising Type B, consist of concordant lenses of bedded or laminated barite-rich sediments. The laminae are marked by either contrasting compositional differences, especially in silica or organic carbon content, or by organic and/or clay-rich partings. At the ORO deposit, a footwall stockwork of quartz-ankerite-pyrite-barite veins may represent a feeder zone (Dawson and Orchard, 1982). At the TEA deposit, a localized footwall fracture zone, infilled with coarsely crystalline barite, quartz and carbonate may have the same origin.

Type C occurrences are represented by elevated concentrations of barite in Lower Earn Group rocks at many localities between Summit Lake and Macmillan Pass. The thickness of the baritic member ranges from just a few metres at some localities (e.g., near Summit Lake) to more than 100 m at others (e.g., near TOM deposit). The barite occurs as scattered small (1-5 mm) barite nodules, discontinuous laminae, or 1-5 cm baritic beds within normal Lower Earn Group carbonaceous siliceous shale, cherty sediments, siltstone and debris flows. It is uncertain whether Type C includes one or more, laterally extensive baritic members. In the Macmillan Pass area, the Type C member appears to form one laterally continuous stratigraphical interval, and appears to encompass the known Type B deposits. In this area, it is of probable Frasnian age.

The geochemical characteristics of the three types of stratiform baritic deposits of the Selwyn Basin were compared on the basis of complete chemical analysis of about 15 samples, from each of ten localities (three of Type A, five of Type B and two of Type C). The samples, each representing about a 10 cm thickness were taken from representative baritic strata of each locality.

The major result of the analyses is that geochemically both Type A and Type B deposits contrast completely with normal Selwyn Basin sediments. This contrast is the expected result if both are sedimentary-exhalative types of deposits, because both the provenance of components (from hydrothermal solutions) and environment of deposition (brine pool or at least highly modified circum-vent bottom conditions) differ from those of normal marine sediments and bottom waters. Type C occurrences, on the other hand, are normal Lower Earn Group sediments to which only barite has been added in significant amounts.

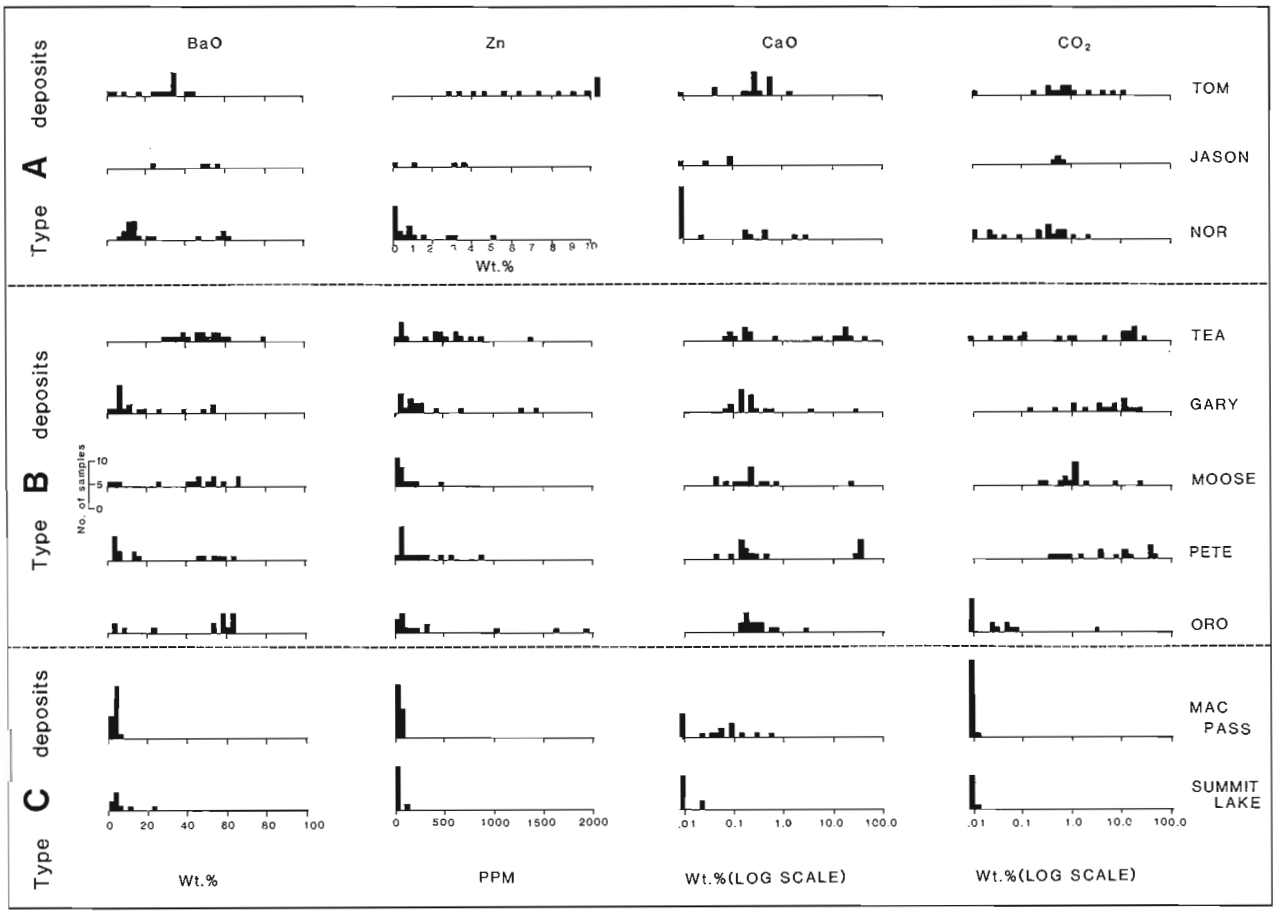

Figure 76.3. *Frequency distributions of Ba, Zn, Ca and CO_2 in samples from the baritic deposits indicated. Vertical scale indicates number of samples.*

The main differences between Type A and Type B deposits, are that the former contains much higher concentrations of sulphide sulphur and chalcophile elements (e.g., Zn, Pb, Ag, Sb, Cd, Hg), but much lower concentrations of CaO, compared to the latter. These differences are illustrated as frequency distribution diagrams in Figure 76.3. The pattern for Zn is similar to the pattern shown by sulphide sulphur and other chalcophile elements. The pattern for CO_2 illustrates that both Type A and Type B have elevated carbonate contents compared to the chemistry of normal sediments, as shown by Type C. In addition, Type B also contains higher absolute amounts of carbonate than Type A, and the CaO/CO_2 ratio for Type B is higher than Type A, because a significant proportion of carbonate in Type A is contained in siderite or ankerite.

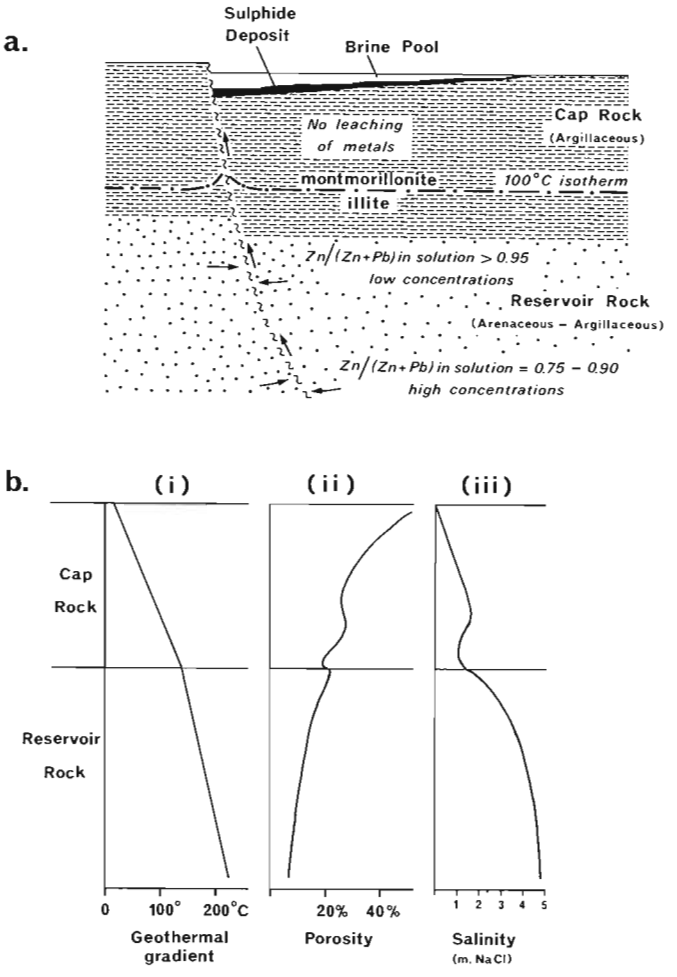

Figure 76.4. *Diagram illustrating the essential features of optimum conditions for the generation of metalliferous pore waters in sedimentary rocks (after Lydon, 1983).*

a) Geological relationships, illustrating that a high geothermal gradient promotes temperature dependent pliogenetic mineralogical changes at relatively shallow depth which allows leaching of ore metals into pore solutions. The Zn/(Zn + Pb) ratio of saturated solutions will systematically increase with depth of reservoir in response to increasing temperature and increasing salinity.

b) Vertical profiles through the section illustrated in 'a', showing the variations in the parameters illustrated.

General genetic model

Lydon (1983) identified the optimal conditions for the generation of ore-forming hydrothermal solutions within sedimentary rocks as part of a comprehensive genetic model for sediment-hosted stratiform Zn-Pb deposits. He argued that the ore solutions were evolved connate waters, and that leaching of metals from a sedimentary pile is significant only during episodes of mineralogical transformations, particularly of clay minerals, which occur at stages during first cycle burial and compaction of the sediments. As illustrated in Figure 76.4, optimum conditions for the generation of large volumes of saline metalliferous formational waters occur where a compacting sedimentary pile, that consists of a dominantly arenaceous sequence is overlain by a dominantly argillaceous sequence, occupies a large region of high geochemical gradient. The role of the upper argillaceous sequence or "cap rock" is to:

1. act as a thermal insulator to the lower arenaceous sequence or "reservoir rock" (Fig. 76.4a, b(i)).
2. retard the dewatering of the reservoir rock, thereby preserving large volumes of pore fluids within geopressured reservoirs (Fig. 76.4b(ii)).
3. act as a semi-permeable barrier which promotes ion filtration and consequently the enhancement of salinities within the geopressured reservoirs (Fig. 76.4b(iii)).

According to this genetic model, metals were leached from the arenaceous sequence by stagnant geopressured pore solutions and discharged to the palaesurface when the geopressured reservoir was ruptured by faulting.

Comparison of Figures 76.2 and 76.4 shows that during the Paleozoic, the Selwyn Basin possessed all the essential features of this model. The uppermost Proterozoic argillaceous rocks and the Paleozoic basinal carbonaceous, siliceous shales and cherts are modelled as cap rocks to the underlying, arenaceous to argillaceous, Late Proterozoic Grit Unit. The sporadic but repetitive tectonic and volcanic activity throughout the Paleozoic as noted above, is compatible with the high regional geothermal gradients during parts of the Paleozoic. Direct application of this genetic model to the Selwyn Basin predicts that the metals and gangue components of the stratiform sulphidic and baritic deposits were leached from the Grit Unit. This prediction is consistent with the conclusions of Godwin and Sinclair (1982) that the lead isotope data for Selwyn Basin stratiform sulphide deposits are most consistent with a source rock that has been directly derived from Hudsonian basement, as is the case for the Grit Unit.

Lydon et al. (1979) argued that, based on analogy to modern hydrothermal systems and the similarity in chemical composition of contemporaneously formed clusters of the volcanogenic massive sulphide type of exhalative deposits, hydrothermal systems of the same age and same area tend to be derived from the same reservoir units and consequently have the same base temperature and same chemistry. These authors therefore suggested that the difference between Type A and Type B deposits in the Macmillan Pass area was essentially that Type B deposits formed in more oxic environments than Type A. Fundamentally their argument was that the more oxic environment of Type B deposits would lead to greater oxidation versus cooling rates of the hydrothermal solutions after discharge than that for Type A deposits, and therefore the more rapid and complete oxidation of H_2S to SO_4, and the conversion of CH_3 to CO_2 would promote the deposition of limestone.

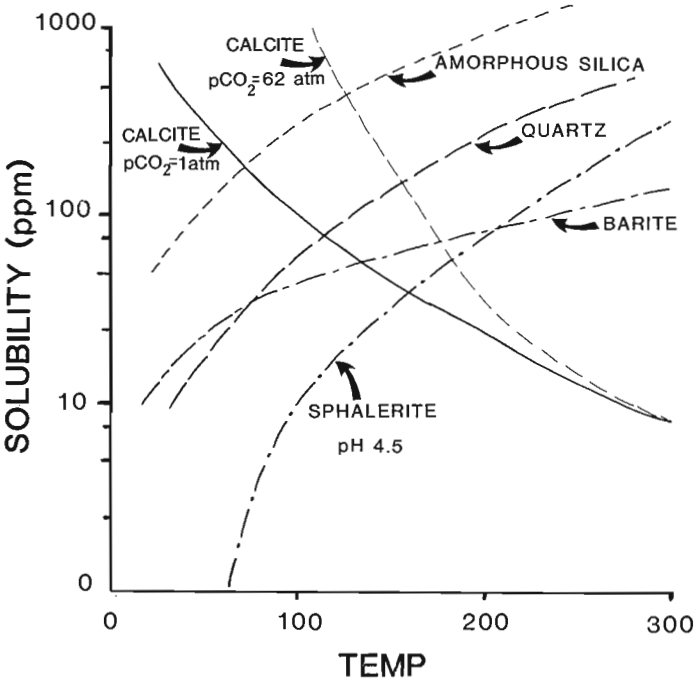

Figure 76.5. *Experimental stoichiometric solubilities of barite, calcite, sphalerite, quartz and amorphous silica in 3m NaCl solutions as functions of temperature. Data from Blount (1977), Ellis (1963), Barrett (1974) and Holland (1967) respectively.*

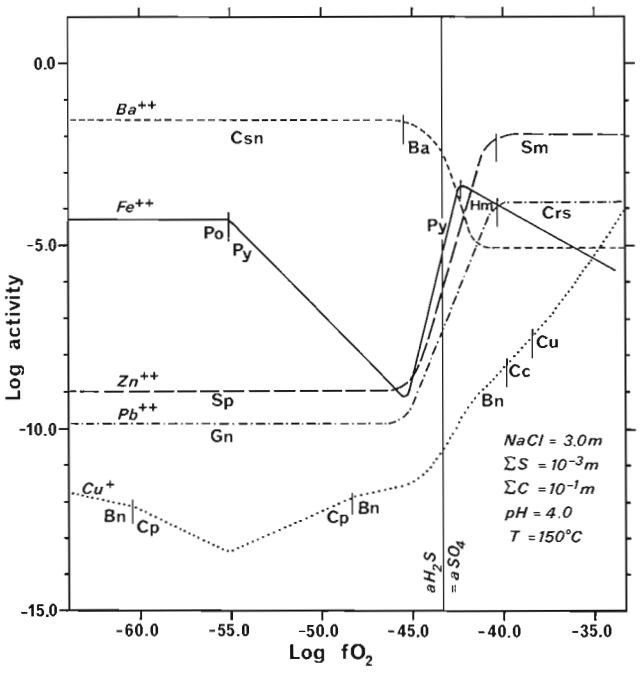

Figure 76.6. *Calculated activities of Pb^{++}, Cu^{+}, Zn^{++}, Fe^{++}, Ba^{++} and in a 3m NaCl solution as a function of fO_2, at a temperature of 150°C, and pH 4, $\Sigma mS. = 10^{-3}$. Bars on activity curves indicate boundaries between mineral stability fields. Key to mineral abbreviations: Ba – barite; Bn – bornite; Csn – celsian; Crs – cerussite; Cu – copper; Cc – chalcocite; Cp – chalcopyrite; Gn – galena; Hm – hematite; Py – pyrite; Po – pyrrhotite; Sp – sphalerite; Sm – smithsonite. The activity for Ba^{++} within the stability field of celsian was calculated assuming log K dissociation of celsian is similar to that for microcline. From Lydon (1983).*

However, chemical data obtained since that time indicate that the differences between Type A and Type B deposits go beyond merely the presence of limestone and absence of sulphides in Type B compared to Type A. These new data indicate:

1. Both Type A and Type B contain significant carbonate.
2. Type A is depleted only in CaO compared to Type B, and not both CaO and CO_2 (calcite) as assumed by Lydon et al. (1979).
3. The average SiO_2/Al_2O_3 ratio of Type A deposits is significantly higher than that of Type B deposits. If Al_2O_3 contents are assumed to be directly proportional to a non-hydrothermal clastic component of the sedimentary mineralization, then this would indicate that the SiO_2 flux of the ore solutions for Type A deposits was higher than for Type B deposits.
4. Sulphur isotope data indicate that the degree of mixing with coeval seawater and hence oxidation of the ore solutions was comparable for Type A and Type B deposits. The absence of significant base metal sulphides in Type B deposits therefore probably reflects original low concentrations of Zn and Pb in the ore solutions.

The concentrations of all major components of a natural hydrothermal dissolution are determined by equilibrium with respect to rock forming minerals in the reservoir. For hydrothermal solutions generated in sedimentary rocks, the concentrations of silicon, calcium, carbonate, barium and zinc in solution can be expected to be determined by saturation with respect to quartz, calcium carbonate, barite or barium feldspar and sphalerite respectively (Lydon, 1983). Figure 76.5 shows that in order to generate the element associations typical of Type A deposits (high Zn, high Ba, relatively high Si, low Ca), the base temperature of the hydrothermal system must be at least 100°C higher than for the Type B association (low Zn, high Ba, relatively lower Si, high Ca).

Because both Type A and Type B deposits formed during the same time interval, at least in the Macmillan Pass area, the lower base temperatures of the reservoirs to Type B deposits indicate that they occurred at shallower depths, i.e., within stratigraphically higher horizons, than the reservoirs to Type A deposits. If, for the reasons outlined above, the reservoirs for Type A deposits were within the Grit Unit, then the reservoirs for Type B deposits must have been within the upper part of the Grit Unit or the lower part of the Paleozoic carbonaceous siliceous shale sequence (i.e., Road River Group and perhaps the lower part of the Lower Earn Group). Road River Group reservoirs are favoured for two main reasons:

1. A genetic affiliation between Type B deposits and a stratigraphically underlying carbonaceous shale sequence readily explains the extremely high incidence of stratiform barite deposits in the Paleozoic of western North America, compared to otherwise geologically similar environments elsewhere in the world, especially those that contain stratiform baritic sulphide deposits, e.g., Ireland, Germany.
2. Type B deposits have a much higher BaO/SiO_2 ratio compared to Type A deposits than Figure 76.5 would predict. This suggests that the barium content of Type B reservoirs was controlled by a more soluble barium mineral than barite.

With regard to the latter point, there is evidence that the pO_2 of the pore waters of the Road River Group was lower than the minimum required to stabilize barite, and

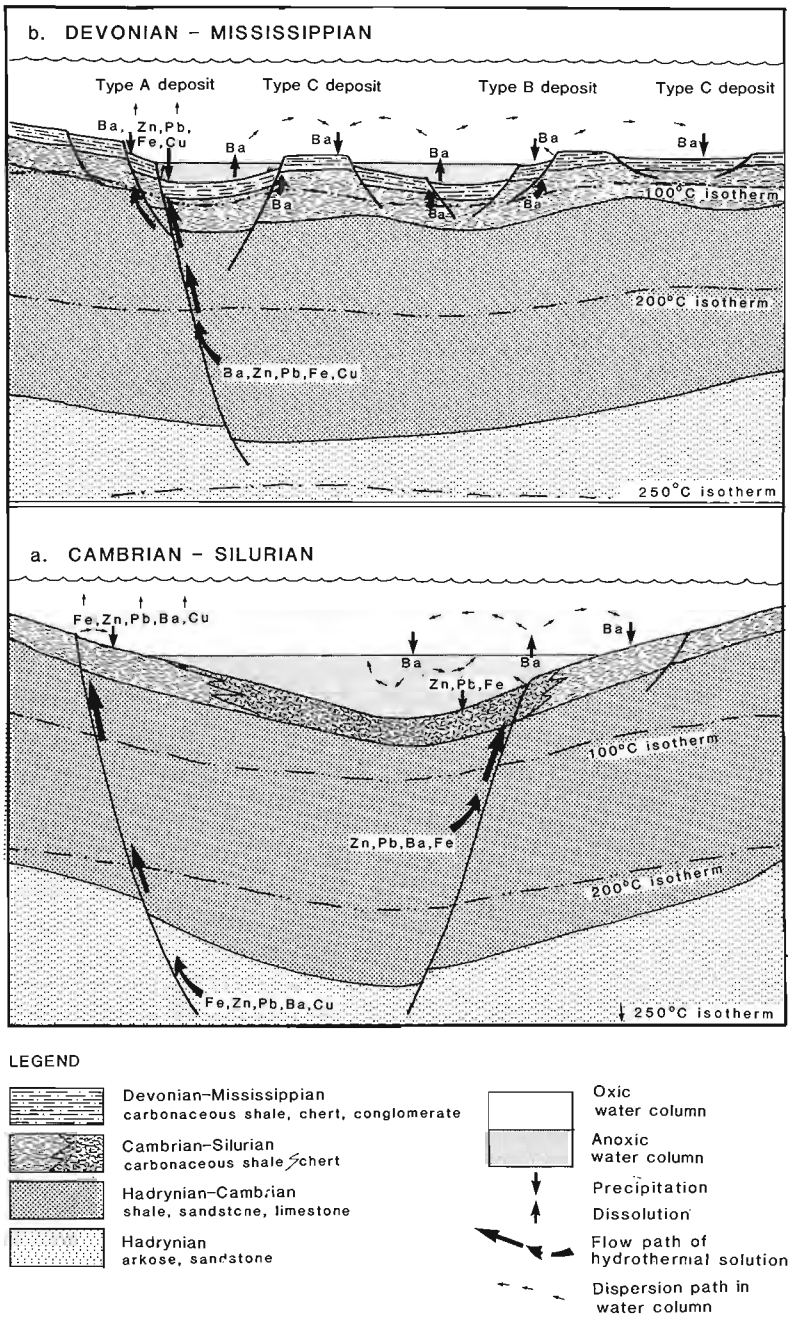

Figure 76.7. *Schematic representation of the major processes controlling the distribution of barium in sedimentary rocks from the Selwyn Basin during (a) Cambrian-Silurian and (b) Devonian-Mississippian. Not to scale and no representation of the specific timing of hydrothermal events in Selwyn Basin.*

hence within the stability field of different barium minerals such as celsian, cymrite or hyalophane. Barite is very rare as a primary or authigenic mineral in the Road River Group within the area shown in Figure 76.1. Even where anomalously high Ba concentrations have been found, such as the orange weathering silty mudstone (Unit Sp), which averages 2.8% Ba at Howards Pass, the main barium mineral is a K-Ba-feldspar (Goodfellow and Jonasson, in press). As can be seen from Figure 76.6, the presence of a barium feldspar in a system containing sulphur (remembering the ubiquitous presence of rock pyrite in the Road River rocks) indicates a low pO_2. The anomalously low pO_2 values during diagenesis of the Road River Group sediments is attributed to the consumption of oxygen by the oxidation of the high organic carbon content.

Figure 76.6 also shows that for comparable temperature and pH the concentration of barium in pore waters will be many times higher if a barium feldspar is the stable authigenic barium mineral than if barite is the stable barium phase. The conclusion is that the pore waters of the Road River Group had an anomalously high barium concentration during its burial history. Direct evidence for this high barium mobility in the Road River Group includes the barium metasomatism of intercalated basic volcanics to give Ba contents higher than 4% (Goodfellow et al., 1980). Expulsion of these barium-rich formational waters from Lower Paleozoic carbonaceous siliceous shale units, particularly during periods of tectonic activity could have given rise to Type B and Type C deposits.

Evolution of exhalative activity and barium mobility in Selwyn Basin

The deposition of baritic sediments in the Selwyn Basin took place during two main time intervals (Fig. 76.7). Optimum conditions for the generation and exhalation of metalliferous hydrothermal solutions existed, in a general sense, during both time intervals.

From Late Proterozoic to Late Silurian (Fig. 76.7a), the dominantly arenaceous and arkosic lower part of the Grit Unit (Hsp) was successively buried and capped by the dominantly argillaceous upper part of the Grit Unit (HI€p) and Early Cambrian (l€p), the thin bedded argillaceous limestones, silty limestones and calcareous shales of the Rabbit Kettle (u€lOl) and the dominantly carbonaceous siliceous shales and cherts of the Road River Group (Osp, Ost, Sp). Initiation of extensional tectonics and volcanic activity in the earliest Cambrian to produce the Selwyn Basin aulacogen indicates a high geothermal gradient during that time. The deposits of the Anvil camp are the major examples of hydrothermal discharge accompanying the tectonic activity during the Cambrian (Jennings and Jilsen, 1983). Sea floor conditions appear to have been oxic to some degree at the discharge sites, because barite forms a significant proportion of the Anvil deposits. All stratiform Zn-Pb deposits of the Anvil camp conform chemically with the high Fe, high Ba, sub-type of sediment-hosted stratiform Zn-Pb deposits, indicating hydrothermal solution generation within a sequence of normal or average clastic rocks (pO_2 in range of pyrite stability and $H_2S > SO_4^{--}$) (Lydon, 1983). The presence of only small quantities of copper in these deposits indicates solution temperatures in the range of 200-250°C (Lydon, 1983, Fig. 6.29), and the hydrothermal reservoirs are presumed to have been the Lower Grit Unit.

From late Cambrian through Ordovician, sulphur isotopes of pyrite (Fig. 76.2) indicate the Selwyn Basin became increasingly restricted, so that by early Silurian there was virtually complete depletion of seawater sulphate,

especially in localized deeps such as the Howards Pass subbasin (Goodfellow and Jonasson, 1984). The limited data available indicate that the barium content of chert in the Road River Group averages about 250 ppm, but shales in the area of Figure 76.1 average more than 3000 ppm (Goodfellow et al., 1983) which is five times higher than shales of the same age in the Misty Creek embayment (Goodfellow et al., 1980). The reason for this distribution is not clear. Perhaps in the central, deeper, chert-rich part of the Selwyn Basin, bottom conditions were more anoxic and suppressed the precipitation of barium as trace barite grains, or perhaps the lack of alumina allowed almost total mobility of barium and its escape with expelled pore waters during compaction. In the shales, on the other hand, a large proportion of the original minor barium content of the sediment became fixed as authigenic barium aluminum silicate during diagenesis. Whatever the reason, it is evident that the Road River Group shales of the area shown in Figure 76.1 have an anomalously high barium content. This is attributed both to the restricted nature of this part of the Selwyn Basin, which conserved any barium released during the compaction and dewatering of the underlying rock column, and also a high level of hydrothermal discharge accompanying presumed higher incidences of tectonic activity in this part of the Selwyn Basin.

The barium content of the Silurian Howards Pass Zn-Pb sulphide deposits averages less than 400 ppm, otherwise the chemistry of these deposits is similar to the Devonian TOM deposit, which belongs to a high-barium, low-iron, carbonate-rich sub-type of sediment-hosted stratiform Zn-Pb deposits. It is presumed therefore that any barium discharged with the ore solutions at Howards Pass remained in solution in the sulphate-free water column overlying the sub-basin This dissolved barium probably contributed to the anomalously high barium content of the shales in the more oxic areas surrounding the sub-basin (Goodfellow and Jonasson, 1984).

The orange-weathering silty mudstone (Sp), which was deposited during the period of Selwyn Basin ventilation, averages more than 1% Ba. At least some of this barium enrichment, because of the regional nature of the anomaly, was probably due to precipitation from the previously sulphate-depleted, barium-enriched, Selwyn Basin water column, due to the effects of gradual oxidation and incursion of fresh marine sulphate. However, localized areas of barium enrichment, such as above the Howards Pass sub-basin where the Sp Unit averages about 6% Ba, suggest that hydrothermal activity continued to add barium to the sedimentary succession during this time interval (Goodfellow and Jonasson, in press).

During the second major time interval, from about Late Silurian to Mississippian (Fig. 76.7), the mobility and deposition of barium was dominated by two major factors. The first was that the Road River Group shales had been buried to sufficient depths, and hence heated to sufficient temperatures, to maximize the diagenetic reactions discussed earlier that produced barium-rich pore waters. The second was the intense localized vertical tectonic movements that produced a horst and graben topography and gave rise to the chert pebble conglomerates and related rock types. Lower to Middle Devonian cherts average about 0.2% Ba, but sections through Middle to Upper Devonian sediments (i.e., those deposited synchronously prior or later than "black clastics") commonly average about 5% Ba. This indicates that tectonic activity played an important role in increasing the supply of barium during the second major time interval. Type B deposits are confined to Devonian or younger host rocks, and the background barium content of Lower Earn Group basinal clastic rocks is much higher than similar rock types of presumed similar or lower depositional rates in the Road River Group. This indicates that the barium concentration of hydrothermal solutions discharged into the Selwyn Basin was higher during the second major time interval than during the first. This would further indicate that a different or an additional barium source existed during deposition of the Lower Earn Group than that existed during the first major time interval (Fig. 76.7a). As suggested above, this additional source of barium was probably pore waters derived from carbonaceous siliceous shales of the Road River Group.

Focussed discharge of these barium-rich pore waters along zones of cross-stratal permeability related to faulting probably led to the formation of Type B deposits (Fig. 76.7b). It is inferred that most of this faulting was of the listric type, and because of its relatively shallow depth penetration, resulted in the release of pore waters from only the Paleozoic substrate. Faulting associated with major tectonic features like the Macmillan Pass graben, was much deeper seated, and caused the release of solutions from geopressured aquifers present in the Proterozoic Grit Unit. Focussed discharge of these higher temperature hydrothermal solutions probably gave rise to Type A deposits. The presence of Cu mineralization in the stockwork of the TOM deposit suggests that, like the deposits of the Anvil camp, hydrothermal temperatures were above 200°C (Lydon, 1983). However, the relatively low iron content of the TOM deposit suggests that the ore solutions were more alkaline and perhaps more sulphur-rich than those that formed the Anvil deposits, indicating a mineralogically different reservoir rock type (perhaps a feldspar-clay assemblage for TOM as opposed to a clay-clay assemblage for the Anvil deposits). It is possible that the barium contained in Type A deposits was derived from aquifers within the Paleozoic substrate, but in view of the over-pressured nature of the hydrothermal system, most of the fluid would be expected to flow away from, rather than into, the conduit system. However, shallow fault systems, spatially associated with the deep-seated fault system, could have contributed to the total barium content of Type A deposits.

Barium released to the seawater by dispersion away from the focussed discharge of the exhalative vents responsible for Type A and Type B deposits, or added to seawater by diffuse discharge and seepage related to normal dewatering processes of the Paleozoic substrate, is suggested to be responsible for the high background levels of barium in Lower Earn Group sediments. Type C deposits are suggested to represent anomalously high concentrations of barite precipitated by these mechanisms, and would therefore indicate periods of more intense tectonic activity and more rapid dewatering of the Paleozoic substrate, than was generally the case. Recent conodont dating reported by Dawson and Orchard (1982) and Gordey et al. (1982) indicates that the Type C stratigraphic interval in the Macmillan Pass area is of Frasnian age. This corresponds to a period of ventilation of the Selwyn Basin, succeeding the stratified and bottom-anoxic conditions of the Givetian and perhaps early Frasnian (Goodfellow et al., in press). This Frasnian ventilation (Fig. 76.2), which corresponds to a global ventilation of the oceans, may have contributed to the formation of the Macmillan Pass Type C mineralization by precipitation of barite from the previously sulphate depleted, barium enriched Selwyn Basin water column, similar to the event that occurred during the deposition of the Sp unit in the Silurian. There is not sufficient biostratigraphic control to determine whether Type C occurrences observed in the upper part of the Lower Earn Group elsewhere occupies the same stratigraphic interval as that at Macmillan Pass.

Conclusions

During unique periods in the Paleozoic, the Selwyn Basin maintained a geological configuration and environment that provided optimum conditions for the generation of metalliferous hydrothermal solutions and the formation of sediment-hosted stratiform Zn-Pb deposits. We speculate that baritic deposits characterized by high Zn-Pb contents (Type A) were probably formed by the release of formational waters from the upper Proterozoic Grit Unit along deep-seated, synsedimentary fault zones. Much smaller, though more numerous, barren baritite deposits (Type B) of Devonian-Mississippian age, are postulated to have formed by the release of formational waters from the carbonaceous shale succession of the Ordovician-Silurian Road River Group, by shallow-seated listric fault systems. Type C deposits represent periods of anomalously rapid barite precipitation that accompanied higher levels of tectonic activity, dewatering of the Paleozoic substrate, and ventilation of the Selwyn Basin during the late Devonian. This coincidence in time and space of sea floor hydrothermal discharge from unrelated hydrothermal systems that gave rise to deposits of totally different economic significance, requires caution be exercised in the interpretation of synsedimentary, hydrothermal activity in the Selwyn Basin for the purposes of mineral exploration.

Further documentation and testing of the genetic model presented here is continuing.

Acknowledgments

This work has drawn on the information supplied by many people who have worked in the Selwyn Basin, without whose help and co-operation comprehensive genetic modelling of the type presented is not possible. In particular we wish to acknowledge the contributions by mineral exploration companies in supplying material, information, and help in field logistics, particularly Placer Development, Aberford Resources, Hudson Bay Exploration and Development, Noranda Exploration, and our colleagues at the GSC who participated in the Nahanni IMPP. This paper benefitted from the critical reading and suggestions of C.W. Jefferson.

References

Barret, T.J.
1974: Solubility of galena and sphalerite in sodium chloride brines up to 95°C; unpublished MSc Thesis, University of Toronto, 157 p.

Blount, C.W.
1977: Barite solubilities and thermodynamic quantities up to 300°C and 1400 bars; American Mineralogist, v. 62, p. 942-957.

Carne, R.C.
1979: Geological setting and stratiform lead-zinc-barite mineralization, Tom Claims, Macmillan Pass, Yukon Territory; Department of Indian and Northern Affairs, Whitehorse, Report 1979-4, 30 p.

Cecile, M.P.
1982: The Lower Paleozoic Misty Creek Embayment, Selwyn Basin, Yukon and Northwest Territories; Geological Survey of Canada, Bulletin 335, 78 p.

Dawson, K.M. and Orchard, M.J.
1982: Regional metallogeny of the Northern Cordillera: biostratigraphy, correlation and metallogenic significance of bedded barite occurrences in eastern Yukon and western District of Mackenzie; in Current Research, Part C, Geological Survey of Canada, Paper 82-1C, p. 31-38.

Ellis, A.J.
1963: The solubility of calcite in sodium chloride solutions at high temperatures; American Journal of Science, v. 261, p. 259-267.

Godwin, C.I. and Sinclair, A.J.
1982: Average lead isotope growth curves for shale-hosted zinc-lead deposits, Canadian Cordillera; Economic Geology, v. 77, p. 675-690.

Goodfellow, W.D., Jonasson, I.R., and Cecile, M.P.
1980: Nahanni Integrated Multidisciplinary Pilot Project Geochemical Studies Part 1: Geochemistry and mineralogy of shales, cherts, carbonates and volcanic rocks from the Road River Formation, Misty Creek Embayment, Northwest Territories; in Current Research, Part B, Geological Survey of Canada, Paper 80-1B, p. 149-161.

Goodfellow, W.D., Jonasson, I.R., and Morganti, J.M.
1983: Zonation of chalcophile elements about the Howard's Pass (XY) Zn-Pb deposit, Selwyn Basin, Yukon; Journal of Geochemical Exploration, v. 19, p. 503-542.

Goodfellow, W.D. and Jonasson, I.R.
1984: Ocean stagnation and ventilation defined by $\delta^{34}S$ secular trends in pyrite and barite, Selwyn Basin, Yukon; Geology, v. 12.

– Environment of formation of the Howards Pass (XY) Zn-Pb deposit, Selwyn Basin, Yukon; in Mineral Deposits of Northern Cordillera, Canadian Institute of Mining and Metallurgy, Special Volume. (in press)

Gordey, S.P.
1981: Geology of Nahanni map-area (105I), Yukon Territory and District of Mackenzie; Geological Survey of Canada, Open File 780.

Gordey, S.P., Wood, D., and Anderson, R.G.
1981: Stratigraphic framework of southeastern Selwyn Basin, Nahanni Map Area, Yukon Territory and District of Mackenzie; in Current Research, Part A, Geological Survey of Canada, Paper 81-1A, p. 395-398.

Gordey, S.P., Abbott, J.G., and Orchard, M.J.
1982: Devono-Mississippian (Earn Group) and younger strata in east-central Yukon; in Current Research, Part B, Geological Survey of Canada, Paper 82-1B, p. 93-100.

Holland, H.D.
1967: Gangue minerals in hydrothermal deposits; in Geochemistry of Hydrothermal Ore Deposits, ed. H.L. Barnes; Holt, Rinehart and Winston Inc., New York, p. 382-436.

Jennings, D.S. and Jilson, G.A.
1983: Geology and sulphide deposits of Anvil Range, Yukon Territory (abstract); in Symposium on Mineral Deposits of Northern Cordillera, Abstracts, Joint Canadian Geological Association of Canada Meeting, Whitehorse, December, 1983, p. 11.

Lydon, J.W.
1983: Chemical parameters controlling the origin and deposition of sediment-hosted stratiform lead-zinc deposits; in Mineralogical Association of Canada Short Course Handbook, v. 8, Sediment-hosted stratiform lead-zinc deposits, ed. D.F. Sangster; p. 175-250.

Lydon, J.W., Lancaster, R.D., and Karkkainen, P.
1979: Genetic controls of Selwyn Basin stratiform barite/sphalerite/galena deposits: an investigation of the dominant barium mineralogy at the TEA deposit, Yukon; in Current Research, Part B, Geological Survey of Canada, Paper 79-1B, p. 223-229.

Lydon, J.W., Jonasson, I.R., and Goodfellow, W.D.
1982: Some geochemical aspects of stratiform baritic deposits of Selwyn Basin (abstract); International Association of Sedimentologists, Eleventh International Congress, Hamilton, Ontario, Abstracts of Papers, v. 11, p. 18.

Lydon, J.W., Jonasson, I.R., and Hudson, K.A.
1985: The distribution of gold in the TEA barite deposit, Yukon; in Current Research, Part A, Geological Survey of Canada, Paper 85-1A, report 77.

Norford, B.S. and Orchard, M.J.
1983: Early Silurian age of lead-zinc mineralization at Howards Pass, Yukon Territory and District of Mackenzie; review of local biostratigraphy of Road River Formation and Earn Group; Geological Survey of Canada, Paper 83-18, 36 p.

Tempelman-Kluit, D.
1981: CRAIG Claims; in Yukon Geology and Exploration 1979-80, Department of Northern Affairs, Whitehorse, p. 225-230.

THE DISTRIBUTION OF GOLD IN THE TEA BARITE DEPOSIT, YUKON TERRITORY

Projects 770063 and 740081

John W. Lydon[1], Ian R. Jonasson[2], and Karen A. Hudson[3]

Lydon, J.W., Jonasson, I.R., and Hudson, K.A., The distribution of gold in the TEA barite deposit, Yukon Territory; in Current Research, Part A, Geological Survey of Canada, Paper 85-1A, p. 661-667, 1985.

Abstract

Although there is some doubt as to the age of the TEA barite deposit, its chemistry and geological setting is very similar to other stratiform "barren" baritite deposits of the Lower Earn Group in the Selwyn Basin. Chemical thermodynamic modelling of a general genetic model for these deposits indicates that the chemical composition of the ore solution was at optimum conditions for the mobilization of gold. Chemical analyses of previously collected samples indicate that the average gold content of baritite from the TEA deposit is 4 ppb compared to average contents of ≤ 1 ppb for other basinal lithologies of the Selwyn Basin. Maximum gold concentration in the TEA deposit occurred at the end of hydrothermal exhalative cycles, when rates of baritite deposition were lowest and the abundance of suitable synsedimentary gold collectors, particularly organic carbon and pyrite, was at a maximum.

Résumé

Bien qu'il subsiste quelques doutes sur l'âge du gîte de barytine TEA, sa chimie et son cadre géologique ressemblent beaucoup à ceux d'autres gîtes de barytine stratiformes "stériles" du groupe inférieur d'Earn, dans le bassin de Selwyn. En faisant appel à la réalisation thermodynamique et chimique d'un modèle général de genèse de ces gisements, on a constaté que la composition chimique de la solution minéralisée créait des conditions optimales pour la mobilistion de l'or. L'analyse chimique d'échantillons recueillis auparavant indique que la teneur moyenne en or de la barytine du gîte TEA est de 4 ppb, alors que les teneurs moyennes sont inférieures à 1 ppb dans les autres types de strates d'eau profonde du bassin de Selwyn. Dans le gîte TEA, la concentration maximale d'or a eu lieu à la fin des cycles hydrothermaux de type exhalatif, durant lesquels le rythme de mise en place de la barytine a été le plus lent, et l'abondance de collecteurs appropriés de l'or synsédimentaire, en particulier du carbone organique et de la pyrite, a été maximale.

[1] Economic Geology and Mineralogy Division
[2] Resource Geophysics and Geochemistry Division
[3] Queen's University, Kingston, Ontario K7L 3N6

Introduction

Over the past six years, field and laboratory studies have been carried out at the Geological Survey of Canada aimed at understanding the distribution and genesis of stratiform barite deposits of the Selwyn Basin. These studies formed part of the Nahanni Integrated Multidisciplinary Pilot Project, under the general direction of J.E. Reesor. A preliminary report synthesizing the results to date by Lydon et al. (1985) presents a general genetic model for the various types of stratiform baritic deposits of the Selwyn Basin.

During the conceptual development of this genetic model, thermodynamic modelling of the postulated environments of ore solution generation predicted that the theoretical ore solutions for the formation of the Type B deposits (localized lensoid deposits of barite-silica-calcite) were very favourable for the mobilization of gold. To test whether there was any indication of gold enrichment that would verify the model, selected samples of a previously collected suite from the TEA barite deposit were analyzed for gold.

This preliminary report on the results obtained to date also serves to illustrate the usefulness of thermodynamics in understanding the genesis of ore deposits. Neither the Selwyn Basin nor the known ore deposit types that it contains have the reputation of potential repositories of economically recoverable gold concentrations. Although the extent and concentration of gold mineralization in the TEA deposit reported here is far from being of economic significance, the fact that processes leading to gold concentration have operated in the Selwyn Basin may warrant reconsideration of the gold potential of this area.

Geological setting of the TEA barite deposit

The TEA barite deposit is located about 20 km southwest of the airstrip at Macmillan Pass, and can be reached by a 12 km access road that branches off the Canol Road near mile 254 (Fig. 77.1). The TEA claims were staked in August 1975 (Carne, 1976), and since that time activities to evaluate and develop the TEA deposit for commercial purposes, especially since the fall of 1980 (Coolen, 1982), have included bulldozer trenching, road construction and blasting of a quarry face. This new exposure has provided more opportunity for extending geological investigations than the original natural exposure allowed.

Published geological studies of the TEA deposit include geological mapping by Carne (1976) and Coolen (1982), mineralogical investigations by Lydon et al. (1979), and biostratigraphic age dating by Dawson (1977) and Dawson and Orchard (1982).

On the basis of lithological comparison to the geology at Macmillan Pass, Carne (1976) assigned the carbonaceous siliceous shale of his Unit 2, which hosts the statiform massive barite mineralization, to the then assumed Canol Formation equivalent (now part of the Middle and Upper Devonian Lower Earn Group of Gordey et al., 1982). Carne (1976) assigned the overlying sequence of sandstone, siltstone and mudstone, comprising his units 3 and 4, to the then assumed Imperial Formation equivalent (now part of the post-mid Famennian to pre-Late Mississipian Upper Earn Group of Gordey et al., 1982).

Dawson (1977) reported that a sample of limestone from "within the thick TEA barite sequence contained Devono-Mississippian conodonts and a brachiopod tentatively assigned to the same broad range". Dawson and Orchard (1982) reported that a re-examination of the same sample (GSC Loc. No. C-087721) yielded a definitive conodont fauna of Osagean age (late Lower Mississipian). A sample of limestone containing brachiopods collected by two of the present authors (JWL and IRJ) in 1979 from a bulldozer trench more than 100 m laterally away from the nearest exposure typical of the the main baritite sequence of the TEA deposit, also yielded a conodont fauna of Osagean age (Sample GSC Loc. No. C-086426 in Dawson and Orchard, 1982).

Thus, there appears to be an apparent conflict in the evidence for the age of the TEA deposit. On the one hand, the correlation of Carne's (1976) unit 2 and units 3 and 4 with the Lower Earn Group and Upper Earn Group, respectively, at Macmillan Pass, is very convincing both in terms of lithologies and thicknesses. On the other hand, the biostratigraphic correlation by conodont dating of Carne's (1976) unit 2 with the Upper Earn Group, seems unquestionable.

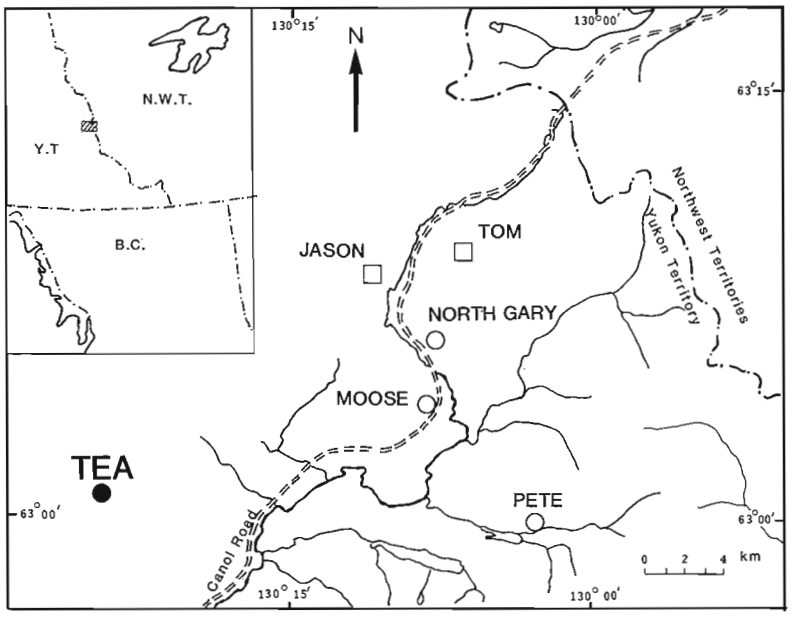

Figure 77.1

Location of the TEA deposit with respect to other baritic deposits of the Macmillan Pass area.

During the 1984 field season two of the current authors (JWL and KAH) utilizing the new exposures created since 1979, attempted to define the stratigraphic relationship of the brachiopod-containing limestone (Sample GSC Loc. No. C-086426) to the main baritite sequence on the TEA property. Due to the structural complexity of the local geology, the field investigations were inconclusive in resolving the problem, but they did not preclude the possibility that the brachiopod-containing limestone actually occurs at the base of Carne's (1976) unit 3. The limestone is overlain by a 10 m sequence of black mudstone and impure baritite, that distinctly contrasts in appearance to the main baritite sequence on the property. Thus, although the brachiopod-containing limestone of Osagean age can be described as occurring within the naturally exposed section of baritite on the TEA property, it may actually rest unconformably on the main baritite sequence. If this viewpoint is correct, the brachiopod-containing limestone may represent the basal beds of the Upper Earn Group, and the overlying impure baritite a local clastic derivative from the main baritite sequence below the sub-Upper Earn Group erosion surface. Investigation of this problem is continuing.

Thermodynamic prediction for a gold association with the TEA baritite deposit

Although there is some doubt as to the age of the main baritite sequence of the TEA property, this does not materially affect the interpretation as to the nature of the substrate to the deposit at the time of its deposition. The main baritite sequence rests on at least 60 m of carbonaceous siliceous shale and chert pebble conglomerate (Carne, 1976). Regardless of whether this footwall sequence forms the lower part of the Upper Earn Group or occurs within the Lower Earn Group, it must rest on a dominantly carbonaceous siliceous shale and chert sequence of older Palaeozoic rocks, because these are the dominant lithologies of both the Lower Earn Group and Road River Group in this part of the Selwyn Basin (Gordey, 1981; Gordey et al., 1982).

Lydon et al. (1985) suggested that localised stratiform barite-silica-calcite deposits in the Lower Earn Group were due to the focussed discharge of formational waters from carbonaceous shales of the Road River Group along relatively shallow-seated listric faults. The essence of this model is that, because of their relatively shallow depth at the time of their dewatering, hydrothermal reservoirs within the Road River Group would have relatively low temperatures of about 100°C. Furthermore, because of the highly carbonaceous nature of the reservoir rocks, the hydrothermal solutions would be depleted in oxygenated species such as sulphate and, because of the ubiquitous presence of pyrite in the reservoir rocks, would also be sulphurous.

These reservoir conditions are described by Figure 77.2, in which the pO_2 of the hydrothermal solution is determined by equilibrium with respect to carbon (graphite) and the maximum sulphur content of the solution is assumed to be 0.1 m. The range of bulk compositions of Road River Group and Lower Earn Group carbonaceous shales corresponds to the range of illite composition on an Al_2O_3-K_2O-MgO ternary diagram, and it is assumed that illite was the main aluminum silicate mineral during early diagenesis at temperatures of about 100°C. This assumption is in accord with observations on the mineralogy of more recent argillaceous successions during their burial and compaction history (Burst, 1969). For the simplicity of calculation, it is assumed that the pH of the hydrothermal reservoir solution is controlled by the co-existence of muscovite (rather than illite) and adularia (rather than the observed authigenic K-Ba-feldspar reported by Goodfellow and Jonasson, in preparation). These assumptions do not materially affect the values calculated for pH.

Within the range of permissible reservoir conditions shown in Figure 77.2, the maximum concentration possible of both zinc and lead in solution is very low, but that of barium is relatively high (see Fig. 76.5, 76.6, Lydon et al., 1985). The solubility of gold, which forms a very strong bisulphide complex (Seward, 1973), is at a maximum for the very pH and pO_2 ranges buffered by the mineral assemblage of the reservoir rocks. These are determined by the maximum range of K^+ contents (40-4000 ppm) of modern formational waters from argillaceous rocks (e.g., Carpenter et al., 1974) and the abundance of carbonate in Type B deposits (Lydon et al., 1985) which indicates pO_2 close to the C-CO_2 buffer. If the general genetic model of Lydon et al. (1985), is correct and that sufficient gold is present in the reservoir rocks, it would therefore seem reasonable to expect a significant gold enrichment in their Type B "barren" baritite deposits.

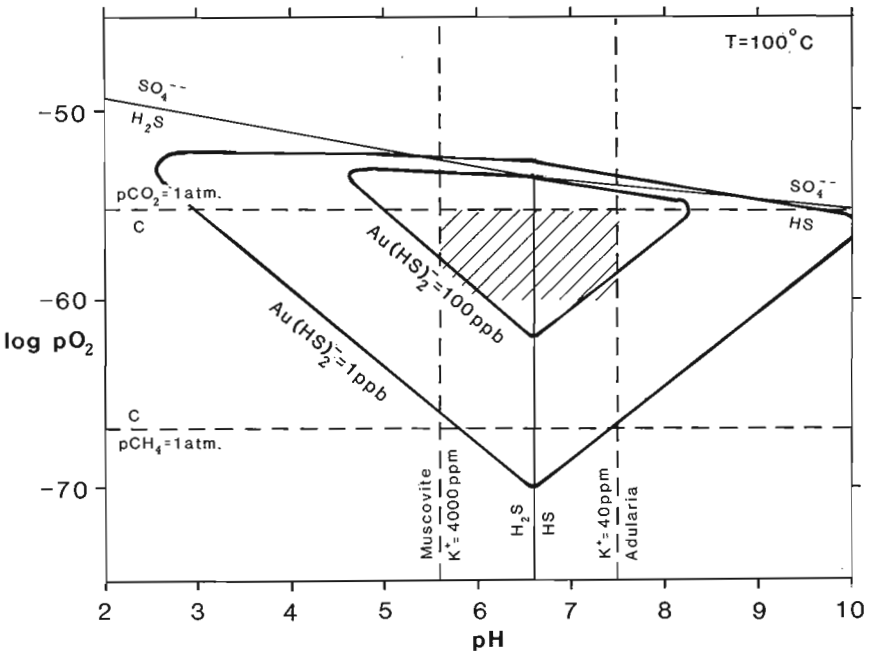

Figure 77.2

Calculated approximate solubilities of gold as the $Au(HS)_2^-$ complex in aqueous solutions at 100°C, 1 atmosphere pressure, and maximum ΣS=0.1 m. Activity coefficients for all species are assumed to be 1.0. Hatched area is maximum range of permissible reservoir conditions for the generation of Type B (Lydon et al., 1985) barite deposits. See text for explanation. Data from Seward (1973), Helgeson (1969), and Robie and Waldbaum (1968).

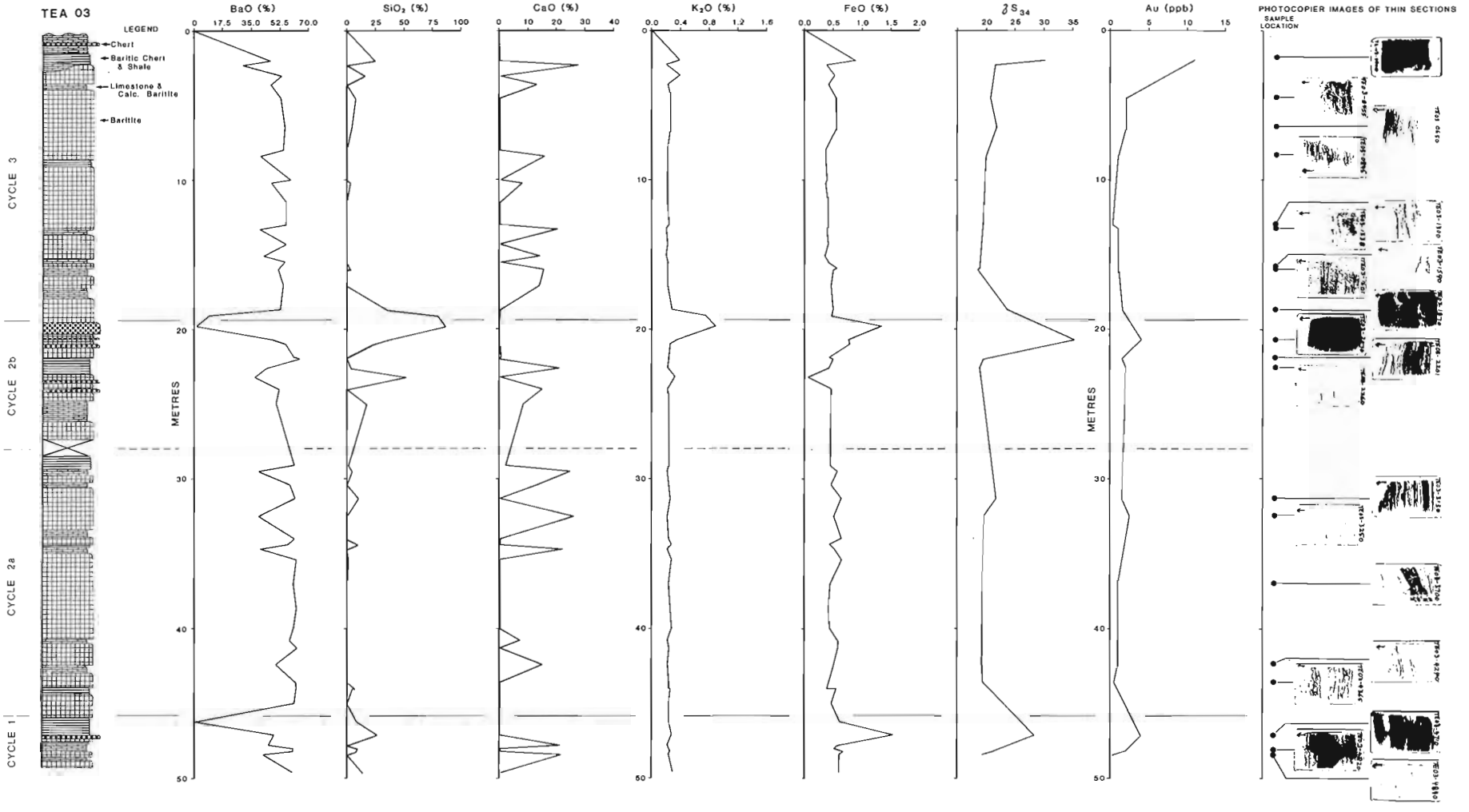

Figure 77.3. *Composite measured section through the main baritite member of the TEA deposit showing lithologies and geochemical profiles of the indicated components. Cycles refer to depositional cycles referred to in text.*

In order to test this hypothesis, selected samples of a suite collected from the TEA deposit by JWL and IRJ in 1979 were analyzed for gold by a fire assay-atomic absorption method in the laboratories of Bondar-Clegg & Co., Ottawa.

Results

Figure 77.3 summarizes some of the geological and geochemical data of part of a composite section measured and sampled by two of the authors (JWL and IRJ) through the TEA deposit in 1979. The part of this section that is illustrated is that of the main natural exposure of the main baritite sequence in the cliff on the northern side of the hill containing the deposit. Whereas the top of the section illlustrated corresponds to the top of the main baritite sequence, the basal part of the main sequence was not exposed at the time. It is estimated that about 5 m of massive baritite exists below the bottom of the section shown in Figure 77.3. This section is on the northern limb of a tight westerly-plunging syncline. Bedding plane faults are common in the massive baritite, especially near the axis of the fold. In the section measured these faults have the tendency to suppress rather than repeat the stratigraphy. The main lithology in this section is massive to laminated baritite interbedded with subordinate amounts of limestone and calcareous baritite, baritic siliceous shale, and chert. Much of the limestone is baritic and would appear to be calcareous concretions that are concentrated within specific beds of baritite. Contacts of this limestone type with contiguous baritite are usually undulatory or cross-cutting. However, some of the limestone appears to represent beds of originally calcareous sediment. Siliceous beds range in composition from black, siliceous, baritic shale, consisting of 0.1-0.5 mm nodules and lamellae of barite in a fissile shaley matrix, to massive black chert with few barite nodules. Disseminated small white prismatic crystals of celsian and/or cymrite (largely altered to kaolinite in surface samples) are common in the more argillaceous baritite types.

The section appears to consist of at least three major geochemical cycles, most obviously shown by the variation in sulphur isotope ratios of barite (Fig. 77.3). Cycle 1 extends stratigraphically upwards from the unexposed base to the 48 m section depth. The small increase in ^{34}S, Au and organic carbon values around 31 m section depth may indicate the upper part of a succeeding depositional cycle, but the absence of analytical data about the unexposed interval at 27-28 m section depth precludes a positive diagnosis. On the basis of current analytical data, the interval from the 48 m section depth stratigraphically upwards to the 20 m section depth is designated as Cycle 2, which is divided into lower (2A) and upper (2B) sub-cycles by at least a minor resurgence of the depositional cycle at the 28 m section depth. Cycle 3 extends from the 20 m section distance level to the top of the section.

Each cycle is characterized by a basal sequence of thick massive baritite beds which become more laminated and more carbonaceous upwards. This phenomenon is illustrated by the series of photocopier images of thin sections shown in Figure 77.3. Limestone beds and calcareous concretions also increase in their frequency upwards. The uppermost part of each cycle is marked by:

1. Maximum content of organic carbon in the baritite (shown by the very dark shade of the thin section photocopier images).
2. A dramatic increase in $\delta^{34}S$ values of the barite.
3. An increase in the SiO_2 (chert) content of the sediments.
4. An increase in the proportion of normal marine sedimentation (represented in Fig. 77.3 by the K_2O component), as opposed to hydrothermal chemical sedimentation.
5. Maximum content of pyrite (represented by the FeO component in Fig. 77.3).
6. Maximum content of gold.

Discussion

As diagrammatically depicted in Figure 77.4, the depositional cycles within the main baritite section of the TEA deposit is interpreted to be due to repeated episodes of the high volume discharge of hydrothermal solutions onto the sea floor separated by periods of relative quiescence in hydrothermal discharge activity. The bulk of hydrothermal discharge during one discharge episode (Fig. 77.4a) is envisaged to have taken place within a relatively short time span, in perhaps an analogous fashion and for similar reasons to the catastrophic discharge of $10^7 m^3$ of saline groundwaters within a year during the 1966 Matsushiro swarm earthquakes (Tsuneishi and Nakamura, 1970). Focussed discharge of volumes of groundwater of this magnitude within a short time span into a submarine environment would be expected to result in forced pluming and turbulent mixing throughout a considerable volume of ambient seawater. If the discharge temperature of the hydrothermal solution was about 100°C and its salinity more than 50% greater than the ambient seawater, the brine resulting from the mixing would tend to sink. This sinking action of the brine would tend to act as a confining blanket in preventing the dispersal of barite nucleated within the turbulent cloud of mixing. Barite formed rapidly as the result of reaction between barium of the hydrothermal solution and sulphate of the seawater would have sulphur isotope values essentially identical to that of the seawater sulphate. It is suggested that the massive to laminated baritite that occupies the basal part of each depositional cycle represents the rapid accumulation of barite in the circum-vent area during this stage of high volume discharge. The uniformity of the chemical composition and sulphur isotope values of this part of the depositional cycle are consistent with this interpretation. It is suggested that the laminations in the massive baritite section reflect the pulsatory nature of barite deposition in a high volume turbulent environment, and is envisaged as successive accumulations from squalls of barium "snow" that move across the depositional basin.

As the hydrothermal discharge flux waned the rate of barite sedimentation decreased, and the proportion of other components of the hydrothermal solution such as silica and calcium carbonate, whose nucleation and precipitation rates were less efficient than that of barite, increased correspondingly. Hence the increasing frequency of occurrence of these components upwards in each cycle (Fig. 77.3).

The end stage of each cycle is envisaged as a stable, perhaps stratified, brine pool (Fig. 77.4b), into which only relatively small quantities of barium were added, either through episodic pulses of focussed discharge of fresh hydrothermal solution or continuous seepage of pore waters from the underlying baritite muds. It is only during this stage of very low hydrothermal sedimentation rates that a component of normal Selwyn Basin sedimentation is geochemically evident, as illustrated by the K_2O concentrations in Figure 77.3.

The relatively high organic carbon of the baritite at the top of each cycle indicates high levels of organic activity within or surrounding the brine pool. Some of these organic-rich layers at the top of each cycle have the appearance of algal mats, and in thin section structures with the appearance of algal filaments extend from the carbon-rich layers downwards into underlying barite laminae. This suggests that although a brine pool may have existed, at least periodically or in some places it was sufficiently oxic to support algal life. The dramatic increase in $\delta^{34}S$ values of barite at

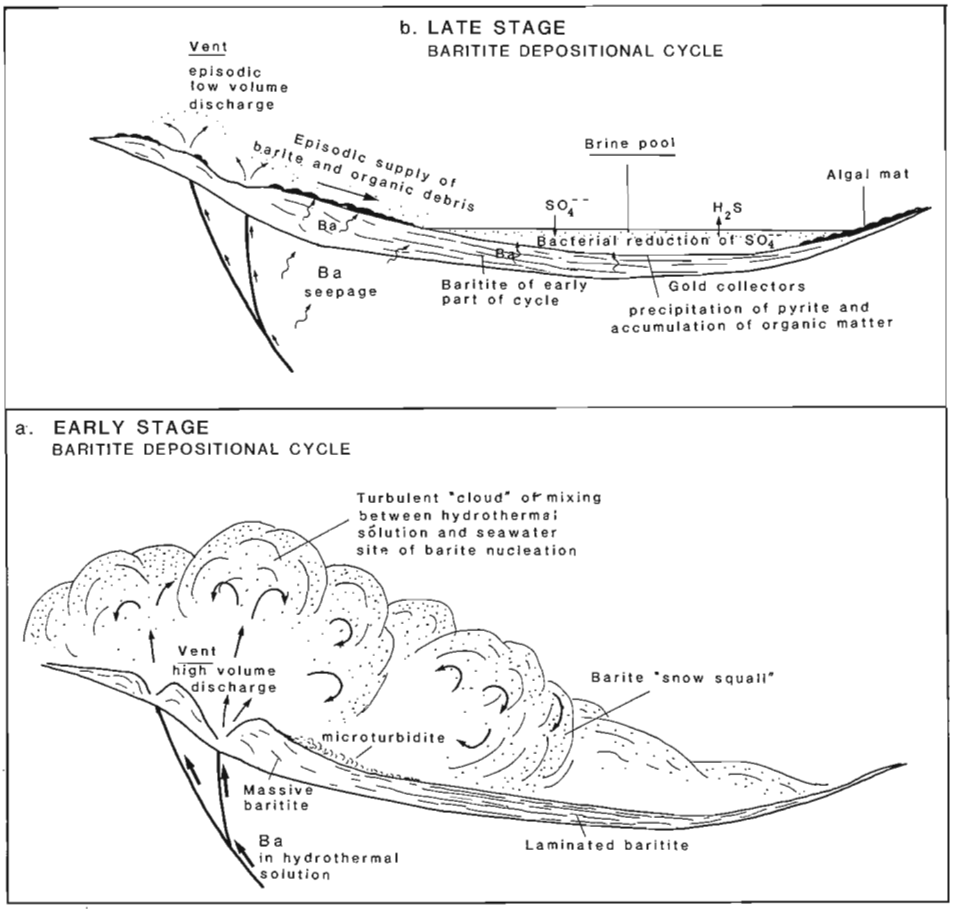

Figure 77.4

Schematic representation of processes during early (a) and late (b) stages of baritite depositional cycles shown in Figure 77.3. Stippling denotes sites of barite precipitation.

the top of each cycle is attributed to the bacterial reduction of sulphate to sulphide accompanying this high organic activity. Some of the sulphide produced was fixed by combining with iron present in solution to form pyrite. This accounts for the increase in FeO content at the top of each cycle (Fig. 77.3). Small quantities of zinc also present in solution were similarly precipitated as sphalerite, which has been seen in thin section as small grains scattered along organic carbon-rich layers. However, most of the sulphide produced must have been lost to the system, presumably as H_2S, preferentially removing ^{32}S and leaving the sulphate remaining in the brine pool enriched in ^{34}S. It is possible that some of the heavy sulphate was derived by the oxidation of hydrothermal H_2S, which if derived from Road River Group rock pyrite, could have been as heavy as $^{34}S=+30‰$ (Goodfellow and Jonasson, in prep.). The bacterial action in the brine pool and its sediments may also have been responsible for the production of CO_2 by the oxidation of organic matter, thereby contributing to the fixing of calcium as a carbonate in the upper part of each depositional cycle.

Based on the analysis of a limited number of samples, background values of gold in Selwyn Basin carbonaceous shales are below analytical detection limits of 1 ppb. The average gold content of the analyzed baritite samples from the TEA deposit is 4 ppb and therefore significantly higher than rocks resulting from normal basinal sedimentation in the Selwyn Basin. This indicates that the observed enrichment in gold in the TEA deposit was due to its supply by the hydrothermal solutions responsible for the barite mineralization, which substantiates the prediction made by the chemical thermodynamic model. The good correlation between the concentration of gold with organic carbon and synsedimentary pyrite content of the baritite (see Fig. 77.3 and interpretations above) suggests that an important limiting factor to the concentration of gold was the availability of suitable synsedimentary gold collectors. The nucleation of gold presumably as a colloid, due to the oxidation of the aurous bisulphide complex, would obviously require an abundance of suitable collectors in order to remain near the site of nucleation. The absolute abundances of both organic carbon (maximum 0.8%) and pyrite iron (maximum 1.5%) in the baritite samples analyzed are very low. It is therefore possible that gold concentrations above the maximum 12 ppb so far detected may exist in rocks within or associated with, "barren" baritic deposits of the Selwyn Basin having higher abundances of suitable synsedimentary gold collectors. Investigation of this possibility is continuing.

Conclusions

The gold content of the TEA barite deposit is significantly higher than values obtained for Paleozoic basinal facies rocks of the Selwyn Basin. The gold enrichment is due to hydrothermal activity associated with the formation of "barren" barite (Type B, Lydon et al., 1975) deposits. The gold concentration in the samples analyzed appears to be proportional to the concentration of suitable synsedimentary gold collectors, particularly organic carbon and pyrite. Although the gold concentrations detected are

far below those of direct economic interest, the observation that synsedimentary processes leading to the concentration of gold have operated within the Selwyn Basin has mineral exploration significance from two perspectives:

1. Given the presence of sufficient quantities and extent of suitable synsedimentary gold collectors around the hydrothermal vent areas responsible for the formation of Type B stratiform barite deposits, haloes of economically significant gold concentrations could have formed.
2. Of perhaps more realistic potential is that the barium-enriched part of the Lower Earn Group (Lydon et al., 1985), may also be enriched in background gold content, thereby becoming a more suitable source rock for later gold-concentrating processes than the remainder of Selwyn Basin sedimentary rocks.

With regard to the latter point, it is interesting to note that the only reported gold occurrence in that part of the Selwyn Basin studied by Lydon et al. (1985) is the gold-bearing quartz veins of the SEL claims, which occur in pyritic black shales of reported Devono-Mississippian age (Sinclair et al., 1976), and therefore presumably form part of the Lower Earn Group. Further investigation of aspects of the geology and distribution of gold in the TEA deposit is being carried out by one of the current authors (KAH) as a B.Sc. Thesis study at Queen's University, Kingston.

Ackowledgments

The contributions of Alan Galley to this study deserve special acknowledgment, particularly in his pointing out and graphically displaying the correlation between the organic content of thin sections with the baritite depositional cycles as illustrated in Fig. 3. A. Galley and J.M. Duke are thanked for critically reading the manuscript and making suggestions which improved its quality. R.D. Lancaster is thanked for his help in drafting the diagrams.

References

Burst, J.F.
1969: Diagenesis of Gulf Coast clayey sediments and its possible relation to petroleum migration; Bulletin of the American Association of Petroleum Geologists, v. 53, p. 73-93.

Carne, R.C.
1976: The TEA deposit; Department of Indian and Northern Affairs, Open File Report EGS 1976-16, p. 20-31.

Carpenter, A.B., Trout, M.L., and Pickett, E.W.
1974: Preliminary report on the origin and chemical evolution of lead- and zinc-rich oil field brines in Central Mississippi, Economic Geology, v. 69, p. 1191-1206.

Coolen, P.R.
1982: A report on the barite potential of the Samovar prospect, TEA claims, Mayo mining district; Indian Minerals (West) Directorate, Department of Indian Affairs and Northern Development, Calgary, 27 p.

Dawson, K.M.
1977: Regional metallogeny of the Northern Cordillera; in Report of Activities, Part A, Geological Survey of Canada, Paper 77-1A, p. 1-4.

Dawson, K.M. and Orchard, M.J.
1982: Regional metallogeny of the Northern Cordillera: Biostratigraphy, correlation and metallogenic significance of bedded barite occurrences in eastern Yukon and western District of Mackenzie; in Current Research, Part C, Geological Survey of Canada, Paper 82-1C, p. 31-38.

Goodfellow, W.D. and Jonasson, I.R.
– Environment of formation of the Howards Pass (XY) Zn-Pb deposit, Selwyn Basin, Yukon; in Mineral Deposits of Northern Cordillera, Canadian Institute of Mining and Metallurgy, Special Volume. (in prep.)

Gordey, S.P.
1981: Geology of Nahanni map-area (105 I), Yukon Territory and District of Mackenzie; Geological Survey of Canada, Open File 780.

Gordey, S.P., Abbott, J.G., and Orchard, M.J.
1982: Devono-Mississippian (Earn Group) and younger strata in east-central Yukon; in Current Research, Part B, Geological Survey of Canada, Paper 82-1B, p. 93-100.

Helgeson, H.C.
1969: Thermodynamics of hydrothermal systems at elevated temperatures and pressures; American Journal of Science, v. 267, p. 729-804.

Lydon, J.W., Lancaster, R.D., and Karkkainen, P.
1979: Genetic controls of Selwyn Basin Stratiform barite/sphalerite/galena/ deposits: an investigation of the dominant barium mineralogy of the TEA deposit, Yukon; in Current Research, Part B, Geological Survey of Canada, Paper 79-1B, p. 223-229.

Lydon, J.W., Goodfellow, W.D., and Jonasson, I.R.
1985: A general genetic model for stratiform baritic deposits of the Selwyn Basin; in Current Research, Part A, Geological Survey of Canada, Paper 85-1A, report 76.

Robie, R.A. and Waldbaum, D.R.
1968: Thermodynamic properties of minerals and related substances at 298.15°K (25°C) and 1 atmosphere (1.013 bars) pressure and at higher temperatures; United States Geological Survey Bulletin 1259, 256 p.

Seward, T.M.
1973: Thio complexes of gold and the transport of gold in hydrothermal ore solutions; Geochimica et Cosmochimica Acta, v. 37, p. 379-399.

Sinclair, W.D., Maloney, J.M., and Craig, D.B.
1975: SEL; in Mineral Industry Report 1974, Yukon Territory, Department of Indian and Northern Affairs, Report EGS 1975-9, p. 165-166.

Tsuneishi, Y. and Nakamura, K.
1970: Faulting associated with the Matsushiro swarm earthquakes; Bulletin of the Earthquake Research Institute, University of Tokyo, v. 48, p. 29-52.

MISE-À-LA-MASSE MAPPING OF GOLD-BEARING ALTERATION ZONES AT THE HOYLE POND GOLD DEPOSIT, TIMMINS, ONTARIO

Project 840031

C.J. Mwenifumbo
Resource Geophysics and Geochemistry Division

Mwenifumbo, C.J., Mise-à-la-masse mapping of gold-bearing alteration zones at the Hoyle Pond Gold deposit, Timmins, Ontario; in Current Research, Part A, Geological Survey of Canada, Paper 85-1A, p. 669-679, 1985.

Abstract

Drillhole mise-à-la-masse measurements were conducted between two holes at the Hoyle Pond Gold deposit, near Timmins, Ontario. Gold mineralization in this deposit occurs in carbonate alteration zones within magnesium-rich tholeiitic basalts. The alteration zones have relatively low resistivities compared to the unaltered basalts. The mise-à-la-masse method was successfully applied in correlating these zones between the holes. The limited mise-à-la-masse measurements between the two holes indicated that there are two possible orientations of the alteration zones, one nearly vertical which is concordant with the primary structures (foliation and in situ brecciation) within the basalts and another one which transects these primary structures.

Résumé

Au moyen de la méthode de la mise-à-la-masse, on a pris des mesures entre deux trous de forage localisés dans le gisement d'or de Hoyle Pond près de Timmins, en Ontario. L'or se presente dans des zones d'altération carbonatées contenues à l'intérieur de basaltes tholéiitiques riches en magnésium. Ces zones d'altération font preuve d'une faible résistivité par rapport aux basaltes non altérés. La méthode de la mise-à-la-masse a permis la corrélation de zones d'altération entre les trous. Les quelques mesures effectuées entre les trous de forage ont demontré que les zones d'altération se présentent selon deux orientations, soit (1) une première parallèle à la foliation et à la bréchification primaires dans les basaltes et, (2) une plus jeune qui recoupe ces structures primaires.

Introduction

Recent applications of borehole geophysics to gold exploration have indicated that significant geophysical anomalies may be observed in gold-bearing horizons. The single-hole geophysical logging methods that give promising results with respect to outlining gold-bearing alteration zones include gamma ray spectrometry, IP and resistivity (Mwenifumbo et al., 1983; Urbancic and Mwenifumbo, 1984). These single-hole geophysical logging techniques, however, provide information on the changes in the physical and chemical properties of the rock mass in the immediate vicinity of the drillhole. Geophysical anomalies observed in a number of holes are often difficult to correlate from hole to hole. This is mainly due to lack of characteristic signatures because of geological changes from one hole to the next. To provide information on the nature of the rock mass between holes and to determine whether anomalous features continue from hole-to-hole, techniques such as the mise-a-la-masse method are employed. The mise-à-la-masse method is a cross-hole or hole-to-surface electrical technique. With this technique, the potential field distribution is studied along a drillhole or on the surface while a current source is emplaced at an intersection of a conductive mineralization or structure. It is mainly used for mapping size and orientation of a conductor and for hole-to-hole correlation of the conductive structures.

The mise-à-la-masse method has been extensively and successfully applied during detailed mapping of massive sulphide ore bodies with high electrical conductivity (eg. McMurray and Hoagland, 1956; Parasnis, 1967; and Ketola, 1972). More recently the application of the mise-à-la-masse method has been extented to the mapping of fracture zones (relatively poor conductors compared to massive sulphide ores) in connection with the evaluation of areas for possible radioactive waste disposal sites (Jamtlid et al., 1982; Rouhianen and Poikonen, 1982). In this paper we present an example of the application of the mise-à-la-masse method for correlating gold-bearing alteration zones between holes. The study was carried out at the Hoyle Pond Gold deposit near Timmins, Ontario. The Hoyle Pond deposit is located just to the west of the Kidd Creek Metallurgical site, about 18 km northeast of the city of Timmins. Figure 78.1 shows the western part of the deposit and the location of the holes where the present study was carried out.

Geology and structure

The Hoyle Pond Gold deposit lies within the Abitibi Greenstone belt. Stratigraphically the area consists largely of ultramafic flows (komatiites) at the base, magnesium-rich tholeiitic basalts in the middle and sediments in the upper portion of the section.

Gold mineralization is found in carbonate alteration zones within a uniform sequence of magnesium-rich tholeiitic basalts. The zones are identified from the drill core by their distinctive steely blue-black colour and are characterized by the presence of free carbon (Downes et al., 1982). They have diffuse margins and become darker towards the centres that are black. The zones are structurally controlled and are characterized by in-situ brecciation and a strong schistosity in their centres. The foliation which strikes at 60 to 70 degrees and dips nearly vertical, increases in intensity from the margin to the core of the alteration zones. The alteration zones contain 1 to 3 per cent fine grained pyrite in the form of 1 to 5 mm 'snowflake'-like blotches occurring along fine cleavage fractures. Gold is present in quartz veins, 1 cm to 1 m wide, within the alteration zones and is also associated with the fine grained disseminated pyrite. The carbonate alteration zones in the Timmins area are believed to have been developed in a subseafloor volcanic environment by the passage of hydrothermal fluids up through joint or fracture sytems or along flow contacts (Fyon and Crocket, 1981).

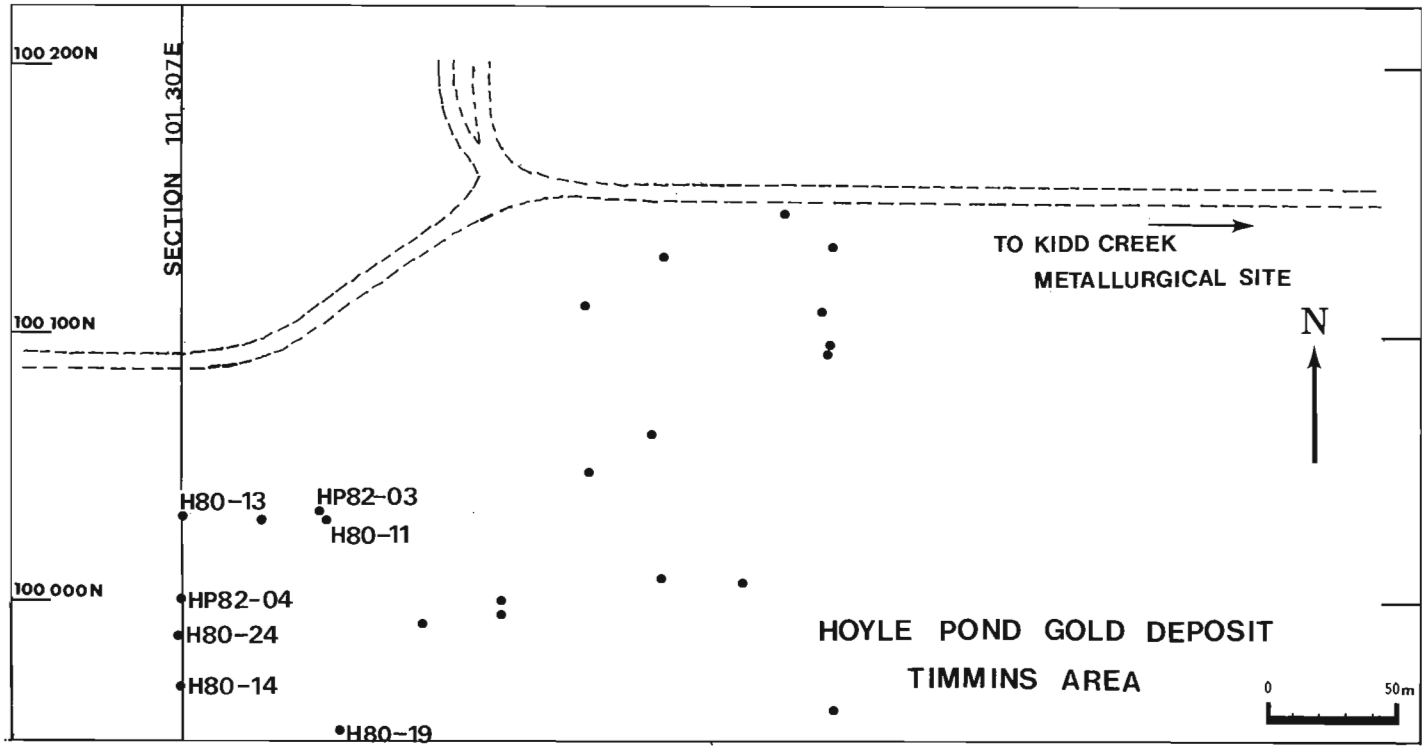

Figure 78.1. Map of the Hoyle Pond Gold Deposit showing the location of the drillholes where mise-à-la-masse data were obtained.

Figure 78.2 based on information provided by Kidd Creek Mines Ltd., shows the geology and structure of section 101,307E of the Hoyle Pond Gold deposit where the mise-à-la-masse measurements were carried out. Four holes were drilled along this section. They intersect about 20 m of glacial overburden and then the magnesium tholeiitic basalt flows. The holes were drilled with initial inclinations ranging from 55 to 65 degrees to intersect the steeply dipping alteration zones. A number of these alteration zones are intersected by drillholes. They vary in width from 5 to 30 m. The location of the zones that were identified in the drill core are displayed along the drillholes as shaded areas. Note the geological interpretation of the presence of alteration zones in areas where they were not identified on the drill core, especially along holes H80-24 and HP82-04. It is clear from the interpretation that even with this number of closely spaced drillholes on this section, the correlation of the alteration zones between the holes is a difficult task. It should be noted, however, that although core recovery was excellent the geological information from the drill core data represents only a small sample volume and the probability of not intersecting the target structure is quite high. The drillhole IP, resistivity and mise-à-la-masse measurements were carried out to outline the zones and to determine their continuity between holes. The measurements were conducted in drillhole H80-14 and HP82-04.

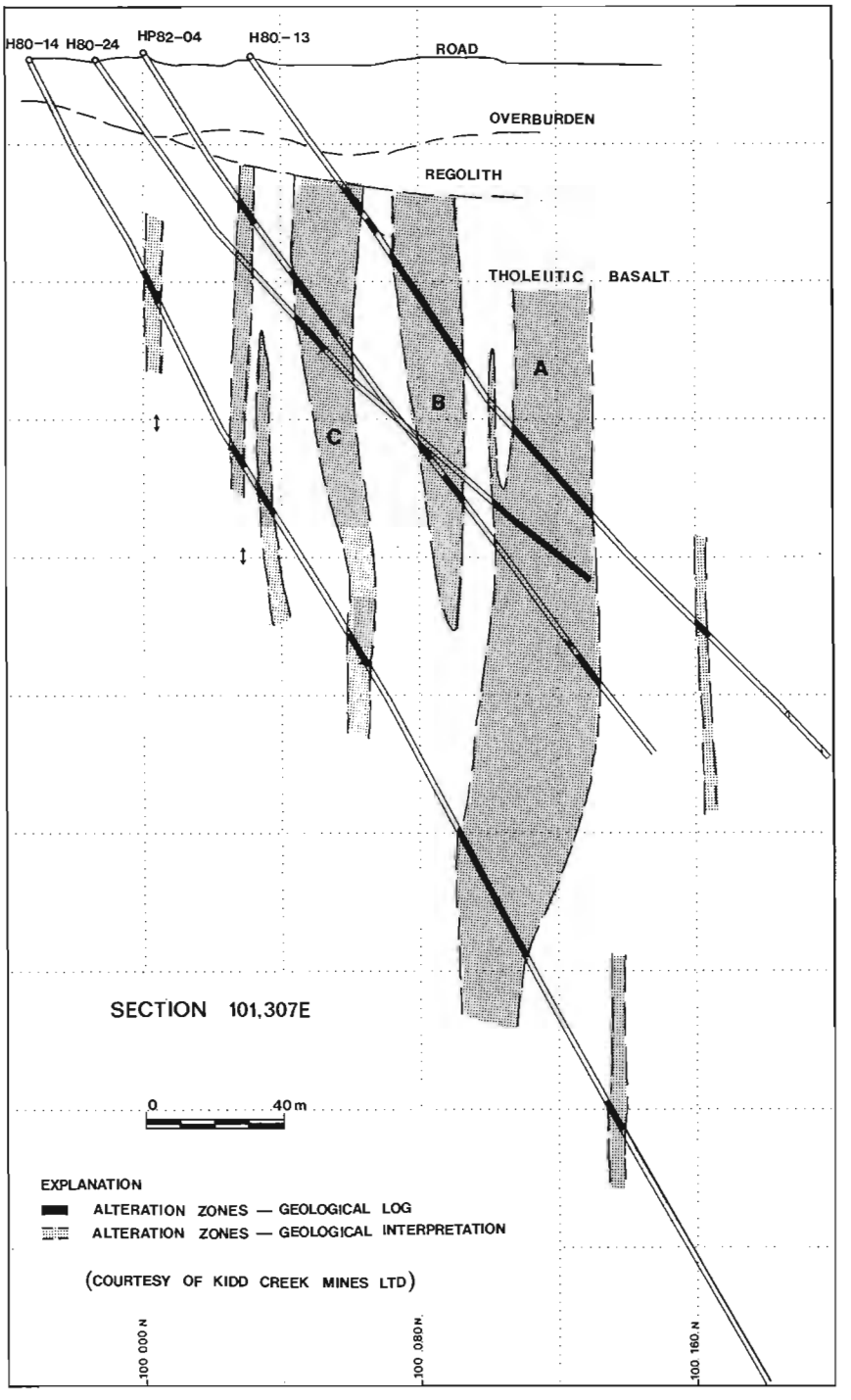

Drillhole IP and resistivity logging

Drillhole induced polarization (IP) and resistivity data were obtained with the lateral (pole-dipole) array. The potential dipole spacing (MN) was 0.4 m and the distance between the current electrode and the potential dipole centre was 2.8 m. The downhole current and potential electrodes consisted of gold-plated brass cylinders, 4 cm in diameter. The surface remote current electrode consisted of 3 steel rods about a metre in length, located approximately 500 m west of section 101,307E. The measurements were carried out with the GSC time domain IP/resistivity logging system (Bristow, 1984). The transmitter on this system is a constant current source, capable of supplying currents up to 250 mA. There are 4 selectable periods for the current waveform; 1, 2, 4 and 8 seconds. In cases where IP logging is done incrementally or continuously over short holes, long period waveforms (normally an 8 s period) are usually employed. However, for continuous logging in deep holes, it is expedient to log the holes with current waveforms of as short a period as possible in order to combine data resolution with reasonable speed. In the present study, IP and resistivity measurements were made using a period of 1 s (ie a current ON time of 0.25 s followed by an equal current OFF time with the polarity reversed during the second half cycle). Complete IP waveforms were recorded on 9 track magnetic tape. The apparent resistivities were computed from the primary voltages, that is, voltages observed during the current ON time, with the appropriate geometric factor. The IP chargeability data are determined from the decay voltages during the current OFF time. It is standard practice to integrate under a portion of the the decay curve and normalize it with the primary voltage.

Figure 78.2

Geological cross section along grid line 101,307E, Hoyle Pond deposit. (Unpublished data, courtesy Kidd Creek Mines Ltd.).

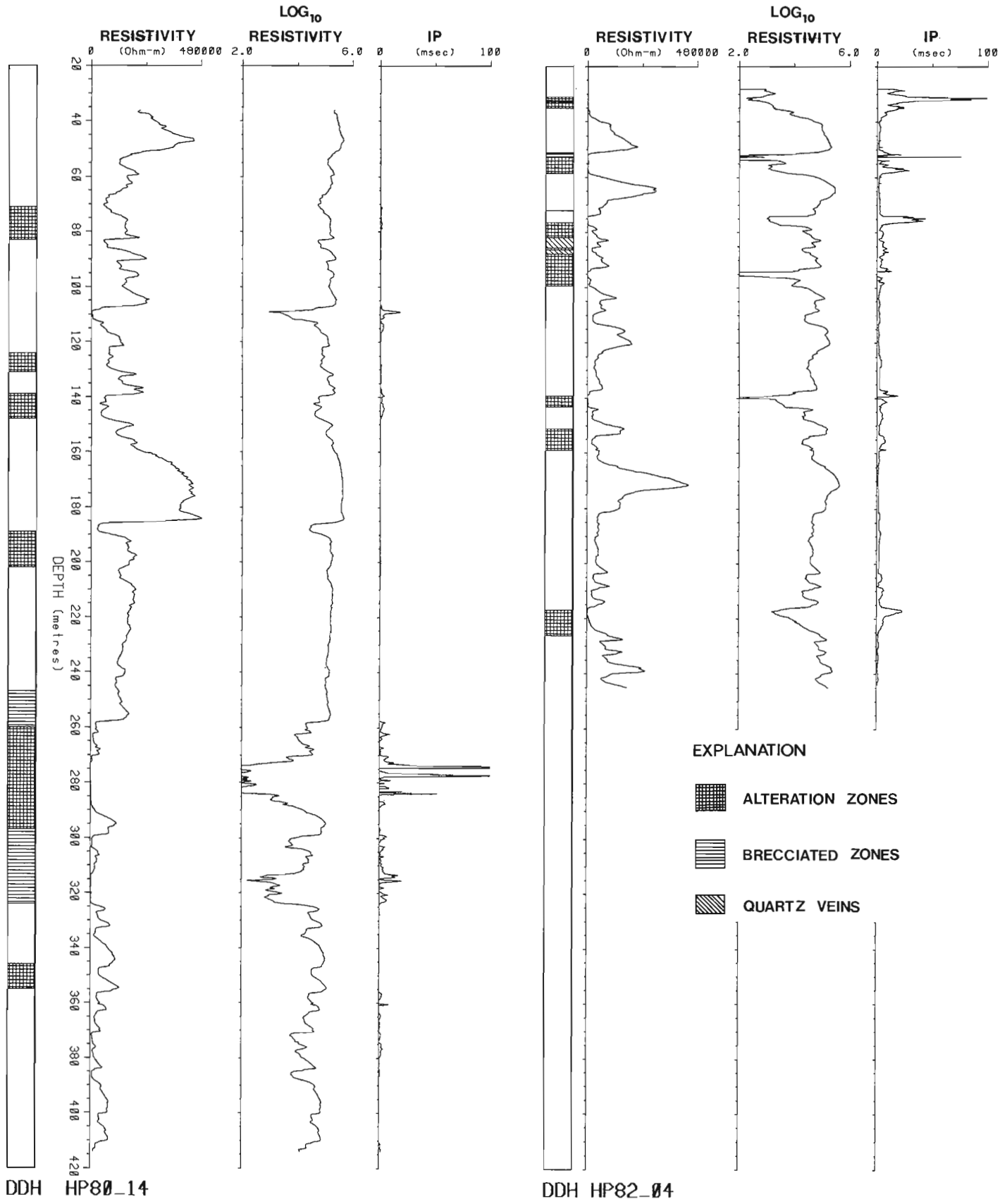

Figure 78.3. *Apparent resistivity and induced polarization logs obtained in holes HP82-04 and H80-14 with the lateral array.*

Since the integration is with respect to time the units of the apparent chargeability parameter are in milliseconds. In the present IP measurements, the chargeabilities were determined by integrating from 62 ms to 138 ms after the current is switched off. The logging speed was 3 m/min with measurements taken every second (equivalent to the hole sampling interval of 5 cm).

Figure 78.3 shows the IP and resistivity logs conducted along drill holes H80-14 and HP82-04. The locations of the alteration zones and in situ brecciated zones that were identified in the drill core are displayed in the columns next to the apparent resistivity log for each hole. The logarithm of the resistivity is also presented in the figure for each hole to enhance the low resistivity variations along the log. Chargeability highs and resistivity lows are observed across the majority of the alteration zones. This excellent correlation between the alteration zones and low resistivity high IP zones makes this type of log quite useful for detecting the alteration zones. There are a few low resistivity zones which do not correspond to any of the mapped alteration zones especially along drillhole H80-14. High chargeabilities and low resistivities are observed at about 110 m and between 370 and 390 m. These zones may correspond to alteration zones narrowly missed by the drill hole. The resistivities for most of the alteration zones vary between 10 000 and 1000 ohm-m except for the wide alteration zone between 260 and 330 m which has apparent resistivities lower than 100 ohm-m. The apparent resistivities of the unaltered basalts are around 100 000 ohm-m. The majority of the alteration zones along hole HP82-04 have apparent resistivities between 10 000 and 1000 ohm-m with some even lower than 1000 ohm-m. The resistivity contrast between the unaltered basalts and the alteration zones is, therefore, a factor of 10 or higher. This resistivity contrast is adequate for the mise-à-la-masse method.

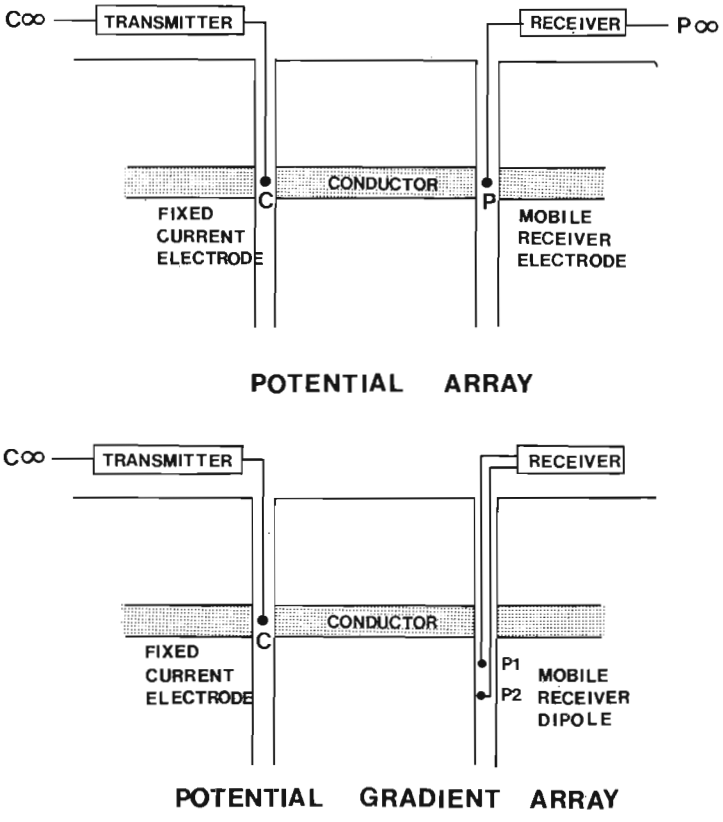

Figure 78.4. *Electrode configurations in drill hole mise-à-la-masse measurements.*

Drill hole mise-à-la-masse measurements

Field equipment and procedure

The mise-à-la-masse measurements were done with the same equipment used in the IP/resistivity logging. The measurements are accomplished by placing a current electrode in one borehole directly in a conductive zone to be studied and measuring the resulting potential field distribution in another borehole. The other return current electrode is located a large distance from the drillhole being studied (essentially at infinity). There are two possible arrays which can be used in drillhole mise-à-la-masse measurements; the potential array and the potential gradient array. Figure 78.4 shows the two electrode configurations. With the potential array one of the potential electrodes is fixed distant from the measurement hole (remote reference electrode placed effectively at infinity). The other potential electrode is moved along the measurement hole continuously or incrementally. In the potential gradient arrangement, the potential difference is measured by a mobile potential dipole, with the dipole spacing ranging from 2.5 to 10 m. The current electrode setup is the same for the two modes of operation. With the potential array, measurements of voltages do not require very sensitive receivers since the voltages are relatively large and directly referenced to a fixed potential electrode. The potential gradient array, however, involves measuring relatively small voltage drops across two closely spaced electrodes that are floating. A very sensitive receiver coupled with a powerful transmitter is required for accurate determination of the voltages. The choice of a particular array for the mise-à-la-masse surveys in typical field conditions is mainly dictated by the power of the transmitter and the sensitivity of the receiver used. The distance between holes and the conductivity contrast between the target structures and the surrounding rocks are also factors which must also be considered. The potential array has received more attention than the potential gradient array mainly because of the ease in interpreting the data. The potential gradient data, however, provide some characteristic features for quantifying the geometrical parameters of the conductive structure, for instance, estimation of the inclination and width of the conductors under study (Mwenifumbo, 1980). Potential gradients can be computed from the potential data if the measurements are taken at very small depth intervals. In the present study the potential array was used.

The downhole current electrode used in this study consisted of a 1 m long copper tube about 4 cm in diameter attached to an insulated copper wire to lower it into the selected drillhole. The lateral resistivity logs and the geological logs were used to locate the conductive zones where the current electrode was emplaced. In order to ensure that the current electrode was placed in zones with the highest conductivity (for maximum signal strength) contact resistances were monitored as the electrode was lowered into the conductive zone. The surface current electrode was placed approximately 500 m from section 101,307E (effectively at infinity). The in-hole potential measuring electrode was a gold-plated brass cylinder, 4 cm in length. The other potential electrode (remote reference electrode) was placed on the surface approximately 100 m away from the drillhole collar. Most of the logging was carried out at 3 m/min with one second data sample interval, giving a measurement every 5 cm. A few logs were obtained at 6 and 9 m/min with a one second data sample interval, giving measurements every 10 and 15 cm respectively. The current intensity was maintained constant during each run. Figure 78.5 shows a vertical section with the locations of the two holes logged and the positions of the energizing current electrodes. The apparent resistivity logs are also diplayed to show their proper depth perspective along the holes.

Presentation of the data

In the present study mise-à-la-masse potential gradients along the drillhole axis are also analyzed. The gradients are computed from the potential measurements using the Savitzky-Golay least squares derivative operator (Madden, 1978; Savitzky and Golay, 1964). The derived gradients are valid since the data sample interval in the hole was small. The mise-à-la-masse potential and the derived potential gradients are plotted for each source location. The potentials are designated as the P logs and the potential gradients as the G logs. In all the logs, the top scale and axis is for the potential data and the bottom scale and axis is for the gradient data. The zero for the gradient data is plotted as dotted lines. The dominant current flow path between the holes is indicated by a solid line between the drill hole geologic columns. This is determined from the maximum amplitudes in the potential logs and the zero-crossover point on the gradient logs. The depth scale on the logs does not represent the true vertical depths but lengths along the drillhole. All the values are normalized with respect to the current intensity in order to facilitate comparision of the amplitudes of the observed measurements for different source locations with different energizing current intensities. The potentials are expressed in volts/ampere and the potential gradients in millivolts/ampere-metre. The column of the holes with the source and the receiver are displayed with the location of the alteration zones identified from the drill core shown in hatched lines.

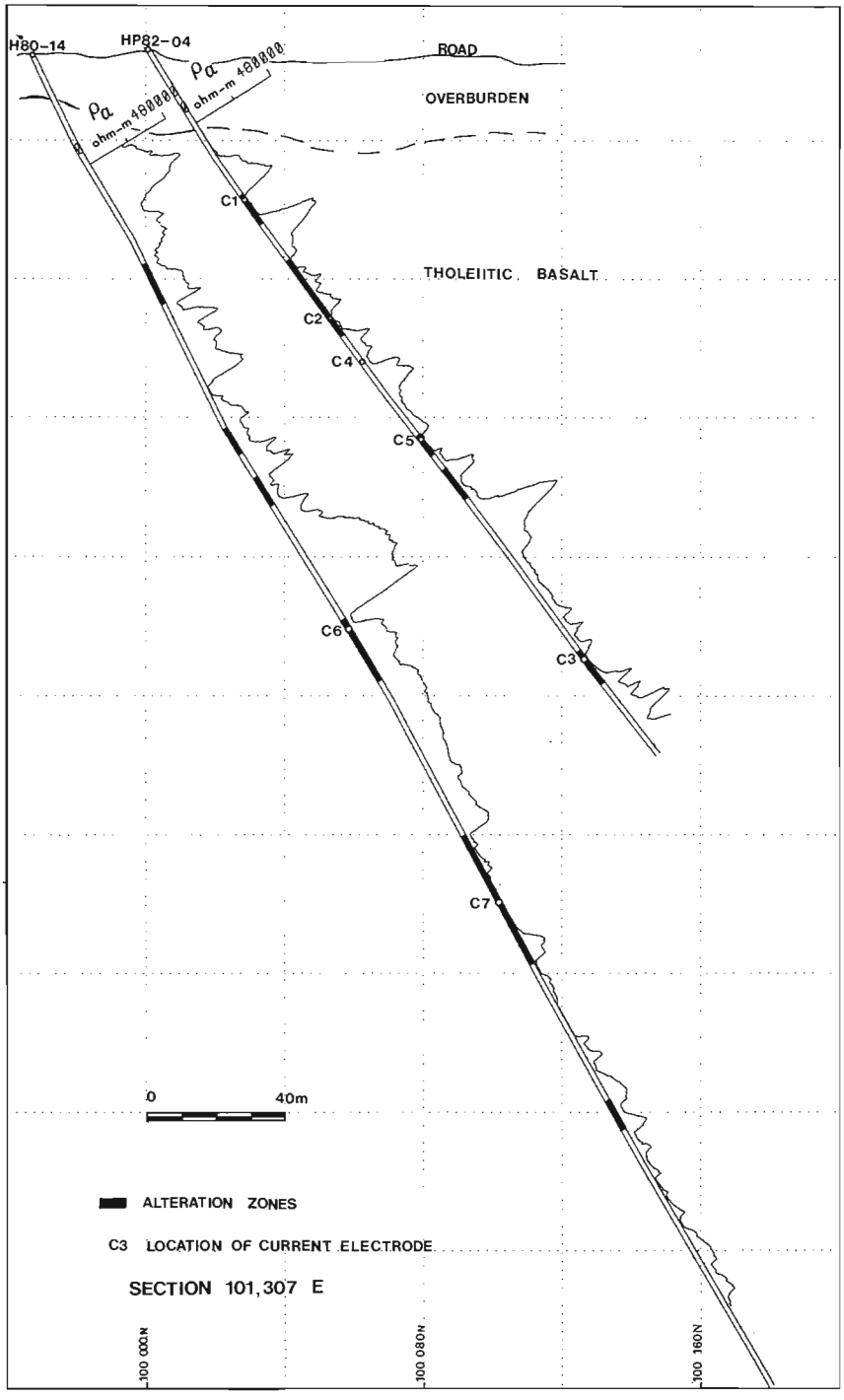

Figure 78.5. Vertical section showing the locations of the current electrodes used during measurements. Apparent resistivity logs are displayed along the drillholes.

For an electrically homogeneous and isotropic medium, the equipotential surfaces resulting from a buried current source are concentric about the source, governed by the equation, $V = \rho I/4 \pi R$ (V = volts, I = current, ρ = resistivity and R = distance from source to measurement point). In this situation, mise-à-la-masse data will indicate maximum potential amplitudes (zero-crossover points in the gradient data) at a point in the measurement hole which is closest to the source. When a current electrode is placed in a conductor, current tends to be channelled along the conductor and observations in a hole that intersects the energized conductor will show a flat potential maximum or zero gradients across the intersection. The intersection is not necessarily the shortest distance from the source. The peak-to-peak amplitude separation on the gradient data gives a rough estimate of the width of the conductor under investigation in the case of a simple, single conductor environment.

Results and discussion

Measurements in H80-14 - current electrodes in HP82-04

Figure 78.6 shows mise-à-la-masse measurements in drillhole H80-14 with the current electrodes implanted at three different low resistivity zones in drillhole HP82-04. C1-LOG, C2-LOG and C3-LOG represent mise-à-la-masse data obtained with the current electrode at C1, C2 and C3 respectively in hole HP82-04. The C1 electrode was placed at approximately 52 m and a current strength of 254 mA was injected into the medium. The C1-LOG shows maximum potential amplitudes and a zero-crossover point in the gradient at approximately 110 m in drillhole H80-14 indicating that electrical continuity exists between the alteration zone energized by C1 in HP82-04 and the location at 110 m in H80-14. No alteration zone has been mapped at this depth but the resistivity log

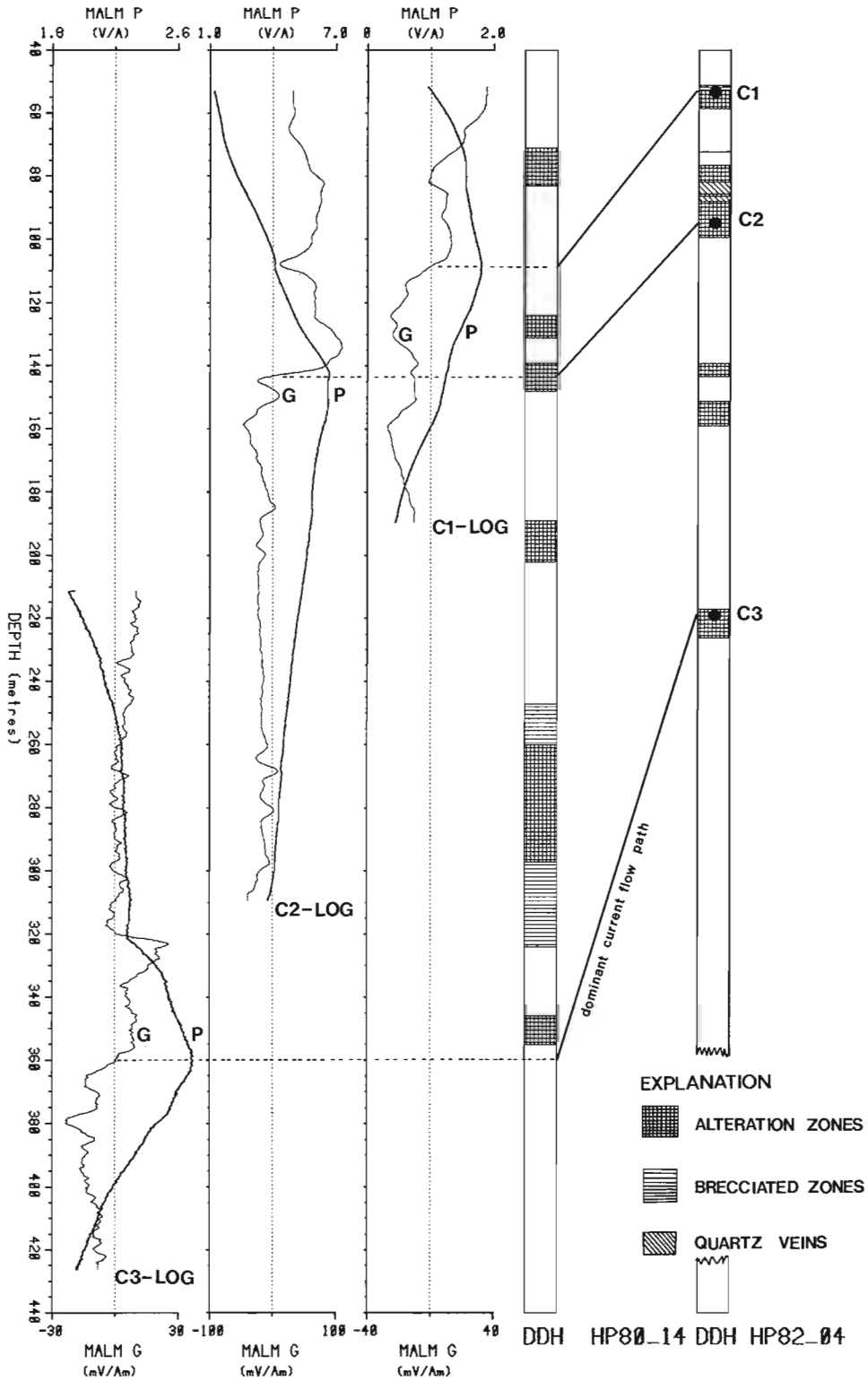

Figure 78.6. *Mise-à-la-masse potential and gradient measurements obtained in drillhole H80-14 with the current electrodes in drillhole HP82-04. The C1-LOG, C2-LOG and C3-LOG represent measurements with the current electrodes located at C1, C2 and C3 respectively. P – potential log; G – gradient log. The solid lines between the geologic columns represent the dominant current flow path.*

indicates a fairly conductive zone around this depth. The mise-a-la-masse potential flattens out and the gradients are fairly low and constant over the regions occurring at approximately 76-83 m and at about 140-150 m. These regions correlate with the low resistivity zones on the lateral resistivity log. This observation is characteristic of an electrically isolated conductor lying parallel to an energized one. It has been numerically modelled by Eloranta (1984) for drillhole mise-à-la-masse data and has been observed in a number of field cases.

The C2-LOGs were obtained with the current electrode placed at approximately 95 m in the lower part of the alteration zone between 75 and 105 m. A maximum current of 180 mA was supplied to the medium. The log exhibits high potentials between 140-150 m. This coincides with the location of an alteration zone. It is interesting to note that the rate of change of the potentials is gradual on the downhole side and rapid on the uphole side. This trend is more evident in the gradient data. This pattern suggests that the conductive structure from C2 intersects H80-14 at a fairly low angle on the downhole side. The main current axis is located at approximately 143 m (zero-crossover point in the gradient data with maximum peak-to-peak amplitude). The upper conductive zone that is electrically continuous with the C1 alteration zone is indicated on the C2-LOGs by the flattening of the potentials and a local minimum in gradients.

A current of 142 mA was injected through the C3 electrode at approximately 218 m down drillhole HP82-04. The C3-LOG indicates that the alteration zone at C3 intersects H80-14 at approximately 360 m. The separation between the peak-to-peak amplitudes around the zero-crossover point is about 10 m. This is approximately the width of the conductor at this location. It is interesting to note the abrupt step-like change in potential at approximately 320 m, above which the potentials are fairly low and flat (almost zero gradients). The conductive zone at 360 is well isolated from the conductive alteration zone above (between 260 and 320), contrary to the interpretation inferred from the drill core log (see Fig. 78.2).

Figure 78.7 shows mise-à-la-masse data along drillhole H80-14 with current electrodes placed at two locations in HP82-04. The C4-LOG represents mise-a-la- masse data with the C4 current electrode located just below the alteration zone with the C2 electrode at about 110 m. The apparent resistivities are not very low at this location (approximately 20 000 ohm-m) and hence a maximum current of about 60 mA could be put into the ground with the present lower-powered transmitter. The reason for putting a current electrode at this location will become clear later in discussion of the measurements in HP82-04 with the current electrodes in hole H80-14. The C4-LOGs indicate a fairly broad zone (from approximately 140 to 190 m) of high potentials. Maximum potentials of almost equal amplitudes are observed at 140 to 155 m and at about 187 m (zero-crossover points in the gradient data at 144 and at 187 m). The lateral resistivity log indicates a zone of high resistivity (greater than 100 000 ohm-m) between the conductive alteration zone at 145 m

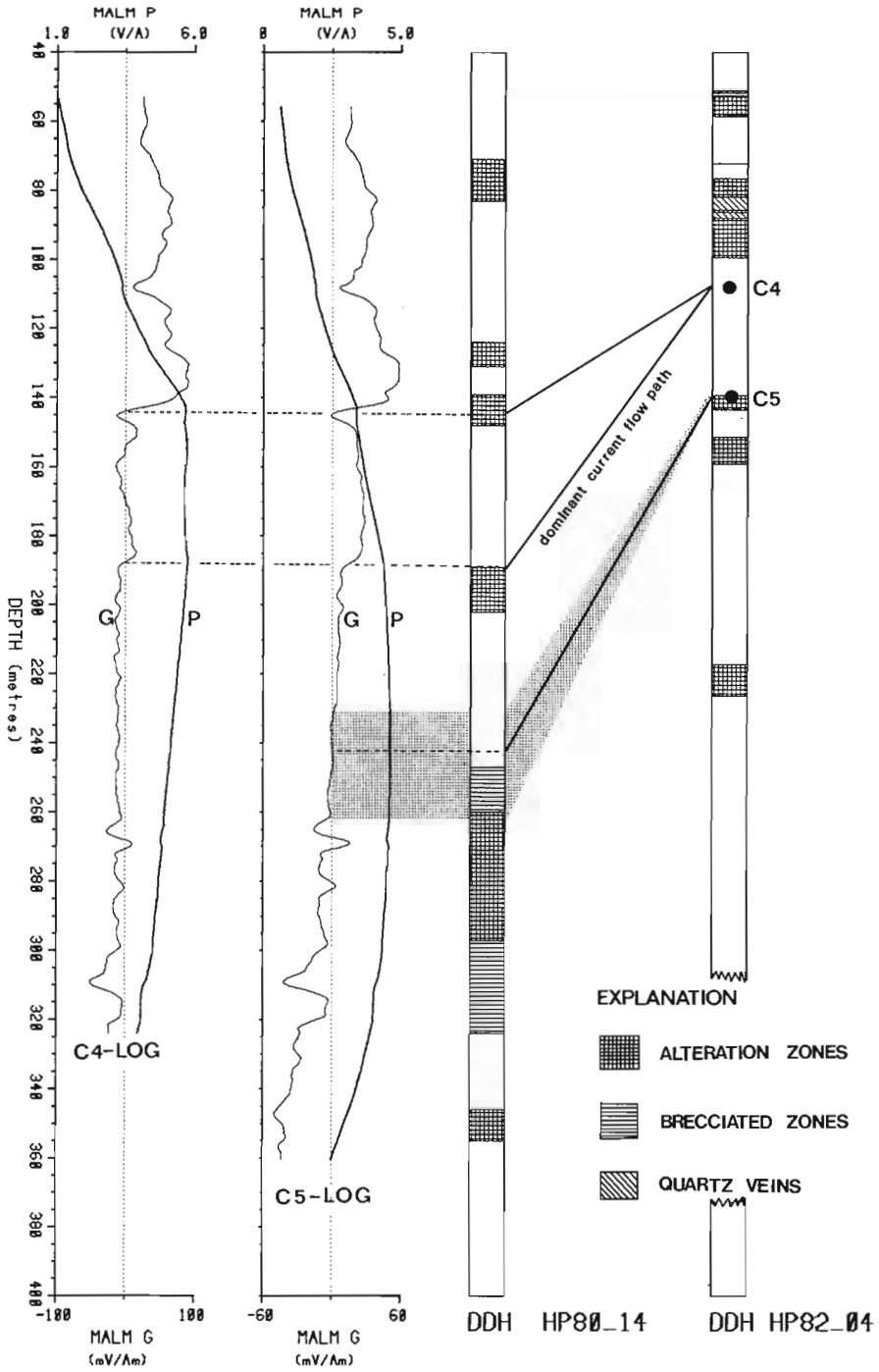

Figure 78.7. Mise-à-la-masse potential and gradient measurements obtained in drillhole H80-14 with the current electrodes in drillhole HP82-04. The C4-LOG and C5-LOG represent measurements with the current electrodes located at C4 and C5 respectively. The solid lines between the geologic columns represent the dominant current flow path.

and that at 187 m. The data indicate that the conductive zone intersected at C4 in HP82-04 splits into two zones; one intersecting H80-14 at approximately 145 m and the other one at approximately 187 m. The data also suggest that the lower conductive zone passes close to H80-14 but not close enough to be detected by the lateral resistivity log. As noted previously the resistivity log only provides information on the resistivity changes in the immediate vicinity of the drillhole.

The C5-LOG represents mise-à-la-masse data along H80-14 with the current electrode at about 139 m in HP82-04. Again we see a broad potential high from approximately 190 m to 270 m. The diffuse nature of the response indicates that the conductor at C5 is not in electrical continuity with any of the conductive zones along H80-14. The gradient data shows the location of maximum current flow at approximately 226-250 m which does not coincide with any of the low resistivity zones on the lateral resistivity log. The conductive zones at about 110 m and 145 m are indicated on the gradient logs as electrically isolated from the energized zone.

In all the above observations, the location of the potential maxima (or zero-crossover points on gradient data) showed considerable displacement from the location of the points along the observation hole with the minimum distance to the current sources. This indicates considerable current channelling along the more conductive paths. Conductive zones above and below the one in electrical continuity with the source are indicated by the flattening of the potentials (or local minima in potential gradients) confirming their electrical isolation from the energized one.

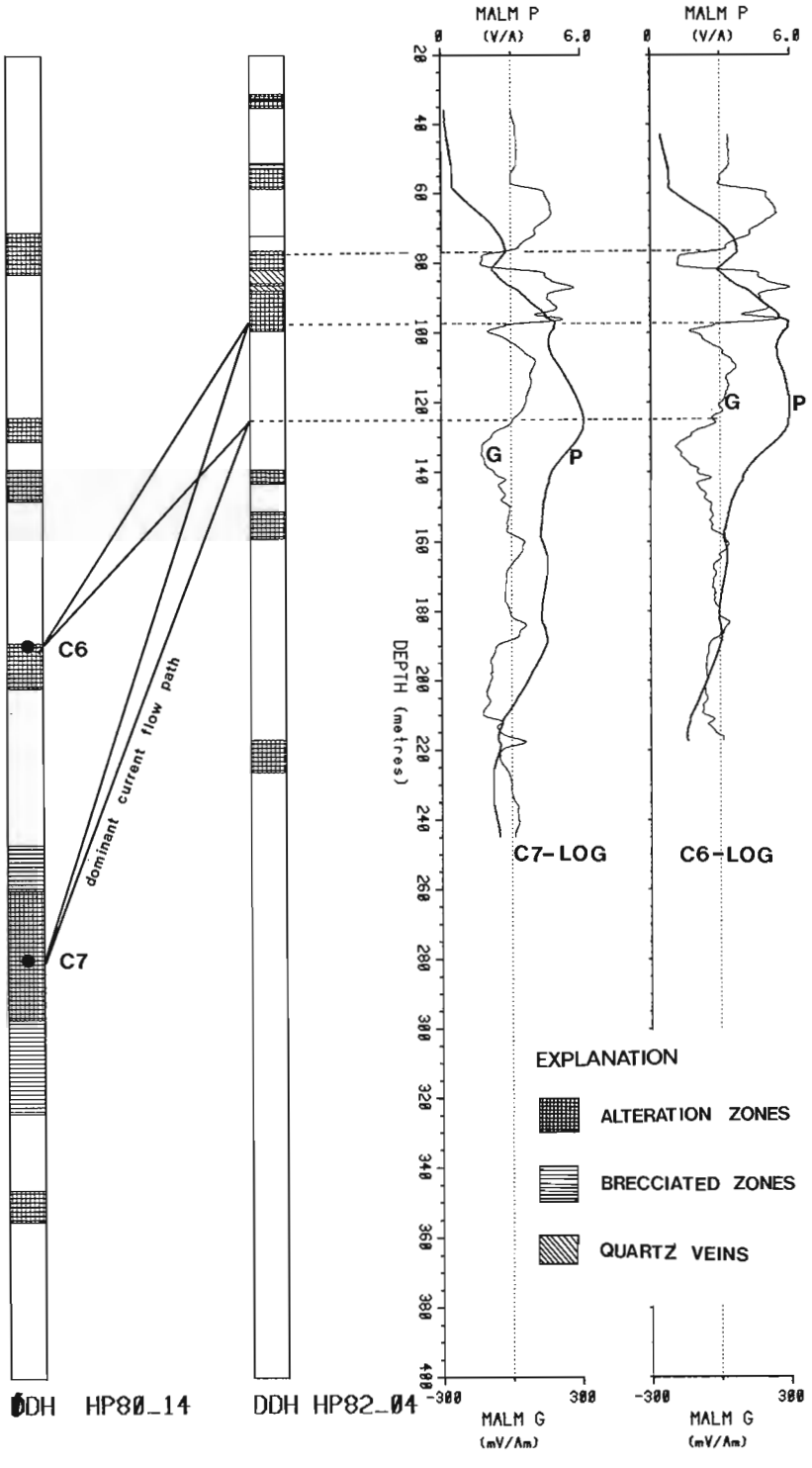

Figure 78.8. Mise-à-la-masse potential and gradient measurements obtained in drillhole HP82-04 with the current electrodes in drillhole H80-14. The C6-LOG and C7-LOG represent measurements with the current electrodes located at C6 and C7 respectively. The solid lines between the geologic columns represent the dominant current flow path.

Measurements in HP82-04 - current electrodes in H80-14

Figure 78.8 shows mise-à-la-masse data obtained in drillhole HP82-04 with the C6 and C7 current electrodes emplaced at 190 m and 280 m, respectively, in H80-14. It is interesting to note the similarities in the observed potentials for the two current electrode positions. The gradients are almost identical. For both of the current electrode positions, the current flow axes are observed at 125 m and 97 m, suggesting that the two energized conductive zones at C6 and C7 converge and intersect hole HP82-04 at the same locations. There is a pronounced potential minimum on both the C6-LOG and C7-LOG at about 82 m followed by a pronounced local maximum at about 77 metres. This suggests that there is a fairly conductive path between the conductive zones at C6 and C7 in hole H80-14 and the location at 77 m in hole HP82-04. This location is the conductive upper part of the alteration zone identified between 75 and 100 m. It is separated by a fairly resistive section (about 100 000 ohm-m) from the lower conductive part at 100 metres and hence a pronounced minimum between the two parts. The observed high potentials between 110 to 130 m in HP82-04 do not coincide with any mapped alteration zones. The indicated current flow path from C7 and C6 to 120 m in HP82-04 is an excellent conductive path. The data suggest that there is strong current channelling along this conductor over a distance greater than 150 m between the holes. The measurements in hole H80-14, with the current electrode placed at about 110 m in hole HP82-04, were conducted to

determine where the zone near 110 m manifests itself in hole HP80-14. The data indicate that the zones at C6 and at C4 are in electrical continuity. There was little indication of electrical continuity between zones at C4 and C7 when the current electrode was at C4. This is probably because the current electrode at C4 was not located in zone with the optimum coupling to C7. This should have been at 125 m, the location of the current flow axis with the current electrode at C7.

The overall interpretation of the mise-à-la-masse observations and the lateral resistivity logs carried out between the drillholes HP82-04 and H80-14 are presented in Figure 78.9. This is a qualitative interpretation of the conductive structure between the two holes and is derived from dominant current flow paths determined by joining the location of the potential maxima (or zero-crossover points in the gradient data) with their respective energizing current sources. The widths of the conductive zones between the holes are speculative at the present time. Theoretical modelling of the structure may provide some realistic widths. As noted previously the observed alteration zones generally show high conductivity. Therefore it is interesting to compare the interpretation of the alteration zones based on the drill core data (Fig. 78.2) and that of the conductive zones based on the mise-à-la-masse data (Fig. 78.9). The most dramatic difference in the interpretation is the orientation of the alteration zones between 260 and 300 m in hole H80-14. This conductive zone intersects hole HP82-04 at about 125 m and dips steeply towards the north (conductive structure from C4 to C7 electrode locations) in contrast to the southerly or nearly vertical dips of the the rest of the conductors. It appears that there are two sets of conductive structures (alteration zones) which may represent two stages of fracturing and alteration. A more complete picture on the conductivity structure between the holes along this section could have been obtained by studying the alteration zones in other holes (holes H80-24 and H80-13). This was unfortunately not done because the holes in the area were not available for geophysical work at the time.

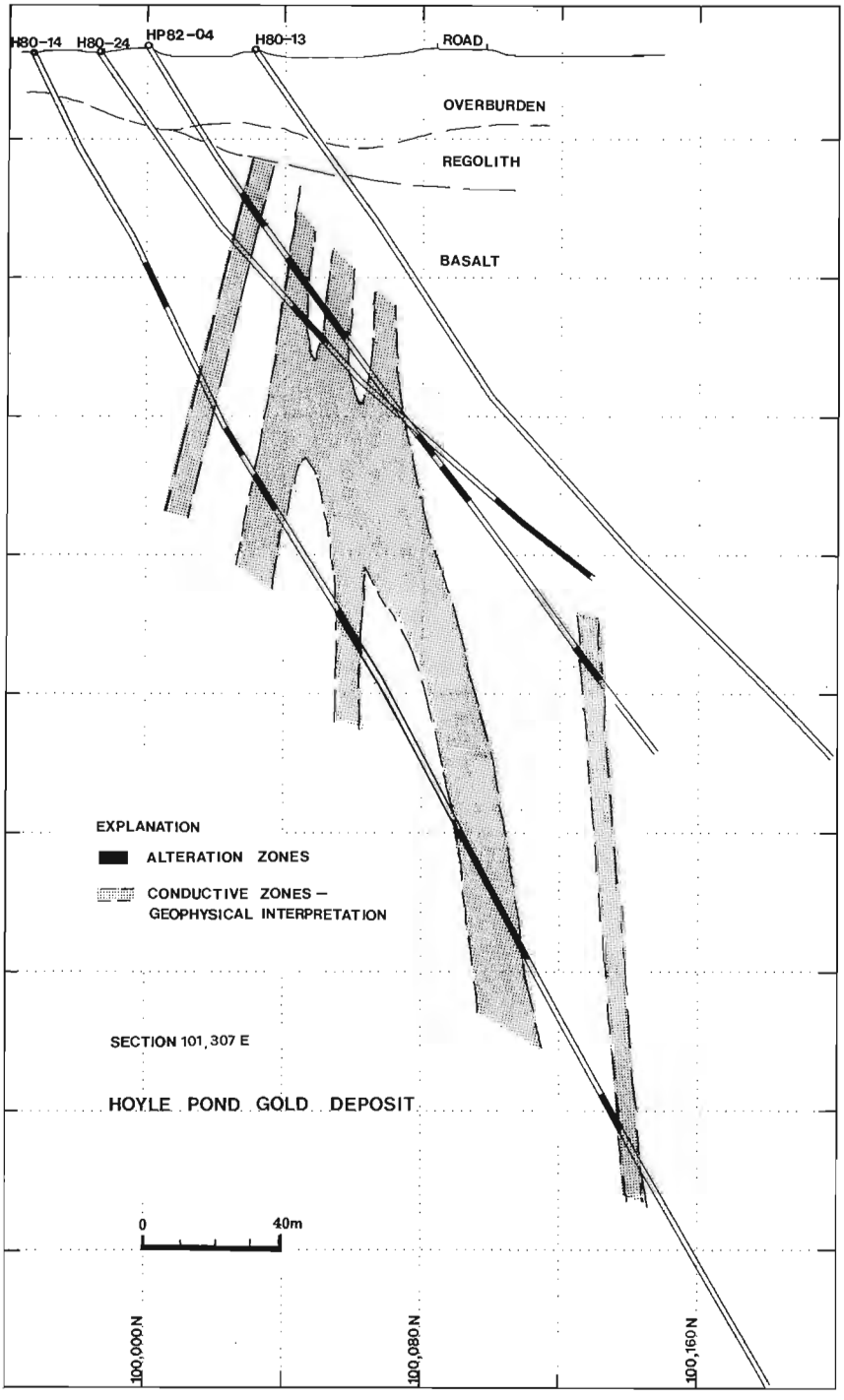

Figure 78.9. Conductivity structure between holes HP82-04 and H80-14 as inferred from the mise-à-la-masse and lateral resistivity logs.

Conclusion

The drill hole mise-à-la-masse measurements carried out between the two holes at the Hoyle Pond Gold deposit were successful in correlating the alteration zones between these holes. The alteration zones are relatively good conductors compared to the unaltered basalt flows and seem to be well suited for investigation by the mise-à-la-masse method.

Acknowledgments

I would like to thank Kidd Creek Mines Ltd. for permission to work on their property and to present these data. Special thanks are due to Dr. J.A. Slankis and D.J. Londry of Kidd Creek Mines who suggested this interesting study. I would also like to thank my colleagues at the GSC, especially, P.G. Killeen, for valuable discussions and comments, Q. Bristow who designed the IP/resistivity logging system and W.G. Hyatt for assistance in field data acquisition.

References

Bristow, Q.
1984: A system for the digital transmission and recording of Induced Polarization Measurements in Boreholes; in Proceedings of the International Symposium and Workshop on Borehole Geophysics: Mining and Geotechnical Applications.

Downes, M.J., Hodges, D., and Derweduwen, J.
1982: A Free Carbon and Carbonate Bearing Alteration Zone Associated with the Hoyle Pond Gold Deposit, Ontario, Canada; in Gold '82: The Geology, Geochemistry and Genesis of Gold Deposits, ed. R.P.Foster; Geological Society of Zimbabwe Special Publication No. 1. p.435-448.

Eloranta, E.
1984: A method for calculating mise-à-la-masse anomalies in the case of high conductivity contrasts by the integral equation technique; Geoexploration, v. 22, p. 77-88.

Fyon, J.A. and Crocket, J.H.
1981: Volcanic Environment of Carbonate Alteration and Stratiform Gold Mineralization, Timmins area; in Genesis of Archean, Volcanic Hosted Gold Deposits, Ontario Geological Survey, Miscellaneous Paper 97.

Jamtlid, A., Magnusson, K.A., and Olsson, O.
1982: Electrical borehole measurements for the mapping of fracture zones in crystalline rock; in Proceedings of a workshop on Geophysical Investigations in Connection with Geological Disposal of Radioactive Waste, Nuclear Energy Agency.

Ketola, M.
1972: Some points of view concerning mise-à-la-masse measurements; Geoexploration, v. 10, p. 1-23.

Madden, H.H.
1978: Comments on the Savatzky-Golay convolution method for least-squares fit smoothing and differentiation of digital data; Analytical Chemistry, v. 50, no. 9, p. 1383-1386.

McMurry, H.V. and Hoagland, A.D.
1956: Three dimensional applied potential studies at Austinville, Virginia; Bulletin Geological Society of America, v. 67, no. 6, p. 683-696.

Mwenifumbo, C.J.
1980: Interpretation of mise-à-la-masse data for vein type bodies; University of Western Ontario, London, Ontario, Ph.D. Dissertation.

Mwenifumbo, C.J., Urbancic, T.I., and Killeen, P.G.
1983: Preliminary Studies in Gamma Ray Spectral Logging in Exploration for Gold; in Current Research, Part A, Geological Survey of Canada, Paper 83-1A, p. 391-397.

Parasnis, D.S.
1967: Three dimensional mise-à-la-masse surveys of an irregular lead-zinc-copper deposit in central Sweden; Geophysical Prospecting, v. 15, no. 3, p. 407-437.

Rouhianen, P. and Poikonen, A.
1982: Geophysical studies in the power plant area of Loviisa in southern Finland; in Proceedings of a workshop on geophysical investigations in connection with geological disposal of radioactive waste, Nuclear Energy Agency.

Savitzky, A. and Golay, J.E.
1964: Smoothing and differentiating of data by simplified least squares procedures; Analytical Chemistry, v. 36, p. 1627-1638.

Urbancic, T.I. and Mwenifumbo, C.J.
1984: Multiparameter Logging Techniques Applied to Gold Exploration; in Proceedings of the International Symposium and Workshop on Borehole Geophysics: Mining and Geotechnical Applications.

PHYSICAL VOLCANOLOGY AND STRATIGRAPHY OF THE SETON FORMATION: FOREDEEP VOLCANISM IN ATHAPUSCOW AULACOGEN, DISTRICT OF MACKENZIE

Gerald M. Ross[1] and Terri L. Smith[1]
Precambrian Geology Division

Ross, G.M. and Smith, T.L., Physical volcanology and stratigraphy of the Seton Formation: foredeep volcanism in Athapuscow Aulacogen, District of Mackenzie; in Current Research, Part A, Geological Survey of Canada, Paper 85-1A, p. 681-692, 1985.

Abstract

The Seton Formation (Great Slave Supergroup) is a succession of volcanic and intrusive rocks composed mostly of basalt and rhyolite with subordinate intermediate rocks. In the Seton Island area, the Seton Formation is interbedded with fluvial-deltaic siliciclastics of the Sosan Group and constitutes a succession of volcaniclastic rocks, lava flows and hypabyssal intrusions. Seton Island is an anticlinorial structure that displays en echelon folds, penetrative flattening cleavage and a strain gradient that is the result of transcurrent movement along an east-trending splay of the McDonald-Wilson Fault system.

In the Pekanatui Point area, the Seton Formation comprises thick (300-1000 m) assemblages of allochthonous volcanic rocks thrust northward from the axial zone of Athapuscow Aulacogen. The allochtons contain a diverse assemblage of volcanic rocks that record shoaling of submarine islands and are intruded by gabbroic rocks and rhyolite porphyry. Each allochthon displays a distinct structural style which may be related to nappe emplacement or a phase of deformation that predates thrusting.

Seton Formation volcanism correlates with a time of plate convergence in Wopmay Orogen (Calderian Orogeny) and probably resulted from the ascent of basaltic magma during periodic extension and fracture of thin lithosphere in Athapuscow Aulacogen as a consequence of oblique plate convergence.

Résumé

Dans le secteur de l'île Seton, de la région du Grand lac des Esclaves, la formation de Seton (supergroupe du Grand lac des Esclaves) est interstratifiée avec les roches siliceuses clastiques et fluvio-deltaïques du groupe de Sosan, et constitue une succession de roches volcanoclastiques, de coulées de laves et d'intrusions hypabyssales. L'île Seton est une structure de type anticlinorium que caractérisent des plis en échelon, une schistosité de flux et un gradient de déformation dû à un mouvement de décrochement le long d'une ramification, dans la direction est, du réseau de failles de McDonald-Wilson.

Dans le secteur de la pointe Pekanatui, la formation de Seton contient d'épais assemblages (300 à 1000 m) de roches volcaniques allochtones poussées vers le nord à partir de la zone axiale de l'aulacogène d'Athapuscow. Les allochtones contiennent un assemblage varié de roches volcaniques, vestiges de la présence en eaux peu profondes d'îles sous-marines, et traversées par des roches gabbroïques et un porphyre rhyolitique. Chaque allochtone présente un style structural précis associé soit à la mise en place de la nappe de charriage, soit à une phase de déformation antérieure au mouvement de charriage.

Le volcanisme de la formation de Seton correspond chronologiquement à la convergence de plaques dans l'orogène de Wopmay (orogenèse caldérienne); il a probablement eu pour origine la remontée de magma basaltique pendant des épisodes périodique de dilatation et de fracturation de la lithosphère mince, à l'intérieur de l'aulacogène d'Athapuscow, par suite de la convergence de plaques obliques.

[1] Earth and Planetary Sciences, Washington University, St. Louis, Missouri 63130

Introduction

Athapuscow Aulacogen contains a diverse assemblage of supracrustal rocks formed during a key period of lithosphere evolution in northwest Canada. Sedimentation and igneous activity can be related to the rifting and subsequent tectonic evolution of the western and southern edges of the Archean Slave Craton during formation of Wopmay Orogen (Hoffman, 1973a, 1980, 1981; Hoffman et al., 1974). The aulacogen records foredeep subsidence during the first collision event in Wopmay Orogen, then northwest-directed thrusting and nappe tectonics localized along the Slave and Churchill province boundary, and finally northeast right-slip faulting related to the terminal collision event in Wopmay Orogen.

The Seton Formation comprises foredeep volcanic rocks within the upper Sosan Group and the Kahochella Group (Hoffman, 1968). References to previous work on the Seton Formation may be found in Hoffman et al. (1977). Based on recent U-Pb zircon geochronology (Bowring and Van Schmus, 1984; Bowring et al., in press) and correlations between Athapuscow Aulacogen and Wopmay Orogen, Seton volcanism probably occurred at 1885 to 1875 Ma.

Field work on the Seton Formation was initiated in 1984 to examine the stratigraphy, volcanic style, paleoenvironment and deformation of these rocks. Mapping was concentrated in the autochthonous, shallow water volcanics of Seton Island and the deeper water allochthons of the Pekanatui Point area (Fig. 79.1).

Seton Island

Seton Formation is the dominant formation in the Seton Island area, for which the formation is named (Hoffman, 1968). Rocks of the Seton Formation comprise non-cyclic deposits of felsic and mafic volcaniclastic rocks and basalt flows that are interlayered with siliciclastic sediments of the Kluziai and Akaitcho River formations (upper Sosan Group) and intrusions of plagioclase porphyry of both mafic and felsic composition. Volcanic activity in this region spanned the time of deposition of upper Sosan Group rocks and is therefore older than Seton Formation in the Pekanatui Point area (Fig. 79.1).

Sosan Group

Nonvolcanogenic rocks in the Seton Island area are composed of quartzose arenites, siltstones and mudstones of the Kluziai and Akaitcho River formations (Fig. 79.2). Lower Kluziai Formation (unit K1, Fig. 79.2) is composed of very well-sorted feldspathic quartz arenite that occurs in sheets (10-100 cm thick) displaying tabular planar crossbeds, parallel lamination or are massive. The base of massive arenite sheets display flute casts, the axes of which are parallel to the southwest paleocurrent azimuths inferred from crossbeds. Arenite sheets are separated by green micaceous mudstone layers, several centimetres thick, that increase in thickness upwards in unit K1.

Lower Kluziai arenites grade upwards into drab olive to maroon fine grained arenites of upper Kluziai Formation (unit K2) that occur in undulose sheets (10-40 cm) that display a normal grade to massive base overlain by laminated siltstone. Sheets are separated by laminated to sand-streaked brown to green micaceous mudstones (Fig. 79.3A).

Akaitcho River Formation gradationally overlies Kluziai Formation and in the Seton Island area the contact is arbitrarily placed at the first occurrence of finely interlayered red mudstone and quartzofeldspathic arenite. The lower Akaitcho River Formation (unit A1) is composed of interbedded sheets of massive to normal graded hematitic arkosic arenite and laminated red mudstone-siltstone couplets. Upper Akaitcho River Formation (unit A2) is distinguished by the occurrence of drab coloured fine grained arenites, mudstones and rare granular cherty ironstone.

Paleobathymetry. The upper Sosan Group has been interpreted as a blanket of siliciclastic sediments deposited in a fluvial-deltaic setting (Hoffman, 1969). Lower Kluziai Formation arenites are largely subaerial fluvial deposits that grade into delta plain and prodelta facies of upper Kluziai and Akaitcho River formations. The water depth is difficult to constrain precisely but the lack of desiccation features and paucity of traction current structures, scour marks and ripple marks, especially in upper Kluziai and Akaitcho River sediments suggests subtidal deposition. The prevalence of turbiditic/density flow bedding structures and absence of slumps favour a low-slope prodeltaic environment.

Volcanic rocks

Volcanic rocks in the Seton Island area include basaltic tuffs, felsic, lithic-rich tuffs, intermediate composition tuff, basaltic lava flows and local dome margin deposits of uncertain composition.

Mafic tuff. Four map units of mafic pyroclastic rock were recognized (unit K2a, K2c, K2e, and A1a; Fig. 79.2). Cleavage is particularly well-developed in mafic tuffs and tuffaceous sediments (Fig. 79.3A) and locally obscures grain characteristics and sedimentary structures. The tuff units display similar assemblages of sedimentary structures but differ in the overall geometry of the deposits, composition (relative proportions of vitric, lithic and crystal fragments) and diagenetic alteration. All tuff successions occur abruptly within the siliciclastic background sediments and are composed of tabular beds of normal graded to massive lapilli tuff and tuff breccia with thin (5-30 cm) interbeds of parallel laminated ash. Units K2a and A1a (Fig. 79.2) are lithic- to formerly vitric-rich, crystal poor (<5% phenocrysts of plagioclase) basaltic tuffs that thicken and coarsen considerably towards the north. Unit K2c is a particularly distinctive uniform sheet of crystal-rich (10-25% plagioclase crystals) lapilli tuff. Unit K2e is a uniform sheet of coarse ash in which cleavage has obliterated internal structures. The lack of control on depositoinal strike makes it difficult to attach genetic significance to the shape and grain size variations in the tuff units. Most tuffs are composed largely of unabraded pyroclasts and display sedimentary structures that suggest deposition by subaqueous pyroclastic flow and/or resedimentation of juvenile tephra.

Lithic-rich felsic tuffs. Units K2b and K2d (Fig. 79.2) are composed of lithic-rich ash-flow tuff and heterolithic conglomerate and arenite. Epiclastic rocks dominate these units along the north part of Seton Island with an increased proportion of ash-flow tuff towards the south. The conglomerates form sheets of subround irregular cobbles and boulders composed of amygdaloidal basalt, ash-flow tuff, feldspar porphyry, rhyolite and various breccias in a granular to sandy matrix (Fig. 79.4A) and are interbedded with massive to normal graded arenites. The ash-flow tuffs are composed of lithic fragments (aphyric to quartz-feldpar phyric felsite, amygdaloidal basalt and sediments) and irregularly-shaped flattened bodies of chloritic material with feldspar phenocrysts (collapsed pumice?) (Fig. 79.4B) in an ashy matrix with about 5% quartz phenocrysts. The ash-flow tuffs range from unwelded to densely welded with well-developed eutaxitic foliation defined by flattened pumice(?). The individual ash-flow tuffs are less than 5 m thick and are interbedded with vitric ash beds and epiclastic rocks.

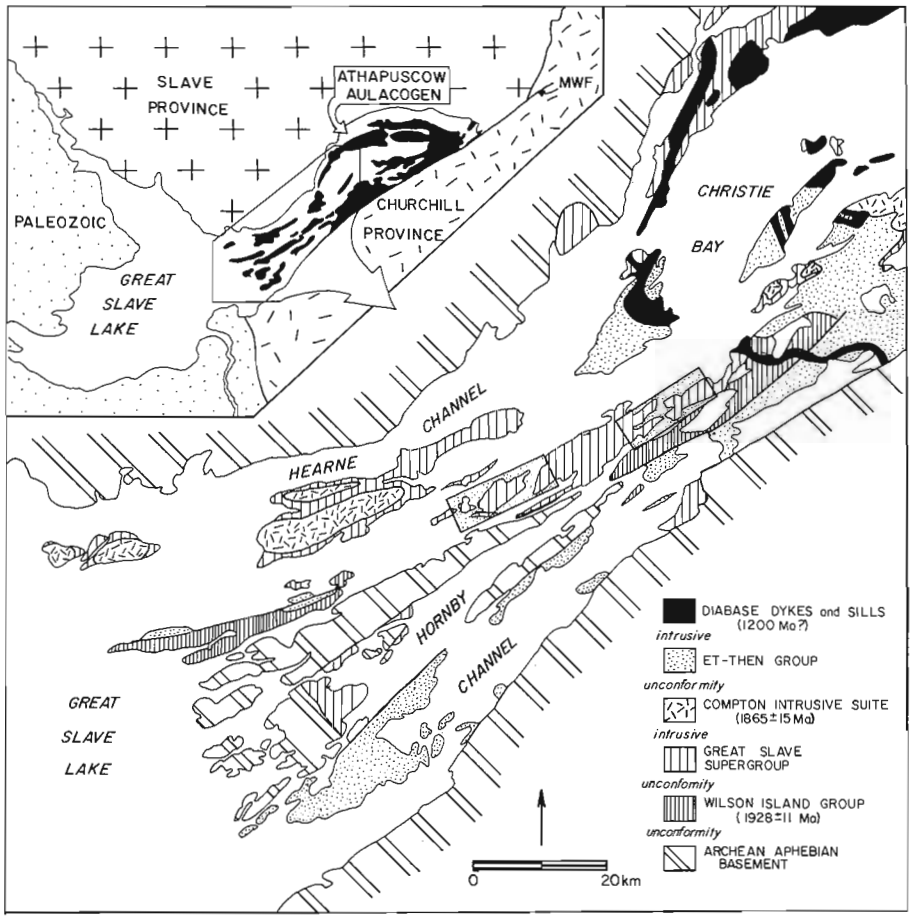

Figure 79.1A

General geology of Athapuscow Aulacogen. Areas in rectangles show location of Seton Formation rocks studied in 1984. MWF: McDonald-Wilson Fault.

***Figure 79.1B** (below)*

Composite stratigraphic section for Athapuscow Aulacogen. The stratigraphic position of Seton Formation on this diagram pertains to the Seton Island area. Seton Formation in the Pekanatui Point area occurs within the Kahochella Group (from Hoffman et al., 1974).

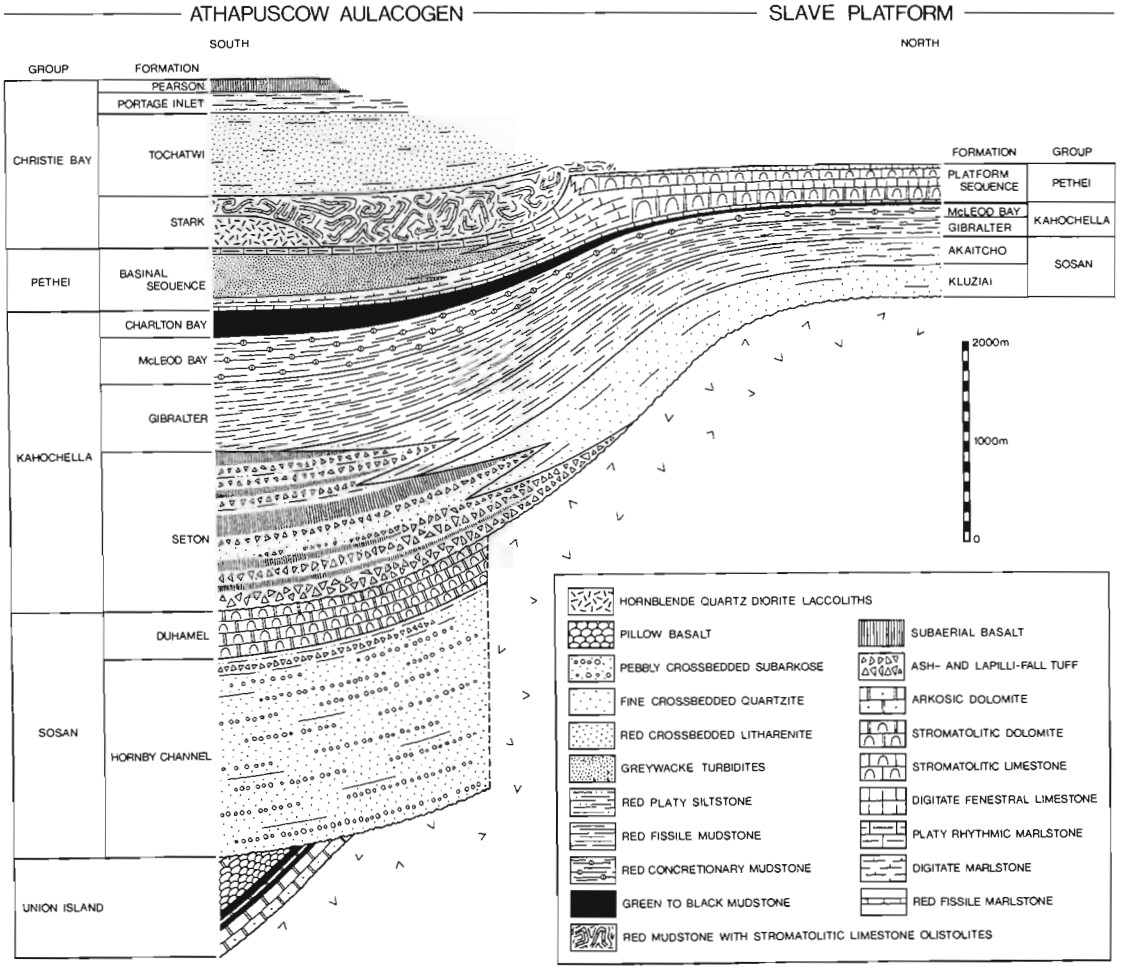

Based on structures in the sedimentary rocks, we tentatively suggest that the ash-flows were both deposited and welded subaqueously.

Lower Kluziai tuffs. Three tuff units (K1a, b, c) of local extent occur within the lower Kluziai Formation (Fig. 79.2). Unit K1a is an intermediate composition tuff to tuff breccia composed of microlitic vesicular basalt clasts, blocks of plagioclase porphyritic basalt and less than 5% subround quartz grains that may be phenocrysts. High initial dips of bedding and the occurrence of bomb impact sags with clasts up to 20 cm in diameter suggest deposition on the proximal cone flank or volcaniclastic apron. Unit K1a underlies intermediate composition tuffs of unit K1b that are distinguished by their purple colour and the presence of broken plagioclase crystals (5-10% with crystals up to 6 cm long) and 1-5% quartz phenocrysts. Relatively distal deposits comprise ash and lapillistone with massive to well developed graded bedding (Fig. 79.3B). These rocks can be traced for about 500 m to the west where they grade into poorly stratified coarse lapilli tuff to breccia with cored to fusiform bombs in addition to scoria and mafic lithic clasts. The well bedded lapillistones (Fig. 79.3B) contain thin (5-20 cm) welded zones that formed during deposition and compactional flattening of hot airfall scoria and pumice (cf. Sparks and Wright, 1979). Units K1a and K1b interfinger and probably represent the deposits of coalesced cinder cones. They are overlain by finely laminated ash beds of lacustrine or airfall origin and are cut by fine grained breccia pipes and plagioclase porphyritic basalts. Unit K1c is a

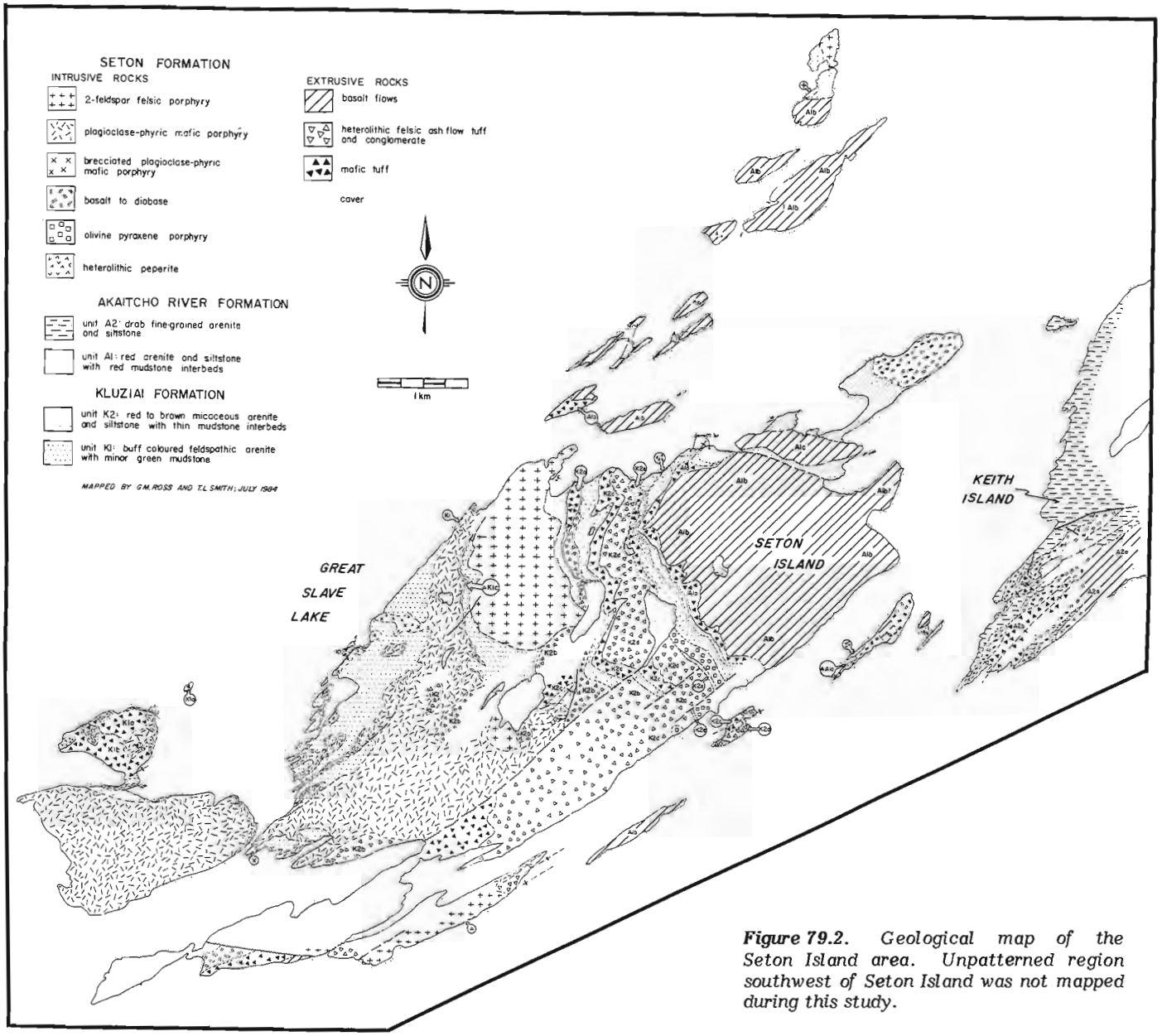

Figure 79.2. Geological map of the Seton Island area. Unpatterned region southwest of Seton Island was not mapped during this study.

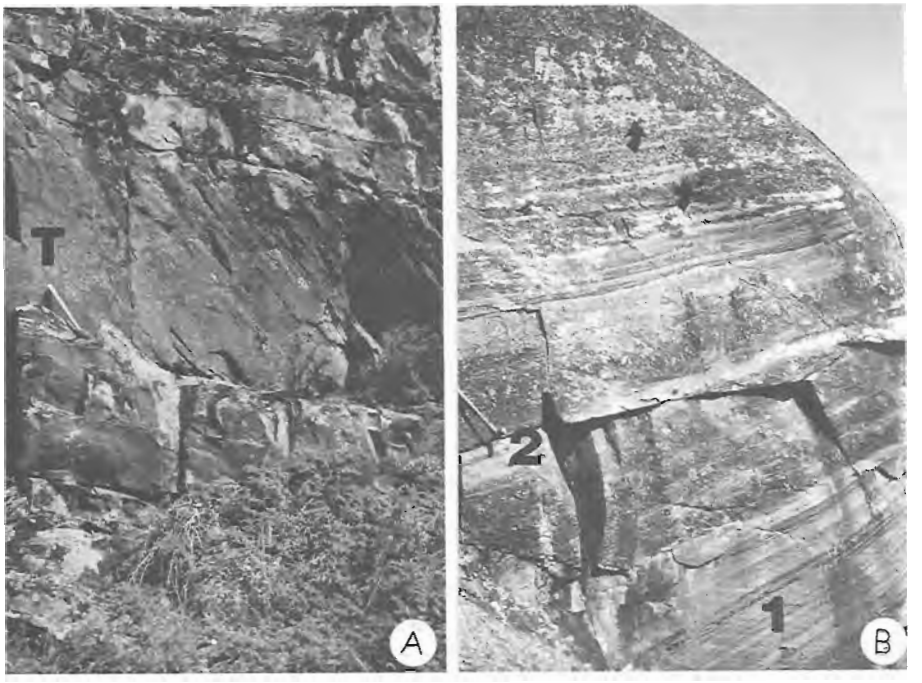

Figure 79.3

A. Mafic lapilli tuff bed (T) within graded to massive sheets of fine grained feldspathic arenite of unit K2. Note pronounced cleavage in tuff (dipping to the right).

B. Well-stratified airfall lapillistone with unit K1b. Laminated fine grained lapillistone at base (1) is overlain by two beds of massive to normal-graded lapillistone (2) that is in turn overlain by stratified lapillistone with welded zones (arrows).

heterolithic lapilli tuff to tuff breccia that occurs in upper unit K1 and contains pumiceous clasts, quartz phenocrysts (5-10%), vein quartz cobbles and pebbles and clasts of sedimentary derivation.

"Dome" breccias. Localized deposits of monolithologic breccia and conglomerate occur on the north shore of Seton Island. The breccias are massive, unstratified(?) units composed of angular, unsorted aphanitic lapilli and blocks (up to 2 m) that are mottled pink and green. Laterally equivalent conglomerates are composed of a well-sorted tight framework of boulders of scoria (up to 1.2 m diameter) and subordinate aphanite in a silica-cemented matrix of volcanic granulestone. The breccia and conglomerate pinches out abruptly to the south. Contemporaneous deposits of laminated purple to red mudstone and siltstone onlap the breccias and infill topographic irregularities. These rocks are tentatively interpreted as breccia lobes deposited during collapse of a thick flow and/or dome and lobes of conglomerate composed of reworked subaerial lava.

Basalt flows. Basalt flows (units A1b and A1c) are widespread in the lower Akaitcho River Formation and constitute a nearly continuous section (about 200 m) of flows and minor interflow sediments exposed over an area of 30 km^2. The basalts are high TiO_2 (1.5-3.4 wt% TiO_2; Olade, 1975) tholeiites and contain microlites and uncommon phenocrysts of plagioclase.

The vertical zonation of a typical flow unit is shown in Fig. 79.4. Most flows are 5-10 m thick and consist of 1) a basal zone of vesicular, locally flow-brecciated basalt with involute selvages, 2) a massive zone with local columnar joints and large (10-20 cm) amygdules in the upper part (Fig. 79.5C), 3) an upper zone of very vesicular (up to 50%) basalt, and 4) an involute to lobate upper surface commonly with strongly elongate vesicles. Flows that exhibit this zonation have a sheet-like geometry with lateral terminations characterized by lobate to pillowed forms. Lava flows composed entirely of pillows (Fig. 79.5D) are interlayered with the sheet flows. The pillows have thin (<2 cm) amygdaloidal selvages and coarse interpillow hyaloclastite that is commonly replaced by jasper cement.

Interflow sediments consist of monolithologic conglomerates and litharenites. The conglomerates are well-sorted, less than 1 m thick and composed of equant, angular to rounded clasts of basalt derived largely from reworking of flow breccia. Litharenites occur as stratified to crossbedded lenses (<1 m) composed of basalt clasts and abraded crystals of feldspar and quartz. Crossbeds in the litharenite indicate northwest transport, parallel to the azimuth of most elongate flow top vesicles.

Intrusive rocks. Mafic plagioclase porphyry forms an irregular sill-like body that occurs on the western third of Seton Island and neighboring islands to the west. Units ranging from lower Kluziai Formation to K2d felsic tuffs are crosscut by the intrusion which is texturally variable with irregular apophyses and satellitic bodies. The porphyry is composed of plagioclase crystals (5-35%) (Fig. 79.5E) in an aphanitic, locally vesicular, groundmass. Contacts with country rock range from sharp, concordant boundaries with little evidence of contact metamorphism to discordant

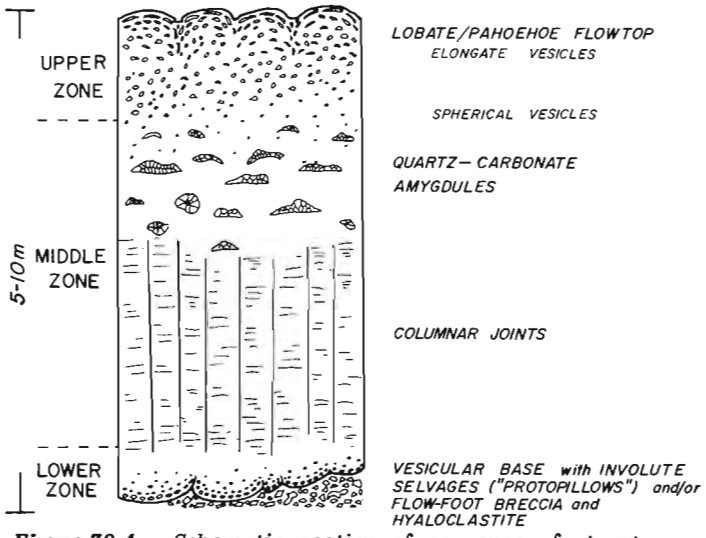

Figure 79.4. *Schematic section of sequence of structures and textures in unit A1b basalt sheet flows.*

fluidized contacts along which porphyry and country rock have been extensively mixed. Irregular pods and lobes of brecciated porphyry occur along the northwest margin of the intrusion (Fig. 79.5F). The breccia is composed of in situ and rotated angular blocks of porphyry in a matrix of quartz sand derived by thorough disaggregation of Kluziai arenite. The sill is tentatively interpreted as a hypabyssal intrusion emplaced during eruption of unit A1b basalt flows.

Stocks of felsic porphyry comprising 5-10% plagioclase and 1-5% alkali feldspar phenocrysts in a granular to aphanitic groundmass occur at different stratigraphic levels. The oldest intrusion crosscuts lower Kluziai Formation sediments that contain an upwardly increasing proportion of volcanogenic material, including crystal-rich felsic tuffs at the top of the preserved section that may be comagmatic with the stock. The youngest intrusion cuts mudstones of lower Akaitcho River Formation. The occurrence of boulders and cobbles of felsic porphyry in epiclastic conglomerates and tuffs of unit K2d, provides evidence of synvolcanic unroofing of some intrusions.

Discussion. The sedimentology of the Kluziai and Akaitcho River formations suggests a gradual deepening of the depositional environment from subaerial/fluvial to quiet water subaqueous conditions. Basaltic and intermediate composition tuffs at units K1a and K1b constitute the only near vent deposits recognized. The unusual occurrence of welded airfall tuff, formed by compaction of hot pumice clasts rather than welding as a result of emplacement of an ash-flow unit on top of airfall, is consistent with a proximal subaerial origin for these tuffs (cf. Sparks and Wright, 1979). All of the mafic tuff units represent nearly two-dimensional cross-sections through aprons of subaqueous deposits formed by gravity flow and to a lesser extent suspension settling. The lack of abrasion and admixture of nonvolcanogenic clasts implies negligible reworking of tephra prior to deposition and hence many of the tuff beds could be subaqueous pyroclastic flows (cf. Fiske, 1963). The relatively thin character of the ash-flow tuff beds of units K2b and K2d suggest that they are probably far removed from the vent or that they represent small volume ash-flows. The southerly increase in relative proportion of ash-flow tuff to epiclastic deposits within these units may be evidence that the eruptive centre was somewhere south of Seton Island. Unit A1b basalt flows are interpreted to be shallow water (tens of metres?) effusive deposits that, based on the lack of coarse breccias and conglomerates, formed low-relief shield volcanoes. In summary, the Seton Island area appears to have been the locus of persistent bimodal igneous activity during the early stages of foredeep evolution. Unfortunately, later dismemberment by thrust faults and transcurrent faults has masked the true regional extent of this phase of volcanism.

Structural geology

The structural fabric of the Seton Island area reflects the proximity of this region to the McDonald-Wilson Fault, a major transcurrent fault system that accommodated at least 70 km of right-slip movement (Hoffman, 1981). The rocks of Seton Island display a marked strain gradient which is recognized by an increase in the intensity of cleavage and decreased interlimb angle of folds towards the McDonald-Wilson Fault. In general bedding in Seton Island area has a gentle dip to the northeast that is locally deflected around weakly plunging, northeast-trending, open folds. Examination of the map pattern (Fig. 79.2) and a stereonet plot (Fig. 79.6) of poles to bedding illustrate the presence of a large amplitude (>5 km), gently northeast plunging (5°-8°) anticlinorial structure with an upright axial plane that strikes 058°. A steep pressure solution(?) flattening cleavage is present in the region and is axial planar to the anticlinorium. The orientation of the folds and cleavage is consistent with formation as en echelon structures within the plane of flattening of a right-lateral shear couple (cf. Wilcox et al., 1973). The strain gradient and deformation are related to movement along a prominent easterly-trending splay off of the main McDonald-Wilson Fault.

Pekanatui Point

In the Pekanatui Point area the Seton Formation occurs as structurally and stratigraphically distinct allochthonous slices that have been thrust northward onto basinal facies of the Pethei Group and lower Stark Formation (Christie Bay Group) (Fig. 79.7). The lack of distinctive marker units, in addition to the insular character of outcrop belts, hampers stratigraphic correlation between thrust sheets and renders paleogeographic reconstructions impossible.

Stratigraphic setting and sedimentology

In the Pekanatui Point area, Seton Formation rocks occur within fine grained basinal facies siliciclastic sediments of the Kahochella Group. In general the volcanic successions overlie green to black siltstones and mudstones, with distinctive large (up to 80 cm) dolomite concretions, that appear to be part of the Ogilvie Formation (lower Kahochella Group; Hoffman, 1977). This stratigraphic distinction is misleading because normally red-colored Kahochella Group lithologies develop a drab pigmentation and contain large dolomite concretions below the occurrence of volcanic rocks. Pending further lithostratigraphic analysis, Seton volcanism occurred sporadically during deposition of the Ogilvie, Gibralter and lower McLeod Bay Formations.

Basinal facies of the Kahochella Group is a monotonous succession of fine-grained, locally concretionary, siliciclastic sediment. Graded quartzose siltstone to mudstone beds (2-10 cm thick), parallel laminated mudstone beds (2-5 cm thick) and siltstone-mudstone laminates predominate. Coarse sand beds and greywacke, apparently derived from a source area composed of felsic volcanic rocks, occur within the Gibralter Formation along the south shore of Christie Bay (Fig. 79.7). With the exception of uncommon climbing ripples, traction current structures are absent, thereby implying subaqueous quiet (deep?) water sedimentation.

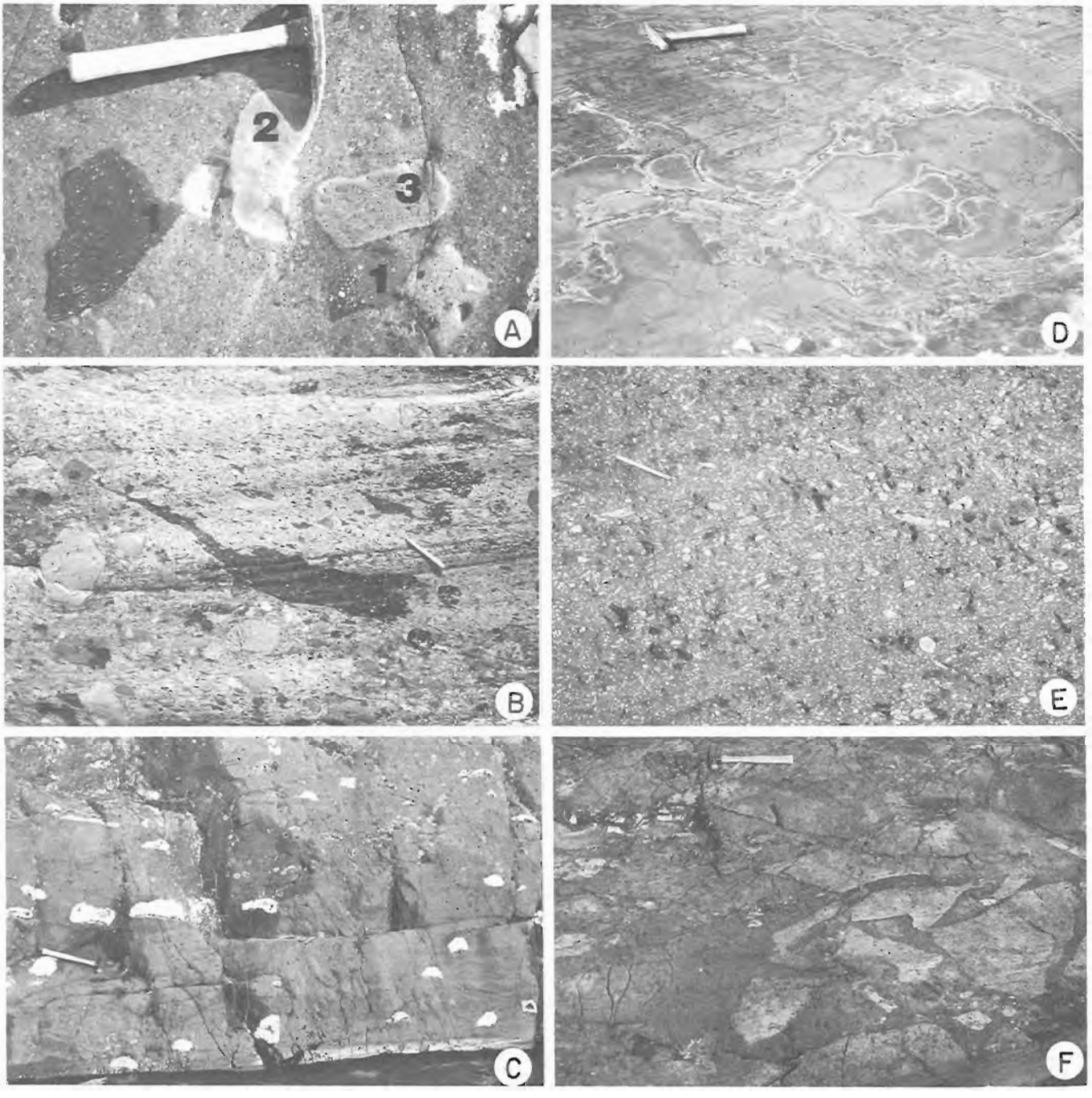

Figure 79.5

A. *Bedding surface exposure of heterolithic paraconglomerate of unit K2d composed of clasts of amygdaloidal basalt(1), felsite (2) and ash-flow tuff (3) in granulestone matrix.*

B. *Lithic-rich ash-flow tuff from unit K2d. Tuff is composed of equant lithic blocks of feldspar porphyry and aphanitic felsite and elongate flattened vitric clasts (dark shapes) of flattened pumice(?). Eutaxitic foliation defined by flattened shards is here indistinguishable from flattening cleavage. Matchstick is 4 cm long.*

C. *Large quartz and dolomite-filled amygdules in upper part of massive zone of a sheet flow basalt (unit A1b).*

D. *Pillowed flow in unit A1b, south shore of Seton Island. Pillows are composed of amygdaloidal basalt with thin (white) selvages. Interpillow areas are composed of hyaloclastite and jasper cement.*

E. *Plagioclase-porphyritic basalt typical of crystal-rich parts of intrusive sill. Pits on outcrop surface are due to weathering and are not vesicles. The elongate plagioclase crystals are aligned parallel to cleavage. Matchstick is 4 cm long.*

F. *Intrusive breccia at margin of basalt sill. Breccia is composed of angular blocks of basalt porphyry in matrix of carbonatized Kluziai sand.*

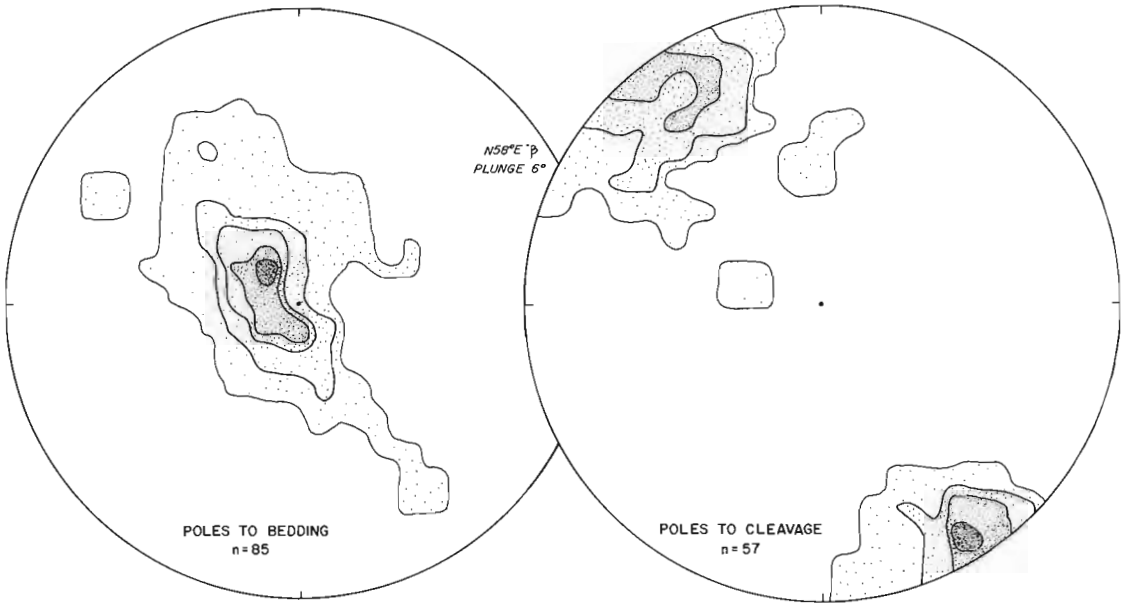

Figure 79.6. *Stereonet plots of poles to bedding and poles to cleavage for measurements made on Seton Island. Weak disperson of poles to bedding reflects open undulose character of folds.*

Pillow lavas

Microphyric to plagioclase-porphyritic pillow lavas and massive lava sheets are common (35%) in the Seton Formation. The lavas are conspicuously vesicular and contain 5-40% carbonate and quartz-filled ovoid amygdules (<1 cm) commonly arranged in trains parallel to flow margins (Fig. 79.8A). Flows (10-60 m thick) are composed of tightly-packed elliptical pillows (<1 m wide) with less than 5% interpillow hyaloclastite. Exhumed three-dimensional pillows display a bifurcating tubular shape, thus clearly indicating that the pillows are cross-sections of tubular flows. Massive flows are subordinate to pillowed flows. The base and upper surface of massive flows are pillowed and/or irregularly involute and grade into massive lava of the flow interior.

Pillow breccia

Pillow breccia, as used here, refers to a breccia composed of angular to amoeboid blocks of vesicular basalt in a hyaloclastic matrix. Pillow breccia occurs at the base and/or top of some pillowed flows and as massive sheets (Fig. 79.8B). In the latter case, successive sheets of hyaloclastite-rich pillow breccia comprise unbroken sequences up to 40 m thick (Fig. 79.7, map 1). Pillow fragments occur both as fracture-bounded clasts formed by brecciation of chilled lava and as amoeboid bodies with vesicle trains that are concentric to the fragment margin, indicative of cooling of a discrete globule of lava.

Hyaloclastites

Accumulations of lapilli to ash-sized, generally aphyric, chloritic fragments that display a blocky to cuspate and platy shape, are referred to as hyaloclastite. Hyaloclastites generally occur only locally in interpillow areas although in one allochthon (Fig. 79.7, map 1) hyaloclastite occurs in bedded sequences up to 20 m thick. In the latter example, hyaloclastite occurs in 0.50-1.5 m thick massive to crudely plane bedded sheets of coarse aphyric basaltic ash that contains 5-30% spherical to elongate vesicles. Broken to amoeboid pillow fragments comprise 0-30% of these units.

Pyroclastic rocks

Lapilli tuffs, ash and uncommon tuff breccia of basaltic composition constitute about 35% of Seton Formation in most allochthons. The tuffs are characteristically heterolithic with respect to the morphology and internal texture of the fragments. Lithic fragments (5-40%) are composed of porphyritic to microlitic vesicular basalt with a granular groundmass and display an angular to rounded shape. Clasts inferred to have been vitric (20-70%) are dark green, generally aphyric (0-5% feldspar microlites) and also range from angular to rounded in shape. Clast margins range in texture from delicate re-entrant to fracture-bounded to abraded and rounded. Cored lapilli (lava coated lapilli) and bombs, and accessory lithoclasts of siltstone, jasper and granite, are locally present.

Tuffs occur mostly in bedded sequences, up to 150 m thick, and uncommonly as interbeds, less than 3 m thick, within pillow lavas. The tuffs are dominantly poorly sorted lapilli tuffs to coarse ash with subordinate interbeds of ash and tuff breccia. Beds are tabular to rarely lenticular in shape and display a massive fabric, uncommon normal and reverse graded bedding (Fig. 79.8C) and in the finer grained tuffs, parallel lamination. No cyclic variations in grain size or the relative abundance of lithic and vitric fragments was observed.

Epiclastic rocks

Epiclastic rocks are deposits of volcaniclastic sediment in which the depositional process was not the direct consequence of a volcanic eruption. These rocks are recognized by the presence of rounded or abraded clasts and the heterolithic composition of the rock, although there are many cases in which the distinction is arbitrary.

Epiclastic conglomerate and granulestone are common along the south shore of Christie Bay (Fig. 79.7) and comprise a thick (>50 m) upward fining sequence of basalt and scoria boulder paraconglomerate that abruptly overlies pillow breccia. Similar conglomerates occur in the Hornby Channel area except that, in one case, the conglomerates contain

blocks and rounded boulders of scoria, aphyric basalt, dolomite and jasper (Fig. 79.8D). Volcanic mudstone to siltstone is locally common (Fig. 79.8E). Epiclastic rocks are massive to normally graded with local parallel lamination in the arenaceous deposits. In general, epiclastic rocks contain clasts that are significantly more rounded and vesicular than underlying or overlying tuffs and basalts, suggesting derivation from a subaerial source area.

Breccias

Monolithologic breccias composed of angular clasts of aphyric to microphyric-porphyritic basalt are locally present in the Seton Formation (Fig. 79.8F). The breccias display intrusive, discordant or extrusive, concordant relationships with associated rocks (Fig. 79.7). Intrusive breccias are generally associated with irregularly shaped intrusions of

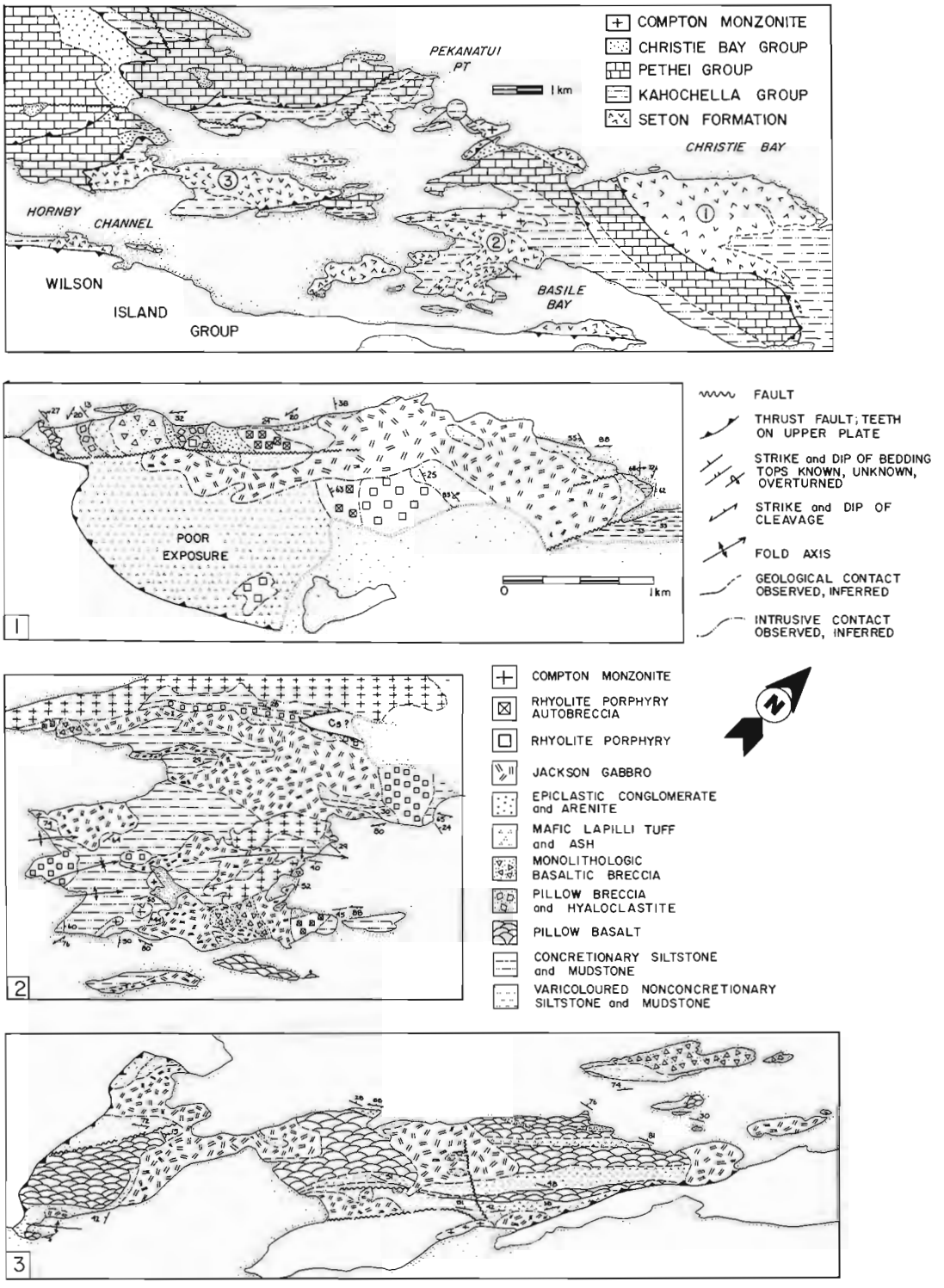

Figure 79.7. *Simplified geology for parts of selected allochthons of Seton Formation rocks in the Pekanatui Point area. Upper panel presents a 1:50 000 scale map modified from Hoffman (1977). In allochthon 2, the unit marked "Cs?" is a fenster of Stark Formation red mudstone and dolostone.*

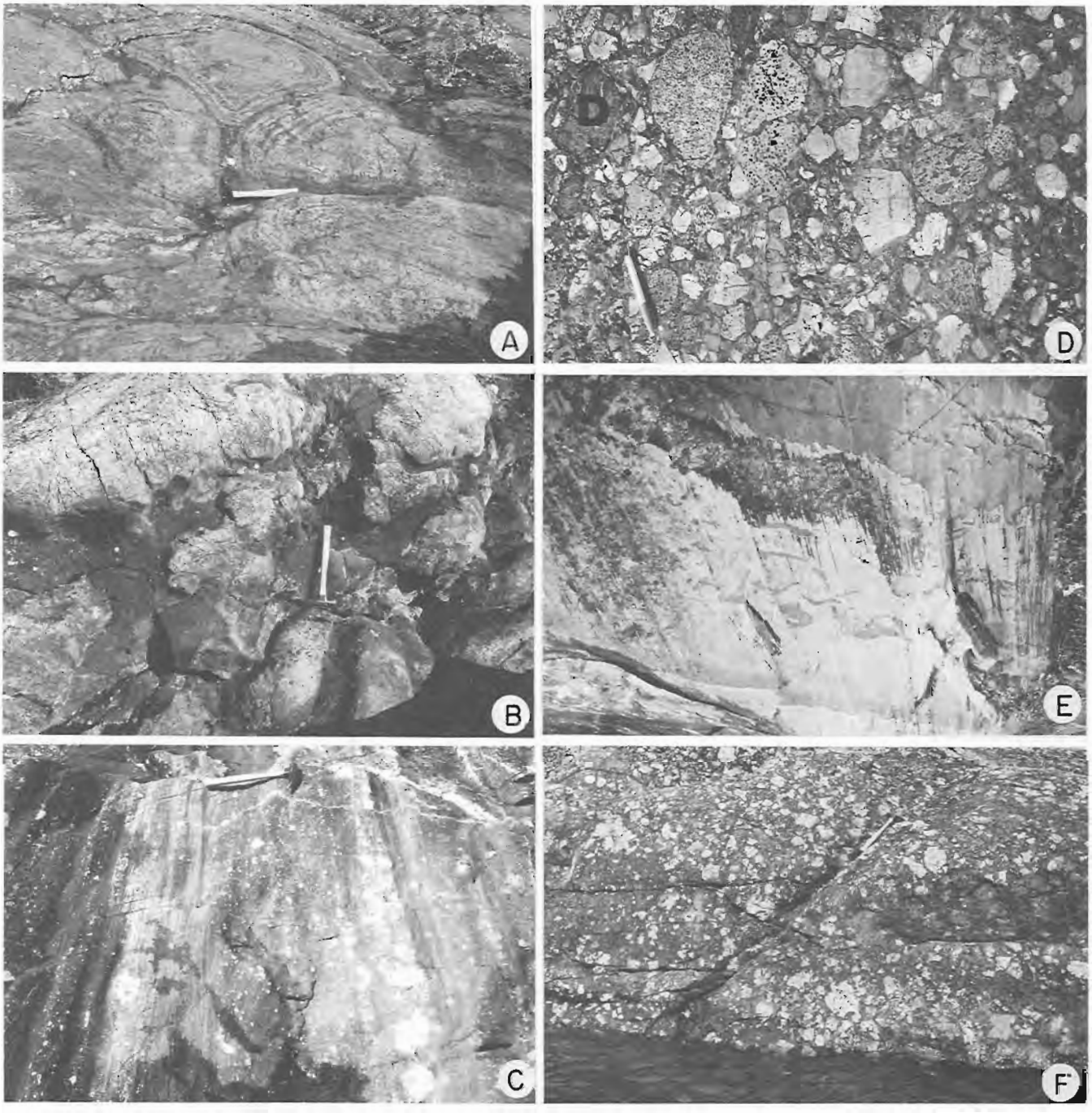

Figure 79.8

A. Pillowed basalt flows with trains of vesicles in bands concentric to pillow margins.

B. Amoeboid pillow breccia composed of amoeboid bodies of vesicular basalt (light coloured) in a matrix of hyaloclastic granules and shards.

C. Bedding in pyroclastic tuffs. Stratified lapilli tuff and coarse ash underlie and overlie a poorly sorted mass flow deposit with coarse blocks at the top of the bed. The stratified beds are suspension deposits formed by settling of tephra through the water column. Note the random distribution of lithic blocks in these tuffs.

D. Epiclastic conglomerate composed of rounded cobbles of coarse scoriaceous basalt, angular clasts of aphyric basalt and blocks of chemogenic dolomite (D) in a carbonate-replaced matrix.

E. Graded volcanic siltstone to mudstone with detached convolute balls of siltstone. Matchstick is 4 cm long.

F. Monolithologic breccia (from allochthon 1, Fig. 79.7) composed of angular blocks of non-vesicular microlitic basalt in a matrix of chloritized basalt lapilli.

massive microphyric basalt. Fragments are composed of weakly vesicular basalt, display an angular blocky shape and are dispersed in a matrix of chloritized granule to sand-sized basalt fragments. In one example (allochthon 3; Fig. 79.7), brecciated basalt porphyry has an intrusive relationship with bedded lapilli tuffs which becomes concordant (extrusive) along strike, reflecting the change from intrusive to extrusive facies of a lava dome.

In the section in allochthon 1 (Fig. 79.7), monolithologic breccia occurs as a stratabound sheet about 85 m thick. The breccia has a sharp, apparently concordant, contact with underlying lithic lapilli tuff and the upper surface of the breccia sheet is composed of a lag of rounded basalt cobbles in a granular sandy basaltic matrix. The breccia is remarkably massive and homogeneous (Fig. 79.8F) with only a rare hint of stratification. Clasts (2-60 cm) of white weathering microlitic basaltic porphyry predominate and are mostly angular in shape although a few amoeboid blocks occur. The groundmass is composed of angular-shards and granules of chloritized aphyric basalt that is locally replaced by carbonate. This unit is tentatively interpreted as a mass flow deposit related to collapse of a volcanic spine, dome or thick lava flow.

Chemogenic sediments

Minor beds (<2 m) of cherty hematitic ironstone (jasper) with nodules and discontinuous beds of sparry ferroginous dolomite and nodular pyrite locally overlie lava flows. Jasper beds display weak parallel stratification and are composed of sand to granule-sized, poorly laminated jasper peloids in a clear to white silica cement. A syngenetic origin of the jasper beds and dolomite is indicated by the occurrence of cobbles of both jasper and dolomite within pyroclastic tuffs and epiclastic conglomerates that overlie the ironstones.

Intrusive rocks

Intrusive basaltic rocks in the Pekanatui Point area comprise irregularly shaped intrusions that display a wide variety of textures and are collectively referred to as Jackson Gabbro (Hoffman, 1977). Textural varieties include gabbroic rock with an equigranular to porphyritic texture with coarse (1-3 cm) glomeritic knots of stellate plagioclase, feldspar porphyry, vesicular diabase and fine-grained basalt. Most intrusions appear to postdate volcanism but predate folding (?) and thrusting.

Rhyolite porphyry is common in allochthons 1 and 2 (Fig. 79.7). For the most part the porphyries are massive and contain 5-15% phenocrysts of quartz, alkali feldspar and biotite. Intrusions range in shape from crudely subcircular to thin (<100 m) dykes or sills with locally autobrecciated margins that crosscut mafic volcanic rocks (cf. allochthon 2). The porphyries predate thrusting and penetrative deformation of the allochthons based on the occurrence of disrupted and boudinaged sills of rhyolite at the northeast end of allochthon 1 (not distinguished in Fig. 79.7).

Discussion

Sedimentary structures within the Kahochella Group suggest depositon by dilute turbidity currents and settling of suspended mud in deep or very quiet water. Comparison of stratigraphic sequences in volcanic rocks in the Pekanatui Point area with those described from Cenozoic seamounts (Staudigel and Schminke, in press) and some Archean volcanic belts (Dimroth and Rocheleau, 1979), reveals similarities that may be used to partially reconstruct the Seton Formation volcanoes.

Pillow lavas and associated pillow breccias and hyaloclastite formed during subaqueous eruptions that probably built low-slope pillow volcanoes. Unstratified pillow breccia and hyaloclastite represent more or less in situ deposits formed by spallation and granulation of glassy basalt contemporaneous with extrusion of thin flows (i.e. amoeboid pillow breccia). Thick sequences of stratified hyaloclastite are inferred to be resedimented deposits formed by downslope movement of granulated basalt associated with flows and/or slurries of basaltic ash formed over a subaqueous vent. The high vesicle content of the pillow selvages of the basalts suggests eruptions took place at water depths of a kilometre or less although the lack of chemical data for these basalts renders such estimates ambiguous.

Heterolithic basaltic lapilli tuffs contain mixtures of pyroclasts bounded by fracture surfaces, which were generated by thermal shock and/or explosive fragmentation of rigid lava, and vesicular pyroclasts with re-entrant margins and cored bombs and lapilli formed by lava fountaining. The morphologies of the pyroclasts could have been generated by subaerial (Walker and Croasdale, 1972) or shallow subaqueous eruptions (Kokelaar and Durant, 1983). Sedimentary structures in the tuffs suggest deposition both by continuous settling of tephra through the water column and by sediment gravity flows (subaqueous pyroclastic flows?).

Epiclastic conglomerate and arenite record mass flow deposition of detritus derived from erosion of emergent volcanic edifices during periods of eruptive quiescence. The coarsely scoriaceous basalt cobbles and boulders were derived from subaerially erupted lavas and the well-rounded character of the fragments indicates subaerial or littoral zone reworking.

Unfortunately the lateral extent of most of the map units, which is critical for paleogeographic reconstruction and recognition of volcanic edifices, is unknown. It is concluded that Seton Formation volcanism constitutes the products of growth and shoaling of marine volcanic islands that culminated with the emplacement of hypabyssal basaltic and rhyolitic intrusions.

Structural geology

Each allochthon in the Pekanatui Point area is characterized by a distinct structural style. Cleavage development is of weak to moderate intensity and consists of a spaced, weakly anastamosing fabric that appears to be the result of pressure solution and/or crenulation of bedding. In allochthons where fold closures and cleavage are both present, the cleavage is axial planar. In the simplest case (allochthon 3; Fig. 79.7) a weak high angle cleavage is consistently steeper than the homoclinal northwest-dipping bedding indicating that the allochthon comprises the limb of an upright, open anticlinal fold. In allochthon 2 (Fig. 79.7) bedding-cleavage relationships, intersection lineations and minor folds delineate a series of moderately plunging (50°-60° NE) tight, reclined folds with steep axial planes. In allochthon 1 (Fig. 79.7) the upright limb of a recumbent anticline (nappe) is inferred from shoreline outcrops on the basis of southeast-dipping low-angle (10°-30°) cleavage that is slightly steeper than bedding. At the northeast end of this allochthon bedding is steep to overturned and boundinage and disruption of bedding is common, possibly indicating that this region is the overturned limb of the anticline.

The relationship between the internal deformation present in the allochthons and northward thrusting is unknown. The variation in structural style may simply represent different levels of a heterogeneously strained sequence of nappes (cf. Helvetic nappes; Ramsay and Huber, 1983, p. 205) or it may indicate thrust dismemberment of an already deformed sequence.

Conclusions

The Seton Formation is a diverse assemblage of bimodal volcanic rocks and intrusions formed during Calderian orogeny of Wopmay Orogen. Allochthons in the Pekanatui

Point region comprise axial zone volcanic rocks of dominantly basaltic composition formed during growth and shoaling of submarine volcanic islands. The significance of the variable fold style and intensity of cleavage development in the allochthons is incompletely understood at present.

In the Seton Island area mafic and felsic volcanic rocks are interbedded with fluvial and deltaic siliciclastic rocks. Volcanism resulted in construction of local tuff cones, deposition of mafic tuff and ash-flow tuff and formation of basaltic shield volcanoes. The structural character of the Seton Island area reflects the proximity of a major transcurrent fault system which caused en echelon folding and locally intense flattening of rocks.

Seton Formation represents intracontinental volcanism that began when Athapuscow Aulacogen was transformed into a foredeep during Calderian Orogeny. Seton volcanism is broadly correlative with the tholeiitic gabbroic rocks (Morel sills) in the foredeep and molasse of Wopmay Orogen (Hoffman, 1980; Hoffman et al., 1984). The composition of these rocks, their stratigraphic position and their location on the lower plate during Calderian Orogeny argues against derivation of these magmas above a subduction zone. Rather it is suggested that these rocks represent mafic melts emplaced in continental crust as a consequence of lithosphere fracture and/or reactivation of basement faults during oblique plate convergence.

Acknowledgments

We would like to thank Paul Hoffman, John McGlynn, and Simon Hanmer (Geological Survey of Canada) for procuring air photos and field equipment. Bill Padgham and the Geology Office of Department of Indian Affairs and Northern Development (Yellowknife) provided logistic support and kept us fueled and fed. Visits in the field by C.E. Chapin, G.R. Osburn (New Mexico Bureau of Mines) and S. Hanmer were particularly helpful as was critical review and discussion of the manuscript by Sam Bowring, Bob Hildebrand, and Paul Hoffman.

References

Bowring, S.A. and Van Schmus, W.R.
1984: U-Pb zircon constraints on evolution of Wopmay Orogen, Northwest Territories; Geological Association of Canada, Program with Abstracts, v. 9, p. 47.

Bowring, S.A., Van Schmus, W.R., and Hoffman, P.F.
– U-Pb zircon ages from Athapuscow Aulacogen, East Arm of Great Slave Lake, Northwest Territories, Canada; Canadian Journal of Earth Sciences. (in press)

Dimroth, E. and Rocheleau, M.
1979: Volcanology and sedimentology of Rouyn-Noranda area, Quebec; Geological Association of Canada, Field Trip Guide A-1, 193 p.

Fiske, R.S.
1963: Subaqueous pyroclastic flows in the Ohanepecosh Formation, Washington; Geological Society of America Bulletin, v. 74, p. 391-406.

Hoffman, P.F.
1968: Stratigraphy of the Lower Proterozoic (Aphebian), Great Slave Supergroup, East Arm of Great Slave Lake, District of Mackenzie; Geological Survey of Canada, Paper 68-42, 93 p.

1969: Proterozoic paleocurrents and depositional history of the East Arm fold belt, Great Slave Lake, Northwest Territories; Canadian Journal of Earth Sciences, v. 6, p. 441-462.

Hoffman, P.F. (cont.)
1973a: Evolution of an early Proterozoic continental margin: The Coronation geosyncline and associated aulacogens of the Northwestern Canadian Shield; Philosophical Transactions of the Royal Society of London, Series A, v. 273, p. 547-581.

1977: Geology of the East Arm of Great Slave Lake, District of Mackenzie; Geological Survey of Canada, Open File 475 (1:50 000 scale).

1980: Wopmay Orogen: A Wilson cycle of early Proterozoic age in the northwest of the Canadian Shield; in The Continental Crust and Its Mineral Deposits, ed. D.W. Strangway; Geological Association of Canada, Special Paper 20, p. 523-552.

1981: Autopsy of Athapuscow Aulacogen: A failed arm affected by three collisions; in Proterozoic Basins of Canada, ed. F.H.A. Campbell; Geological Survey of Canada, Paper 81-10, p. 97-102.

Hoffman, P.F., Bell, I.R., Hildebrand, R.S., and Thorstad, L.
1977: Geology of Athapuscow Aulacogen, East Arm of Great Slave Lake, District of Mackenzie; in Report of Activities, Part A, Geological Survey of Canada, Paper 77-1A, p. 117-129.

Hoffman, P.F., Dewey, J.F., and Burke, K.
1974: Aulacogens and their genetic relation to geosynclines with a Proterozoic example from Great Slave Lake, Canada; in Modern and Ancient Geosynclinal Sedimentation, ed. R.H. Dott, Jr. and R.H. Shaver; Society of Economic Paleontologists and Mineralogists, Special Publication 18, p. 38-55.

Hoffman, P.F., Tirrul, R., Grotzinger, J.P., Lucas, S.B., and Eriksson, K.A.
1984: The Externides of Wopmay Orogen, Takijug Lake and Kikerk Lake map areas, District of Mackenzie; in Current Research, Part A, Geological Survey of Canada, Paper 84-1A, p. 383-395.

Kokelaar, B.P. and Durant, G.P.
1983: The submarine eruption and erosion of Surtla (Surtsey), Iceland; Journal of Volcanology and Geothermal Research, v. 17, p. 238-246.

Olade, M.A.D.
1975: Trace-element and isotopic data and their bearing on the genesis of Precambrian spilites from the Athapuscow Aulacogen, Great Slave Lake, Canada; Geological Magazine, v. 3, p. 283-293.

Ramsay, J.G. and Huber, M.I.
1983: The Techniques of Modern Structural Geology: Volume 1: Strain Analysis; Academic Press, Inc., New York, 307 p.

Sparks, R.S.J. and Wright, J.V.
1979: Welded air-fall tuffs; in Ash-flow Tuffs, ed. C.E. Chapin and W.E. Elston; Geological Society of America, Special Paper 180, p. 155-166.

Staudigel, H. and Schminke, H.-U.
– The Pliocene seamount series of La Palma/Canary Islands; Journal of Geophysical Research. (in press)

Walker, G.P.L. and Croasdale, R.
1972: Characteristics of some basaltic pyroclastics; Bulletin Volcanologique, v. 35, p. 303-317.

Wilcox, R.E., Harding, T.P., and Seely, R.
1973: Basic wrench tectonics; American Association of Petroleum Geologists, v. 57, p. 74-96.

SCIENTIFIC AND TECHNICAL NOTES
NOTES SCIENTIFIQUES ET TECHNIQUES

STRATIGRAPHY OF THE UPPER PART OF THE RAE GROUP, JOHANSEN BAY AREA, NORTHERN CORONATION GULF AREA, DISTRICT OF FRANKLIN

Project 770012

F.H.A. Campbell
Precambrian Geology Division

Campbell, F.H.A., Stratigraphy of the upper part of the Rae Group, Johansen Bay area, northern Coronation Gulf area; in Current Research, Part A, Geological Survey of Canada, Paper 85-1A, p. 693-696, 1985.

Abstract

The Hadrynian Rae Group of the Johansen Bay area consists of a succession of buff-cream and white trough and planar crossbedded quartzites and quartz sandstones, which conformably overlie shallow water, locally stromatolitic, dolomite. The dolomite is ubiquitously intruded by diabase sills and dykes of varying thickness, whereas the overlying quartzite is cut only by rare dykes.

The quartzite is uncomformably overlain by either terrigeneous clastics of Cambrian(?) age or basal quartzose carbonates of Ordovician-Silurian age. The unconformity surface on top of the quartzite is marked by a series of locally steep-sided or broad paleovalleys with relief locally up to 10 m vertically and up to 50 m over a distance of 0.5 km. The Cambrian(?) clastics, which occur only locally in the paleovalleys, are unconformably overlain by Ordovician-Silurian carbonates. This relationship suggests that there was a post-Cambrian(?) period of uplift and erosion prior to deposition of the overlying carbonates.

Résumé

Le groupe hadrynien de Rae, dans la région de la baie Johansen, est constitué d'une succession de quartzites et de grès quartziques de couleurs chamois et crème qui présentent des stratifications croisées courbes et planes. Ces roches reposent en concordance sur de la dolomite d'eau peu profonde, stromatolitique par endroits. Dans la dolomite, des filons-couches et des dykes de diabase d'épaisseur variable sont omnipésents, alors que la quartzite susjacente n'est traversée que par de rares dykes.

Sur la quartzite reposent en discordance soit des roches clastiques terrigènes du Cambrien(?), soit des carbonates quartzeux basals qui datent de l'Ordovicien/Silurien. La surface de discordance au sommet de la quartzite est marquée par une série de paléovallées qui ont par endroits des versants raides ou une grande largeur et dont le relief atteint 10 m localement et 50 m sur une distance de 0,5 km. Les roches clastiques du Cambrien(?), qui ne se rencontrent que par endroits dans les paléovallées, sont surmontées en discordance par des carbonates ordoviciens-siluriens. Ces relations font penser qu'il y a eu une période post-cambrienne(?) de soulèvement et d'érosion avant le dépôt des carbonates susjacents.

Introduction

The Rae Group, initially defined by Baragar and Donaldson (1973) and redefined by Campbell (1983), outcrops throughout the Coronation Gulf area (Fig. 1). Campbell (1983) confirmed the suggestions of earlier workers (Young, 1974, 1977; Young and Jefferson, 1975; Campbell, 1979; Dixon, 1979) that the Rae Group in the type area of the Rae River is lithostratigraphically correlative with the succession in the Johansen Bay area (as originally mapped by Thorsteinsson and Tozer, 1962), across the Duke of York Archipelago.

A brief examination of exposures in the Johansen Bay area was conducted to determine the stratigraphic relationships within the upper part of the Rae Group and to determine the contact relationships between the group and overlying Phanerozoic sediments. As the lowermost Phanerozoic units are commonly quartz sandstones and closely resemble the quartz sandstones of the Rae, the sole means of distinguishing between the two sandstones is the presence or absence of (a) diabase dykes or sills and (b) fossils. During this phase of this study, only the quartzites of the uppermost Rae Group were examined, in particular their relationships with diabase dykes and the overlying Phanerozoic sediments. No mineralization of economic significance was noted.

Rae Group

North of Johansen Bay, the only part of the Rae Group exposed consists of grey-weathering, buff, cream or white, medium- to coarse-grained quartzites. They are locally extremely friable, nearly flat lying, and unmetamorphosed. Trough crossbeds (1-3 m) are locally well-developed, but planar crossbeds of various scales (0.25-2 m) are more common. Pebbles of white quartz (to 1 cm) are locally abundant throughout the sequence, but no other pebble types were observed. The quartzites extend from the northern part of the Richardson Islands, off Johansen Bay, east, west and north to the contact with the overlying Phanerozoic rocks.

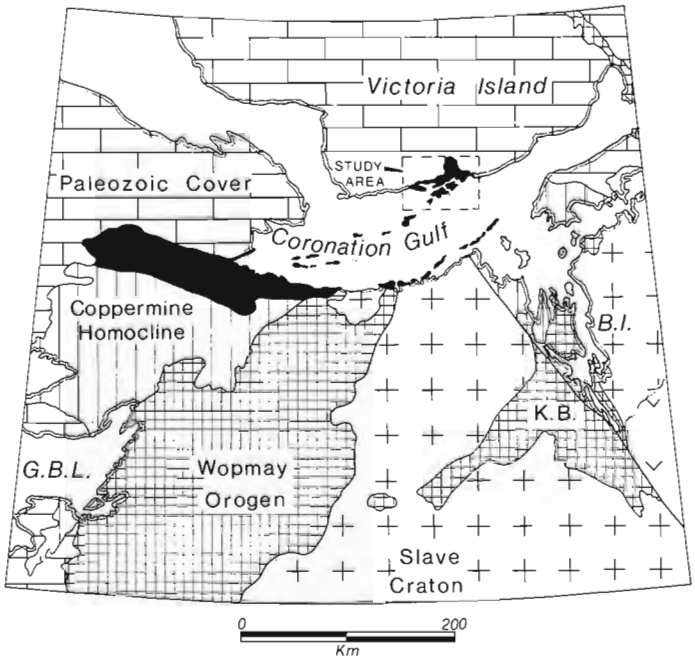

Figure 1. *Distribution of the Rae Group sediments (black) in the northwestern part of the Canadian Shield. The abbreviations are as follows: B.I. for Bathurst Inlet; G.B.L. for Great Bear Lake and K.B. for Kilohigok Basin, which contains the Goulburn Group. The Coppermine Homocline contains the Hornby Bay, Dismal Lakes and Coppermine River groups; the equivalent Ellice, Parry Bay, Kanuyak, Ekalulia and Algik formations occur around the northeast of Bathurst Inlet. Figure 3 shows the stratigraphic relationships between many of these various units and the Rae Group. The area outlined is that shown in Figure 2.*

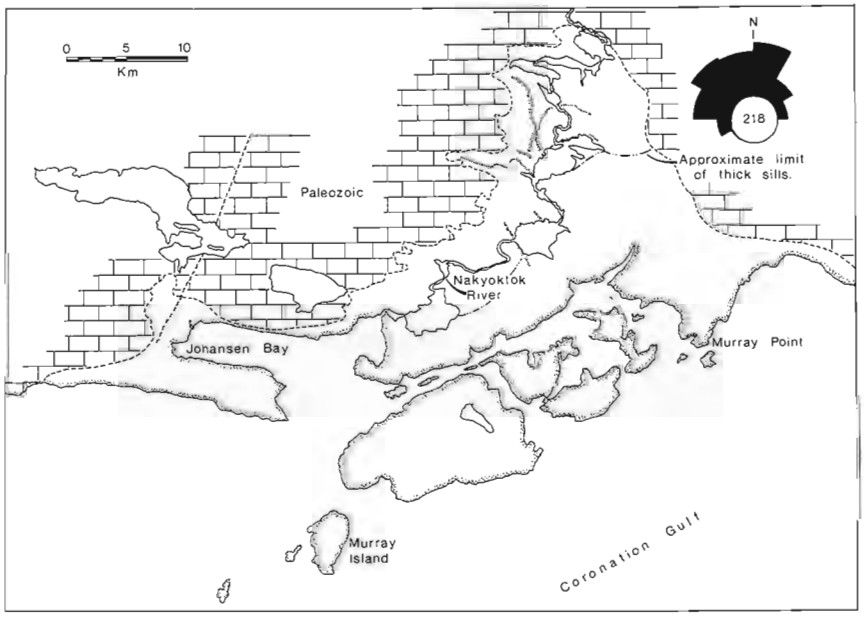

Figure 2

Generalized geological map of the Johansen Bay area, southern shore of Victoria Island. The Rae Group, and its contained diabase sills, are unpatterned. Diabase dykes are shown by the short hachured lines. The rose diagram shows the distribution of trough and planar crossbeds from the quartzites of the area. The number of measurements is as shown and the diameter of the centre circle is 20%.

The only notable feature within this quartzite succession is an apparently continuous unit which contains small disseminated pyrite nodules or concretions up to 3 cm in diameter, but typically 2-5 mm. On weathering, these impart a limonitic stain to the outcrop area and appear to be large gossans from a distance.

Trough and planar crossbeds in the quartzites show a near-unimodal paleocurrent distribution to the northwest-southeast (Fig. 2), consistent with the earlier interpreted east-northeast depositional strike of the basin (Campbell, 1983).

Contact relationships

On Murray Island (Fig. 2), Campbell (1983) noted that locally quartzites of the uppermost Rae Group conformably overlie stromatolitic dolomite of the Rae Group, and both are intruded by diabase sills. To the west of this area, the contact with Paleozoic sediments is not exposed, and thus the age of the upper part of the succession remained uncertain.

Near the west end of Johansen Bay, contact relationships between the quartzites and Paleozoic sediments are well exposed over a series of outcrops in a river gorge and also inland to the west. The upper surface of the Rae Group quartzites is broadly undulating, locally with paleovalleys up to 20 m deep. The unconformity surface, particularly in the valleys, is knobby, fractured and deeply weathered. Fractures and joints, up to 30 cm wide and 2-3 m deep, are filled with carbonate-cemented quartzose detritus. The immediately overlying sediments are typically quartzose carbonates, with rare red sandstone beds to 5 cm. These "valley fills", as well as the remainder of the Rae Group basement in the area, are capped by the ubiquitous thin-bedded, buff-weathering grey limestone (Ordovician).

At the west end of the Johansen Bay, an orange stromatolitic dolomite, interpreted by Campbell (1983) to be correlative with an identical unit of Cambrian(?) age north of the Rae River, is approximately 4 km south of and 80 m topographically below the Cambrian-Precambrian contact. This suggests that the Cambrian(?) terrigeneous clastics and shallow marine carbonates accumulated in paleo-valleys between hills of Rae Group quartzite and were eroded before deposition of the Ordovician carbonates.

North of Nakyotok River (Fig. 2), as elsewhere in the region, the erosion surface at the top of the Rae quartzite defines a series of undulating hills and valleys. In this area, the relief from the top of the "hills" to the "valley" floors is up to 50 m, over a distance of 0.5-1 km. In most cases, the Paleozoic sediments in the "valleys" are carbonate-cemented quartzose sands, or quartzose carbonates. In some cases, however, there are valley-fills which consist of rippled, thin-bedded grey-green siltstones, fine grained sandstones, and rare thick-bedded buff quartzites (2 m). In all cases, these sequences are overlain by monotonous, buff-weathering, grey, thin-bedded carbonates, which typically cap the "hills" of Rae Group quartzites. There was no evidence of a distinct unconformity or regolith between the Paleozoic carbonates and the "valley-fill" siliciclastics in the Nakyotok River area. However, the "pinch-out" of the clastics on the flanks of the Rae Group paleohills, together with the uniform "blanketing" by the Paleozoic carbonates suggests that the valley-fills may be Cambrian(?) in age and not removed by erosion.

These data, together with the uniformity of the Rae quartzite throughout its exposed thickness, strongly suggest that the Cambrian-Precambrian boundary is above and not within the sediments locally identified as possible Rae Group, as suggested by Campbell (1983).

Diabase dykes

Although diabase dykes and sills are ubiquitous throughout most of the Rae Group, they are rare in the Rae quartzite of the Johansen Bay area. However, the relationship is not unequivocal. In the Nakyoktak River area (Fig. 2), the quartzite is in close (10 m) proximity to a 30 m thick, west-dipping (65°) diabase dyke. Together, the two stand some 60 m above the surrounding terrain. To the northwest, the quartzite topographically overlies the projected continuation of the dyke. The quartzite at all locations appears undeformed but contains no dyke-derived detritus. Thus, although the two were nowhere observed in direct contact, it may be reasonably assumed that the dyke intrudes the Rae Group quartzite.

At the west end of Johansen Bay, a narrow (20 m) dyke apparently intrudes the Rae Group, but the two were not observed in direct contact. Within 10 m of the dyke, however, the quartzite is flat lying, apparently undisturbed, and contains no diabase-derived detritus.

Summary

Following a period of terrigenous sedimentation and stabilization of the carbonate-dominated Rae Group platform, uplift in the source area(s) to the east supplied predominantly quartzose detritus to the basin. These relatively coarse clastics spread across the basin and buried the shallow marine carbonates beneath a veneer of quartz sands.

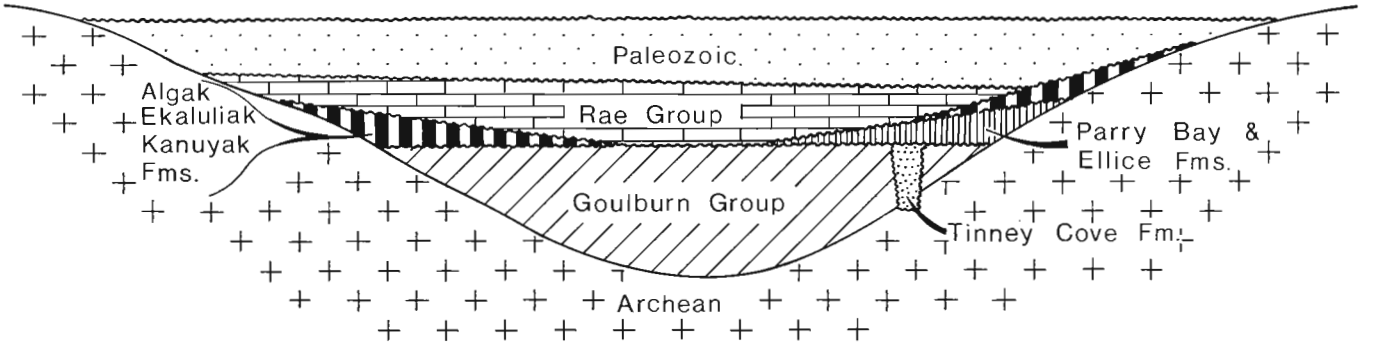

Figure 3. *Diagrammatic sketch of the contact relationships between the Rae Group and the various pre-Rae units in the Bathurst Inlet-Coronation Gulf-Victoria Island area. Depending on location, the Rae Group rests unconformably on all the older units in the region, with the exception of the Tinney Cove Formation. Not to scale.*

As the Rae Group rests unconformably on all older rocks throughout the Coronation Gulf area, the source for these quartzose clastics could have been any of the older successions (Fig. 3). However, the relative purity of the quartz sands, together with the quartz pebbles as the sole large clasts, strongly suggests that the Rae quartzites were derived from an earlier quartz-sand dominated source. As the Archean basement was probably blanketed by sediments of the lower part of the Rae Group, as on the south shore of Coronation Gulf, the source for the upper quartzites probably lay to the east and/or north of the basin. Quartzose sediments in both areas include the Algak and Ellice formations, the quartz sandstones of the Goulburn Group, and the sandstones of unknown age in the Hadley Bay area of northern Victoria Island (Campbell, 1979, 1981; Campbell and Cecile, 1981). While none of these units can be unequivocally identified as the source of the upper Rae Group quartzites, they or their equivalents could have provided the detritus to the basin (Fig. 3).

Acknowledgments

This project was supported through the facilities of the Polar Continental Shelf Project, whose continued assistance is gratefully acknowledged. W.A. Gibbins (Department of Indian and Northern Affairs, Yellowknife) assisted the author throughout the investigation of the Rae Group.

References

Baragar, W.R.A. and Donaldson, J.A.
1973: Coppermine and Dismal Lakes map area; Geological Survey of Canada, Paper 71-39.

Campbell, F.H.A.
1979: Stratigraphy and sedimentation in the Helikian Elu Basin and Hiukitak Platform, Bathurst Inlet-Melville Sound, Northwest Territories; Geological Survey of Canada, Paper 79-8, 18 p.

Campbell, F.H.A. (cont.)
1981: Stratigraphy and tectono-depositional relationships of the Proterozoic rocks of the Hadley Bay area, northern Victoria Island, District of Franklin; in Current Research, Part A, Geological Survey of Canada, Paper 81-1A.

1983: Stratigraphy of the Rae Group, Coronation Gulf area, Districts of Mackenzie and Franklin; in Current Research, Part A, Geological Survey of Canada, Paper 83-1A.

Campbell, F.H.A. and Cecile, M.P.
1981: Evolution of the early Proterozoic Kilohigok Basin, Bathurst Inlet-Victoria Island, Northwest Territories; in Proterozoic Basins of Canada, ed. F.H.A. Campbell; Geological Survey of Canada, Paper 81-10, p. 103-131.

Dixon, J.
1979: Comments on the Proterozoic stratigraphy of Victoria Island and the Coppermine area, Northwest Territories; in Current Research, Part B, Geological Survey of Canada, Paper 79-1B.

Thorsteinsson, R. and Tozer, E.T.
1962: Banks, Victoria and Stefansson Islands, Arctic Archipelago; Geological Survey of Canada, Memoir 330, 83 p.

Young, G.M.
1974: Stratigraphy, paleocurrents and stromatolites of the Hadrynian (Upper Precambrian) rocks of Victoria Island, Arctic Archipelago; Precambrian Research, v. 1, p. 13-41.

1977: Stratigraphic correlation of upper Precambrian rocks of northwestern Canada; Canadian Journal of Earth Sciences, v. 14, p. 1771-1787.

Young, G.M. and Jefferson, C.W.
1975: Late Precambrian shallow water deposits, Banks and Victoria Islands, Arctic Archipelago; Canadian Journal of Earth Sciences, v. 12, p. 1734-1748.

TRIAXIAL SHEAR STRENGTH TESTING FACILITY FOR THE WESTERN ARCTIC

Project 700092

K. Moran and H. Christian[1]
Atlantic Geoscience Centre, Dartmouth

Moran, K. and Christian, H., Triaxial shear strength testing facility for the Western Arctic; in Current Research, Part A, Geological Survey of Canada, Paper 85-1A, p. 697-698, 1985.

Abstract

The geotechnical testing facility at the Inuvik Scientific Resource Centre has been expanded to include triaxial testing. Through cooperation among the Department of Indian and Northern Affairs, the Department of Energy, Mines and Resources, and Gulf Canada Resources Incorporated, the testing equipment was added to the existing laboratory. Triaxial shear strength tests can now be performed on all sensitive Beaufort Sea sediments with a minimum of transportation of the material, thus significantly reducing sample disturbance and improving test quality. Soft surficial sediments collected from the upper continental slope of the Beaufort Sea are currently being tested.

Résumé

L'installation pour les essais géotechniques au Centre des ressources scientifiques d'Inuvik a été agrandie afin de pouvoir y effectuer des essais triaxaux. L'équipement requis a été fourni au laboratoire existant grâce à la collaboration du ministère des Affaires indiennes et du Nord canadien, du ministère de l'Energie, des Mines et des Ressources et de Gulf Canada Ressources Incorporée. Il est maintenant possible d'y effectuer des essais triaxiaux sur tous les sédiments sensibles prélevés de la mer de Beaufort ce qui permet de réduire le temps de transport du matériau et donc de réduire de façon marquée son remaniement et d'améliorer ainsi la qualité de l'essai. Le Centre géoscientifique de l'Atlantique y effectue présentement des essais sur les sédiments superficiels mous prélevés de la partie supérieure du talus continental de la mer de Beaufort.

Introduction

During 1983 and 1984, the Department of Indian and Northern Affairs (INA) and the Geological Survey of Canada (GSC) cooperated in the upgrade of the Soil Mechanics Laboratory at the Inuvik Scientific Resource Centre (ISRC). Prior to upgrading, facilities were limited to classification testing (e.g. Atterberg limits, moisture content) and grain size analysis. The facility now has the capability of testing soil samples for triaxial compression with pore pressure measurement under microcomputer control. Consequently, Mohr-Coulomb shear strength parameters can be determined. In addition to triaxial compression tests, permeability tests may be performed with the same system. The facilities now provide an ability to determine seabed strength properties and the assessment of the interrelationships between these properties and the geological history of the sediments.

Equipment

The triaxial testing apparatus purchased by INA consists of an ELE 50 kN Tritest load frame, a Brainard – Kilman (BK) triaxial cell, and a BK triaxial and permeability panel. This system is capable of testing samples up to 63.5 mm in diameter. The system is presently configured for testing 35.6 mm (1.4") diameter samples and 50.8 mm (2.0") diameter samples. The ISRC maintains an air compressor and vacuum pump which supply maximum pressures of 690 kPa and 207 kPa (vacuum) respectively.

The sensing devices which are used with the triaxial system during backpressure, consolidation, and shear are: Hewlett-Packard DCDT (25.4 mm) for the measurement of axial strain; Dynisco absolute pressure transducers (0-1380 kPa) for cell pressure and pore pressure measurement; and a Sensotec (12.7 mm) LVDT coupled to a proving ring for the measurement of load. Each of these devices is connected to a Mountain Inc. 8 bit analog to digital board on an Apple IIe. The software program which controls the triaxial shear portion of the test is based upon strain as measured with the DCDT. The Applesoft program monitors the strain and samples the rest of the channels (load, pore pressure, and cell pressure) at every 0.2% strain. The program calculates, prints, and stores axial strain, major principal stress, minor principal stress, pore pressure, major to minor stress ratio (Holtz and Kovacs, 1981), and A factor (Skempton, 1954). Four additional channels are available for other measurements (e.g. lateral strain).

In addition to the apparatus mentioned above, Gulf Canada Resources Inc. have loaned their triaxial equipment to the laboratory. The equipment consists of two additional triaxial cells, a cell and back pressure application board, four absolute pressure transducers for monitoring cell and pore pressures, and a 4.5 kN load cell. This additional equipment has been set up and tested at ISRC and adds flexibility and efficiency to the triaxial facility. With the additional cells, three samples may be tested at one time. Consequently, at the same time, one sample may be backpressured, one sample consolidated, and one sample tested in axial compression.

To complete the triaxial facility, the Geological Survey purchased a Nold deairator which has been integrated to both Gulf Canada's pressure board and the B-K panel. At present the deairator is connected to a salt water supply for the testing of marine sediments. However, for the use of the system for testing freshwater samples, a distilled water source is available.

[1] Faculty of Civil Engineering University of Alberta, Edmonton, Alberta

Summary

The triaxial testing facility has been fully calibrated and tested and is presently operational. The Atlantic Geoscience Centre's Beaufort Sea group is using the facility to test soft surficial sediment samples from the Beaufort Sea as input to the stability analysis of the upper continental slope. Due to the sensitive nature of these sediments, the Inuvik facility is ideal as it allows for the testing of the relatively undisturbed samples with a minimum of handling. Thus, samples may be tested under conditions where no transportation disturbance has occurred.

Future plans for the facility include shear and compressional wave velocity measurements of the sediment samples under a consolidation pressure prior to shear, anisotropic consolidation, and temperature control.

Acknowledgments

The Inuvik Scientific Resource Centre's Scientist-in-charge, Dave Sherstone and manager, John Ostrick have been particularly supportive to the Beaufort Sea project. The space made available for our use and the equipment which is key to the triaxial facility were supplied through Dave Sherstone and John Ostrick. Gulf Canada Resource, Inc. through Mike Jefferies loaned additional triaxial equipment and we are most appreciative of this support as well as the enthusiasm which Gulf personnel have given to our project. The Panel on Energy Research and Development (PERD), Task 6 Conventional Energy Systems supported this project as part of its program to investigate seabed stability problems in the Beaufort Sea.

References

Holtz, Robert D. and Kovacs, William, D.
1981: An Introduction to Geotechnical Engineering; Prentice-Hall, Inc., Englewood Cliffs, New Jersey, 733 p.

Skempton, A.W.
1954: "The Pore-Pressure Coefficients A and B", Geotechnique, v. IV, p. 143-147.

DISTINCTION OF EOCAMBRIAN AND LOWER CAMBRIAN REDBEDS, SAINT JOHN AREA, SOUTHERN NEW BRUNSWICK

Project 730044

S.K. Tanoli[1], R.K. Pickerill[1], and K.L. Currie
Precambrian Geology Division

Tanoli, S.K., Pickerill, R.K., and Currie, K.L., Distinction of Eocambrian and Lower Cambrian redbeds, Saint John area, southern New Brunswick; in Current Research, Part A, Geological Survey of Canada, Paper 85-1A, p. 699-702, 1985.

Abstract

Redbed sequences associated with the upper part of the Hadrynian Coldbrook Group have historically been confused with redbeds in the overlying Lower Cambrian Ratcliffe Brook Formation of the Saint John Group. The redbed sequences have previously all been included within the Ratcliffe Brook Formation. The Eocambrian sequences can be distinguished by (i) deformed oriented clasts in conglomerate, (ii) feldspathic matrix to sandstone and conglomerates, (iii) generally coarse grain size, immaturity, and massive character, (iv) paucity of detrital muscovite (v) intensely red to purple colour, and (vi) consistent association with volcanic rocks. The Eocambrian sequence appears to disconformably underlie the Ratcliffe Brook Formation.

Résumé

Les séquences de couches rouges que l'on associe à la partie supérieure du groupe hadrynien de Coldbrook ont été confondues jusqu'ici avec les couches rouges de la formation susjacente de Ratcliffe Brook (groupe de Saint John), du Cambrien inférieur. Toutes les séquences de couches rouges étaient auparavant incluses dans cette formation. Les séquences éocambriennes peuvent se reconnaitre à i) la présence d'intraclastes orientés et déformés dans le conglomérat, ii) la matrice feldspathique des grès et conglomérats, iii) un grain généralement grossier, un manque de maturité et un caractère massif, iv) une pauvreté en muscovite détritique, v) une couleur variant de rouche vif au pourpre, et vi) une association systématique avec des roches volcaniques. La séquence éocambrienne semble reposer en discordance sous la formation de Ratcliffe Brook.

Introduction

The Late Precambrian (Hadrynian) volcanic, sedimentary and hypabyssal rocks of the Coldbrook Group of southern New Brunswick have been subdivided by Giles and Ruitenberg (1977) into three northeasterly-trending belts, each characterized by specific rock assemblages. The Saint John region lies within the Central Volcanic Belt of Giles and Ruitenberg (1977), which is characterized by ca. 10 000 m of basaltic, andesitic and rhyolitic flows, felsic tuffs and minor intercalated volcanogenic sediments. In this region the Cambro-Ordovician Saint John Group unconformably or disconformably overlies the Coldbrook Group (Hayes and Howell 1937; Alcock 1938). Stratigraphic relations between the two units can be observed only in Hanford Brook (Fig. 1C). Elsewhere lack of continuous outcrop, complex structural relations, and/or difficulties in stratigraphic correlation make direct observation and interpretation of the relations difficult, controversial and ambiguous. On the basis of observations in Hanford Brook, and the evidence presented in this note, we believe the contact to be a disconformity rather than an unconformity.

The basic stratigraphy of the Saint John region was established by Hayes and Howell (1937) and Alcock (1938), with some slight modifications by Ruitenberg et al. (1975). However recent mapping by Currie et al. (1981), Currie and Nance (1983) and Currie (1984) has considerably revised some of the stratigraphy on the basis of new exposures. In particular, Currie (1984) recognized a redbed sequence (his unnamed map unit H_{ce}) which on all previous maps had been included within the basal Cambrian redbed sequence of the Ratcliffe Brook Formation of the Saint John Group. Currie (1984) pointed out that despite the similarities between the two sequences, there were obvious contrasts which previous workers (Hayes and Howell 1937; Alcock 1938; Yoon 1970, Ruitenberg et al., 1975; O'Brien, 1976; McCutcheon, 1981) had failed to distinguish. He pointed out that the redbeds of his unit H_{ce} appeared conformable with, and formed the top of, the Coldbrook Group whereas the redbeds of the Ratcliffe Brook Formation lay unconformably or disconformably above this group. The former redbeds he referred to as Eocambrian to clarify that the sequence was intermediate in age between the Hadrynian Coldbrook Group and the Lower Cambrian Ratcliffe Brook Formation. We adopt this terminology.

In this note we document two locations where the distinction between the two redbed sequences can easily be observed in readily accessible outcrop, list the criteria used to make the distinction, and note three additional areas where redbed sequences have historically, and probably erroneously, been referred to the Ratcliffe Brook Formation.

Locations

The detailed locations referred to in this note are shown in Figure 1, which also illustrates the simplified geology at each location. These locations are:

i) the area between Goodrich Street and Paradise Row in the eastern part of the city of Saint John (Fig. 1A, NTS sheet 21 G/8, long. 66° 03'-66°05'W, lat. 45°16'-45°17'N). At this location both the Eocambrian sequence and the Ratcliffe Brook Formation are exposed together with overlying and underlying strata.

ii) the Mystery Lake area in the eastern suburbs of Saint John (Fig. 1B, NTS sheet 21 H/5, long. 65°59'-66°00'W, lat. 45°18'-45°20'N). At this location both units are well exposed.

[1] Department of Geology, University of New Brunswick, Fredericton, N.B. E3B 5A3

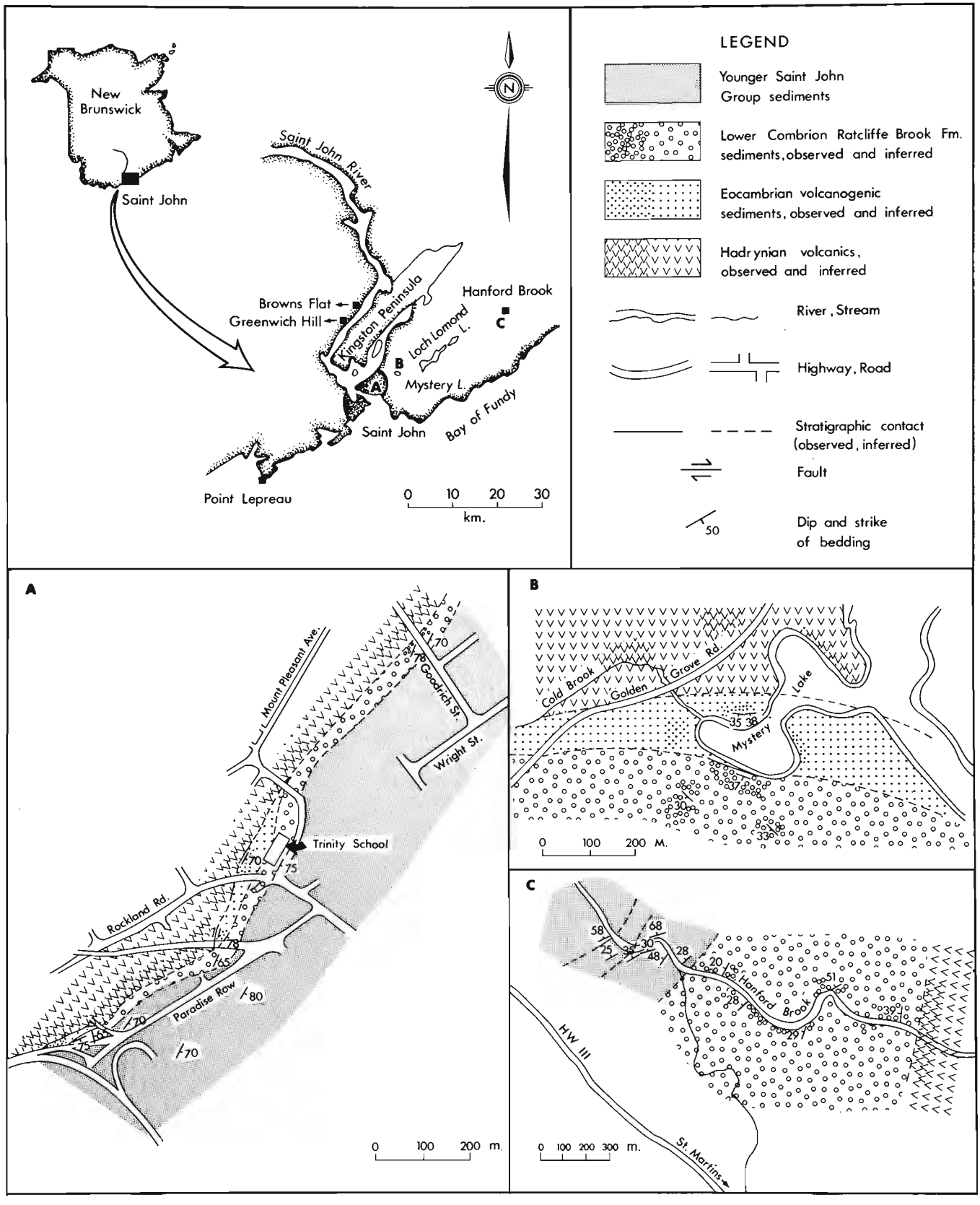

Figure 1. *Location and simplified geological maps.*

iii) Hanford Brook, ca. 45 km northeast of Saint John (Fig. 1C, NTS sheet 21 H5, long. 65°36'-65°37'W, lat. 45°27'-45°28'N). This location exposes the thickest and most continuous known section of Ratcliffe Brook Formation (see Hayes and Howell, 1937).

Discussion

The confusion surrounding the distinction of the Eocambrian sequence and the Ratcliffe Brook Formation apparently stems from three factors.

i) Both are maroon, purple, purple-red or greenish-grey in colour.

ii) Both consist of interbedded conglomerates, sandstones and shales which exhibit similar sedimentary structures.

iii) Both include volcanogenic debris.

The confusion engendered by these similarities is of long standing. For the past fifty years all the redbeds have been lumped in the Ratcliffe Brook, but older workers included all sediments now recognized as belonging to the Ratcliffe Brook within the Coldbrook Group (see Ells, 1908 for review).

The Ratcliffe Brook Formation is best and most continuously exposed in Hanford Brook (Fig. 1C). There the basal conglomerates overlie amygdaloidal basalts and red felsic tuffs of the Coldbrook Group. The pebble- to cobble-conglomerates are massive and poorly sorted with subangular to rounded clasts of quartzite, vein quartz and subordinate deformed volcanic rocks. The matrix consists essentially of fine grained quartz with subsidiary clay. The conglomerates pass upward into a sequence of purplish-red, pale greenish-grey or greyish-green fine grained muscovitic sandstones and maroon, purplish-red, or rare olive-green micaceous shales. Sandstones are commonly parallel or crosslaminated, and rarely massive. In the upper part of the succession individual sandstone layers, not exceeding a few centimetres in thickness, may be feldspathic. Such volcanogenic sandstones normally exhibit grading and parallel or small-scale crosslamination. Exposures of the Ratcliffe Brook elsewhere in the Saint John region display similar, if not identical, lithologies to those observed in Hanford Brook.

The redbed sequence which we attribute to the Eocambrian sequence is well exposed along Rockland Road in Saint John and at Mystery Lake (Figs. 1A, 1B). These sequences were previously assigned to the Ratcliffe Brook because of superficial resemblance to the lithologies in Hanford Brook (Hayes and Howell, 1937; Alcock, 1938; Ruitenberg et al., 1975). The sediments of the Eocambrian at these localities consist of purplish-red conglomerates, sandstones and shales with minor olive-grey interbeds. We established these sequences as clearly belonging to the Eocambrian by the following observations.

i) Clasts within conglomerates of the sequence are generally deformed and exhibit preferred orientation parallel to maximum extension. Ratcliffe Brook conglomerates possess rather rare deformed clasts, but such clasts exhibit no preferred orientation.

ii) The matrix of conglomerates in the unit is highly feldspathic, and the feldspars exhibit alteration to clays and micas. The matrix of Ratcliffe Brook conglomerates is essentially quartz with very minor amounts of clay.

iii) Sandstones of the sequence are typically coarse grained, contain easily identified altered feldspars, rock fragments and quartz grains, and only small amounts of detrital muscovite. Petrographic analysis indicates an average of 40% rock fragments, and consistently less than 30% monocrystalline quartz from a volcanic source. Hematite cement and extensive sericitization are common. Ratcliffe Brook sandstones are typically fine- to meidum-grained and contain 55-60% quartz. Muscovite content is relatively high and easily recognized in specimen. The degree of sericitization is generally low.

iv) Most sandstones in the Eocambrian sequence are massively bedded and crosslamination can only rarely be seen. Massive sandstone beds occur rarely in the Ratcliffe Brook. Typically laminated and crosslaminated layers are present. Bedding planes can be recognized in H_{ce} only with great difficulty, whereas they are extremely well developed in Ratcliffe Brook Formation.

v) Sandstones in the Eocambrian sequence are always purplish-red, whereas purplish red sandstones in Ratcliffe Brook are invariably interbedded with greyish-green or greenish-grey varieties.

vi) Shales in the Eocambrian sequence are never micaceous and exhibit maroon or purplish-red colour. Shales in the Ratcliffe Brook are typically micaceous and paler coloured. The (rather rare) olive-green shales appear distinctive of the latter unit.

vii) The clast population in Eocambrian conglomerates, which varies from angular to rounded, exhibits a significantly higher porportion of rounded clasts.

viii) Sediments in the sequence are invariably spatially associated with volcanogenic mafic flows and tuffs (cf. Currie, 1984), appear to be interbedded with them and in some locations clearly interdigitate with them.

A combination of the above criteria can be used to distinguish redbed sequences of the Eocambrian from those of the Lower Cambrian Ratcliffe Brook. On a regional scale it is apparent that sediments of the Eocambrian succession were only locally developed, probably representing local fluvial sequences formed on the irregular topographic surface of the essentially volcanic Hadrynian Coldbrook Group. The basal Cambrian marine transgression resulted in deposition of a superficially similar redbed sequence but, as demonstrated by the contained faunas (Walcott, 1900) and ichnofaunas, in a marine as distinct from fluvial environment. No unconformity has been observed between the two units, but a disconformity is suggested by a consistent discrepancy in attitude of 15-30° between the two.

In addition to the two locations discussed above, a number of other redbed sequences in the Saint John area appear, on the basis of preliminary examination, to belong to the Eocambrian rather than the Ratcliffe Brook. These include

i) The Browns Flat-Greenwich Hill area northwest of the Long Reach (Fig. 1). McCutcheon (1981) interpreted red-coloured sediments and associated volcanics as Lower Cambrian, and thus equivalent to the Ratcliffe Brook. This led to difficulties in correlation of other units of the Saint John Group. The intense red colour of the sediments, their highly feldspathic character, and close association with volcanic rocks suggests to us that they would be better correlated with the Eocambrian. As pointed out by Currie (1984), this leads to a significant simplification of the stratigraphy and structure.

ii) The Sproul Road area, about 2750 m west northwest of the southwestern end of Loch Lomond (Fig. 1), where feldspathic, red, coarse grained sandstones, massive tuff, and minor pebble conglomerate have historically been regarded as Lower Cambrian in age (Hayes and Howell, 1937), though Currie (1984) mapped them as Eocambrian.

In the Saint John Drydock area, Currie (1984) demonstrated the presence of both the Eocambrian and Ratcliffe Brook Formation.

References

Alcock, F.J.
1938: Geology of the Saint John Region, New Brunswick; Geological Survey of Canada. Memoir 215, 65 p.

Currie, K.L.
1984: A reconsideration of some geological relationships near Saint John, New Brunswick; in Current Research, Part A, Geological Survey of Canada, Paper 84-1A, p. 193-201.

Currie, K.L. and Nance, R.D.
1983: A reconsideration of the Carboniferous rocks of Saint John, New Brunswick; in Current Research, Part A, Geological Survey of Canada, Paper 83-1A, p. 29-36.

Currie, K.L., Nance, R.D., Pajari, G.E., and Pickerill, R.K.
1981: Some aspects of the pre-Carboniferous geology of Saint John, New Brunswick; in Current Research, Part A, Geological Survey of Canada, Paper 81-1A, p. 23-30.

Ells, R.W.
1908: Notes on a proposed new base for the Cambrian rocks of southern New Brunswick. Transactions of the Royal Society of Canada, Section IV, v. 2, p. 113-120.

Giles, P.S. and Ruitenberg, A.A.
1977: Stratigraphy, palaeogeography and tectonic setting of the Coldbrook Group in the Caledonia Highlands of southern New Brunwick; Canadian Journal of Earth Sciences, v. 14, p. 1263-1275.

Hayes, A.O. and Howell, B.F.
1937: Geology of Saint John, New Brunswick; Geological Society of America, Special Paper 5, 146 p.

McCutcheon, S.R.
1981: Revised stratigraphy of the Long Reach area, southern New Brunswick; evidence for major, northwestward-directed Acadian thrusting; Canadian Journal of Earth Sciences, v. 18, p. 646-656.

O'Brien, B.H.
1976: The geology of parts of the Coldbrook Group, southern New Brunswick; unpublished M.Sc. thesis, University of New Brunswick, Fredericton, New Brunswick.

Ruitenberg, A.A., Giles, P.S., Venugopal, D.V.,
Buttimer, S.M., McCutcheon, S.R., and Chandra, J.
1975: Geology and mineral deposits, Caledonia area; Mineral Resources Branch, New Brunswick Department of Natural Resources and Canada Department of Regional Economic Expansion, Memoir 1, 213 p.

Walcott, C.D.
1900: Lower Cambrian terrane in the Atlantic Province; Proceedings of the Washington Academy of Sciences, v. 1, p. 301-339.

Yoon, T.
1970: The Cambrian and Lower Ordovician stratigraphy of the Saint John area, New Brunswick; unpublished M.Sc. thesis, University of New Brunswick, Fredericton, New Brunswick.

EVIDENCE OF ICE RAFTING AND TRACTIVE TRANSFER IN CORES FROM QUEEN CHARLOTTE SOUND, BRITISH COLUMBIA

Project 840033

K.W. Conway[1] and J.L. Luternauer[1]
Cordilleran Geology Division

Conway, K.W. and Luternauer, J.L., Evidence of ice rafting and tractive transfer in cores from Queen Charlotte Sound, British Columbia; in Current Research, Part A, Geological Survey of Canada, Paper 85-1A, p. 703-708, 1985.

Abstract

Sedimentological analysis of six piston cores collected from three major troughs on the central shelf off British Columbia suggests (a) ice rafting was active 13 600 ± 150 BP, but that any ice grounding during the Fraser Glaciation occurred prior to 15 000 BP, (b) debris and grain flows occurred during deglaciation and, (c) postglacial deposition has been concentrated on the inner southeastern and possibly outer northern part of the shelf.

Résumé

L'analyse sédimentologique de six carottes de forage prélevées avec des carottiers à piston dans trois grandes fosses de la plate-forme centrale au large de la Colombie-Britannique semble indiquer (a) que le transport de matériaux par la glace avait encore lieu il y a 13 600 ± 150 BP, mais que tout ancrage des glaces au fond durant la glaciation de Fraser remontait à plus de 15 000 BP, (b) que les coulées de débris et de particules ont eu lieu avant la déglaciation et (c), que le dépôt de sédiments postglaciaires s'est concentré sur la portion intérieure du sud-est et peut-être sur la portion extérieure du nord de la plate-forme.

Introduction

The main physiographic features of Queen Charlotte Sound (Fig. 1, 2) are shallow banks dissected by troughs. In June 1981, six piston cores were taken from three of the major troughs (Fig. 2) to extend an investigation of the late Quaternary history of the region by Luternauer and Murray (1983) which relied mainly on seabed and seismic profiling information. Conway and Luternauer (1984) presented a compilation of the lengths and depths of the cores, a brief description of the longest of these cores and a preliminary interpretation of its lithology. This report examines in more detail evidence obtained from all six cores of sedimentary processes which have been active on the seafloor.

Methods

Cores were taken with a Benthos piston corer from the **CSS Hudson** during 6-8 June 1981. They were maintained in cold storage prior to opening in June and July 1983. Subsamples were analyzed for grain-size distribution at 0.5 ϕ intervals using a settling tube for the -1.0 to 4.0 ϕ fraction and a sedigraph 5000D for the 4.0 and 12.0 ϕ fraction. The greater than -1 ϕ (2.00 mm) or gravel-size fraction was not fractionated but was treated statistically as being 2.00 mm (this applied to only three subsamples all of which contained a maximum of 12.0 weight per cent gravel). Mean size, standard deviation and skewness were calculated using moment measures. The concentration of organic carbon in cores 8 and 12 was determined using a Leco Carbon Analyser. The internal structure of core 8 was examined by X-radiography (power source 180-190 KV; exposure time 1.5 minutes; film type Kodak AA). A subsample of sand from core 2 was studied using the Pacific Geoscience Centre's scanning electron microscope. Photomicrographs were then compared to representative photomicrographs in Krinsley's (1973) Atlas of sand surface textures. Radiocarbon dates on shell material from core 8 were provided by the Geological Survey of Canada's radiocarbon laboratory in Ottawa. The colour of moist sediments was determined using Munsell Soil Colour charts.

Summary of results

Two major sedimentary sequences can be distinguished on the basis of colour, organic content and stiffness/plasticity in all but core 13 where the lower unit is absent (Fig. 3a, b, c). The upper unit is olive green (5Y 4/4) to olive grey (5Y 4/2), is less stiff and plastic, and has a higher organic content (Fig. 3b, c). The thickness and sand content of this unit varies markedly across the Sound.

The dark grey (5Y 4/1) to very dark grey (5Y 3/1) lower unit has matrix supported gravel and sand (fragments distinctly larger than the enclosing sediment) in both cores

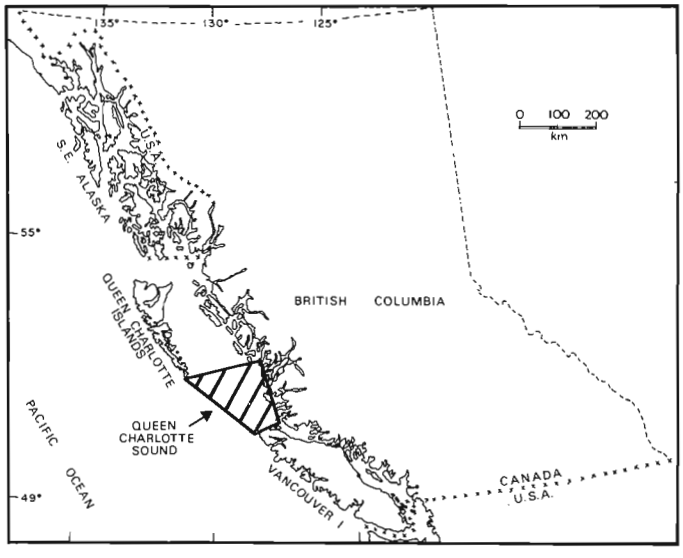

Figure 1. *Location of Queen Charlotte Sound study area.*

[1] Pacific Geoscience Centre, Sidney, British Columbia V8L 4B2

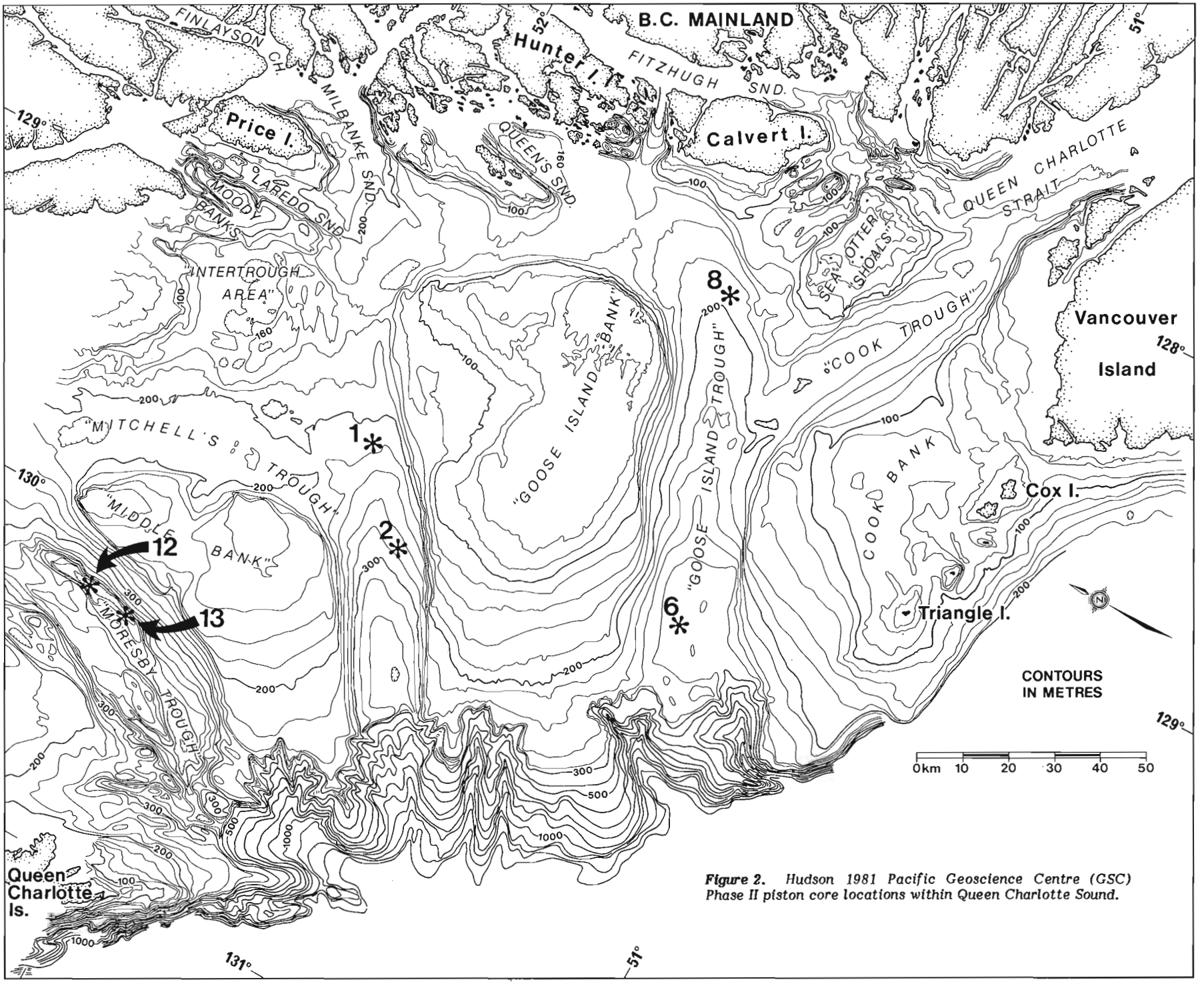

Figure 2. *Hudson 1981 Pacific Geoscience Centre (GSC) Phase II piston core locations within Queen Charlotte Sound.*

collected in Mitchell's Trough (Fig. 3a). These two cores also have the most variable mean size through the sediment column. In core 8 from inner Goose Island Trough the lower unit has matrix-supported gravel but little sand (Fig. 3b). Clean, well sorted sand layers are present only in core 2. The subsamples of a sand layer at 1.43 m (Fig. 4) depth display very good sorting. However, no environmentally diagnostic surface texture assemblage was recognized in scanning electron micrographs of grains from this layer.

The lowermost unit in core 8, which is lithologically similar to the lower units in the other cores, has been dated at 13 600 ± 150 BP (GSC-3711). Shell matter in the uppermost part of the lower unit, however, has been dated at 15 200 ± 490 BP (GSC-3746). This portion of the lower unit is somewhat anomalous because of its blocky texture, the presence of gravelly, shelly sandy mud layers (Fig. 5) and because it is bounded by relatively sharp contacts. It contains a rich fossil fauna including whole barnacles, gastropods, pelecypods and foraminifera.

Discussion and conclusions

On the basis of characteristics such as those identified earlier in this report coupled with mineralogical and fossil analysis, Luternauer and Murray (1983) identified the lower dark grey unit as a glacial marine deposit and the upper, more olive green/olive grey unit as mainly postglacial sediments (i.e. detritus deposited after ice had retreated from the shelf). The matrix-supported grains in the lower sequence are interpreted as ice rafted debris (IRD). This material is evidence that at least floating ice enroached onto this shelf area during the late Wisconsin glaciation of British Columbia. The rich fossil fauna in the coarse, poorly sorted, poorly bedded unit in core 8, from which a radiocarbon date of 15 200 BP was obtained, does suggest, however, that any grounding of ice on the shelf during the late Wisconsin,

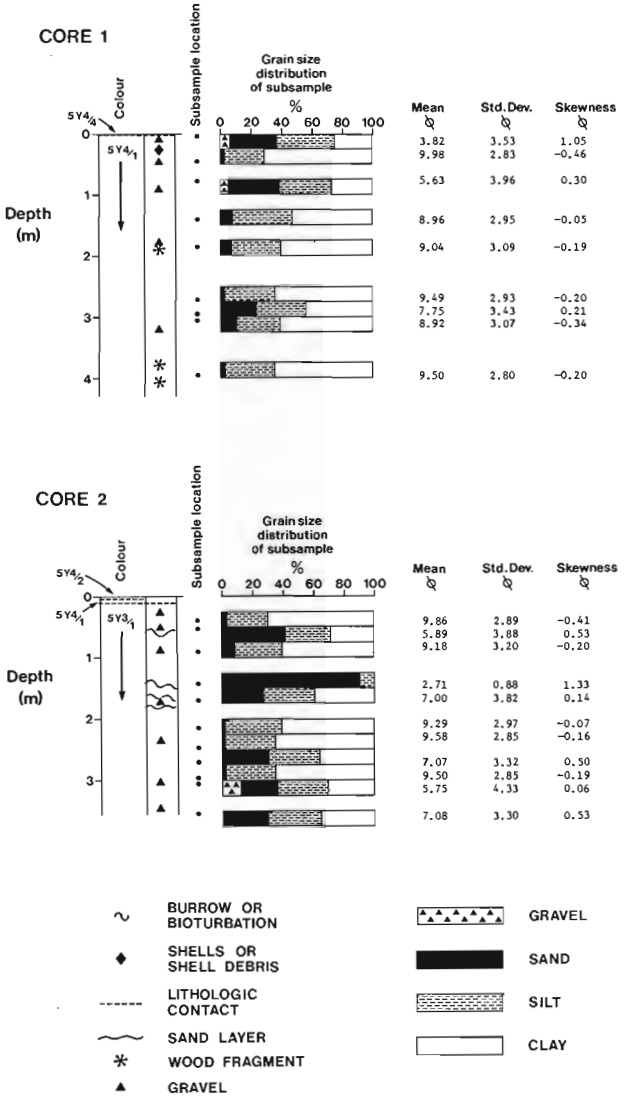

Figure 3a. *Lithology of cores 1 and 2.*

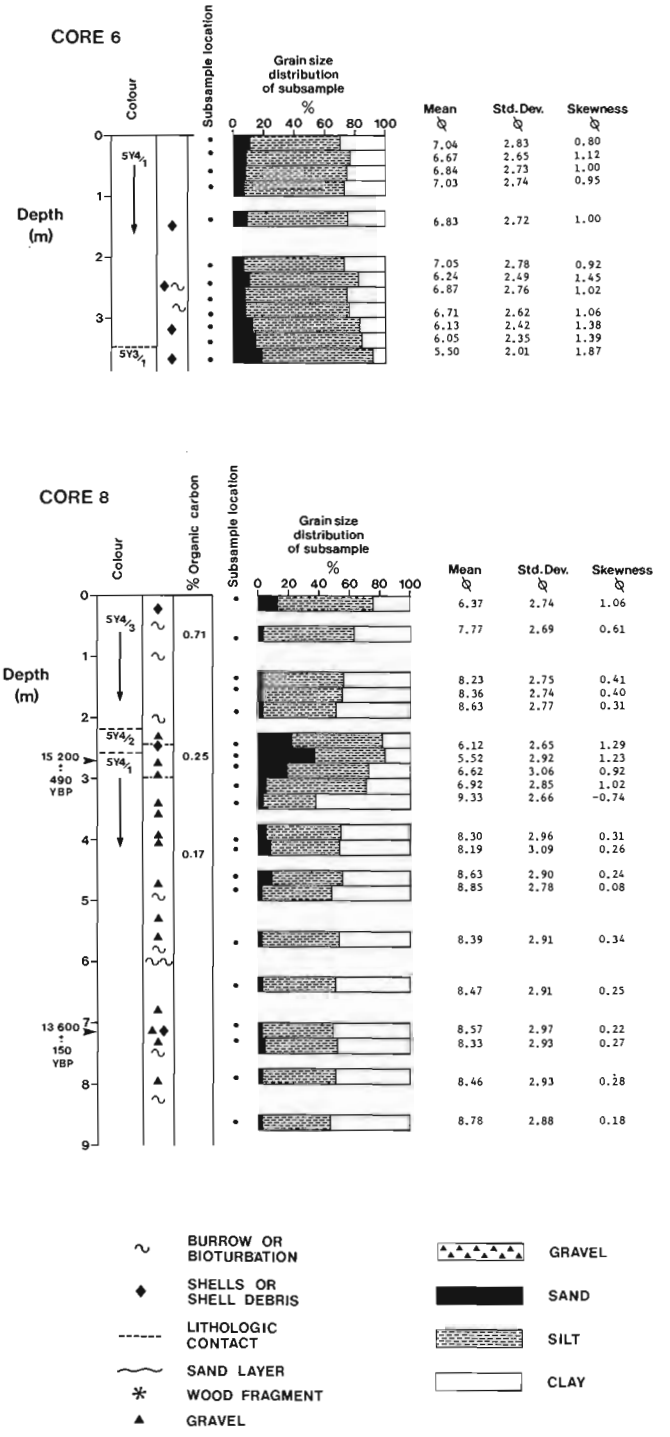

Figure 3b. *Lithology of cores 6 and 8.*

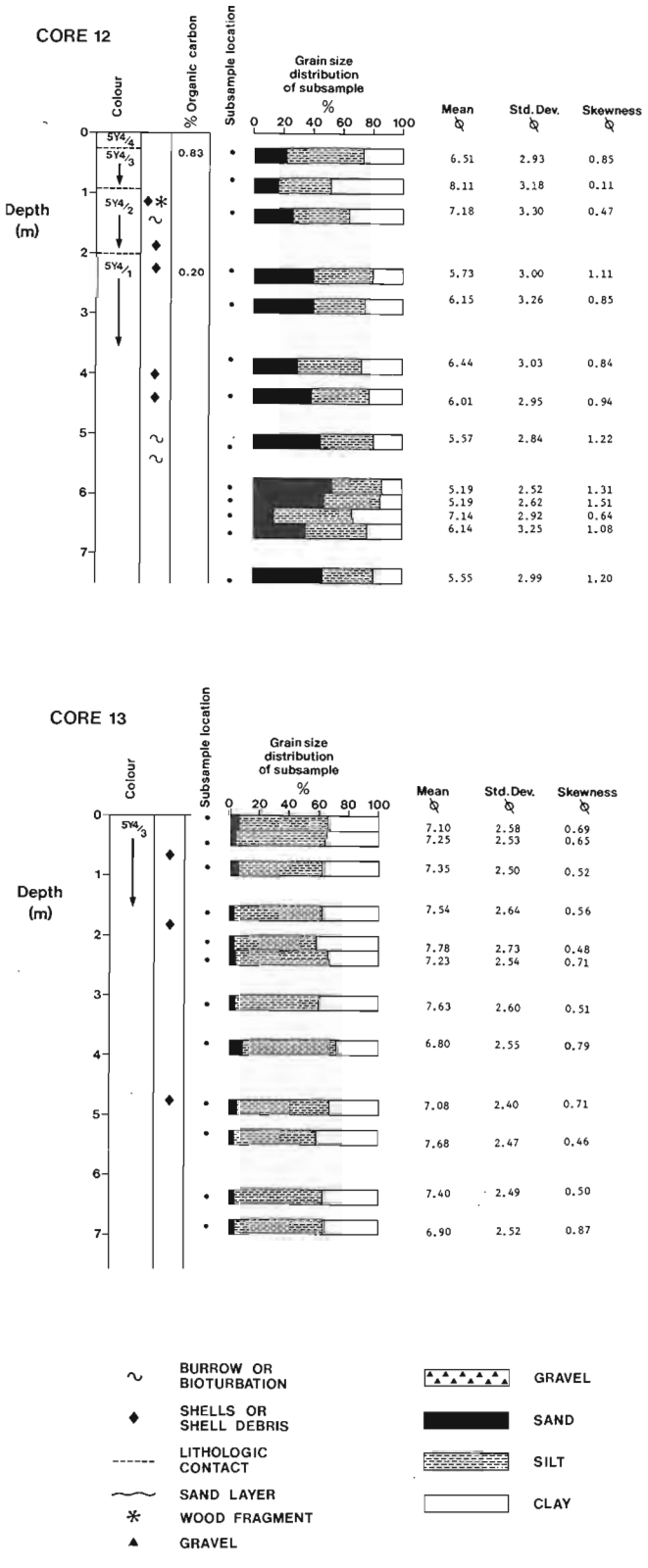

Figure 3c. *Lithology of cores 12 and 13.*

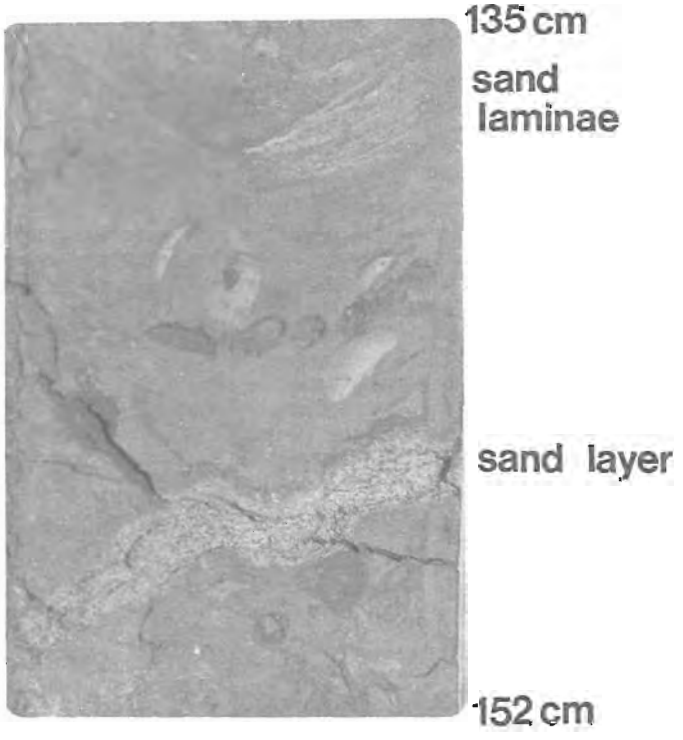

Figure 4. *Clean, well sorted sand layer in sandy mud in core 2. Features immediately above the sand layer are surface gouges resulting from the opening of the core.*

occurred prior to the obtained date. It is possible then, that maximum extension of the Fraser Glaciation in Queen Charlotte Sound preceded that event in the southern mainland which occurred approximately 15 000 BP (Clague et al., 1980). The glacial climax in the sound may have coincided more closely with the time of maximum ice extension in the northern part of the coast which, recent evidence suggests, occurred prior to 16 000 BP (Clague et al., 1982).

The well sorted sand layers in core 2 may represent material mobilized from Goose Island Bank, by storm generated waves, possibly during a period when sea level was at a minimum. However, such grain flows may still recur under the present oceanographic regime as local storm swells are capable of mobilizing coarse sand to at least 100 m below sea level (Luternauer and Murray, 1983). Consideration also should be given to the possibility that intense seismic activity immediately outside the area of the Sound (Milne et al., 1978) may trigger sand flows of this nature.

The anomalous sequence (at the top of the dark grey lower unit) in core 8, which encloses a 15 200 (radiocarbon) year-old shell and overlies 13 600 year-old ice-recessional deposits, probably represents a debris flow. It may have been generated by the collapse of oversteepened side walls from a shelf ice-stream valley, by entrainment of older material in meltwater/tidal current torrents as ice retreated across the shelf, or by seismically triggered failure of older deposits on either Goose Island Bank or the Sea Otter Shoals.

Finally, the cores further support the suggestion by Luternauer and Murray (1983) that postglacial deposition on the shelf has been limited mainly to inner Goose Island Trough and part of Moresby Trough.

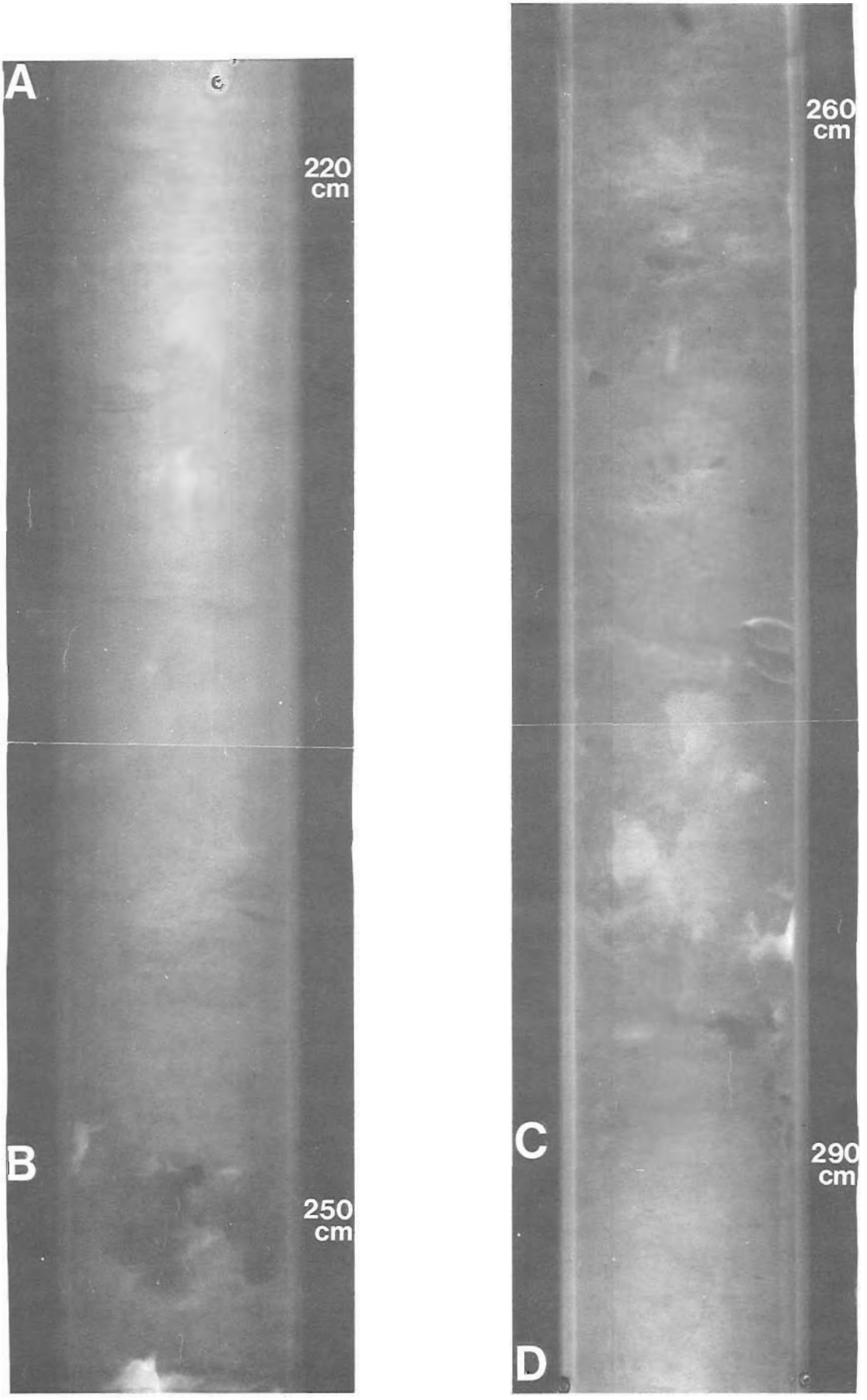

A-B– *finely laminated clayey silt (5Y 4/4, olive green).*
B-C– *shelly gravelly sandy silt (5Y 4/1, dark grey); possible debris flow (note upper and lower contacts).*
C-D– *clayey silt (5Y 4/1, dark grey) with minor gravel.*

Figure 5. *X-ray of possible debris flow in core 8.*

References

Clague, J.J., Armstrong, J.E., and Mathews, W.H.
1980: Advance of the Late Wisconsin Cordilleran Ice Sheet in southern British Columbia since 22 000 yr. BP; Quaternary Research, v. 13, p. 322-326.

Clague, J.J., Mathews, R.W., and Warner, B.G.
1982: Late Quaternary geology of eastern Graham Island, Queen Charlotte Islands, British Columbia; Canadian Journal of Earth Sciences, v. 19, p. 1786-1795.

Conway, K.W. and Luternauer, J.L.
1984: Longest core of Quaternary sediments from Queen Charlotte Sound: preliminary description and interpretation; in Current Research, Part A, Geological Survey of Canada, Paper 84-1A, p. 647-649.

Krinsley, D.H. and Doornkamp, J.C.
1973: Atlas of quartz sand surface textures; Cambridge University Press, New York, N.Y., 91 p.

Luternauer, J.L. and Murray, J.W.
1983: Late Quaternary morphologic development and sedimentation, central British Columbia continental shelf; Geological Survey of Canada, Paper 83-21, 38 p.

Milne, W.G., Rogers, G.C., Riddihough, R.P.,
McMechan, G.A., and Hyndman, R.D.
1978: Seismicity of western Canada; Canadian Journal of Earth Sciences, v. 15, p. 1170-1193.

LICHEN-FREE ZONES AS NEOGLACIAL INDICATORS ON WESTERN MELVILLE ISLAND, DISTRICT OF FRANKLIN

Project 760058

S.A. Edlund
Terrain Sciences Division

Edlund, S.A., Lichen-free zones as neoglacial indicators on western Melville Island, District of Franklin; in Current Research, Part A, Geological Survey of Canada, Paper 85-1A, p. 709-712, 1985.

Abstract

Extensive lichen-free zones occur adjacent to several small glaciers on the plateau of western Melville Island. These zones are generally snow-free for at least a few weeks every summer. It is suggested that the zones developed during a period when perennial snow and ice covered more than six times the present area of ice, down to 400 m elevation. This probably coincided with expansion of ice caps and snow fields during the Little Ice Age elsewhere in the Arctic.

Résumé

De vastes zones dépourvues de lichens sont contiguës à plusieurs petits glaciers dans le plateau de la partie ouest de l'île Melville. Ces zones sont généralement sans neige pendant au moins quelques semaines chaque été. Elles se sont vraisemblablement formées lorsque la neige et la glace pérennes couvraient une surface plus de six fois celle de la région présentement englacée, jusqu'à 400 d'altitude. Cette époque a problablement coïncidée avec l'expansion des calottes glaciaires et des champs de neige au cours du petit Age glaciaire (Little Ice Age) ailleurs dans l'Arctique.

Introduction

The extent of neoglacial ice and snow field expansion in the western Queen Elizabeth Islands, particularly Melville Island, is not well known, although such expansion during the Little Ice Age (16-19th centuries) has been documented in several regions of the eastern Arctic, particularly in mountainous areas with modern ice caps. This report presents observations on probable neoglacial ice and snow fields on the western plateau of Melville Island, an area that also supports a number of small modern ice caps.

One way to delimit the expansion of neoglacial ice and snow fields is to map the lichen-free zones around modern ice fields and ice caps. This technique is restricted to surfaces capable of supporting crustose lichen growth and is based on

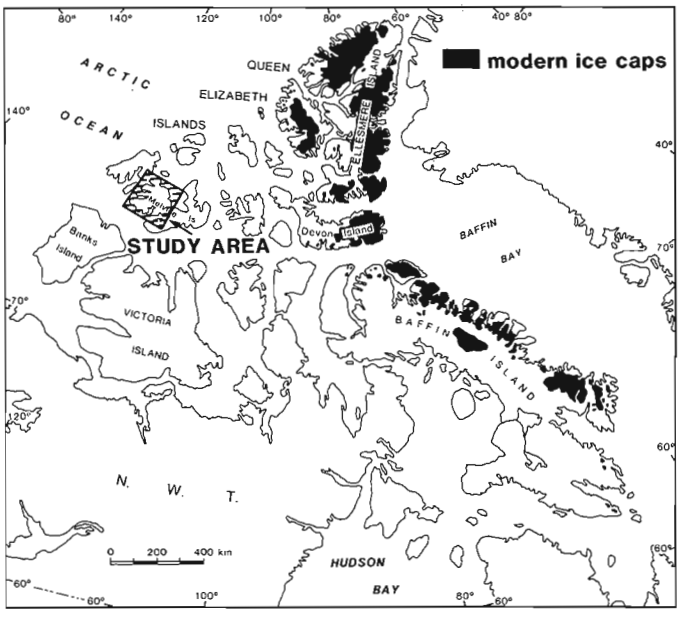

Figure 1: *Modern ice caps in the Canadian Arctic. The study area on western Melville Island is shown.*

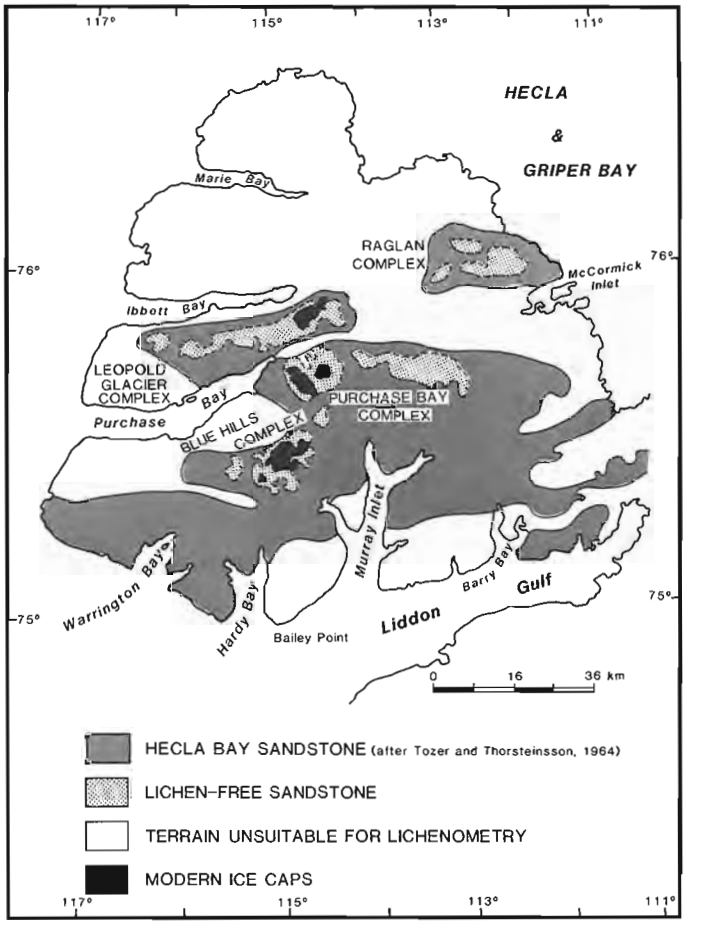

Figure 2. *Western Melville Island showing modern glaciers and lichen-free zones on Hecla Bay sandstone.*

the premise that lichens readily colonize suitable substrates immediately upon exposure from under snow and ice cover for sufficient periods during the year. The length of time before lichens colonize a bared surface varies, but seems to be in the range of at least 100-300 years (Beschel, 1961).

Since large areas that have been recently exposed have different reflectant properties than lichen-covered surfaces, such large areas can be seen readily on satellite and aerial photo imagery (Locke and Locke, 1977). This technique is particularly effective on areas with extensive granitic and gneissic bedrock surfaces and felsenmeer, where lichens readily grow.

Other surfaces are less amenable to lichen growth: in particular the more alkaline carbonate rocks may be toxic or extremely nutrient deficient, or both. Also, rocks that disintegrate into fine particles offer insufficient surface area for attachment of crustose lichen.

Although suitable for lichens are common along the easternmost Arctic Islands, lichen-free areas also occur on these surfaces. Andrews et al. (1975) found lichen-free areas on the summits of northern Labrador. Extensive lichen-free areas occur on north-central Baffin Island (Ives, 1962; Locke and Locke, 1977) and on northern Baffin Island (Falconer, 1966). Dyke (1978) found lichen-free areas on the gneissic plateau of western Somerset Island at elevations of 405 m a.s.l.; on adjacent carbonate rocks, however, neoglacial limits were discerned from meltwater channels and miniature eskers because these carbonates are highly calcareous and do not support lichen growth.

Little data exist on the extent of neoglacial snow and ice from the western Queen Elizabeth Islands (Fig. 1). Much of the terrain is too low to intersect the elevations at which present-day snow and ice persist. In areas of higher elevation, for major parts of Devon, Somerset, Cornwallis, and Bathurst islands, the terrain consists of carbonate rocks that are vegetation free.

Lichen-free zones on Melville Island

On western Melville Island, the plateau, although generally snow-free for a few weeks of the summer, is at sufficiently high elevation to support numerous small ice caps. These vary in size from 5 to 150 km^2 and occur at elevations of greater than 500 to 600 m a.s.l. Together they cover an area of approximately 300 km^2.

Most of the plateau surface is covered with a mantle of resistant Hecla Bay sandstone (Fig. 2) that has weathered into felsenmeer and coarse gravel, which readily support crustose lichen and other cryptogamic communities (Barnett et al., 1975; Edlund, 1982). Surrounding these ice



Figure 3. *Landsat satellite image of northwestern Melville Island showing the lichen-free (L-F) plateaus, light-toned carbonate terrain (C), and poorly vegetated, finely weathered bedrock (Cf) of the Canyon Fiord Formation.*

caps are extensive lichen-free areas, readily detected on both aerial photographs and summer Landsat satellite imagery (Fig. 3). The light grey sandstone surface contrasts sharply with the dark toned lichen-covered sandstone fragments.

The lichen-free zone around the Leopold Glacier complex (Fig. 2) covers roughly 740 km^2; the Blue Hills complex, 560 km^2; and the Purchase Bay complex, 585 km^2. The lichen-free zones occur generally at elevations greater than 400 m a.s.l.

Another extensive lichen-free area, covering approximately 400 km^2, occurs on Hecla Bay sandstone north of McCormick Inlet (Fig. 4). Although no ice caps exist in the area today, numerous perennial snowbeds and snow cornices are common in sheltered locations. Here, too, above 400 m a.s.l., the major lichen-free zones occur.

These data from western Melville Island suggest that in the recent past, probably less than 100 years ago, the snow line rose from 400 m a.s.l. to its present level at 500-600 m a.s.l. At that time, ice and snow fields occupied at least 2200 km^2 of the plateau, a surface area at least six times that of the area now occupied by ice.

Other parts of the plateau intersect the 400 m elevation, and the extent of neoglacial ice and snow fields may have been even greater. However, because the surficial materials are either extremely calcareous (as is the case for some of the Canrobert Hills on the north side of Ibbett Bay) or are composed of sandstone and siltstone that weather into fine particles, the absence of crustose lichen cannot be used as a criterion to delimit former extent of snow and ice cover.

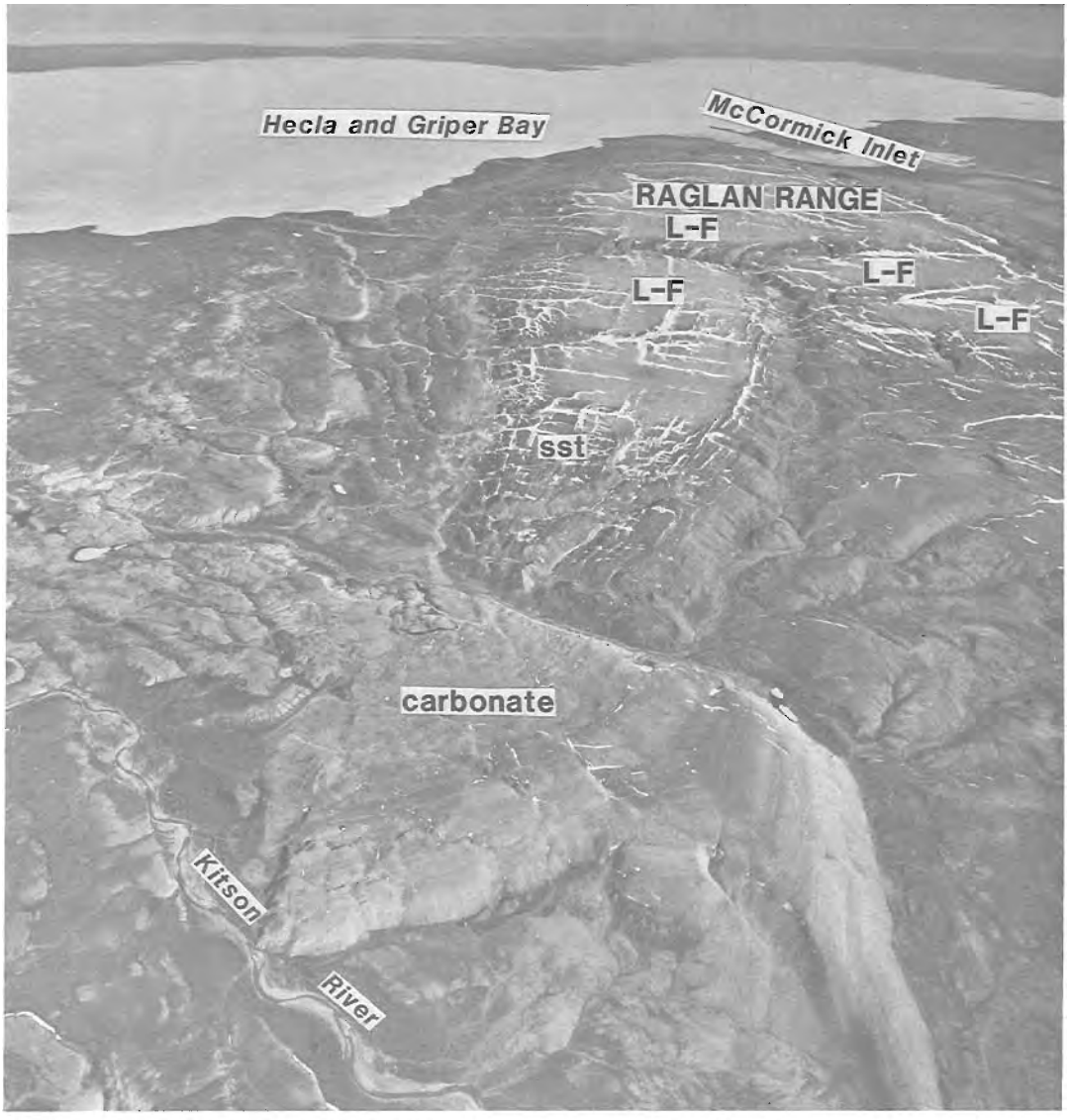

Figure 4. *Aerial view of lichen-free (L-F) zones on Hecla Bay sandstone (sst) on the Raglan Range near McCormick Inlet (cf. Fig. 2).*

Acknowledgments

Appreciation is extended to Polar Continental Shelf Project for field logistical support, and to R.L. Christie from whose field camp this study was conducted. Thanks are also extended to R.L. Christie and C. Harrison; and Q. Goodbody (University of Alberta) for useful discussions in the field. D.A. Hodgson, R.L. Christie, and D.A. St-Onge provided useful comments on an earlier version of this manuscript.

References

Andrews, J.T., Barry, R.G., Davis, T.T., Miller, G.H., and Williams, L.D.
1975: The Laurentide Ice Sheet: Problems of mode and speed of inception; World Meteorological Original Publication No. 421, p. 87-94.

Barnett, D.M., Edlund, S.A., Dredge, L.A., Thomas, D.C., and Prevett, L.S.
1975: Terrain classification and evaluation, Melville Island, N.W.T.; Geological Survey of Canada, Open File 252, 3 maps, expanded legends, 2 volumes, 1318 p.

Beschel, R.E.
1961: Dating rock surfaces by lichen growth and its application to glaciology and physiography (lichenometry); in Geology of the Arctic, ed. E. Raasch; Proceedings of the First Symposium on Arctic Geology, Calgary, Alberta, University of Toronto Press, p. 1044-1062.

Dyke, A.S.
1978: Indications of neoglacierization on Somerset Island, District of Franklin; in Current Research, Part B, Geological Survey of Canada, Paper 78-1B, p. 215-217.

Edlund, S.A.
1982: Vegetation of Melville Island, District of Franklin, Eastern Melville Island and Dundas Peninsula; Geological Survey of Canda, Open File 852.

Falconer, G.
1966: Preservation of vegetation and patterned ground under a thin ice body in northern Baffin Island, N.W.T., Canada; Geographical Bulletin, v. 8, p. 194-200.

Ives, J.D.
1962: Indications of recent extensive glacierization in north-central Baffin Island, N.W.T.; Journal of Glaciology, v. 4, p. 197-205.

Locke, C.W. and Locke, W.W., III
1977: Little Ice Age snow cover extent and paleoglaciation thresholds: north-central Baffin Island, N.W.T., Canada; Arctic and Alpine Research, v. 9, p. 291-300.

Tozer, E.T. and Thorsteinsson, R.
1964: Western Queen Elizabeth Islands, Arctic Archipelago; Geological Survey of Canada, Memoir 332, 242 p.

OCCURRENCE OF COPPER ARSENIDES IN THE EAST ARM AREA, GREAT SLAVE LAKE, DISTRICT OF MACKENZIE

Project 680060

D.C. Harris and R.I. Thorpe
Economic Geology and Mineralogy Division

Harris, D.C. and Thorpe, R.I., Occurrence of copper arsenides in the East Arm area, Great Slave Lake, District of Mackenzie; in Current Research, Part A, Geological Survey of Canada, Paper 85-1A, p. 713-716, 1985.

Abstract

The copper arsenide minerals α-domeykite and β-domeykite, and associated loellingite, kutinaite, native silver and cuprite occur in altered carbonate rock near a monzonitic laccolith in the East Arm area of Great Slave Lake. This is the first reported occurrence of kutinaite in Canada.

Résumé

Les arséniures de cuivre α-domeykite et β-domeykite, ainsi que la loellingite, la kutinaïte, l'argent natif et la cuprite qui lui sont associées, se présentent dans une roche carbonatée altérée à proximité d'un laccolite monzonitique dans la région du bras Est du Grand lac des Esclaves. C'est la première minéralisation de kutinaïte dont on signale l'existence au Canada.

Introduction and General Geology

Thorpe (1966) reported domeykite and at least one other copper arsenide mineral in association with cuprite at the discovery showing on the HAR claim group, East Arm area of Great Slave Lake, District of Mackenzie. Domeykite has previously been reported from Michipicoten Island and Silver Islet in Lake Superior (Traill, 1983). Also, Heslop (1970) and, more recently, Hak et al. (1977) have reported algodonite, domeykite and arsenian copper in a complex mineral assemblage at the Coppercorp deposit, Mamainse Point, about 100 km north-northwest of Sault Ste. Marie, Ontario. The associated minerals at the latter locality include native silver, native gold, clausthalite, wittichenite and other sulphide and sulphosalt minerals. The present note is based on study of specimens from the East Arm locality.

The copper arsenide occurrence consists of copper mineralization in a shear zone that has been traced for 130 m and cuts light-grey-green dolomite and siltstone of the Stark Formation near the contact of these sedimentary rocks with a monzonite intrusion (Fig. 1). Stratified rocks exposed in the area are dominantly Proterozoic (Aphebian) clastic and chemical sedimentary rocks (Hoffman, 1977; Hoffman et al., 1977) that were deposited in the Athapuscow aulacogen as defined by Hoffman (1973). These rocks belong to the Kahochella, Pethei, Christie Bay and Et-Then groups. The host Stark Formation, part of the Christie Bay Group, consists of mudstone, limestone, and dolomite, and includes major megabreccia units in the lower part (Hoffman, 1977). Two of the monzonite-diorite laccoliths in the region, collectively termed the Caribou laccoliths (Hoffman, 1977), have intruded rocks of the Stark Formation in the immediate area of the copper arsenide occurrence. The sedimentary rocks and monzonitic intrusions have been cut by a series of north-northwest trending Mackenzie diabase dykes.

The copper arsenides are located between Wilson Lake and Stark Lake, near the northern contact of a laccolithic body of diorite-monzonite that has a strike length of about 9 km. Two smaller laccoliths in the area, the Regina Bay body 16 km to the southwest and the Meridian Lake body about 32 km to the northeast, have been studied by Gandhi and Prasad (1982). Their petrochemical study demonstrated that the intrusions are subalkaline in character, that they exhibit a small compositional range and a calc-alkaline differentiation trend, and locally show effects of alkali metasomatism. They concluded that the limited in situ differentiation of the intrusions most likely did not lead to the extreme enrichment of iron, phosphorus and other elements necessary to form uraniferous actinolite-apatite-magnetite (+arsenides) veins in the Regina Bay laccolith. They suggested a much deeper magma-chamber source for the vein-forming fluids.

A number of arsenide localities have been known in the East Arm region for many years. All of these are restricted to the margins of high-level intrusions. The older of these intrusions are alkaline (Badham, 1979) and the younger are calc-alkaline (Badham, 1978; Gandhi and Prasad, 1982). These localities include Easter Island, Aristifats Lake, Regina Bay, Labelle Peninsula, Blanchet Island, and Sachowia Lake (Badham, 1978; Muda, 1979; Badham and Muda, 1980). Loellingite, one of the minerals reported in the present study, and associated arsenide minerals occur at Regina Bay (Muda, 1979), Labelle Peninsula, and Blanchet Island.

Regional reconnaissance lake sediment geochemical results have been reported by Maurice (1977, 1984) for the area lying east of 110°W longitude. Arsenic is significantly anomalous and uranium moderately anomalous in association with the monzonite laccolith east of Compston Lake. One of the strongest arsenic anomalies, however, covers a large area about 50 to 90 km to the east. It has associated coincident strong cobalt and nickel anomalies. This anomalous area is southeast of the McDonald Fault and corresponds generally to a mapped quartzite-paragneiss unit.

The present study of copper arsenide material from the East Arm area was undertaken to characterize the arsenides and associated phases. The material examined consists of hand specimens collected from trench No. 2 on the HAR claims at approximately 62°29'07"N, 110°03'25"W (Fig. 1).

Mineralogy

α and β-domeykite are the major phases and occur as coexisting polycrystalline irregular masses interstitial to the

siliceous gangue (Fig. 2). β-domeykite is more abundant than α-domeykite. Both minerals contain numerous inclusions of loellingite and are slightly altered to cuprite.

The compositions of the domeykites were determined by electron microprobe using a natural α-domeykite as a standard. The standard specimen was selected from the National Mineral Reference Collection (No. 19724) from a locality from which material was shown by Skinner and Luce (1971) to have the composition $Cu_{3.0}As$. Attempts to analyze domeykite using synthetic CuS and $FeAs_2$ were not satisfactory and experiments to synthesize a homogeneous Cu_3As were not successful. With the natural mineral as a standard, α-domeykite gave a composition of $Cu_{3.02}As$ and β-domeykite a composition of $Cu_{2.80}As$. No other elements were detected.

Loellingite is very abundant as small (< 50 μm) idiomorphic to lamellar inclusions in grains of α- and β-domeykite (Fig. 2 and 3). Loellingite inclusions are also concentrated along the contacts between domeykite grains and gangue. Microprobe analysis shows that the mineral contains variable copper contents, ranging from 2.3 to 6.4 weight per cent. An average composition for seven larger grains is Cu 4.3%, Fe 23.9%, As 70.7%, total 98.9 weight per cent, corresponding to the formula $Cu._{14}Fe._{91}As_{2.00}$. A similar occurrence of cuprian loellingite in β-domeykite was reported by Picot and Ruhlmann (1978) in a high temperature copper arsenide assemblage from the Ballons granite, southern Vosges.

Cuprite is very common and has generally replaced domeykite grains along fractures and grain boundaries (Fig. 4). Microprobe analysis shows that it contains 0.9 weight per cent As.

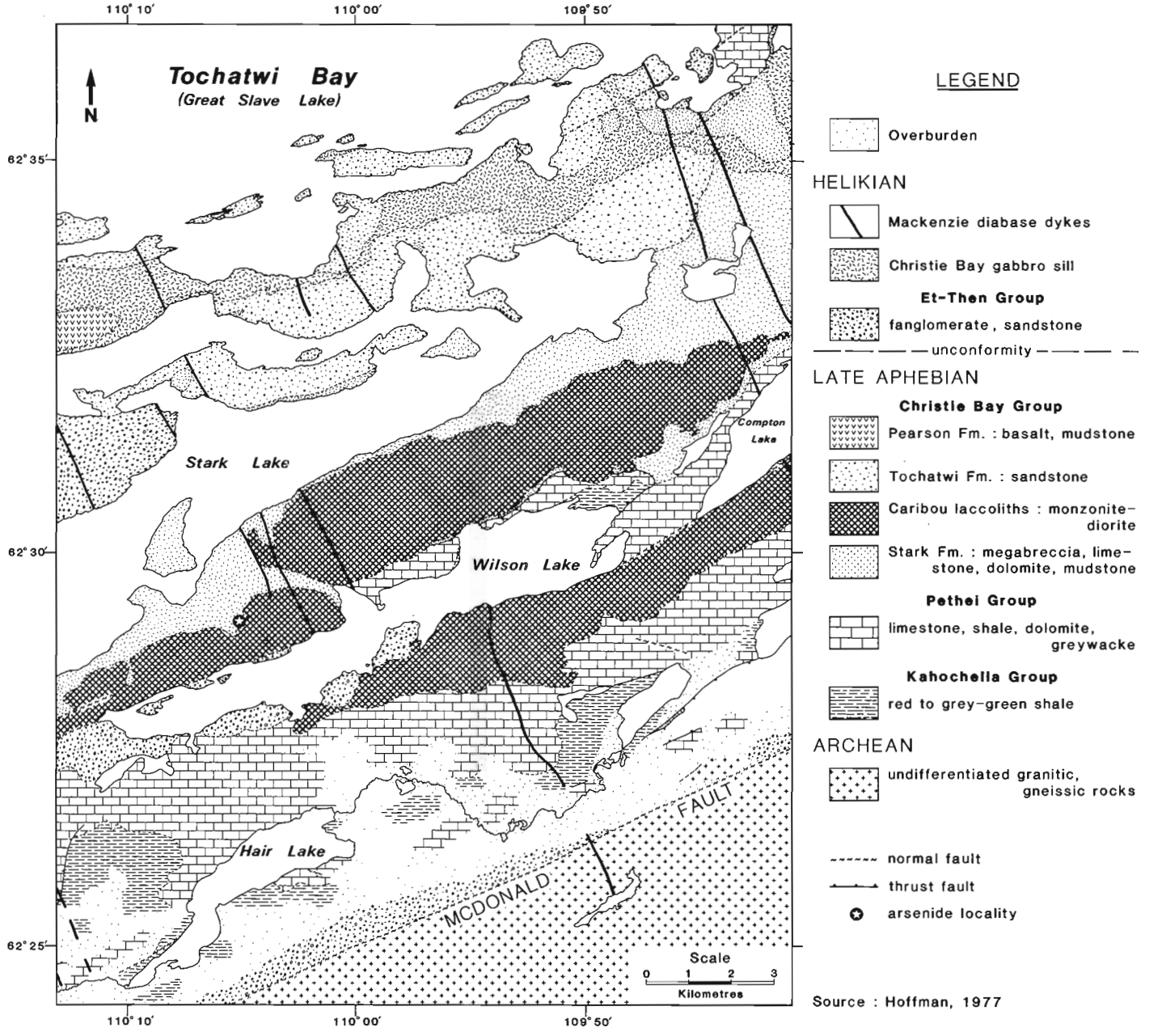

Figure 1. *Geological map, generalized from Hoffman (1977), of an area including the copper arsenide locality.*



Figure 2. *Irregular polycrystalline β-domeykite with selvage of idiomorphic loellingite in siliceous gangue.*



Figure 3. *β-domeykite with inclusions of native silver and idiomorphic to lamellar grains of loellingite.*

Native silver is rare and occurs as fine inclusions smaller than 20 µm in domeykite, in contact with loellingite and in gangue (Fig. 2). Due to the small grain size, accurate analyses could not be obtained, but the larger grains were found to contain traces of mercury.

Kutinaite ($Cu_{2.07}Ag_{.84}As_{1.00}$) was discovered by Hak et al. (1970) in the Cerny Dul ore deposit, Czechoslovakia where it is associated with novakite, koutekite, paxite, arsenolamprite and loellingite in carbonate-rich veins. Picot and Ruhlmann (1978) reported an occurrence of kutinaite in a high temperature copper arsenide assemblage from the Ballons granite, southern Vosges. Their analyses gave a composition of $Cu_{2.14}Ag_{.91}As_{1.00}$ (average of analyses 2 and 3). In our samples, kutinaite is rare and occurs as small grains (15 to 25 µm) in contact with β-domeykite. Its isotropic character and bluish-grey color helps to distinguish it from the creamy α-domeykite and the anisotropic β-domeykite. Analysis gave Cu 42.1, Ag 31.1, As 25.3, total 98.5 weight per cent, corresponding to the composition $Cu_{1.97}Ag_{.85}As_{1.00}$. This is the first reported occurrence of kutinaite in Canada.

Paragenesis

Makovicky (1978) suggested a composition close to $Cu_5Ag_2As_3$ for synthetic kutinaite and reported a stability range between 478°C and approximately 230°C. Skinner and Luce (1971) established that the upper stability of α-domeykite at 1 atmosphere is approximately 90°C. Because of such a low breakdown-temperature, they suspected that much of the β-domeykite described in the literature might have been formed as a consequence of sample handling techniques, particularly those employed

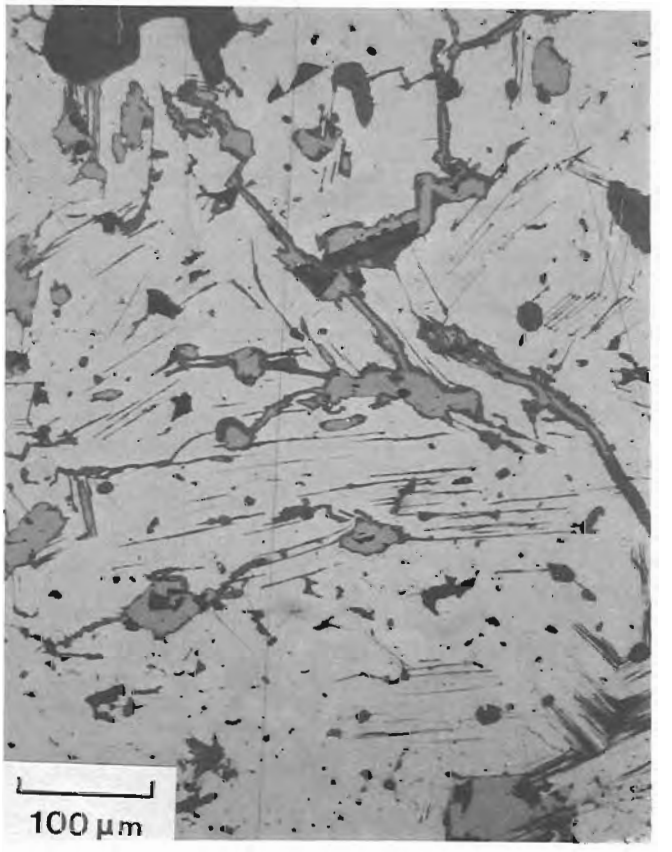

Figure 4. *Polycrystalline β-domeykite with secondary cuprite.*

during mounting and polishing. In our specimens, both minerals have been identified by x-ray diffraction in situ in the hand specimens. Based on the textural relations and stabilities, the following paragenetic sequence is postulated. The selvage of loellingite along the contacts between domeykite and gangue suggests that this mineral probably formed first. The stability range for kutinaite indicates a minimum of 230°C and it may thus have been the second to form. Coexisting α- and β-domeykites with mutual borders suggest co-precipitation, and these were probably the last phases to form at around 90°C.

References

Badham, J.P.N.
1978: Magnetite-apatite-amphibole-uranium and silver-arsenide mineralizations in Lower Proterozoic igneous rocks, East Arm, Great Slave Lake, Canada; Economic Geology, v. 73, no. 8, p. 1474-1491.

1979: Geology and petrochemistry of lower Aphebian (2.4-2.0 Ga) alkaline plutonic and hypabyssal rocks in the East Arm of Great Slave Lake, Northwest Territories; Canadian Journal of Earth Sciences, v. 16, no. 1, p. 60-72.

Badham, J.P.N. and Muda, M.M.Z.
1980: Mineralogy and paragenesis of hydrothermal mineralizations in the East Arm of Great Slave Lake; Economic Geology, v. 75, no. 8, p. 1220-1226.

Gandhi, S.S. and Prasad, N.
1982: Comparative petrochemistry of two cogenetic monzonitic laccoliths and genesis of associated uraniferous actinolite-apatite-magnetite veins, East Arm of Great Slave Lake, District of Mackenzie; in Uranium in Granites, ed. Y.T. Maurice; Geological Survey of Canada, Paper 81-23, p. 81-90.

Hak, J., Johan, Z., and Skinner, B.J.
1970: Kutinaite; a new copper-silver arsenide mineral from Cerny Dul, Czechoslovakia. American Mineralogist, v. 55, p. 1083-1087.

Hak, J., Tupper, W.M., and Heslop, J.B.
1977: The mineralogy of the Coppercorp deposit, Mamainse Point, Ontario, Canada; Acta Universitatis Carolinae – Geologica, Slavik Volume, no. 3-4, p. 267-283.

Heslop, J.B.
1970: Geology, mineralogy and textural relationships of the Coppercorp deposit, Mamainse Point area, Ontario; unpublished M.Sc. thesis, Carleton University, Ottawa.

Hoffman, P.F.
1973: Evolution of an early Proterozoic continental margin: the Coronation geosyncline and associated aulacogens, northwest Canadian Shield; in Evolution of the Precambrian Crust, ed. J. Sutton and B.F. Windley; Philosophical Transactions of the Royal Society of London, Series A, v. 273, p. 547-581.

1977: Preliminary geology of Proterozoic formations in the East Arm of Great Slave Lake, District of Mackenzie; Geological Survey of Canada, Open File 475 – Sheets A to L (NTS 75 E,L,K; 85 H,I) scale 1:50 000.

Hoffman, P.F., Bell, P.R., Hildebrand, R.S., and Thorstad, L.
1977: Geology of the Athapuscow aulacogen, east arm of Great Slave Lake, District of Mackenzie; in Report of Activities, Part A, Geological Survey of Canada, Paper 77-1A, p. 117-129.

Makovicky, M. and Johan, Z.
1978: Reflectivity and microhardness of synthetic and natural koutekite, kutinaite and beta-domeykite. Neues Jahrbuch Fuer Mineralogie, Monatshefte, p. 421-432.

Maurice, Y.T.
1977: Follow-up geochemical activities in the Nonacho Lake area (75 F,K), District of Mackenzie; Geological Survey of Canada, Open File 489, 10 p.

1984: Regional geochemical reconnaissance interpretation of data from Nonacho Lake-East Arm of Great Slave Lake region, District of Mackenzie; Geological Survey of Canada, Paper 84-12, 17 p.

Muda, M.M.Z.
1979: The petrogenesis of host rocks and associated hydrothermal mineralizations of the East Arm of Great Slave Lake, Canada; unpublished M. Phil. thesis, University of Southampton, 201 p.

Picot, P. and Ruhlmann, F.
1978: Présence d'arséniures de cuivre de haute température dans le granite des Ballons (Vosges méridionales); Societe Française de Minéralogie et de Cristallographie, Bulletin, v. 101, p. 563-569.

Skinner, B.J. and Luce, F.D.
1971: Stabilities and compositions of α-domeykite and algodonite; Economic Geology, v. 66, p. 133-139.

Thorpe, R.I.
1966: Mineral industry of the Northwest Territories 1965; Geological Survey of Canada, Paper 66-52, 25 p.

Traill, R.J.
1983: Catalogue of Canadian Minerals; Revised 1980; Geological Survey of Canada, Paper 80-18, 432 p.

SEDIMENTARY FRAMEWORK OF THE FRASER RIVER DELTA, BRITISH COLUMBIA: PRELIMINARY FIELD AND LABORATORY RESULTS

EMR Research Agreement 275-04-84 and Projects 790006 and 690075

M.C. Roberts[1], H.F.L. Williams[1], J.L. Luternauer[2], and B.E.B. Cameron[2]
Cordilleran Geology Division, Vancouver

Roberts, M.C., Williams, H.F.L., Luternauer, J.L., and Cameron, B.E.B., Sedimentary framework of the Fraser River delta, British Columbia: preliminary field and laboratory results; in Current Research, Part A, Geological Survey of Canada, Paper 85-1A, p. 717-722, 1985.

Abstract

Twenty-two cores ranging in length from 3 to 30.5 m were collected from the subaerial part of the Fraser River delta during the summer of 1984 employing a Concore C-68 research drill rig. These and subsequent cores will provide, for the first time, a systematic and detailed basis for establishing the regional stratigraphy and evolution of the delta. Preliminary examination of the lithology, structures and micropaleontology of the cores indicate most of the sediments at all sampled areas and depths represent mainly fluvial and intertidal deposits. The thickness of these deposits suggests that accretion during the latter stages of delta development kept pace with the rapid local relative rise in sea level from approximately 7700 to 5000 BP.

Résumé

Pendant l'été 1984, dans la partie subaérienne du delta du fleuve Fraser, on a recueilli 22 carottes de forage dont la longueur variait entre 3 et 30,5 m, au moyen d'une foreuse expérimentale Concord C-68. Ces carottes de forage et les carottes prélevées ultérieurement, fourniront pour la première fois une base systématique et détaillée qui permettra d'établir la stratigraphie régionale et l'évolution du delta. Les analyses préliminaires de la lithologie, de la structure et de la micropaléontologie de ces carottes de forage ont indiqué que dans tous les secteurs et à toutes les profondeurs d'échantillonnage, la majorité des sédiments étaient principalement des dépôts fluviatiles et intertidaux. La puissance de ces dépôts semble indiquer que l'accrétion survenue pendant les dernières phases de formation du delta a suivi le rythme de l'élévation locale relativement rapide du niveau de la mer, entre approximativement 7700 et 5000 BP.

Introduction

Evolution of the Fraser River delta has been described in broad outline (Clague et al., 1983) but a systematic examination of subsurface sediments has yet to be done. This study is the first to rely on detailed borehole data to reconstruct the history and character of the delta. Specifically, the ultimate objectives of the study are: a) to interpret the nature and origin of sedimentary units on the basis of contemporary sedimentary environments on the delta, b) to establish a geochronology from wood and shell fragments, and c) to provide more accurate information, than is presently available, on the internal structure, composition and relationships of the facies encountered.

The present report describes the 1984 drilling program and presents preliminary determinations of sedimentary environments based on interpretation of core logs and the results of micropaleontological analysis. These interpretations represent the initial results from ongoing analyses designed to meet objective 'a' as outlined above.

Field methods

1. A drilling program was designed with two major objectives: firstly, to drill in sedimentary environments identified by previous research in order to provide drillhole logs that could be used as models or guides in the interpretation of logs from those parts of the delta where the sedimentary environments are unknown, and secondly, to locate drill sites that would provide a regional overview of the deltaic stratigraphy. The drill site locations for the 1984 field season are shown in Figure 1 and listed in Table 1.
2. The drilling was carried out with a Concore C-68 research drill rig (Fig. 2). This rig can drill to a maximum depth of 50 m in one of three modes: rotary, auger and hammer coring.
3. Due to the unconsolidated nature of the deltaic sediments the drillholes were prone to collapse. Considerable time and effort were expended to achieve the most efficient drilling method. The problem was largely overcome by employing a newly available polymer-based drilling mud (GS 550 Polymer) in the rotary drilling mode.
4. The following core properties were logged in the field: grain size, sedimentary structures, colour, and organic content. This information was coupled with micropaleontological data to form a basis for identifying the major paleoenvironments represented in the cores.
5. Wood and shell fragments were retrieved from the cores for ^{14}C dating.

Laboratory methods

Selected subsamples have been submitted for (a) radiocarbon analysis by an accelerator mass spectrometer, (b) detailed grain-size analysis and (c) palynological and micropaleontological analysis by R. Hebda and B.E.B. Cameron, respectively. To date a micropaleontological analysis has been completed on 16 subsamples from a range of depths and locations. This analysis consisted of washing out the 200 µm fraction of the subsample and identifying the organic and inorganic components of the dried residue.

[1] Department of Geography, Simon Fraser University
[2] Pacific Geoscience Centre, Sidney, British Columbia, V8L 4B2

Results

Twenty-two holes were completed during the 1984 field season (Fig. 1) yielding 210 m of recovered core; a core library has been established at Simon Fraser University.

Preliminary examination of the lithology, structures and micropaleontology of the cores established that the two most prevalent sedimentary environments are fluvial and intertidal; in one core, deposits of the upper delta foreslope were encountered. The logs of two cores representing these environments are presented in Figure 3. The presence of frequent shell fragments and shell beds, characteristic of the contemporary intertidal environment, is evident in core SFU (D) 12 which is interpreted as representing dominantly tidal-flat deposits; whereas characteristic fluvial structures, including fining upward sequences, erosional contacts and gravel layers, are apparent in core SFU (D) 11, interpreted as dominantly channel deposits. Both cores, it should be noted, represent more than one environment of deposition. A summary of core information and preliminary interpretation of dominant depositional environments is contained in Table 1.

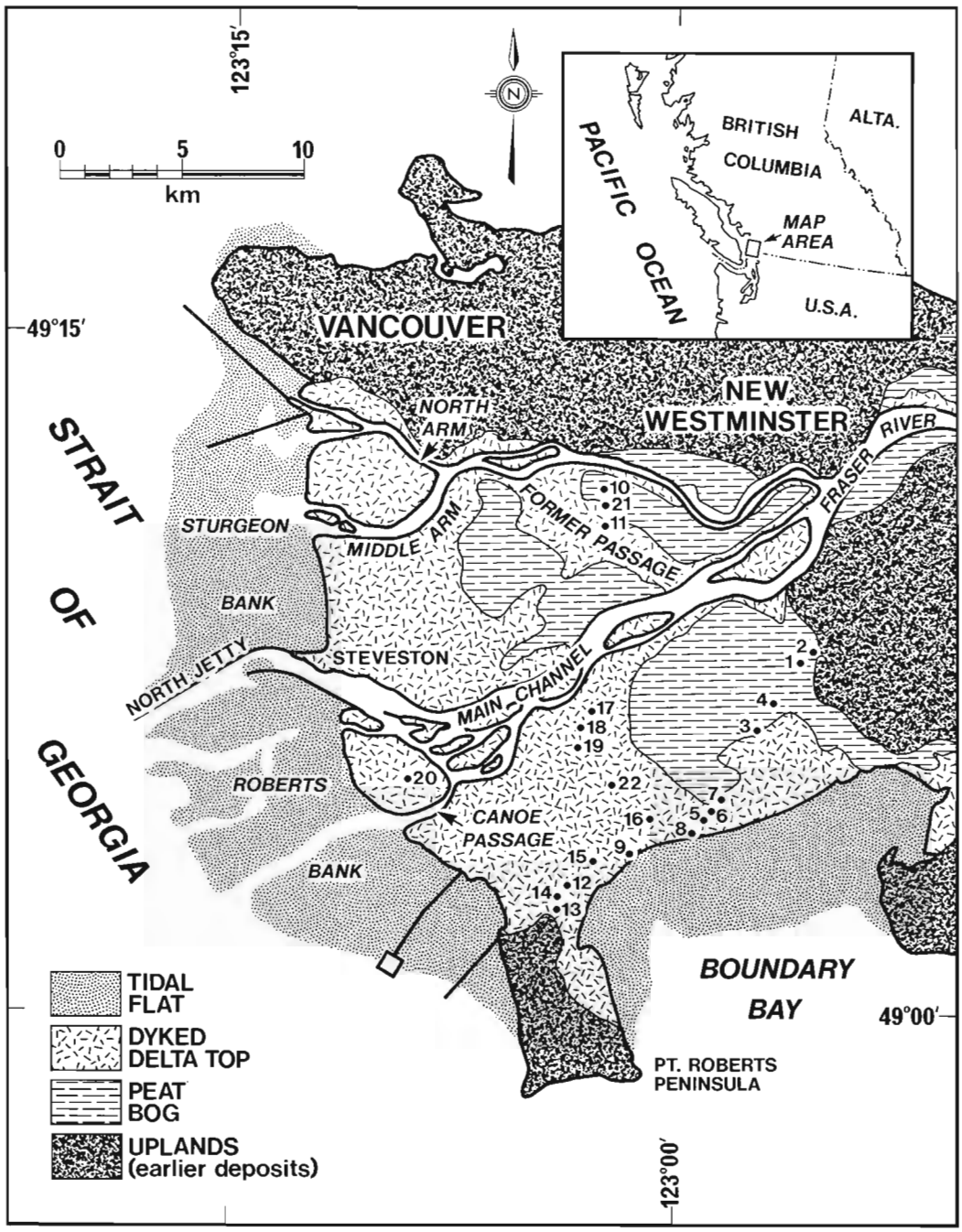

Figure 1. Location of coring sites on the Fraser River delta.

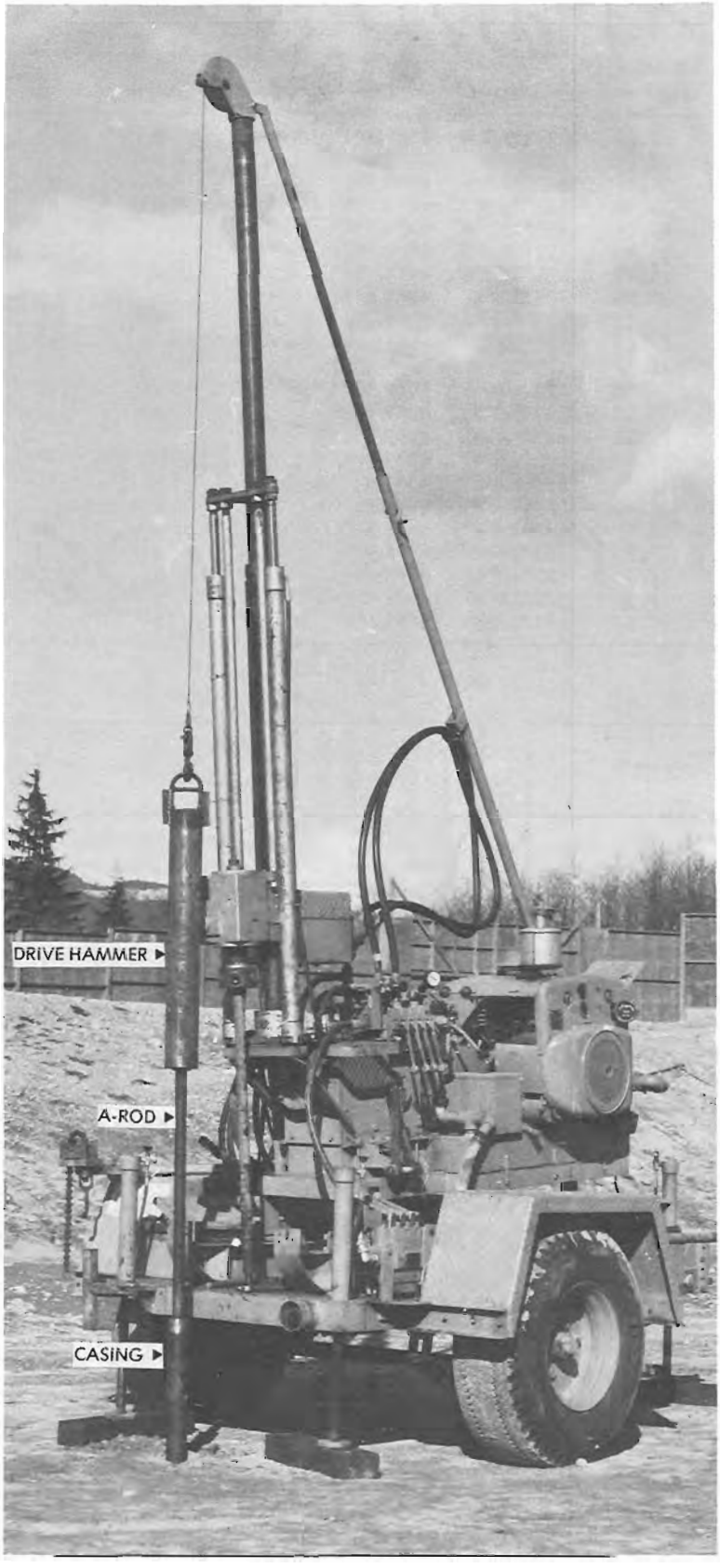

Figure 2. *The Concore C-68 drilling rig in position to set casing. The approximate height of the drill mast is 5 m.*

Table 1. Summary of drillhole data

Drillhole No.	Continuous cored length (m)	Bottom Depth (m)	Location Long.	Location Lat.	Drilling Methods Coring	Drilling Methods Auger	Drilling Methods Rotary	Preliminary Interpretation of dominant depositional environment in core
SFU (D) 1	4.17	7.25	122°55.3'W	49°7.8'N	x	x		Beach
SFU (D) 2	2.7	2.7	122°55'W	49°8'N		x		Beach
SFU (D) 3	10.8	30.5	122°57.4'W	49°6.5'N	x	x	x	Fluvial
SFU (D) 4	12.6	23.18	122°56'W	49°6.7'N	x	x	x	Fluvial
SFU (D) 5	10.86	10.86	122°59.7'W	49°4.2'N	x			Tidal flat
SFU (D) 6	7.44	18.3	122°59.6'W	49°4.5'N	x	x		Tidal flat
SFU (D) 7	8.54	13.73	122°59.4'W	49°4.7'N	x	x		Tidal flat
SFU (D) 8	9.86	9.86	123°0.1'W	49°3.8'N	x			Tidal flat
SFU (D) 9	6.36	14.03	123°1.3'W	49°3.6'N	x	x		Tidal flat
SFU (D) 10	16.52	24.4	123°2.7'W	49°11.2'N	x		x	Fluvial
SFU (D) 11	18.24	28.37	123°2.7'W	49°10.5'N	x		x	Fluvial
SFU (D) 12	14.38	20.94	123°4'W	49°2.5'N	x	x		Tidal flat
SFU (D) 13	4.9	15.56	123°4.1'W	49°2.1'N	x	x		Beach
SFU (D) 14	7.6	18.82	123°4.1'W	49°2.2'N	x	x		Tidal flat
SFU (D) 15	9.6	18.3	123°2.8'W	49°3.2'N	x	x		Tidal flat
SFU (D) 16	9.6	18.3	123°1.4'W	49°4'N	x	x		Fluvial
SFU (D) 17	12.0	18.45	123°2.8'W	49°6.3'N	x	x		Fluvial
SFU (D) 18	10.28	18.3	123°2.8'W	49°5.8'N	x	x		Fluvial
SFU (D) 19	8.15	18.3	123°3'W	49°5.5'N	x	x		Fluvial
SFU (D) 20	8.9	18.3	123°9.5'W	49°5.6'N	x	x		Fluvial
SFU (D) 21	10.52	18.3	123°2.7'W	49°11'N	x	x		Fluvial
SFU (D) 22	8.52	18.3	123°2.8'W	49°4.6'N	x	x		Tidal flat

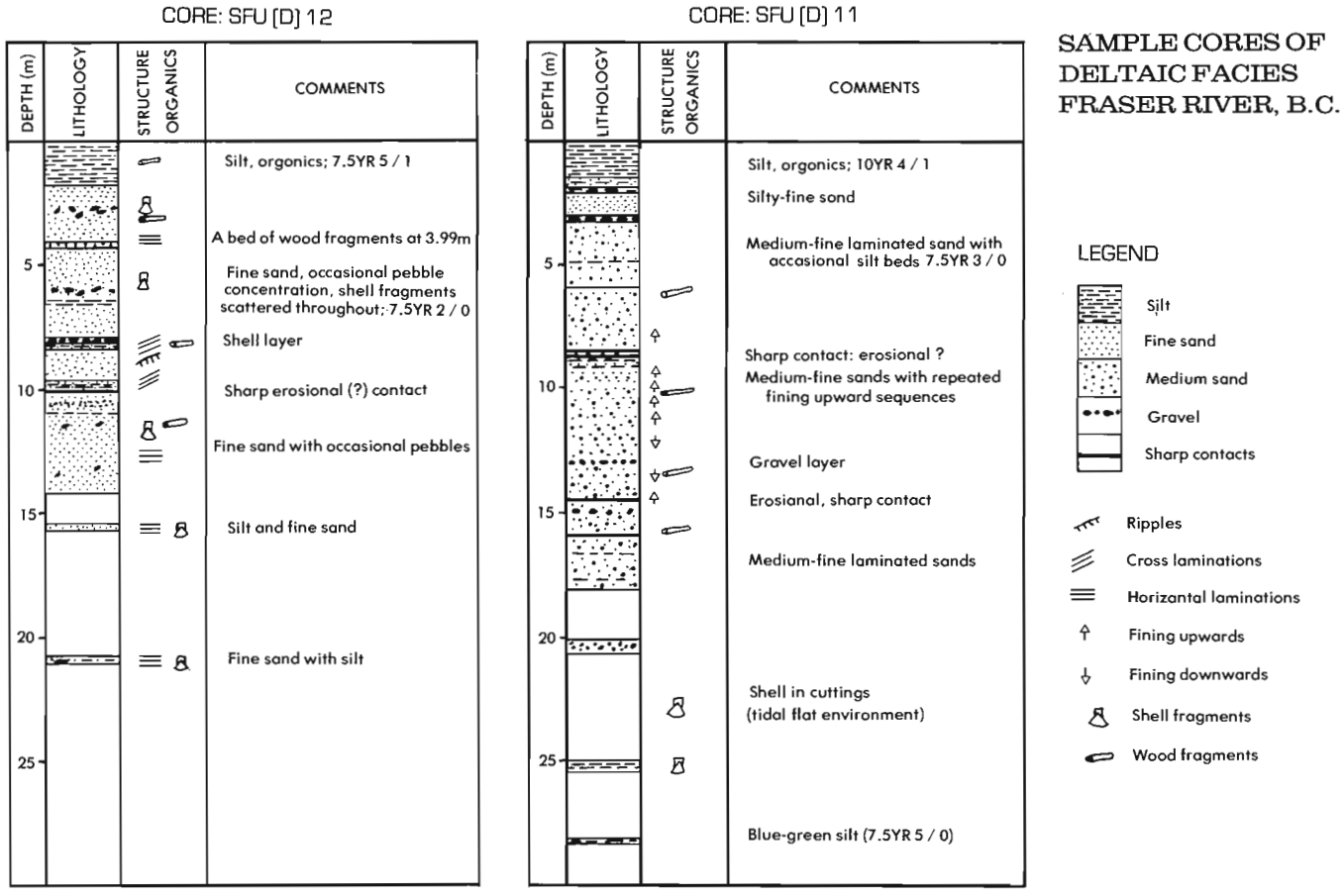

Figure 3. *Field descriptions of two representative cores. Core SFU (D) 12 probably represents a succession from a pro-delta upper slope environment at its base to an intertidal environment. Core SFU (D) 11 probably contains intertidal deposits at its base but fluvial deposits throughout most of the remainder of the core. Both cores are capped by mud derived from Fraser River floods.*

Table 2. Paleoenvironmental analyses of 16 subsamples based on organic/inorganic components of coarse residue

Core SFU (D) 3; sample from 3050 cm.
Residue
- heterogeneous f-c angular to subangular sand
- no microfauna
- presumed environment
  - continental, fluvial

Core SFU (D) 4; sample from 1830 cm.
Residue
- very heterogeneous f-vc angular to subangular sand
- no microfauna
- bivalve fragments; abundant wood fragments
- probable environment
  - very shallow, brackish water, very close to strand line

Core SFU (D) 4; sample from 1861 cm.
Residue
- very heterogeneous, f-vc angular to subangular sand
- no microfauna
- no marine indicators
- common wood fragments and plant tissue
- presumed environment
  - continental, fluvial

Core SFU (D) 4; sample from 2166 cm.
Residue
- very heterogeneous, f-vc angular to subangular sand and small pebbles
- no microfauna
- no marine indicators
- common wood fragments, plant tissue and rootlets
- presumed environment
  - continental, fluvial

Core SFU (D) 10; sample from 1650 cm.
Residue
- heterogeneous f-m angular to subangular sand
- no microfauna
- no marine indicators
- common wood fragments (partly coalified)
- presumed environment
  - continental, fluvial

Core SFU (D) 10; sample from 80 feet (2438.4 cm).
Residue
- heterogeneous f-c angular to subangular sand
- no microfauna
- no marine indicators
- common wood fragments and plant tissue
- rare megaspore
- presumed environment
  - continental, fluvial

Core SFU (D) 11; sample from 1650 cm.
Residue
- heterogeneous f-c angular to subangular sand
- no microfauna
- no marine indicators
- rare coalified wood and plant rootlets
- presumed environment
  - continental, fluvial

Core SFU (D) 11; sample from 93 feet (2834.6 cm).
Residue
- small amount of vf-m angular to subangular sand
- no microfauna
- mussel (**Mytilus** ?) fragment
- rare wood debris
- fairly common limonite (or goethite) crusts
- probable environment
  - very shallow, low energy, brackish water, very close to strand line

Core SFU (D) 12; sample from 1050 cm.
Residue of sediment from within a barnacle encrusted gastropod
- vf-m angular to subangular sand
- common wood fragments (partly coalified), plant tissue, megaspores and rootlets
- rare mussel (**Mytilus** ?) fragments
- Foraminifera
  - **Elphidium incertum** (Williamson) - 1 specimen
  - **Trochammina grisea** Earland - 6 specimens
- Ostracoda
  - **Heterocythereis (Heterocythereis)** sp. - 5 values
  - indet. genus - 2 values
  - **Aurila** ? sp. - 1 juvenile value
- environment
  - shallow marine, somewhat reduced salinity, much continentally derived material (i.e. close to fluvial source).

Core SFU (D) 12; sample from 1218 cm.
Residue from within two bivalve shells
- vf-c angular to subangular sand
- common bivalve, barnacle and gastropod fragments
- common mussel (**Mytilus** ?) fragments
- common wood, plant tissue and rootlets
- rare diatom (**Coscinodiscus** ?)
- Foraminifera
  - **Elphidium incertum** (Williamson) - 1 specimen
  - **Trochammina grisea** Earland - 5 specimens
- Ostracoda
  - **Cyprideis torsa** (Jones) - 5 values
  - **Heterocythereis (Heterocythereis)** sp. - 8 values
  - indet. genus - 2 values
- environment
  - shallow marine, somewhat reduced salinity, much continentally derived material (i.e. close to fluvial source).

Core SFU (D) 12; sample from 68 feet (2072.6 cm).
Residue
- heterogeneous vf-c angular to subangular sand
- common bivalve and barnacle debris
- common mussel (**Mytilus** ?) fragments
- common wood fragments (partly coalified) plant tissue and rootlets
- Foraminifera
  - **Elphidiella hannai** (Cushman & Grant) - 15 specimens
  - **Elphidium incertum** (Williamson) - 1 specimen
- Ostracoda
  - **Radimella** sp. of **R. aurita** (Skogsberg) - 2 values
- environment
  - shallow marine but near normal salinity still with much continentally derived material (i.e. close to fluvial source).

Core SFU (D) 15; sample from 600 cm.
Residue
- very heterogeneous vf-c angular to subangular sand
- common barnacle and bivalve debris
- common wood (partly coalified) and rootlets
- fairly common mussel (**Mytilus** ?) debris
- rare limonite (or goethite crusts)
- probable environment
  - very shallow brackish water, very close to strand line

Core SFU (D) 15; sample from 60 feet (1824.8 cm).
Residue
- heterogeneous f-c angular to subangular sand
- common barnacle and bivalve debris
- common mussel (**Mytilus** ?) fragments
- abundant wood (partly coalified), plant tissue and rootlets
- probable environment
  - very shallow brackish water, very close to strand line

Core SFU (D) 16; sample from 950 cm.
Residue
- heterogeneous vf-m angular to subangular sand
- common wood fragments (partly coalified) & plant tissue
- no microfauna
- no marine indicators
- presumed environment
  - continental, fluvial

Core SFU (D) 18; sample from 580 cm.
Residue
- heterogeneous, vf-m angular to subangular sand
- rare wood fragments
- no microfauna
- no marine indicators
- presumed environment
  - continental, fluvial

Core SFU (D) 22; sample from 550 cm.
Residue
- heterogeneous, vf-m angular to subangular sand
- very rare wood fragments and plant tissue
- fairly common bivalve debris
- no microfauna
- presumed environment
  - very shallow brackish water, very close to strand line

Micropaleontological analysis of an initial set of 16 subsamples from the cores has been completed. These findings along with accompanying paleoenvironmental interpretations are listed in Table 2. These results coincide with preliminary interpretations based on core logs (e.g. SFU (D) 11 – continental, fluvial; SFU (D) 12 – shallow marine).

Discussion and conclusions

The prevalence of shallow-water environments in the upper sediment column is compatible with the pattern of delta development proposed by Clague et al. (1983) which took into consideration the radiocarbon dates and sedimentation rates available for the outer delta (Clague and Luternauer, 1982; Luternauer et al., 1983; Clague et al., 1983). According to this model the sea was at its lowest postglacial position relative to the land at 7000-8000 BP when the front of the Fraser delta probably was far to the southwest of New Westminster and the alluvial surface of the delta was graded to sea level in the Strait of Georgia about 12 m lower than that at present. Between 7700 and 5000 BP sea level appears to have risen relatively rapidly to within 2 m of its present level. The vertical perpetuation of shallow marine depositional environments represented in the cores suggests that the sedimentary accumulation rate kept pace with the rate of submergence. The deposits below 12 m depth, tentatively identified as continental/fluvial, may represent fluvial distributary channels which crossed the alluvial part of the delta. These deposits now lie below the level to which sea level fell relative to land about 7000-8000 BP (i.e. 12 m lower than at present) probably because of compaction and/or subsidence.

The results show that obtaining a more precise definition of the vertical stratigraphy and sedimentary environments of the delta would require: (a) a dense drillhole pattern; (b) that the lithologic descriptions of the cores be supplemented by geophysical logging (resistivity, SP and gamma), shallow seismic surveys; (c) additional micropaleontological analysis, and (d) ^{14}C dates for the establishment of a more detailed geochronology of the delta than presently available.

References

Clague, J.J. and Luternauer, J.L.
1982: Excursion 30A: Late Quaternary sedimentary environments, southwestern British Columbia; 11th International Congress on Sedimentology, Field Excursion Guidebook 30A, 167 p.

Clague, J.J., Luternauer, J.L., and Hebda, R.J.
1983: Sedimentary environments and post glacial history of the Fraser Delta and lower Fraser Valley, B.C.; Canadian Journal of Earth Sciences, v. 20, p. 1314-1326.

Luternauer, J.L., Clague, J.J., and Pharo, C.H.
1983: Substrates of the Strait of Georgia, British Columbia; Canadian Journal of Fisheries and Aquatic Sciences, v. 40, p. 1026-1032.

AN OVERVIEW OF THE SUDBURY-TIMMINS-ALGOMA MINERAL PROGRAM (STAMP), ONTARIO

J.M. Duke
Economic Geology and Mineralogy Division

Duke, J.M., An overview of the Sudbury-Timmins-Algoma Mineral Program (STAMP), Ontario; in Current Research, Part A, Geological Survey of Canada, Paper 85-1A, p. 723-725, 1985.

Abstract

The Sudbury Timmins Algoma Mineral Program was a federal government job creation initiative undertaken in the winter of 1983-84. The program produced both geological and geochemical data which are of interest to the mineral exploration sector. These data are being released by the Geological Survey of Canada as Open Files.

Résumé

Le programme relatif aux minéraux de Sudbury, Timmins et Algoma représentait une initiative du Gouvernement fédéral pour créer des emplois, initiative entreprise pendant l'hiver 1983-1984. Le programme a produit un ensemble de données géologiques et géochimiques certaines d'intéresser le secteur de l'exploration minérale. Les données recueillies paraîtront sous forme de dossiers publics qui seront émis par la Commission géologique du Canada.

Introduction

The Sudbury Timmins Algoma Mineral Program (STAMP) was a federal government job creation initiative designed with two objectives in mind. Firstly it was to provide meaningful short term employment to a significant number of geologists, chemists and other professionals from the mining sector which had been particularly hard hit during the recent recession. Secondly, it was hoped that the program would produce a body of technical data which would be useful in the mineral exploration efforts of the private sector and, depending upon the results, perhaps even stimulate exploration activity.

The program was carried out from 3 October 1983 to 25 May 1984, generating 1792 person-weeks employment. This represents about 90 per cent of the objective set out in the program proposal. Once STAMP was underway, between 43 and 67 individuals were employed at any given time. Altogether, 82 different people were employed at one time or another during the program.

The program was designed and implemented by Energy, Mines and Resources Canada, and managed by Laurentian University. The $1.56 million cost of the program was provided by Employment and Immigration Canada through Section 38 of the Unemployment Insurance Act and the Employment Initiatives Reserve.

Three of the five technical reports resulting from STAMP were released as GSC Open Files during the fall of 1984, and the remaining two are in press. The results described in these reports are outlined briefly below.

Description of the program

Project 1 - mineral data base

The objectives of this project were to collect, code and enter basic information on mineral occurrences in north-central Ontario into the Geological Survey of Canada mineral data bank, specifically the CANMINDEX file (Picklyk et al., 1978); to provide information on these occurrences to the Ontario Geological Survey in their file format, and update information for the EMR National Mineral Inventory (NMI) system; and to compile available rock geochemical data for a file maintained by the Department of Geology, Laurentian University.

A total of 1300 townships in the STAMP area were covered. This resulted in 1110 occurrences being added to the CANMINDEX file and the substantial revision of the records for 1130 occurrences. The CANMINDEX data are incorporated in a report entitled "Mineral Inventory of the Sudbury-Timmins-Sault Ste. Marie Region" (Rose, in press). The report includes index level data for a total of 2240 mineral occurrences. The information includes location of the occurrence, commodities present, a brief geological characterization of the occurrence, and literature and map references.

Project 2 - Swayze Belt overburden geochemistry

The Swayze greenstone belt has been identified as an area worthy of exploration, particularly for gold (e.g., Siragusa, 1983). The objective of this project was to identify target areas for mineral exploration by geochemical sampling and analysis of material from eskers which cross the Swayze belt. Although glacial till has been used extensively as a sampling medium for geochemical exploration in the Canadian Shield, the use of esker material for this purpose has been limited. Base-of-till sampling is normally carried out using drilling equipment and is often very costly. Moreover, interpretation of the data from till sampling presupposes a more detailed knowledge of the local Quaternary geology than is normally available. Eskers typically form well-defined and readily accessible topographical ridges and, because sampling is carried out using hand tools, sample collection is a relatively quick and inexpensive operation.

The results of the project are reported by Richard (in press). Thirteen eskers in the Chapleau-Foyleyet-Gogama area were sampled at 0.5 km intervals yielding 398 samples for chemical analysis. A fine fraction was separated from each sample and analyzed for gold, copper, nickel, lead, zinc, silver, cobalt, iron and manganese. In addition, 302 clast samples were collected for lithological analysis, and in particular were used to estimate the distance of sediment transport by the esker stream. Richard (in press) reported that many samples carried anomalous metal concentrations. Anomalous gold concentrations were observed in samples from the Penhorwood, Groundhog, Mallard, Jerome and Huffman eskers, whereas high silver values were detected in

the Penhorwood, Garnet, and Jerome eskers. Anomalous levels of the base metals, particularly nickel, were observed in many of the eskers sampled.

Project 3 - Lithogeochemistry of the Huronian Supergroup

The objective of this project was to identify areas of anomalous base and precious metal concentrations in upper Huronian sedimentary rocks in the area between Sudbury and Sault Ste. Marie, specifically the Lorrain Formation and the contact of the Lorrain with the overlying Gordon Lake Formation. The Lorrain Formation is known to contain paleo-placer gold concentrations in the area northeast of Sudbury (Colvine, 1981; Long et al., 1982) and it was desired to see whether similar concentrations occur in the STAMP area. Furthermore, the contact between the Lorrain and Gordon Lake formations is the locus of stratabound copper mineralization between Elliot Lake and Sault Ste. Marie (Pearson, 1980).

A total of 2189 samples were collected and analyzed for gold, copper, nickel, zinc, lead, manganese and iron and the results were reported by Tortosa (1984). The results indicate definite stratigraphic and lithological controls on the distribution of gold. The mean gold content was highest in rocks of the upper red quartzite member of the Lorrain Formation where the mean was 10.6 ppb. Similarly, heavy mineral beds and pebbly beds with heavy minerals contained the highest average gold concentration, a distribution consistent with their concentration as placers. Although numerous anomalous concentrations of gold were observed, nowhere did values exceed 250 ppb. Tortosa (1984) concluded that sediments sampled during the program represented distal facies, and that the more proximal facies present in Huronian outliers north of Sault Ste. Marie and Sudbury and in the Rawhide Lake-Wakomata Lake areas would have higher potential for placer gold concentrations. A significant finding was the association of anomalous gold concentrations associated with copper mineralization in the Stag Lake area which, as Tortosa (1984) noted, may indicate that the Lorrain-Gordon Lake contact is a target for gold as well as copper exploration.

Project 4A - mineralization in the Onaping Formation

The Onaping Formation lies at the base of the Early Proterozoic Whitewater Group, the mainly sedimentary sequence which fills the Sudbury basin. Disseminated sulphide minerals are ubiquitously distributed within the Onaping Formation (Rousell, 1983) and stratabound Zn-Pb-Cu deposits occur near the base of the overlying Onwatin Formation (i.e., the Errington and Vermillion deposits). The main objective of this project was to characterize the distribution of copper, nickel, zinc, lead and gold in two representative and well-mapped areas within the Onaping as a basis for further research and exploration of the Whitewater sequence.

A total of 595 samples from Morgan and Dowling townships were collected and analyzed, and the results are described by Bussolaro et al. (1984). They found that the concentrations of Cu, Zn and Ni are generally low (median values <100 ppm) and that there are no significant differences either between the two sample areas or among the three members of the Onaping Formation. Gold was detected in 200 of the 374 samples from Morgan township but the highest concentration was 20 ppb and most were less than 10 ppb. The samples from Dowling township were not analyzed for gold.

Project 4b - metamorphic mineralogy and chemical alteration of the Temagami greenstone belt

The Temagami greenstone belt consists of a succession of Archean metavolcanic rocks, clastic sediments and iron formation which has been intruded by both mafic and felsic plutons. The Archean rocks are unconformably overlain in places by Early Proterozoic sediments of the Gowganda Formation and Nipissing diabase sills. The objective of this project was to identify areas within the Archean metavolcanic sequence that have undergone hydrothermal alteration and therefore constitute targets for base and precious metal exploration. A total of 825 samples were collected at intervals of 300 m or less on traverses separated by about 1 km. The samples were analyzed for major and minor elements by x-ray fluorescence methods, and the resulting data were processed using the discriminant analysis technique outlined by Beswick and Nichol (1980). The mineralogy of the samples was determined by x-ray diffraction techniques.

The results of this project are reported by Beswick and James (1984). The mineralogical studies showed that unaltered mafic rocks were characterized by assemblages containing plagioclase-amphibole-carbonate-quartz whereas hydrothermally altered rocks were dominated by chlorite, carbonate, epidote, and white mica. The relatively less altered felsic rocks contained quartz, plagioclase, white mica, and minor chlorite and epidote. The hydrothermally altered assemblages tend to lack plagioclase and epidote and are dominated by white mica, carbonate, chlorite and quartz. A general correspondence was noted between alteration assemblages and known mineral occurrences in the project area. Ten anomalous areas were identified on the basis of the discriminant analysis of the analytical data. Some of these areas correspond with known mineral occurrences or deposits but others do not. Beswick and James (1984) recommended five of the anomalous areas as potential targets for further exploration.

Project 5 - program administration

The objective of this project was to provide administrative support for the five scientific projects carried out under STAMP. A small administrative and clerical staff was hired under the program in order to reduce the load which would otherwise have fallen on the University.

Conclusion

STAMP achieved its two primary objectives in terms of job creation and the generation of a body of geoscientific data of practical as well as scientific value. It is hoped that the database produced by STAMP will lead to follow-up work by the exploration sector and will also provide a basis for further research. Moreover, STAMP demonstrated the feasibility of mounting, in a very short time period, a useful geoscientific program which involves a number of participating organizations in different jurisdictions.

Acknowledgments

The success of STAMP may be attributed to the co-operative efforts of many individuals including the following who were largely responsible for the design, implementation and management of the program: F.W. Chandler, D.C. Findlay, D.F. Garson, C.R. McLeod, K.H. Poulsen, W.W. Shilts, J. Stapledon, and R.I. Thorpe of the Geological Survey of Canada; C. Bowstead of the Earth Sciences Sector, EMR; R. Keyes of the Mineral Policy Sector, EMR; D. Janes and M. Bozzo of Employment and Immigration Canada in Sudbury; A.E. Beswick and D. Goldsack of Laurentian University. We are indebted to the Resident Geologists of the Ontario Ministry of Natural Resources in Sudbury, Timmins and Sault Ste. Marie for providing work space and access to certain files. Finally, and most importantly, we must acknowledge the conscientious and enthusiastic efforts of the individuals employed under the program.

References

Beswick, A.E. and James, R.S.
1984: The metamorphic mineralogy and chemical alteration of the Temagami greenstone belt; Geological Survey of Canada, Open File 1091.

Beswick, A.E. and Nichol, I.
1980: Alteration in mineralized and unmineralized greenstones; Ontario Geological Survey, Miscellaneous Paper 93, p. 39-47.

Bussolaro, N., Rousell, D.H., and Beswick, A.E.
1984: Mineralization in the Onaping Formation, Sudbury Basin, Ontario; Geological Survey of Canada, Open File 1090.

Colvine, A.C.
1981: Reconnaissance of the Lorrain Formation, Northern Cobalt Embayment; Ontario Geological Survey, Miscellaneous Paper 100, p. 187-190.

Long, D.G.F., Leslie, C., and Colvine, A.C.
1982: Placer Gold in the Huronian of the Cobalt Plain; Ontario Geological Survey, Geoscience Research Seminar 1982, p. 16.

Pearson, W.N.
1980: Copper metallogeny, North Shore region of Lake Huron, Ontario; Ph.D. thesis, Queen's University, Kingston, 403 p.

Picklyk, D.D., Rose, D.G., and Laramee, R.M.
1978: Canadian Mineral Occurrence Index (CANMINDEX) of the Geological Survey of Canada; Geological Survey of Canada, Paper 78-8.

Richard, J.A.
– Geochemistry of eskers of the Swayze Belt; Geological Survey of Canada, Open File 1088. (in press)

Rose, D.G.
– Inventory of the Sudbury-Timmins-Sault Ste. Marie region, Ontario; Geological Survey of Canada, Open File 1087. (in press)

Rousell, D.H.
1983: Nature and origin of mineralization inside the Sudbury Basin; Ontario Geological Survey, Open File 5443.

Siragusa, G.M.
1983: Southern Swayze belt needs more exploration to determine potential; The Northern Miner, April 21, 1983, p. A16.

Tortosa, D.
1984: Lithogeochemistry of Huronian Supergroup, Bruce Mines and Whitefish Falls areas, northern Ontario; Geological Survey of Canada, Open File 1089.

REINTERPRETATION OF THE AGE OF A SUCCESSION OF PALEOZOIC STRATA, DELPHINE CREEK, SOUTHEASTERN BRITISH COLUMBIA

Project 810010

K.G. Root[1]
Institute of Sedimentary and Petroleum Geology, Calgary

Root, K.G., Reinterpretation of the age of a succession of Paleozoic strata, Delphine Creek, southeastern British Columbia; in Current Research, Part A, Geological Survey of Canada, Paper 85-1A, p. 727-730, 1985.

Abstract

Strata in the Delphine Creek area of southeastern British Columbia that were assigned to the Eo-Cambrian Hamill Group, are now reassigned to the Middle Devonian Mount Forster Formation. The Mount Forster Formation at Delphine Creek, and at the type section at Mount Forster, exhibits considerable lateral variation in lithologic character, ranging from dominantly sandstone successions to successions with significant components of argillite. Clasts of fossiliferous dolomite, apparently derived from the Ordovician-Silurian Beaverfoot Formation, are present in conglomerate horizons at various stratigraphic levels in the sandy facies at Delphine Creek and Mount Forster.

Résumé

Les strates de la région du ruisseau Delphine, dans le sud-est de la Colombie-Britannique, assignées au groupe éocambrien de Hamill, sont maintenant placées dans la formation de Mount Forster du Dévonien moyen. La formation de Mount Forster au ruisseau Delphine, et à l'emplacement de la coupe type au mont Forster, manifeste une variation latérale considérable de son caractère lithologique; on y trouve en effet des successions principalement composées de grès, et des successions contenant des quantités notables d'argilite. Dans des horizons conglomératiques, à divers niveaux stratigraphiques des faciès sableux au ruisseau Delphine et au mont Forster, on rencontre des clastes de dolomie fossilifère, apparemment dérivés de la formation ordovicienne et silurienne de Beaverfoot.

Introduction

Root (1983) reported the presence at Delphine Creek of a previously recognized outlier of Paleozoic strata in the Purcell Anticlinorium. In that earlier report, a succession of unfossiliferous clastic rocks, which lies unconformably on the Upper Proterozoic Horsethief Creek Group and is unconformably overlain by the Upper Devonian Starbird Formation, was assigned to the Eo-Cambrian Hamill Group on the basis of rock type. Subsequent fieldwork indicates that the assignment of these strata to the Hamill Group was incorrect, and suggests that the succession is part of the Middle Devonian Mount Forster Formation.

The Mount Forster Formation at Delphine Creek

Strata at Delphine Creek now assigned to the Mount Forster Formation consist of dolomitic and calcareous sandstone, quartzite, dolomitic and calcareous argillite, dolomite, granule and pebble conglomerate, basic volcanic flows, and locally, cobble and boulder conglomerate. The Mount Forster Formation at Delphine Creek outcrops in two areas (Fig. 1). The western exposure is located within the hanging wall of the Delphine Creek thrust fault and comprises mainly medium- to coarse-grained sandstone and quartzite (Fig. 2, Section A). One volcanic flow is present at the location at which Section A was measured (Fig. 1, 2); two additional flows outcrop within this exposure but to the west of Section A. The two flows are lenticular, are up to 1.5 m and 14 m thick respectively, and occur approximately 15 m and 90 m stratigraphically above the level of the flow present in Section A. The flows are locally amygdaloidal and pillowed.

Cobble and boulder conglomerate is present at, or near, the base of the succession, locally in horizons up to 12 m thick. Clasts within the conglomerates are well rounded, range up to 50 cm in diameter, and consist of quartzite, sandy dolomite, and dolomitic sandstone.

Quartz-pebble conglomerate is common throughout the exposure within the Delphine Creek thrust sheet and, in some localities, includes scattered pebbles of light grey dolomite containing crinoid ossicles and coral fragments (Fig. 2, Section A). The fossiliferous clasts are lithologically similar to dolomite of the Upper Ordovician and Lower Silurian Beaverfoot Formation, suggesting that they were derived from it. In easternmost exposures within the Delphine Creek thrust sheet, pebbles and cobbles of this fossiliferous dolomite are very abundant throughout the section and occur in conglomeratic horizons ranging in thickness from several centimetres to about 50 cm. The dolomite clasts occur within a matrix of medium grained dolomitic sandstone, are commonly 1 cm to 3 cm in diameter but range up to 8 cm in diameter, and constitute 20 to 60 per cent of the rock. The majority of the clasts in these conglomerate horizons are the above-mentioned fossiliferous dolomite, but pebbles of brown, nonfossiliferous dolomite and minor pebbles and granules of quartz are also present.

The Mount Forster Formation in the Delphine Creek thrust sheet thins rapidly westward to a zero edge (Root, 1983). Detailed mapping of individual lithostratigraphic units within the succession demonstrates that westward thinning is due largely to depositional thinning. Pre-Starbird Formation erosion and, in westernmost exposures, a probable internal unconformity at the approximate stratigraphic level of the volcanic flow in Section A (Fig. 2) also contribute to the westward thinning.

[1] Department of Geology and Geophysics, The University of Calgary, Calgary, Alberta T2N 1N4

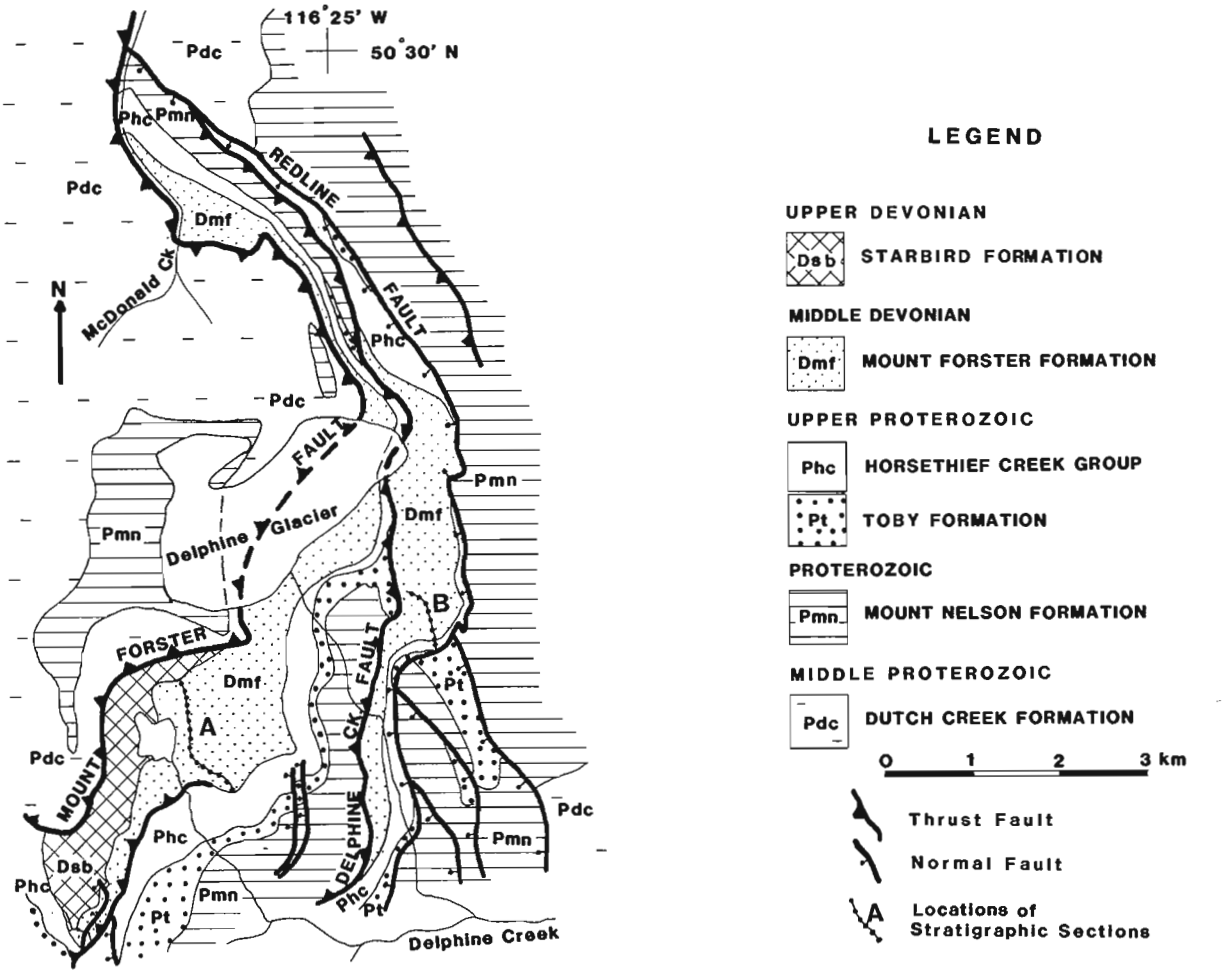

Figure 1. Generalized geological map of the Delphine Creek area. Geology by Freiholz (1983) and the author.

Since the original description of the Paleozoic strata at Delphine Creek by Root (1983), an additional exposure of Mount Forster Formation has been mapped in the footwall of the Delphine Creek thrust fault to the west of the Redline normal fault (Fig. 1). In marked contrast to the succession exposed in the hanging wall of the Delphine Creek thrust sheet, this exposure contains a significantly greater proportion of purple and green, calcareous and dolomitic argillite (Fig. 2, Section B). Horizons of quartz granule-and-pebble conglomerate are present but are relatively rare; no clasts of Beaverfoot Formation dolomite have been recognized.

The Mount Forster Formation at Mount Forster

Published accounts concerning the Mount Forster Formation at the type section on Mount Forster describe the succession as consisting dominantly of red and green, calcareous and dolomitic argillite, and sandy and silty argillite, with subordinate horizons of dolomite, sandy dolomite, and sandstone (Walker, 1926; Reesor, 1973; Norford, 1981). A stratigraphic section measured approximately 2 km southwest of the section measured near the summit of Mount Forster by Norford (1981), however, consists chiefly of sandstone with only minor horizons of red and green argillite, dolomite, and sandy dolomite, and demonstrates considerable variability in lithologic character. Conglomerate horizons, comprising fossiliferous pebbles interpreted as Beaverfoot Formation dolomite in a dolomitic sandstone matrix, are located at about 175 m, 355 m, and 385 m above the base of the 440 m thick section. These conglomerates are virtually identical to those at Delphine Creek in the easternmost exposures of the Delphine Creek thrust sheet.

Discussion

The discovery of clasts of fossiliferous dolomite, apparently derived from the Ordovician-Silurian Beaverfoot Formation, within the sequence of unfossiliferous strata at Delphine Creek indicates that the succession cannot be correlated with the Eo-Cambrian Hamill Group, as previously suggested by Root (1983). The succession at Delphine Creek can, however, be confidently assigned to the Middle Devonian Mount Forster Formation on the basis of the similar rock types and the occurrence of marked lateral lithological variations present in both the Delphine Creek succession and the Mount Forster Formation at Mount Forster. The exposures of Mount Forster Formation at Delphine Creek are the most westerly exposures of the Formation.

Reinterpretation of the strata at Delphine Creek as the Mount Forster Formation, rather than the Hamill Group, indicates that stratigraphic relationships in the region of the Purcell Anticlinorium are not as complex as depicted in a

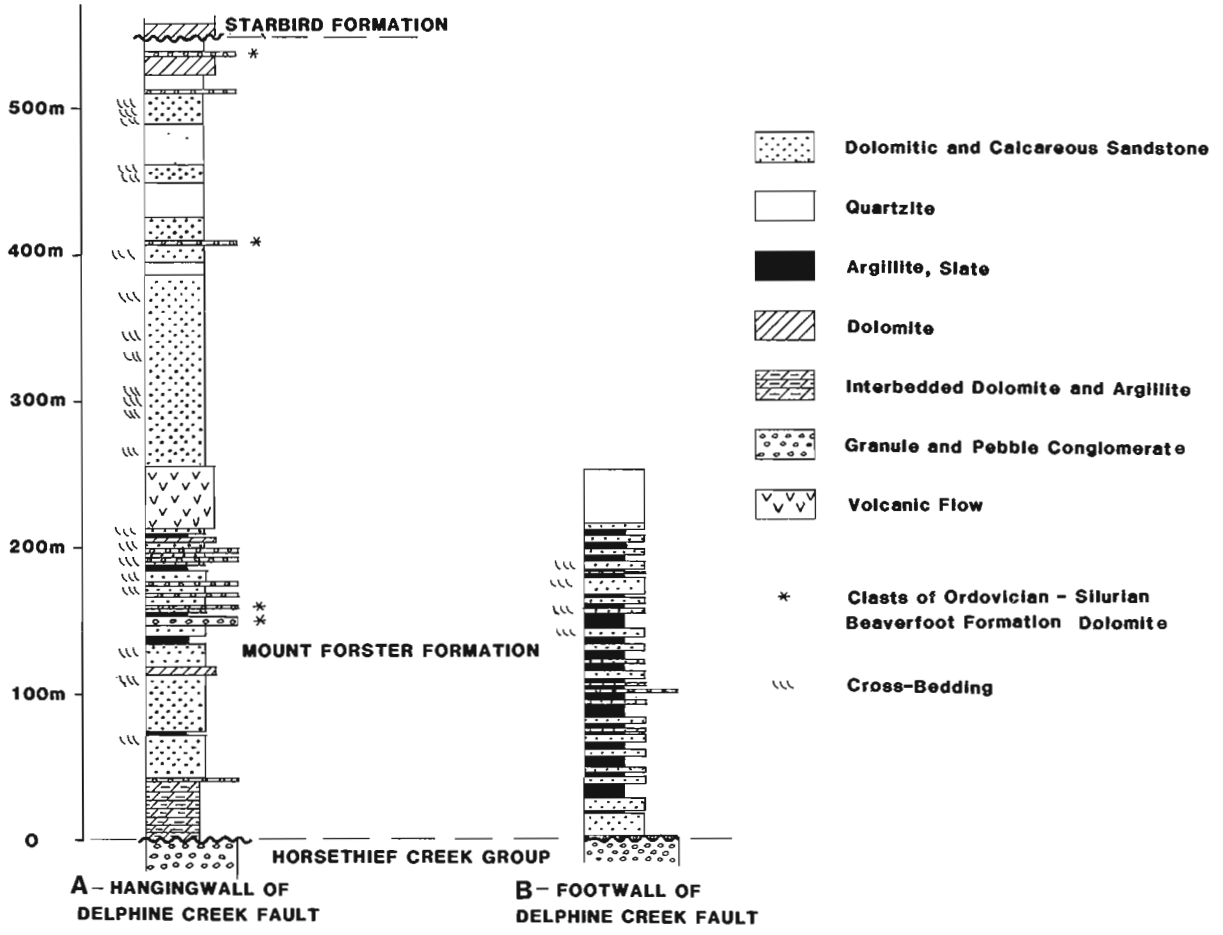

Figure 2. Generalized stratigraphic sections of the Mount Forster Formation in the Delphine Creek area. Section locations are shown in Figure 1.

schematic stratigraphic cross-section by Root (1983). The cross-section illustrates an earlier interpretation that the clastic succession between the Horsethief Creek Group and the Starbird Formation at Delphine Creek is an exposure of Hamill Group strata deposited in a half-graben, and also that the Mount Forster Formation thins to a zero edge between Mount Forster and Delphine Creek. Assignment of the succession at Delphine Creek to the Mount Forster Formation permits simple stratigraphic correlations; the Horsethief Creek Group, the Mount Forster Formation, and the Starbird Formation can be correlated between Mount Forster and Delphine Creek. An 800 m thick succession comprising the Upper(?) Cambrian Jubilee Formation, the Cambro-Ordovician McKay Group, and the Upper Ordovician (and Silurian?) Beaverfoot Formation is present between the Horsethief Creek Group and the Mount Forster Formation on the eastern slopes of Mount Forster (Reesor, 1973). These Lower Paleozoic strata are absent at Delphine Creek due to either nondeposition or to pre-Middle Devonian erosion along a paleo-high termed the Purcell Arch (Douglas et al., 1970) or the Windermere High (Reesor, 1973).

Acknowledgments

The study of the Mount Forster Formation at Delphine Creek constitutes part of a geological investigation carried out under the supervision of P.S. Simony. Many thanks to W.K. Foo for sharing his knowledge of the sandy facies of the Mount Forster Formation at Mount Forster, and for assisting in measuring a stratigraphic section through it. Discussions with W.K. Foo and S. Bennett have been most helpful. H.H.J. Geldsetzer and B.S. Norford critically reviewed an earlier draft of the manuscript and made many useful suggestions.

References

Douglas, R.J.W., Gabrielse, H., Wheeler, J.O., Stott, D.F., and Belyea, H.R.

1970: Geology of western Canada; in Geology and Economic Minerals of Canada, ed. R.J.W. Douglas; Geological Survey of Canada, Economic Geology Report 1, p. 365-488.

Freiholz, G.
1983: The stratigraphic and structural setting of a lead-zinc occurrence near Invermere, southeastern British Columbia; unpublished M.Sc. thesis, the University of Calgary, Calgary, Alberta, 203 p.

Norford, B.S.
1981: Devonian stratigraphy of the margins of the Rocky Mountain Trench, Columbia River, southeastern British Columbia; Bulletin of Canadian Petroleum Geology, v. 29, no. 4, p. 427-448.

Reesor, J.E.
1973: Geology of the Lardeau map area, east half, British Columbia; Geological Survey of Canada, Memoir 369, 129 p.

Root, K.G.
1983: Upper Proterozoic and Paleozoic stratigraphy, Delphine Creek area, southeastern British Columbia: implications for the Purcell Arch; in Current Research, Part B, Geological Survey of Canada, Paper 83-1B, p. 377-380.

Walker, J.F.
1926: Geology and mineral deposits of the Windermere map area, British Columbia; Geological Survey of Canada, Memoir 148, 69 p.

MOLES AS AGENTS OF EROSION IN THE OTTAWA AREA, ONTARIO

Project 810005

P.A. Egginton
Terrain Sciences Division

Egginton, P.A., Moles as agents of erosion in the Ottawa area, Ontario; in Current Research, Part A, Geological Survey of Canada, Paper 85-1A, p. 731-733, 1985.

Abstract

Within the Ottawa region of Ontario, where habitat is favourable and densities are high, moles may be significant agents of erosion, moving 14-28 tonnes/ha/a. Their burrowing activity alters soil permeability and as water table conditions change through the year, their tunnels may become pipes intercepting and channelling subsurface flow.

Résumé

Dans la région d'Ottawa, en Ontario, là où l'habitat est favorable et les populations élevées, les taupes sont parfois des agents importants d'érosion, pouvant déplacer de 14 à 28 tonnes/ha/a. En fouissant la terre, elles modifient la perméabilité du sol et, à mesure que les conditions hydrologiques souterraines se modifient au cours de l'année, leurs tunnels peuvent devenir des puits qui interceptent et dirigent les eaux souterraines.

Introduction

Generally the role of animals as agents of erosion has been overlooked by geomorphologists. Many animals tunnel or burrow, they move material at depth to the surface, alter soil permeability, expose what may be readily eroded material, and displace material downslope.

The quantities of material moved may be prodigious. Darwin (1881), in a classic work, found that earthworms move 18-44 tonnes/ha/a. Ground squirrels in the Yukon displace 18 tonnes/ha/a (Price, 1971) and pocket gophers in alpine tundra zones diplace up to 27.7 tonnes/ha/a (Thorn, 1978, 1982). In favourable areas in Luxembourg, voles and moles raise 20 tonnes/ha/a (Imeson and Kwaad, 1976; Imeson, 1976).

This study was undertaken to provide a preliminary estimate of the quantity of material moved, per unit area, by moles in the Ottawa area.

Study area

The study area is situated along the floodplain of Union Hall Creek located some 56 km west of Ottawa (Fig. 1). Here organic muck and limited quantities of sand and gravel overlie Champlain Sea clays. Molehills and tunnels are common in this area and on the basis of habitat, tunnel size, and trapping, they are related for the most part to the burrowing activity of the star-nosed mole (**Condylura cristata**).

Distribution and habitat of the star-nosed mole

The star-nosed mole has the most extensive distribution of any Canadian mole, ranging from Manitoba to Cape Breton (Fig. 1). It prefers wet places with soils ranging from clay-loam to sand or muck and is most abundant along small streams. The tunnels made by this mole are found 3 to 60 cm below the surface. Nearly all tunnel systems have branches opening at or below water level in adjacent streams or ponds. In swampy ground, tunnels may be below the water table. Excess earth from deeper tunnels is pushed out, forming the familiar molehills (Fig. 2). The distribution of this mole, because of its habitat, is rather patchy. Densities of 25 and 41 animals per hectare have been reported (van Zyll de Jong, 1983).

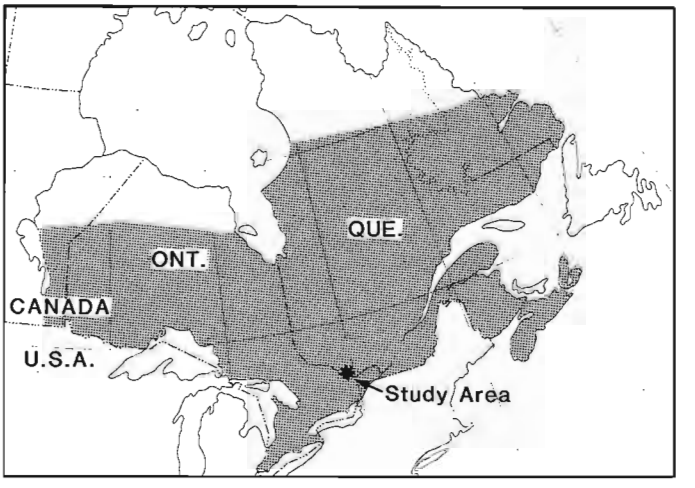

Figure 1. *The location of the study area and the distribution (shaded area) of the star-nosed mole (adapted from van Zyll de Jong, 1983, p. 179).*



Figure 2. *Molehills at the study site; the 100 m^2 plot is bounded by stakes.*

Methodology

Fresh molehills were found in mid April 1984 along a pathway frequented by the author. The hills did not exist in mid October 1983. A 10 by 10 m plot in the middle of this area was staked out and the hills within it were examined (Fig. 2). The muds and muck which comprise the molehills were pushed out over a sod of grasses and legumes. The muds and muck were scraped from the sod surface using a shovel and trowel, then a spring balance was used to determine the weight of material, at field moisture content, comprising each molehill.

Outside the 100 m^2 plot, water was found issuing from several mole tunnels. The discharge was determined by using a pipe to funnel the water into a bucket of known volume and recording the time required to fill the bucket.

Results and discussion

Nineteen distinct molehills were identified within the 100 m^2 plot. The largest contained 20 kg of mud and muck, the smallest, 1 kg. In total 140 kg of material was recovered from the plot. On this basis, over the six-month period October 15, 1983 to April 15, 1984, the moles moved 14 tonnes/ha.

The amount of material moved by the moles over the subsequent six month period, April 15, 1984 to October 15, 1984, coincident with the growing season, is more difficult to assess. Any material pushed to the surface was rapidly vegetated. As a result, an accurate determination of the material moved during this period requires intensive study and a methodology beyond the scope of this study. On the other hand, if it is assumed that similar amounts of material are moved during the two six-month periods, then a reasonable estimate of the quantity of material moved by the



Figure 3. *Molehill with a central tunnel that has become a seepage route. A small delta or fan (arrow) has formed downslope of the hill. The lens cap to the left of the molehill gives scale.*

moles during the 12 month period is 28 tonnes/ha. Conservatively, the moles moved at least 14 tonnes/ha/a and possibly 28 tonnes/ha/a.

Over a number of years moles can essentially rework the entire surface of their preferred habitat, significantly altering runoff characteristics. Burrowing and turning over the soil increases soil permeability, and the microrelief of the molehills diverts and channels surface runoff. The interconnected tunnelways can become local drainageways as they are extensive and commonly extend below the water table. In April 1984 the discharge issuing from three tunnels located less than 10 m apart was measured at 0.3, 1.2, and 2.4 L/minute, respectively. At the latter two sites, discharges of similar magnitude were maintained for 10 days or longer. Substantial quantities of material can move through these tunnels. In some places microdeltas or fans are produced at tunnel outlets (Fig. 3). At one site more than 30 kg of material was so deposited.

Clearly, in eastern Canada, as in the Ottawa region, where habitat is suitable and densities are high, moles can be significant agents of erosion and/or significant biological influences on geomorphic process.

References

Darwin, C.R.
1881: The formation of vegetable mould through the action of worms with observations on their habitats; published in 1945 as "Darwin and the Earthworms"; Faber, London.

Imeson, A.C.
1976: Some effects of burrowing animals on slope processes in the Luxembourg, Ardennes, Part I: The excavation of animal mounds in experimental plots; Geografiska Annaler, v. 58A, no. 1-2, p. 115-125.

Imeson, A.C. and Kwaad, F.J.P.M.
1976: Some effects of burrowing animals on slope processes in the Luxembourg, Ardennes, Part II: The erosion of animal mounds by splash under forest; Geografiska Annaler, v. 58A, p. 317-328.

Price, L.W.
1971: Geomorphic effect of the arctic ground squirrel in an alpine environment; Geografiska Annaler, v. 53A, no. 2, p. 100-105.

Thorn, C.
1978: A preliminary assessment of the geomorphic role of pocket gophers in the alpine zone of the Colorado Front Range; Geografiska Annaler, v. 60A, p. 181-187.

1982: Gopher disturbance: Its variability by Brawn-Blanquet vegetation units in the Niwot Ridge alpine tundra zone, Colorado Front Range, U.S.A.; Arctic and Alpine Research, v. 14, p. 45-51.

van Zyll de Jong, C.G.
1983: Handbook of Canadian Mammals; 1. Marsupials and Insectivores; National Museum of Natural Sciences, National Museums of Canada Publication, p. 176-183.

FEDERAL-PROVINCIAL MINERAL DEVELOPMENT PROGRAMS 1984-89 AND OTHER FEDERAL PROGRAMS

PROGRAMMES FÉDÉRAUX-PROVINCIAUX DE MISE EN VALEUR DES RESSOURCES MINÉRALES, 1984 à 1989, ET AUTRES PROGRAMMES FÉDÉRAUX

THE KING'S POINT COMPLEX, WESTERN NEWFOUNDLAND[1]

Project 730044

B. Mercer[2], D.F. Strong[2], D.H.C. Wilton[2], and D. Gibbons[3]
Precambrian Geology Division

Mercer, B., Strong, D.F., Wilton, D.H.C., and Gibbons, D., The King's Point Complex, western Newfoundland; in *Current Research, Part A, Geological Survey of Canada, Paper 85-1A, p. 737-741, 1985.*

Abstract

The King's Point Complex provides a section across the interface between a high-level granite-syenite complex and its overlying volcanic carapace. The volcanic rocks are dominantly welded silicic ash-flow tuffs, and the plutonic rocks are mainly granite and syenite which are mutually gradational through variations in proportions of quartz and alkali feldspar phenocrysts. Both may be locally metasomatized with the production, or at least enhancement, of peralkaline chemistry and the growth of hydrothermal riebeckite oikocrysts. The lithological assemblages, the elliptical shape of the complex, and the arcuate ring dyke at its northern margin suggest that the Complex may be a site of major surface cauldron subsidence.

Résumé

Le complexe de King's Point nous fit voir une section transversale de la surface de contact entre un complexe de grainite-syénite de niveau élevé et sa carapace volcanique susjacente. Les roches volcaniques sont dominées par des tufs soudés de cendres et de débris de lave siliceux, et les roches plutoniques sont surtout constituées de granite et de syénite, dans des proportions qui varient en fonction de la quantité de quartz et de phénocristaux de feldspath alcalin. Les deux groupes de roches sont métasomatosés par endroits; on y observe alors une production ou, du moins, une accentuation de la peralcalinité et une croissance de cristaux oecillitiques de riébeckite hydrothermale. Les assemblages lithologiques, la forme elliptique du complexe et la présence d'un dyke annulaire arqué à la bordure nord donnent à penser que les roches du complexe de King's Point sont peut-être le théâtre d'un vaste mouvement d'effondrement circulaire en surface.

INTRODUCTION

The King's Point Complex, at the base of Baie Verte Peninsula near the community of King's Point, provides a cross-section through a felsic volcanic-plutonic system. It underlies the main part of the King's Point map sheet (12 H/9; scale 1:50 000) and extends northward into Baie Verte (12 H/16) map sheet; the total area of the Complex is more than 350 km^2 (Fig. 1). The Complex, although not specifically named as such, was first outlined by Neale et al. (1960), and first recognized as containing peralkaline phases by Neale (1962). All subsequent maps of the area were essentially based on this work, although interpretations differed dramatically, apparently depending on the differing views concerning the significance of quartz-feldspar porphyry. For example, the Complex was shown by Williams (1967) as dominantly volcanic, by Kean et al. (1981) as completely intrusive, and by Hibbard (1983) as dominantly intrusive with minor volcanics.

More detailed mapping at a scale of 1:25 000 was begun by the authors during the summer of 1984, in an attempt to resolve these and other questions, and to provide a base for detailed geochemical and petrogenetic studies. This study is part of a larger program of investigation of the petrology and tectonic significance of Paleozoic granitoid rocks of the Canadian Appalachians (Strong, 1980a, b). Interest in the Siluro-Devonian magmatism of western Newfoundland has been particularly stimulated by studies of peralkaline and other granites in the correlative Topsails Complex to the south (Thurlow, 1973; Taylor et al., 1980, 1981; Whalen and Currie, 1982, 1983, 1984) and the La Scie Granite to the north (Degrace et al., 1976).

The term King's Point Complex is here introduced to include the large area of silicic plutonic rocks, and their overlying volcanic equivalents, which are more or less bounded by Southwest Arm in the east, Gull Pond in the south, and Bartletts Pond in the west (Fig. 1). To the north of

[1]Project partly supported by Geological Survey of Canada under Canada-Newfoundland Mineral Development Program 1984-89
[2]Department of Geology, Memorial University of Newfoundland, St. John's, Newfoundland A1B 3X5
[3]Department of Geology, Dalhousie University, Halifax, Nova Scotia B3H 3J5

the area shown by Figure 1, on the Baie Verte map sheet, the northern boundary of the Complex is considered to be marked by the arcuate ring-dyke of quartz-feldspar porphyry which intersects Middle Arm road. Thus the Complex has a near elliptical outline, with axes about 30 by 12 km.

Two assemblages form the basement to the King's Point Complex, rocks equivalent to the Lower Ordovician Betts Cove Ophiolite, and the Middle Ordovician Burlington Granodiorite. No radiometric dates are available for the Complex, but presumed equivalents to the north have apparent ages of 404 ± 25 Ma (Cape St. John Group and Cape Brule Porphyry) and 435 ± 14 Ma (Seal Island Bight Syenite; Hibbard, 1983), and to the south (Springdale Formation and Topsails Complex) have ages between 415 and 430 Ma (Whalen and Currie, 1983; F. Chandler, personal communication). The King's Point Complex is thus inferred to be Middle to Late Silurian in age.

Map units

Unit 1 — Ophiolitic Rocks

These rocks are found along the eastern margin of the Complex, at the extreme northeast corner of the map area (Fig. 1), and represent the southern extremity of rocks included in the Betts Cove Ophiolite by Hibbard (1983). They consist of pillowed and massive basaltic flows, gabbro and trondhjemite. All are metamorphosed at greenschist facies and pervasively epidotized, but primary structures and textures are generally preserved.

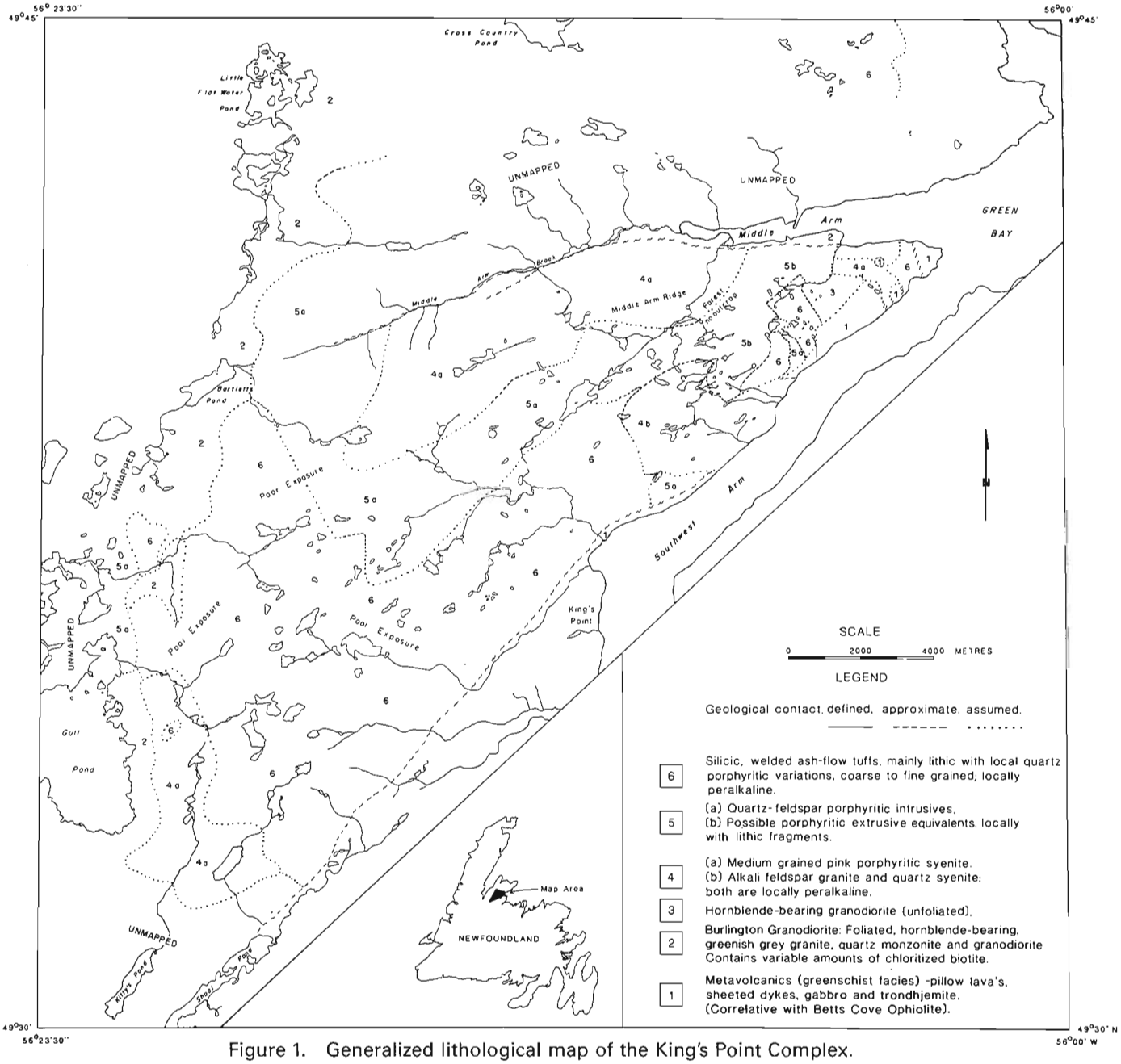

Figure 1. Generalized lithological map of the King's Point Complex.

Unit 2 — Burlington Granodiorite

The Burlington Granodiorite forms a large body almost completely surrounding the King's Point Complex (Fig. 1). Although a great variety of rock types have been reported (Hibbard, 1983), the few outcrops examined in the map area consist of medium- to coarse-grained, roughly equigranular granite, quartz monzonite or granodiorite. It is generally pale green and leucocratic, with about 5% chloritized biotite throughout, and locally with 3-5% hornblende. The chloritized biotite defines a foliation of variable intensity and orientation.

Unit 3 — Undeformed Hornblende Granodiorite

An area of leucocratic, hornblende-bearing granodiorite is present in the extreme northeast corner of the map area. Like the Burlington Granodiorite it is equigranular and is superficially similar to it, but it lacks the green colour and foliation, and is seen to intrude finely laminated welded tuff of the King's Point Complex.

Unit 4 — Syenite

Unit 4 includes dark pink-to-red syenite (4a) where it is exposed in the northwest near Middle Arm Ridge, and alkali feldspar to quartz syenite (4b) in the southeast along Southwest Arm (Fig. 1). As described by Neale (1962), the quartz syenites locally appear to be gradational with the granites of the Complex.

Subunit 4a is medium grained, commonly porphyritic with up to 20% alkali feldspar phenocrysts, and contains less than 5% mafic minerals. It is distinctive in outcrop due to its dark red colour. Subunit 4b is somewhat lighter in colour due to a higher percentage of quartz, and also differs from 4a in being finer grained, equigranular, and containing fewer mafic minerals.

Both units locally display peralkaline varieties, which are distinctive because of extensive albitization of the feldspars, and an abundance of metasomatic riebeckite.

Unit 5 — Quartz-Feldspar Porphyry

Intrusive quartz-feldspar porphyry (subunit 5a) forms a very prominent lithotype in the map area. It has a deep wine to brown matrix with highly variable amounts of quartz and alkali feldspar phenocrysts, the latter being most abundant. The quartz is generally subhedral and averages about 1-2 mm in diameter. The feldspars are mostly euhedral and range in length from 1 mm to 1.5 cm, with an average of 3-4 mm. Subunit 5a is locally in gradational contact with the syenite, subunit 4a, to the northwest.

Subunit 5b appears to be transitional between intrusive rocks like those of subunit 5a, and pyroclastic rocks like the crystal tuffs of unit 6. Although it resembles subunit 5a in most respects, phenocryst content is much lower (<20%) and the matrix also contains a few purple or maroon, felsic fragments.

Unit 6 — Ash-flow Tuffs

Unit 6 is topographically higher than all other units in the map area, and is readily interpreted as being stratigraphically highest. It consists essentially of silicic ash-flow tuffs of great textural variety, but which are dominantly welded and eutaxitic, with spherulitic devitrification textures and lithophysae common. It is dominantly vitric, with quartz phenocrysts and lithic clasts only locally present. Colour is not a distinctive feature of this unit as it can be red, pink, maroon, tan, buff, green, purple or black. In some areas, as along the shore of Southwest Arm and around the benchmark hill north of Middle Arm, the finely laminated ignimbrite is clearly peralkaline, marked by abundant fine riebeckite oikocrysts which overgrow fiamme and other textures.

Other lithologies

A well-known feature of high-level granite suites is the presence of coexisting mafic magma, seen as either composite diabase-rhyolite dykes (e.g. the St. Lawrence Granite; Strong et al., 1978) or intermixed mafic and silicic globules (e.g. the Topsails Complex; Taylor et al., 1980; Furey, 1985), and the King's Point Complex is no exception. Composite dykes are seen along the southwest margin of the Complex along the main logging road to Gull Pond, and Hibbard (1983) has noted mafic globules in the granite of unit 4 along Middle Arm Ridge. Mafic dykes are also common throughout the area, and they are locally very rich in plagioclase phenocrysts.

Geological relationships

The ophiolitic rocks of *unit 1* outcrop in three areas in the extreme northeast of the map area, on the western side of Southwest Arm. The northernmost area, (I, about 1 km^2), and the middle area (II, about 400 m^2) are predominantly gabbro, trondhjemitic, and sheeted diabase dykes. The southernmost area (III, about 1 by 3 km) is predominantly pillow lava and massive basaltic flows which are cut in places by dykes similar to those of the first two areas.

Area I is in contact with unit 6 along a fault trending 167°. The southernmost exposed contact of area III, which strikes approximately 85°, steeply-dipping, irregular and appears to be intrusive with possible syn- and/or post-intrusive faulting. A small body of syenite, unit 4a, separates area II from area III. Its contacts with unit 1 are also intrusive although locally faulted. The northeasternmost and southwesternmost contacts trend about 160° although faulting makes it difficult to measure exactly. The syenite also contains a small inlier of the ophiolitic rocks but no contacts were observed.

Unit 2, the Burlington Granodiorite, outcrops in the western part of the map area and to the north of Middle Arm. From a range of radiometric dates, Hibbard (1983) has chosen an age of ca. 460-465 Ma as most probable for this unit. Outside the map area, it intrudes the Betts Cove Ophiolite, and together they form the basement to the four

units of the King's Point Complex. The Burlington Granodiorite is also usually topographically lower than the extrusives of unit 6, presumably reflecting a nonconformable relationship between them, but the actual contact is not exposed.

Unit 3 is a small (about 1.5 km^2) intrusion of granodiorite located near the ophiolitic rocks of unit 1. No contacts were observed between unit 3 and any of the others, but xenoliths of unit 6 occur in unit 3. This indicates that unit 3 is intrusive into the overlying volcanics of unit 6 and is not related to the granodiorite of unit 2. Other evidence which makes it seem probable that units 2 and 3 are two different bodies is the foliated nature of unit 2 whereas unit 3 is unfoliated.

The granitoid rocks of *unit 4*, like those of unit 3, are unfoliated and appear to be younger than unit 2. Although no clear-cut intrusive relationships were observed, there is some indirect evidence, discussed below, that unit 4 is intrusive into unit 6.

Unit 5 consists of a quartz-feldspar intrusive porphyry (5a) and a problematical subunit (5b). It is unclear if unit 5b is a matrix-rich, high level, intrusive porphyry or if it is an extrusive crystal tuff. Dykes of unit 5a can be seen in unit 2 everywhere near the contact between these units in the western area of the map sheet. They also cut unit 6, and in the same area it appears as if unit 4 may grade into the porphyry. The porphyry intrudes unit 6, altering the overlying volcanic rocks near the north-trending contact.

Unit 6, generally overlies all other units except unit 3 and is clearly intruded by units 3 and 5a and probably by units 4a and 4b.

Contact metasomatism

Peralkaline rhyolite or comendite are recognized in unit 6 by the presence of oikocrysts of hydrothermal riebeckite, presumably the product of sodic metasomatism of "normal" felsic volcanic rocks. In U.T.M. block 560000E/550000N, a section can be seen which displays such contact metasomatism. At the (topographic) base of the section is a peralkaline granite which gives way upwards to a porphyry of suspected peralkaline affinity which in turn is overlain by roughly horizontal welded tuff. At the base of the volcanic sequence is a zone of comendite, 2-3 m thick. Along the stream section in U.T.M. block 549000E/5500000N, the comendite is less than 100 m from a peralkaline granite. Towards the southeast the comendite is oxidized and grades into the welded tuff which still contains oikocrysts of riebeckite, although the percentage decreases to the southeast.

It is clear from these observations that there is a close relationship between the peralkaline granites and metasomatism of the tuffs, although it cannot be said whether the Na-bearing metasomatic fluids were derived from the granite, as suggested for similar features of the Topsails Complex by Taylor et al. (1981) and Strong and Taylor (1984), or were externally derived and affected both equally.

SUMMARY

The King's Point Complex provides a section across the interface between a high-level granite-syenite complex and its overlying volcanic carapace. The volcanic rocks are dominantly welded silicic ash-flow tuffs, and the plutonic rocks are mainly granite and syenite which are mutually gradational through variations in proportions of quartz and alkali feldspar phenocrysts. Both may be locally metasomatized with the production, or at least enhancement, of peralkaline chemistry and the growth of hydrothermal riebeckite oikocrysts. These features are similarly common in the Topsails Complex to the south of the map area, and support suggestions of a similar history and correlation of it with the King's Point Complex. As noted by Neale (1962), the lithological assemblages, the elliptical shape of the Complex, and the arcuate ring dyke at its northern margin are features which suggest that the rocks of the King's Point Complex "represent a site of major surface cauldron subsidence". We anticipate that further studies will demonstrate this to have been a common phenomenon during Siluro-Devonian magmatism in western Newfoundland.

ACKNOWLEDGMENTS

We are grateful for assistance from M. Basha, M. Coyle, K. Currie, W. Epp, B. Kean, E. Lambert, D. Machin, J. Maloney, H. Sandeman, G. Stapleton, and H.S. Swinden. We especially thank A.A. Burgoyne and R. Hewton of Brinco Mining Ltd. for use of their Springdale facilities, and the Springdale office of the Newfoundland Department of Forestry for unlimited access to their aerial photographs.

REFERENCES

DeGrace, J.R., Kean, B.F., Hsu, E., and Green, T.
1976: Geology of the Nippers Harbour map area (2E/13); Newfoundland Department of Mines and Energy, Report 76-3, 73 p.

Furey, D.J.
1985: Geology of the Belleoram pluton, southeast Newfoundland; *in* Current Research, Part A, Geological Survey of Canada, Paper 85-1A, Report 20.

Hibbard, J.
1983: Geology of the Baie Verte Peninsula, Newfoundland; Newfoundland Department of Mines and Energy, Memoir 2, 279 p.

Kean, B.F., Dean, P.L., and Strong, D.F.
1981: Regional geology of the central volcanic belt of Newfoundland; *in* Geological Association of Canada Special Paper 22, p. 65-78.

Neale, W.
1962: King's Point area, Newfoundland; unpublished manuscript.

Neale, W., Nash, W., and Innes, G.M.
1960: Sandy Lake (east half), Newfoundland; Geological Survey of Canada, Paper 62-28, 40 p.

Strong, D.F. and Taylor, R.P.
1984: Magmatic-subsolidus and oxidation trends in composition of amphiboles from silica-saturated peralkaline igneous rocks; Tschermaks Mineralogische Petrographische Mittelungen, v. 32, p. 211-222.

Taylor, R.P., Strong, D.F., and Fryer, B.J.
1981: Volatile control of contrasting trace element distributions in peralkaline granitic and volcanic rocks; Contributions to Mineralogy and Petrology, v. 77, p. 267-271.

Taylor, R.P., Strong, D.F., and Kean, B.F.
1980: The Topsails igneous complex: Silurian-Devonian peralkaline magmatism in western Newfoundland; Canadian Journal of Earth Sciences, v. 17, p. 425-439.

Thurlow, J.G.
1973: Lithogeochemical studies in the vicinity of the Buchans massive sulphide deposits, central Newfoundland; unpublished M.Sc. thesis, Memorial University of Newfoundland, 172 p.

Whalen, J.B. and Currie, K.L.
1982: Volcanic and plutonic rocks in the Rainy Lake area, Newfoundland; *in* Current Research, Part A, Geological Survey of Canada, Paper 82-1A, p. 17-22.

Whalen, J.B. and Currie, K.L. (cont.)
1983: The Topsails igneous terrane of western Newfoundland; *in* Current Research, Part A, Geological Survey of Canada, Paper 83-1A, p. 15-23.

1984: Peralkaline granite near Hare Hill, south of Grand Lake, Newfoundland; *in* Current Research, Part A, Geological Survey of Canada, Paper 84-1A, p. 181-184.

Williams, H.
1967: Island of Newfoundland; Geological Survey of Canada Map 1231A.

SANDSTONE LITHOLOGY IN THE SILVER MINE FORMATION AND ITS RELATION TO GALENA OCCURRENCE IN THE YAVA DEPOSIT, CAPE BRETON ISLAND, NOVA SCOTIA[1]

Project 830012

P.D. Vaillancourt
Economic Geology and Mineralogy Division

Vaillancourt, P.D., Sandstone lithology in the Silver Mine Formation and its relation to galena occurrence in the Yava deposit, Cape Breton Island, Nova Scotia; in *Current Research, Part A, Geological Survey of Canada, Paper 85-1A, p. 743-751, 1985.*
Also in *Mines and Minerals Branch, Report of Activities, 1984; Nova Scotia Department of Mines and Energy, Report 85-1, 1985.*

Abstract

The Yava deposit occurs in an Upper Carboniferous fluviatile sandstone above an unconformity over lower Carboniferous sediments and a Devonian intrusive basement. Yava is situated along the southeast margin of the Glengarry Half-Graben of the Fundy Basin system in the Appalachian Orogen. The deposit is located at an unconformity pinchout in contact with crystalline basement, and consists of three zones of disseminated galena. Each zone overlies a basement depression and is separated from the adjacent zone by an intervening basement high. Mineralization occurs in a 3-7 m thick layer which is discordant to bedding but follows the basement profile.

The mineralized and unmineralized portions of the host sandstone can be subdivided into a grey and a green sandstone respectively. The grey sandstone is a more mature, porous rock containing less clay than the green sandstone, and is also distinguished by the presence of silicified coal, heavily mineralized with galena, pyrite and sphalerite, as well as by the coincidence of detrital heavy minerals in galena-rich, thin, discontinuous bands. The green sandstone is distinctive in colour, uniform composition and appearance, and randomly distributed pyrite clusters. The grey sandstone represents a nearshore equivalent of the green sandstone in a transgressive phase of sedimentation.

Résumé

Le gisement de Yava se manifeste dans un grès fluviatile du Carbonifère supérieur qui repose en discordance sur des sédiments du Carbonifère inférieur et un socle intrusif du Dévonien. Ce gisement longe la marge sud-est du demi-graben Glengarry du bassin de Fundy, dans l'orogène des Appalaches. Il est situé au niveau d'une discordance qui s'amincit progressivement en coin jusqu'au contact du socle cristallin et se compose de trois zones de galène disséminée. Chaque zone repose sur une dépression du socle et se trouve séparée de la suivante par une élévation du socle. La zone minéralisée s'observe dans une couche de trois à sept mètres d'épaisseur qui n'est pas conforme à la stratification mais qui épouse la forme du socle.

Des travaux récents ont démontré que les parties minéralisées et non minéralisées du grès qui agit à titre de roche réservoir peuvent être subdivisées en grès gris et en grès verts. Le grès gris, roche plus mature et poreuse, renferme moins d'argile que le grès vert. Il se distingue également par la présence de charbon silicifié fortement minéralisé en galène, en pyrite et en sphalérite, de même que par la présence de minéraux lourds de nature détritique dans des bandes discontinues, minces et riches en galène. Quant au grès vert, on le reconnaît à sa couleur, à l'unformité de sa composition et de son aspect et à la présence de grappes de pyrite éparpillées. Les auteurs émettent l'hypothèse que le grès gris est l'équivalent littoral du grès vert passant par une phase de sédimentation transgressive.

[1] Contribution to Canada-Nova Scotia Mineral Development Agreement.
Project carried by Geological Survey of Canada.

INTRODUCTION

The Yava deposit in southeast Cape Breton Island, Nova Scotia, is a former lead producer in which galena is hosted in Upper Carboniferous fluviatile sandstone. The sandstone unconformably overlies lower Carboniferous shale and a Devonian quartz-feldspar porphyry basement (Barr et al., 1984). Yava consists of three separate zones overlying basement depressions separated by intervening paleotopographic highs. Ore reserves are estimated at 5.6 million tonnes at 5.3% Pb (Bonham, 1982).

Disseminated ore grade mineralization occurs in a 3-7 m thick zone discordant to bedding but conforming to the basement profile. Although a transgressive sedimentation process has been ascribed to the Yava host rocks (Boehner, 1981), the sedimentology and petrology of this zone of mineralization have not been defined and its relationship to the sandstone lithology was not made clear. This paper reports on the nature of the host rock at Yava, to demonstrate the lithological differences and to relate these to the distribution and grade of mineralization as well as to sedimentation.

Regional geology

The Yava deposit is located in the Glengarry Half-Graben (Prime and Boehner, 1984) which is part of the Fundy Basin system in the Avalon Zone of the Appalachian Orogen (Fig. 1). The Fundy Basin formed as a result of regional subsidence that occurred after the Acadian Orogeny when a relatively stable area with a zone of steep northeasterly trending faults developed in the region (Hacquebard, 1972).

The Fundy Basin system is a series of connected troughs and intermontane basins, interpreted as a rift valley with high-angle faults on both sides which were active during sedimentation (Belt, 1965). It is bounded to the south by the Meguma Platform, to the north and northwest by the New Brunswick Platform and to the northeast by the Newfoundland Platform (McCabe and Schenk, 1982). Continental molasse facies, containing extensive coal deposits in the upper parts, dominate the Carboniferous of eastern Canada. The only marine incursion took place during Visean (Mississippian) time when a cyclic sequence of marine carbonates, evaporites and red siltstone was deposited.

LOCAL AND MINE GEOLOGY

Yava is at the southeastern margin of the Glengarry Half-Graben (Fig. 2) where Carboniferous strata of late Visean to late Westphalian age form an asymmetric syncline with beds dipping gently mainly to the northwest. Near the centre of the basin, a maximum thickness of 2 000 m is projected (Prime and Boehner, 1984). The sediments rest nonconformably upon intrusive rocks of the Loch Lomond plutonic complex (McMullin, 1984).

The Glengarry Half-Graben contains a mixed Carboniferous succession dominated by marginal continental alluvial-fluvial and marine evaporite-carbonate sediments representing molassic deposition. At Yava, the major rock packages (Fig. 3) are marine carbonate of the Uist Formation, the shale-dominated assemblage of the MacKeigan Lake Formation and sandstone of the Silver Mine Formation; towards the centre of the basin, this sequence is overlain by

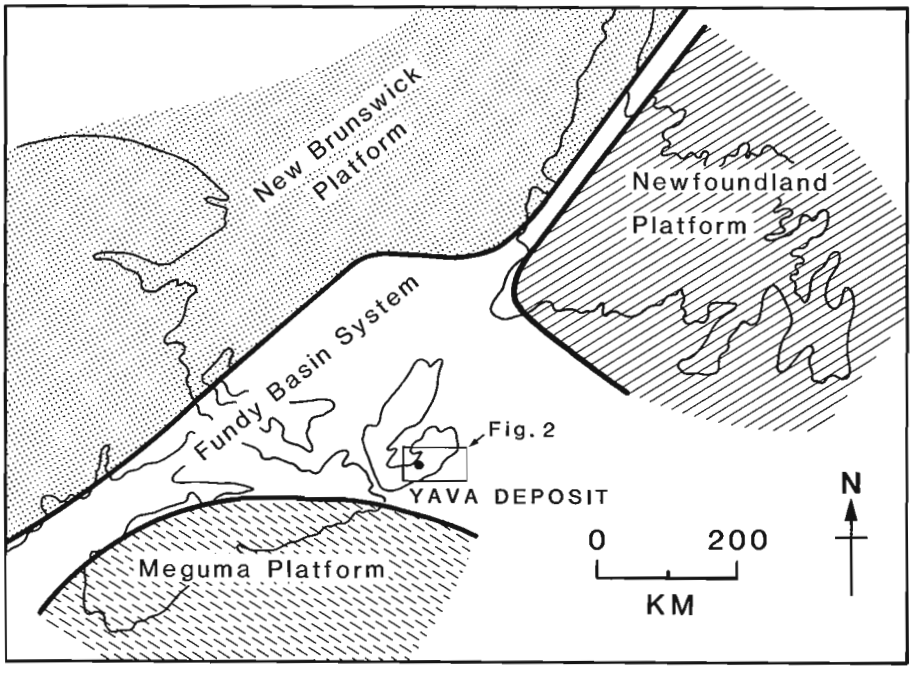

Figure 1. Generalized map of the Fundy Basin system with adjoining platforms (from McCabe and Schenk, 1982).

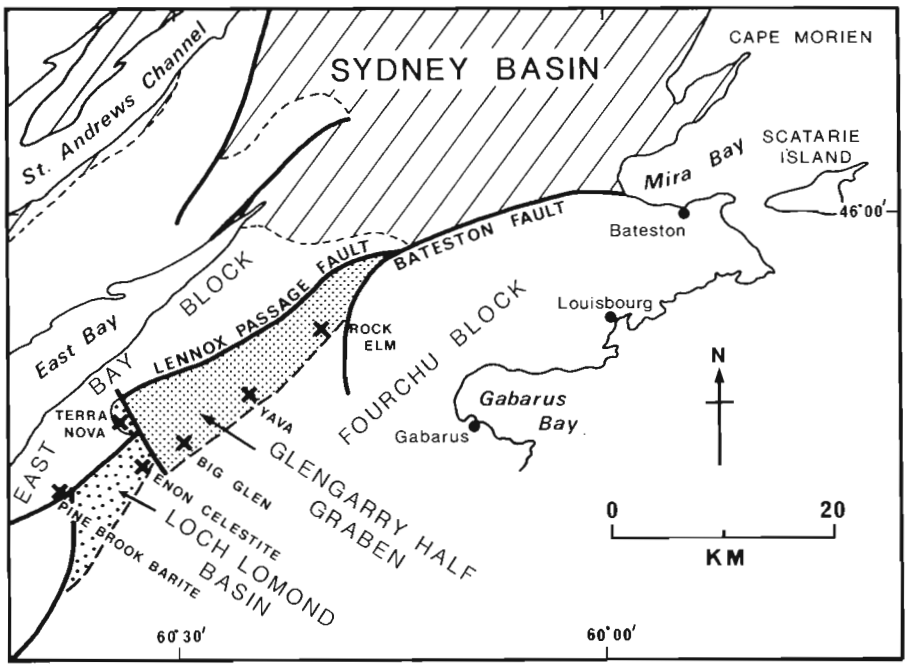

Figure 2. Map showing position of the Glengarry Half-Graben and the location of major sulphide and sulphate mineral occurrences (from Prime and Boehner, 1984).

conglomerate of the Big Barren Formation and by coal-bearing sandstone of the Glengarry Valley Formation. Along the strike of the graben, there is an overstep to the northeast of sedimentary cycles against the crystalline basement, brought about by transgression of the Carboniferous sequence from the southwest following the basal unconformity. Yava and other base metal occurrences in the half-graben are located at or near unconformity pinchouts at several stratigraphic levels in contact with the basement (Fig. 4).

The Yava deposit consists of three zones (West, Central, East) of galena disseminated in sandstone of the Silver Mine Formation (Fig. 5). Each zone overlies a paleotopographic depression in the underlying porphyry basement and is separated from adjacent zones by an intervening basement high. The deposit extends along strike for 3 000 m and extends down dip for 600 m (Bonham, 1982). Ore grade mineralization (cut-off at 4% Pb) is confined to a 3-7 m thick zone of the Silver Mine Formation where it onlaps underlying units at the periphery of the Glengarry Half-Graben. Lower grade material extends upwards for several more metres. The ore zone crosscuts bedding in the sandstone while following the basement profile, although ore-grade galena does not normally extend more than several metres along bedding outward from the basement contact (Fig. 6).

Sedimentology and petrography, Silver Mine Formation

Bonham (1982) identified up to four fining-upward cycles in the Silver Mine Formation. The base of each sedimentary cycle is marked by an erosional contact overlain by an assemblage of shale flake conglomerate, limestone pebble conglomerate or coal lag grading into sandstone and then thin shale beds marking the top of the sequence. Each cycle is rarely complete; most profiles tend to be a continuous succession of sandstone with minor shale and conglomerate interruptions. In the basal 15 m of the west zone, Bonham (1982) observed that sandstone comprises 75% of the profile, limestone pebble conglomerate, shale flake conglomerate and coal lag 14%, and shale 11%. These mine and drillhole observations, along with a coarse to fine sediment ratio of 8:1, led Bonham to conclude that Yava host rock sandstone was deposited in a braided stream environment.

Although sandstone comprises 75% of the clastic assemblage at Yava, galena occurs in each sandstone unit only in a position close to the pinchout against the underlying lithologies (Fig. 4). The galena appears as distorted bands or pods in silicified wood fragments, as disseminations in the sandstone, or in sedimentary features such as laminar bands or clusters.

Bonham (1982) described the host assemblage as a grey-green, moderately-sorted medium- to fine-grained sandstone with a visible clay matrix. Compositionally, the same author reported the sandstone to comprise 80% quartz, 15% rock fragments, 1-3% potassium feldspar, with the remainder being muscovite, chlorite and heavy minerals. Mineralized sandstone is characterized by silicified wood fragments with abundant pyrite and galena. The bulk of the galena occurs as cement between detrital grains in the grey sandstone. Textural studies (Vaillancourt and Sangster, 1984) have shown that the galena was deposited in intergranular open space after secondary silica overgrowths on quartz grains.

Subsequent detailed studies of the Silver Mine Formation, by the present author, have shown that the host sandstone can be divided into two members in the Yava mine area: a lower, grey sandstone and an upper green sandstone. These differences, listed in Table 1, are based on colour, maturity, porosity, clay ratios and mineral components.

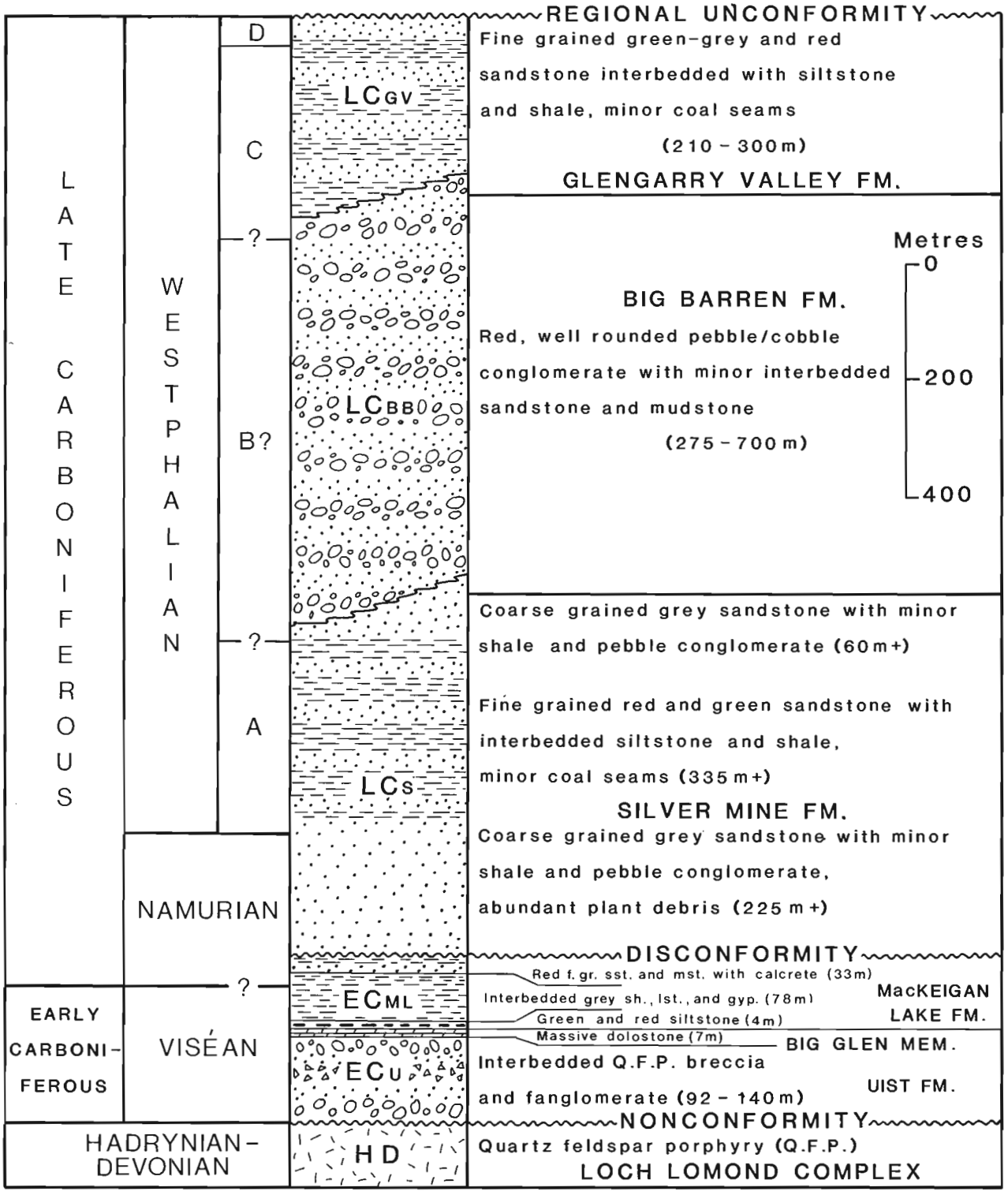

Figure 3. General stratigraphy in the Glengarry Half-Graben (from Prime and Boehner, 1984).

Table 1. Summary of major petrographic and lithologic features characterizing the grey and green sandstone, Silver Mine Formation, Yava mine area

	Porosity	Quartz Grains	Clay Content
Grey sandstone	- 1-5% in galena-rich portion - 15-22% in galena-poor portion	- medium to coarse grained - mature, well rounded - overgrowths common	- 1-15%
Green sandstone	- 8-10%	- medium grained - immature, angular - overgrowths not common	- 15-25%

	Clay Mineralogy	Sulphide, Sulphate Mineralogy	Coal	Other Minerals
Grey sandstone	- high kaolinite/chlorite ratio	- galena - pyrite - sphalerite - barite	- abundant at base of sequence - silicified - associated with abundant pyrite, sphalerite and galena	- rutile, zircon - potassium feldspar } common - detrital muscovite
Green sandstone	- low kaolinite/chlorite ratio	- pyrite	- present in minor amounts - non-silicified - associated with minor pyrite	- rutile, zircon - potassium feldspar } rare - detrital muscovite

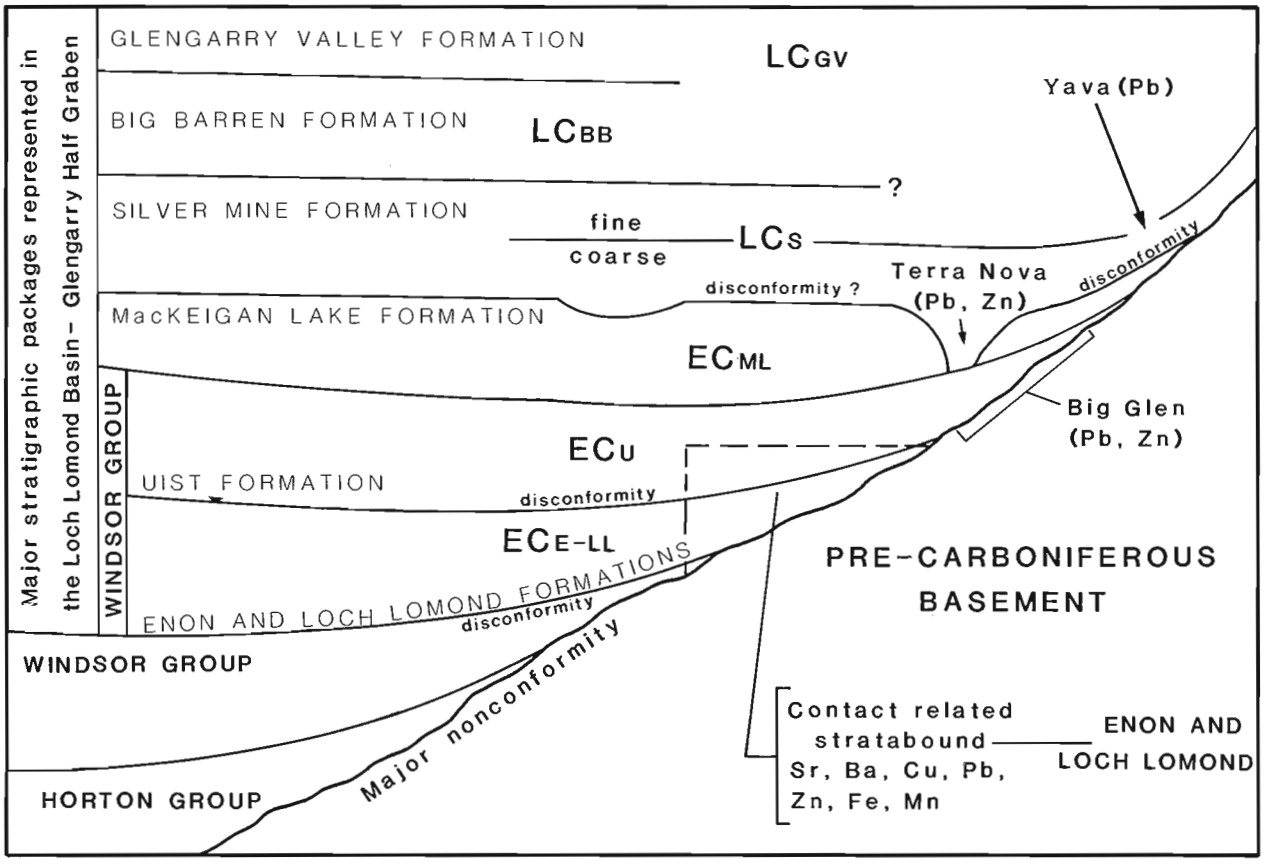

Figure 4. Onlapping relationship of mineral occurrences from southwest to northeast in the Glengarry Half-Graben and the adjoining Loch Lomond basin to the southwest (modified from Prime and Boehner, 1984).

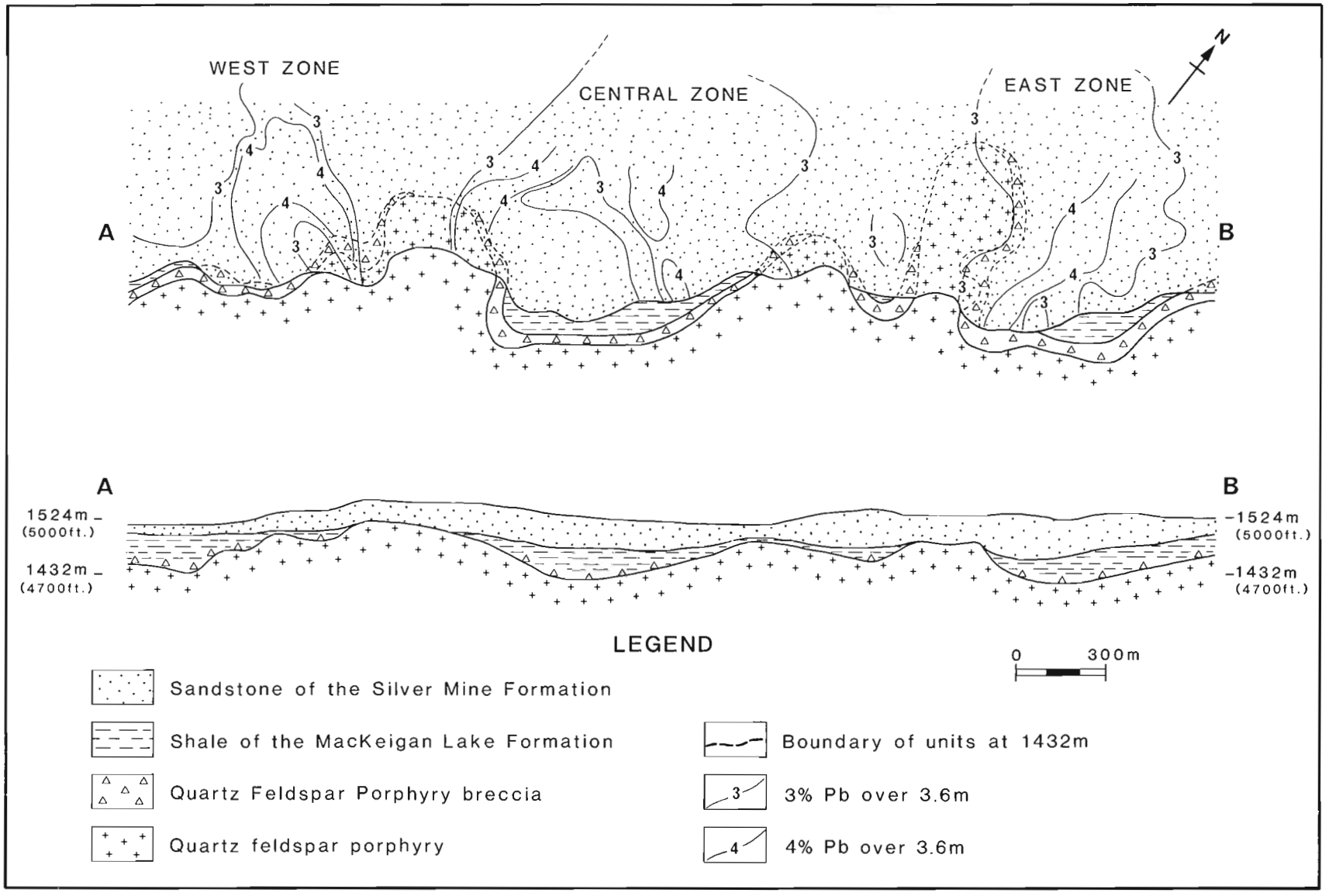

Figure 5. Generalized map and longitudinal section of the Yava deposit (adapted from Bonham, 1982). Note the lithological boundaries below the sandstone cover at 1432 m to show basement highs between zones.

The grey sandstone, occurring immediately in contact with either the MacKeigan Lake Formation or the basement porphyry is mature and medium- to coarse-grained, with well rounded quartz grains. Quartz is the dominant component, and is characteristically overgrown with secondary silica. Within this sandstone, coal fragments, which are particularly abundant at the base of each cycle, are heavily silicified. The clean nature of the rock allows for porosity, determined by image analysis on polished thin sections, to be as great as 15 to 22% in the absence of galena. In the presence of disseminated galena, porosity in the grey sandstone can be less than 1%, thereby supporting the concept of porosity-filling by galena. The clay content is generally low, from 1 to 15% and has a high kaolinite-to-chlorite ratio. Potassium feldspar and large muscovite flakes are common, but not abundant, detrital components of the grey sandstone.

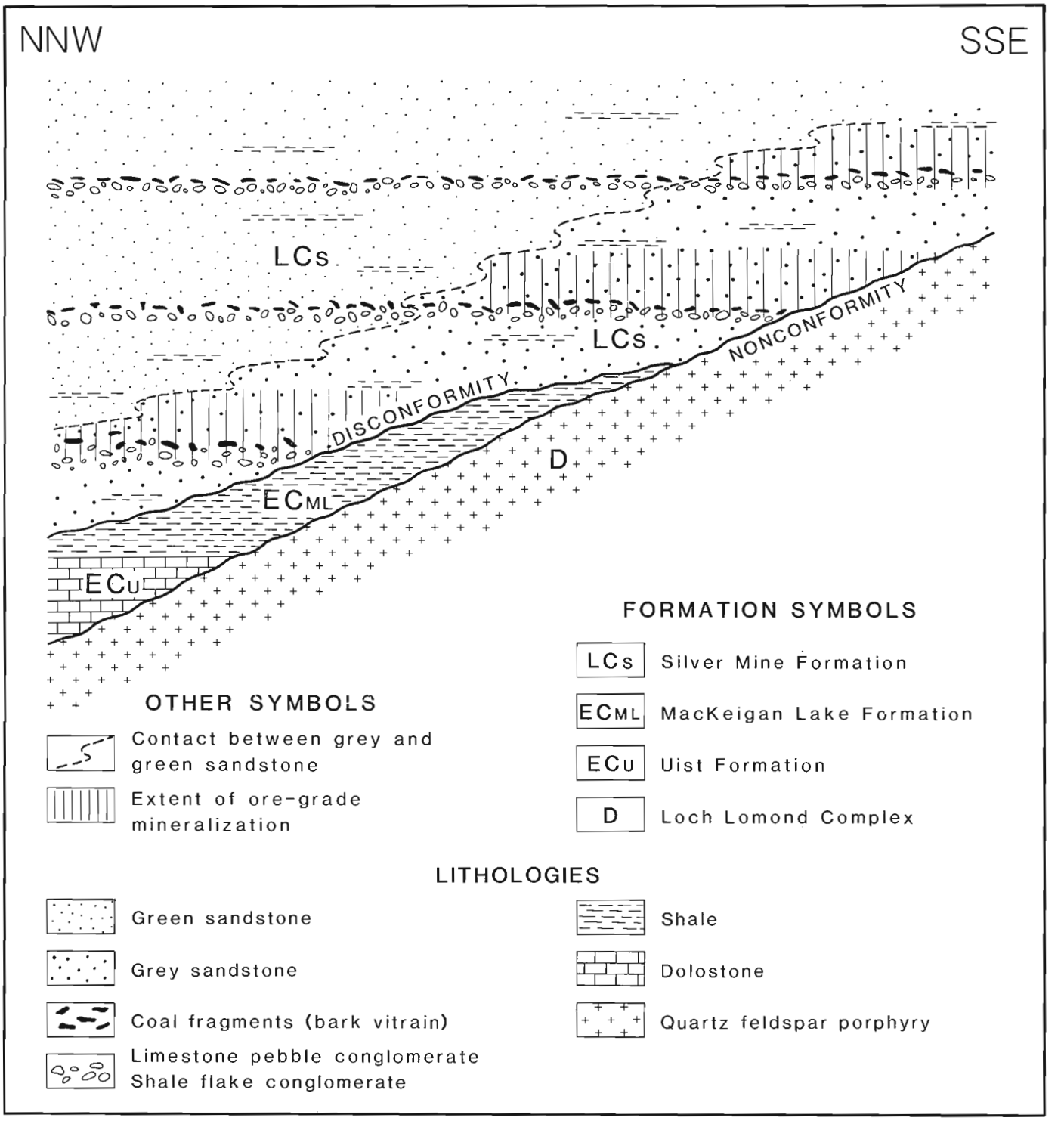

Figure 6. Idealized cross-section of the ore zone, Yava mine.

In contrast to the grey sandstone, the green sandstone is immature, fine- to medium-grained, with subangular quartz grains. Quartz is again the dominant component but is not characterized by pervasive growth of secondary silica around the grains. Where present, secondary quartz overgrowths are very localized and poorly developed. Coal fragments are present in much smaller amounts relative to the grey sandstone and are usually not silicified. Green sandstone contains a greater abundance of clay material and as a result, porosity is generally between 8 and 10% with clay content ranging from 15 to 25%. The kaolinite-to-chlorite ratio is low relative to the grey sandstone and detrital minerals such as potassium feldspar and muscovite are rare.

Significance of sedimentology and petrography to mineralization

The distinction between the two sandstones is important because ore grade galena is restricted to the grey sandstone; only minor galena occurs in the green sandstone. Galena is present throughout the grey unit as disseminations and bands. The galena bands are characterized by important concentrations of detrital heavy minerals (rutile and zircon) and barite. Sphalerite may also occur in association with galena. Pyrite is very abundant in the presence of the silicified coal and may have served to precipitate galena in and around the coal fragments. Sphalerite may also occur with silicified coal but its paragenetic position relative to other sulphide minerals and silicification is unclear.

Galena is also found in the green sandstone but is much less abundant, never reaches ore-grade, is never sufficiently concentrated to form bands, and is generally weakly disseminated where present. Sphalerite is not common. In contrast to coal in grey sandstone, the coal in green sandstone is never galena-bearing although it may contain pyrite. In non-galena-bearing green sandstone, the only visible sulphide mineral is pyrite as spots and clusters, randomly distributed throughout the rock. This type of pyrite has not been observed in the grey sandstone.

The boundary between the two sandstone members is gradational over as much as 5 m and may occur directly above a galena-bearing bed or well beyond any trace of mineralization. Nevertheless, each sandstone is indicative of different conditions of sedimentation and occurrence of galena. The grey sandstone may represent a nearshore equivalent of the green sandstone at the eastern margin of the Glengarry Half-Graben (Fig. 2), where reworking by wave and current action created a well-sorted, clean sediment. The layers containing heavy minerals could be explained by such a process; the abundance of galena and barite in these bands, however, is less well understood and is the subject of continuing study. The green sandstone shows evidence of quieter sedimentation in deeper waters. Reworking of the sediment upon deposition was minimal and, as a result, finer clay particles are more abundant in these sediments.

The sequence within the sandstone suggests a transgressive, onlap succession wherein green sandstone not only overlies the grey sandstone member but represents its lateral, offshore equivalent. A transgressive cycle where coarse sediments (proximal) grade into fine sediments (distal) laterally as well as vertically would best explain the profile of the Yava orebody in Figure 6 where the mineralized zone follows the basement profile across stratigraphy. There is no documentation at present of a lateral transition from coarser grey sandstone to fine grained green sandstone beyond the ore zone, but studies by the author are presently underway to examine this possibility.

CONCLUSIONS

Yava is a deposit which is controlled by paleotopography wherein mineraliza tion preferentially occurs above basement topographic lows at stratigraphic pinchouts. Within the deposit, ore grade galena is confined to a 3-7 m thick discordant zone within the Silver Mine Formation immediately above its contact with underlying units. A detailed petrographic study of the Silver Mine Formation sandstone has shown that:

1. Sandstone of the Silver Mine Formation at Yava can be divided into two distinctive members (grey and green). The grey sandstone represents a mature, well washed sediment which has been extensively reworked, resulting in a sandstone of relatively high porosity. The green sandstone is an immature rock with more angular grains, a higher clay content, lower porosity, and fewer detrital components.
2. The well rounded quartz grains and the abundance of heavy minerals in the grey sandstone suggest that this member formed in a nearshore environment. The higher clay content of the green sandstone suggests that it was deposited in a deeper, more restricted, possibly offshore environment. The ore zone profile in the grey sandstone indicates that precipitation of galena was confined to the nearshore well-washed environment as transgression proceeded, thereby explaining the discordant nature of the ore zone relative to sedimentary layering.
3. The mature, relatively clean grey sandstone, because of its greater porosity, provided more open space for galena deposition than did the less porous green sandstone.

ACKNOWLEDGMENTS

The author thanks the staff of the Nova Scotia Department of Mines and Energy in Halifax and Stellarton for their support throughout the study, in particular, R.C. Boehner for his helpful comments and suggestions. The assistance of Yvonne Brown during the 1984 summer field season is also greatly appreciated. Finally, D.F. Sangster of the Geological Survey of Canada was most helpful in making critical comments and reviewing the text.

REFERENCES

Barr, S.M., Sangster, D.F., and Cormier, R.F.
1984: Petrology of Early Cambrian and Devono-Carboniferous intrusions in the Loch Lomond complex, southeastern Cape Breton Island, Nova Scotia; *in* Current Research, Part A, Geological Survey of Canada, Paper 84-1A, p. 203-211.

Belt, E.S.
1965: Stratigraphy and paleogeography of Mabou Group and related Middle Carboniferous facies; Geological Society of America, Bulletin, v. 76, p. 777-802.

Boehner, R.C.
1981: Preliminary report on the geology and mineral deposits of the Loch Lomond Basin, Cape Breton Island; *in* Mineral Resources Division, Report of Activities, 1980, Nova Scotia Department of Mines and Energy, Report 81-1, p. 153-165.

Bonham, O.J.
1982: Geology of the Yava sandstone-lead deposit, Cape Breton, Nova Scotia; unpublished M.Sc. thesis, Dalhousie University, Halifax, Nova Scotia, 181 p.

Hacquebard, P.A.
1972: The Carboniferous of eastern Canada; International Stratigraphie Géologie du Carbonifère Congress, Trefeld, Compte Rendu, v. 1, p. 69-90.

McCabe, P.J. and Schenk, P.E.
1982: From sabkha to coal swamp — the Carboniferous sediments of Nova Scotia and New Brunswick; Field excursion guidebook, excursion 4A; International Association of Sedimentologists, 11th International Congress on Sedimentology, McMaster University, Hamilton, Canada.

McMullin, D.W.
1984: Geology and geochemistry of the granitoid rocks of the Loch Lomond Irish Cove area, Cape Breton Island; unpublished M.Sc. thesis, Acadia University, Wolfville, Nova Scotia, 239 p.

Prime, G. and Boehner, R.C.
1984: Preliminary report on the geology of the Glengarry Half-Graben and vicinity, Cape Breton Island, Nova Scotia; *in* Mines and Minerals Branch, Report of Activities, 1983, Nova Scotia Department of Mines and Energy, Report 84-1, p. 61-69.

Vaillancourt, P.D. and Sangster, D.F.
1984: Petrography of mineralization at the Yava sandstone-lead deposit, Nova Scotia; *in* Current Research, Part A, Geological Survey of Canada, Paper 84-1A, p. 345-352.

METAMORPHISM AND STRUCTURE OF THE LAURIE LAKE REGION, MANITOBA[1]

S.L. Jackson[2] and *T.M. Gordon*
Precambrian Geology Division

Jackson, S.L. and Gordon, T.M., Metamorphism and structure of the Laurie Lake region, Manitoba; in *Current Research, Part A, Geological Survey of Canada, Paper 85-1A, p. 753-759, 1985.*

Abstract

The Laurie Lake region in west-central Manitoba contains the transition between the Proterozoic Lynn Lake greenstone belt and the Kisseynew metasedimentary gneiss belt. The region is characterized by northeast trending, moderately plunging folds and well developed co-axial lineations. In the Lynn Lake region elongate minerals are either randomly oriented, occur as planar rosettes, or less commonly, define a lineation.

Changes in metamorphic mineral assemblages in metapelites indicate that the following reactions took place with increasing grade between Lynn Lake and the southwest Laurie Lake region:

staurolite + muscovite + quartz = sillimanite + garnet + biotite (1)
muscovite + quartz = K feldspar + sillimanite + H_2O (2)
sillimanite + biotite = cordierite + garnet + K feldspar + H_2O (3).

In metabasites and calcareous psammites two zones have been established; one with epidote bearing assemblages and one with epidote free assemblages.

Dating of concordant and discordant pegmatites may provide tight constraints on the timing of the main tectonometamorphic event in the Laurie Lake region.

Résumé

La transition entre la zone protérozoïque de roches vertes de Lynn Lake et la zone de gneiss métasédimentaire de Kisseynew se trouve dans la région du lac Laurie, dans la partie centrale ouest du Manitoba. Cette région est caractérisée par la présence de plis à orientation nord-est et à plongement modéré et de linéations coaxiales bien développées. Dans la région de Lynn Lake, les minéraux allongés ont soit une orientation aléatoire, soit une forme en rosettes planes, ou moins souvent, définissent une linéation.

Les changements dans les assemblages de minéraux métamorphiques des metapélites indiquent que les réactions suivantes se sont produites de façon directement proportionnelle au degré de métamorphisme, entre Lynn Lake et la région du lac Laurie au sud-ouest:

staurolite + muscovite + quartz = sillimanite + grenat + biotite (1)
muscovite + quartz = feldspath potassique + sillimanite + H_2O (2)
sillimanite + biotite = cordiérite + grenat + feldspath potassique + H_2O (3).

Deux zones ont été reconnues dans les métabasites et les psammites calcaires; l'une contient des assemblages à épidote et l'autre des assemblages sans épidote.

La datation des pegmatites concordantes et discordantes pourraient fournir des limites chronologiques étroites pour la datation de l'évènement tectonométamorphique principal de la région du lac Laurie.

[1]Contribution to Canada-Manitoba Mineral Development Agreement 1984-1989.
[2]Department of Geological Sciences, Queen's University, Kingston, Ontario K7L 3N6

INTRODUCTION

The Laurie Lake area straddles the transition between the Lynn Lake greenstone belt and the Kisseynew sedimentary gneiss belt in northern Manitoba (Fig. 1). Both belts are Proterozoic and belong to the Churchill Structural Province.

In the Lynn Lake belt, the Wasekwan Group consists principally of basaltic to rhyolitic volcanic rocks and mafic to aluminous greywacke-mudstone turbidites. The overlying Sickle Group comprises clastic sediments including siliceous, calcareous and mafic psammites and various conglomerates.

A period of deformation, plutonism and metamorphism of the Wasekwan Group preceded deposition of the Sickle Group. A second period of deformation, plutonism and metamorphism affected both groups. These two periods of tectonic disturbance are readily discernible in some regions but in others, such as the Laurie Lake region, they are difficult to distinguish (Gilbert et al., 1980).

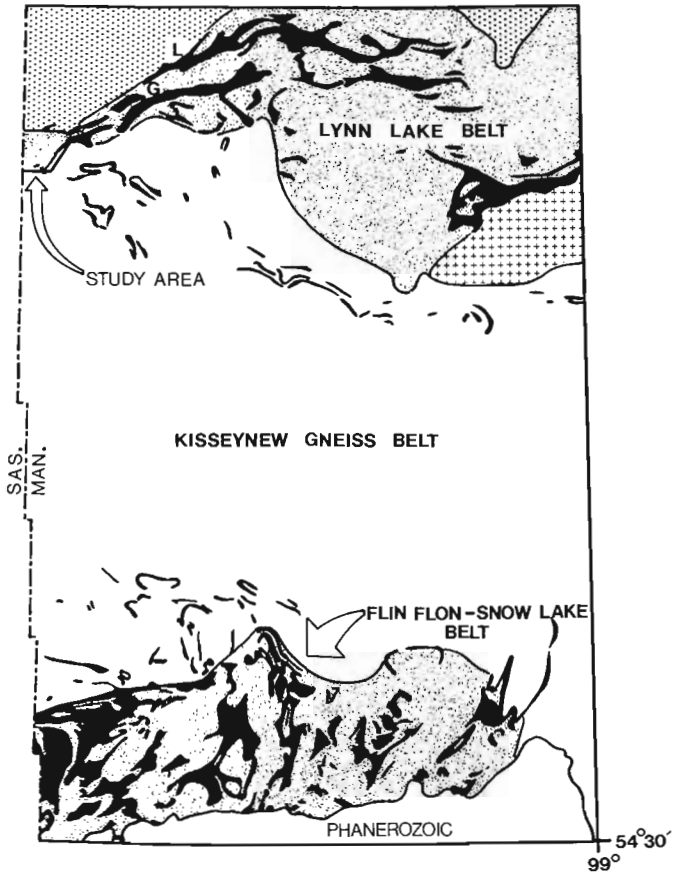

Figure 1. Location map of study area and the major Proterozoic lithostructural belts in west central Manitoba. In addition to the labelled belts the Southern Indian gneiss belt (dotted pattern) and the Baldock Batholith (crossed pattern) are also shown. "L" and "G" represent the approximate locations of Lynn Lake and Gemmel Lake respectively. The solid black regions represent the major areas of metabasites in the two greenstone belts (shaded regions) and the Kisseynew metasedimentary gneiss belt (blank).

The Kisseynew metasedimentary gneiss belt is underlain by metamorphosed psammites and pelites of the Burntwood Metamorphic Suite and metamorphosed psammites of the Sickle Metamorphic Suite. Both suites have been deformed and intruded by various granitic plutons (Baldwin et al., 1979). Metamorphism increases from greenschist facies in the greenstone belt to upper amphibolite facies in the gneiss belt.

The general geology, structure, and metamorphism of the two belts have been described by Baldwin et al. (1979), Lenton (1981), Bailes and McRitchie (1978), Gilbert et al. (1980), Zwanzig et al. (1980), and Thomas (1980).

The Laurie Lake area has been recently mapped by Zwanzig et al. (1980) who successfully extended the stratigraphy of the Lynn Lake belt into the Kisseynew belt. The purpose of this project is to elucidate the physical conditions and timing of metamorphism and deformation in the Lynn Lake Kisseynew transition zone. This summer, a brief reconnaissance established the main elements of structure and metamorphism in the area.

H.V. Zwanzig and D.A. Baldwin of Manitoba Mineral Resources Division provided invaluable advice and assistance during the course of the field studies.

STRUCTURE

The dominant structural elements in the Laurie Lake region are bedding; secondary foliations (schistosity, gneissosity, and migmatitic layering); folds of bedding and secondary foliations; lineations (mineral and mineral aggregate); and boudinage features.

Secondary foliations in the Laurie Lake region are generally subparallel to bedding. In several localities, however, a schistosity defined by the parallel orientation of biotite grains is discordant to bedding and/or migmatitic layering. In these instances the schistosity is parallel to the axial surfaces of local minor folds.

Folding of the Wasekwan and Sickle Group rocks controls the map pattern. The dominant and latest (F_2) folds in the area are northeast trending and moderately plunging with an open to tight interlimb angle. F_2 folds occur at map, outcrop and hand specimen scale. They refold primary bedding, secondary foliations and pre- to syn-tectonometamorphic pegmatites.

Rare folded axial planar fabrics that cut fold noses (Fig. 4) indicate an earlier set of folds (F_1). On the scale of observation of (usually a few square metres) the F_1 folds appear to be isoclinal.

Three main types of lineations are present in the Laurie Lake region: mineral lineations (usually sillimanite, hornblende, cummingtonite and quartz); mineral aggregate lineations (usually faserkiesel, quartz and feldspar, and sillimanite-magnetite intergrowths); and biotite crenulations. These lineations are co-axial with minor F_2 folds throughout the Laurie Lake region (Fig. 3).

Thomas (1980), however, found a reversal in plunge of fold axes in South Bay (Fig. 2). This reversal is likely due to refolding of earlier large scale F_1 folds by the F_2 northeast trending folds. The "dome and basin" map pattern (Fig. 2) is indicative of fold interference and therefore reversals in plunge of fold axes are to be expected. Thomas (1980) and Gilbert et al. (1980) postulated an early episode of nappe style deformation in the area which may explain these observations.

Figure 3 shows an equal area plot of all lineations (fold axes, crenulations, and mineral elongation directions) in the Laurie Lake region. Also shown in Figure 3 are the poles to measured bedding, schistosity, gneissosity and migmatitic layering. The lineations define a pole to the girdle of poles to foliations suggesting that development of the lineations was synchronous with folding of foliations.

Some pegmatites, calcareous layers in metapelites and granitic segregations are boudinaged and are subparallel to secondary foliations and bedding (where present). The timing of these boudinage features with respect to folding is not yet clear.

Zwanzig et al. (1980) mapped a major fault extending from the south end of the Laurie River to the east of the bottom of South Bay (Fig. 2). This fault is inferred to repeat stratigraphy so that Wasekwan basalt structurally overlies younger Sickle sediments. Gilbert et al. (1980), however, pointed out that the contact may be stratigraphic and not structural.

An interesting transition in mineral fabrics occurs between Lynn Lake and Laurie Lake. In the Lynn Lake region metamorphic porphyroblasts such as hornblende tend

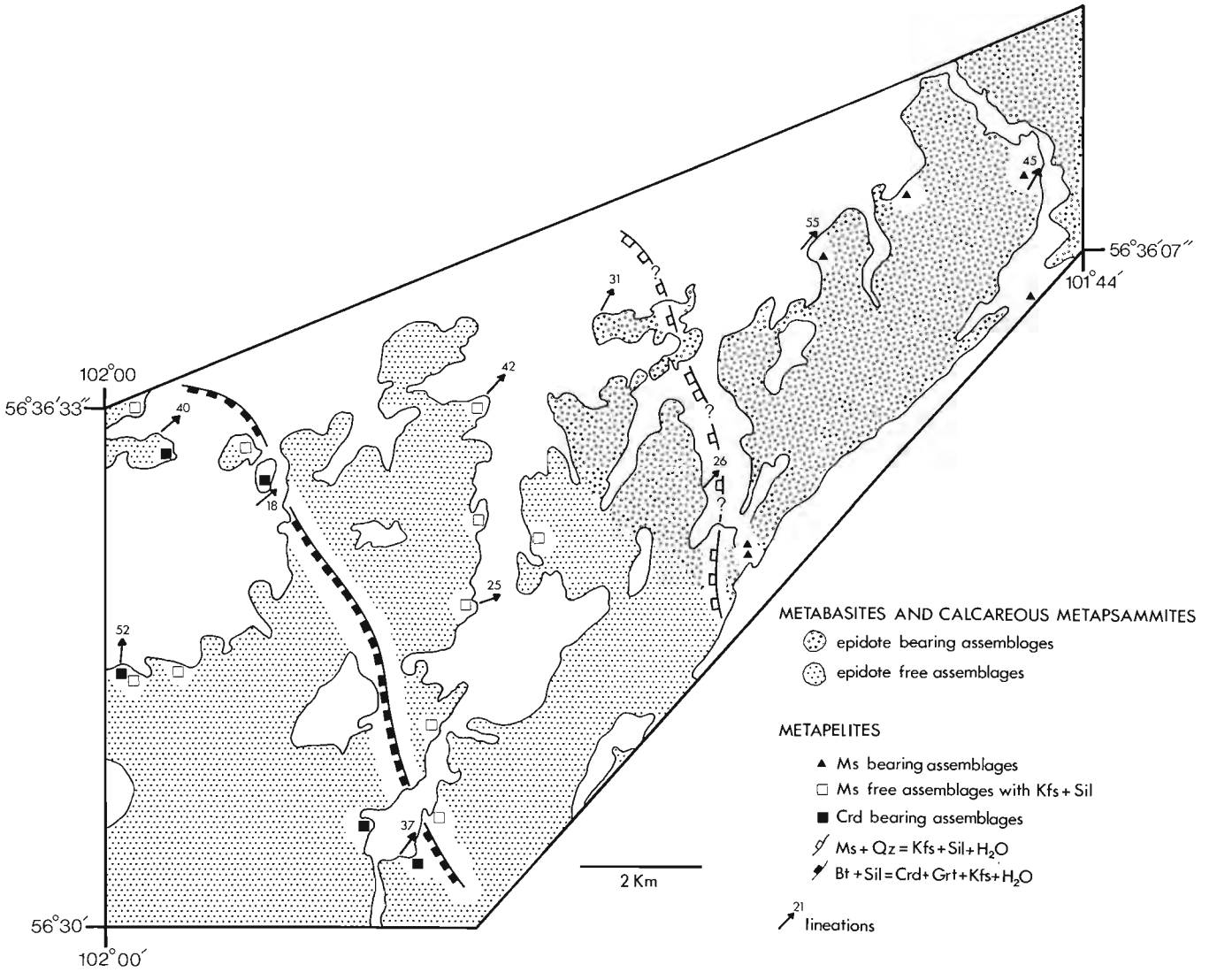

Figure 2. Geological sketch map of the Laurie Lake region. Modified after Zwanzig et al. (1980).

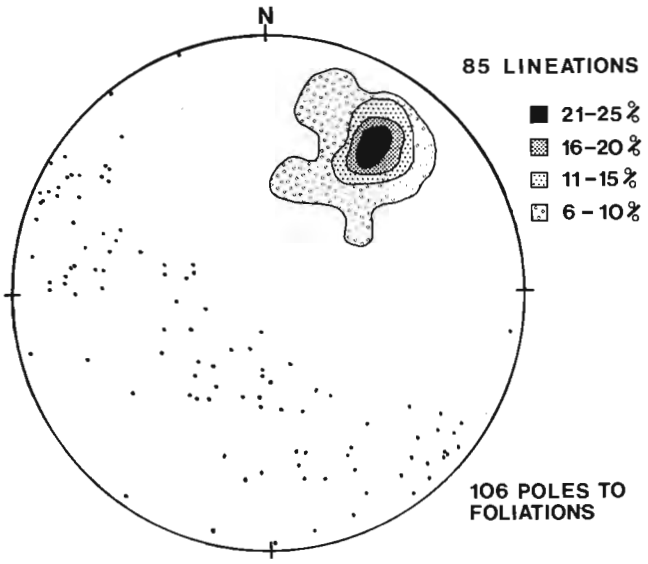

Figure 3. Equal area dot summarizing structural data. Dots represent poles to bedding and secondary foliations. Lineations (mineral elongation, crenulations and minor fold axes) are contoured by per cent of lineations per one per cent area.

to show either random orientations (Fig. 5) or rosettes confined to the foliation plane. They are less frequently lineated. In the Laurie Lake region a pervasive northeast trending lineation dominates the mineral fabrics. Only one locality on Laurie Lake was found to have hornblende forming rosettes. Additional observations of this type may constrain the relative timing of deformation and metamorphism.

METAMORPHISM

Pelitic rocks between Lynn Lake and the southwest portion of Laurie Lake exhibit a variety of mineral assemblages that can be related to isograd reactions. Reactions in pelitic rocks recognized in this study are similar to those mapped by Froese and Gassparini (1975), Bailes (1980), and Gordon (1981) in the Flin Flon-Snow Lake greenstone belt.

Thirty kilometres northeast of the area shown in Figure 6, the maximum phase assemblage is staurolite + garnet + biotite + plagioclase + muscovite + quartz. To the southwest on Laurie River (Fig. 6) the maximum phase assemblage is sillimanite-garnet-biotite-muscovite-plagioclase-quartz. This suggests that the following reaction occurred northeast of Laurie River:

$$\text{staurolite} + \text{muscovite} + \text{quartz} = \text{sillimanite} + \text{garnet} + \text{biotite} \qquad (1)$$

Towards the southwest on Laurie Lake muscovite is not observed in rocks containing potassium feldspar. This may be related to the reaction:

$$\text{muscovite} + \text{quartz} = \text{sillimanite} + \text{K-feldspar} + H_2O \qquad (2)$$

Gilbert et al. (1980) mapped the limit of anatexis in metasedimentary rocks. This boundary approximately coincides with the sillimanite-K-feldspar isograd marked in Figure 6. Pelitic rocks are generally migmatitic south and west of the isograd corresponding to reaction (2).

Farther southwest on Laurie Lake cordierite is observed in granitic segrega tions (Fig. 6). The resultant maximum phase assemblage is cordierite + sillimanite + garnet + biotite + plagioclase + K-feldspar + quartz. The appearance of cordierite might be related to the reaction

$$\text{sillimanite} + \text{biotite} + \text{plagioclase} + \text{quartz} + H_2O = \text{garnet} + \text{cordierite} + \text{K-feldspar} \qquad (3)$$

South of Laurie Lake in the Kisseynew metasedimentary gneiss belt a common assemblage is cordierite + garnet + biotite + K-feldspar + plagioclase + quartz (Baldwin et al., 1980; Bailes and McRitchie, 1979; Gordon et al., 1985). The predominance of this assemblage indicates that reaction (3) has gone to completion. In the Laurie Lake region the reactants and products persist together for several kilometres southwest of the isograd corresponding to reaction (3).

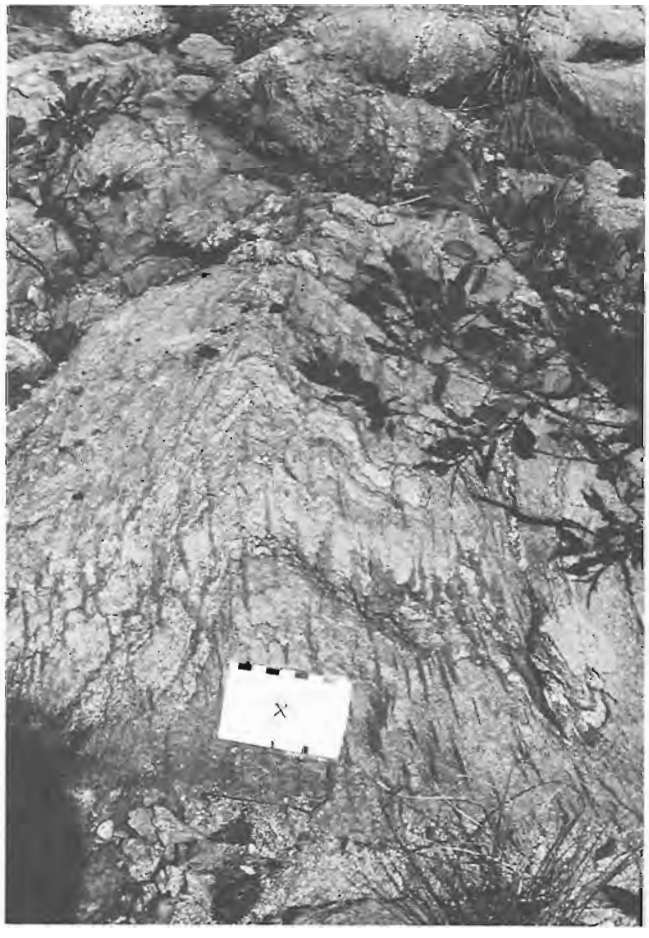

Figure 4. Sillimanite-magnetite dots axial planar to F^1 folds that have subsequently been refolded about northeast trending axes. (GSC 204068-E)

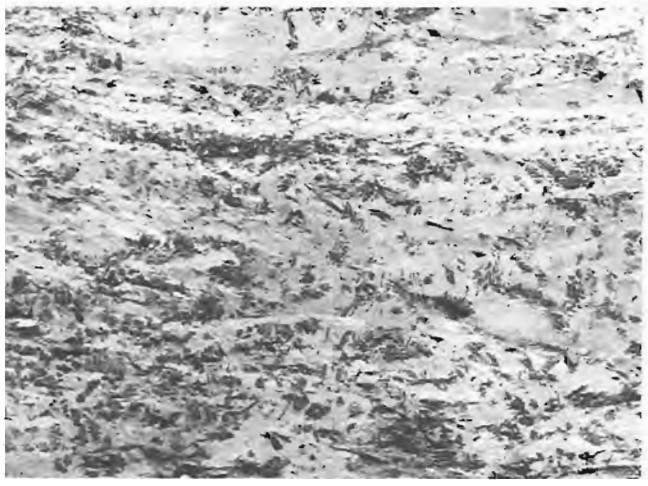

Figure 5. Randomly oriented hornblende porphyroblasts in a metapsammite from near Lynn Lake. Long dimension of photograph is 6 cm. (GSC 204068-G)

Metabasites and calcareous psammites in the Laurie Lake region exhibit a variety of amphibolite and transitional greenschist-amphibolite assemblages. As a first step in recognizing the various metamorphic zones in these rocks they have been tentatively divided into those with epidote bearing and those with epidote free assemblages (Fig. 6).

Below

Figure 6. Metamorphic data collected in metapelites, metabasites, and metacalcareous psammites. This figure is a preliminary outline of mappable isograds in the metapelites and epidote bearing and epidote free assemblages in metabasites and metacalcareous psammites. An increase in the number of data points may change the configuration of the isograds and extent of epidote bearing assemblages. Mineral abbreviations after Kretz (1983).

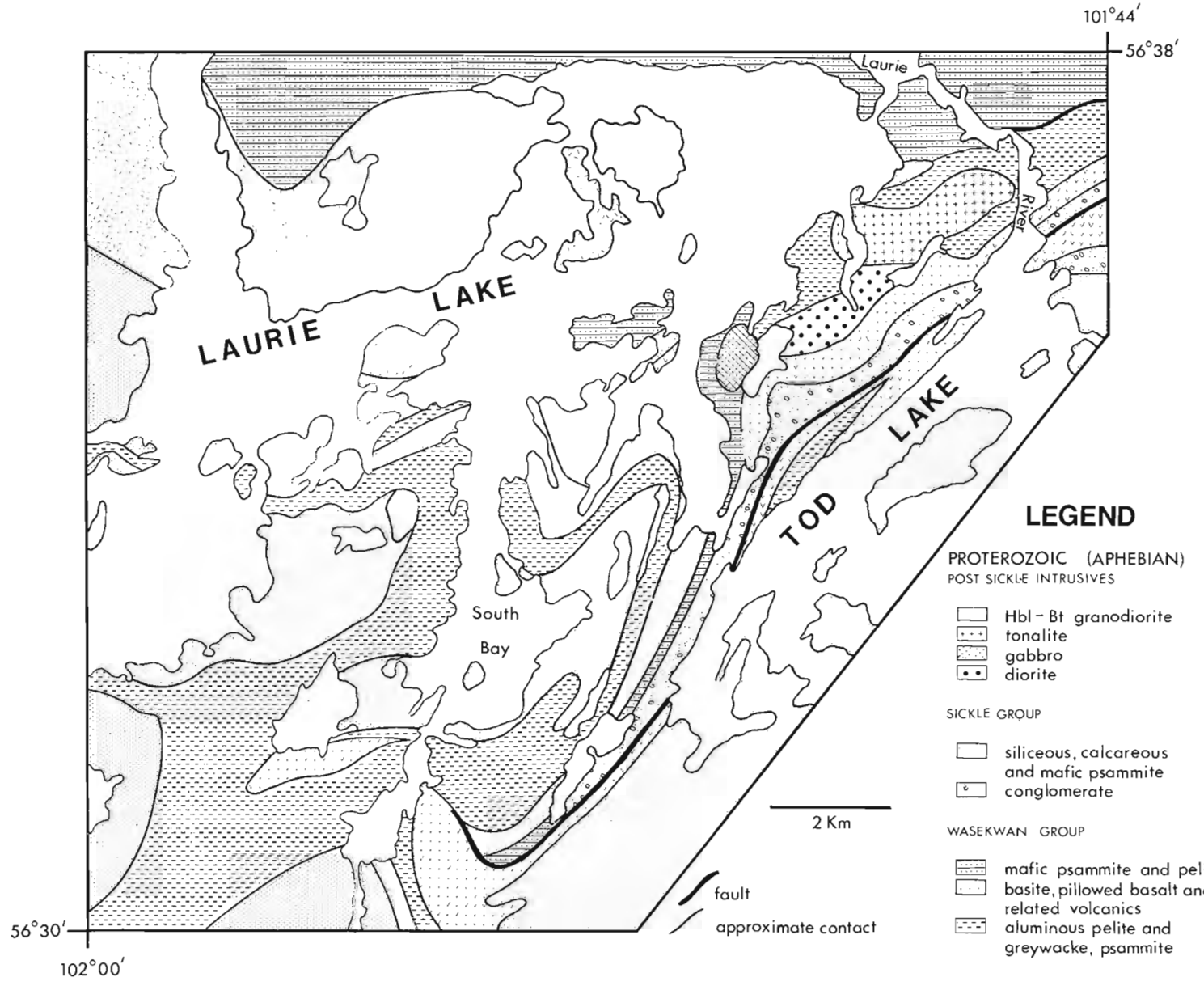

Assemblages in the zone of epidote bearing rocks include:
clinopyroxene + hornblende + epidote + plagioclase + sphene,
hornblende + cummingtonite + plagioclase,
garnet + clinopyroxene + epidote + plagioclase,
hornblende + clinopyroxene + garnet + plagioclase,
hornblende + chlorite + plagioclase + epidote ± actinolite?

These assemblages include varying amounts of biotite and quartz and some may contain K-feldspar.

In the epidote-free zone assemblages are similar to those of the epidote bearing zone. The assemblage hornblende + clinopyroxene + plagioclase is particularly abundant while the assemblage garnet + clinopyroxene + hornblende + plagioclase occurs less commonly. Cummingtonite and hornblende often coexist and one assemblage containing cummingtonite + hornblende and garnet was observed.

Cummingtonite tends to occur in concentrated zones in metabasites, for instance along pillow selvages in metabasalts. These concentrated zones may be sites of Ca depletion and Mg enrichment.

Concordant pegmatites in South Bay have been metamorphosed and deformed and commonly possess the same phase assemblage as the country rock. These pegmatites predate or are synchronous with the main tectonometamorphic event. Discordant, straight sided pegmatites are usually of lower metamorphic grade. For instance discordant pegmatites are muscovite bearing although muscovite is not stable in the country rock. These pegmatites postdate the main tectonometamorphic event and show little or no evidence of post crystallization deformation. Age determinations of these two sets of pegmatites may thus constrain timing of deformation and metamorphism.

SUMMARY

The structure and map pattern of the Laurie Lake region is dominated by northeast trending moderately plunging F_2 folds. Linear minerals such as hornblende in the Lynn Lake region are either randomly oriented or in planar rosettes in contrast to the Laurie Lake region which is dominated by the co-axial lineations.

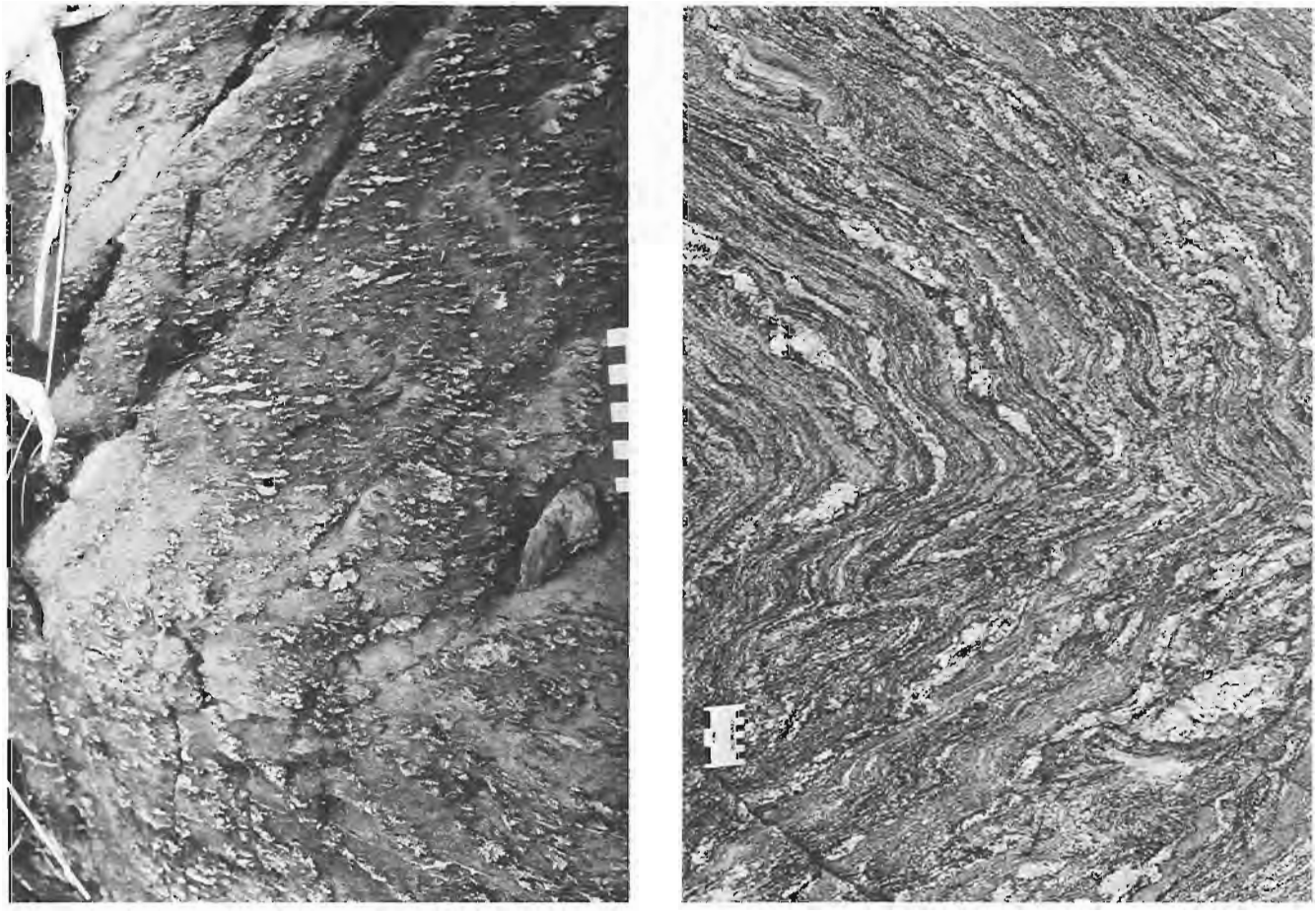

Figure 7. Left: Metapelite with maximum phase assemblage of Grt-Sill-Ms-Bt-Pl-Qtz (low grade side of sillimanite-K-feldspar isograd in Figure 6). White resistant weathering patches are sillimanite-quartz intergrowths. (GSC 204068-I)
Right: Metapelite with maximum phase assemblage of Grt-Sill-Kfs-Bt-Pl-Qtz (high grade side of sillimanite-K-feldspar isograd in Fig. 6).
Note the extent of migmatization in the K-feldspar bearing muscovite free assemblage (right). (GSC 204068-H)

Reactions in pelitic rocks in the Laurie Lake region occur with increasing grade. These reactions result in the disappearance of staurolite, the disappearance of muscovite and the production of cordierite.

Metabasites in the Laurie Lake region may be divided into those with epidote bearing and those with epidote free assemblages. Cummingtonite is a relatively common mineral in the metabasites.

REFERENCES

Bailes, A.H.
1980: Geology of the File Lake area; Manitoba Mineral Resources Division, Geological Report 78-1, 134 p.

Bailes, A.H. and McRitchie, W.D.
1978: The transition from low to high grade metamorphism in the Kisseynew sedimentary gneiss belt, Manitoba; *in* Metamorphism in the Canadian Shield, ed. J.A. Fraser and W.W. Heywood; Geological Survey of Canada, Paper 78-10, p. 155-177.

Baldwin, D.A., Frohlinger, T.G., Kendrick, G., McRitchie, W.D., and Zwanzig, H.V.
1979: Geology of the Nelson House-Pukatawagan region (Burntwood Project); Manitoba Mineral Resources Division, Geological Maps 78-3-1 to 78-3-22.

Froese, E. and Gasparrini, E.
1975: Metamorphic zones in the Snow Lake area, Manitoba; Canadian Mineralogist, v. 13, p. 162-167.

Gilbert, H.P., Syme, E-C., and Zwanzig, H.V.
1980: Geology of the metavolcanic and volcaniclastic metasedimentary rocks in the Lynn Lake area; Manitoba Mineral Resources Division, Geological Paper GP80-1, 118 p.

Gordon, T.M.
1981: Metamorphism in the Crowduck Bay area, Manitoba; *in* Current Research, Part A, Geological Survey of Canada, Paper 81-1A, p. 315-316.

Gordon, T.M., Jackson, S.L., and Zaleski, E.
1985: Metamorphic processes in the Kisseynew metasedimentary gneiss belt; *in* Current Research, Part A, Geological Survey of Canada, Paper 85-1A, report 62.

Kretz, R.
1983: Symbols for rock-forming minerals; American Mineralogist, v. 68, p. 277-279.

Lenton, P.G.
1981: Geology of the McKnight-McCullum Lakes area, Manitoba Mineral Resources Division, Geological Report GR 79-1, 39 p.

Thomas, M.W.
1980: Structural geology of a gneisic terrain, Laurie Lake, northern Manitoba; unpublished M.Sc. thesis, Department of Earth Sciences, University of Manitoba.

Zwanzig, H.V., Thomas, M.W., and Keag, J.P.
1980: Laurie Lake; Manitoba Mineral Resources Division, Map 6P 80-1-3.

PRELIMINARY INVESTIGATION OF GOLD OCCURRENCES IN THE FLIN FLON-SNOW LAKE BELT, MANITOBA AND SASKATCHEWAN[1]

Project 750098

A. Galley, D. Ames, and J.M. Franklin

Galley, A., Ames, D., and Franklin, J.M., Preliminary investigation of gold occurrences in the Flin Flon-Snow Lake Belt, Manitoba and Saskatchewan; in *Current Research, Part A, Geological Survey of Canada, Paper 85-1A, p. 761-771, 1985.*

Abstract

A multiyear study of gold occurrences in the Proterozoic rocks of the Flin Flon-Snow Lake area of Manitoba and Saskatchewan was initiated during the 1984 field season. Areas studied included the Herb Lake gold camp, Snow Lake region, Elbow Lake, Douglas-Phantom Lake area and Amisk Lake. Mapping, detailed structural analyses and sampling for lithogeochemistry were begun on many of the 55 occurrences examined.

A wide variety of gold deposits is recognized. These include quartz vein occurrences in the Herb Lake Camp, disseminated occurrences hosted by carbonatized rocks and showings related to felsic porphyry dykes in the Elbow Lake and Amisk Lake regions and gold-tungsten mineralization related to porphyritic intrusions in the Phantom Lake area.

Résumé

Au cours de la saison sur le terrain de 1984, une étude pluriannuelle des venues aurifères dans les roches protérozoïques de la région de Flin-Flon-Snow Lake, au Manitoba et en Saskatchewan, a été entreprise. Le gisement aurifère du lac Herb, la région du lac Snow, le lac Elbow, la région de Douglas-lac Phantom et le lac Amisk ont été étudiés. La cartographie, les analyses structurales détaillées et l'échantillonnage à des fins d'études lithogéochimiques ont été entreprise pour un grand nombre des 55 venues étudiées.

On a établi la présence d'un grand nombre de gisements aurifères y compris les venues dans les filons de quartz du gisement du lac Herb, les venues disséminées dans les roches carbonatisées et les indices liés aux filons de porphyre felsique dans les régions des lacs Elbow et Amisk ainsi que les minéralisations d'or et de tungstène associées aux intrusions porphyritiques de la région du lac Phantom.

INTRODUCTION

During the 1984 field season, a multiyear study of gold occurrences in the Proterozoic rocks of the Flin Flon-Snow Lake area of Manitoba and Saskatchewan was initiated. This project is being undertaken co-operatively with the geological surveys of Manitoba and Saskatchewan, as the Federal component of new Economic and Regional Development Agreements (ERDA) recently signed with these provinces.

The primary objective of this project is to determine the principal geological controls of gold mineralization in southern Churchill Province. Comparison of the number of gold deposits and occurrences per unit area of greenstone belt terrain reveals that the Churchill Province contains far fewer deposits than the Superior Province (Fig. 1). However, examination of the literature on the deposits in Churchill Province reveals that they share many common geological characteristics with those in Superior Province. Why, then, is this difference so prominent? We hope that through comparison of the local and regional geology around the deposits in Churchill Province with that of more productive areas, some explanation of this difference will become evident. We hope to establish geological criteria for this type of deposit that will aid in the exploration for new resources in northern Manitoba and Saskatchewan. Our preliminary investigations reveal no obvious reason for the differences in past production and number of occurrences between Superior and southern Churchill provinces. This leads to the tentative conclusion that the potential for discovery of major deposits in the latter area is good.

In addition to studying gold deposits, two other possibly related aspects of the regional metallogeny will be examined; occurrences of molybdenum and tungsten that bear a close spatial relationship to many gold occurrences will be mapped and sampled. Alteration associated with volcanic-associated massive sulphide deposits has been the subject of earlier investigations by one of us (Walford and Franklin, 1982); the present program will be extended to include additional types of alteration, normally associated with massive sulphide

[1]Contribution to the Canada-Manitoba and Canada-Saskatchewan mineral development agreements 1984-1989.

deposits, and to compare this alteration with that associated with gold deposits.

GENERAL GEOLOGY AND METALLOGENY

Excellent reviews of the regional geology of the Flin Flon-Snow Lake Belt are available (Byers and Dahlstrom, 1954; Bailes, 1971, 1980; Syme et al., 1982) so that only a brief review of the principal geological elements is necessary here. The Flin Flon-Amisk Lake greenstone segment (Fig. 2) consists of a dominantly subaqueous sequence of volcanic and sedimentary rocks, the Amisk Group (Bruce, 1918), unconformably overlain by terrestrial sandstone and conglomerate of the Missi Group. However, volcanic rocks of the Amisk Lake area contain a significant subaerial component (Ayres, 1978), in contrast to rocks of similar (apparent) age elsewhere in the belt. The unconformity between the two major groups is marked locally by a prominent hematitic paleosol.

The more easterly segments of the belt include the Elbow Lake, File Lake, and Snow Lake areas (Fig. 2). Only in the Snow Lake area do Missi Group rocks constitute a significant component. On the east shore of Wekusko Lake, the

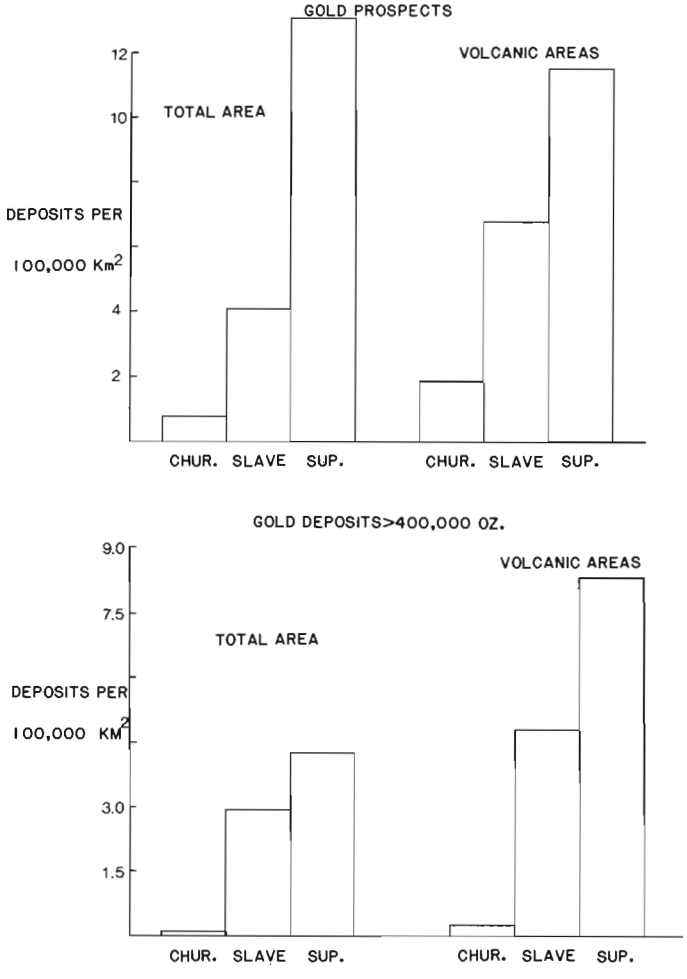

Figure 1. A comparison of the number of gold occurrences per unit area of greenstone belt in the Superior and Churchill provinces.

Missi sequence contains a significant portion of subaerially deposited mafic volcanic and sedimentary strata (Stockwell, 1937; Gordon and Gall, 1982).

At least three phases of deformation have affected the Flin Flon-Snow Lake Belt (Syme et al., 1982). Major faults include late, apparently vertical strike-slip and block faults (Bailes and Syme, 1983), and earlier folded thrust faults (Price, 1977; Gordon and Gall, 1982). Folding is complex, with refolded folds common.

Felsic intrusions include subvolcanic trondhjemitic bodies, (Baldwin, 1980; Walford and Franklin, 1982), and post-Missi granodioritic intrusions. Mafic intrusions also range from synvolcanic to syntectonic in origin.

In the Flin Flon region, the metamorphic grade is typical of lower to upper greenschist facies (Bailes and Syme, 1983), but at Snow Lake, upper greenschist to middle amphibolite facies assemblages are present (Froese and Moore, 1980).

The Flin Flon-Snow Lake Belt contains at least 28 major volcanic-associated massive sulphide deposits (Walford and Franklin, 1982), but has only one major past producer of gold, the Nor-Acme mine at Snow Lake. However, numerous additional small past producers occur in the Flin Flon, Amisk Lake and Elbow Lake areas, and an important discovery has been reported recently near Tartan Lake, north of Flin Flon (Northern Miner, 1984). Minor amounts of tungsten were recovered from the Jacknut and Nor-Acme mines near Snow Lake (Harrison, 1949), and lithium-bearing pegmatites have been intensively explored near Wekusko Lake (Černý et al., 1981). A few porphyry copper occurrences have been described (Baldwin, 1980). Notably, major iron formations are absent, although a few minor occurrences are shown on more recent maps (Bailes and Syme, 1983).

PRESENT WORK

Present work in the Flin Flon Belt was divided into five distinct areas: 1) Herb Lake gold camp, 2) Snow Lake area, 3) Elbow Lake area, 4) Bootleg-Phantom Lake area, and 5) Amisk Lake area (Fig. 2). Fifty-five occurrences and past producers were examined.

Herb Lake Gold Camp

The Herb Lake Gold Camp is located on the east shore of Wekusko Lake (Fig. 3). Gold-bearing veins were discovered in 1914, with the first producing gold mine in Manitoba being the Moosehorn Ballast (Stockwell, 1937; Alcock, 1920). The Rex Laguna and Ferro mines also produced bullion, with the Ferro operating sporadically until 1982.

The area is underlain by Missi Group sedimentary and volcanic rocks intruded by felsic plutons and mafic dykes. The rocks are possibly in fault contact with garnet-biotite-staurolite-bearing metasedimentary rocks of the Amisk Group along the shore of Wekusko Lake (T.M. Gordon, personal communication, 1984).

The Missi Group rocks are folded into a synform that plunges southwest. The core of the synform consists of subaerial mafic lava flows, intercalated felsic pyroclastic rocks

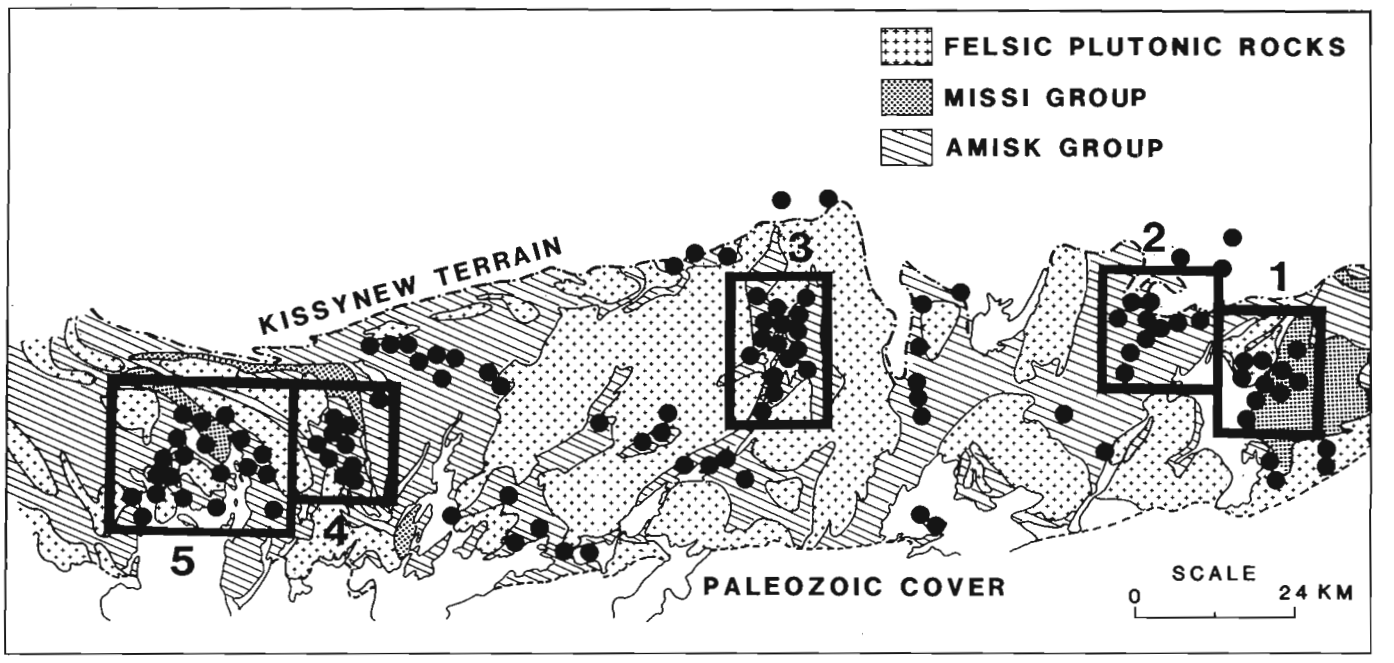

Figure 2. Location of gold occurrences in the Flin Flon-Snow Lake Belt, with areas studied: 1) Herb Lake Camp, 2) Snow Lake, 3) Elbow Lake, 4) Douglas Lake-Phatom Lake, and 5) Amisk Lake.

and chemical sedimentary rocks (Stockwell, 1937; Gordon and Gall, 1982). To the west of these rocks is a sequence of conglomerate and greywacke which contains rhyolite domes and associated pyroclastic and epiclastic rocks. The sequence of sedimentary rocks has been intruded by a series of elongate quartz-feldspar porphyry bodies, which are locally altered to quartz-feldspar sericite schists. Both sedimentary and volcanic rocks have been intruded by dacite and quartz porphyritic granite.

All rocks in the area possess a strong southwest-northeast penetrative foliation that is axial planar to the 'Herb Lake synform'. A second less prominent north-northest-striking foliation was observed near the Rex Mine. Metamorphism in the area ranges from garnet-chlorite zone to garnet-biotite-sillimanite zone, and is highest to the northwest and southeast of the area (Gordon and Gall, 1982).

Gold occurrences

Sampling and mapping was carried out on a series of gold occurrences that are aligned subparallel to the major foliation and are spatially related to the series of quartz-feldspar porphyry bodies that also form a linear array subparallel to the foliation (Fig. 3). These occurrences include the McCafferty, Elizabeth Dauphin, Bingo, Rex-Laguna, Moosehorn-Ballast and Kiski. Farther east, within the core of the Herb Lake synform, are several occurrences aligned parallel to the axial trace of the fold, including the Ferro mine and Rainbow claims. Following a preliminary examination of the district in 1981, work in 1984 was concentrated on detailed lithogeochemical traverses across the mineralized zones and host rocks, plus close examination of the local structure.

The gold occurrences in the Herb Lake Camp consist of gold-tourmaline-quartz veins containing varying amounts of arsenopyrite and pyrite, with minor chalcopyrite, scheelite, galena and sphalerite. Arsenopyrite is ubiquitous within the veins and immediate wallrocks in the western series of deposits (Rex-Laguna etc.), while in the Ferro-Rainbow system pyrite is the principal sulphide. The occurrences commonly consist of one main vein up to 2 m wide, but averaging 1 m. Intense foliation is present in the immediate wallrocks parallel to the veins; wisps and bands of foliated wallrock are incorporated within marginal parts of the veins. Smaller veins at an acute angle to the main vein are intensely folded, whereas smaller veins parallel to the main system are strongly boudinaged.

Alteration is restricted to narrow zones of sulphide-bearing quartz-sericite schist along the margins of the veins. At the Ferro Mine, however, the mafic volcanic wallrocks are foliated and sericitized for distances up to 5 m away from the gold-bearing quartz vein system. Carbonate alteration is notably absent from the vein systems in the Herb Lake Camp.

Snow Lake area

General geology

The geology of the Snow Lake area has been described in detail by Harrison (1949), Russell (1957), Bailes (1980), and Froese and Moore (1980). The area is underlain by a thick sequence of felsic volcanic rocks interlayered with and underlain by mafic volcanic rocks. This sequence of Amisk Group rocks has been intruded by a large body of quartz porphyritic tonalite that may be subvolcanic (Walford and Franklin, 1982) and by various peridotitic and gabbroic intrusions. The

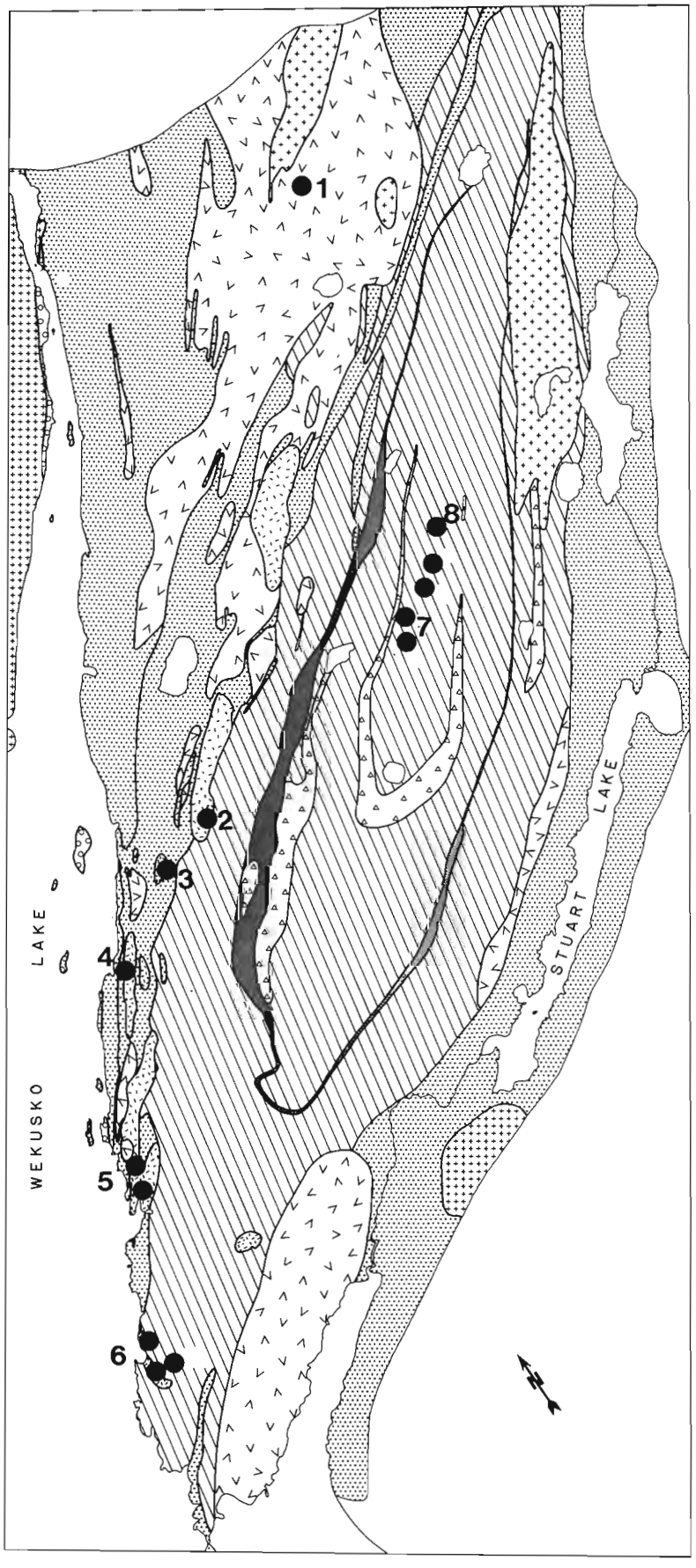

LEGEND

Granite

"Quartz-eye" granite

Quartz-feldspar porphyry

MISSI

Biotite dacite

Rhyolite

Chert, greywacke

Mafic volcanic

Missi metasediment

AMISK

Amisk metasediment

GOLD OCCURRENCES EXAMINED

HERB LAKE AREA

500 0 1000

Metres

Figure 3. Geology of the Herb Lake area, with locations of gold occurrences examined: 1) McCafferty, 2) Elizabeth-Dauphin, 3) Bingo, 4) Rex-Laguna, 5) Moosehorn-Ballast, 6) Kiski, 7) Ferro, and 8) Rainbow Group.

Amisk Group in the area also contains a substantial thickness of turbiditic greywacke that overlies the volcanic rocks (Bailes, 1980; Froese and Moore, 1980). To the north of Snow Lake, the Amisk Group is overlain by meta-arkose of the Missi Group. The rocks have been isoclinally folded and subsequently refolded about the northeast-trending Threehouse synform. Metamorphic assemblages range from those of upper greenschist to upper almandine-amphibolite facies (Froese and Moore, 1980).

Gold occurrences

Although a number of small gold occurrences are scattered throughout the area, our principal interest is in two properties; the Nor Acme Mine and the adjacent Goldfields property directly north of the town of Snow Lake (Fig. 4). A short time was spent logging and sampling drill core at the Goldfields occurrence. The proximity of the Goldfields property to Nor Acme, the largest past gold producer in the belt, and their similarity in structure and mineralization make the two properties a principal target for any gold study in the area.

Detailed mapping and sampling was carried out on the Bounter gold property in the town of Snow Lake (Fig. 4). A shear zone up to 12 m wide crosscuts intermediate to mafic fragmental rocks and gabbro. The zone contains a cherty rock with finely disseminated arsenopyrite and pyrite. Subordinate shears at an acute angle to the main shear also appear to be mineralized, and have been traced through a unit of quartz-feldspar porphyry directly south of the fragmental rocks. The main shear zone would appear to parallel the McLeod Road Thrust which lies along the southern boundary of the property.

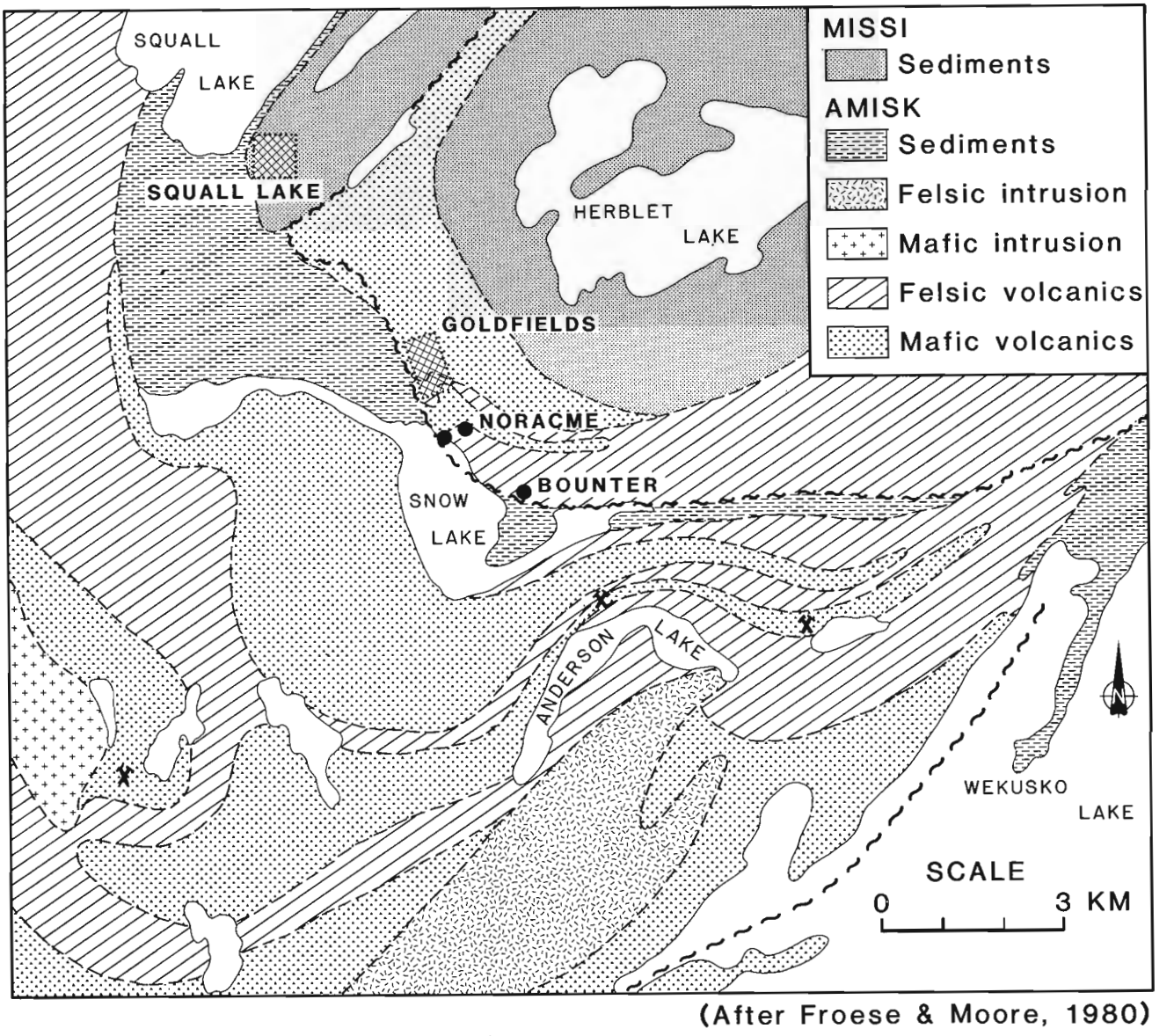

Figure 4. Geology and major gold deposits in the Snow Lake region. Crossed hammers mark volcanogenic massive sulphide deposits in production.

Elbow Lake area

The geology of the region around Elbow Lake was first examined by Bruce (1918). Gold properties in the area were described by Armstrong (1922), Wright (1931) and Stockwell (1935), but no geological mapping of any consequence was carried out until McGlynn (1959) compiled a 1:50 000 sheet in the Elbow-Heming lakes area. Because the detailed stratigraphy and structure within the belt is poorly understood, some selective regional mapping was carried out this summer in order to place the gold occurrences within the context of the surrounding rocks.

General geology

The region around Elbow Lake consists of a segment of a volcano-sedimentary belt striking south through Elbow Lake and then southwest through the Cranberry Lakes system (Fig. 5). The belt is bordered to the east, west and north by

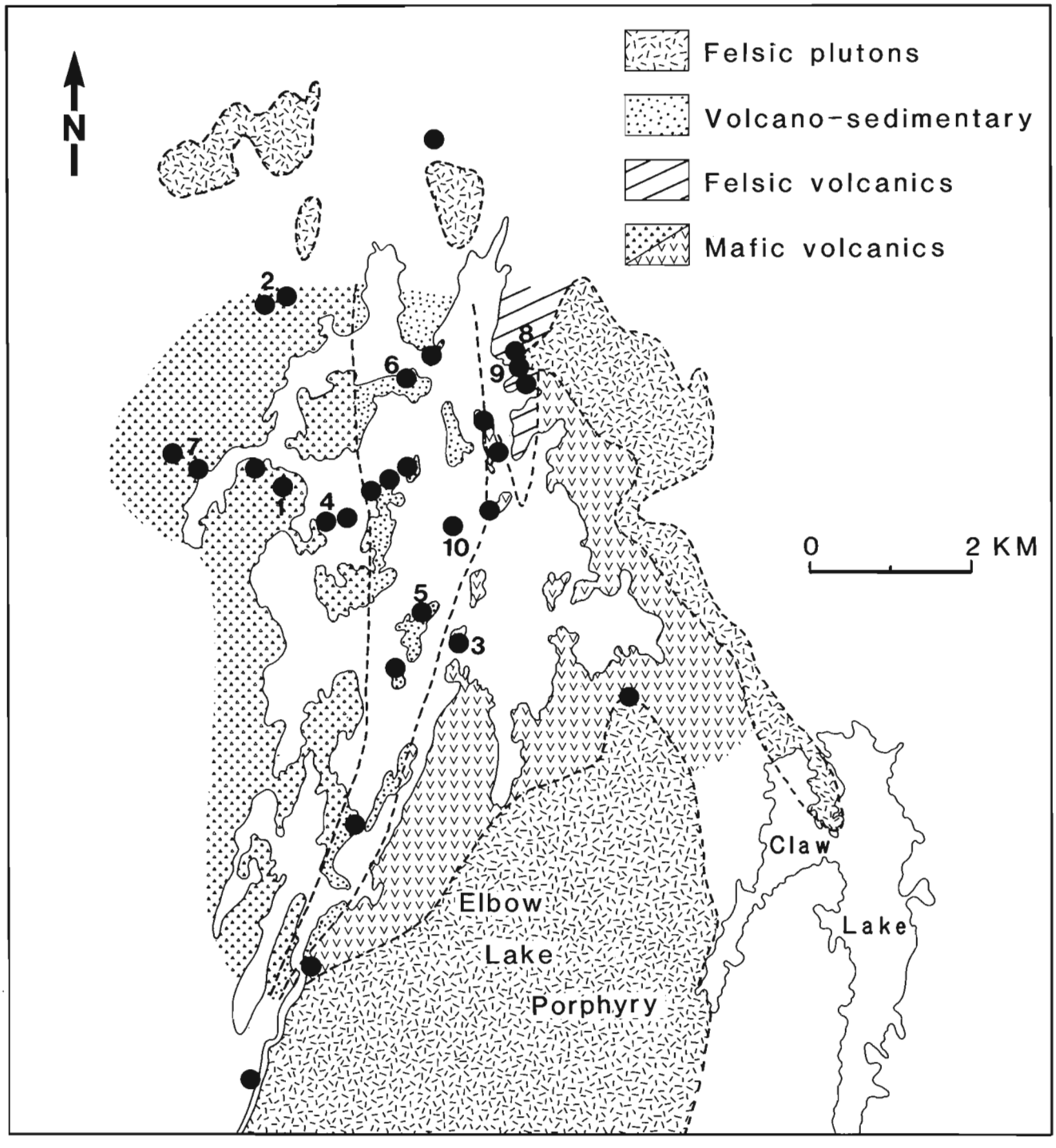

Figure 5. Geology and gold occurrences of the Elbow Lake area. Gold occurrences examined include: 1) GSL, 2) Skogsberg Group, 3) Ding How, 4) Fred, 5) Smith, 6) Century Mine, 7) Gunwar Group, 8) Van No. 2, 9) Mack, and 10) Harbour.

gneissic granodiorite, and to the south by the Elbow Lake Porphyry (McGlynn, 1959; Baldwin, 1980).

From our preliminary mapping, the supracrustal rocks around Elbow Lake can be divided into three zones, each striking north-northeast (Fig. 5). The western zone consists of massive to pillowed mafic flows with subordinate mafic volcaniclastic rocks. A unit of coarse mafic fragmental rock can be traced along the eastern edge of this zone on the north-central part of the lake. The central zone consists primarily of chlorite-sericite-carbonate and chlorite-carbonate schists that, prior to alteration, were most likely fine grained tuffaceous rocks. Lenses of Algoma-type oxide facies iron formation occur on the north central part of the lake, and argillite and cherty argillite are predominant farther south. The iron formation consists of intercalated hematite, magnetite and jasper with interlayered chert beds.

The eastern zone of rocks in the Elbow Lake belt (Fig. 5) contains a sequence of mixed, well layered felsic sericite-quartz tuff and mafic chlorite-amphibole altered tuff in the north, changing to a sequence of intercalated mafic tuff and pillowed flows to the south. The volcanic and sedimentary rocks of the entire Elbow Lake belt are crosscut by numerous intrusions. Diorite dykes, sills and small plugs are common, and a diorite-gabbro complex is present along the east-central shore. A felsic dyke swarm cuts the mafic volcanic flows in the vicinity of the northwestern part of the lake, and several large felsic porphyry dykes underlie the central area of the lake. Small plugs and stocks of orphyritic rhyolite are present along the north shore, and a large quartz porphyritic granite body occurs along the eastern margin of the belt.

Gold occurrences

More than twenty gold occurrences were examined in the area, and can be classified in the following manner:

1. Fault-controlled alteration and stockwork zones.

Many of the occurrences in the Elbow Lake area are characterized by zones of intense carbonate alteration with associated quartz-carbonate veins. Zones up to 20 m wide consisting of fine grained, light grey altered rock occur within mafic volcanic rocks on the GSL and Skogsberg claims (Fig. 5). Quartz-carbonate veins within these zones are strongly folded and boudinaged. At some occurrences, such as the Ding How, the alteration is not as intense or pervasive, but is subordinate to abundant quartz-carbonate veins. This vein network has a short strike length (20-30 m), and the veins are en echelon and parallel to the major foliation. Pyrite is ubiquitous, except at the GSL claim where arsenopyrite predominates. At the Ding How prospect, minor chalcopyrite, sphalerite and galena are present as well as visible gold and green mica.

2. Porphyry-related gold occurrences.

Several types of gold mineralization are spatially related to felsic porphyry dykes. Occurrences on the Fred and Smith claims, (Fig. 5), are associated with single felsic dykes, each more than 10 m wide. Gold mineralization is associated with disseminated arsenopyrite within these dykes, and with pyrite and arsenopyrite along the contacts of the dykes. The Century Mine mineralization (Fig. 5) is associated with a quartz-feldspar porphyry dyke 1-3 m wide that crosscuts carbonatized mafic volcanic rocks. The altered dyke rock is composed of quartz, sericite, carbonate and abundant disseminated pyrite. According to Stockwell (1935), quartz-carbonate veins up to 2 m wide occur in the dyke. The altered dyke, where exposed near the mine dump, contains pyrite, chalcopyrite galena and visible gold associated with a stockwork of quartz veins.

The Gunwar claims (Fig. 5), are underlain by massive to pillowed mafic flows crosscut by a series of felsic porphyry dykes that strike north and east. Spatially associated with these dykes are several sets of quartz-carbonate veins which are subparallel to the dykes, but in most cases are not in contact with them. The veins have envelopes of intensely carbonatized rock, which is fine grained, light grey and well indurated. In the northeast corner of the property where a vein system crosscuts a porphyry dyke, the dyke is intensely carbonatized and brecciated. Mineralization consists of disseminations and veinlets of pyrite and chalcopyrite in the altered wallrocks, and coarse grained aggregates of pyrite in the quartz-carbonate veins.

3. Stratabound occurrences.

Although most stratabound gold occurrences in the Elbow Lake area are obviously related to faulting or shearing in the rocks, there are stratabound occurrences where this is not so evident. The Van No 2 claim (Fig. 5), contains a sulphide-rich unit up to 4 m wide striking parallel to bedding within a series of interbedded, well layered felsic and mafic tuffs. To the east, the sequence has been intruded by a large body of quartz porphyritic granite and associated dykes and sills. The mineralized zone consists of a fine grained cherty rock, with 10 to 15% disseminated fine grained pyrite. The zone can be traced discontinuously 200 m south to the Mack claim (Fig. 4). Here, the unit has abundant carbonate and contains a large quartz-carbonate-tourmaline vein through which an 8 m deep shaft has been sunk. Several of the tuff layers are also cherty and contain finely disseminated pyrite. No assays from the sampling program have yet been received, but the unit averaged 0.20 oz/ton across its width near the Mack shaft (Stockwell, 1935).

Occurrences which may be less definitely classified as stratabound are those associated with lenses of oxide facies iron formation. At the Harbour claim (Fig. 5) magnetite-chert iron formation is lensoid, attains a thickness of 3 m, but diminishes rapidly in thickness along strike due to either primary distribution or subsequent structural modification. The iron formation is in contact with intensely carbonatized wallrocks containing disseminated pyrite and green sericite. A 9 m wide felsic porphyry dyke that has been subjected to pyrite-carbonate alteration occurs 10 m east of the iron formation. The volcanic rocks in the area consist of chlorite-carbonate and chlorite-sericite-carbonate schist. Pyrite is present as small veinlets and fracture fillings as well as in numerous quartz veins that crosscut the iron formation. The iron formation assayed 0.25 oz gold/ton across 2.2 m (Stockwell, 1935). Although the mineralization is stratabound within the iron formation, the distribution of the sulphide and the intensely altered wallrocks to the iron formation suggest that the formation of pyrite postdates the formation of the chemical sedimentary rock.

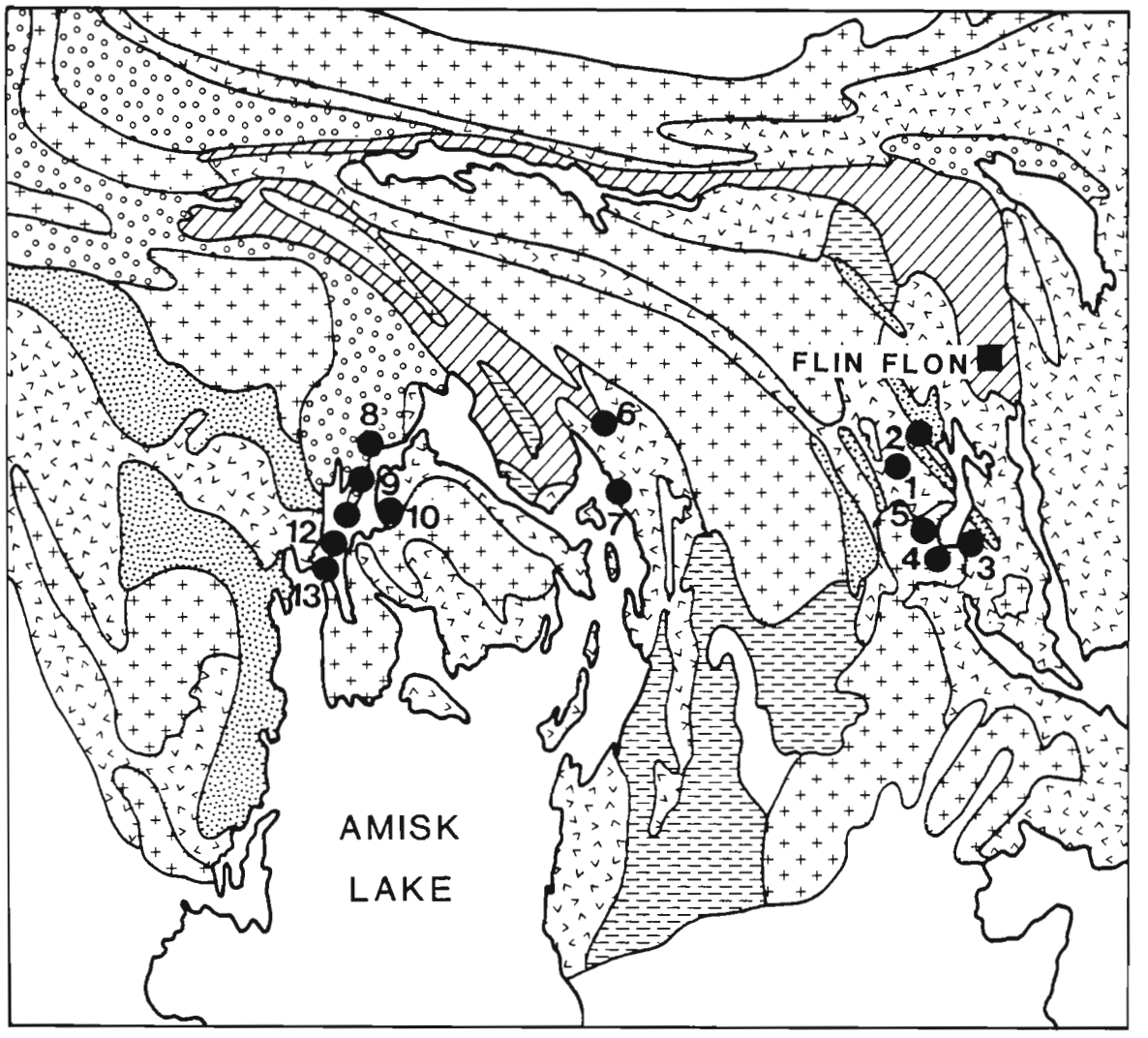

Figure 6. Geology of the western margin of the Flin Flon-Snow Lake Belt. Gold and or tungsten occurrences examined include: 1) Rio Mine, 2) Douglas tungsten, 3) McMillan Mine, 4) Phatom Lake Mine, 5) IMC, 6) Mitchell, 7) Amisk Syndicate, 8) Duplex, 9) Monarch, 10) Laural, 11) Amisk Gold Syndicate, 12) Waverly, and 13) Sonora.

Bootleg – Phantom Lake area

General geology

The rocks in the Bootleg-Phantom Lake area comprise a northeasterly striking, westerly-facing and dipping homoclinal sequence of, principally, subaqueous volcanic rocks. According to Pearson (1983), the lowest stratigraphic unit, which is exposed in the Phantom Lake area, is a massive quartz and/or feldspar porphyritic rhyolite. This is overlain to the west by a thick sequence of tholeiitic basalt, pillowed lava and pillow breccia followed by a thick succession of heterolithic breccia, intermediate to felsic lava capped by a graphite-argilite horizon and a thick sequence of bedded, mafic to felsic aquagene tuff. The Boot Lake Pluton, Reynard Lake Pluton and the Phantom Lake Granite are the latest intrusions; the Phantom Lake Granite, at about 1820 Ma, being the youngest.

Gold-tungsten occurrences

Several weeks were spent examining both gold and tungsten occurrences in the Bootleg-Phantom Lake area and extensive mapping and sampling were completed on surface at the Rio Mine, Flin Flon Gold Mines Ltd. Some spot sampling was completed underground. A study of the geology and structure of the immediate area around the mineralized zone is being completed by T. Middleton (Department of Earth Sciences, University of Waterloo) as a Bachelors dissertation. The relationship between the Rio Mine and several other gold and tungsten occurrences that are all spatially related to the Rio Fault is also being examined. The Douglas tungsten showing (Fig. 6) illustrates an intimate relationship between tungsten emplacement and late stage deformation in the area, with a strong west-northwest shear system causing dilation of an earlier northwest-striking fracture cleavage. It is along these zones of dilation that the carbonate and scheelite are present.

In an attempt to determine the age of gold mineralization in the area, several gold and tungsten occurrences spatially associated with the Phantom Lake Granite were examined. These include the McMillan Mine, Phantom Lake Mine and IMC tungsten showing (Fig. 5). Extensive fracture-controlled alteration is present within the Phantom Lake Granite, and also in the older Boot Lake Granodiorite, where the former intruded the latter. Phyllitic and argillic alteration types are present in the Phantom Lake Granite, whereas in the Boot Lake Granodiorite a zonation from potassic quartz-feldspar-chalcopyrite outwards through quartz-chlorite to epidote-hematite was observed. Dominant fracture sets are west-northwest and north-northeast and appear to control tungsten-gold, and gold- copper-molybdenum mineralization, with the west-northwest fracture set being the youngest.

Hydrothermal alteration associated with the mineralization in these intrusions is similar to the characteristic alteration of porphyry deposits (Lowell and Guilbert, 1970), and has been observed in plutons elsewhere in the Flin Flon-Snow Lake Belt (Baldwin, 1980; Wallster, 1979; Stewart, 1977), and at other locations within Precambrian volcanosedimentary belts (Ayres and Averill, 1974; Cimon, 1973; Findlay, 1976; Kirkham, 1972).

Amisk Lake area

General geology

The following description of the geology of the Amisk Lake area is from Pearson (1983, p. 69-73):

"The Amisk Lake area is underlain by a thick sequence of submarine tholeiitic basalts in the east, which give way westwards to subaerial lava flows, debris flows, fragmental rocks, and finally to submarine intermediate calc-alkaline flows and fragmental rocks on the west side of Amisk Lake. Volcanic rocks on Missi Island have been intruded by a number of porphyritic subvolcanic bodies which range in composition from andesite to rhyolite and form part of a vent complex.

Rocks in the Amisk Lake area have been subjected to at least two periods of folding. The early phase was accompanied by development of major faults, including the West Channel Fault; a system of several subparallel faults".

Gold occurrences

A cursory examination of the gold occurrences on Amisk Lake was carried out in order to assess the direction of more detailed work in the area. Many of the showings are associated with carbonate-rich shear zones, including the Mitchell and Amisk Syndicate showings along the east shore (Fig. 6), and the Monarch, Amisk Gold Syndicate, Duplex and Waverly showings along the West Channel. As many of these faults are believed to have been active for a long period of time, including synvolcanic activity, it is important to determine the relative age of the gold mineralization. F. McDougall (personal communication, 1984) indicated that gold mineralization on the Laural claims (Fig. 6) is strata-bound within a rhyolite dome and associated fragmental rocks, and may be epithermal in origin. It is felt that detailed examination of the structure in the area will assist in determining whether the gold mineralization was synchronous with volcanism and associated intrusive activity, or if it was associated with later metamorphic and tectonic activity.

SUMMARY

An initial examination of gold occurrences in the Flin Flon-Snow Lake Belt, appears to indicate different types of deposit. These include gold-quartz veins of the Herb Lake camp, disseminated gold deposits in the Elbow Lake and Amisk Lake areas that are hosted by carbonate-altered rocks and associated with faults and shears, gold associated with felsic porphyry dykes in the Elbow Lake area and possible epithermal gold mineralization associated with felsic extrusive and subvolcanic rocks on Amisk Lake. In the Phantom Lake area gold-tungsten- molybdenum mineralization may be genetically related to late high-level porphyry intrusions.

In comparing gold deposits in the Flin Flon-Snow Lake Belt with gold camps in the Superior Province, several similarities are evident. The association of extensive carbonate and sericite alteration with gold deposits is well documented in the Timmins area (Pyke, 1975; Fyon and Crockett, 1980; Karvinen, 1980) and at Red Lake (MacGeehan et al., 1982;

Durocher, 1983). The association of felsic porphyritic rocks with gold mineralization is also common in Superior Province gold camps, including Timmins (Kirkham, 1972), Val d'Or (Robert et al., 1983) and Hemlo (Valliant et al., 1984).

Although the settings for gold deposits in the Superior Province are generally similar, the size of known occurrences in the Churchill Province is an order of magnitude smaller. Whether this is a true geological phenomenon or a symptom of the directions pursued in previous gold exploration in the Flin Flon-Snow Lake Belt is still uncertain. A redirection of exploration in the area from gold mineralization of quartz vein type to more disseminated-type occurrences associated with extensive alteration might be a step in the right direction.

ACKNOWLEDGMENTS

Many of the companies in the area were generous in their assistance to the gold project during the 1984 field season. We would particularly like to thank D. Ziehlke and R. McQuarrie of Hudsons Bay Exploration and Development, N. Provens of Hudson Bay Mining and Smelting Ltd., D. Mallo of Goldfields Ltd., G. Pearce of Noranda Exploration Ltd., F. McDougall of SMDC, and John Pearson of the Saskatchewan Geological Survey.

We also thank our assistants, T. Middleton and J. Scoates, for the cheerful and professional way they completed their various duties during the field season.

We thank R. Thorpe for reviewing the manuscript and offering numerous helpful suggestions for its improvement.

REFERENCES

Alcock, F.J.
1920: The Reed-Wekusko map area, northern Manitoba; Geological Survey of Canada, Memoir 119.

Armstrong, P.
1922: Geology and ore deposits of Elbow Lake area, northern Manitoba; Geological Survey of Canada, Summary Report, 1922, Part C, p. 37-44.

Ayres, L.D.
1978: A transition from subaqueous to subaerial eruptive environments in the middle Precambrian Amisk Group at Amisk Lake, Saskatchewan — a progress report; Centre for Precambrian Studies, University of Manitoba, 1977 Annual Report, p. 36-51.

Ayres, L.D. and Averill, S.A.
1974: Setting Net Lake Stock; Centre for Precambrian Studies, University of Manitoba, 1974 Annual Report, p. 202-205.

Bailes, A.H.
1971: Preliminary compilation of the geology of the Snow Lake-Flin Flon-Sherridan area; Manitoba Mines Branch, Geological Paper 1-71, 27 p.

1980: Geology of the File Lake Area, Manitoba; Manitoba Mineral Resources Division, Geological Report 79-1.

Bailes, A.H. and Syme, E.C.
1983: Flin Flon/Schist Lake Project (parts of 63 K/12, 13); Manitoba Mineral Resources Division, Report of Field Activities 1983, p. 23-29.

Baldwin, D.A.
1980: Porphyritic intrusions and related mineralization in the Flin Flon volcanic belt; Manitoba Mineral Resources Division, Economic Geology Report ER 79-4.

Bruce, E.L.
1918: Amisk-Athapapuskow Lake District; Geological Survey of Canada, Memoir 105.

Byers, A.R. and Dahlstrom, C.D.A.
1954: Geology and mineral deposits of the Amisk-Wildnest lakes area, Saskatchewan; Saskatchewan Department of Mineral Resources, Report no. 14, 177 p.

Černý, P., Trueman, D.L., Ziehlke, D.V., Goad, B.E., and Paul, B.J.
1981: The Cat Lake-Winnipeg River and Wekusko Lake pegmatite fields, Manitoba; Manitoba Mineral Resources Division, Economic Geology Report ER 80-1.

Cimon, J.
1973: Possibility of Archean porphyry copper in Quebec; (abstract), Canadian Mining Journal, v. 94, no. 4, p. 97.

Durocher, M.E.
1983: The nature of hydrothermal alteration associated with the Madsen and Staratt-Olsen gold deposits, Red Lake area; *in* The Geology of Gold in Ontario, ed. A.C. Colvine; Ontario Geological Survey, Miscellaneous Paper 110, p. 123-140.

Findlay, D.J.
1976: An Early Precambrian porphyry copper-molybdenum deposit at Lang Lake, northwestern Ontario (a summary); *in* Centre for Precambrian Studies, University of Manitoba, Annual Report 1976, p. 97-98.

Froese, E. and Moore, J.M.
1980: Metamorphism in the Snow Lake area, Manitoba; Geological Survey of Canada, Paper 98-27, 16 p.

Fyon, J.A. and Crockett, J.H.
1980: Volcanic environment of carbonate alteration and stratiform gold mineralization, Timmins area; *in* Genesis of Archean, Volcanic-Hosted Gold Deposits; Ontario Geological Survey, Open File Report 5293, p. 44-65.

Gordon, T.M. and Gall, Q.
1982: Metamorphism in the Crowduck Bay area, Manitoba; *in* Current Research, Part A, Geological Survey of Canada, Paper 82-1A, p. 197-201.

Harrison, J.M.
1949: Geology and mineral deposits of the File-Tramping lakes area, Manitoba; Geological Survey of Canada, Memoir 250.

Kirkham, R.V.
1972: Geology of copper and molybdenum deposits; *in* Current Research, Part A, Geological Survey of Canada, Paper 72-1A, p. 82-87.

Karvinen, W.O.
1980: Geology and evolution of gold deposits, Timmins area, Ontario; *in* Genesis of Archean, Volcanic-Hosted Gold Deposits; Ontario Geological Survey, Open File Report 5293, p. 1-43.

Lowell, J.D. and Guilbert, J.M.
1970: Lateral and vertical alteration-mineralization zoning in porphyry ore deposits; Economic Geology, v. 65, p. 373-408.

MacGeehan, P.J., Sanders, T., and Hodgson, C.J.
1982: Meter-wide veins and a kilometre-wide anomaly: wall-rock alteration at the Campbell Red Lake and Dickenson gold mines, Red Lake District, Ontario; Canadian Institute of Mining and Metallogeny, v. 75, no. 841, p. 90-102.

McGlynn, J.C.
1959: Elbow-Heming lakes area, Manitoba; Geological Survey of Canada, Memoir 305.

Northern Miner
1984: Granges' first hole hits high grade ore; May 17, 1984.

Pearson, J.G.
1983: Gold metallogenic studies: Flin Flon-Amisk Lake area; *in* Summary of Investigations 1983, Saskatchewan Geological Survey, Miscellaneous Report 83-4, p. 67-74.

Price, D.P.
1977: Geology and economic potential of the Flin Flon-Snow Lake area; Centre for Precambrian Studies, University of Manitoba, Annual Report 1977, p. 52-83.

Pyke, D.R.
1975: On the relationship of gold mineralization and ultramafic volcanic rocks in the Timmins area; Ontario Division of Mines, Miscellaneous Paper no. 62.

Robert, F., Brown, A.C., and Audet, A.J.
1983: Structural control of gold mineralization at the Sigma Mine, Val d'Or, Quebec; Canadian Institute of Mining and Metallurgy, Bulletin, v. 76, no. 850, p. 72-80.

Russell, G.A.
1957: Structural studies of the Snow Lake-Herb Lake area, Hab Lake mining division, Manitoba; Manitoba Mines Branch, Publication 55-3.

Stockwell, C.H.
1935: Gold deposits of Elbow-Morton area, northern Manitoba; Geological Survey of Canada, Memoir 186.

1937: Gold deposits of Herb Lake area, northern Manitoba; Geological Survey of Canada, Memoir 208.

Stewart, J.W.
1977: Gold evaluation program; *in* Report of Field Activities 1977, Manitoba Mineral Resources Division, p. 105-109.

Syme, E.C., Bailes, A.H., Price, D.P., and Ziehlke, D.V.
1982: Flin Flon Volcanic Belt: Geology and Ore Deposits at Flin Flon and Snow Lake, Manitoba; Geological Association of Canada, Field Trip Guidebook no. 6.

Valliant, R., Guthrie, A., Bradbrook, C., Motzok, A., McIlveen, D., Kent, C., MacMillan, S., Skecky, G., Wingfield, T., and Sheehan, D.
1984: Field guide to geological setting of Lac Minerals Limited pyritic gold orebodies, Hemlo, Ontario; *in* CIM Geology Divison Guidebook, Hemlo-Manitouwadge-Winston Lake, Metallogenesis of Highly Metamorphosed Archean Gold-Base Metal Terrain, Canadian Institute of Mining and Metallurgy, p. F1-F17.

GEOLOGY OF THE IGNEOUS-METAMORPHIC COMPLEX OF SHELBURNE AND EASTERN YARMOUTH COUNTIES, NOVA SCOTIA[1]

Project 840043

H.D. Rogers[2]
Precambrian Geology Division

Rogers, H.D., Geology of the igneous-metamorphic complex of Shelburne and eastern Yarmouth counties, Nova Scotia; in *Current Research, Part A, Geological Survey of Canada, Paper 85-1A, p. 773-777, 1985.*

Abstract

Three major plutons on shore and a fourth offshore are identified. Related igneous phenomena include numerous stocks and large dioritic xenoliths. Diabase dykes of several different ages are also present. Lithologies in the plutons include diorite, tonalite, granite and minor granodiorite.

Metamorphic rocks consist of metasedimentary rocks ranging from greenschist to upper amphibolite facies. Spectacular occurrences of staurolite-andalusite-cordierite schists and granofelses are common. Poikiloblastic overgrowths on these minerals indicate a contact metamorphic overprint on the porphyroblasts which were developed during regional metamorphism.

A syntectonic foliation is well developed in all plutons except the Seal Island pluton which exhibits a progressive westward increase in ductile post-intrusive deformation. Shear zones were found in other plutons and in the porphyroblastic metamorphic rocks, but measurable offsets are rare, except in the Pubnico area. Fold styles range from overturned isoclinal to irregular open folds. Occurrences of pseudotachylite in pelitic rocks are widespread in the project area.

Résumé

Trois grands plutons sur terre et un quatrième en mer ont été identifiés. Des phénomènes ignés connexes ont produit un grand nombre de massifs et de gros xénolites dioritiques. Des filons de diabase d'âges différents sont également présents. Des plutons se composent de diorite, de tonalite, de granite, et de petites quantités de granodiorite.

Les roches métamorphiques se composent de roches métasédimentaires dont les faciès varient de celui de schistes vers au faciès supérieur d'amphibolites. Des venues spectaculaires de schistes à staurotide, à andalousite et à cordiérite et de roches métamorphiques granoblastiques sont fréquentes. Les cristaux poeciloblastiques sur ces minéraux indiquent qu'il y a eu surimpression par métamorphisme de contact sur les porphyroblastes formés lors du métamorphisme régional.

Tous les plutons sauf selui de Seal Island présentent une foliation syntectonique bien développée. Dans le pluton de Seal Island, il y a accroissement progressif vers l'ouest de la déformation ductile post-intrusive. Des zones de cisaillement sont trouvées dans d'autres plutons et dans les roches métamorphiques porphyroblastiques mais les décalages mesurables sont rares sauf dans la région de Pubnico. Les plis varient des plis isoclinaux déversés aux plis ouverts irréguliers. Des venues de pseudotachylite sont fréquentes dans les roches pélitiques de la région.

[1]Contribution to the Canada-Nova Scotia Mineral Development Agreement 1984-89.
[2]Department of Geology, Acadia University, Wolfville, Nova Scotia, B0P 1X0

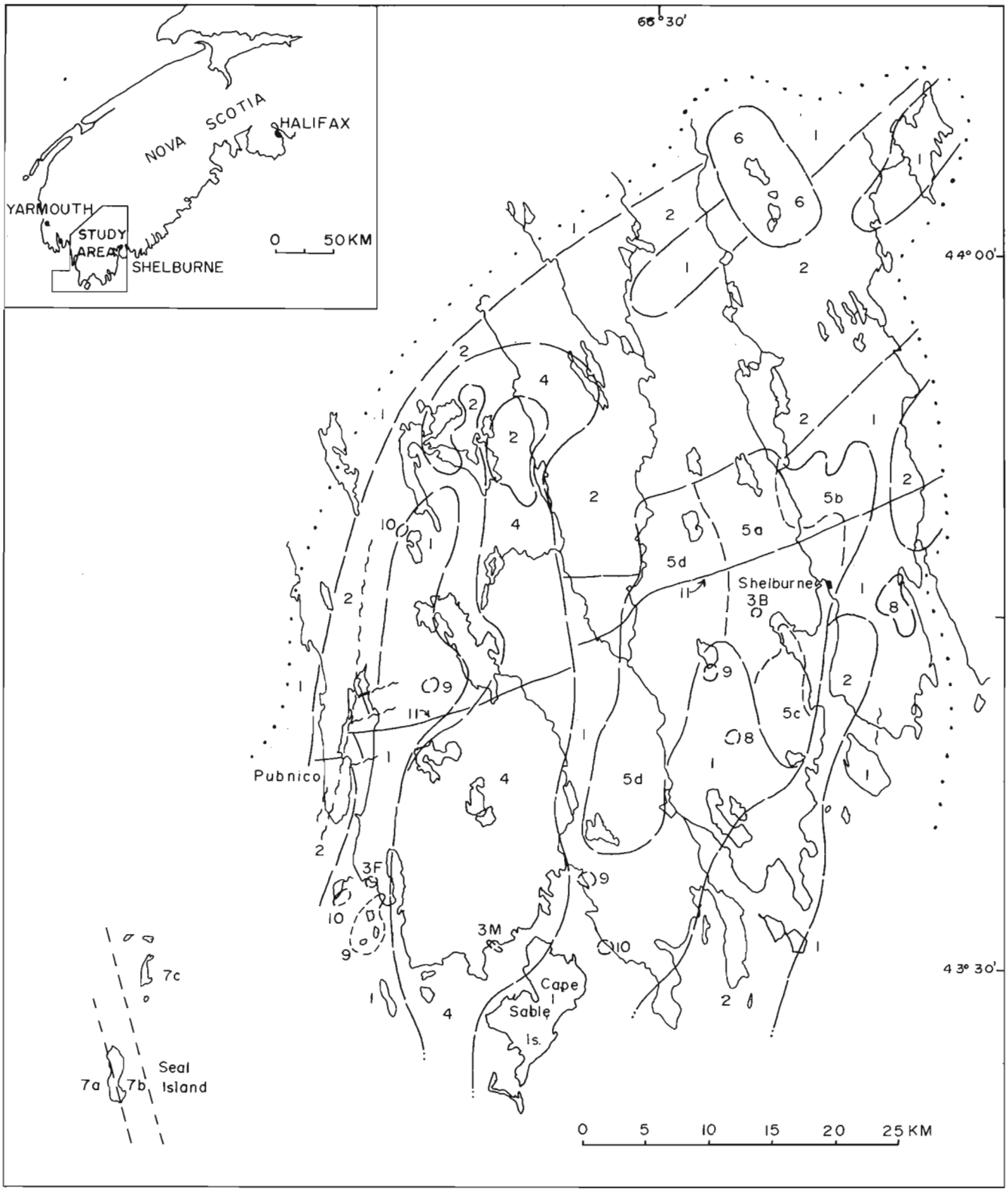

Figure 1. Generalized geology of igneous and metamorphic rocks of Shelburne County and eastern Yarmouth County.

INTRODUCTION

The project area covers 1900 km^2 of southwestern Nova Scotia in Shelburne and Yarmouth counties (Fig. 1) (parts of 21A/3, 20O/8, and 20P/5, 6, 11, 12, 13). Although outcrop is most abundant in coastal areas it is also sufficient along inland waterways and roads to allow mapping. Access to the inland areas has improved considerably during the last 25 years. An extensive network of waterways and trails largely offsets the accessibility problems posed by large areas of swamp and bog.

The geology of the project area is apparently unique within the Meguma Zona of the Appalachians because of the spectacular metamorphic development of porphyroblastic staurolite, andalusite and cordierite. Unusual too is the widespread development of migmatite in the area. Granitoid lithologies are mainly tonalite and mappable units of muscovite, two-mica and biotite monzogranite and syenogranite. Granodiorite occurs only in very small volumes. A few diabase dykes of pre-Jurassic age intrude the granites. The granitoid rocks are also characterized by the pervasive development of an apparently syntectonic foliation. These various features contrast strongly with those of other areas of the Meguma Zona.

The first systematic mapping of the project area was done in 1959 and 1960 on a reconnaissance scale of 1 inch = 4 miles (Taylor, 1967). The geochemistry and evolution of plutonic rocks in the area were described by Albuquerque (1977, 1979). $^{40}Ar/^{39}Ar$ geochronology of these granitoid rocks was reported by Reynolds et al. (1981). These data indicated a significantly younger age (Late Carboniferous) for the plutons of the project area compared to the Early Carboniferous age for the South Mountain Batholith. There is some uncertainty as to whether these new data represent intrusion ages or cooling ages.

The lack of detailed mapping in the area led to the development of this project and field work was conducted in 1983 and 1984. Results of the mapping, combined with petrologic studies emphasizing the granitoid rocks, will form the basis of a M.Sc. thesis. Metamorphic aspects of the area are being studied by students doing B.Sc. (Honours) thesis at Acadia University, e.g. White (1984).

LEGEND

EARLY JURASSIC

11 Shelburne Dyke - diabase

CARBONIFEROUS

no age succession implied

10 granite stocks

9 tonalite and/or granodiorite stocks

8 granodiorite stocks

7 Seal Island Pluton - a) muscovite granite
b) 2-mica granite
c) biotite granite

6 Bald Mountain Pluton - granite

5 Shelburne Pluton - a) 2-mica granite
b) muscovite granite
c) biotite granite
d) undivided granite/tonalite

4 Barrington Passage Pluton - tonalite

SILURO-DEVONIAN (?)

3 xenoliths - F) Forbes Point Diorite
M) Murray Cove Diabase
B) Birchtown Diorite

CAMBRO-ORDOVICIAN

2 Halifax Formation - pelite

1 Goldenville Formation - psammite

METASEDIMENTARY ROCKS

The Cambro-Ordovician rocks of the Goldenville and Halifax formations which outcrop in the area can be relatively easily distinguished at various metamorphic grades (Fig. 1). The older of the two formations, the Goldenville, consists primarily of well-bedded psammites and minor interbedded pelitic schists or slates. It occurs on the outer margins and in the south-central portions of the map area.

A sharp contact between the Goldenville Formation and the overlying Halifax Formation is exposed in Pubnico Harbour. The Halifax Formation, made up of biotite and chiastolite slates, staurolite-andalusite-cordierite granofelses and garnet-sillimanite schists and granofelses, outcrops over most of the northern portion of the area and along the eastern and western margins.

INTRUSIVE ROCKS

Granitoid bodies in the area range from small stocks with areas of less than 1 km^2 up to one as large as 475 km^2. They include four major plutons and a large number of smaller stocks.

The laragest of the major plutons, the Barrington Passage Pluton (Taylor, 1967), which underlies an area of 475 km^2, is made up of medium grained, biotite tonalite. The plagioclase content is relatively constant at nearly 50% but the quartz and biotite contents vary in an apparently unsystematic manner. Potassium feldspar is lacking, except near the contact with the Goldenville Formation where small quantities of microcline make the rock-type granodiorite. The

tonalite has a higher biotite content where it is surrounded by the Halifax Formation rocks.

The Shelburne Pluton (Taylor, 1967) outcrops as a lobed body underlying an area of 285 km^2. Equigranular, medium grained granite comprises most of the pluton. Smaller amounts of tonalite and granodiorite also occur. The higher outcrop density in the eastern portion of the pluton makes subdivision possible. Two-mica granite is the major lithology, with the southeastern lobe being mainly biotite granite and the northeastern area being mainly muscovite granite. Locally, along the margins and near roof pendants, the pluton is granodiorite. A 1 km wide garnetiferous aplite body occurs near Shelburne. In the western part of the pluton, biotite tonalite probably underlies most of the northwest corner. A lower outcrop density the western portion of the pluton may be responsible for the lack of lithologic subdivision. The most notable occurrence in the western part of the pluton is tonalite and granite in single and adjacent outcrops. The absence of observed cross-cutting relationships makes it apparent that both rock types were intruded simultaneously. Large volumes of pegmatite were found along the margin of the pluton, irregardless of the local lithology.

The Bald mountain pluton outcrops north of the Shelburne Pluton and covers an area of 30 km^2. It is similar in appearance to much of the Shelburne Pluton although it is mainly muscovite granite. No pegmatites were noted in this pluton.

The Seal Island pluton outcrops on a group of islands 45 km south of Yarmouth and underlies an area of at least 100 km. Equigranular, coarse grained granite characterizes this pluton. On Seal Island it grades from a tourmaline-bearing, muscovite syenogranite to a two-mica monzogranite on the east side of the island. Biotite granite occurs on the other islands.

The numerous small stocks so far identified in the area can be grouped into three types. Two granodiorite stocks occur in association with the Shelburne Pluton. Four stocks ranging in composition from granodiorite to tonalite occur mainly near the margins of the Barrington Passage Pluton. One is associated with the Shelburne Pluton. Three two-mica granite stocks are spatially associated with the Barrington Passage Pluton. Three small mafic to intermediate bodies, the Birchtown diorite, the Forbes Point diorite and the Murray Cove diabase (Albuquerque, 1979), are thought to be xenolithic.

The Shelburne Dyke is a major geological feature extending for several hundred kilometres across southwestern Nova Scotia (Papezik and Barr, 1981). Additional outcrops of this diabase dyke have been found in the project area and are associated with the axis of the aeromagnetic high associated with other parts of the dyke. Several diabase dykes also occur in the Seal Island pluton.

STRUCTURE

The major folds (F1) in the Meguma Group rocks were formed during the early stages of the Acadian Orogeny (Keppie, 1979). Intrusion of the plutons appears to have had no more than a local effect on their form. These F1 folds outline a relatively simple large scale structural pattern consisting of three synclines and two intervening anticlines which extend north to northeast across the map area. The two outer synclines and the northern portion of the central syncline are cored by Halifax Formation metasedimentary rocks. Along strike the synclines vary from upright to inclined and in some places overturned, often for many kilometres. Along most of their lengths the major folds appear to be tight to isoclinal although the central syncline approaches an open fold style in the north. A second regional fold phase (F2), of minor proportions, was responsible for widespread crenulation and kinking of the pelitic rocks. In a general way it appears that the Barrington Passage Pluton has intruded the axial part of the central syncline whereas the Shelburne Pluton has intruded along the axis of the eastern syncline.

Pseudotachylite occurrences are very numerous. Most of these occur parallel to bedding in rocks of the Halifax Formation. A few have been found in the same situations in psammitic rocks of the Goldenville Formation.

With the exception of the Seal Island pluton, the granitoid plutonic rocks display a syntectonic foliation. This is most obvious over large areas of the Barrington Passage and Bald Mountain plutons as a well developed mineral orientation. In the Bald Mountain pluton this foliation is partly post-tectonic, resulting in strongly sheared rocks. A similar, but weaker, foliation occurs in the Shelburne Pluton. A few instances of flow foliation exist in individual outcrops of the Shelburn Pluton.

The granitoid rocks of the Seal Island pluton exhibit an increase in intensity of ductile deformation from east to west. The muscovite granite zone to the west is intensely deformed and contains numerous mylonite zones. Augen structure is more typical in the granite on the east side of the island.

There is little evidence in most of the area for major faulting. A notable exception is the Pubnico area where biotite and chiastolite slates of the Halifax Formation appear to be in fault contact with higher grade staurolite-andalusite schists and granofelses. This same north-trending fault has also caused sinistral displacement of the Shelburne Dyke. Parallel faults or splays further disrupt the chiastolite slates along the west shore of the Pubnico peninsula. Displacement along this fault system appears to extend for at least 15 km to the north where biotite slates and staurolite-andalusite schists remain in close proximity. A number of northeast-trending faults, which also occur in the Pubnico area, probably predate the main north-trending fault. A north- to northwest-trending system of narrow shear zones in the granitoid rocks of the mainland may be related to the faulting observed in the Pubnico area.

METAMORPHISM

Metamorphic grade ranges from greenschist facies at the margins of the map area to the sillimanite zone of the amphibolite facies over much of the central portion. Intervening isograds occur in close proximity to each other on the western side of the area but are much further apart on the east side. The isograds conform in general outline to the area occupied by the Barrington Passage and Shelburn plutons.

Poikiloblastic overgrowths on porphyroblastic minerals are ubiquitous and are interpreted to indicate two separate metamorphic events. The first was a regional metamorphic event (M1), achieving middle amphibolite facies (staurolite-andalusite-cordierite). A later contact metamorphic event (M2) produced overgrowths on these porphyroblasts and initiated the widespread development of sillimanite zone assemblages along the margins of the major plutons. M2 also resulted in migmatization along the margins of the Barrington Passage Pluton.

DISCUSSION

The plutons of the map area appear to represent a different and probably younger magmatic event than that responsible for the plutons of the South Mountain Batholith. The southern plutons of Nova Scotia described here display a variety of features which contrast with the South Mountain Batholith including the lithologic types present, the textural and mineralogical relationships within the plutons, the nature of the intrusive contacts, the extent and degree of contact metamorphism and the nature of the associated gravity anomaly pattern.

Geochemical data pertaining to major, trace and rare earth element distribution are currently being prepared. This will greatly enlarge the present geochemical data base and provide a basis for investigating the geochemical relationships with the South Mountain Batholith.

Dating studies (Reynolds et al., 1981) to have indicated that the plutons of the area may be significantly younger than those of the South Mountain Batholith. Geochronological studies are continuing to test this possibility.

REFERENCES

Albuquerque, C.A.R. de

1977: Geochemistry of the tonalitic and granitic rocks of the Nova Scotia southern plutons; Geochimica et Cosmochimica Acta, v. 41, P. 1-13

1979: Origin of the mafic plutonic rocks of southern Nova Scotia; Geological Society of America Bulletin, v. 90, Part A, p. 719-731

Keppie, J.D.

1979: Geological map of the Province of Nova Scotia; Nova Scotia Department of Mines and Energy, Halifax, N.S.

Papezik, V.S. and Barr, S.M.

1981: The Shelburne Dyke, an Early Mesozoic diabase dyke in Nova Scotia: mineralogy, chemistry and regional significance; Canadian Journal of Earth Sciences, v. 18, p. 1346-1355

Reynolds, P.H., Zentilli, M. and Muecke, G.K.

1981: K-Ar and Ar40/Ar39 geochemistry of granitoid rocks from southern Nova Scotia: its bearing on the geological evolution of the Meguma Zone of the Appalachians; Canadian Journal of Earth Sciences, v. 18, p. 386-394

Taylor, F.C.

1967: Reconnaissance geology of Shelburne map area, Queens, Shelburne and Yarmouth Counties, Nova Scotia; Geological Survey of Canada, Memoir 349, 82 p.

White, C.E.

1984: Structure and metamorphism of the Jordan River Valley, Shelburne County, Nova Scotia; unpublished B.Sc. (Honours) thesis, Acadia University, Wolfville, Nova Scotia, 74 p.

PETROGENESIS AND ECONOMIC GEOLOGY OF THE SPORTING MOUNTAIN PLUTON, CAPE BRETON ISLAND, NOVA SCOTIA[1]

Project 840044

A.J. Sexton[2] *and A.A. Cotie*[2]
Precambrian Geology Division

Sexton, A.J. and Cotie, A.A., Petrogenesis and economic geology of the Sporting Mountain pluton, Cape Breton Island, Nova Scotia; in *Current Research, Part A, Geological Survey of Canada, Paper 85-1A, p. 779-782, 1985.*

Abstract

Fieldwork completed during 1984 indicated that there is a single Late Hadrynian — Early Cambrian intrusion (Sporting Mountain pluton) that consists mainly of granite and granodiorite with minor diorite, monzodiorite and quartz monzodiorite. Numerous mafic dykes crosscut mainly the granitic and granodioritic phases of the pluton.

Metavolcanic rocks of the Fourchu Group outcrop along the margins of the pluton. Cover rocks consist of Carboniferous sedimentary rocks of the Windsor and Riversdale groups.

The occurrence of significant sulphide mineralization in the plutonic and volcanic rocks on the southeastern margin of the pluton, and their apparent similarity to the Coxheath Hills deposit to the northeast, has resulted in exploration interest in the area.

Résumé

Les travaux sur le terrain achevés en 1984 dans la région du mont Sporting dans le comté de Richmond, en Nouvelle-Écosse, révèlent qu'il existe une seule intrusion d'âge hadrynien récent-cambrien ancien (le pluton du mont Sporting), qui se compose surtout de granite et de granodiorite avec de petites quantités de diorite, de monzodiorite et de monzodiorite quarztique. Un grand nombre de filons intrusifs mafiques recoupent surtout les phases granitiques et granodioritiques du pluton.

Les roches métavolcaniques du groupe de Fourchu affleurent en bordure du pluton. Les roches de couverture se composent de roches sédimentaires carbonifères des groupes de Windsor et de Riversdale.

La présence d'une importante minéralisation sulfurée dans les roches plutoniques et volcaniques de la marge sud-est du pluton et leur similarité apparente au gisement des collines Coxheath au nord-est ont suscité l'intérêt pour l'exploration de la région.

INTRODUCTION

The Sporting Mountain pluton (Fig. 1) is one of several granitoid intrusions in southeastern Cape Breton Island. Weeks (1954) indicated that the northern and southeastern portions of the pluton consists of granitic rocks with minor diorite and quartz diorite near the centre. He assigned a Devonian age to the pluton correlating it with other granitoid plutons in the region. However, subsequent radiometric dating on the major plutons in southeastern Cape Breton Island have given Late Hadrynian to Early Cambrian ages, while only the smaller intrusions to the northeast are Devonian (Cormier, 1972, 1979, 1980, Stevens et al. 1982). It therefore seems probable that the Sporting Mountain pluton is also Late Hadrynian – Early Cambrian in age, especially as it contains granitoid rocks similar to those found in the nearby Late Hadrynian – Early Cambrian Loch Lomond – Irish Cove plutonic complex (McMullin, 1984).

During the 1984 field season the Sporting Mountain pluton and the associated Fourchu Group metavolcanic rocks were mapped and sampled. This report is a preliminary description of the geology and petrography of the rock units encountered.

REGIONAL GEOLOGY

As mapped by Weeks (1954), the Late Hadrynian Fourchu Group occurs in two belts in southeastern Cape Breton Island. A northern belt extends along the southeastern

[1]Contribution to the Canada-Nova Scotia Mineral Development Agreement 1984-89.
[2]Department of Geology, Acadia University, Wolfville, Nova Scotia, B0P 1X0

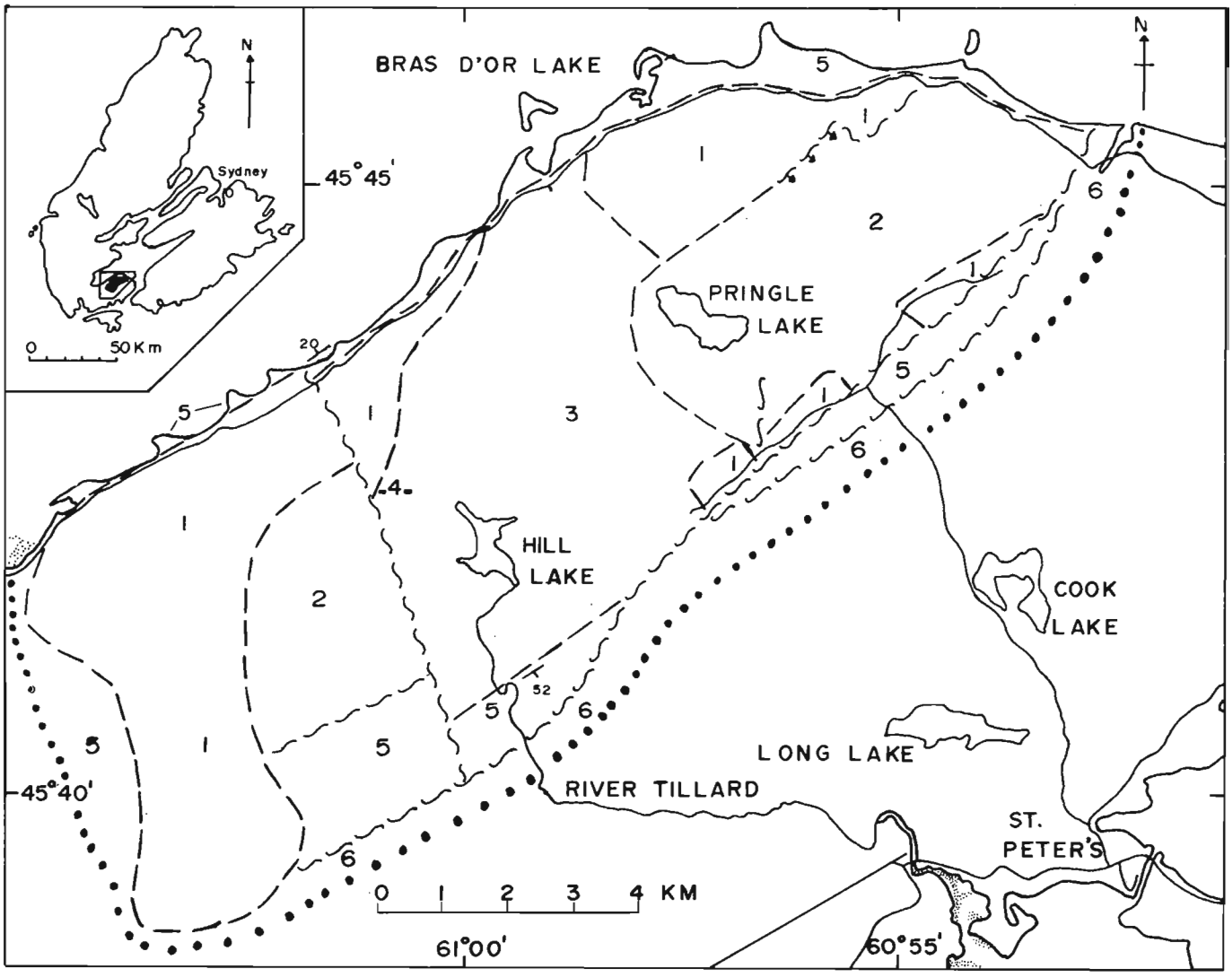

LEGEND

CARBONIFEROUS

6 Riversdale Group

5 Windsor Group

LATE HADRYNIAN - EARLY CAMBRIAN

4 Monzodiorite

3 Granite

2 Granodiorite

} relative age uncertain

LATE HADRYNIAN

1 Fourchu Group

SYMBOLS

geologic contact

fault: approximate

inclined

limit of mapping

bedding 20

Figure 1. Generalized geology of the igneous and volcanic rocks of Sporting Mountain, Richmond County, Nova Scotia.

shores of the Bras D'Or Lakes and East Bay, and a larger southern belt extends along the Atlantic coast of Cape Breton Island, in a broad band that widens to the northeast (Barr et al., 1984). The Fourchu Group consists of varied metavolcanic (predominantly pyroclastic), meta-intrusive, and metasedimentary rocks, interpreted to have formed in an ensialic volcanic arc (Keppie et al., 1979).

The widespread volcanic and sedimentary rocks which flank the Loch Lomond Complex were interpreted by Weeks (1954) to be mainly Cambrian in age and to overlie the Hadrynian Fourchu Group. However Smith (1978) re-interpreted these rocks and placed much of this terrane into the "Giant Lake Complex" which he considered to be time-equivalent to the Fourchu Group.

The Fourchu Group, as well as the granitoid intrusions, are in faulted or unconformable contact with Carboniferous clastic sedimentary rocks. Occurrences of barite, celestite, lead, and zinc in the sedimentary rocks along the western margins of the Loch Lomond plutonic complex and the Sporting Mountain pluton have made these areas a focus for exploration in Cape Breton Island (Felderhof, 1978).

FIELD OBSERVATIONS

The field work concentrated on the granitoid rocks of the Sporting Mountain pluton, which consists mainly of granite (monzogranite) and granodiorite with minor quartz monzodiorite, monzodiorite and diorite. The metavolcanic rocks of the Fourchu Group, which fringe the pluton to the north, west, and southeast, were mapped in less detail than the granitoid rocks.

Contact Relationships

The contact between the granitoid and metavolcanic rocks was not observed. However, in the northeastern part of the study area, the granite closest to the volcanic rocks is a fine grained porphyritic phase which also occurs as dykes from 1 to 15 cm wide within the metavolcanic rocks. It appears therefore that at least the granite phase of the Sporting Mountain pluton has intruded the metavolcanic rocks of the Fourchu Group.

The metavolcanic rocks unconformably lie below the clastic sedimentary rocks of the Windsor and Riversdale groups in the northwestern part of the study area, and are in faulted contact with them in the southeast. The latter contact was observed in diamond drill core. The granitoid rocks of the drill core were also observed to have the same faulted contact with the clastic sedimentary rocks.

The only observed intrusive relationship within the pluton occurs where a monzodiorite dyke cuts the finer grained porphyritic granite.

Lithology

All the granitoid rocks are sheared and partly altered. Alteration consists of saussuritization of the feldspar minerals and chloritization of the mafic minerals.

There are five subdivisions within the pluton – granite (monzogranite), granodiorite, diorite, quartz monzodiorite and monzodiorite. These subdivisions were determined by lithologic variation in outcrop and drill core with granodiorite being more widespread than granite. The three other phases are minor and are found in only a few scattered outcrops. They are not considered to be mappable phases. However, the crosscutting relationship of the monzodiorite and granite is still a significant field relationship.

The granodiorite is a medium grained, red to grey-green rock that varies in texture and mafic mineral content. The mafic minerals are biotite and hornblende. The granite is a medium grained, pink to green rock that varies in texture and mafic mineral content. Biotite is the only mafic mineral. The diorite, quartz monzodiorite and monzodiorite are medium grained, dark gray-green rocks that are less variable in texture and have a higher mafic mineral content (15-20% hornblende and biotite) and a lower quartz content (5-15%) than the two main granitoid phases.

The two main phases locally contain finer grained, more mafic areas (less than 3 cm wide) which may represent digested xenolithic material. Numerous mafic dykes, with random orientation cut the two main phases of the pluton.

STRUCTURE

Several major faults were observerd during the mapping and core logging, the longest of which occurs between the plutonic and metavolcanic rocks of Sporting Mountain and the Carboniferous clastic rocks.

Faulted contacts between the granitoid and metavolcanic rocks were also observed, mainly in the northeastern part of the study area. There is also geophysical evidence for parallel and cross faulting within the plutonic-metavolcanic complex (Leslie 1968, 1969, 1970).

Within the granitoid rocks shear zones occur where the rocks have a cataclastic texture and penetrative foliation. These zones occur throughout the pluton; foliation in them strikes approximately northeast and dips steeply to the northwest or southeast.

The pyroclastic rocks of the Fourchu Group have a penetrative foliation with approximately the same attitude as that found in the granitoid rocks. Locally a steeply plunging, southeast trending mineral lineation is found on the foliation planes of the pyroclastic rocks. Fragments were flattened in the plane of the foliation and were also concentrated in these planes, which may therefore represent bedding.

MINERALIZATION

There is widespread sulphide mineralization in the southeastern portion of the study area. Disseminations and narrow veinlets of chalcopyrite and/or pyrite and minor bornite (?) are associated with sheared metavolcanic and granitoid rocks. Weathering of the copper minerals has resulted in the widespread development of malachite. Molybdenite is present in minor amounts in the granitoid rocks.

From the field observations and core logging there appear to be very few mutual boundaries between sulphide minerals. Where mutual boundaries exist they indicate that chalcopyrite has replaced pyrite. Alteration associated with the mineralization has produced mainly chlorite, epidote, and carbonate.

The close proximity of granitoid rocks to areas of mineralization implies that they were the source of the mineralizing fluids. Mineralization is more widespread in those areas that are intensely sheared. It appears therefore that the shear zones acted as the plumbing system through which the fluids moved and eventually precipitated minerals.

DISCUSSION

The Sporting Mountain pluton comprises five granitoid lithologies and the associated Fourchu Group metavolcanic rocks consist of felsic to mafic pyroclastic and flow rocks.

An intrusive relationship was not observed between the metavolcanic and plutonic rocks. However, the presence of a finer grained porphyritic granite phase in close proximity to the metavolcanic rocks, as well as granite dykes in the metavolcanic rocks, suggests the granite intruded the surrounding Fourchu Group rocks. The only instrusive relationship observed within the pluton consists of a monzodiorite dyke crosscutting the granite.

The study area contains several major faults, the longest of which is at the contact between the Sporting Mountain-Fourchu Group plutonic-metavolcanic complex and the Carboniferous clastic rocks. Some faulted contacts between the granitoid and volcanic rocks are also found. Faults within the plutonic-volcanic complex consist of parallel and cross faults as indicated by detailed geophysics.

Mineralization is associated with a shearing event which was more intense in the metavolcanic rocks than the granitoid rocks, possibly due to the more competent nature of the latter. The shear zones developed by this event acted as the plumbing system for the movement and eventual precipitation of the mineralizing fluids. The mineralization in the Sporting Mountain plutonic-metavolcanic complex may be similar to the Coxheath Hills deposit to the northeast.

The plutonic rocks of the study area appear to be similar to the southeastern part of the Late Hadrynian to Early Cambrian Loch Lomond – Irish Cove plutonic complex. Therefore the Sporting Mountain pluton is probably of a similar age.

ACKNOWLEDGEMENTS

The field work for this project was supported by the Precambrian Geology Division of the Geological Survey of Canada through Project 840044 and by E.M.R. Research Agreement 269 to Dr S.M. Barr.

REFERENCES

Barr, S.M., Sangster, D.F. and Cormier, R.F.
1984: Petrology of Early Cambrian and Devono-Carboniferous intrusions in the Loch Lomond Complex, southeastern Cape Breton Island, Nova Scotia; *in* Current Research, Part A, Geological Survey of Canada, Paper 84-1A, p. 203-211.

Cormier, R.F.
1972: Radiometric ages of granitic rocks, Cape Breton Island, Nova Scotia; Canadian Journal of Earth Sciences, v. 9, p. 1974-1086.

1979: Rubidium/strontium isochron ages of Nova Scotian granitoid plutons; *in* Nova Scotia Department of Mines and Energy, Report 79-1, p. 143-147.

1980: New rubidium/strontium ages in Nova Scotia; *in* Nova Scotia Department of Mines and Energy, Report 80-1, p. 223-233.

Felderhof, G.W.
1978: Barite, celestite and fluorite in Nova Scotia; *in* Nova Scotia Department of Mines Bulletin 4, 463 p.

Keppie, J.D., Dostal, J. and Murphy, J.B.
1979: Petrology of the Late Precambrian Fourchu Group in the Louisbourg area, Cape Breton Island, Nova Scotia; *in* Nova Scotia Department of Mines and Energy, Paper 79-1, 18 p.

Leslie, J.A.
1968: St. Peter's Claim Group; *in* Nova Scotia Department of Mines and Energy, Assessment Report 27-0-21(02), 25 p.

1969: St. Peter's Claim Group; *in* Nova Scotia Department of Mines and Energy, Assessment Report 27-0-21(03), 67 p.

1970: St. Peter's Claim Group; *in* Nova Scotia Department of Mines and Energy, Assessment Report 27-0-21(04), 127 p.

McMullin, D.W.A.
1984: Geology and geochemistry of the granitoid rocks of the Loch Lomond-Irish Cove area, Cape Breton Island; unpublished M.Sc. Thesis, Acadia University, 239 p.

Smith, P.K.
1978: Geology of the Giant Lake Complex area, southeastern Cape Breton Island, Nova Scotia; *in* Nova Scotia Department of Mines and Energy, Paper 78-3.

Stevens, R.D., Delabio, R.N. and Lachance, G.R.
1982: Age determinations and geological studies; Geological Survey of Canada, Paper 81-2, p. 46.

Weeks, L.J.
1954: Southeast Cape Breton Island, Nova Scotia; Geological Survey of Canada, Memoir 277, 112 p.

GEOLOGY OF THE MONT ALBERT REGION, GASPE PENINSULA, QUEBEC[1]

Project 840022

Y. Denis Gagnon[2] and Rebecca A. Jamieson[2]
Precambrian Geology Division

Gagnon, Y. D. and Jamieson, R. A., Geology of the Mont Albert region, Gaspé Peninsula, Quebec; in *Current Research, Part A, Geological Survey of Canada, Paper 85-1A, p. 783-788, 1985.*

Abstract

Mont Albert is a semicircular, partially serpentinized, layered harzburgite massif underlain and surrounded by an arcuate zone of high grade metamorphic rocks which are dominated by garnet amphibolites with well-developed segregation and shear banding interlayered with megascopic metasedimentary quartzofeldspathic lenses. These lenses are subparallel to the foliation plane and compositional banding, and show intense shearing along their borders and transposition into the foliation plane. Metasediments range from muscovite-chlorite schists and phyllites to biotite-garnet-kyanite schists and gneisses near the ultramafic body. The limit of high grade metamorphism is marked by the appearance of banded epidote-bearing amphibolites. The peridotite and metamorphic rocks are surrounded by chloritized, spilitized, moderately deformed metabasalts, greenschists, meta-arkoses, and phyllites of the Shickshock Group. Locally pillow forms are well preserved, but a good foliation and later crenulation are generally present. The peridotite, high grade metamorphic rocks, and Shickshock Group are probably juxtaposed by shearing, possibly during transport and emplacement of the ultramafic rocks.

Résumé

Le mont Albert est un massif semi-circulaire stratifié et partiellement serpentinisé de harzburgite qui est recouvert et entouré d'une zone arquée de roches fortement métamorphisées. Les roches métamorphiques sont surtout des amphibolites grenatifères qui présentent une texture rubannée bien développée due à la ségrégation et au cisaillement; elles sont interstratifiées avec des lentilles quartzofeldspatiques métasédimentaires macroscopiques. Ces lentilles sont à peu près parallèles au plan de foliation et aux bandes de composition; elles sont fortement cisaillées le long de leurs marges et présentent une transposition du plan de foliation. Les métasédiments varient des schistes et des phyllades à muscovite et à chlorite aux schistes et gneiss à biotite, à grenat et à cyanite près de la masse ultramafique. La limite du métamorphisme intense est marquée par l'apparence d'amphibolites zonées à épidote. Les péridotites et les roches métamorphiques sont à leur tour entourées de métabasaltes, de schistes verts, de méta-arkoses et de phyllades chloritisés, spilitisés et modérément déformés du groupe de Shickshock. Les structures en oreillers sont bien conservées par endroits et en général on y trouve une foliation marquée et une crénulation plus récente. Il y a eu vraisemblablement juxtaposition de péridotite, des roches fortement métamorphisées et du groupe de Shickshock par cisaillement, peut-être au cours du transport et de la mise en place des roches ultramafiques.

[1]Contribution to the "Plan de développement économique Canada/Gaspésie et Bas Saint-Laurent."
[2]Department of Geology, Dalhousie University, Halifax, N.S. B3H 3J5

INTRODUCTION

The Mont Albert Peridotite and associated metamorphic rocks are located in the southern Chic-Choc Mountains, in the central Gaspé Peninsula of Quebec (66°10′W longitude; 48°50′ N latitude; NTS 22B/16). The peridotite is a partially serpentinized layered harzburgite massif surrounded on three sides by strongly foliated amphibolites and metasedimentary rocks (Fig. 1). To the north the complex passes into regionally metamorphosed sedimentary and volcanic rocks of the Shickshock Group. It is bounded on the south by the South Chic-Choc Fault, which separates it from the Silurian-Devonian sequences of central Gaspé.

Mont Albert is part of a belt of ophiolites and related ultramafic and metamorphic rocks that extends along the northwestern margin of the Appalachians from Newfoundland to Vermont (Williams and Talkington, 1977). Although originally interpreted as a diapiric intrusion with a high temperature contact aureole (MacGregor, 1962, 1964; MacGregor and Basu, 1976, 1979), recent studies of the Mont Albert area and regional similarities to western Newfoundland (Laurent, 1977; Beaudin, 1983) suggest that the peridotite is the remnant of a transported ophiolite massif with an underlying metamorphic sheet (eg. Williams and Smyth, 1973; Malpas, 1979; Jamieson, 1980; Spray, 1984). Similar metamorphic rocks associated with the Thetford Mines ophiolite have recently been described by Feininger (1981). The present detailed study of the metamorphic rocks is intended to establish their relationship to both the Mont Albert Peridotite and the regionally metamorphosed rocks of the Shickshock Group, and to test the hypothesis that these rocks formed in a high temperature shear zone during ophiolite emplacement, as has been postulated for the St. Anthony Complex of western Newfoundland (Jamieson, 1981, 1984; Craw, 1983).

The Mont Albert Peridotite, two smaller ultramafic bodies to the southwest (Mont Paul and Mont du Sud) and the surrounding Shickshock Group are part of the "internal domain" of the Quebec Appalachians (St. Julien and Hubert, 1975). These rocks consist mainly of transported Cambrian to Lower Ordovician sedimentary, volcanic, and rare plutonic rocks formed at a continental slope and rise, emplaced as thrust sheets during the Taconic Orogeny along with ophiolitic rocks derived from the oceanic crust. The Shickshock Group consists mainly of spilitized tholeiitic basalts and minor alkaline flows interbedded with pyroclastic rocks, and minor arkoses, shales, arenites, and limestones (Alcock, 1925; McGerrigle, 1954; Beaudin, 1983). Both Beaudin (1983) and MacGregor (1964) intepreted the Shickshock Group metavolcanics as the protoliths for the high grade amphibolites immediately surrounding Mont Albert, although they differed in their interpretation of how the peridotite was emplaced. On the basis of chemical differences between the high grade metabasites and the metavolcanics of the Shickshock Group Laurent (1977) intepretred the amphibolites as essentially igneous rocks derived from the oceanic crust. Recently, Trzcienski (1984a,b) has described the petrology of amphibole eclogites from near the peridotite contact, suggesting peak metamorphic conditions of 900°C and 12 kb. Our preliminary results suggest that there are important metamorphic and structural differences between the high grade and low grade rocks, consistent with the chemical differences between the metabasites and the presence of eclogite. This article therefore describes the geology in terms of peridotite, high grade rocks, and lower grade rocks of the Shickshock Group.

Acknowledgments

The authors are grateful for the financial and logistical support of the Geological Survey of Canada, and in particular the assistance of Dr. K.L. Currie and Dr. J. Whalen in organizing the project. RAJ acknowledges support of NSERC through Operating Grants in 1979-1984 for research on the general problem of ophiolite emplacement and associated metamorphism. YDG is supported by a Dalhousie University Graduate Fellowship. The assistance of N. Giguere and G. Lavallee in the field is deeply appreciated.

PERIDOTITE

The Mont Albert Peridotite is a layered semicircular harzburgite massif of about 40 km^2. Its petrology has been described in detail by MacGregor and Basu (1979), who attributed much of the compositional variation to partial melting, differentiation and mechanical segregation of crystals and liquid intrusion. Beaudin (1983) demonstrated that the peridotite was emplaced into its present position in the solid state, undergoing extreme ductile deformation before and during its transport.

The most common rock type, harzburgite, is interlayered with dunite and rare lherzolite on the scale of a few centimetres to a few tens of centimetres. The compositional layering is generally sharply defined and concordant with the foliation. The harzburgite is a brown to orange weathering, hackly rock with elongated orthopyroxene porhyroclasts in a smooth weathering, fine grained, olivine-rich matrix. The dunite contains 1-10 per cent disseminated, fine grained chromite, concentrated in stringers which locally form up to 30 per cent of the rock. Lherzolite is very rare and consists of sparse pale green clinopyroxene with orthopyroxene and olivine. Pyroxenite bands occur within the peridotite, generally strongly attenuated and essentially concordant with the foliation, although locally they truncate the banding. Similar complex relationships between pyroxenite veins, compositional banding, and foliation have been described by Talkington (1981) for the White Hills Peridotite of northwestern Newfoundland.

The peridotite is strongly foliated throughout with a porphyroclastic texture defined by elongated orthopyroxene crystals. Within 40 m of the contact with the surrounding metamorphic rocks, the ultramafic rocks have been mylonitized, resulting in extreme grain size reduction and a finely banded, intensely foliated appearance. Close to the contact no orthopyroxene is preserved and the compositional layering is obliterated. Along the contact the peridotite has been extensively serpentinized, with a whitish colour on the surface suggesting the presence of talc. No petrographic data are yet available to document the detailed metamorphic history

of the contact zone ultramafic mylonites, but given the well-preserved structure, it is likely that serpentinization postdated the development of the mylonitic fabric.

HIGH GRADE METAMORPHIC ROCKS

High grade metabasites and metasediments surround the Mont Albert Peridotite on three sides and generally dip steeply or moderately towards the peridotite contact (Fig. 1). These rocks were studied in detail to determine their relationship both to the peridotite and to the lower grade rocks of the Shickshock Group. The main lithology is strongly foliated garnetiferous amphibolite interbanded with lenses of metasedimentary rocks. Preliminary investigations at Mont Paul and Mont du Sud confirm that high grade metamorphic rocks, including garnet amphibolite, are also associated with these two peridotite outliers.

Amphibolite

Medium- to coarse-grained garnet amphibolite and garnet-clinopyroxene hornblendite constitute the inner part of the metamorphic complex on all sides (areas marked "G" in Fig. 1). Close to the peridotite plagioclase is relatively rare, and many of the "amphibolites", which may contain over 70 per cent black hornblende, are better described as hornblendites. The garnet is generally bright red, fractured and granulated, with a grain size ranging from 1 to 5 mm. Irregularly distributed lenses up to several metres long contain as much as 50 per cent in a black hornblende-rich matrix. Bands of green clinopyroxene are fairly common close to the contact, so that the characteristic mineral assemblage is garnet-hornblende-clinopyroxene. Feldspar, if present, is in reaction rims around garnet, which locally are drawn out into linear aggregates within the foliation plane suggesting shearing during and after retrograde metamorphism. These rocks have been described as amphibole eclogites by Trzcienski (1984a) although more detailed work is required to establish the relationships between metamorphic mineral assemblages of different generations.

Garnet amphibolite is characteristic of the contact zone but is not limited to it; it has been noted up to 700 m from the peridotite contact in the southeastern re-entrant. In the same area, magnetite concentrations have been observed within the amphibolite. This sector is structurally and metamorphically complex and its significance in the overall geological interpretation is not clear.

Epidote occurs throughout the amphibolites, as foliation-parallel bands and crosscutting veins. Its distribution suggests variable retrograde metamorphism during deformation. The external boundary of the amphibolites is marked by the appearance of well banded, epidote-bearing black amphibolite, with layering on the 2 to 5 cm scale defined by variable proportions of epidote, feldspar, hornblende, and quartz, as well as grain size variations.

In general, grain size increases towards the peridotite contact, although fine- and coarse-grained zones are interlayered. Throughout the amphibolites, grain size and mineralogical variations define a lenticular banding which may be related to shearing and associated fluid circulation along foliation planes. The presence of isoclinal transposed folds, good mineral preferred orientations, and abrupt grain-size variations suggest that deformation occurred during and after the peak of metamorphism. Protomylonitic features include elongated feldspar porphyroclasts with granular tails, grain size reduction in felsic bands, strong mineralogic segregation, and good preferred orientation of hornblende (areas marked "P" in Fig. 1). The main foliation is locally crenulated and these minor folds locally have parallel mineral lineations. The lineations generally have moderate to steep plunges, but locally they are nearly horizontal, suggesting the effects of later folding. The foliation bends around metasedimentary lenses which are presumably boudinaged resistant layers.

Metasedimentary rocks

Within the metamorphic complex surrounding Mont Albert the proportion of amphibolite to metasediment is highly variable. Metasediments generally occur as megascopic lenses within the amphibolites; these are particularly prominent in the northeastern sector of the complex, where a staircase-like topography results from differential weathering of resistant metasedimentary layers.

The metasedimentary rocks are psammitic to semipelitic, and commonly have a gneissic appearance. Feldspar is the dominant mineral and the rocks may originally have been arkoses. Some outcrops show compositional layering defined by quartzofeldspathic and phyllitic layers. The mineralogy varies from muscovite-chlorite- and muscovite-biotite-bearing assemblages away from the peridotite to garnet-muscovite-biotite and rare kyanite-bearing assemblages closer to the contact. However, the progression is irregular undoubtedly affected by variable degrees of retrograde overprinting. some biotite-rich rocks associated with garnet amphibolite near the contact may represent K-metasomatized shear zones like those occurring beneath the west Newfoundland ophiolites (Jamieson and Strong, 1981).

All metasedimentary layers and associated fold axes have been transposed in the foliation plane. Local ptygmatic folds and discontinuous feldspathic lenses suggest that partial melting of the metasediments occurred prior to shearing. Rootless folds, pinch and swell structures, and intense shear zones are common throughout the metamorphic sequence, but are particularly evident in the metasediments where they affect compositional layering.

SHICKSHOCK GROUP

The boundary between the higher grade rocks and the Shickshock Group is defined by a well banded epidote amphibolite mylonite. There is an abrupt decrease in grain size across this mylonite zone, as well as a distinct change in metamorphic and lithologic character. The discontinuity is also reflected in a topographic break, with the lower grade rocks forming the low ground at the foot of Mont Albert (Fig. 1).

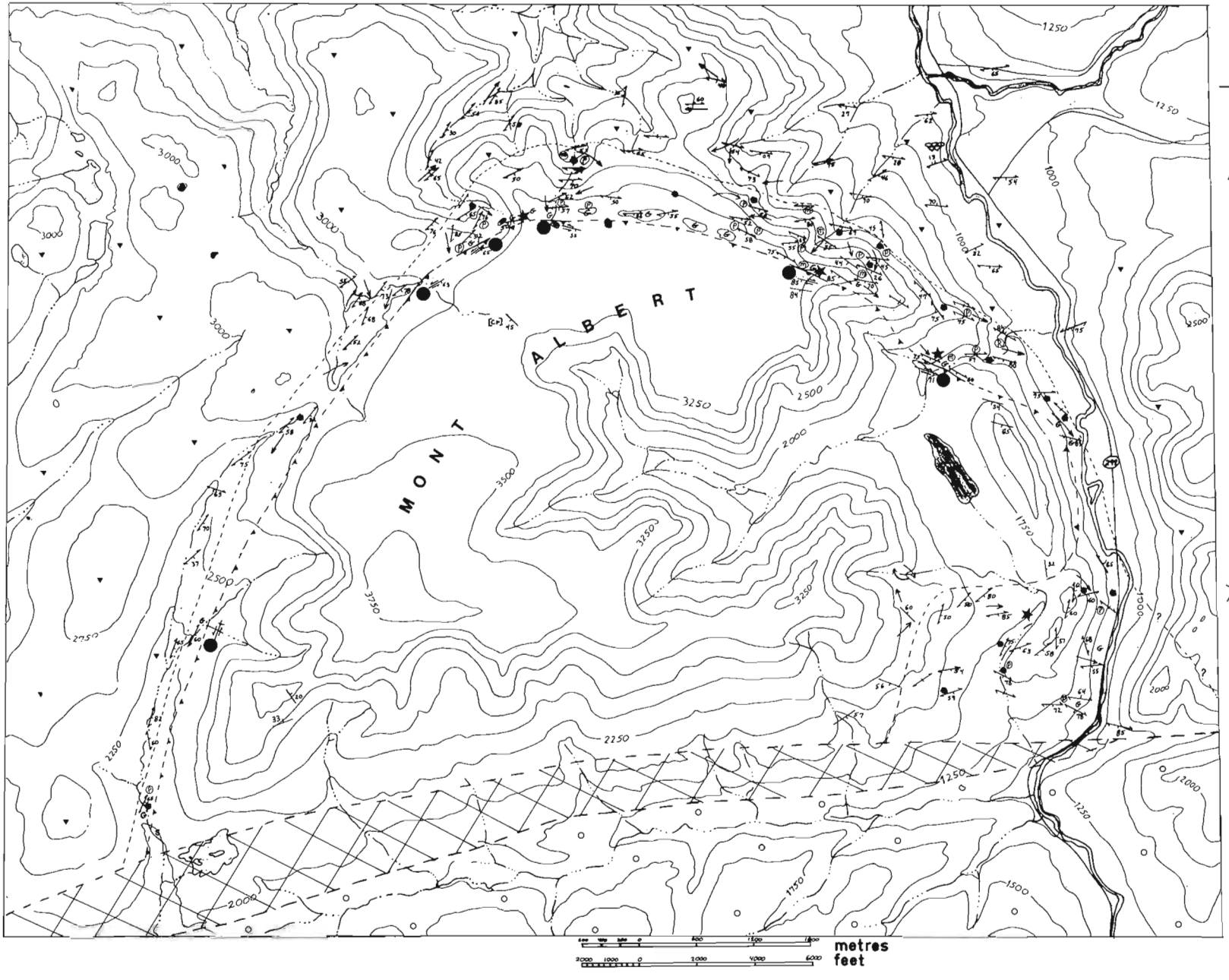

Figure 1. Geological map of the Mont Albert area.

On a regional scale, the metamorphic grade of the Shickshock Group increases from north to south (Beaudin, 1983). In the vicinity of Mont Albert it consists mainly of spilitized metabasalts associated with fine grained phyllites and meta-arkose. The rocks are mainly in the greenschist facies with the assemblage chlorite-albite-epidote in the metavolcanics. The amount of actinolite apparently increases toward the contact with the high grade rocks although a clear mineralogical zonation is difficult to define. In the metasediments muscovite and chlorite occur with quartz, feldspar, epidote and minor biotite, pyrite, and hematite.

Deformation in these rocks is highly variable. Well-preserved, although much elongated, pillows are present within a kilometre of the peridotite (Fig. 1), but highly sheared and fractured schists are far more characteristic. Near the contact with the amphibolites the fine grained schists show evidence of shearing, including intense foliations, transposed banding, and centimetre scale curvilinear folds. Phyllites may show two to four phases of deformation, generally as a strong foliation with one or two later crenulations.

DISCUSSION

This study supports the conclusion of Beaudin (1983), based on structural, petrological, and regional considerations, that the Mont Albert Peridotite is a transported alpine-type peridotite rather than an intrustion. Emplacement of the peridotite was accompanied by mylonitization of the contact zone, followed by serpentinization. The surrounding rocks also show evidence of intense ductile deformation during and after high grade metamorphism.

Metamorphic grade and average grain size both increase toward the contact with the peridotite, but some observations suggest that there is not a simple progression as suggested by both MacGregor (1964) and Beaudin (1983). The distribution of the major metamorphic minerals is irregular in detail and the degree of preservation may depend on later shearing. Retrograde metamorphism has been important, as evident from feldspar rims on garnet, replacement of clinopyroxene by hornblende, and the presence of epidote throughout the high grade rocks. Trzcienski (1984b) has suggested retrograde metamorphic conditions of 600°C and 9 kb.

On a broader scale, although metamorphic grade increases towards the peridotite from the surrounding Shickshock Group, there is no continuous metamorphic gradient toward the contact. The high grade rocks are very different in character from the Shickshock Group metavolcanics. Their bulk compositions are different (cf. Laurent, 1977; Beaudin, 1983), and the coarse black hornblende characteristic of the amphibolites is completely absent from the metavolcanics. The contact of the amphibolites with the lower grade rocks is a mylonitic epidote amphibolite zone, probably formed by downgrading of the coarse grained amphibolites during shearing rather than upgrading of the surrounding, regionally metamorphosed, greenschist facies spilites and phyllites.

It appears from our preliminary results that the Mont Albert region is underlain by three distinctive rock assemblages – peridotite, high grade amphibolites and metasediments, and the Shickshock metavolcanics, and that these were juxtaposed by shearing, possibly during emplacement of the peridotite. Conclusive evidence awaits the results of further petrographic and geochemical studies, which it is hoped will establish the relationships among prograde metamorphism, retrograde metamorphism, and deformation during juxtaposition of these rocks.

REFERENCES

Alcock, F.J.
1925: Shickschock Mountains, central Gaspe, Quebec; Geological Survey of Canada, Summary Report (1924), Part C, p. 127-133.

Beaudin, J.
1983: Analyse structurale du Groupe des Chic-Choc et de la peridotite alpine du Mont Albert, Gaspésie; Unpublished Ph.D. thesis, Universite Laval.

Craw, D.
1983: Structural evolution of a section along the base of the St. Anthony Complex, northwest Newfoundland; Canadian Journal of Earth Sciences, v. 20, p. 1713-1724.

Feininger, T.
1981: Amphibolite associated with the Thetford Mines Ophiolite Complex at Belmina Ridge, Quebec; Canadian Journal of Earth Sciences, v. 18, p. 1878-1892.

Jamieson, R.A.
1980: The formation of metamorphic aureoles beneath ophiolite suites – evidence from the St. Anthony Complex, northwestern Newfoundland; Geology, v.8, p. 151-154.

1981: Metamorphism during ophiolite emplacement – the petrology of the St. Anthony Complex; Journal of Petrology, v. 22, p. 397-449.

1984: Retrograde and prograde metamorphism in the St. Anthony Complex, Newfoundland, and its significance for ophiolite emplacement. International Geological Congress, Moscow, Abstracts, v. 3, p. 241.

Jamieson, R.A. and Strong, D.F.
1981: A metasomatic mylonite zone within the ophiolite aureole, St. Anthony Complex, northwestern Newfoundland; American Journal of Science, v. 281, p. 264-281.

Laurent, R.
1977: Ophiolites from the northern Appalachians of Quebec; *in* North American Ophiolites, R.G. Coleman and W.P. Irwin (editors), Oregon Department of Geology and Mineral Industries, Bulletin 95, p. 25-40.

MacGregor, I.D.
1962: Geology, petrology, and geochemistry of the Mt. Albert and associated ultramafic bodies of central Gaspé, Quebec; Unpublished M.Sc. thesis, Queen's University.

1964: A study of the contact metamorphic aureole surrounding the Mount Albert ultramafic intrusion; Unpublished Ph.D. thesis, Princeton University. 195 pp.

MacGregor, I.D. and Basu, A.R.
1976: Geological problems in estimating mantle geothermal gradients; American Mineralogist, v. 61, p. 715-724.

1979: Petrogenesis of the Mount Albert ultramafic massif, Quebec; Geological Society of America Bulletin, Part II, v. 90, p. 1529-1627.

Malpas, J.G.
1979: The dynamothermal aureole of the Bay of Islands ophiolite suite; Canadian Journal of Earth Sciences, v. 16, p. 2086-2101.

McGerrigle, H.W.
1954: The Tourelle and Courcellette areas, Gaspé Peninsula; Quebec Department of Mines, Geology Report 62.

Spray, J.G.
1984: Possible causes of upper mantle decoupling and ophiolite displacement; *in* Ophiolites and oceanic lithosphere, I.G. Gass, S.J. Lippard, and A.W. Shelton (editors), Geological Society of London Special Publication 13, p. 255-268.

St. Julien, P. and Hubert, C.
1975: Evolution of the Taconian orogen in the Quebec Appalachians; American Journal of Science, v. 275-A, p. 337-362.

Talkington, R.W.
1981: The geology, petrology and petrogenesis of the White Hills Peridotite, St. Anthony Complex, northwestern Newfoundland; Unpublished Ph.D. thesis, Memorial University of Newfoundland, 292 pp.

Trzcienski, W.E.
1984a: Amphibole eclogite from Mt. Albert, Gaspé, Quebec, Canada; Transactions of the American Geophysical Union (Abstract), v. 65, p. 290.

1984b: Paragonite-zoisite-quartz-plagioclase-H_2O equilibria at Mt. Albert, Gaspé, Canada. Geological Society of America Abstracts with Programs, Reno, November, 1984.

Williams, H. and Smyth, W.R.
1973: Metamorphic aureoles beneath ophiolite suites and Alpine peridotites: tectonic implications with west Newfoundland examples; American Journal of Science, v. 273, p. 594-621.

Williams, H. and Talkington, R.W.
1977: Distribution and tectonic setting of ophiolites and ophiolitic melanges in the Appalachian Orogen; *in* North American Ophiolites, R.G. Coleman and W.P. Irwin (editors), Oregon Department of Geology and Mineral Industries, Bulletin 95, p. 1-11.

PRELIMINARY REPORT ON THE GEOLOGY OF THE LAHAVE RIVER AREA, NOVA SCOTIA[1]

Project 760027
Contract 14 SQ.23233-4-0488

Brian H. O'Brien[2]

O'Brien, B.H., Preliminary report on the geology of the LaHave River area, Nova Scotia; in *Current Research, Part A, Geological Survey of Canada, Paper 85-1A, p. 784-794, 1985.*

Abstract

The LaHave River area is underlain by chlorite-grade slates and sandstones belonging to the Cambro-Ordovician Meguma Group of mainland Nova Scotia. The stratigraphical succession is divided into six lithological units comprising green, black and grey beds. These units were folded by generally southwest-trending, gently plunging, major folds and then cross-faulted. Veins in black slate and pyritiferous sandstones contain Au and Wo; Mn is present within laminated fine grained sandstones.

Résumé

La région de la rivière Lahave repose sur des schistes chloriteux et des grès appartenant au groupe de Meguma du Cambrien-Ordovicien en Nouvelle-Écosse. La succession stratigraphique se divise en six unités lithologiques composées de couches vertes, noires et grises. Ces unités ont été plissées, les plis importants étant généralement à orientation sud-ouest et plus inclinés, par la suite elles ont été faillées. Des filons dans les schistes noirs et les grès pyriteux contiennent de l'or et du tungstène; les grès feuilletés à grain fin contiennent du manganèse.

INTRODUCTION

The LaHave River area in southeastern Lunenburg County, Nova Scotia, is underlain by Cambro-Ordovician metasedimentary rocks of the Meguma Group (Fig. 1). During the 1984 field-season approximately 400 km^2 of ground were surveyed using 1:10 000 aerial photographs and a provisional 1:25 000 scale map was prepared.

LITHOSTRATIGRAPHY

Six lithological units belonging to three major divisions of the Meguma Group are identifiable and mappable in the LaHave River area (Fig. 2). Rocks assigned to unit 1 are similar to those seen in the vicinity of Goldenville (i.e., Goldenville Formation), whereas many of the rocks in unit 3 are observable in the Halifax area (i.e., the Halifax Formation). In the LaHave River area, however, a third Meguma Group division is locally well developed as unit 2 which is sharply bounded at its stratigraphical base by unit 1 and at its stratigraphical top by unit 3. Subunits 2A, 2B and 2C are conformable and gradational with each other. Faribault (1929) and Hall (1981) mapped the contact between the Halifax and Goldenville formations near the boundary between units 2A and 2B.

Unit 1 is composed of thickly bedded to massive, buff-weathered, quartz-rich sandstones (Fig. 3). In places, individual beds are up to 12 m thick. They are commonly graded, show incomplete Bouma cycles and probably contain rip-up clasts.

Unit 2A comprises fine grained, rhythmically interbedded, green and grey-green sandstones ranging from 5-10 cm in thickness (Fig. 4). The green sandstones are enriched in chlorite relative to the cross-stratified, grey-green sandstones.

Unit 2B is characterized by prominent, buff-weathered beds of quartz-rich sandstone (Fig. 5). They vary from approximately 25 cm to 1 m in thickness, are graded in places and are similar to the sandstones in unit 1. Such sandstones are interstratified throughout unit 2B with fine grained, rhythmically interbedded, green and grey-green, 5-15 cm thick sandstones. In the extreme southeast of the map area, on the La Have Islands, the buff-weathered sandstones of unit 2B split into two, discrete bodies. Here, the rhythmically layered green beds separating the sandy subunits are thicker than elsewhere, are commonly graded, show partial Bouma cycles and illustrate signs of thixatropic deformation.

Unit 2C is made up of rhythmically laminated and rarer crosslaminated, grey-green and green, fine grained sandstones (Fig. 6). Layering is evident on scales from several millimetres to several centimetres. Small, mineralogically zoned concretions occur in Mn-rich beds which define an excellent 'marker' horizon near the top of the unit.

Unit 3A contains black slate interbedded with pyritiferous, grey coloured, rippled and cross-stratified, fine

[1]Contribution to Canada-Nova Scotia Mineral Development Agreement 1984-89
[2]Hi-Tec Geoconsultants Ltd., P.O. Box 244, Hubbards, Aspotogan, Lunenburg County, Nova Scotia, B0J 1T0

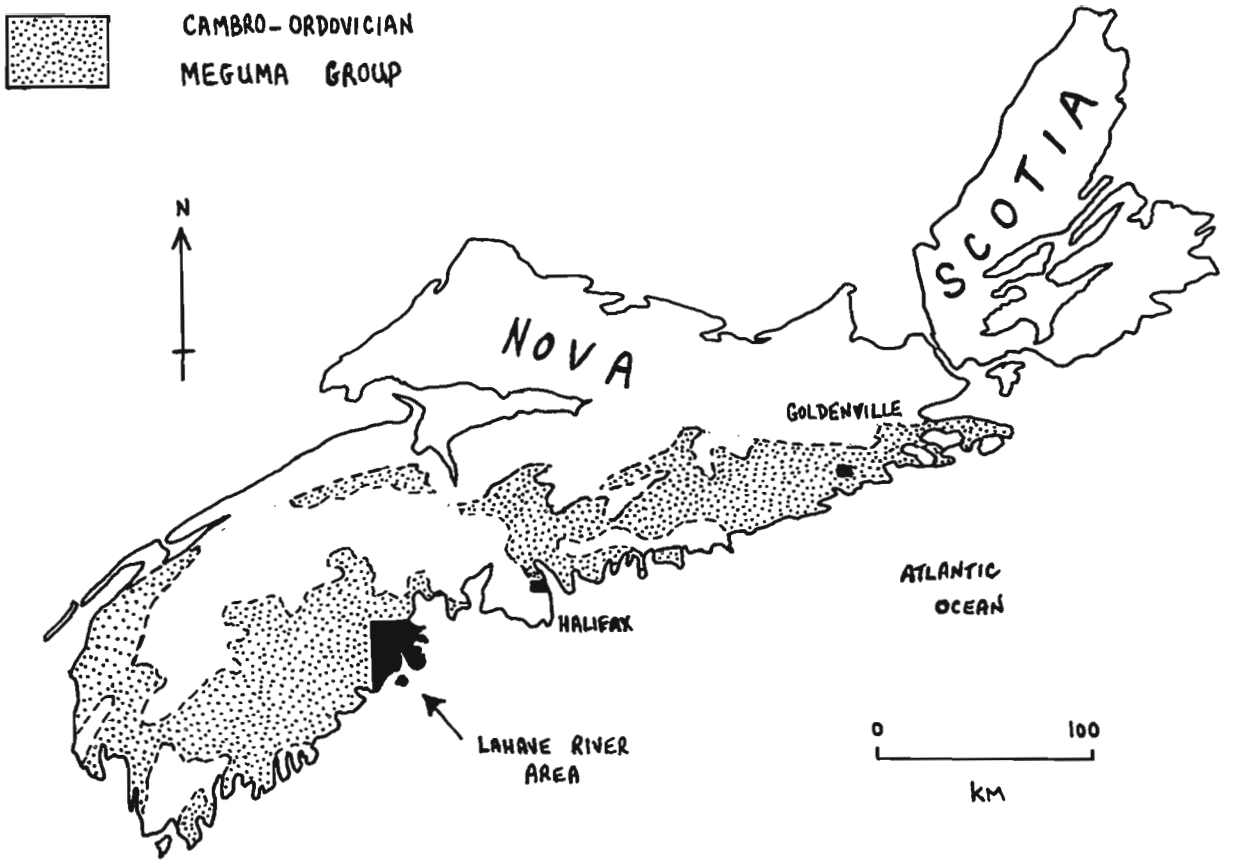

Figure 1. Location map showing the LaHave River area and the distribution of the Meguma Group in Nova Scotia.

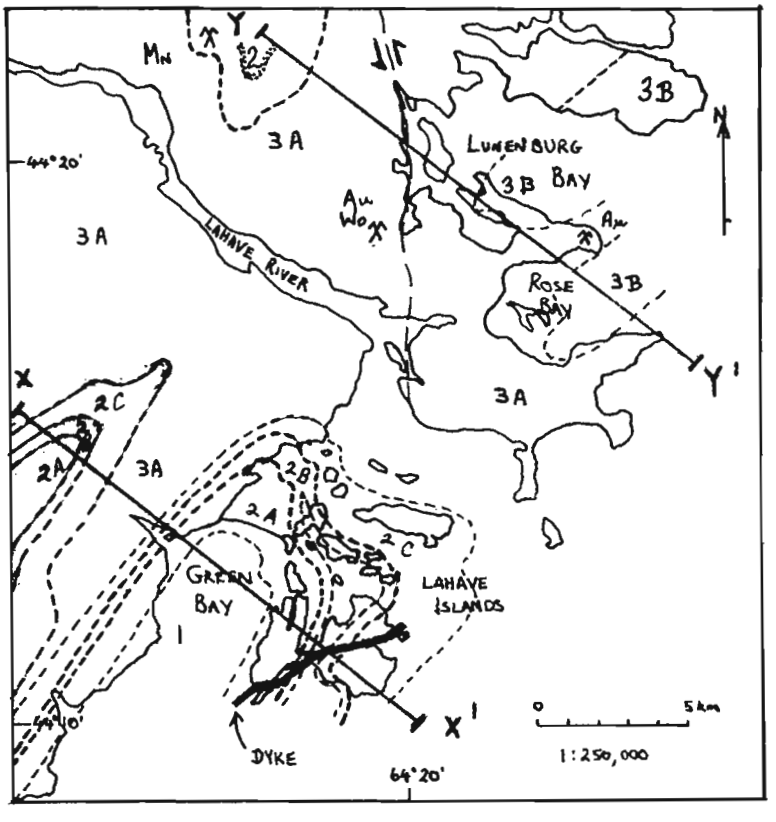

LEGEND

Unit 3B – grey slate and laminated to thinly bedded sandstone

Unit 3A – black slate and thinly to thickly bedded pyritiferous sandstone

Unit 2 – undivided, laminated to thinly bedded, grey and grey-green sandstone and siltstone. Thickly bedded to massive, buff-weathered sandstones are shown in part

Unit 2C – laminated, grey-green and green sandstones

Unit 2B – thinly to thickly bedded, buff-weathered sandstones. Includes thin bedded, green and grey-green sandstones on the La have Islands

Unit 2A – thinly bedded, green and grey-green sandstones

Unit 1 – thickly bedded to massive, buff-weathered sandstones

Figure 2. Generalized geological map of the LaHave River area. Lines of cross-sections XX′ and YY′ are indicated.



Figure 3. Thick bedded, buff-weathered, quartz-rich sandstones of unit 1.

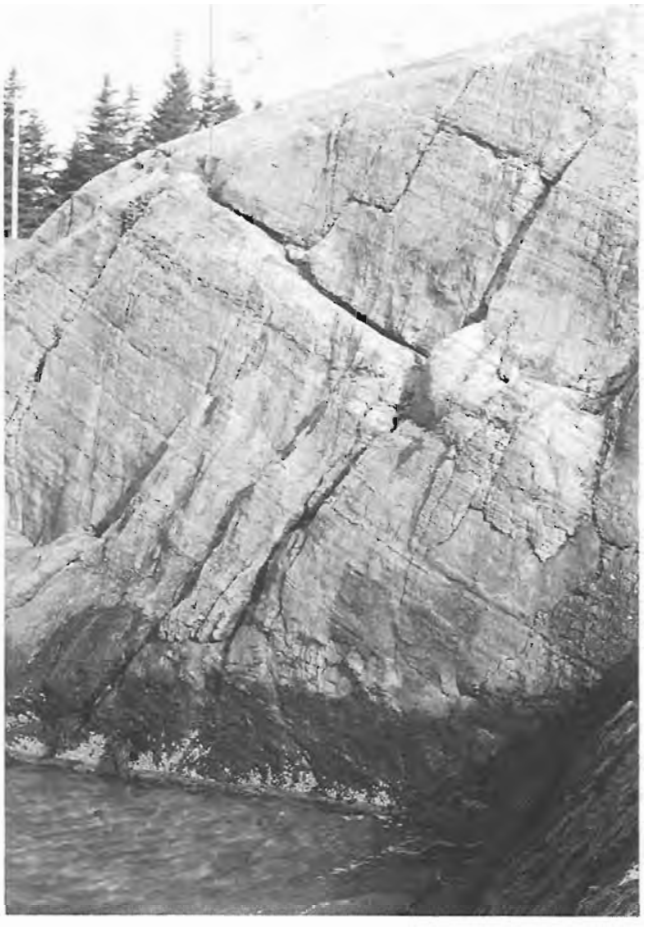

Figure 4. Rhythmically interbedded, green and grey-green sandstones of unit 2A. The vertical face of the exposure is approximately 2.5 m high.



Figure 5. Well bedded, buff-weathered, quartz-rich sandstones of unit 2B.



Figure 6. Laminated, grey-gren and green sandstones of unit 2C.

grained sandstones (Fig. 7). The bed thickness of the sandstones is approximately 20-50 cm and the slate: sandstone ratio is highly variable. Giant, dark coloured nodules up to 75 cm in diameter are observed from place to place within this unit.

Unit 3B comprises light grey, dark grey and blue-grey slate rhythmically interbedded with laminated to thinly bedded, buff-weathered, grey sandstones (Fig. 8). Near the base of the unit cross-stratified sandstones are commonly 5-10 cm thick, whereas 1-2 cm thick, crosslaminated sandstones prevail higher in the stratigraphical sequence.

In general, the colour of the Meguma Group rocks in the LaHave River area varies from green near the lithostratigraphical base through black to grey at the lithostratigraphical top. Sandstones become less notable towards the top of the green beds and the top of the grey beds.

STRUCTURE

The major structures affecting the Meguma Group are outlined by the trace of the lithostratigraphical units (Fig. 2). The major folds generally trend southwest and plunge gently. Individual folds with wavelengths from 1-5 km can be followed for distances in excess of 35 km along their axial traces (Fig., 2, 9). Sinuous tracers are a result of the major folds being asymmetrical or polyclinal and changing their shape both parallel and perpendicular to the plunge (Fig. 9). A conspicious feature of some of the major folds in unit 3A is the fact that the fold axes change from being gently plunging to being locally steeply plunging along the axial trace. A vertical slaty cleavage is developed in association with all of the major folds.

Major faults produce lineaments which can be recognized on the ground and on aerial photographs and magnetic

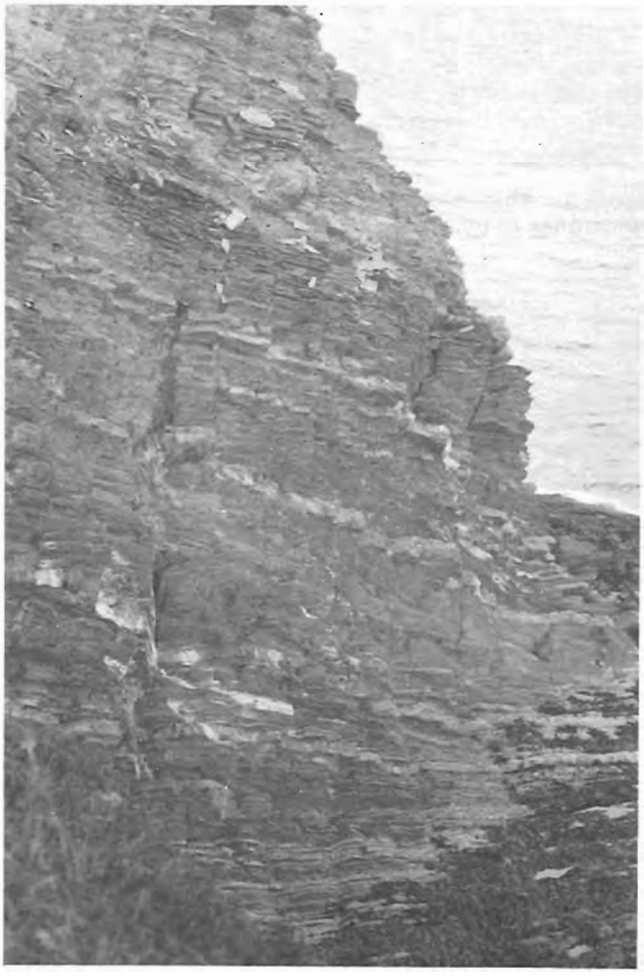

Figure 7. Black slates and rust-weathered, grey sandstones of unit 3A.

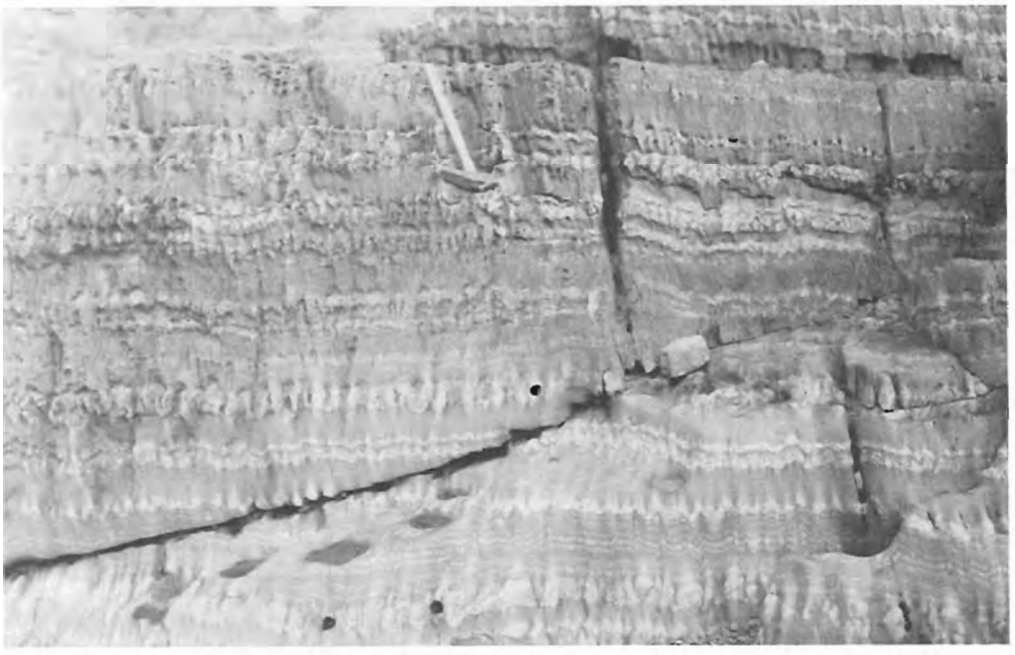

Figure 8. Grey slates and laminated to thin bedded, buff-weathered sandstones of unit 3B.

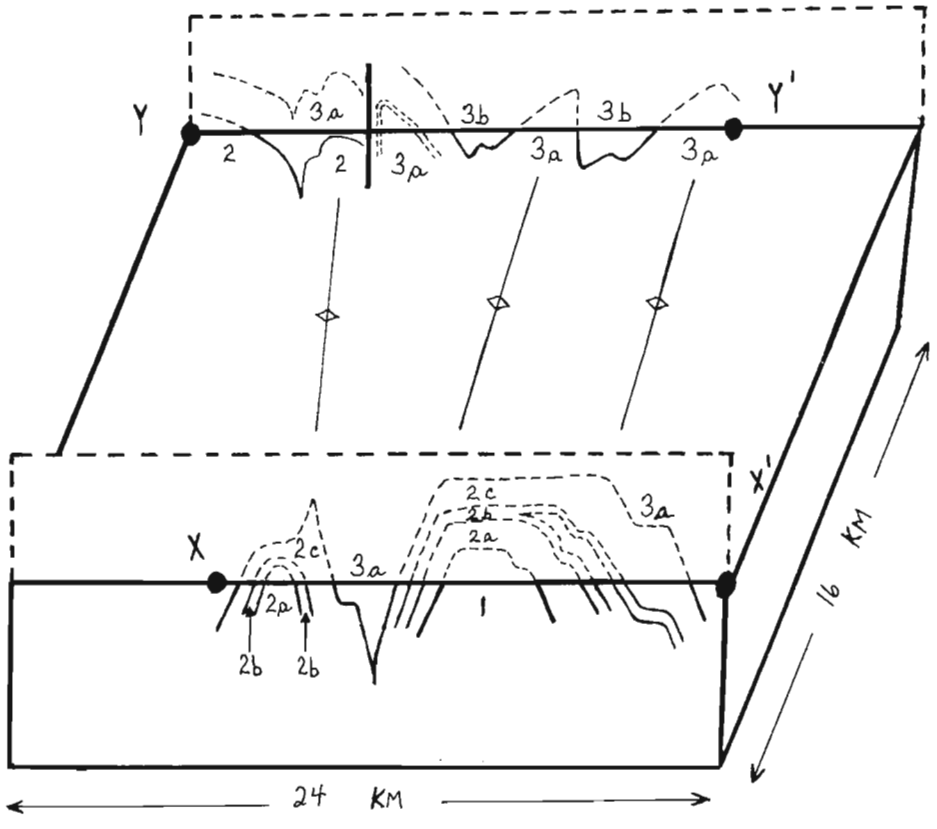

Figure 9. Block diagram illustrating representative cross-sections of the LaHave River area at XX′ and YY′ (Fig. 2). Vertical scale exaggerated.

gradiometer maps of the area. Most faults are subvertical, offset the major folds and have a large strike-slip displacement (e.g., Fig. 9). Kindred minor structures include joints, kink folds and fracture cleavage.

In certain localities there is evidence to suggest that the strata have been tilted, cleaved, and veined prior to the development of the major folds and the regional slaty cleavage.

METAMORPHISM

Regional dynamothermal metamorphism is witnessed by the preferred alignment of chlorites and white micas along the slaty cleavage. Garnet is present in concretions in the manganiferous beds of unit 2C.

Contact metamorphism is restricted to a narrow zone of recrystallization in the wall rock of a fine to medium grained, equigranular, intermediate to basic dyke found on the LaHave Islands (Fig. 2).

Hydrothermal alteration is associated with some of the sulphide-rich quartz veins in the Meguma Group.

MINERAL COMMODITIES

Visible gold is present in the LaHave River area in sulphide-bearing quartz veins injected into the black slates and pyritiferous grey sandstones of unit 3A. Two fundamental types of auriferous quartz veins are distinguishable. The first type is 'laminated', stratabound veins that are folded around some of the major folds. The second type is 'fissure' veins emplaced along faults which displace the major folds.

Scheelite is found in association with certain auriferous quartz veins. During World War II some of these veins were mined for tungsten.

Thin, stratiform, Mn-rich laminae occur within the upper beds of unit 2C. Pyrolusite is also found along joints in the rocks and within overlying strata. Both types of Mn occurrences are present in the area enclosed by undivided unit 2 (Fig. 2).

REFERENCES

Faribault, E.R.
1929: Bridgewater Sheet No. 89; Geological Survey of Canada Map.

Hall, L.R.
1981: Geology of the LaHave River area, Lunenburg County, Nova Scotia; Unpublished M.Sc. thesis, Acadia University, Wolfville, N.S., 161 p.

THE MCGERRIGLE PLUTONIC COMPLEX, GASPÉ, QUEBEC: EVIDENCE OF MAGMA MIXING AND HYBRIDIZATION[1]

Project 840021

J.B. Whalen
Precambrian Geology Division

Whalen, J.B., The McGerrigle plutonic complex, Gaspé, Quebec: evidence of magma mixing and hybridization; in *Current Research, Part A, Geological Survey of Canada, Paper 85-1A, p. 795-800, 1985.*

Abstract

The small (100 km²) Devonian age McGerrigle plutonic complex can be roughly subdivided into a granite and hybrid suites. The granite suite is relatively compositionally homogeneous, whereas the hybrid suite exhibits a large compositional spectrum from gabbro to granite. The hybrid suite is heterogeneous on both a large and an outcrop scale and exhibits spectacular evidence for the coexistence and mixing of mafic and felsic magmas. The mixing features have implications not only for the petrogenesis of this plutonic complex and its associated mineralization but also have a bearing on the controversy of restite unmixing versus magma mixing as the cause of chemical dispersion in granite suites.

Résumé

Le complexe plutonique de McGerrigle, de faible étendue (100 km²) et datant du Dévonien, peut être grossièrement subdivisé en deux suites, l'une granitique et l'autre hybride. La suite granitique présente une composition assez homogène, tandis que l'autre renferme une large variété de roches plutoniques, du gabbro au granite. L'hétérogénéité de la suite hybride s'observe autant dans les affleurements que sur une grande échelle; ici, la coexistence et l'hybridation de magmas mafiques et felsiques se révèlent de façon très nette. Cette manifestation de l'assimilation magmatique peut contribuer à expliquer la pétrogenèse du complexe plutonique et des minéralisations qui lui sont associées, mais elle alimente aussi la controverse entre ceux qui invoquent l'immobilité des restites et ceux qui favorisent plutôt l'assimilation magmatique pour expliquer la dispersion chimique dans les suites granitiques.

INTRODUCTION

Magma mixing, an old concept which has been applied to many types of magmas, has recently received prominent attention as applied to calc-alkaline volcanic associations (Eichelberger, 1975, 1978; Anderson, 1976). Although it has been reported from some plutonic associations (Wiebe, 1974, 1980; Walker and Skelhorn, 1966; Whalen and Currie, in press) magma mixing has received much less attention than restite unmixing (White and Chappell, 1977; 1983; Chappell, 1978; Compston and Chappell, 1979) and crystal fractionation (Bateman and Chappell, 1979; McCarthy and Hasty, 1976) as a cause of chemical dispersion in granites.

The McGerrigle plutonic complex in the Gaspé Peninsula, Quebec (Fig. 1) consists of a large compositional spectrum of plutonic rocks, many of which exhibit spectacular small and large scale evidence of mixing of mafic and felsic magmas. This paper documents these features and discusses their implications.

GENERAL GEOLOGY

The McGerrigle plutonic complex covers a rugged area of about 100 km² in the Gaspé segment of the north-central Appalachian orogenic belt (Fig. 1). This discordant, Devonian (de Romer, 1974) intrusion produced a striking 1.5 to 3 km wide aureole of hornfels and skarn in its host rocks, the Cambro-Ordovician Shickshock and Quebec groups.

The complex can be roughly subdivided into granite and hybrid suites. The bulk of the granite suite occurs in the southern portion of the pluton, but there are areas of mainly granitic rocks in the northern half and granites are also mixed in with the hybrid suite (Fig. 1). The relatively compositionally homogeneous granite suite has been subdivided into different intrusive phases on the basis of grain size, presence of one or two feldspars and on whether equigranular or porphyritic. Contacts between the phases, which are not shown in Figure 1, appear to be mainly gradational. The hybrid suite, though mainly restricted to the northern half of

[1]Contribution to the "Plan de développement économique Canada/ Gaspésie et Bas Saint-Laurent."

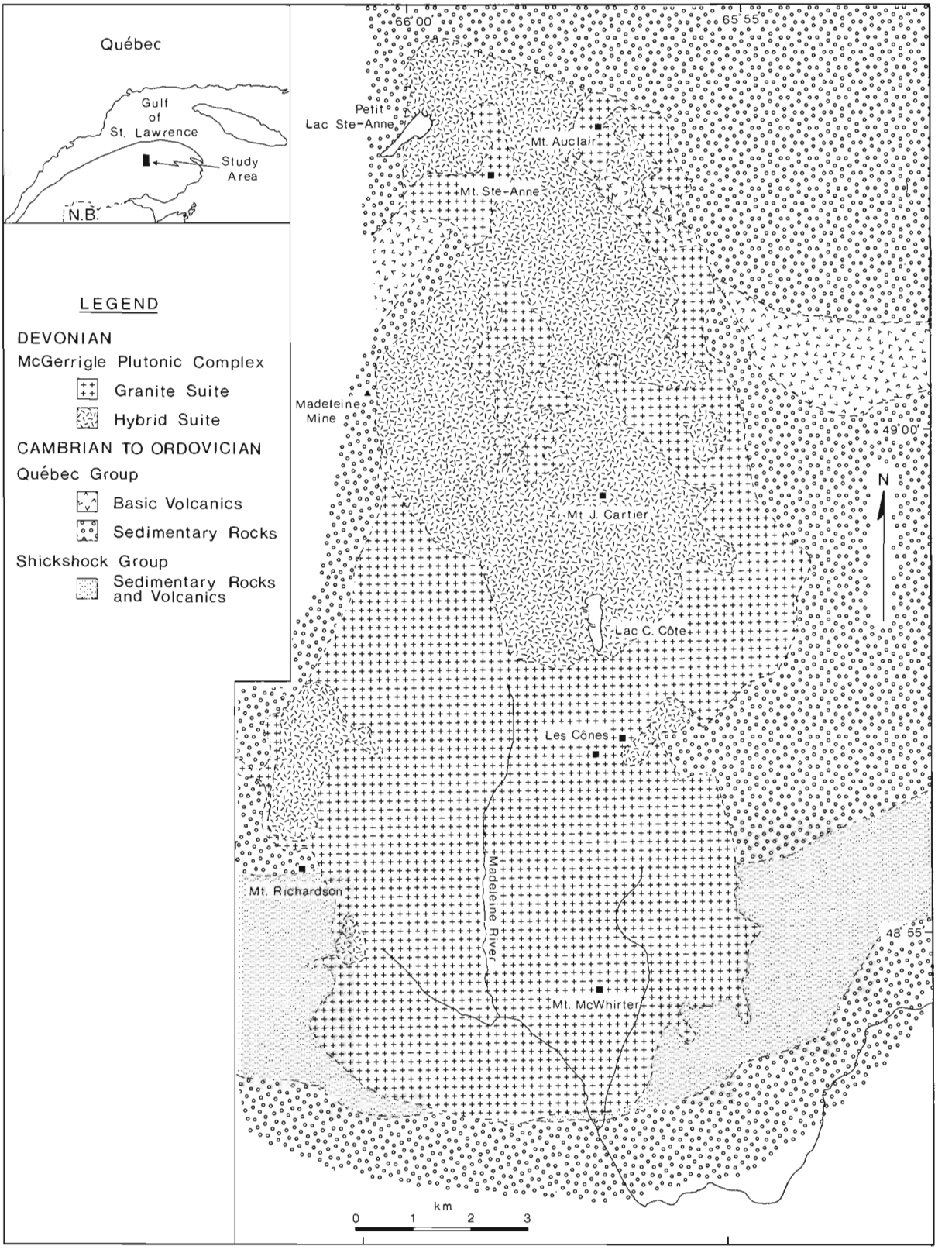

Figure 1. Location of the McGerrigle plutonic complex, Gaspé, Quebec and a generalized geological map of the area.

the pluton, does outcrop north and southeast of Mount Richardson and east of Les Cones (Fig. 1). The suite consists of a geologically complex and compositionally diverse mixture of gabbro, basalt, diorite, quartz diorite, granodiorite, monzonite, quartz monzonite, syenite, quartz syenite, and granite. Although on a scale of 1:25 000 some portions of the hybrid suite have been subdivided into compositionally homogeneous intrusive units, the most striking feature of the suite is its heterogeneity on both an outcrop scale and larger. Even though in most cases the compositionally more mafic rocks appear to be older and included in the felsic rocks, the nature of the contacts suggests that they formed from contemporaneous magmas. Evidence of magma mixing and hybridization within the suite are described below. Field relationships between the hybrid and granite suites are ambiguous. The hybrid suite includes a component lithologically identical to the granite suite rocks and contacts between the two suites appear to be gradational in most areas, being marked by the appearance of mafic inclusions in the granite. However, there are also examples of sharp intrusive relationships between younger granite and hybrid suite rocks. Although apparently volumetrically insignificant, it is notable that in the northern portion of the pluton there are nephline syenite dykes which cut hybrid rocks and also small areas of nepheline syenite which have irregular, probably gradational contacts with the hydrid rocks. This suggests that an undersaturated magma may have been contemporaneous with the magma or magmas that produced the hydrid suite.

DESCRIPTION OF OCCURRENCES

In contrast to much of the pluton, relationships in the hyybrid suite are well exposed on the trail to Mount Jacques-Cartier, along a road above Madelaine Mine, on a trail up Mount Auclair and in a roadcut near Petit Lac Ste-Anne. Of particular interest are the contact relationships between the mafic and felsic components in the hybrid suite. Although fairly large areas of coarse grained gabbro are not uncommon, where mafic and felsic intrusive rocks are in contact, the mafic rocks are almost invasriably fine grained. This appears to be due to chilling of a higher temperature mafic magma in a lower temperature felsic magma. Features such as chilled margins on mafic inclusions (Fig. 2, 3), pillow-like structures of chilled basaltic rock in granite (Fig. 4), highly cuspated irregular margins of mafic inclusions in granite (Fig. 5) and broken-up mafic dykes cutting granite (Fig. 6) indicate the coexistence of mafic and felsic magmas. There are also features such as vesiculated mafic inclusions in granite. On outcrop scale, there is abundant evidence for hybrid rocks produced by mixing (Fig. 7, 8, 9). The field relationships are complex and indicate multiple injection and hybridization.

DISCUSSION

The McGerrigle plutonic complex exhibits convincing observational evidence both for the coexistence of mafic and salic magmas and for mixing of magmas to produce more or less homogeneous hybrids. Similar features have been described elsewhere (eg. Walker and Skelhorn, 1966; Wiebe, 1980; Whalen and Currie, in press). Most of the diversity of igneous rock types in the hybrid suite may reflect magma mixing processes, though it is not clear whether more than a basaltic and a granitic magma were involved. Chemical and petrological work in progress should help to resolve this problem. Previous work by de Romer (1977) recognized the presence of the complex and diverse suite of rocks contained in the hybrid suite and that this suite reflected and probably

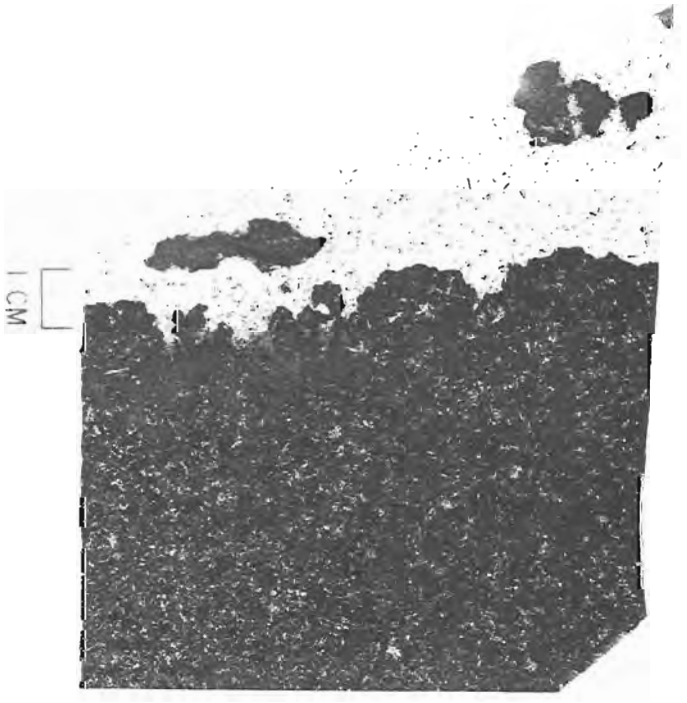

Figure 2. Contact between white, medium grained granite and medium grained gabbro. Note the irregular cuspated contact and the very fine grained "droplets" of basalt in the granite; Mount Auclair trail. (GSC 204184-B)



Figure 3. Basaltic inclusion in medium grained pink syenite, note the chilled margin and the "bread crust" chilling features on the inclusion; Mount Jacques-Cartier trail. (GSC 204123-O)



Figure 4. Pillow-like structures exhibited by basalt included in pink, medium grained granite. Note that there is a thin intermediate composition reaction rim on the inclusions; Mount Auclair trail. (GSC 204123-G)



Figure 6. Broken-up basaltic dyke cutting medium grained white biotite-amphibole granite; Mount Jacques-Cartier trail. (GSC 204123-P).

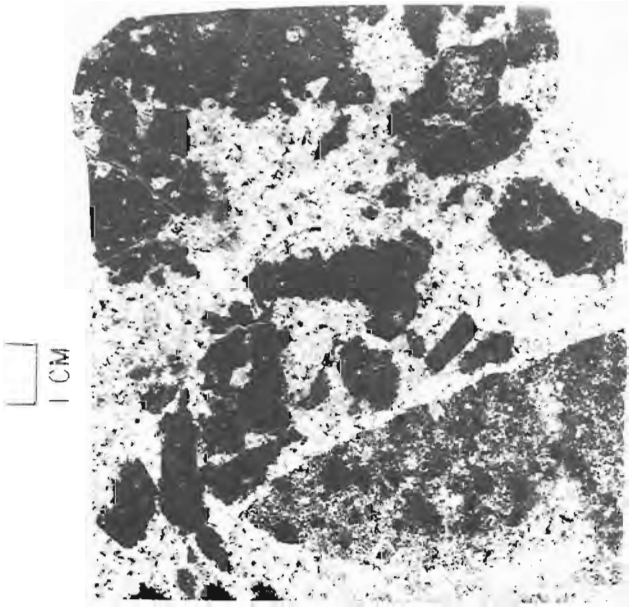

Figure 5. Fine grained mafic inclusions in white, medium grained granite. Note the highly irregular cuspated margins to the inclusions, the composite, angular, intermediate hybrid granite inclusion (lower part of photo) which contains small partially digested mafic inclusions and the mafic inclusion (top right of photo) which contains an inclusion of hybrid granite; roadcut by Petit Lac Ste-Anne. (GSC 204184)

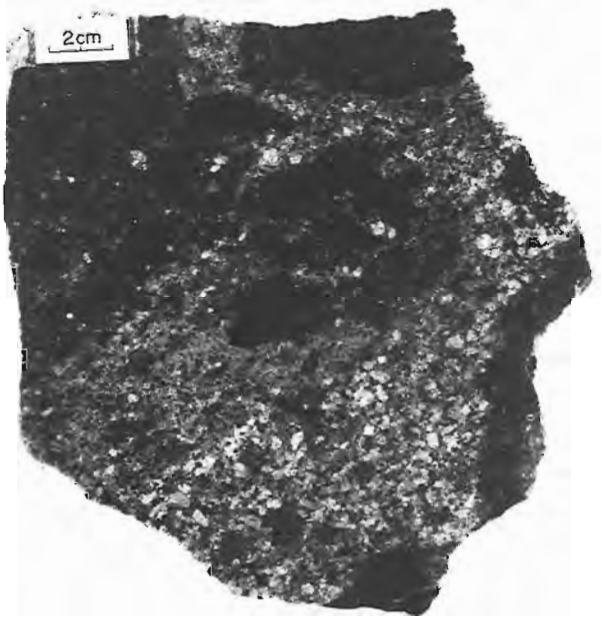

Figure 7. Mafic inclusions in red, medium- to fine-grained granite. The inclusions are largely digested and surrounded by a fine grained, more mafic (hybridized) granite; Mount Jacques-Cartier trail. (GSC 204065-W).

resulted from interaction between mafic and felsic compositions. He did not, however, recognize the evidence for coexistence of magmas, but instead considered the fine grained mafic rocks to be derived from similar parent volcanic and pyroclastic rocks and the coarse grained basic rocks to represent portions of an older mafic intrusion. Recognition of the magma mixing and hybridization features in the McGerrigle plutonic complex is obviously central to an understanding of the formation of the suite and also to other aspects such as dating by the Rb-Sr method. Although the initial ratio may not be very significant, isochrons which include the acid and mafic end members and hybrids can give precise ages for a suite generated by magma mixing (Whalen et al., in prep.). The presence of contemporaneous mafic and felsic magmas



Figure 8. Irregular "pillow-like" contact between diorite (lower right and left of photo) and white, medium grained granite crosscut by granite containing abundant chilled "droplet-like" basalt inclusions; roadcut by Petit Lac Ste-Anne. (GSC 204123).



Figure 9. Complex relationships between mafic to felsic intrusive rocks: a quartz diorite (right side) has an irregular cuspated margin with quartz monzonite (middle) which contains angular, broken-up inclusions of mafic rock (left side). The quartz monzonite, where adjacent to the gabbroic rock, is more mafic and later granitic veins or dyklets crosscut the outcrop; Madelaine Mine road. (GSC 204123-L).

in the McGerrigle pluton is similar to other Devonian igneous suites in the area, such as the bimodal volcanic rocks of the York River Formation, around Mount Lyall and Mount Tuzo. Although it contains a wide spectrum of intrusive rock compositions, the McGerrigle plutonic complex is not a calc-alkaline plutonic suite such as those formed at destructive plate margins (eg. Sierra Nevada and Southern California batholiths). Bimodal suites are generally considered to be typical of extensional tectonic environments.

It is notable that the copper mineralization associated with the pluton occurs in its northern portion at Madelaine Mine, and around Mount Auclair, areas where spectacular features of magma mixing are well exposed. Mixing of a high temperature mafic melt with a granitic magma would be expected to generate a superheated hybrid magma. This hot, probably fairly water-rich magma, would be a very good thermal source to drive a mineralizing hydrothermal system; also, a mafic magma is generally considered to be a better source of copper than a granite.

The restite model (White and Chappell, 1977, 1983; Chappell, 1978; Compston and Chappell, 1979) is a mixing model which has been applied to plutonic rocks. According to this model, granite magmas may be considered as mixtures of refractory solid source residue (restite) and relatively felsic melt. Chemical evolution takes place by unmixing of these two components. Granites, thought to be compositionally controlled by restite separation processes, generally contain mafic xenoliths and clotty mafic mineral aggregates, and exhibit straight-line chemical variation on Harker variation diagrams. The restite model has recently come under increasing criticism. Re-examination of a well exposed part of the Moruya suite of eastern Australia (the "type minimum melt suite" of Compston and Chappell (1979)) found outcrop features such as scalloped contacts and mutual chilling relations between phases which Vernon et al. (1983) intepreted as indicating that magma mixing and fractional crystallization processes, not restite unmixing, controlled chemical variation in the suite. Clemens et al. (1983) contended that chemical variation in many granite suites of the Lachlan Fold Belt of Australia could largely be explained by source-related characters, crystal-liquid fractionation and hybridization processes. Vernon (1983, 1984), mainly on microstructural evidence, contends that the common microgranitoid enclaves (autoliths, cognate xenoliths, mafic inclusions) in high-level granitoid plutons represent globules of mafic magma that have commingled and quenched in the granitoid host magma.

Features exhibited by the McGerrigle plutonic complex have implications for the controversy of restite unmixing versus magma-mixing. Unlike the Lachlan granites, the McGerrigle pluton exhibits unequivocal evidence for mixing and hybridization of coexisting magmas. The great textural and compositional heterogeneity on a large and small scale exhibited by the small (40 km^2) McGerrigle hybrid suite is in very marked contrast to the voluminous (some in excess of 1000 km^2), compositionally restricted, and homogeneous on a large scale "restite controlled" granite suites in the Lachlan Fold Belt. The features of the McGerrigle plutonic suite probably reflect essentially *in situ* magma mixing and hybridization processes and can be visualized as resembling a marble cake or taffy in water. Although this may in part reflect the high-level nature of the mixing process, the poor degree of mixing exhibited by the McGerrigle hybrid suite indicates there may be serious problems in generating relatively homogeneous mixtures on the scale of a batholith. The restite model avoids this difficulty because the mafic restite component is initially embedded in the magma, and needs no mixing. In a discussion of the problem of magma mixing, Whalen and Currie (in press) deduce that tectonic shearing must be the main mechanism in nature of achieving large scale homogenization. A compressive regime such as a destructive plate margin should be a better environment to

achieve large scale mixing than a tensional environment such as that in which the McGerrigle pluton apparently occurs. Nevertheless, some composite model such as the "modified" restite model of Hildreth (1981) may be a more viable model for granitic rocks than magma mixing alone. Hildreth suggested that rising granitoid diapirs consist of felsic melt, refactory source material, and a network of basaltic bodies intruding and hybridizing the salic melt. The "restite" inclusions, according to this model, might represent either remnants of injected basalt, or refractory residues of the source material. Further, the source material could be hybrid, rather than the uniform source implicitly assumed in the original restite model of White and Chappell (1977).

ACKNOWLEDGMENTS

Graeme Wallace and Scott Greene provided able assistance in the field.

REFERENCES

Anderson, A.T.
1976: Magma mixing: petrological process and volcanological tool; Volcanology and Geothermal Research, v. 1, p. 3-33.

Bateman, P.C. and Chappell, B.W.
1979: Crystallization, fractionation, and solidification of the Tuolumne Intrusive Series, Yosemite National Park, California; Geological Society of America, Bulletin 90, p. 465-482.

Chappell, B.W.
1978: Granitoids from the Moonbi District, New England Batholith, Eastern Australia; Journal Geological Society Australia, v. 25, p. 267-283.

Clemens, J.D., Wall, V.J. and Clarke, B.D.
1983: Models for granitoid evolution and source compositions: restite - R.I.P.; *in* Lithosphere Dynamics and Evolution of Continental Crust; Geological Society Australia Abstracts, v. 9, p. 178-179.

Compston, W. and Chappell, B.W.
1979: Strontium isotope evolution of granitoid source rocks; *in* The Earth: Its Origin, Structure and Evolution, ed. M.W. McElhinny; Academic Press; p. 377-424.

de Romer, H.S.
1974: Geology and age of some plutons in north-central Gaspe, Canada; Canadian Journal of Earth Sciences, v. 11, p. 570-582.

1977: McGerrigle Mountains area; Quebec Ministry of Natural Resources, Geological Report 174, 233 p.

Eichelberger, J.G.
1975: Origin of andesite and dacite: evidence of mixing at Glass Mountain in California and at othere circum-Pacific volcanoes; Geological Society of America, Bulletin 86, p. 1381-1391.

1978: Andesitic volcanism and crustal evolution; Nature, v. 275, p. 21-27.

Hildreth, E.W.
1981: Gradients in silicic magma chambers: implications for lithospheric magmatism; Journal of Geophysical Research, v. 86, p. 10153-10192.

McCarthy, T.S., and Hasty, R.A.
1976: Trace element distribution patterns and their relationship to the crystallization of granitic melts; Geochimica Cosmochimica Acta, v. 40, p. 1351-1358.

Vernon, R.H.
1983: Restite, xenoliths and microgranitoid enclaves in granites; Journal and Proceedings, Royal Society of New South Wales, v. 116, p. 77-103.

1984: Microgranitoid enclaves in granites - globules of hybrid magma quenched in a plutonic environment; Nature, v. 309, p. 438-439.

Vernon, R.H., Etheridge, M.A. and Wall, V.J.
1983: Magma mixing in the development of metaluminous granitoid suites of the Moruya Batholith around Tuross Head, N.S.W.; *in* Lithosphere Dynamics and Evolution of Continental Crust; Geological Society of Australia Abstracts, v. 9, p. 185.

Walker, G.P.L. and Skelhorn, R.R.
1966: Some associations of acid and basic igneous rocks; Earth Science Reviews, v. 2, p. 93-109.

Whalen, J.B. and Currie, K.L.
in press: The Topsails igneous terrane, Western Newfoundland: evidence of magma mixing; Contributions to Mineralogy and Petrology, accepted June, 1984.

White, A.J.R. and Chappell, B.W.
1977: Ultrametamorphism and granitoid genesis; Tectonophysics, v. 43, p. 7-22.

1983: Granitoid types and their distribution in the Lachlan Fold Belt, southeastern Australia; Geological Society of America, Memoir 159, p. 21-34.

Wiebe, R.A.
1974: Coexisting intermediate and basic magmas, Ingonish, Cape Breton Island; Journal of Geology, v. 82, p. 74-87.

1980: Commingling of contrasted magmas in the plutonic environment: examples from the Nain Anorthosite Complex; Journal of Geology, v. 88, p. 197-209.

Author Index

	Page
Aitken, J.D.	603
Ames, D.	761
Anderson, T.W.	239
Anglin, C.D.	193
Annesley, I.R.	259
Ashton, K.E.	527
Bardoux, M.	333
Bays, A.R.	523
Bell, R.T.	145
Bertram, M.B.	499
Blasco, S.M.	523
Bolton, T.E.	29
Bower, M.E.	517
Brandon, M.T.	543
Brown, R.L.	81
Buchan, K.L.	131
Buchanan, J.R.	555
Cameron, B.E.B.	717
Campbell, F.H.A.	693
Card, K.D.	131
Carr, S.D.	81,89
Cheadle, S.P.	499
Christian, H.	697
Christie, R.L.	629
Clowes, R.M.	543
Conway, K.W.	703
Connare, K.M.	175
Corriveau, L.	165
Cotie, A.A.	779
Coyle, M.	157
Culshaw, N.	555
Cumming, L.M.	215
Currie, K.L.	73,699
Daudier, B.S.	421
Davidson, A.	463
Delorme, L.D.	239
Dietrich, J.R.	613
Digel, M.R.	385
DiLabio, R.N.W.	117
Dixon, J.	613,629
Doucet, P.	69
Dredge, L.A.	181,247
Duggan, D.M.	317
Duke, J.M.	723
Edlund, S.A.	709
Egginton, P.A.	731
Forest, R.	485
Franklin, J.M.	193,761
French, H.M.	111
Frisch, T.	259
Furey, D.J.	151
Gagnon, Y.D.	783
Galley, A.	761
Gandhi, S.S.	359
Gerasimoff, M.D.	327
Ghent, E.D.	69
Gibbons, D.	157,737
Gilbert, R.	505
Gittins, C.A.	259
Graham, B.W.	431
Grant, S.M.	463
Green, A.G.	543
Grégoire, D.C.	223
Goodbody, Q.H.	629
Goodfellow, W.D.	651
Gordon, T.M.	511, 753
Hardwick, C.D.	517
Harms, T.	301
Harris, D.C.	713
Harrison, J.C.	629
Harry, D.G.	111
Henderson, J.B.	441,455
Hildebrand, R.S.	373
Hofmann, H.J.	603
Hood, P.J.	517
Hudson, K.A.	661
Hughes, O.L.	229
Hyndman, R.D.	543
Iannelli, T.R.	639
Jackson, G.D.	639
Jackson, S.L.	511,753
James, D.T.	449
James, N.P.	399
Jamieson, R.A.	783
Jefferson, C.W.	103,203
Jonasson, I.R.	651,661
Kanasewich, E.R.	543
Kirkham, R.V.	203,573
Klassen, R.W.	187
Klepacki, D.W.	273,277
Knight, R.D.	639
Kumarapeli, P.S.	123
Lambert, E.	157
Lawton, D.C.	491,499
Lebel, D.	639
LeCheminant, G.M.	15
Leonard, R.	485
Long, D.G.F.	97
Loveridge, W.D.	65
Lowey, G.E.	97
Luternauer, J.L.	317,703,717
Lydon, J.W.	651,661
Massey, N.W.D.	543
Macfie, R.I.	441
McGrath, P.H.	455
McNeil, D.H.	613
McNutt, R.H.	175
Mercer, B.	737
Monger, J.W.H.	349
Moran, K.	697
Morency, M.	123
Mountjoy, E.W.	341,485
Mott, R.J.	239
Mwenifumbo, C.J.	651
Nadeau, L.	463
Nance, D.	7
Narbonne, G.M.	603
Nelson, W.E.	203
Nielsen, E.	247
O'Brien, B.H.	789
Orchard, M.J.	287

	Page
Parrish, R.	81
Pedder, A.E.H.	587
Percival, J.A.	1, 385
Pickerill, R.K.	699
Pintson, H.	123
Poley, D.F.	491,523
Pollard, W.H.	111
Pryer, L.L.	463
Read, P.B.	273
Reedman, J.H.	203
Ricketts, B.D.	609
Rimsaite, J.	47
Roberts, M.C.	717
Rogers, H.D.	773
Root, K.G.	727
Roots, C.F.	373
Ross, G.M.	681
Ross, J.R.P.	29
Roscoe, S.M.	141
Ruzicka, V.	15,145
St-Onge, D.A.	181
Scammell, R.J.	311
Schau, M.	527
Schwarz, E.J.	421
Scoates, R.F.J.	303
Sexton, A.J.	779
Sharpe, D.R.	365
Simony, P.S.	69
Smith, S.	229
Smith, T.L.	681
Spencer, C.	543
Stephens, L.E.	431
Stern, R.A.	385
Stevens, R.K.	399
Stevenson, R.K.	23
Strong, D.F.	157,739
Struik, L.C.	267,305
Sutherland-Brown, A.	543
Syvitski, J.P.M.	505
Tarnocai, C.	229
Tanoli, S.K.	699
Taylor, F.C.	65
Taylor, R.B.	505
Teitz, M.	341
Teskey, D.J.	517
Thompson, D.L.	555
Thompson, P.H.	555
Thorpe, R.I.	713
Tirrul, R.	407
Vaillancourt, P.D.	743
Vreeken, W.J.	187
Whalen, J.B.	795
Wheeler, J.O.	273,277
Williams, H.	399
Williams, H.F.L.	717
Wilton, D.H.C.	737
Woods, D.V.	533
Yorath, C.J.	543
Zaleski, E.	511

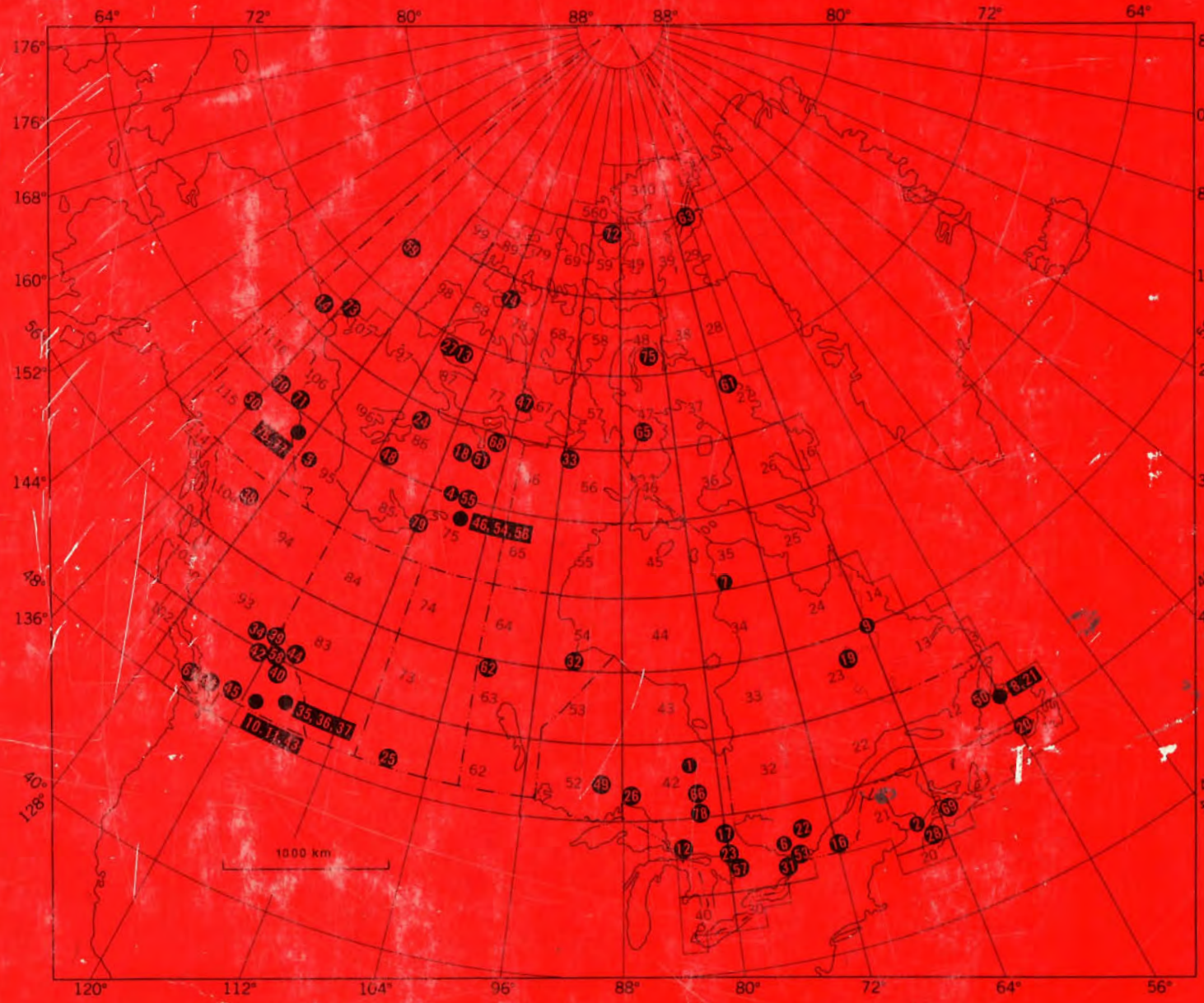

Numbers on index map refer to Scientific and Technical Reports in this volume

Energy, Mines and Resources Canada
Énergie, Mines et Ressources Canada